Patai Series:
The Chemistry of Functional Groups

Series Editor: Zvi Rappoport

Volume Editor: Jacob Zabicky

The Chemistry of Metal Enolates

Part 1

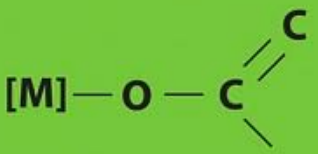

Patai Series online:
http://www.interscience.wiley.com

WILEY

An Interscience® Publication

The chemistry of
Metal Enolates

Part 1

Edited by

JACOB ZABICKY

Ben-Gurion University of the Negev

2009

A John Wiley and Sons, Ltd., Publication

An Interscience® Publication

The chemistry of

Metal Enolates

Patai Series: The Chemistry of Functional Groups

A series of advanced treatises founded by Professor Saul Patai and under the general editorship of Professor Zvi Rappoport

The **Patai Series** publishes comprehensive reviews on all aspects of specific functional groups. Each volume contains outstanding surveys on theoretical and computational aspects, NMR, MS, other spectroscopic methods and analytical chemistry, structural aspects, thermochemistry, photochemistry, synthetic approaches and strategies, synthetic uses and applications in chemical and pharmaceutical industries, biological, biochemical and environmental aspects.
To date, over 120 volumes have been published in the series.

Recently Published Titles

The chemistry of the Cyclopropyl Group (Volume 2)
The chemistry of the Hydrazo, Azo and Azoxy Groups (Volume 2, 2 parts)
The chemistry of Double-Bonded Functional Groups (Volume 3, 2 parts)
The chemistry of Organophosphorus Compounds (Volume 4)
The chemistry of Halides, Pseudo-Halides and Azides (Volume 2, 2 parts)
The chemistry of the Amino, Nitro and Nitroso Groups (2 volumes, 2 parts)
The chemistry of Dienes and Polyenes (2 volumes)
The chemistry of Organic Derivatives of Gold and Silver
The chemistry of Organic Silicon Compounds (2 volumes, 4 parts)
The chemistry of Organic Germanium, Tin and Lead Compounds (Volume 2, 2 parts)
The chemistry of Phenols (2 parts)
The chemistry of Organolithium Compounds (2 volumes, 3 parts)
The chemistry of Cyclobutanes (2 parts)
The chemistry of Peroxides (Volume 2, 2 parts)
The chemistry of Organozinc Compounds (2 parts)
The chemistry of Anilines (2 parts)
The chemistry of Organomagnesium Compounds (2 parts)
The chemistry of Hydroxylamines, Oximes and Hydroxamic Acids (2 parts)

Forthcoming Titles

The chemistry of Organocopper Compounds

The Patai Series Online

Since 2003 the **Patai Series** is available in electronic format on Wiley InterScience. All new titles will be published as online books and a growing list of older titles will be added every year. It is the ultimate goal that all titles published in the **Patai Series** will be available in electronic format.
For more information see under **Online Books** on:

www.interscience.wiley.com

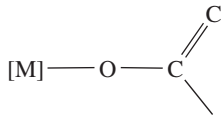

The chemistry of
Metal Enolates

Part 1

Edited by

JACOB ZABICKY

Ben-Gurion University of the Negev

2009

A John Wiley and Sons, Ltd., Publication

An Interscience® Publication

John Wiley & Sons Ltd, The Atrium, Southern Gate, Chichester,
West Sussex PO19 8SQ, England

Telephone (+44) 1243 779777

Email (for orders and customer service enquiries): cs-books@wiley.co.uk
Visit our Home Page on www.wiley.com

Other Wiley Editorial Offices

John Wiley & Sons Inc., 111 River Street, Hoboken, NJ 07030, USA

Jossey-Bass, 989 Market Street, San Francisco, CA 94103-1741, USA

Wiley-VCH Verlag GmbH, Boschstr. 12, D-69469 Weinheim, Germany

John Wiley & Sons Australia Ltd, 42 McDougall Street, Milton, Queensland 4064, Australia

John Wiley & Sons (Asia) Pte Ltd, 2 Clementi Loop #02-01, Jin Xing Distripark, Singapore 129809

John Wiley & Sons Canada Ltd, 6045 Freemont Blvd, Mississauga, Ontario, L5R 4J3, Canada

Wiley also publishes its books in a variety of electronic formats. Some content that appears in print may not be available in electronic books.

Library of Congress Cataloging-in-Publication Data:

The chemistry of metal enolates / edited by Jacob Zabicky.
p. cm.—(Patai series: the chemistry of functional groups)
"Available in electronic format on Wiley InterScience."
Includes bibliographical references and index.
ISBN 978-0-470-06168-8 (cloth : alk. paper) 1. Organometallic compounds. 2. Enols. I. Zabicky, Jacob.
QD411.C46 2009
547′.05–dc22

2009001886

British Library Cataloguing in Publication Data

A catalogue record for this book is available from the British Library

ISBN 978-0-470-06168-8

Typeset in 9/10pt Times by Laserwords Private Limited, Chennai, India
Printed and bound in Great Britain by MPG Biddles Limited, Kings Lynn, Norfolk
This book is printed on acid-free paper responsibly manufactured from sustainable forestry in which at least two trees are planted for each one used for paper production.

Dedicated to

Judith
for the best things life can give

Tali and David
for the realizations of the present

Yael, Noa, Danielle and Jehonathan
for the promise of the future

Contributing authors

Juan Andrés	Departament de Química Física y Analítica, Universitat Jaume I, 12071 Castelló, Spain Fax: +34-96-4728066; e-mail: andres@qfa.uji.es
Ksenija Babić-Samardžija	Chemistry Department, Rice University, 6100 Main St., Houston, TX 77005, USA Present address: Baker Hughes Incorporated, 12645 West Airport Blvd., Sugar Land, TX 77478, USA Fax: +1-281-276-5491; e-mail: ksenija.babic@bakerpetrolite.com
Shmuel Bittner	Department of Chemistry, Ben-Gurion University of the Negev, P.O. Box 653, Beer-Sheva 84105, Israel Fax: +972-77-7575886; e-mail: bittner@bgu.ac.il
Hermi Felinto Brito	Department of Fundamental Chemistry, University of São Paulo, São Paulo-SP, 05508-000, Brazil Fax: +55-11-3815-5579; e-mail: hefbrito@iq.usp.br
Roy Buschbeck	Technische Universität Chemnitz, Fakultät für Naturwissenschaften, Institut für Chemie, Lehrstuhl für Anorganische Chemie, Strasse der Nationen 62, 09111 Chemnitz, Germany Fax: +49-371/531-21219; e-mail: roy.buschbeck@chemie.tu-chemnitz.de
Paola Deplano	Università di Cagliari, Dipartimento di Chimica Inorganica e Analitica, S.S. 554-Bivio per Sestu, I09042 Monserrato-Cagliari, Italy Fax: +39-706754456; e-mail: deplano@unica.it
Luis R. Domingo	Departament de Química Orgánica, Universitat de Valencia, Dr. Moliner 50, 46100 Burjassot, Valencia, Spain Fax: +34-96-3544328; e-mail: domingo@utopia.uv.es
Jason Eames	Department of Chemistry, University of Hull, Cottingham Road, Kingston upon Hull, HU6 7RX, England Fax: +44-1482-464610; e-mail: j.eames@hull.ac.uk
Maria Claudia França Cunha Felinto	Institute of Nuclear Energy and Research, Av. Prof Lineu Prestes 2242 Cidade Universitária, São Paulo-SP. 05508-000, Brazil Fax: +55-11-3133-9249; e-mail: mfelinto@ipen.br

Eli Harlev — Department of Chemistry, Ben-Gurion University of the Negev, P.O. Box 653, Beer-Sheva 84105, Israel
Fax: +972-8-9956713; e-mail: harleve@bezeqint.net

Robert Jérôme — Center for Education and Research on Macromolecules (CERM), University of Liège, Sart-Tilman, B6a, 4000 Liège, Belgium
Fax: +32-4-3663497; e-mail: rjerome@ulg.ac.be

Vladislava M. Jovanović — ICTM-Institute of Electrochemistry, University of Belgrade, Njegoševa 12, P.O. Box 473, 11000 Belgrade, Serbia
Fax: +381-11-337-0389; e-mail: vlad@tmf.bg.ac.rs

Uli Kazmaier — Department of Organic Chemistry, Saarland University, D-66123 Saarbrücken, Germany
Fax: +49-681-3022409; e-mail: u.kazmaier@mx.uni-saarland.de

Heinrich Lang — Technische Universität Chemnitz, Fakultät für Naturwissenschaften, Institut für Chemie, Lehrstuhl für Anorganische Chemie, Strasse der Nationen 62, 09111 Chemnitz, Germany
Fax: +49-371/531-21219; e-mail: heinrich.lang@chemie.tu-chemnitz.de

Philippe Lecomte — Center for Education and Research on Macromolecules (CERM), University of Liège, Sart-Tilman, B6a, 4000 Liège, Belgium
Fax: +32-4-3663497; e-mail: rjerome@ulg.ac.be

Joel F. Liebman — Department of Chemistry and Biochemistry, University of Maryland, Baltimore County, 1000 Hilltop Circle, Baltimore, Maryland 21250, USA
Fax: +1-410-455-2608; e-mail: jliebman@umbc.edu

Oscar Manoel Loureiro Malta — Department of Fundamental Chemistry, Federal University of Pernambuco, CCEN Cidade Universitária, Recife-PE, 50670-901, Brazil
Fax: +55-81-21268442; e-mail: oscar@renami.com.br

M. Laura Mercuri — Università di Cagliari, Dipartimento di Chimica Inorganica e Analitica, S.S. 554-Bivio per Sestu, I09042 Monserrato-Cagliari, Italy
Fax: +39-706754456; e-mail: mercuri@unica.it

Li-June Ming — Department of Chemistry and Institute for Biomolecular Science, University of South Florida, 4202 E. Fowler Avenue, CHE205 Tampa, Florida 33620-5250, USA
Fax: +1-813-974-1733; e-mail: ming@shell.cas.usf.edu

Guido Pampaloni — Università di Pisa, Dipartimento di Chimica e Chimica Industriale, Via Risorgimento 35, I-56126 Pisa, Italy
Fax: +39-50-2219-246; e-mail: pampa@dcci.unipi.it

Luca Pilia — Università di Cagliari, Dipartimento di Chimica Inorganica e Analitica, S.S. 554-Bivio per Sestu, I09042 Monserrato-Cagliari, Italy
Fax: +39-706754456; e-mail: pilialuc@unica.it

Katelyn A. Provencher	Department of Chemistry, Bates College, Lewiston, Maine 04240, USA Fax: +1-207-786-8336; e-mail: twenzel@bates.edu
Angela Serpe	Università di Cagliari, Dipartimento di Chimica Inorganica e Analitica, S.S. 554-Bivio per Sestu, I09042 Monserrato-Cagliari, Italy Fax: +39-0706754456; e-mail: serpe@unica.it
Mitsuru Shindo	Institute for Materials Chemistry and Engineering, Kyushu University, Kasuga-koen, Kasuga 816–8580, Japan Fax: +81-92-583-7875; e-mail: shindo@cm.kyushu-u.ac.jp
Suzanne W. Slayden	Department of Chemistry, George Mason University, 4400 University Drive, Fairfax, Virginia 22030, USA Fax: +1-703-993-1055; e-mail: sslayden@gmu.edu
Sofija P. Sovilj	Faculty of Chemistry, University of Belgrade, Studentski trg 12–16, P.O. Box 158, 11001 Belgrade, Serbia Fax: +381-11-2184-330; e-mail: ssovilj@chem.bg.ac.rs
Daniel Stolz	Department of Organic Chemistry, Saarland University, D-66123 Saarbrücken, Germany Fax: +49-681-3022409; e-mail: u.kazmaier@mx.uni-saarland.de
Ercules Epaminondas de Sousa Teotonio	Department of Chemistry, Federal University of Paraíba Cidade Universitária, Paraíba-PB, 58051-900, Brazil Fax: +55-83-3216-7437; e-mail: teotonioees@quimica.ufpb.br
José Vicente	Grupo de Química Organometálica, Departamento de Química Inorgánica, Facultad de Química, Universidad de Murcia, Apdo. 4021, 30071 Murcia, Spain Fax: +34-868887785; e-mail: jvs1@um.es; http://www.um.es/gqo/
Thomas J. Wenzel	Department of Chemistry, Bates College, Lewiston, Maine 04240, USA Fax: +1-207-786-8336; e-mail: twenzel@bates.edu
Stephen A. Westcott	Department of Chemistry, Mount Allison University, Sackville, NB E4L 1G8, Canada Fax: +1-506-364-2313; e-mail: swestcott@mta.ca
Jacob Zabicky	Department of Chemical Engineering, Ben-Gurion University of the Negev, P.O. Box 653, Beer-Sheva 84105, Israel Fax: +972-8-6472969; e-mail: zabicky@bgu.ac.il
Piero Zanello	Università di Siena, Dipartimento di Chimica, Via De Gasperi 2, I-53100 Siena, Italy Fax: +39-577-234254; e-mail: zanello@unisi.it

Foreword

The present book, *The Chemistry of Metal Enolates*, is unique in 'The Chemistry of Functional Groups' series (Editor-in-chief Zvi Rappoport), for various reasons: (i) the name of the functional group may be a misnomer, as it points to metallorganic compounds derived from deprotonated enols, but the actual structure may preferentially be organometallic, derived from an α-ketocarbanion; (ii) it does not belong to the group of recently published volumes *The Chemistry of Organolithium Compounds, The Chemistry of Organozinc Compounds* and *The Chemistry of Organomagnesium Compounds*, because the scope of the book covers both organic and inorganic chemistry subjects, related to metals over the entire periodic table of the elements, rather than a single metal; (iii) the range of applications focuses not mainly on organic synthesis, but extends to inorganic synthesis and important aspects of modern technology such as catalysis, polymers, metal and oxide deposition, luminescence, electronic and magnetic devices; and (iv) this is the first book ever published dedicated to multiple aspects of the metal enolates. The literature coverage is mostly up to 2007 and the beginning of 2008.

The two parts of the present volume contain seventeen chapters written by experts from eleven countries. They cover computational chemistry, structural chemistry by spectroscopic methods, luminescence, thermochemistry, synthesis, various aspect of chemical behavior such as application as synthons, acid-base properties, coordination chemistry, redox behavior, electrochemistry, analytical chemistry and biological aspects of the metal enolates. Chapters are devoted to special families of compounds, such as the metal ynolates and 1,2-thiolenes and, besides their use as synthons in organic and inorganic chemistry, chapters appear on applications of metal enolates in structural analysis as NMR shift reagents, catalysis, polymerization, electronic devices and deposition of metals and their oxides.

Abbreviations for ligands are used profusely in the field of metal enolates, in a style depending on the author's speciality and personal taste. For example, organic chemists would write 'THF' for tetrahydrofuran, while coordination chemists would usually prefer 'thf'; certain ligands have more than one abbreviation in use. No attempt was made to have a uniform abbreviation style over the entire book, but in each chapter authors adhered to a unique style. Furthermore, under the title 'List of abbreviations used', a few pages below, appear the abbreviations for functional groups and chemical concepts in use in 'The Chemistry of Functional Groups' series, based mainly on IUPAC recommendations. Several new abbreviations were introduced in the present volume, which are expected to gain general acceptance, where 'f' is added at the end of the regular abbreviation to denote a perfluorinated group; for example, Mef (CF_3), Phf (C_6F_5) and Acf (CF_3CO).

Regretfully, the planned chapters on supramolecular structure of metal enolates and the magnetic properties of metal 1,2-enediolates were not delivered. I will be grateful to readers who draw attention to mistakes or omissions in the present volume, and to new topics which deserve to be included in a future volume on the metal enolates.

JACOB ZABICKY

Beer-Sheva, Israel, December 2008
Department of Chemical Engineering
Ben-Gurion University of the Negev

The Chemistry of Functional Groups Preface to the series

The series 'The Chemistry of Functional Groups' was originally planned to cover in each volume all aspects of the chemistry of one of the important functional groups in organic chemistry. The emphasis is laid on the preparation, properties and reactions of the functional group treated and on the effects which it exerts both in the immediate vicinity of the group in question and in the whole molecule.

A voluntary restriction on the treatment of the various functional groups in these volumes is that material included in easily and generally available secondary or tertiary sources, such as Chemical Reviews, Quarterly Reviews, Organic Reactions, various 'Advances' and 'Progress' series and in textbooks (i.e. in books which are usually found in the chemical libraries of most universities and research institutes), should not, as a rule, be repeated in detail, unless it is necessary for the balanced treatment of the topic. Therefore each of the authors is asked not to give an encyclopaedic coverage of his subject, but to concentrate on the most important recent developments and mainly on material that has not been adequately covered by reviews or other secondary sources by the time of writing of the chapter, and to address herself or himself to a reader who is assumed to be at a fairly advanced postgraduate level.

It is realized that no plan can be devised for a volume that would give a complete coverage of the field with no overlap between chapters, while at the same time preserving the readability of the text. The Editors set themselves the goal of attaining reasonable coverage with moderate overlap, with a minimum of cross-references between the chapters. In this manner, sufficient freedom is given to the authors to produce readable quasi-monographic chapters.

The general plan of each volume includes the following main sections:

(a) An introductory chapter deals with the general and theoretical aspects of the group.

(b) Chapters discuss the characterization and characteristics of the functional groups, qualitative and quantitative methods of determination including chemical and physical methods, MS, UV, IR, NMR, ESR and PES — as well as activating and directive effects exerted by the group, and its basicity, acidity and complex-forming ability.

(c) One or more chapters deal with the formation of the functional group in question, either from other groups already present in the molecule or by introducing the new group directly or indirectly. This is usually followed by a description of the synthetic uses of the group, including its reactions, transformations and rearrangements.

(e) Additional chapters deal with special topics such as electrochemistry, photochemistry, radiation chemistry, thermochemistry, syntheses and uses of isotopically labeled compounds, as well as with biochemistry, pharmacology and toxicology. Whenever applicable, unique chapters relevant only to single functional groups are also included (e.g. 'Polyethers', 'Tetraaminoethylenes' or 'Siloxanes').

This plan entails that the breadth, depth and thought-provoking nature of each chapter will differ with the views and inclinations of the authors and the presentation will necessarily be somewhat uneven. Moreover, a serious problem is caused by authors who deliver their manuscript late or not at all. In order to overcome this problem at least to some extent, some volumes may be published without giving consideration to the originally planned logical order of the chapters.

Since the beginning of the Series in 1964, two main developments have occurred. The first of these is the publication of supplementary volumes which contain material relating to several kindred functional groups (Supplements A, B, C, D, E, F and S). The second ramification is the publication of a series of 'Updates', which contain in each volume selected and related chapters, reprinted in the original form in which they were published, together with an extensive updating of the subjects, if possible, by the authors of the original chapters. Unfortunately, the publication of the 'Updates' has been discontinued for economic reasons.

Advice or criticism regarding the plan and execution of this series will be welcomed by the Editors.

The publication of this series would never have been started, let alone continued, without the support of many persons in Israel and overseas, including colleagues, friends and family. The efficient and patient co-operation of staff-members of the Publisher also rendered us invaluable aid. Our sincere thanks are due to all of them.

The Hebrew University
Jerusalem, Israel

SAUL PATAI
ZVI RAPPOPORT

Sadly, Saul Patai who founded 'The Chemistry of Functional Groups' series died in 1998, just after we started to work on the 100th volume of the series. As a long-term collaborator and co-editor of many volumes of the series, I undertook the editorship and I plan to continue editing the series along the same lines that served for the preceding volumes. I hope that the continuing series will be a living memorial to its founder.

The Hebrew University
Jerusalem, Israel
May 2000

ZVI RAPPOPORT

Contents

List of abbreviations used[a]

Ac	acetyl (MeCO)
acac	acetylacetonate
Acf	trifluoroacetyl (CF_3CO, MefCO, Tfa)
Ad	adamantyl
AIBN	azoisobutyronitrile (aibn)
Alk	alkyl
Alkf	perfluoroalkyl
All	allyl
Allf	pentafluoroallyl
An	anisyl[b]
Ar	aryl
Bn	benzyl ($PhCH_2$)
Bu	butyl (C_4H_9)[b]
Buf	nonafluorobutyl (C_4F_9)[b]
Bz	benzoyl (PhCO, C_6H_5CO)
c-	cyclo (-*c*)[c]
CD	circular dichroism
CI	chemical ionization
CNDO	complete neglect of differential overlap
Cp	η^5-cyclopentadienyl anion (C_5H_5)
Cp*	η^5-pentamethylcyclopentadienyl anion (C_5Me_5)
DABCO	1,4-diazabicyclo[2.2.2]octane (dabco)
DBN	1,5-diazabicyclo[4.3.0]non-5-ene (dbn)
DBU	1,8-diazabicyclo[5.4.0]undec-7-ene (dbu)
DIBAH	diisobutylaluminum hydride (dibah)
DIBAlH	diisobutylaluminum hydride (dibalh)
DME	1,2-dimethoxyethane (dme)
DMF	*N*,*N*-dimethylformamide (dmf)
DMSO	dimethyl sulphoxide (dmso)
dr	diastereomeric ratio
DTA	differential thermal analysis
DTG	differential thermogravimetric/thermogravimetry

E-	*entgegen*
ee	enantiomeric excess
EI	electron impact
EPR	electron paramagnetic resonance
ESCA	electron spectroscopy for chemical analysis
ESR	electron spin resonance
Et	ethyl (C_2H_5)
Etf	pentafluoroethyl (C_2F_5)
eV	electron volt
Fc	ferrocenyl ($CpFeC_5H_4$)
FD	field desorption
FI	field ionization
FT	Fourier transform
Fu	furyl (OC4H3)[b]
GLC	gas liquid chromatography
Hex	hexyl(C_6H_{13})[b]
Hexf	tridecafluorohexyl(C_6F_{13})[b]
HMPA	hexamethylphosphortriamide (hmpa)
HOMO	highest occupied molecular orbital
HPLC	high performance liquid chromatography
i-	iso (-*i*)[c]
Ip	ionization potential (IP)
IR	infrared
LAH	lithium aluminum hydride ($LiAlH_4$, lah)
LC	liquid chromatography
LCAO	linear combination of atomic orbitals
LDA	lithium diisopropylamide (*i*-Pr_2NLi, lda)
LUMO	lowest unoccupied molecular orbital
M	metal
[M]	metal with unspecified ligands, molecular species in MS[d]
M	parent molecule
Me	methyl (CH_3)
Mef	trifluoromethyl (CF_3)
Mes	mesityl ($C_6H_2Me_3$-2,4,6)
MNDO	modified neglect of diatomic overlap
MO	molecular orbital
MS	mass spectrum/spectrometry
n-	normal (-*n*)[c]
Naph	naphthyl ($C_{10}H_7$)[b]
NBS	*N*-bromosuccinimide
NCS	*N*-chlorosuccinimide
NIR	near infrared
NMR	nuclear magnetic resonance
NOESY	nuclear Overhauser effect spectroscopy

OTf	triflate (TfO, O_3SCF_3, O_3SMef)
Pen	pentyl (C_5H_{11})[b]
Penf	undecafluoropentyl (C_5F_{11})[b]
Ph	phenyl (C_6H_5)
Phf	pentafluorophenyl (C_6F_5)
Pi	phosphoryl (H_2O_3P, PO_3H_2)
Pip	piperidyl ($C_5H_{10}N$)[b]
ppb	parts per billion[e]
ppm	parts per million
ppt	parts per trillion[e]
Pr	propyl (C_3H_7)[b]
Prf	heptafluoropropyl (C_3F_7)[b]
PTC	phase transfer catalysis or phase transfer conditions[d]
Py	pyridine (C_5H_5N, py)
Pyr	pyridyl (NC_5H_4, C_5H_4N)[b]
R	any radical
Rf	any perfluoro radical
r.t.	room temperature (RT)
RT	room temperature (r.t.)
s-	secondary (-*s*)[c]
SAM	self-assembled monolayer
SBH	sodium boron hydride ($NaBH_4$, sbh)
SET	single electron transfer
SOMO	singly occupied molecular orbital
t-	tertiary (-*t*)[c]
TCNE	tetracyanoethylene (tcne)
TFA	trifluoroacetic acid (CF_3CO_2H, $MefCO_2H$, AcfOH)
Tfa	trifluoroacetyl (CF_3CO, MefCO, Acf)
TfO	triflate (OTf, CF_3SO_3, $MefSO_3$)
TG	thermogravimetric/thermogravimetry
TGA	thermogravimetric analysis
THF	tetrahydrofuran (thf)
Thi	thienyl (SC_4H_3, C_4H_3S)[b]
TLC	thin layer chromatography
TMEDA	*N*,*N*,*N*′,*N*′-tetramethylethylenediamine (tmeda)
TMS	trimethylsilyl or tetramethylsilane[d]
Tol	tolyl (MeC_6H_4, C_6H_4Me)[b]
Tos	tosyl (*p*-toluenesulphonyl, 4-$TolSO_2$)
Ts	tosyl (*p*-toluenesulphonyl, 4-$TolSO_2$)
Trityl	triphenylmethyl (Ph_3C, CPh_3)
UV-vis	ultraviolet–visible
Vi	vinyl (C_2H_3)
Vif	trifluorovinyl (C_2F_3)

XRD	X-ray diffraction
XRF	X-ray fluorescence
Xyl	xylyl ($Me_2C_6H_3$, $C_6H_3Me_2$)[b]
Z-	*zusammen*

[a] Other entries in the following sources can also be used in their unabbreviated or acronym forms, both in the text and in formulae instead of explicitly drawn structures: 'List of Radical Names' in *IUPAC Nomenclature of Organic Chemistry*, 1979 Edition, Pergamon Press, Oxford, 1979, p. 305–322; (http://www.acdlabs.com/iupac/nomenclature/79/r79_1036.htm); 'Acronyms and abbreviations' in the general section of *IUPAC Gold Book* (http://goldbook.iupac.org/list_s.html).
[b] Can be modified by prefixed or suffixed letters or numbers to denote a specifc isomer.
[c] This modifier can be used as prefix or suffix of functional groups in full text or abbreviated form.
[d] This ambiguity should be dispelled by the context.
[e] U.S.A. style: 1 billion $= 1 \times 10^9$, 1 trillion $= 1 \times 10^{12}$.

CHAPTER 1

General and theoretical aspects of the metal enolates

LUIS R. DOMINGO

Departament de Química Orgánica, Universitat de Valencia, Dr. Moliner 50, 46100 Burjassot, Valencia, Spain
Fax: +34 96 3544328; e-mail: domingo@utopia.uv.es

and

JUAN ANDRÉS

Departament de Química Física y Analítica, Universitat Jaume I, 12071 Castelló, Spain
Fax: +34 96 4728066; e-mail: andres@qfa.uji.es

Dedicated to Professor Ramón Mestres on the occasion of his retirement

The chemistry of metal enolates
Edited by Jacob Zabicky

I. GENERAL ASPECTS

The term enolate is applied to an anionic structure with two carbon atoms bound through a double bond and one of them attached to a negatively charged oxygen atom through a single bond, as in structure **1** in equation 1. This structure does not describe properly the electronic distribution of the anion and a resonance hybrid is assumed between the enolate **1** and carbanion **2**, where the negative charge is located on the α-carbon atom. In any case the enolate anion is accompanied by a cationic counterion, generally a metal ion, and the compound can be referred to as a metal enolate.

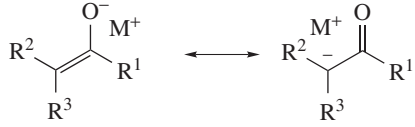

(**1**) (**2**) (1)

Deprotonation at the α-carbon atom of a parent carbonylic compound by an adequate base (equation 2) is the most general method, though not exclusive, for generation of metal enolates, thus they frequently are presented as activated forms of their carbonylic precursors.

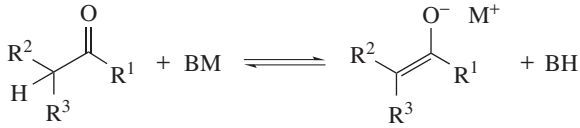

(2)

Metal enolates have basic character, behaving as ambident nucleophiles, and most synthetically valuable reactions of enolates take advantage of the fact that they frequently react with electrophiles through their anionic carbon atom, rather than through the oxygen atom. Selectivity depends both on the nature of the metal ion and the electrophile. Basicity, nucleophilicity and redox potential all depend on both the structure of the enolate and on the accompanying metal ion. Oxidizing reagents can remove one electron of enolates, although synthetic applications of the generated radicals are less common. Regarding the metal, Li(I), Na(I), K(I), Mg(II) and Zn(II) are met while others are rare. Some significant substituent groups of **1** and **2** are shown in Table 1. Their accessibility depends on the availability of their parent carbonyl compound and on the compatibility of their anionic character with reactive sites in the molecule. Geometric *E* and *Z* isomers are possible,

TABLE 1. Some significant groups attached to the enolate structure **1** and **2**

Group type	R^1, R^2 or R^3
H	H
C-substituents	
non-π-delocalizing	alkyl, allyl, propargyl, benzyl
π-delocalizing	alkenyl (e.g. $-CH{=}CH_2$), alkynyl (e.g. $-C{\equiv}CH$), aryl, hetaryl
π-electron-withdrawing	acyl, alkoxycarbonyl, cyano, nitro
O-substituents	anionic oxygen ($-O^-$), alkoxy, acyloxy ($-O_2CR$)
N-substituents	alkylamino ($-NR_2$), acylamino ($-NRC(=O)R'$), *N*-hetaryl onium salt
P-substituents	phosphino (e.g. $-PPh_2$), phosphinium (e.g. $-P^+Ph_3$), phosphonate ($-P(=O)(OR)_2$)
X-substituents	fluoro, chloro, bromo, iodo

whenever R^2 and R^3 are different and R^1 cannot have a second anionic oxygen, as would happen on double deprotonation of a carboxylic acid.

The presence of alkenyl or alkynyl groups at C1 are not relevant on the reactivity of the enolate, while regioselectivity questions arise in reaction with electrophiles when they are placed at C2. Similarly, electron-withdrawing groups located at C2 modify very significantly both the basicity and the nucleophilicity of the enolate anion, while their effect is less significant when they are placed at the C1. O-substituents usually are found at the C1 center when the enolate derives from a carboxylic acid, ester or anhydride and similarly N-substituents from amides. P-substituents at C2 are met in the Wittig and related reactions, whereas the halo groups, most frequently chloro, are found at C2 in the Darzens reaction.

The present chapter focuses on theoretical aspects of the metal enolates and the references are up to the end of 2006. It is clear from the present review that theoretical approaches based on semiempirical, *ab initio* or/and density functional theory (DFT) methods contribute enormously in the study of structure and reactivity of metal enolates. Combination of experimental data, such as spectroscopic and kinetic measurements, and theoretical results allows an understanding of phenomena which in most cases is not feasible from experimental results alone. The chapter is organized into three sections intended to be useful and timely points of entry to the literature of their particular subject Firstly, some relevant theoretical studies devoted to the structure of the metal enolates in solution will be presented, including formation of aggregates. In the second part, theoretical spectroscopic data obtained by calculations are confronted with the experimental data, and they are used to characterize these species in solutions. Specifically, NMR shields are sensitive to the chemical environments of an atom, and therefore, they are used to find specific behaviors of a particular aggregate. Finally, the third part gathers the reactivity of the metal enolates as bases or nucleophile species. The carbanionic character of the enolates enables most of the reactions that experiment as nucleophiles, as addition reactions and substitution reactions, to become one of the selected type of reactions which allow the building of the carbon skeleton via a C−C bond formation. Some of these relevant reactions are collected in the last section. Each section is written with the aim of being a valuable and timely point of entry to the literature that is being covered.

II. STRUCTURE OF THE METAL ENOLATES

Metal enolates are widely used as building blocks in modern organic synthesis. A thorough understanding of their structure and reactivity is important, particularly since many of these

compounds exist as aggregates in solution and in the solid state. A number of fundamental traits remain unclear, but various aspects of reactivity and regio- and stereoselectivity have been attributed to aggregation. Structural details of metal enolates have been obtained from X-ray crystallographic data. Moreover, the structure and aggregation of these species in solution have been widely studied by using semiempirical and *ab initio* methods.

A. Lithium Enolates

Lithium salts of dianions of unsaturated carboxylic acids can adopt the structure of lithium dienolates, **3** or **4** (equation 3), or lithium salts of oxycarbonyl substituted allyl anions, **5** or **6** (equation 4). In any case these formulations provide an oversimplified view of the structures, as these dianions are expected to form ion pairs and aggregates in weakly polar solvents such as diethyl ether or thf[1].

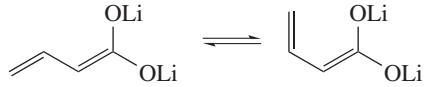

(**3**) *s-trans* (**4**) *s-cis* (3)

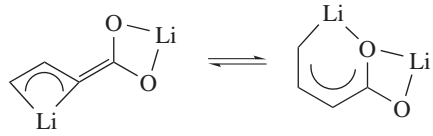

(**5**) *exo* (**6**) *endo* (4)

Bongini and coworkers[2] performed an early *ab initio* (HF/STO-3G)[3] study on the structure of the dienolate of 3-methyl-2-butenoic acid. They found that the ^{13}C NMR spectrum of the corresponding dianion was consistent with a delocalized π system. An *endo* structure (**7**), with a lithium atom placed above the molecular plane and coordinated to one of the oxygen atoms and to both C2 and C4 carbon atoms, was found at the HF/STO-3G computing level. Coordination of each lithium atom with two water molecules, as a model of ether solvent, does not modify substantially the *endo* structure. However, Bongini's model was not capable of explaining the almost exclusive protonation or alkylation processes of the dianion at the C2 center, as the HF/STO-3G calculations give higher negative charge at the C4 center than at the C2 center. Previously, Kaneti, Schleyer and Kos[4] studied the dilithium salt of acetic acid 'dianion' through HF/3-21G calculations and found an 'ate' structure with a lithium atom placed above the molecular plane and coordinated to one of the oxygen atoms and to the C2 center. Again lithium solvation with water did not lead to any important structural change. All these structures showed a higher negative charge at the C center coordinated to the lithium atom.

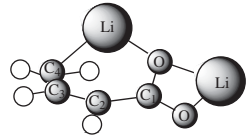

(**7**)

Theoretical studies by Domingo, Mestres and coworkers[5] using semiempirical PM3[6] and *ab initio* HF/3-21G methods confirmed that the dilithium salt of 3-methyl-2-butenoic

'dianion' presents an *endo* conformation in agreement with previous calculations of Bongini[2] at the HF/STO-3G computing level. Further complexation of the lithium atoms with a discrete number of water molecules afforded very similar results to those obtained for the unsolvated species. However, coordination of each lithium atom with three dimethyl ether molecules rendered a planar *s-trans* dienediolate structure (**8**), where each lithium atom is coordinated to four oxygen atoms[5]. The results obtained at the semiempirical PM3 computing level were confirmed by further HF/STO-3G and HF/3-21G *ab initio* calculations[5] of **8**. The charge distribution obtained by the semiempirical PM3 calculations was in agreement with that obtained from ^{13}C NMR data for this lithium 1,3-diene-1,1-diolate[7]. Similar results were obtained for the lithium dianion solvated with thf molecules. A subsequent PM3 semiempirical study[8] of similar methyl-substituted lithium dienediolates, applying both the continuum and the implicit solvation models, emphasizes the importance of including three ether molecules for each lithium atom to obtain structures in good agreement with the experimental ^{13}C NMR spectral data and chemical reactivity.

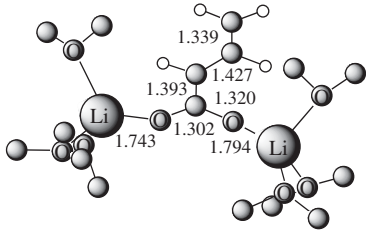

(**8**)

Veya and coworkers[9] found that for M = K the enolates $[Ph_2PCH{=}(Ph){-}O]^-M^+$ and $[Ph_2PCH{=}C(OEt){-}O]^-M^+$ should be much less reactive toward electrophiles (e.g. CO_2, activated alkynes) than for M = Pd[$(NMe_2CHPh)^-$]. These authors performed *ab initio* calculations on both free phosphine enolate anion and when M = Li or Na, to rationalize their reactivity toward electrophiles as a function of their electronic properties.

Three possible geometries, **9**–**11**, were investigated for the Li and Na complexes by using the nonpolarized basis set[9]. Single point energy calculations using the polarized basis set were also performed for the Li phosphine enolate complexes (see Table 2). The computed geometry of **9** was in agreement with the X-ray crystal structure of the title compound and of known Li enolate structure[10–12]. The Li–O bond, however, was longer than the one obtained in similar calculations for the lithium enolate of acetaldehyde[13,14]. The rationale lies in the above mentioned dual interaction of the lithium atom: in the calculations of the lithium enolate of acetaldehyde there is also a lengthening of the Li–O bond when Li has a bridging character. In **10**, where the Li atom is bound only to the oxygen atom, the Li–O bond distance decreases. This structure was considered to check the effect of the conjugation between the phosphorus lone pair and the π system of the enolate moiety (**10′**). The shortening of the Li–O bond and the almost linear arrangement

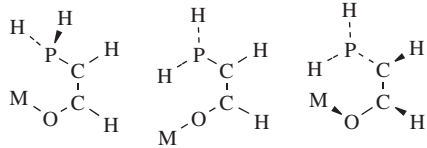

(**9**) (**10**) (**11**)

TABLE 2. Relative energies (in kcal mol^{-1}) of the three optimized geometries of enolates $[PH_2CH{=}CH{-}O]^-$ M^+ (M = Li, Na)

M	Basis set[a]	**9**	**10**	**11**
Li	BS I	0	+9.7	+19.3
Li	BS II	0	+13.9	+14.6
Na	BS I	0	+ll.l	+14.9

[a] BS I denotes the nonpolarized basis set and BS II the polarized one.

of Li−O−C were attributed to the loss of the interaction between Li^+ and the phosphorus lone pair, which is one of the causes for destabilization of **10** (13.9 kcal mol^{-1} with the polarized basis set). Another cause is the destabilization of the HOMO of the system, which has considerable P−C antibonding character, **10′**. Structure **11** allows the interaction of the lithium 2s orbital with both the oxygen atom lone pairs and the π orbital of the carbon−carbon bond. It was derived from a structure computed to be the most stable for the $LiOCH{=}CH_2$ system[13]. As seen in Table 2, **11** turned out to be much less stable than **9**, due in part to the loss of interaction between the phosphine lone pair and the Li^+ empty 2s orbital. The π-type orbitals were quite similar in the free enolate anion (which is highly relevant to the experimental system where the cation has been complexed by a crown ether), in the alkali metal complexes (in their ground state structure **9**) and in the Pd complex. More specifically, the HOMO (which corresponds to the nonbonding orbital of an allylic system) is highly localized on the C2 atom, **9′**.

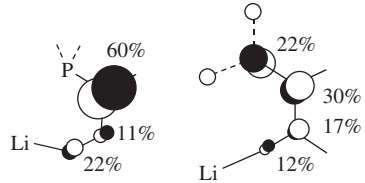

(**9′**) $n\pi$ HOMO (**10′**) $n\pi$ HOMO

Williard and coworkers[15] characterized aggregates of lithium halides with lithium enolates by X-ray crystallography. Two compounds containing both lithium halide and lithium enolate were identified as heterodimers. Using this information, they proposed a reaction sequence for enolization and subsequent aldol addition reactions involving halide-containing aggregates. An *ab initio* (HF/LANL1DZ) theoretical study of model systems showed that solvated heterodimers between LiBr and either $LiNH_2$ (**12**) or $LiOCH{=}CH_2$ (**13**) are favored over the respective homodimers. Single-point MP2/LANL1DZ(POL) energy calculations using the HF/LANL1DZ optimized structures indicate that **13** is only 0.1 kcal mol^{-1} more stable than **12**; in addition, formation of **12** is exothermic, −12.4 kcal mol^{-1}. These facts support the contention that both structures are involved in the reaction sequence[15]. The N−Li bonds were larger in **12** than in the heterodimer **13**, whereas the Li−Br distances were similar: very long, 2.93 Å. This large value and the $Br^{-0.90}$ calculated natural charge at the HF/LANL1DZ(POL) computing level characterize structure **12** as a bromide of the complex cation $[Li(LiNH_2)(NH_3)_4]^+$.

Abbotto, Streitwieser and Schleyer[16] performed an exhaustive study, using the B3LYP[17,18]/6-31+G*//PM3 calculation level, on the effect of dimethyl ether solvation on aggregated forms of the lithium enolate of acetaldehyde $(CH_2{=}CHOLi)_n(Me_2O)_x$,

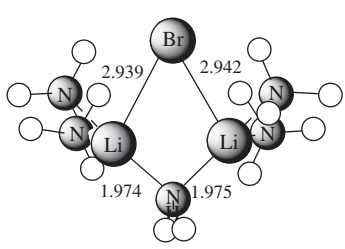

(**12**)

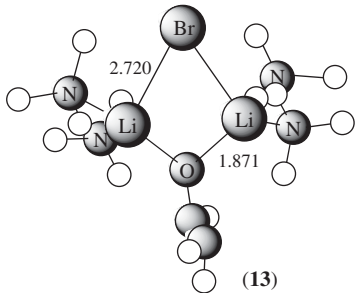

(**13**)

$n = 1–4$, $x = 0–4$. The structures and energies of the aggregates were obtained and the main factors controlling relative stabilities were discussed. Common crystal structure motifs were well reproduced. These authors found that solvation plays a key role in the equilibrium among the aggregated species and the relative stabilities of the tetrameric isomers, but it is balanced by π-interactions between lithium and the enolate double bond. Aggregation and successive solvation energies as well as entropy considerations indicate that solution equilibria are dominated by solvated forms of both monomer **14** and tetramer **15**. The disolvated monomer was remarkably stable; addition of a third solvent was far less exothermic than the first two additions and may not suffice to compensate for the corresponding entropy change. Among the tetramer structures, lithium was tetracoordinated only in the cubic tetramer in its most stable solvated form (**15**). Natural population analysis suggested that polarization rather than delocalization of charge from oxygen into the enolate double bond is the main mechanism of charge distribution. These authors concluded that solvation has a critical role in determining the relative energies of the aggregated species. π-Interaction between Li and the enolate double bond is another factor that helps to determine the relative stabilities of isomers and the degree of solvation. The cubic tetramer **15** is stable because of the electrostatic stabilization of aggregation, but the monomeric species **14** is important in the equilibrium because of its high solvation energies. In contrast, the dimer and, to a greater extent, the trimer are less important. The tendency of lithium cation to reach tetracoordination is shown to be less significant than is commonly believed.

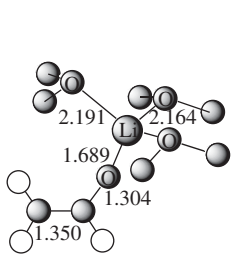

(**14**)

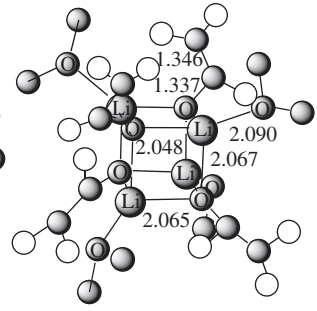

(**15**)

Sgamellotti and coworkers[19] investigated the geometries and electronic structures of lithioacetamide, lithioacetylphosphine, lithioacetophenone and lithiomethylphenylsulfoxide through *ab initio* calculations, including correlation at the MP2 computing level. The different coordination modes, η^1-O (**16**), η^3 (**17**) and η^1-C (**18**), of the lithium center

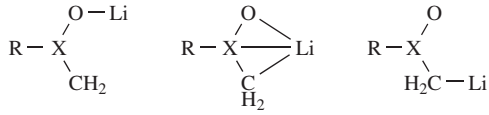

(**16**) (**17**) (**18**)

TABLE 3. Relative energies (in kcal mol^{-1}) of lithium enolates relative to the most stable geometry obtained at different calculation levels[20]

Compound & calculation level	η^1-O (**16**)	η^3 (**17**)	η^1-C (**18**)
Lithioacetamide (R−X = H_2N−C)			
SCF/SV	0.0	1.7	20.8
SCF/DZP	8.0	0.0	18.5
MP2/DZP	9.0	0.0	19.4
Lithioacetylphosphine (R−X = H_2P−C)			
SCF/SV	0.0	10.0	31.4
SCF/DZP	0.9	0.0	20.9
MP2/DZP	2.8	0.0	22.1
Lithioacetophenone (R−X = Ph−C)			
SCF/SV	0.0	6.2	29.4
SCF/DZP	3.4	0.0	21.2
MP2/DZP	5.4	0.0	23.3
Lithiomethylphenylsulfoxide (R−X = Ph−S)			
SCF/SV	14.4	0.0	26.6
SCF/DZP	22.3	0.0	24.3
MP2/DZP	19.6	0.0	21.6

were analyzed. In Table 3 are summarized the energies of three possible coordination patterns of lithium enolates, calculated by various methods. In lithiomethylphenylsulfoxide there is a clear preference for η^3 coordination of lithium with the enolate anion (**17**, R−X = Ph−S), due to delocalization of the negative charge in the enolate fragment on both nucleophilic C and O atoms. It is important to remark that in this anion the delocalization of the negative charge towards the aromatic ring is precluded by the nonplanarity of the sulfoxide group. The situation is different in lithioacetophenone, where the η^1-O (**16**, R−X = Ph−C) and η^3 (**17**, R−X = Ph−C) structures are close in energy. Moreover, the η^3 structure can be seen as a η^1-O one with the lithium also slightly interacting with the carbon center, suggesting that the oxygen is the main nucleophilic center in this enolate anion. The η^1-O (**16**) and η^3 (**17**) coordinations are almost isoenergetic in the lithioacetamide (R−X = H−C) and lithioacetylphosphine (R−X = H_2P−C) systems, where both coordination forms should be stabilized by interaction with the carbon center. Therefore, in these enolate anions, the oxygen atom is the main nucleophilic center, at least as far as the interaction with a lithium cation is concerned. In lithioacetamide the η^3 structure is more stabilized than the η^1-O, suggesting a reduced nucleophilic character of the oxygen center.

Pugh and Streitwieser[20] used semiempirical PM3, *ab initio* (HF/6-31+G(d) and MP2/6-31+G(d)) and density functional calculations (using the perturbative Becke−Perdew model pBP[21,22] together with DN*[23] split valence basis set, both included in the Spartan 5.1 suite of programs) to investigate the rotational barrier of the C−N bond in a simple enolate anion (lithioacetamide, **19**), as shown in Figure 1. For comparison, the amidate anion, vinylamine, and a simulated dimer were also calculated. All the rotational

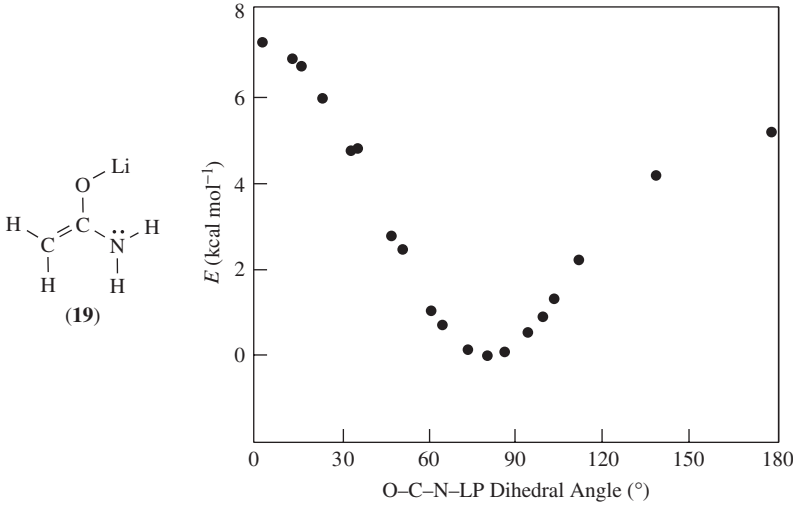

FIGURE 1. Rotation function for the lone pair (LP) of **19** with Li–O–C constrained to 180° at the HF/6-31G(d,s) level. The two barriers are 7.28 and 5.18 kcal mol^{-1}. Reprinted with permission from J. K. Pugh and A. Streitwieser, *J. Org. Chem.*, **66**, 1334. Copyright 2001 American Chemical Society

barriers were less than 10 kcal mol^{-1}, in agreement with the experimental result for *N*,*N*-dimethyldiphenylacetamide[24]. All the computing levels yielded the rotational barrier for the lithium salt **19** somewhat higher than that of the corresponding free anion. The barriers at the correlated levels were somewhat larger than the HF levels, while the PM3 barriers were much lower than the *ab initio* results and are clearly unreliable. Computed geometries and structural changes on rotation were consistent with a model in which conjugation of the amino nitrogen with the double bond was comparable to that in vinylamine, even though charge transfer to an anionic system would be expected to be inhibited and polarization of the double bond is the important feature of the electronic structure.

Pratt and Streitwieser[25] performed *ab initio* (HF/6-31G* and HF/6-311+G*) calculations to examine the formation of mixed dimer and trimer aggregates between the lithium enolate of acetaldehyde (lithium vinyloxide, LiOVi) and lithium chloride, lithium bromide and lithium amides. Gas-phase calculations showed that in the absence of solvation effects, the mixed trimer $(LiOVi)_2$•LiX (**20**) was the most favored species.

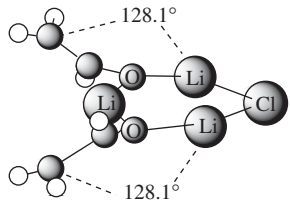

(**20**)

Solvation of lithium enolates in ether solvents was modeled by a combination of specific coordination of dimethyl ether ligands on each lithium and 'dielectric solvation'

followed by immersion of each molecule in a cavity within a continuous dielectric having the dielectric constant of thf at room temperature. Dielectric solvation energies were lower for aggregates (reduced dipoles or quadrupoles) and coordinatively solvated species than for monomers (dipoles). Both specific coordination and dielectric solvation lowered the exothermicity of the aggregation process. In many cases, lithium salts were three- rather than four-coordinate at room temperature. The strongly basic lithium amides preferred forming mixed aggregates with weaker bases instead of homoaggregates[25]. The effects of lithium dialkylamide structure, mixed aggregate formation and solvation on the stereoselectivity of ketone enolization were examined by Pratt and coworkers[26] both experimentally and theoretically using B3LYP/6-31+G* calculations. The results pointed out that lithium tetramethylpiperidide (Litmp) in thf presents the best enolization selectivity. The highest E/Z ratios were obtained with Litmp-butyllithium mixed aggregates in thf, for example R = Bu in equation 5.

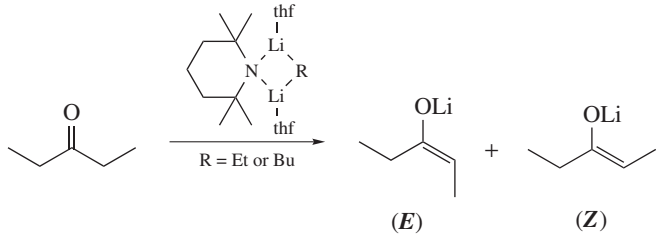

(5)

Equations 6 and 7 show the species in equilibrium in methyl ether solutions containing Litmp, EtLi and acetaldehyde or 3-pentanone, respectively. DFT calculations predicted that such an lda or Litmp system would form mixed cyclic isomers in ether solvents. These results also render that Litmp-alkyllithium mixed aggregates inhibit competitively the formation of less stereoselective Litmp-lithium enolate mixed aggregates. The formation of lithium dialkylamide mixed dimers with ethyllithium was favored by increasing the steric bulk of the lithium amide and by ethereal solvents. The use of microsolvation simulations appeared to be sufficient to represent the solvent effects, as little change in the energies of mixed aggregate formation was found when bulk solvation effects were included. The computational results were consistent with the $^{6}Li-^{15}N$ spin coupling patterns[26].

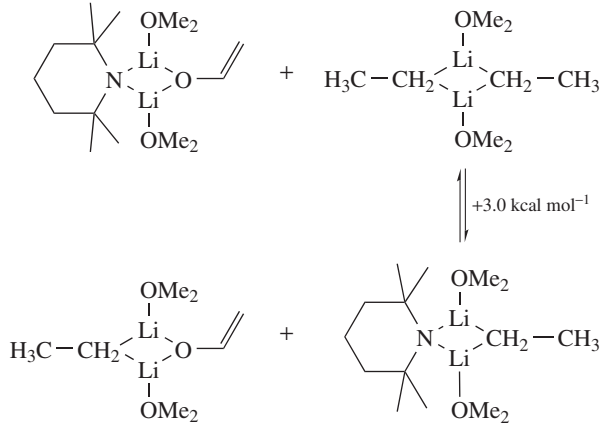

(6)

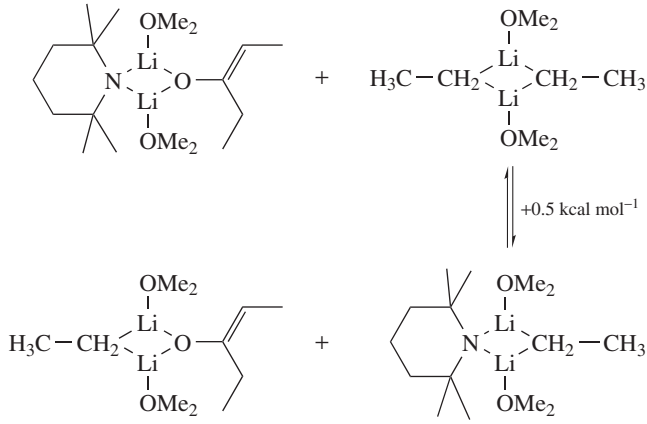

(7)

B. Calcium and Magnesium Enolates

Oviedo and Sanz[27] studied, at the *ab initio* (HF/TZP) level, the adsorption of acetone and 2-propenol on a clean MgO(100) surface model and by means of the embedded-cluster approach in which the environment was described by total ion potentials and point charges. Optimized geometries for both acetone and 2-propenol adsorbed on the surface, **21** and **22**, respectively, were obtained using two basis sets and several cluster models[27]. The adsorbate–surface interaction was found to be weak and electrostatic in nature, although there is a relative stabilization of the enol tautomer. The effect of the surface on the keto–enol equilibrium was analyzed and explained on the basis of this differential adsorption. Surface reconstruction induced by the adsorbate was also considered. While the surface relaxation effects were found to be negligible for acetone, they appear to be larger for 2-propenol, and allowing the surface to relax changes the qualitative description of the enolization process since in this case an enolate species was found to be adsorbed on the surface.

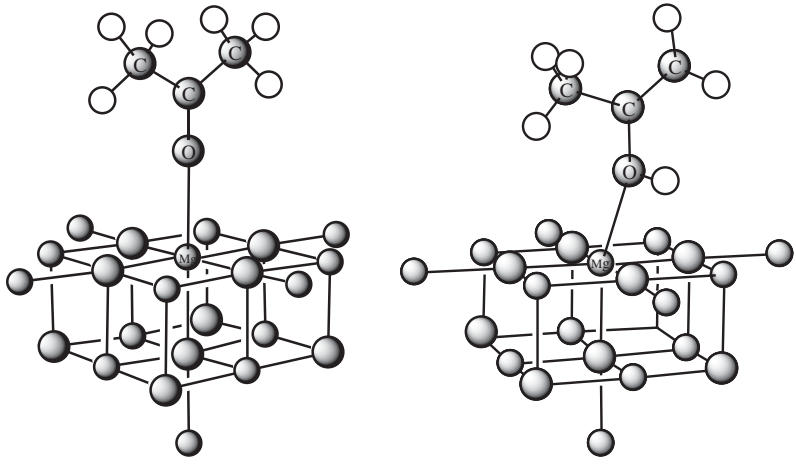

(**21**) (**22**)

The enol form of 3-acetoacetyl-7-methyl-2*H*,5*H*-pyrano(4,3-*b*)pyran-2,5-dione was studied by Fery-Forgues, Lavabre and Rochal[28] both spectroscopically and theoretically using semiempirical PM3 calculations. To analyze its interactions with alkali and alkaline earth perchlorates in acetonitrile, absorption and fluorescence spectroscopies were employed. The presence of salts provokes significant variations in the absorption spectrum and quenching of the fluorescence intensity. The spectrophotometric data, together with NMR and mass spectrometry, showed that in the metal enolate the heterocyclic oxygen atom as well as the two oxygen atoms of the side chain can participate in cation binding, as suggested by semiempirical PM3 calculations of **23** and **24**. The association constants varied over many orders of magnitude, depending on the nature of the salt. The calcium and magnesium complexes were more stable than those usually found for crown-ether-based fluoroionophores in the same solvent.

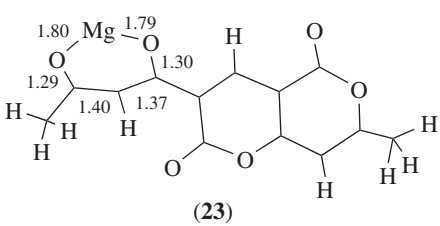

(**23**)

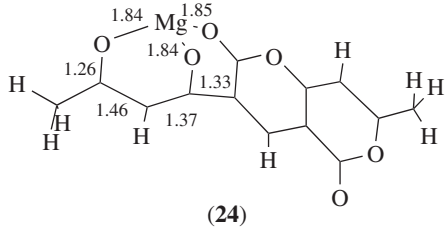

(**24**)

C. Aluminum Enolates

The reactions between trialkylaluminum, R_3Al, and carbonyl-containing species have been the subject of intensive study over many years[29]. These reactions may result in adduct formation, alkylation, reduction or enolate formation, depending on the nature of the ketone and also the alkyl group attached to aluminum (equation 8). Rather surprisingly, there have been relatively few studies on mechanistic and structural aspects of enolization mediated by organoaluminum compounds. In part, this is due to the reported difficulty in the isolation and structural identification of aluminum enolates[30].

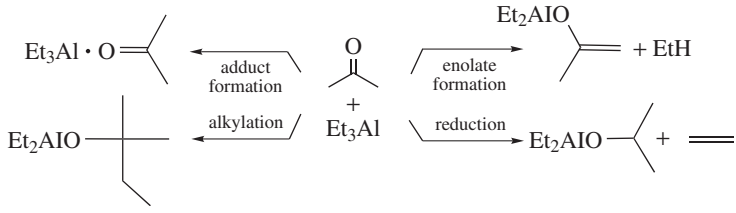

(8)

Henderson and coworkers[31] studied the reaction of Me_3Al with a series of aromatic ketones (**25**, **27**, **29**) to yield the precipitation of either dimethylaluminum enolates or alkoxides (see equations 9–11). *In situ* ^{1}H NMR spectroscopic studies of the reaction between Me_3Al and acetophenone (**29**) revealed a complex mixture of products, whereas under the same conditions 2,4,6-trimethylacetophenone (**25**) reacts cleanly to give the corresponding enolate. The enolate compounds **26** and **28** were isolated and **26** as well as the representative alkoxide **30** were characterized by X-ray crystallography. Both **26** and **30** form dimers with a central Al_2O_2 core. *Ab initio* calculations at the HF/6-31G* level indicated that both **26** and **30** are the thermodynamic products of the reactions[31]. Equation 12 shows the alkylation and enolization reactions for the ketones **25** and **29** and

the relative energies involved for each transformation (dimeric aggregation was assumed for the calculated organometallic species)[32]. Both the alkylation and enolization reactions were highly exothermic for each ketone. However, the enolization route was preferred by 4.70 kcal mol^{-1} for ketone **25**, whereas alkylation was preferred by 25.39 kcal mol^{-1} for ketone **29**. Therefore, the calculations indicated that both **31** and **33**, the dimers of **26** and **30**, were the thermodynamic products of their respective reactions, i.e. the outcome of the reaction (alkylation or enolization) was not necessarily controlled by kinetic factors. Significantly, there is also a large difference in the relative energies within each type of reaction for the ketones. While the energy difference between the enolization reactions was only 6.27 kcal mol^{-1}, the alkylation reactions differed by 23.82 kcal mol^{-1}. The large difference in the relative energies of the alkylation reactions can be attributed to the increased steric bulk of the alkoxide in **32** compared to that in **33**. Steric crowding around the quaternary carbon (O*C*Me$_2$Ar) was significantly greater in **32** compared to **33**, due to the presence of methyl groups in the 2- and 6-positions of the aromatic ring. The difference between the energies of the enolization reactions can be attributed mainly to the higher Bronsted acidity of **25** compared to **29**. The energy required to deprotonate ketones **25** and **29** to form the corresponding enolate anions [MesC(O)=CH$_2$]$^-$ and [PhC(O)=CH$_2$]$^-$ was calculated to be 389.06 and 392.98 kcal mol^{-1}, respectively, i.e. methylation of the aromatic ring increases the acidity of the ketone. The bond lengths associated with the α-carbon (O*C*) decreased significantly comparing the alkoxides and the enolates. As expected, formation of the olefinic bond shortens the C−C bond length and, together with it, also the O–C and C–C(*ipso*) bonds shorten significantly. It is pertinent to note that this contraction is greater for the more substituted anion, i.e. the O–C bonds shorten by 0.078 and 0.064 Å, and the C–C(*ipso*) bonds shorten by 0.063 and 0.045 Å for **31′** and **34′**, respectively. These results support the assessment that steric crowding induced by the *ortho* methyl groups is an important factor in determining the stability of complexes **31** and **34**. The olefinic group of the enolate in **31** sits almost perfectly in the same plane as the dimeric ring (with a torsion angle of 0.0° for Al−O−C−C arrangement between the metal center and the enolate group). When enolate ligands are orthogonal to the Al_2O_2 plane, no local minimum could be found; however, if the enolates are in a *pseudo-syn* orientation with respect to each other, an energy minimum is located, with essentially the same absolute energy as **31′** (with a torsion angle of 19.7° for Al−O−C−C). No minimum was located for an 'in-plane' orientation in **34**. In this case the ligands rotate to adopt staggered conformations with respect to the Al_2O_2 ring (with a torsion angle of 59.5° for Al−O−C−C).

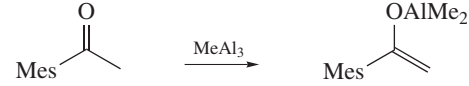

(**25**) (**26**) (9)

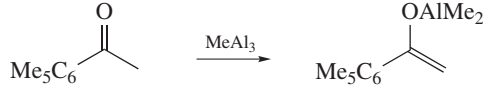

(**27**) (**28**) (10)

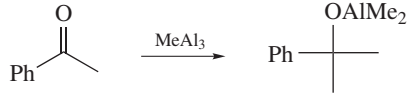

(**29**) (**30**) (11)

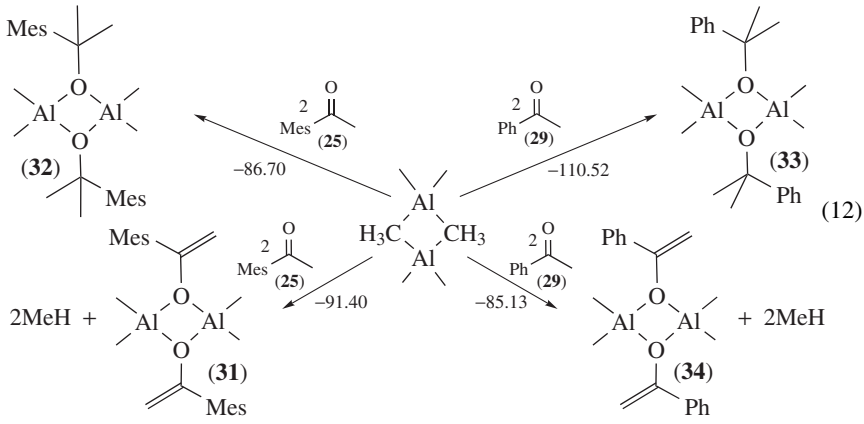

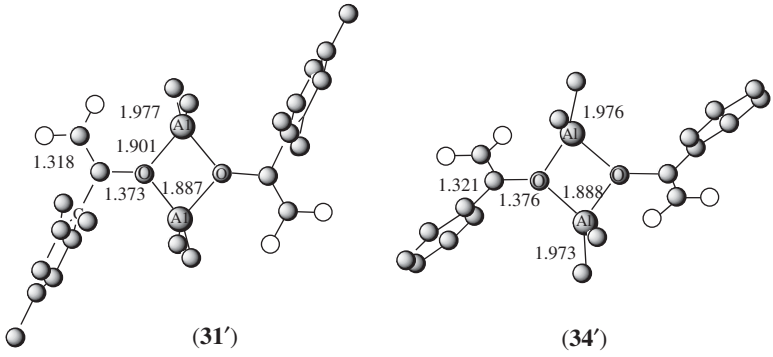

D. Copper and Titanium Enolates

Rosi, Sgamellotti and Floriani investigated by means of *ab initio* calculations the electronic structure and geometry of the trifluorotitanio (TiF_3^+)[33] and phosphinecopper ($CuPH_3^+$)[34] complexes with the enolate anions of acetamide (**35**), acetylphosphine (**36**), acetophenone (**37**) and methylphenylsulfoxide (**38**). The different coordination modes, η^1-O, η^3 and η^1-C, of the TiF_3^+ and $CuPH_3^+$ cations were analyzed (see Scheme 1). For titanium[33], the η^1-O coordination towards the enolate anion was preferred, although in the acetamide enolate anion and the methylphenylsulphoxide enolate anion the η^1-O and η^3 coordinations were almost isoenergetic. The η^1-C coordination was destabilized in all systems. A comparison between TiF_3^+ and Li^+ showed that TiF_3^+ is more oxophilic than Li^+. For copper[34], the η^1-C coordination towards the enolate anion was preferred for acetamide, while the η^3 coordination was the lowest in energy for methylphenylsulfoxide. For the acetylphosphine and the acetophenone enolate anions the η^1-O and η^1-C coordinations were almost isoenergetic, while the η^3 coordination is higher in energy. The comparison between $CuPH_3^+$ and TiF_3^+ interacting with the same enolate anions showed that copper(I) stabilizes the η^1-C coordination, while titanium(IV) prefers the interaction with the other nucleophilic center, i.e. the oxygen.

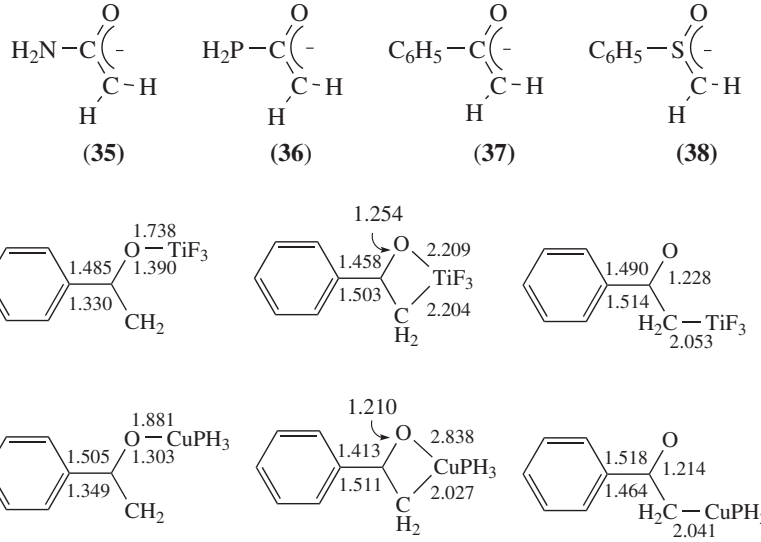

SCHEME 1. Calculated structures of trifluorotitanium (TiF_3^+)[33] and phosphinecopper ($CuPH_3^+$)[34] acetophenonates

E. Cobalt Enolates

Babic-Samardzija and coworkers[35] prepared four new cobalt(II) complexes of formula $[Co_2(dam)(tpmc)](ClO_4)_3$ (**39a**–**d**, tpmc = *N*,*N*′,*N*″,*N*‴-tetrakis(2-pyridylmethyl)-1,4,8,11-tetraazacyclotetradecane, dam = diacylmethanoate), which were characterized by elemental analyses, conductometric measurements, UV/VIS, IR, EPR and mass spectroscopy. Each cobalt(II) ion was coordinated with four nitrogen atoms in an *exo* arrangement of tpmc groups while the additional β-diketone bridges metal-ion centers through both enolate oxygens. The presence of different R-groups on the diketone influence the ν(C-O) and ν(C-C) vibrations in the IR spectra. The corresponding values of these frequencies decrease in the order: hfac (**39c**) > dibzac (**39b**) > acac (**39a**) > tmhd (**39d**) ligands. Semiempirical PM3 and ZINDO/I[36,37] calculations were used to characterize the complex species. According to both methods, cobalt(II) ions are capable of being bound with neighboring N atoms from pyridine and tertuary amine as well as to the O atom of diketone moiety, forming an inner molecule complex with a trigonal bipyramidal geometry. All molecules present high symmetry with typical coordination mode for tpmc along the macrocyclic moiety around cobalt(II) ions. The adjacent oxygen atoms of the β-diketonato ligand were joined to two cobalt atoms occupying *cis* positions.

These results showed that there is some variation in calculated bond lengths around the cobalt (Co–N and Co–O) and the Rac skeleton (O–C and C–C). Slight elongation of hexafluoro β-diketononato ring bonds in **39c** as well as the Co–O_{hfac} coordination bond was a result of the electron-withdrawing effect of the $-CF_3$ groups that lower the negative charge density on the oxygen donors, decreasing the basicity of β-diketone[38]. An opposite effect was found with respect to the methyl substituent diketones in the complexes **39a** and **39d**. The estimated distance between two diketonato oxygens was longer than the experimental value for free β-diketone ligand[39] as a consequence of bridging O,O′-coordination toward both cobalt atoms in octaaza moiety. In complex

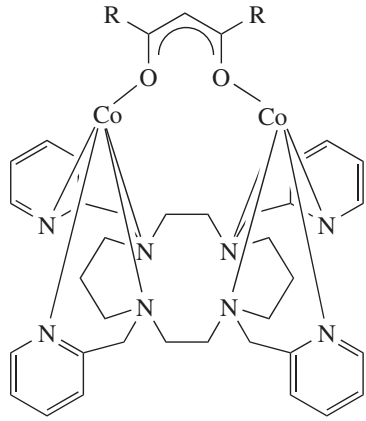

39 (a) R = Me (dam = acac) (see **39′**)
(b) R = Ph (dam = dbzm) (see **39″**)
(c) R = CF_3 (dam = hfac)
(d) R = t-Bu (dam = dpim)

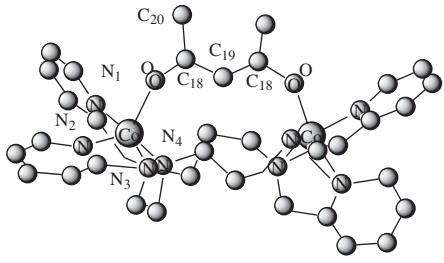

(**39′**)

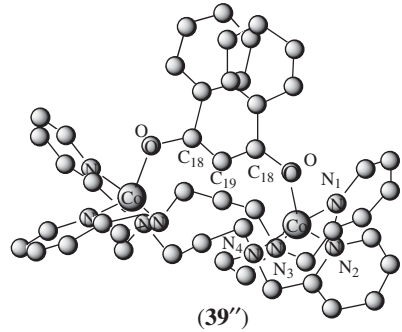

(**39″**)

39a with the corresponding acetylacetone this distance is 4.637 Å (Table 4 and **39**″). This became longer with the bulky terc-butyl group and/or withheld the effect of $-CF_3$ groups in the complexes **39d** and **39c**, while it is shorter in complex **39**″ due to the presence of parallel benzene ring orientation. Consequently, the effect of the bridging ligands on the Co-to-Co distances in these dicobalt compounds is in the same order as well.

III. SPECTROSCOPY OF THE METAL ENOLATES

A. NMR Spectroscopy

Ester enolates can be used as molecular models of the active centers in the anionic polymerization of acrylates and methacrylates. Thus, knowledge of the structure of these models in polar and nonpolar solvents is important for the understanding of the polymerization processes. Earlier ^{13}C and ^{7}Li NMR studies by Wang and coworkers[40] of methyl

TABLE 4. Selected bond distances and angles calculated for complexes **39a–d** by the semiempirical PM3 method

Complex	**39a**	**39b**	**39c**	**39d**
E_{tot} (kcal mol^{-1})	204.2	232.6	262.6	224.2
E_{tot} (kcal mol^{-1})[a]	294.4	337.2	388.2	324.1
Co−N (Å)[b]	1.85–2.10	1.90–1.92	1.92–2.01	1.92–1.99
Co−N (Å)[a, b]	2.05–2.23	2.06–2.16	2.05–2.15	2.04–2.38
Co−O (Å)	1.988	1.994	2.034	1.876
C18−O (Å)	1.396	1.397	1.398	1.386
C18−C19 (Å)	1.455	1.494	1.501	1.413
C18−C20 (Å)	1.504	1.518	1.525	1.520
O--- O (Å)[c]	4.637	4.595	4.683	4.750
Co--- Co (Å)[c]	5.760	5.431	6.146	6.453
∠Co−O−C18(°)	110.15	121.87	108.32	114.57
∠O−C18−C19 (°)	124.75	123.23	126.54	124.90
∠O−C18−C20 (°)	116.59	118.38	117.62	120.00
∠C18−C19−C18 (°)	124.96	116.73	127.90	121.38

[a] Calculated by the ZINDO/1 method.
[b] Range of Co−N1 to Co−N4 distances.
[c] Nonbonded interatomic distance.

α-lithioisobutyrate (mibLi) in thf solution revealed an equilibrium between these species and its dimer. According to osmometry measurements the aggregation degree of mibLi in thf at room temperature is about 3.5[41], therefore they concluded[40] that the equilibrium was between $(mibLi)_2$ and $(mibLi)_4$. Interpretation of the NMR data[42] on aggregation of mibLi in thf was aided by semiempirical MNDO[43] calculations carried out by Dybal and Kriz[44] of several possible dimeric, trimeric and tetrameric structures, both unsolvated and specifically solvated with dimethyl ether (a model for thf). In this work the dimeric and trimeric structures of ester-like units $(CH_3)_2C(Li)CO_2CH_3$ were more stable than the corresponding aggregates of enolate-like units $(CH_3)_2C{=}C(OLi)OCH_3$. However, it is important to note the MNDO tendency to overestimate the strength of the C−Li bond[45, 46].

Weiss, Yakimansky and Müller[47] performed *ab initio* calculations to obtain the equilibrium geometries, energies and ^{13}C NMR shifts of various monomeric, dimeric and tetrameric aggregates of mibLi. The energy values were improved through single-point MP2 calculations. These gas phase results should be compared to the data on the mibLi or ethyl α-lithioisobutyrate (eibLi) state of aggregation in nonpolar solvents like toluene. Both semiempirical MNDO and PM3 calculations of specific and nonspecific solvation energies of mibLi aggregates solvated by thf were carried out and it was found that the solvation effects decrease in the following order: monomer > dimer > tetramer. The calculated total solvation energies for mibLi aggregates were used to estimate the solvent effects on the *ab initio* relative energies of the aggregates. In all considered systems, Weiss and coworkers found at least two stable structures for each aggregate. For monomer and dimer structures, a planar and nonplanar arrangement of the C=C double bond and the Li−O bond were obtained. In the nonplanar structures, there is a direct interaction between the π-system and one lithium atom, whereas this direct (attractive) interaction is missing in the planar systems.

Dybal and Kriz[44] already presented *ab initio* calculations for the planar (**40**) and nonplanar (**41**) mibLi. Calculations at the MP2/SVD//MP2/SVD computing level render **41** as the more stable by 3.3 kcal mol^{-1}, which is too small to allow predictions concerning the stability in polar solvent at ambient temperatures. More pronounced differences were found in the calculated ^{13}C NMR shifts (Table 5). They found a high-field shift of the

TABLE 5. Comparison of calculated (SCF/TZD//SCF/SVD level of theory) and experimental ^{13}C NMR chemical shifts (in ppm with respect to TMS) of mibLi aggregates

C type	Oligomer	Planar[a]	Nonplanar[a]	Experimental[b]	eibLi[c]
C=O	monomer	169.6 (**40**)	176.7(**41**)	—	—
	dimer	164.1 (**42**)	164.5 (**43**)	158.9	163.9[a,d]
	tetramer	161.9 (**44**)	162.3/162.4 (**45**)	160.5	158.5/159.2[e]
Cα	monomer	50.8 (**40**)	44.5 (**41**)	—	—
	dimer	66.8 (**42**)	58.3 (**43**)	65.8	67.2[a,d]
	tetramer	78.8 (**44**)	77.9/78.1 (**45**)	72.5/73.5	76.5/78.5[e]

[a] Calculated at the SCF/TZD//SCF/SVD level of theory.
[b] In thf solution at $-80\,^{\circ}C$.
[c] Selected chemical shifts of ethyl α-lithioisobutyrate for comparison.
[d] For the planar form of eibLi.
[e] Experimental value in toluene solution at $-60\,^{\circ}C$.

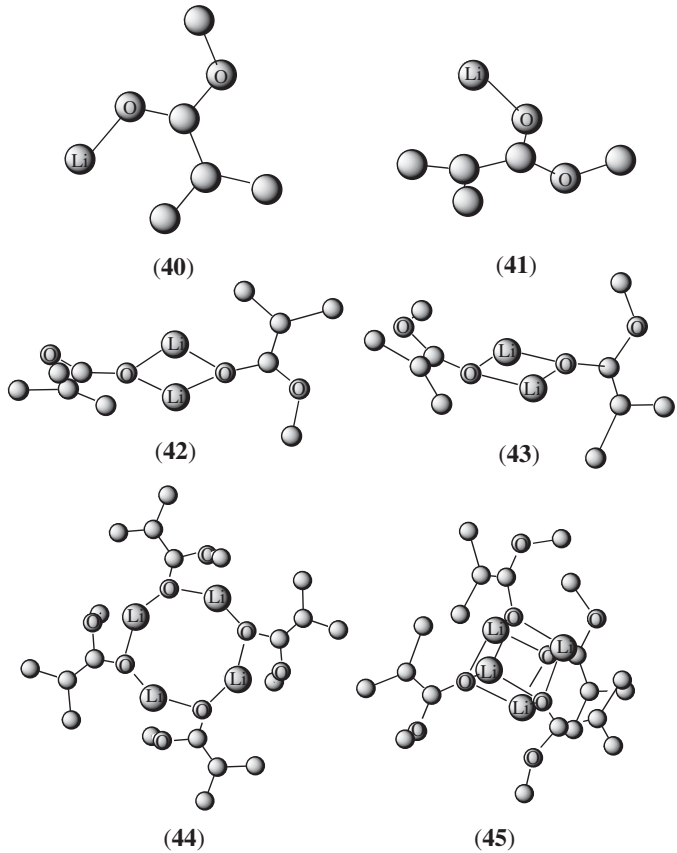

α-carbon (50.8 ppm) with a Mulliken charge of $-0.49e$ for **40** compared to 44.5 ppm and $-0.66e$ for **41**. These results point to the α-carbon of the nonplanar monomer **41** as having a stronger carbanion character than that of the planar **40** and it is thus assumed to have a higher activity in anionic polymerization.

Geometric optimization of the dimeric mibLi systems yielded at the MP2/TZD//SCF/SVP computing level a planar (**42**) and a nonplanar (**43**) structure, which were almost isoenergetic (relative energy *ca* 1 kcal mol^{-1}); in spite of the small calculated energy difference, the authors[44] proposed that the nonplanar structure **43** was the more stable at the correlated level.

The stabilization energy for the dimer formation was ΔE *ca* -28.7 kcal mol^{-1} in the gas phase. Similarly to the monomeric structures, the carbanionic character of the α-carbon was stronger in the nonplanar structure **43** (charge: -0.57e) than in the planar **42** (charge: -0.47e). The corresponding calculated shifts lay at 66.8 ppm (planar) and 58.3 ppm (nonplanar) (see Table 6). The agreement between the calculated shift for the planar structure **42** and the experimental value (65.8 ppm) found by Wang and coworkers[40] was convincing. Thus, the shift of the dimer measured in thf solution belongs to the planar structure.

In the case of the possible tetrameric structures, the concept of filling up the coordination sphere of the electron-deficient Li through electron-richer parts of mibLi becomes more flexible. Weiss and coworkers[47] found as the most stable aggregates a nearly flat eight membered-ring structure (**44**) and a cubic structure (**45**). At the MP2/SVD//SCF/SVD computing level **45** was significantly (*ca* 9.6 kcal mol^{-1}) more stable than **44**, in agreement with the X-ray data for crystalline ester enolates[13,14] and *ab initio* calculations[48] of comparable systems (LiX_4, X = OH, F), where cubic structures were found to be the most stable. The stabilization energies for the tetramers are in the range of -43 to -45 kcal mol^{-1}, which means that at least in the gas phase or in nonpolar solvents like toluene, the tetramers are more stable than the dimers and the monomers. This stabilization of higher aggregates was in accord with experimental osmometry data[42]. Tetramers show shifts at δ equal to *ca* 78 ppm and Mulliken charges of -0.41e and -0.42e. The tetramer structures **44** and **45** have similar values of shifts (Table 6) and charges. The calculated NMR shifts agreed well with those measured by Schlaad and coworkers[49] for eibLi in toluene. The effect of the alky group of the ester on the calculated shifts of the planar mibLi and eibLi dimers was shown to be negligible. The charges on the α-carbon and the NMR shifts (Table 6) clearly showed that the carbanion (or nucleophilic) character of the α-carbon decreases due to aggregation. This trend, observed on going from the monomer through the dimer to the tetramer, was also reflected by the reactivity in anionic polymerization.

Multinuclear ^{7}Li and ^{13}C NMR and quantum-chemical investigations by Müller and coworkers[50] showed that it is possible to determine the structure of active species in methacrylate polymerization in the presence of triethylaluminum ($AlEt_3$) in nonpolar solvents, such as toluene. Reaction of eibLi and trialkylaluminum with methyl pivalate (mpiv), in equimolar amounts, leads to an equilibrium of monomer **46** and dimer **47** complexes (eibLi•mpiv•$AlEt_3$)$_n$ ($n = 1, 2$), consistent with kinetic studies. Methyl pivalate was

TABLE 6. Calculated Cα-NMR shifts, Mulliken charges and C=C bond lengths for the most stable SCF/SVD//SCF/SVD geometries of mibLi aggregates

	Monomer		Dimer		Tetramer	
	40[a]	**41**[b]	**42**[a]	**43**[b]	**44**[a]	**45**[b]
Shift (ppm)	50.8	44.5	66.8	58.3	*ca* 78	*ca* 78
Charge (e)	-0.49	-0.66	-0.47	-0.57	-0.41	-0.42
Bond length (Å)	1.356	1.387	1.342	1.36	1.335	1.335

[a] Planar structure.
[b] Nonplanar structure.

able to fill up the coordination sphere of lithium, leading to highly stabilized active chain ends without the tendency to associate with polymer ester groups, preventing formation of a network. Although excess $AlEt_3$ destroys these species, forming separate adducts of each ester (eibLi•2$AlEt_3$ and mpiv•$AlEt_3$), these authors concluded that this reaction was not important in real polymerization systems, where the concentration of the ester groups is much higher than that of $AlEt_3$.

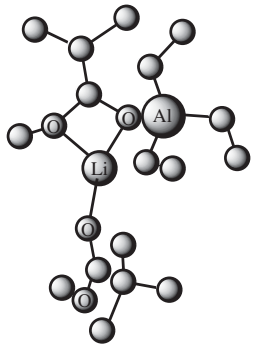

(**46**)

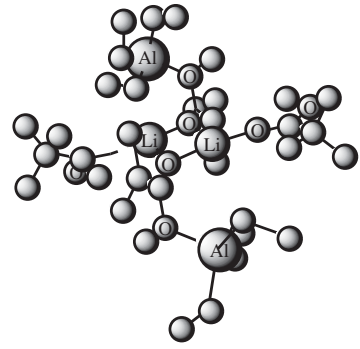

(**47**)

Yakimansky and Müller[51] performed a DFT study on structures of the mibLi in thf solution, in the presence of tmeda, dimethoxyethane (dme), crown ether 12-crown-4 and cryptand-2,1,1, as electron donor ligands (α-ligands). Both specific solvation with thf and/or ligand molecules, and nonspecific solvation by the solvent continuum were taken into account. The possibility of ligand-separated ion-pair formation was analyzed for each of the ligands, including thf alone. The theoretical results obtained by means of DFT calculations, using a basis set similar to the 6-31G*, clearly demonstrated that tmeda, dme and 12-crown-4-separated ion pairs of mibLi are not sufficiently stable in thf solution to provoke an accelerating effect on the anionic polymerization of methyl methacrylate (mma) by mibLi in the presence of these σ-ligands. This result agrees with the experimental data for both tmeda[52] and oligoether ligands[53]. In contrast, the formation of the cryptand-2,1,1-separated triple ion pair of mibLi (**48**) was shown to be energetically quite favorable in thf solution at all considered levels of theory, including the B3LYP/TZVP+ level with diffuse s-functions. These data were in agreement with the experimental ^{13}C and ^{7}Li NMR data reported by Wang and coworkers[53]. It is important to emphasize that the structural features of the ion pair (*C*2-symmetry and interionic separation) were in excellent agreement with those found experimentally for 2,1,1-cryptated lithium iodide[54]. In most cases peripherally solvated dimers were the most stable species. Only in the presence of cryptand-2,1,1 was a ligand-separated triple ion pair, $[Li(2,1,1)_1{}^+]$, $[(mibLi)(mib)(thf)_2]^-$, shown to be comparable in stability to the thf-solvated dimer, $(mibLi)_2thf_4$. These results were in agreement with experimental NMR data on the structure of mibLi in the presence of dme, 12-crown-4 and cryptand-2,1,1. An upfield shift of the ^{13}C NMR signal of the α-carbon of mibLi observed in the presence of cryptand-2,1.1, originally attributed to a ligand-separated monomer, $mibLi(2,1,1)^+$, was well reproduced by HF-calculated NMR shifts for the predicted ligand-separated triple ion pair.

A noticeable increase in rate was also observed in the polymerization of mma in the presence of the $Na^+(2,2,2)$ countercation[55]. Wang and coworkers[53] postulated that

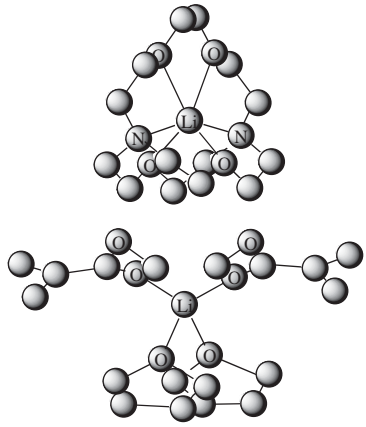

(**48**)

the counteranion within the ion pair formed in the presence of cryptand-2,1,1 was the monomeric mib anion. However, the results reported by Yakimansky and Müller[51] on the calculated stabilities and ^{13}C NMR chemical shifts of α-carbons for the 2,1,1-cryptated complexes of mibLi pointed to the $[Li(2,1,1)]^+$, $[(mibLi)(mib)(thf)_2]^-$ triple ion pair as the most probable one. Moreover, experimental X-ray data confirmed the ability of organolithium compounds to form thf-separated ion pairs containing triple counteranions with respect to the $[Li(thf)_4]^+$ cation[56]. As further arguments for triple anions, it could also be added that solutions of phenyllithium have been postulated to contain Li^+, Ph-Li-Ph$^-$ ion pairs[57], and those of 1:1 PhMPhLi adducts to contain ion pairs M^+, Ph-Li-Ph$^-$ (M = Na, K, Cs)[58], and a crystalline complex with the suggested[59] structure of $[Na(OEt_2)]^+$, Ph-Li-Ph$^-$ was known[58]. Organolithium compounds are strong dipoles which can form aggregates in solution[60]; for example, in coordinating solvents such as ethers, they often present dimeric or tetrameric structures.

The presence of Lewis bases affects the reactivity of organolithium reagents in solution, allowing noncovalently bonded auxiliaries to be used for asymmetric reactions[61]. To obtain a rational design of such chiral additives, a detailed understanding of the thermodynamic and kinetics of ligand exchange is necessary. However, the mechanism of this important process is yet unclear. Hilmersson[62] reported the fruitful combination of experimental and computing methods (semiempirical PM3 and DFT B3LYP/6-31G*) to address this topic. This author used calculated isotropic shielding constants (DFT B3PW91[18,63]/6-31G*) as an additional source for correct assignment of NMR signals of organolithium compounds. Calculations of isotropic shielding constants of ^{13}C nuclei can provide additional support for assignment of a given structure, helping in the choice between closely related structures. Calculation of chemical shifts can provide additional support to the correct assignment. Gauge-invariant atomic orbital[64] (GIAO) DFT calculations of the isotropic shielding constants of ^{13}C nuclei of various compounds have been reported. There are many accurate calculations of ^{13}C chemical shifts[65].

Hilmersson reported several studies on **49** and its solvated and mixed complexes with *n*-BuLi by various NMR spectroscopy methods (equation 13) [66]. The geometries of the structures (**49**)$_2$•dee (dee = diethyl ether) and (**49**)$_2$•thf were optimized using semiempirical PM3 methods. The distances between the lithium and the coordinating oxygen of the ethereal ligands were 2.06 Å (dee) and 2.02 Å (thf). Single-point energy

calculations of the relative solvation energies were performed at the B3LYP/6-31G(d) level of theory for the process $(\mathbf{49})_2 + \text{solvent} \rightleftharpoons (\mathbf{49})_2\bullet(\text{solvent})$. Calculated solvation energies for the equilibrium were $\Delta E_{\text{solv}}(\text{dee}) = -9.15$ kcal mol^{-1} and $\Delta E_{\text{solv}}(\text{thf}) = -10.94$ kcal mol^{-1}.

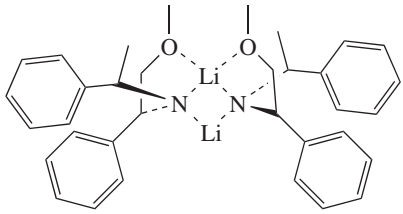

(**49**) dimer

+

solvent

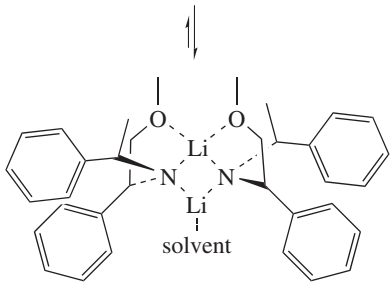

(**49**) dimer complex with solvent

(13)

The dissociation of dee solvent from $(\mathbf{49})_2\bullet$dee was modeled at the semiempirical PM3 level. The calculated Li–O_{dee} distances go from 2.06 Å in the normal state of $(\mathbf{49})_2\bullet$dee to 3.119 Å in the corresponding transition state (**50**). Single-point energy calculations at the B3LYP/6-31G(d)//PM3 level of theory gave an activation energy of 7.3 kcal mol^{-1}, fairly close to the experimentally determined activation enthalpy of 11.0 kcal mol^{-1}. Similar results were obtained for the dissociation the $(\mathbf{49})_2\bullet$thf complex. The calculated activation energy of 9.5 kcal mol^{-1} was close to the 11.2 kcal mol^{-1} obtained by means of a full bandshape analysis of the dynamic NMR spectra. Isotropic shielding values were calculated by the GIAO method at the B3PW91/6-31G(d)//PM3 level of theory. The

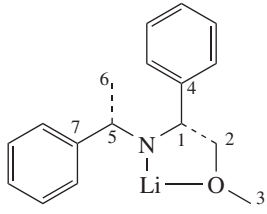

(**49**)

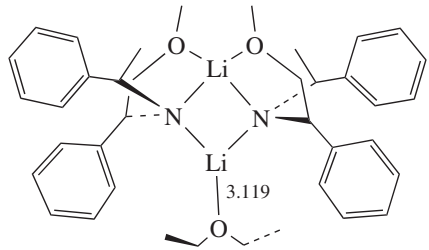

(**50**)

TABLE 7. Experimental (−90 °C) and calculated[a] ^{13}C NMR chemical shifts for selected carbon atoms of $(\mathbf{49})_2$•dee and $(\mathbf{49})_2$•thf

	$(\mathbf{49})_2$•dee		$(\mathbf{49})_2$•thf	
Carbon atom[b]	δ_{exp}	δ_{calc}	δ_{exp}	δ_{calc}
2	77.8[c]		78.4[c]	
6	27.1	29.4	27.2	29.7
3	57.6	55.4	57.5	55.9
5	61.8	64.4	61.0	64.9
1	64.4	67.7	64.8	68.1
4	147.4	142.0	147.3	143.0
7	153.7	148.0	153.4	147.1
Coordinated solvent (α-carbon)	60.0	60.5	68.4	69.2
Coordinated solvent (β-carbon)	11.9	13.1	24.5	25.9

[a] DFT-GIAO at the B3PW91/6-31G(d)//PM3 level of theory.
[b] The ^{13}C NMR signals of the aromatic carbon atoms have not been fully assigned and are therefore excluded.
[c] Reference for the ^{13}C NMR spectrum.

corresponding chemical shifts are presented in Table 7. There is satisfactory agreement between the experimental and the GIAO-DFT computational results and the largest differences between experimental and calculated shifts were ±2 ppm: these results allowed Hilmersson to propose that the GIAO-DFT method can become invaluable as an independent parameter for resonance assignments of complicated structures and aggregates involving organolithium compounds[62].

Szczecinski and coworkers[67] have recently performed ^{1}H, ^{13}C NMR and computational DFT studies on the structure of 2-acylcyclohexane-1,3-diones and their lithium sodium and potassium salt enolates (**51a–c**) in solution. Compound **51c** (ntbc) is a life-saving medicine applied in tyrosinemia type I[68]. The molecular structures of **51a–c** in solutions were obtained using DFT methods with B3LYP functional and 6-31G** and 6-311G(2d,p) basis sets, while the theoretical values of the NMR parameters were calculated by the GIAO-DFT B3LYP/6-311G(2d,p) method (see Table 8). The theoretical data[67] for the triketo compounds **51a–c** supported the contention that the experimental NMR spectra pointed to the endocyclic tautomer as the prevalent one in equilibrium. The differences in

NMR spectra of the salts of **51a** can be rationalized in terms of the size of the cation and the degree of salt dissociation. It seems that in dmso solution the lithium salt exists mainly as an ion pair stabilized by the chelation of a lithium cation with two oxygen atoms. The free energy of activation for rotation of the formyl group for this salt was estimated to be 12.3 kcal mol^{-1}, suggesting that in these systems, including the free enolate ions, all atoms directly bonded to the carbonyl carbons are on the same plane. Some observations concerning the chemical shift changes could indicate strong solvation of the anion of **51a** by water molecules.

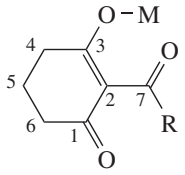

(**51**) (**a**) M = H, Li, Na, K, R = H

(**b**) M = H, R = 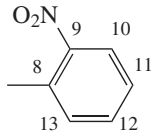

(**c**) M = H, R = 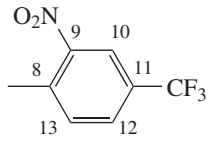

TABLE 8. Experimental and calculated[a] ^{13}C chemical shifts (ppm) for **51a–c** in $CDCl_3$ solution

	Compound **51a**		Compound **51b**		Compound **51c**	
Carbon number	δ_{exp}	δ_{calc}	δ_{exp}	δ_{calc}	δ_{exp}	δ_{calc}
1	195.1	194.4	193.9	192.7	194.1	192.7
2	113.8	112.1	112.8	111.4	112.7	111.5
3	195.6	196.8	195.6	197.3	195.8	197.4
4	31.2	30.8	31.8	32.3	31.6	31.9
5	19.3	20.5	19.1	20.2	19.1	20.1
6	36.5	36.5	37.5	37.2	37.3	36.6
7	191.3	191.8	197.7	198.4	196.3	196.7
8			136.6	138.9	139.7	141.8
9			145.5	144.8	145.5	144.9
10			123.6	123.7	121.1	122.8
11			129.6	127.1	132.0	130.8
12			134.1	135.0	130.8	131.0
13			126.7	125.2	127.7	125.3

[a] Theoretical absolute values of carbon atom shielding constants by the GIAO DFT B3LYP/6-311G(2d,p) PCM method.

B. UV Spectroscopy

Equation 14 shows the reaction of tetramethyl-1,3-cyclobutanedione (**52**) with with various organolithium compounds, opening the cyclobutanedione ring to give the corresponding lithium β-diketonates (**53a**–**d**), which after aqueous work-up gave the corresponding β-diketones (**54a**–**d**). Compounds **54a**–**c** were the first known cases of a β-ketoacylsilane or a β-ketoacylgermane[69]. The UV-visible spectra of the lithium enolates **53a**–**c** exhibit two new transitions: one absorption is 'red' shifted and the other is 'blue' shifted (each by about 40–50 nm) relative to the absorptions of the corresponding β-ketoacylsilanes. *Ab initio* (HF/6-31G*) molecular orbital calculations showed that the 'red-shifted' transitions stem from a low-lying Rydberg-type antibonding O–Li orbital, while the 'blue-shifted' transition results from a weakening (due to Li^+ complexation) of the destabilizing hyperconjugative interactions between the oxygen lone pair (n_O) and the σ_{C-Si} orbital, which leads to a lowering of the energy of the filled $n_O - \sigma_{C-Si}$ orbital relative to its energy in the β-diketones, and thus to a higher $(n_O - \sigma_{C-Si}) \rightarrow \pi$(C-O)* excitation energy than in the corresponding β-diketones.

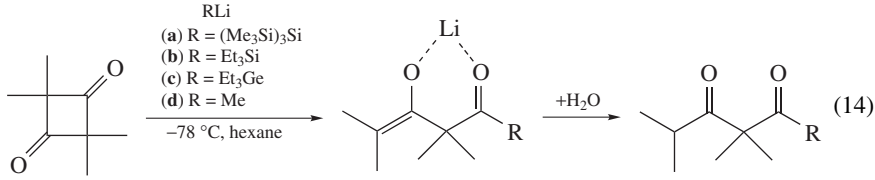

(**52**) (**53a–d**) (**54a–d**) (14)

C. IR Spectroscopy

Depending on the reaction conditions, *n*-BuLi may react as a base both with the reactants and the solvent. Thus, it has been shown that the *n*-BuLi dimer reacts with thf to give acetaldehyde lithium enolate (CH_2=CHOLi). Castella-Ventura and coworkers[70] applied the DFT approach at the B3LYP/6-31+G* level to determine the geometrical, energetic and vibrational characteristics of the different aggregates of the acetaldehyde lithium enolate involved in the cleavage of thf by *n*-BuLi. Calculations showed that two types of anions may be distinguished in these aggregates, the O and π(CC)-Li bound pyramidal structure (**55**) and the O-Li only bound linear structure (**56**). In parallel, IR and FT-Raman spectroscopy allowed one to determine the vibrational properties of the different enolate aggregates and to specify the mechanism of the thf cleavage. The very good agreement between theory and experiment concerning the wavenumbers and the IR intensities allowed one to characterize the structures of the different enolate aggregates.

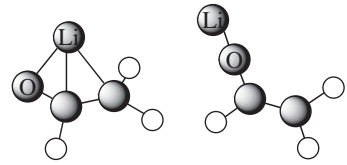

(**55**) (**56**)

The mechanism of the addition of HLi, CH_3Li and their dimers to aldehydes (formaldehyde, acetaldehyde) has been studied by *ab initio* methods[71,72]. For the thf cleavage,

Castella-Ventura and coworkers[70] proposed a similar mechanism (see equations 15–17). The dimer of *n*-BuLi was solvated by four thf molecules (**57**). The oxygen lone pairs of each thf species were coordinated to the Li cations in a plane perpendicular to the COC group. The O–Li bond of one thf molecule rotates in this plane in order to allow the interaction of thf with the butyl carbon bound to the Li cation[72] and the cleavage of the C–Li bond to form an open dimer[71]. Then, the abstraction from the thf molecule of an α-hydrogen followed by a cycloreversion mechanism[73] leads to an ethylene molecule and a butane molecule. The acetaldehyde enolate anion in the CH_2CHOLi mixed aggregate with *n*-BuLi (**58**) (equation 15) probably interacts by its oxygen atom bound to the two lithium cations. Its structure corresponds to a linear enolate anion. Mixed aggregate **58** was characterized by the 1612 cm^{-1} Raman band, and their larger stability was confirmed by *ab initio* calculations[74]. In pure thf or in the presence of only small amounts of hexane, a second thf molecule reacts and gives rise to the *trans* linear–linear enolate dimer **59** (equation 16), the formation of which was associated to the appearance of the 1619 cm^{-1} Raman and the 1608 cm^{-1} IR bands. As the concentration of **59** increases, it dimerizes with desolvation (equation 17) forming tetramers (**60**), where each oxygen atom in the enolate anions coordinates with up to three Li^+ cations. The tetramers were characterized by the 1624 cm^{-1} Raman band and the shoulder around 1616 cm^{-1} in the IR spectrum. Hence, it is not surprising that the concentration of **59** goes through a maximum before decreasing due to the formation of the more stable **60**[75].

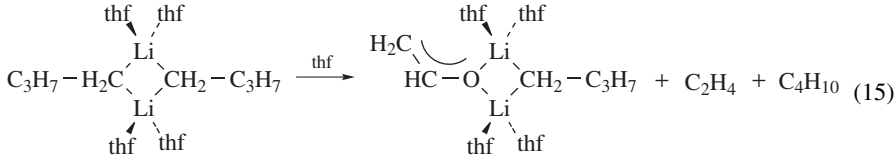

(**57**) (**58**) (15)

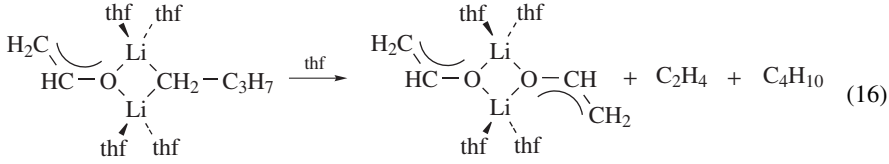

(**58**) (**59**) (16)

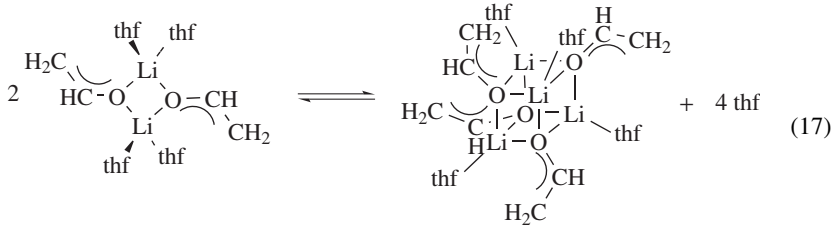

(**59**) (**60**) (17)

The adsorption of acetone on the surface of group 10 hydrogenation catalysts provides a basic model system to study the adsorption and reaction of ketones. The insight provided

by modeling can be used as a starting point for determining the most likely mechanism of the reactive traits related to stereo- and regioselectivity in molecules containing more than one multiple bond. Recently, Willock and coworkers[76] presented a periodic DFT calculation with the generalized gradient approximation[77] (GGA-DFT) for adsorption modes of acetone on the (111) surface of Pt, in various orientations and in three possible isomeric forms. In the gas phase, the ketone was considerably more stable than the enol or enolate, thus any adsorption process will begin with the ketone interacting with the surface. The keto isomer was found to be around 4.5 kcal mol^{-1} more strongly adsorbed in an end-on, η^1(O)configuration (**61**) than the alternative μ_2(C_2,O) adsorption parallel to the surface (**62**). This energy difference is caused by the steric interaction between the methyl groups and the surface and so is likely to be common to any substituted ketone adsorbed parallel to the surface. The agreement between the calculated vibrational modes of **61** and experimental electron energy loss spectroscopy (EELS) data was satisfactory for all the studied skeletal modes of the molecule. Configuration **62** has a considerably longer C−O bond than the gas phase ketone, with a correspondingly lowered C−O stretch frequency. This makes it unlikely that the second species identified in the surface spectroscopy experiments was a ketone adsorbed parallel to the surface. In addition, experimental thermal desorption spectra data suggested that this second species is more strongly bound than **61**, which was not supported by their or earlier calculations. Willock and coworkers[76] concluded that the most likely explanation for the second species observed in the experiments for acetone adsorbed on a Pt(111) surface has the enolate structure **63**. This would mean that deprotonation of acetone can take place on the clean Pt surface even at low temperatures. This explanation seems reasonable since similar species have recently been observed on the (111) surface of Ni[78].

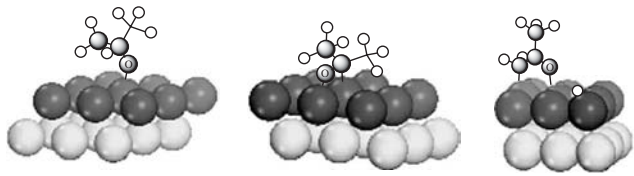

(**61**) (**62**) (**63**)

IV. REACTIVITY OF THE METAL ENOLATES

A. Metalation Reactions

During the last four decades, lithium dialkylamide bases have been the most employed reagents for the formation of lithium enolates and related stabilized carbanions. A plethora of empirical observations have been the basis of frequent mechanistic debates on these types of formation processes. In 1990 Collum and coworkers[79] initiated investigations of the structures and reactivities of lithium dialkylamides in order to establish the lithium dialkylamide structure–reactivity relationships underlying their role as strong Bronsted bases. More recently, they began to employ semiempirical MNDO methods to study a number of issues that could not be adequately addressed by spectroscopic and kinetic works. In 1995 Romesberg and Collum[80] studied the metalation mediated by the lithium amide dimmer (**64**) of carbonyl compounds such as acetaldehyde, acetone and pinacolone (AcBu-*t*), leading to complexes with the amide monomer (**65**) or with the amide open dimer (**66**), applying semiempirical MNDO methods (see equations 18 and 19).

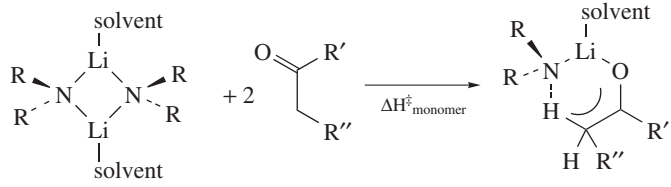

(**64**) (**65**) (18)

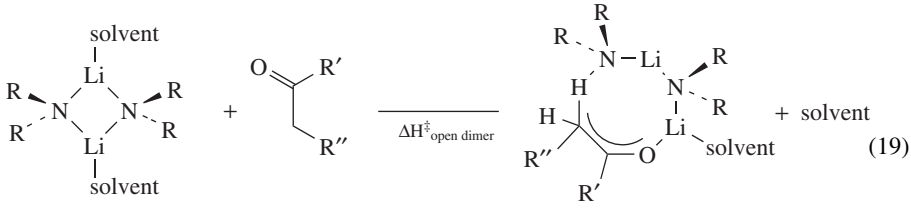

(**64**) (**66**) (19)

The role of lithium amide, solvent and substrate substituents on the absolute and relative stabilities of the monomeric and open dimeric transition **67**, the six-membered ring, bears little resemblance to standard cyclohexane conformation. The ring of the unhindered $LiNH_2$/acetaldehyde/H_2O transition structure displayed a puckering arrangement along the axis between the lithium and the acidic carbon that was unique to the minimally substituted system. The puckered structure resembled the unsolvated $LiNH_2$/acetaldehyde structure calculated with the *ab initio method* by McKee[81]. Inclusion of alkyl groups on the lithium amide, substrate and solvent fragments caused flattening of the ring to near planarity for lda-based transition structures (lda = lithium diisopropylamide) solvated by the bulkier ethereal and amine solvents, for example in the case of **67**, derived from pinacolone and solvated with thf. Both C−O and C−C bond lengths differ only slightly from those observed in the starting carbonyl substrates. The open dimeric transition structure **68** shared several geometrical characteristics with other open dimeric ground states[82] and bear little semblance to the standard carbocyclic eight-membered ring[83]. The ring forms a smooth loop and the lone-pair-bearing nitrogen is close to the acidic proton. The fundamental geometry of the eight-membered ring varied only marginally with changes in the lithium amide, substrate or solvent. The lithium amide *N*-alkyl groups showed some

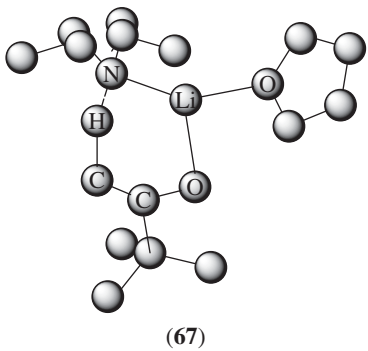

(**67**)

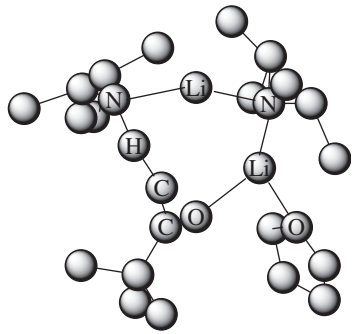

(**68**)

rotation away from being coplanar, presumably to avoid steric interactions. The two alkyl substituents of the ketone substrate were generally free of spatial interactions with the remainder of the transition structure. In the more hindered lda case, the solvent was located away from the bulky *N*-alkyl groups. The relatively uncongested region about the carbonyl oxygen allowed conformational relaxation to both the solvent and ketone substituents. In general, relief of the high steric demands inherent to the disolvated cyclic dimer reactant (**64**) upon proceeding to the transition states was the dominant factor determining the values of the activation enthalpies. The results shed light on a number of issues central to lithium-amide-mediated metalations, such as: (i) the *syn* effect observed in imine metalations, (ii) *E*/*Z* ketone enolization selectivities, (iii) the dramatically reduced kinetic acidities of imines relative to ketones and (iv) the role of the chelate effect in ligand-assisted imine metalations.

Calculated values of activation enthalpies for ketone enolizations via monomeric and open dimeric transition structures are listed in Table 9. Analysis of the results points out that increasing the lithium amide bulk reduces the activation enthalpies. This behavior was consistent with the notion that relief of the high steric congestion in the lithium amide dimers upon proceeding to the transition structure imparts the dialkylamide bases with their high reactivity. Comparison of the activation enthalpies between acetone (AcMe) and pinacolone (AcBu-*t*) indicates that the steric demands of the substrate bulk are not important, a behavior prevalent with monomeric enolization transition structures that are not very sterically congested. Solvent perturbations showed a significant influence on the calculated barriers, with predicted metalation rates following the order: NMe_3 > hmpa > thf ≈ Me_2O > H_2O. Within this series Romesberg and Collum[80] found an interesting result: monomer-based metalations are predicted to be slower for thf than for either the weakly coordinating NMe_3 or strongly coordinating hmpa. NMe_3 and hmpa are both sterically demanding, yet have very different affinities for lithium ion; hmpa imparts stabilization to the transition state that is greater than in the ground state. In contrast, NMe_3 was destabilizing in the ground state, yet less so in the transition state. This is a recurrence of the following principle: *the high reactivities of hindered lithium dialkylamides stem from relief of steric demands*. The open dimer-based enolizations showed an enhanced sensitivity to amide steric bulk relative to the monomer cases. The barriers were predicted to increase marginally with the increased ketone bulk

TABLE 9. Enthalpies of activation ($\Delta H^{\neq}$) for cyclic monomeric- and open dimeric-based transition structures (**65** and **66**) of ketone metalation

Amide/substrate/solvent	$\Delta H^{\neq}_{\text{monomeric}}$	$\Delta H^{\neq}_{\text{open dimeric}}$	$\Delta\Delta H^{\neq a}$
$LiNH_2$/AcH/H_2O	34.5	35.2	0.7
$LiNMe_2$/AcMe/H_2O	37.8	39.7	1.9
$LiNMe_2$/AcMe/Me_2O	37.2	35.7	−1.5
lda/AcMe/H_2O	34.2	34.2	0.0
lda/AcMe/Me_2O	31.8	24.8	−7.0
lda/AcMe/thf	31.8	25.4	−6.4
lda/AcMe/NMe_3	26.6	14.7	−11.9
lda/AcMe/hmpa	27.4	23.4	−4.0
lda/AcBu-*t*/H_2O	34.8	36.9	2.1
lda/AcBu-*t*/Me_2O	32.2	27.7	−4.5
lda/AcBu-*t*/thf	32.4	28.1	−4.3
lda/AcBu-*t*/NMe_3	27.4	18.4	−9.0
lda/AcBu-*t*/hmpa	28.2	26.9	−1.3

[a] $\Delta\Delta H^{\neq} = \Delta H^{\neq}_{\text{open dimeric}} - \Delta H^{\neq}_{\text{monomeric}}$.

(pinacolone *vs*. acetone) for the ethereal solvents, but increase markedly with substrate bulk for the NMe_3 solvation where destabilizing solvent–substrate interactions become substantial. The open dimer-based enolization pathways were predicted to display the same solvent-dependent rates as the monomer-based pathways. The open dimeric transition structures (**66**) were found to be more strongly stabilized by solvation than the dimeric lda reactant (**64**, R = *i*-Pr), yet less dramatically than for the monomeric transition structures (**65**). Structures **66** appeared to be more sterically demanding than **65**. The increased bulk of pinacolone was destabilizing for bulky solvents. However, the desolvation accompanying the open dimer-based metalations magnified the accelerating effects of the weakly coordinating NMe_3 ligands, yet attenuated the acceleration by hmpa.

B. Enolization and Tautomerization Reactions

Several studies have demonstrated the formation of the less stable *E* enolate under kinetic control rather than the more stable *Z* enolate. Mixed aggregate formation between alkyllithiums and lithium iodide was reported in 1968 by McKeever and coworkers[84], while Collum and coworkers[85] demonstrated a remarkably high *E*/*Z* selectivity of 3-pentanone enolization by lithium tetramethylpiperidide (Litmp) in the presence of lithium halides in very dilute solutions, although this selectivity decreased with increasing concentration. This high selectivity was attributed to the formation of various mixed aggregates[86], the synthetic importance of which was reported by Corey and Gross[87] in a study of enolization reactions in the presence of chlorotrimethylsilane, which generates lithium chloride during the course of the reaction. Although the mixed aggregate formation was not yet known, it was noted that the *E*/*Z* enolate selectivity was dependent upon the lithium dialkylamide which was used. Litmp was also shown to form a 1:1 mixed aggregate with ethyllithium and phenyllithium. The ^{7}Li and ^{15}N NMR spectra were consistent with either a cyclic mixed dimer (**69**) or an open mixed dimer (**70**). Semiempirical molecular orbital calculations showed that both mixed dimers are minima on the potential energy surface. Regardless of the actual structure of the major species, the reactive aggregate could be either a spectroscopically unobservable minor species or a small amount of the Litmp in equilibrium with the mixed dimer.

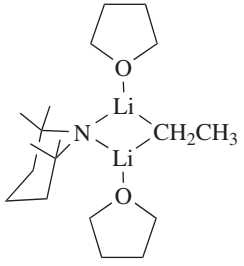

(**69**)

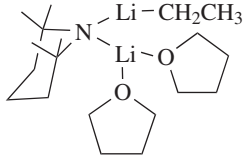

(**70**)

The stereoselective enolization of 3-pentanone by LiTMP mixed aggregates with butyllithium was studied by Pratt and coworkers[88]. The mixed aggregate resulted in a slightly higher stereoselectivity, which increased with decreasing amount of the lithium base. Semiempirical PM3 calculations were used in an attempt to determine the mechanism of ketone deprotonation by the mixed aggregate. Equations 20 and 21 show two alternative mechanisms for the formation of lithium acetone enolate in thf solution, involving

either the cyclic mixed dimmer (**71**) of lithium dimethylamide (Lidma) and ethyllithium or its open form (**74**). Formation of intermediate complexes (**72** or **75**) of acetone with the mixed dimers is assumed, which pass through a transition state (**73** or **76**) of ketone deprotonation by ethyllithium acting as a strong Lewis base. The activation enthalpies were calculated at various levels of refinement, as shown in Table 10, and in all cases there was a large energy difference in favor of transition structure **76**, derived from the open mixed dimer, over transition structure **73**, derived from the cyclic mixed dimmer.

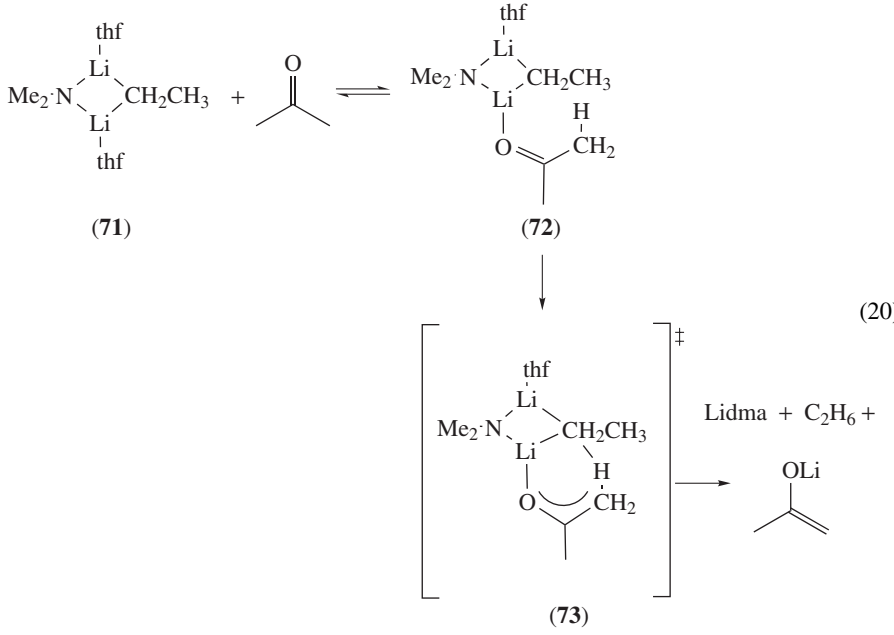

(20)

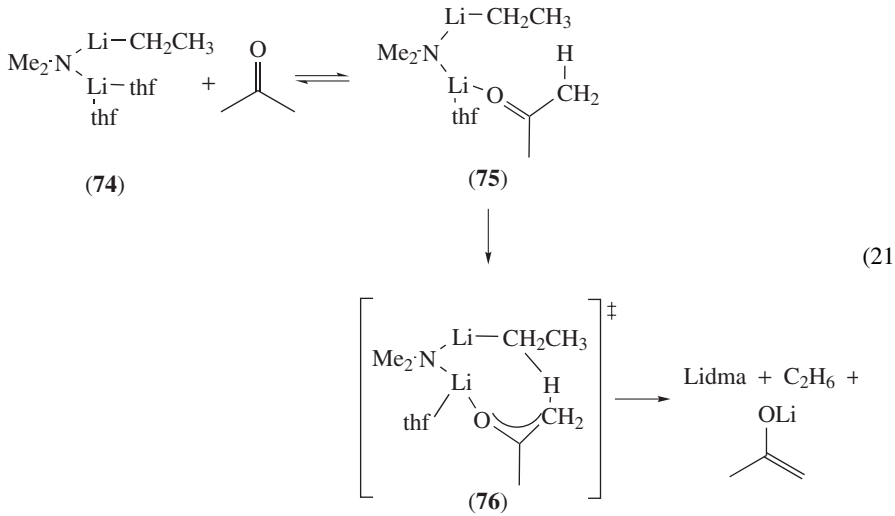

(21)

TABLE 10. Calculated activation energies (in kcal mol^{-1}) for acetone deprotonation by the cyclic and open mixed dimer mechanisms (equations 20 and 21)

Transition state	Calculation method		
	PM3	HF/3-21G	HF/6-31G*//HF/3-21G
Mixed cyclic dimer (**73**)	15.2	18.4	25.2
Mixed open dimer (**76**)	3.0	10.6	16.7

Mechanisms involving both the mixed cyclic (equation 20) and open dimers (equation 21) were considered. Activation enthalpies were calculated for the acetone enolate formation from the ethyllithium-lithium dimethylamide (LiDMA) cyclic and open dimers. For comparison purposes, the semiempirical PM3 geometries were reoptimized by using the HF/3-21G method, and single point energies were calculated at the HF/6-31G*//HF/3-21G level. The results are shown in Table 10. The large difference in calculated energy values indicates that the mixed open dimer pathway via the transition structure **76** is favored over the mixed cyclic dimer mechanism along the transition structure **73**.

Calculations were performed on the deprotonation of 3-pentanone by the mixed open dimers of ethyllithium with both Lidma and Litmp systems. In both cases, the transition structures leading to the *E* enolate were favored over the *Z* enolate formation. For comparison purposes, calculations were also performed on the ground and transition states for the deprotonation of 3-pentanone by the open dimer of Litmp[82, 86]. In the case of the Lidma mixed aggregate, the calculated activation enthalpies for the formation of the *E* and *Z* enolates were 2.95 and 3.89 kcal mol^{-1}, respectively, while a theoretical *E*/*Z* ratio of 11.7 was found at $-78\,^{\circ}$C. With the Litmp mixed aggregate the calculated activation enthalpies were 3.09 and 4.40 kcal mol^{-1} for the *E* and *Z* enolates, respectively, and the theoretical *E*/*Z* ratio was 27.9. For the Litmp open dimer (without mixed aggregation), the calculated activation enthalpy for the *E* enolate formation was only 1.11 kcal mol^{-1}, compared to 5.16 kcal mol^{-1} for the *Z* enolate. These calculations predicted an *E*/*Z* ratio of 3.29×10^4, which was much larger than the highest *E*/*Z* ratio reported for Litmp in very dilute solutions[86]. From the results obtained using these semiempirical and *ab initio* calculations, Pratt and coworkers[88] showed that the most likely mechanism involves a mixed open dimer as either the ground state or a reactive intermediate, and that the reaction proceeds through an open dimer-like transition state. Calculations on the transition structures were consistent with the observed stereoselectivity, and indicated that this selectivity can be associated to greater steric hindrance in the transition state leading to the *Z* enolate.

2-Acylaryl complexes of Ni and Pd containing chelating diphosphines react with KOBu-*t* to give metallacyclic enolate complexes. While C-coordination is preferred in the case of Pd, the nickel O-enolate compounds are formed from the corresponding O-tautomers. Slow equilibration between O- and C-enolate tautomers has been observed for the nickel complex with an unsubstituted enolate function (M$-$O$-$C$=$CH$_2$). To provide theoretical support to the proposed molecular mechanism for the exchange between the tautomeric enolate forms as well as to gain a better understanding of the properties of these complexes, Cámpora and coworkers[89] performed the DFT calculations summarized in Table 11, using the BP86 functional and the numerical basis set DN*. As expected, the C-tautomeric form was strongly favored for Pd. For Ni, the C-enolate was favored by only about 2 kcal mol^{-1}. The presence of alkyl substituents on the P atoms of the phosphine ligand does not significantly change the energy balance, although there seems to be a tendency to favor the O-enolate form when electron-donor alkyl groups replace the hydrogen atoms. Since the energy calculations did not take into account solvation effects, they concluded

TABLE 11. Calculated energy differences and barriers for the tautomerization of divalent metal enolates shown in equation 22

Energy items ($kcal\,mol^{-1}$)	M = R =	(a) Ni H	(b) Pd H	(c) Ni Me	(d) Ni *i*-Pr
$\Delta E = E(\mathbf{79}) - E(\mathbf{77})$		2.07	7.23	2.11	0.03
$\Delta E^{\neq} = E(\mathbf{78}) - E(\mathbf{77})$		25.2	—	25.4	25.4

that the calculations reasonably reproduce the thermoneutral character of the equilibrium between the two tautomeric Ni enolates.

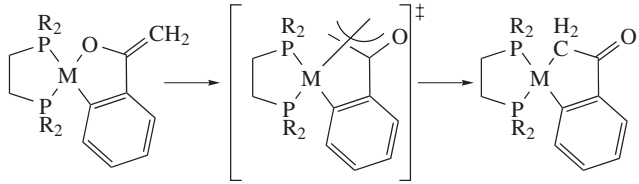

(**77**) (**a**–**d**) O-enolate (**78**) (**a**–**d**) TS (**79**) (**a**–**d**) C-enolate (22)

The experimental data suggested that for the Ni derivatives the equilibration of the tautomers could involve an intermediate η^3-enolate species. Accordingly, Cámpora and coworkers[89] located a transition structure (**80**) in which the Ni atom is interacting. simultaneously with the C and O atoms of the enolate fragment. The O−C−CH_2 unit was approximately perpendicular to the coordination plane (93.3°), allowing a π-interaction with the Ni atom. The lengths of the the Ni−O and Ni−C bonds suggested that the interaction was not symmetrical, and can be considered closer to η^2-C=O than a η^3-pseudoallylic interaction. The energy difference between **80** and the O−Ni enolate, *ca* 25.2 $kcal\,mol^{-1}$ (see entry a in Table 11), is very similar to the experimental value $\Delta G^{\neq} = 25.3\ kcal\,mol^{-1}$, although it was somewhat higher than the activation enthalpy, $\Delta H^{\neq} = 18.5\ kcal\,mol^{-1}$. Introduction of Me or *i*-Pr substituents into the diphosphine did not alter significantly the relative energy of the corresponding transition states. Therefore, the origin of the relatively high barrier to the tautomeric exchange is not steric hindrance caused by the diphosphine ligand, but distortion of the metallacyclic ring during the course of the process. The aryl−CO bond has to bend noticeably (it is nearly perpendicular to the aromatic ring), in order to maintain the M−enolate interaction. No such restriction exists

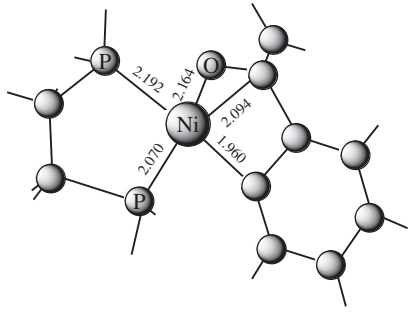

(**80**)

in open chain enolates, where the interconversion is more easy. The presence of bulky substituents on the diphosphine ligand seems to have a small influence on the equilibrium constant or the exchange rate between the two tautomers.

C. Alquilation Reactions

Considerable attention was given to the stereochemistry for the alkylation of metal enolates of γ-butyrolactones[90,91] during the past 1980's decade. It is well recognized that electrophilic attack on the enolates of β-substituted γ-butyrolactones is controlled exclusively by the β-substituent leading to the *trans* addition products[92]. However, Iwasaki and coworkers[93] reported the reverse diastereofacial differentiation in the alkylation of the enolates of α,β-dibenzyl-γ-butyrolactones. These authors proposed that the factor controlling the selectivity in this case was allylic strain. Also, γ-substituted γ-lactones give stereoselective *trans* alkylation[94].

Pellissier and coworkers[95] studied the diastereoselective alkylation of the (±)-spiro-γ-lactones **81** and **82**, which are involved in steroid synthesis. Alkylation of enolate **83** with iodobenzocyclobutene led to only one stereoisomer whose structure was confirmed by X-ray crystal diffraction analysis of the resulting steroid. With the aim of understanding the origin of the diastereofacial selectivity, Pellissier, Michellys and Santelli performed *ab initio* calculations to determine the preferred geometry of the enol **84** and consequently the probable attack mode of the corresponding electrophilic reagent[96]. The HF/4-31G optimized geometry of **84** showed that both diastereotopic faces of the enolate (**83**) are accessible. However, if the angle of attack of about 80° to the plane of **83** occurs, combined with a displacement of the electrophile trajectory away from the oxygen linked to lithium, the face containing the vinyl group *anti* to the lactone ring-oxygen is favored as depicted in structure **83′**. In contrast, attack on the face with the vinyl group *syn* to the lactone ring oxygen should be preferred with an approach along an obtuse angle. HF/STO-3G calculations were performed on enolate **85**, where the lithium ion was encapsulated by three molecules of water as ligands[96]. Calculations indicated that the HOMO coefficient at O(1), −0.565, lies lower than that at O(2), −0.198. As depicted in transition structure **86**, the out-of-phase overlap between the σ*-LUMO of the electrophile and the more contributing oxygen in the HOMO (secondary orbital interaction) pushes the electrophile closer to the cyclopentane ring and increases the π-facial selectivity for acute angles of approach.

The diastereoselectivity associated to the alkylation process of the dianion **88** derived from *N*,*N*-bis(1(*R*)-phenylethyl)-3-(benzyloxycarbonylamino)propionamide (**87**) was studied by Juaristi and coworkers[97] (equation 23). Treatment of (*R*,*R*)-**88** with various alkyl halides afforded the monoalkylated product (**89**) in 24–85% yield and 65–86% diastereoselectivity. Addition of LiCl or hmpa improved the reaction yields but had only a negligible effect on the diastereoselectivity of the alkylation reaction. They performed molecular modeling studies by means of semiempirical PM3 and *ab initio* (HF/3-21G) and DFT (B3LYP/3-21+G(d)) calculations, to rationalize the observed stereoinduction by the chiral bis(1(*R*)-phenylethyl)amino group in dianion (*R*,*R*)-**88**. A 'folded' conformation in the β-aminopropionic segment of monoanion was even more strongly favored. Indeed, compound **90**, involving a six-membered chelate N−Li−O structure, was estimated to be 22.3 kcal mol^{-1} more stable than the extended conformer **91**. Conformer **90** was also stabilized by $\pi-\pi$ attraction[98]. Finally, (*R*,*R*)-**88** could be folded into the lowest-energy structure **92**. Most interestingly, the ion triplet configuration[99] of the dilithium salt **92** was estimated to be a remarkable 33.8 kcal mol^{-1} lower in energy than enolate **93**. From observation of the calculated lowest-energy conformation for (*R*,*R*)- **88** it can be appreciated that enolate face *Si* is less hindered towards electrophilic approach (*syn* to methyl

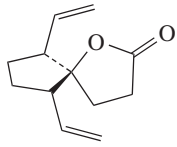

(**81**)

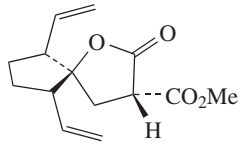

(**82**)

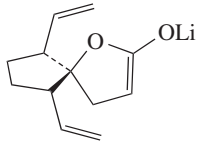

(**83**)

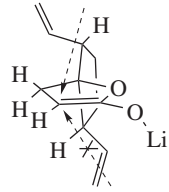

(**83′**)

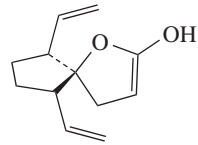

(**84**)

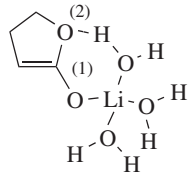

(**85**)

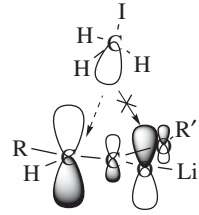

(**86**)

vis-a-vis phenyl groups on the α-phenethyl moieties) relative to the *Re* face, which is *syn* to the phenyl rings. Indeed, predicted addition of the electrophile on the *Si* face should lead to the preferred formation of the experimentally observed (*S*)-stereogenic center.

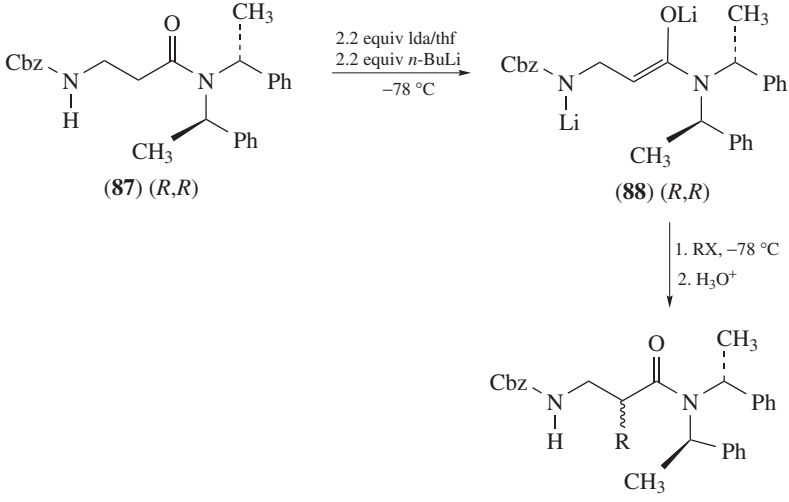

(**87**) (*R*,*R*)

(**88**) (*R*,*R*)

(23)

(**89**) C-alkylation

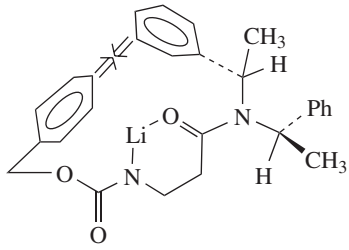

(**90**) (π-π attraction and N–Li–O bond)

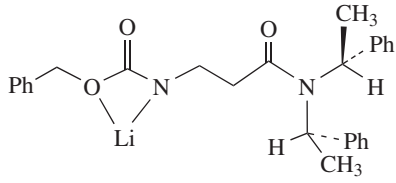

(**91**) (four-membered N–Li–O ring)

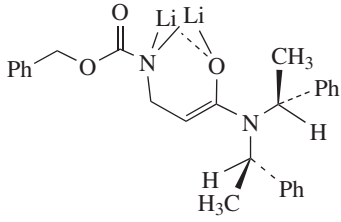

(**92**)

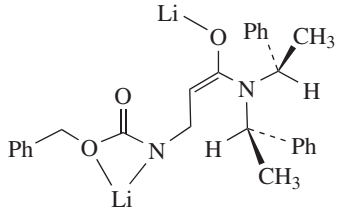

(**93**)

Fujii and coworkers examined the organocopper-mediated reduction–alkylation of γ-acetoxy or α,β-unsaturated γ,γ-difluoro-δ-lactams for the synthesis of (*Z*)-alkene- or (*E*)-fluoroalkene-containing diketopiperazine mimetics[100]. Reduction of acetates **94a**, **94b** and **95** and difluorolactam **96** (equation 24) with higher-order cuprate reagents (Me_3CuLi_2•LiI•3LiBr), followed by trapping the resulting metal dienolate with an electrophile in a one-pot procedure, gave α-alkylated-β,γ-unsaturated-δ-lactams in good yields. Because of side-chain steric repulsion, they found that alkylation using relatively large electrophiles such as BnBr gave mostly 3,6-*trans* isomers (**97**) by kinetic trapping of metal enolates. On the other hand, MeI-mediated alkylations predominantly provided the unexpected 3,6-*cis* isomers (**98**) despite the presence of a bulky benzyl side chain.

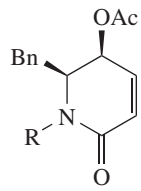

(**94**) (**a**) R = Me
(**b**) R = dmb

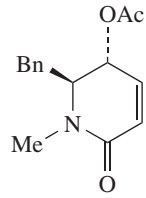

(**95**)

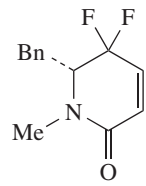

(**96**)

(24)

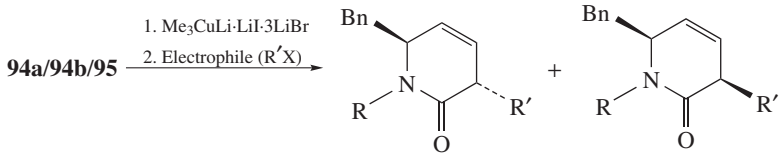

(**97**) 3,6-*trans*

(**98**) 3,6-*cis*

To determine whether the metal dienolate (Cu or Li enolate) played a critical role in the reaction mechanism, Fujii and coworkers[100] examined the alkylation of the Li dienolate (equation 25). Deprotonation of **99a** and **99b** with lda was followed by electrophilic trapping of the Li dienolate with MeI or BnBr[101]. In these reactions, similar trends to those in the organocopper-mediated reduction–alkylation sequence (see equation 26) were observed, where methylation proceeded with high *cis* selectivity (**100a** and **100b**), while benzylation gave predominantly *trans* isomers (**100c** and **100d**). It was therefore concluded[100] that diastereoselectivity in the organocopper-mediated reduction–alkylation was determined at the alkylation step of the metal dienolate (Cu or Li). Additionally, because essentially no differences were observed in the alkylation diastereoselectivity between Li and putative Cu dienolates, they performed DFT (B3LYP/6-31G(d)) calculations on the lithium dienolates to probe the mechanism leading to diastereoselectivity. Reactions of the lithium dienolates from lactam **99a** and fluorolactam **99b** with MeBr were chosen as model systems. First, they examined local energy minima structures of lithium dienolates from lactam **99a**. As a result, two oxa-π-allyllithium complexes **101a** and **102a** were optimized as local minima. It was found that oxa-π-allyllithium complexes **101a** and **102b**, having the lithium cation on the same face of the benzyl side chain, were significantly more stable as compared to the complexes having the lithium cation on the opposite face of the benzyl group (**102a** and **102b**), respectively (energy difference: Y = H, 7.76 kcal mol^{-1}; Y = F, 6.78 kcal mol^{-1}). Calculated charge distributions of the lithium atoms were estimated as follows: **101a** (+0.26e) *vs*. **102a** (+0.38e) and **101b** (+0.27e) *vs*. **102b** (+0.39e), suggesting that the lithium cation interacts with the π-electrons of the phenyl ring.

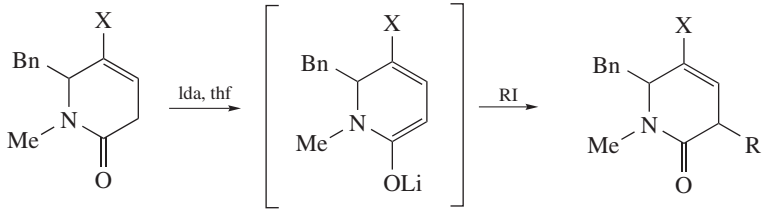

(25)

(**99**) (**a**) X = H
(**b**) X = F

(**100**) (**a**) X = H, R = Me (51%, *trans*:*cis* = 3:7)
(**b**) X = F, R = Me (51%, *trans*:*cis* = 3:7)
(**c**) X = H, R = Bn (69%, *trans*:*cis* = 8.5:1.5)
(**d**) R = F, R = Bn (60%, *trans*:*cis* = 10:0)

Fujii and coworkers carried out DFT calculations on the complexes **101** and **102** further coordinated with MeBr to give **103** and **104**[100]. Local minima for these structures were found and the relative energies were calculated at the B3LYP/6-31G(d) level. The relative energies of complexes **103a** and **103b**, which were derived from the stable oxa-π-allyllithium complexes **101a** and **101b**, were lower than those of complexes **104a** and **104b** (energy difference: Y = H, 4.27 kcal mol^{-1}; Y = F, 3.30 kcal mol^{-1}). From these results they derived a plausible explanation for the observed diastereoselectivity in the organocopper mediated reduction–alkylation system. After reduction of the lactams **94a** and **96** with Me_3CuLi_2•LiI•3LiBr, the thermodynamically stable oxa-π-allylmetal complex **105** exists as the preferred reaction intermediate. The coordination of MeI with **105** gives complex **107**, which is a precursor intermediate of the 3,6-*cis* isomers. Such a reactive channel proceeds via thermodynamically more stable intermediates **105** and **107** leading to the 3,6-*cis* isomers, rather than the reactive channel via the more energetic intermediates **106** and **108** leading to the 3,6-*trans* isomers. This reaction pathway is preferable over alternative routes in the reaction of the resulting metal dienolate with MeI or D_2O.

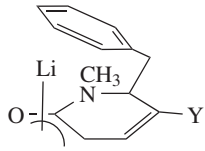

(**101**) (**a**) Y = H
(**b**) Y = F

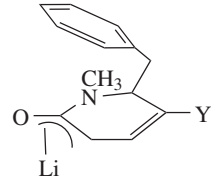

(**102**) (**a**) Y = H
(**b**) Y = F

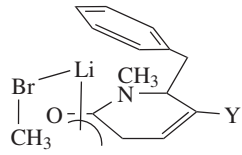

(**103**) (**a**) Y = H
(**b**) Y = F

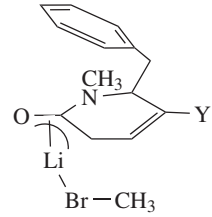

(**104**) (**a**) Y = H
(**b**) Y = F

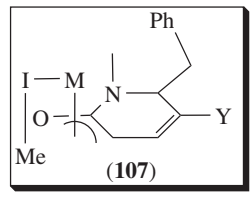

(**107**)

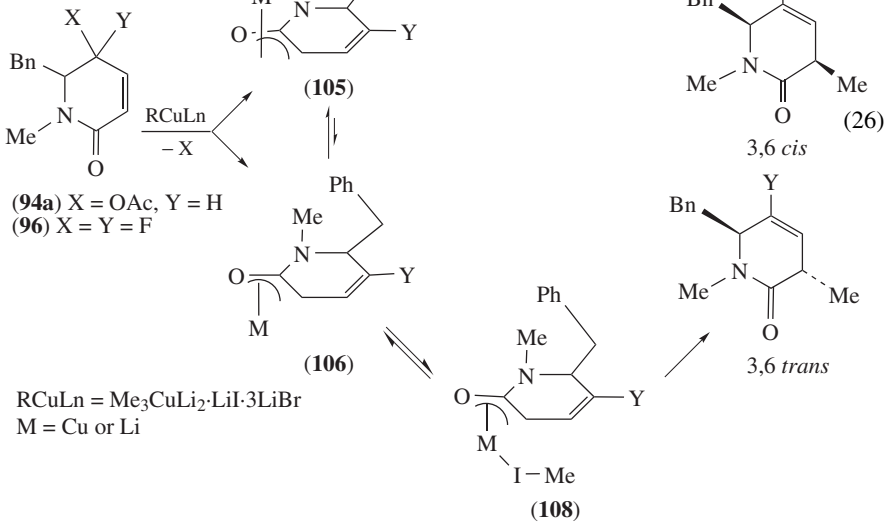

(**94a**) X = OAc, Y = H
(**96**) X = Y = F

(**105**)

(**106**)

(**108**)

RCuLn = $Me_3CuLi_2 \cdot LiI \cdot 3LiBr$
M = Cu or Li

3,6 *cis*

3,6 *trans*

(26)

In contrast, the approach of bulky alkyl halides from the same side of the benzyl side chain would be difficult due to steric repulsion. Then, DFT calculations of complexes coordinated with *i*-PrBr were performed and the results implied that complex derived from the π-allyllithium intermediate **101a** was thermodynamically more stable than complex derived from **102a**[100]. However, the subsequent alkylation step might be disturbed by steric hindrance of the *i*-Pr group, implying that electrophilic trapping with bulky alkyl halides such as *i*-Pr could be controlled in the final step of the alkylation to yield the 3,6-*trans* isomer as the main product.

Recent studies have suggested that coordination with a lithium cation may be responsible for the stereochemical outcome in Meyers-type enolate alkylations[102, 103]. In fact, the hypothesis that the diastereofacial selectivity observed in these reactions might result from specific interactions with a solvated lithium cation was already proposed in 1990[104]. Nevertheless, the potential influence exerted by solvation and lithium cation coordination was not supported by a series of experimental results reported by Romo and Meyers[105], who stated that '*it would appear that neither the aggregation state of the enolate nor the coordination sphere about lithium plays a major role in the observed selectivity*'. This contention is further supported by recent theoretical studies of Ando[106], who carried out a detailed analysis of the potential influence of solvated lithium cation on the stereoselective alkylation of enolates of γ-butyrolactones. The results showed conclusively that complexation with lithium cation had a negligible effect on the relative stability of the transition states leading to *exo* and *endo* addition. The stereochemical outcome in the alkylation of γ-butyrolactones is determined by the different torsional strain in the *endo* and *exo* TSs.

Bosch, Luque and coworkers[107] studied the influence of the lithium cation coordination on diastereoselective alkylation of enolates of oxazolopiperidone **109** (see equation 27). The TSs corresponding to the addition of methyl chloride to the enolate of **109** coordinated to a lithium cation solvated by two thf molecules were determined at the B3LYP/6-31+G(d) level. The length of the C−C forming bond in the solvated *exo* TS (**110**, 2.371 Å) was 0.021 Å shorter than that in the *endo* TS (**111**, 2.350 Å), which agrees with the geometrical difference found from B3LYP/6-31+G(d) geometry optimizations for the attack of methyl chloride to the enolate of **109** (0.031 Å). Moreover, the intermolecular H···H distance between the hydrogen atoms bonded at the enolate C_γ atom and the incoming methyl group amounts to 2.392 Å, as compared to the H···H distance of 2.339 Å found in the absence of the solvated lithium cation. Finally, the *endo* TS **111** was destabilized by 1.2 kcal mol^{-1} relative to the *exo* TS **110**, as compared to the 1.7 kcal mol^{-1} destabilization for the attack of methyl chloride to the enolate of **109**. The relative stability of the two TSs was indeed little affected upon addition of the free energies of solvation, as determined from SCRF calculations in carbon tetrachloride, chloroform, octanol and water solvents. Therefore, these findings suggested that coordination of a solvated lithium cation to the enolate *does not play a crucial role* in modulating the stereochemical outcome of the reaction.

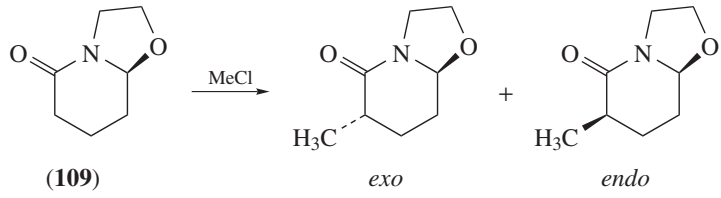

(**109**) *exo* *endo* (27)

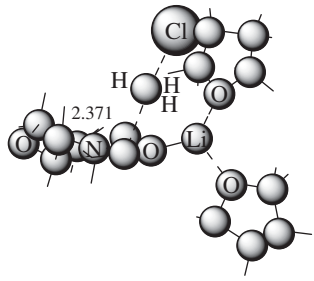

(**110**)

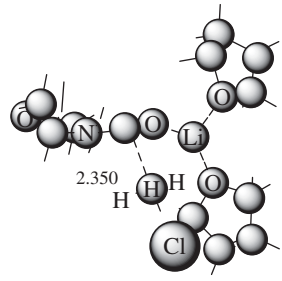

(**111**)

Recently, Pratt and coworkers[108] calculated the gas-phase activation energies for three reactions of lithium acetaldehyde enolate, namely the aldol reaction (equation 28), proton transfer (equation 29) and a bimolecular nucleophilic substitution (equation 30). The purpose of this study was to determine which levels of theory can be used to obtain accurate activation energies in the gas-phase using Hartree–Fock, DFT and MP2 methods. Although organolithium compounds are generally used in solution, solvation is a complex issue and was not treated in this study. Rather, they focused on obtaining one or more acceptable gas-phase methods that would be suitable to be used in conjunction with solvent models in the future. This comparative study showed that the MP2 calculated activation barriers were generally in qualitative agreement with those calculated by using the MP4 or QCISD methods. In contrast, the DFT calculations carried out using B3LYP, MPW1PW91, MPW1K, MPW1B95 and MPW1BK functionals gave erratic activation barriers. Nevertheless, when the energy barriers of transition structures were in reasonable agreement with MP2 estimates, the lengths of the forming or breaking bonds were generally also in good agreement.

Aldol Reaction

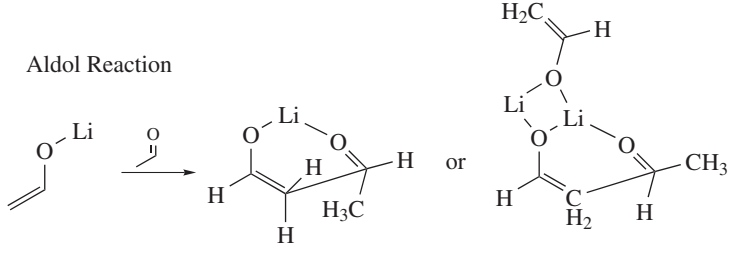

(28)

Monomer Dimer

Proton Transfer

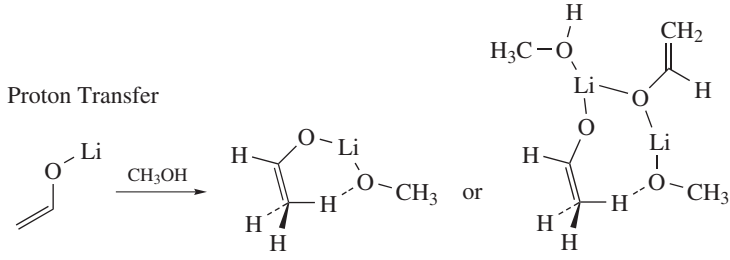

(29)

Monomer Dimer

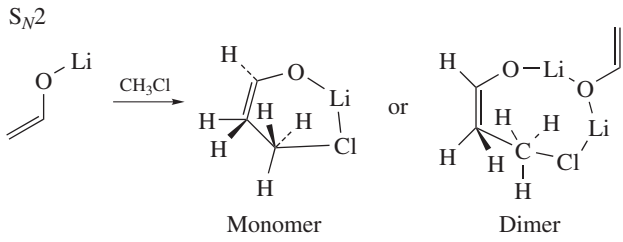

(30)

Good energy estimates could be obtained from single-point MP2//B3LYP calculations, as shown in Table 12, where the values for the barrier heights agree within 1 kcal mol^{-1}, except for the aldol reaction (equation 28), for which the results differed by about 1.8 kcal mol^{-1}. Geometry optimization at the MP2 level renders acceptable results, but it is a very computationally demanding task for large molecules, especially those where solvent ligands are included in the model systems to be optimized. Thus, Pratt and coworkers concluded that a transition structure can be located and characterized by means of the B3LYP method, while a reasonable estimation of lithium enolate activation barriers in the gas phase can be obtained by single point calculations at the MP2//B3LYP level.

D. Addition Reactions

1. Lithium enolates

The carbonyl-carbon kinetic isotope effect (KIE) and the substituent effects for the reaction of lithium pinacolone enolate (**112**) with benzaldehyde (equation 31) were analyzed by Yamataka, Mishima and coworkers[109] and the results were compared with those for other lithium reagents such as MeLi, PhLi and AllLi. *Ab initio* (HF/6-31+G*) calculations were carried out to estimate the equilibrium isotope effect (EIE) on the addition to benzaldehyde. In general, a carbonyl addition reaction (equation 32) proceeds by way of either a direct one-step polar nucleophilic attack (PL) or a two-step process involving electron transfer (ET) and a radical ion intermediate. The carbonyl-carbon KIE was of primary nature for the PL or the radical coupling (RC) rate-determining ET mechanism, while it was considered to be less important for the ET rate-determining mechanism. The reaction of **112** with benzaldehyde gave a small positive KIE ($^{12}k/^{13}k = 1.019$), which is larger than the theoretical EIE ($^{12}k/^{13}k = 1.006$). Thus, there is a reaction-coordinate contribution to the observed KIE. This was in sharp contrast to the absence of

TABLE 12. Comparison of $\Delta E^{\neq}$ and $\Delta G^{\neq}$ calculated at two levels of theory, for intermediates derived from the lithium enolates of acetaldehyde in three reactions carried out at 298.15 K

		$\Delta E^{\neq}$ (kcal mol^{-1})		$\Delta G^{\neq}$ (kcal mol^{-1})	
Equation	Intermediate	Level 1[a]	Level 2[b]	Level 1[a]	Level 2[b]
27 (aldol)	monomer	0.46	4.91	2.24	6.69
27 (aldol)	dimer	6.72	11.0	5.78	10.0
28 (proton transfer)	monomer	8.62	5.48	8.64	5.50
28 (proton transfer)	dimer	17.8	13.5	18.1	13.8
29 (S$_N$2)	monomer	26.4	29.3	26.9	29.8
29 (S$_N$2)	dimer	24.3	27.0	23.9	26.7

[a] Single-point calculations at the MP2//B3LYP level of theory.
[b] Calculations at the MP2/6-31+G(d) and MP2/6-31+G(d)//B3LYP/6-31+G(d) level of theory.

KIE ($^{12}k/^{14}k = 1.000$) measured previously for the MeLi addition. Dehalogenation and enone-isomerization probe experiments showed no evidence for a single electron transfer to occur during the course of the reaction. The primary carbonyl-carbon KIE together with the substituent effect and chemical probe experiments led to the conclusion that equation 31 proceeds via the polar mechanism.

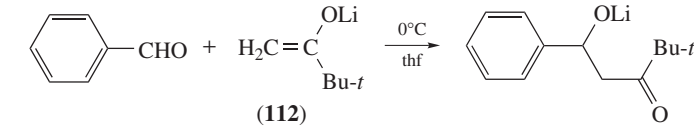

(**112**) (31)

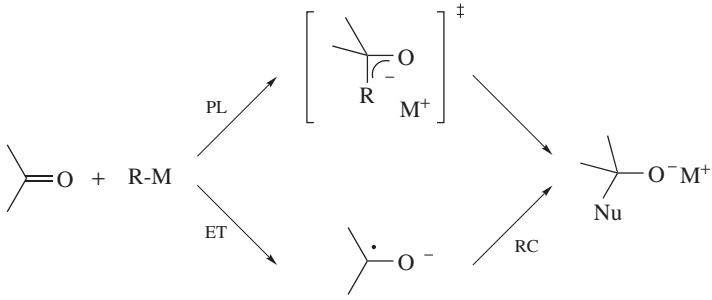

(32)

The mixed Tishchenko reaction involves the reaction of the aldol product **113** from one aldehyde with another aldehyde having no α-hydrogens to yield an ester[110]. The products were proposed to be formed through an aldol step (equation 33), followed by addition of another aldehyde (equation 34) and an intramolecular hydride transfer (equation 35). However, several aspects of this mechanism need to be clarified. As part of the continuing mechanistic studies carried out by Streitwieser and coworkers on reactions of alkali enolates[111], it was found that the aldol–Tishchenko reaction between certain lithium enolates and benzaldehyde proceeded cleanly in thf at room temperature[112]. Reaction of the lithium enolate of isobutyrophenone (Liibp) with 1 equiv of benzaldehyde in thf at $-65\,^{\circ}C$ affords a convenient route to the normal aldol product **113** (R = R″ = Ph, R′ = Me). At room temperature, however, the only product observed after acid workup was the diol-monoester **116**, apparently derived from the corresponding lithium ester alcoholate (**115**, R = R″ = Ph, R′ = Me), which was quantitatively transformed into **116** after quenching. As found in other systems[113], only the *anti* diol-monoester diastereomer was formed.

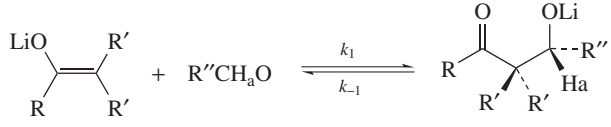

(**113**) (33)

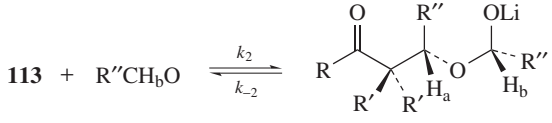

114 (34)

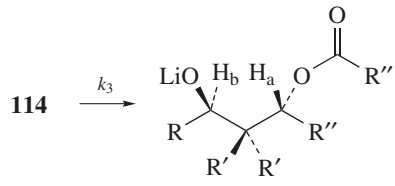

(35)

(**115**)

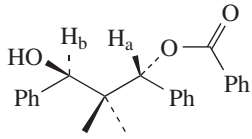

(**116**)

Although the energetics obtained from *ab initio* calculations on a model system consisting of unsolvated formaldehyde and the lithium enolate of acetaldehyde (Lien) (R = Me, R′ = H, in equation 33) as the reacting species is inadequate for describing the energetics of the real reactions in solution, the computed isotope effects should still be useful, since they often are rather insensitive to solvent and substituent effects. The computed reaction barriers, energies as well as the isotope effects of the optimized geometries for equilibrium (**117**, **113**) and transition structures (**118**, **120** and **121**) for the sequence of reactions in equations 33 to 35, are given in Table 13. The computed isotope effects derived only from the zero point energy (ZPE) effects were in excellent agreement with experiment[112]. In particular, the calculated EIE, $K_H/K_D = 0.65$, for addition to the carbonyl group of formaldehyde compares well with the experimental value of 0.74. The computed isotope effect for the rate-determining hydride transfer was normal and substantial, 3.22, in good agreement with the experimental value of 2.9. This agreement indicates that the model system was reasonable, that the proposed reaction mechanism was correct and especially

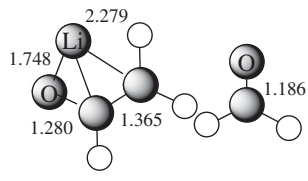

(**117**)

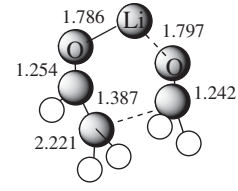

(**118**)

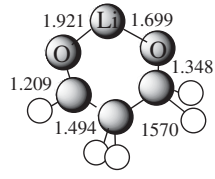

(**119**)

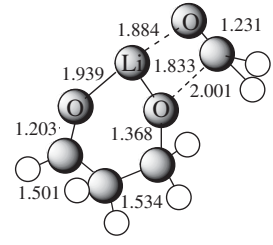

(**120**)

TABLE 13. Computed reaction and activation energies (kcal mol^{-1}) and corresponding kinetic (KIE) and equilibrium (EIE) isotope effects a reaction sequence between lithium acetaldehyde enolate (Lien) and formaldehyde

Reaction	ΔE^a	ΔZPE^b	$\Delta\Delta$ZPE^c	Isotope effect^d
LiEn + $CH_2O \rightleftharpoons$ **117** (complex-1)	−18.4	1.625	0.122	$EIE_{complex\text{-}1} = 0.92$
LiEn + $CH_2O \rightarrow$ **118** (TS1)	−12.2	2.379	0.225	$KIE_1 = 0.84$
LiEn + $CH_2O \rightleftharpoons$ **119**	−26.8	4.138	0.256	$EIE_1 = 0.82$
119 + $CH_2O \rightleftharpoons$ complex-2	−13.8	1.280	0.085	$EIE_{complex\text{-}2} = 0.95$
119+ $CH_2O \rightarrow$ **120** (TS2)	−11.1	2.205	0.225	$KIE_2 = 0.79$
119 + $CH_2O \rightleftharpoons$ **114**	−14.1	4.070	0.293	$EIE_2 = 0.77$
114 $\rightarrow$ **120** (TS3)	25.1	−1.152	−0.654	$KIE_3 = 3.22$
114 $\rightleftharpoons$ **115**	−3.0	0.315	−0.033	$EIE_3 = 1.05$

[a] Energies are given in kcal mol^{-1} and corrected for ΔZPE (scaled by a factor of 0.9).
[b] $\Delta ZPE = ZPE_{product} - {}^a(ZPE)_{reactants}$; or $ZPE_{TS} - {}^a(ZPE)_{reactants}$ (proteo species).
[c] $\Delta\Delta ZPE = \Delta ZPEH - \Delta ZPED$; ΔZPED corresponds to the terms for the reactions of monodeuteriated aldehydes.
[d] Isotope effects were computed at 25 °C. The two hydrogens of formaldehyde cease to be equivalent in the reaction products. Similar isotope effects are obtained when either of the two hydrogens is deuteriated.

that the computed transition structure **121** for the hydride transfer is a suitable model of the chemical reaction.

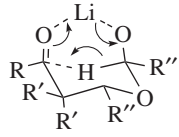

(**121**) (R = Me, R′ = R″ = H)

The Horner–Wadsworth–Emmons (HWE) modification of the Wittig reaction is a widely employed method in organic synthesis for the preparation of α,β-unsaturated esters. The phosphonate anions are strongly nucleophilic and react readily with carbonyl compounds under mild conditions to form olefins and water-soluble phosphate esters in high yields. A characteristic feature of the general HWE reaction is the predominant formation of thermodynamically favored *trans*-olefins. Especially high *trans* selectivity was found in the presence of strongly coordinating counterions such as Li^+[114]. To find the factors which influence its stereochemistry, Ando[115] studied the mechanism of the HWE reaction of lithium enolate **122** derived from trimethyl phosphonoacetate with acetaldehyde, to yield *E*- and *Z*-methyl 2-butenoate (**123** and **124**, respectively), as shown in equation 36. *Ab initio* calculations indicated that the HWE reaction occurs with addition of the phosphonate enolate to the aldehyde, followed by oxaphosphetane formation, pseudorotation, P–C bond cleavage and then O–C bond cleavage. Calculations by the RHF/6-31+G* method showed that the oxaphosphetane formation is the rate-determining step, in which the transition state **125** leading to an *E*-olefin is 2.16 kcal mol^{-1} lower in energy than the transition state **126** leading to a *Z*-olefin. The electronic energy differences between **125** and **126** associated with oxaphosphetane formation were 2.20 and 2.23 kcal mol^{-1}, at the RHF/6-31+G* and B3LYP/6-31+G*//RHF/6-31+G* levels of calculation, respectively. Thus, the usual preference for *E*-olefins in the HWE reaction of dialkylphosphono acetate reagents was predicted by calculations.

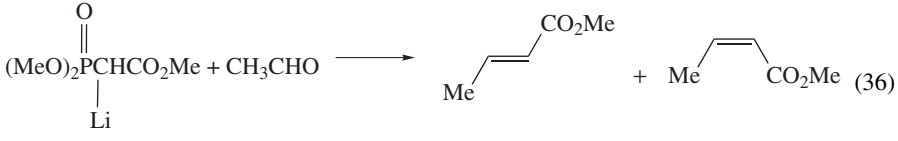

(36)

(**122**) (**123**) (*E*) (**124**) (*Z*)

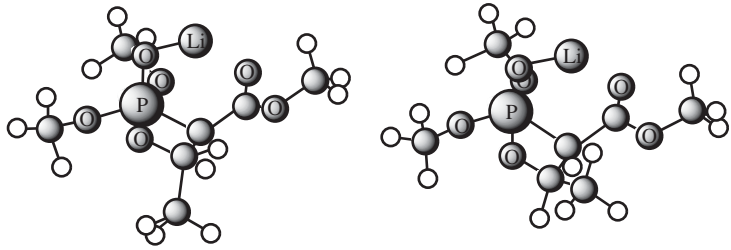

(**125**) (*E* precursor TS) (**126**) (*Z* precursor TS)

Ojea and coworkers[116] investigated the *syn,anti*-selectivity of aldol additions of the lithiated Schollkopf's bislactim ether **127** to 1,3-dioxolane-4-carboxaldehydes such as **128** (equation 37). The reaction involves an initial coordination of the carbonyl oxygen to the lithium atom to form the complex **(129)**. Subsequently, reorganization of this intermediate through competing six-membered transition structures affords mixtures of the lithium aldolates **130**–**133**. The ONIOM method developed by Morokuma and coworkers[117], which has been proven to be a very valuable tool for the theoretical treatment of large molecular systems, was applied for the study of the aldol reaction between **127** and **128**. Within this extrapolation method an *ab initio* semiempirical scheme operated for the description of the system, as depicted in **134**. The *ab initio* part was limited to an 'inner layer' including the critical parts of the reacting system: the atoms directly involved in the breaking and forming bonds and areas sensitive to electronic effects, such as the groups directly bonded to the azaenolate moiety and to the α-position of the aldehyde as well as the oxygen atoms of the solvent molecules coordinated to lithium. Thus, by replacing the groups excluded from the inner layer with hydrogen atoms, the *ab initio* model **135** was reduced to the interaction of a lithiated dihydropyrazinone and (2*S*)-hydroxypropanal in the presence of water molecules, which were treated at the HF level using the 3-21G* and 6-31G* basis sets[116].

The semiempirical MNDO method has the capacity to calculate geometries of chemically realistic reactants and transition structures bearing a full complement of alkyl substituents and solvents, which has been clearly established for organolithium compounds in general and for lithium amides and enolates in particular[80]. The MNDO method was used for the low-level treatment of the entire system shown in equation 37, for which the steric and electrostatic influence of the 'outer layer' was evaluated. In spite of its well known shortcomings, MNDO has been shown to successfully reproduce Li–N and Li–O interactions by comparisons with experimental results and *ab initio* calculations[118]. Thus, ONIOM calculations were performed with the (HF/3-21G*:MNDO) method during the initial conformational searches and with the (HF/6-31G*:MNDO) method for the reoptimization of all located stationary points. These methods were referred to as (I) and (II), respectively. Although the calculated MNDO energies were usually not as accurate as the MNDO geometries, it has been shown that for lithium compounds the

use of MNDO geometries followed by single point *ab initio* energy evaluations yields a potential energy surface which reproduces all the qualitative features of the fully *ab initio* surface[81]. Therefore, Ojea and coworkers[116] also computed B3LYP/6-31+G* energies on the most significant ONIOM geometries. Initial lithium–carbonyl coordination to form a disolvated complex such as **129**, with an energy gain of 4.6–8.4 kcal mol^{-1}, was followed by the rate-determining reorganization to the aldolate products through six-membered chair-like transition structures **136** to **139**. The experimental stereoselectivities of the aldol additions were adequately reproduced. According to the calculations, the most stable transition structures **136** and **137** were characterized by a non-Anh conformation of the aldehyde moiety. In addition, the β-methyl substituent of the aldehyde, *trans* to the carbonyl group, was found to increase the energy barrier of the competitive pathways, thus reinforcing the *syn,anti*-stereoselection of the aldol process.

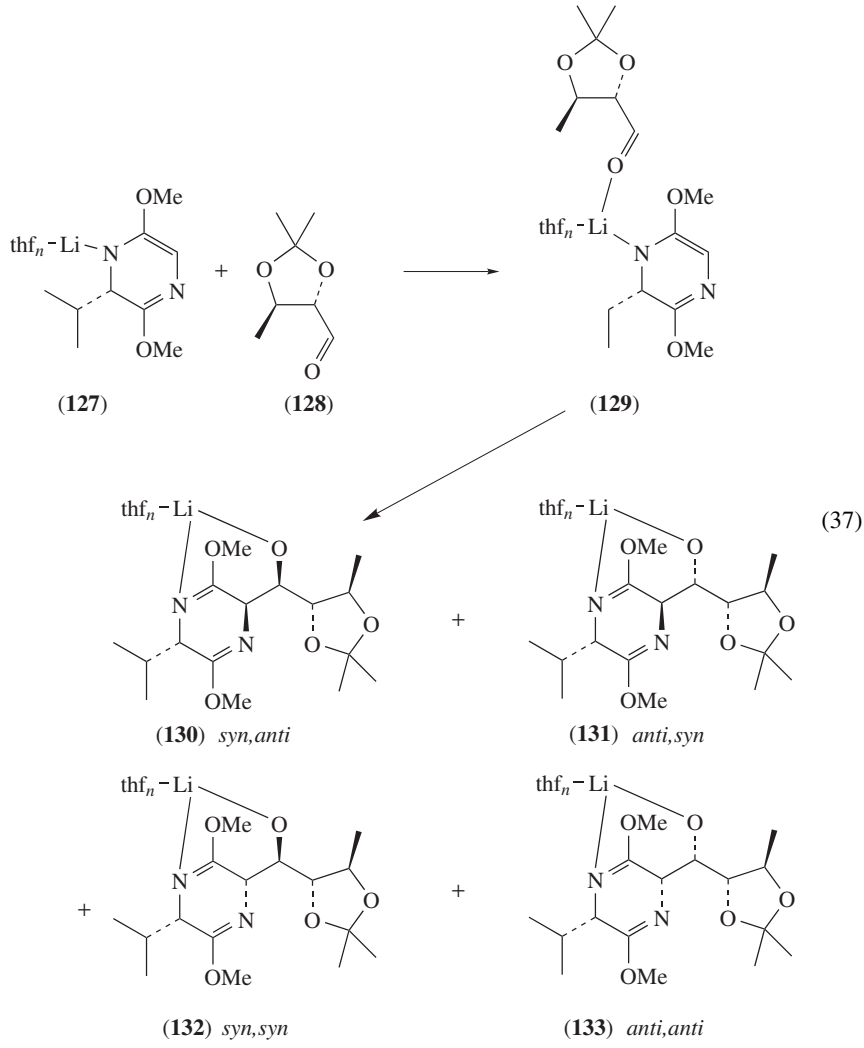

(37)

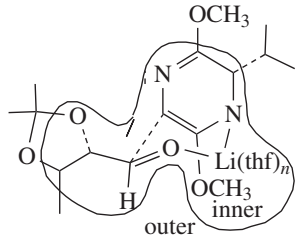

(**134**) 'real' model

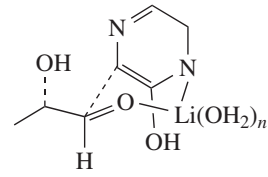

(**135**) *ab initio* model

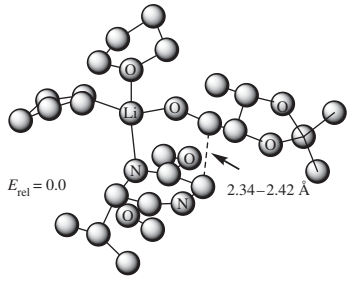

(**136**) ⟶ *syn,anti*

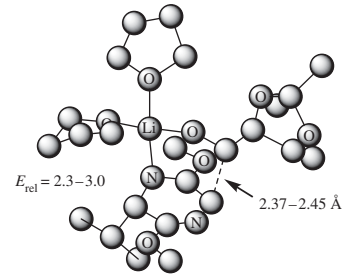

(**137**) ⟶ *anti,syn*

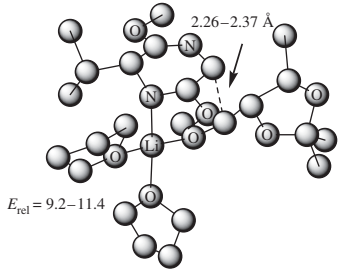

(**138**) ⟶ *syn,syn*

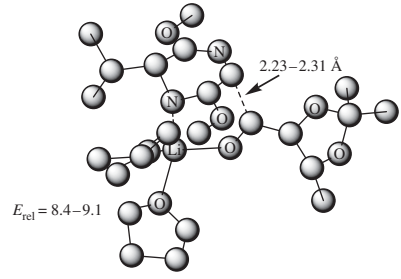

(**139**) ⟶ *anti,anti*

To assess the reliability of the particular ONIOM scheme employed in the analysis of the aldol addition, Ojea and coworkers[116] considered the difference between the activation energies of the most stable transition structures **136** and **137** in the favored disolvated reaction channel (**130** and **131**) as a convenient parameter for the *S*-value test proposed by Morokuma[119]. In this manner the error of the ONIOM(I) and ONIOM(II) extrapolations, with respect to their benchmark calculations at the B3LYP/6-31+G*//HF/6-31G* level, were 0.86 and 0.60 kcal mol^{-1}, respectively. When the geometry optimizations at the ONIOM(II) level were followed by single-point energy evaluations at the B3LYP/6-31+G* level, the error was reduced to less than 0.10 kcal mol^{-1}.

Addition of lithium enolates derived from esters and ketones to epoxides has been the object of some consideration, because it offers a direct route for the synthesis of γ-hydroxy esters and γ-hydroxy ketones, very useful for difunctionalized organic compounds[120]. In fact, more complex molecules can be synthesized by using these compounds as synthons

for polysubstituted lactones and tetrahydrofuranes, or related bicyclic, carbocyclic and heterocyclic compounds[121].

Crotti, Favero and coworkers introduced synthetic methods based on the reaction of lithium enolates of simple ketones with epoxides in the presence of $LiClO_4$, lanthanide salts or $Sc(OTf)_3$[122, 123]. In equation 38 is shown the *in situ* preparation of litium enolate **140** of *Z*-configuration, derived from propiophenone on addition of lithium hexamethyldisilazane (lhmds). Addition of **140** to propene oxide (**141**) in the presence of $Sc(OTf)_3$ as catalyst, in toluene/hexane solvent, afforded a mixture of *syn*- (**142**) and *anti*- (**143**) γ-hydroxy ketones with a slight preference for *anti* (**142**:**143** = 45:55)[123]. The reaction was completely regioselective with an exclusive attack of the enolate on the less substituted oxirane carbon. A rationalization of these experimental results is attained on assuming transition structures such as **144**, leading to the *syn* adduct **142**, and **145**, leading to the *anti* adduct **143**, where the [M] coordinated to the oxirane oxygen is a metal catalyst (Li, Al, Sc) with its associated groups, similar to the analogous addition of aluminum enolates of esters to epoxides[124]. Crotti, Favero and coworkers[125] studied the geometry of the TS involved in equation 38, using the B3LYP/6-31+G(d)//B3LYP/6-31+G(d) computing level in vacuum and in the presence of the solvent, without and with participation of the metal catalyst.

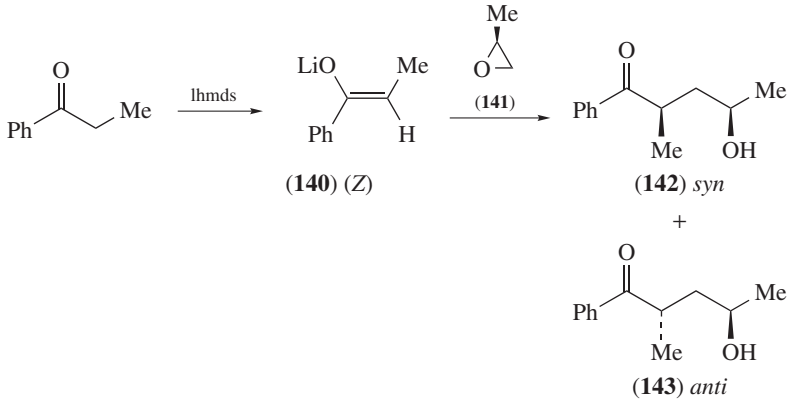

(38)

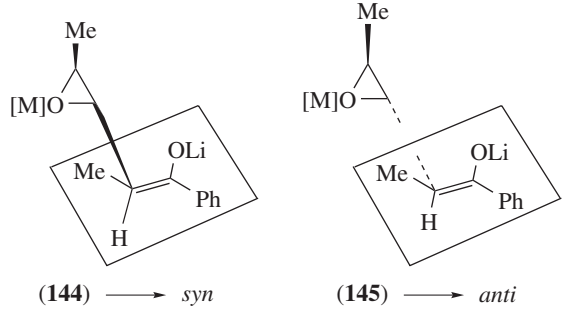

The nucleophilic addition reactions of enolates to imines and related compounds (the so-called Mannich-type reactions, equation 39) are important tools in organic synthesis[126] and a variety of electrophiles have been used to obtain the resulting nitrogen-containing

compounds. The *syn*–*anti* stereoselectivity of the lithium enolate–imine addition reaction has been thoroughly investigated. The rule of thumb is that *E*-OLi enolates and *E*-imines (usually the highly reactive trimethylsilylimines)[127] react to form *syn* products, whereas *Z*–OLi enolates and *E*-imines typically react to form mixtures of *syn* and *anti* products[128]. This rule was contradicted by several important examples where *E*-OLi enolates and *E*-trimethylsilylimines react to form *anti* products with high selectivity[129]. The results have been rationalized using the chair- and boat-like transition structures shown in equations 40 and 41, and the *syn*–*anti* preferences have been discussed examining the steric bias of the imine substituents[128–130].

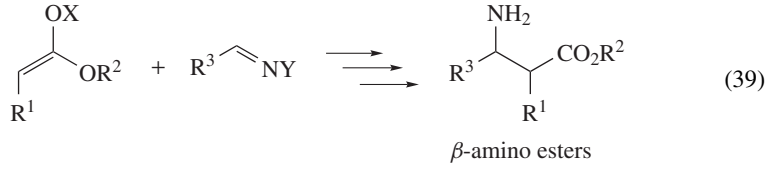

(39)

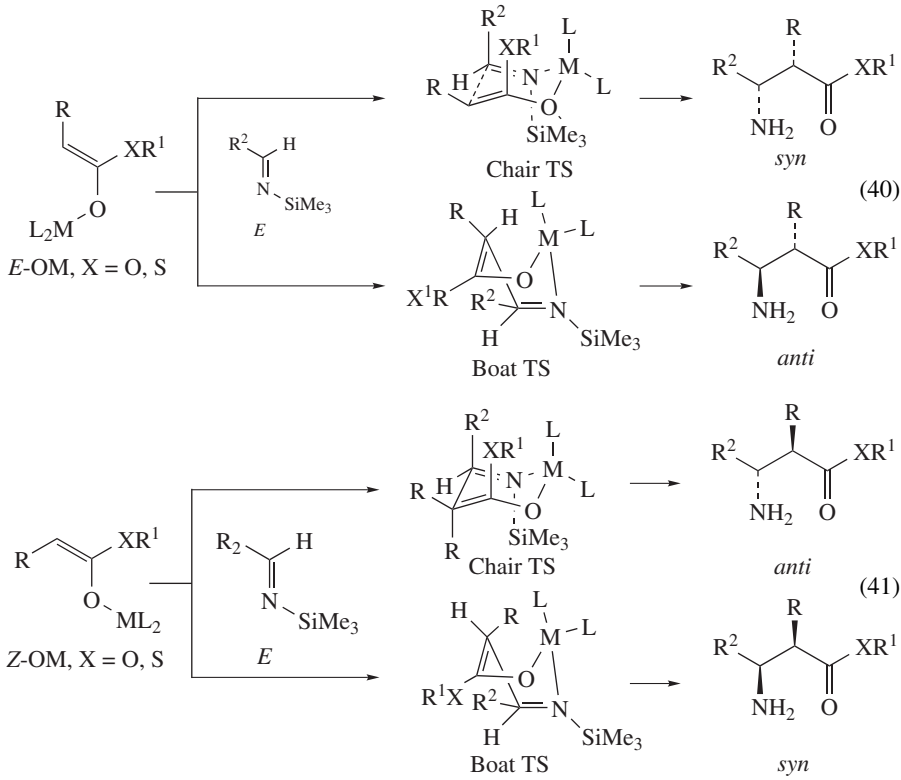

The reaction of a lithium ester enolate (**146**) with a nitrone (**147**) to yield a β-hydroxylamino acid ester (**149**) has been recently investigated by Domingo, Merino and coworkers[131], using DFT (B3LYP/6-31G*) methods, to gain insight on the molecular mechanism. The proposed transition structure (**148**) shown in equation 42 derives from attack of the most nucleophilic center of enolate **146** on the most electrophilic center of

nitrone **147**. Along the reaction channel, the lithium atom was coordinated with two ether molecules to complete a tetrahedral coordination sphere. The activation energy associated with the C−C bond formation process was 1.0 kcal mol^{-1}. Coordination of the lithium atom to the nitrone and the enolate oxygen atoms favored the nucleophilic attack of the enolate **146** on the nitrone **147** along the *gauche* reaction channel by an increase of the electrophilicity of the nitrone; consequently, the lithium atom acts as a Lewis acid catalyst favoring the nucleophilic addition. Formation of the adduct **149** was exothermic by −13.4 kcal mol^{-1}.

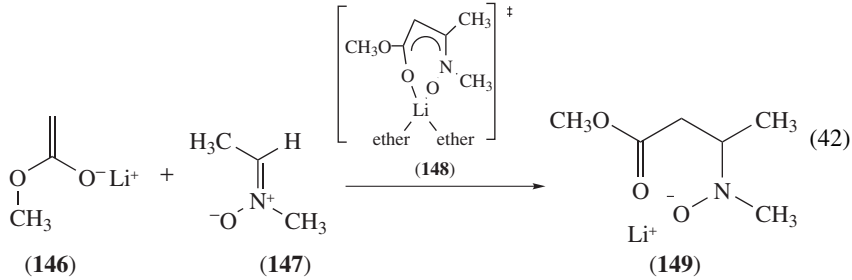

(**146**) (**147**) (**149**) (42)

2. Boron enolates

The Evans aldol reaction readily makes possible the asymmetric synthesis of biologically important compounds. In this reaction aldehyde reacts preferentially on the *re* face of the double bond of boron enolate **150a** to provide the 'normal Evans' **151** *syn* aldol product (see equation 43)[132]. In some cases, alteration of the reaction conditions results in reversal of π-face selectivity of **150a**[133]. Several aldehydes containing fluoral (CF_3CHO) were previously shown to react on the *si* face of **150a** and give the 'non-Evans' **153** *syn* and **154** *anti* aldols[134]. The reversal of stereoselectivity with fluoral was discussed by Makino and coworkers[135] using semiempirical AM1 calculations to obtain the reaction pathways for *re*- and *si*-face attacks.

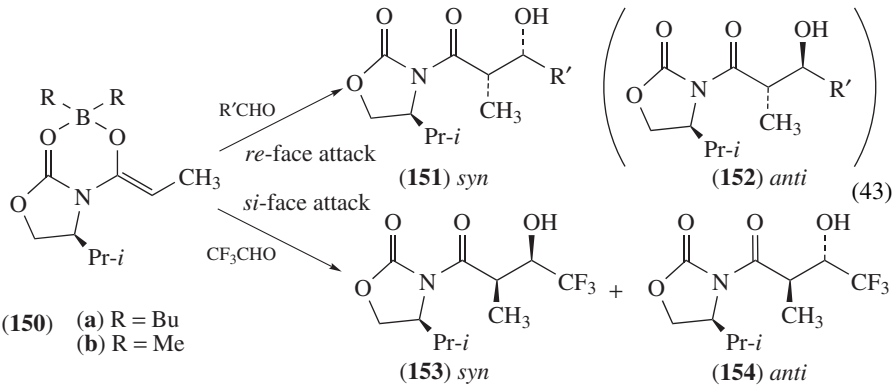

(43)

AM1 calculations were performed to locate the pathway for the *re*-face attack, using the boron enolate **150b** as a model compound for **150a** in the gas phase and acetaldehyde. In transition structure **155**, the forming bond length was 2.19 Å and the heat of formation was −179.6 kcal mol^{-1} (Figure 2). On rotating the oxazolidinone ring in **155** the forming

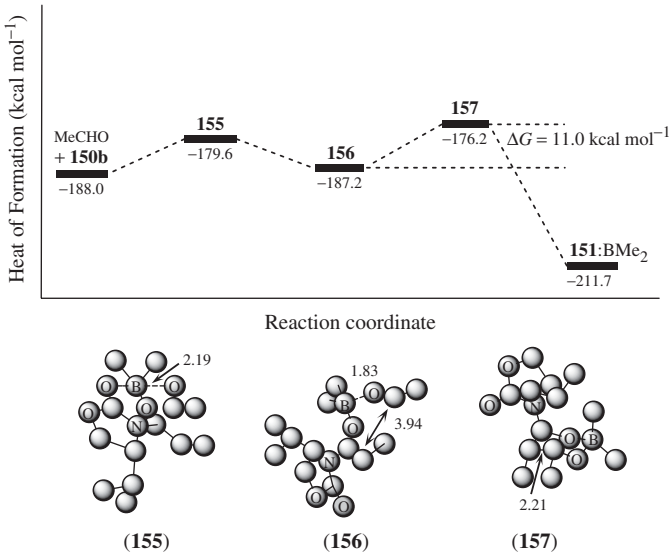

FIGURE 2. AM1-calculated reaction path for the aldol reaction of acetaldehyde with propionaldehyde, using complex **150b** as a model for the intermediate boron enolate complex **150a**. Reproduced from Y. Makino, K. Iseki, K. Fujii, S. Oishi, T. Hirano and Y. Kobayashi, *Tetrahedron Lett.*, **36**, 6527. Copyright 1995, courtesy of Elsevier

B−O bond was shortened and the heat of formation decreased to give a reactant complex **156** with a newly formed B−O bond (1.83 Å) and a value for the heat of formation of −187.2 kcal mol^{-1}. Subsequent calculation by approaching the carbonyl carbon of acetaldehyde to the β-carbon of the enolate double bond provided the second maximal point **157** and a product complex **151**:BMe_2. In the Zimmerman–Traxler chair transition structure **157** the forming C−C bond length was 2.21 Å and the heat of formation was −176.2 kcal mol^{-1}. With fluoral, analogous calculations failed to locate the transition structure corresponding to **155**. Reaction with fluoral thus does not proceed via the closed transition state required for *re*-face attack[132–134].

Figure 3 summarizes pathways for *si*-face attack[133, 134], where a reaction coordinate calculation with fluoral was carried out by approaching the carbonyl carbon of the aldehyde to β-carbon of the enolate double bond of **150b** to give a stationary point. From an open transition structure, **158**, with a value of the forming bond of 1.83 Å, may possibly lead to the formation of a product complex, **154**:BMe_2. Another possible transition structure (an open transition structure **159**) was found by exchanging the hydrogen and oxygen of the fluoral in **158**. In **159**, the forming bond length was 1.82 Å and the heat of formation was −308.1 kcal mol^{-1}. The transition structure **159** should lead to the formation of another product complex, **153**:BMe_2. With acetaldehyde, analogous calculation failed to give an open transition structure such as **158** or **159**, indicating that the reaction with acetaldehyde does not proceed via the open transition state required for *si*-face attack[133, 134].

Reversal of π-face selectivity of the enolate may be possibly due to the low Lewis basicity and high electrophilicity of fluoral. In Table 14, fluoral has lower LUMO (higher electrophilicity) and lower negative charge of the carbonyl oxygen (lower Lewis basicity) than acetaldehyde, showing *re*-face attack. With fluoral the low Lewis basicity prevents the coordination of carbonyl oxygen with boron, and the high electrophilicity promotes

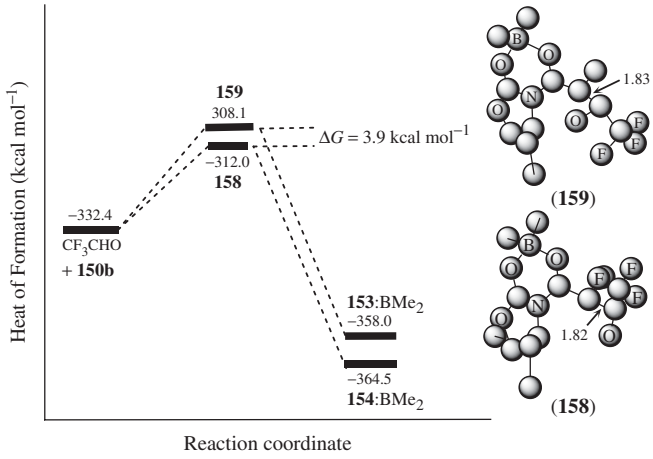

FIGURE 3. AMl-calculated reaction path coordinate for the aldol reaction of **150b** with CF_3CHO. Reproduced from Y. Makino, K. Iseki, K. Fujii, S. Oishi, T. Hirano and Y. Kobayashi, *Tetrahedron Lett.*, **36**, 6527. Copyright 1995, courtesy of Elsevier

TABLE 14. *Ab initio* calculations of carbonyl compounds with the HF/3-21G basis set

Carbonyl compound	MO energy levels (au)		Mulliken atomic charges (e)		Stereoselectivities (boron enolate **122a**)
	HOMO	LUMO	O	C	
CH_3CHO	−0.4145	0.1542	−0.519	+0.520	*re* (normal Evans)
CF_3CHO	−0.4937	0.0699	−0.431	+0.246	*si* (non-Evans)
EtO_2CCHO	−0.4239	0.0807	−0.476	+0.302	*re*:*si* = 21:79

the reaction via an open transition structure, even though the carbonyl does not coordinate with a Lewis acid such as $TiCl_4$[133]. Ethyl glyoxylate (EtO_2CCHO), which reacts on either face of the double bond of the boron enolate **150a** (*re*:*si* = 21:79), shows a LUMO level and a negative charge of the carbonyl oxygen intermediate between those of fluoral and acetaldehyde. The semiempirical AM1 calculations reproduced the experimental results, i.e. acetaldehyde and fluoral react preferentially on *re* and *si* faces of the double bond of the boron enolate, respectively.

The stereochemical analysis of the metal enolate–imine reaction appears to be simpler in the case of boron enolates: *Z*-OB enolates react with *E*-imines leading preferentially to *anti* products[136], while *E*-OB enolates can give either *syn* or *anti* products or *syn*–*anti* mixtures, depending on the particular substrate[136, 137]. The results were rationalized considering a chair-like TS for the *Z*-OB enolates[136] and a chair-like *vs*. a boat-like TS for the *E*-OB enolates (see equations 40 and 41)[137].

Bernardi and coworkers[138] performed an *ab initio* study at the HF/3-21G computing level to gain a better understanding of the stereochemical factors controlling the aldol-type addition of enolborinates to imines. Only two TSs, the chair (**160**) and the boat (**161**), were located. In Table 15 are summarized the relative energies of the chair–boat pairs, as a result of introducing a methyl group in the various positions of **160** and **161**, to yield the fourteen TS structures **162**–**175**. The first interesting result was the negligible energy gap (0.1 kcal mol^{-1}) between the chair (**160**) and boat (**161**) conformations.

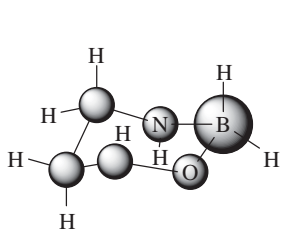

(**160**) chair

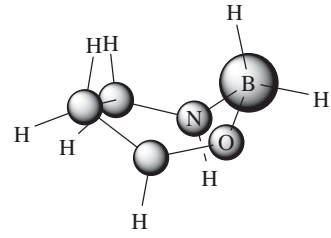

(**161**) boat

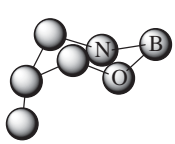

(**162**) chair

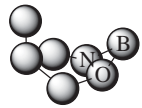

(**163**) boat

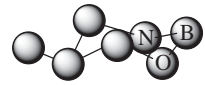

(**164**) chair

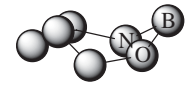

(**165**) boat

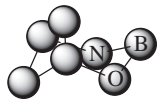

(**166**) chair

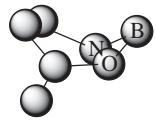

(**167**) boat

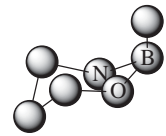

(**168**) chair

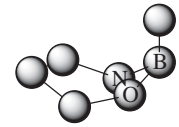

(**169**) boat

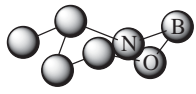

(**170**) chair

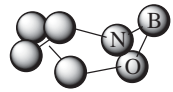

(**171**) boat

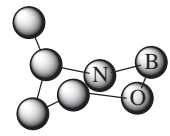

(**172**) chair

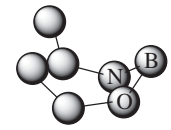

(**173**) boat

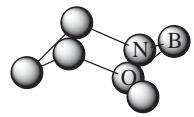

(**174**) chair

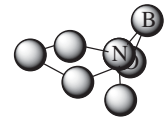

(**175**) boat

In the aldol case the chair was 1.3 kcal mol^{-1} higher in energy than the boat[139], and one would naively expect that in the imine case this gap would increase because of the presence of diaxial interactions of the *N*-substituent which are absent in the aldol chair. However, these interactions were greater in the boat TS[140].

The most striking effect among the TSs listed in Table 15 was the destabilization imparted by the enolate *Z*-methyl group of the boat **163** (4.5 kcal mol^{-1}) compared to the corresponding chair **162** arrangement. Like in the aldol reaction, this fact was clearly due to the interaction between the *Z*-methyl group and the substituent at the B heteroatom in the boat TS, and it is likely to increase in real cases where the substituent at B is not H but

TABLE 15. Relative energies of the conformers obtained after introduction of one Me group in the TSs **156** and **157**

Reagents	TS relative energies (kcal mol^{-1})	
	Chair	Boat[a]
CH_2=NH + H_2BO–CH=CH–CH_3 (*Z*)	**158**: 0.0	**159**: 4.5
CH_2=NH + H_2BO–CH=CH–CH_3 (*E*)	**160**: 0.0	**161**: 1.0
CH_2=NH + H_2BO–C(CH_3)=CH_2	**162**: 0.0	**163:** 1.0
CH_2=NH + H(CH_3)BO–CH=CH_2	**164**: 0.0[b]	**165:** 1.0[c]
CH_3–CH=NH (*Z*) + H_2BO–CH=CH_2	**166**: 0.3	**167**: 0.0
CH_3–CH=NH (*E*) + H_2BO–CH=CH_2	**168**: 0.1	**169**: 0.0
CH_2=NH–CH_3 + H_2BO–CH=CH_2	**170**: 0.3	**171**: 0.0

[a] With the B atom in the bow position.
[b] With the *B*-Me group in the axial position.
[c] With the *B*-Me group in the flagpole position.

a larger group. The effect was much reduced in the case of the corresponding *E*-enolate, where the boat **167**, although higher in energy (1.0 kcal mol^{-1}), is still competitive with the chair **166**. Imine substitution, both at C and at N, had a minor effect on the boat/chair balance: substituted imines stabilize the boats **171**, **173**, **175** only by 0.1–0.3 kcal mol^{-1}, over the corresponding chairs **170**, **172**, **174**. Steric effects in disubstituted TSs, after introducing a second methyl substituent in those of Table 15, were found to be qualitatively a combination. The following rules of thumb were devised from the above discussion: (a) a *Z*-enolate proceeds only through a chair TS; (b) an *E*-enolate proceeds through two competing TSs, the chair and the boat; (c) substituents on the enolate destabilize the boat TS, while substituents on the imine stabilize the boat TS, as compared to the chair. Therefore, *Z*-OB enolates react with *E*-imines via the chair TS shown in equation 40, leading preferentially to *anti* products[136]. *E*-OB enolates give either *syn* or *anti* products or *syn*–*anti* mixtures depending on the particular substrate[136, 137].

The influence of the protecting groups on the *syn*/*anti* stereoselectivity of boron aldol additions with erythrulose derivatives **176** and **178** to aldehydes RCHO (R = Et, *i*-Pr, Ph, 4-ClC_6H_4; equations 44 and 45) was studied by Carda and coworkers[141]. It was found that stereoselectivity depends on the type of protecting groups on the hydroxyl functions at the C3 and C4 atoms. Thus, erythruloses benzylated at these hydroxyl groups gave only *syn* aldols (**177**) while the corresponding benzoylated derivatives gave *anti* aldols (**179**) under the same reaction conditions. The resident chirality of the enolate promoted a complete internal 1,3-induction, which was *syn* in both aldol types.

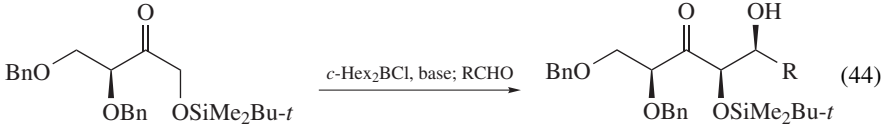

(**176**) (**177**) dr > 19:1 (44)

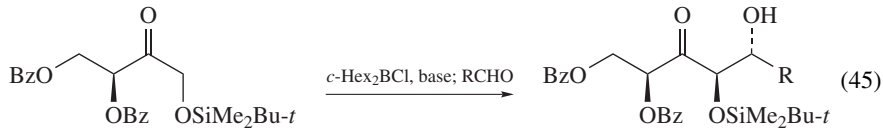

(**178**) (**179**) dr > 9:1 (45)

Carda and coworkers[141] rationalized the experimental results of equations 44 and 45 performing *ab initio* (HF/3-21G) calculations on the system depicted in Scheme 2, where **180** with the protecting group PG = $SiMe_3$ was selected as a model for the enolizing ketone, while benzaldehyde was the reacting aldehyde and the cyclohexyl groups of the enolization reagent were replaced by cyclopropyl groups. The study included the *E*- and *Z*-configurations of the boron enolates, **181** and **182**, and the four diastereoisomeric reactive channels for the aldol reactions, **183** to **186**. Table 16 shows the calculated energies of each molecular complex and of the respective transition structure, which leads to the final aldolate. The energy barrier for the individual process is the difference between these two energy contents. As shown, when boron enolate of *Z* configuration (**182**) reacts with the aldehyde carbonyl, the calculations predicted that the lowest energy barrier (19.8 kcal mol^{-1}) is that leading to the *syn–syn* aldol, in complete agreement with experimental results. For the corresponding transition structure **187**, calculations predicted a half-chair geometry (C=C···C=O dihedral angle, 70.8° *vs*. 60° in an ideal chair). The other three transition structures consisted of another half-chair and two boats of the 'boat A' type[142]. Calculations further predicted that the *anti–anti* aldol was thermodynamically the most stable adduct. All these data confirmed the conclusion that the aldol additions in equations 44 and 45 of ketones **176** and **178** are kinetically controlled processes which yield *syn–syn* aldols via the corresponding *Z* boron enolates.

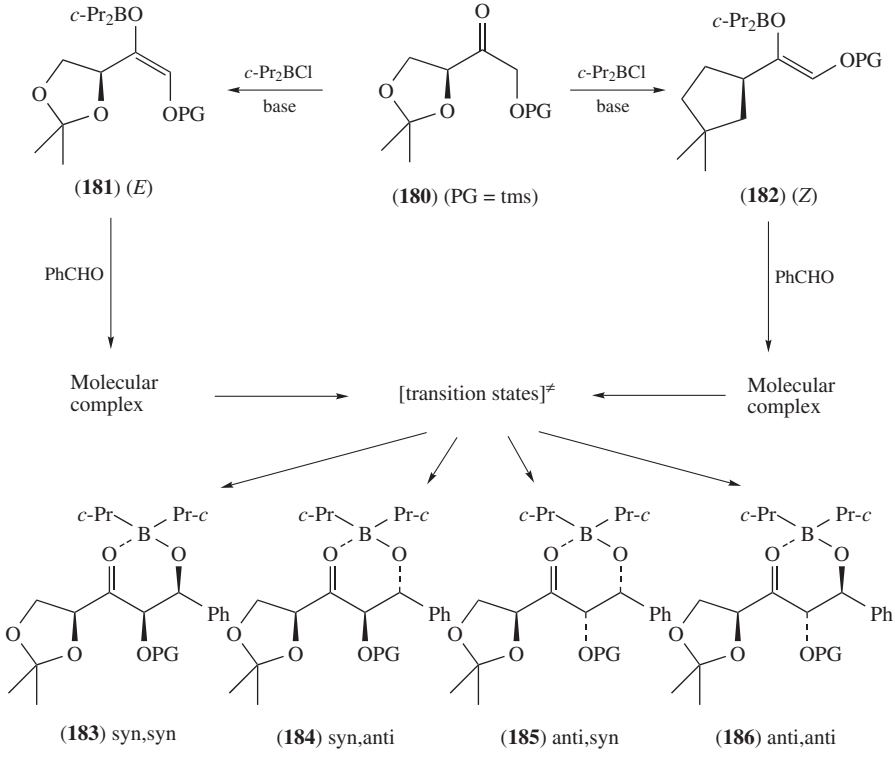

SCHEME 2. Diastereomeric pathways for the aldol reaction of model ketone **180** with benzaldehyde, mediated by *c*-Pr_2BCl

TABLE 16. Energies (in kcal mol^{-1}) of the stationary points in the reaction between the boron enolates **181** or **182** with benzaldehyde (Scheme 2), relative to these reagents, by the HF/6-31G*//HF/3-21G method

Boron enolate	Aldol configuration	Molecular complex	Transition state	Product
181 (*E*)	**183** (*syn*,*syn*)	−6.2	+23.9	−19.3
	184 (*syn*,*anti*)	−10.3	+9.7	−21.2
	185 (*anti*,*syn*)	−15.4	+13.7	−27.0
	186 (*anti*,*anti*)	−9.2	+12.4	−35.3
182 (*Z*)	**183** (*syn*,*syn*)	−7.4	+12.4	−19.9
	184 (*syn*,*anti*)	−14.4	+13.0	−21.8
	185 (*anti*,*syn*)	−14.4	+14.4	−27.5
	186 (*anti*,*anti*)	−16.6	+17.5	−35.9

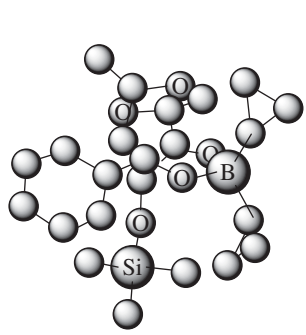

(**187**)

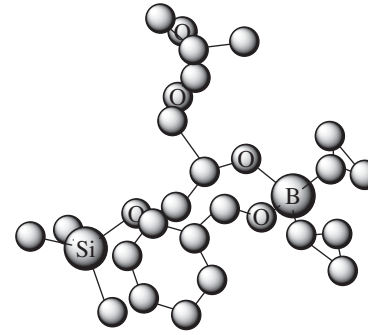

(**188**)

Aldol reactions of α-benzoyloxy ketone **178** afforded *syn*−*anti* aldols **179**. This strongly suggested the intermediacy of an *E* enolate and possibly a nonchair geometry for the key TS. Table 16 shows that the lowest energy barrier leading to the *syn*−*anti* aldol is in fact the *E*-boron enolate **181** (20 kcal mol^{-1}). Furthermore, the corresponding transition structure **188** adopts the 'boat B' type distorted geometry[142]. Three further high energy boat-like TSs were found in the calculations but no chair-like TSs were located. A plausible explanation for a boat-like TS being energetically favored here was that it minimizes the strain within the allylic moiety, as with the H atom at C_α which faces the enolate $OSiMe_2Bu$-*t* group (equation 46). The steric crowding which would exist in the chair TS between the OBz moiety and one of the *B*-cyclohexyl groups in **189** is relieved by rotation of the two B−O bonds and the subsequent spatial separation between these groups in **190**. Apparently, these two favorable steric factors are quantitatively more important than the less favorable, nonanticoplanar alignment of the C−OBz and C−OB dipoles, which occurs in the boat B TS.

3. Titanium enolates

Metal enolates of carbonyl compounds are important nucleophiles in C−C bond-forming reactions for the synthesis of nonfluorinated compounds. However, the metal enolates of fluorinated carbonyl compounds have been severely limited to α-F metal enolates, which can be stabilized by chelate structures containing the M−F moiety. In sharp

contrast, α-CF_3 metal enolates have generally been recognized as unstable and difficult to prepare because of the rapid β-M−F elimination(equation 47)[143].

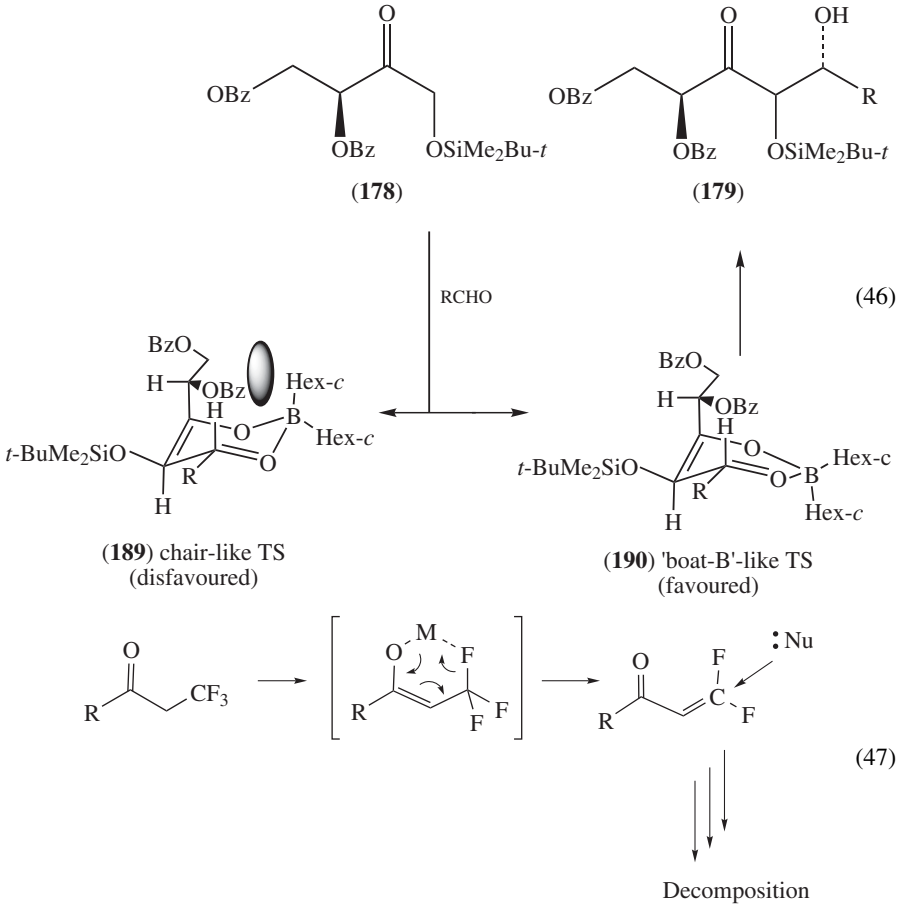

In general, the fluorine atom has been recognized to strongly coordinate with metals. However, the interaction between the metal and F vary widely according to the nature of the metal. α-Mef enolate precursors are, in principle, most effective synthons for compounds containing a Mef group. Mikami and Itoh showed that these enolates can be formed quantitatively by using $TiCl_4$ and Et_3N[144]. According to crystallographic data, Ti rather than Li has a strong affinity for F. Therefore, it seems strange that Ti enolates of α-Mef ketones could be formed without defluorination. To clarify this anomaly, the structures of Ti and Li enolates of 4,4,4-trifluoro-2-butanone (**191** and **192**, respectively) were optimized by B3LYP/631LAN at computing levels LANL2DZ for Ti and 6-31G* for other atoms[144]. In the Li enolate **192** a strong interaction between Li and F was clearly observed, and it can be easily understood that defluorination readily occurs. In contrast, in the Ti enolate **191**, the Ti−O−C angle is almost straight (170.2°), and no Ti−F interaction can be observed. The stability of the $TiCl_3$ enolate of an α-Mef ketone can be explained by the linearity of the Ti−O−C bond, which suppresses any Ti−F

interaction. The linearity of the Ti−O−C angle stems from the multiple bonding nature of the Ti−O bond. Donation of the lone electron pair of the O to an empty d orbital of the Ti causes multiple bonding[144]. This was supported by both the X-ray structure of Ti complexes and computational studies[145].

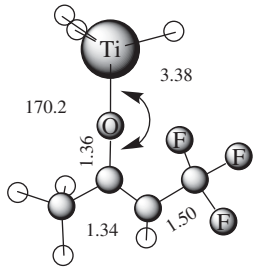

Ti enolate
(**191**)

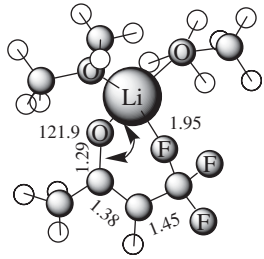

Li enolate
(**192**)

It is well known that the aldol reaction of a titanium enolate of *Z*-configuration would produce a *syn*-aldol via a cyclic transition structure[146]. However, titanium enolates of *Z*-configuration relative to a Mef group undergo anomalous reaction with aldehydes to yield *anti*-aldols with high stereoselectivity, as shown in Table 17 for the reaction depicted in equation 48[144]. For example, upon addition of benzaldehyde (R = Ph) to the *in situ*-generated **193**, the aldol **194** was obtained in moderate yield (46%) but with high diastereoselectivity (anti:syn > 99:1). Several Lewis acids were examined as an additive, and Ti(OPr-*i*)$_4$was found to be very effective for raising the yield without affecting the diastereoselectivity. Similar behavior regarding yields and diastereoselectivity was observed for aliphatic aldehydes (R = *i*-Pr, $PhCH_2CH_2$); however, in the case of fluoral (R = Mef) the presence of the Lewis acid lowered the yield because of significant polymerization. The *anti*-configuration of **194** was confirmed by XR or NMR analysis of its acetonide.

TABLE 17. Reaction of the $TiCl_3$ enolate of an α-Mef ketone (**193**) with an aldehyde RCHO, to yield an *anti*-aldol (**194**)

R	Yield % (dr)[a]	Yield % (dr)[b]
Ph	46 (>99:1)	97 (99:1)
i-Pr	45 (98:2)	80 (99:1)
$PhCH_2CH_2$	42 (98:2)	74 (97:3)
Mef	83 (90:10)	75 (91:9)

[a] For the reaction as shown in equation 48.
[b] For the reaction in equation 48 in the presence of 1.2 equiv of Ti(OPr-*i*)$_4$ as Lewis acid.

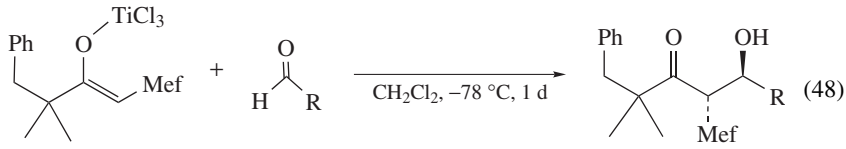

(48)

(**193**) (**194**)

The reaction of 2,2,2-trifluoroethyl *t*-butyl ketone with benzaldehyde, via the intermediate trichlorotitanum enolate, was taken as a model to uncover the origin of the *anti*-selective aldol reaction of α-Mef ketones. Transition structures **195** for the *anti*-aldol and **196** for the *syn*-aldol reaction were optimized at the B3LYP/631LAN level. Energy calculations of both transition structures were in good agreement with the experimental results, that of **196** being 4.1 kcal mol^{-1} higher than that of **195**. Surprisingly, an interaction between Ti and the Mef group, which was not present in the starting Ti enolate, was observed in both **195** and **196**. Owing to the Ti–F interaction, both **195** and **196** are fixed in a boat conformation; the Mef group would be attracted by Ti, thus enhancing the steric repulsion with the equatorial Ph group of **196**. Along with this displacement of the Mef group the *t*-Bu group would move away from the metal six-membered ring, thus reducing the steric repulsion with the axial Ph group of **195**; therefore, the transition structure leading to *anti*-aldol would be stabilized. To confirm the effect of Ti–F interaction at the transition state, the reaction was carried out in the presence of hexamethylphosphoramide (HMPA) to preclude Ti–F coordination, leading to the usual *syn*-selectivity, contrary to what was shown in Table 17 for the aldol reactions of an analogous titanium enolate. Indeed, when HMPA was added to the reaction mixture, *syn* selectivity was obtained (*anti* : *syn* = 20 : 80). Therefore, it could be concluded that the *anti*-selective aldol reaction stems from Ti–F interaction at the aldol transition structure.

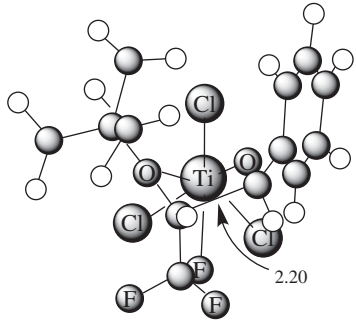

(**195**)

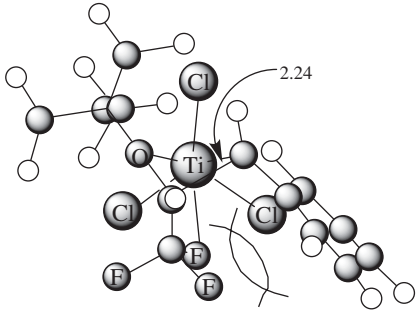

(**196**)

4. Tin enolates

Highly coordinated organometallic reagents often show a change in their reactivity and/or selectivity relative to the original noncoordinated species, partly because of the change in the hybridization states of relevant metals. Organotin(IV) compounds could be easily coordinated by an appropriate ligand, giving a highly coordinated species[147]. A five-coordinated carbon, resembling the well-known transition state in S_N2 reaction, lies on the top of the potential energy surface. On the contrary, a five-coordinated organotin entity **197**, formed as TS in equation 49, could lie at the bottom of the energy surface due to the contribution of their d-orbitals to be rehybridized to a hypercoordination state. Then, the highly coordinated tin(IV) could be used as a unique reagent with far different properties from those of the noncoordinated tin.

Baba and coworkers reported the unusual reactivity of highly coordinated tin compounds such as organotin(IV) enolates[148–151] or organotin(IV) hydrides[152]. NMR studies disclose the existence of five-coordinated tin enolate arising from the addition of certain ligands[148, 150]. In particular, the coordination to tin enolates by a bromide anion (from Bu_4NBr) shows novel types of selective reactions[148].

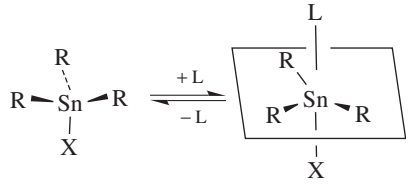

(**197**) (49)

In general, four-coordinated organotin enolates readily add to aldehydes[153] and are inert to organic halides[154]. On the contrary, highly coordinated tin enolates can attain a marked change in chemoselectivity and have higher nucleophilicity toward organic halides, showing at the same time low reactivity toward carbonyl compounds[148]. Thus, the high coordination approach accomplishes a significant change in chemoselectivity even in a competitive reaction system which includes both carbonyl compounds and organic halides[148].

Highly coordinated silyl enolates have been studied more than highly coordinated tin enolates and they are reported to accelerate the reactions with both organic halides[155] and carbonyl compounds[156]. Compared to the silyl moiety, the system using highly coordinated tin enolates has unique characteristics which can be applied to obtain chemoselective reactions. Baba and coworkers[157] reported a computational study of the difference between uncoordinated and highly coordinated tin enolates and their reactivities toward organic halides and carbonyl compounds.

a. Reaction with aldehydes. The calculated potential energy profiles for the reaction of both four-coordinated **198** and five-coordinated **201** tin enolates with an aldehyde (equations 50 and 51) are shown in Figure 4. Both reactions are exothermic; the activation energy of equation 50, 18 kcal mol^{-1}, is lower than that of equation 51, 27 kcal mol^{-1}. This result was explained by comparison of their transition structures **200** and **203**. The cyclic TS **200** established in the aldol reaction between tin enolates with aldehydes has an appropriate Sn−O bond length of 2.24 Å[158]. The six-membered cyclic TS **200** has a peculiar conformation, deviating from either chair or boat types, with five atoms other than the methylene C on the same plane (sled-type), probably because of steric hindrance of the trialkylstannyl group. The TS **203** showed an acyclic structure in which the Sn−O bond length is too long, 4.54 Å. This open structure was associated to the bromide coordinated tin which is reluctant to coordination by another ligand. In both cases, the synclinal arrangement between the C=O group of the aldehyde and the C=C group of the enolate was observed with dihedral angles of 58.6° for **200** and 35.8° for **203**.

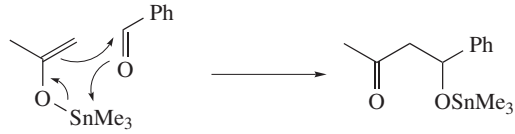

(**198**) (**199**) (50)

b. Reaction with halides. The energy diagrams for the reactions of four-coordinated **198** and five-coordinated **201** tin enolates with an organic halide (equations 52 and 53) are shown in Figure 4. These reactions proceed through two steps involving alkylation along an S_N2-type mechanism (through TS **207** or **211**) and destannylation with formation of bromostannane **206** (through TS **208** or **212**). The system using a bromide coordinated tin

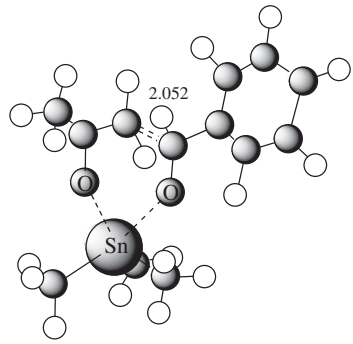

(**200**)

enolate was favored both thermodynamically and kinetically, showing a higher stabilization of the products and a lower activation energy than the system using four-coordinated species. The significant stabilization of organotin bromide by high coordination allows this thermodynamically favored feature. An analyis and comparison of the TSs **207** and **211** shows that the carbon atom at which the atom displacement occurs is more neutral in the high coordination system (partial charge −0.03e for **211**) than in the four coordination system (−0.06e for **207**). Furthermore, the positive charge on C of the C−O link in **211** (+0.57e) was closer to neutral than that in **207** (+0.62e). These neutralization effects caused by an anionic ligand lead to stabilization of the transition structure.

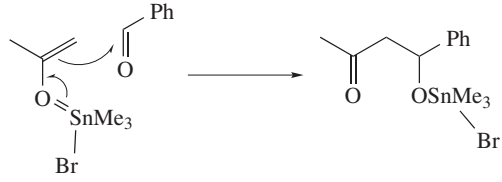

(**201**) (**202**) (51)

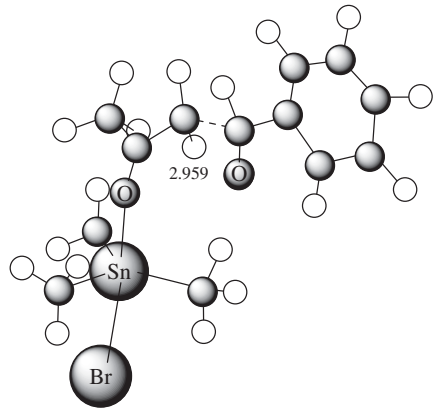

(**203**)

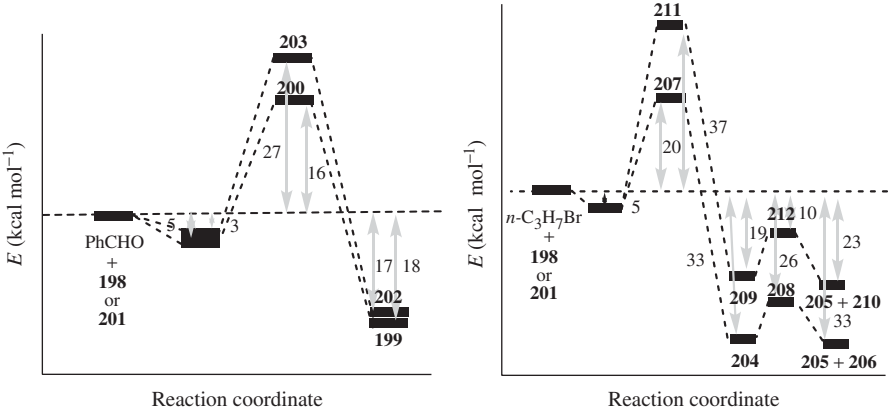

FIGURE 4. Potential energy profiles for the reaction of tin enolates with benzaldehyde according to equations 50 and 51 (left) and with 1-bromopropane according to equations 52 and 53 (right). Reprinted with permission from M. Yasuda, K. Chiba and A. Baba, *J. Am. Chem. Soc.*, **122**, 7549. Copyright 2000 American Chemical Society

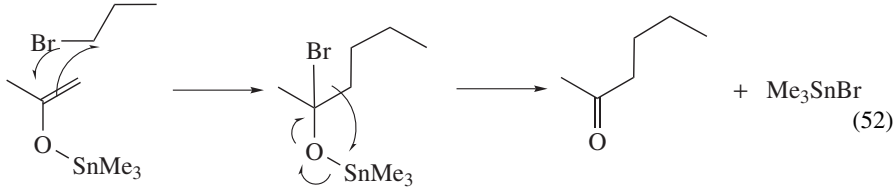

(**198**) (**204**) (**205**) (**206**)

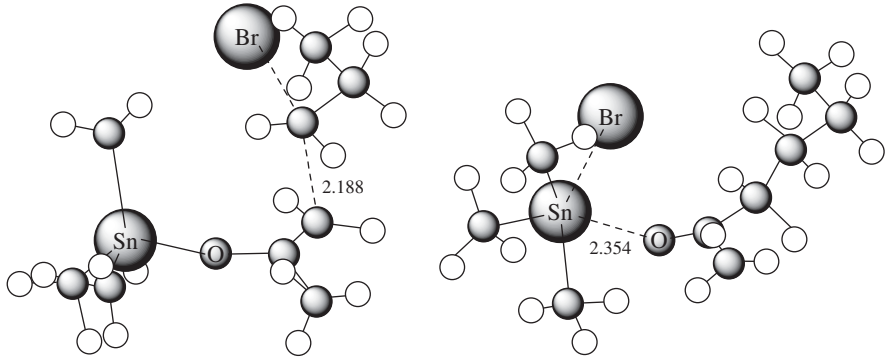

(**207**) (**208**)

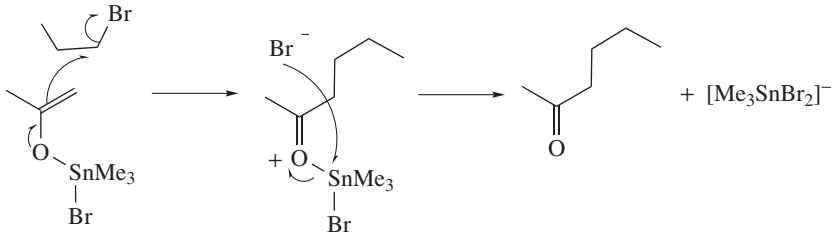

(53)

(**201**) (**209**) (**205**) (**210**)

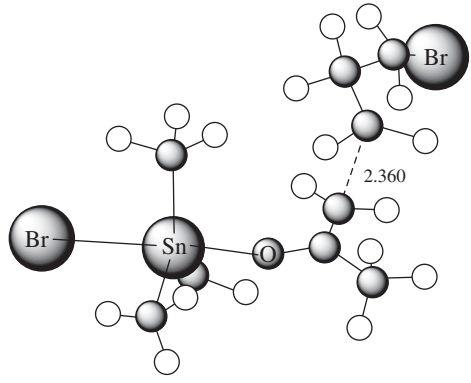

(**211**)

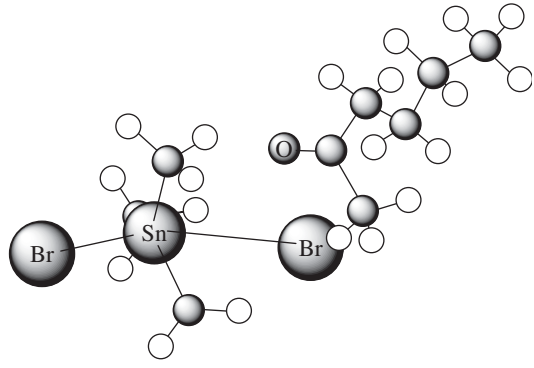

(**212**)

This computational study revealed the mechanism of the reaction between trialkyltin enolates and aldehydes or organic halides, both without and with coordinating ligands. High coordination of trialkyltin enolates causes an increase of their nucleophilicity and decrease of Lewis acidity of the tin center, which control the course of reaction[159]. In the reaction of tin enolates with aldehydes, a noncoordinated tin enolate gives a cyclic TS in sled conformation whereas an acyclic TS leading to deactivation of the process is shown in the case of a highly coordinated enolate. Both theoretical and experimental results of

the system involving trialkyltin enolates point to diminished Lewis acidity as being more important than enhanced nucleophilicity in the reaction with aldehydes. This is probably because the Lewis acidity is effectively reduced by high coordination with increase of nucleophilicity[160]. In the reaction with organic halides, on the contrary, the system of highly coordinated tin enolate was favored both kinetically and thermodynamically. The bromide coordination to tin enolate increases the high nucleophilicity to promote the reaction kinetically. Complexation of Br^- with bromostannane strongly affects stabilization, leading to a thermodynamically favored reaction course.

5. Paladium enolates

Poli and coworkers[161] have recently reported on the regioselective and stereoselective build-up of γ-lactams via the intramolecular 5-*exo* interaction between a stabilized acetamide enolate anion and a properly tethered η^3-allyl-palladium appendage. The palladium-catalyzed intramolecular allylic alkylations of unsaturated amides **213a–f** (equation 54), activated by electron-withdrawing groups (EWG) under phase-transfer conditions or in the presence of a crown ether, took place at room temperature to give the expected γ-lactams **214a–f** in good yields[162].

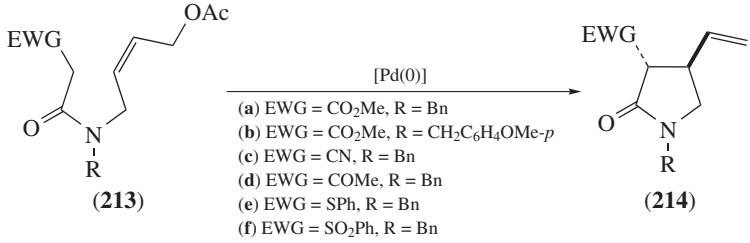

(54)

It was proposed that the remarkable efficacy of these reactions could be directly related to the particular nature of the enolate counterion. Indeed, upon NaH deprotonation, the malonamide substrates are expected to give rise to planar, resonance-stabilized, Na-chelated enolates, which are at the same time conjugated with the intrinsically planar amide function. As a consequence, in the ground-state conformation of the reactive intermediate **215** (equation 55), all twelve atoms making up the Na-chelated malonamide enolate will roughly lie in the same α plane. On the other hand, in an ideal intermolecular enolate/η^3-allyl-PdX interaction, optimal orbital overlap requires a parallel disposition between the plane containing the enolate (α') and that containing the allyl fragment (β).Therefore, the transition state **216** of the cyclization process has to feature a significant loss of conjugation with respect to the Na-chelated ground-state conformation. As a consequence, the remarkable reactivity of these new cyclization conditions is likely to be due to generation of a highly reactive zwitterionic enolate/η-allyl intermediates, that can be achieved either under biphasic phase transfer catalysis or under Na-sequestered homogeneous conditions[163].

To support the above contention, Poli, Norrby and coworkers[162] performed a DFT (B3LYP/LACVP*) computational study using **217** as a model system for the Pd-allyl enolate intermediate. The solvent was simulated as a continuum using the PB-SCRF model in the Jaguar program[164] with parameters appropriate for dichloromethane. Eight possible TSs were located and characterized. In all cases, the *exo* cyclization was favored by more than 7.2 kcal mol^{-1} as compared to the *endo* cyclization pathways. The forming bond at the most accessible *exo* TS **218** has a length of over 2.6 Å, as compared to *ca*

2.4 Å when the Na^+ counterion is included at the TS **219**[165]. This indicated that the free anion **217** is inherently more reactive than the chelated complex, as expected. Looking more closely at the geometries of the transition states, it can be seen that exclusion of the counterion also allows the nucleophile to deviate from planarity. There is substantial strain induced in the planar amide in the transition state; in the absence of Na^+, this strain can be somewhat relieved by a rotation (*ca* 20–25°) of the planar enolate with respect to the amide, leading to a more facile ring closure. It should be noted that in the absence of the chelating counterion, which enforces a (*Z*)-configuration on the enolate, the free form can also exist as the (*E*)-isomer. It was found that, in all cases, the (*E*)-form has a lower barrier to ring closure, by 3–4 kcal mol^{-1}, corresponding to a rate increase of 2 to 3 orders of magnitude. The combination of these three effects fully rationalized the observed rate increase upon exclusion of chelating counterions. The geometrical effects observed may also have a bearing on other cases where strong counterion effects are present[166].

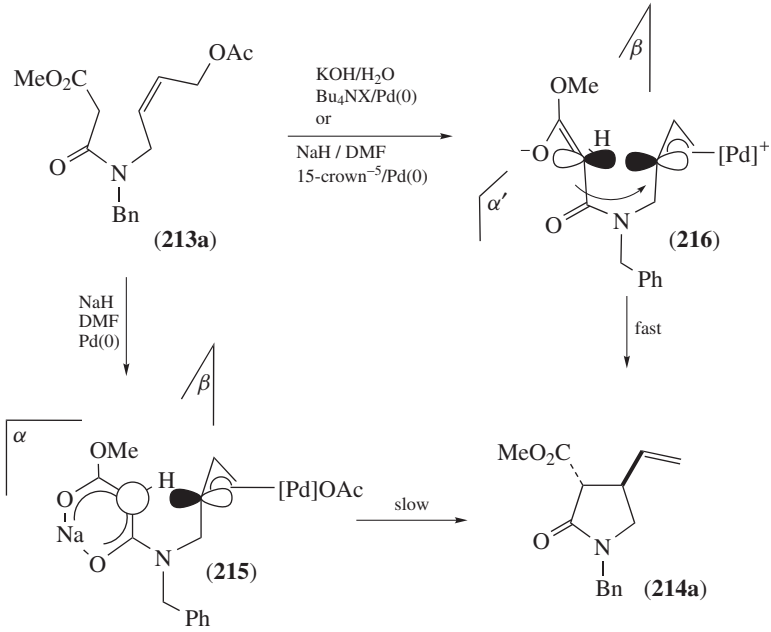

6. Platinum enolates

Recently, Baiker and coworkers[167] have found that in the Pt-catalyzed hydrogenation of 1,1,1-trifluoro-2,4-diketones (**220**, R^1 = Mef, equation 56), the presence of trace amounts of (*R*,*R*)-pantoyl(1-α-naphthylethyl)amine (**221**), cinchonidine (**222a**) or its methyl ether (**222b**) induces up to 93% ee and enhances the chemoselectivity up to 100%. The high chemo- and enantioselectivities were attributed to the formation of an ion pair involving the protonated amine function of the chiral modifier and the enolate form of the substrate. DFT calculations including the simulation of the interaction of a protonated amine with the enolate adsorbed on a Pt_{31} cluster model revealed that only the C−O bond next to the CF_3 group of the substrate is in direct contact with Pt and can be hydrogenated.

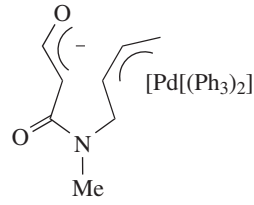

(**217**)

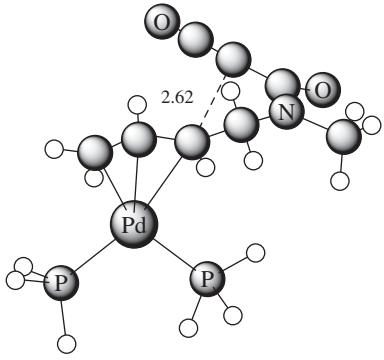

(**218**)

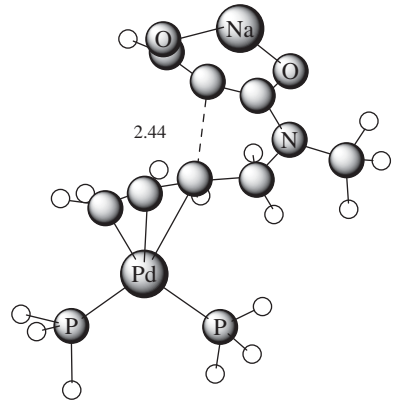

(**219**)

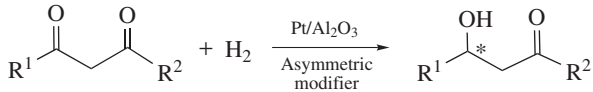

(56)

(**220**)

$R^1 = R^2$ = Me, Mef

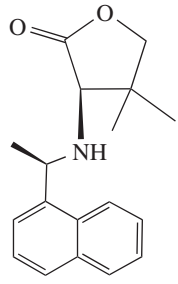

(**221**)

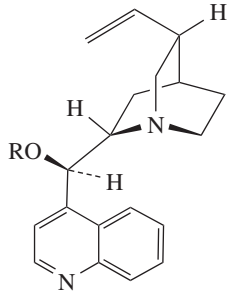

(**222**) (**a**) R = H
(**b**) R = Me

Adsorption of the diketone **223** and its enol forms **224** and **225** (equation 57) was studied using a Pt_{31} cluster model to better understand the catalytic behavior. Structure **226** shows the adsorption mode of **223** in the diketo form, chemisorbed η^2 via the activated C=O adjacent to the CF_3 group. This chemisorption mode of C=O double bonds is also called di-σ to recall the double σ binding of the keto carbonyl moiety to the metal atoms. The η^1 adsorption modes are theoretically possible, but their adsorption energy is much smaller than the η^2 modes and, in particular, in such adsorption modes the carbonyl group is distant from the surface and cannot reach the surface hydrogen, being therefore of less interest to our discussion[168].

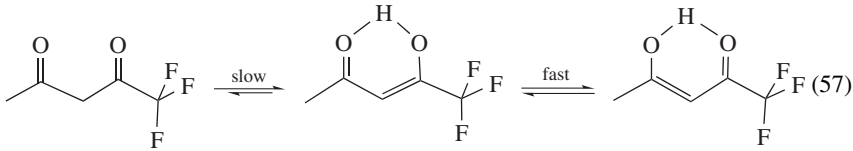

(**223**) (**224**) (**225**)

Energetically, **227** is the most favored adsorbed form for the enols, where the optimal chemisorption of the carbonyl of **225** is attained[167]. The adsorbed enol forms do not involve the expected η^2 interaction of the carbonyl group in **224** with the metal, but rather the formation of a σ-bond between the C adjacent to the CF_3 group and a Pt atom. Competition for surface sites is in favor of the carbonyl of **225** while that of **224** undergoes no evident structural alteration induced by the metal. Both adsorbed enol forms are found to be stabilized by an internal H-bond; however, while in adsorbed **224** the H-bond length is 1.35 Å, it elongates to 1.71 Å in adsorbed **225**, showing the stronger hydrogen-acceptor character of the adsorbed activated carbonyl group. Structure **228** shows the adsorption mode of the enolate, the deprotonated form of the enol, thus it corresponds to a charged species. Unlike the enols, the enolate has a more symmetric adsorption mode where both oxygen atoms are bound to a metal atom, and with a third σ binding site due to a C(3) center that is also bound to a metal atom and rehybridized. The negative charge of the enolate is delocalized on the metal upon adsorption.

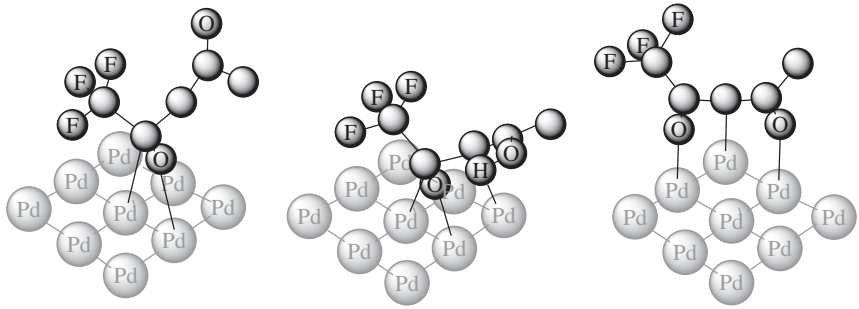

(**226**) (**227**) (**228**)

It was mentioned in the discussion of equation 56 that the presence of certain amines leads to nearly perfect chemoselectivity in the hydrogenation of the C=O group adjacent to a Mef group. It has also been shown that in solution the amine deprotonates the enol and generates an ammonium cation and an enolate anion. This was modeled by the interaction between the trimethylammonium ion and the enolate derived from **223** in the presence of

a Pt surface[167]. A pictorial representation of the adsorbed species is shown in **229**, starting with the trimethylammonium ion positioned close to the adsorbed enolate ion (the H–O distance is 2.5 Å for both N^+ H···O^- and N^+ H···O=C). During minimization, the ammonium ion moves toward the surface and comes closer to the C=O of the enolate derived from **224** (H–O distance 1.8 Å) and farther from the C=O of that derived from **225** (H–O distance 2.3 Å). In this intermediate position, the hydrogen bond formed with the nonactivated moiety was 1.8 Å, while that formed with the activated moiety was 2.3 Å. As the optimization continues, this preferential coordination yields a displacement of the C=O derived from **224** from the surface, and when convergence is reached the ammonium ion coordinated to the C=O derived from **225** changes its adsorption mode to η^2.

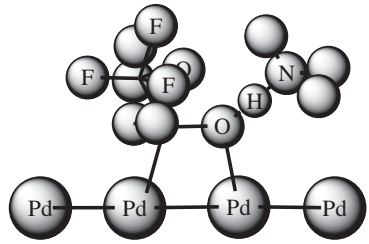

(**229**)

E. Protonation Reactions

Asensio and coworkers studied the effects of solvent, temperature, presence of lithium salts and proton acidity on the enantioselective protonation of enolates **230** to yield (*R*)-2-methyl-1-tetralone (**231**, equation 58) with α-sulfinyl alcohols **232**[169] and 1,2-sulfinyl thiols **233**[170]. Stereoselectivity was generally enhanced when lithium bromide was present in the medium during enolization and also with the use of methylene chloride solutions.

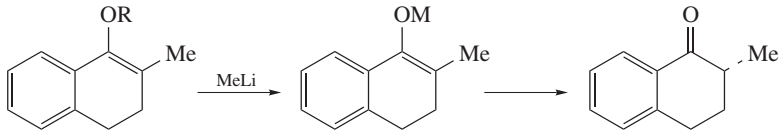

(**230**) (**231**) (58)

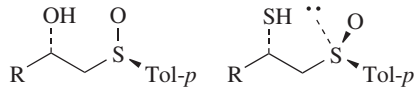

(**232**) (**233**)

A preliminary approach[171] to understand the mechanism of the enantioselective protonation and the role of lithium bromide, based on TSs containing one lithium atom, failed to explain the selectivity enhancement by lithium bromide, and the calculated energies of the TSs did not account for the experimentally observed selectivity. Asensio, Domingo and coworkers studied the molecular process associated with the proton transfer at the semiempirical PM3 level[169]. Based on literature data[91], they defined the structure of a mixed dimer enolate **234** consisting of a four-membered ring where the bromide anion and the oxygen atom of the enolate were connected by two lithium cations. These bridging

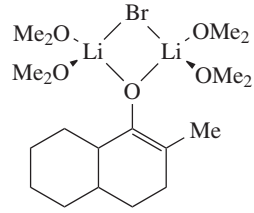

(**234**)

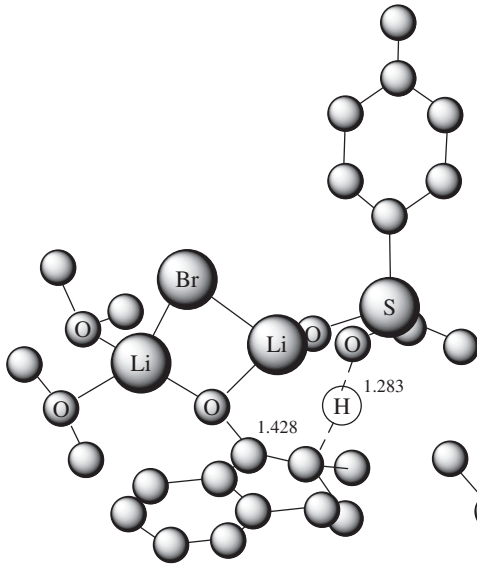

(**235**) (*R*)

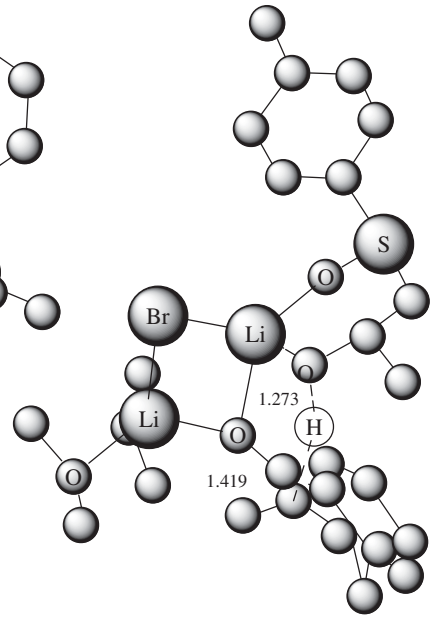

(**236**) (*S*)

cations were in an approximately tetrahedral environment provided by two pairs of oxygen atoms corresponding to two molecules of dimethyl ether, as a reduced model of diethyl ether used experimentally. Subsequent substitution of two solvent molecules of one lithium atom for the chiral alcohol **232** (R = Me) afforded two enolate complexes, which may be considered precursors to the corresponding transition structures. These enolate complexes can be converted into two chiral complexed ketones, via the TSs **235** and **236**, containing a six-membered ring with an OH group from which the proton transfer process takes place via a favorable intramolecular pathway to yield ketone **231** of (*R*) or (*S*) configuration, respectively. In contrast with the very similar energy values calculated for the monolithium TSs, **235** was 3.9 kcal mol^{-1} less energetic than **236**, in good agreement with the experimental results. The breaking O−H (1.283 Å) and forming C−H (1.428 Å) bonds in **235** were larger than in **236** (1.273 and 1.419 Å, respectively). These geometrical values were close to those in monolithium TSs, illustrating the invariance of the geometry relative to the lithium aggregate state. Consequently, the lower activation energy of **235** relative to

236 is responsible for the preferential protonation via the former. Despite the difficulty in studying these chemical processes in solution, where different aggregates are assumed to exist simultaneously, this work provided new insights on the general mechanism of the enantioselective protonation, underpinning the role played by lithium bromide in the formation of mixed dimers. Similar results were obtained for the protonation of enolates **230** with 1,2-sulfinyl thiols **232** at the semiempirical PM3 computational level[170].

F. Polymerization Reactions

The polymerization of alkyl acrylates or methacrylates has industrial significance and, therefore, has been the subject of intensive experimental investigations and practical applications. Zirconocene complexes are used as catalyst or catalyst precursors for the polymerization of methyl methacrylate[172]. Several investigations are based on a modification of dimethylzirconocene or derivatives thereof as catalyst precursors[173–175]. Of particular interest are the generation of the actual catalyst and the nature of the propagation step. Bridged and nonbridged zirconocene derivatives have been studied. Most of these studies have in common that, in the initial preparation of the active catalyst, methyl groups are eliminated from dimethylzirconocene complexes in order to provide a cationic intermediate with a vacant ligand site which can be used by an acrylate molecule or, in view of the catalytic activity, by an ester enolate molecule, which is presumed to be formed *in situ* prior to polymerization.

Three mechanisms have been proposed on the basis of experimental studies, all involving a zirconium ester enolate subunit. The cationic mechanism is based on a positively charged zircocene subunit **237**[173, 174]. Acrylate is attached to zirconium via the carbonyl oxygen atom. The terminal C atom of acrylate forms a C−C bond with the β-C atom of the enolate and in this arrangement the acrylate now becomes the new enolate unit. The catalytic cycle is terminated by removing the methoxycarbonyl group, formerly the enolate, from zirconium. The neutral mechanism is similar but incorporates a neutral zircocene unit **238** bound to an enolate ligand[174]. The bimetallic mechanism is different insofar as two dicyclopentadienyl methylzirconium units are involved, **239**[174], one bearing an ester

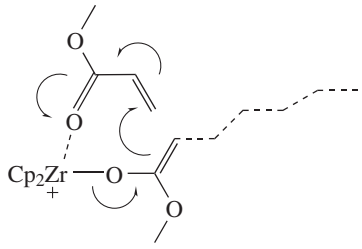

(**237**) cationic mechanism

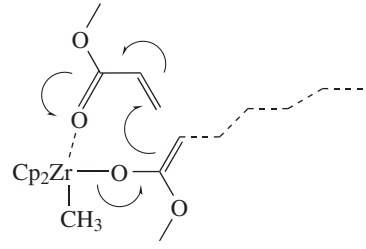

(**238**) neutral mechanism

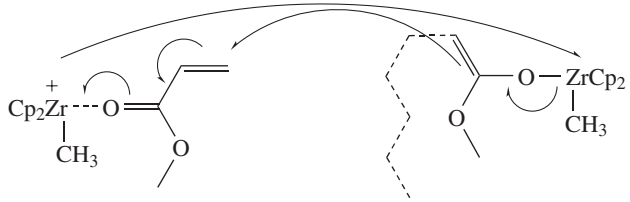

(**239**) bimetallic mechanism

enolate and the other an acrylate molecule. C−C bond formation is a bimolecular reaction. During the process, the positively charged complex becomes neutral and vice versa.

A number of theoretical studies have been carried out on ethene or propene polymerization by metallocene complexes. In part, they are based on HF, DFT calculations or even a hybrid method including force-field procedures[176]. The three possible catalytic mechanisms were shown to be realistic alternatives by Sustmann and coworkers at the B3LYP/3-21G and B3LYP/6-31G*-ECP(S)//B3LYP/3-21G computing levels[177]. The cationic mechanism (**237**) was originally favored by several groups[173, 174], where the cationic species $[Cp_2Zr(OC(OR)=CR_2)]^+$ was assumed to add an acrylate molecule via the TS **240**. The drawback of the cationic mechanism was the breaking of a Zr−O bond, a very energy-consuming process to start a new propagation step. The neutral mechanism, starting with a mononuclear, neutral zirconocene complex formally derived from $[Cp_2ZrMe]^+$ and an ester enolate, yielded the energetically slightly higher TS **241** for

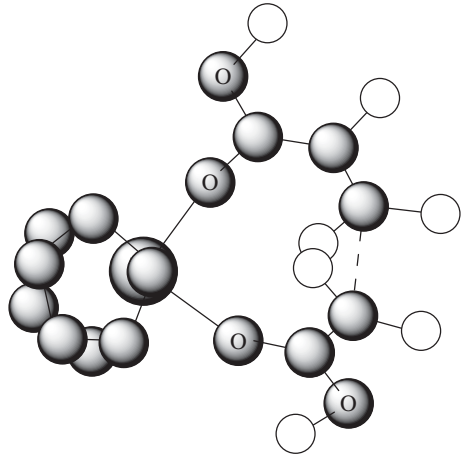

(**240**)

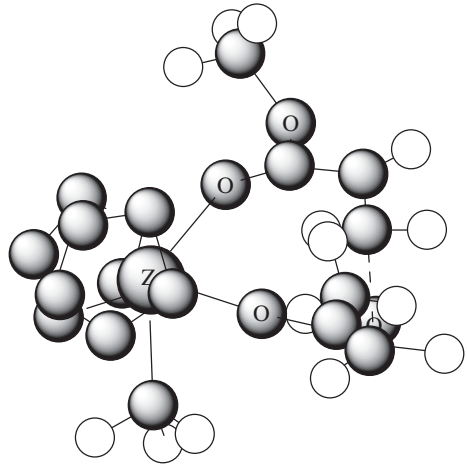

(**241**)

C−C coupling than the cation mechanism, but separation of the newly generated carboxy group from zirconium proved to be exothermic and did not require assistance by an acrylate molecule.

The 'bimetallic' mechanism 3 delineated from experiments by Collins's group[174] presumes that $[Cp_2ZrMe(OC(OR)=CR_2)]$ reacts with $[Cp_2ZrMe(O=C(OR)CH=CH_2)]^+$. C−C coupling by this mechanism requires the lowest activation energy of the three cases considered. A rationalization of the higher reactivity in terms of a Lewis acid function of $[Cp_2ZrMe]^+$ on methyl acrylate was provided. To be competitive with the other two catalytic cycles, the final step, that is the separation of $[Cp_2ZrMe]^+$ from the product complex, must be assisted by acrylate. Both back-side and front-side attack of the carbonyl oxygen of acrylate on the zirconium fragment were found to be possible, although back-side attack was slightly favored.

The influence of bridging by bivalent groups $>SiH_2$, $>CMe_2$ and $-CH_2CH_2-$ on the structure and reactivity of the ester−enolate complex in polymerization has been also studied. A widening of the angle between the planes of the cyclopentadienyl units from 50° to about 70° was observed, with enhanced accessibility of the metal center. Reaction coordinate calculations provided evidence that the neutral mononuclear mechanism profits from the increase in angle widening. Chlorine instead of methyl at zirconium seems to have an activating effect. The bridged single-component zirconocene $[Zr\{(Cp)(Ind)CMe_2\}(Me)(thf)](BPh_4)$ (Ind = inden-1-yl) polymerizes methyl methacrylate (MMA) selectively to isotactic poly(methyl methacrylate) (PMMA) with no cocatalysts or activators. To elucidate the stereoselective steps of the polymerization of MMA by using this catalyst, Holscher and coworkers[178] studied the propagation steps occurring with the derivative $[Zr\{(Cp)(Ind)CH_2\}\{-O-C(OMe)=C(Me)(Et)\}(MMA)]$ by *ab initio* (HF/3-21G) calculations (see Scheme 3). After the initiation step, which consumes the first two MMA molecules, each new catalytic cycle begins with the stereoselective addition of a new MMA molecule at the indenyl side of the zirconocene fragment. At the same time the enolate ring undergoes a stereoselective in-plane ring shift to the side

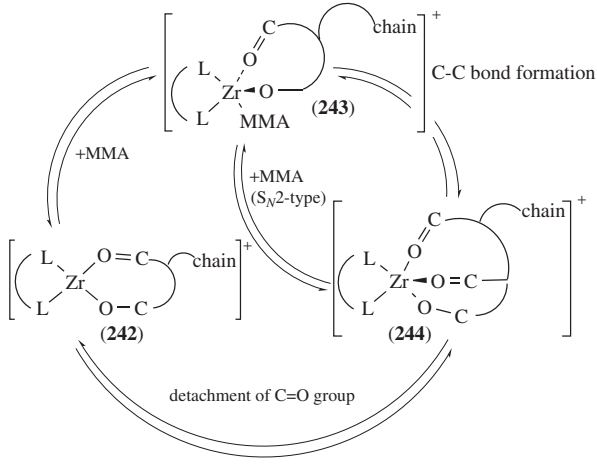

SCHEME 3. Simplified polymerization mechanism showing the stereoselective shift of the enolate ring of **242** away from the indenyl ring (L) system upon addition of MMA to yield **243**. An S_N2-type reaction of **244** with MMA to yield **243** might also be possible

opposite to the indenyl ring. These findings were used to postulate a mechanism for the polymerization that explains the stereoselective synthesis of isotactic PMMA.

Recently, Tomasi and coworkers[179] performed a DFT (BP86/STO) study to explore the mechanism of the group transfer polymerization (GTP) of methyl acrylate (MA), catalyzed by mononuclear Zr-based and Sm-based metallocenes (equations 59 and 60). From their calculations, the process catalyzed by a neutral zirconocene appears to be slower than that catalyzed by a cationic zirconocene. The mechanism of the neutral samarocene-catalyzed GTP[180] showed a close similarity to that catalyzed by the cationic zirconocene because the two systems are isoelectronic. No energy barrier was encountered on the potential energy surface in the C−C coupling reaction catalyzed by these two systems (Figure 5b), whereas when a neutral zirconocene was involved, a moderate activation energy was found (Figure 5a). Also, the products of the reaction were different, since in the GTP catalyzed by a cationic zirconocene or by a neutral samarocene a very stable metallacycle (**251**) was formed (equation 60), which is the resting state in the whole polymerization, while in the GTP catalyzed by the neutral zirconocene the metallacycle was only a high-energy intermediate. A dependence was found of stereoregularity on the relative disposition of the acrylate and enolate ligands, as well as the direction of the incoming acrylate molecule. The first transition state in the opening of the metallacycle resting state, assisted by an incoming acrylate molecule, was the most important elementary step. On the basis of these discoveries a kinetic model for the prediction of stereoregularity was developed, which has been shown to be qualitatively in agreement with the experimental data available for similar systems.

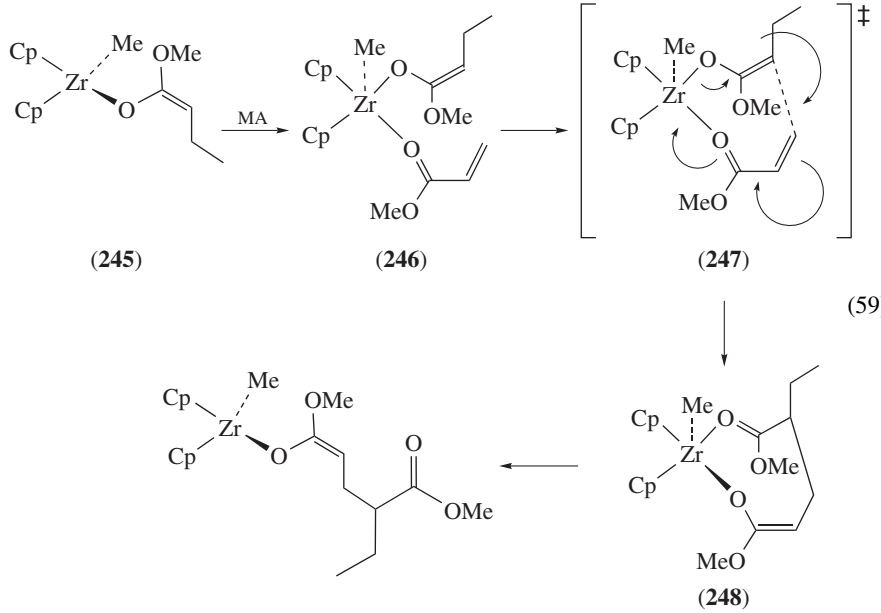

(**245**) (**246**) (**247**) (59)

(**248**)

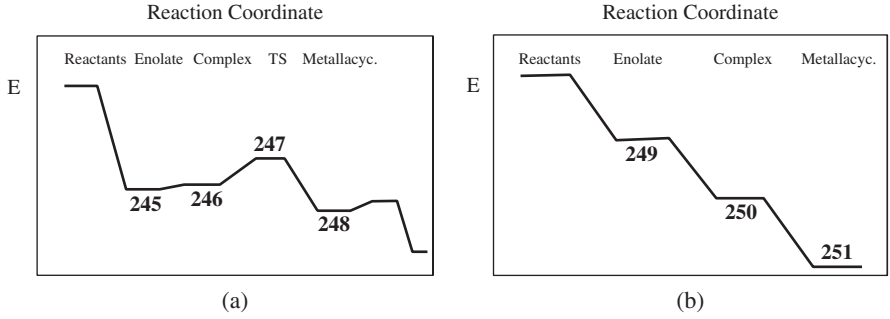

FIGURE 5. Energy profile for GTP catalyzed by (a) a neutral zirconocene, (b) a cationic zirconocene and neutral samarocene. Reprinted with permission from S. Tomasi, H. Weiss and T. Ziegler, *Organometallics*, **25**, 3619. Copyright 2006 American Chemical Society

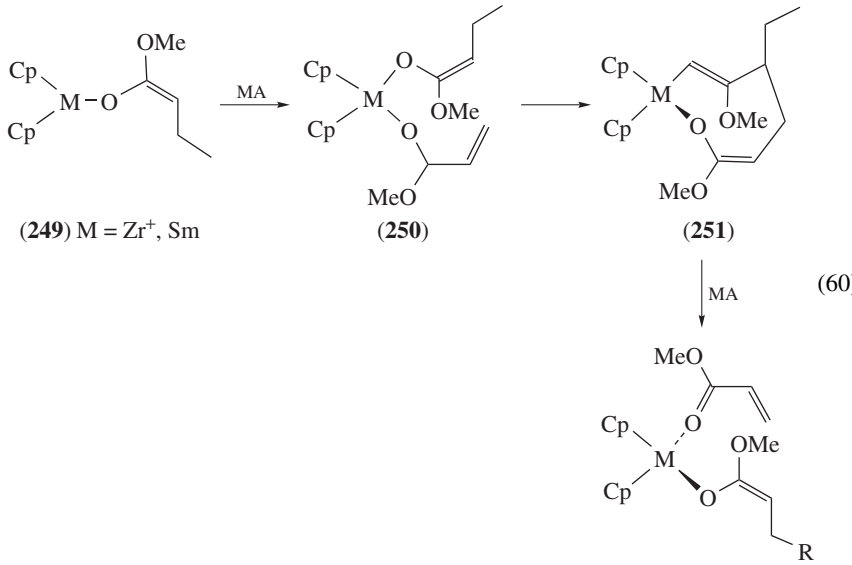

(60)

V. ACKNOWLEDGMENTS

L.R.D. acknowledges the research funds provided by the Ministerio de Educación y Ciencia of the Spanish Government (project CTQ2006-14297/BQU). The research of J.A. was supported by the Ministerio de Educación y Ciencia of the Spanish Government (project CTQ2006-15447-C02-01) and the Universitat Jaume I-Fundacio Bancaixa (Project P1.1B2004-20). We are particularly grateful to J. A. Sáez, M. J. Aurell and P. Domingo-Calap who have read the initial drafts with patience, and helped us to prepare the graphical material in the final version.

VI. REFERENCES

1. (a) R. B. Bates, in *Comprehensive Carbanion Chemistry*, Part A, Chap. 1 (Eds E. Buncel and T. Durst), Elsevier, Amsterdam, 1980.
   (b) P. O'Brien, in *Comprehensive Carbanion Chemistry*, Part A, Chap. 6 (Eds E. Buncel and T. Durst), Elsevier, Amsterdam, 1980.
   (c) C. M. Thompson and D. L. C. Green, *Tetrahedron*, **47**, 4223 (1991).
   (d) L. M. Jackman and J. Bortiatynski, in *Advances in Carbanion Chemistry*, Vol. 1 (Ed. V. Snieckus), JAI Press, Greenwich, 1992, pp. 45–87.
2. A. Bongini, M. Orena and S. J. Sandri, *J. Chem. Soc., Chem. Commun.*, 50 (1986).
3. W. J. Hehre, L. Radom, P. v. R. Schleyer and J. A. Pople, in *Ab Initio Molecular Orbital Theory*, John Wiley & Sons, Inc., New York, 1986.
4. J. Kaneti, P. v. R. Schleyer and A. J. Kos, *J. Chem. Soc., Chem. Commun.*, 1014 (1985).
5. L. R. Domingo, S. Gil, R. Mestres and M. T. Picher, *Tetrahedron*, **51**, 7207 (1995).
6. J. J. P. Stewart, *J. Comput. Chem.*, **10**, 209 (1989).
7. M. J. Aurell, S. Gil, R. Mestres, M. Parra and A. Tortajada, *Tetrahedron*, **50**, 5109 (1994).
8. L. R. Domingo, S. Gil, R. Mestres and M. T. Picher, *Tetrahedron*, **52**, 11105 (1996).
9. P. Veya, C. Floriani, A. Chiesivilla, C. Guastini, A. Dedieu, F. Ingold and P. Braunstein, *Organometallics*, **12**, 4359 (1993).
10. P. G. Williard and G. B. Carpenter, *J. Am. Chem. Soc.*, **108**, 462 (1986).
11. T. Maetzke, C. P. Hidber and D. Seebach, *J. Am. Chem. Soc.*, **112**, 8248 (1990).
12. D. Seebach, R. Amstutz, T. Laube, W. B. Schweizer and J. D. Dunitz, *J. Am. Chem. Soc.*, **107**, 5403 (1985).
13. T. J. Lynch, M. Newcomb, D. E. Bergbreiter and M. B. Hall, *J. Org. Chem.*, **45**, 5005 (1980).
14. R. Leung-Toung and T. T. Tidwell, *J. Am. Chem. Soc.*, **112**, 1042 (1990).
15. K. W. Henderson, A. E. Dorigo, Q. Y. Liu, P. G. Williard, P. v. R. Schleyer and P. R. Bernstein, *J. Am. Chem. Soc.*, **118**, 1339 (1996).
16. A. Abbotto, A. Streitwieser and P. v. R. Schleyer, *J. Am. Chem. Soc.*, **119**, 11255 (1997).
17. A. D. Becke, *J. Chem. Phys.*, **98**, 5648 (1993).
18. C. Lee, W. Yang and R. G. Parr, *Phys. Rev. B*, **37**, 785 (1988).
19. M. Rosi, A. Sgamellotti and C. Floriani, *Theochem—J. Mol. Struct.*, **431**, 33 (1998).
20. J. K. Pugh and A. Streitwieser, *J. Org. Chem.*, **66**, 1334 (2001).
21. A. D. Becke, *Phys. Rev. A*, **38**, 3089 (1988).
22. J. P. Perdew, *Phys. Rev. B*, **33**, 8822 (1986).
23. W. J. Hehre and L. Lou, *A Guide to Density Functional Calculations in Spartan*, Wavefunction, Inc., Irvine, CA, 1997.
24. Y. J. Kim, A. Streitwieser, A. Chow and G. Fraenkel, *Org. Lett.*, **1**, 2069 (1999).
25. L. M. Pratt and A. Streitwieser, *J. Org. Chem.*, **68**, 2830 (2003).
26. L. M. Pratt, A. Newman, J. St Cyr, H. Johnson, B. Miles, A. Lattier, E. Austin, S. Henderson, B. Hershey, M. Lin, Y. Balamraju, L. Sammonds, J. Cheramie, J. Karnes, E. Hymel, B. Woodford and C. Carter, *J. Org. Chem.*, **68**, 6387 (2003).
27. J. Oviedo and J. F. Sanz, *Surf. Sci.*, **397**, 23 (1998).
28. S. Fery-Forgues, D. Lavabre and A. D. Rochal, *New J. Chem.*, **22**, 1531 (1998).
29. J. R. Zietz, G. C. Robinson and K. L. Lindsay, in *Comprehensive Organometallic Chemistry*, Vol. 7, Chap. 46 (Eds G. Wilkinson, F. G. A. Stone and E. W. Abel), Pergamon, Oxford, 1983.
30. F. H. van der Steen, G. P. M. van Mier, A. L. Spek, J. Kroon and G. van Koten, *J. Am. Chem. Soc.*, **113**, 5742 (1991).
31. J. F. Allan, W. Clegg, M. R. J. Elsegood, K. W. Henderson, A. E. McKeown, P. H. Moran and I. M. Rakov, *J. Organomet. Chem.*, **602**, 15 (2000).
32. E. A. Jeffery, A. Meisters and T. Mole, *J. Organomet. Chem.*, **74**, 365 (1974).
33. M. Rosi, A. Sgamellotti and C. Floriani, *Theochem—J. Mol. Struct.*, **459**, 47 (1999).
34. M. Rosi, A. Sgamellotti and C. Floriani, *Theochem—J. Mol. Struct.*, **459**, 57 (1999).
35. K. Babic-Samardzija, S. P. Sovilj and N. Katsaros, *J. Mol. Struct.*, **694**, 165 (2004).
36. W. D. Edwards and M. C. Zerner, *Theor. Chim. Acta*, **72**, 347 (1987).
37. W. P. Anderson, W. D. Edwards and M. C. Zerner, *Inorg. Chem.*, **25**, 2728 (1986).
38. S. J. Eng, R. J. Motekaitis and A. E. Martell, *Inorg. Chim. Acta*, **278**, 170 (1998).
39. S. Umetani, Y. Kawase, Q. T. H. Le and M. Matsui, *Inorg. Chim. Acta*, **267**, 201 (1998).

40. J. S. Wang, R. Jerôme, R. Warin and P. Teyssié, *Macromolecules*, **26**, 1402, (1993).
41. V. Halaska and L. Lochmann, *Collect. Czech. Chem. Commun.*, **38**, 1780 (1973).
42. J. Kriz, J. Dybal, P. Vlcek and M. Janata, *Macromol. Chem. Phys.*, **195**, 3039 (1994).
43. M. J. S. Dewar and W. Thiel, *J. Am Chem. Soc.*, **99**, 4899 (1977).
44. J. Dybal and J. Kriz, *Collect. Czech. Chem. Commun.*, **59**, 1699 (1994).
45. E. Kaufmann, K. Raghavachari, A. E. Reed and S. P. v. R. Schleyer, *Organometallics*, **7**, 1597 (1988).
46. W. N. Setzer and P. v. R. Schleyer, *Adv. Organomet. Chem.*, **24**, 353 (1985).
47. H. Weiss, A. V. Yakimansky and A. H. E. Müller, *J. Am. Chem. Soc.*, **118**, 8897 (1996).
48. A. M. Sapse, K. Raghavachari, P. v. R. Schleyer and E. Kaufmann, *J. Am. Chem. Soc.*, **107**, 6483 (1985).
49. H. Schlaad, H. Kolshorn and A. H. E. Müller, *Macromol. Rapid Commun.*, **15**, 517 (1994).
50. B. Schmitt, H. Schlaad, A. H. E. Müller, B. Mathiasch, S. Steiger and H. Weiss, *Macromolecules*, **32**, 8340 (1999).
51. A. V. Yakimansky and A. H. E. Müller *J. Am. Chem. Soc.*, **123**, 4932 (2001).
52. D. Baskaran, A. H. E. Müller and S. Sivaram, *Macromol. Chem. Phys.*, **201**, 1901 (2000).
53. J. S. Wang, R. Jerôme, R. Warin, H. Zhang and P. Teyssié, *Macromolecules*, **27**, 3376 (1994).
54. D. Moras and R. Weiss, *Acta Crystallogr., Sect. B*, **29**, 400 (1973).
55. C. Johann and A. H. E. Müller, *Makromol. Chem., Rapid Commun.*, **2**, 687 (1981).
56. (a) C. Eaborn, P. B. Hitchcock, J. D. Smith and A. C. Sullivan, *J. Chem. Soc., Chem. Commun.*, 827 (1983).
    (b) C. Eaborn, P. B. Hitchcock, J. D. Smith and A. C. Sullivan, *J. Organomet. Chem.*, **263**, C23 (1984).
57. G. Wittig, F. J. Meyer and G. Lange, *Liebigs Ann. Chem.*, **571**, 167 (1951).
58. (a) G. Wittig and F. Bickelhaupt, *Chem. Ber.*, **91**, 865 (1958).
    (b) G. Wittig, R. Ludwig and R. Postler, *Chem. Ber.*, **88**, 294 (1955).
59. G. Wittig, *Angew. Chem.*, **70**, 65 (1958).
60. (a) W. Bauer and P. v. R. Schleyer, in *Advances in Carbanion Chemistry*, Vol. 1 (Ed. V. Snieckus), JAI Press, Greenwich, 1992, pp. 89–175.
    (b) H. Gunther, in *Advanced Application of NMR to Organometallic Chemistry*, Vol. 1 (Eds M. Gielen, R. Willem and B. Wrackmeyer), John Wiley & Sons, Ltd, Chichester, 1996, pp. 247–290.
61. (a) M. B. Eleveld and H. Hogeveen, *Tetrahedron Lett.*, **25**, 5187 (1984).
    (b) L. Colombo, C. Gennari, G. Poli and C. Scolastico, *Tetrahedron*, **38**, 2725 (1982).
62. G. Hilmersson, *Chem. Eur. J.*, **6**, 3069 (2000).
63. J. P. Perdew and Y. Wang, *Phys. Rev. B*, **45**, 13244 (1992).
64. R. Ditchfield, *Mol. Phys.*, **27**, 789 (1974).
65. (a) J. R. Cheeseman, G. W. Trucks, T. A. Keith and J. M. Frisch, *J. Phys. Chem.*, **104**, 5497 (1996).
    (b) W. B. Smith, *Magn. Reson. Chem.*, **37**, 103 (1999).
66. (a) P. I. Arvidsson, G. Hilmersson and O. Davidsson, *Chem. Eur. J.*, **5**, 2348 (1999).
    (b) G. Hilmersson, P. I. Arvidsson, O. Davidsson and M. Hakansson, *J. Am. Chem. Soc.*, **120**, 8143 (1998).
67. P. Szczecinski, A. Gryff-Keller and S. Molchanov, *J. Org. Chem.*, **71**, 4636 (2006).
68. (a) S. Lindstedt and E. Holme, *Lancet*, **340**, 813 (1992).
    (b) E. Holme and S. Lindstedt, *J. Inherited Metab. Dis*, **21**, 507 (1998).
69. Y. Apeloig, I. Zharov, D. Bravozhivotovskii, Y. Ovchinnikov and Y. Struchkov, *J. Organomet. Chem.*, **499**, 73 (1995).
70. J. Corset, M. Castella-Ventura, F. Froment, T. Strzalko and L. Wartski, *J. Raman Spectrosc.*, **33**, 652 (2002).
71. E. Kaufmann, P. v. R. Schleyer, K. N. Houk and Y. D. Wu, *J. Am. Chem. Soc.*, **107**, 5560 (1985).
72. M. Nakamura, E. Nakamura, N. Koga and K. Morokuma, *J. Am. Chem. Soc.*, **115**, 11016 (1993).
73. (a) R. B. Bates, L. M. Kroposki and D. E. Potter, *J. Org. Chem.*, **37**, 560 (1972).
    (b) A. Maercker and W. Theysohn, *Liebigs Ann. Chem.*, **747**, 70 (1971).
74. T. Kremer, S. Harder, M. Junge and P. v. R. Schleyer, *Organometallics*, **15**, 585 (1996).
75. J. F. McGarrity, C. A. Ogle, Z. Brich and H. R. Loosli, *J. Am. Chem. Soc.*, **107**, 1810 (1985).

76. E. L. Jeffery, R. K. Mann, G. J. Hutchings, S. H. Taylor and D. J. Willock, *Catal. Today*, **105**, 85 (2005).
77. (a) G. Kresse and J. Furthmuller, *Phys. Rev. B*, **54**, 11169 (1996).
(b) G. Kresse and J. Furthmuller, *Comput. Mater. Sci.*, **6**, 15 (1996).
78. W. S. Sim, T. C. Li, P. X. Yang and B. S. Yeo, *J. Am. Chem. Soc.*, **124**, 4970 (2002)
79. D. B. Collum, *Acc. Chem. Res.*, **25**, 448, (1992).
80. F. E. Romesberg and D. B. Collum, *J. Am. Chem. Soc.*, **117**, 2166, (1995).
81. M. L. McKee, *J. Am. Chem. Soc.*, **109**, 559 (1987).
82. F. E. Romesberg and D. B. Collum, *J. Am. Chem. Soc.*, **114**, 2112 (1992).
83. E. J. Corey and R. A. Sneen, *J. Am. Chem. Soc.*, **78**, 6269 (1956).
84. L. D. McKeever, R. Waack, M. A. Doran and E. B. Baker, *J. Am. Chem. Soc.*, **90**, 3244 (1968).
85. P. L. Hall, J. H. Gilchrist, A. T. Harrison, D. J. Fuller and D. B. Collum, *J. Am. Chem. Soc.*, **113**, 9575 (1991).
86. P. L. Hall, J. H. Gilchrist and D. B. Collum, *J. Am. Chem. Soc.*, **113**, 9571 (1991).
87. E. J. Corey and A. W. Gross, *Tetrahedron Lett.*, **25**, 495 (1984).
88. Y. Balamraju, C. D. Sharp, W. Gammill, N. Manuel and L. M. Pratt, *Tetrahedron*, **54**, 7357 (1998).
89. J. Cámpora, C. M. Maya, P. Palma, E. Carmona, E. Gutiérrez, C. Ruiz, C. Graiff and A. Tiripicchio, *Chem. Eur. J.*, **11**, 6889 (2005).
90. D. Evans, in *Asymetric Synthesis*, Vol. 3 (Ed. J. D. Morrison), Academic Press, Orlando, 1984, pp. 1–110.
91. D. Seebach, *Angew. Chem., Int. Ed. Engl.*, **27**, 1624 (1988).
92. (a) A. R. Chamberlin, M. Dezube, S. H. Reich and D. J. Sall, *J. Am. Chem. Soc.*, **111**, 6247 (1989).
(b) D. L. J. Clive, H. W. Manning, T. L. B. Boivin and M. H. D. Postema, *J. Org. Chem.*, **58**, 6857 (1993).
93. (a) Y. Moritani, T. Ukita, T. Nishitani, M. Seki and T. Iwasaki, *Tetrahedron Lett.*, **31**, 3615 (1990).
(b) Y. Moritani, C. Fukushima, T. Ukita, T. Miyagishima, H. Ohmizu and T. Iwasaki, *J. Org. Chem.*, **61**, 6922 (1996).
94. (a) K. Tomioka, Y.-S. Cho, F. Sato and K. Koga, *J. Org. Chem.*, **53**, 4094 (1988).
(b) A. K. Ghosh, S. P. McKee and W. J. Thompson, *J. Org. Chem.*, **56**, 6500 (1991).
(c) T. Yamazaki, K. Mizutani and T. Kitazume, *J. Org. Chem.*, **58**, 4346 (1993).
95. P. Y. Michellys, P. Maurin, L. Toupet, H. Pellissier and M. Santelli, *J. Org. Chem.*, **66**, 115 (2001).
96. H. Pellissier, P. Y. Michellys and M. Santelli, *J. Org. Chem.*, **62**, 5588 (1997).
97. V. M. Gutiérrez-Garcéa, G. Reyes-Rangel, O. Muñoz-Muñiz and E. Juaristi, *J. Braz. Chem. Soc.*, **12**, 652 (2001).
98. W. L. Jorgensen and D. L. Severance, *J. Am. Chem. Soc.*, **112**, 4768 (1990).
99. (a) A. Streitwieser, *Acc. Chem. Res.*, **17**, 353 (1984).
(b) A. Streitwieser, S. M. Bachrach, A. Dorigo and P. v. R. Schleyer, in *Lithium Chemistry: A Theoretical and Experimental Overview* (Eds A. M. Sapse and P. v. R. Schleyer), John Wiley & Sons, Inc., New York, 1995, pp. 12–15.
100. A. Niida, M. Mizumoto, T. Narumi, E. Inokuchi, S. Oishi, H. Ohno, A. Otaka, K. Kitaura and N. Fujii, *J. Org. Chem.*, **71**, 4118 (2006).
101. T. F. Anderson, J. G. Knight and K. Tchabanenko, *Tetrahedron Lett.*, **44**, 757 (2003).
102. Y. Ikuta and S. Tomoda, *Tetrahedron Lett.*, **44**, 5931 (2003).
103. Y. Ikuta and S. Tomoda, *Org. Lett.*, **6**, 189 (2004).
104. K. A. Durkin and D. Liotta, *J. Am. Chem. Soc.*, **112**, 8162 (1990).
105. D. Romo and A. I. Meyers, *Tetrahedron*, **47**, 9503 (1991).
106. K. Ando, *J. Am. Chem. Soc.*, **127**, 3964 (2005).
107. I. Soteras, O. Lozano, A. Gómez-Esqué, C. Escolano, M. Orozco, M. Amat, J. Bosch and F. J. Luque, *J. Am. Chem. Soc.*, **128**, 6581 (2006).
108. L. M. Pratt, N. Van Nguyen and B. Ramachandran, *J. Org. Chem.*, **70**, 4279 (2005).
109. (a) H. Yamataka, D. Sasaki, Y. Kuwatani, M. Mishima and Y. Tsuno, *J. Am. Chem. Soc.*, **119**, 9975 (1997).

(b) H. Yamataka, D. Sasaki, Y. Kuwatani, M. Mishima and Y. Tsuno, *Chem. Lett.*, 271 (1997).
110. I. Lin and A. R. Day, *J. Am. Chem. Soc.*, **74**, 5133, (1952).
111. (a) J. A. Krom and A. Streitwieser, *J. Am. Chem. Soc.*, **114**, 8747 (1992).
(b) A. Abbotto and A. Streitwieser, *J. Am. Chem. Soc.*, **117**, 6358 (1995).
(c) F. Abu-Hasanayn, M. Stratakis and A. Streitwieser, *J. Org. Chem.*, **60**, 4688 (1995).
112. F. Abu-Hasanayn and A. Streitwieser, *J. Org. Chem.*, **63**, 2954 (1998).
113. (a) D. Evans and A. H. Hoveyda, *J. Am. Chem. Soc.*, **112**, 6447 (1990).
(b) E. Burkhardt, R. Bergman and C. Heathcock, *Organometallics*, **9**, 30 (1990).
(c) Y. Aoki, K. Oshima and K. Utimoto, *Chem. Lett.*, 463 (1995).
114. (a) J. Boutagy and R. Thomas, *Chem. Rev.*, **74**, 87 (1974).
(b) B. E. Maryanoff and A. B. Reitz, *Chem. Rev.*, **89**, 863 (1989).
115. K. Ando, *J. Org. Chem.*, **64**, 6815 (1999).
116. M. Ruiz, V. Ojea and J. M. Quintela, *Tetrahedron: Asymmetry*, **13**, 1863 (2002).
117. M. Svensson, S. Humbel, R. D. J. Froese, T. Matsubara, S. Sieber and K. Morokuma, *J. Phys. Chem.*, **100**, 19357 (1996).
118. E. Kaufmann, J. Gose and P. v. R. Schleyer, *Organometallics*, **8**, 2577 (1989).
119. T. Vreven and K. Morokuma, *J. Comput. Chem.*, **21**, 1419 (2000).
120. M. Watanabe and K. Soai, *J. Chem. Soc., Perkin Trans. 1*, 3125 (1994).
121. J. C. Harmange and B. Figadere, *Tetrahedron: Asymmetry*, **4**, 1711 (1993).
122. (a) M. Chini, P. Crotti, L. Favero and M. Pineschi, *Tetrahedron Lett.*, **32**, 7583 (1991).
(b) P. Crotti, V. Di Bussolo, L. Favero, F. Macchia and M. Pineschi, *Tetrahedron Lett.*, **35**, 6537 (1994).
123. P. Crotti, V. Di Bussolo, L. Favero, M. Pasero and M. Pineschi, *J. Org. Chem.*, **61**, 9548 (1996).
124. S. K. Taylor, *Tetrahedron*, **56**, 1149 (2000).
125. C. S. Pomelli, A. M. Bianucci, P. Crotti and L. Favero, *J. Org. Chem.*, **69**, 150 (2004).
126. (a) A. Cordova, *Acc. Chem. Res.*, **37**, 102 (2004).
(b) M. Arend, B. Westermann and N. Risch, *Angew. Chem. Int. Ed.*, **37**, 1045 (1998).
(c) E. F. Kleinman, in *Comprehensive Organic Synthesis*, Vol. 2 (Eds B. M. Trost and I. Fleming), Pergamon Press, Oxford, 1991, pp. 893–951.
127. (a) F. Bernardi, A. Bongini, G. Cainelli, M. A. Robb and G. Suzzi Valli, *J. Org. Chem.*, **58**, 750 (1993).
(b) A. Bongini, D. Giacomini, M. Panunzio, G. Suzzi-Valli and P. Zarantonello, *Spectrochim. Acta*, **51A**, 563 (1995).
128. G. I. Georg, G. C. B. Harriman, M. Hepperle, J. S. Clowers, D. G. Vander Velde and R. H. Himes, *J. Org. Chem.*, **61**, 2664 (1996).
129. G. Cainelli, M. Panunzio, E. Bandini, G. Martelli and G. Spunta, *Tetrahedron*, **52**, 1685 (1996).
130. (a) T. Ishihara, K. Ichihara and H. Yamanaka, *Tetrahedron*, **52**, 255 (1996).
(b) R. Annunziata, M. Benaglia, M. Cinquini, F. Cozzi, O. Martini and V. Molteni, *Tetrahedron*, **52**, 2583 (1996).
(c) S. Itsuno, K. Watanabe, K. Ito, A. A. El-Shehawy and A. A. Sarhan, *Angew. Chem., Int. Ed. Engl.*, **36**, 109 (1997).
131. L. R. Domingo, M. Arno, P. Merino and T. Tejero, *Eur. J. Org. Chem.*, 3464 (2006).
132. (a) D. A. Evans, J. Bartroli and T. L. Shih, *J. Am. Chem. Soc.*, **103**, 2127 (1981).
(b) D. A. Evans, *Aldrichimica Acta*, 318 (1982).
133. (a) M. A. Walker and C. H. Heathcock, *J. Org. Chem.*, **56**, 5747 (1991).
(b) K. Chibale and S. Warren, *Tetrahedron Lett.*, **33**, 4369 (1992).
134. K. Iseki, S. Oishi, T. Taguchi and Y. Kobayashi, *Tetrahedron Lett.*, **34**, 8147 (1993).
135. Y. Makino, K. Iseki, K. Fujii, S. Oishi, T. Hirano and Y. Kobayashi, *Tetrahedron Lett.*, **36**, 6527 (1995).
136. (a) T. Iimori and M. Shibasaki, *Tetrahedron Lett.*, **26**, 1523 (1985).
(b) T. Iimori and M. Shibasaki, *Tetrahedron Lett.*, **27**, 2149 (1986).
(c) M. Shibasaki, Y. Ishida, G. Iwasaki and T. Iimori, *J. Org. Chem.*, **52**, 3488 (1987).
(d) M. Mori, K. Kagechika, H. Sasai and M. Shibasaki, *Tetrahedron*, **47**, 531 (1991).
137. (a) C. Gennari and G. Pain, *Tetrahedron Lett.*, **37**, 3747 (1996).

(b) C. Gennari, A. Vulpetti, M. Donghi, N. Mongelli and E. Vanotti, *Angew. Chem., Int. Ed. Engl.*, **35**, 1723 (1996).
138. A. Bernardi, C. Gennari, L. Raimondi and M. B. Villa, *Tetrahedron*, **53**, 7705 (1997).
139. A. Bernardi, C. Gennari, J. M. Goodman and I. Paterson, *Tetrahedron: Asymmetry*, **6**, 2613, (1995).
140. (a) Y. Li, M. N. Paddon-Row and K. N. Houk, *J. Org. Chem.*, **55**, 481 (1990).
(b) Y. Li and K. N. Houk, *J. Am. Chem. Soc.*, **111**, 4505 (1989).
141. J. Murga, E. Falomir, F. González, M. Carda and J. A. Marco, *Tetrahedron*, **58**, 9697 (2002).
142. A. Bernardi, A. M. Capelli, C. Gennari, J. M. Goodman and I. Paterson, *J. Org. Chem.*, **55**, 3576 (1990).
143. (a) T. Ishihara, M. Kuroboshi and K. Yamaguchi, *Chem. Lett.*, 211 (1990).
(b) M. Kuroboshi and T. Ishihara, *Bull. Chem. Soc. Jpn.*, **63**, 1191 (1990).
144. K. Mikami and Y. Itoh, *Chem. Rec.*, **6**, 1 (2006).
145. (a) A. J. Nielson, P. Schwerdtfeger and J. M. Waters, *J. Chem. Soc., Dalton Trans.*, 529 (2000).
(b) J. A. Dobado, J. M. Molina, R. Uggla and M. R. Sundberg, *Inorg. Chem.*, **39**, 2831 (2000).
146. Y. Itoh, M. Yamanaka and K. Mikami, *Org. Lett.*, **5**, 4807 (2003).
147. (a) P. G. Harrison, *Chemistry of Tin*, Blackie, Glasgow and London, 1989.
(b) R. Hulme, *J. Chem. Soc.*, 1524 (1963).
148. M. Yasuda, K. Hayashi, Y. Katoh, I. Shibata and A. Baba, *J. Am. Chem. Soc.*, **120**, 715 (1998).
149. M. Yasuda, Y. Katoh, I. Shibata, A. Baba, H. Matsuda and N. Sonoda, *J. Org. Chem.*, **59**, 4386 (1994).
150. M. Yasuda, T. Oh-hata, I. Shibata, A. Baba and H. Matsuda, *J. Chem. Soc., Perkin Trans. 1*, 859 (1993).
151. M. Yasuda, N. Ohigashi, I. Shibata and A. Baba, *J. Org. Chem.*, **64**, 2180 (1999).
152. (a) T. Kawakami, I. Shibata and A. Baba, *J. Org. Chem.*, **61**, 82 (1996).
(b) T. Suwa, I. Shibata and A. Baba, *Organometallics*, **18**, 3965 (1999).
153. (a) Y. Yamamoto, H. Yatagai and K. Maruyama, *J. Chem. Soc., Chem. Commun.*, 162 (1981).
(b) S. S. Labadie and J. K. Stille, *Tetrahedron*, **40**, 2329 (1984).
154. Y. Odic and M. Pereyre, *J. Organomet. Chem.*, **55**, 273 (1973).
155. (a) I. Kuwajima and E. Nakamura, *J. Am. Chem. Soc.*, **97**, 3257 (1975).
(b) I. Kuwajima, E. Nakamura and M. Shimizu, *J. Am. Chem. Soc.*, **104**, 1025 (1982).
(c) G. A. Kraus, B. Roth, K. Frazier and M. Shimagaki, *J. Am. Chem. Soc.*, **104**, 1114 (1982).
156. (a) E. Nakamura, M. Shimizu, I. Kuwajima, J. Sakata, K. Yokoyama and R. Noyori, *J. Org. Chem.*, **48**, 932 (1983).
(b) R. Noyori, I. Nishida and J. Sakata, *J. Am. Chem. Soc.*, **103**, 2106 (1981).
157. M. Yasuda, K. Chiba and A. Baba, *J. Am. Chem. Soc.*, **122**, 7549 (2000).
158. H. E. Zimmerman and M. D. Traxler, *J. Am. Chem. Soc.*, **79**, 1920 (1957).
159. M. Kira, K. Sato and H. Sakurai, *J. Am. Chem. Soc.*, **110**, 4599 (1988).
160. (a) S. E. Denmark, S. B. D. Winter, W. X. Su and K.-T. Wong, *J. Am. Chem. Soc.*, **118**, 7404 (1996).
(b) K. Miura, H. Sato, K. Tamaki, H. Ito and A. Hosomi, *Tetrahedron Lett.*, **39**, 2585 (1998).
161. (a) G. Poli and G. Giambastiani, *J. Org. Chem.*, **67**, 9456 (2002).
(b) S. Thorimbert, G. Giambastiani, C. Commandeur, M. Vitale, G. Poli and M. Malacria, *Eur. J. Org. Chem.*, 2702 (2003).
(c) S. Lemaire, G. Giambastiani, G. Prestat and G. Poli, *Eur. J. Org. Chem.*, 2840 (2004).
162. D. Madec, G. Prestat, E. Martini, P. Fristrup, G. Poli and P. O. Norrby, *Org. Lett.*, **7**, 995 (2005).
163. (a) A. Gobbi, D. Landini, A. Maia and S. Petricci, *J. Org. Chem.*, **63**, 5356 (1998).
(b) B. Lygo and B. Andrews, *Acc. Chem. Res.*, **37**, 518 (2004).
164. *Jaguar 4.2*; Schrodinger, Inc., Portland, OR, 2000. (http://www.schrodinger.com./ProductDescription.php?mID=6&sID=9&cID=0).
165. P. O. Norrby, M. M. Mader, M. Vitale, G. Prestat and G. Poli, *Organometallics*, **22**, 1849 (2003).
166. B. M. Trost and C. B. Lee, *J. Am. Chem. Soc.*, **123**, 3671 (2001).
167. S. Diezi, D. Ferri, A. Vargas, T. Mallat and A. Baiker, *J. Am. Chem. Soc.*, **128**, 4048 (2006).

168. A. Vargas, T. Burgi and A. Baiker, *J. Catal.*, **222**, 439 (2004).
169. G. Asensio, P. Alemán, J. Gil, L. R. Domingo and M. Medio-Simón, *J. Org. Chem.*, **63**, 9342 (1998).
170. G. Asensio, P. Gaviña, A. Cuenca, M. C. R. de Arellano, L. R. Domingo and M. Medio-Simón, *Tetrahedron: Asymmetry*, **11**, 3481 (2000).
171. G. Asensio, P. A. Alemán, L. R. Domingo and M. Medio-Simón, *Tetrahedron Lett.*, **39**, 3277 (1998).
172. W. B. Farnham and W. R. Hertler, *US Patent* 4,728,706 (1988).
173. S. Collins and D. G. Ward, *J. Am. Chem. Soc.*, **114**, 5460 (1992).
174. (a) S. Collins, D. G. Ward and K. H. Suddaby, *Macromolecules*, **27**, 7222 (1994).
(b) Y. Li, D. G. Ward, S. S. Reddy and S. Collins, *Macromolecules*, **30**, 1875 (1997).
175. (a) H. Deng and K. Soga, *Macromolecules*, **29**, 1847 (1996).
(b) Y. X. Chen, M. V. Metz, L. T. Li, C. L. Stern and Z. J. Marks, *J. Am. Chem. Soc.*, **120**, 6287 (1998).
176. (a) M. R. Bray, R. J. Deeth and V. Paget, *J. Prog. React. Kinet.*, **21**, 169 (1996).
(b) J. Endo, N. Koga and K. Morokuma, *Organometallics*, **12**, 2777 (1993).
(c) Y. van der Leek, K. Angermund, M. Reffke, R. Kleinschmidt, R. Goretzki and F. G. Fink, *Chem. Eur. J.*, **3**, 585 (1997).
(d) P. Margl, L. Deng and T. Ziegler, *J. Am. Chem. Soc.*, **121**, 154 (1999).
177. R. Sustmann, W. Sicking, F. Bandermann and M. Ferenz, *Macromolecules*, **32**, 4204 (1999).
178. M. Holscher, H. Keul and H. Hocker, *Chem. Eur. J.*, **7**, 5419 (2001).
179. S. Tomasi, H. Weiss and T. Ziegler, *Organometallics*, **25**, 3619 (2006).
180. (a) L. S. Boffa and B. M. Novak, *Chem. Rev.*, **100**, 1479 (2000).
(b) H. Yasuda, *J. Organomet. Chem.*, **647**, 128 (2002).

CHAPTER **2**

Molecular structure of metal enolates

KSENIJA BABIĆ-SAMARDŽIJA

Chemistry Department, Rice University, 6100 Main St., Houston, TX 77005, USA
Present address: Baker Hughes Incorporated, 12645 West Airport Blvd., Sugar Land, TX 77478, USA
Fax: (+1)-281-276-5491; e-mail: ksenija.babic@bakerpetrolite.com

SOFIJA P. SOVILJ

Faculty of Chemistry, University of Belgrade, Studentski trg 12-16, P.O. Box 158, 11000 Belgrade, Serbia
Fax: (+381)-11-184-330; e-mail: ssovilj@chem.bg.ac.rs

and

VLADISLAVA M. JOVANOVIĆ

ICTM-Institute of Electrochemistry, University of Belgrade, Njegoševa 12, P.O. Box 473, 11000 Belgrade, Serbia
Fax: (+381)-11-337-0389; e-mail: vlad@tmf.bg.ac.rs

The chemistry of metal enolates
Edited by Jacob Zabicky

I. ACRONYMS

acac	acetylacetonate	hfac	hexafluoroacetylacetonate
bipy	2,2′-bipyridine	ILCT	intraligand charge transfer
bzac	1-phenylbutane-1,3-dionate	LLCT	ligand-to-ligand charge transfer
bzq	benzoquinoline	MLCT	metal-to-ligand charge transfer
CFSE	crystal field stabilization energies	MOCVD	metallorganic chemical vapor deposition
CR	charge reversed	OLED	organic light-emitting diode
CT	charge transfer	phen	1,10-phenanthroline
diam	diamine	Racac	substituted acetylacetonate
dibzm	1,3-diphenyl-1,3-propanedionate	$^{SC}CO_2$	supercritical CO_2
dik	β-diketonate	tfac	trifluoroacetylacetonate
dpm	dipivaloylmethanoate	thp	2-(2′-thienyl)pyridine
en	ethylenediamine	tmeda	*N*,*N*,*N*′,*N*′-tetramethylethylenediamine
GED	gas electron diffraction	tpy	2-(4-tolyl)pyridine

II. INTRODUCTION

Ligand properties such as coordination activity, bond length and orientation of donor atoms are among the key functions in designing organic structures. β-Diketones and their metal complexes are among the first groups studied. Numerous classes of various metal complexes are the product of their versatility and flexibility to adopt different coordination modes. They typically act in monoanionic form as bidentate oxygen donor in enol form or in keto form as neutral molecule[1]. In that form ligand coordination can take place through the carbon atom or as a monodentate oxygen donor in enol form, or as bridging ligand donor.

Enolate ions are most important intermediates in synthetic organic chemistry. The preferred reaction path of an enolate is influenced by the nature of the generating functional group. Most of the aldehyde and ketone enolates react through oxygen while ester enolates, amide enolates and enolates with electronegative substituents react preferentially through carbon[2]. Ring size has a significant effect in bond selectivity; small-ring enolates react preferably through carbon while large-ring enolates react through

oxygen. Another parameter is the enthalpy of the keto–enol transformation, ΔH_{K-E}, which determines whether bonding will preferably take place through oxygen if its value is low (10–15 kcal mol^{-1}) or through carbon if its value is high (30–40 kcal mol^{-1}).

Acetylacetone has been studied as a prototype molecule for keto–enol tautomerization. In Scheme 1 are presented enolic and ketonic forms of acetylacetonate with structure transition forms from C_{2v} to C_s. It has been agreed that enol I and keto I forms are the two of lowest energy while the other structures are expected to have higher energies[3]. Complete agreement was found in data with a potential of the enolic proton exhibiting a single symmetric minimum; thus the observed C_{2v} species in the enol I structure are as predicted with a global minimum energy.

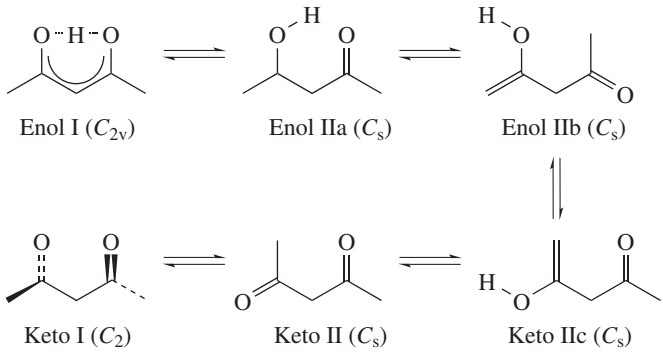

SCHEME 1. Enolic and ketonic forms of acetylacetone. The enolic conformations shown are plausible lowest-energy forms. Reprinted with permission from Reference 3. Copyright 2006 American Chemical Society

Earlier studies have disclosed that the coordination mode of the enolate ligands exerts a strong influence in its reactivity[4,5]. For instance, in contrast to *O*-enolates, coordination through carbon atom often causes low enolate-like reactivity and a chemical behavior more similar to that of alkylmetals, for example, toward migratory insertion[6,7], although some aldol-type additions of *C*-bonded enolates are known[8,9]. The active participation of the *O*-bonded tautomer in these transformations cannot be ruled out, as the two forms may have similar energies. Both *O*- and *C*-binding have been ascertained for late transition metals[10–12] but the latter is more common for the softer Lewis acids derived from the heavier elements of these groups[13,14]. In some cases both tautomeric *C*- and *O*-enolate forms have been detected[12].

Preference of the enol or the keto tautomeric form depends strongly on the substituents. According to structural studies in the gas phase on compounds of general formula $XC(O)CH_2C(O)Y$ the enol tautomer is present when X = Y = H, Me, *i*-Pr, Mef. On the other hand, when X = Y = F, Cl, OMe, NH_2 the diketo form prevails. There are two enol and three possible conformers of the diketo tautomer of $XC(O)CH_2C(O)Y$ type compounds. It was found by GED that methyl acetoacetate ($MeC(O)CH_2C(O)OMe$) containing Me and OMe substituents shows a mixture of $80 \pm 7\%$ enol and $20 \pm 7\%$ diketo tautomers, while some theoretical predictions and calculations pointed to 92% or 87% of enol tautomer or a strong preference for the diketo form[15]. Experiments and calculations on acetoacetamide ($MeC(O)CH_2C(O)NH_2$) show a mixture of $63 \pm 7\%$ enol and $37 \mp 7\%$ diketo forms at the gas phase. In the aqueous solution 90% of diketo tautomer is present, probably due to stabilizing intermolecular interactions with water molecules.

It is hard to predict tautomeric properties of dicarbonyl compounds, and an intuitive way is based on the nature of the substituents and their electronegativity. For example, substituents of group I with $\chi_{BB} < 2.88$ (Boyd and Boyd χ_{BB} values) as H (2.10), Me (2.55), *i*-Pr (2.55), CF_3 (2.71) favor enol tautomer and Cl (3.00), NH_2 (3.12), OMe (3.53) and F (4.00) with $\chi_{BB} \geqslant 3.00$ favor the diketo form[15]. An alternative consideration is the presence or absence of a nonbonding electron. Alkyl groups do not contain a lone pair and favor the enol tautomer, whereas the others possess nonbonding one, two or three electron pairs. In disagreement with this aproach are substituents with lone pairs and low electronegativity, such as $-SH$ or $-SCH_3$ group with $\chi_{BB} = 2.65$. Quantum chemical calculations predict a strong preference for the diketo tautomer but, based on electronegativity, enol is the expected tautomer. Apparently, conjugation between a lone pair of the substituent and the C=O π-bond, i.e. a resonance structure of the $X^+ = C-O^-$, stabilizes the keto structure.

The chemistry of late transition metal enolates is a subject of considerable synthetic interest due to the high levels of selectivity that such compounds introduce in many organic reactions. A detailed study of these complexes is essential for the development of new synthetic applications[16]. Thus, transition metal enolates have become crucial in a number of valuable synthetic methodologies. Optimization of these methodologies demands a deeper understanding of their mechanistic details.

III. VIBRATIONAL SPECTRA

IR spectra are the most important spectral technique for detecting the β-diketonate moiety and type of bonding. The most characteristic peaks in the IR spectra of β-diketonates[17] belong to the following groups: (i) The skeletal vibrations of acetylacetone derived from the coupling of two acetone molecules linked by a common methylene group: for example, the bands of $Fe(acac)_3$ are found around 1272 and 1186 cm^{-1}, 799 and 769 cm^{-1}, and 548, 434 and 412 cm^{-1}. (ii) The characteristic vibrations of the C−H bonds found at 1419, 1355, 1021 and 927 cm^{-1}. (iii) The C=O group vibrations near 1575 and 1522 cm^{-1}, pointing to coordination through the enol form when both oxygen atoms are involved in coordination. The first band assigned to C=O has reduced bond order. Appearance of a band at 1385 cm^{-1} is characteristic for C−O increased bond order. Vibrations at 1522 cm^{-1} correspond to C=C reduced or perturbed bond due to the enol coordination[17]. In case of absence of this band, coordination is probably realized through both carbonyl groups. Therefore, absorption in the OH region is considered as evidence for the enol form, since ν(O−H) is significantly weakened and broadened by intramolecular hydrogen bonding. Absorptions in the 1700–400 cm^{-1} region are common to the spectra of most metal acetylacetonates. Position and number of these bands depend on the nature of the coordinated central metal ion. (iv) The band around 1425 cm^{-1} was found to be present only in acac and metal complexes with basic acetylacetonate or other β-diketonates containing the acetyl moiety. This band corresponds to methyl deformation vibrations, together with a band near 800 cm^{-1}, assigned either to out-of-plane C−H deformation or π(C−H). (v) There are three bands around 3000 cm^{-1} in spectra of β-diketones and their metal β-diketonates that are unaffected by the metal ion, corresponding to ν(C−H) of the methylene group, as well as asymmetric and symmetric vibrations of the methyl group, ν(C−H), at 2970 and 2870 cm^{-1}.

IR data show that the metal–ligand bond is partially ionic since ν(C−O) is relatively high (e.g. at 1593 cm^{-1} for Mn−O) and the fairly low value of the crystal field splitting parameter (Dq) is also consistent with the ionic character of the Mn−O bond[18]. In the case of Co(III), Dq is very high suggesting strong π-bonding and, consequently, the relatively high stretching M−O and C−O frequencies. Acceptor π-bonding provides the major

contribution to the total π-interaction, raising the d-orbital level and decreasing Dq. On the other hand, donor π-bonding lowers the d-orbital level and increases Dq. For instance, Ti(III) is a strong donor and weak acceptor thus resulting in the π-interaction being weak; Cr(III) is moderate as donor and acceptor and total π-interaction is strong. Also, in case of Co(III) ion, the strong donor role and absence of an acceptor contribution will produce total strong π-interaction.

Substituents on β-diketonate have a considerable effect on spectral data. Fluorine is known as the strongest electron-withdrawing element with three lone electron pairs and the ability to form strong intramolecular hydrogen bonding is reflected in its capabilities[19].

A. Metal–Oxygen Frequencies

1. Metal(III) diketonates

Theoretically, there are three IR active stretching modes for metal(III) acetylacetonates[17]. Band assignments were investigated using the normal coordinate analysis, oxygen ^{18}O labeling and metal labeling. There is a couple of sections within the 700–250 cm^{-1} region assigned to (i) ν(M–O) stretching + ring deformation, (ii) ν(M–O) stretching + δ(C–CH_3) in-plane bending, (iii) ν(M–O) stretching + ν(C–CH_3) stretching, (iv) π, out-of-plane bending, ring deformation and in-plane bending δ(O–M–O) and (v) ν(M–O) stretching vibrations.

Crystal field stabilization energies (CFSE) of the complexes with trivalent metals follow the sequence for metal–ligand (oxygen) bonds in the order Sc < V < Cr, followed by Cr > Mn > Fe and Fe < Co. Metal–oxygen stretching bands, ν(M–O), are of similar vibrational purity, but it is observed that CFSEs have an effect on these frequencies[17]. This is the case of Mn(III), with high spin d^4 configuration and intensive Jahn–Teller distortion. It is clear that CFSEs can affect not only metal–ligands bonds but also C–O bonds of Racac-type ligands.

Co(III) acetylacetonates show frequencies closer to the low spin d^6-ion configuration than to the high spin. Co(tfac)$_3$ has an even lower ν(Co–O) band than calculated for low spin, i.e. 445 *vs.* 451 cm^{-1}, respectively[17]. Therefore, metal–ligand vibrations for a series of octahedral metal complexes are in order Co(II) < Ni(II) and Zn(II) < Ni(II) within the same ligand system. Fe(III) < Mn(III) < Cr(III) is observed, as expected from crystal field theory[17].

A series of tris(acetylacetonato)metal(III) complexes (Co, Cr, Ru and Rh) has revealed a new aspect concerning the effect of the central metal ion on the vibrational energy levels split by interligand interactions (Figure 1)[20]. Correlated vibrational motions of vicinal ligands are affected by the d-electron configuration of a central metal ion. All IR spectra in the 1700–1000 cm^{-1} range have a similar form. Differences seen in the 1500–1300 cm^{-1} range corresponds to C–O stretching vibrations. The two oppositely signed peaks in the VCD spectra are caused by the splitting of the vibrational energy level due to interaction of vicinal ligands. In the case of the Δ-enantiomer of Co and Rh complexes, the negative peak appears at the higher frequency with the residual positive peak at the lower frequency, whereas the Cr and Ru complexes have the opposite appearance. This behavior can be attributed to the electronic configuration of the central metal ion. Co(III) and Rh(III) have diamagnetic (e_g^6) d-electron configuration, while Cr(III) and Ru(III) have paramagnetic (e_g^5) d-electron configuration. Accordingly, the diamagnetic configuration has a symmetric distribution of d-electrons that stabilizes in-phase motion of vicinal ligands more than the out-of-phase motion, and vice versa for the paramagnetic species.

Since the strength of the metal–ligand bond is directly related to the metal–ligand stretching constant, it is expected that the ν(M–O) vibrations will be in the order Al, Ga, In > alkali earth > alkali metals[21]. Correlations were found between the stability constants

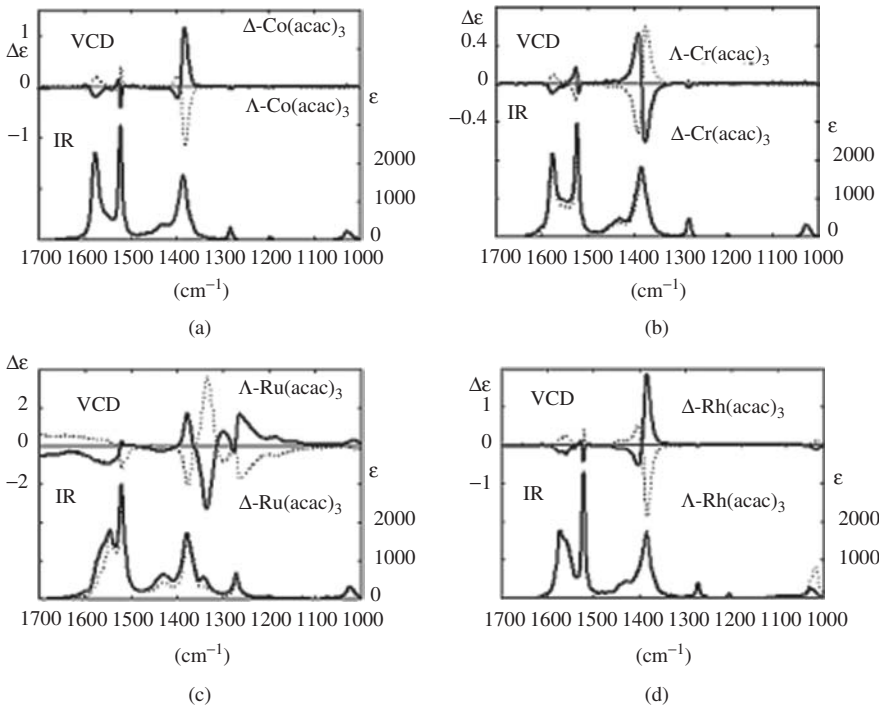

FIGURE 1. FT-IR (lower traces) and VCD (vibrational circular dichroism, upper traces) spectra of $M(acac)_3$ complexes: (a) M = Co, (b) M = Cr, (c) M = Ru and (d) M = Rh. In the VCD spectra the solid and dotted curves correspond to the Δ- and Λ-enantiomers, respectively. Reproduced with permission from Reference 20

and energetic parameters for molecular complexes, for example the force constant and the frequency of the M−O stretching vibrations. The M−O normal vibrations of $M(acac)_3$ show strong isotope effects for M = Al, Ga and In. Unfortunately, no satisfactory correlation can be established for the metal isotopes between the experimental IR frequencies and either the force constant of the M−O bond or the stability constants.

2. Metal(II) diketonates

$M(dik)_2$ complexes are not as straightforward structurally as $M(dik)_3$ complexes; most of them are with polymeric structure (e.g. Ca, Mn, Fe, Co, Ni, Zn) but, interestingly, $Cu(dik)_2$ complexes are monomeric, square planar[22].

An almost linear relationship is observed between the *d*-orbital population and the ν(M−O) frequencies, from Mn (d^5) toward Fe (d^6), Co (d^7), Ni (d^8), Cu (d^9) and Zn (d^{10}), increasing from *ca* 540 to 615 cm^{-1}, respectively. The value for Cr (d^4) is the same as for the Ni (d^8), while the Cu (d^0) vibrations appear at lower frequencies than all the d^4–d^{10} transition ions. The particularly high ν(Cu−O) frequency is a consequence of a change to coordination number 4, producing strong Jahn–Teller distortion in the Cu(II)

complexes[23]. The effect of the metal ion is related to the degree of ionic character in the metal–ligand bond[23]. These complexes show low ν(M–O) and high ν(C–O) frequencies, which will be reversed in the case of complexes with more covalent character of the metal–ligand bond. In the case of transition metals this effect is usually associated with crystal field and ion configuration: thus, large CFSE produce high ν(M–O) and low ν(C–O) frequencies. Both effects are independent of ligand substituents.

B. Carbonyl Frequencies

Incorporation of electron-releasing substituents is related to the increase of metal–oxygen bond frequency ν(M–O) and the decrease of ν(C–O) and ν(C–C) in the following order: hexafluoroacetylacetonates < trifluoroacetylacetonates < acetylacetonates < pivaloylacetonates < dipivaloylmethanoates. The ligand substituent is associated with field and resonance contributions, therefore electron-releasing or electron-withdrawing substituents will have opposite effects on metal–ligand and other molecular frequencies[17].

The ν(C=O) frequencies are dependent on the R groups attached to the carbonyl group, i.e. methyl, phenyl, trifluoromethyl etc. The possible interaction of the C=O group with adjacent π- or d-orbitals and the relative electron density over the σ bonds also depend on the R substituents. Electronegative groups, such as trifluoromethyl and hexafluromethyl, tend to raise the ν(C=O) frequencies while coordinated benzoylacetonates have frequencies considerably lower than acetylacetonate. For example, in the case of Cu(bzac)$_2$, ν(C=O) is shifted by 19 cm^{-1} relative to acac (1561 *vs.* 1580 cm^{-1}, respectively) while with Cu(hfac)$_2$ this frequency is moved up to 1655 cm^{-1}. The ν(C=O) frequencies of Cu(dik)$_2$ depend on the R groups of the dik ligand, and are in the order: Cu(dibzm)$_2$ < Cu(acac)$_2$ < Cu(tfa)$_2$ < Cu(hfac)$_2$. Bands at 680, 654 and 455 cm^{-1} are assigned to ν(Cu–O) stretching mode vibrations. For ν(M–O) vibrations in the 600–290 cm^{-1} region the order is Cu > Ni > Co > Zn. Metals capable of forming M(dik)$_2$ and M(dik)$_3$ complexes have the ν(M–O) vibrations at similar frequencies for both oxidation states. The carbonyl group frequencies for these metal acetylacetonates are in a similar range and follow CFSE order Co < Ni and Ni > Cu > Zn[23].

Fluoro-containing ligands are expected to change the stability of coordinatively unsaturated metal complexes. Combination of geometrically defined pyridine-containing organic ligands and coordinatively unsaturated Cu(II)-hexafluoroacetylacetonate moieties leads to formation of a porous metal–organic hybrid structure[24]. In main Cu(hfac)$_2$ complex primary frequencies from IR spectra correspond to: ν(C=O) at 1647 cm^{-1}, ν(C=C) + ν(C=O) at 1561 and 1535 cm^{-1}; δ(CH) 1484–1468 cm^{-1}; ν(C=C) 1257 cm^{-1}; ν(CF$_3$) at 1345, 1229 and 1145 cm^{-1}; δ(CF$_3$) at 807 cm^{-1}; δ(chelate ring) at 676 cm^{-1} and δ_{sym}(CF$_3$) at 594 cm^{-1}. In saturated complexes[24] frequencies that correspond to C–C and C–O vibrations from the chelate ring are shifted to slightly higher wave numbers while the CF$_3$ group shows lower frequencies.

Not only the metal ion but also substituents in the ligands have a strong effect on the characteristic frequencies. For example, the presence of the electron-withdrawing group Mef in tfac or hfac yields the lowest M–O frequencies and highest C–O frequencies. On the other hand, electron-releasing subsitituents such as Me or t-Bu lower the C–C bond strength and will result in the highest M–O and the lowest C–C frequencies. In the case of Cu(hfac)$_2$[17], ν(M–O) is located at 427 cm^{-1}, ν(C–O) at 1655 cm^{-1} and ν(C–C) at 1618 cm^{-1}. For the Cu(acac)$_2$ complex these frequencies are at 455, 1582 and 1536 cm^{-1}, respectively. For Cu(dpm)$_2$ they are located at 496, 1571 and 1504 cm^{-1} while for Cu(dibzm)$_2$ they are shifted to 465, 1549 and 1535 cm^{-1}. Similarly, the corresponding

ν(M−O) frequencies of Fe(hfac)$_3$[17] are shifted to 421 cm^{-1}, ν(C−O) is at 1647 cm^{-1} and ν(C−C) at 1623 cm^{-1}. For Fe(*i*-PrCOCHCOPr-*i*)$_3$ the corresponding frequencies are at 437, 1575 and 1530 cm^{-1}, respectively, for Fe(dpm)$_3$ 479, 1563 and 1510 cm^{-1}, while with Fe(dibzm)$_3$ they are located at 455, 1533 and 1528 cm^{-1}.

C. Scandium and Yttrium Diketonates

β-Diketonates have received much attention because of their stability, volatility and ability to serve as metal source in chemical vapor deposition under mild conditions. The symmetry of Sc(dik)$_3$ complexes[25], dik = dpm, acac, hfac, is essentially D_3 (Figure 2). The six oxygen atoms surrounding the scandium atom are defined in distored antiprismatic coordination. Replacement of organic groups such as Me, *t*-Bu or Mef with one another will not change the chelate ring structure but will affect the bond distances. The electron-withdrawing Mef group weakens the metal−ligand bond and increases this distance. In contrast, the *t*-Bu group could cause shortening of the M−O bond. It seems that the MO_6 polyhedron structure largely depends on the type of metal ion and also on the presence of different substituent groups. Based on GED measurements, a 36.4(63)° rotation angle for the CH_3 groups in Sc(acac)$_3$ points to almost free rotation, whereas the 19.8(17)° value for the CF_3 groups in Sc(hfac)$_3$ indicates restricted rotation[25].

Simultaneous electron diffraction and MS investigation of Sc(acac)$_3$ saturated vapor shows that the vapor contains only monomeric molecules[25]. The heaviest ion in mass spectra is the molecular ion, $[M]^+ = [Sc(hfac)_3]^+$. Also, $[CF_3]^+$ appears to be of high intensity. While the geometrical parameters of the ligand agree fairly well, those of the coordination polyhedron of the Sc(acac)$_3$ molecule differ widely between the crystalline state[26] and the free molecules in the gaseous state[27]. Moreover, the structure of the coordination polyhedron ScO_6 conflicts with Kepert's model[28], based on the idea that the stereochemical distribution of ligands around the central atom depends on mutual repulsion between the central bonds of the ligands and the central atom. In this model, the bidentate ligands are approximated by diatomic molecules with one parameter—the normalized coordination size, b. For metal β-diketonates, $b = r(O\cdots O)/r(M\cdots O)$.

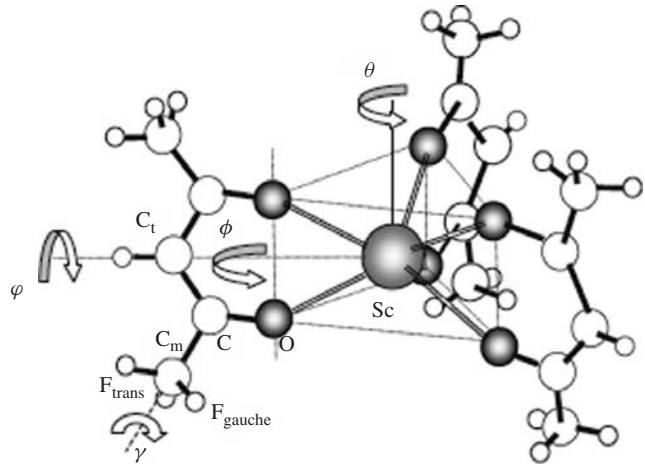

FIGURE 2. Structure of the Sc(hfac)$_3$ molecule, showing definitions of some geometrical parameters. Reproduced with permission from Reference 25

The $Sc(acac)_3$ molecule possesses D_3 symmetry[29]. The barrier to internal rotation of the Me groups (γ axis in Figure 2) estimated from the effective rotation angle is low at the temperature of the GED experiment, $V_0 = 3.6$ kJ mol^{-1}, therefore the rotation may be considered as virtually free.

The dipole moments of six scandium complexes $Sc(RCOCHCOR')_3$, R, R′ = Me, Mef, increase from 4.34 to 6.18 D[30] when Mef groups gradually replace Me groups. Introduction of Mef instead of Me lengthens the adjacent C−O bond and shortens the nearest O−Sc bond (Figure 3). Shorter C−H bonds appear due to the shift of electron density as the number of Mef groups increases in the complex.

The structure of $Sc(mda)_3$[31] (mda = malondialdehyde) and $Sc(acac)_3$[32] was determined by *ab initio* methods. In both cases, the energy minimum corresponds to a D_3 symmetry configuration with a nearly octahedral surrounding of the central atom and a planar configuration of the chelate rings. It can be assumed that replacement of the substituent radical in the chelate by bulky substituents such as *t*-Bu results in additional steric effects[33]. The effect of bulky substituents on the structure of the complexes should weaken in the series $Sc(dpm)_3$–$Y(dpm)_3$–$La(dpm)_3$ with an increase in the r(M−O) distance and the distance between the *t*-Bu groups of neighboring ligands. Replacement of the substituent is not accompanied by substantial structural changes in the MO_6 coordination polyhedron or internuclear distances in the ligand[33].

$Y(dpm)_3$ has been used as molecular precursor for deposition of high-temperature superconducting $YBa_2Cu_3O_{7-x}$ films, due to its high volatility and thermal stability[34]. The advantage of the anhydrous lanthanide β-diketonate and related elements is based on a study where the lack of volatility is attributed to the fact that only hydrates decompose at elevated temperatures, forming the polymeric compounds. In the monohydrate,

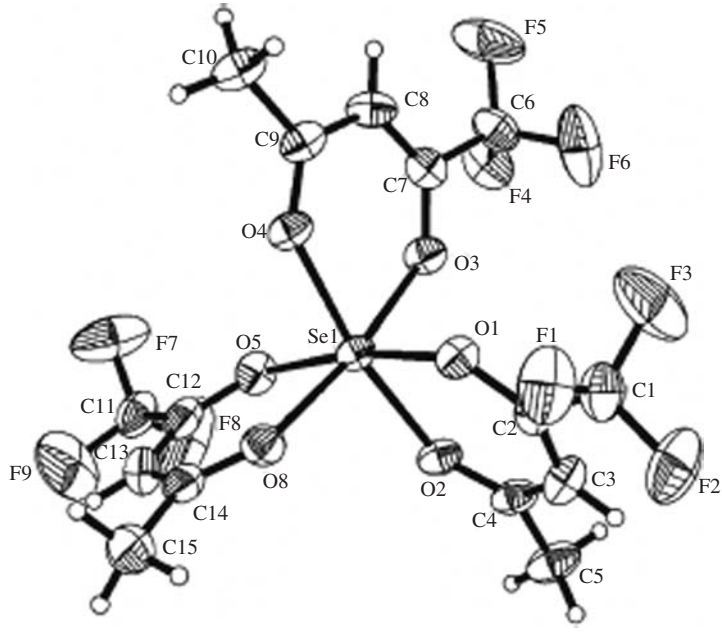

FIGURE 3. Molecular structure of *mer*-$Sc(tfac)_3$. Ellipsoids are shown at the 50% probability level. Reproduced with permission from Reference 30

$Y(thd)_3(H_2O)$, hydrogen bonding between the water molecules and ketonic oxygen atoms occurs. The IR spectrum of $Y(dpm)_3$[34] explains the structure as a symmetrically *O*-coordinated β-diketonate, for bands $\nu_{sym}(C-O)$ at 1597–1575 cm^{-1}, $\nu_{sym}(C-C)$ at 1554 cm^{-1}, $\nu_{asym}(C-O)$ at 1407 cm^{-1}, $\delta(C-H)$ at 1189 cm^{-1}, $\pi(C-H)$ at 800 cm^{-1}, $\nu_{asym}(Y-O)$ at 614 cm^{-1}, $\nu_{sym}(Y-O)$ at 491–475 cm^{-1}, $\pi(C-H)$ of *t*-Bu at 1378–1359 cm^{-1} and $\nu_{sym}(C-C)$ at 1247–1229 cm^{-1}.

In the monomeric structure of $Y(dpm)_3$, all three dpm rings occupy a terminal chelating positions. The reaction of $Y(dpm)_3$ and $Cu(dpm)_2$ with BaX_2, X = *t*-BuO or $Me_2NCH_2CH(Me)$, gives mixed metal complexes[35]. The IR spectra show that $\nu(C{=}O)$ and $\nu(C{=}C)$ vibrations differ in mixed complexes, e.g. $[YBa_3(OBu\text{-}t)_6(thd)_3]$ has two intense absorption bands at 1595 and 1578 cm^{-1} and two weaker ones at 1543 and 1538 cm^{-1}. The frequencies of the M–O vibrations with the dpm ligand are also different from those of the starting complexes.

D. Titanium Diketonates

The nature of β-diketonates, with oxygen donors and substituents pulled back by the chelate geometry, makes these systems very effective for electronic and steric observations. In the d^0-orbital of Ti in $Ti(Racac)_2(OR)_2$ complexes[36], each β-diketonate has only the π-nonbonding HOMO to engage in effective π-donation. Monomeric titanium complexes were investigated as possible antitumor agents. The anticancer activity of budotitane, $Ti(bzac)_2(OEt)_2$, depends on the presence of the phenyl groups of bzac and the spatial distribution of the ligands[37]. If these are replaced with methyl groups, activity completely disappears. In any case, spatial arrangement of Ti complex and/or resulting hydrolyzed species seems to be important for anticancer activity. Figure 4 presents the five possible diastereomeric configurations (barring chirality) of complexes $Ti(Racac)_2X_2$[37], in the particular case of Racac = bzac. The three *cis*-X_2 diastereoisomers are chiral and the *trans*-X_2 ones are achiral. According to spectroscopy data, in $CDCl_3$ solution the *cis-cis-trans* configuration of budotitane with benzoylacetonate ligands in *trans*-position occurs only to a 19% extent. According to NMR spectra and force field calculation, coordination with the X-ligands in the *trans*-position is not expected. Only those benzoylacetonato complexes with bulky hydrolyzable groups X^- such as iodide or *p*-dimethylaminophenoxy have *trans*-configuration[38].

Titanium tetraalkoxides react with β-diketones to give products formulated as (dik)$Ti(OR)_3$ and $(dik)_2Ti(OR)_2$[39,40]. Qualitatively, the *cis*-configurations are more strained but are preferred due to electronic effects caused by $p_\pi - d_\pi$ (t_{2g}) bonding of the β-diketonato ligand[41,42]. Complex $[TiO(acac)_2]_2$ is a cyclic dimer with the Ti centers linked by oxygen atoms[42]. Positive electrospray MS of complexes indicate that, in solution, these derivatives lose anionic ligands that immediately interact with H, Na and/or K ions, yielding polynuclear monocharged species. The *cis*-stereoisomer of a mononuclear species can have three conformers[43].

E. Vanadium Diketonates

Vanadium(III) is reported to form neutral, cationic, anionic and oxo-bridged complexes[44]. The vanadium ion is in a distorted octahedral environment with an O–V–O bite angle in the acetylacetonate chelate ring moiety of 88.37(9)°. The hexacoordinated V(III) complexes with *o*-phenantroline and acetylacetonate show intense IR peaks at 1521 and 1526 cm^{-1} that correspond to the $\nu(CO)$ stretching vibration of planar acac ligands. Substitution of the acac ligand with phenantroline or another slim ligand will allow the approach of another atom for coordination with vanadium, which will become

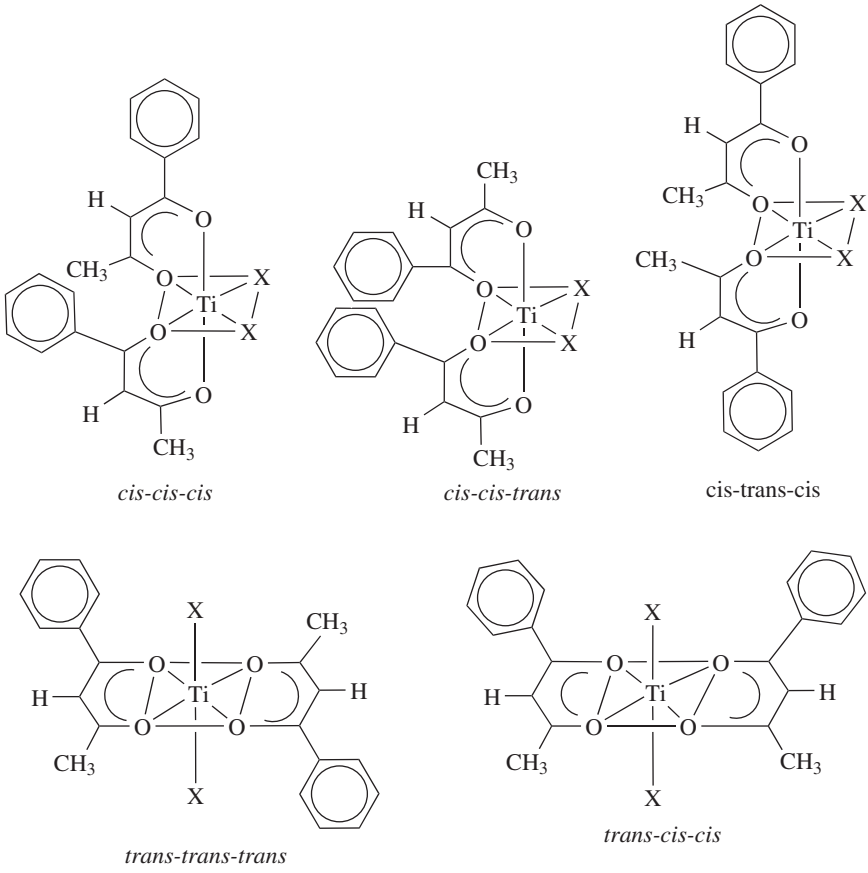

FIGURE 4. Diastereoisomers of octahedrally coordinated $Ti(bazc)_2X_2$ complexes. Reproduced with permission from Reference 37

heptacoordinated. Counterions such as ClO_4^- or BF_4^- may interact with the acac group through hydrogen bonding, which stabilizes solid-state structures.

Vanadyl β-diketonato complexes in a distorted square-pyramidal structure have a strong V=O bond sticking out from the basal plane and four oxygen atoms from β-diketonato anions forming a square plane. Consequently, there is a strong effect on the V=O and V−O bonds by ligand subsituents. Bond lengths of 1.57 Å for V=O and 1.97 Å for V−O in complexes[45,46] point to very strong bonding, which can be probably associated with a partial ionic contribution of the V−O bond[47,48]. The difference is seen by comparing the coordinated acac, tfac and dpm in $[(VO)L_2]$ complexes: ν(V=O) and ν(V−O) are located at 999, 611 and 488 cm^{-1} for L = acac, at 931, 602 and 449 cm^{-1} for L = tfac and 1006, 648 and 490 cm^{-1} for L = dpm. The last two values of every such triplet are ν(V−O) frequencies. In the vanadyl series there is a partial ionic contribution to V−O bonds, and an electron-releasing group will promote polarization of this bond and thereby a ν(V=O) frequency increase. The presence of a trifluoromethyl group shifts the vanadium−oxygen frequencies to lower wave numbers, whereas the electron-releasing *t*-butyl group has the

opposite effect on these frequencies. On the other hand, the opposite effect is observed for these groups on ν(C−O) and ν(C−C) bonds inside the chelate ring.

Complexes (VO)L_2 with L = acac, 3,5-heptanedionate, dpm, bzac, dibzm and acac NMe_2 show a shift to the blue of the absorption band[49] as the axial interaction increases. Also, IR spectroscopy points to changes in strength of the V=O bond. For example, in noncoordinating solvents (e.g. methylene chloride or chloroform) the absorption spectra are the same as for the pentacoordinated VO(acac)$_2$ complex (i.e. $\lambda_{max} = 676$ nm and ν(V=O) = 1003 cm^{-1}), while in strongly or moderately coordinating solvent (e.g. dioxane or thf) the corresponding values are $\lambda_{max} = 731$ nm and ν(V=O) = 991 cm^{-1}. Very strongly coordinating agents will have an even stronger effect on these bands relative to a nonbonded one. Pyridine can be strongly attached to a square-pyramidal VO(acac)$_2$ molecule probably at the sixth coordinating position, which is stable only in the solid state. The *cis-trans* isomerism and solution chemistry of VO(dik)$_2$ complexes is influenced by factors such as the ligand strength, the size of the chelate structure, the type of donor atoms and solvation effects.

M(acac)$_3$ complexes, M = V, Ti, Mn and Co, were studied for ligand coordination, Jahn–Teller distortion and bonding features in organometallic systems[50], as shown in Table 1 for M = V and Ti. The low-spin D_3 structure is indeed a minimum energy for both located high-spin D_3 and C_2 structures. In V(acac)$_3$ the lowest energy corresponds to a C_2 structure that is accordance with the rule that a d-orbital (t_{2g} parentage) shows less Jahn–Teller distortion than an antibonding e_g orbital. In IR spectra it is possible to distinguish the difference between C_2 and D_3 symmetry: a new band around 280 cm^{-1} and a group of three bands instead of two for D_3 symmetry at 400–500 cm^{-1}.

F. Chromium and Molybdenum Diketonates

Two mechanisms have been proposed for the racemization of ΔΔ-binuclear species in a homogeneous solvent[51]: one takes into account inversion of the coordination sphere when a new metal-to-ligand bond is formed and the other includes conversion to its opposite enantiomer by the pseudorotation. The second mechanism seems to be more feasable in homogeneous systems such as hexane solutions or liquid crystals. In hexane, enantiomeric [Cr(acac)$_3$] undergoes recemization by photoisomerization, giving a mixture of the Δ,Δ-, Δ,Λ- and Λ,Λ-isomers. Spectral assignments were followed by changes in CD and UV-Vis spectra.

A new type of catalyst with high conversion, selectivity and reusability was designed by grafting polyamine-functionalized polystyrene (PS) on zirconium oligo(styrenylphosphonate) hydrogen phosphate (ZrP) and subsequently coordinating with MoO_2(acac)$_2$[52], as shown in Scheme 2. Intense symmetric and asymmetric stretching modes of Mo=O double bonds were observed in IR spectra, but also peaks at 1680–1700 cm^{-1} due to carbonyl absorption are an indication that parts of acac had not been replaced by polyamines.

G. Manganese Diketonates

The synergistic interaction between Mn(III) tris(acetylacetonate) with organic acid leads to the ligand exchange and to the formation of mixed-ligand Mn(III) bis(acetylacetonate)–carboxylate chelates[53]. These types of complexes increase catalytic activity due to chelate electronic structure change. The unfilled d-orbitals in the d^4 electron system cause in these complexes a typical Jahn–Teller distortion, dark discoloration and magnetic moments in the range of 4.76–4.9 μ_B.

Mn(CO)$_4$(hfac) represents an interesting example of manganese(I) complex with two equivalent 'hard' oxygen atoms in conjunction with 'soft' carbonyls[54]. IR spectra exhibit

TABLE 1. Scaled quantum mechanical (SQM) force-field-calculated infrared frequencies (cm^{-1}) and intensities ($km\,mol^{-1}$) for $V(acac)_3$ and $Ti(acac)_3$. Reproduced with permission from Reference 50

$V(acac)_3$				$Ti(acac)_3$		
Int	Calc	Exp	TED assignment	Int	Calc	TED assignment
21	235		ν(M−O)	9	242	ν(M−O), δ(CH_3−C=C), δ(M−O=C)
64	304		ν(M−O), δ(O−M−O)	7	322	ν(M−O)
33	335	366	δ(O−M−O)	83	336	δ(O−M−O)
2	341		ν(M−O)			
35	417		δ(CH_3−C=C)	102	409	δ(CH_3−C=C), ν(M−O),
3	418		δ(CH_3−C=C), δ(O=C=C), δ(M−O=C)			δ(O=C=C, δ(M−O=C)
11	421		δ(CH_3−C=C), δ(O=C=C), δ(M−O=C)	16	419	δ(CH_3−C=C)
119	434	426	ν(M−O), δ(O−M−O)	140	430	ν(M−O)
13	446	465	ν(M−O), ν(C=C)			
94	450	484	ν(M−O)			
5	557		δ(CH_3−C=O)	40	554	δ(CH_3−C=O), ν(M−O)
15	562	563	Mixed	35	566	δ(CH_3−C=O)
6	574		Mixed			
25	577		Mixed			
30	591	611	δ(CH_3−C=O), ν(M−O), δ(M−O=C)			
69	647	660	ν(C−CH_3)	70	640	ν(C−CH_3), δ(O=C=C)
40	660		ν(C−CH_3)			
2	665		ν(C−CH_3)			
2	670		π_{ring}	8	661	π_{ring}
4	674		π_{ring}	6	663	π_{ring}
23	676	686	π_{ring}			
23	774	793	π(C−H)	8	778	π(C−H)
11	778	798	π(C−H)	9	778	π(C−H)
3	914	937	ν(C−CH_3)	29	915	ν(C−CH_3)
37	916		ν(C−CH_3)	9	915	ν(C−CH_3)
8	949		ν(C=C), δ(C=C=C)	4	952	ν(C=C), δ(C=C=C)
14	1021	999	ρr(CH_3)	7	1017	ρr(CH_3)
71	1027	1021	ρr(CH_3)	9	1019	ρr(CH_3), ν(C=O)
31	1029		ρr(CH_3), ν(C=O), ν(C−CH_3)	84	1027	ρr(CH_3)
15	1036		ρr(CH_3)	16	1036	ρr(CH_3), π_{ring}
34	1037		ρr(CH_3)	26	1036	ρr(CH_3), π_{ring}
12	1193	1190	δ(C=CH)			
2	1194		δ(C=CH)	6	1191	ν(C=O), δ(C=CH)
24	1196		δ(C−CH), ν(C−O)	25	1192	δ(C=CH)
289	1269	1288	ν(C=C), ν(C=CH_3)	273	1270	ν(C=C), ν(C−CH_3)
60	1365	1363	ν(C=O), δ(CH_3)	23	1367	δ(CH_3)
47	1366		δ(CH_3)	67	1369	δ(CH_3)
45	1367		δ(CH_3)			
5	1369		δ(CH_3)			
9	1370		δ(CH_3)			
181	1406		ν(C=O), ν(C=C)	220	1377	ν(C=O), ν(C=C)
485	1412	1419	ν(C=O)	475	1406	ν(C=O)
11	1441		δ(CH_3)			
19	1442		δ(CH_3)	21	1442	δ(CH_3)
12	1443		δ(CH_3)	11	1443	δ(CH_3)
210	1448		δ(CH_3)	185	1446	δ(CH_3)
4	1449		δ(CH_3)			
4	1458		δ(CH_3), ρr(CH_3)	40	1464	δ(CH_3), ν(C=O)
22	1466		δ(CH_3)			
69	1466		Mixed			
662	1522	1535	ν(C=C), δ(C=CH)	319	1523	ν(C=C), δ(C=CH)
390	1524		ν(C=C), δ(C=CH)	718	1525	ν(C=C), δ(C=CH)

(*continued overleaf*)

TABLE 1. (*continued*)

$V(acac)_3$				$Ti(acac)_3$		
Int	Calc	Exp	TED assignment	Int	Calc	TED assignment
628	1575	1568	ν(C=O)			
840	1583		ν(C=O), nu(C=C)	875	1561	ν(C=O), ν(C=C)
23	1605		ν(C=O)			
20	2927		ν(C−H)	21	2931	ν(C−H)
34	2928		ν(C−H)	36	2931	ν(C−H)
16	2984		ν(C−H)	5	2983	ν(C−H)
16	2985		ν(C−H)	17	2983	ν(C−H)
16	2986		ν(C−H)	26	2983	ν(C−H)
115	3016	3003	ν(C−H)	109	3015	ν(C−H)
14	3085		ν(C−H)			
25	3086		ν(C−H)	44	3086	ν(C−H)
	17.06		rms deviation			
	14.14		avg deviation			

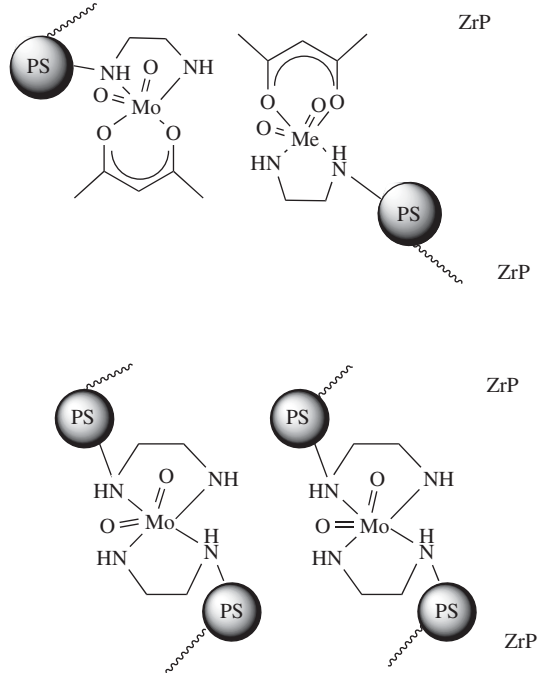

SCHEME 2. Possible structure of a catalyst derived from $MoO_2(acac)_2$ supported on zirconium oligo(styrenylphosphonate) hydrogen phosphate (ZrP) grafted with polyamine-functionalized polystyrene (PS). Reproduced with permission from Reference 52

typical bands determined as hfac carbonyl stretch bands, different from metal carbonyl stretches. In complexes of this type they are assigned to the 1616–1635 cm^{-1} region, while others were present as two to three intense bands at higher wave numbers.

Manganese(I) carbonyl complexes[55] with a tfac ligand show three strong and one weak bands in the ν(C=O) region, similar to the spectrum in the presence of *cis*-tetracarbonyl moiety. The IR bands at 1615 cm^{-1} and 1201 cm^{-1} correspond to the trifluoroacetylacetonate carbonyl stretching and C−H in-plane bending absorptions that support a bidentate, oxygen-bonded structure. In ^{1}H NMR spectra, resonances at 7.77 and 4.12 ppm assigned to CH_3 and ring CH protons are proposed as well as an *O*-bonded chelate structure.

In a substitution reaction the $Mn(CO)_4$(tfac) complex in the presence of one monodentate ligand, such as py, $AsPh_3$ or PPh_3, undergoes CO replacement and with two similar ligands, e.g. P(*n*-Bu)$_3$ or PPh_3, gives *trans*-ligand octahedral complexes, while tfac in both cases remains as *cis*-bonded bidentate ligand[55]. In the case when another bidentate ligand, such as bipy, phen or two molecules of py, are bonded to a Mn−carbonyl complex, the substitution reaction with hfac proceeds to monodentate replacement and Mn−C coordination or *cis*-Mn−*O*,*O*′-tfac bidentate coordination, leaving only one molecule of pyridine when this ligand was present. In all substituted tfac manganese complexes, carbonyl stretching frequencies of β-diketonato ligand are found to be in the range of 1620–1610 cm^{-1}. The observed differences between tfac and hfac complexes may be ascribed to their different degrees of fluoronation, in which more fluorinated ligand hfac is a poorer electron donor to manganese. Also, the relative stability of carbonyl as a function of the bidentate ligand is larger for hfac, due to its stronger electron-withdrawing ability and steric effects. It appears that the above trend is directed by electronic factors. The solid-state structure of [Mn(acac)$_2$(bipy)][56] presents a trigonal-prismatic geometry (Figure 5) and bands in the IR spectrum at ν(C−O) 1604, 1578 cm^{-1}, ν(C−C) 1516 cm^{-1}, ν(M−O) 647, 536, 415 cm^{-1} and ν(Mn−O) 403, 228 cm^{-1}.

A manganese bis(acetylacetonato)−ethylenediamine complex[57] was employed in the preparation of supramolecular assemblies with an octahedral niobium cyanochloride cluster, $[Nb_6Cl_{12}(CN)_6]^{4-}$. These assemblies range in size from 1.5 to 2.4 nm and their charge varies between −3 and +2, depending on the number of Mn units per cluster.

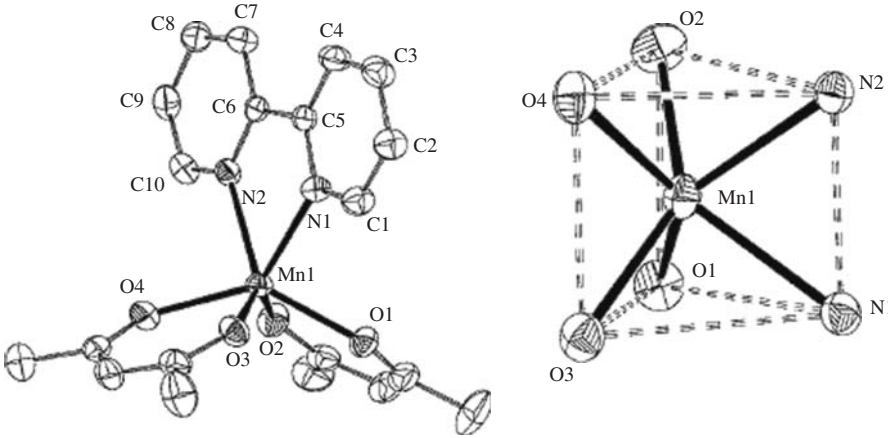

FIGURE 5. ORTEP plot of [Mn(acac)$_2$(bpy)] (left) and its trigonal-prismatic geometry in detail (right). Ellipsoids are shown at 50% probability. Hydrogen atoms are omitted for clarity. Reproduced with permission from Reference 56

Reaction of the alkoxo-containing niobium complexes $[NbCl_3(OR)_2]_2$ (R = Me, Et, *i*-Pr) with β-diketonates such as acac, dpm and dibzm, in a 1:2 molar ratio, afforded the corresponding alkoxo–β-diketonato complexes[58] $[NbCl_2(OR)_2(O,O'\text{-R}'\text{COCHCOR}')]$ (R = R′ = Me; R = Et, R′ = Me; R = *i*-Pr, R′ = Me; R = Me, R′ = *t*-Bu; R = Et, R′ = *t*-Bu; R = *i*-Pr, R′ = *t*-Bu; R = Me, R′ = Ph; R = Et, R′ = Ph; R = *i*-Pr, R′ = Ph). The complexes are described as a pseudooctahedral Nb(V) containing two *trans*-chloride ligands in the axial positions; two *cis*-ethoxide ligands and a β-diketonate ligand are placed in the equatorial plane. The β-diketonate group is coordinated to the Nb center through both oxygen atoms, forming a six-membered ring. The metallacycle ring is reasonably planar and the parameters within this ring suggest significant delocalization. As a result, both C–O distances are intermediate between the single- and double-bond extremes. Similarly, the C–C distances are intermediate between single- and double-bond distances involving sp^2 carbons. Chelate rings are displaced slightly on opposite sides of the metallacycle plane, thereby minimizing contacts between each other. Their IR spectra exhibit characteristic bands that correspond to the ν(C–C) and ν(C–O) of a β-diketonate unit coordinated in a bidentate fashion. ^{1}H- and ^{13}C{^{1}H}-NMR spectra show only one set of highly resolved resonances for the alkoxide groups, indicating that the units are equivalent. In addition, one set of resonances is also present for the alkyl or aryl groups of the β-diketonate ligand.

H. Ruthenium Diketonates

The chemistry of transition-metal allenylidene complexes has been the subject of special attention in recent years due to their applications in stoichiometric[59] and catalytic reactions[60]. The diphenylallenylidene complex $[Ru(=C=C=CPh_2)(PPh_3)_2][PF_6]$ (C_9H_7 = indenyl anion) reacts regioselectively at the C_γ atom with the lithium enolate derived from (1*R*)-(+)-camphor ($C_{10}H_{16}O$) to yield the σ-alkynyl derivative $[Ru\{C{\equiv}CCPh_2(C_{10}H_{15}O)\}(PPh_3)_2]$. Indeed, the unsaturated character of the M=C=C=C chain as well as its alternating array of electrophilic/nucleophilic carbon sites[61] makes allenylidene complexes unique organometallic reagents for use in C–C and C-heteroatom coupling processes.

The dicyanamidobenzene-bridged diruthenium complex $[\{Ru(tpy)(dpm)\}_2(\mu\text{-dicyd})][PF_6]$ (tpy = 2,2′:6′,2″-terpyridine, dicyd = 1,4-dicyanamidobenzene) and its mononuclear counterpart were synthesized and characterized[62]. The average *g* value of 2.16 for a low-spin d^5-Ru(III) ion is a bit smaller than that obtained for a $[Ru(tpy)(acac)(ipcyd)]^+$ complex (ipcd = 4-iodophenylcyanamide anion), which can be attributed to the stronger donor character of dpm compared to the acac ligand.

I. Cobalt Diketonates

IR spectra of Co(III) β-diketonates with the Co(cyclam)Racac chromophore[63] (cyclam = 1,4,8,11-tetraazacyclotetradecane) are characteristic in view of the Racac anion being bonded to the metal through both oxygens[64]. The ν(CC) and ν(CO) bands of the chelate β-diketonates are in the 1507–1627 cm^{-1} range and indicate charge delocalization with resultant coordination via both oxygen atoms[65]. In the $[Co(cyclam)dibzm]^{+2}$ complex, apparently a combination of negative inductive and positive resonance effects of the phenyl group is present. The CF_3 group of hfac much more affects the electronic density decreasing due to its electron-withdrawing effect[66], and consequently results in a shift of ν(CC) and ν(CO) bands toward higher frequencies. On the other hand, because of the positive inductive effect of the methyl group which increases the electronic density, the complex with dpm causes a large displacement of these bands to lower wave numbers. These frequencies of the coordinated β-diketonate are in the order hfac > dibzm > dpm.

There are several regions in the IR spectra of considerable interest for Racac coordination. The 1556–1500 cm^{-1} region is associated primarily with vibrations attributed to ν(CO) and ν(CC). Due to the keto–enolate ring, high electron density via the π-system produces a greater double-bond character in complexes with bridged β-diketonate in binuclear Co(II)[67]. This results in higher frequencies in comparison with free β-diketonate ligands, but the electron-releasing ability of the β-diketonate R-group could produce an additional effect. All these complexes exhibit ν(CO) bands in the 1529–1500 cm^{-1} range, which lie between ν(C=O) and ν(C–O), and this confirms *O*,*O*′-bridge coordination to both Co(II) ions. Further evidence of such behavior in the 1556–1540 cm^{-1} range gives the position of the C–C bond vibrations from the enolate ring, which have the same bond character. The absorption frequencies of R groups, i.e. $\nu_{asym}(CH_3)$, $\nu_{sym}(CH_3)$, $\gamma(CH_3)$, $\nu(CF_3)$ and $\gamma(CF_3)$, are unchanged compared to the free ligands.

J. Iridium Diketonates

A group of iridium β-diketonate complexes with 1,3,4-oxadiazole and acetylacetonate as ancillary ligands conforms to a ^{1}H NMR signal at 5.27 ppm for CH and 2.47 ppm for CH_3. The complexes have a distorted octahedral coordination geometry at the iridium center by three chelating ligands with *cis*-C–C and *trans*-N–N dispositions[68]. The similarity of bond lengths indicates that the negative charge of the acac ligand is delocalized over both oxygen atoms. This complex undergoes two reversible reduction processes at potentials that correspond to the reduction of two oxadiazole ligands. The LUMO energy of these complexes is little affected by the nature of the ancillary acac ligand. For example, the dithiolate ligands with stronger ligand field strength than the ligand acac result in higher oxidation potentials and lower HOMO energy levels of complexes than acac itself.

K. Nickel and Palladium Diketonates

The structure of some cobalt and nickel complexes clearly indicates the formation of enolato complexes, where negative charge is delocalized over the chelate ring structure[69]. Electron density is located mainly on electronegative oxygen atoms, causing an increase of single-bond character of C–O moiety. Also, the C–O and C–C lengths in chelate rings are between single-bond and double-bond lengths that are typical for an acetylacetonato type of complex. This flexible structure of the six-membered ring should be favorable in terms of energetic as well as entropic parameters.

Cyclic Pd-enolates stabilized by either PMe_3 or *i*-$Pr_2PCH_2CH_2PPr$-*i*$_2$ (dippe) auxiliary ligands can be arranged only as *C*-enolate tautomers[16]. Isolation of analogous Ni-enolates has only been possible when the chelating diphosphine dippe is employed. The failure to obtain Ni-enolates containing monodentate phosphine ligands could be due to the formation of binuclear *O*-bridged species with phosphine dissociation. While *C*-coordination is favored for the Pd-enolate complex, the Ni complexes prefer *O*-coordination[13]. Nonetheless, for a compound which features primary alkyl coordination in the *C*-bonded form, equilibrium mixtures of the two tautomers may be generated. Still, the *O*-enolate predominates. DFT calculations suggest that the tautomeric exchange is hindered by the incorporation of the enolate functionality into a rigid metallacyclic fragment. The parent *O*-enolate complex reacts with enolizable and nonenolizable aldehydes, giving products that retain the enolate functionality. Interestingly, the *C*-enolate tautomer does not react with aldehydes, illustrating the relationship between coordination mode and reactivity in this class of compounds.

Adducts of Ni(II) square-planar complexes of general formula $[Ni(dik)(tmeda)]^+$ (dik = acac, bzac) with a series of bidentate ligands (tmeda, bipy, en, $C_2O_4^{2-}$) have been synthesized and characterized by spectral, thermal and magnetic measurements[70]. In the

IR spectra of the isolated adducts, the frequencies of the asymmetric stretching vibration combination $\nu_{asym}(CO) + \nu_{asym}(CC)$[71,72] have been shifted to higher frequencies than those of their mother chelates. The enhanced π-interactions appeared within the adduct complexes because of hyperconjugation, which result in an increased C−O bond strength. The same reasons can be applied to the shift in lowering the stretching frequencies, ν(Ni−O), compared to those assigned to the mother chelates.

Isolation and identification of surface-bonded acetone enolate on Ni(111) surfaces show that metal enolate complexes are key intermediates in carbon–carbon bond-forming reactions in both organometallic chemistry and heterogeneous catalysis[73]. Based on studies on powdered samples of defined surface structure and composition, most of the results were reported for acetone condensation over transition-metal oxide catalysts, as surface intermediate in industrially important processes. With the exception of a preoxidized silver surface, all other metal single-crystal surfaces have suggested that the main adsorption occurs via oxygen lone-pair electrons or di-σ bonding of both the carbonyl C and O atoms.

Exposing acetone to a Ni(111) surface[73] yields three absorption bands at 1260, 1353 and 1545 cm^{-1} that are assigned to ν(CC) stretching vibration, symmetric deformation $\delta(CH_3)$ and stretching vibration ν(CO), respectively. Acetone enolate can be synthesized using the acetylacetonate as precursor molecule. Based on DFT frequency calculations the other surface complexes can be effectively ruled out, i.e. a vibrational mode of ν(CO) can be detected at 1638, 1670, 1665 and 1690 cm^{-1} on Pt(111), Pd(111), Rh(111) and Ru(001) surfaces, respectively. In addition, this vibration mode was found to be in the 1680–1694 cm^{-1} range for Mn, Fe, Co, Ni, Zn and Cu surfaces. These are all η^1(O) assignments, while η^2(CO)-acetone was shifted to around 1200–1435 cm^{-1}. In the case of η^1C-acetyl the calculated ν(CO) frequency is 1634 cm^{-1}, and it is a very small range for most of the metal single-crystal surfaces. The mechanism of adsorption is based on the hydroxyl proton of the enol tautomer by Ni or basic oxygen atoms from a preoxidized crystal surface which yield the enolate and H or OH, respectively. In the case of acetylacetonate, C−C bond cleavage occurs to give acetone enolate and acetyl.

The reaction between $Pd(acac)_2$ and lithium β-diketiminate, a nitrogen derivative of acac, gives a mixed-ligand and homoleptic complex[74]. Interestingly, these complexes are stable at ambient temperature, but in acetonitrile solution they decompose to elemental Pd presumably due to reaction of Pd(II) and the acac ligand. Furthermore, in pentane or ether solution the complex can isomerize into the thermodynamically stable form. Both isomers are similar, but their NMR spectra are inequivalent due to an asymmetric structure with nonrotating substituents. Since one of the imine groups is coordinated to the Pd ion, this isomerization results in the formation of a chiral center at the coordinated C atom.

L. Copper Diketonates

$Cu(acac)_2$ is unique among the metal complexes of acetylacetonate so far investigated[75]. The bivalent metal complexes of M = Ca, Mn, Fe, Co, Ni and Zn are polymeric with general formula $[M(dik)_2]_n$ except for the square-planar monomeric copper(II) complex[76].

In the case of complex $[\{Cu(acac)(phen)(ClO_4)\}\{Cu(phen)(\mu_{1,3}\text{-}N_3)_2]_2$, the Cu(II) ions are ferromagnetically coupled, as expected for the bridging mode of azido ligands. The Cu(II) ion is in square-pyramidal coordination, achieved with chelating ligands and the azido bridge to the other part of the molecule[77]. Significant $\pi-\pi$ stacking interaction occurs between these two units and the presence of extended π-systems like acac, phen or bipy favors this interaction. The strongest interaction takes place between acac ligands. The crystal structure of $[\{Cu(acac)(bipy)\}_2(\mu_{1,3}\text{-}N_3)]_3(ClO_4)_3 \bullet 3.75H_2O$ can be described as a 3D supramolecular structure consisting of parallel layers, which are formed by a $\pi-\pi$ stacking interaction between [Cu(acac)(bipy)] fragments of the *trans*-isomers and

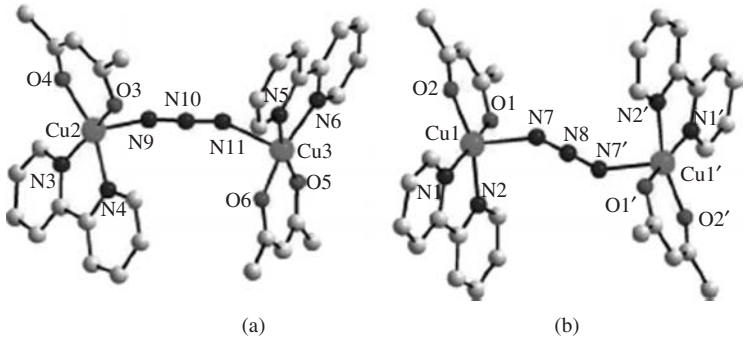

FIGURE 6. View of the *cis* (a) and *trans* (b) isomers of the binuclear complex $[\{Cu(acac)(bipy)\}_2(\mu_{1,3}\text{-}N_3)]^+$. Reproduced with permission from Reference 77

the [Cu(acac)(bipy)] fragments from one head of the *cis*-isomers (Figure 6). Basically, each *trans*-isomer interacts with two *cis*-isomers through an acac ligand and each *cis*-isomer interacts with another *cis*-isomer through the bipy ligand and one *trans*-isomer. The magnetic properties of this type of complexes are devoid of any magnetic interaction between copper ions. This behavior can be attributed to the $d_{x^2-y^2}$ orbital that prevents intramolecular exchange interactions realized by the bridging ligands. The linear decrease in magnetic moment with temperature can be ascribed to temperature-independent paramagnetism.

Two other copper complexes[78], mononuclear $[Cu(acac)(phen)(H_2O)]ClO_4$ and one-dimensional polynuclear $[Cu(acac)(bipy)(ClO_4)]_n$, have square-pyramidal structure. The latter complex has fragments bridged by perchlorate anions resulting in neutral polynuclear chains. The solid-state spectra exhibit a broad d–d band and intraligand $\pi-\pi^*$ transitions. IR data show that C−O vibrations correspond to a very strong intensity band at 1585 cm^{-1}, as well as 1578 and 1525 cm^{-1}.

For some planar Cu(II) β-diketonates, the HOMO energy is determined mainly by the interaction of the metal atom with the oxygen atoms of the chelating ligands[79]. For example, for $Cu(hfac)_2$ it is 3.2 eV while for the other complexes with an additional chelating ligand beside hfac, of structure similar to $Cu(hfac)_2L$ (L = imidazoline), it can be as high as 5.4–5.7 eV. Structural changes should result in broadening of the X-ray emission spectrum, involving the valence electrons and shorter wavelengths of the spectrum from the HOMO of these complexes. In case of the presence of a nitroxyl group the multiple splitting (ΔE) obtained from experimental Cu_{3s} X-ray photoelectron spectra shows an increase, which indicates delocalization of odd electron density toward the central metal ion.

$Cu(hfac)_2$ chain polymer heterospin complexes with pyrazole-substituted nitronyl nitroxides exhibit structural rearrangements with magnetic effects in the solid state at reduced temperature[80]. The most important structural features of this type of complexes are short Cu−O and Cu−N axial distances. As the temperature decreases, the $Cu-O_{hfac}$ distances along the $O_{hfac}-Cu-O_{hfac}$ directions decrease and all $Cu-O_{hfac}$ bond lengths in the CuO_6 core become equal at low temperatures. In case of an additional pyrazole ligand, these distances are equal in the equatorial plane and donor atoms from other ligands are in the axial plane. The 'head-to-tail' motif of the structure $Cu(hfac)_2L$ allows this molecule to be an exchange-coupled cluster $Cu(II)-{}^{-\bullet}ON<$ with net spin $S_\Sigma = 1$. In this case the cluster will have $S = 0$ (antiferromagnetic exchange) or $S = 1$ (ferromagnetic exchange), depending on the sign of the exchange interaction in the ground state. Thus

magnetic resonance spectra indicate two types of structurally nonequivalent CuO_5N-type coordination units coexisting in $Cu(hfac)_2L$ over a range of temperature.

Monocondensation products of various diamines and benzoylacetonate are readily involved in the basal–apical type of oxo-bridging complexes resulting in the formation of trinuclear complexes with partial cubane structure[81]. However, replacing the acac by bzac makes the ligand sterically more demanding, and as a result Cu–O–Cu angles become significantly greater and axial Cu–O bonds weaker. Such complexes show antiferromagnetic coupling, which corresponds to the assumption that the greatest coplanarity of the three principal ligand planes and the lowest distance with a bridging ligand provides stronger antiferromagnetic coupling.

The influence of fluorine substitution effects on the properties of $Cu(dik)_2$ was seen in the spectra[82] when dik = acac, tfac and hfac. The presence of an OH stretching vibration in IR spectra of the free ligands is an indication of strong enolization. It is interesting that the presence of a CF_3 group causes the shift of the OH band from 3550 cm^{-1} in acac to 3360 cm^{-1} in tfac. This correlates with the fact that the enol of tfac is more acidic than that of acac. In the case of their complexes, absence of the OH band indicates coordination of enolate. In the case of a carbonyl group, free ligands show normal carbonyl frequencies of 1708 and 1725 cm^{-1} for acac, and shifted to 1775 and 1745 cm^{-1} for tfac or 1790 and 1765 cm^{-1} for hfac. For all three ligands there is a strong, broad band, approximately 70–90 cm^{-1} below the free carbonyl band, which is assigned to a conjugated hydrogen-bonded carbonyl group characteristic for the enolic form of the β-diketone. Another band at 1633 cm^{-1} for acac is assigned to C=C stretching frequencies. The lower wave number bands at 1300–1500 cm^{-1} are due to CH_3 deformation vibrations.

Cu-chelate spectra[82] show the absorption bands of $Cu(acac)_2$ at 1582 and 1530 cm^{-1} assigned to chelated carbonyl and C=C stretching, respectively. The first band is shifted from 1582 cm^{-1} for acac to 1615 and 1643 cm^{-1} in case of coordinated tfac and hfac, respectively. Increase in frequency means decrease in stability of the metal chelate with fluorinated substituents. The effect on C=C stretching vibrations is lower, the frequency increasing very slightly when a methyl group is replaced with trifluoromethyl.

The structure of $Cu(acac)_2$ was determined by XRD[83]. The metal–oxygen distance of about 1.93 Å is considerably shorter than 2.01 Å for $[Ni(acac)_2]_3$[84], 2.02 Å for $Ni(acac)_2 \cdot 2H_2O$[85], 2.03 Å for $Zn(acac)_2 \cdot H_2O$[86] and 2.05 Å for $Co(acac)_2 \cdot 2H_2O$[87,88]. This contraction is attributed to the smaller repulsion between the copper and oxygen atoms in the tetracoordinate square-planar structure than in the hexacoordinate octahedron.

The calculated frequencies and isotopic shifts are slightly higher than the observed values for the majority of the normal modes[75]. Two factors may be responsible for such discrepancy in the case of $Cu(acac)_2$. The first is caused by the environment, and the second by the fact that the experimental value relates to an anharmonic frequency while the calculated value relates to a harmonic frequency. For $Cu(acac)_2$ only three bands were observed. According to theoretical calculations, the weak IR and Raman bands at about 3000 and 2970 cm^{-1} are assigned to asymmetric CH_3 stretching modes. The Raman spectrum of $Cu(acac)_2$ shows a strong band at about 2910 cm^{-1}, which is assigned to symmetric CH_3 stretching modes[89–92]. It is expected that the stretching vibrational wave numbers of the methine groups occur at higher frequency than those of the methyl groups. Theoretical calculations suggest that the observed bands can be assigned to ν(CH) of the methine group. In the 1700–1000 cm^{-1} region, in addition to the CH_3 deformation, rocking and –CH in-plane bending modes, one can expect to observe four bands due to the C–O and C–C stretching. In the IR spectrum, three bands at 1578, 1554 and 1534 cm^{-1} appear and the Raman spectrum shows two bands at 1586 and 1566 cm^{-1}, which are inactive in the IR spectrum. The IR band at 1554 cm^{-1} and the Raman band at 1566 cm^{-1} are mainly due to asymmetric (C2–C3, C3–C4) stretching (49%), which are

coupled to the $-CH_\alpha$ in-plane bending mode (27%). The weakness of the Raman band at 1566 cm^{-1} has been considered[93,94] as a measure of delocalization of the π-system of the chelate ring. The IR of $Cu(acac)_2$ shows a medium band at 1415 cm^{-1} of asymmetric C−O stretching (57%), which is coupled to the asymmetric CH_3 deformation mode (21%). The Raman spectrum shows a strong band at 1270 cm^{-1} due to the symmetric (C2−C3, C3−C4) stretching (56%), which is slightly coupled to the symmetric CH_3 deformation mode (9%). This band is absent in the IR, but theoretical calculations predict a strong IR band at 1275 cm^{-1}. The IR and Raman spectra show two relatively strong bands at about 1190 and 1180 cm^{-1} of the CH_α in-plane bending modes. In the IR of $Cu(acac)_2$ only two $\delta(CH_3)$ vibrational modes could be identified at 1534 and 1356 cm^{-1}. Theoretical calculation predicts $\delta_a(CH_3)$ (53%), which is coupled to $\delta(CH_\alpha)$ (17%). Two other bands at 1503 and 1497 cm^{-1} are assigned to $\delta(CH_3)$ and the last band at 1356 cm^{-1} to $\delta_{sym}(CH_3)$. Below 1000 cm^{-1} one expects to observe $C-CH_3$ and Cu−O stretching, −CH out-of-plane bending and in-plane and out-of-plane ring deformation modes. For the $Cu(acac)_2$ complex, two Raman bands at 942 and 928 cm^{-1} are observed; in the IR spectrum a band at 937 cm^{-1} is assigned to $C-CH_3$ stretching. The band at 782 cm^{-1} and the Raman band at 769 cm^{-1} are assigned to $\gamma(CH_\alpha)$. According to theoretical calculation, the infrared band at 651 cm^{-1} is mainly due to in-plane ring deformation (51%), which is coupled to $\delta(C-CH_3)$ (25%).

The Raman spectrum of $Cu(acac)_2$ shows two bands at 437 and 396 cm^{-1}; the IR spectrum shows two bands at 455 and 429 cm^{-1}. The IR and Raman bands at 429 and 396 cm^{-1} are assigned to ν(Cu−O) coupled with $\nu(C-CH_3)$. Pinchas and coworkers[95,96] believed that the M−O stretching of metal acetylacetonate complexes appears in the 500–600 cm^{-1} region. A consideration of M−O in metal acetylacetonate complexes could be used as a measure of complex stability, since in this vibrational mode the metal is not moving, therefore its frequency depends on the M−O bond strength and not on the metal ion.

The structural parameters, vibrational frequencies, IR and Raman intensities of the vibrational bands were calculated by DFT. The predicted frequencies were compared with experimental data in the solid state. The short M−O distance in $Cu(acac)_2$ suggests a strong metal–ligand bond.

M. Zinc, Cadmium and Mercury Diketonates

Interest in zinc enolates[97], compared to alkaline or alkaline earth enolates, is growing due to their ideal combination of reactivity and tolerance of many functional groups. The form and structural motifs of complexes depend on the type of metal, solvents and bulkiness of the ligands. Generally, enolates of electropositive metals prefer *O*-coordination; however, even *C*-coordinated metal enolates usually rearrange to *O*-bonded ones.

The main Zn_2O_2 core is symmetrical with respect to the four Zn−O bonds[97], the lengths of which vary slightly in a geometry that appears to minimize the steric repulsion between the enolates and other parts of the molecule.

β-Diketonates and O_2N_2-type Schiff bases incorporated in bond formation with a Zn ion are interesting for the study of enantiomerization processes. Intramolecular enantiomerization of Zn(II) complexes occurs via a diagonal twist pathway in the gas phase[98]. On going toward cadmium and mercury, the energy barrier decreases due to smaller overlap populations of M−O and M−N bonds, which indicates weaker interactions between the metal ions and the ligands, making the diagonal twist more easy. Similar trends were observed in solution even though the energy barriers were significantly reduced.

Structurally, complexes of malonaldehyde and acetylacetonate with Zn(II) ion show very similar Zn−O bond lengths[99]. The cadmium complexes have similar structures but

they have longer Cd−O bonds. This structural change is due to the bigger size of the Cd(II) ion in which the more diffuse electron cloud pushes away the ligands to alleviate the large ring strain. The Hg(II) complexes, however, are very different. With malonaldehyde, the molecular structure and symmetry are similar to those of the Cd(II) analog because of the similar covalent radii. Besides, in HgL_2 analogous linear arrangements of ligands are a consequence of mixing the $5d_{z^2}$ and 6*s* orbitals, resulting in the hybrid orbital oriented along the *z*-axis and in the $x - y$ plane. In order to minimize negative charge on oxygen, the ligand adopts the planar geometry wherein two oxygen atoms are farthest apart. Thus the metal–ligand (M−O) bond strength stands in the order Zn ≫ Cd ≈ Hg.

N. Lanthanide Diketonates

Lanthanide(III) complexes demand special attention in view of the specific spectra–structure relationship for biological applications, chiral catalysis, molecular magnetism and luminescence. One unique chiral stereochemistry is realized by the combination of labile Ln complexes and weak Na^+-fluorocarbon interaction[100], which show intense CD (circular dichroism) with variation of Ln(III) and/or M(I) ions to chiroptical spectra–structure relations and an important role in configurational chirality for chemical sensors, NMR shift reagents or chiral catalysis. Trivalent lanthanides are also found to be incorporated into heterobimetallic complexes[101] showing intramolecular energy transfer processes.

Newly prepared Ln(III) complexes with β-diketonate, such as 3-heptafluorobutyryl-(+)-camphorate or tfac, give labile lanthanide complexes[100]. The proposed structure in a solution of Δ-[Ln((+)-hfbc)$_4$]Na shows a configuration of four bidentate chelates with a trapped sodium ion as well as Na^+-fluorocarbon interactions realized by three n-C_3F_7 groups of hfbc. By analyzing the bond lengths and angles, a decrease was found from La to Er due to the lanthanide contraction. The data on the molecular structure show that these types of complexes can be divided in two groups with respect to the metal ion present in their Ln(dik)$_3$ complexes. The first group demonstrates the La(dpm)$_3$ type of complexes with structurally triangular prismatic polyhedrons and chelate rings folded around the O···O axes. The other group includes La(dmp)$_3$ and the M(hfac)$_3$ (M = Al, Ga, In, Cr) complexes. These molecules have the structure of triangular anti-prismatic polyhedrons and planar chelate rings. The heaviest ion in the mass spectrum is $[La(dmp)_3]^+$ but the ion of highest abundance is $[La(dmp)_2]^+$.

Most of the lanthanides form stable and volatile complexes with dipivaloymethane; most of them were found to have C_3 symmetry[102]. The special feature of their molecular structure is a folding of the chelate rings around the O···O axes. Kepert's model[103] assumes a simple pairwise metal–bidentate interaction while ligand and the total interaction energy between the ligands is minimal.

Acetylacetonate and substituted acac derivatives are attractive because of their versatility and stability under normal conditions, as well as their ability to deposit metals cleanly under relatively mild conditions[104]. The dipivaloylmethanato (dpm) derivative from stable and volatile lanthanide compounds, e.g. Lu(dpm)$_3$, have in the gas phase D_3 symmetry of the coordination polyhedron. According to Kepert's model, bidentate ligands can be approximated by diatomic molecules and it is completely predictable for the structures of these complexes in the gas phase, but the solid-state structures might be different.

Lanthanide *tris*-β-diketonates[105] form stable 1:1 highly coordinated complexes with amino alcohols with specific, largely enhanced fluorescence and intense induced circular dichroism signals. Since these types of complexes exhibit versatile coordination modes, which involve reorganization of β-diketonate chelate rings, often leading to fluorescence and CD spectral changes and concentration-dependent behavior, they are not applicable in practical sensing and probing systems.

Volatile complexes $M(dpm)_n$ (M = Ce, Gd, Y, Zr; $n = 3, 4$) were synthesized[106]. These chelates exhibit high volatility and air stability, so they can be used as precursors in metallorganic chemical vapor deposition (MOCVD) of thin oxide films in electrochemical devices. The highest volatility is attained with fluorinated β-diketonato ligands, but their use is limited because of contamination of the deposited films and the production of toxic gases. The volatility and thermal stability of this group of the dpm complexes are affected by the radius of the metal ion, the number of ligands attached to it (3 or 4) and other properties. The IR spectra of complexes $M(dpm)_n$ (M = Ce, Gd, Y, Zr; $n = 3, 4$) are presented in Figure 7.

Zr and Ce complexes with four coordinated dpm molecules exhibit abnormal volatilities. Their thermal stability is found to be in the order Zr > Ce coordinated with four dpm and Gd > $Y(dpm)_3$ for three. In these spectra, the three bands in the 1500–1600 cm^{-1} range belong to the stretching vibrational mode of C−O, C−C and the bending vibration of C−H in the ring structure, which contribute to the tautomeric keto–enol form of β-diketonate. At 500–600 cm^{-1} two well-resolved bands are due to the stretching mode of the M−O bond. The metal–oxygen distance in β-diketonate molecules passing from the crystal to the gas phase is expected to be much shorter if the coordination number of the central atom changes[29]. For example, the $Pr(dpm)_3$ complex in the crystal is dimerized and $r(Pr{-}O) = 2.41(2)$ Å[107]. For the monomeric molecule in the gas phase, $r(Pr{-}O)$ decreases to 2.331(7) Å[108]. For $Er(dpm)_3$, which is monomeric in both phases, this transition is not accompanied by any substantial change in the Er−O bond, namely $r(Er{-}O) = 2.212(45)$ Å in the crystal[109] and $r(Er{-}O) = 2.218(5)$ Å in the gas phase. The $Sc(acac)_3$ crystal is composed of monomeric molecules[110] and transition into the gas phase is not accompanied by changes of the coordination number of the central atom; there are no substantial changes in the internuclear Sc−O distance. The γ angle of ligand

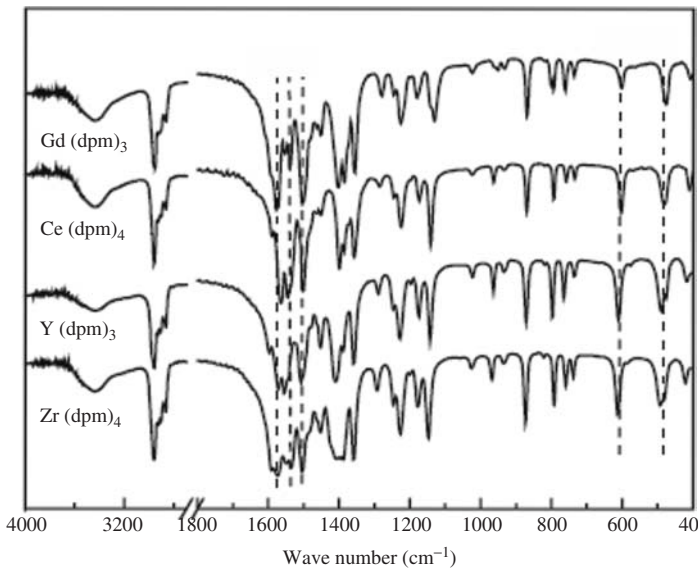

FIGURE 7. IR spectra of freshly prepared $M(dpm)_n$ complexes. Reproduced with permission from Reference 106

rotation in the crystal may differ from that in free molecules because of internuclear interaction forces. However, the unit cell dimensions of $Sc(acac)_3$[27,111] are rather large (compared to $Er(dpm)_3$)[109], meaning that the molecules are far from each other. Since the coordination polyhedron in *tris*-complexes is strongly screened, one can expect that the structure of the ScO_6 fragment will not differ strongly between the crystal and the gas phase.

Simultaneous electron diffraction and mass spectrometric studies of saturated vapor of $Er(dpm)_3$ showed that vapor consists solely of such molecules[112]. Two alternative models (of C_3 and D_3 symmetry) may describe the electron diffraction data. Structural analysis has established that a strong correlation between the dihedral and torsion angles, determining the structure of the coordination polyhedron and ligands, leads to the different molecular models. The C_3 model is characterized by a nearly prismatic structure of the MO_6 fragment. The D_3 model has a planar structure of ligands and the coordination polyhedron is shaped as an antiprism. Testing the D_3 model with planar ligands led to slightly better agreement between the experimental and theoretical functions. The structural parameters of the molecule in this model are comparable to the parameters of free Sc[113] and La[102,114] dipivaloylmethanate molecules, as well as to Al[115], Ga and In[116] hfac complex molecules. The unit cell of $Sc(acac)_3$ is significantly larger than that of $Er(dpm)_3$, although the volume of the individual $Sc(acac)_3$ molecule is much smaller than that of the $Er(dpm)_3$ molecule, the latter having bulkier ligands and larger r(M−O).

O. Uranyl Diketonates

$UO_2(acac)_2$ is known as an ahydrous or monohydrate molecule. In the IR spectra the main sharp intense band near 900 cm^{-1} corresponds to the asymmetric uranyl stretching frequency, ν_{asym}(U=O). The other assignment of ν(U−O) from acetylacetonate is hardly determined, but it is expected to be at lower frequencies than for other metal ions because of the greater mass and higher coordination number of the uranium atom[117]. These frequencies are usually around 528, 555 and 606 cm^{-1}, and the other region is 403, 413 and 430 cm^{-1} for coordinated acetylacetone, benzoylacetonate and dibenzoylmethanoate, respectively. In case of uranium complexes there is repulsion between the U atom and two oxygens in the O=U=O bonds, leading to a decrease in ν(U=O) in the presence of electron-releasing substituents. Electron-withdrawing substituents will decrease the donor ability of the carbonyl groups. This will affect U → O π-bonding and facilitate a positive contribution to ν(U−O). Thus, the electron-releasing substituents will minimize π-interaction and increase the ν(U−O) frequencies.

Corresponding ν(C−O) wave numbers for β-diketonates, i.e. acac, bzac and dibzm, are in decreasing order, from 1565, 1552 to 1541 cm^{-1}, respectively. The relevant IR frequencies (Table 2) and NMR chemical shifts vary systematically for these ligands. Other spectroscopy data[117] show that vibrations which correspond to ν(C−C) and ν(C−O) bands are in the same region for UO_2-complexes, which implies that they are *O*-bonded ligands. The most intense band at 1597 cm^{-1} corresponds to stretching vibrations of the benzene ring from the benzoylacetonato ligand. Generally, in this type of system, the uranium atom is surrounded by seven oxygen atoms, i.e. four from two bidentate β-diketonates, one from an oxygen-containing ligand of another type and two uranyl oxygen atoms.

Solvent–solvent and solvent–solute interactions were examined by measuring the Raman spectrum of CO_2 in neat $^{SC}CO_2$ and in solutions of β-diketones (acacH, tfacH and hfacH) or the complex $[UO_2(hfac)_2DMSO]$[118]. It was found that the Raman bands of $^{SC}CO_2$ containing β-diketones are shifted to lower wave numbers compared to neat CO_2 and no shift to lower wave numbers was observed for the uranyl complex solution. Acid–base interactions between the carbonyl oxygen atoms of diketonato ligand and

TABLE 2. IR data for uranyl β-ketoenolates $[UO_2(dik)_2]$

dik	ν(U=O) (cm^{-1})	ν(U–O) (cm^{-1})		ν(C–O) (cm^{-1})
acac	928	528	403	1565
bzac	918	555	413	1552
dibzm	904	606	430	1541

the CO_2 carbon, and hydrogen bonding between enolic OH and the CO_2 oxygen occur in $^{SC}CO_2$ containing β-diketones. It was suggested that an increase in concentration of β-diketones in $^{SC}CO_2$ causes the increase in the number of carbonyl and OH groups interacting with $^{SC}CO_2$. See further discussion on UO_2-CO_2 interactions in Section VIII.

P. Enolates of Miscellaneous Elements

Alkali metal enolates show varying reactivity, which has been attributed to structural changes due to the metal. The stabilization energy of the enolate anion, 33 kcal mol^{-1} (*vs.* OH^-), is drastically reduced to 9–14 kcal mol^{-1} (*vs.* CH_3OH) in the metal complexes[119]. In bridged enolates, the negative charge on the oxygen is smaller, and larger on the carbon, than in the linear isomers. The negative charge on the oxygen repels both σ and the π electrons of the adjacent carbon and polarizes the double bond. Alkali metal M–O bonds possess an ionic character.

The saturated vapors of β-diketonates of Group 2 elements[120–122] contain a mixture of $[M(dik)_2]_n$ molecules with different degrees of oligomerization. The ratio between the forms in vapor depends on the metal atom, the type of ligand, the vapor temperature and the total pressure. It seems natural to start by investigating the structure of the monomeric form, having created the necessary conditions for sample evaporation. As shown for $Ca(dpm)_2$ and $Ba(dpm)_2$[121, 122], when superheating increases, the composition contains only the monomeric form.

It was established structurally that the chelate framework of the monomeric molecule $Ba(dpm)_2$ has D_{2d} symmetry, the two equivalent ligands having a common twofold symmetry axis and the ligand planes being mutually perpendicular[120]. No pronounced folding of ligands along the O···O axis has been found. The *t*-Bu groups are rotated through an angle $\gamma = 38.4^\circ$ arising from the hindered rotation of the Me groups. The r(Ba–O) distance was determinated in β-diketonate complexes involving a tetracoordinated Ba atom. Structural analysis of $Ba(dpm)_2$[123–125] shows that the unit cell of an anhydrous crystal is a tetramer $Ba_4(dpm)_8$. It was stated that four Ba atoms form a rhombus, in which the six O atoms of three β-diketonate ligands coordinate two of the Ba atoms and the other two are heptacoordinated. The compound contains both Ba–O chelate bonds, which are analogous to those in the monomeric molecule, and Ba–O bridging bonds, where one oxygen atom is linked to two Ba atoms. The average length of the Ba–O bonds involving the heptacoordinated Ba atom is 2.775 Å, while that of the tetracoordinated one is only 2.535 Å, which may be indicative of steric hindrances in the coordination sphere of BaO_7 compared to BaO_4 due to the great rigidity of the chelate rings. The molecular structure of $Ba_4(dpm)_8$[123–125] contains chelate rings analogous to those found in the monomeric molecule $Ba(dpm)_2$.

It was established that the $Sr(dpm)_2$ monomeric molecule as well as the $Ca(dpm)_2$ and $Ba(dpm)_2$ molecules have D_{2d} symmetry when the two equivalent planar ligand rings are perpendicular to each other[126]. A comparison of structural parameters in the series $Ca(dpm)_2-Sr(dpm)_2-Ba(dpm)_2$ shows that r(M–O) is lengthened and the O–M–O angle

decreases when the central alkaline earth metal is a large one. The geometrical structure of the ligand does not change. In contrast to alkaline earth dipivaloylmethanates, $Cu(dpm)_2$ has a planar structure of the bicyclic fragment, which is possibly provided by the participation of the *d*-atomic orbitals of the copper atom in the formation of a unified π-conjugate system with the ligands[127, 128]. This is also supported by the internuclear distances r(C−C) and r(C−O), which are slightly shorter in $Cu(dpm)_2$ than in Group 2 metal dipivaloylmethanates. When the π-system of the ligand is not conjugated to the central atom, the ligands occupy a position with the four oxygen atoms lying at maximal distances from each other.

Bidentate β-diketonates usually have symmetric structure, and many crystal structures show sets of equal M−O, C−C and C−O bonds. Alkali metal enolate structures are symmetric as well as those for the Pd, Rh and Al enolates. Few structures show unequal M−O distances; these enolate complexes (M = Ge, Sn and Sb) are asymmetric as the metal atom is not located at equal distances from the nearest oxygen atoms[129].

Acetylacetone is usually coordinated in the enolate form and rarely as the neutral ketone or enol molecules or via the γ-carbon atom of the acac ligand. MNDO calculations for $Pb(acac)_2$ indicate equal Pb−O bonds. In this case[130] (Figure 8), differences in coordination number and Pb−O distances were observed in solution and the solid state, which depend on different chemical states of acac ligand in these two systems. First, relatively long and weak electrostatic bonds of lead(II) in the solvate raise the coordination number to 10. On the contrary, the negatively charged acac ligands in $Pb(acac)_2$ interact more strongly, especially around the Pb−O bonds, making the $6s^2$ electron pair stereochemically active and lowering the coordination number to 4. Acetylacetone in solution shows bands corresponding to asymmetric and symmetric carbonyl stretching vibrations in the keto form, at 1730 and 1710 cm^{-1}. The dominant band at 1613 cm^{-1} originates from C=O and C=C vibrations of the enol form. In case of $Pb(acac)_2$ in solution, the appearance of this band is significantly lower, at 1559 cm^{-1}, while for the solid compounds only one band at 1584 cm^{-1} of coordinated enolate is distinguished.

The hfac ligand forms very stable and volatile complexes, therefore there is an opportunity for their use in separation and metal vapor deposition reactions. An analogous reaction with PbO will lead to the formation of dimer complexes, which exist in the solid state as a chiral enantiomer connected with the third diglyme oxygen of one unit oriented toward the Pb center of the other unit[131]. Despite the dimer structure, this complex is

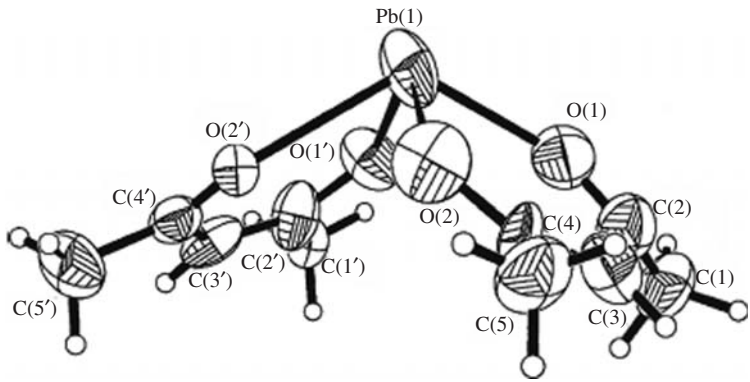

FIGURE 8. Molecular structure of $Pb(acac)_2$. Non-hydrogen atoms are shown as 30% probability ellipsoids. Reproduced with permission from Reference 130

volatile. In the complex with diglyme the Pb−O distances are longer than in the complex with hfac. Reaction of K(hfac) with 18-crown-6 forms a new structure, which exists in the solid state as a linear polymeric chain, interacting through the CF_3 group with K (Figure 9).

The versatility of the thallium ion, its coordination number and its geometry are responsible for many properties and, in particular, for the use of Tl(I)−β-diketonato complexes as

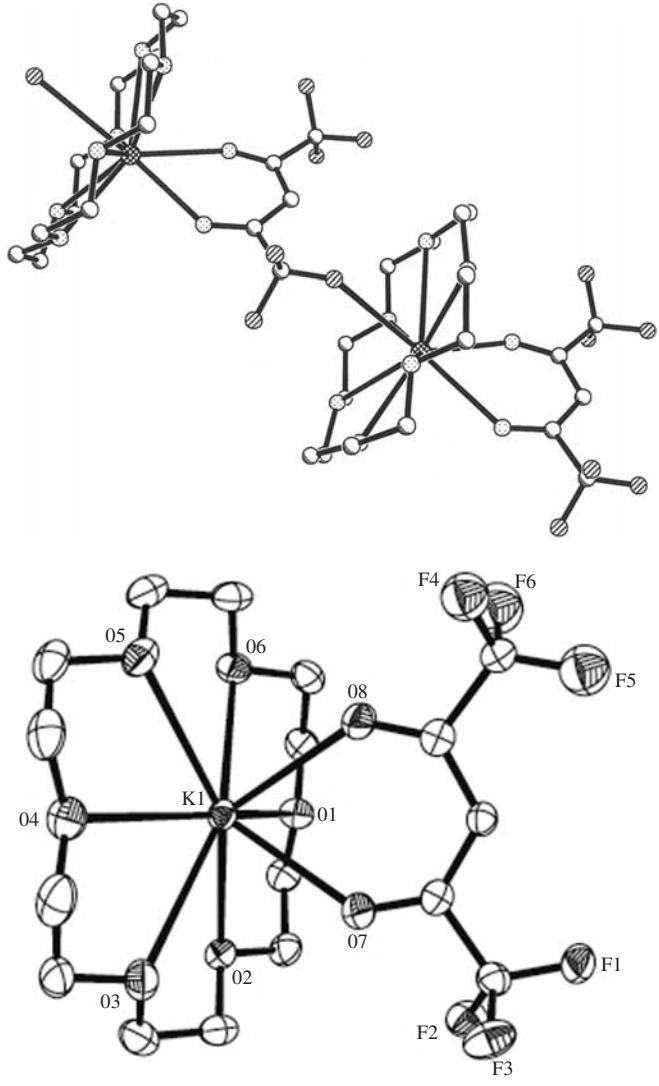

FIGURE 9. Ball-and-stick representation of the polymer chain of $[(18\text{-crown-6})K(hfac)]_n$. Thermal ellipsoids are shown at 50% probability for the monomer [(18-crown-6)K(hfac)] with hydrogen atoms omitted for clarity. Reproduced with permission from Reference 131

precursors in the synthesis of metallorganic liquid crystals[132]. The heteropolynuclear complexes of stoichiometry $[AuTl_2(acac)(C_6Cl_5)_2]$ or $[AuTl_3(acac)_2(C_6F_5)_2]$ consist of neutral $Tl_2(acac)_2$ units acting as bridges between linear oligomeric chains of $[AuTl((C_6Cl_5)_2)_2]_n$ or between $[AuTl(C_6F_5)_2]$ units, respectively. In both cases, strong ionic Au···Tl interactions and Tl(I)···Tl(I) contacts are present, which are considered to be in part responsible for luminescense. The chemical shifts at 5.0 (CH) and 1.72 (CH_3) ppm are different from those of a typical ionic derivative at 4.7 and 1.56 ppm. These two types of complexes with gold are formed as infinite chains via unsupported Au···Tl interactions and as a double-chain one-dimensional polymer. Both complexes show luminescence in acetonitrile solution, with a single high-energy emission and virtually identical profiles. The [Tl(acac)] complex itself is luminescent, showing a blue shift on decreasing the temperature, probably due to the rigidity or luminescent dichroism observed in its two-dimensional structure in the solid state; the excitation profiles of the heteronuclear complexes originates from the $d^{10} - s^2$ interaction between gold(I) and thallium(I) centers. TD-DFT calculations point to $Tl_2(acac)_2$ units as responsible for the luminescent behavior of Tl(acac) and the heteronuclear complexes in acetonitrile solution. A study of their molecular orbitals shows HOMO contribution from acac ligand, with an important contribution of oxygen atoms bonded to Tl(I) centers. The shape of the LUMO involves Tl centers. Transitions responsible for the luminescent behavior arise from ligand-based acac orbitals while thallium MOs have LMCT character.

The molecular structure of $Sn(acac)_2Cl_2$ was determinated by XRD crystallography[133]. In the Raman spectrum, three coincident bands were correlated[134] with the IR bands at 1554, 1535 and 1517 cm^{-1}. For the rocking vibrations, only one infrared band centered at 1024 cm^{-1} could be assigned. The skeletal stretching vibrational modes ν(C=O), ν(C=C) or ν(O−C−C), assuming a 'benzenoid resonance' structure of the ligands by coordination with $SnCl_2$, can be considered as equivalent internal coordinates for the C−O and C−C bonds. In the IR spectrum only two bands at 1620 and 1574 cm^{-1} are observed. Deconvolution analysis also gives absorption bands at 1597, 1594 and 1581 cm^{-1}; that at 1597 cm^{-1}, corresponding to the observed band at 1620 cm^{-1}, can be assigned to the coupled mode ν(C=C) + δ(CCH) + $\nu(CH_{methine})$. The value at 1594 cm^{-1} was described as the very complex mode ν(C=C) + δ(O=C−CH_3) + β(H−CH).

For ν(C−CH_3) stretching modes of $Sn(acac)_2Cl_2$ with two Raman bands at 986 and 939 cm^{-1}, in the IR spectrum a band was observed at 938 cm^{-1} that can be assigned as the coupled mode ν(C−CH_3) + ν(O−C−C). Concerning this assignment, the DFT calculations indicate two wave numbers at 963 and 960 cm^{-1}. It is expected[135, 136] that the ν(C−H) of methine groups will be at higher wave numbers than those of methyl groups. The observed bands at 3108 cm^{-1} (IR, Raman) and at 3070 cm^{-1} (IR) are assigned to $\nu(CH_{methine})$.

The bending in-plane vibrations of the acac ligands of $Sn(acac)_2Cl_2$ are: α(O−Sn−O), β(C−O−Sn or O−C−C), γ(O−C−CH_3 or C−C−CH_3), ε(C−C−H) and α(O−Sn−O). The calculated wave numbers at 278 and 257 cm^{-1} for these vibrations can be correlated with the experimental values found at 292 and 247 cm^{-1} (IR) or 288 and 238 cm^{-1} (Raman)[135, 136] and assigned as the coupled modes α(O−Sn−O)(63%) + ν(Sn−O)(23%) and α(O−Sn−O) + δ(O−Sn−Cl)(27%).

IV. UV-VIS SPECTRA

The position of acac ion in the spectrochemical series involves weaker metal ligand π-bonding (close to water) than the relatively high $\pi - \pi^*$ transition energies would suggest[18]. This assessment is based on Hückel's LCAO theory. In MO levels of the acac ion the $\pi 3$ orbital is occupied and the $\pi 4^*$ unoccupied antibonding MO is energetically suitable for overlap with the metal d-orbital. The reason is that both donor–acceptor

combinations, i.e. π^*–M and π–M bonding, are possible. Coordination with metal ion shows that π metal–ligand interaction increases splitting between the $\pi 3$ and $\pi 4^*$ levels and thus moves up the $\pi-\pi^*$ transition energy. In these terms a bathochromic shift of the $\pi-\pi^*$ bands through the series of transition metal ions was found to be in order Co > Cr ≈ Fe > Mn ≈ V by stating that the total π-interaction increases with the *d*-orbital population, except that it is particularly large on the Cr(III) and particularly small in the Mn(III) complexes. The energy of the $\pi-\pi^*$ transition depends not only on the metal ion but also on the substituent groups of the β-diketonato ligands: in case of $M(acac)_3$ the $\pi-\pi^*$ transition energy is high, and higher than in the case of using tfac, bzac or dibzm. The relatively high $\pi-\pi^*$ transition energy implies that the donor π-bonding is strong.

The interpretation of photoelectron spectra of metal acetylacetonates, based on theoretical modeling, shows that oxygen *n*-orbitals make the usual contribution in the metal–ligand covalent interaction[137]. Introduction of substituents in the ligands causes changes in the transition energy: the presence of fluorine implies an electron-withdrawing effect that increases $\pi-\pi^*$ transition energies, i.e. it displaces the σ-electron density toward fluorine and the π-electron density toward carbon[18]. Generally, the $\pi-\pi^*$ band is more sensitive, in particular it is more affected by the different substituents present and the effect is more pronounced in the nontransition metal complexes. For example, comparison between benzyl and methyl substituent being replaced and introduced in the Mn(III) coordination sphere, respectively, show a very high degree of subsitituent sensitivity or shift in $\pi-\pi^*$ transition energy, which is consistent with the fact of some degree of ionic character present in the Mn–O bond. Moreover, in the case of Co(III) minimum sensitivity is observed, which is correlated with a maximum of the metal–ligand bond.

UV spectra of β-diketonate ligands are high-intensity bands arising from electronic transitions in the conjugated system. The difference in spectra between acac, tfac and hfac is noticeable[82]. The maximum of the intense absorption band of acac is shifted to higher wavelengths and becomes intensified by the presence of an electron-withdrawing CF_3 group at one end of the conjugated system, which increases the preference for the enolate tautomer over the α-keto carbanion form. In the case of hfac, frequency and intensity are considerably decreased and the enolate form is 100%.

The square-planar $[Ni(dik)(diam)]^+$ cationic complexes show a strong band near 490 nm assigned to a $^1A_{1g} \rightarrow {}^1A_{2g}$ transition[138,139]. This band was found in the spectra of the adducts near 950 nm, indicating an octahedral Ni(II) complex. This band can be assigned to a $^3A_{2g} \rightarrow {}^3T_{2g}$ that corresponds directly to a $d_{xy} \rightarrow d_{x^2-y^2}$ transition. The small absorption band observed for the octahedral complexes at 800 nm may be assigned to a $^1A_{2g} \rightarrow {}^1E_g$ transition. The *d*–*d* band positions and the corresponding molar absorptions are shifted by a change in the concentration of the bidentate ligand as well as by a change in the substituents at the β-diketonate or diamine moieties on the square-planar chelate.

The *meso*-aryldipyrrylmethanoato (adpm) acetylacetonato Cu(II) complexes (**1**)[140] show in the UV-vis spectra the characteristic charge-transfer band at 494 nm[141] of heteroleptic [Cu(adpm)(acac)] complexes. For $Cu(dik)_2$ type of complexes[142] solid-state electronic spectra show the intraligand $\pi-\pi^*$ transitions of the acac ligand in the 270–340 nm region, whereas LMCT transitions appear in the 400–420 nm range.

The type 1:1 donor–acceptor complex between $Co(acac)_3$ and iodine (σ-acceptor) shows a strong absorption band at 360 nm, which has been assigned as a charge-transfer band[143]. In IR spectra, compared to $Co(acac)_3$, frequencies are slightly shifted in addition to three new bands of triiodide ion that are not observed in the spectrum of the donor.

Cobalt(III) β-diketonato complexes[63] (**2**), with the CoN_4O_2 chromophore, have similar electron absorption spectra, indicating that the central ion and ligands are coordinated in a similar mode. In the visible region they exhibit two maxima which correspond to the spin-allowed *d*–*d* transitions, $^1A_{1g} \rightarrow {}^1T_{1g}$ and $^1A_{1g} \rightarrow {}^1T_{2g}$. A third very intense

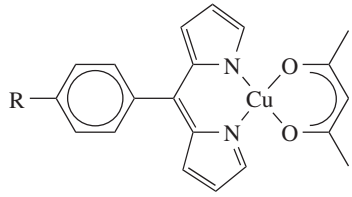

(**1**) R = MeO_2C, *i*-PrNHC(O), O_2N

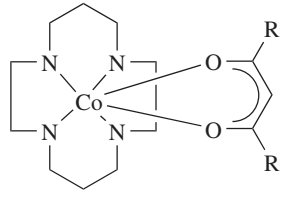

(**2**) R = Me, Mef, *t*-Bu, Ph

band appearing in the near-ultraviolet region (230–240 nm) is thought to correspond to an $n \rightarrow \pi^*$ transition in the enolate ring[144] and some degree of 'benzenoid' resonance in addition to the enolate-type resonance in which the main π-delocalization occurs. Upon introduction of phenyl groups, as in the case of the complex with dibzm, the bands at 305 and 269 nm correspond to $\pi \rightarrow \pi$ and $\pi \rightarrow \pi^*$ transitions, respectively, which is consistent with the possibility for enhanced delocalization of π-electrons. Since the metal and ligand π-levels are mixed, these bands may have some charge-transfer character. The large value of molar absorption coefficients supports the resonance form of the dik structure, indicating its symmetric coordination. Generally, β-diketonate on chelation to cobalt causes a bathochromic shift in the wavelength of maximum absorption[145].

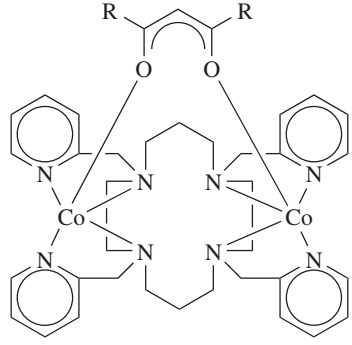

(**3**) R = Me, Mef, *t*-Bu, Ph

The electronic absorption spectrum of the binuclear Co(II) complex ion $[Co_2(dik)tpmc]^{3+}$ (**3**, dik = acac, dibzm, hfac, dpm; tpmc = 1,4,8,11-tetrakis(2-pyridylmethyl)-1,4,8,11-tetraazacyclotetradecane)[67] shows a single coordination mode with one well-resolved band in the 522–540 nm range. In the 254–344 nm UV region these appear

absorption maxima stemming from π-electrons and unpaired electron spins of the chromophore groups, with very high molar absorption coefficients as a consequence of a symmetric coordination mode of resonance of the β-diketonato ligand. The presence of Mef substituents on the β-diketonato bridge destabilizes metal-ion levels relative to the Me group while Ph substituents stabilize them. Absorption maxima at about 260 nm belong to the $n \rightarrow \pi^*$ transition and that at 344 nm comes from $\pi \rightarrow \pi$ and $\pi \rightarrow \pi^*$ intraligand transitions in the case of coordinated dibzm. Similarly, the hfac ligand gives a maximum at 300 nm as a consequence of $n \rightarrow \sigma^*$ transition[146]. Because of the mixed and overlayed π-levels of the β-diketonato and cobalt atoms, these bands are charge-transfer bands from the ligand to the metal ion.

Transition metals can form tris(acetylacetonato) complexes with strong metal–ligand covalent bonds, which enhance molecular stability and support the sublimation process without dissociation. These MO_6 arrangement forms[147] in an octahedral coordination polyhedron are in the solid state usually in an α (orthorhombic, P_{bca}) or β (monoclinic, $P_{21/c}$) structure. The XRF spectrum of $Fe(acac)_3$ powder and thin film show the appearance of a FeK_α signal that confirms the stability of the crystalline molecular structure during sublimation at about 150 °C. The UV-vis absorption spectral assignments show two distinguishable maxima at 355 nm and 435–440 nm, both due to the existence of a Fe ion coordinated to an acac ligand, since the pure ligand will not show any of these absorptions: d–d transitions in the case of d^5-Fe^{3+} are spin-forbidden transitions, therefore intense absorption peaks are a result of LMCT transitions. This characteristic of the $Fe(dik)_3$ complex shows that films grown on p-Si display a low dielectric constant and are promising materials for dielectric applications.

The molecular structure of some non-heme iron(III) complexes of general formula $[L(dik)Fe(\mu\text{-}O)Fe(dik)L](ClO_4)_2$ (dik = acac, bzac) was characterized as hexacoordinated and *O*-bridged diiron complexes[148]. They are chemically and electrochemically very reactive and can be oxidized to the Fe(IV) diamagnetic species $[Fe(\mu\text{-}O)Fe]^{6+}$. Complexes with a diiron oxygen-bridged core were obtained from mononuclear Fe(II) species. Electrochemically, it is possible to react and generate mixed-valence complexes as a product of a one-electron reversible redox reaction. Its electronic spectrum shows three charge transfer bands, and one at 365 nm assigned to acac-to-Fe CT or p_x,p_y-(oxo) $\rightarrow$ d_{xz},d_{yz}-Fe(III), having two acac ligands coordinated independently to the two iron ions.

Iridium(III) β-diketonates[68] show a relatively week absorption in the 350–400 nm range, that can be ascribed to spin-allowed MLCT transitions. Electroluminescent spectra (EL) show green light emission. In electronic spectra of Ir(III)), Pt(II), Ru(II) and Os(II) β-diketonates[149] weak absorption bands between 330 and 560 nm can be assigned to singlet and triplet MLCT transitions. The $\pi \rightarrow \pi^*$ transition from the complexes are blue-shifted for about 20 nm compared with the free ligands.

The Ir(III) complex (**4**) was the first six-membered chelated iridium complex found fit for application in organic light-emitting diode (OLED) devices[150]. The coordination geometry of iridium is approximately octahedral, with two quinoline nitrogen atoms *trans* to each other, whereas the two acetylacetonate oxygen atoms lie *trans* to the ligating carbon atoms of the phenyl groups. The molecule has near-C_2-symmetry. Notably, the six-membered chelated iridium geometry is not coplanar and is close to a twisted boat form[150]. These species show strong low-lying absorption bands with a mixed MLCT/π-π^* character, indicating an unusually strong spin–orbit coupling due to the heavy atom (Ir) effect and, perhaps, the short six-membered coordinating distance. Complexes of this type show deep red phosphorescent emission (650–680 nm) in deareated acetonitrile.

Ir(III) cyclometalated complexes, $[Ir(C^\wedge N)_2acac]$, where C^N is thp, tpy or bzq, show low-energy absorptions at 450 and 500 nm of MLCT/ILCT character[151], $\{[d_{z^2}(Ir) + d_{x^2-y^2}(Ir) + \pi(C^\wedge N)] \rightarrow \pi^*(C^\wedge N)\}$, while a complex with dbm shows an extra lower energy weak absorption at 536 nm that can be attributed to $\{[d_{z^2}(Ir) + d_{x^2-y^2}(Ir) + \pi(C^\wedge N)] \rightarrow$

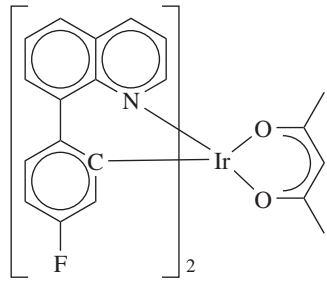

(4)

π^*(dbm)}, of MLCT/LLCT character. The intense participation of a conjugated phenyl group remarkably stabilizes the molecular orbital. Calculations of the isolated ligands show that the intraligand $\pi \rightarrow \pi^*$ transition occurs at $\lambda < 300$ nm, while coordination between metal and ligands produces lower-energy absorptions due to the presence of the metal and spin-forbidden singlet–triplet transitions. The lower lying absorption energies are in opposite order from π-conjugation effect, but introducing the phenyl group enhances the conjugation effect and significantly lowers the LUMO energy level, resulting in a considerable decrease of the HOMO–LUMO energy gap (Figure 10). The LUMO energy levels of the complexes are little disturbed by variation of the ancillary ligand, whereas the HOMO energy levels can be tuned by interaction of ancillary ligands with iridium *d*-orbitals. The stronger ligand field strength of the dithiolate ancillary ligands leads to lower HOMO energy levels of complexes than acetylacetonate. Correspondingly, the energy gap of the complexes increases when dithiolate ancillary ligands replace acetylacetonate, which is correlated with the hypsochromic shift of the emitting wavelength of the complexes.

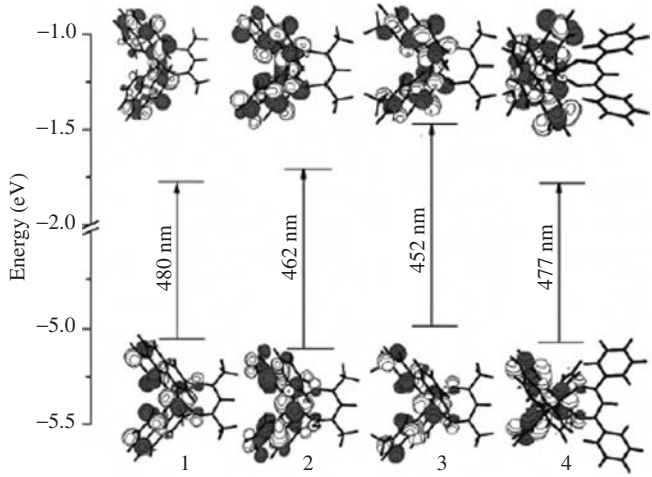

FIGURE 10. Transitions contributing to the absorptions at 480, 462, 452 and 477 nm for the iridium(III) complexes [Ir(C^N)$_2$(L)] (C^N = benzoquinoline, L = acac, 1; C^N = 2-Thi-Pyr-2, L = acac, 2; C^N = 4-Tol-Pyr-2, L = acac, 3; C^N = benzoquinoline, L = dibzm, 4) in THF solution. Reproduced with permission from Reference 151

Ir(III) complexes in photoluminescence spectra emit red light at 617 and 613 nm. The presence of a Mef group on napy (2-(1-naphthyl)pyridine) to afford the 4-fnapy (2-(1-naphthyl)-4-trifluoromethylpyridine) ligand changes the $\pi-\pi$ conjugation on the ligand, lowers the LUMO level of the complex and finally emits orange light at 595 nm. HOMO and LUMO data show that the trifluoromethyl group lowers more efficiently the LUMO than the HOMO energy levels. The crystal structure[149] of $(napy)_2Ir(acac)$ and $(4\text{-fnapy})_2Ir(acac)\bullet CH_2Cl_2$ shows that the Ir−O bond lengths and the O−Ir−O bond angle in the chelate are reduced to some degree on changing the other ligand from napy (2.130(4) and 2.160(4) Å, 87.9(2)°) to fnapy (2.129(2) and 2.142(2) Å, 87.55(8)°).

The relatively simple structure of $Cr(acac)_3$ was used as a model for electronic structure evaluation[152]. This molecule has a high degree of photostability and opportunity for excitation to both ligand-field and charge-transfer states. The lowest-energy state corresponds to ^2E. The $^2E \rightarrow {}^4A_2$ transition is responsible for the static emission line at 794 nm. The ligand-field $^4A_2 \rightarrow {}^4T_2$ transition shows a maximum at 560 nm, which involves a change in orbital population, i.e. one electron from the nonbonding t_{2g} orbital transfers to the antibonding e_g* orbital. Then, below 400 nm the absorption spectrum corresponds to CT processes.

Electrogenerated chemiluminescence (ECL) involves the formation of excited states at or near electrode surfaces. Recent reviews of 2,2′-bipyridine−ruthenium(II) complexes have highlighted the use of metal chelate systems in ECL[153]. UV-vis spectra depend on the nature of the β-diketonato ligand (Table 3), and show absorption intensities between 481 and 502 nm that are characteristic for ruthenium MLCT transitions. This absorption is red-shifted relative to the $(bipy)_2Ru^{2+}$ complex without a dik ligand. In the presence of β-diketonato ligands with electron-donating substituents, the absorption maxima appear at lower energies. This observation correlates with another parameter, that the presence of more electron-withdrawing substituents results in a larger HOMO−LUMO energy gap and higher absorption energies.

The symmetrical binuclear diamagnetic $[(bpy)_2Ru(\mu\text{-}H_2L)Ru(bpy)_2](ClO_4)_2$ and paramagnetic $[(acac)_2Ru(\mu\text{-}H_2L)Ru(acac)_2]$[154] (L = 2,5-dioxido-1,4-benzoquinone diimine) complexes show that electron transfer occurs largely at the bridging ligand. In contrast, the higher oxidation states Ru(III) and Ru(IV) seem to be favored by the binuclear bis(acetylacetonato)−ruthenium complexes, leading to more involved and ambivalent oxidation-state combinations. Intense long-wavelength absorption bands point to mixed-valent binuclear configurations.

The luminescent cyclometalated Pt(II) complexes **5**[155], with absorption maxima around 520 nm, exhibit similarly structured emission bands, independent of the nature of the β-diketonato ligand. A representative complex of this type (R = H, R′ = Me) in a frozen EPA (ether−isopentane−alcohol) glass at 77 K has two sets of vibrationally structured bands (460−560 nm, 570−800 nm), due to the presence of two emitting isomeric species,

TABLE 3. Absorption spectra of $[(bipy)_2Ru(dik)](PF_6)$ complexes. Reproduced with permission from Reference 153

dik[a]	λ_{max} (nm)	ε (L mol^{-1} cm^{-1})
bzac	502	11000
dibzm	493	12000
ttfa	489	13000
tfpb	482	8400
tfac	481	16000

[a] ttfa = thenoyltrifluoroacetonate, tfpb = 1-phenyl-4,4,4-trifluoro-1,3-butanedionate.

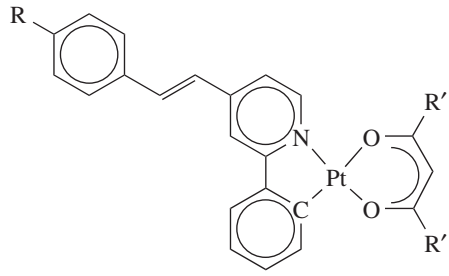

(**5**) R = H, MeO, Et_2N, O_2N, R′ = Me, *t*-Bu

which have significantly different triplet excited-state energies. The other acetylacetonates (R′ = Me) studied show a similar behavior, but the low-energy emission bands are progressively red-shifted for the R group in the order H < OMe < NO_2 < NEt_2. The very large red-shift compared to related unsubstituted complexes (e.g. [Pt(C∧N-ppy)(O∧O-acac)$_2$]) is the result of the extension of the π-conjugated system and the electronic effects of the R substituent.

The reaction of tetramethyl-1,3-cyclobutanedione with $LiSiR_3$ (R = $SiMe_3$, Et) or $LiGeEt_3$ results in the opening of the cyclobutanedione ring to give β-ketoacylsilane lithium enolates (**6**)[156]. The UV-visible spectra of these enolates exhibit two new transitions: one absorption is red-shifted and the other is blue-shifted (each by about 40–50 nm) relative to the absorptions of the corresponding β-ketoacylsilanes. *Ab initio* MO calculations show that the red-shifted transitions result from the presence of a low-lying Rydberg-type antibonding O–Li orbital. The blue-shifted transition, on the other hand, results from a weakening due to Li^+ complexation and destabilizing hyperconjugative interactions between the oxygen lone pair and the σ-(C–Si) orbital. This leads to a lowering of the energy of the filled *n*-O–σ-(C–Si) orbital, relative to its energy in the acylsilanes, and thus to a higher *n*-O–σ-(C–Si) → π*-(C–O) excitation energy than in the corresponding acylsilanes.

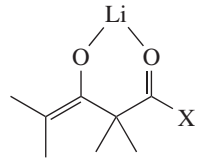

(**6**) X = $Si(SiMe_3)_3$, $SiEt_3$, $GeEt_3$

One of the most intriguing properties of acylsilanes is their color, showing absorption around 370 nm. However, the lithium enolates exhibit two new interesting absorption maxima: one near 335 nm and the other at 410 nm. Acylsilanes absorb at about 370 nm whereas the corresponding *n*-O → π*-(C=O) transition in simple ketones is at about 280 nm[157]. This large drop in the excitation energy, when silyl groups are attached to the carbonyl carbon, is because the excited state of acylsilanes is stabilized by participation of *d*-orbitals on silicon and inductive destabilization of the oxygen lone pairs by the electropositive silicon[158]. However, later photoelectron spectroscopy studies and CNDO/2 calculations[159] have shown that the main reason for the observed shifts is strong mixing between the in-plane lone-pair orbital on oxygen (*n*-O) and the σ-(C–Si) bond, which

pushes the filled antibonding combination of these orbitals (i.e. n-O$-\sigma$-(C$-$Si)) to a higher energy (hyperconjugative destabilization), reducing the gap with the empty π*-(C=O) orbital[159]. More recent molecular orbital analysis suggested that other contributing factors are the similarity of the vertical and the adiabatic excitation energies of acylsilanes[160] and the dative bonding between the R_3Si and C=O groups.

A new class of ligands, the sila-β-diketones, 2,2,6,6-tetramethyl-2-sila-3,5-heptanedione (tmshdH), has been developed. The UV spectra of the homoleptic Cu(II) complex, Cu(tmshd)$_2$[161,162], exhibits absorption at 276 nm that is slightly less intense than that for nonsilylated β-diketonate analogs. The lack of the expected bathochromic shift or hyperchromic effect expected for an acylsilane is consistent with the predominant enolic tautomer being on the silicon side[161]; the green complex coloration is generally due to a broad, moderately intense CT band in the electronic spectrum that occurs at 360$-$370 nm (ε *ca* 9000) tailing into the blue portion of the visible region, in combination with weak d–d transitions at 520 (ε *ca* 100) and 655 nm (ε *ca* 50)[162].

Ultrafast time-resolved spectroscopic methods have been used to probe the dynamics associated with ligand-field excited states in Cr(III) and Fe(II) complexes. Cr(acac)$_3$ serves as a prototype for studying the $^4T_2 \rightarrow {}^2E$ conversion characteristic of Cr(III) complexes[163]. The data reveal that formation of the ^2E state occurs faster than the instrumental time resolution, implying a rate constant for intersystem crossing of at least 10^{13} s^{-1}. Slight changes observed in the differential absorption spectra were attributed to vibrational cooling in the ^2E state. The role of low-lying ligand-field states as highly efficient deactivation pathways for higher-lying charge-transfer states was demonstrated in low-spin Fe(II)$-$polypyridyl complexes. Following $^1A_1 \rightarrow$ MLCT excitation, the ligand-field manifold is accessed with a time constant of *ca* 100 fs. This pattern was observed for several complexes, suggesting a general feature of this class of molecules. Subsequent to populating the ligand-field states, dynamics ultimately leads, on the subpicosecond time scale, to formation of the $^5T_2$ state as the lowest-energy excited state. This observation has important implications for the use of such complexes as sensitizers in photovoltaic applications.

The presence of ligand-field states—electronic states that derive largely from the d-orbitals—is a unique defining feature of the photophysics and photochemistry of transition metal complexes[164,165]. Excited ligand-field states are responsible for a wide range of reactivity, most notably photosubstitution and photoisomerization. Although charge-transfer states are most commonly associated with excited-state electron transfer, ligand-field states can also engage in photoredox chemistry[166]. The study of transition metal photophysics on the subpicosecond time scale is a rapidly developing area of physical inorganic chemistry[167,168] and holds considerable promise for advanced fundamental understanding of excited-state electronic structure and reactivity. To date, the overwhelming majority of work in this field has involved the study of CT chromophores and new developments focus on the ligand-field excited states of coordination compounds[163] such as Cr(acac)$_3$.

V. NMR SPECTRA

NMR spectroscopy and DFT computations were employed to study the structure of 2-acylcyclohexane-1,3-diones and their alkali metal salts in solution[169]. It was found that these triketones prefer an *endo*-enol tautomer configuration. In ^{1}H NMR spectra, separate signals of protons attached to C1, C2, C3 and C4 indicate that no rotation takes place around the C2$-$C7 bond and intermolecular hydroxyl proton exchange occurs despite the existence of the strong intramolecular hydrogen bonding. At $-90\,^\circ$C the spectra gave no evidence of restriction of cyclohexane ring inversion. Calculations show that enolic protons exist and the calculated energy of the *exo*-enol is higher by 2.8 kJ mol^{-1} than

that of the *endo*-enol, which favors the *endo*-form in solution. Experimental results and calculation of the corresponding alkali metal enolates show that the ^{13}C chemical shifts of the salt or the free anion depend on the population of these two species[169]. Compared with the Li salt, in the free anion sp^2 carbon atoms are deshielded whereas sp^3 atoms are shielded; all three oxygen atoms are coplanar and, except for C5, the other C atoms of the cyclohexane ring and the C of the exocyclic carbonyl group also lie on the same plane. A strong interaction between water in the solvent and the carbonyl oxygens is observed. Considering literature data about β-dicarbonyl and tricarbonyl compounds, no simple differentiation between tautomers by NMR spectra should be expected because of fast tautomerization.

NMR data (Table 4) show that the presence of different substituents on the β-deketonate chelate ring has a high impact on the electronic effects in the ring and also affects the chemical shift of the protons. With acac the >CH resonance is found at δ 5.85 ppm while for tfac and dibzm it is at δ 6.28 and 7.24 ppm, respectively.

The ^1H NMR spectrum of linear tetranuclear complex (**7**)[170], bridged by enolato ligands derived from mesityl metyl ketone and capped by bidentate tmeda molecules, displays two sets of olefinic signals, one at δ 5.01 and 4.20 ppm, for enolato bridging two Mg nucleii, which are downfield to the ones at δ 4.81 and 4.01 ppm, for enolato connecting Na and Mg nucleii. The *o*-Me group signals are shifted downfield for the Mg−Mg enolate bridge (δ 2.87 ppm) relative to those of Na−Mg bridges (δ 2.49 ppm). The *p*-Me group

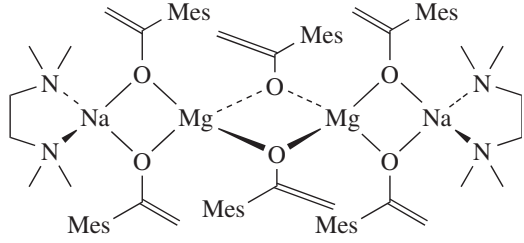

(**7**)

TABLE 4. IR and NMR spectra[a] of uranyl β-diketoenolates $[UO_2(dik)_2(py)]$[a] [17]

dik[b]	ν(U=O)[c] (cm^{-1})	ν(U−O)[d] (cm^{-1})		ν(C−O) (cm^{-1})	δ(2-H)[e] (ppm)	δ(3-H)[e] (ppm)	δ(4-H)[e] (ppm)	δ(>CH) (ppm)
tfac	922	562	408	1621	9.20	7.75	8.12	6.28
eaa	918	571	423	1605	9.47	7.72	7.98	5.31
acac	913		403	1570	9.57	7.73	7.96	5.85
bzac	911	553	412	1555	—	—	—	—
dibzm	909	605	453, 428	1539	9.63	7.73	7.88	7.24
pa	916	621	479, 416	1584	9.46	7.73	7.98	5.96
mac	907	653	541, 452	1582	9.59	7.73	7.95	—
dpm	917	607	479, 409	1560	9.36	7.73	8.00	6.11

[a] IR spectra of the solid complex; NMR spectra in $DCCl_3$ solution, relative to TMS.
[b] eaa = ethyl acetylacetate enolate; mac = 3-methyl-1,3-pentanedionate.
[c] Of the uranyl ion.
[d] Of the chelate.
[e] Proton of the pyridine ring.

signals are almost the same in both cases (δ 2.15 and 2.11 ppm, respectively). In the ^{13}C NMR spectra, the relative downfield–upfield relation of the enolate signals is not always the same for Mg–Mg and Na–Mg bridges: δ(C–O) 161.23 and 163.12 ppm, $\delta(C_{ipso})$ 140.51 and 143.14 ppm and $\delta(=CH_2)$ 89.74 and 87.04 ppm, respectively.

The ^{13}C NMR spectrum of the homobinuclear Zn enolate **8** in CD_2Cl_2 solvent[97] shows resonances at δ 157.2 and 102.1 ppm, corresponding to Cα and Cβ, respectively, on the main enolate chain M–O–Cα=Cβ. These resonances and analogous ones of similar complexes (e.g. **9**) are related to others reported for *O*-bonded enolates, such as δ 160.0 and 104.6 ppm for the Zn enolate **10** and δ 146.6 and 106.8 ppm for the heteronuclear sodium zincate **11**. Other features seen in NMR spectra are consistent with sp^2-hybridized vinylic C–H bonds: Two doublets at δ 4.46 and 3.57 ppm (2*H* each) are assigned to two inequivalent vinylic hydrogen atoms of each enolate, which are in correlation with sp^2-hybridized vinylic bonds. Most notably, the difference between resonances assigned to Cα and Cβ atoms were proposed to predict bonding, reactivity and the degree of polarization of the C=C bond.

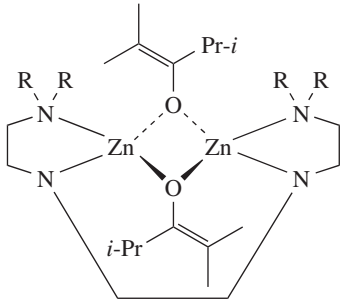

(**8**) R = Me, *i*-Pr

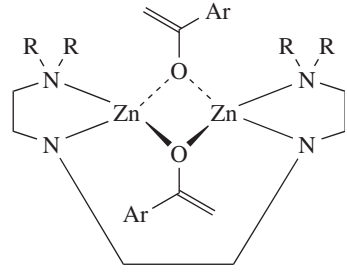

(**9**) R = Me, *i*-Pr, Ar = C_6Me_5

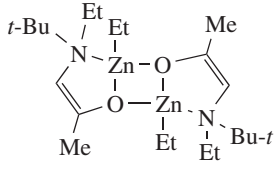

(**10**)

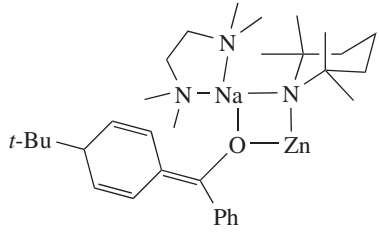

(**11**)

The chemical shifts of chelated β-diketonato protons are due to the 'aromatic' nature of the ring[171] or to its magnetic anisotropy[172] and others related to the nature of the central atom and the orbitals if used in σ and π bonding to the ring[171]. The chemical shift of the CH group depends mainly on the electrical symmetry of the complexes, and in the case of cobalt(III) compounds[63] it moves to the δ 6.50–6.21 ppm range relative to the enolate form of the free dik anion. This effect may be a function of the symmetric Racac coordination, suggesting that strong cobalt–oxygen bonding occurs[173]. The high symmetry of the complexes is reflected in the ^{13}C NMR spectra. The powerful efficacy of the six fluor atoms of the hfac ligand moves chemical shifts strongly downfield in

comparison with dibzm and dpm. Carbonyl carbons are under the strong influence of electronic effects of the R-groups attached to them, with chemical shifts as ligands of complexes in the order dpm > dibzm > hfac. A triple chelate complex of C_1 symmetry, such as $[Co(acac)_2(pdmp)]^+$, pdmp = $H_2NCH_2CH_2Ch_2PMe_2$, shows in ^1H NMR two doublets for *P*-CH_3 and four singlets (δ 1.90, 1.92, 1.93 ppm for each 3*H*, s, *C*-CH_3), and in ^{13}C NMR two doublets (δ 23.09 and 26.29 ppm, d, *C*-CH_3 and δ 26.51 and 26.89 ppm, s, *C*-CH_3), coupled very weakly with the P nucleus[174].

Reaction of the non-oxo V(IV) species $[VCl_2(dik)_2]$ (dik = acac, bzac) with a chelate nitrogen-donor ligand leads to reduction of V(IV) to V(III) compounds[175]. The diketonate ligand of the V(IV) precursor is the more probable reducing agent in the preparations of that type of complex. The two geometrical isomers of $V(acac)_3$ and the three isomers of $V(bzac)_3$ are resolved in their ^1H NMR spectra in $CDCl_3$ or CD_2Cl_2 solution. Based on the thermodynamic parameters, the greater stability of the *cis*-isomer is achieved due to better solvation in polar solvents. The CH_3 protons of the acac ligand in complexes of $HB(pz)_3VO(acac)$ type (**12**)[176] appear at δ 1.57 and 1.59 ppm. The signals of the CH_3 group of the acac ligand in ^{13}C NMR spectra of the hexacoordinated V(III) complexes[44] with *o*-phenantroline and acetylacetonate, $[V(acac)_2(phen)]^+$, appear at δ 68.12 and 68.53 ppm, which is considerably downfield with respect to $V(acac)_3$. The CH shows up at δ 40.41 ppm.

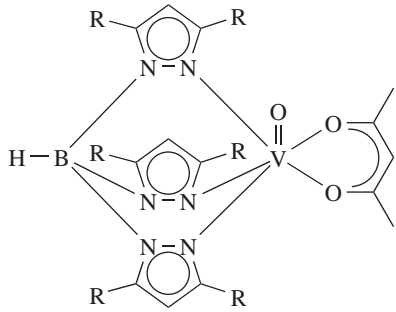

(**12**) R = H, Me

NMR spectra show a single average environment for $Y(dpm)_3$ complexes[34]: ^1H NMR in $CDCl_3$: δ 5.7 ppm (CH, 1*H*) and δ 1.13 ppm (CH_3, 18*H*); ^{13}C NMR: δ 201.5 ppm (CO), δ 91.6 ppm (CH) and 40.6 ppm (CH_3 in *t*-Bu); 28.3 ppm (CH_3); the ^{89}Y NMR spectrum in CD_2Cl_2 exhibits a single signal at δ 163 ppm, which indicates that the complex is monomeric in solution. The electron-impact mass spectral (EIMS) data exhibit the parent molecular ion and the base peak belongs to the fragment $[M - dpm]^+$.

Consecutive nuclear Overhauser enhancement spectroscopy (NOESY) experiments allowed one to calculate the distance between the enolate proton and other protons in the octahedrally coordinated titanium enolate **13**[177]. The H^1-H^2 and H^1-H^3 distances calculated from NMR spectra are 0.2 Å longer or 0.5 Å shorter, respectively, than those in the model structures. Using modeling studies, the same prediction can be observed, indicating that one side of the Ti enolate complex is less sterically hindered than the other side. This is due to the efficient diffusion pathway formed by the enolate H (H^1), the protons on the *i*-Pr group (H^2, Me) and the protons on the selone heterocycle (H^3, H^4). These distances confirm that the enolate oxygen atoms are *cis* to each other and their orientation should promote a strong facial preference upon subsequent reaction with an aldehyde or ketone.

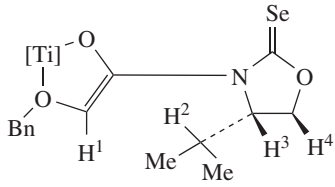

(**13**)

Application of triorganostannyl enolates[178] to organic synthesis was investigated on *O*-stannyl and *C*-stannyl enolates. ^{119}Sn NMR spectra showed that tributylstannyl enolate is a mixture of both enolate kinds at lower temperature. The *O*- to *C*-stannyl enolate ratio is temperature-dependent and it was confirmed to be reversible.

VI. EPR SPECTRA

The average bite angle for the acac ligands (81.81°) in $[Mn(acac)_2(bipy)]$[56] is among the lowest found for 2,4-pentanedionate coordinated to Mn(II)[179]. The only other case found in the literature where the pentanedionate ligand coordinated to Mn(II) has a bite angle smaller than 82° is in the Mn(II) trinuclear complex $[Mn\{Mn(acac)_3\}_2]$, in which the two peripheral Mn(II) ions have a trigonal prismatic geometry[180]. The high spin d^5 Mn(II) ion has no ligand-field stabilization and no large degree of π-bonding, since the magnetic data show both complexes to have a spin state of $S = {}^5/_2$. This value would be lower if π-bonding would take place to the extent found in rhenium dithiolene complexes, for example[181]. The solid-state EPR spectra for the two complexes are of quite different coordination symmetries, leading to a difference in the zero-field splitting parameters. The symmetry of the trigonal prismatic complex is rhombic, which is the cause of the large EPR signal at $g = 3.25$. The complex $[Mn(acac)_2(phen)]$ has a fairly regular octahedral coordination environment, which gives small zero-field splitting parameters, thus a resonance signal near the free electron value of $g = 2$ is observed[182]. Since the rigidity of the dinitrogen diimine ligand does not seem to play a role and the energy difference between different ligand environments for the complexes in vacuum is quite small, packing effects in the crystal lattice must play an important role in determining the solid-state structure.

A number of well-known Cu(II) complexes[183], for which structural and spectroscopic data are available, e.g. $Cu(acac)_2$, $[Cu(C_2O_4)_2]^{2-}$ and $[Cu(py)_4]^{2+}$, show the correlation between calculated and observed g values to be satisfactory, given the complexity of the task and the simplicity of the model. Moderate accuracy predictions can be afforded with the INDO/S CI model, but it is clearly recognized that the g tensor is a quantity that is difficult to model accurately by theoretical methods. It appears that the simple INDO/S CI model places the metal and ligand orbitals at realistic relative energies and thereby produces realistic metal–ligand covalent bonds. This is especially remarkable for sulfur-containing ligands that have orbitals quite close to the metal orbitals and therefore very strong covalent bonds, e.g. $Cu(Me_2NCS_2)_2$. Well-resolved electron spin resonance spectra of a series of stable dianion radicals are observed in solution[184] when a variety of metal β-diketonates, such as $Fe(dik)_3$, $Co(acac)_2$ and $Mn(acac)_3$, are reduced with Grignard reagents. The structure of acetylacetonate is related to a chelate model based on INDO molecular orbital calculations by fitting the observed proton hyperfine splitting.

Isotropic EPR measurements of the VO(IV)–acac system in aqueous solution[49] point to an equilibrium between the *cis*- and *trans*-isomers. Anisotropic EPR analysis allows one

to obtain information on the symmetry and coordination geometry of a complex and the character of the ligands, and detecting the presence of minor species in solution. The solid pentacoordinate compound $VO(acac)_2$ can give rise to *cis–trans* isomerism in solution because the metal has a free coordination place to react with a solvent molecule. The experimental data indicate that only the *trans*-isomer is formed and that can be simply confirmed using UV-vis and IR spectra. The energy of the e^*_π orbitals (d_{xz}, d_{yz}) is sensitive to perturbations along the *z*-axis, which can be effected by coordination with a solvent molecule. EPR spectra are defined by *g* and *A* values. Due to the splitting of the d_{xz} and d_{yz} orbital energy, four transition bands can be resolved, associated with the distortion of square-pyramidal to trigonal-bipyramidal geometry. Three bands can be seen from electronic spectra, suggesting that the $x-y$ anisotropy is small, as is the energy difference between the d_{xz} and d_{yz} orbitals.

Vanadyl complexes[185] coordinated by two pyrazole nitrogens and two oxygens from an acac ligand show that every complex has the same N_2O_4 donor sphere dominated by the axial oxo group, therefore the isotropic g_0 and A_0 values in EPR spectra are all similar. The visible spectra contain three or less distinct bands in the range of 350–800 nm, consistent with the Ballhausen and Gray assignments[186].

The EPR spectra of binuclear Co(II) complexes[67], e.g. $[Co_2(dik)tpmc](ClO_4)_3$ (**3** perchlorate, R = Me, Mef, *t*-Bu, Ph), show a symmetrical signal with no hyperfine splitting, with insignificant differences of electron g_e factors and band shapes. The antiferromagnetic coupling between the Co(II) centers that occurs through the bridging system of β-diketonato ligand is anticipated[187]. The decrease of the g_e factors at higher temperature suggests that magnetic interactions create weak intramolecular spin–spin and intermolecular interactions. It can be seen that the bridging ligand significantly reduces the distance between the two metal-ion centers and makes possible indirect spin exchange interaction between the d^7 electrons.

β-Diketonates exist in solution as metal chelates[188,189] and it would certainly be expected that the corresponding doubly charged anion radicals also exist in a similar form. The review of Dessy[190] demonstrated that generally the spin density in anion radical metal complexes could be largely localized on the ligand and the charge density on the metal. EPR studies indicate high localization of unpaired spin density in an orbital of predominantly ligand character[191].

VII. MASS SPECTRA

Negative chemical ionization (NCI) is a useful technique for determination of the molecular mass of compounds with distinct electron affinities yielding $[M]^{-\bullet}$ or of acidic compounds yielding $[M-H]^-$, usually as base peaks. A tandem combination of NCI and CID (collision induced dissociation) mass spectrometry usually affords poor results for structural analysis, because the main reaction is loss of an electron from the negative ions and few fragments derived from them[192]. On the other hand, the charge-reversed CID technique is a good method for assigning structures to nondecomposing negative ions.

Enolate ions are generated from carbonyl compounds by deprotonation with OH^- in a chemical ionization source producing the $[M-H]^-$ ions. Specific fragmentation of enolates corresponds to the loss of CO or the alkyl substituents and remaining fragments to produce ions of *m/z* 29 and 28. The main fragments in the CR spectrum of $[M-H]^-$ are ions with *m/z* 43 $[CH_3CO]^+$ and 42 $[C_2H_2O]^{+\bullet}$, obtained by α-cleavage of the ligand and further deprotonation to the ketene radical cation, respectively. Generally, CR enolate ions accommodate sufficient excess energy for extensive fragmentations. In case of open-chain enolates, characteristic fragmentations are α-cleavages giving rise to acylium ions

and ketene radical cations. These ions and the other fragments formed by loss of CO can be used to establish the structure of the parent carbonyl compound from which the enolate was derived.

Mass spectroscopy is widely used in the study of volatile metal β-diketonate complexes and, in particular, the saturated vapors of Al, Ga and In complexes with acac and its fluorinated derivatives[193], while dipivaloymethanato complexes were studied less extensively than the others. In case of $Al(acac)_3$, the threshold temperature at which the base peak attributed to $Al(acac)_2^+$ begins to decrease is 290 °C. Some metal complexes of this type, e.g. $Y(dpm)_2$, can undergo thermolysis and form new molecular entities at temperatures above 300 °C. The heaviest ion detected in saturated vapors of $M(dpm)_3$ complexes is $M(dpm)_3^+$, thus discarding the possible presence of oligomeric species. Further superheating of the vapors results in a decrease in intensity of metal-containing species and an increase of ion fragments of the organic ligand. The relative peak intensities for Ga and Al complexes with dpm remain unchanged up to temperatures of total decomposition.

The mass spectra of *sp*-elements differ significantly from *d*-elements. Studies of Ca, Sr, Ba, Y and Cu found that electron-induced fragmentation primarily results in the formation of ions with the loss of one ligand in the case of *sp*-elements or the formation of ions similar to the molecular ion for *d*-elements. This difference in mass spectra reflects metal–ligand bond features. In the case of *d*-elements, participation of a *d*-orbital in coordination results in more pronounced delocalization of electron density due to six oxygen atom donors. Therefore, fragmentation requires higher energy consumption and redistribution of electron density in the molecule. This process is less favorable compared to elements such as Al, Ga and In, in which the metal does not form π-bonds and ligands are easier to activate. $Al(dpm)_3$ and $Ga(dpm)_3$ complexes in the gas phase remain unchanged to the thermal stability limits at *ca* 600 °C, whereas $In(dpm)_3$ vapor at *ca* 550 °C shows an In(dpm) entity due to thermal decomposition. This tendency is consistent with changes in chemical properties within a series of this group of compounds. Therefore, one can detect temperature limits or the temperature at which metal-containing ions are no longer observed in the superheated vapors.

A mass-spectral study performed on $Sc(acac)_3$, $Sc(dpm)_3$ and $La(dpm)_3$ vapors[194] shows that, due to volatility and thermal stability, this group of β-diketonates is suitable for low-temperature gas-phase transport of metals. The similarity of the mass spectra of Sc, Y and La β-diketonates may point to a similarity of the processes involved in the thermal destruction of the molecular species present in vapor. Within the framework of crystal field theory, an unpaired electron of a central metal ion (Sc^{2+}, Y^{2+} or La^{2+} with the nd^1 configuration) occupies a d_{z^2} orbital, which has the lowest energy in D_{2h} symmetry. This results in stabilization of the ML_2 radical and enhances the thermal stability of the complex.

Mass fragmentation was followed in a series of Co(III)–amine–β-diketonato complexes[63]. Fragmentation starts from bond cleavage α to the carbonyl group and the charge remaining with the oxygenated fragment. Further fragmentation involves charge migration through the 'pseudoaromatic' ring of the β-diketonate chelate, with simultaneous formation of a C=O bond. The presence of these peaks is conclusive evidence for β-diketonato coordination through oxygen and seems to be a convincing approach to elucidation of the molecular structure. Further steps include cleavage of the cobalt–oxygen bond leaving a positive charge on the acyl fragment $(RC{=}O)^+$. The most intense peaks in the mass spectra of metal β-diketonates belong to β-diketonato fragments, i.e. $R(CO)CH_2(CO)R^+$, $R(CO)CH_2(CO)^+$, $R(CO)CH_2^+$ and $R(CO)^+$. The relative instability of the β-diketonato ion is due to weak C–R bonds, especially in the case of the electron-withdrawing groups[146,195].

VIII. MOLECULAR CHARACTERISTICS AND APPLICATION PERSPECTIVES

The ability to control chemical and structural properties of surfaces is crucial for new technologies. Direct implementation of transition-metal β-diketonates on some inorganic surfaces, such as silica, alumina or zeolites, is a matter of great interest in catalysis and interface processes[196]. On the other hand, SAMs (self-assembled monolayers) allow a large variety of molecules to be attached by chemisorption to different types of surfaces. For example, $Ni(acac)_2$ can be attached to grafted carboxylate, which involves substitution of one acac group with a CO_2H group on the surface. Spectral regions show bands characteristic for both environments. It was possible to control the surface density of the Ni complex by modifying the surface concentration of the grafted carboxylate groups. This is a promising perspective for controlled modification of substrates of technological relevance.

Complexes of uranium with β-diketonates were extensively studied because of their importance in the processes of solvent extraction and separation of uranium[117]. Uranyl(VI) complexes are active materials of the uranium redox-flow battery, where high solubility in an aprotic solvent is required[197]. $UO_2(dik)_2dmso$ (dik = acac, tfac, hfac) complexes are used for uranium extraction into a $^{SC}CO_2$ phase[198]. This group of ligands was found to be the most efficient for extraction of uranyl and lanthanide ions from radioactive wastes. The solubility of these compounds is related to the number of CO_2 molecules associated with metal chelate complexes and a temperature-dependent constant, C, in the correlation $\ln S = k\ln\rho + C$, where S is the solubility ($g\,L^{-1}$), k is the number of CO_2 molecules associated with the metal chelate ν and ρ is the density of $^{SC}CO_2$ ($g\,L^{-1}$). The C values are found for the UO_2 complexes to be in the order acac > tfac > hfac, which is opposite to the solubility of the corresponding complexes. Chemical shifts of CO_2 in ^{13}C NMR spectra of $^{SC}CO_2$ containing a β-diketone are found to be displaced to lower fields relative to neat $^{SC}CO_2$. The $\Delta\delta_C$ values decrease in the order Htfac > Hhfac > Hacac, suggesting that interaction with CO_2 and β-diketonate decrease from tfac to acac. This is the main interaction that characterizes the solubility of uranyl complexes. ^1H and ^{19}F NMR spectra for CH, CH_3 and CF_3 groups of β-diketonato ligands show that shifting tendency is due to the difference in strength of the van der Waals interaction between $^{SC}CO_2$ and specific sites of the β-diketonate. This interaction is stronger for CF_3 than for CH and CH_3. It is generally recommended to use the more soluble fluorine-containing UO_2 complexes.

Novel Zr, Hf, Y and Cu 2,7,7-trimethyl-3,5-octanedionates (tod) were used as precursors for the deposition of oxide films and compared with conventional dpm precursors[199]. Monoclinic ZrO_2, HfO_2 and cubic yttria-stabilized HfO_2 films were deposited by pulsed liquid injection MOCVD on sapphire and silicon substrates. Films on sapphire lead to significantly higher growth rates at lower temperatures and give smoother films containing less carbon compared to the $M(tod)_4$ type being more attractive for MOCVD applications. Higly fluorinated $Cu(hfac)_2$ and $Cu(tdf)_2$ (tdf = n-PrfC(O)CH=C(O^-)Prf-n) have been investigated as potential precursors for MOCVD of copper[200–204] due to their high volatility. The hfac ligand has become a common building block in MOCVD precursor design, in spite of the limitations associated with its restricted functionality and the potential for fluorine contamination of the thin film[205].

Silicon-containing β-diketonate anions (**14**) provides an attractive, novel approach to modification of the thermal stability and volatility of Cu(II) MOCVD precursors based on β-diketonato ligands[206]. Multinuclear NMR studies suggest that the sila-β-diketons exist as the enolic tautomer with a C=C−Si structure.

β-Diketonates are used as model systems for syntheses and calculations because of their similarity to the active sites of metalloproteins, where metal ions are coordinated to nitrogen, oxygen and sulfur atoms of amino acid residues[207]. Heavy metal complexes are efficient phosphors in organic light-emitting diodes (OLEDs) and have attracted much

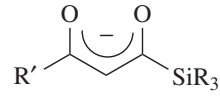

(**14**) R′ = Me, Et, *n*-Pr, *i*-Pr, *n*-Bu, *i*-Bu, *s*-Bu, *t*-Bu,
SiR_3 = $SiMe_3$, $SiEt_3$, $SiMe_2$Bu-*t*, $SiMe_2$Hex-*t*, Si(Pr-*i*)$_3$

attention due to the strong spin–orbit coupling by the metal ions[208]. This results in efficient intersystem crossing from the singlet to triplet excited states, enabling utilization of both[209]. Especially, iridium(III) complexes with cyclometalated ligands show intense phosphorescence at room temperature and this behavior is very promising for application as phosphor dyes in OLEDs[210]. Ir(III), Pt(II), Ru(II) and Os(II) complexes are the major triplet emitters that have been studied for application in OLEDs[149]. Ir(III) complexes were found to be superior to the other metal complexes due to the relatively short lifetime of their triplet state.

Homoleptic Ir($F_n$ppy)$_3$ (**15**, $n = 3$, X = H; $n = 4$, X = F) and heteroleptic ($F_n$ppy)$_2$Ir (acac) complexes (**16**, $n = 3$, X = H; $n = 4$, X = F) complexes[211] were shown as the most challenging materials for high emission and good stability for highly efficient OLEDS. Due to the presence of fluoro substituents the HOMO energy is decreased and, consequently, the HOMO–LUMO gap will shift the emission to a higher frequency. All complexes exhibit broad emissions in the 'light blue' region. Replacement of one $F_n$ppy ligand with acac shifts the emission of the complexes bathochromically by *ca* 10 nm regardless of the number of fluorine atoms. The triplet level of the acac ligand lies above the phenylpyridine levels, therefore acac perturbs the HOMO or LUMO but it is not directly involved in the luminescence. The disturbing nature of the acac ligand is due to shifting of the *d*-orbitals of the metal ion. The decrease of oxidation potential of complexes **16** is due to the lower back-bonding nature of the acac ligand *vs*. the fluorinated phenylpyridine carbanion ligands.

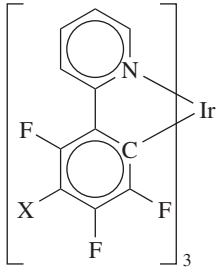

(**15**) X = H, F

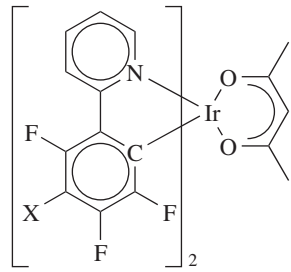

(**16**) X = H, F

The novel luminescent metalapyrrole platinum(II) complexes **5**[212] (Section IV) have coordinated acac and dpm beside styrylphenylpyridine carbanions and have found potential application in the conversion of light to chemical energy–artificial photosynthesis, OLEDs and biological labels.

Metal(III) acetylacetonates can be used to assemble organic monolayers on the surface of porous H-capped silicon (PS), that will generally improve its electric, optical and magnetic characteristics and therefore increase its range of potential application[213]. The proposed mechanism of adsorption consists of a couple of steps that include production of an acetylacetonato free radical that attacks an Si–H bond, yielding a silicon free

radical; in the second step, the silicon free radical is available to bind to a carbon of $M(acac)_3$ and an acetylacetonato free radical is regenerated to propagate the adsorption. As an intermediate, a $M(acac)O_2$ peroxide layer is formed which is unstable and easily polymerizes to a structure with M(acac)−O units (Scheme 3). Domains of different sizes were observed and show that the surfaces covered by Mn and Fe acetylacetonates are crystal-like with sharp edges and are much larger than Co and Ni acetylacetonate surfaces.

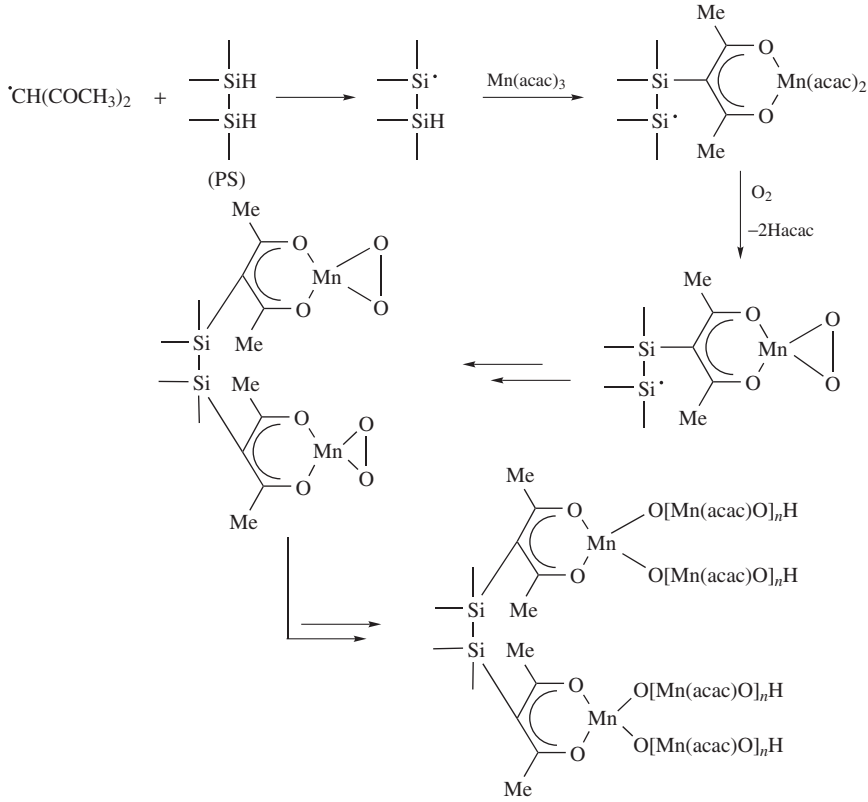

SCHEME 3. Proposed reaction mechanism for the chemisorption of $Mn(acac)_3$ on H-end-capped porous silicon (Si atoms on the surface carry an H). Reproduced with permission from Reference 213

Enolate ions are known as key intermediates in numerous transformations including Michael and aldol additions, alkylation, protonation and acylation. A remarkable reactive Mg enolate[214] intermediate (**17**) of the aldol addition of methyl mesityl ketone has been identified, containing four metal centers, eight enolato ligands of which six are bridging and two are terminally bonded, as well as two unenolized ketones. The linearity of the metal ions in the tetranuclear complex represents a new structural motif in Mg coordination chemistry. The central Mg_2O_2 ring is planar, whereas the two terminal rings are buckled, deviating from the main plane.

Homopolynuclear copper acetylacetonate complexes containing phen or bipy bridges[77] play an important role in sustaining supramolecular solid-state architectures. A group of

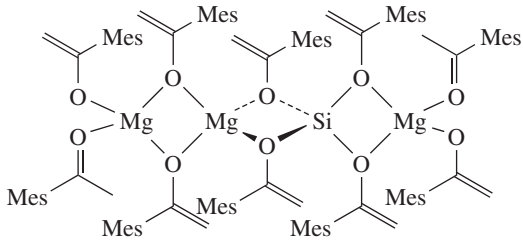

(**17**)

manganese(III) complexes with 1,5-bis(2-hydroxyanil)pentane-2,4-dionate was characterized as homogeneous and encapsulated into the nanocavity of the faujasite zeolites[215]. One advantage of encapsulation is the absence of major irreversible catalyst deactivation.

IX. ACKNOWLEDGMENTS

Dr. Ksenija Babić-Samardžija wishes to express her gratitude to the late Distinguished Professor Emeritus Norman Hackerman of Rice University for his assistance and encouragement during the preparation of this work. Dr. Sofija P. Sovilj thanks the Ministry of Science of the Republic of Serbia for its support of this work (Project 142028).

X. REFERENCES

1. R. C. Mehrotra, R. Bohra and D. P. Gaur, *Metal β-Diketones and Allied Derivatives*, Academic Press, New York, 1978.
2. M. D. Brickhouse and R. R. Squires, *J. Phys. Org. Chem.*, **2**, 389 (1989).
3. W. Caminati and J.-U. Grabow, *J. Am. Chem. Soc.*, **128**, 854 (2006).
4. G. A. Slough, R. G. Bergman and C. H. Heathcock, *J. Am. Chem. Soc.*, **111**, 938 (1989).
5. D. A. Culkin and J. F. Hartwig, *J. Am. Chem. Soc.*, **123**, 5816 (2001).
6. J. G. Stack, J. J. Doney, R. G. Bergman and C. H. Heathcock, *Organometallics*, **9**, 453 (1990).
7. P. Veya, R. G. Gozzi, C. Floriani, F. P. Rotzinger, A. Chiesi-Villa and C. Rizzoli, *Organometallics*, **14**, 4101 (1995).
8. E. R. Burkhardt, R. G. Bergman and C. H. Heathcock, *Organometallics*, **9**, 30 (1990).
9. E. R. Burkhardt, J. J. Doney, R. G. Bergman and C. H. Heathcock, *J. Am. Chem. Soc.*, **109**, 2022 (1987).
10. J. F. Hartwig, R. A. Andersen and R. G. Bergman, *J. Am. Chem. Soc.*, **112**, 5670 (1990).
11. J. F. Hartwig, R. G. Bergman and R. A. Andersen, *Organometallics*, **10**, 3344 (1991).
12. J. F. Hartwig, R. G. Bergman and R. A. Andersen, *Organometallics*, **10**, 3326 (1991).
13. P. Dotta, R. G. A. Kumar, P. S. Pregosin, A. Albinati and S. Rizzato, *Organometallics*, **22**, 5345 (2003).
14. P. Veya, R. G. Gozzi, C. Floriani, F. P. Rotzinger, A. Chiesi-Villa and C. Rizzoli, *Organometallics*, **12**, 489 (1993).
15. N. V. Belova, G. V. Girichev, S. A. Shlykov and H. Oberhammer, *J. Org. Chem.*, **71**, 5298 (2006).
16. J. Cámpora, C. M. Maya, P. Palma, E. Carmona, E. Gutiérrez, C. Ruiz, C. Graff and A. Tiripicchio, *Chem. Eur. J.*, **11**, 6889 (2005).
17. D. A. Thornton, *Coord. Chem. Rev.*, **104**, 173 (1990).
18. R. D. Hancock and D. A. Thornton, *Theor. Chim. Acta*, **18**, 67 (1970).
19. T. Yamazaki and T. Kitazume, *Enantiocontrolled Synthesis of Fluoro-Organic Compounds: Stereochemical Challenges and Biomedical Targets*, John Wiley & Sons, Ltd, Chichester, 1999, pp. 575–600.

20. H. Sato, T. Taniguchi, K. Monde, S.-I. Nishimura and A. Yamagishi, *Chem. Lett.*, **35**, 364 (2006).
21. S. N. Slabzhennikov, O. B. Ryabchenko and L. A. Kuarton, *Russ. J. Coord. Chem.*, **32**, 545 (2006).
22. K. Nakamoto and A. E. Martell, *J. Chem. Phys.*, **32**, 588 (1960).
23. R. D. Hancock and D. A. Thornton, *J. S. Afr. Chem. Inst.*, **23**, 71 (1970).
24. S. Winter, E. Weber, L. Eriksson and I. Csöregh, *New J. Chem.*, **30**, 1808 (2006).
25. N. V. Belova, G. V. Girichev, S. L. Hinchley, N. P. Kuzmina, D. W. H. Rankin and I. G. Zaitzeva, *J. Mol. Struct.*, **779**, 23 (2005).
26. T. J. Anderson, M. A. Neuman and G. A. Melson, *Inorg. Chem.*, **12**, 927 (1973).
27. Yu. S. Ezhov, S. A. Komarov and V. G. Sevast'yanov, *Zh. Strukt. Khim.*, **39**, 633 (1998); *Chem. Abstr.*, **131**, 87991 (1999).
28. D. Kepert, *Inorganic Stereochemistry* (Russian transl.), Mir, Moscow, 1985.
29. N. V. Belova, N. I. Giricheva, G. V. Girichev, S. A. Shlykov, N. V. Tverdova, N. P. Kuz'mina and I. G. Zaitseva, *J. Struct. Chem.*, **43**, 56 (2002).
30. D. W. Bennett, T. A. Siddiquee, D. T. Haworth and S. V. Lindeman, *J. Chem. Crystallogr.*, **37**, 207 (2007).
31. V. V. Sliznev, S. B. Lapshina and G. V. Girichev, *Abstracts of the IIIrd Fock Conference in Quantum and Computational Chemistry*, Nizhniy Novgorod, 2001, pp. 128–129.
32. I. Díaz-Acosta, J. Baker, W. Cordes and P. Pulay, *J. Phys. Chem. A*, **105**, 238 (2001).
33. N. V. Belova, N. I. Giricheva, G. V. Girichev, S. A. Shlykov, N. V. Tverdova, N. P. Kuz'mina and I. G. Zaitseva, *J. Struct. Chem.*, **43**, 925 (2002).
34. A. Gleizes, S. Sans-Lenain, D. Medus, N. Hovnanian, P. Miele and J.-D. Foulon, *Inorg. Chim. Acta*, **209**, 47 (1993).
35. F. Labrize, L. G. Hubert-Pfalzgraf, J. Vaissermann and C. B. Knobler, *Polyhedron*, **15**, 577 (1996).
36. S. N. Brown, E. T. Chu, M. W. Hull and B. C. Noll, *J. Am. Chem. Soc.*, **127**, 16010 (2005).
37. E. Dubler, R. Buschmann and H. W. Schemalle, *J. Inorg. Biochem.*, **95**, 97 (2003).
38. B. K. Keppler, C. Friesen, H. G. Moritz, H. Vongerichten and E. Vogel, *Struct. Bond.*, **78**, 97 (1991).
39. F. Schmidt, *Angew. Chem.*, **64**, 536 (1952).
40. A. Yamamoto and S. Kambara, *J. Am. Chem. Soc.*, **79**, 4344 (1957).
41. D. C. Bradley and C. E. Holloway, *J. Chem. Soc. A*, 282 (1969).
42. G. D. Smith, C. N. Caughlan and J. A. Campbell, *Inorg. Chem.*, **11**, 2989 (1972).
43. F. Caruso, L. Massa, A. Gindulyte, C. Pettinari, F. Marchetti, R. Pettinari, M. Ricciutelli, J. Costamagna, J. C. Canales, J. Tanski and M. Rossi, *Eur. J. Inorg. Chem.*, 3221 (2003).
44. S. J. Kavitha, K. Panchanatheswaran, M. R. J. Elsegood and S. H. Dale, *Inorg. Chim. Acta*, **359**, 1314 (2006).
45. R. P. Dodge, D. H. Templeton and A. Zalkin, *J. Chem. Phys.*, **35**, 55 (1961).
46. P. K. Hon, R. L. Belford and C. E. Pfluger, *J. Am. Chem. Soc.*, **43**, 1323, 3111 (1965).
47. C. Furlani, *Coord. Chem. Rev.*, **3**, 141 (1968).
48. J. Selbin, *Coord. Chem. Rev.*, **1**, 293 (1966).
49. E. Garribba, G. Micera and D. Sanna, *Inorg. Chim. Acta*, **359**, 4470 (2006).
50. I. Díaz-Acosta, J. Baker, J. F. Hinton and P. Pulay, *Spectrochim. Acta A*, **59**, 363 (2003).
51. Y. Furuno, H. Sato, J. Yoshida, N. Hoshino, Y. Fukuda and A. Yamagishi, *J. Phys. Chem. B*, **111**, 521 (2007).
52. Y. Sui, X. Fang, R. Hu, Y. Xu, X. Zhou and X. Fu, *Mater. Lett.*, **61**, 1354 (2007).
53. S. Cakić, E. Lačnjevac, G. Nikolić, J. Stamenković, M. B. Rajković, M. Gligorić and M. Barac, *Sensors*, **6**, 1708 (2006).
54. F. A. Hartman, M. Kilner and A. Wojcicki, *Inrog. Chem.*, **6**, 34 (1967).
55. P. J. Parker and A. Wojcicki, *Inorg. Chim. Acta*, **11**, 9 (1974).
56. R. van Gorkum, F. Buda, H. Koojman, A. L. Spek, E. Bouwman and J. Reedijk, *Eur. J. Inorg. Chem.*, 2255 (2005).
57. H. Zhou and A. Lachgar, *Cryst. Growth Des.*, **6**, 2384 (2006).
58. A. Antinolo, F. Carrillo-Hermosilla, J. Fernández-Baeza, S. García-Yuste, A. Otero, E. Palomares, A. M. Rodríguez and L. F. Sánchez-Barba, *J. Organomet. Chem.*, **603**, 194 (2000).
59. H. Le Bozec and P. H. Dixneuf, *Russ. Chem. Bull.*, **44**, 801 (1995).

60. L. Jafarpour, J. Huang, E. D. Stevens and S. P. Nolan, *Organometallics*, **18**, 3760 (1999).
61. V. Cadierno, M. P. Gamasa, J. Gimeno, M. González-Cueva, E. Lastra, J. Borge, S. García-Granda and E. Pérez-Carreño, *Organometallics*, **15**, 2137 (1996).
62. M. Fabre, J. Jaud, M. Hliwa, J.-P. Launay and J. Bonvoisin, *Inorg. Chem.*, **45**, 9332 (2006).
63. S. P. Sovilj, K. Babić-Samardžija and D. Stojšić, *Spectrosc. Lett.*, **36**, 183 (2003).
64. M. J. Seco, *Chem. Educ.*, **66**, 779 (1989).
65. L. Yang, W. Jin and J. Lin, *Polyhedron*, **19**, 93 (2000).
66. S. J. Eng, R. J. Motekaitis and A. E. Martell, *Inorg. Chim. Acta*, **278**, 170 (1998).
67. K. Babić-Samardžija, S. P. Sovilj and N. Katsaros, *J. Mol. Struct.*, **694**, 165 (2004).
68. L. Chen, C. Yang, J. Qin, J. Gao, H. You and D. Ma, *J. Organomet. Chem.*, **691** 3519 (2006).
69. M. Kujime, S. Hikichi and M. Akita, *Inorg. Chim. Acta*, **350**, 163 (2003).
70. A. A. Soliman, A. Taha and W. Linert, *Spectrochim. Acta, Part A*, **64**, 1058 (2006).
71. D. P. Gardon and K. B. Heng, *Aust. J. Chem.*, **24**, 1059 (1971).
72. K. Nakamoto, *Infrared and Raman Spectra of Inorganic and Coordination Compounds*, 4th edn, Wiley, New York, 1986.
73. W.-S. Sim, T.-C. Li, P.-X. Yang and B.-S. Yeo, *J. Am. Chem. Soc.*, **124**, 4970 (2002).
74. X. Tian, R. Goddard and K.-R. Pörschke, *Organometallics*, **25**, 5854 (2006).
75. H. Raissi, A. R. Nowroozi, F. Farzad and M. S. Hosseini Bojd, *Spectrochim. Acta, Part A*, **62**, 343 (2005).
76. J. P. Fackler, *Prog. Inorg. Chem.*, **7**, 361 (1966).
77. A. M. Madalan, M. Noltemeyer, M. Neculai, H. W. Roesky, M. Schmidtmann, A. Müller, Y. Journaux and M. Andruh, *Inorg. Chim. Acta*, **359**, 459 (2006).
78. A. M. Madalan, C. Ruiz-Pérez, V. Kravtsov, Y. A. Simonov and M. Andruh, *Rev. Roum. Chim.*, **50**, 11 (2005).
79. L. N. Mazalov, S. V. Trubina, G. K. Parygina, I. M. Oglezneva, E. A. Aseeva, N. V. Brenner, E. Yu. Fursova and V. I. Ovcharenko, *J. Struct. Chem.*, **47**, 558 (2006).
80. G. A. Petrakovskii, A. M. Vorotynov, D. A. Velikanov, Ya. G. Shiyan, V. I. Ovcharenko, V. N. Ikorskii, G. V. Romanenko, E. Yu. Fursova and R. Szimczak, *J. Struct. Chem.*, **47**, 447 (2006).
81. B. Sarkar, M. S. Ray, M. G. B. Drew, A. Figuerola, C. Díaz and A. Ghosh, *Polyhedron*, **25**, 3084 (2006).
82. R. L. Belford, A. E. Martell and M. Calvin, *J. Inorg. Nucl. Chem.*, **2**, 11 (1956).
83. H. Koyama, Y. Saito and K. Kuroya, *J. Inst. Polytech., Osaka City Univ.*, **C4**, 43 (1953).
84. F. A. Cotton and J. J. Wise, *Inorg. Chem.*, **5**, 1200 (1966).
85. H. Montgomery and E. C. Lingafelter, *Acta Crystallogr.*, **17**, 1481 (1964).
86. H. Sonohara, S. Takata and H. Sato, *Jpn. J. Appl. Phys.*, **33**, L743 (1994).
87. L. M. Shkolnikova and E. A. Shugam, *Zh. Strukt. Khim.*, **2**, 72 (1961); *Chem. Abstr.*, **55**, 122303 (1961).
88. A. Camerman, D. Mastropalo and N. Camerman, *J. Am. Chem. Soc.*, **105**, 1584 (1983).
89. S. F. Tayyari, H. Raissi, F. Milani-Nejad and I. S. Butler, *Vib. Spectrosc.*, **26**, 187 (2001).
90. S. F. Tayyari and F. Milani-Nejad, *Spectrochim. Acta*, **56**, 2679 (2000).
91. S. F. Tayyari, H. Raissi and F. Tayyari, *Spectrochim. Acta*, **58A**, 1681 (2002).
92. H. Raissi, S. F. Tayyari and F. Tayyari, *J. Mol. Struct.*, **613**, 195 (2002).
93. S. F. Tayyari, Th. Zeegers-Huyskens and J. L. Wood, *Spectrochim. Acta*, **35A**, 1265 (1979).
94. S. F. Tayyari and F. Milani-Nejad, *Spectrochim. Acta*, **56**, 2679 (2000).
95. S. Pinchas, B. L. Silver and I. Laulicht, *J. Chem. Phys.*, **46**, 1506 (1967).
96. S. Pinchas and J. Shamir, *J. Chem. Soc., Perkin Trans. 2*, 1098 (1974).
97. M. L. Hlavinka and J. R. Hagadorn, *Organometallics*, **25**, 3501 (2006).
98. J. M. H. Lo and M. Klobukowski, *Inorg. Chim. Acta*, **353**, 15 (2003).
99. R. L. Belford, A. E. Martell and M. Calvin, *J. Inorg. Nucl. Chem.*, **2**, 11 (1956).
100. D. Shirotani, T. Suzuki and S. Kaizaki, *Inorg. Chem.*, **45**, 6111 (2006).
101. M. Cantuel, F. Gumy, J.-C. G. Bünzli and C. Piguet, *Dalton Trans.*, 2647 (2006).
102. N. I. Giricheva, N. V. Belova, S. A. Shlykov, G. V. Girichev, N. Vogt, N. V. Tverdova and J. Vogt, *J. Mol. Struct.*, **605**, 171 (2002).
103. D. L. Kepert, *Inorganic Stereochemistry*, Springer-Verlag, Berlin–Heidelberg–New York, 1982.
104. N. V. Belova, G. V. Girichev, S. L. Hinchley, N. P. Kuzmina, D. W. H. Rankin and I. G. Zaitzeva, *Dalton Trans.*, 1715 (2004).

105. H. Tsukube, M. Hosokubo, M. Wada, S. Shinoda and H. Tamiaki, *Inorg. Chem.*, **40**, 740 (2001).
106. H. Song, Y. Jiang, C. Xia, G. Meng and D. Peng, *J. Cryst. Growth*, **250**, 423 (2003).
107. C. S. Erasmus and J. C. A. Boeyens, *Acta Crystallogr., Sect. B*, **26**, 1843 (1970).
108. S. Shibata, K. Lijita and T. Inuzuka, *J. Mol. Struct.*, **140**, 65 (1986).
109. J. P. R. De Villiers and J. C. A. Boeyens, *Acta Crystallogr., Sect. B*, **28**, 2335 (1972).
110. T. J. Anderson, M. A. Neuman and G. A. Melson, *Inorg. Chem.*, **12**, 927 (1973).
111. J. Narbutt and J. Krejzler, *Inorg. Chim. Acta*, **286**, 175 (1999).
112. N. I. Giricheva, N. V. Belova, G. V. Girichev, N. V. Tverdova, S. A. Shlykov, N. P. Kuz'mina and I. G. Zaitseva, *J. Struct. Chem.*, **44**, 771 (2003).
113. N. V. Belova, N. I. Giricheva, G. V. Girichev, S. A. Shlykov, N. V. Tverdova, N. P. Kuz'mina and I. G. Zaitseva, *Zh. Strukt. Khim.*, **43**, 1001 (2002); *Chem. Abstr.*, **139**, 297265 (2003).
114. M. Morissette, S. Haufe, R. McDonald, G. M. Ferrence and J. Takats, *Polyhedron*, **23**, 263 (2004).
115. M. L. Moris and R. L. Hildebrandt, *J. Mol. Struct.*, **53**, 69 (1979).
116. P. T. Brain, M. Buhl, H. E. Robertson, A. D. Jackson, P. D. Lickiss, D. MacKerracher, D. W. H. Rankin, D. Shah and W. Thiel, *J. Chem. Soc., Dalton Trans.*, 545 (1998).
117. K. Umeda, J. Zukerman-Schpector and P. C. Isolani, *Polyhedron*, **25**, 2447 (2006).
118. Y. Kachi, T. Tsukahara, Y. Kayaki, T. Ikariya, J. Sato and Y. Ikeda, *J. Supercrit. Fluids*, **40**, 20 (2007).
119. T. Kremer and P. v. R. Schleyer, *Organometallics*, **16**, 737 (1997).
120. N. I. Giricheva, G. V. Girichev, N. V. Belova, N. A. Isakova, N. P. Kuzmina, A. R. Kaul and V. M. Petrov, *J. Struct. Chem.*, **40**, 527 (1999).
121. N. I. Giricheva, N. A. Isakova, N. P. Kuzmina, G. V. Girichev, V. M. Petrov and A. R. Kaul, *Zh. Neorg. Khim.*, **41**, 1523 (1996); *Chem. Abstr.*, **126**, 80270 (1997).
122. N. I. Giricheva, N. A. Isakova, N. P. Kuz'mina, G. V. Girichev, V. M. Petrov and A. R. Kaul', *Zh. Neorg. Khim.*, **41**, 1694 (1996); *Chem. Abstr.*, **126**, 149997 (1997).
123. A. A. Drozdov and S. I. Trojanov, *Polyhedron*, **11**, 2877 (1992).
124. A. Gleises, S. Sans-Lenain, D. Medus and C. R. Hebd., *Séances Acad. Sci. Ser.*, **313**, 761 (1991).
125. D. J. Otway and W. S. Rees Jr, *Coord. Chem. Rev.*, **210**, 279 (2000).
126. N. I. Giricheva, G. V. Girichev, N. V. Belova, N. A. Isakova and N. P. Kuzmina, *J. Struct. Chem.*, **40**, 862 (1999).
127. N. I. Giricheva, N. A. Isakova, G. V. Girichev, V. M. Petrov and N. P. Kuzmina, *Zh. Strukt. Khim.*, **40**, 468 (1999); *Chem. Abstr.*, **132**, 83991 (2000).
128. N. I. Giricheva, G. V. Girichev, N. V. Belova, N. A. Isakova, N. P. Kuzmina, A. R. Kaul and V. M. Petrov, *Zh. Strukt. Khim.*, **40**, 647 (1999); *Chem. Abstr.*, **132**, 113336 (2000).
129. C. L. Perrin and Y.-J. Kim, *Inorg. Chem.*, **39**, 3902 (2000).
130. K. Lyczko, J. Narbutt, B. Paluchowska, J. K. Maurin and I. Persson, *Dalton Trans.*, 3972 (2006).
131. W. J. Evans, D. B. Rego and J. W. Ziller, *Polyhedron*, **25**, 2691 (2006).
132. E. J. Fernández, A. Laguna, J. M. López-de-Lazuriaga, M. Monde, M. Montiel, E. Olmos and J. Pérez, *Organometallics*, **23**, 774 (2004).
133. G. A. Miller and E. O. Schlemper, *Inorg. Chim. Acta*, **30**, 131 (1978).
134. C. A. Téllez, S. E. Hollauer, M. I. Pais da Silva, M. A. Mondragón, I. Haiduc and M. Curtui, *Spectrochim. Acta, Part A*, **57**, 1149 (2001).
135. S. C. Téllez and J. Gómez Lara, *Spectrochim. Acta*, **51A**, 395 (1995).
136. S. C. Téllez and J. Gómez Lara, *Spectrosc. Lett.*, **27**, 209 (1994).
137. V. I. Vovna, I. B. Lvov, Y. V. Ivanov, S. N. Slabzhennikov, A. I. Streltsov and A. Yu. Ustinov, *J. Electron. Spectrosc. Relat. Phenom.*, **96**, 141 (1998).
138. M. Mikami, I. Nakagava and T. Shimanouchi, *Spectrochim. Acta*, **23A**, 1037 (1967).
139. W. Linert, B. Pouresmaeil, V. Gutmann, K. Mafune, Y. Fukuda and K. Sone, *Monatsh. Chem.*, **121**, 765 (1990).
140. K. Heinze and A. Reinhart, *Inorg. Chem.*, **45**, 2695 (2006).
141. S. R. Halper, M. R. Malachowski, H. M. Delaney and S. M. Cohen, *Inorg. Chem.*, **43**, 1242 (2004).

142. A. M. Madalan, C. Ruiz-Perez, V. Kravtsov, Y. A. Simonov and M. Andruh, *Rev. Roum. Chim.*, **50**, 11 (2005).
143. H. A. Hashem and M. S. Refat, *Surf. Rev. Lett.*, **13**, 439 (2006).
144. R. C. Fay and T. S. Piper, *J. Am. Chem. Soc.*, **84**, 2303 (1962).
145. H. Irving and R. J. P. Williams, *J. Chem. Soc.*, 3192 (1953).
146. K. C. Joshi and V. N. Pathak, *Coord. Chem. Rev.*, **22**, 37 (1977).
147. A. A. Dakhel and A. Y. Ali-Mohamed, *J. Phys. Chem. Solids*, **68**, 162 (2007).
148. T. Justel, M. Muller, T. Weyhermuller, C. Kressl, E. Bill, P. Hildebrandt, M. Lengen, M. Grodzicki, A. X. Trautwein, B. Nuber and K. Wieghardt, *Chem. Eur. J.*, **5**, 793 (1999).
149. C.-H. Yang, C.-H. Chen and I.-W. Sun, *Polyhedron*, **25**, 2407 (2006).
150. H.-C. Li, P.-T. Chou, Y.-H. Hu, Y.-M. Cheng and R.-S. Liu, *Organometallics*, **24**, 1329 (2005).
151. T. Liu, B.-H. Xia, X. Zhou, H.-X. Zhang, Q.-J, Pan and J.-S. Gao, *Organometallics*, **26**, 143 (2007).
152. E. A. Juban and J. K. McCusker, *J. Am. Chem. Soc.*, **127**, 6857 (2005).
153. S. C. Brooks, D. J. Vinyard and M. M. Richter, *Inorg. Chim. Acta*, **359**, 4635 (2006).
154. S. Kar, B. Sarkar, S. Ghumaan, D. Janardanan, J. van Slagere, J. Fiedler, V. G. Puranik, R. B. Sunoj, W. Kaim and G. K. Lahiri, *Chem. Eur. J.*, **11**, 4901 (2005).
155. B. Yin, F. Niemeyer, J. A. G. Williams, J. Jiang, A. Boucekkine, L. Toupet, H. Le Bozec and V. Guerchais, *Inorg. Chem.*, **45**, 8584 (2006).
156. Y. Apeloig, I. Zharov, D. Bravo-Zhivotovskii, Y. Ovchinnikov and Y. Struchkov, *J. Organomet. Chem.*, **499**, 73 (1995).
157. P. C. B. Page, S. S. Klair and S. Rosenthal, *Chem. Soc. Rev.*, **19**, 147 (1990).
158. A. G. Brook, M. A. Quigley, G. J. D. Peddle, N. V. Schwartz and C. H. Warner, *J. Am. Chem. Soc.*, **82**, 5102 (1960).
159. B. G. Ramsey, A. G. Brook, A. R. Bassindale and H. Bock, *J. Organomet. Chem.*, **74**, C41 (1974).
160. R. S. Grev and H. F. Schaefer III, *J. Am. Chem. Soc.*, **111**, 6137 (1989).
161. K. K. Banger, A. Kornilov, R. U. Claessen, E. T. Eisenbraun, A. E. Kaloyeros, P. J. Toscano and J. T. Welch, *Inorg. Chem. Commun.*, **4**, 496 (2001).
162. K. K. Banger, S. C. Ngo, S. Higashiya, R. U. Claessen, K. S. Bousman, P. N. Lim, P. J. Toscano and J. T. Welch, *J. Organomet. Chem.*, **678**, 15 (2003).
163. E. A. Juban, A. L. Smeigh, J. E. Monat and J. K. McCusker, *Coord. Chem. Rev.*, **250**, 1783 (2006).
164. G. J. Ferraudi, *Elements of Inorganic Photochemistry*, John Wiley & Sons, Inc., New York, 1988.
165. D. M. Roundhill, *Photochemistry and Photophysics of Metal Complexes*, Plenum Press, New York, 1994.
166. B. Brunschwig and N. Sutin, *J. Am. Chem. Soc.*, **100**, 7568 (1978).
167. J. K. McCusker, *Acc. Chem. Res.*, **36**, 876 (2003).
168. A. Vlček, *Coord. Chem. Rev.*, **200–202**, 933 (2000).
169. P. Szczecinski, A. Gryff-Keller and S. Molchanov, *J. Org. Chem.*, **71**, 4636 (2006).
170. E. Hevia, K. W. Henderson, A. R. Kennedy and R. E. Mulvey, *Organometallics*, **25**, 1778 (2006).
171. R. H. Holm and F. A. Cotton, *J. Am. Chem. Soc.*, **80**, 5658 (1958).
172. J. A. S. Smith and J. D. Thwaites, *Discuss. Faraday Soc.*, **34**, 143 (1962).
173. K. Nakamoto, P. J. McCarthy, A. Ruby and A. E. Martell, *J. Am. Chem. Soc.*, **83**, 1066 (1961).
174. T. Suzuki, K. Fujiiwara, H. D. Takagi and K. Kashiwabara, *Dalton Trans.*, 308 (2007).
175. M. Rikkou, M. Manos, E. Tolis, M. P. Sigalas, T. A. Kabanos and A. D. Keramidas, *Inorg. Chem.*, **42**, 4640 (2003).
176. Y. H. Xing, Z. Sun, W. Zou, J. Song, K. Aoki and M. F. Ge, *J. Struct. Chem.*, **47**, 913 (2006).
177. D. B. Kimball, R. Michalczyk, E. Moody, M. Ollivault-Shiflett, K. De Jesus and L. A. "Pete" Silks, III, *J. Am. Chem. Soc.*, **125**, 14666 (2003).
178. K. Kobayashi, M. Kawanisi, T. Hitomi and S. Kozima, *Chem. Lett.*, 497 (1984).
179. F. H. Allen, *Acta Crystallogr., Sect. B*, **58**, 380 (2002).
180. S. Shibata, S. Onuma and H. Inoue, *Inorg. Chem.*, **24**, 1723 (1985).

181. E. I. Stiefel, R. Eisenberg, R. C. Rosenberg and H. B. Gray, *J. Am. Chem. Soc.*, **88**, 2956 (1966).
182. R. D. Dowsing, J. F. Gibson, D. M. Goodgame, M. Goodgame and P. J. Hayward, *Nature*, **219**, 1037 (1968).
183. F. Neese, *Int. J. Quantum Chem.*, **83**, 104 (2001).
184. C. L. Kwan and J. K. Kochi, *J. Am. Chem. Soc.*, **98**, 4903 (1976).
185. V. Manivannan, J. T. Hffman, V. L. Dimayuga, T. Dwight and C. J. Carrano, *Inorg. Chim. Acta*, **360**, 529 (2007).
186. C. J. Ballhausen and H. B. Gray, *Inorg. Chem.*, **1**, 111 (1972).
187. J. A. Weil, J. R. Bolton and J. E. Wertz, *Electron Paramagnetic Resonance: Elementary Theory and Practical Applications*, Wiley-Interscience, New York, 1994.
188. J. P. Fackler, Jr., *Prog. Inorg. Chem.*, **7**, 361 (1966).
189. H. E. Zaugg and A. D. Schaefer, *J. Am. Chem. Soc.*, **87**, 1857 (1965).
190. R. E. Dessy and L. A. Bares, *Acc. Chem. Res.*, **5**, 415 (1972).
191. N. Hirota, in *Radical Ions* (Eds E. T. Kalser and C. Kevan), Interscience, New York, 1968, p. 35.
192. T. Surig and H.-F. Grutzmacher, *Org. Mass Spectrosc.*, **25**, 446 (1990).
193. G. V. Girichev, N. V. Belova, S. A. Shlykov, N. I. Giricheva, N. P. Kuz'mina, I. G. Zaitseva, T. N. Strenalyuk and I. E. Galanin, *Russ. J. Inorg. Chem.*, **46**, 1711 (2001).
194. G. V. Girichev, N. V. Belova, S. A. Shlykov, N. I. Giricheva, N. P. Kuz'mina, I. G. Zaitseva, T. N. Strenalyuk and I. E. Galanin, *Russ. J. Inorg. Chem.*, **48**, 556 (2003).
195. S. Kawaguchi, *Coord. Chem. Rev.*, **70**, 51 (1986).
196. G. G. Condorelli, A. Motta, C. Bedoya, A. Di Mauro, G. Pellegrino and E. Smecca, *Inorg. Chim. Acta*, **360**, 170 (2007).
197. K. Shirasaki, T. Yamamura and Y. Shiokawa, *J. Alloys Compd.*, **408–412**, 1296 (2006).
198. T. Tsukahara, Y. Kachi, Y. Kayaki, T. Ikariya and Y. Ikeda, *J. Supercrit. Fluids*, **39**, 6 (2006).
199. S. V. Pasko, L. G. Hubert-Pfalzgraf, A. Abrutis, P. Richard, A. Bartasyte and V. Kazlauskiene, *J. Mater. Chem.*, **14**, 1245 (2004).
200. P. Doppelt, *Coord. Chem. Rev.*, **178–180**, 1785 (1998).
201. R. E. Sievers and J. E. Sadlowski, *Science*, **201**, 217 (1978).
202. B. D. Fahlman and A. R. Barron, *Adv. Mater. Opt. Electron.*, **10**, 223 (2000).
203. P. Mushak, M. T. Glenn and J. Savory, *Fluorine Chem. Rev.*, **6**, 43 (1973).
204. K. I. Pashkevich, V. I. Saloutin and I. Y. Postovskii, *Russ. Chem. Rev.*, **50**, 180 (1981).
205. M. L. Hitchman, S. H. Shamlian, D. D. Gilliland, D. J. Cole-Hamilton, J. A. P. Nash, S. C. Thompson and S. L. Cook, *J. Mater. Chem.*, **5**, 47 (1995).
206. K. K. Banger, S. C. Ngo, S. Higashiya, R. U. Claessen, K. S. Bousman, P. N. Lim, P. J. Toscano and J. T. Welch, *J. Organomet. Chem.*, **678**, 15 (2003).
207. J. M. H. Lo and M. Klobukowski, *Inorg, Chim. Acta*, **353**, 15 (2003).
208. L. Chen, C. Yang, J. Qin, J. Gao, H. You and D. Ma, *J. Organomet. Chem.*, **691**, 3519 (2006).
209. S. Lamansky, P. Djurovich, D. Murphy, F. Abdel-Razzaq, R. Kwong, I. Tsyba, M. Bortz, B. Mui, R. Bau and M. E. Thompson, *Inorg. Chem.*, **40**, 1704 (2001).
210. W. Chien, A. T. Hu, J. Duan, D. K. Raybarapu and C. Chien, *J. Organomet. Chem.*, **689**, 4882 (2004).
211. R. Ragni, E. A. Plummer, K. Brunner, J. W. Hofstraat, F. Babudri, G. M. Farinola, F. Naso and L. De Cola, *J. Mater. Chem.*, **16**, 1161 (2006).
212. B. Yin, F. Niemeyer, J. A. G. Williams, J. Jiang, A. Boucekkine, L. Toupet, H. Le Bozec and V. Guerchais, *Inorg. Chem.*, **45**, 8584 (2006).
213. J. Chao, H.-T. Wang, B. Xia, H.-B. Liu, Z.-D. Xiao and S.-J. Xiao, *J. Phys. Chem. B*, **110**, 24565 (2006).
214. J. F. Allan, K. W. Henderson, A. R. Kennedy and S. J. Teat, *Chem. Commun.*, 1059 (2000).
215. M. Salavati-Niasari, *Microporous Mesoporous Mater.*, **95**, 248 (2006).

CHAPTER 3

Luminescence phenomena involving metal enolates

HERMI FELINTO BRITO

Department of Fundamental Chemistry, University of São Paulo, São Paulo-SP, 05508-000, Brazil
Fax: +55-11-3815-5579; e-mail: hefbrito@iq.usp.br

OSCAR MANOEL LOUREIRO MALTA

Department of Fundamental Chemistry, Federal University of Pernambuco, CCEN Cidade Universitária, Recife-PE, 50670-901, Brazil
Fax: +55-81-21268442; e-mail: oscar@renami.com.br

MARIA CLAUDIA FRANÇA CUNHA FELINTO

Institute of Nuclear Energy and Research, Av. Prof Lineu Prestes 2242 Cidade Universitária, São Paulo-SP. 05508-000, Brazil
Fax: +55-11-3133-9249; e-mail: mfelinto@ipen.br

and

ERCULES EPAMINONDAS DE SOUSA TEOTONIO

Department of Chemistry, Federal University of Goiás, Av. Dr. Lamartine P. de Avelar, 1120, Catalão-GO, 75704-020, Brazil
Fax: +55-64-3441-1500; e-mail: ercteot@gmail.com

The chemistry of metal enolates
Edited by Jacob Zabicky

I. ABBREVIATIONS

aap	4-aminoantipyrine
acac	acetylacetonate
aind	2-acetyl-1,3-indandionate
Alq_3	tris(8-hydroxyquinoline)aluminum
anl	acetanilide
atfa	9-antroyltriflusoroacetonate
azt	3′-azidothymidine (zidovudine)
bath	4,7-diphenyl-1,10-phenanthroline (bathophenanthroline)
bbind	2-(4-bromobenzoyl)-1,3-indandionate
bbpo	2-(4-biphenyl)-5-(4-*t*-butylphenyl)-1,3,4-oxadiazole
bcp	2,9-dimethyl-4,7-diphenyl-1,10-phenylanthroline (bathocuproin)
bind	2-benzyl-1,3-indandionate
bipy	2,2-bipyridine
bt	2-(2-benzotiazolyl-$\kappa N3$)phenyl-κC
bta	bis(trimethylsilyl)acetylene
btfa	benzoyltrifluoroacetonate
btfmp	2-benzo[*b*]thiophen-2-yl-5-trifluoromethyl-pyridine
btp	2-(2-benzo[*b*]thienyl)pyridinato
bza	benzamide
bzac	benzoylacetonate

cbind	2-(4-chlorobenzoyl)-1,3-indandionate
cbp	4,4′-*N*,*N*′-dicarbazolylbiphenyl
CIE	Commission International de l'Eclairage
Cupc	copper phthalocyanine
dbm	dibenzoylmethanate
dbq	dibenzo[*f*,*h*]-quinoxaline
dbso	dibenzyl sulfoxide
dcm	[2-[2-[4-(dimethylamino)phenyl]ethenyl]-4*H*-pyran-4-ylidene] propanedinitrile
dfpp	2-(2,4-difluorophenyl)pyridine
dgeba	diglycidyl ether of bisphenol-A
dia	4,5-diazafluoren-9-one
dmac	*N*,*N*-dimethylacetamide
dmbp	4,4′-dimethyl-2,2'-bipyridine
dmbpy	4,4′-dimethoxy-2,2'-bipyridine
dmbz	*N*,*N*-dimethylbenzamide
dmfa	*N*,*N*-dimethylformamide
dmpy	dimethylpyridine
dmso	dimethyl sulfoxide
dnm	dinaphthoylmethanate
dpac	*N*,*N*-diphenylacetamide
dpfa	diphenylformamide
dpi	1,4-diphenylimidazole
dpm	dipivaloylmethanate
dpso	diphenyl sulfoxide
DU600	diureasil organic–inorganic hybrid
EL	electroluminescence
EP	eletrophosphorescence
ET	energy transfer
ETL	electron transport layer
facam	3-(trifluoroacetyl)-*d*-camphor
fnapy4	4-trifluoromethyl-2-(1-naphthyl)pyridine
fnapy5	5-trifluoromethyl-2-(1-naphthyl)pyridine
fod	6,6,7,7,8,8,8-heptafluoro-2,2-dimethyl-3,5-octanedionato
hcpybm	9-[6-[2-(2-pyridinyl)-1*H*-benzimidazol-1-yl]hexyl]-9*H*-carbazole
hfa	hexafluoroacetylacetonate
hfnh	4,4,5,5,6,6,6-heptafluoro-1-(2-naphthyl)hexane-1,3-dione
hfth	4,4,5,5,6,6,6-heptafluoro-1-(2-thienyl)-1,3-hexanedione
HTL	hole transport layer
IC	internal conversion
ISC	intersystem crossing
isovind	2-*i*-valeryl-1,3-indandionate
ito	indium tin oxide
LMCT	ligand-to-metal charge transfer
mbind	2-(4-metylbenzoyl)-1,3-indandionate
mk	4,4′-bis(*N*,*N*-dimethylaminobenzophenone)
mtcd	1-(3-methylphenyl)-1,2,3,4-tetrahydroquinoline-6-carboxyaldehyde diphenylhydrazone
napy	2-(1-naphthyl)pyridine
nind	2- anthracyl-1,3-indandionate
nphen	5-nitro-1,10-phenanthroline
ntfa1	1-naphthoyltrifluoroacetone

ntfa2	2-naphthoyltrifluoroacetone
OLED	organic light emitting device
pbi	3-phenyl-4-benzoyl-5-*i*-oxazolone
pc	polycarbonate
pCNmhp	poly[2-(6-cyano-6-methyl-heptyloxy)-1,4-phenylene]
pedot	3,4-polyethylene-dioxythiophene-polystyrene sulfonate
pha	*N*-phenylacetamide
phen	1,10-phenanthroline
phenNO	1,10-phenanthroline-*N*-oxide
PL	photoluminescence
pmap	1-phenyl-3-methyl-4-acetyl-5-pyrazolone
pmbp	1-phenyl-3-methyl-4-benzoyl-5-pyrazolone
pmip	1-phenyl-3-methyl-4-*i*-butyryl-5-pyrazolone
pmma	poly(methyl methacrylate)
pmnp	1-phenyl-3-methyl-4-neovaleryl-5-pyrazolone
pmpp	1-phenyl-3-methyl-4-propionyl-5-pyrazolone
ppa	3-phenyl-2,4-pentanedionate
ppbtfa	*p*-phenylbenzoyltrifluoroacetonate
ppy	2-phenylpyridine.
$ppyF_2MeO$	2-(2,4-difluorophenyl)-4-metoxypyridine
ptfa	phenantroyltrifluoroacetonate
ptso	*p*-tolyl sulfoxide
pvk	poly(*N*-vinylcarbazole)
pybm	2-(2-pyridyl)benzimidazole
pyNO	pyridine *N*-oxide
pza	pyrazinamide
qh	2,3-diphenylquinoxaline
qipr	*i*-propyl-acylpyrazolone
SMLC/AM1	Sparkle Model for the Calculation of Lanthanide Complexes/ Austin Model 1
tatbp	*meso*-tetraalkyltetrabenzoporphyrin
tfa	trifluoroacetylacetonate
tfnb	4,4,4-trifluoro-1-(2-naphthyl)-1,3-butanedionate
TL	triboluminescence
tmpy	trimethylpyridinium
tmspi	1-trimethylsilyl-4-phenylimidazole
topo	trioctylphosphine oxide
tpbi	1,3,5-tris(*N*-phenylbenzimidazol-2-yl)benzene
tpd	*N*,*N*′-diphenyl-*N*,*N*′-bis(3-methylphenyl)-1,10-biphenyl-4,40-diamine
tpi	3-phenyl-4-(4toluoyl-)5-*i*-oxazolone
tpip	(2-4′-triphenylamino)imidazo[4,5-*f*]1,10-phenanthroline
tppo	triphenylphosphine oxide
tta	1-(2-thienoyl)-3,3,3-trifluoroacetonate
VR	vibrational relaxation
XRD	X-ray diffraction

II. INTRODUCTION

The design of highly luminescence trivalent rare earth (RE^{3+}) complexes containing enolates as ligands, in particular, β-diketonates, is the most intensively investigated among

the RE^{3+} coordination compounds[1]. The great interest in research on the luminescence properties of rare-earth 1,3-diketonate complexes is mainly due to their potential practical applications such as medical diagnosis[2–4], electroluminescence[5,6], triboluminescence[7,8], optical markers and even laser materials[9,10]. The importance of optical spectroscopy of RE^{3+} ions is associated mainly with their narrow emission bands arising from the intraconfigurational 4f–4f transitions and long lifetimes, which make these ions unique among the luminescent coordination compounds[11]. Laporte's rule is slightly relaxed for these transitions due to the mixing of opposite parity electronic configurations, produced by the odd components of a non-centrosymmetric ligand field. Moreover, the ligand polarization effects have been shown to be of considerable importance for the f–f transitions. Because of the great importance of RE^{3+} β-diketonate complexes as luminescent materials, a large part of this chapter is devoted to their luminescent properties.

Luminescence originating from intraconfigurational d–d transitions is quite different from that of the 4f–4f ones. The spectra of d metals are much poorer in the number of observed pure zero-phonon transitions, since d^N configurations have less microstates by far than the $4f^N$ ones. The vibronic interaction is much stronger than in the case of 4f–4f transitions. Besides, for d transition elements, the ligand field interaction is at least one order of magnitude great, due to the non-screened and more extended d radial distribution. These facts produce very broad d–d bands. Transition metal complexes have usually lower coordination numbers (4 and 6) than the f elements. In the case of four-fold tetrahedral coordination d–p mixing relaxes Laporte's rule allowing the d–d transitions, while in the case of octahedral coordination Laporte's rule is not relaxed, except for the vibronic interaction that instantaneously breaks down the center of inversion and allows the d–d transitions, with much weaker intensities than in the tetrahedral case[12]. Ligand polarization effects on the d–d transitions, to our knowledge, have not yet been investigated.

The luminescence phenomenon is an emission process of ultraviolet, visible or infrared photons from an electronically excited species. The term luminescence was introduced by Eilhardt Wiedemann in 1888—'all those phenomena of light which are not solely conditioned by the rise in temperature'[13]. Therefore, luminescence is cold light while incandescence is hot light. There are several types of luminescence which depend on the mode of excitation (given in parenthesis): (i) *Photoluminescence* (absorption of photons)—fluorescence and phosphorescence are particular cases; (ii) *radioluminescence* (ionizing radiation X-, α-, β- and γ-rays); (iii) *cathodoluminescence* (cathode rays–electron beams); (iv) *electroluminescence* (electric field); (v) *thermoluminescence* (heating after prior storage of energy); (vi) *chemiluminescence* (chemical process); (vii) *bioluminescence* (biochemical process); (viii) *triboluminescence* (frictional and electrostatic forces) and (ix) *sonoluminescence* (ultrasound).

In this chapter we focused on the investigation of photoluminescence, electroluminescence and triboluminescence phenomena involving metal enolates[14].

III. METAL ENOLATES

A. The Chemistry of Metal β-Diketonate Complexes

In the last decades there has been a growing interest in coordination compounds with diketonate ligands. These systems have attracted the interest of both the organic and inorganic chemical communities[1,15]. Here we very briefly describe the chemistry of β-diketone ligands which are capable of keto–enol tautomerism (Scheme 1).

The hydrogen atom on the α-carbon is activated by the C=O groups, and a conjugate system is formed. Under appropriate conditions the enolic hydrogen atom of β-diketone can be replaced by a metal ion (M^{n+}) to produce a six membered chelate ring (**1**) thereby shifting the keto–enol equilibrium favoring the enol form.

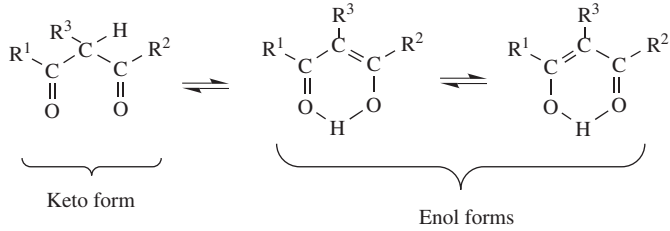

SCHEME 1. Tautomerism of β-diketones

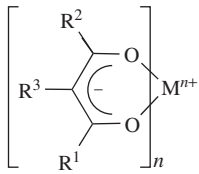

(**1**)

It is observed that in most β-diketones the substituents on the α-carbon are hydrogen atoms. Consequently, only very few examples of luminescent rare-earth α-substituted β-diketonate complexes are known. The β-diketonates are good chelating ligands forming highly stable RE^{3+} complexes.

Rare earth β-diketonate complexes[15] usually are synthesized using the RE^{3+} chloride and ammonium or sodium β-diketonate in water or ethanol solvent. Rare earth chlorides are preferred over nitrate or acetates due to the lower coordination power of chloride anion. Binnemans[1], Mehrotra[15], Thompson[16], Joshi[17] and Mañas[18] give an overview of the synthesis of rare earth ion complexes with β-diketonate ligands including different RE^{3+}-(1,3-diketonate) coordination compounds.

1. Ligand luminescence

Molecular radiative decay is a process in which a molecule releases its excitation energy as a photon. A more common process is the non-radiative decay, in which the excess energy is transferred to vibration, rotation and translation of the surrounding molecules[19]. The relaxation pathways for molecules are shown in Figure 1. Assume that a molecule has been excited, by absorption of a photon or by other means, to a high vibrational state belonging to an excited electronic singlet state such as S_2. In a time interval of the order of 10^{-12} s the molecule will drop to the lowest vibrational state by non-radiative processes that are mediated by molecular collisions. Quite often there is considerable overlap between excited vibrational states of S_2 and S_1 singlets. This occurs when the potential energy surfaces of S_2 and S_1 intersect. This is known as *internal conversion* (IC) which is defined as a non-radiative transition between electronic states of the same multiplicity. The rate constant associated to this process is typically $10^9 - 10^{10}$ s^{-1}, which is several orders of magnitude larger than the rate constant for photon emission from S_2 to a lower singlet state (S_1). The molecule, having crossed over from S_2 and S_1 states, undergoes further vibrational relaxation and may continue by IC to the ground state S_0 which is also assumed to be a singlet[14].

Considering that S_1 is the first excited singlet state, well separated from the ground S_0 state, and that IC, together with vibrational relaxation (VR), have brought the molecule

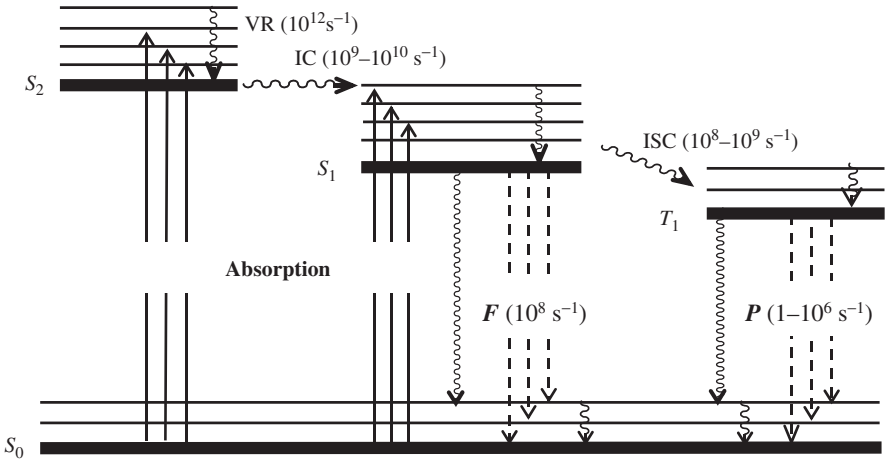

FIGURE 1. Jablonski diagram for the relative positions of the electronic energy levels of a molecule, where $\boldsymbol{F}$ = fluorescence rate, $\boldsymbol{P}$ = phosphorescence rate and VR = vibrational relaxation

to the vibrational ground state of S_1, two pathways are considered: (i) a singlet–singlet transition ($S_1 \rightarrow S_0$) with emission of photons, called *fluorescence*, the spontaneous emission taking place without change in spin, typically within 10^{-8} s after the exciting radiation is extinguished, and (ii) the non-radiative transition from singlet to triplet states ($S_1 \rightarrow T_1$) known as *intersystem crossing* (ISC).

If the radiative transition occurs from the first excited triplet to the singlet ground state ($T_1 \rightarrow S_0$, a spin-forbidden transition $\Delta S \neq 0$), the phenomenon is called *phosphorescence*. The spontaneous emission may persist for long periods, even hours, but the lifetimes usually last milliseconds to seconds.

2. Ligand electronic properties based on Gd^{3+} complexes

The luminescence properties of rare-earth enolate complexes are largely dependent on the position of the excited electronic states (singlet and triplet) of the ligands. The experimental S states are usually obtained from the electronic absorption spectra of the metal complex in solution[15]. On the other hand, the phosphorescence spectra of solid state Gd^{3+} complexes, obtained from the broad emission bands assigned to $T_1 \rightarrow S_0$ transitions, give information about the triplet state position of the enolate ligands (Figure 2).

As the ligand phosphorescence is, in general, completely quenched at room temperature, for these coordination compounds[20], it is necessary to record the spectra at low temperature (77 K), otherwise the T states are deactivated by non-radiative processes. In this case, trivalent gadolinium complexes are generally used due to the intrinsic spectroscopic characteristics of the Gd^{3+} ion (Figure 2).

Since there is a large energy gap (*ca* 32000 cm^{-1}) between the $^8S_{7/2}$ ground state and the first $^6P_{7/2}$ excited state of the Gd^{3+} ion[23], it cannot be widened by energy from the lower-laying first excited T_1 state of the β-diketonate ligands via intramolecular ligand-to-metal energy transfer (Figure 2)[24]. Furthermore, the paramagnetic RE^{3+} ions, and in particular the Gd^{3+} ion that has the $4f^7$ configuration, induce an increase in the intersystem crossing from the singlet state to the triplet state owing to the increase

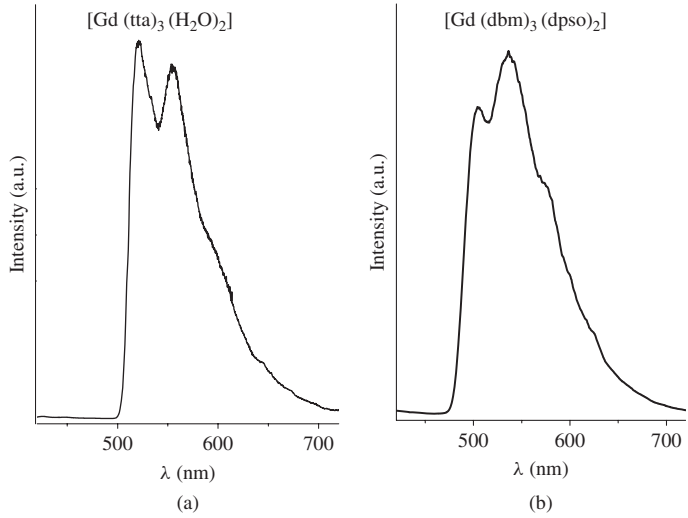

FIGURE 2. Phosphorescence spectra of Gd^{3+} β-diketonate complexes in the solid state, under excitation at around 375 nm, at 77 K: (a) $[Gd(tta)_3(H_2O)_2]$[21] and (b) $[Gd(dbm)_3(dpso)_2]$[22]. (a) Reproduced with permission from Reference 21, Copyright 2003 Taylor & Francis, and (b) reproduced with permission from Reference 22, Copyright 2005 Elsevier

in the S and T mixing (heavy ion effect)[25]. Table 1 presents the molecular structures and triplet state energies of some Gd^{3+} β-diketonate complexes. de Sá and coworkers[20] used phosphorescence spectroscopy to obtain the energy values of the T state of several Gd^{3+} β-diketonate compounds, allowing for the test of the accuracy of their theoretically calculated energies.

B. Experimental and Theoretical Structures of RE^{3+} β-Diketonates

The structural information of the rare-earth β-diketonates is of crucial importance in the evaluation of their luminescence properties. More than two hundred crystal structures of RE^{3+} β-diketonates determined by single crystal X-ray diffraction (XRD) have been reported in the literature and deposited in the database of the Cambridge Crystallographic Data Center[1]. In addition, theoretical methods have been used to predict the structures of diketonate compounds. Among them, the SMLC/AM1 method[20,31–34] has been successfully used in the determination of coordination geometries from calculations on the isolated single RE^{3+} diketonate complex[35].

The existence of RE^{3+} diketonate complexes with large coordination number is due to the large size, steric factors and ionic bond character of these systems. Although six-, seven- and eight-coordination are known, each of these complexes with higher coordination number depends critically on the size of the RE^{3+} ion as well as the nature of the ligands[16]. The number of six-coordination complexes determined by XRD is small, for example *tris*-bidentate complexes[2], $[Er(dpm)_3]$. There is a significant number of RE^{3+} β-diketonate complexes with seven-coordination number with the basic formulation [RE^{3+} (β-diketonate)$_3$(unidentate)], showing three-coordination polyhedra: mono-capped octahedron—$[Ho(dbm)_3(H_2O)]$, mono-capped trigonal prism—$[Yb(acac)_3(H_2O)]$ and pentagonal bipyramid—$[Eu(dpm)_3(dmso)]$, where dmso acts as a monodentate ligand[16].

TABLE 1. Excitation energy of the T_1 triplet state of Gd^{3+} enolate complexes

Complex	T (cm^{-1}) [a]	Reference
$Gd(atfa)_3$	13600	26
$Gd(pmbp)_3$ [b]	18180	27
$Gd(pmnp)_3$ [c]	19340	27
$Gd(ntfa1)_3$	19400	26
$Gd(ntfa2)_3$	19600	26
$Gd(ptfa3)_3$	19800	26
$Gd(tta)_3$	20300	26
$Gd(pmip)_3$ [d]	20370	27
$Gd(ppbtfa)_3$	20400	26
$Gd(pmap)_3^e$	20580	27
$Gd(ptfa)_3$	20600	26
$Gd(dbm)_3$	20660	28
$Gd(pmpp)_3$ [f]	20750	27
$Gd(btfa)_3$	21400	26
$Gd(bzac)_3$	21460	28
$Gd(hfa)_3$	22000	28
$Gd(pbi)_3$ [g]	22220	30
$Gd(tpi)_3$ [h]	22620	30
$Gd(fod)_3$	22711	29
$Gd(tfa)_3$	23000	28
$Gd(dpm)_3$	23530	29
$Gd(acac)_3$	26000	28

[a] Energy in increasing order; 10000 cm^{-1} = 1.23984 eV = 119.62656 kJ mol^{-1}.
[b] Structure **2**, R = Ph.
[c] Structure **2**, R = *n*-Bu.
[d] Structure **2**, R = *i*-Pr.
[e] Structure **2**, R = Me.
[f] Structure **2**, R = Et.
[g] Structure **3**, R = Ph.
[h] Structure **3**, R = 4-Tol.

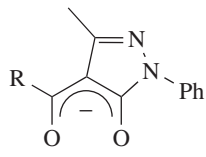

(**2**)

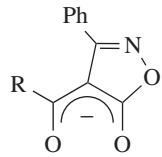

(**3**)

The most common coordination numbers shown by RE^{3+} β-diketonate complexes is eight, where the two most frequent chemical formulae are $[RE(\beta\text{-diketonate})_4]^-$ and $[RE(\beta\text{-diketonate})_3(\text{unidentate})_2]$ corresponding to dodecahedron and square antiprism polyhedra, respectively. It is noted that the number of crystal structures presented for the *tetrakis* complexes is very low compared with the *tris* complexes. The majority of the *tetrakis* complexes have square antiprism polyhedron structure[2, 16] $[Ce(acac)_4]$. On the other hand, a number of rare earth β-diketonate complexes has the dodecahedral coordination polyhedron.

If a RE^{3+} ion occupies a symmetry site with a center of inversion, its intraconfigurational 4f transitions are rigorously forbidden by the electric dipole mechanism (Laporte's

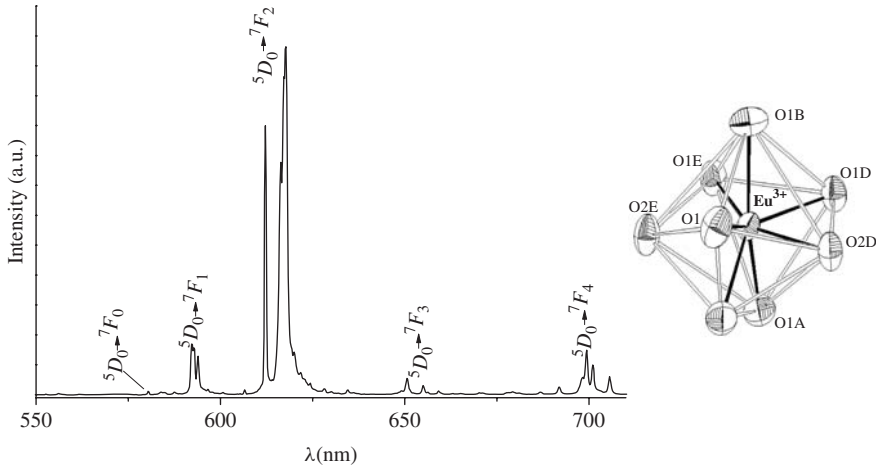

FIGURE 3. Emission spectrum and eight-fold coordination polyhedron of $[Eu(tta)_2(NO_3)(tppo)_2]$[38]. Reproduced with permission from Reference 38, Copyright 2008 Elsevier

rule). However, if there is no center of inversion at the symmetry site of these ions, the 4f–4f transitions are allowed by the forced electric dipole mechanism and absorption and emission bands appear in the spectra[36,37], from which structural information may be extracted. For example, when the Eu^{3+} ion displays the $^5D_0 \rightarrow {}^7F_2$ transition with a much higher emission intensity than the $^5D_0 \rightarrow {}^7F_1$ transition (allowed by the magnetic dipole mechanism), one may conclude that the symmetry of the chemical environment around the Eu^{3+} ion is very low. In this case, the degeneracies of the energy level manifolds are totally raised by the ligand field. Consequently, good correlations between spectral and structural data can be made. Figure 3 shows the emission spectrum and experimental eight-coordination polyhedron of $[Eu(tta)_2(NO_3)(tppo)_2]$, which can be described by a distorted dodecahedron with point symmetry close to D_{2d}[38].

Quantum chemical calculations on RE^{3+} β-diketonate complexes are presently restricted to two approaches: the effective core potential (ECP) and the SMLC/AM1 method[31–35]. The SMLC/AM1 method is a very powerful addition to the semi-empirical molecular orbital method AM1 in that it allows the prediction of geometric parameters of rare-earth β-diketonate complexes of very difficult experimental determination. In this method the RE^{3+} ion is a sparkle represented by a +3e charge in the center of a repulsive spherical potential of the form $\exp(-\alpha r)$. Recently, *ab initio* effective core potential calculations have also succeeded in reproducing the coordination polyhedron geometries of RE^{3+} β-diketonate complexes with high accuracy[39].

The structural data determined by the SMLC/AM1 method for $[Eu(tta)_2(NO_3)(tppo)_2]$ are in agreement with the experimental data (Figure 4). In addition, comparisons between crystallographic and calculated coordination polyhedron geometries are consistent with a very low symmetry of the chemical environment around the Eu^{3+} ion, described by a distorted dodecahedron with symmetry close to D_{2d}, showing an unsigned minor error (UME)[38] of 0.0583.

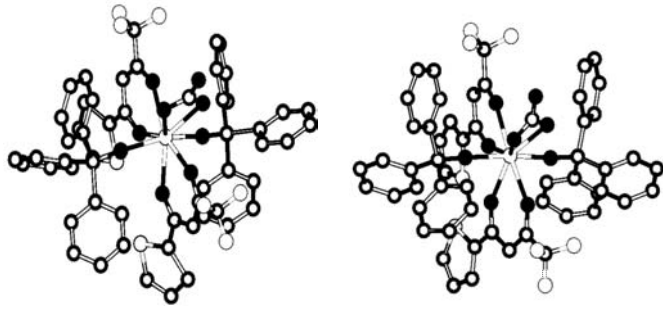

FIGURE 4. Experimental and theoretical structures of $[Eu(tta)_2(NO_3)(tppo)_2]$[38]. Reproduced with permission from Reference 38, Copyright 2008 Elsevier

IV. LUMINESCENCE OF RARE-EARTH ENOLATES

A. General Considerations

The ionic radii of RE^{3+} ions are large (Table 2), with the exception of the value for Sc^{3+}, denoting that the charge-to-radius ratio is relatively low, resulting in a very low polarizability which reflects the rather ionic nature of the metal ligand bonds. The large ionic radii lead to RE^{3+} complexes with coordination numbers higher than six, which is common for d-transition metals. Although the Y^{3+} ion has no 4f electrons, it presents coordination chemistry similar that of the Ln^{3+} ions, because yttrium has ionic radius between those of the Ho^{3+} and Er^{3+} ions[2, 16, 40]. The electronic configurations of the RE^{3+} ions together with their ground-state spectroscopic terms are shown in Table 2. The more common oxidation states are +3, +2 and +4. However, the +3 oxidation state is characteristic for all rare-earth ions that present a $4f^N$ configuration (N = number of electrons).

The most important attribute that characterizes the RE^{3+} ions is the small radial extension of the 4f sub-shell and their electronic energy levels which are only little affected by their chemical environments (e.g. diketonates), due to the effective shielding of the 4f electrons from the external filled 5s and 5p sub-shells. In particular, the solid state spectra of RE^{3+} ions retain more or less their atomic character, which can act as local structural probes, presenting usually quite narrow absorption and emission bands, in contrast to the case of d-transition metal ions[41].

The $4f^N$ configuration of the RE^{3+} ions give rise to several spectroscopic terms whose energy components are in the following order: central field (10^5 cm^{-1}) > interelectronic repulsion (10^4 cm^{-1}) > spin–orbit coupling (10^3 cm^{-1}) > ligand field (10^2 cm^{-1}). The ligand field interaction removes the $^{2S+1}L_J$ levels degeneracy of the free ion into a number of ligand field sublevels (Stark levels) which depend on the symmetry around the RE^{3+} ion[42]. The 4f–4f transitions are parity forbidden by Laporte's rule and their emission and absorption spectra exhibit weak intensity under excitation monitored on the $^{2S+1}L_J$ levels of the RE^{3+} ion, with molar absorption coefficients around 1.0 M^{-1} cm^{-1}. However, some organic ligands in coordination compounds can act as an 'antenna', absorbing

TABLE 2. Properties of trivalent rare earths. Adapted by permission from Reference 2, Copyright 2005 the Royal Society of Chemistry

Element	Configuration (spectroscopic terms)	RE^{3+} radius (Å)	Luminescence	$\lambda_{emission}$ (nm)
^{21}Sc	$[Ar]3d^0$ ($^1S_0$)	0.68	—	—
^{39}Y	$[Kr]4d^0$ ($^1S_0$)	0.88	—	—
^{57}La	$[Xe]4f^0$ ($^1S_0$)	1.06	—	—
^{58}Ce	$[Xe]4f^1$ ($^2F_{5/2}$)	1.03	—	—
^{59}Pr	$[Xe]4f^2$ ($^3H_4$)	1.01	$^3P_0 \rightarrow {}^3H_6$	610
			$^1D_2 \rightarrow {}^3F_4$	1060
			$^1G_4 \rightarrow {}^3H_5$	1300
^{60}Nd	$[Xe]4f^3$ ($^4I_{9/2}$)	0.99	$^4F_{3/2} \rightarrow {}^4I_{9/2}$	1060
^{61}Pm	$[Xe]4f^4$ ($^5I_4$)	0.98	$^5F_1 \rightarrow {}^5I_J$	
^{62}Sm	$[Xe]4f^5$ ($^6H_{5/2}$)	0.96	$^4G_{5/2} \rightarrow {}^6H_{9/2}$	590
^{63}Eu	$[Xe]4f^6$ ($^7F_0$)	0.95	$^5D_0 \rightarrow {}^7F_2$	615
^{64}Gd	$[Xe]4f^7$ ($^8S_{7/2}$)	0.94	$^6P_{7/2} \rightarrow {}^8S_0$	311
^{65}Tb	$[Xe]4f^8$ ($^7F_6$)	0.92	$^5D_4 \rightarrow {}^7F_5$	550
^{66}Dy	$[Xe]4f^9$ ($^6H_{15/2}$)	0.91	$^4F_{9/2} \rightarrow {}^6H_{13/2}$	570
^{67}Ho	$[Xe]4f^{10}$ ($^5I_8$)	0.89	$^5F_5 \rightarrow {}^5I_{7,6}$	970,1450
			$^5S_2 \rightarrow {}^5I_8$	550
^{68}Er	$[Xe]4f^{11}$ ($^4I_{15/2}$)	0.88	$^4S_{3/2} \rightarrow {}^4I_{15/2}$	545
			$^4I_{13/2} \rightarrow {}^4I_{15/2}$	1500
^{69}Tm	$[Xe]4f^{12}$ ($^3H_6$)	0.87	$^1G_4 \rightarrow {}^3H_6$	480
^{70}Yb	$[Xe]4f^{13}$ ($^2F_{7/2}$)	0.86	$^3F_{5/2} \rightarrow {}^2F_{7/2}$	980
^{71}Lu	$[Xe]4f^{14}$ ($^1S_0$)	0.85	—	—

and transferring energy efficiently to the rare-earth ion and consequently increasing their luminescence quantum yield[11]. Figure 5 shows the typical energy level diagram for the RE^{3+} ions and the first excited triplet state for some diketonate ligands.

From the point of view of 4f–4f luminescence the RE^{3+} ions can be divided into four groups depending on their optical characteristics[2,41,43]: (i) Sc^{3+} ($3d^0$), Y^{3+} ($4d^0$), La^{3+} ($4f^0$) and Lu^{3+} ($4f^{14}$), which exhibit no luminescence because they contain no optically active electrons. (ii) Gd^{3+} ($4f^7$) ion is a special case, since there is a large energy gap between the $^8S_{7/2}$ ground state and first $^6P_{7/2}$ excited state (*ca* 32000 cm^{-1}). As a result this ion emits in the ultraviolet region. In general, it cannot accept energy from the lower line excited states of the organic ligands (diketonates) via intramolecular ligand-to-metal energy transfer. (iii) Sm^{3+} ($4f^5$), Eu^{3+} ($4f^6$), Tb^{3+} ($4f^8$) and Dy^{3+} ($4f^9$) ions have relatively large energy gaps between their excited and ground states. Complexes of these ions generally show strong luminescence because the excited energy levels of the ion lie just below that of the ligand triplet state. (iv) Ce^{3+} ($4f^1$), Pr^{3+} ($4f^2$), Nd^{3+} ($4f^3$), Ho^{3+} ($4f^{10}$), Er^{3+} ($4f^{11}$), Tm^{3+} ($4f^{12}$) and Yb^{3+} ($4f^{13}$), the complexes of which usually show only weak 4f–4f luminescence, as a consequence of the small energy gap between their emitting and lower energy levels; this increases the probability of non-radiative transitions through coupling with vibrational modes in the ligands.

B. Photoluminescence of Rare-earth β-Diketonates

1. Energy transfer between organic ligands and rare earth ions

Investigation of rare earth β-diketonate photoluminescence began in 1942 with Weissman's work[44], which was the first observation of the indirect excitation arising from the

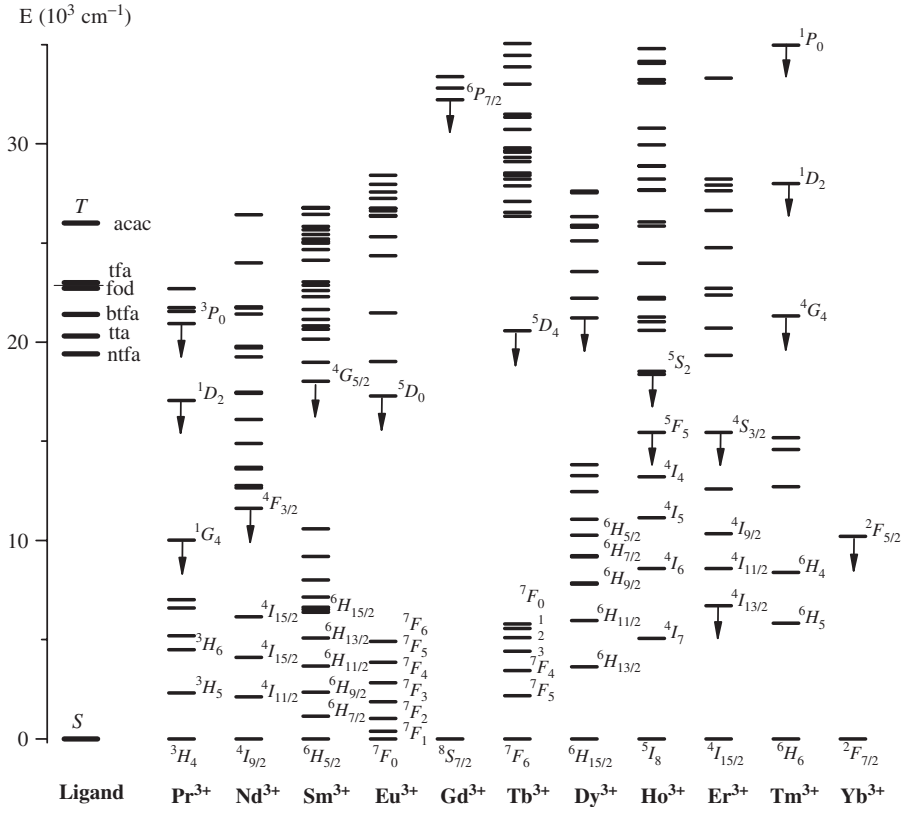

FIGURE 5. Partial energy level diagram of RE^{3+} ions. Some triplet states of diketonate ligands are shown on the left. Arrows indicate emitting levels. Reproduced with permission from Reference 42, Copyright 1989 American Institute of Physics

organic moiety (chromophores) in certain RE^{3+} complexes, resulting in narrow emission bands characteristic of the intraconfigurational 4f–4f transitions of the metal ion.

Interest in the photoluminescence properties of rare-earth β-diketonates has grown considerably since they can be seen as UV-visible light conversion molecular systems, where the ligand acts as a sensitizer. The term 'antenna effect'[11] has been used to denote the efficient absorption by the ligands, intramolecular energy transfer and emission by the metal ion, thus overcoming the typically very small absorption coefficients of the RE^{3+} ions (Figure 6). The luminescence quantum yield is given by a balance between radiative and non-radiative transition and transfer rates in the complex, including intramolecular energy transfer.

After the initial strong absorption by the ligand, three pathways, shown schematically in Figure 7, have been considered by which the excitation energy can be transferred to the rare-earth ion[41,45–47]: (i) The donor $|S_1\rangle$ state transfers energy to a higher excited 4f state $|4\rangle$ which then decays non-radiatively, finally populating the state $|2\rangle$. (ii) State $|4\rangle$ transfers energy back to a lower ligand triplet state $|T_1\rangle$ which then transfers energy to

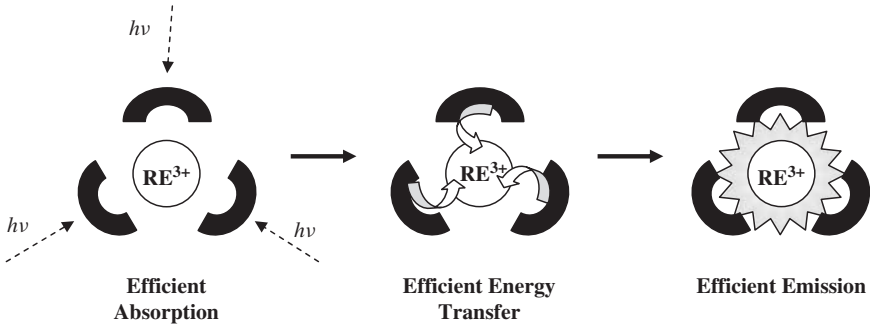

FIGURE 6. The antenna effect in the luminescence of rare-earth complexes. Reproduced by permission from Reference 2, Copyright 2005 the Royal Society of Chemistry

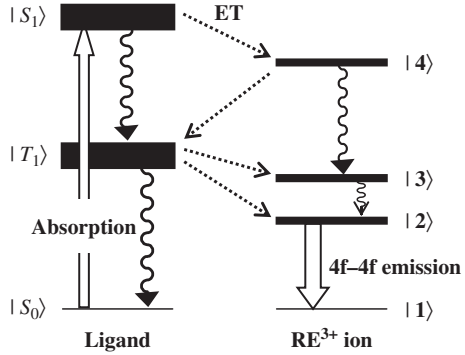

FIGURE 7. Schematic energy level diagram showing the possible energy transfer processes in a rare-earth ion coordination compound. Dashed arrows indicate energy transfer and wavy arrows indicate non-radiative decays. Reproduced with permission from Reference 20, Copyright 2000 Elsevier

the lower 4f states $|3\rangle$ or $|2\rangle$. (iii) State $|S_1\rangle$ decays non-radiatively to the state $|T_1\rangle$ which then transfers energy to the states $|3\rangle$ or $|2\rangle$. In the case of Eu^{3+} and Tb^{3+} ions there is experimental and theoretical evidence that process (iii) is dominant[41,44,48,49], although in some cases direct energy transfer from singlet state $|S_1\rangle$ (process i) is of importance[50].

Luminescence decay curves of the RE^{3+} β-diketonates are usually fitted by a single exponential decay curve $I(t) = I(0)\exp(-t/\tau)$, where $I(t)$ is the radiation intensity at time t after the excitation source is extinguished and τ is the luminescence lifetime. Generally, the shorter lifetime of the $^5D_0$ level in hydrated rare-earth β-diketonates are associated to the non-radiative decay channel due to vibronic coupling with the vibrations of the water molecules (Table 3). Luminescence decay times (τ) of selected transitions of [RE(tta)$_3$(phen)] complexes attached to a Merrifield resin with $RE^{3+} = Nd^{3+}$, Sm^{3+}, Eu^{3+}, Tb^{3+}, Er^{3+} and Yb^{3+} ions are 0.4, 75, 500, 800, 1.4 and 10 μs, respectively, at room temperature[51]. The lifetimes of the green broad-band emission arising from the Gd^{3+} β-diketonate complexes, recorded at 77 K, are consistent with emission from a state with strong triplet character and indicate that intersystem crossing to the singlet ground state is reduced at low temperature[25].

TABLE 3. Lifetime values (τ, in ms) of emitting levels of Sm^{3+}, Eu^{3+} and Gd^{3+} complexes[52]

RE^{3+} β-diketonate	Sm^{3+}	Eu^{3+}	Ligand (T) [a]
$[RE(tta)_3(H_2O)_2]$	0.030	0.260	1.520
$[RE(tta)_3(pha)_2]$	0.068	0.507	4.736
$[RE(tta)_3(bza)_2]$	0.054	0.676	3.278
$[RE(tta)_3(pza)_2]$	0.052	0.409	1.533
$[RE(tta)_3(dmac)_2]$	0.048	0.558	2.328
$[RE(tta)_3(dmfa)(H_2O)]$	0.049	0.643	3.374
$[RE(tta)_3(dmbz)_2]$	0.062	0.489	2.584
$[RE(tta)_3(dpac)_2]$	0.089	0.736	1.860
$[RE(tta)_3(dpfa)_2]$	0.099	0.656	3.055
$[RE(dbm)_3(H_2O)]$	0.083	0.351	0.694
$[RE(dbm)_3(dmac)]$	0.054	0.344	1.002
$[RE(tta)_3(dmfa)]$	0.021	0.410	0.862

[a] Triplet state of diketonate ligand, RE = Gd.

2. Europium intraconfigurational transition intensities and emission quantum yields

The narrow absorption and emission bands of rare-earth β-diketonates in the visible, near ultra-violet and near infra-red is attributed to 4f–4f transitions. These transitions are electric dipole forbidden to first order, but are allowed by the electric quadrupole, vibronic, magnetic dipole and forced electric dipole mechanisms[53]. The magnetic dipole character of the $^5D_0 \rightarrow {}^7F_1$ transition of the Eu^{3+} ion was demonstrated in 1939 by Deutschbein[54]. Most of the intraconfigurational 4f transitions in the RE^{3+} ions, however, cannot be accounted for by the magnetic dipole mechanism, not only because the predicted oscillator strengths are in general smaller than 10^{-6}, but also due to the restrictive selection rules on the total angular momentum J, $|\Delta J| = 0, 1$ ($0 \leftrightarrow 0$ excluded), as far as J is considered to be a good quantum number.

In the standard theory the integrated coefficient of spontaneous emission ($A_{JJ'}$) of a transition between two manifolds J and J' is given by equation 1[36,37], where ω is the angular frequency of the transition, e is the electron charge, c is the velocity of light, h is Planck's constant divided by 2π and n is the refractive index of the medium. The electric and magnetic dipole strengths, respectively, S_{ED} and S_{MD} (in units of e^2), are given by equations 2 and 3, where the quantities Ω_λ are the so-called Judd–Ofelt intensity parameters[36,37], m is the electron mass, J is the total angular momentum quantum number of the rare-earth ion and α stands for the 4f spectroscopic term. The quantity $\langle \alpha' J' || U^{(\lambda)} || \alpha J \rangle$ is the reduced matrix element, in the intermediate coupling scheme, of the unit irreducible tensor operator[57] $U^{(\lambda)}$, and the angular momentum operators L and S are in units of h. The corresponding expression for the oscillator strength ($P_{J'J}$) is given by equation 4.

$$A_{JJ'} = \frac{4e^2\omega^3}{3\hbar c^3}\left[\frac{n(n+2)^2}{9}S_{ED} + n^3 S_{MD}\right] \tag{1}$$

$$S_{ED} = \frac{1}{2J+1}\sum_{\lambda=2,4,6}\Omega_\lambda \langle \alpha' J' \| U^{(\lambda)} \| \alpha J \rangle^2 \tag{2}$$

$$S_{MD} = \frac{\hbar^2}{4mc^2}\langle \alpha' J' \| L + 2S \| \alpha J \rangle^2 \tag{3}$$

$$P_{J'J} = \frac{2J+1}{2J'+1}\frac{mc^2}{2\omega^2 e^2 n^2} A_{JJ'} \tag{4}$$

Among the rare-earth β-diketonate complexes that present characteristic 4f–4f intraconfigurational narrow lines, those of Eu^{3+} exhibit strong red monochromatic emission color (*ca* 615 nm) and a reasonably large gap between the main emitting level and the lower energy, separated by at least 12000 cm^{-1} (Figure 2). They also have been amply used as an efficient luminescent probe due to the following characteristics[55]: (i) the emitting $^5D_0$ and the ground $^7F_0$ levels are non-degenerate and, therefore, the $^5D_0 \rightarrow {}^7F_0$ transition displays a single peak when the Eu^{3+} ion occupies only one site of C_s, C_n or C_{nv} symmetry; (ii) long luminescence decay time for the emitting $^5D_0$ level (milliseconds); (iii) exceptionally large Stokes shift when the emission spectra are obtained through direct excitation of the $^5L_6$ level (*ca* 394 nm); (iv) the radiative rate of the $^5D_0 \rightarrow {}^7F_1$ transition, allowed by the magnetic dipole, is formally insensitive to the ligand field environment and consequently can be used as a reference transition[56]. Besides, from the emission and excitation spectra of the compounds containing europium ions, a larger amount of information about ligand field splitting, energy transfer processes and quantum efficiencies of the emitting levels can be obtained. In the case of other rare-earth chelates, it has not been possible to establish the presence of more than one crystallographic; phase from the spectroscopic data because of absence of the appropriate energy level structures.

a. Experimental intensity parameters for Eu^{3+} β-diketonates. From the emission spectra of Eu^{3+} β-diketonates experimental intensity parameters Ω_2 and Ω_4 may be estimated using the $^5D_0 \rightarrow {}^7F_2$ and $^5D_0 \rightarrow {}^7F_4$ transitions, respectively, and expressing the emission intensity in terms of the area under the emission curve. The Ω_6 intensity parameter is not included in this study since the $^5D_0 \rightarrow {}^7F_6$ transition is usually not observed for these complexes. The emission intensity is defined as $I = \hbar\omega AN$, where $\hbar\omega$ is the transition energy, N is the population of the emitting level ($^5D_0$) and the coefficient of spontaneous emission, A, is given by equation 5, where $\chi = n\ (n+2)^2/9$ is the Lorentz local field correction and n is the index of refraction of the medium. An average index of refraction equal to 1.5 has been used for these complexes. The quantities $\langle {}^7F_J||U^{(\lambda)}||{}^5D_J\rangle^2$ are the square reduced matrix elements and are equal to 0.0032 and 0.0023 for $J = 2$ and 4, respectively[57]. Since the intensity of the magnetic dipole transition $^5D_0 \rightarrow {}^7F_1$ is relatively insensitive to the chemical environment of the Eu^{3+} ion, it may be used as the internal standard (reference transition) to avoid the difficulties in the experimental measurement of absolute emission intensities. The experimental coefficients of spontaneous emission (A) to be used in equation 5 are then obtained according to equation 6, where B_{01} and B_{0J} are the integrated areas under the emission curves of the $^5D_0 \rightarrow {}^7F_1$ and $^5D_0 \rightarrow {}^7F_J$ transitions ($J = 2$ and 4) with ν_{01} and ν_{0J} being their energy baricenters, respectively. The coefficient of spontaneous emission, A_{01}, in equation 6 is given by the expression[20] $A_{01} = 0.31 \times 10^{-11} n^3 \nu_{01}^3$, and its value is estimated to be around 50 s^{-1} for the index of refraction $n = 1.5$.

$$A = \frac{4e^2\omega^3}{3\hbar c^3}\chi \sum_{\lambda} \Omega_\lambda \langle {}^7F_J \| U^{(\lambda)} \| {}^5D_0\rangle^2 \tag{5}$$

$$A_{0J} = A_{01}\left(\frac{B_{0J}}{B_{01}}\right)\left(\frac{\nu_{01}}{\nu_{0J}}\right) \tag{6}$$

From all the A_{0J}, it is possible to calculate the total spontaneous emission for the emitting $^5D_0$ level, in this case given by $A_{rad} = \sum A_{0J} = A_{00} + A_{01} + A_{02} + A_{03} + A_{04}$.

Moreover, it is possible to determine the emission efficiency $\eta = A_{rad}/A_{nrad}$ of the $^5D_0$ emitting level, where the total decay rate is $A_{tot} = 1/\tau = A_{rad} + A_{nrad}$, and where the non-radiative component A_{nrad} depends on the vibronic coupling between the Eu^{3+} ion and its chemical environment and τ is the lifetime of the $^5D_0$ emitting level. It may be determined from lifetime measurements and the experimentally determined radiative component A_{rad}. The hydrated Eu^{3+} β-diketonates tend to present lower values of emission quantum efficiencies, and emission quantum yields, in agreement with the well known effect of luminescence quenching due to the vibrational modes of the water molecule.

Values of experimental intensity parameters Ω_λ ($\lambda = 2$ and 4), radiative rates (A_{0J}) for the $^5D_0 \rightarrow {}^7F_2$ and $^5D_0 \rightarrow {}^7F_4$ transitions and emission efficiencies (η) for Eu^{3+} β-diketonate complexes are presented in Table 4. The high values of the intensity Ω_2 parameter ($\gg 1 \cdot 10^{-20}$ cm^2) might be interpreted as a consequence of two concurrent factors. The first one is the very low symmetry around the Eu^{3+} ion, allowing the appearance of all odd-rank components in the sums-over-ligands as discussed in Section IV.B.2.b. The second factor is related to the hypersensitive behavior of the $^5D_0 \rightarrow {}^7F_2$ transition[20], suggesting that the dynamic coupling mechanism is operative and that the chemical environment around metal ion is highly polarizable, possibly due to the strong delocalization of the enolate oxygen charge.

b. Theoretical intensity parameters. The intensity parameters Ω_λ depend on both the chemical environment and the rare-earth ion, and theoretically they are given by equation 7[20]. The quantities $B_{\lambda tp}$, which have been described in detail elsewhere[69,70], are known as the intensity parameters of individual transitions between Stark levels and are calculated according to equation 8, where ΔE is the energy difference between the baricenters of the excited $4f^5 5d$ and ground $4f^6$ configurations, $\langle r^\lambda \rangle$ is a radial expectation value, $\theta(t, \lambda)$ is a numerical factor, σ_λ is a shielding factor and $C^{(\lambda)}$ is a Racah tensor operator of rank λ. The first term in the right-hand side of equation 8 corresponds to the forced electric dipole mechanism, as expressed by the average energy denominator method, and the dynamic coupling mechanism within the point dipole isotropic ligand polarizability approximation. From the experimental Ω_λ intensity parameters one cannot distinguish between these two mechanisms. This is one of the reasons that justify the efforts invested in the theoretical calculations of these quantities.

$$\Omega_\lambda = (2\lambda + 1) \sum_{t,p} \frac{|B_{\lambda tp}|^2}{(2t + 1)} \tag{7}$$

$$B_{\lambda tp} = \frac{2}{\Delta E} \langle r^{t+1} \rangle \theta(t, \lambda) \gamma_p^t - \left[\frac{(\lambda + 1)(2\lambda + 3)}{(2\lambda + 1)} \right]^{1/2} \langle r^\lambda \rangle (1 - \sigma_\lambda) \langle 3 \| C^{(\lambda)} \| 3 \rangle \Gamma_p^t \delta_{t,\lambda+1} \tag{8}$$

The sums-over-ligands γ_p^t and Γ_p^t are ligand field parameters and contain the dependence on the coordination geometry and on the nature of the chemical environment around the rare-earth ion. The latter is given by equation 9, where α_j is the isotropic polarizability of the j-th ligand atom, or group of atoms, at position R_j and Y_p^t is a spherical harmonic of rank t, where the asterisk denotes a complex conjugate. The ligand field parameters, γ_p^t, are those given by equation 10, according to the simple overlap model (SOM)[71], where ρ is the magnitude of the total overlap between 4f and ligand wavefunctions, $\beta_j = 1/(1 + \rho_j)$ and γ_p^t (P.C.,j), calculated according to equation 11, is the ligand field

TABLE 4. Experimental intensity parameters, lifetimes, radiative and non-radiative rates, and emission efficiencies, η, for Eu^{3+} β-diketonate complexes[a]

Eu^{3+} diketonate complex	Ω_2 (10^{-20} cm^2)	Ω_4 (10^{-20} cm^2)	A_{rad} (s^{-1})	A_{nrad} (s^{-1})	τ (ms)	η (%)	q_{exp} (%)	Reference
$[Eu(tta)_3(H_2O)_2]$	33	5	1110	2730	0.260	29	23	58
$[Eu(tta)_3(dbso)_2]$	29	4	980	420	0.714	70	85	58
$[Eu(tta)_3(pza)]$	19	9	751	1670	0.413	31	26	21
$[Eu(tta)_3(anl)]$	35	11	1256	705	0.510	64	58	21
$[Eu(tta)_3(tppo)_2]$	42	10	1444	560	0.499	72	73	38
$[Eu(tta)_2(NO_3)(tppo)_2]$	22	6	780	446	0.816	63	68	38
$[Eu(tta)_3(bza)_2]$	24	11	923	557	0.676	62	54	52
$[Eu(tta)_3(dmac)_2]$	37	9	1295	498	0.558	72	78	52
$[Eu(tta)_3(dmfa)(H_2O)]$	24	9	904	651	0.643	58	45	52
$[Eu(tta)_3(dpfa)_2]$	21	5	758	1905	0.376	28	40	52
$[Eu(tta)_3(dmbz)_2]$	36	8	1255	269	0.656	82	81	52
$[Eu(tta)_3(azt)_2]$	20	9	778	2179	0.338	26		59
$[Eu(dbm)_3(H_2O)]$	37	2	1200	3093	0.233	37	1	22
[Ee(dbm)$_3$(dmac)]	51	7	1752	1189	0.340	60	45	52
$[Eu(dbm)_3(dmfa)]$	44	7	1491	947	0.410	61	43	52
$[Eu(dbm)_3(dmbz)]$	47	9	1488	2442	0.254	38	20	52
$[Eu(dbm)_3$ (dpso)]	43	11	1508	1754	0.307	62	16	22
$[Eu(dbm)_3$ (dbso)]	34	11	1217	1204	0.413	67	62	22
$[Eu(dbm)_3$ (dmso)]	45	10	1538	1887	0.292	60	49	22
$[Eu(dbm)_3(ptso)]$	62	13	2098	1763	0.259	72	70	22
$[Eu(btfa)_3(bipy](EtOH)]$	29	7	1033	1189	0.450	46	38	60
d-U(600)AA:Eu-(btfa)-	31	7	1094	692	0.560	63	49	60
d-U(600): Eu-(btfa)-	24	7	884	783	0.600	53	51	60
$[Eu(tpi)_3(H_2O)_3]$	8	6	381	2952	0.300	13	1	61
$[Eu(tpi)_3(topo)_2]$	21	6	773	242	0.985	76	50	61
$[Eu(tpi)_3(tphpo)_2(H_2O)_2]$	18	6	658	1265	0.520	34	8.3	62
$[Eu(tpi)_3(phen)(H_2O)]$	6	7	335	1304	0.610	20	6	62
$[Eu(aind)_3(H_2O)_2]$	42	15	1532	7739	0.108	16		24
$[Eu(aind)_3(tppo)_2]$	36	9	1255	628	0.531	67		24
$[Eu(isovind)_3(H_2O)_2]$	40	16	1499	24330	0.039	6		24
$[Eu(isovind)_3(tppo)_2]$	35	11	1283	688	0.507	65		24

[Eu(bind)$_3$(H$_2$O)$_2$]	41	14	1482	17080	0.054	8		24
[Eu(bind)$_3$(tppo)$_2$]	29	16	1165	1978	0.318	37		24
Epoxy:1%[Eu(tta)$_3$]	28	10	1034	1229	0.442	46		63
[Eu(acac)$_3$(H$_2$O)$_3$]	30	12	1127	2522	0.274	33		64
Polymer:Eu(acac)$_3$1%	18	10	750	2244	0.334	24		64
[Eu(nta)$_3$(H$_2$O)$_2$]	30	5	832	2025	0.350	29	13	65
[Eu(nta)$_3$(dmso)$_2$]	36	5	1070	654	0.580	62	75	65
[Eu(pbi)$_3$(EtOH)(H$_2$O)]	27	14	1059	2941	0.250	26	2	66
[Eu(pbi)$_3$ (bipy)]	19	3	6911	3314	0.098	68	15	66
[Eu(pbi)$_3$(dmbpy)]	17	2	6094	2373	0.118	72	18	66
[Eu(pbi)$_3$(phen)]	16	2	5543	4213	0.103	57	11	66
[Eu(pbi)$_3$(bath)]	20	2	7023	2878	0.101	71	15	66
[Eu(btfa)$_3$(H$_2$O)]	21	4	349	2283	0.380	13	22	67
[Eu(btfa)$_3$(phenNO)]	29	4	760	786	0.647	49	65	67
[Eu(mbind)$_3$(H$_2$O)$_2$]	40	13.5	1456	17050	0.054	9		68
[Eu(mbind)$_3$(tppo)$_2$]	37	10	1310	2152	0.289	39		68
[Eu(cbind)$_3$(H$_2$O)$_2$]	38	11	1350	11130	0.080	11		68
[Eu(cbind)$_3$(tppo)$_2$]	40	11	1396	2019	0.293	41		68
[Eu(bbind)$_3$(H$_2$O)$_2$]	21	12	854	12340	0.076	7		68
[Eu(bbind)$_3$(tppo)$_2$]	38	13	1380	1186	0.390	54		68
[Eu(nind)$_3$(H$_2$O)$_2$]	22	13	888	19730	0.048	5		68
[Eu(nind)$_3$(tppo)$_2$]	32	12	1161	18810	0.050	6		68
[Eu(pind)$_3$(tppo)$_2$]	36	11	1236	1873	0.322	41		68

[a] For the sake of comparison with η, values of the experimental emission quantum yields, q_{exp} (see Section IV.B.2.d), are also given.

parameter due to the j-th ligand with charge $-g_j$ as given by the point charge (P.C.) electrostatic model. Equation 10 should be interpreted as a ligand field parameter produced by effective charges $-\rho_j g_j e$ located close to the midpoints of the rare-earth–ligand chemical bonds. In this way the charge factors g_j are more appropriately treated as parameters which no longer have to be given by the valencies of the ligand atoms. It has been assumed that the overlap ρ_j varies ρ_j varies as $\rho_j = \rho_0(R_0/R_j)^n$, where R_0 is the smallest among the R_j's, $\rho_0 = 0.05$ and $n = 3.5$[72].

$$\Gamma_{\mathrm{p}}^{t} = \left(\frac{4\pi}{2t+1}\right)^{1/2} \sum_j \frac{\alpha_j}{R_j^{t+1}} Y_{\mathrm{p}}^{t^*}(\Omega_j) \tag{9}$$

$$\gamma_{\mathrm{p}}^{t} = \sum_j \rho_j (2\beta_j)^{t+1} \gamma_{\mathrm{p}}^{t}(\mathrm{P.C.}, j) \tag{10}$$

$$\gamma_{\mathrm{p}}^{t}(\mathrm{P.C.}, j) = \left(\frac{4\pi}{2t+1}\right)^{1/2} \frac{g_j e^2}{R_j^{t+1}} Y_{\mathrm{p}}^{t^*}(\Omega_j) \tag{11}$$

In order to investigate the nature of the chemical environment around the RE^{3+} ion, the intensity parameters Ω_λ were calculated using the coordination geometry (in spherical coordinates) obtained from the DRX structure or sparkle model[20]. The isotropic polarizability (α_j) and the charge factor (g_j) of the j-th donor atom, at position R_j, have been treated as freely varying parameters within ranges of physically acceptable values by assuming two types of oxygen donor atoms from β-diketonates and ligand L. The ligand field parameters have been obtained from the simple overlap model (SOM)[71]. The values of the intensity parameters together with the values obtained for g_1(diketonates), g_2(L), α_1(diketonates) and α_2(L) are presented in Table 5.

Table 5 also gives the contributions from the forced electric dipole mechanism ($\Omega_\lambda^{\mathrm{e.d.}}$, $\alpha_j = 0$) and dynamic coupling mechanism ($\Omega_\lambda^{\mathrm{d.c.}}$, $g_j = 0$). The values of $\Omega_2^{\mathrm{d.c.}}$ and $\Omega_4^{\mathrm{d.c.}}$ parameters are higher than $\Omega_2^{\mathrm{e.d.}}$ and $\Omega_4^{\mathrm{e.d.}}$, suggesting that the dynamic coupling is by far the dominant mechanism to the radiative transitions in the Eu^{3+} β-diketonates. Since in this mechanism the intensity of the hypersensitive transitions is related explicitly to the polarizabilities of the ligands, the $\Omega_2^{\mathrm{d.c.}}$ values of Eu^{3+} β-diketonates give evidence of a highly polarizable chemical environment around the Eu^{3+} centers in complexes containing β-diketonate ligands (Table 5).

c. Diketonate ligand–rare-earth ion energy transfer rates. Rates of intramolecular energy transfer in RE^{3+} coordination compounds have been estimated experimentally to be in the range from 10^5 to 10^{12} s^{-1}. The experimental procedure adopted is in general based on lifetime and/or luminescence quenching measurements. Theoretically, the transfer rates may be determined from Fermi's golden rule and the Born–Oppenheimer approximation according to the general equation 12, where ψ and ϕ' are the initial electronic states of the rare-earth ion and of the ligand, respectively. After the energy transfer takes place these species are found in the electronic states ψ' and ϕ. The temperature-dependent factor F contains a sum over Franck–Condon factors and the appropriate energy mismatch condition for the transfer process, which is mediated by the interaction hamiltonian H between the electronic clouds of the RE^{3+} ion and the β-diketonate ligand. The hamiltonian H can be split into two parts, one corresponding to the direct Coulomb interaction and the other to the exchange interaction. The first part leads to the lowest-order contributions to the transfer rates, as shown in equation 13, which corresponds to the dipole-2^λ–pole mechanism, with $\lambda = 2$, 4 and 6, and equation 14, corresponding to the dipole–dipole

TABLE 5. Theoretical intensity parameters[a] (Ω_λ^{theo} and $\Omega_\lambda^{d.c.}$), charge factors and ligating atom polarizabilities calculated for Eu^{3+} β-diketonate complexes

Compounds	Ω_2^{theo} (10^{-20} cm^2)	$\Omega_2^{d.c.}$ (10^{-20} cm^2)	$\Omega_2^{e.d.}$ (10^{-20} cm^2)	Ω_4^{theo} (10^{-20} cm^2)	$\Omega_4^{d.c.}$ (10^{-20} cm^2)	$\Omega_4^{e.d.}$ (10^{-20} cm^2)	g_1 (Å^3)	g_2 (Å^3)	α_1 (Å^3)	α_2 (Å^3)	Reference
[Eu(tta)$_3$(H$_2$O)$_2$]	20	19	0.1	5	7	0.3	1.0	2.0	4.0	1.0	58
[Eu(tta)$_3$(dbso)$_2$]	26	27	0.1	3	5	0.5	1.8	1.4	1.8	4.5	58
[Eu(tta)$_3$(dmso)$_2$]	22	20	0.3	5	7	0.6	1.5	1.7	4.5	0.5	73
[Eu(tta)$_3$(ptso)$_2$]	25	26	0.2	8	12	0.3	1.6	0.8	4.0	4.5	73
[Eu(tta)$_3$(fso)$_2$]	22	26	0.3	5	8	0.3	0.9	1.5	2.5	4.5	73
[Eu(tta)$_3$(dmac)$_2$]	35	36	1.8	9	0.2	18	0.8	1.8	4.3	4.5	52
[Eu(tta)$_3$(dmbz)$_2$]	36	40	1.3	11	13	0.2	0.9	0.5	4.0	4.2	52
[Eu(tta)$_3$(dpac)$_2$]	24	25	1.2	5	7	0.1	0.9	1.5	4.0	2.0	52
[Eu(tta)$_3$(dpfa)$_2$]	22	23	0.5	5	6	0.05	0.5	1.0	3.5	0.5	52
[Eu(dbm)$_3$(dmac)]	21	23	0.3	12	14	0.06	0.5	0.4	2.8	4.4	52
[Eu(tta)$_3$(tppo)$_2$]	40	43	1.4	15	16	0.1	0.7	1.0	4.8	2.8	38
[Eu(tta)$_2$(NO$_3$)(tppo)$_2$][b]	20	19	3.2	11	14	0.2	1.4	1.0	4.0	4.5	38
[Eu(btfa)$_3$(bipy](EtOH)][c]	27	27	0.04	3	3.0	0.01	0.8	0.3	0.9	5.2	60
[Eu(aind)$_3$(H$_2$O)$_2$]	40	41	0.8	6	7	0.05	0.5	0.8	4.4	2.0	68
[Eu(pind)$_3$(H$_2$O)$_2$]	47	53	3.3	2	2	0.03	1.2	1.2	3.7	2.0	68
[Eu(bind)$_3$(H$_2$O)$_2$]	41	42	0.6	12	13	0.1	0.6	0.7	4.7	1.5	68
[Eu(mbind)$_3$(H$_2$O)$_2$]	40	40	1.3	13	14	0.1	0.5	1.3	4.0	2.0	68
[Eu(cbind)$_3$(H$_2$O)$_2$]	28	29	2.0	17	20	0.2	1.2	0.8	5.5	2.0	68
[Eu(bbind)$_3$(H$_2$O)$_2$]	20	20	1.7	7	9	0.1	0.6	1.4	3.0	2.0	68
[Eu(nind)$_3$(H$_2$O)$_2$]	21	22	0.9	8	9	0.1	0.8	0.5	4.0	3.5	68
[Eu(aind)$_3$(tppo)$_2$]	36	38	1.5	5	6	0.1	0.6	1.4	3.8	3.0	68
[Eu(isovnd)tppo)$_2$]	9	9	1.1	6	7	0.04	0.8	0.8	5.0	4.0	68
[Eu(bind)$_3$(tppo)$_2$]	26	28	1.2	4	4	0.1	0.6	1.7	4.5	4.0	68
[Eu(mbind)$_3$(tppo)$_2$]	32	33	0.8	12	14	0.05	0.6	0.7	5.5	4.0	68
[Eu(cbind)$_3$(tppo)$_2$]	33	34	0.7	12	14	0.04	0.6	0.6	5.5	4.5	68
[Eu(bbind)$_3$(tppo)$_2$]	35	36	0.6	13	14	0.04	0.5	0.6	5.5	4.8	68
[Eu(nind)$_3$(tppo)$_2$]	30	31	0.8	9	10	0.06	0.7	0.6	4.5	4.5	68

[a] theo = theoretical, d.c. = dynamic coupling, e.d. = electric dipole.
[b] For NO_3^-, $g_3 = 1.0$ and $\alpha_3 = 1.0$.
[c] For bipy, $g_3 = 1.0$ and $\alpha_3 = 0.6$.

mechanism, also with $\lambda = 2$, 4 and 6; G is the degeneracy of the ligand initial state, S_L is the dipole strength associated with the $\phi \rightarrow \phi'$ transition in the ligand and R_L is the distance from the rare-earth ion to the region of the ligand molecule in which the ligand donor (or acceptor) state is localized. The $\Omega_\lambda^{\text{e.d.}}$ quantities are the electric dipole contribution to the so-called intensity parameters which appear in the theory of 4f–4f intensities[53], and the γ_λ's are given by equation 15, where $\langle r^\lambda \rangle$ is the radial expectation value of r^λ for 4f electrons, $\langle 3||\mathrm{C}^{(\lambda)}||3\rangle$ is a reduced matrix element of the Racah tensor operator[74] $\mathrm{C}^{(\lambda)}$ and the σ_λ's are screening factors due to the 5s and 5p filled sub-shells of the rare earth ion. The second part of the hamiltonian H (the exchange interaction) leads to the lowest-order contribution to the transfer rates shown in equation 16, where S is the total spin operator of the rare-earth ion, μ_z is the z component of the electric dipole operator and s_m ($m = 0, \pm 1$) is a spherical component of the spin operator, both for the ligand electrons; σ_0 is also a screening factor of the same nature as those which appear in equation 15, and it has been estimated to be $\geqslant 0.9$.

$$W_{\text{ET}} = \frac{2\pi}{\hbar} |\langle \psi' \phi | H | \psi \phi' \rangle|^2 F \tag{12}$$

$$W_{\text{ET}} = \frac{2\pi}{\hbar} \frac{e^2 S_L}{(2J+1)G} F \sum_\lambda \gamma_\lambda \langle \alpha' J' \| U^{(\lambda)} \| \alpha J \rangle^2 \tag{13}$$

$$W_{\text{ET}} = \frac{2\pi}{\hbar} \frac{e^2 S_L}{(2J+1)G R_L^6} F \sum_\lambda \Omega_\lambda^{\text{e.d.}} \langle \alpha' J' \| U^{(\lambda)} \| \alpha J \rangle^2 \tag{14}$$

$$\gamma_\lambda = (\lambda + 1) \frac{\langle r^\lambda \rangle^2}{(R_L^{\lambda+2})^2} \langle 3 \| C^{(\lambda)} \| 3 \rangle^2 (1 - \sigma_\lambda)^2 \tag{15}$$

$$W_{\text{ET}} = \frac{8\pi}{3\hbar} \frac{e^2 (1-\sigma_0)^2}{(2J+1) R_L^4} F \langle \alpha' J' \| S \| \alpha J \rangle^2 \sum_m |\langle \phi | \sum_k \mu_z(k) s_m(k) | \phi' \rangle|^2 \tag{16}$$

An approximate expression for the F factor appearing above is given by equation 17, where γ_{L} is the ligand state band width at half-height and Δ is the difference between the donor and acceptor transition energies involved in the transfer process[20].

$$F = \frac{1}{\hbar \gamma_{\text{L}}} \sqrt{\frac{\ln 2}{\pi}} \exp\left[- \left(\frac{\Delta}{\hbar \gamma_{\text{L}}} \right)^2 \ln 2 \right] \tag{17}$$

From the rare-earth-ion side the selection rules for the transfer process may be derived from the reduced matrix elements of the tensor operator $\mathrm{U}^{(\lambda)}$, appearing in equations 13 and 14, expressing the multipolar mechanism and the spin operator S appearing in equation 16, expressing the exchange mechanism. The selection rules are $J + J' \geqslant \lambda \geqslant |J - J'|$ ($J = J' = 0$ excluded) for the former mechanism and $\Delta J = 0, \pm 1$ for the latter. These rules are, therefore, complementary and are operative as long as the total angular momentum J can be taken as a good quantum number. From the diketone ligand side the selection rules are derived from the dipole strength S_{L}, for the multipolar mechanism, and from the matrix element involving the coupled dipole and spin operators in equation 16 for the exchange mechanism. These quantities, as well as the distance R_{L}, may be calculated by quantum chemical methods as, for example, the method based on the sparkle model for rare-earth compounds recently introduced in the literature[31]. Calculated values of transfer rates[49] are consistent with the range of experimental estimates.

The influence of ligand-to-metal charge transfer (LMCT) states on the intramolecular energy transfer processes in rare-earth coordination compounds has been analyzed[75,76]. It has been shown that, depending on the relative energy position of the LMCT state, important luminescence quenching effects may be operative. The quenching process may occur through intramolecular energy transfer channels either from ligand excited states or from excited 4f states to the LMCT state, or both channels simultaneously. Low-lying energy (near UV-visible) LMCT states occur when the metal ion has a high electron affinity and the ligand has a low ionization potential. Reports on the observation of charge transfer bands in rare-earth β-diketonates are rather scarce. However, evidence of luminescence quenching through LMCT states in some of these compounds may be found in the literature[77–79].

d. Experimental emission quantum yield (q_{exp}) measurements. The emission quantum yield can be defined for all practical purposes as the ratio between the number of photons emitted by the rare-earth ions and the number of photons absorbed by the ligand[80]. Bril and coworkers[81–84] used the q_{exp} values for a given solid state sample which can be determined by comparison with standard phosphors. This method provides absolute yields while avoiding absolute measurements, which are in general complicated. The experimental quantum yield q_{exp} of a sample is thus determined as shown in equation 18, where r_{st} and r_x are the amount of exciting radiation reflected by the standard and by the sample, respectively, and q_{st} is the quantum yield of the standard phosphor. The terms $\Delta\phi_x$ and $\Delta\phi_{st}$ give the integrated photon flux (photon s^{-1} cm^{-2}) for the sample and the standard phosphor, respectively. The values of r_{st}, r_x, $\Delta\phi_x$ and $\Delta\phi_{st}$ must be obtained for the same excitation wavelength, geometry and instrumental conditions. The values of $\Delta\phi_x$ and $\Delta\phi_{st}$ are determined by integrating the emission intensity over the total spectral range in the emission spectra, plotted as quanta per wavelength interval (photon s^{-1} nm^{-1}) versus wavelength (nm). The reflection coefficients (r) are established by scanning the emission monochromator through the excitation wavelength region, and integrating the intensities of the spectra thus obtained. In order to have absolute r values, MgO is used as a reflectance standard[81] ($r = 0.91$).

$$q_{exp} = \frac{(1 - r_{st})}{(1 - r_x)} \frac{(\Delta\phi_x)}{(\Delta\phi r_{st})} q_{st} \tag{18}$$

Sodium salicylate has been used as a standard emission quantum yield, exhibiting a broad emission band around 450 nm and $q_{st} = 60\%$ at room temperature[83]. de Mello Donegá and coworkers[85–88] have reported some commercial phosphors as standards, such as Y_2O_3 doped with 3% Eu (Philips YOX-U719, $\lambda_{emiss} = 610$ nm, $q = 99\%$) for Eu^{3+} samples and $GdMgB_5O_{10}$ doped with Tb and Ce (Philips CBTU734, $\lambda_{emiss} = 542$ nm, $q = 95\%$) for Tb^{3+} samples. However, sodium salicilate is better suited as a standard, since it is readily available and presents a nearly constant quantum yield for excitation wavelengths around 380 nm, with accuracy to within 10%[82].

e. Theoretical emission quantum yield (q_{theo}). The emission quantum yield (q value) can be defined either as the ratio between the intensities (in units of power) of emitted and absorbed light or the ratio between the numbers of emitted and absorbed photons. In the latter case, for the diagram shown in Figure 7, the theoretical quantum yield is given by equation 19[20,49], where N_2 and A are the population and total radiative rate of emission from level $|2\rangle$, respectively, and N_{S_0} and Φ are the population and absorption rate from level $|S_0\rangle$, respectively. The level populations are obtained from a set of appropriate rate equations of the type shown in equation 20, where P_{ij} represents a transition or energy

transfer rate starting from state $|j\rangle$ and P_{ji} represents a transition or transfer rate ending in this state. In the steady state regime all $dN_j/dt = 0$. The level populations must also satisfy the condition $\sum N_j = N$, where N is the total number of emitting species. The rate equations could also be established in terms of the so-called normalized populations (η) defined by $N_i = N\eta_i$.

$$q_{\text{theo}} = \frac{AN_2}{\Phi N_{S_0}} = \frac{\text{number of emitted photons}}{\text{number of absorbed photons}} \tag{19}$$

$$\frac{dN_j}{dt} = -\left(\sum_{i\neq j} P_{ij}\right) N_j + \sum_{i\neq j} P_{ji} N_i \tag{20}$$

Efficient light-conversion molecular systems can thus be designed on the basis of the electronic structures of the rare-earth ion and the ligands, and the rather weak interaction between them, which allow control of the parameters governing the intramolecular energy transfer process and the absorption and decay rates in the compound. For this purpose different classes of molecules, as for example β-diketones, have been shown to be promising as efficient ligands, though in the case of macrocyclic ligands the emission quantum yield tends to be smaller than in the case of β-diketone ligands, possibly due to the presence of low-lying LMCT states.

Table 6 presents calculated transfer rates and theoretical emission quantum yields of Eu^{3+} β-diketonates, which are in agreement with rough estimates based on experimental values, as mentioned at the beginning of Section IV.B.2.e. The transfer rates to the $^5D_0$ and $^5D_1$ levels are dominated by the exchange mechanism, while those to the $^5D_4$ level are dominated by the multipolar mechanism. In the case of the $^5D_0$ level, the thermal population of the $^7F_1$ manifold is required; otherwise a smaller contribution from the multipolar mechanism may be operative through J-mixing effects with the $^7F_2$ level. Details of the calculations may be found elsewhere[20,49]. The calculated values of energy differences, intramolecular energy transfer and back transfer rates and theoretical quantum yield of several Eu^{3+} diketonate complexes (tpi[62], tta[60], pbi[89], fod[90], hfc[91]) have been reported.

3. Terbium

The luminescence spectra of Tb^{3+} β-diketonates ($4f^8$ configuration) generally exhibit bands arising from the $^5D_4 \rightarrow {}^7F_J$ transitions ($J = 0$–6) in the metal ion assigned as: $^5D_4 \rightarrow {}^7F_0$ (682 nm), $^5D_4 \rightarrow {}^7F_1$ (669 nm), $^5D_4 \rightarrow {}^7F_2$ (653 nm), $^5D_4 \rightarrow {}^7F_3$ (621 nm), $^5D_4 \rightarrow {}^7F_4$ (587 nm), $^5D_4 \rightarrow {}^7F_5$ (545 nm) and $^5D_4 \rightarrow {}^7F_6$ (490 nm) with the $^5D_4 \rightarrow {}^7F_5$ hypersensitive transition as the dominant one. The large gaps between the emitting $^5D_4$ levels and final ^7F_J levels are around 15000 cm^{-1} (Figure 8). Consequently, Tb^{3+} compounds generally exhibit a green color in the presence of UV radiation. In contrast to the Eu^{3+} ion, detailed analyses of energy level structure and symmetry site around the Tb^{3+} ion are complicated since the $^5D_4$ emitting level is nine-fold degenerate[55]. The hypersensitive $^5D_4 \rightarrow {}^7F_5$ transition is the best luminescence probe for the terbium ion[92]. In the case of the acac ligand, for example, the spectral data do not exhibit a broad band from the triplet state of the ligand in the range of 370–550 nm, showing an efficient energy transfer from the ligand to the emitting $^5D_4$ level of the terbium ion. Generally, the sensitization pathway in luminescent Tb^{3+} complexes is similar to those of Eu^{3+} complexes. However, the triplet state of the β-diketonate ligands has to be above or in resonance with the excited $^5D_4$ level (*ca* 20400 cm^{-1})[55].

TABLE 6. Calculated values of energy differences, intramolecular energy transfer rates and theoretical and experimental quantum yields of Eu^{3+} β-diketonate complexes

Eu^{3+} β-diketonate complex	Transition	ΔE (cm^{-1})	Transfer rate (s^{-1})	q_{theo} (%)	q_{exp} (%)	Reference
$[Eu(dbm)_3(H_2O)]$	$S \rightarrow {}^5D_4$	2118	$8.2 \cdot 10^6$			52
	$T \rightarrow {}^5D_1$	1464	$2.1 \cdot 10^{10}$	25	1	
	$T \rightarrow {}^5D_0$	3334	$1.0 \cdot 10^{10}$			
$[Eu(dbm)_3(dmac)]$	$S \rightarrow {}^5D_4$	2118	$8.2 \cdot 10^6$			52
	$T \rightarrow {}^5D_1$	2116	$1.8 \cdot 10^{10}$	59	45	
	$T \rightarrow {}^5D_0$	3986	$7.2 \cdot 10^9$			
$[Eu(dbm)_3(dmfa)]$	$S \rightarrow {}^5D_4$	2162	$8.7 \cdot 10^6$			52
	$T \rightarrow {}^5D_1$	2116	$1.8 \cdot 10^{10}$	61	43	
	$T \rightarrow {}^5D_0$	3986	$7.2 \cdot 10^9$			
$[Eu(tta)_3(H_2O)_2]$	$S \rightarrow {}^5D_4$	1898	$9.2 \cdot 10^6$			52
	$T \rightarrow {}^5D_1$	1255	$2.2 \cdot 10^{10}$	29	23	
	$T \rightarrow {}^5D_0$	3125	$1.2 \cdot 10^{10}$			
$[Eu(tta)_3(bza)_2]$	$S \rightarrow {}^5D_4$	2162	$8.3 \cdot 10^6$			52
	$T \rightarrow {}^5D_1$	1872	$1.9 \cdot 10^{10}$	62	54	
	$T \rightarrow {}^5D_0$	3742	$8.3 \cdot 10^9$			
$[Eu(tta)_3(pza)]$	$S \rightarrow {}^5D_4$	2430	$7.6 \cdot 10^6$			52
	$T \rightarrow {}^5D_1$	1173	$2.3 \cdot 10^{10}$	24	26	
	$T \rightarrow {}^5D_0$	3043	$1.2 \cdot 10^{10}$			
$[Eu(tta)_3(dmac)_2]$	$S \rightarrow {}^5D_4$	1640	$9.6 \cdot 10^6$			52
	$T \rightarrow {}^5D_1$	1851	$1.9 \cdot 10^{10}$	72	78	
	$T \rightarrow {}^5D_0$	3721	$8.4 \cdot 10^9$			
$[Eu(tta)_3(dmfa)(H_2O)]$	$S \rightarrow {}^5D_4$	1898	$9.0 \cdot 10^6$			52
	$T \rightarrow {}^5D_1$	1677	$2.0 \cdot 10^{10}$	58	45	
	$T \rightarrow {}^5D_0$	3547	$9.3 \cdot 10^9$			
$[Eu(tta)_3(dmbz)_2]$	$S \rightarrow {}^5D_4$	1683	$9.5 \cdot 10^6$			52
	$T \rightarrow {}^5D_1$	1763	$2.0 \cdot 10^{10}$	82	81	
	$T \rightarrow {}^5D_0$	3633	$8.9 \cdot 10^9$			
$[Eu(tta)_3(dpac)_2]$	$S \rightarrow {}^5D_4$	729	$1.1 \cdot 10^7$			52
	$T \rightarrow {}^5D_1$	1591	$2.1 \cdot 10^{10}$	42	—	
	$T \rightarrow {}^5D_0$	3461	$9.7 \cdot 10^9$			
$[Eu(tta)_3(dpfa)_2]$	$S \rightarrow {}^5D_4$	1726	$9.4 \cdot 10^6$			52
	$T \rightarrow {}^5D_1$	930	$2.3 \cdot 10^{10}$	28	40	
	$T \rightarrow {}^5D_0$	2800	$1.3 \cdot 10^{10}$			
$[Eu(bzac)_3(bipy)]$	$S \rightarrow {}^5D_4$	4847	$2.3 \cdot 10^7$			35
	$T \rightarrow {}^5D_1$	3138	$1.2 \cdot 10^{11}$	41	30	
	$T \rightarrow {}^5D_0$	5008	$3.7 \cdot 10^{10}$			
$[Eu(btfa)_3(bipy)]$	$S \rightarrow {}^5D_4$	4456	$3.4 \cdot 10^6$			35
	$T \rightarrow {}^5D_1$	2472	$1.1 \cdot 10^{11}$	58	43	
	$T \rightarrow {}^5D_0$	4342	$6.3 \cdot 10^9$			

(*continued overleaf*)

TABLE 6. (*continued*)

Eu^{3+} β-diketonate complex	Transition	ΔE (cm^{-1})	Transfer rate (s^{-1})	q_{theo} (%)	q_{exp} (%)	Reference
$[Eu(bzac)_3(phen)]$	$S \rightarrow {}^5D_4$	3924	$1.1 \cdot 10^7$			35
	$T \rightarrow {}^5D_1$	3157	$3.3 \cdot 10^{10}$	28	18	
	$T \rightarrow {}^5D_0$	5027	$9.9 \cdot 10^9$			
$[Eu(btfa)_3(phen)]$	$S \rightarrow {}^5D_4$	3852	$5.6 \cdot 10^6$			35
	$T \rightarrow {}^5D_1$	2553	$1.2 \cdot 10^{11}$	50	50	
	$T \rightarrow {}^5D_0$	4287	$6.7 \cdot 10^9$			
$[Eu(btfa)_3(H_2O)_2]$	$S \rightarrow {}^5D_4$	5490	$1.9 \cdot 10^6$			35
	$T \rightarrow {}^5D_1$	1221	$3.4 \cdot 10^{10}$	24	24	
	$T \rightarrow {}^5D_0$	3091	$1.8 \cdot 10^{10}$			
$[Eu(bzac)_3(H_2O)_2]$	$S \rightarrow {}^5D_4$	5574	$1.4 \cdot 10^6$			35
	$T \rightarrow {}^5D_1$	2401	$2.1 \cdot 10^{10}$	21	21	
	$T \rightarrow {}^5D_0$	4271	$7.7 \cdot 10^9$			

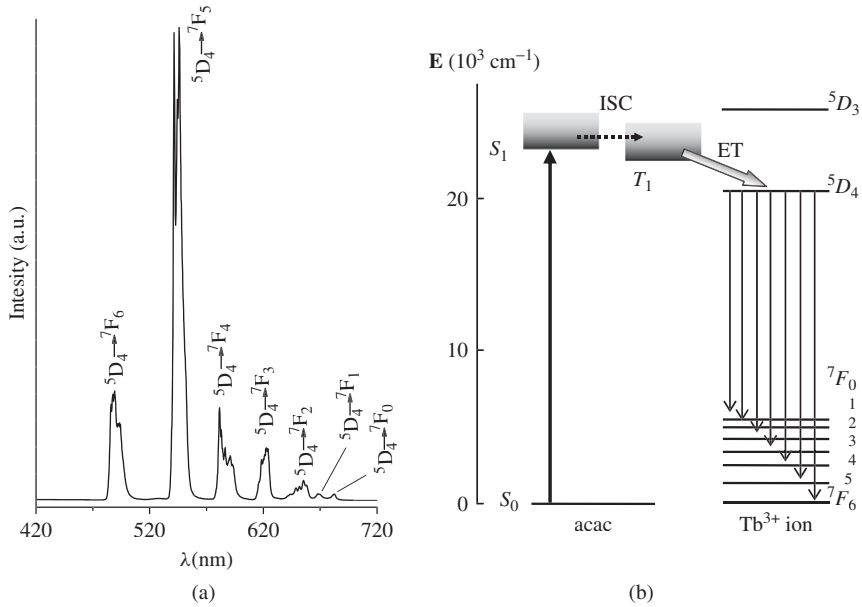

FIGURE 8. Emission spectrum (a) and energy level diagram (b) of epoxy:10% $Tb(acac)_3$. Reproduced with permission from Reference 92, Copyright 2004 John Wiley & Sons, Ltd

According to Reinhoudt's empirical rule[93] the intersystem crossing process will be effective when the energy gap between S and T states of the ligands, ΔE $[S(^1\pi\pi) - T(^3\pi\pi)]$, is around 5000 cm^{-1}. In addition, Latva and coworkers[94] reported that the best intramolecular energy transfer from a ligand to Tb^{3+} occurs when the energy gap between the T state of the ligand and the first emitting $^5D_4$ level of the Tb^{3+} is higher than

2000 cm^{-1}. Biju and coworkers[30] observed that ΔE for pbi and tpi diketonate ligands is 5180 and 5160 cm^{-1}, respectively. The energy transfer process for $[Tb(tpi)_3(H_2O)_2]$ has ΔE $[T(^3\pi\pi) - ^5 D_4 = 22620 - 20400 = 2220\ cm^{-1}]$, indicating an efficient energy transfer from the tpi ligand to the Tb^{3+} ion. However, the value ΔE $[T(^3\pi\pi) - ^5 D_4] =$ 1880 cm^{-1} for $[Tb(pbi)_3(H_2O)_2]$ indicates that the T state (22220 cm^{-1}) of pbi is close to the emitting $^5D_4$ level (20400 cm^{-1}) of Tb^{3+}, suggesting an energy back transfer from the metal ion to the pbi ligand ($^5D_4 \rightarrow T$)[30].

$[Tb(acac)_3]$, $[Tb(4,4'\text{-}F_2dbm)_3]$ and $[Tb(tfa)_3]$ show high luminescence intensity[95], the first one being the strongest[96,97]. Other luminescent Tb^{3+} aromatic β-diketonates are those with 1-indoleacetylacetonate and 3-indoleacetylacetonate ligands[98–100]. In this case, the T state of the indole group has a higher energy than the T state of the phenyl group, leading to a better energy transfer from the ligand to the Tb^{3+} ion. In addition, the presence of a rigid planar structure in the complex favors a higher luminescence intensity[96,97]. For determination of the luminescence quantum yield for Tb^{3+} complexes in solution, quinine sulfate (54.6%, in 0.5 M aqueous H_2SO_4) and 9,10-diphenylanthracene (90% in cyclohexane) can be used as standard[101]; Tb^{3+} tris(dipicolinate) complex has also been used as secondary standard[101,102]. The dendritic Tb^{3+} complexes with 1-phenyl-3-[**G**-n]-4-phenylacetyl-5-pyrazolone ($n = 0$–3), where **G** stands for polyaryl ether, showed luminescence quantum yields increasing from 0.1 to 2.26% with an increase of the dendritic generation from 0 to 3, which is associated with an energy transfer from the ligand to Tb^{3+} and is due to both an 'antenna effect' and a 'shell effect'[103].

The energy transfer from Tb^{3+} to Eu^{3+} ion in the $[Eu/Tb(tfa)_3(tppo)_2]$ pure chelate and the *in situ* chelate doped in gel glass indicates that the Dexter exchange mechanism is operative in the energy transfer process between ions[104]. Pettinari and coworkers[105,106] showed terbium 4-acylpyrazol-5-onate and its derivatives are luminescent materials, also pointing to the importance of properties such as hydrophobicity, solubility in non-polar solvents and large size of the molecule.

Zhou and coworkers[107] studied a series of 4-acylpyrazolone terbium complexes, $[Tb(\beta\text{-diketonate})_3(H_2O)_2]$. The triplet states of pmap (20580 cm^{-1}), pmpp (20750 cm^{-1}) and pmip (20370 cm^{-1}) are slightly higher or close to the emitting $^5D_4$ level (20400 cm^{-1}) of Tb^{3+}, thereby increasing the efficiency of energy transfer and yielding a strong luminescence. On the other hand, the triplet states of pmnp (19300 cm^{-1}) and pmbp (18180 cm^{-1}) are lower than the first emitting excited $^5D_4$ level, and thus the energy transfer cannot be operative. The first absorption band of a series of 1-phenyl-3-methyl-4-RCO-5-pyrazolone compounds gradually shifts toward the shorter wavelength region as the R group changes from an electron acceptor to an electron donor. In the same way, the photoluminescence quantum efficiency of the terbium complexes increases[108].

A novel bis-β-diketone 2,6-bis(3-phenyl-3-ketopropionyl)pyridine with Eu, Tb, Sm and Gd ions is luminescent. All these rare-earth ions could be sensitized to some extent by the ligand. In particular, the Tb^{3+} complex is an excellent green emitter and may find application in organic light-emitting devices (OLEDs) and medical diagnosis[109].

The complex of N-(2-pyridinyl)-3-ketobutyramide with Tb^{3+} in methanol solution can emit the intrinsic fluorescence of Tb^{3+}. When Et_3N and Zn^{2+} are added to the solution, the fluorescence ($\lambda_{ex} = 329$ nm, $\lambda_{fl} = 546$ nm) is significantly enhanced. This sensitive fluorescence enhancement system can be used for the determination of terbium ion[110].

4. Samarium

Sm^{3+} β-diketonates show intense luminescence of orange color[57]. Sm^{3+} has an odd-electron configuration ($4f^5$) and it is labeled, therefore, as a Kramer ion due to its electronic

states that are at least doubly degenerated in any ligand field[111]. The maximum number of the Stark components for Kramer ions with $^{2S+1}L_J$ state is $J+1/2$ for any symmetry lower than cubic[112]. Detailed analyses of the energy levels of Sm^{3+} in several hosts have been reported[113,114]. The emitting $^4G_{5/2}$ state of the Sm^{3+} ion (*ca* 18021 cm^{-1}) is resonant with a great number of triplet states of several β-diketonate ligands, which allows an efficient energy transfer from the ligand to the rare earth ion ($T \rightarrow Sm^{3+}$). The sharp bands in the luminescence spectra of samarium complexes consists of transitions from the $^4G_{5/2}$ excited state to the lower energy levels ^6H_J ($J = 5/2$, 7/2, 9/2, 11/2, 13/2 and 15/2) and ^6F_J ($J = 1/2$ and 3/2). The $^4G_{5/2} \rightarrow {}^6H_{9/2}$ transition (*ca* 642 nm) is the hypersensitive and intermediate gaps between the emitting $^4G_{5/2}$ level and final ^6H_J levels are around 7500 cm^{-1}. Because of the Kramer degeneracy, the low temperature emission pattern should consist of 3, 4, 5, 6, 7, 8, 1 and 2 lines, respectively, for each aforementioned manifold, when Sm^{3+} ions occupy a site of low symmetry in the ligand field[115].

In a recent PL study, Sm^{3+} β-diketonates with sulfoxide, phosphine oxide and amide ligands showed the characteristic orange emission color of the Sm^{3+} ion[116]. The emission spectra of these complexes present narrow bands arising from the $^4G_{5/2} \rightarrow {}^6H_J$ ($J = 5/2$, 7/2, 9/2, 11/2) transitions with the hypersensitive $^4G_{5/2} \rightarrow {}^6H_{9/2}$ transition as a prominent group. An efficient intramolecular energy transfer from the T state of the tta ligand to the emitting $^4G_{5/2}$ state of Sm^{3+} has been observed (Figure 9). The lifetimes (τ) of the emitting level $^4G_{5/2}$ of the Sm complexes are approximately ten times longer than in the

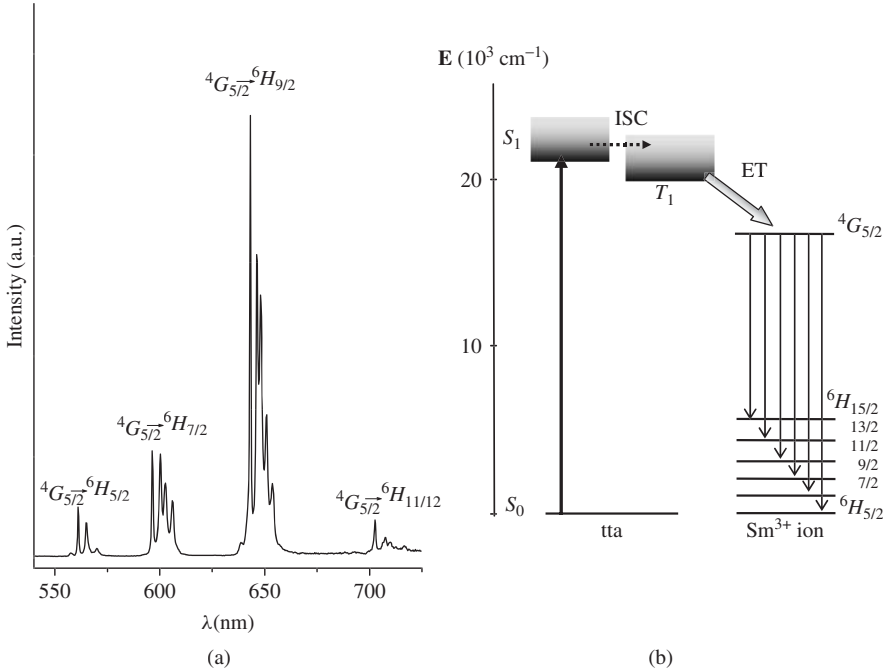

FIGURE 9. Emission spectrum (a) and energy level diagram (b) of the $[Sm(tta)_3(H_2O)_2]$ complex. Reproduced with permission from Reference 116, Copyright 2002 Elsevier

precursor hydrate $[Sm(tta)_3(H_2O)_2]$, indicating that radiative processes are operative in all the compounds due to the absence of multiphonon relaxation by coupling with the OH oscillators. The transition $^4G_{5/2} \rightarrow {}^6H_{5/2}$ (*ca* 560 nm) is taken as the reference due to its predominant magnetic dipole character ($\Delta J = 0$). On the other hand, the $^4G_{5/2} \rightarrow {}^6H_{9/2}$ transition is magnetic-dipole forbidden and electric-dipole allowed. From this transition the intensity parameter (η_{Sm}) has been determined for $[Sm(tta)_3(L)_2]$ complexes, where L = dbso, ptso, tppo and pha; η_{Sm} is the ratio between the intensities of the $^4G_{5/2} \rightarrow {}^6H_{9/2}$ and $^4G_{5/2} \rightarrow {}^6H_{5/2}$ transitions, pointing to the highly polarizable chemical environment around Sm^{3+} in the complexes[116].

Fabrication of luminescent polymeric nanoparticles doped with a Sm^{3+} β-diketonate compound by self-organized particle precipitation methods has been recently reported by Tamaki and coworkers[117]. They point to the importance of miscibility of the lanthanide complex dopant with the polymeric matrix to the particle luminescence. Polystyrene nanoparticles doped with a lanthanide β-diketonate complex possessing phenyl groups present highly uniform luminescence under UV irradiation. The increase of the emission intensities of uncured and cured $[Sm(tta)_3(phen)]$/nitrite rubber composites with increase of the complex content has been recently observed. Given the same complex content, the cured composites were found to have higher luminescence intensity. This was attributed to the cross-linking network helping to stabilize the coordination environment of the central Sm^{3+} and improving the energy transfer efficiency to it[118]. The PL and EL properties of a pmma film doped with the newly synthesized $[Sm(hfa)_3(phen)_2(MeOH)]$ were studied. The film shows peaks around 564, 598, 645 and 710 nm, characteristic of Sm^{3+}. Due to its good PL properties this composite has been tested for OLED devices[119].

An innovative near-infrared-luminescent mesoporous material has been prepared by linking trivalent rare-earth ion complexes ($RE^{3+} = Pr^{3+}$, Nd^{3+}, Sm^{3+}, Er^{3+} and Yb^{3+}) to the ordered mesoporous MCM-41 through 5-(*N*,*N*-bis-(3-(triethoxysilyl)propyl)ureyl)-1,10-phenanthroline. These materials have the characteristic NIR luminescence of the corresponding RE^{3+} ions, by sensitization from the organic ligands moiety, upon excitation at the absorption wavelengths of the organic ligands. Their good luminescence performance makes them of potential application in optical amplification (operating at 1300 or 1500 nm), laser systems and medical diagnosis[120]. $[RE(hfnh)_3(phen)]$ complexes, where RE = Eu and Sm, exhibit bright PL due to the characteristic emission from the Eu^{3+} and Sm^{3+} ions. Devices using the two complexes as emitting layers have been fabricated[121].

Organized molecular films of $[RE(\beta\text{-diketonate})_3(phen)]$ complexes have been fabricated by the Langmuir–Blodgett films (LB) technology, where RE^{3+} = Sm, Eu and Tb, and β-diketonate = acac, tfa, hfa and tta[122]. The luminescence lifetimes of these complexes were measured by the laser-induced luminescence decay and it was observed that the lifetimes of the complexes in LB films were longer than that in solution and solid powder[122]. A new methodology for the rapid optimization of the luminescence conditions of the thin-film sample in arrays of microwells has been used. The results have shown that a multi-parallel approach is a valid possibility for luminescence measurements and represents a tool to rapidly optimize the luminescence conditions. The intramolecular and intermolecular energy transfer processes in aggregates of $[Sm(dbm)_3phen]$ and $[RE(dbm)_3phen]$ (RE = La, Gd, Tb, Y) co-doped pmma films make the cofluorescence effect operative[123].

5. Dysprosium

The PL spectrum of the recently synthesized $[Dy(pm)_3(tppo)_2]$ shows the characteristic yellow emission band at 572 nm and blue emission band at 480 nm, corresponding to the

$^4F_{9/2} \rightarrow {}^6H_{13/2}$ and $^4F_{9/2} \rightarrow {}^6H_{15/2}$ transitions of Dy^{3+}, respectively. The antenna effect was adduced to discuss the energy transfer mechanism between the ligand and the central Dy^{3+} ion[124].

The luminescence of [Dy(acac)$_3$tatbp] was investigated, where the alkyl substituents on the tatpb porphyrin ligand ranged from C_6H_{13} to $C_{18}H_{37}$[125]. Quantum yields of the $S_1 \rightarrow S_0$ fluorescence are in the range 0.26–0.28 and the fluorescence lifetimes are in the range 0.013–0.019 ms at room temperature. The phosphorescence bands of the complex at 77 K appear at 714 nm. The phosphorescence of the ligand at low and room temperature did not appear in the spectra. These materials are of potential application in extremely high-density optical recording, frequency domain optical storage, optical frequency conversion, superconductivity, information processing and transmission.

6. Thulium

The photophysical analysis of the excitation and absorption spectra of [Tm(ppa)$_3$ $(H_2O)_2$], an α-substituted β-diketonate investigated by Serra and coworkers[126,127], showed a broad band centered around 335 nm, which is ascribed to the complex, since the ppa absorbance maximum is centered at 296 nm. The emission spectra ($\lambda_{exc} = 335$ nm) presented the characteristic bands of Tm^{3+} due to the $^1G_4 \rightarrow {}^3H_6$ (478 nm), $^1G_4 \rightarrow {}^3F_4$ (650 nm), $^1G_4 \rightarrow {}^3H_5$ (770 nm) and $^3H_4 \rightarrow {}^3H_6$ (790 nm) transitions. The PL spectrum of [Gd(ppa)$_3$(H_2O)$_2$] shows the triplet state of the ppa transition at 19200 cm^{-1}.

The spectral hole-burning properties of Tm^{3+} β-diketonates blended in a pmma matrix has been reported. Persistent spectral hole burning was observed for the $^3H_4(1) \rightarrow {}^3H_6(1)$ transition of Tm^{3+} near 795 nm in these materials. The holewidth was found to be in the range 180–360 MHz and the hole lifetime is longer than 10 h at 1.4 K. A complex hole profile which is best described by the superposition of two Lorentzians has been observed. Temperature cycling experiments have been performed. The maximum annealing temperature was determined for the complexes, and its correlation with the size of the side groups has been established. Spectroscopic results indicate glass-like properties for these materials, i.e. a high degree of disorder in the Tm^{3+} coordination surroundings. The materials have large inhomogeneous broadening, and certainly deserve further investigation for possible hole-burning frequency- and time-domain storage and other applications[128].

C. Electroluminescence of RE^{3+} β-Diketonates

Electroluminescence (EL) is defined as a non-thermal generation of light resulting from the application of an electric field to a substance[129]. This phenomenon was first observed by Destriau in 1936 when a large electric field was applied to ZnS[130]. Since the work of Tang and VanSlyke[131] in 1987 and Burroughes and coworkers[132] in 1990, EL was observed in a multilayer device containing an organic compound as emitting layer (OLED); this field has rapidly established itself as a new branch of applied science. The first organic light-emitting device containing RE^{3+} β-diketonate complexes was reported by Kido and coworkers[5] using the Tb^{3+}-acac as emitting layer[5].

The simplest OLED is a device consisting of a single organic layer sandwiched between the anode and the cathode. For a compound to be used in a single-layer device it must have high PL quantum efficiency and good bipolar charge-transport properties of holes and electrons through the organic layer. However, to improve the charge transport and injection in devices additional layers are generally necessary of a hole and/or of an electron-transport material[131,133], leading to the two-layer or three-layer OLED (Figure 10). It is important to mention that the hole transport layer (HTL) can also help to block the migration of excitons from the emitting layer. The most extensively used molecules as electron

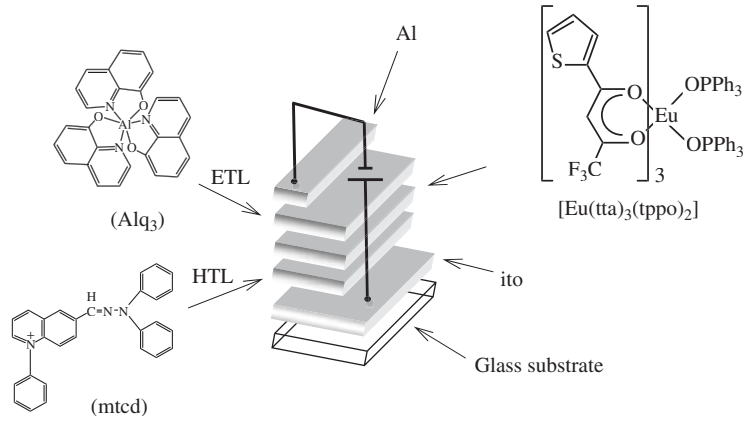

FIGURE 10. $[Eu(tta)_3(tppo)_2]$ complex used as the emitter in a three-layer OLED cell structure, sandwiched between an ito cathode and an aluminum anode[134]. Reproduced with permission from Reference 134, Copyright 2002 Sociedade Brasileira de Física

transport materials in OLEDs are bbpo and Alq_3. However, pvk, mtcd and tpd have been also used as hole-transport materials.

The fabrication and characterization of red emitting triple-layer electroluminescent organic devices using vacuum deposited $[Eu(tta)_3(tppo)_2]$ as emitting layer has been described[134]. Figures 11a and 11b shown a comparison between the EL spectrum of the ito/mtcd/$[Eu(tta)_3(tppo)_2]$/Alq_3/Al OLED device and the PL spectrum taken from a $[Eu(tta)_3(tppo)_2]$ thermally deposited thin film, under excitation at 350 nm. These spectra recorded at room temperature are similar. Moreover, the typical Alq_3 wide emission band, peaked at 520 nm, is absent in the PL spectrum, indicating that the energy transfer process from the triplet of tta ligand to the Eu^{3+} ion is quite efficient.

Although several methods may be used to fabricate the organic layers in OLEDs, such as thermal evaporation, Langmuir–Blodget deposition or spin coating from solutions, RE^{3+} β-diketonates usually are deposited by thermal evaporation techniques, under high vacuum (*ca* 10^{-5} Pa); thus, volatility and thermal stability of the diketonates are required[5].

The operating mechanism in OLEDs is described as the injection of electrons from the cathode (usually a low-work-function metal such as Al or an alloy such as Mg:Ag), which are transported into the organic layer via the LUMO, whereas holes from the anode (usually ito) are injected and transported via the HOMO. Electrons and holes recombine within the organic emitting layer. In these devices the energy gap and ionization potential of RE^{3+} compounds are generally estimated by optical and electrochemical techniques, as described by Hümmelgen and coworkers[135]. Based on these results it has been possible to construct the energy level diagrams of HOMO and LUMO states for device components, which were correlated to useful quantities such as the Al and ito electrode work functions. The energy diagram is important for further understanding and optimization of the device performance.

OLEDs are nowadays the most important type of light source for artificial lighting, making them potential candidates in the development of full-color flat panel display devices. Challenging problems to be addressed are emission color, emission efficiency and device lifetime. The emission color problem results from the broad emission bands exhibited by electroluminescent devices containing organic emitting layers, since pure and sharp emission bands from these materials, a requisite for display applications, are

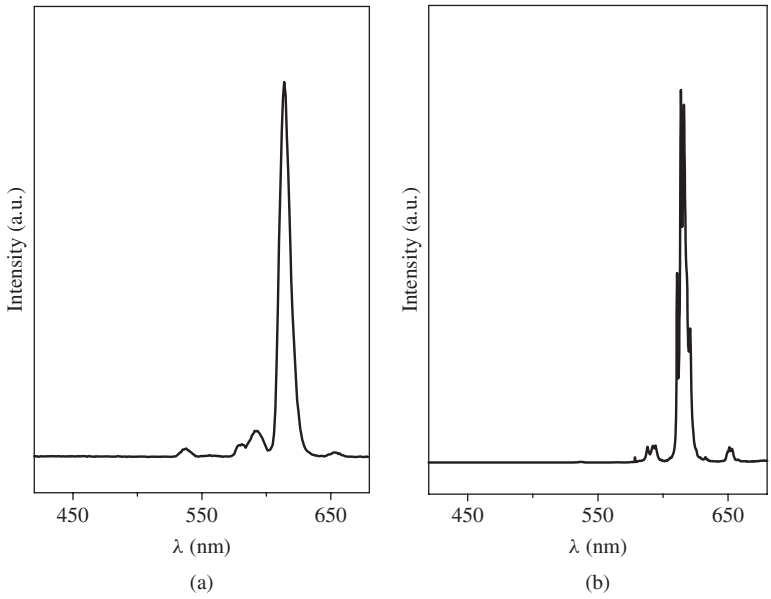

FIGURE 11. (a) EL spectrum of a Eu^{3+} complex as emitting layer in the ito/mtcd/[$Eu(tta)_3(tppo)_2$]/Alq/Al OLED device with bias voltage of 22 V and (b) PL spectrum of the [$Eu(tta)_3(tppo)_2$] complex thin film. Reproduced with permission from Reference 134, Copyright 2002 Sociedade Brasileira de Física

difficult to obtain, and consequently, OLEDs based on these materials usually exhibit no pure emission colors. To overcome this problem, OLEDs using RE^{3+} compounds as the emitting layer have been extensively investigated[5]. As discussed in Section IV.B.1, the most important emission bands in RE^{3+} ions arise from intraconfigurational transitions which are extremely sharp, leading to almost monochromatic light emission[20]. Besides, RE^{3+} β-diketonates provide a significant improvement in the internal quantum efficiencies. In OLEDs using fluorescent organic compounds as emitting layers, the energy of the excited T states usually are completely degraded by thermal deactivation without light emission, limiting the internal quantum efficiency. On the other hand, for devices using RE^{3+} β-diketonates as emitting layer, the theoretical quantum efficiencies may be extremely high because the T states of the ligand may be closely matched to or slightly above the RE^{3+} emitting levels (Figure 7). These excited ligand states that are generated by carrier recombination may transfer their energy efficiently to the central RE^{3+} ion, which undergoes the characteristic radiative emitting process[26]. In this case, the diketonate ligands may act as an 'antenna' sensitizing the luminescence of the RE^{3+} ions. These properties make RE^{3+} β-diketonates promising candidates for full color flat-panel displays, which require pure red, green and blue emissions.

The biggest challenge today for the EL devices containing RE^{3+} β-diketonates is the increase of efficiency and stability of the devices. Double layer devices, such as ito/tpd/[Eu β-diketonate]/Al, have demonstrated the ability of the RE^{3+} β-diketonates to act also as electron transporters, despite the large electron energy barrier between the Al electrode Fermi level and the RE^{3+} β-diketonate LUMO level.

In RE^{3+} β-diketonates certain neutral Lewis base ligands coordinated to the central metal ions act as synergic agents, which not only saturate the first coordination sphere of the RE^{3+} ions but also improve the fluorescence intensity, volatility and stability of the rare-earth complex. For EL applications these ligands also improve the charge mobility of the RE^{3+} complexes in the devices. For example, in EL devices of Tb^{3+} acylpyrazolonates having a neutral ligand, the EL spectra exhibit both the light-emitting layer and the hole-transport layer, while the EL devices without a neutral ligand display a pure green color, coming solely from the light-emitting layer, thus demonstrating the higher electron-transport ability of the compounds with neutral Lewis bases[136]. Zhang and coworkers[137] fabricated a novel OLED containing a complex functionalized by a carbazole fragment, [Eu(dbm)$_3$(hcpybm)], showing improved hole transporting ability as compared to a device based on the unfunctionalized complex [Eu(dbm)$_3$pybm]. This demonstrates that chemical modification of the neutral ligand may improve the balancing injection, transport and recombination of charge carriers in OLEDs containing RE^{3+} β-diketonates as emitting layers. The most frequently used neutral ligands are tppo, bipy, phen and their derivatives. New β-diketones and neutral ligands are being synthesized, to fabricate high performance OLEDs. Recently, 1-(4′-(5-(4-tolyl)-1,3,4-oxadiazol-2-yl)biphenyl-4-yl)-4,4,4-trifluorobutane-1,3-dione (mpbdtfa) with an electro-transporting oxadiazole group has been prepared. Its europium complex exhibits high yield and high thermal stability, which makes it a potential candidate for fabrication of red-emitting OLEDs[138].

Bian and coworkers[139] reported the fabrication of a four-layer device by using the vacuum deposited film of the Eu^{3+} complex as the emitting layer, Alq_3 as electron-transporting layer, bcp as hole-blocking layer and tpd as a hole-transporting layer. This device, with a luminance of *ca* 230 cd m^{-2}, was more efficient than the more common ones containing two or three layers.

Thermal evaporation is one of the most efficient methods for the preparation of diketonate complexe layers. However, many of these compounds are thermally unstable at high temperature and require an alternative method. Milder conditions are attained on incorporating such compounds into polymer host materials, followed by thin film deposition by the spin coating method. In these cases, the luminance of OLED devices is comparable to those measured for devices fabricated using small molecules and polymer blends.

Other advantages in using RE^{3+} β-diketonates doped into polymers are: (i) the polymer matrices generally form better films than the small molecules; (ii) some polymers can act as charge transporters, improving the EL phenomenon—for example, poly(*N*-vinylcarbazole) (pvk) acts as a hole transporter exhibiting a mobility comparable to the hole mobilities of small molecule materials such as tpd[139]; and (iii) the polymer-RE^{3+} energy transfer may be observed when there is an overlap between the emission spectrum of the polymer used as matrix and the absorption spectrum of the antenna ligand coordinated to the RE^{3+} ion. It is important to mention that the electron mobility of pvk is negligible and, consequently, it is also employed as an electron blocking layer[140]. In contrast, the higher electron mobility of Alq_3 makes OLED devices fabricated with small molecules often exhibiting higher performance than using polymers.

The most popular among the polymer matrices used for RE^{3+} diketonate doping in EL devices is pvk[140–143]. An efficient energy transfer from the pvk host to the Eu^{3+} ion in the [Eu(fod)$_3$mk] complex, leading to high intensity electroluminescence, has been reported by Wang and Samuel[142] . This behavior reflects the spectral overlap between pvk and the mk ligand. Acylpyrazolones are an interesting class of β-diketones, containing a pyrazole ring fused to a chelating arm[136]. A bilayer OLED, using the blue-fluorescent [Y(qipr)$_3$(bipy)] complex as emitting material and pvk as hole-transporting material, emits bright green light instead of blue light, which has been attributed to the exciplex

formation at the solid interface between the pvk matrix and [Y(qipr)$_3$(bipy)] dopant[136, 140]. O'Riordan and coworkers[144] reported on fabrication of devices presenting the configuration ito/pedot/pvk/Al and ito/pedot/pvk:[Eu(dbm)$_3$(phen)]/Ca/Al using polymer solution spin coating techniques. The benefits caused by pedot are planarization of the ito layer and reduction in the hole injection barrier at the pvk/anode interface. When polymers are used as host, the concentration of doping RE^{3+} compounds is usually required to be low for both EL and PL processes due to the interaction between molecules that cause luminescence quenching[59, 65, 145]. Furthermore, in some cases the rare-earth emission overlaps with the emission from the host polymer, leading to a broadened band.

Some devices using RE^{3+} diketonate doping in the hole or electron transporter layers of small molecular materials have also been fabricated[146]. However, in contrast to polymer doped devices, the organic layers are sequentially deposited under high vacuum. OLEDs containing RE^{3+} diketonates doped in the bcp layer have been fabricated to take advantage of the wide energy gap in cbp which supports bipolar carrier transport. Only a few studies of dinuclear luminescent compounds as emitting layer in OLEDs have been reported, probably due to the close proximity between RE^{3+} centers in the complexes which leads to cross-relaxation luminescence quenching[141].

One of the most interesting features observed in OLEDs based on RE^{3+} diketonate complexes is the presence of electrophosphorescence (EP). This phenomenon occurs in electroluminescent devices when the emission arises from a T state[147]. It is noted that the emitted color by this device depends on the ratio between the rare-earth EL sharp peaks and the EP broad emission band from the $T \rightarrow S$ transition of the tta ligand. An advantage of this system is that it can be used to obtain different colors by simply changing the applied voltage.

OLEDs have been fabricated based on the RE^{3+} *tetrakis*(β-diketonate) anionic complexes as emitting layers (e.g. Li[Eu(tta)$_4$], Na[Eu(tta)$_4$], K[Eu(tta)$_4$] and (pyH)$^+$[Eu(tta)$_4$])[148, 149]. Most EL investigations in RE^{3+} β-diketonates are centered on Eu^{3+}, Tb^{3+} and Sm^{3+} compounds with acac, dbm or tta as ligands, whereas works reporting the fabrication of OLEDs based on Nd^{3+}, Er^{3+}, Tm^{3+}, Pr^{3+} and Yb^{3+} ions are rather scarce[1]. OLEDs based on Nd^{3+} and Er^{3+} β-diketonates as emitting layers exhibit infrared emission at 1340 and 1530 nm, respectively, that are assigned to the intraconfigurational $^4F_{3/2} \rightarrow {}^4I_{11/2}$ and $^4I_{13/2} \rightarrow {}^4I_{15/2}$ transitions[150, 151]. Of particular importance is the emission at 1530 nm of Er^{3+} due to its high relevance to optical-fiber communication.

[Dy(acac)$_3$(phen)] and [Dy(pm)$_3$(tppo)$_2$], where pm = 1-phenyl-3-methyl-4-*i*-butyryl-5-pyrazolone, have been used as emitting layer in OLEDs[151, 152]. The EL spectra of these devices consist of a yellow emission band at 572 nm and a blue one at 480 nm, corresponding to the $^4F_{9/2} \rightarrow {}^6H_{13/2}$ and $^4F_{9/2} \rightarrow {}^6H_{15/2}$ transition of the Dy^{3+} ion, respectively. An appropriate tuning of the blue/yellow intensity ratio can presumably accomplish a white luminescence.

A significant step in the development of highly efficient OLEDs consists of the addition of phosphorescent dopants to generate both the singlet and triplet excitons as photons[137–140]. This innovation has led to near-quantitative internal emission efficiencies in OLEDs that are based on small organic molecules.

Bazan and coworkers[153] incorporated Eu^{3+} β-diketonates (acac, dbmim, dmn and bzac) into conjugated polymers. Pure red-emitting LEDs with a quantum efficiency of 1.1% have been made by doping pCNmhp with [Eu(dnm)$_3$phen]. Blue- and green-emitting LEDs have also been made using pCNmhp doped and doped with coumarin 6, respectively. The research could lead to the fabrication of high quality full color displays. Furthermore, RE^{3+} polymer blends could be quite useful as a source of monochromatic emission in photonic crystals. Kuzmina and Eliseeva[154] designed OLEDs based on Eu^{3+}, Tb^{3+} and Tm^{3+} ions with various β-diketonate ligands and noted that the electroluminescence efficency

TABLE 7. Some OLED configurations and their luminance under optimal conditions

OLED configuration[a]	Maximum luminance ($cd\,m^{-2}$)	Reference
ito/tpd/cbp:dcjtb:[Eu(tta)$_3$tmphen]1:0.2:5%/bcp/Li:bcp(2%)/V_2O_5/ tpd/cbp:dcjtb:[Eu(tta)$_3$tmphen](1:0.2:5%)/bcpAlq$_3$/LiF/Al	3000	155
ito/tpd/[Tb(pmip)$_3$(tppo)$_2$]/Alq$_3$/LiF/Al	2500	156
ito/tpd/dcjtb:[Eu(dbm)$_3$tmphen]:cbp(0.2%,5%:1)/bcpAlq$_3$/LiF/Al	2300	155
ito/tapc/[Eu(dbm)$_3$]:bcp(1:1)/bcp/Alq$_3$/ Mg:Ag(10:1)/Ag	2123	157
ito/npb/[Eu(tta)$_3$(dppz)]:cbp (2%)/bcp/Alq$_3$/ Mg0.9:Ag0.1	2046	158
ito/tpd/[Eu(dbm)$_3$(Bath)]:dcm(0.8 wt%)/Mg0.9:Ag0.1	2000	159
ito/tpd/[Eu(dbm)$_3$(tpip)]/bcp/Alq$_3$/ Mg0.9:Ag0.1/Ag	1305	160
ito/tpd/[Eu(hfnh)$_3$(phen)]:cbp(10%)/bcp/Alq$_3$/LiF/Al	1132	146
ito/tpd/cbp:[Eu(tta)$_3$tmphen](1%:1)/bcp/Li:bcp(2%)/V_2O_5/ tpd/cbp:[Eu(tta)$_3$tmphen](1%:1)/bcpAlq$_3$/LiF/Al	1005	155
ito/tpd/[Eu(dbm)$_3$tmphen]:cbp(5%:1)/bcpAlq$_3$/LiF/Al	930	155
ito/tpd/[Tb(pmip)$_3$(tppo)$_2$]/Alq$_3$/Al	920	161
ito/tpd/cpb:[Eu(tta)$_3$nphen]/bcp/Alq$_3$/LiF/Al	800	162
ito/Cupc/[Dy(pm)$_3$(tppo)$_2$]/bcp/Alq$_3$/LiF/Al	524	163
ito/tpd/[Eu(dbm)$_3$phen]:pbd/Alq$_3$/ Mg:Ag.	460	5
ito/tpd/[Eu(dbm)$_3$(bath)]/oxd7/Al[b]	460	133
ito/tpd/[Eu(dtp)$_3$(bath)]/Alq$_3$/Al:Li	450	164
ito/pvk:pbd:[Eu(tta)$_3$(Phen)](0.7 mol%)/bcp/Ca:Al	417	165
ito/tpd/Eu(tta)$_3$ Eu(pyNO)$_2$ Eu(tta)$_3$:cbp/bcp/(Alq$_3$/LiF/Al	340	166
ito/tpd/[Eu(dbm)$_3$(oxd-pybm)]/LiF/Al[c]	322	167
ito/tpd/[Eu(dbm)$_3$L]/bcp/Alq$_3$/ Mg:Ag/Ag	230	139
ito/tpd/[Eu(dbm)$_3$car−pybm]/tpbi/LiF/Al	200	137
ito/pvk/[Tb(mtp)$_3$phen]/Alq$_3$/Al.	152	5
ito/pedot/pvk:[Eu(dbm)$_3$phen/Ca/Al	130	144
ito/[Eu(tta)$_3$phen]:pvk/Mg:In	100	5
ito/[Tb(acac)$_3$(Cl-phen)]/Be(bq)$_2$/Al:Li/Al	95	168
ito/tpd/[Tb(acac)$_3$(bath)]/Alq$_3$/Al	77	169
ito/pvk/pvk:pbd:[Eu(tfa)$_3$(Phen)](10:6:6)/pbd/Al	68	170
ito/tpd/pvk:pbd:[Eu(tfa)$_3$(Phen)](10:6:5)/pbd/Al	63	171
ito/pedot/pvk:[Eu(dbm)$_3$phen)]/Al	62	144
ito/pvk/pvk:pbd:[Tb(tfa)$_3$phen]/pbd/Al	58	172
ito/tpd/[Tb(acac)$_3$(aap)]/Alq$_3$/Al	56	173
ito/pvk:Na[Eu(tta)$_4$](5wt%)/oxd7/Alq$_3$/Al[b]	37	174

[a] Layers are ordered from the cathode to the anode and are separated by a solidus; the components of a mixed layer are separated by a colon.
[b] oxd7 = 1,3-bis[4-(*t*-butylphenyl)-1,3,4-oxadiazolyl]benzene.
[c] oxd = 2-(2-pyridyl)benzimidazole.

depends on factors such as the structure of new highly luminescent RE^{3+} compounds, the OLED architecture (ETL, HTL, cathode, layer quality and thickness) and the chemical, thermal and electrochemical stability of all the materials used in the EL devices. In Table 7 are listed diverse OLED configurations and their luminance under optimal conditions.

D. Triboluminescence of RE^{3+} β-Diketonate Complexes

Triboluminescence (TL) is the phenomenon of light emission during the application of a mechanical stress or by fracture of crystals in a solid sample[175]. The materials presenting this behavior are promising for application in real-time structural damage sensors[176].

However, up to now, no fully clear mechanism by which TL occurs has been presented. Some works suggest that TL is a consequence of a recombination of charges separated during fracture of a crystal belonging to a non-centrosymmetric space group[177]. On the other hand, Cotton and coworkers[7,178] showed that centric compounds can exhibit TL, and they pointed to two non-centric compounds, at least, which show no TL at room temperature. However, TL in centrosymmetric compounds have been generally assigned to impurities or disorder of some atoms in the molecular structure[1,8,179].

Most TL studies are centered on enolate compounds, in particular, rare-earth β-diketonates. Present evidence points to morpholinium tetrakis(dibenzoylmethanato)europate (III) and triethylammonium tetrakis(dibenzoylmethanato)europate(III) as the first and second most efficient triboluminescent compounds, respectively[1]. In these cases the coexistence of disorder in the chelating ring and the non-centrosymmetric crystal structures may contribute to major charge separation upon cleavage and, consequently, to higher luminescence intensity.

Generally, TL spectra of diketonate complexes are characterized by the metal ion-centered transitions, which exhibit similar position and spectral profiles as those photoluminescent ones[180]. The TL spectra of trivalent europium diketonates usually display only those intraconfigurational $^5D_0 \rightarrow {}^7F_J$ ($J = 0$–4) transitions which are dominated by the hypersensitive $^5D_0 \rightarrow {}^7F_2$ transition. In general, the PL is stronger than the TL and as a consequence only the high intensity transitions are observed in the TL spectra.

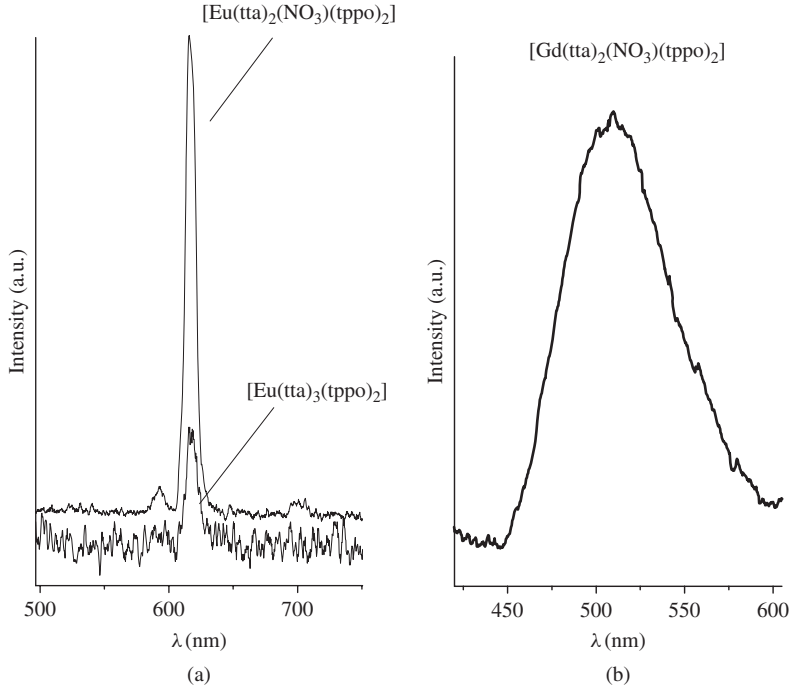

FIGURE 12. Triboluminescence spectra recorded for the sample in solid state, at *ca* 298 K: (a) TL spectra of $[Eu(tta)_2(tppo)_2]$ and $[Eu(tta)_2(tppo)_2(NO_3)]$, and (b) TL spectrum of $[Gd(tta)_2(tppo)_2(NO_3)]$. Reproduced with permission from Reference 38, Copyright 2008 Elsevier

TL phenomena in RE^{3+} β-diketonates have been explained as a result of intramolecular energy transfer from the ligand excited states to the RE^{3+} ion during the fracture process (Section IV.A). However, only recently Teotonio and coworkers[38] have presented experimental data that confirm this mechanism. The TL spectrum of $[Gd(tta)_2(tppo)_2(NO_3)]$ is the first reported tribophosphorescence (TP) spectrum of a diketonate complex (Figure 12). According to the experimental evidence presented by the Gd^{3+} complex, TL for europium complexes may be occurring by the following processes: (i) breakage of crystals, (ii) ligand excitation, (iii) energy transfer from the ligand to the europium ion and (iv) emission from the Eu^{3+} ion. Tribophosphorescence from the $[Gd(tta)_2(tppo)_2(NO_3)]$ complex also suggests that, at least for the similar $[Eu(tta)_2(tppo)_2(NO_3)]$ complex, the energy transfer from the ligand to the Eu^{3+} ion is primarily involving the tta triplet state and one excited $^{2S+1}L_J$ level of the Eu^{3+} ion as energy donor and acceptor, respectively. However, the excitation process of diketonate ligands in the Eu^{3+} complexes is not fully clear. One proposed mechanism suggests that the voltage developed during the fracture is sufficient to promote a gas discharge that is followed by the emission of light, exciting β-diketonate ligands coordinated to the Eu^{3+} ion[181]. Table 8 summarizes some triboluminescent rare-earth diketonates reported in the literature. It is worth mentioning that most of these works deal with TL of Eu^{3+} β-diketonates emitting red light when fractured. In fact, TL studies of other complexes, such as the green-emitting Tb^{3+} enolates and the orange-emitting Sm^{3+} enolates, are rather scarce.

TABLE 8. Triboluminescent RE^{3+} diketonates

RE^{3+} diketonate[a]	TL emission transition (λ_{max}, nm)	Reference
$(dmpy)^+$ $[Sm(tta)_4]^-$	$^4G_{5/2} \rightarrow {}^6H_{9/2}$ (645.4)	182
$(tmpy)^+$ $[Sm(tta)_4]^-$	$^4G_{5/2} \rightarrow {}^6H_{9/2}$ (645.5)	182
$(Et_3NH)^+$ $[Eu(dbm)_4]^-$	$^5D_0 \rightarrow {}^7F_2$ (613.0)	183
$(HOCH_2CH_2)_2NH_2)^+$ $[Eu(dbm)_4]^-$	$^5D_0 \rightarrow {}^7F_2$ (613.0)	184
$(Me)_2NH)^+$ $[Eu(dbm)_4]^-$	$^5D_0 \rightarrow {}^7F_2$ (614.0)	184
$(BnMe_2NH)^+$ $[Eu(dbm)_4]^-$	$^5D_0 \rightarrow {}^7F_2$ (613.0)	184
$(C_4H_8NH_2)^+$ $[Eu(dbm)_4]^-$	$^5D_0 \rightarrow {}^7F_2$ (616.0)	184
$(imdz)^+$ $[Eu(dbm)_4]^-$	$^5D_0 \rightarrow {}^7F_2$ (612.9)	185
$(dmpy)^+$ $[Eu(tta)_4]^-$	$^5D_0 \rightarrow {}^7F_2$ (612.7)	186
$(4\text{-}mpy)^+$ $[Eu(tta)_4]^-$	$^5D_0 \rightarrow {}^7F_2$ (612.5)	186
$(miq)^+$ $[Eu(tta)_4]^-$	$^5D_0 \rightarrow {}^7F_2$ (612.6)	186
$(1,2,6tmpy)^+$ $[Eu(tta)_4]^-$	$^5D_0 \rightarrow {}^7F_2$ (611.7)	186
$(morph)^+$ $[Eu(tta)_4]^-$	$^5D_0 \rightarrow {}^7F_2$ (614.0)	187
$[Eu(acac)_3(H_2O)]$	$^5D_0 \rightarrow {}^7F_2$ (613.0)	181
$[Eu(tta)_3bipy]$	$^5D_0 \rightarrow {}^7F_2$ (611.2)	188
$[Eu(tta)_3dia]$	$^5D_0 \rightarrow {}^7F_2$ (611.2)	188
[Eu(tta)$_3$(5-phenyl-phen)]	$^5D_0 \rightarrow {}^7F_2$ (611.1)	189
$[Eu(tta)_3(tppo)_2]$	$^5D_0 \rightarrow {}^7F_2$ (616.0)	38
$[Eu(tta)_2(tppo)_2(NO_3)]$	$^5D_0 \rightarrow {}^7F_2$ (618.0)	38
$[Gd(tta)_2(tppo)_2(NO_3)]$	$T_1 \rightarrow S_0$ (510.0)	38
$[Tb(acac)_3(H_2O)]$	$^5D_4 \rightarrow {}^7F_5$ (545.0)	181
$[Tb(btfa)_2(tppo)_2(NO_3)]$	$^5D_4 \rightarrow {}^7F_5$ (552.0)	190

[a] $C_4H_8NH_2$ = pyrrolidinium; dia = 4,5-diazafluoren-9-one; dmpy = 1,2-dimethylpyridinium; imdz = imidazolium; miq = *N*-methylisoquinolinium; morph = morpholinium; mpy = 1-methylpyridinium; tmpy = 1,2,6-trimethylpyridinium.

Rare-earth diketonates incorporated into polymers that result in new triboluminescent materials have been investigated by Takada and coworkers[189]. Although some RE^{3+} compounds exhibit no TL in powder form, the TL phenomenon has been observed when these compounds are dispersed in a polymer matrix and the TL mechanism is adduced to electron impact caused by discharge due to a high electric field arising from frictional electrification between the film and the substrate.

V. LUMINESCENCE INVOLVING s, p AND d METAL BLOCK ENOLATES

A. d-Transition Metal Compounds

1. Photoluminescence of d-transition metal enolates

The luminescence spectral data of d-transition elements are very different from those of the RE^{3+} ions. Ligand field interactions have typically the following magnitudes: $3d^N$ (*ca* 15000 cm^{-1}), $4d^N$ (*ca* 20000 cm^{-1}) and $5d^N$ (*ca* 25000 cm^{-1}), while for RE^{3+} ions *ca* 200 cm^{-1} is the typical value. Vibronic interactions are also considerably larger in compounds with these elements, usually leading to a strong coupling regime. These facts produce considerable homogeneous broadening of d–d absorption and emission bands. On the other hand, the spin–orbit interaction is rather small, mainly in the first-row transition metal ions, meaning that the total spin and orbital angular momentum quantum numbers S and L, respectively, behave as good quantum numbers. Therefore, in the presence of a spin-independent ligand field, the usual electric dipole selection rule on the multiplicity applies.

The transition d-metal β-diketonates present absorption bands in the UV-visible region assigned to the following electronic transitions (Figure 13): (i) d–d transitions arising from ligand field interactions, (ii) intraligand transition ($\pi \rightarrow \pi^*$) arising from molecular orbitals localized on the β-diketonate ligand and (iii) charge transfer transitions (LMCT or MLCT) involving an electron transition from the ligand to the metal ion or from the metal ion to the ligand, respectively[191,192].

The transition d-metal enolate complexes generally exhibit no luminescence, and as a consequence there are few studies reported in the literature about the photoluminescence properties of these compounds. Indeed, the d-metal β-diketonate complexes are

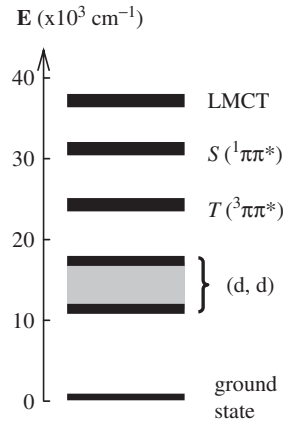

FIGURE 13. Typical energy level diagram of the main excited states of a d-metal complex[192]. Reproduced with permission from Reference 192, Copyright 1997 Elsevier

characterized by different types of electronic states and by inefficient radiative processes. The excited state of a complex populated by direct excitation or by a sensitization process can be deactivated by an efficient non-radiative process or by a photochemical reaction. Nevertheless, the use of β-diketonate chelates as luminescent sensitizers for the rare-earth complexes that have been extensively studied[1] has encouraged the investigation of the photoluminescence and electroluminescence properties of the d-metal β-diketonate complexes.

The emission spectra of chromium acetylacetonate and several derivatives in dilute crystals have been obtained at 4 K. Intramolecular vibrations of energies 270, 360, 459 and 630 cm^{-1} have been identified. Evidence for the absence of thermal equilibrium in the 2E state has been presented[193]. Room and low temperature magnetic circular dichroism in the intraligand spin-forbidden singlet–triplet $\pi-\pi^*$ transition for the coordinated diketonate ligands were observed for the $Ni^{2+}\beta$-diketonate with a chelated imino or nitronyl nitroxide radical, but not for the $Ni^{2+}\beta$-diketonate without the radical ligands. This is elucidated by the borrowing mechanism from the singlet–singlet $\pi-\pi^*$ transition through the hypothetical interligand β-diketonate-to-radical charge transfer (LLCT) in contrast to the Cr^{3+} complexes[194–196].

The last decade has seen great interest in the study of RE^{3+} β-diketones which show luminescence in the near-infrared (NIR) region[197]. Recently, Ward[198] presented a review on the PL properties of d–f heteronuclear assemblies in which a strong light absorbing d-block chromophore is used as an antenna group to generate sensitized luminescence from NIR emitting Yb^{3+}, Nd^{3+} and Er^{3+} ions following $d \rightarrow f$ photoinduced energy transfer. The ability of strongly absorbing d-block chromophores to sensitize low-energy 4f–4f transitions of NIR emitting RE^{3+} ions has been well established and important criteria for optimizing the energy-transfer process have been established. Major goals now include (i) using the tricks that have been developed for dramatically extending the NIR luminescence lifetime in other situations, and (ii) making water-stable d–f systems which allow long-wavelength excitation (700 nm or longer) to be used to generate long-lived NIR luminescence for biological imaging.

Kunkely and Vogler[199] reported on the excited state properties of [Cu(hfa)bta], with the absorption at 324 nm assigned to a spin-allowed $Cu^+ \rightarrow \pi^*$ bta MLCT transition. The solid state complex shows a broad emission band at 601 nm arising from MLCT. Besides, the photochemical behavior of this complex is in accordance with MLCT instead of LMCT.

In the last decade, several compounds based on heavy metal ions, such as Ir^{3+}, have attracted attention due to their potential applications as dopant in OLEDs[200], producing blue emission with relatively short excited-state lifetime, high PL efficiency and tunable emission wavelengths. In particular, there is a current effort to synthesize blue-emitting Ir^{3+}-based complexes. Among these compounds, those containing the acac ligand are notable examples for blue-emitting materials with potential application as emitting layer in OLEDs. Ir^{3+} β-diketonates play an important role as a layer in the development of highly efficient OLEDs due to the possibility of harvesting both the singlet and triplet excitons as light emission[201]. However, for fabrication of efficient electrophosphorescence devices the T state of the phosphorescent heavy metal ions guest should be below the one of the conjugated polymer host[202].

The excited state properties of $[Ir(CO)_2acac]$ have also been studied in dilute solutions that absorbs only in the UV region, exhibiting a greenish luminescence (*ca* 480 nm) which arises from the intraligand T state of the acac ligand. At 77 K these solutions turn blue owing to the presence of oligomers which are characterized by strong metal–metal interactions and display a red emission at 662 nm (fluorescence) and 815 nm (phosphorescence)[203].

Recently Zhao and coworkers[204] investigated a series of new Ir^{3+} complexes based on quinoline derivatives and different β-diketonate ligands. It has been observed that the PL efficiency is improved on replacing acac with pmip. This behavior has also been observed for the electrophosphorescence properties. The explanation is that the T state of pmip (*ca* 23000 cm^{-1}) is higher than the one for acac (*ca* 22200 cm^{-1}). Consequently, for Ir^{3+} complexes containing the pmip ligand the emission is dominated by MLCT $d\pi(Ir)-\pi^*(C\wedge N)$, where $(C\wedge N)$ represents the quinoline derivatives.

Rho and Ha[205] synthesized a series of Ir^{3+} complexes with a variety of imidazole-based ligands (L = dpi, tmspi). The $[Ir(acac)(L)_2]$ complexes do not exhibit emission. DFT calculations show that the LUMO energy levels of dpi and tmspi are similar to that of acac in these complexes, leading to an ET process involving the dpi and tmspi ligands and landing on a non-radiative channel that quenches the emission.

A DFT study was carried out[206] on the ground and low-lying excited states of blue phosphorescent cyclometalated Ir^{3+} complexes [*fac*-$Ir(dfpp)_3$], $[Ir(acac)(dfpp)_2]$ and [Ir(pic)(F)], where *fac* is facial and pic is picolinic acid. Nearly all of the low-lying calculated excitations have been categorized as MLCT transitions because the HOMOs are strongly mixed between the p orbital of the dfpp ligand and the d orbital of the central Ir atom.

Relaxation processes in the triplet state T_1 of $Ir(acac)(btp)_2$ doped in pc and cbp fluorescent materials have been investigated by Tsuboi and Aljaroudi[207]. They found good agreement between the calculated and observed temperature dependence of the PL lifetime and intensity for these doped materials.

Chou and Chi[208] studied the Os^{2+} complexes with dbm, quinolinate, diazene and C-linked pyridyl azolates and reported the spectroscopic and dynamic measurements, in combination with theoretical analyses. This work has provided the electronically excited state properties of these complexes, such as the energy gap and nature of the lower lying states, the rate of intersystem crossing, and the efficiency of corresponding radiative decay and non-radiative deactivation processes.

2. Electroluminescence of the d-transition metal enolates

Evans and coworkers[6] carried out a systematic analysis of main-group, d-transition metal and rare-earth complexes exhibiting room temperature phosphorescence from the T state as emitting level in OLEDs. Phosphorescence at room temperature is not common for first-row transition metal complexes, due to the weak spin–orbit coupling. However, it is more frequent for complexes of the second- and third-row transitions metals, due to strong spin–orbit coupling induced by the heavy atoms, leading to an efficient $T_1 \rightarrow S_0$ radiative transition and resulting in high phosphorescence quantum yields. A large number of second- and third-row transition metal ions (d^6, d^8 and d^{10} configurations) exhibit luminenscence. The heavy metal (Pt^{2+}, Os^{2+} and Ir^{3+}) complexes[209] have been widely employed as emitters in EL devices. Among these materials, iridium complexes seem the most effective. For example, a highly efficient green device using $[Ir(acac)(ppy)_2]$ as the emitting layer has been reported. Devices with emission in other regions of the visible spectrum have also been prepared, for example $[Ir(bt)_2(acac)]$ and $[Ir(btp)_2(acac)]$ used as emitting layers in OLED devices exhibit yellow and red emissions, respectively[210,211]. Laskar and coworkers prepared three EL devices using $[Ir(F_2MeOppy)_2(acac)]$ as a dopant in three different hole blockers cbp, ([1,1′-biphenyl]-4-olato)bis(2-methyl-8-quinolinato-$\kappa N1$, $\kappa O8$)aluminum (bAlq) and *N*,*N*′-dicarbazolyl-3,5-benzene (mcp) hosts. Blue emission at 472 nm and a luminance of 133 and 327 cd m^{-2} at 20 mA cm^{-2} have been reached for the devices ito/CHF_3/npb/Host+7% $[Ir(acac)(F_2MeOppy)_2]$/bAlq/Alq_3/LiF/Al, where Host = cbp or mcp, respectively[200].

The nature of Dexter triplet energy transfer between bonded systems of a red phosphorescent Ir^{3+} complex and a conjugated polymer, polyfluorene, has been investigated in electrophosphorescence OLEDs[202]. Red-emitting phosphorescence has been described based on the [Ir(btp)$_2$(acac)] fragment attached either directly (spacerless) or through a $-(CH_2)_8-$ chain (octamethylene-tethered) at the 9-position of a 9-octylfluorene host. Xu and coworkers[212] reported that an efficient red EP with CIE chromaticity coordinates $x = 0.69$, $y = 0.29$, independent on current density, was obtained from [Ir(acac)(btfmp)$_2$] doped devices. The EL spectrum has a maximum at 648 nm. A maximum external quantum efficiency of 9.6%, at current density of 0.125 mA cm^{-2}, and a maximum luminance of 4200 cd m^{-2}, at $J = 552$ mA cm^{-2}, have been obtained.

The ultimately pure red elephosphorescence diode using new compound [(qh)$_2$Ir(acac)] is described elsewhere[213]. The EP peak wavelength has been reported at 680 nm, with full width at half maximum of 89 nm by doping [(qh)$_2$Ir(acac)] into a light-emitting electron transport layer composed of 3-(4-biphenylyl)-4phenyl-5-(4-*t*-butylphenyl)-1,2,4-triazole. A bright red EP with CIE chromaticity coordinates better than $x = 0.70$ and $y = 0.28$. This is the closest to the ultimate limit of pure red among reported OLEDs, and holds even in luminance brighter than 600 cd m^{-2}. A very high maximum external EP quantum efficiency of 10.2% has also been obtained.

Three iridium complexes of formula [Ir(acac)(L)$_2$] have been synthesized, [Ir(dpp)$_2$(acac)], [Ir(bpp)$_2$(acac)] and [Ir(fpp)$_2$(acac)], where L is a substituted arylpyridine (dpp = 2,4-diphenylpyridine; bpp = 2-(4-*t*-butylphenyl)-4-phenylpyridine; fpp = 2-(4-fluorophenyl)-4-phenylpyridine). The OLEDs based on these materials, with structure ito/Ir complex:pvk/F-tbb/Alq$_3$/LiF/Al (F-tbb = 1,3,5-tris(4-fluorobiphenyl-4′-yl)benzene), showed maximum luminances of 8776, 8838 and 14180 cd m^{-2}, and maximum external efficiencies of 11.5, 12.9 and 17.0 cd A^{-1}, repectively[209].

Iridium complexes with a series of trifluoromethyl-substituted 1-naphthylpyridine ligands have been synthesized and, upon excitation at 470 nm, [Ir(acac)(fnapy4)$_2$] and [Ir(acac)(fnapy5)$_2$] emit red photoluminescence at 617 and 613 nm, respectively. Compared to [Ir(acac)(napy)$_2$], the incorporation of trifluoromethyl substituents resulted in a significant bathochromic shift caused by a lowering of the LUMO levels. It has been proposed that the bathochromic effect of the nitrogen atom in the pyridine ring should be much weaker than expected. For a blend of cbp with 6 wt% of [Ir(acac)(fnapy5)$_2$], a brightness of 8600 cd m^{-2} at 10.5 V is reached with CIE chromaticity coordinates of $x = 0.65$ and $y = 0.35$[214].

Polymer light-emitting devices (PLEDs) have attracted considerable interest because of their potential use in portable electronic devices. PLEDs have improved the performance of devices by increasing the device stability and efficiency. Chang and coworkers[215] fabricated an efficient PLED using [Ir(acac)(dbq)$_2$] as the phosphorescent dopant of a pvk matrix layer and bbpo as the electron transport material. Trapping of charge carriers at the [Ir(acac)(dbq)$_2$] dopant sites dominates the EL of the device. This is the first PLED that emits red electrophosphorescence centered at 610 nm, exclusively from the dopant and an EL efficiency of 8.5 cd A^{-1} (luminance 1287 cd m^{-2}) biased at 14.5 mA cm^{-2}.

B. Alkali, Alkaline Earth and Main Group Compounds

Extensive research has been carried out on the luminescence of the Alq$_3$ complex which is used as an electron transport emitting layer in OLEDs, with strong green emission at 532 nm and phosphorescence quantum efficiency around 32%[5,6,216,217].

Heavy main group metal ions with s^2 electronic configuration, such as Tl^+, Pb^{2+} and Bi^{3+}, may enhance spin–orbit coupling in the ligands. The intraligand phosphorescence

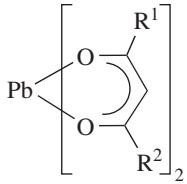

(**4**) (**a**) $R^1 = R^2 =$ Me (acac)
(**b**) $R^1 = R^2 =$ Mef (hfa)
(**c**) $R^1 =$ Mef, $R^2 = 2$-Thi (tta)
(**d**) $R^1 = R^2 =$ Ph (dbm)
(**e**) $R^1 = R^2 = t$-Bu (dpm)

from several Pb^{2+} diketonates (**4a–4e**) show a weak emission in the spectral range from 400 to 500 nm, in the solid state at room and low temperatures, which is related to the $^3\pi\pi^*$ state of the β-diketonate ligand as a consequence of the 'heavy atom effect'. Depending on the substituent groups in the ligands, the phosphorescence emission band shifts from the blue to the green region[218]. Comparison between the spectral profiles of these complexes shows that [Pb(acac)$_2$] exhibits a typical intraligand phosphorescence spectrum from vibronic structure. Also [Tl(hfa)] and [Bi(hfa)$_3$] exhibit phosphorescence at ambient conditions with emission maxima at 477 and 472 nm, respectively[219].

It has been reported that the heteropolynuclear complexes [AuTl(L)$_2$]$_n$, with L = C_6Cl_5, C_6F_5 react with [Tl(acac)] in 1:1 or 1:2 molar ratios, leading to products of [AuTl$_2$(acac)(C_6Cl_5)$_2$] (**5**) and [AuTl$_3$(acac)$_2$(C_6F_5)$_2$] (**6**) stoichiometry. These new complexes display Tl$_2$(acac)$_2$ units acting as bridges between linear chains of [AuTl(C_6Cl_5)$_2$]$_n$ in **5** or between [AuTl(C_6F_5)$_2$] units in **6**. In both structures, in addition to Au–Tl interactions, Tl(I)–Tl(I) contacts also exist, which are considered to be responsible in part for the luminescence behavior. Comparison between the properties of **5** and **6** in solution with those of [Tl(acac)] point to the presence of Tl(I)–Tl(I) interactions also in solution. Time-dependent DFT calculations show that the Tl$_2$(acac)$_2$ units would affect the luminescence behavior of [Tl(acac)], **5** and **6** in acetonitrile solution[220].

Energy transfer and light yield properties of a new highly loaded In^{3+} β-diketonate organic scintillator system with 2-(4-biphenylyl)-5-phenyloxazole (bpo) and 2,5-diphenyloxazole (ppo) fluor systems have been reported by Buck and coworkers[221,222]. A notable luminescence light yield using [In(acac)$_3$]-doped organic liquid scintillator systems, even at reasonably high loadings of In, has been achieved.

Highly efficient orange emitting OLEDs based on phosphorescence Pt^{2+} acac complexes, employing a series of 2-phenylbenzothiazolato ligands, have been studied. The EL devices have been fabricated by doping Pt^{2+} acac complexes (5, 7 and 9%) in the host cbp. The EL performance of two of these complexes was exceptionally high (luminances 10550 and 11320 cd m^{-2})[223].

VI. APPLICATIONS

A. Time-resolved Detection of Luminescence for Bioassays

Luminescent RE^{3+} chelates have been successfully developed as labels and probes for highly sensitive and selective bioassays in the past two decades. Time-resolved luminescence detection[224,225] has been widely applied in fluoroimmunoassay, DNA hybridization assay, enzyme assay, cell activity assay and fluorescence imaging microscopy[226].

The intrinsic advantages of luminescent RE ions, and especially Eu^{3+} β-diketonates, have led to the development of time-resolved luminescence immunoassay techniques[4,227–231]. Among the advantages one counts (i) high oxidation potential, (ii) almost total compound-independent narrow emission lines, (iii) large Stokes shift upon ligand excitation, (iv) high emission quantum yields obtained upon ligand sensitization in certain complexes and (v) long lifetime of the emitting state (Figure 14).

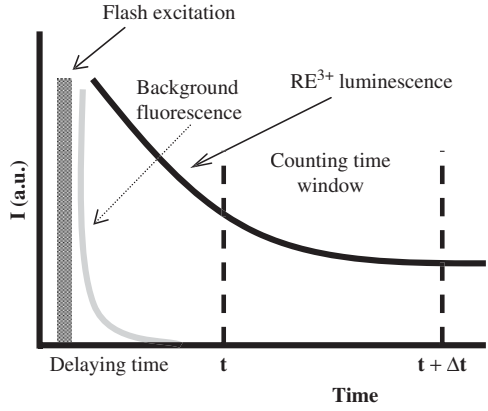

FIGURE 14. Principle of the time-resolved (gated) luminescence assay. Reproduced with permission from Reference 2, Copyright 2005 the Royal Society of Chemistry

Immunoassays are based on the immunoreaction between an antibody that is used as the immunoreagent and the antigen that has to be analyzed. In the dissociation-enhanced rare-earth fluoroimmunoassay (DELFIA), the immunoreagent is labeled for immunoreactions with an isothiocyanatophenyl-EDTA-RE^{3+} or N^1-(*p*-isothiocyanatobenzyl)diethylene-triamine-N^1,N^2,N^3,N^4-tetraacetate-RE^{3+} by binding to an amino group of the antibody. After the immunoreaction and separation of the labeled immunocomplex, the RE^{3+} ions are released from the complex by lowering the pH (2–3). By treatment of the RE^{3+}-containing solution with a mixture of ntfa2H, topo and their Triton X-100 or nonaoxyethylene dodecylether (BL-9EX), the strongly luminescent $[RE(ntfa2)_3(topo)_2]$ is formed. The function of the non-ionic surfactants Triton X-100 or BL-9EX is to disperse the hardly soluble Eu^{3+} complex in a micellar phase. The function of topo is to shield the RE^{3+} from water molecules by occupying the vacant coordination sites in the β-diketonate complex. The luminescence is measured in a time-resolved mode, discarding the background fluorescence of the organic compounds present in solution[232,233].

Research is going on to improve the DELFIA system[234,235], because of drawbacks such as the time-consuming conversion of the non-fluorescent RE^{3+} label into a luminescent complex, or the system vulnerability to contamination by RE^{3+} due to the excess of the reagents ntfa and topo. An alternative is the use of a β-diketone that can be covalently bonded to proteins such as 5-(4,4,4-trifluoro-1,3-dioxobutyl)-2-thiophenesulfonyl chloride (ctta)[96,97,236,237]. Since the stability of the RE^{3+} complexes formed by this ligand is quite low, a large excess of RE^{3+} has to be used to shift the equilibrium to the rare-earth complex. More stable europium complexes can be obtained by the use of tetradentate β-diketonates, such as **7a**–**7d**, anchored on a functionalized *o*-terphenyl skeleton, or **8a**–**8c**, anchored on a biperfluorobutadiene skeleton[238–242].

Addition of tta anions to a Eu^{3+}-containing Schiff's base macrocycle increases the luminescence intensity markedly[243]. The tta anion coordinates to the europium macrocycle without disrupting the macrocyclic structure. A protocol for the use of these systems as luminescent markers for cytological imaging has been developed. A new β-diketone that can be used to determine estrogens was developed by Matsumoto and coworkers[244] and had detection limits between 0.60 and 0.65 ng mL^{-1}.

Lanthanide chelates can be also packed inside a nanoscale polymer shell to produce a particulate fluorescent label. Commercially available Eu^{3+} chelate dyed nanoparticles

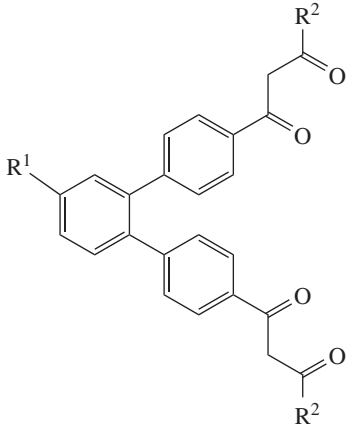

(**7**) (**a**) $R^1 = SO_2Cl$, $R^2 = CF_3$ (btbct)

(**b**) $R^1 = SO_2Cl$, $R^2 = C_2F_5$ (bppct)

(**c**) $R^1 = SO_2Cl$, $R^2 = C_3F_7$ (bhhct)

(**d**) $R^1 =$ 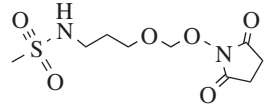 , $R^2 = C_3F_7$ (bhhst)

(Seradyn Inc., Indianapolis, IN) contain several thousands of different Eu^3-β-diketone chelates inside a single polystyrene shell[245]. Also, particles dyed with Tb^{3+}, Sm^{3+} and Dy^{3+} chelates have been used as immunoassay labels[246]. The shell produces a hydrophobic environment protecting the chelates from the quenching effect of water molecules. The carboxy groups on the surface of the particle enable covalent conjugation of proteins, e.g. antibodies or streptavidin[245]. Eu^{3+} chelate dyed nanoparticles have been used successfully as labels in both heterogeneous and homogeneous immunoassays. In heterogeneous immunoassay the use of nanoparticle labels increases the sensitivity of clinical[247–249] and food[250] analyses.

In homogeneous immunoassays based on fluorescence resonance energy transfer (FRET), the Eu^{3+} chelate dyed nanoparticles have been used as donor labels with a short-lifetime near-infrared fluorophore acting as an acceptor label. When the donor and the acceptor are in close proximity, the emission of the donor label can excite the acceptor label and sensitized emission is generated. Because the donor label has slow luminescence decay, the sensitized emission can also be measured using time-resolved detection. Homogeneous assays using nanoparticles as donors (see Figure 15) include both sandwich-type non-competitive assays for proteins[251] and competitive assays for haptens, and were applied in automated high-throughput screening of novel drugs[252, 253].

B. Laser Materials

In the early 1960s the possibility to use rare-earth β-diketonate complexes for the design of lasers gave a strong impulse to the spectroscopic study of these compounds.

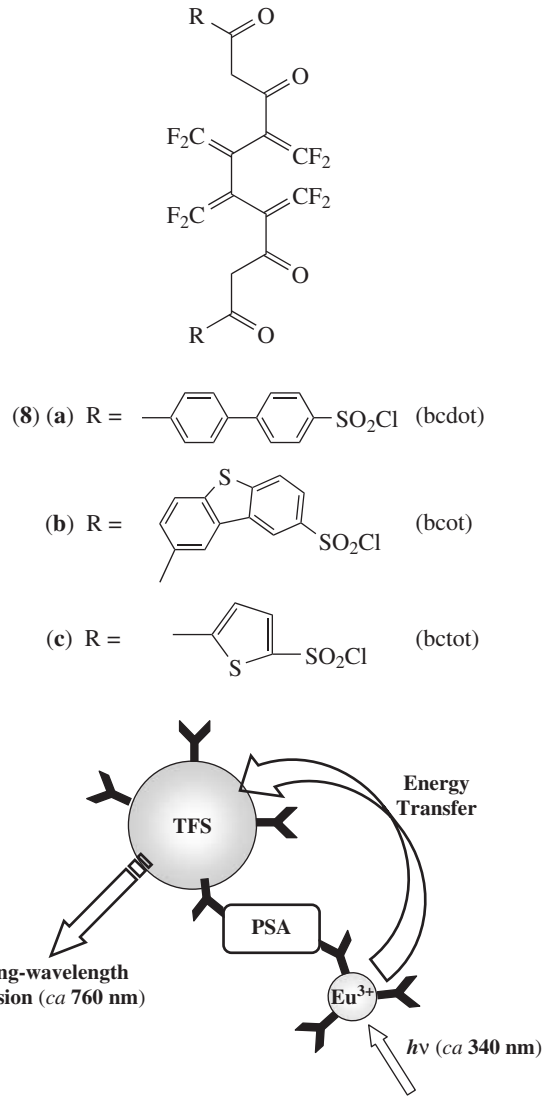

FIGURE 15. Luminescence energy transfer from Eu^{3+} complex doped in polystyrene particle to TFS particles[240] (PSA = prostatic specific antigen, TFS = transfluosphere^{TM}). Reproduced with permission from Reference 240, Copyright 2006 Elsevier

In 1962, it was pointed out that europium complexes dissolved in organic solvents or in a polymer matrix have optical properties that make them potential candidates for laser materials[254]. At the same time, Whan and Crosby[47] and Filipescu and coworkers[255] have also suggested the potential application of rare-earth chelates in lasers. Lempicki and Samelson[256] in 1963 were the first researchers to obtain stimulated emission at

613.1 nm ($^5D_0 \rightarrow {}^7F_2$ transition) from an alcohol solution of europium benzoylacetonate by pumping this solution with a xenon flash lamp with threshold energy between 1790 and 1920 J. This threshold is the amount of energy that must be delivered to the laser device to bring it to the point at which the onset of laser action is observed. Samelson and coworkers[257] have observed a room temperature operation of a Eu^{3+}-chelate laser. Subsequently, a significant number of studies on laser action of Eu^{3+} and Tb^{3+} β-diketonates in frozen organic solutions and in polymeric matrix were reported[256, 258–281]. Among the enolate ligands, the β-diketones like bzac, dbm, tfa, tta and btfa have been the most frequently used. It has been shown that the active components in most successful laser systems are the RE^{3+} tetrakis(β-diketonate) anionic complexes[282]. Although in most studies on laser chelates, Eu^{3+} has been chosen as the emitting ion, some studies report on laser action of Tb^{3+} complexes[257, 268, 272, 283], whereas observation of laser action by Nd^{3+} in a tetrakis(tta) complex, prepared from a didymium salt (mixture of Pr and Nd salts), has been reported[284].

Strong light absorption by the β-diketonate ligands is an advantage for sensitizing the luminescence of lanthanide ions by the antenna effect, but this property limits the usefulness of these complexes as laser materials. To achieve uniform excitation of the solutions containing the rare-earth chelate at the concentration required for laser action (*ca* 0.01 M), only thin samples (*ca* 1–6 mm) could be used[259, 280]. Therefore, most studies about liquid lasers have been performed on laser solutions in a capillary tube or on rare-earth doped polymers drawn to fibers. Another problem with the chelate lasers is the low photostability of the rare-earth β-diketonate complexes under UV irradiation, severely limiting the lifetime of the laser systems. Furthermore, the lasing thresholds are high for these chelate lasers at room temperature (1000–3000 J), causing excessive heating of the laser solutions. Circulation of the liquid through the cell and cooling with an external heat exchanger have been proposed to solve this problem[263]. Finally, the energy output of the rare-earth chelate lasers is low, because of the efficient pathways of the radiationless deactivation of the excited states. The most commonly used solvents for the study of the laser action are a 2:1:1 mixture of 3-ethoxypropionitrile, 2-ethoxyethanol and acetonitrile (EAA), a 1:1:1 mixture of proprionitrile, butyronitrile and isobutyronitrile ('nitrile solvent'), a 3:1 ethanol–methanol mixture, a 3:1 ethanol–DMF mixture and acetonitrile. Some of the mixed solvent systems remain liquid to temperatures as low as $-150\,^{\circ}C$. However, the β-diketonate complexes are not always stable for a long time in such solutions, for instance Eu^{3+} β-diketonates degrade in the 3:1 ethanol:methanol mixture[262]. Fry and Pirie[285] have found that in this alcohol mixture $[Eu(bzac)_3(H_2O)]$ decomposes upon heating the solution to $70\,^{\circ}C$ or upon UV irradiation. The main decomposition products are ethyl acetate and acetophenone, which indicates that benzoylacetonate undergoes a reverse Claisen condensation. Brecher and coworkers[283] have discussed the dissociation in solution of the tetrakis complexes into mixtures of non-lasing tris complexes and free β-diketonate anions. For a long time after 1970, no research was conducted on rare-earth chelate lasers. In 1995, Taniguchi and coworkers[286] demonstrated ultra-low threshold lasing due to morphology-dependent resonances from $[Eu(dbm)_3(phen)]$ dissolved in liquid microdroplets of *ca* 90 μm diameter. These microdroplets consist of a viscous ethanol–glycerol mixture. The same year, authors from the same research group[287] described a solid chelate laser based on $[Eu(dbm)_3(phen)]$ dispersed into polystyrene spheres, which is free of the solvent effects encountered with the liquid chelate laser.

C. Miscellaneous

New near-infrared-luminescent mesoporous materials have been prepared by linking ternary rare-earth (Er^{3+}, Nd^{3+}, Yb^{3+}, Sm^{3+}, Pr^{3+}) complexes to the ordered mesoporous MCM-41 functionalized with a phen derivative group. The resulting materials

have been denoted as RE(hfth)$_3$phen–M41 and RE(tfnb)$_3$phen–M41. Upon excitation at the absorption wavelengths of the organic ligands, all these materials show the characteristic NIR luminescence of the corresponding rare-earth ions by sensitization from the organic ligands. The good luminescent performances enable these NIR-luminescent mesoporous materials to have possible applications in optical amplification (operating at 1.3 or 1.5 μm), laser systems and medical diagnosis[288].

VII. ACKNOWLEDGMENTS

The authors thank Fundação de Amparo à Pesquisa do Estado de São Paulo (FAPESP), Conselho Nacional de Desenvolvimento Científico e Tecnológico (CNPq), RENAMI and IM^{2}C projects for financial support.

VIII. REFERENCES

1. K. Binnemans, in *Handbook on the Physics and Chemistry of Rare Earths*, Vol. 35, *Rare-Earth Beta-Diketonates* (Eds K. A. Gschneidner, Jr., J.-C. G. Bünzli and V. K. Pecharsky), Elsevier, Amsterdam 2004, pp. 107–272.
2. J.-C. G. Bünzli and C. Piguet., *Chem. Soc. Rev.*, **34**, 1048 (2005).
3. J.-C. G. Bünzli and G. R. Choppin (Eds), *Lanthanide Probes in Life, Chemical and Earth Sciences—Theory and Practice*, Elsevier, Amsterdam, 1989.
4. I. A. Hemmilä, *Application of Fluorescence in Immunoassays*, John Wiley & Sons, Inc., New York, 1991.
5. J. Kido and Y. Okamoto, *Chem. Rev.*, **102**, 2357 (2002).
6. R. C. Evans, P. Douglas and C. J. Winscom, *Coord. Chem. Rev.*, **250**, 2093 (2006).
7. F. A. Cotton and P. L. Huang, *Inorg. Chem. Acta*, **346**, 223 (2003).
8. L. M. Sweeting, *J. Am. Chem. Soc.*, **109**, 2652 (1987).
9. S. P. Sinha, *Europium*, Springer-Verlag, New York, 1967.
10. C. N. R. Rao and J. R. Ferraro (Eds), *Spectroscopy in Inorganic Chemistry*, Vol. 2, Academic Press, New York, 1971.
11. N. Sabbatini, M. Guardigli and J. M. Lehn, *Coord. Chem. Rev.*, **123**, 201 (1993).
12. D. F. Shriver and P. W. Atkins, *Inorganic Chemistry*, 3rd edn, Oxford University Press, 1999, pp. 450–453.
13. E. N. Harvey, *History of Luminescence*. The American Philosophical Society, Philadelphia, 1957.
14. B. Valeur, *Molecular Fluorescence: Principles and Applications*, Wiley-VCH, Weinheim, 2001.
15. R. C. Mehrotra, R. Bohra and D. P. Gaur, *Metal ß-Diketonates and Allied Derivatives*, Academic Press, London, 1978.
16. L. C. Thompson, in *Handbook on the Physics and Chemistry of Rare Earths*, Vol. 3; *Complexes* (Eds K. A. Gschneidner Jr. and L. R. Eyring), North-Holland, Amsterdam, 1979, pp. 209–297.
17. K. C. Joshi and V. N. Pathak, *Coord. Chem. Rev.*, **22**, 37 (1977).
18. M. M. Mañas, J. Marquet and A. Vallribera, *Tetrahedron*, **52**, 3377 (1996).
19. J. R. Lakowicz, *Principles of Fluorescence Spectroscopy*, Plenum Press, New York, 2006.
20. G. F. de Sá, O. L. Malta, C. de Mello Donegá, A. M. Simas, R. L. Longo, P. A. Santa-Cruz and E. F. da Silva Jr., *Coord. Chem. Rev.*, **196**, 165 (2000).
21. E. E. S. Teotonio, H. F. Brito, M. C. F. C. Felinto, C. A. Kodaira and O. L. Malta, *J. Coord. Chem.*, **10**, 913 (2003).
22. E. Niyama, H. F. Brito, M. Cremona, E. E. S. Teotonio, R. Reyes, G. E. S. Brito and M. C. F. C. Felinto, *Spectrochim. Acta A*, **61**, 2643 (2005).
23. H. F. Brito and G. K. Liu, *J. Chem. Phys.*, **112**, 4334 (2000).
24. E. E. S. Teotonio, H. F. Brito, H. Viertler, W. M. Faustino, O. L. Malta, G. F. de Sá, M. C. F. C. Felinto, R. H. A. Santos and M. Cremona, *Polyhedron*, **25**, 3488 (2006).
25. S. Tobita, M. Arakawa and I. Tanaka, *J. Phys. Chem.*, **89**, 5649 (1985).
26. S. Sato and M. Wada, *Bull. Chem. Soc. Jpn.*, **43**, 1955 (1970).

27. C. Pettinari, F. Marchetti, R. Pettinari, P. Natanti, A. Drozdov, S. Semenov, S. I. Troyanov and V. Zolin, *Inorg. Chim. Acta*, **359**, 4062 (2006).
28. W. R. Dawson, J. L. Kropp and M. W. Windsor, *J. Chem. Phys.*, **45**, 2409 (1966).
29. V. Tsaryuk, V. Zolin and J. Legendziewicz, *J. Lumin.*, **102–103**, 744 (2003).
30. S. Biju, M. L. P. Reddy and R. O. Freire, *Inorg. Chem. Commun.*, **10**, 393 (2007).
31. A. V. M. Andrade, N. B. Jr. Costa, A. M. Simas and G. F. de Sá, *Chem. Phys. Lett.*, **227**, 349 (1994).
32. A. V. M. Andrade, N. B. Jr. Costa, A. M. Simas and G. F. de Sá, *J. Alloys Compd.*, **225**, 55 (1995).
33. A. V. M. Andrade, R. L. Longo, A. M. Simas and G. F. de Sá, *J. Chem. Soc., Faraday Trans.*, **92**, 1835 (1996).
34. G. B. Rocha, M. E. de Mesquita, A. M. Simas and G. F. de Sá, *Mater. Sci. Forum*, **315**, 400 (1999).
35. W. M. Faustino, S. A. Junior, L. C. Thompson, G. F. de Sá, O. L. Malta and A. M. Simas, *Int. J. Quantum Chem.*, **103**, 572 (2005).
36. B. R. Judd, *Phys. Rev.*, **127**, 750 (1962).
37. G. S. Ofelt, *J. Chem. Phys.*, **37**, 511 (1962).
38. E. E. S. Teotonio, G. M. Fett, H. F. Brito, W. M. Faustino, G. F. de Sá, M. C. F. C. Felinto and R. H. A. Santos, *J. Lumin.*, **128**, 190 (2008).
39. R. O. Freire, G. B. Rocha and A. M. Simas, *J. Mol. Model.*, **12**, 373 (2006).
40. F. A. Hart, in *Comprehensive Coordination Chemistry*, Vol. 3 (Eds G. Wilkinson, R. D. Guillard and J. A. McClevert), Pergamon, Oxford, 1987, pp. 1059–1127.
41. G. E. Buono-Core, H. Li and B. Marciniak, *Coord. Chem. Rev.*, **99**, 55 (1990).
42. W. T. Carnall, G. L. Goodman, K. Rajnak and R. S. Rana, *J. Chem. Phys.*, **90**, 3443 (1989).
43. J. H. Forsberger, *Coord. Chem. Rev.*, **10**, 195 (1973).
44. S. I. Weissman, *J. Chem. Phys.* **10**, 214 (1942).
45. G. A. Crosby and M. Kasha, *Spectrochim. Acta*, **10**, 377 (1958).
46. G. A. Crosby, R. E. Whan and R. M. Alire, *J. Chem. Phys.*, **34**, 743 (1961).
47. R. E. Whan and G. A. Crosby, *J. Mol. Spectrosc.*, **8**, 315 (1962).
48. G. A. Crosby, *Mol. Cryst.*, **1**, 37 (1966).
49. O. L. Malta and F. R. Gonçalves e Silva, *Spectrochim. Acta A*, **54**, 1593 (1998).
50. I. M. Alaoui, *J. Phys. Chem.*, **99**, 13280 (1995).
51. P. Leanaerts, K. Driensen, R. V. Deun and K. Binnermans, *Chem. Mater.*, **17**, 2148 (2005).
52. E. E. S. Teotonio, *Síntese e investigação das propriedades fotoluminescentes de dispositivos moleculares conversores de luz (DMCL) de complexos dicetonatos de terras raras com ligantes amidas*, PhD thesis, Institute of Chemistry, University of São Paulo, São Paulo, Brazil (2004).
53. P. D. Peacock, *Struct. Bond.*, **22**, 83 (1975).
54. O. Deutschbein, *Ann. Phys.*, **36**, 183 (1939).
55. F. S. Richardson, *Chem. Rev.*, **82**, 541 (1982).
56. H. F. Brito, O. L. Malta and J. F. S. Menezes *J. Alloys Compd.*, **303–304**, 364 (2000).
57. W. T. Carnall, H. Crosswithe and H. M. Crosswithe, *Energy Level Structure and Transition Probabilities of the Trivalent Lanthanide in* LaF_3, Argonne National Laboratory. Argonne, Illinos, 4493 (1977).
58. O. L. Malta, H. F. Brito, J. F. S. Menezes, F. R. Gonçalves e Silva, S. Alves Jr, F. S. Farias and A. V. M. Andrade, *J. Lumin.*, **75**, 255 (1997).
59. A. A. S. Araújo, H. F. Brito, O. L. Malta, J. R. Matos, E. E. S. Teotonio, S. Storpirtis and C. M. S. Izumi, *J. Inorg. Biochem.*, **88**, 87 (2002).
60. P. P. Lima, R. A. S. Ferreira, R. O. Freire, F. A. A. Paz, L. Fu, S. A. Junior, L. D. Carlos and O. L. Malta, *Chem. Phys. Chem.*, **7**, 735 (2006).
61. P. P. Lima, R. S. A. Junior, O. L. Malta, L. D. Carlos, R. A. S. Ferreira, R. Pavithran and M. L. P. Reddy, *Eur. J. Inorg. Chem.*, **19**. 3923 (2006).
62. R. Pavithran, M. L. P. Reddy, S. A. Junior, R. O. Freire, G. B. Rocha and P. P. Lima, *Eur. J. Inorg. Chem.*, 4129 (2005).
63. D. F. Parra. H. F. Brito. J. R. Matos and L. C. Dias. *J. Appl. Polym. Sci.*, **83**, 2716 (2002).
64. D. F. Parra. A. Mucciolo. H. F. Brito and L. C. Thompson, *J. Solid State Chem.*, **171**, 412 (2003).
65. L. D. Carlos, C. de Mello Donegá, R. Q. Alburquerque, S. A. Junior, J. F. S. Menezes and O. L. Malta, *Mol. Phys.*, **101**, 1037 (2003).

66. S. Biju, D. B. A. Raj, M. L. P. Reddy and B. M. Kariuki, *Inorg. Chem.*, **45**, 10651 (2006).
67. C. de Mello Donegá, S. Alves Jr., O. L. Malta and G. F. de Sá, *Mater. Sci. Forum*, **315–317**, 204 (1999).
68. E. E. S. Teotonio, *Preparação e investigação eletroluminescente de novos dispositivos contendo complexos β-dicetonatos de terras raras com ligantes fosfinóxidos*, FAPESP-Report No 04/01479-9, Universidade de São Paulo, IQUSP, São Paulo, Brazil (2006).
69. O. L. Malta, S. J. L. Ribeiro, M. Faucher and P. Porcher, *J. Phys. Chem. Solids*, **52**, 587 (1991).
70. O. L. Malta, M. A. Couto dos Santos, L. C. Thompson and N. K. Ito, *J. Lumin.*, **69**, 77 (1996).
71. O. L. Malta, *Chem. Phys. Lett.*, **88**, 353 (1982).
72. C. K. Jorgensen, *Modern Aspects of Ligand Field Theory*, North-Holland, Amsterdam, 1971.
73. H. F. Brito, *Propriedades espectroscópicas de elementos do bloco-f*, Livre docência Thesis, Universidade de São Paulo, IQUSP, São Paulo, Brazil (2000).
74. B. R. Judd, *Operator Techniques in Atomic Spectroscopy*, 2nd edn, McGraw-Hill, Princeton, 1998.
75. W. M. Faustino, O. L. Malta and G. F. Sá, *J. Chem. Phys.*, **122**, 109 (2005).
76. W. M. Faustino, O. L. Malta and G. F. Sá, *Chem. Phys. Lett.*, **429**, 595 (2006).
77. G. D. R. Napier, J. D. Neilson and T. M. Shepherd, *Chem. Phys. Lett.*, **31**, 328 (1975).
78. P. Gawryszewska, J. Sokolnicki and J. Legendziewicz, *Coord. Chem. Rev.*, **249**, 2489 (2005).
79. B. N. Nelson, A. G. Caster and M. T. Berry, *Chem. Phys. Lett.*, **396**, 256 (2004).
80. O. L. Malta, H. F. Brito, J. F. S. Menezes, F. R. Gonçalves e Silva, C. de Mello Donegá and S. Alves Jr., *Chem. Phys. Lett.*, **282**, 233 (1998).
81. A. Bril, in *Luminescence of Organic and Inorganic Materials* (Eds H. P. Kallman and G. M. Spruch), Wiley, Eindhoven, 1962, pp. 479–493.
82. A. Bril and A. W. De Jager-Veens, *J. Res. Natl. Bureau Stand.*, **80 A**, 401 (1976).
83. A. Bril and A. W. De Jager-Veens, *J. Electrochem. Soc.*, **123**, 396 (1976).
84. A. W. De Jager-Veens and A. Bril, *Philips J. Res.*, **33**, 124 (1978).
85. C. de Mello Donegá, S. Alves Jr. and G. F. de Sá, *Chem. Commun.*, **10**, 1199 (1996).
86. C. de Mello Donegá, S. J. L. Ribeiro, R. R. Gonçalves and G. Blasse, *J. Phys. Chem. Solids*, **57**, 1727 (1996).
87. C. de Mello Donegá, S. Alves Jr. and G. F. Sá, *J. Alloys Compd.*, **250**, 422 (1997).
88. S. Alves Jr., F. V. Almeida, G. F. Sá and C. de Mello Donegá, *J. Lumin.*, **72**, 478 (1997).
89. R. Pavithran, N. S. S. Kumar, S. Biju, M. L. P. Reddy, S. A. Junior and R. O. Freire, *Inorg. Chem.*, **5**, 2184 (2006).
90. M. E. de Mesquita, S. A. Junior, N. B. C. Junior, R. O. Freire, F. R. G. e Silva and G. F. de Sá, *J. Solid State Chem.*, **171**, 181 (2003).
91. M. E. de Mesquita, S. A. Junior, F. R. G. e Silva, M. A. Couto dos Santos, R. O. Freire, N. B. C. Junior and G. F. de Sá, *J. Alloys Compd.*, **374**, 320 (2004).
92. D. F. Parra. A. Mucciolo and H. F. Brito, *J. Appl. Polym. Sci.*, **94**, 865 (2004).
93. F. J. Steemers, W. Verboon, D. N. Reinhoudt, E. B. Vander Tol and J. W. Verhoeven, *J. Am. Chem. Soc.*, **117**, 9408 (1995).
94. M. Latva, H. Takalo, V. M. Mukalla, C. Matachescu, J. C. Rodríguez-Ubis and J. Kanakare, *J. Lumin.*, **75**, 149 (1997).
95. N. Filipescu, W. F. Sager, and F. A. Serafin, *J. Phys. Chem.*, **68**, 3324 (1964).
96. X. D. Yang, Y. Y. Ci and W. B. Chang, *Anal. Chem.*, **66**, 2590 (1994).
97. Y. S. Yang, M. L. Gong, Y. Y. Li, H. Y. Lei and S. L. Wu, *J. Alloys Compd.*, **207/208**, 112 (1994).
98. S. L. Wu, Y. L. Wu and Y. S. Yang, *J. Alloys Compd.*, **180**, 391 (1992).
99. S. L. Wu, Y. L. Wu and Y. S. Yang, *J. Alloys Compd.*, **180**, 399 (1992).
100. S. L. Wu, and Y. S. Yang, *J. Alloys Compd.*, **180**, 403 (1992).
101. D. F. Eaton, *Pure Appl. Chem.*, **60**, 1107 (1998).
102. A. S. Chauvin, F. Gumy, D. Imbert and J.-C. G. Bünzli, *Spectrosc. Lett.*, **37**, 517 (2004).
103. L. Shen, M. Shi, F. Li, D. Zhang, X. Li, E. Shi, T. Yi, Y. Du and C. Huang, *Inorg. Chem.*, **45**, 6188 (2006).
104. Y. Liu, Y. Yang, G. Qian, Z. Wang and M. Wang, *Mater. Sci. Eng. B.*, **137**, 74 (2007).
105. C. Pettinari, F. Marchetti, R. Pettinari, A. Cingolani A. Drozdov, I. Tomokhin, S. I. Troyanov, V. Tsaryuk and V. Zolin, *Inorg. Chim. Acta*, **357**, 4181 (2004).

106. C. Pettinari, F. Marchetti, R. Pettinari, P. Natanti, A. Drozdov, S. Semenov, S. I. Troyanov and V. Zolin, *Inorg. Chim. Acta*, **359**, 4062 (2006).
107. D. Zhou, Q. Li, C. Huang, G. Yao, S. Umetani, M. Matsui, L. Ying, A. Yu and X. Zhao, *Polyhedron*, **16**, 1381 (1997).
108. X. Gao, H. Cao, C. Huang, S. Umitani, G. Chen and P. Jiang, *Synth. Met.*, **99**, 127 (1999).
109. Y. M. Luo, Z. Chen, R. R. Tang, L. X. Xiao and H. J. Peng, *Spectrochim. Acta A*, (2007). In press.
110. F. Dang, Y. Li and W. Liu., *Spectrochim. Acta A*, **66**, 676 (2007).
111. P. S. May, D. H. Metcalf, F. S. Richardson, R. C. Carter and C. E. Miller, *J. Lumin.*, **51**, 249 (1992).
112. L. Beaury, J. Hölsä, J. Korventausta, J. C. Krupa, R. J. Lamminmäki, P. Porcher, H. Rahiala and E. Säilynoja, *Acta Phys. Pol. A*, **90**, 1203 (1997).
113. J. B. Gruber, Z. Bahram and M. F. Reid, *Phys. Rev.*, **60**, 15643 (1999).
114. S. B. Stevens, C. A. Morrison, M. D. Seltezer, M. E. Hills and J. B. Gruber, *J. Appl. Phys.*, **70**, 948 (1991).
115. X. Y. Chen, M. P. Jensen and G. K. Liu, *J. Phys. Chem. B*, **109**, 13991 (2005).
116. H. F. Brito, O. L. Malta, M. C. F. C. Felinto, E. E. S. Teotonio, J. F. S. Menezes, C. F. B. Silva, C. S. Tomiyama and C. A. A. Carvalho, *J. Alloys Compd.*, **344**, 293 (2002).
117. K. Tamaki, H. Yabua, T. Isoshima, M. Hara and M. Shimomura, *Colloids and Surfaces A: Physicochem. Eng. Aspects*, **284–285**, 355 (2006).
118. L. Liu, W. Zhang, X. Li, X. F. Wu, C. Yang, Y. D. Liu, L. He, Y. L. Xu, X. J. Zhang, L. Q. Zhang and R. G. Jin, *Compos. Sci. Technol.*, **67**, 2199 (2007).
119. Z. Kin, H. Kajii, Y. Hasegawa, T. Kawai and Y. Ohmori, *Thin Solid Films*, (2008). In press.
120. L. N. Sun, J. B. Yu, H. J. Zhang, Q. G. Meng, E. Ma, C. Y. Peng and K. Y. Yang, *Micropor. Mesopor. Mater.*, **98**, 156 (2007).
121. J. Yu, L. Zhou, H. Zhang, Y. Zheng, H. Li, R. Deng, Z. Peng and Z. Li, *Inorg. Chem.*, **44**, 1611 (2005).
122. R. J. Zhang, K. Z. Yang, A. C. Yu and X. S. Zhao, *Thin Solid Films*, **36**, 275 (2000).
123. H. Jiu, J. Ding, J. Bao, Q. Zhang and C. Gao, *Spectrochim. Acta A*, **61**, 3150 (2005).
124. Z. F. Li, L. Zhou, J. B. Yu, H. J. Zhang, R. P. Deng, Z. P. Peng, and Z. Y. Guo, *J. Phys. Chem. C*, **111**, 2295 (2007).
125. M. H. Qi and G. F. Liu, *Solid State Sci.*, **6**, 287 (2004).
126. O. A. Serra, E. J. Nassar, P. S. Calefi and I. L. V. Rosa, *J. Alloys Compd.*, **275–277**, 838 (1998).
127. O. A. Serra, E. J. Nasser, C. A. Kodaira, C. R. Neri, P. S. Cazlefi and I. L. V. Rosa, *Spectrochim. Acta A*, **54**, 2077 (1998).
128. A. V. Turukhin, A. V. Carpenter, A. A. Gorokhovsky, T. Chu and Y. Okamoto, *J. Lumin.*, **86**, 333 (2000).
129. Y. A. Ono, *Electroluminescent Displays*, World Scientific, Singapore, 1995.
130. G. Destriau, *J. Chim. Phys.*, **33**, 587 (1936).
131. C. W. Tang and S. A. VanSlyke, *Appl. Phys. Lett.*, **51**, 913 (1987).
132. J. H. Burroughes, D. D. C. Bradly, A. R. Brown, N. Marks, K. Mackay, R. H. Friend, P. L. Burn and A. B. Holmes, *Nature*, **347**, 539 (1990).
133. L. Liu, W. Li, Z. Hong, J. Peng, X. Liu, C. Liang, Z. Liu, J. Yu and D. Zhao, *Synth. Met.*, **91**, 267 (1997).
134. R. Reyes, C. F. B. da Silva, H. F. Brito and M. Cremona, *Braz. J. Phys.*, **32**, 535 (2002).
135. L. Micaroni, F. C. Nart and I. A. Hümmelgen, *J. Solid State Electrochem.*, **7**, 55 (2002).
136. F. Marchetti, C. Pettinari and R. Pettinari, *Coord. Chem. Rev.*, **249**, 2909 (2005).
137. L. Zhang, T. Li, B. Li, B. Lei, S. Yue and W. Li, *J. Lumin.*, **126**, 682 (2007).
138. N. J. Xiang, L. M. Leung, S. K. So and M. L. Gong, *Spectrochim. Acta A*, **65**, 907 (2006).
139. Z. Bian, D. Gao, K. Wang, L. Jin and C. Huang, *Thin Solid Films*, **460**, 237 (2004).
140. J. Kido, W. Ineda, M. Kimura and K. Nagai, *Jpn. J. Appl. Phys.*, **35**, L394 (1996).
141. Y. Liang, Q. Lin, H. Zhang and Y. Zheng, *Synth. Met.*, **123** 377 (2001).
142. Z. Wang and D. W. Samuel, *J. Lumin.*, **111**, 199 (2005).
143. Y. Lv, J. Zhang, W. Cao, J. C. Juan, F. Zhang and Z. Xu, *J. Photochem. Photobiol. A: Chem.*, **188**, 155 (2007).
144. A. O'Riordan, E. O'Connor, S. Moynihan, X. Llinares, R. V. Deun, P. Fias, P. Nockemann, K. Binnemans and G. Redmond, *Thin Solid Films*, **491**, 264 (2005).

145. M. A. Baldo, C. Adachi and S. R. Forrest, *Phys. Rev. B*, **62**, 10967 (2001).
146. J. Yu, L. Zhou, H. Zhang, Y. Zheng, H. Li, R. Deng, Z. Peng and Z. Li, *Inorg. Chem.*, **44**, 1611 (2005).
147. R. Reyes, M. Cremona, E. E. S. Teotonio, H. F. Brito and O. L. Malta, *Chem. Phys. Lett.*, **396**, 54 (2004).
148. G. Yu, Y. Liu, X. Wu, D. Zhu, H. Li, L. Jin and M. Wang, *Chem. Mater.*, **12**, 2537 (2000).
149. C. Liang, W. Li, Z. Hong, X. Liu, J. Peng, L. Liu, Z. Lu, M. Xie, Z. Liu, I. Yu and D. Zhao, *Synth. Met.*, **91**, 151 (1997).
150. Y. Kawamura, Y. Wada, Y. Hasegawa, M. Iwamuro, T. Kitamura and S. Yanagira, *Appl. Phys. Lett.*, **74**, 3245 (1999).
151. R. G. Sun, Y. Z. Wang, Q. B. Zheng, H. J. Zhang and A. J. Epstein, *J. Appl. Phys.*, **87**, 7589 (2000).
152. Z. R. Hong, W. L. Li, D. X. Zhao, C. J. Liang, X. Y. Liu, J. B. Peng and D. Zhao, *Synth. Met.*, **111–112**, 43 (2000).
153. G. C. Bazan, T. Bergstedt, M. D. McGehee, A. J. Heeger, C. Zhang, M. B. O'Regan, A. P. Saab and V. I. Srdanov, *Adv. Mater.*, **11**, 1349 (1999).
154. N. P. Kuzmina and S. V. Eliseeva, *Russ. J. Inorg. Chem.*, **51**, 73 (2006).
155. H. You, J. Fang, Y. Xuan and D. Ma, *Mater. Sci. Eng. B*, **131**, 252 (2006).
156. X. C. Gao, H. Cao, C. H. Huang, B. G. Li, K. Ibrahim, F. K. Liu and S. Umitani, *Chem. Phys. Lett.*, **297**, 530 (1998).
157. T. Oyamada, Y. Kawamura, T. Koyama, H. Sasabe and C. Adachi., *Adv. Mater.*, **16**, 1082 (2004).
158. P. P. Sun, J. P. Duan, J. J. Lih and C. H. Cheng, *Adv. Funct. Mater.*, **13**, 683 (2003).
159. Z. R. Hong, O. Lengye, C. S. Lee, and S. T. Lee, *Org. Electron.*, **4**, 149 (2003).
160. M. Sun, H. Xin, K. Wang, Y. Zhang, L. Jin and C. Huang, *J. Chem. Soc., Chem. Commun.*, **6**, 702 (2003).
161. X. C. Gao, H. Cao, C. Huang, B. G. Li and S. Umitani, *Appl. Phys. Lett.*, **72**, 2217 (1998).
162. J. Fang, H. You, J. Gao, W. Lu and D. Ma, *J. Lumin.*, **124**, 157 (2007).
163. Z. F. Li, L. Zhou, J. B. Yu, H. J. Zhang, R. P. Deng, Z. P. Peng and Z. Y. Guo, *J. Phys. Chem. C*, **111**, 2295 (2007).
164. K. Okada, Y. Wang, T. Chen, M. Kitamura, T. Nakaya and H. Inoue, *J. Mater. Chem.*, **9**, 3023 (1999).
165. N. A. H. Male, O. V. Salata and V. Christou, *Synth. Met.*, **126**, 7 (2002).
166. H. You, J. Fang, L. Wang, X. Zhu, W. Huang and D. Ma, *Opt. Mater.*, **29**, 1514 (2007).
167. F. Liang, Q. Zhou, Y. Cheng, L. Wang, D. Ma, X. Jing and F. Wang., *Chem. Mater.*, **15**, 1935 (2003).
168. Y. K. Kim, S. W. Pyo, D. S. Choi, H. S. Hue, S. H. Lee, Y. K. Ha, H. S. Lee, J. S. Kim and W. Y. Kim, *Synth. Met.*, **111/112**, 113 (2000).
169. Y. Zheng, H. Lin, Y. Liang, X. Zheng, J. Lin, Y. Liang, Q. Lin, Y. Yu, S. Wang, C. Guo and H. Zhang, *Opt. Mater.*, **20**, 273 (2002).
170. Y. Zheng, H. Lin, Y. Liang, Y. Yu, Y. Zhou, C. Guo, S. Wang and H. Zhang, *J. Alloys. Compd.*, **336**, 114 (2002).
171. Y. Zeng, Y. Liang and H. Zhang, *Mater. Lett.*, **53**, 52 (2002).
172. Y. Zheng, H. Lin, Y. Liang, Y. X. Zheng, J. Lin, Y. J. Liang, Q. Lin, Y. N. Lin, Q. G. Meng, Y. H. Zhou, S. B. Wang and H. J. Zhang, *J. Mater. Chem.*, **11**, 2615 (2001).
173. Y. Zheng, H. Lin, Y. Liang, B. Li and S. Umitani., *Mater. Lett.*, **54**, 424 (2002).
174. D. Zhu, Y. Liu and F. Bai, *Thin Solid Films*, **363**, 51 (2000).
175. L. M. Sweeting, in *Spectroscopic Characterization of Minerals and Their Surfaces* (Eds L. M. Coyne, D. F. Blake, S. W. McKeever and S. W. S. McKeever), *Am. Chem. Soc. Symps. Ser.*, **415**, 245 (1989).
176. I. Sage, R. Badcock, L. Humberstone, N. Geddes, M. Kemp and G. Bourhill, *Smart Mater. Struct.*, **8**, 504 (1999).
177. M. B. Hocking, F. W. Vandervoort-Maarschalk, J. McKiernan and J. I. Zink, *J. Lumin.*, **51**, 323 (1992).
178. F. A. Cotton, L. M. Daniels and P. L. Huang, *Inorg. Chem. Commun.*, **4**, 319 (2001).
179. L. M. Sweeting, *Chem. Mater.*, **13**, 854 (2001).
180. J. P. Duignan, I. D. H. Oswald, I. C. Sage, L. M. Sweeting, K. Tanaka, T. Ishihara, K. Hirao and G. Bourhill, *J. Lumin.*, **97**, 115 (2002).

181. R. G. Bulgakov, S. P. Kuleshov, A. N. Zuzlov and R. R. Vafin, *Russ. Chem. Bull.*, **53**, 2712 (2004).
182. X. F. Chen, X. H. Zhu, W. Chen, J. J. Vittal, G. K. Tan, J. Wu and X. Z. You, *J. Coord. Chem.*, **52**, 97 (2000).
183. C. R. Hurt, N. McAvoy, S. Bjorklund and N. Filipescu, *Nature*, **212**, 179 (1966).
184. R. G. Xiong and X. Z. You, *Inorg. Chem. Commun.*, **5**, 677 (2002).
185. X. F. Chen, S. H. Liu, Z. Yu, K. K. Cheung, J. Ma, N. B. Min and X. Z. You, *J. Coord. Chem.*, **47**, 349 (1999).
186. X. F. Chen, C. Y. Duan, X. H. Zhu, X. Z. You, S. S. S. Raj, H. K. Fun and J. Wu, *Mater. Chem. Phys.*, **72**, 11 (2001).
187. X. R. Zeng, R. G. Xiong, X. Z. You and K. K. Cheung, *Inorg. Chem. Commun.*, **3**, 341 (2000).
188. X. F. Chen, X. H. Zhu, Y. H. Xu, S. S. S. Raj, S. Oztürk, H. K. Fun, J. Ma and X. Z. You, *J. Mater. Chem.*, **9**, 2919 (1999).
189. N. Takada, J. I. Sugiyama, R. Katoh, N. Minami and S. Hieda, *Synth. Met.*, **91**, 351 (1997).
190. A. G. Mirochnik, B. V. Bukvetskii, P. A. Zhikhareva, N. V. Polyyakova and V. E. Karasev, *Russ. J. Inorg. Chem.*, **51**, 717 (2006).
191. B. Marciniak and G. E. Buono-Core, *J. Photochem. Photobiol. A*, **52**, 1 (1990).
192. B. Marciniak and G. L. Hug, *Coord. Chem. Rev.*, **159**, 55 (1997).
193. M. Courtois and L. S. Forster, *J. Mol. Spectrosc.*, **18**, 396 (1965).
194. S. Kaizaki and T. Yamauchi, *Inorg. Chim. Acta*, **360**, 649 (2007).
195. Y. Yamamoto and Y. Shimura, *Bull. Chem. Soc. Jpn.*, **54**, 3351 (1981).
196. T. Ohno, S. Kato, S. Kaizaki and I. Hanazaki, *Chem. Phys. Lett.*, **102**, 471 (1983).
197. N. M. Shavaleev, S. J. A. Pope, Z. R. Bell, S. Faulkner and M. D. Ward, *Dalton Trans.*, 808 (2003).
198. M. D. Ward, *Coord. Chem. Rev.*, **251**, 1663 (2007).
199. H. Kunkely and A. Vogler, *Inorg. Chem. Commun.*, **6**, 543 (2003).
200. I. R. Laskar, S. F. Hsu and T. M. Chen, *Polyhedron*, **24**, 189 (2005).
201. C. Adachi, R. C. Kwong, P. Djurovich, V. Adamovich, M. A. Baldo, M. E. Thompson and S. R. Forrest, *Appl. Phys. Lett.*, **79**, 2082 (2001).
202. N. R. Evans, L. S. Devi, C. S. K. Mak, S. E. Watkins, S. I. Pascu, A. Köhler, R. H. Friend, C. K. Williams and A. B. Holmes, *J. Am. Chem. Soc.*, **128**, 6647 (2006).
203. H. Kunkely and A. Vogler, *Inorg. Chem. Commun.*, **8**, 119 (2005).
204. Q. Zhao, C. Y. Jiang, M. Shi, F. Y. Li, T. Yi, Y. Cao and C. H. Huang, *Organometallics*, **25**, 3631 (2006).
205. H. H. Rho and Y. Ha, *Curr. Appl. Phys.*, **6**, 706 (2006).
206. N. G. Park, G. C. Choi, Y. H. Lee and Y. S. Kim, *Curr. Appl. Phys.*, **6**, 620 (2006).
207. T. Tsuboi and N. Aljaroudi, *J. Lumin.*, **119–120**, 127 (2006).
208. P. T. Chou and Y. Chi, *Eur. J. Inorg. Chem.*, 3319 (2006).
209. P. Sun, C. Li, Y. Pan and Y. Tao, *Synth. Met.*, **156**, 525 (2006).
210. S. Lamansky, P. Djurovich, D. Murphy, F. Abdel-Razzaq, H. E. Lee, C. Adachi, P. E. Burrows, S. R. Forrest and M. E. Thompson, *J. Am. Chem. Soc.*, **123**, 4304 (2001).
211. S. Lamansky, P. Djurovich, F. Abdel-Razzaq, S. Garon, D. Murphy and M. E. Thompson, *J. Appl. Phys.*, **92**, 1570 (2002).
212. M. L. Xu, M. T. Li, Z. R. Hong, W. L. Li, Z. W. An and Q. Zhou, *Opt. Mater.*, **28**, 1025 (2006).
213. H. Fujii, H. Sakurai, K. Tani, K. Wakisaka and T. Hirao, *IEICE Electronics Express*, **2**, 260 (2005).
214. C. H. Yang, C. H. Chen and I. W. Sun, *Polyhedron*, **25**, 2407 (2006).
215. C. Y. Chang, S. N. Hsieh, T. C. Wen, T. F. Guo and C. H. Cheng, *Chem. Phys. Lett.*, **418**, 50 (2006).
216. C. H. Chen and J. Shi, *Coord. Chem. Rev.*, **171**, 161 (1998).
217. S. Wang, *Coord. Chem. Rev.*, **215**, 79 (2001).
218. A. Strasser and A. Vogler, *J. Photochem. Photobiol. A: Chem.*, **165**, 115 (2004).
219. A. Strasser and A. Vogler, *Inorg. Chem. Commun.*, **7**, 528 (2004).
220. E. J. Fernández, A. Laguna, J. M. López-de-Luzuriaga, M. Monge, M. Montiel, M. E. Olmos and J. Pérez, *Organometallics.*, **23**, 774 (2004).

221. C. Buck, F. X. Hartmann, T. Lasserre, D. Motta, S. Schoenert and U. Schwan, *J. Lumin.*, **106**, 57 (2004).
222. C. Buck, F. X. Hartmann, D. Motta and S. Schoenert, *Chem. Phys. Lett.*, **435**, 252 (2007).
223. I. R. Laskar, S. F. Hsu and T. M. Chen, *Polyhedron*, **24**, 881 (2005).
224. E. F. G. Dickson, A. Pollak and E. P. Diamandis, *J. Photochem. Photobiol. B: Biol.*, **27**, 3 (1995).
225. M. Elbanowski and B. Makowska., *J. Photochem. Photobiol. A*, **99**, 85 (1996).
226. V. S. Sastri, J.-C. G. Bünzli, V. R. Rao, G. V. S. Rayudu and J. R. Perumareddi, *Modern Aspects of Rare Earths and Their Complexes*, Elsevier, Amsterdam, 2003.
227. E. Soini and T. Lovgren, *CRC Crit. Rev. Anal. Chem.*, **18**, 105 (1987).
228. I. Hemmilä, S. Dakubu, V. Mukkala, H. Siitari and T. Lövgren, *Anal. Biochem.*, **137**, 335 (1984).
229. N. Sabbatini, M. Guardigli and I. Manet, in *Handbook on the Physics and Chemistry of Rare Earths*, Vol. 23 (Eds K. A. Gschneidner Jr. and L. Eyring), North-Holland, Amsterdam, 1996.
230. I. Hemmilä, *J. Alloys Compd.*, **225**, 480 (1995).
231. I. Hemmilä and V. M. Mukkala, *Crit. Rev. Lab. Clin. Sci.*, **38**, 441 (2001).
232. S. Petoud, S. M. Cohen, J.-C. G. Bünzli and K. N. Raymond, *J. Am. Chem. Soc.*, **125**, 13324 (2003).
233. Y. Y. Xu and I. Hemmilä, *Talanta*, **39**, 759 (1992).
234. E. P. Diamandis, *Clin. Biochem.*, **21**, 139 (1988).
235. G. Mathis, *Clin. Chem.*, **39**, 1953 (1993).
236. Y. X. Ci and X. D. Yang, *Chin. Chem. Lett.*, **3**, 1007 (1992).
237. Y. X. Ci, X. D. Yang and W. B. Chang, *J. Immunol. Methods*, **179**, 233 (1995).
238. J. Yuan and K. Matsumoto, *J. Pharm. Biomed. Anal.*, **15**, 1397 (1997).
239. J. Yuan, K. Matsumoto and H. Kimura, *Anal. Chem.*, **70**, 596 (1998).
240. J. Yuan and G. Wang, *Trends Anal. Chem.*, **25**, 490 (2006).
241. F. B. Wu and C. Zhang, *Anal. Biochem.*, **311**, 57 (2002).
242. F. B. Wu, S. Q. Han, C. Zhang and Y. F. He, *Anal. Chem.*, **74**, 5882 (2002).
243. L. M. Vallarino, *J. Alloys Compd.*, **249**, 69 (1997).
244. K. Matsumoto, Y. Tsukahara, T. Uemara, K. Tsunoda, H. Kume, S. Kawasaki, J. Tadano and T. Matsuya, *J. Chromatogr. B*, **773**, 135 (2002).
245. H. Harma, T. Soukka and T. Lovgren, *Clin. Chem.*, **47**, 561 (2001).
246. P. Huhtinen, M. Kivela, O. Kuronen, V. Hagren, H. Takalo, H. Tenhu, T. Lovgren and H. Harma, *Anal. Chem.*, **77**, 2643 (2005).
247. T. Soukka, J. Paukkunen, H. Harma, S. Lonnberg, H. Lindroos and T. Lovgren, *Clin. Chem.*, **47**, 1269 (2001).
248. A. Valanne, S. Huopalahti, T. Soukka, R. Vainionpaa, T. Lovgren and H. Harma, *J. Clin. Virol.*, **33**, 217 (2005).
249. A. Valanne, S. Huopalahti, R. Vainionpaa, T. Lovgren and H. Harma, *J. Virol. Methods*, **129**, 83 (2005).
250. S. Jaakohuhta, H. Harma, M. Tuomola and T. Lovgren, *Int. J. Food Microbiol.*, **114**, 288 (2007)
251. A. Valanne, H. Lindroos, T. Lovgren and T. Soukka, *Anal. Chim. Acta*, **539**, 251 (2005).
252. L. Kokko, N. Johansson, T. Lovgren and T. Soukka, *J. Biomol. Screen.*, **10**, 348 (2005).
253. L. Kokko, S. Jaakohuhta, P. Lindroos and T. Soukka, *ASSAY Drug Dev. Technol.*, **4**, 671 (2006).
254. E. J. Schimitschek and E. G. K. Schwarz, *Nature*, **196**, 832 (1962).
255. N. Filipescu, M. R. Kagan, N. McAvoy and F. A. Serafin., *Nature*, **196**, 467 (1962).
256. A. Lempicki and H. Samelson, *Phys. Lett.*, **4**, 133 (1963).
257. H. Samelson, A. Lempicki, C. Brecher and V. A. Brophy, *Appl. Phys. Lett.*, **5**, 173 (1964).
258. H. Samelson, A. Lempicki, V. A. Brophy and C. Brecher, *J. Chem. Phys.*, **40**, 2547 (1964).
259. H. Samelson, A. Lempicki and C. Brecher, *J. Chem. Phys.*, **40**, 2553 (1964).
260. H. Samelson, A. Lempicki and C. Brecher, *J. Chem. Phys.*, **41**, 1214 (1964).
261. A. Lempicki and K. H. Weise, US Patent 3,319,183 (1967).
262. E. J. Schimitschek, R. B. Nehring and J. A. Trias, *J. Chem. Phys.*, **42**, 788 (1965).
263. E. J. Schimitschek, R. B. Nehring and J. A. Trias, *Appl. Phys. Lett.*, **9**, 1031 (1966).
264. E. J. Schimitschek, R. N. Nehring and J. A. Trias, *J. Chim. Phys.*, **64**, 173 (1967).
265. E. J. Schimitschek, R. N. Nehring and J. A. Trias, US Patent 3,450,641 (1969).

266. C. Brecher, A. Lempicki and H. Samelson, US Patent 3,405,372 (1968).
267. N. E. Wolff and R. J. Pressley, *Appl. Phys. Lett.*, **2**, 152 (1963).
268. E. H. Huffmann, *Nature*, **200**, 158 (1963).
269. E. H. Huffmann, *Nature*, **203**, 1373 (1964).
270. M. L. Bhaumik, P. C. Fletcher, L. J. Nugent, S. M. Lee, S. Higa, C. L. Telk and M. Weinberg, *J. Phys. Chem.*, **68**, 1490 (1964).
271. P. A. Bazhulin, L. D. Derkacheva, B. G. Distanov, G. V. Peregudov, A. P. M. Prokhorov, A. I. Sokolovskaya and D. N. Shigorin, *Opt. Spectrosc.*, **18**, 298 (1965).
272. S. Bjorklund, G. Kellmeyer, C. R. Hurt, N. McAvoy and N. Filipescu, *Appl. Phys. Lett.*, **10**, 160 (1967).
273. Y. Meyer, R. Astier and J. Simon, *Compt. Rend.*, **259**, 4604 (1964).
274. Y. Meyer, *J. Phys. (Paris)*, **26**, 558 (1965).
275. R. Seitz, US Patent 3,477,037 (1969).
276. M. Verron and Y. Meyer, Fr. Patent 1453474 (1966); *Chem. Abstr.*, **67**, 16686 (1967).
277. O. de Witte and Y. Meyer., *J. Chim. Phys.*, **64**, 186 (1967).
278. P. Crozet and Y. Meyer, *Nature*, **213**, 1115 (1967).
279. D. E. Altman and M. Geller, US Patent 3,470,493 (1969).
280. D. L. Ross and J. Blanc, *Europium Chelates as Laser Materials*, in *Lanthanide/Actinide Chemistry*, *Advances in Chemistry Series* (Ed. R. F. Gould), Vol. 71, Am. Chem. Soc., Washington, 1967, p. 155.
281. I. M. Batyaev, *Russ. Chem. Rev.*, **40**, 622 (1971).
282. C. Brecher, H. Samelson and A. Lempicki, *J. Chem. Phys.*, **42**, 1081 (1965).
283. H. Samelson, C. Brecher and A. Lempicki, *J. Chim. Phys.*, **64**, 165 (1967).
284. B. Whittaker, *Nature*, **228**, 157 (1970).
285. F. H. Fry and W. R. Pirie, *J. Chem. Phys.*, **43**, 3761 (1965).
286. H. Taniguchi, H. Tomisawa and J. Kido, *Appl. Phys. Lett.*, **66**, 1578 (1995).
287. H. Taniguchi, J. Kido, M. Nishiya and S. Sasaki., *Appl. Phys. Lett.*, **67**, 1060 (1995).
288. L. N. Sun, J. B. Yu, H. J. Zhang, Q. G. Meng, E. Ma, C. Y. Peng and K. Y. Yang, *Micropor. Mesopor. Mater.*, **98**, 156 (2007).

CHAPTER 4

Thermochemical considerations of metal enolates

JOEL F. LIEBMAN

Department of Chemistry and Biochemistry, University of Maryland, Baltimore County, 1000 Hilltop Circle, Baltimore, MD 21250, USA
Fax: 410-455-2608; e-mail jliebman@umbc.edu

and

SUZANNE W. SLAYDEN

Department of Chemistry, George Mason University, 4400 University Drive, Fairfax, VA 22030-4444, USA
Fax: 703-993-1055; e-mail sslayden@gmu.edu

The chemistry of metal enolates
Edited by Jacob Zabicky

I. INTRODUCTION

Data for enthalpies of formation and combustion for most classes of metal enolates are scant in the literature. It is only for β-diketonates and related complexes (e.g. 2-ketiminoenolates, β-thiodiketonates) that these thermochemical data are extensively available[1–5]. This precludes taking the approach of other chapters of ours on organic thermochemistry in the Patai–Rappoport series[6,7]. In the present chapter we will make thermochemical inferences from the available data, hoping to gain new qualitative understanding for a wide variety of species, as well as to encourage more experimental determinations.

This chapter deals with metal enolates of the type $RR^1C{=}C(R^2){-}O{-}M$ or their isomeric α-metalloketones $RR^1C(M)C(O)R^2$, where R, R^1 and R^2 are hydrogen, alkyl and/or aryl groups. The enolates of carboxylic esters (e.g. the zinc derivatives involved in the Reformatzky reaction) are outside our scope. Other modes of coordination of the metal to the C–C–O framework that define enolates, such as enediolates, oxocarbons, semidiones, tropolonates, ynolates and related species, will also be discussed. We will generally ignore β-diketonates (derivatives of acetylacetone and the like). Unlike all other classes of metal enolates discussed in this chapter, enthalpy of combustion and/or reaction measurements and derived enthalpies of formation for this class of compounds are numerous: desired data for them are found and they have been reviewed before[8,9]. The organization scheme for the chapter follows the periodic table, first through the main group elements and then through the transition elements. Following thermochemical convention, the energy unit is $kJ\,mol^{-1}$ (4.184 kJ $\equiv$ 1 kcal). The standard symbol η^n ($n \geqslant 2$) is used to designate the number of sites on any ligand that are bonding to the metal. For the Cp and Cp* ligands, η^5 will be implicitly assumed.

II. GROUP 1: LITHIUM, SODIUM, POTASSIUM, RUBIDIUM AND CESIUM

Lithium enolates have been actively investigated, including reaction rates and equilibria. Sodium enolates, more ionic than their lithium analogs, more covalent than their heavier alkali metal counterparts, have been studied less while potassium appears frequently. Rubidium enolates have been almost totally ignored. Cesium and lithium enolate chemistry are often compared. We know of no francium enolate chemistry.

It was found[10] from calculations that alkali metal cation-acetaldehyde enolate ion pairs are less stable compared to the free anions by about 30–60 $kJ\,mol^{-1}$: the metal cations, all with charges of nearly +1, comparably increase localization of negative charge on the enolate oxygen. The cations also influence the geometry and reaction energies of the anions. The enthalpies of the exothermic acid/base reaction (equation 1) for Li, Na, K, Rb and Cs are −34, −51, −56, −60 and −47 $kJ\,mol^{-1}$, respectively. Except for lithium, these values do not differ much from each other. The isomerization reaction (equation 2) favors the bridged η^3 species on the right over the singly oxygen-attached isomer by a nearly constant 8 $kJ\,mol^{-1}$ for all the alkali elements.

$$CH_2{=}CHOH + MOH \longrightarrow CH_2CHOM + H_2O \qquad (1)$$

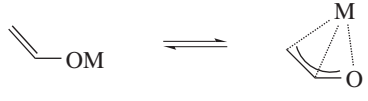

(2)

Elemental lithium, sodium and potassium react[11] with CO to form the isomeric ynediolate (MOC≡COM) and ketenolate (MOC(M)=C=O) of unknown relative stability.

A combined theoretical and experimental study[12] showed that solid complexes of Li, Na, K and Rb with the squarate ion (**1**) are neither isostructural nor similarly hydrated. As the size of the cation increases, the C−C bond lengths tend to equalize, which was interpreted by the original authors as an enhancement of aromatic delocalization. Croconates (**2**) appear more stable than rhodizonates (**3**)[13].

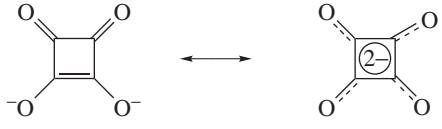

(**1**)

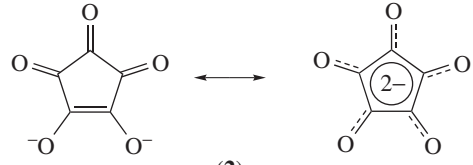

(**2**)

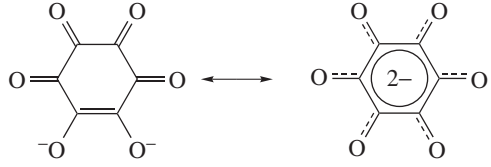

(**3**)

KH is exceptionally reactive compared to LiH and NaH in the formation of enolates from acyclic ketones in ether[14]. The IR absorption stretching frequency for the enolate O−M bond suggests a tighter coordination for the Li^+ than for the K^+ enolate.

A systematic study[15] of some monosubstituted solvent-separated cyclopentadienide salts of Group 1 cations (Li, Na, K, Cs) in DMSO revealed the bonding preferences for the fulvenoid (**4**) over the cyclopentadienyl isomer (**5**). Three of the substituents contained an α-carbonyl group: formyl, acetyl and benzoyl. From the viewpoint of the anions, there is a conflict between the inherent greater stability of oxyanions over carbanions and the aromaticity associated with the 6 π-electron carbocyclic system. The authors demonstrated that the fulvenoid interaction is favored by strong electron-accepting substituents and

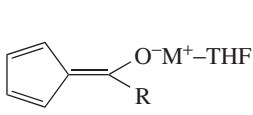

(**4**)

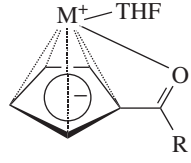

(**5**)

hard Lewis acid cations; conversely, the cyclopentadienyl interaction is favored by weak electron-accepting substituents and soft Lewis acid cations. The alkali cation-carbonyl substituent pairs were generally equally distributed between forms **4** and **5**, except for K^+ $[BzC_5H_4]^-$ which favors **5**. A study[16] of Na^+ $[AcC_5H_4]^-$ shows some structural ambivalence in the solid (as the THF monosolvate) where the Na is bonded to the acyl group oxygen, the THF oxygen and the five carbons of the cyclopentadienide ring. In solution, $K^+[AcC_5H_4]^-$ undergoes rapid equilibrium between diverse ion pair structures[16].

Relatedly, there is the temperature-dependent equilibration in THF of the sodium salt of 1-methylnonafulvene-1-oxide or acetyl-[9]-annulenide (equation 3)[17]. As the temperature is lowered to $-52\,^{\circ}C$, equilibrium shifts to the right and the sodium cation in the contact ion pair acquires another solvent molecule to form a solvent-separated ion pair. At $-52\,^{\circ}C$, the rate constant of the reaction from left to right is $\geqslant 330\ s^{-1}$ with $\Delta G^{\neq} \leqslant 43\ kJ\,mol^{-1}$ and $\Delta H = -29\ kJ\,mol^{-1}$. Analysis of the species involved in the base-catalyzed rearrangement of equation 3 would be most informative since data for 1-methylheptafulvene-1-oxide may point to enhanced stability over the tropenide, with its antiaromatic 8-π-electrons carbocyclic system[18–21].

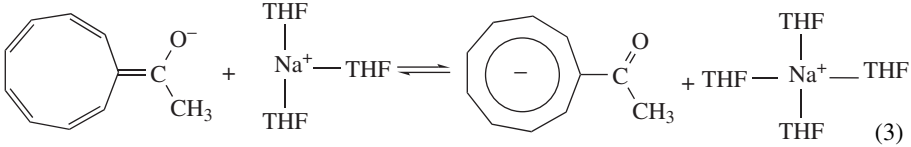

(3)

2,4,6-Trimethylacetophenone forms a dimeric sodium enolate with two chelating TMEDA ligands (**6**). There is significant π-electron interaction of the metal ion with the olefinic carbons but no evidence of π-bonding with the aromatic rings[22].

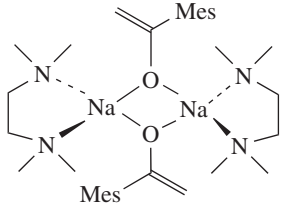

(**6**)

Acyclic semidiones (RC(O)=C(O$^-$) R) and their metal complexes exhibit rapid $E - Z$ equilibration[23] where the E/Z ratio is determined by the extent of ion pairing. The E/Z ratio changes directly with the alkali metal cation radius or the solvent dielectric constant. Both K^+ and Rb^+ dimethylsemidione prefer the (E)-conformation. The free energy of the (E) rubidium species is lower by *ca* 2 kJ mol^{-1} than that of the potassium species. As the size of the R group increases, the proportion of E increases[24]. In DMSO in the presence of potassium ion, the (E)-dimethylsemidione is more stable than the (Z)-isomer by 10.5 kJ mol^{-1}. For comparison, dimethylethylene (i.e. 2-butene) is more stable[25] as the (E)-form by 4.3 kJ mol^{-1}.

The enolates of the largest and smallest alkali metals of 6-phenyl-1-tetralone (**7**) have been found[26] to have comparable monomer–tetramer equilibration constants in THF ($K^{Cs}_{1,4} = 2.3 \times 10^{11}$, $K^{Li}_{1,4} = 4.7 \times 10^{10}\ M^{-3}$). By contrast, the p$K$ values of the monomers differ by a bit more than 10^9 (p$K^{monomerCs} = 23.39$, p$K^{monomerLi} = 14.22$). The

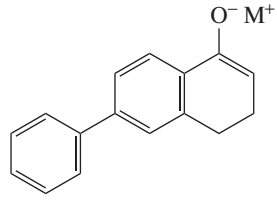

(**7**)

original authors state that the pK values are not pK_a's, but are referred to an arbitrary (but convenient) standard[26]. The comparable equilibration constants are presumably a balance between the ion pair aggregation which is reduced for the larger cesium ion and the stabilization of the monomer by solvation which is more important for the smaller lithium. We would like to compare these results with corresponding ones for the enolates of 2-tetralone and ring-varied[20,27,28] benzocyclobutenone, indanones and benzosuberones. However, we are thwarted in doing so because no association data are available for any metal enolates of these last ketones, and indeed, even the simpler comparison of the basicity of the enolates themselves is frustrated because the studies referred to were done in different media.

In the lithium and cesium enolates of *o*-methoxyacetophenone, the methoxy oxygen coordinates with the smaller lithium cation but not with the cesium cation[29]. Other examples of lithium enolate chemistry include a thermochemical analysis of the aldol reaction of lithiopinacolonate with pivalaldehyde[30] and a comparison of the proton affinities and aggregation states of lithium alkoxides, phenolates, enolates, β-dicarbonyl enolates, carboxylates and amidates[31]. Although the lithium enolate of cyclopropanone itself remains unknown, derivatives (accompanied by their allenoxide isomer) have been implicated in the reaction of α-(trimethylsilyl) vinyl lithium with CO[32]. That both species are seemingly formed is surprising because cyclopropanone enolate is expected to be much less stable than its acyclic isomer: cyclopropene is less stable[25] than allene by almost 90 kJ mol^{-1}.

Another relevant phenomenon is the reaction of carbon monoxide with the lithium trimethylsilyldiazomethanide (Me_3SiCN_2Li) to form either an ynolate ($Me_3SiC{\equiv}COLi$) or a ketenide ($Me_3SiC(Li){=}C{=}O$) derivative[33]. The corresponding neutral species Me_3SiCHN_2 reacts with CO, in the presence of $Co_2(CO)_8$, to form $Me_3SiCH{=}C{=}O$[34]. Neither reaction was studied calorimetrically. Accordingly, they cannot be compared with the energetics of the reaction of HCN_2^- with CO to form $HCCO^-$ and N_2, a quantity indirectly obtainable from the deprotonation enthalpies of diazomethane[35,36] and ketene[37].

We note the reaction[38] of *in situ* generated, suitably activated, LiH with the lithium alkynolate $PhCH_2C{\equiv}COLi$, to form the (*Z*)-α,*O*-dilithioenolate, $PhCH_2C(Li){=}CHOLi$. The addition is stereospecific with Li and OLi *cis* to each other, thus suggesting stabilization from Li$\cdots$O bonding. Also known as α-keto dianions, these dilithioenolates seem surprisingly stable as they are also formed[39] by chlorine–lithium exchange of lithium α-chloroenolates with *t*-BuLi. It would be interesting to vary the α-halogen and the alkyl group of the organolithium reactant. Related experimental results for the isomeric 'ketone α,β dianions' with a $-CHLiC{=}C(OLi)-$(or $-CHLiCHLiC(O)-$) substructure[40] (and 'ketone α, δ dianions'[41]) are also desirable.

Ring opening to form potassium 1,ω-diphenylenolates occurs upon deprotonation of 1,2-diphenylcycloalkanols and a related chain cleavage occurs in the acyclic 3,4-diphenyl-3-hexanol[42]. With reactivities spanning a 10^6 range (c-C_8 > c-C_9 > c-C_7 > c-C_5 > c-C_6),

the reaction rates only poorly correlate with estimates of strain energy release. Kinetic isotope effects suggest a different rate-limiting step for c-C_8 and c-C_5.

Some bimetallic enolate systems were studied: Reaction[43] in THF solution of either CH_2=C(t-Bu)OK and t-BuOLi or CH_2=C(t-Bu)OLi and t-BuOK results in a crystallographically defined complex containing four units of each of the enolato, alkoxido, Li^+ and K^+ species, five units of THF and an additional KOH species. We have no idea what governs this precise composition. Potassium and calcium hexamethyldisilazide (HMDS) react stoichiometrically with 2,4,6-trimethylacetophenone to form a diverse set of oligomeric homo- and heterometallic enolates depending on the K:Ca ratio[44]. While crystallographically documented species exhibit an enolate oxygen bridging two metal atoms (as follows from the two in-plane lone pairs on oxygen), species with triple bridging oxygen are also characterized (befitting a negative oxygen as found in alkoxides with three tetrahedrally coordinating lone pairs) with the coordination number of the metal atoms ranging from three to six. It is found in one complex that toluene binds K^+ more strongly than does a lone pair of oxygen electrons of THF[45]. Of thermochemical relevance is the comparison of the ligand binding affinities of these metals. The gas phase binding of K^+ to toluene (80 kJ mol^{-1} [46]) is found to be somewhat weaker than to diethyl ether (93 kJ mol^{-1}[47]), there being no data for binding to THF. It is surprising that given π complexation is so powerful that we found no evidence for π complexation of K^+ using the formal C=C double bond in the enolate.

Finally, consider the crystal structure of the rubidium salt of 5,5-dimethyl-1,3-cyclohexanedione-2-sulfonic acid[48]. This species exists as the ketoenol wherein the rubidium ion is surrounded by seven oxygen atoms in pentagonal bipyramidal coordination. We know of no ketoenolate (and hence dianionic) salt of this 'sulfo-dione' with any cation. Perhaps some more highly charged cation would allow for this—note the significantly enhanced stability of rare earth complexes of 2-acetyl-5,5-dimethyl-1,3-cyclohexanedione over the parent diketone[49].

III. GROUP 2: BERYLLIUM, MAGNESIUM, CALCIUM, STRONTIUM AND BARIUM

There are few studies that compare two or more of the group 2 metal enolates. One is an ESR study of the bis(semidione) of 1,1,4,4-tetramethyltetralin-2,3-dione (**8**) where M = Be^{2+}, Mg^{2+}, Ca^{2+}, Sr^{2+}, Ba^{2+} and Zn^{2+}, and the analogous tris-complex of Al^{3+} in frozen solutions of 2-methyltetrahydrofuran[50]. Be^{2+}, Ba^{2+} and Zn^{2+} form only one kind of complex **8**, while there are four types for Mg^{2+} and Ca^{2+} and three types with Sr^{2+}. All group 2 cation complexes are in their triplet state; that of Al is likely a quartet-state complex. Another study discusses the use of the rhodizonate ion (**3**) as reagent for the detection of Sr^{2+}, with stronger enolate–metal binding than with Ca^{2+} and Ba^{2+} [51].

Beryllium chemistry includes its β-diketonate complexes formed from dimedone (**9**), acetylacetone[4, 52, 53] and some other β-diketones such as α,α,α-trifluoroacetylacetone[54]. However, unlike the monomeric chelate products from acetylacetone and its fluorinated derivative, the enolate species of dimedone (**9**) cannot form chelates and as the complex is polymeric, it cannot be distilled and is more labile to hydrolysis, as might be expected for an unstabilized alkoxide[55]. However, dimedone has a gas phase deprotonation enthalpy of 1418 ± 9 kJ mol^{-1} while acetylacetone enol (the more stable tautomer) is somewhat less acidic with a deprotonation enthalpy of 1438 ± 10 kJ mol^{-1} [56]. Accordingly, had beryllium acetylacetonate not been a chelate, this species would have been more, not less, susceptible to hydrolysis. There is a formal similarity (roughly π-isoelectronic structures) between cyclic β-diketonates and complexes of dimedone with benzene and polyacetylene (**10**). The difference between the enthalpies of formation of these hydrocarbons[57] is *ca*

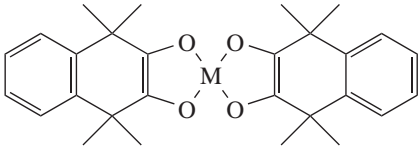

(**8**)

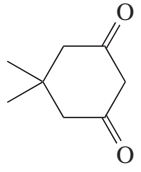

(**9**)

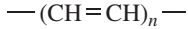

(**10**)

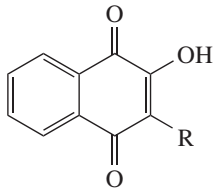

(**11**) (**a**) R = $CH_2CH{=}CMe_2$
(**b**) R = CH_2CH_2Pr-*i*

70 kJ mol^{-1}: what remains unmeasured is the enthalpy of formation of the two beryllium complexes from which their difference can be calculated. Indeed, we know of no enthalpy of formation measurement for any other dimedone complex.

Beryllium forms an enolate complex with lapachol (**11a**), a versatile ligand that also forms complexes with a variety of other divalent cations[58], e.g. Pd(II) and ZrO(II), and trivalent metallic cations[59], e.g. In(III) and Rh(III), for which there is quantitative stability data. There are no data on related saturated derivatives, e.g. the analogous species **11b**, to assess additional stabilization due to π-metal interactions.

The bromomagnesium enolate *n*-BuC(=CH_2)OMgBr•HMPA is an oxygen bridged dimer[60] while *i*-PrC(=CMe_2)OMgBr•HMPA is monomeric, probably due to steric hindrance. A study of the monomer/dimer equilibrium for ROMgBr•HMPA (R = Me, Et, *i*-Pr, *t*-Bu, Vi, isopropenyl etc.) would be desirable.

Grignard reagents (RMgX) react with carbon suboxide (C_3O_2) to form simple ketones of the type RAc and also cyclic dimers and trimers of acylketenes. An intermediate has been suggested where both O=C=C=C(R)O$^-$ and RC(O)C≡CO$^-$ are plausible descriptions[61–64]. Localized magnesium enolates such as O=C=C=C(R)OMgX and RC(O)C≡COMgX are reasonable, while the benzyne-like cyclic magnesium enolate **12** is very much less so.

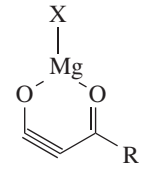

(**12**)

Addition of a second molecule of Grignard reagent to the terminal carbon to form a bisenolate RC(OMgX)=C=C(OMgX)R is not expected; however, formation of β-diketones RC(=O)CH_2C(=O)R by the addition of organolithium compounds (RLi) to carbon suboxide has been observed, suggesting such lithium bisenolate intermediates[65]. In these reactions, the number of keto groups, whether found in neutral starting materials or as product ligands, or as deprotonated enolate anionic products, always exceeds the number of magnesiums. As an example of the opposite situation where the number of magnesium atoms exceeds that of keto or enolate groups, the adsorption of acetone on solid MgO has been suggested by spectroscopic evidence to form a surface enolate[66]. Theoretical calculations suggest the carbonyl compound (at least acetone) is more stable as the enol than as the ketone when adsorbed on the MgO surface[67]. Such calculations[68] also show that the ionic charges on oxygen in MgO are more likely to be -1 than -2. Singly charged oxygen, the radical anion $O^{\bullet -}$ reacts with ketones to afford products formed by 1,1 and 1,3-dehydrogenation[69,70] rather than by loss of a single proton by reaction with O^{2-}. The resulting formation of a stable surface-bonded oxyallyl radical anion, here found as a η^4 metal enolate, is plausible because it is also known that the oxyallyl radical anion, and by implication its metal enolate derivatives, is stable to rearrangement or subsequent reaction, unlike singlet oxyallyl which rapidly closes to form the more stable cyclopropanone[71,72].

Solutions of calcium dienolate ([$Ca(OR)_2$]) and calcium diamide ([$Ca(NRR^1)_2$]) contain also the mixed complex ([$Ca(OR)(NRR^1)$])[73], and therefore, presumably their Gibbs free energy differences are small. The calcium enolates in this study are monomeric and their magnesium analogues are dimeric. The propiophenonate complex [$(HMDS)_2Mg_2(\mu$-HMDS)$\{\mu$-OC(Ph)=$CHCH_3\}$] in solution, with bridging enolate and HMDS ligands, has an E:Z ratio close to 3:1, while the Ca analog prefers the Z configuration. We would like to be able to make comparisons with the equilibrium E:Z ratio of other propiophenone enolates, as the reversal of the relative stability of the E and Z isomers is unexpected. We recognize the $-$C(Ph)=$CHCH_3$ substructure as part of 1-phenylpropene. Except for 1-phenylpropene[74], no data are available for the relative E–Z stability of compounds RC(Ph)=$CHCH_3$ with R $\neq$ H. The enthalpy of formation of the metal enediolate, calcium bis(ascorbate) tetrahydrate, was recently determined[75] by reaction calorimetry, -3945.1 kJ mol^{-1}. Unfortunately, there is virtually nothing with which to compare and evaluate this result.

Strontium enolate chemistry is almost nonexistent; barium enolate chemistry is rare; radium enolate chemistry is unknown. Allyl chlorides react with barium to form the corresponding organometallics, which in turn react with α,β-unsaturated ketones to form the metal enolate[76]. These enolates may also be formed *in situ* by the reaction of α-chloroketones with barium metal in the presence of an aldehyde, resulting in addition products[77]. These reactions and the enthalpies of formation of the precursor α-haloketones and enones are seemingly ideal candidates for calorimetric investigation.

IV. GROUP 13: ALUMINUM, GALLIUM, INDIUM AND THALLIUM

Trimethylaluminum was shown[78] to prefer formation of the corresponding dimethylaluminum enolate by deprotonation of o,o'-disubstituted acetophenones (equation 4a), while acetophenone itself or more remotely substituted acetophenones undergo addition to the carbonyl group with formation of the dimethylaluminum alkoxide (equation 4b). These results were explained in terms of steric hindrance of the products—the enolate appears not that much more strained than the parent ketone that also has a trigonal carbon attached to the substituted phenyl ring[79]. By contrast, the alkoxide addition product is expected to have considerable strain arising from a substituted ring bonded to a quaternary carbon, as

is found in the structurally related *o*-*t*-butyltoluene[80] which is strained by *ca* 25 kJ mol^{-1} relative to its *m*- and *p*-isomers. Aluminum enolates can also be synthesized by reaction of highly halogenated ketones with activated metal[81]. From a thermochemical perspective, $CF_3C(=O)CF_2X$ (X = Cl, Br, O_3SF) results in loss of the X group (weaker C−X bond but also weaker Al-X bond) and fluorinated enols are often more stable than the corresponding ketones[82], unlike their hydrocarbon counterparts where CH_2 replaces C=O.

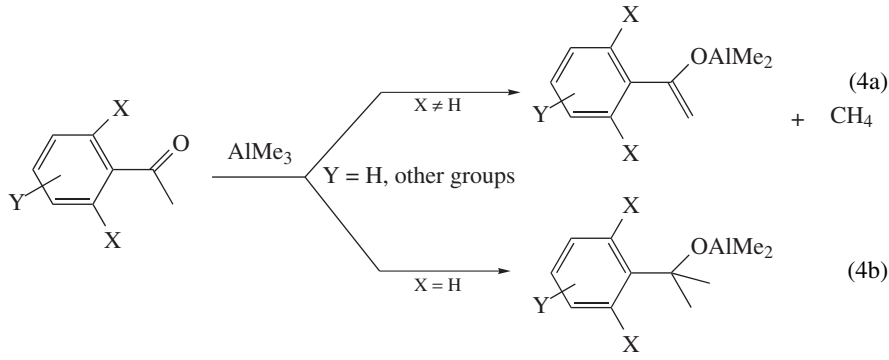

(4a)

(4b)

Direct reaction of cyclic ketones with triethylgallium forms the kinetically-favored metal enolate without seeming complication from carbonyl addition[83]. Conversely, triethylaluminum preferably gave the thermodynamically preferred hydride and ethyl addition products.

The $InCl_3$/In coupling reaction[84] of benzaldehydes with enones forms 5-aryl-4-pentenones as shown in equation 5. The authors invoke the $InCl_3$ Lewis acid adduct of the aldehyde reacting with the In-derived enone/enolate radical anion. The observed product is less stable than its α,β-unsaturated isomer, the 5-aryl-3-pentenone; this conclusion is derived by comparing the hydrogenation enthalpies[85] of styrene and crotonaldehyde that are taken as analogs of the ArC=C and C=C–C(O) fragments of the formed and unformed pentenones respectively.

$$ArCHO + CH_2{=}CHCOCH_3 \longrightarrow ArCH{=}CHCH_2COCH_3 \qquad (5)$$

Carbon-bonded enolate thallium species, e.g. $ClTl(CH_2COCH_3)_2$ and $[Cl_2Tl(CH_2COCH_3)_2]^-$, are seemingly stable[86]. However, the related monoketonyl thallium species such as $Cl_2TlCH_2COCH_2R$ (R = H, Me, Ac), readily formed by reaction of the parent ketone with $TlCl_3$, eliminate TlCl to form α-chloroketones in a synthetically useful reaction[87]. The origin of this difference between mono- and diorganyl derivatives remains unexplained but well-precedented: for example, alkylthallium dibromides readily disproportionate to form dialkylthallium bromides[88]. *C*-Enolates of thallium may be novel, but their relative energetics are long-known.

V. GROUP 14: TIN AND LEAD

Proceeding from left to right in the periodic table, metallic character decreases and so there are fewer elements to consider in ever rightmost columns. An aspect of comparative tin and lead enolate chemistry involves the reaction[89] of the diketoamine chelating ligand $HN[CH_2C(O)Bu\text{-}t]_2$. As an anionic dienolate, it readily complexes Sn^{4+} to form a conjugated bicyclic chelate which then undergoes intramolecular electron transfer to give the Sn^{2+} compound **13**. We recognize **13** as isolobal with highly stable, delocalized

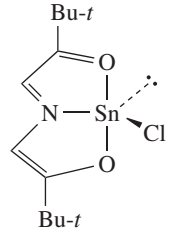

(13)

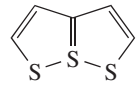

(14)

1,6,6*a*-λ^4-trithiapentalene (6*a*-thiathiophthene, **14**)[90]. Unlike Sn^{2+}, which forms a stable complex, reaction of the ligand with Pb^{2+} reduces the metal cation.

Tin enolate chemistry is quite sparse and thermochemical data generally lacking. One of the few examples arises from the addition of Bu_3SnH to ketenes $RR^1C{=}C{=}O$ to form enolates. While the enthalpies of formation of few ketenes are known, and thereby provide little guidance as to the enthalpy of formation of these enolates, *Z*/*E*-equilibration of the final enolates where $R \neq R^1$ tells us about isomers. With R = Me and R^1 = Ph, the enolate $MePhC{=}CHOSnBu_3$ is formed[91] in a 7:3 *Z*/*E* ratio; the *Z* isomer is almost 2 kJ mol^{-1} more stable than its *E* counterpart.

One may ask about the R−O−Sn bond strength in enolates and alkoxides. Direct hydrogenation of the double bond of such enolates has not been reported; tin damages the platinum catalyst. However, direct transfer from enoxyl to alkoxyl oxygen has been observed as part of the reaction of *t*-butoxyl radicals with glycidol O−Sn derivatives and enolates. The reaction directly forms an α-alkoxyglycidyl radical which spontaneously and sequentially rearranges to form an alkoxyl radical + tin enolate, and then the enoxyl radical + tin alkoxide[92]. Accordingly, enolate–Sn bonds are weaker than alkoxide–Sn bonds. The same rearrangement was observed for enolate and alkoxide bonds to hydrogen. Now, enolates bonded to hydrogen normally rearrange to form carbonyl compounds—the tin rearrangement was slow enough to study it. What about enolate–tin species and the corresponding α-stannylated carbonyl compounds? Examples of both isomers have been observed: it is rare, however, that actual dynamic equilibria have been monitored. Not surprisingly, this metalotropic isomerization observed by variable temperature ^{119}Sn NMR spectroscopy is both substitution-[93] and solvent-dependent[94].

Enediolates of Sn(II) are not expected to have this structural ambiguity. We note the facile formation of such a species by reaction of methylglyoxal with activated elemental tin[95]. Assumed monomeric, we note that this metallocycle **15** is formally a 6π-system analogous to 1,3-dioxolen-2-one (vinylene carbonate). Whether it is aromatic like the more classical heterocycle[96] or how it compares with the tetracoordinate 1,3-dioxastannolane (enediolates of tin(IV)) formed from an analogous reaction of biacetyl with dimethylstannylene[97] is not known.

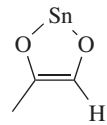

(15)

From well-established enthalpies of formation[98] it is readily deduced that the reaction in equation 6 is significantly endothermic. By contrast, the corresponding tropolonato

reaction in equation 7 proceeds readily, and presumably exothermically, in the pure condensed phase (in both solid and liquid) and in solution[99]. The mechanism, enthalpy and entropy of this reaction remain unknown.

$$2Me_3SnCl \longrightarrow Me_2SnCl_2 + Me_4Sn \quad (6)$$

$$2Me_3Sn(trop) \longrightarrow Me_2Sn(trop)_2 + Me_4Sn \quad (7)$$

Lead, like its neighbor tin, enjoys both the +2 and +4 oxidation state. In this case, Pb(II) is the normal metallic cation and the Pb(IV) state is rather unstable and very often oxidizing. As such, any species that might contain a bonded Pb(IV) and an enolate anion may mimic Pb(II) and an enoxyl cation. Metal-metal exchange reactions of lead enolates show both enolate and enoxyl cation behavior[100], depending on what is affixed to the metal. This quasi-enolate vs. enoxyl cation dichotomy is also seen for suitable mercury- and thallium-containing species.

VI. GROUP 11: COPPER, SILVER AND GOLD

Copper enolates may be *C*- or *O*-bonded. For example, the isomeric species Li[CH_2=CMeCH(CuMe)C(=O)CH_2Ph] and Li[CH_2=CMeCH=C(CH_2Ph)OCuMe] have been characterized in dynamic equilibrium[101]. Equilibration has also been seen for related complexes formed by organocuprate addition to polyunsaturated ketones where the formal Cu(III)-containing group migrates along the carbon chain unless stopped by an intervening C≡C bond[102]. This was attributed to lack of effective conjugation of an enyne. However, there is insufficient thermochemistry for enynes[103] to show this and the validity of this assertion for di- and polyynes has been questioned[104, 105].

Examples of thermochemical considerations of cupric enolates include the study of the binding of Cu^{2+} with kojic acid (**16**), a cyclic α-ketoenol. Comparison[106] was made between the divalent cations of UO_2^{2+}, Cu^{2+}, Zn^{2+}, Ni^{2+}, Co^{2+}, Cd^{2+}, Ca^{2+} where these metals are listed in decreasing order of binding constants over 6 powers of 10. In this case carbon-bonded metal seems most unreasonable because it would ruin the chelation as well as any aromaticity in the pyrone ring. It is admittedly an assumption that pyrones are aromatic. There are no one-ring pyrones for which there are enthalpy of formation data for gas phase species, as opposed to the benzoannelated compounds coumarin (**17**)[107a, 107b], chromone (**18**)[107b, 107c] and xanthone (**19**)[107c]. Plausible, but unstable, Cu(II) enolates eliminate copper and form the 1,4-dicarbonyl compounds[108] as shown in equation 8.

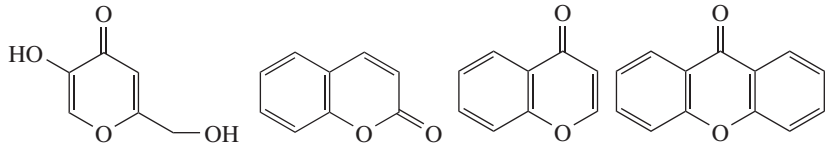

(16) **(17)** **(18)** **(19)**

$$2RCCH_2Cu \longrightarrow RCCH_2CH_2CR + 2Cu(s) \quad (8)$$

Silver enolates are not expected to be particularly stable. Indeed, the sole silver enolate of thermochemical relevance that has an enthalpy of formation data is silver squarate[109],

determined via the enthalpy of its thermal decomposition. The value of -665 ± 20 kJ mol^{-1} may be compared with these authors' value of -580 ± 10 kJ mol^{-1} for the parent squaric acid: this latter value is in reasonable accord with the -598.2 ± 0.4 kJ mol^{-1} determined by direct enthalpy of combustion[25]. It is surprising that the silver salt is more stable than the parent acid by *ca* 80 kJ mol^{-1} because silver oxalate is *ca* 150 kJ mol^{-1} less stable than oxalic acid. It is doubtful that either the strength of silver π-complexes and/or squarate anion stabilization could account for the difference.

Useful gold(I) enolates are surprisingly easy to make by reaction of silyl enolates with CsF and Ph_3PAuCl[110], and are known to be *C*-bonded rather than *O*-enolates like their synthetic precursors[111]. Gold(III) enolates also prefer *C*-bonding over *O*-bonding[112]. However, in no case are the enthalpies of *C*-bonded to *O*-bonded interconversion in a 'simple' enolate seemingly known. The *O*,*O*′-bonded acetylacetonate complex of Au(III), $Me_2Au(acac)$, has been shown to combine reversibly[113] with triarylphosphines to form the *C*-bonded complex $Me_2Au(PAr_3)CHAc_2$ with an enthalpy change of *ca* 50 kJ mol^{-1} and an entropy change of *ca* -160 J mol^{-1} K^{-1}; a Hammett constant $\rho = -1.6$ was also shown.

VII. GROUP 12: ZINC, CADMIUM AND MERCURY

Zinc enolate chemistry is rich and was recently reviewed[114]. However, it is dominated by species with α-alkoxy groups, i.e. the enolate of carboxylic acid esters, and so these studies are not relevant in the current context. Acetophenone, 2-acetylthiophene and 3-acetylthiophene form enolate complexes with Zn^{2+} and Cd^{2+} [115,116]. The degree of enolization of these ketones is quite independent of the metal. Accordingly, sulfur cannot be assisting the enolization by chelation in the 2-acetylthiophene compound.

As part of a biomimetic study for the enzyme class II aldolase[117] the equilibrium was reported for the cyclen complex, hydroxo-Zn(II)-1-(4-bromophenacyl)-1,4,7,10-tetraaza-cyclododecane and the intramolecular enolate **20**, formed from Zn(II) and the enolate of 1-(4-bromophenacyl)cyclen. This cyclization reaction was shown to be endothermic by 8.7 kJ mol^{-1}. However, with an entropy of 19 J mol^{-1} K^{-1} it proceeds readily enough to show facile H/D exchange from the CH_2 group of the exocyclic ligand. We wonder about the enthalpy and entropy changes associated with a different choice of other polyamines and/or central metals.

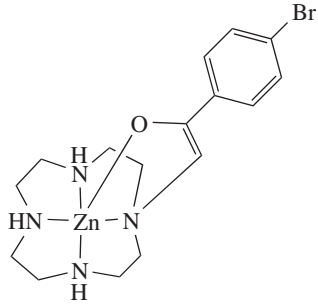

(20)

Reaction calorimetry results[118] in the enthalpy of formation of zinc bisquarate, i.e. Zn $[HC_4O_4]_2$, of -1436.7 kJ mol^{-1}. Unfortunately, we do not know of any other relevant zinc salts with which to compare this enthalpy of formation. Indeed, among the

very few zinc enolate derivatives for which we know the enthalpy of formation is zinc bis(ascorbate) tetrahydrate, recently determined[119] by reaction calorimetry to be $-3528.9\ kJ\,mol^{-1}$. Recall that the corresponding calcium species has an enthalpy of formation of $-3945.1\ kJ\,mol^{-1}$, some $416\ kJ\,mol^{-1}$ more negative. The only species for which we can make meaningful comparison are the related hydrated calcium and zinc acetate salts, $M(OAc)_2{\bullet}H_2O$ (M = Ca, Zn), for which the difference is not dissimilar, $396\ kJ\,mol^{-1}$ [120].

Cadmium enolate chemistry is considerably unexplored compared to that of Zn. These metals have comparable binding to the acetyl isomeric thiophene enolates[116]. In the case of metal kojic acid complexes[106] the Zn complex is more stable than the corresponding Cd complex regardless of choice of 1:1, 1:2 or 1:3 ratio of the metal and ligand. However, one should not deduce that cadmium always binds ligands less tightly than zinc. Were that the case, Cd(II) would be expected to be rather nontoxic.

Mercurous enolates are all but unknown—attempts to form them result in the Hg(II) complex and elemental Hg[121]: we recall the general finding that 'organic calomels', R_2Hg_2, are unstable relative to the free metal and the diorganomercury R_2Hg[122] while mercurous inorganic derivatives such as Hg_2Cl_2 and $HgCl_2$ have the reverse order of stability. Hg(II), like its heavy (and isoelectronic) counterparts Tl(III) and Pb(IV), provides examples of the ambiguity of enolate vs. enoxyl cation behavior, and like the enolates of the latter species, they are better understood as *C*-bonded α-mercurated ketones rather than their *O*-bonded metal enolate isomers[100]. Indeed, structural determinations show carbon bonding in 1-(acetoxymercuriobutanone) as opposed to its enolate isomer[123]. Also, the di- and trimercurated ketones involve C−Hg bonding[123]. These polymetallated species have the two or three mercury atoms on the same carbon, namely the methyl adjacent to the carbonyl. The driving force for having so many large groups geminally arranged may be ascribed to 'mercurophilicity', an example of the generally found stabilization between pairs of closed shell atoms and ions of high atomic number[124], especially gold, mercury's periodic table neighbor[125, 126].

VIII. GROUP 3: SCANDIUM, YTTRIUM AND THE LANTHANIDES

Scandium enolate chemistry is quite limited. The complex (nacnac)Sc(NHAr)($HBEt_3$) where nacnac = **21** and Ar = 2,6-(i-Pr_2)$_2C_6H_3$) reacts[127] with THF to form the enolate (nacnac)Sc(NHAr)OCH=CH_2 while diethyl ether forms the related alkoxide (nacnac)Sc(NHAr)OEt. This suggests considerable stabilization due to the Sc−O bond. After all, ring opening of THF is energetically unfavorable (THF → EtOVi; $\Delta H > 40$ kJ mol^{-1}).

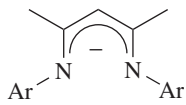

(**21**) nacnac

Yttrium enolate chemistry is discussed in the context of other metal enolates in a report[128] of the synthesis of the oxygen bridge dimer of $Cp_2Y(OCH{=}CH_2)_2$ and its bis(monomethylcyclopentadienyl) analog. The molecular geometry of this species is compared with other metal enolates. There are insufficient data to discuss the effect of the choice of metal on the conjugation of their C−O and C=C bonds; indeed, much remains to be learned even about simple 'all-organic' enol ethers[129]. Yttrium enolates

also appear during the synthesis of the furyl-functionalized [Y{η^5:η^1-$C_5Me_4SiMe_2$(2-Fu)}$(CH_2SiMe_3)_2$(THF)] and the attempted synthesis of the 5-methylfuryl counterpart of this species[130]. The former species can be synthesized by metallation of the parent cyclopentadiene; the latter species yields the ring opened [Y{η^5:η^1-$C_5Me_4SiMe_2$C≡CCH=C(Me)O}$(CH_2SiMe_3)]_2$ yne-enolate instead. While the enthalpy of formation of HC≡CCH=CHOH is unknown, that of its isomer HC≡CC(OH)=CH_2 has been found[131] to be *ca* 145 kJ mol^{-1} higher than that of furan, possibly pointing to the yne-enolate synthesis as being energetically unfavorable had it not been for the concomitant formation of a very strong oxygen–metal bond.

Cp*$_2$La{$CH(SiMe_3)_2$} reacts[132] with 3-pentanone to form the solvated enolate, Cp*$_2$La–O–C(Et)=CHMe•Et_2CO (equation 9a), while with acetone it forms a chelate (equation 9b) after intramolecular aldol condensation. The reaction of the precursor bistrimethylsilylmethyl organometallic with hydroxyketone, preformed from the pentanone, yields the enolate ketone solvate. This difference between acetone and 3-pentanone presumably reflects the difference in strain in the condensation product because the ethyl groups in 3-pentanone are rather much bigger than the methyl groups in acetone.

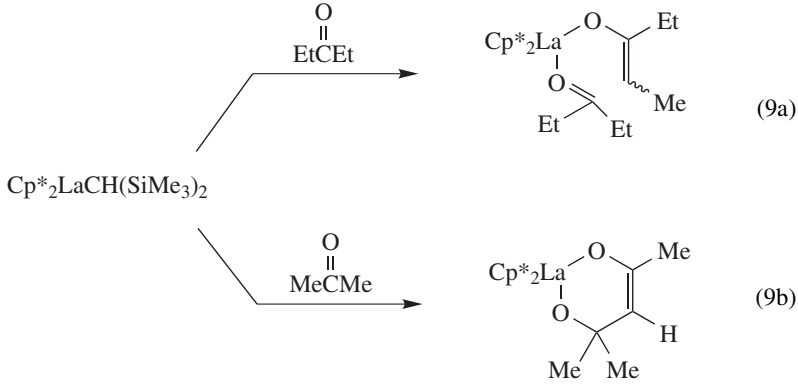

(9a)

(9b)

The chemistry of Cp*$_2$Ce$CH(SiMe_3)_2$ with acetone and 3-pentanone is the same as that of its La(III) counterpart[132]. Ce(III) enolates, generated from $CeCl_3$ and Li enolates, undergo aldol condensation with ketones or sterically crowded aldehydes to give the corresponding β-hydroxy ketones in good to high yields[133]. Cerium(III) enolates are plausibly implicated in the study[134] of the reaction of Ce(III) species with α-haloketones and aldehydes to yield β-hydroxyketones or α,β-unsaturated ketones depending on the cerium reagent employed. The Ce(IV) complex $(NH_4)_2Ce(NO_3)_6$ readily oxidizes silyl enolates to form the corresponding enoxy radical[135]. However, we know of no cerium(IV) enolate arising from subsequent reaction chemistry.

Samarium has two common oxidation states +2 and +3. Upon solution in toluene under nitrogen, an anionic Sm(II) species, {[(–CH_2–)$_5$]$_4$–calix–tetrapyrrole}Sm(THF)[Li(THF)]$_2$[Li(THF)$_2$]Cl, forms, in part, the compound {[(–CH_2–)$_5$]$_4$–calix–tetrapyrrole}Sm(THF)Li_2[Li(THF)](μ^3-OCH=CH_2)[136]. However, this compound is a lithium enolate derived by elimination of THF. In that the metalloorganic reagent is rather similar to what will be discussed in Section XI as part of vanadium enolate chemistry[137], we fail to understand why in the former case with Sm a lithium enolate is formed but in the latter with V it is an ynolate that is produced. Almost nothing is known to allow comparing the energetics of metal enolates and related ynolates. We note from the enthalpies of

formation of ethenol[131] and ethynol[138] that equation 10 is seemingly endothermic by only 5 kJ mol^{-1}.

$$EtC{\equiv}CH + CH_2{=}CHOH \longrightarrow EtCH{=}CH_2 + HC{\equiv}COH \qquad (10)$$

Elemental samarium in HMPA reacts[139, 140] with benzophenone to form the samarium benzophenone dianion species. Subsequent reaction with the hindered phenols, ArOH (Ar = 2,6-*t*-Bu$_2$C$_6$H$_4$ and its 4-methyl analog) forms Sm(III) enolate complexes **22a** by dearomatization of two benzene rings. Complex **23** is a minor byproduct. Is the presence of the dearomatized enolato ligand in **22** due to thermodynamics or kinetics? We remember the 'hexaphenylethane riddle'[141], i.e. Ph_3CCPh_3 remains unknown and the dearomatized *p*-isotoluene derivative **24** is the isolated, and (as confirmed by quantum chemical calculations[142]) more stable, isomer. On the other hand, the simplest and unstrained methylenecyclohexadiene, *p*-isotoluene itself, is shown by experiment[143] to be less stable than its aromatic isomer by *ca* 100 kJ mol^{-1}.

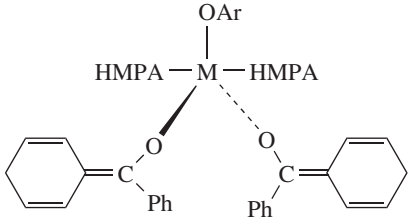

(22) **(a)** M = Sm, **(b)** M = Yb

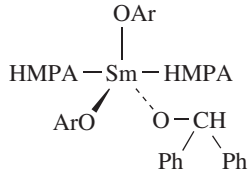

(23)

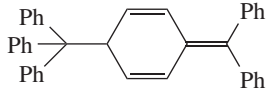

(24)

Dysprosium might appear to be a rather unexceptional, generally trivalent element. For example, we are not surprised that Cp_3Dy reacts[144] with 2-butanol to yield the oxygen bridged dimeric alkoxide $[Cp_2Dy(\mu^2\text{-}OCH(Me)CH_2CH_3)]_2$. What is surprising, however, is its facile dehydrogenation on refluxing in THF solution to yield the corresponding enolate dimer. Other than the corresponding ytterbium alkoxide and corresponding enolate, we do not know of any other facile thermal dehydrogenation of alkoxides. Also, what remains unexplained is why the enolate is solely the $[Cp_2Dy(\mu^2\text{-}OC(Me){=}CHCH_3)]_2$ and not the isomeric $[Cp_2Dy(\mu^2\text{-}OC(Et){=}CH_2]_2$ or 'mixed' enolate. After all, equilibration reactions[145] show the corresponding methyl enolates (i.e. Me in lieu of Cp_2Dy) have enthalpies of formation differing by only 0.5 ± 0.4 kJ mol^{-1}.

Ytterbium has the oxidation states +2 and +3. A stereochemical dichotomy exists in their enolate chemistry[146]. Yb(II) enolates react with aldehydes to form the *erythro*-β-hydroxyketones while Yb(III) enolates yield the *threo* stereoisomers. We fail to understand this by either thermodynamic or mechanistic reasoning. Analogous to corresponding reaction chemistry for samarium, preformed ytterbium benzophenone dimer, $[Yb(Ph_2CO)(HMPA)_2]_2$, reacts[140] with sterically crowded phenols to form in low yield (5%) the enolate complex **22b** by dearomatization of benzophenone. The major product (80%) is the

ytterbium aryloxide $(ArO)_2Yb(HMPA)_2$, accompanied by hydrogen transfer from the phenol to the *p*-position of the benzophenone of the enolate byproduct. It is unequivocal, however, that Yb-enolate bonding is strong because of dehydrogenation of a ytterbium alkoxide to form the enolate, analogous to what was found for Dy[144]. Both the dimeric ytterbium propoxide and allyloxide spontaneously dehydrogenate[147] on reflux in THF to form the corresponding allenolate $Cp_2YbOCHC{=}CH_2$ in what would be expected to be an even more endothermic process. Mimicking Cp_2YbO by Et in the absence of any published thermochemical data for allene ethers, the dehydrogenation of pentane to 1-pentene is endothermic by 115 kJ mol^{-1} and to form 1,2-pentadiene, the allene analog, the reaction is endothermic by 173 kJ mol^{-1}.

Lutetium enolate chemistry mimics that of yttrium[128, 130]. Lu(III) is the smallest of all of the trivalent lanthanide cations, and so the chemistry of Lu(III) is more similar to that of its 4*d* congener Y(III).

Since tropolones and 3-hydroxy-4-pyrones are taken in this chapter to be enols, we now cite their binding as enolato ligands to lanthanum and all the other trivalent lanthanides (save the radioactive promethium)[148, 149]. Likewise, we note such studies for complexes with enolato ligands derived from 3-acetyl-4-hydroxycoumarin, dehydroacetic acid and their oximes[150], and with the aromatic enediolates, squarate[151] and croconate[152]. Periodic trends in thermodynamic parameters were reported and analyzed in these studies.

IX. ACTINIDES

The formation constants of an actinium isopropyltropolonate complex were determined[153]. Thermochemically relevant studies of thorium enolates generally involve bis(pentamethylcyclopentadienyl)thorium derivatives. $Cp^*_2Th(Cl)(C(O)CH_2Bu\text{-}t)$ with an anionic acyl group that readily rearranges to the isomeric enolate $Cp^*_2Th(Cl)OCH{=}CHBu\text{-}t$. The *Z*-isomer is formed upon heating[154] and the *E*-isomer upon catalysis with $Cp^*_2ThH_2$[155]. Is the *E* or *Z* enolate thermodynamically more stable? For the simple 'alkyl enolates' MeCH=CHOR, the equilibration reaction of the *Z*- and *E*-isomers is nearly thermoneutral[156]. Consider the two species $Cp^*_2Th(H)OCH(Bu\text{-}t)_2$ and $Cp^*_2Th(H)O\text{-}2,6\text{-}C_6H_3(Bu\text{-}t)_2$. The reversible addition[157] of CO yields the η^2 formyl derivative in reactions that are 19 ± 4 and 25 ± 6 kJ mol^{-1} exothermic. These formyl species dimerize to form the classical enediolate, $Cp^*_2Th(OR)OCH{=}CHO(OR)ThCp^*_2$. This product is formed as the *Z*-isomer, plausibly thermodynamically preferred over the *E*-isomer, much as (*Z*)-MeOCH=CHOMe is preferred over its *E*-counterpart[158] by 6.0 ± 0.2 kJ mol^{-1}.

The aforementioned monomeric species $Cp^*_2Th(Cl)(CH_2Bu\text{-}t)(CO)$ reacts with additional CO to form a dimeric *E*-enedionediolate ligand bridging two metal centers (**25**). A similar reaction of CO takes place with complex $Cp_2LuCOBu\text{-}t$, yielding the binuclear enediolate **26**[159]. Complex **25**, with its two 5-membered unsaturated rings bridged by an ethene moiety, resembles fulvalene, whereas **26**, with its pair of condensed 6-membered unsaturated rings, resembles naphthalene. Fulvalene is much less stable than naphthalene[160]; the reverse is presumably true for their dianions[161]. In fact, there are no measured enthalpies of formation for either fulvalene or for any of its derivatives. Measurement of the enthalpy of hydrogenation of heptafulvalene stopped at the reduction of the tetrasubstituted olefin, cycloheptylidenecycloheptane[160].

Various tropolonato complexes of protoactinium have been synthesized and characterized[162, 163]. However, no thermochemical data (including emf and hence ΔG) are seemingly available, even though there are simple redox reactions interrelating these species.

Uranium, whose radioactive isotopes have half-lives measured in billions of years, is a rather well-studied element. Cp_3U, as its THF complex, reacts with simple ketones to form alkoxide and enolate products in a 1:1 ratio by transfer of an α-hydrogen[164].

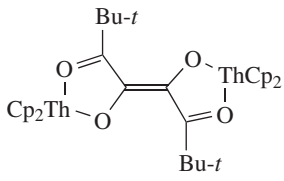

(25)

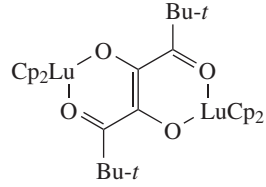

(26)

We consider this reaction to be calorimetrically useful, especially given the interest in Cp_3UX derivatives by the thermochemical community[165]. Like its Th analog, the reaction of $Cp^*_2UMe_2$ with CO quantitatively yields dimeric **27**, a *Z*-enediolate[166] with a 10-membered ring. We may then ask about the enthalpies of interconversion with the respective monomer, noting that Zr and Hf form[167] the monomeric 2-metala-1,3-dioxolenes, **27′**[167]. The corresponding carbocycles are (*Z*,*Z*)-1,6-cyclodecadiene and cyclopentene. From the enthalpy of hydrogenation[168] of the former species and the enthalpies of formation of their saturated cycloalkane products[25], the conversion of 1,6-cyclodecadiene to two cyclopentenes is found to be endothermic by some 30 kJ mol^{-1}.

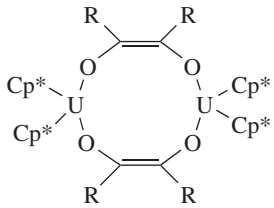

(27)

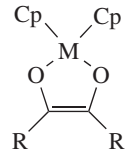

(27′) M = Zr, Hf

Uranium(VI) strongly bonds squarate (**1**), second in strength only to Fe(III)[169] among the metal cations studied, and likewise rhodizonate (**3**), second only to Cu(II)[170], again among the metals of interest, which did not include Fe(III). The order of binding strength of the various metals to these oxocarbon anions remains unexplained.

Finally, we note the formation of complexes of uranium with tropolones with multiple stoichiometries and oxidation states. Letting Trop be tropolone and/or its 3-isopropyl derivative, these include $U(Trop)_{4-n}Cl_n$ $(0 \leqslant n < 4)$ ($n = 0$[171], $n = 1$, 2, 3[172]), $U(Trop)_{5-n}Cl_n$ ($n = 0$, 1)[173], $U(Trop)_5^{-}$[171], $UO_2(Trop)_2$[174], $UO_2(Trop)^+$[175] and $UO_2(Trop)_2$(TropH) (but not the conjugate base)[174]. However, thermochemistry has rarely been of explicit interest.

Equilibrium constants for complexes of tropolones with UO_2^{2+}[176], NpO_2^+[176,177], Pu^{4+}[178], Pu^{3+}[176], Am^{3+}[177], Cm^{3+}[177] and Cf^{3+}[177] have all been investigated. While neptunium and plutonium enjoy high oxidation states like uranium, there are seemingly no thermochemically related data for complexes with PuO_2^{2+} despite the apparent stability of such tropolonate species[179]. Tropolone reduces NpO_2^{2+} rather than forming neptunyl tropolonates[180].

X. GROUP 4: TITANIUM, ZIRCONIUM AND HAFNIUM

Titanium has more than one common oxidation state and a rich organometallic chemistry dominated by π bonding ligands such as cyclopentadienyl. The two chloro ligands

in Cp_2TiCl_2 are readily displaced, leading to a relatively lush derivative chemistry and an extensive thermochemistry, or at least thermochemical reasoning[181]. It is customary to posit an oxidation state of +4 for Ti in derivatives for singly anionic ligands, X, such as Cp_2TiCl_2, Cp_2TiClX and Cp_2TiX_2. The radical cation of these species, however generated—say electrochemically, does not contain Ti(V). For example, the electrochemical oxidation[182] of the Cp_2TiCl enolates **28** results in substituted benzofurans and 1,4-butanediones, depending on the substituents, e.g. $R = R^1 = Mes$, $R^2 = H$ forms a benzofuran while $R = Me$, $R^1 = H$, $R^2 = Ph$ forms a 1,4-butanedione. Both products arise from cleavage of the Ti−OR bond to form enoxy radicals, as shown in equation 11. Unfortunately, the enthalpy of formation data for benzofurans is limited to the parent heterocycle and appears only in a rather inaccessible report[183]. Enthalpy of formation data for butanediones are limited to the 1,4-diphenyl derivative[25], the monocyclic 1,4-cyclohexanedione[184] and a cage species[185].

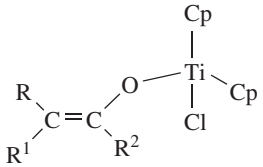

(28)

$$(Cp_2TiClOR) \xrightarrow{-e^-} (Cp_2TiClOR)^+ \longrightarrow Cp_2TiCl^+ + RO^\bullet \qquad (11)$$

C-Trifluoromethylation of titanium enolates by CF_3I was recently compared[186] to that of lithium enolates. Given that CF_3 derivatives do not undergo substitution reactions by either S_N1 or S_N2 reactions, a chain reaction involving CF_3 and/or CF_3I^- has been suggested. To understand this, thermochemical considerations include the strengths of Ti−I and Li−I bonds, and barriers for loss of Ti(III) and Li(0) from ketyl radicals.

Zr and Hf tetraphenylporphin imido complexes (**29**) and pinacolone react in a condensation and deprotonation reaction[187] to form the cyclic dimeric enolate **30**. For the lack of thermochemical data on dimerization of pinacolone and addition of lithium pinacolonate and pinacolone, take for comparison the exothermic reaction of lithium pinacolonate and pivalaldehyde, which has been experimentally measured in hexane[188] (-126 ± 3 kJ mol^{-1}). Zirconium and hafnium chemistry are generally quite similar, as evidenced by the above; however, a significant difference[189] is found for $Cp^*_2MH(i\text{-Bu})$ reactions involving CO. At low temperature, both species reacted with CO to form the derivative $Cp^*_2M(H)(\eta^2\text{-COBu-}i)$ with an anionic acyl group. Warming to room temperature resulted in the formation of the carbonyl-aldehyde complex $Cp^*_2M(CO)(\eta^2\text{-O=CHBu-}i)$. However, on standing, this M = Zr carbonyl-aldehyde species slowly lost CO to form the enolate which is presumably more stable than the starting acyl species with which it is isomeric. In the case of M = Hf, the corresponding carbonyl-aldehyde species rearranged to form an enediolate. This provides thermochemical information as to the relative stability of isomers and some otherwise related species.

How does one describe the enediolates of Zr and Hf? Plausibly they are 2-metala-1,3-dioxolenes (**31**). However, structural determinations[190] show **31** with M = Zr to be planar for two abutting R = *t*-Bu groups but significantly nonplanar for R = Me. Is this to allow for C=C···Zr interaction for the smaller R = Me, or is this to minimize repulsion between substituents on the cyclopentadienyl and 1,3-dioxa-2-zirconacyclopent-4-ene rings that

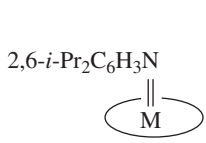

(29) M = Zr, Hf

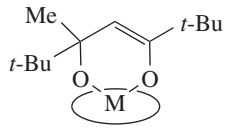

(30) M = Zr, Hf

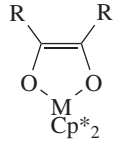

(31) M = Zr, Hf, U

would be quite severe for *t*-butyl in the latter? We note that R–R repulsion between the two R = Me groups themselves is most assuredly small; the difference between the enthalpies of formation of disubstituted benzenes such as the xylenes is *ca* 1 kJ mol^{-1}, while the difference for 1,2-di-*t*-butylbenzene and its other two isomers is *ca* 95 kJ mol^{-1}, as shown by reaction calorimetry[191].

XI. GROUP 5: VANADIUM, NIOBIUM AND TANTALUM

An example of fortuitous vanadium enolate chemistry is the CO addition reaction to a silylamido vanadium species in which the dimeric metallocycle **32** is transformed[192] into the corresponding cyclic enolate **33**, as shown in equation 12. Given silicon's profound oxophilicity, the absence of the Si–O moieties in **33** is surprising. For example, the liquid phase reaction shown in equation 13 is exothermic by *ca* 420 kJ mol^{-1}, as determined from the enthalpies of formation of tetramethoxymethane[193, 194] and the silicon compounds[120].

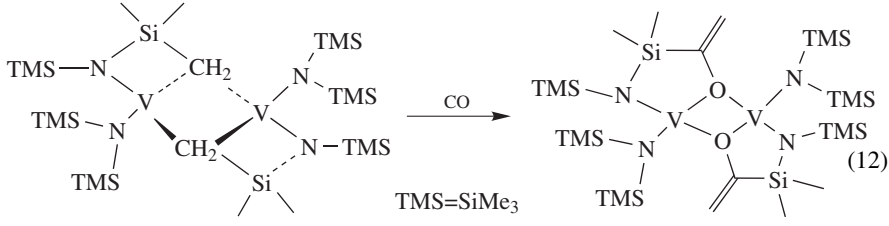

(32) **(33)** (12)

$$SiMe_4 + C(OMe)_4 \longrightarrow CMe_4 + Si(OMe)_4 \qquad (13)$$

More conventional species[195] are the spectroscopically, magnetically and structurally characterized vanadyl bis(picolinylketone) enolate complexes **34**, and the related complexes formed by their protonation. These species have also been converted into their VCl_2 derivatives **35**. The dependence of the V–O and V–Cl bond strengths on the substituent X would provide insight into metal–oxygen bonding. We also recognize in these enolates the *p*-XC_6H_4–C=C–Pyr-2 framework, for which the energetics of some of their *o*-X isomers was of interest in the past[196]. Vanadium(V) is well-known to react with the enediol ascorbic acid and ascorbate by electron transfer reactions. While kineticists and spectroscopists have dominated these studies showing multiple reaction products and processes[197], thermochemists have also shown interest[198].

Niobium enolate chemistry is largely unexplored. A seemingly unambiguous case involves the reaction of the highly sterically hindered Nb(IV) species [3,5-$Me_2C_6H_3N$(Ad)]$_3$NbCl with PhLi or MeLi to form [$Me_2C_6H_3N$(Ad)]$_3$NbR, R = Ph or Me. However, the neophyl complex (R = CH_2CMe_2Ph) could not be made because this group is seemingly too big; instead the *O*-bonded enolate group R = OCH=CH_2 was found

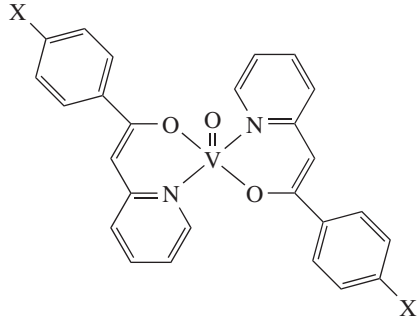

(**34**) X = H, Me, OMe, Cl, NO_2

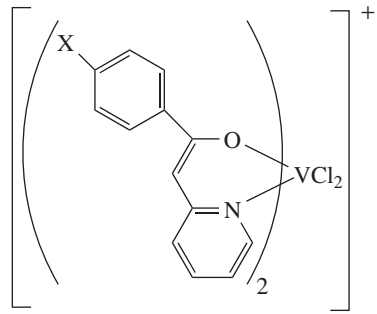

(**35**) X = H, Me, OMe, Cl, NO_2

attached to the metal. This was understood in terms of ring cleavage of THF, serving both as solvent and as ligand[199]. Why some transition metal assisted decompositions of THF result in vinyloxy and others in ethynyloxy complexes remains unknown.

Tantalum enolate chemistry shows the dichotomy for the carbonylation reaction[200] of $Cp^*Ta(CH_2R)Cl_3$ with CO which results in the mono-THF adduct of η^2-acyl complex $Cp^*Ta(O{=}CCH_2R)Cl_3(THF)$ for R = *t*-Bu (the acyl group is anionic) but the isomeric enolate $Cp^*Ta((Z)\text{-}\eta^1\text{-}OCH{=}CHR)Cl_3$ for R = *p*-Tol. This invites the question of the relative thermodynamic stabilities of metal complexes of RCH_2CO and RCHCHO and additionally the question of *Z* vs. *E* enolate stabilities. Only for organometallic compounds (X = [M]) do we find examples where RCH_2COX is less stable than RCH=CHOX.

Pentamethyltantalum(V) also forms the bis-enolate $TaMe_3[OC(=Ad)Ar]_2$ where Ad = is 2-adamantylidene and Ar = 3,5-$Me_2C_6H_3$[201]. These large groups affixed to the metal are found where they can be furthest apart, the diapical isomer. This complex reacts with pyridine to form the mixed Py and 2,2′-bipyridyl complex by loss of ethane. Now why are there no terpyridyl-containing species? From the data found elewhere[202], it can be concluded that the dimerization reaction of pyridine to form 2,2′-$(C_5H_4N)_2$ is exothermic while the related reaction of benzene to form biphenyl is endothermic. Benzene, biphenyl, the terphenyls and quaterphenyls form a homologous series, i.e. these species have very nearly constant enthalpy of formation differences[57]. Do pyridine, the isomeric bipyridines and terpyridines also form a homologous series, and why isn't the 2:2′,6′:2″-terpyridine complex formed instead of a mixed bipyridine/pyridine complex? The entropy gain by loss of an additional H_2 molecule should further drive the reaction.

XII. GROUP 6: CHROMIUM, MOLYBDENUM AND TUNGSTEN

Chromium enolate chemistry exhibits diverse thermochemical facets. For example, contrast the energetics of enolate addition reactions to benzaldehyde and to benzaldehyde π-bonded to $Cr(CO)_3$ and of the enolate addition reactions to acetophenone and to acetophenone π-bonded to $Cr(CO)_3$. Thermochemical analysis is still unreported, although the reactions are synthetically useful[203, 204]. It is clear that the organic ligands are electronically coupled to the metallic center—$PhCHO{\bullet}Cr(CO)_3$ is red, $PhCH(OEt)_2{\bullet}Cr(CO)_3$ is yellow[205] but benzaldehyde and its diethyl acetal are both colorless. It is well established[206] that acetophenone, and presumably other acylated benzenes such as benzaldehyde, binds $Cr(CO)_3$ rather more weakly than does toluene, and presumably other alkylated benzenes such as the aforementioned benzaldehyde acetal. The enthalpy of hydrolysis of the metallated acetal remains unknown other than it is therefore smaller than that of the unmetallated species[207].

Consider the reaction[208] of bis(1-bromocyclopropyl) ketone with $[Cr(CO)_4NO]^-$ to form the bicyclic 2-metalafuran derivative **36**, which may be considered as a chromium enolate in two contexts. The first one relates to the endocyclic 2-chromafuran. The second one relates to the O−C=C−CH_2−O substructure of the bicyclic system. We may also ask questions about the relative aromaticity of chromafuran and furan by thermochemical criteria where we note that delocalization is suggested for both species by structural criteria.

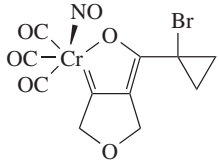

(36)

Molybdenum forms both η^1-*C*-bonded and η^3-*C*,*C*,*O*-bonded enolates in low oxidation states, as evidenced by the reaction of $CpMo(CO)_3^-$ with $ClCH_2COMe$ to form[209] the *C*-bonded $CpMo(CO)_3CH_2COCH_3$ with no formation of the isomeric *O*-bonded η^1-$CpMo(CO)_3OC(Me)=CH_2$. Heating the *C*-bonded product results in loss of CO and rearrangement to the *O*-bonded η^3-$CpMo(CO)_2OC(Me)=CH_2$. From this we may deduce that the *C*-bonded enolate is more stable than its *O*-isomer. Conversely, Mo(IV) as found in the complex $(Ad=C(Mes)O)_4Mo$ (where Ad=is 2-adamantylidene) is isolable[210] with no evidence of *C*-bonded enolate. Admittedly, this does not really show that higher valence molybdenum prefers *O*-bonded enolates in that the *C*-bonded ligand, 2-mesitoyl-adamant-2-yl, is highly sterically hindered and the presence of more than one of these groups on a central metal adds additional strain. Despite the seeming congestion in the observed tetraenolate, nonetheless it readily forms a stable NCN (cyanimide) derivative containing Mo(VI) for which a Mo−N bond energy of 435 kJ mol^{-1} has been suggested[210].

Molybdenum has yet other oxidation states. For example, kojic acid (**16**) has been reported to form 1:1 complexes with Mo(V)[211] and with Mo(VI)[212]. What is the redox potential connecting these two species? While the latter species has been crystallographically determined to have a *cis*-MoO_2^{2+} metal center[213], no structural data are available for the former species. Other ketopyran enolate derivatives of MoO_2^+ exhibit[214] the doubly oxygen bridged dimer, singlet paired, $Mo_2O_4^{2+}$ (**37**). Unexpected complications were found for the redox behavior of edta complexes of Mo(V) and Mo(VI) even though the complexing agent is electronically innocuous[215].

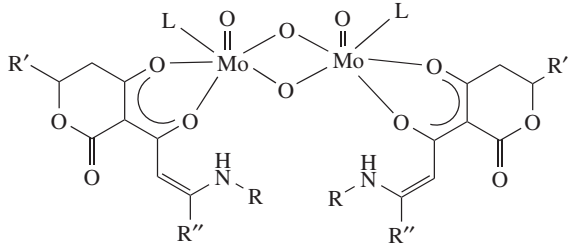

(**37**) R = *n*-Bu, Ph, 1-Naph
R′ = Me, R″ = CO_2Et; R′ = CO_2Et, R″ = Me
L = MeOH, EtOH, *i*-PrOH

As tungsten and molybdenum are congeners, it should not be surprising that there are some similarities between their enolate chemistry. Earlier acetylcyclopentadienide species were referred to as enolates. We now note that $AcC_5H_4W(CO)_3^-$ (and the related W complex) reacts with diphenyltin dihalides (Cl, Br) to form the monosubstituted derivatives, $AcC_5H_4M(CO)_3SnPh_2X$ (M = Mo, W; X = Cl, Br), without any accompanying formation of either *O*-acetyl or ring-stannylated or trinuclear products[216] $[AcC_5H_4M(CO)_3]_2SnPh_2$. The corresponding deacetylated $[CpM(CO)_3]_2SnPh_2$ species are well-established[217]. While the lack of formation of these alternative products was ascribed in the literature[216] to the electron-withdrawing power of the acetyl group, steric hindrance might also play a role. Bond length is often related to bond order, and hence is assumed to relate to bond strength. All of the above species likely contain a Mo−Sn single bond. Recently, a suitable $CpMo(CO)_3SnAr$ (and also W) was synthesized[218] for which multiple bond character was suggested. However, with such extensively substituted aryl groups as the Ar of **38**, we wonder how meaningful is any comparison between the two types of M−Sn bonds.

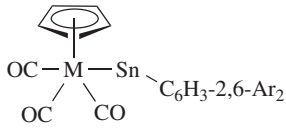

(**38**) M = Mo, W, Ar = C_6H_2-2,4,6-Me_3, C_6H_2-2,4,6-(*i*-Pr)$_3$

Suitable zero-valent Mo and W species react[219] with enones to form species of the formal stoichiometry and structure $M(C{=}C{-}C{=}O)_3$, or rather, the tris-enolate $M(C{-}C{=}C{-}O)_3$.

XIII. GROUP 7: MANGANESE AND RHENIUM

Manganese forms compounds with a variety of oxidation states from −1 to +7. Enolate ligands phenylsquarate ($PhC_4O_3^{2-}$) and diphenylaminosquarate ($Ph_2NC_4O_3^{2-}$) form electrochemical couples[220] involving Mn(II)/Mn/(0), Mn(III)/Mn(II), Mn(IV)/Mn(III) and Mn(V)/Mn(IV). How can the electronic coupling between substituent, ring and metal be disentangled? Multiple patterns of hydrogen bonding in the hydrates of these species (each oxygen may be unbonded, singly or doubly hydrogen bonded) may be invoked[221] as well as charge states for the oxocarbon ring (−1, the semitrione with −2, or the antiaromatic cyclobutadienetriolate with −3)[222]. It is not obvious that Mn has to be bonded to O. There is also a low oxidation state possibility involving π-bonding to C=C of the cyclobutene ring and even σ-bonding as in $(Mn(CO)_5)_2C_4O_2$[223]. The energetics of the interconversion of these diverse structures remains unexplored except for some emf values, and hence Gibbs free energies, that correspond to processes that reversibly interconnect a few of the diverse oxidation and charge states.

Similarly to the 2-chromafuran derivative **36**[208] discussed in Section XII, where Cr was also bonded to CO and NO, the same study refers to a related reaction involving the isoelectronic $Mn(CO)_5^-$, for which a 2-manganesafuran was observed wherein the metal-bonded substituents were solely CO. The analysis continues with an additional adjustment on the aromaticity of furan by replacement of C^2 by a substituted manganese. The same questions brought up in Section XII about the aromaticity of the 2-metalafuran system are valid here too.

That manganese enjoys a variety of oxidation states means Mn(II) enolates may be obtained from ketones by deprotonation or from α-haloketones by redox reactions[224]. (*Z*)-Mn(II) enolates seem to be preferentially formed over their (*E*)-isomers. This has been

ascribed to kinetic factors[225], without thermochemical data on the relative stability of the two isomers. Mn(III) enolates are also known. The reaction[226] of diketene and manganic acetate yields products corresponding to conjugated and unconjugated manganic enolates from acetoacetic acid derivatives.

The 2-rhenafuran-3-ol **39** is in equilibrium[227] with the corresponding 3*H*-furanone **40** ($K_{eq} = 1.5$) while the equilibrium constant is much more on the side of the furanone when the ring Re is replaced by Mn or in the absence of the metal heteroatom. For example, no 5-methyl-2-furanol (**41**) is detected in the rearrangement of γ-methylene-γ-butyrolactone (**42**) to α-angelicalactone (**43**)[228]. Understanding the contribution to aromaticity of Re in the 2-rhenafurans (**39**, **40**) and the exocyclic and endocyclic methylene groups in **42** and **43** would be most instructive.

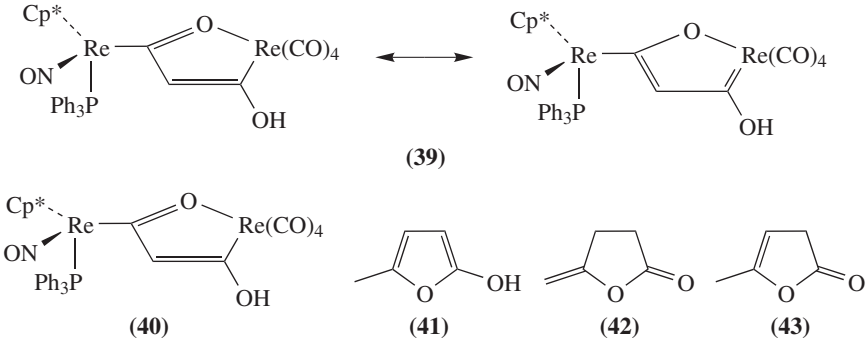

(39)

(40) **(41)** **(42)** **(43)**

Trimethylphosphine reacts[227, 229] with Cp*Re(CO)(NO)Me to produce $(Me_3P)_3Re(O)C{=}C_5H_4(NO)$, which may be recognized variously as a cyclic metal enolate, oxarhenirane or a cyclopentadienylideneketene derivative. The acetyl rhenium complex CpRe(Ac))(NO)(PPh_3) deprotonates[230] on the cyclopentadienyl ring and then rearranges to form $\{(C_5H_4Ac)Re(NO)(PPh_3)]^-$, and in turn is methylated on the Re with methyl iodide. The corresponding Cp* species produces the related propionyl complex via deprotonation of the acetyl group, i.e. the classical enolato ligand $[C_5Me_4C(O){=}CH_2]^{2-}$. Thermodynamic vs kinetic factors in solution were discussed—comparison of the intrinsic (gas phase) acidities of the diverse sites for deprotonation is welcomed. It is likewise welcomed for ligands themselves—cyclopentadiene, acetylcyclopentadiene and their methylated derivatives. The closest we get to relevant data is found for the reverse situation—the effect of an acetyl group on the acidity of cyclopentadienyl metal-containing carboxylic acids. In the case of ferrocenecarboxylic acid and its 1′-acetyl derivative[231], the gas-phase acid dissociation constants are 8.1 to 25.7×10^{-7} corresponding to a more favorable Gibbs free energy of deprotonation change of *ca* 2.7 kJ mol^{-1} upon acetylation.

XIV. GROUP 8: IRON, RUTHENIUM AND OSMIUM

As was discussed in Section VI for the reactions of enolates with the oxidizing cation Cu(II), Fe(III) also oxidizes enolates to form products associated with formal radical dimerization[232]. The presumed intermediate enoxyl radicals react with $FeCl_3$, not by formation of Fe(IV) enolates[233], but rather from an α-chlorinated ketone product + $FeCl_2$, thereby providing a thermochemical upper bound for the enthalpy of formation of these haloketones.

More is known about the thermochemistry of 1-acetylferrocene and 1,1′-diacetylferrocene than about many other more classical organic compounds, including experimental

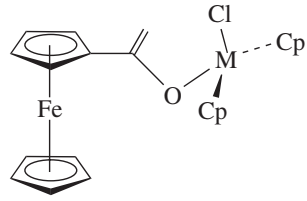

(44) M = Ti, Zr

data for their enthalpies of formation[234] and of sublimation[235], heat capacities[236], cyclodextrin inclusion parameters[237] and torsional barriers[238]. Indeed, to the extent that ferrocene may be recognized as aromatic as is benzene, then acetylferrocene relates to acetophenone. Thus, one can mention the formation of the acetylferrocene potassium enolate and and its transformation into oxygen-bridged titanium and zirconium derivatives[239] (**44**), for which the direct comparison with those of acetophenone and other ketones is rather immediately suggested. Based on knowledge of benzenes with electronegative substituents[25] we would expect *o*-diacetylbenzene to be less stable than its *m*- and *p*-isomers. Why then is 1,2-diacetylferrocene seemingly more stable[240] than its 1,3- and 1,1′-isomers?

4,6-Cycloheptadiene-1,3-dione iron tricarbonyl and the related 5,7-cyclooctadiene-1,4-dione complex were readily prepared[241]. It is not surprising that these species do not tautomerize to form the enol–iron tricarbonyl complexes, i.e. of 3-hydroxytropone and 1,4-dihydroxycyclooctatetraene, because the dienes conform to the '18-electron rule' while their tautomers would not.

Fe(II) forms the enolate cation $[FeOC(Me)=CH_2]^+$ in the gas phase[242] in the reaction of diverse FeX^+ (X = H, Me, All, NH_2, OH, F) ions with acetone. Other products are also observed. The relative reactivities of the FeX^+ cations relate to electronic and thermodynamic properties of the displaced substituent X.

Comparison of corresponding ruthenium and iron enolates are rare. A particularly evocative one deals with the mass spectra of acetyl and diacetylferrocene and the corresponding ruthenocene derivatives. Scission of bonds within the ligands attached to Ru is relatively facile[243]: diacetylruthenocene undergoes fragmentation to form CH_3, two CO and a derived ion that was presumed to be $CpRu(C_6H_6)^+$. Measurement of the threshold energies of this rearrangement is welcomed. Another structural feature deals with the torsional barriers associated with acetyl- and diacetylruthenocene[244].

Among the more classical enolates, the complex $Me[\eta^1\text{-}CH_2{=}C(Me)O]Ru(PMe_3)_4$ and its *C*-bonded isomer (more stable by 6 kJ mol^{-1}) have been observed[245] in THF solution. Also, complexes of double-deprotonated acetone ligands were present, such as the 2-ruthenacyclobutanone **45** and $[\eta^4\text{-}(CH_2)_2CO]Ru(PMe_3)_3$ (**46**); however, no methyleneruthenaoxetane complex (**47**) could be detected.

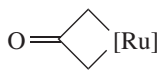

(45)

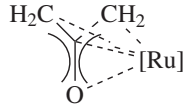

(46)

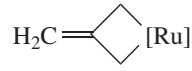

(47)

As the triosmium carbonyl cluster, we find examples of neutral single oxygen, oxygen-bridged $\eta^1, \mu^2 - O$-bonded enolates[246] with ten CO ligands accompanied by Os−H−Os bonds, e.g. **48**, and deprotonated anionic η^1 and nonbridging carbon-bonded species[247] with eleven CO ligands, e.g. **49**. Why are these species so different from each other from a structural vantage point and why should protonation effect such a major change? Osmium carbonyl hydrides have been thermochemically investigated[248], and understood within the context of other metal carbonyl clusters[249]. However, the effect of enolate 'substitution' remains unexplored.

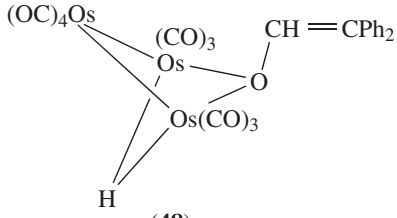

(**48**)

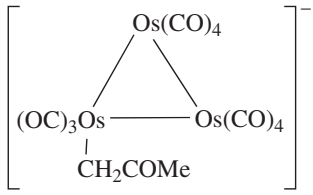

(**49**)

XV. GROUP 9: COBALT, RHODIUM AND IRIDIUM

There are few examples of classical cobalt enolates. The reaction of CH_2=CHOLi with $CoCl_2$ and Cp*Li yields the binuclear bridged complex $Co_2Cp^*_2(\mu\text{-}CH_2)(\mu\text{-}CO)$ (**50**) resulting from cleavage of the enolate C=C double bond[250]. The initial reaction step was postulated to be formation of the dilithium enolate. The one-carbon fragments are reminiscent of those from ketene. The cleavage of ketene to form CH_2 and CO is endothermic by 348 kJ mol^{-1}, using 390 kJ mol^{-1} for the enthalpy of formation of CH_2[120]. There are no measured enthalpies of formation of CHOLi or $COLi_2$, nor their dilithium enolate precursor. However, consider the fragmentation reaction of the enolate anion in equation 14.

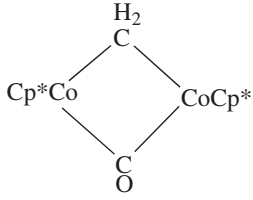

(**50**)

While this process is not directly observable, Hess' Law says that the endothermicity of this reaction is the sum of the next three reactions, equations 15–17. The sum[251–253] is 566 kJ mol^{-1}, some 215 kJ mol^{-1} more endothermic than the aforementioned ketene cleavage. We can conclude that lithiation and dianion formation significantly weaken the CC bond in the dilithium enolate as the lithium enolate has a considerably stronger CC bond than ketene.

$$CH_2{=}CHO^- \longrightarrow CH_2 + HCO^- \quad (14)$$

$$CH_3CHO \longrightarrow CH_2 + CH_2O \quad (15)$$

$$CH_2O \longrightarrow CHO^- + H^+ \quad (16)$$

$$CH_2{=}CHO^- + H^+ \longrightarrow CH_3CHO \quad (17)$$

The Co(III) complex cobalamin (**51a**) and the synthetic Co(II) complex cobaloxime (**52a**) exhibit diverse enolate chemistry. *C*-Bonded phenacylcobalamin (**51b**)[254] and phenacylcobaloxime (**52b**)[255] derivatives decompose in acid to form acetophenone, presumably by protonation, π-enol complex formation and decomposition and tautomerism of the enol. No evidence is offered for *O*-bonded enolate in either case, suggesting it is less stable than either *C*- or π-complexed ketone or enol. By contrast, β-hydroxyethylcobalamin (**51c**) decomposes in base to form enol-related products while its homolog, the γ-hydroxypropyl species (**51d**), cyclizes to form a 5-membered oxametallocycle[256]. While the strain energy difference between this last species and the unknown 4-membered oxacobaletane is unknown, the corresponding THF and oxetane differ by *ca* 80 kJ mol^{-1}. Cobalt-alkylated porphyrins with a vinylogous *C*-enolate substituent, $CH_2CH{=}CHCHO$, were easily made[257]. No sign of the tautomeric enolic—$CH{=}CHCH{=}CHOH$ or the cyclic enolate 2-cobalta-2*H*-pyran was observed. Note that the corresponding 1,3-butadien-1-ol ($CH_2{=}CHCH{=}CHOH$) is *ca* 12 ± 10 kJ mol^{-1} less stable[258] than crotonaldehyde ($CH_3CH{=}CHCHO$); no experimental enthalpy of formation data exist for the heterocyclic species 2*H*-pyran or 4*H*-pyran.

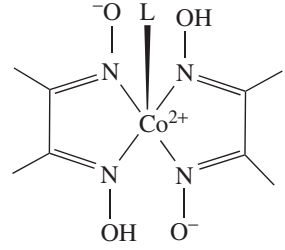

(**51**) (**a**) L = nil
(**b**) L = $CH_2C(Ph){=}O$
(**c**) L = CH_2CH_2OH
(**d**) L = $CH_2CH_2CH_2OH$

(**52**) (**a**) L = nil
(**b**) L = $CH_2C(Ph){=}O$

The η^5 derivatives of acylcyclopentadienides were referred to in Section II as enolates. Again, we note the dichotomy[259] between 1-formyl-1′,2′,3′,4′,5′-pentamethylcobaltocene and some related species. This species undergoes an auto-redox reaction to form pinacol-like dimers of the corresponding cobaltocinium ion. No such reaction is seen for 1-formyl-1′,2′,3′,4′,5′-pentamethylferrocene[260] or 1,1′-diacetylcobaltocene[261] (no formylcobaltocenes are known). It would appear that the ionization energies of the acylated metallocenes are too high, and/or their electron affinities insufficient to allow electron transfer and disproportionation to ensue. For comparison, the ionization energy of ferrocene itself is *ca* 125 kJ mol^{-1} higher than that of cobaltocene[262]. While we do not know of the corresponding values for the pentamethyl ferrocene or cobaltocene, there is a nearly identical drop of *ca* 80 kJ mol^{-1} on decamethylation for both species. These ionization energies were determined by photoelectron spectroscopy, electron impact measurements

having earlier been made. Electron impact experiments with 1,1'-diacetylferrocene and its cobaltocene analog led to rearranged products[263].

There are several relevant aspects of rhodium enolate chemistry. Rh(I) catalyzes[264] the isomerization of allylic alkoxides to enolates. We welcome this reaction done in a direct thermochemical context analogous to the related isomerizations of allyl halides[265], ethers[266] and allyl amines[267]. From the enthalpies of formation of allyl alcohol and propanal (-185.6 and -124.5 kJ mol^{-1}), and their respective gas phase deprotonation enthalpies (1564[268] and 1530 kJ mol^{-1} [252, 253]), it can be concluded that the rearrangement of the allyloxide to propen-1-olate is exothermic by 95 kJ mol^{-1}.

Cp*RhH$_2$(PMe$_3$) reacts[269] with ethylene oxide to form isomeric oxiranyl and the *C*-enolate CH_2CHO derivatives. There are few examples where both oxirane and aldehyde isomers have been thermochemically characterized (only the organic examples of the epoxides of ethylene, propene and 1-butene come to mind). Although this is disproportionation rather than isomerization, we recall the multidentate rhodium enolate complexes (Ph$_3$P)$_2$Rh[η^3-$CH_2C(R)O$] (R = Ph, *t*-Bu) and their catalytic conversion[270] of aldehydes to the corresponding ester (Tischenko reaction) in a highly energetically favorable process (the reaction of acetaldehyde to form ethyl acetate is exothermic by *ca* 110 kJ mol^{-1}).

The reaction of [Cp*(PMe$_3$)M(η^3-All)]$^+$ (M = Rh, Ir) with alkali metal enolates has been demonstrated to be a reversible nucleophilic addition[271]. There is a kinetic preference for addition to the central carbon of the allyl ligand to give the 3-(*C*-enolato)metallacyclobutane **53**. The thermodynamically more stable product is the lower valent metal–olefin π complex, **54**.

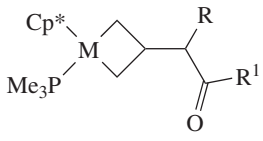

(**53**) M = Rh, Ir

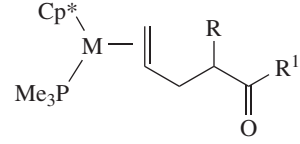

(**54**) M = Rh, Ir

A variety of 3-iridacyclobutanes, Ir(H)(PMe$_3$)$_3$(CH_2XCH_2) (X = CO), including the doubly *C*,*C*′-bridged enolate, are formed easily[272] from Ir(PMe$_3$)$_4$Cl and $MeXCH_2Li$ (X can also be Me_2C and Me_2Si). It would be most informative to know the difference between the strain energies of these irida-heterocycles and the corresponding species with Ir replaced by CH_2 (there is some controversy about the enthalpy of formation, and hence the strain energy, of cyclobutanone itself[273]). The 3-iridacyclobutan-1-one[274] ring system in Ir(CO)$_2$(PPh$_3$)$_2$)($CH_2C(O)CH_2$) is significantly nonplanar and so nonbonded Ir$\cdots$CO interactions are entirely plausible. Indeed, cyclohexanone substituted at position 2 with {Cp*Ir(PMe$_3$)[$(CH_2)_2CH$]} shows the 3-iridacyclobutyl group to be axially positioned on the 6-membered ring[275], allowing a longer range Ir$\cdots$CO interaction.

Related to that described above[264], reactions of Rh(I) and Ir(I) with allylic alcohols yields enols. From a study[276] using the iridium catalyst it was concluded that 1-propenol is more stable as the *E* rather than the *Z* configuration, despite the initial preponderance of the latter prior to equilibration of the products, in contradiction to the gas phase results reported elsewhere[258].

XVI. GROUP 10: NICKEL, PALLADIUM AND PLATINUM

As seen in the previous sections, both *C*- and *O*-enolates of metals have been observed, the dominant species depending on the metal and on its oxidation state. Nickel is outstanding

in having the two coexisting isomeric forms. The 3-nickela-1-indanone complex **55** (*C*-bonded) and the isomeric 3-methylene-1-nickela-isobenzofuran complex **56** (*O*-bonded) are in equilibrium with each other[277] in approximately equal amounts and so necessarily they have nearly equal Gibbs free energies. Temperature-dependent measurements show the *C*-isomer is more stable by 1.1 ± 0.4 kJ mol^{-1}. By contrast, compare the nonmetallic (1-ring) analogs of these species, cyclopentanone and 2-methylenetetrahydrofuran. From the enthalpy of formation of the former, the isomerization[232] and formation[278,279] of the latter, we conclude that the former is 70 ± 5 kJ mol^{-1} more stable than the latter. This metallocyclic/'organic' difference is consonant with the conclusion that while C–C and C–O bonds are of comparable strength, the Ni–C bond is much weaker than the Ni–O bond. This is not surprising, but suggests care must be taken when applying reasoning from carbocycles and 'ordinary' heterocycles to metallocycles. In contradistinction to the above case of 3-nickela-1-indanone and the nearly isoenergetic isomeric 3-methylene-1-nickela-isobenzofuran, the isoelectronic Pd species uneqivocally prefers the carbon-bonded enolate[277].

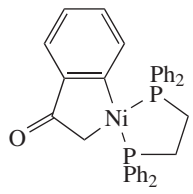

(**55**)

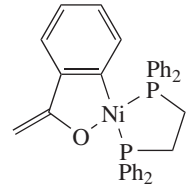

(**56**)

The Ni(II)-catalyzed decarboxylation of the dienol dihydroxyfumaric acid[280] proceeds sequentially to form 2,3-dihydroxyacrylic acid and hydroxyacetaldehyde. Each of these three species has thermochemical relevance. We ask: what is the difference between the enthalpy of formation of dihydroxyfumaric acid and its (*Z*)-isomer, dihydroxymaleic acid? We note that fumaric acid is more stable than maleic acid in the solid phase by *ca* 12 kJ mol^{-1}. Is the *E* isomer dihydroxyfumaric acid more stable than dihydroxy-maleic acid? While the difference between the enthalpies of formation of (*Z*)- and (*E*)-dihydroxyethylene is not known from experiment, the corresponding difference for the dimethoxyethylenes favors the *Z* configuration[158] by 6 kJ mol^{-1}: is not the (*Z*)-dihydroxy acid the more stable? And so, we repeat the question: which isomer is more stable, dihydroxyfumaric or maleic acid? Reaction chemistry suggests the fumaric acid[281]. 2,3-Dihydroxyacrylic acid ((*Z*)- and/or (*E*)-isomer) is of comparable stability to its tautomer hydroxymalonic acid semialdehyde[282]. While the enthalpy of formation of hydroxyac-etaldehyde remains unknown from experiment, quantum chemical calculations suggest[283] -316 kJ mol^{-1}, the same as its (*Z*)-1,2-ethene-diol isomer[258] as shown by ion chemical experiments; studies in aqueous solution show them to be in equilibrium[284].

For the binuclear Pd(I) dienolate [μ-$CH_2C(O)CHCH_2Pd_2(PPh_3)_2(\mu$-Cl)] there is spectroscopic and crystallographic evidence[285] that suggests resonance between the *C*- and π-olefin-bonded enolate structures. This and an earlier discussion invites the question about the relative stability of the 1- and 2-enolates, $CH_2{=}CHCH{=}CHO^-$ and $CH_2{=}C(O^-)CH{=}CH_2$, and indeed other conjugated and cross-conjugated species. From the enthalpies of formation of their conjugate acids[34,286] and their acidities[287], we conclude that 1-enolate is *ca* 25 kJ mol^{-1} more stable—the corresponding neutral enols differ by very much the same value[258]. In contrast, the enthalpies of formation of $CH_2{=}CHCH{=}CHMe$ and $CH_2{=}C(Me)CH{=}CH_2$ differ only by 6 kJ mol^{-1}.

The 2,4-disubstituted derivatives of the aforementioned 3-metallacyclobutanones allow for *cis* and *trans* isomers, much as for cyclobutanone and cyclobutane. It is found that the diphenyl species [Pt{CHPhC(O)CHPh}$(PPh_3)_2$] is synthesized with predominantly *cis* stereochemistry[288]. This is consistent with stereochemical expectations—however, disconcertingly, there are no examples of disubstituted cyclobutanes (or derivatives) for which the enthalpy of formation of both the *cis* and *trans* isomers are both known[273] to confirm this expectation. Gibbs free energy differences have been determined for the dimethyl[289], dichloro, dibromo and diiodo[290] species, again in the expected order[290]. Indeed, the only case where the *trans* isomer is known to be more stable than the *cis* is the enigmatic bis-phenylsulfonyl species for which no explanation has been offered[291, 292].

Pt(II), bonded to two Ph_3P ligands, exhibits a profound difference[293] in its bis-enolate complexes with the doubly deprotonated triones $RC(O)CH_2C(O)CH_2C(O)R$, R = Me and Ph. For R = Me, a highly puckered 2,4-diacetylated 3-platinacyclobutanone, **57**, is formed with a weak transannular Pt–C bond. For R = Ph, the more usual 1:1 O,O'-chelate is formed and the product is isolated as the dienediolate complex **58**. What would be the product if the two substituent groups were different, R = Me and R^1 = Ph? Would a 2-acetyl-4-benzoyl-3-platinacyclobutanone be formed; would a 6-membered-ring β-diketonate be formed with one Me and a PhCOCH substituent apiece or such a species with one Ph and an MeCOCH, or would an unprecedented 1,3-dioxa-2-platinacyclooctadienone (**59**) result?

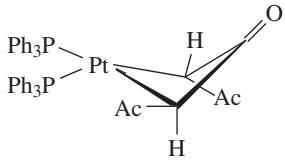

(**57**)

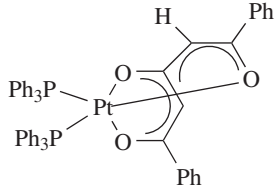

(**58**)

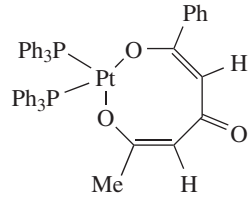

(**59**)

XVII. REFERENCES

1. A. I. Gubareva, P. A. Gerasimov, O. L. Chernysheva, T. V. Trusova, N. G. Malyuta and I. K. Igumenov, *Sibir. Khim. Zh.*, 112 (1992); *Chem. Abstr.*, **116**, 263492 (1992).
2. J. O. Hill and R. J. Irving, *J. Chem. Soc. A*, 971 (1966).
3. K. K. Cavell and G. Pilcher, *J. Chem. Soc., Faraday Trans. 1*, **73**, 1590 (1977).
4. M. A. Ribeiro da Silva, G. Pilcher and R. J. Irving, *J. Chem. Thermodyn.*, **20**, 95 (1988).
5. M. A. V. Ribeiro da Silva, M. L. C. C. H. Ferrao, R. M. C. Marques and J. M. T. Lima, *J. Chem. Thermodyn.*, **24**, 595 (1992).
6. S. W. Slayden and J. F. Liebman, in *The Chemistry of Organolithium Compounds* (Eds Z. Rappoport and I. Marek), John Wiley & Sons, Ltd, Chichester, 2004, pp. 121–136.
7. J. F. Liebman and S. W. Slayden, in *The Chemistry of Organozinc Compounds* (Eds Z. Rappoport and I. Marek), John Wiley & Sons, Ltd, Chichester, 2006, pp. 135–145.
8. M. A. V. Ribeiro da Silva and M. L. C. C. H. Ferrao, *Pure Appl. Chem.*, **60**, 1225 (1988).
9. J. O. Hill and J. P. Murray, *Rev. Inorg. Chem.*, **13**, 157 (1993).
10. T. Kremer and P. v. R. Schleyer, *Organometallics*, **16**, 737 (1997).
11. (a) O. Ayed, A. Loutellier, L. Manceron and J. P. Perchard, *J. Am. Chem. Soc.*, **108**, 8138 (1986).
    (b) O. Ayed, L. Manceron and B. Silvi, *J. Phys. Chem.*, **92**, 37 (1988).
12. S. L. Georgopoulos, R. Diniz, M. I. Yoshida, N. L. Speziali, H. F. Dos Santos, A. G. M. Junqueira and L. F. C. De Oliveira, *J. Mol. Struct.*, **794**, 63 (2006).
13. D. Braga, L. Maini and F. Grepioni, *Chem. Eur. J.*, **8**, 1804 (2002).

14. C. A. Brown, *J. Org. Chem.*, **39**, 1324 (1974).
15. M. Arthurs, J. C. Bickerton, G. Hogarth, D. A. Morton-Blake, G. Kubal and M. R. Truter, *J. Organometal. Chem.*, **571**, 43 (1998).
16. R. D. Rogers, J. L. Atwood, M. D. Rausch, D. W. Macomber and W. P. Hart, *J. Organometal. Chem.*, **238**, 79 (1982).
17. M. Arthurs, H. K. Al-Daffaee, J. Haslop, G. Kubal, M. D. Pearson, P. Thatcher and E. Curzon, *J. Chem. Soc., Dalton Trans.*, 2615 (1987).
18. G. Boche and F. Heidenhain, *J. Am. Chem. Soc.*, **101**, 738 (1979).
19. G. Linstrumelle, *Bull. Soc. Chim. Fr.*, 920 (1970).
20. (a) K. M. Broadus and S. R. Kass, *J. Chem. Soc., Perkin Trans. 2*, 2389 (1999).
    (b) K. M. Broadus and S. R. Kass, *J. Chem. Soc., Perkin Trans. 2*, 603 (2000).
    (c) R. W. Nagorski, A. D. DeAtley and K. M. Broadus, *J. Am. Chem. Soc.*, **123**, 8428 (2001).
21. R. Breslow and M. Douek, *J. Am. Chem. Soc.*, **90**, 2698 (1968).
22. E. Hevia, K. W. Henderson, A. R. Kennedy and R. E. Mulvey, *Organometallics*, **25**, 1778 (2006).
23. G. A. Russell and C. E. Osuch, *J. Am. Chem. Soc.*, **104**, 3353 (1982).
24. G. A. Russell, D. F. Lawson, H. L. Malkus, R. D. Stephens, G. R. Underwood, T. Takano and V. Malatesta, *J. Am. Chem. Soc.*, **96**, 5830 (1974).
25. J. B. Pedley, *Thermochemical Data and Structures of Organic Compounds*, *TRC Data Series*, Vol. 1, College Station, TX, 1994.
26. D. Z. Wang and A. Streitwieser, *J. Org. Chem.*, **68**, 8936 (2003).
27. (a) A. M. Ross, D. L. Whalen, S. Eldin and R. M. Pollack, *J. Am. Chem. Soc.*, **110**, 1981 (1988).
    (b) S. Eldin, D. L. Whalen and R. M. Pollack, *J. Org. Chem.*, **58**, 3490 (1993).
28. N. L. Allinger and E. S. Jones, *J. Org. Chem.*, **27**, 70 (1962).
29. M. J. Kaufman and A. Streitwieser, Jr, *J. Am. Chem. Soc.*, **109**, 6092 (1987).
30. E. M. Arnett, F. J. Fisher, M. A. Nichols and A. A. Ribeiro, *J. Am. Chem. Soc.*, **112**, 801 (1990).
31. E. M. Arnett and D. Moe, *J. Am. Chem. Soc.*, **113**, 7288 (1991).
32. I. Ryu, Y. Hayama, A. Hirai, N. Sonoda, A. Orita, K. I. Ohe and S. Murai, *J. Am. Chem. Soc.*, **112**, 7061 (1990).
33. H. Kai, K. Iwamoto, N. Chatani and S. Murai, *J. Am. Chem. Soc.*, **118**, 7634 (1996).
34. N. Ungvari, T. Kegl and F. Ungvary, *J. Mol. Catal.*, **219A**, 7 (2004).
35. C. H. DePuy, J. M. Van Doren, S. Gronert, S. R. Kass, E. L. Motell, G. B. Ellison and V. M. Bierbaum, *J. Org. Chem.*, **54**, 1846 (1989).
36. E. P. Clifford, P. G. Wenthold, W. C. Lineberger, G. A. Peterssom, K. M. Broadus, S. R. Kass and S. Kato, *J. Phys. Chem. A*, **102**, 7100 (1998).
37. J. M. Oakes, M. E. Jones, V. M. Bierbaum and G. B. Ellison, *J. Phys. Chem.*, **87**, 4810 (1983).
38. C. J. Kowalski and G. S. Lal, *J. Am. Chem. Soc.*, **108**, 5356 (1986).
39. C. J. Kowalski, M. L. O'Dowd, M. C. Burke and K. W. Fields, *J. Am. Chem. Soc.*, **102**, 5411 (1980).
40. I. Ryu, H. Nakahira, M. Ikebe, N. Sonoda, S.-Y. Yamato and M. Komatsu, *J. Am. Chem. Soc.*, **122**, 1219 (2000).
41. S.-Y. Yamato, G. Yamamura, M. Komatsu, M. Arai, T. Fukuyama and I. Ryu, *Org. Lett.*, **7**, 2489 (2005).
42. S. M. Moosavi, R. S. Beddoes and C. I. F. Watt, *J. Chem. Soc., Perkin Trans. 2*, 1585 (1997).
43. P. G. Williard and G. J. MacEwan, *J. Am. Chem. Soc.*, **111**, 7671 (1989).
44. X. He, B. C. Noll, A. Beatty, R. E. Mulvey and K. W. Henderson, *J. Am. Chem. Soc.*, **126**, 7444 (2004).
45. S. E. Baillie, E. Hevia, A. R. Kennedy and R. E. Mulvey, *Organometallics*, **26**, 204 (2007).
46. R. Amunugama and M. T. Rodgers, *J. Phys. Chem. A*, **106**, 5529 (2002).
47. W. R. Davidson and P. Kebarle, *J. Am. Chem. Soc.*, **98**, 6133 (1976).
48. S. Apinitis, A. S. Antsyshkina and A. Ievins, *Latv. PSR Zin. Akademijas Vest., Kim. Ser.*, 643 (1969); *Chem. Abstr.*, **73**, 29751 (1970).
49. I. I. Zheltvai, S. S. Alam and M. A. Tishchenko, *Ukrain. Khim. Zh.*, **58**, 289 (1992); *Chem. Abstr.*, **117**, 77638 (1992).
50. M. Brustolon, L. Pasimeni and C. Corvaja, *J. Chem. Soc., Dalton Trans.*, 604 (1981).
51. A. J. Llacer, *Microchim. Acta*, 921 (1955).

52. Ya. Kh. Grinberg, V. V. Petukhov, G. Ya. Novikova, V. A. Bogdanov, G. A. Sharpataya and Z. P. Ozerova, *Zh. Fiz. Khim.*, **61**, **2894** (1987); *Chem. Abstr.*, **108**, 63557 (1970).
53. S. Murata, M. Sakiyama and S. Seki, *J. Chem. Thermodyn.*, **20**, 1203 (1988).
54. R. J. Irving and M. A. V. Ribeiro da Silva, *J. Chem. Soc., Dalton Trans.*, 413 (1977).
55. C. Weygand and H. Forkel, *Ber. Dtsch. Chem. Ges.*, **59B**, 2243 (1926).
56. J. B. Cumming and P. Kebarle, *Can. J. Chem.*, **56**, 1 (1978).
57. S. W. Slayden and J. F. Liebman, *Chem. Rev.*, **101**, 1541 (2001).
58. B. M. L. Bhatia and S. S. Sawhney, *Thermochim. Acta*, **45**, 121 (1981).
59. S. S. Sawhney and B. M. L. Bhatia, *Thermochim. Acta,* **42**, 105 (1980).
60. J. F. Allan, W. Clegg, K. W. Henderson, L. Horsburgh and A. Kennedy, *J. Organomet. Chem.,* **559**, 173 (1998).
61. J. H. Billman and C. M. Smith, *J. Am. Chem. Soc.,* **61**, 457 (1939).
62. J. H. Billman and C. M. Smith, *J. Am. Chem. Soc.,* **74**, 3174 (1952).
63. D. J. Cram and R. L. Zimmerman, *J. Am. Chem. Soc.*, **74**, 2646 (1952).
64. L. B. Dashkevich and B. E. Kuvaev, *Zh. Obshch. Khim.*, **29**, 2368 (1959); *Chem. Abstr.*, **54**, 55853 (1960).
65. L. B. Dashkevich and L. N. Kuz'menkov, *Zh. Obshch. Khim.*, **29**, 2367 (1959); *Chem. Abstr.*, **54**, 55852 (1960).
66. J. F. Santz, J. Ovideo, A. Márquez, J. A. Odriozola and M. Montes, *Angew. Chem., Int. Ed.*, **38**, 506 (1999).
67. R. Kakkar, P. N. Kapoor and K. J. Klabunde, *J. Phys. Chem. B*, **110**, 25941 (2006).
68. A. I. Boldyrev and J. Simons, *J. Phys. Chem.*, **100**, 8023 (1996).
69. A. G. Harrison and K. R. Jennings, *J. Chem. Soc., Faraday Trans. 1*, **72**, 1601 (1976).
70. M. Lin and J. J. Grabowski, *Int. J. Mass Spectrom.*, **237**, 149 (2004).
71. P. G. Wenthold, J. Hu, B. T. Hill and R. R. Squires, *Int. J. Mass Spectrom.*, **179/180**, 173 (1998).
72. C. A. Schalley, S. Blanksby, J. N. Harvey, D. Schroeder, W. Zummack, J. H. Bowie and H. Schwarz, *Eur. J. Org. Chem.*, 987 (1998).
73. X. He, J. F. Allan, B. C. Noll, A. R. Kennedy and K. W. Henderson, *J. Am. Chem. Soc.*, **127**, 6920 (2005).
74. E. Taskinen and N. Lindholm, *J. Phys. Org. Chem.*, **7**, 256 (1994).
75. J. Qu, J. Dong, M. Liu and S. Qu, *Huaxue Tongbao*, **69**, 544 (2006); *Chem. Abstr.*, **146**, 433370 (2006).
76. A. Yanagisawa, S. Habaue, K. Yasue and H. Yamamoto, *J. Am. Chem. Soc.*, **116**, 6130 (1994).
77. A. Yanagisawa, H. Takahashi and T. Arai, *Chem. Commun.*, 580 (2004).
78. J. F. Allan, W. Clegg, M. R. J. Elsegood, K. W. Henderson, A. E. McKeown, P. H. Moran and I. M. Rakov, *J. Organomet. Chem.*, **602**, 15 (2000).
79. S. Böhm, J.-F. Gal, P.-C. Maria, J. Kulhanek and O. Exner, *Eur. J. Org. Chem.*, 2580 (2005).
80. H. C. Brown and L. Domash, *J. Am. Chem. Soc.,* **78**, 5384 (1956), citing unpublished calorimetric studies by E. J. Prosen and his colleagues.
81. Yu. V. Zeifman, S. A. Postovoi, I. M. Vol'pin and L. S. German, *Dokl. Akad. Nauk SSSR*, **307**, 1385 (1989); *Chem. Abstr.,* **112**, 178011 (1990).
82. P. E. Lindner and D. M. Lemal, *J. Am. Chem. Soc.*, **119**, 3267 (1997).
83. Y. Nishimura, Y. Miyake, R. Amemiya and M. Yamaguchi, *Org. Lett.*, **8**, 5077 (2006).
84. S. Kang, T.-S. Jang, G. Keum, S. B. Kang, S.-Y. Han and Y. Kim, *Org. Lett.*, **2**, 3615, (2000).
85. D. W. Rogers, *Heats of Hydrogenation: Experimental and Computational Hydrogen Thermochemistry of Organic Compounds*, World Scientific, Hackensack, 2006.
86. J. Vicente, J. A. Abad, G. Cara and J. F. Gutierrez-Jugo, *J. Chem. Soc., Dalton Trans.*, 2481 (1992).
87. J. Glaser and I. J. Toth, *J. Chem. Soc., Chem. Commun.*, 1336 (1986).
88. A. McKillop, L. F. Elsom and E. C. Taylor, *J. Organomet. Chem.*, **15**, 500 (1968).
89. M. Driess, N. Dona and K. Merz, *Chem. Eur. J.*, **10**, 5971 (2004).
90. J. K. Bjernemose, E. Frandsen, F. Jensen and C. T. Pedersen, *Tetrahedron*, **59**, 10255 (2003).
91. A. S. Hneihen, J. W. Bruno and J. C. Huffman, *J. Organomet. Chem.*, **382**, 361 (1990).
92. A. G. Davies and M.-W. Tse, *J. Organomet. Chem.*, **155**, 25 (1978).
93. K. Kobayashi, M. Kawanisi, T. Hitomi and S. Kozima, *Chem. Lett.*, 497 (1984).
94. M. Yasuda, Y. Katoh, I. Shibata, A. Baba, H. Matsuda and N. Sonoda, *J. Org. Chem.*, **59**, 4386 (1994).

95. T. Mukaiyama, R. Tsuzuki and J. Kato, *Chem. Lett.*, 1825 (1983).
96. R. S. Hosmane and J. F. Liebman, *Tetrahedron Lett.*, **33**, 2303 (1992).
97. A. F. El Farargy, H. Fobbe, R. Marx and W. P. Neumann, *Silicon, Germanium, Tin and Lead Compounds,* **9**, 71 (1986).
98. J. F. Liebman, J. A. Martinho Simões and S. W. Slayden, in *The Chemistry of Organic Germanium, Tin and Lead Compounds* (Ed. S. Patai), John Wiley & Sons, Ltd, Chichester, 1995, pp. 245–266.
99. A. Deak, P. Kiraly and G. Tarkanyi, *J. Chem. Soc., Dalton Trans.*, 234 (2007).
100. R. M. Moriarty, R. Penmasta, I. Prakash and A. K. Awasthi, *J. Org. Chem.*, **53**, 1022 (1988).
101. J. Berlan, J. P. Battioni and K. Koosha, *J. Organomet. Chem.*, **152**, 359 (1978).
102. N. Yoshikai, T. Yamashita and E. Nakamura, *Asian J. Chem.*, **1**, 322 (2006).
103. W. R. Roth, O. Adamczak, R. Breuckmann, H. W. Lennartz and R. Boese, *Chem. Ber.*, **124**, 2499 (1991).
104. (a) D. W. Rogers, N. Matsunaga, A. A. Zavitsas, F. J. McLafferty and J. F. Liebman, *Org. Lett.*, **5**, 2373 (2003).
(b) D. W. Rogers, N. Matsunaga, F. J. McLafferty, A. A. Zavitsas and J. F. Liebman, *J. Org. Chem.*, **69**, 7143 (2004).
105. (a) P. D. Jarowski, M. D. Wodrich, C. S. Wannere, P. v. R. Schleyer and K. N. Houk, *J. Am. Chem. Soc.*, **126**, 15036 (2004).
(b) M. D. Wodrich, C. S. Wannere, Y. Mo, P. D. Jarowski, K. N. Houk and P. v. R. Schleyer, *Chem. Eur. J.*, **13**, 7731 (2007).
106. B. E. Bryant and W. C. Fernelius, *J. Am. Chem. Soc.*, **76**, 5351 (1954).
107. (a) L. El Watik and R. Sabbah, *Bull. Soc. Chim. Fr.*, 344 (1991).
(b) M. Agostinha R. Matos, personal communication.
(c) R. Sabbah and L. El Watik, *Bull. Soc. Chim. Fr.*, 688 (1988).
108. Y. Ito, T. Konoike, T. Harada and T. Saegusa, *J. Am. Chem. Soc.*, **99**, 1487 (1977).
109. M. E. Brown, H. Kelly, A. K. Galwey and M. A. Mohamed, *Thermochim. Acta*, **127**, 139 (1988).
110. (a) M. Murakami, M. Inouye, M. Suginome and Y. Ito, *Bull. Chem. Soc. Jpn.*, **51**, 3649 (1988).
(b) Y. Ito, M. Inouye, M. Suginome and M. Murakami, *J. Organomet. Chem.*, **342**, C41 (1988).
111. E. G. Perevalova, I. G. Bolesov, Y. T. Struchkov, I. F. Leschova, Y. S. Kalyuzhnaya, T. I. Voyevodskaya, Y. L. Slovokhotov and K. I. Grandberg, *J. Organomet. Chem.*, **286**, 129 (1985).
112. J. Vicente, M. D. Bermúdez, M. P. Carrillo and P. G. Jones, *J. Chem. Soc., Dalton Trans.*, 1975 (1992).
113. S. Komiya and J. K. Kochi, *J. Am. Chem. Soc.*, **99**, 3695 (1977).
114. M. Lombardo and C. Trombini, in *The Chemistry of Organozinc Compounds* (Eds Z. Rappoport and I. Marek), John Wiley & Sons, Ltd, Chichester, 2006, pp. 797–861.
115. M. V. Roux, M. Temprado, P. Jiménez, R. Notario, J. S. Chickos, A. F. L. O. M. Santos and M. A. V. Ribeiro da Silva, *J. Phys. Chem. A*, **111**, 11084 (2007).
116. P. De Maria, A. Fontana and D. Spinelli, *J. Chem. Soc., Perkin Trans. 2*, 1067 (1991).
117. E. Kimura, T. Gotoh, T. Koike and M. Shiro, *J. Am. Chem. Soc.*, **121**, 1267 (1999).
118. Y.-P. Zhou, R. Zhang, F. Xu, H.-W. Wan and M.-L. Wu, *Huazhong Shifan Daxue Xuebao Zirankexueban*, **35**, 189 (2001); *Chem. Abstr.,* **137**, 175612 (2002).
119. J. Qu, J. Dong, Y. Liu and S. Qu, *Huaxue Tongbao*, **69**, 544 (2006); *Chem. Abstr.*, **146**, 433370 (2006).
120. D. D. Wagman, W. H. Evans, V. B. Parker, R. H. Schumm, I. Halow, S. M. Bailey, K. L. Churney and R. L. Nuttall, 'The NBS tables of chemical thermodynamic properties: Selected values for inorganic and C_1 and C_2 organic substances in SI units', *J. Phys. Chem. Ref. Data*, **11** (Supplement No. 2) (1982).
121. E. V. Zappi and A. Manini, *An. Asoc. Quim. Argent.*, **26**, 89 (1938); *Chem. Abstr.*, **33**, 13854 (1939).
122. K. P. Butin, V. V. Strelets, A. N. Kashin, I. P. Beletskaya and O. A. Reutov, *J. Organomet. Chem.*, **64**, 181 (1974).
123. Z. Popović, B. Korpar-Eolig, D. MatkoviČ-Calogovic, D. Vikić-Topić and M. Sikirica, *Main Group Chemistry*, **1**, 373 (1996).

124. P. Pyykkö, *Chem. Rev.*, **97**, 597 (1997).
125. (a) P. Pyykkö, *Angew. Chem. Int. Ed.*, **43**, 4412 (2004).
(b) P. Pyykkö, *Inorg. Chim. Acta*, **358**, 4113 (2005).
126. O. Steigelmann, P. Bissinger and H. Schmidbauer, *Angew. Chem., Int. Ed. Engl.*, **29**, 1399 (1990).
127. F. Basuli, J. Tomaszewski, J. C. Huffman and D. J. Mindiola, *Organometallics*, **22**, 4705 (2003).
128. W. J. Evans, R. Dominguez and T. Hanusa, *Organometallics*, **5**, 1291 (1986).
129. E. Taskinen, T. Alanko and J. F. Liebman, *Struct. Chem.*, **17**, 323 (2006).
130. S. Arndt, T. P. Spaniol and J. Okuda, *Organometallics*, **22**, 775 (2003).
131. F. Tureček and Z. Havlas, *J. Org. Chem.*, **51**, 4066 (1986).
132. H. J. Heeres, M. Maters, J. H. Teuben, G. Helgesson and S. Jagner, *Organometallics*, **11**, 350 (1992).
133. (a) T. Imamoto, T. Kusumoto, Y. Sugiura, N. Suzuki and N. Takiyama, *Nippon Kagaku Kaishi*, 445 (1985); *Chem. Abstr.*, **104**, 88215 (1986).
(b) T. Imamoto, T. Kusumoto and M. Yokoyama, *Tetrahedron Lett.*, **24**, 5233 (1983).
134. S. Fukuzawa, T. Tsuruta, T. Fujinami and S. Sakai, *J. Chem. Soc., Perkin Trans. 1*, 1473 (1987).
135. A. B. Paolobelli, P. Ceccherelli, F. Pizzo and R. Ruzziconi, *J. Org. Chem.*, **60**, 4954 (1995).
136. J. Guan, T. Dube, S. Gambarotta and G. P. A. Yap, *Organometallics*, **19**, 4820 (2000).
137. (a) J. Jubb and S. Gambarotta, *J. Am. Chem. Soc.*, **115**, 10410 (1993).
(b) J. Jubb and S. Gambarotta, *J. Am. Chem. Soc.*, **116**, 1167 (1994).
138. V. M. Orlov, A. A. Krivoruchko, A. D. Misharev and V. V. Takhistov, *Izv. Akad. Nauk SSSR, Ser. Khim.*, 2619 (1986); *Chem. Abstr.*, **106**, 213345 (1987).
139. Z. Hou, T. Yoshimura and Y. Wakatsuki, *J. Am. Chem. Soc.*, **116**, 11169 (1994).
140. T. Yoshimura, Z. Hou and Y. Wakatsuki, *Organometallics*, **14**, 5382 (1995).
141. J. M. McBride, *Tetrahedron*, **30**, 2009 (1974).
142. T. Vreven and K. Morokuma, *J. Phys. Chem A*, **106**, 6167 (2002).
143. J. E. Bartmess, *J. Am. Chem. Soc.*, **104**, 335 (1982).
144. Z. Wu, Z. Xu, X. You, X. Zhou and X. Huang, *J. Organomet. Chem.*, **483**, 107 (1994).
145. E. Taskinen, *J. Chem. Thermodyn.*, **6**, 345 (1974).
146. S.-I. Fukuzawa, T. Tsuchimoto and T. Kanai, *Bull. Chem. Soc. Jpn.*, **67**, 2227 (1994).
147. Z. Wu, Z. Xu, X. You, X. Zhou, Y. Xing and Z. Yan, *J. Chem. Soc., Chem. Commun.*, 1494 (1993).
148. D. L. Campbell and T. Moeller, *J. Inorg. Nucl. Chem.*, **32**, 945 (1970).
149. R. Petrola, *Ann. Acad. Sci. Fenn., Ser. A2*, 215 (1987).
150. G. S. Manku, *Aust. J. Chem.*, **24**, 925 (1971).
151. E. Orebaugh and G. R. Choppin, *J. Coord. Chem.*, **5**, 123 (1976).
152. G. R. Choppin and E. Orebaugh, *Inorg. Chem.*, **17**, 2300 (1978).
153. C. Keller and H. J. Schreck, *Inorg. Nucl. Chem.*, **31**, 1121 (1969).
154. P. J. Fagan, J. M. Manriquez, T. J. Marks, V. W. Day, S. H. Vollmer and C. Day, *J. Am. Chem. Soc.*, **102**, 5393 (1980).
155. E. A. Maatta and T. J. Marks, *J. Am. Chem. Soc.*, **103**, 3576 (1981).
156. T. Okuyama, T. Fueno and J. Furukawa, *Tetrahedron*, **25**, 5409 (1969).
157. P. J. Fagan, K. G. Moloy and T. J. Marks, *J. Am. Chem. Soc.*, **103**, 6959 (1981).
158. J. T. Waldron and W. H. Snyder, *J. Am. Chem. Soc.*, **95**, 5491 (1973).
159. W. J. Evans, A. L. Wayda, W. Hunter and J. L. Atwood, *J. Chem. Soc., Chem. Commun.*, 706 (1981).
160. R. B. Turner, W. R. Meador, W. v. E. Doering, L. H. Knox, J. R. Mayer and D. W. Wiley, *J. Am. Chem. Soc.*, **70**, 4127 (1957).
161. (a) G. R. Stevenson and R. T. Hashim, *J. Phys. Chem.*, **90**, 1896 (1986).
(b) N. S. Mills and M. Benish, *J. Org. Chem.*, **72**, 2207 (2006).
162. D. Brown and C. E. F. Rickard, *J. Chem. Soc. A*, 3373 (1970).
163. K. W. Bagnall, A. M. Bhandari, D. Brown, P. E. Lidster and B. Whittaker, *J. Chem. Soc., Dalton Trans.,* 1249 (1975).
164. R. Adam, C. Villiers and M. Ephritrikhine, *Tetrahedron Lett.*, **35**, 573 (1994).
165. V. I. Tel'noi, I. B. Rabinovich, V. N. Larina, R. M. Leonov and G. V. Solov'eva, *Radiokhimiya*, **31**, 38 (1989); *Chem. Abstr.,* **113**, 24103 (1990).

166. J. M. Manriquez, P. J. Fagan, T. J. Marks, C. S. Day and V. W. Day, *J. Am. Chem. Soc.*, **100**, 7112 (1978).
167. J. M. Manriquez, D. R. McAlister, R. D. Sanner and J. E. Bercaw, *J. Am. Chem. Soc.*, **100**, 2716 (1978).
168. R. B. Turner, B. J. Mallon, M. Tichy, W. v. E. Doering, W. R. Roth and G. Schroder, *J. Am. Chem. Soc.*, **95**, 8605 (1973).
169. P. H. Tedesco and H. F. Walton, *Inorg. Chem.*, **8**, 932 (1969).
170. S. Mukherjee and N. S. Rawat, *J. Ind. Chem. Soc.*, **56**, 413 (1979).
171. E. L. Muetterties, *J. Am. Chem. Soc.*, **88**, 305 (1966).
172. P. Zanella, G. Rossetto, A. Berton and G. Paolucci, *Inorg. Chim. Acta*, **95**, 263 (1984).
173. A. M. Bhandari and D. K. Kulkarni, *Curr. Sci.*, **48**, 577 (1979).
174. D. L. Plymale and W. H. J. Smith, *Inorg. Nucl. Chem.*, **30**, 2267 (1968).
175. J. P. Shukla, P. M. Ravi and M. S. Subramanian, *Thermochim. Acta*, **99**, 79 (1986).
176. L. Magon, A. Bismondo, G. Bandol and R. Portanova, *J. Inorg. Nucl. Chem.*, **35**, 1995 (1973).
177. L. G. Cilindro and C. Keller, *Radiochim. Acta*, **21**, 29 (1974).
178. H. Metivier and R. Guillaumont, *Radiochem. Radioanal. Lett.*, **10**, 27 (1972).
179. D. L. Plymale and W. H. Smith, *J. Inorg. Nucl. Chem.*, **31**, 233 (1969).
180. G. R. Choppin and W. H. Kim, *Radiochim. Acta*, **48**, 153 (1989).
181. M. J. Calhorda, R. Gomes da Costa, A. R. Dias and J. A. Martinho Simões, *J. Chem Soc., Dalton Trans.*, 2327 (1982); M. J. Calhorda, A. R. Dias, A. M. Galvao and J. A. Martinho Simões, *J. Organomet. Chem.*, **307**, 167 (1986); M. J. Calhorda, M. E. Minas da Piedade, M. S. Salema and J. A. Martinho Simões, *Organometallics*, **6**, 734 (1987); M. A. V. Ribeiro da Silva and M. D. M. C. Ribeiro da Silva, *J. Organomet. Chem.*, **393**, 359 (1990); P. M. Nunes and M. E. Minas da Piedade, *J. Chem. Thermodyn.*, **36**, 321 (2004).
182. M. Schmittel and R. Söllner, *Angew. Chem. Int. Ed.*, **35**, 2107 (1996).
183. W. V. Steele and R. D. Chirico, *Thermodynamics and the Hydrodeoxygenation of 2,3-Benzofuran*, Cooperative Agreement No. FC22-83FE60149 (NIPEP-457), IIT Research Institute, NIPEP, Bartlesville, OK 74005, 1990.
184. G. Pilcher, O. G. Parchment, I. H. Hillier, F. Heatley, D. Fletcher, M. A. V. Ribeiro da Silva, M. L. C. C. H. Ferrao, J. S. Monte and F. Jiye, *J. Phys. Chem.*, **97**, 243 (1993).
185. I. de P. R. Moreira, J. M. Bofill, J. M. Anglada, J. G. Solsona, J. Nebot, P. Romea and F. Urpí, *J. Am. Chem. Soc.*, **130**, 3242 (2008).
186. Y. Itoh, K. N. Houk and K. Mikami, *J. Org. Chem.*, **71**, 8918 (2006).
187. J. L. Thorman, I. A. Guzei, V. G. Young, Jr. and L. K. Woo, *Inorg. Chem.*, **39**, 2344 (2000).
188. E. M. Arnett, F. J. Fisher, M. A. Nichols and A. A. Ribeiro, *J. Am. Chem. Soc.*, **111**, 748 (1989).
189. D. M. Roddick and J. E. Bercaw, *Chem. Ber.*, **122**, 1579 (1989).
190. P. Hofmann, M. Frede, P. Stauffert, W. Lasser and U. Thewalt, *Angew. Chem.*, **97**, 693 (1985).
191. E. M. Arnett, J. C. Sanda, J. M. Bollinger and M. Barber, *J. Am. Chem. Soc.*, **89**, 5389 (1987).
192. P. Berno, R. Minhas, S. Hao and S. Gambarotta, *Organometallics*, **13**, 1052 (1994).
193. J. Hine and A. W. Klueppet, *J. Am. Chem. Soc.*, **96**, 2924 (1974).
194. K. B. Wiberg and R. R. Squires, *J. Chem. Thermodyn.*, **11**, 773 (1979).
195. B. J. A. Jeragh and A. El-Dissouky, *Transition Metal Chem.*, **29**, 579 (2004).
196. R. Schubert, D. V. Ramana and H.-F. Grutzmacher, *Chem. Ber.*, **113**, 3758 (1980).
197. P. C. Wilkins, M. D. Johnson, A. A. Holder and D. C. Crans, *Inorg. Chem.*, **45**, 1471 (2006).
198. L. Jansson, H. Nilsson, C. Silvegren, B. Tornell, *Thermochim. Acta*, **118**, 97 (1987).
199. K. B. P. Ruppa, S. Gambarotta, G. P. A. Yap, *Inorg. Chim. Acta*, **280**, 143 (1998).
200. T. Y. Meyer, L. R. Garner, N. C. Baenziger and L. Messerle, *Inorg. Chem.*, **29**, 4045 (1990).
201. H. S. Soo, P. L. Diaconescu and C. C. Cummins, *Organometallics*, **23**, 498 (2004).
202. M. A. V. Ribeiro da Silva, V. M. F. Morais, M. A. R. Matos and C. M. A. Rio, *J. Org. Chem.*, **60**, 5291 (1995).
203. J. Brocard, M. Mahmoudi, L. Pelinski and L. Maciejewski, *Tetrahedron*, **46**, 6995 (1990).
204. M. Uemura, T. Minami, M. Shiro and Y. Hayashi, *J. Org. Chem.*, **57**, 5590 (1992).
205. E. Mostardini, F. Calderazzo and R. Ercoli, *Chim. Ind.*, **42**, 1231 (1960); *Chem. Abstr.*, **56**, 2497 (1962).

206. G. Al-Takhin, J. A. Connor, H. A. Skinner and M. T. Zafarani-Moattar, *J. Organomet. Chem.*, **260**, 189 (1984).
207. S. P. Verevkin, B. Dogan, J. Hdrich, H.-D. Beckhaus and C. Ruchardt, *J. Prakt. Chem.*, **337**, 93 (1995).
208. A. P. Masters, M. Parvez, T. S. Sorensen and F. Sun, *Can. J. Chem.*, **71**, 230 (1993).
209. E. R. Burkhardt, J. J. Doney, R. G. Bergman and C. H. Heathcock, *J. Am. Chem. Soc.*, **109**, 2022 (1987).
210. H. S. Soo, J. S. Figueroa and C. C. Cummins, *J. Am. Chem. Soc.*, **126**, 11370 (2004).
211. V. P. R. Rao and K. V. Rao, *Curr. Sci.*, **39**, 210 (1970).
212. V. P. R. Rao and K. V. Rao, *Curr. Sci.*, **37**, 696 (1968).
213. S. J. Lord, N. A. Epstein, R. L. Paddock, C. M. Vogels, T. L. Hennigar, M. J. Zaworotko, N. J. Taylor, W. R. Driedzic, T. L. Broderick and S. A. Westcott, *Can. J. Chem.*, **77**, 1249 (1999).
214. M. Cindric, V. Vrdoljak, N. Strukan, P. Tepes, P. Novak, A. Brbot-Saranovic, G. Giester and B. Kamenar, *Eur. J. Inorg. Chem.*, 2128 (2002).
215. A. H. Khan, K. Mahmood and Z. Mehmood, *J. Chem. Soc. Pakistan*, **19**, 87 (1997).
216. J.-T. Wang, H.-Y. He, Y.-M. Xu, J. Sun and X.-F. Kong, *Heteroatom Chem.*, **9**, 169 (1998).
217. (a) A. N. Nesmeyanov, K. N. Anisimov, N. E. Kolobova and M. Y. Zakharova, *Dokl. Akad. Nauk SSSR*, **156**, 612 (1964); *Chem. Abstr.*, **61**, 29886 (1964).
(b) H. R. H. Patil and W. A. G. Graham, *Inorg. Chem.*, **5**, 1401 (1966).
(c) Y. T. Struchkov, K. N. Anisimov, O. P. Osipova, N. E. Kolobova and A. N. Nesmeyanov, *Dokl. Akad. Nauk SSSR*, **172**, 107 (1967); *Chem. Abstr.*, **66**, 119626 (1967).
218. B. E. Eichler, A. D. Phillips, S. T. Haubrich, B. V. Mork and P. P. Power, *Organometallics*, **21**, 5622 (2002).
219. T. Schmidt, S. Neis and R. Goddard, *Z. Naturforsch., B*, **50**, 315 (1995).
220. E. Iwuoha, A. R. Williams-Dottin and L. A. Hall, *Inorg. Chim. Acta*, **331**, 1 (2002).
221. O. M. Yaghi, G. Li and T. L. Groy, *J. Chem. Soc., Dalton Trans.*, 727 (1995).
222. G. A. Russell, V. Malatesta and R. A. Blankespoor, *J. Org. Chem.*, **43**, 1837 (1978).
223. W. Beck, M. J. Schweiger and G. Mueller, *Chem. Ber.*, **120**, 889 (1987).
224. M. Hojo, H. Harada, H. Ito and A. Hosomi, *J. Am. Chem. Soc.*, **119**, 5459 (1987).
225. G. Cahiez, M. Kanaan and P. Clery, *Synlett*, 191 (1995).
226. H. Nishino, V.-H. Nguyen, S. Yoshinaga and K. Kurosawa, *J. Org. Chem.*, **61**, 8264 (1996).
227. J. M. O'Connor and R. Uhrhammer, *J. Am. Chem. Soc.*, **110**, 4448 (1988).
228. L. U. Gron, K. J. Haller and A. B. Ellis, *J. Organomet. Chem.*, **323**, 207 (1987).
229. (a) C. P. Casey, J. M. O'Connor and K. J. Haller, *J. Am. Chem. Soc.*, **107**, 3172 (1985).
(b) J. M. O'Connor, R. Uhrhammer, A. L. Rheingold and D. M. Roddick, *J. Am. Chem. Soc.*, **113**, 4530 (1991).
230. P. C. Heah, A. T. Patton and J. A. Gladysz, *J. Am. Chem. Soc.*, **108**, 1185 (1986).
231. S. P. Gubin, K. I. Grandberg, E. G. Perevalova and A. N. Nesmeyanov, *Dokl. Akad. Nauk SSSR*, **159**, 1075 (1964); *Chem. Abstr.*, **62**, 43411 (1965).
232. R. H. Frazier, Jr. and R. L. Harlow, *J. Org. Chem.*, **45**, 5408 (1980).
233. Y. Ito, M. Nakatsuka and T. Saegusa, *J. Org. Chem.*, **45**, 2022 (1980).
234. L. G. Domracheva, N. V. Karyakin, M. S. Sheiman, G. V. Kamelova, V. N. Larina, O. N. Suvorova and G. A. Domrachev, *Russ. Chem. Bull.*, **48**, 1647 (1999).
235. M. Pelino, M. Tomassetti, V. Piacente and G. D'Ascenzo, *Thermochim. Acta*, **44**, 89 (1981).
236. M. Tomassetti, R. Curini, G. D'Ascenzo and G. Ortaggi, *Thermochim. Acta*, **48**, 333 (1981).
237. V. I. Sokolov, V. L. Bondareva and G. Shustov, *Metalloorg. Khim.*, **4**, 697 (1991); *Chem. Abstr.*, **116**, 21369 (1992).
238. L. Bencivenni, D. Ferro, M. Pelino and R. Teghil, *J. Ind. Chem. Soc.*, **57**, 1062 (1980).
239. P. Veya, P. G. Cozzi, C. Floriani, F. P. Rotzinger, A. Chiesi-Villa and C. Rizzoli, *Organometallics*, **14**, 4101 (1995).
240. A. N. Nesmeyanov, E. V. Leonova, N. S. Kochetkova and A. I. Malkova, *J. Organomet. Chem.*, **96**, 271 (1975).
241. N. Morita, S. Ito and T. Asao, *J. Organomet.Chem.*, **460**, 67 (1993).
242. D. Schroeder, J. Hrusak and H. Schwarz, *Ber. Bunsenges. Phys. Chem.*, **97**, 1085 (1993).
243. R. Davis and D. J. O'Reardon, *J. Ind. Chem. Soc.*, **59**, 1270 (1982).

244. J. Sandstrom and J. Seita, *Acta Chem. Scand.*, **B31**, 86 (1977).
245. J. F. Hartwig, R. A. Andersen and R. G. Bergman, *J. Am. Chem. Soc.*, **112**, 5670 (1990).
246. K. A. Azam, A. J. Deeming and I. Rothwell, *J. Chem. Soc., Dalton Trans.*, 91 (1981).
247. S. L. Bassner, E. D. Morrison, G. L. Geoffroy and A. Rheingold, *J. Am. Chem. Soc.*, **108**, 5358 (1986).
248. A. K. Hughes, K. L. Peat and K. Wade, *J. Chem. Soc., Dalton Trans.,* 4639 (1996).
249. A. K. Hughes and K. Wade, *Coord. Chem. Rev.*, **197**, 191 (2000).
250. T. R. Halbert, M. E. Leonowicz and D. J. Maydonovitch, *J. Am. Chem. Soc.*, **102**, 5101 (1980).
251. K. K. Murray, T. M. Miller, D. G. Leopold and W. C. Lineberger, *J. Chem. Phys.*, **84**, 2520 (1986).
252. J. B. Cumming and P. Kebarle, *Can. J. Chem.*, **56**, 1 (1978).
253. J. E. Bartmess, J. A. Scott and R. T. McIver, Jr., *J. Am. Chem. Soc.*, **101**, 6047 (1979).
254. K. L. Brown, M. M. L. Chu and L. L. Ingraham, *Biochemistry*, **15**, 1402 (1976).
255. Y. Y. P. Wo and K. L. Brown, *J. Organomet. Chem.*, **329**, 115 (1987).
256. W. L. Mock and C. Bieniarz, *Organometallics*, **4**, 1917 (1985).
257. J. Watanabe and J. Setsune, *Organometallics*, **16**, 3679 (1997).
258. F. Turecek, Z. Havlas, F. Maquin, N. Hill and T. Gaumann, *J. Org. Chem.*, **51**, 4061 (1986).
259. B. Bildstein, A. Hradsky, K. Ongania and K. Wurst, *J. Organomet. Chem.*, **563**, 219 (1998).
260. G. E. Herberich, A. Gaffke and H. Eckenrath, *Organometallics*, **17**, 5931 (1998).
261. W. P. Hart, D. W. Macomber and M. D. Rausch, *J. Am. Chem. Soc.*, **102**, 1196 (1980).
262. C. Cauletti, J. C. Green, M. R. Kelly, P. Powell and J. Van Tilborg, *J. Electron Spectrosc. Relat. Phenom.*, **19**, 327 (1980).
263. Y. Andrianov and A. S. Smirnov, *Metalloorg. Khim.*, **6**, 312 (1993); *Chem. Abstr.*, **120**, 134798 (1994).
264. L. J. Gazzard, W. B. Motherwell and D. A. Sandham, *J. Chem. Soc., Perkin Trans.* **1**, 979 (1999).
265. Z. B. Alfassi, D. M. Golden and S. W. Benson, *J. Chem. Thermodyn.*, 411 (1973).
266. E. Taskinen, *Tetrahedron*, **49**, 11389 (1993).
267. W. von E. Doering, L. Birladeanu, D. W. Andrews and M. Pagnotta, *J. Am. Chem. Soc.*, **107**, 428 (1985).
268. S. T. Graul, M. E. Schnute and R. R. Squires, *Int. J. Mass Spectrom. Ion Processes*, **96**, 181 (1990).
269. J. Wu and R. G. Bergman, *J. Am. Chem. Soc.,* **111**, 7628 (1989).
270. G. A. Slough, J. R. Ashbaugh and L. A. Zannoni, *Organometallics*, **13**, 3587 (1994).
271. E. B. Tjaden and J. M. Stryker, *J. Am. Chem. Soc.,* **112**, 6420 (1990).
272. T. H. Tulip and D. L. Thorn, *J. Am. Chem. Soc.*, **103**, 2448 (1981).
273. J. F. Liebman and S. W. Slayden, in *The Chemistry of Cyclobutanes* (Eds Z. Rappoport and J. F. Liebman), John Wiley & Sons, Ltd, Chichester, 2005, pp. 133–175.
274. M. D. Jones, R. D. W. Kemmitt, J. Fawcett and D. R. Russell, *J. Chem. Soc., Chem. Commun.*, 427 (1986).
275. E. B. Tjaden, K. E. Schwiebert and J. M. Stryker, *J. Am. Chem. Soc.*, **114**, 1100 (1992).
276. C. S. Chin, B. Lee, S. Kim and J. Chun, *J. Chem. Soc., Dalton Trans.*, 443 (1991).
277. J. Cámpora, C. M. Maya, P. Palma, E. Carmona, E. Gutiérrez, C. Ruiz, C. Graiff and A. Tiripicchio, *Chem. Eur. J.*, **11**, 6889 (2005).
278. K. Pihlaja and J. Heikkila, *Suom. Kemistil. B*, **42**, 338 (1969); *Chem Abstr.*, **71**, 117119 (1969).
279. A. T. Cocks and K. W. Egger, *J. Chem. Soc., Perkin Trans.* **2**, 197 (1973).
280. R. W. Hay and S. J. Harvie, *Aust. J. Chem.*, **18**, 1197 (1965).
281. E. F. Hartree, *J. Am. Chem. Soc.*, **75**, 6244 (1953).
282. M. B. Fleury and D. Fleury, *Experientia, Suppl.*, **18**, 289 (1971).
283. J. Espinosa-García and S. Dobe, *THEOCHEM*, **713**, 119 (2005).
284. V. A. Yaylayan, S. Harty-Majors and A. A. Ismail, *Carbohydr. Res.*, **309**, 31 (1998).
285. T. Murahashi and H. Kurosawa, *J. Organomet Chem.*, **574**, 142 (1999).
286. J. P. Guthrie, *Can. J. Chem.*, **56**, 962 (1978).
287. J. E. Bartmess and J. P. Kiplinger, *J. Org. Chem.*, **51**, 2173 (1986).

288. K. W. Chiu, W. Henderson, R. D. W. Kemmitt, L. J. S. Prouse and D. R. Russell, *J. Chem. Soc., Dalton Trans.,* 427 (1988).
289. N. L. Allinger and L. A. Tushaus, *J. Org. Chem.*, **30**, 1945 (1965).
290. K. B. Wiberg and G. M. Lampman, *J. Am. Chem. Soc.*, **88**, 4429 (1966).
291. A. Sella, S. Cohen and S. Hoz, *Can. J. Chem.*, **76**, 828 (1998).
292. A. Sella, S. Cohen and S. Hoz, *Can. J. Chem.*, **76**, 1108 (1998).
293. A. Imran, R. D. W. Kemmitt, A. J. W. Markwick, P. McKenna, D. R. Russell and L. J. S. Sherry, *J. Chem. Soc., Dalton Trans.*, 549 (1985).

CHAPTER 5

Synthesis of metal enolato complexes

JOSÉ VICENTE

Grupo de Química Organometálica, Departamento de Química Inorgánica, Facultad de Química, Universidad de Murcia, Apdo. 4021, 30071 Murcia, Spain
Fax: +34968367785; e-mail: jvs1@um.es; http://www.um.es/gqo/

The chemistry of metal enolates
Edited by Jacob Zabicky

I. INTRODUCTION

When a carbonyl compound capable of undergoing the keto–enol tautomerization (**1** $\rightleftharpoons$ **2**) loses the α-proton, the resulting anionic ligand is ambidentate and can coordinate to a metal via the O, **3**, or the α-C atom, **4**, depending mainly on the nature of the metal. If the cation is hard, derived from representative, early transition, lantanide or actinide element, it is oxophilic and will result in an enolato complex (**3**). If the cation is soft, the ligand will coordinate through the softer C atom to give a 2-oxoalkyl complex (**4**). Metals with an intermediate character give both complex types or show equilibria of both species in solution (Section II.C of Chapter 6[1]).

The subject of this Chapter is the synthesis of species having at least one [M]OCC group with the oxygen atom bearing a negative formal charge and an electronic structure

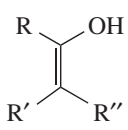

(**1**)

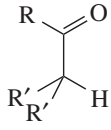

(**2**)

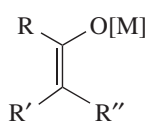

(**3**) Enolato complex

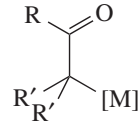

(**4**) 2-Oxoalkyl complex

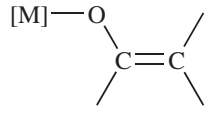

(**5**)

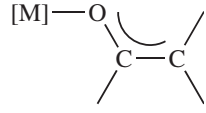

(**6**)

described by **5** or **6**, except for those prepared from other enolato complexes which will be treated in Section III of Chapter 6[1]. The synthesis of enolato complexes of B, Si, Ge, P, As, Sb and those with phenolato and related ligands will not be considered.

A 2-oxoalkyl complex (**4**) can act as an oxygen donor metalaligand towards another metal center M' but, provided it keeps the σ-M−C bond, the resulting species continues to be a 2-oxoalkyl complex, i.e. it can be formulated as [M]{μ-*C*,*O*-CR′R″C(=O[M′])R}. The best known example of this type of complex is the Reformatsky reagent **7**, prepared from $BrCH_2CO_2Bu$-*t* and Zn in thf, which has been structurally characterized[2]. Recently, a related complex [Zn_2{*C*,*O*-$CH_2C(O)NMe_2$}$_2$L], in which L is a dianionic tetradentate ligand, has been prepared by reaction of [Zn_2Ph_2L] with $AcNMe_2$[3]. In these complexes electron delocalization over the CCO moiety is difficult to accept, considering the known structural parameters. These reagents are dimeric, e.g. **7**, except in strongly polar solvents where they are monomeric. Therefore, in the solid state and in solution, complexes with μ-*C*,*O*-CR′R″C(O)R ligands are not actually enolato but 2-oxoalkyl complexes. Related palladium complexes have also been reported[4,5].

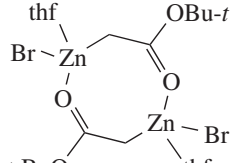

(**7**)

Empirical observations and calculations suggest that some 2-oxoalkyl complexes rearrange to *O*-bonded structures in solution (Section II.C, Chapter 6)[1,6]. This is probably the reason why many authors still name species [M]−$CH_2C(O)R$ as *C*−enolato complexes, although it is both incorrect and confusing.

As the nature of most enolato complexes in solution is strongly dependent on the solvent and it is not always well established, and the enormous amount of enolato complexes reported exceeds the limits assigned to this chapter, we have restrained its content to the synthesis of isolated, mainly fully characterized, enolato complexes.

The synthesis of metal enolato complexes will be presented in sections according to the type of reagent supplying the oxygen atom of the enolato ligand and in each section the different types of metals will be considered separately.

The following abbreviations are used in the chapter. Unless otherwise stated, the diketonato ligands are assumed to be *O*,*O*-dicoordinated.

acac	acetylacetonato	LTMP	lithium 2,2,6,6-tetramethylpiperidide
cod	1,5-cyclooctadiene		
DBU	1,8-diazabicyclo(5.4.0)undec-7-ene	Me_6acac	1,1,1,3,3,3-hexamethyl-acetylacetonato
dik	β-diketonato	nbd	norbornadiene
dme	1,2-dimethoxyethane	phen	1,10-phenanthroline
dpk	diphenylketene	py	pyridine
dppe	1,2-bis(diphenylphosphino) ethane	tmeda	*N*,*N*,*N*′,*N*′-tetra-methylethylenediamine
F_3acac	1,1,1-trifluoroacetylacetonato	TMP	2,2,6,6-tetramethylpiperidide
F_6acac	1,1,1,3,3,3-hexafluoro-acetylacetonato	Tol	4-tolyl (unless Tol-2 is stated)
		$Tp^{Me,Me}$	hydrotris(3,5-dimethyl-pyrazolyl)borate
HMDS	hexamethyldisilazanide		
HMPA	hexamethylphosphoramide	trimeda	*N*,*N*,*N*′-trimethyl ethylenediamine
LDA	lithium diisopropylamide		
LHMDS	lithium hexamethyldisilazanide	Xyl	2,6-dimethylphenyl

II. SYNTHESIS FROM KETONES, ALDEHYDES AND ESTERS

The most general and well-known methods for the synthesis of metal enolato complexes involve the use of the conjugated acid of the enolato ligand, i.e. the corresponding ketone, aldehyde or ester. However, although the enolato ligand is usually regarded as the result of the deprotonation of these compounds, this path (Section II.A) is only one of the possible ways to generate it (Sections II.B and II.C).

A. Deprotonation and Transmetalation Reactions

This method consists in the generation of the enolato ligand by deprotonation of the corresponding carbonyl compound RC(O)CHR′R″ in the presence of a metal (M) salt or complex. However, frequently the deprotonating agent is a compound of a different metal, M′X (M′ = alkali, alkaline-earth, Tl(I), etc., X = amide, hydride, acetate, etc.). In this case, the synthesis of the desired complex is a one-pot, two-step process consisting of [M′]−OC(=CR′R″)R formation followed by transmetalation of the enolato ligand from [M′] to [M].

1. Enolato complexes from monoketones

a. Group 1 elements. Monoketone enolates are very important reagents in a wide variety of organic processes such as aldol and Michael additions, alkylations, acylations, etc.[7]. Most of the metal enolates employed in organic synthesis are alkali metal derivatives, particularly lithium, sodium or potassium enolates, which are easily obtained by reacting the corresponding ketone with metal derivatives of sterically hindered amides such as LDA, LTMP and Li, Na or K derivatives of HMDS in thf. The structure, synthesis and properties of lithium enolates[8] and the structure and reactivity of alkali metal enolates have been reviewed[9].

Although it is usual to represent the alkali and alkaline-earth derivatives as MOC(=CRR′)R′, i.e. as they were mononuclear metal enolates (**3**), they are actually dinuclear, tetranuclear or hexanuclear aggregates in the solid state and in solution through bridging

enolato ligands[8]. The exceptions are a few potassium derivatives $[K(L_n)]\{OC(=CHR)R'\}$ (L_n = crown ether, R = H, Me, R′ = Ph)[10] obtained from KH, the crown ether and acetophenone or propiophenone in thf, in which the metal-to-ligand interaction is mainly ionic[10].

The aggregation extent of lithium enolates in the solid state depends mainly on the solvent and the ligands used for their isolation. Thus, the lithium enolato complex of AcBu-*t* crystallizes in the presence of trimeda as dimeric $[Li_2\{\mu\text{-}OC(=CH_2)Bu\text{-}t\}_2(trimeda)_2]$ (type **8**)[11], as tetrameric $[Li_4\{\mu_3\text{-}OC(=CH_2)Bu\text{-}t\}_4(thf)_4]$ in thf (type **9**)[12] or as hexameric $[Li_6\{\mu_3\text{-}OC(=CH_2)Bu\text{-}t\}_6]$ in heptane (type **10**, without L)[13,14]. Also type **8** are the tmeda complexes of the lithium enolates of $EtCO_2Bu\text{-}t$ and $i\text{-}PrCO_2Bu\text{-}t$[15], the trimeda complex of the enolate of *N*,*N*-dimethylpropionamide[11] and the thf complex of 8-(dimethylamino)-8-heptafulvenolato[16]. Type **9** is also the py complex $[Li_4\{\mu_3\text{-}O(=CH_2)Bu\text{-}t\}_4(py)_4]$[17], obtained by reacting AcBu-*t* with LHMDS and an excess of py. If a 1:1:0.65 molar ratio is used, the resulting complex $[Li_4\{\mu_3\text{-}O(=CH_2)Bu\text{-}t\}_4(py)_3]$ has a similar structure but with one tricoordinated lithium atom[17].

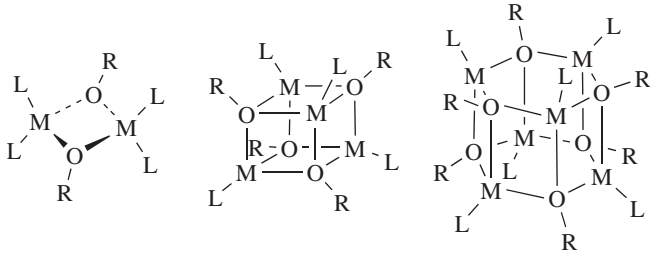

(**8**) (**9**) (**10**)

In some cases, dinuclear enolato complexes bear both enolato and non-enolato bridging ligands. Thus, AcBu-*t* reacts with LHMDS and dme to afford $[Li_2\{\mu\text{-}O(=CH_2)Bu\text{-}t\}\{\mu\text{-}N(SiMe_3)_2\}(dme)_2]$. Similarly, $i\text{-}PrCO_2Bu\text{-}t$ reacts with one equivalent of NaHMDS and tmeda to give the dimer $[Na_2\{\mu\text{-}OC(=CMe_2)OBu\text{-}t\}(\mu\text{-}NSiMe_3)(tmeda)_2]$[18] and $i\text{-}Pr_2C(O)$ reacts with a mixture of *n*-BuBr, $i\text{-}Pr_2NH$, tmeda and LiBu-*n* or with 2,2,6,6-tetramethylpiperidinium bromide or iodide, tmeda and LiBu-*n* to give $[Li_2\{\mu\text{-}OC(=CMe_2)Pr\text{-}i\}(\mu\text{-}X)(tmeda)_2]$ (X = Br, I)[19].

Co-crystallization of a mixture of LiBr, LHMDS, $LiOC(=CH_2)Bu\text{-}t$ and tmeda in a 1:1:1:2 molar ratio gives **11**[20]. Similarly, a mixture of MOBu-*t* and $M'\{O(=CH_2)Bu\text{-}t\}$ or of M′OBu-*t* and $M\{O(=CH_2)Bu\text{-}t\}$ (M = Li, M′ = K) in the presence of thf yields a unique aggregate of composition $[Li_4K_5(OBu\text{-}t)_4\{\mu\text{-}O(=CH_2)Bu\text{-}t\}_4(OH)(thf)]$[21].

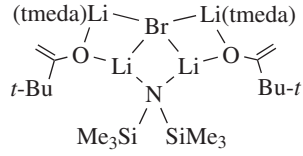

(**11**)

12 and **13** reacts with LDA to give **14**[22] and **15**[23], respectively. Reaction of an equimolar mixture of sodium diisopropylamide and LDA with two equivalents of AcBu-*t* affords crystals of **16**[24].

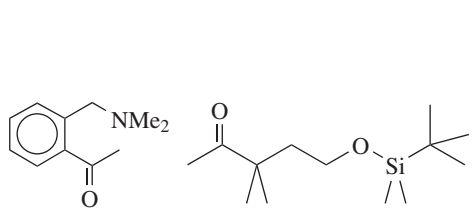

(**12**) (**13**)

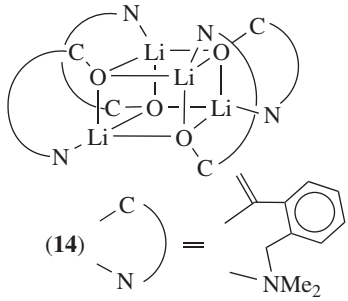

(**14**)

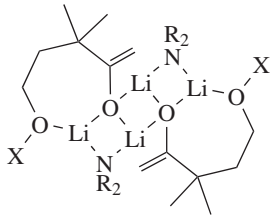

(**15**) R = *i*-Pr, X = $SiMe_2Bu$-*t*

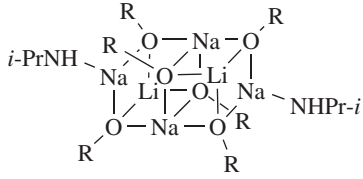

(**16**) R = $C(=CH_2)Bu$-*t*

The reaction of AcBu-*t* with NaHMDS gives the tetranuclear compound [Na{μ_3-$O(=CH_2)Bu$-*t*}$(AcBu$-*t*$)]_4$, a type **9** structure like that of its thf lithium analogue. However, the potassium complex crystallizes with thf and its structure is hexameric type **10** [K_6{μ_3-$OC(Bu$-*t*$)=CH_2$}$_6(thf)_6$][14].

AcMes has been chosen as a model ketone for deprotonation since its enolato complexes have excellent crystallization properties with a variety of cations. Thus, the reaction of AcMes with KHMDS in PhMe gives the type **9** complex [K_4{μ_3-$OC(=CH_2)Mes$}$_4$ $(PhMe)_4$] (type **9**)[25] and with NaBu-*n* and tmeda leads to the sodium enolato complex [Na_2{μ-$OC(=CH_2)Mes$}$_2(tmeda)_2$] (type **8**)[26].

b. Group 2 and 12 elements. The reaction of AcMes with $Ca(HMDS)_2$ in Et_2O/hexane affords **17**[25] and with $Mg(HMDS)_2$ in hexane gives **18**[27]. The latter result is in contrast with that reported in the reaction with one equivalent of PhC(O)Et in thf, which gives **19**. This, in turn, is in contrast with the reaction between the same ketone and $Ca(HMDS)_2$, which gives **20**[28]. If this reaction is carried out in the presence of one equivalent of $Me_2N(CH_2)_2N(Me)(CH_2)_2NMe_2$ the mononuclear complex **21** is obtained[28]. $Mg(HMDS)_2$ reacts with substoichiometric amounts of PhC(O)Et at room temperature to form a 74:26 mixture of the enolates *E*- and *Z*-**22**[29]. [MgBr{N(Pr-*i*)$_2$}] reacts with AcBu-*t* and HMPA to give [MgBr{μ-$OC(=CH_2)Bu$-*t*}$(HMPA)]_2$[30].

Complex **23** is an enolising reagent toward aliphatic ketones such as $(Bn)_2CO$, $AcCHPh_2$ or camphor, giving enolato complexes **24**[31].

The syntheses of mixed Na/Mg metal enolato complexes **25**–**27** (RO = $O(=CH_2)Mes$) have been reported by mixing the metal alkyl reagents NaBu-*n* and Mg(*n*-Bu)$_2$ in the desired stoichiometry with the required amount of AcMes and tmeda[26].

Mixtures of MM′$(HMDS)_3$ (M = K, M′ = Ca[25], Zn[32]; M = Na, M′ = Zn[32]) and $K_2Ca(HMDS)_4$[25] with AcMes give **28**–**30** (X = $OC(=CH_2)Mes$), respectively. The special synergic reactivity of these heterobimetallic ate compounds MM′$(HMDS)_n$ has been reviewed[33].

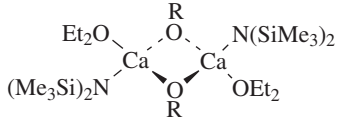

(**17**) R = C(=CH2)Mes

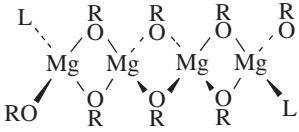

(**18**) L = Ac(Mes), R = C(=CH_2)Mes

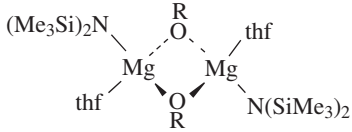

(**19**) R = C(=CHMe)Ph

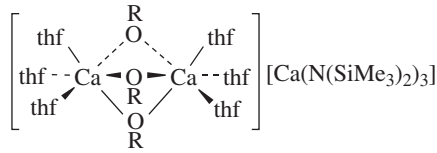

(**20**) R = C(=CHMe)Ph

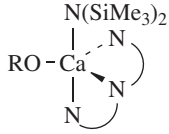

(**21**) R = C(=CHMe)Ph

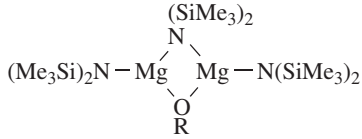

(**22**) R = C(=CHMe)Ph

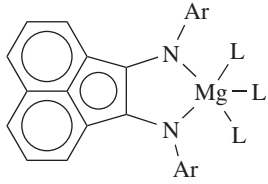

(**23**) Ar = 2,6-(*i*-Pr)$_2$C$_6$H$_3$, L = thf, py

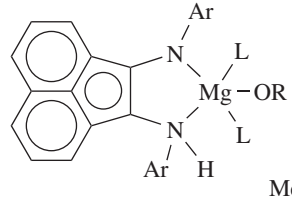

(**24**) R = C(=CHPh)Bn, C(=CH_2)CPh$_2$,

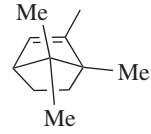

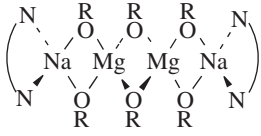

(**25**)

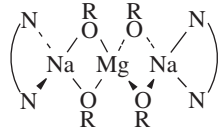

(**26**)

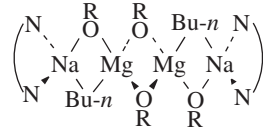

(**27**)

The deprotonation of a series of ketones by [$Zn_2(Ph)_2$L], where L^{2-} represent various bis(amidoamine) ligands, gives the corresponding enolato complexes. Their crystal structures show some of them to be dimers [Zn_2{OC(=CR_2)$_2$R′}$_2$L] (R = Me, R′ = *i*-Pr; R = H, R′ = C_6Me_5)[34]. Li enolates of *N*,*N*-disubstituted glycine esters $MeO_2CCH_2N(R)R'$ react with [Zn(Et)Cl] to give **31**[35].

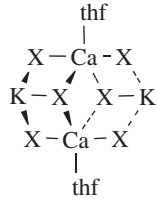

(**28**)

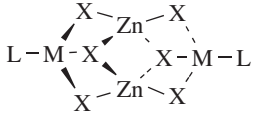

(**29**) (**a**) M = K, L = PhMe
(**b**) M = Na, L = Ac(Mes)

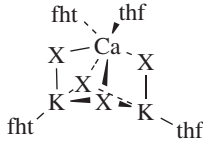

(**30**)

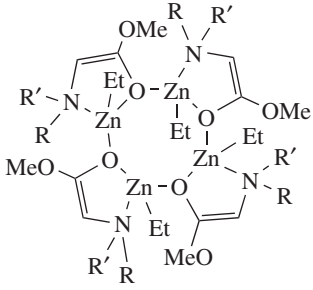

(**31**) R = Me, R′ = Me, *t*-Bu; R = R′ = Et

c. Group 13 elements. Trialkylaluminum compounds react with ketones leading to adduct formation, alkylation, reduction or enolization products, depending on the ketone and the alkyl group attached to aluminum. In particular, the reaction of AlR_3 (R = Me, Ph) with ketones AcAr (Ar = Mes, $C_6H_2(i\text{-Pr})_3$-2,4,6) gives $[AlR_2\{\mu\text{-OC}(=CH_2)Ar\}]_2$[36].

N,*N*-disubstituted glycine esters $R'_2NCH_2CO_2R''$ react with LDA to give complexes **32**. The complex with R′ = R″ = Et has a type **10** hexagonal prismatic structure, in which the chelating enolato ligand plays the role of both OR and L[37]. **32** transmetalates the enolato ligand to alkyl Al compounds $[AlR_2Cl]_2$ (R = R′ = R″ = Me, Et; R = R′ = Et, R″ = *t*-Bu; R = R″ = Me, R′ = Me, *t*-Bu) to give **33** (1:1 molar ratio) or **34** (1:2 molar ratio)[38].

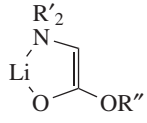

(**32**)

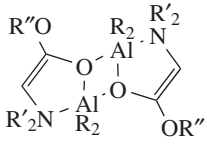

(**33**)

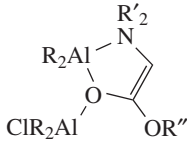

(**34**)

d. Group 4 elements. The reaction of $[Ti(\eta^5\text{-Cp})_2Cl_2]$ with potassium enolates of AcAr (Ar = An-2, Mes) gives the corresponding metal enolato complexes $[Ti(\eta^5\text{-Cp})_2\{OC(=CH_2)Ar\}Cl]$ or $[Ti(\eta^5\text{-Cp})_2\{OC(=CH_2)An\text{-}2\}_2]$ depending on the reagents' molar ratio[39]. $[Ti\{\eta^5,N\text{-}C_5Me_4(SiMe_2NBu\text{-}t)\}Cl(X)]$ reacts with the ester enolate $LiOC(=CMe_2)OPr\text{-}i$ to give $[Ti\{\eta^5,N\text{-}C_5Me_4(SiMe_2NBu\text{-}t)\}\{OC(=CMe_2)OPr\text{-}i\}(X)]$ (X = Cl, Me)[40]. Some enolizable ketones RR′CHC(O)R″ react with $[Ti(\eta^5\text{-Cp})_2(=CH_2)]$, formed *in situ* by

thermolysis of [Ti(η^5-Cp)$_2$Me$_2$], to give regio- and stereoselectively the enolato complexes [Ti(η^5-Cp)$_2$Me{OC(=CRR′)R″}][41].

LiOCH=CMe$_2$, prepared from LiMe and Me$_3$SiOCH=CMe$_2$, reacts with [M(η^5-Cp)$_2$XCl] (M = Ti, Zr; X = Me, Cl) to render the corresponding enolato complexes [M(η^5-Cp)$_2$Me(OCH=CMe$_2$)] and [M(η^5-Cp)$_2$(OCH=CMe$_2$)$_2$][42]. Similarly, [{Zr(η^5-Cp)$_2$Cl}$_2$(μ-O)] reacts with two equivalents of LiOC(=CMe$_2$)OR (R = *t*-Bu, Me) to give [{Zr(η^5-Cp)$_2$\{OC(=CMe$_2$)OR\}}$_2$(μ-O)][43]. The stable enols Mes$_2$C=C(R)OH react with [Ti(η^5-Cp)$_2$Cl$_2$] and NaH to give [Ti(η^5-Cp)$_2$\{OC(=C(Mes)$_2$)OR\}$_2$] (R = H, Ph)[44].

The K$^+$ Li$^+$ salt of **35** reacts with [Zr(η^5-Cp)$_2$Cl$_2$] to give **36**[45].

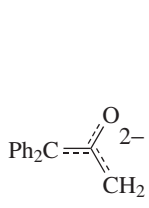

(**35**)

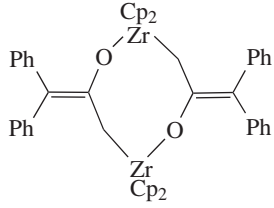

(**36**)

2-Acetylpyridine reacts with KH and [MCl$_2$(NEt$_2$)$_2$] to afford complexes **37** which transmetalate the enolato ligand to [AlMe$_3$]$_2$, affording complex **38**[46].

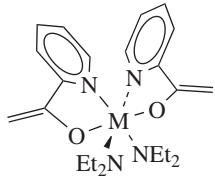

(**37**) M = Ti, Zr

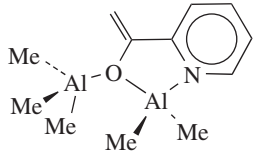

(**38**)

The Li$^+$ Na$^+$ salt of **39**, prepared by reacting NaCp with AcOEt and LDA, reacts with [MCl$_2$(NR$_2$)$_2$] (1:1) to give complexes **40**[47].

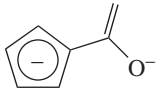

(**39**)

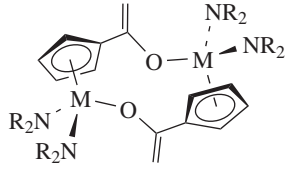

(**40**) M = Ti, R = Me; M = Zr, R = Et

Potassium complex **41** reacts with one equivalent of [M(η^5-Cp)$_2$Cl$_2$] to afford **42**[48]. Complex **43** adds KOC(=CH$_2$)Ph to give the heteronuclear complex **44**[49].

Complexes bearing ligands that can be protonated react with ketones without the necessity of a base. Thus, [Zr(η^5-Cp*)$_2$(=E)(py)] (E = O, S, Se, Te) reacts with AcR (R = Me, *t*-Bu, Ph) to give complexes [Zr(η^5-Cp*)$_2$(EH)\{OC(=CH$_2$)R\}][50]. Similarly, the

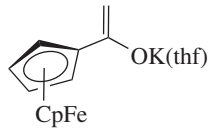

(**41**)

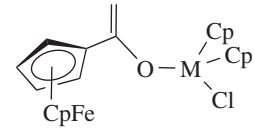

(**42**) M = Ti, Zr

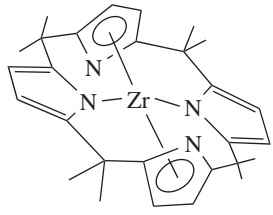

(**43**)

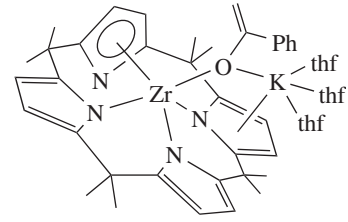

(**44**)

imido complex [Zr(η^5-Cp)$_2$(=NBu-*t*)(thf)] reacts with moderately hindered ketones to afford [Zr(η^5-Cp)$_2$(NHBu-*t*){OC(=CR′R″)R}] (R = R′ = (CH$_2$)$_3$CHBu-*t*, R″ = H; R = *t*-Bu, R′ = R″ = H, Me[51]). Complexes **45** (R = *i*-Pr, *c*-Hex) react with diazo compounds AcC(=N$_2$)CO$_2$Et to give complexes **46**, probably through **47**[52]. Enolizable ketones RC(O)CH$_2$R′ react with [Ti(η^5-Cp*)$_2$(=C=CH$_2$)] to give [Ti(η^5-Cp*)$_2$(CH=CH$_2$){OC(=CHR′)R}][53].

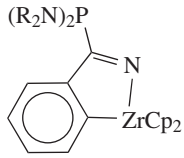

(**45**)

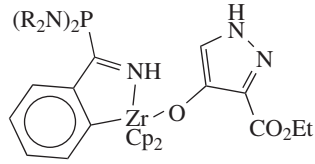

(**46**)

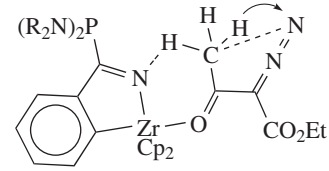

(**47**)

Equimolar amounts of LDA and **48** give the corresponding lithium enolato complex which, by means of a Claisen-type condensation, leads to **49**, which, in turn, reacts with [Zr(η^5-Cp)$_2$(Me)Cl] to give **50**[54].

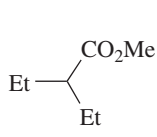

(**48**)

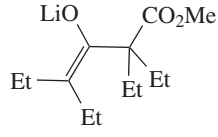

(**49**)

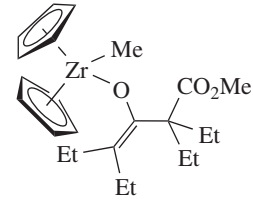

(**50**)

The reaction of the lithium phosphinoenolato complex [Li{μ-OC(=CHR)PPh$_2$}(thf)$_2$] with [Zr(η^5-Cp)$_2$Cl$_2$] leads to the corresponding complexes [Zr(η^5-Cp)$_2$(OC(=CHR)PPh$_2$}Cl] (R = H, Me)[55].

Reaction of **51** with lithium isopropylisobutyrate produces complex **52**[56]. Similarly, the addition of $LiOC(=CMe_2)OMe$ to $[Ti(\eta^5\text{-}Cp)_2Cl_2]$ gives the enolato complex $[Ti(\eta^5\text{-}Cp)_2Cl\{OC(=CMe_2)OMe\}]$[57] and complexes $[M(\eta^5\text{-}Cp)_2Cl_2]$ (M = Ti, Zr, Hf) react with two equivalents of $Li\{OC(=CH_2)Me\}$ to give $[M(\eta^5\text{-}Cp)_2\{OC(=CH_2)Me\}_2]$[58]. Deprotonation of $AcNPh_2$ with LDA, followed by reaction with $[Zr(\eta^5\text{-}Cp)_2Cl_2]$, gives the complex $[Zr(\eta^5\text{-}Cp)_2Cl\{OC(=CH_2)NPh_2\}]$[59].

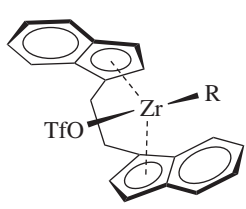

(**51**) R = Me, TfO

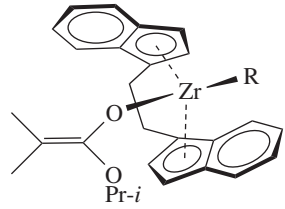

(**52**) R = Me, $OC(=CMe_2)OPr\text{-}i$

Complexes $[M]-C(=CR_2)OLi$, obtained by treating an alkyllithium compound with an acyl complex, react with electrophiles to give new acyl complexes that can be used in organic synthesis[60] or to transmetalate the metalaenolato ligand to another metal center [M′] to give $[M]-C(=CR_2)O[M']$. Thus, addition of LiBu-*n* to [Fe]Ac ($[Fe] = Fe(\eta^5\text{-}Cp)(CO)(PPh_3)$) gives $[Fe]\{C(=CH_2)OLi\}$, which reacts with $[Zr(\eta^5\text{-}Cp)Cl_2]$ to give $[Fe]\{C(=CH_2)O[Zr(\eta^5\text{-}Cp)Cl]\}$[61].

e. Group 5, 6 and 7 elements. Treatment of $[TaMe_3Cl_2]$ with two equivalents of KOC(ad)(Mes) (ad = adamanten-2-yl) leads to $[TaMe_3\{OC(ad)(Mes)\}_2]$[62]. Similarly, reaction of $[MoCl_4(thf)_2]$ with four equivalents of KOC(ad)(Mes) gives $[Mo\{OC(ad)(Mes)\}_4]$[63]. The complex $[M\{\eta^3\text{-}CH_2C(R)CH_2\}Cl(CO)_2(phen)]$ reacts with one equivalent of $KOC(=CH_2)Ar$ to give $[M\{OC(=CH_2)Ar\}\{\eta^3\text{-}CH_2C(R)CH_2\}(CO)_2(phen)]$ (M = Mo, R = Me, Ar = Ph, Naph; R = H, Ar = Naph; M = W, R = H, Ar = Ph)[64].

The reaction of **53** with **54** gives the dimetalafuran complex **55** (Section IV.E)[65].

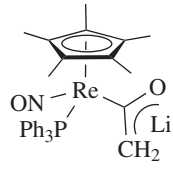

(**53**)

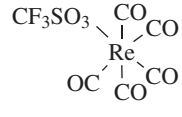

(**54**)

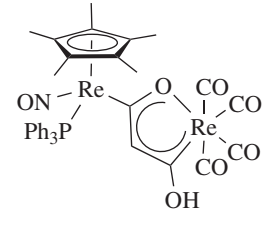

(**55**)

f. Group 8 elements. The reaction of $FeBr_2$ with **56** in the presence of KH leads to **57**[66].

Benzyne complex **58** (L = PMe_3) reacts with AcR′ (R′ = Me, Ph) to afford the cyclometalated complex **59** plus methane or benzene, respectively[67], and with Me_3NHCl and $KOC(=CH_2)Me$ to give **60a**, for which intermediate **61a** has been isolated. Complex **60a** rearranges in solution at room temperature to give the oxametalacyclobutane **62**, which at 45 °C leads to **59** and methane, providing strong evidence that **60a** and **62** are intermediates in the reaction of **58** with AcMe to give **59**[68,69]. Furthermore, **62** reacts with

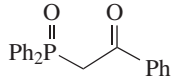

(**56**)

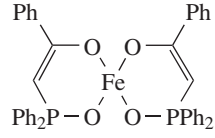

(**57**)

AcPh to give also **59**[68]. Complexes **61a**–**c** react with KOC(=CH_2)R′ to afford enolato complexes **60a**, **60b**, **60c**[70]. The reaction of **61d** with KOC(=CH_2)CH_2Bu-*t* gives **63**, containing a dianionic enolato ligand[69,70].

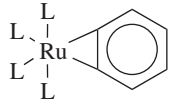

(**58**)

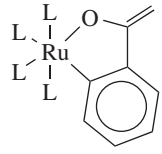

(**59**)

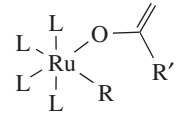

(**60**) (**a**) R = Ph, R′ = Me
(**b**) R = Me, R′ = H, Bu-*t*
(**c**) R = H, R′ = Me

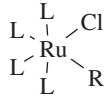

(**61**) (**a**) R = Ph
(**b**) R = Me
(**c**) R = H
(**d**) R = OAc

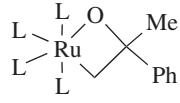

(**62**)

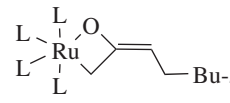

(**63**)

g. Group 9 elements. Potassium enolates react with *trans*-[RhX(CO)$(PR_3)_2$] (X = Cl, R = Me; X = F, R = Ph) to afford the corresponding enolato complexes *trans*-[Rh{OC(=CHR″)R′}(CO)$(PR_3)_2$] (R = R″ = Me, R′ = Ph, Mes, *t*-Bu; R′ = Ph, R″ = H, R = Me, Ph). $AcC_6H_4NO_2$-4 replaces the less acidic EtC(O)Bu-*t* from [Rh{OC(=CHMe)Bu-*t*}(CO)$(PMe_3)_2$] to give [Rh{OC(=CH_2)$C_6H_4NO_2$-4}(CO)$(PMe_3)_2$][71]. Treatment of **64** (L = PPh_3) with NaOMe affords the acyl enolato complex **65**[72].

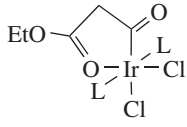

(**64**)

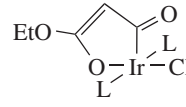

(**65**)

h. Group 10 elements. [Fe]{$C(O)CH_2PPh_2$} ([Fe] = Fe(η^5-Cp)(CO)(PPh_3)) reacts with LiBu-*n* and $NiCl_2$ to afford the trinuclear phosphinoenolato complex *cis*-[Ni{*O*,*P*-OC(=$CHPPh_2$)[Fe]}$_2$][73].

Complexes **66**–**68** react with KOBu-*t* to give **69**, **70**[74] and **71**[75], respectively.

[NiMe(μ-OMe)$(PMe_3)]_2$ causes double deprotonation of 2-formylketones **72**–**74** to give CH_4, MeOH and the corresponding acylenolato complexes **75**[76] which (i) give

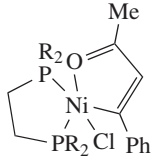

(**66**) R = *i*-Pr

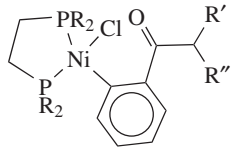

(**67**) R = *i*-Pr, R′ = R″ = H
R = *i*-Pr, R′ = Me, R″ = H, Me

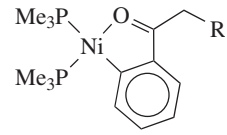

(**68**) R = H, Me

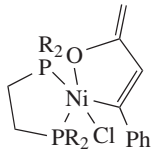

(**69**) R = *i*-Pr

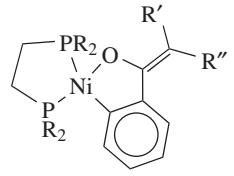

(**70**) R = *i*-Pr, R′ = R″ = H
R = *i*-Pr, R′ = Me, R″ = H, Me

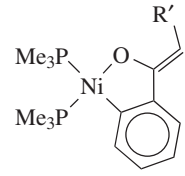

(**71**) R′ = H, Me

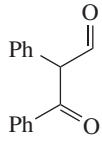

(**72**)

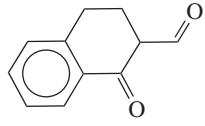

(**73**)

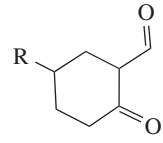

(**74**) R = H, Ph, Bu-*t*

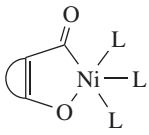

(**75**)

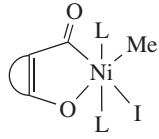

(**76**)

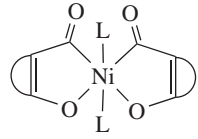

(**77**)

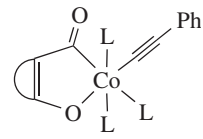

(**78**)

Ni(IV) complexes **76** or **77** by oxidative addition of MeI or I_2 (alternatively $C_2H_4I_2$ or CH_2I_2), respectively, or (ii) transmetalate the enolato ligand to the Co(I) complex $[Co(C{\equiv}CPh)(PMe_3)_4]$ leading to Co(III) complexes **78** and $[Ni(PMe_3)_4]$[77].

Imidazolium salts **79** (Ar = Mes, $C_6H_2R'_2$-2,6-R″-4, R′ = *i*-Pr, R″ = H) react (i) with $[Ni(cod)_2]$, PhCl, py and two equivalents of NaHMDS at −195 °C to afford **80**, which is active for linear polyethylene and polypropylene synthesis[78], or (ii) when Ar = Mes, with $[Pd(\eta^3\text{-allyl})(\mu\text{-Cl})]_2$ and KOBu-*t* to afford **81**[79].

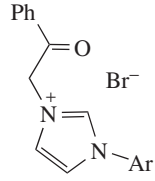

(**79**)

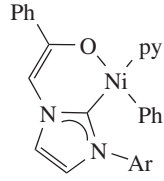

(**80**)

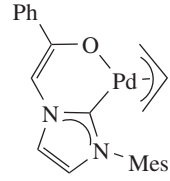

(**81**)

The 2-oxoalkyl polymer **82**[5] reacts with isocyanides RNC to give **83**, probably through the insertion product **84**, followed by a tautomerization[80].

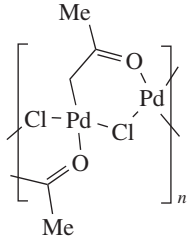

(**82**)

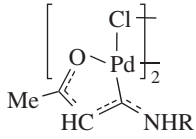

(**83**) R = *t*-Bu, Xyl-2,6

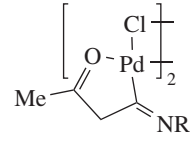

(**84**)

Pd(I) complex **85** has been prepared by reacting $Me_3SiOC(=CH_2)Vi$ and Et_3N (i) with **86** and $[Pd_2(dba)_3]$•dba (dba = dibenzylidenacetone) or (ii) with **87**[81].

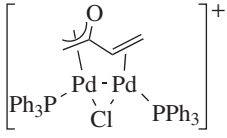

(**85**)

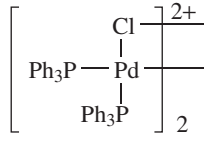

(**86**)

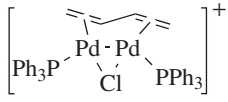

(**87**)

i. Rare-earth elements. Addition of ROH to a mixture of $Ph_2C{=}O$ and Sm or Yb in thf/HMPA affords the enolato complexes **88**[82].

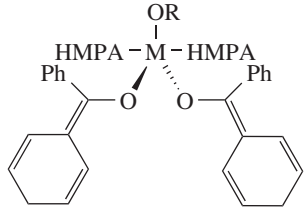

(**88**) (**a**) M = Sm, R = C_6H_2Me-4-(*t*-Bu)$_2$-2,6
(**b**) M = Sm, R = C_6H_3(*t*-Bu)$_2$-2,6
(**c**) M = Yb, R = C_6H_2Me-4-(*t*-Bu)$_2$-2,6

Reaction of $Li(OCH{=}CH_2)$ with $[Ln_2(\eta^5\text{-}C_5H_4R)_4(\mu\text{-}Cl)_2]$ (R = H, Me[83], $SiMe_3$[84]; Ln = Lu, Yb[83], Y[83,84]) leads to $[Ln_2(\eta^5\text{-}C_5H_4R)_4(\mu\text{-}OCH{=}CH_2)_2]$.

2. Enolato complexes from diketones and their derivatives

In this section we will deal with complexes obtained by deprotonation or transmetalation from compounds containing two carbonyl groups. Although derivatives of aldehydes and esters are also included, they all will be addressed as diketonato. Various organic parent compounds can be distinguished: (i) the most important are α-, β- and other diketones; (ii) compounds in which one or two of the keto forms are less important than the enol

form, therefore, they are better named ketoenols (e.g. tropolone) or enediols (e.g. ascorbic acid); (iii) ketoimines or thioketones, considered as derived from diketones.

a. α-Diketonato complexes. In this family of enolato complexes are included species that actually or formally can be derived from an α-diketone. The most important ones are those derived from cyclic α-hydroxy ketones such as the tropolones (**89a,b**), the 3-hydroxy-4-pyrones (**90a**–**f**) (e.g. maltol (**90a**), kojic acid (**90d**) or allixin (**90e**)), 3-hydroxy-4-pyridinones (**91**), the 3-hydroxy-2-pyridinones (**92**), the hydroxyquinones (**93**, **94**), etc., which find use as complexing agents[85–87] and, along with their metal complexes, have actual or potential applications in medicine[88–97] and as functional materials[87]. In these compounds, the α-diketone tautomeric form is less important than the corresponding α-hydroxyketone form[96,98].

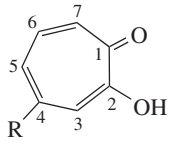

(**89**) (**a**) R = H (tropolone)
(**b**) R = *i*-Pr
(hinokitiol or thujaplicin)

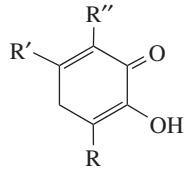

(**90**) (**a**) R = Me, R′ = R″ = H (maltol)
(**b**) R = R″ = H, R′ = Me (isomaltol)
(**c**) R = Et, R′ = R″ = H (ethylmaltol)
(**d**) R = R″ = H, R′ = CH_2OH (kojic acid)
(**e**) R = Me, R′ = $(CH_2)_4Me$,
R″ = OMe (allixin)
(**f**) R = Ph, R′,
R″ = C_6H_4-1,2 (3-hydroxyflavone)

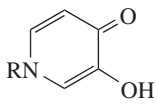

(**91**)

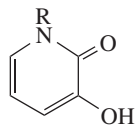

(**92**)

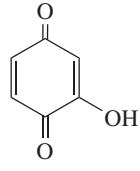

(**93**)

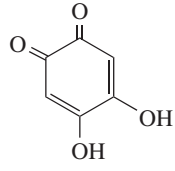

(**94**)

i. Tropolonato complexes. Upon deprotonation, tropolones can be used as bidentate five-membered *O*,*O*-enolato chelates to give tropolonato complexes [M](tropo)$_n$ (**95**). Thus, neutral, cationic and anionic complexes of most elements have been isolated by reacting tropolone or its Li, Na or Ag salt with the metal or its halide, nitrate, oxide, acetate,

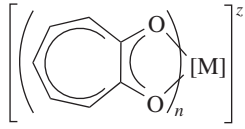

(**95**) n = 1–5, z = 0, ± 1

etc. Some anionic complexes have also been prepared by reacting tropolonato complexes with alkali tropolonates. Thus, [M(tropo)$_4$] (M = Th, U, tropo = *O*,*O*-tropolonato ligand and ring-substituted derivatives)[99–102] reacts with Q(tropo) to give Q[M(tropo)$_5$] (Q = Li, Na, K)[100]; in the case of [U(tropo)$_4$] the Li salt is required. However, attempts to prepare [M(tropo)$_5$]$^-$ with other cations (M = Zr, Hf, Ce) were unsuccessful[100]. Similarly, [M(tropo)$_3$][99] (M = Sc, Y, In and rare-earth trivalent ions) react with Na(tropo) in polar media to form Na[M(tropo)$_4$]. Attempts to extend this chemistry to other trivalent ions (Fe(III), Ga(III), Rh(III)) failed[99, 103].

Some of the isolated simple tropolonato complexes grouped by their charge, metal oxidation state and stoichiometry are listed in Tables 1–3.

Other tropolonato complexes of Mo[125], Re[126], Ru[127, 128], Co[129], Rh[130], Ir[131], Ni[132], Pd[133], Cu[123, 132] and Sn[134] have also been isolated.

ii. Complexes derived from hydroxpyrones, hydroxypyridinones and related species. Some of the isolated complexes of cyclic α-hydroxy ketones **90**–**92** are listed in Table 4.

TABLE 1. Neutral tropolonato complexes

Metal oxidation state	Stoichiometry	Examples
M(I)	[M(tropo)]$_2$	[Ag$_2$(tropo)$_2$][104]
M(II)	[M(tropo)$_2$]	M = Be, Mg, Ca, Sr, Ba, Mn, Fe[105], Cu[105, 106], Co, Ni[105, 107], Pd[105, 108], Zn[89, 105], Ge[109], Pb[105], Hg[105], Sn[89]
M(III)	[M(tropo)$_3$]	M = Al, Ga[103, 110], In, Tl[103], Bi[105], Ti[99], Mn[111], Rh[99], Ir[112], Sc[99, 113], La[87, 103, 105], Eu[87, 103, 105, 114], Y, Ce, Tb[87, 99, 105, 114], Pr, Nd, Dy, Tm[99], Sm[99, 115], Yb[87, 99], Gd[87, 99, 105, 114], Ho[87, 99, 105], Er[87, 99, 105], Lu[99, 105]
M(III)	[M(tropo)$_2$X]	M = Bi, X = Cl, ONO$_2$, Ph[91, 103]
M(III)	[M(tropo)R$_2$]	M = Al, R = Me, Et[116]
M(IV)	[M(tropo)$_4$]	M = Sn[99, 103, 105, 117], Pb[103], Zr, Hf[99, 110], Nb[118], Ce[99], U[100, 101], Th[99–101, 110], Pa, Np, Pu[101]
M(IV)	[M(tropo)$_3$X]	M = Sn, X = Cl[103, 105, 110], Ph[103], OH[99]; M = Zr, X = η^5-Cp[119]
M(IV)	[{M(tropo)$_3$}$_2$O]	M = Ti[99]
M(IV)	[M(tropo)$_2$XY]	M/X/Y = Sn/Cl/Cl[103, 105], Sn/Br/Br, Sn/Cl/Ph[103], Sn/Me/Me[120], Ti/Cl/Cl[99]
M(IV)	[M(tropo)X$_2$Y]	M = Sn, X = Y = Me[120], X = Me, Y = Cl[105]
M(V)	[M(tropo)$_4$X]	M = Pa, X = Cl, Br[101]; M = Ta, X = Cl[110]
M(V)	[MO(tropo)$_3$]	M = V[99, 105], Nb[99]
M(V)	[M(tropo)$_2$R$_3$]	M = Bi, R = Ph[90, 121]
M(V)	[MO(tropo)$_2$X]	M = V, Mo, X = Cl[99]
M(V)	M$_4$O$_8$(tropo)$_4$(L)$_4$]	M = Mo, L = EtOH[122]

TABLE 2. Cationic tropolonato complexes

Metal oxidation state	Type	Examples
M(II)	[M(tropo)L$_2$]X	M = Cu, L$_2$ = tmeda, X = BPh$_4$[123]
M(V)	[M(tropo)$_4$]X	M = Nb, Ta, Q = Cl, PF$_6$; M = Nb, X = I[99]

TABLE 3. Anionic tropolonato complexes

Metal oxidation state	Type	Examples
M(III)	$Q[M(tropo)_4]$	Q = H, M = Sc, Y, Tm, Yb, Lu; Q = Li, M = La, Ce; Q = Na, M = Sc, Y, La, Pr, Nd, Sm, Eu, Gd, Tb, Dy, Ho, Er, Tm, Yb, Lu, In[99,103], Bi[105]; Q = K, M = La, Pr, Nd, Sm, Eu, Gd, Tb, Dy, Ho, Er, Tm, Yb, Lu[86]; Q = NH_4, M = Dy, Ho, Tm, Yb[99,103]
	$Q_2[M(tropo)_4]_2$	Q = H, M = Sc[113,124]
M(IV)	$Q[M(tropo)_5]$	Q = Li, M = Th, Pa, U; Q = Na, K, M = Th[101]

TABLE 4. Complexes derived from hydroxypyrones, hydroxypyridinones and related species

Metal oxidation state	Examples
M(VI)	$[MO_2]^{2+}$, M = Mo[135,136], Os, U[135]
M(V)	V[137], Tc[138], Re[126,138,139]
M(IV)	Ce[140], Ti[141], $[VO]^{2+}$[94,142–144], Hf[145], Ge[146], Sn[134,146,147]
M(III)	V[95], Cr[148–150], Mn[151], Tc[152], Fe[92,93,153–155], Ru[126,128,135,156], Rh[135,157], Ir[158], Al[155,159–161], Ga[97,159], Ln[162]
M(II)	Be[163], Ca[164], Mn[165,166], Co[149,166], Ru[167], Ni[166], Pd[135,168], Pt[135,169], Cu[145,149,166,170], Zn[89,145,166,171–173], Cd[145], Hg[145,172,174], Sn[89,175], Pb[172]

These complexes have been synthesized in water, aqueous EtOH or non-aqueous solvents, by reaction of the ligand with metal halides[92,135,145,148,176,177], nitrates[160,176], sulfates[94,142,171], oxo[126] or acac[144] complexes in the absence[126,135,145,152] or the presence of a base (NH_4OH[92,176], NaOH[142,153,176], KOH[94], NaOMe[177], Et_3N[148]).

iii. Enolato complexes derived from hydroxyquinone and related species. These complexes have been prepared by reacting 2-hydroxy-*p*-quinone (**93**) or 4,5-dihydroxy-*o*-quinone (**94**) with metal acetates[178], sulfates[178,179] or nitrates[180,181], metal chlorides in the presence of NaAcO[182], oxometalates[183], or the sodium salts of the ligands with metal chlorides[184] in water or aqueous MeOH[185] or MeCN[180]. Complexes of types **96** (M = Cu[186]), **97** (M = Fe[187], Co, Ni[178], Cu[178,182,184,185], Zn[178,184,188]), **98** (M = Ag[180]), **99** (M = Ca[189], Mo[183], Y, La, Gd, Yb, Lu, Ce[181]), **100** (M = Cu[190]) and **101** (M = Hg[191], Pt[192]) have been reported.

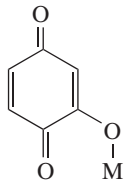

(**96**)

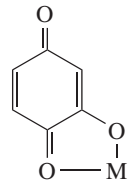

(**97**)

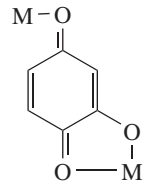

(**98**)

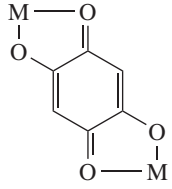

(**99**)

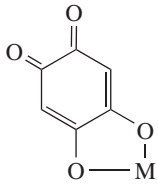

(**100**)

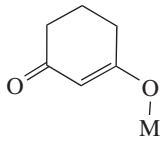

(**101**)

iv. Metal complexes of oxocarbon ligands $C_nO_n^{2-}$. These cyclic dianions[193] have an extensive π-electronic delocalization over the ring and the oxygen atoms and are known for $n = 3$ (deltate, **102**)[194], 4 (squarate, **103**), 5 (croconate, **104**) and 6 (rhodizonate, **105**)[195]. However, their coordination chemistry is almost limited to squarato and some croconato complexes. They usually coordinate to one or several metal ions as terminal or bridging ligands frequently giving 2-D and 3-D complex networks. They have been prepared, generally in water, by reaction of a metal salt or complex with the acid[196, 197], or its alkali or alkaline-earth salt. Croconato complexes of Ca[198], Mo[199], Mn[198, 200, 201], Fe[198, 201, 202], Co[198, 203], Ni[198, 204, 205], Pt[206], Cu[198, 201, 204, 207–210], Ag[211], Zn[198, 207], Cd[211], lantanide and actinide elements[197, 210, 212] have been isolated and characterized by X-ray diffraction.

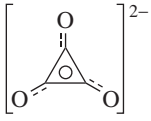

(**102**)

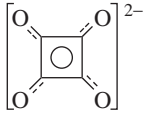

(**103**)

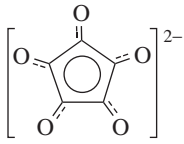

(**104**)

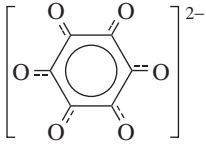

(**105**)

Squarato complexes have been widely studied. Thus, mononuclear complexes of Ba[213], V[214, 215], Cr[216], Mo[215, 217], Mn[218–221], Fe[220, 222–224], Co[219, 220, 224–228], Ni[220, 224, 226–230], Pd[231], Pt[206, 232], Cu[208, 210, 222, 228, 233], Zn[219, 220, 227, 228, 230, 234, 235], Cd[227, 236], Ga[237], Sn[238], Pb[239], Y[240], La[241, 242], Pr[243], Nd[244], Eu[241, 243–245], Gd[241], Tb[241], Yb[243], U[246] as well as dinuclear complexes of Ba/Cu[247], Cu/Ce[248], Ni/Ce[249], Cu/La[250], Cu/Gd[250] have been fully characterized.

Many metal complexes of squarate-related ligands like $RC_4O_3^-$ have also been characterized. Some examples are those with R = OH[235, 251, 252], Me[253], Ph[241, 254, 255], An-4[256], NMe_2[257], NHPh[256, 258], NPh_2[245, 259, 260], $N(PO_3H^-)_2$[221], $NHCH_2CH(NH_3)CO_2^-$[261], OMe[262], and M = Na[261], Mo[252], Mn[235, 254, 258, 260, 262], Ru[255, 256], Co[251, 254, 258, 260, 262], Ni[254, 258, 262], Cu[221, 258, 260], Zn[254, 258, 260, 262], La[241, 253], Eu[241, 245, 253, 259], Gd[241, 253], Tb[241, 253, 255, 259], Ga[259], Pb[257], or with $(O_3C_4S(CH_2)_2SC_4O_3)^{2-}$ and M = Pb[263].

Squaraines are a class of 1,3-derivatives of squaric acid in which the substituents are amino or highly electron-releasing aromatic or heterocyclic groups. The squaraine ligand **106** (Ar = $C_6H_3(i\text{-Pr})_2$-2,6) yields with $AlMe_3$ in thf a dimeric tetranuclear complex (**107**)[264].

A special mention deserves the synthesis of a uranium squarato[265] and the first deltato complex, using CO as the only source of the oxocarbon ligands (Section IV.D).

The crystal structures of three metal rhodizonato complexes were determined: $Rb_2C_6O_6$[266], prepared by reacting anhydrous rhodizonic acid with RbOH, and the other two[267], **108**, prepared by reacting aqueous $Na_2C_6O_6$, with 2,2′-bipyrimidine and either $Cd(NO_3)_2 \cdot 4H_2O$ or $MnCl_2$.

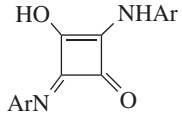

(**106**)

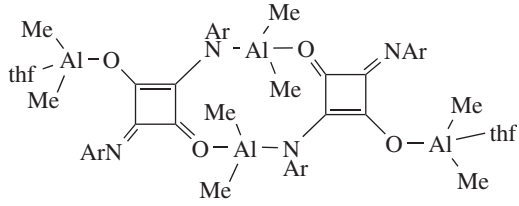

(**107**)

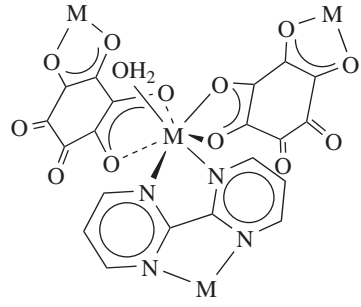

(**108**) M = Cd, Mn

v. L-Ascorbato complexes. The coordination chemistry of vitamin C has recently been reviewed[268]. There have been few reports on the isolation of ascorbato complexes, and their structures have been the subject of some controversy due to the unstable nature of the molecule and the hydrolytic instability of complexes. However, L-ascorbic acid (**109**) reacts with $[Pt(OH)_2(N\hat{}N)]$ ($N\hat{}N$ = diamines) to give a mixture of the 2,5-dioxoalkyl complex **110** and the enolato complex **111**[269].

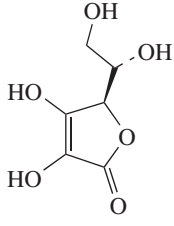

(**109**)

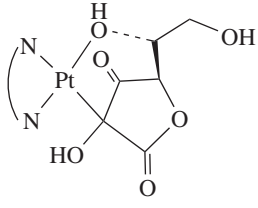

(**110**)

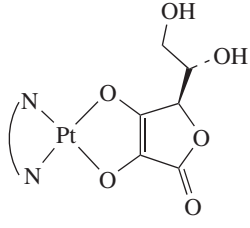

(**111**)

vi. Miscellaneous complexes of α-diketones. The cyclic diketones **112** react with an excess of Ag_2O and complexes $[M]Cl_2$ to afford **113a**[270] or **113b**[271].

Although many complexes containing an enediolato ligand (O,O-OC{=C(R)O}R)$^{2-}$ have been obtained by reduction of the corresponding α-diketones (Section II.B.2) or by using CO or carbonyl complexes (Section IV.B), a few have been obtained by a double deprotonation process. Thus, PhC(O)CH(Ph)OH reacts (i) with $[SnBu_2(O)]_n$ or $[SnBu_2(OMe)_2]$ to give $[SnBu_2\{O,O\text{-OC}\{=C(Ph)O\}Ph\}]$[272] and (ii) with $[SnBu_3(NEt_2)]$

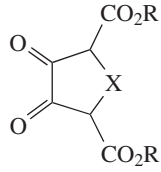

(**112**) X = O, S, CH_2 R = Me, Et

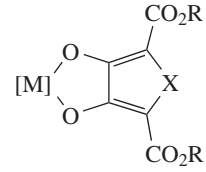

(**113**) (**a**) X = O, S, CH_2, R = Me, Et, [M] = [PtL_2], L = PPh_3, L_2 = cod
(**b**) X = O, S, R = Et, [M] = [Rh(η^5-Cp*)L], L = PPh_3, py, $P(OPh)_3$

to afford first the monoenolato complex [$SnBu_3${OCH(Ph)C(O)Ph}] and then [($SnBu_3$)$_2$ {μ-*O*,*O*-OC{=C(Ph)O}Ph}][273]. Analogous complexes have been prepared photochemically[274].

Complex [Zn($Tp^{Me,Me}$)(OH)] reacts with AcC(O)Et to give complex **114**. However, the corresponding derivative from AcC(O)Ph is not stable, decomposing to **115** and [Zn($Tp^{Me,Me}$)(O_2CPh)][275].

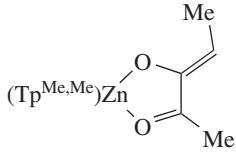

(**114**)

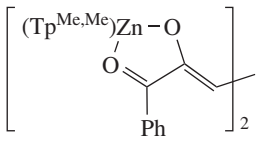

(**115**)

b. β-Diketonato complexes. The β-diketonato ligands (dik) are probably the best known monoanionic chelating ligands. Neutral, cationic and anionic, homo and heteroleptic complexes containing these ligands with nearly all metals and metalloids are known. Although the best known β-diketonato metal complexes are those containing acetylacetonato (acac), hexafluoro acetylacetonato (F_6acac)[276] or hexamethyl acetylacetonato (Me_6acac) ligands, others derived from β-diketones RC(O)CH(R″)C(O)R′ with R or R′ = Me, Mef, Ph, *t*-Bu, and R″ generally H, but also many other substituents (see below), have been reported. The synthesis, structure and reactivity of these complexes have been widely reviewed[277–284]. Many of these complexes are commercially available and have found technological applications, as discussed elsewhere in this book.

β-Diketonato complexes can be prepared (i) by a one-pot reaction between the diketone, a base (MB = Na_2CO_3[285,286], $NaHCO_3$[287], KOH[288], NaOAc[288–290], NaOMe[291], NH_3[283,288,290], Et_3N[289], $BaCO_3$[289]) and a halocomplex or a metal salt (halide[283,286,289,290], nitrate[287,288], sulfate[290]) or between the diketone and the metal[283,290,292–294] or a metal acetate[283,290,292,295,296], carbonate[283,288,293,297], oxide[283], hydroxide[283,288,289], hydride[289,290,292], carbide[283], halide[289,291,298], alkyl[289], alkoxide[284,289,299,300] or acetylacetonato complex[301] or (ii) by a two-step process involving the synthesis of a metal β-diketonato complex, M(dik) (M = Na[286,290,302–304], K[290], Tl[283,286,293,304,305] or others[306,307]) and then a transmetalation reaction between M(dik) and a halocomplex[293] or a metal salt[290]. Depending on the solubility and stability of the reagents and products, the reactions can be carried out in water, aqueous ethanol or dioxane, in organic solvents or even in inmiscible mixtures of water and organic solvents[283].

In some cases, to prepare a β-diketonato complex of a metal in an oxidation state higher than usual, the addition of an oxidizing agent is required. Thus, β-diketonato Mn(III) or Mn(III)/Mn(IV) complexes are obtained from $MnCl_2$ or $MnSO_4$, $KMnO_4$, NH_4OH and the β-diketone; similarly Co(III) β-diketonato complexes can be prepared from $CoCO_3$, the β-diketone and H_2O_2[290,308,309].

Carbonyl β-diketonato complexes can be prepared by heating a mixture of a carbonyl complex and the β-diketone in an autoclave. Under these conditions, $H(R_6acac)$ (R = F, Me) reacts with $M_3(CO)_{12}$ (M = Ru, Os) to give $[Ru(F_6acac)_2(CO)_2]$[310], $[Os(F_6acac)(O_2CMef)(CO)_3]$[311] or $[Os_4(Me_6acac)_4(CO)_{10}]$[312].

Some diketonato complexes substituted at position 4 of the 1-metala-2,6-dioxacyclohexane rings, usually denominated the γ-position, are prepared by electrophilic substitution (Section III.C in Chapter 6[1]) but others are synthesized using the corresponding diketone, for example complexes $[VO(\gamma\text{-R-acac})_2]$ (R = Me, Et)[313] or tetrathiafulvalene-substituted acetylacetonato derivatives such as **116**[295].

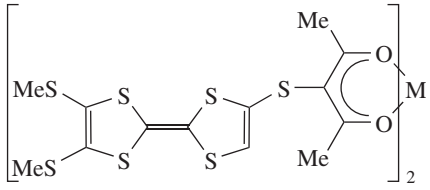

(**116**) M = Mn, Cu

An unexpected result is the interchange of NR_2 ligands with OR″ substituents in the reaction of complexes $[Ti(NR_2)_4]$ with two equivalents of $R'C(O)CH_2CO_2R''$ (R = Me, Et, R′ = *t*-Bu, R″ = Me; R = R′ = Me, R″ = *t*-Bu) to give **117**, probably through intermediates **118** and **119**[314].

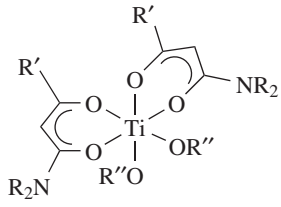

(**117**)

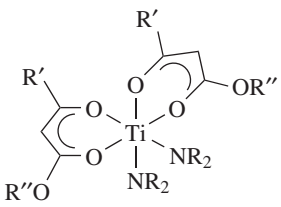

(**118**)

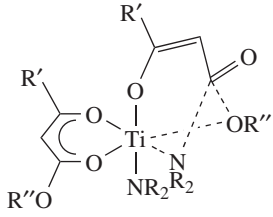

(**119**)

i. Families of β-diketonato complexes. The syntheses and properties of the following families of β-diketonato complexes have been reported: metal[288] and non-metal[281] acetylacetonates, fluorinated acetylacetonates[276,301,315], dipivaloylmethanates $[M(Me_6acac)_n]$[290,316], benzoylpivaloylmethanates $[M\{O,O\text{-OC(Bu-}t\text{)CHC(O)Ph}\}_n]$[290] and *p*-substituted dibenzoylmethyl derivatives[317,318].

The reactions of diferrocenoylmethane and of spacer-bridged bis-, tris- and tetrakis (ferrocenoyl)-1,3-diketones with NaOMe, KH or chloro complexes of Pd(II), Ru(II), Rh(III) and Ir(III) in the presence of K_2CO_3 afford a series of mono-, bis-, tris- and tetrakis(β-diketonato) complexes[319].

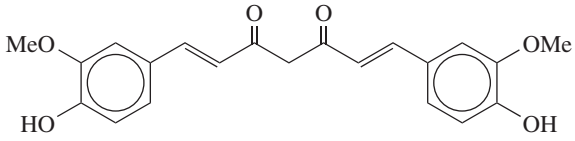

(**120**)

[Ga(cur)$_3$], [In(cur)$_3$][320], [Cu(cur)$_2$][321], [VO(cur)$_2$][320,322] and [Mn(cur)$_2$][323] (Hcur = curcumin (**120**) and some derivatives or analogues) have been obtained by reacting **120** with [VO(acac)$_2$] or $VOSO_4$, M(NO$_3$)$_3$ (M = Ga, In) or M(OAc)$_2$ (M = Cu, Mn), respectively, and tested as therapeutic agents.

(−)-[Cr(acac)$_3$] and enriched samples of (+)-[Ru(acac)$_3$] have been isolated by treatment of aqueous solutions of the corresponding (+)-tartrate complexes with Hacac at high pH followed by recrystallization of the partially resolved mixture[324]. Partial resolution of the tris(acetylacetonates) of Cr, Co, Ru and Rh, and also the *cis* and *trans* isomers of cobalt benzoylacetonate have been achieved by column chromatography on D-(+)-lactose[325].

ii. β-Diketonato complexes of specific groups of elements. Studies have been published in the past[280,283]similar to the general methods outlined above. However, since the number of β-diketonato complexes is so large, account will be given only of the most recent work where detailed syntheses and properties of β-diketonato complexes are reported.

Group 1 elements. Li, Na and K acetylacetonates have been prepared by reacting Hacac with LiBu-*n* in benzene, NaH in benzene or pentane, and KOH in MeOH, respectively[326,327]. They have also been prepared by treating the corresponding metal hydroxide with acetylacetone in methanol or water solution[288]. [Na(acac)] has been prepared by reacting Hacac with NaOEt, prepared *in situ* from Na and EtOH. The Li, K and Cs compounds can be prepared by the same method but, in the case of [Cs(acac)], Cs amalgam is used[327]. Direct reaction between Na sand and Hacac in toluene has also been used[328]. The reaction of ethyl acetoacetate with LiOEt, NaOBu-*t* and NaOBu-*t* affords the corresponding enolates[329]. Addition of L = 18-crown-6 or criptand (2.2.2) to the K enolate leads to [K{O,O^2-OC(=CH$_2$)CH$_2$C(O)OEt}(L)][330]. [Rb(acac)] and [Cs(acac)] have also been prepared from the corresponding carbonates[331]. The alkali β-diketonates can be used for the synthesis of other metal β-diketonates; for example, Ag(acac) was prepared by mixing equimolar quantities of *ca* 1 M solutions of $AgNO_3$ and Na(acac) dissolved in oxygen-free water[327].

Group 2 elements. The asynthesis and structure of β-diketonato complexes of Group 2 elements have been reviewed[282]. [Ca(acac)$_2$] and [Sr(acac)$_2$] have been obtained by reacting the metal nitrates, acetylacetone and the stoichiometric quantity of KOH in water[288]. [Ba(acac)$_2$] has been prepared by treating the corresponding metal hydroxide with acetylacetone in methanol or water solution[288]. Alkaline-earth fluorinated acetylacetonates [M(dik)$_2$] (M = Ca, Sr, Ba, dik = F$_3$acac, F$_6$acac), some of which have proved to be useful as MOCVD (Metal-Organic Chemical Vapor Deposition)[332,333] materials, have been prepared by reacting the corresponding metal with the β-diketone[333]. These complexes are not suitable for the preparation of superconducting metal oxides due to MF_2 formation during deposition. An alternative to these complexes are the dipivaloylmethanato complexes, for example [Ba(Me$_6$acac)$_2$(NH$_3$)$_2$] prepared by reacting [Ba(Me$_6$acac)$_2$][290] with NH_3[334].

A literature listing for the synthesis of many main group and transition metals appears in Table 5.

TABLE 5. Synthesis of M(dik)$_n$ complexes of metals belonging to various groups of the periodic table

Group	M
2	Be[335], Mg[336], Ca[337], Sr[294,338], Ba[294]
3, Ln, An[a]	Sc[124], Y[339], La[340–342], Ce[341,343,344], Pr[341,345–347], Nd[277,301,340,341,345,348–350], Pm[340], Sm[301,316,340,341,345,346,351,352], Eu[277,301,316,340,349,352–357], Gd[301,316,340,349,352,358], Tb[316,340,344,349,354,357], Dy[277,316,340,341,352], Ho[316,340,341,359], Er[340,341,346,349,352], Tm[340,354], Yb[341,348,349,353,360,361], Lu[360,362], Th[363], Pa[364], U[365], Np[366], Pu[364], Am[356]
4	Ti[367,368], Zr[369], Hz[370]
5	V[368,371], Nb[368,372], Ta[306,372,373]
6	Cr[374], Mo[368,375,376], W[376,377]
7	Mn[296,309,378], Tc[379], Re[380]
8	Fe[381–385], Ru[302,386], Os[304,311,387]
9	Co[296,381,382,388–391], Rh[392], Ir[393]
10	Ni[296,318,381,389,391,394–396], Pd[397,398], Pt[397,399]
11	Cu[296,381,382,384,389,395,400], Ag[401], Au[402], Ag[327]
12	Zn[300,318,381,403], Cd[404], Hg[390,405]
13	Al[287,306,307,383,406], Ga[384,407], In[303,408], Tl[293,297,409]
14	Sn[410], Pb[411]
15	Bi[381]

[a]Ln = lanthanoid, An = actinoid.

iii. Complexes with bridging β-diketonato ligands. In a few dinuclear complexes the two metal centers are bridged by a non-chelating β-diketonato. Thus the complex [{Mn(CO)$_3$(dppe)}$_2$(μ-acac)], in which the acac ligand is monocoordinated to each Mn atom, is obtained by reacting [Mn(CO)$_3$(dppe)(OClO$_3$)] with Hacac and Et$_3$N[412]. Similarly, the reaction of Ag$_2$O with hexafluoroacetylacetone and cod in a 1:2:2 molar ratio affords [Ag(μ-F$_6$acac)(cod)]$_2$[413].

One of the few examples in which an aryl ligand acts as the deprotonating agent to form an enolato ligand is the reaction of **121** with ethyl acetate to afford a rare example of a complex, **122**, with a bridging instead of chelating diketonato ligand. In addition, a condensation reaction takes place[414].

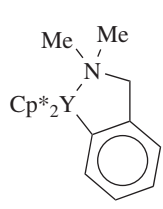

(**121**)

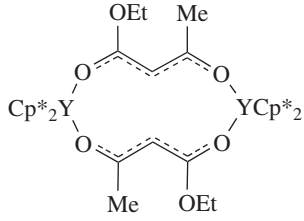

(**122**)

In some cases, complexes with a monocoordinated β-diketonato ligand are obtained by substitution of other monodentate terminal ligands. Thus, PhCH(CHO)$_2$ reacts with [SnPh$_3$(OEt)] to afford the polymer [SnPh$_3${OCH=C(Ph)CHO}]$_n$[289].

iv. Complexes derived from miscellaneous β-diketones. Among the non-classical β-diketonato complexes the best studied are those derived from 4-acyl-5-pyrazolones

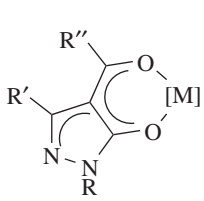

(**123**)

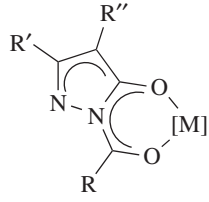

(**124**)

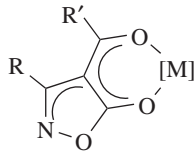

(**125**)

123–**125**. As the synthesis of these complexes has been reviewed widely and recently[277] we will only include here some selected and recent publications.

The reaction of $[M(\eta^5\text{-Cp}^*)Cl(\mu\text{-Cl})]_2$ with **126** leads to complexes **127**[415].

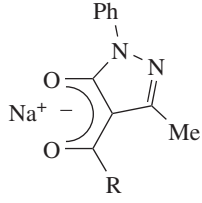

(**126**) R = Me, Et, CH_2Bu-*t*, $CHPh_2$

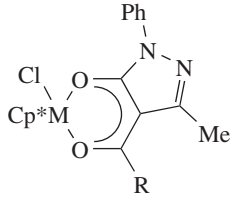

(**127**) M = Rh, Ir

Cyclometalated Ir(III) chloro-bridged dimers $[Ir(C\hat{}N)(\mu\text{-Cl})]_2$ react with Na_2CO_3 and various 4-acyl-5-pyrazolones (Hap) to afford $[Ir(C\hat{}N)(ap)]$[416]. The reaction of $AgNO_3$ with **128**, NaOMe and trimeda gives **129**[417].

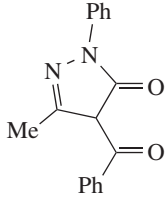

(**128**)

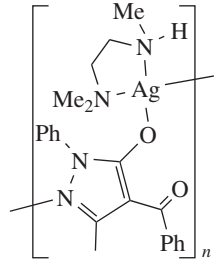

(**129**)

The reaction of **130**, neutralized by NaOH, with an aqueous solution of $TbCl_3$ affords the dendritic complex **131**[418].

Electron-poor and electron-rich 4-acyl substituted pyrazolones (Hap) react with NaOH and $M(NO_3)_3$ (M = Eu, Gd) to afford $[M(ap)_3(OH_2)_2]$[419]. The analogous $[Tb(ap)_3(OPPh_3)]$ (Hap = 1-phenyl-3-methyl-4-(2-ethylbutyryl)-5-pyrazolone) shows high electroluminiscence performance[420].

1,3-Dibenzoylacetone (**132**) reacts with $[Pt(CO_3)L_2]$ (L = PPh_3, $AsPh_3$) to give complex **133** containing a dianionic β,β'-bis(diketonato) ligand[421].

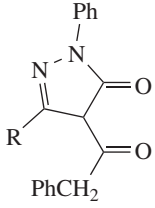

(**130**)

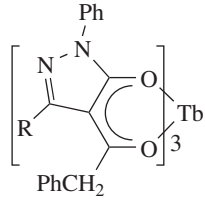

(**131**)

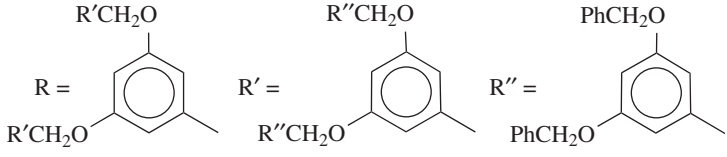

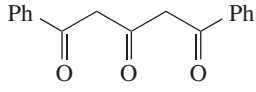

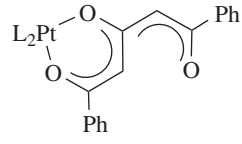

(**132**) (**133**)

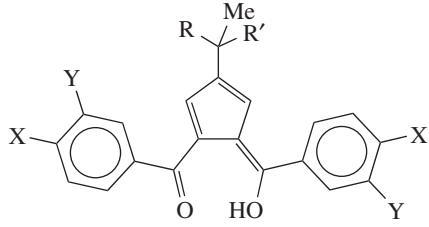

(**134**)

The fulvene-type organic ligands **134** react with $M(OAc)_2 \cdot 2H_2O$ (M = Cu, Co, Mn) in EtOH to give **135**[422].

The ylide **136** reacts in thf with LiBu-*n* to give **137**[423].

3. Polyketonato complexes

These complexes result from the coordination of tri-, tetra- or polyketonates to two or more metal centers (**138**–**140**). Because these topics have been reviewed widely and recently[277, 278] and, in addition, the methods of synthesis are not different from those outlined above, only a few of them will be discussed.

The actual synthetic challenge in this chemistry is more the preparation of new and interesting β-diketones than that of their metal complexes. Thus, the β-diketone **141** reacts with CaH_2 or Mg to afford the corresponding β-diketonato complex **142** which, in turn, reacts with LDA and $(Tos(CH_2)_2)_2O$, followed by aqueous HCl to give the macrocyclic

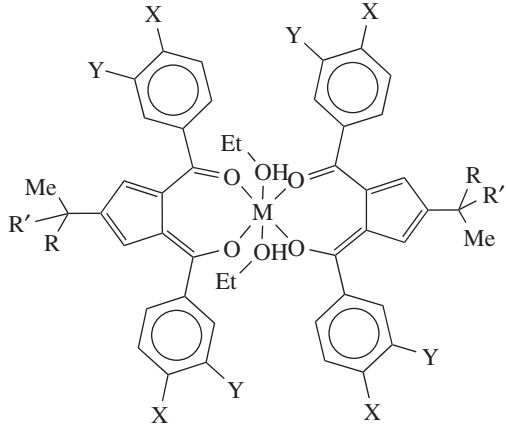

(**135**) (**a**) M = Cu, Co, Mn, R = Me, R′ = Ph, X = H, Y = CN
(**b**) M = Co, R = Et, R′ = Ph, X = H, Y = CN
(**c**) M = Co, R = R′ = Me, X = CN, Y = H

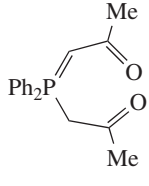

(**136**)

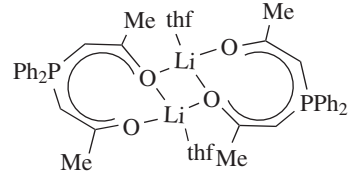

(**137**)

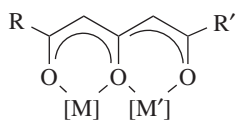

(**138**)

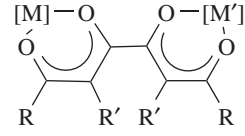

(**139**)

bis(β-diketone) ligand **143**. Complexes of Cu(II), Co(II) and UO_2^{2+} with macrocyclic polyether β-diketone ligands have been isolated[292].

Some interesting tetraketones synthesized recently allow one to prepare the corresponding mononuclear Ti(IV) ketonato complexes[424]. In some cases polyketonato ligands can coordinate different metal centers. Thus, some complexes containing Cu(II)/Ca[425], Cu(II)/Na[426], Cu(II)/Y(III))[427], Cu(II)/Ln(III)) (Ln = La, Ce, Pr, Nd, Sm, Eu, Gd, Tb, Dy, Ho, Er, Tm, Yb, Lu)[427], Cu(II)/Gd(III)[427,428], Cu(II)/M(II) (M = Mn, Fe, Co)[429], Ni(II)/UO_2^{2+} [429], Co(II)/La(III)[430] have been characterized. Other recent results can be found elsewhere[431].

Tetraketone **144** reacts with *cis*-[$PtCl_2L_2$] and $AgBF_4$ to afford complex **145**[432].

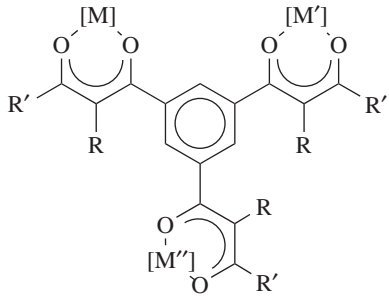

(**140**)

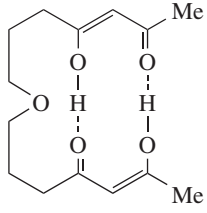

(**141**)

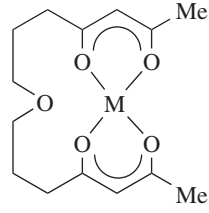

(**142**)

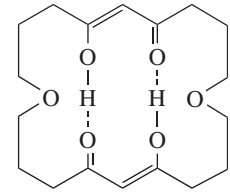

(**143**)

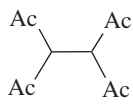

(**144**)

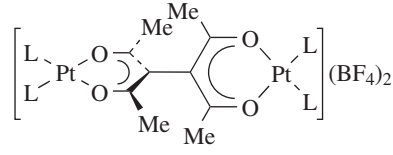

(**145**) L = SEt_2, PMe_2Ph, L_2 = cod

4. Complexes derived from ketimines and ketohydrazones

The *N*,*O*-enolato ligands **146** are usually prepared by deprotonation of the corresponding conjugated acids which, for ketimines, can be formulated as consisting of the tautomeric forms **147**–**149**. However, some of them have been prepared (i) by reacting nitriles with the corresponding β-diketonato complexes, or with 2-oxoalkyl or enolato complexes (Section III.C, Chapter 6[1]) or (ii) by oxidation of diketoamines with metal complexes in the presence of a base (Section II.B.3). Although the most abundant tautomeric form of a β-ketimine depends on the nature of the substituents, they will be represented as **148**.

Complex **150** is obtained by reacting first the corresponding ketimine with LiBu-*n* and then with $TiCl_4$[433].

By reacting β-diketodiimines **151** with metal hydroxides or with NaH and halo complexes, families of β-diketodiiminato metal complexes **152a** or **152b**, respectively, have been prepared[434]. Other related complexes with [M] = VX(thf) (X = Cl[435], PhO, NCS[436]), $NbCl_2$[437], $[Cr(py)_2]^{+}$[438], $MoCl_2$[439], Mn[440] have been prepared similarly.

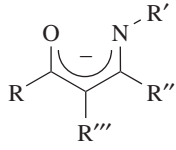

(**146**)

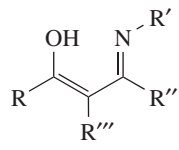

(**147**)

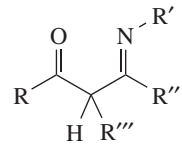

(**148**)

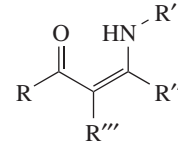

(**149**)

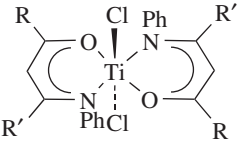

(**150**) R = Ph, 2-Thi, 2-Fu, R′ = Mef
R = Mef, Ph, R′ = Me

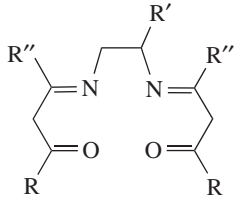

(**151**)

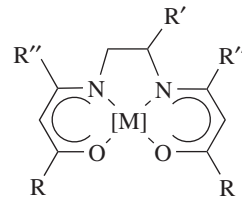

(**152**) (**a**) [M] = Co, Ni, Pd, Pt, Cu, R = Me, Mef,
R′ = H, Me, R″ = Me, Ph, $C_6H_4Br^{-2}$
(**b**) [M] = $TiCl_2$, TiCl(thf), R = R″ = Me, R′ = H

Complex **153** has been prepared by reacting the diketimine with Et_3N and $Ni(NO_3)_2$•$6H_2O$, $PdCl_2$•2MeCN, $Cu(NO_3)_2$•$3H_2O$[441].

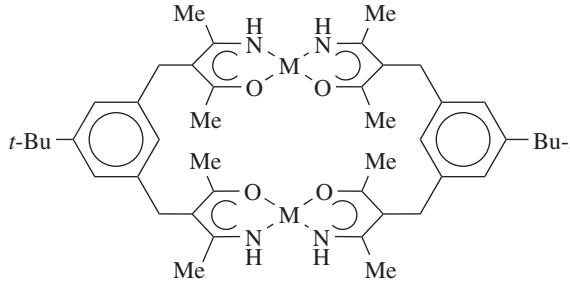

(**153**)

Complexes **154** have been obtained by reacting the ketimines with $[Ti(OR)_4]$[442].

Tetraketodiimines react with $M(OAc)_2$ to form mononuclear complexes **155** or **156**, and homo- or hetero-dinuclear complexes **157** (M(II)/M′(II) = Cu/Cu, Ni/Ni Cu/Zn, Ni/Cu,

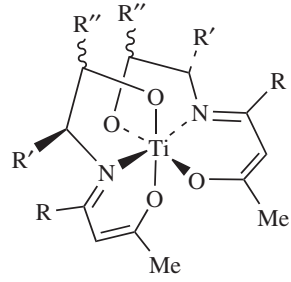

(**154**) (**a**) R = Me, R′ = Et, R″ = H
(**b**) R = *t*-Bu, R′ = H, R″ = Me

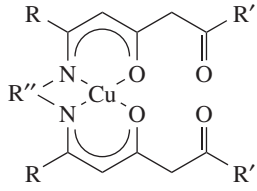

(**155**)

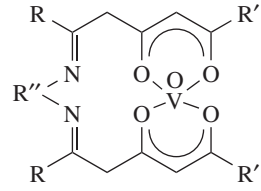

(**156**)

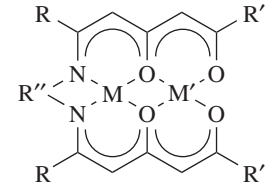

(**157**)

Ni/Co, Ni/Mn, Ni/Zn; M(II)/MO_x^{2+} = Cu/UO_2, Cu/VO, Ni/UO_2, Ni/VO; M(II)/M′(III) = Ni/Fe)[443].

The diiminoketone **158** reacts with two equivalents of [$ZnEt_2$] to afford the ketodiiminato complex **159**[444].

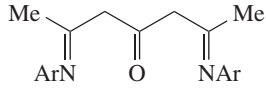

(**158**) Ar = $C_6H_3(i\text{-Pr})_2$-2,6

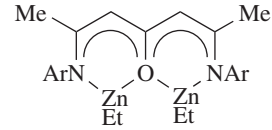

(**159**)

Ketimines **160** react with NaH and [Ni(Ph)Cl(PPh_3)$_2$][445] or with [$NiMe_2$(tmeda)] and py[446] to afford complexes **161a,b** or **161c**, respectively.

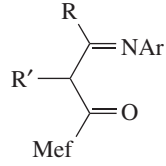

(**160**) Ar = $C_6H_3(i\text{-Pr})_2$-2,6

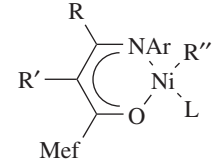

(**161**) (**a**) L = PPh_3, R = Me, R′ = Acf, R″ = Ph
(**b**) L = PPh_3, R = Acf, R′ = H, R″ = Ph
(**c**) L = py, R = H, R′ = Acf, R″ = Me

TABLE 6. Synthesis of β-diketiminato complexes of metals belonging to various groups of the periodic table

Group	Metal
1	Li[448], Na[449]
2	Mg[450], Ba[451]
Ln, An[a]	La[452–454], Ce[455], Pr[452], Nd[453,455,456], Sm[452,456,457], Eu[454], Gd[452,454,455], Tb[454], Dy[452,454], Ho[454], Er[452,454–457], Yb[452,458], U[459]
4	Ti[460,461], Zr[461,462]
5	V[463]
6	Cr[464,465], Mo[466]
7	Mn[467], Tc[468], Re[469]
8	Fe[464,470], Ru[471], Os[472]
9	Co[473–475], Rh[476]
10	Ni[394,475,477–480], Pd[479–482], Pt[481]
11	Cu[455,464,474,475,477,479,483]
12	Zn[464,484]
13	Al[485], Ga[486,487], In[487,488]
14	Sn[489]

[a]Ln = lanthanoid, An = actinoid.

The diketoamine **162** reacts with $Sn(HMDS)_2$, giving complex **163**[447].

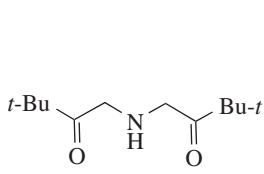

(**162**)

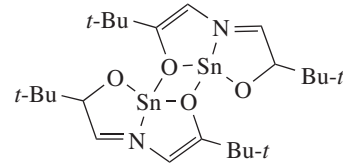

(**163**)

Many other β-ketiminato complexes have been prepared, as listed in Table 6.

The ligands **164** react with $NiCl_2 \cdot H_2O$ and various additional ligands to give enolato complexes **165**[490].

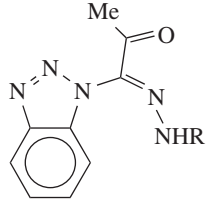

(**164**) R = C_6H_4X-4, X = H, Cl, Br, Me

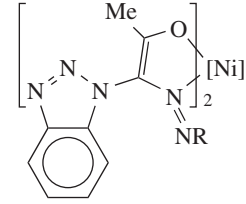

(**165**) [Ni] = *trans*-NiL_2; L = py, *n*-$PrNH_2$

5. Metal complexes with P,O- and As,O-enolato ligands

Metal complexes with *P,O*- and *As,O*-enolato ligands are of interest because the Ni(II) complex [NiPh{*O*,*P*-OC(=CHPPh_2)Ph}(PPh_3)] is successfully used in the Shell Higher

Olefin Process (SHOP). Although this Ni complex is prepared by oxidative addition reaction (Section II.B.4), most other phosphinoenolato complexes are prepared by deprotonation of the corresponding phosphines $R_3PCH(R')C(O)R''$[491] or by other methods, as discussed in Sections III.A and IV.A.

$[Zr(\eta^5\text{-}Cp)_2Cl_2]$ reacts with $[Li\{OC(=CH_2)PPh_2\}(thf)_2]$ (prepared from $AcPPh_2$ and LiBu-*n* in thf) to give the metalaligand **166**[492]. The titanium enolate **167** reacts either with $[MCl_2(cod)]$ (M = Pd, Pt), transmetalating both enolato ligands to give **168**, or with $[Pt(\eta^2\text{-}C_2H_2)(PPh_3)_2]$ to afford the Ti(III)/Pt(I) complex **169**[493].

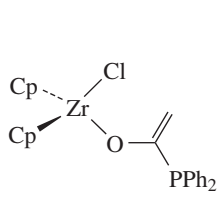

(**166**)

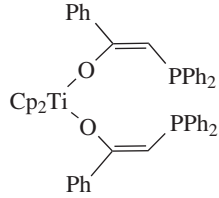

(**167**)

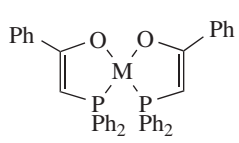

(**168**)

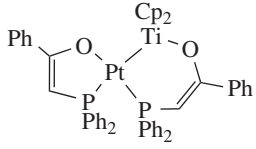

(**169**)

The α-phosphinoketone **170** reacts with LiBu-*n* and $[Zr(\eta^5\text{-}Cp)_2Cl_2]$ to give the zirconium enolate **171**, which behaves as a diphosphine toward AgOTf or $[Cu(NCMe)_4]PF_6$ to give $[Ag(P,P\text{-}\mathbf{171})(OTf)]$ or $[Cu(P,P\text{-}\mathbf{171})(NCMe)_2]$, respectively, or as a transmetalating agent toward $[Pd(C_6H_4CH_2NMe_2\text{-}2)(\mu\text{-}Cl)]_2$ or $[PdCl_2(SEt_2)_2]$ to give **172** or **173**[494], respectively.

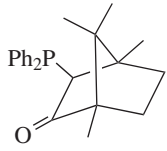

(**170**)

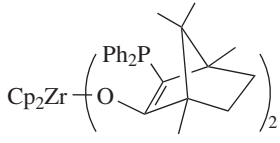

(**171**)

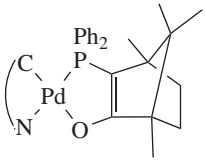

(**172**)

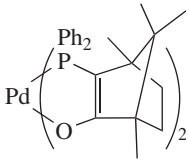

(**173**)

The reaction of $[M(\eta^5\text{-}C_5R_4R')Cl_4]$ (R = R′ = H, M = Nb, Ta; R = R′ = Me, M = Ta; R = H, R′ = *i*-Pr; M = W) with $Ph_2PCH_2C(O)Ph$ affords phosphinoenolato complexes $[M(\eta^5\text{-}C_5R_5)Cl_3\{O,P\text{-}OC(=CHPPh_2)Ph\}]$[495].

The complex $[Mo(\eta^3\text{-}C_3H_5)(\mu\text{-}Cl)(\eta^6\text{-}C_6H_5R)]_2$ (R = H, Me) reacts with $Ph_2PCH_2C(O)R'$ (i) in a 1:1 molar ratio in the presence of an excess of Et_3N to afford $[Mo(\eta^3\text{-}C_3H_5)\{O,P\text{-}OC(=CHPPh_2)R'\}(\eta^6\text{-}C_6H_5R)]$ (R′ = Ph, NPh_2), and (ii) in a 1:2 molar ratio in refluxing ethanol to yield $[Mo\{O,P\text{-}OC(=CHPPh_2)Ph\}_2(\eta^6\text{-}C_6H_5R)]$[496].

By refluxing EtOH solutions of $Ph_4As[Re(=O)Cl_4]$ or $[Re(\equiv N)Cl_2(PPh_3)_2]$ with $Ph_2PCH_2C(O)Ph$, in the presence of Et_3N, complexes $[Re(=O)Cl\{O,P\text{-}OC(=CHPPh_2)Ph\}_2]$ or $[Re(\equiv N)\{O,P\text{-}OC(=CHPPh_2)Ph\}_2(PPh_3)]$ have been isolated, respectively. Similar complexes have been reported[497] recently.

Complex $[FeBr_2(CO)_2\{PPh_2CH_2C(O)Ph\}_2]$ reacts with NaOH to give $[Fe(CO)_2\{O,P\text{-}OC(=CHPPh_2)Ph\}_2]$[66]. **174** reacts with $[Sn(n\text{-}Bu)_2(OAc)_2]$ to afford **175**[498]. The reaction of **176** with $Ph_2PCH(R)C(O)R'$ and KOH in EtOH gives **177**[499]. Treatment of **178** with KOBu-*t* affords **179**[500].

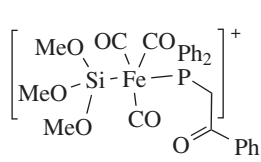

(**174**)

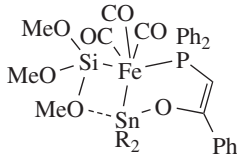

(**175**) R = Bu-*n*

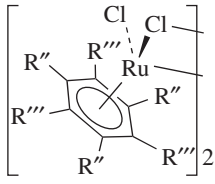

(**176**) R″ = R‴ = Me, H
R″ = Me, R‴ = H

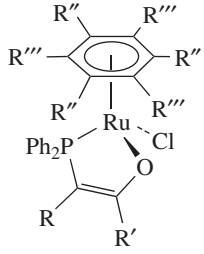

(**177**) R = H, Me, R′ = Ph, *t*-Bu

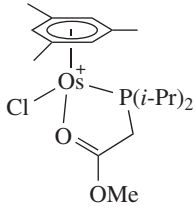

(**178**)

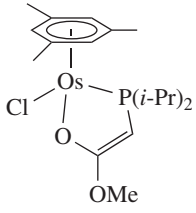

(**179**)

A CH_2Cl_2 solution of the cluster $[Ru_3(CO)_{10}\{PPh_2CH_2C(O)Ph\}_2]$ yields after a week a moderate amount of $[Ru(\mu\text{-}Cl)\{O,P\text{-}OC(=CHPPh_2)Ph\}(CO)_2]_2$. The corresponding iodo

complex is obtained in good yield by reacting $[Ru_3(CO)_9\{PPh_2CH_2C(O)Ph\}_3]$ with I_2[501]. The homoleptic *fac*- and *mer*-$[Ru\{O,P\text{-}OC(=CHPPh_2)Ph\}_3]^-$ have been isolated by reacting *mer*-$[RuCl\{O,P\text{-}PPh_2CH_2C(O)Ph\}_2\{PPh_2CH_2C(O)Ph\}]^+$ with NaH[502].

The homoleptic Co(III) complexes *fac*- and *mer*-$[Co\{O,P\text{-}OC(=CHPPh_2)Ph\}_3]$ have been prepared from $[CoCl_2\{PPh_2CH_2C(O)Ph\}_2]$ and NaOMe[503].

The Rh(I) complexes $[Rh(\mu\text{-}Cl)(\eta^2\text{-}CH_2{=}CH_2)\{PPh_2CH_2C(O)Ph\}]_2$ and $[RhCl\{O,P\text{-}PPh_2CH_2C(O)Ph\}\{PPh_2CH_2C(O)Ph\}]$ react with $TlPF_6$ in thf to give, respectively, $[Rh\{O,P\text{-}OC(=CHPPh_2)Ph\}(thf)_2]$ and $[Rh\{O,P\text{-}OC(=CHPPh_2)Ph\}_2]$. $[Rh\{O,P\text{-}PPh_2CH_2C(O)Ph\}(L)(PPh_3)]PF_6$ reacts with NaOMe to afford $[Rh\{O,P\text{-}OC(=CHPPh_2)Ph\}(L)(PPh_3)]$ (L = CO, PPh_3). Similarly, $[M(\mu\text{-}Cl)(\eta^2\text{-coe})]_2$ (coe = cyclooctene) reacts (i) with $Ph_2PCH_2C(O)Ph$, PR_3, CO and NaOMe or (ii) with a diene, $R_2PCH_2C(O)R'$ and NaOMe to give $[M\{O,P\text{-}OC(=CHPPh_2)Ph\}LL']$ (M = Rh, R = R′ = Ph, L = CO, L′ = PR_3; M = Rh, Ir, R = R′ = Ph, LL′ = cod; M = Rh, R = R′ = Ph, LL′ = nbd; R = Ph, R′ = Me, C_6H_4F-4; R = *i*-Pr, R′ = Ph). The Ir complex $[Ir\{O,P\text{-}OC(=CHPPh_2)Ph\}(cod)]$ reacts with H_2 to give $[Ir\{O,P\text{-}OC(=CHPPh_2)Ph\}H_2(cod)]$[504].

The reaction of $[RhCl(PPh_3)_3]$ with three equivalents of $Ph_2PCH_2C(O)Ph$ gives $[RhCl\{O,P\text{-}OC(=CHPPh_2)Ph\}_2\{P,O\text{-}PPh_2CH_2C(O)Ph\}]$ and, probably, H_2. This Rh(III) complex reacts with NaOMe to give the homoleptic complex $[Rh\{O,P\text{-}OC(=CHPPh_2)Ph\}_3]$. The reaction of $[RhCl_2\{P,O\text{-}PPh_2CH_2C(O)Ph\}_2]PF_6$ with NaH affords $[Rh(\mu\text{-}Cl)\{O,P\text{-}OC(=CHPPh_2)Ph\}_2]_2$[505]. A family of Rh(III) complexes $[RhI\{O,P\text{-}OC(=CHPPh_2)Ph\}(R)(CO)(PPh_3)]$ has been prepared by oxidative addition of RI (R = I, Me, Ph) to the Rh(I) complex $[Rh\{O,P\text{-}OC(=CHPPh_2)Ph\}(CO)(PPh_3)]$[506].

$[Pd(C\text{^}N)Cl\{PPh_2CH_2R\}]$ (C^N = *C*,*N*-cyclometalated ligand, R = CO_2Et, C(O)Ph) reacts with NaH[507,508] or $[Pd(C\text{^}N)(\mu\text{-}Cl)]_2$ with $Li(PPh_2CHCO_2Et)$[508] to give $[Pd(C\text{^}N)\{O,P\text{-}OC(=CHPPh_2)R\}]$ (R = Ph, OEt). The homoleptic *cis*-$[M\{O,P\text{-}OC(=CHPPh_2)Ph\}_2]$ (M = Ni, Pd, Pt) can be prepared by reacting $Li_2[PdCl_4]$ with $Ph_2PCH_2C(O)Ph$ and Et_3N[507] or $[MCl_2\{PPh_2CH_2C(O)Ph\}_2]$ (M = Ni, Pd, Pt) with a base (NaOEt, NaH) or, for M = Ni, by reacting the phosphine with $[Ni(cod)_2]$. Similarly, $[Pd(\mu\text{-}Cl)\{O,P\text{-}OC(=CHPPh_2)Ph\}]_2$ is obtained by deprotonation of $[PdCl(\mu\text{-}Cl)\{PPh_2CH_2C(O)Ph\}]$ with NaH or by reacting *cis*-$[Pd\{O,P\text{-}OC(=CHPPh_2)Ph\}_2]$ with $[PdCl_2(SEt_2)_2]$[509].

6. Thioenolato complexes

The synthesis of monothio-β-diketonato complexes has been reviewed[510].

The reaction between $[Mo(\eta^5\text{-}Cp)_2(S_4)]$, Et_3N and **180** leads to **181** and **182**. Similar complexes have been prepared from $[Ti(\eta^5\text{-}Cp)_2(S_5)]$, $[Pd(dppe)(S_4)]$ and $[Pt(dppe)(S_4)]$[511].

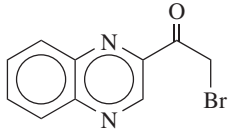

(**180**)

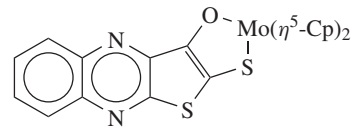

(**181**)

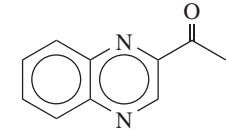

(**182**)

Flavothionato ligands L^-, prepared by reacting HL (**183**–**186**) with a MeOH/H_2O NaOH solution, react with transition metal salts to afford complexes **187** (M/*n*/HL = Co, Fe/3/**183**; Cu, Ni, Zn, Cd/2/**183**[512]; Co, Cu, Zn/2/**184**; Ni, Cu, Zn/2/**185**, **186**; Fe/3/**185**, **186**[513]). Complexes of Zn, Cd, Hg, Ga, In, Sn, Pb, V, Mo, Fe, Co, Ni, Cu, La, Pr, Nd, Sm, Gd, Ho, Yb, Lu with these and similar thiono ligands have been prepared using the same synthetic method[514]. Other thio-β-diketonato complexes have been reported[515].

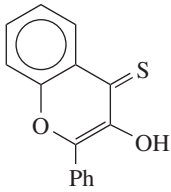
(**183**)

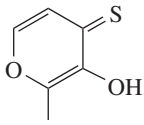
(**184**)

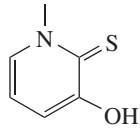
(**185**)

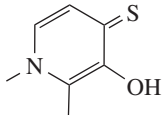
(**186**)

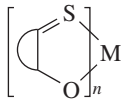
(**187**)

B. Redox Reactions

Three main types of redox reactions of keto compounds leading to the formation of metal enolates have been reported: (i) two-electron reduction of diketones or α,β-unsaturated ketones or esters (equation 1), (ii) oxidative addition reactions (equation 2) and (iii) threefold deprotonation of diketoamines followed by a two-electron oxidation of the trianion by the metal (equation 3).

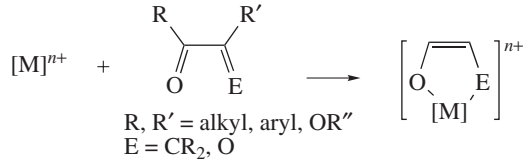
(1)

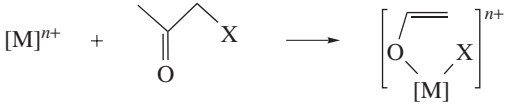
(2)

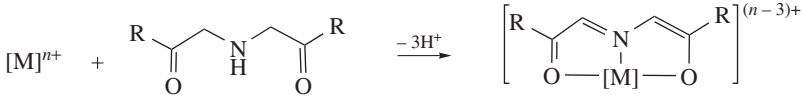
(3)

1. Reduction of enones

Two-electron reduction of an α,α-unsaturated ketone or ester leads to a chelate C,O-ligand that can coordinate to a metal as a κ^2-C,O (e.g. **189** or **190**) or, additionally, as an η^2-C,C ligand (e.g. **196** or **197**).

Stannylenes **188a** and **188b** react with $MeO_2CCH{=}CHCO_2Me$ to afford the corresponding Sn(IV) enolato complex **189**[516], while **188a** reacts with α,β-unsaturated aldehydes, ketones or esters to give **190** (R = H, Me, CH=CHPh, OMe; R′, R″, R‴ = H, Me, Ph; R = Et, R′ = R″ = R‴ = H)[516, 517].

A reductive coupling of some α,β-unsaturated ketones in the presence of [Ti(η^5-Cp)$_2$(CO)$_2$] gives **191**[518]. α,β-Unsaturated ketones $H_2C{=}CHC(O)R$ react with η^5-Cp′ complexes **192** to give **193** or **194** depending on R and Cp′[519].

High-pressure carbonylation of [Ta(η^5-Cp)Cl$_4$] in the presence of Na followed by treatment with $AcCH{=}CMe_2$ gives **195**[520]. $RC(=CH_2)CO_2Me$ is reduced by the Ta(III) complex [Ta(η^5-Cp*)Cl$_2$(CO)$_2$(thf)] or [Ta(η^5-Cp*)Cl(μ-Cl)]$_2$ to afford the Ta(V) derivative **196** (R = H[521], Me[522]). The reaction between the W(0) complex [W(CO)$_3$(NCMe)$_3$]

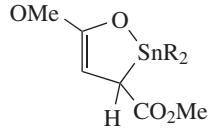

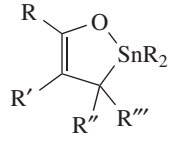

(**188**) (**a**) R = $CH(SiMe_3)_2$ (**189**) (**190**)

(**b**) R2 =

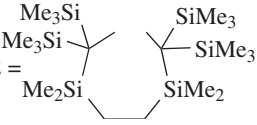

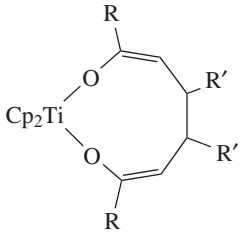

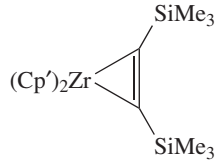

(**191**) R = R′ = Ph
R = *t*-Bu, R′ = Ph
R = Ph, R′–R′ = $(CH_2)_3$

(**192**) Cp′ = Cp
$(Cp')_2$ = ind =

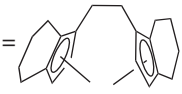

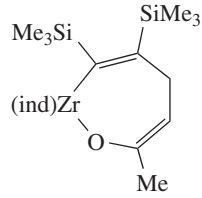

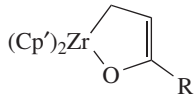

(**193**) Cp′ = Cp, R = Me
$(Cp')_2$ = ind, R = OBu-*t*

(**194**)

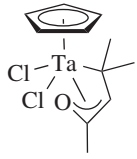

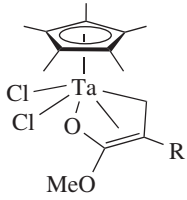

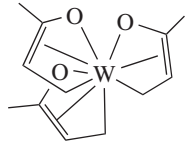

(**195**) (**196**) (**197**)

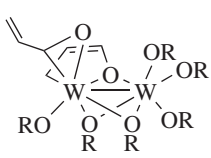

(**198**)

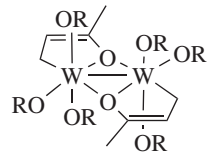

(**199**)

and AcCH=CH_2 gives the W(VI) complex **197**[523]. [$W_2(OCH_2Bu\text{-}t)_6(py)_2$] reacts with acrylaldehyde (CH_2=CHCHO) to afford **198** or methyl vinyl ketone (CH_2=CHAc) to yield **199**[524].

The Os(II) complex **200**•BF_4^- reacts at low temperature with $TlPF_6$ to give the Os(IV) complex **201**•PF_6^- which, in turn, transforms in solution into the metalafuran **202**•PF_6^- (R = H, Section IV.E) by a 1,2-hydrogen shift from the CH_2 group to the metal center. Complexes **202**•BF_4^- have been prepared by reacting **203**•BF_4^- with AcCH=CHR[525].

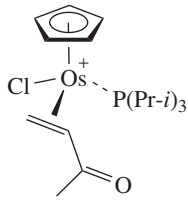

(**200**)

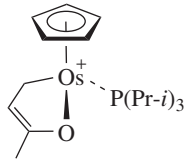

(**201**)

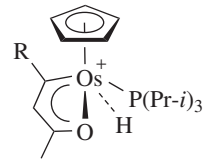

(**202**) R = H, Ph

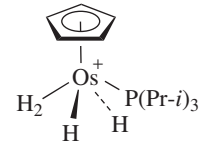

(**203**)

[M(cod)$_2$] (M = Ni, Pt) reduces (i) PhC(O)CH=C(Mef)$_2$ in the presence of *t*-BuNC to give **204**[526], (ii) alkynylenal **205** in the presence of tmeda (L^L) to afford **206**[527] and (iii) Acf_2CH_2 to give **207**[528].

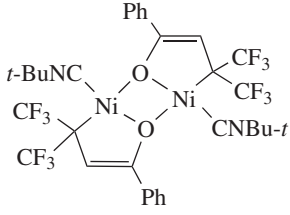

(**204**)

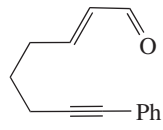

(**205**)

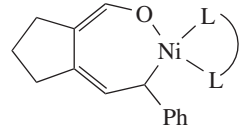

(**206**)

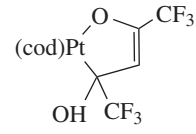

(**207**)

2. Enediolato complexes by reduction of α-diketones and reductive coupling

Enediolato complexes have been prepared by deprotonation of α-diketones (Section II.A.2.a) or by using CO or carbonyl complexes (Section IV.B).

Benzil (Bz–Bz) and other α-diketones react (i) with the aluminum hydride complex **208** to afford **209** (the diketone is reduced by the hydrido ligand)[529], (ii) with Green's 'GaI' (predominately consisting of the salt, $Ga(I)_2[Ga(II)_2I_6]$) to give **210**[530] or (iii) with stannylenes **188** to afford **211**[517,531].

Reductive coupling of PhCHO by the Cr(II) complex **212** affords the Cr(III) enediolato **213**[532]. The α-diketones RC(O)C(O)R (R = Me, Ph, Tol) are reduced (i) by $[W(OR')_3]_2$

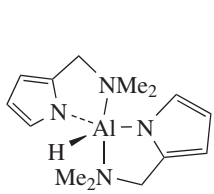

(**208**)

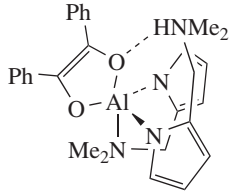

(**209**)

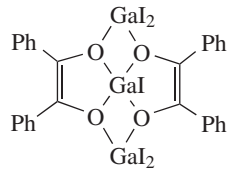

(**210**)

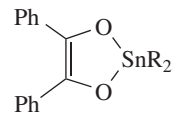

(**211**)

($R' = t$-Bu, i-Pr) to give **214**[533], (ii) by the dinitrogen complex [{Zr(η^5-Cp*)$_2$(N$_2$)}$_2$N$_2$] to afford [Zr(η^5-Cp*)$_2${*O*,*O*-OC{=C(R)O}R}] (R = Me, t-Bu)[534], (iii) by 'Ti(η^5-Cp)$_2$' to give [Ti(η^5-Cp)$_2${*O*,*O*-OC{=C(Ph)O}Ph}][535] or (iv) by [VCl$_2$(tmeda)] to give [V{*O*,*O*-OC{=C(Ph)O}Ph}$_2$(tmeda)][536].

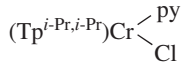

(**212**)

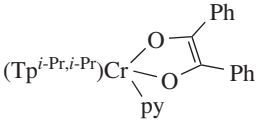

(**213**)

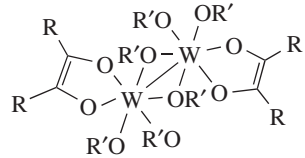

(**214**) R = Me, Ph, tol; R′ = t-Bu, i-Pr

3. Oxidation of deprotonated diketoamines

The diketoamine HN{CH$_2$C(O)Bu-t}$_2$ is threefold deprotonated by triethylamine and two-electron oxidized (i) by BiCl$_3$ to give the nine-coordinated Bi(III) complex **215** and Bi(0)[537], (ii) by SnCl$_4$ to give the Sn(II) complex **216**[538] or (iii) by two equivalents of LDA and one equivalent of PbCl$_2$ to give **217**, where the O^N^O ligands are the same as those in **215** and **216**, and Pb[447].

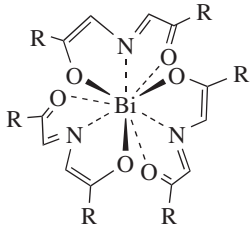

(**215**) R = t-Bu

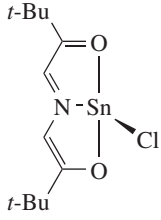

(**216**)

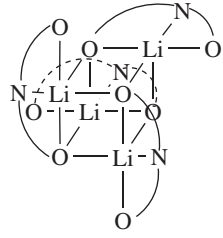

(**217**)

4. Oxidative addition reactions

The reaction of t-BuC(O)CH(Br)Me with Mg in Et$_2$O gives [MgBr{μ-OC(=CHMe)Bu-t}(OEt$_2$)]$_2$[539]. The Ti(III) complex [Ti{N(Bu-t)Ar}$_3$] oxidatively adds [RC(O)CH$_2$]$_2$ to give the Ti(IV) enolato complex [Ti{N(Bu-t)Ar}$_3${OC(=CH$_2$)R}] (Ar = C$_6$H$_3$Me$_2$-3,5; R = Tol, An-4, OC$_6$H$_3$(Bu-t)$_2$-3,5, NPhMe)[540].

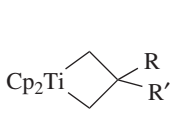

(**218**)

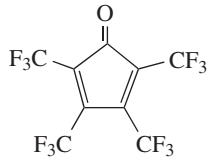

(**219**)

(**220**)

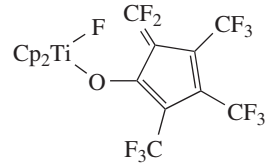

(**221**)

The reaction of titanacyclobutanes **218** (R = H, R′ = *t*-Bu, *i*-Pr; R = R′ = Me) with **219** occurs with the reductive elimination of cyclopropanes **220** and a C–F oxidative addition to the resulting Ti(II) complex 'Ti(η^5-Cp)$_2$' to give **221**[541].

Complexes [M(CO)$_4$(NO)]$^-$ react with **222** to give **223**[542]. Dicarbonyl compounds RC(O)CH$_2$C(O)R′ (R = R′ = Me, OMe; R = Me, R′ = OMe) react with [Fe(N$_2$)(depe)$_2$] (depe = 1,2-bis(diethylphosphino)ethane) to afford **224**, as a result of a C–H oxidative addition reaction[543]. [Fe(CO)$_2$(PEt$_3$)$_2$(N$_2$)] oxidatively adds XCH$_2$CO$_2$R (R = Me, Et) to give the mixture of isomers **225** and **226**; the latter reacts with DBU and [SiMe$_3$Cl] to afford the metalafuran **227** (Section IV.E)[544].

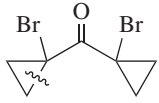

(**222**)

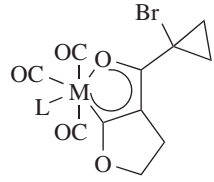

(**223**) M/L = Cr/NO, Mn/CO

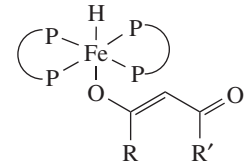

(**224**)

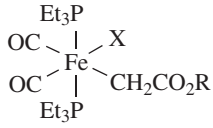

(**225**)

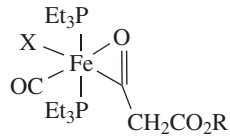

(**226**)

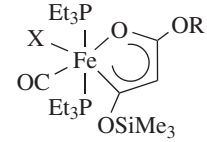

(**227**) R/X = Me/Cl, Br; Et/I

Ir(I) complex **228**•BF$_4^-$ rearranges at room temperature to give the Ir(III) metalafuran **229**•BF$_4^-$ (Section IV.E) after a C–H oxidative addition[545].

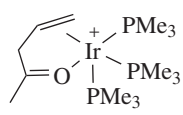

(**228**)

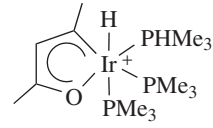

(**229**)

The oxidative addition reaction of the ylide **230** to [Ni(cod)$_2$] gives Ni(II) complex **231**, which is successfully used in the Shell Higher Olefin Process (SHOP)[546]. Similar reactions have been used to prepare [NiPh{*O*,*E*-OC(=C(R′)EPh$_2$)R}(PPh$_3$)] (E = P, As)[547,548], [Ni{η^3-CH$_2$C(R)CHR′}{*O*,*P*-OC(=CHPPh$_2$)Ph}] (from [Ni{η^3-CH$_2$C(R)CHR′}$_2$] and the

ylide) and [Ni{η^5-Cp}{*O*,*P*-OC(=CHPPh$_2$)Ph}] (from [Ni(η^5-Cp)$_2$] and the ylide)[547]. However, most of the other phosphinoenolato complexes have been prepared by deprotonation of the corresponding phosphines R$_2$PCH(R′)C(O)R″ (Section II.A.5). [Pt{P(*c*-Hex)$_3$}$_2$] reacts quantitatively with two equivalents of AcCO$_2$Et to yield **232** (L = P(*c*-Hex)$_3$). A mechanism proposed for the formation of **232** consists of a C−H oxidative addition reaction giving **233**, insertion of a second pyruvate unit into the C−Pt bond to give **234**, followed by cyclization with EtOH elimination[549]. Refluxing a thf solution of [Ru$_3$(CO)$_{11}$(PPh$_2$CH$_2$C(O)Ph)] gives **235** after a C−H oxidative addition reaction[550].

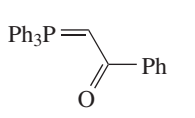

(**230**)

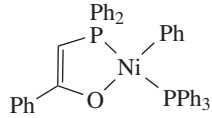

(**231**)

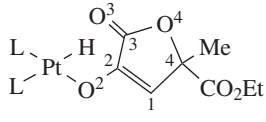

(**232**)

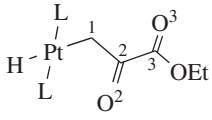

(**233**)

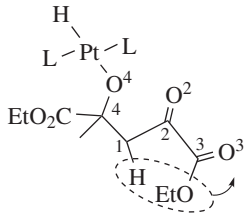

(**234**)

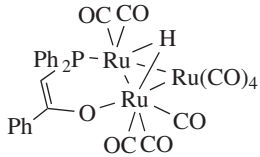

(**235**)

C. Insertion/Migration/Cleavage Reactions

The reaction of **236** with LiR (R = Si(SiMe$_3$)$_3$, SiEt$_3$, GeEt$_3$) occurs with opening of the cyclobutanedione ring to give **237** (equation 4)[551].

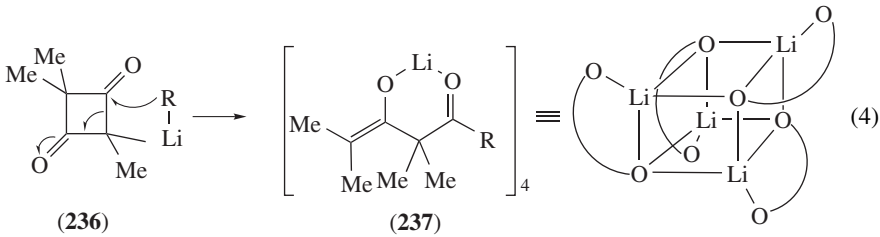

(4)

(**236**) (**237**)

The 1:1 reaction of ZnR$_2$ with α-imino ketones R′N=C(R″)C(O)R‴ leads to quantitative formation of the dinuclear complexes [ZnR{μ-*N*,*O*-N(R)(R′)C(R″)=C(R‴)O}]$_2$. The crystal structure of the derivative **238** has been reported[552]. The reaction of [ZnEt(Cp)] and Et$_2$NCH$_2$CO$_2$Et gives **239**, probably through the intermediate **240**[553]. The sodium dialkylamidozincate [(tmeda)Na(μ-Bu-*t*)(μ-TMP)Zn(Bu-*t*)] reacts with benzophenone to give **241**[554].

[Ti(η^5-Cp*)$_2$(=S)(py)] reacts with unsaturated aldehydes RCH=C(R′)CHO to afford [Ti(η^5-Cp*)$_2${*O*,*S*-OCH=C(R′)CH(R)S}][555]. The reaction of **242** with *i*-PrCO$_2$Me gives **243**, after β-elimination of MeOH from the intermediate **244**[556].

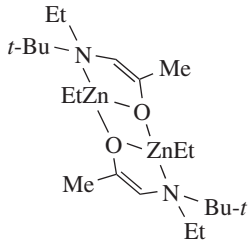

(**238**)

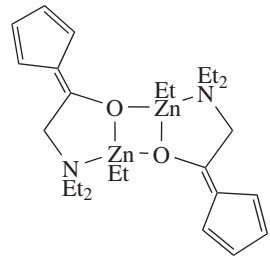

(**239**)

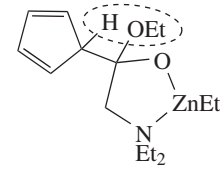

(**240**)

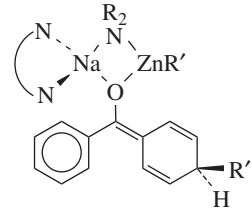

(**241**) R_2N = TMP, R′ = *t*-Bu

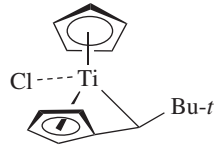

(**242**)

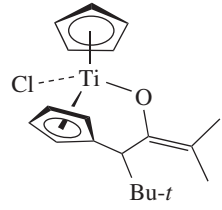

(**243**)

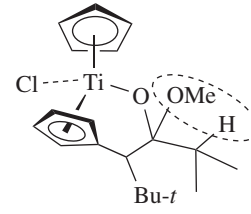

(**244**)

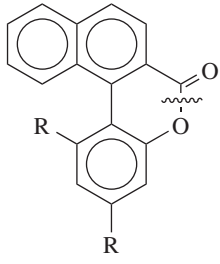

(**245**) R = H, OMe, Me

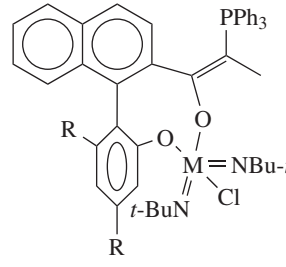

(**246**) M = Mo, W

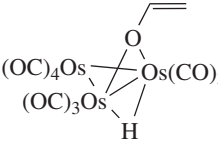

(**247**)

The imido complexes [M(NBu-*t*)$_2$(CH=PPh$_3$)Cl] (M = Mo, W) react with **245** to afford complexes **246** resulting after a C−O bond cleavage and the migration of the ylide ligand to the carbonyl carbon atom[557]. [$Os_3H_2(CO)_{10}$] reacts with maleic anhydride or ketene to give **247**[558].

Addition of $MeO_2CC{\equiv}CCO_2Me$ to $[Re(N{=}CPh_2)(bpy)(CO)_3]$ affords the metalafuran **248** (Section IV.E)[559]. Reactions of enaminones **249** with carbene complex **250** afford complexes **251**[560]. The carbene porphyrin complex **252** reacts with CO to give **253**[561].

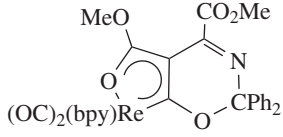

(**248**)

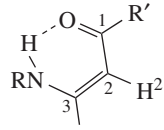

(**249**)

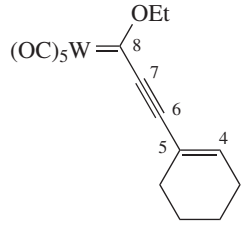

(**250**)

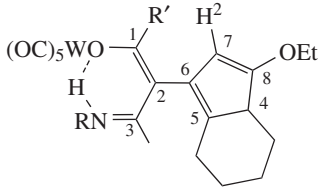

(**251**)

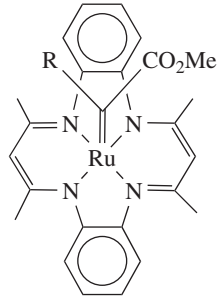

(**252**) R = Me, Ph

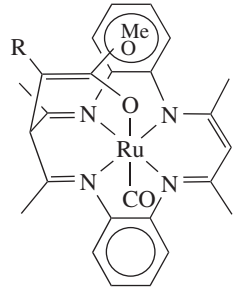

(**253**)

Complex **254**•BF_4^- rearranges upon heating to give the metalafuran **255**•BF_4^- (Section IV.E)[545]. The reaction of $[Sm(\eta^5\text{-}Cp^*)_2H]_2$ with two equivalents of $MeC(=CH_2)CO_2Me$ affords **256**[562].

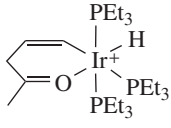

(**254**)

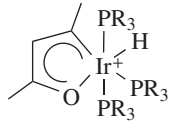

(**255**)

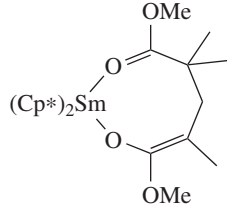

(**256**)

III. SYNTHESIS FROM KETENES, ISOCYANATES AND ACYL HALIDES

A. Ketenes

In Section IV.D we describe the synthesis of complexes containing the dianionic enolato η^2-*C*,*O*-ketenido ligand, which usually are not prepared from ketenes. In this section we will show how ketenes are useful reagents to prepare other enolato complexes. In most cases a ketene $RR'C{=}C{=}O$ inserts into a M−C bond of a [M]−R″ complex to give

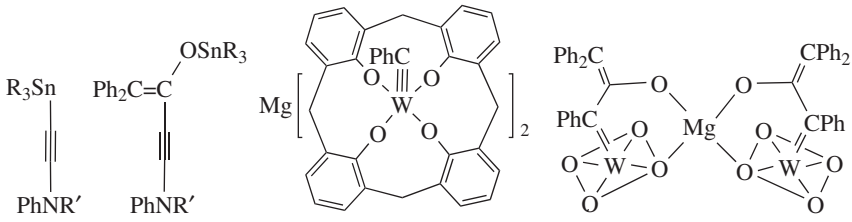

(**257**) (**258**) (**259**) (**260**)

[M]−OC(=CRR′)R″. Thus, dpk inserts into the C−Sn bond of **257** (R, R′ = Me, Bu, Ph) to give **258**[563] and reacts with the carbyne complex **259** to give **260**[564].

When ketenes $R_2C{=}C{=}O$ (R = *t*-Bu[565], Ph[566]) are heated with **261**, complexes **262** and ethylene are obtained, but at room temperature dpk leads to **263**[567]. The ketenido complex **264** (Section IV.D) reacts with one equivalent of dpk to afford **265**[568].

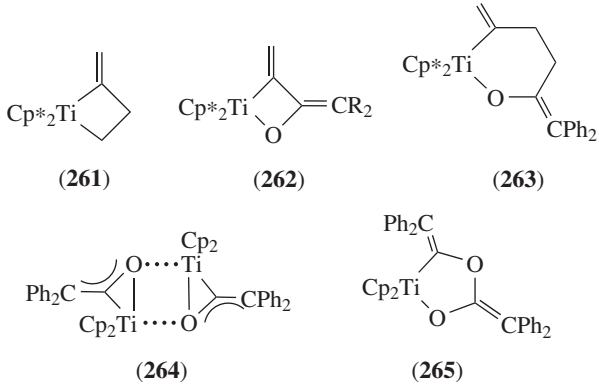

(**261**) (**262**) (**263**)

(**264**) (**265**)

Complex [Ti(nacnac)(μ_2-O)(μ_2-OTf)]$_2$ (**266**) reacts with dpk or *t*-BuCH=C=O to afford **267**[569]. A similar reaction takes place between [Ti(nacnac)(=NC_6H_3(Pr-*i*)$_2$-2,6)(OTf)] and dpk[570]. The imido complex **268** reacts with an excess of dpk to afford **269** and $Ph_2C{=}C{=}NBu$-*t*[51]. The reaction of dpk with [Zr(η^5-Cp)$_2$R$_2$] gives **270** or **271**, depending on R and the reaction conditions[571].

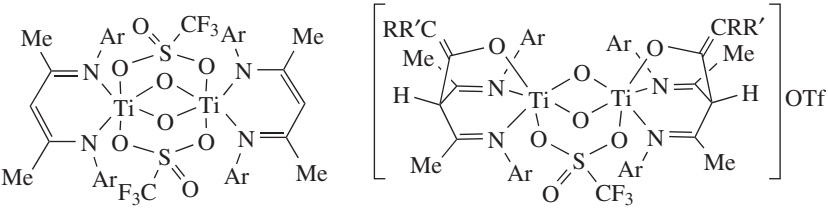

(**266**) Ar = C_6H_3(*i*-Pr)$_2$-2,6 (**267**) R = R′ = Ph, R = H, R′ = *t*-Bu

The isoprene derivative **272** reacts with dpk to afford **273**[572]. Complexes **274** react with dpk to give **275**[573].

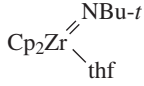

(**268**)

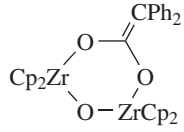

(**269**)

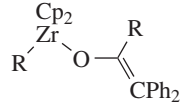

(**270**) R = Me, Bn, Ph

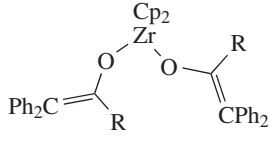

(**271**) R = Me, Ph

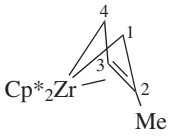

(**272**)

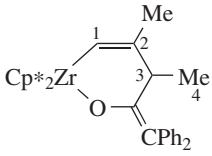

(**273**)

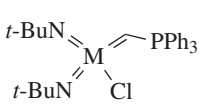

(**274**) M = Cr, Mo, W

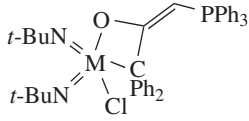

(**275**)

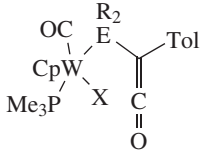

(**276**) X = Cl, E = P, R = Ph
X = I, E = As, R = Me

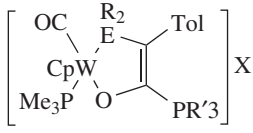

(**277**) R′ = Me, Et, *i*-Pr, *n*-Bu

Nucleophilic attack of trialkylphosphines PR'_3 at the central ketene carbon in complexes **276** affords the phosphino- and arsino-enolato complexes **277** (Section II.A.5)[574].

The oxorhenium complex $[Re(\eta^5\text{-Cp}^*)(=O)(\mu\text{-O})]_2$ reacts with dpk to give the product of a formal [2 + 2]-cycloaddition $[Re(\eta^5\text{-Cp}^*)(=O)(O,O\text{-O}_2C{=}CPh_2)]$[575]. $[Os_3H_2(CO)_{10}]$ reacts with ketenes to give **278**[558, 576] (see **247**). Complex **279** reacts with dpk to give

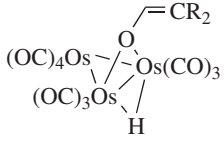

(**278**) R = H, Me, Ph

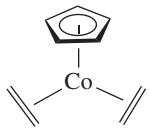

(**279**)

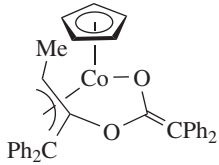

(**280**)

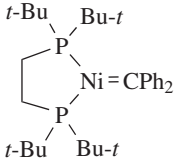

(**281**)

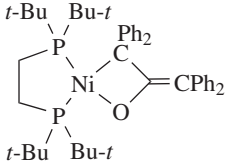

(**282**)

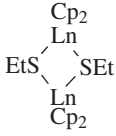

(**283**)

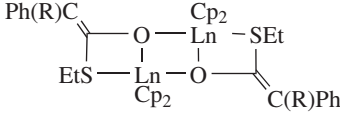

(**284**) Ln = Yb, Er, Sm, Y, R = Ph
Ln = Er, R = Et

complex **280**, which contains a new ligand formed by condensation of two molecules of dpk and one of ethylene[577]. In this process, Co(I) is oxidized to Co(III). Insertion of dpk into the Ni carbene bond of complex **281** affords **282**[578]. Ph(R)C=C=O inserts into the metal–sulfur bonds of **283** to give **284**[579].

The reaction of dpk with *trans*-[PtH_2{P(*c*-Hex)$_3$}$_2$] gives *trans*-[PtH{OC(=CPh_2)H}{P(*c*-Hex)$_3$}$_2$][580].

B. Isocyanates

The reaction of [$MgCp_2$] with four equivalents of PhNCO in thf gives **285**[581].

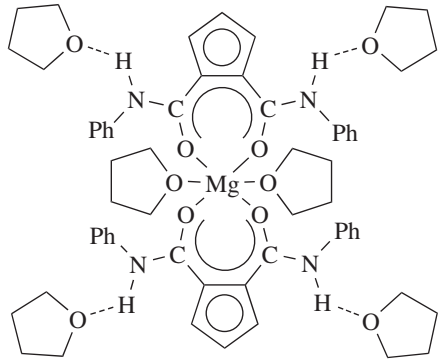

(**285**)

Complexes **286** react with N_2=$CHCO_2Et$ and R′NCO to afford **287**[52]. The reaction of equimolar amounts of PhNCO and **288** affords **289**[582].

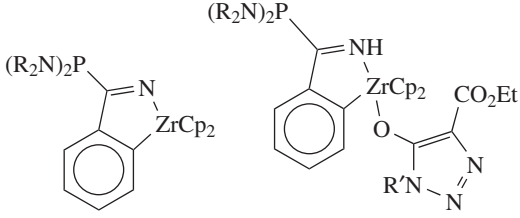

(**286**) R = *i*-Pr, *c*-Hex (**287**) R = *i*-Pr, *c*-Hex; R′ = Ph, α-naphtyl (**288**) R/R′ = Me/Ph, Ph/Me (**289**)

C. Acyl Halides

Complex **290** reacts with 4-$MeC_6H_4C(O)Cl$ to give LiCl and **291**[583]. Carbene complexes [Ta(CH_2Bu-*t*)$_3$(=CHBu-*t*)][584] or [Ti(η^5-Cp)$_2$(=CH_2)][585] react with RC(O)Cl (R = Me, Et, Ph, *t*-Bu) to give [Ta(CH_2Bu-*t*)$_3$Cl{OC(=CHBu-*t*)R}] or [Ti(η^5-Cp)$_2$Cl{OC(=CH_2)R}], respectively.

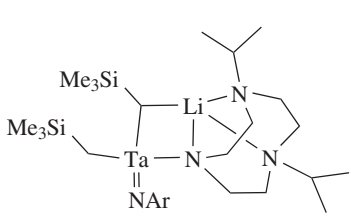

(**290**) Ar = $C_6H_3(i\text{-Pr})_2$-2,6

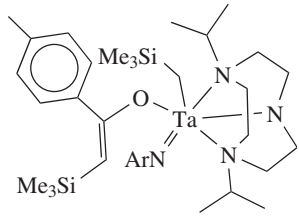

(**291**)

IV. SYNTHESIS FROM CARBON MONOXIDE AND CARBONYL COMPLEXES

Carbon monoxide and its metal complexes are of widespread use as the source of enolato ligands in the synthesis of transition metal enolato complexes.

A. Insertion/Migration Reactions

Carbon monoxide can be inserted into some metal−C bonds to give metal acyl complexes [M]C(O)R. However, early transition, lantanide and actinide metals usually afford [M](κ^2-O=CR) complexes. When R is an alkyl group (CR′R″R‴), a 1,2-shift of some of its substituents can give rise to an enolato complex (equation 5).

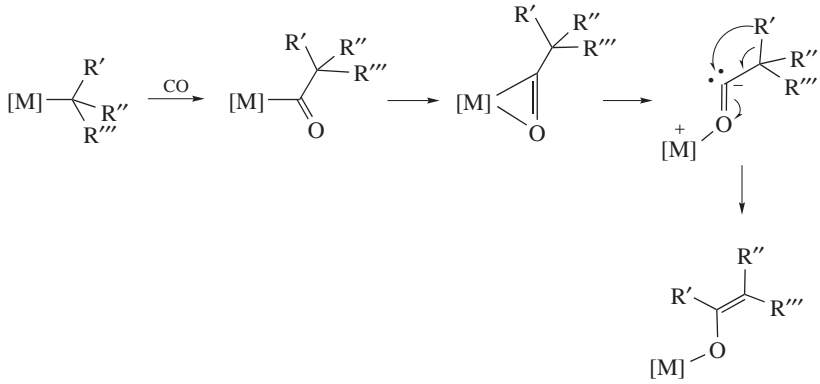

(5)

Complex **292a** reacts with CO to give **293**[586]. A similar reaction occurs in the carbonylation of [Zr(η^5-Cp)$_2${CH(Ar)SiMe$_3$}Cl] (Ar = 9-anthryl) to give [Zr(η^5-Cp)$_2${OC(=CHAr)SiMe$_3$}Cl][587] or that of [Lu(η^5-Cp*)(CH$_2$SiMe$_3$)$_2$(bpy)] to give [Lu(η^5-Cp*){OC(=CH$_2$)SiMe$_3$}(bpy)][588]. However, carbonylation of **292b** gives **294**, which decomposes upon heating at 100 °C to afford **295** after a 1,2-hydrogen shift[589]. Similarly, the enolato complex [Hf(OCH=CH$_2$)Me(N^C^N)] (N^C^N is a chelating diamido-N-heterocyclic-carbene ligand; see hafnium complexes at the end of Section IV.B) is obtained when [Hf(η^2-O=CMe)Me(N^C^N)] decomposes at room temperature[590]. Carbonylation of [Ta(η^5-Cp*)Cl$_3$(CH$_2$R)] in the presence of the ligand L affords [Ta(η^5-Cp*)Cl$_3$(OCH=CHR)(L)] (R = Tol, L = thf[591]; R = *t*-Bu, L = py[592]). Carbonylation of **296** affords the phosphinoenolato complex **297** (Section II.A.5)[593].

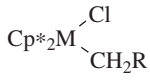

(**292**) (**a**) M = Th, U, R = $SiMe_3$
(**b**) M = Th, R = *t*-Bu

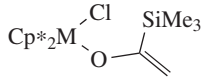

(**293**) M = Th, U

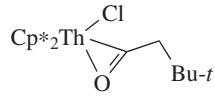

(**294**)

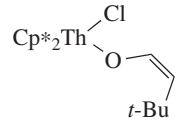

(**295**)

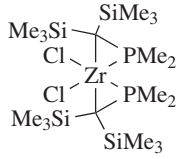

(**296**)

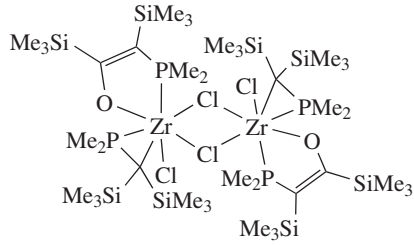

(**297**)

Carbonylation of **298** gives the dienolato complex **299**[594]. Complex **300** absorbs CO rapidly to yield **301**, while **302** reacts with CO to form **303**[595].

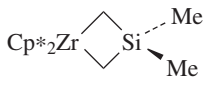

(**298**)

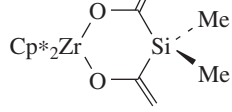

(**299**)

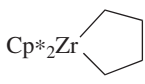

(**300**)

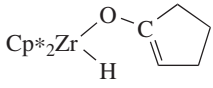

(**301**)

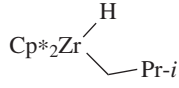

(**302**)

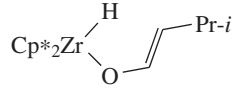

(**303**)

Reaction of **304** with CO affords an equimolecular mixture of **305** and the enolato complex **306**, implying an interesting build-up of the 3-methyl-2-buten-2-olato ligand from two CO molecules and three methyl groups[596].

Complex **307** reacts with CO to give **308**, probably by insertion into the Zr−Si bond to afford **309** that rearranges to the intermediate **310**[597]. The dinuclear complex **311** reacts with CO differently, namely by insertion into the V−C and Si−C bonds to give **312**[598].

Carbonylation of the yttrium complex **313** gives the dinuclear enolato complex **314**[599]. The lutetium complex **315** reacts with two molecules of CO to give **316**, a process which can be formally viewed as the result of (i) a CO insertion into a Lu−C bond to give an η^2-acyl complex, followed by acyl insertion into a 2,2′-bipyridine C−H bond, and (ii) a second CO insertion followed by $SiMe_3$ migration[588].

The migrating group can be part of a ligand. Thus, carbonylation of **317** affords **318** (X = Cl, Me), which can be the result of insertion of CO into the Me−Ta bond, C−N bond cleavage and migration of the CMe_2 group taking place in succession[600].

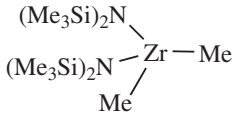

(**304**)

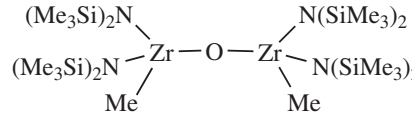

(**305**)

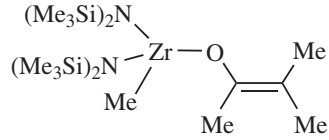

(**306**)

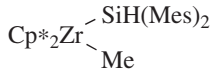

(**307**)

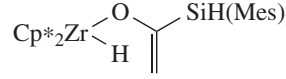

(**308**)

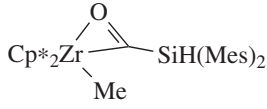

(**309**)

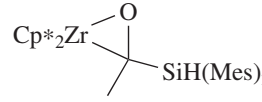

(**310**)

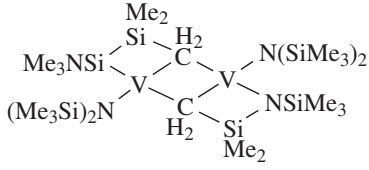

(**311**)

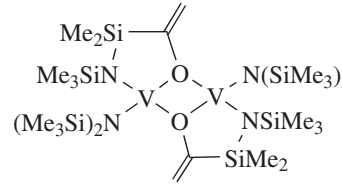

(**312**)

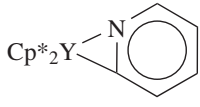

(**313**)

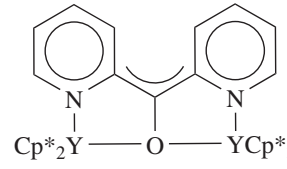

(**314**)

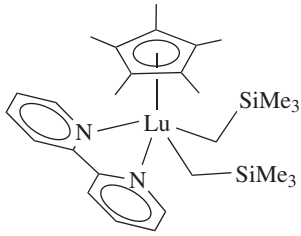

(**315**)

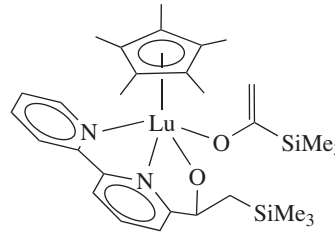

(**316**)

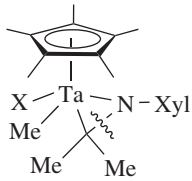

(**317**)

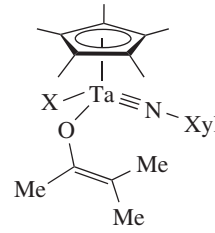

(**318**)

The carbyne complex **319** reacts with CO to give **320**[601], which results from a double CO insertion and PMe_3 migration, while **321** reacts with the manganese carbonyl complex **322** in refluxing toluene to give **323**[602].

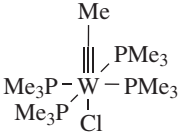

(**319**)

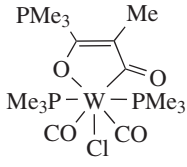

(**320**)

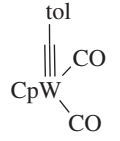

(**321**)

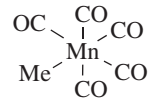

(**322**)

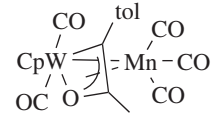

(**323**)

The metalaenolato complexes **324** (M = Cr, Mo, W), prepared *in situ* from $[M(CO)_6]$, EtOC≡CH and LiBu-*n*[603], react with $[Re(CO)_5(FBF_3)]$ to give **325**[604].

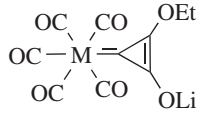

(**324**)

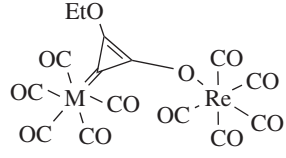

(**325**)

The reaction of $[MnMe(CO)_5]$ with **326** leads to a mixture of products containing **327**. Probably, complexes **328** and **329** are intermediates in this process[605].

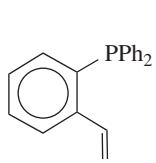

(**326**)

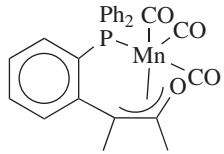

(**327**)

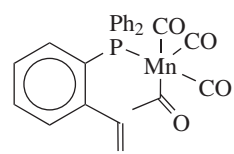

(**328**)

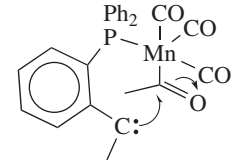

(**329**)

B. Enediolato Complexes

Complexes of this type have been prepared from carbonyl compounds by deprotonation (Section II.A.2.a) and redox reactions (Section II.B.2). Complex **330** decomposes above −50 °C to give **331**. Complexes **332** react with CO to afford **333**[586, 595]. The latter (M = Zr) has also been obtained from [{Zr(η^5-Cp*)$_2$(N$_2$)}$_2$N$_2$] and MeC(O)C(O)Me (Section II.B.2)[534].

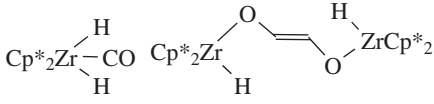

(**330**)

(**331**)

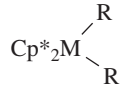

(**332**) M = Zr, R = Me
M = Th, U, R = Me, CH_2SiMe_3

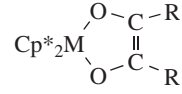

(**333**)

Treatment of [Zr(η^5-Cp*)$_2$(CO)$_2$] with **334** at −78 °C gives **335**, which, in turn, reacts with MeI to afford **336** or with py to give **337**[606].

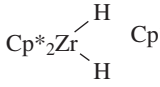

(**334**)

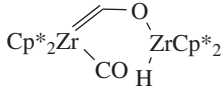

(**335**)

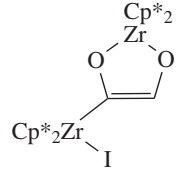

(**336**)

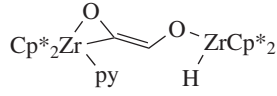

(**337**)

Carbonylation of **338** produces complex **339**[607], a compound of a type different from that obtained from its Zr homologue (**300**).

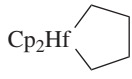

(**338**)

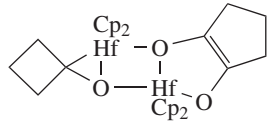

(**339**)

Reaction of equimolecular amounts of **340** and P(*c*-Hex)$_3$ or 2,6-lutidine in a CO atmosphere under pressure gives **341**[592]. Complex **342** reacts with CO to afford **343**[600].

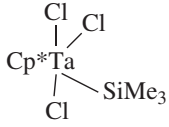

(**340**)

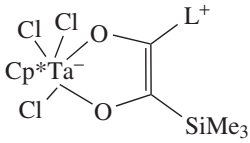

(**341**) L = P(*c*-Hex)$_3$, 2,6-Me$_2$C$_5$H$_3$N

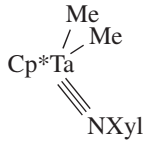

(**342**)

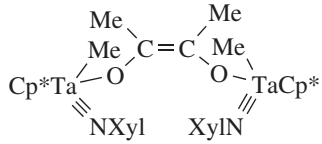

(**343**)

[Th(η^5-Cp*)$_2$H(OR)] reacts with CO to give [{Th(η^5-Cp*)$_2$(OR)}$_2${μ-*O*,*O*-*Z*-OCH=CHO}][608]. [Sm(η^5-Cp*)$_2$H]$_2$ reacts with CO and OPPh$_3$ to give [{Sm(η^5-Cp*)$_2$(OPPh$_3$)}$_2${μ-*O*,*O*-*Z*-OCH=CHO}], which, in turn, isomerizes in solution at room temperature to the complex with the *E*-OCH=CHO ligand[609]. Complexes [Ln(η^5-Cp*)$_3$] (Ln = Sm[610], Nd[611]) react with CO to form the pentamethylnorbornadienyliumdiolato complex **344.**

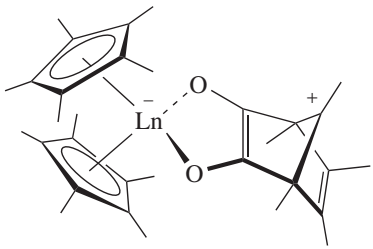

(**344**)

The U(III) complex **345a** reacts with CO at atmospheric pressure to give the U(IV) complex **346**, which is the first reported deltato complex[612]. The same authors have reported the surprising formation of the squarato complex **347** from CO and **345b**[265]. In both cases, CO is the only source of the dianionic oxocarbon ligands.

Isolated η^2-acyl complexes, which are probably intermediates in many of the above reactions, can further react with CO to give a variety of C−C coupling products. Thus, the acyl complex **348a** reacts with CO to afford **349**[589], but in the presence of PR$_3$ the reaction gives **350**[613]. Similarly, CO reacts with **348b** to give **351**[614] or with **352** to afford **353**[590].

C. Amidoenolato Complexes

The η^2-iminoacyl complexes **354** react with CO to give the corresponding amidoenolato complexes **355**[615]. Similarly, the reaction between **356** and CO gives **357**[590].

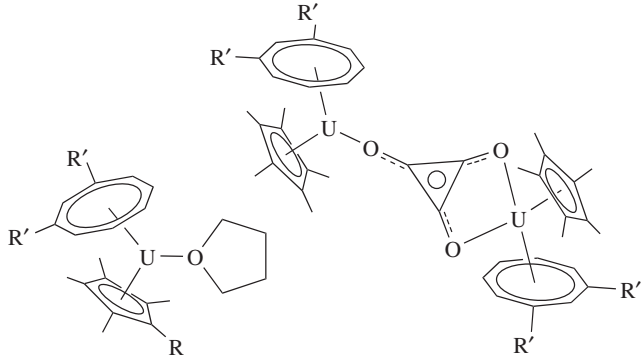

(**345**) (**a**) R = Me, R′ = Si(Pr-*i*)$_3$
(**b**) R = H, R′ = Si(Pr-*i*)$_3$

(**346**)

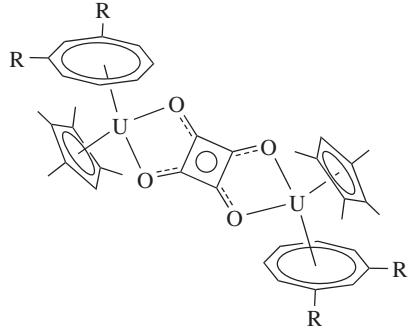

(**347**)

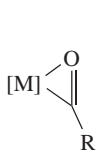

(**348**) (**a**) [M] = Cp*$_2$Th, R = CH_2Bu-*t*
(**b**) [M] = Cp_2Lu, R = Bu-*t*

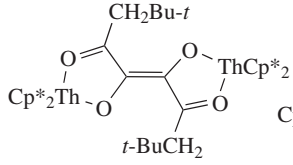

(**349**)

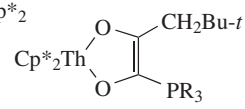

(**350**) R = Ph, Me

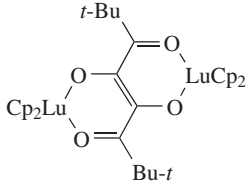

(**351**)

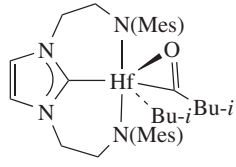

(**352**)

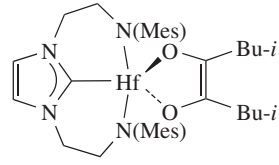

(**353**)

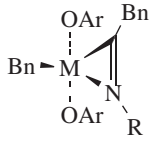

(**354**) M = Ti, Ar = C_6H_3(Pr-*i*)$_2$-2,6, R = Xyl
M = Zr, Ar = C_6H_3(Bu-*t*)$_2$-2,6, R = Bu-*t*

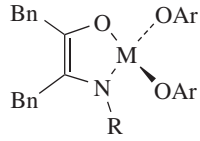

(**355**)

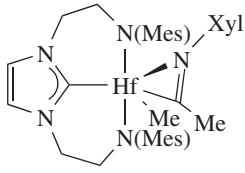

(**356**)

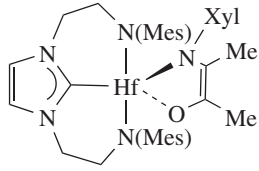

(**357**)

D. Ketenido Complexes

When a ketene is coordinated to a metal through both C and O atoms, two extreme resonance forms can be considered: that containing the ketene as a neutral ligand (**358**) and that with a ketenide dianion (**359**). The contribution of the enolato form **359** can be estimated by the C−O bond distance (d) and the O−C−C angle (α). In some complexes, a ketenido ligand can bridge two metal centers, as in **360**.

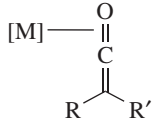

(**358**)

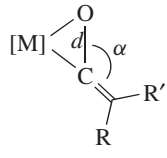

(**359**)

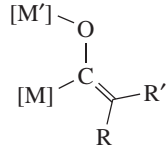

(**360**)

A search of the Cambridge Crystallographic Database shows the expected inverse relationship between d and α. Complexes prepared by reacting a ketene and [Ti(η^5-Cp)$_2$(CO)$_2$][568,616], [V(η^5-Cp)$_2$][617], [Nb(η^5-$C_5H_4SiMe_3$)$_2$Cl]$_2$[618], [RhCl{P(Pr-*i*)$_3$}]$_2$[619], [OsCl(NO){P(Pr-*i*)$_2$R}$_2$][620], or [Ni{P(*t*-Bu)$_2$CH$_2$P(Bu-*t*)$_2$}(olefin)][621] show smaller d (1.25–1.33 Å) and larger α (129–140°) values than those in which the ligand originates by deprotonation of an acyl ligand (Section IV.D.1) or by insertion of CO into into a vinyl–, carbene–or methylene–metal bond (Section IV.D.2). In the latter, d and α values are in the 1.32–1.44 Å and 117–127° ranges, respectively. Therefore, complexes in the first group could be classified as ketene complexes (**358**) and the other as ketenido complexes (**359**). However, some exceptions can be found in the borderline between the two ranges. Thus, complex **361**, for which $d = 1.27$ Å and $\alpha = 131°$ (R = Me), is obtained along with the acyl enolato complex **362**, in the reaction of the mixture of isomers **225** and **226** (Section II.B.4; R = Me, Et) with DBU and CO[544]. These data suggest that the ranges for ketenido complexes should be slightly extended to $d = 1.27$–1.44 Å and $\alpha = 117$–$131°$. Complex **264** (Section III.A) is another exception because it is prepared

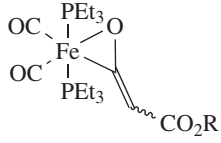

(**361**)

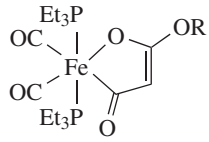

(**362**)

by reacting $[Ti(\eta^5\text{-}Cp)_2(CO)_2]$ with one equivalent of dpk, but the structural parameters ($d = 1.311$ Å, $\alpha = 128.8°$) suggest that it is a ketenido complex.[568].

Therefore, it seems that the α angle is the best parameter to distinguish between formally ketene (129–140°, **358**) and ketenido (117–131°, **359**) complexes, because there is only a small overlap between these ranges (129° and 131°) while it is larger for distances (1.27–1.33 Å). In agreement with the above data, a theoretical study shows the complex $[Ni(\kappa^2\text{-}C,O\text{-}OC{=}CPh_2)\{P(t\text{-}Bu)_2CH_2P(Bu\text{-}t)_2\}]$ ($d = 1.298$ Å, $\alpha = 132.763°$) to be a ketene Ni(0) complex[621]. In some cases the reactivity of the ketene complexes proves that the oxidation state of the metal center is the same as that in the starting complex[619].

Terminal and bridging ketenido complexes are prepared by deprotonation of acyl complexes or by insertion of CO into a vinyl–, carbene–or methylene–metal bond.

1. Deprotonation of acyl complexes

The synthesis of complexes **363** was reported almost simultaneously by three different groups. **363a** is prepared by reacting PMe_3 with LiBu-*n*, $[Zr(\eta^5\text{-}Cp)_2Cl_2]$ and CO, with complex **364a** postulated as an intermediate in this reaction[622]. **363b** was synthesized by reacting **364b** with CO[623]. The deprotonation of the acyl complexes **365** with NaHMDS affords Na•**366**[624].

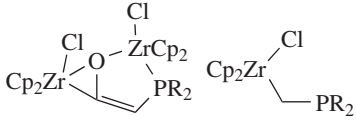

(**363**) (**a**) R = Me (**b**) R = Ph

(**364**) (**a**) R = Me (**b**) R = Ph

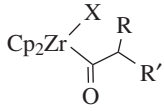

(**365**) X = Me, R = H, Me, R′ = H, Me
X = Cl, R = t-Bu, R' = H
X = Br, R = R' = H

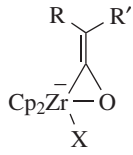

(**366**)

The acetyl complex [Fe]{C(O)Me} ([Fe] = $Fe(\eta^5\text{-}Cp)(CO)(PPh_3)$) reacts with LiBu-*n* and $ClPPh_2$ to give $Li[Fe]\{C(O)CHPPh_3\}$[73].

2. Carbon monoxide insertion reactions

Reaction of CO with the vinyl complex **367** gives **368**[625] and with **369** affords **370**[626].

Treatment of $[Ru_3(CO)_{10}\{(PPh_2)_2CH_2\}]$ with CH_2N_2 affords a mixture containing complex **371**, which has the simplest ketenido as a μ_3-bridging ligand[627]. The tantalum–lithium complex **372** reacts with CO to afford **373**[628].

Insertion of a terminal carbonyl ligand [M]CO into a metal carbene [M′]=CRR′ bond can generate a complex containing a bridging ketenido ligand (**374**)[629].

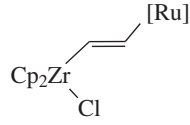

(**367**) [Ru] = Ru(η^5-Cp)$_2$(PMe$_3$)$_2$

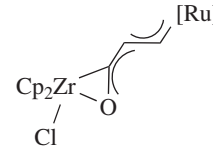

(**368**)

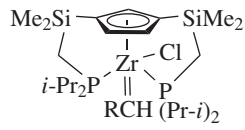

(**369**) R = Ph, SiMe$_3$

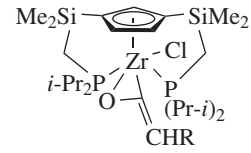

(**370**)

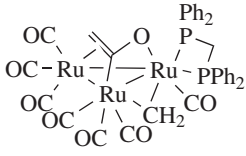

(**371**)

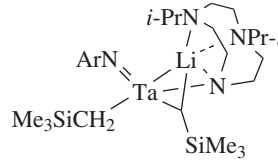

(**372**) C$_6$H$_3$(*i*-Pr$_2$)-2,6

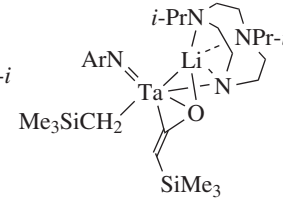

(**373**)

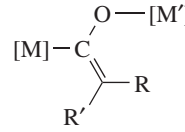

(**374**) (**a**) [M] = W(CO)$_5$, Mn(η^5-Cp)(CO)$_2$, Co(η^5-Cp)(CO);
[M′] = U(η^5-Cp)$_3$; R = H, R′ = PR″$_3$
(**b**) [M] = Re(R‴)(CO)$_4$ (R‴ = Me, Ph), Re(Prf)(CO)$_4$,
[M′] = Ta(η^5-Cp)$_2$Me, R = R′ = H

E. Metalafuran Complexes

Compounds in which a CH group of furan is replaced by a metal moiety are named metalafurans. However, X-ray and spectroscopic data suggest the electronic structure of these complexes to be a resonance hybrid of a metalafuran (**375**) and a metalavinylketone (**376**). Therefore we will formulate the *C*,*O* ligand as OC(R)C(R′)C(R″) and graphically as **377**. The synthesis of many of these compounds involves the use of carbonyl complexes or CO; however, other reagents have been used, as in the preparation of **57** (Section II.A.1), **204a** (Section II.B.1), **227**, **229** (Section II.B.), **248**, **255** (Section II.C) and others (Section VII). Alkynes are also key reagents in the preparation of many metalafurans as shown in equations 6 and 7, although they do not always involve CO or a carbonyl complex.

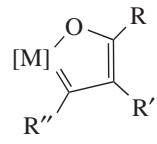

(**375**)

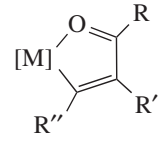

(**376**)

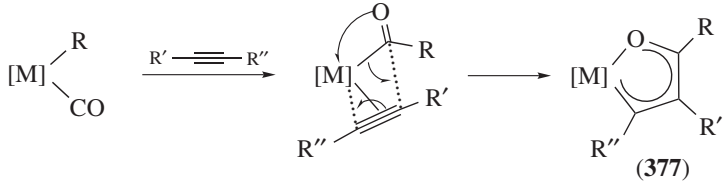

(**377**) (6)

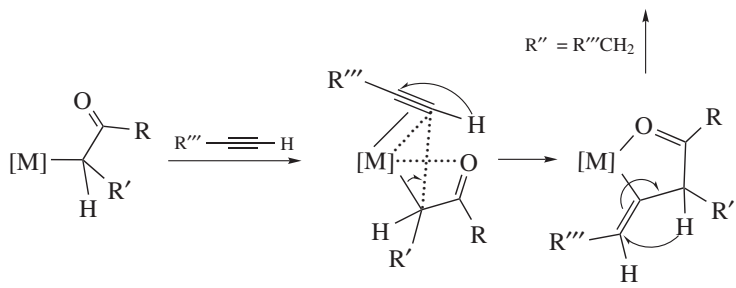

(7)

The first family of metalafurans was prepared by heating or irradiating a mixture of $[M(\eta^5\text{-Cp})(R)(CO)_3]$ and but-2-yne ($R' = R'' = Me$) to give **377** ([M] = $M(\eta^5\text{-Cp})(CO)_2$, M = Mo, R = Mef, Me, Bn; M = W, R = Mef, Me; equation 6)[630]. Many metalafurans ([M] = $M(\eta^5\text{-Cp}')(CO)_2$, M = Cr, Mo, W) have been prepared by this method: M = W, Cp′ = Cp, R = CH_2CO_2Et, R′ = H, R″ = Ph[631]; M = Mo, W, Cp′ = Cp, R, R′ = *c*-Pr, *c*-Bu, *c*-Pen, R″ = Me[632]; M = Cr, Mo, W, Cp′ = Cp, Cp*, C_5H_4Me, indenyl, R = Me, Et, *n*-Pr, *n*-Bu, R′ = R″ = H, Me, Ph[633]; M = Cr, Mo, Cp′ = Cp*, R = Me, R′ = Ph, R″ = H and M = Mo, W, Cp′ = Cp*, R = Me, R′ = H, R″ = Ph[634]. Other metalafurans have neither Cp or related η^5-ligands nor is M a group 6 element: [M] = $Fe(CO)_4$, R = Me, R′ = $SiMe_3$, H, CO_2Et, R″ = Ph; R′ = H, Ph, R″ = CO_2Et; R = Bn, R′ = H, R″ = *n*-Bu, CO_2Et[635] and [M] = $Re(CO)_3(PPh_3)$, R″ = Me, Et, *n*-Pr, CH_2Pr-*i*, CH_2Bu-*i*, Bn, CH_2SiMe_3, CH_2CO_2Me, CH_2CO_2Et, $(CH_2)_7Me$, R = OEt, R′ = H, Me; R = NEt_2, R′ = H (obtained according to equation 7 by reacting the 2-oxoalkyl complex $[Re\{CH(R')C(O)R\}(CO)_4(PPh_3)]$ with Me_3NO and R″C≡CH)[636].

Protonation with HBF_4 (i) of **378** at 183 K < *T* < 193 K leads to **379**, which inserts CO at *T* > 193 K to afford **380**[637] or (ii) of the carbyne complex $[W(Tp^{Me,Me})(\equiv CO-Tol)(CO)_2]$ in the presence of PhC≡CH gives the metalafuran complex $[W(Tp^{Me,Me})(CO)_2\{C,O\text{-}OCHCHC(Ph)\}]$[638]. Its isomer $[W(Tp^{Me,Me})(CO)_2\{C,O\text{-}OC(Ph)CHCH\}]$ is obtained by rearrangement in solution of $[W(Tp^{Me,Me})(CO)_2\{\equiv CCH_2C(O)Ph\}]$[639].

Treatment of the acetylide complexes $Li[W(\eta^5\text{-Cp})(C\equiv CR)(CO)(NO)]$ with ethyl iodoacetate gives, after protonation, the metalafuran with [M] = WI(NO), R = CH_2CO_2Et, R′ = H, R″ = *t*-Bu, Ph, Tol[640].

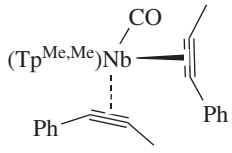

(**378**)

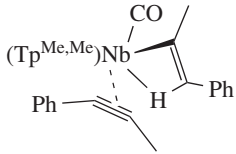

(**379**)

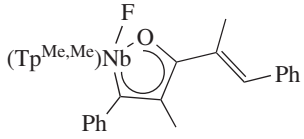

(**380**)

Reaction of **381** with one equivalent of CO gives the metalafuran **382** in high yield[641]. Similarly, the reaction between $[Mo(\eta^5\text{-Cp})(CO)(\eta^2\text{-R}'C{\equiv}CR'')_2]BF_4$ (R′ = Me, R″ = Me, Et) and K{BH(Bu-*n*)$_3$} in the presence of CO gives metalafuran complexes with [M] = $Mo(\eta^5\text{-Cp})(CO)_2$, R = *E*-C(=CHR‴)Me (R‴ = Me, Et), R′ = R″ = Me; R = *E*-C(=CHEt)Me, R′, R″ = Et[642]. Complex **383** decomposes at room temperature in CH_2Cl_2 to afford the metalafuran **384**[643].

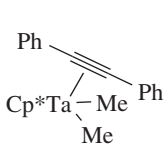

(**381**)

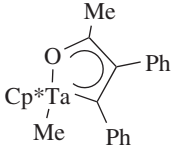

(**382**)

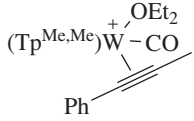

(**383**)

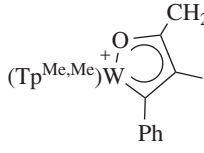

(**384**)

The reaction of $[W(Tp^{Me,Me})(\equiv NPh)(CO)(\eta^2\text{-PhC}{\equiv}CMe)]^+$ with MeMgBr affords the metalafuran complex $[W(Tp^{Me,Me})(=NHPh)\{C,O\text{-OC(Me)C(Me)C(Ph)}\}]^+$, resulting after methylation at the carbonyl carbon and protonation (presumably from water introduced in the workup) at the nitrene nitrogen[644].

V. SYNTHESIS VIA CLEAVAGE OF ETHERS AND RELATED COMPOUNDS

It has long been known that alkali metals (mainly Li) and some of their derivatives are able to cleave ethers[645]. The resulting fragments can coordinate metal complexes. However, other metals have also the same behavior.

A. Cleavage of the Tetrahydrofuran Ring

Cleavage of thf by LiR occurs with formation of ethylene and the metal enolate of acetaldehyde (ethenolate), the simplest enolate anion. For example, Li(OCH=CH_2) results from the reaction of LiR (R = *n*-Bu[646], *t*-Bu[646,647]) with thf and it has been used in the synthesis of other metal enolato complexes.

In some cases, the reaction between lithium compounds and metal complexes in thf leads to the unexpected formation of ethenolato complexes. Thus, the reaction of $[Li_2\{(NBu\text{-}t)_3S\}(thf)]_2$ with LiBu-*t* in thf gives **385**[648].

β-trans-$[N_4\{P(Ph)\{(c\text{-Hex})NH\}\}_4]$ can be deprotonated using an excess of LiBu-*n* in the presence of thf, to give the lithium ethenolato complex $[Li_6\{\mu_6\text{-}\beta\text{-}trans\text{-}[N_4\{P(Ph)\{(c\text{-Hex})N\}\}_4](\mu_3\text{-OCH=CH}_2)_2\}(thf)_2]$[649]. The phosphazene $H_6A = (2\text{-TolNH})_6P_3N_3$ reacts with twelve equivalents of LiBu-*n* in thf to give the monomeric dodecanuclear complex $[Li_{12}(A)(OCH{=}CH_2)_6(thf)_6]$ containing six enolato anions resulting from thf fragmentation[650].

The reaction of $[Li(thf)_2][Y(oepg)(\mu\text{-OEt})Li(thf)]$ (H_4oepg = octaethylporphyrinogen) with $LiCH(SiMe_3)_2$ or $LiBEt_3H$ affords the unexpected lithium complex [{Li(thf)}$_4$(oepg)]

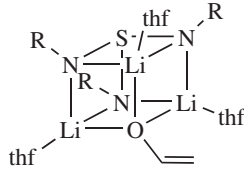

(**385**) R = *t*-Bu

$[Li(OCH{=}CH_2)(thf)]_2$[651]. The lithium derivative $[Li_4(oepg)]$ gives, when refluxed in thf, the enolato complex $[Li_6(oepg)(OCH{=}CH_2)_2(thf)_4]$[652].

LiBu-*n* reacts with the tripodal ligand **386** (Ar = Tol), $AlCl_3$ and thf to give a mixture from which **387** has been isolated in low yield[653].

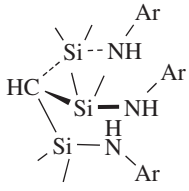

(**386**)

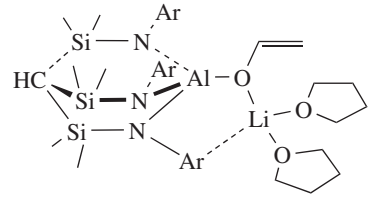

(**387**)

The tetranuclear complex $[Sm_2\{\mu\text{-}[(CH_2)_4]\text{-calix-tetrapyrrole}\}\{(\mu\text{-}Me)_2[Li(thf)_2]\}_2]$ (**388**) reacts with $PhSiH_3$ in thf to afford a mixture of compounds from which the hydrido ethenolato complex **389** has been isolated[654]. The calix-tetrapyrrole complex $[Sm\{\mu_4\text{-}[(CH_2)_4]\text{-calix-tetrapyrrole}\}(thf)\{Li_3(thf)_4\}(\mu_3\text{-}Cl)]$ decomposes in toluene to give the product of thf cleavage $[Sm\{\mu_4\text{-}[(CH_2)_4]\text{-calix-tetrapyrrole}\}(thf)\{Li_3(thf)\}(\mu_3\text{-}OCH{=}CH_2)]$[655]. Similar calix-tetrapyrrole complexes with ethenolato ligands have been reported[656].

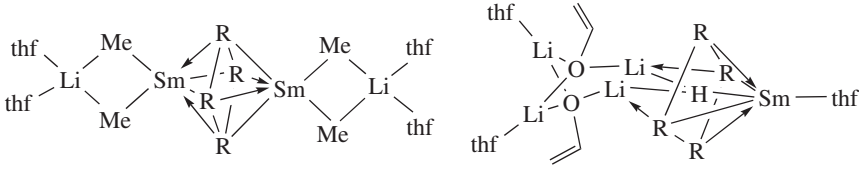

(**388**)

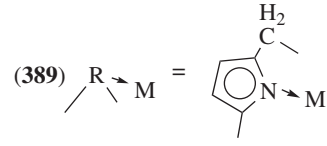

(**389**)

In the presence of [18]crown-6 (18-C-6), the reaction in thf of (i) $[Sr(Bn)_2]$ with two equivalents of Ph_2CH_2 gives **390** and (ii) $[Ba_6(OBu\text{-}t)_{12}]$ with two equivalents of $Ph_2CHSiMe_3$ and LiBu-*n* affords **391**[657].

$LiOCH{=}CH_2$, prepared from LiBu-*n* and thf, reacts readily with $[M(\eta^5\text{-}Cp)_2XCl]$ (M = Ti, Zr; X = Me, Cl) to give the corresponding enolato complexes $[M(\eta^5\text{-}Cp)_2Me(OCH{=}$

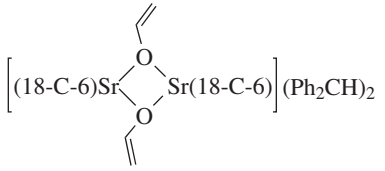

(**390**)

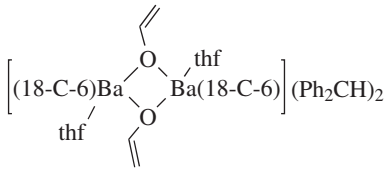

(**391**)

CH_2)] and [M(η^5-Cp)$_2$(OCH=CH_2)$_2$], which are thermally quite stable and show no tendency to eliminate aldehyde to form ketene complexes[42]. [NbCl{N($C_6H_3Me_2$-3,5)(adamantyl)}$_3$] reacts with thf to give [Nb{N($C_6H_3Me_2$-3,5)(adamantyl)}$_3$(OCH=CH_2)][658].

The triethylborohydride adduct **392** reacts with thf to yield the ethenolato complex **393**[659]. [$Y_2(\eta^5$-$C_5H_4R)_4(\mu$-OCH=$CH_2)_2$] can be prepared by thermolysis of [Y(η^5-$C_5H_4R)_2(CH_2SiMe_3)$(thf)] (R = H, Me) or from [$Y_2(\eta^5$-Cp)$_4Me_2$] in the presence of LiCl and thf[83].

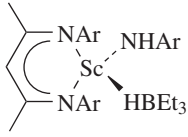

(**392**) Ar = C6H3(i-Pr)2-2,6

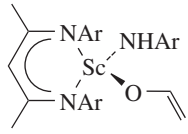

(**393**)

The reaction of [Li_3{N($CH_2CH_2NSiMe_3)_3$}] with YCl_3 in thf leads to a Li_3Y_2 cluster containing one 'Y{N($CH_2CH_2NSiMe_3)_3$}' fragment, as well as one μ_5-O^{2-}, two ethenolato ligands and the modified ligand N($CH_2CH_2SiMe_3)_2CH_2CH_2N(SiMe_3)CH=CH_2$, all derived from the cleavage of thf[660]. La reacts with [Hg(Bn)$_2$] in thf to give [La(Bn)H(OCH=CH_2)(thf)$_2$][661]. $CeCl_3$ reacts with an excess of LTMP in thf to afford [Ce(μ-OCH=CH_2)(TMP)$_2$]$_2$[662].

B. Cleavage of the Furan Ring

The reaction of [LnR_3(thf)$_2$] with $Me_2Si(C_5Me_4H)$(2-Fu) and its 5-Me derivative at the furyl group affords complex **394**, which decomposes to give **395** and two equivalents of $SiMe_4$[663]. The reaction between **396** and *t*-BuOH opens up one of the furyl rings, leading to the 2-furyl complex **397**[664]. Decomposition of **398** affords **399**[665]. Thermolysis of **400** (R = Me, 2-Fu, $SiMe_3$) affords complexes **401**[666].

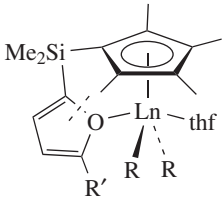

(**394**) Ln = Sc, Y, Lu, R = CH_2SiMe_3, R′ = H, Me

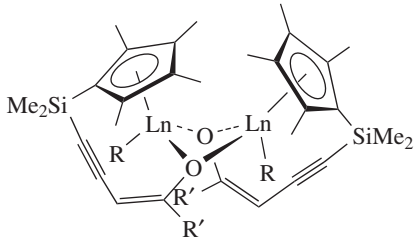

(**395**)

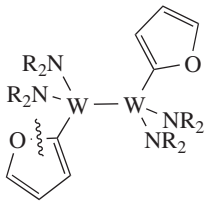

(**396**) R = Me

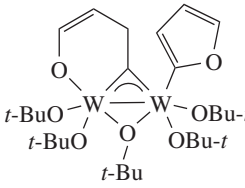

(**397**)

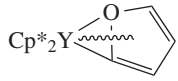

(**398**)

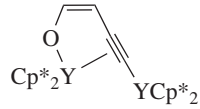

(**399**)

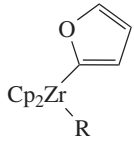

(**400**)

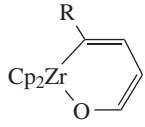

(**401**)

C. Cleavage of an Epoxide Ring

Cyclohexene oxide reacts with **402** to afford **403**[667]. Reaction of tetracyanoethylene oxide with low-valent metal complexes $[Pd(PAr_3)_n]$ (Ar/n = Ph/4, Tol/3) or $[Pt(PPh_2Me)_4]$ leads to complexes **404**[668].

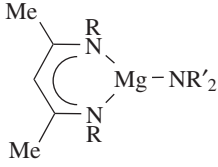

(**402**) R = $C_6H_3(i\text{-Pr})_2$-2,6; R′ = $SiMe_3$

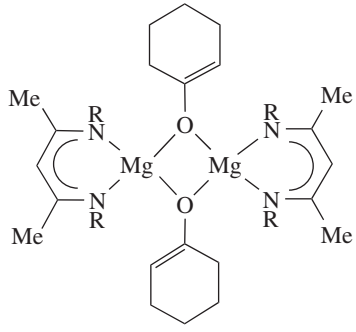

(**403**)

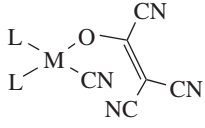

(**404**)

VI. SYNTHESIS FROM OXO, HYDROXO OR ALKOXO COMPLEXES

The alkoxo complex **405** decomposes (170 °C, 10^{-4} torr) to give H_2 and **406**[669].

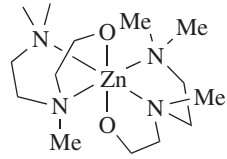

(**405**)

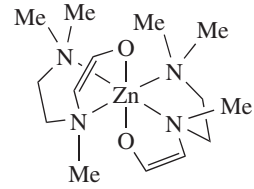

(**406**)

The oxo complexes **407** react with RC≡CR′ to give **408a**[670] or with allene to afford complex **409**[671]. Heating solutions of **410** (i) with alkynes RC≡CR (R = Ph, Tol) leads to benzene and [ZrO(η^5-Cp*)$_2$], which inserts the alkyne into the Zr=O bond to afford **408b** or **408c**, which, in turn, undergoes orthometalation to give **411** or (ii) with PhC≡CC≡CPh affords **412**[672]. Complex **408b** has been isolated from the reaction of [Zr(η^5-Cp*)$_2$(η^2-PhC≡CPh)] with N_2O (Section VII)[673].

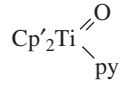

(**407**) Cp′ = Cp, Cp*

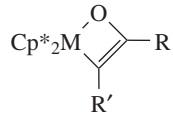

(**408**) (**a**) M = Ti, R = R′ = Ph;
R = Ph, Tol, Me, *t*-Bu, R′ = H
(**b**) M = Zr, R = R′ = Ph
(**c**) M = Zr, R = R′ = Tol

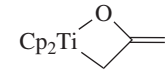

(**409**)

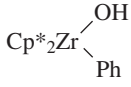

(**410**)

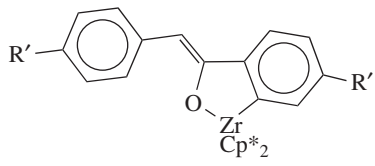

(**411**) R′ = H, Me

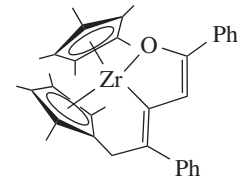

(**412**)

Complex **408b** reacts (i) with H_2 or protic acids HX to give **413** (X = H, OH, OPh, OC(=CH_2)Me, C≡CR (R = H, Ph, *t*-Bu)), (ii) with C≡E to afford **414**, (iii) with Ph_2CN_2 or (Tol)N_3 to give **415** and (iv) with RCHO to form **416** (R = H, Tol, $(CH_2)_5$Me)[674].

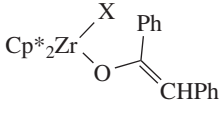

(**413**)

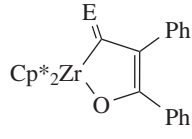

(**414**) E = O, NBu-*t*

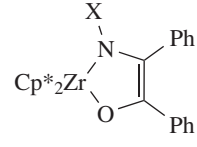

(**415**) X = N=CPh$_2$, N=NTol

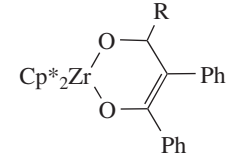

(**416**)

Reaction of **417** (Me-6) with NaH and [$CrCl_2$(thf)] affords Cr(II) complexes **418** and [$CrCl_2$(2-methylpyridine)$_2$]. When the methyl substituent is in position $x = 3$, 4,

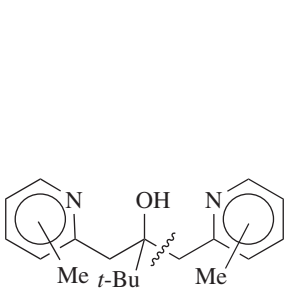

(**417**)

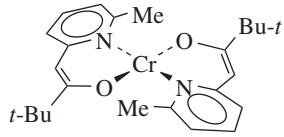

(**418**)

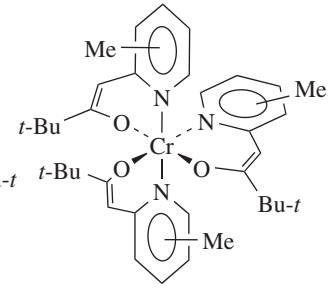

(**419**)

5, the corresponding Cr(III) complexes **419** and $[CrCl_2(x\text{-methylpyridine})_2]$ ($x = 3, 4$) are obtained[675].

Addition of $MeO_2CC{\equiv}CCO_2Me$ to a solution of $[Re(OH)(bpy)(CO)_3]$ or $[Mo(OH)(\eta^3\text{-}C_3H_4Me\text{-}2)(CO)_2(phen)]$ affords **420**[676].

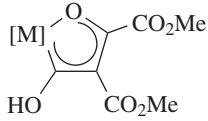

(**420**) (**a**) $Re(bpy)(CO)_2$
(**b**) $Mo(\eta^3\text{-}C_3H_4Me\text{-}2)(CO)(phen)$

The oxaruthenacylobutane complex **62** (L = PMe_3) decomposes at 45 °C to give CH_4 and the cyclometalated complex **59**[68,69] (Section II.A.1). The monohydride complex $[OsClH(CO)\{P(Pr\text{-}i)_3\}_2]$ reacts with PhCH(OH)C≡CH to give a mixture of products, from which the metalafuran complex $[Os\{C,O\text{-}OC(Ph)CHCH\}Cl(CO)\{P(Pr\text{-}i)_3\}_2]$ (Section IV.E) can be isolated[677]. By refluxing a thf solution of alkoxides $[Ln(\eta^5\text{-}Cp)_2\{\mu\text{-}OCH(Et)Me\}]_2$ (Ln = Dy, Yb), the dehydrogenated products $[Ln(\eta^5\text{-}Cp)_2\{\mu\text{-}E\text{-}OC(=CHMe)Me\}]_2$ are obtained[678].

VII. OXYGENATION REACTIONS

Nitrous oxide reacts at room temperature with **421** to afford **422** with N_2 and PMe_3 loss[679]. Similarly, **423** reacts with N_2O to give **408b**[673]. The intermediate **424** has been isolated at low temperature in solution or even in a solid/gas reaction and it undergoes N_2 loss at room temperature to give **408b**[674].

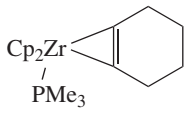

(**421**)

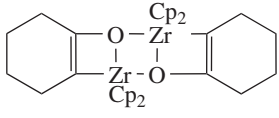

(**422**)

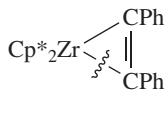

(**423**)

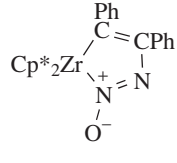

(**424**)

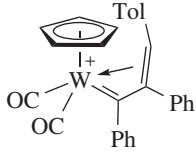

(**425**)

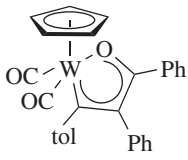

(**426**)

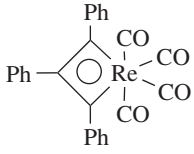

(**427**)

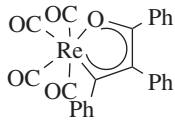

(**428**)

The vinylcarbene complex **425**•BF_4^- reacts with nitrone PhCH=N(O)Me to give the metalafuran complex **426**[680] (Section IV.E). Complex **427** reacts with Me_3NO to give the metalafuran **428**[681].

Complex **429** is obtained by reaction of [Pt{P(*c*-Hex)$_3$}$_2$(κ^2-O_2)] with $MeO_2CC{\equiv}CCO_2Me$[682].

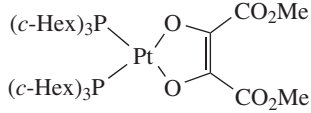

(**429**)

VIII. MISCELLANEOUS REACTIONS

Complex **430** reacts with $Ph_3P{=}CH_2$ to afford **431**[683]. When complexes **432** are heated in aqueous thf, complexes **433** are obtained[684].

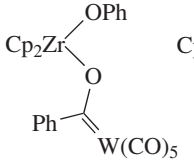

(**430**)

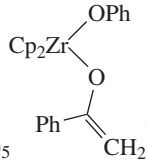

(**431**)

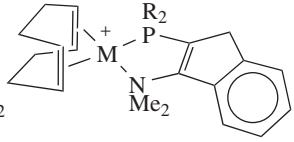

(**432**) M = Rh, Ir, R = *i*-Pr

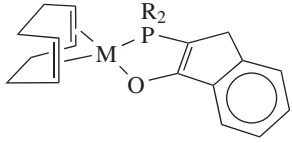

(**433**)

The metalacyclic complex **434** reacts with $HO(CH_2)_nC{\equiv}CH$ and $AgBF_4$ to give the Ir(III) π-allyl enolato complex **435** when $n = 2$ and the Ir(I) alkene enolato complex **436** when $n = 3$[685].

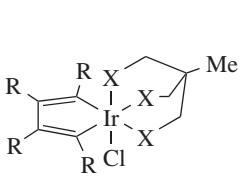

(**434**) R = CO_2Me, X = PPh_2

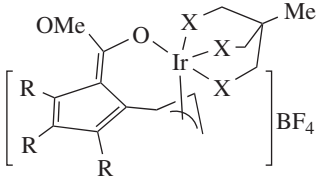

(**435**)

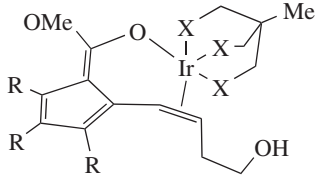

(**436**)

The enolato complex [Cu{OC(=C(CN)$_2$)CN}$_2${*N*,*N*-(Pyr-2)$_2$NH}] has been isolated by reacting stoichiometric amounts of an aqueous solution of [$CuCl_2${*N*,*N*′-(Pyr-2)$_2$NH}]

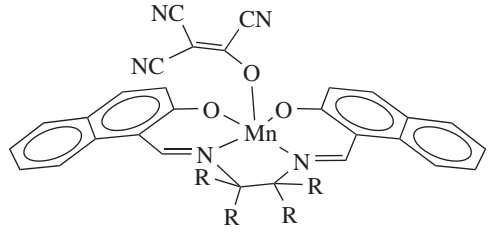

(**437**) R = Me

with tetracyanoethylene in butyl alcohol[686]. Similarly, Mn(III) complexes [Mn(L)(NCO)], where L is the tetradentate dianion derived from a double Schiff base, react with tetracyanoethylene to give the corresponding tricyanoethenolato complex **437**[687].

Diazo compounds have been used in the synthesis of enolato complexes. Thus, for example, $(EtO_2C)_2C{=}N_2$ reacts with **438** to give the adduct **439**[688].

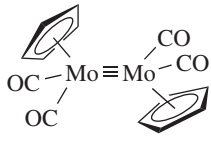

(**438**)

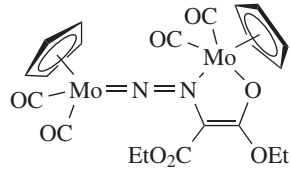

(**439**)

$(RO_2C)_2C{=}N_2$ reacts with $[Ti(\eta^5\text{-}Cp)_2(CO)_2]$ at 0 °C to give **440**, or with $[Ti(\eta^5\text{-}Cp^*)_2(CO)_2]$ at room temperature to afford **441** (R = Ph)[689].

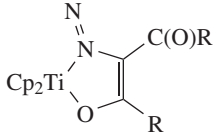

(**440**) R = Me, Ph

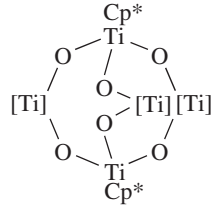

(**441**) [Ti] =

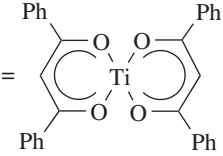

IX. ACKNOWLEDGMENTS

The author thanks Dirección General de Investigación, Ministerio de Educación y Ciencia (Spain, Grant CTQ2007-60808/BQU), FEDER and Fundación Séneca for financial support and Drs. A. Arcas, M. T. Chicote, A. Guirado and I. Saura-Llamas for their suggestions.

X. REFERENCES

1. J. Vicente, Chap. 6 in *The chemistry of Metal Enolates* (Ed. J. Zabicky), John Wiley & Sons, Ltd, Chichester, 2009, pp. 313–354.
2. J. Dekker, P. H. M. Budzelaar, J. Boersma, G. J. M. van der Kerk and A. J. Spek, *Organometallics*, **3**, 1403 (1984).
3. M. L. Hlavinka and J. R. Hagadorn, *Organometallics*, **24**, 4116 (2005).
4. N. Masciocchi, F. Ragaini and A. Sironi, *Organometallics*, **21**, 3489 (2002); P. Veya, C. Floriani, A. Chiesi-Villa and C. Rizzoli, *Organometallics*, **12**, 4899 (1993).
5. J. Vicente, A. Arcas, J. M. Fernández-Hernández and D. Bautista, *Organometallics*, **20**, 2767 (2001).
6. M. J. S. Dewar and K. M. Merz, *J. Am. Chem. Soc.*, **109**, 6553 (1987); W. R. Vaughan and H. P. Knoess, *J. Org. Chem.*, **35**, 2394 (1970); W. R. Vaughan, S. C. Bernstein and M. E. Lorber, *J. Org. Chem.*, **30**, 1790 (1965).
7. H. B. Mekelburger and C. S. Wilcox, in *Comprehensive Organic Synthesis*, Vol. 1, Chap. 1 (Eds B. M. Trost, I. Fleming), Pergamon, Oxford, 1990.
8. D. Seebach, *Angew. Chem., Int. Ed. Engl.*, **27**, 1624 (1988).
9. L. M. Jackman and B. C. Lange, *Tetrahedron*, **33**, 2737 (1977).
10. P. Veya, C. Floriani, A. Chiesi-Villa and C. Rizzoli, *Organometallics*, **13**, 214 (1994).
11. T. Laube, J. D. Dunitz and D. Seebach, *Helv. Chim. Acta*, **68**, 1373 (1985).
12. R. Amstutz, W. B. Schweizer, D. Seebach and J. D. Dunitz, *Helv. Chim. Acta*, **64**, 2617 (1981).
13. P. G. Williard and G. B. Carpenter, *J. Am. Chem. Soc.*, **107**, 3345 (1985).
14. P. G. Williard and G. B. Carpenter, *J. Am. Chem. Soc.*, **108**, 462 (1986).
15. D. Seebach, R. Amstutz, T. Laube, W. B. Schweizer and J. D. Dunitz, *J. Am. Chem. Soc.*, **107**, 5403 (1985).
16. W. Bauer, T. Laube and D. Seebach, *Chem. Ber.*, **118**, 764 (1985).
17. P. J. Pospisil, S. R. Wilson and E. N. Jacobsen, *J. Am. Chem. Soc.*, **114**, 7585 (1992).
18. P. G. Williard and M. J. Hintze, *J. Am. Chem. Soc.*, **112**, 8602 (1990).
19. K. W. Henderson, A. E. Dorigo, Q. Y. Liu, P. G. Williard, P. v. R. Schleyer and P. R. Bernstein, *J. Am. Chem. Soc.*, **118**, 1339 (1996).
20. K. W. Henderson, A. E. Dorigo, P. G. Williard and P. R. Bernstein, *Angew. Chem., Int. Ed. Engl.*, **35**, 1322 (1996).
21. P. G. Williard and G. J. Macewan, *J. Am. Chem. Soc.*, **111**, 7671 (1989).
22. J. T. B. H. Jastrzebski, G. van Koten, M. J. N. Christophersen and C. H. Stam, *J. Organomet. Chem.*, **292**, 319 (1985).
23. P. G. Williard and M. J. Hintze, *J. Am. Chem. Soc.*, **109**, 5539 (1987).
24. K. W. Henderson, P. G. Williard and P. R. Bernstein, *Angew. Chem., Int. Ed. Engl.*, **34**, 1117 (1995).
25. X. Y. He, B. C. Noll, A. Beatty, R. E. Mulvey and K. W. Henderson, *J. Am. Chem. Soc.*, **126**, 7444 (2004).
26. E. Hevia, K. W. Henderson, A. R. Kennedy and R. E. Mulvey, *Organometallics*, **25**, 1778 (2006).
27. J. F. Allan, K. W. Henderson, A. R. Kennedy and S. J. Teat, *Chem. Commun.*, 1059 (2000).
28. X. Y. He, J. F. Allan, B. C. Noll, A. R. Kennedy and K. W. Henderson, *J. Am. Chem. Soc.*, **127**, 6920 (2005).
29. X. He, J. J. Morris, B. C. Noll, S. N. Brown and K. W. Henderson, *J. Am. Chem. Soc.*, **128**, 13599 (2006).
30. J. F. Allan, W. Clegg, K. W. Henderson, L. Horsburgh and A. R. Kennedy, *J. Organomet. Chem.*, **559**, 173 (1998).
31. I. L. Fedushkin, A. A. Skatova, G. K. Fukin, M. Hummert and H. Schumann, *Eur. J. Inorg. Chem.*, 2332 (2005).
32. S. E. Baillie, E. Hevia, A. R. Kennedy and R. E. Mulvey, *Organometallics*, **26**, 204 (2007).
33. R. E. Mulvey, *Organometallics*, **25**, 1060 (2006).
34. M. L. Hlavinka and J. R. Hagadorn, *Organometallics*, **25**, 3501 (2006).
35. F. H. van der Steen, J. Boersma, A. L. Spek and G. van Koten, *Organometallics*, **10**, 2467 (1991).
36. J. F. Allan, W. Clegg, M. R. J. Elsegood, K. W. Henderson, A. E. McKeown, P. H. Moran and I. M. Rakov, *J. Organomet. Chem.*, **602**, 15 (2000); A. R. Kunicki, A. Chojecki, J. Zachara

and M. Glinski, *J. Organomet. Chem.*, **664**, 136 (2002); Z. S. Sales, R. Nassar, J. J. Morris and K. W. Henderson, *J. Organomet. Chem.*, **690**, 3474 (2005).
37. J. T. B. H. Jastrzebski, G. van Koten and W. F. van de Mieroop, *Inorg. Chim. Acta*, **142**, 169 (1988).
38. F. H. van der Steen, G. P. M. van Mier, A. L. Spek, J. Kroon and G. van Koten, *J. Am. Chem. Soc.*, **113**, 5742 (1991).
39. P. Veya, C. Floriani, A. Chiesi-Villa and C. Rizzoli, *Organometallics*, **12**, 4892 (1993).
40. A. Rodríguez-Delgado, W. R. Mariott and E. Y. X. Chen, *Macromolecules*, **37**, 3092 (2004).
41. S. H. Bertz, G. Dabbagh and C. P. Gibson, *Organometallics*, **7**, 563 (1988).
42. M. D. Curtis, S. Thanedar and W. M. Butler, *Organometallics*, **3**, 1855 (1984).
43. G. Stojcevic, H. Kim, N. J. Taylor, T. B. Marder and S. Collins, *Angew. Chem. Int. Ed.*, **43**, 5523 (2004).
44. M. Schmittel, A. Burghart, H. Werner, M. Laubender and R. Sollner, *J. Org. Chem.*, **64**, 3077 (1999).
45. D. Seyferth, T. Wang and W. M. Davis, *Organometallics*, **13**, 4134 (1994).
46. U. G. Joung, T. H. Kim, D. J. Joe, B. Y. Lee, D. M. Shin and Y. K. Chung, *Polyhedron*, **23**, 1587 (2004).
47. K. Kunz, G. Erker, G. Kehr, R. Fröhlich, H. Jacobsen, H. Berke and O. Blacque, *J. Am. Chem. Soc.*, **124**, 3316 (2002).
48. P. Veya, P. G. Cozzi, C. Floriani, F. P. Rotzinger, A. Chiesi-Villa and C. Rizzoli, *Organometallics*, **14**, 4101 (1995).
49. G. Solari, E. Solari, C. Floriani, A. Chiesi-Villa and C. Rizzoli, *Organometallics*, **16**, 508 (1997).
50. W. A. Howard and G. Parkin, *J. Am. Chem. Soc.*, **116**, 606 (1994); W. A. Howard, T. M. Trnka, M. Waters and G. Parkin, *J. Organomet. Chem.*, **528**, 95 (1997).
51. S. Y. Lee and R. G. Bergman, *J. Am. Chem. Soc.*, **118**, 6396 (1996).
52. V. Cadierno, M. Zablocka, B. Donnadieu, A. Igau and J.-P. Majoral, *Angew. Chem. Int. Ed.*, **39**, 4524 (2000).
53. R. Beckhaus, I. Strauss and T. Wagner, *J. Organomet. Chem.*, **464**, 155 (1994).
54. T. Stuhldreier, H. Keul, H. Höcker and T. Englert, *Organometallics*, **19**, 5231 (2000).
55. P. Veya, C. Floriani, A. Chiesi-Villa and C. Guastini, *Organometallics*, **13**, 208 (1994).
56. A. D. Bolig and E. Y.-X. Chen, *J. Am. Chem. Soc.*, **126**, 4897 (2004).
57. K. Hortmann, J. Diebold and H. H. Brintzinger, *J. Organomet. Chem.*, **445**, 107 (1993).
58. W. Spaether, K. Klass, G. Erker, F. Zippel and R. Fröhlich, *Chem. Eur. J.*, **4**, 1411 (1998).
59. P. Veya, C. Floriani, A. Chiesi-Villa and C. Guastini, *J. Chem. Soc., Chem. Commun.*, 1166 (1991); P. G. Cozzi, P. Veya, C. Floriani, F. P. Rotzinger, A. Chiesi-Villa and C. Rizzoli, *Organometallics*, **14**, 4092 (1995).
60. S. G. Davies, J. Dupont, R. J. C. Easton, O. Ichihara, J. M. McKenna, A. D. Smith and J. A. A. de Sousa, *J. Organomet. Chem.*, **689**, 4184 (2004); L. S. Liebeskind, M. E. Welker and R. W. Fengl, *J. Am. Chem. Soc.*, **108**, 6328 (1986).
61. I. Weinstock, C. Floriani, A. Chiesi-Villa and C. Guastini, *J. Am. Chem. Soc.*, **108**, 8298 (1986).
62. H. S. Soo, P. L. Diaconescu and C. C. Cummins, *Organometallics*, **23**, 498 (2004).
63. H. S. Soo, J. S. Figueroa and C. C. Cummins, *J. Am. Chem. Soc.*, **126**, 11370 (2004).
64. D. Morales, M. E. N. Clemente, J. Pérez, L. Riera, V. Riera and D. Miguel, *Organometallics*, **22**, 4124 (2003).
65. J. M. O'Connor, R. Uhrhammer, A. L. Rheingold and D. M. Roddick, *J. Am. Chem. Soc.*, **113**, 4530 (1991).
66. P. Braunstein, S. C. Cea, A. Decian and J. Fischer, *Inorg. Chem.*, **31**, 4203 (1992).
67. J. F. Hartwig, R. A. Andersen and R. G. Bergman, *J. Am. Chem. Soc.*, **111**, 2717 (1989); J. F. Hartwig, R. G. Bergman and R. A. Andersen, *J. Am. Chem. Soc.*, **113**, 3404 (1991).
68. J. F. Hartwig, R. G. Bergman and R. A. Andersen, *J. Am. Chem. Soc.*, **112**, 3234 (1990).
69. J. F. Hartwig, R. G. Bergman and R. A. Andersen, *Organometallics*, **10**, 3344 (1991).
70. J. F. Hartwig, R. G. Bergman and R. A. Andersen, *Organometallics*, **10**, 3326 (1991).
71. G. A. Slough, R. G. Bergman and C. H. Heathcock, *J. Am. Chem. Soc.*, **111**, 938 (1989).
72. E. Lippmann, J. Milke, K. Sunkel and W. Beck, *J. Organomet. Chem.*, **479**, 221 (1994).
73. P. Berno, P. Braunstein, C. Floriani, A. Chiesi-Villa and C. Guastini, *Inorg. Chem.*, **30**, 1407 (1991).

74. J. Cámpora, C. M. Maya, P. Palma, E. Carmona, E. Gutiérrez, C. Ruiz, C. Graiff and A. Tiripicchio, *Chem. Eur. J.*, **11**, 6889 (2005).
75. J. Cámpora, I. Matas, C. M. Maya, P. Palma and E. Álvarez, *Organometallics*, **25**, 3124 (2006).
76. H. F. Klein, A. Bickelhaupt, M. Lemke, H. Sun, A. Brand, T. Jung, C. Rohr, U. Florke and H. J. Haupt, *Organometallics*, **16**, 668 (1997).
77. H. F. Klein, X. Li, H. Sun, A. Brand, M. Lemke, U. Florke and H. J. Haupt, *Inorg. Chim. Acta*, **298**, 70 (2000).
78. B. E. Ketz, X. G. Ottenwaelder and R. M. Waymouth, *Chem. Commun.*, 5693 (2005).
79. B. E. Ketz, A. P. Cole and R. M. Waymouth, *Organometallics*, **23**, 2835 (2004).
80. J. Vicente, A. Arcas, J. M. Fernández-Hernández, D. Bautista and P. G. Jones, *Organometallics*, **24**, 2516 (2005).
81. T. Murahashi and H. Kurosawa, *J. Organomet. Chem.*, **574**, 142 (1999).
82. Z. M. Hou, T. Yoshimura and Y. Wakatsuki, *J. Am. Chem. Soc.*, **116**, 11169 (1994); T. Yoshimura, Z. M. Hou and Y. Wakatsuki, *Organometallics*, **14**, 5382 (1995).
83. W. J. Evans, R. Domínguez and T. P. Hanusa, *Organometallics*, **5**, 1291 (1986).
84. E. Ihara, M. Morimoto and H. Yasuda, *Macromolecules*, **28**, 7886 (1995).
85. I. Kojima, H. Fukumori and C. Iida, *Anal. Sci.*, **8**, 533 (1992).
86. J. Zhang, P. D. Badger, S. J. Geib and S. Petoud, *Angew. Chem. Int. Ed.*, **44**, 2508 (2005).
87. L. Bertolo, S. Tamburini, P. A. Vigato, W. Porzio, G. Macchi and F. Meinardi, *Eur. J. Inorg. Chem.*, 2370 (2006).
88. Y. Inamori, S. Shinohara, H. Tsujibo, T. Okabe, Y. Morita, Y. Sakagami, Y. Kumeda and N. Ishida, *Biol. Pharmacol. Bull.*, **22**, 990 (1999); S. C. Liu and H. Yamauchi, *Biochem. Biophys. Res. Commun.*, **351**, 26 (2006); E. Matsumura, Y. Morita, T. Date, H. Tsujibo, M. Yasuda, T. Okabe, N. Ishida and Y. Inamori, *Biol. Pharmacol. Bull.*, **24**, 299 (2001); D. Miyamoto, N. Endo, N. Oku, Y. Arima, T. Suzuki and Y. Suzuki, *Biol. Pharmacol. Bull.*, **21**, 1258 (1998); Y. Morita, E. Matsumura, T. Okabe, M. Shibata, M. Sugiura, T. Ohe, H. Tsujibo, N. Ishida and Y. Inamori, *Biol. Pharmacol. Bull.*, **26**, 1487 (2003); V. Badmaev, S. Prakash and M. Majeed, *J. Altern. Complement Med.*, **5**, 273 (1999); G. G. Briand and N. Burford, *Chem. Rev.*, **99**, 2601 (1999); S. M. Cohen, B. O'Sullivan and K. N. Raymond, *Inorg. Chem.*, **39**, 4339 (2000); R. A. Yokel, *Coord. Chem. Rev.*, **228**, 97 (2002); M. Yamane, Y. Adachi, Y. Yoshikawa and H. Sakurai, *Chem. Lett.*, **34**, 1694 (2005); R. Bhat and S. M. Hadi, *Mutagenesis*, **7**, 119 (1992); L. Novotny, P. Rauko, M. Abdel-Hamid and A. Vachalkova, *Neoplasma*, **46**, 89 (1999); M. Kawase, N. Kagaya, S. Akamatsu, A. Kamiyoshi, S. Muto, Y. Tagawa and K. Yagi, *Exp. Anim.*, **53**, 1 (2004); B. D. Liboiron, K. H. Thompson, G. R. Hanson, E. Lam, N. Aebischer and C. Orvig, *J. Am. Chem. Soc.*, **127**, 5104 (2005); P. Caravan, L. Gelmini, N. Glover, F. G. Herring, H. L. Li, J. H. McNeill, S. J. Rettig, I. A. Setyawati, E. Shuter, Y. Sun, A. S. Tracey, V. G. Yuen and C. Orvig, *J. Am. Chem. Soc.*, **117**, 12759 (1995); K. H. Thompson and C. Orvig, *Dalton Trans.*, 761 (2006); K. H. Thompson, C. A. Barta and C. Orvig, *Chem. Soc. Rev.*, **35**, 545 (2006); N. Kaneko, J. Takada, H. Yasui and H. Sakurai, *Biometals*, **19**, 83 (2006); H. Sakurai and Y. Adachi, *Biometals*, **18**, 319 (2005); R. Tsubouchi, H. H. Htay, K. Murakami, M. Haneda and M. Yoshino, *Biometals*, **14**, 181 (2001).
89. M. C. Barret, M. F. Mahon, K. C. Molloy, J. W. Steed and P. Wright, *Inorg. Chem.*, **40**, 4384 (2001).
90. U. Dittes, E. Vogel and B. K. Keppler, *Coord. Chem. Rev.*, **163**, 345 (1997).
91. R. Diemer, B. K. Keppler, U. Dittes, B. Nuber, V. Seifried and W. Opferkuch, *Chem. Ber.*, **128**, 335 (1995).
92. J. J. Molenda, M. A. Basinger, T. P. Hanusa and M. M. Jones, *J. Inorg. Biochem.*, **55**, 131 (1994).
93. M. A. Santos, *Coord. Chem. Rev.*, **228**, 187 (2002); M. T. Ahmet, C. S. Frampton and J. Silver, *J. Chem. Soc., Dalton Trans.*, 1159 (1988).
94. Y. Adachi, J. Yoshida, Y. Kodera, A. Katoh, J. Takada and H. Sakurai, *J. Med. Chem.*, **49**, 3251 (2006).
95. M. Melchior, S. J. Rettig, B. D. Liboiron, K. H. Thompson, V. G. Yuen, J. H. McNeill and C. Orvig, *Inorg. Chem.*, **40**, 4686 (2001).
96. K. Zborowski, R. Grybos and L. M. Proniewicz, *J. Mol. Struct. (Theochem)*, **639**, 87 (2003).

97. P. Collery, B. Keppler, C. Madoulet and B. Desoize, *Crit. Rev. Oncol./Hematol.*, **42**, 283 (2002).
98. G. Steyl and A. Roodt, *S. Afr. J. Chem.*, **59**, 21 (2006).
99. E. L. Muetterties and C. M. Wright, *J. Am. Chem. Soc.*, **87**, 4706 (1965).
100. E. L. Muetterties, *J. Am. Chem. Soc.*, **88**, 305 (1966).
101. D. Brown and C. E. F. Rickard, *J. Chem. Soc. A*, 3373 (1970).
102. E. L. Muetterties and C. M. Wright, *J. Am. Chem. Soc.*, **87**, 21 (1965).
103. E. L. Muetterties and C. M. Wright, *J. Am. Chem. Soc.*, **86**, 5132 (1964).
104. K. Nomiya, A. Yoshizawa, K. Tsukagoshi, N. C. Kasuga, S. Hirakawa and J. Watanabe, *J. Inorg. Biochem.*, **98**, 46 (2004).
105. E. L. Muetterties, H. Roesky and C. M. Wright, *J. Am. Chem. Soc.*, **88**, 4856 (1966).
106. K. Nomiya, A. Yoshizawa, N. C. Kasuga, H. Yokoyama and S. Hirakawa, *Inorg. Chim. Acta*, **357**, 1168 (2004); A. Mori, R. Mori, M. Takemoto, S. Yamamoto, D. Kuribayashi, K. Uno, K. Kubo and S. Ujiie, *J. Mater. Chem.*, **15**, 3005 (2005); G. M. Arvanitis, M. E. Berardinia and D. M. Hob, *Acta Crystallogr., Sect. C*, **60**, m126 (2004); D. Miyamoto, Y. Kusagaya, N. Endo, A. Sometani, S. Takeo, T. Suzuki, Y. Arima, K. Nakajima and Y. Suzuki, *Antiviral Res.*, **39**, 89 (1998); M. C. Barret, M. F. Mahon, K. C. Molloy, P. Wright and J. E. Creeth, *Polyhedron*, **21**, 1761 (2002); J. R. Chipperfield, S. Clark, J. Elliott and E. Sinn, *Chem. Commun.*, 195 (1998); M. Hasegawa, Y. Inomaki, T. Inayoshi, T. Hoshi and M. Kobayashi, *Inorg. Chim. Acta*, **257**, 259 (1997).
107. R. J. Irving, M. L. Post and D. C. Povey, *J. Chem. Soc., Dalton Trans.*, 697 (1973).
108. G. Steyl, *Acta Crystallogr., Sect. E*, **61**, m1860 (2005).
109. A. Rodgers and S. R. Stobart, *J. Chem. Soc., Chem. Commun.*, 52 (1976).
110. E. L. Muetterties and C. W. Acegranti, *J. Am. Chem. Soc.*, **91**, 4420 (1969).
111. T. S. Davis, J. P. Fackler, Jr. and M. J. Weeks, *Inorg. Chem.*, **7**, 1994 (1968); A. Avdeef, J. A. Costamagna and J. P. F. Junior, *Inorg. Chem.*, **13**, 1854 (1974).
112. W. P. Griffith, C. A. Pumphrey and A. C. Skapski, *Polyhedron*, **6**, 891 (1987).
113. A. R. Davis and F. W. B. Einstein, *Inorg. Chem.*, **13**, 1880 (1974).
114. B. S. Santos, C. D. Donega, G. F. de Sa, L. F. C. de Oliveira and P. S. Santos, *Spectrochim. Acta A*, **54**, 2237 (1998).
115. J. S. Gu, J. Y. Tong, M. H. Ma and D. G. Tuck, *Chin. Chem. Lett.*, **6**, 259 (1995).
116. J. Lewinski, J. Zachara and I. Justyniak, *Organometallics*, **16**, 4597 (1997).
117. M. Kira, L. C. Zhang, C. Kabuto and H. Sakurai, *Organometallics*, **17**, 887 (1998).
118. A. R. Davis and F. W. B. Einstein, *Inorg. Chem.*, **14**, 3030 (1975).
119. M. McPartlin and J. D. Matthews, *J. Organomet. Chem.*, **104**, C20 (1976).
120. A. Deák, P. Király and G. Tárkányi, *Dalton Trans.*, 234 (2007).
121. U. Dittes, B. K. Keppler and B. Nuber, *Angew. Chem., Int. Ed. Engl.*, **35**, 67 (1996).
122. S. Takekuma, K. Tomoda, M. Sasaki, T. Minematsu and H. Takekuma, *Bull. Chem. Soc. Jpn.*, **77**, 1935 (2004).
123. A. Camard, Y. Ihara, F. Murata, K. Mereiter, Y. Fukuda and W. Linert, *Inorg. Chim. Acta*, **358**, 409 (2005).
124. T. J. Anderson, M. A. Neuman and G. A. Melson, *Inorg. Chem.*, **13**, 1884 (1974).
125. S. C. Liu and J. Zubieta, *Polyhedron*, **7**, 1129 (1988).
126. C. F. Edwards, W. P. Griffith, A. J. P. White and D. J. Williams, *J. Chem. Soc., Dalton Trans.*, 957 (1992).
127. M. Melchart, A. Habtemariam, S. Parsons, S. A. Moggach and P. J. Sadler, *Inorg. Chim. Acta*, **359**, 3020 (2006).
128. A. M. El-Hendawy, S. Y. Alqaradawi and H. A. Al-Madfa, *Transition Metal Chem.*, **25**, 572 (2000).
129. R. J. Irving, M. L. Post and R. W. Baker, *J. Chem. Soc., Dalton Trans.*, 1898 (1975); A. Bencini, A. Beni, F. Costantino, A. Dei, D. Gatteschia and L. Soracea, *Dalton Trans.*, 722 (2006).
130. J. G. Leipoldt, L. D. C. Bok, S. S. Basson and H. Meyer, *Inorg. Chim. Acta*, **42**, 105 (1980); G. Steyl, G. J. Kruger and A. Roodt, *Acta Crystallogr., Sect. C*, **60**, m473 (2004); G. Steyl and A. Roodt, *Acta Crystallogr., Sect. C*, **60**, m324 (2004).
131. G. Bhalla, J. Oxgaard, W. A. Goddard and R. A. Periana, *Organometallics*, **24**, 3229 (2005); G. Bhalla and R. A. Periana, *Angew. Chem. Int. Ed.*, **44**, 1540 (2005).
132. Y. Ihara, S. Kurose and T. Koyama, *Monatsh. Chem.*, **132**, 1433 (2001).

133. G. Steyl, *Acta Crystallogr., Sect. E*, **62**, m974 (2006).
134. M. C. Barret, M. F. Mahon, K. C. Molloy and P. Wright, *Main Group Metal Chem.*, **23**, 663 (2000).
135. S. J. Greaves and W. P. Griffith, *Polyhedron*, **7**, 1973 (1988).
136. N. A. Epstein, J. L. Horton, C. M. Vogels, N. J. Taylor and S. A. Westcott, *Aust. J. Chem.*, **53**, 687 (2000); M. K. J. Gagnon, T. R. S. Germain, C. M. Vogels, R. A. McNamara, N. J. Taylor and S. A. Westcott, *Aust. J. Chem.*, **53**, 693 (2000); S. J. Lord, N. A. Epstein, R. L. Paddock, C. M. Vogels, T. L. Hennigar, M. J. Zaworotko, N. J. Taylor, W. R. Driedzic, T. L. Broderick and S. A. Westcott, *Can. J. Chem.*, **77**, 1249 (1999); N. C. Tam, S. P. Fletcher, C. M. Vogels, S. A. Westcott and A. Decken, *Transition Metal Chem.*, **28**, 103 (2003); E. J. Brown, A. C. Whitwood, P. H. Walton and A.-K. Duhme-Klair, *Dalton Trans.*, 2458 (2004).
137. F. Avecilla, C. Geraldes and M. Castro, *Eur. J. Inorg. Chem.*, 3135 (2001).
138. H. Y. Luo, S. J. Rettig and C. Orvig, *Inorg. Chem.*, **32**, 4491 (1993).
139. C. M. Archer, J. R. Dilworth, P. Jobanputra, M. E. Harman, M. B. Hursthouse and A. Karaulov, *Polyhedron*, **10**, 1539 (1991).
140. J. D. Xu, E. Radkov, M. Ziegler and K. N. Raymond, *Inorg. Chem.*, **39**, 4156 (2000).
141. P. Sobota, K. Przybylak, J. Utko, L. B. Jerzykiewicz, A. J. L. Pombeiro, M. da Silva and K. Szczegot, *Chem. Eur. J.*, **7**, 951 (2001).
142. K. Saatchi, K. H. Thompson, B. O. Patrick, M. Pink, V. G. Yuen, J. H. McNeill and C. Orvig, *Inorg. Chem.*, **44**, 2689 (2005).
143. Y. Sun, M. Melchior, D. A. Summers, R. C. Thompson, S. J. Rettig and C. Orvig, *Inorg. Chem.*, **37**, 3119 (1998); J. Burgess, B. DeCastro, C. Oliveira, M. Rangel and W. Schlindwein, *Polyhedron*, **16**, 789 (1997); V. G. Yuen, P. Caravan, L. Gelmini, N. Glover, J. H. McNeill, I. A. Setyawati, Y. Zhou and C. Orvig, *J. Inorg. Biochem.*, **68**, 109 (1997); R. Shukla, V. Barve, S. Padhye and R. Bhonde, *Bioorg. Med. Chem. Lett.*, **14**, 4961 (2004); P. Buglyo, T. Kiss, E. Kiss, D. Sanna, E. Garribba and G. Micera, *J. Chem. Soc., Dalton Trans.*, 2275 (2002); M. Rangel, A. Leite, M. J. Amorim, E. Garribba, G. Micera and E. Lodyga-Chruscinska, *Inorg. Chem.*, **45**, 8086 (2006); K. H. Thompson, B. D. Liboiron, Y. Bellman, I. A. Setyawati, B. O. Patrick, V. Karunaratne, G. Rawji, J. Wheeler, K. Sutton, S. Bhanot, C. Cassidy, J. H. McNeill, V. G. Yuen and C. Orvig, *J. Biol. Inorg. Chem.*, **8**, 66 (2003).
144. S. J. Kavitha, K. A. B. Panchanatheswaran, J. N. Low and C. Glidewell, *Acta Crystallogr., Sect. C*, **62**, m116 (2006).
145. E. Malhotra, N. K. Kaushik and G. S. Sodhi, *J. Therm. Anal. Cal.*, **65**, 859 (2001).
146. D. Fregona, G. Faraglia and S. Sitran, *J. Coord. Chem.*, **30**, 221 (1993).
147. C. I. F. Denekamp, D. F. Evans, A. M. Z. Slawin, D. J. Williams, C. Y. Wong and J. D. Woollins, *J. Chem. Soc., Dalton Trans.*, 2375 (1992); D. Fregona, Z. J. Guo, G. Faraglia and S. Sitran, *J. Coord. Chem.*, **28**, 73 (1993); R. Jain and N. K. Kaushik, *J. Therm. Anal.*, **49**, 713 (1997).
148. W. Y. Hsieh and S. Liu, *Synth. React. Inorg. Met.-Org. Nano-Metal Chem.*, **35**, 61 (2005).
149. K. H. Thompson, J. Chiles, V. G. Yuen, J. Tse, J. H. McNeill and C. Orvig, *J. Inorg. Biochem.*, **98**, 683 (2004).
150. J. Burchfield, P. Telehowski, R. C. Rosenberg, S. S. Eaton and G. R. Eaton, *J. Magn. Reson. Ser. B*, **104**, 69 (1994); V. M. Deflon, D. M. de Oliveira, G. F. de Sousa, A. A. Batista, L. R. Dinelli and E. E. Castellano, *Z. Anorg. Allg. Chem.*, **628**, 1140 (2002).
151. W.-Y. Hsieh and S. Liu, *Inorg. Chem.*, **44**, 2031 (2005).
152. J. R. Dilworth, P. Jobanputra, R. M. Thompson, D. C. Povey, C. M. Archer and J. D. Kelly, *J. Chem. Soc., Dalton Trans.*, 1251 (1994).
153. J. Charalambous, A. Dodd, M. McPartlin, S. O. C. Matondo, N. D. Pathirana and H. R. Powell, *Polyhedron*, **7**, 2235 (1988).
154. W. Schlindwein, E. Waltham, J. Burgess, N. Binsted, A. Nunes, A. Leite and M. Rangel, *Dalton Trans.*, 1313 (2006); E. T. Clarke, A. E. Martell and J. Reibenspies, *Inorg. Chim. Acta*, **196**, 177 (1992); G. Xiao, D. van der Helm, R. C. Hider and P. S. Dobbin, *J. Chem. Soc., Dalton Trans.*, 3265 (1992); T. A. Hamor and D. J. Watkin, *J. Chem. Soc. D*, 440 (1969); P. S. Dobbin, R. C. Hider, A. D. Hall, P. D. Taylor, P. Sarpong, J. B. Porter, G. Xiao and D. v. d. Helm, *J. Med. Chem.*, **36**, 2448 (1993).
155. M. Odoko, K. Yamamoto, M. Hosen and N. Okabe, *Acta Crystallogr., Sect. C*, **59**, m121 (2003).

156. D. C. Kennedy, A. Wu, B. O. Patrick and B. R. James, *Inorg. Chem.*, **44**, 6529 (2005); D. C. Kennedy, B. R. James and B. O. Patrick, *J. Inorg. Biochem.*, **96**, 167 (2003); D. C. Kennedy, A. Wu, B. O. Patrick and B. R. James, *J. Inorg. Biochem.*, **100**, 1974 (2006).
157. A. P. Abbott, G. Capper, D. L. Davies, J. Fawcett and D. R. Russell, *J. Chem. Soc., Dalton Trans.*, 3709 (1995).
158. M.-L. Lehaire, R. Scopelliti, H. Piotrowski and K. Severin, *Angew. Chem. Int. Ed.*, **41**, 1419 (2002).
159. M. M. Finnegan, T. G. Lutz, W. O. Nelson, A. Smith and C. Orvig, *Inorg. Chem.*, **26**, 2171 (1987).
160. M. M. Finnegan, S. J. Rettig and C. Orvig, *J. Am. Chem. Soc.*, **108**, 5033 (1986).
161. J. Burgess and M. S. Patel, *Inorg. Chim. Acta*, **170**, 241 (1990).
162. D. Fregona, G. Faraglia, R. Graziani, U. Casellato and S. Sitran, *Gazz. Chim. Ital.*, **124**, 153 (1994); R. C. Agarwal, S. P. Gupta and D. K. Rastogi, *J. Inorg. Nucl. Chem.*, **36**, 208 (1974).
163. F. Cecconi, C. A. Ghilardi, A. Ienco, P. Mariani, C. Mealli, S. Midollini, A. Orlandini and A. Vacca, *Inorg. Chem.*, **41**, 4006 (2002).
164. M. Odoko, K. Yamamoto and N. Okabe, *Acta Crystallogr., Sect. C*, **58**, m469 (2002).
165. W. Y. Hsieh, C. M. Zaleski, V. L. Pecoraro, P. E. Fanwick and S. A. Liu, *Inorg. Chim. Acta*, **359**, 228 (2006); O. Vajragupta, P. Boonchoong, Y. Sumanont, H. Watanabe, Y. Wongkrajang and N. Kammasud, *Bioorg. Med. Chem.*, **11**, 2329 (2003).
166. C. Gerard, *Bull. Soc. Chim. Fr.*, I451 (1979).
167. A. Wu, D. C. Kennedy, B. O. Patrick and B. R. James, *Inorg. Chem.*, **42**, 7579 (2003); M. D. Fryzuk, M. J. Jonker and S. J. Rettig, *Chem. Commun.*, 377 (1997).
168. R. Lang, A. Schorwerth, K. Polborn, W. Ponikwar, W. Beck, T. Severin and K. Severin, *Z. Anorg. Allg. Chem.*, **625**, 1384 (1999).
169. M. Carland, K. J. Tan, J. M. White, J. Stephenson, V. Murray, W. A. Denny and W. D. McFadyen, *J. Inorg. Biochem.*, **99**, 1738 (2005).
170. M. Odoko, K. Yamamoto and N. Okabe, *Acta Crystallogr., Sect. C*, **58**, m506 (2002); M. Czaun, G. Speier and L. Parkanyi, *Chem. Commun.*, 1004 (2004); A. El-Jammal, P. L. Howell, M. A. Turner, N. Li and D. M. Templeton, *J. Med. Chem.*, **37**, 461 (1994).
171. S. I. Ahmed, J. Burgess, J. Fawcett, S. A. Parsons, D. R. Russell and S. H. Laurie, *Polyhedron*, **19**, 129 (2000).
172. F. R. Abreu, D. G. Lima, E. H. Hamu, S. Einloft, J. C. Rubim and P. A. Z. Suárez, *J. Am. Oil Chem. Soc.*, **80**, 601 (2003).
173. Y. Adachi, J. Yoshida, Y. Kodera, A. Kato, Y. Yoshikawa, Y. Kojima and H. Sakurai, *J. Biol. Inorg. Chem.*, **9**, 885 (2004).
174. S. S. Marwaha, J. Kaur and G. S. Sodhi, *J. Inorg. Biochem.*, **54**, 67 (1994); K. K. Dahiya, M. P. Singh and N. K. Kaushik, *Synth. React. Inorg. Met.-Org. Chem.*, **20**, 65 (1990).
175. A. B. de Oliveira, I. F. Jorge, P. A. Z. Suárez, N. R. D. S. Basso and S. Einloft, *Polym. Bull.*, **45**, 341 (2000).
176. W. O. Nelson, T. B. Karpishin, S. J. Rettig and C. Orvig, *Inorg. Chem.*, **27**, 1045 (1988).
177. L. Carter, D. L. Davies, J. Fawcett and D. R. Russell, *Polyhedron*, **12**, 1599 (1993).
178. K. Yamada, S. Yagishita, H. Tanaka, K. Tohyama, K. Adachi, S. Kaizaki, H. Kumagai, K. Inoue, R. Kitaura, H.-C. Chang, S. Kitagawa and S. Kawata, *Chem. Eur. J.*, **10**, 2647 (2004).
179. S. Padhye, P. Garge and M. P. Gupta, *Inorg. Chim. Acta*, **152**, 37 (1988); P. Garge, S. Padhye and J. P. Tuchagues, *Inorg. Chim. Acta*, **157**, 239 (1989).
180. M.-L. Tong, X.-L. Yu and X.-M. Chen, *Inorg. Chem. Commun.*, **3**, 694 (2000).
181. B. F. Abrahams, J. Coleiro, K. Ha, B. F. Hoskins, S. D. Orchard and R. Robson, *J. Chem. Soc., Dalton Trans.*, 1586 (2002).
182. N. H. Gokhale, S. B. Padhye, S. L. Croft, H. D. Kendrick, W. Davies, C. E. Anson and A. K. Powell, *J. Inorg. Biochem.*, **95**, 249 (2003).
183. S. Liu and S. N. Shaikh, *Chem. Commun.*, 1017 (1988).
184. C. L. Foster, X. Liu, C. A. Kilner, M. Thornton-Pett and M. A. Halcrow, *J. Chem. Soc., Dalton Trans.*, 4563 (2000).
185. S. Salunke-Gawali, S. Y. Rane, V. G. Puranik, C. Guyard-Duhayon and F. Varret, *Polyhedron*, **23**, 2541 (2004).
186. E. H. de Oliveira, G. E. A. Medeiros, C. Peppe, M. A. Brown and D. G. Tuck, *Can. J. Chem.*, **75**, 499 (1997).

187. P. Garge, R. Chikate, S. Padhye, J.-M. Savariault, P. d. Loth and J.-P. Tuchagues, *Inorg. Chem.*, **29**, 3315 (1990).
188. M. A. Martínez, M. C. L. De Jiménez, E. E. Castellano, O. E. Piro and P. J. Aymonino, *J. Coord. Chem.*, **56**, 803 (2003).
189. C. Robl and W. F. Kuhs, *J. Solid State Chem.*, **79**, 46 (1989).
190. S. Decurtins, H. W. Schmalle, P. Schneuwly and L.-M. Zheng, *Acta Crystallogr., Sect. C*, **52**, 561 (1996).
191. S. S. Sawhney, *Thermochim. Acta*, **74**, 361 (1984).
192. H. Yuge and T. K. Miyamoto, *Acta Crystallogr., Sect. C*, **55**, 1617 (1999).
193. R. West, *Oxocarbons*, Academic Press, New York, 1980; R. West and J. Niu, in *The Chemistry of the Carbonyl Group*, Vol. 2 (Ed. J. Zabicky), John Wiley & Sons, Ltd, London, 1970, pp. 241–275.
194. D. Eggerding and R. West, *J. Am. Chem. Soc.*, **98**, 3641 (1976).
195. L. Gmelin, *Ann. Phys.*, 431 (1825); L. F. C. Oliveira and P. S. Santos, *J. Mol. Struct.*, **263**, 59 (1991); R. B. Wyrwas and C. C. Jarrold, *J. Am. Chem. Soc.*, **128**, 13688 (2006).
196. R. Nietzki, *Ber. Dtsch. Chem. Ges.*, **20**, 1617 (1998); K. Yamada and Y. Hirata, *Bull. Chem. Soc. Jpn.*, **31**, 55 (1958).
197. C. Brouca-Cabarrecq and J.-C. Trombe, *Inorg. Chim. Acta*, **191**, 227 (1992).
198. R. West and H. Y. Niu, *J. Am. Chem. Soc.*, **85**, 2586 (1963).
199. Q. Chen, S. Liu and J. Zubieta, *Inorg. Chim. Acta*, **175**, 241 (1990).
200. M. D. Glick and L. F. Dahl, *Inorg. Chem.*, **5**, 289 (1966); D. Deguenon, G. Bernardinelli, J. P. Tuchagues and P. Castan, *Inorg. Chem.*, **29**, 3031 (1990).
201. A. Cornia, A. C. Fabretti, A. Giusti, F. Ferraro and D. Gatteschi, *Inorg. Chim. Acta*, **212**, 87 (1993).
202. S. Curreli, P. Deplano, C. Faulmann, M. L. Mercuri, L. Pilia, A. Serpe, E. Coronado and C. J. Gómez-García, *Inorg. Chim. Acta*, **359**, 1177 (2006); C. J. Gómez-García, E. Coronado, S. Curreli, C. Giménez-Saiz, P. Deplano, M. L. Mercuri, L. Pilia, A. Serpe, C. Faulmann and E. Canadell, *Chem. Commun.*, 4931 (2006).
203. F. Dumestre, B. Soula, A. M. Galibert, P. L. Fabre, G. Bernardinelli, B. Donnadieu and P. Castan, *J. Chem. Soc., Dalton Trans.*, 4131 (1998).
204. C. C. Wang, C. H. Yang and G. H. Lee, *Inorg. Chem.*, **41**, 1015 (2002).
205. M. L. Calatayud, J. Sletten, M. Julve and I. Castro, *J. Mol. Struct.*, **741**, 121 (2005).
206. N. Das, A. Ghosh, A. M. Arif and P. J. Stang, *Inorg. Chem.*, **44**, 7130 (2005).
207. M. D. Glick, G. L. Downs and L. F. Dahl, *Inorg. Chem.*, **3**, 1712 (1964).
208. I. Castro, J. Sletten, J. Faus, M. Julve, Y. Journaux, F. Lloret and S. Alvarez, *Inorg. Chem.*, **31**, 1889 (1992).
209. I. Castro, J. Sletten, J. Faus and M. Julve, *J. Chem. Soc., Dalton Trans.*, 2271 (1992); I. Castro, M. L. Calatayud, F. Lloret, J. Sletten and M. Julve, *J. Chem. Soc., Dalton Trans.*, 2397 (2002); J. Carranza, J. Sletten, C. Brennan, F. Lloret, J. Cano and M. Julve, *Dalton Trans.*, 3997 (2004).
210. J. Carranza, C. Brennan, J. Sletten, B. Vangdal, P. Rillema, F. Lloret and M. Julve, *New J. Chem.*, **27**, 1775 (2003).
211. T. K. Maji, S. Konar, G. Mostafa, E. Zangrando, T.-H. Lu and N. R. Chaudhuri, *Dalton Trans.*, 171 (2003).
212. C. Brouca-Cabarrecq and J.-C. Trombe, *Inorg. Chim. Acta*, **191**, 241 (1992).
213. R. Koferstein and C. Robl, *Z. Anorg. Allg. Chem.*, **629**, 371 (2003).
214. C. Brouca-Cabarrecq, A. Mohanu, P. Millet and J. C. Trombe, *J. Solid State Chem.*, **177**, 2575 (2004); A. Mohanu and J.-C. Trombe, *Acta Crystallogr., Sect. C*, **62**, m16 (2006); K.-J. Lin and K.-H. Lii, *Angew. Chem., Int. Ed. Engl.*, **36**, 2076 (1997); A. Muller, R. Rohlfing, E. Krickemeyer and H. Bogge, *Angew. Chem., Int. Ed. Engl.*, **32**, 909 (1993); M. I. Khan, Y.-D. Chang, Q. Chen, J. Salta, Y.-S. Lee, C. J. O'Connor and J. Zubieta, *Inorg. Chem.*, **33**, 6340 (1994).
215. M. Hilbers, M. Meiwald and R. Mattes, *Z. Naturforsch., Sect. B*, **51**, 57 (1996).
216. J. P. Chesick and F. Doany, *Acta Crystallogr., Sect. B*, **37**, 1076 (1981); E. Bang, K. Michelsen, K. M. Nielsen and E. Pedersen, *Acta Chem. Scand.*, **43**, 748 (1989).
217. B. Modec, J. V. Brencic, E. M. Burkholder and J. Zubieta, *Dalton Trans.*, 4618 (2003); Q. Chen, L. Ma, S. Liu and J. Zubieta, *J. Am. Chem. Soc.*, **111**, 5944 (1989); Q. Chen, S. Liu

and J. Zubieta, *Inorg. Chim. Acta*, **164**, 115 (1989); L. Lisnard, P. Mialane, A. Dolbecq, J. Marrot and F. Secheresse, *Inorg. Chem. Commun.*, **6**, 503 (2003).
218. A. K. Ghosh, D. Ghoshal, E. Zangrando, J. Ribas and N. R. Chaudhuri, *Dalton Trans.*, 1554 (2006); D. S. Yufit, D. J. Price, J. A. K. Howard, S. O. H. Gutschke, A. K. Powell and P. T. Wood, *Chem. Commun.*, 1561 (1999); A. Weiss, E. Riegler and C. Robl, *Z. Naturforsch., Sect. B*, **41**, 1333 (1986); J. Greve and C. Nather, *Acta Crystallogr., Sect. E*, **58**, m625 (2002).
219. S. Neeraj, M. L. Noy, C. N. R. Rao and A. K. Cheetham, *Solid State Sci.*, **4**, 1231 (2002).
220. A. Weiss, E. Riegler, I. Alt, H. Bohme and C. Robl, *Z. Naturforsch., Sect. B*, **41**, 18 (1986).
221. B.-P. Yang and J.-G. Mao, *Inorg. Chem.*, **44**, 566 (2005).
222. G. M. Frankenbach, M. A. Beno, A. M. Kini, J. M. Williams, U. Welp, J. E. Thompson and M.-H. Whangbo, *Inorg. Chim. Acta*, **192**, 195 (1992).
223. S. Konar, M. Corbella, E. Zangrando, J. Ribas and N. R. Chaudhuri, *Chem. Commun.*, 1424 (2003); J. Sletten, H. Daraghmeh, F. Lloret and M. Julve, *Inorg. Chim. Acta*, **279**, 127 (1998); F. Lloret, M. Julve, J. Faus, X. Soláns, Y. Journaux and I. Morgenstern-Badarau, *Inorg. Chem.*, **29**, 2232 (1990); C. Nather, J. Greve and I. Jess, *Acta Crystallogr., Sect. E*, **58**, m507 (2002).
224. C.-R. Lee, C.-C. Wang and Y. Wang, *Acta Crystallogr., Sect. B*, **52**, 966 (1996).
225. R. Kirchmaier, E. Altin and A. Lentz, *Z. Kristallogr.*, **219**, 29 (2004); I. Ucar and A. Bulut, *Acta Crystallogr., Sect. E*, **61**, m1320 (2005); A. Ludi and P. Schindler, *Angew. Chem.*, **80**, 664 (1968); H.-A. Hosein, L. A. Hall, A. J. Lough, W. Desmarais, M. J. Vela and B. M. Foxman, *Inorg. Chem.*, **37**, 4184 (1998).
226. B. D. Alleyne, H.-A. Hosein, H. Jaggernauth, L. A. Hall, A. J. P. White and D. J. Williams, *Inorg. Chem.*, **38**, 2416 (1999).
227. M. Dan, K. Sivashankar, A. K. Cheetham and C. N. R. Rao, *J. Solid State Chem.*, **174**, 60 (2003).
228. C.-C. Wang, C.-H. Yang, G.-H. Lee and H.-L. Tsai, *Eur. J. Inorg. Chem.*, 1334 (2005).
229. R. Kirchmaier, E. Altin and A. Lentz, *Z. Kristallogr.*, **218**, 541 (2003); R. Soules, F. Dahan, J.-P. Laurent and P. Castan, *J. Chem. Soc., Dalton Trans.*, 587 (1988); J. Greve and C. Nather, *Acta Crystallogr., Sect. E*, **58**, m653 (2002); J. A. C. van Ooijen, J. Reedijk and A. L. Spek, *Inorg. Chem.*, **18**, 1184 (1979); R. Kirchmaier, E. Altin and A. Lentz, *Z. Kristallogr.*, **219**, 135 (2004); I. Castro, M. L. Calatayud, J. Sletten, F. Lloret and M. Julve, *J. Chem. Soc., Dalton Trans.*, 811 (1997); M. L. Calatayud, I. Castro, J. Sletten, J. Cano, F. Lloret, J. Faus, M. Julve, G. Seitz and K. Mann, *Inorg. Chem.*, **35**, 2858 (1996).
230. A. Weiss, E. Riegler and C. Robl, *Z. Naturforsch., Sect. B*, **41**, 1329 (1986).
231. A. Crispini, D. Pucci, I. Aiello and M. Ghedini, *Inorg. Chim. Acta*, **304**, 219 (2000).
232. S. Grabner, B. Modec, M. Cemazar and N. Bukovec, *J. Inorg. Biochem.*, **99**, 1465 (2005); G. Bernardinelli, P. Castan and R. Soules, *Inorg. Chim. Acta*, **120**, 205 (1986).
233. I. Ucar, A. Bulut and O. Buyukgungor, *Acta Crystallogr., Sect. C*, **61**, m218 (2005); J. Sletten and O. Bjorsvik, *Acta Chem. Scand.*, **52**, 770 (1998); I. Castro, M. L. Calatayud, J. Sletten, F. Lloret and M. Julve, *Inorg. Chim. Acta*, **287**, 173 (1999); X. Soláns, M. Aguiló, A. Gleizes, J. Faus, M. Julve and M. Verdaguer, *Inorg. Chem.*, **29**, 775 (1990); I. Castro, J. Faus, Y. Journaux and J. Sletten, *J. Chem. Soc., Dalton Trans.*, 2533 (1991); E. Krupicka and A. Lentz, *Z. Kristallogr.*, **216**, 287 (2001); E. Krupicka and A. Lentz, *Z. Kristallogr.*, **216**, 289 (2001); A. Bulut, I. Ucar, O. Z. Yesilel, H. Icbudak, H. Olmez and O. Buyukgungor, *Acta Crystallogr., Sect. C*, **60**, m526 (2004); H. Grove, J. Sletten, M. Julve, F. Lloret, L. Lezama, J. Carranza, S. Parsons and P. Rillema, *J. Mol. Struct.*, **606**, 253 (2002); C. E. Xanthopoulos, M. P. Sigalas, G. A. Katsoulos, C. A. Tsipis and A. Terzis, *Polyhedron*, **11**, 2819 (1992); I. Castro, J. Sletten, M. L. Calatayud, M. Julve, J. Cano, F. Lloret and A. Caneschi, *Inorg. Chem.*, **34**, 4903 (1995).
234. R. Kirchmaier, E. Altin and A. Lentz, *Z. Kristallogr.*, **219**, 31 (2004); C. Robl and W. F. Kuhs, *J. Solid State Chem.*, **75**, 15 (1988).
235. O. M. Yaghi, G. Li and T. L. Groy, *J. Chem. Soc., Dalton Trans.*, 727 (1995).
236. C.-C. Wang, C.-H. Yang, S.-M. Tseng, G.-H. Lee, H.-S. Sheu and K. Phyu, *Inorg. Chim. Acta*, **357**, 3759 (2004); T. K. Maji, G. Mostafa, S. Sain, J. S. Prasad and N. R. Chaudhuri, *CrystEngComm*, **3**, 155 (2001).
237. W. Uhl, L. Cuypers, M. Prott and K. Harms, *Polyhedron*, **21**, 511 (2002).
238. Q. Chen, S. Liu and J. Zubieta, *Inorg. Chim. Acta*, **175**, 269 (1990).
239. I. Ucar, A. Bulut and C. Kazak, *Acta Crystallogr., Sect. C*, **61**, m428 (2005).

240. N. Mahe and T. Bataille, *Inorg. Chem.*, **43**, 8379 (2004).
241. P. M. T. Piggott, L. A. Hall, A. J. P. White and D. J. Williams, *Inorg. Chem.*, **42**, 8344 (2003).
242. A. Dolbecq, P. Mialane, L. Lisnard, J. Marrot and F. Secheresse, *Chem. Eur. J.*, **9**, 2914 (2003); U. Heinl, P. Hinse and R. Mattes, *Z. Anorg. Allg. Chem.*, **627**, 2173 (2001).
243. J.-F. Petit, A. Gleizes and J.-C. Trombe, *Inorg. Chim. Acta*, **167**, 51 (1990).
244. E. Huskowska, T. Glowiak, J. Legendziewicz and G. Oremek, *J. Alloys Compd.*, **179**, 13 (1992).
245. B. D. Alleyne, L. A. Hall, I. A. Kahwa, A. J. P. White and D. J. Williams, *Inorg. Chem.*, **38**, 6278 (1999).
246. A. S. Wilson, *Cryst. Struct. Commun.*, **11**, 809 (1982).
247. A. Bouayad, J.-C. Trombe and A. Gleizes, *Inorg. Chim. Acta*, **230**, 1(1995).
248. S. W. Ng, S.-Z. Hu, I. A. Razak and H.-K. Fun, *Acta Crystallogr., Sect. E*, **57**, **m28** (2001).
249. J.-F. Petit, J.-C. Trombe, A. Gleizes and J. Galy, *C. R. Seances Acad. Sci., Ser. II*, **304**, 1117 (1987).
250. A. Bouayad, C. Brouca-Cabarrecq, J.-C. Trombe and A. Gleizes, *Inorg. Chim. Acta*, **195**, 193 (1992).
251. D. Braga, C. Bazzi, L. Maini and F. Grepioni, *CrystEngComm*, **1**, 15 (1999).
252. Q. Chen, S. Liu and J. Zubieta, *Angew. Chem., Int. Ed. Engl.*, **29**, 70 (1990).
253. B. D. Alleyne, A. R. Williams, L. A. Hall, A. J. P. White and D. J. Williams, *Inorg. Chem.*, **40**, 1045 (2001).
254. A. Williams, B. D. Alleyne, H.-A. Hosein, H. Jaggernauth, L. A. Hall, B. M. Foxman, L. K. Thompson and C. Agosta, *Inorg. Chim. Acta*, **313**, 56 (2001).
255. A. R. Williams, L. A. Hall, A. J. P. White and D. J. Williams, *Inorg. Chim. Acta*, **314**, 117 (2001).
256. P. M. T. Piggot, L. A. Hall, A. J. P. White and D. J. Williams, *Inorg. Chim. Acta*, **357**, 207 (2004).
257. L. A. Hall, D. J. Williams, S. Menzer and A. J. P. White, *Inorg. Chem.*, **36**, 3096 (1997).
258. P. M. T. Piggot, L. A. Hall, A. J. P. White, D. J. Williams and L. K. Thompson, *Inorg. Chem.*, **43**, 1167 (2004).
259. B. D. Alleyne, L. S. Bernard, H. Jaggernauth, L. A. Hall, I. Baxter, A. J. P. White and D. J. Williams, *Inorg. Chem.*, **38**, 3774 (1999).
260. A. R. Williams, B. D. Alleyne, L. A. Hall, A. J. P. White, D. J. Williams and L. K. Thompson, *Inorg. Chem.*, **39**, 5265 (2000).
261. P. C. M. Chan, R. J. Roon, J. F. Koerner, N. J. Taylor and J. F. Honek, *J. Med. Chem.*, **38**, 4433 (1995).
262. H.-A. Hosein, H. Jaggernauth, B. D. Alleyne, L. A. Hall, A. J. P. White and D. J. Williams, *Inorg. Chem.*, **38**, 3716 (1999).
263. M. Plitzner, U. Heinl, R. Mattes and R. Frohlich, *Z. Anorg. Allg. Chem.*, **627**, 1426 (2001).
264. J. Rong, Y. Peng, H. W. Roesky, J. Li, D. Vidovic and J. Magull, *Eur. J. Inorg. Chem.*, 3110 (2003).
265. O. T. Summerscales, F. G. N. Cloke, P. B. Hitchcock, J. C. Green and N. Hazari, *J. Am. Chem. Soc.*, **128**, 9602 (2006).
266. D. Braga, G. Cojazzi, L. Maini and F. Grepioni, *New J. Chem.*, **25**, 1221 (2001).
267. C.-C. Wang, C.-T. Kuo, P.-T. Chou and G.-H. Lee, *Angew. Chem. Int. Ed.*, **43**, 4507 (2004).
268. B. Zümreoglu-Karan, *Coord. Chem. Rev.*, **250**, 2295 (2006).
269. H. Yuge and T. K. Miyamoto, *Inorg. Chim. Acta*, **329**, 66 (2002); L. S. Hollis, E. W. Stern, A. R. Amundsen, A. V. Miller and S. L. Doran, *J. Am. Chem. Soc.*, **109**, 3596 (1987); H. Yuge and T. K. Miyamoto, *Acta Crystallogr., Sect. C*, **52**, 3002 (1996); H. Yuge and T. K. Miyamoto, *Chem. Lett.*, 375 (1996).
270. J. A. Daldy, J. Fawcett, W. Henderson, R. D. W. Kemmitt and D. R. Russell, *J. Chem. Soc., Dalton Trans.*, 3383 (1994).
271. W. Henderson, J. Fawcett, R. D. W. Kemmitt and D. R. Russell, *J. Chem. Soc., Dalton Trans.*, 3007 (1995).
272. A. G. Davies and J. A. A. Hawari, *J. Chem. Soc., Perkin Trans. 1*, 875 (1983).
273. S. Sakai, M. Murata, N. Wada and T. Fujinami, *Bull. Chem. Soc. Jpn.*, **56**, 1873 (1983).
274. W. P. Neumann and A. Schwarz, *Angew. Chem., Int. Ed. Engl.*, **14**, 812 (1975); I. Wakeshima and I. Kijima, *Bull. Chem. Soc. Jpn.*, **54**, 2345 (1981).

275. T. Tekeste and H. Vahrenkamp, *Eur. J. Inorg. Chem.*, 5158 (2006).
276. K. C. Joshi and V. N. Pathak, *Coord. Chem. Rev.*, **22**, 37 (1977).
277. C. Pettinari, F. Marchetti and A. Drozdov, 'ß-Diketones and Related Ligands', in *Comprehensive Coordination Chemistry II*, Vol. 1 (Eds J. McCleverty and T. Meyer), 2nd edn, Elsevier, Amsterdam, 2003, pp. 97–115.
278. A. R. Siedle, 'Diketones and Related Ligands', in *Comprehensive Coordination Chemistry*, Vol. 2 (Eds G. Wilkinson, R. D. Gillard and J. A. McCleverty), Pergamon, Oxford, 1987, pp. 365–412.
279. G. T. Morgan, *J. Chem. Soc.*, **105**, 189 (1914); D. Gibson, *Coord. Chem. Rev.*, **4**, 225 (1969); J. P. Collman, *Angew. Chem., Int. Ed. Engl.*, **4**, 132 (1965); D. P. Graddon, *Coord. Chem. Rev.*, **4**, 1 (1969); J. Selbin, *Chem. Rev.*, **65**, 153 (1965); R. C. Mehrotra, R. Bohra, D. P. Gaur, *Metal-Diketonates and Allied Derivatives*, Academic Press, London,1978.
280. J. P. Fackler, Jr., *Prog. Inorg. Chem.*, **7**, 361 (1966).
281. R. M. Pike, *Coord. Chem. Rev.*, **2**, 163 (1967).
282. D. J. Otway and W. S. Rees, *Coord. Chem. Rev.*, **210**, 279 (2000).
283. W. C. Fernelius and B. E. Bryant, *Inorg. Synth.*, **5**, 105 (1957).
284. R. C. Mehrotra, *Pure Appl. Chem.*, **60**, 1349 (1988).
285. R. Ragni, E. A. Plummer, K. Brunner, J. W. Hofstraat, F. Babudri, G. M. Farinola, F. Naso and L. De Cola, *J. Mater. Chem.*, **16**, 1161 (2006).
286. W. Rigby, H. B. Lee, P. M. Bailey, J. A. McCleverty and P. M. Maitlis, *J. Chem. Soc., Dalton Trans.*, 387 (1979).
287. L. G. Mackay, H. L. Anderson and J. K. M. Sanders, *J. Chem. Soc., Perkin Trans. 1*, 2269 (1995).
288. R. G. Charles and M. A. Pawlikowski, *J. Phys. Chem.*, **62**, 440 (1958).
289. C. L. Perrin and Y.-J. Kim, *Inorg. Chem.*, **39**, 3902 (2000).
290. G. S. Hammond, D. C. Nonhebel and C.-H. S. Wu, *Inorg. Chem.*, **2**, 73 (1963).
291. R. Ueeda, Y. Kawasaki, T. Tanaka and R. Okawara, *J. Organomet. Chem.*, **5**, 194 (1966).
292. A. H. Alberts and D. J. Cram, *J. Am. Chem. Soc.*, **101**, 3545 (1979).
293. J. Vicente and M. Chicote, *Inorg. Synth.*, **32**, 172 (1998).
294. C. Pettinari, F. Marchetti, R. Pettinari, V. Vertlib, A. Drozdov, I. Timokhin, S. Troyanov, Y.-S. Min and D. Kim, *Inorg. Chim. Acta*, **355**, 157 (2003).
295. Q. Y. Zhu, G. Q. Bian, Y. Zhang, J. Dai, D. Q. Zhang and W. Lu, *Inorg. Chim. Acta*, **359**, 2303 (2006).
296. G. Aromi, C. Boldron, P. Gamez, O. Roubeau, H. Kooijman, A. L. Spek, H. Stoeckli-Evans, J. Ribas and J. Reedijk, *Dalton Trans.*, 3586 (2004).
297. G. Malandrino, A. M. Borzi, F. Castelli, I. L. Fragala, W. Dastru, R. Gobetto, P. Rossi and P. Dapporto, *Dalton Trans.*, 369 (2003).
298. T. N. Srivastava and K. L. Saxena, *Indian J. Chem.*, **9**, 601 (1971).
299. R. C. Mehrotra and V. D. Gupta, *J. Organomet. Chem.*, **4**, 237 (1965); V. M. DePalma and E. M. Arnett, *J. Am. Chem. Soc.*, **100**, 3514 (1978).
300. H. Brombacher and H. Vahrenkamp, *Inorg. Chem.*, **43**, 6054 (2004).
301. W. J. Evans, D. G. Giarikos, M. A. Johnston, M. A. Greci and J. W. Ziller, *J. Chem. Soc., Dalton Trans.*, 520 (2002).
302. R. Fernández, M. Melchart, A. Habtemariam, S. Parsons and P. L. Sadler, *Chem. Eur. J.*, **10**, 5173 (2004).
303. O. T. B. Junior, J. R. Gardinier and M. R. Churchill, *Organometallics*, **22**, 1145 (2003).
304. B. Weberndorfer, G. Henig, D. C. R. Hockless, M. A. Bennett and H. Werner, *Organometallics*, **22**, 744 (2003).
305. N. Serpone and K. A. Hersh, *J. Organomet. Chem.*, **84**, 177 (1975); W. H. Nelson and D. F. Martin, *J. Inorg. Nucl. Chem.*, **27**, 89 (1965).
306. V. G. Kessler, S. Gohil and S. Parola, *Dalton Trans.*, 544 (2003).
307. E. Suslova, G. A. Seisenbaeva and V. G. Kessler, *Inorg. Chem. Commun.*, **5**, 946 (2002).
308. G. H. Cartledge, *J. Am. Chem. Soc.*, **73**, 4416 (1951); G. Aromi, M. J. Knapp, J.-P. Claude, J. C. Hoffman, D. N. Hendrickson and G. Christou, *J. Am. Chem. Soc.*, **121**, 5489 (1999).
309. G. Aromi, S. Bhaduri, P. Artus, K. Folting and G. Christou, *Inorg. Chem.*, **41**, 805 (2002).
310. F.-J. Lee, Y. Chi, C.-S. Liu, P.-F. Hsu, T.-Y. Chou, S.-M. Peng and G.-H. Lee, *Chem. Vap. Deposition*, **7**, 99 (2001).
311. H.-L. Yu, Y. Chi, C.-S. Liu, S.-M. Peng and G.-H. Lee, *Chem. Vap. Deposition*, **7**, 245 (2001).

312. M.-D. Su, H.-Y. Liao, S.-Y. Chu, Y. Chi, C.-S. Liu, F.-J. Lee, S.-M. Peng and G.-H. Lee, *Organometallics*, **19**, 5400 (2000).
313. S. S. Amin, K. Cryer, B. Y. Zhang, S. K. Dutta, S. S. Eaton, O. P. Anderson, S. M. Miller, B. A. Reul, S. M. Brichard and D. C. Crans, *Inorg. Chem.*, **39**, 406 (2000).
314. F. Gornshtein, M. Kapon, M. Botoshansky and M. S. Eisen, *Organometallics*, **26**, 497 (2007).
315. C. T. Vogelson, C. L. Edwards, A. N. Kobylivker, S. B. Chacko, C. E. Moran, K. Dalton, S. M. Stewart, B. C. Werner, S. G. Bott and A. R. Barron, *J. Chem. Crystallogr.*, **28**, 815 (1998).
316. V. A. Mode and G. S. Smith, *J. Inorg. Nucl. Chem.*, **31**, 1857 (1969).
317. M. G. Murray and D. C. Nonhebel, *J. Chem. Soc. C*, 1172 (1970).
318. D. V. Soldatov, A. T. Henegouwen, G. D. Enright, C. I. Ratcliffe and J. A. Ripmeester, *Inorg. Chem.*, **40**, 1626 (2001).
319. O. E. Woisetschlager, A. Geisbauer, K. Polborn and W. Beck, *Z. Anorg. Allg. Chem.*, **626**, 766 (2000).
320. K. H. Thompson, K. Bohmerle, E. Polishchuk, C. Martins, P. Toleikis, J. Tse, V. Yuen, J. H. McNeill and C. Orvig, *J. Inorg. Biochem.*, **98**, 2063 (2004); K. Mohammadi, K. H. Thompson, B. O. Patrick, T. Storr, C. Martins, E. Polishchuk, V. G. Yuen, J. H. McNeill and C. Orvig, *J. Inorg. Biochem.*, 2217 (2005).
321. V. D. John and K. Krishnankutty, *Appl. Organomet. Chem.*, **20**, 477 (2006); A. Barik, B. Mishra, L. Shen, H. Mohan, R. M. Kadam, S. Dutta, H.-Y. Zhang and K. I. Priyadarsini, *Free Radic. Biol. Med.*, **39**, 811 (2005).
322. J. B. Majithiya, R. Balaraman, R. Giridhar and M. R. Yadav, *J. Trace Elem. Med. Biol.*, **18**, 211 (2005).
323. O. Vajragupta, P. Boonchoong, H. Watanabe, M. Tohda, N. Kummasud and Y. Sumanont, *Free Radic. Biol. Med.*, **35**, 1632 (2003).
324. S. F. Mason, R. D. Peacock and T. Prosperi, *J. Chem. Soc., Dalton Trans.*, 702 (1977); R. Kuroda and S. F. Mason, *J. Chem. Soc., Dalton Trans.*, 273 (1979).
325. R. C. Fay, A. Y. Girgis and U. Klabunde, *J. Am. Chem. Soc.*, **92**, 7056 (1970).
326. A. J. Carty, D. G. Tuck and E. Bullock, *Can. J. Chem.*, **43**, 2559 (1965).
327. R. West and R. Riley, *J. Inorg. Nucl. Chem.*, **5**, 295 (1958).
328. R. West, *J. Am. Chem. Soc.*, **80**, 3246 (1958).
329. F. Guibe, P. Sarthou and G. Bram, *Tetrahedron*, **30**, 3139 (1974).
330. C. Riche, C. Pascardbilly, C. Cambillau and G. Bram, *J. Chem. Soc., Chem. Commun.*, 183 (1977); C. Cambillau, G. Bram, J. Corset, C. Riche and C. Pascard-Billy, *Tetrahedron*, **34**, 2675 (1978).
331. C. R. Bhattacharjee, M. Bhattacharjee, M. K. Chaudhuri and H. Sangchungnunga, *J. Chem. Res.-S*, 250 (1991).
332. R. E. Sievers, S. B. Turnipseed, L. Huang and A. F. Lagalante, *Coord. Chem. Rev.*, **128**, 285 (1993).
333. A. P. Purdy, A. D. Berry, R. T. Holm, M. Fatemi and D. K. Gaskill, *Inorg. Chem.*, **28**, 2799 (1989).
334. W. S. Rees Jr., M. W. Carris and W. Hesse, *Inorg. Chem.*, **30**, 4479 (1991).
335. V. D. Vreshch, A. B. Lysenko, A. N. Chernega, J. Sieler and K. V. surDomasevitch, *Polyhedron*, **24**, 917 (2005); V. D. Vreshch, A. N. Chernega, J. A. K. Howard, J. Sieler and K. V. Domasevitch, *Dalton Trans.*, 1707 (2003); I. Boldog, E. B. Rusanov, A. N. Chernega, J. Sieler and K. V. Domasevitch, *Angew. Chem. Int. Ed.*, **40**, 3435 (2001).
336. L. Wang, Y. Yang, J. Ni, C. L. Stern and T. J. Marks, *Chem. Mater.*, **17**, 5697 (2005); H. O. Davies, A. C. Jones, T. J. Leedham, M. J. Crosbie, P. J. Wright, N. M. Boag and J.R. Thompson, *Chem. Vap. Deposition*, **6**, 71 (2000).
337. M. Westerhausen, S. Schneiderbauer, A. N. Kneifel, Y. Soltl, P. Mayer, H. Noth, Z. Zhong, P. J. Dijkstra and J. Feijen, *Eur. J. Inorg. Chem.*, 3432 (2003).
338. H. O. Davies, J. J. Brooks, A. C. Jones, T. J. Leedham, J. F. Bickley, A. Steiner, P. O'Brien, A. J. P. White and D. J. Williams, *Polyhedron*, **20**, 2397 (2001).
339. P. W. Roesky, G. Canseco-Melchor and A. Zulys, *Chem. Commun.*, 738 (2004); G. Malandrino, R. L. Nigro, I. L. Fragala and C. Benelli, *Eur. J. Inorg. Chem.*, 500 (2004); F. A. Cotton and P. Legzdins, *Inorg. Chem.*, **7**, 1777 (1968); A. Gleizes, S. Sans-Lenain, D. Medus, N. Hovnanian, P. Miele and J.-D. Foulon, *Inorg. Chim. Acta*, **209**, 47 (1993); H. A. Luten,

W. S. R. Junior and V. L. Goedken, *Chem. Vap. Deposition*, **2**, 149 (1996); M. J. Bennett, F. A. Cotton, P. Legzdins and S. J. Lippard, *Inorg. Chem.*, **7**, 1770 (1968).
340. Y. Fukuda, A. Nakao and K. Hayashi, *J. Chem. Soc., Dalton Trans.*, 527 (2002).
341. D. R. van Staveren, G. A. van Albada, J. G. Haasnoot, H. Kooijman, A. M. M. Lanfredi, P. J. Nieuwenhuizen, A. L. Spek, F. Ugozzoli, T. Weyhermuller and J. Reedijk, *Inorg. Chim. Acta*, **315**, 163 (2001).
342. S. Bruck, M. Hilder, P. C. Junk and U. H. Kynast, *Inorg. Chem. Commun.*, **3**, 666 (2000); T. Phillips, D. E. Sands and W. F. Wagner, *Inorg. Chem.*, **7**, 2295 (1968); M. D. Danford, J. H. Burns, C. E. Higgins, J. R. S. Junior and W. H. Baldwin, *Inorg. Chem.*, **9**, 1953 (1970).
343. S. Suh, J. Guan, L. A. Miinea, J.-S. M. Lehn and D. M. Hoffman, *Chem. Mater.*, **16**, 1667 (2004); D. L. Kepert, J. M. Patrick and A. H. White, *J. Chem. Soc., Dalton Trans.*, 567 (1983); I. Baxter, J. A. Darr, M. B. Hursthouse, K. M. A. Malik, J. McAleese and D. M. P. Mingos, *Polyhedron*, **17**, 1329 (1998); T. Behrsing, A. M. Bond, G. B. Deacon, C. M. Forsyth, M. Forsyth, K. J. Kamble, B. W. Skelton and A. H. White, *Inorg. Chim. Acta*, **352**, 229 (2003); M. Becht, K.-H. Dahmen, V. Gramlich and A. Marteletti, *Inorg. Chim. Acta*, **248**, 27 (1996).
344. W. C. Andersen, B. C. Noll, S. P. Sellers, L. L. Whildin and R. E. Sievers, *Inorg. Chim. Acta*, **336**, 105 (2002).
345. V. Baskar and P. W. Roesky, *Z. Anorg. Allg. Chem.*, **631**, 2782 (2005).
346. A. Lennartson, M. Vestergren and M. Hakansson, *Chem. Eur. J.*, **11**, 1757 (2005).
347. S. G. Davies, J. Dupont, R. J. C. Easton, O. Ichihara, J. M. McKenna, A. D. Smith and J. A. A. de Sousa, *J. Organomet. Chem.*, **689**, 4184 (2004).
348. L.-N. Sun, H.-J. Zhang, Q.-G. Meng, F.-Y. Liu, L.-S. Fu, C.-Y. Peng, J.-B. Yu, G.-L. Zheng and S.-B. Wang, *J. Phys. Chem. B*, **109**, 6174 (2005).
349. G. M. Davies, R. J. Aarons, G. R. Motson, J. C. Jeffery, H. Adams, S. Faulkner and M. D. Ward, *Dalton Trans.*, 1136 (2004).
350. A. F. Kirby and R. A. Palmer, *Inorg. Chem.*, **20**, 1030 (1981); O. Poncelet and L. G. Hubertpfalzgraf, *Polyhedron*, **8**, 2183 (1989).
351. A. Volpe, G. Bombieri and N. Marchini, *J. Alloys Compd.*, **408**, 1046 (2006).
352. G. Xu, Z.-M. Wang, Z. He, Z. Lu, C.-S. Liao and C.-H. Yan, *Inorg. Chem.*, **41**, 6802 (2002).
353. M. Volpe, G. Bombieri and N. Marchini, *J. Alloys Compd.*, **408**, 1046 (2006).
354. V. A. Petrov, W. J. Marshall and V. V. Grushin, *Chem. Commun.*, **520** (2002).
355. R.-G. Xiong and X.-Z. You, *Inorg. Chem. Commun.*, **5**, 677 (2002); X.-R. Zeng, R.-G. Xiong, X.-Z. You and K.-K. Cheung, *Inorg. Chem. Commun.*, **3**, 341 (2000); A. L. Rheingold and W. King, *Inorg. Chem.*, **28**, 1715 (1989); L. M. Sweeting and A. L. Rheingold, *J. Am. Chem. Soc.*, **109**, 2652 (1987); T. Moriguchi, K. Uchiyama, M. Yasutake, T. Shinmyozu, K. Sakata and A. Tsuge, *Polyhedron*, **19**, 785 (2000); J. P. Leonard, C. M. G. dos Santos, S. E. Plush, T. McCabe and T. Gunnlaugsson, *Chem. Commun.*, 129 (2007).
356. J. H. Burns and M. D. Danford, *Inorg. Chem.*, **8**, 1780 (1969).
357. J. Kido and Y. Okamoto, *Chem. Rev.*, **102**, 2357 (2002).
358. I. Baxter, S. R. Drake, M. B. Hursthouse, K. M. A. Malik, J. McAleese, D. J. Otway and J. C. Plakatouras, *Inorg. Chem.*, **34**, 1384 (1995).
359. A. Zalkin, D. H. Templeton and D. G. Karraker, *Inorg. Chem.*, **8**, 2680 (1969).
360. V. Baskar and P. W. Roesky, *Dalton Trans.*, 676 (2006).
361. J. A. Cunningham, D. E. Sands, W. F. Wagner and M. F. Richardson, *Inorg. Chem.*, **8**, 22 (1969); L. Shi, H. Ma, Y. Yu and Z. Ye, *J. Organomet. Chem.*, **339**, 277 (1988); Z. Ye, Y. Yu, S. Wang and X. Jin, *J. Organomet. Chem.*, **448**, 91 (1993).
362. S. J. S. Wasson, D. E. Sands and W. F. Wagner, *Inorg. Chem.*, **12**, 187 (1973).
363. R. C. Young and J. Kovitz, *Inorg. Synth.*, **36**, 123 (1946); P. J. Reeves and A. J. Smith, *Inorg. Chim. Acta*, **139**, 51 (1987).
364. D. Brown, B. Whittaker and J. Tacon, *J. Chem. Soc., Dalton Trans.*, 34 (1975).
365. A. E. Comyns, B. M. Gatehouse and E. Wait, *J. Chem. Soc.*, 4655 (1958); J. C. Taylor, A. Ekstrom and C. H. Randall, *Inorg. Chem.*, **17**, 3285 (1978); S. Kannan, M. R. A. Pillai, V. Venugopal, P. A. Droege and C. L. Barnes, *Inorg. Chim. Acta*, **254**, 113 (1997).
366. B. Allard, *Acta Chem. Scand.*, **26**, 3492 (1972); A. Nakamura, M. Nakada, T. Nakamoto, T. Kitazawa and M. Takeda, *J. Magn. Magn. Mater.*, **310**, 1447 (2007).
367. S. N. Brown, E. T. Chu, M. W. Hull and B. C. Noll, *J. Am. Chem. Soc.*, **127**, 16010 (2005); E. Dubler, R. Buschmann and H. W. Schmalle, *J. Inorg. Biochem.*, **95**, 97 (2003); H. M.

Lindemann, M. Schneider, B. Neumann, H.-G. Stammler, A. Stammler and P. Jutzi, *Organometallics*, **21**, 3009 (2002); S.-S. Yun, I.-H. Suh, E. H. Kim, B.-J. Choi and S. Lee, *J. Organomet. Chem.*, **631**, 16 (2001).
368. F. Calderazzo, U. Englert, G. Pampaloni and M. Volpe, *J. Organomet. Chem.*, **690**, 3321 (2005).
369. R. C. Young and A. Arch, *Inorg. Synth.*, **35**, 121 (1946); G. I. Spijksma, H. J. M. Bouwmeester, D. H. A. Blank and V. G. Kessler, *Chem. Commun.*, 1874 (2004); B. Moraru, G. Kickelbick, M. Battistella and U. Schubert, *J. Organomet. Chem.*, **636**, 172 (2001); J. V. Silverton and J. L. Hoard, *Inorg. Chem.*, **2**, 235 (1963); M. Elder, *Inorg. Chem.*, **8**, 2103 (1969); R. B. Von Dreele, J. J. Stezowski and R. C. Fay, *J. Am. Chem. Soc.*, **93**, 2887 (1971); B. Allard, *J. Inorg. Nucl. Chem.*, **38**, 2109 (1976); J. J. Stezowski and H. A. Eick, *J. Am. Chem. Soc.*, **91**, 2890 (1969).
370. L. G. Hubert-Pfalzgraf, N. Touati, S. V. Pasko, J. Vaissermann and A. Abrutis, *Polyhedron*, **24**, 3066 (2005); S. V. Pasko, L. G. Hubert-Pfalzgraf, A. Abrutis, P. Richard, A. Bartasyte and V. Kazlauskiene, *J. Mater. Chem.*, **14**, 1245 (2004).
371. S. J. Kavitha, K. Panchanatheswaran, M. R. J. Elsegood and S. H. Dale, *Inorg. Chim. Acta*, **359**, 1314 (2006); R. A. Rowe and M. M. Jones, *Inorg. Synth.*, **5**, 113 (1957); K. S. Dichmann, G. Hamer, S. C. Nyburg and W. F. Reynolds, *J. Chem. Soc. D*, 1295 (1970); M. M. Musiani, F. Milani, R. Graziani, M. Vidali, U. Casellato and P. A. Vigato, *Inorg. Chim. Acta*, **61**, 115 (1982); F. L. Jiang, O. P. Anderson, S. M. Miller, J. Chen, M. Mahroof-Tahir and D. C. Crans, *Inorg. Chem.*, **37**, 5439 (1998); S. Lee, K. Nakanishi, M. Y. Chiang, R. B. Frankel and K. Spartalian, *Chem. Commun.*, 785 (1988); T. W. Hambley, C. J. Hawkins and T. A. Kabanos, *Inorg. Chem.*, **26**, 3740 (1987); J. G. Reynolds, E. L. Jones, J. C. Huffman and G. Christou, *Polyhedron*, **12**, 407 (1993).
372. P. A. Williams, A. C. Jones, P. J. Wright, M. J. Crosbie, J. F. Bickley, A. Steiner, H. O. Davies and T. J. Leedham, *Chem. Vap. Deposition*, **8**, 110 (2002).
373. H. O. Davies, T. J. Leedham, A. C. Jones, P. O'Brien, A. J. P. White and D. J. Williams, *Polyhedron*, **18**, 3165 (1999).
374. L. R. Ocone and B. P. Block, *Inorg. Synth.*, **8**, 125 (1966); F. A. Cotton, C. E. Rice and G. W. Rice, *Inorg. Chim. Acta*, **24**, 231 (1977); W. C. Fernelius and J. E. Blanch, *Inorg. Synth.*, **5**, 130 (1957); T. Birk and J. Bendix, *Inorg. Chem.*, **42**, 7608 (2003); M. Nakahanada, T. Fujihara, A. Fuyuhiro and S. Kaizaki, *Inorg. Chem.*, **31**, 1315 (1992); P. G. Jessop, M. M. Olmstead, C. D. Ablan, M. Grabenauer, D. Sheppard, C. A. Eckert and C. L. Liotta, *Inorg. Chem.*, **41**, 3463 (2002); O. Heinemann, P. W. Jolly, C. Kruger and G. P. J. Verhovnik, *J. Organomet. Chem.*, **553**, 477 (1998); H. R. Fischer, D. J. Hodgson and E. Pedersen, *Inorg. Chem.*, **23**, 4755 (1984).
375. P. Werndrup, G. A. Seisenbaeva, G. Westin, I. Persson and V. G. Kessler, *Eur. J. Inorg. Chem.*, 1413 (2006); T. Shima, J. Ito and H. Suzuki, *Organometallics*, **20**, 10 (2001); R. D. Rogers, E. Carmona, A. Galindo, J. L. Atwood and L. G. Canada, *J. Organomet. Chem.*, **277**, 403 (1984); M. H. Chisholm, K. Folting, J. C. Huffman and A. L. Ratermann, *Inorg. Chem.*, **23**, 613 (1984); M. H. Chisholm, J. F. Corning, K. Folting, J. C. Huffman, A. L. Ratermann, I. P. Rothwell and W. E. Streib, *Inorg. Chem.*, **23**, 1037 (1984).
376. R. Hernández-Molina, M. Sokolov, W. Clegg, P. Esparza and A. Mederos, *Inorg. Chim. Acta*, **331**, 52 (2002).
377. M. G. B. Drew, G. W. A. Fowles, D. A. Rice and K. J. Shanton, *J. Chem. Soc., Chem. Commun.*, 614 (1974).
378. R. van Gorkum, F. Buda, H. Kooijman, A. L. Spek, E. Bouwman and J. Reedijk, *Eur. J. Inorg. Chem.*, 2255 (2005); S. Geremia and N. Demitri, *J. Chem. Educ.*, **82**, 460 (2005); R. G. Charles, *Inorg. Synth.*, **6**, 164 (1960); G. L. Abbati, A. Cornia, A. C. Fabretti, A. Caneschi and D. Gatteschi, *Inorg. Chem.*, **37**, 1430 (1998); G. L. Abbati, A. Cornia, A. C. Fabretti, A. Caneschi and D. Gatteschi, *Inorg. Chem.*, **37**, 3759 (1998); G. L. Abbati, A. Caneschi, A. Cornia, A. C. Fabretti and D. Gatteschi, *Inorg. Chim. Acta*, **297**, 291 (2000); G. Aromi, P. Gamez, O. Roubeau, P. C. Berzal, H. Kooijman, A. L. Spek, W. L. Driessen and J. Reedijk, *Inorg. Chem.*, **41**, 3673 (2002); J. R. Bryant, J. E. Taves and J. M. Mayer, *Inorg. Chem.*, **41**, 2769 (2002); S. Shibata, S. Onuma and H. Inoue, *Inorg. Chem.*, **24**, 1723 (1985); S. Koda, S. Ooi, H. Kuroya, Y. Nishikawa, Y. Nakamura and S. Kawaguchi, *Inorg. Nucl. Chem. Lett.*, **8**, 89 (1972); H. Adams, N. A. Bailey, D. E. Fenton and R. A. Khalil, *Inorg. Chim. Acta*, **209**, 55 (1993); E. Bouwman, K. G. Caulton, G. Christou, K. Folting, C. Gasser,

D. N. Hendrickson, J. C. Huffman, E. B. Lobkovsky, J. D. Martin, P. Michel, H.-L. Tsai and Z. Xue, *Inorg. Chem.*, **32**, 3463 (1993); G. Aromi, M. W. Wemple, S. J. Aubin, K. Folting, D. N. Hendrickson and G. Christou, *J. Am. Chem. Soc.*, **120**, 5850 (1998); A.-L. Barra, D. Gatteschi, R. Sessoli, G. L. Abbati, A. Cornia, A. C. Fabretti and M. G. Uytterhoeven, *Angew. Chem., Int. Ed. Engl.*, **36**, 2329 (1997).

379. D. S. Brown, J. L. Newman, J. R. Thornback, R. M. Pearlstein, A. Davison and A. Lawson, *Inorg. Chim. Acta*, **150**, 193 (1988).
380. M. Ganesan, P. N. Kapoor, P. E. Fanwick and R. A. Walton, *Inorg. Chem. Commun.*, **5**, 1073 (2002); M. Leeaphon, P. E. Fanwick and R. A. Walton, *Inorg. Chem.*, **29**, 4348 (1990); P. E. Fanwick, M. Leeaphon and R. A. Walton, *Inorg. Chem.*, **29**, 676 (1990).
381. E. V. Dikarev, H. Zhang and B. Li, *J. Am. Chem. Soc.*, **127**, 6156 (2005).
382. J. K. Clegg, L. F. Lindoy, J. C. McMurtrie and D. Schilter, *Dalton Trans.*, **857** (2005).
383. V. D. Vreshch, A. B. Lysenko, A. N. Chernega, J. A. K. Howard, H. Krautscheid, J. Sieler and K. V. Domasevitch, *Dalton Trans.*, 2899 (2004).
384. J. K. Clegg, L. F. Lindoy, B. Moubaraki, K. S. Murray and J. C. McMurtrie, *Dalton Trans.*, 2417 (2004).
385. J. M. Manríquez, E. E. Bunel, B. Oelckers and E. Roman, *Inorg. Synth.*, **31**, 267 (1997); A. Cornia, A. C. Fabretti, P. Garrisi, C. Mortalo, D. Bonacchi, D. Gatteschi, R. Sessoli, L. Sorace, W. Wernsdorfer and A.-L. Barra, *Angew. Chem. Int. Ed.*, **43**, 1136 (2004); C. E. Pfluger and P. S. Haradem, *Inorg. Chim. Acta*, **69**, 141 (1983); P. F. Lindley and A. W. Smith, *J. Chem. Soc. D*, 1355 (1970); A. L. Barra, A. Caneschi, A. Cornia, F. Fabrizi de Biani, D. Gateschi, C. Sangregorio, R. Sessoli and L. Sorace, *J. Am. Chem. Soc.*, **121**, 5302 (1999); H. Müller, W. Seidel and H. Görls, *Z. Anorg. Allg. Chem.*, **623**, 155 (1997); H. Müller, W. Seidel and H. Görls, *Z. Anorg. Allg. Chem.*, **622**, 1968 (1996).
386. A. A. Rachford, J. L. Petersen and J. J. Rack, *Inorg. Chem.*, **44**, 8065 (2005); S. Kar, B. Sarkar, S. Ghumaan, D. Janardanan, J. van Slageren, J. Fiedler, V. G. Puranik, R. B. Sunoj, W. Kaim and G. K. Lahiri, *Chem. Eur. J.*, **11**, 4901 (2005); P. Govindaswamy, S. M. Mobin, C. Thöne and M. R. Kollipara, *J. Organomet. Chem.*, **690**, 1218 (2005); J. Shono, Y. Nimura, T. Hashimoto and K. Shimizu, *Chem. Lett.*, **33**, 1422 (2004); H. Matsuzawa, Y. Ohashi, Y. Kaizu and H. Kobayashi, *Inorg. Chem.*, **27**, 2981 (1988); E. Meléndez, R. Ilarraza, G. P. A. Yap and A. L. Rheingold, *J. Organomet. Chem.*, **522**, **1**(1996).
387. A. F. A. Peacock, A. Habtemariam, R. Fernández, V. Walland, F. P. A. Fabbiani, S. Parsons, R. E. Aird, D. I. Jodrell and P. J. Sadler, *J. Am. Chem. Soc.*, **128**, 1739 (2006); Y.-L. Chen, C. Sinha, I.-C. Chen, K.-L. Liu, Y. Chi, J.-K. Yu, P.-T. Chou and T.-H. Lu, *Chem. Commun.*, 3046 (2003); Y. Chi, J.-W. Lan, S.-M. Peng and G.-H. Lee, *J. Cluster Sci.*, **12**, 421 (2001); K. Dallmann and W. Preetz, *Z. Anorg. Allg. Chem.*, **623**, 1991 (1997).
388. J. F. Berry, F. A. Cotton, C. Y. Liu, T. Lu, C. A. Murillo, B. S. Tsukerblat, D. Villagran and X. Wang, *J. Am. Chem. Soc.*, **127**, 4895 (2005); F. A. Cotton and R. C. Elder, *Inorg. Chem.*, **5**, 423 (1966); F. A. Cotton and R. C. Elder, *Inorg. Chem.*, **4**, 1145 (1965); F. A. Cotton, C. Y. Liu, C. A. Murillo and X. Wang, *Inorg. Chem.*, **42**, 4619 (2003); L. C. Wang, H. Y. Jang, Y. Roh, V. Lynch, A. J. Schultz, X. P. Wang and M. J. Krische, *J. Am. Chem. Soc.*, **124**, 9448 (2002); F. A. Cotton and R. Eiss, *J. Am. Chem. Soc.*, **90**, 38 (1968); J. A. Bertrand and A. R. Kalyanaraman, *Inorg. Chim. Acta*, **5**, 167 (1971); R. B. V. Dreele and R. C. Fay, *J. Am. Chem. Soc.*, **93**, 4936 (1971); P. Comba, H. Jakob, B. Nuber and B. K. Keppler, *Inorg. Chem.*, **33**, 3396 (1994); O. Angelova, J. Macicek, M. Atanasov and G. Petrov, *Inorg. Chem.*, **30**, 1943 (1991).
389. T. Shiga, T. Nakanishi, M. Ohba and H. Okawa, *Polyhedron*, **24**, 2732 (2005).
390. M. Hassanein and I. F. Hewaidy, *Z. Anorg. Allg. Chem.*, **373**, 81 (1970).
391. D. V. Soldatov and J. A. Ripmeester, *Chem. Eur. J.*, **7**, 2979 (2001).
392. X. Y. Liu, W. J. Tenn, G. Bhalla and R. A. Periana, *Organometallics*, **23**, 3584 (2004); U. Herber, T. Pechmann, B. Weberndorfer, K. Ilg and H. Werner, *Chem. Eur. J.*, **8**, 309 (2002); J. M. Burke, R. B. Coapes, A. E. Goeta, J. A. K. Howard, T. B. Marder, E. G. Robins and S. A. Westcott, *J. Organomet. Chem.*, **649**, 199 (2002); J. G. Leipoldt, S. S. Basson and J. H. Potgieter, *Inorg. Chim. Acta*, **117**, L3 (1986); H. J. McCarthy and D. A. Tocher, *Inorg. Chim. Acta*, **145**, 171 (1988); Z. Duan, M. J. Hampden-Smith, E. N. Duesler and A. L. Rheingold, *Polyhedron*, **13**, 609 (1994).
393. W. J. Tenn III, K. J. H. Young, G. Bhalla, J. Oxgaard, W. A. Goddard III and R. A. Periana, *J. Am. Chem. Soc.*, **127**, 14172 (2005); G. Bhalla, X. Y. Liu, J. Oxgaard, W. A. Goddard and

R. A. Periana, *J. Am. Chem. Soc.*, **127**, 11372 (2005); G. Bhalla, J. Oxgaard, W. A. Goddard III and R. A. Periana, *Organometallics*, **24**, 5499 (2005); V. A. Bhirud, A. Uzun, P. W. Kletnieks, R. Craciun, J. F. Haw, D. A. Dixon, M. M. Olmstead and B. C. Gates, *J. Organomet. Chem.*, **692**, 2107 (2007); M. A. Bennett and T. R. B. Mitchell, *Inorg. Chem.*, **15**, 2936 (1976); T. Matsumoto, D. J. Taube, R. A. Periana, H. Taube and H. Yoshida, *J. Am. Chem. Soc.*, **122**, 7414 (2000).

394. X. He, Y. Yao, X. Luo, J. Zhang, Y. Liu, L. Zhang and Q. Wu, *Organometallics*, **22**, 4952 (2003).
395. R. W. Saalfrank, H. Maid, N. Mooren and F. Hampel, *Angew. Chem. Int. Ed.*, **41**, 304 (2002).
396. F. Benvenuti, C. Carlini, F. Marchetti, M. Marchionna, A. M. R. Galletti and G. Sbrana, *J. Organomet. Chem.*, **622**, 286 (2001); J. H. Binks, G. J. Dorward, R. A. Howie and G. P. McQuillan, *Inorg. Chim. Acta*, **49**, 251 (1981); M. B. Hursthouse, M. A. Laffey, P. T. Moore, D. B. New, P. R. Raithby and P. Thornton, *J. Chem. Soc., Dalton Trans.*, 307 (1982); G. J. Bullen, R. Mason and P. Pauling, *Inorg. Chem.*, **4**, 456 (1965); M. Urrutigoity, C. Cecutti, F. Senocq, J.-P. Gorrichon and A. Gleizes, *Inorg. Chim. Acta*, **248**, 15 (1996); A. Dohring, R. Goddard, P. W. Jolly, C. Kruger and V. R. Polyakov, *Inorg. Chem.*, **36**, 177 (1997).
397. E. Alonso, J. Forniés, C. Fortuño, A. Martín and A. G. Orpen, *Organometallics*, **22**, 5011 (2003).
398. M. Nowotny, U. Hanefeld, H. van Koningsveld and T. Maschmeyer, *Chem. Commun.*, 1877 (2000); O. E. Woisetschlager, A. Geisbauer, K. Polborn and W. Beck, *Z. Anorg. Allg. Chem.*, **626**, 766 (2000); M. R. Churchill, *Inorg. Chem.*, **5**, 1608 (1966); M. Horike, Y. Kai, N. Yasuoka and N. Kasai, *J. Organomet. Chem.*, **72**, 441 (1974); A. R. Siedle and L. H. Pignolet, *Inorg. Chem.*, **21**, 3090 (1982); A. R. Siedle, R. A. Newmark, A. A. Kruger and L. H. Pignolet, *Inorg. Chem.*, **20**, 3399 (1981); A. R. Siedle, R. A. Newmark and L. H. Pignolet, *Inorg. Chem.*, **22**, 2281 (1983); S. Okeya, H. Asai, S. Ooi, K. Matsumoto, S. Kawaguchi and H. Kuroya, *Inorg. Nucl. Chem. Lett.*, **12**, 677 (1976); G. J. Baker, J. B. Raynor, J. M. M. Smits, P. T. Beurskens, H. Vergoossen and C. P. Keijzers, *J. Chem. Soc., Dalton Trans.*, 2655 (1986); B. F. Straub, F. Rominger and P. Hofmann, *Inorg. Chem. Commun.*, **3**, 358 (2000); J. P. Wolkowski and J. F. Hartwig, *Angew. Chem. Int. Ed.*, **41**, 4289 (2002).
399. G. Raper and W. S. McDonald, *J. Chem. Soc., Dalton Trans.*, 265 (1972); A. Robson and M. R. Truter, *J. Chem. Soc.*, 630 (1965); W. Lin, S. R. Wilson and G. S. Girolami, *Inorg. Chem.*, **36**, 2662 (1997); S. A. De Pascali, P. Papadia, A. Ciccarese, C. Pacifico and F. P. Fanizzi, *Eur. J. Inorg. Chem.*, 788 (2005).
400. S. Schneider, J. A. S. Roberts, M. R. Salata and T. J. Marks, *Angew. Chem. Int. Ed.*, **45**, 1733 (2006); S. Delgado, A. Muñoz, M. E. Medina and C. J. Pastor, *Inorg. Chim. Acta*, **359**, 109 (2006); J. Kaizer, R. Csonka, G. Speier, M. Giorgi and M. Reglier, *J. Mol. Catal. A: Chem.*, **235**, 81 (2005); B. Chen, F. R. Fronczek and A. W. Maverick, *Inorg. Chem.*, **43**, 8209 (2004); A. M. Madalan, V. C. Kravtsov, D. Pajic, K. Zadro, Y. A. Simonov, N. Stanica, L. Ouahab, J. Lipkowski and M. Andruh, *Inorg. Chim. Acta*, **357**, 4151 (2004); M. F. Farona, D. C. Perry and H. A. Kuska, *Inorg. Chem.*, **7**, 2415 (1968); S. K. Dey, B. Bag, Z. Zhou, A. S. C. Chan and S. Mitra, *Inorg. Chim. Acta*, **357**, 1991 (2004); T. Y. Chen, L. Omnes, J. Vaisserman and P. Doppelt, *Inorg. Chim. Acta*, **357**, 1299 (2004); V. Pawlowski, H. Kunkely, M. Zabel and A. Vogler, *Inorg. Chim. Acta*, **357**, 824 (2004); B. Chen, F. R. Fronczek and A. W. Maverick, *Chem. Commun.*, 2166 (2003); S. Higashiya, K. K. Banger, S. C. Ngo, P. N. Lim, P. J. Toscano and J. T. Welch, *Inorg. Chim. Acta*, **351**, 291 (2003); B. Croxtall, J. Fawcett, E. G. Hope and A. M. Stuart, *J. Fluorine Chem.*, **119**, 65 (2003); A. W. Maverick, F. R. Fronczek, E. F. Maverick, D. R. Billodeaux, Z. T. Cygan and R. A. Isovitsch, *Inorg. Chem.*, **41**, 6488 (2002); T. C. Higgs, S. Parsons, P. J. Bailey, A. C. Jones, F. McLachlan, A. Parkin, A. Dawson and P. A. Tasker, *Organometallics*, **21**, 5692 (2002); T. C. Higgs, S. Parsons, A. C. Jones, P. J. Bailey and P. A. Tasker, *J. Chem. Soc., Dalton Trans.*, 3427 (2002); G. Aromi, P. Gamez, O. Roubeau, H. Kooijman, A. L. Spek, W. L. Driessen and J. Reedijk, *Angew. Chem. Int. Ed.*, **41**, 1168 (2002); D. V. Soldatov, J. A. Ripmeester, S. I. Shergina, I. E. Sokolov, A. S. Zanina, S. A. Gromilov and Y. A. Dyadin, *J. Am. Chem. Soc.*, **121**, 4179 (1999); L. A. Batory, C. E. McInnis and J. T. Njardarson, *J. Am. Chem. Soc.*, **128**, 16054 (2006); J. Hirsch, H. Paulus and H. Elias, *Inorg. Chem.*, **35**, 2343 (1996); J. A. P. Nash, S. C. Thompson, D. F. Foster, D. J. Cole-Hamilton and J. C. Barnes, *J. Chem. Soc., Dalton Trans.*, 269 (1995); H. Irngartinger, A. Altreuther, T. Sommerfeld and T. Stojanik, *Eur. J. Org. Chem.*, 4059 (2000); J. A. Campo, M. Cano, J. V. Heras, M. C. Lagunas, J. Perles, E. Pinilla and M. R. Torres,

Helv. Chim. Acta, **84**, 2316 (2001); S. S. Turner, D. Collison, F. E. Mabbs and M. Halliwell, *J. Chem. Soc., Dalton Trans.*, 1117 (1997); M. R. Kidd, R. S. Sager and W. H. Watson, *Inorg. Chem.*, **6**, 946 (1967); R. U. Claessen, A. M. Kornilov, K. K. Banger, S. C. Ngo, S. Higashiya, C. C. Wells, E. V. Dikarev, P. J. Toscano and J. T. Welch, *J. Organomet. Chem.*, **689**, 71 (2004); J. K. Bjernemose, C. J. McKenzie, P. R. Raithby and S. J. Teat, *Dalton Trans.*, 2639 (2003); M. R. Truter and B. L. Vickery, *J. Chem. Soc., Dalton Trans.*, 395 (1972); I. Robertson and M. R. Truter, *J. Chem. Soc. A*, 309 (1967); T. J. Wenzel, E. J. Williams, R. C. Haltiwanger and R. E. Sievers, *Polyhedron*, **4**, 369 (1985); W. S. Rees Jr., C. R. Caballero and W. Hesse, *Angew. Chem., Int. Ed. Engl.*, **31**, 735 (1992); S. Sans-Lenain and A. Gleizes, *Inorg. Chim. Acta*, **211**, 67 (1993); P. Hon, C. E. Pfluger and R. L. Belford, *Inorg. Chem.*, **5**, 516 (1966); C. L. Modenbach, F. R. Fronczek, E. W. Berg and T. C. Taylor, *Inorg. Chem.*, **22**, 4083 (1983); B. Corain, M. Basato, G. Visentin and G. Zanotti, *J. Chem. Soc., Dalton Trans.*, 1217 (1983); K. K. Banger, S. C. Ngo, S. Higashiya, R. U. Claessen, K. S. Bousman, P. N. Lim, P. J. Toscano and J. T. Welch, *J. Organomet. Chem.*, **678**, 15 (2003); K.-M. Chi, H. K. Shin, M. J. Hampden-Smith, T. T. Kodas and E. N. Duesler, *Inorg. Chem.*, **30**, 4293 (1991); P. Doppelt and T. H. Baum, *J. Organomet. Chem.*, **517**, 53 (1996); G. Pampaloni, R. Peloso, C. Graiff and A. Tiripicchio, *Organometallics*, **24**, 4475 (2005); G. Schmidt and U. Behrens, *J. Organomet. Chem.*, **509**, 49 (1996); H. K. Shin, M. J. Hampdensmith, E. N. Duesler and T. T. Kodas, *Polyhedron*, **10**, 645 (1991); R. Kumar, F. R. Fronczek, A. W. Maverick, A. J. Kim and L. G. Butler, *Chem. Mater.*, **6**, 587 (1994); G. D. Fallon, B. Moubaraki, K. S. Murray, A. M. van den Bergen and B. O. West, *Polyhedron*, **12**, 1989 (1993); G. Doyle, K. A. Eriksen and D. V. Engen, *Organometallics*, **4**, 830 (1985); K. M. Chi, H. K. Shin, M. J. Hampdensmith, E. N. Duesler and T. T. Kodas, *Polyhedron*, **10**, 2293 (1991).

401. L. Zanotto, F. Benetollo, M. Natali, G. Rossetto, P. Zanella, S. Kaciulis and A. Mezzi, *Chem. Vap. Deposition*, **10**, 207 (2004); W. J. Evans, D. G. Giarikos, D. Josell and J. W. Ziller, *Inorg. Chem.*, **42**, 8255 (2003); S. C. Ngo, K. K. Banger, P. J. Toscano and J. T. Welch, *Polyhedron*, **21**, 1289 (2002); A. J. Blake, N. R. Champness, S. M. Howdle, K. S. Morley, P. B. Webb and C. Wilson, *CrystEngComm*, **4**, 88 (2002); K.-M. Chi and Y.-H. Lu, *Chem. Vap. Deposition*, **7**, 117 (2001); M. E. Fragala, G. Malandrino, O. Puglisi and C. Benelli, *Chem. Mater.*, **12**, 290 (2000).
402. G. I. Zharkova, I. A. Baidina and I. K. Igumenov, *J. Struct. Chem.*, **47**, 1117 (2006).
403. J. Ni, H. Yan, A. Wang, Y. Yang, C. L. Stern, A. W. Metz, S. Jin, L. Wang, T. J. Marks, J. R. Ireland and C. R. Kannewurf, *J. Am. Chem. Soc.*, **127**, 5613 (2005); G. Malandrino, M. Blandino, L. M. S. Perdicaro, I. L. Fragala, P. Rossi and P. Dapporto, *Inorg. Chem.*, **44**, 9684 (2005); J. Pradilla-Sorzano and J. P. F. Junior, *Inorg. Chem.*, **12**, 1174 (1973); R. P. Adams, H. C. A. Junior, U. Rychlewska and D. J. Hodgson, *Inorg. Chim. Acta*, **119**, 67 (1986); F. A. Cotton and J. S. Wood, *Inorg. Chem.*, **3**, 245 (1964); J. Boersma, A. L. Spek and J. G. Noltes, *J. Organomet. Chem.*, **81**, 7 (1974); R. L. Belford, N. D. Chasteen, M. A. Hitchman, P.-K. Hon, C. E. Pfluger and I. C. Paul, *Inorg. Chem.*, **8**, 1312 (1969); G. Voutsas, L. C. Tzavellas and C. Tsiamis, *Struct. Chem.*, **10**, 53 (1999); D. V. Soldatov, P. Tinnemans, G. D. Enright, C. I. Ratcliffe, P. R. Diamente and J. A. Ripmeester, *Chem. Mater.*, **15**, 3826 (2003); E. L. Lippert and M. R. Truter, *J. Chem. Soc.*, 4996 (1960); A. Gulino, F. Castelli, P. Dapporto, P. Rossi and I. Fragala, *Chem. Mater.*, **12**, 548 (2000).
404. G. Malandrino, S. T. Finocchiaro, P. Rossi, P. Dapporto and I. L. Fragala, *Chem. Commun.*, 5681 (2005); A. Gulino, P. Dapporto, P. Rossi and I. Fragala, *Chem. Mater.*, **14**, 1441 (2002); E. N. Maslen, T. M. Greaney, C. L. Raston and A. H. White, *J. Chem. Soc., Dalton Trans.*, 400 (1975); T. M. Greaney, C. L. Raston, A. H. White and E. N. Maslen, *J. Chem. Soc., Dalton Trans.*, 876 (1975).
405. M. F. Mahon, K. C. Molloy, B. A. Omotowa and M. A. Mesubi, *J. Organomet. Chem.*, **525**, 239 (1996).
406. G. Li, H. Hou, Y. Zhu, X. Meng, L. Mi and Y. Fan, *Inorg. Chem. Commun.*, **5**, 929 (2002).
407. G. L. Abbati, L.-C. Brunel, H. Casalta, A. Cornia, A. C. Fabretti, D. Gatteschi, A. K. Hassan, A. G. M. Jansen, A. L. Maniero, L. Pardi, C. Paulsen and U. Segre, *Chem. Eur. J.*, **7**, 1796 (2001); O. T. B. Junior, J. R. Gardinier and M. R. Churchill, *Organometallics*, **19**, 4544 (2000).
408. O. T. B. Junior, D. J. MacRae, M. R. Churchill, A. Y. Kovalevsky and E. S. Robirds, *Organometallics*, **22**, 3991 (2003); W. Tyrra and M. S. Wickleder, *J. Organomet. Chem.*, **677**,

28 (2003); J. H. Park, G. A. Horley, P. O'Brien, A. C. Jones and M. Motevalli, *J. Mater. Chem.*, **11**, 2346 (2001).
409. A. Askarinejad, A. Morsali and L.-G. Zhu, *Solid State Sci.*, **8**, 537 (2006); E. J. Fernández, A. Laguna, J. M. López de Luzuriaga, M. Monge, M. Montiel, M. E. Olmos and J. Pérez, *Organometallics*, **23**, 774 (2004).
410. V. Briois, S. Belin, M. Z. Chalaca, R. H. A. Santos, C. V. Santilli and S. H. Pulcinelli, *Chem. Mat.*, **16**, 3885 (2004); H. Reuter, *Z. Kristallogr.*, **219**, 109 (2004).
411. J. M. Harrowfield, F. Marandi and A. A. Soudi, *Inorg. Chim. Acta*, **358**, 4099 (2005); G. Malandrino, R. L. Nigro, P. Rossi, P. Dapporto and I. L. Fragala, *Inorg. Chim. Acta*, **357**, 3927 (2004).
412. B. Alvarez, C. Bois, Y. Jeanin, D. Miguel and V. Riera, *Inorg. Chem.*, **32**, 3783 (1993).
413. P. Doppelt, T. H. Baum and L. Ricard, *Inorg. Chem.*, **35**, 1286 (1996); A. Bailey, T. S. Corbitt, M. J. Hampden-Smith, E. N. Duesler and T. T. Kodas, *Polyhedron*, **12**, 1785 (1993).
414. B. J. Deelman, F. Wierda, A. Meetsma and J. H. Teuben, *Appl. Organomet. Chem.*, **9**, 483 (1995).
415. C. Pettinari, R. Pettinari, M. Fianchini, F. Marchetti, B. W. Skelton and A. H. White, *Inorg. Chem.*, **44**, 7933 (2005).
416. Q. Zhao, C. Y. Jiang, M. Shi, F. Y. Li, T. Yi, Y. Cao and C. H. Huang, *Organometallics*, **25**, 3631 (2006).
417. A. Cingolani, Effendy, F. Marchetti, C. Pettinari, R. Pettinari, B. W. Skelton and A. H. White, *Inorg. Chem.*, **41**, 1151 (2002).
418. L. Shen, M. Shi, F. Li, D. Zhang, X. Li, E. Shi, T. Yi, Y. Du and C. Huang, *Inorg. Chem.*, **45**, 6188 (2006).
419. M. Shi, F. Li, T. Yi, D. Zhang, H. Hu and C. Huang, *Inorg. Chem.*, **44**, 8929 (2005).
420. H. Xin, F. Y. Li, M. Shi, Z. Q. Bian and C. H. Huang, *J. Am. Chem. Soc.*, **125**, 7166 (2003).
421. A. Imran, R. D. W. Kernmitt, A. J. W. Markwick, P. McKenna, D. R. Russell and L. J. S. Sherry, *J. Chem. Soc., Dalton Trans.*, 549 (1985).
422. Y.-B. Dong, X. Zhao, G.-X. Jin, R.-Q. Huang and M. D. Smith, *Eur. J. Inorg. Chem.*, 4017 (2003); Y.-B. Dong, J.-P. Ma, G.-X. Jin, R.-Q. Huang and M. D. Smith, *Dalton Trans.*, 4324 (2003); Y.-B. Dong, P. Wang, R.-Q. Huang and M. D. Smith, *Inorg. Chem.*, **43**, 4727 (2004).
423. O. Angelova, E. M. G. Kirilov, M. Kirilov, G. Petrov, J. Kaneti and J. Macicek, *J. Chem. Soc., Perkin Trans. 2*, 1405 (1989).
424. V. Ugrinova, B. C. Noll and S. N. Brown, *Inorg. Chem.*, **45**, 10309 (2006).
425. R. W. Saalfrank, N. Low, S. Kareth, V. Seitz, F. Hampel, D. Stalke and M. Teichert, *Angew. Chem. Int. Ed.*, **37**, 172 (1998).
426. R. W. Saalfrank, N. Low, B. Demleitner, D. Stalke and M. Teichert, *Chem. Eur. J.*, **4**, 1305 (1998).
427. T. Shiga, M. Ohba and H. Okawa, *Inorg. Chem.*, **43**, 4435 (2004).
428. T. Shiga, M. Ohba and H. Okawa, *Inorg. Chem. Commun.*, **6**, 15 (2003).
429. R. L. Lintvedt, B. A. Schoenfelner, C. Ceccarelli and M. D. Glick, *Inorg. Chem.*, **23**, 2867 (1984).
430. T. Shiga, H. Okawa, S. Kitagawa and M. Ohba, *J. Am. Chem. Soc.*, **128**, 16426 (2006).
431. S. Biju, D. B. A. Raj, M. L. P. Reddy and B. M. Kariuki, *Inorg. Chem.*, **45**, 10651 (2006); R. Pavithran, M. L. P. Reddy, S. Alves, Jr., R. O. Freire, G. B. Rocha and P. P. Lima, *Eur. J. Inorg. Chem.*, **20**, 4129 (2005); R. Pavithran, N. S. Saleesh Kumar, S. Biju, M. L. P. Reddy, S. Alves, Jr. and R. O. Freire, *Inorg. Chem.*, **45**, 2184 (2006); A. Cingolani, Effendy, F. Marchetti, C. Pettinari, R. Pettinari, B. W. Skelton and A. H. White, *Inorg. Chem.*, **43**, 4387 (2004).
432. S. Yamazaki, T. Ama and Z. Taira, *Polyhedron*, **7**, 353 (1988); T. Sakai, Z. Taira and S. Yamazaki, *Polyhedron*, **12**, 2133 (1993).
433. X.-F. Li, K. Dai, W.-P. Ye, L. Pan and Y.-S. Li, *Organometallics*, **23**, 1223 (2004).
434. P. J. McCarthy, R. J. Hovey, K. Ueno and A. E. Martell, *J. Am. Chem. Soc.*, **77**, 5820 (1955); M. Mazzanti, J.-M. Rosset, C. Floriani, A. Chiesi-Villa and C. Guastini, *J. Chem. Soc., Dalton Trans.*, 953 (1989); F. Corazza, E. Solari, C. Floriani, A. Chiesi-Villa and C. Guastini, *J. Chem. Soc., Dalton Trans.*, 1335 (1990).
435. S. Gambarotta, M. Mazzanti, C. Floriani, A. Chiesi-Villa and C. Guastini, *Chem. Commun.*, 829 (1985).
436. M. Mazzanti, C. Floriani, A. Chiesi-Villa and C. Guastini, *Inorg. Chem.*, **25**, 4158 (1986).

437. C. Floriani, M. Mazzanti, S. Ciurli, A. Chiesi-Villa and C. Guastini, *J. Chem. Soc., Dalton Trans.*, 1361 (1988).
438. P. J. Toscano, P. T. DiMauro, S. Geremia, L. Randaccio and E. Zangrando, *Inorg. Chim. Acta*, **217**, 195 (1994).
439. G. Pennesi, F. Corazza, C. Floriani, A. Chiesi-Villa and C. Guastini, *J. Chem. Res.*, **86**, 601 (1989).
440. E. Gallo, E. Solari, C. Floriani, A. Chiesi-Villa and C. Rizzoli, *Inorg. Chem.*, **36**, 2178 (1997).
441. J. R. Bradbury, J. L. Hampton, D. P. Martone and A. W. Maverick, *Inorg. Chem.*, **28**, 2392 (1989).
442. S. Lim, B. Choi, Y. S. Min, D. Kim, I. Yoon, S. S. Lee and I. M. Lee, *J. Organomet. Chem.*, **689**, 224 (2004).
443. D. E. Fenton and S. E. Gayda, *J. Chem. Soc., Dalton Trans.*, 2109 (1977); H. Adams, N. A. Bailey, D. E. Fenton, M. S. L. Gonzalez and C. A. Phillips, *J. Chem. Soc., Dalton Trans.*, 371 (1983); R. L. Lintvedt, M. D. Glick, B. K. Tomlonovic and D. P. Gavel, *Inorg. Chem.*, **15**, 1646 (1976); R. L. Lintvedt, L. S. Kramer, G. Ranger, P. W. Corfield and M. D. Glick, *Inorg. Chem.*, **22**, 3580 (1983); N. A. Bailey, D. E. Fenton, S. E. Gayda and C. A. Phillips, *J. Chem. Soc., Dalton Trans.*, 2289 (1984); R. L. Lintvedt, K. A. Rupp and M. J. Heeg, *Inorg. Chem.*, **27**, 331 (1988); M. D. Glick, R. L. Lintvedt, D. P. Gavel and B. Tomlonovic, *Inorg. Chem.*, **15**, 1654 (1976).
444. S. D. Allen, D. R. Moore, E. B. Lobkovsky and G. W. Coates, *J. Organomet. Chem.*, **683**, 137 (2003).
445. L. Zhang, M. Brookhart and P. S. White, *Organometallics*, **25**, 1868 (2006).
446. S. M. Yu, A. Berkefeld, I. Göttker-Schnetmann, G. Müller and S. Mecking, *Macromolecules*, **40**, 421 (2007).
447. M. Driess, N. Dona and K. Merz, *Chem. Eur. J.*, **10**, 5971 (2004).
448. M. Brehon, E. K. Cope, F. S. Mair, P. Nolan, J. E. Obrien, R. G. Pritchard and D. J. Wilcock, *J. Chem. Soc., Dalton Trans.*, 3421 (1997).
449. Y. Chi, S. Ranjan, P.-W. Chung, C.-S. Liu, S.-M. Peng and G.-H. Lee, *J. Chem. Soc., Dalton Trans.*, 343 (2000).
450. F. Corazza, C. Floriani, A. Chiesi-Villa, C. Guastini and S. Ciurli, *J. Chem. Soc., Dalton Trans.*, 2341 (1988).
451. D. B. Studebaker, D. A. Neumayer, B. J. Hinds, C. L. Stern and T. J. Marks, *Inorg. Chem.*, **39**, 3148 (2000); D. L. Schulz, B. J. Hinds, C. L. Stern and T. J. Marks, *Inorg. Chem.*, **32**, 249 (1993).
452. D. J. Berg, S. J. Rettig and C. Orvig, *J. Am. Chem. Soc.*, **113**, 2528 (1991).
453. S. A. Schuetz, V. W. Day, A. L. Rheingold and J. A. Belot, *Dalton Trans.*, 4303 (2003).
454. Z.-Y. Yang, R.-D. Yang, F.-S. Li and K.-B. Yu, *Polyhedron*, **19**, 2599 (2000).
455. N. L. Edleman, A. Wang, J. A. Belot, A. W. Metz, J. R. Babcock, A. M. Kawaoka, J. Ni, M. V. Metz, C. J. Flaschenriem, C. L. Stern, L. M. Liable-Sands, A. L. Rheingold, P. R. Markworth, R. P. H. Chang, M. P. Chudzik, C. R. Kannewurf and T. J. Marks, *Inorg. Chem.*, **41**, 5005 (2002).
456. S. A. Schuetz, M. A. Erdmann, V. W. Day, J. L. Clark and J. A. Belot, *Inorg. Chim. Acta*, **357**, 4045 (2004).
457. S. A. Schuetz, C. M. Silvernail, C. D. Incarvito, A. L. Rheingold, J. L. Clark, V. W. Day and J. A. Belot, *Inorg. Chem.*, **43**, 6203 (2004).
458. W. S. Rees Jr., O. Just, S. L. Castro and J. S. Matthews, *Inorg. Chem.*, **39**, 3736 (2000).
459. C. C. Gatto, E. S. Lang and U. Abram, *Inorg. Chem. Commun.*, **6**, 1001 (2003).
460. S. Doherty, R. J. Errington, N. Housley, J. Ridland, W. Clegg and M. R. J. Elsegood, *Organometallics*, **18**, 1018 (1999); S.-H. Hsu, J.-C. Chang, C.-L. Lai, C.-H. Hu, H. M. Lee, G.-H. Lee, S.-M. Peng and J.-H. Huang, *Inorg. Chem.*, **43**, 6786 (2004); L.-M. Tang, T. Hu, Y.-J. Bo, Y.-s. Li and N.-H. Hu, *J. Organomet. Chem.*, **690**, 3125 (2005).
461. L. Kakaliou, W. J. Scanlon IV, B. Qian, S. W. Baek, M. R. Smith III and D. H. Motry, *Inorg. Chem.*, **38**, 5964 (1999).
462. P. L. Franceschini, M. Morstein, H. Berke and H. W. Schmalle, *Inorg. Chem.*, **42**, 7273 (2003); A. Bastianini, G. A. Battiston, F. Benetollo, R. Gerbasi and M. Porchia, *Polyhedron*, **16**, 1105 (1997); J. Scholz, G. A. Hadi, K.-H. Thiele, H. Gorls, R. Weimann, H. Schumann and J. Sieler, *J. Organomet. Chem.*, **626**, 243 (2001); E. B. Tjaden, D. C. Swenson, R. F. Jordan and J. L. Petersen, *Organometallics*, **14**, 371 (1995).

463. S. Gao, L.-H. Huo, H. Zhao and S. W. Ng, *Acta Crystallogr., Sect. E*, **61**, m325 (2005).
464. D. H. Gerlach and R. H. Holm, *Inorg. Chem.*, **9**, 588 (1970).
465. L. F. Larkworthy, D. C. Povey and B. Sandell, *Inorg. Chim. Acta*, **83**, L29 (1984).
466. F. A. Cotton, W. H. Ilsley and W. Kaim, *Inorg. Chim. Acta*, **37**, 267 (1979).
467. D. Xu, B. Chen, K. Chen, C. Chen, K. Miki and N. Kasai, *Bull. Chem. Soc. Jpn.*, **62**, 2384 (1989); N. Matsumoto, Z. J. Zhong, H. Okawa and S. Kida, *Inorg. Chim. Acta*, **160**, 153 (1989); R. Mukhopadhyay, S. Bhattacharjee, C. K. Pal, S. Karmakar and R. Bhattacharyya, *J. Chem. Soc., Dalton Trans.*, 2267 (1997).
468. G. F. Morgan, U. Abram, G. Evrard, F. Durant, M. Deblaton, P. Clemens, P. Van den Broeck and J. R. Thornback, *Chem. Commun.*, 1772 (1990); S. Liu, S. J. Rettig and C. Orvig, *Inorg. Chem.*, **30**, 4915 (1991); S. S. Jurisson, K. Dancey, M. McPartlin, P. A. Tasker and E. Deutsch, *Inorg. Chem.*, **23**, 4743 (1984); S. Jurisson, L. F. Lindoy, K. P. Dancey, M. McPartlin, P. A. Tasker, D. K. Uppal and E. Deutsch, *Inorg. Chem.*, **23**, 227 (1984).
469. P. D. Benny, C. L. Barnes, P. M. Piekarski, J. D. Lydon and S. S. Jurisson, *Inorg. Chem.*, **42**, 6519 (2003); P. D. Benny, J. L. Green, H. P. Engelbrecht, C. L. Barnes and S. S. Jurisson, *Inorg. Chem.*, **44**, 2381 (2005); M. A. A. F. de C. T. Carrondo, A. R. Middleton, A. C. Skapski, A. P. West and G. Wilkinson, *Inorg. Chim. Acta*, **44**, L7 (1980).
470. S. Gambarotta, F. Corazza, C. Floriani and M. Zehnder, *Chem. Commun.*, 1305 (1984); F. Corazza, C. Floriani and M. Zehnder, *J. Chem. Soc., Dalton Trans.*, 709 (1987); N. R. Sangeetha, C. K. Pal, P. Ghosh and S. Pal, *J. Chem. Soc., Dalton Trans.*, 3293 (1996).
471. S. A. Serron, C. M. Haar, S. P. Nolan and L. Brammer, *Organometallics*, **16**, 5120 (1997).
472. W. E. Lynch, R. L. Lintvedt and X. Q. Shui, *Inorg. Chem.*, **30**, 1014 (1991).
473. I. Levitin, M. Tsikalova, N. Sazikova, V. Bakhmutov, Z. Starikova, A. Yanovsky and Y. Struchkov, *Inorg. Chim. Acta*, **270**, 169 (1998); A. Böttcher, T. Takeuchi, K. I. Hardcastle, T. J. Meade, H. B. Gray, D. Cwikel, M. Kapon and Z. Dori, *Inorg. Chem.*, **36**, 2498 (1997); T. Yamada, T. Nagata, T. Ikeno, Y. Ohtsuka, A. Sagara and T. Mukaiyama, *Inorg. Chim. Acta*, **296**, 86 (1999).
474. N. A. Stephenson, S. J. Dzugan, J. C. Gallucci and D. H. Busch, *J. Chem. Soc., Dalton Trans.*, 733 (1991).
475. J. T. Pulkkinen, R. Laatikainen, M. J. Ahlgrén, M. Peräkylä and J. J. Vepsäläinen, *J. Chem. Soc., Perkin Trans. 2*, 777 (2000).
476. F. Bonati and G. Wilkinson, *J. Chem. Soc.*, 3156 (1964).
477. H. Adams, N. A. Bailey, I. S. Baird, D. E. Fenton, J.-P. Costes, G. Cros and J.-P. Laurent, *Inorg. Chim. Acta*, **101**, 7(1985).
478. D. Ramprasad, W.-K. Lin, K. A. Goldsby and D. H. Busch, *J. Am. Chem. Soc.*, **110**, 1480 (1988); Y. Chen, G. Wu and G. C. Bazan, *Angew. Chem. Int. Ed.*, **44**, 1108 (2005); S. Doherty, J. G. Knight, T. H. Scanlan, M. R. J. Elsegood and W. Clegg, *J. Organomet. Chem.*, **650**, 231 (2002); M. E. Bluhm, C. Folli, D. Pufky, M. Kroger, O. Walter and M. Doring, *Organometallics*, **24**, 4139 (2005); H.-Y. Wang, J. Zhang, X. Meng and G.-X. Jin, *J. Organomet. Chem.*, **691**, 1275 (2006); R. P. Scaringe and D. J. Hodgson, *Inorg. Chem.*, **15**, 1193 (1976); K. C. Joshi, R. Bohra and B. S. Joshi, *Inorg. Chem.*, **31**, 598 (1992); M. Mikuriya, K. Minowa and N. Nagao, *Inorg. Chem. Commun.*, **4**, 441 (2001); A. Mukhopadhyay, G. Padmaja, S. Pal and S. Pal, *Inorg. Chem. Commun.*, **6**, 381 (2003).
479. M. Basato, U. Vettori, A. C. Veronese, A. Grassi and G. Valle, *Inorg. Chem.*, **37**, 6737 (1998).
480. N. T. S. Phan, D. H. Brown, H. Adams, S. E. Spey and P. Styring, *Dalton Trans.*, 1348 (2004).
481. M. D. Milton, J. D. Singh and R. J. Butcher, *Tetrahedron Lett.*, **45**, 6745 (2004).
482. H. Iida, Y. Yuasa, C. Kibayashi and Y. Iitaka, *J. Chem. Soc., Dalton Trans.*, 2212 (1981); Y.-L. Tung, W.-C. Tseng, C.-Y. Lee, P.-F. Hsu, Y. Chi, S.-M. Peng and G.-H. Lee, *Organometallics*, **18**, 864 (1999); J. Ruiz, V. Rodríguez, G. López, P. A. Chaloner and P. B. Hitchcock, *J. Organomet. Chem.*, **523**, 23 (1996).
483. H.-K. Shin, M. J. Hampden-Smith, T. T. Kodas and A. L. Rheingold, *Chem. Commun.*, 217 (1992); N. Matsumoto, T. Tsutsumi, A. Ohyoshi and H. Okawa, *Bull. Chem. Soc. Jpn.*, **56**, 1388 (1983); G. R. Clark, D. Hall and T. N. Waters, *J. Chem. Soc. A*, 223 (1968); Y.-C. Shi, H.-M. Yang, W.-B. Shen, C.-G. Yan and X.-Y. Hu, *Polyhedron*, **23**, 15 (2004); M. Becht, T. Gerfin and K.-H. Dahmen, *Helv. Chim. Acta*, **77**, 1288 (1994); R. Wegner, M. Gottschaldt, H. Gorls, E.-G. Jager and D. Klemm, *Angew. Chem. Int. Ed.*, **39**, 595 (2000); A. Mukherjee, M. Nethaji and A. R. Chakravarty, *Angew. Chem. Int. Ed.*, **43**, 87 (2004);

R. Wegner, M. Gottschaldt, H. Gorls, E.-G. Jager and D. Klemm, *Chem. Eur. J.*, **7**, 2143 (2001); Y. Nishida, M. Takeuchi, K. Takahashi and S. Kida, *Chem. Lett.*, 1815 (1983); A. R. Paital, T. Mitra, D. Ray, W. T. Wong, J. Ribas-Arino, J. Novoa, J. Ribas and G. Aromi, *Chem. Commun.*, 5172 (2005); M. S. Ray, A. Ghosh, R. Bhattacharya, G. Mukhopadhyay, M. G. B. Drew and J. Ribas, *Dalton Trans.*, 252 (2004); E. Solari, M. Latronico, P. Blech and C. Floriani, *Inorg. Chem.*, **35**, 4526 (1996).

484. M. Mikuriya and K. Minowa, *Inorg. Chem. Commun.*, **3**, 227 (2000).
485. S. Doherty, R. J. Errington, N. Housley and W. Clegg, *Organometallics*, **23**, 2382 (2004); R.-C. Yu, C.-H. Hung, J.-H. Huang, H.-Y. Lee and J.-T. Chen, *Inorg. Chem.*, **41**, 6450 (2002); P.-C. Kuo, I.-C. Chen, J.-C. Chang, M.-T. Lee, C.-H. Hu, C.-H. Hung, H. M. Lee and J.-H. Huang, *Eur. J. Inorg. Chem.*, 4898 (2004); P. Shukla, J. C. Gordon, A. H. Cowley and J. N. Jones, *J. Organomet. Chem.*, **690**, 1366 (2005).
486. J. K. Vohs, D. O. Miller, D. R. Denomme, J. W. Ziller and B. D. Fahlman, *Acta Crystallogr., Sect. C*, **61**, m287 (2005).
487. Y. Shen, J. Han, H. Gu, Y. Zhu and Y. Pan, *J. Organomet. Chem.*, **689**, 3461 (2004).
488. T.-Y. Chou, Y. Chi, S.-F. Huang, C.-S. Liu, A. J. Carty, L. Scoles and K. A. Udachin, *Inorg. Chem.*, **42**, 6041 (2003).
489. P. F. R. Ewings, P. G. Harrison and A. Mangia, *J. Organomet. Chem.*, **114**, 35 (1976); D. K. Dey, A. Lycka, S. Mitra and G. M. Rosair, *J. Organomet. Chem.*, **689**, 88 (2004).
490. N. Al-Awadi, N. M. Shuaib and A. El-Dissouky, *Spectrochim. Acta A*, **65**, 36 (2006).
491. P. Braunstein, *Chem. Rev.*, **106**, 134 (2006).
492. P. Veya, C. Floriani, A. Chiesi-Villa and C. Guastini, *Organometallics*, **10**, 2991 (1991).
493. P. Braunstein, X. Morise, M. Benard, M.-M. Rohmer and R. Welter, *Chem. Commun.*, 610 (2003).
494. C. Mattheis, P. Braunstein and A. Fischer, *J. Chem. Soc., Dalton Trans.*, 800 (2001).
495. X. Morise, M. L. H. Green, P. Braunstein, L. H. Rees and I. C. Vei, *New J. Chem.*, **27**, 32 (2003).
496. N. G. Jones, M. L. H. Green, I. C. Vei, L. H. Rees, S. I. Pascu, D. Watkin, A. Cowley, X. Morise and P. Braunstein, *J. Chem. Soc., Dalton Trans.*, 2491 (2002).
497. F. Connac, Y. Lucchese, M. Dartiguenave and A. L. Beauchamp, *Inorg. Chem.*, **36**, 256 (1997); X. Couillens, M. Gressier, R. Turpin, M. Dartiguenave, Y. Coulais and A. L. Beauchamp, *J. Chem. Soc., Dalton Trans.*, 914 (2002).
498. P. Braunstein, C. Charles, A. Tiripicchio and F. Ugozzoli, *J. Chem. Soc., Dalton Trans.*, 4365 (1996).
499. P. Crochet, B. Demerseman, C. Rocaboy and D. Schleyer, *Organometallics*, **15**, 3048 (1996); B. Demerseman, B. Guilbert, C. Renouard, M. González, P. H. Dixneuf, D. Masi and C. Mealli, *Organometallics*, **12**, 3906 (1993).
500. H. Werner, G. Henig, B. Windmüller, O. Gevert, C. Lehmann and R. Herbst-Irmer, *Organometallics*, **18**, 1185 (1999).
501. P. Braunstein, S. C. Cea, M. I. Bruce, B. W. Skelton and A. H. White, *J. Chem. Soc., Dalton Trans.*, 2539 (1992).
502. P. Braunstein, Y. Chauvin, J. Nahring, Y. Dusausoy, D. Bayeul, A. Tiripicchio and F. Ugozzoli, *J. Chem. Soc., Dalton Trans.*, 851 (1995).
503. P. Braunstein, D. G. Kelly, A. Tiripicchio and F. Ugozzoli, *Inorg. Chem.*, **32**, 4845 (1993).
504. P. Braunstein, Y. Chauvin, J. Nahring, A. DeCian, J. Fischer, A. Tiripicchio and F. Ugozzoli, *Organometallics*, **15**, 5551 (1996).
505. P. Braunstein, Y. Chauvin, J. Nahring, A. Decian and J. Fischer, *J. Chem. Soc., Dalton Trans.*, 863 (1995).
506. P. Braunstein, Y. Chauvin, J. Fischer, H. Olivier, C. Strohmann and D. V. Toronto, *New J. Chem.*, **24**, 437 (2000).
507. S. E. Bouaoud, P. Braunstein, D. Grandjean, D. Matt and D. Nobel, *Inorg. Chem.*, **25**, 3765 (1986).
508. P. Braunstein, D. Matt, Y. Dusausoy, J. Fischer, A. Mitschler and L. Ricard, *J. Am. Chem. Soc.*, **103**, 5115 (1981).
509. P. Braunstein, D. Matt, D. Nobel, F. Balegroune, S.-E. Bouaoud, D. Grandjean and J. Fischer, *J. Chem. Soc., Dalton Trans.*, 353 (1988).
510. M. Cox and J. Darken, *Coord. Chem. Rev.*, **7**, 29 (1971); S. E. Livingstone, *Coord. Chem. Rev.*, **7**, 59 (1971).

511. S. P. Kaiwar, J. K. Hsu, A. Vodacek, G. Yap, L. M. Liable-Sands, A. L. Rheingold and R. S. Pilato, *Inorg. Chem.*, **36**, 2406 (1997).
512. B. L. Tran and S. M. Cohen, *Chem. Commun.*, 203 (2006).
513. J. A. Lewis, B. L. Tran, D. T. Puerta, E. M. Rumberger, D. N. Hendrickson and S. M. Cohen, *Dalton Trans.*, 2588 (2005).
514. D. Brayton, F. E. Jacobsen, S. M. Cohen and P. J. Farmer, *Chem. Commun.*, 206 (2006); V. Monga, B. O. Patrick and C. Orvig, *Inorg. Chem.*, **44**, 2666 (2005); V. Monga, K. H. Thompson, V. G. Yuen, V. Sharma, B. O. Patrick, J. H. McNeill and C. Orvig, *Inorg. Chem.*, **44**, 2678 (2005); J. A. Lewis, D. T. Puerta and S. M. Cohen, *Inorg. Chem.*, **42**, 7455 (2003); K. Schuknecht, E. Uhlemann and G. Wilke, *Z. Chem.*, **15**, 285 (1975); E. Uhlemann, W. Petzold and M. Raab, *Z. Anorg. Allg. Chem.*, **508**, 191 (1984); V. E. Uhlemann, H. Motzny and G. Wilke, *Z. Anorg. Allg. Chem.*, **401**, 255 (1973).
515. M. Das and D. T. Haworth, *Transition Metal Chem.*, **21**, 442 (1996); B. Kamenar, B. Korparcolig, M. Penavic and M. Cindric, *J. Cryst. Spectrosc. Res.*, **22**, 391 (1992); R. C. Mehrotra, S. K. Saini and V. D. Gupta, *Indian J. Chem., Sect. A*, **28**, 614 (1989); R. C. Mehrotra, S. K. Saini and V. D. Gupta, *Indian J. Chem., Sect. A*, **28**, 715 (1989); K. Nag and M. Chaudhury, *Inorg. Nucl. Chem. Lett.*, **12**, 307 (1976); S. K. Saini, V. D. Gupta and R. C. Mehrotra, *Indian J. Chem., Sect. A*, **26**, 165 (1987); S. K. Saini, V. D. Gupta and R. C. Mehrotra, *J. Indian Chem. Soc.*, **59**, 1424 (1982); S. K. Saini, V. D. Gupta and R. C. Mehrotra, *Aust. J. Chem.*, **35**, 2215 (1982); O. Siiman, D. D. Titus, C. D. Cowman, J. Fresco and H. B. Gray, *J. Am. Chem. Soc.*, **96**, 2353 (1974); R. P. Singh, *J. Coord. Chem.*, **44**, 101 (1998); R. P. Singh, V. D. Gupta, E. N. Duesler and C. K. Narula, *J. Chem. Soc., Dalton Trans.*, 1289 (1988); C. Sreelatha, D. K. Srivastava, V. D. Gupta and H. Noth, *J. Chem. Soc., Dalton Trans.*, 407 (1988); C. H. Sreelatha and V. D. Gupta, *Curr. Sci.*, **53**, 858 (1984).
516. K. Hillner and W. P. Neumann, *Tetrahedron Lett.*, **27**, 5347 (1986).
517. A. Asadi, C. Eaborn, M. S. Hill, P. B. Hitchcock, M. M. Meehan and J. D. Smith, *Organometallics*, **21**, 2430 (2002).
518. F. Hampel, N. van Eikema Hommes, S. Hoops, F. Maaref and R. Schobert, *Eur. J. Inorg. Chem.*, 1253 (1998); R. Schobert, C. Melanophy, F. Maaref and F. Hampel, *Inorg. Chim. Acta*, **355**, 454 (2003).
519. H. Sun, V. V. Burlakov, A. Spannenberg, W. Baumann, P. Arndt and U. Rosenthal, *Organometallics*, **21**, 3360 (2002).
520. E. Guggolz, M. L. Ziegler, H. Biersack and W. A. Herrmann, *J. Organomet. Chem.*, **194**, 317 (1980).
521. D. Kwon and M. D. Curtis, *Organometallics*, **9**, 1(1990).
522. Y. Matsuo, K. Mashima and K. Tani, *Angew. Chem. Int. Ed.*, **40**, 960 (2001).
523. R. B. King and A. Fronzaglia, *Inorg. Chem.*, **5**, 1837 (1966); R. E. Moriarty, R. D. Ernst and R. Bau, *Chem. Commun.*, 1242 (1972).
524. M. H. Chisholm, E. A. Lucas, A. C. Sousa, J. C. Huffman, K. Folting, E. B. Lobkovsky and W. E. Streib, *Chem. Commun.*, 847 (1991).
525. M. A. Esteruelas, Y. A. Hernández, A. M. López, M. Oliván and E. Oñate, *Organometallics*, **24**, 5989 (2005).
526. H. H. Karsch, A. W. Leithe, M. Reisky and E. Witt, *Organometallics*, **18**, 90 (1999).
527. K. K. D. Amarasinghe, S. K. Chowdhury, M. J. Heeg and J. Montgomery, *Organometallics*, **20**, 370 (2001).
528. M. Green, D. M. Grove, J. L. Spencer and F. G. A. Stone, *J. Chem. Soc., Dalton Trans.*, 2228 (1977).
529. C.-Y. Lin, C.-F. Tsai, H.-J. Chen, C.-H. Hung, R.-C. Yu, P.-C. Kuo, H. M. Lee and J.-H. Huang, *Chem. Eur. J.*, **12**, 3067 (2006).
530. S. P. Green, C. Jones, A. Stasch and R. P. Rose, *New J. Chem.*, **31**, 127 (2007).
531. M. Saito, N. Tokitoh and R. Okazaki, *Organometallics*, **15**, 4531 (1996); N. Tokitoh, M. Sato and R. Okazaki, *J. Am. Chem. Soc.*, **115**, 2065 (1993).
532. K. Sugawara, S. Hikichi and M. Akita, *J. Chem. Soc., Dalton Trans.*, 4514 (2002).
533. M. H. Chisholm, J. C. Huffman and A. L. Ratermann, *Inorg. Chem.*, **22**, 4100 (1983).
534. P. Hofmann, M. Frede, P. Stauffert, W. Lasser and U. Thewalt, *Angew. Chem., Int. Ed. Engl.*, **24**, 712 (1985).
535. L.-C. Song, P.-C. Liu, C. Han and Q.-M. Hu, *J. Organomet. Chem.*, **648**, 119 (2002).
536. M. Farahbakhsh, H. Schmidt and D. Rehder, *Chem. Commun.*, 2009 (1998).

537. C. A. Stewart, J. C. Calabrese and A. J. Arduengo, *J. Am. Chem. Soc.*, **107**, 3397 (1985).
538. G. Bettermann and A. J. Arduengo III, *J. Am. Chem. Soc.*, **110**, 877 (1988).
539. P. G. Williard and J. M. Salvino, *J. Chem. Soc., Chem. Commun.*, 153 (1986).
540. T. Agapie, P. L. Diaconescu, D. J. Mindiola and C. C. Cummins, *Organometallics*, **21**, 1329 (2002).
541. M. J. Burk, D. L. Staley and W. Tumas, *Chem. Commun.*, 809 (1990).
542. A. P. Masters, M. Parvez, T. S. Sorensen and F. Sun, *Can. J. Chem.*, **71**, 230 (1993).
543. S. Kiyota, J. Tamuki, N. Komine, M. Hirano and S. Komiya, *Chem. Lett.*, **34**, 498 (2005).
544. H. Kandler, W. Bidell, M. Janicke, M. Knickmeier, D. Veghini and H. Berke, *Organometallics*, **17**, 960 (1998).
545. J. R. Bleeke, P. R. New, J. M. B. Blanchard, T. Haile and A. M. Rohde, *Organometallics*, **14**, 5127 (1995).
546. W. Keim, F. H. Kowaldt, R. Goddard and C. Krüger, *Angew. Chem., Int. Ed. Engl.*, **17**, 466 (1978).
547. W. Keim, A. Behr, B. Gruber, B. Hoffmann, F. H. Kowaldt, U. Kuerschner, B. Limbaecker and F. P. Sistig, *Organometallics*, **5**, 2356 (1986).
548. P. Braunstein, Y. Chauvin, S. Mercier, L. Saussine, A. Decian and J. Fischer, *J. Chem. Soc., Chem. Commun.*, 2203 (1994).
549. A. Grassi, P. Longo, A. Musco, W. Porzio and A. Scrivanti, *J. Organomet. Chem.*, **289**, 439 (1985).
550. P. Braunstein, S. C. Cea, M. I. Bruce, B. W. Skelton and A. H. White, *J. Organomet. Chem.*, **423**, C38 (1992).
551. Y. Apeloig, I. Zharov, D. Bravo-Zhivotovskii, Y. Ovchinnikov and Y. Struchkov, *J. Organomet. Chem.*, **499**, 73 (1995).
552. M. R. P. van Vliet, G. van Koten, P. Buysingh, J. T. B. H. Jastrzebski and A. L. Spek, *Organometallics*, **6**, 537 (1987).
553. J. T. B. H. Jastrzebski, J. Boersma, G. van Koten, W. J. J. Smeets and A. L. Spek, *Recl. Trav. Chim. Pays-Bas*, **107**, 263 (1988).
554. E. Hevia, G. W. Honeyman, A. R. Kennedy and R. E. Mulvey, *J. Am. Chem. Soc.*, **127**, 13106 (2005).
555. Z. K. Sweeney, J. L. Polse, R. A. Anderson and R. G. Bergman, *J. Am. Chem. Soc.*, **120**, 7825 (1998).
556. J. Stroot, R. Beckhaus, W. Saak, D. Haase and A. Lutzen, *Eur. J. Inorg. Chem.*, 1729 (2002).
557. J. Sundermeyer, K. Weber, H. Werner, N. Mahr, G. Bringmann and O. Schupp, *J. Organomet. Chem.*, **444**, C37 (1993).
558. A. J. Arce and A. J. Deeming, *J. Chem. Soc., Chem. Commun.*, 364 (1982).
559. L. Cuesta, E. Hevia, D. Morales, J. Pérez, V. Riera, M. Seitz and D. Miguel, *Organometallics*, **24**, 1772 (2005).
560. R. Aumann, I. Gottker-Schnetmann, R. Fröhlich, P. Saarenketo and C. Holst, *Chem. Eur. J.*, **7**, 711 (2001).
561. A. Klose, E. Solari, C. Floriani, S. Geremia and L. Randaccio, *Angew. Chem. Int. Ed.*, **37**, 148 (1998).
562. H. Yasuda, H. Yamamoto, M. Yamashita, K. Yokota, A. Nakamura, S. Miyake, Y. Kai and N. Kanehisa, *Macromolecules*, **26**, 7134 (1993).
563. G. Himbert, L. Henn and R. Hoge, *J. Organomet. Chem.*, **184**, 317 (1980).
564. L. Giannini, E. Solari, S. Dovesi, C. Floriani, N. Re, A. Chiesi-Villa and C. Rizzoli, *J. Am. Chem. Soc.*, **121**, 2784 (1999).
565. R. Beckhaus, I. Strauss, T. Wagner and P. Kiprof, *Angew. Chem., Int. Ed. Engl.*, **32**, 264 (1993).
566. R. Beckhaus, I. Strauss and T. Wagner, *Z. Anorg. Allg. Chem.*, **623**, 654 (1997).
567. R. Beckhaus, T. Wagner, C. Zimmermann and E. Herdtweck, *J. Organomet. Chem.*, **460**, 181 (1993).
568. G. Fachinetti, C. Biran, C. Floriani, A. Chiesi-Villa and C. Guastini, *Inorg. Chem.*, **17**, 2995 (1978).
569. F. Basuli, B. C. Bailey, L. A. Watson, J. Tomaszewski, J. C. Huffman and D. J. Mindiola, *Organometallics*, **24**, 1886 (2005).
570. F. Basuli, J. C. Huffman and D. J. Mindiola, *Inorg. Chem.*, **42**, 8003 (2003).

571. S. Gambarotta, S. Strologo, C. Floriani, A. Chiesi-Villa and C. Guastini, *Inorg. Chem.*, **24**, 654 (1985).
572. H. Yasuda, T. Okamoto, Y. Matsuoka, A. Nakamura, Y. Kai, N. Kanehisa and N. Kasai, *Organometallics*, **8**, 1139 (1989).
573. J. Sundermeyer, K. Weber and H. Pritzkow, *Angew. Chem., Int. Ed. Engl.*, **32**, 731 (1993).
574. F. R. Kreissl, M. Wolfgruber and U. Thewalt, *J. Organomet. Chem.*, **317**, 175 (1986).
575. U. Kusthardt, W. A. Herrmann, M. L. Ziegler, T. Zahn and B. Nuber, *J. Organomet. Chem.*, **311**, 163 (1986).
576. K. A. Azam, A. J. Deeming and I. P. Rothwell, *J. Chem. Soc., Dalton Trans.*, 91 (1981).
577. S. Gambarotta, S. Stella, C. Floriani, A. Chiesi-Villa and C. Guastini, *J. Chem. Soc., Dalton Trans.*, 1789 (1987).
578. D. J. Mindiola and G. L. Hillhouse, *J. Am. Chem. Soc.*, **124**, 9976 (2002).
579. C. M. Zhang, R. T. Liu, X. G. Zhou, Z. X. Chen, L. H. Weng and Y. H. Ling, *Organometallics*, **23**, 3246 (2004).
580. A. Musco, W. Porzio, S. Destri, G. Gatti, A. Grassi and P. Longo, *J. Organomet. Chem.*, **301**, 237 (1986).
581. R. A. Layfield and S. M. Humphrey, *Organometallics*, **24**, 6063 (2005).
582. R. E. Cramer, J. H. Jeong and J. W. Gilje, *Organometallics*, **6**, 2010 (1987).
583. J. A. R. Schmidt and J. Arnold, *Organometallics*, **21**, 3426 (2002).
584. R. R. Schrock and J. D. Fellmann, *J. Am. Chem. Soc.*, **100**, 3359 (1978).
585. J. R. Stille and R. H. Grubbs, *J. Am. Chem. Soc.*, **105**, 1664 (1983).
586. J. M. Manriquez, P. J. Fagan, T. J. Marks, C. S. Day and V. W. Day, *J. Am. Chem. Soc.*, **100**, 7112 (1978).
587. M. F. Lappert, C. L. Raston, L. M. Engelhardt and A. H. White, *J. Chem. Soc., Chem. Commun.*, 521 (1985).
588. T. M. Cameron, J. C. Gordon, B. L. Scott and W. Tumas, *Chem. Commun.*, 1398 (2004).
589. P. J. Fagan, J. M. Manriquez, T. J. Marks, V. W. Day, S. H. Vollmer and C. S. Day, *J. Am. Chem. Soc.*, **102**, 5393 (1980).
590. L. P. Spencer and M. D. Fryzuk, *J. Organomet. Chem.*, **690**, 5788 (2005).
591. T. Y. Meyer, L. R. Garner, N. C. Baenziger and L. Messerle, *Inorg. Chem.*, **29**, 4045 (1990).
592. J. Arnold, T. D. Tilley, A. L. Rheingold, S. J. Geib and A. M. Arif, *J. Am. Chem. Soc.*, **111**, 149 (1989).
593. H. H. Karsch, G. Grauvogl, M. Kawecki, P. Bissinger, O. Kumberger, A. Schier and G. Muller, *Organometallics*, **13**, 610 (1994).
594. J. L. Petersen and J. W. E. Junior, *Organometallics*, **6**, 2007 (1987).
595. J. M. Manriquez, D. R. McAlister, R. D. Sanner and J. E. Bercaw, *J. Am. Chem. Soc.*, **100**, 2716 (1978); P. T. Wolczanski and J. E. Bercaw, *Acc. Chem. Res.*, **13**, 121 (1980).
596. R. P. Planalp and R. A. Andersen, *J. Am. Chem. Soc.*, **105**, 7774 (1983).
597. D. M. Roddick, R. H. Heyn and T. D. Tilley, *Organometallics*, **8**, 324 (1989).
598. P. Berno, R. Minhas, S. K. Hao and S. Gambarotta, *Organometallics*, **13**, 1052 (1994).
599. B.-J. Deelman, W. M. Stevels, J. H. Teuben, M. T. Lakin and A. L. Spek, *Organometallics*, **13**, 3881 (1994).
600. M. Gómez, P. Gómez-Sal, G. Jimónez, A. Martín, P. Royo and J. Sánchez-Nieves, *Organometallics*, **15**, 3579 (1996).
601. L. M. Atagi and J. M. Mayer, *Organometallics*, **13**, 4794 (1994).
602. I. J. Hart, J. C. Jeffery, R. M. Lowry and F. G. A. Stone, *Angew. Chem., Int. Ed. Engl.*, **27**, 1703 (1988).
603. K. N. Juneau, L. S. Hegedus and F. W. Roepke, *J. Am. Chem. Soc.*, **111**, 4762 (1989).
604. P. M. Fritz, J. Breimair, B. Wagner and W. Beck, *J. Organomet. Chem.*, **426**, 343 (1992).
605. G. B. Robertson and P. O. Whimp, *Inorg. Chem.*, **12**, 1740 (1973); M. A. Bennett and R. Watt, *Chem. Commun.*, 95 (1971).
606. P. T. Barger, B. D. Santarsiero, J. Armantrout and J. E. Bercaw, *J. Am. Chem. Soc.*, **106**, 5178 (1984).
607. G. Erker, P. Czisch, R. Schlund, K. Angermund and C. Kruger, *Angew. Chem., Int. Ed. Engl.*, **25**, 364 (1986).
608. P. J. Fagan, K. G. Moloy and T. J. Marks, *J. Am. Chem. Soc.*, **103**, 6959 (1981).
609. W. J. Evans, J. W. Grate and R. J. Doedens, *J. Am. Chem. Soc.*, **107**, 1671 (1985).
610. W. J. Evans, K. J. Forrestal and J. W. Ziller, *J. Am. Chem. Soc.*, **117**, 12635 (1995).

611. W. J. Evans, S. A. Kozimor, G. W. Nyce and J. W. Ziller, *J. Am. Chem. Soc.*, **125**, 13831 (2003).
612. O. T. Summerscales, F. G. N. Cloke, P. B. Hitchcock, J. C. Green and N. Hazari, *Science*, **311**, 829 (2006).
613. K. G. Moloy, T. J. Marks and V. W. Day, *J. Am. Chem. Soc.*, **105**, 5696 (1983).
614. W. J. Evans, A. L. Wayda, W. E. Hunter and J. L. Atwood, *J. Chem. Soc., Chem. Commun.*, 706 (1981).
615. A. K. McMullen, I. P. Rothwell and J. C. Huffman, *J. Am. Chem. Soc.*, **107**, 1072 (1985); L. R. Chamberlain, L. D. Durfee, P. E. Fanwick, L. M. Kobriger, S. L. Latesky, A. K. McMullen, B. D. Steffey, I. P. Rothwell, K. Folting and J. C. Huffman, *J. Am. Chem. Soc.*, **109**, 6068 (1987).
616. G. Fachinetti, C. Biran, C. Floriani, A. Chiesi-Villa and C. Guastini, *J. Am. Chem. Soc.*, **100**, 1921 (1978).
617. S. Gambarotta, M. Pasquali, C. Floriani, A. C. Villa and C. Guastini, *Inorg. Chem.*, **20**, 1173 (1981); J. M. Galante, J. W. Bruno, P. N. Hazin, K. Folting and J. C. Huffman, *Organometallics*, **7**, 1066 (1988); M. Wiederhold and U. Behrens, *J. Organomet. Chem.*, **476**, 101 (1994).
618. S. E. Halfon, M. C. Fermin and J. W. Bruno, *J. Am. Chem. Soc.*, **105**, 2068 (1983); M. C. Fermin, A. S. Hneihen, J. J. Maas and J. W. Bruno, *Organometallics*, **12**, 1845 (1993); A. Antiñolo, A. Otero, M. Fajardo, R. Gil-Sanz, M. J. Herranz, C. López-Mardomingo, A. Martín and P. Gómez-Sal, *J. Organomet. Chem.*, **533**, 87 (1997).
619. E. Bleuel, M. Laubender, B. Weberndorfer and H. Werner, *Angew. Chem. Int. Ed.*, **38**, 156 (1999).
620. R. Flugel, O. Gevert and H. Werner, *Chem. Ber.*, **129**, 405 (1996).
621. P. Hofmann, L. A. Perez-Moya, O. Steigelmann and J. Riede, *Organometallics*, **11**, 1167 (1992).
622. L. M. Engelhardt, G. E. Jacobsen, C. L. Raston and A. H. White, *J. Chem. Soc., Chem. Commun.*, 220 (1984).
623. S. J. Young, H. Hope and N. E. Schore, *Organometallics*, **3**, 1585 (1984); R. Choukroun, F. Dahan and D. Gervais, *J. Organomet. Chem.*, **266**, C33 (1984).
624. S. C. H. Ho, D. A. Straus, J. Armantrout, W. P. Schaefer and R. H. Grubbs, *J. Am. Chem. Soc.*, **106**, 2210 (1984); E. J. Moore, D. A. Straus, J. Armantrout, B. D. Santarsiero, R. H. Grubbs and J. E. Bercaw, *J. Am. Chem. Soc.*, **105**, 2068 (1983).
625. F. R. Lemke, D. J. Szalda and R. M. Bullock, *J. Am. Chem. Soc.*, **113**, 8466 (1991).
626. M. D. Fryzuk, P. B. Duval, S. Mao, S. J. Rettig, M. J. Zaworotko and L. R. MacGillivray, *J. Am. Chem. Soc.*, **121**, 1707 (1999).
627. J. S. Holmgren, J. R. Shapley, S. R. Wilson and W. T. Pennington, *J. Am. Chem. Soc.*, **108**, 508 (1986).
628. J. A. R. Schmidt and J. Arnold, *J. Am. Chem. Soc.*, **123**, 8424 (2001).
629. R. E. Cramer, J. H. Jeong, P. N. Richmann and J. W. Gilje, *Organometallics*, **9**, 1141 (1990); R. E. Cramer, J. H. Jeong and J. W. Gilje, *Organometallics*, **5**, 2555 (1986); R. E. Cramer, K. T. Higa and J. W. Gilje, *J. Am. Chem. Soc.*, **106**, 7245 (1984); G. Proulx and R. G. Bergman, *J. Am. Chem. Soc.*, **118**, 1981 (1996).
630. M. Green, J. Z. Nyathi, C. Scott, F. G. A. Stone, A. J. Welch and P. Woodward, *J. Chem. Soc., Dalton Trans.*, 1067 (1978).
631. E. R. Burkhardt, J. J. Doney, R. G. Bergman and C. H. Heathcock, *J. Am. Chem. Soc.*, **109**, 2022 (1987).
632. P. L. Watson and R. G. Bergman, *J. Am. Chem. Soc.*, **101**, 2055 (1979).
633. H. G. Alt, H. E. Engelhardt, U. Thewalt and J. Riede, *J. Organomet. Chem.*, **288**, 165 (1985).
634. H. G. Alt, G. S. Herrmann, H. E. Engelhardt and R. D. Rogers, *J. Organomet. Chem.*, **331**, 329 (1987).
635. P. DeShong, D. R. Sidler, P. J. Rybczynski, G. A. Slough and A. L. Rheingold, *J. Am. Chem. Soc.*, **110**, 2575 (1988).
636. J. G. Stack, R. D. Simpson, F. J. Hollander, R. G. Bergman and C. H. Heathcock, *J. Am. Chem. Soc.*, **112**, 2716 (1990).
637. M. Etienne, C. Carfagna, P. Lorente, R. Mathieu and D. de Montauzon, *Organometallics*, **18**, 3075 (1999).

638. K. C. Stone, G. M. Jamison, P. S. White and J. L. Templeton, *Organometallics*, **22**, 3083 (2003).
639. B. E. Woodworth, D. S. Frohnapfel, P. S. White and J. L. Templeton, *Organometallics*, **17**, 1655 (1998).
640. J. Ipaktschi, F. Mirzaei, K. Reimann, J. Beck and M. Serafin, *Organometallics*, **17**, 5086 (1998).
641. W. Hirpo and M. D. Curtis, *Organometallics*, **13**, 2706 (1994).
642. S. R. Allen, M. Green, N. C. Norman, K. E. Paddick and A. G. Orpen, *J. Chem. Soc., Dalton Trans.*, 1625 (1983).
643. T. B. Gunnoe, J. L. Caldarelli, P. S. White and J. L. Templeton, *Angew. Chem. Int. Ed.*, **37**, 2093 (1998).
644. L. W. Francisco, P. S. White and J. L. Templeton, *Organometallics*, **16**, 2547 (1997).
645. A. Maercker, *Angew. Chem., Int. Ed. Engl.*, **26**, 972 (1978).
646. R. B. Bates, D. E. Potter and L. M. Kroposki, *J. Org. Chem.*, **37**, 560 (1972); M. E. Jung and R. B. Blum, *Tetrahedron Lett.*, 3791 (1977).
647. P. Tomboulian, D. Amick, S. Beare, K. Dumke, D. Hart, R. Hites, A. Metzger and R. Nowak, *J. Org. Chem.*, **38**, 322 (1973).
648. B. Walfort, S. K. Pandey and D. Stalke, *Chem. Commun.*, 1640 (2001).
649. A. Steiner and D. S. Wright, *Chem. Commun.*, 283 (1997).
650. F. Rivals and A. Steiner, *Chem. Commun.*, 1426 (2001).
651. J. Jubb, S. Gambarotta, R. Duchateau and J. H. Teuben, *Chem. Commun.*, 2641 (1994).
652. S. De Angelis, E. Solari, C. Floriani, A. Chiesi-Villa and C. Rizzoli, *J. Chem. Soc., Dalton Trans.*, 2467 (1994).
653. H. Zhu and E. Y. X. Chen, *Inorg. Chem.*, **46**, 1481 (2007).
654. T. Dube, S. Gambarotta and G. P. A. Yap, *Organometallics*, **19**, 817 (2000).
655. J. W. Guan, T. Dube, S. Gambarotta and G. P. A. Yap, *Organometallics*, **19**, 4820 (2000).
656. T. Dube, J. W. Guan, S. Gambarotta and G. P. A. Yap, *Chem. Eur. J.*, **7**, 374 (2001); T. Dube, S. Gambarotta and G. P. A. Yap, *Angew. Chem. Int. Ed.*, **38**, 1432 (1999).
657. J. S. Alexander and K. Ruhlandt-Senge, *Chem. Eur. J.*, **10**, 1274 (2004).
658. K. B. P. Ruppa, S. Gambarotta and G. P. A. Yap, *Inorg. Chim. Acta*, **280**, 143 (1998).
659. F. Basuli, J. Tomaszewski, J. C. Huffman and D. J. Mindiola, *Organometallics*, **22**, 4705 (2003).
660. H. C. Aspinall and M. R. Tillotson, *Inorg. Chem.*, **35**, 2163 (1996).
661. K. H. Thiele, K. Unverhau, M. Geitner and K. Jacob, *Z. Anorg. Allg. Chem.*, **548**, 175 (1987).
662. S. D. Daniel, J.-S. M. Lehn, J. D. Korp and D. M. Hoffman, *Polyhedron*, **25**, 205 (2006).
663. S. Arndt, T. P. Spaniol and J. Okuda, *Organometallics*, **22**, 775 (2003); J. Hitzbleck and J. Okuda, *Organometallics*, **26**, 3227 (2007).
664. M. H. Chisholm, S. T. Haubrich, J. C. Huffman and W. E. Streib, *J. Am. Chem. Soc.*, **119**, 1634 (1997).
665. S. N. Ringelberg, A. Meetsma, S. I. Troyanov, B. Hessen and J. H. Teuben, *Organometallics*, **21**, 1759 (2002).
666. G. Erker, R. Petrenz, C. Kruger and M. Nolte, *J. Organomet. Chem.*, **431**, 297 (1992); G. Erker, R. Petrenz, C. Kruger, F. Lutz, A. Weiss and S. Werner, *Organometallics*, **11**, 1646 (1992).
667. M. H. Chisholm, J. Gallucci and K. Phomphrai, *Inorg. Chem.*, **41**, 2785 (2002).
668. M. Lenarda, R. Ros, O. Traverso, W. D. Pitts, W. H. Baddley and M. Graziani, *Inorg. Chem.*, **16**, 3178 (1977).
669. S. C. Goel, M. Y. Chiang and W. E. Buhro, *Inorg. Chem.*, **29**, 4646 (1990).
670. J. L. Polse, R. A. Andersen and R. G. Bergman, *J. Am. Chem. Soc.*, **117**, 5393 (1995).
671. D. J. Schwartz, M. R. Smith and R. A. Andersen, *Organometallics*, **15**, 1446 (1996).
672. M. J. Carney, P. J. Walsh, F. J. Hollander and R. G. Bergman, *J. Am. Chem. Soc.*, **111**, 8751 (1989); M. J. Carney, P. J. Walsh, F. J. Hollander and R. G. Bergman, *Organometallics*, **11**, 761 (1992).
673. G. A. Vaughan, C. D. Sofield, G. L. Hillhouse and A. L. Rheingold, *J. Am. Chem. Soc.*, **111**, 5491 (1989).
674. G. A. Vaughan, G. L. Hillhouse and A. L. Rheingold, *J. Am. Chem. Soc.*, **112**, 7994 (1990).
675. V. C. Gibson, C. Newton, C. Redshaw, G. A. Solan, A. J. P. White and D. J. Williams, *Dalton Trans.*, 4612 (2003).

676. L. Cuesta, D. C. Gerbino, E. Hevia, D. Morales, M. E. N. Clemente, J. Pérez, L. Riera, V. Riera, D. Miguel, I. del Rio and S. García-Granda, *Chem. Eur. J.*, **10**, 1765 (2004).
677. M. A. Esteruelas, F. J. Lahoz, E. Oñate, L. A. Oro and B. Zeier, *Organometallics*, **13**, 1662 (1994).
678. Z. Z. Wu, Z. Xu, X. Z. You, X. G. Zhou and X. Y. Huang, *J. Organomet. Chem.*, **483**, 107 (1994).
679. G. A. Vaughan, G. L. Hillhouse, R. T. Lum, S. L. Buchwald and A. L. Rheingold, *J. Am. Chem. Soc.*, **110**, 7215 (1988).
680. K. E. Garrett, J. B. Sheridan, D. B. Pourreau, W. C. Feng, G. L. Geoffroy, D. L. Staley and A. L. Rheingold, *J. Am. Chem. Soc.*, **111**, 8383 (1989).
681. C. Löwe, V. Shklover and H. Berke, *Organometallics*, **10**, 3396 (1991).
682. A. B. Goel and S. Goel, *Angew. Chem., Int. Ed. Engl.*, **23**, 375 (1984).
683. G. Erker, U. Dorf, R. Lecht, M. T. Ashby, M. Aulbach, R. Schlund, C. Krueger and R. Mynott, *Organometallics*, **8**, 2037 (1989).
684. J. Cipot, R. McDonald and M. Stradiotto, *Organometallics*, **25**, 29 (2006).
685. J. M. O'Connor, K. Hiibner, R. Merwin, P. K. Gantzel, B. S. Fong, M. Adams and A. L. Rheingold, *J. Am. Chem. Soc.*, **119**, 3631 (1997).
686. C. C. Fuller and R. A. Jacobson, *Inorg. Chim. Acta*, **48**, 191 (1981).
687. Y. Sato, H. Miyasaka, N. Matsumoto and H. Okawa, *Inorg. Chim. Acta*, **247**, 57 (1996).
688. M. D. Curtis, L. Messerle, J. J. D'Errico, W. M. Butler and M. S. Hay, *Organometallics*, **5**, 2283 (1986).
689. M. Nieuwenhuyzen, R. Schobert, F. Hampel and S. Hoops, *Inorg. Chim. Acta*, **304**, 118 (2000).

CHAPTER 6

Coordination chemistry of metal enolato complexes

JOSÉ VICENTE

Grupo de Química Organometálica, Departamento de Química Inorgánica, Facultad de Química, Universidad de Murcia, Apdo. 4021, 30071 Murcia, Spain
Fax: +34-868887785; e-mail: jvs1@um.es; http://www.um.es/gqo/

The chemistry of metal enolates
Edited by Jacob Zabicky

I. INTRODUCTION

As defined in Chapter 5[1], an enolato complex contains a [M]OCC group with the oxygen atom bearing a negative formal charge and its electronic structure can be described as **1** or **2**, where [M] is a metal ion with all the other ligands. However, complexes with phenolato, oxalato or related ligands will not be considered. Neither will the enolates of B, Si, Ge, P, As, Sb and elements of Groups 16 and 17 be treated. The content of this chapter is restricted mainly to the chemistry of enolato complexes that were isolated and fully characterized: Section II deals with the factors that promote formation of enolato (**3**) or 2-oxoalkyl (**4**) complexes, in Section III the equilibrium between complexes of type **3** and **4** is discussed, Section IV deals with reactions in which enolato complexes are converted into complexes bearing a different enolato ligand and the rest of the chapter is devoted to reactions in which an enolato ligand is replaced or transformed into a nonenolato ligand. This chapter is strongly linked to Chapter 5[1], on the synthesis of metal enolates.

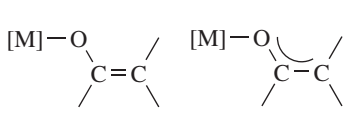

(**1**) (**2**)

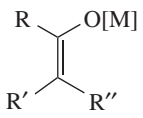

(**3**) Enolato complex

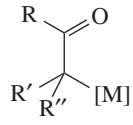

(**4**) 2-Oxoalkyl complex

The abbreviations listed below are used in the chapter. Unless otherwise stated, the diketonato ligands are assumed to be O,O'-dicoordinated.

acac	acetylacetonato
bipy	2,2′-bipyridine
cod	1,5-cyclooctadiene
dik	diketonato
dpk	diphenylketene
dppe	1,2-bis(diphenylphosphino)ethane
dppm	bis(diphenylphosphino)methane
F_6acac	1,1,1,3,3,3-hexafluoroacetylacetonato
F_3acac	1,1,1-trifluoroacetylacetonato
LDA	lithium diisopropylamide
Me_6acac	1,1,1,3,3,3-hexamethyacetylacetonato
nbd	norbornadiene
phen	1,10-phenanthroline
py	pyridine
TfO	triflate
tol	*p*-tolyl
$Tp^{R,R'}$	hydrotris(3-R-5-R′-pyrazolyl)borate (R and R′ are substituent groups)

II. ENOLATO *VERSUS* 2-OXOALKYL COORDINATION

A. Pd(II) and Pt(II) Enolato Complexes

These complexes are obtained (i) by reacting Pd(II) or Pt(II) complexes with ketones and a base[2], (ii) by transmetalating the ligand from a 2-oxoalkyl mercury derivative to a halo complex[3–5] or (iii) by an oxidative addition reaction using an α-haloketone or $[Hg(CH_2C(O)Me)_2]$[5] and a Pd^0 or Pt^0 complex[6,7]; however, instead of enolato complexes, 2-oxoalkyl derivatives usually form because Pd(II) and Pt(II) are more carbophilic than oxophilic[2,3,7–9], namely these metal ions are soft acids that preferentially bond to soft C-donor rather than to hard O-donor ligands. Nevertheless, Pd(II) enolates exist containing chelating ligands derived from diketones, ketoimines, carbonyl-functionalized phosphines (Sections II.A.2, 4 and 5, respectively, in Chapter 5[1]), phosphorus ylides (Section II.B) and a few containing unidentate enolato ligands described here. The O-coordination of these ligands is due to their chelating nature, to the transphobia[10] between P- or C-donor ligands toward C-donor ligands or to steric hindrance of their substituents[8]. Thus, complex *trans*-$[Pd(tol)Br(PPh_2Et)_2]$ reacts with KOC(=CHR)Ar to give *trans*-$[Pd(tol)\{OC(=CHR)Ar\}(PPh_2Et)_2]$ (R = Me, Ar = Ph) or a mixture of the enolato and the 2-oxoalkyl isomers (R = H, Ar = tol)[8]. The reactions of *cis*-[PdBr(Ar)(dpb)] (dpb = 1,2-bis-(diphenylphosphino)benzene) with the appropriate potasium enolates give a family of 2-oxoalkyl complexes *cis*-$[Pd(Ar)\{CRR'C(O)R''\}(dpb)]$[8] and only in the case of R = R′ = Me and R″ = Ph was the enolato complex the most stable isomer. The stabilization of these few enolato complexes has been attributed to the steric hindrance.

B. Carbonyl-stabilized Phosphorus Ylide Complexes

The electronic structure of these neutral ligands is intermediate between those of resonance forms **5**–**7**. In accordance with their ν(CO) IR absorption, the enolato character of these ylides, or the relative weight of resonance form **7**, increases in the order R = OMe ≪ Me < Ph[11]. Therefore, these ligands are expected to coordinate in the enolato form when R = Ph, Me or when the coordination position available has a crowded environment. In addition, as most reported carbonyl-stabilized phosphorus ylide complexes are Pd(II) or Pt(II) derivatives[12], the enolato coordination of these ligands is preferred when the ligand in *trans* position is C- or P-donor, due to the transphobia between these ligands and the ylide coordinate through the carbon atom. Thus, *cis*-$[PtCl_2(P\,P)]$ (P P = dppe or *Z*-1,2-bis(diphenylphosphino)ethene) reacts with $Ph_3PCHC(O)R$ and $AgBF_4$ (1:1:1) to give **8** or **9**, i.e. depending on R[13].

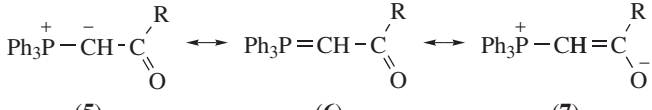

(**5**) (**6**) (**7**)

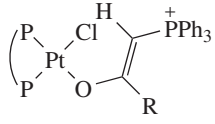

(**8**) R = Me, Ph

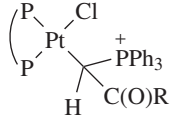

(**9**) R = OMe

The reactions of *trans*-[Pt(Mef)Br(PPh_3)$_2$] with $AgBF_4$ and $Ph_3ECHC(O)R$ (E = P, R = Me, OMe, Ph; E = As, R = Me) afford only *trans*-[Pt(Mef){OC(=CHEPh_3)R}(PPh_3)$_2$] because the *C*-alkyl/*C*-ylide transphobia is greater than the *C*-alkyl/*O*-ylide transphobia and also because of the lower steric requirement of the *O*-ylide ligand. Contrarily, [Pt(η^3-C_3H_5)(μ-Cl)]$_2$ or [Pt(*C*,*P*-{$CH_2C(Me)_2P(t$-Bu)$_2$}(μ-Cl)]$_2$ reacts with $Ph_3ECHC(O)R$ to give complexes containing the *C*-ylide ligand, [Pt(η^3-C_3H_5)Cl{CH{C(O)R}PPh_3}] (R = Me, OMe, Ph) or *cis*-[Pt(*C*,*P*-{$CH_2C(Me)_2P(t$-Bu)$_2$}Cl{CH{C(O)R}EPh_3}] (E = P, As; R = Me, OMe, Ph)[13]; in the isolated isomer of the last reaction the ylide is *cis* to the CH_2 group, i.e. *cis* to the atom to which the ligand has the greater transphobia and in the less hindered coordination site. In the case of the η^3-allyl complex, the π-C/C- and P/C-ylide transphobia are probably similar and the metal center environment is not too crowded as to prevent the preferred *C*-coordination of the ylide. Similar results have been reported for reactions of ylides with [Pd(η^3-C_3H_5)(μ-Cl)]$_2$[14], K[$PtCl_3$(η^2-C_2H_4)][15] and [Pt(μ-Cl)(dppe)]$_2$(BF_4)$_2$[16].

Reactions of Pd organometallic complexes **10a** and **10b** with ylides $Ph_3PCHC(O)R$ (R = Me, Ph or OMe)[17] can afford the *O*-isomers **11a–c** or the *C*-isomers **12a** and **12b**, with the ylide *trans* to N. The first possibility goes against the soft character of Pd(II), but it should be expected when the L ligand has a great C/L transphobia, as in **11a** (L = PPh_3), which requires L being *trans* to N and the ylide *trans* to the aryl group and *O*-coordinated due to the greater C/C than O/C transphobia. The *O*-isomer is also expected when the ylide is a better O- than C-donor ligand as in **11b** (R = Me). In agreement with these assumptions, a mixture of *O*- and *C*-isomers is isolated when L = MeCN and R = Me or Ph (**11c**, **12b**). In the case of **12a** (R = OMe and L = py or MeCN), only the *C*-isomer is obtained[17,18]. Similarly, [Pt(C∧P){OC(=CHPPh_3)R}(PPh_3)]$^+$ (C∧P = *C*,*P*-$CH_2C_6H_4${P(C_6H_4Me-2)$_2$}-2) has been obtained for R = Me, OMe and [Pt(C∧P){CH{C(O)R}PPh_3}(NCMe)]$^+$ for R = Me, Ph, OMe. When the starting complex is [Pt(C∧P)(μ-Cl)]$_2$, the products are [Pt(C∧P)Cl{CH{C(O)R}PPh_3}], with the ylide *trans* to P. The complex with R = Me reacts with $TlClO_4$ and one equivalent of the same ylide, which is the most prone to coordinate through the oxygen, to afford [Pt(C∧P){OC(=CHPPh_3)R}$_2$]ClO_4[19].

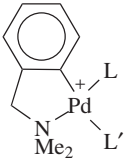

(**10**) (**a**) L = PPh_3, py; L′ = thf
(**b**) L = L′ = MeCN

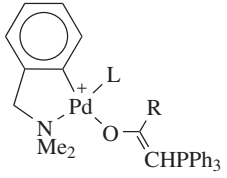

(**11**) (**a**) L = PPh_3, R = Me, Ph, OMe
(**b**) L = py, R = Me
(**c**) L = MeCN, R = Me, Ph

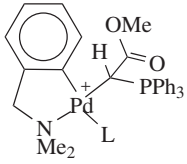

(**12**) (**a**) L = py, MeCN
(**b**) L = MeCN, R = Me, Ph

The ylide $Ph_3PCHC(O)CH_2CO_2Et$ reacts with *cis*-$[M(C{\sim}E)(thf)_2]^+$ (M = Pd, C∼E = $C_6H_4CH_2NMe_2$-2, $CH_2C_6H_4P(tol)_2$-2; M = Pt, *C*∼E = $CH_2C_6H_4P(tol)_2$-2) to afford *cis*-$[M(C{\sim}E)(O,O^2\text{-}OC(=CHC(O)OEt)CH_2PPh_3)_2]^+$, in which the enolato ligand has undergone a proton migration[20]. The same ligand reacts with [AuCl(tetrahydrothiophene)] or $[Au(OCMe_2)(PPh_3)]^+$ to give complexes with the C-bonded ylide [AuCl{$CH(PPh_3)C(O)CH_2CO_2Et$}] or [Au{$CH(PPh_3)C(O)CH_2CO_2Et$}PPh_3]$^+$, respectively[20]. This is not unexpected since no enolato Au(I) complex is known. In fact, all Au(I) complexes with carbonyl-stabilized phosphorus ylide ligands are *C*-bonded[11,21,22].

The ylide $Ph_3PC\{C(O)Me\}C(O)Ph$ reacts with HgX_2 to afford monomeric **13** or dimeric **14**, depending on the halide[23].

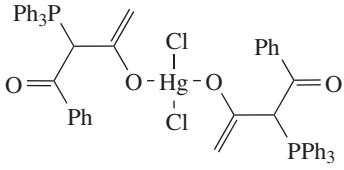

(**13**)

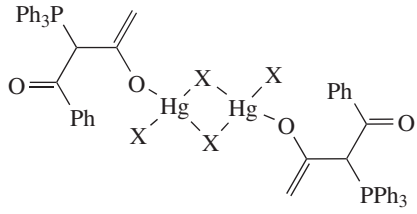

(**14**) X = Br, I

Early transition elements coordinate carbonyl-stabilized ylides through the oxygen atom because they are harder (more oxophilic) than Pd(II) and Pt(II). Thus, the reaction of $[Ti(NMe_2)_4]$ with two equivalents of $[Ph_3PCH_2C(O)Ph]Br$ gives the complex $[TiBr_2(NMe_2)_2\{OC(=CHPPh_3)Ph\}]$[24]. $[NbCl_3(dme)(\eta^2\text{-}PhC{\equiv}CSiMe_3)]$ reacts with ylides $Ph_3PCHC(O)R$ to give $[NbCl_2(\mu\text{-}Cl)(\eta^2\text{-}PhC{\equiv}CSiMe_3)\{OC(=CHPPh_3)R\}]_2$ (R = Me, Ph)[24] or $[NbCl_3\{O,N\text{-}OC(R){=}CHPPh_3\}(\eta^2\text{-}PhC{\equiv}CSiMe_3)]$ (R = 2-thiazolyl)[25]. $Ph_3PCHC(O)R$ reacts with MCl_4 in thf to give $[MCl_4\{OC(=CHPPh_3)R\}(thf)]$ (R = Me, Ph; M = Ti, Zr, Hf)[26].

One of the products of the reaction of $Ph_3PCHCHO$ with $[Os_3(CO)_{10}(NCMe)_2]$, **15**, is the result of a C–H oxidative addition reaction. Complex **15** decomposes at room temperature, under daylight, to give a mixture of isomers of complex **16**, one of which has been studied by X-ray diffraction[27]. Similarly, the Ru complex analogous to **16** has been prepared by reacting $[Ru_3(CO)_{12}]$ with the same ylide or with $Ph_3P{=}CH_2$[28].

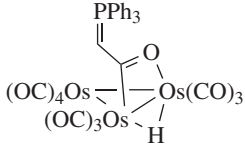

(**15**)

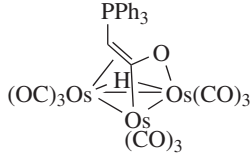

(**16**)

The cobalt perfluoro phthalocyanide complex **17** reacts with PPh_3 in the presence of atmospheric oxygen to give **18**. Therefore, PPh_3 couples with acetone according to equation 1[29].

$$PPh_3 + MeC(O)Me + {}^1/_2\ O_2 \longrightarrow Ph_3PCHC(O)Me + H_2O \qquad (1)$$

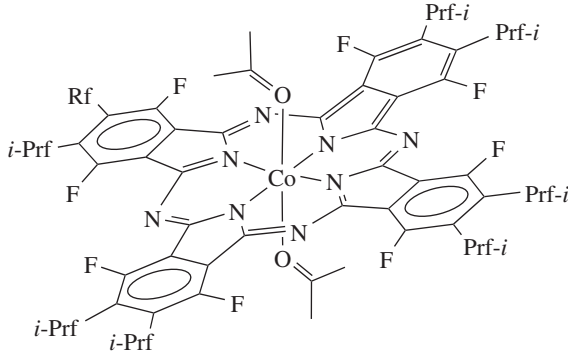

(**17**)

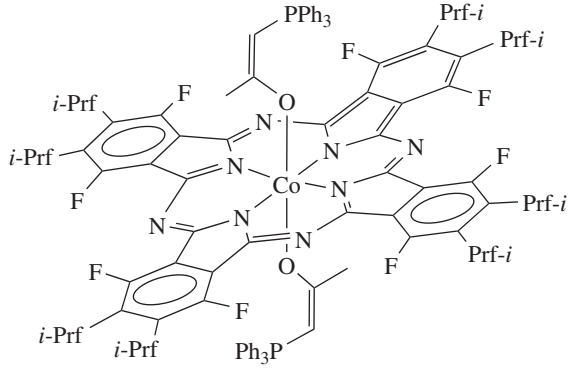

(**18**)

C. 2-Oxoalkyl to Enolato Rearrangements and Equilibria

In a few cases a 2-oxoalkyl ligand transforms into an enolato ligand upon thermal treatment, irradiation or ligand addition. Thus, ultraviolet irradiation of complexes **19** results in the loss of CO to afford **20** (M = W, R = H, R′ = Me, Ph, OEt, NEt_2; M = W, R = Me, R′ = OEt; M = Mo, R = H, R′ = Me, OEt)[30]. Reaction of **21** with excess of PMe_3 affords complex **22**[31].

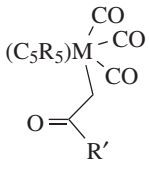

(**19**)

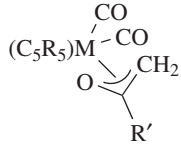

(**20**)

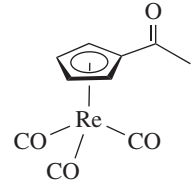

(**21**)

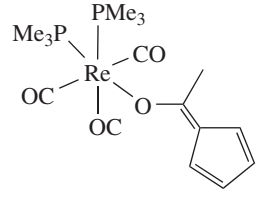

(**22**)

Complex **23a** (L = PMe_3) reacts with $KOC(=CH_2)Me$ to afford a 70:30 mixture of **24a** and **25a** which, upon thermolysis, leads to methane and a mixture of **26** and the product of phosphine dissociation **27**[32,33]. **23a** and $KOC(=CH_2)CH_2Bu\text{-}t$ also provide an equilibrium mixture of enolato and 2-oxoalkyl complexes **24b** and **25b**[33], which has also been observed between complexes *trans*-$[Rh\{OC(=CHR'')R'\}(CO)(PR_3)_2]$ (R = R′ = Ph, R″ = H and R = R″ = Me, R′ = *t*-Bu) and their 2-oxoalkyl isomers[34]. Complex **28**, containing a dianionic enolato ligand, reacts with $AcCH_2Bu\text{-}t$ at 110 °C to afford the β-diketonato complex **29**[33,35], which can also be obtained by reacting **23b** with two equivalents of $KOC(=CH_2)CH_2Bu\text{-}t$[35].

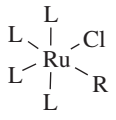

(**23**) (**a**) R = Me
(**b**) R = OAc

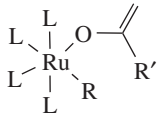

(**24**) (**a**) R = R′ = Me
(**b**) R = Me, R′ = $CH_2Bu\text{-}t$

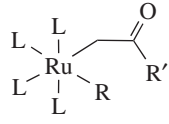

(**25**) (**a**) R = R′ = Me
(**b**) R = Me, R′ = $CH_2Bu\text{-}t$

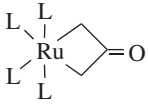

(**26**)

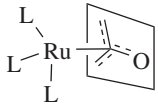

(**27**)

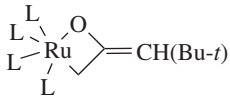

(**28**)

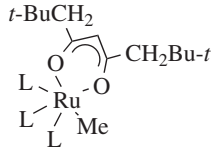

(**29**)

D. Enolato to 2-Oxoalkyl Isomerization

Complex **30** isomerizes in solution to the corresponding 2-oxoalkyl complex **31**[36]. This isomerization is catalyzed by LiCl. The η^3-enolato complex **32**, detected in solution, reacts with PPh_3 to afford complex **33**[30].

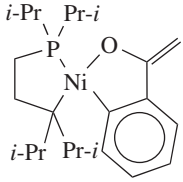

(**30**)

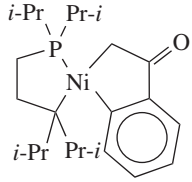

(**31**)

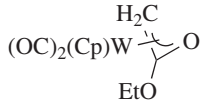

(**32**)

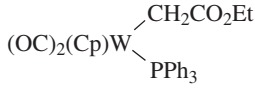

(**33**)

O,*O*-β-diketonato complexes react with strong nucleophiles L (phosphines[37], carbenes[38], phen[39], py[40,41] and other nitrogen donor ligands[42–44]) to give *C*-β-diketonato derivatives (**34**).

There are many complexes containing a *C*,*O*,*O*-β-diketonato ligand. The best known example is **35**, which can be prepared by reacting $PtMe_3X$ with M(acac) (M/X = H/$^1/_2$ SO_4[45], Na/$^1/_2SO_4$[46], Tl/I[47]). Replacement of a ligand in a β-diketonato complex by a weakly bonded ligand usually affords a di- or polynuclear complex containing bridging

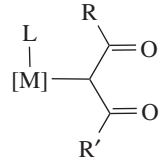

(**34**)

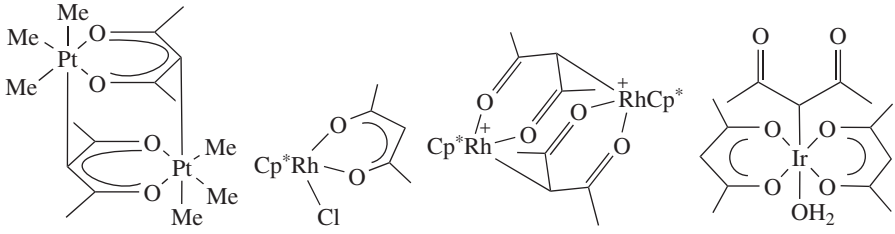

(**35**) (**36**) (**37**) (**38**)

C,*O*,*O*-β-diketonato ligands. Thus, complex **36** reacts with $AgBF_4$ to give **37**[48]. [MR_2] (M = Zn, Hg, R = Me, Et, $PhCH_2CH_2$) transfers the R group to **38** affording the dinuclear complex **39**[49]. Similarly, the Ru(II) complex [$Ru(acac)_2(NCMe)_2$] reacts with thiouracils **40**, in the presence of NEt_3, to give **41**[50].

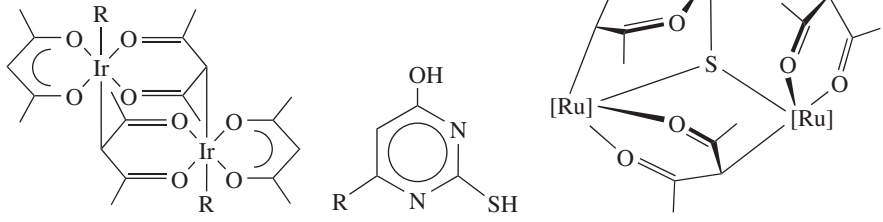

(**39**) (**40**) R = H, Me (**41**) [Ru] = Ru(acac)

The reaction of [Rh(acac)(η^2-CH_2=CH_2)$_2$] with tetraarylcyclopentadienones affords dinuclear complexes **42**[51].

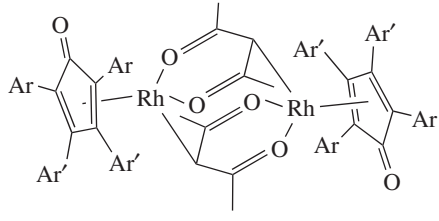

(**42**) Ar = Ar′ = Ph; Ar = $C_6H_3R_2$-3,5, R = H, Me, Ar′ = 2-Naph

$[PdPhf_2(acac)]^-$ reacts with $AgClO_4$ or $[Au(OClO_3)(PPh_3)]$ to afford **43**[52] or **44**[53], respectively. $[MPhf_2(\mu\text{-}PPh_2)_2M'(acac)]^-$ reacts with $AgClO_4$ to give hexanuclear complexes containing two trinuclear metal clusters **45**[54].

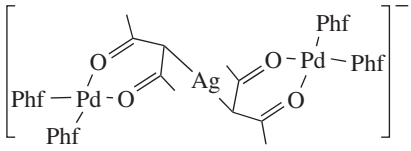

(**43**)

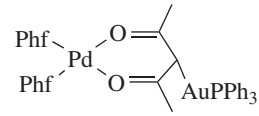

(**44**)

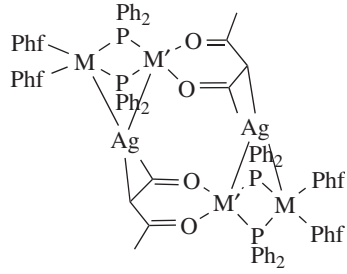

(**45**) M/M′ = Pt/Pt, Pt/Pd, Pd/Pd

Other reported examples of dinuclear complexes containing μ-*C*,*O*,*O*-β-diketonato ligands are $[Ru(\eta^5\text{-}Cp^*)(\mu\text{-}C,O,O\text{-acac})]_2$[55] and $[Ru(\eta^6\text{-}C_6Me_6)(\mu\text{-}C,O,O\text{-acac})]_2{}^{2+}$[56].

III. REACTIONS OF ENOLATO COMPLEXES TO GIVE OTHER ENOLATO COMPLEXES

A. Complexes with κ^1-*O*-Diketonato Ligands

Reaction of *O*,*O*-diketonato complexes with strong nucleophiles can replace one coordinated oxygen to give a complex with a κ^1-*O*-diketonato ligand. Thus, addition of P(*c*-Hex)$_3$ to an acetone solution of tropolonato (tropo) complex **46** gives **47**[57]. Similarly, Ag(tropo) reacts with P(Bu-*n*)$_3$ to give $[Ag(O\text{-tropo})P(Bu\text{-}n)_3]$[58].

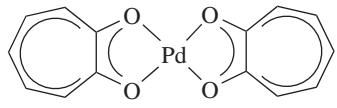

(**46**)

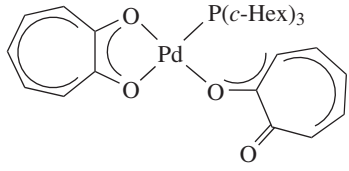

(**47**)

$[Zn(acac)_2(OH_2)]$ reacts with Hpko (di-2-pyridyl ketone oxime) and NH_4PF_6 to afford $NH_4[Zn_5(O\text{-acac})_2(pko)_6](PF_6)_3$[59] and $[GaMe_2(F_6acac)]$ reacts with py to give $[GaMe_2(O\text{-}F_6acac)(py)]$[60].

$[Pd(acac)_2]$ reacts with 1.1 equivalents of PEt_3 to give $[Pd(acac)\{C\text{-}CHAc_2\}(PEt_3)]$ whereas $[Pt(acac)_2]$ renders $[Pt(acac)(\kappa^1\text{-}O\text{-}acac)(PEt_3)]$[61]. The latter reacts with two equivalents of PEt_3 to give *trans*-$[Pt(\kappa^1\text{-}O\text{-}acac)_2(PEt_3)_2]$[62]. However, several $[M(\beta\text{-}dik)(O\text{-}F_3acac)(PR_3)]$ (M = Pd, Pt, β-dik = acac, F_3acac, R = Et, Ph, *c*-Hex) have been obtained by reacting $[M(\beta\text{-}dik)(F_3acac)]$ with phosphines[61,63]. The variety in the coordination modes of β-diketonato ligands has been reviewed[64].

Tetrakis(2-pyridyl)methane, $C(Pyr)_4$, reacts with $[Cu(F_6acac)_2]$ to give a mixture of $[Cu(F_6acac)(N,N,N\text{-}C(Pyr)_4)][Cu(F_6acac)_3]$ and $[Cu(F_6acac)(O\text{-}F_6acac)(N,N\text{-}C(Pyr)_4)]$[65]. The reaction of $[Cu(F_6acac)_2]$ with four equivalents of 3-methyl-1*H*-pyrazole (Hmpz) (1:4 molar ratio) gives the octahedral *trans*-$[Cu(O\text{-}F_6acac)_2(Hmpz)_4]$[66]. The complex **48** has been isolated by reacting equimolar amounts of the diprotonated imino ligand and $[Cu(O\text{-}F_6acac)_2(OH_2)_2]$[67].

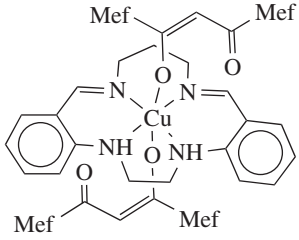

(**48**)

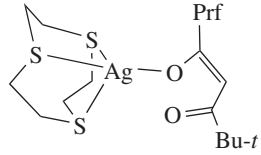

(**49**)

Complex **49** is obtained by reacting $[Ag_2\{O,O\text{-}OC(t\text{-}Bu)CHC(O)Prf\}_2(OH_2)]$ with the thioether macrocycle [9]aneS_3. The strong preference of this ligand to impose threefold S-donor coordination and the resultant large steric demand of this macrocyclic ligand favors the monodentate coordination of the β-diketonato ligand[68]. On the other hand, in the related complex $[Cu\{O,O\text{-}OC(t\text{-}Bu)CHC(O)Prf\}(PMe_3)]$, prepared by the reaction of $Na(OC(t\text{-}Bu)CHC(O)Prf)$ with CuCl in the presence of the appropriate amount of PMe_3, the β-diketonato ligand adopts the usual chelating coordination[69].

The addition of $P(i\text{-}Pr)_3$ to $[Rh(acac)(CO)_2]$ or PPh_3 to $[Pd(F_6acac)_2]$ gives *trans*-$[Rh(O\text{-}acac)(CO)\{P(i\text{-}Pr)_3\}_2]$[70] or $[Pd(F_6acac)(O\text{-}F_6acac)(PPh_3)]$, respectively[71].

B. Synthesis of Homodinuclear, Heterodinuclear and Polynuclear β-Diketonato Complexes

For metal ions M^{q+} that usually have coordination numbers toward oxygen greater than $2q$, the neutral $[M(\beta\text{-}dik)_q]$ complexes are coordinatively unsaturated and, in order to complete the coordination sphere, they can coordinate additional ligands (water, ammonia, py, ... (L) or an additional β-diketonato ligand to give, respectively, $[M(\beta\text{-}dik)_qL_2]$ or $[M(\beta\text{-}dik)_{q+1}]^-$[72]), or oligomerize through bridging β-diketonato ligands. This is the reason why most syntheses of β-diketonato complexes in water give hydrated species; for example, complexes of Co(II) and Ni(II) are usually obtained as the dihydrates **50**. Removal of H_2O from this adduct leaves the anhydrous complex **51** that meets its usual coordination numbers 5 or 6 by self-association[73]. Complex $(Ph_3PNPPh_3)[\{Mg(acac)(\mu\text{-}acac)\}_2(\mu\text{-}O,O\text{-}AcO)]$ contains terminal and bridging acac ligands[74].

The Lewis acidity of the β-diketonato complexes is affected by the nature of the substituents, being the strongest for fluoro derivatives. Thus, $[Cu(acac)(F_6acac)]$ and $[Cu(F_3acac)(F_6acac)]$ readily form complexes $[Cu(\beta\text{-}dik)(\beta\text{-}dik)'L_2]$ where L_2 = phen bipy or TMEDA, whereas $[Cu(acac)(F_3acac)]$ gives only the corresponding complexes

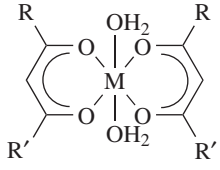

(**50**)

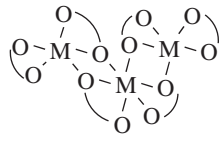

(**51**)

$[Cu(F_3acac)_2(L_2)]$[75]. The acidic character of $[La(F_6acac)_3(H_2O)]$ favors its reaction with $[Cu(acac)_2]$ to give the heterodinuclear adduct $[La(F_6acac)_3(\mu\text{-}OH_2)(\mu\text{-}acac)_2Cu]$ in which La reaches the coordination number nine by forming two additional La–O bonds with the acac ligands[76]. A similar adduct forms both in solution and in the solid state when equimolar amounts of the lantanide shift reagent $[Eu(fod)_3]$ (fod = *t*-BuC(O)CHC(O)Prf) reacts with $[Co(acac)_3]$[77]. Trinuclear complexes $[\{Bi(\mu\text{-}F_6acac)_3\}_2\{[M(F_6acac)_2]\}]$ form by reacting $[Bi(F_6acac)_3]$ with $[M(F_6acac)_2]$ (M = Cu, Zn) or with $[M(F_6acac)_2(OH_2)_2]$ (M = Co, Ni, Cu) or in the solid state with M = Mn, Fe, Co, Ni, Cu, Zn in a 2:1 molar ratio[78]. Grignard compounds react in thf with $[Co(acac)_3]$ or $[M(acac)_2]$ (M = Fe, Ni) affording $[\{Mg(\mu\text{-}acac)_2(thf)_2\}(MX_2)]$ (X = Cl, Br)[79]. Slow evaporation of a nitromethane solution containing $[Pt(acac)_2]$ and [Ag(OTf)] in a 1:2 molar ratio affords the 2-D sheet complex containing a $[Ag_2(\mu_3\text{-}OTf)_4]^{2-}$ central unit bridging two $[Ag(H_2O)]^+$ groups, through four triflato oxygens, and each one is additionally coordinated to two oxygens of $[Pt(acac)_2]$[80].

C. Electrophilic and Nucleophilic Substitution Reactions

In 1945 Calvin postulated that the six-membered ring formed by a metal center and the acac ligand has, as an important resonance form, a fully conjugated six-membered ring analogous to benzene, pyridine or the pyrylium salts[81]. In fact, many acetylacetonato complexes have remarkable stabilities and show various properties similar to aromatic compounds. However, Cotton showed later that the NMR spectra of diamagnetic acetylacetonate complexes do not support the claim of a benzenoid resonance in the chelate rings[82]. An excellent article by Collman reviewed this chemistry[83]. In the past decade, there has been renewed interest in the concept of metalloaromaticity due to the advances in the synthesis, theory and recognition of its relevance in reaction mechanisms[84].

From a synthetic point of view, the above studies have stimulated the synthesis of new types of β-diketonato complexes. Thus, reactions at position 4 of the 1-metalla-2,6-dioxacyclohexane rings, usually denominated the γ-position[85] (equation 2), such as halogenation[48,86,87], thiocyanogenation, chlorosulfenylation[86,88], arylsulfenylation, acylation[88], nitration, formylation[89], chloromethylation and dimethylaminomethylation (equation 2)[90] have been performed as well as Suzuki coupling reactions (equation 3)[91], or an aldol reaction with *p*-nitrobenzaldehyde under Lewis acidic conditions (equation 4)[92].

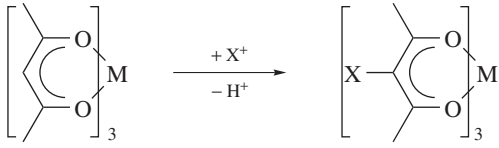

(2)

X = I, Br, Cl, SCN, SAr, SCl, NO_2, CH_2Cl, CH_2NMe_2, C(O)R, CHO

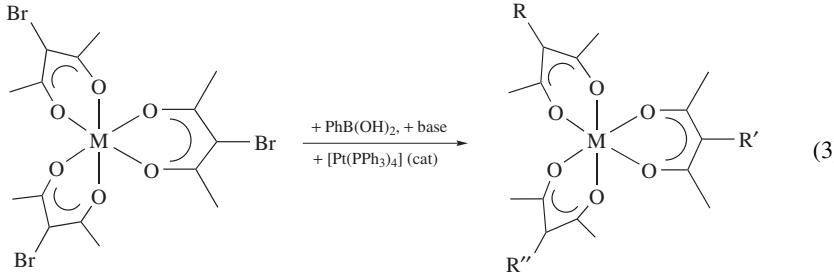

(3)

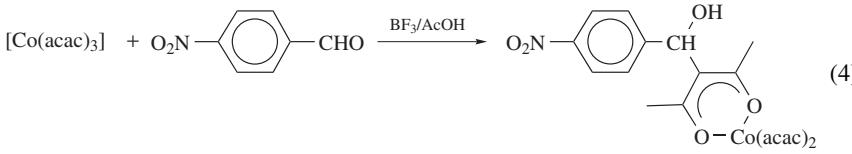

(4)

These studies have been almost restricted to relatively inert tris-acetylacetonato complexes of Cr(III), Co(III) and Rh(III) allowing the synthesis of a variety of mixed substituted β-diketonato complexes in various steps, using limited amounts of electrophilic reagents (e.g. *N*-halogenosuccinimide), as shown, for example, in equation 5[93]. The X and Y substituent groups in these metal acetylacetonates are sometimes very resistant to nucleophilic displacement[86]. Thus, all attempts to prepare Grignard or lithium reagents from halogenated chelates or oxime, hydrazone and semicarbazone derivatives of formyl aldehyde substituted chelates failed, and the starting complexes were recovered. However, catalytic hydrogenation of nitro compound **52a** affords the amino derivative **52b** which autoxidizes readily and should be handled under nitrogen. The amino group behaves like a typical aromatic amine: it is reversibly protonated and can be acetylated and readily converted into a stable diazonium salt **53** which undergoes reduction with ethanol, coupling with β-naphthol, and solvolysis in water or methanol to give **52c**[94]. Mono-9-anthrylmethyl- and -9-anthroyl-substituted β-diketonato derivatives of Rh(III) and Ir(III), with interesting chemical and photophysical properties, have been prepared by alkylation or acylation of the corresponding tris-acetylacetonates under Friedel–Crafts conditions[95].

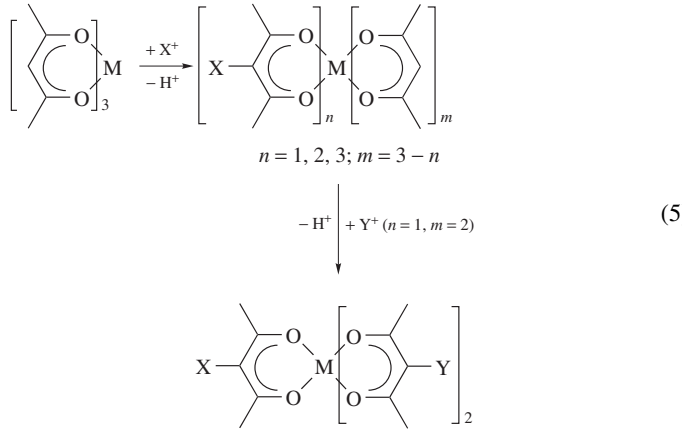

(5)

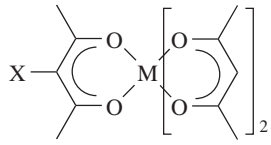

(**52**) (**a**) X = NO_2
(**b**) X = NH_2
(**c**) X = OH

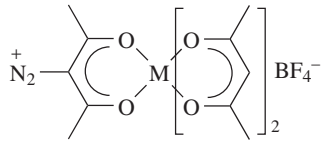

(**53**)

A palladium-catalyzed copolymerization of the iridium complex **54** (R = C_8H_{17}), containing a dibromo-functionalized acac ligand, with **55** affords phosphorescent copolymers of stoichiometry **56**[96].

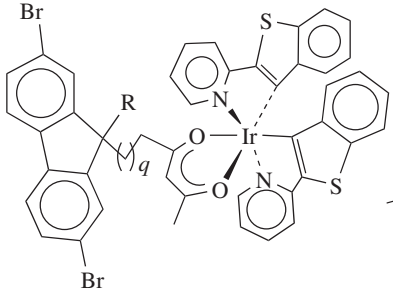

(**54**)

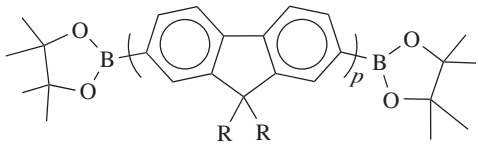

(**55**)

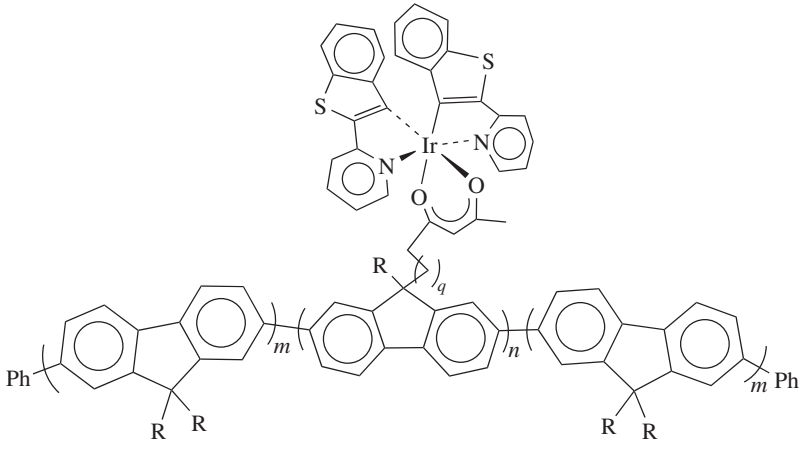

(**56**)

Complex **57** reacts with nucleophiles X^- to afford **58**[97]. A similar reaction occurs between $AlMe_3$ and two equivalents of [$AlMe_2$(acac)] giving the trinuclear complex [($AlMe_2$)$_2$(MeAl){μ_3-*O*,*O*-OC(=CHCMe_2CO)Me}$_2$], the result of the carbonyl methylation of two acac ligands by one $AlMe_3$ molecule[98]. Dimanganese macrocyclic complex

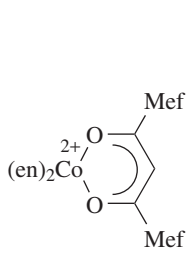

(**57**)

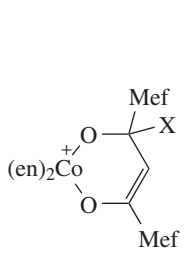

(**58**) X = OH, OMe

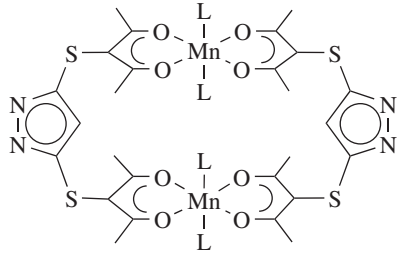

(**59**) L = Me_2SO, Me_2NCHO

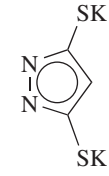

(**60**)

59 can be obtained by aerobic assembly reaction of $MnCl_2$, **60** and acetylacetone. These and similar Ni(II) and Fe(II) dinuclear complexes have a host cavity sufficiently large to trap solvent molecules or a sulfate anion[99].

Ketiminato complexes **61** can be obtained by reacting β-diketonato complexes with nitriles, involving elimination of an acetyl group. Thus, addition of BF_3•$2MeCO_2H$ to a mixture of [$Co(acac)_3$] and RCN leads to **61** ([M] = $Co(acac)_2$) via intermediate **62**, which is isolated in low yield. When R = CO_2Et an intermediate in the synthesis of **62**, complex **63**, has also been obtained (2% yield)[100]. Similarly, nitriles RCN react with [$M(acac)_2$] to give ketiminato complexes **64**, with no acetyl group elimination[101]. *trans*-[$PtCl_2(NCPh)_2$] reacts with two equivalents of [Tl(acac)] to afford a mixture of **65** and **66**[102]. Analogous complexes are obtained using *cis*-[$PtCl_2(NCPh)_2$] or [Tl(benzoylacetonato)].

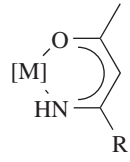

(**61**)

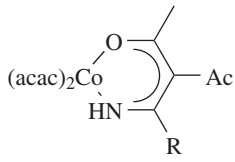

(**62**) R = Me, Et, CH_2OEt, Bn, CH_2CO_2Et, C(CN)=CHOEt, C(CN)=C(Et)OEt, $C(CO_2Et)$=CHOEt

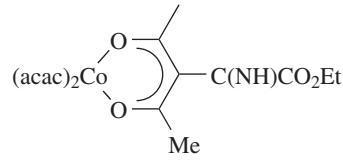

(**63**)

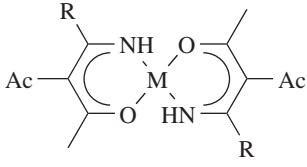

(**64**) M = Ni, Cu, R = CN; M = Ni, R = PhC(O)

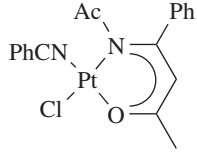

(**65**)

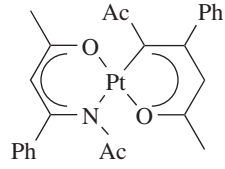

(**66**)

Similarly, nitrilo ligands are attacked by enolato anions. So, reaction of [$Ru(acac)_2(NCR)_2$] with various ketones R′C(O)CH_2R″ gives rise to β-ketiminato complexes **67**[103]. However, it is not clear which reagents are responsible for the deprotonation and oxidation that takes place in this process. The reaction between [$Zn(Tp^{Ph,Me})(CH_2CN)$] and acetone to give **68** could occur through the enolato complex **69**[104].

Nucleophilic attack of an enolato or a 2-oxoalkyl ligand to the carbon atom of a cyano group can also give ketiminato complexes. In fact, **70** reacts with AgTfO and RCN to

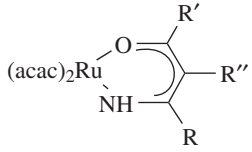

(**67**) R = Me, Ph, R′ = Me, Et, R″ = H, Cl, Ac

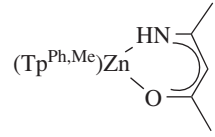

(**68**)

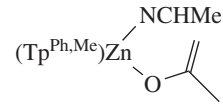

(**69**)

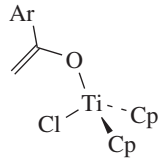

(**70**) Ar = C_6H_4OMe-2, $C_6H_2Me_3$-2,4,6

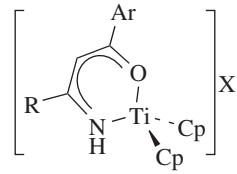

(**71**) R = Me, Ph, X = TfO

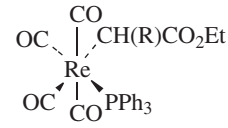

(**72**) R = H, Me

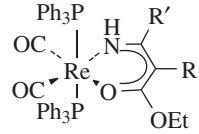

(**73**) R = H, R′ = Me, Et, Pr-*i*, Ph; R = Me, R′ = Et

give **71**[105]. When Re complexes **72** and an excess of PPh_3 are heated at *ca* 110 °C in nitrile solvents (R′CN), ketiminato complexes **73** are obtained[106].

D. Condensation Reactions. Synthesis of Ketohydrazonato Complexes

The reaction of acylhydrazines with β-diketonato complexes allows one to prepare *O*,*N*,*O*-enolato complexes containing the condensed hydrazones. Thus, [VO{OC(R)CHC(R′)O}$_2$] reacts with $ArC(O)NHNH_2$ in EtOH to give **74**[107]. However, V(III) complex [V(acac)$_3$] reacts with $H_2NNHC(O)C_6H_4OH$-2 in EtOH to afford V(V) complex [VO{*O*,*N*,*O*-OC(Me)CHC(Me)NNC(C_6H_4OH-2)O}(OEt)] as a result of condensation, deprotonation of the NH group and air oxidation[108]. If the reaction is carried out with a limited amount of oxygen, the V(IV) complex [V{*O*,*N*,*O*-OC(Me)CHC(Me)NNC(C_6H_4OH-2)O}$_2$] can be isolated[109]. The analogous complex derived from phenylhydrazine is obtained from [VO(acac)$_2$]. Both V(IV) complexes have a trigonal prismatic structure[110].

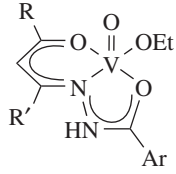

(**74**)

E. Miscellaneous Reactions

Complex **75** reacts with SO_2Cl_2 to afford the ketoiminoenolato Sn(IV) complex **76**[111].

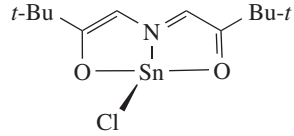

(**75**)

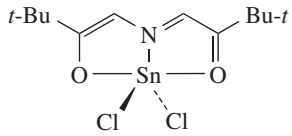

(**76**)

Complexes **77** (see **270** in Chapter 5[1]) add a molecule of dpk to afford **78**[112].

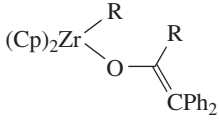

(**77**) R = Me, Bn, Ph

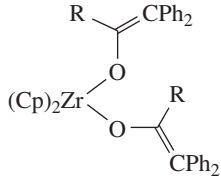

(**78**) R = Me, Bn, Ph

Hydrogenation of ketenido complexes **79** (Section IV.D in Chapter 5[1]) affords **80**, which in turn reacts with MeI to give [Zr(η^5-Cp*)$_2$(I){*Z*-OCH=CHBu-*t*}]. This complex isomerizes to [Zr(η^5-Cp*)$_2$I(*E*-OCH=CHBu-*t*)] after heating[113].

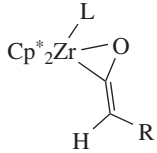

(**79**) R = *t*-Bu, L = CO, CH_2PMe_3; R = H, L = py

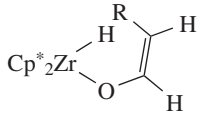

(**80**) R = *t*-Bu, H

The Na salt of **81**[113, 114] reacts with [MCl(Me)L$_2$] to give **82**[114]. Similarly, deprotonation of [Cr{η^6-ArC(O)Me}(CO)$_3$] (Ar = Ph, 2-Tol, 2,4-Xyl, Mes) with LDA in thf, followed by reaction with [M]X ([M] = Ti(η^5-Cp)$_2$Cl, Zr(η^5-Cp)$_2$Cl, X = Cl; [M] = $SiMe_3$, X = Cl, OTf), affords the dimetallic enolates [Cr{η^6-ArC(=CH_2)O[M]}(CO)$_3$][115].

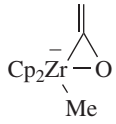

(**81**)

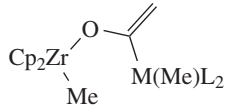

(**82**) M = Zr, L = η^5-Cp; M = Pt, L = PMe_3

83 inserts ethylene to afford **84**. This metalacycle reacts with CO to afford **85** after CO insertion and C–P coupling[116].

Complex **86** reacts with CO to give $Ru_3(CO)_{12}$ and the dinuclear complex **87** containing the dianion resulting from the double deprotonation of an acetone molecule[117].

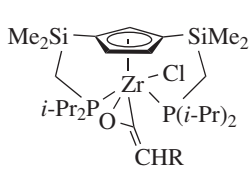

(**83**) R = Ph, $SiMe_3$

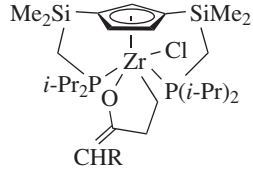

(**84**) R = Ph, $SiMe_3$

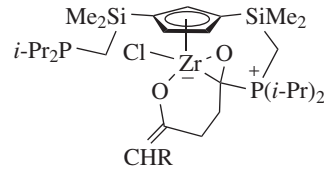

(**85**) R = Ph, $SiMe_3$

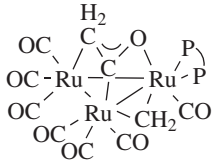

(**86**) P⌒P = dppm

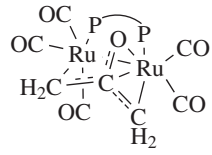

(**87**) P⌒P = dppm

The Os(IV) enolato complex **88**•PF_6 is converted in solution into the metalafuran **89**•PF_6 by a intramolecular C–H oxidative addition reaction[118].

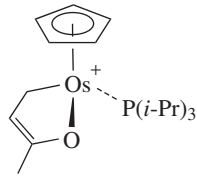

(**88**)

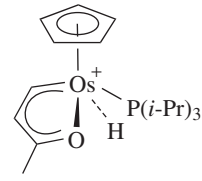

(**89**)

[$IrClL_3$] reacts with **90** to afford **91** (Scheme 1; L = PMe_3, R = H, R′ = Me), which is stable enough to be isolated and characterized. Its homologous complexes with L = PEt_3, R = R′ = H, Me; R = H, R′ = Me, are proposed as intermediates in the synthesis of the corresponding hydridoiridapyrans **92** after an intramolecular C–H oxidative addition reaction (see **228** and **229** in Chapter 5[1]). However, **91** (L = PMe_3, R = H, R′ = Me) slowly undergoes a different C–H oxidative addition to afford **93**. The analogous **93** (L = PEt_3) is obtained by decomposition of the corresponding hydrido complex **92**[119–121]. When **92** (L = PEt_3, R = R′ = Me) reacts with $AgBF_4$, an equimolar mixture of the iridapyrylium complexes **94** and **95** is obtained. Deprotonation of **95** allows one to recover half of **92** which, after solvent extraction, can be reused to prepare new amounts of **94**. Reactions of **94** with neutral or anionic ligands afford new enolato complexes **96** and **97**[122, 123].

Complexes **93** (R′ = Me, L = PMe_3, PEt_3) react with HBF_4•OEt_2 to give the metalafuran **98**•BF_4, which reacts with Br_2 or I_2 to give **99** or **100**, respectively[120].

[$Pt(F_3acac)_2$] reacts with two equivalents of neutral ligands (L = PAr_3, $AsPh_3$, py) to give **101**[124] and [$Pt(acac)_2$] reacts with two equivalents of PPh_3 in hot MeOH to afford **102**[125] containing, respectively, a di- or trianionic β-diketonato ligand. The latter also contains a noncoordinated acac counterion (Section VIII.A.)

The dinuclear complex **103** (L = SEt_2) reacts with the dipotassium salt of 1,1,2,2-tetraacetylethane to give the mononuclear complex **104**[126].

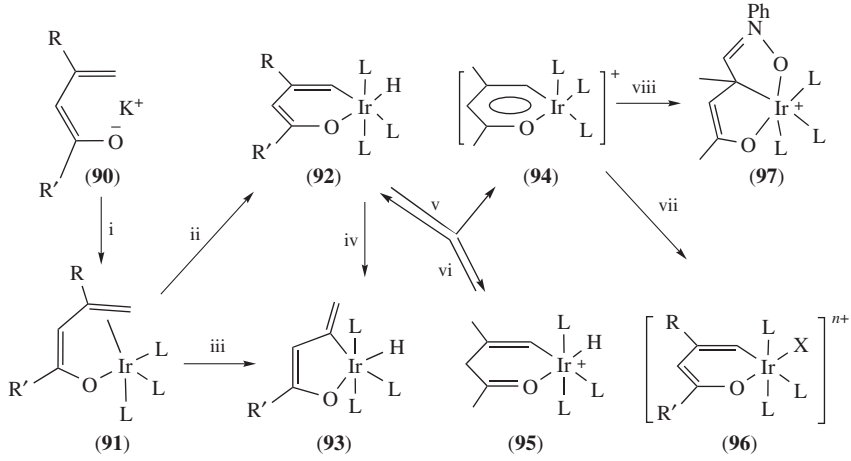

SCHEME 1. Reagents and conditions: (i) $[IrClL_3]$; (ii) 0 °C; (iii) slow decomposition (L = PMe_3, R = H, R′ = Me); (iv) decomposition; (v) $AgBF_4$; (vi) LDA; (vii) X^{n-1} ($n = 0$, L = PEt_3, X = Me, Cl; $n = 1$, L = X = PMe_3); (viii) PhN = O

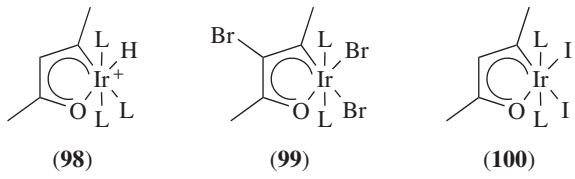

(**98**) (**99**) (**100**)

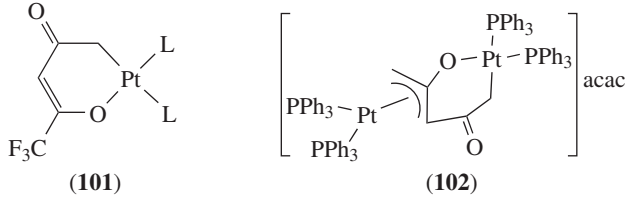

(**101**) (**102**)

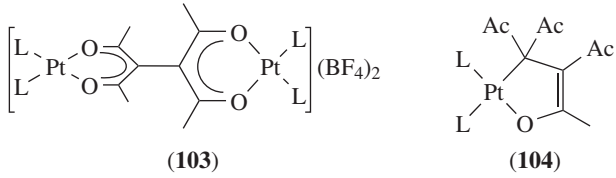

(**103**) (**104**)

IV. ALDOL REACTIONS

In this section are included aldol and aldol-like reactions in which an aldehyde or a ketone adds to an enolato ligand. Most of the products of these reactions are alkoxo complexes **105** (equation 6) that can be viewed as the result of the insertion of the carbonyl compound into the C–[M] bond of the 2-oxoalkyl isomer of the enolato complex. Thus, reaction of

$LiOC(=CH_2)Bu\text{-}t$ with *t*-BuCHO at 0 °C in pentane leads to the tetranuclear aldol product **106**[127]. Complexes **107** and **108** react with benzaldehyde to give the corresponding aldol condensation products **109**[128] and **110**[129], respectively.

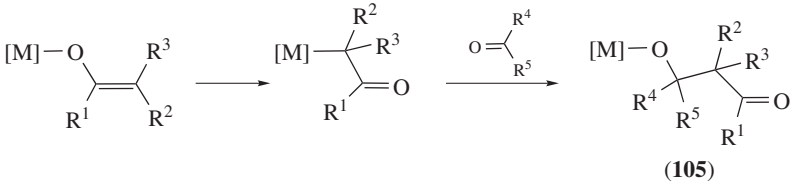

(6)

(**105**)

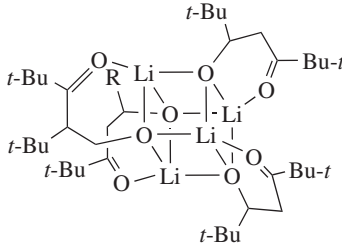

(**106**)

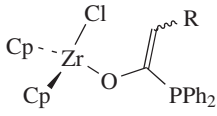

(**107**) R = H, Me

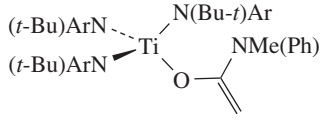

(**108**)

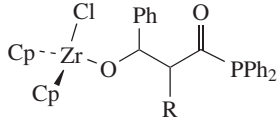

(**109**)

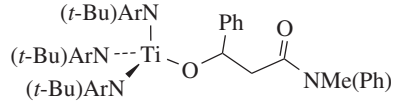

(**110**)

Complex **111** reacts with PhCHO to give the aldolato complex **112**[130] and the heteronuclear complex **113** reacts with AcPh to afford the polymeric complex **114**[131].

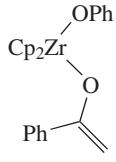

(**111**)

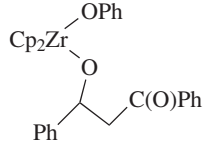

(**112**)

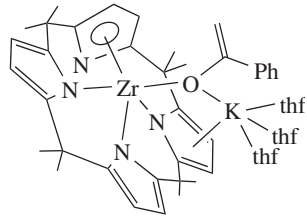

(**113**)

The dinuclear complexes $[M(\eta^5\text{-}Cp)_2Cl\{OC(=CH_2)(\eta^5\text{-}C_5H_4)Fe(\eta^5\text{-}Cp)\}]$ (M = Ti, Zr) react with benzaldehyde to give the corresponding metal aldolato derivatives $[M(\eta^5\text{-}Cp)_2Cl(OCHPhCH_2CO(C_5H_4\text{-}\eta^5)Fe(\eta^5\text{-}Cp)]$[132]. Similarly, the complex *trans*-[Rh{OC(=CHMe)Bu-*t*}(CO)$(PMe_3)_2$] reacts with PhCHO to give *trans*-[Rh{OCH(Ph)CH(Me)C(O)Bu-*t*}(CO)$(PMe_3)_2$][34].

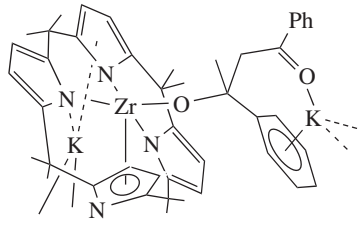

(**114**)

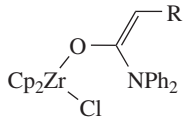

(**115**)

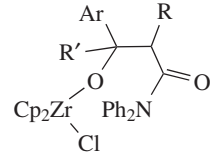

(**116**)

The amine enolato complex **115** (R = H, Me) reacts with variously substituted benzaldehydes or acetophenones (ArC(O)R′, Ar = C_6H_4X-4, X = H, Me, F, Cl, NO_2, R′ = H, Me) to give **116**[133].

Iridapyrylium complex **94** (L = PEt_3) reacts with acetone to afford the [4 + 2] cycloaddition product **117**[123].

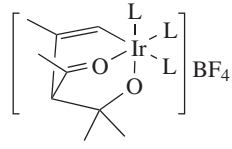

(**117**)

Complex **118a** reacts with traces of water to afford the aldol-like alkoxo-hydroxo derivative **119**[134]. [2 + 4] Cycloaddition of methyl vinyl ketone to **118b–d** affords the corresponding bicyclic complexes **120**[135].

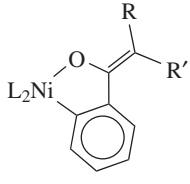

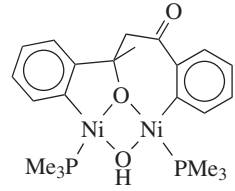

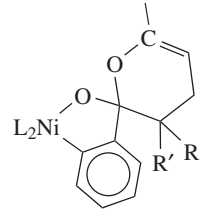

(**118**) (**a**) L = PMe_3, R = R′ = H (**119**) (**120**)
(**b**) L_2 = P^P, R = R′ = Me
(**c**) L_2 = P^P, R = Me, R′ = H
(**d**) L_2 = P^P, R = $CH_2CH_2C(O)Me$, R′ = H
P^P = *i*-$Pr_2PCH_2CH_2P$(*i*-Pr)$_2$

Complex **121** (P∧P = *i*-$Pr_2PCH_2CH_2PPr_2$-*i*) reacts with MeCHO or MeC(O)CH=CHR (R = H, Me) to afford **122**[36] or mixtures of complexes **123**–**126**, respectively[135].

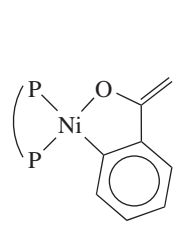

(**121**)

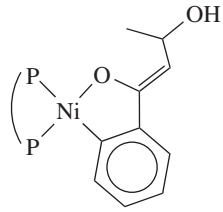

(**122**)

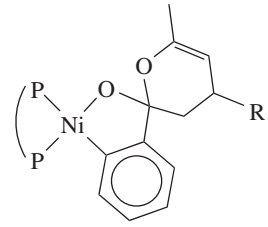

(**123**)

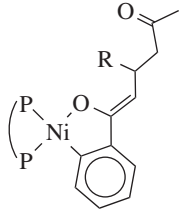

(**124**)

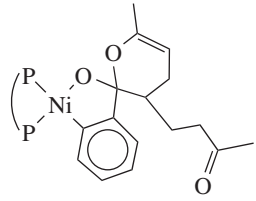

(**125**)

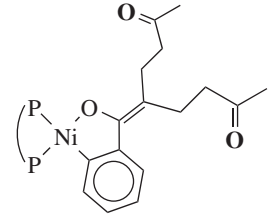

(**126**)

V. PROTONATION REACTIONS

Protonation of enolato complexes can lead to the corresponding ketone derivatives. Thus, **127a** reacts with HBF_4•OEt_2 to give the protonated product **128**[119,121]. Its homologue **127b** is unstable and rapidly rearranges to give **129**. The protonation of **130** with the same acid affords **131**•BF_4[120].

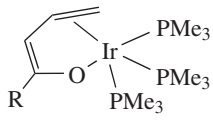

(**127**) (**a**) R = Me
(**b**) R = H

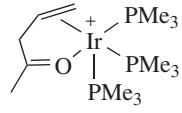

(**128**)

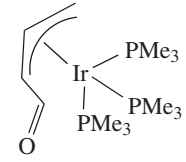

(**129**)

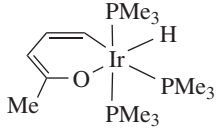

(**130**)

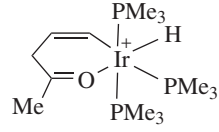

(**131**)

Protic acids HX (e.g. HCl, CF_3CO_2H) add at low temperature to the ethenolato ligand in **132** to afford the alkoxo complexes **133**, which at room temperature decompose to MeCHO and **134a**. The reaction with HBF_4•Et_2O in the presence of different anions X^-

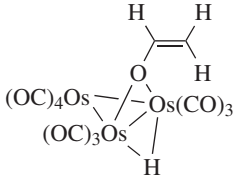

(**132**)

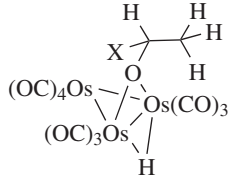

(**133**) X = Cl, AcfO

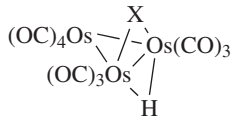

(**134**) (**a**) X = Cl or AcfO
(**b**) X = Cl, Br, I, $EtOCS_2$,Et_2NCS_2
(**c**) X = OMe
(**d**) X = OH

leads to complexes **134b**; when X = OH the reaction in MeOH gives **134c**; when no anion is added, the product reacts with H_2O to give **134d**[136].

Nevertheless, replacement of an enolato ligand by the anion of the acid occurs in most protonation reactions. This makes enolato complexes interesting intermediates in coordination chemistry. Thus, $[VO(acac)_2]$[137] or [Au(III)](acac)[22] complexes have been used to prepare other vanadium or gold complexes. $[VO(acac)_2]$ easily exchanges one or both acetylacetonato groups by organic ligands to give V(IV) complexes that usually are stabilized as $[VO]^{2+}$ derivatives. However, under aerobic conditions, V(V) complexes can be obtained with $[VO]^{3+}$, $[VO_2]^+$ or $[V_2O_3]^{4+}$ cores.

In the Au(III) complex **135** the acac ligand can be replaced by neutral or anionic ligands in several ways: (i) Reaction with ammonium salts containing noncoordinating anions (LH)X, for example, with bibenzimidazolium perchlorate, $(H_3bibim)ClO_4$, to yield the cationic complex **136** and with NH_4ClO_4 or $(Hpy)BF_4$ in the presence of PPh_3 to afford the cationic complexes **137a** or **137b**, respectively; (ii) reaction with diprotic acids, for example, oxalic acid or H_2bibim, to afford the neutral complexes **138** or **139**, respectively, containing the corresponding tetradentate anions as ligands; (iii) reaction with ammonium salts (LH)X containing coordinating anions, for example, NH_4OAc or (Hpy)OAcf, to give the neutral complexes **140a** or **140b**, respectively[138].

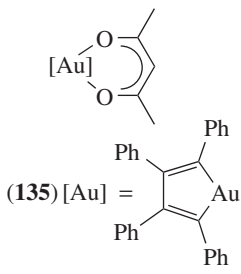

(**135**) [Au] =

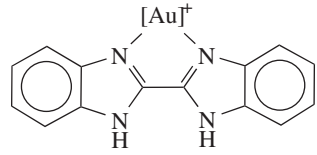

(**136**)

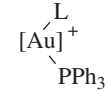

(**137**) (**a**) L = NH_3
(**b**) L = py

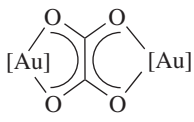

(**138**)

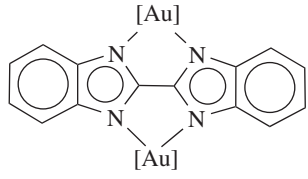

(**139**)

(**140**) (**a**) X = OAc, L = NH_3
(**b**) X = OAcf, L = py

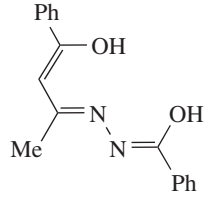

(**141**)

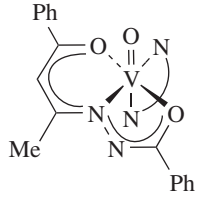

(**142**)

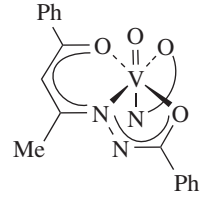

(**143**)

tetrafluorobenzobarrelene) and *O*-, *N*- and *S*-donor ligands containing acidic hydrogen atoms[141]. Likewise, by reacting [$PdPhf_2$(acac)] or [$Pd(C_6X_5)$(acac)(PPh_3)] (X = F, Cl) with LH_2 (LH_2 = H_2bibim, 2,2-biimidazol, tetramethylbiimidazol) dinuclear complexes containing bridging ligands L^{2-} have been obtained[142]. The hexanuclear Au(I)/Pd(II) complex [{(dppm)Au_2(μ-bibim)Pd}$_2$(μ-bibim)]$^{2+}$ has been obtained by reacting [(dppm)Au_2(μ-bibim)Pd(acac)]$^+$ with H_2bibim[143]. Complexes [$AuPhf_2$(acac)], [PdPhf(acac)(PPh_3)] and [$Pd(acac)_2$] react with $(Ph_2P)_3CH$ to give [$AuPhf_2${*P*,*P*-$(Ph_2P)_2C(PPh_2)$}][144], [PdPhf{*P*,*P*-$(PPh_2)_2C(PPh_2)$}(PPh_3)][145] and [Pd{*P*,*P*-$(PPh_2)_2C(PPh_2)$}$_2$][146], respectively. Similarly, [$M(acac)_2$] (M = Pd, Pt) and dppm react to give [M{*P*,*P*-$(PPh_2)_2CH$}$_2$][147].

Oxalic amidines **144** react (i) with two equivalents of [$M(acac)_2$] to give **145**, (ii) with one equivalent each of [Zn(acac)(Et)]$_2$ and [$Ni(acac)_2$] leading to **146** and (iii) with one equivalent of $ZnEt_2$ and two of [$M(acac)_2$] to afford **147**[148].

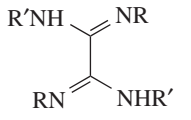

(**144**) R = R′ = Tol, Mes;
R = Mes, R′ = Ph

(**145**) M = Ni, Pd

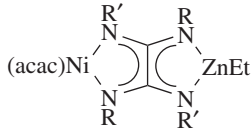

(**146**)

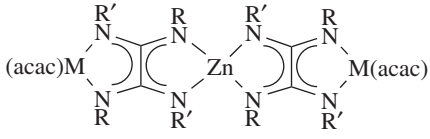

(**147**) M = Ni, Pd

Reactions of **148**, containing a variety of N∧N bridges, with [$M(acac)_4$] in refluxing pyridine give complexes **149**[149].

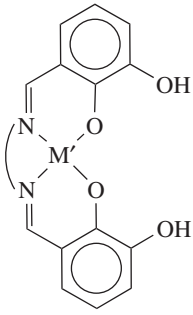

(**148**) M′ = Cu, Zn

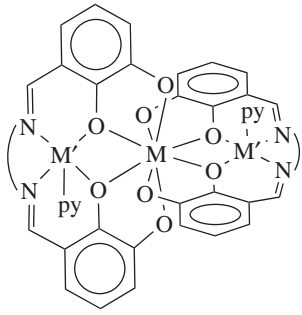

(**149**) M = U, Th, M′ = Cu, Zn

Complex **150** reacts with an excess of $HClO_4$ in H_2O/Me_2CO in the presence of two equivalents of PPh_3 to afford **151**•ClO_4; the strong C/P transphobia[10] favors the coordination of the weak donor acetone instead of PPh_3. In CH_2Cl_2 (Pd:PPh_3 = 1:3 molar ratio), **150** gives a mixture of the C–P coupling product **152**•ClO_4 (probably the coordination of PPh_3 *trans* to C destabilizes the complex) and **153**•ClO_4[150].

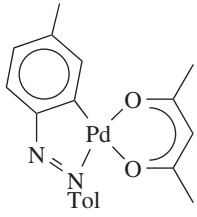

(**150**)

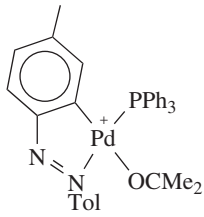

(**151**)

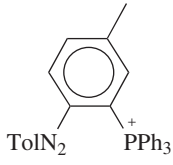

(**152**)

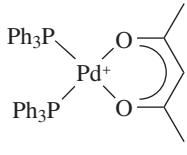

(**153**)

The enolato complex **154** reacts with the nonprotected OH group at the partially methylated glucopyranose **155** to form **156** and acetone[151].

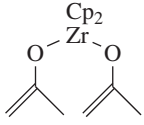

(**154**)

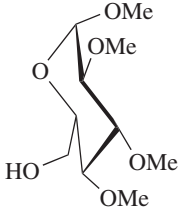

(**155**)

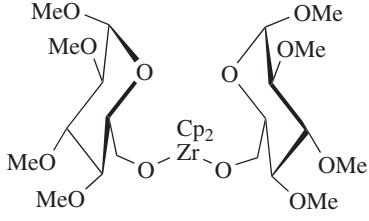

(**156**)

By hydrolyzing $Ln(acac)_3$•$4H_2O$ (Ln = Tb, Eu) with the base 2,2′-dipyridyl sufide, the tetradecanuclear complexes $[Ln_{14}(\mu_4\text{-}OH)_2(\mu_3\text{-}OH)_{16}(\mu\text{-}acac)_8(acac)_{16}$ (Ln = Tb, Eu) have been isolated and the Tb derivative fully characterized[152].

VI. COORDINATION CHEMISTRY OF PHOSPHINOENOLATO COMPLEXES

The coordination chemistry of phosphinoenolato complexes has been reviewed[153]. In certain cases the phosphinoenolate complex acts as a plain phosphine ligand; for example,

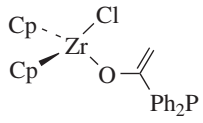

(**157**)

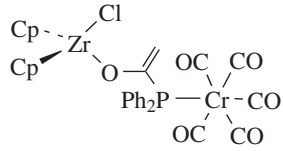

(**158**)

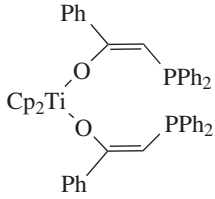

(**159**)

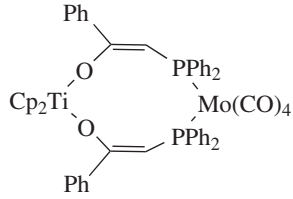

(**160**)

the unidentate metalaligand **157** reacts with $[Cr(CO)_5(thf)]$ leading to **158**[154]. Similarly, the bidentate ligand **159** reacts with $[Mo(CO)_4(nbd)]$ to give **160**[155].

The reaction between the phosphinoenolato complexes **161**, $Me_3SiC{\equiv}CH$ and NH_4PF_6 in methanol gives the corresponding metalafuran complexes **162** through the intermediates **163**[156, 157].

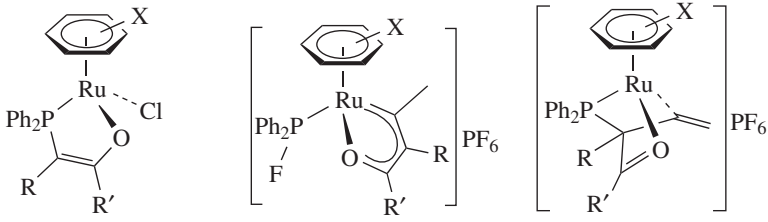

(161) η^6-arene = C_6Me_6, R = H, R′ = *t*-Bu; (**162**) (**163**)
η^6-arene = MesH, R = Me, R′= *t*-Bu, Ph

The reaction of **164** with KOAc or K_2CO_3 in refluxing methanol gives **165** or **166**, respectively[156, 158].

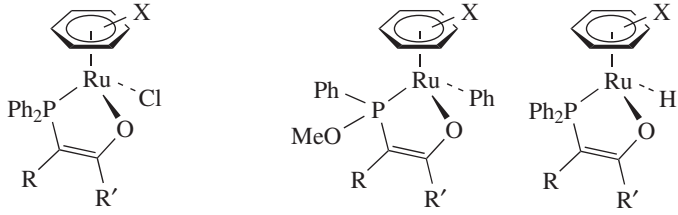

(**164**) η^6-arene = PhH, MesH, C_6Me_6, (**165**) (**166**)
R = H, Me, R′ = *t*-Bu, Ph

Complex **167** reacts with PhNCO to give **168**[159].

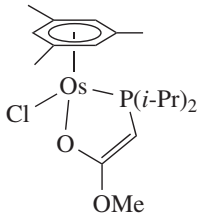

(**167**)

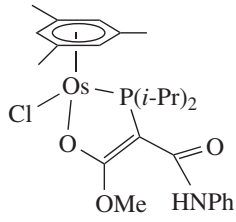

(**168**)

Phosphinoenolato complexes **169a**–**c** (*C*,*N*-cycloPd = Pd(*C*,*N*-$C_6H_4CH_2NMe_2$-2) and related cyclopalladated moieties) react with X=C=O (X = O, PhN) to give complexes **170a**–**c**, respectively, with a new phosphinoenolato ligand. The platinum complex **169d** reacts with PhN=C=O leading to **171**[160,161].

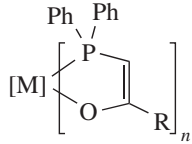

(**169**) (**a**) $n = 1$, [M] = C,*N*-cycloPd, R = OEt
(**b**) $n = 2$, [M] = Ni, R = Ph
(**c**) $n = 1$, [M] = $Rh(PPh_3)_2$, R = Ph
(**d**) $n = 2$, [M] = Pt, R = Ph

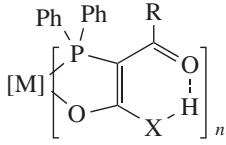

(**170**) (**a**) $n = 1$, [M] = C,*N*-cycloPd, X = O, PhN, R = OEt
(**b**) $n = 2$, [M] = Ni, X = PhN, R = Ph
(**c**) $n = 1$, [M] = $Rh(PPh_3)_2$, X = PhN, R = Ph

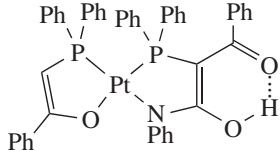

(**171**)

Complex **172** reacts with dpk to give **173**[159].

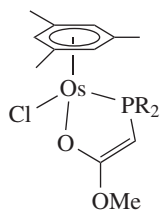

(**172**)

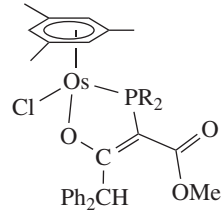

(**173**)

Phosphinoenolato complexes **174a–b** react with Ph_2PCl to afford **175a–b**, respectively, while **176** gives **177**[161]. Complex **174a** or **178** reacts with $PhPCl_2$ in the presence of py to give **179** or **180**, respectively[162].

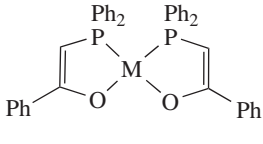

(**174**) (**a**) M = Ni
(**b**) M = Pd, Pt

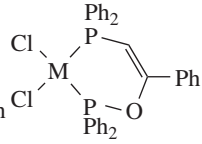

(**175**) (**a**) M = Ni
(**b**) M = Pd, Pt

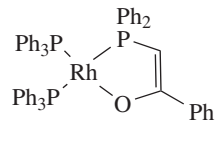

(**176**)

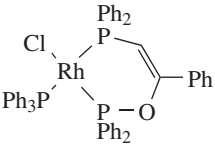

(**177**)

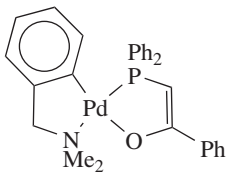

(**178**)

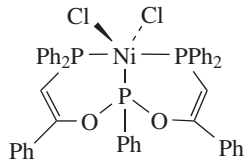

(**179**)

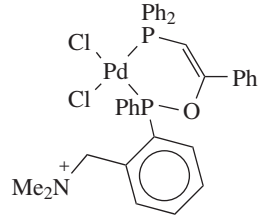

(**180**)

Phosphinoenolato complexes **181** and **181′** react with $MeO_2CC{\equiv}CCO_2Me$ to give **182** and **182′**, respectively[163]. Complexes **183** react with terminal alkynes $R''C{\equiv}CH$ and PF_6^- in methanol to give complexes **184**•PF_6, although when η^6-arene = MesH, C_6Me_6, R = Me, R′ = *t*-Bu and R″ = Me_3Si a different type of product, **185**•PF_6, forms instead[156–158].

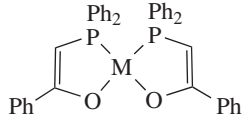

(**181**) M = Ni, Pd

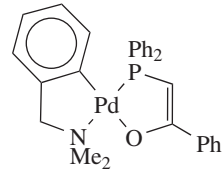

(**181′**)

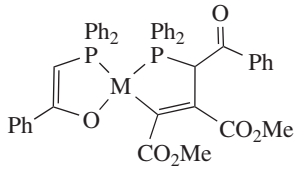

(**182**) M = Ni, Pd

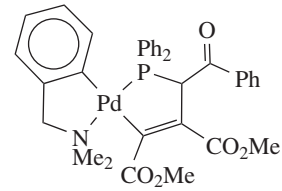

(**182′**)

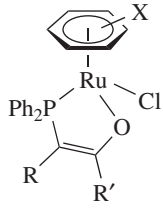

(**183**) η^6-arene = *i*-PrTol-4, MesH, C_6Me_6, R = Me, Et, *t*-Bu, R′= H, Me, *t*-Bu

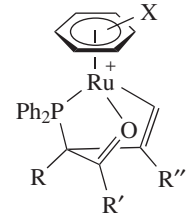

(**184**) η^6-arene = *i*-PrTol-4, MesH, C_6Me_6, R = Me, Et, *t*-Bu, R′ = H, Me, *t*-Bu, R″ = H, Me, $SiMe_3$

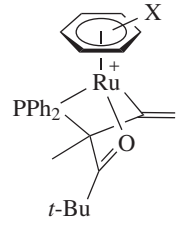

(**185**) η^6-arene = MesH, C_6Me_6

Protonation of [Mo(η^3-C_3H_5){*O*,*P*-OC(=CHPPh$_2$)Ph}(η^6-C_6H_5R)] (R = H, Me) with pyH(PF_6) affords the ketophosphino complex [Mo(η^3-C_3H_5){*O*,*P*-O=C(Ph)CH_2PPh$_2$}(η^6-C_6H_5R)]PF_6[164].

VII. COORDINATION CHEMISTRY OF METALAFURANS

The chemistry of metalafurans has been reviewed[165]. The metalafurans **186** react in various ways, depending on the metal and on the substituents, as shown in Table 1[165].

The metalafuran [Pt{*C*,*O*-OC(Me)CHC(Ph)}Cl(CO)] reacts with PPh_3 to give first [Pt{*C*,*O*-OC(Me)CHC(Ph)}Cl(PPh_3)] and then *trans*-[Pt{C(=CHC(O)Me)Ph}Cl(PPh_3)$_2$]. The former two react with aniline to give imino complexes [Pt{*C*,*N*-N(Ph)C(Me)CHC(Ph)}Cl(L)] (L = CO, PPh_3) but the latter does not[166].

TABLE 1. Chemical behavior of metalafurans (**186**) in the presence of various reagents[164]

Precursor 186					Reagents	Products
M	X	R	R′	R″		
W	Me	Ph	H	Me	ClNO	**187**
W	Me	Me	Me	Me	ClNO	**188**
W	H	Me	H	H	ClNO	**189** + **190**
Cr	Me	Me	Ph	H	ClNO	**191** + **192**
W	H	Alkyl	H	H	PMe_3	**193**
Cr	Me	Me	Ph	H	NO	**194** + **195**
W	Me	Me	H	H	NO	**196** + **197** + **198**
W	H		$(CH_2)_4$	Me	CO + AcfOH	**199** + **200**
W	H	Me	H	H	2 AcfOH	**201** + **202**
W	H	Me	H, Me	Ph, Me	HBF_4	**203**•BF_4

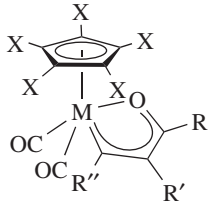

(**186**)

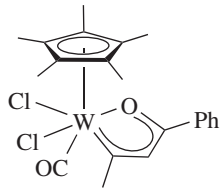

(**187**)

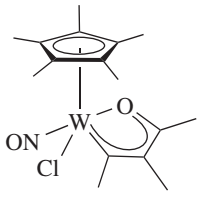

(**188**)

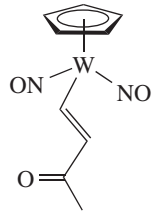

(**189**)

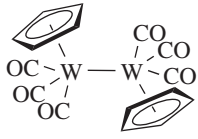

(**190**)

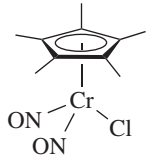

(**191**)

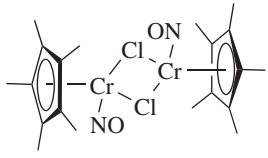

(**192**)

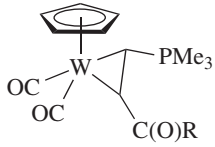

(**193**)

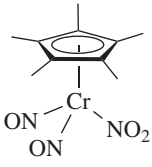

(**194**)

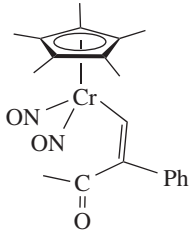

(**195**)

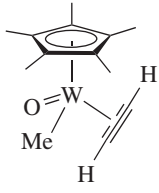

(**196**)

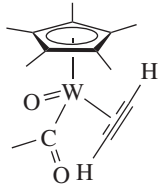

(**197**)

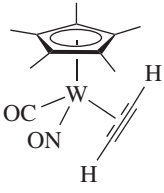

(**198**)

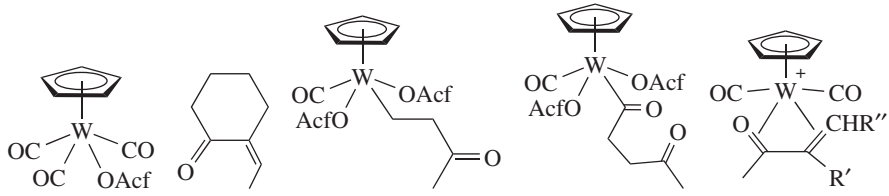

(**199**) (**200**) (**201**) (**202**) (**203**)

VIII. MISCELLANEOUS REACTIONS

A. Formation of Complexes with Noncoordinated β-Diketonato Ligands

The ease of displacement of a β-diketonato ligand (β-dik) out of the coordination sphere of a complex depends on the nature of the ligand (F_6acac > F_3acac > benzoylacetonato ≈ acac) and on the entering ligand (alkylamines > benzylamine > py). Thus, by reacting secondary amines or pyridine with [Pt(acac)(F_3acac)] only complexes [Pt(acac)L_2](F_3acac) were obtained. Furthermore, although [Pt(β-dik)$_2$] reacts with pyridine to give [Pt(py)$_4$](β-dik)$_2$ (β-dik = F_3acac, F_6acac), with 4-cyanopyridine only [PtL_4](F_6acac)$_2$ could be obtained[43]. When [Pd(acac)$_2$] is heated with Et_2NH and the mixture cooled, [Pd(acac)($NHEt_2$)$_2$](acac) is obtained[44]. However, when the solution is kept at room temperature, [Pd(*C*-acac)(acac)($NHEt_2$)] is isolated[40]. Kinetic studies have shown that the former is an intermediate in the formation of the latter[167]. In Section III.E the case of complex **102** was mentioned.

B. Oxidative Cleavage of a C–C Bond in β-Diketonato Complexes

The acac ligand in complex **204** is readily oxidized by atmospheric oxygen upon irradiation in acetone solution, to give the corresponding acetato derivative **205**, providing a model for some chemical and biological processes. In the presence of ligands (py, MeCN, dmso) no photooxidation occurs. Spectroscopic data suggest that these ligands inhibit this photochemical oxidation because they change the type of coordination of the azobenzene chromophore (antenna) and/or the acac ligands, inducing a disconnection between them[168]. A similar cleavage process has been recently reported between **206**•ClO_4 ($N(CH_2Pyr)N(CH_2Pyr)_2$), O_2 and Me_4NOH to give **207**•ClO_4 and CO[169]. In absence of the base, the reaction affords **208**•ClO_4, CO, PhC(O)C(O)Ph, benzoic acid and other minor products[170].

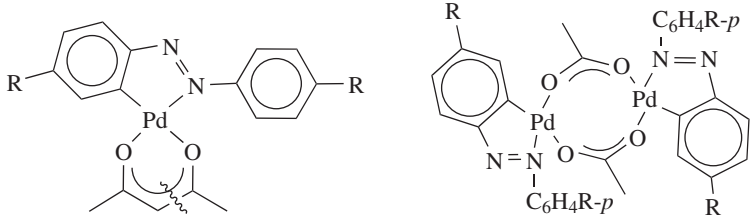

(**204**) R = H, Me, OMe (**205**) R = H, Me, OMe

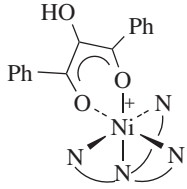

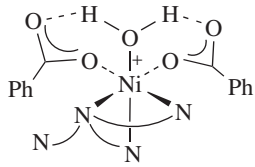

(**207**)

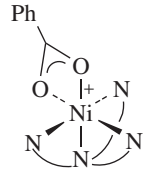

(**208**)

(**206**) N(N N)$_3$ =

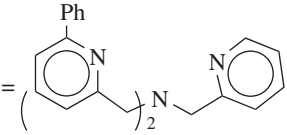

C. Reactions Giving Alkoxides

Heating **209** at 180 °C the enolato ligand isomerizes to give **210**[171].

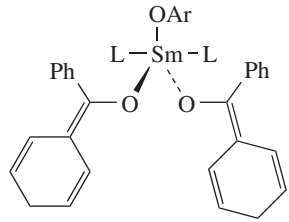

(**209**) L = OP(NMe$_2$)$_3$, Ar = C$_6$H$_2$Me-4-(Bu-*t*)$_2$-2,6, C$_6$H$_3$(Bu-*t*)$_2$-2,6

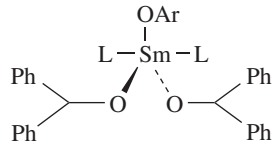

(**210**)

Complex **211** rearranges in solution at room temperature to give **212**[172].

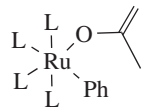

(**211**)

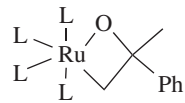

(**212**)

D. Reactions with Lewis Acids

[Ti(C,N-η^5-$C_5Me_4SiMe_2NBu$-t){OC(=CMe_2)OPr-i}X] reacts with $AlMe_3$ when X = Cl to give [Ti(C,N-η^5-$C_5Me_4SiMe_2NBu$-t){OC(=CMe_2)OPr-i}Me] or with [$BPhf_3$(thf)] when X = Me to afford [Ti(C,N-η^5-$C_5Me_4SiMe_2NBu$-t){OC(=CMe_2)OPr-i}(thf)] $MeBPhf_3$[173].

Reaction of **213a** with one equivalent of $MPhf_3$ gives **214** (M = Al) or **213b**•$MeBPhf_3$ (M = B)[174]. However, complexes **215** react with $BPhf_3$ to afford successively **216** and **217**. When the latter are heated they decompose through an intramolecular aldol reaction to give **218**[175].

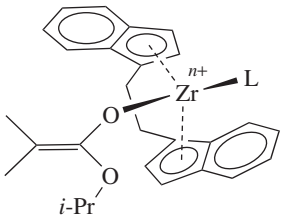

(**213**) (**a**) L = Me, n = 0
(**b**) L = thf, n = 1

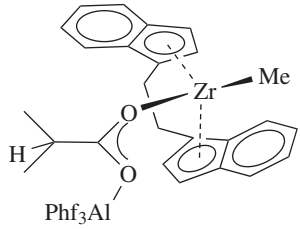

(**214**)

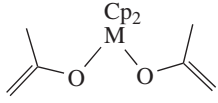

(**215**) M = Ti, Zr, Hf

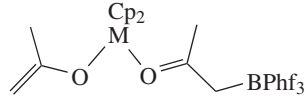

(**216**) M = Ti, Zr, Hf

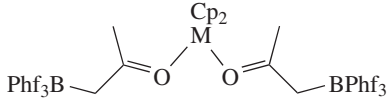

(**217**) M = Ti, Zr, Hf

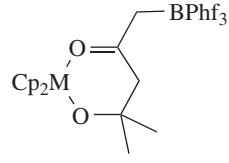

(**218**) M = Ti, Zr

The reaction between **219** and $BPhf_3$ in thf gives $Me_2C{=}CH_2$ and **220**•$MeBPhf_3$, probably through **221**•$MeBPhf_3$. The reaction in CH_2Cl_2 affords **222**[176] and in the presence of one equivalent of acetone or acetophenone gives **223**[177]. The μ-oxo enolato complex **224** reacts with $(PhNHMe_2)[BPhf_4]$ to give **225** and $Me_2C{=}CH_2$[178].

E. Cleavage of the C–O Bond in Enolato Complexes

Thermolysis of the oxatitaniacyclobutene complexes [Ti(η^5-Cp*)$_2${C,O-OC(=CR′)R}] (R = R′ = Ph; R = Ph, Tol, Me, t-Bu, R′ = H) in the presence of pyridine gives [TiO(η^5-Cp*)$_2$py] and the alkynes RC≡CR′. The process is reversible. In the absence of pyridine,

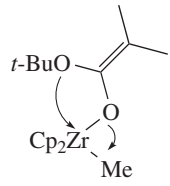

(**219**)

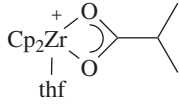

(**220**)

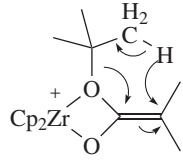

(**221**)

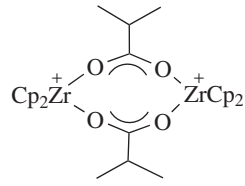

(**222**)

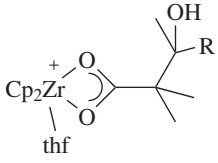

(**223**) R = Me, Ph

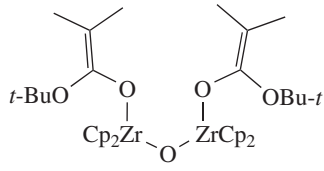

(**224**)

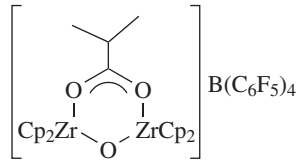

(**225**)

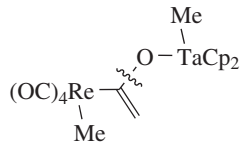

(**226**)

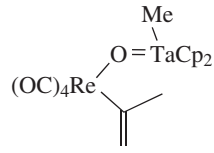

(**227**)

when R′ = H, the hydroxo acetylides [Ti(η^5-Cp*)$_2$(OH)(C≡CR)] are formed[179]. Complex **226** decomposes at room temperature to give **227**[180].

F. Cycloaddition Reactions

228 decomposes at room temperature to give **229**[33].

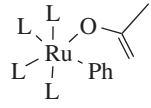

(**228**) L = PMe3

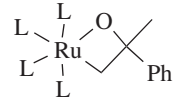

(**229**)

Iridapyrylium complex **230** reacts with RC≡CH, CH_2=$CHCO_2Me$ or SO_2 to afford [4 + 2] cycloaddition products **231**–**233**, respectively[123].

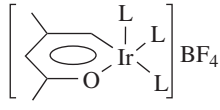

(**230**)

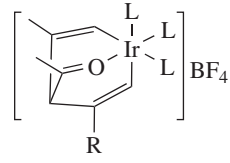

(**231**) R = CO_2Me, $SiMe_3$, Ph

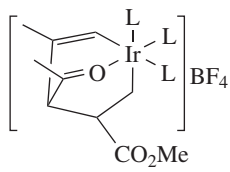

(**232**)

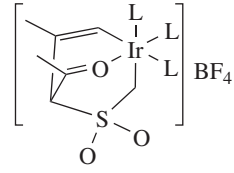

(**233**)

G. Various Reactions

Complex **234** rearranges in solution to give **235**[181].

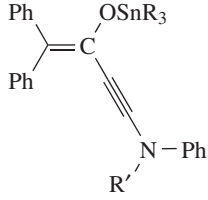

(**234**)

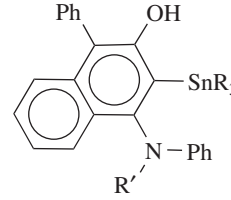

(**235**)

[Ti(η^5-Cp)$_2${OC(=CH$_2$)Ar}Cl] (Ar = An-2, Mes) reacts with AgX (X = BF_4, TfO) and cyclohexanone to give ArC(O)CH=C_6H_{10} and [(η^5-Cp)$_2$Ti(μ-O)Ti(η^5-Cp)$_2$]X_2[105]. Upon heating in cyclohexane **236** is converted into **237**[28].

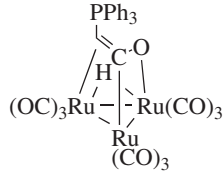

(**236**)

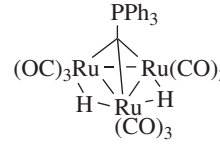

(**237**)

[Al(tpp){OC(=CHMe)Ph}] (tpp = 5,10,15,20-tetraphenylporphinato) reacts with CO_2 and 1-methylimidazol (meim) under irradiation to afford [Al(tpp){OC(O)CH(Me)C(O)Ph}(meim)] which is, formally, the result of insertion of CO_2 into the C–Al bond of the 2-oxoalkyl isomer of the starting complex[182].

The aminoenolato complex **238** reacts with [Cr(CO)$_5$(thf)] to give **239**[133, 183].

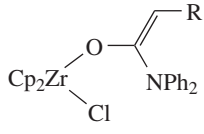

(**238**) R = H, Me

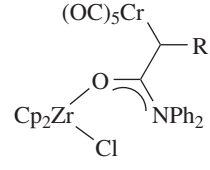

(**239**)

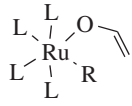

(**240**) (**a**) L = PMe_3 R = Ph
(**b**) L = PMe_3 R = Me

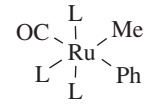

(**241**)

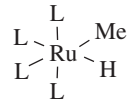

(**242**)

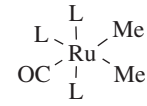

(**243**)

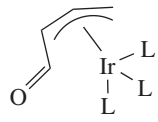

(**244**) L = PMe_3

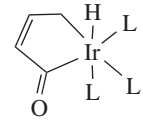

(**245**) (**a**) L = PMe_3
(**b**) L = PEt_3

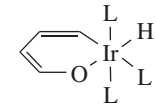

(**246**) L = PEt_3

Complexes **240a** and **240b** decompose at 65°C to afford **241** or a mixture of **242** and **243**, respectively[33].

Complex **244** undergoes a C–H oxidative addition reaction to afford **245a**. Its homologous **245b** is obtained by rearrangement of the iridapyran **246**[121].

IX. ACKNOWLEDGMENTS

The author thanks Dirección General de Investigación, Ministerio de Educación y Ciencia (Spain, Grant CTQ2004-05396), FEDER and Fundación Séneca for financial support and Drs A. Arcas, M. T. Chicote, A. Guirado and I. Saura-Llamas for their suggestions.

X. REFERENCES

1. J. Vicente, Chap. 5 in *The chemistry of Metal Enolates* (Ed. J. Zabicky), John Wiley & Sons, Ltd, Chichester, 2009, pp. 223–312.
2. J. Vicente, J. A. Abad, R. Bergs, P. G. Jones and D. Bautista, *J. Chem. Soc., Dalton Trans.*, 3093 (1995); J. Vicente, J. A. Abad, M. T. Chicote, M. D. Abrisqueta, J. A. Lorca and M. C. Ramírez de Arellano, *Organometallics*, **17**, 1564 (1998); J. Vicente, M. T. Chicote, C. Rubio, M. C. Ramírez de Arellano and P. G. Jones, *Organometallics*, **18**, 2750 (1999).
3. J. Vicente, A. Arcas, J. M. Fernández-Hernández and D. Bautista, *Organometallics*, **20**, 2767 (2001).
4. J. Vicente, A. Arcas, J. M. Fernández-Hernández, A. Sironi and N. Masciocchi, *Chem. Commun.*, 1267 (2005).
5. J. Vicente, A. Arcas, J. M. Fernández-Hernández and D. Bautista, *Organometallics*, **25**, 4404 (2006).
6. V. De Felice, B. Giovannitti, A. Derenzi, D. Tesauro and A. Panunzi, *J. Organomet. Chem.*, **594**, 445 (2000); R. Bertani, C. B. Castellani and B. Crociani, *J. Organomet. Chem.*, **269**, C15 (1984); K. Suzuki and H. Yamamoto, *Inorg. Chim. Acta*, **208**, 225 (1993).
7. A. Ohsuka, T. Hirao, H. Kurosawa and I. Ikeda, *Organometallics*, **14**, 2538 (1995); A. C. Albéniz, N. M. Catalina, P. Espinet and R. Redón, *Organometallics*, **18**, 5571 (1999).
8. D. A. Culkin and J. F. Hartwig, *Organometallics*, **23**, 3398 (2004).
9. P. Veya, C. Floriani, A. Chiesi-Villa and C. Rizzoli, *Organometallics*, **12**, 4899 (1993).
10. J. Vicente, A. Arcas, D. Bautista and P. G. Jones, *Organometallics*, **16**, 2127 (1997); J. Vicente, J. A. Abad, A. D. Frankland and M. C. Ramírez de Arellano, *Chem. Eur. J.*, **5**, 3066 (1999); J. Vicente, J. A. Abad, F. S. Hernández-Mata and P. G. Jones, *J. Am. Chem. Soc.*, **124**, 3848 (2002); J. Vicente, A. Arcas, M. D. Gálvez-López and P. G. Jones, *Organometallics*, **25**, 4247

(2006); J. Vicente, J. A. Abad, E. Martínez-Viviente and P. G. Jones, *Organometallics*, **21**, 4454 (2002).
11. J. Vicente, M. T. Chicote, I. Saura-Llamas, J. Turpín and J. Fernández-Baeza, *J. Organomet. Chem.*, **333**, 129 (1987).
12. R. Navarro and E. P. Urriolabeitia, *J. Chem. Soc., Dalton Trans.*, 4111 (1999).
13. U. Belluco, R. A. Michelin, R. Bertani, G. Facchin, G. Pace, L. Zanotto, M. Mozzon, M. Fyrlan and E. Zangrando, *Inorg. Chim. Acta*, **252**, 355 (1996).
14. G. Facchin, R. Bertani, M. Calligaris, G. Nardin and M. Mari, *J. Chem. Soc., Dalton Trans.*, 1381 (1987).
15. G. Facchin, L. Zanotto, R. Bertani and G. Nardin, *Inorg. Chim. Acta*, **245**, 157 (1996).
16. G. Facchin, L. Zanotto, R. Bertani, L. Canovese and P. Uguagliati, *J. Chem. Soc., Dalton Trans.*, 2871 (1993).
17. L. R. Falvello, S. Fernández, R. Navarro, I. Pascual and E. P. Urriolabeitia, *J. Chem. Soc., Dalton Trans.*, 763 (1997).
18. L. R. Falvello, S. Fernández, R. Navarro and E. P. Urriolabeitia, *Inorg. Chem.*, **35**, 3064 (1996).
19. S. Fernández, M. M. García, R. Navarro and E. P. Urriolabeitia, *J. Organomet. Chem.*, **561**, 67 (1998).
20. M. Carbó, L. R. Falvello, R. Navarro, T. Soler and E. P. Urriolabeitia, *Eur. J. Inorg. Chem.*, 2338 (2004).
21. J. Vicente, M. T. Chicote, R. Guerrero and P. G. Jones, *J. Am. Chem. Soc.*, **118**, 699 (1996); J. Vicente, M. T. Chicote, I. Saura-Llamas and M. C. Lagunas, *J. Chem. Soc., Chem. Commun.*, 915 (1992); J. Vicente, M. T. Chicote, I. Saurallamas, P. G. Jones, K. Meyerbase and C. F. Erdbrugger, *Organometallics*, **7**, 997 (1988); J. Vicente, M. T. Chicote, J. A. Cayuelas, J. Fernandezbaeza, P. G. Jones, G. M. Sheldrick and P. Espinet, *J. Chem. Soc., Dalton Trans.*, 1163 (1985); J. Vicente, M. T. Chicote and M. C. Lagunas, *Helv. Chim. Acta*, **82**, 1202 (1999); J. Vicente, M. T. Chicote, M. C. Lagunas and P. G. Jones, *J. Chem. Soc., Chem. Commun.*, 1730 (1991); J. Vicente, M. T. Chicote and I. Saura-Llamas, *J. Chem. Soc., Dalton Trans.*, 1941 (1990); J. Vicente, M. T. Chicote, M. C. Lagunas and P. G. Jones, *J. Chem. Soc., Dalton Trans.*, 2579 (1991); J. Vicente, M. T. Chicote and M. C. Lagunas, *Inorg. Chem.*, **32**, 3748 (1993); J. Vicente, M. T. Chicote, M. D. Abrisqueta, M. M. Alvarez-Falcon, M. C. R. de Arellano and P. G. Jones, *Organometallics*, **22**, 4327 (2003); J. Vicente, M. T. Chicote, M. C. Lagunas, P. G. Jones and B. Ahrens, *Inorg. Chem.*, **36**, 4938 (1997); J. Vicente, A. R. Singhal and P. G. Jones, *Organometallics*, **21**, 5887 (2002).
22. J. Vicente and M. T. Chicote, *Coord. Chem. Rev.*, **193–195**, 1143 (1999).
23. P. Laavanya, U. Venkatasubramanian, K. Panchanatheswaran and J. A. K. Bauer, *Chem. Commun.*, 1660 (2001).
24. A. Spannenberg, W. Baumann and U. Rosenthal, *Appl. Organomet. Chem.*, **14**, 611 (2000).
25. E. Diez-Barra, J. Fernández-Baeza, M. M. Kubicki, A. Lara-Sánchez, A. Otero, N. Poujaud and J. Tejeda, *J. Organomet. Chem.*, **542**, 291 (1997).
26. J. A. Albanese, D. L. Staley, A. L. Rheingold and J. L. Burmeister, *Inorg. Chem.*, **29**, 2209 (1990).
27. A. J. Deeming, D. Nuel, N. I. Powell and C. Whittaker, *J. Chem. Soc., Dalton Trans.*, 757 (1992).
28. D. S. Bohle, D. Heineke, A. Tiripicchio, M. Tiripicchio-Camellini and H. Vahrenkamp, *Angew. Chem., Int. Ed. Engl.*, **29**, 896 (1990).
29. B. A. Bench, W. W. Brennessel, H.-J. Lee and S. M. Gorun, *Angew. Chem. Int. Ed.*, **41**, 750 (2002).
30. E. R. Burkhardt, J. J. Doney, R. G. Bergman and C. H. Heathcock, *J. Am. Chem. Soc.*, **109**, 2022 (1987).
31. L. U. Gron, K. J. Haller and A. B. Ellis, *J. Organomet. Chem.*, **323**, 207 (1987).
32. J. F. Hartwig, R. A. Andersen and R. G. Bergman, *J. Am. Chem. Soc.*, **112**, 5670 (1990).
33. J. F. Hartwig, R. G. Bergman and R. A. Andersen, *Organometallics*, **10**, 3326 (1991).
34. G. A. Slough, R. G. Bergman and C. H. Heathcock, *J. Am. Chem. Soc.*, **111**, 938 (1989).
35. J. F. Hartwig, R. G. Bergman and R. A. Andersen, *Organometallics*, **10**, 3344 (1991).
36. J. Cámpora, C. M. Maya, P. Palma, E. Carmona, E. Gutiérrez, C. Ruiz, C. Graiff and A. Tiripicchio, *Chem. Eur. J.*, **11**, 6889 (2005).

37. J. Vicente, M. D. Bermúdez, F. J. Carrión and P. G. Jones, *J. Organomet. Chem.*, **508**, 53 (1996); J. P. Wolkowski and J. F. Hartwig, *Angew. Chem. Int. Ed.*, **41**, 4289 (2002); T. Ito, T. Kiriyama and A. Yamamoto, *Bull. Chem. Soc. Jpn.*, **49**, 3250 (1976).
38. O. Navarro, N. Marion, N. M. Scott, J. González, D. Amoroso, A. Bell and S. P. Nolan, *Tetrahedron*, **61**, 9716 (2005).
39. L. A. Oro, D. Carmona, M. A. Esteruelas, C. Foces-Foces and F. H. Cano, *J. Organomet. Chem.*, **307**, 83 (1986); J. Forniés, F. Martínez, R. Navarro and E. P. Urriolabeitia, *J. Organomet. Chem.*, **495**, 185 (1995); J. Vicente, A. Arcas, M. A. Blasco, J. Lozano and M. C. Ramírez de Arellano, *Organometallics*, **17**, 5374 (1998).
40. S. Baba, T. Ogura and S. Kawaguchi, *Bull. Chem. Soc. Jpn.*, **47**, 665 (1974).
41. M. Horike, Y. Kai, N. Yasuoka and N. Kasai, *J. Organomet. Chem.*, **72**, 441 (1974); T. Ito, T. Kiriyama, Y. Nakamura and A. Yamamoto, *Bull. Chem. Soc. Jpn.*, **49**, 3257 (1976); S. Komiya and J. K. Kochi, *J. Am. Chem. Soc.*, **99**, 3695 (1977).
42. A. R. Siedle and L. H. Pignolet, *Inorg. Chem.*, **20**, 1849 (1981); S. Okeya, H. Sazaki, M. Ogita, T. Takemoto, Y. Onuki, Y. Nakamura, B. K. Mohapatra and S. Kawaguchi, *Bull. Chem. Soc. Jpn.*, **54**, 1978 (1981); S. Okeya and S. Kawaguchi, *Inorg. Chem.*, **16**, 1730 (1977).
43. S. Okeya, Y. Nakamura and S. Kawaguchi, *Bull. Chem. Soc. Jpn.*, **55**, 1460 (1982).
44. S. Okeya, H. Yoshimatsu, Y. Nakamura and S. Kawaguchi, *Bull. Chem. Soc. Jpn.*, **55**, 483 (1982).
45. P. J. Heard, K. Kite and A. E. Aliev, *Polyhedron*, **17**, 2543 (1998).
46. J. R. Hall and G. A. Swile, *J. Organomet. Chem.*, **47**, 195 (1973).
47. R. C. Menzies, *J. Chem. Soc.*, **130**, 565 (1928).
48. W. Rigby, H. B. Lee, P. M. Bailey, J. A. McCleverty and P. M. Maitlis, *J. Chem. Soc., Dalton Trans.*, 387 (1979).
49. G. Bhalla, X. Y. Liu, J. Oxgaard, W. A. Goddard and R. A. Periana, *J. Am. Chem. Soc.*, **127**, 11372 (2005).
50. S. Patra, B. Mondal, B. Sarkar, M. Niemeyer and G. K. Lahiri, *Inorg. Chem.*, **42**, 1322 (2003).
51. L. E. Harrington, J. F. Britten, D. W. Hughes, A. D. Bain, J. Y. Thepot and M. J. McGlinchey, *J. Organomet. Chem.*, **656**, 243 (2002); H. K. Gupta, N. Rampersad, M. Stradiotto and M. J. McGlinchey, *Organometallics*, **19**, 184 (2000).
52. J. Forniés, R. Navarro, M. Tomás and E. P. Urriolabeitia, *Organometallics*, **12**, 940 (1993).
53. J. Forniés, F. Martínez, R. Navarro and E. P. Urriolabeitia, *Organometallics*, **15**, 1813 (1996).
54. E. Alonso, J. Forniés, C. Fortuño, A. Martín and A. G. Orpen, *Organometallics*, **22**, 5011 (2003).
55. M. E. Smith, F. J. Hollander and R. A. Andersen, *Angew. Chem., Int. Ed. Engl.*, **32**, 1294 (1993); U. Koelle, C. Rietmann and G. Raabe, *Organometallics*, **16**, 3273 (1997).
56. P. Govindaswamy, S. M. Mobin, C. Thöne and M. R. Kollipara, *J. Organomet. Chem.*, **690**, 1218 (2005).
57. G. Steyl, *Acta Crystallogr., Sect. E*, **62**, m650 (2006).
58. A. Jakob, H. Schmidt, B. Walfort, G. Rheinwald, S. Fruhauf, S. Schulz, T. Gessner and H. Lang, *Z. Anorg. Allg. Chem.*, **631**, 1079 (2005).
59. M. Alexiou, E. Katsoulakou, C. Dendrinou-Samara, C. P. Raptopoulou, V. Psycharis, E. Manessi-Zoupa, S. P. Perlepes and D. P. Kessissoglou, *Eur. J. Inorg. Chem.*, 1964 (2005).
60. O. T. Beachley Jr., J. R. Gardinier, M. R. Churchill and L. M. Toomey, *Organometallics*, **17**, 1101 (1998).
61. S. Okeya, Y. Nakamura and S. Kawaguchi, *Bull. Chem. Soc. Jpn.*, **54**, 3396 (1981).
62. T. Ito, T. Kiriyama and A. Yamamoto, *Chem. Lett.*, 835 (1976).
63. S. Ooi, T. Matsushita, K. Nishimoto, S. Okeya, Y. Nakamura and S. Kawaguchi, *Bull. Chem. Soc. Jpn.*, **56**, 3297 (1983).
64. S. Kawaguchi, *Coord. Chem. Rev.*, **70**, 51 (1986).
65. A. Okazawa, T. Ishida and T. Nogami, *Polyhedron*, **24**, 2584 (2005).
66. T. Kogane, M. Ishii, K. Harada, R. Hirota and M. Nakahara, *Bull. Chem. Soc. Jpn.*, **62**, 2524 (1989).
67. G. Brewer, P. Kamaras, S. Prytkov, M. Shang and W. R. Scheidt, *J. Chem. Soc., Dalton Trans.*, 4511 (1999).
68. A. J. Blake, N. R. Champness, S. M. Howdle, K. S. Morley, P. B. Webb and C. Wilson, *CrystEngComm*, **4**, 88 (2002).

69. K. M. Chi, T. S. Corbitt, M. J. Hampden-Smith, T. T. Kodas and E. N. Duesler, *J. Organomet. Chem.*, **449**, 181 (1993).
70. S. Yoshida, Y. Ohgomori, Y. Watanabe, K. Honda, M. Goto and M. Kurahashi, *J. Chem. Soc., Dalton Trans.*, 895 (1988).
71. A. R. Siedle, R. A. Newmark and L. H. Pignolet, *J. Am. Chem. Soc.*, **104**, 6584 (1982).
72. D. P. Graddon, *Coord. Chem. Rev.*, **4**, 1 (1969).
73. G. J. Bullen, R. Mason and P. Pauling, *Inorg. Chem.*, **4**, 456 (1965).
74. P. G. Jones and M. M. Álvarez-Falcón, *Acta Crystallogr., Sect. E*, **59**, m192 (2003).
75. N. A. Bailey, D. E. Fenton, M. V. Franklin and M. Hall, *J. Chem. Soc., Dalton Trans.*, 984 (1980).
76. A. Y. Rogachev, A. V. Mironov and A. V. Nemukhin, *J. Mol. Struct.*, **831**, 46 (2007).
77. L. F. Lindoy, H. C. Lip, H. W. Louie, M. G. B. Drew and M. J. Hudson, *J. Chem. Soc., Chem. Commun.*, 778 (1977).
78. E. V. Dikarev, H. Zhang and B. Li, *J. Am. Chem. Soc.*, **127**, 6156 (2005).
79. M. Doring, E. Uhlig and L. Dahlenburg, *Z. Anorg. Allg. Chem.*, **578**, 58 (1989).
80. T. Yamaguchi, F. Yamazaki and T. Ito, *J. Chem. Soc., Dalton Trans.*, 273 (1999).
81. M. Calvin and R. H. Bailes, *J. Am. Chem. Soc.*, **68**, 949 (1946); M. Calvin and K. W. Wilson, *J. Am. Chem. Soc.*, **67**, 2003 (1945); R. B. Duffield and M. Calvin, *J. Am. Chem. Soc.*, **68**, 557 (1946).
82. R. H. Holm and F. A. Cotton, *J. Am. Chem. Soc.*, **80**, 5658 (1958).
83. J. P. Collman, *Angew. Chem., Int. Ed. Engl.*, **4**, 132 (1965).
84. H. Masui, *Coord. Chem. Rev.*, **219**, 957 (2001).
85. J. P. Collman, R. A. Moss, S. D. Goldby and W. S. Trahanovsky, *Chem. Ind.*, 1213 (1960).
86. J. P. Collman, H. Maltz, C. C. Heindel and R. A. Moss, *J. Am. Chem. Soc.*, **83**, 531 (1961).
87. R. W. Kluiber, *J. Am. Chem. Soc.*, **82**, 4839 (1960); V. G. Isakova, I. A. Baidina, N. B. Morozova and I. K. Igumenov, *Polyhedron*, **19**, 1097 (2000).
88. R. W. Kluiber, *J. Am. Chem. Soc.*, **83**, 3030 (1961).
89. J. P. Collman, S. D. Goldby, W. L. Young and R. L. Marshall, *Inorg. Chem.*, **1**, 704 (1962).
90. R. H. Barker, R. L. Marshall and J. P. Collman, *J. Org. Chem.*, **29**, 3216 (1964).
91. Y. Nakano, A. Baba, T. Adachi and T. Noguchi, *Inorg. Chim. Acta*, **321**, 149 (2001).
92. T. Noguchi, F. B. Yuki and Y. Nakano, *Inorg. Chim. Acta*, **359**, 2268 (2006).
93. J. P. Collman, R. L. Marshall and W. L. Young, *Chem. Ind.*, 1380 (1962).
94. J. P. Collman and M. Yamada, *J. Org. Chem.*, **28**, 3017 (1963).
95. M. Carano, F. Cicogna, J. L. Houben, G. Ingrosso, F. Marchetti, L. Mottier, F. Paolucci, C. Pinzino and S. Roffia, *Inorg. Chem.*, **41**, 3396 (2002).
96. N. R. Evans, L. S. Devi, C. S. K. Mak, S. E. Watkins, S. I. Pascu, A. Kohler, R. H. Friend, C. K. Williams and A. B. Holmes, *J. Am. Chem. Soc.*, **128**, 6647 (2006).
97. S. Aygen, Y. Kitamura, K. Kuroda, R. Kume, H. Kelm and R. van Eldik, *Inorg. Chem.*, **24**, 423 (1985); S. Aygen, E. F. Paulus, Y. Kitamura and R. van Eldik, *Inorg. Chem.*, **26**, 769 (1987); W. Purcell, J. G. Leipoldt and Y. Kitamura, *Inorg. Chim. Acta*, **177**, 151 (1990).
98. J. Lewinski and J. Zachara, *J. Organomet. Chem.*, **560**, 89 (1998).
99. X. F. Zhang, H. Chen, C. B. Ma, C. N. Chen and Q. T. Liu, *Dalton Trans.*, 4047 (2006).
100. Y. Nakano, T. Noguchi, H. Kondo, T. Ishiwata and S. Sato, *Inorg. Chim. Acta*, **358**, 513 (2005).
101. M. Basato, B. Corain and G. Zanotti, *J. Chem. Soc., Dalton Trans.*, 3003 (1992).
102. T. Uchiyama, K. Takagi, K. Matsumoto, S. Ooi, Y. Nakamura and S. Kawaguchi, *Bull. Chem. Soc. Jpn.*, **54**, 1077 (1981).
103. T. Hashimoto, S. Hara, Y. Shiraishi, M. Yamauchi, K. Natarajan and K. Shimizu, *Inorg. Chim. Acta*, **358**, 2207 (2005).
104. H. Brombacher and H. Vahrenkamp, *Inorg. Chem.*, **43**, 6054 (2004).
105. P. Veya, C. Floriani, A. Chiesi-Villa and C. Rizzoli, *Organometallics*, **12**, 4892 (1993).
106. J. G. Stack, J. J. Doney, R. G. Bergman and C. H. Heathcock, *Organometallics*, **9**, 453 (1990).
107. C. Tsiamis, B. Voulgaropoulos, D. Charistos, G. P. Voutsas and C. A. Kavounis, *Polyhedron*, **19**, 2003 (2000).
108. M. Moon, M. Pyo, Y. C. Myoung, C. I. Ahn and M. S. Lah, *Inorg. Chem.*, **40**, 554 (2001).
109. Y. Jin and M. S. Lah, *Eur. J. Inorg. Chem.*, 4944 (2005).
110. A. A. Diamantis, M. R. Snow and J. A. Vanzo, *Chem. Commun.*, 264 (1976).

111. G. Bettermann and A. J. Arduengo III, *J. Am. Chem. Soc.*, **110**, 877 (1988).
112. S. Gambarotta, S. Strologo, C. Floriani, A. Chiesi-Villa and C. Guastini, *Inorg. Chem.*, **24**, 654 (1985).
113. E. J. Moore, D. A. Straus, J. Armantrout, B. D. Santarsiero, R. H. Grubbs and J. E. Bercaw, *J. Am. Chem. Soc.*, **105**, 2068 (1983).
114. S. C. H. Ho, D. A. Straus, J. Armantrout, W. P. Schaefer and R. H. Grubbs, *J. Am. Chem. Soc.*, **106**, 2210 (1984).
115. P. Veya, P. G. Cozzi, C. Floriani, A. Chiesi-Villa and C. Rizzoli, *Organometallics*, **13**, 4939 (1994).
116. M. D. Fryzuk, P. B. Duval, S. Mao, S. J. Rettig, M. J. Zaworotko and L. R. MacGillivray, *J. Am. Chem. Soc.*, **121**, 1707 (1999).
117. J. S. Holmgren, J. R. Shapley, S. R. Wilson and W. T. Pennington, *J. Am. Chem. Soc.*, **108**, 508 (1986).
118. M. A. Esteruelas, Y. A. Hernández, A. M. López, M. Oliván and E. Oñate, *Organometallics*, **24**, 5989 (2005).
119. J. R. Bleeke, T. Haile and M. Y. Chiang, *Organometallics*, **10**, 19 (1991).
120. J. R. Bleeke, P. R. New, J. M. B. Blanchard, T. Haile and A. M. Rohde, *Organometallics*, **14**, 5127 (1995).
121. J. R. Bleeke, T. Haile, P. R. New and M. Y. Chiang, *Organometallics*, **12**, 517 (1993).
122. J. R. Bleeke and J. M. B. Blanchard, *J. Am. Chem. Soc.*, **119**, 5443 (1997).
123. J. R. Bleeke, J. M. B. Blanchard and E. Donnay, *Organometallics*, **20**, 324 (2001).
124. S. Okeya, Y. Nakamura, S. Kawaguchi and T. Hinomoto, *Inorg. Chem.*, **20**, 1576 (1981); S. Okeya, Y. Kawakita, S. Matsumoto, Y. Nakamura, S. Kawaguchi, N. Kanehisa, K. Miki and N. Kasai, *Bull. Chem. Soc. Jpn.*, **55**, 2134 (1982).
125. S. Okeya, Y. Kusuyama, K. Isobe, Y. Nakamura and S. Kawaguchi, *J. Organomet. Chem.*, **551**, 117 (1998).
126. S. Yamazaki, T. Ama and Z. Taira, *Polyhedron*, **7**, 353 (1988); T. Sakai, Z. Taira and S. Yamazaki, *Polyhedron*, **12**, 2133 (1993).
127. P. G. Williard and J. M. Salvino, *Tetrahedron Lett.*, **26**, 3931 (1985).
128. P. Veya, C. Floriani, A. Chiesi-Villa and C. Guastini, *Organometallics*, **13**, 208 (1994).
129. T. Agapie, P. L. Diaconescu, D. J. Mindiola and C. C. Cummins, *Organometallics*, **21**, 1329 (2002).
130. G. Erker, U. Dorf, R. Lecht, M. T. Ashby, M. Aulbach, R. Schlund, C. Krueger and R. Mynott, *Organometallics*, **8**, 2037 (1989).
131. G. Solari, E. Solari, C. Floriani, A. Chiesi-Villa and C. Rizzoli, *Organometallics*, **16**, 508 (1997).
132. P. Veya, P. G. Cozzi, C. Floriani, F. P. Rotzinger, A. Chiesi-Villa and C. Rizzoli, *Organometallics*, **14**, 4101 (1995).
133. P. G. Cozzi, P. Veya, C. Floriani, F. P. Rotzinger, A. Chiesi-Villa and C. Rizzoli, *Organometallics*, **14**, 4092 (1995).
134. J. Cámpora, I. Matas, C. M. Maya, P. Palma and E. Álvarez, *Organometallics*, **25**, 3124 (2006).
135. J. Cámpora, C. M. Maya, P. Palma, E. Carmona, C. Graiff and A. Tiripicchio, *Chem. Commun.*, 1742 (2003); C. M. Maya, J. Cámpora, E. Carmona, I. Matas, P. Palma, E. Gutiérrez-Puebla and A. Monge, *Chem. Eur. J.*, **13**, 3675 (2007).
136. A. J. Arce, A. J. Deeming, S. Donovan-Mtunzi and S. E. Kabir, *J. Chem. Soc., Dalton Trans.*, 2479 (1985).
137. M. R. Maurya, *Coord. Chem. Rev.*, **237**, 163 (2003).
138. R. Usón, J. Vicente and M. T. Chicote, *J. Organomet. Chem.*, **209**, 271 (1981).
139. J. Chakravarty, S. Dutta, A. Dey and A. Chakravorty, *J. Chem. Soc., Dalton Trans.*, 557 (1994).
140. G. Aromi, S. Bhaduri, P. Artus, K. Folting and G. Christou, *Inorg. Chem.*, **41**, 805 (2002).
141. M. A. Calvo, A. M. M. Lanfredi, L. A. Oro, M. T. Pinillos, C. Tejel, A. Tripicchio and F. Ugozzoli, *Inorg. Chem.*, **32**, 1147 (1993); D. Carmona, J. Ferrer, R. Atencio, F. J. Lahoz, L. A. Oro and M. P. Lamata, *Organometallics*, **14**, 2057 (1995); D. Carmona, J. Ferrer, A. Mendoza, F. Lahoz, L. A. Oro, F. Viguri and J. Reyes, *Organometallics*, **14**, 2066 (1995); D. Carmona, J. Ferrer, F. J. Lahoz, L. A. Oro, J. Reyes and M. Esteban, *J. Chem. Soc., Dalton Trans.*, 2811 (1991); P. Cornago, C. Escolástico, M. D. S. María,

R. M. Claramunt, D. Carmona, M. Esteban, L. A. Oro, C. Foces-Foces, A. L. Llamas-Saiz and J. Elguero, *J. Organomet. Chem.*, **467**, 293 (1994); A. Elduque, F. Aguilera, F. J. Lahoz, J. A. López, L. A. Oro and M. T. Pinillos, *Inorg. Chim. Acta*, **274**, 15 (1998); A. Elduque, L. A. Oro, M. T. Pinillos, C. Tejel, A. Tiripicchio and F. Ugozzoli, *J. Chem. Soc., Dalton Trans.*, 2807 (1991).
142. R. Usón, J. Gimeno, J. Forniés and F. Martínez, *Inorg. Chim. Acta*, **50**, 173 (1981).
143. R. Usón, J. Gimeno, J. Forniés, F. Martínez and C. Fernández, *Inorg. Chim. Acta*, **63**, 91 (1982).
144. E. J. Fernández, M. C. Gimeno, P. G. Jones, B. Ahrens, A. Laguna, M. Laguna and J. M. López de Luzuriaga, *J. Chem. Soc., Dalton Trans.*, 3487 (1994).
145. J. Forniés, F. Martínez, R. Navarro and E. P. Urriolabeitia, *Polyhedron*, **9**, 2181 (1990).
146. J. Forniés, F. Martínez, R. Navarro, M. Tomás and E. P. Urriolabeitia, *J. Chem. Soc., Dalton Trans.*, 505 (1994).
147. H. Hashimoto, Y. Nakamura and S. Okeya, *Inorg. Chim. Acta*, **120**, L25 (1986).
148. D. Walther, T. Döhler, N. Theyssen and H. Görls, *Eur. J. Inorg. Chem.*, 2049 (2001); S. Rau, K. Lamm, H. Görls, J. Schöffel and D. Walther, *J. Organomet. Chem.*, **689**, 3582 (2004).
149. L. Salmon, P. Thuery, E. Riviere and M. Ephritikhine, *Inorg. Chem.*, **45**, 83 (2006).
150. J. Vicente, A. Arcas, D. Bautista, A. Tiripicchio and M. Tiripicchio-Camellini, *New J. Chem.*, **20**, 345 (1996).
151. B. Meyer zu Berstenhorst, G. Erker, G. Kehr and R. Fröhlich, *Dalton Trans.*, 3200 (2006).
152. R. Y. Wang, D. T. Song and S. M. Wang, *Chem. Commun.*, 368 (2002).
153. P. Braunstein, *Chem. Rev.*, **106**, 134 (2006).
154. P. Veya, C. Floriani, A. Chiesi-Villa and C. Guastini, *Organometallics*, **10**, 2991 (1991).
155. P. Braunstein, X. Morise, M. Benard, M.-M. Rohmer and R. Welter, *Chem. Commun.*, 610 (2003).
156. P. Crochet, B. Demerseman, C. Rocaboy and D. Schleyer, *Organometallics*, **15**, 3048 (1996).
157. P. Crochet and B. Demerseman, *Organometallics*, **14**, 2173 (1995).
158. B. Demerseman, B. Guilbert, C. Renouard, M. González, P. H. Dixneuf, D. Masi and C. Mealli, *Organometallics*, **12**, 3906 (1993).
159. H. Werner, G. Henig, B. Windmüller, O. Gevert, C. Lehmann and R. Herbst-Irmer, *Organometallics*, **18**, 1185 (1999).
160. P. Braunstein, D. Matt, Y. Dusausoy, J. Fischer, A. Mitschler and L. Ricard, *J. Am. Chem. Soc.*, **103**, 5115 (1981); S. E. Bouaoud, P. Braunstein, D. Grandjean, D. Matt and D. Nobel, *Inorg. Chem.*, **27**, 2279 (1988); S.-E. Bouaoud, P. Braunstein, D. Grandjean, D. Matt and D. Nobel, *Chem. Commun.*, 488 (1987).
161. P. Braunstein, Y. Chauvin, J. Nahring, A. DeCian, J. Fischer, A. Tiripicchio and F. Ugozzoli, *Organometallics*, **15**, 5551 (1996).
162. F. Balegroune, P. Braunstein, D. Grandjean, D. Matt and D. Nobel, *Inorg. Chem.*, **27**, 3320 (1988).
163. P. Braunstein, T. M. G. Carneiro, D. Matt, F. Balegroune and D. Grandjean, *Organometallics*, **8**, 1737 (1989).
164. N. G. Jones, M. L. H. Green, I. C. Vei, L. H. Rees, S. I. Pascu, D. Watkin, A. Cowley, X. Morise and P. Braunstein, *J. Chem. Soc., Dalton Trans.*, 2491 (2002).
165. H. G. Alt, *J. Organomet. Chem.*, **383**, 125 (1990).
166. C. Allevi, L. Garlaschelli, M. C. Malatesta and F. Ganazzoli, *Organometallics*, **9**, 1383 (1990).
167. S. Matsumoto and S. Kawaguchi, *Bull. Chem. Soc. Jpn.*, **53**, 1577 (1980).
168. J. Vicente, A. Arcas, D. Bautista and G. B. Shulpin, *J. Chem. Soc., Dalton Trans.*, 1505 (1994).
169. E. Szajna, A. M. Arif and L. M. Berreau, *J. Am. Chem. Soc.*, **127**, 17186 (2005).
170. E. Szajna-Fuller, K. Rudzka, A. M. Arif and L. M. Berreau, *Inorg. Chem.*, **46**, 5499 (2007).
171. Z. M. Hou, T. Yoshimura and Y. Wakatsuki, *J. Am. Chem. Soc.*, **116**, 11169 (1994); T. Yoshimura, Z. M. Hou and Y. Wakatsuki, *Organometallics*, **14**, 5382 (1995).
172. J. F. Hartwig, R. G. Bergman and R. A. Andersen, *J. Am. Chem. Soc.*, **112**, 3234 (1990).
173. A. Rodríguez-Delgado, W. R. Mariott and E. Y. X. Chen, *Macromolecules*, **37**, 3092 (2004).
174. A. D. Bolig and E. Y.-X. Chen, *J. Am. Chem. Soc.*, **126**, 4897 (2004).
175. W. Spaether, K. Klass, G. Erker, F. Zippel and R. Fröhlich, *Chem. Eur. J.*, **4**, 1411 (1998).
176. B. Lian, L. Toupet and J. F. Carpentier, *Chem. Eur. J.*, **10**, 4301 (2004).

177. B. Lian, C. W. Lehmann, C. Navarro and J. F. Carpentier, *Organometallics*, **24**, 2466 (2005).
178. G. Stojcevic, H. Kim, N. J. Taylor, T. B. Marder and S. Collins, *Angew. Chem. Int. Ed.*, **43**, 5523 (2004).
179. J. L. Polse, R. A. Andersen and R. G. Bergman, *J. Am. Chem. Soc.*, **117**, 5393 (1995).
180. G. Proulx and R. G. Bergman, *J. Am. Chem. Soc.*, **118**, 1981 (1996).
181. G. Himbert, L. Henn and R. Hoge, *J. Organomet. Chem.*, **184**, 317 (1980).
182. Y. Hirai, T. Aida and S. Inoue, *J. Am. Chem. Soc.*, **111**, 3062 (1989).
183. P. Veya, C. Floriani, A. Chiesi-Villa and C. Guastini, *J. Chem. Soc., Chem. Commun.*, 1166 (1991).

CHAPTER 7

Metal enolates as synthons in organic chemistry

DANIEL STOLZ and ULI KAZMAIER

Department of Organic Chemistry, Saarland University, D-66123 Saarbrücken, Germany
Fax: +49 681 3022409; e-mail: u.kazmaier@mx.uni-saarland.de

The chemistry of metal enolates
Edited by Jacob Zabicky

I. ACRONYMS

BINAP	2,2′-(diphenylphosphino)-1,1′-bisnaphthyl	LA	Lewis acid
BOC	*t*-butoxycarbonyl	LDA	lithium diisopropylamide
CBZ	benzyloxycarbonyl	LiHMDS	lithium hexamethyldisilazide
cee	conservation of enantiomeric excess	LTMP	lithium 2,2,6,6-tetramethylpiperidide
DBA	dibenzylideneacetone	MOM	methoxymethyl
DIBAlH	diisobutylaluminium hydride	NaHMDS	sodium hexamethyldisilazide
DIPEA	*N*-ethyldiisopropylamine	PG	protecting group
DME	1,2-dimethoxyethane	PMB	*p*-methoxybenzyl
DMF	*N*,*N*-dimethylformamide	rs	regioselectivity
DMPU	*N*,*N*′-dimethylpropyleneurea	TBAF	tetra-*n*-butylammonium fluoride
DPEphos	bis[(2-diphenylphosphino) phenyl] ether	TBDPS	*t*-butyldiphenylsilyl
DPPE	1,2-bis(diphenylphosphino) ethane	TBME	*t*-butyl methyl ether
dr	diastereomeric ratio	TBS	*t*-butyldimethylsilyl
ds	diastereoselectivity	TES	triethylsilyl
ee	enantiomeric excess	Tfa	trifluoroacetyl
ent-	enantiomer of . . .	TFA	trifluoroacetic acid
HMDS	hexamethyldisilazane	TMEDA	*N*,*N*,*N*′,*N*′-tetramethylethyl enediamine
		TMS	trimethylsilyl
		TMSCl	trimethylsilyl chloride

II. C–C BOND FORMATION BY α-SUBSTITUTION OF KETONE ENOLATES

A. Control of Stereo- and Regioselectivity in Enolate Preparation

The regio- and stereoselectivity of enolate formation has been discussed in many reviews[1,2]. In general, the stereo- and regioselectivity of ketone deprotonation can be *thermodynamically* or *kinetically* controlled. Conditions for the *kinetic* control of enolate formation are achieved by slow addition of the ketone to an excess of strong base in an aprotic solvent at low temperature. In this case the deprotonation occurs directly, irreversibly and with high regioselectivity (equation 1)[3]. By using a proton donor (solvent or excess of ketone) or a weaker base, an equilibration between the enolates formed may

TABLE 1. Conditions for the *kinetic* or *thermodynamic* control of enolate formation from 2-methylcyclohexanone[4a]

Conditions	Control	**1**:**2**[a]	Yield (%)
LDA, DME, 15 min, 0 °C	*kinetic*	1:99	74
Et_3N, DMF, 48h, reflux	*thermodynamic*	78:22	80

[a] Isomeric ratios were determined by GC analysis of the corresponding silyl enol ethers.

occur producing a *thermodynamically* controlled equilibrium. Thus, under *kinetic* control the formation of the less substituted enolate **2** is preferred; on the other hand, the more highly substituted enolate **1** arises in the equilibrium mixture. Typical examples are the enolizations of 2-substituted cyclic ketones summarized in Table 1[4,5].

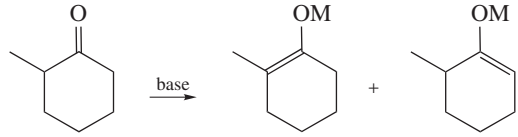

(**1**) (**2**) (1)

The *E*/*Z*-selectivity with acyclic ketones (equation 2) can be explained assuming a chair-like transition-state (**3** or **4**, respectively)[1,6]. Thereby, the (*E*)-configured enolate **5** is formed preferentially under *kinetic* control via transition-state **3**. However, by using side chains R that are sterically more demanding, the interactions in the transition-state increase significantly. Therefore, in some cases mainly the (*Z*)-configured isomer **6** is obtained, as shown in Table 2 for R = phenyl[7]. This reversal in selectivity is also achieved by adding polar aprotic solvents, such as DMSO, HMPA or DMPU, which are able to coordinate alkali metal ions: despite *kinetically* controlled reaction conditions the (*Z*)-configured ketone enolate **6** is formed preferentially in this case[8]. This effect is attributed to a disruption of the pericyclic transition-state model, resulting from complexation of the metal cation by the cosolvent[1].

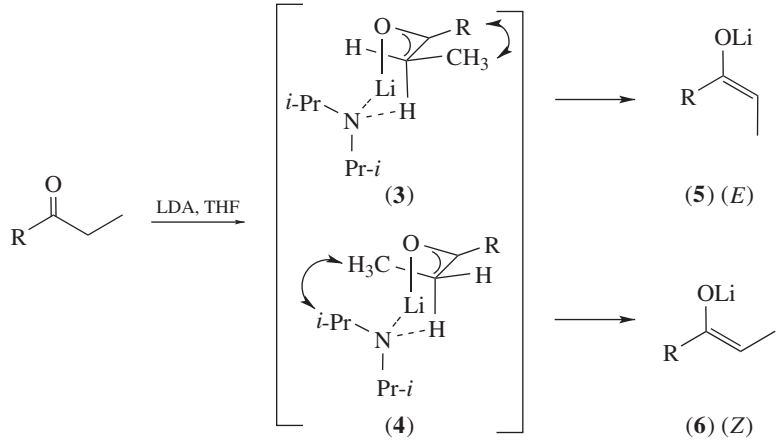

(2)

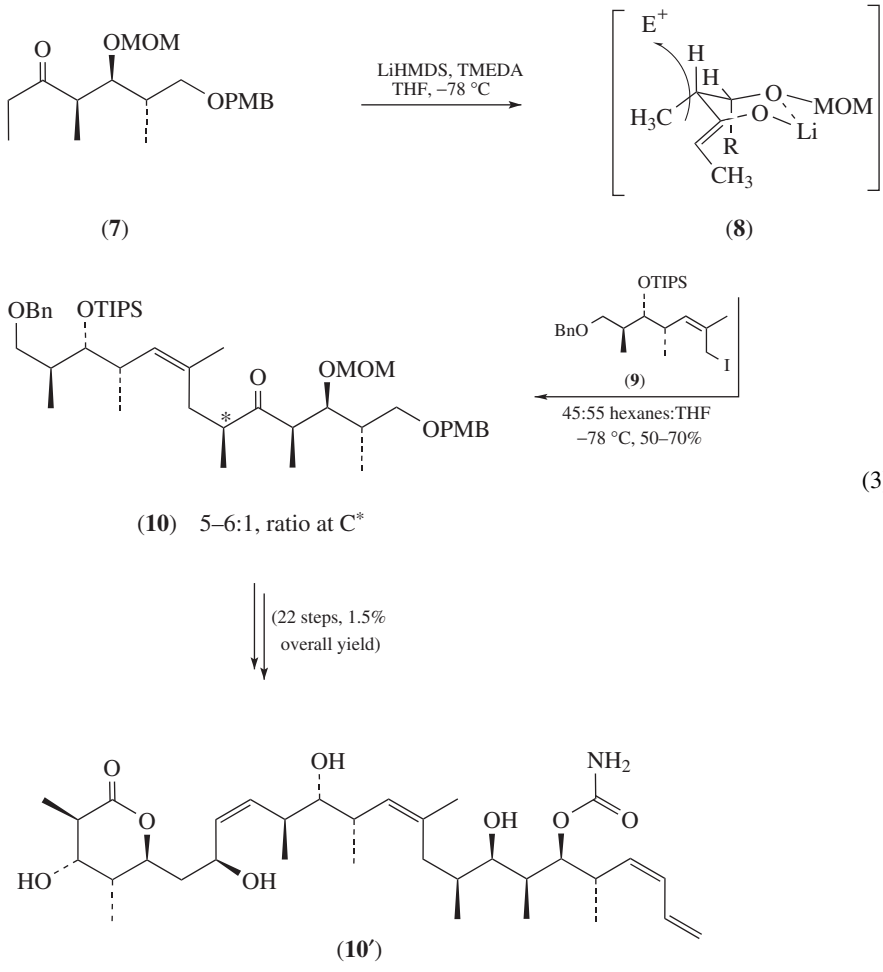

(**7**) (**8**)

(**9**)

(3)

(**10**) 5–6:1, ratio at C*

(**10′**)

TABLE 2. Conditions for the stereoselective enolate formation of acyclic ketones according to equation 2

R	Conditions	Cosolvent	**5**:**6** (*E*:*Z*)	Reference
i-Pr	LDA, THF, −72 °C	—	44:56	7
Ph	LDA, THF, −72 °C	—	<1:>99	7
Et	LDA, THF, −78 °C	—	77:23	8a
Et	LDA, THF, −78 °C	HMPA	5:95	8a

TABLE 3. Synthesis of α-benzylated ketones starting from enol ethers

R	Lewis acid	Product	Yield (%) [a]
Me	1 mol% $B(C_6F_5)_3$	**13a**	84
Me	5 mol% $Cu(OTf)_2$	**13a**	77
c-Hex	1 mol% $B(C_6F_5)_3$	**13b**	71

[a] Reactions were carried out in CH_2Cl_2 at r.t. (5–10 min).

Similar conditions for the formation of a (*Z*)-configured ketone enolate (**6**) at low temperature were applied by Myles and coworkers in their total synthesis of (+)-discodermolide (**10′**, equation 3)[9]. Deprotonation of the ethyl ketone **7** with LiHMDS as base at −78 °C and addition of TMEDA delivered a (*Z*)-configured enolate (**8**), which was subsequently alkylated with allyl iodide **9**. Thereby, chelation of the lithium enolate with the adjacent MOM protecting group led to a conformationally stable chair-like transition-state **8**, in which the attack of the alkylation reagent **9** (represented in **8** by E^+) could only occur from the site opposite to the bulky group R. Thus, the alkylation product **10** was obtained with a good diastereomeric selectivity at C* of 83–85% ds.

B. Alternative Methods for Enolate Formation

The base-induced abstraction of a proton α to a carbonyl group is not the only method for the preparation of ketone enolates; alternative methods also can provide good regio- and stereoselectivities. Enol ethers **11** can be converted on addition of a Lewis acid into the corresponding enolates **12**, which can attack the liberated benzyl cation under formation of α-benzylated ketones **13** (equation 4) in good yields (Table 3)[10].

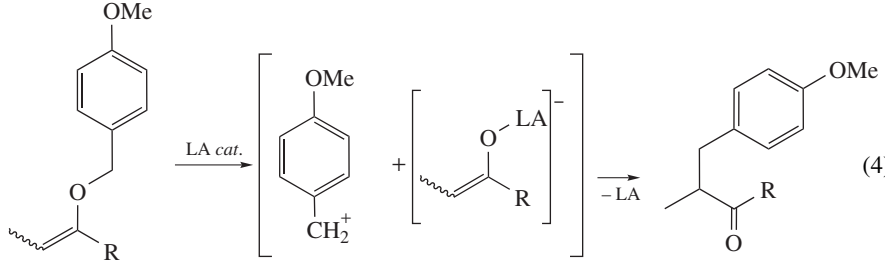

(4)

(**11**) (**12**) (**13**) (**a**) R = Me (**b**) R = *c*-Hex

Enolates can also be prepared by rhodium-catalyzed isomerization of allylic lithium alcoholates, such as **14** (equation 5)[11]. Subsequent treatment of the intermediately formed rhodium hydride complexes (**15** and **16**) with an electrophile led to the formation of various products. For example, alkyl halides gave α-alkylated ketones (**17**) in good yields, as shown in Table 4. Interestingly, addition of benzaldehyde under *kinetically* controlled

TABLE 4. Rhodium-catalyzed enolate alkylations

Catalyst	RX	Product	Yield (%)
$[Rh(dppe)(THF)_2]ClO_4$	BnBr	**17a**	75
$[Rh(dppe)(THF)_2]ClO_4$	MeI	**17b**	62
$[Rh(dppe)(THF)_2]ClO_4$	AllBr	**17c**	82
$RhCl(PPh_3)_3$	AllBr	**17c**	68

conditions gave the aldol products *syn* (**18**) and *anti* (**19**) aldol products with a good preference for the formation of the *syn* diastereomer, which indicates that the reaction preferentially proceeds via the (*Z*)-enolate **16**.

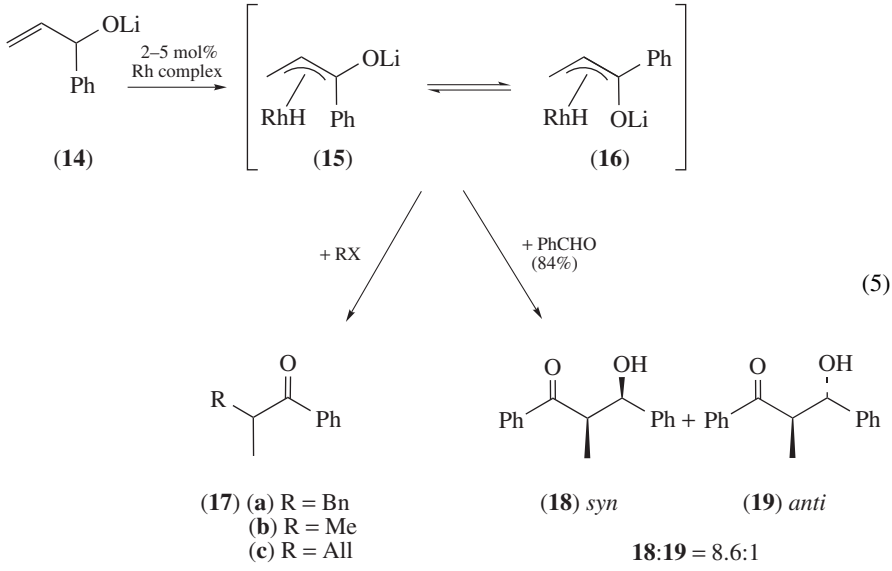

(**14**) (**15**) (**16**) (5)

(**17**) (**a**) R = Bn
(**b**) R = Me
(**c**) R = All

(**18**) *syn* (**19**) *anti*

18:**19** = 8.6:1

C. Substrate-controlled α-Alkylations of Ketone Enolates

Many applications for substrate-induced diastereoselective alkylations are reported in the literature. For a general overview of the different methods available see References 1, 12 and 13. In general, excellent diastereoselectivities were obtained by using conformationally fixed and sterically demanding ring systems, as illustrated in numerous highly stereoselective syntheses of 17α-alkylated progesterone derivatives **21** (equation 6)[14]. In this case the lithium enolate was created by reduction of enone **20** with elementary lithium in liquid ammonia. Subsequent alkylation *anti* to the methyl group delivered ketone **21** as a single diastereomer.

High diastereoselecivities are normally observed in the alkylation of five-membered ring enolates (equations 7 and 8), implying that the alkylation is mainly controlled by steric factors. Thus, with 3-substituted cyclopentanones formation of only the *trans*-product (**23** and **25**, respectively) is preferred. Representative examples are the alkylations of lithium enolates derived from ketones **22**[15] and **24**[16]. Before the electrophiles were added, the enolate solutions were stirred at higher temperature for a longer time to secure the

generation of the *thermodynamical* enolate at the more substituted carbon. Moreover, for deprotonation of ketone **22** less than one equivalent of LDA was used to produce a *thermodynamically* controlled equilibrium, in which the more highly substituted enolate is favored.

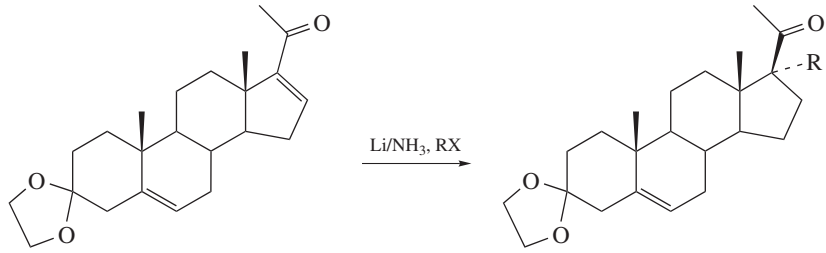

(**20**) (6)

only one diastereomer formed:

(**21**) (**a**) RX = MeI, 65%
(**b**) RX = EtI, 43%
(**c**) RX = AllBr, 17%

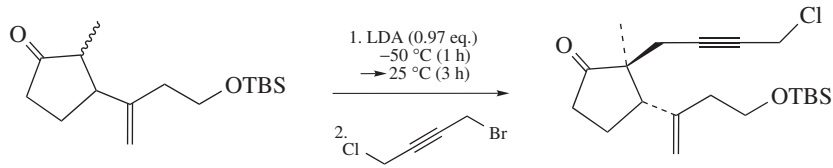

(**22**) 86% (**23**) (7)

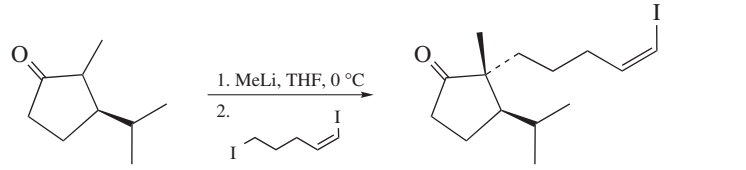

(**24**) 63–72% (**25**) (8)

α,β-Dialkylations of enones (three-component couplings)[17] are one of the most elegant methods for the diastereoselective construction of highly functionalized small rings, mainly because only one enolate can be created in the first addition step[18]. Thus, problems associated with *kinetically* or *thermodynamically* controlled enolate formation can be avoided completely. Fürstner and coworkers described a tandem organozincate conjugate addition–alkylation for the synthesis of the prostaglandin intermediate **28** starting from vinyl stannane **26** (equation 9)[19]. The transmetalation (Sn → Li → Zn) afforded a zincate intermediate that underwent a smooth Michael addition in a highly stereoselective fashion and enhanced the efficiency of the subsequent alkylation of the intermediary formed zinc enolate **27**.

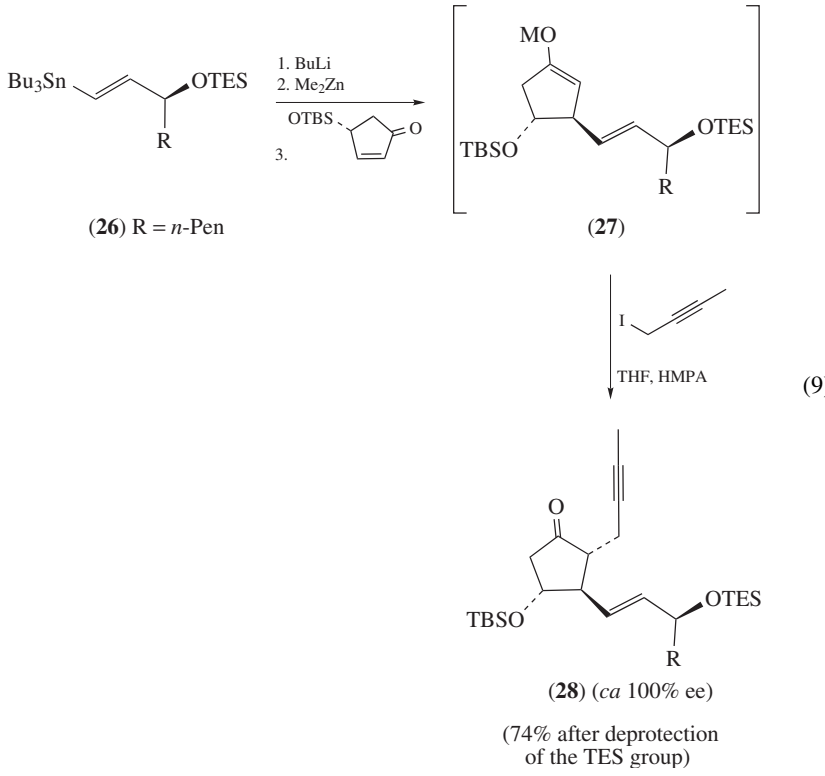

(**26**) R = *n*-Pen

(**27**)

(**28**) (*ca* 100% ee)

(74% after deprotection of the TES group)

(9)

Kibayashi and coworkers described a similar approach to a 2,3,4-trisubstituted cyclopentanone (**29**) in their total synthesis of (−)-incarvilline (**30**, equation 10)[20]. The reaction proceeded with all-*trans* stereoselection with respect to the stereocenters of the cyclopentane ring.

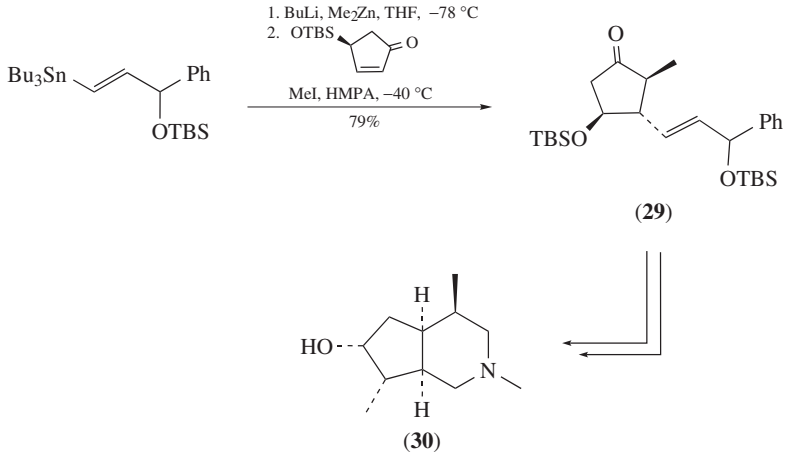

(**29**)

(**30**)

(10)

D. Asymmetric α-Alkylation with a Chiral Lewis Acid

Enolates, which are associated with an optically active bulky Lewis acid (equation 11), can be alkylated in a regio- and enantioselective manner as reported by Yamamoto and coworkers (Table 5)[21]. After precomplexation of the ketones **31a** or **31b** with aluminum tris((*R*)-1-α-naphthyl-3-phenylnaphthoxide) (**32′**) in toluene and treatment with a THF–pentane solution of LDA/*t*-BuLi, addition of TBSOTf caused ring-opening of THF and butylation at the more congested α-site of the enolate, to give **32** predominantly with good enantiomeric excesses. Thereby, the productivity of the reaction depends strongly on the molar ratio of the ketone, the Lewis acid (**32′**) and the base used.

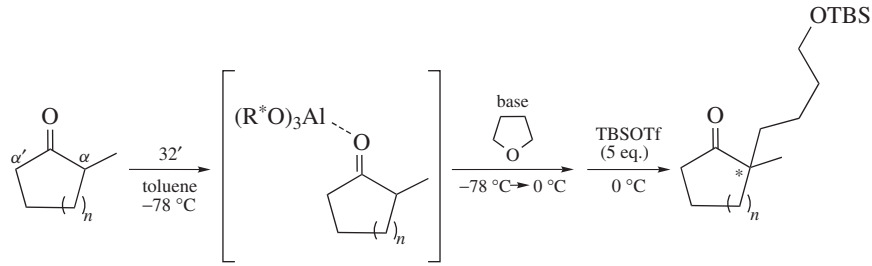

(**31**) (**a**) $n = 1$
(**b**) $n = 2$

(**32**) (11)

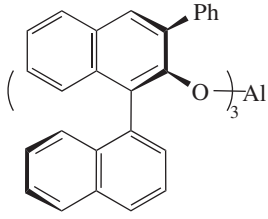

(**32′**)

E. Ketone Enolates as Nucleophiles in Transition-metal Catalyzed Allylic Alkylations

In 1980 Trost and Keinan reported on allylic alkylations of tin enolates such as **33** catalyzed by tetrakis(triphenylphosphine)palladium (equation 12)[22]. The stannyl ethers led to a rapid and clean monoalkylation with high regioselectivity. Thereby, alkylation generally occurred at the less substituted end of the allyl moiety with formation

TABLE 5. Regio- and enantioselective alkylation of 2-methylcyclopentanone (**31a**) and 2-methylcyclohexanone (**31b**) with an optically active Lewis acid

n	Base	Yield (%)	Ratio α:α′	ee (%)
1	LDA (4 eq.)	93	>20:1	89
2	LDA (1 eq.)/*t*-BuLi (1 eq.)	56	>99:1	78
2	LDA (2 eq.)/*t*-BuLi (2 eq.)	90	>99:1	77

of the (*E*)-isomers **34** and **35**, independently of the olefin geometry in the starting allylic acetates.

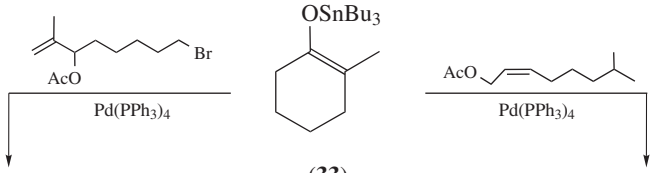

(**33**)

(12)

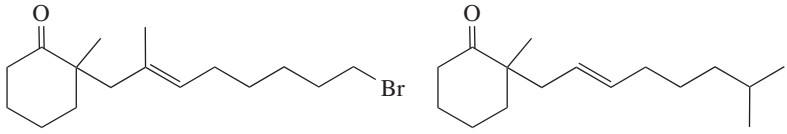

(**34**) 89% (**35**) 96%

The *kinetic* tin enolates, e.g. **36a**, can be generated *in situ* from the lithium enolate of ketone **36** and tributyltin chloride, as illustrated in equation 13a. Under these conditions the allylic alkylation with cinnamyl acetate (**37**) led only to the 2,6-disubstituted product **38**[22]. The *in situ* generation of tin enolates (**36b**) by treatment of the lithium enolate with tri-*n*-butyltin or trimethyltin trifluoroacetate is also possible (equation 13b); using the allylic acetate **39**, this method delivered the *kinetically controlled* alkylation product **40** regioselectively, but in moderate yield[23]. Negishi and coworkers showed that allylation of zinc enolates (**36c**) or potassium enoxyborates (**36d**) derived from **36** proceeded well in the presence of palladium phosphine complexes (equations 13c and 13d). Various allylic halides, such as **41**, and acetates (**43**) could be used and the regioselectivities observed for the substitution products **42** and **44** were in the range of 95%. Remarkably, the alkylation of neryl acetate (**43**) led to a nearly complete retention (⩾98%) of the olefin configuration (**44**). A wide range of other counterions were also tested, but they gave either unsatisfying results (35% yield with Bu_3Sn^+) or did not show any reaction at all ($ClMg^+$, Me_2Al^+, Me_3Si^+, Cp_2ClTi^+)[24].

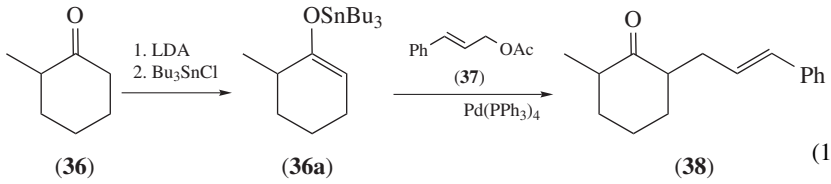

(**36**) (**36a**) (**38**)

(13a)

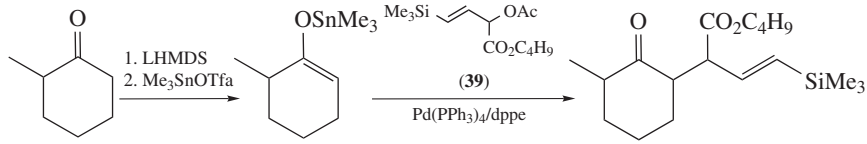

(**36**) (**36b**) (**40**) 49%

(13b)

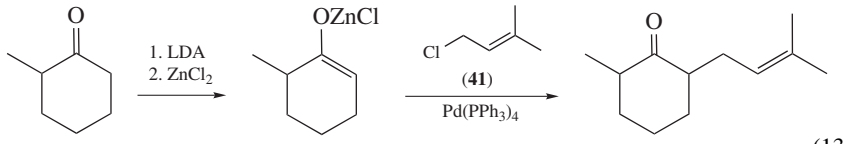

(**36**) (**36c**) (**42**) 92%, 95% rs (13c)

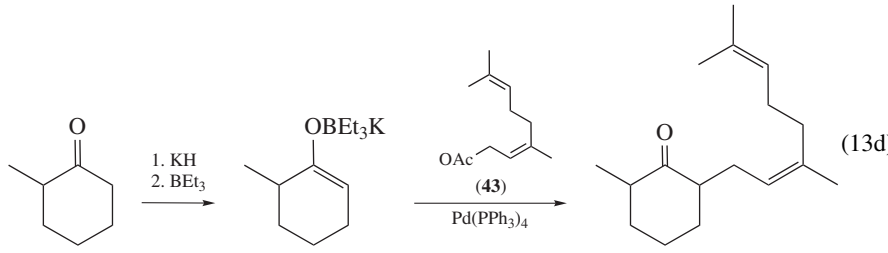

(**36**) (**36d**) (**44**) 73%, 95% rs (13d)

In 1999 Trost and Schröder reported on the first asymmetric allylic alkylation of nonstabilized ketone enolates of 2-substituted cyclohexanone derivatives, e.g. 2-methyl-1-tetralone (**45**), by using a catalytic amount of a chiral palladium complex formed from π-allylpalladium chloride dimer and the chiral cyclohexyldiamine derivative **47** (equation 14)[25]. The addition of tin chloride helped to 'soften' the lithium enolate by transmetalation and a slight increase in enantioselectivity and yield for the alkylated product **46** was observed. Besides allyl acetate also linearly substituted or 1,3-dialkyl substituted allylic carbonates functioned well as electrophiles. A variety of cyclohexanones or cyclopentanones could be employed as nucleophiles with comparable results[26]. Hou, Dai and coworkers reported comparable results for **45**, using ferrocene-modified chiral ligands similar to **47**[27]. Their results were comparable to those obtained by Trost.

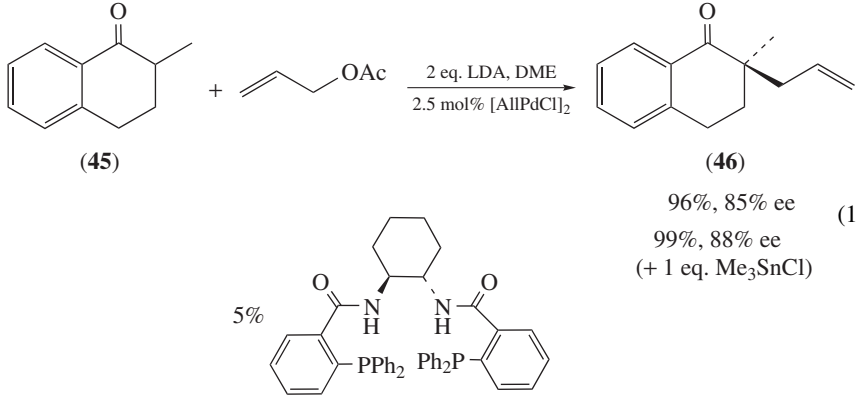

(**45**) (**46**) 96%, 85% ee
99%, 88% ee
(+ 1 eq. Me_3SnCl) (14)

(**47**) (*S*,*S*)

The efficiency of the palladium-catalyzed asymmetric alkylation of ketone enolates was shown by Trost and coworkers in their synthesis of hamigeran B (**50**), a potent antiviral agent with low cytotoxicity to host cells (equation 15)[28]. The quaternary center

of compound **49** was generated in 93% ee by asymmetric allylation of the ketone enolate derived from **48**. This stereocenter controls the relative configuration of the contiguous two stereocenters of **50**, so that only one asymmetric step was necessary in the whole synthesis.

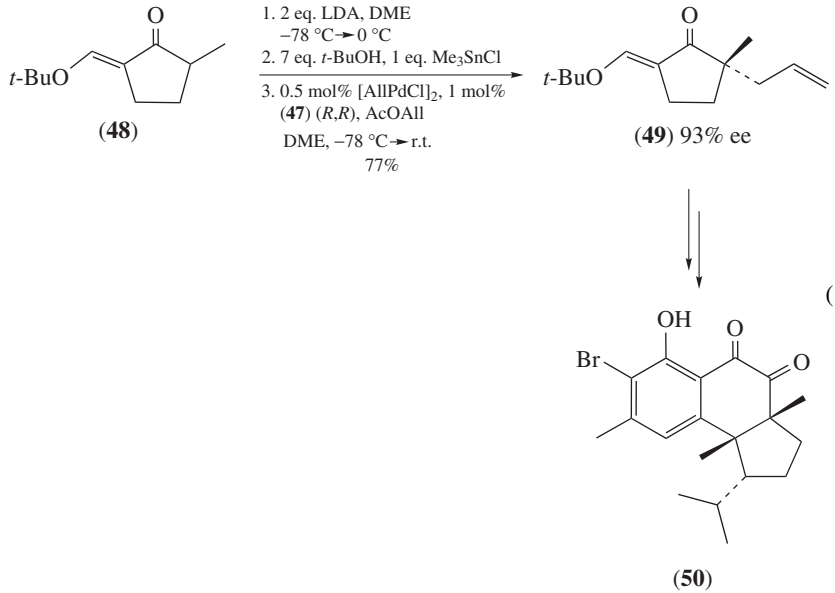

(15)

Interesting investigations were carried out by Braun and coworkers in diastereoselective and enantioselective palladium-catalyzed allylic substitutions with the nonstabilized magnesium enolate of cyclohexanone (**51**, equation 16)[29]. With (*R*)-BINAP as chiral ligand and the *syn* product **53** was obtained nearly exclusively with high enantiomeric excess and quantitative conversion of the starting material **52**.

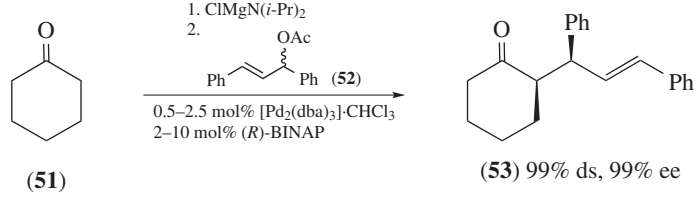

(16)

An intramolecular palladium-mediated allylic alkylation via a ketone enolate of piperidinone **54** was reported by Williams and coworkers for the synthesis of (*R*)-7-hydroxyquinine **57** (equations 17 and 18)[30]. The key step involves a palladium-mediated S_N2'-type cyclization reaction of enol ether **55** in the presence of Bu_3SnF, giving rise to a quinuclidine ketone, which was immediately reduced to **56** to avoid equilibration and β-elimination. Interestingly, none of the undesired C3-vinyl stereoisomer was observed,

which could be explained either by formation of a palladium complex **58** undergoing allylic alkylation to ketone **61** or a palladium-mediated etherification (**55** → **59** → **60**), followed by a Claisen rearrangement (**60** → **61**).

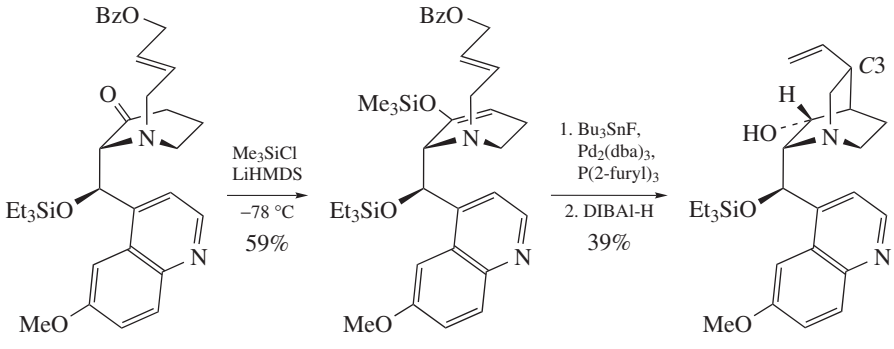

(**54**) (**55**) (**56**)

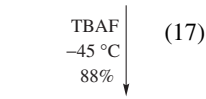

(17)

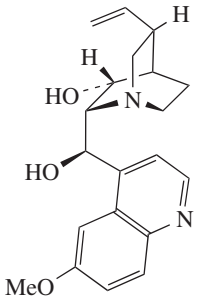

(**57**)

Evans and Leahy reported on a method for the rhodium-catalyzed allylic alkylation using copper enolates, generated by transmetalation of the corresponding lithium enolates (equation 19)[31]. These enolates are softer and less basic nucleophiles than lithium enolates and therefore problems typically associated with enolate nucleophiles in metal-allyl chemistry can be avoided[32]. A copper(I) enolate, derived from acetophenone derivative **63**, was used as nucleophile in a regio- and stereoselective rhodium-catalyzed alkylation of the *in situ* activated allylic alcohol **62**. Thereby, the synthesized ketone **64**, a key intermediate in the total synthesis of (−)-sugiresinol dimethyl ether (**65**), was produced as the only detectable regioisomer with complete conservation of enantiomeric excess.

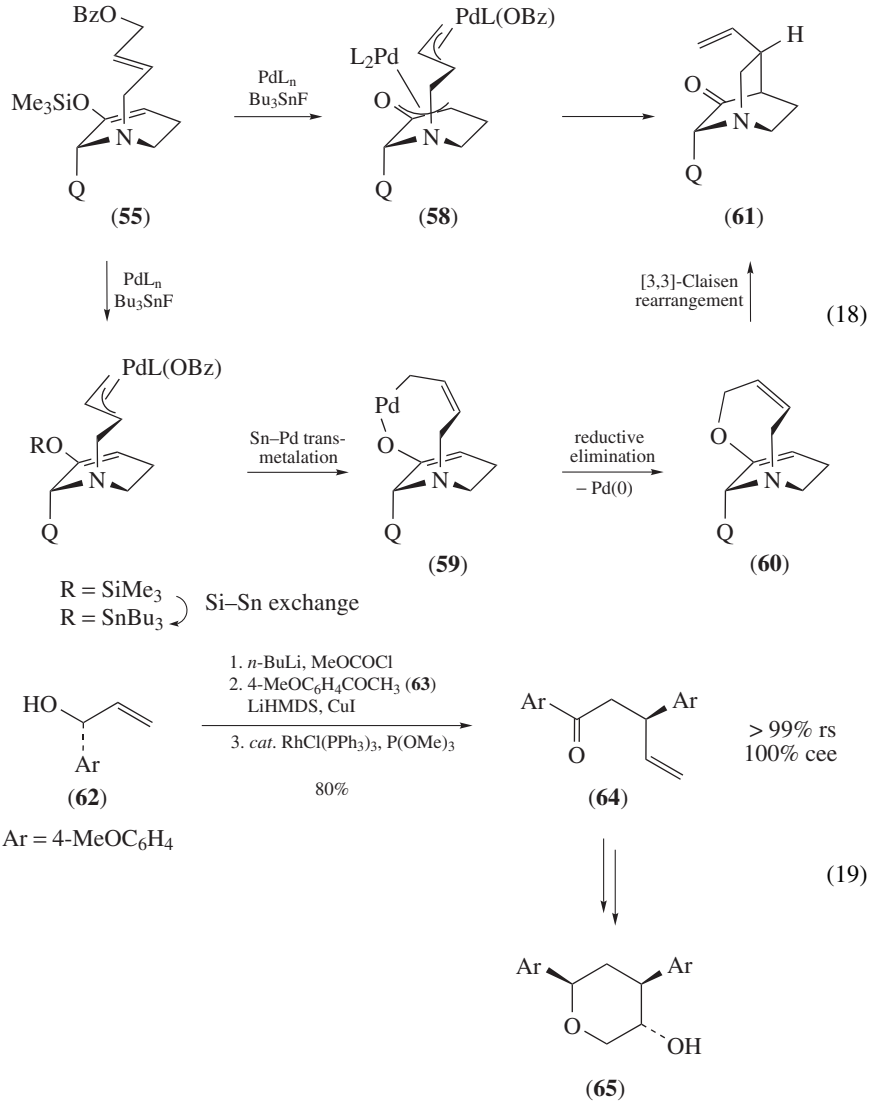

F. Cross-coupling Reactions of Enolate Nucleophiles

In the last years several publications appeared describing palladium-catalyzed α-arylations of ketone enolates for the synthesis of α-aryl ketones, involving ketone enolates[33], silyl enol ethers[34] and intramolecular α-arylation of ketone enolates[35]. In this process, an enolate is generated from a ketone in the presence of an aryl halide, and a palladium catalyst couples this enolate with the aryl halide. Iwama and Rawal proposed

TABLE 6. Arylations via cyclohexanone stannyl enolates (**68**)

Product	R′	R	X	Yield (%)
69a	H	4-MeO	I	82
69b	H	4-MeO	Br	64
69c	H	4-NO_2	Br	71
69d	H	2-MeO	I	71
69e	Me	4-MeO	I [a]	72 [a]

[a] Only the *trans*-isomer was formed.

a general procedure taking advantage of the *in situ* formation of cyclohexanone stannyl enolates (**68**) (equation 20)[36]. It allows regiospecific inter- and intramolecular arylation of silyl enol ethers (**66**) with a wide range of electron-poor and electron-rich aryl halides (**67**). Remarkably, the arylation of a 3-methyl substituted enol ether (**66**, R′ = Me) gave the arylated product **69e** as a single regio- and stereoisomer (Table 6). Obviously no equilibration of the putative tin or palladium enolate intermediate to the regioisomeric, less-hindered enolate took place. The investigations showed that satisfactory yields were obtained if the silyl enol ether **66** and tin fluoride were used in excess (2 eq. each).

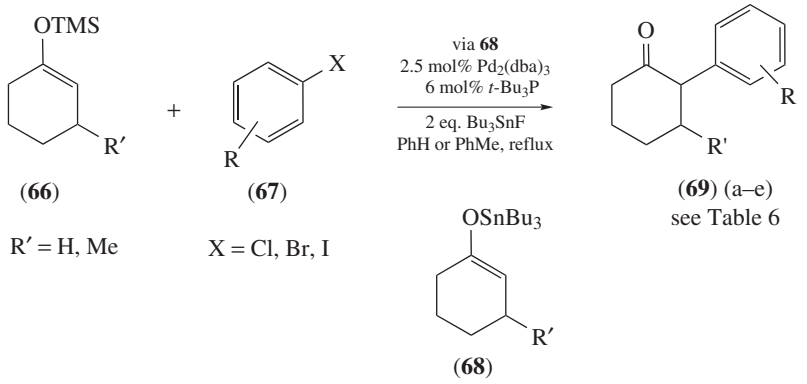

(**66**) (**67**) (**69**) (a–e) see Table 6 (20)

R′ = H, Me X = Cl, Br, I (**68**)

The synthetic utility of this method was further developed through investigation of substrates in which the arylation took place intramolecularly. Treatment of the TMS enol ether **70** with 2.5 mol% of $Pd_2(dba)_3$ and 6 mol% of t-Bu_3P in the presence of 1 eq. Bu_3SnF afforded the bicyclic arylation product **71** in 84% yield (equation 21)[36].

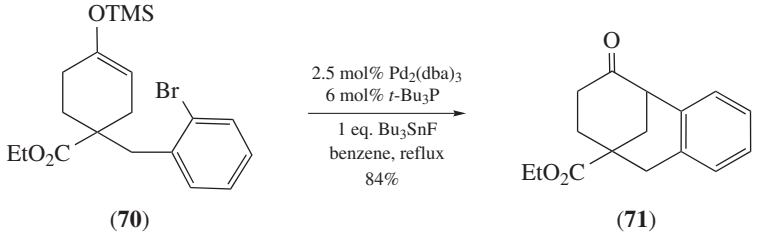

(**70**) (**71**) (21)

The group of Willis and coworkers reported on palladium-catalyzed intramolecular *O*-arylation[37] of enolates and *S*-arylation[38] of thioenolates. The process tolerates many variations in both the ketone and aryl fragments and delivers the cyclization precursors and heterocyclic products in good yields. As an illustrative example the reaction sequence starting from cyclohexanone **72** is used for benzo[*b*]furan (**78**) and benzo[*b*]thiophene (**79**) synthesis (equations 22 and 23)[38]. The α-(*o*-bromoaryl)-substituted ketone **75** was prepared through an intermolecular α-arylation of a cesium ketone enolate using 1-bromo-2-iodobenzene **73**, $Pd_2(dba)_3$ and xantphos (**74**) as ligand. After purification, thioketone **76**, which was required for the synthesis of benzothiophene **79**, was obtained by treatment of **75** with P_2S_5. Although trace amounts of benzo[*b*]furan **78** could be detected already during preparation of the α-arylated ketone **75**, the use of DPEphos (**77**) was necessary to achieve optimal yields in the cyclization step. Lowering the temperature or using a stronger base (NaOBu-*t*) resulted in poorer conversions.

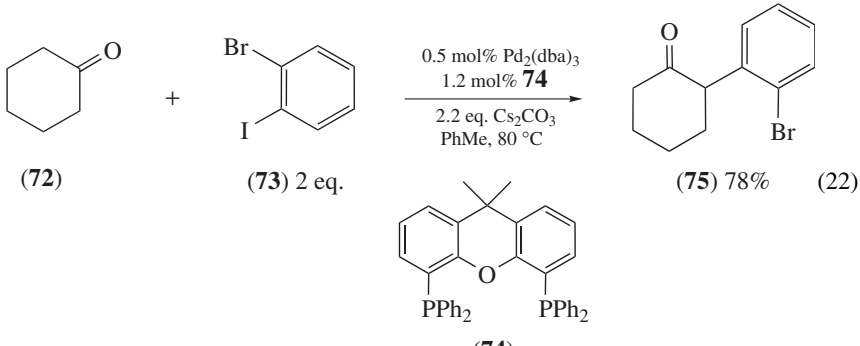

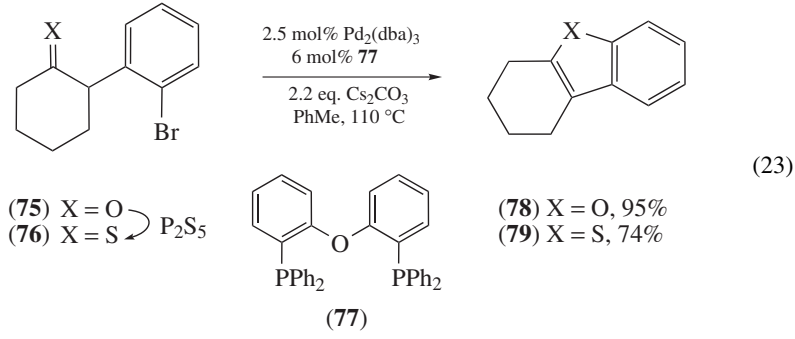

Combining both ligands **74** and **77** in a single reaction led to a one-pot cascade process in which the cyclohexane-fused benzo[*b*]furan **78** was formed directly in 51% overall yield[38]. Screening of different catalysts under various reaction conditions (ligand loading, solvent, temperature) showed that the yield could be significantly increased (up to 100%) by using 12 mol% of the dimethoxy-substituted dicyclohexylphosphine ligand **80** at higher temperature in toluene (equation 24). Unfortunately, these conditions were not transferable to alternative substrates: only low yields of mixtures of arylated ketone and benzofuran were obtained in almost all cases.

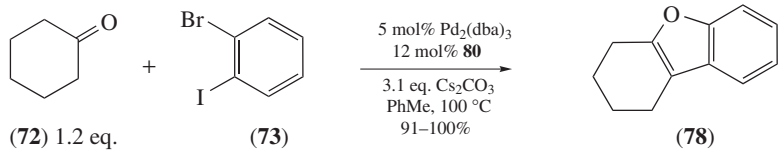

(**72**) 1.2 eq. (**73**) (**78**)

(24)

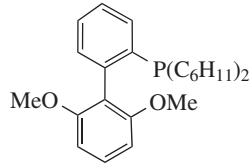

(**80**)

A reaction sequence comparable to the enolate-driven cross-coupling process was described by Cook and coworkers for the enantiospecific total synthesis of (+)-macroline (**84**) (equation 25)[39]. The key step (**82** → **83**) involved an intramolecular Pd(0)/DPEphos-catalyzed α-vinylation of a ketone enolate under formation of the pentacyclic ketone **83**, whereby best results were obtained with NaOBu-*t* as base. Using a weaker base such as K_3PO_4 or increasing the DPEphos/Pd ratio, the yield of **83** decreased distinctly. Probably an excess of ligand reduces the amount of catalytically active Pd(0) species, leading to a retardation of the oxidative-addition step. Thus, a base-mediated E_2-elimination could occur to provide an alkyne byproduct from vinyl iodide **82** resulting in lower yields for the cyclization product **83**. Finally, further modifications of **83** led to the desired (+)-macroline (**84**) in good overall yield (17.5% starting from tryptophan methyl ester **81**).

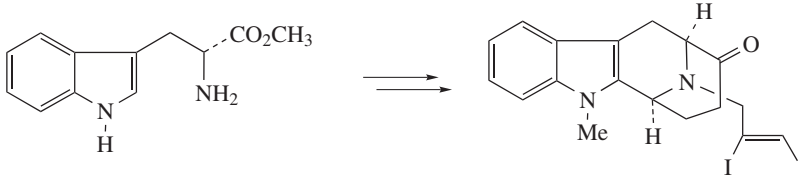

(**81**) (**82**)

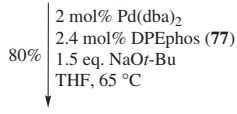

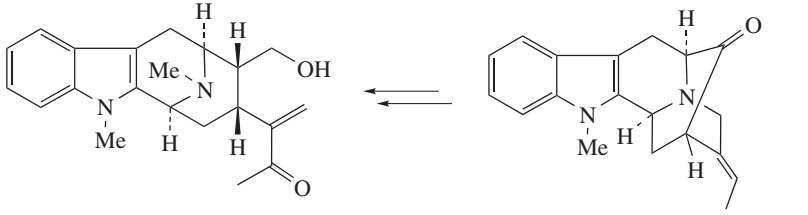

(**84**) (**83**)

(25)

III. C–C BOND FORMATION BY ADDITION OF KETONE ENOLATES TO CARBONYL GROUPS

A. Introduction

The aldol addition is one of the most powerful transformations in organic synthesis for the generation of 1,3-dioxygen relationships in organic molecules[40]. New, and particularly stereoselective variants of this reaction have been developed during the last decades and found many applications for the synthesis of a wide range of natural products with biological and pharmacological significance[41]. This section presents a short overview of modern versions and latest developments of the aldol reaction, illustrated by selected syntheses of natural products. One of the most important aspects in aldol reactions is described, namely the influence of the metal enolate structure on reactivity and diastereoselectivity.

B. Substrate-controlled Stereoselective Aldol Reactions

1. Simple diastereoselectivity

Simple diastereoselectivity is generally related to the enolate geometry[42,43]: (*E*)-ketone enolates predominantly furnish *anti*-aldol products **86** and (*Z*)-enolates give *syn*-aldols **88** as the main products, especially with a sterically demanding substituent R at the carbonyl group[7]. This observation can be explained by assuming a six-membered chair-like assembly (**85** and **87**) of the reactants (Zimmerman–Traxler model, equations 26a and 26b)[44]. However, many exceptions to this general rule are also known. Especially for aldol additions with lithium or magnesium enolates (M = Li, Mg), this transition-state hypothesis is a rough simplification, because lithium enolates form aggregates, even in solution, so that the reactive species in aldol additions are not monomeric but oligomeric lithium enolates[45]. This observation is underpinned by the fact that boron enolates, which are known to be monomeric, show a stronger (*Z*)-*syn* and (*E*)-*anti* correlation[46].

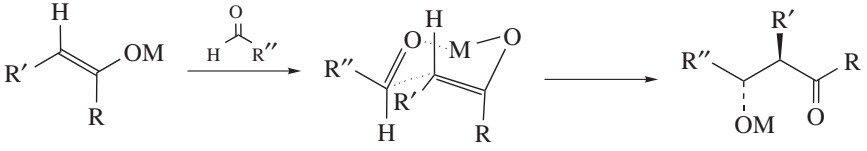

(*E*)-enolate (**85**) (**86**) (*anti*) (26a)

M = Li, Mg, Ti, Sn, B

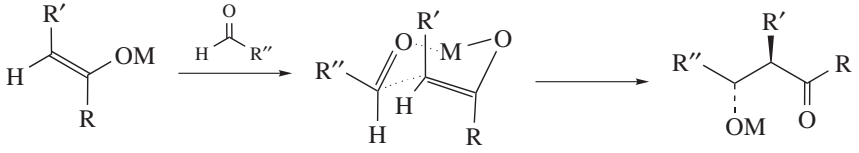

(*Z*)-enolate (**87**) (**88**) (*syn*) (26b)

M = Li, Mg, Ti, Sn, B

2. Induced diastereoselectivity

The addition of a chiral ketone enolate to an aldehyde displays not only simple diastereoselectivity, but also highly induced stereoselectivity, as shown by Fecik and coworkers for the formal total synthesis of the polyketide macrolactone narbonolide (**92**, equation 27)[47]. This reaction demonstrates the successful application of titanium in aldol additions for the highly stereoselective construction of two new stereogenic centers: by addition of aldehyde **90** to the titanium enolate of Evans' β-keto imide **89**[48a] the *syn*-aldol product **91** was obtained exclusively in 74% yield. Interestingly, there is no detectable loss of stereochemistry via enolization at the potentially labile C2-methyl-bearing stereocenter in **89**[48b].

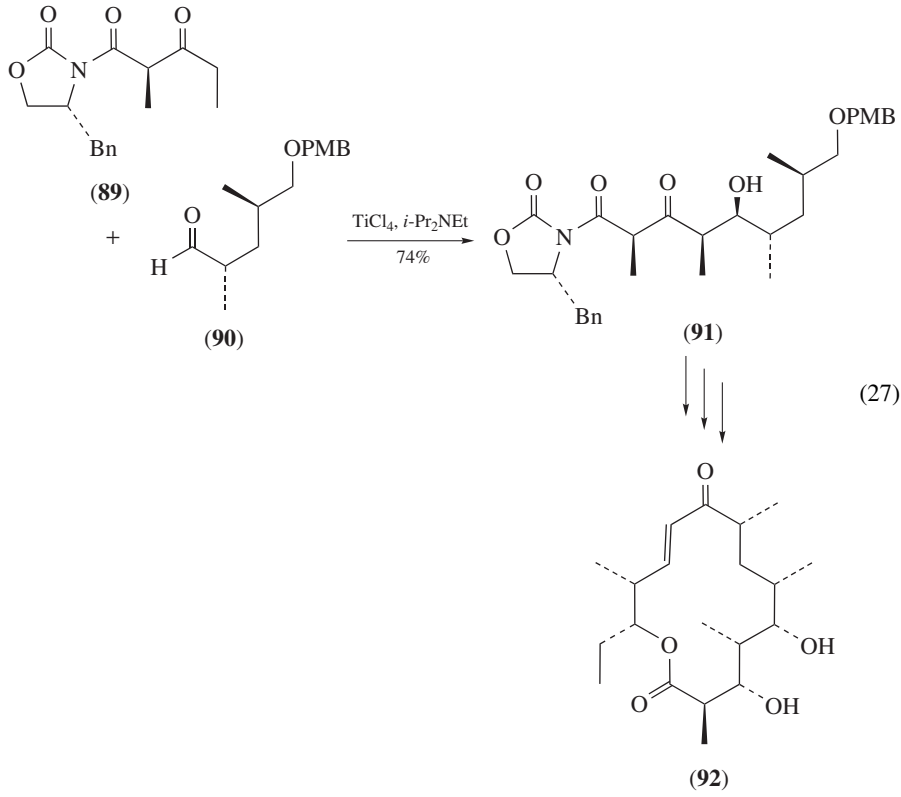

Also, Urpí and coworkers reported on stereoselective aldol reactions based on titanium enolates, both from chiral ethyl ketones **93**[49] (equation 28) and lactate-derived ketones[50]. High yields and diastereoselectivities, preferring the 2,4-*syn*-4,5-*syn* diastereomer **95**, were obtained by using (i-PrO)$TiCl_3$ as soft Lewis acid and i-Pr_2NEt as base. The stereochemical outcome of the process is consistent with a selective formation of a (*Z*)-enolate (affected by a coordination of the β-chelating *O*-protecting group to titanium), as illustrated in transition-state **94**. Replacement of the benzyl-protecting group by a silyl group in **93** also gave rise to high (*Z*)-enolate selectivity, but unfortunately the aldol products were obtained as a mixture of diastereomers with up to 20% of the diastereomer **96** (Table 7,

TABLE 7. Stereoselective aldol reactions with titanium ketone enolates

PG	R	**95**:**96**	Yield (%)
PMB	*i*-Pr	95:5	88
Bn	*i*-Pr	97:3	95
Bn	Ph	94:6	87
Bn	$CH_2{=}CCH_3$	97:3	91
TBDPS	*i*-Pr	80:20	65

entry 5). This result is attributed to a weaker coordination ability of the β-OTBDPS protecting group to titanium in the transition-state. Alternatively, $Sn(OTf)_2$ can be used as Lewis acid for preparation of the *syn* aldol product **95**, since tin(II) also forms (*Z*)-enolates preferentially with ethyl ketone **93** and takes advantage of the coordinating ability of the benzyloxy group[51].

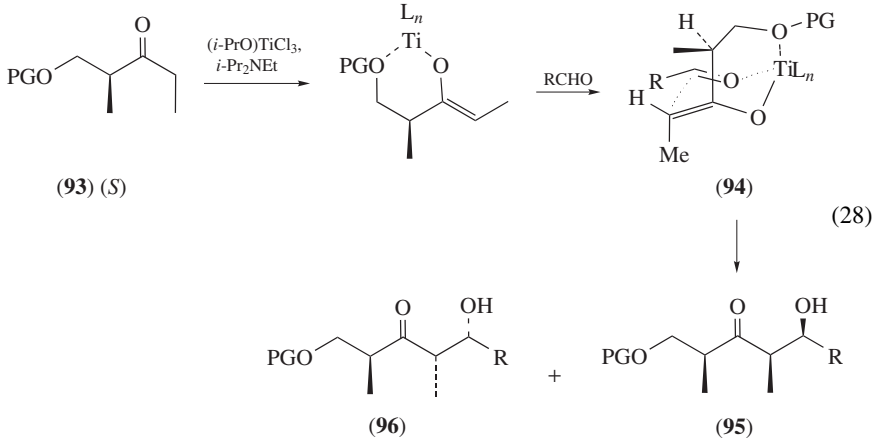

The (*R*)-enantiomer of benzyl protected ethylketone **93** was used by Perkins and Sampson for a total synthesis of (−)-membrenone *C* (**99**, equation 29)[52a]. Two aldol additions were performed in the presence of $TiCl_4$ and diisopropylethylamine during this synthesis, whereby the aldol adducts **97** and **98** were obtained with a high degree of *syn* selectivity (**97** with >95% ds and **98** with >90% ds). Also, a boron enolate approach was done for the synthesis of **99**[52b] and a tin(II)-mediated aldol for (−)-membrenone *A* (**100**) and (−)-membrenone *B* (**100′**)[52c].

Besides tin(II) or titanium enolates the boron enolates play an important role in aldol chemistry[53]. As mentioned above, the configuration of the aldol products strongly depends on the geometry of the boron enolates: (*E*)-enolates give *anti* aldols whereas (*Z*)-enolates give *syn* aldols. These results can be explained by the transition-states shown in equation 26. Evans established that simple diastereoselectivity is enhanced in aldol reactions of boron enolates compared to lithium enolates, owing to the considerably shorter B−O and B−C bond lengths that lead to much tighter transition-states[54].

Perkins and coworkers reported on stereoselective aldol reactions with boron and titanium ketone enolates (equations 30 and 31) for the construction of a spiroacetaldihydropyrone (**108**) related to natural products auripyrone *A* and *B*[55]. Both are cytotoxic

polypropionates with activity against HeLa S_3 cells (IC_{50} values of 0.26 and 0.48 μg/mL, respectively)[56]. *Anti*-configured boron aldolate **103** was obtained by treating the boron enolate of ketone **101** with methacrolein (**102**). *In situ* reduction of **103** with $LiBH_4$ furnished the aldol product **104** with a high degree of diastereoselectivity (>95% ds). The coupling of aldehyde **105** with the titanium enolate of racemic ketone **106** yielded the *syn*-configured aldol **107** as a racemic mixture of a single diastereomer. Formation of the single racemic product **107** from the coupling of two racemic fragments is an unusual example of mutual *kinetic* diastereoselection. In this case a large *anti*-Felkin preference[57] of the aldehyde **105** is matched in a fast reaction with the *syn-syn* preference of the ketone **106**. Thus, each enantiomer of the titanium enolate of ketone **106** selectively reacts with the correct enantiomer of aldehyde **105**[55].

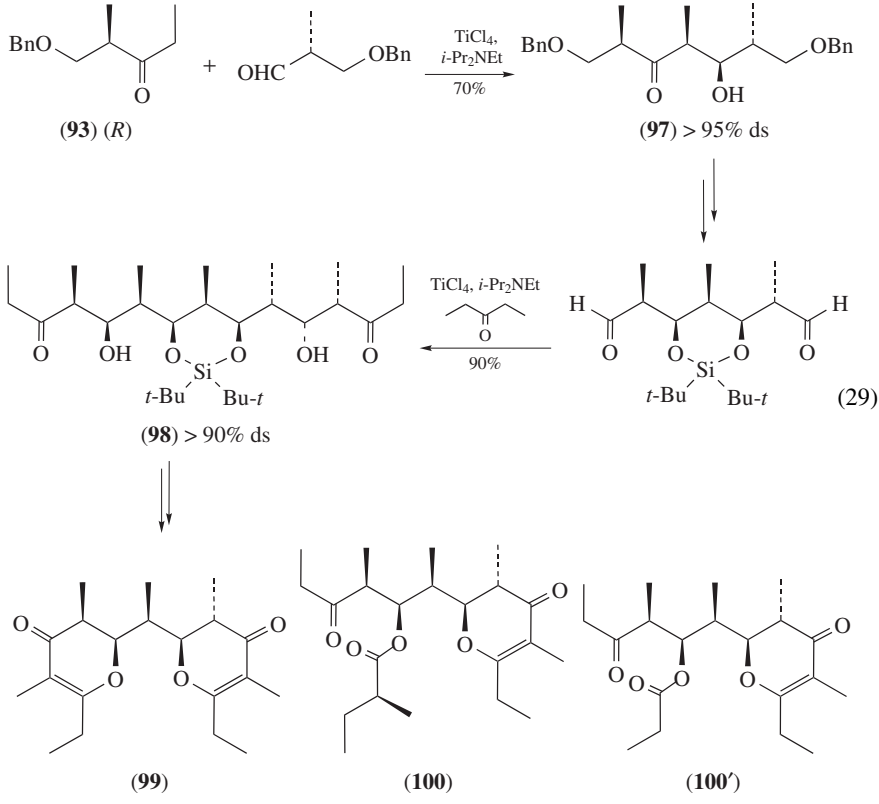

Perkins and coworkers also synthesized eight isomers of maurenone (**116**) to elucidate the unknown structure of the natural product (−)-maurenone, a marine polypropionate from the pulmonate mollusc *Siphonaria maura* (equations 32a–32d, 33a, 33b and 34)[58]. The required pairs of enantiomeric chiral aldehydes **110**, *ent*-**110**, **112** and *ent*-**112** as well as chiral ketones **113** and **114** were synthesized using a cascade of highly diastereoselective *syn* and *anti* boron aldol reactions. Notably, the change in protecting group from benzyl (in **109** and *ent*-**109**) to benzoyl (in **111** and *ent*-**111**) and the use of slightly modified enolization conditions (Me_2NEt instead of NEt_3 as base and warming up the boron enolate mixtures to 0 °C) generates the *trans* boron enolates selectively.

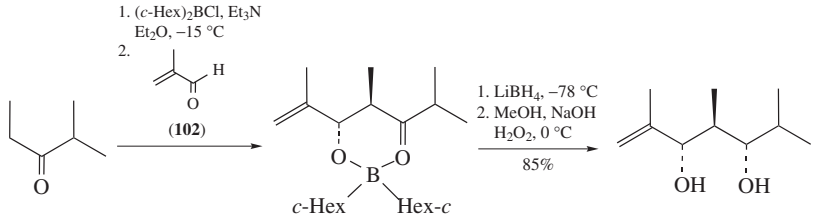

(**101**) (**103**) (**104**) > 95% ds

(30)

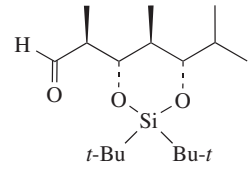

(**105**)

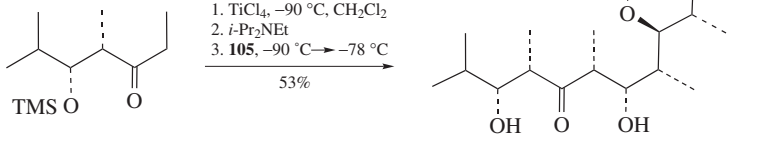

(**106**) *rac* (**107**) only diastereomer observed

(31)

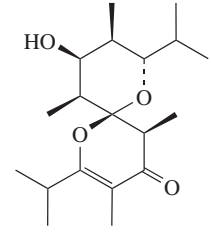

(**108**)

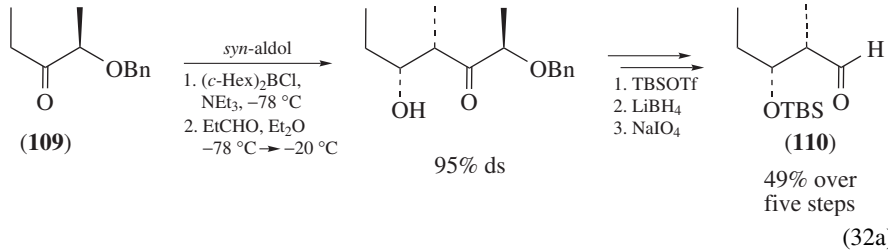

(32a)

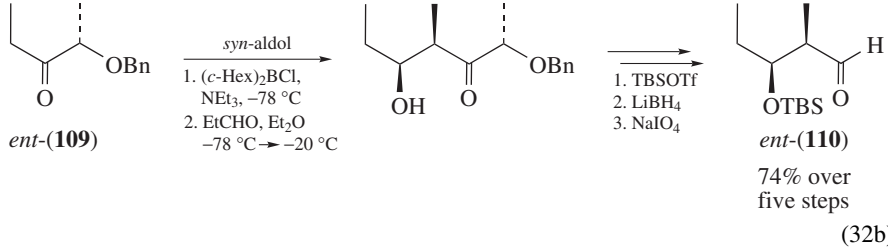

(32b)

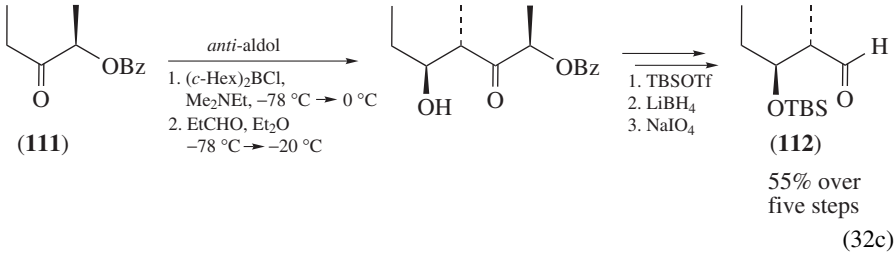

(32c)

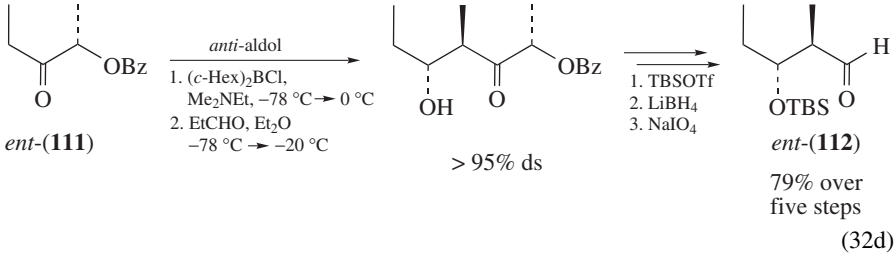

(32d)

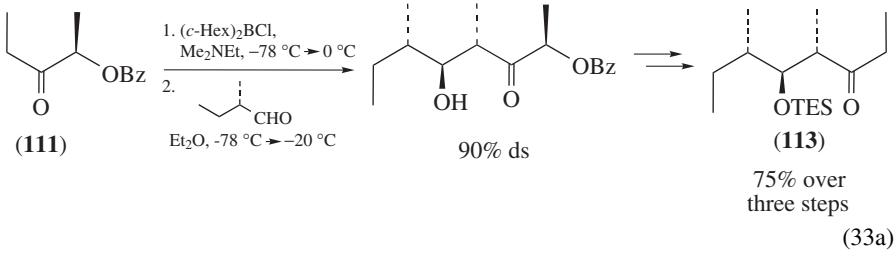

(33a)

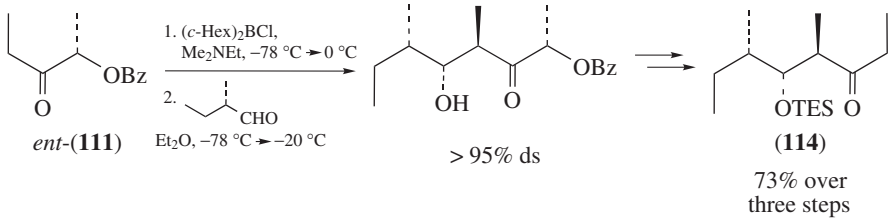

(33b)

The synthesis of eight isomers of maurenone **116** proceeded by coupling of each of the four aldehyde isomers **110**, *ent*-**110**, **112** and *ent*-**112** with the two ketone isomers **113** and **114**. Attempts to couple the titanium enolate ($TiCl_4$, *i*-Pr_2NEt) of ketone **113** with aldehyde **110** proved troublesome, because of desilylation taking place during enolization of ketone **113**. Better results were achieved by means of lithium enolates, on treatment of ethyl ketone **113** with LiHMDS and subsequent addition of aldehyde **110**, yielding the isomer **115** with an acceptable diastereoselectivity of 74% ds (equation 34). Separation of the isomers and further transformations gave (−)-maurenone (**116**), which NMR data showed to be an almost perfect correlation with all the peaks reported for the natural product maurenone[58].

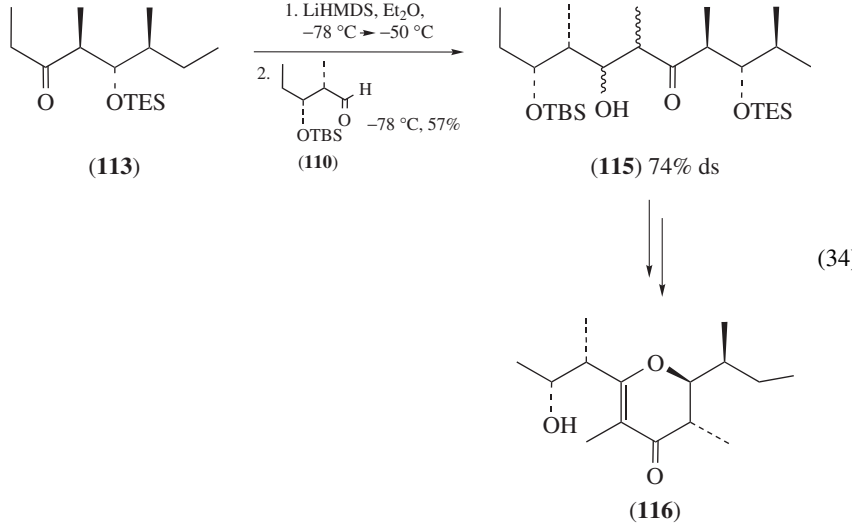

(34)

C. Alternative Methods for Enolate Preparation

Recently, Yamaguchi and coworkers reported on enolate formation from ketones under *kinetic* control by using triethylgallium as a nonnucleophilic base (equation 35)[59]. The reaction of 4-(*t*-butyl)cyclohexanone (**117**) with triethylgallium at 125 °C followed by subsequent addition of benzaldehyde (**118**) at −40 °C gave the aldol products with a remarkable preference for the equatorial isomer (**119**) over the axial one (**120**), which appears to be a general feature of gallium enolates[60]. This stereochemical outcome is highly contrasted with those of lithium enolates exhibiting axial preferences[61].

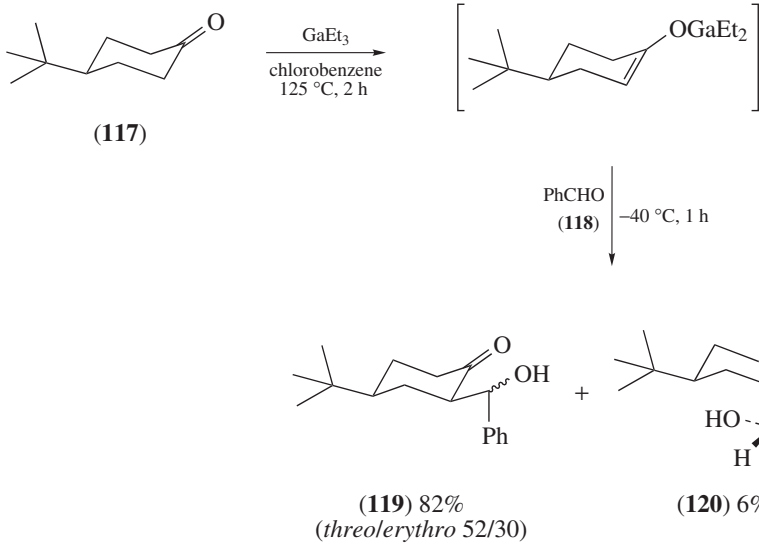

(35)

An alternative method for the preparation of a *kinetic* zinc ketone enolate (**123**) from an arene thiol ester **121** and bis(iodozincio)methane (**122**) in the presence of a palladium(0) catalyst was developed by Matsubara and coworkers (equation 36)[62]. The modest reactivity of the zinc reagent **122** makes this transformation highly chemo- and regioselective: neither isomerization of the *kinetic* enolate **123** nor a palladium-catalyzed coupling with the thiol ester **121** could be observed. Thus, treatment of zinc enolate **123** with various aldehydes or ketones led regioselectively to one aldol product **124**. The method provides access to reactive functionalized zinc enolates which are otherwise hard to obtain.

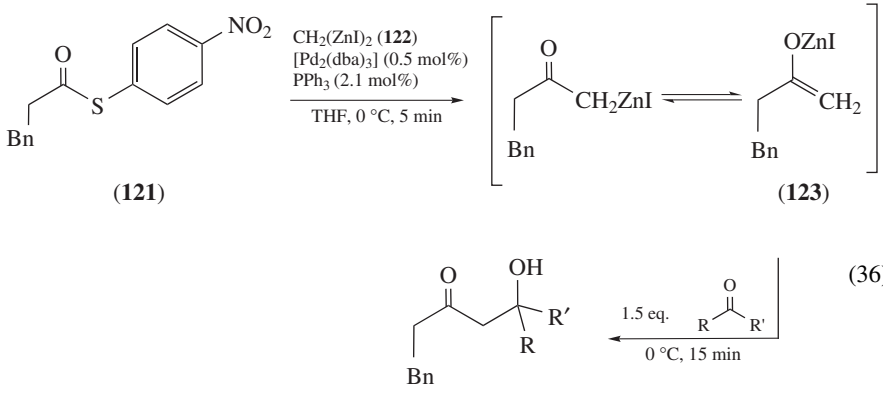

(36)

(**124**) (**a**) R = Ph, R′ = H, > 99%
(**b**) R = Et, R′ = H, > 99%
(**c**) R = Ph, R′ = CH_3, 86%
(**d**) R = Ph, R′ = (*E*)-CH_3CH=CH, 62%

TABLE 8. Conditions for the Michael addition of ketone enolates to α,β-unsaturated esters, according to equation 37

M	Additive	Conditions	Yield (%)
Li	none	THF, −78 °C, 48 h	0
$SnBu_3$	none	THF, 63 °C, 12 h	0
$SiMe_3$	$TiCl_4$ (1.0 eq.)	CH_2Cl_2, −78 °C, 15 min	81

IV. C–C BOND FORMATION BY MICHAEL ADDITION OF METAL ENOLATES

A. Introduction

Michael addition of metal enolates to α,β-unsaturated carbonyls has been intensively studied in recent years and provides an established method in organic synthesis for the preparation of a wide range of 1,5-dicarbonyl compounds (**128**) under neutral and mild conditions[63]. Metal enolates derived from ketones or esters typically act as Michael donors, and α,β-unsaturated carbonyls including enoates, enones and unsaturated amides are used as Michael acceptors. However, reaction between a ketone enolate (**125**) and an α,β-unsaturated ester (**126**) to form an ester enolate (**127**, equation 37) is not the thermodynamically preferred one, because ester enolates are generally more labile than ketone enolates. Thus, this transformation does not proceed well under thermal or catalytic conditions: more than equimolar amounts of additives (mainly Lewis acids, such as $TiCl_4$) are generally required to enable satisfactory conversion, as shown in Table 8. Various groups have developed synthons as unsaturated ester equivalents (ortho esters[64], thioesters[65]) and β-lithiated enamines[66] as ketone enolate equivalents to afford a conjugate addition with acceptable yields.

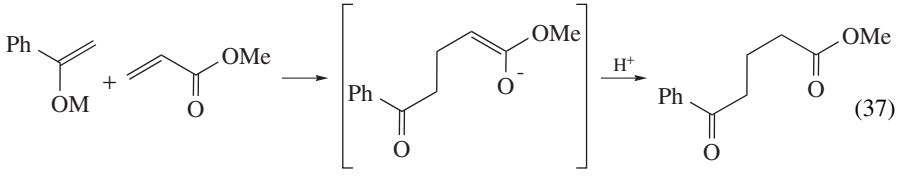

(37)

(**125**) (**126**) (**127**) (**128**)

B. Michael Additions of Ketone Enolates

In 2003, Baba and coworkers reported first examples of a catalytic Michael addition of stannyl ketone enolates (**129**) to α,β-unsaturated esters (**131**) using a catalytic amount of tetrabutylammonium bromide (equation 38)[67]. Their investigations showed that the

TABLE 9. Michael additions of stannyl ketone enolates catalyzed by Bu_4NBr (equation 38)

Product	R	R^1	R^2	R^3	Yield (%)
134a	Ph	H	H	Me/Et/*t*-Bu	>99
134b	2-Thi	H	H	Me	91
134c	Ph	Me	H	Me	86
134d	*t*-Bu	H	H	Et	70
134e	Ph	H	CF_3	Et	64

bromide anion from Bu_4NBr coordinates to the tin center under formation of a five-coordinated tin species (**130**)[68]. Thus, the nucleophilicity of the tin enolate is enhanced resulting in a significant acceleration of the subsequent conjugate addition to **131**. Because the reaction is *thermodynamically* disfavored, as mentioned above, the authors proposed a further step for stabilization by a special feature of tin enolate species, namely tautomerization of the stannyl ester enolate **132** into the *C*-stannylated form **133**. This transformation releases the bromide anion and completes the catalytic cycle. The method was applied to a variety of tin enolates and Michael acceptors, whereby the δ-keto esters **134** were usually obtained in high yields (Table 9). Furthermore, all the single steps of the reaction course were corroborated by detailed *ab initio* calculations. Recently, a similar approach to δ-keto esters and amides using *in situ* generated lithium salts for enolate activation was published by the same group[69].

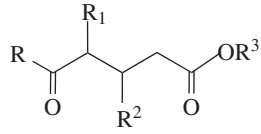

(**134**) (**a**–**e**, Table 9)

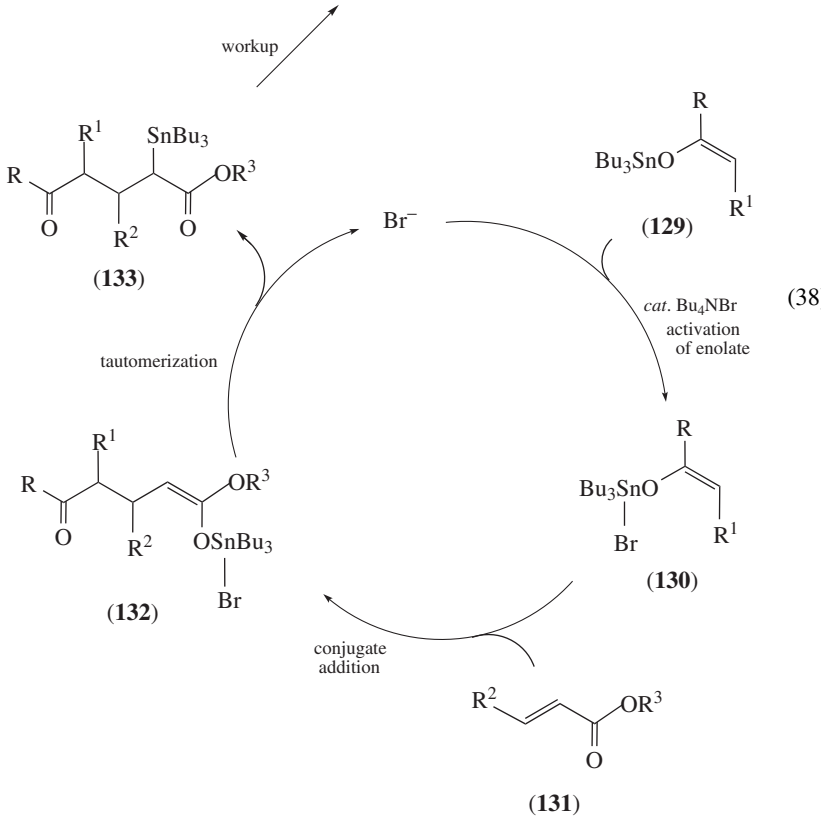

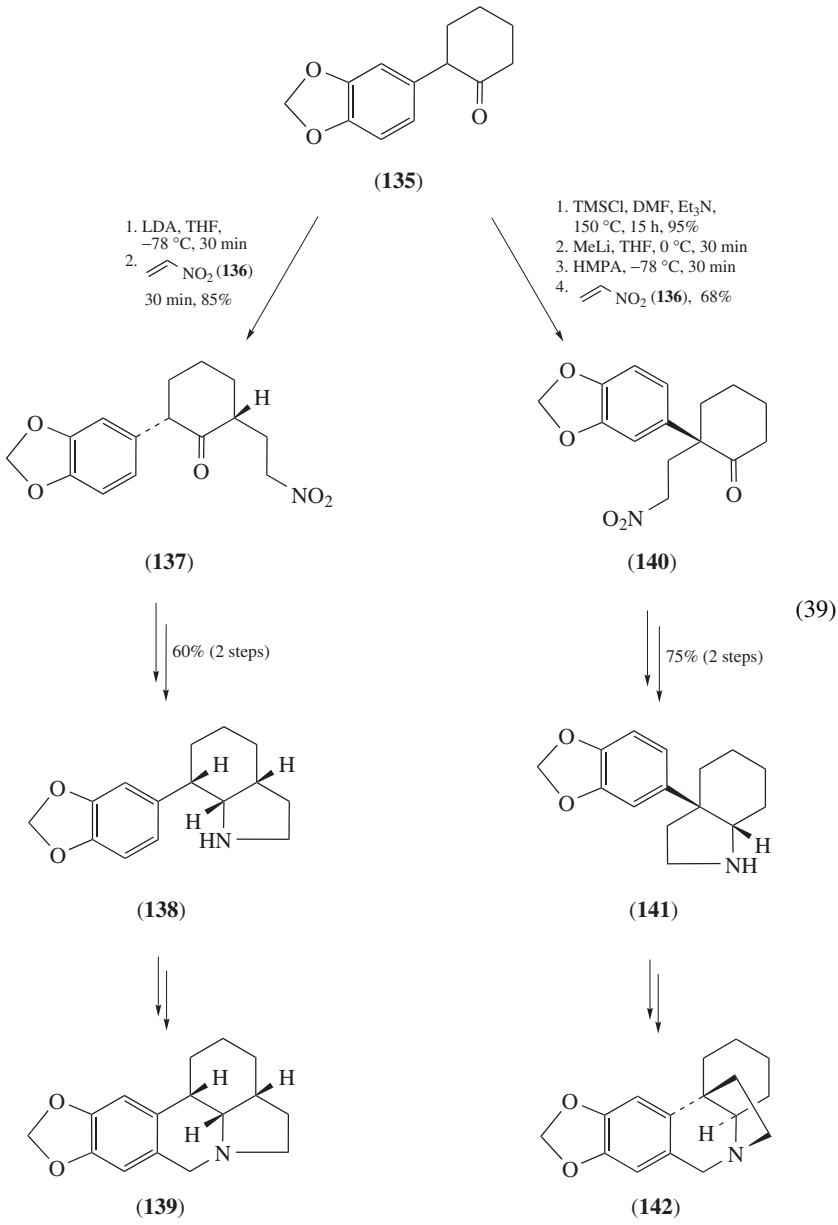

(39)

Tu and coworkers reported on both kinetically and thermodynamically controlled Michael addition of the lithium enolates of ketone **135** to nitroethylene **136** as the key step in the total syntheses of the alkaloids (±)-γ-lycorane (**139**) and (±)-crinane (**142**) (equation 39)[70]. Both reactions started from the same Michael donor (**135**) with nitroethylene (**136**) as a C–C–NH_2 synthon for the construction of aryl-substituted

octahydroindole derivatives (**138** and **141**, respectively), which are central substructures of the two natural products. In a first step, reaction of the kinetically controlled lithium enolate of **135** with **136** delivered γ-nitro carbonyl compound **137** as a 25:1 mixture of diastereoisomers (85% yield), which could be easily isolated by column chromatography. The thermodynamically controlled lithium enolate, instead, was formed by Li–Si exchange of the corresponding silyl enol ether, and subsequent Michael addition to **136** led to the intermediate **140**. Further similar transformations in both cases gave rise to (±)-γ-lycorane (**139**) and (±)-crinane (**142**) in high overall yields (22% and 36%, respectively).

Recently, Shchepin and coworkers described Michael addition reactions with zinc ketone enolates (**144**) for the preparation of chroman-2-one derivatives **146**. The enolates were generated *in situ* from α-bromo ketones **143** by addition of excess zinc (equation 40), and subsequent conjugate addition to α,β-unsaturated ketones (**145**) (equation 40′) provided chroman-2-ones (**146a**, **b**) in yields up to 82%[71].

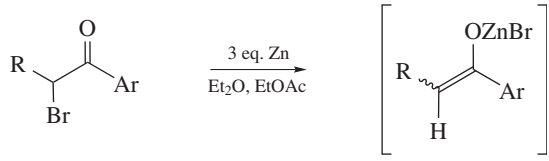

(40)

(**143**) (**144**)

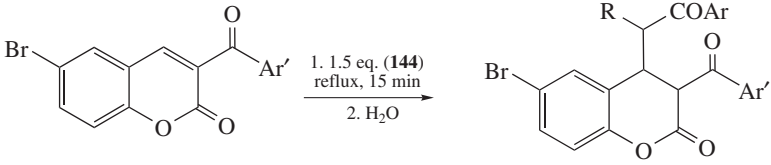

(40′)

(**145**) (**146**) (**a**) R = Me, Ar = 4-MeC_6H_4, Ar′ = 4-BrC_6H_4, 43%

(**b**) R = *i*-Pr, Ar = 4-BrC_6H_4, Ar′ = Ph, 82%

C. Enantioselective Michael Reactions

In recent years, many chiral catalysts for the enantioselective synthesis of optical active 1,5-dicarbonyl compounds have been developed[72], such as chiral crown ethers with potassium salt bases[73] and chiral palladium complexes[74], including bimetallic systems[75]. Nakajima and coworkers reported on enantioselective Michael reactions of β-keto esters to α,β-unsaturated carbonyl compounds in the presence of a chiral biquinoline *N*,*N*′-dioxide–scandium complex, which catalyzed the additions in high yields and with enantioselectivities up to 84% ee[76]. Kobayashi and coworkers found that the combination of $Sc(OTf)_3$ with the chiral bipyridine ligand **149** (equation 41) was also effective as a chiral catalyst for asymmetric Michael additions of 1,3-dicarbonyl compounds **147** to α,β-unsaturated ketones **148**. The corresponding Michael adducts **150** were obtained in good to high yields with excellent enantiomeric excesses in most cases (Table 10).

The authors proposed an intermediate complex **150′** in which the chiral induction occurs by reaction of the scandium ketone enolate with the α,β-unsaturated ketone **148** (equation 42). The absolute configuration of the Michael adduct **150a** can be explained by coordination of the hydroxy groups of **149** to Sc^{3+} in a tetradentate manner and shielding of the *si*-face of the scandium enolate by an adjacent *t*-butyl group. Therefore, the enolate attacks the Michael acceptor preferably at the *re*-face[77].

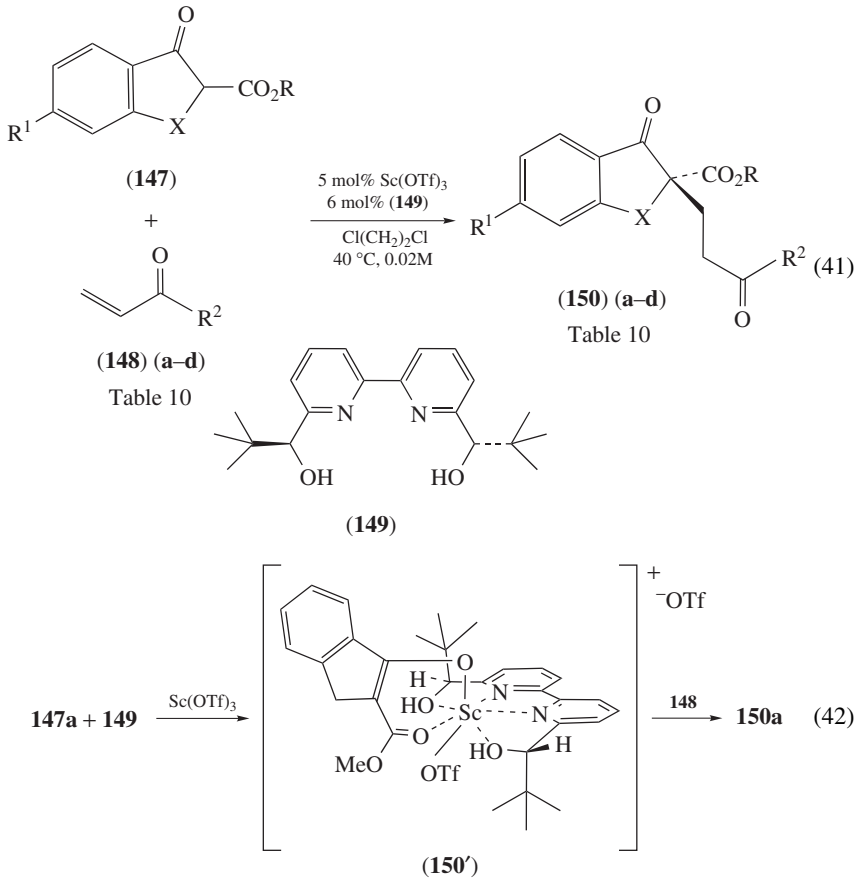

D. Michael-initiated Ring Closure Reactions with Ketone Enolates

An interesting feature of Michael addition reactions is that Michael acceptors with a leaving group (mostly halides) in γ-position can be used for the synthesis of cyclopropanes. The so-called Michael-initiated ring closure reaction (MIRC reaction) starts with an addition of a nucleophile to the α,β-unsaturated carbonyl, and afterwards the intermediate enolate displaces the leaving group to give the desired cyclopropanes[78].

TABLE 10. Asymmetric Michael additions catalyzed by the chiral scandium–bipyridine complex **149** (equation 41)

	β-Keto ester			R^2	Time (h)	Product	Yield (%)	ee (%)
	R	R^1	X					
147a	Me	H	CH_2	Et	48	**150a**	98	93
147b	Et	H	CH_2	Et	38	**150b**	95	93
147c	Et	OMe	CH_2	Me	13	**150c**	88	95
147d	Me	H	O	Me	24	**150d**	72	94

Shchepin and coworkers showed that bromine-containing zinc enolates are suitable nucleophiles in Michael additions (equation 43′) for the synthesis of cyclopropanederivatives. The nucleophiles **152** were derived *in situ* from 1-aryl-2,2-dibromoalkanones **151** by addition of zinc (equation 43). Their attack at the double bond of α,β-unsaturated amides (**153**) shown in equation 43′ delivered the intermediates **154** bearing a leaving group in γ-position to the amide enolate, which can undergo stereoselective intramolecular ring closure under formation of the cyclopropane derivatives **155**. After aqueous work-up the products **156a–c** were obtained in good yields and always as a single diastereomer[79].

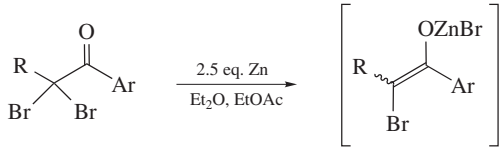

(43)

(**151**) (**152**)

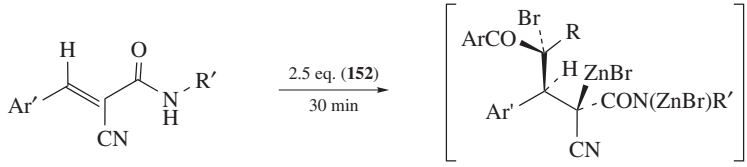

(**153**) (**154**)

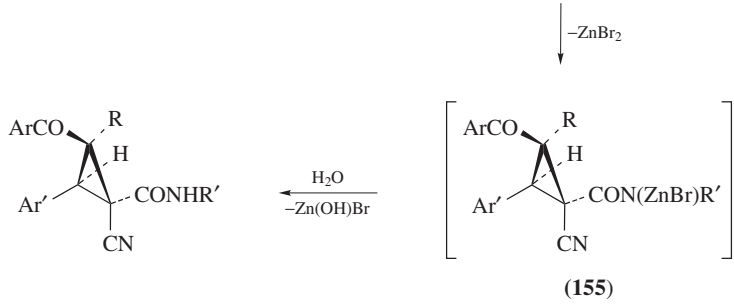

(43′)

(**155**)

(**156**) (**a**) R = Me, R′ = 3-MeC_6H_4, Ar = Ph, Ar′ = 4-ClC_6H_4, 72%

(**b**) R = Me, R′ = *c*-Hex, Ar = Ph, Ar′ = 3-BrC_6H_4, 68%

(**c**) R = Et, R′ = *c*-Hex, Ar = 4-ClC_6H_4, Ar′ = 3-BrC_6H_4, 64%

V. ESTER ENOLATES

A. General Aspects

The preparation of ester enolates, their subsequent alkylation and their use as nucleophiles in aldol or Michael reactions are standard procedures in synthesis today. Normally, these are high yield reactions and their stereochemical course can be predicted with confidence, due to the intense investigation effort invested in recent years in this research area.

The mostly used reagents for deprotonation and formation of metalated ester enolates are sterically hindered nonnucleophilic amide bases, such as LDA or the less basic lithium and sodium hexamethyldisilazides. Both amide bases are strong enough to deprotonate all

α-acidic esters quantitatively. As reported before for ketone enolates, the enolate geometry is of fundamental interest in order to control the steric course in ester enolate chemistry. In this context rearrangement experiments of trimethylsilyl enol esters showed that the (*E*)/(*Z*) diastereoselectivity of enolate formation strongly depends on the solvent system used: deprotonation of the allylic ester **157** with LDA in tetrahydrofuran in the presence of HMPA delivered, after reaction with trimethylsilyl chloride, predominantly the (*Z*)-silylketene acetal **158**, the geometry of which has been deduced from the *syn*-configuration of its Claisen rearrangement product **159** (equation 44). In contrast, treatment of **157** with LDA in tetrahydrofuran without adding HMPA led to the formation of a (*E*)-configured silyl enol ether **160**, which rearranged to the *anti*-configured product **161**. In both cases the stereochemical outcome could be explained by assuming a six-membered chair-like transition-state[8a].

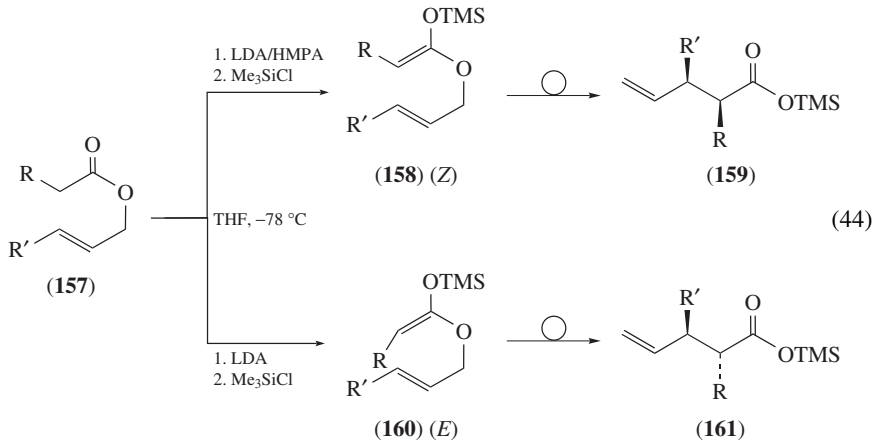

(44)

B. Diastereoselective Additions of Ester Enolates to Carbonyl Groups

An effective control of the simple diastereoselectivity in boron-mediated aldol reactions of various propionate esters (**162**) was achieved by Abiko and coworkers (equation 45)[80]. They could show that under usual enolization conditions (dialkylboron triflate and amine) enol borinates are formed, which allowed the selective synthesis of *syn*-configured aldol products (Table 11). The enolization at low temperature (−78 °C) generated a (*Z*)-enolate selectively, which afforded mainly the *syn* diastereomer **164** after reaction with isobutyraldehyde (**163**), following a Zimmerman–Traxler transition-state. The *anti* diastereomer **164′** instead was obtained only in small amounts (5–20%).

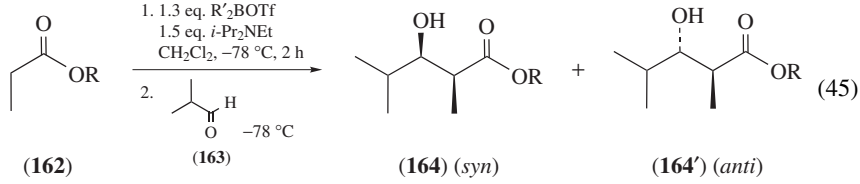

(45)

Recently, Charette and coworkers reported on a similar approach to β-hydroxy esters (equation 46) in their synthesis of (±)-coronafacic acid, a natural component of the phytotoxin coronatin[81]. They studied the effect of various aldehydes on the diastereoselectivity

TABLE 11. Diastereoselective boron-mediated aldol reactions of propionate esters (equation 45)

R	R′ = Bu		R′ = *c*-Hex	
	Yield (%)	**164**:**164′**	Yield (%)	**164**:**164′**
Me	85	>95:5	75	95:5
Et	81	95:5	72	>95:5
CH_2Hex-*c*	89	80:20	73	>95:5
Bn	97	95:5	84	90:10

TABLE 12. Diastereoselective syntheses of β-hydroxy esters

Aldehyde	Yield (%)	*syn*:*anti*	Major product
163	87	98:2	**169**
166	82	22:78	**170′**
167	66	18:82	**171′**
168	85	13:87	**172′**

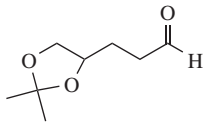

(**166**)

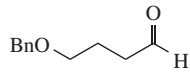

(**167**)

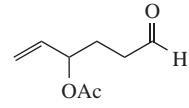

(**168**)

in the aldol reaction with the β,γ-unsaturated ester **165**. Their results indicated that the nature of the aldehyde had a considerable effect on diastereoselectivity, as only the α-branched isobutyraldehyde (**163**) appeared to afford high *syn* selectivity, as shown in Table 12. Reactions with linear aldehydes, such as **166**–**168**, led to a reversal in selectivity, whereby the *anti* products **170′**–**172′** were formed as major diastereomers (up to 87% ds). The authors postulated that the aldol reactions with linear aldehydes possibly proceed through an open transition-state.

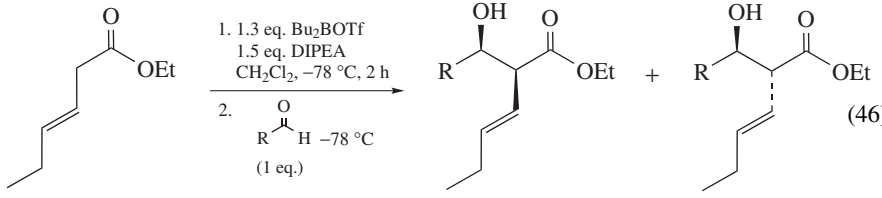

(46)

(**165**) 1.3 eq. (**169**)–(**172**) (*syn*) (**169′**)–(**172′**) (*anti*)

An interesting base-free method for enolate preparation was described by Baba and coworkers (equation 47)[82]. They generated (*E*)-configured indium enolates (**174**) selectively by adding elementary indium to an α-bromo ethyl ester **173**. Reactions of these enolates with α-hydroxy ketones (**175**) furnished highly diastereoselective five-membered lactones (**177**) with three contiguous stereogenic centers, as shown in Table 13. Remarkably, no protecting group for the free hydroxy group of the ketone **175** was necessary. The observed perfect diastereoselectivities of lactones **177** could be explained by assuming a

TABLE 13. Diastereoselective lacton syntheses using indium enolates

R^1	R^2	R^3	Conditions	Product	Yield (%)	ds (%)[a]
c-Pen	Ph	Ph	r.t., 1.5 h	**177a**	69	99
n-Hex	4-ClC_6H_4	4-ClC_6H_4	reflux, 5.5 h	**177b**	65	98
Me	4-MeC_6H_4	4-MeC_6H_4	r.t., 1.5 h	**177c**	73	93

[a] The stereochemistry between C^β and C^γ has been completely controlled, the values of ds are related C^α/C^β.

boat-like bicyclic transition-state **176**, in which the hydroxyl moiety is coordinated to the indium atom.

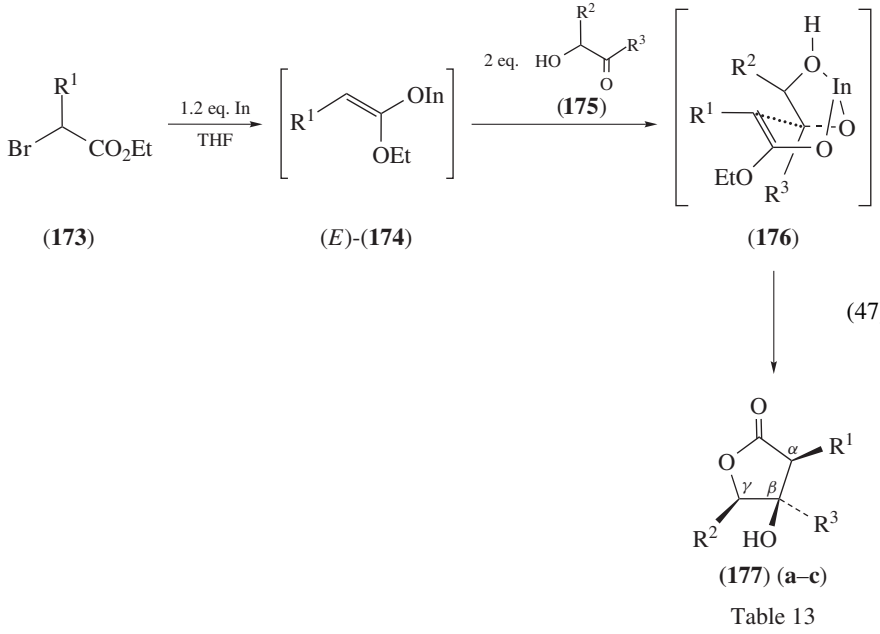

Table 13

Reissig and coworkers reported on a further unusual method for enolate preparation using samarium diiodide and indole derivatives with a methyl ester functionality in 3-position (**178**, equation 48)[83]. In the presence of an aldehyde or ketone and with HMPA as additive, a samarium enolate intermediate (**179**) was formed, which could be protonated by addition of phenol giving rise to dehydroindole derivates **180a** and **180b** in a highly stereoselective manner. Intermediate **179** could also be trapped with allyl iodide as electrophile resulting in the formation of a *cis*-configured intermediate **181** exclusively. By intramolecular transesterification, **181** was converted *in situ* into the tricyclic lactones **182a** and **182b** in good yields.

Feringa and coworkers developed a protocol for the first catalytic asymmetric 1,4-addition of Grignard nucleophiles to acyclic α,β-unsaturated thioester substrates **183** using (*R*,*S*)-Josiphos as chiral ligand (equation 49)[84a]. The intermediate magnesium enolate **184** showed high reactivity toward aldol coupling, and the tandem reaction products (**185**–**187**) were obtained with excellent control of relative and absolute stereochemistry across the three newly formed stereogenic centers (Table 14)[84b]. Numerous aldehydes were tested

and in all cases aldol product **185** was formed as the major diastereomer, which indicated that the initial 1,4-addition reaction furnished the magnesium enolate **184** with a high (*Z*)-selectivity.

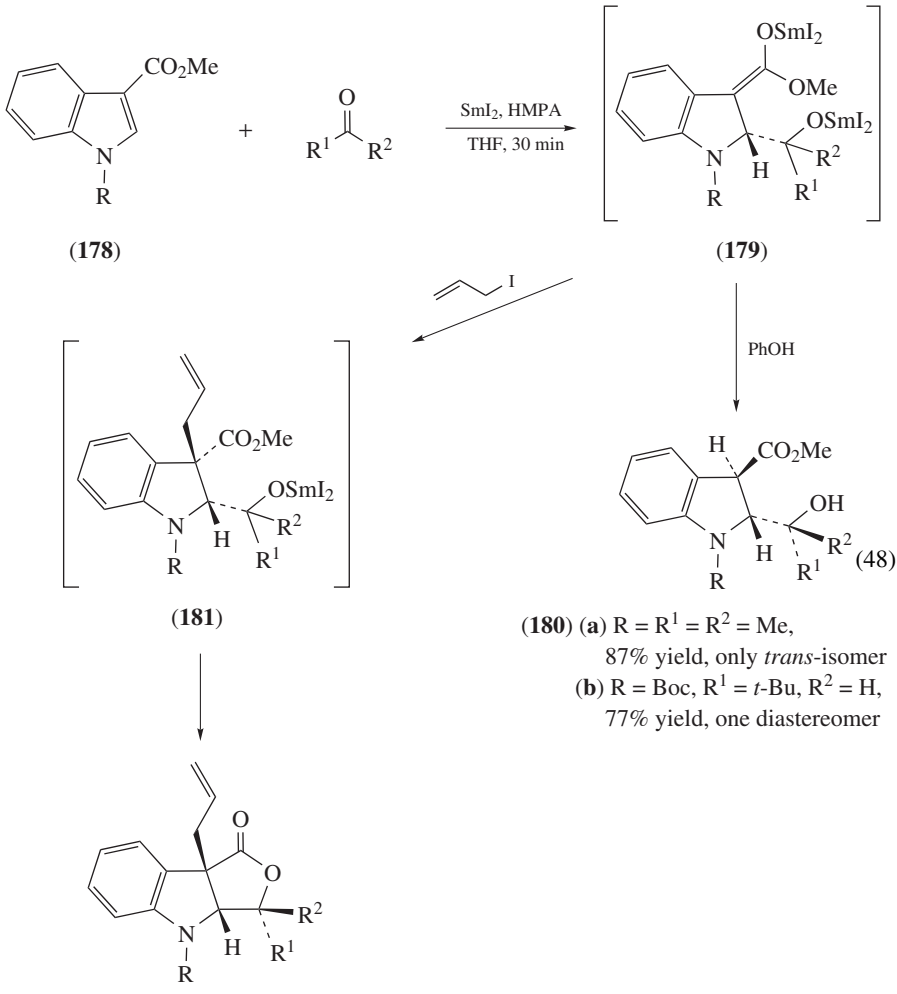

(**178**) (**179**)

(**181**)

(**180**) (**a**) R = R^1 = R^2 = Me, 87% yield, only *trans*-isomer
(**b**) R = Boc, R^1 = *t*-Bu, R^2 = H, 77% yield, one diastereomer (48)

(**182**) (**a**) R = Me, R^1 = *t*-Bu, R^2 = H, 94% yield, one diastereomer
(**b**) R = R^1 = Me, R^2 = Ph, 87% yield, one diastereomer

The versatility and efficiency of this method were demonstrated in the first catalytic asymmetric synthesis of (−)-phaseolinic acid **188**[84b], a biologically active compound of the paraconic acid family (equation 50)[85]. Using the 1,4-addition-aldol pathway, the paraconic acid skeleton could be synthesized in only four synthetic transformations with excellent stereoselectivities and 54% overall yield.

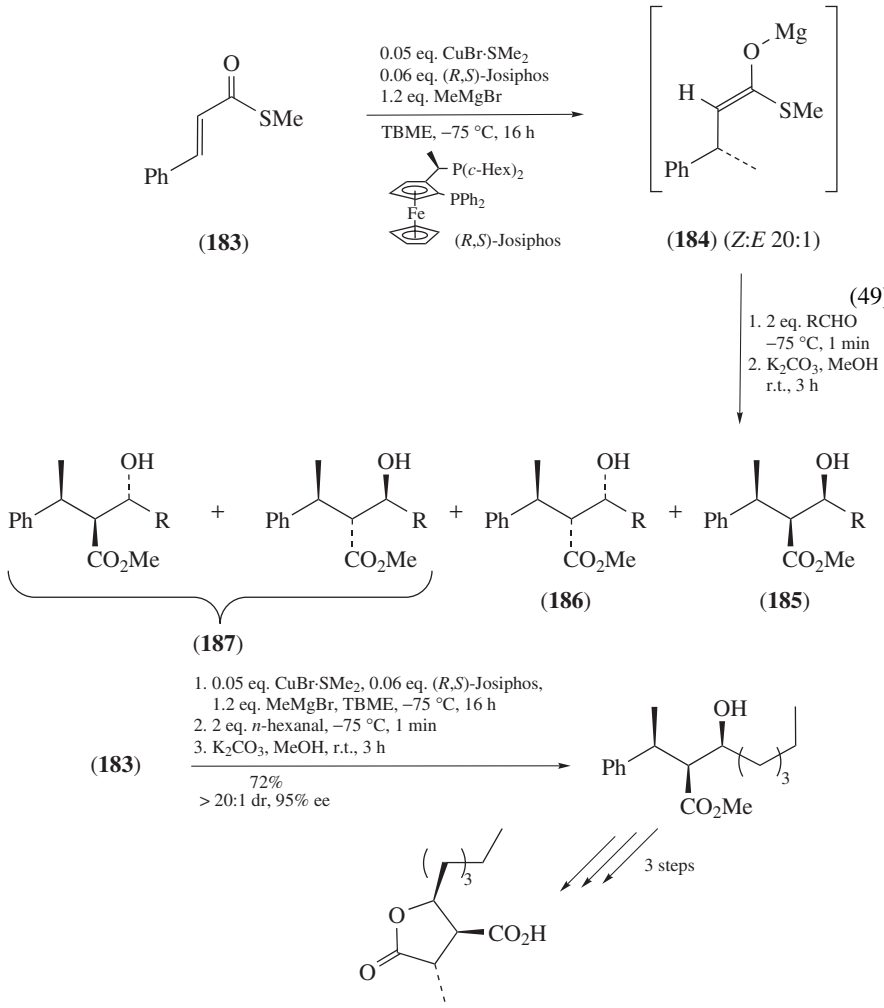

TABLE 14. Stereoselective aldol couplings using magnesium enolates (equation 49)

R	Conversion (%)	Ratio	Ratio	**185**	
		185:**186**:**187**	(**185** + **186**):**187**	Yield (%)	ee (%)
Ph	>95	85:10:5	>20:1	66	95
4-MeOC$_6$H$_4$	>95	80:15:5	>20:1	54	95
n-Pen	>95	90:5:5	>20:1	74	95
c-Hex	>95	>95:5:0	>20:1	76	95

C. Conjugate Additions of Ester Enolates

1. Asymmetric Michael reactions in presence of chiral amides

The formation of carbon–carbon bonds by conjugate addition of carbonucleophiles to α,β-unsaturated systems has been studied intensively and reviewed over the past few years[86]. Interestingly, applications with simple, unstabilized lithium enolates are relatively rare. Most reported examples are limited to the addition of stabilized enolates, such as those derived from malonates or acetoacetates. Nevertheless, some diastereo- and enantioselective versions of the conjugate addition, even with unstabilized lithium enolates, are well known[87]. In 2004, Tomioka and coworkers studied the influence of a chiral diether (**191**) on the 1,4-addition of lithium ester enolates (**189**) to α,β-unsaturated ketones (equation 51)[87b]. Their investigations showed that good enantioselectivities were obtained with cyclic enones, like 2-cyclopentenone (**190**); addition to a mixture of **189** and **191** gave the desired 1,4-adduct (*R*)-**192** with 74% ee, but only 47% yield. Unfortunately, also the Peterson product **193** was formed in a yield of 22% by initial 1,2-addition of the enolate to the Michael acceptor.

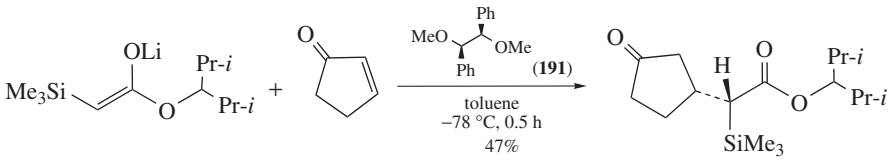

(**189**) (**190**) (**192**) (*R*), 74% ee (51)

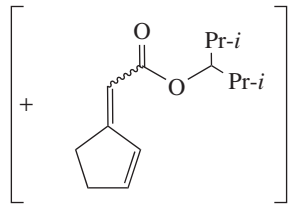

(**193**)

The group of Maddaluno and coworkers also reported on enantioselective Michael additions of ester enolates (equations 52 and 53)[88]. Thereby, lithium enolate **195** was generated by deprotonation of the corresponding ester with chiral lithium amide **194**, which was already known to form 1:1 noncovalent aggregates with lithium organyles[89]. Subsequent deprotonation of the resulting 3-aminopyrrolidine by addition of 1 equivalent of *n*-BuLi delivered a mixed aggregate between chiral amide and lithium enolate (**194** + **195**), which was used for enantioselective conjugate addition on various α,β-unsaturated esters. Detailed investigations with crotyl ester (**196**) showed that best results for yield and enantioselectivity (up to 76% ee in **197**) were obtained when increasing both the amide and enolate concentrations (Table 15, entries 1–3)[88]. Interestingly, changing the solvent from THF to toluene reversed the sense of the induction, albeit the yield and selectivity were somewhat decreased. However, the reaction seems highly substrate-sensitive and works well only with crotyl ester **196**, with satisfactory yield and enantioselectivity. With sterically more demanding substrates, such as *t*-butyl cinnamate, the enantioselectivities dropped dramatically[88].

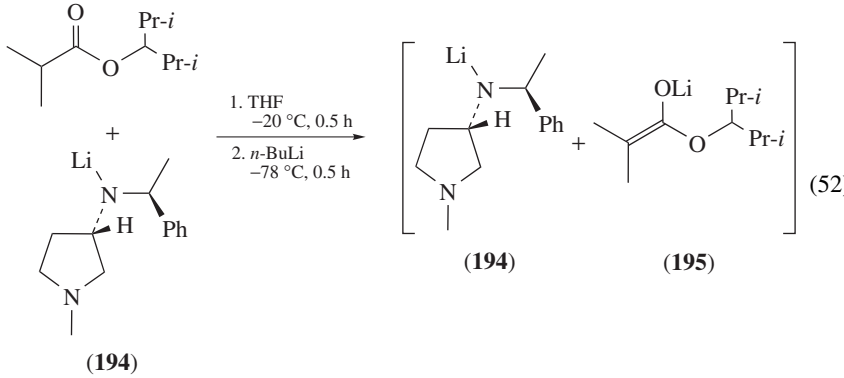

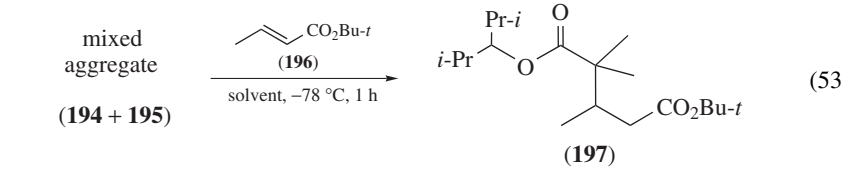

2. Asymmetric additions using chiral substrates

Pedro and coworkers developed a strategy for asymmetric Michael additions of a masked benzoyl anion equivalent (**199**) to α,β-unsaturated carbonyl compounds (equation 54)[90]. With (*S*)-mandelic acid (**198**) as a source for the benzoyl anion and chiral information, the corresponding Michael adducts were obtained in good yields and with high

TABLE 15. Enantioselective Michael additions of ester enolates using chiral amides (equation 53)

Amide:Enolate:**196**	Solvent	**197**	
		Yield (%)	ee (%)
1.3:1.3:1.0	THF	68	72 (+)
1.7:1.3:1.0	THF	83	74 (+)
2.4:2.0:1.0	THF	82	76 (+)
1.7:1.3:1.0	toluene	52	62 (−)

TABLE 16. Asymmetric Michael additions with masked benzyl anion equivalents (equation 54)

R^1	R^2	HMPA (eq.)	Yield (%)	**200**:**201**
Me	Et	0	60	30:70
Ph	Me	0	34	35:65
Me	Et	3	85	100:0
Ph	Me	3	85	98:2
i-Pr	Me	3	73	98:2
4-$MeOC_6H_4$	Me	3	76	99:1

diastereoselectivities, as shown in Table 16. First, **198** was transformed into the (2*S*,5*S*)-1,3-dioxolan-4-one derivative **199** by addition of pivalaldehyde. This preserves the chiral information of mandelic acid[91], although the subsequent formation of the lithium enolate led to loss of chirality at the stereogenic center. Indeed, the Michael additions provided the adducts **200** and **201** in acceptable diastereoselectivities and yields, preferring diastereomer **201** (Table 16, first two entries). Interestingly, the diastereoselectivity and yield could be significantly increased by adding 3 equivalents of HMPA, which was already known to improve the nucleophilicity and reactivity of carbanions. Furthermore, the addition of HMPA caused a change in the diastereomer distribution[92] and so Michael product **200** was formed predominantly, without any influence of the aliphatic or aromatic nature of the substituents R^1 and R^2 (Table 16, entries 3–6). Subsequent basic hydrolysis and Co(III)-catalyzed oxidative decarboxylation of the hemiacetal acids **202** led to the formation of chiral, nonracemic 2-substituted-1,4-diketones **203** with excellent enantiomeric excesses (equation 54′)[93]. Pedro and coworkers also reported an extension of this methodology to the diastereoselective benzylation of (*S*)-mandelic acid (**198**) through the sodium enolate of dioxolanone **199**, using various substituted *o*-nitrobenzyl bromides[94].

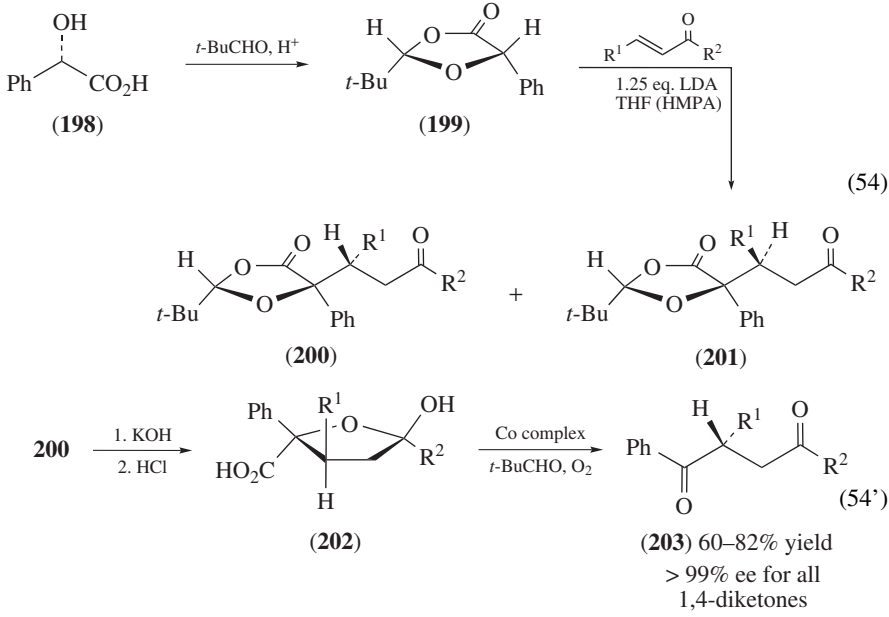

D. Amino Acid Enolates

The great importance of nonproteinogenic amino acids including α-substituted derivatives led to numerous investigations of modified amino acid enolates as nucleophiles in both 'classical' alkylation or Mannich reactions and palladium-catalyzed allylic alkylations.

1. Asymmetric syntheses with amino acid enolates

A new camphor-derived auxiliary was developed by Dixon and coworkers as a stereodirecting group for highly diastereoselective alkylations of an attached glycinamide residue

(equation 55)[95]. Remarkably, the complete chiral building block **207** could be obtained in a simple one-pot synthetic procedure on multigram scale, consisting of rhodium-catalyzed hydroformylation of the homoallylic alcohol **204** in the presence of glycine dimethylamide (**205**) to afford intermediate **206** selectively, which was subsequently *N*-protected with the Cbz group. Alkylations of lithium or sodium enolates of **207** were carried out with a wide range of alkyl halides (**208**) and furnished the alkylation products **210** in excellent diastereoselectivities as well as good to excellent yields (Table 17). The stereochemical outcome was explained by formation of a seven-membered ring chelate (**209**), in which alkylation can only occur from the sterically less hindered *re*-face of the (*Z*)-configured enolate ion. Removal of the camphor auxiliary in **210** using acidic conditions afforded the *N*-protected amino amides (**210′**) in high enantiomeric excesses (94–97% ee) without loss of stereochemical purity. Moreover, the lithium enolate of glycinamide **207** was also used as nucleophile in diastereoselective Michael additions to nitro olefins and α,β-unsaturated carbonyls[96].

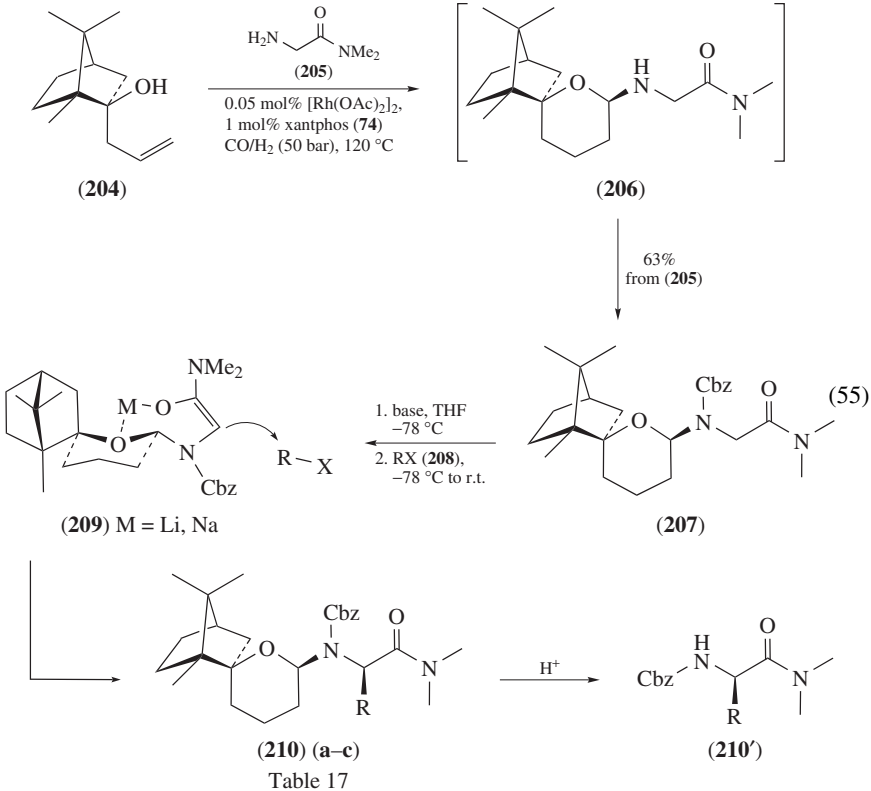

Table 17

Enolates from *N*-(diphenylmethylene)glycine esters (**211**) were also used as nucleophiles in Mannich reactions with chiral *N*-sulfinyl imines (**212**), as reported by Davis and coworkers (equation 56)[97]. They found that the simple *anti*/*syn* selectivity of the formed 2,3-diamino esters **213** and **214** was strongly influenced by the water content in the THF solvent. In the absence of water both 2,3-diamino ester isomers were equally obtained (first entry of Table 18), but by changing the H_2O/LDA ratio the formation of the

TABLE 17. Diastereoselective alkylations of glycinamides

Base	RX	Product	Yield (%)	ds (%)
LiHMDS	MeI	**210a**	80	>99
LiHMDS	*n*-PrI	**210b**	88	>99
NaHMDS [a]	BnBr	**210c**	94	97.5

[a] Toluene as solvent.

anti product **213** dramatically increased (second and third entries). When the H_2O/LDA ratio was enhanced to 1.35:1, **213** was formed in 86% yield with an excellent *anti*/*syn* ratio of 33:1 (fourth entry). A further increase of the H_2O/LDA ratio to *ca* 4:1 did not affect the *anti*/*syn* ratio but diminished the yield (fifth entry), mainly because the intermediary enolate was quenched, albeit slowly. These results were explained by assuming that the (*Z*)-enolate of **211** adds to (*S*)-sulfinimine **212** to give an *anti*-configured 2,3-diamino ester anion, which is the *kinetically* favored intermediate. This one is apparently stabilized by the H_2O–LDA species inhibiting a retro-Mannich fragmentation and leading to *anti*-**213** after workup.

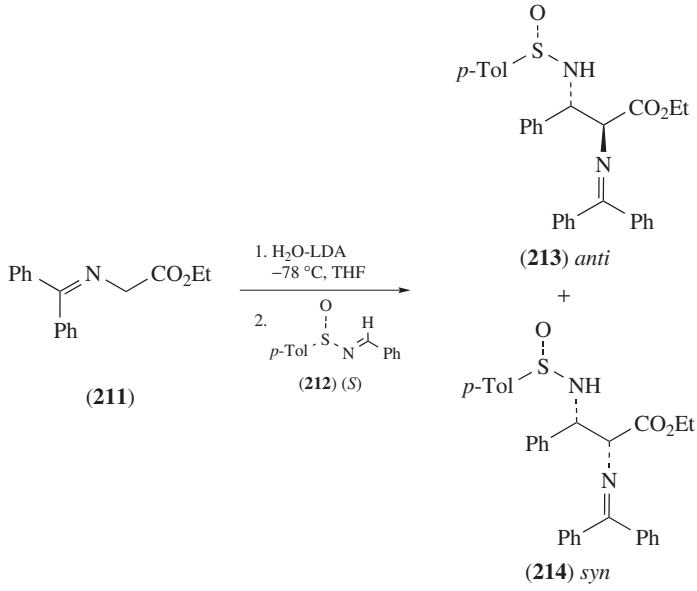

(56)

Besides stereoselective alkylations of glycine-derived enolates, enantioselective construction of chiral quaternary carbon centers from α-amino acids is one of the most challenging topics in current organic synthesis[98], since nonproteinogenic α,α-disubstituted amino acids often show a remarkable influence on the conformation of peptides. Moreover, they can act as enzyme inhibitors or as building blocks for the synthesis of a wide range of natural products[99].

A remarkable method for the enantioselective synthesis of cyclic α,α-disubstituted amino acids (**218** and **220**) from natural (*S*)-α-amino acids (**215**) was developed by Kawabata and coworkers (equation 57)[100]. It provides a concise and simple entry to both enantiomers of cyclic amino acids, since the absolute configuration of the newly

TABLE 18. Asymmetric Mannich reactions using chiral *N*-sulfinyl imines

H_2O:LDA ratio [a]	**213**:**214** (*anti:syn*) [b]	Yield (%) [c]
0:1	1:1	n.d.
0.98:1	25:1	86
1.09:1	33:1	86
1.35:1	33:1	86
3.9:1	33:1	60

[a] The water content was determined by Karl Fischer titration.
[b] Determined by ^{1}H NMR on the crude reaction mixture.
[c] Isolated yield of the major diastereomer.

formed tetrasubstituted stereocenter is controlled only by the solvent and the base used for the enolate preparation. With lithium amide bases, cyclization proceeds with inversion of configuration (**218**), while retention (**220**) was observed with potassium or sodium amide bases (Table 19). In both cases the memory of chirality[101] was explained by assuming the formation of chiral nonracemic enolate intermediates with chiral C-N axes (**217** for M = Li and **219** for M = K, Na). Intermediate **217** was formed predominantly with lithium amide bases, because lithium cations enforce chelation with the carbonyl group of Boc (**216**), so that a subsequent intramolecular alkylation gave the cyclization products **218** with inversion of configuration.

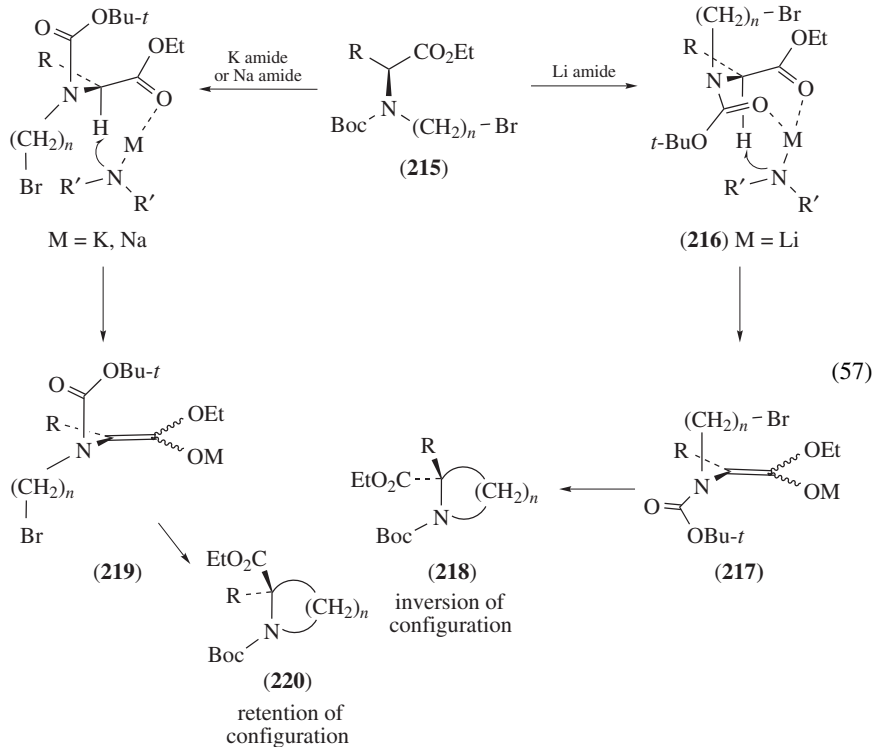

(57)

TABLE 19. Enantioselective synthesis of cyclic α,α-disubstituted amino acids (equation 57)

n	R	Base, solvent, temp	Product	Yield (%)	ee (%)
3	Bn	LTMP, THF, 20 °C	**218**	93	91 (*R*)
3	Me	LTMP, THF, 20 °C	**218**	91	87 (*S*)
2	$MeS(CH_2)_2$	LTMP, THF, 0 °C	**218**	66	83 (*R*)
3	Bn	KHMDS, DMF, −60 °C	**220**	94	98 (*S*)
3	Me	KHMDS, DMF, −60 °C	**220**	91	95 (*R*)
2	$MeS(CH_2)_2$	KHMDS, DMF, −60 °C	**220**	98	97 (*S*)

TABLE 20. Diastereoselective α-alkylations of 4-fluoro-proline esters (equation 58′)

	AllBr	BnBr	MeI
Yield (%)	93	97	72
225:**226**	3:97	98:2	53:47

Numerous investigations have been carried out to rationalize the stereochemical outcome of the α-alkylation of amino acid enolates such as those derived from chiral 4-silyloxy-*L*-proline esters[102]. The diastereoselectivity was found to be dependent on the alkylation reagent and the *N*-protecting group on proline[103]. Recently, similar reactions with 4-fluoro-*L*-proline methyl esters (**221** and **222**, equations 58 and 58′) were reported by Filosa and coworkers.[104]. They demonstrated the strong influence of the fluorine atom in controlling the reactivity and selectivity of the lithium enolate, leading with allyl or benzyl bromide to alkylated prolines (**223**–**226**) in excellent overall yields and a particularly high degree of facial diastereoselectivity (Table 20). In contrast, when MeI was used as a 'smaller' alkylation agent, the reaction yielded a mixture of diastereomers.

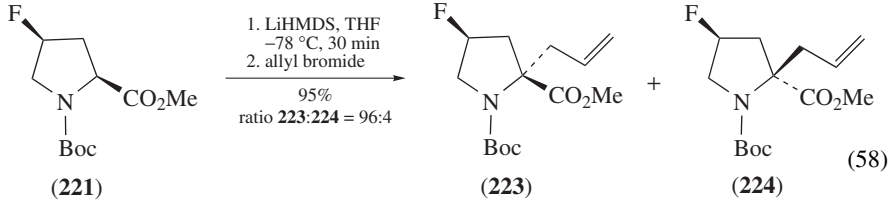

(**221**) (**223**) (**224**) (58)

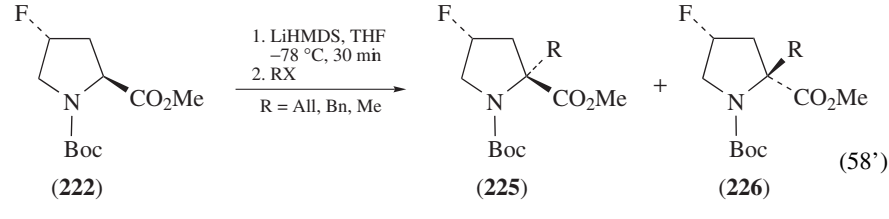

(**222**) (**225**) (**226**) (58')

2. Allylic alkylation reactions with amino acid enolates

α-Substituted derivatives of amino acids can be synthesized by palladium-catalyzed allylic alkylations of modified amino acid ester enolates acting as nucleophiles. In 1998,

Nájera and coworkers introduced a new class of cyclic alanine templates (**227**, equation 59), the structure of which was anchored on Schöllkopf's bislactim ether[105]. Palladium-catalyzed allylations of the chiral pyrazinone derivative **227** with allylic carbonates (**228**) as substrates led to the formation of γ,δ-unsaturated amino acids (**229a–c**) under very mild and neutral reaction conditions, whereas the required base for enolate preparation has been generated *in situ* from the allylic carbonate during π-allyl complex formation. With this protocol in hand, the alkylated pyrazinones **229** were obtained with excellent regio- and diastereoselectivities (>98% ds). Finally, hydrolysis with 6 N aqueous HCl under relatively drastic conditions (150 °C) led to the free amino acids.

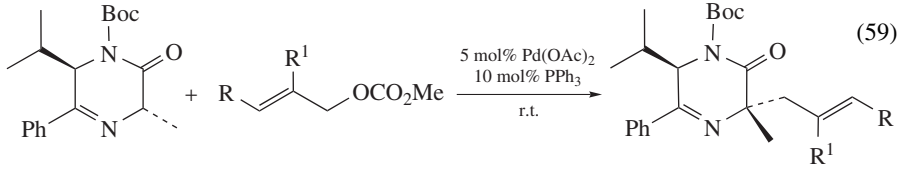

(59)

(**227**) (**228**) (**229**) (**a**) R = R^1 = H, 75%
(**b**) R = H, R^1 = Me, 85%
(**c**) R = Ph, R^1 = H, 78%

γ,δ-Unsaturated amino acids, even without a methyl group in the α-position, can be synthesized if chelated amino acid ester enolates are used as nucleophiles (equation 60)[106]. Investigations by Kazmaier and coworkers showed that chelation in zinc complex **231** causes a marked enhancement of thermal stability without having any negative influence on the reactivity. Due to the fixed enolate geometry, conversion of such complexes often proceeds with a high degree of stereoselectivity. If amino acid esters such as **230** were deprotonated with excess LiHMDS in the presence of zinc chloride, a chelated ester enolate (**231**) would be formed, which could be trapped, e.g. with allyl acetates or carbonates (**232**) in the presence of palladium(0). As a result of the high reactivity of the chelated enolates, the allylations proceeded under very mild reaction conditions at −78 °C, giving rise to monoallylated *anti*-configured amino acid derivative **233** in a highly stereoselective fashion; the diastereomerically pure product was accessible after a single crystallization step. Most common *N*-protecting groups could be used with comparable success, although the Tfa-protected derivatives gave the best selectivities[107].

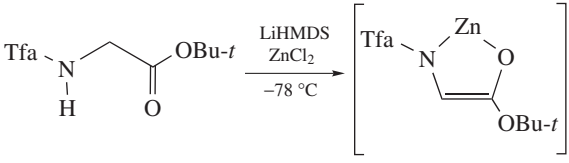

(**230**) (**231**)

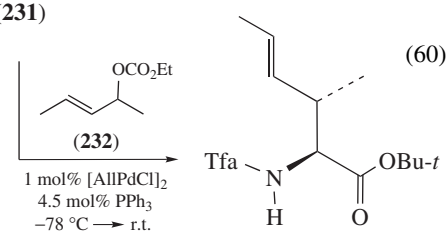

(60)

(**233**) 74%, 96% ds

Also, the allylic substitutions with chiral allyl substrates (such as **234** or **235**) proceeded cleanly and with good yields (equation 61). In both cases the chirality could be transferred almost completely from the allyl derivatives to the substitution products **236** and **236′**, respectively[107]. The diastereoselectivities depended on the substitution pattern at the allyl moiety: the results with carbonates were slightly better than those obtained with acetates (**235**). Further investigations by Kazmaier and coworkers showed that even isomerization-free allylic alkylations with (*Z*)-configured allyl substrates are possible, since the reactions with the zinc ester enolates **231** already proceed at −78 °C. Thus, π-σ-π-isomerization can be suppressed almost completely and alkylation of the (*Z*)-configured carbonate **237** (97% ee) yielded almost exclusively the (*Z*)-substitution product **238** with excellent selectivities ($Z{:}E > 99{:}1$)[108]. Interestingly, alkylation of the chiral and symmetrically substituted (*Z*)-carbonate **239** provided the optically active (*E*)-configured substitution product **240** as only isomer in good yields. The almost complete transfer of chirality indicates that the reaction has to proceed via an *anti-syn* complex, in which the more reactive *anti*-position[109] is attacked by the zinc enolate. In contrast, reactions via a *syn-syn* complex would lead inevitably to racemization of the optically active starting material.

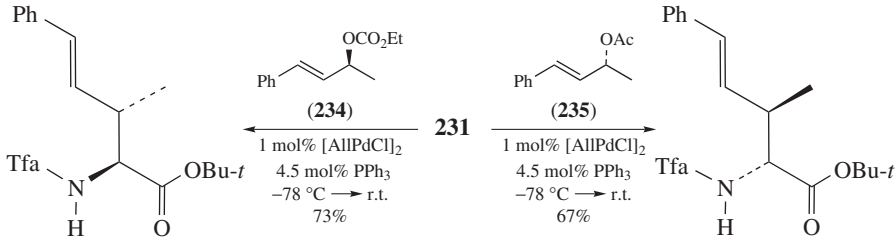

(**236**) 91% ds, 96% ee

(**236′**) = *ent*-(**236**)
83% ds, 96% ee (61)

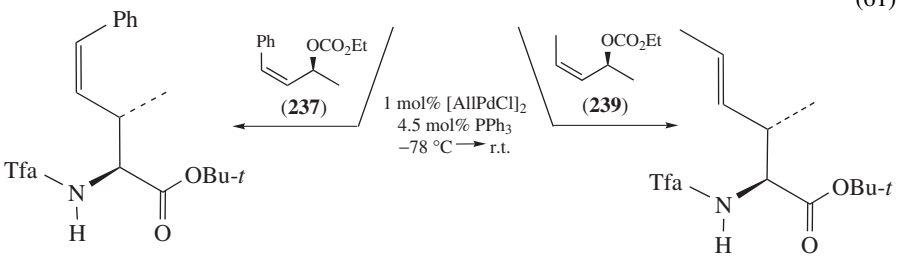

(**238**) 73%,
98% ds, 97% ee

(**240**) 81%,
96% ds, 96% ee

Changing the transition-metal from palladium to rhodium (equation 62) makes possible, in addition to the straight-chain alkylation product (**243**), the regio- and stereoselective synthesis of amino acid derivatives with a terminal double bond (**242**), starting from optically active branched allylic substrates **241** (Table 21)[110]. Remarkably, the substitution products were obtained with high enantiomeric excesses, what might result from a slow isomerization of the intermediary formed allyl rhodium complexes[111].

Besides allylic alkylation reactions chelated zinc ester enolates **231** also give good results in various types of standard enolate reactions, including alkylations, aldol reactions[112] and Michael additions[113].

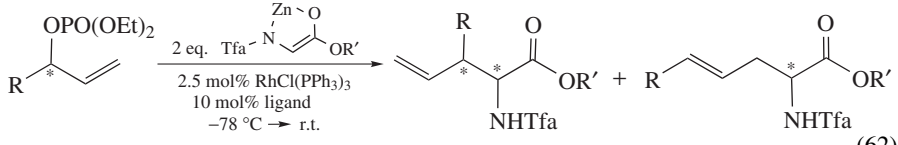

(**241**) (**242**) (**243**) (62)

3. Chelate enolate Claisen rearrangements of α-amido substituted allylic esters

Kazmaier and coworkers reported on chelated enolates of allylic esters **245**, which undergo Claisen rearrangement upon warming to room temperature, giving rise to γ,δ-unsaturated amino acids **246** (equation 63)[114]. Many different metal salts MX_n ($CoCl_2$, $MgCl_2$, $ZnCl_2$, $Al(OPr\text{-}i)_3$, $Ti(OPr\text{-}i)_4$) could be used for chelation, but normally the best results are obtained with zinc chloride (M = Zn) as chelating metal salt, as shown in Table 22. The yields and selectivities were generally quite independent of the protecting groups (PG) used and the substitution pattern of the allylic double bond. Using substituted (*E*)-allylic esters **244**, products with *syn*-configuration (**246**) are obtained diastereoselectively, which can be explained by a preferential rearrangement via a chair-like transition-state. The corresponding (*Z*)-isomers give rise to the *anti* products[115], but in this case the selectivity is dependent on the substitution pattern[116].

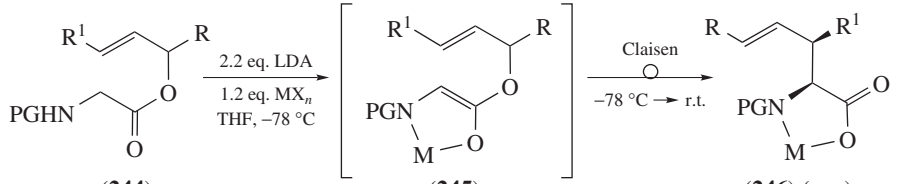

(**244**) (**245**) (**246**) (**a**–**c**)

Table 22

(63)

Switching from glycine esters to allylic esters of other amino acids (**247**) allows the synthesis of various α-alkylated amino acids, such as **248** or **249**, with high selectivities (equation 64)[117]. The last example had been chosen, because especially the lysine

TABLE 21. Regio- and stereoselective synthesis of amino acids by rhodium-catalyzed allylic alkylation (equation 62)

Substrate (**241**)			Ligand	Yield (%)	**242**:**243**	**242**
Configuration	R	R′				
(*R*), 99% ee	*n*-Pr	Me	$P(OEt)_3$	76	85:15	(2*R*,3*R*) 92% ds, 95% ee
(*S*), 95% ee	Me	*t*-Bu	$P(OPr\text{-}i)_3$	95	98:2	(2*S*,3*S*) 94% ds, 93% ee
(*R*), 99% ee [a]	Ph	*t*-Bu	$P(OMe)_3$	52	99:1	(2*R*,3*R*) 59% ds, 99% ee

[a] In this case allyl acetate was used instead of allyl phosphate.

TABLE 22. Diastereoselective synthesis of γ,δ-unsaturated amino acids by a Claisen rearrangement (equation 63)

MX_n	PG	R	R^1	Product	Yield (%)	ds (%)
$CoCl_2$	Cbz	H	Me	**246a**	78	93
$MgCl_2$	Cbz	H	Me	**246a**	85	91
$ZnCl_2$	Cbz	H	Me	**246a**	90	95
$ZnCl_2$	Cbz	Et	Me	**246b**	98	95
$ZnCl_2$	Tfa	H	Pr	**246c**	79	95

derivative **249** is a critical substrate for α-alkylation reactions[118]. In summary, two different procedures for the synthesis of substituted γ,δ-unsaturated amino acids are available with chelated amino acid ester enolates, which complement one another: the *anti* diastereomers can be obtained via palladium-catalyzed allylic substitution (see Section V.D.2), and the *syn* diastereomers by ester enolate Claisen rearrangement.

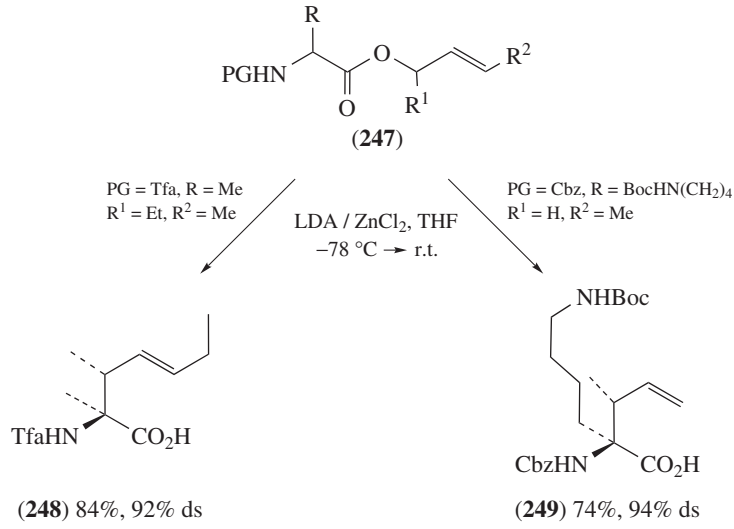

(64)

F. Backbone Modifications of Peptide Enolates

In principle, *C*-terminal glycine units of a peptide chain **250** can be deprotonated selectively by strong lithium bases such as LiHMDS or LDA, without affecting other α-CH groups in the peptide backbone, because these units are protected by deprotonation of the adjacent amide NHs (**251**). Treatment of **251** with an electrophile (EX), followed by hydrolysis, leads to the peptide chain **252**, α-substituted at the *C*-terminal glycine unit (equation 65).

Ager, McIntosh and coworkers applied this methodology to the benzylation of tosyl-protected Phe-Gly esters **253** (equation 66)[119]. With 3 eq. of LDA and TMEDA as additive, the alkylation products **254** were obtained in good yields and diastereoselectivities. By using the methyl ester **253a** mainly the (*S*,*R*)-diastereomer **254a** was formed (controlled by the adjacent stereogenic center in phenylalanine), while the (−)-menthylester **253b** induced the opposite stereochemistry in the **254b** product.

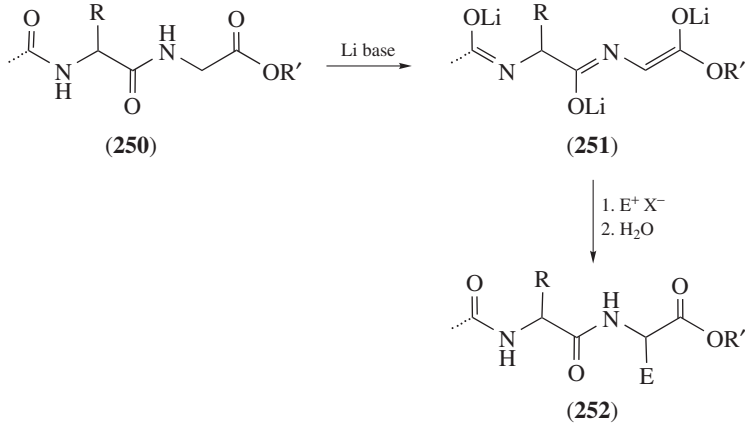

(**250**) (**251**) (**252**) (65)

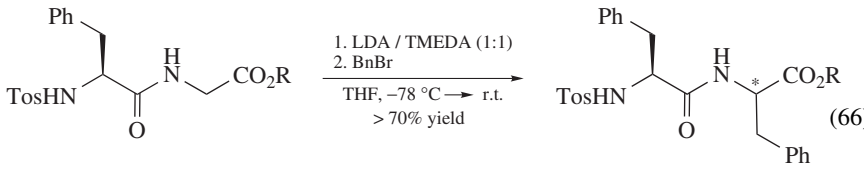

(66)

(**253**) (**a**) R = Me
(**b**) R = (−)-menthyl

(**254**) (**a**) (*S*,*R*):(*S*,*S*) = 80:20
(**b**) (*S*,*R*):(*S*,*S*) = 30:70

Better inductions by a vicinal amino acid were observed by Ojima and coworkers in the benzylation of chiral β-lactam ester enolates (**255**, equation 67)[120]. Interestingly, the enolate formation occurred at an uncommonly high temperature (0 °C) to form the *thermodynamic* Li-chelated enolate **256**, which allowed a stereoselective attack of the electrophile, while the diastereoselectivity with the nonchelated *kinetic* enolate **259** was significantly lower. Subsequent hydrogenolytic cleavage of lactam **257** delivered (*S*)-α-methylphenylalanine derivative **258** in nearly quantitative yield and high diastereoselectivity.

Another route to chelated peptide enolates was developed by Kazmaier and coworkers. They showed that treatment of peptide esters with lithium bases led to formation of polylithiated peptide enolates, which could be transmetalated by addition of metal salts, giving rise to multiply coordinated peptide metal complexes (Section V.D.2). Depending on the *N*-protecting group and the metal salt used, coordination of the adjacent amide group to the metal is assumed, resulting in shielding of one face of the enolate. As shown in equation 68, addition of $ZnCl_2$ to the deprotonated *N*-tosyl-protected dipeptide methylester **260** delivered alkylation (**261**) and aldol (**262**) products with high diastereoselectivities and good yields[121].

These peptide enolates could also be used as excellent nucleophiles in palladium-catalyzed allylic alkylations[121]. Reactions of numerous dipeptides (e.g. **263**) with different allylic substrates (e.g. **264**) and $[AllPdCl]_2$ as catalyst delivered (*S*,*R*)-configured peptides with γ,δ-unsaturated side chains (**265**), usually in high yields and diastereoselectivities (equation 69).

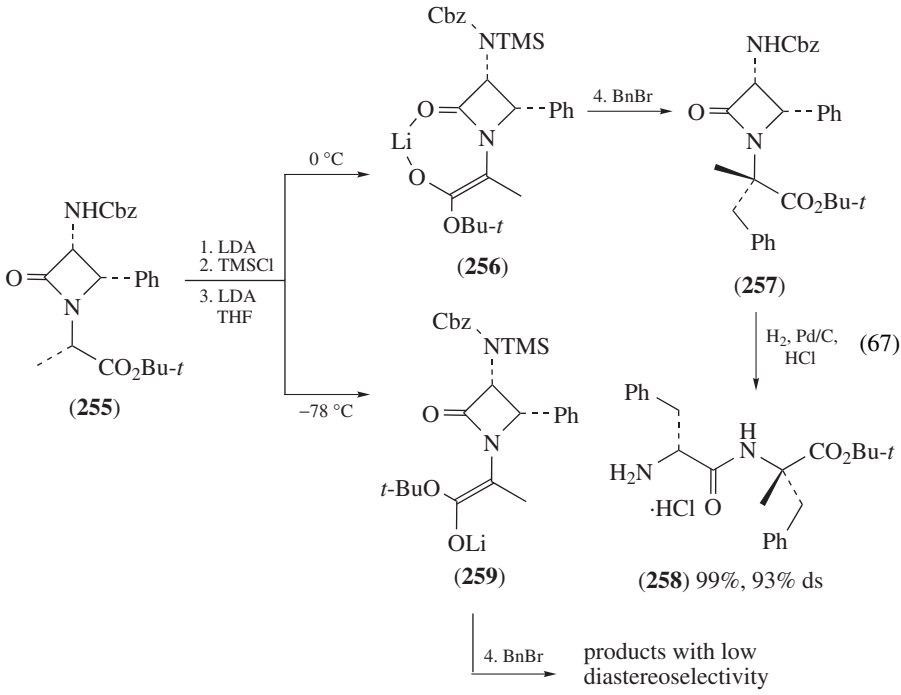
NHCbz
O
Ph
N
CO2Bu-t
(255)
1. LDA
2. TMSCl
3. LDA
THF
0 °C
–78 °C
Cbz
NTMS
O
Ph
N
Li
O
OBu-t
(256)
4. BnBr
NHCbz
O
Ph
N
CO2Bu-t
Ph
(257)
H2, Pd/C,
HCl
(67)
Ph
H2N
·HCl
H
N
O
CO2Bu-t
Ph
(258) 99%, 93% ds
Cbz
NTMS
O
Ph
N
t-BuO
OLi
(259)
4. BnBr
products with low
diastereoselectivity

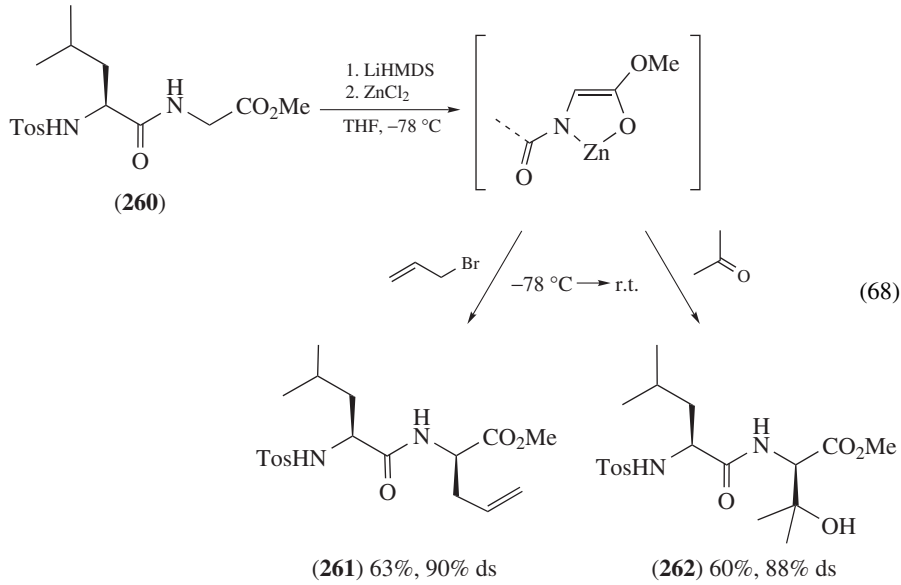
TosHN
H
N
O
CO2Me
(260)
1. LiHMDS
2. ZnCl2
THF, –78 °C
OMe
N
O
Zn
O
Br
–78 °C → r.t.
O
(68)
TosHN
H
N
O
CO2Me
(261) 63%, 90% ds
TosHN
H
N
O
CO2Me
OH
(262) 60%, 88% ds

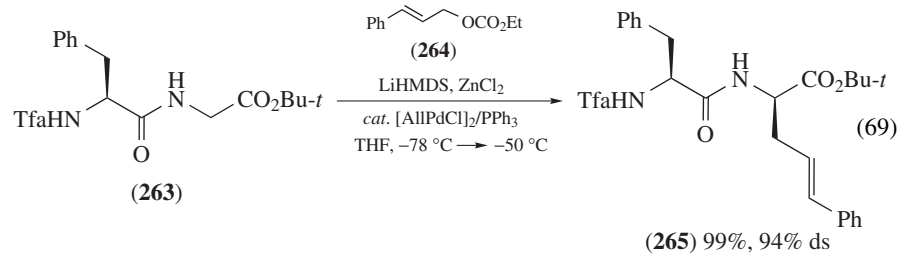

The use of chelated peptide enolates is not restricted to intermolecular reactions, as demonstrated for the [3,3]-sigmatropic Claisen rearrangement of allylic esters (**266**, equation 70)[122]. Based on the fixed enolate geometry and a chair-like transition-state, the β-branched γ,δ-unsaturated rearrangement products **267** were obtained with high *syn* diastereoselectivities (Section V.D.3). Thereby, the side-chain-induced stereoselectivity strongly depended on the metal salt added: only a slight selectivity was observed in reactions of manganese enolates (**267a**), while the addition of $NiCl_2$ or $Ti(OPr\text{-}i)_4$ provided the corresponding (*R*)-configured isoleucine derivative **267b** with excellent diastereoselectivity.

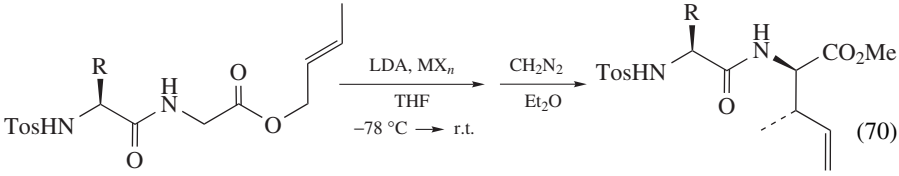

(**266**) (**a**) R = Bn
(**b**) R = *i*-Pr

(**267**) (**a**) R = Bn, $MX_n = MnCl_2$, 92%, 56% ds
(**b**) R = *i*-Pr, $MX_n = NiCl_2$, 66%, 93% ds;
$MX_n = Ti(OPr\text{-}i)_4$, 60%, 96% ds

For the rearrangement of higher peptides, tin chloride proved to be the chelating agent of choice[122]. Tos-protected derivatives gave best yields and high diastereoselectivities, even in the case of Val-Gly-Gly crotylester (**268**), where five atoms separate the directing and the newly formed stereogenic center (**269**, equation 71). Incorporation of secondary amino acids, like proline (**270**), disrupted the successive coordination of the peptide chain to the metal, resulting in a complete loss of chiral induction in tetrapeptide **271** (equation 72).

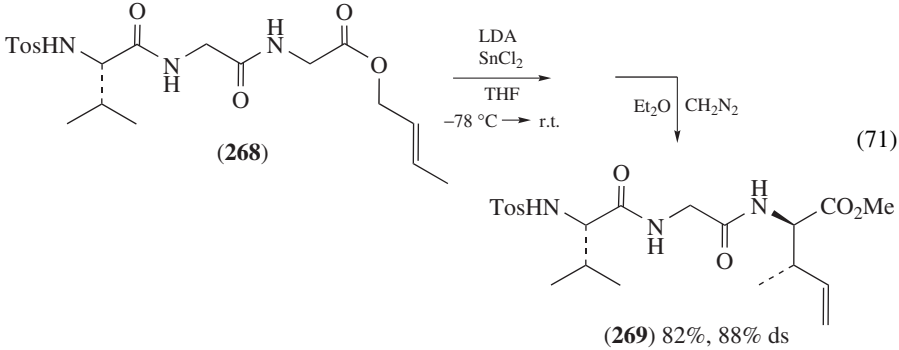

(**269**) 82%, 88% ds

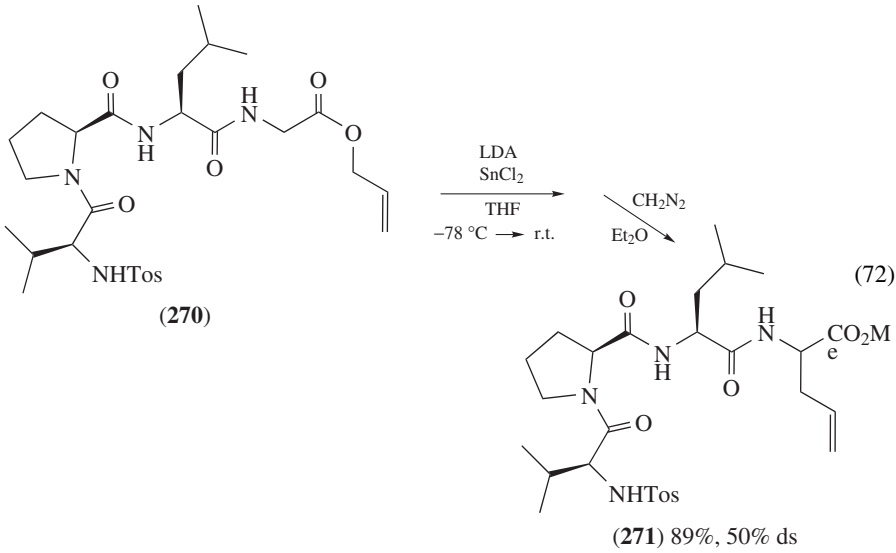

(**270**) (72)

(**271**) 89%, 50% ds

VI. REFERENCES

1. D. A. Evans, in *Asymmetric Synthesis* (Ed. J. D. Morrison), Academic Press, New York, 1983, pp. 1–110.
2. (a) D. Caine, in *Comprehensive Organic Synthesis* (Eds B. M. Trost and I. Fleming), Pergamon, Oxford, 1991, pp. 1–63.
   (b) D. L. Hughes, in *Comprehensive Asymmetric Catalysis* (Eds E. N. Jacobsen, A. Pfaltz and H. Yamamoto), Springer, Berlin, 1999, pp. 1273–1294.
3. J. d'Angelo, *Tetrahedron*, **32**, 2979 (1976).
4. (a) H. O. House, L. J. Czuba, M. Gall and H. D. Olmstead, *J. Org. Chem.*, **34**, 2324 (1969).
   (b) H. O. House, M. Gall and H. D. Olmstead, *J. Org. Chem.*, **36**, 2361 (1971).
5. (a) E. Vedejs, *J. Am. Chem. Soc.*, **96**, 5944 (1974).
   (b) H. J. Reich, J. M. Renga and I. L. Reich, *J. Am. Chem. Soc.*, **97**, 5434 (1975).
6. M. J. Munchhof and C. H. Heathcock, *Tetrahedron Lett.*, **33**, 8005 (1992).
7. C. H. Heathcock, C. T. Buse, W. A. Kleschick, M. C. Pirrung, J. E. Sohn and J. Lampe, *J. Org. Chem.*, **45**, 1066 (1980).
8. (a) R. E. Ireland, R. H. Müller and A. K. Willard, *J. Am. Chem. Soc.*, **98**, 2868 (1976).
   (b) Z. A. Fataftah, I. E. Kopka and M. W. Rathke, *J. Am. Chem. Soc.*, **102**, 3959 (1980).
9. S. S. Harried, C. P. Lee, G. Yang, T. I. H. Lee and D. C. Myles, *J. Org. Chem.*, **68**, 6646 (2003).
10. A. Gansäuer, D. Fielenbach, C. Stock and D. Geich-Gimbel, *Adv. Synth. Catal.*, **345**, 1017 (2003).
11. G. L. Edwards, W. B. Motherwell, D. M. Powell and D. A. Sandham, *J. Chem. Soc., Chem. Commun.*, 1399 (1991).
12. D. Caine, in *Carbon–Carbon Bond Formation* (Ed. R. L. Augustine), Marcel Dekker, New York, 1979, pp. 85–352.
13. H. E. Radunz, V. Eiermann, G. Schneider and A. Riethmueller, *Tetrahedron*, **47**, 1887 (1991).
14. (a) R. Deghenghi, C. Revesz and R. Gaudry, *J. Med. Chem.*, **6**, 301 (1963).
    (b) R. Joly, *Bull. Soc. Chim. Fr.*, 2694 (1973).
    (c) M. J. Weiss, R. E. Schaub, G. R. Allen, Jr., J. F. Poletto, C. Pidacks, R. B. Conrow and C. J. Coscia, *Tetrahedron*, **20**, 357 (1964).
15. K. Narkunan, L.-H. Shiu and R.-S. Liu, *Synlett*, 1300 (2000).
16. M. Mandal and S. J. Danishefsky, *Tetrahedron Lett.*, **45**, 3827 (2004).

17. R. Noyori, in *Asymmetric Catalysis in Organic Synthesis* (Ed. R. Noyori), John Wiley & Sons, Inc., New York, 1994, pp. 298–322.
18. (a) M. Suzuki, A. Yanagisawa and R. Noyori, *J. Am. Chem. Soc.*, **110**, 4718 (1988).
(b) Y. Morita, M. Suzuki and R. Noyori, *J. Org. Chem.*, **54**, 1785 (1989).
(c) J Otera, Y. Niibo and H. Nozaki, *Tetrahedron Lett.*, **33**, 3655 (1992).
(d) B. H. Lipshutz and M. R. Wood, *J. Am. Chem. Soc.*, **116**, 11689 (1994).
19. A. Fürstner, K. Grela, C. Mathes and C. W. Lehmann, *J. Am. Chem. Soc.*, **122**, 11799 (2000).
20. M. Ichikawa, S. Aoyagi and C. Kibayashi, *Tetrahedron Lett.*, **46**, 2327 (2005).
21. S. Saito, M. Nakadai and H. Yamamoto, *Synlett*, 1107 (2000).
22. B. M. Trost and E. Keinan, *Tetrahedron Lett.*, **21**, 2591 (1980).
23. B. M. Trost and C. R. Self, *J. Org. Chem.*, **49**, 468 (1984).
24. E.-i. Negishi and R. A. John, *J. Org. Chem.*, **48**, 4098 (1983).
25. B. M. Trost and G. M. Schröder, *J. Am. Chem. Soc.*, **121**, 6759 (1999).
26. B. M. Trost and G. M. Schröder, *Chem. Eur. J.*, **11**, 174 (2005).
27. S.-L. You, X.-L. Hou, L.-X. Dai and X.-Z. Zhu, *Org. Lett.*, **3**, 149 (2001).
28. B. M. Trost, C. Pissot-Soldermann and I. Chen, *Chem. Eur. J.*, **11**, 951 (2005).
29. (a) M. Braun, F. Laicher and T. Meier, *Angew. Chem. Int. Ed.*, **39**, 3494 (2000).
(b) M. Braun and T. Meier, *Angew. Chem. Int. Ed.*, **45**, 6952 (2006).
30. D. M. Johns, M. Mori and R. M. Williams, *Org. Lett.*, **8**, 4051 (2006).
31. P. A. Evans and D. K. Leahy, *J. Am. Chem. Soc.*, **125**, 8974 (2003).
32. P. A. Evans, in *Modern Rhodium-Catalyzed Organic Reactions* (Ed. P. A. Evans), Wiley-VCH, Weinheim, 2005, pp. 191–214.
33. (a) M. Miura and M. Nomura, *Top. Curr. Chem.*, **219**, 211 (2002).
(b) A. Ehrentraut, A. Zapf and M. Beller, *Adv. Synth. Catal.*, **344**, 209 (2002).
(c) J. L. Rutherford, M. P. Rainka and S. L. Buchwald, *J. Am. Chem. Soc.*, **124**, 15168 (2002).
(d) M. S. Viciu, R. F. Germaneau and S. P. Nolan, *Org. Lett.*, **4**, 4053 (2002).
(e) T. Hamada, A. Chieffi, J. Åhman and S. L. Buchwald, *J. Am. Chem. Soc.*, **124**, 1261 (2002).
(f) D. A. Culkin and J. F. Hartwig, *Acc. Chem. Res.*, **36**, 234 (2003).
34. (a) J. Chae, J. Yun and S. L. Buchwald, *Org. Lett.*, **6**, 4809 (2004).
(b) W. Su, S. Raders, J. G. Verkade, X. Liao and J. F. Hartwig, *Angew. Chem. Int. Ed.*, **45**, 5852 (2006).
35. (a) D. Solé, L. Vallverdú, X. Solans, M. Font-Bardia and J. Bonjoch, *J. Am. Chem. Soc.*, **125**, 1587 (2003).
(b) T. Honda and Y. Sakamaki, *Tetrahedron Lett.*, **46**, 6823 (2005).
36. T. Iwama and V. H. Rawal, *Org. Lett.*, **8**, 5725 (2006).
37. M. C. Willis, D. Taylor and A. T. Gillmore, *Org. Lett.*, **6**, 4755 (2004).
38. M. C. Willis, D. Taylor and A. T. Gillmore, *Tetrahedron*, **62**, 11513 (2006).
39. X. Liao, H. Zhou, J. Yu and J. M. Cook, *J. Org. Chem.*, **71**, 8884 (2006).
40. A. T. Nielsen and W. J. Houlihan, *Org. React.*, **16**, 1 (1968).
41. (a) C. H. Heathcock, in *Comprehensive Organic Syntheses* (Eds B. M. Trost, I. Fleming and C. H. Heathcock), Pergamon, Oxford, 1993, pp. 181–238.
(b) A. S. Franklin and I. Paterson, *Contemp. Org. Synth.*, **1**, 317 (1994).
(c) C. J. Cowden and I. Paterson, *Org. React.*, **51**, 1 (1997).
(d) B. Schetter and R. Mahrwald, *Angew. Chem. Int. Ed.*, **45**, 7506 (2006).
42. D. A. Evans, J. M. Takacs, L. R. McGee, M. D. Ennis, D. J. Mathre and J. Bartroli, *Pure Appl. Chem.*, **53**, 1109 (1981).
43. D. A. Evans, J. V. Nelson and T. R. Taber, *Top. Stereochem.*, **13**, 1 (1982).
44. H. E. Zimmerman and M. D. Traxler, *J. Am. Chem. Soc.*, **79**, 1920 (1957).
45. D. Seebach, *Angew. Chem. Int. Ed.*, **27**, 1624 (1988).
46. E. J. Corey and S. S. Kim, *J. Am. Chem. Soc.*, **112**, 4976 (1990).
47. (a) L. Venkatraman, C. C. Aldrich, D. H. Sherman and R. A. Fecik, *J. Org. Chem.*, **70**, 7267 (2005).
(b) C. C. Aldrich, B. J. Beck, R. A. Fecik and D. H. Sherman, *J. Am. Chem. Soc.*, **127**, 8441 (2005).
48. (a) D. A. Evans, H. P. Ng, J. S. Clark and D. L. Rieger, *Tetrahedron*, **48**, 2127 (1992).
(b) D. A. Evans, M. D. Ennis, T. Le, N. Mandel and G. Mandel, *J. Am. Chem. Soc.*, **106**, 1154 (1984).

49. J. G. Solsona, J. Nebot, P. Romea and F. Urpí, *J. Org. Chem.*, **70**, 6533 (2005).
50. J. Nebot, S. Figueras, P. Romea, F. Urpí and Y. Ji, *Tetrahedron*, **62**, 11090 (2006).
51. I. Paterson and R. D. Tillyer, *Tetrahedron Lett.*, **33**, 4233 (1992).
52. (a) M. V. Perkins and R. A. Sampson, *Org. Lett.*, **3**, 123 (2001).
    (b) M. V. Perkins and R. A. Sampson, *Tetrahedron Lett.*, **39**, 8367 (1998).
    (c) R. A. Sampson and M. V. Perkins, *Org. Lett.*, **4**, 1655 (2002).
53. T. Mukaiyama and J.-I. Matsuo, in *Modern Aldol Reactions* (Ed. R. Mahrwald), Wiley-VCH, Weinheim, 2004, pp. 127–160.
54. D. A. Evans, E. Vogel and J. V. Nelson, *J. Am. Chem. Soc.*, **101**, 6120 (1979).
55. M. V. Perkins, S. Jahangiri and M. R. Taylor, *Tetrahedron Lett.*, **47**, 2025 (2006).
56. K. Suenaga, H. Kigoshi and K. Yamada, *Tetrahedron Lett.*, **37**, 5151 (1996).
57. W. R. Roush, *J. Org. Chem.*, **56**, 4151 (1991).
58. J. S. Crossman and M. V. Perkins, *J. Org. Chem.*, **71**, 117 (2006).
59. Y. Nishimura, Y. Miyake, R. Amemiya and M. Yamaguchi, *Org. Lett.*, **8**, 5077 (2006).
60. R. Amemiya, Y. Miyake and M. Yamaguchi, *Tetrahedron Lett.*, **47**, 1797 (2006).
61. M. Majewski and D. M. Gleave, *Tetrahedron Lett.*, **30**, 5681 (1989).
62. Z. Ikeda, T. Hirayama and S. Matsubara, *Angew. Chem. Int. Ed.*, **45**, 8200 (2006).
63. B. L. Feringa and J. F. G. A. Jansen, in *Stereoselective Synthesis* (Eds G. Helmchen, R. W. Hoffmann, J. Mulzer and E. Schaumann), Thieme, Stuttgart, 1996, pp. 2104–2155.
64. S. Kobayashi and T. Mukaiyama, *Chem. Lett.*, **16**, 1183 (1987).
65. S. Kobayashi, M. Tamura and T. Mukaiyama, *Chem. Lett.*, **17**, 91 (1988).
66. D. Enders and W. Karl, *Synlett*, 895 (1992).
67. M. Yasuda, K. Chiba, N. Ohigashi, Y. Katoh and A. Baba, *J. Am. Chem. Soc.*, **125**, 7291 (2003).
68. (a) M. Yasuda, K. Chiba and A. Baba, *J. Am. Chem. Soc.*, **122**, 7549 (2000).
    (b) M. Yasuda and A. Baba, *J. Synth. Org. Chem. Jpn.*, **59**, 697 (2001).
69. M. Yasuda, Y. Shigeyoshi, I. Shibata and A. Baba, *Synthesis*, 233 (2005).
70. S. Gao, Y. Q. Tu, Z. Song, A. Wang, X. Fan and Y. Jiang, *J. Org. Chem.*, **70**, 6523 (2005).
71. (a) V. V. Shchepin, A. E. Korzun, M. I. Vakhrin, P. S. Silaichev, M. A. Ezhikova and M. I. Kodess, *Russ. J. Org. Chem.*, **42**, 1344 (2006).
    (b) V. V. Shchepin, A. E. Korzun, S. N. Shurov, M. I. Vakhrin and N. Yu. Russkikh, *Russ. J. Gen. Chem.*, **74**, 1410 (2004).
72. M. Yamaguchi, in *Comprehensive Asymmetric Catalysis*, Supplement 1 (Eds E. N. Jacobsen, A. Pfaltz and H. Yamamoto), Springer, Berlin, 2004, pp. 151–159.
73. D. J. Cram and G. D. Y. Sogah, *J. Chem. Soc., Chem. Commun.*, 625 (1981).
74. (a) J. Christoffers, *Eur. J. Org. Chem.*, 1259 (1998).
    (b) Y. Hamashima, D. Hotta and M. Sodeoka, *J. Am. Chem. Soc.*, **124**, 11240 (2002).
    (c) Y. Hamashima, D. Hotta, N. Umebayashi, Y. Tsuchiya, T. Suzuki and M. Sodeoka, *Adv. Synth. Catal.*, **347**, 1576 (2005).
75. (a) M. Shibasaki and N. Yoshikawa, *Chem. Rev.*, **102**, 2187 (2002).
    (b) V. Annamalai, E. F. DiMauro, P. J. Carroll and M. C. Kozlowski, *J. Org. Chem.*, **68**, 1973 (2003).
76. M. Nakajima, S. Yamamoto, Y. Yamaguchi, S. Nakamura and S. Hashimoto, *Tetrahedron*, **59**, 7307 (2003).
77. C. Ogawa, K. Kizu, H. Shimizu, M. Takeuchi and S. Kobayashi, *Chem. Asian J.*, **1–2**, 121 (2006).
78. (a) R. D. Little and J. R. Dawson, *Tetrahedron Lett.*, **21**, 2609 (1980).
    (b) P. Prempree, S. Radviroongit and Y. Thebtaranonth, *J. Org. Chem.*, **48**, 3553 (1983).
    (c) R. A. Bunce, *Tetrahedron*, **51**, 13103 (1995).
    (d) H. Lebel, J.-F. Marcoux, C. Molinaro and A. B. Charette, *Chem. Rev.*, **103**, 977 (2003).
    (e) M. Pohlman, U. Kazmaier and T. Lindner, *J. Org. Chem.*, **69**, 6909 (2004).
79. V. V. Shchepin, P. S. Silaichev, Yu. G. Stepanyan, M. M. Kalyuzhnyi, N. Yu. Russkikh and M. I. Kodess, *Russ. J. Org. Chem.*, **42**, 973 (2006).
80. A. Abiko, J.-F. Liu and S. Masamune, *J. Org. Chem.*, **61**, 2590 (1996).
81. B. Moreau, M. Ginisty, D. Alberico and A. B. Charette, *J. Org. Chem.*, **72**, 1235 (2007).
82. S. A. Babu, M. Yasuda, Y. Okabe, I. Shibata and A. Baba, *Org. Lett.*, **8**, 3029 (2006).
83. V. Blot and H.-U. Reissig, *Synlett*, 2763 (2006).

84. (a) R. Des Mazery, M. Pullez, F. López, S. R. Harutyunyan, A. J. Minnaard and B. L. Feringa, *J. Am. Chem. Soc.*, **127**, 9966 (2005).
(b) G. P. Howell, S. P. Fletcher, K. Geurts, B. ter Horst and B. L. Feringa, *J. Am. Chem. Soc.*, **128**, 14977 (2006).
85. R. Bandichhor, B. Nosse and O. Reiser, *Top. Curr. Chem.*, **243**, 43 (2005).
86. (a) O. M. Berner, L. Tedeschi and D. Enders, *Eur. J. Org. Chem.*, 1877 (2002).
(b) A. Duursma, A. J. Minnaard and B. L. Feringa, *J. Am. Chem. Soc.*, **125**, 3700 (2003).
(c) J. Christoffers and A. Baro, *Angew. Chem. Int. Ed.*, **42**, 1688 (2003).
(d) J.-A. Ma and D. Cahard, *Angew. Chem. Int. Ed.*, **43**, 4566 (2004).
(e) O. Andrey, A. Alexakis, A. Tomassini and G. Bernardinelli, *Adv. Synth. Catal.*, **346**, 1147 (2004).
(f) D. A. Evans and D. Seidel, *J. Am. Chem. Soc.*, **127**, 9958 (2005).
(g) A. Lattanzi, *Tetrahedron: Asymmetry*, **17**, 837 (2006).
87. (a) E. Juaristi, A. K. Beck, J. Hansen, T. Matt, T. Mukhopadhyay, M. Simson and D. Seebach, *Synthesis*, 1271 (1993).
(b) M. Iguchi, H. Doi, S. Hata and K. Tomioka, *Chem. Pharm. Bull.*, **52**, 125 (2004).
88. N. Duguet, A. Harrison-Marchand, J. Maddaluno and K. Tomioka, *Org. Lett.*, **8**, 5745 (2006).
89. (a) K. Flinois, Y. Yuan, C. Bastide, A. Harrison-Marchand and J. Maddaluno, *Tetrahedron*, **58**, 4707 (2002).
(b) Y. Yuan, A. Harrison-Marchand and J. Maddaluno, *Synlett*, 1555 (2005).
90. G. Blay, I. Fernández, B. Monje, M. C. Muñoz, J. R. Pedro and C. Vila, *Tetrahedron*, **62**, 9174 (2006).
91. D. Seebach, A. R. Sting and M. Hoffmann, *Angew. Chem. Int. Ed.*, **35**, 2708 (1996).
92. W. H. Sikorski and H. J. Reich, *J. Am. Chem. Soc.*, **123**, 6527 (2001).
93. G. Blay, I. Fernández, P. Formentin, B. Monje, J. R. Pedro and R. Ruiz, *Tetrahedron*, **57**, 1075 (2001).
94. G. Blay, L. Cardona, L. Torres and J. R. Pedro, *Synthesis*, 108 (2007).
95. D. J. Dixon, R. A. J. Horan and N. J. T. Monck, *Org. Lett.*, **6**, 4423 (2004).
96. D. J. Dixon, R. A. J. Horan, N. J. T. Monck and P. Berg, *Org. Lett.*, **6**, 4427 (2004).
97. F. A. Davis, Y. Zhang and H. Qiu, *Org. Lett.*, **9**, 833 (2007).
98. (a) J. Christoffers and A. Mann, *Angew. Chem. Int. Ed.*, **40**, 4591 (2001).
(b) J.-A. Ma, *Angew. Chem. Int. Ed.*, **42**, 4290 (2003).
99. (a) T. Wirth, *Angew. Chem. Int. Ed.*, **36**, 225 (1997).
(b) J. M. Humphrey and A. R. Chamberlin, *Chem. Rev.*, **97**, 2243 (1997).
100. T. Kawabata, S. Matsuda, S. Kawakami, D. Monguchi and K. Moriyama, *J. Am. Chem. Soc.*, **128**, 15394 (2006).
101. (a) T. Kawabata, S. Kawakami and S. Majumdar, *J. Am. Chem. Soc.*, **125**, 13012 (2003).
(b) T. Kawabata, S. Majumdar, K. Tsubaki and D. Monguchi, *Org. Biomol. Chem.*, **3**, 1609 (2005).
(c) H. Zhao, D. Hsu and P. R. Carlier, *Synthesis*, 1 (2005).
102. (a) D. Seebach and R. Naef, *Helv. Chim. Acta*, **64**, 2704 (1981).
(b) T. Sato, Y. Kugo, E. Nakaumi, H. Ishibashi and M. Ikeda, *J. Chem. Soc., Perkin Trans. 1*, 1801 (1995).
103. S. Nagumo, M. Mizukami, N. Akutsu, A. Nishida and N. Kawahara, *Tetrahedron Lett.*, **40**, 3209 (1999).
104. R. Filosa, C. Holder and Y. P. Auberson, *Tetrahedron Lett.*, **47**, 8929 (2006).
105. T. Abellán, C. Nájera and J. M. Sansano, *Tetrahedron: Asymmetry*, **9**, 2211 (1998).
106. (a) U. Kazmaier, *Recent Res. Dev. Org. Chem.*, **2**, 351 (1998).
(b) U. Kazmaier, in *Bioorganic Chemistry* (Eds U. Diederichsen, T. K. Lindhorst, B. Westermann and L. A. Wessjohann), Wiley-VCH, Weinheim, 1999, pp. 201–206.
(c) U. Kazmaier and T. Lindner, *Angew. Chem. Int. Ed.*, **44**, 3303 (2005).
(d) U. Kazmaier and K. Krämer, *J. Org. Chem.*, **71**, 8950 (2006).
107. (a) U. Kazmaier and F. L. Zumpe, *Angew. Chem. Int. Ed.*, **38**, 1468 (1999).
(b) U. Kazmaier and F. L. Zumpe, *Angew. Chem. Int. Ed.*, **39**, 802 (2000).
108. U. Kazmaier and M. Pohlman, *Synlett*, 623 (2004).
109. B. Åkermark, S. Hansson and A. Vitagliano, *J. Am. Chem. Soc.*, **112**, 4587 (1990).
110. U. Kazmaier and D. Stolz, *Angew. Chem. Int. Ed.*, **45**, 3072 (2006).

111. (a) P. A. Evans and J. D. Nelson, *Tetrahedron Lett.*, **39**, 1725 (1998).
(b) P. A. Evans and L. J. Kennedy, *J. Am. Chem. Soc.*, **123**, 1234 (2001).
112. (a) U. Kazmaier and R. Grandel, *Synlett*, 945 (1995).
(b) U. Kazmaier and R. Grandel, *Eur. J. Org. Chem.*, 1833 (1998).
113. (a) M. Pohlman and U. Kazmaier, *Org. Lett.*, **5**, 2631 (2003).
(b) B. Mendler and U. Kazmaier, *Org. Lett.*, **7**, 1715 (2005).
114. (a) U. Kazmaier, *Angew. Chem. Int. Ed.*, **33**, 998 (1994).
(b) U. Kazmaier, *Liebigs Ann. Chem.*, 285 (1997).
(c) U. Kazmaier, *J. Indian Chem. Soc.*, **76**, 631 (1999).
(d) H. Mues and U. Kazmaier, *Synthesis*, 487 (2001).
(e) U. Kazmaier, H. Mues and A. Krebs, *Chem. Eur. J.*, **8**, 1850 (2002).
115. H. Y. Kim, K. Stein and P. L. Toogood, *J. Chem. Soc., Chem. Commun.*, 1683 (1996).
116. (a) U. Kazmaier, *Tetrahedron*, **50**, 12895 (1994).
(b) U. Kazmaier, *J. Org. Chem.*, **61**, 3694 (1996).
117. (a) U. Kazmaier and S. Maier, *J. Chem. Soc., Chem. Commun.*, 1991 (1995).
(b) U. Kazmaier and S. Maier, *Tetrahedron*, **52**, 941 (1996).
118. M. Gander-Coquoz and D. Seebach, *Helv. Chim. Acta*, **71**, 224 (1988).
119. D. J. Ager, D. E. Froen, R. C. Klix, B. Zhi, J. M. McIntosh and R. Thangarasa, *Tetrahedron*, **50**, 1975 (1994).
120. I. Ojima and X. Qiu, *J. Am. Chem. Soc.*, **109**, 6537 (1987).
121. U. Kazmaier, J. Deska and A. Watzke, *Angew. Chem. Int. Ed.*, **45**, 4855 (2006).
122. (a) U. Kazmaier and S. Maier, *J. Org. Chem.*, **64**, 4574 (1999).
(b) U. Kazmaier, S. Maier and F. L. Zumpe, *Synlett*, 1523 (2000).

CHAPTER 8

Acid–base properties of enols and enolates

JASON EAMES

Department of Chemistry, University of Hull, Cottingham Road, Kingston upon Hull, HU6 7RX, England
Fax: +44-1482-464610; e-mail: j.eames@hull.ac.uk

I. ACRONYMS

ACAC	acetylacetonate anion
BINAP	2,2′-bis(diphenylphosphino)-1,1′-binaphthyl
DIFLUORPHOS	2,2,2′,2′-tetrafluoro(4,4′-bi(1,3-benzodioxole)-5,5′-diyl)bis (diphenylphosphine)
DKR	dynamic kinetic resolution
KHMDS	potassium hexamethyldisilazane
LDA	lithium diisopropylamide
LiTMP	lithium tetramethylpiperidide
PyBox	2,6-bis[oxazolin-2′-yl]pyridine
TBAF	tetrabutylammonium fluoride

The chemistry of metal enolates
Edited by Jacob Zabicky

II. INTRODUCTION

The chemistry of enolates is extremely well documented[1–3]. Enolates are generally formed by simple deprotonation of carbonyl-containing compounds using a Brønsted base[4,5]. However, competitive nucleophilic addition to the carbonyl group can occur due to its Lewis acidity[6–8]. Enolates can be synthesized[9–11] and isolated[12–14] or used *in situ*[3,4,15,16] efficiently under kinetic control[17], whereas under thermodynamic control[18] enolate formation is reversible[19–22], and therefore for efficient product formation the product(s) generally needs to be more stable than the starting precursor(s)[23]. By far, the majority of enolate chemistry is dominated by the reformation of the more thermodynamically favoured (typically by *ca* 40 kJ mol^{-1} for simple aldehydes and ketones)[24] carbonyl (C=O) group through either reprotonation[25–27] or by addition to an electrophile[28–35]. The chemistry of carbonyl groups and their enolates are a near-perfect marriage where neither can be divorced from one another[36].

This chapter is primarily concerned with keto–enol equilibrium and the chemistry of dissociated enols (enoxides)[37] and lithium enolates. The acid–base aspects of the chemistry of other metal enolates (e.g. silyl enol ethers[38–43], boron enol ethers[44–51], aluminium[52], tin[53–55], gallium[56], bismuth[57,58], zinc[59–70], rhodium[71], palladium[72–82], manganese[83,84], copper[85], nickel[86,87], magnesium[88–90], titanium[91–108], molybdenum[109], zirconium[110,111] and ammonium[112,113] enolates) have been reported elsewhere.

III. CHEMISTRY OF ENOLS AND ENOLATES

A. Enol Formation

Carbonyl-containing molecules, such as **1**, with an α-carbon–hydrogen C($2sp^3$)–H($1s$) hybridized bond can exist as an enol tautomer **2**, and their relative proportions depend on the relative stability of each tautomeric component (Scheme 1)[114–120]. For saturated carbonyl-containing molecules, like **1**, the amount of enol content **2** is quite low (<1%; $K_E \ll 1$; $pK_E \gg 0$)[24,121,122]. By simply stabilizing the enol component (relative to the carbonyl group) through resonance[123–125], hyperconjugation[126], aromatization[127–129] and solvation[130], the relative stability of enols can be controlled by the relative position of the enol double bond (e.g. endocyclic versus endocyclic)[131]. For example, phenol is the stable enolic form of cyclohexa-2,4-dienone [$pK_a^E(H_2O) = 9.95$ and $pK_a^K(H_2O) = -3 \pm 1$][132] due to its continuous (aromatic) conjugation. In comparison, intrinsically unstable enols can be made under kinetic control[133], generally using indirect methodology[134], such as photolysis[135–137]. These kinetic enols have been shown to tautomerize[138–141] to give the corresponding carbonyl-containing compounds under acidic and/or basic conditions[142].

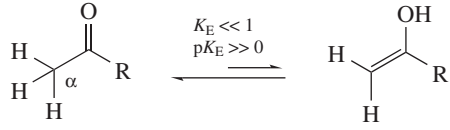

(**1**) (**2**)

B. Enol Formation and Proton Transfer

Enolates, such as **3**, are generally formed by direct deprotonation of either its carbonyl (**1′**) or enol tautomer (**2′**), using a Brønsted base :B (Scheme 1). The relative proportion of this enolate to the corresponding parent carbonyl and enol components is largely dependent

on the strength of the Brønsted base, :B[3–5, 143], the nature of the solvent[144], associated additives[145, 146] and metal ions[147–149]. Regarding the solvent, it is interesting to note that no comparison can be made between the acidity of acetophenone in DMSO, $pK_a = -\log_{10}([eneO^-][H^+]/[eneOH])$, and in other solvents, such as benzene or a polyether, $pK_a = -\log_{10}([eneOM^*][H^+]/[eneOH][M^{*+}])$, because in the latter the metal enolate is present as an ion pair, where M* denotes a metal cation, possibly coordinated to other ligands, including enolato ones. For example, acetophenone is a stronger acid than fluorene in benzene (by 10^6) but a weaker one in DMSO (by 10^2)[144]. Enolates by their very nature are ambident Brønsted bases[150–152] and Lewis bases[153–160]. *O*-Protonation of enolates to give enols, using strong Brønsted acids, has been shown to be kinetically preferred over *C*-protonation[161, 162]. Tautomerization of the enol generally occurs to give the more thermodynamically stable carbonyl compound. *C*-Protonation by electrophilic attack on the C=C double bond leads directly to the more stable carbonyl group[163–165]. Intriguingly, under certain conditions, deprotonation and subsequent reaction with an acid HA can lead to proton exchange (**1′** → **1″**) or (**2′** → **2″**) (Scheme 1)[166–168].

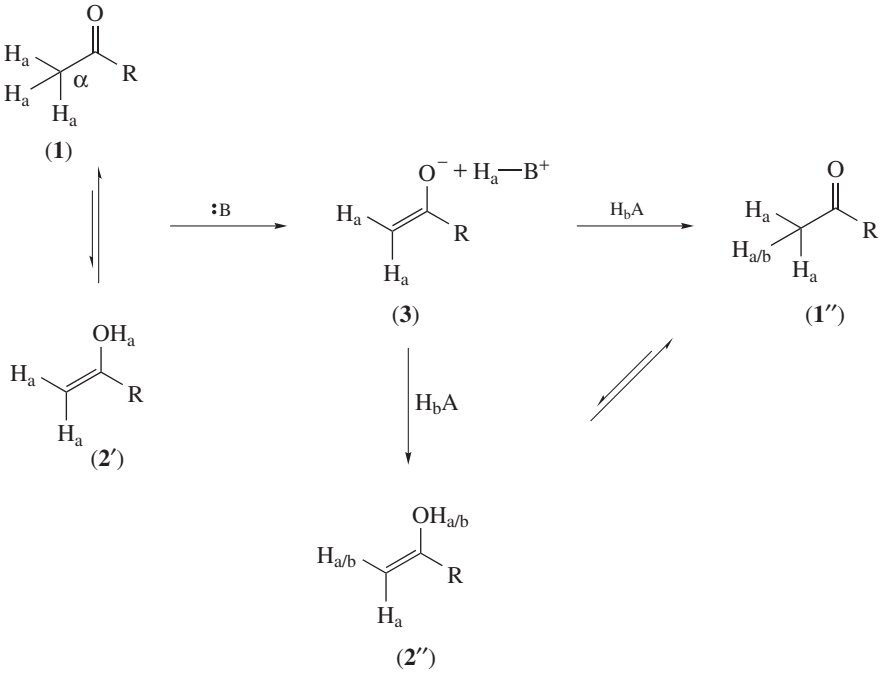

SCHEME 1. Formation and protonation pathways for enolate (**3**)

IV. ACIDITY OF CARBONYL COMPOUNDS AND ASSOCIATED ENOLS

Over the last twenty years[169], there has been a resurgence into the measurement of acidity of organic molecules[170] and its associated solvent effects (e.g. in heptane[171], cyclohexane[172], THF[173] and cyclohexylamine[174]). These have generally been measured[175] using close comparison indicators[176, 177] of known pK_a determined by colorimetric, spectroscopic and polarimetric methods[178–183]. The carbonyl (C=O) group with its σ- and

π-electron-withdrawing nature has attracted a large proportion of this attention[184–186]; the related C=S compounds are known to be more acidic[185]. The acidity of organic compounds is universally quoted as a function of its pK_a ($-\log_{10} K_a$) value[187,188]; the smaller the pK_a (or larger K_a) the more acidic the Brønsted acid[189]. For example, for acetophenone **4**, the pK_a values of the keto and enol components (in water) are 18.31 and 10.34, respectively [$pK_a^K(H_2O) = 18.31$[190], $pK_a^E(H_2O) = 10.34$[190]] (equation 1). In equation 1 are shown the equilibrium constant of enolization (pK_E) of acetophenone in water, as well as the acidities of the keto (**4**[190], pK_a^K) and enol (**5**[190], pK_a^E) tautomers. Clearly, the keto form (**4**) is less acidic than the solvent, water ($pK_a = 15.74$[191]), whereas the enol form (**5**) is more acidic. The use of traditional inorganic bases, such as sodium hydroxide (NaOH) [$pK_aH_2O(H_2O) = 15.74$[191]] and sodium amide ($NaNH_2$) [$pK_aNH_3(H_2O) = 38$[191]], as Brønsted bases for enolate formation is largely dependent on the acidity of the cabonyl derivative concerned. For acetophenone, LiOH and $NaNH_2$ would allow approximately 0.5% and 99.9999999999998% enolate **6** formation, respectively, whereas for a more acidic carbonyl compound, such as 2-acetyl cyclohexanone (**7**)[192] which has similar acidity to its enol form (**8**), near-exclusive enolate (**9**) formation is expected for both inorganic bases (equation 2). The resulting enolate (**9**) was shown to be less basic than enolate **6**. Interestingly, to ensure 99.99% enolate formation under equilibrium conditions, the Brønsted base needs to be at least four pK_{HA} units higher than the pK_a^K of the carbonyl compound. For synthetic ease, most enolates are formed under kinetic control[3,4] at low temperature by deprotonation of the carbonyl compound, with $pK_a^K(H_2O) = 17–30$[4], using a sterically demanding metal amide (MNR_2, R = *i*-Pr, $SiMe_3$) with pK_{HA} (H_2O) *ca* 33[5].

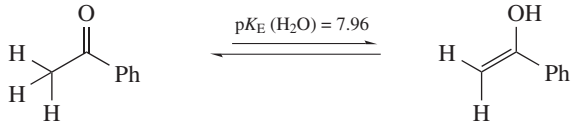

(**4**) (**5**)

$pK_a^K(H_2O) = 18.31$ $pK_a^E(H_2O) = 10.34$ (1)

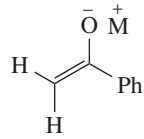

(**6**)

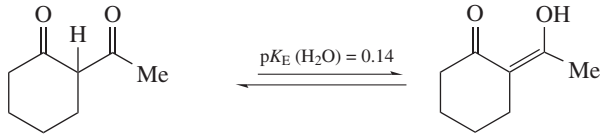

(**7**) (**8**)

$pK_a^K(H_2O) = 9.62$ $pK_a^E(H_2O) = 9.47$ (2)

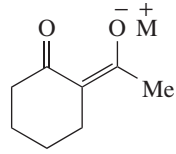

(**9**)

The relative stability and reactivity[193–199] of enolates (versus their parent carbonyl compounds) can be controlled through solvation[200–203]. In polar protic solvents, such as H_2O, enolates are more stable due to hydrogen-bonding between the enolic oxy-anion and the neighbouring water molecules[148, 204]. By comparison, in polar aprotic solvents, such as DMSO, this type of stabilization is impossible and consequently the stability and availability of the enolate is lower. This can be seen by closer examination of the relative acidity of a particular carbonyl-containing molecule, such as acetophenone (**4**), in a variety of solvents: it is more acidic in H_2O ($pK_a^K = 18.31$[190]) than in Et_2O ($pK_a^K = 19.0$[205]), which in turn is more acidic than in DMSO ($pK_a^K = 24.7$[206]). By gradually replacing the solvent from DMSO to H_2O, the relative acidity of acetophenone can be increased by up to 2.5×10^6 times! With the enormous amount of information and pK_a data available since the 1930s[205, 207], a great deal of time and effort has been spent creating mathematical models and algorithms for predicting the theoretical pK_a of organic molecules with some successes[208–210].

The rate of enolate–carbonyl equilibration[211, 212] is dependent on the forward and backward rates of proton exchange. Proton exchange from a carbon-based acid is known to be slower than that of a more electronegative atom donor (in particular, O and N atoms)[162, 213]. For a series of closely related molecules usually the more acidic a given molecule is, the faster the rate of proton transfer (high k_{rel}, note that thermodynamic and kinetic parameters are not related). For example, benzocyclobutanone (**10**) is less acidic and the rate of deprotonation is substantially slower[214] (10^6 times) than the related benzocyclopentanone (**12**)[215] due to its enolate (**11**) having unfavourable anti-aromatic character. Deprotonation of the simplest cyclobutanone (**13**)[215] clearly does not lead to an unfavourable anti-aromatic enolate (**14**)[216]. By assuming the internal strain of **14** is similar to that of **11**, cyclobutanone (**13**) is evidently $10^{7.7}$ times more acidic than benzocyclopentanone (**12**). By the same vain, the more acidic propanone (**15**)[215] has a faster rate of deprotonation (10^3 times) than the less acidic ethyl acetate (**16**)[127].

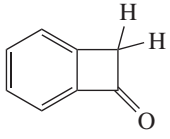

(**10**)

pK_a^K (H_2O) = 27

$k_{rel} = 1$

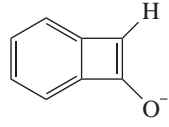

(**11**)

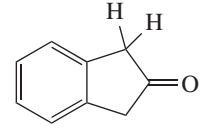

(**12**)

pK_a^K (H_2O) = 12.2

$k_{rel} = 3.1 \times 10^6$

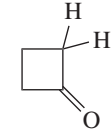

(**13**)

pK_a^K (H_2O) = 19.3

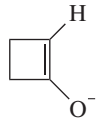

(**14**)

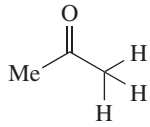

(**15**)

pK_a^K (H_2O) = 19.3

$k_{rel} = 1.6 \times 10^3$

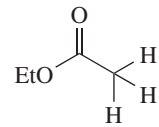

(**16**)

pK_a^K (H_2O) = 25.6

$k_{rel} = 1.7$

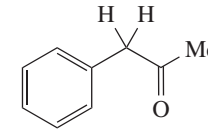

(**17**)

pK_a (H_2O) = 19.4

Formation of the antiaromatic enolate **11** from the low acidity ketone **10**[214] is evidently unfavourable compared with its acyclic variant **17**[217]. Attempts at isolating a stable enol derivative of **10**, such as its silyl enol ether, have proved unsuccessful[214]. Treatment of benzocyclobutanone (**10**) with LiTMP in THF at −78 °C, followed by the addition of trimethylsilyl chloride (Me_3SiCl), gave the corresponding *C*-silylated benzocyclobutanone **18** (equation 3)[214]. The non-aromatic *C*-lithiated ketone **20** appears to be more preferred than its related *O*-lithiated enolate **11**. Unlike traditional lithium enolates, this particular lithium enolate reacts *in situ* with its parent compound, benzocyclobutanone (**10**), to give the diketone **19** (equation 3). In comparison, bridgehead enolates have also been shown to be similarly reactive[218–226].

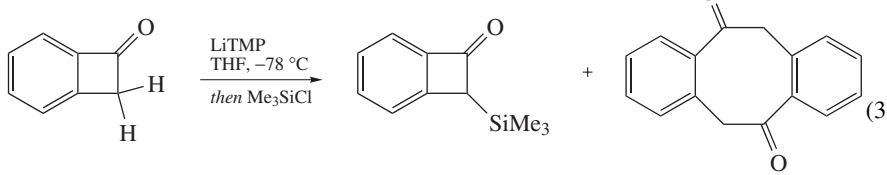

(**10**)

pK_a (H_2O) = 27

(**18**) 89:11 (**19**)

combined 52% yield

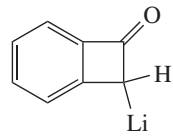

(**20**)

The acidity of carbonyl-containing compounds and their solvent effects have been well documented[148, 204]. Typically, enolate formation is less favoured in DMSO than H_2O due to lower stabilization of its oxy-anion (i.e. the pK_a of the corresponding carbonyl compound in DMSO is higher than in H_2O)[227]. However, under certain circumstances, the reverse can be true[228, 229], as with certain ammonium salts[230, 231], for ethyl 2-trifluoromethylsulfonylacetate (**21**) was found to be more acidic in DMSO [pK_a(DMSO) = 6.40[232]] than in H_2O[232]. This unusual behaviour is presumably due to the corresponding enolate existing as a carbanion as opposed to its normal enolic form[147]. In comparison, for ethyl nitro-acetate (**22**) and ethyl cynanoacetate (**23**) the usual trend returns, even

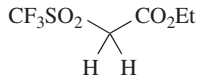

(**21**)

pK_a^K (H_2O) = 6.83
pK_a^K (H_2O, 30% DMSO) = 6.36
pK_a^K (H_2O, 50% DMSO) = 5.84
pK_a^K (H_2O, 70% DMSO) = 5.56
pK_a^K (H_2O, 90% DMSO) = 6.00
pK_a^K (DMSO) = 6.40

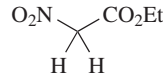

(**22**)

pK_a^K (H_2O) = 5.82
pK_a^K (H_2O, 30% DMSO) = 5.78
pK_a^K (H_2O, 50% DMSO) = 6.00
pK_a^K (H_2O, 70% DMSO) = 6.55
pK_a^K (H_2O, 90% DMSO) = 8.31
pK_a^K (DMSO) = 9.08

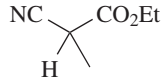

(**23**)

pK_a^K (H_2O) = 10.17
pK_a^K (H_2O, 30% DMSO) = 10.63
pK_a^K (H_2O, 50% DMSO) = 10.83
pK_a^K (H_2O, 70% DMSO) = 11.30
pK_a^K (H_2O, 90% DMSO) = 11.68
pK_a^K (DMSO) = 12.48

though the nitro group in **22** allows for greater stabilization and subsequent acidity[232]. These solvent effects are clearly non-linear for H_2O–DMSO mixtures in all proportions.

The conformation and the resulting polarity of enolates can play an important role in their stability[233], as in the case of diethyl malonate (**24**), with apparent pK_a(DMSO) = 16.4. However, its acidity was found to be largely dependent on the conformation of its resonance-stabilized enolate **25**. The conformation of the resulting enolate can be altered by chelation of a Lewis acid metal and/or by minimization of electrostatic C–O

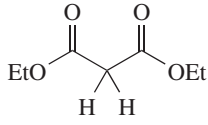

(**24**)

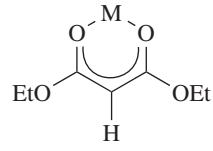

(**25**)

pK_a (DMSO) = 16.4

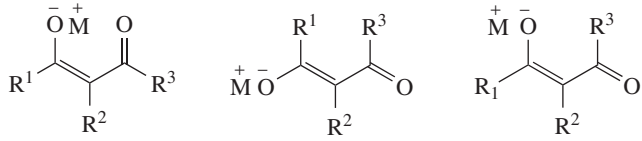

(**26**) (*Z*,U) 'U' shape

(**26**') (*E*,W) 'W' shape

(**26**") (*Z*,S) 'S' shape

bond repulsion. The (*Z*,U shape)-conformation (**26**) can be accessible for coordinating metals (e.g. Li^+ chelate formation), whereas the (*E*,W shape)-conformation (**26**′) should be favoured for both coordinating and non-coordinating metal ions, such as Li^+ and K^+, due to minimization of C−O bond repulsion. The remaining (*Z*,S shape)-conformation (**26**″) has neither internal metal coordination nor minimal C−O repulsion.

For weakly coordinating potassium K^+ counter-ions, the acidity of diethyl malonate (**24**) (in DMSO) increased by increasing the fraction of ion pairing, as shown in Table 1 for three counter-ions in DMSO solution (Table 1). This trend also continued by increasing the coordinating ability of the metal counter-ions from sodium to lithium counter-ions. From this study, it appears the (*E*,W)-conformer (**26**′) is more preferred over the (*Z*,U)-conformer (**26**) as the repulsion between the C−O bonds is more energetically unfavourable than chelate formation might be favourable.

These effects can be seen more clearly by probing the relative acidity of conformationally flexible (**24**, **27** and **28**) and locked (**30**–**34**) 1,3-dicarbonyl-containing molecules.

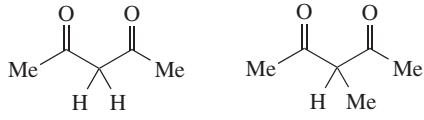

(**27**) pK_a (DMSO) = 13.3

(**28**) pK_a (DMSO) = 15.1

TABLE 1. Effect of metal ion pairing on the apparent experimental pK_a value of diethylmalonate (**24**). Reprinted with permission from Reference 233. Copyright 1980 American Chemical Society

Metal ion	% ion pairing	pK_a
Li^+	94.1	15.16
Li^+	90.2	15.37
Li^+	86.0	15.53
Li^+	72.3	15.82
Li^+	64.3	15.94
Na^+	81.8	15.64
Na^+	75.9	15.76
Na^+	65.0	15.92
Na^+	57.0	16.01
Na^+	46.9	16.10
K^+	65.8	15.91
K^+	57.8	16.00
K^+	47.1	16.09
K^+	39.0	16.16
K^+	16.1	16.30

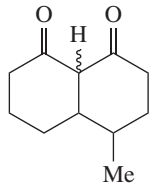

(**29**)

pK_a (DMSO) = 18.2

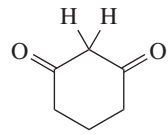

(**30**)

pK_a (DMSO) = 10.3

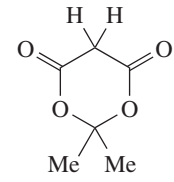

(**31**)

pK_a (DMSO) = 7.32

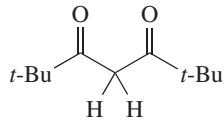

(**32**)

pK_a (DMSO) = 15.4

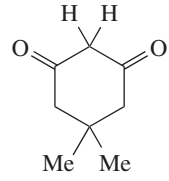

(**33**)

pK_a (DMSO) = 11.2

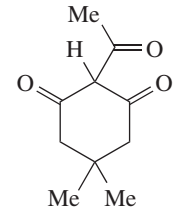

(**34**)

pK_a (DMSO) = 9.8

For molecules with locked 'U'- and 'W'-shaped carbonyl groups, such as **29** and **30**, their relative acidity difference is surprisingly large (nearly 8 logarithmic units in favour of the latter[233]). For Meldrum's acid (**31**), the locked conformation further enhances the acidity due to lower conjugation of the 'lactone' oxygen atoms[234–236] with the neighbouring C=O bonds[148]. In comparison, for the conformationally flexible diethylmalonate (**24**), where the conjugation is not disrupted, the relative acidity is significantly higher (nearly 9 logarithmic units[233]). The association constants of various enolates of alkali metal ions are summarized in Table 2.

The extent of ion pairing shown in Table 2 is greatly influenced by the conformation of the 1,3-dicarbonyl compound. For **29**, with a locked 'U'-shape conformation, there is significant ion pairing (log K_{as} for Li+, Na+ and K+ is >7, 4.93 and 3.39, respectively), whereas for **33**, with a locked 'W' conformation, there is significantly lower ion-pairing (1.58, 1.05 and <1, respectively). For conformationally labile 1,3-dicarbonyl compounds, the diester **24** has been shown to have higher levels of ion pairing than the diketones **27** and **28**, as the ester functional group is known to be more Lewis basic[237] than the ketone functional group. Interestingly, the more sterically demanding 1,3-dicarbonyl compound **32**[148] is noticeably less acidic than its analogue **27**[233]. This is in part due to the *t*-Bu groups in **32** being less able to hyperconjugate with the adjacent carbonyl groups than the related Me groups in **27**.

Recent attention has focussed on the solvation of neutral enolates formed through the deprotonation of α-ammonio[230–238], α-pyridinio[231–238] and α-imino carbonyl compounds[228, 229, 239, 240]. A trimethylammonio (Me_3N^+-) group has been shown to stabilize in water-adjacent enolates more dominantly than an unsubstituted ammonio group (H_3N^+-). For example, α-trimethylammonio ester **35**[206] is about 1000 times more acidic than the simple α-ammonio ester **36**[206]. This is presumably due to the highly solvated ammonio (H_3N^+-) group having a lower charge effect in water than the less solvated and more

TABLE 2. Ion pair association constants ($\log K_{as}$ in DMSO at 25 °C)[a] for enolates derived from 1,3-dicarbonyl compounds with alkali metal cations. Reprinted with permission from Reference 233. Copyright 1980 American Chemical Society

1,3-Dicarbonyl compound	Li^+	Na^+	K^+
2,4-Pentanedione (**27**)	4.77 ± 0.01	2.60 ± 0.06	1.39 ± 0.05
3-Methyl-2,4-pentanedione (**28**)	3.38 ± 0.14	1.52 ± 0.09	0.79 ± 0.10
Diethyl malonate (**24**)	5.86 ± 0.11	3.30 ± 0.06	2.31 ± 0.02
4-Methyl-1,8-decalinedione (**29**)	>7	4.93 ± 0.14	3.39 ± 0.04
5,5-Dimethyl-1,3-cyclohexanedione (**33**)	1.58 ± 0.03	1.05 ± 0.14	<1

[a] K_{as} in L mol^{-1}.

hydrophobic trimethylammonio (Me_3N^+-) group. This effect was found to be less dominant for the zwitterionic ammonio carboxylates **37** and **38**[230], as the resulting enolates were negatively charged. The presence of a trimethylammonio (Me_3N^+-) group in **35** lowers the relative acidity of methyl acetate (**39**)[230] by 7.6 pK_a units.

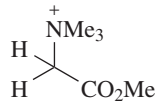

(**35**)

pK_a (H_2O) = 18.0 ± 1

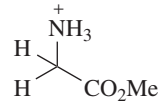

(**36**)

pK_a (H_2O) = 21.0 ± 1

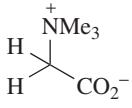

(**37**)

pK_a (H_2O) = 27.3 ± 0.5

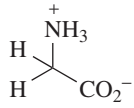

(**38**)

pK_a (H_2O) = 28.9 ± 0.5

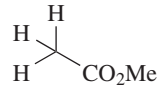

(**39**)

pK_a (H_2O) = 25.6 ± 1

By comparison, the α-pyridio group in **40**[231] lowers the relative acidity by 3.9 pK_a units relative to the α-ammonio group in **41**. This is somewhat unexpected as this additional enolate stabilization is presumably due to resonance stabilization of the α-ketocarbanion tautomer with the neighbouring π-system of the pyridinium ring. The charge effect associated with the α-ammonio group in **41** is considerable as the associated hydrophobic character of the methyl groups must disfavour enolate formation. This can be inferred from ketone **42**[238], containing a *t*-Bu group as a hydrophobic model for a Me_3N^+ group, being less acidic than the less hydrophobic acetophenone (**42′**)[233].

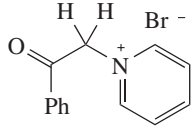

(**40**)

pK_a (DMSO) = 10.7

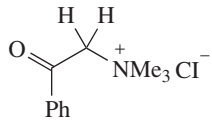

(**41**)

pK_a (DMSO) = 14.6

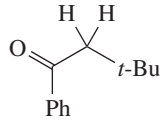

(**42**)

pK_a (DMSO) = 25.3

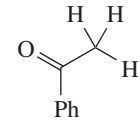

(**42′**)

pK_a (DMSO) = 24.7

Charge effects have been shown to play an important role in enolate formation. For example[241], a lithium carboxylate group (CO_2Li) in **43** stabilizes enolate through aggregation more so than the related ester motif (CO_2Me) in **44**. This acidifying effect of the OLi group vs. the OMe group in DMSO was found to be surprisingly similar to that of nitrile (CN) and sulfonyl (SO_2R) groups[241].

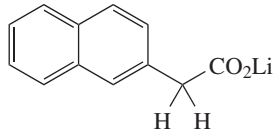

(**43**)

pK_a (H_2O) = 21.4

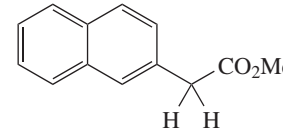

(**44**)

pK_a (H_2O) = 22.7

Enols are generally more acidic (pK_a *ca* 11–12) than their corresponding carbonyl tautomer (pK_a *ca* 17–25). Exceptions to this arise when the carbonyl derivative is either destabilized relative to the enol component, or when the enol is exceptionally stable, as in the case of phenol [pK_a^E(H_2O) = 9.95][132] vs. cyclohexa-2,4-dienone [pK_a^K(H_2O) = -3 ± 1][132]. Enol acidity can be controlled by O–H bond strength. In certain cases, the relative proportion of enol content can be determined by the relative strengths of the C=O and C–H bonds in the carbonyl tautomer versus the C=C and O–H bonds in the enol[132].

Enols (pK_a *ca* = 11–12)[132] are usually more acidic than alcohols [e.g. EtOH; pK_a (H_2O) = 15.9[242]] but are less acidic than phenols [e.g. PhOH; pK_a(H_2O) = 9.95[132, 191]]. The acidity of enols (and the basicity of the corresponding enolate) is surprisingly uniform when considering the relative acidity of the carbonyl derivative. The majority of enols derived from saturated aldehydes and ketones have pK_a^E *ca* 11–12. For simple aldehydes and ketones, such as acetaldehyde (**45**) and acetone (**45′**), their enol acidity (pK_a^E) in water is similar even when their keto acidity (pK_a^K) is moderately different[243]. It is interesting to note that relative enol stability (pK_E) plays little or no role in the relative acidity of enols for example, as is the case of **45** and **45′**[243].

Promoting enol stabilization by increasing the level of substitution at the α-carbon atom of a carbonyl-containing compound has little or no influence on its acidity. For example, the enol stability (pK_E) of isobutyraldehyde (**46**) is greater than that of acetaldehyde (**45**), whereas its enol is only slightly less acidic (pK_a^E). Increasing the enol substitution at C1 by changing from aldehyde (**46**) to ketone (**47**) can lower the relative amount (pK_a^E) slightly and the stability (pK_E) to a great extent of the resulting enol, through steric congestion[244]. In the case of methyl trimethylsilyl ketone (**48**), the pK_a^E was similar to that of its carbon analogue **45′**, but the stability (pK_E) was enhanced[244].

Enol acidity can be increased (or enolate basicity lowered) by increasing the conjugation of the resulting enolate. Interestingly, the enol of pentane-2,4-dione (**48′**)[245] was found to

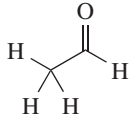

(**45**)

pK_a^K (H_2O) = 16.5
pK_a^E (H_2O) = 11.2
pK_E (H_2O) = 5.3

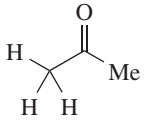

((**45′**)

pK_a^K (H_2O) = 19.0
pK_a^E (H_2O) = 11.8
pK_E (H_2O) = 7.2

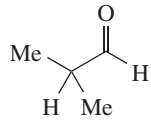

46)

pK_a^K (H_2O) = 14.6
pK_a^E (H_2O) = 11.8
pK_E (H_2O) = 2.8

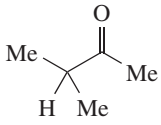

(**47**)

pK_a^K (H_2O) = 21.0
pK_a^E (H_2O) = 12.4
pK_E (H_2O) = 7.9

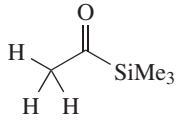

(**48**)

pK_a^K (H_2O) = 16.44
pK_a^E (H_2O) = 11.54
pK_E (H_2O) = 4.9

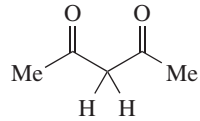

(**48′**)

pK_a^K (H_2O) = 8.9
pK_a^E (H_2O) = 4.7

be more acidic than phenol [$pK_a(H_2O) = 9.95$] and similar to acetic acid [$pK_a(H_2O) = 4.76$][245]. The extra conjugation and coordination of the adjacent acetyl group in the enol of **48′** is predominant over the aromaticity of phenol itself.

Enol acidity can be increased by simply ensuring that conjugation is present in the enolic form but not the carbonyl form. 2-Indanone (**49**) has greater enolic acidity than both 2-tetralone (**50**) and 2-benzosuberone (**51**) due to more efficient π-overlap with the adjacent aryl ring[246]. By comparison, conjugation present in both the ketonic and enolic forms, such as in 1-tetralone (**52**)[247] and 4-chromanone (**52′**)[247], increases enol acidity relative to saturated compounds such as acetone (**45′**).

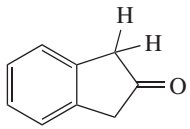

(**49**)

pK_a^K (1% MeOH/H_2O) = 12.1
pK_a^E (1% MeOH/H_2O) = 8.3
pK_E (1% MeOH/H_2O) = 3.8

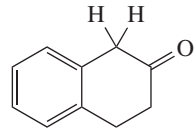

(**50**)

pK_a^K (1% MeOH/H_2O) = 12.8
pK_a^E (1% MeOH/H_2O) = 9.2
pK_E (1% MeOH/H_2O) = 3.6

Isomeric enols have different acidity. The more stable (*E*)-enol of phenylacetaldehyde (**53**) was found to be more acidic (pK_a^E) than its less stable (pK_E) stereoisomeric (*Z*)-enol. This was presumably due to the less sterically demanding (*E*)-enol or (*E*)-enolate being better solvated in water than the corresponding (*Z*)-stereoisomers. Increasing the

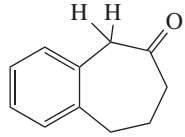

(**51**)

pK_a^K (1% MeOH/H_2O) = 14.9
pK_a^E (1% MeOH/H_2O) = 10.0
pK_E (1% MeOH/H_2O) = 4.9

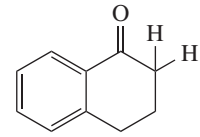

(**52**)

pK_a^K (H_2O) = 18.1
pK_a^E (H_2O) = 10.8
pK_K (H_2O) = 7.31

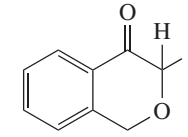

(**52′**)

pK_a^K (H_2O) = 15.3
pK_a^E (H_2O) = 10.1
pK_K (H_2O) = 5.26

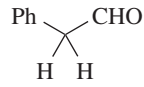

(**53**)

pK_a^K (H_2O) = 12.43
pK_a^E (H_2O) = 9.46 (*E*)
pK_a^E (H_2O) = 9.76 (*Z*)
pK_E (H_2O) = 3.07 (*E*)
pK_E (H_2O) = 3.35 (*Z*)
pK_E (H_2O) = 2.88 (overall)

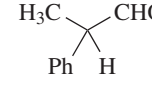

(**54**)

pK_a^K (H_2O) = 10.4
pK_a^E (H_2O) = 9.40
pK_E (H_2O) = 0.98

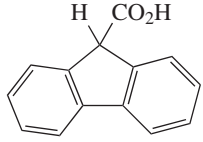

(**55**)

pK_a^K (H_2O) = 11.7
pK_a^E (H_2O) = 2.2
pK_E (H_2O) = 9.5

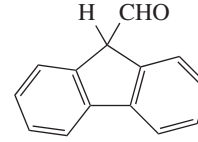

(**56**)

pK_a^K (H_2O) = 6.2
pK_a^E (H_2O) = 7.4
pK_E (H_2O) = –1.22

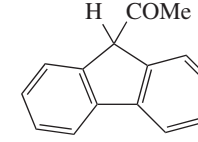

(**57**)

pK_a^K (H_2O) = 9.4
pK_a^E (H_2O) = 7.6
pK_E (H_2O) = 2.3

potential conjugation at the C2 position of **53** with an additional Ph group, as in diphenylacetaldehyde (**54**), lowers its keto acidity (pK_a^E) and increased its relative enol stability (pK_E)[248, 249]. Both enolic forms of **53** and **54** have similar acidity (pK_a^E).

The enols of **55**–**57** owe much of their acidity (pK_a^E)[128] to formation of an aromatic fulvenoid on deprotonation. 9-Carboxyfluorene (**55**) is surprisingly less acidic (pK_a^E) than both the 9-formyl- (**56**) and 9-acetyl (**57**) analogues[128], but its enolic form was found to be substantially more acidic. The enol form of the aldehyde 9-formylfluorene (**56**) is thermodynamically (pK_E) preferred over its keto tautomer, whereas the enolic forms of **55** and **57** are thermodynamically less stable[128]. Rates of base-mediated enolization are

TABLE 3. Acidity (pK_a) and relative stability (pK_E) data for carbonyl compounds and their corresponding enols

Carbonyl compound	pK_a^K (H_2O)[a]	pK_a^E (H_2O)	pK_K (H_2O)	pK_a (DMSO)[a]
Ethanal	16.7[127]			
(Acetaldehyde)	16.5[243]	11.2[243]	5.3[243]	
	19.7[258]			
	16.73[259]	10.50[259]	6.23[259]	
2-Phenylethanal	13.1[127]	(*E*) 9.46[249]	(*E*) 3.07[249]	
(Phenylacetaldehyde)	12.43[249]	(*Z*) 9.76[249]	(*Z*) 3.35[249]	
			gross 2.88[249]	
2,2′-Diphenylethanal	10.4[127]			
(Diphenylacetaldehyde)	10.4[248]	9.40[248]	0.98[248]	
2-Methylpropanal	14.6[243]	11.8[243]	2.8[243]	
(Isobutyraldehyde)				
Propan-2-one	19.3[127]			26.5[206, 263, 264]
(Acetone)	19.3[215]			
	19.0[243]	11.8[243]	7.2[243]	
	19.3[245]			
	20.0[258]			
	19.16[260]			
	19.27[260, 261]	10.94[260]	8.22[260]	
	18.79[262]	10.94[260, 261]	8.33[260, 261]	
	19.36[262]			29.9[265]
1-Methoxypropan-2-one	18.7[258]			
1-Chloropropan-2-one	16.5[258]			
1,1-Dichloropropan-2-one	14.9[258]			
Butan-2-one	20.5[243]	12.1[243]	8.3[243]	24.4[206]
1-Phenylpropan-2-one	19.4[217]			19.9[206]
2-(2-Oxopropyl)benzaldehyde	19.6[230]			
3-Methylbutan-2-one	21.0[266]	12.4[266]	7.9[266]	
Pentan-3-one				27.1[129]
				27.1[204]
2,4-Dimethylpentan-3-one	21.8[267]			28.2[206]
	21.5[268]	12.4[268]	9.1[268]	
2,6-Dimethylheptan-4-one	21.0[267]			

3,3-Dimethylbutan-2-one	20.8[267]			
2,2-Dimethylpentan-3-one	21.3[267]			
2,2-Dimethylhexan-3-one	21.6[267]			
2,2,4-Trimethylpentan-3-one	23.5[267]			
1-Trimethylsilylethan-1-one	16.44[244]	11.54[244]	4.89[244]	
1-Phenylethan-1-one	18.31[190]	10.34[190]	7.96[190]	24.7[204, 206, 231, 263, 271–273]
(Acetophenone)	18.24[269]	11.0[270]	7.92[269]	
	19.2[258]			27.0[265]
	17.7[243]	11.0[243]	6.7[243]	
	19.2[258]			(DMSO/H_2O) 21.5[252]
	19.1[267]			(Et_2O) 19[175]
				(Et_2O) 20[205]
				(5% EtOH/H_2O) 15.8[274]
AcC_6H_4X (substituted acetophenone)				
X = 4-NMe_2				27.48[144]
X = 4-OMe				25.70[144]
X = 4-Me				25.19[144]
X = 3-Me				25.95[144]
X = 4-Ph				24.51[144]
X = 4-F				24.45[144]
X = 3-OMe				24.52[144]
X = 4-Br				23.81[144]
X = 3-F				23.45[144]
X = 3-Cl				23.18[144]
X = 3-Br				23.19[144]
X = 3-CF_3				22.76[144]
X = 4-CF_3				22.69[144]
X = 3-SO_2Ph				22.32[144]
X = 4-SO_2Ph				24.12[144]
1-(2,4,6-Trimethylphenyl)ethan-1-one	17.61[190]	10.69[190]	6.92[190]	
1-(4-Pyridyl)ethan-1-one				21.8[206]
1-Fluoro-2-phenylethan-2-one				21.7[206]
(α-Fluoroacetophenone)				

(*continued overleaf*)

TABLE 3. (*continued*)

Carbonyl compound	pK_a^K (H_2O)[a]	pK_a^E (H_2O)	pK_K (H_2O)	pK_a (DMSO)[a]
1-Methoxy-2-phenylethan-2-one				22.8[126, 272]
1-Phenoxy-2-phenylethan-2-one				21.1[206]
1-Amino-2-phenylethan-2-one				*ca* 24[126]
1-Pyrrolidinyl-2-phenylethan-2-one				24.0[126]
1-Dimethylamino-2-phenylethan-2-one				23.5[126, 272]
1-Diphenylamino-2-phenylethan-2-one				20.3[206]
1-Phenylmethylsulfanyl-2-phenylethan-2-one				19.0[206]
1-Phenylsulfanyl-2-phenylethan-2-one				17.1[206]
1-Phenylselenyl-2-phenylethan-2-one				18.6[206]
1-Cyano-2-phenylethan-2-one				10.2[238]
1-Nitro-2-phenylethan-2-one				7.1[238]
1-Phenylsulfonyl-2-phenylethan-2-one				11.4[206, 238]
1-Trifluoromethylsulfonyl-2-phenylethan-2-one				5.1[206]
(2-Oxo-2-phenylethyl) triphenylphosphonium salts				6.1[206]
1-Phenylpropan-1-one				24.4[204, 275]
1-Phenylbutan-1-one	18.6[267]			
3,3-Dimethyl-1-phenyl-butan-1-one				25.3[238]
1,2-Diphenylethan-1-one	16.1[267]			17.5[206]
1,2,2-Triphenylethan-1-one				18.7[206]
2,2-Difluoro-1-phenylethan-1-one				20.2[206]
2-Methyl-1-phenylpropan-1-one	19.5[267]			26.2[206]
Cyclopentyl phenyl ketone				25.8[206]
Cyclobutyl phenyl ketone				26.1[206]
Cyclopropyl phenyl ketone				28.2[206]
4-Benzhydrylbenzophenone				22.4[276]
9-Acetylfluorene	9.9[127]			
	9.4[128]	7.6[128]	2.3[128]	
Methyl fluorene-9-thiocarboxylate	10.5[127]			
Methyl fluorene-9-thionocarboxylate	7.4[128]	1.6[128]	5.8[128]	
Methyl fluorene-9-carboxylate	11.5[128]			10.35[277]
				(DME) 9.20[206]

Fluorene-9-carboxylic acid	11.7[128]	2.2[128]	9.5[128]	
Fluorene-9-carboxaldehyde	6.2[128]	7.4[128]	−1.22[128]	
1-(2′-Furyl)-2-phenylethan-1-one	14.4[278]	8.5[278]	5.88[278]	
1-(2′-Thienyl)-2-phenylethan-1-one	14.6[291]	8.15[291]	6.45[291]	
Cyclobutanone	19.3[215]			25.0[206]
Cyclopentanone				25.8[129, 206]
Cyclohexanone	18.1[246]		6.4[246]	26.45[206]
Cycloheptanone				27.8[206]
Cyclodecanone				26.8[206]
Benzocyclobutanone	27[214]			
Indan-1-one				23.0[206]
Tetral-1-one	18.1[247]	10.8[247]	7.31[247]	
Tetral-2-one	12.9[246]			
	12.8[246] (1% MeOH)	9.2[246] (1% MeOH)	3.6[246] (1% MeOH)	
Isochroman-4-one	15.3[247]	10.1[247]	5.26[247]	
Benzosuber-1-one	14.9[246]			
Benzosuber-2-one	14.9[246] (1% MeOH)	10.0[246] (1% MeOH)	4.9[246] (1% MeOH)	
Indan-2-one	12.2[215]			16.9[129, 206]
	12.1[246] (1% MeOH)	8.3[246] (1% MeOH)	3.8[246] (1% MeOH)	
Indan-2-thione				10.0[129]
1,1-Dimethylindan-2-one				18.5[129]
1,3-Diphenylpropan-2-one	16.9[267]			18.6[129]
				18.1[206]
Cyclohex-3-en-1-one	15.2[246]		5.3[246]	
Cyclohexa-3,5-dien-1-one	−3 ± 1[132]	9.95[132]	11.0 ± 0.8[132]	
3,4,4*a*,5,6,7-Hexahydro-1*H*-5,6-dimethylnaphthalen-2-one	12.7[246]		2.7[246]	
N-Phenylacetamide				26.5[206]
N,*N*-Diethylacetamide				35[231]
Ethanoic acid (Acetic acid)	22.7[245]			
Methyl ethanoate	25.6[127, 230, 245]			29.5[231]
S-Ethyl thioethanoate	21.0[127]			
Ethyl 2-nitroethanoate	5.82[232]			9.08[232]

(*continued overleaf*)

TABLE 3. (*continued*)

Carbonyl compound	pK_a^K (H_2O)[a]	pK_a^E (H_2O)	pK_K (H_2O)	pK_a (DMSO)[a]
Ethyl 2-cyanoethanoate	10.17[232]			12.48[232]
Ethyl 2-(trifluoromethylsulfonyl)ethanoate	6.83[232]			6.40[232]
Ethyl 2-phenylethanoate				22.6[206]
Phenyl 2-phenylethanoate				18.7 [129]
S-Phenyl 2-phenylthioethanoate				16.9[129]
3*H*-Benzofuran-2-one				13.6[129]
3*H*-Benzothiophen-2-one				10.7[129]
1,3-Dihydroindol-2-one				18.2[129]
N-Methylindolin-2-one				18.5[129]
N-Methylindolin-2-thione				10.0[129]
N,*N*-Dimethyl-2-phenylthioacetamide				21.3[129]
Methyl 2-(2′-naphthyl)ethanoate	22.7[241]			
Lithium 2-(2′-naphthyl)ethanoate	21.4[241]			
N-Isopropylideneglycine methyl ester hydrochloride	14[229]			
Methyl 2-trimethylammonio ethanoate salts	18.0 ± 1[230] 21[229] 21.0 ± 1[230]			8.7[206]
Glycine	28.9 ± 0.5[230]			
2-Trimethylammonioethanoate salts	27.3 ± 0.5[230]			
Proline methyl ester hydrochloride	21[279, 280]			
Proline	29[279, 280]			
Proline methyl ester hydrochloride	22[239]			
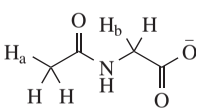	30.3[240] (H_a) 30.8[240] (H_b)			
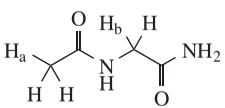	29.1[240] (H_a) 23.9[240] (H_b)			

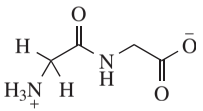	26.7[240]			
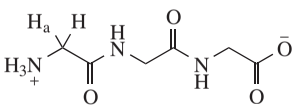	25.1[240] (H_a)			
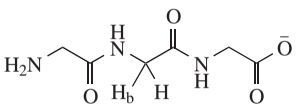	25.9[240] (H_b)			
2-Trimethylammonio-*N*,*N*′-diethylacetamide chloride				24.9[231]
Ethyl 2-trimethylammonioethanoate chloride				20.0[231]
1-(Ethoxycarbonylmethyl)pyridinium chloride				14.1[231]
1-Trimethylammoniopropion-2-one perchlorate				16.3[231]
1-Phenyl-2-trimethylammonioethan-1-one chloride				14.6[231]
1-Phenacylpyridinium bromide				10.7[231]
Ethyl 2-trimethylammonio-2-ethyloxycarbonyl-ethan-1-one bromide				11.8[231]
Ethyl 2-pyridino-2-ethyloxycarbonyl-ethan-1-one bromide				5.6[231]
Alanine	16.5[281]			
Valine	17.0[281]			
Leucine	16.7[281]			
Phenylglycine	14.9[281]			
Phenylalanine	16.2[281]			
Trimethyl methanetricarboxylate	7.8[268]	4.75[268]		
3-Acetylpentan-2,4-dione (Triacetylmethane)	8.4[148, 206]			
2-Acetylcyclopentanone	8.12[282]	7.72[282]	0.40[282]	

(*continued overleaf*)

TABLE 3. (*continued*)

Carbonyl compound	pK_a^K (H_2O)[a]	pK_a^E (H_2O)	pK_K (H_2O)	pK_a (DMSO)[a]
2-Acetylcyclohexanone	9.62[192]	9.47[192]	0.14[192]	
	9.90[268]	4.75[268]		
2-(Ethyloxycarbonyl)cyclohexanone	10.94[268]	4.75[268]		
Diethyl malonate	12.9[258]			16.4[206, 263]
				16.4[231]
				16.4[233]
Diethyl 2-isopropylmalonate				20.5[206]
1-Phenylsulfonylpropan-2-one				22.1[206]
Ethyl acetoacetate	10.68[268, 283]	4.75[268]		14.4[206]
	10.70[258]			
Ethyl 2-methylacetoacetate	12.70[268]	4.75[268]		
Ethyl 2-bromoacetoacetate	8.5[258]			
N,*N*′-Dimethylacetoacetamide				18.2[129]
3-Methylpentane-2,4-dione				15.0[206]
				15.1[233]
3-Bromopentane-2,4-dione	7.00[268]	4.75[268]		
Pentane-2,4-dione	9.3[258]			13.3[206, 233, 263]
	8.87[268]	4.75[268]		14.6[265]
	8.93[283]			
1,1,1-Trifluoropentane-2,4-dione	6.30[284]			
1-Phenyl-butane-1,3-dione	8.52[268]	4.75[268]		
	8.93[283]			
1,3-Diphenylpropane-1,3-dione				13.5[206, 263]
2,2,6,6-Tetramethylheptane-3,5-dione				15.4[148]
1-Cyclohexyl-2-phenylbutane-1,3-dione	9.73[285]			
2,2,5-Trimethyl-1,3-dioxan-4,6-dione (Methyl Meldrum's acid)				7.4[148, 206]
5,5-Dimethylcyclohexane-1,3-dione				11.2[206, 233]
5,5-Dimethyl-2-acetylcyclohexane-1,3-dione				9.8[148]
Cyclohexane-1,3-dione				10.3[206]
4-Methyldecalin-1,8-dione				18.2[233]

[a] Keto-form acidity data (pK_a^K) are commonly measured in H_2O and/or DMSO. However, H_2O has been more extensively used to measure enol acidity (pK_a^E) and its associated stability (pK_E).

well known[250]. A large proportion of these processes has been studied using isotopic incorporation[251–257].

The carbonyl (pK_a^K) and enol (pK_a^E) acidity and associated equilibrium constant of a variety of structurally related carbonyl-containing compounds are given in Table 3.

V. BASICITY OF CARBONYL COMPOUNDS

A carbonyl (C=O) group is intrinsically basic[286–290], as measured by the formation of its conjugate acid ($K_{HA} = [HA]/[H^+][A^-]$), where A^- represents the carbonyl compound acting as a base. For ordinary ketones $pK_{HA} < 0$, as is the case of acetophenone (**58**)[291], signifying that acetophenone itself and the solvated proton are more stable than the corresponding oxonium ion (protonated form). The kinetic[292] and thermodynamic[293, 294] consequences of carbonyl basicity have been extensively studied. For increased carbonyl group basicity, the carbonyl oxygen atom has to be electron rich. Carbamates, like **58′**, are known to be more basic than simple aldehydes and ketones [$pK_{HA}(H_2SO_4/H_2O) = -4$ to -8] as their conjugate acids are weaker acids[295]. The kinetic[296, 297] and thermodynamic protonation[298] of these and related ambident carbonyl groups[299], such as amides[300–302], have attracted significant attention[303, 304]. The carbonyl basicity of a variety of structurally related carbonyl-containing compounds is outlined in Table 4 as a function of its conjugate acid acidity (pK_{HA}).

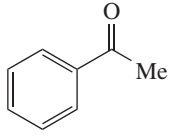

(**58**)

pK_{HA} (H_2SO_4/H_2O) = –4.08

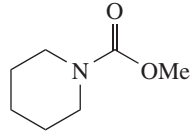

(**58′**)

pK_{HA}^N (H_2SO_4/H_2O) = –4.9
pK_{HA}^O (H_2SO_4/H_2O) = –2.8

VI. STEREOSELECTIVE PROTON TRANSFER

A. *In situ* Racemization

Racemization of carbonyl compounds which contain a single stereogenic centre is well documented[308–314]. These processes have generally been used to convert enantiomerically pure compounds into the opposite enantiomer or the racemic form. However, in certain cases unwanted racemization has been shown to occur[315–317].

Synthetically, *in situ* racemization has been shown to play an important role in biological[318–322] and chemical[323–328] dynamic kinetic resolution of carbonyl compounds[329–333]. Generally, if the required *in situ* racemization is faster than the kinetic resolution (derivatization step), this process can allow the conversion of a racemic substrate into a single enantiomeric product in quantitative yield[329–335]. This strategy has found industrial application in the synthesis of Levobupivacaine[336], Bupivacaine[337] and Roxiban[338].

rac-Ibuprofen (**59**) racemizes during esterification with the enantiomerically pure secondary alcohol (*S*)-**60** by a DCC–DMAP (**61**)-assisted coupling procedure (equation 4)[339], giving a mixture of diastereoisomeric esters (*S*,*S*)- and (*R*,*S*)-**62** in 71% yield with dr 85:15[339]. The faster reacting enantiomer appears to be the activated pyridinium intermediate (*S*)-**63**, derived from (*S*)-**59** by coupling with DMAP (**61**) in the presence of DCC, and as addition of alcohol (*S*)-**60** leads to the major diastereoisomeric adduct (*S*,*S*)-**62**.

TABLE 4. Basicity (pK_{HA}) of carbonyl compounds

Carbonyl compound	pK_{HA} (H_2SO_4/H_2O)
Benzaldehyde	−7.20[305]
4-XC_6H_4CHO (substituted benzaldehyde)	
X = MeO	−5.54[305]
X = Me	−6.32[305]
X = Cl	−7.26[305]
X = NO_2	−8.45[305]
1-Phenylethan-1-one	−4.08[299]
(Acetophenone)	−6.17[306]
4-XC_6H_4Ac (substituted acetophenone)	
X = MeO	−4.81[306]
X = Me	−5.47[306]
X = Cl	−6.52[306]
X = NO_2	−8.04[306]
Benzophenone	−5.70[307]
4-XC_6H_4Bz (substituted benzophenone)	
X = MeO	−4.93[307]
X = Me	−5.43[307]
X = Cl	−5.24[307]
$(4\text{-}XC_6H_4)_2C{=}O$ (disubstituted benzophenone)	
X = MeO	−4.41[307]
X = Cl	−6.46[307]
3-Acetylthiophene	−3.52[291]
2-Acetylthiophene	−4.20[291]
Methyl 2-tolyl ketone	−4.10[291]
Methyl 2,6-xylyl ketone	−4.85[291]
Indan-1-one	−3.65[291]
7-Methylindan-1-one	−3.23[291]
Tetral-1-one	−3.72[291]
2-Acetylcyclohexanone	< −5[192]
Methyl *N*-piperidinylformate	*N* − 4.9[295]
	O − 2.8[295]
1-Naphthalenecarboxamide	−2.73[298]
2-Naphthalenecarboxamide	−2.50[298]
N,*N*-Dimethyl-1-naphthalenecarboxamide	−1.93[298]
N,*N*-Dimethyl-2-naphthalenecarboxamide	−1.67[298]

As *ca* 60% of (*S*,*S*)-**62** is derived from (*S*)-**63**, it appears that competitive racemization via (*R*)-**63** occurs under the time frame of this reaction (equation 5).[339]

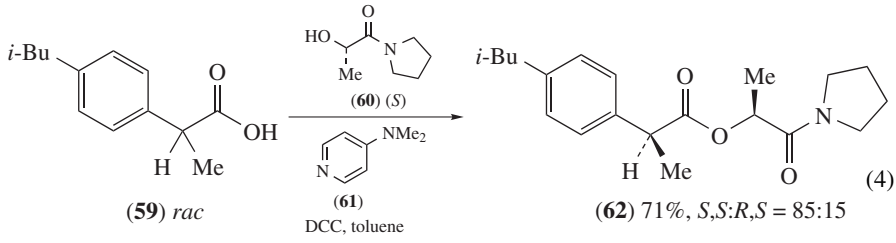

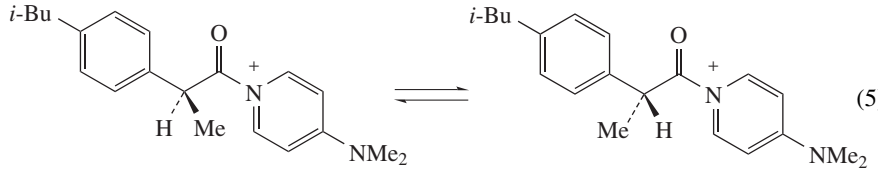

(**63**) (*S*) (**63**) (*R*) (5)

The asymmetric phosphonate **65** is an efficient agent for dynamic kinetic resolution (DKR) of aldehyde *rac*-**64** by Horner–Wadsworth–Emmons reaction (equation 6)[340]. In the presence of 18-crown-6 a slight excess of KHMDS **65** undergoes deprotonation and forms an ion pair with potassium, which reacts preferentially with (*R*)-**65** to give a single diastereoisomeric enone **66** in 78% yield. However, on purification the stereochemical integrity of the alkene motif is slightly lowered to (*E*: *Z* = 85:15). The remaining (*S*)-**64** racemizes by a deprotonation–reprotonation mechanism in the presence of a slight excess of KHMDS via enolate **67** (equation 7)[340].

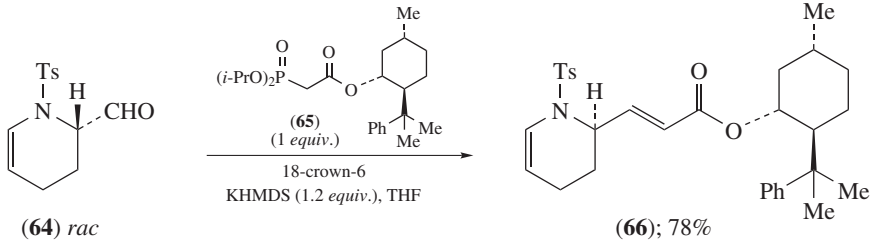

(**64**) *rac* (1.4 *equiv*.)

(**66**); 78%
E:*Z* = 99:1 crude
E:*Z* = 85:15 purified (6)

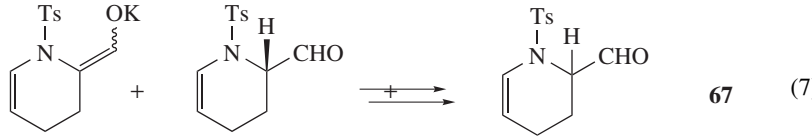

(**67**) (**64**) (*S*) (**64**) *rac* **67** (7)

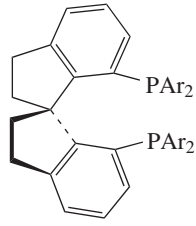

(**68**)
Ar = 3,5-Me_2-4-$MeOC_6H_2$

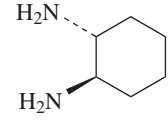

(**69**)

Dynamic kinetic resolutions involving enantioselective reductions have attracted significant attention[341]. Hydrogenation of aldehyde *rac*-**70** using substoichiometric amounts of $RuCl_2$ and chiral mediators **68** and **69** has been shown to be highly enantioselective for (*S*)-**70**, leading to the primary alcohol (*S*)-**71** in 96% ee (equation 8)[342]. The unreacted (*R*)-**70** racemises via enolate formation to give *rac*-**70** under the prevailing basic conditions of equation 8.[342]

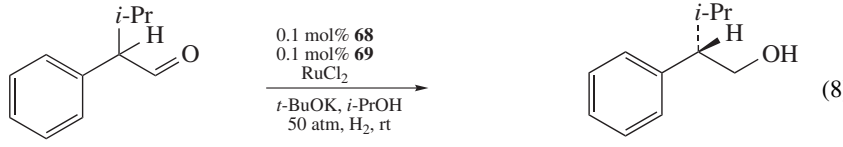

(8)

(**70**) *rac* (**71**) (*S*), ee 96%

This reaction type has also been used for the diastereoselective reduction of a variety of structurally related α-amino-β-keto esters (equations 9 and 10). Treatment of *rac*-**73** with a substoichiometric amount of chiral mediator **72**, using formic acid and triethylamine as the hydrogen source, gave the enantiomerically pure α-amino-β-hydroxy ester (*R*,*S*)-*syn*-**74** in 100% yield with 95:5 dr and 99% ee (equation 9)[343], via the diastereoselective reduction of (*S*)-**73**. The unreacted (*R*)-**73** efficiently racemizes through tautomerization under these reaction conditions.

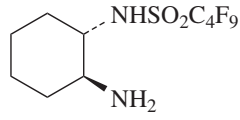

(**72**)

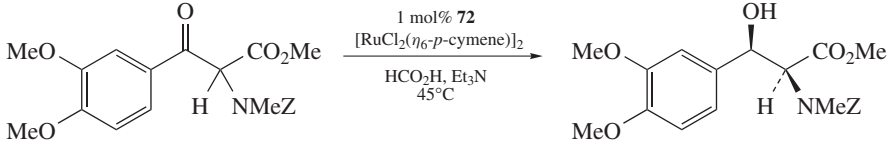

(**73**) *rac*, Z = CO_2Bn (**74**) (*R*,*S*)-*syn*, 100% dr 95:5, ee 99%

(9)

This particular methodology has been used extensively for the DKR of a wide variety of structurally related β-keto-esters to give β-hydroxy-esters, such as *rac*-**75** yielding (*S*,*S*)-**76** (equation 10)[344] and *rac*-**77** yielding (*R*,*R*)-**79** (equation 11)[345], with excellent diastereo- and enantioselectivities. The diastereoselectivity can be influenced using reagent control.

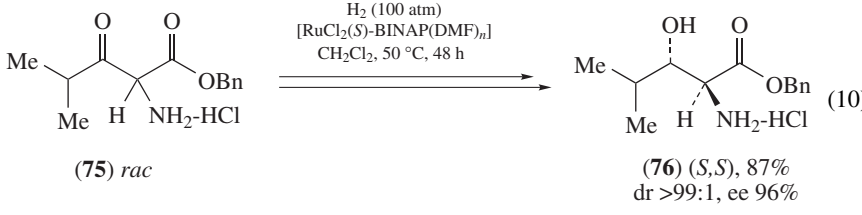

(**75**) *rac*

(**76**) (*S,S*), 87%
dr >99:1, ee 96%

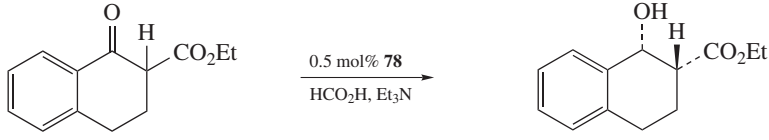

(**77**) *rac*

(**79**) (*R,R*), 90%
dr >99:1, ee 99%

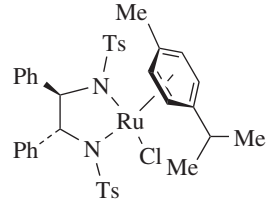

(**78**)

Racemic chiral enones are versatile substrates for DKR[346]. Reduction of *rac*-**80** with (*S*)-[*p*-TolCuCl(BINAP)], polymethylhydrosiloxane and *t*-BuONa/*t*-BuOH in toluene, followed by TBAF, yields diastereoselectively (*R,R*)-**81** (equation 12)[346]. The chiral copper mediator preferentially reduces the (*R*)-enantiomer of enone **80**, whereas the unreacted (*S*)-**80** efficiently racemizes via an enolate by deprotonation–reprotonation under the basic conditions of the reaction.

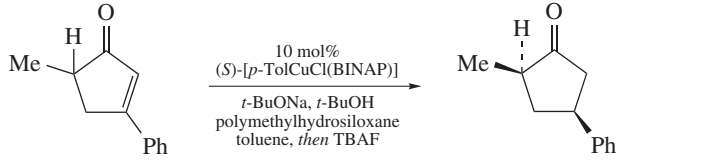

(**80**) *rac*

(**81**) (*R,R*)
90%, 96.5:3.5, ee 91%

DKR of the mixed anhydride *rac*-**82** has been achieved on addition to a solution of the covalent nucleophilic mediator $(DHQD)_2AQN$ (**83**) in EtOH–Et_2O (equation 13)[347], to yield the ethyl ester (*R*)-**84**. The remaining (*S*)-enantiomer of **82** is efficiently racemized through enolization by deprotonation–reprotonation, under basic conditions by **83**.

Interestingly, DKR of a propargylic phosphate, such as *rac*-**85**, to give the enantiomerically enriched allene (*R*)-**87**, has been achieved by a samarium(II) iodide-mediated

reduction in the presence of α-hydroxy γ-lactone (*R*)-**86** as a chiral Brønsted acid and a palladium complex as catalyst (equation 14)[348]. Racemization of propargylic phosphate (*S*)-**85** takes place via two interconverting enantiomeric allenylsamarium(III) intermediates.

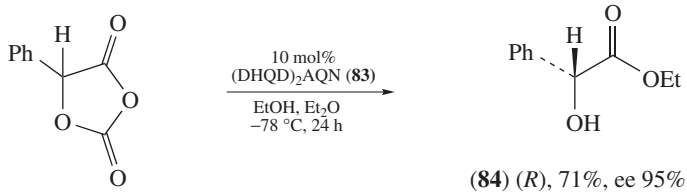

(**82**) *rac* (**84**) (*R*), 71%, ee 95%

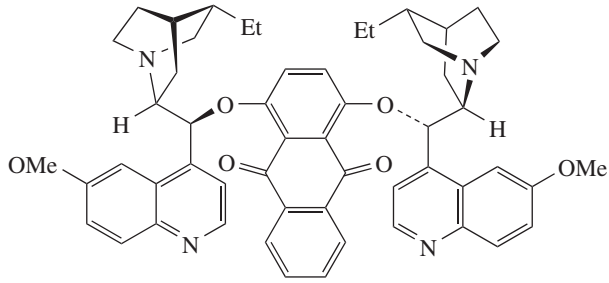

(**83**) $(DHQD)_2AQN$ (13)

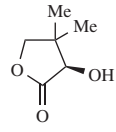

(**86**) (*R*)

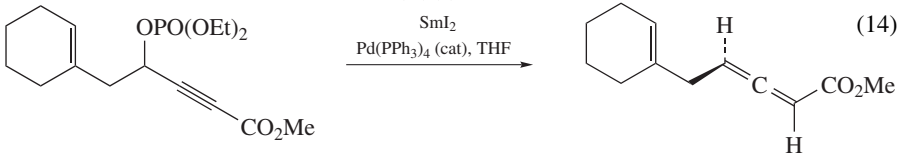

(**85**) *rac* (**87**) (*R*), 68%, ee 95% (14)

B. Enantioselective Proton Transfer

Enantioselective protonation of enols[349], silyl enol ethers[350] and enolate ions[351] to give enantiomerically enriched carbonyl compounds containing a single stereogenic centre is well documented[151,352]. This reaction type can be considered as a stereochemical resolution, involving deprotonation of a racemic carbonyl compound to give an intermediate achiral enolate, followed by enantioselective protonation which can lead to one of the original single stereoisomeric carbonyl compounds in 100% yield[353–363]. For this process to be efficient, the resulting enolate must be either achiral or interconversion between enantiomeric enolate conformers must be rapid in the time frame of proton transfer[151,364].

In certain cases, seemingly simple enolates can have a chiral memory effect[365–368]. For example, treatment of α-imino lactam (*S*)-**88** with *t*-BuOK in CD_3OD for 6–13 days at 25 °C gave the corresponding enantiomerically deuteriated α-imino lactam 1-*d*-(*S*)-**89** in quantitative yield with 98% D incorporation and ee 97% (equation 15)[369], via a conformationally chiral enolate. This methodology has been extended towards enantioselective alkylation of enolates. Excellent levels of enantioselectivity (ee 88%) were achieved for α-imino lactam (*S*)-**88** using KHMDS as Brønsted base and benzyl iodide as the electrophile[369]. Interestingly, to prevent unwanted racemization of the intermediate enolate, the reaction time for deprotonation was lowered to 10 seconds, and to ensure rapid alkylation, 20 equivalents of BnI were used[369].

(**88**) (*S*) (**89**) (*S*), 100%, ee 97%
98% D-incorporation (15)

In comparison, configurationally stable enolates can be formed through enantioselective deprotonation of *meso*-[370–375], chiral[376] and mixed aggregate[377] carbonyl-containing compounds. For example, treatment of *meso*-imide **90** with an enantiomerically pure lithium amide (*R*,*R*)-**91** in the presence of LiCl, in THF at −105 °C, followed by the addition of methyl iodide, gave the almost pure imide enantiomer **92** (equation 16)[378]. This reaction must proceed via enantioselective deprotonation of *meso*-**90** to a *C*- and/or *O*-enolate, which undergoes *C*-alkylation to **92**. Simple alkylation of this enolate with methyl iodide leads to the enantiomerically enriched imide **92**[378].

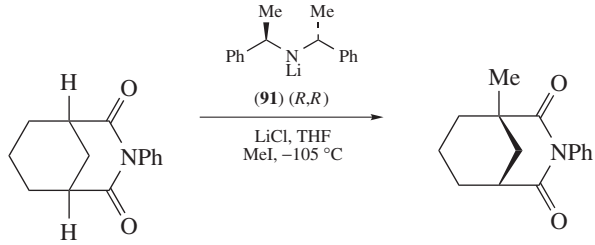

(**90**) *meso* (**92**) 57%, ee 97% (16)

There are two distinct approaches[151] for the enantioselective protonation of prostereogenic enolates: those that use an enantiomerically pure Brønsted acid[379–386], and those that use an enantiomerically pure mediator in combination with an achiral Brønsted acid[387, 388]. High levels of enantiomeric excesses have been achieved using both approaches[151]; however, the former has become more popular.

rac-2-Methyltetralone (*rac*-**93**) has been efficiently deracemized using the chiral triamine (*R*)-**96** as mediator and acetic acid as achiral Brønsted acid (equation 17)[389]. After total loss of chirality in *rac*-**93** by a two-step conversion to a silyl enol ether (**94**) and a 'base-free' lithium enolate–LiBr complex (**95**), addition of acetic acid in the presence of

(*R*)-**96** results in a good yield of the (*S*)-**93** enantiomer (ee 91%). Using a substoichiometric amount (0.1 equiv.) of chiral mediator (*R*)-**96** lowered the enantiomeric excess of (*S*)-**93** to 28%. However, using a large excess of a heterogeneous proton source, such as 10 equiv. of succinimide, and 0.2 equiv. of (*R*)-**96** restored the ee of (*S*)-**93** to 83%.

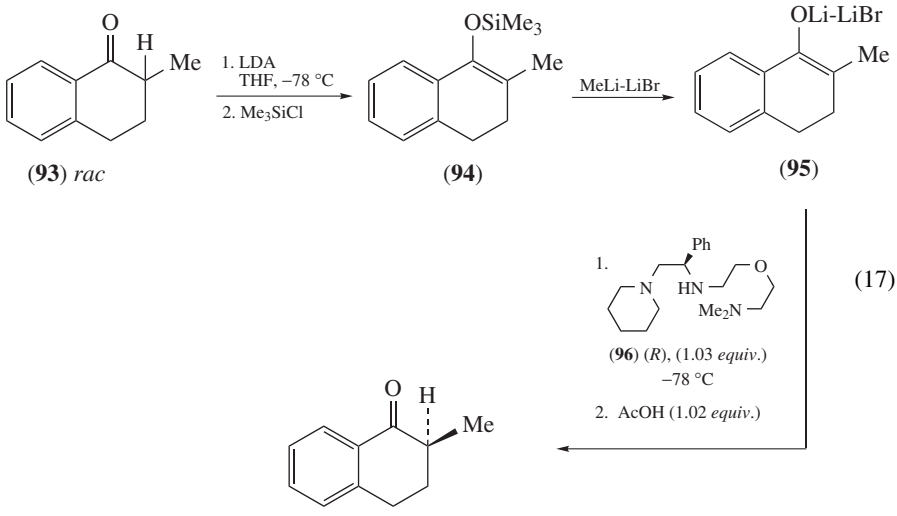

(17)

The alternative method shown in equation 18, using a chiral alcohol, like (*S*,*S*)-**97**, as the chiral Brønsted acid, affords a high level of facial selectivity for the enantioselective protonation of lithium enolate **95** to give the required 2-methyltetralone (*S*)-**93** in yields and enantiomeric purity similar to those of equation 17[390]. The concept of internal versus external proton delivery has been probed[390–392]. The use of disulfonamide (*R*,*R*)-**98** as chiral Brønsted acid leads to the (*R*)-**93** enantiomer (equation 19), whereas using as chiral scaffold (*R*,*R*)-**99**, the *N*,*N*′-dilithio salt of (*R*,*R*)-**99** and acetic acid (as external proton source) gives (*S*)-**93** (equation 20)[393], however, in poorer yield and enantiomeric purity than in equation 18. From this study, it appears that external protonation with AcOH occurs on the face away from the chiral scaffold (*R*,*R*)-**99** to give (*S*)-**93**, whereas for internal protonation with (*R*,*R*)-**98**, this occurs on the same face as the chiral scaffold to give (*R*)-**93**[393]. This type of behaviour has previously been shown to occur with protonation versus alkylation processes[389, 394, 395].

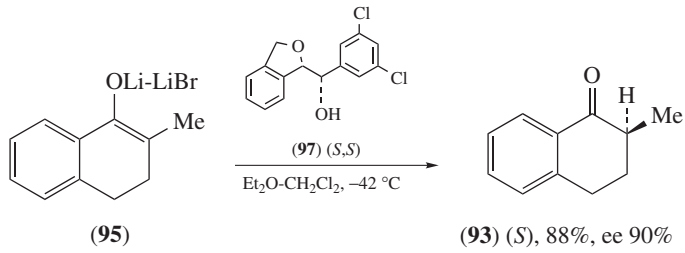

(18)

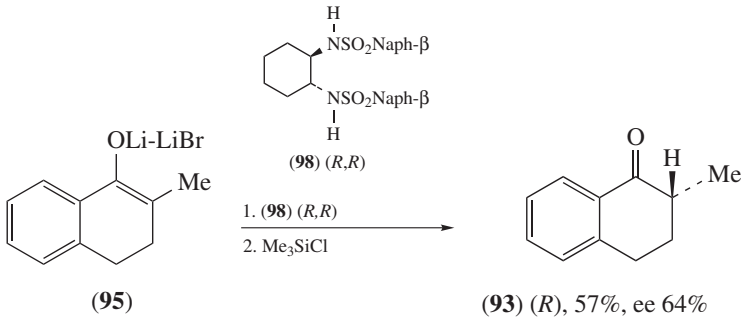

(19)

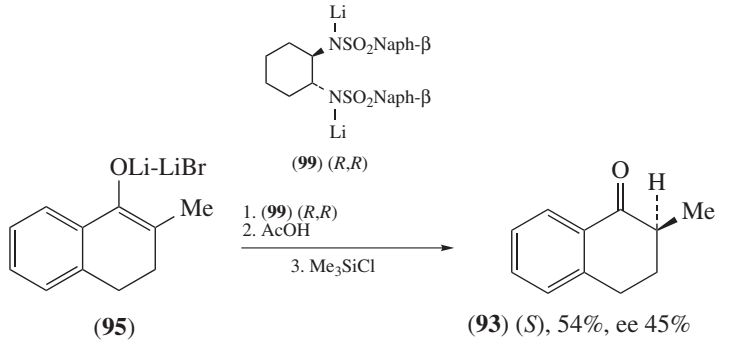

(20)

Prostereogenic enolates can be formed by nucleophilic 1,4-additions to the carbon–carbon double bonds of α,β-unsaturated aldehydes, ketones and esters[396–398], yielding an intermediate enolate ion that becomes protonated and tautomerizes to the final 'keto' form, leaving the product of an apparent 1,2-addition to the carbon–carbon double bond. For example, treatment of ester **100** with 2-naphthylboronic acid (**101**) in the presence of Rh(acac)(ethylene)$_2$ and (*S*)-DIFLUORPHOS acting as chiral scaffold and a Brønsted acid, such as phthalimide, gave the enantiomerically enriched ester **102** in high yield and enantiomeric purity (equation 21)[399]. In addition, phenylthiol (PhSH) has been shown to enantioselectively add to **100** in the presence of a chiral mediator (**103**, 10 mol%) to give ester (*S*)-**104** in high yield and enantiomeric purity (equation 22)[400]. Interestingly, protonation in this reaction was performed by PhSH or Brønsted acids derived from this thiol.

Less obvious enantioselective protonation processes have been investigated; for example, the unusual conversion of a simple achiral α,α-dichloro aldehyde (**105**) into the enantiomerically enriched α-chloro ester (*S*)-**109**, as shown in Scheme 2[401]. Treatment of **105** with a substoichiometric amount of covalent nucleophilic carbene (derived from **106** and KH) leads to formation of enolate intermediate **107**, which undergoes protonation to gyral ketonic intermediate **108** in the presence of an excess of phenol (acting as Brønsted acid), followed by nucleophilic displacement by phenol/phenolate (acting as nucleophile) to gyral α-chloroester (*S*)-**109** and regeneration of **106**.

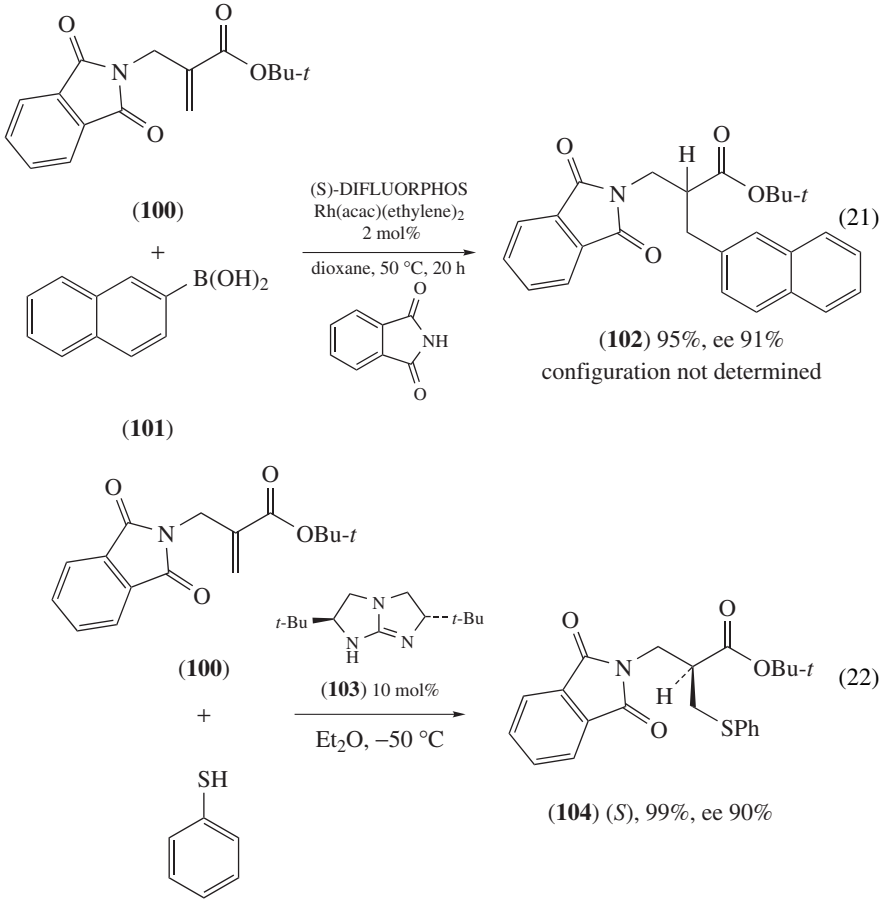

C. Diastereoselective Proton Transfer

Diastereoselective protonation[402] of enolates has been extensively documented[152, 165]. Conversion of a diastereoisomeric mixture of carbonyl-containing compounds into a single diastereoisomer through deprotonation[403] (enolate formation) and re-protonation is well known[152, 165].

The rate of epimerization of an α-stereogenic centre within a carbonyl-containing compound with several stereogenic centres depends on the acidity of the enolizable proton. Diastereoselectivity depends on kinetic[404–418] and/or thermodynamic effects[419–423] (reagent and substrate control)[152, 424].

For example, treatment of β-thiolactone **110** with Et_3N in $CDCl_3$ gives a thermodynamic mixture of two diastereoisomeric β-thiolactones (**110:100′** = 60 : 40, equation 23)[425]. In comparison, treatment of β-lactam **111** with NaOD in D_2O gives the deuteriated β-lactam **111′** as a single diastereoisomer in quantitative yield with retention of

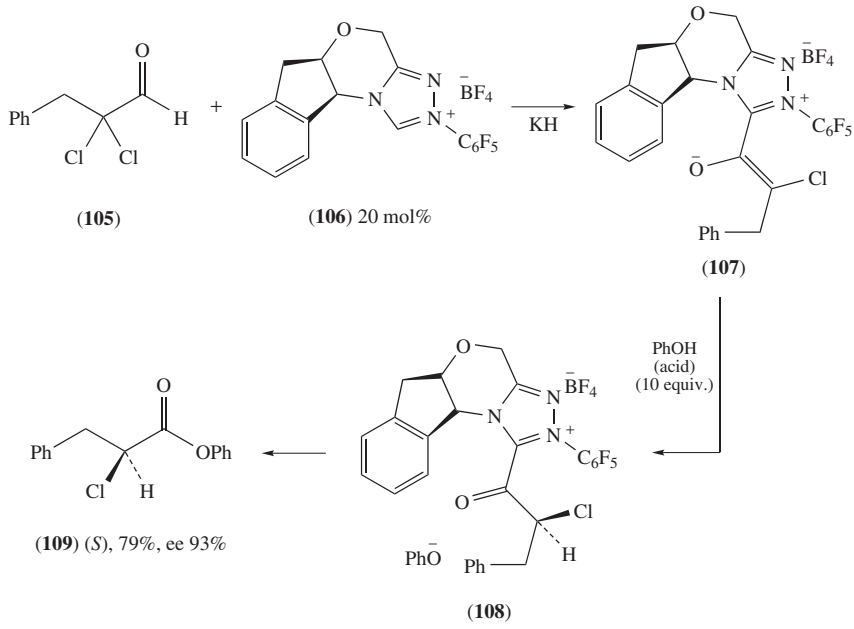

SCHEME 2. Mechanism for the formation of chiral α-chloroester (*S*)-**109** from achiral 2,2-dichloro-3-phenylpropanal (**105**)

configuration (equation 24)[426]. Deprotonation of **111** with NaOD, and deuteriation of the resulting enolate with D_2O, leads to the thermodynamically more stable 2-*d*-deuterio-β-lactam **111′** with perfect substrate control (equation 24)[426].

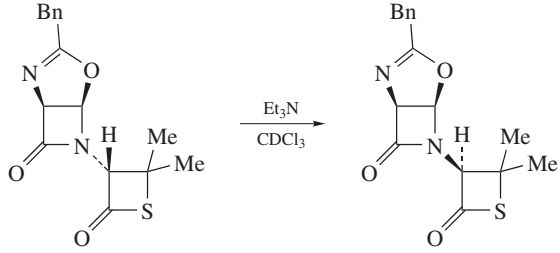

(23)

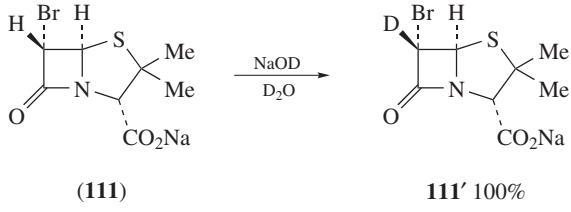

(24)

Epimerization of the *cis*-**112** ketone using NaOMe in MeOH gives the more thermodynamically stable ketone of *trans*-**112** configuration (equation 25)[427]. This stereoisomer is clearly more stable than *cis*-**112**, as both methyl substituents occupy less sterically demanding equatorial positions. However, *cis*-**112** can be synthesized with high levels of configurational control by quenching the lithium enolate (**115**), formed by Me_2CuLi addition to enone **113** under kinetic control using a chelating proton donor[428–430], like ethyl salicylate (**114**, equation 26)[431]. Regioselective protonation of the lithium enolate **115** occurs on its less hindered face (via a chair transition state) leading to the kinetically controlled ketone *cis*-**112** in good yield and excellent stereoselectivity.

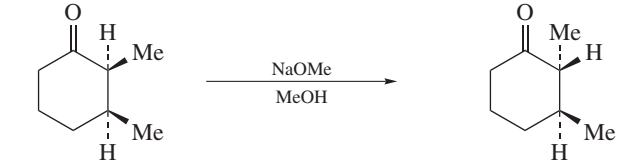

(**112**) *cis*
de *cis*:*trans* = 60:40

(**112**) *trans*
de *cis*:*trans* = 19:81

(25)

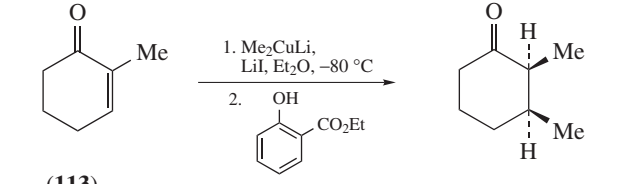

(**113**)

(**114**)

(**112**) *cis*, 76%
de *cis*:*trans* = 96:4

(26)

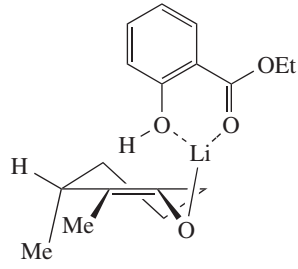

(**115**)

Diastereoselective protonation under kinetic control is a useful strategy for allowing access to particular diastereoisomeric carbonyl derivatives[432]. For example, deprotonation of γ-lactone **116** with excess LiHMDS in THF at $-78\,^{\circ}C$, and quenching the resulting lithium enolate with saturated aqueous solution of sodium sulfate, gave the diastereoisomerically pure γ-lactone **116**′ (equation 27)[433]. The diastereoselective protonation of the intermediate lithium enolate with H_2O must occur on its less hindered face, controlled by the γ-benzyloxymethyl substituent of the γ-lactone residue to give the required **116**′.

This strategy has been used to control a variety of tandem addition reactions to α,β-unsaturated ketones[396–398]. Single electron reduction of enone **117** using lithium in

ammonia, followed by the addition of ammonium chloride, gave a diastereoisomeric mixture of ketones *cis*- and *trans*-**119** with preference for *cis* (equation 28)[434]. This reaction proceeds via the initial formation of an intermediate chiral lithium enolate **118** which, on quenching with ammonium chloride mainly on its less hindered face, away from the *C*3-phenyl substituent, leads to the major diastereoisomer form *cis*-**119**. Evidently this is the kinetic product, as it can be converted into the more stable ketone *trans*-**119** under equilibrating conditions (NaOEt in EtOH, equation 29)[434].

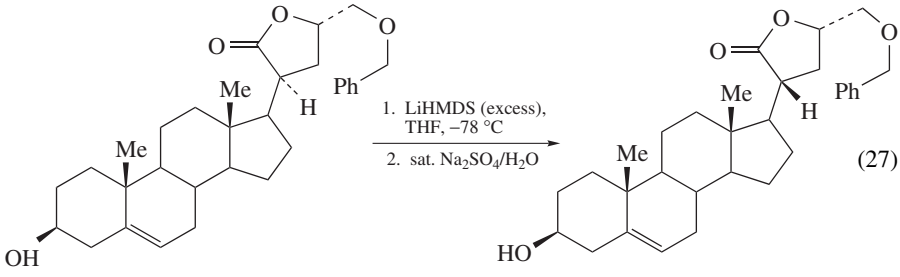

(27)

(**116**) (**116′**) 75%

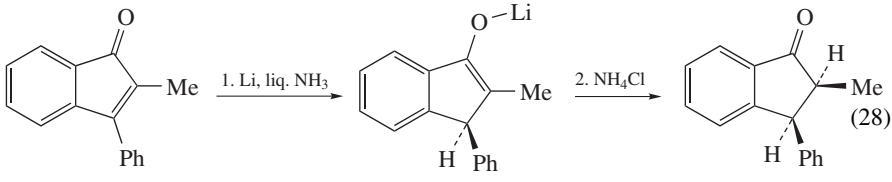

(28)

(**117**) (**118**) (**119**) *cis*, 40%
dr *cis*:*trans* = 80:20

(29)

syn-(**119**) (**119**) *trans*, 100%
dr *cis*:*trans* = 21:79, d.e. 58%

Michael additions have been extensively used as a method for intermediate formation of chiral enolates derived from α,β-unsaturated carbonyl-containing compounds[396–398, 435,436]. For example, treatment of acyclic ester **120** with lithium bis(phenyldimethylsilyl) cuprate [$(PhMe_2Si)_2CuLi$] and quenching the resulting chiral enolate **121** with ammonium chloride gave the *threo*-diastereoisomeric ester **122** in moderate yield with a high level of configurational control (equation 30)[437]. The relative stereochemistry was controlled by protonation on the intermediate lithium enolate **121** on the less hindered face (away from the more sterically demanding $PhMe_2Si$ group) while adopting the more energetically favourable Houk conformation.

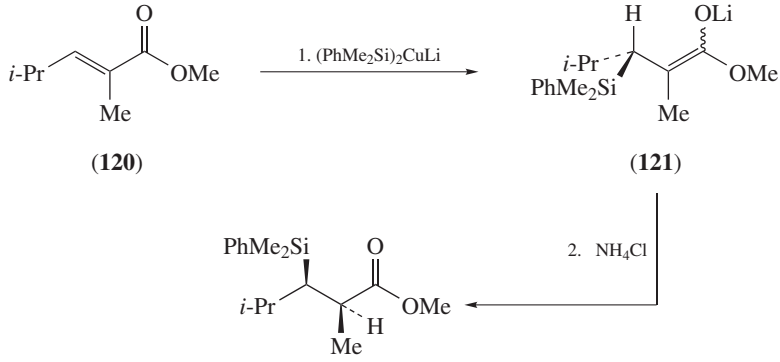

(**120**) (**121**)

(30)

threo-(**122**) 56%
dr *threo*:*erythro* = 96:4

A high level of diastereoselective protonation was achieved for the rigid bicyclic enone **123** in the presence of a Cu(I) mediator and quenching the resulting magnesium enolate with acid gave the corresponding bicyclic ketone **124** in moderate yield and almost perfect configurational purity (equation 31)[438], because protonation takes places on the less hindered face of the conformationally rigid magnesium enolate intermediate[438].

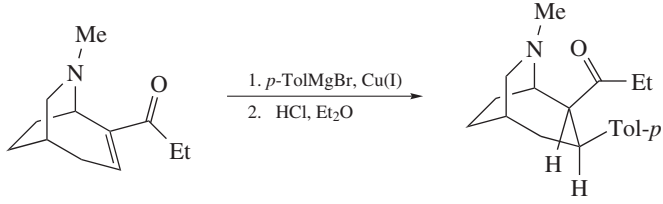

(**123**) (**124**); 67%; 98% *d.e.*

(31)

This strategy has been used extensively to synthesize esters of β-amino acids with controlled configuration[439]. Treatment of enoate **125** with an enantiomerically pure lithium amide **126**, and quenching the resulting lithium enolate with 2,6-di-*t*-butylphenol (**127**), gives the *cis*-β-amino ester **128**, in moderate yield with superb levels of diastereomeric control, preserving the configuration of the alkyl groups of **126** (equation 32)[440]. Formation of this kinetic product must have occurred by protonation of the less hindered face of the intermediate enolate. The *cis*-β-amino ester can be efficiently converted into the epimeric *trans*-β-amino ester **128** in THF under thermodynamic control by addition of KHMDS in *t*-BuOH[440].

Intermediate enolates derived from Michael-type processes can be isolated. For example, enantiomerically pure enolate (*S*)-**131** can be isolated, as is the case of the almost enantiomerically pure enolate (*S*)-**131**, prepared by 1,4-addition of the phenyl-substituted borane **130** to enone **129**, in the presence of a substoichiometric amount of the chiral rhodium mediator $[Rh(OMe)(COD)]_2$–(*S*)-BINAP (COD = 1,5-cyclooctadiene, equation 33)[441]. Protonation of (*S*)-**131** with methanol leads to cyclohexanone (*S*)-**132** in good yield with no loss of enantiomeric purity (equation 34)[441]. The protonation is presumably diastereoselective, taking place on the less hindered face of (*S*)-**131**, away from the neighbouring phenyl group, as can be inferred from the stereochemical outcome (**133**)

of deuteriation with MeOD, giving the *trans*-deuteriated ketone in good yield and excellent diastereomeric ratio (equation 34)[441].

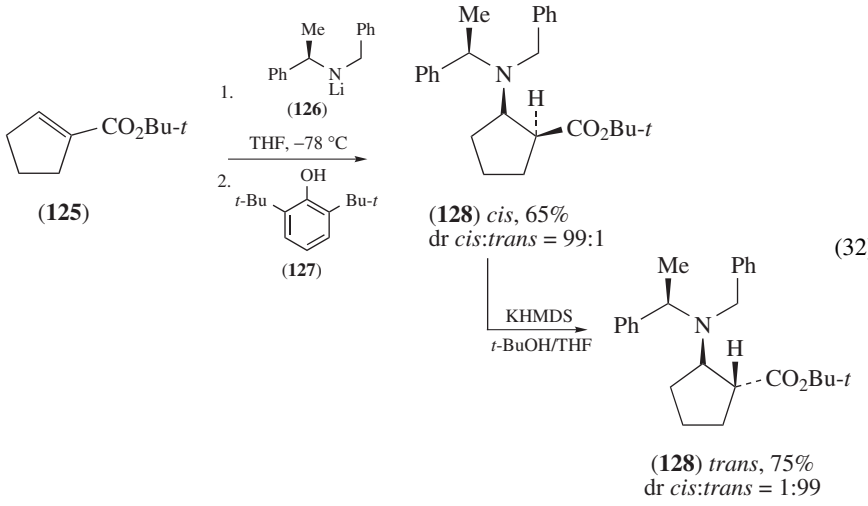

(32)

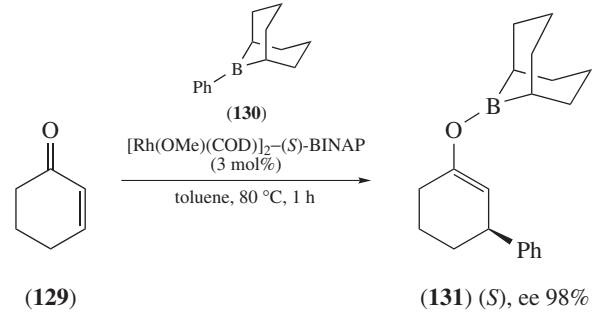

(33)

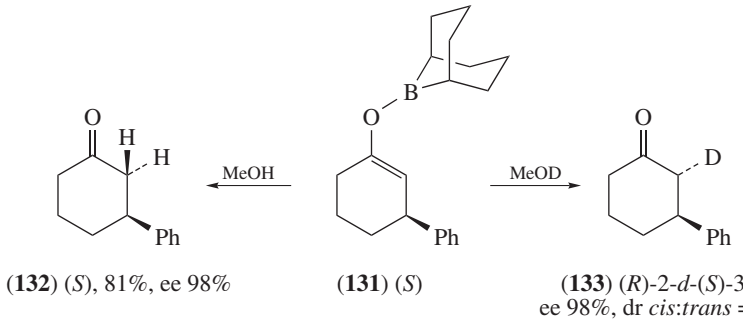

(34)

Nazarov processes have allowed access to intermediate cyclic enolates[442–444]. Enone **134** undergoes a Nazarov cyclization catalysed by a Lewis acid [e.g. $Cu(OTf)_2$] to give the intermediate enol complex **135**, which undergoes tautomerization to the diastereoisomerically pure cyclic enone *trans*-**136** in almost quatitative yield (equation 35)[445,446].

The diastereoselective protonation leading to the keto form occurs on the more hindered face of **135**, close to the phenyl group, so that the phenyl and ethoxycarbonyl groups end up *trans* to each other, in the less sterically strained configuration. This reaction type has also been shown to be highly enantioselective when using an enantiomerically pure Lewis acid. Treatment of enone **137** with a substoichiometric amount of chiral scandium–diindanopybox complex **138** gives the cyclic enone (*S*)-**139** in excellent yield and enantiomeric purity (equation 36)[447]. This enantioselective Nazarov reaction is of mechanistic interest in its own right[447].

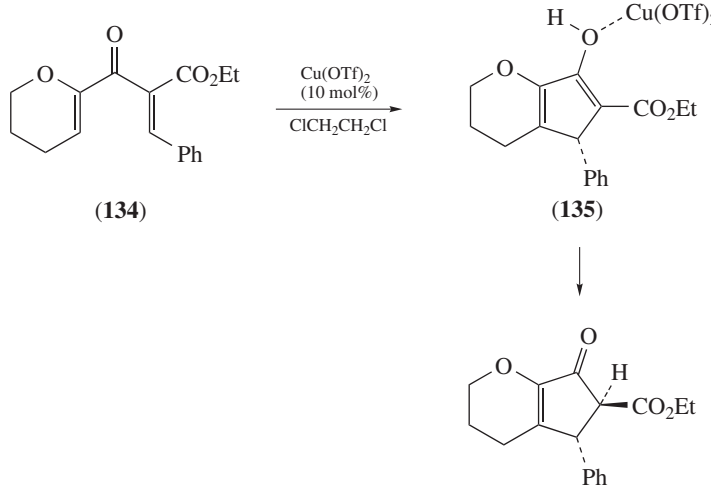

(**134**) (**135**) (**136**) *trans*, 99%

(35)

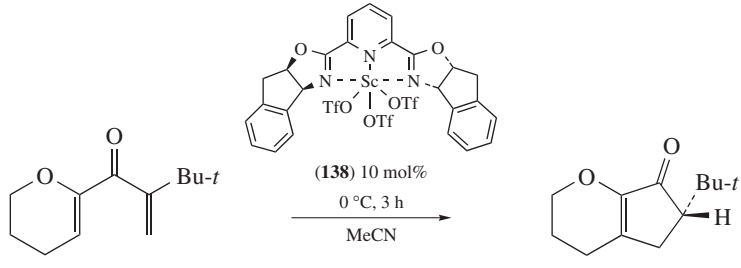

(**137**) (**139**) (*S*), 94%, ee 97%

(36)

The β-keto ester *trans*-**140** undergoes deprotonation by Lewis base NaH, followed by reduction with AlH_3 to an intermediate aluminum enolate (**141**), which on subsequent protonation with *t*-BuOH yields the β-hydroxy ketone *cis*-**142** in good yield and configurational purity (equation 37)[448]. Diastereoselective protonation to the *cis* product allows both the 2-(hydroxymethyl) and the 4-methyl groups to be in axial positions for minimal steric interaction.

Remote stereocentres have been shown to influence the facial preference for the diastereoselective protonation of enolates. Deprotonation of an equimolar diastereoisomeric mixture of δ-lactams (α-*S*, *N*-*R*)-**143** and (α-*R*, *N*-*R*)-**143** with *n*-BuLi, followed by the

addition of ammonium chloride, gives the single diastereoisomer (α-*S*, *N*-*R*)-**143** in very good yield (equation 38)[449]. Diastereoselective protonation appears to occur on the less hindered face of the enolate complex **144** with potential coordination/delivery from the neighbouring CH_2OLi tether[449]. The (α-*S*, *N*-*R*)-**143** diastereoisomer can be deuteriated in the α-position, with some loss of configuration purity, by the same deprotonation with *n*-BuLi, followed by deuteriation with EtOD (equation 39)[449].

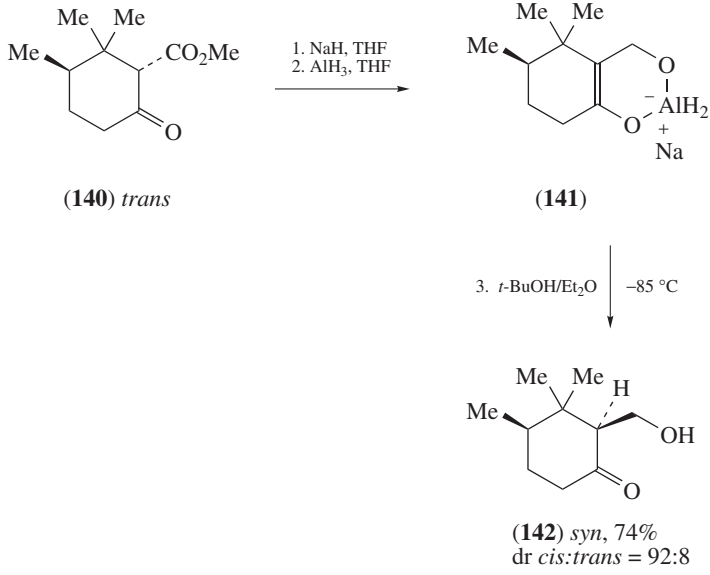

(**140**) *trans* (**141**)

(**142**) *syn*, 74%
dr *cis*:*trans* = 92:8

(37)

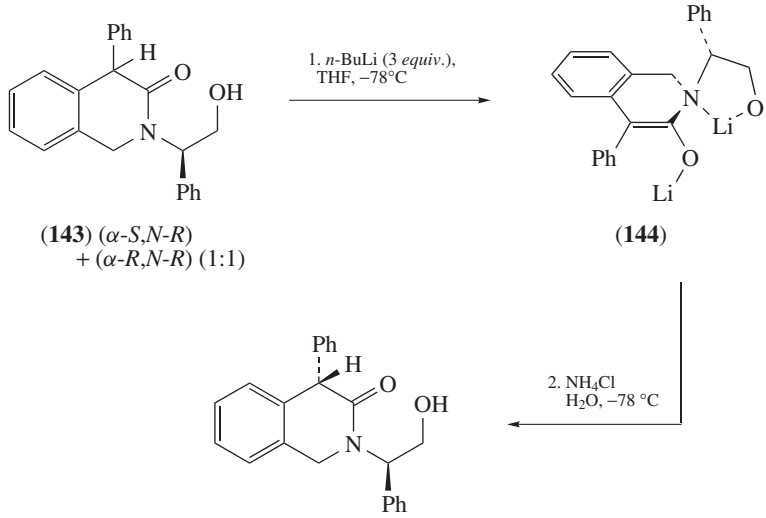

(**143**) (α-*S*,*N*-*R*)
+ (α-*R*,*N*-*R*) (1:1)

(**144**)

(**143**) (α-*S*,*N*-*R*), 92%
dr (α-*S*,*N*-*R*):(α-*R*,*N*-*R*) = 98.5:1.5

(38)

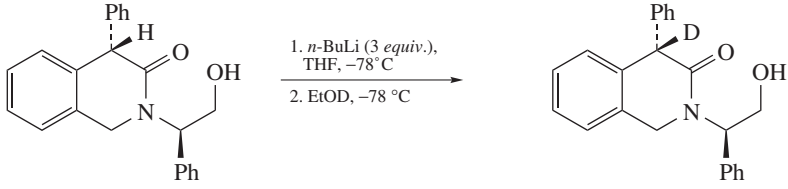

(39)

(**143**) (*α*-*S*,*N*-*R*)

(**143**) (*α*-*S*,*N*-*R*)-*α*-d, 85%
90% D incorporation
dr (*α*-*S*,*N*-*R*):(*α*-*R*,*N*-*R*) > 92.5:7.5

Significant progress has been made towards the understanding of proton delivery[151, 152, 165]. Diastereomeric silyl ethenyl ethers **145** and **148** decompose on addition of TBAF and AcOH into the corresponding enols **146** and **149**, which yield with AcOH two complementary bicyclic ketones (**147** and **150**, respectively), in different degrees of diastereomeric purity (equations 40 and 41)[450]. Two different proton transfer processes take place: Bicyclic ketone **147** is formed by external delivery of a proton to **146** on its less hindered face (equation 40); the complementary ketone **150** is formed by protonation of **149** on its more hindered face (equation 41)[450], invoking internal proton delivery from the intermediate pyridinium acetate **151**. For a more sterically demanding and weaker acid, such as phenol, the diastereoselectivity increased for **147** but reversed for **150**[450].

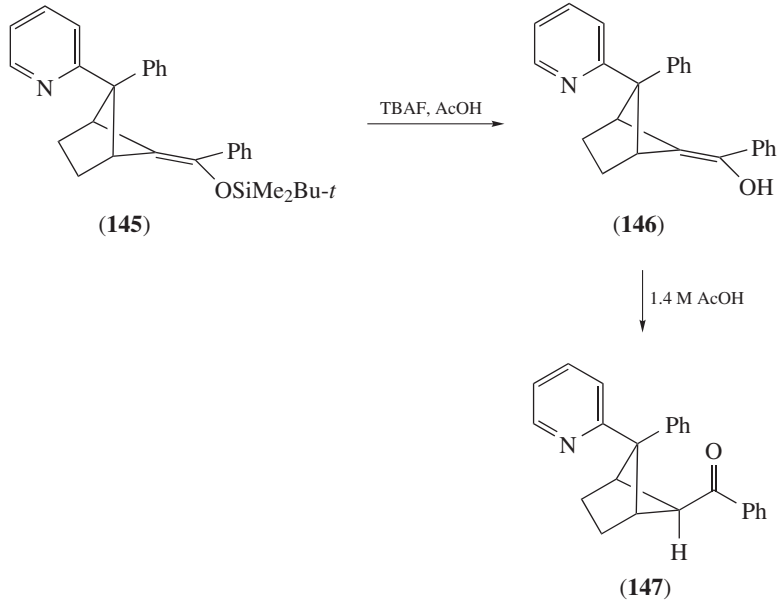

(40)

(**145**)

(**146**)

(**147**)

dr 88:12 (AcOH)
dr 95:5 (PhOH)

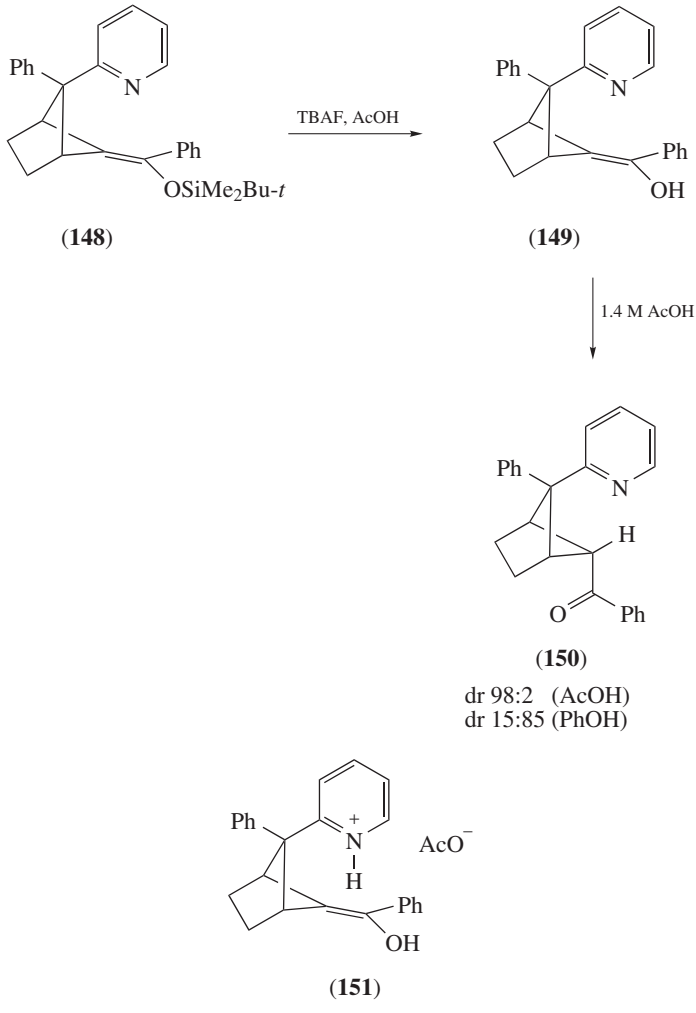

(**148**) (**149**)

(41)

(**150**)

dr 98:2 (AcOH)
dr 15:85 (PhOH)

(**151**)

This change from an external versus an internal proton delivery mechanism has also been shown to occur for a pair of complementary ethenyl silyl ethers with tethered hydroxylmethyl and aminomethyl groups (**152** and **155**, equations 42 and 43)[451]. On treatment of the silyl enolates with TBAF and acetic acid they give the corresponding enols (**153**, **156**), which undergo protonation by different routes, to yield their respective ketone diastereomeric tautomer (**154**, **157**). Protonation of enol **153** occurs through external proton transfer on its less hindered face to give exclusively the ketone **154**, the level of diastereoselectivity being independent of the concentration of acetic acid used. On the other hand, protonation of enol **156** occurs on the more hindered face through internal proton transfer

involving an intermediate ammonium ion, with the levels of diastereoselectivity found to be highly dependent on the concentration of acetic acid; at low concentration external protonation of the less hindered face was dominant, as in equation 42, whereas at higher concentrations internal protonation was preferred due to efficient ammonium ion formation.

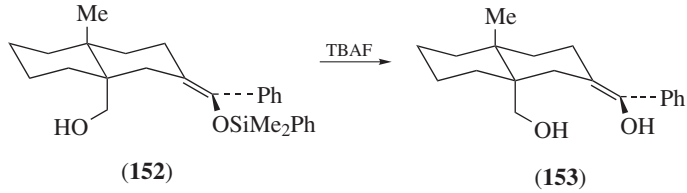

(**152**) (**153**)

(42)

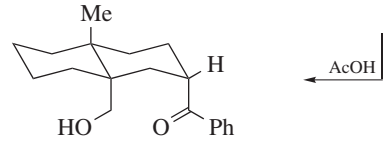

(**154**) dr 99:1

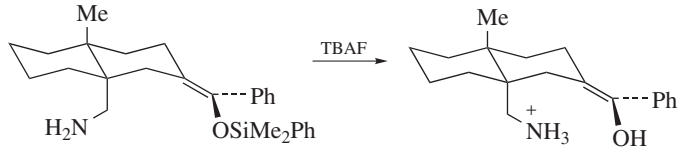

(**155**) (**156**)

(43)

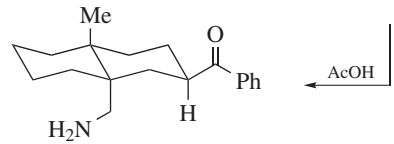

(**157**)

dr 47:53 (0.05 M AcOH)
dr 93:7 (0.73 M AcOH)

VII. REFERENCES

1. L. M. Jackman and B. C. Lange, *Tetrahedron*, **33**, 2737 (1977).
2. D. Seebach, *Angew. Chem., Int. Ed. Engl.*, **27**, 1624 (1988).
3. D. Caine, in *Comprehensive Organic Synthesis*, Vol. 1, Chap. 1 (Eds I. Fleming and B. M. Trost), Pergamon, Oxford, 1991, pp. 1–59.
4. H. B. Mekelburger and C. S. Wilcox, in *Comprehensive Organic Synthesis*, Vol. 1, Chap. 4 (Eds I. Fleming and B. M. Trost), Pergamon, Oxford, 1991, pp. 99–131.
5. J. Eames, *Science of Synthesis*, Vol. 8a, Chap. 6, Georg Thieme Verlag, Stuttgart, 2006, pp. 173–242.
6. T. J. Fleck, W. W. McWhorter Jr, R. N. DeKam and B. A. Pearlman, *J. Org. Chem.*, **68**, 9612 (2003).

7. N. S. Nudelman and G. E. G. Linares, *J. Org. Chem.*, **65**, 1629 (2000).
8. T. Nemoto, T. Ohshima and M. Shibasaki, *J. Am. Chem. Soc.*, **123**, 9474 (2001).
9. M. Suzuki, H. Koyama and R. Noyori, *Tetrahedron*, **60**, 1571 (2004).
10. A. J. McNeil, G. E. S. Toombes, S. V. Chandramouli, B. J. Vanasse, T. A. Ayers, M. K. O'Brien, E. Lobkovsky, S. M. Gruner, J. A. Marohn and D. B. Collum, *J. Am. Chem. Soc.*, **126**, 5938 (2004).
11. L. M. Pratt and A. Streitwieser, *J. Org. Chem.*, **68**, 2830 (2003).
12. Y.-J. Kim, M. P. Bernstein, A. S. Galiano Roth, F. E. Romesberg, P. G. Williard, D. J. Fuller, A. T. Harrison and D. B. Collum, *J. Org. Chem.*, **56**, 4435 (1991).
13. C. Riche, C. Pascard-Billy, C. Cambillau and G. Bram, *J. Chem. Soc., Chem. Commun.*, 183 (1977).
14. P. G. Williard and J. M. Salvino, *J. Chem. Soc., Chem. Commun.*, 153 (1986).
15. M. J. Munchhof and C. H. Heathcock, *Tetrahedron Lett.*, **33**, 8005 (1992).
16. E. J. Corey and A. W. Gross, *Tetrahedron Lett.*, **25**, 495 (1984).
17. L. Xie, K. M. Isenberger, G. Held and L. M. Dahl, *J. Org. Chem.*, **62**, 7516 (1997).
18. C. H. Heathcock, C. T. Buse, W. A. Kleschick, M. C. Pirrung, J. E. Sohn and J. Lampe, *J. Org. Chem.*, **45**, 1066 (1980).
19. G. Stork and P. F. Hudrlik, *J. Am. Chem. Soc.*, **90**, 4462 (1968).
20. F. A. Carey and R. J. Sundberg, *Advanced Organic Chemistry, Part A: Structure and Mechanism* (5th Edition), Chap. 6, Springer, Berlin, 2007, pp. 595.
21. H. O. House, L. J. Czuba, M. Gall and H. D. Olmstead, *J. Org. Chem.*, **34**, 2324 (1968).
22. P. Duhamel, D. Cahard, Y. Quesnel and J.-M. Poirier, *J. Org. Chem.*, **61**, 2232 (1996).
23. A. T. Nielsen and W. J. Houlihan, *Org. React.*, **16**, 1 (1968).
24. J. Clayden, N. Greeves, S. Warren and P. Wothers, *Organic Chemistry*, Oxford University Press, Oxford, 2001, pp. 524–525.
25. S. V. Ley, D. J. Dixon, R. T. Guy, F. Rodríguez and T. D. Sheppard, *Org. Biomol. Chem.*, **3**, 4095 (2005).
26. K. Mitsuhashi, R. Ito, T. Arai and A. Yanagisawa, *Org. Lett.*, **8**, 1721 (2006).
27. T. Kotake, Y. Hayashi, S. Rajesh, Y. Mukai, Y. Takiguchi, T. Kimura and Y. Kisu, *Tetrahedron*, **61**, 3819 (2005).
28. Y. Jin and R. M. Coates, *Chem. Commun.*, 2902 (2006).
29. R. Green, A. T. Merritt and S. D. Bull, *Chem. Commun.*, 508 (2008).
30. D. Z. Wang, Y.-J. Kim and A. Streitwieser, *J. Am. Chem. Soc.*, **112**, 10764 (2000).
31. A. Abiko, T. Inoue and S. Masamune, *J. Am. Chem. Soc.*, **124**, 10759 (2002).
32. M. Jorgensen, S. Lee, X. Liu, J. P. Wolkowski and J. F. Hartwig, *J. Am. Chem. Soc.*, **124**, 12557 (2002).
33. P. A. Evans and D. K. Leahy, *J. Am. Chem. Soc.*, **125**, 8974 (2003).
34. Y. Itoh, M. Yamanaka and K. Mikami, *J. Am. Chem. Soc.*, **126**, 13174 (2004).
35. L. Yao, B. T. Smith and J. Aube, *J. Org. Chem.*, **69**, 1720 (2004).
36. I. O. Sutherland (Ed.), *Comprehensive Organic Chemistry*, Vol. 2 (Series Eds D. H. R. Barton and W. D. Ollis), Pergamon, Oxford, 1979.
37. W. J. Layman, T. D. Greenwood, A. L. Downey and J. F. Wolfe, *J. Org. Chem.*, **70**, 9147 (2005).
38. M. Schmittel, A. Burghart, W. Malisch, J. Reising and R. Söllner, *J. Org. Chem.*, **63**, 396 (1998).
39. C. Wiles, P. Watts, S. J. Haswell and E. Pombo-Villar, *Lab on a Chip*, **1**, 100 (2001).
40. K. Mikami and H. Ohmura, *Chem. Commun.*, 2626 (2002).
41. J. O. Bunte, S. Rinne, C. Schäfer, B. Neumann, H.-G. Stammler and J. Mattay, *Tetrahedron Lett.*, **44**, 45 (2003).
42. D. A. Walthall, J. M. Karty, B. Römer, O. Ursini and J. I. Brauman, *J. Phys. Chem. A*, **109**, 8785 (2005).
43. D. Alonso, E. Caballero, M. Medarde and F. Tomé, *Tetrahedron Lett.*, **46**, 4839 (2005).
44. E. Negishi, H. Matsushita, S. Chatterjee and R. A. John, *J. Org. Chem.*, **47**, 3188 (1982).
45. K. Iseki, S. Oishi and Y. Kobayashi, *Tetrahedron*, **52**, 71 (1996).
46. K.-H. Baringhaus, H. Matter and M. Kurz, *J. Org. Chem.*, **65**, 5031 (2000).
47. J. Murga, E. Falomir, M. Carda and J. A. Marco, *Tetrahedron*, **57**, 6239 (2001).
48. M. Suginome, L. Uehlin, A. Yamamoto and M. Murakami, *Org. Lett.*, **6**, 1167 (2004).
49. L. C. Dias and A. M. Aguilar, *Org. Lett.*, **8**, 4629 (2006).

50. L. Ma, R. Hopson, D. Li, Y. Zhang and P. G. Williard, *Organometallics*, **26**, 5834 (2007).
51. J. Bai, L. D. Burke and K. J. Shea, *J. Am. Chem. Soc.*, **129**, 4981 (2007).
52. H. N. Borah, R. C. Boruah and J. S. Sandhu, *J. Chem. Soc., Chem. Commun.*, 154 (1991).
53. I. Shibata, M. Nishio, A. Baba and H. Matsuda, *J. Chem. Soc., Chem. Commun.*, 1067 (1993).
54. M. Yasuda, K. Chiba, N. Ohigashi, Y. Katoh and A. Baba, *J. Am. Chem. Soc.*, **125**, 7291 (2003).
55. V. K. Yadav and R. Balamurugan, *Org. Lett.*, **5**, 4281 (2003).
56. Y. Nishimura, Y. Miyake, R. Amemiya and M. Yamaguchi, *Org. Lett.*, **8**, 5077 (2006).
57. P. K. Koech and M. J. Krische, *J. Am. Chem. Soc.*, **126**, 5350 (2004).
58. D. H. R. Barton, J.-C. Blazejewski, B. Charpiot, J.-P. Finet, W. B. Motherwell, M. T. B. Papoula and S. P. Stanforth, *J. Chem. Soc., Perkin Trans. 1*, 2667 (1985).
59. K. Fuji, N. Kinoshita and K. Tanaka, *Chem. Commun.*, 1895 (1999).
60. S. Lai, C. K. Zercher, J. P. Jasinski, S. N. Reid and R. J. Staples, *Org. Lett.*, **3**, 4169 (2001).
61. O. Knopff and A. Alexakis, *Org. Lett.*, **4**, 3835 (2002).
62. T. D. Weiß, G. Helmchen and U. Kazmaier, *Chem. Commun.*, 1270 (2002).
63. E. Hevia, G. W. Honeyman, A. R. Kennedy and R. E. Mulvey, *J. Am. Chem. Soc.*, **127**, 13106 (2005).
64. X. Rathgeb, S. March and A. Alexakis, *J. Org. Chem.*, **71**, 5737 (2006).
65. M. L. Hlavinka and J. R. Hagadorn, *Organometallics*, **25**, 3501 (2006).
66. T. Hama, D. A. Culkin and J. F. Hartwig, *J. Am. Chem. Soc.*, **128**, 4976 (2006).
67. L.-T. Yu, M.-T. Ho, C.-Y. Chang and T.-K. Yang, *Tetrahedron: Asymmetry*, **18**, 949 (2007).
68. S. E. Baillie, E. Hevia, A. R. Kennedy and R. E. Mulvey, *Organometallics*, **26**, 204 (2007).
69. J. F. Greco, M. J. McNevin, R. K. Shoemaker and J. R. Hagadorn, *Organometallics*, **27**, 1948 (2008).
70. J. R. DeBergh, K. M. Spivey and J. M. Ready, *J. Am. Chem. Soc.*, **130**, 7828 (2008).
71. P. K. Koech and M. J. Krische, *Org. Lett.*, **6**, 691 (2004).
72. D. A. Culkin and J. F. Hartwig, *J. Am. Chem. Soc.*, **123**, 5816 (2001).
73. F. Churruca, R. SanMartin, I. Tellitu and E. Domínguez, *Org. Lett.*, **4**, 1591 (2002).
74. T. Hamada, A. Chieffi, J. Ahman and S. L. Buchwald, *J. Am. Chem. Soc.*, **124**, 1261 (2002).
75. J. L. Portscheller, S. E. Lilley and H. C. Malinakova, *Organometallics*, **22**, 2961 (2003).
76. D. Solé, F. Diaba and J. Bonjoch, *J. Org. Chem.*, **68**, 5746 (2003).
77. T. Honda and Y. Sakamaki, *Tetrahedron Lett.*, **46**, 6823 (2005).
78. M. C. Willis, D. Taylor and A. T. Gillmore, *Tetrahedron*, **62**, 11513 (2006).
79. N. Kinoshita, T. Kawabata, K. Tsubaki, M. Bando and K. Fuji, *Tetrahedron*, **62**, 1756 (2006).
80. S. R. Taylor, A. T. Ung and S. G. Pyne, *Tetrahedron*, **63**, 10889 (2007).
81. B. M. Trost, J. Xu and M. Reichle, *J. Am. Chem. Soc.*, **129**, 282 (2007).
82. W.-H. Zheng, B.-H. Zheng, Y. Zhang and X.-L. Hou, *J. Am. Chem. Soc.*, **129**, 7718 (2007).
83. G. Dessole, L. Bernardi, B. F. Bonini, E. Capitò, M. Fochi, R. P. Herrera, A. Ricci and G. Cahiez, *J. Org. Chem.*, **69**, 8525 (2004).
84. C. Tanyeli and D. Özdemirhan, *Tetrahedron*, **61**, 8212 (2005).
85. D. Zhao, K. Oisaki, M. Kanai and M. Shibasaki, *Tetrahedron Lett.*, **47**, 1403 (2006).
86. J. Cámpora, I. Matas, P. Palma, E. Álvarez, C. Graiff and A. Tiripicchio, *Organometallics*, **26**, 5712 (2007).
87. G. M. Mahandru, A. R. L. Skauge, S. K. Chowdhury, K. K. D. Amarasinghe, M. J. Heeg and J. Montgomery, *J. Am. Chem. Soc.*, **125**, 13481 (2003).
88. S. Tanaka, T. Anai, M. Tadokoro and T. Satoh, *Tetrahedron*, **64**, 7199 (2008).
89. A. D. William and Y. Kobayashi, *Org. Lett*, **3**, 2017 (2001).
90. A. P. Dove, V. C. Gibson, E. L. Marshall, A. J. P. White and D. J. Williams, *Chem. Commun.*, 1208 (2002).
91. J. R. Stille and R. H. Grubbs, *J. Am. Chem. Soc.*, **105**, 1664 (1983).
92. S. H. Bertz, G. Dabbagh and C. P. Gibson, *Organometallics*, **7**, 563 (1988).
93. P. Veya, C. Floriani, A. Chiesi-Villa and C. Rizzoli, *Organometallics*, **12**, 4892 (1993).
94. D. K. Dikshit and S. N. Bajpai, *Tetrahedron Lett.*, **36**, 3231 (1995).
95. M. T. Crimmins, B. W. King and E. A. Tabet, *J. Am. Chem. Soc.*, **119**, 7883 (1997).
96. K. Maeda, H. Shinokubo and K. Oshima, *J. Org. Chem.*, **63**, 4558 (1998).
97. Z. Han, S. Uehira, T. Tsuritani, H. Shionkubo and K. Oshima, *Tetrahedron*, **57**, 987 (2001).
98. J. W. B. Cooke, M. B. Berry, D. M. Caine, K. S. Cardwell, J. S. Cook and A. Hodgson, *J. Org. Chem.*, **66**, 334 (2001).

99. D. B. Kimball, R. Michalczyk, E. Moody, M. Ollivault-Shiflett, K. D. Jesus and L. A. Silks, *J. Am. Chem. Soc.*, **125**, 14666 (2003).
100. D. M. Casper and S. R. Hitchcock, *Tetrahedron: Asymmetry*, **14**, 517 (2003).
101. Y. Sawada, T. Mori and A. Oku, *J. Org. Chem.*, **68**, 10040 (2003).
102. M. Hayashi, N. Nakamura and K. Yamashita, *Tetrahedron*, **60**, 6777 (2004).
103. Y.-S. Lee, W.-K. Choung, K. H. Kim, T. W. Kang and D.-C. Ha, *Tetrahedron*, **60**, 867 (2004).
104. E. Barrágan, H. F. Olivo, M. Romero-Ortega and S. Sarduy, *J. Org. Chem.*, **70**, 4214 (2005).
105. J. G. Solsona, J. Nebot, P. Romea and F. Urpí, *J. Org. Chem.*, **70**, 6533 (2005).
106. C. Dong, G. Deng and J. Wang, *J. Org. Chem.*, **71**, 5560 (2006).
107. I. de P. R. Moreira, J. M. Bofill, J. M. Anglada, J. G. Solsona, J. Nebot, P. Romea and F. Urpí, *J. Am. Chem. Soc.*, **130**, 3243 (2008).
108. A. Olivella, C. Rodríguez-Escrich, F. Urpí and J. Vilarrasa, *J. Org. Chem.*, **73**, 1578 (2008).
109. P. A. Cameron, G. J. P. Britovsek, V. C. Gibson, D. J. Williams and A. J. P. White, *Chem. Commun.*, 737 (1998).
110. A. D. Bolig and E. Y.-X. Chen, *J. Am. Chem. Soc.*, **126**, 4897 (2004).
111. A. Kasatkin and R. J. Whitby, *Tetrahedron*, **59**, 9857 (2003).
112. V. Petrik and D. Cahard, *Tetrahedron Lett.*, **48**, 3327 (2007).
113. M. J. Gaunt and C. C. C. Johansson, *Chem. Rev.*, **107**, 5596 (2007).
114. H. Yamataka and Z. Rappoport, *J. Am. Chem. Soc.*, **122**, 9818 (2000).
115. J. Song, Y. X. Lei and Z. Rappoport, *J. Org. Chem.*, **72**, 9152 (2007).
116. E. Rochlin and Z. Rappoport, *J. Org. Chem.*, **68**, 1715 (2003).
117. D. H. Flint, A. Nudelman, J. C. Calabrese and H. E. Gottlieb, *J. Org. Chem.*, **57**, 7270 (1992).
118. E. Rochlin and Z. Rappoport, *J. Org. Chem.*, **68**, 216 (2003).
119. Y. X. Lei and Z. Rappoport, *J. Org. Chem.*, **67**, 6971 (2002).
120. Y. X. Lei, G. Cerioni and Z. Rappoport, *J. Org. Chem.*, **85**, 4028 (2000).
121. W. L. Jorgensen, J. M. Briggs and J. Gao, *J. Am. Chem. Soc.*, **109**, 6857 (1987).
122. C. D. Johnson and B. Stratton, *J. Org. Chem.*, **52**, 4798 (1987).
123. F. G. Bordwell and G. J. McCollum, *J. Org. Chem.*, **41**, 2391 (1976).
124. D. Algrim, J. E. Bares, J. C. Branca and F. G. Bordwell, *J. Org. Chem.*, **43**, 5025 (1978).
125. F. G. Bordwell and A. V. Satish, *J. Am. Chem. Soc.*, **116**, 8885 (1994).
126. F. G. Bordwell and T.-Y. Lynch, *J. Am. Chem. Soc.*, **111**, 7558 (1989).
127. T. L. Amyes and J. P. Richard, *J. Am. Chem. Soc.*, **118**, 3129 (1996).
128. Y. Chiang, J. Jones and A. J. Kresge, *J. Am. Chem. Soc.*, **116**, 8353 (1994).
129. F. G. Bordwell and H. E. Fried, *J. Org. Chem.*, **56**, 4218 (1991).
130. F. G. Bordwell, J. C. Branca, D. L. Hughes and W. N. Olmstead, *J. Org. Chem.*, **45**, 3305 (1980).
131. H. C. Brown, J. H. Brewster and H. Shechter, *J. Am. Chem. Soc.*, **76**, 467 (1954).
132. M. Capponi, I. Gut and J. Wirz, *Angew. Chem., Int. Ed. Engl.*, **25**, 344 (1986).
133. J. L. Holmes and F. P. Lossing, *J. Am. Chem. Soc.*, **104**, 2648 (1982).
134. B. Urwylet and J. Wirz, *Angew. Chem., Int. Ed. Engl.*, **29**, 790 (1990).
135. F. Turecek, L. Brabec and J. Korvola, *J. Am. Chem. Soc.*, **110**, 7984 (1988).
136. P. J. Wagner and B. Zhou, *J. Am. Chem. Soc.*, **110**, 611 (1988).
137. J. L. Holmes and F. P. Lossing, *J. Am. Chem. Soc.*, **102**, 1591 (1980).
138. F. C. Kohesh, *J. Org. Chem.*, **41**, 3593 (1976).
139. N. Sleszynski and P. Zuman, *J. Org. Chem.*, **52**, 2622 (1987).
140. R. J. Highet and I. V. Ekhato, *J. Org. Chem.*, **53**, 2843 (1988).
141. K. Kamiya, M. Boero, K. Shiraishi and A. Oshiyama, *J. Phys. Chem. B*, **110**, 4443 (2006).
142. D. A. Makeiff, K. Vishnumurthy and J. C. Sherman, *J. Am. Chem. Soc.*, **125**, 9558 (2003).
143. P. F. Godenschwager and D. B. Collum, *J. Am. Chem. Soc.*, **130**, 8726 (2008).
144. F. G. Bordwell and F. J. Cornforth, *J. Org. Chem.*, **43**, 1763 (1978).
145. T. S. Snowden, A. P. Bisson and E. V. Anslyn, *J. Am. Chem. Soc.*, **121**, 6324 (1999).
146. L. Xie, K. M. Isenberger, G. Held and L. M. Dahl, *J. Org. Chem.*, **62**, 7516 (1997).
147. N. S. Simpkins, *Sulphones in Organic Synthesis*, Pergamon, Oxford, 1993.
148. E. M. Arnett, S. G. Maroldo, S. L. Schilling and J. A. Harrelson, *J. Am. Chem. Soc.*, **106**, 6759 (1984).
149. P. R. Rablen and K. H. Bentrup, *J. Am. Chem. Soc.*, **125**, 2142 (2003).
150. J. Eames, N. Weerasooriya and G. S. Coumbarides, *Eur. J. Org. Chem.*, 181 (2002).

151. C. Fehr, *Angew. Chem., Int. Ed. Engl.*, **35**, 2566 (1996).
152. N. Krause, S. Ebert and A. Haubrich, *Liebigs Ann./Recueil*, 2409 (1997).
153. R. G. Dozent, *Angew. Chem., Int. Ed. Engl.*, **3**, 560 (1964).
154. M. Celina, R. L. R. Lazana, M. L. T. M. B. Franco and B. J. Herold, *J. Chem. Soc., Perkin Trans. 2*, 1399 (1987).
155. F. Méndez and J. L. Gázquez, *J. Am. Chem. Soc.*, **116**, 9298 (1994).
156. P. Sarthou, F. Guibe and G. Bram, *J. Chem. Soc., Chem. Commun.*, 377 (1974).
157. K. L. Shepard and J. L. Stevens, *Chem. Commun.*, 951 (1971).
158. S. J. Rhoads and R. W. Holder, *Tetrahedron*, **25**, 5443 (1969).
159. E. V. Dehmlow, M. Kaiser and J. Bollhofer, *New J. Chem.*, **25**, 588 (2001).
160. S. J. Rhoads and A. W. Decora, *Tetrahedron*, **19**, 1645 (1963).
161. The Kinetics of Proton Transfer Processes, conference reports, *Angew. Chem., Int. Ed. Engl.*, **4**, 791 (1965).
162. M. Eigen, *Angew. Chem., Int. Ed. Engl.*, **3**, 1 (1964).
163. H. Morrison, S. R. Kurowsky, *Chem. Commun.*, 1098 (1967). For additional information, see References 151 and 152.
164. J. Eames, G. S. Coumbarides, M. J. Suggate and N. Weerasooriya, *Eur. J. Org. Chem.*, 634 (2003).
165. H. E. Zimmerman, *Acc. Chem. Res.*, **20**, 263 (1987).
166. T. Laube, J. D. Dunitz and D. Seebach, *Helv. Chim. Acta*, **68**, 1373 (1985).
167. D. Seebach, M. Boes, R. Naef and W. B. Schweizer, *J. Am. Chem. Soc.*, **105**, 5390 (1983).
168. G. S. Coumbarides, J. Eames, M. J. Suggate and N. Weerasooriya, *J. Labelled Compd. Radiopharm.*, **49**, 641 (2006).
169. E. P. Serjeant and B. Dempsey, in *Ionisation Constants of Organic Acids in Aqueous Solution* (*IUPAC Chemical Data Series*, Num. 23), Pergamon, Oxford, 1979, pp. 9–765.
170. A. Albert and E. P. Serjeant, in *Ionisation Constants of Acids and Bases: A Laboratory Manual*, Butler & Tanner, London, 1962.
171. E.-I. Room, I. Kaljurand, I. Leito, T. Rodima, I. A. Koppel and V. M. Vlasov, *J. Org. Chem.*, **68**, 7795 (2003).
172. A. Streitwieser Jr, J. H. Hammons, E. Ciuffarin and J. I. Brauman, *J. Am. Chem. Soc.*, **89**, 59 (1967).
173. G. Garrido, E. Koort, C. Rafols, E. Bosch, T. Rodima, I. Leito and M. Roses, *J. Org. Chem.*, **71**, 9062 (2006).
174. A. Streitwieser Jr., J. I. Brauman, J. H. Hammons and A. H. Pudjaatmaka, *J. Am. Chem. Soc.*, **87**, 384 (1965).
175. W. K. McEwen, *J. Am. Chem. Soc.*, **58**, 1124 (1936).
176. E. C. Steiner and J. M. Gilbert, *J. Am. Chem. Soc.*, **87**, 382 (1965).
177. E. C. Steiner and J. D. Starkey, *J. Am. Chem. Soc.*, **89**, 2751 (1967).
178. J. P. Collman, Z. Wang, M. Zhong and L. Zeng, *J. Chem. Soc., Perkin Trans. 1*, 1217 (2000).
179. J. O. Stoffer, D. R. Strait, D. L. Filger, E. T. Lloyd and C. Crain, *J. Org. Chem.*, **43**, 1812 (1978).
180. J. M. B. Fernandes Diniz and T. M. Herrington, *J. Chem. Eng. Data*, **38**, 109 (1993).
181. K. Box, C. Bevan, J. Comer, A. Hill, R. Allen and D. Reynolds, *Anal. Chem.*, **75**, 883 (2003).
182. W. C. Barrette Jr, H. W. Johnson Jr and D. T. Sawyer, *Anal. Chem.*, **56**, 1890 (1984).
183. M. Mofaddel, N. Bar, D. Villemin and P. L. Desbene, *Anal. Bioanal. Chem.*, **380**, 664 (2004).
184. C. D. Ritchie and R. E. Uschold, *J. Am. Chem. Soc.*, **89**, 2752 (1967).
185. F. G. Bordwell and H. E. Fried, *J. Org. Chem.*, **56**, 4218 (1991).
186. F. G. Bordwell, D. J. Algrim and J. A. Harrelson, Jr, *J. Am. Chem. Soc.*, **110**, 5903 (1988).
187. K. Bowden, *Chem. Rev.*, **66**, 119 (1966).
188. W. Simon, *Angew. Chem., Int. Ed. Engl.*, **3**, 661 (1964).
189. N. Isaacs, *Physical Organic Chemistry* (2nd Edition), Longman Group Limited, Harlow, 1995, pp. 259–269.
190. A. J. Kresge and N. P. Schepp, *J. Chem. Soc., Chem. Commun.*, 1548 (1989).
191. J. March, *Advanced Organic Chemistry* (4th Edition), John Wiley & Sons, Ltd, Chichester, 1992, p. 250.
192. E. Iglesias, *J. Org. Chem.*, **68**, 2680 (2003).
193. A. Streitwieser, E. Juaristi, Y.-J. Kim and J. K. Pugh, *Org. Lett.*, **2**, 3739 (2000).
194. A. Streitwieser, Y.-J. Kim and D. Z.-R. Wang, *Org. Lett.*, **3**, 2599 (2001).

195. Y.-J. Kim and A. Streitwieser, *Org. Lett.*, **4**, 573 (2002).
196. D. Z. Wang and A. Streitwieser, *J. Org. Chem.*, **68**, 8936 (2003).
197. J. A. Miller and H. D. Zook, *J. Org. Chem.*, **42**, 2629 (1977).
198. S. Saito and H. Yamamoto, *Acc. Chem. Res.*, **37**, 570 (2004).
199. S. E. Denmark and G. L. Beutner, *Angew. Chem. Int. Ed.*, **47**, 1560 (2008).
200. H. D. Zook and T. J. Russo, *J. Am. Chem. Soc.*, **82**, 1258 (1960).
201. H. D. Zook, T. J. Russo, E. F. Ferrand and D. S. Stotz, *J. Org. Chem.*, **33**, 2222 (1968).
202. H. D. Zook and J. A. Miller, *J. Org. Chem.*, **36**, 1112 (1971).
203. L. R. Liou, A. J. McNeil, A. Ramírez, G. E. S. Toombes, J. M. Gruver and D. B. Collum, *J. Am. Chem. Soc.*, **130**, 4859 (2008).
204. W. S. Matthews, J. E. Bares, J. E. Bartmess, F. G. Bordwell, F. J. Cornforth, G. E. Drucker, Z. Margolin, R. J. McCallum, G. J. McCollum and N. R. Vanier, *J. Am. Chem. Soc.*, **97**, 7006 (1975).
205. J. B. Conant and G. W. Wheland, *J. Am. Chem. Soc.*, **54**, 1212 (1932).
206. F. G. Bordwell, *Acc. Chem. Res.*, **21**, 456 (1988).
207. W. K. McEwen, *J. Am. Chem. Soc.*, **58**, 1124 (1936).
208. R. Partasarathi, J. Padmanabhan, M. Elango, K. Chitra, V. Subramanian and P. K. Chattaraj, *J. Phys. Chem. A*, **110**, 6540 (2006).
209. K. E. Gutowski and D. A. Dixon, *J. Phys. Chem. A*, **110**, 12044 (2006).
210. L. Xing and R. C. Glen, *J. Chem. Inf. Comput. Sci.*, **42**, 796 (2002).
211. R. G. Pearson and R. L. Dillon, *J. Am. Chem. Soc.*, **75**, 2439 (1953).
212. R. G. Pearson and J. M. Mills, *J. Am. Chem. Soc.*, **72**, 1692 (1950).
213. F. Hibbert, in *Advances in Physical Organic Chemistry* (Eds V. Gold and D. Bethell), Vol. 22, Academic Press, London, 1986, pp. 113–212. For additional information see Reference 162.
214. K. M. Broadus and S. R. Kass, *J. Chem. Soc., Perkin Trans. 2*, 2389 (1999).
215. J. R. Keeffe and A. J. Kresge, in *The Chemistry of Enols* (Ed. Z. Rappoport), John Wiley & Sons, Ltd, Chichester, 1990, p. 399.
216. H. Shechter, M. J. Collins, R. Dessy, Y. Okuzumi and A. Chen, *J. Am. Chem. Soc.*, **84**, 2905 (1962).
217. F. G. Bordwell, J. E. Bartmess, G. E. Drucker, Z. Margolin and W. S. Matthews, *J. Am. Chem. Soc.*, **97**, 3226 (1975).
218. P. D. Bartlett and G. F. Woods, *J. Am. Chem. Soc.*, **62**, 2933 (1940).
219. K. W. Turnball, S. J. Gould and D. Arigoni, *J. Chem. Soc., Chem. Commun.*, 597 (1972).
220. D. H. Bowen and J. MacMillan, *Tetrahedron Lett.*, **13**, 4111 (1972).
221. C. S. Shiner, A. H. Berks and A. M. Fisher, *J. Am. Chem. Soc.*, **110**, 957 (1988).
222. K. S. Feldman, J. H. Come, B. J. Kosmider, P. M. Smith, D. P. Rotella and M.-J. Wu, *J. Org. Chem.*, **54**, 592 (1989).
223. P. Magnus, D. Parry, T. Iliadis, S. A. Eisenbeis and R. A. Fairhurst, *J. Chem. Soc., Chem. Commun.*, 1543 (1994).
224. A. J. Blake, G. M. P. Giblin, D. T. Kirk, N. S. Simpkins and C. Wilson, *Chem. Commun.*, 2668 (2001).
225. G. M. P. Giblin, D. T. Kirk, L. Mitchell and N. S. Simpkins, *Org. Lett.*, **5**, 1673 (2003).
226. N. M. Ahmad, V. Rodeschini, N. S. Simpkins, S. E. Ward and A. J. Blake, *J. Org. Chem.*, **72**, 4803 (2007).
227. F. B. Bordwell and H. E. Fried, *J. Org. Chem.*, **46**, 4327 (1981).
228. A. Rios, J. Crugeiras, T. L. Amyes and J. P. Richard, *J. Am. Chem. Soc.*, **123**, 7949 (2001).
229. J. Crugeiras, A. Rios, E. Riveiros, T. L. Amyes and J. P. Richard, *J. Am. Chem. Soc.*, **130**, 2041 (2008).
230. A. Rios, T. L. Amyes and J. P. Richard, *J. Am. Chem. Soc.*, **122**, 9373 (2000).
231. X.-M. Zhang, F. G. Bordwell, M. Van Der Puy and H. E. Fried, *J. Org. Chem.*, **58**, 3060 (1993).
232. R. Goumont, E. Magnier, E. Kizilian and F. Terrier, *J. Org. Chem.*, **68**, 6566 (2003).
233. W. N. Olmstead and F. G. Bordwell, *J. Org. Chem.*, **45**, 3299 (1980).
234. R. Huisgen, *Angew. Chem.*, **69**, 341 (1957).
235. R. Huisgen and H. Ott, *Tetrahedron*, **6**, 253 (1959).
236. P. Deslongchamps, *Stereoelectronic Effects in Organic Chemistry*, Pergamon, Oxford, 1983, pp. 52–53.

237. A. J. Kirby, *Stereoelectronic Effects*, Oxford Chemistry Primer, Oxford University Press, Oxford, 1996, Number 36.
238. F. G. Bordwell, M. Van Der Puy and N. R. Vanier, *J. Org. Chem.*, **41**, 1883 (1976).
239. G. Williams, E. P. Maziarz III, T. L. Amyes, T. D. Wood and J. P. Richard, *Biochemistry*, **42**, 8354 (2003).
240. A. Rios, J. P. Richard and T. L. Amyes, *J. Am. Chem. Soc.*, **124**, 8251 (2002).
241. S. Gronert and A. Streitwieser, *J. Am. Chem. Soc.*, **110**, 4418 (1988).
242. P. Ballinger and F. A. Long, *J. Am. Chem. Soc.*, **82**, 795 (1960).
243. J. P. Guthrie and P. A. Cullimore, *Can. J. Chem.*, **57**, 240 (1979).
244. A. J. Kresge and J. B. Tobin, *J. Org. Chem.*, **58**, 2652 (1993).
245. J. J. Grabowski, *Chem. Commun.*, 255 (1997).
246. S. Eldin, R. M. Pollack and D. L. Whalen, *J. Am. Chem. Soc.*, **113**, 1344 (1991).
247. Y. Chiang, A. J. Kresge, Q. Meng, R. A. M. O'Ferrall and Y. Zhu, *J. Am. Chem. Soc.*, **123**, 11562 (2001).
248. Y. Chiang, A. J. Kresge and E. T. Krogh, *J. Am. Chem. Soc.*, **110**, 2600 (1988).
249. Y. Chiang, A. J. Kresge, P. A. Walsh and Y. Yin, *J. Chem. Soc., Chem. Commun.*, 869 (1989).
250. D. J. Cram, B. Rickborn, C. A. Kingsbury and P. Haberfield, *J. Am. Chem. Soc.*, **83**, 3678 (1961).
251. W. D. Emmons and M. F. Hawthorne, *J. Am. Chem. Soc.*, **78**, 5593 (1956).
252. D. W. Earls, J. R. Jones and T. G. Rumney, *J. Chem. Soc., Perkin Trans. 1*, 878 (1975).
253. J. R. Jones, R. E. Marks and S. C. Subba Rao, *Trans. Faraday Soc.*, **63**, 111 (1967).
254. H. P. Beutelman, L. Xie and W. H. Saunders Jr., *J. Org. Chem.*, **54**, 1703 (1989).
255. D. J. Miller and W. H. Saunders Jr., *J. Org. Chem.*, **47**, 5039 (1982).
256. O. Miyara and R. R. Schmidt, *Angew Chem., Int. Ed. Engl.*, **21**, 637 (1982).
257. L. Zhang and J. J. Grabowski, *J. Chem. Soc., Chem. Commun.*, 1819 (1989).
258. R. P. Bell, *Trans. Faraday Soc.*, **39**, 253 (1943).
259. Y. Chiang, M. Hojatti, J. R. Keeffe, A. J. Kresge, N. P. Schepp and J. Wirz, *J. Am. Chem. Soc.*, **109**, 4000 (1987).
260. Y. Chiang, A. J. Kresge and Y. S. Tang, *J. Am. Chem. Soc.*, **106**, 460 (1984).
261. Y. Chiang, A. J. Kresge and N. P. Schepp, *J. Am. Chem. Soc.*, **111**, 3977 (1989).
262. J. P. Guthrie, J. Cossar and A. Klym, *J. Am. Chem. Soc.*, **104**, 895 (1982).
263. F. G. Bordwell, J. A. Harrelson and X. Zhang, *J. Org. Chem.*, **56**, 4448 (1991).
264. F. G. Bordwell, J.-P. Cheng and J. A. Harrelson, *J. Am. Chem. Soc.*, **110**, 1229 (1988).
265. G. I. Almerindo, D. W. Tondo and J. R. Pliego Jr, *J. Phys. Chem. A*, **108**, 166 (2004).
266. J. Warkentin and C. Barnett, *J. Am. Chem. Soc.*, **90**, 4629 (1968).
267. H. D. Zook, W. L. Kelly and I. Y. Posey, *J. Org. Chem.*, **33**, 3477 (1968).
268. J. P. Guthrie, *Can. J. Chem.*, **57**, 1177 (1979).
269. Y. Chiang, A. J. Kresge and J. Wirz, *J. Am. Chem. Soc.*, **106**, 6392 (1984).
270. M. Novak and G. M. Loudon, *J. Am. Chem. Soc.*, **98**, 3591 (1976).
271. F. G. Bordwell, J. E. Bartmess and J. A. Hautala, *J. Org. Chem.*, **43**, 3095 (1978).
272. F. G. Bordwell, J. A. Harrelson and T.-Y. Lynch, *J. Org. Chem.*, **55**, 3337 (1990).
273. F. G. Bordwell and D. Algrim, *J. Org. Chem.*, **41**, 2507 (1976).
274. M. Novak and G. M. Loudon, *J. Org. Chem.*, **42**, 2494 (1977).
275. F. G. Bordwell, J. E. Bares, J. E. Bartmess, G. J. McCollum, M. Van Der Puy, N. R. Vanier and W. S. Matthews, *J. Org. Chem.*, **42**, 321 (1977).
276. X.-M. Zhang and F. G. Bordwell, *J. Am. Chem. Soc.*, **114**, 9787 (1992).
277. I. M. Kolthoff and M. K. Chantooni Jr, *J. Am. Chem. Soc.*, **87**, 4428 (1965).
278. P. De Maria, A. Fontana, C. Gasbarri and G. Siani, *Tetrahedron*, **61**, 7176 (2005).
279. A. Rios, T. L. Amyes and J. P. Richard, *J. Am. Chem. Soc.*, **122**, 9373 (2000).
280. A. Rios and J. P. Richard, *J. Am. Chem. Soc.*, **119**, 8375 (1997).
281. E. D. Stround, D. J. Fife and G. G. Smith, *J. Org. Chem.*, **48**, 5368 (1983).
282. E. Iglesias, *New. J. Chem.*, **26**, 1352 (2002).
283. M. L. Eidinoff, *J. Am. Chem. Soc.*, **67**, 2072 (1945).
284. J. C. Reid and M. Calvin, *J. Am. Chem. Soc.*, **72**, 2948 (1950).
285. M. J. Zapatero, M. P. Elizalde and J. M. Castresana, *Anal. Sci.*, **7**, 935 (1991).
286. M. Tamres and S. Searles, *J. Am. Chem. Soc.*, **81**, 2100 (1959).
287. E. F. Pratt and K. Matsuda, *J. Am. Chem. Soc.*, **75**, 3739 (1953).
288. S. Searles, M. Tamres and G. M. Barrow, *J. Am. Chem. Soc.*, **75**, 71 (1953).

289. L. B. Krivdin, S. V. Zinchenko, G. A. Kalabin, J. C. Facelli, M. F. Tufro, R. H. Contreras, A. Y. Denisov, O. A. Gavrilyuk and V. I. Mamatyuk, *J. Chem. Soc., Trans. Faraday Soc.*, **88**, 2459 (1992).
290. D. R. Clark, J. Emsley and F. Hibbert, *J. Chem. Soc., Chem. Commun.*, 1252 (1988).
291. R. Noto, F. D'Anna, M. Gruttadauria, P. L. Meo and D. Spinelli, *J. Chem. Soc., Perkin Trans. 2*, 2043 (2001).
292. E. F. Pratt and K. Matsuda, *J. Am. Chem. Soc.*, **75**, 3739 (1953).
293. A. Koeberg-Telder, T. A. Kortekass and H. Cerfontain, *J. Chem. Soc., Perkin Trans. 2*, 851 (1979).
294. T. G. Bonner and J. Phillips, *J. Chem. Soc. (B)*, 650 (1966).
295. P. J. Battye, J. F. Cassidy and R. B. Moodie, *J. Chem. Soc., Chem. Commun.*, 68 (1981).
296. R. A. McClelland and W. F. Reynolds, *J. Chem. Soc., Chem. Commun.*, 824 (1974).
297. B. G. Cox and P. De Maria, *J. Chem. Soc., Perkin Trans. 2*, 942 (1975).
298. R. B. Homer and R. B. Moodie, *J. Chem. Soc.*, 4377 (1963).
299. M. Allard and J. Levisalles, *J. Chem. Soc., Chem. Commun.*, 1515 (1969).
300. M. Miler, *J. Chem. Soc., Chem. Commun.*, 115 (1971).
301. H. Benderly and K. Rosenheck, *J. Chem. Soc., Chem. Commun.*, 179 (1972).
302. R. B. Martin, *J. Chem. Soc., Chem. Commun.*, 793 (1972).
303. J. L. Sudmeier and K. E. Schwartz, *J. Chem. Soc., Chem. Commun.*, 1646 (1968).
304. A. Taskinen, V. Nieminen, E. Toukoniitty, D. Y. Murzin and M. Hotokka, *Tetrahedron*, **61**, 8106 (2005).
305. K. Yates and R. Stewart, *Can. J. Chem.*, **37**, 644 (1959).
306. R. Stewart and K. Yates, *J. Am. Chem. Soc.*, **80**, 6355 (1958).
307. T. G. Bonner and J. Phillips, *J. Chem. Soc. (B)*, 650 (1966).
308. A. McKenzie and S. T. Widdows, *J. Chem. Soc., Trans.*, **107**, 702 (1915).
309. A. McKenzie and H. Wren, *J. Chem. Soc.*, 602 (1919).
310. J. Read and H. G. Smith, *J. Chem. Soc., Trans.*, 2267 (1923).
311. S. K. Hsu and C. L. Wilson, *J. Chem. Soc.*, 623 (1936).
312. C. K. Ingold and C. L. Wilson, *J. Chem. Soc.*, 93 (1939).
313. J. Kenyon and D. P. Young, *J. Chem. Soc.*, 216 (1940).
314. M. K. Hargreaves and M. A. Khan, *J. Chem. Soc., Perkin Trans. 2*, 1204 (1973).
315. I. Antonovics and G. T. Young, *Chem. Commun.*, 398 (1965).
316. C. Di Bello, F. Filira, V. Giormani and F. D'Angeli, *J. Chem. Soc. (C)*, 350 (1969).
317. P. Watts, C. Wiles, S. J. Haswell and E. Pombo-Villar, *Lab on a Chip*, **2**, 141 (2002).
318. C. Kobler and F. Effenberger, *Tetrahedron: Asymmetry*, **15**, 3731 (2004).
319. T. A. Paal, E. Forro, A. Liljeblad, L. T. Kanerva and F. Fulop, *Tetrahedron: Asymmetry*, **18**, 1428 (2007).
320. M. R. Atuu and M. M. Hossain, *Tetrahedron Lett.*, **48**, 3875 (2007).
321. T. Cazetta, I. Lunardi, G. J. A. Conceicao, P. J. S. Moran and J. A. R. Rodrigues, *Tetrahedron: Asymmetry*, **18**, 2030 (2007).
322. P. Hoyos, M. Fernández, J. V. Sinisterra and A. R. Alcántara, *J. Org. Chem.*, **71**, 7632 (2006).
323. A. Kubo, H. Kubota, M. Takahashi and K. Nunami, *J. Org. Chem.*, **62**, 5830 (1997).
324. K. Makino, T. Fujii and Y. Hamada, *Tetrahedron: Asymmetry*, **17**, 481 (2006).
325. H. J. Kim, Y. Kim, E. T. Choi, M. H. Lee, E. S. No and Y. S. Park, *Tetrahedron*, **62**, 6303 (2006).
326. J. Chang, E. Shin, H. J. Kim, Y. Kim and Y. S. Park, *Tetrahedron*, **61**, 2743 (2005).
327. S. Caddick, C. A. M. Afonso, S. X. Candeias, P. B. Hitchcock, K. Jenkins, L. M. D. Pardoe, A. G. Santos, N. R. Treweeke and R. Weaving, *Tetrahedron*, **57**, 6589 (2001).
328. O. Labeeuw, P. Phansavath and J.-P. Genet, *Tetrahedron: Asymmetry*, **15**, 1899 (2004).
329. R. S. Ward, *Tetrahedron: Asymmetry*, **6**, 1475 (1995).
330. R. Sturmer, *Angew. Chem., Int. Ed. Engl.*, **36**, 1173 (1997).
331. F. F. Huerta, A. B. E. Minidis and J.-E. Backvall, *Chem. Soc. Rev.*, **30**, 321 (2001).
332. H. Pellissier, *Tetrahedron*, **59**, 8291 (2003).
333. H. Pellissier, *Tetrahedron*, **64**, 1563 (2008).
334. U. T. Strauss and K. Faber, *Tetrahedron: Asymmetry*, **10**, 107 (1999). For additional information see References 329–333.
335. J. A. Andraos, *J. Phys. Chem. A*, **107**, 2374 (2003).

336. M. Langston, U. C. Dyer, G. A. C. Frampton, G. Hutton, C. J. Lock, B. M. Skead, M. Woods and H. S. Zavareh, *Org. Process Res. Dev.*, **4**, 530 (2000).
337. A. J. Blacker, M. J. Stirling and M. I. Page, *Org. Process Res. Dev.*, **11**, 642 (2007).
338. J. A. Pesti, J. Yin, L. Zhang, L. Anzalone, R. E. Waltermire, P. Ma, E. Gorke, P. N. Confalone, J. Fortunak, C. Silverman, J. Blackwell, J. C. Chung, M. D. Hrytsak, M. Cooke, L. Powell and C. Ray, *Org. Process Res. Dev.*, **8**, 22 (2004).
339. A. Ammazzalorso, R. Amoroso, G. Bettoni, B. de Filippis, L. Giampietro, M. Pierini and M. L. Tricca, *Tetrahedron Lett.*, **43**, 4325 (2002).
340. T. Rein, R. Kreuder, P. von Zezschwitz, C. Wulff and O. Reiser, *Angew. Chem., Int. Ed. Engl.*, **34**, 1023 (1995).
341. R. Noyori, *Asymmetric Catalysis in Organic Synthesis*, John Wiley & Sons, Ltd, Chichester, 1993, pp. 16–94.
342. J.-H. Xie, Z.-T. Zhou, W.-L. King and Q.-L. Zhou, *J. Am. Chem. Soc.*, **129**, 1868 (2007).
343. B. Mohar, A. Valleix, J.-R. Desmurs, M. Felemez, A. Wagner and C. Mioskowski, *Chem. Commun.*, 2572 (2001).
344. K. Makino, T. Goto, Y. Hiroki and Y. Hamada, *Angew. Chem. Int. Ed.*, **43**, 882 (2004).
345. A. Ros, A. Magriz, H. Dietrich, J. M. Lassaletta and R. Fernández, *Tetrahedron*, **63**, 7532 (2007).
346. V. Jurkauskas and S. L. Buchwald, *J. Am. Chem. Soc.*, **124**, 2892 (2002).
347. L. Tang and L. Deng, *J. Am. Chem. Soc.*, **124**, 2870 (2002).
348. K. Mikami and A. Yoshida, *Tetrahedron*, **57**, 889 (2001).
349. M. A. Baur, A. Riahi, F. Henin and J. Muzart, *Tetrahedron: Asymmetry*, **14**, 2755 (2003).
350. K. Ishihara, D. Nakashima, Y. Hiraiwa and H. Yamamoto, *J. Am. Chem. Soc.*, **125**, 24 (2003).
351. G. S. Coumbarides, J. Eames, J. E. W. Scheuermann, K. F. Sibbons, M. J. Suggate and M. Watkinson, *Bull. Chem. Soc. Jpn.*, **78**, 906 (2005).
352. J. Eames and N. Weerasooriya, *Tetrahedron: Asymmetry*, **12**, 1 (2001).
353. R. Melgar-Fernández, R. González-Olvera and E. Juaristi, *Tetrahedron*, **61**, 4329 (2005).
354. O. Munoz-Muniz and E. Juaristi, *Tetrahedron*, **59**, 2023 (2003).
355. O. Munoz-Muniz and E. Juaristi, *Tetrahedron*, **59**, 4233 (2003).
356. Y. Ohtsuka, T. Ikeno and T. Yamada, *Tetrahedron: Asymmetry*, **14**, 967 (2003).
357. K. Flinois, Y. Yuan, C. Bastide, A. Harrison-Marchand and J. Maddaluno, *Tetrahedron*, **58**, 4707 (2002).
358. W. Wang, M.-H. Xu, X.-S. Lei and G.-Q. Lin, *Org. Lett.*, **2**, 3773 (2000).
359. G. R. Allan, A. J. Carnell and W. Kroutil, *Tetrahedron Lett.*, **42**, 5959 (2001).
360. D. R. Carbery and T. J. Donohoe, *Chem. Commun.*, 722 (2004).
361. K. Futatsugi, A. Yanagisawa and H. Yamamoto, *Chem. Commun.*, 566 (2003).
362. G. S. Coumbarides, J. Eames, S. Ghilagaber and M. J. Suggate, *Tetrahedron Lett.*, **45**, 9469 (2004).
363. D. E. Ward, O. T. Akinnusi, I. Q. Alarcon, V. Jheengut, J. Shen and J. W. Quail, *Tetrahedron: Asymmetry*, **15**, 2425 (2004).
364. L. Duhamel, P. Duhamel and J.-C. Plaquevent, *Tetrahedron: Asymmetry*, **15**, 3653 (2004).
365. T. Kawabata, S. Kawakami and K. Fuji, *Tetrahedron Lett.*, **43**, 1465 (2002).
366. T. Kawabata, S. Kawakami, S. Shimada and K. Fuji, *Tetrahedron*, **59**, 965 (2003).
367. J. Eames and M. Suggate, *Angew. Chem. Int. Ed.*, **44**, 186 (2005).
368. T. Kawabata, O. Ozturk, J. Chen and K. Fuji, *Chem. Commun.*, 162 (2003).
369. P. R. Carlier, P. C.-H. Lam, J. C. DeGuzman and H. Zhao, *Tetrahedron: Asymmetry*, **16**, 2998 (2005).
370. B. J. Bunn, N. S. Simpkins, Z. Spavold and M. J. Crimmin, *J. Chem. Soc., Perkin Trans. 1*, 3113 (1993).
371. J. Busch-Petersen and E. J. Corey, *Tetrahedron Lett.*, **41**, 6941 (2000).
372. K. Bambridge, B. P. Clark and N. S. Simpkins, *J. Chem. Soc., Perkin Trans. 1*, 2535 (1995).
373. V. K. Aggarwal, P. S. Humphries and A. Fenwick, *J. Chem. Soc., Perkin Trans. 1*, 2883 (1999).
374. D. J. Adams, A. J. Blake, P. A. Cooke, C. D. Gill and N. S. Simpkins, *Tetrahedron*, **58**, 4603 (2002).
375. L. M. Murray, P. O'Brien, R. J. K. Taylor and S. Wunnemann, *Tetrahedron Lett.*, **45**, 2597 (2004).
376. C. Sun and P. G. Williard, *J. Am. Chem. Soc.*, **122**, 7829 (2000).

377. M. Majewski and D. M. Gleave, *J. Org. Chem.*, **57**, 3599 (1992).
378. G. M. P. Giblin, D. T. Kirk, L. Mitchell and N. S. Simpkins, *Org. Lett.*, **5**, 1673 (2003).
379. A. Yangagisawa, T. Kikuchi, T. Kuribayashi and H. Yamamoto, *Tetrahedron*, **54**, 10253 (1998).
380. H. Kosugi, K. Hoshino and H. Uga, *Tetrahedron Lett.*, **38**, 6861 (1997).
381. T. Takahashi, N. Nakao and T. Koizumi, *Tetrahedron: Asymmetry*, **8**, 3293 (1997).
382. Y. Nakamura, S. Takeuchi, Y. Ohgo, M. Yamaoka, A. Yoshida and K. Mikami, *Tetrahedron Lett.*, **38**, 2709 (1997).
383. G. Asensio, P. A. Aleman, L. R. Domingo and M. Medio-Simón, *Tetrahedron Lett.*, **39**, 3277 (1998).
384. E. Vedejs, A. W. Kruger and E. Suna, *J. Org. Chem.*, **64**, 7863 (1999).
385. E. Vedejs, A. W. Kruger and E. Suna, *J. Org. Chem.*, **63**, 2792 (1998).
386. S. J. Aboulhoda, I. Reiners, J. Wilken, F. Henin, J. Martens and J. Muzart, *Tetrahedron: Asymmetry*, **9**, 1847 (1998).
387. M. Sugiura and T. Nakai, *Angew. Chem., Int. Ed. Engl.*, **36**, 2366 (1997).
388. Y. Yamashita, Y. Emura, K. Odashima and K. Koga, *Tetrahedron Lett.*, **41**, 209 (2000).
389. P. Riviere and K. Koga, *Tetrahedron Lett.*, **38**, 7589 (1997).
390. B. M. Kim, H. Kim, W. Kim, K. Y. Im and J. K. Park, *J. Org. Chem.*, **69**, 5104 (2004).
391. J. Eames and N. Weerasooriya, *Chirality*, **11**, 787 (1999).
392. G. S. Coumbarides, J. Eames and N. Weerasooriya, *Tetrahedron Lett.*, **41**, 5753 (2000).
393. E. Boyd, G. S. Coumbarides, J. Eames, A. Hay, R. V. H. Jones, R. A. Stenson and M. J. Suggate, *Tetrahedron Lett.*, **45**, 9465 (2004).
394. J. Matsuo, S. Kobayashi and K. Koga, *Tetrahedron Lett.*, **39**, 9723 (1998).
395. T. Yasukata and K. Koga, *Tetrahedron: Asymmetry*, **4**, 35 (1993).
396. J. A. Kozloski, in *Comprehensive Organic Synthesis*, Vol. 4, Chap. 4 (Eds I. Fleming and B. M. Trost), Pergamon, Oxford, 1991, pp. 169–198.
397. H.-G. Schmalz, in *Comprehensive Organic Synthesis*, Vol. 4, Chap. 5 (Eds I. Fleming and B. M. Trost), Pergamon, Oxford, 1991, pp. 199–236.
398. M. Hulce and M. J. Chapdelaine, in *Comprehensive Organic Synthesis*, Vol. 4, Chap. 6 (Eds I. Fleming and B. M. Trost), Pergamon, Oxford, 1991, pp. 238–268.
399. M. P. Sibi, H. Tatamidani and K. Patil, *Org. Lett.*, **7**, 2571 (2005).
400. D. Leow, S. Lin, S. K. Chittimalla, X. Fu and C.-H. Tan, *Angew. Chem. Int. Ed.*, **47**, 1 (2008).
401. N. T. Reynolds and T. Rovis, *J. Am. Chem. Soc.*, **127**, 16406 (2005).
402. U. Lüning and M. Müller, *Angew. Chem., Int. Ed. Engl.*, **31**, 80 (1992).
403. D. Kim, J. Lee, J. Chang and S. Kim, *Tetrahedron*, **57**, 1247 (2001).
404. D. A. Carcache, Y. S. Cho, Z. Hua, Y. Tian, Y.-M. Li and S. J. Danishefsky, *J. Am. Chem. Soc.*, **128**, 1016 (2006).
405. C. Cativiela, M. D. Diaz-de-Villegas and J. A. Galvez, *Can. J. Chem.*, **70**, 2325 (1992).
406. A. Ortiz, H. Hernández, G. Mendoza, L. Quintero and S. Bernès, *Tetrahedron Lett.*, **46**, 2243 (2005).
407. P. Barraclough, C. A. Spray and D. W. Young, *Tetrahedron Lett.*, **46**, 4653 (2005).
408. A. R. Rodríguez and B. W. Spur, *Tetrahedron Lett.*, **43**, 9249 (2002).
409. J. Clayden, R. Turnbull and I. Pinto, *Tetrahedron: Asymmetry*, **16**, 2235 (2005).
410. M. Calmès, F. Escale and J. Martinez, *Tetrahedron: Asymmetry*, **13**, 293 (2002).
411. S. Comesse and O. Piva, *Tetrahedron: Asymmetry*, **10**, 1061 (1999).
412. Y. Hu, R. L. Bishop, A. Luxenburger, S. Dong and L. A. Paquette, *Org. Lett.*, **8**, 2735 (2006).
413. D. T. Witiak, R. J. Patch, S. J. Enna and Y. K. Fung, *J. Med. Chem.*, **29**, 1 (1986).
414. R. Grigg, H. Q. N. Gunaratne and V. Sridharan, *J. Chem. Soc., Chem. Commun.*, 1183 (1985).
415. J. Eames, *Tetrahedron Lett.*, **40**, 5787 (1999).
416. H. E. Zimmerman and P. Wang, *J. Org. Chem.*, **68**, 9226 (2003).
417. A. Yanagisawa, T. Watanabe, T. Kikuchi, T. Kuribayashi and H. Yamamoto, *Synlett*, 956 (1997).
418. T. Sugimura, W. H. Kim, M. Kagawa and T. Okuyama, *Org. Lett.*, **4**, 2059 (2002).
419. A. K. Bose, C. S. Narayanan and M. S. Manhas, *Chem. Commun.*, 975 (1970).
420. P. W. Hickmott and K. N. Woodward, *J. Chem. Soc., Chem. Commun.*, 275 (1974).
421. R. A. Firestone and B. G. Christensen, *J. Chem. Soc., Chem. Commun.*, 288 (1976).
422. C. M. Pant and R. J. Stoodley, *J. Chem. Soc., Chem. Commun.*, 57 (1977).
423. A. Malkawi, *Int. J. Appl. Chem.*, **4**, 15 (2008).

424. N. Krause and M. Mackenstedt, *Tetrahedron Lett.*, **39**, 9646 (1998); F. Cavelier, S. Gomez, R. Jacquier and J. Verducci, *Tetrahedron Lett.*, **35**, 2891 (1994).
425. S. D. Carter and R. J. Stoodley, *J. Chem. Soc., Chem. Commun.*, 92 (1977).
426. J. P. Clayton, J. H. C. Nayler, R. Southgate and E. R. Stove, *Chem. Commun.*, 129 (1969).
427. P. E. Pfeffer and S. F. Osman, *J. Org. Chem.*, **37**, 2425 (1972).
428. J. E. Beddow, S. G. Davies, K. B. Ling, P. M. Roberts, A. J. Russell, A. D. Smith and J. E. Thomson, *Org. Biomol. Chem.*, **5**, 2818 (2007).
429. G. S. Coumbarides, J. Eames and N. Weerasooriya, *Can. J. Chem.*, **78**, 935 (2000).
430. S. Ebert and N. Krause, *Eur. J. Org. Chem.*, 3831 (2001).
431. N. Krause, *Angew. Chem., Int. Ed. Engl.*, **33**, 1764 (1994).
432. N. Krause and S. Ebert, *Eur. J. Org. Chem.*, 3837 (2001).
433. S. Takano, S. Yamada, H. Numata and K. Ogasawara, *J. Chem. Soc., Chem. Commun.*, 760 (1983).
434. H. E. Zimmerman, *J. Am. Chem. Soc.*, **78**, 1168 (1956).
435. J. G. Urones, N. M. Garrido, D. Diez, M. E. El Hammoumi, S. H. Dominguez, J. A. Casaseca, S. G. Davies and A. D. Smith, *Org. Biomol. Chem.*, **2**, 364 (2004).
436. T. J. Fleck, W. W. McWhorter Jr, R. N. DeKam and B. A. Pearlman, *J. Org. Chem.*, **68**, 9612 (2003).
437. I. Fleming, J. H. M. Hill, D. Parker and D. Waterson, *J. Chem. Soc., Chem. Commun.*, 318 (1985).
438. H. M. L. Davies, L. M. Hodges and T. M. Gregg, *J. Org. Chem.*, **66**, 7898 (2001).
439. S. G. Davies, A. D. Smith and P. D. Price, *Tetrahedron: Asymmetry*, **16**, 2833 (2005).
440. S. G. Davies, O. Ichihara, I. Lenoir and I. A. S. Walters, *J. Chem. Soc., Perkin Trans. 1*, 1411 (1994).
441. K. Yoshida, M. Ogasawara and T. Hayashi, *J. Org. Chem.*, **68**, 1901 (2003).
442. A. J. Frontier and C. Collison, *Tetrahedron*, **61**, 7577 (2005).
443. G. Liang, S. N. Gradl and D. Trauner, *Org. Lett.*, **5**, 4931 (2003).
444. V. K. Aggarwal and A. J. Belfield, *Org. Lett.*, **5**, 5075 (2003).
445. W. He, X.-F. Sun and A. J. Frontier, *J. Am. Chem. Soc.*, **125**, 14278 (2003).
446. M. Janke, W. He, A. J. Frontier and R. Eisenberg, *J. Am. Chem. Soc.*, **126**, 6846 (2004).
447. G. Liang and D. Trauner, *J. Am. Chem. Soc.*, **126**, 9544 (2004).
448. G. Laval, G. Audran, J.-M. Galano and H. Monti, *J. Org. Chem.*, **65**, 3551 (2000).
449. N. Philippe, V. Levacher, G. Dupas, G. Queguiner and J. Bourguignon, *Org. Lett.*, **2**, 2185 (2000).
450. H. E. Zimmerman and P. Wang, *J. Org. Chem.*, **67**, 9216 (2002).
451. H. E. Zimmerman and J. Cheng, *J. Org. Chem.*, **71**, 873 (2006).

CHAPTER 9

Redox chemistry and electrochemistry of metal enolates

GUIDO PAMPALONI

Università di Pisa, Dipartimento di Chimica e Chimica Industriale, Via Risorgimento 35, I-56126 Pisa, Italy
Fax: +39 50 2219 246; e-mail: pampa@dcci.unipi.it

and

PIERO ZANELLO

Università di Siena, Dipartimento di Chimica, Via De Gasperi 2, I-53100 Siena, Italy
Fax: +39 577 234233; e-mail: zanello@unisi.it

The chemistry of metal enolates
Edited by Jacob Zabicky

I. LIST OF ABBREVIATIONS

acac	acetylacetonato (2,4-pentanedionato) anion
acacCN	3-cyano-2,4-pentanedionato anion
bpyn	*N*-*tert*-butyl-*a*-(2-pyridyl)nitrone
bqdi	*o*-benzoquinonediimine
bzac	benzoylacetonato anion
cod	1,5-cyclooctadiene
coe	cyclooctene
cpba	*m*-chloroperbenzoic acid

CV	cyclic voltammetry
CVD	chemical vapour deposition
c-Hex	cyclohexyl
dbm	dibenzoylmethanato anion
dca	9,10-dicyanoanthracene
ddq	2,3-dichloro-5,6-dicyano-1,4-benzoquinone
DFT	density functional theory
dik	β-diketonato anion
dipy	2,2′-dipyridyl
dme	1,2-dimethoxyethane
dpb	1,1′-(1,3-phenylene)bis(4,4-dimethyl-1,3-pentanedionato) dianion
dpm	dipivaloylmethanato anion
dppz	dipyridophenazine
ECE	electrochemical chemical electrochemical
en	ethylenediamine
hfacac	1,1,1,6,6,6-hexafluoroacetylacetonato anion
hmpa	hexamethylphosphortriamide
lda	lithium *N*,*N*-diisopropylamide
lhmds	lithium hexamethyldisilazide
LMCT	ligand-to-metal charge transfer band
MLCT	metal-to-ligand charge transfer band
mob	1,1′-(1,3-phenylene)bis(7-methyl-1,3,5-octanetrionato) tetranion
NIS	*N*-iodosuccinimide
NXS	*N*-halosuccinimide
opda	*o*-phenylenediamide dianion
Pc	phthalocyaninato dianion
PET	photoinduced electron transfer
phen	1,10-phenathroline
prc	propylene carbonate
py	pyridine
SCE	saturated calomel electrode
sqdi	*o*-benzosemiquinonediimide anion
tmeda	*N*,*N*,*N*′,*N*′-tetramethylethylenediamine
ttfs	tetrathiofulvenylthiol

II. INTRODUCTION

The first volume devoted to the chemistry of enols appeared in 1990[1]. The present chapter on the redox properties of metal enolates aims to show or confirm how the redox concepts, which play an important role in inorganic chemistry, may find useful application also in organic chemistry.

Considering that the volume on enols[1] did not refer specifically to redox processes and that the one-electron oxidation of enols produces enol radical cations which are more stable than the corresponding tautomeric ketone ions, in distinct contrast to the thermochemistry of the neutral species[2–4], this chapter will deal also with the reactivity of electrogenerated enol radical cations[5].

In view of the profusion of material concerning metal enolates as intermediates in the organic synthesis, the chapter has been organized as follows: (i) enolates of main group elements will be treated separately from those of the transition metals; (ii) the redox reactions will be organized according to the nature of the triggered process (cyclization, coupling etc.); (iii) silyl enolates will receive particular attention in Section III.B;

(iv) β-diketonates, which represent a milestone in the evolution of the coordination chemistry of transition metals, will be addressed separately for redox reactions involving the transition metal or the β-diketonato ligand or both, whereas the large amount of electrochemical processes, which generally occur on the metal, will be discussed in Sections IV–VI; (v) it was considered useful to discuss some related derivatives such as substituted β-diketonates and polyketonates; (vi) the redox chemistry of complexes containing ligands strictly related to β-diketonates but not containing the dionato functionality such as mono- and dithio-β-diketonates[6] or acylpyrazolon-5-onates[7] will not be included in this chapter.

III. METAL ENOLATES MO–C=C

A. Redox Reactions of Enolates of Main Group Elements

Most metal enolates which participate in a wide variety of fundamental processes involving C–C bond formation, such as alkylations, aldol additions, Michael reactions and acylations[8], are alkali-metal enolates, particularly lithium enolates. The decisive role of the metal for these reactions was first appreciated when Stork[9] demonstrated that an enolato anion can be transformed into silyl enolates, purified by distillation or chromatography, and then converted back to the anion. Recently new reagents containing main group elements, such as magnesium, or alkali metals and magnesium or zinc couples have been considered as alternative bases, showing in some cases higher selectivity with respect to the related lithium amides[10]. In the following sections, redox reactions of metal enolates of main group elements will be presented with particular reference to the two pivotal species in this field, i.e. lithium and silyl enolates.

1. Synthesis of α-hydroxy carbonyl compounds

α-Hydroxy carbonyl compounds are valuable intermediates in organic synthesis and are key structural units of many biologically active natural products such as sugars, pherormones, antibiotics, terpenes and alkaloids. Many routes to their synthesis have been developed. In the present section reactions involving oxidation of enolates to α-hydroxy carbonyl derivatives will be considered.

The reaction of lithium enolates with molecular oxygen has been used for the α-hydroxylation of several substrates. The carbanion generated in the reaction of *N*,*N*-dialkylamides or esters with alkyl lithium reagents undergoes rapid oxidation under mild conditions when treated with molecular oxygen. The reaction produces an α-hydroperoxide intermediate which is cleanly reduced with sodium sulphite to the α-hydroxo derivatives[11] (equation 1).

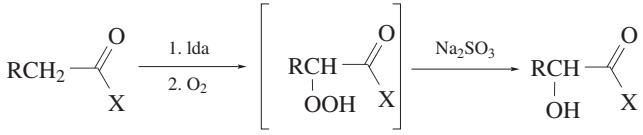

X = NR_2, OR (1)

As shown in equation 2, the lithium enolate oxidation with O_2, followed by sodium sulphite reduction, has been applied with success to oxidation of the enolate derived from **1**: the nature of the reducing agent has been decisive for the direct preparation of the hepatoprotective agent Clausenamide (**2**)[12]. As a matter of fact, **2** forms when the treatment with O_2 is done in the presence of triethyl phosphite as reducing agent, whereas sodium sulphite reduction affords compound **3**. It has been postulated that the transformation **1** → **3** occurs through the intermediacy of the peroxide **4**.

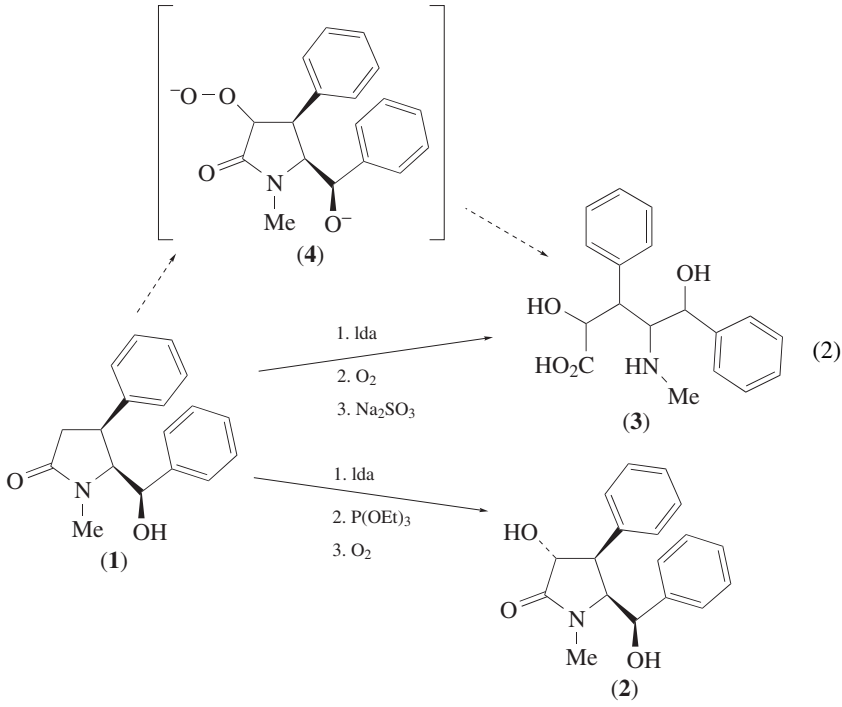

(2)

The sodium enolate **5a** undergoes oxidation in air giving the δ-hydroxy-γ-keto-carboxylic acid **6** in high yields after acid hydrolysis: this compound can be further transformed into the methyl ester of (*d*,*l*)-*trans*-chrisantemic acid (**7**, equation 3)[13]. Compound **6** can also be obtained from the potassium enolate **5b** but only under slight pressure of pure oxygen[13].

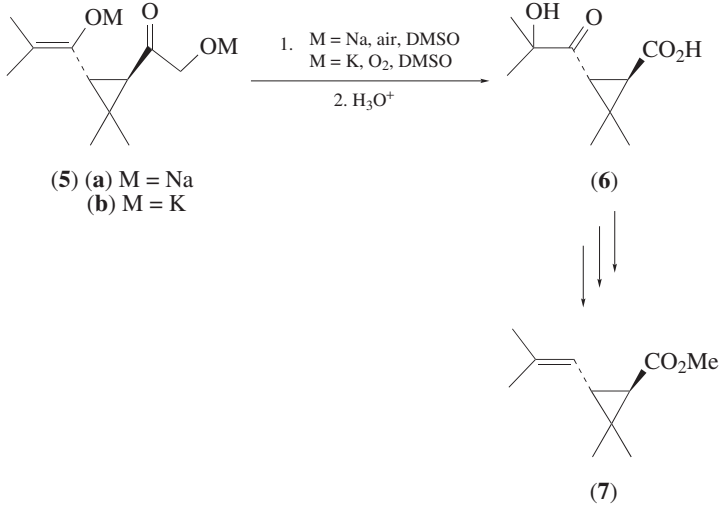

(3)

Although enolates can be directly oxidized to α-hydroxo derivatives by shaking solutions of the enolate under an O_2 atmosphere[14], the absence of an added reducing agent makes the dioxygen oxidation inapplicable to systems containing an enolizable methyl or methylene group because of the formation of complex product mixtures. Enolates of ketones, esters and lactones having α-methylene or α-methyne groups, **8**, can be oxidized to α-hydroxocarbonyl compounds by the molybdenum(VI) peroxo complex $MoO(O_2)_2$•py•HMPA (MoOPH, equation 4)[15]. Thus, the treatment of the carbonyl compound with a 5–10% excess of lda followed by addition of crystalline MoOPH at low temperature and washing with sodium sulphite affords the α-hydroxy-substituted products. The intermediate formation of **9** is based on the known tendency of 'MoO_5' chelates such as MoOPH to transfer one of the peroxidic oxygens rather than the oxo ones[16]. 3-Phenylpropionates of chiral alcohols derived from (+)-camphor behave similarly and are oxidized by MoOPH with high diastereoselectivity[17].

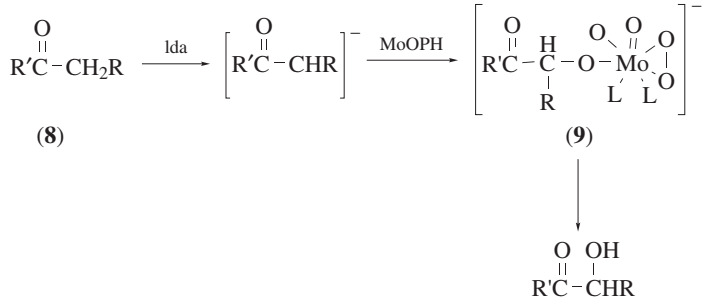

(**8**) (**9**) (4)

Dibenzyl peroxydicarbonate has been used for the oxidation of both chiral and achiral lithium or potassium enolates to form carbonates of α-hydroxy carbonyl compounds. Dibenzyl peroxydicarbonate, prepared from aqueous hydrogen peroxide and benzyl chloroformate under basic conditions[18], was preferred for mechanistic studies to the commonly used MoOPH in view of the easier preparation of ^{18}O-labelled compounds[19].

Another route to the preparation of α-hydroxy derivatives consists of the transformation of enolates into silyl enolates and their subsequent oxidation. Oxidation of trialkylsilyl enolates with peroxyacids, most frequently cpba, has been applied for preparation of α-hydroxy- and α-acetoxy aldehydes or ketones. Reactions require mild conditions and generally give good yields of the expected compound[20]. Mechanistic investigations suggest the intermediate formation of epoxides which evolve to the final products via 1,4-silyl group migration.

Evolution of the method has allowed the insertion of two oxygen atoms in a single step (e.g. preparation of α-α'-dihydroxy ketones)[21]. Depending on the structural features of the silyl enolate, treatment of a mixture of enolate and solid $KHCO_3$ with cpba, followed by acidification, affords the α-α'-dihydroxy ketone in good yields. When bulky tripropylsilyl groups are present (equation 5a), the hydroxy siloxy ketone **10** is the major product. The conversion of **11** to **12** shown in equation 5b is highly chemoselective.

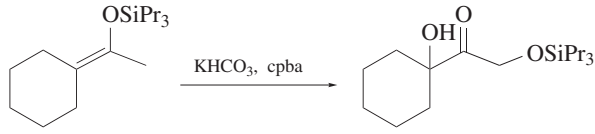

(**10**) (5a)

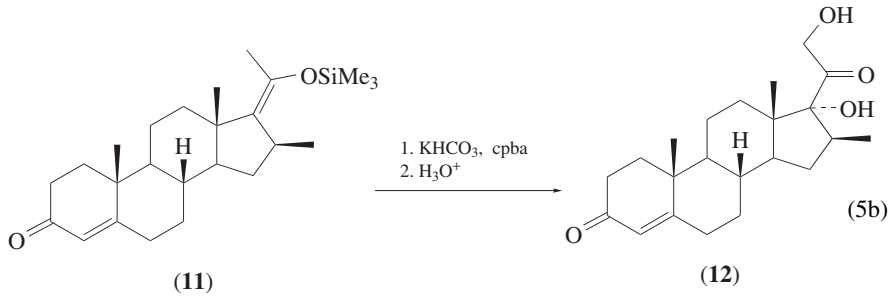

(**11**) (**12**) (5b)

Another interesting example taken from the synthesis of natural products is reported in equation 6. Epoxidation of **13** with cpba affords a mixture of **14a** and **14b**, which can be directly desilylated with tetrabutylammonium fluoride to give *d*,*l*-isospongiadiol (**15**)[22].

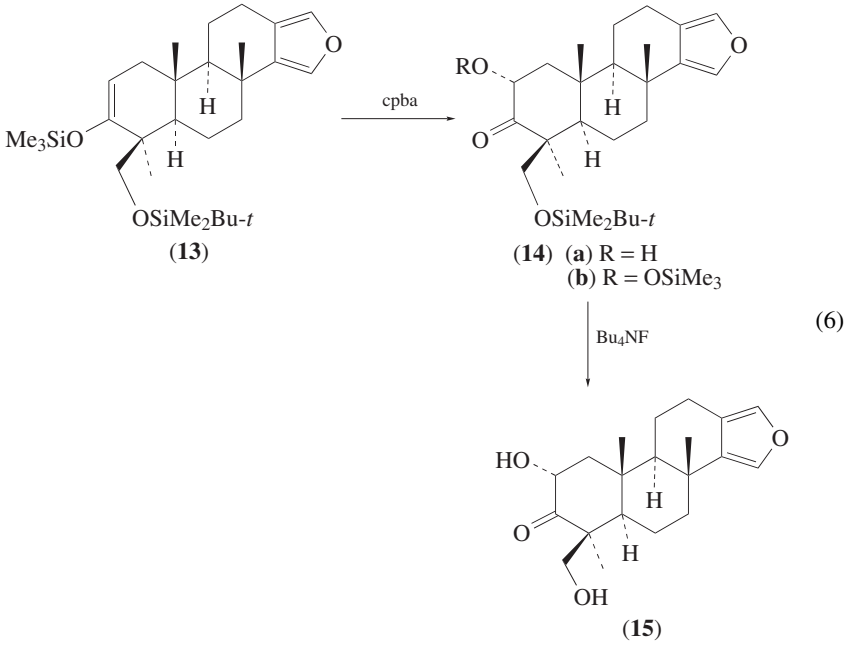

(**13**) (**14**) (**a**) R = H (**b**) R = $OSiMe_3$ (6)

(**15**)

Hydrogen peroxide in the presence of catalytic amounts of methyltrioxorhenium(VII), $ReMeO_3$, is a convenient and efficient method for the α-hydroxylation of ketones[23]. Particularly interesting is the H_2O_2/cetylpyridinium peroxotungstophosphate system which, under phase transfer conditions, provides a facile method for preparing aldehydes with one carbon atom less than the parent precursors[24]. The ratio of the products changes with the experimental conditions.

Other oxidizing agents capable of converting silyl enolates into α-hydroxy carbonyl derivatives are OsO_4/4-hydroxymorpholine[25] or the HOF•MeCN complex prepared by bubbling nitrogen-diluted fluorine into aqueous acetonitrile[26], which has the advantage of short reaction times and high yields, at least on the substrate reported in the study.

An hydroxy group may be introduced into the α'-position of α,β-unsaturated diketones using triphenylphosphite ozonide[27], a well known chemical source of singlet oxygen[28a]. Singlet oxygen in the presence of tetraphenylporphirine as sensitizer has been used to convert the trimethylsilyl enolates of pinacolone or of isopropyl phenyl ketone to the corresponding α-hydroxy ketones (via the intermediacy of an α-trimethylsilyl peroxy ketone)[28b].

Optically active α-hydroxy-keto functional units are widespread in natural products and have been frequently used for convenient building blocks in organic synthesis[29]. Adam and coworkers reported that optically active α-hydroxy ketones can be obtained by oxidation of the corresponding silyl enolates with various oxidizing agents in the presence of manganese(III) adducts of optically active Shiff bases[30], or with *in situ* generated dioxirane from a fructose-derived ketone (equation 7)[31].

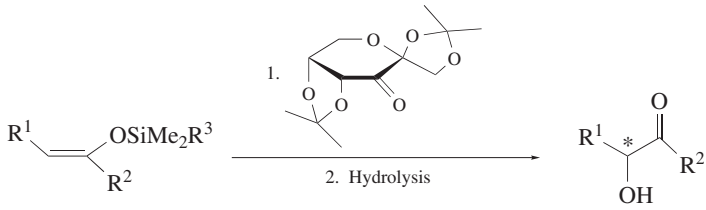

(7)

The great diversity of metal enolates makes their oxidation one of the most versatile methods for the preparation of species containing the α-hydroxy carbonyl functionality, and some attention should be paid to examine how the nature of the oxidizing agent affects the diastereoselectivity of the reaction. In 1984, Davis and coworkers[32] introduced racemic *trans*-(±)-2-(phenylsulphonyl)-3-phenyloxaziridines (**16**), for the asymmetric hydroxylation of enolates. The availability of *N*-sulphonyloxaziridines, e.g. **17** and **18**, as pure enatiomers makes control of the stereoselectivity by the reagent possible[33]. Oxidation is fast even at low temperature: however, lithium enolates give lower yields than the sodium and potassium analogues, probably due to the counteranion dependency of the ionic hemiaminal intermediate **19**, which is thought to be involved in the oxidation (equation 8)[32,34]. The synthesis and application of oxaziridines in organic synthesis has been exhaustively reviewed[33].

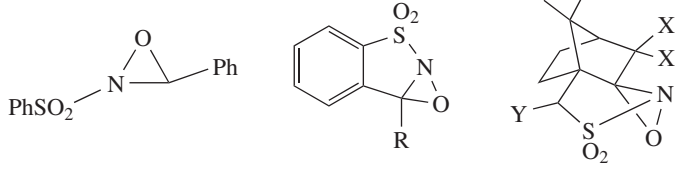

(**16**) (**17**) (**18**)

Oxaziridines are unique among nitrogen-containing compounds in having a configurationally stable nitrogen atom at ordinary temperature[33], making possible asymmetric oxidations. Moreover, the nitrogen and carbon stereocentres are adjacent to the active-site oxygen atom, thus the asymmetric induction is postulated to be high. As a matter of fact, the enantioselective oxidation of prochiral enolates with (camphorylsulphonyl)oxaziridine (**18**, Y = H) produces the corresponding α-hydroxy carbonyl derivative in good yields and high enantiomeric excess[33]. For example, hydroxylation of the sodium enolate of deoxybenzoin **20a** with (+)-**18** (X = Y = H) at −78 °C affords (+)-(*S*)-benzoin **21** in 84%

yield and >95% enantiomeric excess (equation 9)[35]. Similarly, (*S*)-2-hydroxy-1-phenyl-1-propanone (**22**) is produced in 95% enantiomeric excess by oxidation of the sodium enolate of propiophenone **20b**, using (+)-**18** (X = Cl, Y = H)[36] as oxidizing agent.

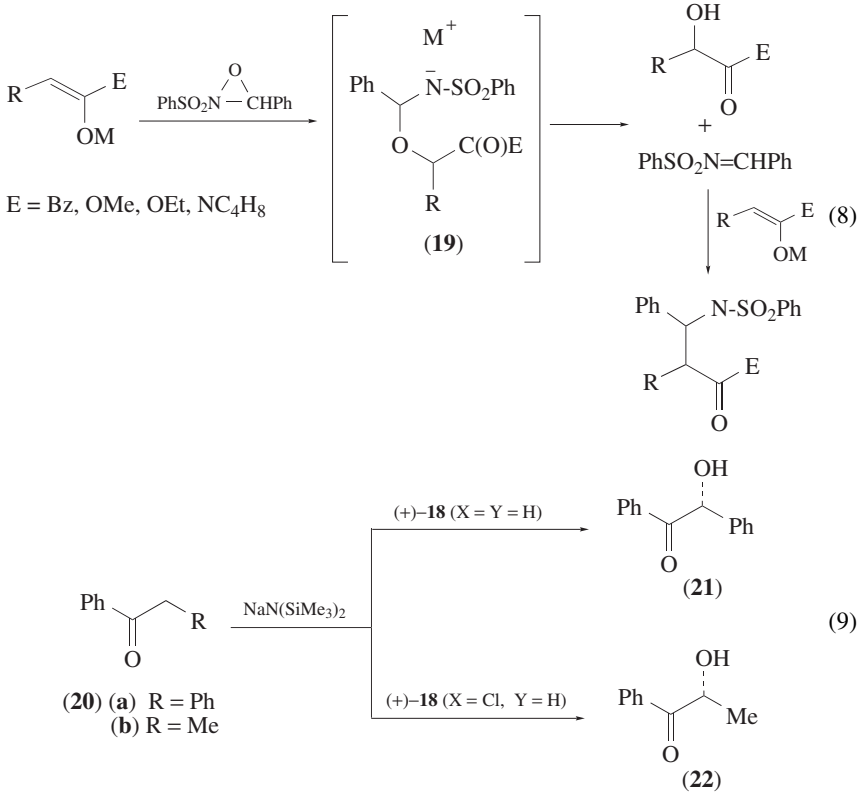

Oxidation of the lithium enolate of 1-tetralone **23** to (−)-2-hydroxy-1-tetralone **24**, the AB ring synthon of the antitumour antibiotic rhodomycinones, with (+)-**18** (X = OMe, Y = H, equation 10) resulted in much better enantiomeric excess values (ee >94%) than hydroxylation with other oxaridines[37].

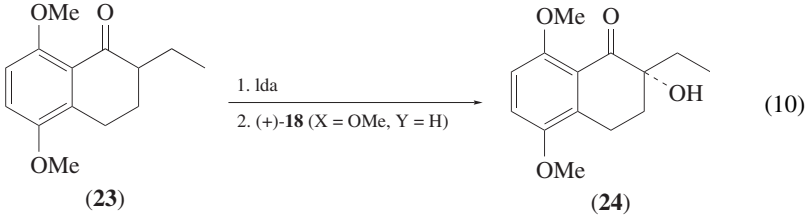

2. Oxidative coupling

The oxidative coupling of enolates, reported for the first time in 1935[38], represents an interesting application of enolates in organic synthesis. Examples of these reactions,

which can proceed through intra- and intermolecular paths, are shown in equations 11a–c. Most commonly, lithium enolates were treated with oxidants such as iron(III), copper(II), cerium(IV) salts or halogens. Examples of both types of coupling reactions are discussed in this section.

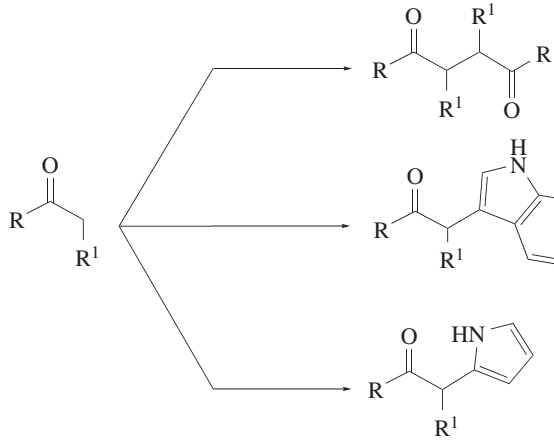

(11a)

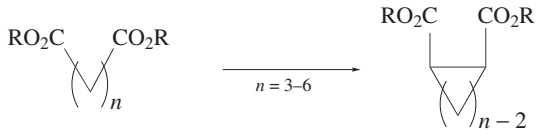

(11b)

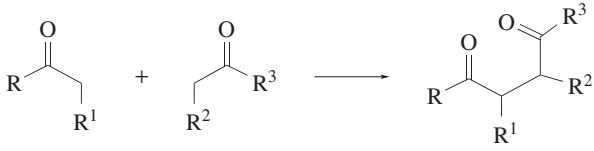

(11c)

a. Intramolecular oxidative cyclization. The intramolecular oxidative coupling of bis-enolates is an attractive alternative to the well known Dieckman cyclization[39] or to the acyloin condensation[40] and has been successfully applied for the preparation of three-, four-, five- and six-membered rings[41]. Copper(I), copper(II), nickel(II), silver and iron(II) salts have been used as oxidizing agents. For example, 2,2-dialkyl-1,3-cyclopentanedione and functionalized *spiro*[4.*n*] ring systems can be obtained by oxidative coupling of dilithium enolates of 3,3-dialkyl-2,4-pentanedione with copper(II) triflate[42].

The oxidative cyclization by copper(II) chloride of the ketone diolate derived from 1,8 diacetylbiphenylene (equation 12) represents a key step in the preparation of cycloocta [*def*]biphenylene-1,4-dione (**25**)[43].

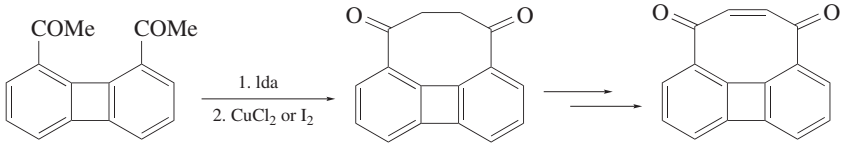

(12)

(**25**)

The experience acquired on the manganese(III)-based free radical cyclizations[44] suggested to Snider and coworkers that these salts could not be used for the cyclization of ε,ζ-unsaturated enolates due to further oxidation of the desired product. On changing the oxidant from $Mn(OAc)_3 \bullet 2H_2O$ to $(NH_4)_2[Ce(NO_3)_6]$ or to $Cu(OTf)_2$, δ,ε- and ε,ζ-unsaturated silyl enolates could be obtained in good yields (equation 13). It is interesting to note that the oxidation of lithium enolates affords the dimeric 1,4-diketone because intramolecular coupling of the enol radical with the alkene cannot compete with intermolecular coupling of the very reactive enolate[45].

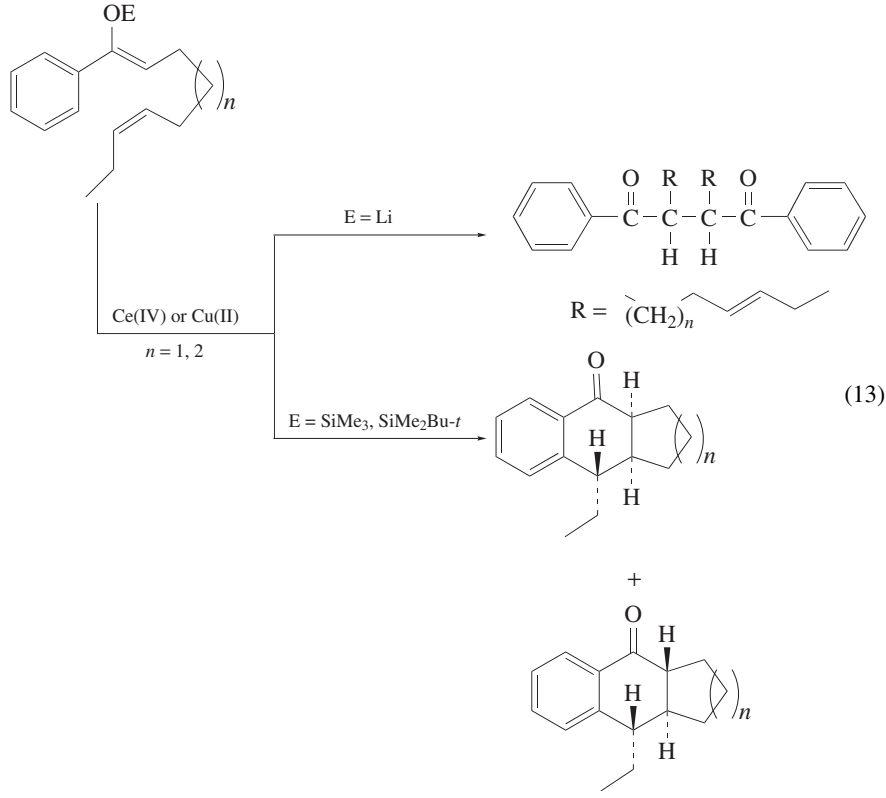

(13)

Kende[46–49] and Whiting[50] reported radical cyclizations of equilibrium-generated enolates onto phenolates induced by $K_3[Fe(CN)_6]$; however, these cyclizations were limited to the most acidic carbonyl precursors such as 1,3-diketones (equation 14a) or nitroalkyl compounds (equations 14b and 14c).

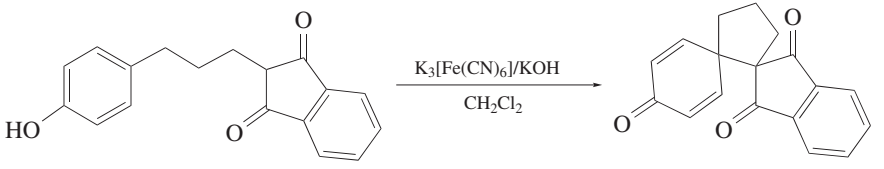

(14a)

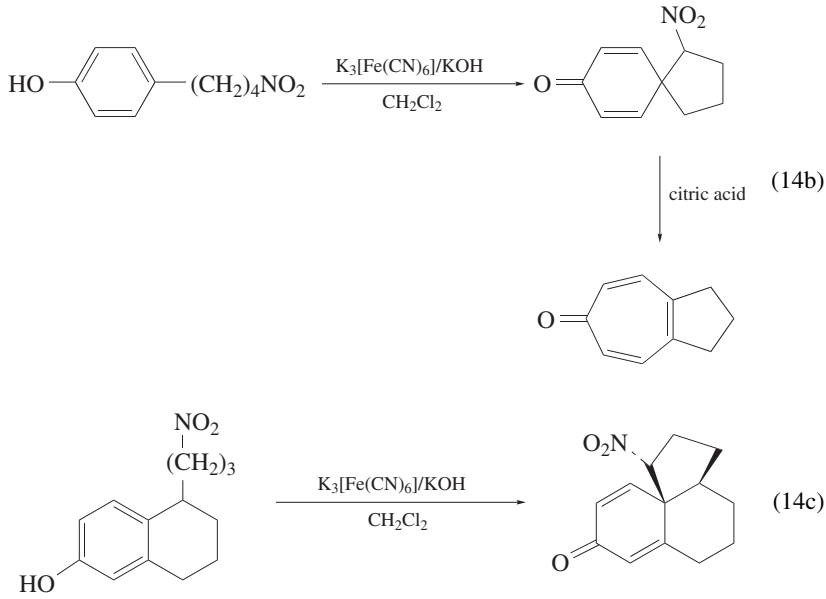

In a series of papers on the total syntheses of alkaloids, Baran and coworkers have recently reported that enolates of carbonyl compounds undergo oxidative coupling with indoles and pyrroles in the presence of oxidants such as copper(II) and iron(III) salts[51–53]. A detailed study of the oxidative cyclization reported in equation 15 has shown that **26** is converted into **27** with the highest yields when $Fe(acac)_3$ is the oxidant, presumably due to its high redox potential (+1.1 V vs. the ferrocenium/ferrocene couple in THF solution[54]), which is the most positive among all the oxidizing agents tested for the transformation.

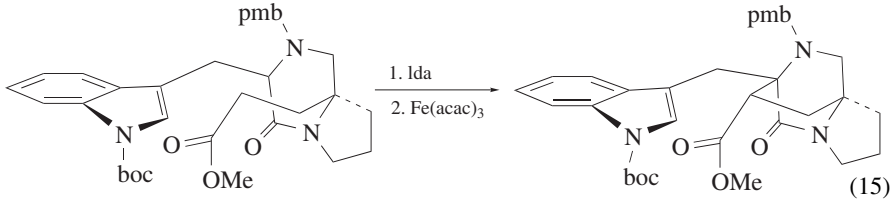

(**26**) (**27**)

pmb = *p*-methoxybenzyl
boc = *t*-butoxycarbonyl

Paquette has reported[55] an intramolecular oxidative coupling using ferric chloride to prepare the intermediate **30** for the synthesis of cerorubenic acid-III. Addition of the dienolate of **28** to $FeCl_3$ in dmf at −78 °C produced the cyclopropane intermediate **29** in 54% yield (equation 16). Although the mechanism of this oxidative cyclization is not discussed in the paper, it is likely that a one-electron transfer pathway is involved. Copper(II) salts have also been utilized for intramolecular enolate coupling, but they proved to be somewhat less effective in the present context.

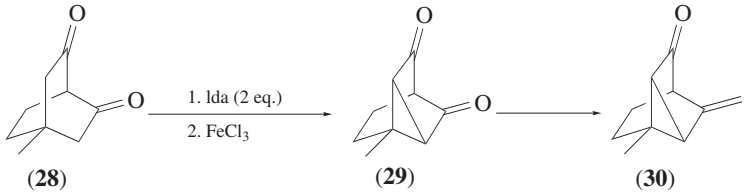

(**28**) (**29**) (**30**) (16)

An elegant synthesis of (±)-hirsutene (**32**) was developed by Cohen and coworkers[56]. The key step of the synthesis is the one pot, completely stereoselective, oxidative cyclopentannulation of dienolate **31** with two equivalents of $FeCl_3$ in dmf (equation 17). $CuCl_2$ was also tested, but proved inferior. The formation of a single diastereoisomer of the triquinane intermediate (**31′**) is useful and suggests that stereochemical equilibration may occur at some stage. This annulation procedure can also be extended to cyclohexanone enolates.

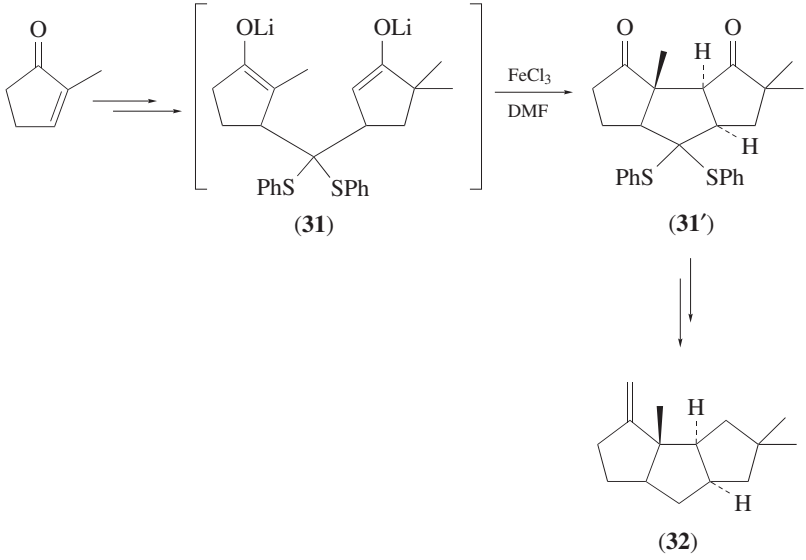

(**31**) (**31′**) (17)

(**32**)

b. Intermolecular couplings. Intermolecular oxidative coupling of enolato anions has been studied extensively especially as far as their oxidation to 1,4-dicarbonyl compounds is concerned[57], which are important precursors for the synthesis of cyclopentanones, furan, thiophene and pyrrole ring systems. Several oxidizing agents such as halogens (bromine[57,58] and iodine[57,58]), lead(IV) acetate[59], copper(II)-, iron(III)- and silver salts[60], $(NR_4)_2[Ce(NO_3)_6]$, R = H[61], Bu[62] and early transition metal derivatives such as $TiCl_4$[63,64], vanadium(V) alkoxide $VO(OR)Cl_2$[65] and $Mn(OAc)_3{\bullet}2H_2O$ were used[66]. Titanium enolates derived from organometallic or coordination compounds of titanium(IV) such as $Ti(OR)_4$, $TiCp_2Cl_2$, will be discussed in Section III.C. Although an oxidizing agent of general use is yet to be found, some of the mentioned ones allow preparation of the desired compound with high stereoselectivity and high yields.

In 1995, Helmchen and coworkers[58i] reported that no stereoselectivity was observed when the achiral deprotonated substrates shown in equation 18 were oxidized by copper(II) pentanoate or diiodine to the carbonyl derivatives, the *rac*/*meso* ratio of **33a** being 57/43 and of **33b** 48/52. However, when chiral amides were subjected to the same reaction conditions, the (*S*,*S*) isomer **33c** was formed with a diastereoselectivity higher than 99%.

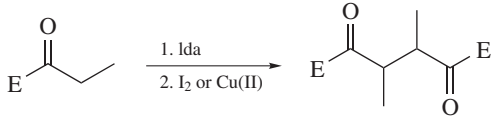

(**33**) (**a**) E = *t*-BuO

(**b**) E = 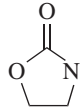

(**c**) E = 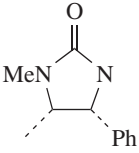

(18)

Analogously, after enolization with lhmds, hypervalent iodine compounds such as $PhI(OAc)_2$ have been used for the stereoselective synthesis of 2,3-disubstituted succinates by using the chiral oxazolidinone auxiliary (4*S*)-4-(phenylmethyl)-2-oxazolidinone (equation 19)[58e].

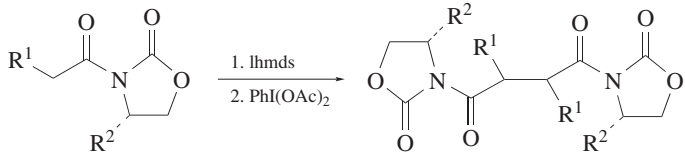

(19)

A wide series of oxidants, spanning from $TiCl_4$ to iodine, has been used in the oxidative homocoupling of chiral 3-arylpropionic acid derivatives aimed at the preparation of lignans[58f]. The *R*,*R*-selectivity in the reactivity of **34** has been explained by a radical coupling mechanism (equation 20). The initially formed lithium (*Z*)-enolate may transform into the titanium enolate **35**, which undergoes oxidation to the radical intermediate **36** via a single electron transfer process. The *syn*-*Z*-type radicals **36** couple each other at the less hindered β-side (*si* face) to give the *R*,*R*-isomers **37** stereoselectively.

The same research group has recently reported[58g] that the oxidative homocoupling of chiral aroylacetic acid derivatives proceeds stereoselectively when the sodium enolate derived from **38** is oxidized with bromine (equation 21). Good stereoselectivity was also observed in the oxidative homo- and heterocoupling reactions of the lithium enolates of chiral 3-phenylpropionamides with iodine, copper(II) pentanoate and ferrocenium hexafluorophosphate[58h].

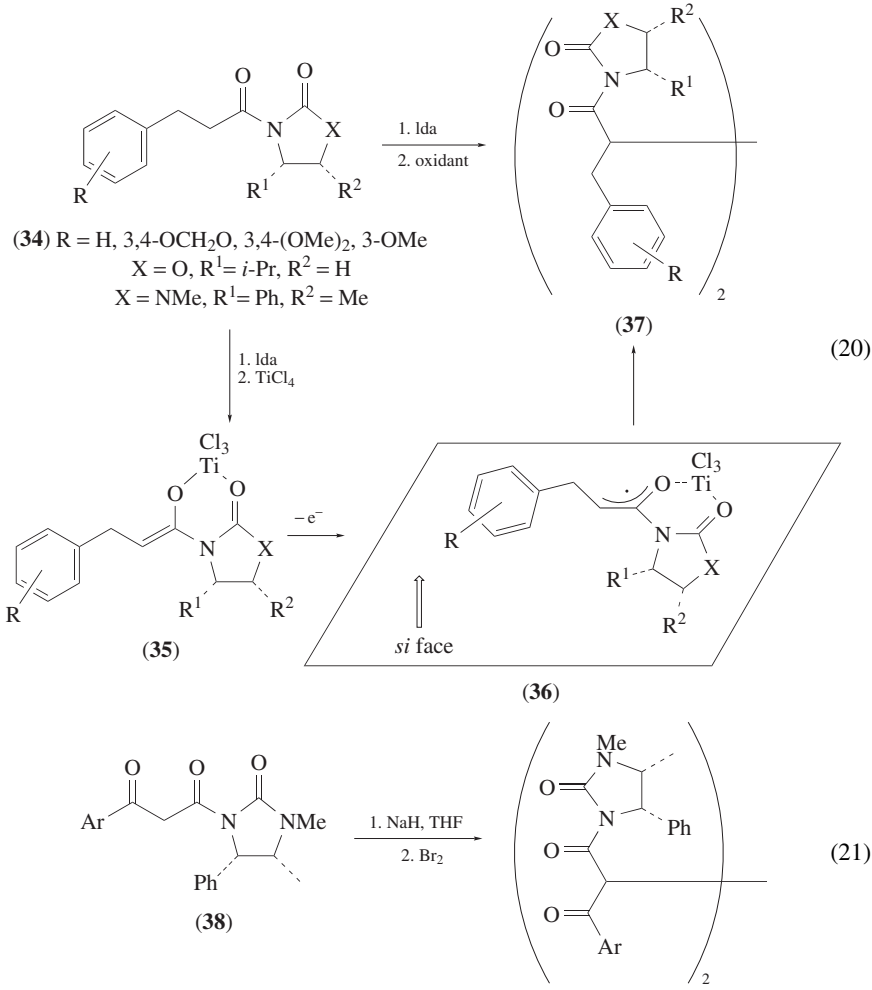

(20)

(21)

Symmetrical (equation 22a) and unsymmetrical 1,4-diketones (equations 22b and 22c) are obtained in good yield with the vanadium(V) alkoxo derivatives $VO(OR)Cl_2$ (R = Et, *i*-Pr)[65]. The same reagent induces cross coupling between allyl silanes and silyl enolates to γ,δ-unsaturated ketones. Noteworthy is the fact that only traces of the homocoupled 1,4-diketones and 1,5-hexadienes are produced.

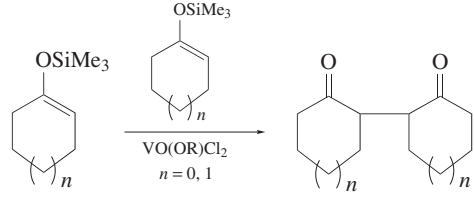

(22a)

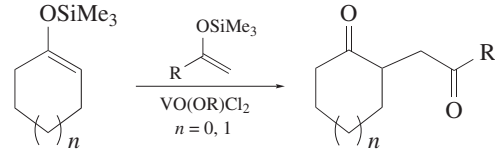

(22b)

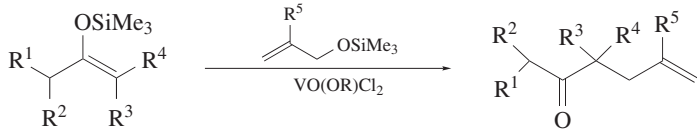

(22c)

Titanium tetrachloride in dichloromethane behaves similarly and succinates can be obtained starting from lithium or silyl enolates[63a]. For example, as shown in equation 23, the ketene silyl acetals **40**, obtained from the lithium enolate **39**, undergo smooth oxidative dimerization in the presence of $TiCl_4$ to give the succinates **41** in high yields, regardless of the substitution pattern at the α-position of the starting esters[63b]. It is interesting to observe that Lewis acids such as BF_3•OEt_2 or $SnCl_4$ do not promote these reactions to any extent and $ZrCl_4$ acts as Lewis acid to promote Claisen condensation, strongly suggesting that the reaction described by equation 23 proceeds via an electron transfer process.

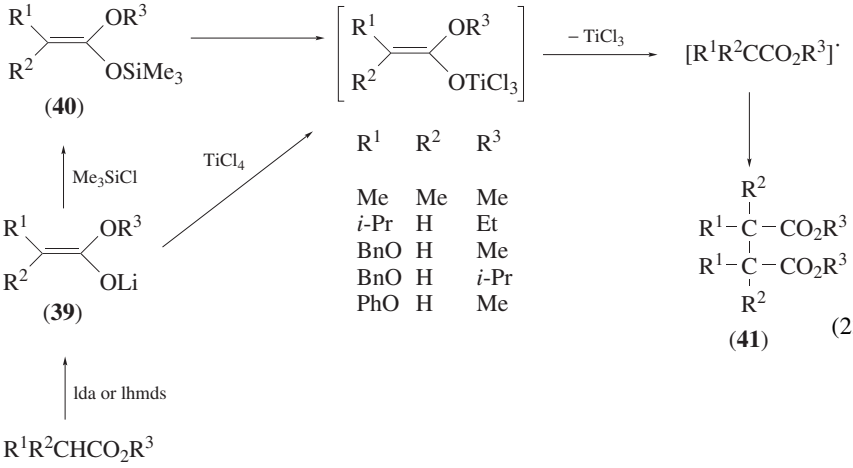

(23)

Silver enolates are proposed as reactive intermediates in the reaction of silyl enolates with Ag_2O in dmso. An important feature of the reaction is the regiospecific formation of 1,4-diketones[60j]. Sessler and coworkers reported[60e] that the key step in the preparation of β-substituted tetra- and hexaalkylterpyrrols is the copper(II) triflate-mediated oxidative coupling of the lda-derived enolates of α-keto pyrrols. The coupling reaction shown in equation 24 produces a mixture of distereoisomers which does not require separation and can be directly converted to the corresponding terpyrroles.

Oxidative coupling of silyl bis-enolates to 1,4-diketones (equation 25) occurs with a variety of oxidizing agents such as $[Fe(phen)_3](PF_6)_3$, $(NH_4)_2[Ce(NO_3)_6]$ and $Cu(OTf)_2$[67]. The high *d*,*l*-diastereoselectivity of the coupling is attributed to the energy difference in the transition states of the two diastereomorphic approaches. The steric interactions between

the phenyl and the methyl groups are smaller for the *lk*-conformation (equation 26a) than for the *ul*-one (equation 26b), thus the preferred formation of the *rac*- over the *meso*-diastereomer is evident. The steric influence of the substituents at the silicon atom on the diastereoselectivity can be additionally observed by considering that the reaction of the tris enolate $[Me_2C{=}C(Ph)O]_3SiMe$ with $(NH_4)_2[Ce(NO_3)_6]$ affords the *rac*-isomer of the 1,4-diketone in 64% yield and 97% stereoselectivity[68].

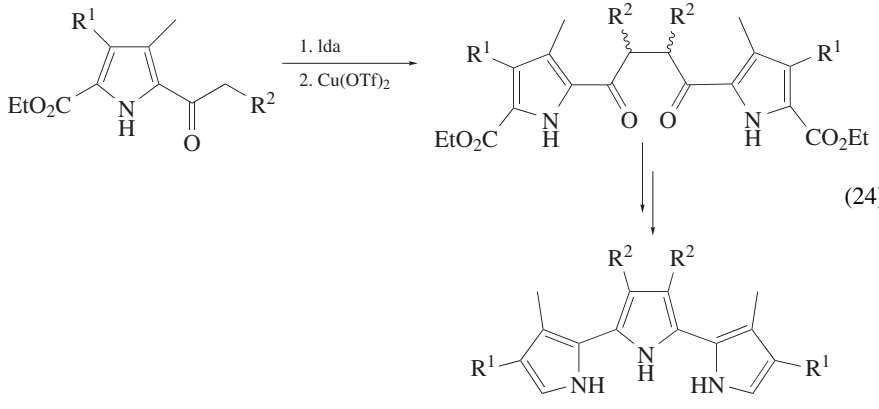

(24)

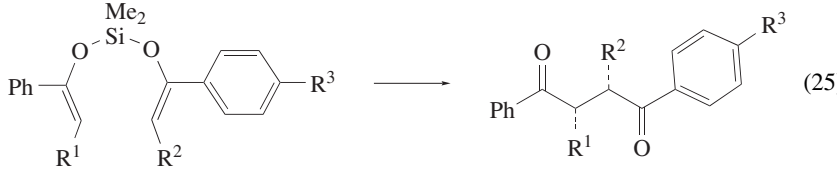

(25)

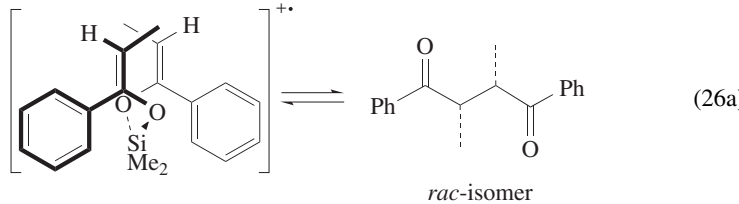

(26a)

rac-isomer

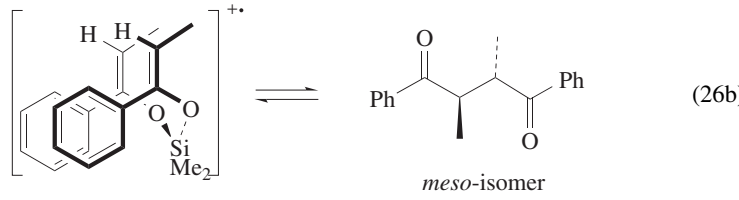

(26b)

meso-isomer

Unsymmetrical 1,4-diketones have been prepared in good yields by $(NH_4)_2[Ce(NO_3)_6]$ oxidative cross coupling between 1,2-disubstituted and 1-substituted trimethylsilyl enolates[61a]. The same cerium(IV) compound has been also applied to the preparation of 6-oxo-α,β-unsaturated carbonyl compounds: trimethylsilyl dienolates are easily oxidized

to α-carbonylallyl radicals which add to enolic C−C double bonds with high γ-regioselectivity (equation 27)[61b].

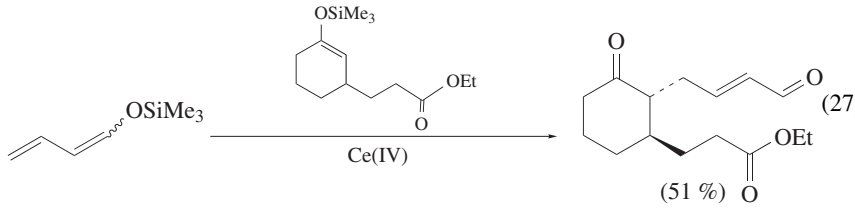

(27)

Ruzziconi and coworkers used the ceric ammonium nitrate promoted C−C forming reaction to prepare polycyclic homo- and heteroaromatics starting from aryl-substituted silyl enolates[61c,d] and, more recently, the same strategy has been applied to the preparation of fluorinated naphthaldehydes and naphthyl ketones[61e].

B. Silyl Enolates: A Class of 'Masked Enolates'

Silyl enolates are a class of electron-rich, non aromatic compounds which can be described as 'masked enols or enolates' since hydrolysis following their reaction yields ketones[69]; they can be purified by distillation or chromatography, and then converted back to the enolate anion. The electron-rich character of these species can be used for oxidation reactions and examples have been described in the preceding sections. In this section, additional examples of chemical, PET and electrochemical redox reactions involving silyl enolates will be discussed, for a better appreciation of these interesting species in organic synthesis.

1. Chemical oxidation methods

Chemical oxidation of silyl enolates has been performed with a variety of inorganic and organic oxidants such as ozone, copper(II) salts, $Pb(OAc)_4$, Ag_2O, hypervalent iodine compounds such as iodosobenzene in methanol, $(NH_4)_2[Ce(NO_3)_6]$, xenon difluoride, tetranitromethane, halogens, nitronium-, diazonium- and triphenylmethyl salts, chloranil and ddq.

Ozonolysis results in cleavage of the double bond as in the case of **42** (equation 28)[70]. Other examples are the syntheses of the ambrosia bettle pheromone lineatin (**43**, equation 29)[71] and vernolepin (**44**, equation 30)[72].

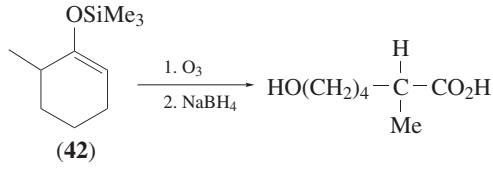

(**42**)

(28)

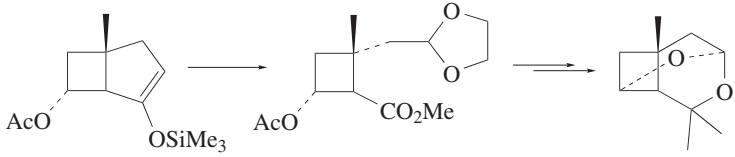

(**43**)

(29)

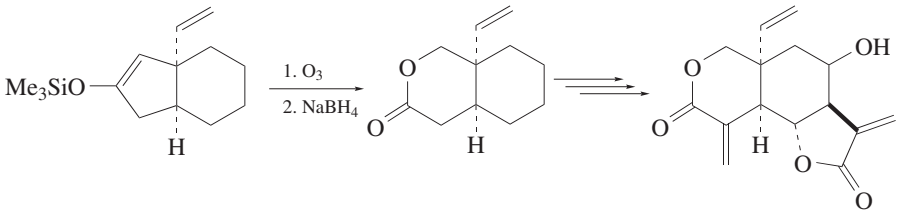

(**44**) (30)

Another reagent suitable for this transformation is *t*-butyl peroxide in the presence of catalytic amounts of $MoO_2(acac)_2$ (equation 31)[73] or titanium silicalite-1[74]. Considering that regiospecific generation of silyl enolates can be achieved under kinetic or thermodynamic control, the reaction paths shown in equation 31 constitute an interesting method for regiospecific α-cleavage of ketonic precursors.

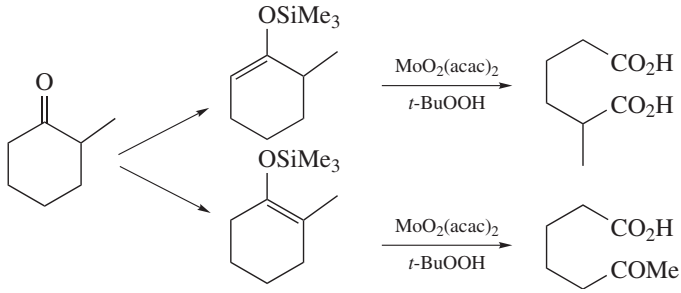

(31)

Sensitized photooxidation of silyl enolates with singlet oxygen followed by reduction of the hydroperoxides with PPh_3 in methanol has been used for the preparation of chiral and achiral ketones such as (*R*)-6-methyl-2-cyclohexen-1-one starting from (*R*)-2-methylcyclohexanone[75].

As it will be pointed out in more detail in Section III.D, the keto–enol tautomerization effectively converts a relatively electron-poor carbonyl acceptor into the correspondingly electron-rich olefinic donor[5a]. Such an *umpolung*[76] allows the conventional nucleophilic additions at the carbonyl centre (e.g. Grignard reaction) to be readily replaced by electrophilic substitution at the α-carbon of ketones, aldehydes and esters[77]. α-Methoxylation of aliphatic, aromatic and hetorocyclic ketones was achieved via oxidation of the corresponding silyl enolates with iodosobenzene–$BF_3(OEt_2)$[78]. For example, cyclohexanone silyl enolate and the sterically hindered species *t*-butyl methyl ketone (pinacolone) silyl enolate were converted into the corresponding α-methoxy ketones in almost quantitative yields. The reactions are considered to take place through the addition of PhI–O–BF_2 [generated from $(PhIO)_n$ and $BF_3(OEt_2)$][78] to the silyl enolate with formation $RC(=O)CH_2-I(Ph)(OBF_2)$, which is the synthetic equivalent of the carbocation $[RC(=O)CH_2]^+$.

Silyl enolates are useful starting materials for the smooth α-halogenation of ketones, which can be carried out by oxidation with *N*-halosuccinimides[79], halogens[80] and iodobenzenedifluoride or xenon difluorides[81]. As shown in equation 32[81d], the reaction of **45** with XeF_2 gives a 1:1 mixture of α-fluoroketone diastereoisomers **46a** and **46b**.

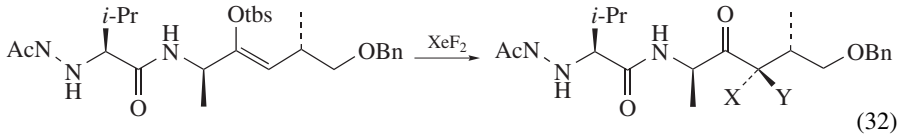

(**45**) (**46**) (**a**) X = H, Y = F (**b**) X = F, Y = H (32)

Various α-nitro ketones, widely used as synthetic intermediates, have been prepared by reaction of silyl enolates with tetranitromethane in the dark at room or low temperature or under photochemical conditions[82]. The highly coloured solutions are due to intermolecular 1:1 electron donor–acceptor complexes formed between the enolate and tetranitromethane. The formation of similar vividly coloured complexes with electron acceptors such as chloranil, tetracyanobenzene and tetracyanoquinonedimethane readily establishes silyl enolates as electron donors[83]. The formation of radical cations as reactive intermediates has been confirmed.

Another α-nitrating agent of silyl enolates is nitronium tetrafluoborate, NO_2BF_4, which reacts with cyclic ketones such as cyclohexanone or cycloheptanone affording α-nitro ketones in *ca* 40% yield. On the other hand, the bicyclic silyl enolates reported in equation 33 are formed in high yields (R = H, 90%; R = CO_2Me, 86%)[84].

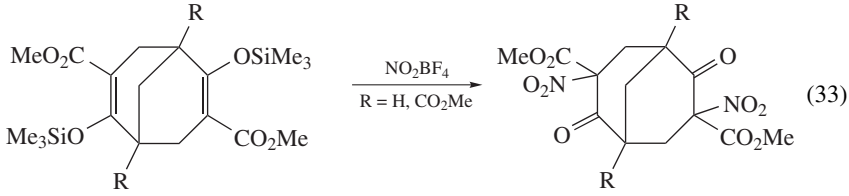

(33)

α-Arylation of silyl enolates with aryldiazonium tetrafluoborate, $[PhN{=}N]BF_4$, proceeds smoothly in pyridine with dinitrogen evolution[85]. Substituents on silyl enolates exhibited quite a large influence on the yield of α-aryl ketones. By taking into consideration that the reaction of metal enolates with aryl halides, a well established method for the formation of C–C bonds, cannot be applied to the insertion of an aryl group (aryl halides are generally resistant to nucleophilic substitution), the importance of this class of enolates in organic synthesis is enhanced.

Hydroboration–oxidation of cyclic silyl enolates provides a simple way to *trans*-1,2-diols; the intermediate monosylilated, α'-hydroxysilylenolate may be isolated under appropriate working conditions (equation 34)[86].

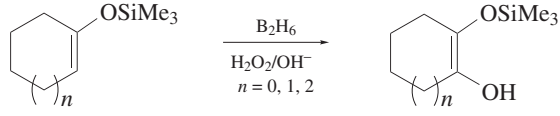

(34)

Trialkylsilyl enolates can be oxidized to the corresponding α,β-unsaturated ketones with trityl tetrafluoborate or trityl methyl ether in the presence of BF_3OEt_2[87]. It has been observed that the use of trityl cations often leaves substantial amounts of saturated ketones. The amount of these species can be reduced by the use of ddq as in the case of

the preparation of cholest-1-en-3-one (**48**) from the $\Delta^{2,3}$-silyl enolate of cholestan-3-one (**47**, equation 35)[88].

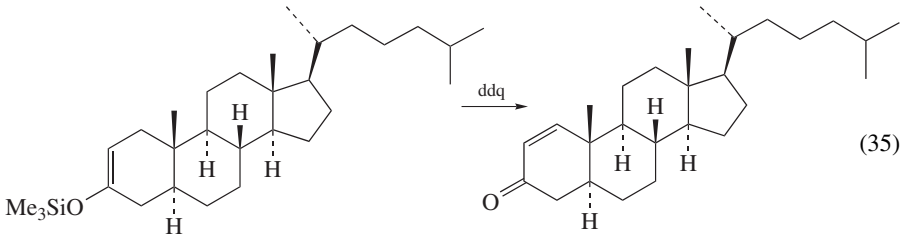

(35)

(**47**) (**48**)

The reaction of the silyl enolate of cyclohexanone with ddq, initially believed to involve allylic hydride abstraction, was later established to involve two substrate–quinone adducts: the thermally stable **49** and the thermally unstable **50** (equation 36)[89].

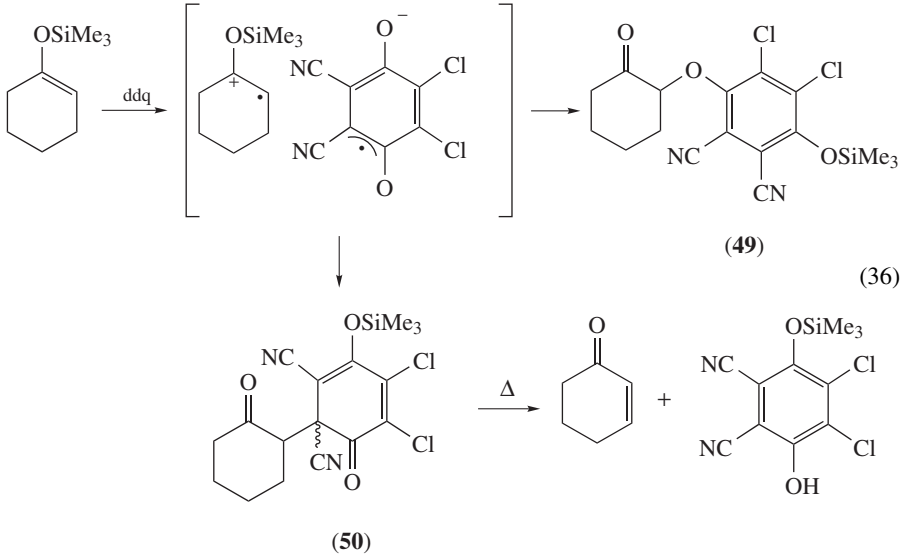

(**49**)

(36)

(**50**)

2. Photoinduced electron transfer reactions

Because of the high selectivity often observed and the mild reaction conditions required, PET provides a powerful tool for carrying out single electron transfer reactions[90]. By photochemical oxidation excitation of either the electron donor or the acceptor, the redox properties of the respective species change. For example, 9,10-dicyanoanthracene in its singlet state (dca*) is a powerful oxidant ($E_{1/2}^{red} = +1.28$ V vs. $Ag/AgNO_3$ with an electronic excitation energy of the singlet state E_{S1} of 2.89 eV in acetonitrile)[91,92];

1,4-dicyanonaphthalene behaves similarly ($E_{1/2}^{red} = +1.67$ V vs. $Ag/AgNO_3$; E_{S1} of 3.74 eV in acetonitrile)[93]. Mattay and coworkers reported about the PET-oxidative cyclization of various alkyl- and aryl-substituted 1-triethylsilyloxy-1,6-heptadienes[92] and monocyclic silyl enolates tethered to an olefinic (equations 37a and 37b) or to a silylacetylenic side chain (equation 37c)[94] to the corresponding ketones with catalytic amounts of sensitizer like dca. The PET cyclization strategy has been also applied to the synthesis of novel steroid backbones[95].

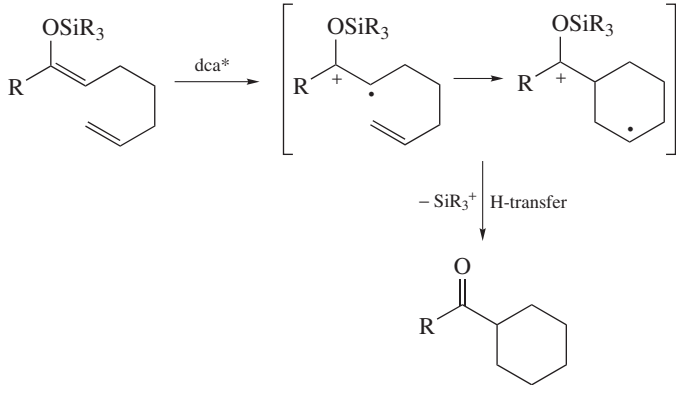

(37a)

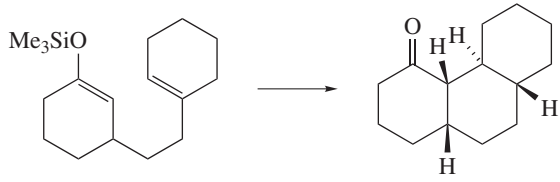

(37b)

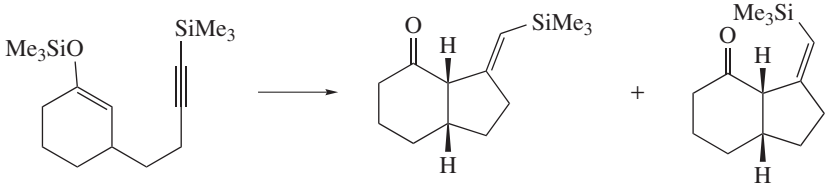

(37c)

Detailed studies of the mechanism of these reactions have been performed by Mattay[96] and by Kochi[97]. The former has shown that the *endo*/*exo* regiochemistry of the ring closure reaction can be controlled either by variation of the silyl group or by addition of polar molecules such as alcohols (probably the source of hydrogen in equations 37a–c). Based on solvent and salt effects, Kochi has proposed[97b,c] that the oxidation of enols to ketones in the presence of activated chloranil proceeds via photoactivation of chloranil which reacts with the silyl enolate through two competing pathways, namely oxidative elimination to the ketone and oxidative addition to the adduct **51** (equation 38). Non-polar solvents such as dichloromethane favour the oxidative eliminations, while polar solvents such as acetonitrile direct the reaction towards the oxidative addition. More strikingly,

the presence of an inert electrolyte such as $[Bu_4N]PF_6$ in CH_2Cl_2 diverts the predominant pathway towards the oxidative elimination with respect to oxidative addition.

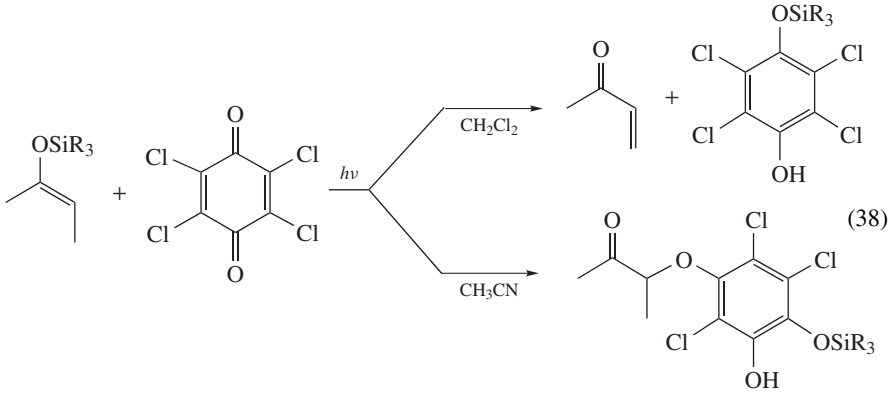

(38)

(**51**)

Noteworthy is the identification of the intermediate **52** in the oxidation of the trimethyl silyl enolate of cyclohexanone with photoactivated chloranil[97a]. Compound **53** has been isolated and characterized by X-ray diffraction methods[97b].

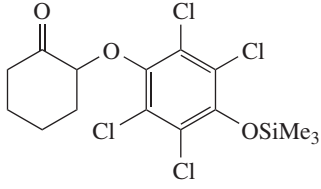

(**52**)

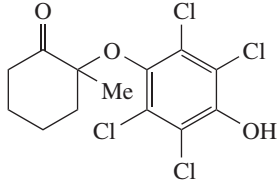

(**53**)

On the basis of the results of cyclization reactions on model compounds, accompanied by a number of DFT calculations, Mattay and coworkers have established that radical cations are reactive intermediates in the PET-mediated oxidative cyclization of the silyl enolates, although the contribution of a radical pathway could not be excluded[98].

3. Electrochemical syntheses

As far as the use of electrochemical oxidation of metal enolates in organic synthesis is concerned, more than 30 years ago the electrochemical oxidation of lithium ester enolates was used for the preparation of succinate esters[99]. An excellent review on the applications of anodic electrochemistry in organic synthesis has been published[100].

In a recent study[101], Wright and coworkers described the preparation of annulated furan systems through a two-step annulation reaction involving an electrochemically-induced ring closure between a furan and a silyl enolate. The reaction is quite general for the formation of six-membered rings in good yields and can be applied in the presence of different functional groups, such as acyclic or five-, six-, seven-membered

bicyclic- (equation 39) and acyclic trimethylsilyl enolates. It is interesting to observe that these reactions do not proceed to any extent when using chemical oxidants such as $(NH_4)_2[Ce(NO_3)_6]$, $VO(OCH_2CF_3)Cl_2$ and $Mn(OAc)_3 \cdot 2\ H_2O$, which react with electron-rich olefins. The only alternative to electrochemical oxidation is the use of the stable [tris(*p*-bromophenyl)aminium] hexachloroantimoniate[102]. Unfortunately, the amine byproducts are removed with difficulty from the primary products of the reaction. The best results for the conversion of enol ethers to annulated furans are attained with the use of direct anodic oxidation at a carbon anode in CH_3CN in the presence of $LiClO_4$ as supporting electrolyte, 2,6-dimethylpyridine as acid scavenger and 2-propanol as cation trap[103].

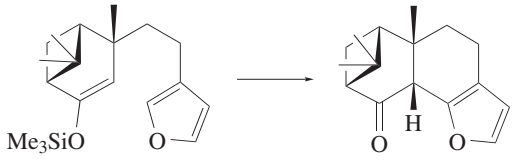

(39)

Anodic oxidation couples the pendant arm and the silyl enolate fragments of **54** to give the annulated product **55** (equation 40)[104], a key intermediate in the synthesis of hamigerans, an unusual halogenated marine natural product[105].

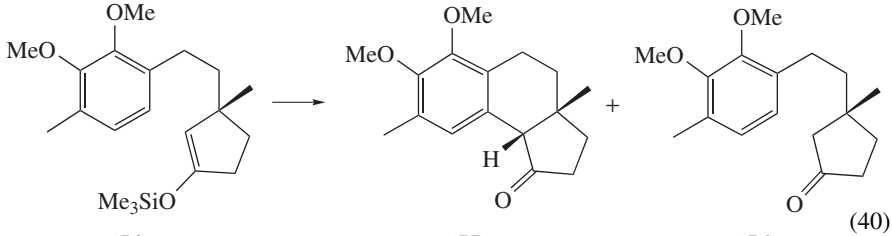

(**54**) (**55**) (**56**)

(40)

The surprising factor of the reaction, which shows how intriguing and constantly innovative synthetic chemistry can be, is the fact that the annulation reaction reported in equation 40 occurs in satisfactory yields in the absence of an alcohol additive (the cation scavenger), which is normally used in these reactions[100]. As a matter of fact, when the reaction was performed at a carbon anode and current density of 0.5 mA cm^{-2}, the hydrolysed ketone **56** was formed as the main product and the yield of **55** was only 5% when using a 4/1 CH_3CN/*i*-PrOH mixture as solvent. The **55/56** molar ratio turned 6.5/1 (67% yield) in the absence of alcohol, the other experimental condition being essentially the same[104].

C. Redox Reactions of Enolates of Transition Metals and Lanthanides

Transition metal enolates were introduced into organic synthesis in 1981 by Reetz and Peter, who reported that titanium enolates *are easily accessible using cheap reagents, distillable and miscible in THF, ether, methylene chloride or pentane, and display pronounced erithro selectivity in reactions with aldehydes*[106]. Since then, the importance of these versatile nucleophiles has steadily increased and compounds which can be represented as **57** or **58** have been identified.

Due to their oxophilic nature, early transition metals show general properties which somehow recall those of the main group elements and lanthanides[107] and afford *O*-bonded

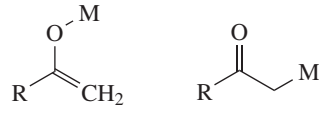

(**57**) (**58**)

enolates **57**. On the other hand, middle-to-late transition elements are expected to have the carbon-bound structure **58**. This is especially true when the enolates of heavier metals are concerned due to the generally observed increase of the M−C bond energy on descending a vertical sequence of transition elements[107]. Thus, transition metal enolates may provide a unique system for comparing the structure and reactivity of metal−oxygen to metal−carbon bonds. In this section are presented some redox reactions involving transition metal enolates, mainly of titanium; however, other systems such as zirconium and middle-to-late transition metal enolates are also considered.

The most studied *O*-bonded transition metal enolates are titanium enolates[106]. The reason for their success has been recognized in the fact that titanium enolates show an enhanced stereochemical control in C−C bond-forming reactions over simple lithium enolates and the possibility of incorporating chiral ligands at the titanium centre, a possibility which has lead to enantioselective aldol reactions with excellent enantiomeric excess. Moreover, titanium enolates have been used in oxidation reactions with remarkable diastereoselectivity.

In a series of papers, Itoh and Mikami have reported the high yield, radical α-trifluoromethylation of ketones using titanium enolates and MefI/BEt_3 as free radical generator[108] and trifluoromethylating agent[109]. The use of excess lda and Ti(OPr-*i*)$_4$ in the preparation of the titanium enolate represents the key to the success of the reaction (equation 41). Interest in this reaction stems from the fact that in general, the radical α-trifluoromethylation of ketones via lithium enolates is complicated by the easy defluorination of the α-CF_3 ketone by the parent enolate[109]. For this reason, less reactive enolates such as silyl or germyl enolates have been initially used instead of lithium enolates[110].

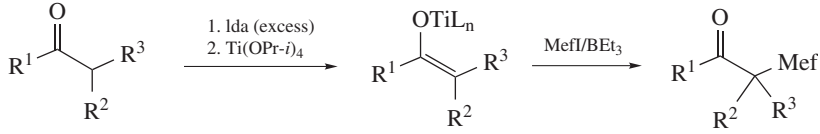

(41)

More recently Ito and Mikami observed[111] that the titanium reagent is not indispensable in the case of highly basic lithium enolates derived from cyclic ketones or silyl enolates, for which the reactions are very fast (ending in *ca* 1s to 5 min) and afford high yields of the α-trifluoromethylation products. A tentative radical mechanism has been proposed for these processes[110a] involving reaction of the Mef$^\bullet$ free radical with the enolate to give a radical intermediate which reacts with another MefI molecule to afford Mef$^\bullet$ and the *a*-trifluoromethylation product (equation 42).

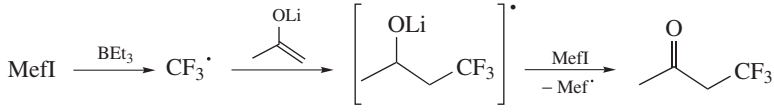

(42)

Based on the optimization of the structures of titanium and lithium enolates, it has been shown that, although Ti−F bonds are stronger than Li−F bonds[112], the stability of

the titanium enolate, i.e. the success of the radical *a*-trifluoromethylation, comes from the linearity of the Ti−O−C bond with consequent reduction of M · · · · F interactions: the calculated M−O−C bond angles are in fact 170.2 and 121.9° in the titanium and the lithium enolates **59** and **60**, respectively[109a].

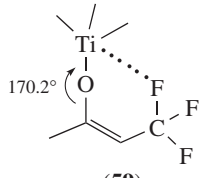

(**59**)

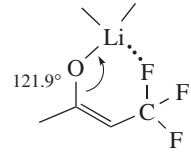

(**60**)

Titanium enolates deriving from titanium(IV) alcoholates, amido or mixed chlorocyclopentadienyl derivatives of general formula $R^1R^2C{=}C(R^3)COTiL_3$ have been oxidized to α-hydroxyketones by several oxidizing agents such as dioxygen[113], dimethyldioxirane[114], *t*-BuOOH and its lithium salt[115], the diastereoselectivity of the reactions depending on the substituents on titanium and the oxidizing agent. For example, high yields but low stereoselectivity occurs in the oxidation of the trisalkoxyenolate **61** with O_2 (equation 43), while the oxidation of mixed ligand chlorotitanocene and alkoxy enolates derived from camphor with *t*-BuOOH[115] or with dimethyloxirane, racemic oxaziridine or molybdenum peroxides[114c] affords the corresponding α-hydroxyketones with high (>95%) diastereomeric excess (equations 43a–d).

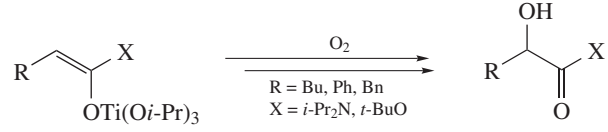

(**61**) (43)

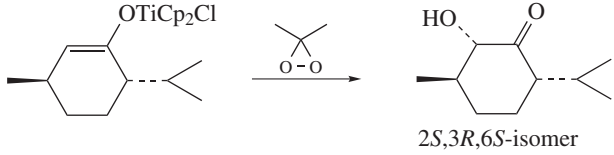

2*S*,3*R*,6*S*-isomer (43a)

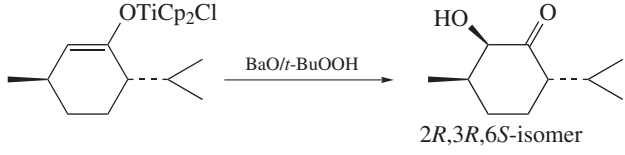

2*R*,3*R*,6*S*-isomer (43b)

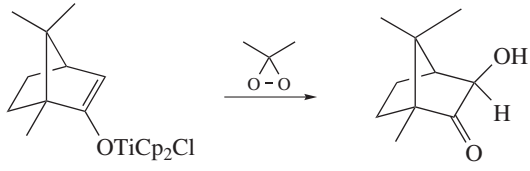

exo-isomer (43c)

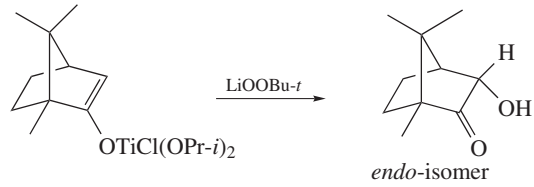

(43d)

Adam and Korb have attributed the higher stereoselectivity of titanium enolates relative to the corresponding lithium enolates in the oxidations with dimethyldioxirane to the steric demand of the oxidizing agent: for the chlorotitanocene enolate, the high preference of the *exo*-isomer for all the oxidants is due to the presence of the steric demanding titanium fragment ligated to the enolate[114c]. Remarkably, the nature of the oxidant determines the stereochemistry of the product: in the case of dimethyldioxirane, the 2*S*,3*R*,6*S*-isomer of menthone (equation 43a) and the *exo*-isomer of camphor (equation 43c) were formed with dimethyldioxirane as oxidant. On the other hand, the use of *t*-butylperoxides provided high stereoselectivity for the 2*R*,3*R*,6*S*-isomer (equation 43b) and for the *endo*-isomer (equation 43d). The difference in the behaviour of the two oxidants has been attributed to the different modes of attack of the oxidant on the titanium enolate. In the case of the peroxide, the first step of the reaction involves ligand exchange and the peroxy function activates a titanium-assisted oxygen transfer[115]. By contrast, dimethyldioxirane probably does not coordinate to titanium[114b] and the TiL_3 fragment behaves as a bulky substituent favouring the formation of the *exo*-isomer.

In the attempt to oxidize allenyl enolates derived from the allenyl ester **62** to α-hydroxyallenes following the procedure used by Adam and coworkers[114a–c] (i.e. deprotonation of the substrate with lda, *trans*-metallation of the lithium enolate with $TiCp_2Cl_2$ and treatment of the titanium enolate with dimethyldioxirane), Hoffmann-Röder and Krause found that the procedure suffers from the poor reactivity of the titanium enolate towards dimethyldioxirane[116], thus leading to unsatisfactory conversion of the substrate (equation 44). Transmetallations to the corresponding zinc, boron or aluminium enolates with $ZnCl_2$, $Zn(OTf)_2$, BBu_2OTf or $AlEt_2Cl$ did not give better yields. Using $ZrCp_2Cl_2$ instead of $TiCp_2Cl_2$ led to good yields of ethyl 2-hydroxy-3,4-dienoates, which are valuable precursors of chiral 2,5-dihydrofurans[117].

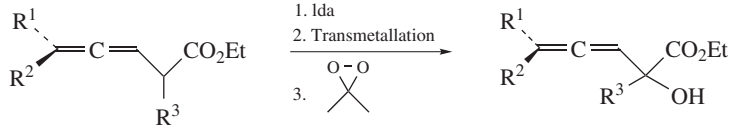

(**62**) (44)

Copper(I)-catalysed conjugate additions to zirconocene are supposed to have zirconium enolates as intermediates, which can be oxidized with *N*-halosuccinimides (equation 45)[118].

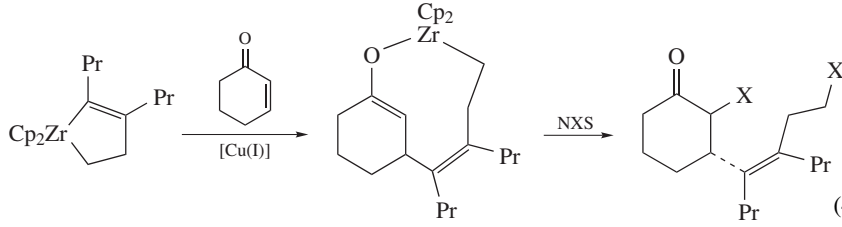

(45)

Another example of zirconium enolate oxidation is the facile reaction of the enolate **63** with molecular oxygen to give a mixture of α-hydroxy ketone **64** and hydroperoxide **65** (equation 46)[119].

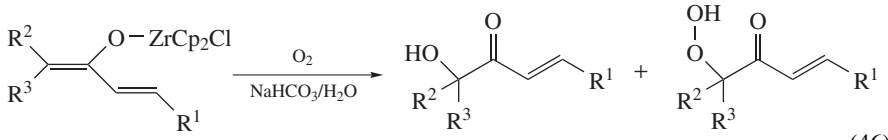

(**63**) (**64**) (**65**) (46)

Oxidation reactions of isolated titanium and zirconium enolates are rather uncommon, examples being the reaction of **66** with $[Fe(phen)_3](PF_6)_3$ (equation 47a)[120] and oxidation of the thermally stable five-membered chelate **67** with dioxygen or bromine (equation 47b)[121].

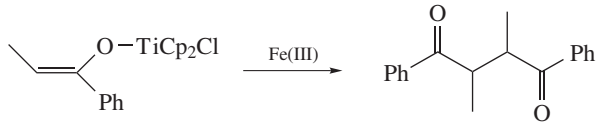

(**66**) (47a)

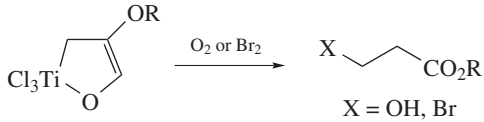

(**67**) (47b)

For the sake of completeness, it should be mentioned that at variance with the corresponding silyl enolates, the oxidation of titanium bis(enolates) with a variety of oxidants does not show any diastereoselectivity in the formation of the enolate coupling product[67b]. On the basis of crossover experiments, it has been shown that the C−C bond formation occurs via an intramolecular route in the case of the silyl derivatives and intermolecularly in the case of the titanium derivatives.

Although several research groups have been interested in transition metal enolates to use the metal centre as a potential site of asymmetry in the design of chiral catalysts, examples of well defined redox reaction involving middle to late transition elements and lanthanides are scarce in the literature. Based on Pearson's theory of hard and soft acids and bases[122], it has been proposed that combining a hard ligand with a soft late transition metal centre may lead to weak metal–heteroatom links, resulting in reactive late metal–heteroatom bonds.

The *O*-bonded ruthenium(II) enolato derivatives **68** undergo thermal reductive elimination under carbon monoxide atmosphere to give acetone and the carbonyl derivative **69** (equation 48)[123].

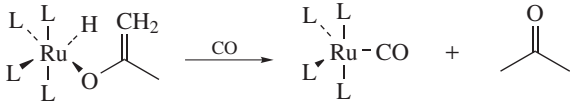

(**68**) (**69**) (48)

A C−C coupling reaction has been observed in the reaction of $LnCp^*_2CH(SiMe_3)_2$ (Ln = La, Ce) with enolizable ketones such as acetone or 3-pentanone[124]. A plausible mechanism for this reaction, which proceeds with elimination of one mole of $CH_2(SiMe_3)_2$, invokes formation of the lanthanide enolate **70**, coordination of a second molecule of ketone to the metal centre to give **71** and C−C coupling with the enolate to yield the final product (equation 49).

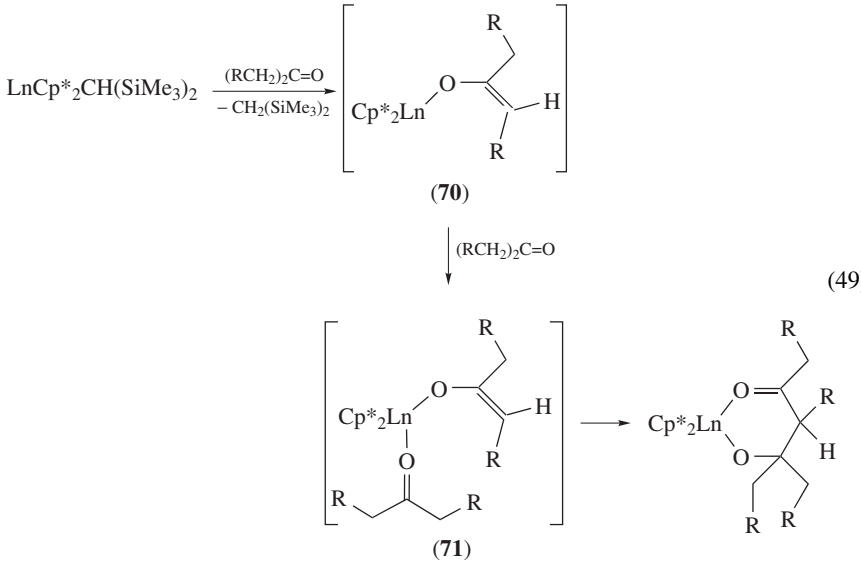

(49)

As far as late-transition elements are concerned, it is worthwhile to discuss some reactions occurring at *C*-bonded nickel and palladium enolates. Treatment of the nickel complex **73**, derived from the alkynylenone **72** and $Ni(cod)_2$, with dry dioxygen yielded the [3.1.0]bicyclohexane derivative **75** (equation 50), with the carbene species **74** as possible intermediate[125].

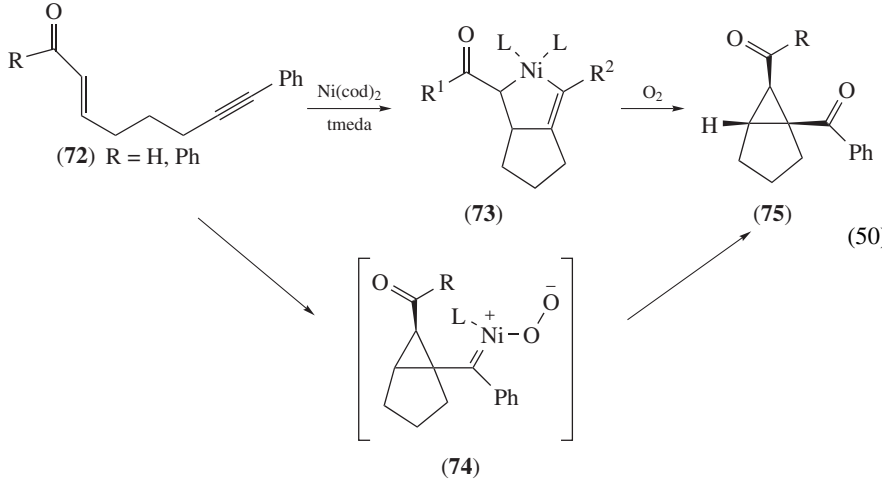

(50)

Recently, Culkin and Hartwig reported examples of arylpalladium enolates that are sufficiently stable to be isolated in pure form, but reactive to undergo reductive elimination of α-aryl carbonyl compounds in high yields (equations 51a and 51b)[126]. Of special interest is that the isolation of a large number of palladium(II) enolates has allowed one to account for the dependence of the enolate coordination to palladium on the ancillary ligands. For example, it happens that the *C*-bound isomer is favoured if the enolate is located *trans* to a phosphine (equation 51a), but the *O*-bound form if favoured if located *trans* to an aryl group (equation 51b).

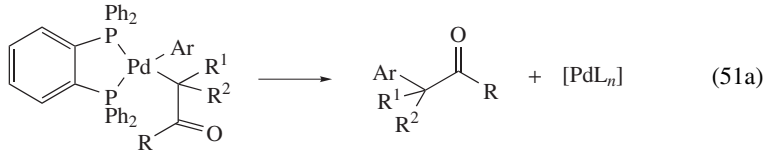

(51a)

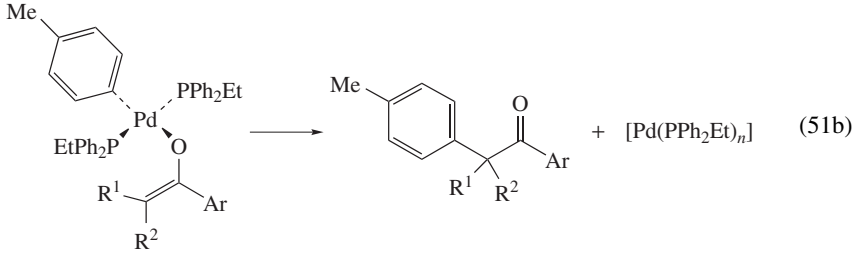

(51b)

D. Electrochemistry of Enols and Enolato Derivatives

The discovery that sterically crowded β-carbon enols are kinetically stable constitutes the milestone towards the elucidation of the electron transfer ability of enolates[127,128]. Based on this, Schmittel and coworkers started an accurate examination of their redox aptitude, and how it could be reflected on their chemical reactivity. In particular, they pointed out how the predominance of ketones over enols in the neutral keto/enol equilibrium could be inverted upon one-electron oxidation[5a]. These findings opened up interesting possibilities for new synthetic procedures. Starting from available ketones, the small amount of enol present in equilibrium can be oxidized by suitable oxidants and the resulting radical cation can be trapped by nucleophiles. For example, 1-(*p*-methoxyphenyl)propan-2-one, which has an enol [1-(*p*-methoxyphenyl)propen-2-ol] content of only about 0.0001%[129], reacts with tris(*p*-methoxyphenyl)aminium hexachloroantimonate in methanol to give the α-methoxyketone **76**[130]. Comparable yields are obtained with $[Fe(phen)_3](PF_6)_3$. The products isolated in the reactions are consistent with the mechanism reported in equation 52.

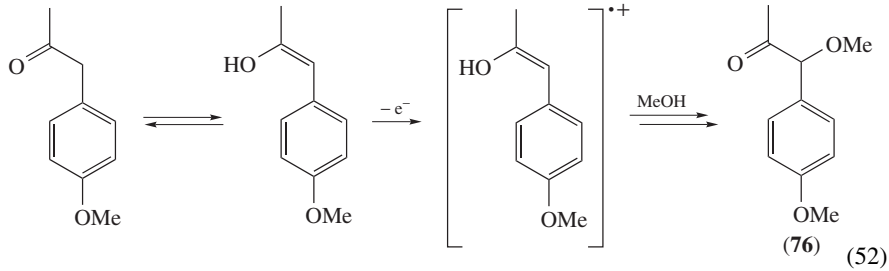

(**76**) (52)

1. Enols and enolato anions

The archetype of stable enols is represented by the 2,2-dimesityl enols **77**, which undergo oxidation to the corresponding benzofurans **78** (equation 53)[131–136]. Electrochemical studies allowed one to ascertain that the commonest and simplest mechanism involved in such electron-transfer-induced conversion is that shown in equation 54. As a matter of fact, the step triggering the enol → benzofuran conversion resides in the first one-electron oxidation, which is accompanied by a chemical transformation leading to a product which undergoes a further one-electron oxidation (the ECE mechanism)[137] to the α-carbonyl cation **79**, which rapidly cyclizes. Schematically, the two-electron transfers involved in the ECE process can proceed at the same potential value (peak A + B in Figure 1)[134], or, in the case of the deprotonated enolates, at separated potential values (peaks A and B in Figure 2)[131c]. In both cases, the most anodic step C is assigned to the reversible benzofuran ⇌ benzofuran monocation oxidation. The fact that the enolato anions exhibit separate anodic processes is not unexpected when considering that the well known sequence catecholate dianion → semiquinonate → quinone proceeds through separate reversible one-electron removals[137], whereas catechol is oxidized in a single two-electron step, which possesses features of chemical reversibility only under adequate pre-treatment of electrode surfaces[138].

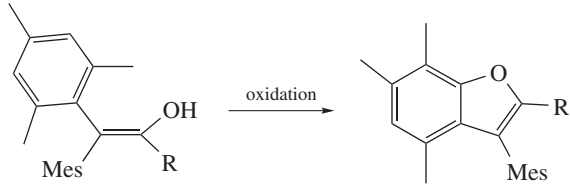

(53)

(**77**) (**78**)

The extent of chemical reversibility of the ECE electron transfers depends either on the type of enol or on the solvent. In general, non-coordinating dichlomethane favours the chemical reversibility as opposed to the coordinating acetonitrile. Furthermore, the ECE mechanism can be in some cases enriched or complicated by further intermediates, thus making in some cases the voltammetric profiles more intriguing. Such a complication can be observed in the redox mechanism involved in the oxidation pathway of the dimesityl

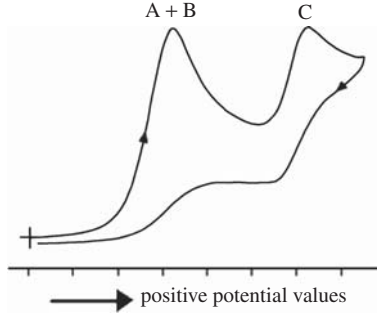

FIGURE 1. Representative cyclic voltammogram of a 2,2-dimesityl enol in which the two electron removals involved in the ECE determining steps proceed at the same potential value[134]. Reproduced from Reference 134 by permission of Wiley-VCH

enol bearing an ethynylferrocenyl substituent[139]. The formal electrode potentials for the ECE process exhibited by the 2,2-dimesitylenols and the respective benzofurans oxidation are compiled in Table 1.

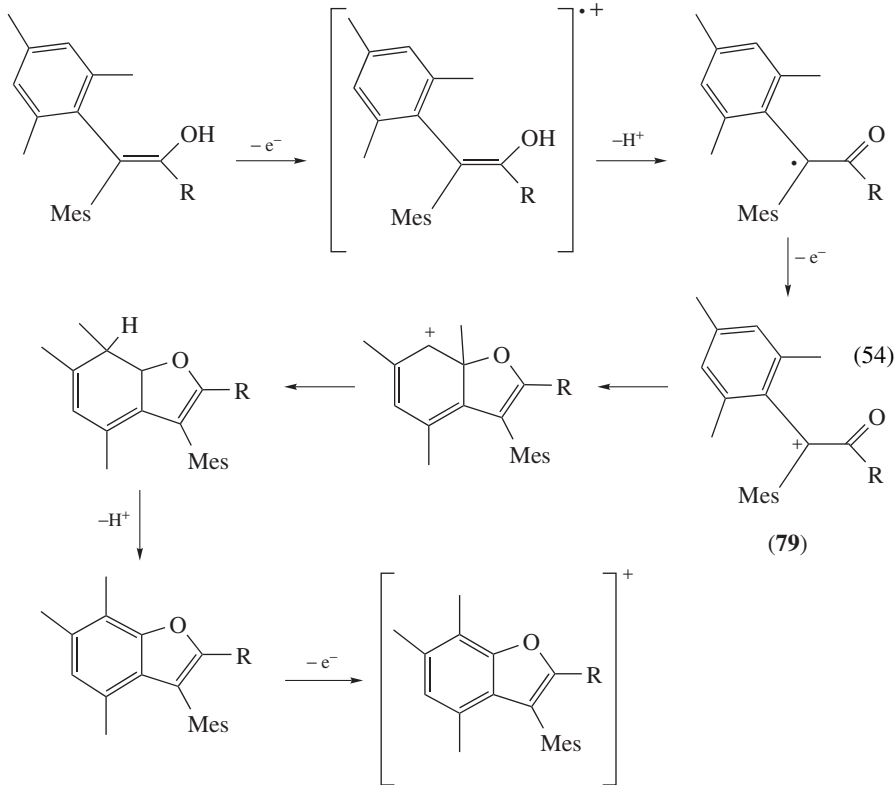

Enols sterically protected at the β-carbon have also been investigated. In general, the cyclic voltammetric response exhibits only the already mentioned ECE process, while the reversible benzofuran oxidation is not detected. The pertinent electrode potentials are compiled in Table 2. In the case of the enolato species, the ECE process probably proceeds through separated one-electron oxidations as those of Table 1.

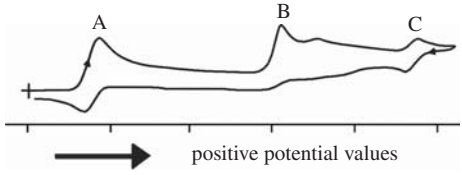

FIGURE 2. Representative cyclic voltammogram of a 2,2-dimesityl enolate in which the two electron removals involved in the ECE determining steps proceed at different potential values[131c]. Reproduced from Reference 131c by permission of the Royal Society of Chemistry

TABLE 1. Formal electrode potentials (vs. SCE) for the enol-centred oxidations exhibited by the 2,2-dimesityl enols (**77**) and their derived benzofurans (**78**)

R	$E^{\circ\prime}$ (V) 1st oxidation	$E^{\circ\prime}$ (V) 2nd oxidation	$E^{\circ\prime}$ (V) (benzofuran oxidation)	Solvent	Reference
H	+1.00 [a]	+1.00 [a]	—	MeCN	131a,b
	−0.34 [b], +1.06 [a]	+0.75 [a,b], +1.06 [a]	+1.41		131b
Me	−0.51 [b], +1.07 [a]	+0.60 [a,b], +1.07 [a]	+1.38	MeCN	131b
t-Bu	+0.97 [a]	+0.97 [a]	—	MeCN	131
	−0.62 [b], +1.03 [a]	+0.54 [a,b], +1.03 [a]	+1.32		131b
Vi	+1.08 [a]	+1.08 [a]	—	MeCN	134
CH=CHMe	+1.03 [a]	+1.03 [a]	+1.16 [a]	MeCN	134
$CH{=}CMe_2$	+0.90 [a]	+0.90 [a]	—	MeCN	132
C≡CPh	+1.11 [a]	+1.11 [a]	+1.40 [a]	MeCN	134
C≡C-C_6H_4OMe-4	+1.07 [a]	+1.07 [a]	+1.25	MeCN	134
Ph	−0.44 [b], +1.00 [a]	+0.63 [a,b], +1.00 [a]	+1.26	MeCN	131c
	+1.06	+1.06	—	MeCN or CH_2Cl_2	131d
4-Tol	−0.47 [b], +0.96 [a]	+0.61 [a,b], +0.96 [a]	+1.20	MeCN	131c
	+1.03	+1.03	—	MeCN or CH_2Cl_2	132
Mes	−0.36 [b], +1.15 [a]	+0.65 [a,b], +1.15 [a]	+1.33	MeCN	131c
	+1.15	+1.15	—	MeCN or CH_2Cl_2	132
4-An	+0.96	+0.96	—	MeCN or CH_2Cl_2	132
	+0.90	+0.90	+1.08	MeCN	132, 134, 136
4-C_6H_4-NMe_2	+0.52 [a]	+0.52 [a]	+0.62	MeCN	135, 136
3,4-$C_6H_3(OMe)_2$	+0.90 [a]	+0.90 [a]	+1.08	MeCN	136
	+0.97 [a]	+0.97 [a]	—	CH_2Cl_2	
α-$C_{10}H_6$OMe-5	+0.91 [a]	+0.91 [a]	+1.04	MeCN	136
	+1.03 [a]	+1.03 [a]	—	CH_2Cl_2	
2-Thi	−0.39 [b], +0.92 [a]	+0.63 [a,b], +0.92 [a]	+1.10	MeCN	136, 140
	+1.03 [a]	+1.03 [a]	—	CH_2Cl_2	
3-Thi	−0.60 [b], +0.92 [a]	+0.92 [a]	—	MeCN	136, 140
2-C_8H_9S [c]	−0.38 [b], +0.85 [a]	−0.66 [a,b], +0.85 [a]	—	MeCN	140
2-Fu	−0.39 [b], +0.92 [a]	+0.66 [a,b], +0.92 [a]	+1.07	MeCN	140
	+1.02 [a]	+1.02 [a]		CH_2Cl_2	
C≡C-Fc	+0.56 [a,d]	+0.56 [a,d]	+1.30 [a,e]	MeCN	139

[a] Peak-potential values for irreversible processes.
[b] Deprotonated enol.
[c] 2-C_8H_9S = 2-tetrahydrobenzothienyl.
[d] Partially overlapped by the ferrocene-centred oxidation.
[e] Followed by an irreversible oxidation to benzofuran dication.

2. Group 4 enolates

As for stable enols or enolates, the kinetic stability of metal enolates is obtained by shielding the 2,2-β-carbon atom of the enol core. The stable titanium enolates **80**–**83** have been studied electrochemically up to the present[67b, 68, 120a,b, 143]. As illustrated representatively in Figure 3 for a titanium monoenolate[120b], the most stable titanium enolates undergo a first oxidation to the corresponding unstable monocations (peak A), followed by a second oxidation of the pertinent enols formed by mesolytic cleavage of the O−Ti bond consequent to the first electron removal (peak B, equation 55). This redox process is followed by a third oxidation of the corresponding benzofurans generated by the usual cyclization of the α-carbonyl monocations (equation 54), peak C. The formal electrode potentials of the redox processes are summarized in Table 3. It should be noted that oxidation of the titanium enolate with R = CH_3, $R^1 = R^2 = H$, does not undergo cyclization to a benzofuran.

TABLE 2. Formal electrode potentials (vs. SCE) for the first oxidation of the substituted enols of general formula 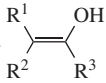

R^1	R^2	R^3	$E^{\circ\prime}$ (V)	Solvent	Reference
Mes	Me	Mes	+1.26 [a]	MeCN	131a,b
Mes	Ph	H	+1.08 [a]	MeCN	131a,b
Ph	H	Ph	−0.14 [a,b]	thf	141
Ph	Ph	Ph	−0.23 [b,c]	thf	141
Ph	C≡N	H	−0.42 [b]	dmso	142
4-C_6H_4Cl	C≡N	H	−0.38 [b]	dmso	142
4-Tol	C≡N	H	−0.51 [b]	dmso	142
4-An	C≡N	H	−0.60 [b]	dmso	142
Ph	C≡N	Me	−0.51 [b]	dmso	142
4-C_6H_4Cl	C≡N	Me	−0.46 [b]	dmso	142
4-Tol	C≡N	Me	−0.55 [b]	dmso	142
4-An	C≡N	Me	−0.66 [b]	dmso	142

[a] Peak-potential values for irreversible processes.
[b] Deprotonated enol.
[c] Partial chemical reversibility.

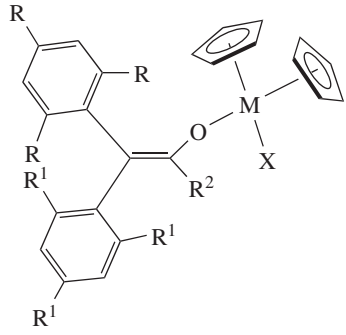

(**80**) (**a**) M = Ti, X = Cl
(**b**) M = Zr, X = Cl, Me, R^1 = Me

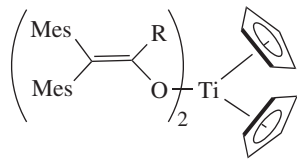

(**81**)

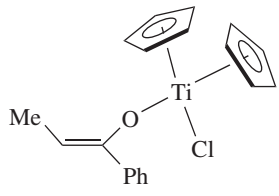

(**82**)

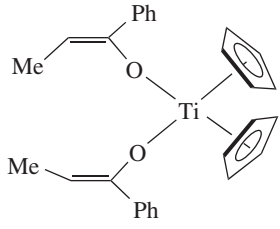

(**83**)

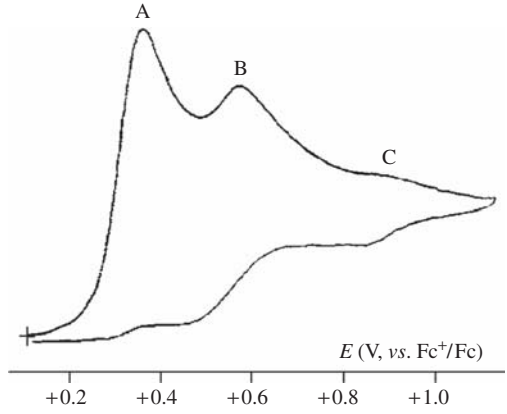

FIGURE 3. Cyclic voltammogram of the titanium mono-2,2-dimesitylenolate **80** ($R = R^1 = Me$, $R^2 = Ph$, Pt electrode, MeCN, scan rate 0.2 $V\,s^{-1}$)[120b]. Reproduced from Reference 120b by permission of Wiley-VCH

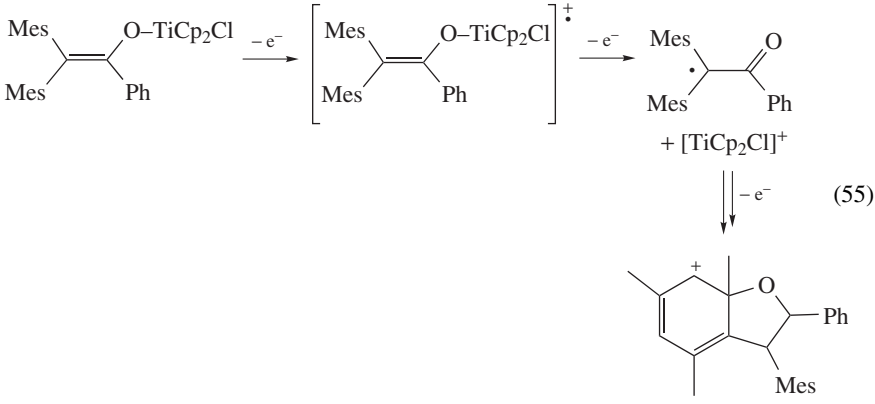

(55)

Titanium dienolates display cyclic voltammetric profiles more complicated than those of the monoenolates. In Figure 4[143] process A + B consists of oxidation to the corresponding dienolato monocation overlapping with oxidation of the α-carbonyl radical formed by mesolytic cleavage of the O−Ti bond; process C arises from oxidation of the cationic titanium monoenolate formed on O−Ti cleavage; process D is oxidation of the generated enol, and process E is assigned to oxidation of the final benzofuran product. Table 3 lists the oxidation potentials of the most important steps.

Regarding the sterically unprotected complexes **82** and **83**, either the monoenolato or the dienolato derivatives display an irreversible oxidation in MeCN solution ($E_p = +0.93$ V for **82**; $E_p = +0.74$ V for **83**; vs. SCE)[67b, 120b, 143], which in both cases ultimately leads to 2,3-dimethyl-1,4-diphenyl-1,4-butanedione.

Electrochemical studies have been also devoted to zirconium enolates[68, 120c]. All complexes undergo one-electron oxidation followed by the usual path to the corresponding

TABLE 3. Formal electrode potentials (vs. SCE) for the redox processes of the titanium monoenolates **80a** and dienolates **81**

R	R^1	R^2	$E^{\circ\prime}$ (V) titanium enolate oxidation	$E^{\circ\prime}$ (V) enol oxidation	$E^{\circ\prime}$ (V) benzofuran oxidation	Solvent	Reference
Titanium monoenolates **80a**							
H	H	H	+0.79 [a]	—	—	MeCN	120a,b
			+0.88 [b]	—	—	CH_2Cl_2	
Me	H	H	+0.83 [a]	—	—	MeCN	120a,b
Me	Me	H	+0.83 [a]	+1.06 [a]	+1.45	MeCN	68, 120a,b
			+0.89 [b]	—	—	CH_2Cl_2	
Me	Me	*t*-Bu	+0.69 [a]	+1.03 [a]	+1.32	MeCN	68, 120b
			+0.55 [b]	—	—	CH_2Cl_2	
Me	Me	Ph	+0.77 [a]	+0.99 [a]	+1.26	MeCN	68, 120b
			+0.70 [b]	—	—	CH_2Cl_2	
Titanium dienolates **81**							
H	—	—	+0.66 [a]	+1.11 [a]	+1.47	MeCN	68, 143
			+0.66 [b]	+1.24 [a]	+1.44	CH_2Cl_2	
Ph	—	—	+0.66 [a]	+0.94 [a]	+1.26	MeCN	68, 143
			+0.58 [b]	—	—	CH_2Cl_2	

[a] Irreversible process.
[b] Partial chemical reversiblity.

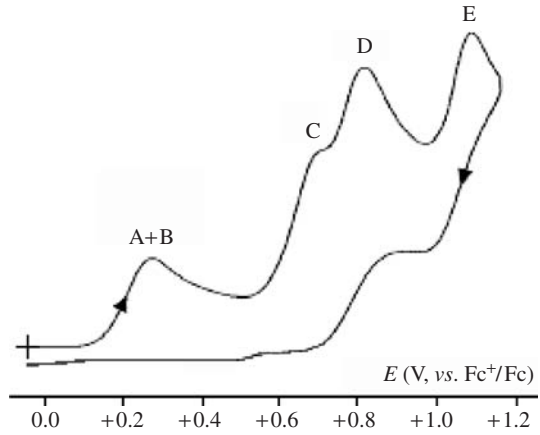

FIGURE 4. Cyclic voltammogram of the titanium bis-2,2-dimesitylenolate **81** (R = H, Pt electrode, CH_2Cl_2, scan rate 0.2 V s^{-1})[143]. Reproduced from Reference 143 with permission. Copyright 1999 American Chemical Society

benzofurans. As in previous cases, the anodic process is irreversible in acetonitrile solution, whereas partial chemical reversibility is apparent in dichloromethane (Table 4). In agreement with the higher electron density on zirconium relative to titanium, the zirconium enolates are easier to oxidize by about 0.1 V with respect to the corresponding titanium enolates.

TABLE 4. Formal electrode potentials (vs. SCE) for the one-electron oxidation of the zirconium enolates **80b**[68, 120c]

X	R	E_p (V)/MeCN	$E^{\circ\prime}$ (V)/CH_2Cl_2 [a]
Cl	H	+0.84	+0.96
Cl	*t*-Bu	+0.71	+0.82
Cl	Ph	+0.80	+0.83
Me	H	+0.90	+0.85
Me	*t*-Bu	+0.69	+0.74
Me	Ph	+0.74	+0.75

[a] Partial chemical reversibility.

TABLE 5. Formal electrode potentials (V, vs. SCE) for the one-electron oxidation of shielded silyl enolates $[Mes_2C{=}C(R^1)O]_nSiMe_{4-n}R^2$ [68, 120c]

n	R^1	R^2	E_p (V)/MeCN	$E^{\circ\prime}$ (V)/CH_2Cl_2 [a]
1	Ph	Me	+1.04	+1.08
1	Ph	*t*-Bu	+1.12	+1.06
1	Ph	4-An	+1.07	—
2	H	Ph	+1.29	+1.27
2	Ph	Me	+1.14	—
2	Ph	Ph	+1.20	+1.13
3	Ph	—	+1.18	+1.14

[a] Partial chemical reversibility.

TABLE 6. Formal electrode potentials (vs. SCE, in acetonitrile) for the irreversible oxidation of unshielded silyl enolates $[MeCH{=}C(Ph)O]_2SiR^1R^2$ [67b]

R^1	R^2	E_p (V)
Me	H	+1.68
Me	Me	+1.50
MeCH=C(Ph)O−	Me	+1.52
MeCH=C(Ph)O−	MeCH=C(Ph)O−	+1.55

3. Silyl enolates

The electrochemistry of the shielded and unshielded silyl enolates has been investigated[67b, 68, 143, 144]. As in the case of the shielded titanium analogues, all the dimesitylsilyl enolates display the usual oxidation to the corresponding benzofurans. In some cases, reversible oxidation of the latter is also detectable[68]. The pertinent oxidation potentials are reported in Table 5.

As in the case of the related titanium complexes, the oxidation of the unshielded silyl enolates affords the related 1,4-diketones[67b] (Table 6).

IV. SIMPLE β-DIKETONATES

β-Dicarbonyl compounds have been of considerable interest to inorganic, organic and physical chemists. β-Diketonates (especially the acetylacetonato anion) have been appreciated by inorganic chemists as useful chelating ligands. Organic chemists have used them

in reactions such as the malonic synthesis, the Knoevenagel condensation, the Michael addition etc. Physical chemists have used β-dicarbonyl compounds to study the keto/enol equilibrium which, due to a 1,3 hydrogen shift, affords in solution mixtures of the keto and of the enol form **84** and **85**, respectively. Exhaustive review papers have dealt with this topic[145].

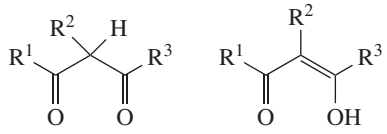

(**84**) (**85**)

As Section IV will be mostly devoted to 2,4-pentanedione, acacH, it is worthwhile to dwell on this well studied species. The rate of interconversion between the keto and the enol form of acacH is rather slow at room temperature[146], thus they can be simultaneously detected by NMR spectroscopy: it has been observed that the lower the polarity of the solvent, the higher the percentage of the enol tautomer[145c]. Electron diffraction studies[147] indicate that in the gas phase acacH adopts the enol configuration with a keto/enol ratio of 8/92. More recently, an X-ray analysis of acacH, carried out at 110 K[148], showed that it exists as a mixture of the two enol forms **86** and **87**, with the enolic hydrogen atom equally distributed over two positions close to the oxygen atoms as in **88**. It should be noted that inclusion compounds containing different host molecules show different ratios of acacH in the enol form. For example, acacH exists as a dynamically averaged 1:1 mixture of **86** and **87** in an inclusion complex with 1,1′-binaphthyl-2,2′-dicarboxylic acid as host[149], while 1,1-bis(*p*-hydroxyphenyl)cyclohexane and (4*R*,5*R*)-*trans*-4,5-bis(hydroxydiphenylmethyl)-2,2-dimethyl-1,3-dioxolane include acacH in pure enolic form[150].

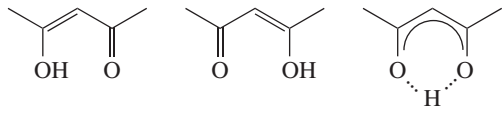

(**86**) (**87**) (**88**)

The proton in position 3 in the keto form and the hydroxyl proton in the enol form of β-diketones are acidic and their removal generates β-diketonato anions, forming the broad class of the β-diketonates with every main group and transition element, the lanthanides and the actinides. Beyond the academic interest, β-diketonato complexes have been used as extracting and complexing agents, for chromatographic separations, as molecular precursors in CVD techniques and as liquid crystal phases (metallamesogens). Several reviews have been published on this topic[151].

A. Redox Reactions

1. Reactions involving the metal

a. Reductions, oxidations and oxidative addition reactions. Transition metal β-diketonates are interesting starting materials for the preparation of organometallic compounds due to their easy preparation from readily available starting materials. Alkyl complexes

of iron(II) have been obtained in good yields by reaction of $Fe(acac)_3$ with trialkylaluminium or alkoxodialkylaluminium compounds in the presence of triphenylphosphine[152a], dppe, dppe = 1,2-bis(diphenylphosphino)ethane[152b], or dipy[153] (equation 56) and have been used as catalytic precursors for the oligomerization of butadiene[153] and the polymerization of styrene, methylmetacrylate and acrylonitrile[152].

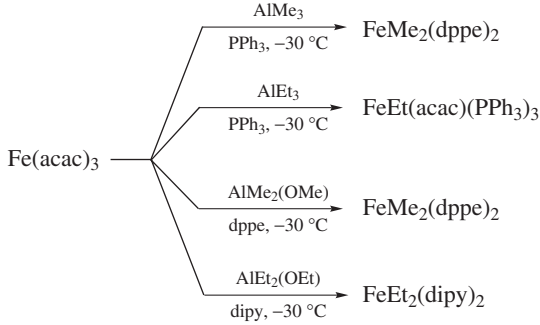

(56)

The $Fe(acac)_3$ reduction with alkylaluminium compounds in the presence of phosphines strongly depends on the reaction conditions (equation 57). Control of the reductant-to-iron molar ratio and the reaction temperature allows the isolation of intermediates such as $FeEt_2(dppe)_2$, which converts into the dihydride $FeH_2(dppe)_2$ on increasing the temperature[154].

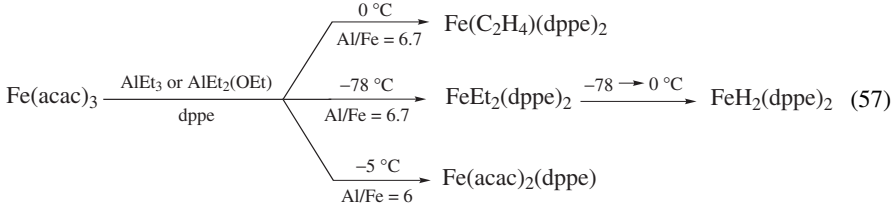

(57)

Alkylaluminium compounds in the presence of the proper ligands have been used as reducing agents for molybdenum(III), manganese (II) and nickel(II) acetylacetonates in the preparation of $MoH(acac)(dppe)_2$[155], $Mn_2(CO)_{10}$[156], $Ni(PPh_3)_2(C_2H_4)$[157] and the nitrogen-bridged $[Ni(PHex\text{-}c_3)_2]_2N_2$[158]. Dihydrogen as reductant of $Ru(acac)_3$ in the presence of carbon monoxide has been used for the preparation of $Ru_3(CO)_{12}$[159].

Alkyllithium compounds smoothly reduce $Ce(acac)_4$ to the cerium(III) derivative $Li[Ce(acac)_4]$. On increasing the Li/Ce molar ratio, organocerium compounds of composition $Li_3[CeR_3(acac)_3]$ are formed. With Grignard reagents, products of the type $Ce(acac)_3{\bullet}RMg(acac)$ are obtained[160].

Bis(cyclopentadienyl)cobalt(II), $CoCp_2$, or hexacarbonylmetalate anions of niobium and tantalum, $[M(CO)_6]^-$, have been used as reducing agents for the preparation of titanium(III)[161], and niobium(I) and tantalum(I) derivatives[162].

Zinc amalgam reduction of $Ru(acac)_3$ in the presence of olefinic *N*- or *O*-donor chelating ligands affords the corresponding complexes **89** of ruthenium(II)[163].

Well resolved EPR spectra of stable dianion radicals of β-diketonate have been observed in the reaction of transition metal β-diketonates of manganese(III), iron(III), cobalt(III) and copper(II) with Grignard reagents[164]. On the basis of the spectral pattern and of

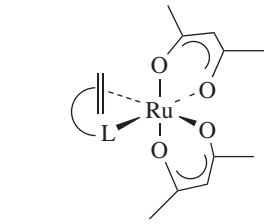

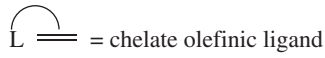

(**89**)

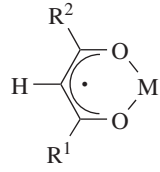

(**90**)

deuteriation experiments, it has been proposed that stable dianion radicals of the β-diketonate exist as the metal complexes **90** ($R^1 = R^2 =$ Me, Ph, *t*-Bu; $R^1 =$ Me, $R^2 =$ Ph).

More recently, Ingrosso and coworkers have studied the reaction of some cobalt(III) β-ketoenolates with trifluoroacetic acid[165] observing a ligand-to-metal electron transfer process which affords radical species and cobalt(II) derivatives. Depending upon the nature of the β-ketoenolates, the radicals can be described as the cationc cobalt(III) derivatives containing a β-ketoenolyl radical **91**, or as cationic β-ketoenolates of cobalt(IV), $[CoL_3]^+$. On the basis of detailed synthetic and EPR studies, it has been shown that trifluoroacetic acid promotes the formation of strong oxidant, cationic cobalt(III) centres by the gradual removal of β-ketoenolate ligands from the coordination sphere of the starting CoL_3 species. The proposed electron transfer steps, protonation and loss of one diketonate followed by Co(III) to Co(II) reduction closely resembles that reported by McKellar and West in 1974[166].

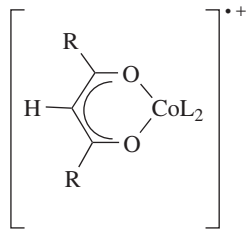

(**91**)

Metal acetylacetonates $M(acac)_n$ (M = Mn, Fe, Co, Al, Cr, $n = 3$; M = Zn, Cu, $n = 2$) react with the stable 2,2-diphenyl-1-picrylhydrazyl (dpph) free radical, with formation of

2,2-diphenyl-1-picrylhydrazine and reduction of the metal[167]. In the case of $Cu(acac)_2$, a copper(I) derivative formulated as Cu(dpph)(acac) was obtained: on the basis of IR, NMR and UV-VIS spectra, the authors propose that the coordination of dpph to copper occurs through the picryl ring[168].

Oxidative addition reactions of dihydrogen[169], iodine[170], alkyl halides[171] and $Hg(CN)_2$[172] to carbonyl, olefin or phosphine substituted derivatives of rhodium(I) and iridium(I) have been described. In order to determine the effect on the rate of the reaction, the kinetics of the oxidative addition of $Hg(CN)_2$ to $Rh(dik)(P(OPh)_3)_2$ has been studied[172]. A second-order rate law coupled to large negative values of the activation entropy suggest an associative mechanism which probably proceeds via a cyclic three-centred transition state (equation 58). Analogous results were obtained with Ir(dik)(cod)[173].

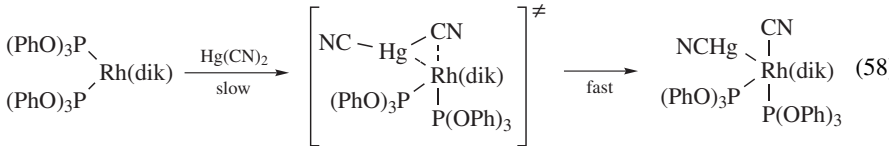

(58)

The hydrido-vinyl species of iridium(III), $Ir(acac)(H)(C_2H_3)L(Pi\text{-}Pr_3)$, L = py, $i\text{-}Pr_3$, obtained from $Ir(acac)(C_2H_4)(Pi\text{-}Pr_3)$ via intramolecular oxidative addition of a coordinated ethylene ligand under UV irradiation[169a], represents a useful starting material for the preparation of vinylidene iridium complexes.

The oxidative additions of alkynes, hydrosilanes and hydrostannanes to M(acac)(coe)P(Hex-*c*)$_3$, M = Rh, Ir, have been studied by Esteruelas and coworkers[169b,c]. Particularly interesting is the reaction of **92** with dihydrogen (equation 59), affording a rare example of a silyl trihydride derivative, and shows that the acetylacetonato ligand is able to stabilize either the +3 or the +5 oxidation states of iridium.

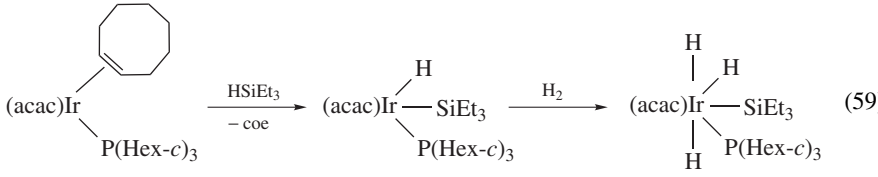

(59)

(**92**)

Cobalt(III) 1,5-dialkyl-2,4-pentanedionate derivatives have been obtained by oxidation of CoL_2 with hydrogen peroxide in water[174]. Analogously, the vanadium(IV) derivative $VO(acac)_2$ is oxidized by I_2 to the polyiodide $[VO(acac)_2]I_5$[175]. Charge transfer complexes of general formula $[M(acac)_nI]I_3$ (M = Fe[176], Co[177], $n = 3$; M = Ni, $n = 2$[178]) have been isolated and characterized from the reaction of $M(acac)_n$ with diiodine.

b. Reactions induced by amines or phosphines. Goswami and coworkers have shown that $Ru(acac)_3$ reacts with arylamines at *ca* 130 °C with oxidative dimerization of the arylamine and formation of diimine complexes of ruthenium(II) (equation 60)[179]. The overall transformation **93** → **94** (equation 61) consists of the oxidative dimerization of **93**, followed by oxidation of the resulting dimer to the diimine ligand **94**. The production of H^+ during the oxidative dimerization justifies the yield increase on addition of triethylamine.

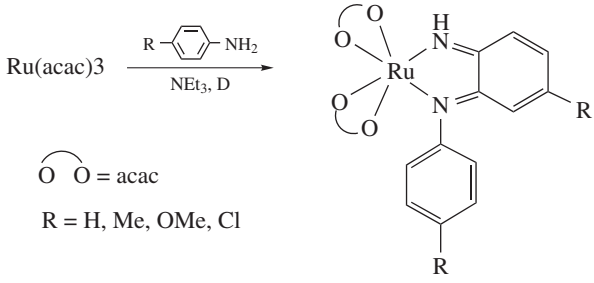

(60)

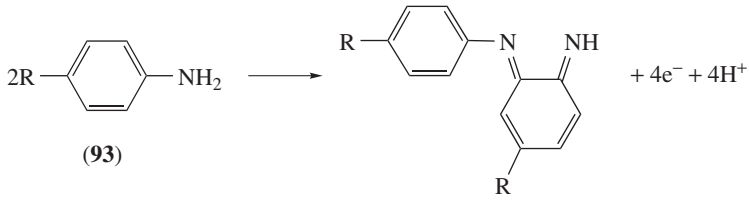

(**93**) (**94**)

(61)

In the course of studies on the design and synthesis of new metal compounds containing labile ligands in *cis*-positions as antitumour agents, Kabanos and coworkers[180] reported a series of dichelates of vanadium(III) containing two terminal chlorine atoms, prepared by reaction of a vanadium(IV) precursor with dipy or phen in acetonitrile (equation 62). Although the *cis*- and the *trans*-isomers of VCl_2(dik)(N N) were observed in solution, only the *cis*-isomer was obtained in the solid state. On the basis of the thermodynamic parameters obtained from variable temperature ^{1}H NMR experiments and DFT studies, this finding has been attributed to the greater stability of the *cis*-isomer due to better solvation by polar molecules such as acetonitrile. In view of the detection of 3-chloro-2,4-pentanedione in solution, it has been suggested that the reaction in equation 62 takes place with formation of diketonato radicals.

$$\begin{gathered} VCl_2(dik)_2 + N\text{^}N \longrightarrow VCl_2(dik)(N\text{^}N) + [dik]^{\bullet} \\ dik = acac, bzac \\ N\text{^}N = phen, dipy, 5,5'\text{-}Me_2dipy, 4,4'\text{-}t\text{-}Bu_2dipy \end{gathered} \tag{62}$$

Other reactions dealing with the reduction of β-diketonates by amines have been reported by Nemykin and coworkers, such as the reduction of $LnPc(dik)_2$, Ln = Sm, Eu, Gd and Lu, with aliphatic amines with formation of amine radicals identified by EPR[181], and by Yamamoto and coworkers[182], stating that pyridine promotes the reduction of $NiR(acac)(PPh_3)$, R = Me, Et, to $Ni(PPh_3)_2(C_2H_4)$ with formation of methane or ethane, depending on R.

As far as the reactions with phosphines are concerned, hexacoordinated rhodium(III) complexes *cis*-$[RhMe(dik)(PPh_3)(CH_3CN)]BPh_4$, dik = acac, bzac, are reduced by PPh_3, the $[MePPh_3]^+$ cation being formed as a result of intramolecular methyl transfer from Rh(III)[183].

The reaction of $Pd(acac)_2$ with PBu_3 proceeds with addition of the phosphine and change of the coordination mode of one of the two acetylacetonato ligands from the

O,*O*′-coordinated to the *C*-bonded mode form **95** (equation 63)[184]. Reduction of **95** to $Pd(PBu_3)_4$ is observed in the presence of adventitious water, PBu_3 being the oxygen acceptor giving the phosphine oxide $OPBu_3$.

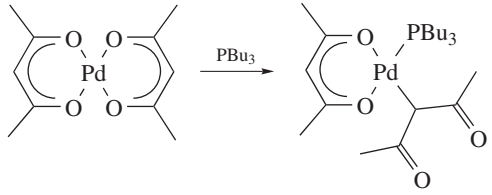

(**95**) (63)

The reaction of the dinuclear Rh(I) acetylacetonate carbene derivatives **96** with tertiary phosphines gives the mixed 0- and +2-valent compound **97** (equation 64)[185], a rare combination of two atoms of the same metal in different oxidation states. Such complexes, containing a d^9-Rh(0) and a d^7-Rh(II) metal centre, are diamagnetic and are characterized by a metal–metal single bond.

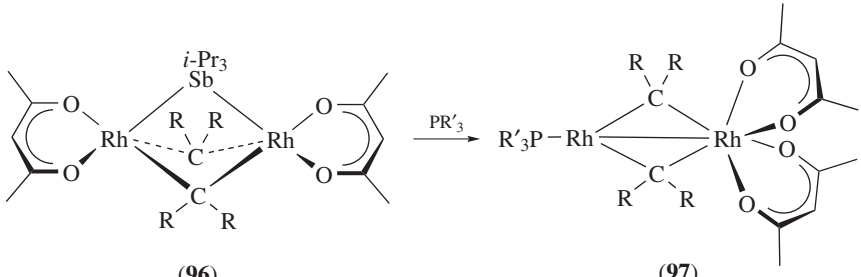

(**96**) (**97**) (64)

R = Ph, *p*-Tol; $PR'_3 = PPh_{3-n}i\text{-}Pr_n$; *n* = 0–3

It has been observed that a series of 2,4-alkanedionato adducts of cobalt(III)(salen), salen = bis(salicylideneaminato) dianion, undergo a thermally induced, intramolecular one-electron transfer reaction to cobalt(II)bis(salicylideneaminato)[186]. The concomitant formation in the gas phase of a mixture of the β-diketone (not more than 50%), methanol, ethanol and acetone has been explained as follows[186]: the thermally induced, homolytic fission of the $Co-O_{dik}$ bond gives a β-diketonato radical which abstracts a hydrogen atom from a second β-diketonate to form the corresponding diketone, whereas the dehydrogenated β-diketonato radical decomposes into compounds of lower molecular weight.

Shimizu and coworkers have recently reported that the Ru(II) → Ru(III) oxidation takes place when $Ru(acac)_2(CH_3CN)_2$ is refluxed in 2-methyl-propanol for 24 h with formation of the μ-oxo derivatives as described in equation 65[187]. The authors do not point to the source of the oxygen atom but it is reasonable that it comes from the solvent or from adventitious air. The structure of **98** has been determined by single-crystal X-ray diffraction and it has been found that it contains a $[Ru_4(\mu_3\text{-}O)_2]^{8+}$ core where two acetylacetonates, coordinated to Ru^1 via oxygen atoms, link to Ru^3 and Ru^4 with the 3-carbon atom of the acetylacetonate. This fact, together with the values of the bond distances and angles, suggests that the acetylacetonato ligands bonded to Ru^1 are in the ketonic form

with sp^3-hybridized methyne carbon atom, thus justifying the boat conformation assumed by these ligands.

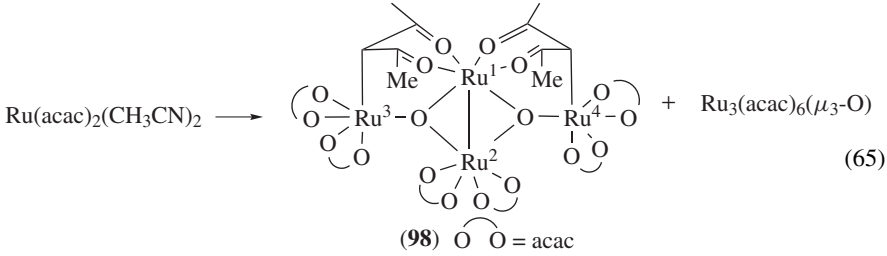

(65)

The first example of a symmetric triangular mixed-valent triruthenium complex **99** has been obtained by thermal treatment of $Ru(acac)_2(MeCN)_2$ with substituted 2-thiouracil (equation 66)[188]. Although the usual coordination mode of the acetylacetonate is present in the trinuclear compound, the γ-carbon atom of one of the coordinated acetylacetonato units of the parent $Ru(acac)_2(MeCN)_2$ links to a ruthenium atom forming the trinuclear network. The factors which are primarily involved in the ruthenium-mediated C−S bond cleavage of the stable thiouracyl are not clear. It was suggested that the process starts with the initial coordination of thiouracyl to ruthenium followed by cleavage of the C−S bond and subsequent nucleation[188].

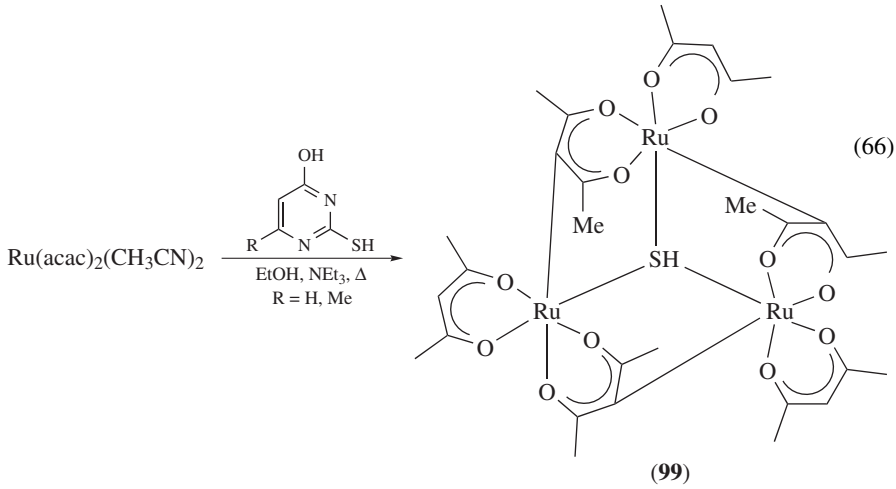

(66)

c. Photochemical reductions. Quantitative photochemical studies of metal diketonates began in the late 1960s and were concerned with metals such as chromium(III)[189], manganese(III)[190], iron(III)[190], cobalt(III)[191], rhodium(III)[192], nickel(II)[193], copper(II)[194] and platinum(II)[195]. In general, UV irradiation in solution leads to the photoreduction of the complex[196]. For example, copper(II) and nickel(II) diketonates in deoxygenated ethanolic solutions are photoreduced by 254 nm irradiation (excitation at the LMCT) and the overall reaction can be presented as in equation 67. The main photoproducts are metallic copper or nickel and β-diketone. However, the reaction pattern is more complex and

proceeds by a photochemical reduction from ML_2 to ML followed by a thermal reaction to M(0).

$$ML_2 \xrightarrow[EtOH]{h\nu\ (254\ nm)} M + 2HL \tag{67}$$

In the case of trivalent transition metal diketonates, ML_3, such as manganese, iron or cobalt, photolysis at the LMCT band in hydrogen-atom-donating solvents (*S*H) leads to the formation of a ML_2 derivative and β-diketone, the quantum yield depending on the excitation wavelength and the solvent. The mechanism reported in equations 68a–c has been postulated, where $[ML_2L]^\bullet$ represents the species which formally contains the M(II) cation bound to the β-diketonato radical $[L]^\bullet$.

$$ML_3 \overset{h\nu}{\rightleftharpoons} [ML_2L]^\bullet \tag{68a}$$

$$[ML_2L]^\bullet + SH \rightleftharpoons ML_2 + [S]^\bullet + HL \tag{68b}$$

$$ML_2 + 2SH \rightleftharpoons ML_2(SH)_2 \tag{68c}$$

The reactions reported above can explain most experimental results for ML_n photolysis[189d]. However, it has been observed that flash photolysis of tris(1,1,1-trifluoroacetylacetonato)cobalt produces $[ML_2L]^\bullet$ species which can undergo intramolecular rearrangment and additional reaction with the solvent[191b].

Recently, the formation of both colloidal copper and films on the nanometer scale by irradiation of ethanol solutions of commercially available $Cu(acac)_2$ has been described[194b]. During the optimization of the experimental conditions, the authors could demonstrate that some of the mechanisms of photoreduction should be reformulated. In particular, the authors did not get evidence of copper(I) derivatives and their eventual thermal dismutation reaction. It appeared that the photoreduction is sensitized by the acacH released during the reaction.

Kunkely and Vogler have shown[194c] that Cu(hfacac)(cod) in hexane undergoes photochemical release of cod, induced by a Cu(I) $\rightarrow \pi^*$(cod) MLCT excitation, with formation of Cu(hfacac), which rapidly disproportionates to copper metal and copper(II), a well known reaction in the field of copper(I) chemistry and especially easy to carry out in the case of copper(I) fluoro-substituted diketonates[197].

Traverso and coworkers reported[198] that the irradiation of $U(dik)_4$, dik = acac, dbm, at the wavelengths of the intraligand and LMCT transitions causes the reduction of U(IV) to U(III) as the primary photoprocess. Reoxidation of U(III) to U(IV) due to halogen abstraction takes place in halocarbon solvents. When $U(acac)_4$ was photolysed at the wavelengths of the *f–f* transitions in dichloromethane in the presence of dioxygen (equations 69a–d), a photooxygenation reaction was observed forming bis(dik)dioxouranium(VI) and acetylacetone (equation 69c). These compounds probably arise from the unstable peroxo derivative formed by the oxidative addition of dioxygen to the eight-coordinated uranium(IV) (equation 69b)[198].

$$U(acac)_4 \xrightarrow{h\nu} [U(acac)_4]^* \tag{69a}$$

$$[U(acac)_4]^* + O_2 \rightarrow \left[(acac)_4U\begin{smallmatrix}O\\|\\O\end{smallmatrix}\right] \tag{69b}$$

$$\left[(acac)_4U\begin{matrix}\diagup O \\ \\ \diagdown O\end{matrix}\right] \rightarrow [UO_2(acac)_2] + 2(acac)^- \quad (69c)$$

$$2(acac)^- + CH_2Cl_2 \rightarrow 2acacH + \text{products} \quad (69d)$$

d. Kinetic studies in solution. The kinetics of homogeneous redox reactions involving β-diketonato complexes has been studied by several groups. Examples are (i) the reaction of $[Mn(acac)_2(H_2O)_2]^+$ with thiosulphate in perchloric acid medium showing first-order kinetics with respect to the complex and fractional order with respect to both thiosulphate and H^+ [199], (ii) the reduction of $M(acac)_3$ (M = Mn, Co) with $[Fe(dmf)_6]^{2+}$ in propandiol-1,2-carbonate involving an intramolecular electron transfer through a binuclear intermediate $[(acac)_2Mn{-}acac{-}Fe(dmf)_5]^{2+}$ and formation of Mn(II) and $Fe(acac)_3$ [200] and (iii) reduction of $Ru(acac)_3$ in acidic medium, involving an outer-sphere electron transfer with $[Ti(H_2O)_6]^{3+}$ and $[Ti(H_2O)_5(OH)]^{2+}$ as reductants[201] (the latter Ti(III) complex cation acting when the Ru(III) complex does not contain good bridging ligands such as NH_3 [202]). An inner-sphere mechanism has been observed[203] when a formyl substituent is introduced in the γ-position of the β-diketonate (e.g. 3-formyl-2,4-pentanedionate = facac), thus the reaction of $Ru(facac)(acac)_2$ and Ti(III) involves formation of a binuclear Ru(III)/Ti(III) intermediate (equations 70a and 70b) and a subsequent rate-determining electron transfer within the conjugated base of the intermediate (equation 70c).

$$Ru(facac)(acac)_2 + [Ti(H_2O)_6]^{3+} \longrightarrow [(acac)_2Ru(III)(facac)Ti(III)(H_2O)_6]^{3+} \quad (70a)$$

$$[(acac)_2Ru(III)(facac)Ti(III)(H_2O)_6]^{3+} \longrightarrow [(acac)_2Ru(III)(facac)Ti(III)(H_2O)_5OH]^{2+} + H^+ \quad (70b)$$

$$[(acac)_2Ru(III)(facac)Ti(III)(H_2O)_5OH]^{2+} \longrightarrow [(acac)_2Ru(II)(facac)Ti(IV)(H_2O)_5OH]^{2+} \quad (70c)$$

A similar mechanism has been proposed for the reaction of titanium(III) salts with $[Co(N\text{-acacCN})(NH_3)_5]^{2+}$, where *N*-acacCN is coordinated to cobalt through the N atom[204, 205].

The reduction of cobalt(III) acetylacetonates with chromium(II) salts has been studied in detail. In particular, a series of mixed chelates has been investigated to elucidate changes of the rate constants and mechanisms based on ligand field effects[206]. As far as chromium(II) salts are concerned, the rate constants of the reduction of $[Co(acac)_{3-n}en_n]^{m+}$ vary approximately as predicted from ligand field arguments, with the weaker field acetylacetonate conferring a faster rate of reduction, $k_{obs} = 28.5\ M^{-1}\,s^{-1}$ for $n = 0$, than the stronger field ethylenendiamine, $k_{obs} = 1.1 \times 10^{-4}\ M^{-1}\,s^{-1}$ for $n = 3$.

In general, it has been observed[206, 207] that mixed [Co(III)(dik)bis(ethylendiamine)] complexes of general formula **100** react with chromium(II) salts at least partially via inner-sphere attack of the reducing agent either at the coordinated oxygen of the β-diketonate or at the substituent X. In the case of $[Co(acac)_2(en)]^+$ both inner- and outer-sphere mechanisms are involved with formation of different chromium(III) compounds and the transition state **101** has been proposed[208].

The 1,3-phenyl-substituted compound $[Co(dbm)(en)_2]^+$ reacts with Cr(II) according to a different mechanism: the attack of chromium(II) occurs on the central carbon atom affording the transition state **101′** [208].

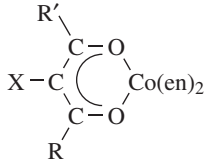

(**100**)

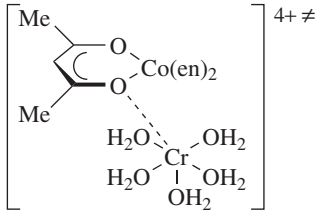

(**101**)

R = R′ = Me, X = H, CHO, Ac , Cl, Br, I
R = Me, R′ = H, X = Ac

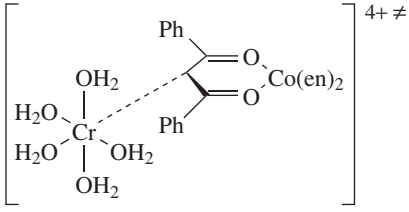

(**101′**)

An inner-sphere intramolecular electron transfer has been observed also in the reaction of chromium(II) salts with $[Co(N\text{-acacCN})(NH_3)_5]^{2+}$ [204]. This reaction proceeds via the binuclear intermediate $[(NH_3)_5Co(N\text{-acacCN})Cr]^{4+}$, which evolves to $[Co(NH_3)_5(H_2O)]^{2+}$ and $[Cr(O,O'\text{-acacCN})(H_2O)_4]^{2+}$ [204, 209]. The mechanism is supported by the observation that addition of non-reducing metal ions such as Zn(II), Ni(II) or Ba(II) to the reaction mixture causes a decrease of the rate constant[204].

2. Reactions involving the diketonate

Reactions at the β-diketonato ligand can involve either a simple attack at the carbon 3 of the diketonate or C−C bond formation or total degradation of the ligand.

Johnson and Lewis reported[210] that thallium(I) β-diketonates react with $Pd(cod)X_2$ or $Pt(cod)X_2$, X = Cl, Br, I, SCN, to give β-diketonyl cyclo-ene derivatives (**102**), the structure of which was assigned on the basis of NMR and IR spectroscopies (equation 71).

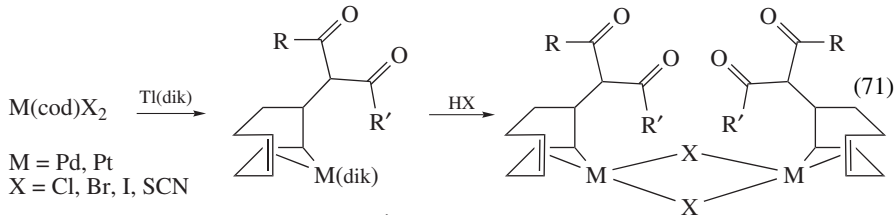

(**102**) R = Me, Ph, R′ = Me, Ph

Carbon−carbon bond formation involving the C-atom in position 3 of the acac ligand has been observed in the reaction of $Pd(acac)_2$ with hexafluoro-2-butyne (equation 72)[211].

The square-planar coordination geometry of palladium is retained but two *O*-donor atoms have been replaced by two carbon atoms.

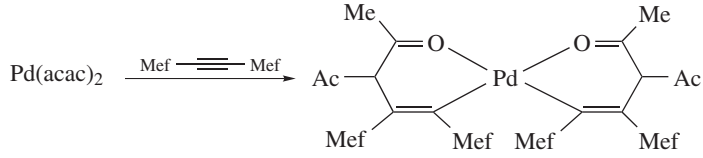

(72)

Hexafluoro-2-butyne undergoes 1,4 addition by reaction with Rh(dik)(diolefin) (dik = acac[212], dpm[213], dbm[214]; diolefin = cod, norbornadiene), with formation of a C−C bond between the alkyne and the methyne carbon atom of the β-diketonate. Additional trimerization of hexafluoro-2-butyne to hexakis(trifluoromethyl)benzene and η^4-arene coordination of the latter to rhodium affords **103** (equation 73).

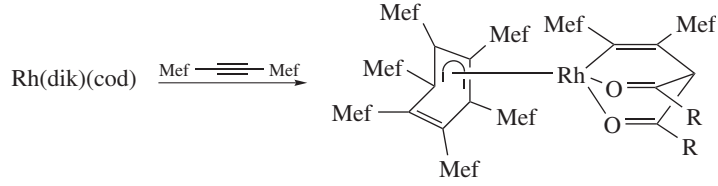

(73)

(**103**) R = Me, *t*-Bu, Ph

The reaction between Rh(dpm)$(CO)_2$ and hexafluoro-2-butyne at room temperature gives the dicarbonyl derivative **104**, which transforms into **103**, R = *t*-Bu[214], at high temperature in the presence of hexafluoro-2-butyne. The same compound **103**, R = *t*-Bu, is formed on heating Rh(dpm)$(CO)_2$ and the alkyne (equation 74).

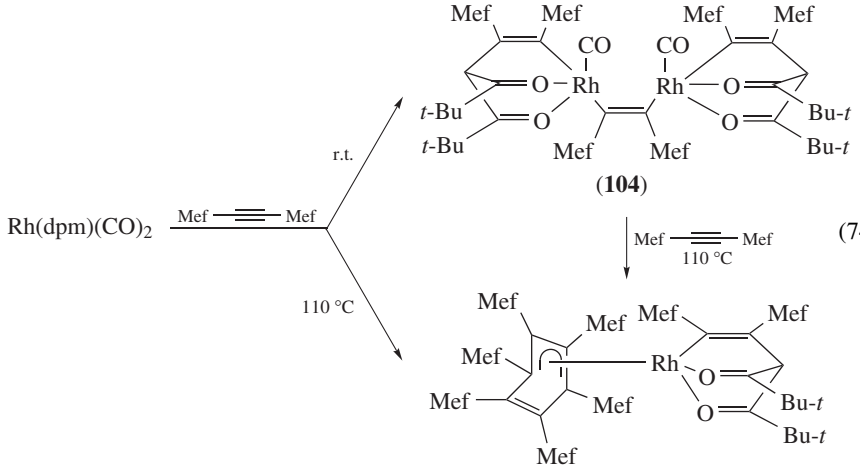

(74)

A similar C−C bond coupling involving the methyne carbon atom of the metal-coordinated β-diketonate is observed when (η^4-cyclohexadienyl)tricarbonyliron tetrafluoborate is treated with Co$(acac)_3$ in the presence of triethylamine as proton acceptor. The reaction is fast at room temperature but gives only low yields of **105** (equation 75)[215].

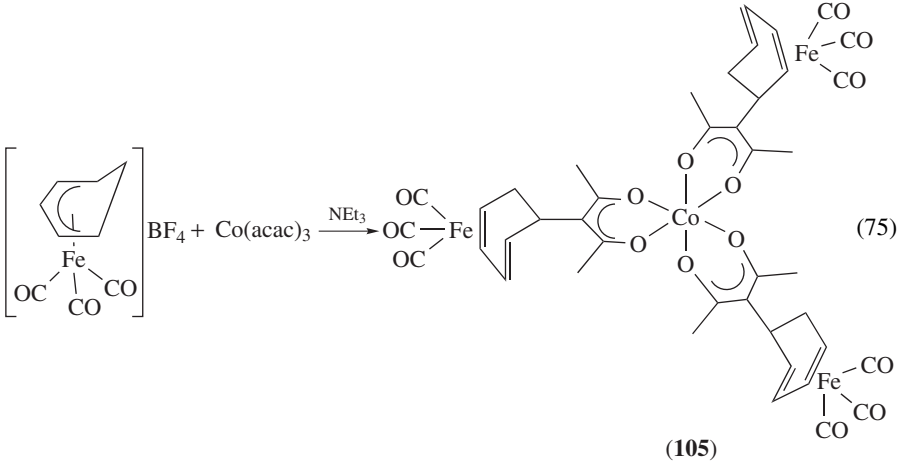

(75)

Examples of aliphatic C−C bond cleavage at the methyne carbon atom of a β-diketonate have been reported. For example, when **106** is reacted with dioxygen in the presence of tetramethylammonium hydroxide (equation 76), cleavage of the bond between the carbonylic and the methyne carbon atoms and activation of O_2 produces the dibenzoato derivative **107**, the structure of which is stabilized by H-bonding to an oxygen atom of the benzoates and the hydrogen atoms of a nickel-coordinated water molecule[216]. When the reaction is performed under an atmosphere of $^{18}O_2$, labelled oxygen atoms are incorporated into the carboxylate ligand and carbon monoxide is found in the gas phase, thus suggesting that the C−C bond cleavage occurs twice at the methyne carbon atom[216].

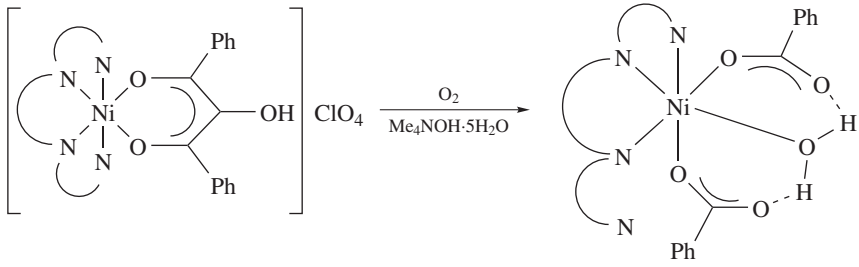

(**106**) (**107**) (76)

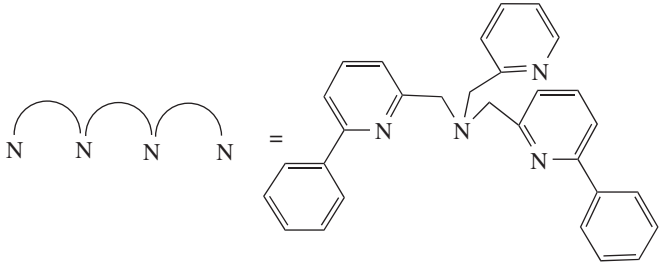

Another example of C−C bond cleavage at the methyne carbon atom has been found when arylazo derivatives of palladium(II) acetylacetonate **108** are photolyzed in air (equation 77)[217]. Since $Pd(acac)_2$ does not undergo C−C bond cleavage on irradiation under the same experimental conditions, a reaction mechanism involving the azo derivative has been postulated (equation 78) based on a kinetic study. The energy absorbed by the azo ligand is transferred to palladium and the excited palladium promotes the electron transfer from an acetylacetonato group. The acetylacetonato radical species **109** thus produced reacts rapidly with molecular oxygen giving the intermediate **110**, which decomposes through C−C and C−O bond cleavages[217] to a dinuclear Pd(II) compound (**108′**) with bridging acetato groups.

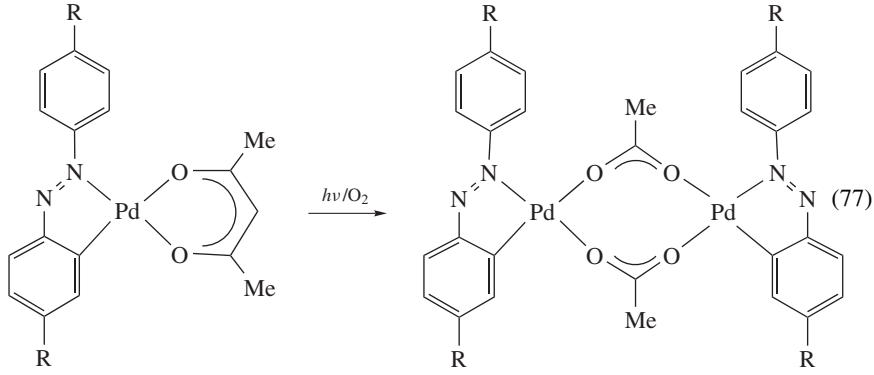

(77)

(**108**) R = H, Me, OMe (**108′**)

In a series of papers published more than forty years ago, Arnett and coworkers reported the reactions of several metal β-diketonates with dioxygen at 100 °C in diphenylether[218]. The exhaustive oxidation of $Fe(acac)_3$ produced water, CO_2, biacetyl, acetic acid, acetylacetone, mesityl oxide and an iron-containing amorphous residue. It was observed that the rate of decomposition depended upon the β-diketonate: taking acac as 1, the relative rates changed from 7.1 for dbm to very small values for 3-phenylacetylacetonate and dpm. The inertness of the 3-phenyl (and 3-benzyl) derivatives was interpreted as evidence that the methyne hydrogen is the site of attack in the rate-determining step and that this pathway is blocked by its replacement. The inertness of the dpm chelate may be the result of the steric hindrance of the flanking *t*-butyl groups on attack at the methyne position[218a,b]. A weak dependence of the decomposition rate on the metal was also observed[218a].

The reaction of metal diketonates with NO_x ($x = 1, 2$) has been reported[219]. NO_2 reacts with substituted $M(acac)_n$ derivatives of Fe(III), Mn(II) and Cu(II) affording the iminoxy radical **111**. The radicals presumably are formed after decomposition of the chelate complex, in view of the fact that the EPR parameters of the free radical are not influenced by the metal ion and that the same radical is also obtained by reaction of the corresponding free ligand and NO_2[219].

On the basis of an EPR analysis, the reaction of $M(acac)_n$ with NO_2 (at room temperature it is present as N_2O_4) has been proposed to occur via a step-by-step oxidation of the metal complex with final formation of metal nitrates and the iminoxy free radical **111** (equation 79). The presence of a donor–acceptor complex between $M(acac)_n$ and N_2O_4 has been postulated for the electron transfer to dinitrogen tetroxide.

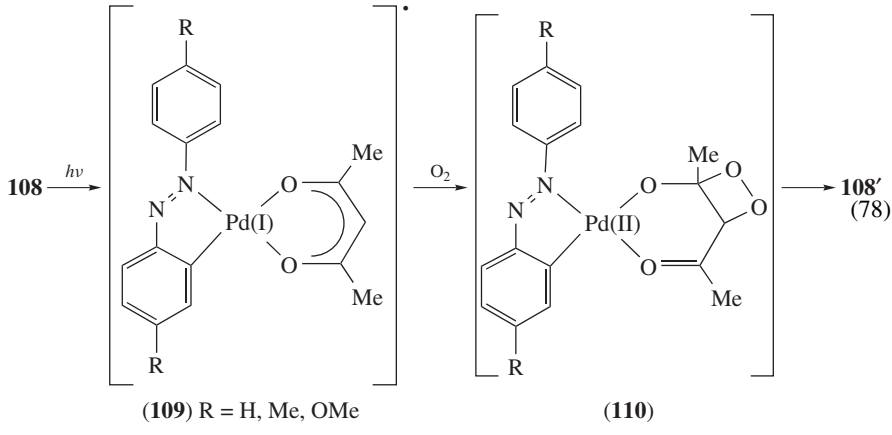

(**109**) R = H, Me, OMe (**110**)

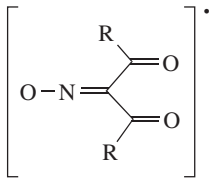

(**111**)

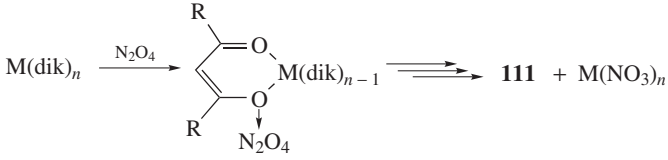

A similar reaction mechanism (donor–acceptor complex followed by the formation of a free radical from the diketonate) has been postulated also in the reaction of metal diketonates with ozone[220], which is very fast. In the case of $Co(acac)_2$, formation of the $Co(acac)_3$ complex was detected by UV-VIS spectroscopy while formation of Cr(V) species was observed by EPR during ozonation of $Cr(acac)_3$ solutions.

According to Collman and coworkers[221] and Calvin and coworkers[222], each chelating ring in metal β-diketonates has a cyclic π-orbital formed by the combination of a vacant d-orbital of the central metal atom with the 6π-electron orbital of the ligand. In spite of some doubts about this bonding situation in metal β-diketonates[223], these systems undergo typical electrophilic substitution reactions at the methyne sp^2 carbon atom. As a matter of fact, as early as 1925, the first electrophilic substitution reactions of metal β-diketonates were reported[224] and tris(3-bromo-acetylacetonato)chromium(III) was isolated by treating chromium(III) acetylacetonate with bromine in chloroform. However, this sytem went unnoticed until 1959, when $Cu(acac)_2$ was nitrated with N_2O_4 at the methyne carbon atom[225]: since then numerous reports[226–228] have appeared concerning halogenation, nitration, etc. of β-diketonates.

NCS, NBS and NIS are the best reagents for halogenation of metal β-diketonates[226, 229], the rate of bromination being much faster than that of iodination and chlorination[228]. Two reaction mechanisms have been proposed to explain the halogenation: an ionic mechanism, which is operative in polar solvents like chloroform, methanol and acetic acid[226], and a free radical one occurring in non-polar solvents like carbon tetrachloride[230].

The usual nitrating mixture (sulphonitric acid) is not a good reagent for nitration of chelate rings, as the latter undergo fast degradation; dinitrogen tetroxide nitrates in low yields[227]. The 3-nitro-β-diketonates of copper(II), manganese(II), iron(III), cobalt(II) and nichel(II) have been obtained in good yields in a direct, single-step process using the corresponding metal nitrate, acetic acid anhydride and acacH or dbmH[227b,d]. The reaction proceeds with formation of acetylnitrate ($CH_3CO_2NO_2$) followed by its decomposition to acetate and nitronium (NO_2^+) ions. Sometimes, as in the case of the nitration of berillium acetylacetonate with copper nitrate trihydrate, formation of copper(3-nitroacetylacetonate)$_2$ takes place[227d].

The rate of the electrophilic substitutions at the methyne carbon atom is higher in methyl-substituted metal β-diketonates compared to their phenyl-substituted analogues. The steric effect of a bulky group can also be illustrated by chlorination and nitration reactions of Cr(dpm)$_3$, which undergoes diketonate oxidation very slowly under forcing conditions. The rate of the reactions also falls sharply when the methyl groups of metal β-diketonates are replaced by CF_3 groups and in some instances no reaction takes place[228]. Joshi and Pathak[231] reported the first electrophilic substitution reactions at chromium(III) fluorinated diketonates: under controlled conditions, halogenation or nitration of the diketonate was performed in good yields.

B. Electrochemistry

1. β-Diketones

It is long known that β-diketones, which exist as keto–enol tautomers, have a well defined electron transfer ability[232]. In general, they exibit a first, partially chemically reversible, one-electron reduction to the corresponding enolato monoanion (minor amounts of the corresponding dimer are also formed), which in turn undergoes either a reduction process or an irreversible oxidation. The electrode potentials of a selection of symmetrically substituted ($R^1 = R^3$) β-diketones are reported in Table 7.

2. Transition metal β-diketonates

a. Group 5 elements. Vanadium(III) derivatives with the general formula V(dik)$_3$ exhibit in non-aqueous solutions either a chemically reversible one-electron reduction or two sequential one-electron oxidations which, in spite of the redox activity of the ligands, have been considered as metal-centred processes. The pertinent electrode potentials are compiled in Table 8, together with those of related VO^{2+} complexes.

The electrochemical measurements indicate that the vanadium(IV) oxidation state of the mentioned complexes is not indefinitely stable, probably because of homogeneous reactions triggered by traces of water present in the nominally anhydrous solvents[232a, 232f]. Nevertheless, the [V(dik)$_3$]SbCl$_6$ (dik = acac, bzac) derivatives have been structurally characterized[233b] so that their geometrical features can be compared with those of the corresponding neutral complexes[233f, 233g].

TABLE 7. Formal electrode potentials (vs. SCE) for the redox processes [a] exhibited by a selection of β-diketones (**84**) in various solvents

$R^1 = R^3$	R^2	$E^{\circ\prime}$ (V) (1st reduction)	E_p (V) (2nd reduction)	E_p (V) (oxidation)	Solvent	Reference
Me	H	—	−2.4 [b,c]	–0.45	MeCN	232e
		—	−2.06 [b,c]	+0.44	dmso	232f
		—	—	+0.49	dmso	232g
		—	−2.25 [c]	—	thf	232h
Ph	H	−1.42	−2.28	+0.5	dmso	232a, d
		−1.20	−2.06	+0.81	MeCN	232i
Mef	H	−0.62	−2.24	+1.32	MeCN	232i
4-C_6H_4F	H	−1.41	−2.3	—	dmso	232a
Me	$C_{12}H_{25}$	—	−2.31 [c]	—	thf	232h
Me	$C_{16}H_{33}$	—	−2.47 [c]	—	thf	232h
Me	$C_{18}H_{37}$	—	−2.52 [c]	—	thf	232h

[a] The following formal electrochemical transformations take place:

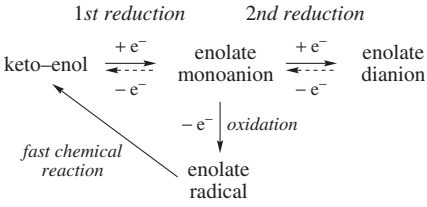

[b] Irreversible process.
[c] We assume that β-diketones are already converted into their enolate monoanions under the cited experimental conditions.

TABLE 8. Formal electrode potentials (vs. SCE) for the redox changes of $[V(dik)_3]^z$ [a] and $[VO(dik)_2]^z$ [b] complexes in various solvents

Complex	$E^{\circ\prime}$ (V) (z: 2+ → +)	$E^{\circ\prime}$ (V) (z: + → 0)	$E^{\circ\prime}$ (V) (z: 0 → −)	$E^{\circ\prime}$ (V) (z: − → 2−)	Solvent	Reference
$[V(acac)_3]^z$	—	+0.76	−1.42	—	dmso	232f
	—	+0.93	−1.37	—	Me_2CO	233a
	—	—	−1.38	—	MeCN	234a
	+1.14	+0.82	—	—	CH_2Cl_2	234b
$[V(bzac)_3]^z$	+1.14	+0.82	—		CH_2Cl_2	234b
$[VO(acac)_2]^z$	—	+0.81	−1.85 [c]	−1.95 [c]	dmso	232c
	—	—	−1.53	—	MeCN	234a

[a] The redox processes are: $[V(dik)_3]^{2+} \underset{-e^-}{\overset{+e^-}{\rightleftharpoons}} [V(dik)_3]^{+} \underset{-e^-}{\overset{+e^-}{\rightleftharpoons}} V(dik)_3 \underset{-e^-}{\overset{+e^-}{\rightleftharpoons}} [V(dik)_3]^{-}$.

[b] The redox processes are: $[VO(dik)_2]^{+} \underset{-e^-}{\overset{+e^-}{\rightleftharpoons}} VO(dik)_2^{+} \underset{-e^-}{\overset{+e^-}{\rightleftharpoons}} [VO(dik)_2]^{-} \underset{-e^-}{\overset{+e^-}{\rightleftharpoons}} [VO(dik)_2]^{2-}$.

[c] Irreversible process.

A few electrochemical studies have been also addressed to the structurally characterized (XRD[235]) $VO(acac)_2$[232e,f,234]. It undergoes oxidation to $[VO(acac)_2]^+$ by a process which seems to be reversible in the short times of cyclic voltammetry, but coupled to chemical complications in the longer times of exhaustive electrolysis[232f]. One of its salts has been spectroscopically identified as $[VO(acac)_2](I_5)$[175]. $VO(acac)_2$ also undergoes irreversible or partially reversible reduction processes, particularly in the presence of uncomplexed acac, which ultimately afford $[V(acac)_3]$[232f,234a]. The pertinent electrode potentials are listed in Table 8.

b. Group 6 elements. Most of the electrochemical investigations have dealt with $Cr(dik)_3$ complexes[234b,236]. Such chromium(III) complexes display the sequential Cr(III) → Cr(II) → Cr(I) reductions which, in spite of features of chemical reversibility in the time scales of polarography or cyclic voltammetry, are accompanied by slow release of ligand[236c,h]. However, no experimental measurement on the lifetimes of such reduction products has been carried out in the longer times of exhaustive electrolysis; this is probably due to the markedly negative potential values at which the reduction occurs. Moreover, no crystal structures of compounds containing the $[Cr(dik)_3]^{n-}$ anions are available, whereas a number of structural data are available for the neutral chromium(III) complexes[237]. The formal electrode potentials of the redox changes exhibited by representative, symmetrically substituted, $Cr(dik)_3$ complexes are reported in Table 9. Complexes containing different substituents in the R^2 position have been also examined[236b,h], from which it is evident that the redox potentials are quite sensitive to the electronic effects of the substituents. It has been shown that linear relationships hold between the formal electrode

TABLE 9. Formal electrode potentials (vs. SCE) for the redox changes of selected $[Cr(dik)_3]^z$ complexes in various solvents

dik	$E^{\circ\prime}$ (V) (z: 0 → −)	$E^{\circ\prime}$ (V) (z: − → 2−)	Solvent	Reference
$CH(CHO)_2^-$	−1.32	−1.82	dmso	236b
	−1.52	—	CH_2Cl_2	236g
acac	−1.73	−2.16	dmso	236b
	−1.94	−2.40	MeCN or Me_2CO	236h
	−1.72	—	Me_2CO	236c
	−1.85	−2.10	MeCN	234b
	−1.81	−2.10	MeCN	236a
	−1.86	−2.15	MeCN	236f
	−2.12[a]	—	CH_2Cl_2	236e
	−2.04	—	CH_2Cl_2	236g
	−1.94	−2.31	dmf	236i
hfacac	−0.40	−1.48	dmso	236b
	−0.40	—	CH_2Cl_2	236g
	−0.20	−0.86	MeCN or Me_2CO	236h
	−0.15	−0.84	MeCN	234b
dbm	−1.26	−1.72	dmso	236b
	−1.48	—	CH_2Cl_2	236g
	−1.63	−2.13	MeCN or Me_2CO	236h
dpm	−2.12	—	MeCN or Me_2CO	236h

[a] Partially overlapped by the solvent discharge.

TABLE 10. Formal electrode potentials (vs. SCE) for the redox changes of $[Mn(acac)_3]^z$ in various solvents

$E^{\circ\prime}$ (V) (z: 0 → +)	$E^{\circ\prime}$ (V) (z: 0 → −)	Solvent	Reference
	+0.03	Me_2CO	236c
+0.97	−0.09	MeCN	234b, 238a
+0.97	−0.13		238c
—	−0.2	thf	238d
+0.95	−0.05	prc	238a
—	−0.07		238b

potentials of the first reduction and the Hammett σ constants of the substituents[236b,h], implying that also the frontier orbitals are affected by the ligand.

c. Group 7 elements. To the best of our knowledge, $Mn(acac)_3$ is the only tris(β-diketonate) complex of manganese which has been studied by electrochemical techniques[234b, 236c, 238]. It exhibits in non-aqueous solvents either a one-electron oxidation or a one-electron reduction, which display a prevailing character of chemical reversibility (Table 10). While the crystal structure of the neutral manganese(III) complex is available[237], there are no structural data either on $[Mn(acac)_3]^+$ or $[Mn(acac)_3]^-$ containing species which could be used to support the chemical reversibility of the pertinent electron transfers. It is in fact expected that the chemical reversibility of an electrochemical process is associated to small changes of the structural parameters of the reduced and oxidized species[137] (as obtained via a XRD study of the species involved in the redox process). Crystal data are available instead for the neutral $Mn(hfacac)_3$[239] and the ionic $[Mn(bpyn)_2(hfacac)][Mn(hfacac)_3]$[240a] and $[FeCp_2][Mn(hfacac)_3]$[240b] derivatives[240], the electrochemical behaviour of which is still unknown (although it has been estimated that the pertinent formal electrode potential is about +0.5 V (vs. SCE) in CH_2Cl_2 solution[240b]).

A number of $Mn(dik)_2$ complexes have been also prepared, which are best described as $[Mn(dik)_2(X)_2]$, X = *N*- or *O*-donor ligand. The crystal structures of the neutral species $Mn(acac)_2(H_2O)_2$ and of the oxidized one, $[Mn(acac)_2(H_2O)_2]ClO_4$, have been reported[241], but no pertinent electrochemical investigations have been performed.

d. Group 8 elements. As easily predictable, electrochemical investigation on $Fe(dik)_3$ complexes in various solvents revealed the Fe(III) → Fe(II) reduction[234b, 236a,c,f, 237, 242], which in most cases appeared as chemically reversible. The respective electrode potentials are compiled in Table 11. It has to be noted that $Fe(acac)_3$ also undergoes an irreversible oxidation[236f, 242d]. As in the case of manganese β-diketonates (see Section IV.B.2.c), crystallographic data involving iron(III) and iron(II) β-diketonates are available only in the case of the fluorinated derivatives $Fe(hfacac)_3$[243] and $[Fe(bpyn)_2(hfacac)][Fe(hfacac)_3]$[240a].

The $Ru(dik)_3$ complexes have been the subject of numerous electrochemical investigations in different media (from aqueous to non-aqueous solvents, to molten salts)[236d, 242c, 244]. Their typical electron transfer ability is illustrated in Figure 5, which refers to $Ru(acac)_3$ in MeCN solution[242c]. In most solvents $Ru(dik)_3$ complexes display either a one-electron oxidation or a one-electron reduction, both the processes exhibiting features of chemical reversibility in the short times of cyclic voltammetry. However, the Ru(III) →

TABLE 11. Formal electrode potentials (vs. SCE) for the redox changes of selected $[Fe(dik)_3]^z$ complexes in various solvents

dik	$E^{\circ\prime}$ (V) (z: 0 → −)	Solvent	Reference
acac	−0.67	MeCN	236a, 237
	−0.64	MeCN	236f
	−0.69	MeCN	242b
	−0.65	MeCN	242c
	−0.62	MeCN	242d
	−0.69	prc	242b
	−0.58	Me_2CO	236c
	−0.66	Me_2CO	242b
	−0.64	dmf	242b
	−0.67	CH_2Cl_2	242e
hfacac	+0.02	MeCN	237b
	+0.03	MeCN	242d
	−0.02	CH_2Cl_2	242e
dbm	−0.49	MeCN	242d
	−0.54	CH_2Cl_2	242e
dpm	−0.87	prc	242b

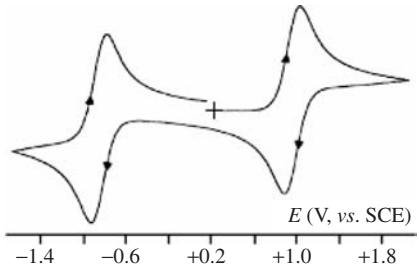

FIGURE 5. Cyclic voltammogram of $Ru(acac)_3$ (Pt electrode, MeCN)[242c]. Reproduced from Reference 242c by permission of Elsevier

Ru(IV) oxidation seems to be coupled to chemical complications in the longer times of bulk electrolysis. Table 12 summarizes the formal electrode potentials for the sequence Ru(IV) → Ru(III) → Ru(II) of symmetric $Ru(dik)_3$ complexes.

As in the case of the chromium(III) derivatives, a linear relationship between the Ru(III) → Ru(IV) and Ru(III) → Ru(II) formal electrode potentials and the electronic effects of the substituents[244a,d,f,g,j,k,l] has been observed for the $Ru(dik)_3$ complexes. In spite of the preparation of some ruthenium(II) compounds containing the $[Ru(dik)_3]^-$ monoanion[244a,b,k,245], no crystal structure is available for ruthenium(II) or ruthenium(IV) congeners.

The intramolecular electron exchanges among the different metal sites of polynuclear β-diketonate–metal complexes are a matter of intrinsic interest, especially as far as the stabilization of mixed-valent oxidation states is concerned[246]. Obviously, the pertinent electrochemical pattern, while becoming richer and richer, also tends to become more

TABLE 12. Formal electrode potentials (vs. SCE) for the redox changes of selected $[Ru(dik)_3]^z$ complexes in various solvents

dik	$E^{\circ\prime}$ (V) (z: 0 → +)	$E^{\circ\prime}$ (V) (z: 0 → −)	Solvent	Reference
acac	+1.09	−0.75	CH_2Cl_2	242c
	+0.94	−0.89	CH_2Cl_2	244o
	+1.14	−0.70	thf	242c
	+1.00	−0.74	MeCN	242c
	—	−0.72	MeCN	244c
	+1.03	−0.74	MeCN	244d,f,g,i–k
	+0.98	−0.78	MeCN	244n, o
	—	−0.79	dmf	242c
	—	−0.73	dmf	236d, 244a
	+1.11	−0.70	dmf	244m
	+0.68	—	$MeNO_2$	244j
hfacac	—	+0.73	MeCN	236d, 244a
	—	+0.76	MeCN	244g,j,k
	—	+0.67	dmf	244j
	—	+0.27	$MeNO_2$	244j
dbm	—	−0.50	dmf	236d, 244a
	+1.04	−0.52	MeCN	244d,g,j
dpm	+0.92	−1.04	dmf	236d, 244a,j
	+0.97	−1.00	dmf	244m
	+0.85	−1.05	MeCN	244d,g,j,k
	+0.43	—	$MeNO_2$	244j

complicated. The discussion will be limited to a series of binuclear ruthenium(III) tris(β-diketonate) complexes **112**, in which the two ruthenium centres are separated by substantially linear spacers. Binuclear ruthenium complexes with more complex connecting bridges[247] or formed by heteroleptic mononuclear units[248] have also been reported.

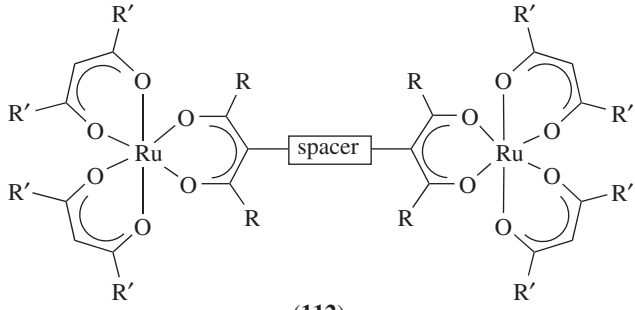

(**112**)

Let us start with the complex in which the two ruthenium(III) tris(β-diketonate) centres are directly connected by an LL bridge with no spacer (R = R′ = CH_3, $(acac)_2Ru(LL)Ru(acac)_2$; R = CH_3, R′ = *t*-Bu, $(dpm)_2Ru(LL)Ru(dpm)_2)^{244n}$. As illustrated in Figure 6, which refers to $(acac)_2Ru(LL)Ru(acac)_2$, such complexes undergo two stepwise oxidations and two stepwise reductions, all having features of chemical reversibility. The involved

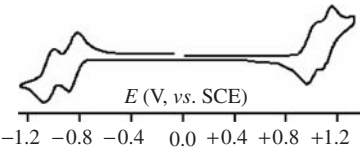

FIGURE 6. Cyclic voltammogram of $(acac)_2Ru(LL)Ru(acac)_2$ (Pt electrode, CH_2Cl_2, scan rate 0.1 $V\,s^{-1}$)[244n]. Reproduced from Reference 244n with permission. Copyright 2004 American Chemical Society

electron transfer sequence is shown in equation 80. A qualitatively similar electrochemical response is given by the complexes having a sulphide or a disulphide spacer[244o].

$$\begin{array}{l} \mathrm{Ru(IV)-Ru(IV)} \underset{-e^-}{\overset{+e^-}{\rightleftharpoons}} \mathrm{Ru(IV)-Ru(III)} \underset{-e^-}{\overset{+e^-}{\rightleftharpoons}} \mathrm{Ru(III)-Ru(III)} \underset{-e^-}{\overset{+e^-}{\rightleftharpoons}} \mathrm{Ru(III)-Ru(II)} \\ \qquad\qquad\qquad\qquad\qquad\qquad\qquad\qquad\qquad\qquad\qquad\qquad\qquad\qquad\qquad\qquad \Big\updownarrow {\scriptstyle -e^- \;\; +e^-} \\ \qquad\qquad\qquad\qquad\qquad\qquad\qquad\qquad\qquad\qquad\qquad\qquad\qquad\qquad\qquad\qquad \mathrm{Ru(II)-Ru(II)} \end{array} \tag{80}$$

A somewhat different picture (Figure 7) is given by **112** (R = CH_3, R′ = *t*-Bu, spacer = $-C{\equiv}C-C{\equiv}C-$)[249], exhibiting the usual stepwise reduction pattern Ru(IV)−Ru(IV) → Ru(III)−Ru(IV) → Ru(III)−Ru(III). Instead of the two-step reduction from Ru(III)−Ru(III) to Ru(II)−Ru(II) shown in equation 80, this proceeds in a single two-electron step, which means that the mixed valent Ru(III)−Ru(II) form is quite unstable. The same behaviour is exhibited by the related complexes having a 1,6-hexatriynediyl, a 2,5-thiophenediyldi(2,1-ethynediyl) or a 9,10-anthracenediyldi(2,1-ethynediyl) spacer[250]. The formal electrode potentials of the redox changes discussed above for all the binuclear complexes are reported in Table 13.

The stability of the mixed-valent species Ru(IV)−Ru(III) and Ru(III)−Ru(II) can be at first determined by the separation of the respective oxidation or reduction sequences, i.e. the higher the separations between the two stepwise processes, the higher the stability of the mixed-valent systems. In all cases, but for those in which a single two-electron step was detected, the Ru(IV)−Ru(III) and Ru(III)−Ru(II) systems belong to the partially delocalized mixed-valent systems.

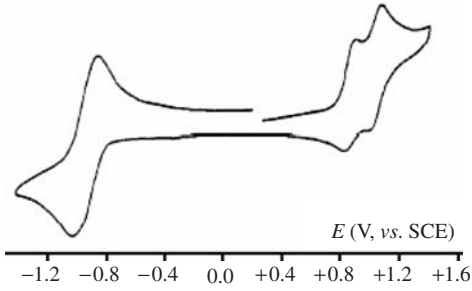

FIGURE 7. Cyclic voltammogram of **112** (R = CH_3, R′ = *t*-Bu, spacer = $-C{\equiv}C-C{\equiv}C-$) (Pt electrode, CH_2Cl_2, scan rate 0.1 $V\,s^{-1}$)[249]. Reproduced from Reference 249 with permission. Copyright 1992 American Chemical Society

TABLE 13. Formal electrode potentials (vs. SCE) and relative separations for the sequential oxidations and reductions of the binuclear ruthenium complexes [**112**]^z in CH_2Cl_2 solution as a function of the spacer

Spacer	R	R′	$E^{\circ\prime}$ (V) (z: 2+ → +)	$E^{\circ\prime}$ (V) (z: + → 0)	$\Delta E^{\circ\prime}$ (V)	$E^{\circ\prime}$ (V) (z: 0 → −)	$E^{\circ\prime}$ (V) (z: − → 2−)	$\Delta E^{\circ\prime}$ (V)	Reference
none	Me	Me	+1.04	+0.92	0.12	−0.92	−1.10	0.18	244n
none	Me	*t*-Bu	+0.93	+0.73	0.20	−1.16	−1.34	0.18	244n
−S−	Me	Me	+1.15	+0.95	0.20	−0.83	−1.04	0.21	244o
−S−S−	Me	Me	+1.17[a]	+1.01	—	−0.78	−0.93	0.15	244o
−C≡C−C≡C−	Me	*t*-Bu	+0.88	+1.11	0.23	−0.94	−0.94	0	249
−C≡C−C≡C−C≡C−	Me	*t*-Bu	+0.86	+0.98	0.13	−0.96	−0.96	0	250
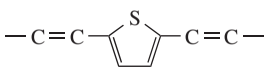	Me	*t*-Bu	+0.77	+0.95	0.18	−0.98	−0.98	0	250
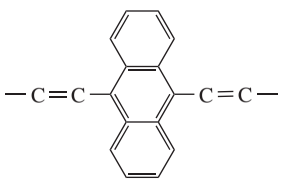	Me	*t*-Bu	+0.67	+0.85	0.18	−0.99	−0.99	0	250

[a] Peak-potential value for irreversible processes.

As far as the $Os(dik)_3$ complexes are concerned, to the best of our knowledge the only electrochemical investigation reported to date deals with $Os(acac)_3$[251], which undergoes the reversible Os(III) → Os(II) reduction at $E^{\circ\prime} = -1.24$ V, vs. SCE, in MeCN solution[244a]. Significantly, the reduction potential is more negative than the corresponding process for the iron(III) and ruthenium(III) homologues, in agreement with the higher stability of the high oxidation states on descending a vertical sequence of transition elements[107].

e. Group 9 elements. Many electrochemical studies have focussed on $Co(dik)_3$ complexes[234b, 236a,f, 238b, 242c, 252]. Generally, they display two reduction processes: the first is attributed to the Co(III) → Co(II) passage, whereas the second process should afford cobalt(0) via ligand release. It is commonly accepted that also the Co(III) → Co(II) reduction is coupled to release of ligands, affording $Co(dik)_2$, in different solvents. It should be noted that conflicting results have been obtained in MeCN: some reports describe the process as followed by chemical complications[234b, 242c, 252e], whereas other reports state its chemical reversibility[238b, 252c,e]. Table 14 compiles the formal electrode processes, limited to the symmetrically substituted derivatives. Crystallographic data are available[237] for neutral or reduced β-diketonate species such as $Co(acac)_3$[253], $E[Co(acac)_3]$, $E = NBu_4^+$[254a], Na^+[254b], and $[Co(bpyn)_2(hfacac)][Co(hfacac)_3]$[240a].

Electrochemical investigations have been carried out on $Co(dik)_2$ complexes in various solvents[236a, 238b, 252a,b, 255]. As can be seen in Table 15, most derivatives undergo irreversible electron transfer processes. Partially chemically reversible reduction processes have been detected only for $Co(dbm)_2$ complex. In fact, the slow release of ligand upon reduction is assumed from the appearance of the voltammetric profile of the free ligand at potential values more negative than those of the metal-centred processes[255]. Further support to the chemical irreversibility of these redox changes has been adduced from the fact that only crystal structures of neutral Co(II) complexes are available[237], suggesting that the reduced species are probably not stable. It should be noted that in coordinating solvents it is unlikely that the investigated complexes might maintain their solid state tetrahedral geometry.

TABLE 14. Formal electrode potentials (vs. SCE) for the redox changes of selected $[Co(dik)_3]^z$ complexes in various solvents

dik	$E^{\circ\prime}$ (V) (z: 0 → −)	$E^{\circ\prime}$ (V) (z: − → 2−)	Solvent	Reference
acac	−0.38	—	MeCN	238b
	−0.27	—	MeCN	252a
	−0.43 [a]	—	MeCN	234b
	−1.15 [a,b]	—	MeCN	242c
	−0.90 [a,b]	—	MeCN	236f
	−0.34	—	MeCN	252c,e,f
	−0.25 [a]	—	Me_2CO	236c
	−0.80 [a]	—	dme	252a
	−0.64 [a]	—	dmf	252d
$hfacac_3$	+0.50	−1.25 [b]	MeCN	252c,f
dbm	−0.13	−1.95	MeCN	252c,f
	−0.05	−1.85	dmf	252b
dpm	−0.40	—	MeCN	252c,f

[a] Coupled to chemical complications.
[b] Peak-potential value for irreversible processes.

TABLE 15. Formal electrode potentials (vs. SCE) for the redox changes of selected $[Co(dik)_2]^z$ complexes in various solvents

dik	E_p (V) (z: $+ \rightarrow 0$)	$E^{\circ\prime}$ (V) (z: $0 \rightarrow -$)	$E^{\circ\prime}$ (V) (z: $- \rightarrow 2-$)	Solvent	Reference
acac	+0.32	−1.84 [a,b]	−1.98 [a,b]	MeCN	236a
	—	−1.95 [a,b]	—	MeCN	238b
	—	−1.96 [a,b]	—	dmf	252b
	—	−2.2 [c]	—	dme	252a
dbm	—	−1.58 [c]	−1.80 [c]	dmf	252b
	—	−1.59 [c]	−1.78 [c]		255

[a] Coupled to fast chemical complications.
[b] Peak-potential value for irreversible processes.
[c] Coupled to slow chemical complications.

The only electrochemically studied rhodium derivative, $Rh(acac)_3$, exhibits an irreversible one-electron oxidation ($E_p = +1.70$ V, vs. SCE, in MeCN solution)[242c] and an irreversible two-electron reduction ($E_p = -2.21$ V, in THF solution)[256]. The same situation holds for $Ir(dik)_3$ complexes. At variance with the rhodium derivative, $Ir(acac)_3$ shows a chemically reversible one-electron oxidation ($E^{\circ\prime} = +1.15$ V, vs. SCE, in MeCN solution)[242c] and an irreversible two-electron reduction ($E_p = -2.60$ V, in THF solution). No crystallographic data of species containing the $[Ir(acac)_3]^+$ cation are available[237].

f. Group 10 elements. The crystal structures of derivatives containing the $[Ni(dik)_3]^-$ anion are known[237], but no pertinent electrochemical data are available. Electrochemical investigations have been carried out only on $Ni(acac)_2$[234b, 236a,f, 238b, 252a], which exhibits irreversible electron transfer processes (Table 16). In particular, it is assumed that it undergoes a two-electron reduction with separation of nickel metal. Moreover, it is evident from the data of Table 16 that the investigations carried out in MeCN solution do not refer to the original molecule but to the solvated species $Ni(acac)_2(MeCN)_2$.

The only electrochemical study available on palladium derivatives reports that $Pd(acac)_2$ in acetonitrile undergoes an irreversible two-electron reduction to palladium metal ($E_p = -0.97$ V, vs. SCE)[236a].

g. Group 11 elements. Compounds containing the $[Cu(hfacac)_3]^-$ anion have been isolated and characterized[237], but no pertinent electrochemical data are available, apart from the attempt to attribute to the couple $[Cu(hfacac)_3]^- \rightarrow [Cu(hfacac)_3]^{2-}$ a reduction potential similar to that of the $[Cu(hfacac)_2] \rightarrow [Cu(hfacac)_2]^-$ [257]couple. The redox activity of a number of copper(II) β-diketonates has been studied by electrochemical

TABLE 16. Formal electrode potentials (vs. SCE) for the redox changes of $Ni(acac)_2$ in different solvents

E_p (V) (z: $+ \rightarrow 0$)	E_p (V) (z: $0 \rightarrow -$)	E_p (V) (z: $- \rightarrow 2-$)	Solvent	Reference
	−1.8	—	dme	252a
+0.28	−1.30	−1.47	MeCN	236a
—	−1.47	−1.47	MeCN	238b
+0.15	−1.50	−1.50	MeCN	236f
—	−0.72	−1.01	MeCN	234b

TABLE 17. Formal electrode potentials (vs. SCE) for the redox changes of selected $[Cu(dik)_2]^z$ complexes in different solvents

dik	$E^{\circ\prime}$ (V) (z: 0 → −)	$E^{\circ\prime}$ (V) (z: − → 2−)	Solvent	Reference
acac	−0.61 [b]	—	MeCN	234b
	−0.61 [a]	−0.61 [a]	MeCN	236a
	−1.05 [a]	−1.53 [a]	MeCN	236f
	−0.67 [b]	−0.67 [b]	MeCN	238b
	−0.67 [b]	−0.67 [b]	MeCN	258b
	−0.50 [a]	−0.50 [a]	Dioxane:H_2O (3:1)	258a
	−1.34 [a]	−1.34 [a]	CH_2Cl_2	236e
hfacac	−0.40 [b]	—	MeCN	234b
	−0.36 [b]	−0.65 [b]	MeCN	258b
	+0.04 [a]	+0.04 [a]	Dioxane:H_2O (3:1)	258a
dpm	−0.82 [b]	−1.61 [a]	MeCN	258b
	−0.69 [a]	−0.69 [a]	Dioxane:H_2O (3:1)	258a
dbm	−0.38 [a]	−0.38 [a]	Dioxane:H_2O (3:1)	258a

[a] Coupled to fast chemical complications.
[b] Coupled to slow chemical complications.

techniques[234b, 236a,e,f, 238b, 258]. Depending upon the nature of the β-diketonato ligand, they may exhibit a single two-electron reduction or two separate one-electron reductions. In any case, the electron transfer processes are coupled to more or less fast release of the diketonato ligand, which means that copper(II) is the only stable oxidation state in the system. Table 17 summarizes the formal electrode potentials for the Cu(II) → Cu(I) → Cu(0) reductions of selected copper(II) β-diketonates.

h. Lanthanides. The electrochemical investigation of lanthanides β-diketonates is scarcely developed and the studies are limited to cerium and europium.

Electrochemical investigation of $Ce(acac)_3$[234b, 238b] have been performed, but the existence of such species in solution is doubted because of its high reactivity towards hydrolysis or dioxygen. In addition, no crystal structure is available for $Ce(dik)_3$ derivatives[237]. A couple of investigations have been concerned with the octacoordinated $Ce(acac)_4$[259], which undergoes reduction to the corresponding cerium(III) monoanion $[Ce(acac)_4]^-$ at potentials between −0.02 and −0.06 V (vs. SCE). Although the process seems to be accompanied by a rather slow release of diketonate, a number of compounds containing the $[Ce(dik)_4]^-$ anion has been isolated and structurally characterized[237], showing that these species are stable, at least in the solid state. In particular, the crystal structures of the unsymmetrically substituted redox couples $Ce(dik)_4$, dik = MefC(O)CHC(O)Bu-t[260], MefC(O)CHC(O)Thi-2[261], are available. At variance with cerium complexes, the existence of $Eu(dik)_3$ is established, even if the pertinent crystal structures show the presence of water or pyridine molecules to complete the octacoordination of the central europium(III) ion[237]. The scanty electrochemical investigations indicate that $Eu(acac)_3$ displays the Eu(III) → Eu(II) reduction with features of chemical reversibility in the short times of voltammetric techniques, even if no data are available on the stability of $[Eu(acac)_3]^-$ at longer times. The marked difference of the redox potentials in MeCN (−0.67 V vs. SCE) or dmf (−1.55 V vs. SCE) is probably due to the different coordinating ability of the two solvents.

A number of crystal structures of derivatives containing the $[Eu(dik)_4]^-$ are available[237] but, at variance with the cerium complexes, the electrochemical investigation of a number

of europium compounds in MeCN solution revealed that they only display ligand-centred processes[232g]. It is likely that the strong coordination of the central europium(III) causes the Eu(III) → Eu(II) reduction to shift beyond the potential at which the solvent itself becomes redox active (the cathodic discharge of the solvent).

i. Actinides. The thorium(IV) complex, $Th(acac)_4$, is the only β-diketonate studied by electrochemical techniques[238d]. It exhibits a first Th(IV) → Th(III) reduction ($E^{\circ\prime} = -2.16$ V, vs. SCE, THF solution) with features of partial chemical reversibility due to the probable release of $[acac]^-$ ligand, followed by an ill-defined cathodic step attributed to the reduction of $[Th(acac)_4]^-$ and/or $[acac]^-$, which almost overlaps with the solvent discharge.

Electrochemical investigations have dealt with either $UO_2(dik)_2$, or $U(dik)_4$ complexes. Most investigations on $UO_2(dik)_2$ derivatives have been carried out in coordinating solvents such as dmso or dmf, so that they actually refer to solvated molecules such as $UO_2(dik)_2(solvent)_2$[262a–e]. Only in $CHCl_3$ solution[262f] has it been assumed that the complex under study is actually $UO_2(dik)_2$. In this medium, both $UO_2(acac)_2$ and $UO_2(dbm)_2$ undergo a chemically reversible U(VI) → U(V) reduction. On the other hand, in coordinating solvents such as dmso or dmf, the one-electron reduction of most complexes is accompanied by chemical complications, which are probably due to the competitive coordination of the solvent itself (it is assumed that the diketonate may act as unidentate ligand in the uranium(V) species). The formal electrode potentials of the U(VI) → U(V) process for selected complexes in various solvents are compiled in Table 18.

No crystal structure of derivatives containing the $[UO_2(dik)_2]^-$ anion is available[237]. Like $Th(acac)_4$, the uranium analogue, $U(acac)_4$, in thf solution exhibits the U(IV) → U(III) reduction at very negative potential values ($E^{\circ\prime} = -2.2$ V, vs. SCE), which is partially chemically reversible[238d]. A previous report stated that in propylene carbonate or MeCN solution, $U(acac)_4$ exhibited two reduction steps at about -0.8 V and -1.2 V, vs. SCE, respectively[263], but the purity of the sample has been questioned[238d]. The presence of chemical complications following the U(IV) → U(III) step has been also pointed out for the unsymmetric $U(dik)_4$ with dik = MefC(O)CHC(O)Bu-*t* in dmso or dmf solution[262c].

TABLE 18. Formal electrode potentials (vs. SCE) for the one-electron reduction of $[UO_2(dik)_2]^z$ complexes in various solvents

dik	$E^{\circ\prime}$ (V) (z: 0 → −)	Solvent	Reference
acac	−0.71	$CHCl_3$	262f
	−0.95[a,b]	dmso	262a
	−1.06[a,b]	dmso	262c
	−1.06[a,b]	dmso	262e
	−1.01[a,b]	dmf	262d
hfacac	−0.49[b]	dmso	262b
	−0.57[b]	dmso	262c
dpm	−1.22[b,c]	dmso	262c
dbm	−0.67	$CHCl_3$	262f
	−0.89[a,b]	dmso	262b

[a] Coupled to slow chemical complications.
[b] $[UO_2(dik)_2(solvent)_2]$, see text.
[c] Coupled to fast chemical complications.

V. FUNCTIONALIZED β-DIKETONATES

A. Redox Reactions

Many efforts have been made in the last decades to modify the electronic and steric properties of β-diketones by synthesizing derivatives of **84** with R^1, R^2 and R^3 substituents other than alkyl or aryl groups, to prepare polyfunctional coordinating ligands with higher complexity and functionality. The examples reported in this section have been limited to cases which have been studied from the redox viewpoint and, in particular, β-diketonates derived from **113**–**116**.

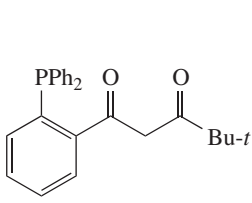

(**113**)

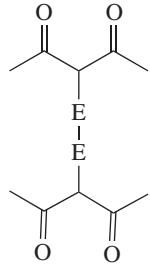

(**114**) E = S, Se

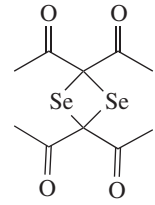

(**115**)

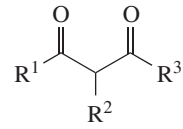

(**116**) (**a**) R^1 = Fc
(**b**) R^2 = Fc
(**c**) $R^1 = R^3$ = Fc

The diketone *o*-(diphenylphosphino)benzoylpinacolone (**113**, dpbpH) exists in the enol form in dichloromethane solution and its enolato anion (dpbp) behaves as tridentate *P*,*O*,*O*-ligand, affording homodinuclear (Cu(I) or Ag(I)) and heterodinuclear (Cu(II) together with Ir(I), Pt(II) or Ru(III)) complexes[264]. The dinuclear complex $Cu_2(dpbp)_2$ (**117**) reacts with dibenzoyl peroxide or *m*-chloroperbenzoic acid yielding the mixed-valence Cu(I)−Cu(II) complexes **118** (equation 81)[264b]. Moreover, oxygenation of **117** in dichloromethane involves both ligand and metal-centred oxidations and gives two products: the dinuclear Cu(II) complex **119** containing a trigonally planar copper(I) linked to a square-pyramidal copper(II) by two dpbp ligands (equation 82), and the methoxy-bridged derivative **120**, obtained by fractional crystallization of **119** from methanol[264d].

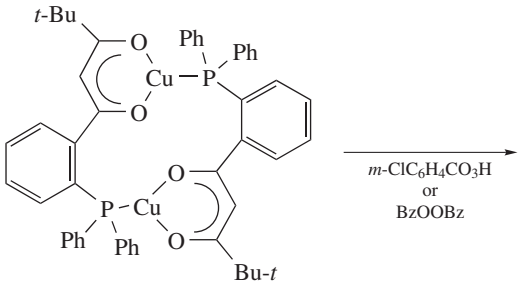

(81)

(**117**)

(**118**) X = H, Cl

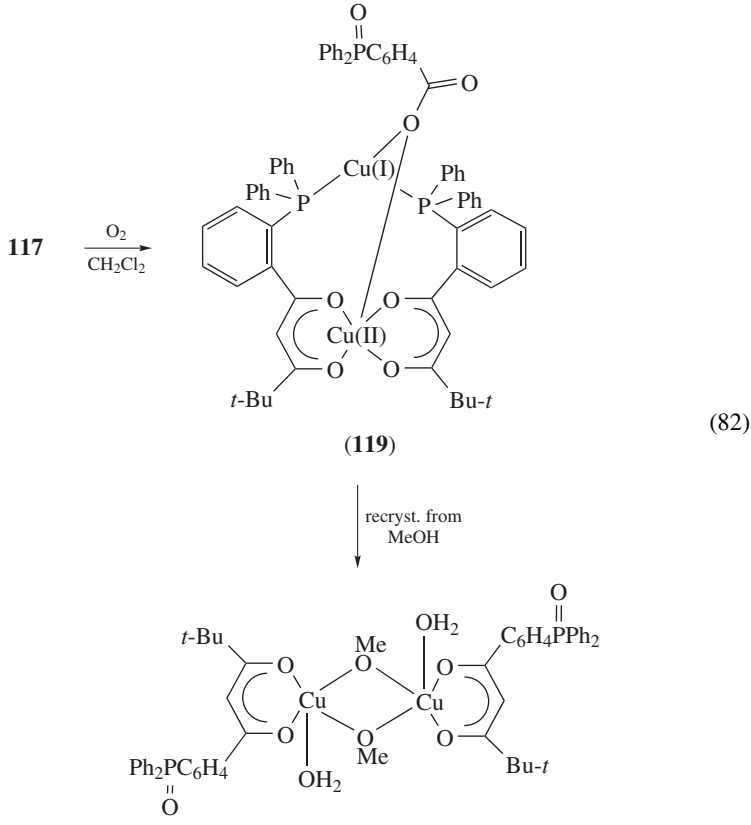

(82)

The bis-β-diketones linked by sulphur or selenium, **114**, which are present in the enol form in solution[265] react with transition metal cations to give the ligand (acetonitrile) substitution products[266] and S−S, S−C and Se−C bond cleavages[247a, 267]. For example, the ruthenium(II) complexes $Ru(dik)_2(NCMe)_2$ (dik = acac, dpm) react at room temperature with **114** (E = S), to give the ruthenium(II) compound **121** (equation 83), following an S−S bond fission. When the reaction is performed in refluxing acetone, addition of **114** to the fragment $Ru(dik)_2$, formed on the dissociation of acetonitrile from $Ru(dik)_2(NCMe)_2$, takes place and the sulphur-bridged dinuclear derivative **122** is formed[247a].

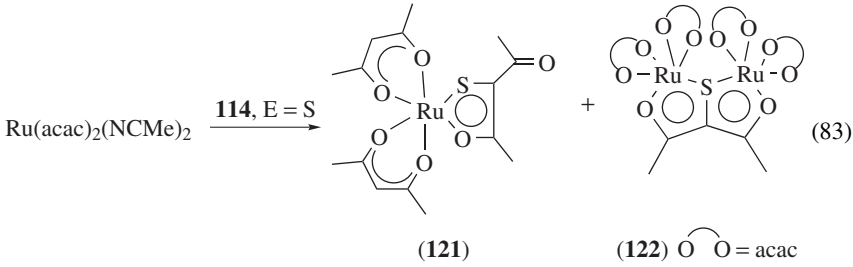

(83)

Yamazaki and coworkers have observed S−S (equation 84a) and S−C or Se−C (equation 84b) bond fission in the reaction of **114** (E = S, Se) with $[PtCl(PMe_2Ph)_3]PF_6$[267a] or *cis*-$PtCl_2(PMe_2Ph)_2$[267b], respectively. On the other hand, **115**, which exists in the keto form[268], reacts with $Pt(PPh_3)_4$ producing the *Se,O*-bonded platinum(II) chelate **123**: two possible intermediates, evolving into **123** via Se−Se bond fission and Pt(I) nuclei or Se−C bond fission and Pt(0) nuclei have been proposed (equation 85).

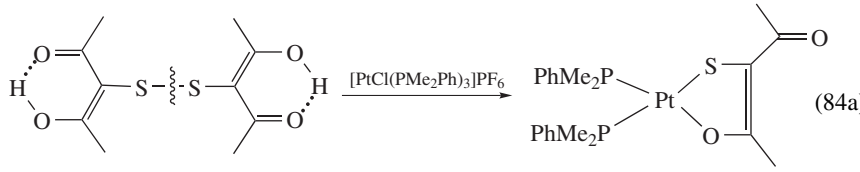

(**114**) (84a)

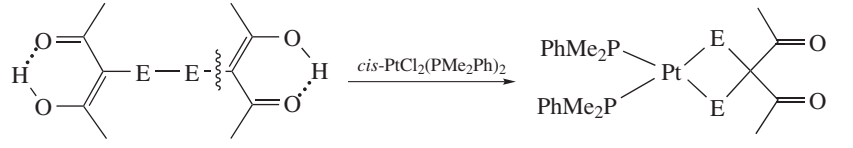

(**114**) E = S, Se (84b)

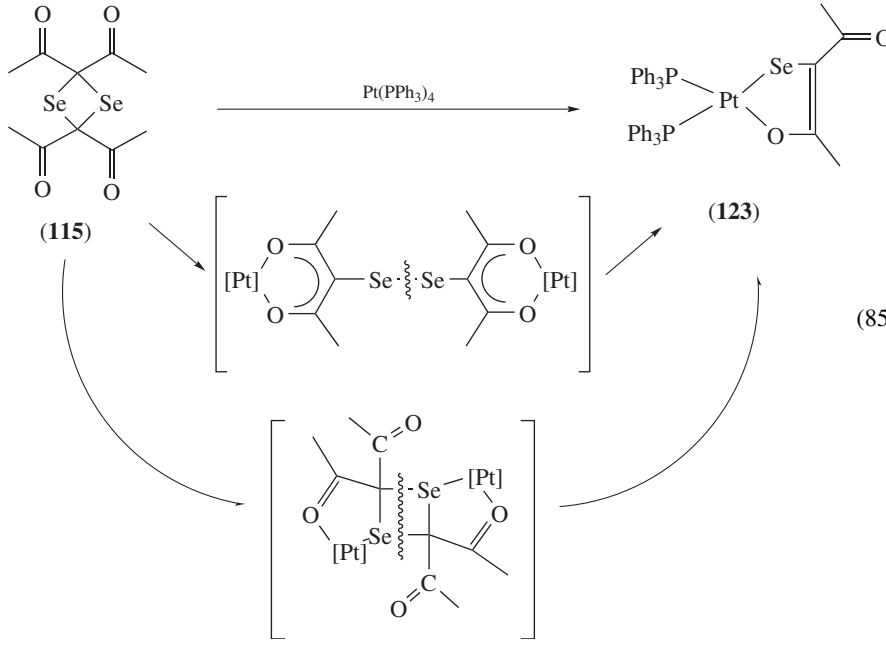

(**115**) (**123**) (85)

Perhaps the most notorious metal-containing dicarbonyl ligands are the ferrocenyl diketonates derived from **116a–c**, first synthesized by Hauser in 1958–1961[269]. Their metal derivatives show interesting electrochemical properties (see Section V.B). As far as the

redox reactions of ferrocenyl diketones are concerned, it has been reported that the manganese(II) complex $Mn(dik)_2$, dik = FcC(O)CHC(O)Me, is oxidized by stoichiometric amounts of permanganate ion to the manganese(III) derivative $Mn(dik)_3$ in the presence of excess diketone (**116a**, R^3 = Me)[270a].

A detailed kinetic study of the oxidative reaction of MeI to Rh(dik)(CO)(PPh_3), dik = FcC(O)CHC(O)Mef has appeared[270b].

Treatment of palladium(II) β-diketonates or PdCl(diferrocenyl-β-diketonato)PPh_3 with NBS affords γ-bromo substituted species[271].

B. Electrochemistry

Insertion of redox-active functions in β-diketonato–metal complexes increases their redox activity. Particularly useful has been the introduction of ferrocenyl or tetrathiofulvenyl substituents; other redox active fragments such as benzoquinone diimines or polypyridines have been also exploited. Frequently, the electrochemical investigation has been focussed on such redox-active substituents rather than on the whole metal–diketonato framework. This section will be limited to well known, representative, mononuclear complexes, but we shall omit complexes such as $MCp_2(acac)$ (M = Ti[272], V[273]), the electrochemistry of which is typical of metal-sandwich complexes[137], as well as complexes of metals in low oxidation states containing π-acids as ligands, such as $Rh(dik)(CO)_2$[274]. In addition, we will limit our survey to well known, representative, mononuclear complexes.

1. Group 6 elements

The octahedral complex $Cr[CH_3C(O)CHC(O)Fc]_3$ displays a single ferrocenyl oxidation at +0.58 V, vs. SCE (CH_2Cl_2 solution), which is lower by about 60 mV than that of the free 1-ferrocenyl-1,3-butanedionato ligand, thus suggesting that the chromium(III) diketonate donates electron density to the ferrocenyl appendices[270a]. As a consequence, the Cr(III) → Cr(II) reduction, which is partially overlapped by the solvent discharge[236e] in $Cr(acac)_3$, cannot be detected. The simultaneous oxidation of the three ferrocenyl units means that they are electronically isolated from each other.

2. Group 7 elements

The manganese derivative $Mn[CH_3C(O)CHC(O)Fc]_3$ is oxidized at potential values 50 mV lower than that of the free ferrocenyl ligand. In addition, it exhibits the chemically reversible Mn(III) → Mn(II) reduction at −0.36 V[270a] which, as expected, appears slightly more negative than that of $Mn(acac)_3$ (Section IV.B.2.c.).

The electrochemistry of manganese(II) complexes bearing functionalized tetrathiafulvalene (ttf) ligands directly linked to the manganese(II) centre, *trans*-$Mn(dik)_2(ttf)_2$, or as substituents in the β-diketonate itself, Mn(ttf-substituted-β-diketonate)$_2$, has been reported. In benzonitrile solution, the complex with 4,5-ethylenedioxy-4′,5′-(4-pyridylethylene-1,2-dithio)tetrathiafulvalene (**124**), *trans*-Mn(hfacac)$_2$(**124**)$_2$, exhibits two reversible oxidation processes at the same potential values of the free ttf-based ligand ($E^{\circ\prime}$ = +0.52 V and +0.83 V, vs. SCE, respectively), thus indicating that no significant flow of electron density between the {Mn(hfacac)$_2$} fragment and the axially coordinated **124** is operative[275].

A slightly different behaviour is observed for the complex with the 3-(4,5-bis(methylthio)tetrathiafulvalen-4-ylthio)-2,4-pentanedionato anion (**125**), Mn(**125**)$_2$[276]. It undergoes two oxidation processes ($E^{\circ\prime}$ = +0.50 V and +0.79 V, vs. SCE, in 4:1 CH_2Cl_2:C_2H_5OH) which are shifted towards less negative potential values by about 30 mV relative to those of the protonated **125**, thus indicating that the functional group attached to acac

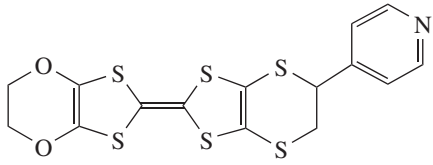

(**124**)

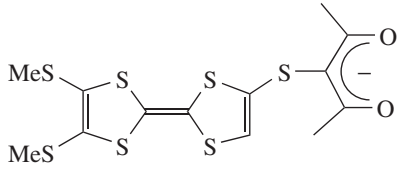

(**125**)

as a substituent withdraws electron density from the rest of the complex framework. No electrochemical data involving the {Mn(dik)$_2$}fragments are reported.

Insertion of ferrocenyl substituents is a common way of increasing the redox activity of metal β-diketonates (see also Section V.A), as is the case of Mn(hfacac)$_2$L$_2$ complexes where L = 5-ferrocenylpyrimidine (**126**) or ferrocenylpyrazine (**126′**)[277]. Because of the instability of the *cis*- (**127**) and *trans*- (**127′**) forms of Mn(hfacac)$_2$L$_2$ in organic solvents, their redox activity has been studied in the solid state. They undergo a single ferrocene-based oxidation at potential values slightly lower than that exhibited by the respective uncoordinated ligands (+0.32 vs. +0.37 V in the case of **127** vs. **126** and +0.35 vs. +0.38 V in the case of **127′** vs. **126′**). At variance with *trans*-Mn(hfacac)$_2$(**124**)$_2$, some electronic effects seem to be operative between the {Mn(hfacac)$_2$} fragment and the ferrocenyl ligands. The appearance of a single oxidation process suggests that the two ferrocenyl groups are electronically independent.

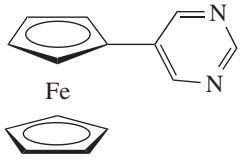

(**126**)

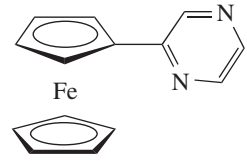

(**126′**)

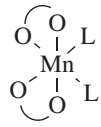

(**127**) *cis*-Mn(hfacac)$_2$L$_2$
L = **126**, **126′**

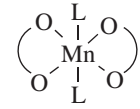

(**127′**) *trans*-Mn(hfacac)$_2$L$_2$
L = **126**, **126′**

3. Group 8 elements

The ferrocenyl-substituted complex $Fe[CH_3C(O)CHC(O)Fc]_3$ is more easily oxidized by about 60 mV (CH_2Cl_2) than the diketone $CH_3C(O)CH_2C(O)Fc$ itself[270a]. It also undergoes the Fe(III) → Fe(II) reversible reduction at $E^{\circ\prime} = -0.88$ V (vs. SCE) which, as a consequence of the increase of electron density on the iron-diketonato fragment, is slightly shifted towards more negative potential values with respect to that of $Fe(acac)_3$ ($E^{\circ\prime} = -0.67$ V)[242e].

The ruthenium(III) β-diketonato **128** exemplifies well how the electron transfer activity of β-diketonato metal complexes can be increased by the proper insertion of redox-active groups[244e]. **128** undergoes the following electrochemical processes (Figure 8): (i) the reversible (in the cyclic voltammetric time scale) one-electron reduction steps Ru(III) → Ru(II) → Ru(I) → Ru(0) ($E^{\circ\prime} = -0.47$, -0.65, -0.80 V, respectively, vs. SCE); (ii) the Ru(III) → Ru(IV) oxidation ($E^{\circ\prime} = +1.03$ V); (iii) the concurrent one-electron oxidation of the three ferrocenyl units ($E^{\circ\prime} = +0.45$ V); (iv) the acetylacetonate-centred oxidation ($E^{\circ\prime} = +0.64$ V).

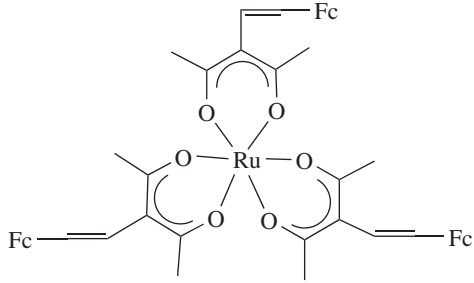

(**128**)

A more limited reversible redox chemistry is displayed by $Ru(dik)_3$ where one of the β-diketonato groups is $[FcC{\equiv}CC{\equiv}CCAc_2]^-$ [249]. It undergoes the ferrocenyl oxidation at $E^{\circ\prime} = +0.55$ V (vs. SCE, MeCN), followed by the Ru(III) → Ru(IV) process at $E^{\circ\prime} = +1.01$ V. The Ru(III) → Ru(II) reduction occurs at $E^{\circ\prime} = -0.81$ V.

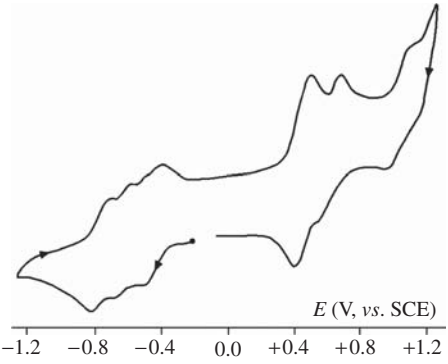

FIGURE 8. Cyclic voltammogram of $Ru[CH_3C(O)C(CH{=}CHFc)C(O)CH_3]_3$ (**128**) (Pt electrode, MeCN)[244e]. Reproduced from Reference 244e by permission of the Royal Society of Chemistry

TABLE 19. Formal electrode potentials (vs. SCE) for the redox changes exhibited by $Ru(acac)_2$(bqdi), bqdi = *o*-HN=(C_6H_3R)=NR′, complexes in acetonitrile

R	R′	$E^{\circ\prime}$ (V) Ru(IV) → Ru(III) [a]	$E^{\circ\prime}$ (V) Ru(III) → Ru(II) [b]	$E^{\circ\prime}$ (V) bqdi/sqdi [c]	$E^{\circ\prime}$ (V) sqdi/opda [d]	Reference
H	H	+1.56 [e]	+0.38	−1.13	−2.10 [e]	179
H	Ph	+1.60 [e]	+0.41	−1.05	−2.04 [e]	179
p-Me	*p*-Tol	+1.53 [e]	+0.33	−1.14	−2.09 [e]	179
p-MeO	*p*-$MeOC_6H_4$	+1.48 [e]	+0.27	−1.17	−2.15 [e]	179
p-Cl	*p*-ClC_6H_4	+1.66 [e]	+0.52	−0.87	−1.94 [e]	179
m-NH_2	*m*-$H_2NC_6H_4$	—	+0.35	−1.14	−1.82 [e]	278

[a] For the process $[Ru(IV)(acac)_2(bqdi)]^{2+} \underset{-\,e^-}{\overset{+\,e^-}{\rightleftharpoons}} [Ru(III)(acac)_2(bqdi)]^{+}$.

[b] For the process $[Ru(III)(acac)_2(bqdi)]^{+} \underset{-\,e^-}{\overset{+\,e^-}{\rightleftharpoons}} Ru(II)(acac)_2(bqdi)$.

[c] The process consists of the one-electron reduction of the diimine.

[d] The process consists of the one-electron reduction of the *o*-benzosemiquinonediimide anion.

[e] Peak-potential value for irreversible processes.

A series of *N*-substituted *o*-benzoquinonediimines, *o*-HN=*p*-C_6H_3R=NR′, adducts of $Ru(acac)_2$, have been characterized from the electrochemical viewpoint[179,278]. Since the ligand is able to undergo reversible stepwise reduction to sqdi and opda, the adducts exhibit in MeCN solution either the Ru(II) → Ru(III) → Ru(IV) oxidations or the benzoquinonediimine-centred reductions (Table 19). When using dppz (**129**)[279] as ligand, the adduct $Ru(acac)_2$(dppz) undergoes the stepwise Ru(II) → Ru(III) → Ru(IV) oxidation at $E^{\circ\prime} = -0.03$ V and +1.49 V (vs. SCE, MeCN), respectively, and the monoelectronic dppz reduction at $E^{\circ\prime} = 1.15$ V.

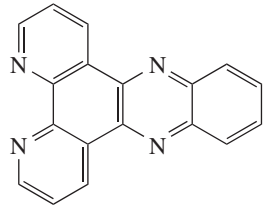

(**129**)

Table 20 compares the formal electrode potential of the Ru(II) → Ru(III) redox change in $Ru(acac)_3$ and the complexes obtained on replacement of one acac anion for *o*-benzoquinonediimines and dppz, It is evident that all the redox-active ligands are more electron-withdrawing than acac, and the benzoquinonediimine ligands are much more electron-withdrawing than dppz.

4. Group 9 elements

From a qualitative viewpoint, the electrochemical behaviour of $Co[CH_3C(O)CHC(O)Fc]_2$ is substantially similar to that of the previously described chromium, manganese

TABLE 20. Formal electrode potential (vs. SCE) for the Ru(III) → Ru(II) redox change in $Ru(acac)_3$ and $Ru(acac)_2(L)$ complexes in acetonitrile

Complex	$E^{\circ\prime}$ (V) Ru(III) → Ru(II)	Reference
$Ru(acac)_3$ [a]	−0.74	242c
$Ru(acac)_2(o\text{-}HN{=}C_6H_4{=}NH)$ [b]	+0.38	179
$Ru(acac)_2(o\text{-}HN{=}C_6H_4{=}NPh)$ [b]	+0.41	179
$Ru(acac)_2(dppz)$ [b]	−0.03	279

[a] For the process $[Ru(III)(acac)_3] \rightarrow [Ru(II)(acac)_3]^-$.
[b] For the process $[Ru(III)(acac)_2(L)]^+ \rightarrow [Ru(II)(acac)_2(L)]$.

and iron complexes (Sections V.B.1, V.B.2 and V.B.3, respectively), with one ferrocenyl centred oxidation ($E^{\circ\prime} = +0.59$ V, vs. SCE) and one metal-centred reduction (partially reversible at $E^{\circ\prime} = -0.90$ V)[270a]. Unexpectedly, the reduction process seems to occur at potential values markedly less negative that that of $Co(acac)_2$ (Section IV.B.2.e), even if the pertinent data in CH_2Cl_2 solution are lacking.

As illustrated in Section IV.B.2.e, $Rh(acac)_3$ exhibits an irreversible one-electron oxidation and an irreversible two-electron reduction in MeCN solution. The introduction of an anthrylmethyl group in the γ-position of one of the acac ligands as in **130** modifies the redox activity of the entire complex[256]. The irreversible two-electron reduction of $Rh(acac)_3$ ($E_p = -2.21$s V, vs. SCE, thf) moves anodically by about 0.3 V ($E_p = -1.88$ V) and is followed by a reversible, anthryl-centred reduction ($E^{\circ\prime} = -2.14$ V). In addition, no rhodium-centred oxidation is detected. Since the anodic shift of the Rh(III) → Rh(I) step indicates that the anthrylmethyl group pushes electron density towards the rhodium(III) core, it does not seem possible that the lack of the Rh(III) → Rh(IV) process might be due to its anodic shift beyond the solvent discharge.

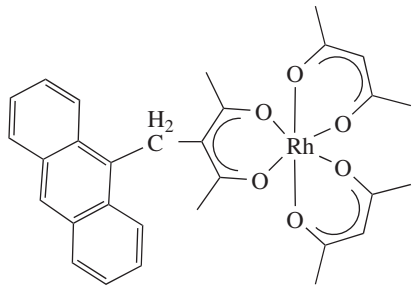

(**130**)

5. Group 10 elements

The nickel(II) derivative, $Ni[CH_3C(O)CHC(O)Fc]_2$, displays the usual ferrocenyl-centred oxidation ($E^{\circ\prime} = +0.58$ V, vs. SCE) and the partially reversible metal-centred reduction ($E^{\circ\prime} = -0.88$ V)[270a], which occurs at potential values less negative than that of $Ni(acac)_2$ (Section IV.B.2.f.).

The solid state electrochemistry of $Ni(hfacac)_2L_2$ complexes (L = **126**, **126′**) shows that the ferrocene-based oxidations occur at potential values lower by about 50 mV than

those exhibited by the corresponding uncomplexed ligands L[277], thus confirming the slight interaction of the {Ni(hfacac)$_2$} unit with the ferrocenyl subunits.

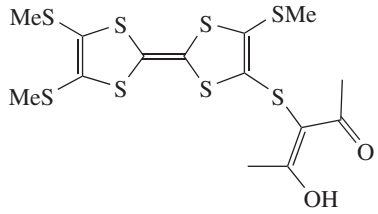

(**131**)

The β-diketone ttfs-acac-H **131** has been prepared and the electrochemistry of the nickel(II) complex *trans*-Ni(ttfs-acac)$_2$(py)$_2$ has been studied in CH_2Cl_2 solution[280]. It shows two, almost overlapping, one-electron oxidations at about +0.4 V, vs. SCE, followed by a single two-electron oxidation at +0.72 V. All the processes have features of chemical reversibility and are considered as ttf centred. In particular, the first two electrons should be removed stepwisely from the two ttf units.

6. Group 11 elements

The copper(II) complex *trans*-Cu(hfacac)$_2$(**124**)$_2$ exhibits two reversible oxidation processes at the same potential values of the uncomplexed ttf-based ligand **124**[275] in benzonitrile solution.

Solid state electrochemistry studies on Cu(hfacac)$_2$L$_2$ (L = **126**, **126′**) show that the ferrocenyl subunits are easier to oxidize by about 30 mV than in the free ligand. A copper(II)-centred reduction is present at about +0.07 V, vs. SCE[277].

Finally, the copper(II) β-diketonate Cu(**125**)$_2$ displays two oxidation processes at potential values less positive by about 50 mV (4:1 CH_2Cl_2:EtOH) with respect to those of protonated **125**[276].

7. Actinides

The electrochemistry of the uranium(IV) and thorium(IV) complexes M(acac)$_2$L (L = Pc, oep dianions) has been studied in benzonitrile solution[281]. In the complexes of both elements, a series of reversible redox processes have been detected, most of which are centred on the macrocyclic rings (Table 21).

TABLE 21. Formal electrode potentials (vs. SCE) for the redox changes exhibited by actinide complexes [M(acac)$_2$L]^z in PhCN

M	L	$E^{\circ\prime}$ (V) (z: 2+ → +)	$E^{\circ\prime}$ (V) (z: + → 0)	$E^{\circ\prime}$ (V) (z: 0 → −)	$E^{\circ\prime}$ (V) (z: − → 2−)[a]	Reference
Th	Pc	+1.12[a,b]	+0.73[a]	−0.85[a]	−1.29[a]	281a
	oep	+1.15[a]	+0.76[a]	−1.57[a]	—	281b
U	Pc	+1.26[a,b]	+0.79[a]	−0.83[a]	−1.28[a]	281a
	oep	+1.26[a,b]	+0.58[c]	−1.56[a]	—	281b

[a] Ring-centred process.
[b] Peak-potential value for irreversible processes.
[c] Metal-centred process.

VI. POLYKETONATES

A. Redox Reactions

The presence of β-carbonyl groups with at least one proton on the carbon between them allows a keto/enol tautomerism to occur and, under appropriate conditions, the enolic proton can be removed. The β-δ-tricarbonyl compounds are the higher analogues of the β-diketonates and can take triketone, monoenol and dienol forms in their tautomeric equilibrium[282] (equation 86); accordingly, they can behave as bidentate or tridentate ligands to form metal chelate complexes[283].

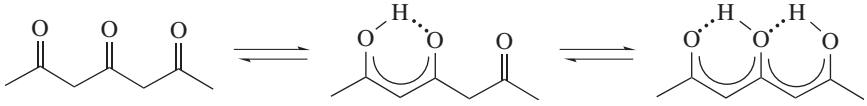

(86)

The 1,3,5-triketones are potentially dinegative, tridentate ligands and the well-developed π-system of the dianion gives to the ligands a preference for a planar configuration, thus precluding tridentate coordination to one metal ion. For example, copper(II) and heptane-2,4,6-trione give mononuclear (**132**) and dinuclear complexes (**133**)[284].

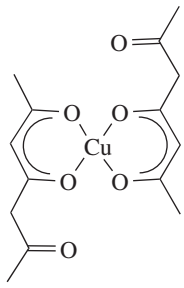

(**132**)

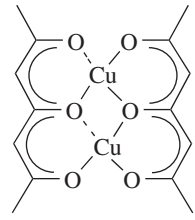

(**133**)

The tetraketone 1,7-diphenyl-1,3,5,7-heptanetetraone (dbbaH$_3$, **134**), containing three enolizable protons, has been prepared[284b] and several heterotrinuclear metal complexes **135**, containing the uranyl cation UO_2^{2+} and other bivalent metal cations, have been isolated and characterized[285].

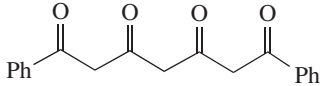

(**134**)

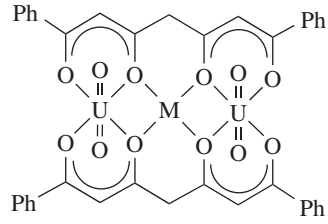

(**135**) M = Fe(II), Mn(II), Ni(II), Co(II), Cu(II)

To the best of our knowledge, only two papers on the oxidation of polyketonates have been published. Lintvedt and coworkers have observed[286] that the binuclear complex $Co_2(dbba)_2py_4$ (**136**) reacts with O_2 in pyridine/benzene affording the binuclear derivative **137**, derived from the oxidation of the 4-methyne carbon of both ligands to carbonyl groups (equation 87). At variance with the β-diketonates, which are decomposed upon oxidation at the methyne carbon atom (Section IV.A.2), the $CH_2 \rightarrow C{=}O$ oxidation at C4 in the tetraketonato complex does not destroy the dianion character of the ligand, preserving the complex coordination.

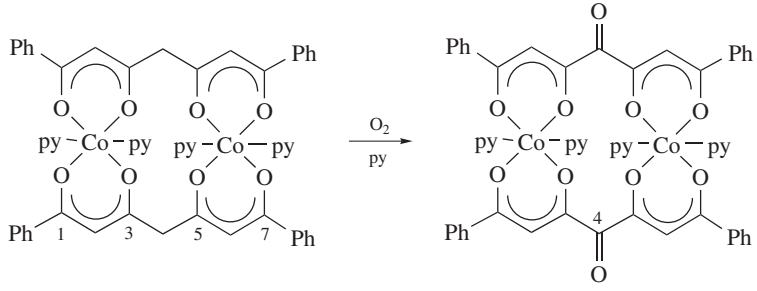

(**136**) (**137**) (87)

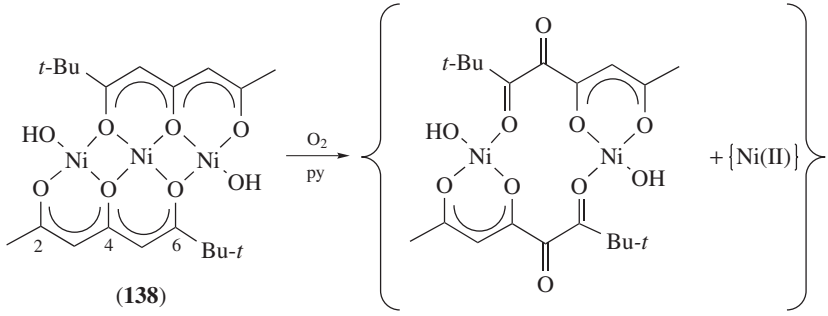

(**138**) (88)

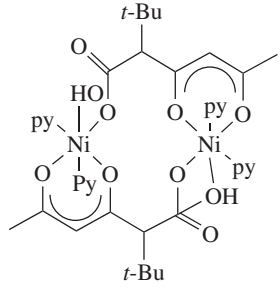

(**139**)

Ligand oxidation and rearrangement together with loss of one metal cation is observed in the reaction of dioxygen with the trinuclear nickel(II) complex $Ni_3(dmot)_2(OH)_2$

$(MeOH)_4$ (**138**) in pyridine (equation 88, MeOH has been omitted for the sake of clarity)[287]. Product **139** of equation 88 clearly shows that one nickel(II) cation is lost and that dmot was converted into 2-*t*-Bu-2-hydroxy-3,5-dioxohexanoate(2−). The ligand has undergone both an oxidation and migration of the *t*-butyl group from the terminal carbonyl at C6 to the adjacent C5. In addition, a hydroxy group is found on C6 in the final product. The authors explain these changes by considering an oxidation at C5 of the original ligand and attack by OH^- on the C6 carbonyl, followed by a benzylic acid type rearrangement[287].

B. Electrochemistry

1. Metal triketonates

As pointed out some time ago[288], the electrochemistry of the dicopper complex of the series M_2(1,3,5-triketonate)$_2$ (**140**) posed some problems of interpretation. It was at first thought that the copper(II) complexes should display a single two-electron reduction [Cu(II)−Cu(II) → Cu(I)−Cu(I)], with features of chemical reversibility in the short reaction times of cyclic voltammetry[284c,d, 289a]. Later, it was stated that they undergo a single two-electron reduction only in the presence of alkali metal ions. In the absence of such cations, the Cu_2(1,3,5-triketonate)$_2$ derivatives undergo the stepwise sequence Cu(II)−Cu(II) → Cu(II)−Cu(I) → Cu(I)−Cu(I), the second one-electron reduction being irreversible and located at rather negative potential values[284e, 289b,c].

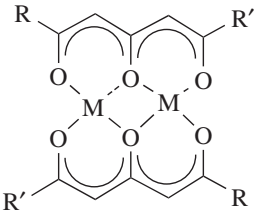

(**140**)

In contrast, the Ni_2(1,3,5-triketonate)$_2$ derivatives display two relatively close-spaced one-electron reductions [Ni(II)−Ni(II) → Ni(II)−Ni(I) → Ni(I)−Ni(I)][290]. For both copper and nickel the mixed-valent species [M(II)−M(I)] were unstable, in spite of the potentially higher stability of the [Cu(II)−Cu(I)] intermediate. The formal electrode potentials of the reduction processes of the Cu_2- and Ni_2(1,3,5-triketonate) complexes are compared in Table 22.

TABLE 22. Formal electrode potentials (vs. SCE) for the redox changes exhibited by [M_2(1,3,5-triketonate)$_2$]^z complexes **140**

M	R	R′	$E^{\circ\prime}$ (V) (z: 0 → −)	$E^{\circ\prime}$ (V) (z: − → 2−)	Solvent	Reference
Cu(II)	Me	*t*-Bu	−0.87	—	dmf	284e
Cu(II)	Me	Ph	−0.82	—	dmf	284e
			−0.85	−1.35 [a]	dmso	289c
			−0.79	−1.4 [a]	py	289c
Ni(II)	Me	Ph	−1.59	−1.77	dmf	290

[a] Irreversible process.

2. Metal tetraketonates

Although tetraketonates can give mono-, di- and trinuclear metal complexes, most investigations have dealt with uranyl-based complexes as, for example, the dianions derived from **141a**, dopb (*m*-bis(3,5-dioxohexyl)benzene dienolate), and **141b**, dpb (1,1′-(1,3-phenylene)bis(4,4-dimethyl-1,3-pentanedionato) dianion). The mononuclear U(VI) complex UO_2(dopb)[262e] in dmso solution undergoes a reversible U(VI) → U(V) reduction at potential values very similar to that of $UO_2(acac)_2$ ($E^{\circ\prime} == -1.06$ V), but free from the chemical complications accompanying the reduction of the latter: a half-life of 3.7 hours has been assigned to the uranium(V) monoanion $[UO_2(dopb)]^-$ [262e]. As far as the dinuclear complexes are concerned, the uranyl complex $[(UO_2)_2(dpb)_2(py)_2]$ is the only dinuclear complex studied from the electrochemical viewpoint[291]. The complex undergoes a partially chemically reversible two-electron reduction ($E^{\circ\prime} = -1.17$ V, vs. SCE, py). The fact that the two uranium(VI) centres undergo the U(VI) → U(V) reduction at the same potential value suggests that they are electronically independent.

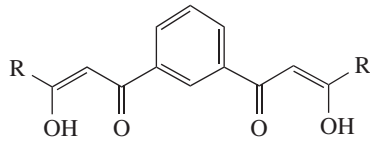

(**141**) (**a**) R = Me
(**b**) R = *t*-Bu

A series of heterotrinuclear complexes of the tetraketone **134** has been characterized. In such complexes the two outer O_4 compartments are occupied by a $[UO_2]^{2+}$ ion, whereas the central O_4 compartment is occupied by a M(II) ion (M = Mn, Co, Ni, Cu, Zn)[285]. As a typical example of the electrochemical behaviour of such complexes, Figure 9 compares the cyclic voltammetric response of $(UO_2)_2Zn(dbba)_2(py)_4$ with that of $(UO_2)_2Ni(dbba)_2(py)_4$[285]. The complex containing the redox-inactive zinc(II) centre, $(UO_2)_2Zn(dbba)_2(py)_4$, affords two separate reductions at about −1.1 and −1.3 V (vs. SCE), which are assigned to the U(VI) → U(V) reduction of each uranyl ion. The insertion of the redox-active nickel(II) as central metal ion causes the appearance of the further Ni(II) → Ni(I) reduction at about −1.5 V. A similar behaviour is exhibited by $(UO_2)_2Cu(dbba)_2(py)_4$, with the only difference that the Cu(II) → Cu(I) reduction occurs at about −0.5 V, thus preceding the two separate UO_2^{2+} reductions.

The trinuclear complexes containing manganese(II), iron(II) or cobalt(II) as central ions, apart from the two uranyl-centred reductions, gave only irreversible oxidation steps. It is evident that, at variance with $(UO_2)_2(dpb)_2(py)_2$, in this case the presence of the central M(II) ion favours the electronic interaction between the two outer uranium(VI) centres.

3. Metal hexaketonates

Both heterotetranuclear $(UO_2)_2M_2(mob)_2(py)_6$ (**142**) and homotetranuclear $Cu_4(mob)_2(py)_4$ (**143**) complexes have been prepared from 1,1′-(1,3-phenylene)bis(7-methyl-1,3,5-octanetrione)[291, 292].

Complex **142** (M = Zn) exhibits only a single two-electron reduction with features of chemical reversibility ($E^{\circ\prime} = -1.06$ V, vs. SCE, py), attributed to the simultaneous U(VI) → U(V) transition of the two not-interacting uranyl ions[291]. A similar behaviour is exhibited by **142** (M = Co) and **142** (M = Ni) in pyridine solution ($E^{\circ\prime} = -1.12$

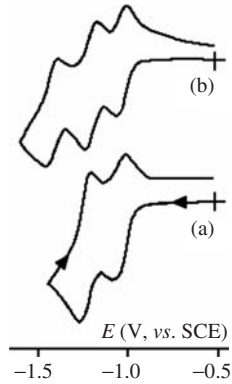

FIGURE 9. Cyclic voltammetric responses of (a) $(UO_2)_2Zn(dbba)_2(py)_4$ and (b) $(UO_2)_2Ni(dbba)_2(py)_4$ (Hg electrode, dmf, scan rate 0.2 V s^{-1})[285]. Reproduced from Reference 285 with permission. Copyright 1984 American Chemical Society

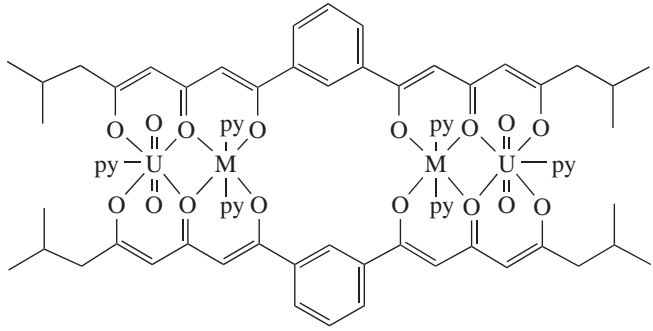

(**142**) M = Co(II), Ni(II), Cu(II), Zn(II)

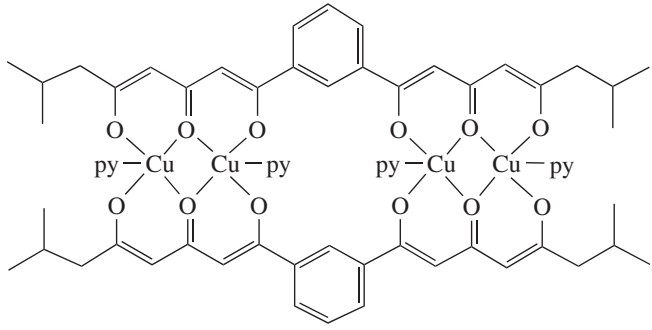

(**143**)

and $E^{\circ\prime} = 1.18$ V, respectively). Changing the solvent to dmso, which allows a larger cathodic window, the simultaneous Ni(II) → Ni(I) reduction of the two Ni(II) centres can be observed ($E^{\circ\prime} = -1.82$ V); see Figure 10[291]. The fact that both the two couples of uranyl and nickel(II) centres (and probably uranyl and cobalt(II) centers too) undergo single two-electron steps indicates that, at variance with the heterometallic triketonates $(UO_2)_2M(dbba)_2(py)_6$ discussed in Section VI.B.2, the interposition of the phenylene moiety between the two triketonato compartments creates a barrier to their mutual electronic communication.

A rather different behaviour is attributed to **142** (M = Cu), exhibiting a single four-electron reduction ($E^{\circ\prime} = -0.82$ V, py) which suggests that, for some unclear synergistic interaction, the two uranyl ions and the two copper ions undergo their simultaneous one-electron reduction at about the same potential value. It is hence implied that the copper(II) reductions induce the two uranyl ions to anticipate by about 0.3 V their one-electron additions relative to the other heteronuclear complexes **142**. In this connection it is also useful to consider the voltammetric behaviour of the homonuclear complex **143** (Figure 11)[292], undergoing two partially overlapping two-electron reductions at about $E^{\circ\prime} = -0.7$ and

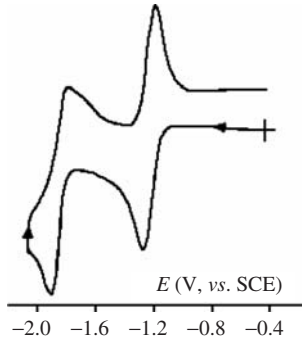

FIGURE 10. Cyclic voltammogram of $(UO_2)_2Ni_2(mob)_2(py)_6$ (Hg electrode, dmso:py = 95:5, scan rate 0.5 V s^{-1})[291]. Reproduced from Reference 291 with permission. Copyright 1990 American Chemical Society

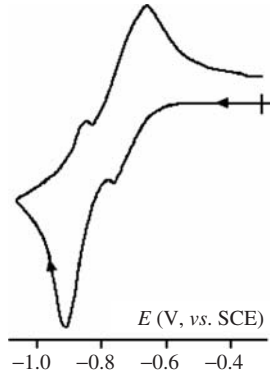

FIGURE 11. Cyclic voltammogram of $Cu_4(mob)_2(py)_4$ (Hg electrode, py, scan rate 0.5 V s^{-1})[292]. Reproduced from Reference 292 with permission. Copyright 1990 American Chemical Society

−0.9 V, which suggests a very weak interaction between the two Cu_2 halves. Such an interaction could be responsible for the unexpected behaviour of $(UO_2)_2Cu_2(mob)_2(py)_6$.

VII. ACKNOWLEDGMENTS

The authors gratefully acknowledge the financial support of the University of Pisa (G.P.) and of the University of Siena (P.Z.). G.P. thanks Dr Simona Samaritani (University of Pisa) for her critical reading of the manuscript.

VIII. REFERENCES

1. Z. Rappoport (Ed.), *The Chemistry of Enols*, John Wiley & Sons, Ltd, Chichester, 1990.
2. (a) W. J. Bouma, J. K. MacLeod and L. Radom, *J. Am. Chem. Soc.*, **101**, 5540 (1979).
   (b) J. L. Holmes and J. P. Lossing, *J. Am. Chem. Soc.*, **104**, 2648 (1982).
   (c) N. Heinrich, W. Koch, G. Frenking and H. Schwarz, *J. Am. Chem. Soc.*, **108**, 593 (1986).
   (d) N. Heinrich, F. Louage, C. Lifshitz and H. Schwarz, *J. Am. Chem. Soc.*, **110**, 8183 (1988).
3. (a) J. L. Holmes, J. K. Terlouw and F. P. Lossing, *J. Phys. Chem.*, **80**, 2860 (1976).
   (b) J. L. Holmes and J. P. Lossing, *J. Am. Chem. Soc.*, **102**, 1591 (1980).
   (c) B. Albrecht, M. Allan, E. Haselbach, L. Neuhaus and P.-A. Carrupt, *Helv. Chim. Acta*, **67**, 220 (1984).
4. (a) G. Frenking, N. Heinrich, J. Schmidt and H. Schwarz, *Z. Naturforsch.*, **37b**, 1597 (1982).
   (b) G. Frenking and H. Schwarz, *Z. Naturforsch.*, **37b**, 1602 (1982).
   (c) M. J. Frisch, K. Raghavachari, J. A. Pople, W. J. Bouma and L. Radom, *Chem. Phys.*, **75**, 323 (1983).
5. (a) M. Schmittel, *Top. Curr. Chem.*, **169**, 183 (1994).
   (b) M. Schmittel and A. Burghart, *Angew. Chem., Int. Ed. Engl.*, **36**, 2550 (1997).
6. T. N. Lockyer and R. L. Martin, *Prog. Inorg. Chem.*, **27**, 223 (1980).
7. F. Marchetti, C. Pettinari, A. Cingolati, D. Leonesi, A. Drozdov and S. I. Troyanov, *J. Chem. Soc., Dalton Trans.*, 3325 (1998).
8. D. Seebach, *Angew. Chem., Int. Ed. Engl.*, **27**, 1624 (1988).
9. (a) G. Stork and P. F. Hudrlik, *J. Am. Chem. Soc.*, **90**, 4462 (1979).
   (b) G. Stork and P. F. Hudrlik, *J. Am. Chem. Soc.*, **90**, 4464 (1979).
   (c) I. Kuwajima and E. Nakamura, *Acc. Chem. Res.*, **18**, 181 (1985).
10. (a) E. Hevia, K. W. Henderson, A. R. Kennedy and R. E. Mulvey, *Organometallics*, **25**, 1778 (2006).
    (b) S. E. Baillie, E. Hevia, A. R. Kennedy and R. E. Mulvey, *Organometallics*, **26**, 204 (2007).
11. H. H. Wasserman and B. H. Lipshuts, *Tetrahedron Lett.*, **16**, 1731 (1975).
12. W. Hartwig and L. Born, *J. Org. Chem.*, **52**, 4352 (1987).
13. A. Krief and S. Jeanmart, *Tetrahedron Lett.*, **43**, 6167 (2002).
14. E. J. Bailey, D. H. R. Barton, J. Elks and J. F. Templeton, *J. Chem. Soc.*, 1578 (1962).
15. E. Vedejs, D. A. Engler and J. E. Telschow, *J. Org. Chem.*, **43**, 188 (1978).
16. K. B. Sharpless, J. M. Townsend and D. R. Williams, *J. Am. Chem. Soc.*, **94**, 295 (1972).
17. R. Gamboni, P. Mohr, N. Waespe-Sarcevic and C. Tamm, *Tetrahedron Lett.*, **26**, 203 (1985).
18. F. Strain, W. E. Bissinger, W. R. Dial, H. Rudoff, B. J. DeWitt, H. C. Stevens and J. H. Langston, *J. Am. Chem. Soc.*, **72**, 1254 (1950).
19. M. P. Gore and J. C. Vederas, *J. Org. Chem.*, **51**, 3700 (1986).
20. (a) G. M. Rubottom, M. A. Vazquez and D. R. Pelegrina, *Tetrahedron Lett.*, **15**, 4319 (1974).
    (b) A. G. Brook and D. M. Mcrae, *J. Organomet. Chem.*, **77**, C19 (1974).
    (c) G. M. Rubottom and J. M. Gruber, *J. Org. Chem.*, **43**, 1599 (1978).
    (d) G. M. Rubottom, J. M. Gruber, R. K. Boeckman, Jr., M. Ramaiah and J. B. Medwid, *Tetrahedron Lett.*, **19**, 4603 (1978).
    (e) A. Hassner, R. H. Reuss and H. W. Pinnick, *J. Org. Chem.*, **40**, 3427 (1975).
21. Y. Horiguchi, E. Nakamura and I. Kuwajima, *Tetrahedron Lett.*, **30**, 3323 (1989).
22. P. A. Zoretic, M. Wang, Y. Zhang and Z. Shen, *J. Org. Chem.*, **61**, 1806 (1996).
23. S. Stankovic and J. H. Espenson, *J. Org. Chem.*, **63**, 4129 (1998).

24. (a) H. Yamamoto, M. Tsuda, S. Sakaguchi and Y. Ishii, *J. Org. Chem.*, **62**, 7174 (1997).
(b) S. Sakaguchi, Y. Yamamoto, T. Sugimoto, H. Yamamoto and Y. Ishii, *J. Org. Chem.*, **64**, 5954 (1999).
25. J. P. McCormick, W. Tomasik and M. W. Johnson, *Tetrahedron Lett.*, **22**, 607 (1981).
26. S. Rozen and Y. Bareket, *J. Chem. Soc., Chem. Commun.*, 627 (1996).
27. C. Iwata, Y. Takemoto, A. Nakamura and T. Imanishi, *Tetrahedron Lett.*, **26**, 3227 (1985).
28. (a) W. A. Pryor and C. K. Govindan, *J. Org. Chem.*, **46**, 4679 (1981).
(b) G. M. Rubottom and M. I. Lopez Nieves, *Tetrahedron Lett.*, **13**, 2423 (1972).
29. S. Hanessian, *Total Synthesis of Natural Products: The Chiron Approach*, Chap. 2, Pergamon Press, New York, 1983.
30. W. Adam, R. T. Fell, C. Moch-Knoblauch and C. R. Saha-Möller, *Tetrahedron Lett.*, **37**, 6531 (1996).
31. W. Adam, R. T. Fell, C. R. Saha-Möller and C.-G. Zhao, *Tetrahedron: Asymmetry*, **9**, 397 (1998).
32. F. A. Davis, L. C. Vishwakarma, J. M. Billmers and J. Finn, *J. Org. Chem.*, **49**, 3241 (1984).
33. (a) F. A. Davis and A. C. Sheppard, *Tetrahedron*, **45**, 5703 (1989).
(b) F. A. Davis and B.-C. Chen, *Chem. Rev*, **92**, 919 (1992).
(c) F. A. Davis, *J. Org. Chem.*, **71**, 8993 (2006).
34. D. A. Evans, M. M. Morrissey and R. L. Dorow, *J. Am. Chem. Soc.*, **107**, 4346 (1985).
35. (a) F. A. Davis, M. S. Haque and R. M. Przelawski, *J. Org. Chem.*, **54**, 2021 (1989).
(b) F. A. Davis and M. S. Haque, *J. Org. Chem.*, **51**, 4083 (1986).
(c) F. A. Davis, A. C. Sheppard, B.-C. Chen and M. S. Haque, *J. Am. Chem. Soc.*, **112**, 6679 (1990).
36. F. A. Davis and M. C. Weismiller, *J. Org. Chem.*, **55**, 3715 (1990).
37. F. A. Davis, A. Kumar and B.-C. Chen, *J. Org. Chem.*, **56**, 1143 (1991).
38. D. Ivanoff and A. Spassoff, *Bull. Soc. Chim. Fr.*, **2**, 76 (1935).
39. J. P. Schaefer and J. J. Bloomfield, *Org. React.*, **1**, 15 (1967).
40. J. J. Bloomfields, D. C. Owsley and J. M. Nelke, *Org. React.*, **23**, 259 (1976).
41. (a) S. K. Chung and L. B. Dunn, Jr., *J. Org. Chem.*, **48**, 1125 (1983).
(b) J. H. Babler and S. J. Sarussi, *J. Org. Chem.*, **52**, 3462 (1987).
42. Y. Kobayashi, T. Taguchi and T. Morikawa, *Tetrahedron Lett.*, **19**, 3555 (1978).
43. C. F. Wilcox, Jr., K. R. Lassila, G. VanDuyne, H. Lu and J. Clardy, *J. Org. Chem.*, **54**, 2190 (1989).
44. B. B. Snider, *Chem. Rev.*, **96**, 339 (1996).
45. B. B. Snider and T. Kwon, *J. Org. Chem.*, **57**, 2399 (1992).
46. A. S. Kende, K. Koch and C. A. Smith, *J. Am. Chem. Soc.*, **110**, 2210 (1988).
47. A. S. Kende and K. Koch, *Tetrahedron Lett.*, **27**, 6051 (1986).
48. A. S. Kende, F. H. Ebatino and T. Ohta, *Tetrahedron Lett.*, **26**, 3063 (1985).
49. A. Leboff, A.-C Carbonnelle, J.-P. Alazard, C. Thal and A. S. Kende, *Tetrahedron Lett.*, **28**, 4163 (1987).
50. D. Hobbs-Mallyon and D. A. Whiting, *J. Chem. Soc., Chem. Commun.*, 899 (1991).
51. P. S. Baran and J. M. Richter, *J. Am. Chem. Soc.*, **126**, 7450 (2004).
52. P. S. Baran and J. M. Richter, *J. Am. Chem. Soc.*, **127**, 15394 (2005).
53. P. S. Baran, J. M. Richter and D. W. Lin, *Angew. Chem. Int. Ed.*, **44**, 609 (2005).
54. P. S. Baran, B. D. Hafensteiner, N. B. Ambhaikar, C. A. Guerrero and J. D. Gallagher, *J. Am. Chem. Soc.*, **128**, 8678 (2006).
55. M.-A. Poupart and L. A. Paquette, *Tetrahedron Lett.*, **29**, 269 (1988).
56. T. Cohen, K. McNamara, M. A. Kuzemko, K. Ramig, J. J. Landi, Jr. and Y. Dong, *Tetrahedron*, **49**, 7931 (1993).
57. (a) H. Hart and R. Willer, *Tetrahedron Lett.*, **18**, 2307 (1977).
(b) M. P. DeMartino, K. Chen and P. S. Baran, *J. Am. Chem. Soc.*, **130**, 11546 (2008).
58. (a) J. L. Belletire and D. F. Fry, *J. Org. Chem.*, **52**, 2549 (1987).
(b) J. L. Belletire and D. F. Fry, *J. Org. Chem.*, **53**, 4724 (1988).
(c) T. J. Brocksom, N. Petragnani, R. Rodriguez and H. La Scala Teixeira, *Synthesis*, 396 (1975).
(d) N. A Porter, Q. Su, J. J. Harp, I. J. Rosenstein and A. T. McPhail, *Tetrahedron Lett.*, **34**, 4457 (1993).
(e) J. W. Kim, J.-J. Lee, S.-H. Lee and K.-H. Ahn, *Synth. Commun.*, **28**, 1287 (1998).

(f) N. Kise, T. Ueda, K. Kumada, Y. Terao and N. Ueda, *J. Org. Chem.*, **65**, 464 (2000).
(g) N. Kise, A. Fujimoto and N. Ueda, *Tetrahedron: Asymmetry*, **13**, 1845 (2002).
(h) T. Langer, M. Illich and G. Helmchen, *Synlett*, 1137 (1996).
(i) T. Langer, M. Illich and G. Helmchen, *Tetrahedron Lett.*, **36**, 4409 (1995).
59. (a) R. M. Moriarty, R. Penmasta and I. Prakash, *Tetrahedron Lett.*, **28**, 873 (1987).
(b) P. Baierweck, U. Simmross and K. Müllen, *Chem. Ber.*, **121**, 2195 (1988).
60. (a) M. W. Rathke and A. Lindert, *J. Am. Chem. Soc.*, **93**, 4605 (1971).
(b) Y. Ito, T. Konoike, T. Harada and T. Saegusa, *J. Am. Chem. Soc.*, **99**, 1487 (1977).
(c) Y. Ito, T. Konoike and T. Saegusa, *J. Am. Chem. Soc.*, **97**, 2912 (1975).
(d) Y. Kobayashi, T. Taguchi and E. Tokuno, *Tetrahedron Lett.*, **18**, 3741 (1977).
(e) J. L. Sessler, S. J. Weghorn, Y. Hiseada and V. Lynch, *Chem. Eur. J.*, **1**, 56 (1995).
(f) Y. Kobayashi, T. Taguchi, T. Morikawa, E. Tokuno and S. Sekiguchi, *Chem. Pharm. Bull.*, **28**, 262 (1980).
(g) R. Quermann, R. Maletz and H. J. Schäfer, *Liebigs Ann. Chem.*, 1219 (1993).
(h) L. A. Paquette, E. I. Bzowej, B. M. Branan and K. J. Stanton, *J. Org. Chem.*, **60**, 7277 (1995).
(i) R. H. Frazier, Jr. and R. L. Harlow, *J. Org. Chem.*, **45**, 5408 (1980).
(j) Y. Ito, T. Konioke and T. Saegusa, *J. Am. Chem. Soc.*, **97**, 649 (1975).
(k) M. J. Aurell, S. Gil, A. Tortajada, R. Mestres and A. García-Raso, *Tetrahedron Lett.*, **29**, 6181 (1988).
61. (a) E. Baciocchi, A. Casu and R. Ruzziconi, *Tetrahedron Lett.*, **30**, 3707 (1989).
(b) A. Belli Paolobelli, D. Latini and R. Ruzziconi, *Tetrahedron Lett.*, **34**, 721 (1993).
(c) P. Lupattelli, R. Ruzziconi, P. Scafato, S. Alunni and A. Belli Paolobelli, *J. Org. Chem.*, **63**, 4506 (1998).
(d) A. Belli Paolobelli, R. Ruzziconi, P. Lupattelli, P. Scafato and C. Spezzacatena, *J. Org. Chem.*, **64**, 3364 (1999).
(e) J.-P. Gourvés, R. Ruzziconi and L. Vilarroig, *J. Org. Chem.*, **66**, 617 (2001).
62. Y. Kohno and K. Narasaka, *Bull. Chem. Soc. Jpn.*, **68**, 322 (1995).
63. (a) I. Ojima, S. M. Brandstadter and R. J. Donovan, *Chem. Lett.*, **21**, 1591 (1992).
(b) S. Inaba and I. Ojima, *Tetrahedron Lett.*, **18**, 2009 (1977).
(c) N. Kise, K. Tokioka, Y. Aoyama and Y. Matsumura, *J. Org. Chem.*, **60**, 1100 (1995).
(d) Y. Matsumura, M. Nishimura, H. Hiu, M. Watanabe and N. Kise, *J. Org. Chem.*, **61**, 2809 (1996).
(e) N. Kise, K. Kumada, Y. Terao and N. Ueda, *Tetrahedron*, **54**, 2697 (1998).
64. P. Q. Nguyen and H. J. Schäfer, *Org. Lett.*, **3**, 2993 (2001).
65. (a) T. Fujii, T. Hirao and Y. Ohshiro, *Tetrahedron Lett.*, **33**, 5823 (1992).
(b) T. Hirao, T. Fujii and Y. Ohshiro, *Tetrahedron*, **50**, 10207 (1994).
66. R. M. Dessau and E. I. Heiba, *J. Org. Chem.*, **39**, 3457 (1974).
67. (a) M. Schmittel and A. Haeuseler, in *Elektronenübertragung in Chemie und Biochemie* (Eds J. Russow and H. J. Schäfer), GDCh, Frankfurt, 2002, p. 31.
(b) M. Schmittel, A. Burghart, W. Malish, J. Reising and R. Söllner, *J. Org. Chem.*, **63**, 396 (1998).
68. M. Schmittel and A. Haeuseler, *J. Organomet. Chem.*, **661**, 169 (2002).
69. (a) P. Brownbridge, *Synthesis*, 1 (1983).
(b) P. Brownbridge, *Synthesis*, 85 (1983)
(c) I. Fleming, A. Barbero and D. Walter, *Chem. Rev.*, **97**, 2063 (1997).
70. J. K. Rasmussen, *Synthesis*, 91 (1977) and references cited therein.
71. K. Mori and M. Sasaki, *Tetrahedron Lett.*, 1329 (1979).
72. R. D. Clark and C. H. Heathcock, *Tetrahedron Lett.*, **15**, 1713 (1974).
73. K. Kaneda, N. Kii, K. Jutsukawa and S. Teranishi, *Tetrahedron Lett.*, **22**, 2595 (1981).
74. S. V. N. Raju, T. T. Upadhya, S. Ponrathnam, T. Daniel and A. Sudalai, *J. Chem. Soc., Chem. Commun.*, 1969 (1996).
75. E. Friedrich and W. Lutz, *Angew. Chem., Int. Ed. Engl.*, **16**, 413 (1977).
76. (a) D. Seebach and M. Kolb, *Chem. Ind. (London)*, 687 (1974).
(b) D. Seebach, *Angew. Chem., Int. Ed. Engl.*, **18**, 239 (1979).
(c) H. J. Schäfer, *Angew. Chem., Int. Ed. Engl.*, **20**, 911 (1981).
77. J. March, *Advanced Organic Chemistry*, 4th Edn, Chap. 12, John Wiley & Sons, Inc., New York, 1992.

78. (a) R. M. Moriarty, O. Prakash, M. P. Duncan, R. K. Vaid and H. A. Musallam, *J. Org. Chem.*, **52**, 150 (1987).
(b) R. M. Moriarty and O. Prakash, *Acc. Chem. Res.*, **19**, 244 (1986).
79. G. F. Hambly and T. H. Chan, *Tetrahedron Lett.*, **27**, 2563 (1986).
80. R. H. Reuss and A. Hassner, *J. Org. Chem.*, **39**, 1785 (1974).
81. (a) C. A. Ramsden and R. G. Smith, *J. Am. Chem. Soc.*, **120**, 6842 (1998).
(b) C. A. Ramsden and R. G. Smith, *Org. Lett.*, **1**, 1591 (1999).
(c) T. Tsushima, K. Kawada and T. Tsuji, *Tetrahedron Lett.*, **23**, 1165 (1982).
(d) G. S. Garrett, T. J. Emge, S. C. Lee, E. M. Fischer, K. Dyehouse and J. M. McIver, *J. Org. Chem.*, **56**, 4823 (1991).
82. R. Rathore and J. K. Kochi, *J. Org. Chem.*, **61**, 627 (1996).
83. R. Rathore and J. K. Kochi, *Tetrahedron Lett.*, **35**, 8577 (1994).
84. H. Fischer and H. M. Weitz, *Synthesis*, 261 (1980).
85. T. Sakakura, M. Hara and M. Tanaka, *J. Chem. Soc., Perkin Trans. 1*, 283 (1994).
86. (a) J. Klein, R. Levene and E. Dunkelblum, *Tetrahedron Lett.*, **13**, 2845 (1972).
(b) G. L. Larson, D. Hernandez and A. Hernandez, *J. Organomet. Chem.*, **76**, 9 (1974).
87. M. E. Jung, Y.-G. Pan, M. W. Rathke, D. F. Sullivan and R. P. Woodbury, *J. Org. Chem.*, **42**, 3961 (1977).
88. I. Fleming and I. Paterson, *Synthesis*, 736 (1979).
89. A. Bhattacharya, L. M. DiMichele, U.-H. Dolling, E. J. J. Grabowski and V. J. Grenda, *J. Org. Chem.*, **54**, 6118 (1989).
90. (a) J. Mattay, *Angew. Chem., Int. Ed. Engl.*, **26**, 825 (1987).
(b) J. Mattay and M. Vondenhof, *Top. Curr. Chem.*, **159**, 219 (1991).
(c) F. Müller and J. Mattay, *Chem. Rev.*, **93**, 99 (1993).
91. J. Eriksen and C. S. Foote, *J. Phys. Chem.*, **82**, 2659 (1978).
92. A. Heidbreder and J. Mattay, *Tetrahedron Lett.*, **33**, 1973 (1992).
93. D. R. Arnold and A. J. Maroulis, *J. Am. Chem. Soc.*, **98**, 5931 (1976).
94. (a) S. Hintz, R. Fröhlich and J. Mattay, *Tetrahedron Lett.*, **37**, 7349 (1996).
(b) S. Hintz, J. Mattay, R. van Eldik and W.-F. Fu, *Eur. J. Org. Chem.*, 1583 (1998).
95. (a) J. O. Bunte, S. Rinne, C. Schäfer, B. Neumann, H.-G. Stammler and J. Mattay, *Tetrahedron Lett.*, **44**, 45 (2003).
(b) J. O. Bunte, S. Rinne and J. Mattay, *Synthesis*, 619 (2004).
96. L. Ackermann, A. Heidbreder, F. Wurche, F.-G. Klärner and J. Mattay, *J. Chem. Soc., Perkin Trans. 2*, 863 (1999).
97. (a) T. M. Bockman, S. Perrier and J. K. Kochi, *J. Chem. Soc., Perkin Trans. 2*, 595 (1993).
(b) T. M. Bockman, D. Shukla and J. K. Kochi, *J. Chem. Soc., Perkin Trans. 2*, 1623 (1996).
(c) T. M. Bockman and J. K. Kochi, *J. Chem. Soc., Perkin Trans. 2*, 1633 (1996).
98. J. O. Bunte, E. K. Heilmann, B. Hein and J. Mattay, *Eur. J. Org. Chem.*, 3535 (2004).
99. M. Tokuda, T. Shigei and M. Itoh, *Chem. Lett.*, **4**, 621 (1975) and references cited therein.
100. K. D. Moeller, *Tetrahedron*, **56**, 9527 (2000).
101. J. B. Sperry, C. R. Whitehead, I. Ghiviriga, R. M. Walczak and D. L. Wright, *J. Org. Chem.*, **69**, 3726 (2004).
102. (a) R. I. Walter, *J. Am. Chem. Soc.*, **88**, 1923 (1966).
(b) D. Gao and N. L. Bauld, *J. Org. Chem.*, **65**, 6276 (2000).
103. (a) D. L. Wright, C. R. Whitehead, E. H. Sessions, I. Ghiviriga and D. A. Frey, *Org. Lett.*, **1**, 1535 (1999).
(b) C. R. Whitehead, E. H. Sessions, I. Ghiviriga and D. L. Wright, *Org. Lett.*, **4**, 3763 (2002).
104. J. B. Sperry and D. L. Wright, *Tetrahedron Lett.*, **46**, 411 (2005).
105. K. D. Wellington, R. C. Cambie, P. S. Rutledge and P. S. Bergquist, *J. Nat. Prod.*, **63**, 79 (2000).
106. M. T. Reetz and R. Peter, *Tetrahedron Lett.*, **22**, 4691 (1981).
107. F. A. Cotton, G. Wilkinson, C. A. Murillo and M. Bochmann, *Advanced Inorganic Chemistry*, 6th Edn., Chaps. 16–18, John Wiley & Sons, Inc., New York, 1999.
108. K. Nozaki, K. Oshima and K. Utimoto, *J. Am. Chem. Soc.*, **109**, 2547 (1987).
109. (a) Y. Itoh, M. Yamanaka and K. Mikami, *J. Am. Chem. Soc.*, **126**, 13174 (2004).
(b) Y. Itoh and K. Mikami, *Org. Lett.*, **7**, 649 (2005).
(c) Y. Itoh and K. Mikami, *J. Fluorine Chem.*, **127**, 539 (2006).

110. (a) K. Miura, M. Taniguchi, K. Nozaki, K. Oshima and K. Utimoto, *Tetrahedron Lett.*, **31**, 6391 (1990).
(b) K. Miura, Y. Takeyama, K. Oshima and K. Utimoto, *Bull. Chem. Soc. Jpn.*, **64**, 1542 (1991).
111. (a) Y. Itoh and K. Mikami, *Org. Lett.*, **7**, 4883 (2005).
(b) Y. Itoh and K. Mikami, *Tetrahedron*, **62**, 7199 (2006).
112. (a) H. Plenio, *Chem. Rev.*, **97**, 3363 (1997).
(b) E. F. Murphy, R. Murugavel and H. W. Roesky, *Chem. Rev.*, **97**, 3425 (1997).
113. W. Adam, M. Metz, F. Prechtl and M. Renz, *Synthesis*, 563 (1994).
114. (a) W. Adam and F. Prechtl, *Chem. Ber.*, **127**, 667 (1994).
(b) W. Adam, M. Müller and F. Prechtl, *J. Org. Chem.*, **59**, 2358 (1994).
(c) W. Adam and M. N. Korb, *Tetrahedron*, **52**, 5487 (1996).
(d) N. Krause, M. Laux and A. Hoffmann-Röder, *Tetrahedron Lett.*, **41**, 9613 (2000).
115. M. Schulz, R. Kluge, M. Schüßler and G. Hoffmann, *Tetrahedron*, **51**, 3175 (1995).
116. A. Hoffmann-Röder and N. Krause, *Synthesis*, 2143 (2006).
117. N. Krause, A. Hoffmann-Röder and J. Canisius, *Synthesis*, 1759 (2002) and references cited therein.
118. B. H. Lipshutz and M. Segi, *Tetrahedron*, **59**, 4407 (1995).
119. A. Kasatkin and R. J. Whitby, *Tetrahedron*, **59**, 9857 (2003).
120. (a) M. Schmittel and R. Söllner, *Angew. Chem., Int., Ed. Engl.*, **35**, 2107 (1996).
(b) M. Schmittel and R. Söllner, *Chem. Ber./Recueil*, **130**, 771 (1997).
(c) M. Schmittel and R. Söllner, *Chem. Commun.*, 565 (1998).
(d) M. Schmittel and R. Söllner, *J. Chem. Soc., Perkin Trans. 2*, 515 (1999).
121. E. Nakamura, H. Oshino and I. Kawajima, *J. Am. Chem. Soc.*, **108**, 3745 (1986).
122. (a) R. G. Pearson, *J. Am. Chem. Soc.*, **85**, 3533 (1963).
(b) H. E. Bryndza and W. Tam, *Chem. Rev.*, **88**, 1163 (1988).
123. J. F. Hartwig, R. G. Bergman and R. A. Andersen, *Organometallics*, **10**, 3326 (1991).
124. H. J. Heeres, M. Maters, J. H. Teuben, G. Helgesson and S. Jagner, *Organometallics*, **11**, 350 (1992).
125. S. K. Chowdhuri, K. K. D. Amarasinghe, M. J. Heeg and J. Montgomery, *J. Am. Chem. Soc.*, **122**, 6775 (2000).
126. (a) D. A. Culkin and J. F. Hartwig, *J. Am. Chem. Soc.*, **123**, 5816 (2001).
(b) D. A. Culkin and J. F. Hartwig, *Organometallics*, **23**, 3398 (2004).
127. H. Hart, *Chem. Rev.*, **79**, 515 (1979).
128. Z. Rappoport and S. E. Biali, *Acc. Chem. Res.*, **21**, 442 (1988).
129. J. R. Keefe, A. J. Kresge and Y. Yin, *J. Am. Chem. Soc.*, **110**, 8201 (1988).
130. M. Schmittel, A. Abufarag, O. Luche and M. Levis, *Angew. Chem., Int. Ed. Engl.*, **29**, 1144 (1990).
131. (a) M. Schmittel and U. Baumann, *Angew. Chem., Int. Ed. Engl.*, **29**, 541 (1990).
(b) M. Schmittel and M. Röck, *Chem. Ber.*, **125**, 1611 (1992).
(c) M. Röck and M. Schmittel, *J. Chem. Soc., Chem. Commun.*, 1739 (1993).
132. M. Schmittel, G. Gescheidt and M. Röck, *Angew. Chem., Int. Ed. Engl.*, **33**, 1961 (1994).
133. M. Röck and M. Schmittel, *J. Prakt. Chem.*, **336**, 325 (1994).
134. M. Schmittel and A. Langels, *Liebigs Ann.*, 999 (1996).
135. M. Schmittel and A. Langels, *Angew. Chem., Int. Ed. Engl.*, **36**, 392 (1997).
136. M. Schmittel and A. Langels, *J. Org. Chem.*, **63**, 7328 (1998).
137. P. Zanello, *Inorganic Electrochemistry. Theory, Practice and Application*, Royal Society of Chemistry, Cambridge, 2003, pp. 49–135.
138. S. H. DuVall and R. L. McCreery, *Anal. Chem.*, **71**, 4594 (1999).
139. M. Schmittel and A. Langels, *J. Chem. Soc., Perkin Trans. 2*, 565 (1998).
140. M. Schmittel, M. Lal, W. A. Schenk, M. Hagel, N. Burzlaff and A. Langels, *Z. Naturforsh., B: Chem. Sci.*, **58**, 877 (2003).
141. S. R. Ruberu and M. A. Fox, *J. Am. Chem. Soc.*, **114**, 6310 (1992).
142. J. M. Kern, J. D. Sauer and P. Federlin, *Tetrahedron*, **38**, 3023 (1982).
143. M. Schmittel, A. Burghart, H. Werner, M. Laubender and R. Söllner, *J. Org. Chem.*, **64**, 3077 (1999).
144. M. Schmittel, M. Keller and A. Burghart, *J. Chem. Soc., Perkin Trans. 2*, 2327 (1995).

145. (a) S. Forsén and M. Nilsson, in *The Chemistry of the Carbonyl Group*, Vol. 2 (Ed. J. Zabicky), John Wiley & Sons, Ltd, Chichester, 1970, pp. 157–240.
(b) J. Toullec, in *The Chemistry of Enols* (Ed. Z. Rappoport), John Wiley & Sons, Ltd, Chichester, 1990, pp. 323–398.
(c) J. Emsley, *Struct. Bonding*, **57**, 147 (1984).
146. (a) D. P. Fay, A. R. Nichols, Jr. and N. Sutin, *Inorg. Chem.*, **10**, 2096 (1971).
(b) M. J. Hynes and M. T. O'Shea, *Inorg. Chim. Acta*, **73**, 201 (1983).
147. (a) A. H. Lowrey, C. George, P. D'Antonio and J. Karle, *J. Am. Chem. Soc.*, **93**, 6399 (1971).
(b) A. L. Andreassen and S. H. Bauer, *J. Mol. Struct.*, **12**, 381 (1972).
148. R. Boese, M. Yu. Antipin, D. Bläser and K. A. Lyssenko, *J. Phys. Chem. B*, **102**, 8654 (1998).
149. O. Gallardo, I. Csöregh and E. Weber, *J. Chem. Crystallogr.*, **25**, 769 (1995).
150. Z. Urbanczyk-Lipkowska, K. Yoshizawa, S. Toyota and F. Toda, *Cryst. Eng. Commun.*, **5**, 114 (2003) and references cited therein.
151. C. Pettinari, F. Marchetti and A. Drozdov, in *Comprehensive Coordination Chemistry II*, Vol. 1 (Eds J. A. McCleverty and T. J. Meyer), Elsevier, 2003, pp. 97–115 and references cited therein.
152. (a) Y. Kubo, A. Yamamoto and S. Ikeda, *J. Organomet. Chem.*, **46**, C50 (1972).
(b) T. Ikariya and A. Yamamoto, *J. Chem. Soc., Chem. Commun.*, 720 (1974).
153. A. Yamamoto, K. Morifuji, S. Ikeda, T. Saito, Y. Uchida and A. Misono, *J. Am. Chem. Soc.*, **90**, 1878 (1968).
154. (a) S. D. Ittel, *Inorg. Chem.*, **16**, 1245 (1977).
(b) G. Hata, H. Kondo and A. Miyake, *J. Am. Chem. Soc.*, **90**, 2278 (1968).
155. T. Ito, T. Kobuko, T. Yamamoto, A. Yamamoto and S. Ikeda, *J. Chem. Soc., Dalton Trans.*, 1783 (1974).
156. H. E. Podall, J. H. Dunn and H. Shapiro, *J. Am. Chem. Soc.*, **80**, 1325 (1960).
157. G. Wilke and G. Herrmann, *Angew. Chem.*, **74**, 693 (1972).
158. P. W. Jolly, K. Jonas, C. Krüger and Y.-H. Tsay, *J. Organomet. Chem.*, **33**, 109 (1971).
159. G. Braca, G. Sbrana and P. Pino, *Chim. Ind. (Milan)*, **50**, 121 (1968).
160. K. Jacob and K.-H. Thiele, *Z. Anorg. Allg. Chem.*, **543**, 192 (1986).
161. P. Biagini, F. Calderazzo, G. Pampaloni and P. F. Zanazzi, *Gazz. Chim. Ital.*, **117**, 27 (1987).
162. F. Calderazzo, G. Pampaloni and P. F. Zanazzi, *Chem. Ber.*, **119**, 2796 (1986).
163. M. A. Bennet, G. A. Heath, D. C. R. Hockless, I. Kovacik and A. C. Willis, *J. Am. Chem. Soc.*, **120**, 932 (1998).
164. C. L. Kwan and J. K. Kochi, *J. Am. Chem. Soc.*, **98**, 4903 (1976).
165. M. Bruni, P. Diversi, G. Ingrosso, A. Lucherini, C. Pinzino and A. Raffaelli, *J. Chem. Soc., Dalton Trans.*, 1035 (1995)
166. J. R. McKellar and B. O. West, *J. Chem. Soc., Dalton Trans.*, 796 (1974).
167. K. Uehara, K. Kamei, M. Tanaka and N. Murata, *Bull. Chem. Soc. Jpn.*, **45**, 540 (1972).
168. F. Leh and J. K. S. Wan, *Can. J. Chem.*, **50**, 999 (1972).
169. (a) B. Papenfuhs, N. Mahr and H. Werner, *Organometallics*, **12**, 4244 (1993).
(b) M. A. Esteruelas, F. J. Lahoz, E. Oñate, L. A. Oro and L. Rodríguez, *Organometallics*, **15**, 823 (1996).
(c) M. A. Esteruelas, F. J. Lahoz, E. Oñate, L. A. Oro, L. Rodríguez, P. Steinert and H. Werner, *Organometallics*, **15**, 3436 (1996).
170. (a) E. P. Shestakova, T. G. Cherkasova and Yu. S. Varshavsky, *Rhodium Express*, 6 (1995); *Chem. Abstr.*, **125**, 47254 (1996).
(b) L. A. Oro, D. Carmona, M. A. Estruelas, C. Foces-Foces and F. H. Cano, *J. Organomet. Chem.*, **307**, 83 (1986).
171. (a) A. Roodt, J. M. Botha, S. Otto, E. P. Shestakova and Yu. S. Varshavsky, *Rhodium Express*, 4 (1996); *Chem. Abstr.*, **127**, 58419 (1997).
(b) S. S. Basson, J. G. Leipoldt, A. Roodt, J. A. Venter and T. J. Van der Walt, *Inorg. Chim. Acta*, **119**, 35 (1986).
(c) S. S. Basson, J. G. Leipoldt and J. T. Nel, *Inorg. Chim. Acta*, **84**, 167 (1984).
(d) G. Doyle, *J. Organomet. Chem.*, **132**, 243 (1977).
(e) G. Doyle, *J. Organomet. Chem.*, **61**, 235 (1973).
172. G. J. van Zyl, G. J. Lamprecht and J. G. Leipoldt, *Transition Met. Chem.*, **15**, 170 (1990).
173. G. J. J. Steyn, S. S. Basson, J. G. Leipoldt and G. J. van Zyl, *J. Organomet. Chem.*, **418**, 113 (1991).

174. I. Yoshida, H. Kobayashi and K. Ueno, *Bull. Chem. Soc. Jpn.*, **45**, 2768 (1972).
175. M. A.-Z. Eltayeb, K. A. Al-Saad and E. M. Nour, *Pol. J. Chem.*, **79**, 1525 (2005).
176. S. M. Teleb and M. S. Refat, *Spectrochim. Acta, Part A*, **60**, 1579 (2004).
177. H. A. Hashem and M. S. Refat, *Surf. Rev. Lett.*, **13**, 439 (2006).
178. E.-M. Nour, S. M. Teleb, M. A. F. Elmosallamy and M. S. Refat, *S. Afr. J. Chem.*, **56**, 10 (2003); *Chem. Abstr.*, **139**, 156654 (2003).
179. K. N. Mitra, S. Choudhury, A. Castiñeiras and S. Goswami, *J. Chem. Soc., Dalton Trans.*, 2901 (1998).
180. M. Rikkou, M. Manos, E. Tolis, M. P. Sigalas, T. A. Kabanos and A. D. Keramidas, *Inorg. Chem.*, **42**, 4640 (2003).
181. V. N. Nemykin, V. Y. Chernii and S. V. Volkov, *J. Chem. Soc., Dalton Trans.*, 2995 (1998).
182. A. Yamamoto, T. Yamamoto, T. Saruyama and Y. Nakamura, *J. Am. Chem. Soc.*, **95**, 4073 (1973).
183. E. P. Shestakova, Yu. S. Varshavsky and A. B. Nikolskii, *J. Organomet. Chem.*, **690**, 3397 (2005).
184. F. K. Schmidt, L. B. Belykh and T. V. Goremyka, *Russ. J. Coord. Chem.*, **28**, 92 (2002).
185. U. Herber, T. Pechmann, B. Weberndörfer, K. Ilg and H. Werner, *Chem. Eur. J.*, **8**, 309 (2002).
186. S. Kinoshita, K. Miyokawa, H. Wakita and I. Masuda, *Bull. Chem. Soc. Jpn.*, **57**, 381 (1984).
187. J. Shono, Y. Nimura, T. Hashimoto and K. Shimizu, *Chem. Lett.*, **33**, 1422 (2004).
188. S. Patra, B. Mondal, B. Sarkar, M. Niemeyer and G. K. Lahiri, *Inorg. Chem.*, **42**, 1322 (2003).
189. (a) K. L. Stevenson, *J. Am. Chem. Soc.*, **94**, 6652 (1972).
    (b) S. S. Minor and G. W. Everett, Jr., *Inorg. Chem.*, **15**, 1526 (1976).
    (c) E. Zinato, P. Riccieri and P. S. Sheridan, *Inorg. Chem.*, **18**, 720 (1979).
    (d) C. Kutal, D. B. Yang and G. Ferraudi, *Inorg. Chem.*,**19**, 2907 (1980).
190. H. D. Gafney, R. L. Lintvedt and I. S. Yaworiwsky, *Inorg. Chem.*, **9**, 1728 (1970).
191. (a) N. Filipescu and H. Way, *Inorg. Chem.*,**8**, 1863 (1969).
    (b) G. Ferraudi, P. A. Grutsch and C. Kutal, *Inorg. Chim. Acta*, **59**, 249 (1982).
192. (a) P. A. Grutsch and C. Kutal, *J. Am. Chem. Soc.*, **99**, 7397 (1977).
    (b) C. Kutal, P. A. Grutsch and G. Ferraudi, *J. Am. Chem. Soc.*, **101**, 6884 (1979).
    (c) X. Yang and C. Kutal, *J. Am. Chem. Soc.*, **105**, 6038 (1983).
193. H. D. Gafney and R. L. Lintvedt, *J. Am. Chem. Soc.*, **92**, 6996 (1970).
194. (a) H. D. Gafney and R. L. Lintvedt, *J. Am. Chem. Soc.*, **93**, 1623 (1971).
    (b) S. Giuffrida, G. G. Condorelli, L. L. Costanzo, I. L. Fragalà, G. Ventimiglia and G. Vecchio, *Chem. Mat.*, **16**, 1260 (2004).
    (c) H. Kunkely and A. Vogler, *Z. Naturforsch., B: Chem. Sci.*, **58**, 704 (2003).
195. R. J. Lavalee, B. J. Palmer, R. Billing, H. Henning, G. Ferraudi and C. Kutal, *Inorg. Chem.*, **36**, 5552 (1997).
196. B. Marciniak and G. E. Buono-Core, *J. Photochem. Photobiol., A*, **52**, 1, 1990.
197. (a) G. Doyle, K. A. Eriksen and D. Van Engen, *Organometallics*, **4**, 830 (1985).
    (b) K. M. Chi, H.-K. Shin, M. J. Hampden-Smith, E. N. Duesler and T. T. Kodas, *Polyhedron*, **10**, 2293 (1991).
    (c) P. Doppelt and T. H. Baum, *J. Organomet. Chem.*, **517**, 53 (1996).
    (d) Y. Shen, T. Rüffer, S. E. Shulz, T. Gessner, L. Wittenbecher, H.-J. Sterzel and H. Lang, *J. Organomet. Chem.*, **690**, 3878 (2005).
    (e) G. Pampaloni, R. Peloso, A. Tiripicchio and C. Graiff, *Organometallics*, **24**, 4475 (2006).
198. S. Sostero, O. Traverso, L. Magon, P. Zanella and G. Scibona, *J. Chem. Soc., Dalton Trans.*, 1324 (1980).
199. M. A. Farrukh and I. I. Naqvi, *J. Indian Chem. Soc.*, **80**, 156 (2003).
200. R. Schmid, *Ber. Bunsenges. Phys. Chem.*, **83**, 522 (1979).
201. J. E. Earley, R. N. Bose and B. H. Berrie, *Inorg. Chem.*, **22**, 1836 (1983).
202. (a) P. Chalilpoyil, K. M. Davies and J. E. Earley, *Inorg. Chem.*, **16**, 3344 (1977).
    (b) K. M. Davies and J. E. Earley, *Inorg. Chem.*, **17**, 3350 (1978).
203. B. H. Berrie and J. E. Earley, *Inorg. Chem.*, **23**, 774 (1984).
204. R. J. Balahura, G. Ferguson, A. Johnston and B. L. Ruhl, *Polyhedron*, **5**, 2075 (1986).
205. R. J. Balahura and A. Johnston, *Inorg. Chem.*, **25**, 652 (1986).
206. R. J. Balahura and N. A. Lewis, *J. Am. Chem. Soc.*, **99**, 4716 (1977).
207. (a) R. J. Balahura and N. A. Lewis, *Can. J. Chem.*, **53**, 1154 (1975).

(b) R. J. Balahura and N. A. Lewis, *Can. J. Chem.*, **57**, 1765 (1979).
208. N. A. Lewis, C. Friesen, P. S. White and R. J. Balahura, *Inorg. Chem.*, **27**, 1662 (1988).
209. R. J. Balahura and A. J. Johnston, *Inorg. Chem.*, **22**, 3309 (1983).
210. B. F. G. Johnson, J. Lewis and M. S. Subramanian, *J. Chem. Soc. (A)*, 1993 (1968).
211. D. R. Russell and P. A. Tucker, *J. Chem. Soc., Dalton Trans.*, 1743 (1975).
212. D. M. Barlex, A. C. Jarvis, R. D. W. Kemmitt and B. Y. Kimura, *J. Chem. Soc., Dalton Trans.*, 2549 (1972).
213. A. C. Jarvis, R. D. W. Kemmitt, D. R. Russell and P. A. Tucker, *J. Organomet. Chem.*, **159**, 341 (1978).
214. A. C. Jarvis and R. D. W. Kemmitt, *J. Organomet. Chem.*, **136**, 121 (1977).
215. O. E. Woisetschläger, A. Geisbauer, K. Polborn and W. Beck, *J. Organomet. Chem.*, **599**, 238 (2000)
216. E. Szajna, A. M. Arif and L. M. Berrau, *J. Am. Chem. Soc.*, **127**, 17186 (2005).
217. J. Vicente, A. Arcas, D. Bautista and G. B. Shul'pin, *J. Chem. Soc., Dalton Trans.*, 1505 (1994).
218. (a) M. A. Mendelsohn, E. M. Arnett and H. Freiser, *J. Phys. Chem.*, **64**, 660 (1960).
(b) E. M. Arnett, H. Freiser and M. A. Mendelsohn, *J. Am. Chem. Soc.*, **84**, 2482 (1962).
(c) E. M. Arnett and M. Mendelsohn, *J. Am. Chem. Soc.*, **84**, 3821 (1962).
(d) E. M. Arnett and M. A. Mendelsohn, *J. Am. Chem. Soc.*, **84**, 3824 (1962).
219. (a) N. D. Yordanov, V. Terziev and B. G. Zhelyazkova, *Inorg. Chim. Acta*, **58**, 213 (1982).
(b) N. D. Yordanov, V. Iliev, D. Shopov, A. Jezierski and B. Jezowska-Trzebiatowska, *Inorg. Chim. Acta*, **60**, 9 (1982).
220. N. D. Yordanov and Y. Karadzhov, *Transition Met. Chem.*, **10**, 15 (1985).
221. J. P. Collman, R. L. Marshall and W. L. Young (III), *Chem. Ind. (London)*, 1380 (1962).
222. M. Calvin and K. W. Wilson, *J. Am. Chem. Soc.*, **67**, 2003 (1945).
223. (a) D. M. G. Lloyd and D. R. Marshall, *Chem. Ind. (London)*, 1760 (1964).
(b) R. H. Holm and F. A. Cotton, *J. Am. Chem. Soc.*, **80**, 5658 (1958).
224. H. Reihlen, R. Illig and R. Wittig, *Ber. Dtsch. Chem. Ges.*, **58**, 12 (1925).
225. C. Djordjevic, J. Lewis and R. S. Nyholm, *Chem. Ind. (London)*, 122 (1959).
226. (a) R. W. Kluiber, *J. Am. Chem. Soc.*, **82**, 4839 (1960).
(b) J. P. Collman, R. A. Moss, H. Maltz and C. C. Heindel, *J. Am. Chem. Soc.*, **83**, 531 (1961).
(c) P. R. Singh and R. Sahai, *Aust. J. Chem.*, **20**, 639 (1967).
227. (a) J. P. Collman, R. A. Moss, S. D. Goldby and W. S. Trahanovsky, *Chem. Ind. (London)*, 1213 (1960).
(b) J. P. Collman, R. L. Marshall, W. L. Young (III) and S. D. Goldby, *Inorg. Chem.*, **1**, 704 (1962).
(c) J. P. Collman and M. Yamada, *J. Org. Chem.*, **28**, 3017 (1963).
(d) P. R. Singh and R. Sahai, *Aust. J. Chem.*, **20**, 649 (1967).
228. K. C. Joshi and V. N. Pathak, *Coord. Chem. Rev.*, **22**, 37 (1977).
229. W. Rigby, H.-B. Lee, P. M. Bailey, J. A. McCleverty and P. M. Maitlis, *J. Chem. Soc., Dalton Trans.*, 387 (1979).
230. F. Dewhurst and P. K. J. Shah, *J. Chem. Soc. (C)*, 1737 (1970).
231. K. C. Joshi and V. N. Pathak, *J. Chem. Soc., Perkin Trans. 1*, 57 (1973).
232. (a) D. H. Evans and E. C. Woodbury, *J. Org. Chem.*, **32**, 2158 (1967).
(b) R. C. Buchta and D. H. Evans, *Anal. Chem.*, **40**, 2181 (1968).
(c) R. C. Buchta and D. H. Evans, *J. Electrochem. Soc*,, **117**, 1494 (1970).
(d) H. W. VandenBorn and D. H. Evans, *J. Am. Chem. Soc*,, **96**, 4296 (1974).
(e) M. Kitamura, K. Sasaki and H. Imai, *Bull. Chem. Soc. Jpn.*, **50**, 3199 (1977).
(f) M. A. Nawi and T. L. Riechel, *Inorg. Chem.*, **20**, 1974 (1981).
(g) F. G. Bordwell, J. A. Harrelson, Jr. and A. V. Satish, *J. Org. Chem.*, **54**, 3101 (1989).
(h) A. Kuncaka, A. Louati, M. Gross and Y. Frère, *J. Electroanal. Chem.*, **338**, 213 (1992).
(i) M. M. Richter and A. J. Bard, *Anal. Chem.*, **68**, 2641 (1996).
233. (a) P. D. W. Boyd, J. Hope and R. L. Martin, *J. Chem. Soc., Dalton Trans.*, 887 (1986).
(b) T. W. Hambley, C. J. Hawkins and T. A. Kabanos, *Inorg. Chem.*, **26**, 3740 (1987).
(c) B. Morosin and H. Montgomery, *Acta Crystallogr., Sect. B*, **25**, 1354 (1969).
(d) C. A. L. Filgueiras, A. Horn, Jr., R. A. Howie, J. M. S. Skakle and J. L. Wardell, *Acta Crystallogr., Sect. E*, **57**, m157 (2001).

(e) S. J. Kavitha, K. Panchanatheswaran, J. N. Low and C. Glidewell, *Acta Crystallogr., Sect. E*, **61**, m1326 (2005).
(f) F. Calderazzo, U. Englert, G. Pampaloni and M. Volpe, *J. Organomet. Chem.*, **690**, 3321 (2005).
(g) V. I. Lisoivan and S. A. Gromilov, *Russ. J. Inorg. Chem.*, **31**, 2539 (1986).
234. (a) M. Kitamura, K. Yamashita and H. Imai, *Bull. Chem. Soc. Jpn.*, **49**, 97 (1976).
(b) G. Gritzner, H. Murauer and V. Gutmann, *J. Electroanal. Chem.*, **101**, 177 (1979).
(c) W. Linert, E. Herlinger, P. Margl and R. Boča, *J. Coord. Chem.*, **28**, 1 (1993).
(d) M. A.-Z. Eltayeb, K. A. Al-Saad and E. M. Nour, *Pol. J. Chem.*, **79**, 1525 (2005).
235. (a) R. P. Dodge, D. H. Templeton and A. Zalkin, *J. Chem. Phys.*, **35**, 55 (1961).
(b) P. K. Hon, R. L. Belford and C. E. Pfluger, *J. Chem. Phys.*, **43**, 3111 (1965).
(c) K. S. Dichman, G. Hamer, S. C. Nyburg and W. F. Reynolds, *J. Chem. Soc., D*, 1295 (1970).
(d) E. Shuter, S. J. Rettig and C. Orvig, *Acta Crystallogr., Sect. C*, **51**, 12 (1995).
(e) A. H. Mahmoudkhani, B. Casari and V. Langer, *Z. Kristallogr. New Cryst. Struct.*, **216**, 205 (2001).
(f) M. A. K. Ahmed, H. Fjellvag, A. Kjekshus and B. Klewe, *Z. Anorg. Allg. Chem.*, **630**, 2311 (2004).
(g) M. Hoshino, A. Sekine, H. Uekusa and Y. Ohashi, *Chem. Lett.*, **34**, 1228 (2005).
236. (a) R. W. Murray and L. K. Hiller, Jr., *Anal. Chem.*, **39**, 1221 (1967).
(b) R. F. Handy and R. L. Lintvedt, *Inorg. Chem.*, **13**, 893 (1974).
(c) A. M. Bond, R. L. Martin and A. F. Masters, *Inorg. Chem.*, **14**, 1432 (1975).
(d) R. L. Lintvedt and D. E. Fenton, *Inorg. Chem.*, **19**, 569 (1980).
(e) B. D. Beaver, L. C. Hall, C. M. Lukehart and L. D. Preston, *Inorg. Chim. Acta*, **47**, 25 (1981).
(f) C. W. Anderson, K. R. Lung and T. A. Nile, *Inorg. Chim. Acta*, **85**, 33 (1984).
(g) R. E. Gamache, Jr., R. A. Rader and D. R. McMillin, *J. Am. Chem. Soc.*, **107**, 1141 (1985).
(h) C. Tsiamis, C. C. Hadjikostas, S. Karageorgiou and G. Manoussakis, *Inorg. Chim. Acta*, **143**, 17 (1988).
(i) J. Saar, *Inorg. Chim. Acta*, **155**, 175 (1989).
237. Cambridge Crystallographic Data Center (CCDC), 12 Union Road, Cambridge CB2 1EZ, UK.
238. (a) G. Gritzner, H. Murauer and V. Gutmann, *J. Electroanal. Chem.*, **101**, 185 (1979).
(b) O. Sock, P. Lemoine and M. Gross, *Electrochim. Acta*, **26**, 99 (1981).
(c) K. Yamaguchi and D. T. Sawyer, *Inorg. Chem.*, **24**, 971 (1985).
(d) A. Vallat, E. Laviron and A. Dormond, *J. Chem. Soc., Dalton Trans.*, 921 (1990).
239. E. Bouwman, K. G. Caulton, G. Christou, K. Folting, C. Gasser, D. N. Hendrickson, J. C. Huffman, E. B. Lobkovsky, J. D. Martin, P. Michel, H.-L. Tsai and Z. Xue, *Inorg. Chem.*, **32**, 3463 (1993).
240. (a) F. A. Villamena, M. H. Dickman and D. R. Crist, *Inorg. Chem.*, **37**, 1446 (1998).
(b) J. R. Bryant, J. E. Taves and J. M. Mayer, *Inorg. Chem.*, **41**, 2769 (2002).
241. (a) S. Onuma and S. Shibata, *Bull. Chem. Soc. Jpn.*, **43**, 2395 (1970).
(b) S. Swarnabala, K. R. Reddy, J. Tirunagar and M. V. Rajasekharan, *Transition Met. Chem.*, **19**, 506 (1994).
242. (a) S. Misumi, M. Aihara and Y. Nonaka, *Bull. Chem. Soc. Jpn.*, **43**, 774 (1970).
(b) M. K. Kalinowski and A. Ćmiel, *Inorg. Chim. Acta*, **49**, 179 (1981).
(c) J. H. Tocher and J. P. Fackler, Jr., *Inorg. Chim. Acta*, **102**, 211 (1985).
(d) C. Tsiamis, C. Michael, A. D. Jannakoudakis and P. D. Jannakoudakis, *Inorg. Chim. Acta*, **120**, 1 (1986).
(e) H. J. McCarthy and D. A. Tocher, *Polyhedron*, **6**, 1421 (1987).
243. (a) C. E. Pfluger and P. S. Haradem, *Inorg. Chim. Acta*, **69**, 141 (1983).
(b) I. A. Baidina, P. A. Stabnikov, I. K. Igumenov and S. V. Borisov, *Koord. Khim.*, **12**, 258 (1986); *Chem. Abstr.*, **104**, 159925 (1986).
244. (a) G. S. Patterson and R. H. Holm, *Inorg. Chem.*, **11**, 2285 (1972).
(b) G. W. Everett, Jr. and R. R. Horn, *J. Am. Chem. Soc.*, **96**, 2087 (1974).
(c) A. Endo, M. Watanabe, S. Hayashi, K. Shimizu and G. P. Satô, *Bull. Chem. Soc. Jpn.*, **51**, 800 (1978).
(d) A. Endo, *Bull. Chem. Soc. Jpn.*, **56**, 2733 (1983).
(e) N. A. Lewis and B. K. P. Sishta, *J. Chem. Soc., Chem. Commun.*, 1428 (1984).

(f) A. Endo, K. Shimizu and G. P. Satô, *Chem. Lett.*, **14**, 581 (1985).
(g) Y. Takeuchi, A. Endo, K. Shimizu and G. P. Satô, *J. Electroanal. Chem.*, **185**, 185 (1985).
(h) S. Aynetchi, P. B. Hitchcock, E. A. Seddon, K. R. Seddon, Y. Z. Yousif, J. A. Zora and K. Stuckey, *Inorg. Chim. Acta*, **113**, L7 (1986).
(i) Y. Hoshino, A. Endo, K. Shimizu and G. P. Satô, *J. Electroanal. Chem.*, **246**, 225 (1988).
(j) A. Endo, Y. Hoshino, K. Hirakata, Y. Takeuchi, K. Shimizu, Y. Furushima, H. Ikeuchi and G. P. Satô, *Bull. Chem. Soc. Jpn.*, **62**, 709 (1989).
(k) Y. Hoshino, Y. Yukawa, T. Maruyama, A. Endo, K. Shimizu and G. P. Satô, *Inorg. Chim. Acta*, **174**, 41 (1990).
(l) J. Tang, K. Shimizu and R. A. Osteryoung, *Inorg. Chem.*, **31**, 2328 (1992).
(m) P. Sharpe, N. G. Alameddin and D. E. Richardson, *J. Am. Chem. Soc.*, **116**, 11098 (1994).
(n) T. Koiwa, Y. Masuda, J. Shono, Y. Kawamoto, Y. Hoshino, T. Hashimoto, K. Natarajan and K. Shimizu, *Inorg. Chem.*, **43**, 6215 (2004).
(o) A. Endo, M. Sibasaki, H. Nagao and K. Shimizu, *Inorg. Chim. Acta*, **357**, 3443 (2004).
245. (a) A. Endo, M. Kajitani, M. Mukaida, K. Shimizu and G. P. Satô, *Inorg. Chim. Acta*, **150**, 25 (1988).
(b) I. R. Baird, S. J. Rettig, B. R. James and K. A. Skov, *Can. J. Chem.*, **77**, 1821 (1999).
246. (a) W. Kaim, A. Klein and M. Glöckle, *Acc. Chem. Res.*, **33**, 755 (2000).
(b) K. D. Demadis, C. M. Hartshorn and T. J. Meyer, *Chem. Rev.*, **101**, 2655 (2001).
(c) Y. Hoshino, S. Higuchi, J. Fiedler, C.-Y. Su, A. Knödler, B. Schwederski, B. Sarkar, H. Hartmann and W. Kaim, *Angew. Chem. Int. Ed.*, **42**, 674 (2003).
247. (a) T. Hashimoto, A. Endo, N. Nagao, G. P. Satô, K. Natarajan and K. Shimizu, *Inorg. Chem.*, **37**, 5211 (1998).
(b) S. Patra, T. A. Miller, B. Sarkar, M. Niemeyer, M. D. Ward and G. K. Lahiri, *Inorg. Chem.*, **42**, 4707 (2003).
248. (a) R. Karvembu, C. Jayabalakrishnan and K. Natarajan, *Transition Met. Chem.*, **27**, 574 (2002).
(b) P. Viswanathamurthi and K. Natarajan, *Transition Met. Chem.*, **25**, 311 (2000).
249. Y. Kasahara, Y. Hoshino, M. Kajitani, K. Shimizu and G. P. Satô, *Organometallics*, **11**, 1968 (1992).
250. Y. Hoshino, T. Susuki and H. Umeda, *Inorg. Chim. Acta*, **245**, 87 (1996).
251. K. Dallmann and W. Preetz, *Z. Naturforsch.*, **B53**, 232 (1998).
252. (a) R. E. Dessy, F. E. Stary, R. B. King and M. Waldrop, *J. Am. Chem. Soc.*, **88**, 471 (1966).
(b) V. H. Matschiner, H. Tanneberg and H.-H. Rüttinger, *Z. Phys. Chem. (Leipzig)*, **260**, 538 (1979).
(c) A. D. Jannakoudakis, C. Tsiamis, P. D. Jannakoudakis and E. Theodoridou, *J. Electroanal. Chem.*, **184**, 123 (1985).
(d) J. Saar, D. E. Smith and M. Cais, *J. Am. Chem. Soc.*, **107**, 6807 (1985).
(e) C. Tsiamis, S. Karageorgiou, M. Lalia-Kantouri and G. Manoussakis, *Gazz. Chim. Ital.*, **117**, 317 (1987).
(f) C. Tsiamis, S. Cambanis and C. Hadjikostas, *Inorg. Chem.*, **26**, 26 (1987).
253. (a) V. M. Padmanabhan, *Proc. Indian Acad. Sci.*, **A47**, 329 (1958).
(b) L. M. Shkol'nikova and E. A. Shugam, *Zh. Strukt. Khim.*, **2**, 72 (1961); *Chem. Abstr.*, **55**, 122303 (1961).
(c) R. B. Von Dreele and R. C. Fay, *J. Am. Chem. Soc.*, **93**, 4936 (1971).
(d) P. K. Hon and C. E. Pfluger, *J. Coord. Chem.*, **3**, 67 (1973).
(e) G. J. Kruger and E. C. Reynhardt, *Acta Crystallogr., Sect. B*, **30**, 822 (1974).
(f) V. P. Nikolaev, L. A. Putman, M. A. Porai-Koshits, V. I. Sokol, V. A. Avilov and I. I. Moiseev, *Koord. Khim.*, **5**, 882 (1979); *Chem. Abstr.*, **91**, 101269 (1979).
(g) W. B. Wright and E. A. Meyers, *Cryst. Struct. Commun.*, **9**, 1173 (1980).
254. (a) B. D. Santarsiero, A. Esmaili, V. Schomaker and E. C. Lingafelter, *Acta Crystallogr., Sect. A*, **37**, C234 (1981).
(b) X. Li, G. Musie and D. R. Powell, *Acta Crystallogr., Sect. E*, **59**, m717 (2003).
255. S. Kudo, A. Iwase and N. Tanaka, *Inorg. Chem.*, **24**, 2388 (1985).
256. M. Carano, F. Cicogna, J. L. Houben, G. Ingrosso, F. Marchetti, L. Mottier, F. Paolucci, C. Pinzino and S. Roffia, *Inorg. Chem.*, **41**, 3396 (2002).
257. V. Pawlowski, H. Kunkely, M. Zabel and A. Vogler, *Inorg. Chim. Acta*, **357**, 824 (2004).
258. (a) R. L. Lintvedt, H. D. Russell and H. F. Holtzclaw, Jr., *Inorg. Chem.*, **5**, 1603 (1966).

(b) C. Tsiamis, S. Cambanis, A. D. Jannakoudakis and E. Theodoridou, *J. Electroanal. Chem.*, **252**, 109 (1988).
259. (a) M. Matsumoto, H. Kodama, S. Funahashi and H. D. Takagi, *Inorg. React. Mech.*, **2**, 19 (2000).
(b) T. Behrsing, A. M. Bond, G. B. Deacon, C. M. Forsyth, M. Forsyth, K. J. Camble, B. W. Skelton and A. H. White, *Inorg. Chim. Acta*, **352**, 229 (2003).
260. M. Becht, K.-H. Dahmen, V. Gramlich and A. Marteletti, *Inorg. Chim. Acta*, **248**, 27 (1996).
261. (a) Y. Baskin and N. S. K. Prasad, *J. Inorg. Nucl. Chem.*, **25**, 1011, (1963).
(b) A. T. McPhail and P.-S. W. Tschang, *J. Chem. Soc., Dalton Trans.*, 1165 (1974).
262. (a) S.-H. Lee, K. Mizuguchi, H. Tomiyasu and Y. Ikeda, *J. Nucl. Sci. Technol.*, **33**, 190 (1996).
(b) K. Mizuguchi, S.-H. Lee, Y. Ikeda and H. Tomiyasu, *J. Alloys Compd.*, **271–273**, 163 (1998).
(c) T. Yamamura, Y. Shiokawa, H. Yamana and H. Moriyama, *Electrochim. Acta*, **48**, 43 (2002).
(d) S.-Y. Kim, H. Tomiyasu and Y. Ikeda, *J. Nucl. Sci. Technol.*, **39**, 160 (2002).
(e) K. Shirasaki, T. Yamamura and Y. Shiokawa, *J. Alloys Compd.*, **408–412**, 1296 (2006).
(f) M. H. Pournaghi-Azar and J. Ordoukhanian, *Talanta*, **38**, 1469 (1991).
263. E. Graf, A. Giraudeau and M. Gross, *Inorg. Chem.*, **22**, 3233 (1983).
264. (a) T. B. Rauchfuss, S. R. Wilson and D. A. Wrobleski, *J. Am. Chem. Soc.*, **103**, 6769 (1981).
(b) D. A. Wrobleski, S. R. Wilson and T. B. Rauchfuss, *Inorg. Chem.*, **21**, 2114 (1982).
(c) D. A. Wrobleski and T. B. Rauchfuss, *J. Am. Chem. Soc.*, **104**, 2314 (1982).
(d) D. A. Wrobleski, T. B. Rauchfuss, A. L. Rheingold and K. A. Lewis, *Inorg. Chem.*, **23**, 3124 (1984).
265. D. H. Dewar, J. E. Fergusson, R. P. Hentshell, C. J. Wilkins and P. P. Williams, *J. Chem. Soc.*, 688 (1964).
266. R. Grybos and W. Paw, *Polyhedron*, **9**, 1397 (1990).
267. (a) S. Yamazaki, T. Ama, M. Hojo and T. Ueno, *Bull. Chem. Soc. Jpn.*, **62**, 4036 (1989).
(b) S. Yamazaki, T. Ueno and M. Hojo, *Bull. Chem. Soc. Jpn.*, **64**, 1404 (1991).
268. S. Yamazaki, *Chem. Lett.*, **20**, 1299 (1991).
269. (a) C. R. Hauser and C. E. Cain, *J. Org. Chem.*, **23**, 1142 (1958).
(b) C. E. Cain, T. A. Mashburn, Jr. and C. R. Hauser, *J. Org. Chem.*, **26**, 1030 (1961).
270. (a) P. Zanello, F. Fabrizi de Biani, C. Glidewell, J. Koenig and S. J. Marsh, *Polyhedron*, **17**, 1795 (1998).
(b) J. Conradie, G. J. Lamprecht, A. Roodt and J. C. Swarts, *Polyhedron*, **26**, 5075 (2007).
271. O. E. Woisetschläger, A. Geisbauer, K. Polborn and W. Beck, *Z. Anorg. Allg. Chem.*, **626**, 766 (2000).
272. A. M. Bond, R. Colton, U. Englert, H. Hügel and F. Marken, *Inorg. Chim. Acta*, **235**, 117 (1995).
273. A. T. Kotchevar, P. Ghosh, D. D. DuMez and F. M. Uckun, *J. Inorg. Biochem.*, **83**, 151 (2001).
274. J. Conradie, T. S. Cameron, M. A. S. Aquino, G. J. Lamprecht and J. C. Swarts, *Inorg. Chim. Acta*, **358**, 2530 (2005).
275. A. Ota, L. Ouahab, S. Golhen, O. Cador, Y. Yoshida and G. Saito, *New J. Chem.*, **29**, 1135 (2005).
276. Q.-Y. Zhu, G.-Q. Bian, Y. Zhang, J. Dai, D.-Q. Zhang and W. Lu, *Inorg. Chim. Acta*, **359**, 2303 (2006).
277. R. Horikoshi, C. Nambu and T. Mochida, *Inorg. Chem.*, **42**, 6868 (2003).
278. P. Majumdar, L. R. Falvello, M. Tomás and S. Goswami, *Chem. Eur. J.*, **7**, 5222 (2001).
279. R. B. Nair, L. K. Yeung and C. J. Murphy, *Inorg. Chem.*, **38**, 2536 (1999).
280. J. Massue, N. Bellec, S. Chopin, E. Levillain, T. Roisnel, R. Clérac and D. Lorcy, *Inorg. Chem.*, **44**, 8740 (2005).
281. (a) R. Guilard, A. Dormond, M. Belkalem, J. E. Anderson, Y. H. Liu and K. M. Kadish, *Inorg. Chem.*, **26**, 1410 (1987).
(b) K. M. Kadish, Y. H. Liu, J. E. Anderson, A. Dormond, M. Belkalem and R. Guilard, *Inorg. Chim. Acta*, **163**, 201 (1989).
282. (a) C. W. Dudley, T. N. Huckerby and C. Oldham, *J. Chem. Soc. (A)*, 2605 (1970).
(b) F. Sagara, H. Kobayashi and K. Ueno, *Bull. Chem. Soc. Jpn.*, **45**, 900 (1972).
283. U. Casellato, P. A. Vigato and M. Vidali, *Coord. Chem. Rev.*, **23**, 31 (1977).

284. (a) F. Sagara, H. Kobayashi and K. Ueno, *Bull. Chem. Soc. Jpn.*, **41**, 266 (1968).
(b) B. Andrelczyk and R. L. Lintvedt, *J. Am. Chem Soc.*, **94**, 8633 (1972).
(c) D. E. Fenton, R. R. Schroeder and R. L. Lintvedt, *J. Am. Chem. Soc.*, **100**, 1931 (1978).
(d) R. L. Lintvedt and L. S. Kramer, *Inorg. Chem.*, **22**, 796 (1983).
(e) R. L. Lintvedt, G. Ranger and B. A. Schoenfelner, *Inorg. Chem.*, **23**, 688 (1984).
285. R. L. Lintvedt, B. A. Schoenfelner, C. Ceccarelli and M. D. Glick, *Inorg. Chem.*, **23**, 2867 (1984).
286. R. L. Lintvedt, C. Ranger and C. Ceccarelli, *Inorg. Chem.*, **24**, 456 (1985).
287. R. L. Lintvedt, G. Ranger and C. Ceccarelli, *Inorg. Chem.*, **24**, 2359 (1985).
288. P. Zanello, S. Tamburini, P. A. Vigato and G. A. Mazzocchin, *Coord. Chem. Rev.*, **77**, 165 (1987).
289. (a) D. E. Fenton and R. L. Lintvedt, *J. Am. Chem. Soc.*, **100**, 6367 (1978).
(b) R. L. Lintvedt, B. A. Schoenfelner and K. A. Rupp, *Inorg. Chem.*, **25**, 2704 (1986).
(c) J. K. Zehetmair and R. L. Lintvedt, *Inorg. Chem.*, **29**, 2201 (1990).
290. R. L. Lintvedt, G. Ranger and L. S. Kramer, *Inorg. Chem.*, **25**, 2635 (1986).
291. R. L. Lintvedt, W. E. Linch and J. K. Zehetmair, *Inorg. Chem.*, **29**, 3009 (1990).
292. R. L. Lintvedt and J. K. Zehetmair, *Inorg. Chem.*, **29**, 2204 (1990).

CHAPTER **10**

Catalysis using β-diketonato metal complexes

STEPHEN A. WESTCOTT

Department of Chemistry, Mount Allison University, Sackville, NB E4L 1G8, Canada
Fax: +1 506 364 2313; e-mail: swestcott@mta.ca

I. INTRODUCTION

Transition metals have been used as catalysts for industrial processes as early as the 19th century[1−4] and are currently used in the manufacture of bulk chemicals such as *n*-butanal (hydroformylation) and acetic acid (carbonylation), as well as in the generation of fine or specialty chemicals. While the development of novel catalysts is the subject of intense research, metal enolate complexes have always played a predominant role in this economically and environmentally important area of chemistry. The purpose of this chapter is to provide a short and concise review on the recent advancements of several catalytic reactions employing well-defined β-diketonato metal complexes. As enolates are among the most utilized reactive intermediates in organic synthesis[5−9], their role as intermediates in catalytic transformations is widespread and beyond the scope of this chapter. However, the reader is encouraged to peruse several excellent reviews for a more detailed account of this exciting area of catalysis[10−12]. Likewise, metal enolates are frequently used as precursors to impregnate heterogenous catalysts. As the active catalytic species in these

The chemistry of metal enolates
Edited by Jacob Zabicky

systems does not usually contain a metal enolate fragment, these systems are not discussed in any detail in this chapter. The use of metal enolates as polymerization catalysts will be discussed in another chapter. Although metal enolates have been investigated for every conceivable catalytic reaction, this review focuses on those where these easily prepared and readily available complexes have made a considerable impact in catalysis in the past few years.

Metal enolates are used in a plethora of catalyzed reactions and the following examples are meant to show the immense utility of these remarkable compounds. As with all catalytic processes, a number of different metal complexes can also be used to facilitate the desired transformation. Several catalytic reactions have been highlighted in this review to show where metal enolate complexes have played a significant role in recent years. Many stimulating developments remain to be discovered, however, and publications using these complexes are coming out even as this chapter is being finalized. Clearly, the ease of synthesis and availability of metal enolates makes them extremely attractive complexes for any number of catalyzed reactions. The following acronyms are in use throughout the chapter:

acac	acetylacetonato	eda	ethylenediamine
AHF	asymmetric hydroformylation	EXAFS	extended X-ray absorption fine structure
bom	benzyloxymethyl		
cat	catecholato, $C_6H_4O_2^{2-}$	hfac	hexafluoroacetylacetonato
cod	1,5-cyclooctadiene	ipr	*N*,*N*′-bis-(2,6-diisopropylphenyl) imidazol-2-ylidene
coe	cyclooctene		
dce	dichloroethane		
dcpb	1,4-bis(dicyclohexylphosphino) butane	nbd	norbornadiene
		pin	pinacolato
dibalh	diisobutylaluminum hydride	pmb	*p*-methoxybenzyl
dpm	2,2,6,6-tetramethylheptane-3,5-dionate	py	pyridine
		quinap	1-(2-diphenylphosphino-1-naphthyl)-isoquinoline
dppbenz	1,2-bis(diphenylphosphino) benzene		
		tbs	*t*-butyldimethylsilyl
dppe	1,2-bis(diphenylphosphino) ethane	XANES	X-ray absorption near edge structure

II. HYDROFORMYLATION

One of the areas where β-diketonato metal complexes have made significant contributions in the last few years has been catalyzed hydroformylations. Hydroformylation is one of the most industrially important catalyzed reactions, covering an annual product of almost eight million tons of aldehydes and alcohols. This reaction is used to convert light alkenes (**1**, mainly C_2 and C_3) into C_3 and C_4 aldehydes by reaction with syn-gas, CO/H_2. A generic metal catalyzed hydroforymlation reaction showing both branched (**2**) and linear (**3**) products is illustrated in equation 1. Subsequent conversion of these aldehydes into the corresponding alcohols provides feedstock for the generation of polyvinyl chloride (PVC) plasticizers and detergents. Although initial catalysts were derived from cobalt, rhodium catalysts are used at present, as they require lower pressures and afford higher selectivities. Recent applications of this reaction have extended to producing intermediates for fine chemicals (vitamins, flavors and fragrances) and pharmaceuticals (ibuprofen).

Several excellent reviews on the rhodium catalyzed hydroformylation have recently been published[13–19].

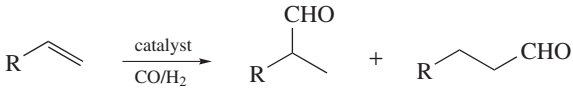

(1)

(**1**) (**2**) (**3**)

Although $RhH(CO)(PPh_3)_3$ (**4**) is widely recognized as one of the most versatile catalysts for the hydroformylation reaction, the ease of synthesis, stability and ability to fine tune the electronic and steric environments around the metal center by the addition of ligands makes complexes of the type $Rh(acac)(CO)_2$ (**5**) and $Rh(acac)(H_2C{=}CH_2)_2$ (**6**) very valuable precatalysts for this reaction[20,21]. To improve selectivities and activities for these systems it is critical to have a detailed knowledge of the nature of the catalytic intermediates and the kinetics of the catalytic cycle. While the catalytic mechanism proposed by Wilkinson in 1968[22] is still generally accepted as being correct, key intermediates in the reaction have remained elusive. Likewise, van Leeuwen and Claver have noted that the kinetics of the hydroformylation reaction has not been discussed in much detail[13]. Work by Poliakoff and George has shown that *in situ* FT-IR and polymer matrix techniques can be used in the hydroformylation of 1-octene, 1-butene, propene and ethene, using either **5** or $Rh(acac)(CO)(PPh_3)$ (**7**), to characterize acyl rhodium intermediates[23]. The kinetics of the hydroformylation of soybean oil by ligand-modified $Rh(acac)(CO)_2$ (**5**) catalysts has also been examined[24]. More recently, Rosales and coworkers have conducted a kinetic study of the hydroformylation of 1-hexene using **5** and one equivalent of dppe. The reaction proceeded with good selectivity to give linear to branched ratios close to 2. The initial rate was found to be first-order with respect to [Rh] and a fractional order with respect to substrate concentration. The kinetic and mechanistic work in this study suggested a mechanism involving RhH(CO)(dppe) (**8**) as the active catalytic species with hydrogenolysis of the acyl intermediate (dppeRhC(O)H, **8′**) as the rate-determining step at low hydrogen pressure and migratory insertion of the alkene into the Rh−H bond at high hydrogen pressures[25].

Other metal enolates are still being examined for equation 1[26], yet the most common catalyst systems are based on $Rh(acac)L_2$[27–35]. For instance, the interaction between **5** and human serum albumin has been found to be an active hydrosoluble nanostructured biocatalyst for the hydroformylation reaction[36]. Most of the work in this area, however, has involved reactions using modified phosphine and phosphite derivatives. Indeed, van Leeuwen and coworkers found that bulky monodentate phosphite/rhodium systems are highly active and selective hydroformylation catalysts for a wide range of substrates, including di- and trisubstituted alkenes[37]. An interesting study by Reetz and Li, outlined in equation 2, demonstrated that mixtures of monodentate achiral ligands could be used to improve product selectivites. For instance, reactions of *t*-butyl methacrylate (**9**) using $Rh(acac)(CO)_2$ (**5**) and two equivalents of phosphite (**12**) gave predominately a branched (**10**) to linear (**11**) ratio of 2.7:1, but with a considerable amount of hydrogenation product (33%). Changing to a heterocombination of ligands including one equivalent of **12** and one of phosphine **13** increased the branched to linear ratio to 6.4:1 and reduced the amount of hydrogenation product to 5%. Unfortunately, while selectivities increased in this mixed reaction, conversion of starting material was only 32% compared to 55% for the homocombination using the phosphite ligands[38]. The electronic effects induced by two identical or

two different phosphorus ligands on the regioselectivity of the rhodium-catalyzed hydroformylation of propene has been investigated using DFT-based calculations[39].

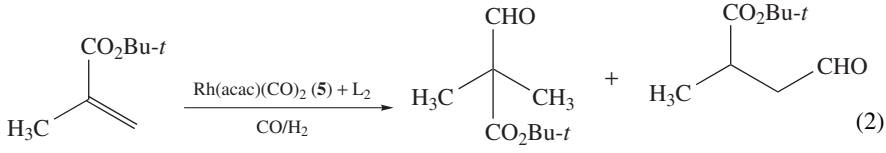

(**9**) (**10**) (**11**) (2)

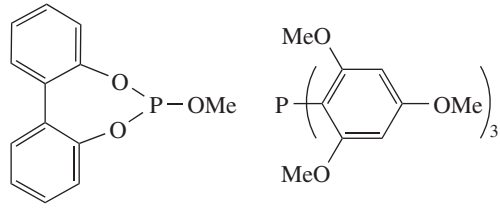

(**12**) (**13**)

In a related study, Klosin, Whiteker and coworkers have reported a correlation between the dihedral angle in a series of biaryl-bridged bisphosphite Rh(acac) complexes and selectivities for the hydroformylation of allyl cyanide and vinyl acetate[40]. Smaller dihedral angles were found to generate products with increased regio- and enantioselectivity. DFT calculations suggested that the decreased dihedral angles led to smaller P-Rh-P bite angles. These results were somewhat surprising, as large bite angles have previously been correlated with increased hydroformylation regioselectivity[41].

As phosphonites and phosphites are susceptible to degradation, a number of studies have focused on developing new phosphine ligands. For instance, Breit and coworkers have designed a class of phosphabarrelene (**16**) based rhodium catalysts for the effective hydroformylation of cyclohexene (**14a**) and cycloheptene (**14b**) (equation 3) to give cyclohexane products (**15**). Of singular interest is the observation that these catalyst systems enable a selective hydroformylation of an endocyclic C=C double bond without generating any products arising from a competing alkene isomerization[42]. In another study, the hydroformylation of 1-octene occurs rapidly (rates up to 800 h^{-1}) when carried out in supercritical CO_2 using the catalyst system derived from $Rh(acac)(CO)_2$ (**5**) and [1-propyl-3-methylimidazolium][$Ph_2P(3\text{-}C_6H_4SO_3)$] (**17**). The catalyst system was stable for at least 40 h with very low levels of metal leaching (0.5 ppm)[43].

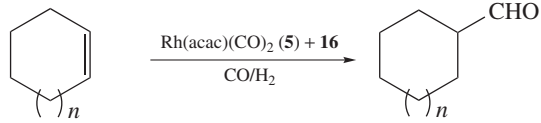

(**14**) (**a**) $n = 1$ (**b**) $n = 2$ (**15**) (**a**) $n = 1$ (**b**) $n = 2$ (3)

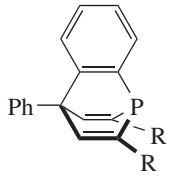

(**16**) R = Ph, *i*-Pr, 2,4-xylyl

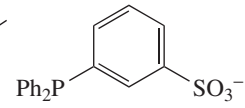

(**17**)

One of the most important breakthroughs in this area has been the development of chiral catalysts for enantioselective hydroformylation. Although Consiglio and coworkers[44] reported the first highly enantioselective variant in 1991 using a bisphosphine $PtCl_2/SnCl_2$ system, rhodium acac complexes containing phosphinophosphite ligands were later found to catalyze the hydroformylation of styrene with excellent selectivity (up to 95% ee)[20,45]. Since this seminal work, a considerable amount of research has focused on the AHF reaction[46–48]. For instance, Huang, Bunel and coworkers have reported that the combination of $Rh(acac)(CO)_2$ (**5**) and TangPhos (**20**) is an active catalyst for the AHF of norbornylene (**18**) under mild conditions to give **19** with ee up to 93% (equation 4)[46].

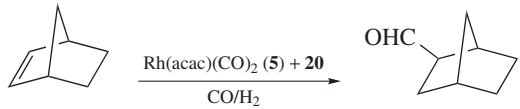

(**18**) (**19**) (4)

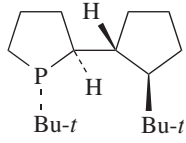

(**20**)

Another area of interest has included modifying phosphine and related ligands so that reactions can be conducted in non-traditional media, especially those solvents that play a critical role in green chemistry[49–62]. A number of excellent and comprehensive reviews are now available that provide a detailed summary of work in this area[63,64].

One of the crowning achievements of catalysis occurs when the reaction is used in the synthesis of natural products, pharmaceuticals, fine chemicals or other industrially relevant compounds[65–68]. Tolterodine (**23**), an important drug used to treat urinary incontinence, has been prepared in high yields[66], utilizing the rhodium-catalyzed hydroformylation of a 1,1′-bisarylalkene (**21**) to give **22** as a key step in the synthesis (equation 5). Likewise, catalyzed hydroformylation of glycals (**24**) using **5** gave low yields of 2-formylpyrans (**25a**, **25b**) and high yields of 3-formylpyrans (**26a**, **26b**) (equation 6). C-branched sugars are key components in many natural products and antibiotics[67]. Lastly, this versatile catalytic reaction has also been applied to the synthesis of a potential BC-ring subunit

of bryostatin (**28**), a remarkably potent anticancer agent, via the hydroformylation of **27** (equation 7)[68].

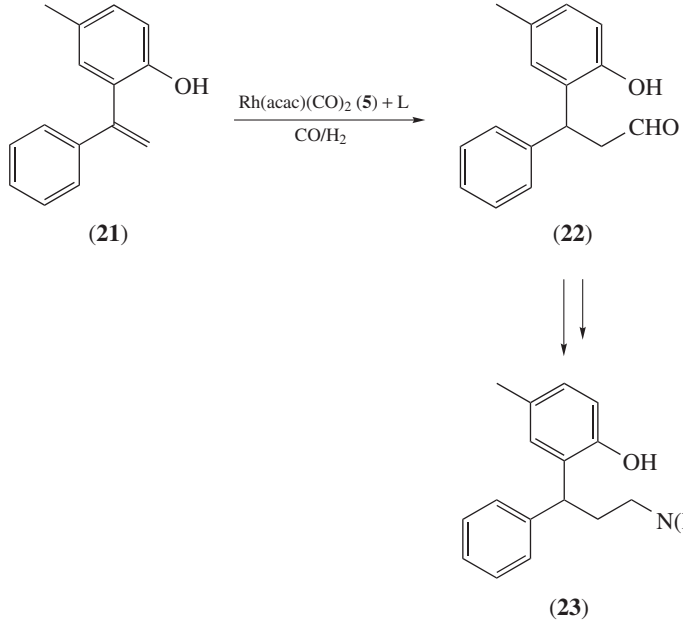

(5)

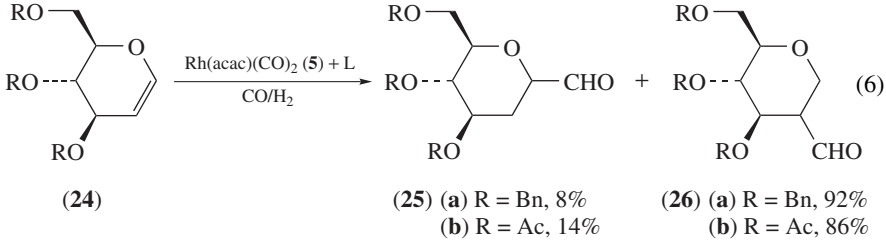

(6)

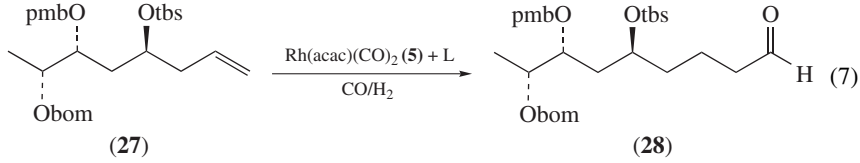

(7)

III. OXIDATION

Another area where metal β-diketonates have made a significant impact is in the oxidation of alkanes[69–74], alkenes[75–78] and alcohols[79–84]. A number of different metal complexes have been used in these reactions, including Pd(acac)$_2$ (**29**)[85], Co(acac)$_3$ (**30**)[69,76], Fe(acac)$_3$ (**31**)[72], a bimetallic Pd(II) complex containing a 1,3,5-triketone ligand[77], MCl(acac)(PPh$_3$) (**32**) where M = Ni, Co, Cu[78], Mn(acac)$_3$ (**33**)[79], MoO$_2$(acac)$_2$ (**34**)[83], VO(acac)$_2$ (**35**)[74,75,84] and VO(hfac)$_2$ (**36**)[82]. In the latter study, the oxidation of α-acetylenic

alkanols (**37**) to the corresponding ketones (**38**) was improved by using **36** as a catalyst instead of **35** (equation 8). Addition of excess hexafluoroacetylacetone was also required to improve product yields[82]. A remarkable study by Fürstner and Nagano reported the oxidation of a furyl alcohol (**39**) using *t*-BuOOH and catalytic amounts of **35** to give **40** in the total synthesis of ipomoeassin B and E (equation 9). Ipomoeassin B and E are extracts from morning glory (*Ipomoea aquamosa*), which are harvested from the Suriname rainforest, and have displayed considerable cytotoxicity[86].

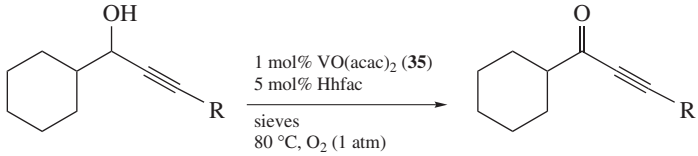

(8)

(**37**) R = H, *n*-C_4H_9, *n*-C_6H_{13} (**38**) R = H, *n*-C_4H_9, *n*-C_6H_{13}

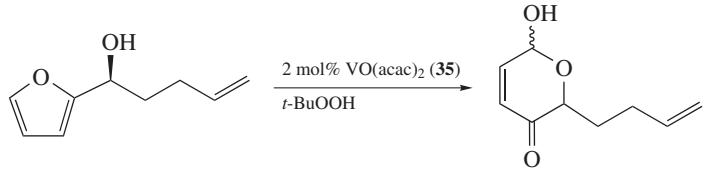

(9)

(**39**) (**40**) 71%

A considerable amount of work in this area has also focused on using Schiff base complexes derived from diketonato precatalysts[87–91] as well as heterogeneous β-diketonates complexes[92–95]. Peyrovi and coworkers reported that the oxidation of alcohols using *t*-butyl hydroperoxide could be catalyzed with $Co(acac)_3$ (**30**) immobilized between layers of bentonite[92]. Interestingly, complex **30** has also been used as an anti-skinning agent in oxidative crosslinking reactions[96]. To avoid skinning in the can, the cobalt-catalyzed decomposition of hydroperoxides has been used in the paint industry to promote the drying of paint. In a related study, $Mn(acac)_3$ (**33**) was found to function as both a radical initiator and as a catalyst for hydroperoxide decomposition for the autooxidation of ethyl linoleate, a model compound for the active binding molecule in alkyd paints[97]. The oxidation of ^{13}C-labelled ethyl linoleate has been monitored by ^{13}C-NMR spectroscopy and **33** appears to be less effective in decomposing ROOH than the combination of **33** and 2,2′-bipyridine[98]. $Mn(acac)_3$ (**33**) has also been found to catalyze the oxidation of *N*-alkyl amides using microwave irradiation with *t*-BuOOH[99].

A number of metal β-diketonates have been used to catalyze the oxidation of sulfides to sulfoxides, important synthetic intermediates for the construction of various biologically active molecules[100–105]. For example, an elegant study by Ishii and coworkers demonstrated that $VO(acac)_2$ (**35**) selectively catalyzed the sulfoxidation of adamantane (**41**) by SO_2/O_2 to give 1-adamantane sulfonic acid (**42**) (equation 10)[105]. Although a number of metal acac complexes were examined as catalysts for this reaction, all but the vanadium compound failed to promote the sulfoxidation. The catalytic oxidation of triarylphosphines using the palladium complex $Pd(acac)_2$ (**29**) has also been investigated[106].

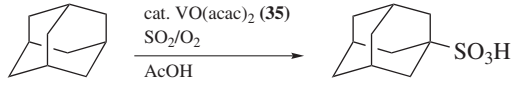

(10)

(**41**) (**42**)

As with all catalytic reactions, recent advances in oxidation chemistry have been used in developing systems that use environmentally benign water[107] or ionic liquids[108–111] as solvents. The economical, soluble and easily prepared complex $Cu(acac)_2$ (**43**) is an active and selective catalyst for the oxidation of secondary alcohols in ionic liquids at room temperature[110]. Further discussion of these reactions can be found in several excellent reviews[111–114].

Epoxides are versatile intermediates that have great value in synthetic organic chemistry and chemical technology and are readily prepared by the oxidation of alkenes with various oxygen sources in the presence of a catalyst. A number of metal enolate complexes are effective catalysts for this reaction, including $MoO_2(acac)_2$ (**34**)[115,116] and $VO(acac)_2$ (**35**)[117]. The vanadium complex is an active and selective catalyst for the epoxidation of α-hydroxyl vinyl sulfoxides (**44**), which proceeds via initial oxidation to give the corresponding unsaturated sulfones, followed by an unusual regio- and stereoselective epoxidation to give *anti*-oxiranes (equation 11). This methodology was subsequently applied to the preparation of carbohydrate derivatives. Interestingly, β-diketonates zirconium complexes, such as $[Zr(acac)_3]ClO_4$ (**46**), have been used in the catalytic ring opening of the resulting oxiranes[118].

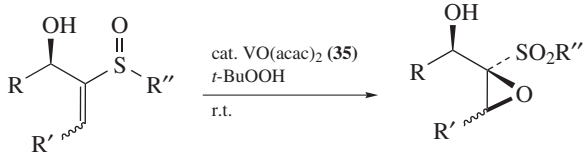

(**44**) (**45**) 54–91% (11)

β-Diketonate epoxidation catalysts have also been successfully grafted onto polymer supports[119–123]. Grafting $Ni(acac)_2$ (**47**) complexes onto polybenzimidazole resulted in active catalysts whereas no activity was observed in reactions using an aminomethylpyridine methacrylate-type resin[119]. EXAFS results and XANES simulations suggested that use of rigid polybenzimidazole results in vacancies in the metal-coordination sphere, allowing for catalysis to occur. A proposed mechanism for this reaction is based on transfer of an oxygen atom to the alkene by an acylperoxy radical. This radical arises from the reaction of molecular oxygen (or a peroxide) with a transient acyl radical generated by a Ni(III) intermediate and an aldehyde, commonly used as a coreactant[124].

Aziridation of alkenes (**48**), the nitrogen atom transfer process analogous to epoxidation, is also of considerable interest, as the resulting aziridanes (**49**) are useful intermediates in organic synthesis of pharmaceuticals and agrochemicals. A number of Lewis acids are known to catalyze this reaction, including $Cu(acac)_2$ (**43**). Recent developments in this area include immobilizing this precatalyst using an amine-functionalized hexagonal silica support[125] or activated carbon[126] and polymer supports[127]. Likewise, copper complex **43** dissolved in an ionic liquid has been reported to be an active and recyclable catalyst system for the aziridation of alkenes using PhI=NTs as the nitrene donor. The ionic liquid phase containing the catalyst was recovered and reused for several cycles without any appreciable drop in activity, as shown for the aziridation of styrene (equation 12)[128]. In a related study, Mancheño and Bolm have shown that the iron complex $Fe(acac)_3$ (**31**) can be used to catalyze the imination of sulfides and sulfoxides in the presence of iodinanes[129].

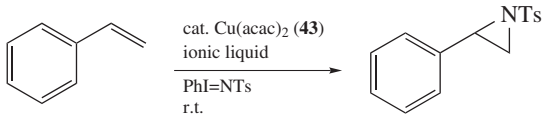

(48) (49) (12)

IV. HYDROGENATION

The ability of transition metals to catalyze the addition of dihydrogen to unsaturated organic molecules has many industrial applications. Unlike oxidations that primarily use either early or middle group metals, late metals are particularly active for catalyzed hydrogenations. Although not particularly common, metal enolates such as $Pd(acac)_2$ (**29**)[130], $Co(acac)_3$ (**30**)[131], $Fe(acac)_3$ (**31**)[132], $Ni(acac)_2$ (**47**)[133,134], Rh(hfac)(dcpb) (**50**)[135] and $Ru(acac)_3$ (**51**)[136] have also been used for this reaction. The ruthenium catalyst system consisting of **51**, $P(octyl)_3$ and *p*-toluenesulfonic acid (*p*-TsOH) was effective in the reduction of succinic anhydride (**52**) to give γ-butyrolactone (**53**) (equation 13). *p*-TsOH was found to enhance reaction rates and increase selectivites to give the desired product in up to 95% yield[136]. Considerably more effort has focused on using heterogeneous systems derived from these metal enolates[137–144]. For instance, supported iridium catalysts prepared by atomic layer deposition of $Ir(acac)_3$ were found to be effective for the hydrogenation of toluene[137]. Hydrogen transfer reactions have also been reported using iron[145] and ruthenium[146] acac catalyst systems.

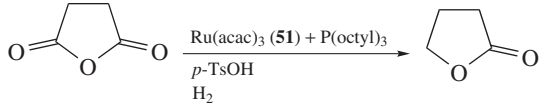

(52) (53) (13)

V. ADDITION OF MAIN GROUP COMPOUNDS

A considerable amount of research has focused on using metal enolates as catalysts for the addition of main group hydrides to unsaturated organic molecules. Indeed, some of the most active and selective catalysts for the metal-catalyzed hydroboration reaction are based on the addition of diphosphine ligands (L_2) to $Rh(acac)(coe)_2$ (**54**). This is the only catalyst system known to facilitate the addition of catecholborane (HBcat) to a tetrasubstituted alkene[147]. A reaction mechanism is shown in Scheme 1 and is believed to proceed via initial oxidative addition of catecholborane to give a putative hydrido boryl intermediate (i). Coordination of the alkene to the metal center (ii) followed by insertion into the Rh−H in either an anti-Markovnikov (iii) or Markovnikov (iv) fashion with subsequent reductive elimination gives the corresponding organoboronate ester products (v) and (vi), respectively. The unusual regioselectivity in favor of branched products (vi) observed in hydroborations of vinylarenes (R = Ar) is believed to arise when the rhodium center can best stabilize a benzylic intermediate (iv).

Hydroboration of $Rh(acac)(coe)_2$ (**54**) + L_2 with excess HBcat affords acacBcat and the zwitterionic complex $Rh(\eta_6\text{-catBcat})L_2$ (**55**), which is believed to be the catalyst resting state in these reactions. Variation of the ligands has a profound effect on these

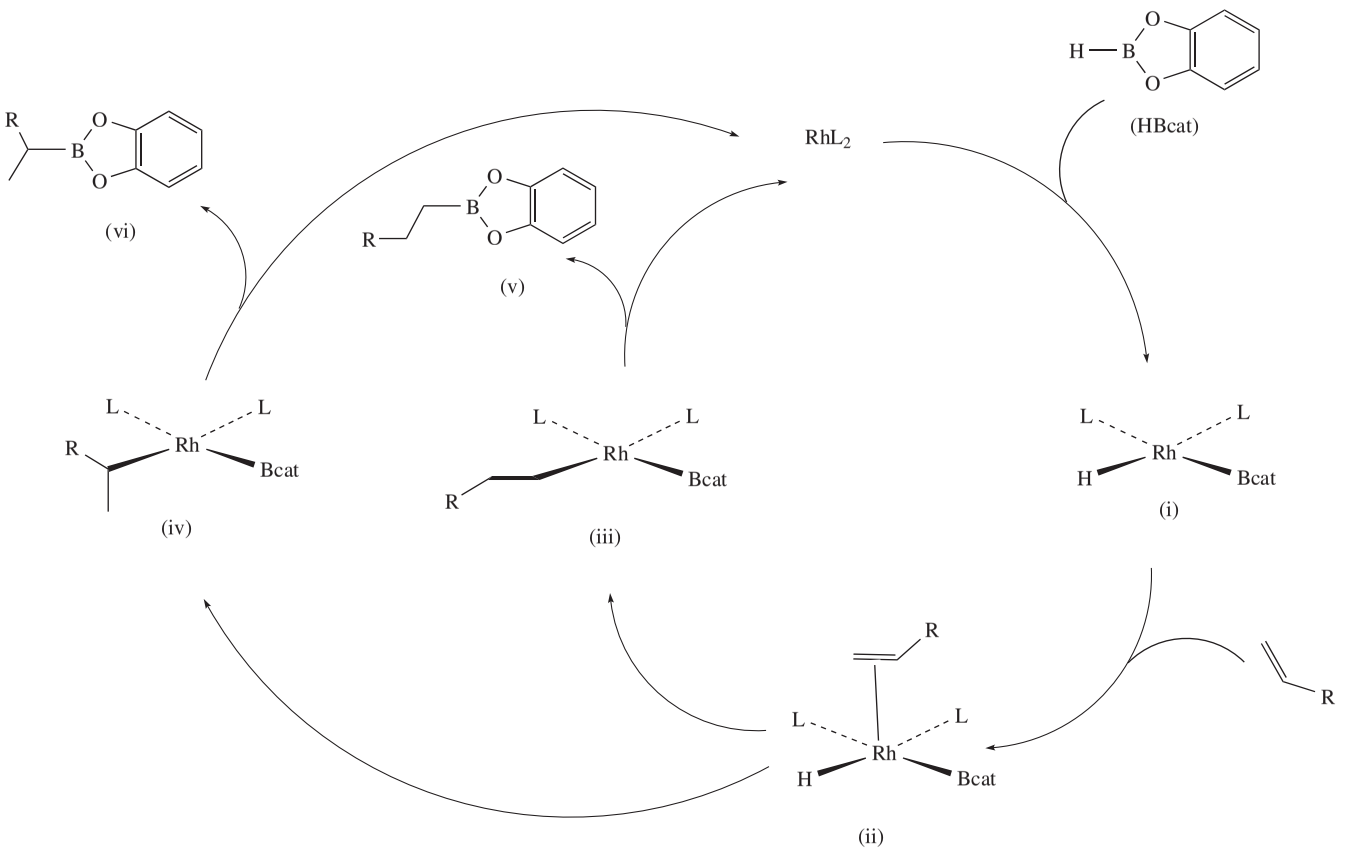

SCHEME 1. A mechanism for the rhodium-catalyzed hydroboration of alkenes using catecholborane (HBcat)

reactions and products derived from a competing dehydrogenative borylation pathway can sometimes dominate[148–152]. Enhanced regioselectities for the hydroboration of vinylarenes in supercritical CO_2 using Rh(hfac)(coe)$_2$ (**56**) and phosphine ligands have been observed with monodentate phosphines[153]. An excellent review by Crudden and Edwards describes recent advances in the metal-catalyzed hydroboration reaction[154].

The diboration (addition of B−B bonds) of alkenes has also been the subject of considerable effort[155] and an elegant review by Beletskaya and Moberg has recently appeared on the metal-catalyzed element–element addition to alkenes and alkynes[156]. Of particular importance in this area is the work by Morken and coworkers who designed the catalytic asymmetric carbohydroxylation of alkenes using a domino diboration cross-coupling oxidation reaction[157–159]. The addition of B_2cat_2 was accomplished using a chiral catalyst system derived from Rh(acac)(nbd) (**57**)/(*S*)-quinap and the resulting 1,2-diboron compounds (**58**) were reacted *in situ* with aryl halides. The less hindered B−C bond was selectively transformed into the corresponding cross-coupled product whereupon the remaining B−C bond was subsequently oxidized to give the corresponding alcohols (**59**) (equation 14).

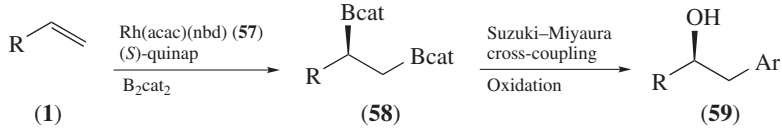

(**1**) (**58**) (**59**) (14)

The addition of B−Si bonds to dienes has also been catalyzed by a number of metal enolate complexes[156, 160–164]. Although early work by Ito and coworkers used a nickel system consisting of Ni(acac)$_2$ (**47**) and dibalh[161], recent studies by Gerdin and Moberg have found that Pt(acac)$_2$ (**60**), dibalh and a chiral phosphoramidite catalyzed the enantioselective silaboration of 1,3-cyclohexadiene (**61**) using $PhMe_2SiBpin$ (**62**) to give **63** with 70% ee (equation 15)[162]. Related nickel catalyst systems gave essentially racemic products and palladium complexes were inactive. Interestingly, attempts to catalyze the silaboration of acyclic 1- and 1,4-substituted 1,3-dienes (**64**) resulted in a new disproportionation reaction with equimolar mixtures of allylsilanes (**65**) and dienylboranes (**66**) (equation 16)[163].

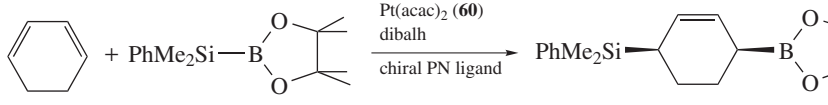

(**61**) (**62**) (**63**) (15)

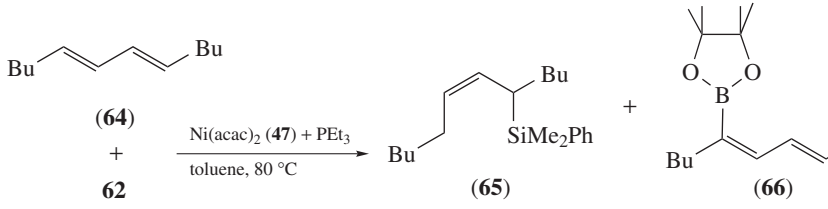

(**65**) (**66**) (16)

Highly enantioenriched (*E*)-allylic silanes have been generated from optically active allylic alcohols using a palladium catalyzed intramolecular bis-silylation (Si−Si addition) with a subsequent and highly stereospecific Si−O elimination[165]. The overall reaction proceeded with nearly complete conservation of the enantiopurity of the starting allylic alcohol (**67**) (equation 17) to give **68** in high yields. Other metal complexes such as $Rh(acac)(CO)_2$ (**5**)[166–168] and $MoO_2(acac)_2$ (**34**)[169] have been used in the related hydrosilation reactions (addition of Si−H bonds). While much less is known about the addition of Sn−H bonds to alkenes using metal enolates, this may be due to the observation that the platinum complex $Pt(acac)_2$ (**60**) catalyzes the dehydrogenative stannylation of tin hydrides to give dihydrogen and distannanes[170]. The carbamoylstannation (addition of $Sn-CONR_2$) of alkynes (**69**) using $Rh(acac)(CO)_2$ (**5**), however, afforded (Z)-β-stannyl-α,β-unsaturated amides (**70**) selectively[171]. Reactions using $Ni(cod)_2$ (**72**) resulted in products with a reversal of regioselectivity (**71**) (equation 18).

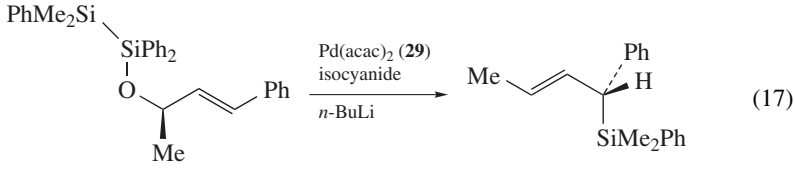

(17)

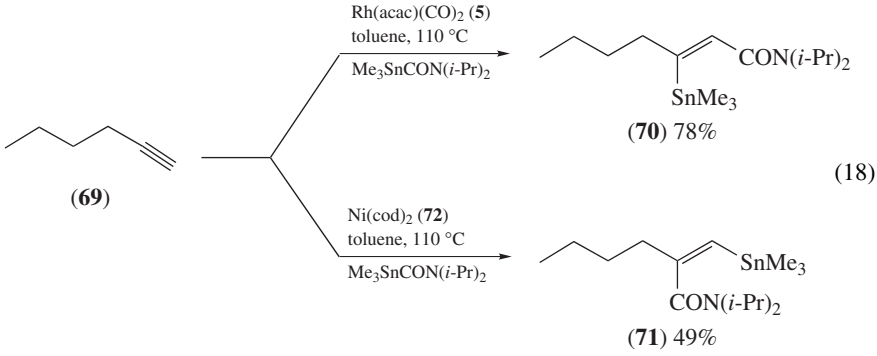

(18)

The addition of N−H bonds to unsaturated organic molecules using metal enolates has also received considerable attention. Recoverable and reusable catalyst systems based on the copper complex $Cu(acac)_2$ (**43**) immobilized in ionic liquids have been used for the insertion of α-diazo compounds into amines[172] and for the aza-Michael reaction[173]. A related hydroaminomethylation (tandem alkene hydroformylation followed by reductive amination) reaction using $Rh(acac)(CO)_2$ (**5**) and a bisphosphite catalyst system has been used to synthesize biologically active tertiary amines (**75**) from the addition of allyl ether (**73**) and secondary amine (**74**) (equation 19)[174]. This reaction is highly regiospecific in favor of the linear products and tolerant of many functional groups including aryl chlorides. Hydrogenation is believed to occur using a rhodium species where the phosphite ligands are not coordinated to the metal center. The hydroaminocarbonylation of alkynes to give the corresponding 1,4-diamide derivatives could also be catalyzed by $Rh(acac)(CO)_2$ (**5**); however, yields were considerably lower than with other rhodium catalysts[175].

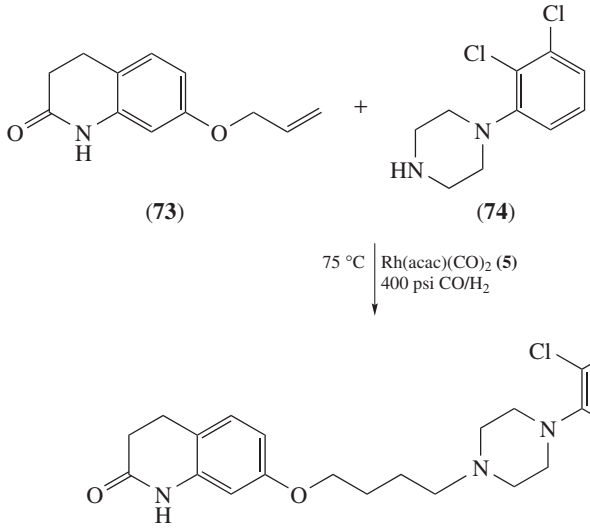

(19)

(**75**) 67%
branched:linear 37:1

The intermolecular hydrophosphination of phenylacetylene (**76**, equation 20) with diphenylphosphine using $Ni(acac)_2$ (**47**) and $(EtO)_2P(O)H$ has been reported to give alkenylphosphine (**77**) in high yields[176]. Alkenylphosphines are an important class of ligands whose applications have been limited by the lack of a simple and convenient synthetic procedure. This reaction gave the corresponding *syn*-addition products with a mixture of α- and β-adducts. Selectivities could be fine-tuned by judicious choice of catalyst precursor used to facilitate this reaction.

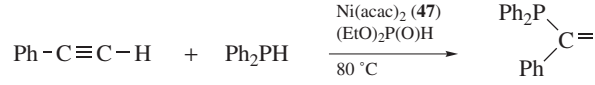

(**76**) (**77**) 90%

(20)

The hydration of nitriles (**78**, equation 21) is another area of intense interest for the preparation of industrially and pharmaceutically important amides (**80**) and carboxylic acids (**81**). Although a number of transition metals can be used to catalyze this important reaction[177], recent work has shown that $Ru(acac)_2$ (**79**) complexes with diphenyl-2-pyridylphosphine (PPh_2py) ligands were extremely active catalysts with turnover frequencies of up to 20,900 h^{-1} [178,179]. This reaction is believed to proceed via initial activation of the nitrile by coordination to the Lewis acidic metal, where a vacant coordination site arises from a $\eta^2 \rightarrow \eta^1$ acac isomerization. Nucleophilic addition of water is then promoted by hydrogen bonding with the Lewis basic pyridine moiety of the PPh_2py ligand.

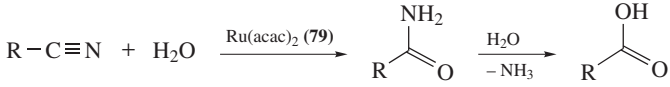

(**78**) (**80**) (**81**)

(21)

The addition of O−H bonds to alkenes has been accomplished with $Ru(acac)_3$ (**51**) for the chemoselective tetrahydropyranylation of *n*-butanol (**82**) with 3,4-dihydro-2*H*-pyran (**83**) and other alcohols under solvent-free conditions to give **84** in high yields (equation 22)[180]. While a number of other metal enolates, including $Pd(acac)_2$ (**29**), $Co(acac)_3$ (**30**) and $VO(acac)_2$ (**35**), were also effective in catalyzing this reaction, highest yields were achieved with the ruthenium complex. In a related study, the same ruthenium catalyst was also active in the solvent-free acylation of alcohols and amines[181]. The addition of methanol to propylene oxide to give 2-methoxy-1-propanol derivatives has been catalyzed using a clay-supported $Zr(acac)_3^+$ (**46**) catalyst system[182]. This heterogeneous system showed a rate increase and improved selectivities compared with the analogous homogeneous catalyst system.

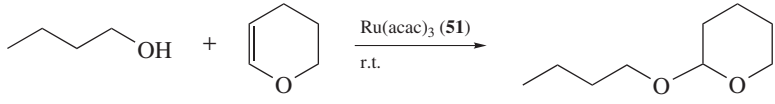

(**82**) (**83**) (**84**) 99% (22)

β-Vinyl sulfides have been prepared by the catalytic addition of the S−H bond of thiols (**85**) to terminal alkynes (**86**) under solvent-free conditions using the nickel complex $Ni(acac)_2$ (**47**)[183]. High alkyne conversions (up to 99%) were achieved after 30 min at 40 °C in favor of the corresponding Markovnikov products (**87**) (equation 23). Other metal acetylacetonate complexes were examined for this reaction, but none showed any improvement over the nickel catalyst. Mechanistic details suggest that alkyne insertion into the Ni−S bond is important to the catalytic cycle and that nanosized structural units comprised of $[Ni(SAr)_2]_n$ represent the active form of the catalyst. Isothiocyanates[184] and vinyl sulfides[185] have been produced in related $Rh(acac)(H_2C{=}CH_2)_2$ (**6**) and $VO(acac)_2$ (**35**) catalyzed sulfenylation reactions of aryl cyanides and aryl acetylenes, respectively.

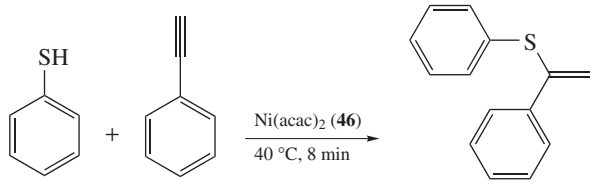

(**85**) (**86**) (**87**) 82% (23)

Enantioselective fluorination reactions catalyzed by chiral palladium enolate complexes have been the subject of considerable research[186–188]. For instance, the fluorination of acyclic β-ketoester (**88**, equation 24) using *N*-fluorobenzenesulfonimide (NFSI) gave product **89** in high yields and with excellent enantioselectivity (ee up to 94%)[186]. This reaction can be carried out in environmentally benign alcoholic solvents and provides valuable synthetic building blocks that find applications in medicinal chemistry, chemical biology and material sciences.

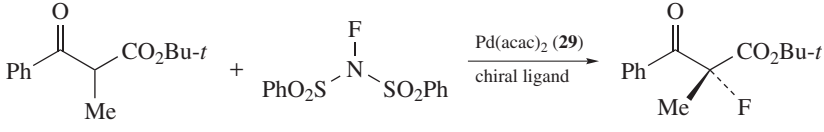

(**88**) NFSI (1.5 equiv) (**89**) (24)

VI. C–C BOND FORMATION

Catalytic carbon–carbon bond-forming reactions are among the most important types of transformations in organic synthesis and metal enolate complexes have played an important role in this field[189–195]. Of significance is the recent discovery that iridium acetylacetonato complexes catalyze the intermolecular hydroarylation[196–198] and hydrovinylation[199] of unactivated alkenes. The active catalyst is a unique complex [Ir(μ-acac-O,O',C^3)(acac-O,O')(acac-C^3)]$_2$ (**90**) and the reaction is believed to proceed via arene C–H activation[200–204] to generate a bis-acac, phenyl-Ir(III) intermediate. Hydroarylations proceed to give the anti-Markovnikov straight-chain alkyl benzenes (**91**) with high selectivity (equation 25), and only minor amounts of the branched product (**92**).

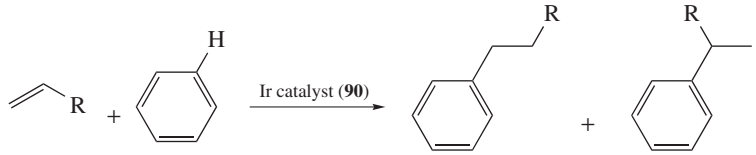

(25)

(**1**) (**91**) major (**92**) minor

Metal enolate complexes have also been used to catalyze the allylation of carbonyl compounds[205–207], addition of aldehydes to 1,3-dienes[208] and alkynes[209] as well as the addition of alkenes to alkynes[210] and indoles[211]. In the latter study, 5 mol% of Pd(acac)$_2$ (**29**) and 10 mol% of PPh_3 were found to be an effective catalyst system for the coupling of *N*-methylindole (**93**) with a variety of 2-acetoxymethyl-substituted electron-deficient alkenes, including methyl 2-(acetoxymethyl)acrylate (**94**) (equation 26). Substituted indoles (**95**) constitute an important class of biologically active natural products and synthetic routes to these valuable compounds have therefore attracted considerable attention.

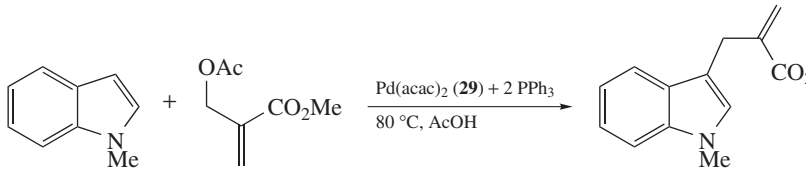

(26)

(**93**) (**94**) (**95**) 84%

Other palladium acetylacetonate complexes have also been developed for cross-coupling reactions. Indeed, an acac palladacycle complex has recently been observed to effectively catalyze both the Suzuki–Miyaura and Heck reactions[212]. Likewise, the *N*-heterocyclic carbene complex Pd(acac)Cl(ipr) (**96**) is an excellent catalyst for the formation of C–N and C–C bonds (equation 27)[213,214]. These catalysts were effective for coupling of ketones (**97**) with a wide range of substrates, including unreactive aryl halides such as **98** and sterically hindered and heterocyclic aryl chlorides, to give products like **99** in high yields. The catalyst precursor was readily prepared from commercially available Pd(acac)$_2$ (**29**) and ipr·hydrochloride.

There has also been interest in using metal enolate complexes to catalyze cross-coupling reactions with organoantimony compounds[215], organophosphanes[216], organosilanes (Hiyama couplings)[217,218] and organotin compounds (Stille cross-coupling reactions)[219]. The palladium complex Pd(acac)$_2$ (**29**), along with an appropriate ligand, such as PPh_3, PMe_3, $AsPh_3$, $SbPh_3$, $P(OPh)_3$ etc., were employed for the Stille reaction of

dihalogen pyridine derivatives (**100**) with a number of substituted thienyl organotin compounds (**101**) to give **102** (equation 28). Also of considerable interest is the cobalt[220,221] or iron[222–228] catalyzed coupling of Grignard reagents. An elegant study by Itami, Yoshida and coworkers[223] has shown the first examples of a catalyzed cross-coupling of alkenyl sulfides (**103**) with Grignard reagents (**104**). This reaction proceeded selectively at the S–alkenyl bonds (equation 29) to give the desired styrenes (**105**) with almost no cross-coupling (**106**) taking place at the competing S–aryl bonds.

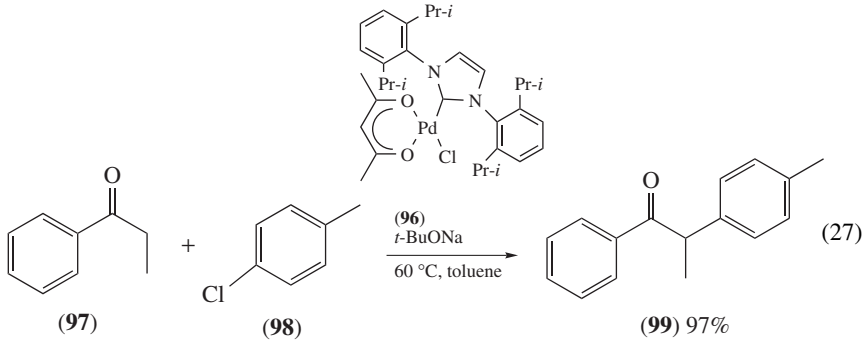

(27)

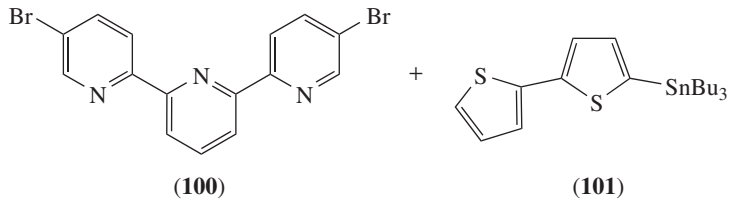

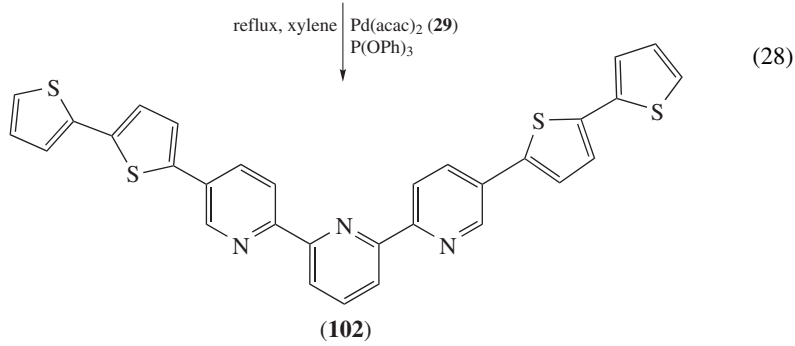

(28)

The cross-coupling of organozinc compounds has been accomplished using a number of metal enolate complexes, namely Rh(acac)($H_2C{=}CH_2$)$_2$ (**6**)[229], Co(acac)$_3$ (**30**)[230], Ni(acac)$_2$ (**47**)[231–233], Li(acac) (**107**)[234,235] and Cr(acac)$_3$ (**108**)[236]. For instance, complex **47** proved to be an extremely effective catalyst system for the Negishi cross-coupling of arylzinc halides (**109**) with aryl (**110**), heteroaryl and alkenyl halides, triflates and nonaflates to give the corresponding biaryl compounds (**111**) (equation 30). The solvent played an important role in these reactions and optimal conditions were found with 8:1 mixtures of THF and *N*-ethylpyrrolidinone (nep). Only 0.05 mol% of the nickel complex

was required to successfully catalyze these reactions[236]. Similar reactions with binuclear magnesium–copper reagents[237–239] and other couplings have also been reported[240].

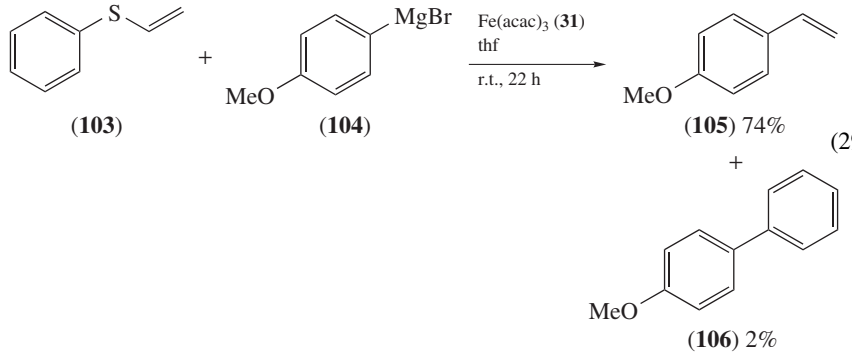

(**103**) (**104**) (**105**) 74% (29)

(**106**) 2%

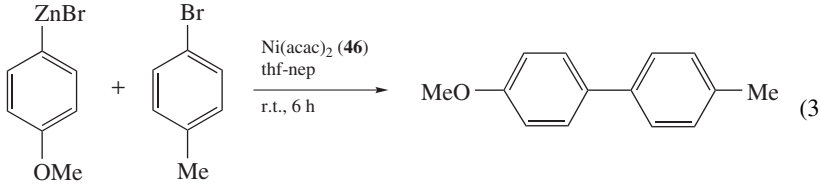

(**109**) (**110**) (**111**) 88% (30)

Metal enolate complexes are well known to play a major role in a number of catalyzed addition reactions[241–247]. For instance, Lerum and Chisholm have reported that the combination of Rh(acac)$(CO)_2$ (**5**) and tris(*o*-methoxyphenyl)phosphine was an excellent catalyst system for the 1,4-addition of alkynes (**112**) to unsubstituted vinyl ketones (**113**) to give the corresponding substituted alkynes (**114**)[247]. Both aryl and alkyl alkynes were effective in this reaction and, unlike most organometallic addition reactions, this reaction also proceeded in aqueous solvent mixtures and reactions were tolerant of functional groups such as primary alcohols and alkyl chlorides (equation 31). The mechanism of the reaction is proposed to start by ligand substitution of CO with the phosphine, followed by coordination and oxidation of the C–H bond of the alkyne. This is followed by coordination of the vinyl ketone with subsequent insertion of the alkene group into the rhodium–carbon bond to give a transient oxo-allylic-type intermediate, whereby reductive elimination of the C–H bond gives the corresponding product.

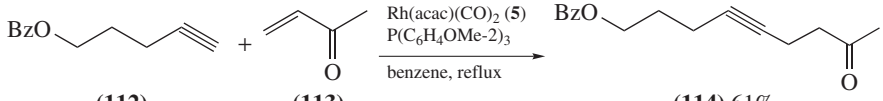

(**112**) (**113**) (**114**) 61% (31)

One of the most important contributions in metal enolate catalysis is the conjugate addition of arylboronic acids (**115**) to vinyl ketone derivatives (**116**) to give the corresponding aryl ketones (**117**) (equation 32)[248–259]. A number of advances have recently been reported[260–262], including reactions with imine derivatives[263, 264] and asymmetric 1,4-addition reactions[264–269]. Indeed, the asymmetric addition of arylboronic acids (**115**) to *N*-*t*-butanesulfinylimino esters (**118**) has been catalyzed by Rh(acac)$(coe)_2$ (**54**) and

dppbenz in an effort to generate protected arylglycines (**119**), important components in several drugs (equation 33). The reaction is tolerant of many functional groups and selective cleavage of the sulfinyl group or ester can be readily accomplished without loss in stereochemical purity[264]. The rhodium-catalyzed asymmetric conjugate addition of arylboronic acids to coumarins (**120**) using Rh(acac)($H_2C{=}CH_2$)$_2$ (**6**) was also found to proceed with excellent enantioselectivity (>99% ee) to give the corresponding (*R*)-4-arylchroman-2-ones (**121**) (equation 34). Optimal conditions were found in reactions using the chiral biarylbisphosphine ligand (*R*)-Segphos (**122**). This methodology has been successfully applied to the synthesis of (*R*)-tolterodine (**23**), as an alternate synthetic route to this important urological drug[265]. Excellent reviews on these conjugate additions have already appeared and the reader is encouraged to read these articles for a deeper insight of these interesting rhodium-catalyzed reactions[270–274].

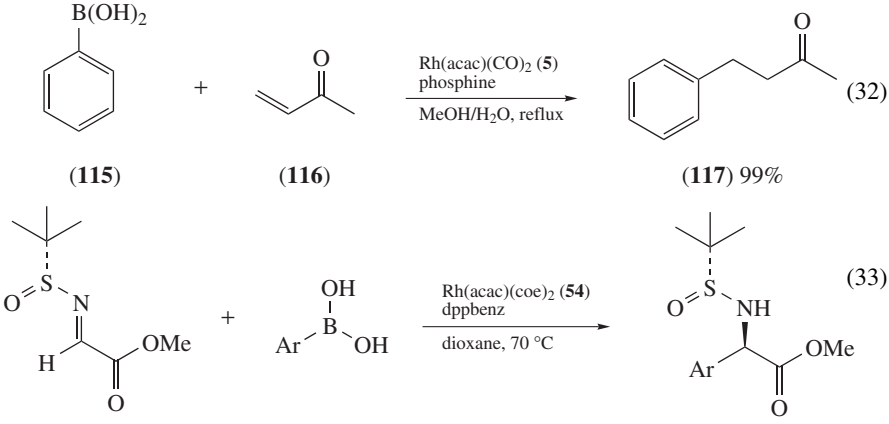

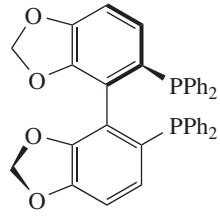

(**122**)

Another area of considerable interest in this field is the metal-catalyzed cyclization or cycloaddition reactions[275–286]. For example, Ojima and coworkers have reported that **5** catalyzed the silane-initiated cyclization of enediynes (**123**)[279,280] to give the corresponding bicyclopentyl products (**124**) in excellent yields (equation 35). Reactions with alkatriynes gave fused tricyclic compounds via a silylcarbotricyclization process. Related studies by Krische and coworkers describe the diastereoselective cycloreduction and cycloaddition reactions using a $Co(dpm)_2$-silane catalyst system[281,282]. Likewise, Mori and coworkers have found that a nickel catalyst system effectively catalyzed the asymmetric carboxylative cyclization of bis-1,3-dienes (**125**). High enantioselectivites for **126** were achieved when (*S*)-MeO-MOP (**127**) was used as a chiral ligand (equation 36). Unsymmetrical bis-1,3-dienes were also used in this study and reactions proceeded with high selectivity[283,284].

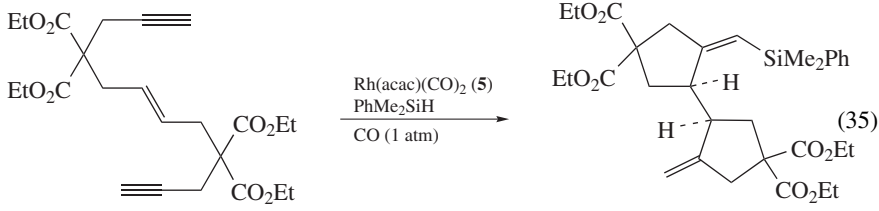

(**123**) (**124**) 55% (35)

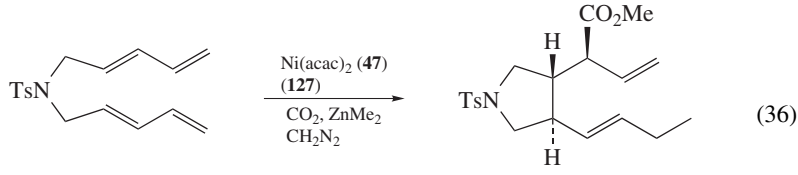

(**125**) (**126**) 71%
> 93% ee (36)

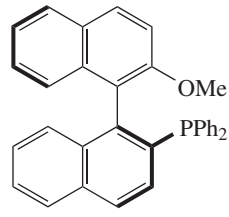

(**127**)

Related cyclopropanation reactions have also been reported using metal enolate catalysts[287–289]. In a recent study, Aggarwal and Grange[289] found that $Cu(acac)_2$ (**43**) was an excellent catalyst for the asymmetric sulfonium-ylide-mediated cyclopropanation reaction, which was used to prepare an important precursor to pharmacologically active (+)-LY354740 from the addition of **128** to give a mixture of *exo* (**129**) and *endo* (**130**) products (equation 37). In these reactions, a chiral sulfide was used and high enantioselectivies were obtained (95% ee) but with relatively low diastereocontrol. Metal enolates could also be used to catalyze the asymmetric ring opening of bicyclic hydrazines[290].

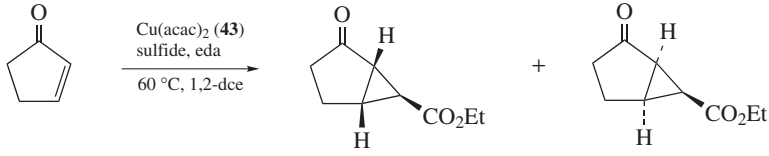

(37)

(**128**) (**129**) *exo* (**130**) *endo*

VII. ISOMERIZATION

Metal enolates have played a limited role in the metal-catalyzed isomerization of alkenes[291,292]. As illustrated in a comprehensive review by Bouwman and coworkers, ruthenium complex $Ru(acac)_3$ (**51**) has been used to isomerize a wide range of substituted double bonds, including allylic alcohols (**131**), to the corresponding ketones (**132**) (equation 38)[293]. The isomerization of allylic alcohols affords products that have useful applications in natural product synthesis and in bulk chemical processes[294]. An elegant review by Fogg and dos Santos shows how these complexes can be used in tandem catalysis, where an alkene is subjected to an initial isomerization followed by a hydroformylation reaction[295].

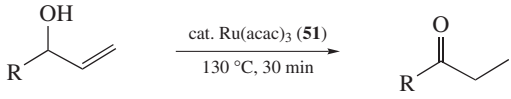

(38)

(**131**) (**132**)

VIII. ACKNOWLEDGMENT

The author thanks the Canada Research Chairs Programme, Canadian Foundation for Innovation-Atlantic Innovation Fund, Natural Science and Engineering Research Council of Canada and Mount Allison University for financial support.

IX. REFERENCES

1. G. W. Parshall and S. D. Ittel, *Homogeneous Catalysis*, 2nd edn., John Wiley & Sons, Inc., New York, 1992.
2. I. Ojima (Ed.), *Catalytic Asymmetric Synthesis*, 2nd edn., Wiley-VCH, New York, 2000.
3. B. Cornils and W. A. Herrmann (Eds), *Applied Homogeneous Catalysis with Organometallic Compounds*, Wiley-VCH, Weinheim, 2002.
4. R. H. Crabtree, *The Organometallic Chemistry of the Transition Metals*, 4th edn., Wiley-Interscience, New York, 2005.
5. M. Sodeoka and M. Shibasaki, *Pure Appl. Chem.*, **70**, 411 (1998).
6. E. R. Burkhardt, J. J. Doney, G. A. Slough, J. M. Stack, C. H. Heathcock and R. G. Bergman, *Pure Appl. Chem.*, **60**, 1 (1988).
7. J. Barluenga, I. Pérez-Sánchez, M. G. Suero, E. Rubio and J. Flórez, *Chem. Eur. J.*, **12**, 7225 (2006).
8. P. A. Evans and M. J. Lawler, *J. Am. Chem. Soc.*, **126**, 8642 (2004).
9. Y. Hamashima, T. Suzuki, H. Takano, Y. Shimura, Y. Tsuchiya, K. Moriya, T. Goto and M. Sodeoka, *Tetrahedron*, **62**, 7168 (2006).
10. T. Mukaiyama, *Pure Appl. Chem.*, **55**, 1749 (1983).
11. M. Mikami and Y. Itoh, *Chem. Rec.*, **6**, 1 (2006).
12. Y. Hamashima and M. Sodeoka, *Chem. Rec.*, **4**, 231 (2004).
13. P. W. N. M. van Leeuwen and C. Claver (Eds), *Rhodium Catalyzed Hydroformylation*, Kluwer Academic, Dordrecht, 2000.

14. C. Claver, M. Diéguez, O. Pàmies and S. Castillón, *Top. Organomet. Chem.*, **18**, 35 (2006).
15. L. Damoense, M. Datt, M. Green and C. Steenkamp, *Coord. Chem. Rev.*, **248**, 2393 (2004).
16. M. Beller, J. Seayad, A. Tillack and H. Jiao, *Angew. Chem. Int. Ed.*, **43**, 3368 (2004).
17. J.-C. Wasike, S. J. Obrey, R. T. Baker and G. Bazan, *Chem. Rev.*, **105**, 1001 (2005).
18. M. L. Clarke, *Curr. Org. Chem.*, **9**, 701 (2005).
19. A. Behr, B. Turkowski, R. Roll, R. Schöbel and G. Henze, *Top. Organomet. Chem.*, **19**, in press (DOI 10.1007/3418_2006_057) (2007).
20. N. Sakai, S. Mano and K. Nozaki, *J. Am. Chem. Soc.*, **115**, 7033 (1993).
21. G. D. Cuny and S. L. Buchwald, *J. Am. Chem. Soc.*, **115**, 2066 (1993).
22. D. Evans, J. A. Osborn and G. Wilkinson, *J. Chem. Soc., A*, 3133 (1968).
23. J. Zhang, M. Poliakoff and M. W. George, *Organometallics*, **22**, 1612 (2003).
24. E. A. Karakhanov, Yu. S. Kardasheva, E. A. Runova, D. A. Sakharov and M. V. Terenina, *Petrol. Chem.*, **46**, 264 (2006).
25. M. Rosales, A. González, Y. Guerrero, I. Pacheco and R. A. Sánchez-Delgado, *J. Mol. Catal. A: Chem.*, **270**, 241 (2007).
26. K. Okabe, I. Takahara, M. Inaba, K. Murata and Y. Yoshimura, *J. Jpn. Petrol. Inst.*, **50**, 65 (2007).
27. C. Li, M.-L. Yuan, H.-Y. Fu, H. Chen and X.-J. Li, *Sichuan Daxue Xuebao, Gongcheng Kexueban*, **38**, 102 (2006); *Chem. abstr.*, 1341735 (2006).
28. E. A. Karakhanov, Yu. S. Kardasheva, E. A. Runova, D. A. Sakharov and M. V. Terenina, *Petrol. Chem.*, **46**, 264 (2006).
29. R. P. J. Bronger, J. P. Bermon, J. Herwig, P. C. J. Kamer and P. W. N. M. van Leeuwen, *Adv. Synth. Catal.*, **346**, 789 (2004).
30. O. Artyushin, I. Odinets, E. Goryunov, I. Fedyanin, K. Lyssenko, T. Mastryukova, G.-V. Röschenthaler, T. Kégl, G. Keglevichm and L. Kollár, *J. Organomet. Chem.*, **691**, 5547 (2006).
31. E. Schwab and S. Mecking, *Organometallics*, **24**, 3758 (2005).
32. A. M. Trzeciak, E. Mieczyńska and J. J. Ziołkowski, *Top. Catal.*, **11/12**, 461 (2000).
33. A. M. Trzeciak, P. Štěpnička, E. Mieczyńska and J. J. Ziołkowski, *J. Organomet. Chem.*, **690**, 3260 (2005).
34. I. Odinets, T. Körtvélyesi, T. Kégl, L. Kollár and G. Keglevich, *Trans. Met. Chem.*, **32**, 299 (2007).
35. M. Rosales, A. González, B. González, C. Moratinos, H. Pérez, J. Urdaneta and R. A. Sánchez-Delgado, *J. Organomet. Chem.*, **690**, 3095 (2005).
36. S. Crobu, M. Marchetti and G. Sanna, *J. Inorg. Biochem.*, **100**, 1514 (2006).
37. T. Jongsam, G. Challa and P. W. N. M. van Leeuwen, *J. Organomet. Chem.*, **421**, 121 (1991).
38. M. T. Reetz and X. Li, *Angew. Chem. Int. Ed.*, **44**, 2962 (2005).
39. E. Zuidema, E. Daura-Oller, J. J. Carbó, C. Bo and P. W. N. M. van Leeuwen, *Organometallics*, **26**, 2234 (2007).
40. C. J. Cobley, R. D. J. Froese, J. Klosin, C. Qin, G. T. Whiteker and K. A. Abboud, *Organometallics*, **26**, 2986 (2007).
41. P. C. J. Kamer, P. W. N. M. van Leeuwen and J. N. H. Reek, *Acc. Chem. Res.*, **34**, 895 (2001).
42. E. Fuchs, M. Keller and B. Breit, *Chem. Eur. J.*, **12**, 6930 (2006).
43. U. Hintermair, G. Zhao, C. C. Santini, K. J. Muldoon and D. J. Cole-Hamilton, *Chem. Commun.*, 1462 (2007).
44. G. Consiglio, S. C. A. Nefkens and A. Borer, *Organometallics*, **10**, 2046 (1991).
45. K. Nozaki, T. Matsuo, F. Shibahara and T. Hiyama, *Adv. Synth. Catal.*, **343**, 61 (2001).
46. J. Huang, E. Bunel, A. Allgeier, J. Tedrow, T. Storz, J. Preston, T. Correll, D. Manley, T. Soukup, R. Jensen, R. Syed, G. Moniz, R. Larsen, M. Martinelli and O. J. Reider, *Tetrahedron Lett.*, **46**, 7831 (2005).
47. A. T. Axtell, J. Klosin and K. A. Abboud, *Organometallics*, **25**, 5003 (2006).
48. M. R. Axet, S. Castillón and C. Claver, *Inorg. Chim. Acta*, **359**, 2973 (2006).
49. C. Deng, G. Ou, J. She and Y. Yuan, *J. Mol. Catal. A: Chem.*, **270**, 76 (2007).
50. S. L. X. Martina, R. B. C. Jagt, J. G. de Vries, B. L. Feringa and A. J. Minnaard, *Chem. Commun.*, 4093 (2006).
51. Z. Jingchang, W. Hongbin, L. Hongtao and C. Weiliang, *J. Mol. Catal. A: Chem.*, **260**, 95 (2006).

52. M. G. Pedrós, A. M. Masdeu-Bultó, J. Bayardon and D. Sinou, *Catal. Lett.*, **107**, 205 (2006).
53. H. Jin, B. Subramaniam, A. Ghosh and J. Tunge, *AIChE J.*, **52**, 2575 (2006).
54. K. Kunna, C. Müller, J. Loos and D. Vogt, *Angew. Chem. Int. Ed.*, **45**, 7289 (2006).
55. H. Jin and B. Subramaniam, *Chem. Eng. Sci.*, **59**, 4887 (2004).
56. D. Guha, H. Jin, M. P. Dudukovic, P. A. Ramachandran and B. Subramaniam, *Chem. Eng. Sci.*, **62**, 4967 (2007).
57. Q. Peng, C. Deng, Y. Yang, M. Dai and Y. Yuan, *React. Kinet. Catal. Lett.*, **90**, 53 (2007).
58. J. Dupont, S. M. Silva and R. F. de Souza, *Catal. Lett.*, **77**, 131 (2001).
59. M. Giménez-Pedrós, A. Aghmiz, N. Ruiz and A. M. Masdeu-Bultó, *Eur. J. Inorg. Chem.*, 1067 (2006).
60. A. C. J. Koeken, M. C. A. van Vliet, L. J. P. van Broeke, B.-J. Deelman and J. T. F. Keurentjes, *Adv. Synth. Catal.*, **348**, 1553 (2006).
61. D. R. Palo and C. Erkey, *Organometallics*, **19**, 81 (2000).
62. A. M. Scurto and W. Leitner, *Chem. Commun.*, 3681 (2006).
63. S. Liu and J. Xiao, *J. Mol. Catal. A: Chem.*, **270**, 1 (2007).
64. P. G. Jessop, *J. Supercrit. Fluids*, **38**, 211 (2006).
65. S. Cossu, P. Peluso, E. Alberico and M. Marchetti, *Tetrahedron Lett*., **47**, 2569 (2006).
66. C. Botteghi, T. Corrias, M. Marchetti, S. Paganelli and O. Piccolo, *Org. Proc. Res. Dev.*, **6**, 379 (2002).
67. M. Seepersaud, M. Kettunen, A. S. Abu-Surrah, W. Voelter and Y. Al-Abed, *Tetrahedron Lett.*, **43**, 8607 (2002).
68. G. E. Keck and A. P. Truong, *Org. Lett.*, **7**, 2149 (2005).
69. A. Pokutsa, J. Le Bras and J. Muzart, *Kinet. Catal.*, **48**, 26 (2007).
70. L. I. Matienko and L. A. Mosolova, *Kinet. Catal.*, **46**, 328 (2005).
71. A.-J. Hu, C.-X. Lu, B.-D. Li and T. Huo, *Chin. J. Org. Chem.*, **26**, 1083 (2006).
72. L. I. Matienko and L. A. Mosolova, *Petrol. Chem.*, **47**, 39 (2007).
73. A.-J. Hu, C.-X. Lu, B.-D. Li and T. Huo, *Youji Huaxe*, **26**, 1083 (2006); *Chem. abstr.*, 202974 (2007).
74. H. Kobayashi and I. Yamanaka, *Chem. Lett.*, **36**, 114 (2007).
75. L. J. Csányi, K. Jáky and G. Galbács, *J. Mol. Catal. A: Chem.*, **179**, 65 (2002).
76. T. Tokuyasu, S. Kunikawa, A. Masuyama and M. Nojima, *Org. Lett.*, **4**, 3595 (2002).
77. A. El-Qisairi and P. M. Henry, *J. Organomet. Chem.*, **603**, 50 (2000).
78. V. G. Gnanasoundari and K. Natarajan, *Trans. Met. Chem.*, **30**, 433 (2005).
79. R. I. Khusnutdinov, N. A. Shchadneva, A. R. Baiguzina, Y. Y. Lavrentieva and U. M. Dzhemilev, *Russ. Chem. Bull.*, **51**, 2074 (2002).
80. G. S. Singh and D. S. Mahajan, *Oxid. Commun.*, **28**, 555 (2005).
81. R. Karvembu and K. Natarajan, *Polyhedron*, **21**, 1721 (2002).
82. Y. Maeda, N. Kakiuchi, S. Matsumura, T. Mishimura, T. Kawamura and S. Uemura, *J. Org. Chem.*, **67**, 6718 (2002).
83. C. Y. Lorber, S. P. Smidt and J. A. Osborn, *Eur. J. Inorg. Chem.*, 655 (2000).
84. L. Rout, P. Nath and T. Punniyamurthy, *Adv. Synth. Catal.*, **349**, 846 (2007).
85. D. L. Rodman, N. A. Carrington and Z.-L. Xue, *Talanta*, **70**, 426 (2006).
86. A. Fürstner and T. Nagano, *J. Am. Chem. Soc.*, **129**, 1906 (2007).
87. I. Mohammadpoor-Baltork, M. Hill, L. Caggiano and R. F. W. Jackson, *Synlett*, 3540 (2006).
88. P. R. Blakemore and M. S. Burge, *J. Am. Chem. Soc.*, **129**, 3068 (2007).
89. C. Drago, L. Caggiano and R. F. W. Jackson, *Angew. Chem. Int. Ed.*, **44**, 7221 (2005).
90. M. R. Maurya, U. Kumar and P. Manikandan, *Dalton Trans.*, 3561 (2006).
91. M. R. Maurya and A. Kumar, *J. Mol. Catal. A: Chem.*, **250**, 190 (2006).
92. M. H. Peyrovi, V. Mahdavi, M. A. Salehi and R. Mahmoodian, *Catal. Commun.*, **6**, 476 (2005).
93. M. C. Brasil, E. V. Benvenutti, J. R. Gregório and A. E. Gerbase, *React. Funct. Polym.*, **63**, 135 (2005).
94. J. C. Fierro-Gonzalez and B. C. Gates, *Langmuir*, **21**, 5693 (2005).
95. S. R. Cicco, M. Latronico, P. Mastrorilli, G. P. Suranna and C. F. Nobile, *J. Mol. Catal. A: Chem.*, **165**, 135 (2001).
96. S. Tanase, E. Bouwman and J. Reedijk, *Appl. Catal. A: Gen.*, **259**, 101 (2004).
97. R. van Gorkum, E. Bouwman and J. Reedijk, *Inorg. Chem.*, **43**, 2456 (2004).
98. Z. O. Oyman, W. Ming and R. van der Linde, *Eur. Polym. J.*, **42**, 1342 (2006).

99. A. A. Taherpour, A. Abramian and H. Kardanyazd, *Chin. J. Org. Chem.*, **27**, 123 (2007).
100. K. L. Prasanth and H. Maheswaran, *J. Mol. Catal. A: Chem.*, **268**, 45 (2007).
101. G. Hua, Q. Zhang, D. McManus, A. M. Z. Slawin and J. D. Woolins, *Dalton Trans.*, 1147 (2006).
102. M. Hinch, O. Jacques, C. Drago, L. Caggiano, R. F. W. Jackson, C. Dexter, M. S. Anson and S. J. F. Macdonald, *J. Mol. Catal. A: Chem.*, **251**, 123 (2006).
103. A. Basak, A. U. Barlan and H. Yamamoto, *Tetrahedron: Asymmetry*, **17**, 508 (2006).
104. M. L. Kantam, B. Neelima, C. V. Reddy, M. K. Chaudhuri and S. K. Dehury, *Catal. Lett.*, **95**, 19 (2004).
105. Y. Ishii, K. Matsunaka and S. Sakaguchi, *J. Am. Chem. Soc.*, **122**, 7390 (2000).
106. O. V. Tyukalova, G. V. Ratovskii and F. K. Shmidt, *Russ. J. Gen. Chem.*, **71**, 888 (2001).
107. A. Behr and M. Urschey, *Adv. Synth. Catal.*, **345**, 1242 (2003).
108. N. Jiang and A. J. Ragauskas, *Tetrahedron Lett.*, **48**, 273 (2007).
109. M. Johansson, A. A. Lindén and J.-E. Bäckvall, *J. Organomet. Chem.*, **690**, 3614 (2005).
110. C. Liu, J. Han and J. Wang, *Synlett*, 643 (2007).
111. J. Muzart, *Adv. Synth. Catal.*, **348**, 275 (2006).
112. M. J. Schultz and M. S. Sigman, *Tetrahedron*, **62**, 8227 (2006).
113. T. Punniyamurthy, S. Velusamy and J. Iqbal, *Chem. Rev.*, **105**, 2329 (2005).
114. R. A. Sheldon and I. W. C. E. Arends, *Adv. Synth. Catal.*, **346**, 1051 (2004).
115. J. A. Gnecco, G. Borda and P. Reyes, *J. Chil. Chem. Soc.*, **49**, 179 (2004).
116. M. G. Topuzova, S. V. Kotov and T. M. Kolev, *Appl. Catal. A: Gen.*, **281**, 157 (2005).
117. R. F. de la Pradilla, A. Castellanos, J. Fernández, M. Lorenzo, P. Manzano, P. Méndez, J. Priego and A. Viso, *J. Org. Chem.*, **71**, 1569 (2006).
118. Y. Permana, S. Shimazu, N. Ichikuni and T. Uematsu, *Catal. Commun.*, **6**, 426 (2005).
119. M. C. Feiters, G. A. Metselaar, B. B. Wentzel, R. J. M. Nolte, S. Nikitenko, D. C. Sherrington, Y. Joly, G. Y. Smolentsev, A. N. Kravtsova and A. V. Soldatov, *Ind. Eng. Chem. Res.*, **44**, 8631 (2005).
120. Y. Sui, X. Fang, R. Hu, Y. Xu, X. Zhou and X. Fu, *Mater. Lett.*, **61**, 1354 (2007).
121. T.-J. Wang, Y.-Y. Yan, M.-Y. Huang and Y.-Y. Jiang, *React. Funct. Polym.*, **29**, 145 (1996).
122. P. Reyes, G. Borda, J. Gnecco and B. L. Rivas, *J. Appl. Polym. Sci.*, **93**, 1602 (2004).
123. K. Dallmann, R. Buffon and W. Loh, *J. Mol. Catal. A: Chem.*, **178**, 43 (2002).
124. B. B. Wentzel, P. L. Alsters, M. C. Feiters and R. J. M. Nolte, *J. Org. Chem.*, **69**, 3453 (2004).
125. A. R. Silva, K. Wilson, A. C. Whitwood, J. H. Clark and C. Freire, *Eur. J. Inorg. Chem.*, 1275 (2006).
126. A. R. Silva, J. L. Figueiredo, C. Freire and B. de Castro, *Catal. Today*, **102–103**, 154 (2005).
127. M. L. Kantam, B. Kavita, V. Neeraja, Y. Haritha, M. K. Chaudhuri and S. K. Dehury, *Tetrahedron Lett.*, **44**, 9029 (2003).
128. M. L. Kantam, V. Neeraja, B. Kavita and Y. Haritha, *Synlett*, 525 (2004).
129. O. G. Mancheño and C. Bolm, *Org. Lett.*, **8**, 2349 (2006).
130. L. B. Belykh, T. V. Goremyka, L. N. Belonogova and F. K. Shmidt, *J. Mol. Catal. A: Chem.*, **231**, 53 (2005).
131. C. S. Consorti, A. P. Umpierre, R. F. de Souza, J. Dupont and P. A. Z. Suarez, *J. Braz. Chem. Soc.*, **14**, 401 (2003).
132. J. J. Eisch and J. N. Gitua, *Organometallics*, **26**, 778 (2007).
133. Y. Mata, M. Diéguez, O. Pàmies and S. Woodward, *J. Org. Chem.*, **71**, 8159 (2006).
134. X. Xiao, H. Wang, Z. Huang, J. Yang, X. Bian and Y. Qin, *Org. Lett.*, **8**, 139 (2006).
135. P. J. Jessop, F. Joó and C.-C. Tai, *Coord. Chem. Rev.*, **248**, 2425 (2004).
136. Y. Hara, H. Kusaka, H. Inagaki, K. Takahashi and K. Wada, *J. Catal.*, **194**, 188 (2000).
137. R. J. Silvennoinen, O. J. T. Jylhä, M. Lindlad, H. Österholm and A. O. I. Krause, *Catal. Lett.*, **114**, 135 (2007).
138. A. Akao, K. Sato, N. Nonoyama, T. Mase and N. Yasuda, *Tetrahedron Lett.*, **47**, 969 (2006).
139. L. B. Belykh, T. V. Goremyka, N. I. Skripov, V. A. Umanets and F. K. Shmidt, *Kinet. Catal.*, **47**, 367 (2006).
140. L. O. Nindakova, F. K. Shmidt, V. V. Saraev, B. A. Shainyan, N. N. Chipanina, V. A. Umanets, L. N. Belonogova and D.-S. D. Toryashinova, *Kinet. Catal.*, **47**, 54 (2006).
141. F. K. Shmidt, L. O. Nindakova, B. A. Shainyan, V. V. Saraev, N. N. Chipanina and V. A. Umanetz, *J. Mol. Catal. A: Chem.*, **235**, 161 (2005).

142. P. Kuotrowski, Y. Segura, L. Chmielarz, J. Surman, R. Dziembaj, P. Cool and E. F. Vansant, *Catal. Today*, **114**, 307 (2006).
143. A. J. Liang, V. A. Bhirud, J. O. Ehresmann, P. W. Kletnicks, J. F. Haw and B. C. Gates, *J. Phys. Chem. B*, **109**, 24236 (2005).
144. L. B. Backman, A. Rautiainen, M. Lindblad and A. O. I. Krause, *Appl. Catal. A: Gen.*, **191**, 55 (2000).
145. S. Enthaler, B. Hagemann, G. Erre, K. Junge and M. Beller, *Chem. Asian J.*, **1**, 598 (2006).
146. K. Nomura and Y. Kuromatsu, *J. Mol. Catal. A: Chem.*, **245**, 152 (2006).
147. S. A. Westcott, H. P. Blom, T. B. Marder and R. T. Baker, *J. Am. Chem. Soc.*, **114**, 8863 (1992).
148. S. J. Geier, E. E. Chapman, D. I. McIsaac, C. M. Vogels, A. Decken and S. A. Westcott, *Inorg. Chem. Commun.*, **9**, 788 (2006).
149. D. I. McIsaac, S. J. Geier, C. M. Vogels, A. Decken and S. A. Westcott, *Inorg. Chim. Acta*, **359**, 2771 (2006).
150. C. M. Vogels, A. Decken and S. A. Westcott, *Tetrahedron Lett.*, **47**, 2419 (2006).
151. C. M. Vogels, A. Decken and S. A. Westcott, *Can. J. Chem.*, **84**, 146 (2006).
152. N. A. Wynberg, L. J. Leger, M. L. Conrad, C. M. Vogels, A. Decken, S. J. Duffy and S. A. Westcott, *Can. J. Chem.*, **83**, 661 (2005).
153. C. A. G. Carter, R. T. Baker, S. P. Nolan and W. Tumas, *Chem. Commun.*, 347 (2000).
154. C. M. Crudden and D. Edwards, *Eur. J. Org. Chem.*, 4695 (2003).
155. C. Dai, E. G. Robins, A. J. Scott, W. Clegg, D. S. Yufit, J. A. K. Howard and T. B. Marder, *Chem. Commun.*, 1983 (1998).
156. I. Beletskaya and C. Moberg, *Chem. Rev.*, **106**, 2320 (2006).
157. S. Trudeau, J. B. Morgan, M. Shrestha and J. P. Morken, *J. Org. Chem.*, **70**, 9540 (2005).
158. J. B. Morgan, S. P. Miller and J. P. Morken, *J. Am. Chem. Soc.*, **125**, 8702 (2003).
159. S. P. Miller, J. B. Morgan, F. J. Nepveux V and J. P. Morken, *Org. Lett.*, **6**, 131 (2004).
160. M. Suginome, T. Matsuda and Y. Ito, *Organometallics*, **17**, 5233 (1998).
161. M. Suginome and Y. Ito, *J. Organomet. Chem.*, **680**, 43 (2003).
162. M. Gerdin and C. Moberg, *Adv. Synth. Catal.*, **347**, 749 (2005).
163. M. Gerdin and C. Moberg, *Org. Lett.*, **8**, 2929 (2006).
164. J. Montgomery, *Angew. Chem. Int. Ed.*, **43**, 3890 (2004).
165. M. Suginome, T. Iwanami, Y. Ohmori, A. Matsumoto and Y. Ito, *Chem. Eur. J.*, **11**, 2954 (2005).
166. B. Marciniec, *Coord. Chem. Rev.*, **249**, 2374 (2005).
167. S.-K. Kang, Y.-T. Hong, J.-H. Lee, W.-Y. Kim, I. Lee and C.-M. Yu, *Org. Lett.*, **5**, 2813 (2003).
168. S. P. Shum, S. D. Pastor and G. Rihs, *Inorg. Chem.*, **41**, 127 (2002).
169. P. M. Reis, C. C. Romão and B. Royo, *Dalton Trans.*, 1842 (2006).
170. S. M. Thompson and U. Schubert, *Inorg. Chim. Acta*, **350**, 329 (2003).
171. R. Hua, S.-Y. Onozawa and M. Tanaka, *Organometallics*, **19**, 3269 (2000).
172. M. L. Kantam, B. Neelima and C. V. Reddy, *J. Mol. Catal. A: Chem.*, **256**, 269 (2006).
173. M. L. Kantam, V. Neeraja, B. Kavita, B. Neelima, M. K. Chaudhuri and S. Hussain, *Adv. Synth. Catal.*, **347**, 763 (2005).
174. J. R. Briggs, J. Klosin and G. T. Whiteker, *Org. Lett.*, **7**, 4795 (2005).
175. Q. Huang and R. Hua, *Adv. Synth. Catal.*, **349**, 849 (2007).
176. M. A. Kazankova, I. V. Efimova, A. N. Kochetkov, V. V. Afanas'ev and I. P. Beletskaya, *Russ. J. Org. Chem.*, **38**, 1465 (2002).
177. V. Y. Kukushkin and A. J. L. Pombeiro, *Inorg. Chim. Acta*, **358**, 1 (2005).
178. T. Oshiki, H. Yamashita, K. Sawada, M. Utsunomiya, K. Takahashi and K. Takai, *Organometallics*, **24**, 6287 (2005).
179. T. Šmejkal and B. Breit, *Organometallics*, **26**, 2461 (2007).
180. R. Varala and S. R. Adapa, *Can. J. Chem.*, **84**, 1174 (2006).
181. R. Varala, A. Nasreen and S. R. Adapa, *Can. J. Chem.*, **85**, 148 (2007).
182. Y. Permana, S. Shimazu, N. Ichikuni and T. Uematsu, *J. Mol. Catal. A: Chem.*, **221**, 141 (2004).
183. V. P. Ananikov, N. V. Orlov and I. P. Beletskaya, *Organometallics*, **25**, 1970 (2006).
184. M. Arisawa, M. Ashikawa, A. Suwa and M. Yamaguchi, *Tetrahedron Lett.*, **46**, 1727 (2005).
185. Y. Maeda, M. Koyabu, T. Nishimura and S. Uemura, *J. Org. Chem.*, **69**, 7688 (2004).

186. Y. Hamashima, T. Suzuki, H. Takano, Y. Shimura, Y. Tsuchiya, K. Moriya, T. Goto and M. Sodeoka, *Tetrahedron*, **62**, 7168 (2006).
187. Y. Hamashima and M. Sodeoka, *Synlett*, 1467 (2006).
188. D. Nama, P. S. Pregosin, A. Albinati and S. Rizzato, *Organometallics*, **26**, 2111 (2007).
189. F. Alonso, I. Beletskaya and M. Yus, *Tetrahedron*, **61**, 11771 (2005).
190. G. Hilt and F. Galbiati, *Synthesis*, 3589 (2006).
191. D.-R. Hwang and B.-J. Uang, *Org. Lett.*, **4**, 463 (2002).
192. L. Huang, Z. Wang, T. P. Ang, J. Tan and P. K. Wong, *Catal. Lett.*, **112**, 219 (2006).
193. A. Novak, R. Fryatt and S. Woodward, *C. R. Chimie*, **10**, 206 (2007).
194. T. Hashimoto, S. Hara, Y. Shiraishi, M. Yamauchi, K. Natarajan and K. Shimizu, *Inorg. Chim. Acta*, **358**, 2207 (2005).
195. J. Handzlik, J. Ogonowski, J. Stoch, M. Mikołajczyk and P. Michorczk, *Appl. Catal. A: Gen.*, **312**, 213 (2006).
196. T. Matsumoto, R. A. Periana, D. J. Taube and H. Yoshida, *J. Mol. Catal. A: Chem.*, **180**, 1 (2002).
197. R. A. Periana, X. Y. Liu and G. Bhalla, *Chem. Commun.*, 3000 (2002).
198. G. Bhalla, J. Oxgaard, W. A. Goddard, III and R. A. Periana, *Organometallics*, **24**, 3229 (2005).
199. J. Oxgaard, G. Bhalla, R. A. Periana and W. A. Goddard, III, *Organometallics*, **25**, 1618 (2006).
200. W. J. Tenn, III, K. J. H. Young, J. Oxgaard, R. J. Nielsen, W. A. Goddard, III and R. A. Periana, *Organometallics*, **25**, 5173 (2006).
201. R. A. Periana, G. Bhalla, W. J. Tenn, III, K. J. H. Young, X. Y. Liu, O. Mironov, C. J. Jones and V. Ziatdinov, *J. Mol. Catal. A: Chem.*, **220**, 7 (2004).
202. J. M. Gonzales, J. Oxgaard, R. A. Periana and W. A. Goddard, III, *Organometallics*, **26**, 1505 (2007).
203. J. Oxgaard, W. J. Tenn, III, R. J. Nielsen, R. A. Periana and W. A. Goddard, III, *Organometallics*, **26**, 1565 (2007).
204. T. Matsumoto, R. A. Periana, D. J. Taube and H. Yoshida, *J. Catal.*, **206**, 272 (2002).
205. T. Hirashita, S. Kambe, H. Tsuji, H. Omori and S. Araki, *J. Org. Chem.*, **69**, 5054 (2004).
206. M. K. Chaudhuri, S. K. Dehury and S. Hussain, *Tetrahedron Lett.*, **46**, 6247 (2005).
207. M. Kimura, A. Ezoe, M. Mori, K. Iwata and Y. Tamaru, *J. Am. Chem. Soc.*, **128**, 8559 (2006).
208. T. Hirashita, S. Kambe, H. Tsuji and S. Araki, *Chem. Commun.*, 2595 (2006).
209. P. K. Dhondi and J. D. Chisholm, *Org. Lett.*, **8**, 67 (2006).
210. T. Nishimura, H. Araki, Y. Maeda and S. Uemura, *Org. Lett.*, **5**, 2997 (2003).
211. S. Ma, S. Yu, Z. Peng and H. Guo, *J. Org. Chem.*, **71**, 9865 (2006).
212. F. K. Friedlein, K. Kromm, F. Hampel and J. A. Gladysz, *Chem. Eur. J.*, **12**, 5267 (2006).
213. O. Navarro, N. Marion, N. M. Scott, J. González, D. Amoroso, A. Bell and S. P. Nolan, *Tetrahedron*, **61**, 9716 (2005).
214. N. Marion, E. C. Ecarnot, O. Navarro, D. Amoroso, A. Bell and S. P. Nolan, *J. Org. Chem.*, **71**, 3816 (2006).
215. G. Schröder, T. Okinaka, Y. Mimura, M. Watanabe, T. Matsuzaki, A. Hasuoka, Y. Yamamoto, S. Matsukawa and K. Akiba, *Chem. Eur. J.*, **13**, 2517 (2007).
216. I. P. Beletskaya, V. V. Afanasiev, M. A. Kazankova and I. V. Efimova, *Org. Lett.*, **5**, 4309 (2003).
217. M. Murata, H. Yamasaki, T. Ueta, M. Nagata, M. Ishikura, S. Watanabe and Y. Masuda, *Tetrahedron*, **63**, 4087 (2007).
218. J. Ju, H. Nam, H. M. Jung and S. Lee, *Tetrahedron Lett.*, **47**, 8673 (2006).
219. S. Krompiec, M. Krompiec, H. Ignasiak, M. Łapkowski, S. Baj and D. Grabarczyk, *Catal. Commun.*, **8**, 1457 (2007).
220. B. Hölzer and R. W. Hoffmann, *Chem. Commun.*, 732 (2003).
221. A. Kuno, N. Saino, T. Kamachi and S. Okamoto, *Tetrahedron Lett.*, **47**, 2591 (2006).
222. L. Boully, M. Darabantu, A. Turck and N. Ple, *J. Heterocycl. Chem.*, **42**, 1423 (2005).
223. K. Itami, S. Higashi, M. Mineno and J.-I. Yoshida, *Org. Lett.*, **7**, 1219 (2005).
224. T. Nagano and T. Hayashi, *Org. Lett.*, **6**, 1297 (2004).
225. A. Fürstner and A. Leitner, *Angew. Chem. Int. Ed.*, **41**, 609 (2002).
226. X. Xu, D. Cheng and W. Pei, *J. Org. Chem.*, **71**, 6637 (2006).
227. G. Berthon-Gelloz and T. Hayashi, *J. Org. Chem.*, **71**, 8957 (2006).

228. G. Cahiez, V. Habiak, C. Duplais and A. Moyeux, *Angew. Chem. Int. Ed.*, **46**, 4364 (2007).
229. L. Dong, Y.-J. Xu, W.-C. Yuan, X. Cui, L.-F. Cun and L.-Z. Gong, *Eur. J. Org. Chem.*, 4093 (2006).
230. G. Dunet and P. Knochel, *Synlett*, 1383 (2007).
231. K. Kojima, M. Kimura, S. Ueda and Y. Tamaru, *Tetrahedron*, **62**, 7512 (2006).
232. M. Piber, A. E. Jensen, M. Rottländer and P. Knochel, *Org. Lett.*, **1**, 1323 (1999).
233. A. Gavryushin, C. Kofink, G. Manolikakes and P. Knochel, *Tetrahedron*, **62**, 7521 (2006).
234. F. F. Kneisel, M. Dochnahl and P. Knochel, *Angew. Chem. Int. Ed.*, **43**, 1017 (2004).
235. L.-Z. Gong and P. Knochel, *Synlett*, 267 (2005).
236. T. Kawasaki, T. Omine, M. Sato, Y. Morishita and K. Soai, *Chem. Lett.*, **36**, 30 (2007).
237. I. Sapountzis, W. Lin, C. C. Kofink, C. Despotopoulou and P. Knochel, *Angew. Chem. Int. Ed.*, **44**, 1654 (2005).
238. T. J. Korn, M. A. Schade, S. Wirth and P. Knochel, *Org. Lett.*, **8**, 725 (2006).
239. G. Dunet and P. Knochel, *Synlett*, 407 (2006).
240. O. Sirkeciouglu, B. Karliga and N. Talinli, *Tetrahedron Lett.*, **44**, 8483 (2003).
241. M. Kimura, M. Mori, N. Mukai, K. Kojima and Y. Tamaru, *Chem. Commun.*, 2813 (2006).
242. K.-I. Shimizu, M. Miyagi, T. Kan-no, T. Hatamachi, T. Kodama and Y. Kitayama, *J. Catal.*, **229**, 470 (2005).
243. S. Dagorne, S. Bellemin-Laponnaz and A. Maisse-François, *Eur. J. Inorg. Chem.*, 913 (2007).
244. Y.-S. Kwak and E. J. Corey, *Org. Lett.*, **6**, 3385 (2004).
245. A. S. ElDouhaibi, M. Lozanov and J. Montgomery, *Tetrahedron*, **62**, 11460 (2006).
246. H. Pellissier, *Tetrahedron*, **63**, 1297 (2007).
247. R. V. Lerum and J. D. Chisholm, *Tetrahedron Lett.*, **45**, 6591 (2004).
248. T. Yanagi, H. Sasaki, A. Suzuki and N. Miyaura, *Synth. Commun.*, **26**, 2503 (1996).
249. T. Senda, M. Ogasawara and T. Hayashi, *J. Org. Chem.*, **66**, 6852 (2001).
250. T. Hayashi, K. Inoue, N. Taniguchi and M. Ogasawara, *J. Am. Chem. Soc.*, **123**, 9918 (2001).
251. S. Sakuma, M. Sakai, R. Itooka and N. Miyaura, *J. Org. Chem.*, **65**, 5951 (2000).
252. A. Takezawa, K. Yamaguchi, T. Ohmura, Y. Yamamoto and N. Miyaura, *Synlett*, 1733 (2002).
253. R. A. Batey, A. N. Thadani and D. V. Smil, *Org. Lett.*, **1**, 1683 (1999).
254. Y. Takaya, M. Ogasawara and T. Hayashi, *Chirality*, **12**, 469 (2000).
255. Q. Shi, L. Xu, X. Li, X. Jia, R. Wang, T. T.-L. Au-Yeung, A. S. C. Chan, T. Hayashi, R. Cao and M. Hong, *Tetrahedron Lett.*, **44**, 6505 (2003).
256. Y. Takaya, M. Ogasawara and T. Hayashi, *Tetrahedron Lett.*, **39**, 8479 (1998).
257. K. Yoshido, M. Ogasawara and T. Hayashi, *J. Org. Chem.*, **68**, 1901 (2003).
258. C. J. Chapman, K. J. Wadsworth and C. G. Frost, *J. Organomet. Chem.*, **680**, 206 (2003).
259. J.-G. Boiteau, A. J. Minnaard and B. L. Feringa, *J. Org. Chem.*, **68**, 9481 (2003).
260. S. Miyamura, T. Satoh and M. Miura, *J. Org. Chem.*, **72**, 2255 (2007).
261. H. Noguchi, K. Hojo and M. Suginome, *J. Am. Chem. Soc.*, **129**, 758 (2007).
262. G. Abbiati, A. Arcadi, F. Marinelli, E. Rossi and M. Verdecchia, *Synlett*, 3218 (2006).
263. K. Ueura, S. Miyamura, T. Satoh and M. Miura, *J. Organomet. Chem.*, **691**, 2821 (2006).
264. M. A. Beenen, D. J. Weix and J. E. Ellman, *J. Am. Chem. Soc.*, **128**, 6304 (2006).
265. G. Chen, N. Tokunaga and T. Hayashi, *Org. Lett.*, **7**, 2285 (2005).
266. C. G. Frost, S. D. Penrose, K. Lambshead, P. R. Raithby, J. E. Warren and R. Gleave, *Org. Lett.*, **9**, 2119 (2007).
267. R. B. C. Jagt, J. G. de Vries, B. L. Feringa and A. J. Minnaard, *Org. Lett.*, **7**, 2433 (2005).
268. C. Monti, C. Gennari and U. Piarulli, *Chem. Eur. J.*, **13**, 1547 (2007).
269. R. T. Stemmler and C. Bolm, *Synlett*, 1365 (2007).
270. T. Hayashi and K. Yamasaki, *Chem. Rev.*, **103**, 2829 (2003).
271. J. Christoffers, G. Koripelly, A. Rosiak and M. Rössle, *Synthesis*, 1279 (2007).
272. G. K. Friestad and A. K. Mathies, *Tetrahedron*, **63**, 2541 (2007).
273. K. Yoshida and T. Hayashi, in *Boronic Acids* (Ed. D. G. Hall), Wiley-VCH, Weinheim, 2005, pp. 171–203.
274. Y. Yamamoto, T. Nishikata and N. Miyaura, *J. Synth. Org. Chem. Jpn.*, **64**, 1112 (2006).
275. O. Anaç, F. S. Güngör and G. Merey, *Helv. Chim. Acta*, **89**, 1231 (2006).
276. X. Han and R. A. Widenhoefer, *J. Org. Chem.*, **69**, 1738 (2004).
277. H. W. Lam, P. M. Joensuu, G. J. Murray, E. A. F. Fordyce, O. Prieto and T. Luebbers, *Org. Lett.*, **8**, 3729 (2006).
278. N. Maezaki, H. Sawamoto, H. Ishihara and T. Tanaka, *Chem. Commun.*, 3992 (2005).

279. I. Ojima, A. C. Moralee and V. C. Vassar, *Top. Catal.*, **19**, 89 (2002).
280. B. Bennaccer, M. Fujiwara, S.-Y. Lee and I. Ojima, *J. Am. Chem. Soc.*, **127**, 17756 (2005).
281. L.-C. Wang, H.-Y. Jang, Y. Roh, V. Lynch, A. J. Schultz, X. Wang and M. J. Krische, *J. Am. Chem. Soc.*, **124**, 9448 (2002).
282. R. R. Huddleston and M. J. Krische, *Synlett*, 12 (2003).
283. M. Takimoto and M. Mori, *J. Am. Chem. Soc.*, **124**, 10008 (2002).
284. M. Takimoto, Y. Nakamura, K. Kimura and M. Mori, *J. Am. Chem. Soc.*, **126**, 5956 (2004).
285. G. Gerstberger and R. Anwander, *Micropor. Mesopor. Mater.*, **44–45**, 303 (2001).
286. S.-I. Ikeda, H. Miyashita, M. Taniguchi, H. Kondo, M. Okano, Y. Sato and K. Odashima, *J. Am. Chem. Soc.*, **124**, 12060 (2002).
287. J. D. Dudones and P. Sampson, *Tetrahedron*, **56**, 9555 (2000).
288. M. A. Celik, M. Yurtsever, N. Ş. Tüzün, F. Ş. Güngör, Ö. Sezer and O. Anaç, *Organometallics*, **26**, 2978 (2007).
289. V. K. Aggarwal and E. Grange, *Chem. Eur. J.*, **12**, 568 (2006).
290. F. Bertolini, F. Macchia and M. Pineschi, *Tetrahedron Lett.*, **47**, 9173 (2006).
291. F. Wang and D. C. Neckers, *J. Org. Chem.*, **68**, 634 (2003).
292. V. S. Tkach, D. S. Suslov, M. Gomboogiin, G. V. Ratovskii and F. K. Shmidt, *Russ. J. Appl. Chem.*, **79**, 85 (2006).
293. R. C. van der Drift, E. Bouwman and E. Drent, *J. Organomet. Chem.*, **650**, 1 (2002).
294. P. B. Keller, *Org. Proced. Res. Dev.*, **7**, 342 (2003).
295. D. E. Fogg and E. N. dos Santos, *Coord. Chem. Rev.*, **248**, 2365 (2004).

CHAPTER **11**

Biological aspects of metal enolates

LI-JUNE MING

Department of Chemistry and Institute for Biomolecular Science, University of South Florida, 4202 E. Fowler Avenue, CHE205, Tampa, Florida 33620-5250, USA
Fax: +1-813-974-1733; e-mail: ming@shell.cas.usf.edu

To
my mom and Shu-Ching
for their endless love and support throughout my career

The chemistry of metal enolates
Edited by Jacob Zabicky

I. ABBREVIATIONS

*	When it appears after a boldface number it denotes an anion derived from a molecule by deprotonation.
**	When it appears after a boldface number it denotes a dianion derived from a molecule by double deprotonation.
2,5-HDMF	4-hydroxy-2,5-dimethyl-3(2*H*)-furanone
3,4-HP	3-hydroxy-4(1*H*)-pyridinone
AA	ascorbic acid
ACC	1-aminocyclopropane-1-carboxylate
CoA	Coenzyme A
COX	cyclooxygenase
DAS645	1-*t*-butyl-3-(2,4-dichlorophenyl)-5-hydroxy-1*H*-pyrazol-4-yl-2-chloro-4-methylsulfonylphenyl methanone
DAS869	1-*t*-butyl-5-hydroxy-1*H*-pyrazol-4-yl-6-methylsulfonyl-4′-methoxy-2-methyl-1,1′-biphenyl-3-yl-methanone
DFT	density function theory
EI	enzyme–inhibitor complex
EPR	electron paramagnetic resonance
ES	enzyme–substrate
EXAFS	extended X-ray absorption fine structure
HEMF	4-hydroxy-5-(or 2)-ethyl-2(or 5)-methyl-3(2*H*)-furanone
HMS	hydroxymandelate synthase
HPPD	4-hydroxyphenylpyruvate dioxygenase
IC_{50}	the concentration required for 50% inhibition
KA	kojic acid
mer	meridional
NSAID	non-steroid anti-inflammatory drug
PDB	Protein Databank

PEP	phosphoenolpyruvate
PG	phosphoglycerate
PGA	2-phospho-D-glyceric acid
PGI	phosphoglucose isomerase
PMI	phosphomannose isomerase
PPA	polyporic acid (2,5-dihydroxy-3,6 diphenyl-1,4-benzoquinone)
QD	quercetin 2,3-dioxygenase
ROS	reactive oxygen species
shmt1	serine hydroxymethyltransferase gene
TIM	triosephosphate isomerase
TPQ	2,4,5-trihydroxyphenylalanine quinone
UMP	uridine monophosphate
XANES	X-ray absorption near edge spectrum

II. INTRODUCTION

A. Scope of the Chapter

The enol functionality is one of the most widely distributed and diverse groups found in chemical and biological systems and processes. This functional group is a chemical Janus in terms of its specific interactions due to its capability to form two tautomers. With these 'two faces' it can act both as H-bond-acceptor (keto form) and donor (enol form). Although the keto form is the more stable tautomer, the enol form can be stabilized greatly at the transition state in many enzymatic transformations, via H-bonding and coordination to metal ions. Thus, the enol functionality can serve as a template for design of transition-state analogues toward specific enzymes for the treatment of metabolism-related disorders or for organism-specific inhibitors.

The chemical, physical, structural and spectroscopic aspects of enols and metal enolate complexes can be found in several chapters in this volume. This chapter offers an overview about the biological aspect of enols and metalloenolates, providing a broad view about their significance, structure, function and reactions in the biological systems and in medicine. To improve the understanding of the special interactions of metal enolates in such systems, most figures and a few chemical structures of this chapter are shown also as color stereoplot plates designed for 'relaxed eye viewing'. This can be achieved by placing the figure at arms-length distance (*ca* 0.5 m) and focusing at a point *ca* 2 m away, whereby the reader can see three images, with the central one in stereo view. More about stereo viewing can be found elsewhere (http://en.wikipedia.org/wiki/Stereoscopy).

B. Enol-containing Natural Products

Many enol-containing compounds show broad bioactivities, serving as enzyme cofactors, antibiotics, enzyme inhibitors, antioxidants and potential pharmaceuticals. A few examples are discussed in this section, wherein the enol moieties in the structures and the enolate metal-binding sites are highlighted. The enediol-containing vitamin C (ascorbic acid, **1**) plays an important role in photosynthesis and serves as a cofactor for enzymes involved in the biosynthetic pathways of collagen in animals and ethylene and anthocyanines in plants[1]. These functions are mainly attributed to its high reduction potential to keep the metal center in several enzymes at reduced states, such as the Fe-containing enzymes prolyl hydroxylase for the production of hydroxyproline and 1-aminocyclopropane-1-carboxylate (ACC) oxidase for ethylene synthesis. The ubiquitous flavonoid family is comprised of thousands of compounds with a three-ring molecular framework (**2**) and can carry the enol moiety, wherein the rings may be derivatized,

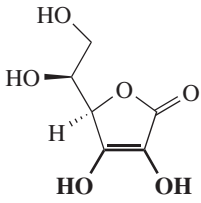

(**1**)

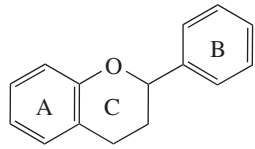

(**2**)

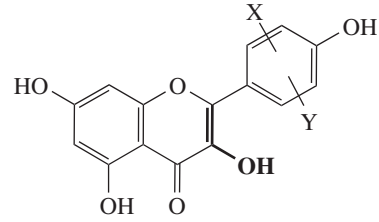

(**3**) (**a**) X = 3-OH, Y = H
(**b**) X = Y = H
(**c**) X = 3-OH, Y = 5-OH

such as the flavonols quercetin (**3a**), kaempferol (**3b**) and myricetin (**3c**). Many of them have been demonstrated to exhibit antibacterial, antiviral and antiprotozoan activities and are well established antioxidants and free radical scavengers[2]. Flavonoids are thus proposed to be beneficiary toward oxidative stress-related disorders and diseases[2, 3], including inflammation, cardiovascular diseases, cancer and neurodegenerative diseases.

A number of marine natural products containing the enol functional group exhibit bioactivities. For example, (a) sorbicillactone A (**4**) from *Penicillium chrysogenum* separated from the interior of the sponge *Ircinia fasciculata* was active against HIV, showed neuroprotective potential and was selectively active against L5178y lymphoma cells[4], while its multi-enol dimeric derivative bisorbicillinoid (**5**) from *P. terrestre* was found to be antiproliferative[5]; (b) a couple of hydroxybenzoquinone derivatives, e.g. the cytotoxic 2-(2,3-dihydrosorbyl)-3,6-dimethyl-5-hydroxy-1,4-benzoquinone (**6**), are also metabolites from the latter fungus[6]; (c) the marine fungal diterpenoids libertellenones (e.g. **7**) are found to be cytotoxic against the colonic epithelial HCT-116 cell lines; and (d) the

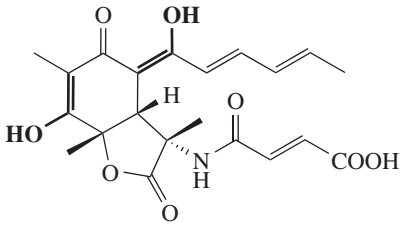

(**4**)

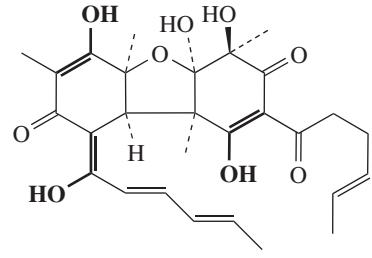

(**5**)

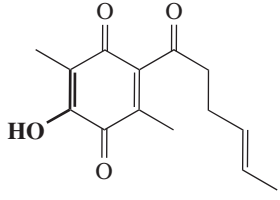

(**6**)

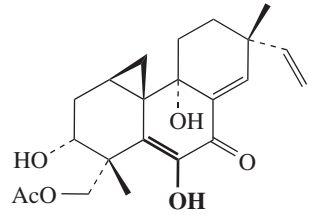

(**7**)

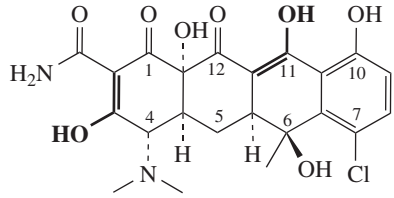

(**8**)

tetracyclines (such as Aureomycin®, **8**) isolated from various *Streptomyces* species are broad-spectrum antibiotics which act against protein synthesis through binding to ribosomes (Section IV.H)[7,8].

Mimosine (**9**) is a natural occurring amino acid with a hydroxypyridone residue isolated from many species (e.g. *Leucaena* leguminous trees) of the *Mimosoideae* subfamily. It exhibits a wide range of bioactivities, including anticancer[9], anti-inflammatory[10], antifungal and antibacterial[11], metabolic antagonism[12] and enzyme inhibition[13]. Kojic acid (**10a**), a secondary metabolite of fungal fermentation in the Japanese koji process[14], is an inhibitor of the dinuclear Cu(II)-containing enzymes tyrosinase and polyphenol oxidase[15] and the mononuclear Cu(II)-containing quercetin 2,5-dioxygenase[16] and has served as a potential lead for antineoplastic drug discovery[17]. Kojic acid has been utilized as the precursor for the production of the flavoring food additives maltol (**10b**), also natural-occurring in beer, coffee, roasted malt and the genus *Cichorium*, and ethyl maltol (**10c**). The five-member ring D-glucose/fructose metabolite 2,5-HDMF (furaneol, **11**) and analogues afford a pleasant aroma in fruits such as banana and strawberry[18,19] and have been used as flavoring food additives.

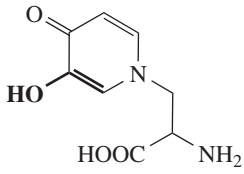

(**9**)

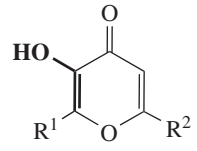

(**10**) (**a**) $R^1 = H$, $R^2 = CH_2OH$
(**b**) $R^1 = Me$, $R^2 = H$
(**c**) $R^1 = Et$, $R^2 = H$

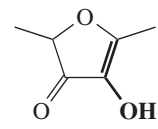

(**11**)

The 'alpha acids' in hops and their isomeric forms 'iso-alpha acids' are enol-containing compounds which include humulone (**12a**), cohumulone (**12b**) and adhumulone (**12c**) and their corresponding isomers such as *cis*-isohumulone (**13**). The latter is formed at high temperatures from **12a**[20] and is the key ingredient for the bitter taste of beers. These compounds were found to inhibit angiogenesis[21], induce differentiation[22], suppress cyclooxygenase-2 gene transcription[23], inhibit bone reabsorption[24], show antibacterial activities[25] and improve insulin sensitivity[26], thus offering significant medicinal values.

Mushrooms and various fungi and lichens are rich in enol metabolites and many exhibit significant bioactivities[27], such as usnic acid (**14**)[28] which serves as a regulator for plant growth and shows antitumor and antibiotic activities[29,30]. The widely distributed quinone polyporic acid (**15a**, PPA) from the Purple-Dye Polypore mushroom (*Hapalopilus nidulans*) and other sources is a weak inhibitor ($IC_{50} = 0.1$ to >1.5 mM[31,32]) of dihydroorotate

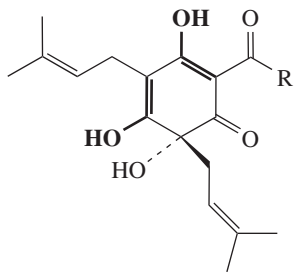

(**12**) (**a**) R = *i*-Bu
(**b**) R = *i*-Pr
(**c**) R = *s*-Bu

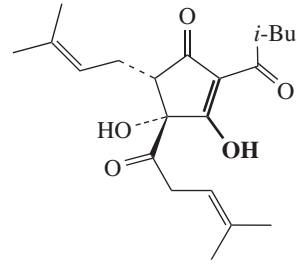

(**13**)

dehydrogenase (an enzyme involved in the synthesis of the uridine nucleotide, UMP). This compound and its derivatives are widely distributed in various fungi and lower plants such as lichens, and have been shown in some early studies to exhibit anticancer[33] and antioxidant[34] activities. The PPA derivatives atromentin (**15b**) and leucomelone (**15c**) are found to be specific inhibitors ($IC_{50} = 0.24$ and 1.57 μM, respectively) toward the enoyl-acyl-carrier protein reductase, FabK, during fatty acid synthesis in *Streptococcus pneumoniae*, but not the enzyme from either *Escherichia coli* or *Staphylococcus aureus* even at 200 μM[35]. PPA is also considered the precursor for other enol metabolites in various mushrooms, such as suillusin (**16**) isolated from the edible mushroom *Suillus granulatus*[36]. The fungal meroterpenoids boviquinone-3 (**17a**) and boviquinone-4 (**17b**) originating from 3,4-dihydroxylbenzoic acid contain the same dihydoxyquinone core as PPA, but with a farnesyl and a geranylgeranyl side chain, respectively, and follow different biosynthetic pathways[37]. The grevillins A, B and D (**18a**–**c**, respectively) are a group of pyrandione pigments present in certain toadstools of the genus *Suillus*. Syntheses of this family of pigments have been attempted to obtain potential pharmaceuticals[38]; however, no bioactivity has been as yet reported.

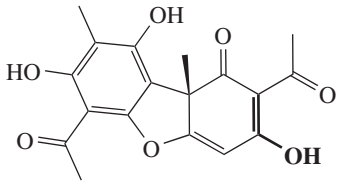

(**14**)

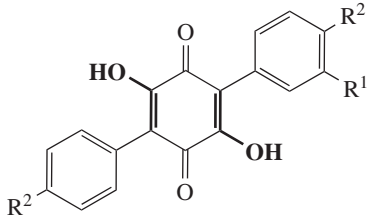

(**15**) (**a**) $R^1 = R^2 = H$
(**b**) $R^1 = H$, $R^2 = OH$
(**c**) $R^1 = R^2 = OH$

In addition to the above examples, there are still a large number of bioactive natural products and various synthetic and semisynthetic enol-containing compounds that serve as potential and promising drugs for various therapeutic purposes such as the non-peptidyl HIV inhibitor Aptivus® (tipranavir; Section IV.I) and the third-generation tetracycline antibiotics (Section IV.H). The structure and function of the metal complexes of some

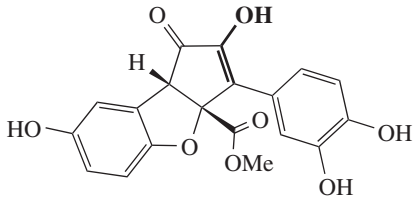

(**16**)

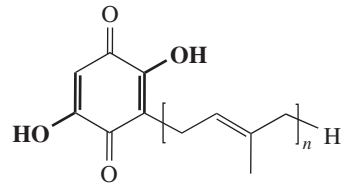

(**17**) (**a**) $n = 3$
(**b**) $n = 4$

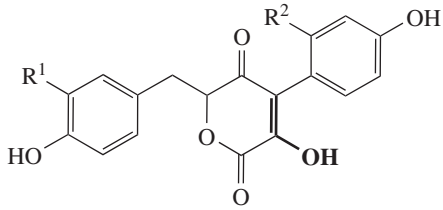

(**18**) (**a**) $R^1 = R^2 = H$
(**b**) $R^1 = OH$, $R^2 = H$
(**c**) $R^1 = R^2 = OH$

enol-containing natural products and (semi)synthetic compounds are further discussed in Section III. It is worth noting that not all enol-containing natural products, biochemicals and pharmaceuticals have been reported to form metal complexes despite the fact that many of them are comprised of well defined metal binding site(s), such as the α-ketoenol and β-ketoenol moieties in the above compounds. Whether or not metal ions are involved in the bioactivities of these potential metal-binding enolates should be further explored in future investigations.

C. Enols and Enolates in Chemical Reactions

Many chemical reactions and biological processes are associated with the formation and utilization of enols and enolates. A π-bonded enol intermediate is proposed to be an important step in the catalytic mechanism of the well known Wacker process for the preparation of acetaldehyde from ethylene. Enols (**19′**) are the first product during the hydration of alkynes, frequently catalyzed by Hg^{2+}, which eventually convert into ketones (**19**) through proton migration. Such proton-mediated enol–ketone isomerization is called tautomerization (equation 1) which dominates the chemistry of ketones and aldehydes, as well as their involvements in biological processes. Several crystal structures discussed in this chapter show a metal–enolate bond distance shorter than that of metal–keto, reflecting higher stability of the former when formed. In a simple case such as acetone, the tautomerism is highly unfavorable toward enol, with an equilibrium constant in the order of 10^{-9}. Thus, enols are usually only the intermediates in many reactions associated with ketones and aldehydes discussed below. When the enol intermediates can be stabilized through H-bonding or by deprotonation and binding to one or more metal ions, particularly in β-diketones, reactions can be greatly accelerated as seen in enzyme-catalyzed reactions with an enol or a metal enolate intermediate discussed in later sections. In the case of

β-diketones, both electronic and steric effects can affect the tautomeric equilibrium, wherein the enol form is frequently stabilized via the internal hydrogen bond between the ketone and the enol[39]. The natural product curcumin from the curry spice is a good example for the tautomerism between β-diketone **20** and β-ketoenol **20′** (equation 2), with the latter suggested to be the predominant form[40].

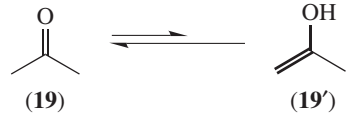

(**19**) (**19′**) (1)

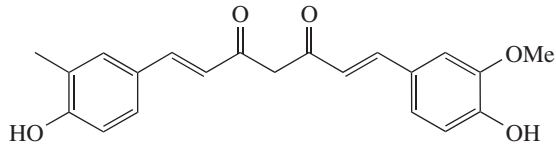

(**20**)

(2)

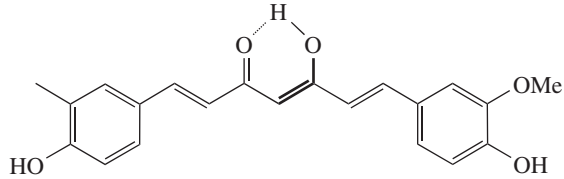

(**20′**)

The formation of a C–C bond in chemical reactions can take place by means of Claisen (equations 3 and 4) or aldol (equation 5) condensation, which are the foundations for many biosynthetic processes while their reverse reactions serve as the basis for many metabolic pathways. In the former case, two esters or one ester and a carbonyl compound react in the presence of a strong base to yield β-ketoesters (equation 3) or β-diketons (equation 4), whereas two carbonyl compounds are used in the latter reaction to yield α,β-unsaturated ketones (equation 5).

(3)

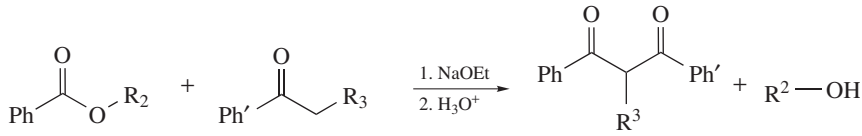

(4)

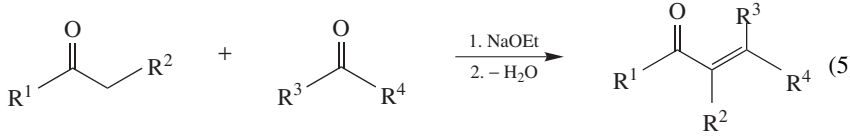

(5)

In these condensations, the deprotonation of the α proton of a carbonyl-containing molecule by a strong base results in the formation of an enolate (a tautomeric form of α-ketocarbanion; equation 6) which performs nucleophilic attack at the carbonyl group of a second molecule to form β-ketoester, β-ketoaldehyde or β-diketon, which are the tautomeric forms of β-ketoenols. Moreover, several other reactions such as isomerization of α-substituted ketones, halogenation of aldehydes and ketones, Michael addition of ketones and alkylation of ketones also take place through an enolate intermediate. The keto–enol conversion (equation 6) can be either base- or acid-catalyzed, wherein a Lewis acid interacts first with the keto moiety followed by deprotonation in the latter case. Since metal ions are Lewis acids, the acid-catalyzed keto–enol conversion can thus be expected to be mediated by metal ions. The role of metal ions as Lewis acids in biological systems is well established via the formation of coordination bonds or charge interactions, which will be further discussed in the following sections.

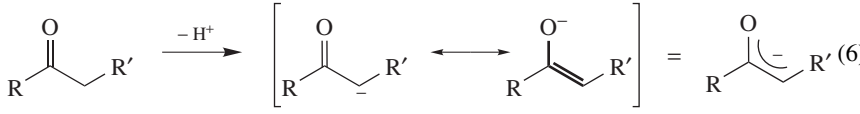

(6)

D. Stabilization of the Enol Functional Group in Biological Processes

In addition to serving as structural motifs, enols and enolates are involved in diverse biological processes. Several enol/enolate intermediates have been proposed to be involved in glycolysis (Section IV.A), wherein *cis*-enediol **21** is proposed to be an intermediate in the catalytic mechanism of phosphohexose isomerase and an enol-containing enamine intermediate (**22**) has been proposed in the catalytic pathway of class I aldolase. In the case of glucose–fructose (aldose–ketose) isomerization, removal of the proton on C1–OH produces the aldose while deprotonation of C2–OH yields the ketose, which is accompanied by protonation at the C2 and C1 positions, respectively. There are several cofactors that are involved in various biological reactions, such as NAD(H)/NADP(H) in redox reaction and coenzyme A in group transfer reactions. Pyridoxal phosphate (PLP, **23**) is a widely distributed enzyme cofactor involved in the formation of α-keto acids, L/D-amino

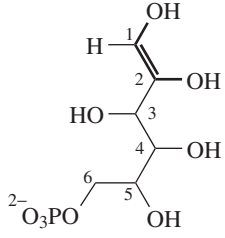

(**21**)

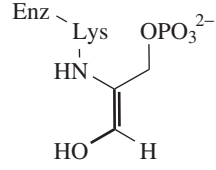

(**22**)

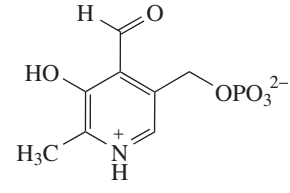

(**23**)

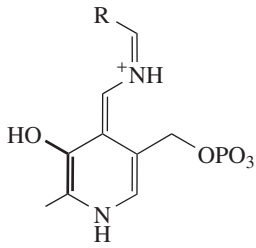

(**24**)

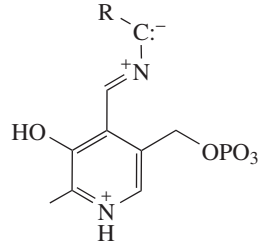

(**25**)

acid isomerization, decarboxylation and group transfer reactions in many enzymes. During the catalysis of a specific PLP-dependent enzyme, a Schiff base is first formed through condensation between the active aldehyde group of PLP and a lysine side chain in the active site. This covalently linked enzyme–cofactor is then followed by decarboxylation or deprotonation to yield a quinonoid intermediate (**24**), which is a resonance form of its corresponding carbanion (**25**).

The Lewis acidity of a functional group in the biological systems can be significantly affected by H-bonding or binding to one or more metal ions, wherein the apparent ionization constant pK_a^{app} is greatly controlled by the binding constant pK_f in the form of $pK_a^{app} = pK_f + pK_a$, where pK_a is the intrinsic ionization constant. Thus, the function of a H-bond donor in one system may be equivalent to that of a metal ion in another system, such as the similar role of proton and metal ions as Lewis acids which has been suggested in the tautomerization of certain α-heterocyclic ketones[41]. Because either a metal ion or a general acid can interact with a Lewis base, such as an enolate, in different systems, examples about both cases are given to provide a clear picture about the functions of the metal ion and Lewis acid in the systems. The nucleophile in the active site of serine protease (a serine residue) is H-bonded to a histidine residue, whereas the nucleophile in the active site of metalloproteases (a water molecule) is bound to a metal. The nucleophilicity and the Lewis acidity of the serine in serine protease is enhanced via H-bonding with the histidine (as reflected by the decrease in its pK_a^{app}), which in turn is H-bonded to an aspartate (i.e. Ser195, His57 and Asp102 as the 'catalytic triad'; Figure 1A)[42]. In all metallohydrolases, except alkaline phosphate, a coordinated water serves as the nucleophile with its nucleophilicity greatly enhanced by the metal center to give a pK_a^{app} value about 7 or much lower in case of acid metallohydrolases, affording the better OH^- nucleophile under physiological conditions or acidic environments. The nucleophilicity of the coordinated water is also further enhanced by H-bonding with a general base such as an aspartate or a glutamate, wherein the nucleophilic water is sandwiched by the metal and the H-bond acceptor glutamate and was dubbed 'metallotriad'[43] to reflect the three-party H-bonding network and the key role of the metal center. Serralysin in Figure 1B is an example[44]. In alkaline phosphatase, it is Ser102 that serves as the primary nucleophile, not a water molecule. The nucleophilicity of this Ser is greatly enhanced via binding to a Lewis acidic Zn(II) ion in the active site, as opposed to the H-bonding to a Lewis basic His in the case of serine proteases. In the case of the catalytic triad in serine protease and the metal–serine active center in alkaline phosphatase, the Lewis basicity of the nucleophilic Ser is greatly enhanced to perform the primary nucleophilic attack at the scissile peptide or phosphoester bond, followed by secondary nucleophilic water attack to complete the hydrolytic cycle.

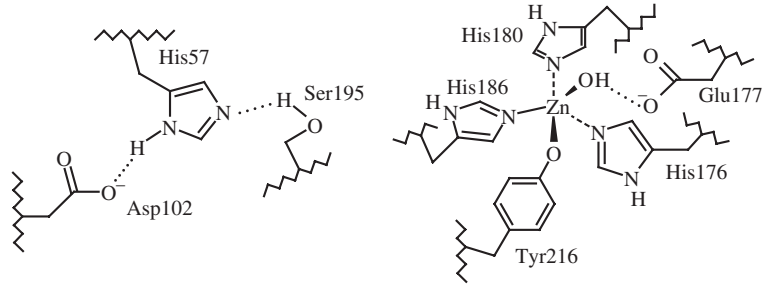

FIGURE 1. (A) Catalytic triad in the serine protease trypsin (PDB ID 1AKS), wherein the nucleophilicity of the nucleophilic Ser195 is dramatically enhanced by H-bonding (dotted lines) with H57. (B) The 'metallotriad' active site in serralysin (PDB ID 1SRP), showing the sandwiched nucleophilic water (in the form of hydroxide) by the active-site Zn(II) and Glu177 via a coordination bond and a H-bond

In some extreme cases, such stabilization in the biological systems may have significant consequences. For example, the tautomeric imine–enol form of thymine enables it to form H-bonding with guanine (**26**, dR = deoxyribose) instead of the normal adenine pair (**27**), wherein the enol is stabilized via H-bonding with the keto group on guanine which causes mismatch in the structure of the DNA double helix.

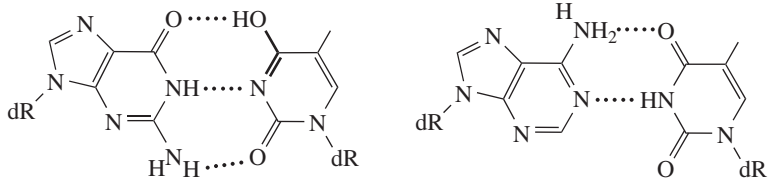

(**26**) (**27**)

Similarly, the enol and enolate configurations can be stabilized by a H-bonding donor (**28**; such as an Arg side chain), by interacting with a metal ion (**28′**) and/or by a H-bonding acceptor (**28″**; such as a His imidazole ring). An example is given in a recent structural study[45] about the biosynthesis of the fluorophore in the green fluorescent protein (GFP) from the jellyfish *Aequorea victoria*[46] that is formed through cyclization and oxidation of an internal tripeptide motif of Ser65, Tyr66 and Gly67. The mature form of GFP exhibits intense fluorescence at 508 nm when excited with UV light that can be monitored to learn about the folding of the protein and formation of the fluorophore, as shown in a recent mutagenesis study[46a]. On the basis of the crystal structure[45], an intermediate enolate is formed upon reduction and is H-bonded with Arg96 (Figure 2). The participation of Lewis acid/base in enol/enolate function is also observed in the conversion of glucose-6-phosphate to fructose-6-phosphate by phosphoglucose isomerase during glycolysis, wherein an intermediate (*Z*)-1,2-enediolate is proposed which is stabilized by the positive side chain of Arg272 (Section IV.A.1)[47]. The proposed mechanism for the production of the mature form of GFP based on the crystal structure of the

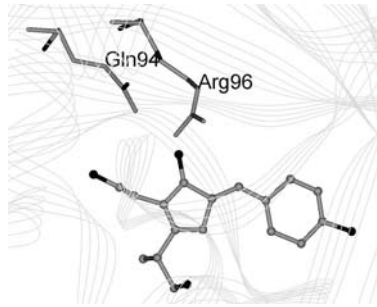

FIGURE 2. The active center of the wild-type GFP (PDB ID 1W7U), showing H-bonding of the fluorophore, where Arg96 stabilizes the intermediate enolate form during formation of the oxidized fluorescent form (Plate I)

reduced variant Ser65-His66-Gly67 (2FZU) is shown in equation 7, with the following steps: (a) cyclization, (b) dehydration, (c) enolization and stabilization via H-bonding with Arg96, (d) peroxidation and (e) removal of hydrogen peroxide.

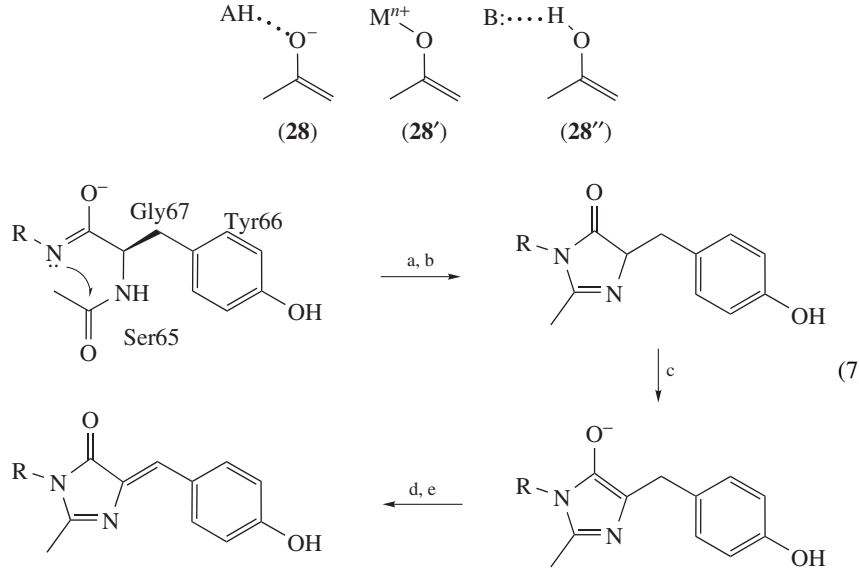

Coenzyme A (CoA) is broadly involved in various biological group-transfer processes, such as the biosynthesis of polyketides. The fungal and bacterial metabolite 1,3,6,8-tetrahydroxy-naphthalene (THN, **29**) is biosynthesized from polyketide intermediates[48]. In some fungi, THN eventually polymerizes to form 1,8-dihydroxynaphthalene-melanin which is a virulent factor in the cell walls of the fungus *Wangiella dermatitidis*, causing phaeohyphomycosis in humans[49]. After oxidation into the enol-containing flaviolin (**30**) by a monooxygenase, THN can also be incorporated into pharmacologically active meroterpenoids (natural hybrid compounds of polyketide and terpenoid) by bacteria, such as the neomarinone (**31**)[50] from *Streptomyces* species. During the synthesis of polyketides by

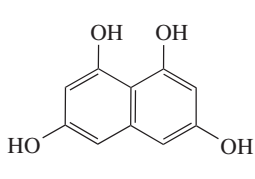

(**29**)

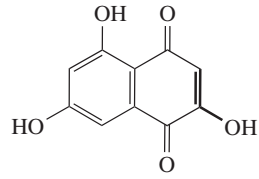

(**30**)

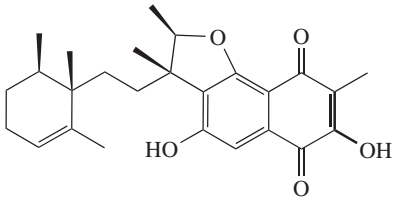

(**31**)

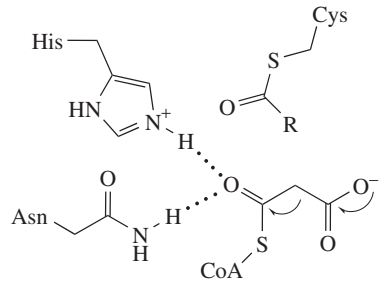

(**32**)

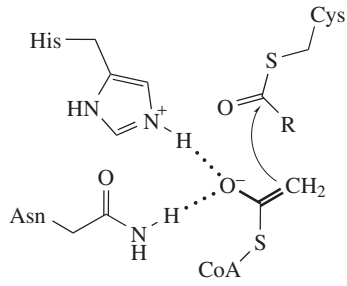

(**33**)

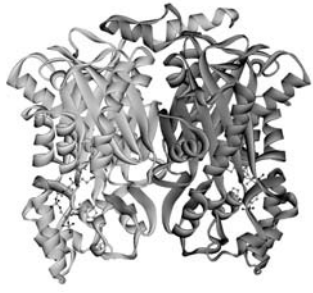

(A)

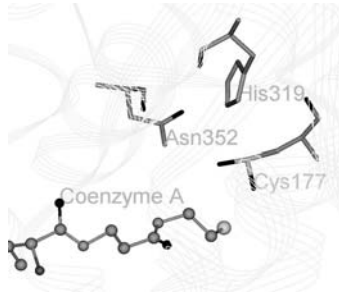

(B)

FIGURE 3. (A) Crystal structure of pentaketide chromone synthase with a bound CoA in the active site (2D3M, Plate II). (B) The active site showing part of the bound CoA and the three catalytically significant side chains. The Cys side chain is oxidized to $-SO_2^-$ in the crystal structure (Plate III). The reduced $-$SH group of Cys177 is needed for catalysis

polyketide synthases (Figure 3)[51], an acyl group is transferred to and from the active-site Cys with the assistance of malonyl-CoA via a geminal thioenolate intermediate. Herein, malonyl-CoA and the intermediate are further stabilized by H-bonding with a His and an Asn side chain in the active site (Figure 3B). The mechanism for the formation of polyketide is proposed to follow two steps: Formation of malonyl-CoA follows the transfer of the acyl group from acyl-CoA to the Cys side chain (**32**), which is followed by decarboxylation to form the enolic thiocarboxylate intermediate **33**. It is followed by acyl transfer from the acylated Cys to result in polyketide extension.

Like the H-bonding in the above examples, metal ions also serve as general acids and are involved in stabilization of enolate intermediates in many biological processes which are discussed in the following sections.

III. METAL ENOLATES IN BIOLOGICAL SYSTEMS

A. Metal Complexes of Enolates

The enol tautomer is usually a stronger acid than the keto tautomer as reflected by the small keto-to-enol equilibrium constant. Upon deprotonation, however, the resulting enolate is stabilized via resonance structures analogous to the resonance in carboxylate with a higher charge density on the carbonyl O due to its larger electronegativity. Consequently, metal ions are expected to interact with enolates through the more electronegative O. A number of metal complexes of enolate-containing compounds and metal enolate reaction intermediates are known or proposed and structures determined wherein the binding of metal ions to the oxygen is revealed. In rare cases such as the enol intermediate proposed in the well known Wacker Process for the production of aldehyde from ethylene and dioxygen on a Pd(II) catalyst, the enol is bound to the metal as a π-base (**34**)[52].

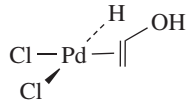

(**34**)

Stable metal complexes can be favorably formed when a bidentate metal-binding site is available, such as α- and β-diketone moieties which are the tautomeric forms of α- and β-ketoenols. Some β-diketonate complexes of paramagnetic lanthanides such as Pr(III), Eu(III) and Yb(III) have been extensively utilized as paramagnetic shift reagents for structural assignment of molecules with complicated stereochemistry prior to 2D techniques in NMR spectroscopy[53]. Their syntheses and application are discussed in separate chapters in this volume. The examples below provide some dynamic and structural basis for better understanding of metal enolates in biomolecules and biochemical processes.

B. Enol-containing Biochemicals and Pharmaceuticals and Their Metal Complexes

There are many biochemicals and drugs that contain the enol functional group. Some examples of enol-containing natural products are given in Section II.B (**1–18**). The enol group is commonly found in drugs, of which many are inhibitors toward specific enzymes. For example, among the enolic thiofuranones **35**, containing the 4-hydroxybutenolide moiety in vitamin C (**1**), antibiotic thiolactomycin[54] (**36**) slows down the proliferation of the protozoan *Plasmodium falciparum* at IC_{50} *ca* 50 μM. This was suggested to take

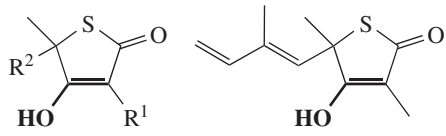

(**35**) (**36**)

place via inhibition of type-II fatty acid synthase ($IC_{50} = 5$ to >25 μM), but not of β-ketoacyl acyl-carrier-protein synthases ($IC_{50} > 330$ μM)[55]. The type-II fatty acid synthase in *P. falciparum* is different from the type-I enzyme in human, thus serves as a valid target for chemotherapy and drug discovery toward malaria. The side chains of the thiofuranone ring can be modified to afford various derivatives with different activities toward protozoans[55,56], such as the derivative with $R^1 = n$-propyl and $R^2 = n$-decyl, showing inhibition toward *P. falciparum* cultured in red blood cells ($IC_{50} = 10$ μM), *Trypanosoma cruzi* ($IC_{50} = 56$ μM) and *T. brucei* (21 μM)[56].

The carbonyl functionality is one of the most abundant functional groups in biomolecules and pharmaceuticals, including many α- and β-carbonyl derivatives of ketones and aldehydes and their enol tautomers, which upon deprotonation can form entropy-favored 5-membered (**37**) and 6-membered (**38**) chelates with metal ions. In this section, the role of metal ions in the action of some enol-containing biochemicals and pharmaceuticals and the structures of their metal complexes are discussed.

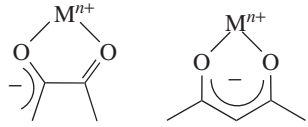

(**37**) (**38**)

1. Biochemicals

a. Ascorbic acid. The antioxidant D-ascorbic acid (AA, **1**, vitamin C) is a lactone of D-glucose origin. AA is a ubiquitous molecule in eukaryotes, except a few species including humans who cannot synthesize this molecule in their body. It is a multifunctional molecule[57], serving as an antioxidant, a precursor for oxalate and tartrate synthesis and a cofactor for numerous enzymes including Cu- and Fe-containing oxygenases and the recently discovered hypoxia-inducible factor-1-modifying hydroxylase[58]. It participates in a variety of processes in plants, including photosynthesis, photoprotection, cell growth and syntheses of many important plant molecules including the hormones ethylene and gibberellins as well as the plant pigments and antioxidants anthocyanins. It is involved in the synthesis of hydroxyproline for cell division and expansion and hydroxylation of lysine in collagen cross-linkage. Despite its biochemical and medicinal significance, its synthetic pathway in plants was not fully understood until very recently[59]. The most recent discovery that ascorbate serves as a reducing agent toward the peroxidase peroxiredoxin 1-Cys family pointed to another previously unidentified biological redox couple[60], wherein a Cys side chain in the active center undergoes a redox cycle between the reduced thiol group (−SH) of Cys and its corresponding oxidized sulfenic acid (−SOH) instead of the more common disulfide (−S−S−) oxidized form of Cys.

The molecular structure of AA provides a few preferred bidentate metal-binding sites, which have been demonstrated in a few crystal structures of metal-ascorbate complexes.

Along with penicillic acid, AA is the prototypical member of the tetronic acid (TA) family which contains a 4-hydroxybutenolide moiety (and its tautomer, equation 8). The hydroxybutenolide moiety is also found in the yellow/orange pigment pulvinic acid (**39**) and various derivatives in many lichens and fungi which were observed to exhibit anti-inflammatory and antimicrobial activities[61, 62]. Several tetronic acid derivatives have been synthesized and shown to exhibit significant inhibitory activities toward bacterial peptidoglycan biosynthesis[63]. As in the case of β-diketones and 3-ketoenols, TA compounds have tautomeric equilibrium between their enol and keto forms. For AA, there is tautomerism between the ene-diol form (**1**) with the acidic OH protons and the β-ketolactone form (**40**) with an acidic $C2$–H proton ($pK_a = 4.25$), resulting in some unique metal-binding configurations.

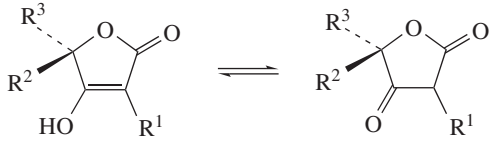

(8)

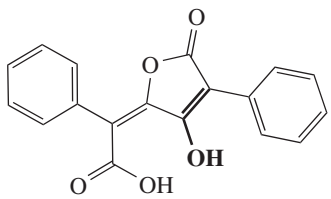

(**39**)

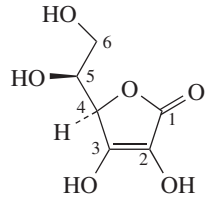

(**1**)

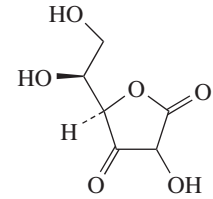

(**40**)

The coordination chemistry of various metal complexes of AA has recently been reviewed[64]. Many metal complexes of AA have been investigated with various spectroscopic methods; however, only a small number of complexes have been characterized with X-ray crystallography. Early spectroscopic studies of mono- and divalent metal binding of AA did not provide conclusive metal-binding modes. However, it seemingly has a preferred binding toward the C2–C3 enediol site for transition metal binding, yet no crystal structures were determined in those studies[65, 66]. The binding of alkali and alkaline earth metal ions with ascorbic acid has been investigated with DFT[67]. The preferred binding of alkali metal ions in water is through $C2$-O and $C3$-O, while the alkaline earth metal ions Be(II), Mg(II) and Ca(II) prefer binding with $C1$-O and $C2$-O of the ascorbate anion.

Metal ascorbates are frequently associated with redox chemistry, particularly when the metal is redox active, which includes most transition metal ions[68]. The redox activity of AA also leads to decomposition of its Co(II) and Gd(III) complexes into oxalate complexes[69]. AA is considered a major reductant for Cr(IV) to yield Cr(III)[70]. Reduction of CrO_3 with excess of AA affords a Cr(III)–ascorbate complex[71]. However, the structure of this complex was not determined. Since Cr(III) has been demonstrated to play a role in glucose metabolism[72], it is thus important to investigate further the reduction of high-valent Cr species by AA and binding of AA to Cr(III).

The Fenton reaction was discovered more than a century ago, wherein a potent oxidation chemistry is taking place by Fe(II) in the presence of H_2O_2. The reaction cycle can be described in equations 9 and 10 under reduction conditions, wherein AA can

serve as the reducing agent toward Fe(III) reduction[73]. Thus, the attempt to prepare an Fe(III)–ascorbate complex may result in the Fenton reaction. Nevertheless, Fe(II)–ascorbate complexes may be prepared under anaerobic conditions and Fe(III)–ascorbate complexes may also be obtained at low temperatures. Iron ascorbates were prepared and their stoichiometry proposed to be Fe(III):ascorbate = 1:2[74], a polymeric Fe(II)–ascorbate complex[75] and a dinuclear and a trinuclear mixed-valence Fe(II)–Fe(III) complex[76] with bridging hydroxo ligands. The oxidation states, ligand binding and electron configuration of the metal centers in these complexes were determined with magnetism measurements, EPR, X-ray absorption spectroscopy (EXAFS and XANES) and Mössbauer spectroscopy. The oxidative activity of these complexes was also revealed from oxidative DNA cleavage. However, the lack of crystal structure of these complexes prevents any conclusion to be made about their structures. Dietary AA shows mild pro-oxidant properties at low Fe concentrations, yet serves as a strong antioxidant against oxidative stress and DNA damage in the liver induced by high concentrations of dietary Fe[77].

$$\mathrm{Fe(II)} + \mathrm{H_2O_2} \longrightarrow \mathrm{Fe(III)} + \mathrm{HO^{\bullet}} + \mathrm{OH^-} \tag{9}$$

$$\mathrm{Fe(III)} + \mathrm{e^-} \longrightarrow \mathrm{Fe(II)} \tag{10}$$

Fenton chemistry is also observed for the Cu(I)–Cu(II) redox cycle with AA as a reducing agent. Free radicals formed in Fe and/or Cu Fenton chemistry have been considered the cause of oxidative stress in living systems due to damage to proteins, nucleic acids and membranes[78], related to cancer, aging, heart diseases, arthritis, diabetes and neurodegenerative disorders such as Parkinson's and Alzheimer's diseases. The non-specific cleavage of nucleic acids by the Fenton chemistry renders DNA footprinting to provide structural insight into DNA and its protein and drug complexes[79]. Under anaerobic conditions, a polymeric Cu(II)–AA complex was obtained, presumably containing enolate binding and alkoxide bridging from AA[80]. However, the lack of crystal structure prevents conclusive assignment of its structure.

Pt complexes of AA represent a group of medicinally significant metal complexes. Cisplatin (*cis*-diamminedichloroplatinum) is one of the most prescribed anticancer drugs used for various types of tumors and cancers[81]. The coordination chemistry and reactivity of cisplatin and its interaction with DNA have been extensively investigated with various methods and reviewed[82]. Pt–AA complexes are also of medical significance. The structures of a few *cis*-diaminoplatinum(II)–ascorbate complexes have been determined with spectroscopic and crystallographic methods[83], showing a *cis* configuration due to the bidentate nature of AA and the associated ligands. These complexes were found to be highly active in the S180a tumor screening. The *cis*-1,2-diaminocyclohexane–Pt complex **41** is organometallic, binding ascorbate through C2 and the deprotonated C5-hydroxyl group. Such a binding pattern reflects the significant acidity of the C2-H proton that is attributable to its position next to two carbonyl groups. ^{195}Pt NMR reveals the (*trans*-1,2-diaminocyclohexane)–Pt complex also binds AA through C2 in a similar fashion[83], Crystallographic and ^{195}Pt and ^{1}H NMR analyses suggest that the binding of AA to various Pt complexes of ethylenediamine and its *N*,*N*′-methyl-substituted derivatives follows the same pattern as **41**, whereas a few diphosphine ($R_2P^{\cap}PR_2$)–Pt complexes, $R_2P^{\cap}PR_2$ = bis(diphenylphosphino)methane, bis(diphenylphosphino)ethane or bis(diphenylphosphino) propane, bind AA as in **42**[84].

A few metalloenzymes are involved in AA metabolism or require AA as a cofactor, including ascorbate oxidase and prolyl and lysyl hydroxylase. The structure and function of these enzymes are discussed in Section IV.C.

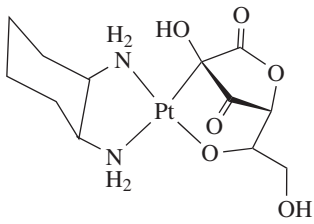

(**41**)

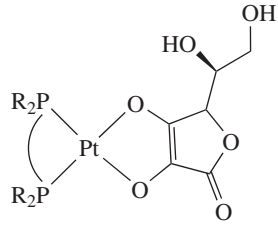

(**42**)

b. Flavonoids. The anthocyanin pigments and flavonoids (e.g. hydroxyl derivatives of **2** and **3**) are ubiquitously distributed in plants. They display antimicrobial and antifungal properties, which largely contribute toward growth and development of plants[85]. Some of these compounds are also antiprotozoal agents with IC_{50} in the low μM range through inhibition of the fatty acid biosynthetic pathway of the parasites[86]. Flavonoids show various beneficial activities to human health[87], such as antihepatotoxic, anti-inflammatory, antiatherogenic, antiallergenic, antiosteoporotic, anticancer and neuroprotective properties[85,88]. These biological activities can be credited to their involvement in signaling[89], interaction with enzymes, ability to scavenge reactive oxygen species (ROS) and free radicals and chelate metal ions[90–92].

The involvement of metal ions in the color of anthocyanins and flavonoids was discovered almost a century ago, whereby the different colors of flowers originated from the same molecules under different conditions[93]. The crystal structure of the pigment complex affords better understanding of the color and the role of metal ions[94], where Fe(III) and Mg(II) bind anthocyanins via the catechol moiety and Ca(II) binds flavone glycosides through a vicinal diol on the glycone.

Many flavonoids are highly hydroxylated on all the three rings, such as quercetin (**43**), which created a few potential metal-binding sites, including α-ketoenolate (site II on ring C), β-ketophenolate (site I from rings A and C[95]) and catechol (site III on ring B). Formation of 1:1 Cu and Fe complexes with several flavonoids was shown by EI-MS, along with 1:2 (e.g. **44** and **45**), 2:2 and 2:3 metal-to-flavonoid complexes less frequently[96]. Rutin contains a disaccharide side chain linked via the enol moiety, leaving only 'site I' for metal-binding to form complexes with various metal-to-flavonoid ratios[97].

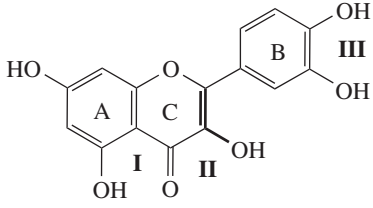

(**43**)

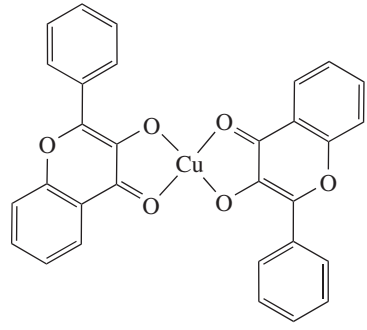

(**44**)

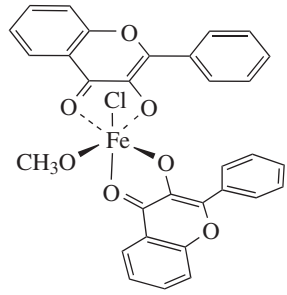

(**45**)

Metal binding causes changes in the antioxidant properties and the color of flavonoids from yellow to green, due to shift in the charge-transfer transition from λ_{max} *ca* 380 to *ca* 450 nm (Figure 4). Quercetin (**43**) and baicalin (from the Chinese medicinal herb *Scutellaria baicalensis*) alleviate mouse liver injury caused by Fe overload, presumably due to their metal-binding capability that attenuates the oxidative stress caused by the excess Fe[98]. Metal chelation by the catechol moiety, which is converted to a quinone form, has been proposed for the mechanism of antioxidation[99]. Moreover, the Fe(III) and Cu(II) complexes of flavonoids with 1:2 metal-to-flavonoid ratio were found to be more effective than the bare flavonoids in scavenging superoxide generated by xanthine/xanthine oxidase reaction[100] and by the use of the DPPH (1,1-diphenyl-2-picrylhydrazyl) radical scavenging method on Fe, Cu, Zn and Al complexes of a few flavonoids[101]. Spectrophotometric and electrochemical methods show that quercetin (**43**) binds Cu(II) and Fe(II) in a lipid bilayer[102], which presumably plays a role in protecting the cell membrane from peroxidation.

Cu(I) and Cu(II) ions bind 3-hydroxyflavone to form a square-planar complex **44** with *trans* configuration[103] (EPR spectrum of the Cu(II) complex: $g_{||} = 2.252$, $g_{\perp} = 2.085$; UV-vis spectrum, λ_{max} nm (ε M^{-1} cm^{-1}): 268 (3470), 433 (28180) and 719 (53)[104]). Tetragonally distorted octahedral and square-planar configurations of Cu(II) complexes are common, due to the Jahn–Teller distortion of d^9 Cu(II) complexes and a large gain

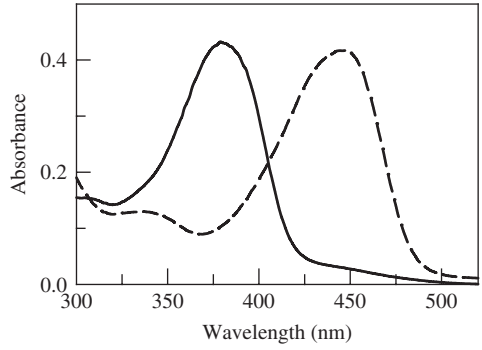

FIGURE 4. Electronic spectra of quercetin (solid trace; $\lambda_{max} = 383$ nm) and its Co(II) complex (dashed trace; $\lambda_{max} = 448$ nm) in DMSO. (Dr. W. Tay is acknowledged for acquiring the spectra in the laboratory.)

of ligand field stabilization energy. In the presence of pyridine, six-coordinate Cu(II) and Ni(II) complexes are formed with two flavonolate anions in the equatorial positions with a *trans* configuration and two pyridines in the axial positions[105]. When equimolar amounts of flavonol, 2,2′-bipyridine (bipy) and metallic copper in acetonitrile are mixed at room temperature, a mixture of several compounds is produced with an average stoichiometry of [Cu(I)(flavonolate)(bipy)][106]. Upon standing at room temperature, red crystals of $[Cu(I)(bipy)_2]_2[Cu(I)(flavonolate)_3]$ are obtained, in which the Cu–O(keto) bond (2.151 Å) is longer than the Cu–O(alkoxo) bond (2.069 Å).

These Cu–flavonol complexes were utilized as model systems for the investigation of the metal active site of the Cu-containing quercetin 2,3-dioxygenase (Section IV.E). In the Cu(II) complex of 3-hydroxyflavone and bipy (**46**, perchlorate salt)[107], bipy can mimic the N-rich metal coordination in the active site of the enzyme (see Section IV.E). The complex has a square-pyramidal coordination sphere with the flavone, which is bound to the Cu(II) via its α-ketoenolate moiety, and bipyridine at the basal positions and a perchlorate weakly bound at the apical position (Cu–O(perchlorate) = 2.425 Å). In DMF solution the complex undergoes oxygenation reaction to yield the oxygenated product Cu(*O*-benzoylsalicylate)$_2$ with a rate constant of 8.7×10^{-3} M^{-1} s^{-1} at 373 K[104]. Several analogous Cu(I) and Cu(II) complexes of flavonolate have been prepared and characterized to show the α-ketoenolate binding mode[108], including a Cu(II)–*N*,*N*,*N*-tribenzyl-1,4,7-triazacyclononane complex which binds a flavonolate to form a 5-coordinate ternary complex[108a].

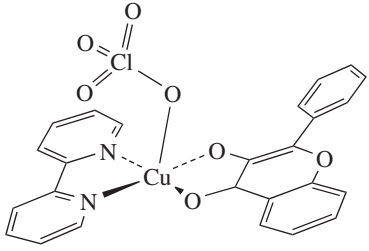

(**46**)

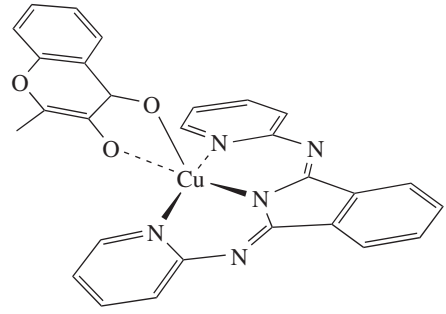

(**47**)

Oxygenation and cleavage of the flavonolate in these complexes are observed which mimic that of quercetin 2,3-dioxygenase. For example, the red complex $[Cu(I)(bipy)_2]_2$ $[Cu(I)(flavonolate)_3]$ turns into green with absorptions 421 and 615 nm (ε = 14,100 and 54 $M^{-1}\,cm^{-1}$, respectively) upon exposure to O_2 to yield [Cu(II)(bipy)(flavonolate)(2-$HOC_6H_4COCO_2$)] of square pyramid structure with the oxidatively cleaved and hydrolyzed product 2-$HOC_6H_4COCO_2^-$ bound at the axial position via the carboxylate group (Cu–O = 2.231 Å); the chelate contains a Cu–O(keto) bond of 2.190 Å and a very short Cu–O(alkoxo) bond of 1.760 Å[106]. A ternary Cu(II) complex of 3-hydroxy-4*H*-benzopyran-4-one and 1,3-bis(2-pyridylimino)isoindoline (**47**)[109] has a distorted square-pyramidal geometry with the tridentate 1,3-bis(2-pyridylimino)isoindoline ligand occupying three of the basal positions, the enolate at the fourth basal position (M–O = 1.95 Å) and the keto at the apical position with a longer M–O bond (2.30 Å) as in other metal enolates. Treatment of **47** at 100 °C with O_2 yields acetylsalicylate which binds to the Cu(II) center, analogous to the reaction catalyzed by quercetin dioxygenase; however, no control experiments were reported under the same conditions.

The Cu(II)–quercetin complex shows DNA cleavage activity[110]. Its structure was not determined and cannot be compared with the simple 3-hydroxyflavonone complexes (**44, 46, 47**) described above owing to the three potential metal-binding sites in quercetin (**43**). The uniform cutting pattern suggests the lack of preferred binding sites on DNA for the complex, making this complex a potential DNA footprinting reagent.

The crystal structure of the purple Fe(III) complex of 3-hydroxyflavone (**45**) has an octahedral coordination sphere with a 1:2 Fe(III)-to-flavone ratio and a Cl^- ion at an axial position[111]. Similar to the Cu(II) complexes, the Fe(III)–O(enolate) bond distances (1.935 and 1.981 Å) are significantly shorter than the Fe(III)–O(keto) bond distances (2.136 and 2.119 Å). The Fe(III) center has a rhombic magnetic environment based on EPR studies. Complete cleavage of pUC18 plasmid DNA by this Fe(III)–flavonoid complex (30 μM) took place in 15 minutes in the presence 1 equivalent of ascorbate/H_2O_2 and was still observable without ascorbate, which is attributed to the reduction capability of the bound flavonoid to yield Fe(II) and initiate the oxidative DNA cleavage[110].

The Zn(II)–flavonolate complex undergoes oxidative cleavage analogous to the Cu complexes[112]. This is adduced to a charge redistribution on the flavonolate ligand taking place upon Zn(II) binding, allowing oxygen attack at the enolate moiety with subsequent oxygenation and cleavage of the 2,3-bond, as observed in quercetin dioxygenase.

Quercetin (**43**) forms a 1:1 complex with vanadyl, VO^{2+} ($S = 1/2$), as shown by electronic spectroscopy[113]. The change in the charge transfer band of quercetin upon VO^{2+} binding is similar to that of Co^{2+} binding (Figure 4). The EPR spectrum of this complex at 140 K displays the typical eight-line pattern (due to $I = {}^7/_2$ of ^{51}V) for the axial V(IV) center with $g_{||} = 1.940$, $g_\perp = 1.979$, $A_{||} = 174 \times 10^{-4}$ cm^{-1} and $A_\perp = 64 \times 10^{-4}$ cm^{-1}, similar to those of the VO^{2+}–maltol and related complexes discussed below. No significant antitumor activity of this complex against osteoblasts was observed; however, the complex stimulates type-I collagen production and slightly inhibits alkaline phosphatase specific activity, two biomarkers of osteoblastic differentiation. This complex stimulates the phosphorylation of extracellular regulated kinase (ERK) in a dose–response manner, suggesting a possible mechanism in its bioactivity and for promoting osteoblast differentiation.

Flavonoids and their metal complexes exhibit a unique redox chemistry, acting both as antioxidants to protect against potential oxidative damage, e.g. in the presence of ROS, and as prooxidant that may result in oxidative damage, depending on the reaction conditions. A fine balance of these two pathways thus determines the characteristic role of this biologically and medicinally important family of natural products.

c. Mimosine and analogues. The naturally occurring amino acid mimosine (**9**), first isolated from *Mimosa pudica*, is produced in large quantities in the seeds and foliage of the leguminous tree subfamily *Mimosoideae* and the genus *Leucaena*[114]. This enol-containing natural product exhibits a potential allelopathic effect (inhibition of the growth of other plants)[115], antineoplastic and other bioactivities (e.g. serving as a product-like inhibitor toward the dinuclear Cu enzymes catechol oxidase and tyrosinase)[9–13, 116] and has been reported to be toxic to animals (e.g. inhibition of wool growth)[117]. The toxic effect of mimosine in *Leucaena* leaf meal and its analogue 2,3-dihydroxypyridine on livestock can be greatly decreased by adding mineral supplements (especially $Fe_2(SO_4)_3$)[118], presumably because the metal binding can prevent their binding to and inhibition of some metalloenzymes.

Mimosine is metabolized into 2,3-dihydroxypyridine, which can be detected at concentrations of up to 1.1 mM, and 3-hydroxy-4(1*H*)-pyridinone (3,4-HP) at up to 0.96 mM in ruminants fed with *L. leucocephala*[119]. The latter can be further degraded by ruminants in some part of the world, indicating that location-specific microbes may be involved in

the degradation process. Obligatorily anaerobic, Gram-negative, rod-shaped bacteria were isolated from the rumen contents of a goat in Hawaii which can use both 3,4-HP and its isomer 3-hydroxy-2(1*H*)-pyridone (3,2-HP) as well as arginine and histidine as substrates for growth[120]. Comparisons of the 16S rRNA sequence of one strain of the ruminant bacteria revealed it to be a new genus and species, named *Synergistes jonesii*.

Mimosine blocks cell cycle progression in the late G_1 phase, thus inhibiting DNA replication in the chromosomes of mammalian nuclei at the replication forks by repressing deoxyribonucleotide metabolism via inhibition of the enzyme ribonucleotide reductase[121] and iron chelation[122]. Mimosine is also able to inhibit the activity of the transcription of the cytoplasmic serine hydroxymethyltransferase gene (*shmt1*)[123]. A mimosine-responsive transcriptional element is found within the first 50 base pairs of the human *shmt1* promoter, wherein a consensus Zn-sensing metal regulatory element (MRE) is located at positions 44–38. Mutation of the MRE attenuated the transcription repression induced by mimosine, whereas introduction of mimosine eliminates MRE-binding activity in nuclear extracts from MCF-7 cells attributed to mimosine chelation of Zn. Moreover, this compound induces apoptosis in the HL60 human tumor cell line[124].

The speciation and stability constants of the Cu(II), Ni(II), Zn(II) and VO(II) complexes of mimosine (**9**) were determined[125]. The Cu(II) and VO(II) complexes adopt a coordination chemistry analogous to the those of maltol (discussed below). The Zn(II) complex of the deprotonated mimosine analogue **48** has a 1:2 distorted square-pyramidal structure with *trans* configuration and a water molecule at the apex (**49**)[126]. Pb(II) forms a 1:2 complex with **48**, which further interacts with one enolate of an adjacent Pb(II) center via Pb–O bridges (2.64 Å) to yield a dinuclear Pb complex (**50**)[126]. Vanadate (with a +5 oxidation state on V) forms with **48** the 1:1 $[VO_2(\mathbf{48}^*)(OH)(H_2O)]^-$ and 1:2 $[VO_2(\mathbf{48}^*)_2]^-$ complex anions, as shown by potentiometry, cyclic voltammetry and NMR and EPR spectroscopies[127], with ^{51}V NMR peaks at −502 and −476 ppm, respectively, similar to the maltol complexes (peaks at −509 and −496 ppm) discussed in the next section.

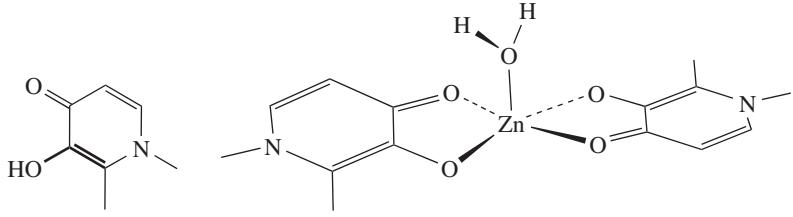

(**48**) (**49**)

The tetradentate ligand **51** shows much better binding affinities with Ni(II), Cu(II) and Zn(II) than **48**, from which it was derived[128]. A wide variety of mimosine (**9**) analogues are at positions 1 and 2[129], such as 2-ethyl-3-hydroxy-1-(3-pyridylmethyl)-4(1*H*)-pyridinonate (EPyHP) that forms a six-coordinate complex with Mo(VI) of formula $[MoO_2(EPyHP^*)_2]$ (**52**, EPyHP* = conjugate base of EPyHP). The complexes of M^+ $(CO)_3$ cores with a few carbohydrate-conjugated derivatives of **48** have been prepared, for example **53**[130]. These complexes are stable up to 24 h in the presence of excess cysteine and histidine. There is no substrate or inhibitory activity observed at the concentrations tested. Nevertheless, these complexes may still have potential as imaging and therapy agents since they might be able to interact with glucose transporters in certain tumor types or accumulate in tumor cells.

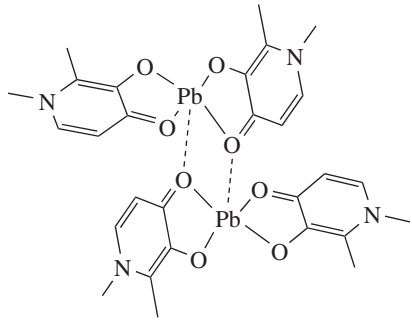

(**50**)

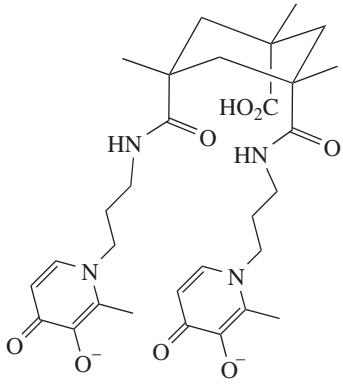

(**51**)

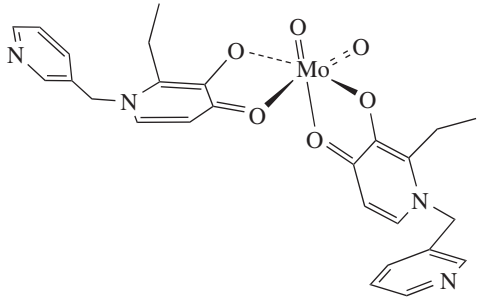

(**52**)

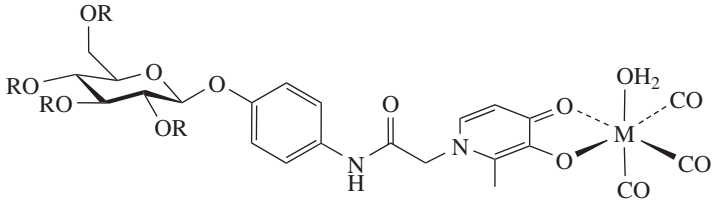

(**53**) M = Re, ^{99m}Tc, ^{186}Re, R = H, Ac

In the 1:1 Pt(II) complex with mimosine (**9**), the Pt ion is coordinated to the N atom of the ring and an O atom of the carboxylate group in a square-planar geometry, as deduced from ^{13}C and ^{15}N NMR and IR spectroscopies[131], with no confirmation by crystallographic analysis. However, the N atom in the pyridinone moiety of the ligand in the crystal structures of **49**, **50** and **52** adopts a trigonal planar bonding configuration (sp^2 hybridization) without an available lone pair, making this N less likely to serve as a ligand in the case of this Pt(II) complex. Since *cis*-dichloro complexes of Pt(II) are clinically important drugs in cancer chemotherapy[8], the Pt(II) complexes of the pyridinones are of great interest as lead drugs.

A few multidentate ligands with 3,2-HP connected to a polyaza cycle have been synthesized and their Cu(II) and Zn(II) binding determined[132]. The crystal structure of the Cu(II) complex shows a square-planar coordination sphere of the Cu(II) center with two coordinated 3,2-HP moieties (**54**). The cyclic amine in this complex is not bound to the metal. The Cu–O (enolate) distance is shorter than the Cu–O (keto) distance by 0.04 Å, similar to other complexes of keto-enolate ligand. Another chelating ligand (**54′**) derived from 3,4-HP and iminodiacetic exhibits strong binding of trivalent metal ions such as Fe(III), Ga(III) and Al(III), but significantly weaker of the divalent Zn(II)[133]. The ^{67}Ga complex of this ligand is cleaned from most tissues faster than the complex of the drug deferriprone (**48**), mostly through the kidneys, making **54′** a potential drug for treating metal overload without affecting essential metal ions like Zn(II).

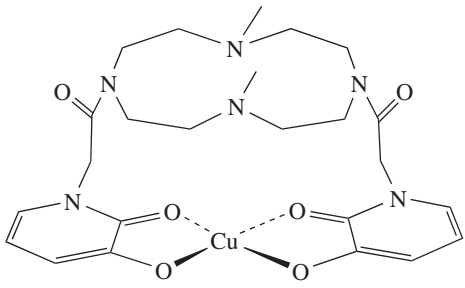

(**54**)

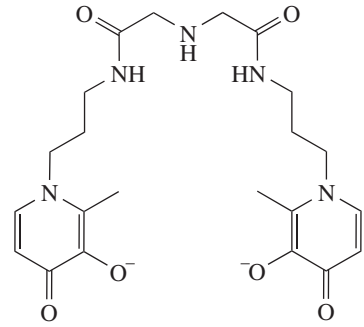

(**54′**)

The condensation of 3,4-HP with deoxyribonucleotide results in a unique metal-binding nucleotide (**55**) which can be incorporated into an oligonucleotide chain[134]. This oligonucleotide has higher thermostability in the presence of Cu(II) compared with an A–T pair, wherein Cu(II) binds to 3,4-HP from each strand to form a double helix (**56**). When the Fe(II)–mimosine complex is introduced to plasmid DNA, cleavage of the supercoiled form is observed in the presence of H_2O_2 and dithiothreitol[135]. The observations described in this section point to mimosine (**9**) and its analogues as the leads for further exploration of their potential application as metal chelators and therapeutics.

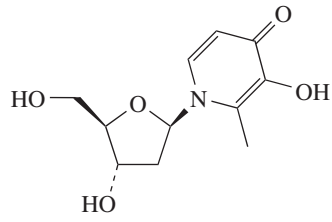

(**55**)

d. Kojic acid and pyranones. The derivatives of 3-hydroxy-4-pyranone, including kojic acid (KA; **10a**) and maltol (**10c**), and their metal complexes are well known for their various bioactivities[136]. KA, found in some traditional Asian fermented foods[14] (soy sauce, miso and sake), is the prototype member of this family. The metal-binding capability of

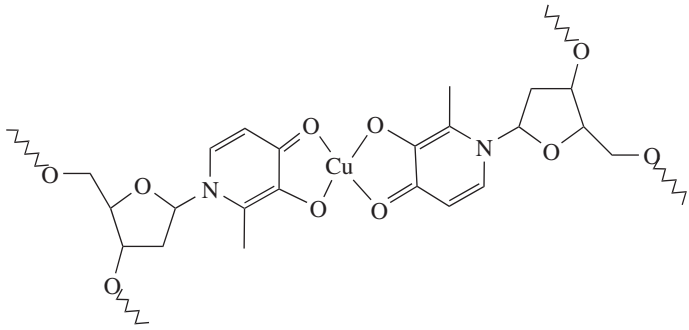

(**56**)

kojic acid renders it a potent inhibitor toward several metalloenzymes, including Cu(II)-containing (polyphenol) oxidases/oxygenases[15] which are the key enzymes for biological synthesis of the melanin pigments. Thus, KA has been widely used as a food additive for preventing enzymatic browning and as a cosmetic agent for skin whitening. Owing to its potential use as a drug lead, several derivatives of KA have been prepared[137, 138], including some peptide derivatives at the 6-hydroxylmethyl group which serve as tyrosinase inhibitors about 100 times more effective than KA itself with higher stability and lower toxicity[139].

The KA crystal consists of an extended H-bonding framework between the hydroxymethyl and the 4-keto groups of contiguous molecules[140]. The high acidity of the α-ketoenol moiety (pK_a *ca* 7) makes it a good metal-binding site. The stoichiometry of the complexes M(**10a***)$_2$ (M = Zn(II), Sn(II), **10a*** = conjugate base of **10a**) was based on elemental analysis with no crystallographic confirmation[141]. Nevertheless, the α-ketoenolate moiety is expected to be the metal-binding site in these complexes as in the case of maltol complexes discussed below. The organometallic KA complex (Me)$_2$Sn(**10a***)$_2$[142] shows C_v mirror symmetry with *cis*-dimethyl octahedral geometry and a Me–Sn–Me angle of 148°, as opposed to the pseudo-C_2 symmetry of the maltol complex Zn(**10b***)$_2$(H$_2$O)$_2$ (see below). Estimates of the Me–Sn–Me angle were also obtained in DMSO solution on the basis of the coupling constants: $^2J(^{119}\text{Sn}, ^1\text{H}) = 83.3$ Hz (143°) and $^1J(^{119}\text{Sn}, ^{13}\text{C}) = 746$ Hz (135°). The Mn(II) and Zn(II) complexes of KA exhibit significant radioprotective effects against lethal doses of γ-irradiation in mice[143]. The crystal of Ca(**10a***)$_2$(**10a**)$_2$ (**57**) has an octacoordinated Ca(II) center of pseudo-D_{2d} symmetry, with the kojinate and KA ligands distinguished by their different Ca–O bond lengths[144]. A high coordination number, frequently 7–8, is quite common in Ca(II) complexes and proteins.

Many metal complexes of the food flavoring natural product maltol (**10b**) and its analogues have been synthesized and characterized[136]. The Zn(II) complexes Zn(**10b***)$_2$(H$_2$O) and Zn(**10b***)$_2$(H$_2$O)$_2$ have 5- and 6-coordination spheres, respectively, with two chelating maltol conjugated bases (**10b***)[126, 145]. The hexacoordinated complex (**58**) has a distorted octahedral coordination sphere with two water molecules occupying the axial position. The two bound **10b*** ligands are *trans* to each other and are slightly skewed from the metal center (**59**). This structure is different from that of pentacoordinated square-pyramidal **49**. Since Zn(II) was found to normalize blood sugar levels in chemically induced and genetically obese (ob/ob) mice[146], the antidiabetic activity of this complex was checked. This complex was determined to exhibit a significant insulin-mimetic activity through *in vitro* assay of inhibited free fatty acids release from the epinephrine-stimulated rat adipocytes,

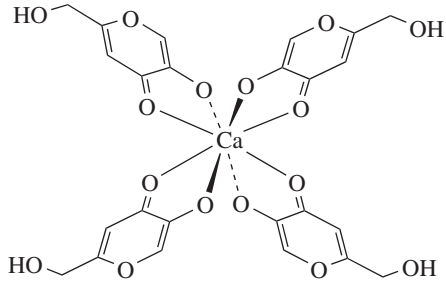

(**57**)

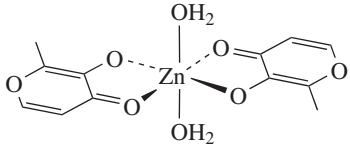

(**58**)

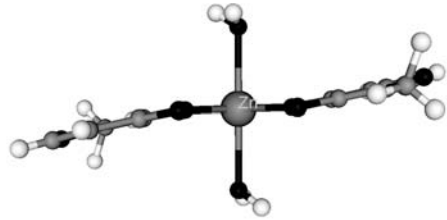

(**59**)

showing $IC_{50} = 0.59$ mM which is lower than the control of $VOSO_4$ (1.00 mM) and $ZnSO_4$ (0.81 mM)[145].

Fe(III) and Al(III) can bind three **10b*** anions to form a distorted octahedral complex of *mer* configuration (**60**, with one of the Me groups pointing in the opposite direction of the other two)[147], with the Fe–O enolate bond distances (average 1.987 Å) shorter than the Fe–O keto ones (average 2.065 Å). The Fe complex **60** has been considered as a potential drug for the treatment of iron-deficient anemia due to its large formation constant, neutral charge, solubility in the pH 6–9 range and lack of toxicity. However, a recent study of **60** revealed its apoptotic activity toward HL60 cells[148], attributed to the production of ROS which explained the prooxidant activity and cytotoxicity of maltol and limited its clinic use.

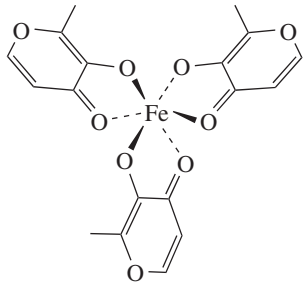

(**60**)

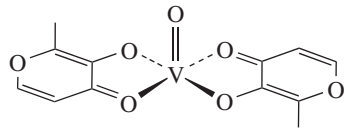

(**61**)

The vanadyl complex of maltol (**10b**) adopts a square-pyramidal coordination sphere with two coplanar **10b*** anions chelating the V atom in *trans* configuration and the

O of VO^{2+} in the apex (**61**) at a short bond distance (1.596 Å)[149]. The ligand configuration of this complex was suggested to undergo *trans–cis* equilibrium in solution. ^{51}V NMR shows the binding of maltol (**10b**) to vanadate (VO_4^{3-}) to form complexes $[VO_2(\mathbf{10b^*})(OH)(H_2O)]^-$ ($\delta = -509$ ppm) and $[VO_2(\mathbf{10b^*})_2]^-$ ($\delta = -496$ ppm), the signals of which are distinctly different from those of vanadate and its oligomeric forms at −559, −572, −576 and −584 ppm under the same conditions. The latter vanadate complex is also formed via aerobic oxidation of **61** in the presence of excess amount of **10b**. The change in oxidation states was confirmed by electrochemical and EPR measurements. Dimaltolato complexes of vanadyl and vanadate supported on carbamated silica gel show catalytic activity in the oxidation of cyclopentane and cyclooctane with O_2 (*ca* 10–14 atm at 150–160 °C) to yield the corresponding ketones as the main products and alcohols in smaller amounts[150]. The results suggest metal complexes of natural products should be further explored as catalysts for catalytic transformations of organic compounds.

V complexes are known to exhibit insulin-mimetic properties from *in vivo* and *in vitro* studies[151]. Because non-insulin-dependent type II diabetes is insulin resistant, but not insulin deficient as in type I diabetes, it is highly significant that V complexes can stimulate glucose metabolism without changing insulin concentration. For example, **61** exhibits insulin-mimetic activities in lowering glucose and lipids and was found to be 2–3 times more effective than $VOSO_4$[152]. More significantly, it is active when administrated orally. Several metal complexes of maltolate, including $[MoO_2]$(II), Co(II), Cu(II), Cr(III) and Zn(II), were tested for their insulin-enhancing activities in streptozotocin-diabetic rats[153]. The first two complexes were shown to exhibit hypoglycemic activity.

Mn(II) complexes of this family of ligands and their analogues were prepared and investigated with various physical methods, including X-ray crystallography, for the purpose of finding potential therapeutics for the treatment of chronic Mn(II) overload (see Section III.B.2.c)[154]. Mn(II) forms a dinuclear complex with ethyl maltol, determined to be $[Mn(\mathbf{10c^*})_2(H_2O)]_2$ **62** by crystallography[154]. Magnetic susceptibility measurement of this complex in the temperature range of 5–300 K revealed a very weak ferromagnetic coupling between the two Mn(II) centers, with a J value of 0.5 cm^{-1}. The crystal structure of the Mn(II) complex of **10b** could not be determined due to low solubility of the complex, which shows a $Mn(\mathbf{10b^*})_2$ stoichiometry and is suspected to adopt a polymeric chain structure in the solid state[154]. However, the **10b** and **10c** complexes of Mn(II) in solution must have an analogous monomeric structure on the basis of their similar spectroscopic and electrochemical properties, showing a ligand-to-metal charge transfer transition at 330–340 nm, monomeric EPR spectra of $g = 2.03$ and $A = 86$ G, ESI-MS spectra consistent with MnL_2 and redox potential at $\Delta E_{1/2}$ *ca* 400 mM[154].

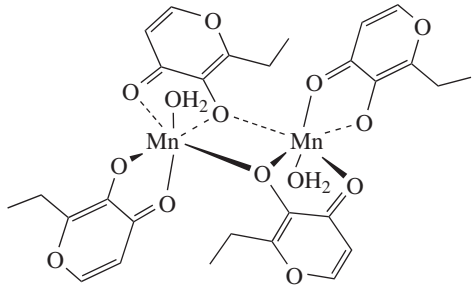

(**62**)

Anions **10a*–c*** form complexes with various first- and second-row transition metal ions. Their Mo(VI) complexes have MoO_2L_2 stoichiometry and crystal structures similar to **52**, as the **10c*** complex **63**[129,155], which was effective in lowering blood glucose and free fatty acid levels similar to $NaMoO_4$. Ru(III) forms 1:3 complexes with **10**, analogous to the Fe(III) complex. However, Ru(III)(**10b***)$_3$ adopt a mixed *mer* configuration (**64**, Plate IV)[156]. The reduction potentials of Ru(**10a***)$_3$ and Ru(**10b***)$_3$ are virtually identical at −1.13 and −1.14 V, respectively, for Ru(III) → Ru(II) and 0.52 V for Ru(IV) → Ru(III) in acetonitrile due to the similar structure of the ligands, which also indicates the complex favors the Ru(III) oxidation state. The Ru(III) complexes of **10b** and**10c** show antiproliferatory activity against the human breast cancer cell line MDA-MB-435S, with IC_{50} values of 140 and 90 μM, respectively. A few Ru(III) complexes coordinated with two **10b*** ligands were characterized by X-ray crystallography[157]. The axial positions are occupied by solvent molecules or other monodentate ligands. These complexes are kinetically inert, thus the axial ligands are not prone to undergo exchange with the solvent. The complexes also exhibit potential antitumor activity against the human breast cancer cell line MDA-MB-435S with the MTT [3-(4,5-Dimethylthiazol-2-yl)-2,5-diphenyltetrazolium bromide] assay in phosphate-buffered saline.

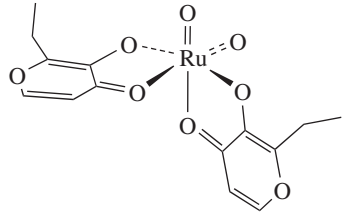

(**63**)

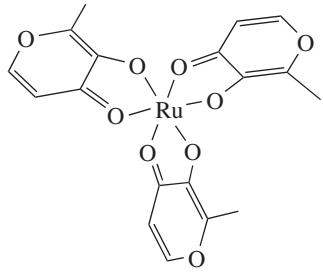

(**64**) Plate IV

Organometallic complexes of Ru and other metals have been prepared and characterized for the purpose of finding potential anticancer drugs[158]. Ru(II) enolate complexes of the **10** family with a bound η^6-arene such as mesitylene or *p*-cymene and a chloride or CO were characterized with crystallography[159], e.g. **65** derived from **10b**[159a]. The Os(II)–**10c** analogue of **65** is also known[159a]. The structures of Ru(II)(**10c***)$_2$L, L = cod, $(PPh_3)_2$, $(Me_2SO)_2$, complexes were determined[160]. NMR and crystallographic analyses point to a mixture of different stereo isomers for the phosphine complex, whereas the cod complex shows only one form. The former one is a catalyst for the dimerization of phenylacetylene

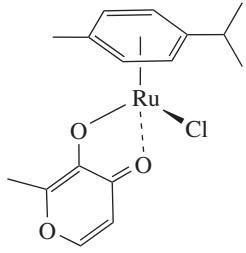

(**65**)

in toluene at 50 °C. Further R&D of the metal complexes of pyranones will lead to new drugs and catalysts.

Titanocene dichloride (Cp_2TiCl_2) exhibits anticancer activity, which triggered wide investigation of Ti complexes for medicinal application[161]. Treatment of Cp_2TiCl_2 with maltol (**10b**) affords a mixture of monomeric *cis*- and *trans*-Ti(**10b***)$_2$(OH)$_2$ in 1:4 ratio[162]. Crystallization of the complex at pH 8.4 affords the tetranuclear [Ti_4(**10b***)$_8$(μ-O)$_4$]•18H_2O. As shown by X-ray crystallography, it consists of an 8-membered Ti_4O_4 ring with four oxide bridges and pseudo-octahedral coordination for the titanium atoms. **66** and **66′** (Plate V) are two different views of the complex without water of crystallization.

(**66**)

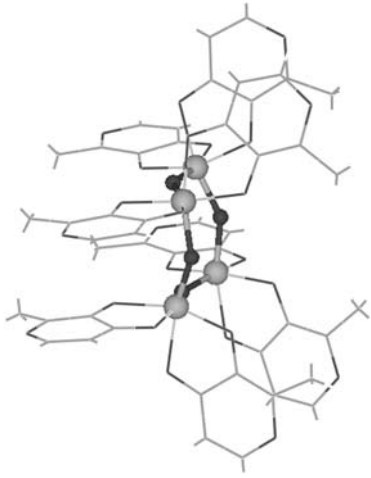

(**66′**) Plate V

e. Furanones. These compounds are comprised of a large number of sugar metabolites in the form of 3-(2*H*)-furanones (e.g. **67a,b**) and 2-(5*H*)-furanones (e.g. **68a,b**)[163]. Ascorbic acid (**1** = **68a**, Section III.B.1.a) is the most studied member of the furanone family which is involved in a number of significant biological processes as enzyme cofactors. Many compounds of this family are key sweet and aroma ingredients in ripe fruits[18, 19, 164], beers[165], wines[166], soy souce[167] and miso[168], such as 2,5-HDMF (**11** = **67a**), 4,5-HDMF (sotolon, **68b**), 4-hydroxy-5-methyl-3(2*H*)-furanone (HMF, norfuraneol, **67b**) and 4-hydroxy-5-ethyl-2-methyl-3(2*H*)-furanone (HEMF, homofuraneol, **69**) and its tautomer 4-hydroxy-2-ethyl-5-methyl-3(2*H*)-furanone (**69′**). HEMF originates from ribose (the ring and the methyl group) and glucose (the ethyl group), as determined using stable isotopes as tracers[168]. These compounds have a very low odor threshold of 20 ppb for **69**, 60 ppb (pH 7) and 21 ppb (pH 3) for **67a** and 23 ppm (pH 7) and 2.5 ppm (pH 3) for **67b**, greatly rendering their use as flavor enhancer in food industry[163, 164].

In addition to their pleasant aroma, these compounds also exhibit various biological activities[163], including serving as possible signaling molecules[169] and antimicrobial activities[170]. An isotope-tracing experiment on ripe strawberries pointed to glucose and fructose as precursors of 2,5-HDMF (**11** = **67a**). Therein, D-glucose-1-*d*, -2-*d* and -6,6-d_2 as well as D-fructose-*1,2,3,4,5,6*-$^{13}C_6$, -1-^{13}C, -1-*d* and -6,6-d_2 are converted into **67a** and its 4-methoxyl derivative[18] through HMF (**67b**) and then the intermediate 4-hydroxy-5-methyl-2-methylene-3(2*H*)-furanone (HMMF) that is reduced by an enone oxidoreductase to yield **67a** as determined by D-glucose-6-^{13}C tracer[171]. More specifically, D-glucose-2-*d*

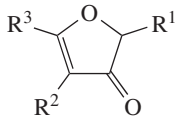

(**67**) (**a**) $R^1 = R^3 = Me$, $R^2 = OH$
(**b**) $R^1 = H$, $R^2 = OH$, $R^3 = Me$

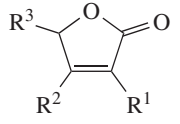

(**68**) (**a**) $R^1 = R^2 = OH$, $R^3 = CH(OH)CH_2OH$
(**b**) $R^1 = OH$, $R^2 = R^3 = Me$

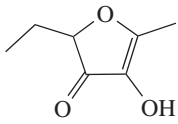

(**69**)

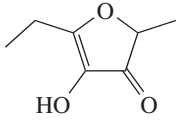

(**69′**)

is converted to **11**-1-*d* or **11**-6-*d* and the 4-methoxyl derivative, whereas D-glucose-4-*d* is not converted. HMF (**67b**) yields several 2-substituted furanones by coupling with various aldehydes and ketones[164].

Structures of metal complexes of these furanone derivatives have not been reported, despite the presence of the potential metal-binding α-ketoenolate moiety in these compounds. Nevertheless, Cu(II) seems to be involved in the DNA cleavage activity of furanones[172], wherein **67a** exhibits a high activity while **68b** does not under the same conditions (20 μM Cu(II) and $\geqslant$20 μM furanone). Unlike Cu(II), addition of Fe(III) to **67a** does not result in DNA cleavage[172]. This DNA cleavage activity was considered to be the reason for the mutagenic activity of **67a**. The DNA cleavage activity and degradation of these compounds seems to be correlated with their activity toward the reduction of Cu(II). In a different study, **69** (0.6 mM) was found to perform single-strained DNA cleavage in the presence of 1 mM Fe(III). Spin-trapping experiments monitored with EPR revealed the generation of hydroxyl radicals[173]. The furanone **67a** inhibits aconitase (an enzyme indicator for ROS) in the presence of Fe(II), possibly due to the production of hydroxyl radicals, while **68b** does not[174]. These studies suggest furanone compounds may serve as prooxidants. Conversely, **69** was also found to be an inhibitor toward iron-induced oxidation when using human erythrocyte membranes and low density lipoprotein (LDL) as substrates under aerobic conditions. Western blot analysis indicated that aggregates of band 3 protein and the level of thiobarbituric acid-reactive substances in LDL caused by Fe ions decreased in the presence of **69**[175]. Furanones exhibit antioxidative activity toward free radical-induced lipid peroxidation and Cu-induced LDL oxidation[176]. These results indicate that **69** protects against Fe- and Cu-induced oxidative modification of biomolecules and cells.

No conclusive mechanisms mechanism can be adduced for the opposite prooxidative and antioxidative activities observed for the metal complexes of these furanones owing to the lack of both detailed structural and kinetic analyses. Whether the opposite results can be attributed to different experimental conditions is also moot. Nevertheless, it is reasonable to expect that the structures of metal–furanone complexes are similar to those of the analogous metal–pyranone complexes discussed in Section III.B.1.d.

f. Quinone derivatives. There is a large number of hydroxyquinone and hydroxynaphthoquinone natural products[27], such as PPA and derivatives (**15a–c**), the boviquinones (**17a,b**) and flaviolin (**30**). Many members of this family of compounds are involved in varied biological functions, e.g. serving as enzyme cofactors and as intermediates in the production of bioactive compounds, and are potential candidates for drug discovery. For example, topaquinone (**70**, see Section IV.D) in amine oxidase is involved in amine metabolism; 7-hydroxymitomycins are precursors of the DNA-alkylation agents mitomycins catalyzed by a methyltransferase[177] (mitomycin C is clinically used as an antitumor agent); and the ubiquinone-like 5-*n*-heptyl-6-hydroxy-4,7-dioxobenzothiazole is a competitive inhibitor toward the multisubunit membrane protein complex ubiquinol:cytochrome *c*

oxidoreductase in respiratory and photosynthetic electron transfer chains[178]. The metabolite ilimaquinone (**71**) from the sponge *Hippospongia metachromia* shows broad bioactivities, including influence on Golgi structure and function[179], antiviral activity[180], anticancer activity[181], inhibition of protein toxins like ricin[182] and interaction with enzymes[183]. Despite the presence of the potential metal-binding α-ketoenolate functionality in these compounds, the roles of metal ions in the activities of many of these compounds are largely unexplored.

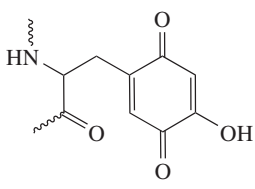

(**70**)

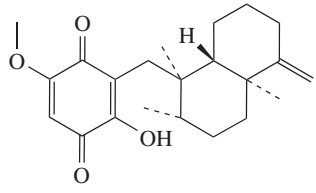

(**71**)

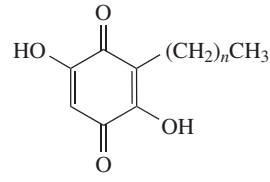

(**72**)

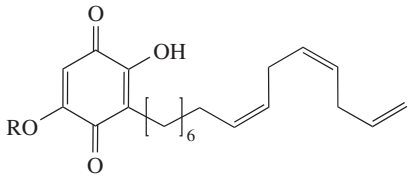

(**73**) (**a**) R = Me
(**b**) R = Et

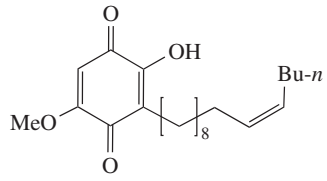

(**73′**)

The hydroxyquinone lipids are a unique group of the hydroxyquinone family which contains a linear hydrocarbon chain. Typical examples are the boviquinones (**17**), embelin (**72**, $n = 10$) and rapanone (**72**, $n = 12$) from the *Myrsinaceae* family, sorgoleone (**73a**) from the *Sorghum* species and maesanin (**73′**) and its derivatives from *Maesa lanceolata*. Embelin is isolated from species in the *Myrsinaceae* family, including *Ardisia japonica* used in traditional Chinese medicine, and is antifertile and anthelminthic. The ethnomedical natural product rapanone from *Myrsine guianensis*[184a] and *Lysimachia* species[184b] is antiparasitic[184a] and antifertile[184c] and an inhibitor[185] toward degranulation ($IC_{50} = 9.8\ \mu M$) and superoxide production ($IC_{50} = 3.0\ \mu M$) in human neutrophils, phospholipase A_2 ($IC_{50} = 2.6\ \mu M$) in human synovial fluid, as well as chronic and acute inflammation in mouse and rat models. Sorgoleone is an allelochemical, a natural herbicide repressing the growth of other plants present in their surroundings[186]. Several analogues with various substitutions (e.g. ethoxysorgoleone **73b**) and chain lengths are found in root exudates. Maesanin and analogues such as dihydromaesonin and maesanol inhibit the metalloenzymes lipoxygenase and 4-hydroxyphenylpyruvate dioxygenase as well as the NADPH-dependent aldose reductase and aldehyde reductase[187].

The naphthoquinone lawsone (**74**, hennotannic acid, natural orange 6) is a red–orange pigment present in the leaves of henna (*Lawsonia inermis*) and the annual flower balsam (*Impatiens balsamica*). Like flaviolin (**30**) and its oxidation product mompain, lawsone is also an oxidative product of the naphthalene derivatives **29** and 1,3-dihydroxynaphthalene[188]. These molecules are precursors for some pigments in various organisms, including *Streptomyces* species. The α-ketoenol group of lawsone is highly accessible to Michael addition. Thus, protein molecules can be modified by lawsone via nucleophiles such as a Lys side chain, which permanently stains skin and hair by reacting with keratin. This

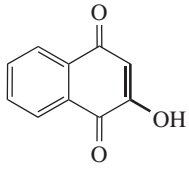

(**74**)

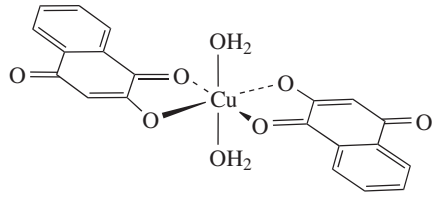

(**75**)

staining technique has been utilized for thousands of years. The capability of lawsone to form complexes with amino acids has recently been investigated for use in forensic detection of latent fingerprints on paper surfaces[189].

The binding properties of Fe(II) and Fe(III) to 3-substituted derivatives of **74** were studied with Mössbauer spectroscopy, showing a small effect by the substituents[190]. The binding of Fe(II) with **74** and its semiquinone was further investigated with electrochemical and electronic spectroscopy, showing a 1:2 stoichiometry and a large formation constant (3.5×10^{25} M^{-2}) for the semiquinone [Fe(III)(**74***)(**74**$^{\bullet}$*)] complex[191]. The Eu(III) complexes of several compounds of this family have been investigated when seeking further application[192], although there is potential for lanthanide(III) luminescence-related applications.

The Cu(II) complex [Cu(**74***)$_2$(H_2O)$_2$] (**75**) has a typical tetragonally distorted octahedral geometry, with two *trans* bidentate **74*** in the equatorial positions[193]. The crystal lattice of **75** has a layered structure, where each coordinated water molecule is H-bonded to a coordinated enolate of one complex and the unbound 4-keto group of an adjacent complex in the next layer. Dideprotonated 3,3′-bilawsone, 2,2′-bis(3-hydroxy-1,4-naphthoquinone), binds Cu(II) to form an extended *trans* complex framework (**76**, Plate VI)[194]. With Cd(II), a one-dimensional linear coordination polymer is formed[195].

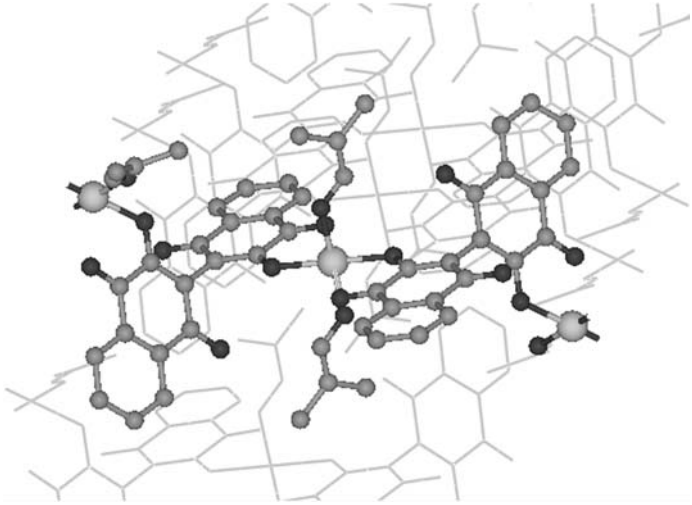

(**76**) Plate VI

Since the hydroxyquinone center of lawsone is redox active, binding of Cu(I) to this compound results in internal electron transfer from Cu(I) to the quinone to afford a magnetically coupled Cu(II)–hydroxysemiquinone (Cu-**74**$^{\bullet}$) center, suggested to be dimeric $[Cu^{II}(\mathbf{74}^{\bullet})\ (\mathbf{74}^{*})]_2$[196]. Based on EPR and magnetic susceptibility studies, a ferromagnetic coupling with a coupling constant of 28 cm^{-1} was suggested to be due to an exchange coupling within Cu(II)–**74**$^{\bullet}$ while an antiferromagnetic coupling with a coupling constant of -50 cm^{-1} was attributed to interdimer exchange coupling. Since the magnetic orbital in Cu(II) is $d_{x^2-y^2}$, the presence of ferromagnetic coupling within the Cu(II)–**74**$^{\bullet}$ unit indicates that the free radical in **74**$^{\bullet}$ does not interact directly with the $d_{x^2-y^2}$ orbital. The lack of crystal structure to date does not allow a correlation between the magnetic interaction and structure to be established. Since the quinone moiety is involved in several copper enzymes, investigation of Cu–quinone and Cu–semiquinone complexes may provide further insight into the role of the quinone cofactors in the actions of these enzymes. A number of derivatives of 2-hydroxy-1,4-naphthoquinone also show various biological activities (Section III.B.2.d).

g. Tropolones. Tropolone (**77**) is a hydroxyl derivative of the unique 7-membered tropone (2,4,6-cycloheptatrien-l-one) and is a functional moiety found in a large number of natural products[197], such as colchicine (**78**) from plants of the genus *Colchicum* for the treatment of gout, stipitatic acid (**79a**,) stipitatonic acid (**80**) from *Penicillium stipitatum* (*Talaromyces stipitatus*)[197,198], puberulic acid (**79b**) and puberulonic acid (**81**) from several *Penicillium* species[199]. The aromatic structure of **79a** was correctly deduced by Dewar[200]; meanwhile, Nozoe was also accredited to the proposal of the aromaticity in tropolone derivatives independently[197]. Many compounds of this family are found to be antimicrobial agents in plants and fungi and also exhibit antiviral, antitumor, antioxidant, antiinflammatory, insecticidal and/or enzyme inhibitor activities[201]. For example, β-thujaplicin (**79c**, hinokitiol[197]) and γ-thujaplicin (**79d**) isolated from *Chamaecyparis taiwanesis* (Taiwanese cypress/hinoki) and *Thuja plicata* (western red cedar) exhibit antibacterial and antifungal activities, improving the resistance of the wood to decay[202]. Production of **79c** occurs in response to oxidative stress by H_2O_2 but not by $O_2^{\bullet-}$[203].

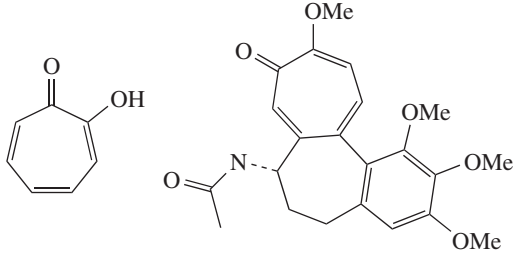

(**77**) (**78**)

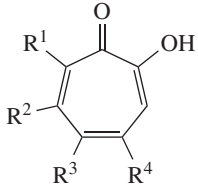

(**79**) (**a**) $R^1 = R^3 = H$, $R^2 = OH$, $R^4 = CO_2H$
(**b**) $R^1 = R^2 = OH$, $R^3 = H$, $R^4 = CO_2H$
(**c**) $R^1 = R^2 = R^4 = H$, $R^3 = i$-Pr
(**d**) $R^1 = R^2 = R^3 = H$, $R^4 = i$-Pr

The tropolones form transition-metal complexes of high affinity constants, for example $[M(\mathbf{77}^{*})_3]^-$ with M = Co(II), Ni(II) and Zn(II), but $M(\mathbf{77}^{*})_2$ with M = Cu(II)[204]. Moreover, these compounds form complexes with heavy metals (Os, Ir, Pt, Mo and W)[205], the lanthanides(III)[206] and main-group metal ions (Ga, In, Sn, Sb and Pb)[207–209]; many have crystal structures determined and some show biological activities and potential

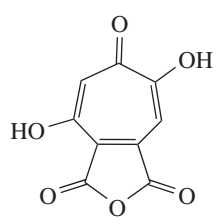

(**80**)

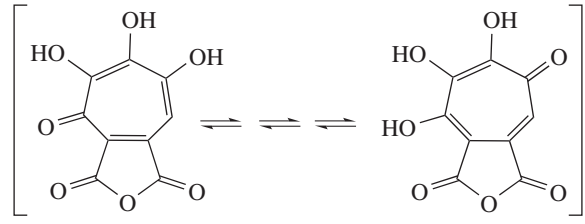

(**81**)

medicinal applications. The first-row transition metal complexes of **77** and derivatives have octahedral geometry, with the ligands bound in the equatorial positions in case of the 1:2 complexes. The stoichiometry and structure of the heavy-metal complexes vary, affording Os(**77***)$_3$, Ir(**77***)$_3$, [Pt(**77***)(PPh$_3$)$_2$]BPh$_4$, OsO_2(**77***)$_2$, MoO_2(**77***)$_2$ and W_2O_5(**77***)$_2$. The crystal structure of MoO_2(**77***)$_2$ has a distorted octahedral geometry with the two O atoms at *cis* positions, analogous to the structures of the MoO_2 complexes of mimosine (**52**) and KA (**63**). The tropolone–lanthanide complexes, [Ln(**77***)$_4$]$^-$, have an eight coordination sphere which is quite common for lanthanide complexes[206]. Moreover, these ligands have been demonstrated to form organometallic compounds with Rh^+ as in the case of Rh(**77***)(CO)PPh$_3$[210]. Those tropolones with a long hydrocarbon chain bind Co(II), Ni(II), Cu(II), Zn(II), UO_2(IV) and VO(II) to form metallomesogens[211], the metal-containing liquid crystals. The metal–tropolone core assists the alignment of the molecules to afford the long-range orientation order of the mesomorphic properties (e.g. **82**, a Cu–hexadecyloxytropolone complex, Plate VII). The tropolones are effective inhibitors for several metalloenzymes, presumably attributed to their metal-binding capability (Section IV.I).

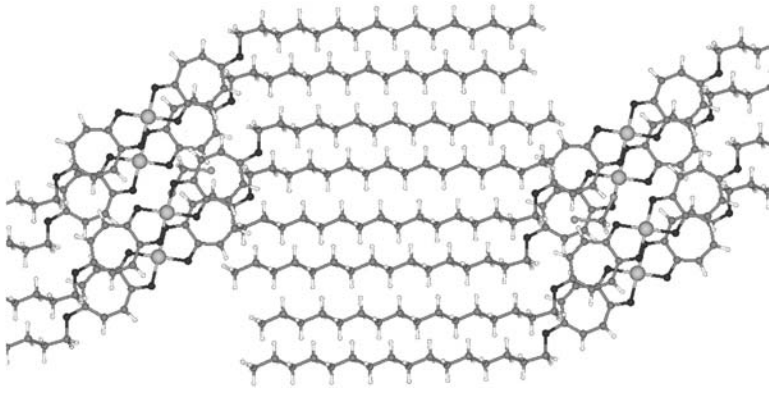

(**82**) Plate VII

2. Pharmaceuticals

a. Antibiotic tetracyclines. The broad-spectrum antibiotic activity of the tetracyclines (TC)[7,212] is attributed to inhibition of protein synthesis upon binding to ribosomes[213]. There are two enol moieties in these antibiotics. The acidic oxy-groups at positions 1, 3, 10, 11 and 12 (see **8**) of this antibiotic family are the potential metal binding sites, among

which the 11,12-β-ketoenol functionality is the primary one[214]. The crystal structure of the drug-bound ribosome subunit has been determined with X-ray crystallography[215]. Many Mg(II) ions are revealed in the structure, of which one that is associated with the nucleotides C1054, G1197 and G1198 may also be involved in the interaction with a bound TC via the 11,12-β-ketoenol functionality. This functionality has also been determined to be the Mg(II) binding site in the repressor TetR–Mg(II)–TC ternary complex of tetracycline resistance in bacteria, where the TC–Mg(II) complex is anchored to the TetR protein through His100 and a few H-bonds (**83**, see Section IV.H). Binding of the Mg(II)–TC complex to the TetR protein turns on the TC-resistance mechanism in bacteria, with efflux of the drug through the membrane as the Mg(II)–TC complex.

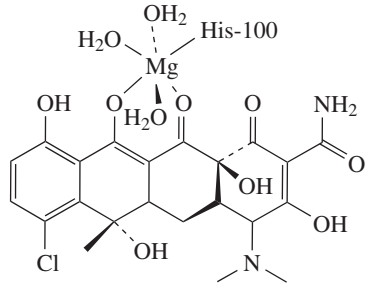

(**83**)

TCs are well documented to bind various metal ions, including alkaline earth metals, Al(III) and transition metals VO(II), Cr(III), Mn(II), Fe(II/III), Co(II), Ni(II), Cu(II) and Zn(II)[216–220]. TC can form 2:1 TC–metal complexes with 3*d* transition metal ions in non-aqueous solution, in which the metal is bound at the 2-amido and 3-enolate chelating sites[216]. TCs are present in plasma mainly in the Ca(II)-bound form or Mg(II)-bound form to a lesser extent, when they are not bound to proteins such as serum albumin. Thus, the bioavailability of TCs should be dependent upon the physical and biochemical properties of their metal complexes instead of their metal-free form.

b. Oxicam anti-inflammatory drugs. The family of the non-steroid anti-inflammatory drugs (NSAID) comprises a large number of compounds, such as oxicams, salicylate derivatives, ibuprofen, diclofenac and their analogues, indomethacin, some cyclooxygenase-2 (COX-2) inhibitors, etc. The Cu(II) complexes of several NSAIDs exhibited better therapeutic activities relative to the free drugs, which triggered an extensive investigation of the physical, structural and spectroscopic properties and biological activities of the metal complexes of this family of drugs[221].

Piroxicam (**84**, Feldene® in the US), a non-selective COX inhibitor with both analgesic and antipyretic properties, is one of the most used NSAIDs and serves as prototype of the oxicam family. This drug is utilized to relieve the symptoms of arthritis, menstrual pains or cramps and fever. It is also used in veterinary medicine to treat certain neoplasias expressing COX receptors, such as bladder, colon and prostate cancers[222]. Variation on the structure of piroxicam has produced several other analogues with the benzene ring replaced by a thiophene ring and/or derivatives of the amide moiety, including meloxicam (**85**, a thiazole amide), isoxicam (**86**, an isoxazole amide), tenoxicam (**87a**, a thiophene derivative) and lornoxicam (**87b**, a chlorothiophene derivative).

The oxicams have several potential metal-binding sites, i.e. the enolate, the carbonyl-O of the amide, the deprotonated amido-N and the N atom on the pyridine/thiazole/isoxazole

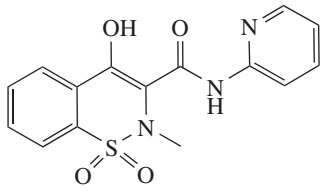

(**84**)

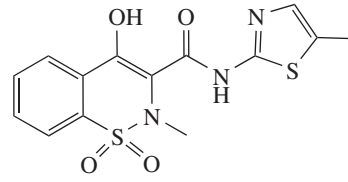

(**85**)

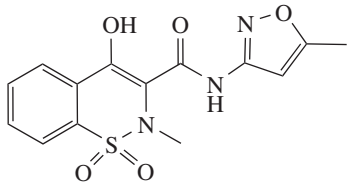

(**86**)

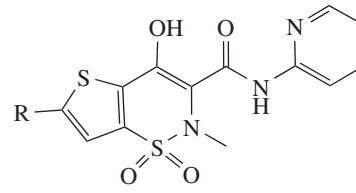

(**87**) (**a**) R = H
(**b**) R = Cl

ring. Bidentate metal binding with these groups is also possible. The crystal structures of a number of metal complexes reveal various metal-binding modes. A monodentate N–Pt bond is formed by the pyridyl group of **84** in the complex *trans*-dichloro-η^2-ethylene-(**84**)Pt(II)[223]. An early study revealed that both **84** in the complex [Cu(**84**)$_2$(DMF$_2$)]$^{2+}$ are coordinated to the metal via the N of the pyridyl group and the O of the amide with a *trans* configuration. The two DMF molecules in this complex occupy the axial positions to afford a tetragonally distorted octahedral geometry[224], showing a typical EPR spectrum of $g_{||} = 2.06$ and $g_{\perp} = 2.29$ and a superoxide dismutase-like activity[225]. However, a square pyramidal geometry is adopted in the Cu(II)–**85** complex with only one DMF ligand at the axial position[226].

Isoxicam (**86**) forms a 2:1 complex with Cu(II) (**88**)[226] where the two coordinated **86** anions have different binding modes: one through the isoxazole N heteroatom and the O of amidate, and the other through the O of the amide (1.90 Å) and enolate (1.88 Å). The crystal shows π-stacking. An attempt to prepare the Cu(II) complex of piroxicam-cinnamate (cinnamic ester of **84** at the enol site) resulted in an unexpected complex (**89**)[226], which is not simply a cleaved product of the ligand. A mechanism was proposed to involve methanolysis of the amide moiety of a coordinated piroxicam by the Lewis acidic Cu(II) to afford a methyl ester and 2-aminopyridine; attack of the latter at the cinnamate ester bond affords *N*-2-pyridylcinnamide. The final complex (**89**) has two coordinated methyl ester molecules through enolate in a *trans* configuration and a coordinated N from a pyridyl moiety at the axial position, attaining a square-pyramidal geometry.

The complex Cu(**84**)$_2$(DMF)$_2$ was found to exhibit antiproliferation activity[226]. Cytotoxic tests of this complex against about 50 human cancer cells showed an average growth inhibition factor GI$_{50}$ value of 54 μM, and was as low as 20 μM against several cancer lines. Higher activities were found toward ovarian, non-small lung, melanoma and central nervous system cancer cell lines, better than the widely used anticancer cisplatin analogue carboplatin (GI$_{50}$ = 102 μM). Direct binding of Cu–**84** and Cu–**85** complexes with DNA proceeds probably through intercalation, suggesting a possible mechanism for the anticancer activity of these complexes[227].

Several organotin complexes of the oxicams and other NSAIDs have been tested against *Mycobacterium tuberculosis*[228]. The complexes *n*-Bu$_2$Sn(**84****), *n*-Bu$_2$Sn(**87a****) (**90**)[229],

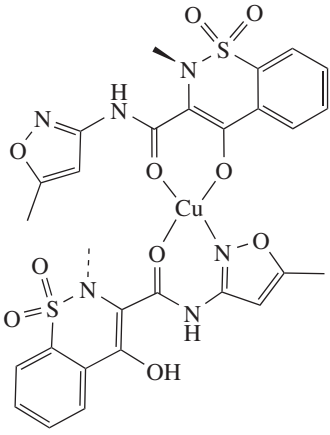

(**88**)

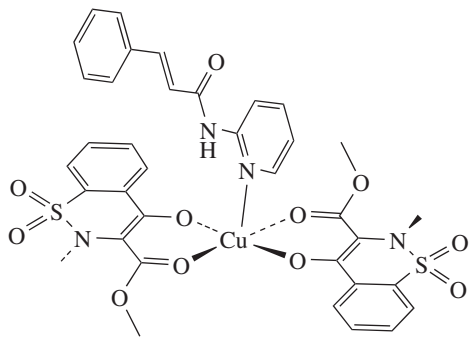

(**89**)

Me_2Sn(**87b****) and n-Bu_2Sn(**87b****)[230] have a unique tridentate binding mode through the pyridyl N, the enolate O and the amidate N. In contrast, the organotin complex with **84**, Ph_2Sn(**84***)$_2$[231], has octahedral geometry with the *trans* ligands bound through the enolate O and amide O atoms.

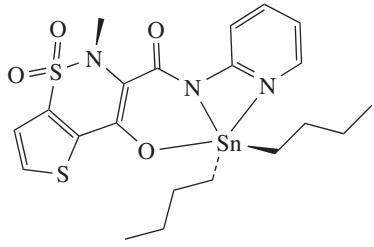

(**90**)

c. Deferiprone for iron overload. Mimosine analogues have high affinity toward Fe(III) due to the 3-hydroxy-4-pyridinone moiety (**9** and analogues in Section III.B.1.c), showing a high affinity constant log(β_3) in the range of 34.7–37.7[232]. They have been investigated as potential clinical chelating agents[233] for the treatment of iron overload[234]. Deferiprone (**48**, Ferriprox®) is used clinically as an orally administered chelating agent for the treatment of transfusional iron overload and as alternative therapy in patients with thalassemia major when there is deferoxamine intolerance or unavailability[235, 236]. Despite its wide use in the rest of the world, it has limited accessibility in the US due to failed phase III trial and controversies. It is quickly absorbed through the stomach into the blood stream within minutes to a couple of hours, and is cleared after 8 hours[237]. Recently, a combined chelation treatment of iron overload in juvenile hemochromatosis with **48** and desferrioxamine B has been demonstrated to effectively prevent heart failure[238].

The 3-hydroxy-4-pyridinone moiety in the mimosine drug family is responsible for metal binding (Section III.B.1.c). The structure of a number of such complexes was determined by X-ray crystallography. The 3:1 complexes of **48** with Fe(III)[239], Al(III), Ga(III)

and In(III)[240] have virtually the same crystal structure[241], with a distorted octahedral coordination sphere and the M–O(enolate) bond shorter by *ca* 0.03 Å than the M–O(keto) bond. The crystal structure of the complexes may vary significantly, depending on the metal nucleus, for example **49**–**51** for the Zn and Pb complexes.

There are a few analogues of hydroxy pyridinone with substituents at positions 1, 2 and/or 6, for example Me, CONHMe and Me in **CP502**, Me, $CONMe_2$ and Me in **CP509** and the much improved second-generation analogue **L1All** with All, Me and H, respectively[242]. Fe(III) binds three **CP502*** anions to form a complex with *mer* configuration (**91**)[243]. Two of the ligands form internal H-bond (dotted line) between the amide NH and the coordinated enolate-O. The same structure is preserved when *N*-Me is replaced by *N*-*c*-Pr[244]. The complexes Fe(**48***)$_3$[239] and Mn(**48***)$_3$[245] have a similar octahedral geometry, however with a *fac* configuration. Mn(**48***)$_2$Cl, on the other hand, has a square pyramidal geometry with both **48*** on the base in *cis* configuration and the chloride ion at the apex[245].

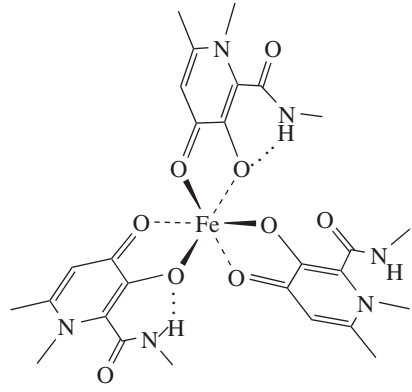

(**91**)

Besides its use for treatment of iron overload, **48** has recently been recognized to improve experimental autoimmune encephalomyelitis in mice, a model for multiple sclerosis and is under pilot trials for this disease[246]. This agent does not affect cell proliferation or viability. A number of derivatives (**92**)[247] of **48** were prepared, by inserting at the N1 position a covalently substituted phenol with various linkers (L), for the purpose of iron chelation (by the hydroxypyridinone moiety) and antioxidation (by the phenol moiety). The six reported derivatives are more potent inhibitors against lipid peroxidation and four of the derivatives exhibit better protection of cells from iodoacetate-induced toxicity at lower concentrations than **48**[248] and the antioxidants 2,6-di-*t*-butyl-4-methylphenol (butylated hydroxytoluene; BHT), Trolox® and the BHT analogue LY231617[249]. One of the derivatives ($L = CH_2$ and $R = t$-butyl) also exhibits better neuroprotection over the combination of **48** and phenol. The Fe-binding properties of these derivatives were not investigated. Owing to their similar metal-binding motifs, these derivatives can be expected to show similar Fe-binding characteristics and affinities as Deferiprone (**48**).

d. Antimalarial hydroxynaphthoquinones and analogues. A number of naphthoquinone derivatives have long been investigated for their therapeutic potential, particularly as antimalaria agents[250]. Atovaquone (**93**) is a clinically promising drug for the treatment of malaria, the AIDS-associated *Pneumocystis carinii* pneumonia and protozoan-caused

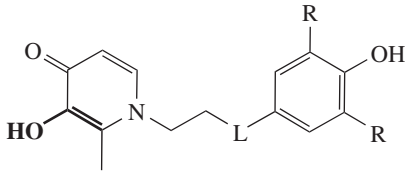

(**92**)

toxoplasmosis[251,252]. It selectively inhibits the electron transport chain of parasites by binding to the mitochondrial metalloprotein complex cytochrome bc_1 as a ubiquinone antagonist, collapsing the membrane potential at concentrations far lower than those affecting the mammalian system[253] The drug has been shown to block the iron–sulfur protein subunit in cytochrome *b*-binding conformation, which prevents the necessary domain movement of the iron–sulfur protein for electron transfer from cytochrome *b*-bound ubihydroquinone to cytochrome c_1 in the cytochrome bc_1 complex[178,254]. Failure of this specific interaction due to mutation of the cytochrome bc_1 complex thus accounts for the resistance toward this drug[255]. Atovaquone (**93**) is suggested to be H-bonded with the coordinated His181 in the Fe–S center when the Fe–S subunit is docked onto the cytochrome complex (Figure 5). The ubiquinone-like enol competitive inhibitor 5-*n*-heptyl-6-hydroxy-4,7-dioxobenzothiazole (**94**) also interacts with the Fe–S center via the coordinated His181. Although there is no direct interaction between atovaquone and the metal center, this interaction is expected to change the Lewis basicity of the coordinated His, which in turn can affect the redox potential of the Fe–S center (e.g. **93** binding raises the midpotential by 75 mV[256]). In addition, inhibition of ubiquinone synthesis has also been attributed to the drug resistance[257].

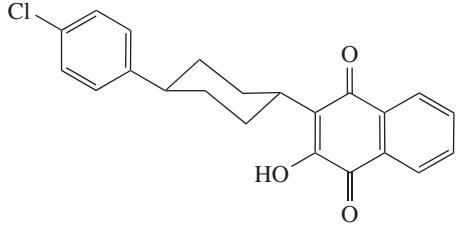

(**93**)

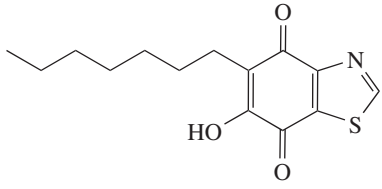

(**94**)

Atovaquone (**93**) exhibits a high inhibitory activity (K_i *ca* 1–10 μM) toward the uridine phosphate-synthesizing enzyme dihydroorotate dehydrogenase[32]. This enzyme is FMN-dependent and does not require a metal cofactor to catalyze the oxidation of dihydroorotate to orotate in the biosynthesis of UMP. Inhibition of this enzyme by **93** has been investigated with crystallography to reveal a specific interaction between the keto-enol moiety of **93** and Arg136 of the enzyme (Figure 5). It has been a promising target for drug design[258] against cancer and arthritis and for development of new antibiotics toward *Helicobacter pylori* (stomach ulcers and cancer) and *Plasmodium* (malaria).

Lapachol (**95**, from the lapacho tree, genus *Tabebuia*, family of the catalpa trees, *Bignoniaceae*) and its analogues show very broad therapeutic capabilities[259], including activity against cancer which results in apoptosis and inhibition in metastasis, antimicrobial, antifungal, antimalarial and other activities[260]. However, clinical application of lapachol is limited by its high toxicity. Lapachol forms complexes with many metal ions,

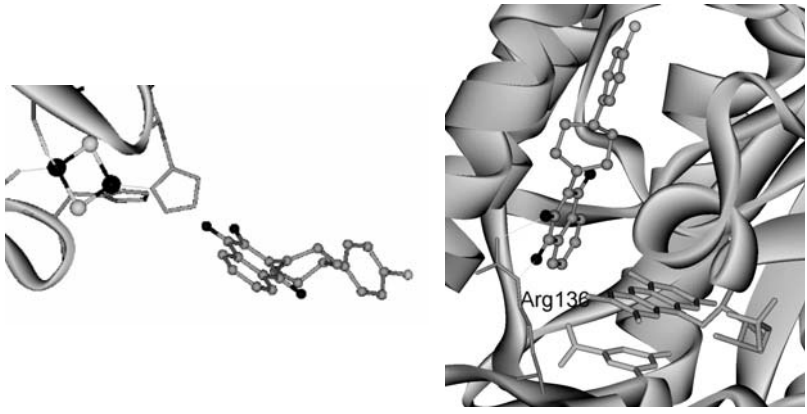

(A) (B)

FIGURE 5. (A) Interaction of atovaquone with the Fe–S center (on left) in the cytochrome bc_1 complex via H-bonding with the coordinated His (Plate VIII). (B) The active center of a class 2 dihydroorotate dehydrogenase (PDB ID 1UUM) with a bound inhibitor atovaquone (top ball-and-stick structure), orotic acid (green) and riboflavin 5′-(dihydrogen phosphate) (FMN, pink) (Plate IX)

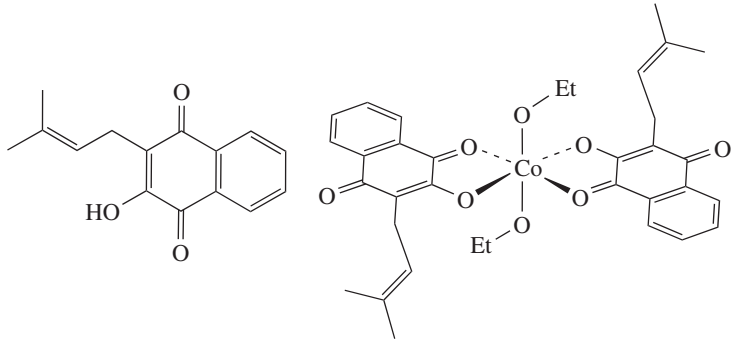

(**95**) (**95′**)

including transition metals[261], main group metals[262] and lanthanides[192, 263]. The crystal structures of the Co(II), Ni(II), Cu(II) and Zn(II) complexes of **95** show 1:2 stoichiometry, chelating through the keto–enolate functionality and *trans* configuration, e.g. the Co(II) complex (**95′**) with two axially coordinated ethanol molecules.

3. Miscellaneous applications of metal enolates

a. Antitumor agents. Several metalloenolates are potential therapeutic agents for the treatment of cancers. For example, some *cis*-diaminoplatinum complexes of ascorbic acid (**41**, **42**) were found to be highly active in the S180a tumor screening[83]. Moreover, pyranone derivatives are synthesized for the development of inhibitors toward matrix metalloproteases (MMPs) as potential chemotherapeutic agents against cancers owing to their strong affinity toward metal ions. New 5-carboxamido-3-hydroxy-4-pyrone

derivatives have been synthesized and their activities toward MMPs checked[264]. The *N*-biphenylylamide derivative **96a** exhibits 21, 34, 34 and 33% inhibition at 100 μM against MMP-1 (collagenase), MMP-2 (gelatinase A), MMP-3 (stromelysin) and MMP-9 (gelatinase B), respectively, while the thiopyranone analogue **96b** exhibits more efficient 52, 94, 45 and 54% inhibition at 50 μM, respectively, and shows IC_{50} of 23 μM against MMP-2. The Ni(II) complex of lapachol (**95**) was reported to exhibit significant radiosensitization, which may enhance cell killing by irradiation during radiation therapy[265].

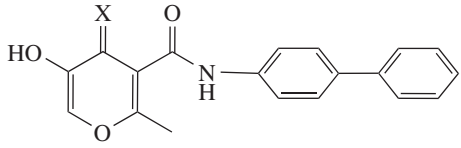

(**96**) (**a**) X = O
(**b**) X = S

A number of organometallic compounds have been recognized to exhibit significant antitumor activities[158], including Ru/Os-arene compounds of pyranones (**10**)[159] (e.g. **65**, Section III.B.1.b). The antitumor activities of metal complexes are largely attributed to their DNA binding capability[266]. The affinity of these organometallic Ru/Os–**10b** compounds toward nucleotides was investigated by NMR spectroscopy. Purine bases (A and G) were found to bind selectively, but not pyrimidine bases (C and T), with binding constants of 7400 and 25700 M^{-1} for 9-Et-G binding to the Ru compound **65** and its Os analogue, respectively[159a]. However, despite their nucleotide binding capability, these Ru/Os(*p*-cymene)(**10b**)Cl complexes were found ineffective toward the human lung A549 and ovarian A2780 cancer cell lines at concentrations up to 50 μM. These organometallic Ru/Os–**10b** complexes undergo hydrolysis to afford a dimer of $[Ru/Os(p\text{-cymene})]_2(OH)_3$ under the biological testing conditions[159a].

The β-diketone functionality undergoes tautomerism with the β-ketoenolate functionality, e.g. acetylacetone and curcumin in equation 2, and becomes a very good metal chelating agent upon deprotonation. A number of organometallic compounds containing β-diketonate chelating ligands as 'tuning agents' to adjust the antitumor activity have attracted much attention[267]. For example, changing the chelating ligand from ethylenediamine (en) to acac in the Ru(η^6-arene) core significantly affects the nucleobase binding selectivity[268]. The en complex binds selectively to guanine (via N7), but not adenine, and to cytosine and thymine in the absence of guanine, but still not adenine. Conversely, the acac complex has comparable affinity toward guanosine and adenine (via N1 and N7), but little to cytidine and thymine. The crystal structures of the Ru(η^6-arene)L (L = acac and analogues) complexes with the N-7-bound adenine have been resolved (e.g. the biphenyl derivative **97**)[268a]. Organometallic Ru(II)–arene complexes comprise a large pool of potential chemotherapeutic drugs[158], including $[Ru(arene)(\beta\text{-diketonate})Cl]^+$, that are as active as the cisplatin analogue carboplatin[269]. These compounds target DNA via binding to nucleobases. The structure–activity correlation of several compounds of this family has also been investigated[270]. Some show a lack of cross-resistance with the commonly used anticancer drugs cisplatin and adriamycin from cancer cells.

b. Biosensors and imaging agents. Biological luminescent sensors have been widely utilized for the visualization of fine structures in cells, recognition of specific biological processes such as signaling[271], investigation of protein/enzyme functions and ion

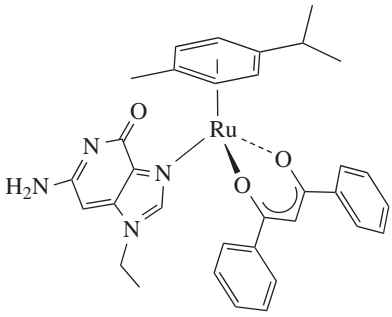

(**97**)

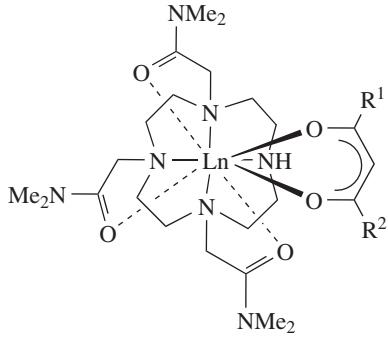

(**98**) (**a**) R^1 = Mef, R^2 = 2-Naph
(**b**) R^1 = Me, R^2 = Ph
(**c**) $R^1 = R^2$ = Ph

sensing under various conditions[272]. A few luminescent macrocyclic complexes of lanthanide(III) β-diketonates (e.g. **98a–c**) have been recently synthesized[273]. For example, **98a**, Ln = Eu(III) and triflate counterions, emits red fluorescence at pH 7.4. The β-diketonate ligand dissociates in acidic or alkaline solutions, quenching the complex emission and exhibiting blue fluorescence due to the dissociated diketone ligand. The biologically important anions bicarbonate and lactate bind more strongly to Eu(III) and can replace the β-diketonate ligand, quenching the red Eu(III) luminescence. An analogue of this complex (which, however, does not contain an enolate moiety) with Tb(III) in place of Eu(III) was also synthesized by the same research group and was demonstrated to sense monobasic phosphate ion ($H_2PO_3^-$)[274].

N-substituted 3-hydroxy-4-pyridinones (such as mimosine **9**) form complexes with Ga(III), suggesting that the ^{67}Ga complexes have potential application as a nuclear imaging agent[275]. Tc-99m compounds have been widely used as diagnostic nuclear imaging agents. The glycoside complex **53** and its ^{99m}Tc(I) analogue have potential as imaging and therapeutic agents, since they may interact with glucose transporters in certain tumor types or accumulate in tumor cells. Tropolone (**77**) forms complexes with ^{99m}Tc[276], ^{111}In[277] and ^{67}Ga[208] which have been verified as a hydrophilic blood labeling agent (Tc), as tracer for platelets labeling (In) and as radiopharmaceutical agents (In and Ga).

IV. METALLOENOLATES AND ASSOCIATED ENZYMES

Enols are involved in many biological processes as inhibitors, cofactors, substrates, intermediates or products. When serving as inhibitors, they frequently are drugs and/or can be the leads for the design of more potential drugs, such as the inhibiting effects of atovaquone (**93**) on cytochrome bc_1 and dihydroorotate dehydrogenase mentioned in Section III.B.2.d[254]. Enols are intermediates in many biological processes such as in sugar metabolism (e.g. during glucose isomerization, triosephosphate isomerization and formation of phosphoenolpyruvate and pyruvate), tryptophan biosynthesis (i.e. during formation of 1-*O*-carboxyphenylamino-1-deoxyribulose-5-phosphate from *N*-5′-phosphoribosylanthranilate) and catalysis by the members of the crotonase (enoyl-CoA hydratase) superfamily through an enolate-CoA thioester intermediate (e.g. reverse Dieckmann conversion of 2-ketocyclohexanecarboxyl-CoA to pimelyl-CoA in the anaerobic degradation of benzoate by *Rhodopseudomonas palustris*). Stabilization of these enol intermediates in enzymes thus accounts for the significant enhancement of the reaction rates. Formation and

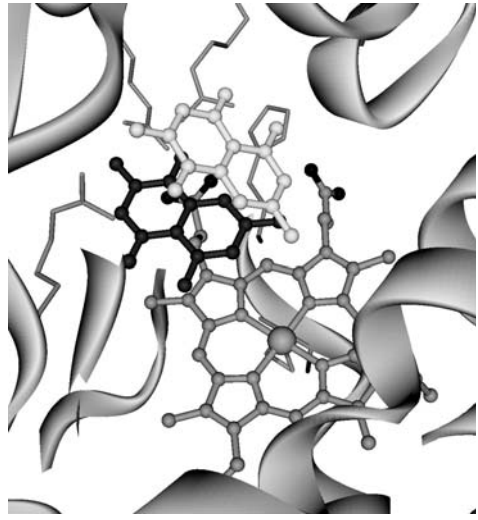

FIGURE 6. Crystal structure of the active center of cytochrome P450 with two bound flaviolin molecules in the active site (PDB ID 1T93, Plate X). The heme is coordinated to the protein chain via Cys353 and H-bonded to Arg71, Arg295 and His351 via the two propionate groups. The two flaviolin molecules are observed on the top of the heme in green and pink, the former is H-bonded to Arg288

further reactions of enol-containing biomolecules and secondary metabolites frequently require involvement of a metal center, wherein interaction of the enol moieties with the metal to afford a metalloenolate is the key step. For example, the oxidation of flaviolin (**30**) by the heme-containing oxidase cytochrome P450 158A2 from *Streptomyces coelicolor* yields a polymer which is assumed to protect the bacterium from UV damage[278]. The crystal structure of the ES complex revealed two flaviolin molecules in the active site, presumably arranged for oxidative coupling between them (Figure 6)[279]. Formation of oxidized flaviolin dimers was confirmed by NMR. When an electron-transfer chain can be established, direct interaction of the enol moieties with the redox-active metal center may not be necessary. There are many metabolic pathways wherein enolates are suggested to be intermediates which are stabilized by H-bonding with protein side chains or by binding to a Lewis acidic metal center. In this section, the metalloenolate centers in enzyme catalysis are discussed.

A. Enols and Associated Enzymes in Glycolysis and Other Sugar Metabolisms

The glycolysis of glucose proceeds through several steps involving enol intermediates to afford pyruvate, which can be converted into acetyl coenzyme A (acetyl-CoA) to participate in the Krebs cycle. Kinetic and crystal structure studies point to the key role played in enzyme catalysis by the stabilization of such intermediates on binding of enolate to the metal ion(s) of the enzymes.

1. Enols in ketose–aldose isomerization

Ketose–aldose isomerases catalyze the interconversion of aldose and ketose in sugar metabolism. Owing to their value in the sugar industry for the preparation of high-fructose

(a ketose) syrup from the more readily available glucose (an aldose) from starch[280], these enzymes have been extensively investigated and a large number of crystal structures of the enzymes from various sources have been solved. Xylose isomerase is a prototype of this enzyme family which primarily catalyzes the interconversion of D-xylose to D-xylulose as well as D-glucose to D-fructose under certain conditions *in vitro*. The catalytic domain has the common structural motif of the eight-stranded α/β barrel (Figure 7A) and contains a well conserved active site with two divalent metal ions (Figure 7B–D)[281], of which Mg(II), Co(II) and Mn(II) ions can activate the enzyme, whereas Ni(II), Ca(II), Ba(II), Zn(II), Cu(II) and Hg(II) ions cannot[282]. Direct binding of substrate and analogues to the metal center has been demonstrated by X-ray crystallography (Figures 7B,C, showing binding of two hydroxylate groups to the metal)[283] and EPR spectroscopy[284], wherein only one of the metal ions is involved in such binding as shown by site-directed mutagenesis with one metal site abolished[285]. The sugar-like ascorbic acid has also been found to bind to one of the metal ions via the 3,4-enediolate moiety (Figure 7D). The mechanism proposed for the aldose (an α-hydroxy aldehyde, **99**) to ketose (an α-hydroxy ketone, **101**)

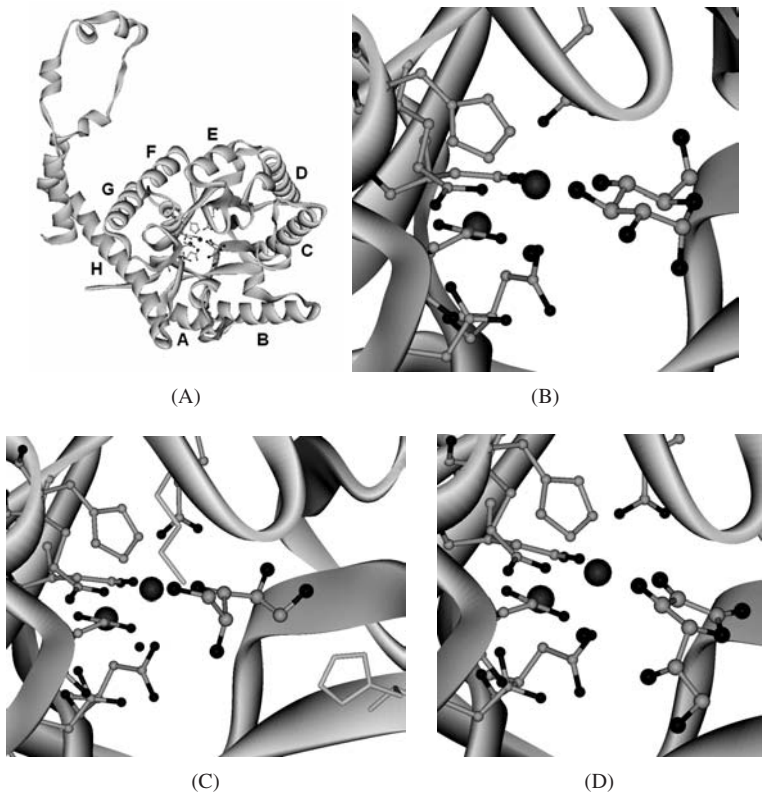

FIGURE 7. (A) Crystal structure of xylose isomerase. The 8 α-helices comprised of the α/β barrel are labeled A–H (PDB ID 1XID, Plate XI). (B) The active site of xylose isomerase with a bound cyclic glucose (1XIF, Plate XII). (C) The active site of xylose isomerase with a bound xylose in linear form (8XIA) and the catalytically important Lys and His (green, Plate XIII). (D) The active site of xylose isomerase with a bound ascorbate via its 3,4-enediolate site (1XID, Plate XIV)

isomerization involves transfer of two hydrogens, taking place in either of two ways: path *a* consisting of proton removal from C2 to yield an enediolate intermediate (**100**) followed by a proton transfer from O2 to O1 and electrophilic attack of a proton at C1, through an enediol intermediate as with triose phosphate isomerase (Section IV.A.3), or path *b* consisting of a direct transfer of a hydride ion from C2–H onto the electropositive C1=O carbon to yield an intermediate carbonium ion (**100′**) and a proton transfer from O2 to O1[283a, 286]. The ketose to aldose conversion involves reversal of these steps. However, the crystallographic studies did not reveal an appropriate base for proton removal from C2 (path *a*), whereas a hydride shift (path *b*) has gained further evidence from kinetic studies[287]. A Lys and a His in the active site are considered important in the catalysis (Figure 7C)[288]. Nevertheless, binding of substrates and analogues to the metal active center in this enzyme (including enediolate binding of ascorbic acid, Figure 7D) points to a possible stabilization mechanism of **100** or **100′**, where an enol with a lower pK_a than an alkoxyl seems to be a more favorable state for binding to the metal center. Moreover, metal binding can lower the apparent pK_a, rendering deprotonation at a lower pH possible even without an assistance of a general base.

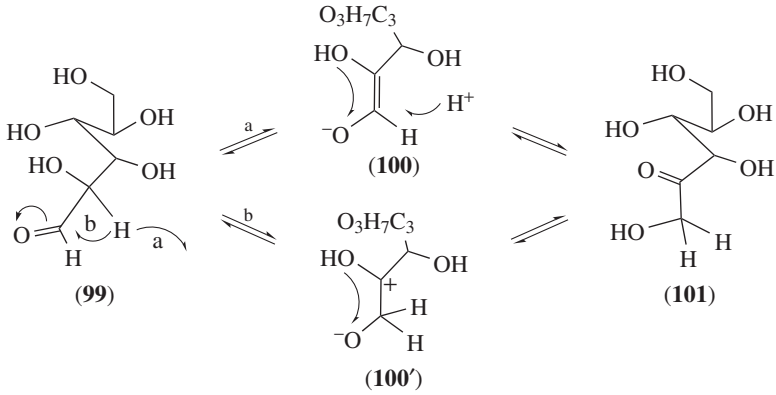

Some rare carbohydrates of significance in industry and medicine, such as D-tagatose as a sweetener and an additive in many products[289], can be produced from more abundant sugars. For example, the conversion of D-galactose to D-tagatose and L-arabinose to L-ribulose can be achieved by L-arabinose isomerase (AI)[290]. This enzyme from *Escherichia coli* has a quaternary structure of a dimer of a trimer (Figure 8A) and a folding different from the $(\alpha/\beta)_8$ barrel folding of xylose isomerase (Figure 7A) and the α/β folding of phosphoglucose isomerase (PGI, Figure 9A), but is analogous to that of the metalloenzyme fucose isomerase from *E. coli* (PDB ID 1FUI, active site shown in Figure 8C) which nevertheless has a very low sequence homology (9.7%)[291]. A putative metal binding site is observed in the AI structure, with ligands from the side chains of Glu306, Glu333, His350 and His450 and two coordinated water molecules, analogous to that of fucose isomerase (Figures 8B,C). However, the electron density at the putative metal site in AI could not be fitted to a metal ion during refinement in the crystallographic study, yet the conservation and similarity between His450, Glu306 and Glu333 with the metal-binding ligands in fucose isomerase (His528, Glu337 and Asp361) suggest this site to be a metal-binding site. It is quite intriguing that this metal binding site has no similarity to the active-site metal centers in all the other sugar-metabolizing enzymes discussed herein, such as xylose isomerase, *Pyrococcus* phosphoglucose isomerase and phosphomannose isomerase. Nevertheless, kinetic studies of AI and its mutants from different sources do

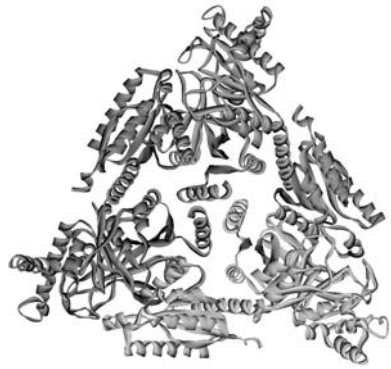

(A)

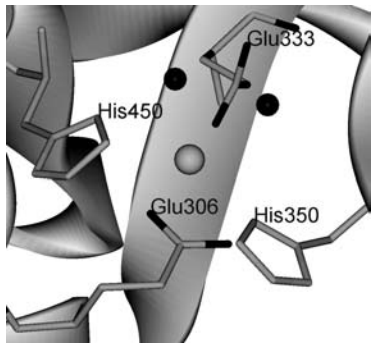

(B)

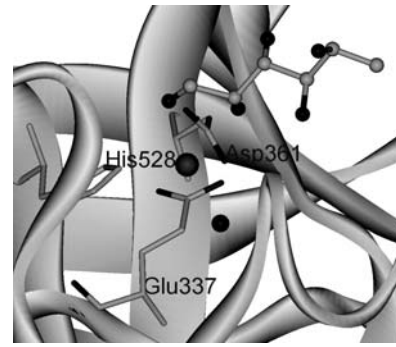

(C)

FIGURE 8. (A) Crystal structure of the trimeric half of hexameric L-arabinose isomerase (AI, PDB ID 2HXG, Plate XV). (B) Putative metal-binding active site of AI. However, Nε and Nδ of His350 do not point toward the proposed metal and may not be a ligand (Plate XVI). (C) Crystal structure of the Mn(II)-binding site of L-fucose isomerase with a bound substrate analogue fucitol replacing two coordinated water molecules seen in the structure of AI (PDB ID 1FUI, Plate XVII). The coordinated water in this structure is at the location of the Nε atom of His350 in AI. The largest red circles in Plates XVI and XVII represent coordinated water molecules

not reveal an essential role of Mn(II) for catalysis[292]. Further mechanistic studies and structural studies with bound substrate or intermediate analogues are needed to reveal the controversy about the putative metal-binding active site in AI.

During the classic Embden–Meyerhof pathway of glycolysis, glucose is first phosphorylated by hexakinase to yield glucose-6-phosphate (**102**), which is then catalyzed by PGI to form fructose-6-phosphate (**104**). Fructose-6-phosphate is further phosphorylated and then cleaved by aldolase (discussed in the next section). PGI catalyzes the interconversion of the two sugar phosphate isomers. Interestingly, the PGI gene was found to be homologous to cytokine neuroleukin[293], the differentiation and maturation mediator of myeloid leukemia cells[294] and the autocrine motility factor[295]. The serum activity of human PGI also serves as a tumor marker in cancers[296]. Purified PGI has been demonstrated to be able to cause the same changes in tumor cell motility and leukemia cell differentiation.

The mechanism for the action of PGI is suggested to involve an enol intermediate (**103**). The structure of rabbit PGI has been determined with or without a bound substrate or analogue[297]. PGI from rabbit is a homodimer with each subunit containing two α/β sandwich domains of 557 amino acids. However, as opposed to xylose/glucose isomerase discussed above, PGI is not a metalloenzyme. The mechanism of catalysis, based on the crystal structure of the rabbit and mouse enzymes[297,298], comprises ring opening of the cyclic sugar substrate, isomerization of the linear form and ring closure to form the cyclic sugar product. The ring opening is assisted by the general acid His388 (sequence of the mouse enzyme) and the general base Lys518 to yield the linear form of the sugar substrate (**102**), followed by a rotation of the C3–C4 bond and proton abstraction by the general base Glu357 to afford an enol intermediate (**103**) which is stabilized by H-bonding interaction with Arg272, protonation at C1 of the enol, wherein isomerization to **104** occurs, followed by C3–C4 bond-rotation and cyclization to the final product.

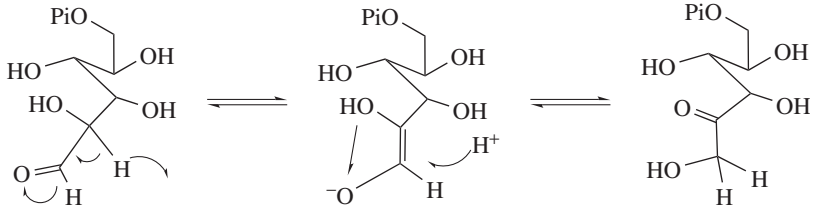

(**102**) (**103**) (**104**)

Archaea metabolize sugars through a modified Embden–Meyerhof pathway[299]. The PGIs from hyperthermophilic archaea *Pyrococcus furiosus*[300] and *Thermococcus litoralis*[301] are quite different from their eukaryote counterpart discussed above. The PGI from *P. furiosus* is a homodimer of two 21.5 kDa subunits (Figure 9A), shares no sequence similarity with the eukaryotic and bacterial counterparts, and is a metalloenzyme. The enzyme can be deactivated by EDTA and fully recovered with $ZnCl_2$[302], wherein the metal is bound to the protein via His and Glu residues (Figures 9B–9D)[302,303]. The *cis*-enediol-mimicking 5-phospho-D-arabinonohydroxamate is a potent inhibitor, suggesting that catalysis goes through a *cis*-enediol pathway. NMR experiments point to chemical exchange between C1 and C2 protons of the substrate and solvent during the catalysis by the enzyme, which also reflects the formation of a *cis*-enediol intermediate since direct hydride transfer would not allow such exchange to occur.

In the crystal structure of the substrate/product complex of the *P. furiosus* enzyme, one carboxylate oxygen of Glu97 is 3.16 and 2.66 Å from C1 and C2, respectively, pointing directly toward the C2H proton (Figure 9B). Similar distances (2.86 and 2.94 Å, respectively) are seen in the corresponding structure of the hydroxamate-bound enzyme (Figure 9C), suggesting that Glu97 may act as the catalytic base in this enzyme. This side chain has also been determined to occupy a similar position as the general base Glu357 in rabbit PGI with respect to the bound 5-phospho-D-arabinonohydroxamate inhibitor, further suggesting the role of Glu97 as a general base in *P. furiosus* PGI and that the enzyme follows a *cis*-enediol mechanism. A schematic presentation of the mechanism is shown below, wherein the metal-bound enolate (**106**) is formed by abstraction of the proton on the C1 (**105**) or C2 (**107**) position by Glu97 which is followed by ketose–aldose isomerization of the sugar.

The ring structure is the predominant form of the substrates glucose and fructose in solution. Ring opening of a sugar substrate prior to isomerization catalyzed by the other PGIs discussed above is assisted by a His side chain. The structure of a bound substrate

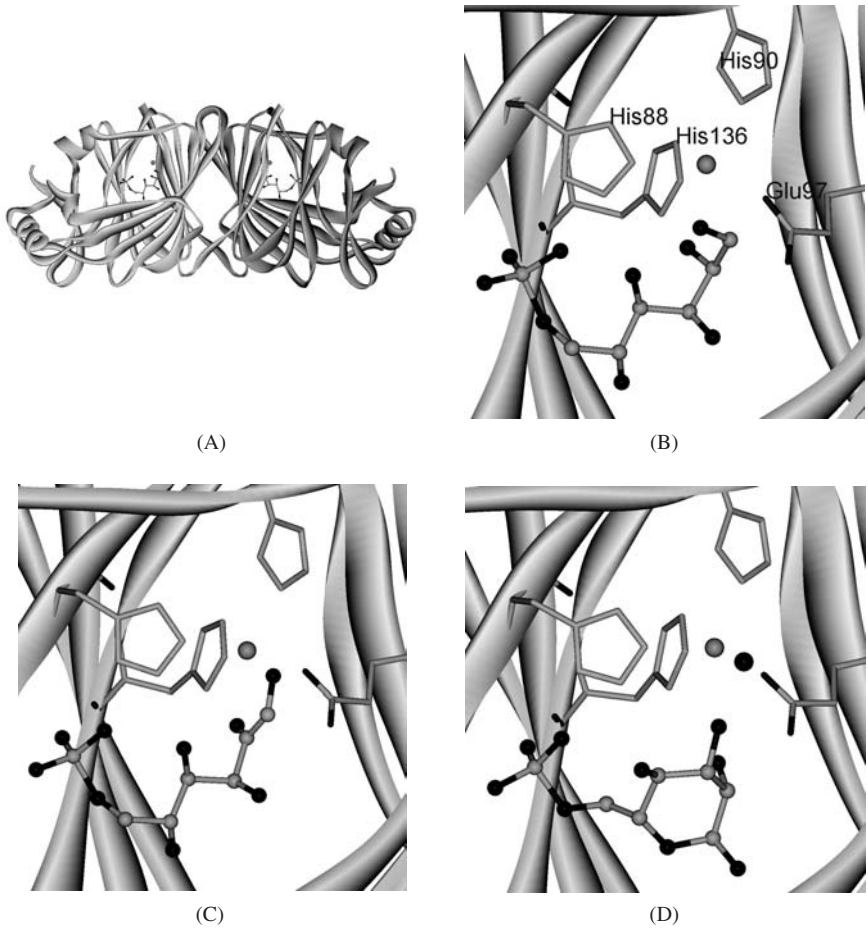

FIGURE 9. (A) Crystal structure of the phosphoglucose isomerase (PGI) dimer from *Pyrococcus furiosus* (PDB ID 2GC2, Plate XVIII). (B) The Zn(II) active site of PGI and a bound phosphofrucose (2GC2, Plate XIX). (C) PGI with a bound 5-phospho-D-arabinonohydroxamate inhibitor (2GC0, Plate XX). (D) PGI with a bound substrate mimic mannose 6-phosphate (2GC3, Plate XXI)

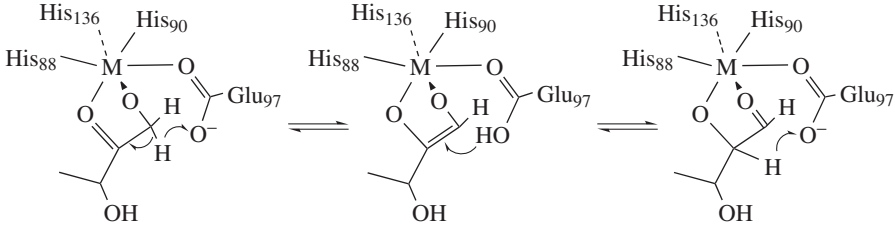

mimic, mannose-6-phosphate, has been determined (Figure 9D). The overall structure of the enzyme remains the same and the configuration of the phosphate moiety of the substrate mimic and its interactions with the enzyme are also preserved, as compared to those of the complex of a linear substrate. However, the metal is bound to a water molecule instead of the ring moiety of the mimic. There is no side chain in *P. furiosus* PGI which seems to play the same role as the His in other PGIs for ring opening. Since the active center of this enzyme can accommodate a sugar of a closed-ring structure, its mechanism is speculated to first bind a sugar substrate with its regular ring structure and then catalyzes the ring opening prior to isomerization. The bound mannose-6-phosphate in Figure 9D may be a 'pre-Michaelis–Menten' ES complex, which may be followed by metal binding. More studies are needed to demonstrate such a hypothesis of the ring-opening step in the action of this enzyme.

Isomerization is an important metabolic pathway for other sugar molecules, such as the conversion of ribose-5-phosphate to ribulose-5-phosphate and vice versa by ribose-5-phosphate isomerase. The latter is involved in CO_2 fixation upon further phosphorylation to generate ribulose-1,5-bisphosphate (Section IV.C). An enediolate is proposed to be an intermediate during this isomerization, which is stabilized by H-bonding to some side chains rather than metal ions discussed above[304]. Similar sugar-metabolizing enzymes in bacteria are potential drug targets, such as the enzyme GmhA that catalyzes the conversion of D-sedoheptulose-7-phosphate into D-glycero-D-mannoheptose-7-phosphate in the guanosine diphosphate (GDP)–heptose pathway for the synthesis of lipopolysaccharide in the outer membrane of Gram-negative bacteria. The structure of this enzyme has been determined, from which an enediol has been proposed to be an intermediate during the isomerization[305]. Once again, Asp65 and His180 serve as general bases for the catalysis, rather than metal ion(s) as Lewis acid(s). Nevertheless, the significance of the enol intermediate in isomerization reactions of carbohydrates is clearly demonstrated.

2. Stabilization of enol intermediates in aldolases and epimerases

Fructose-6-phosphate formed from the isomerization discussed above is further phosphorylated during glycolysis to fructose-1,6-diphosphate (**108**), which is then cleaved by fructose-1,6-bisphosphate aldolase to afford dihydroxyacetone phosphate (**109**) and glyceraldehyde-3-phosphate (**110**). This cleavage reaction is the reverse of an aldol condensation discussed in Section II.C and during gluconeogenesis. In the latter case, fructose-1,6-bisphosphate aldolase catalyzes the reverse reaction herein via aldol condensation of the ketose **109** and the aldose **110** to form linear fructose-1,6-bisphosphate (**108**)[280b].

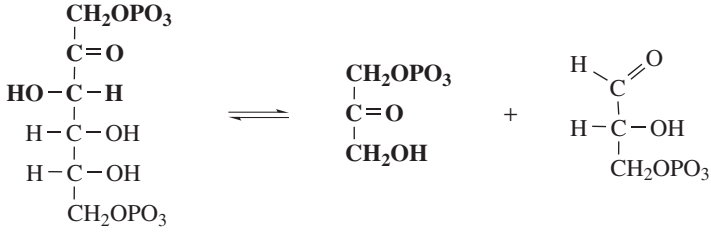

(**108**) (**109**) (**110**)

There are two types of aldolase, type I in animals, plants, protozoa and algae and type II in most bacteria, fungi, yeast, blue-green algae and the parasitic protozoan *Giardia lamblia*. In type I aldolase, the cleavage is enabled by converting the carbonyl group to

the more reactive Schiff base by a Lys side chain in the active site, which is followed by C3–C4 bond cleavage to form glyceraldehyde-3-phosphate and an enol intermediate covalently linked to the enzyme through the Lys. The enol intermediate is then converted back to a Schiff base upon receiving a proton from a His side chain and followed by cleavage of the Schiff base to yield the product dihydroxyacetone phosphate.

Type II aldolases are metalloenzymes which use Zn(II) to polarize the carbonyl group next to the scissile site[306]. The Zn(II) ion in the active site can be replaced by other transition metal ions, Mn(II), Fe(II), Co(II) and Ni(II), to exhibit activities to different extents, attributed to different V_{max} values and similar K_m values[306]. Since $K_m = (k_{-1} + k_{cat})/k_1$, wherein k_{-1}/k_1 is the dissociation constant of the ES complex, the correlation between K_m, k_{cat} and the dissociation constant can be determined. For example, a larger k_{cat} (i.e. V_{max}/[E]) yet similar K_m value of a metal derivative relative to other derivatives indicates that the dissociation constant k_{-1}/k_1 must be smaller correspondingly, reflecting better binding of the substrate to this derivative. Thus, the different V_{max} but similar K_m values from the different metal derivatives of aldolase indicate different dissociation constants for the ES complex of the derivatives, pointing to the importance of the metal in substrate binding and catalysis. Crystal structures of the enzyme from *E. coli* (Figure 10A) and the complex of the enzyme with the transition-state inhibitor phosphoglycolohydroxamate show a dimeric structure with the $(\alpha/\beta)_8$-barrel folding pattern for each subunit and the active-site metal bound to the enzyme through three His side chains (Figure 10B)[307, 308]. The very specific interaction of the enolate-mimicking inhibitor with the enzyme suggests that a metal-bound enolate is likely to be the intermediate in the catalytic pathway of the enzyme. The identity of the metal as Zn(II) is verified with its X-ray absorption edge at 9674.2 eV and the essential role of the residue Asp-83 (Asp-109 in the *E. coli* enzyme[309]) in the active site during catalysis has also been demonstrated with D83A mutant in the enzyme from the human parasite *Giardia lamblia*[308]. Recently, an aldolase isolated from *Deinococcus* was determined to be a Mn(II)-specific enzyme[310]. Based on crystal structure studies, an aldol condensation mechanism mediated by type II aldolase was proposed[308] wherein Glu182 acts as a general base (**111**) to form an enolate intermediate bound to the active-site metal (**112**, **113**), followed by condensation (**113**, **114**).

L-Ribulose-5-phosphate 4-epimerase catalyzes epimerization at the C4 position of L-ribulose-5-phosphate to form D-xylulose-5-phosphate, allowing bacteria to utilize arabinose as an energy source in the pentose phosphate pathway[311]. The enzyme from *E. coli* is comprised of four equal 25.5 kDa subunits and shows very close resemblance to the

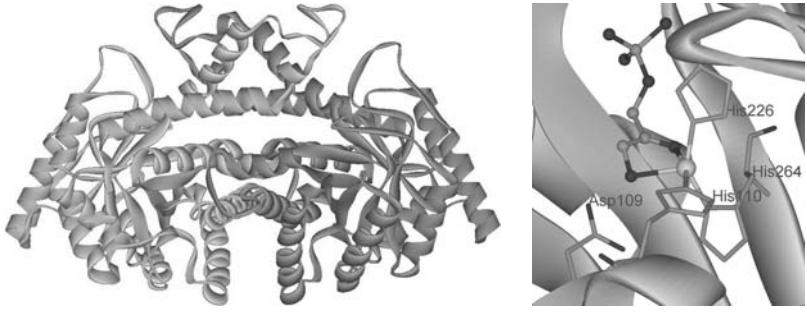

(A) (B)

FIGURE 10. (A) Dimeric structure of *E. coli* type II aldolase (PDB ID 1B57, Plate XXII). (B) The active site showing a bound transition-state inhibitor (phosphoglycolohydroxamate), Zn(II), the coordinated ligands and the catalytically important Asp (Plate XXIII)

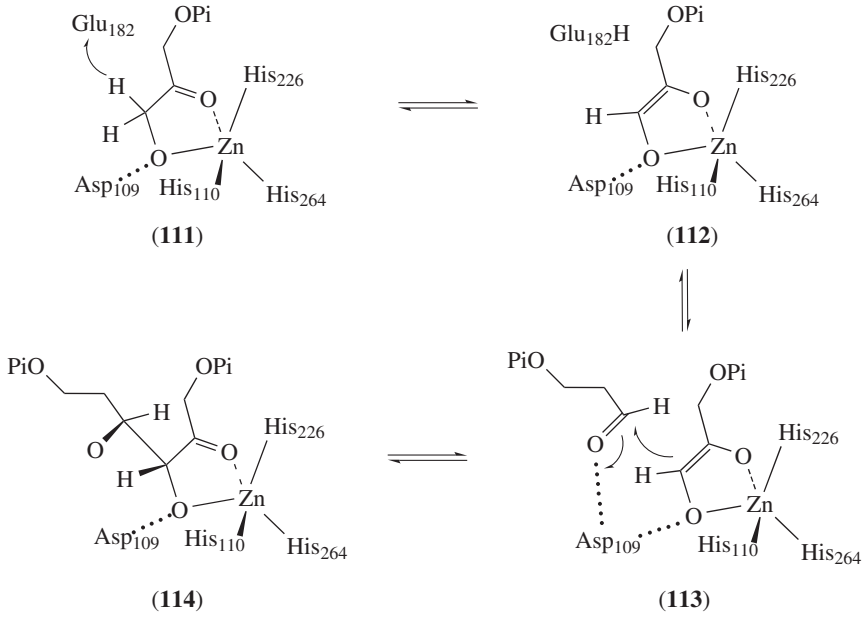

structure of L-fuculose-1-phosphate aldolase discussed above[312]. Like the aldolase, each subunit of the epimerase is comprised of a typical α/β fold (nine β sheets are located between 5 and 3 α helices) with one bound transition metal ion through three His residues (His95, His97 and His171). The activity of the enzyme can be modified by replacing the metal ion in the following increasing order: Mn(II), Co(II), Ni(II), Ca(II), Zn(II) and Mg(II)[313].

One mechanism proposed earlier was the formation of metal-bound enolate intermediate via deprotonation at C3 position. However, a recent study failed to detect a significant deuterium primary kinetic isotope effect which excludes this pathway and suggested an aldolase cleavage mechanism[314], where deprotonation of the substrate (**115**) is followed by bond cleavage (**116**), analogous to the reversed reaction in aldose mechanism (**114** → **113**) discussed above. Cleavage is followed by reposition of the fragments (**117**) and aldol condensation (**118**) to complete the epimerization.

Recently, the crystal structure of epimerases from *Agrobacterium tumefaciens*[315] and *Pseudomonas cichorii*[316] have been determined. These enzymes belong to the family of D-tagatose 3-epimerase (D-TE), which can efficiently catalyze the epimerization of D-tagatose to D-sorbose and D-fructose to D-psicose. The *Agrobacterium* enzyme is specific toward D-psicose, and was dubbed D-psicose 3-epimerase. However, distinct from the epimerases toward phosphorylated sugars discussed above, D-TEs catalyze the steric conversion of non-phosphorylate sugar substrates. These enzymes have an overall $(\alpha/\beta)_8$ folding pattern with similar active site configuration, but different tertiary structure (i.e. a tetramer for the *A. tumefaciens* enzyme and a dimer for the *P. cichorii* enzyme). However, the protein folding pattern and the active-site structure of D-TE are quite different from those of the epimerases discussed above. The active-site Mn(II) in D-psicose 3-epimerase is coordinated by Glu150, Asp183, His209, Glu244 and two water molecules (Figure 11) while the metal active site in *Pseudomonas* D-TE is also conserved with coordinated

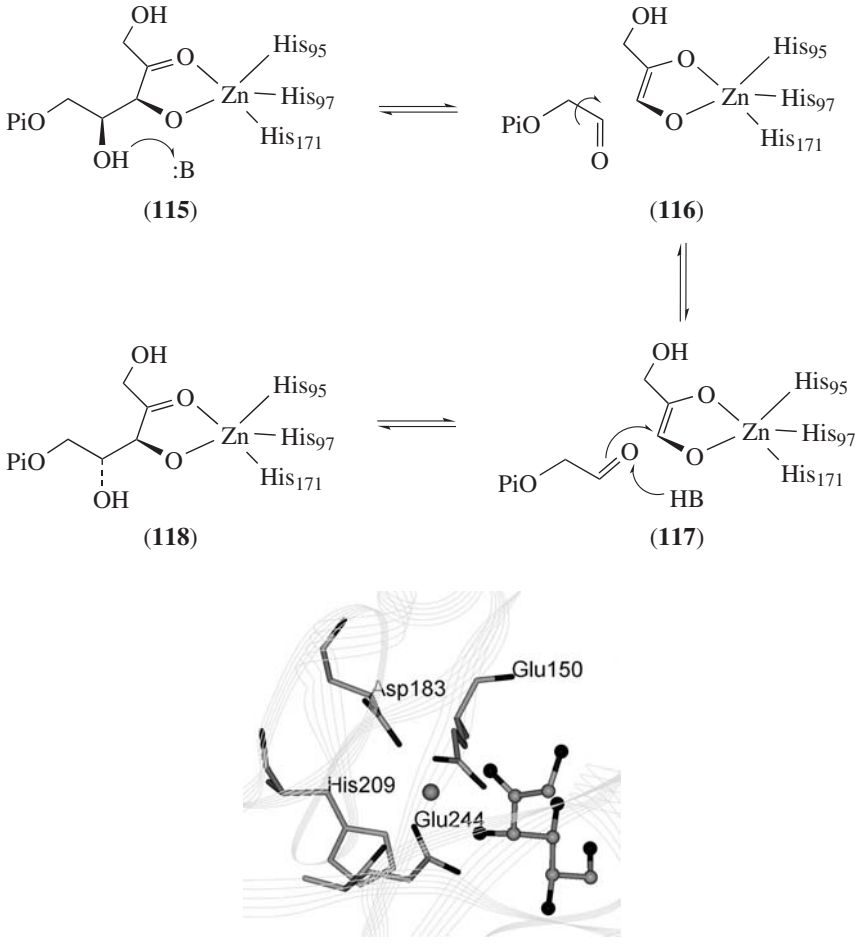

FIGURE 11. Active site of *Agrobacterium* D-psicose-3-epimerase (PDB ID 2HK1, Plate XXIV) with a D-fructose substrate bound to Mn(II) through the hydroxylate groups at C2 and C3

amino acid side chains of Glu152, Asp185, His211 and Glu246. The catalytic mechanism of D-TE is suggested to follow a deprotonation and proton transfer pathway[315,316], different from the aldolase-like mechanism of the epimerases discussed above. Herein, proton abstraction by a general base (**119**) takes place to form a metalloenolate intermediate (**120**), which is then attacked by a general acid from the opposite side (**121**). Upon binding to metal, the apparent pK_a of a ligand would drop significantly. The coordinated Glu244 thus might be too acidic to accept a proton. The general acid in the second step is the coordinated Glu150, which is also too acidic to accept a proton in the first step at neutral pH. This increase in acidity of the coordinated ligands may be partially compensated by a possible lowering of the pK_a of the α-proton and hydroxyl proton on C3 upon metal binding. The E150Q and E244Q mutants did not show activities[315], corroborating the roles of Glu150 and Glu244 in the acid–base reaction mechanism. However, whether

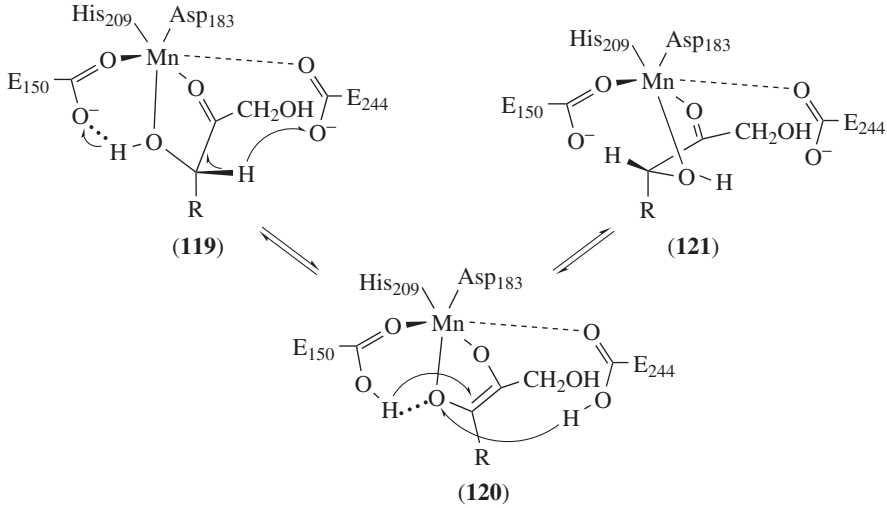

or not metal binding was affected by such mutations was not reported. Further studies are needed to reveal the mechanism of these enzymes of wide potential application.

3. Enolates in triosephosphate isomerase

After fructose-1,6-bisphosphate is cleaved by aldolase to afford dihydroxyacetone phosphate (**122**) and glyceraldehyde-3-phosphate (**124**), the former is further converted to the latter by triosephosphate isomerase (TIM). The structure of this enzyme has the prototypical 'TIM fold' as an $(\alpha/\beta)_8$ barrel (Figure 12), with the active site in one side of the barrel. This protein folding pattern is also found in the structures of hexose isomerases.

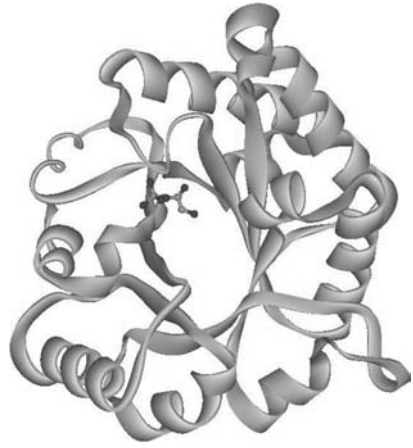

FIGURE 12. Prototypical $(\alpha/\beta)_8$ barrel of the 'TIM fold' of triose phosphate isomerase, containing a transition-state analogue phosphoglycohydroxamate inhibitor (PDB ID 3YPI, Plate XXV)

The detection of tight binding for the inhibitors phosphoglycohydroxamate and phosphoglycolate suggest that the transition state is an enolate intermediate. In the mechanism for TIM action[317] a Glu side chain acts as a general base catalyst, abstracting a proton from **122** to form an enol intermediate (**123**), which is stabilized by H-bonding with a His side chain. Further proton transfer yields **124**, which is subsequently oxidized by glyceraldehyde phosphate dehydrogenase and phosphorylated to afford 1,3-bisphosphoglycerate, dephosphorylated to yield 3-phosphoglycerate and rearranged to 2-phosphoglyceric acid (PGA) by phosphoglycerate mutase. All this is followed by the next unique conversion into phosphoenolpyruvate (PEP) by enolase discussed below. No metal ion is involved in the action of TIM and there is no metallo-counterpart of TIM to date to perform metal-mediated isomerization of trioses.

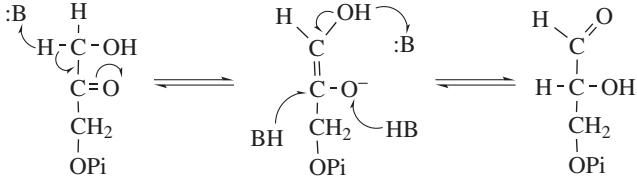

4. Role of metal ions in enolases and the enolase superfamily

Yeast enolase (2-phospho-D-glycerate hydrolyase)[318] is a dimeric enzyme of two identical 46,700 Da subunits. Like the structure of other sugar-metabolizing enzymes, the overall feature of enolase is also an $(\alpha/\beta)_8$-barrel structure along with an $\alpha_4\beta_3$-domain at the *N*-terminus[319]. The active site is located at the center of the barrel (Figure 13A). The high affinity Mg(II)-binding active site is coordinated to Asp246, Glu295, Asp320 and three water molecules. Upon binding of the transition-state inhibitor phosphonoacetohydroxamate, two of the coordinated water molecules are displaced (Figure 13B)[320]. Another Mg(II) is also found in this crystal structure to bind to the inhibitor via one carboxylate oxygen and one phosphate oxygen, 4.19 Å away from the high-affinity Mg(II). This binding mode was further confirmed by the use of Mn(II) as a paramagnetic probe and monitored with EPR spectroscopy on the electron-nuclear magnetic interaction upon binding of ^{17}O-labeled (^{17}O, $I = \frac{5}{2}$) phosphopyruvate[321]. The substrate analogue phosphoglycolate is bound directly to the active-site metal in the yeast enzyme (Figure 13C)[322], different from the lobster enzyme (discussed below) which suggests different possible pathways or different snapshots of the EI complexes.

The enzyme catalyzes the interconversion by dehydration and hydration reactions between PGA and PEP in glycolysis and gluconeogenesis, respectively. In the conversion of PGA to PEP, the reaction is initiated by abstraction of the α-proton of the carboxylate group to generate a phosphoenediolate intermediate that is stabilized by the Mg(II) ions. The activation profiles and deuterium kinetic isotope effects[321] suggest an ordered mechanism, wherein the PGA substrate binds to the enzyme before the second metal ion does, while the release of the PEP product occurs after the departure of the second metal ion. A unique crystal structure of an asymmetric dimer of yeast enolase was resolved with the PGA substrate bound in one subunit (Figure 13D) and the PEP product in the other one (Figure 13E)[323]. A mechanism on the basis of the crystallographic studies consists of removal of the acidic C2–H proton of the substrate by a general base (**125**) to form a *gem*-enediolate that is stabilized by the metal(s) (**126**), followed by β-elimination of the C2–OH hydroxyl group to yield the phosphoenol ester product PEP (**127**).

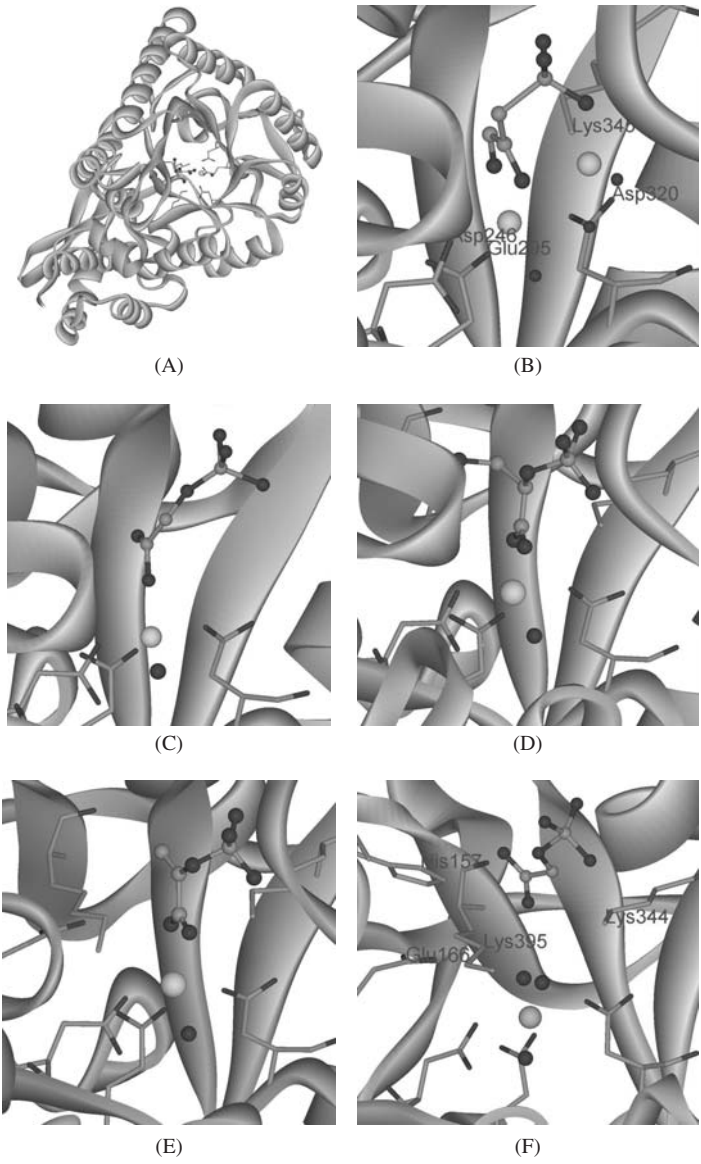

FIGURE 13. Yeast enolase and its active site. (A) One subunit of the enzyme viewed from the top of the $(\alpha/\beta)_8$ barrel and the active site (PDB ID 2ONE, Plate XXVI). (B) The active site shows the coordinated ligands, a bound phosphonoacetohydroxamate and the second metal on the right (1EBG, Plate XXVII). (C) The active site with the bound substrate analogue phosphoglycolate (6ENL, Plate XXVIII). (D) The enzyme has a bound PGA substrate in one subunit (2ONE, Plate XXIX) and (E) the PEP product in another subunit (Plate XXX) to form a mechanistically asymmetric dimer. (F) Active site of lobster enolase with a bound phosphoglycolate inhibitor and those side chains involved in specific interactions (1PDZ, Plate XXXI), showing an EI structure slightly different from that of the yeast enzyme bound with the same inhibitor in (C), wherein the inhibitor is bound to the metal

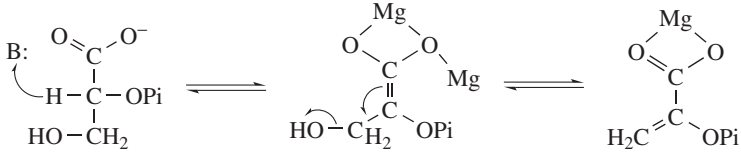

(**125**) (**126**) (**127**)

The enolase from lobster has been expressed and the crystal structures of the apoenzyme and a ternary complex with Mn(II) and the inhibitor phosphoglycolate determined[324]. The Mn(II) ion is bound to three carboxylate side chains and three water molecules as found in the crystal structure of yeast enolase. As opposed to the yeast enzyme shown in Figure 13C, the phosphoglycolate inhibitor does not bind to the metal, but is H-bonded to a coordinated water, and is next to His157, possibly the base that abstracts the C2–H proton, which is followed by removal of the C2–OH hydroxyl group by the metal to form the PEP product (Figure 13F). This suggested mechanism is different from that proposed on the basis of the crystal structure of the yeast enzyme, but consistent with earlier biochemical and spectroscopic data.

There are many enzymes in the functionally diverse enolase superfamily[325]. The overall structural features of these enzymes are similar to the enolase structures, with an α/β barrel active domain and a smaller domain (left lower domain, Figure 13A) where the essential Mg(II) bound to two Asp and one Glu side chains on the third, fourth and fifth β strands. In some cases, however, the active domain is better described as an $(\alpha/\beta)_7\beta$ barrel (e.g. Figure 14A). The enzymes in this superfamily include *O*-succinylbenzoate synthase[326], epimerases[327], racemases[328], the muconate and carboxy lactonizing enzymes (cycloisomerases) in bioconversion of catechol and protocatechuate, respectively[329], acid-sugar

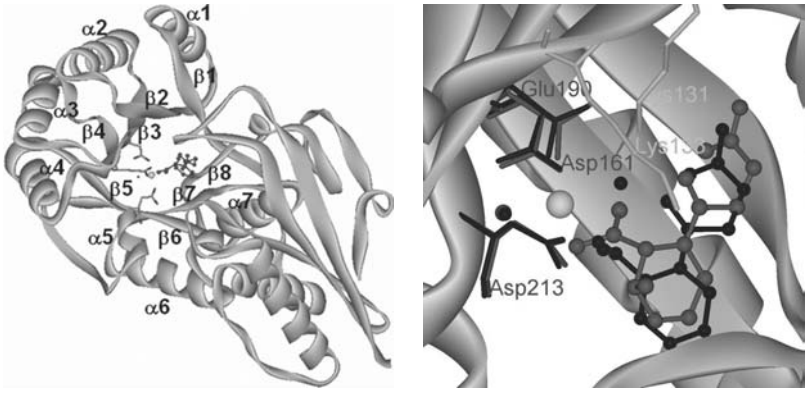

(A) (B)

FIGURE 14. (A) Structure of *O*-succinylbenzoate synthase of the enolase superfamily with an $(\alpha/\beta)_7\beta$ barrel active-site domain as labeled and an α/β domain at the lower-right side (PDB ID 1FHV, Plate XXXII). (B) The product *O*-succinylbenzoate (blue ball-and-stick structure in Plate XXXIII) is bound to the active-site Mg(II) via the carboxylate functionality. The structure with a bound substrate 2-succinyl-6-hydroxy-2,4-cyclohexadiene-1-carboxylate (1R6W, red ball-and-stick structure in Plate XXXIII) is superimposed onto the structure 1FHV to reveal the difference in binding. One of the coordinated water molecules is replaced by the bidentate carboxylate of the substrate

dehydratases found in both bacteria and eukaryotes with six- and five-carbon sugars as substrates[330]. The closeness of these enzymes has also been demonstrated by the easy creation of a 'new activity' via simple mutation, such as the detection of *O*-succinylbenzoate synthase activity on the D297G mutant of L-Ala-D/L-Glu epimerase[331]. Members of this superfamily catalyze reactions of diverse carbon-acid substrates by removal of the α-proton of the substrates, first by a general base of a Lys side chain to form Mg(II)-stabilized enediolate intermediates, followed by various reactions to complete the catalytic pathways for different substrates. The crystal structures of the substrate- and product-bound complexes of *O*-succinylbenzoate synthase have been resolved to show a binding difference of the carboxylate functionality of the substrate and the product (Figure 14B)[326,332]. A metal-bound bidentate *gem*-diolate is proposed to be the transition state on the basis of these structures.

5. Metal–enolate interaction in pyruvate kinase

Dephosphorylation of PEP and transfer of the phosphate to ADP catalyzed by pyruvate kinase is the last step in glycolysis. The structures of this enzyme from various species, bacteria and eukaryotes, are very similar. The catalytic domain of pyruvate kinase (Figure 15) has an overall structural feature of the TIM-fold $(\alpha/\beta)_8$ barrel similar to the structures of triosephosphate isomerase and enolase (Figure 12), with the active site inside the barrel[333]. However, there is an extra all-β-strand subdomain in the structure of pyruvate kinase between the β_3 strand and the α_3 helix. The active center is located within the barrel comprised of a metal ion coordinated to Glu271 and Asp295 in the rabbit enzyme (Glu315 and Asp339 in the human enzyme, Figure 15B). According to the crystal structure of the enzyme with the bound substrate analogue 2-phosphoglycolic acid (Figure 15C)[334], the catalytic activity depends on a monovalent cation interacting with the phosphate group of the substrate. Interaction of a divalent metal ion Mn(II) or Mg(II) and an arginine side chain can further polarize the phosphate group of the substrate to assist the phosphoryl transfer process by the enzyme. The structural similarity suggests that enolase and pyruvate kinase may have evolved from a common ancestral multifunctional enzyme[335].

Pyruvate kinase-catalyzed removal of phosphate from PEP (**128**) yields the unstable intermediate enol form of pyruvate (**129**), presumably stabilized by metal binding (Figure 15B)[336]. The intermediate **129** undergoes fast acid-catalyzed conversion to the keto form of pyruvate (**130**) ($k_{H^+} = 1.7 \times 10^2\ M^{-1}\ s^{-1}$) and can be further enhanced by a general acid or base such as acetic acid ($k_{HOAC} = 0.13\ M^{-1}\ s^{-1}$) and acetate ($k_{OAc^-} = 0.65\ M^{-1}\ s^{-1}$)[337]. One ATP molecule is generated for each pyruvate produced. Pyruvate undergoes oxidative decarboxylation to yield acetyl-CoA and enter the citric acid cycle.

B. Rubisco

Ribulose-1,5-diphosphate carboxylase/oxygenase (Rubisco) is the key enzyme for biofixation of CO_2 in the Calvin cycle taking place in the chloroplasts[338]. Rubisco catalyzes two competing reactions, carboxylation and oxygenation. During carboxylation (which has a relatively small k_{cat}), CO_2 is added to C2 of the pentose substrate, followed by cleavage of the C2–C3 bond to yield two molecules of 3-phosphoglycerate, passing through a metal-stabilized enolate intermediate. In the presence of O_2, the competing photorespiration takes place, wherein O_2 instead of CO_2 attacks the C2 position to finally yield one molecule each of 3-phosphoglycerate and 2-phosphoglycolate.

Over two dozen crystal structures of Rubisco have been resolved. For most cases, the enzyme is assembled into a large complex with 4 large subunits (L; 475 residues) and 4 small subunits (S; 123 residues) assembled as a dimer $(L_4S_4)_2$ of *ca* 550 kDa (Figure 16).

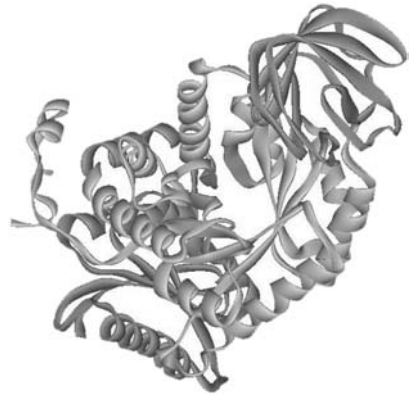

(A)

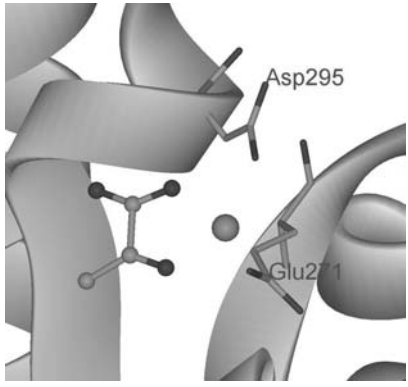

(B)

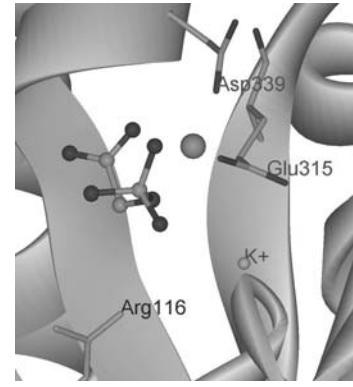

(C)

FIGURE 15. (A) Structure of rabbit muscle pyruvate kinase (PDB ID 1PKN) showing three subdomains: the all-β-strain domain (upper right in the structure, lavender in Plate XXXIV), the catalytic domain (center, cyan in Plate XXXIV) and the α/β domain (lower-left back, brown in Plate XXXIV). (B) The active site of the rabbit enzyme with a bound Mn(II) and the product pyruvate coordinated to the metal (Plate XXXV). (C) The active site of the human enzyme with a bound Mn(II) and the substrate analogue 2-phosphoglycolic acid coordinated to the metal and the essential K^+ and H-bonded to Arg116 (2VGB, Plate XXXVI)

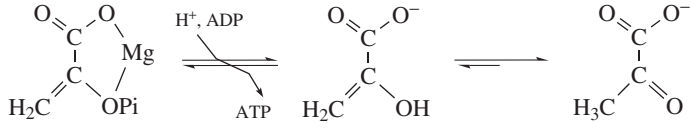

(**128**) (**129**) (**130**)

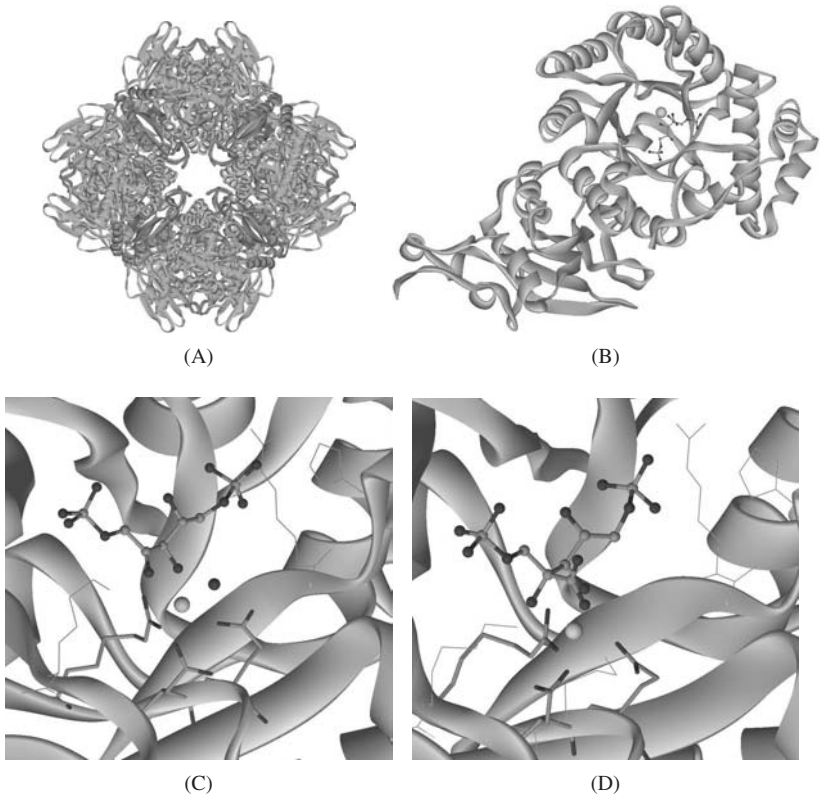

FIGURE 16. (A) Crystal structure of the Ca^{2+}-substituted and inhibitor-bound 'closed state' of spinach Rubisco showing the 16 subunits $(L_4S_4)_2$ of the tertiary structure (PDB ID 1UPM, in Plate XXXVII, L subunits in green/front and cyan/back and S subunits in purple/front and orange/back). (B) The catalytic subunit showing the prototypical enolase folding pattern of an $(\alpha/\beta)_8$-barrel domain and an α/β domain (Plate XXXVIII). (C) Active site of Rubisco with a bound substrate (1RXO) occupying two of the coordination sites of Mg^{2+}, in addition to the specific interactions with Lys175, Arg295 and His298 (thin-line structures, Plate XXXIX). (D) Active site of Rubisco with a bound transition-state analogue 2-carboxyarabinitol-1,5-bisphosphate (1IR2), wherein all the three coordinated water molecules are replaced by the inhibitor (Plate XL)

Variations of the tertiary structure are also observed in different organisms such as algae, dinoflagellates and archaea[338a, 339]. The active-site subunit of Rubisco has a prototypical enolase fold with an $(\alpha/\beta)_8$-barrel subdomain and an α/β subdomain (Figure 16B). The active site of the enzyme is comprised of a Mg(II) ion anchored to the protein backbone via Asp203, Glu204 and the very unique carbamated Lys201 ($-NH-COO^-$) in an octahedral coordination sphere with three coordinated sites occupied by water molecules which can be replaced upon substrate binding (Figure 16C). The post-translational modification of Lys201 by a CO_2 molecule to afford the carbamate is essential for the activation of the enzyme. Herein, CO_2 serves dual roles in the action of Rubisco, for the modification of Lys201 to activate the enzyme and as ribulose carboxylation reagent. Other enzymes also undergo carboxylation at Nζ of a Lys side chain that is involved in metal binding

and catalysis[340], for example, urease[341] and phosphotriesterase[342]. Occupation by Mg(II), Mn(II), Fe(II), Co(II), Ni(II), Cu(II) or Ca(II) in the active site yields the carbamated Lys201[343]; however, Ca(II) fails to catalyze carboxylation[344].

The reaction mechanism for the carboxylation and cleavage of the substrate ribulose-1,5-bisphosphate has been extensively investigated (Figure 17)[345]. Upon substrate binding, the 'open structure' of the active site of Rubisco becomes partially closed; during binding of a transition-state inhibitor the active site adopts a 'closed state', which may reflect the configuration of the transition state of the enzyme during catalysis[346]. Upon binding to the active-site Mg(II), the substrate replaces two of the coordinated water molecules (Figure 17**a**). Herein, the substrate-bound crystal structure of the enzyme reveals that the C3 carbon retains its tetrahedral sp^3 character and the substrate is bound to the metal via the C3–O moiety, i.e. the substrate is bound in its 2-keto form rather than the 2,3-enediolate[347]. Deprotonation of C3–H with the aid of the Lewis acidic Mg(II) and the general base carbamated Lys201 affords an enolate (step ***i*** leading to **b**) accessible to attack by CO_2. The formation of an enolate intermediate was originally proposed by Calvin[348], which was later demonstrated by means of hydrogen isotope exchange experiments[349]. A water molecule is displaced in step ***ii*** from **b** by CO_2 to yield **c**, followed by step ***iii***, a base-promoted attack on the proximal enolate C=C double bond leading to complex **d**, derived from a keto acid, which undergoes bond cleavage at C2–C3 (step ***iv***) to yield a 3-phospho-D-glycerate (3-PG) product and an enediolate product intermediate complex **e**, which in step ***v*** undergoes protonation of the latter to yield 3-PG (**f**), to complete the catalytic cycle. The formation of a 2-carboxyl intermediate has been verified by means of crystallography with the transition-state analogue 2-carboxy-D-arabinitol-1,5-bisphosphate (Figure 16D)[350]. The structure of the product-bound Rubisco has also been resolved to further support the proposed mechanism[351].

In the oxygenation reaction, O_2 attacks at the C2 position of the enolate intermediate and forms an 'eneperoxide' (=C–OOM) intermediate analogous to the metalloenolate

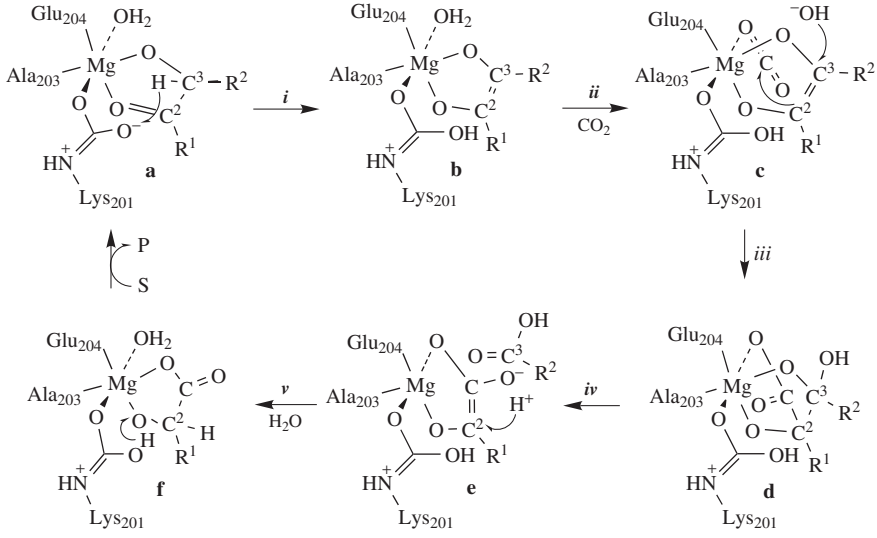

FIGURE 17. Mechanism for the Rubisco-catalyzed carboxylation and cleavage of ribulose 1,5-diphosphate

center in the carboxylation process shown in Figure 17, which undergoes hydration and release of water to yield one molecule each of 3-PG and 2-phosphoglycolate instead of two 3-PG molecules as in the case of carboxylation pathway. In addition to the carboxylation/oxygenation pathway, the enzymes of the Rubisco superfamily exhibit a wide mechanistic diversity[352], including the catalysis of the enolization of 2,3-diketo-5-methylthiopentanyl 1-phosphate to afford phosphoacireductone in the methionine salvage pathway (Section IV.F)[353], wherein 5′-methylthioadenosine is converted to methionine. In this case the enol intermediate is also expected to be stabilized by the active-site Mg(II) ion.

C. Ascorbic Acid Biosynthesis and Biological Roles

Ascorbic acid (**1**) is a prototypical enolic compound with a variety of metal complexes and plays a key role in biological redox reactions. Despite its significance and popularity, the synthetic pathway of AA in higher plants has only very recently been revealed[354], showing that the plant pathway is different from that in mammals. The ultimate precursor for ascorbic acid is glucose. In animals, glucose is eventually converted into L-gulono-1,4-lactone (**131a**), followed by oxidation by gulonolactone oxidase to yield the keto tautomeric form of ascorbic acid 3-keto-gulonolactone (**40**). Humans cannot synthesize ascorbic acid for the lack of this enzyme. In plants[355], glucose is converted to fructose, mannose and then to galactose, which is oxidized to L-galactono-1,4-lactone (**131b**) and then oxidized by galactonolactone oxidase to yield ascorbic acid. Upon further oxidation, dehydroascorbic acid is formed and is commonly referred to as the 'tricarbonyl form (**132**); however, it is not supposed to be stable and has been suggested to adopt a hemiacetal form (**132′**)[356] under physiological conditions. Accordingly, the biosynthesis of AA requires sugar-metabolizing enzymes, including phosphoketose and phosphoaldose isomerases (Section IV.A) such as phosphomannose isomerase (PMI).

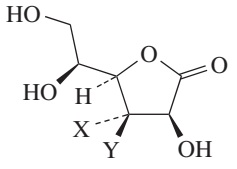

(**131**) (**a**) X = H, Y = OH
(**b**) X = OH, Y = H

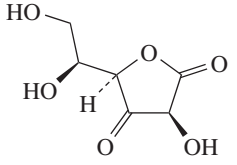

(**40**)

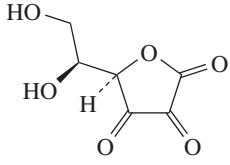

(**132**)

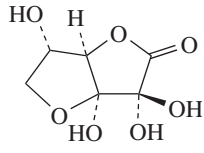

(**132′**)

PMI from the fungus *Candida albicans* is a metalloenzyme of 48.7 kDa, which catalyzes the interconversion of phosphofructose and phosphomannose. The structure of this enzyme is different from that of rabbit PGI (with an α/β-fold and not a metalloenzyme) and those of the few metallo-(phospho-)ketose/aldose isomerases discussed in

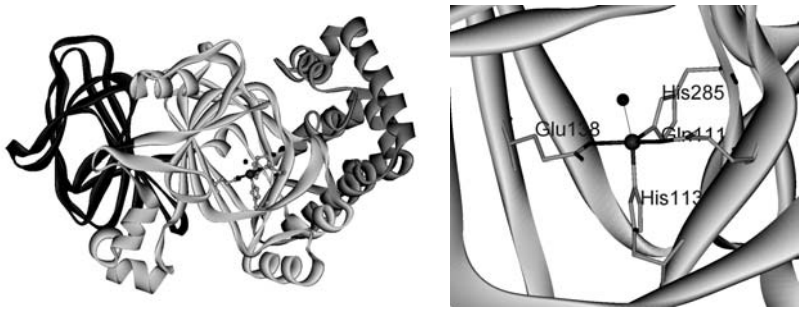

(A) (B)

FIGURE 18. (A) Crystal structure of phosphomannose isomerase from *Candida albicans* (1PMI, 48.7 kDa), comprised of a central catalytic domain (Plate XLI, cyan), a β-roll domain (pink) and a helices domain (brown). (B) The trigonal bipyramidal Zn(II) active site of the enzyme, showing the coordinated water molecule and ligands (Plate XLII)

Section IV.A, such as xylose isomerase (Figure 7) and PGI from *Pyrococcus* (Figure 9). The structure of *Candida* PMI is comprised of three domains (Figure 18A), two cupin-fold domains ('*cupa*' as a small barrel with an extensive β-roll structure)[357], of which one is the catalytic domain and the other an extra β-roll domain, and a helix domain of 8 helices. The catalytic domain contains a Zn(II) ion bound to the protein via Gln111, His113, Glu138 and His285 and a coordinated water molecule to afford a trigonal bipyramidal coordination sphere (Figure 18B). The PMI from *Bacillus subtilis* has a similar overall structure (PDB ID 1qwr), but with a much shorter helix domain of only one helix; the Zn(II) is bound to the protein via His98, Glu116 and His173 and a coordinate water molecule to afford a trigonal bipyramidal coordination sphere, while the Gln111 of *Candida* PMI is replaced by unbound Lys96. This comparison suggests that Gln111 and Lys96 may not play the role of metal binding, but may serve as a general acid or base. Reaction mechanisms with hydride transfer or enediolate intermediate have been proposed. However, the former one has been rejected based on the kinetic isotope effect. Thus, the catalytic mechanism might involve metal binding of the substrate and stabilization of the presumably enediolate intermediate as in other sugar-metabolizing metalloenzymes. A recent theoretical study also suggests such a binding pattern and mechanism[358].

AA (**1**) serves as a reducing agent in many biological processes. When an electron-transfer chain can be established, direct interaction of the enol moieties of AA with the redox-active metal center may not be necessary. In the case of ascorbate peroxidase, the crystal structure of the ascorbate-bound complex reveals that the ascorbate molecule is H-bonded to the 6-propionate group of the heme which presumably mediates electron transfer from the bound ascorbate to the Fe-heme center in the enzyme (Figure 19)[359]. The bound ascorbate is also H-bonded to Lys30 and Arg172. The former one undergoes a significant conformational change upon ascorbate binding.

Ascorbate oxidase is a tetramer; each subunit has 552 amino acids and contains 4 copper ions, the type-I 'blue copper' center and the adjacent 'trinuclear center' (arranged as a type-II center and a type-III dinuclear center) separated by β-sheets (Figure 20)[360]. Ascorbate is oxidized to dehydroascorbate by dioxygen; however, it is not bound directly to the metal center to be oxidized, but is proposed to bind near the type-I Cu site which may facilitate electron transfer to oxygen, presumably in the tri-Cu cluster site. Since humans cannot synthesize ascorbic acid, conservation of this important compound is highly regulated. For example, the oxidized ascorbate can be transported into red blood

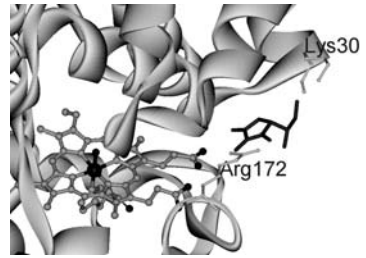

FIGURE 19. Active site of ascorbate peroxidase (1OAF) with the heme anchored to the protein via His163, containing a bound ascorbic acid substrate (pink molecule in Plate XLIII). Ascorbate is H-bonded to the 6-propionate group of the heme and to Lys30 and Arg172 (orange)

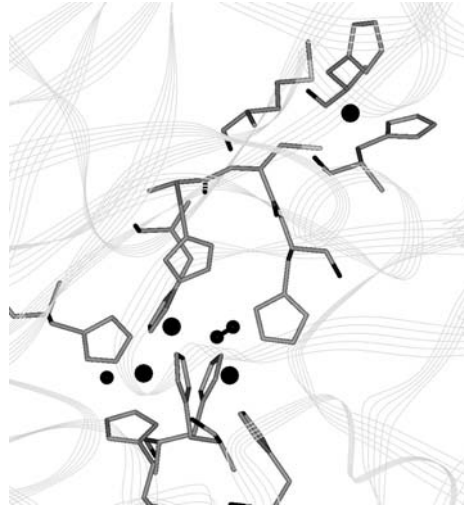

FIGURE 20. Active center of ascorbate oxidase (PDB ID 1ASP, Plate XLIV) showing the blue copper type-I site on the upper-right and the trinuclear center with a bound hydrogen peroxide that mimics dioxygen binding. An electron is expected to be transferred from the bound substrate to the type-I site, then to the trinuclear site and finally to the bound dioxygen which is eventually reduced to water by two molecules of ascorbate

cells via a glucose transport protein which is expressed in humans to a larger extent than in mammals that can synthesize AA[361]. Therefore, humans need only about 1 mg ascorbic acid per kg of body mass per day whereas goats synthesize 200-fold that amount to fulfill their need.

AA serves as an important cofactor for enzymes. Lack of AA in food causes scurvy in humans due to inefficient collagen synthesis, caused by the inactivation of the Fe(II)-activating prolyl hydroxylase and lysyl hydroxylase which catalyze the formation of hydroxyproline and hydroxylysine as essential components for collagens. Prolyl hydroxylases can also hydroxylate conserved prolyl residues in the alpha subunit of the hypoxia-inducible transcription factor, which signals for proteasomal degradation of the transcription factor[362]. The proper action of these hydrolases requires dioxygen, thus they can act

as oxygen-sensors for transcriptional regulation of cellular response to chronic hypoxia. AA is also a cofactor of the Fe-containing ACC oxidase[363] for the production of the plant hormone ethylene (with concomitant production of HCN and H_2O) from ACC and the Fe-containing anthocyanidin synthase[364] during the biosynthesis of the flower-coloring agents anthocyanidins from hydroflavonols (see Section IV.E).

D. Amine Oxidases

Amine oxidases (AOs) are a group of ubiquitous enzymes which catalyze the oxidative deamination of amines, including amino acids and some neurotransmitters, to the corresponding aldehydes with reduction of O_2 to H_2O_2 as illustrated in equation 11 for a primary amine[365]. The ammonia therein is generated as the nitrogen source in microorganisms when amines are the sole nitrogen source. An important case in mammalians is the oxidation of lysine side chains in tropocollagen, catalyzed by lysyl oxidase, a lysine-specific AO, to yield an aldehyde, followed by cross-linking via aldol condensation and dehydration to form an α,β-unsaturated aldehyde linkage.

$$RCH_2NH_3^+ + O_2 + H_2O \longrightarrow RCHO + NH_4^+ + H_2O_2 \qquad (11)$$

The copper-containing AOs catalyze deamination of primary amines by a mono-Cu(II) center (EPR signals at $g_\perp = 2.06$, $g_{||} = 2.30$ and $A_{||} = 152$ G, coordinated by three His residues, Figure 21) in the active site in association with a post-transcriptionally modified tyrosine side chain (Figures 21 and 22A), the *p*-quinone derived from 2,4,5-trihydroxyphenylalanine (topaquinone or TPQ, Figure 22A, **f**), an α-ketoenolate moiety showing an absorption at 472 nm ($\varepsilon = 2400\ M^{-1}\ cm^{-1}$)[366]. The formation of TPQ is self-sustainable by the copper in the active site in the form of Cu(II) or Cu(I) and dioxygen from the air (Figure 22A)[367]. The crystal structures of AO from the various species *Escherichia coli*[368], *Pisum sativum*[369], *Arthrobacter globiformis*[370] and *Hansenula polymorpha*[371] and lysyl oxidase from *Pichia pastoris*[372] have been resolved to provide molecular features of the intrinsic cofactor TPQ, wherein the Cu is shown to bind to the protein through three His side chains and is 2.37 Å from the enolate moiety of TPQ. This conformation results in a non-productive enzyme as the active hydroxyquinone moiety is blocked. The mechanism of TPQ formation in Figure 22A involves binding of the Tyr side chain to the active-center Cu(II) (**a**); electron transfer from the bound phenolate to Cu(II) to afford a phenol cation free radical and Cu(I) (step ***i*** leading to **b**); in step ***ii*** dioxygen

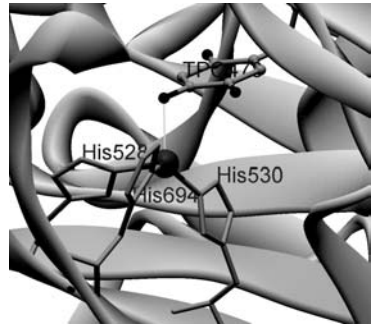

FIGURE 21. Active site structure of amine oxidase (PDB ID 1RKY, Plate XLV), showing the coordinated ligands and the catalytically essential TPQ

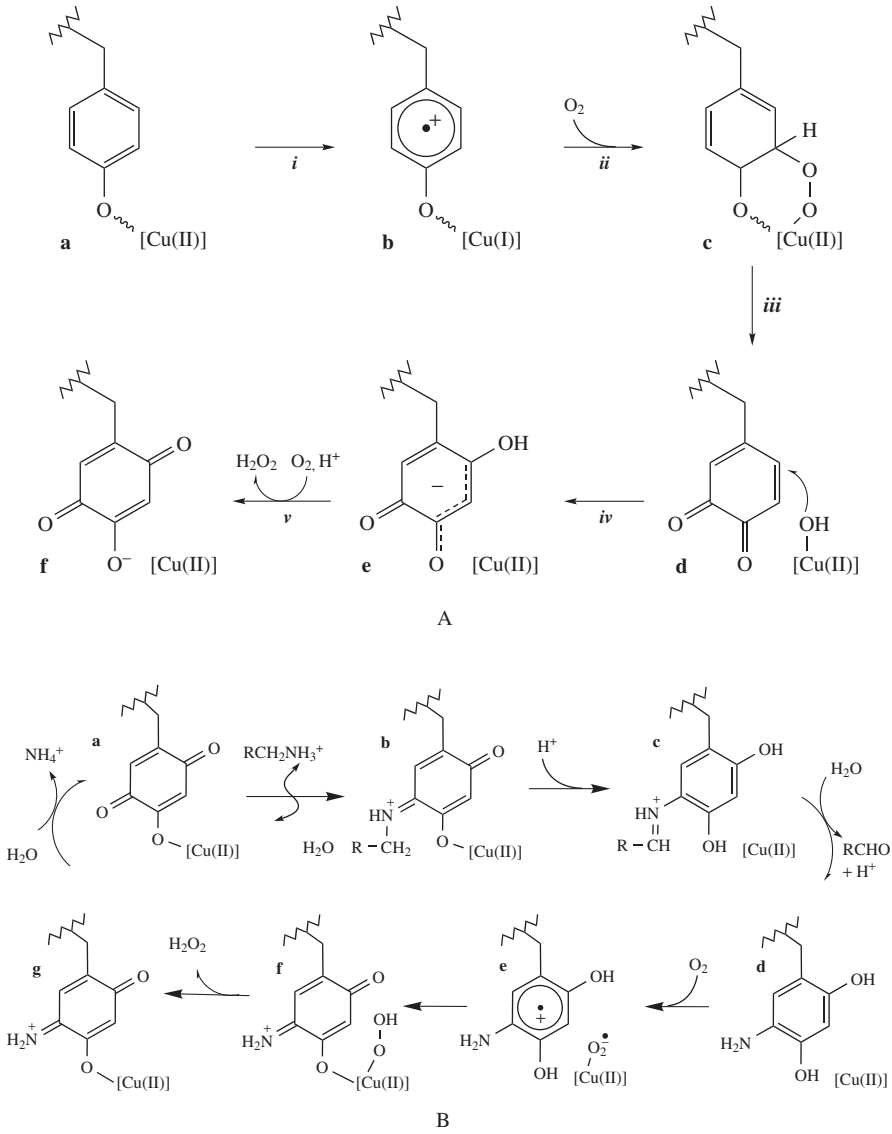

FIGURE 22. (A) O_2-dependent mechanism for the production of TPQ from Tyr478 in amine oxidase, mediated by the active-site Cu(II). (B) Mechanism for the oxidation of amine to aldehyde catalyzed by activated amine oxidase, and regeneration of the TPQ–Cu(II) enolate in the active center

binds to Cu(I) to afford a Cu(II) superoxide center (**c**) coordinated to the phenoxy free radical, which on step ***iii*** rearranges to *o*-quinone **d**; hydroxylation of **d** by Michael addition (step ***iv***) yields intermediate **e**, which is further oxidized (step ***v***) to generate TPQ (**f**) and H_2O_2. Formation of TPQ has been investigated by means of spectroscopic and crystallographic methods and chemical modeling[373]. Optical and crystallographic studies of the mutant D298K (Asp298 is near the TPQ site) reveal the formation of Lys298-modified TPQ[374], further suggesting the self-formation mechanism of the cofactor in AO initiated by the active-site copper.

The mechanism shown in Figure 22B has been proposed for the catalytic action of AOs[376]. Once TPQ is generated by the Cu center, the enzyme becomes active when it adopts a conformation with the 3-keto moiety pointing away from the Cu center (**a**, Figure 22B). A Schiff base salt (**b**) is formed between a primary ammonium salt substrate and the TPQ enolate anion; after proton transfer to neutralize the enolate moiety (**c**) followed by hydrolysis, an aldehyde, the aminocatechol **d** and a Cu(II) center are formed, in equilibrium with aminoquinone and Cu(I). Dioxygen binds to the Cu(I) center to form Cu(II)-superoxide along with the aminoquinone **e**; $H^{\bullet}$ transfer from **e** to the superoxide yield Cu(II) hydroperoxide and TPQ monoimine (**f**), which transfers a proton to the hydroperoxide to release H_2O_2 and form the Cu(II) enolate monoimine **g**; hydrolysis of **g** yields an ammonium salt and regenerates the TPQ–Cu(II) enolate complex of the active enzyme. In an alternative mechanism, dioxygen binds elsewhere and is reduced directly by reduced TPQ and then binds to the Cu(II) center (**e**). The superoxide is further reduced by reduced TPQ (**f**) to yield peroxide and subsequently released; meanwhile an iminoenolate intermediate is formed (**f** → **g**), which is finally hydrolyzed to release ammonia and regenerate the active enzyme.

E. Quercetin 2,5-Dioxygenase

The flavonoids are a most diverse group of natural products with a three-ring molecular framework (**2**), many of which exhibit biological activities, for example, as antioxidants and free radical scavengers, thus being beneficial for oxidative stress-related disorders (Section III.B.1.b). Phenylalanine and malonyl coenzyme A are the two primary precursors for the biosynthesis of flavonoids via the common intermediate metabolites 2′,4′,4-trihydroxychalcone and 2′,4′,6′,4-tetrahydroxychalcone[375]. The latter is the precursor for the flower-coloring anthocyanins and proanthocyanidins as well as the enolic flavonols quercetin (**3a**), kaempferol (**3b**) and myricetin (**3c**). In the case of the flavonols, the α-keto enol moiety is a potential metal-binding site (Section III.B.1.b). The oxidation of leucoanthocyanidins to form anthocyanidins is the penultimate step in the anthocyanin biosynthetic pathway which is catalyzed by Fe-containing anthocyanidin synthase[376]. The metabolisms of these aromatic natural products require dioxygenases to open the stable aromatic ring structures and insert oxygen atom(s). In this section, oxidation of enol-containing flavonoid substrates by quercetin 2,5-dioxygenase and analogous enzymes and the interaction of the enol moiety of the substrates and inhibitors with the metal center in the enzymes are discussed.

Quercetin 2,3-dioxygenase (QD) is the only mononuclear Cu-containing dioxygenase to date which catalyzes the cleavage of ring-C and incorporation of dioxygen into a flavonol substrate such as quercetin (**3a**), to yield 2-protocatechuoyl phloroglucinol carboxylic acid (**133**, Figure 23) with concomitant production of CO. The mechanism in Figure 23 goes through an electron transfer from the bound substrate to the active-site Cu(II) via the ketoenolate functionality (**a**) to generate a free radical at C2 and a Cu(I) center (**b**), which then can bind oxygen in two ways. Attack on the substrate by coupling of the spin-doublet substrate and spin-triplet dioxygen (step ***i***) forms an endoperoxide at C2 and C4 (**c**) followed by oxidative cleavage and removal of CO to yield **133**. Attack of

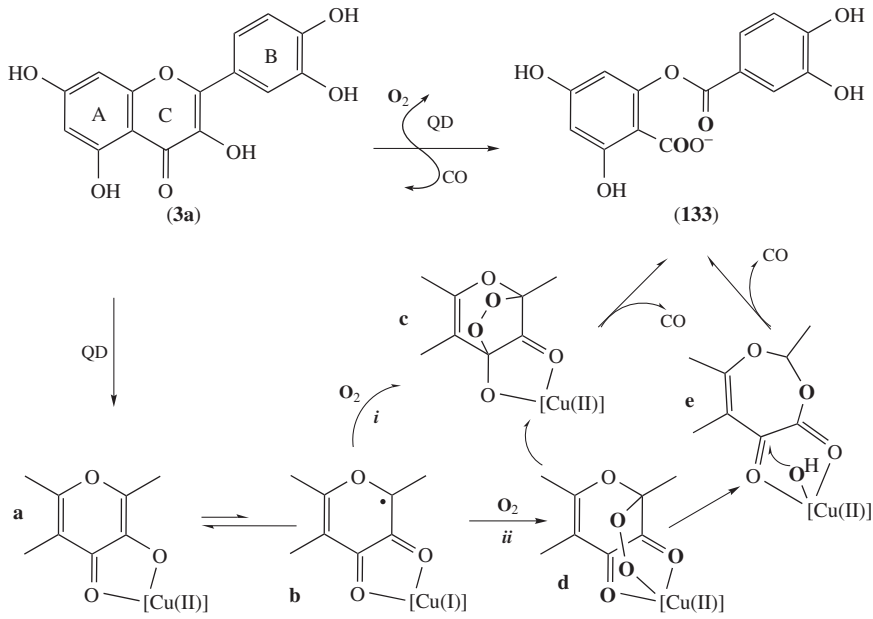

FIGURE 23. Oxidation mechanism of quercetin catalyzed by quercetin 2,3-dioxygenase with ^{18}O shown in boldface

dioxygen on Cu(I) (step ***ii***)[377–379] yields a Cu(II) superoxide intermediate, like in the case of Cu(II)-mediated phenol oxidation[380], followed by coupling with the substrate free radical (**d**), which undergoes rearrangement to form a lactone (**e**), similar to the mechanism for extradiol catechol oxidase, or undergoes nucleophilic attack at the C4 carbonyl as in step ***i***[381] and finally bond cleavage takes place with CO elimination to yield **133**.

Several QDs from different sources have been isolated and characterized, including those from a few *Aspergillus* species[382]. QD from *Penicillium olsonii* has been isolated and sequence determined to be like those from *Aspergillus*[383]. A QD from *Bacillus subtilis* as the YxaG gene product has recently been characterized as an iron-containing enzyme[384]. This enzyme can be activated by various metals (Fe, Cu, Co and Mn), with the highest activity found for the Mn derivative which can be formed stoichiometrically by growing the bacteria in Mn(II)-containing media[385]. The turnover number of this Mn-QD (25 s^{-1}) is nearly 40-fold higher than the corresponding Fe-QD and is similar to the *Aspergillus* enzyme. In an earlier study, the introduction of various metal ions into *Bacillus* apo QD, however, has shown that the Co(II) and Cu(II) derivatives exhibit the highest activities, whereas the Fe(II) reconstituted enzyme shows a much lower activity[386]. Further research is needed to clarify the nature of metal binding and activation.

3-Hydroxyflavone and its derivatives form α-ketoenolate (L) complexes with metals (M) of ML, ML_2 and ML_3 stoichiometry (Section III.B.1.b). Since QD from various sources can be activated by different metal ions, the catalysis of QD has been mimicked with mononuclear Mn(II) and Fe(III) complexes of flavonols, $Mn(II)(L)_2(py)_2$ and $Fe(III)(L)_3$[387]. Upon exposure of these complexes to dioxygen at 95 °C, CO production and the formation of the *O*-benzoylsalicylic acid methylester can be detected with GC-MS, analogous to the products found with QD catalysis. Using *ca* 60% $^{18}O_2$ in the thermal

reaction yields a product where *ca* 60% of the molecules have both carboxylates labeled and the rest is completely unlabeled, while CO is completely unlabeled. These model reactions afford the same products as the QDs and are therefore assumed to proceed via an endoperoxide intermediate.

The crystal structures of QD from *Aspergillus japonicus* and its substrate- and inhibitor-bound forms have been determined[378, 388]. This enzyme is a dimeric protein, wherein each subunit of 350 amino acids has a bicupin folding pattern (Figure 24A)[357], reminiscent of the structure of PMI in ascorbic acid biosynthesis (Section IV.C). The N-terminal cupin domain is the active domain which is comprised of a type-II copper center, whereas the C-terminal cupin domain does not bind a metal ion. The copper in the active site is coordinated to His66, His68, His112 and a water molecule with a distorted tetrahedral geometry (Figure 24B) in the major conformer in the crystals, while the metal is also coordinated with Glu73 to acquire a distorted trigonal bipyramidal coordination geometry in the minor conformer. Glu73 is shown as a general base H-bonded to the coordinated water in the major conformer. There are also two EPR-active species in the enzyme at pH 6.0, a major species with $g_{||} = 2.330$ and $A_{||} = 13.7$ mT and minor species with $g_{||} = 2.290$ and $A_{||} = 12.5$ mT; but only one species is observed at pH 10.0, which suggests a pH-dependent conformational change at the active-site metal center[389]. Such pH-dependent change was also observed in other metalloenzymes, such as the Cu(II) derivative of isopenicillin N synthase[390], wherein only one species at pH 6.0 but two species at pH 7.1 are shown in the EPR spectrum.

Under anaerobic conditions, a substrate can bind to the active-site Cu(II) without being converted to the product. The crystal structure of QD with bound quercetin (**3a**) or kaempferol (**3b**) has been determined under anaerobic conditions (Figure 24C)[391]. The substrate binds to the metal as a monodentate enolate ligand. The binding of a substrate to the enzyme under anaerobic conditions was also investigated with EXAFS, wherein a monodentate binding mode of the substrate was also suggested[379]. Conversely, the inhibitor KA (**10a**) has been determined by crystallography to bind to the enzyme as a bidentate α-ketoenolate ligand (Figure 24D). The binding of quercetin to QD under anaerobic conditions results in a single-species EPR spectrum with $g_{||} = 2.336$ and $A_{||} = 11.4$ mT[389]. The spectrum undergoes further change after substrate turnover, possibly due to a carboxylate-bound product.

The crystal structure of the Fe-containing QD from *B. subtilis* (PDB ID 1Y3T)[386] is very similar to that of *A. japonicus*, in spite of having only 19% sequence identity and 39% similarity. As opposed to the *Aspergillus* enzyme, both cupin domains in the *Bacillus* enzyme contain a metal binding site, coordinated to His62, His64, Glu69 and His103 in one domain and His234, His236, Glu241 and His275 in the other domain. Herein, the Glu is bound to the metal and also H-bonded to the coordinated water. Whether both metal-binding sites function as the active sites and, if so, how these two active sites act cooperatively during catalysis remains to be explored. Similar two-domain structures with two active centers are also observed in the Fe-transport protein transferrin[392] and the bicupin enzyme oxalate decarboxylase[393]. The crystal structures of human (PDB ID 1J1L) and *E. coli* (YhhW gene; 1TQ5) pirin have also been resolved to have a structure similar to that of QD[394, 395]. On the basis of structures and sequence homology, pirin has been assigned to be in the cupin superfamily. Pirin is identified to be a nuclear protein widely expressed in dot-like subnuclear structures in human tissues, proposed to be a transcription cofactor and may be involved in apoptosis, seed germination and seedling development[394, 396]. Pirins are found in a wide variety of organisms, ranging from mammals, plants, fungi and even prokaryotes, and are highly conserved. The human protein contains iron bound to three His and one Glu side chains, while the *E. coli* protein was determined with a Cd ion in the metal-binding site to have only three His side-chain

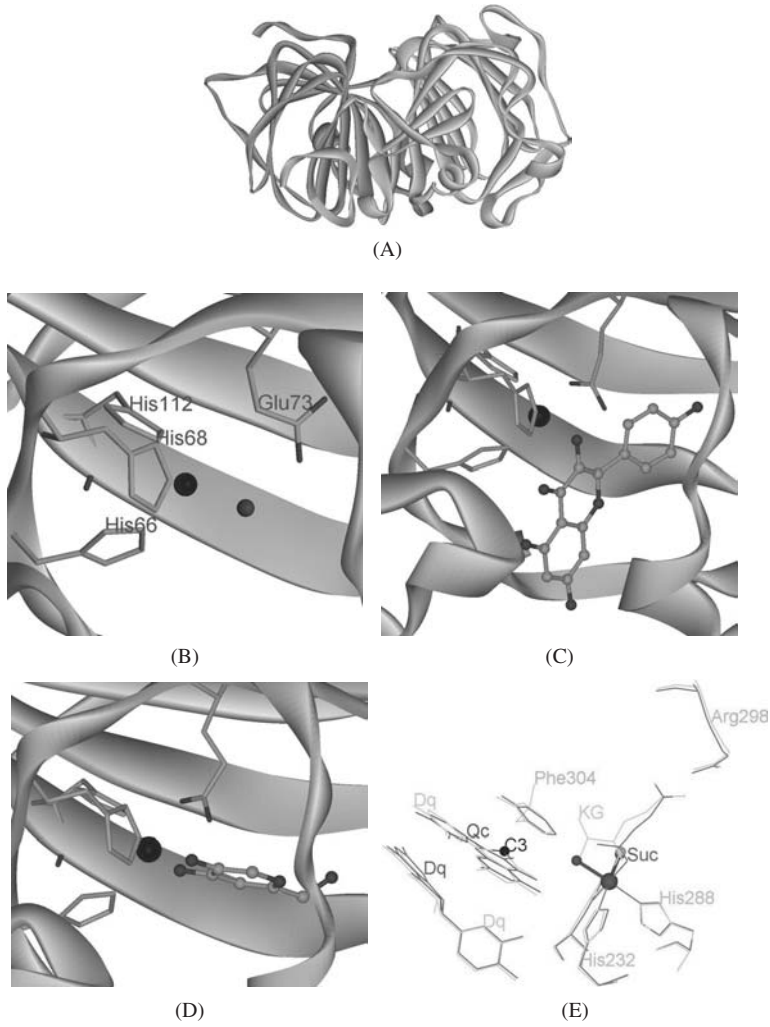

FIGURE 24. (A) Crystal structure of a subunit of the dimeric Cu-containing quercetin 2,5-dioxygenase from *Aspergillus japonicus* (PDB ID 1JUH, Plate XLVI), (B) its active site (Plate XLVII) and (C) its complex with the substrate kaempferol under anaerobic conditions (1H1M, Plate XLVIII). The substrate quercetin is bound in a similar fashion as kaempferol (1H1I). Glu73 is not bound to the metal, but H-bonded to the coordinated water (red sphere in Plate XLVII) in the resting enzyme (B), with a coordinated ligand upon substrate binding. (D) Kojic acid binding of this enzyme (1GQH, Plate XLIX). (E) The active site of anthocyanidin synthase (1GP5, cyan in Plate L) with a coordinated cofactor α-ketoglutamate (KG) H-bonded to Arg298 and two bound substrate molecules (Dq). One substrate is oxidized in the active site after 30-minute exposure to oxygen (1GP6, pink and red in Plate L). Herein the proximal substrate is oxidized to quercetin (Qc) and α-ketoglutamate is decarboxylated into succinate (Suc) and bound to the metal

ligands, despite the presence of a conserved Glu, possibly due to the different metal ion. Both enzymes exhibit QD activity[394].

Conversion of gentisic acid (**134**) to the enolic maleylpyruvic acid (**135**) is part of the flavonone metabolic pathway, catalyzed by the Fe-containing gentisate 1,2-dioxygenase[397]. The *E. coli* enzyme has an overall bicupin structure (2D40)[398], like the structures of human homogentisate 1,2-dioxygenase (1EY2)[399] and QD. The metal is bound to the protein framework through His104, His106 and His145 and three coordinated water molecules, but not a Glu side chain. An EPR study with ^{17}O-labeled substrates revealed significant signal broadening upon binding of substrates labeled with ^{17}O-carboxylate or 2-^{17}OH, but not with 5-^{17}OH, indicating direct binding of the former groups with the metal[400]. Docking of the substrate into the active site of the *E. coli* and the human enzymes also suggests such a binding mode for the substrate[398].

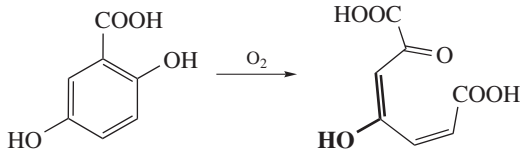

(**134**) (**135**)

Another important enzyme in flavonoid biosynthesis is the Fe-containing anthocyanidin synthase[376]. The crystal structure of this enzyme was solved with two molecules of the substrate analogue *trans*-2,3-dihydroquercetin bound in the active site next to Phe304 via hydrophobic interaction (Dq; Figure 24E)[401], but not coordinated to the metal ion. In one of the substrates the C4=O moiety points to Fe at a distance of 4.14 Å and the proton on the oxidizable C3 carbon is situated 6.18 Å from the metal. Upon exposure to oxygen, the C2–C3 bond of the proximal substrate is oxidized to C2=C3–OH to yield quercetin while α-ketoglutamate is decarboxylated to form succinate and bound to the metal through one carboxylate (KG and Suc; Figure 24E). Despite the metal-binding capability of the α-ketoenolate moiety, the quercetin product is not coordinated to the metal but is situated at the same position as the original substrate (Qc; Figure 24E). The catalysis is proposed to go through an active Fe(IV)=O center, followed by abstraction of the C3H proton, hydroxylation and dehydration to yield the product[401].

F. Acireductone Dioxygenase

Since cellular proliferation requires elevated levels of polyamines, the polyamine biosynthetic pathway has thus become a therapeutic target for proliferative diseases such as cancers[402]. During the synthesis of polyamines, the propylamine moiety from *S*-adenosyl-3-methylthiopropanamine (Figure 25**b**), formed by decarboxylation of *S*-adenosylmethionine (Figure 25**a**), is transferred to putrescine, $H_2N(CH_2)_4NH_2$, to form spermidine, $H_2N(CH_2)_4NH(CH_2)_3NH_2$ or to spermidine to yield spermine, $H_2N(CH_2)_3HN(CH_2)_4NH(CH_2)_3NH_2$, with concomitant production of 5′-methylthioadenosine (Figure 25**c**). *S*-adenosylmethionine is also the precursor of ACC in plants for the synthesis of the universal plant hormone ethylene (Section IV.C)[363]. Thus, a buildup of **c** may have a feedback effect on polyamine and ethylene biosynthesis. It is removed through the 'methionine salvage' pathway wherein **c** is converted to methylthioribose, undergoes phosphorylation, isomerization to the corresponding 5′-methylthioribulose-1-phosphate (Section IV.A.1), dehydration, enolation (Sections IV.A.4 and IV.B) and dephosphorylation to the dienol intermediate acireductone (Figure 25**d**),

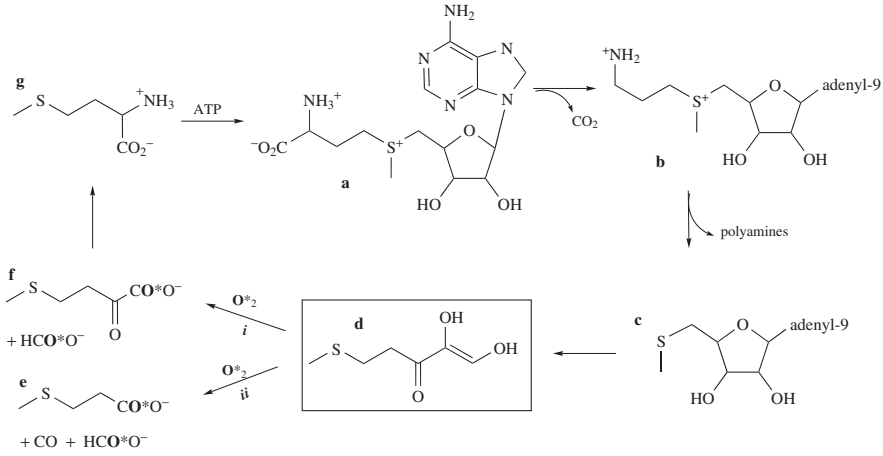

FIGURE 25. Pathways for formation and decomposition of acireductone (**d**)

which is followed by methionine (**g**) regeneration (path ***i***) via oxidative cleavage to 2-keto-4-methylthiobutyrate (**f**) and transamination[352].

The alternative oxidative cleavage of acireductone (Figure 25, path ***ii***) produces 3-methylthiopropanoate (**e**) along with formate and CO[403], and cannot maintain regular polyamine and ethylene synthesis due to methionine depletion. Interestingly, both oxidative paths are catalyzed by the same enzyme, acireductone dioxygenase; however, the pathway ***i*** is catalyzed by the enzyme when Fe(II) is in the active site while the pathway ***ii*** is catalyzed by the enzyme when Ni(II) or Co(II) is in the active site. This enzyme was thus referred to as 'one protein, two enzymes'[404]. Since different metal ions have different structural and chemical properties, changing of the active-site metal ion or ions in metalloenzymes can be expected to alter the catalytic properties of the enzymes which may potentially broaden the applications of metalloenzymes[405]. Two recent examples are the replacement of the native Zn(II) ion in carbonic anhydrase with the redox-active Mn(II) ion to afford peroxidase activity[406] and the substitution of the redox-active Cu(II) for the Zn(II) in dinuclear aminopeptidase to exhibit catechol oxidase activity[407].

A mechanism for acireductone (**a** in Figure 26) oxidation catalyzed by acireductone dioxygenase was proposed[408] wherein dioxygen attacks at position 1 (**h**) closes to 1,2-endoperoxide **d** and yields 2-keto-3-methylthiopropanoate (**g**), or alternatively, closes to 1,3-endoperoxide **i** yielding 3-methylthiopropanoate (**j**); however, the role of different metal ions in the process was not discussed. Later kinetic studies[403] revealed that the enzymes do not bind dioxygen in the absence of the substrate. Conversely, the substrate can bind to the enzyme without dioxygen, most likely as a dianion, based on the UV-vis spectrum of the ES complex. Free radical generation during catalysis was also excluded from the studies therein by the use of a cyclopropyl substrate analogue. Whether or not the substrate is bound to the metal was not certain in the studies. However, it has been demonstrated that metal binding and deprotonation of a ligand can cause the same change in spectral properties as shown by the orange-to-purple change for anthracyclines and their metal binding[409]. Moreover, because metal ions can stabilize the enolate form during catalysis, as with the metalloenzymes discussed in the preceding sections, inclusion of a metal ion can be proposed with slight modification of the previously proposed mechanism[403,410]. In path ***i*** for the Fe(II) enzyme, binding of the substrate to the metal

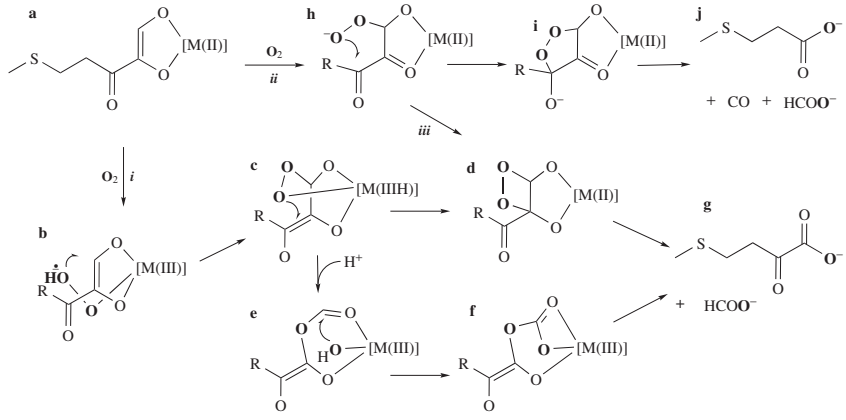

FIGURE 26. Mechanism of acireductone oxidation catalyzed by acireductone dioxygenase, with the atoms from O_2 in boldface

precedes dioxygen binding to afford a transient Fe(III)–O–O$^{\bullet}$ moiety (**b**), followed by attack at C1 (**c**), then at C2 to afford the 1,2-endoperoxide **d**, which then decomposes to yield **g** and methanoate. Alternatively, a Baeyer–Villiger rearrangement of **c**, as in the case of catechol dioxygenase[381], affords intermediate **e**, which undergoes nucleophilic attack by a metal-bound oxide to **f**, followed by reduction–hydrolysis steps to yield the final products. In path ***ii*** for the Ni(II) or Co(II) enzymes, the active-site metal may be restricted to a divalent oxidation state. Nevertheless, binding of the substrate to the metal center may polarize the enol moiety and render dioxygen attack possible (**h**), which is followed by a further nucleophilic attack to afford the 1,3-endoperoxide **i** (as the 'metallo counterpart' suggested above[403]), from which CO is generated as a byproduct, as in the mechanism for oxygenation and cleavage of quercetin by QD (Section IV.E).

Despite the fact that the metal can facilitate oxidative cleavage via polarization of the enolate group, the substrate is known to undergo autooxidation and cleavage in the absence of the enzyme, reflecting a non-metal-mediated reaction pathway. A recent DFT calculation of the autooxidation of acireductone indicates possible involvement of a free radical[411]. Path ***iii*** was proposed for the non-metal-mediated catalysis by the Fe(II) enzyme, with intermediate **h** yielding the 1,2-endoperoxide **d** and the products of path ***i***[410]. Presumably, the C1–C2 bond cleavage could also be achieved through an exodiol catalytic mechanism of dioxygenase by means of the binding of the 2,3-ketoenolate functionality. The intrinsic roles of the different metal ions in the proposed pathways ***i*** and ***ii*** and the substrate-binding coordination chemistry are inconclusive at this stage, and await future exploration of structures of the enzymes with bound substrate or transition-state analogues.

The Ni(II) and Fe(II) forms of the enzyme are separable on an anion exchange or a hydrophobic column[404]. The crystal structure of the Ni(II) form from house mouse (PDB ID 1VR3)[412] and the solution structures of both the Ni(II) (1ZRR)[410,413] and the Fe(II) (2HJI)[414] forms of the enzyme from *Klebsiella pneumoniae* have been resolved to be comprised of a cupin-fold β-barrel (Figure 27A). The active-site metal (Figure 27B) has a distorted octahedral coordination sphere and is bound to the protein framework via three His and one Glu side chains, leaving two sites for water binding which presumably can be replaced by substrate during catalysis. Future structural studies about substrate binding modes in the ES complexes and the transition state are expected to provide further insight

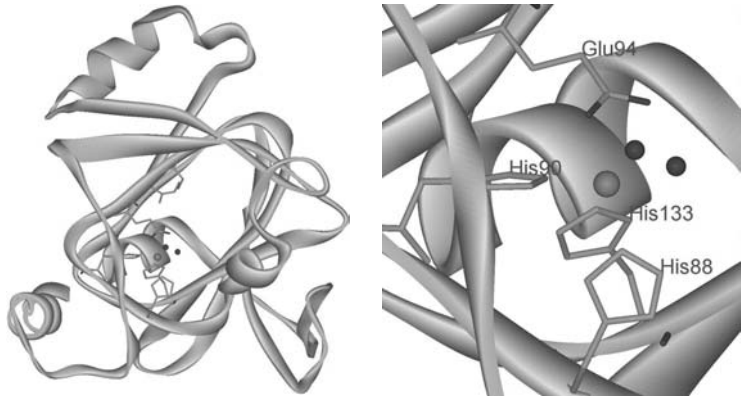

(A) (B)

FIGURE 27. (A) Crystal structure (1VR3) of house mouse acireductone dioxygenase showing a cupin fold (Plate LI). (B) The active site showing a bound Ni(II) and two coordinated water molecules (red sphere, Plate LII)

into the mechanisms for the two different pathways by the two different metal forms of the enzyme.

A Ni(II) complex of tetradentate ligand **136** serves as a chemical model for the Ni form of acireductone dioxygenase[415]. It can bind the substrate-analogous β-diketonate **137** to form a ternary complex with a distorted octahedral coordination sphere (Figure 28)[415a]. The crystal structure of this complex confirms the formation of a delocalized β-diketonate structure since the two Ni−O distances are the same. In this case, the β-diketonate ligand would bind to the metal as a monoanion, as opposed to the dianionic form of the substrate upon binding to the enzyme[403]. CO is produced upon addition of O_2 to the complex in MeCN solution at room temperature. The final product of the reaction is the parent complex with two coordinated benzoate anions. Further analysis of the products revealed the presence of benzil (diphenylethanedione) which was suggested to be produced by a path different from that of benzoate and CO[415b]. When $^{18}O_2$ is used in the experiment, one ^{18}O atom is incorporated into the benzoate product which indicates a dioxygenase activity. If the β-ketoenolate binding mode of the substrate is indeed the reactive species, the reaction at the step from **h** to **i** in the reaction mechanisms of the enzyme would undergo a rearrangement of the coordination from 1,2-enediolate to β-diketonate. It was noted in this

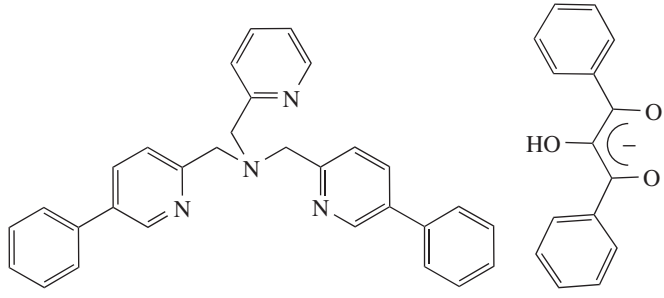

(**136**) (**137**)

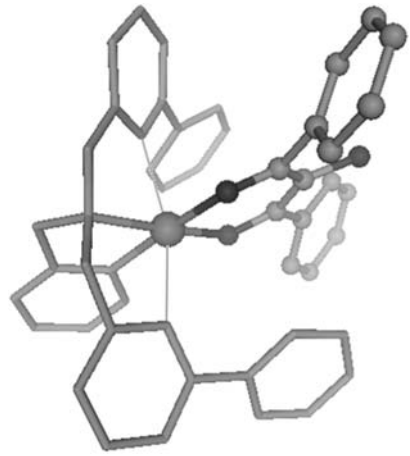

FIGURE 28. Structure of a chemical model complex of the Ni(II) variant of acireductone dioxygenase: Tetradentate *N*,*N*-bis(6-phenyl-2-pyridylmethyl)-*N*-(2-pyridylmethyl)amine (**136**) coordinated to a Ni(II) chelate of monoanionic 2-hydroxy-1,3-diphenylpropan-1,3-dionate (**137**, on the right side) acting as substrate analogue. In the distorted tetragonal bipyramidal complex, the tertiary amine, the pyridine and the chelate (Ni–O bond lengths of 1.95 and 1.99 Å) are in the equatorial positions while the two phenylpyridine moieties occupy the axial positions (Ni–N bond lengths of 2.27 and 2.32 Å)

modeling study that the dianionic form of the complex offered a 'cleaner reaction with O_2' with a higher yield of labeled benzoate product, which was also proposed as an alternative pathway avoiding generation of products such as benzil. These observations indicate the binding mode, i.e. a monoanionic β-ketoenolate versus a dianionic 1,2-dienolate binding, of the substrate may be of significance for the catalysis. Moreover, chemical modeling of the corresponding catalysis by the Fe form of the enzyme is needed to provide further mechanistic insight into the action of the enzyme in the methionine salvage pathway.

G. β-Diketone-cleaving Enzymes

The β-diketone and β-ketocarboxyl functional groups are commonly seen in natural products, such as the tetracycline antibiotics (**8**), the beer ingredient humulone (**12**) and the food spice curcumin (**20**), in intermediate metabolites, such as those obtained after cleavage of gentisate and other polyphenols as well as the oxidation product of polyvinylalcohol[416], and the products of Claisen condensation (equations 2 and 4); all these compounds containing the β-diketo moiety coexist with their β-ketoenol tautomer. Due to the acidic nature of the α-proton(s) and the polarity of the C=O bond, the β-diketone moiety can be attacked by a general base and/or nucleophile and the intermediate stabilized by one or more metal ions and/or via H-bonding during hydrolytic or oxidative cleavage of the β-diketone moiety by several enzymes[417].

1. Hydrolytic cleavage

The C–C bond is commonly considered inert toward hydrolysis relative to the more hydrolytically accessible ester (C–O), thioester (C–S) and phosphoester (P–O) bonds, and thus its hydrolysis has been considerably less studied. However, due to the acidity

of the α-protons of a β-diketone or β-ketoester, the O=C–CH_nC=O, $n = 1, 2$, bond is prone to hydrolysis by several enzymes, by a retro-Claisen reaction (e.g. reversal of equations 3 and 4), either by a hydroxide or another nucleophile, to produce a carboxylate anion and a ketone[418]. Despite the lack of broad investigation, these unique hydrolytic enzymes are ubiquitous.

The enzymes of the crotonase (enoyl-CoA hydratase) superfamily[419] catalyze the hydrolyses of β-ketocarboxy-CoA substrates at the Cα–Cβ bond by a retro-Claisen pathway via nucleophilic attack at the keto group, bond cleavage to form an enolate and proton transfer to form the products with $-COO^-$ and $-C^*H_2CO$-CoA moieties. An inversion takes place at C*, verified using D_2O as the nucleophile to produce $-C^*HDCO$-CoA[420]. These enzymes are not metalloenzymes, wherein the stabilization of the enolate intermediates is through H-bonding with well-oriented peptide NH protons. Recently, a new member of this superfamily from *Rhodococcus* was found to catalyze the conversion of the bicyclic diketone 6-oxocamphor to R-campholinic acid[421]. An enzyme from *Anabaena* catalyzes the convertion of 1-methylbicyclo[2.2.2]octane-2,6-dione (**138**) to (*S*)-(4-methyl-3-oxocyclohexyl)acetic acid (**141**)[422]. Both enzymes act on substrates that lack the acyl-CoA thioester moiety, but contain a β-diketone moiety and, according to the crystal structures, the enolate intermediates are stabilized by H-bonding with a His side chain rather than peptidyl NH groups. In the case of the *Anabaena* enzyme, the nucleophilic water shown besides **138** is H-bonded to the dyad His144–Asp141, which greatly enhances the nucleophilicity of water, analogous to nucleophilic Ser in the Ser–His–Asp catalytic triad of serine proteases. Nucleophilic attack by water yields **139**, which is followed by bond cleavage and formation of enolate **140**, stabilized by the His121 side chain. The interactions and stabilization described herein are also seen in β-diketone metallohydrolases, wherein the metal ions serves as the Lewis acids, analogous to the protons in the non-metalloenzymes.

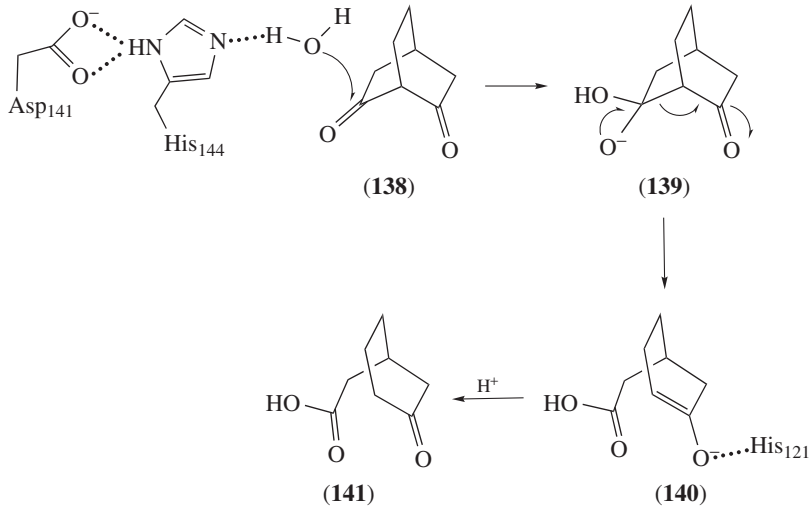

The cleavage of β-diketo acid is commonly seen in polyphenol metabolism and degradation such as orcinol (5-methylbenzene-1,3-diol) catabolism in *Pseudomonas putida*. Acetylpyruvate hydrolase (*ca* 38 kDa) is the terminal enzyme of orcinol catabolism, catalyzing the conversion of acetylpyruvate into acetate and pyruvate (equation 12)[423].

However, the analogous maleylpyruvate, fumarylpyruvate, acetoacetate, oxalacetate and acetylacetonate are not hydrolyzed by this enzyme. Mg(II), Mn(II), Co(II), Ca(II) or Zn(II) enhance the enzyme activity, while Cu(II) is inhibitory. Three forms of acetylpyruvate can be differentiated in aqueous solution by the ^{1}H NMR signal of the methyl group, namely diketone (2.21 ppm), enol (2.13 ppm) and hydrate (2.11 ppm) and also for the similar 4-*t*-butyl-2,4- diketobutanoate, with much clearer methyl signals for quantitative determination[424]. The enol signal undergoes the fastest decrease upon introduction of the enzyme, pointing to the enol as the 'true substrate'. A reaction mechanism was proposed to involve binding of Mg(II) to deprotonated α-enolcarboxylate to form the ES complex (**142**). The keto group is attacked by nucleophilic water to form a tetrahedral transition state (**143**), followed by cleaving to yield the final products. This mechanism is analogous to the hydrolytic pathways of various esters.

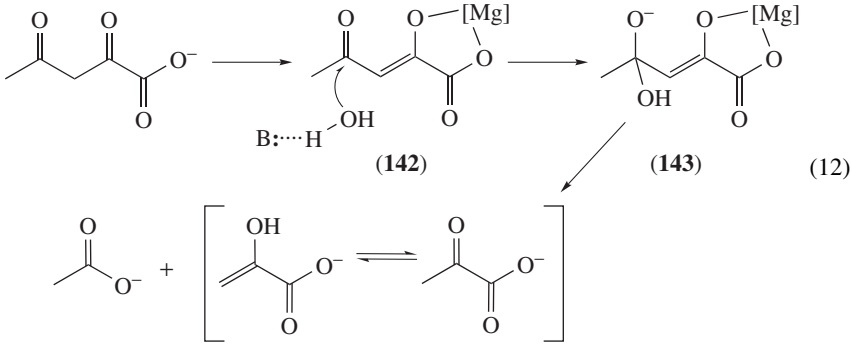

(12)

Fumarylacetoacetate hydrolase (Figure 29A) hydrolyzes catalyzes the last step of the tyrosine catabolism to produce fumarate and acetoacetate (equation 13). Mutations in this enzyme result in the hereditary type-1 tyrosinemia with severe clinical abnormalities in the liver, kidney and nervous system[425]. The mechanism for the hydrolysis of β-diketones has been better revealed from the crystal structures of the Mn(II)-dependent fumarylacetoacetate hydrolase with a bound transition-state (**144**) analogue **145**′ and with the two products bound in the active site before being released[426] (Figure 29). Compounds **145** and **145**′ are transition-state analogues with inhibition constants $K_i = 12$ and 41 nM, respectively, indicating the double bond may be important for recognition and binding of the substrates and inhibitors. The deprotonated phosphinic acid functionality in **145** and **145**′ mimics the deprotonated *gem*-diol functionality of **144** after nucleophilic attack at the scissile carbonyl group. The significance of the fumaryl moiety in substrate specificity was suggested from the inhibition by the transition-state analogue 4-(hydroxy-methylphosphinoyl)-3-oxobutanoic acid with a much higher K_i value of 85 μM[426a]. According to the crystal structure of the transition-state EI complex, the substrate is expected to bind to the Mn(II) center via the ketoacetate functionality and H-bonded to Arg142. As opposed to the metallohydrolases, wherein the nucleophilic water is activated by the metal center, the nucleophilic water in this enzyme is activated by the dyad of His133–Glu364 analogous to the catalytic triad Ser–His–Asp in serine hydrolases. Herein, the acidity of the substrate is expected to be enhanced by the metal center, making the products better leaving groups. The transition state is further stabilized by interacting with the side chains of Arg237, Gln240 and Lys253 (Figure 29B). After the cleavage of the β-diketone functionality, the acetoacetate

product is still bound to the metal while the nucleophilic water seems to be regenerated and is H-bonded with His133 and Glu199 as well as the carboxylate of fumarate product (Figure 29C).

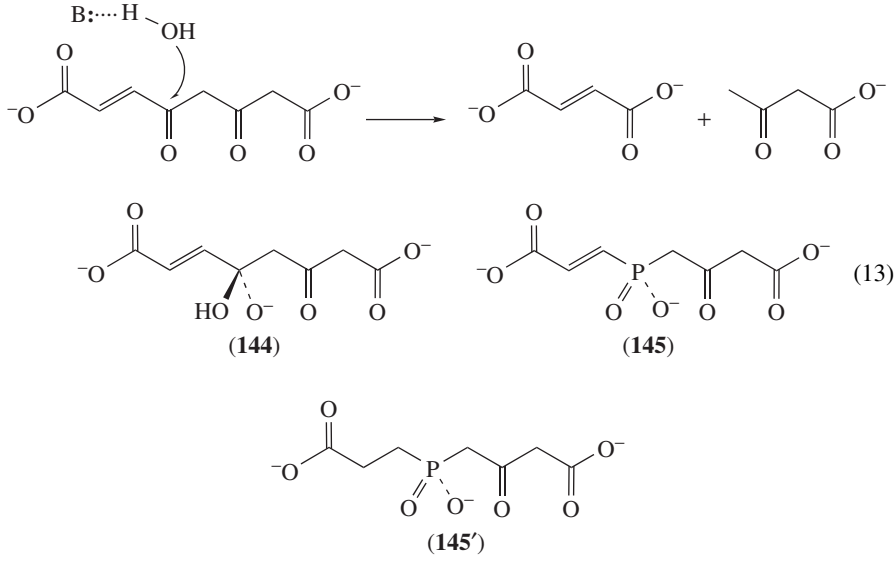

(13)

2. Oxidative cleavage

m-Dihydroxybenzenes can be oxidized and cleaved to yield β-diketones or β,δ-triketones. Catabolism of these products can be carried out by β-diketone hydrolases (preceding section) or undergo further oxidative cleavage. The substrates for hydrolytic cleavage by metallo-β-diketone hydrolases require a pyruvate moiety for binding to the active-site metal; however, the β-diketone can be hydrolyzed by a non-metal hydrolase. Cell extracts of a strain of *Acinetobacter johnsonii*, grown with acacH as the sole carbon source, could convert acacH to acetate, lactate and pyruvate, with the latter two possibly derived from methylglyoxal[427]. Involvement of a β-diketohydrolase was excluded since acacH would be hydrolyzed to produce acetone, which, however, was not the case. The isolated enzyme contains Fe and Zn and has molecular mass 16.6 kDa on SDS-PAGE, but 64 kDa by native gel electrophoresis, suggesting a homotetrameric metalloprotein. Various diketones were used as substrates but acacH was the most specific substrate. Dioxygen is required in the cleavage of acacH and is incorporated into the products in 1:1 stoichiometry, whereas no H_2O_2 is produced[428]. Thus, the enzyme is an acetylacetone dioxygenase. Replacement of a Me group of acacH by a larger one, such as Ph in benzoylacetone and *t*-Bu in pivaloylacetone, affords activities as low as *ca* 5% that of acacH; however, 2-acetylcyclohexanone and the linear caproylacetone show significant activity (56% and 30%, respectively). Acetylpyruvic acid and *o*-hydroxyacetophenone are unaffected by this enzyme. The cleavage products of acacH are acetate and methylglyoxal

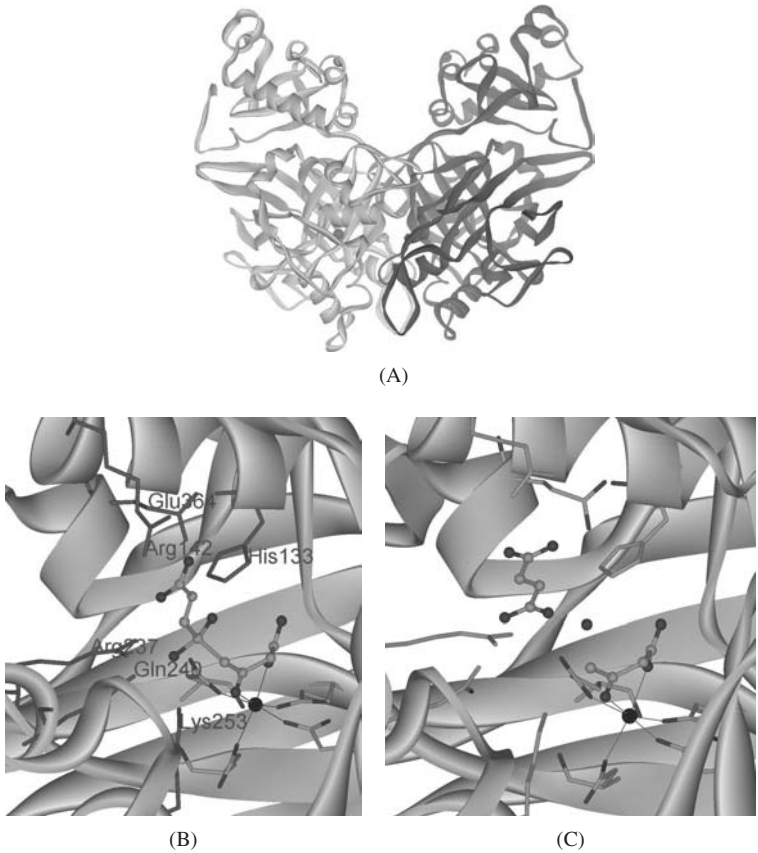

(A) (B) (C)

FIGURE 29. (A) Crystal structure of fumarylacetoacetate hydrolase showing the Mn(II) ion bound to the protein (PDB ID 2HZY, Plate LIII). (B) Active site showing the ligands (from upper left and clockwise) Glu199, Glu201, Asp126 and Asp233, and catalytically important residues (pink, Plate LIV) and a bound transition-state mimic **145′** (stick-and-ball). (C) Active site with bound fumarate and acetoacetonate products (1QCO) before release (Plate LV)

in its monohydrate and dehydrate forms (^{1}H NMR) and the latter are further oxidized to pyruvate (equation 14)[427,428]. Use of labeled $^{18}O_2$ results in 97% incorporation of ^{18}O into acetate and 70% into methylglyoxal[429]. The less-than-stoichiometric incorporation in the latter case can be attributed to the exchange of the oxygen in methylglyoxal with water via its mono- and dehydrated forms.

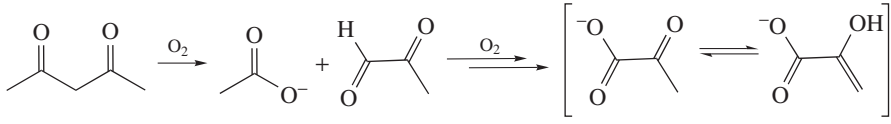

(14)

Cleavage of asymmetric β-diketones occurs at the bond adjacent to the more electron-deficient carbonyl carbon. For example, equation 15 shows that replacement of the methyl group in 1-phenyl-1,3-butanedione by a trifluoromethyl group results in a reversal of cleavage of the bond next to the benzoyl moiety from 83% (path ***i***) to 8% (path ***ii***). A mechanism for this cleavage was proposed[430] whereby the substrate is attacked by metal-bound dioxygen (probably a superoxide) at the acidic Cα carbon of the substrate to form a peroxo-β-diketonate intermediate (equation 15), followed by intramolecular nucleophilic attack by the peroxo anion at the more electronegative carbonyl to generate a dioxetane intermediate, which then undergoes rearrangement and elimination to yield the products. Herein, reaction coordinate analysis of the catalysis suggests that the peroxo intermediate is formed via concerted dioxygen reduction and C–O bond formation, aided by the metal center. A recent chemical model study on oxidative cleavage of phenylpyruvate by a few Fe(II) complexes suggests direct dioxygen attack at the enol double bond without interacting with the metal[431].

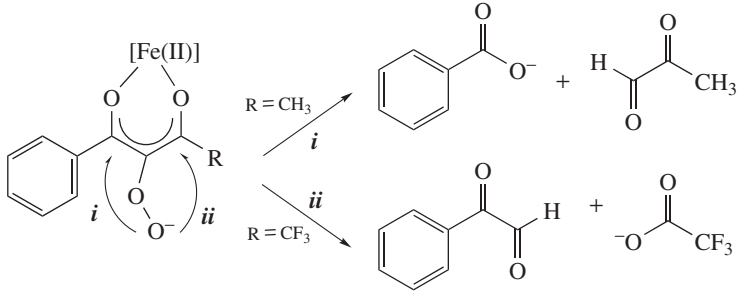

(15)

The gene that encodes the *A. johnsonii* acetylacetone dioxygenase has been cloned and the enzyme expressed and characterized to be the same as isolated before[428]. The enzyme is deactivated by metal chelators and can gain partial activity by introducing Fe(II) to the apo enzyme, while Fe(III), Mn(II), Co(II), Ni(II), Cu(II) and Zn(II) cannot regenerate the activity. Sequence alignment and secondary structure prediction did not result in any analogous metallodioxygenase. Nevertheless, it is not unexpected that proteins in the same superfamily have very different sequences owing to divergent evolution. An unpublished crystal structure of this enzyme was deposited in the Protein Databank (PDB ID 3BAL). Previous biochemical investigations suggested that this enzyme functions as a tetramer[427,428], which is confirmed by the stable tetrameric structure of the enzyme wherein the C-terminus of each subunit interacts with two other subunits of which one forms a stable β-sheet interaction (Figure 30A). The folding pattern classifies this enzyme to be in the cupin superfamily, analogous to the folding of acireductone dioxygenase and quercetin dioxygenase discussed above. The active site of this enzyme (Figure 30B) also bears the consensus His-x-His-x_4-Glu sequence (x and x_4 are non-conserved amino acids) which provides the metal-binding ligands in the other metallo-cupin enzymes. However, a site-specific mutagenesis study of this enzyme reveals the change of Glu69 to a Gln does not significantly affect substrate binding, reduction of dioxygen and C–C bond cleavage[432]. The crystal structure of the wild-type enzyme shows the side chain of Glu69 is on the other side of the β-sheet, pointing away from the active-site metal as opposed to the coordinated Glu found in the other metallo-cupin enzymes. This may explain the small influence caused by Glu69 $\rightarrow$ Gln mutation. Which residue plays the role of this consensus Glu69 as in the other enzymes deserves further investigation.

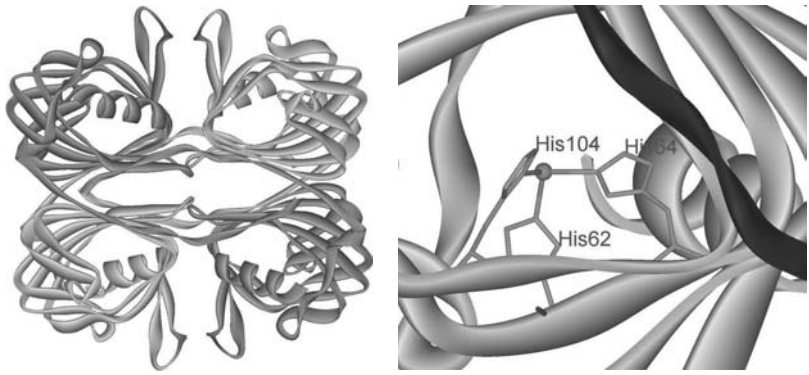

(A) (B)

FIGURE 30. (A) Structure of acetylacetone dioxygenase (PDB ID 3BAL), showing the C-terminal interactions among the subunits (Plate LVI). (B) The active site of the enzyme (Plate LVII). Whether or not there is any coordinated water was not revealed in the structure. The β strand from another subunit is shown as the first strand (purple) in the extended β sheet

H. TetA and Tetracycline Resistance

The broad-spectrum TC antibiotics (e.g. **8**) have gained limited usage in recent years due to side effects and bacterial resistance[433]. Nevertheless, recent studies of the mechanism for bacterial resistance of TCs have provided new insight into rational design of analogues and new directions for finding new analogues of this antibiotic family. The antibiotic activity of TCs is attributed to their binding to the ribosomes which inhibits protein synthesis[434,435]. TCs have been reported to bind different forms of RNA, including ribosome, bulk RNA, rRNA and ribozymes[436]. The low-affinity ($K_d = 1-20$ mM) TC binding to ribosomes at the 30S subunit can induce a conformational change that prevents tRNA from binding to the ribosome and results in interference of protein synthesis[437]. The binding of TCs with 16S rRNA has been identified with photo-modification, activity assay, mutation and crystallography[436,438,439], which further confirms the significance of such binding in the action of this antibiotic family. Two TC molecules can be bound to the RNA[439a], of which one involves a Mg(II) ion binding the drug at the 11,12-ketoenolate site. UV-vis spectroscopic studies show that the Cu(II) complexes of TCs can interact with DNA by intercalation and electrostatic interactions[440].

TCs are well documented to bind metal ions[441], such as VO(II), Cr(III), Mn(II), Fe(II), Fe(III), Co(II), Ni(II), Cu(II), Zn(II) and Al(III) (Section III.B.2.a)[442–446]. TCs are present mainly as Ca(II) complexes, and Mg(II) complexes to a lesser extent, in the plasma when they are not bound to proteins such as serum albumin. Thus, the bioavailability of TCs is supposed to be highly dependent upon the physical and biochemical properties of their metal complexes. The slight variation in metal binding of different TCs has been correlated to their pharmacodynamic behavior[217b]. The 11,12-β-ketoenol functionality of TCs has been considered the primary metal binding site[447], which has also been determined to be the Mg(II) binding site in their RNA complexes discussed in the preceding paragraph and in the repressor TetR-Mg(II)-TC ternary complex discussed in the next one. A recent study indicated that TC forms 2:1 TC:metal complexes with 3*d* transition metal ions in non-aqueous solutions, in which the metal is bound at the 2-carboxamido-3-enol chelating site[216]. Moreover, formation of metal–TC complexes with different stoichiometries, including 2:1, 1:1 and 1:2 TC:metal ratios, has been suggested in previous studies.

Xanthate-modified cellulose binds metal–TC tetracycline complexes and is evaluated to be an effective controlled release system for TCs complexes, owing to the metal-binding properties of these antibiotics[448].

The predominant TC-resistance mechanism in Gram-negative bacteria is active efflux of the Mg(II) complex of the drug by the antiporter membrane protein TetA coupled with proton uptake[449]. The expression of TetA is controlled by the repressor protein TetR. Binding of TetR to the *tet*-operator prevents transcription of both *tet*R and *tet*A genes. A conformational change of the TetR repressor occurs upon binding of metallo-TC[450], which results in the release of the repressor from the operator and initiation of TetA expression. The crystal structures of the repressor TetR and the ternary complex TetR-Mg(II)-TC (Figure 31A) have been resolved, confirming the induction of the conformational change of the repressor upon binding of the Mg(II)–TC complex[451–453]. The *tet*-operator (**146**) is composed of 15 base pairs, with a peculiar kind of 2-fold symmetry with respect to the central T-A base pair (boxed sequences in **146**). Upon Mg(II)-TC binding, significant conformational changes of TetR are observed, including the DNA binding site[451]. Significant changes are also observed at helix-9, suggesting that the opening at the C-terminus of helix-9 serves as the entrance for the drug as this opening is significantly narrowed after TC binding[451,452].

T C T A T C A T T G A T A G G
A G A T A G T A A C T A T C C

(**146**)

Mg(II) in the ternary TetR-Mg(II)-TC complex has an octahedral geometry; it is bonded to the drug at the 11,12-β-ketoenolate functionality, as suggested in early metal-binding studies, and to TetR via the imidazolyl side group of His100 (Figure 31B). Three water molecules occupy the rest of the coordination sphere, of which two form H-bonds with Thr103 and Glu147. The transition metal Ni(II) was also determined to occupy the same

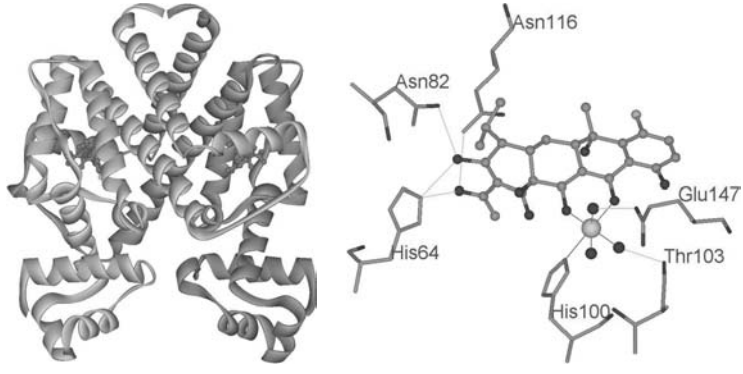

(A) (B)

FIGURE 31. (A) TetR as a dimeric protein with ten α-helical structures (PDB ID 1BJY), of which the first three helical bundles from the N-terminus of each subunit serve as the DNA binding site (bottom part in the structure, Plate LVIII). (B) Metal binding via 11,12-ketoenolate of TC and other specific interactions of tetracycline in TetR (Plate LIX)

metal-binding site and retain the same coordination chemistry as Mg(II) in the TetR-Ni(II)-TC complex[454]. Fe(II) can also form a ternary complex with TC and TetR in place of Mg(II)[450,455]. An *in vitro* induction assay shows that Fe(II)-TC is a stronger inducer of the Tet repressor than Mg(II)-TC by more than 1,000 times, suggesting that Fe(II) may play a role in TC resistance *in vivo*[455a]. Understanding the specificity of TC binding to TetR and the determination of the role of metal ions in the structure of the TC-M(II)-TetR ternary complex is expected to lead to rational design of TC analogues that exhibit broad-spectrum antibiotic activities yet are devoid of bacterial resistance, such as the third-generation TCs of the glycylcycline family[456].

I. Enols in Enzyme Inhibition

Owing to their H-bonding and metal-binding capabilities, the enol/enolate functionality is found in a number of potent inhibitors toward enzymes. For example, the pyranone-containing tipranavir (**147**, Aptivus by Boehringer–Ingelheim) is a unique member of the inhibitors toward HIV protease since it does not contain a symmetric structure (as opposed to the homodimeric structure of the protease) nor is it a peptide analogue (thus would not be easily digested as those peptide inhibitors). Nevertheless, it is a very potent inhibitor ($K_i = 19$ pM) with its enolic 4-hydroxyl group capable of H-bonding with the active-site carboxylates in the protease (Figure 32). The hydroxyquinones atromentin (**15b**) and leucomelone (**15c**) have been found to be specific inhibitors during bacterial fatty acid synthesis in *Streptococcus pneumoniae*, but not in *Escherichia coli* or *Staphylococcus aureus*[35]. The enolic thiofuranone derivatives **35** (e.g. $R^1 = n$-propyl and $R^2 = n$-decyl) and **36** are also inhibitors of fatty acid synthase and have served as drug leads against *Plasmodium falciparum* (malaria) and *Trypanosoma* (sleeping sickness)[55,56]. Several tetronic acid derivatives exhibit significant inhibition toward bacterial peptidoglycan synthesis ($K_d = 0.19$ μM for the derivative R^1 = 2-naphthalene and (R^2, R^3) = vinyl-1-naphthalene in equation 8 analogous to **39**)[63].

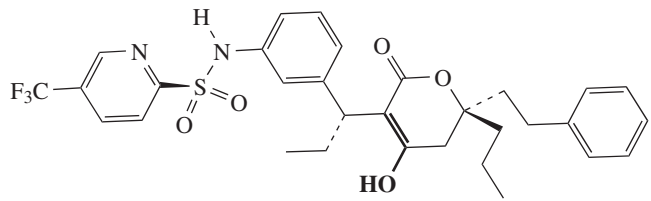

(**147**)

In the case of metalloenzymes, the enolate functional group in inhibitors can bind directly to the active-site metal center to afford stable enzyme–inhibitor complexes. The 2-substituted derivatives of the unique amino acid mimosine (**9**) are found to be inhibitors toward the Fe(II)-containing metalloenzymes lipoxygenase and ribonucleotide reductase[457], wherein the derivatives with a large group are found to be weaker inhibitors toward 5-lipoxygenase, suggesting that this family of compounds inhibits the enzyme by the size and shape of the molecules in addition to their hydrophobicity. The hydroxyquinone derivative maesanin (**73c**) and some of its derivatives are inhibitors of lipoxygenase, presumably due to the hydrophobic long chain present in these compounds[458].

Mimosine (**9**) is an agonist in folate metabolism[459] and suggested to be an inhibitor toward the iron-containing ribonucleotide reductase[121], the activity of the transcription of the cytoplasmic serine hydroxymethyltransferase gene (*shmt1*)[123] and the copper enzymes

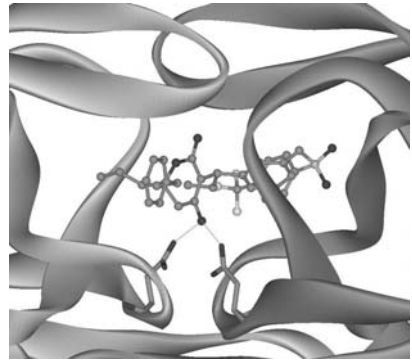

FIGURE 32. Crystal structure of dimeric HIV protease with the bound inhibitor tipranavir (Q7K) viewed from the direction perpendicular to the pseudo-twofold axis, wherein the enolic 4-hydroxyl functionality is H-bonded to the active-site aspartate side chains (Plate LX)

tyrosinase[157,460] and dopamine β-hydroxylase[461]. The binding of mimosine to oxytyrosinase replaces the bound peroxide as shown by the disappearance of the intense O_2^{2-}-to-Cu(II) charge-transfer transition at 345 nm ($\varepsilon = 170{,}000\ M^{-1}\ cm^{-1}$) and its binding to mettyrosinase is demonstrated by the appearance of a charge-transfer transition at 420 nm ($\varepsilon = 800\ M^{-1}\ cm^{-1}$)[462]. The mimosine-like kojic acid (**10a**) was also found to be an inhibitor for the dicopper enzyme tyrosinase[463] and the monocopper enzyme quercetin 2,3-dioxygenase (the structure of its EI complex is shown in Figure 24D)[378].

The cyclic α-ketoenol tropolone (**77**) and some of its derivatives are inhibitors toward several metalloenzymes. A few monoaryl- and bisaryldihydroxytropolones are found to be potent inhibitors toward inositol monophosphatase with IC_{50} values in the low μM range[464]. The crystal structure of this enzyme reveals three metal ions, Mg(II) or Ca(II), in the active site involved in substrate binding and hydrolysis[465]. A modeling study shows that the tropolone derivative puberulonic acid (**81**) binds to all the three metal ions in the active site of this enzyme via the keto-enolate oxygens at 1, 2 and 3 positions as chelating or bridging ligands[466]. Herein, 3-hydroxytropolone, with oxygen groups on three contiguous positions of the cycle, binds two of the metal ions separated by 3.73 Å. Similarly, 2,7-dihydroxytropone is found to be also an inhibitor with $IC_{50} = 75\ \mu M$, while tropolone which lacks the three binding oxygens abreast is not inhibitory. The carboxylate in **81** herein plays little role in the inhibition. Conversely, the 6-membered pyrogallol (1,2,3-trihydroxybenzene), which has the three contiguous oxygens superimposable to those of 3- and 7-hydroxyltropolone, does not inhibit the enzyme. Tropolone and derivatives are also effective inhibitors toward alkaline phosphatase which contains three Zn(II) ions in the active site[466], dopamine β-monooxygenase with two Cu(II) ions in the active site[467], the dinuclear Cu tyrosinase[468] and polyphenol oxidase[469], the mononuclear Mg(II)-containing catechol-*O*-methyltransferase[470] and the dinuclear Mg(II) ribonuclease H[471].

We end this section on enzyme inhibition with a case study about 4-hydroxyphenylpyruvate dioxygenase (HPPD) and disorders in tyrosine catabolism. After transamination of tyrosine, 4-hydroxyphenylpyruvate (**148**) is formed which is then decarboxylated, isomerized and oxygenated by HPPD[472] to yield homogentisate (**149**) or by hydroxymandelate synthase (HMS) to yield *p*-hydroxymandelate (**150**). **149** serves as the precursor for plastoquinones and tocopherols in plants[473]. Thus, inhibitors of HPPD have been designed

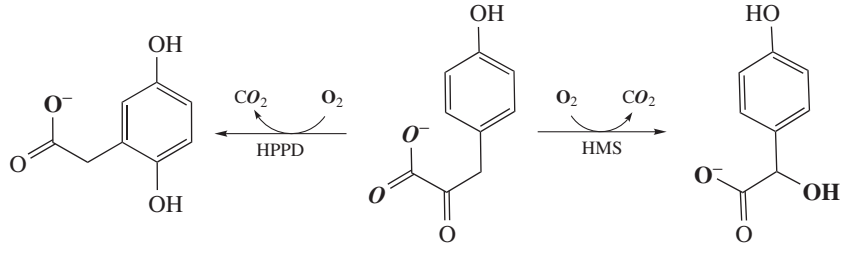

(**149**) (**148**) (**150**)

and utilized as herbicides which result in loss of chlorophyll in treated plants. In mammals, homogentisate may undergo oxidative ring-opening by homogentisate 1,2-dioxygenase to afford maleylacetoacetate, then to fumarylacetoacetate which can be further cleaved by fumarylacetoacetase to yield acetoacetate and fumarate (Section IV.G.1). Imbalance at different stages of tyrosine catabolism may result in various diseases, including three types of tyrosinemia, hawkinisinuria and alkaptonuria, among which type II tyrosinemia is attributed to deficiency in tyrosine aminotransferase, type III tyrosinemia and hawkinisinuria are attributed to imperfection in HPPD, alkaptonuria is due to defect in homogentisate 1,2-dioxygenase and type I tyrosinemia (the most severe tyrosine catabolic defect) stems from fumarylacetoacetase dysfunction.

The crystal structures of HPPD from several different organisms have been determined, including those from *Pseudomonas fluorescens* (PDB ID 1CJX)[474], *Arabidopsis thaliana* (1SP9 and 1SQD)[475,476], *Zea mays* (maize; 1SP8)[475], *Streptomyces avermitilis* (1T47)[477] and rat (1SQI)[476]. HPPD from *A. thaliana* is dimeric with 377 amino acids in each subunit. Each subunit is comprised of two topologically similar domains of β-barrel-like structure nearly perpendicular to each other (Figure 33). The C-terminal domain contains an Fe(II) in the active center bound to the protein via one Glu and two His side chains in a distorted octahedral geometry, leaving three open coordination sites occupied by water molecules. In the structure of the *Pseudomonas* enzyme, the open sites are occupied by a bidentate acetate to afford a 5-coordinate geometry.

Owing to the importance of HPPD for biosynthesis in plants, this enzyme has been a target for herbicides[472,478]. The triketone herbicide NTBC (**151a**), which is present together with its tautomeric forms **152–154**), mesotrione (**151b**), sulcotrione (**151c**) and several natural and synthetic triones (**155**–**158**) have been utilized as herbicides for their capability to inhibit HPPD. The structures of the EI complexes were also resolved for the enzyme from *Streptomyces* with a bound molecule of the trione herbicide NTBC (**151a**, Figure 33B)[477] and for the one from *Arabidopsis* with a bound molecule of the experimental herbicide DAS645 (**155**, Figure 33C) or DAS869 (**156**, Figure 33D)[476]. Herein, the inhibitors are all bound via their β-ketoenolate functionality.

HPPD can be inhibited by natural-occurring β-ketoenolate- or trione-containing allelopathic compounds[479], such as leptospermone (**157a**, $IC_{50} = 3.14$ μg/mL), isoleptospermone (**157b**) and grandiflorone (**157c**, $IC_{50} = 0.22$ μg/mL), but not flavesone (**157d**), in the manuka oil from *Leptospermum scoparium*[480] as well as (−)-usnic acid (**158**, $IC_{50} = 50$ nM) from lichen, which also shows a bleaching effect on plant cotyledonary tissues[481]. Hydrophobicity and size thus seem to be important for inhibition, as shown by molecular modeling on the active site of the enzyme. Moreover, several α-ketoenol natural products exhibit potent inhibition toward HPPD[479], such as the benzoquinones

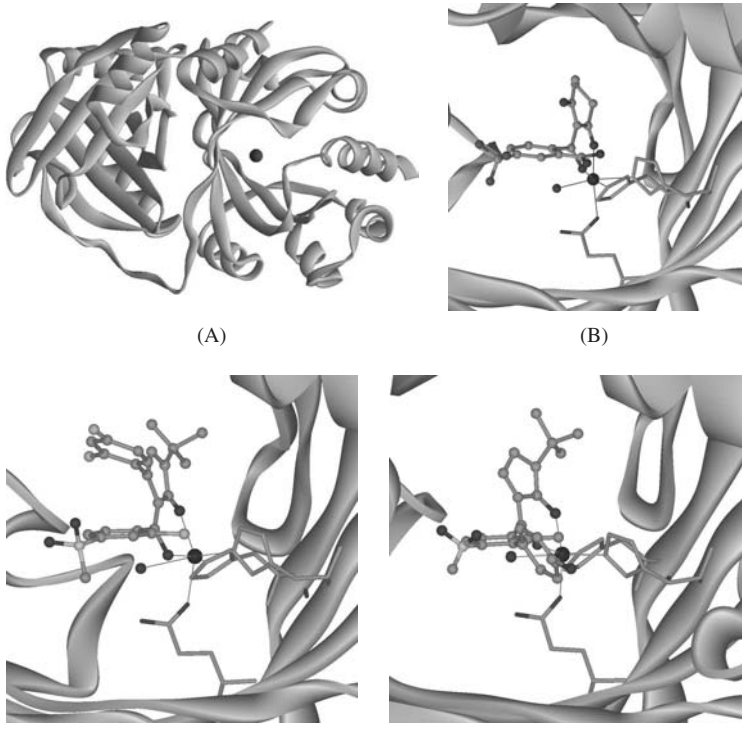

FIGURE 33. 4-Hydroxylphenylpyruvate dioxygenase (HPPD), Fe(II) ions are shown as a solid sphere. (A) One of the subunits (PDB ID 1T47) of the dimeric enzyme of *Streptomyces* (Plate LXI). (B) Active site of the *Streptomyces* enzyme (1T47) with a bound molecule of triketone herbicide NTBC (**151a**, Plate LXII). (C) Active site of the *Arabidopsis* enzyme (1TG5) with a bound molecule of dione herbicide DAS645 (**155**, Plate LXIII). (D) Active site of the rat enzyme (1SQI) with the bound dione herbicide DAS869 (**156**, Plate LXIV)

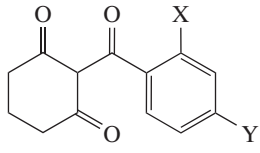

(**151**) (**a**) X = NO_2, Y = Mef
(**b**) X = NO_2, Y = SO_2Me
(**c**) X = Cl, Y = SO_2Me

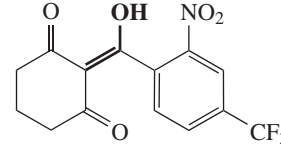

(**152**)

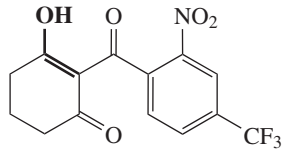

(**153**)

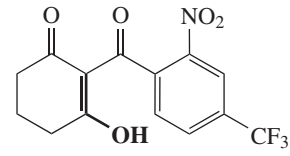

(**154**)

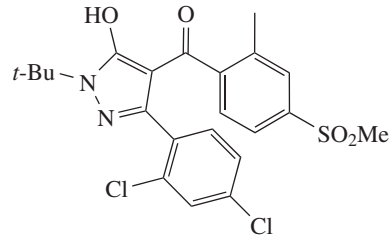

(**155**)

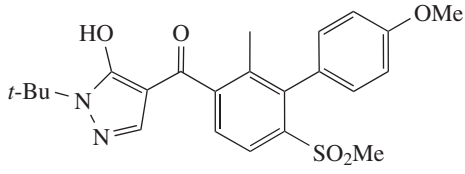

(**156**)

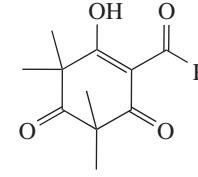

(**157**) (**a**) R = *i*-Bu
(**b**) R = *s*-Bu
(**c**) R = Bn
(**d**) R = *i*-Pr

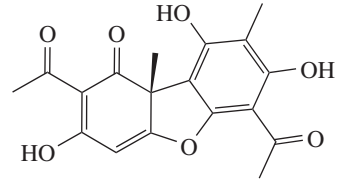

(**158**)

sorgoleone (**73a**), ethoxysorgoleone (**73b**), maesanin (**73′**), dihydromaesonin and maesanol, $IC_{50} = 0.4$, 3, 0.3, 2 and 1.5 μM, respectively, which presumably can be attributed to their metal-binding capability (Section III.B.1.f). However, despite the presence of the metal-binding α-ketoenolate functionality, lapachol (**95**), 2-hydroxy-*p*-naphthoquinone and 2,5-dihydroxy-*p*-naphthoquinone do not exhibit significant inhibition toward HDDP ($IC_{50} > 100$ μM).

Tyrosinemia is caused by defects in various enzymes during tyrosine catabolism discussed above. Inhibition of HPPD thus can be expected to alleviate the symptoms of tyrosinemia and alkaptonuria and prevent tissue damage caused by the fatal type I tyrosinemia, and presumably can also improve hawkinisinuria[472]. The HPPD inhibitor NTBC (**151a**) has been successfully utilized as a therapeutic agent for this purpose[482]. The β-ketoenolate functionality in NTBC, which is analogous to the α-ketocarboxyl group that presumably binds to the active-site metal in HPPD, has been determined to chelate the active-site metal in HPPD according to the crystal structures (Figure 33B). Synthetic triketo compounds analogous to NTBC exhibit significant inhibition toward HPPD, wherein modification at the β-ketoenolate functionality results in decrease in or lack of activity[483]. NTBC shows high affinity toward Fe(III) ion, suggesting its binding to the oxidized form of the enzyme. However, a later study suggested that NTBC interacted only with the ferrous form of HPPD, wherein a metal-to-ligand charge transfer was detected at 450 nm when NTBC was added to reduced HPPD anaerobically, whereas there was no change in the electronic and EPR spectra upon adding NTBC to oxidized HPPD[484]. The crystal structure comparison between the *Arabidopsis* and the rat enzyme revealed possible specific recognition that may allow inhibitors to differentiate these two enzymes[476]. DAS645 (**155**, Figure 33C) has been screened to exhibit high selectivity toward the plant enzyme with $IC_{50} = 12$ nM, whereas no significant inhibition toward the rat enzyme could be detected at concentrations up to 20 μM, while the inhibitor DAS869 (**156**, Figure 33D) exhibits potent inhibition toward both plant ($IC_{50} = 7$ nM) and rat ($IC_{50} < 20$ nM) enzymes. These studies have provided clues for future design of effective HPPD inhibitors for the treatment of disorders associated with tyrosine catabolism.

In a different pathway, 4-hydroxyphenylpyruvate can be decarboxylated and oxygenated to afford *p*-hydroxymandelate (**150**) by hydroxymandelate synthase[485]. The product is converted to hydroxyphenylglycine, suggesting that the reaction goes through dehydrogenation and transamination[485], and then can be incorporated into antibiotics such as vancomycin[486]. The crystal structure of HMS shows an overall folding similar to that of HPPD, with a root-mean-square deviation of 1.85 Å for the α-carbons and a similar six-coordinate metal-binding environment of one coordinated Glu and two His side chains[487]. The potent herbicide NTBC (**151a**) is also an inhibitor toward HMS which is attributed to the structural similarity between this enzyme and HPPD and their use of the same substrate, presumably also due to the binding of the β-ketoenolate functionality of the inhibitor to the active-site metal ion[488].

V. REFERENCES

1. N. Smirnoff and G. L. Wheeler, *Crit. Rev. Biochem. Mol. Biol.*, **35**, 291 (2000); R. D. Hancock and R. Viola, *Crit. Rev. Plant Sci.*, **24**, 167 (2005).
2. B. H. Havsteen, *Pharmacol. Ther.*, **96**, 67 (2002).
3. S. Mandel, T. Amit, L. Reznichenko, O. Weinreb and M. B. H. Youdim, *Mol. Nutr. Food Res.*, **50**, 229 (2006).
4. G. Bringmann, G. Lang, T. A. M. Gulder, H. Tsuruta, J. Mühlbacher, K. Maksimenka, S. Steffens, K. Schaumann, R. Stöhr, J. Wiese, J. F. Imhoff, S. Perovic-Ottstadt, O. Boreiko and W. E. G. Müller, *Tetrahedron*, **61**, 7252 (2005).
5. W. Z. Liu, Q. Q. Gu, W. M. Zhu, C. B. Cui and G. T. Fan, *J. Antibiot.*, **58**, 621 (2005).
6. W. Z. Liu, Q. Q. Gu, W. M. Zhu, C. B. Cui and G. T. Fan, *J. Antibiot.*, **58**, 441 (2005).
7. I. Chopra and M. Roberts, *Microbiol. Mol. Biol.*, **65**, 232 (2001); I. Chopra, P. M. Hawkey and M. Hinton, *J. Antimicrob. Chemother.*, **29**, 245 (1992).
8. L.-J. Ming, *Med. Res. Rev.*, **23**, 697 (2003).
9. H. C. Chang, T. H. Lee, L. Y. Chuang, M. H. Yen and W. C. Hung, *Cancer Lett.*, **145**, 1 (1999); F. Reno, A. Tontini, S. Burattini, S. Papa, E. Falcieri and G. Tarzia, *Apoptosis*, **4**, 469 (1999); A. Zalatnai and J. Bocsi, *Antican. Res.*, **23**, 4007 (2003); A. Zalatnai, *Pathol. Oncol. Res.*, **11**, 164 (2005).

10. S. Frydas, N. Papaioannou, M. Papazahariadou, M. Hatzistilianou, E. Karagouni, M. Trakatelli, G. Brellou, C. Petrarca, M. L. Castellani, P. Conti, G. Riccioni, A. Patruno and A. Grilli, *Int. J. Immunopathol. Pharmacol.*, **18**, 85 (2005).
11. R. Anitha, S. Jayavelu and K. Murugesan, *Phytother. Res.*, **19**, 992 (2005).
12. E. W. Oppenheim, I. M. Nasrallah, M. G. Mastri and P. J. Stover, *J. Biol. Chem.*, **275**, 19268 (2000).
13. M. E. Winkler, K. Lerch and E. I. Solomon, *J. Am. Chem. Soc.*, **103**, 7001 (1981); C. Perry, R. Sastry, I. M. Nasrallah and P. J. Stover, *J. Biol. Chem.*, **280**, 396 (2005).
14. R. Bentley, *Nat. Prod. Rep.*, **23**, 1046 (2006).
15. J. S. Chen, C.-i Wei and M. R. Marshall, *J. Agric. Food Chem.*, **39**, 1897 (1991); T. Tanaka, M. Takeuchi and E. Ichishima, *Agric. Biol. Chem.*, **53**, 557 (1989).
16. R. A. Steiner, I. M. Kooter and B. W. Dijkstra, *Biochemistry*, **41**, 7955 (2002).
17. L. Novotny, P. Rauko, M. Abdel-Hamid and A. Vachalkova, *Neoplasma*, **46**, 89 (1999).
18. M. Wein, E. Lewinsohn and W. Schwab, *J. Agric. Food Chem.*, **49**, 2427 (2001).
19. I. Ménager, M. Jost and C. Aubert, *J. Agric. Food Chem.*, **52**, 1248 (2004); V. De Boishebert, L. Urruty, J.-L. Giraudel and M. Montury, *J. Agric. Food Chem.*, **52**, 2472 (2004).
20. M. G. Malowicki and T. H. Shellhammer, *J. Agric. Food Chem.*, **53**, 4434 (2005).
21. M. Shimamura, T. Hazato, H. Ashino, Y. Yamamoto, E. Iwasaki, H. Tobe, K. Yamamoto and S. Yamamoto, *Biochem. Biophys. Res. Commun.*, **289**, 220 (2001).
22. Y. Honma, H. Tobe, M. Makishima, A. Yokoyama and J. Okabe-Kado, *Leuk. Res.*, **22**, 605 (1998).
23. K. Yamamoto, J. Wang, S. Yamamoto and H. Tobe, *FEBS Lett.*, **465**, 103 (2000).
24. H. Tobe, Y. Muraki, K. Kitamura, O. Komiyama, Y. Sato, T. Sugioka, H. B. Maruyama, E. Matsuda and M. Nagai, *Biosci. Biotechnol. Biochem.*, **61**, 158 (1997).
25. M. Teuber, *Appl. Microbiol.*, **19**, 871 (1970); W. J. Simpson and A. R. Smith, *J. Appl. Bacteriol.*, **72**, 327 (1992).
26. H. Yajima, E. Ikeshima, M. Shiraki, T. Kanaya, D. Fujiwara, H. Odai, N. Tsuboyama-Kasaoka, O. Ezaki, S. Oikawa and K. Kondo, *J. Biol. Chem.*, **279**, 33456 (2004).
27. M. Gill, *Aust. J. Chem.*, **54**, 721 (2001); M. Gill, *Nat. Prod. Rep.*, **11**, 67 (1994).
28. M. Cocchietto, N. Skert and P. L. Nimis, *Naturwissenschaften*, **89**, 137 (2002); K. Ingolfsdottir, *Phytochemistry*, **61**, 729 (2002).
29. M. Takai, Y. Uehara and J. A. Beisler, *J. Med. Chem.*, **22**, 1380 (1979); G. Hardardottir, H. M. Ogmundsdottir and K. Ingolfsdottir, *Plant. Med.*, **72**, 998 (2006).
30. H. Elo, J. Matikainen and E. Pelttari, *Naturwissenschaften*, **94**, 465 (2007).
31. J. Kraft, S. Bauer, G. Keilhoff, J. Miersch, D. Wend, D. Riemann, R. Hirschelmann, H.-J. Holzhausen and J. Langner, *Arch. Toxicol.*, **72**, 711 (1998).
32. W. Knecht, J. Henseling and M. Löffler, *Chem.-Biol. Interact.*, **124**, 61 (2000).
33. J. F. Burton and B. F. Cain, *Nature*, **184**, 1326 (1959); B. F. Cain, *J. Chem. Soc., C*, 1041 (1966) and Parts 1–3 cited therein; K. Y. Zeecheng and C. C. Cheng, *J. Med. Chem.*, **13**, 264 (1970).
34. G. J. Bennett and N. Uri, *Nature*, **192**, 354 (1961).
35. C.-J. Zheng, M.-J. Sohn and W.-G. Kim, *J. Antibiot.*, **59**, 808 (2006).
36. B.-S. Yun, H.-C. Kang, H. Koshino, S.-H. Yu and I.-D. Yoo, *J. Nat. Prod.*, **64**, 1230 (2001).
37. A. Muhlbauer, J. Beyer and W. Steglich, *Tetrahedron Lett.*, **39**, 5167 (1998).
38. G. Patternden, N. A. Pegg and R. W. Kenyon, *J. Chem Soc., Perkin Trans. 1*, 2363 (1991); M. Gill, M. J. Kiefel, D. A. Lally and A. Ten, *Aust. J. Chem.*, **43**, 1497 (1990).
39. V. Bertolasi, V. Ferretti, P. Gilli, X. Yao and C. J. Lib, *New J. Chem.*, **32**, 694 (2008).
40. F. Payton, P. Sandusky and W. L. Alworth, *J. Nat. Prod.*, **70**, 143 (2007).
41. S. J. Eustace, G. M. McCann, R. A. More O'Ferrall, M. G. Murphy, B. A. Murray and S. M. Walsh, *J. Phys. Org. Chem.*, **11**, 519 (1998).
42. A. Johnson, S. Krishnaswamy, P. V. Sundaram and V. Pattabhi, *Acta Crystallogr., Sect. D*, **53**, 311 (1997).
43. H. I. Park and L.-J. Ming, *J. Biol. Inorg. Chem.*, **7**, 600 (2002).
44. U. Baumann, *J. Mol. Biol.*, **242**, 244 (1994).
45. D. P. Barondeau, J. A. Tainer and E. D. Getzoff, *J. Am. Chem. Soc.*, **128**, 3166 (2006).
46. (a) B. G. Reid and G. C. Flynn, *Biochemistry*, **36**, 6786 (1997).

(b) D. C. Prasher, V. K. Eckenrode, W. W. Ward, F. G. Prendergast and M. J. Cormier, *Gene*, **111**, 229 (1992); M. Ormo, A. B. Cubitt, K. Kallio, L. A. Gross, R. Y. Tsien and S. J. Remington, *Science*, **273**, 1392 (1996).
47. J. T. G. Solomons, E. M. Zimmerly, S. Burns, N. Krishnamurthy, M. K. Swan, S. Krings, H. Muirhead, J. Chirgwin and C. Davies, *J. Mol. Biol.*, **342**, 847 (2004).
48. M. B. Austin, M. Izumikawa, M. E. Bowman, D. W. Udwary, J.-L. Ferrer, B. S. Moore and J. P. Noel, *J. Biol. Chem.*, **279**, 45162 (2004).
49. B. Feng, X. Wang, M. Hauser, S. Kaufmann, S. Jentsch, G. Haase, J. M. Becker and P. J. Szaniszlo, *Infect. Immun.*, **69**, 1781 (2001).
50. J. A. Kalaitzis, Y. Hamano, G. Nilsen and B. S. Moore, *Org. Lett.*, **5**, 4449 (2003).
51. H. Morita, S. Kondo, S. Oguro, H. Noguchi, S. Sugio, T. Kohno, I. Abe and T. Kohno, *Chem. Biol.*, **14**, 359 (2007).
52. P. E. M. Siegbahn, *J. Phys. Chem.*, **100**, 14672 (1996); R. L. DeKock, I. H. Hristov, G. D. W. Anderson, I. Göttker-Schnetmann, S. Mecking and T. Ziegler, *Organometallics*, **24**, 2679 (2005); S. A. Beyramabadi, H. Eshtiagh-Hosseini, M. R. Housaindokht and A. Morsali, *Organometallics*, **27**, 72 (2008).
53. L.-J. Ming, in *Physical Methods in Bioinorganic Chemistry, Spectroscopy and Magnetism*, Chap. 8 (Ed. L. Que, Jr.), University Science Books, Sausalito, 2000; T. J. Wenzel and K. A. Provencher, in *The Chemistry of Metal Enolates*, Chap. 14 (Ed. J. Zabicky), John Wiley & Sons, Ltd, Chichester, 2009.
54. S. M. Jones, J. E. Urch, M. Kaiser, R. Brun, J. L. Harwood, C. Berry and I. H. Gilbert, *J. Med. Chem.*, **48**, 5932 (2005).
55. R. F. Waller, P. J. Keeling, R. G. Donald, B. Striepen, E. Handman, N. Lang-Unnasch, A. F. Cowman, G. S. Besra, D. S. Roos and G. I. McFadden, *Proc. Natl. Acad. Sci. U.S.A.*, **95**, 12352 (1998); S. T. Prigge, X. He, L. Gerena, N. C. Waters and K. A. Reynolds, *Biochemistry*, **42**, 1160 (2003); J. L. Harwood, *Biochim. Biophys. Acta*, **1301**, 7 (1996).
56. S. M. Jones, J. E. Urch, R. Brun, J. L. Harwood, C. Berry and I. H. Gilbert, *Bioorg. Med. Chem.*, **12**, 683 (2004).
57. C. L. Linster and E. Van Schaftingen, *FEBS J.*, **274**, 1 (2007).
58. M. A. McDonough, V. Li, E. Flashman, R. Chowdhury, C. Mohr, B. M. Lienard, J. Zondlo, N. J. Oldham, I. J. Clifton, J. Lewis, L. A. McNeill, R. J. Kurzeja, K. S. Hewitson, E. Yang, S. Jordan, R. S. Syed and C. J. Schofield, *Proc. Nat. Acad. Sci. U.S.A.*, **103**, 9814 (2006).
59. N. Smirnoff and G. L. Wheeler, *Crit. Rev. Biochem. Mol. Biol.*, **35**, 291 (2000); R. D. Hancock and R. Viola, *Crit. Rev. Plant Sci.*, **24**, 167 (2005).
60. G. Monteiro, B. B. Horta, D. C. Pimenta, O. Augusto and L. E. S. Netto, *Proc. Nat. Acad. Sci. U.S.A.*, **104**, 4886 (2007).
61. K. Müller, *Appl. Microbiol. Biotechnol.*, **56**, 9 (2001).
62. Y. S. Rao, *Chem. Rev.*, **76**, 625 (1976); Z. Ahmed and P. Langer, *Tetrahedron*, **61**, 2055 (2005).
63. T. S. Mansour, C. E. Caufield, B. Rasmussen, R. Chopra, G. Krishnamurthy, K. M. Morris, K. Svenson, J. Bard, C. Smeltzer, S. Naughton, S. Antane, Y. Yang, A. Severin, D. Quagliato, P. J. Petersen and G. Singh, *ChemMedChem.*, **2**, 1414 (2007).
64. B. Zumreoglu-Karan, *Coord. Chem. Rev.*, **250**, 2295 (2006).
65. H. A. Tajmir-Riahi and D. M. Boghai, *J. Inorg. Biochem.*, **45**, 73 (1992); H. A. Tajmir-Riahi, *J. Inorg. Biochem.*, **44**, 39 (1991); H. A. Tajmir-Riahi, *J. Inorg. Biochem.*, **42**, 47 (1991).
66. W. Jabs, W. Gaube, C. Fehl and R. Lukowski, *Inorg. Chim. Acta*, **175**, 273 (1990).
67. R. N. Allen, M. K. Shukla and J. Leszczynski, *Int. J. Quantum Chem.*, **106**, 2366 (2006).
68. M. B. Davies, *Polyhedron*, **11**, 285 (1992).
69. C. Ünaleroğlu, B. Zumreoğlu-Karan, Y. Zencir and T. Hökelek, *Polyhedron*, **16**, 2155 (1997).
70. D. M. Stearns and K. E. Wetterhahn, *Chem. Res. Toxicol.*, **7**, 219 (1994).
71. A. Adach and M. Cieslak-Golonka, *Transition Met. Chem.*, **30**, 323 (2005).
72. K. Schwarz and W. Mertz, *Arch. Biochem. Biophys.*, **85**, 292 (1959).
73. B. Bänsch, P. Martinez, D. Uribe, J. Zuluaga and R. van Eldik, *Inorg. Chem.*, **30**, 4555 (1991).
74. P. Martinez and D. Uribe, *J. Chem Sci.*, **37**, 1446 (1982).
75. W. Jabs, G. Krüger, A. X. Trautwein, V. Schünemann and E. Bill, in *Transition Metals in Biology and Their Coordination Chemistry* (Ed. A. X. Trautwein), Wiley–VCH, Weinheim, 1997, p. 468.

76. C. P. Rao, K. Geethea, M. S. S. Raghavan, A. Sreedhara, K. Tokunaga, T. Yamaguchi, V. Jadhav, K. N. Ganesh, T. Krishnamoorthy, K. V. A. Ramaiah and R. K. Bhattacharyya, *Inorg. Chim. Acta*, **297**, 373 (2000).
77. K. Premkumar, K. Min, Z. Alkan, W. C. Hawkes, S. Ebeler and C. L. Bowlus, *J. Nutr. Biochem.*, **18**, 272 (2007).
78. A. J. Núñez-Sellés, *J. Braz. Chem. Soc.*, **16**, 699 (2005); M. Valko, M. Izakovic, M. Mazur, C. J. Rhodes and J. Telser, *Mol. Cell. Biochem.*, **266**, 37 (2004); A. C. Maritim, R. A. Sanders and J. B. Watkins, *J. Biochem. Mol. Toxicol.*, **17**, 24 (2003); L. Kruidenier and H. W. Verspaget, *Alim. Pharmacol. Ther.*, **16**, 1997 (2002); A. Spector, *J. Ocul. Pharmacol. Ther.*, **16**, 193 (2000).
79. M. W. van Dyke and P. B. Dervan, *Biochemistry*, **22**, 2373 (1983); D. S. Sigman, *Acc. Chem. Res.*, **19**, 180 (1986); M. J. Guille and G. G. Kneale, *Mol. Biotechnol.*, **8**, 35 (1997); F. Vigneault and S. L. Guerin, *Exp. Rev. Proteom.*, **2**, 705 (2005); K. J. Hampel and J. M. Burke, *Methods*, **23**, 233 (2001).
80. C. Unaleroglu, Y. Mert and B. Zumreoglu-Karan, *Syn. React. Inorg. Met.-Org. Chem.*, **31**, 1531 (2001).
81. A. W. Prestayko, S. T. Crooke and S. K. Carter, *Cisplatin, Current Status and New Developments*, Academic Press, New York, 1980; B. Rosenberg, *Met. Ions Biol. Syst.*, **11**, 127 (1980); B. Rosenberg, *Cancer*, **55**, 2303 (1985); C. Mascaux, M. Paesmans, T. Berghmans, F. Branle, J. J. Lafitte, F. Lemaître, A. P. Meert, P. Vermylen and J. P. Sculier, *Lung Cancer*, **30**, 23 (2000); I. E. Smith and D. C. Talbot, *Br. J. Cancer*, **65**, 787 (1992); E. F. McClay and S. B. Howell, *Gynecol. Oncol.*, **36**, 1 (1990).
82. S. J. Lippard, in *Bioinorganic Chemistry* (Eds. I. Bertini, H. B. Gray, S. J. Lippard and J. S. Valentine), University Science Books, Mill Valley, 1994; M. J. Bloemink and J. Reedijk, *Met. Ions Biol. Syst.*, **32**, 641 (1996); E. Wong and C. M. Giandomenico, *Chem. Rev.*, **99**, 2451 (1999); J. M. Pérez, M. A. Fuertes, C. Alonso and C. Navarro-Ranninger, *Crit. Rev. Oncol. Hematol.*, **35**, 109 (2000); I. Judson and L. R. Kelland, *Drugs*, **59**, 29 (2000); S. M. Cohen and S. J. Lippard, *Prog. Nucl. Acid Res.*, **67**, 93 (2001); T. Boulikas and M. Vougiouka, *Oncol. Rep.*, **10**, 1663 (2003); T. Boulikas and M. Vougiouka, *Oncol. Rep.*, **11**, 559 (2004); G. D. Wang, E. Reed and Q. Q. Li, *Oncol. Rep.*, **12**, 955 (2004); A. M. Havelka, M. Berndtsson, M. H. Olofsson, M. C. Shoshan and S. Linder, *Mini-Rev. Med. Chem.*, **7**, 1035 (2007); B. Lippert (Ed.), *Cisplatin: Chemistry and Biochemistry of a Leading Anticancer Drug*, Wiley, New York, 1999.
83. L. S. Hollis, A. R. Amundsen and E. W. Stern, *J. Am. Chem. Soc.*, **107**, 274 (1985).
84. M. J. Arendse, G. K. Anderson and N. P. Rath, *Inorg. Chem.*, **38**, 5864 (1999).
85. B. H. Havsteen, *Pharmacol. Ther.*, **96**, 67 (2002).
86. H. Kirmizibekmez, I. Calis, R. Perozzo, R. Brun, A. A. Donmez, A. Linden, P. Rudi and D. Tasdemir, *Planta Med.* **70**, 711 (2004).
87. C. A. Rice-Evans and L. Packer, *Flavonoids in Health and Disease*, Dekker, New York, 1998.
88. S. M. Kuo, *Cancer Lett.*, **110**, 41 (1996); G. Cao, E. Sofic and R. L. Prior, *Free Rad. Biol. Med.*, **22**, 749 (1997); G. D. Carlo, N. Mascolo, A. A. Izzo and F. Capasso, *Life Sci.*, **65**, 337 (1999); I. Erlund, *Nutr. Res.*, **24**, 851 (2004); S. Mandel, T. Amit, L. Reznichenko, O. Weinreb and M. B. H. Youdim, *Mol. Nutr. Food Res.*, **50**, 229 (2006).
89. R. J. Williams, J. P. E. Spencer and C. A. Rice-Evans, *Free Rad. Biol. Med.*, **36**, 838 (2004).
90. E. L. Da Silva, T. Tsushida and J. Terao, *Arch. Biochem. Biophys.*, **349**, 313 (1998); A. Nagao, M. Seki and H. Kobayashi, *Biosci. Biotechnol. Biochem.*, **63**, 1787 (1999).
91. M. Furusawa, T. Tanaka, T. Ito, A. Nishikawa, N. Yamazaki, K.-I. Nakaya, N. Matsuura, H. Tsuchiya, M. Nagayama and M. Iinuma, *J. Heal. Sci.*, **51**, 376 (2005).
92. M. E. Bodini, G. Copia, R. Tapia, F. Leighton and L. Herrera, *Polyhedron*, **18**, 2233 (1999); A. Bravo and J. R. Anacona, *Transition Met. Chem.*, **26**, 20 (2001); J. Zhou, L.-f. Wang, J.-y. Wang and N. Tang, *J. Inorg. Biochem.*, **83**, 41 (2001); G. Le Nest, O. Caille, M. Woudstra, S. Roche, F. Guerlesquin and D. Lexa, *Inorg. Chim. Acta*, **357**, 775 (2004); G. Le Nest, O. Caille, M. Woudstra, S. Roche, B. Burlat, V. Belle, B. Guigliarelli and D. Lexa, *Inorg. Chim. Acta*, **357**, 2027 (2004); I. Esparza, I. Salinas, C. Santamaría, J. M. García-Mina and J. M. Fernández, *Anal. Chim. Acta*, **543**, 267 (2005); A. Torreggiani, M. Tamba, A. Trinchero and S. Bonora, *J. Mol. Struct.*, **744**, 759 (2005).
93. K. Shibata, Y. Shibata and I. Kashiwagi, *J. Am. Chem. Soc.*, **41**, 208 (1919).
94. M. Shiono, N. Matsugaki and K. Takeda, *Nature*, **436**, 791 (2005).

95. Y.-B. Zeng, N. Yang, W.-S. Liu and N. Tang, *J. Inorg. Biochem.*, **97**, 258 (2003).
96. M. T. Fernandez, M. L. Mira, M. H. Florêncio and K. R. Jennings, *J. Inorg. Biochem.*, **92**, 105 (2002).
97. Y. Bai, F. R. Song, M. L. Chen, J. P. Xing, Z. Q. Liu and S. Y. Liu, *Anal. Sci.*, **20**, 1147 (2004).
98. Y. Zhang, H. L. Li, Y. L. Zhao and Z. H. Gao, *Eur. J. Pharmacol.*, **535**, 263 (2006).
99. L. Mira, M. T. Fernandez, M. Santos, R. Rocha, M. H. Florencio and K. R. Jennings, *Free Rad. Res.*, **36**, 1199 (2002).
100. M. Y. Moridani, J. Pourahmad, H. Bui, A. Siraki and P. J. O'Brien, *Free Rad. Biol. Med.*, **34**, 243 (2003).
101. R. F. V. de Souza and W. F. De Giovani, *Redox Rep.*, **9**, 97 (2004).
102. M. Soczyńska-Kordala, A. Bakowska, J. Oszmiański and J. Gabrielska, *Cell. Mol. Biol. Lett.*, **6**, 277 (2001).
103. G. Speier, V. Fülöp and L. Párkányi, *J. Chem. Soc., Chem. Commun.*, 512 (1990); E. Balogh-Hergovich, G. Speier and G. Argay, *J. Chem. Soc., Chem. Commun.*, 551 (1991).
104. E. Balogh-Hergovich, J. Kaizer, G. Speier, G. Argay and L. Párkányi, *J. Chem. Soc., Dalton Trans.*, 3847 (1999).
105. Y. Farina, B. M. Yamin, H.-K. Fun, B.-C. Yip and S.-G. Teoh, *Acta Crystallogr., Sect. C*, **51**, 1537 (1995); N. Okabe, E. Yamamoto and M. Yasunori, *Acta Crystallogr., Sect. E*, **59**, m715 (2003).
106. I. Lippai, G. Speier, G. Huttner and L. Zsolnai, *Chem. Commun.*, 741 (1997).
107. I. Lippai, G. Speier, G. Huttner and L. Zsolnai, *Acta Crystallogr., Sect. C*, **53**, 1547 (1997).
108. (a) J. Kaizer, G. Speier, J. Pap and L. Párkányi, *Eur. J. Inorg. Chem.*, 2253 (2004).
(b) J. Kaizer, E. Balogh-Hergovich, M. Czaun, T. Csay and G. Speier, *Coord. Chem. Rev.*, **250**, 2222 (2006); E. Balogh-Hergovich, J. Kaizer, J. Pap, G. Speier, G. Huttner and L. Zsolnai, *Eur. J. Inorg. Chem.*, **9**, 2287 (2002); L. Barhacs, J. Kaizer, J. Pap and G. Speier, *Inorg. Chim. Acta*, **320**, 83 (2001); E. Balogh-Hergovich, J. Kaizer, G. Speier, G. Huttner and A. Jacobi, *Inorg. Chem.*, **39**, 4224 (2000); E. Balogh-Hergovich, J. Kaizer, G. Speier, V. Fulop and L. Párkányi, *Inorg. Chem.*, **38**, 3787 (1999).
109. J. Kaizer, J. Pap, G. Speier, M. Réglier and M. Giorgi, *Transition Met. Chem.*, **29**, 630 (2004).
110. M. S. Ahmed, V. Ramesh, V. Nagaraja, J. H. Parish and S. M. Hadi, *Mutagenesis*, **9**, 193 (1994).
111. F. B. A. El Amrani, L. Perelló, J. A. Real, M. González-Alvarez, G. Alzuet, J. Borrás, S. García-Granda and J. Montejo-Bernardo, *J. Inorg. Biochem.*, **100**, 1208 (2006).
112. L. Barhacs, J. Kaizer and G. Speier, *J. Mol. Catal. A: Chem.*, **172**, 117 (2001).
113. E. G. Ferrer, M. V. Salinas, M. J. Correa, L. Naso, D. A. Barrio, S. B. Etcheverry, L. Lezama, T. Rojo and P. A. M. Williams, *J. Biol. Inorg. Chem.*, **11**, 791 (2006).
114. J. F. Thompson, C. J. Morris and I. K. Smith, *Ann. Rev. Biochem.*, **38**, 137 (1969).
115. T. D. Xuan, A. A. Elzaawely, F. Deba, M. Fukuta and S. Tawata, *Agron. Sustain. Dev.*, **26**, 89 (2006).
116. B. Singh, T. K. Bhat and B. Singh, *J. Agric. Food Chem.*, **51**, 5579 (2003); A. Zalatnai, *Pathol. Oncol. Res.*, **11**, 164 (2005); A. Zalatnai and J. Bocsi, *Anticancer Res.*, **23**, 4007 (2003); H. C. Chang, C. F. Weng, M. H. Yen, L. Y. Chuang and W. C. Hung, *Int. J. Oncol.*, **17**, 659 (2000); P. Conti, S. Frydas, M. Reale, R. C. Barbacane, M. Di Gioacchino, M. Felaco and A. Trakatellis, *Mol. Cell. Biochem.*, **229**, 129 (2002); Y. Samuni, W. DeGraff, M. Chevion, J. B. Mitchell and J. A. Cook, *Rad. Res.*, **155**, 304 (2001).
117. R. L. N. Harris, *Aust. J. Chem.*, **29**, 1329 (1976).
118. G. H. Laswai, J. N. Ocran, F. P. Lekule and F. Sundstøl, *Anim. Feed Sci. Technol.*, **65**, 45 (1997); R. Puchala, T. Sahlu, J. J. Davis and S. P. Hart, *Anim. Feed Sci. Technol.*, **55**, 253 (1995).
119. M. G. Domínguez-Bello and C. S. Stewart, *FEMS Microbiol. Lett.*, **73**, 283 (1990).
120. M. J. Allison, W. R. Mayberry, C. S. McSweeney and D. A. Stahl, *Syst. Appl. Microbiol.*, **15**, 522 (1992); M. G. DominguezBello, M. Lovera and M. T. Rincon, *FEMS Microbiol. Ecol.*, **23**, 361 (1997).
121. Y. Dai, B. Gold, J. K. Vishwanatha and S. L. Rhode, *Virology*, **205**, 210 (1994); D. M. Gilbert, A. Neilson, H. Miyazawa, M. L. DePamphilis and W. C. Burhans, *J. Biol. Chem.*, **270**, 9597 (1995); R. F. Kalejta and J. L. Hamlin, *Exp. Cell Res.*, **231**, 173 (1997); R. Kayyali,

J. B. Porter, Z. D. Liu, N. A. Davies, J. H. Nugent, C. E. Cooper and R. C. Hider, *J. Biol. Chem.*, **276**, 48814 (2001).
122. K. S. Kulp and P. R. Vulliet, *Toxicol. Appl. Pharmacol.*, **139**, 356 (1996).
123. C. Perry, R. Sastry, I. M. Nasrallah and P. J. Stover, *J. Biol. Chem.*, **280**, 396 (2005).
124. F. Reno, A. Tontini, S. Burattini, S. Papa, E. Falcieri and G. Tarzia, *Apoptosis*, **4**, 469 (1999).
125. E. Chruscinska, E. Garribba, G. Micera and A. Panzanelli, *J. Inorg. Biochem.*, **75**, 225 (1999); H. Stunzi, R. L. N. Harris, D. D. Perrin and T. Teitei, *Aust. J. Chem.*, **33**, 2207 (1980).
126. S. I. Ahmed, J. Burgess, J. Fawcett, S. A. Parsons, D. R. Russell and S. H. Laurie, *Polyhedron*, **19**, 129 (2000).
127. M. M. C. A. Castro, C. F. G. C. Geraldes, P. Gameiro, E. Pereira, B. Castro and M. Rangel, *J. Inorg. Biochem.*, **80**, 177 (2000).
128. M. A. Santos, R. Grazina, P. Buglyo, S. Gama and E. Farkas, *Polyhedron*, **21**, 2609 (2002).
129. N. A. Epstein, J. L. Horton, C. M. Vogels, N. J. Taylor and S. A. Westcott, *Aust. J. Chem.*, **53**, 687 (2000); E. J. Brown, A. C. Whitwood, P. H. Walton and A.-K. Duhme-Klair, *Dalton Trans.*, 2458 (2004); N. C. Tam, S. P. Fletcher, C. M. Vogels, S. A. Westcott and A. Decken, *Transition Met. Chem.*, **28**, 103 (2003).
130. C. L. Ferreira, S. R. Bayly, D. E. Green, T. Storr, C. A. Barta, J. Steele, M. J. Adam and C. Orvig, *Bioconjugated Chem.*, **17**, 1321 (2006).
131. P. P. Corbi, A. C. Massabni and C. M. Costa-Neto, *J. Coord. Chem.*, **58**, 1477 (2005).
132. G. Ambrosi, M. Formica, V. Fusi, L. Giorgi, A. Guerri, S. Lucarini, M. Micheloni, P. Paoli, P. Rossi and G. Zappia, *Inorg. Chem.*, **44**, 3249 (2005).
133. M. A. Santos, S. Gama, L. Gano, G. Cantinho and E. Farkas, *Dalton Trans.*, 3772 (2004).
134. K. Tanaka, A. Tengeiji, T. Kato, N. Toyama, M. Shiro and M. Shionoya, *J. Am. Chem. Soc.*, **124**, 12494 (2002); K. Tanaka, A. Tengeiji, T. Kato, N. Toyama and M. Shionoya, *Science*, **299**, 1212 (2003).
135. I. Mikhailov, P. Ninova, G. Russev and B. Anachkova, *Z. Naturforsch., C: Biosci.*, **55**, 849 (2000).
136. K. H. Thompson, C. A. Barta and C. Orvig, *Chem. Soc. Rev.*, **35**, 545 (2006).
137. J. Kadokawa, T. Nishikura, R. Muraoka, H. Tagaya and N. Fukuoka, *Synth. Commun.*, **33**, 1081, (2003).
138. Y.-L. Chen, P.-H. Chen, C.-H. Chung, K.-C. Li, H.-Y. Jeng and C.-C. Tzeng, *Helv. Chim. Acta*, **778**, 778 (2003).
139. H. Kim, J. Choi, J. K. Cho, S. Y. Kim and Y.-S. Lee, *Bioorg. Med. Chem. Lett.*, **14**, 2843 (2004).
140. J. Lokaj, J. Kožíšek, B. Koreň, M. Uher and V. Vrábel, *Acta Crystallogr., Sect. C*, **47**, 193 (1991).
141. M. C. Barret, M. F. Mahon, K. C. Molloy, J. W. Steed and P. Wright, *Inorg. Chem.*, **40**, 4384 (2001).
142. T. P. Lockhart and F. Davidson, *Organometallics*, **6**, 2471 (1987).
143. S. Emami, S. J. Hosseinimehr, S. M. Taghdisi and S. Akhlaghpoor, *Bioorg. Med. Chem. Lett.*, **17**, 45 (2007).
144. M. Odoko, K. Yamamoto and N. Okabe, *Acta Crystallogr., Sect. C*, **58**, m469 (2002).
145. Y. Yoshikawa, E. Ueda, K. Kawabe, H. Miyake, H. Sakurai and Y. Kojima, *Chem. Lett.*, **8**, 874 (2000).
146. L. Coulston and P. Dandona, *Diabetes*, **29**, 665 (1980); A. Shisheva, D. Gefel and Y. Schechter, *Diabetes*, **41**, 982 (1992); M. D. Chen, S. J. Liou, P. Y. Lin, V. C. Yang, P. S. Alexander and W. H. Lin, *Biol. Trace Elem. Res.*, **61**, 303 (1998).
147. M. T. Ahmet, C. S. Frampton and J. Silver, *J. Chem. Soc., Dalton Trans.*, 1159 (1988).
148. K. Murakami, K. Ishida, K. Watakabe, R. Tsubouchi, M. Naruse and M. Yoshino, *Toxicol. Lett.*, **161**, 102 (2006).
149. P. Caravan, L. Gelmini, N. Glover, F. G. Herring, H. Li, J. H. McNeill, S. J. Rettig, I. A. Setyawati, E. Shuter, Y. Sun, A. S. Tracey, V. G. Yuen and C. Orvig, *J. Am. Chem. Soc.*, **117**, 12759 (1995).
150. G. S. Mishra, J. J. R. Fráusto da Silva and A. J. L. Pombeiro, *J. Mol. Catal. A: Chem.*, **265**, 59 (2007).
151. C. J. Bailey and P. R. Flatt, (Eds.), *New Antidiabetic Drugs*, Smith Gordon, London, 1990; C. Orvig, K. H. Thompson, M. Battell and J. H. McNeill, *Met. Ions Biol. Syst.*, **31**, 575 (1995); Y. Shechter, *Diabetes*, **39**, 1 (1990).

152. J. H. McNeill, V. G. Yuen, H. R. Hoveyda and C. Orvig, *J. Med. Chem.*, **35**, 1489 (1992); V. G. Yuen, C. Orvig and J. H. McNeill, *Can. J. Physiol. Pharmacol.*, **71**, 263 (1993); V. G. Yuen, C. Orvig, K. H. Thompson and J. H. McNeill, *Can. J. Physiol. Pharmacol.*, **71**, 270 (1993).
153. K. H. Thompson, J. Chiles, V. G. Yuen, J. Tse, J. H. McNeill and C. Orvig, *J. Inorg. Biochem.*, **98**, 683 (2004).
154. W. Y. Hsieh, C. M. Zaleski, V. L. Pecoraro, P. E. Fanwick and S. A. Liu, *Inorg. Chim. Acta*, **359**, 228 (2006).
155. S. J. Lord, N. A. Epstein, R. L. Paddock, C. M. Vogels, T. L. Hennigar, M. J. Zaworotko, N. J. Taylor, W. R. Driedzic, T. L. Broderick and S. A. Westcott, *Can. J. Chem.*, **77**, 1249 (1999).
156. D. C. Kennedy, A. Wu, B. O. Patrick and B. R. James, *Inorg. Chem.*, **44**, 6529 (2005).
157. D. C. Kennedy, A. Wu, B. O. Patrick and B. R. James, *J. Inorg. Biochem.*, **100**, 1974 (2006).
158. W. H. Ang and P. J. Dyson, *Eur. J. Inorg. Chem.*, **20**, 4003 (2006).
159. (a) A. F. A. Peacock, M. Melchart, R. J. Deeth, A. Habtemariam, S. Parsons and P. J. Sadler, *Chem. Eur. J.*, **13**, 2601 (2007).
(b) G. Capper, L. C. Carter, D. L. Davies, J. Fawcett and D. R. Russell, *J. Chem. Soc., Dalton Trans.*, 1399 (1996).
160. M. D. Fryzuk, M. J. Jonker and S. J. Rettig, *Chem. Commun.*, 377 (1997).
161. M. J. Clarke, F. Zhu and D. R. Frasca, *Chem. Rev.*, **99**, 2511 (1999).
162. J. L. Lamboy, A. Pasquale, A. Rheingold and E. Meléndez, *Inorg. Chim. Acta*, **360**, 2115 (2007).
163. J. C. Slaughter, *Biol. Rev.*, **74**, 259 (1999).
164. W. Schwab and R. Roscher, *Rec. Res. Dev. Phytochem.* **1**, 643 (1997).
165. A. E. Mackie and J. C. Slaughter, *J. Inst. Brew.*, **106**, 209 (2000); I. Techakriengkrai, A. Paterson and J. R. Piggott, *J. Inst. Brew.*, **110**, 360 (2004).
166. E. Sarrazin, D. Dubourdieu and P. Darriet, *Food Chem.*, **103**, 536 (2007); A. C. S. Ferreira, J. C. Barbe and A. Bertrand, *J. Agric. Food Chem.*, **51**, 4356 (2003); Y. Kotseridis, A. Razungles, A. Bertrand and R. Baumes, *J. Agric. Food Chem.*, **48**, 5383 (2000).
167. N. Nunomura, M. Sasaki, Y. Asao and T. Yokotsuka, *J. Agric. Food Chem.*, **40**, 491 (1976).
168. M. Ohata, K. Kohama, Y. Morimitsu, K. Kubota and E. Sugawara, *Biosci. Biotech. Biochem.*, **71**, 407 (2007).
169. M. Ndagijimana, M. Vallicelli, P. S. Cocconcelli, F. Cappa, F. Patrignani, R. Lanciotti and M. E. Guerzoni, *Appl. Environ. Microbiol.*, **72**, 6053 (2006).
170. W. S. Sung, H. J. Jung, K. Park, H. S. Kim, I.-S. Lee and D. G. Lee, *Life Sci.*, **80**, 586 (2007).
171. D. Klein, B. Fink, B. Arold, W. Eisenreich and W. Schwab, *J. Agric. Food. Chem.*, **55**, 6705 (2007).
172. N. Yamashita, M. Murata, S. Inoue, Y. Hiraku, T. Yoshinaga and S. Kawanishi, *Mutat. Res.*, **397**, 191 (1998).
173. X. Li, K. Hiramoto, M. Yoshida, T. Kato and K. Kikugawa, *Food Chem. Toxicol.*, **36**, 305 (1998).
174. K. Murakami, M. Haneda, T. Makino and M. Yoshino, *Food Chem. Toxicol.*, **45**, 1258 (2007).
175. K. Ando, K. Ogawa, X. H. Li and K. Kikugawa, *Biol. Pharmac. Bull.*, **23**, 689 (2000).
176. T. Koga, K. Moro and T. Matsudo, *J. Agric. Food. Chem.*, **46**, 946 (1998).
177. S. Grüschow, L.-C. Chang, Y. Mao and D. H. Sherman, *J. Am. Chem. Soc.*, **129**, 6470 (2007).
178. H. Palsdottir, C. G. Lojero, B. L. Trumpower and C. Hunte, *J. Biol. Chem.*, **278**, 31303 (2003).
179. P. A. Takizawa, J. K. Yucel, B. Veit, D. J. Faulkner, T. Deerinck, G. Soto, M. Ellisman and V. Malhotra, *Cell*, **73**, 1079 (1993); B. Veit, J. K. Yucel and V. Malhotra, *J. Cell Biol.*, **122**, 1197 (1993); V. Cruciani, E. Leithe and S. O. Mikalsen, *Exp. Cell Res.*, **287**, 130 (2003).
180. L. A. Tziveleka, C. Vagias and V. Roussis, *Curr. Top. Med. Chem.*, **31**, 512 (2003).
181. P.-H. Lu, S.-C. Chueh, F.-L. Kung, S.-L. Pan, Y.-C. Shen and J.-H. Guh, *Eur. J. Pharmacol.*, **556**, 45 (2007).
182. M. P. Nambiar and H. C. Wu, *Exp. Cell Res.*, **219**, 671 (1995).
183. H. S. Radeke, C. A. Digits, R. L. Casaubon and M. L. Snapper, *Chem. Biol.*, **6**, 639 (1999); H. S. Radeke and M. L. Snapper, *Bioorg. Med. Chem.*, **6**, 1227 (1998).
184. (a) V. Shah, R. Sunder and N. J. de Souza, *J. Nat. Prod.*, **50**, 730 (1987).
(b) I. Podolak and M. Strzalka, *Chromatographia*, **67**, 471 (2008).

(c) J. Calle, J. Olarte, R. Pinzon, L. F. Ospina, M. C. Mendoza and M. J. Orozco, *J. Ethnopharmacol.*, **71**, 521 (2000).
185. L. F. Ospina, J. Calle, L. Arteaga, R. Pinzon, M. J. Alcaraz and M. Paya, *Planta Med.*, **67**, 791 (2001).
186. F. E. Dayan, *Planta*, **224**, 339 (2006)
187. H. Haraguchi, I. Ohmi and I. Kubo, *Bioorg. Med. Chem.*, **4**, 49 (1996).
188. N. Funa, M. Funabashi, E. Yoshimura and S. Horinouchi, *J. Biol. Chem.*, **280**, 14514 (2005).
189. R. Jelly, S. W. Lewis, C. Lennard, K. F. Lim and J. Almog, *Chem. Commun.*, 3513 (2008).
190. A. Dufresne, C. G. De Lima, J. Knudsen and J. E. Moreira, *J. Inorg. Nucl. Chem.*, **35**, 789 (1973).
191. M. E. Bodini, P. E. Bravo and V. Aranciba, *Polyhedron*, **13**, 497 (1994).
192. S. S. Sawhney and R. Jain, *Thermochim. Acta*, **75**, 347 (1984).
193. S. Salunke-Gawali, S. Y. Rane, V. G. Puranik, C. Guyard-Duhayon and F. Varret, *Polyhedron*, **23**, 2541 (2004).
194. K. Yamada, H. Tanaka, S. Yagishita, K. Adachi, T. Uemura, S. Kitagawa and S. Kawata, *Inorg. Chem.*, **45**, 4322 (2006).
195. L. Han, Y. Zhou and W. N. Zhao, *Crys. Growth Des.*, **8**, 2052 (2008).
196. S. Salunke-Gawali, S. Y. Rane, K. Boukheddaden, E. Codjovi, J. Linares, F. Varret and P. P. Bakare, *J. Therm. Anal. Calorim.*, **79**, 669 (2005).
197. R. Bentley, *Nat. Prod. Rep.*, **25**, 118 (2008).
198. J. H. Birkinshaw, A. R. Chambers and H. Raistrick, *Biochem. J.*, **36**, 242 (1942); R. Bentley, *J. Biol. Chem.*, **238**, 1895 (1963).
199. J. H. Birkinshaw and H. Raistrick, *Biochem. J.*, **26**, 441 (1932).
200. M. J. S. Dewar, *Nature*, **155**, 50 (1945).
201. J. Zhao, *Curr. Med. Chem.*, **14**, 2597 (2007).
202. H. Erdtman and J. Gripenberg, *Nature*, **161**, 719 (1948); A. J. Baillie, G. G. Freeman, J. W. Cook and A. R. Somerville, *Nature*, **166**, 65 (1950); Y. Arima, Y. Nakai, R. Hayakawa and T. Nishino, *J. Antimicrob. Chemother.*, **51**, 113 (2003).
203. J. Zhao, K. Fujita and K. Sakai, *Biotechnol. Bioeng.*, **90**, 621 (2005).
204. B. E. Bryant, W. C. Fernelius and B. E. Douglas, *J. Am. Chem. Soc.*, **75**, 3784, (1953); B. E. Bryant and W. C. Fernelius, *J. Am. Chem. Soc.*, **76**, 1696, (1954); B. E. Bryant and W. C. Fernelius, *J. Am. Chem. Soc.*, **76**, 3783, (1954); B. E. Bryant and W. C. Fernelius, *J. Am. Chem. Soc.*, **76**, 4864, (1954).
205. W. P. Griffith, C. A. Pumphrey and A. C. Skapski, *Polyhedron*, **6**, 891 (1987).
206. J. Zhang, P. D. Badger, S. J. Geib and S. Petoud, *Inorg. Chem.*, **46**, 6473 (2007).
207. M. C. Barret, M. F. Mahon, K. C. Molloy, J. W. Steed and P. Wright, *Inorg. Chem.*, **40**, 4384 (2001).
208. F. Nepveu, F. Jasanada and L. Walz, *Inorg. Chim. Acta*, **211**, 141 (1993).
209. K. Lyczko, W. Starosta and I. Persson, *Inorg. Chem.*, **11**, 4402 (2007); R. Diemer, B. K. Keppler, U. Dittes, B. Nuber, V. Seifried and W. Peferkuch, *Chem. Ber.*, **128**, 335 (1995).
210. G. Steyl, *Polyhedron*, **18**, 5324 (2007).
211. J. R. Chipperfield, S. Clark, J. Elliott and E. Sinn, *Chem. Commun.*, 195 (1998); J. M. Elliott, J. R. Chipperfield, S. Clark and E. Sinn, *Inorg. Chem.*, **40**, 6390 (2001); S. Clark, J. M. Elliott, J. R. Chipperfield, P. Styring and E. Sinn, *Inorg. Chem. Commun.*, **5**, 249 (2002); J. M. Elliott, J. R. Chipperfield, S. Clark and E. Sinn, *Inorg. Chem. Commun.*, **5**, 99 (2002); J. M. Elliott, J. R. Chipperfield, S. Clark, S. J. Teat and E. Sinn, *Inorg. Chem.*, **41**, 293 (2002).
212. I. Chopra, P. M. Hawkey and M. Hinton, *J. Antimicrob. Chemother.*, **29**, 245 (1992).
213. J. R. Smythies, F. Benington and R. D. Morin, *Experientia*, **28**, 1253 (1972).
214. K. H. Jogun and J. J. Stezowski, *J. Am. Chem. Soc.*, **98**, 6018 (1976); M. Celotti and G. V. Fazakerley, *J. Chem. Soc. Perkin Trans. 2*, 1319 (1977); M. Schnarr, M. Matthies and W. Lohmann, *Z. Naturforsch.*, **34**, 1156 (1979).
215. D. E. Brodersen, W. M. Clemons, Jr., A. P. Carter, R. J. Morgan-Warren, B. T. Wimberly and V. Ramakrishnan, *Cell*, **103**, 1143 (2000); M. Pioletti, F. Schlunzen, J. Harms, R. Zarivach, M. Gluhmann, H. Avila, A. Bashan, H. Bartels, T. Auerbach, C. Jacobi, T. Hartsch, A. Yonath and F. Franceschi, *EMBO J.*, **20**, 1829 (2001).
216. C. M. Mikulski, J. Fleming and D. Fleming, *Inorg. Chim. Acta*, **144**, 9 (1988).

217. (a) M. Novák-Pékli, M. E.-H. Mesbah and G. Pethö, *J. Pharm. Biomed. Anal.*, **14**, 1025 (1996).
(b) T. Ohyama and J. A. Cowan, *Inorg. Chem.*, **34**, 3083 (1995); L. Lambs and G. Berthon, *Inorg. Chim. Acta*, **151**, 33 (1988); J. M. Wessels, W. E. Ford, W. Szymczak and S. Schneider, *J. Phys. Chem. B*, **102**, 9323 (1998).
218. F. C. S. de Paula, S. Carvalho, H. A. Duarte, E. B. Paniago, A. S. Mangrich and E. C. Pereira-Maia, *J. Inorg. Biochem.*, **76**, 221 (1999).
219. M. Jeżowska-Bojczuk, L. Lambs, H. Kozłowski and G. Berthon, *Inorg. Chem.*, **32**, 428 (1993).
220. F. C. Machado, C. Demicheli, A. Garnier-Suillerot and H. Beraldo, *J. Inorg. Biochem.*, **60**, 163 (1995); H. F. Dos Santos, E. S. Xavier, M. C. Zerner and W. B. De Almeida, *J. Mol. Struct. (Theochem)*, **527**, 193 (2000); G. Berthon, M. Brion and L. Lambs, *J. Inorg. Biochem.*, **19**, 1 (1983); M. Brion, G. Berthon and J. B. Fourtillan, *Inorg. Chim. Acta*, **55**, 47 (1981).
221. R. Cini, *Comments Inorg. Chem.*, **22**, 151 (2000); J. E. Weder, C. T. Dillon, T. W. Hambley, B. J. Kennedy, P. A. Lay, J. R. Biffin, H. L. Regtop and N. M. Davies, *Coord. Chem. Rev.*, **232**, 95 (2002).
222. D. W. Knapp, R. C. Richardson, T. C. K. Chan, G. D. Bottoms, W. R. Widmer, D. B. Denicola, R. Teclaw and P. L. Bonney, *J. Vet. Intern. Med.*, **8**, 273 (1994).
223. D. Di Leo, F. Berrettini and R. Cini, *J. Chem. Soc., Dalton Trans.*, 1993 (1998).
224. R. Cini, G. Giorgi, A. Cinquantini, C. Rossi and M. Sabat, *Inorg. Chem.*, **29**, 5197 (1990).
225. R. Cini, R. Basosi, A. Donati, C. Rossi, L. Sabadini, L. Rollo, S. Lorenzini, R. Gelli and R. Marcolongo, *Met. Based Drugs*, **2**, 43 (1995).
226. R. Cini, G. Tamasi, S. Defazio and M. B. Hursthouse, *J. Inorg. Biochem.*, **101**, 1140 (2007).
227. S. Roy, R. Banerjee and M. Sarkar, *J. Inorg. Biochem.*, **100**, 1320 (2006).
228. D. Kovala-Demertzi, *J. Organomet. Chem.*, **691**, 1767 (2006).
229. S. K. Hadjikakou, M. A. Demertzis, J. R. Miller and D. Kovala-Demertzi, *J. Chem. Soc., Dalton Trans.*, 663 (1999); M. A. Demertzis, S. K. Hadjikakou, D. Kovala-Demertzi, A. Koutsodimou and M. Kubicki, *Helv. Chim. Acta*, **83**, 2787 (2000).
230. A. Galani, M. A. Demertzis, M. Kubicki and D. Kovala-Demertzi, *Eur. J. Inorg. Chem.*, **9**, 1761 (2003).
231. D. Kovala-Demertzi, A. Koutsodimou, A. Galani, S. K. Hadjikakou, M. A. Demertzis, M. Xanthopoulou, J. R. Miller and C. S. Frampton, *Appl. Organomet. Chem.*, **18**, 501 (2004).
232. R. Ma, J. J. Reibenspies and A. E. Martell, *Inorg. Chim. Acta*, **223**, 21 (1994).
233. R. C. Hider and A. D. Hall, *Prog. Med. Chem.*, **28**, 41 (1991).
234. P. S. Dobbin, R. C. Hider, A. D. Hall, P. D. Taylor, P. Sarpong, J. B. Porter, G. Xiao and D. van der Helm, *J. Med. Chem.*, **36**, 2448 (1993); Z. D. Liu, H. H. Khodr, D. Y. Liu, S. L. Lu and R. C. Hider, *J. Med. Chem.*, **42**, 4814 (1999).
235. A. Maggio, *Br. J. Haematol.*, **138**, 407 (2007).
236. G. J. Kontoghiorghes, *Drugs Today*, **37**, 23 (2001); G. J. Kontoghiorghes, K. Pattichis, K. Neocleous and A. Kolnagou, *Curr. Med. Chem.*, **11**, 2161 (2004); P. V. Bernhardt, *Dalton Trans.*, 3214 (2007).
237. G. J. Kontoghiorghes, J. G. Goddard, A. N. Bartlett and L. Sheppard, *Clin. Pharmacol. Ther.*, **48**, 255 (1990).
238. G. Fabio, F. Minonzio, P. Delbini, A. Bianchi and M. D. Cappellini, *Blood*, **109**, 362 (2007).
239. E. T. Clarke, A. E. Martell and J. Reibenspies, *Inorg. Chim. Acta*, **196**, 177 (1992); J. Charalambous, A. Dodd, M. McPartlin, S. O. C. Matondo, N. D. Pathirana and H. R. Powell, *Polyhedron*, **7**, 2235 (1988).
240. M. A. Santos, *Coord. Chem. Rev.*, **228**, 187 (2002); Z. Zhang, S. J. Rettig and C. Orvig, *Inorg. Chem.*, **30**, 509 (1991).
241. C. A. Matsuba, W. O. Nelson, S. J. Rettig and C. Orvig, *Inorg. Chem.*, **27**, 3935 (1988); W. O. Nelson, T. B. Karpishin, S. J. Rettig and C. Orvig, *Inorg. Chem.*, **27**, 1045 (1988).
242. G. J. Kontoghiorghes, E. Eracleous, C. Economides and A. Kolnagou, *Curr. Med. Chem.*, **12**, 2663 (2005).
243. T. F. Tam, R. Leung-Toung, Y. Wang, M. Spino, G. Williams and A. J. Lough, *Acta Cryst. E*, **61**, m2055 (2005).
244. T. F. Tam, R. Leung-Toung, Y. Wang, M. Spino and A. J. Lough, *Acta Crystallogr., Sect. E*, **61**, m2601 (2005).
245. W.-Y. Hsieh and S. Liu, *Inorg. Chem.*, **44**, 2031 (2005).

246. K. M. Mitchell, A. L. Dotson, K. M. Cool, A. Chakrabarty, S. H. Benedict and S. M. LeVine, *Mult. Scler.*, **13**, 1118 (2007).
247. D. Bebbington, N. J. T. Monck, S. Gaur, A. M. Palmer, K. Benwell, V. Harvey, C. S. Malcolm and R. H. P. Porter, *J. Med. Chem.*, **43**, 2779 (2000).
248. P. S. Dobbin, R. C. Hider, A. D. Hall, P. D. Taylor, P. Sarpong, J. B. Poter, G. Xiao and D. van der Helm, *J. Med. Chem.*, **36**, 2448 (1993).
249. M. J. O'Neill, C. Hicks, M. Ward and J. A. Panetta, *Brain Res.*, **760**, 170 (1997).
250. L. F. Fieser, E. Berliner, F. J. Bondhus, F. C. Chang, W. G. Dauben, M. G. Ettlinger, G. Fawaz, M. Fields, M. Fieser, C. Heidelberger, H. Heymann, A. M. Seligman, W. R. Vaughan, A. G. Wilson, E. Wilson, M.-i Wu, M. T. Leffler, K. E. Hamlin, R. J. Hathaway, E. J. Matson, E. E. Moore, M. B. Moore, R. T. Rapala and H. E. Zaugg, *J. Am. Chem. Soc.*, **70**, 3151 (1948).
251. J. J. Kessl, S. R. Meshnick and B. L. Trumpower, *Trends Parasitol.*, **23**, 494 (2007); A. T. Hudson, *Parasitol. Today*, **9**, 66 (1993).
252. J. A. Kovacs, *Lancet*, **340**, 637 (1992).
253. M. Fry and M. Pudney, *Biochem. Pharmacol.*, **43**, 1545 (1992); I. K. Srivastava, H. Rottenberg and A. B. Vaidya, *J. Biol. Chem.*, **272**, 3961 (1997); E. Suswam, D. Kyle and N. Lang-Unnasch, *Exp. Parasitol.*, **98**, 180 (2001).
254. M. W. Mather, E. Darrouzet, M. Valkova-Valchanova, J. W. Cooley, M. T. McIntosh, F. Daldal and A. B. Vaidya, *J. Biol. Chem.*, **280**, 27458 (2005); J. J. Kessl, N. V. Moskalev, G. W. Gribble, M. Nasr, S. R. Meshnick and B. L. Trumpower, *Biochim. Biophys. Acta Bioenerg.*, **1767**, 319 (2007); H. Palsdottir, C. G. Lojero, B. L. Trumpower and C. Hunte, *J. Biol. Chem.*, **278**, 31303 (2003).
255. D. Syafruddin, J. E. Siregar and S. Marzuki, *Mol. Biochem. Parasitol.*, **104**, 185 (1999); J. J. Kessl, K. H. Ha, A. K. Merritt, S. R. Meshnick and B. L. Trumpower, *Mol. Biochem. Parasitol.*, **146**, 255 (2006); J. J. Kessl, P. Hill, B. B. Lange, S. R. Meshnick, B. Meunier and B. L. Trumpower, *J. Biol. Chem.*, **279**, 2817 (2004); J. E. Siregar, D. Syafruddin, H. Matsuoka, K. Kita and S. Marzuki, *Parasitol. Int.*, **57**, 229 (2008).
256. J. R. Bowyer, C. A. Edwards, T. Ohnishi and B. L. Trumpower, *J. Biol. Chem.* **257**, 8321 (1982).
257. E. S. Kaneshiro, *Drug Resistance Updates*, **4**, 322 (2001).
258. L. D. Fairbanks, M. Bofill, K. Ruckemann and H. A. Simmonds, *J. Biol. Chem.*, **270**, 29682 (1995).
259. H. Hussain, K. Krohn, V. U. Ahmad, G. A. Miana and I. R. Green, *ARKIVOC*, **2007-II**, 145 (2007).
260. I. T. Balassiano, S. A. De Paulo, N. Henriques Silva, M. C. Cabral and M. da Gloria da Costa Carvalho, *Oncol. Rep.*, **13**, 329 (2005); A. Esteves-Souza, K. A. Lucio, A. S. Da Cunha, A. Da Cunha Pinto, E. L. Da Silva Lima, C. A. Camara, M. D. Vargas and C. R. Gattass, *Oncol. Rep.*, **20**, 225 (2008).
261. M. A. Martínez, M. C. L. de Jiménez, E. E. Castellano, O. E. Piro and P. J. Aymonino, *J. Coord. Chem.*, **56**, 803 (2003); R. Hernández-Molina, I. Kalinina, P. Esparza, M. Sokolov, J. Gonzalez-Platas, A. Estévez-Braun and E. Pérez-Sacau, *Polyhedron*, **26**, 4860 (2007).
262. B. M. L. Bhatia and N. Vohra, *Thermochim. Acta*, **53**, 361 (1982).
263. M. Kumar, A. Kamra and N. S. Rathee, *Asian J. Chem.*, **19**, 653 (2007).
264. Y.-L. Yan and S. M. Cohen, *Org. Lett.*, **9**, 2517 (2007).
265. K. A. Skov, H. Adomat and N. P. Farrell, *Int. J. Radiat. Biol.*, **64**, 707 (1993).
266. C. X. Zhang and S. J. Lippard, *Curr. Opin. Chem. Biol.*, **7**, 481 (2003).
267. N. Farrall, *Tranistion Metal Complexes as Drugs and Chemotherapeutic Agents*, Kluwer, Dordrecht, 1989; M. J. Clarke, F. Zhu and D. R. Frasca, *Chem. Rev.*, **99**, 2511 (1999); R. H. Fish and G. Jaouen, *Organometallics*, **22**, 2166 (2003); M. F. R. Fouda, M. M. Abd-Elzaher, R. A. Abdelsamaia and A. A. Labib, *Appl. Organomet. Chem.*, **21**, 613 (2007).
268. (a) M. Melchart, A. Habtemariam, S. Parsons and P. J. Sadler, *J. Inorg. Biochem.*, **101**, 1903 (2007).
(b) R. Fernández, M. Melchart, A. Habtemariam, S. Parsons and P. J. Sadler, *Chem. Eur. J.*, **10**, 5173 (2004); F. Y. Wang, A. Habtemariam, E. P. L. van der Geer, R. Fernandez, M. Melchart, R. J. Deeth, R. Aird, S. Guichard, F. P. A. Fabbiani, P. Lozano-Casal, I. D. H. Oswald, D. I. Jodrell, S. Parsons and P. J. Sadler, *Proc. Natl. Acad. Sci. U.S.A.*, **102**, 18269 (2005).

269. R. E. Morris, R. E. Aird, P. D. Murdoch, H. M. Chen, J. Cummings, N. D. Hughes, S. Parsons, A. Parkin, G. Boyd, D. I. Jodrell and P. J. Sadler, *J. Med. Chem.*, **44**, 3616 (2001).
270. A. Habtemariam, M. Melchart, R. Fernández, S. Parsons, I. D. H. Oswald, A. Parkin, F. P. A. Fabbiani, J. E. Davidson, A. Dawson, R. E. Aird, D. I. Jodrell and P. J. Sadler, *J. Med. Chem.*, **49**, 6858 (2006).
271. A. P. de Silva, H. Q. N. Gunaratne, T. Gunnlaugsson, A. J. M. Huxley, C. P. McCoy, J. T. Rademacher and T. E. Rice, *Chem. Rev.*, **97**, 1515 (1997).
272. T. Gunnlaugsson, M. Glynn, G. M. Tocci (née Hussey), P. E. Kruger and F. M. Pfeffer, *Coord. Chem. Rev.*, **250**, 3094 (2006).
273. J. P. Leonard, C. M. G. dos Santos, S. E. Plush, T. McCabe and T. Gunnlaugsson, *Chem. Commun.*, 129 (2007).
274. C. M. G. dos Santos, P. B. Fernández, S. E. Plush, J. P. Leonard and T. Gunnlaugsson, *Chem. Commun.*, 3389 (2007).
275. M. A. Santos, R. Grazina, A. Q. Neto, G. Cantinho, L. Gano and L. Patrício, *J. Inorg. Biochem.*, **78**, 303 (2000).
276. J. Baldas and J. Bonnyman, *J. Radioanal. Nucl. Chem. Lett.*, **105**, 267 (1986).
277. M. K. Dewanjee, S. A. Rao, J. A. Rosemark, S. Chowdhury and P. Didisheim, *Radiology*, **145**, 149 (1982).
278. J. Cortés, J. Velasco, G. Foster, A. P. Blackaby, B. A. Rudd and B. Wilkinson, *Mol. Microbiol.* **44**, 1213 (2002).
279. B. Zhao, F. P. Guengerich, A. Bellamine, D. C. Lamb, M. Izumikawa, L. Lei, L. M. Podust, M. Sundaramoorthy, L. M. Reddy, S. L. Kelly, J. A. Kalaitzis, D. Stec, M. Voehler, J. R. Falck, B. S. Moore, T. Shimada and M. R. Waterman, *J. Biol. Chem.*, **280**, 11599 (2005).
280. (a) F. H. Verhoff, G. Bogulawski, O. J. Lantero, S. T. Schlager and Y. C. Jao, in *Comprehensive Biotechnology*, Vol. 3 (Eds H. W. Balanch, S. Drew and D. I. C. Wang), Pergamon Press, Oxford, 1985, pp. 837–885.
(b) D. L. Nelson and M. M. Cox, *Lehninger Principles of Biochemistry*, 4th Ed., Chap. 14, Freeman, New York, 2005.
281. H. Van Tilbeurgh, J. Jenkins, M. Chiadmi, J. Janin, S. J. Wodak, N. T. Mrabet and A.-M. Lambeir, *Biochemistry*, **31**, 5467 (1992).
282. M. Callens, H. Kersters-Hilderson, O. Van Opetal and C. K. De Bruyne, *Enzyme Microb. Technol.*, **8**, 696 (1986).
283. (a) T. D. Fenn, D. Ringe and G. A. Petsko, *Biochemistry*, **43**, 6464, (2004).
(b) H. L. Carrell, J. P. Glusker, V. Burger, F. Manfre, D. Tritsch and J. F. Biellmann, *Proc. Natl. Acad. Sci. U.S.A.*, **86**, 4440 (1989); H. L. Carrell, H. Hoier and J. P. Glusker, *Acta Crystallogr., Sect. D*, **50**, 113 (1994).
284. R. Kappl, K. Ranguelova, B. Koch, C. Duboc and J. Huttermann, *Magn. Reson. Chem.*, **43**, S65 (2005).
285. (a) K. N. Allen, A. Lavie, A. Glasfeld, T. N. Tanada, D. P. Gerrity, S. C. Carlson, G. K. Farber, G. A. Petsko and D. Ringe, *Biochemistry*, **33**, 1488 (1994).
(b) J. Jenkins, J. Janin, F. Rey, M. Chiadmi, H. van Tilbeurgh, I. Lasters, M. De Maeyer, D. Van Belle, S. J. Wodak, M. Lauwereys, P. Stanssens, N. T. Mrabet, J. Snauwaert, G. Matthyssens and A.-M. Lambeir, *Biochemistry*, **31**, 5449 (1992).
286. M. Garcia-Viloca, C. Alhambra, D. G. Truhlar and J. L. Gao, *J. Comput. Chem.*, **24**, 177 (2003).
287. C. Lee, M. Bagdasarian, M. Meng and J. G. Zeikus, *J. Biol. Chem.*, **265**, 19082 (1990); M. Meng, M. Bagdasarian and J. G. Zeikus, *Proc. Natl. Acad. Sci. U.S.A.*, **90**, 8459 (1993).
288. A. K. Katz, X. M. Li, H. L. Carrell, B. L. Hanson, P. Langan, L. Coates, B. P. Schoenborn, J. P. Glusker and G. J. Bunick, *Proc. Natl. Acad. Sci. U.S.A.*, **103**, 8342 (2006).
289. D.-K. Oh, *Appl. Microbiol. Biotechnol.*, **76**, 1 (2007).
290. B. A. Manjasetty and M. R. Chance, *J. Mol. Biol.*, **360**, 297 (2006).
291. J. E. Seemann and G. E. Schulz, *J. Mol. Biol.*, **273**, 256 (1997).
292. D. W. Lee, E. A. Choe, S. B. Kim, S. H. Eom, Y. H. Hong, S. J. Lee, H. S. Lee, D. Y. Lee and Y. R. Pyun, *Arch. Biochem. Biophys.*, **434**, 333 (2005); M. Rhimi and S. Bejar, *Biochim. Biophys. Acta*, **1760**, 191 (2006); M. Rhimi, M. July, N. Aghajari, R. Haser and S. Bejar, *J. Bacteriol.*, **189**, 3556 (2007).

293. M. Chaput, V. Claes, D. Portetelle, I. Cludts, A. Cravador, A. Burny, H. Gras and A. Tartar, *Nature*, **332**, 454 (1988); P. Faik, J. I. Walker, A. A. Redmill and M. J. Morgan, *Nature*, **332**, 455 (1988).
294. W. Xu, K. Seiter, E. Feldman, T. Ahmed and J. W. Chiao, *Blood*, **87**, 4502 (1996).
295. H. Watanabe, K. Takehana, M. Date, T. Shinozaki and A. Raz, *Cancer Res.*, **56**, 2960 (1996); Y. Niinaka, S. Paku, A. Haga, H. Watanabe and A. Raz, *Cancer Res.*, **58**, 2667 (1998).
296. M. Baumann, A. Kappl, T. Lang, K. Brand, W. Siegfried and E. Paterok, *Cancer Invest.*, **8**, 351 (1990).
297. J. H. Lee, K. Z. Chang, V. Patel and C. J. Jeffery, *Biochemistry*, **40**, 7799 (2001); C. J. Jeffery, R. Hardre and L. Salmon, *Biochemistry*, **40**, 1560 (2001); C. J. Jeffery, B. J. Bahnson, W. Chien, D. Ringe and G. A. Petsko, *Biochemistry*, **39**, 955 (2000); C. C. Chou, Y. J. Sun, M. Meng and C. D. Hsiao, *J. Biol. Chem.*, **275**, 23154 (2000).
298. J. T. G. Solomons, E. M. Zimmerly, S. Burns, N. Krishnamurthy, M. K. Swan, S. Krings, H. Muirhead, J. Chirgwin and C. Davies, *J. Mol. Biol.*, **342**, 847 (2004).
299. C. H. Verhees, S. W. M. Kengen, J. E. Tuininga, G. J. Schut, M. W. W. Adams, W. M. De Vos and J. Van der Oost, *Biochem. J.*, **375**, 231 (2003).
300. T. Hansen, M. Oehlmann and P. Schönheit, *J. Bacteriol.*, **183**, 3428 (2001).
301. J. J. Jeong, S. Fushinobu, S. Ito, B. S. Jeon, H. Shoun and T. Wakagi, *FEBS Lett.*, **535**, 200 (2003).
302. J. M. Berrisford, A. M. Hounslow, J. Akerboom, W. R. Hagen, S. J. J. Brouns, J. van der Oost, I. A. Murray, G. M. Blackburn, J. P. Waltho, D. W. Rice and P. J. Baker, *J. Mol. Biol.*, **358**, 1353 (2006).
303. M. K. Swan, J. T. Solomons, C. C. Beeson, T. Hansen, P. Schönheit and C. Davies, *J. Biol. Chem.*, **278**, 47261 (2003); J. M. Berrisford, J. Akerboom, S. Brouns, S. E. Sedelnikova, A. P. Turnbull, J. van der Oost, L. Salmon, R. Hardré, I. A. Murray, G. M. Blackburn, D. W. Rice and P. J. Baker, *J. Mol. Biol.*, **343**, 649 (2004).
304. A. K. Roos, E. Burgos, D. J. Ericsson, L. Salmon and S. L. Mowbray, *J. Biol. Chem.*, **280**, 6416 (2005).
305. P. L. Taylor, K. M. Blakely, G. P. De Leon, J. R. Walker, F. McArthur, E. Evdokimova, K. Zhang, M. A. Valvano, G. D. Wright and M. S. Junop, *J. Biol. Chem.*, **283**, 2835 (2008).
306. R. D. Kobes, R. T. Simpson, B. L. Vallee and W. J. Rutter, *Biochemistry*, **8**, 585 (1969).
307. N. S. Blom, S. Tetreault, R. Coulombe and J. Sygusch, *Nat. Struc. Biol.*, **3**, 856 (1996).
308. D. R. Hall, G. A. Leonard, C. D. Reed, C. I. Watt, A. Berry and W. N. Hunter, *J. Mol. Biol.*, **287**, 383 (1999).
309. A. Plater, S. M. Zgiby, G. J. Thomson, S. Qamar, C. W. Wharton and A. Berry, *J. Mol. Biol.*, **285**, 843 (1999).
310. Y. M. Zhang, J. K. Liu, M. R. Shouri and T. Y. Wong, *Biometals*, **19**, 31 (2006).
311. N. Lee, J. W. Patrick and M. Masson, *J. Biol. Chem.*, **243**, 4700 (1968).
312. Y. Luo, J. Samuel, S. C. Mosimann, J. E. Lee, M. E. Tanner and N. C. J. Strynadka, *Biochemistry*, **40**, 14763 (2001).
313. J. D. Deupree and W. A. Wood, *J. Biol. Chem.*, **247**, 3093 (1972).
314. L. V. Lee, M. V. Vu and W. W. Cleland, *Biochemistry*, **39**, 4808 (2000).
315. K. Kim, H. J. Kim, D. K. Oh, S. S. Cha and S. Rhee, *J. Mol. Biol.*, **361**, 920 (2006).
316. H. Yoshida, M. Yamada, T. Nishitani, G. Takada, K. Izumori and S. Karnitori, *J. Mol. Biol.*, **374**, 443 (2007).
317. Q. Cui and M. Karplus, *J. Am. Chem. Soc.*, **123**, 2284 (2001).
318. J. M. Brewer and L. Lebioda, *Adv. Biophys. Chem.*, **6**, 111 (1997); J. M. Brewer, *CRC Crit. Rev. Biochem.*, **11**, 209 (1981).
319. J. E. Wedekind, G. H. Reed and I. Rayment, *Biochemistry*, **34**, 4325 (1995).
320. J. E. Wedekind, R. R. Poyner, G. H. Reed and I. Rayment, *Biochemistry*, **33**, 9333 (1994).
321. R. R. Poyner, W. W. Cleland and G. H. Reed, *Biochemistry*, **40**, 8009 (2001).
322. L. Lebioda, B. Stec, J. M. Brewer and E. Tykarska, *Biochemistry*, **30**, 2823 (1991).
323. E. Zhang, J. M. Brewer, W. Minor, L. A. Carreira and L. Lebioda, *Biochemistry*, **36**, 12526 (1997).
324. S. Duquerroy, C. Camus and J. Janin, *Biochemistry*, **34**, 12513 (1995).
325. P. C. Babbitt, M. S. Hasson, J. E. Wedekind, D. R. Palmer, W. C. Barrett, G. H. Reed, I. Rayment, D. Ringe, G. L. Kenyon and J. A. Gerlt, *Biochemistry*, **35**, 16489 (1996); D. M. Z. Schmidt, E. C. Mundorff, M. Dojka, E. Bermudez, J. E. Ness, S. Govindarajan,

P. C. Babbitt, J. Minshull and J. A. Gerlt, *Biochemistry*, **42**, 8387 (2003); J. A. Gerlt and F. M. Raushel, *Curr. Opin. Chem. Biol.*, **7**, 252 (2003); J. A. Gerlt, P. C. Babbitt and I. Rayment, *Arch. Biochem. Biophys.*, **433**, 59 (2005).
326. T. B. Thompson, J. B. Garrett, E. A. Taylor, R. Meganathan, J. A. Gerlt and I. Rayment, *Biochemistry*, **39**, 10662 (2000); J. B. Thoden, E. A. Taylor-Ringia, J. B. Garrett, J. A. Gerlt, H. M. Holden and I. Rayment, *Biochemistry*, **43**, 5716 (2004).
327. D. M. Schmidt, B. K. Hubbard and J. A. Gerlt, *Biochemistry*, **40**, 15707 (2001).
328. D. J. Neidhart, P. L. Howell, G. A. Petsko, V. M. Powers, R. S. Li, G. L. Kenyon and J. A. Gerlt, *Biochemistry*, **30**, 9264 (1991); A. Sakai, D. F. Xiang, C. Xu, L. Song, W. S. Yew, F. M. Raushel and J. A. Gerlt, *Biochemistry*, **45**, 4455 (2006).
329. S. E. Williams, E. M. Woolridge, S. C. Ransom, J. A. Landro, P. C. Babbitt and J. W. Kozarich, *Biochemistry*, **31**, 9768 (1992); P. Mazur, W. A. Pieken, S. R. Budihas, S. E. Williams, S. Wong and J. W. Kozarich, *Biochemistry*, **33**, 1961 (1994); S. Helin, P. C. Kahn, B. L. Guha, D. G. Mallows and A. Goldman, *J. Mol. Biol.*, **254**, 918 (1995); M. S. Hasson, I. Schlichting, J. Moulai, K. Taylor, W. Barrett, G. L. Kenyon, P. C. Babbitt, J. A. Gerlt, G. A. Petsko and D. Ringe, *Proc. Natl. Acad. Sci. U.S.A.*, **95**, 10396 (1998); T. Kajander, L. Lehtio, M. Schlomann and A. Goldman, *Prot. Sci.*, **12**, 1855 (2003); J. Yang, Y. Wang, E. M. Woolridge, V. Arora, G. A. Petsko, J. W. Kozarich and D. Ringe, *Biochemistry*, **43**, 10424 (2004); S. Halak, L. Lehtio, T. Basta, S. Buerger, M. Contzen, A. Stolz and A. Goldman, *FEBS J.*, **273**, 5169 (2006).
330. W. S. Yew, A. A. Fedorov, E. V. Fedorov, J. F. Rakus, R. W. Pierce, S. C. Almo and J. A. Gerlt, *Biochemistry*, **45**, 14582 (2006); W. S. Yew, A. A. Fedorov, E. V. Fedorov, S. C. Almo and J. A. Gerlt, *Biochemistry*, **46**, 9564 (2007); J. F. Rakus, A. A. Fedorov, E. V. Fedorov, M. E. Glasner, J. E. Vick, P. C. Babbitt, S. C. Almo and J. A. Gerlt, *Biochemistry*, **46**, 12896 (2007).
331. J. E. Vick and J. A. Gerlt, *Biochemistry*, **46**, 14589 (2007).
332. V. A. Klenchin, E. A. Taylor Ringia, J. A. Gerlt and I. Rayment, *Biochemistry*, **42**, 14427 (2003).
333. T. M. Larsen, L. T. Laughlin, H. M. Holden, I. Rayment and G. H. Reed, *Biochemistry*, **33**, 6301 (1994); T. M. Larsen, M. M. Benning, G. E. Wesenberg, I. Rayment and G. H. Reed, *Arch. Biochem. Biophys.*, **345**, 199 (1997).
334. G. Valentini, L. R. Chiarelli, R. Fortin, M. Dolzan, A. Galizzi, D. J. Abraham, C. Wang, P. Bianchi, A. Zanella and A. Mattevi, *J. Biol. Chem.*, **277**, 23807 (2002).
335. L. Lebioda and B. Stec, *Nature*, **333**, 683 (1988).
336. S. H. Seeholzer, A. Jaworowski and I. A. Rose, *Biochemistry*, **30**, 727 (1991).
337. B. A. Miller and D. L. Leussing, *J. Am. Chem. Soc.*, **107**, 7146 (1985).
338. (a) I. Andersson and T. C. Taylor, *Arch. Biochem. Biophys.*, **414**, 130 (2003).
(b) F. C. Hartman and M. C. Harpel, *Annu. Rev. Biochem.*, **63**, 197 (1994); R. J. Spreitzer and M. E. Salvucci, *Annu. Rev. Plant Biol.*, **53**, 449 (2002).
339. T. C. Taylor, A. Backlund, K. Bjorhall, R. J. Andersson and I. Spreitzer, *J. Biol. Chem.*, **276**, 48159 (2001); K. Kitano, N. Maeda, T. Fukui, H. Atomi, T. Imanaka and K. Miki, *Structure*, **9**, 473 (2001).
340. J. Li, J. B. Cross, T. Vreven, S. O. Meroueh, S. Mobashery and H. B. Schlegel, *Prot. Struc. Func. Bioinfo.*, **61**, 246 (2005).
341. E. Jabri, M. B. Carr, R. P. Hausinger and P. A. Karplus, *Science*, **268**, 998 (1995).
342. M. M. Benning, J. M. Kuo, F. M. Raushel and H. M. Holden, *Biochemistry*, **34**, 7973 (1995).
343. M. Wishnick, D. Lane and M. C. Scrutton, *J. Biol. Chem.*, **245**, 4939 (1970); P. D. Robinson, M. N. Martin and F. R. Tabita, *Biochemistry*, **18**, 4453 (1979).
344. S. Karkehabadi, T. C. Taylor and I. Andersson, *J. Mol. Biol.*, **334**, 65 (2003).
345. W. W. Cleland, T. J. Andrews, S. Gutteridge, F. C. Hartman and G. H. Lorimer, *Chem. Rev.*, **98**, 549 (1998).
346. H. A. Schreuder, S. Knight, P. M. G. Curmi, I. Andersson, D. Cascio, C.-I. Brändén and D. Eisenberg, *Proc. Natl Acad. Sci. U.S.A.*, **90**, 9968 (1993); T. C. Taylor and I. Andersson, *Nature Struct. Biol.*, **3**, 95 (1996).
347. T. C. Taylor and I. Andersson, *J. Mol. Biol.*, **265**, 432 (1997).
348. A. T. Wilson and M. Calvin, *J. Am. Chem. Soc.*, **77**, 5948 (1955).
349. B. G. Saver and J. R. Knowles, *Biochemistry*, **21**, 5398 (1982); J. M. Sue and J. R. Knowles, *Biochemistry*, **21**, 5404 (1982).

350. K. Y. Zhang, D. Cascio and D. Eisenberg, *Prot. Sci.*, **3**, 64 (1994); E. Mizohata, H. Matsumura, Y. Okano, M. Kumei, H. Takuma, J. Onodera, K. Kato, N. Shibata, T. Inoue, A. Yokota and Y. Kai, *J. Mol. Biol.*, **316**, 679 (2002).
351. T. Lundqvist and G. Schneider, *J. Biol. Chem.*, **264**, 3643 (1989).
352. F. R. Tabita, T. E. Hanson, H. Li, S. Satagopan, J. Singh and S. Chan, *Microbiol. Mol. Biol. Rev.*, **71**, 576 (2007).
353. H. Ashida, Y. Saito, C. Kojima, K. Kobayashi, N. Ogasawara and A. Yokota, *Science*, **302**, 286 (2003); H. J. Imker, A. A. Fedorov, E. V. Fedorov, S. C. Almo and J. A. Gerlt, *Biochemistry*, **46**, 4077 (2007).
354. G. L. Wheeler, M. A. Jones and N. Smirnoff, *Nature*, **393**, 365 (1998).
355. N. Smirnoff, P. L. Conklin and F. A. Loewus, *Annu. Rev. Plant Physiol. Plant Mol. Biol.*, **52**, 437 (2001).
356. R. C. Kerber, *J. Chem. Educ.*, **85**, 1237 (2008).
357. J. M. Dunwell, A. Purvis and S. Khuri, *Phytochemistry*, **65**, 7 (2004).
358. C. Roux, N. Gresh, L. E. Perera, J.-P. Piquemal and L. Salmon, *J. Comput. Chem.*, **28**, 938 (2007).
359. K. H. Sharp, M. Mewies, P. C. Moody and E. L. Raven, *Nat. Struct. Biol.*, **10**, 303 (2003).
360. A. Messerschmidt, R. Ladenstein, R. Huber, M. Bolognesi, L. Avigliano, R. Petruzzelli, A. Rossi and A. Finazzi-Agró, *J. Mol. Biol.*, **224**, 179 (1992); A. Messerschmidt, H. Luecke and R. Huber, *J. Mol. Biol.*, **230**, 997 (1993).
361. A. Montel-Hagen, S. Kinet, N. Manel, C. Mongellaz, R. Prohaska, J.-L. Battini, J. Delaunay, M. Sitbon and N. Taylor, *Cell*, **132**, 1039 (2008).
362. M. A. McDonough, V. Li, E. Flashman, E. Flashman, R. Chowdhury, C. Mohr, B. M. R. Lienard, J. Zondlo, N. J. Oldham, I. J. Clifton, J. Lewis, L. A. McNeill, R. J. M. Kurzeja, K. S. Hewitson, E. Yang, S. Jordan, R. S. Syed and C. J. Schofield, *Proc. Natl. Acad. Sci. U.S.A.*, **103**, 9814 (2006).
363. P. John, *Physiol. Plant.*, **100**, 583 (1997).
364. K. Saito, M. Kobayashi, Z. Z. Gong, Y. Tanaka and M. Yamazaki, *Plant J.*, **17**, 181 (1999).
365. M. Mure, *Acc. Chem. Res.*, **37**, 131 (2004); E. Agostinelli, F. Belli, L. D. Vedova, S. Longu, A. Mura and G. Floris, *Eur. J. Inorg. Chem.*, 1635 (2005).
366. M. Mure, S. A. Mills and J. P. Klinman, *Biochemistry*, **41**, 9269 (2002).
367. J. E. Dove, B. Schwartz, N. K. Williams and J. P. Klinman, *Biochemistry*, **39**, 3690 (2000); J. L. DuBois and J. P. Klinman, *Arch. Biochem. Biophys.*, **433**, 255 (2005); N. M. Samuels and J. P. Klinman, *J. Biol. Chem.*, **281**, 21114 (2006).
368. M. R. Parsons, M. A. Convery, C. M. Wilmot, K. D. Yadav, V. Blakeley, A. S. Corner, S. E. Phillips, M. J. McPherson and P. F. Knowles, *Structure*, **3**, 1171 (1995).
369. V. Kumar, D. M. Dooley, H. C. Freeman, J. M. Guss, I. Harvey, M. A. McGuirl, M. C. J. Wilce and V. M. Zubak, *Structure*, **4**, 943 (1996).
370. M. C. J. Wilce, D. M. Dooley, H. C. Freeman, J. M. Guss, H. Matsunami, W. S. McIntire, C. E. Ruggiero, K. Tanizawa and H. Yamaguchi, *Biochemistry*, **36**, 16116 (1997).
371. R. Li, J. P. Klinman and F. S. Mathews, *Structure*, **6**, 293 (1998).
372. A. P. Duff, A. E. Cohen, P. J. Ellis, J. A. Kuchar, D. B. Langley, E. M. Shepard, D. M. Dooley, H. C. Freeman and J. M. Guss, *Biochemistry*, **42**, 15148 (2003); A. P. Duff, A. E. Cohen, P. J. Ellis, K. Hilmer, D. B. Langley, D. M. Dooley, H. C. Freeman and J. M. Guss, *Acta Crystallogr., Sect. D*, **62**, 1073 (2006).
373. S. X. Wang, M. Mure, K. F. Medzihradszky, A. L. Burlingame, D. E. Brown, D. M. Dooley, A. J. Smith, H. M. Kagan and J. P. Klinman, *Science*, **273**, 1078 (1996); A. C. Rinaldi, C. M. Porcu, S. Oliva, N. Curreli, A. Rescigno, F. Sollai, A. Rinaldi, A. Finazzi-Agró and E. Sanjust, *Eur. J. Biochem.*, **251**, 91 (1998); M. Kim, T. Okajima, S. Kishishita, M. Yoshimura, A. Kawamori, K. Tanizawa and H. Yamaguchi, *Nat. Struct. Biol.*, **9**, 591 (2002); M. Mure, S. X. Wang and J. P. Klinman, *J. Am. Chem. Soc.*, **125**, 6113 (2003); J. A. Bollinger, D. E. Brown and D. M. Dooley, *Biochemistry*, **44**, 11708 (2005).
374. R. H. Moore, M. A. Spies, M. B. Culpepper, T. Murakawa, S. Hirota, T. Okajima, K. Tanizawa and M. Mure, *J. Am. Chem. Soc.*, **129**, 11524 (2007).
375. B. Winkel-Shirley, *Plant Physiol.*, **126**, 485 (2001).
376. K. Saito, M. Kobayashi, Z. Z. Gong, Y. Tanaka and M. Yamazaki, *Plant J.*, **17**, 181 (1999).
377. G. Speier, in *Dioxygen Activation and Homogeneous Catalytic Oxidation* (Ed. L. I. Simándi), Elsevier, Amsterdam, 1991, pp. 269–278.

378. R. A. Steiner, I. M. Kooter and B. W. Dijkstra, *Biochemistry*, **41**, 7955 (2002).
379. R. A. Steiner, W. Meyer-Klaucke and B. W. Dijkstra, *Biochemistry*, **41**, 7963 (2002).
380. G. F. Z. da Silva and L.-J. Ming, *Angew. Chem. Int. Ed.*, **44**, 5501 (2005).
381. M. Costas, M. P. Mehn and M. P. Jensen, L. Que, *Chem. Rev.*, **104**, 939 (2004).
382. T. Oka and F. J. Simpson, *Biochem. Biophys. Res. Commun.*, **43**, 1 (1971); H.-K. Hund, J. Breuer, F. Lingens, J. Huttermann, R. Kappl and S. Fetzner, *Eur. J. Biochem.*, **263**, 871 (1999).
383. S. Tranchimand, G. Ertel, V. Gaydou, C. Gaudin, T. Tron and G. Iacazio, *Biochimie*, **90**, 781 (2008).
384. B. M. Barney, M. R. Schaab, R. LoBrutto and W. A. Francisco, *Prot. Express. Purif.*, **35**, 131 (2004); L. Bowater, S. A. Fairhust, V. J. Just and S. Bornemann, *FEBS Lett.*, **557**, 45 (2004).
385. M. R. Schaab, B. M. Barney and W. A. Francisco, *Biochemistry*, **45**, 1009 (2006).
386. B. Gopal, L. L. Madan, S. F. Betz and A. A. Kossiakoff, *Biochemistry*, **44**, 193 (2005).
387. J. Kaizer, G. Baráth, J. Pap, G. Speier, M. Giorgi and M. Réglier, *Chem. Commun.*, 5235 (2007).
388. F. Fusetti, K. H. Schroter, R. A. Steiner, P. I. van Noort, T. Pijning, H. J. Rozeboom, K. H. Kalk, M. R. Egmond and B. W. Dijkstra, *Structure*, **10**, 259 (2002).
389. I. M. Kooter, R. A. Steiner, B. W. Dijkstra, P. I. van Noort, M. R. Egmond and M. Huber, *Eur. J. Biochem.*, **269**, 2971 (2002).
390. F. Jian, J. Peisach, L.-J. Ming, L. Que, Jr. and V. J. Chen, *Biochemistry*, **30**, 11437 (1991).
391. R. A. Steiner, K. H. Kalk and B. W. Dijkstra, *Proc. Natl. Acad. Sci. U.S.A.*, **99**, 16625 (2002).
392. P. Aisen, in *Biological Inorganic Chemistry: Structure and Reactivity* (Eds H. B. Gray, E. I. Stiefel, J. S. Valentine and I. Bertini), Chap. VIII.1, Sausalito, CA, 2007.
393. R. Anand, P. C. Dorrestein, C. Kinsland, T. P. Begley and S. E. Ealick, *Biochemistry*, **41**, 7659 (2002).
394. H. Pang, M. Bartlam, Q. Zeng, H. Miyatake, T. Hisano, K. Miki, L. L. Wong, G. F. Gao and Z. Rao, *J. Biol. Chem.*, **279**, 1491 (2004).
395. M. Adams and Z. Jia, *J. Biol. Chem.*, **280**, 28675 (2005).
396. Y. R. Lapik and L. S. Kaufman, *Plant Cell*, **15**, 1578 (2003).
397. M. R. Harpel and J. D. Lipscomb, *J. Biol. Chem.*, **265**, 6301 (1990).
398. M. A. Adams, V. K. Singh, B. O. Keller and Z. Jia, *Mol. Microbiol.*, **61**, 1469 (2006).
399. G. P. Titus, H. A. Mueller, J. Burgner, S. Rodríguez de Córdoba, M. A. Peñalva and D. E. Timm, *Nat. Struct. Biol.*, **7**, 542 (2000).
400. M. R. Harpel and J. D. Lipscomb, *J. Biol. Chem.*, **265**, 22187 (1990).
401. R. Wilmouth, J. Turnbull, R. Welford, I. Clifton, A. Prescott and C. Schofield, *Structure*, **10**, 93 (2002).
402. R. A. Casero, Jr. and L. J. Marton, *Nat. Rev. Drug Dis.*, **6**, 373 (2007).
403. Y. Dai, T. C. Pochapsky and R. H. Abeles, *Biochemistry*, **40**, 6379 (2001).
404. Y. Dai, P. C. Wensink and R. H. Abeles, *J. Biol. Chem.*, **274**, 1193 (1999).
405. K. Hult and P. Berglund, *Trends Biotech.*, **25**, 232 (2007).
406. K. Okrasa and R. J. Kazlauskas, *Chem. Eur. J.*, **12**, 1587 (2006).
407. G. F. Z. da Silva and L.-J. Ming, *J. Am. Chem. Soc.*, **127**, 16380 (2005).
408. J. W. Wray and R. H. Abeles, *J. Biol. Chem.*, **268**, 21466 (1993); J. W. Wray and R. H. Abeles, *J. Biol. Chem.*, **270**, 3147 (1995).
409. X. Wei and L.-J. Ming, *Inorg. Chem.*, **37**, 2255 (1998).
410. T. C. Pochapsky, S. S. Pochapsky, T. Ju, H. Mo, F. Al-Mjeni and M. J. Maroney, *Nat. Struct. Biol.*, **9**, 966 (2002).
411. T. Borowski, A. Bassan and P. E. M. Siegbahn, *J. Mol. Struct. (Theochem.)*, **772**, 89 (2006).
412. Q. Xu, R. Schwarzenbacher, S. S. Krishna, D. McMullan, S. Agarwalla, K. Quijano, P. Abdubek, E. Ambing, H. Axelrod, T. Biorac, J. M. Canaves, H. J. Chiu, M. A. Elsliger, C. Grittini, S. K. Grzechnik, M. DiDonato, J. Hale, E. Hampton, G. W. Han, J. Haugen, M. Hornsby, L. Jaroszewski, H. E. Klock, M. W. Knuth, E. Koesema, A. Kreusch, P. Kuhn, M. D. Miller, K. Moy, E. Nigoghossian, J. Paulsen, R. Reyes, C. Rife, G. Spraggon, R. C. Stevens, H. van den Bedem, J. Velasquez, A. White, G. Wolf, K. O. Hodgson, J. Wooley, A. M. Deacon, A. Godzik, S. A. Lesley and I. A. Wilson, *Proteins*, **64**, 808 (2006).
413. T. C. Pochapsky, S. S. Pochapsky, T. Ju, C. Hoefler and J. Liang, *J. Biomol. NMR*, **34**, 117 (2006).

414. T. Ju, R. B. Goldsmith, S. C. Chai, M. J. Maroney, S. S. Pochapsky and T. C. Pochapsky, *J. Mol. Biol.*, **363**, 823 (2006).
415. (a) E. Szajna, A. M. Arif and L. M. Berreau, *J. Am. Chem. Soc.*, **127**, 17186 (2005).
(b) E. Szajna-Fuller, K. Rudzka, A. M. Arif and L. M. Berreau, *Inorg. Chem.*, **46**, 5499 (2007).
416. J. R. Haines and M. Alexander, *Appl. Microbiol.*, **29**, 621 (1975).
417. G. Grogan, *Biochem. J.*, **388**, 721 (2005).
418. D. Pokorny, W. Steiner and D. W. Ribbons, *Trends Biotech.*, **15**, 291 (1997); G. Grogan, *J. Mol. Catal. B: Enzymatic*, **19–20**, 73 (2002).
419. H. M. Holden, M. M. Benning, T. Haller and J. A. Gerlt, *Acc. Chem. Res.*, **34**, 145 (2001).
420. E. D. Eberhard and J. A. Gerlt, *J. Am. Chem. Soc.*, **126**, 7188 (2004).
421. G. Grogan, G. A. Roberts, D. Bougioukou, N. J. Turner and S. L. Flitsch, *J. Biol. Chem.*, **276**, 12565, (2001); G. Grogan, J. Graf, A. Jones, S. Parsons, N. J. Turner and S. L. Flitsch, *Angew. Chem. Int. Ed.*, **40**, 1111 (2001).
422. J. P. Bennett, J. L. Whittingham, A. M. Brzozowski, P. M. Leonard and G. Grogan, *Biochemistry*, **46**, 137 (2007).
423. J. F. Davey and D. W. Ribbons, *J. Biol. Chem.*, **250**, 3826 (1975).
424. D. Pokorny, L. Brecker, M. Pogorevc, W. Steiner, H. Griengl, T. Kappe and D. W. Ribbons, *J. Bacteriol.*, **181**, 5051 (1999).
425. E. A. Kvittingen, *Scand. J. Clin. Lab. Invest. Suppl.*, **184**, 27 (1986); E. A. Kvittingen, *J. Inherit. Metab. Dis.* **14**, 554 (1991); E. A. Kvittingen, *J. Inherit. Metab. Dis.*, **18**, 375 (1995); S. T. Pitkänen, M. K. Salo and M. Heikinheimo, *Ann. Med.*, **32**, 530 (2000); F. Endo and M. S. Sun, *J. Inherit. Metab. Dis.*, **25**, 227 (2002).
426. (a) R. L. Bateman, P. Bhanumoorthy, J. F. Witte, R. W. McClard, M. Grompe and D. E. Timm, *J. Biol. Chem.*, **276**, 15284 (2001).
(b) R. L. Bateman, J. Ashworth, J. F. Witte, L.-J. Baker, P. Bhanumoorthy, D. E. Timm, T. D. Hurley, M. Grompe and R. W. McClard, *Biochem. J.*, **402**, 251 (2007).
427. G. Straganz, L. Brecker, H.-J. Weber, W. Steiner and D. W. Ribbons, *Biochem. Biophys. Res. Commun.*, **297**, 232 (2002).
428. G. D. Straganz, A. Glieder, L. Brecker, D. W. Ribbons and W. Steiner, *Biochem. J.*, **369**, 573 (2003).
429. G. D. Straganz, H. Hofer, W. Steiner and B. Nidetzky, *J. Am. Chem. Soc.*, **126**, 12202, (2004).
430. G. D. Straganz and B. Nidetzky, *J. Am. Chem. Soc.*, **127**, 12306, (2005).
431. T. K. Paine, J. England and L. Que, *Chem. Eur. J.*, **13**, 6073 (2007).
432. G. D. Straganz, S. Egger, G. Aquino, S. D'Auria and B. Nidetzky, *J. Mol. Catal. B: Enzymol.*, **39**, 171 (2006).
433. B. S. Speer, N. B. Shoemaker and A. A. Salyers, *Clin. Microbiol. Rev.*, **5**, 387 (1992); D. Schnappinger and W. Hillen, *Arch. Microbiol.*, **165**, 359 (1996); H. C. Neu, *Science*, **29**, 245 (1992).
434. J. R. Smythies, F. Benington and R. D. Morin, *Experientia*, **28**, 1253 (1972).
435. J. P. White and C. R. Cantor, *J. Mol. Biol.*, **58**, 397 (1971).
436. C. Berens, in *RNA-Binding Antibiotics* (Eds. R. Schroeder and M. G. Wallis), Chap. 6, Landes Bioscience, Austin, TX, 2001.
437. G. Fey, M. Reiss and H. Kersten, *Biochemistry*, **12**, 1160 (1973).
438. D. Moazed and H. F. Noller, *Nature*, **327**, 389 (1987); R. Oehler, N. Polacek, G. Steiner and A. Barta, *Nucl. Acids Res.*, **25**, 1219 (1997); J. I. Ross, E. A. Eady, J. H. Cove and W. J. Cunliffe, *Antimicrob. Agents Chemother.*, **42**, 1702 (1998).
439. (a) D. E. Brodersen, W. M. Clemons, Jr, A. P. Carter, R. J. Morgan-Warren, B. T. Wimberly and V. Ramakrishnan, *Cell*, **103**, 1143 (2000).
(b) M. Pioletti, F. Schlunzen, J. Harms, R. Zarivach, M. Gluhmann, H. Avila, A. Bashan, H. Bartels, T. Auerbach, C. Jacobi, T. Hartsch, A. Yonath and F. Franceschi, *EMBO J.*, **20**, 1829 (2001).
440. M. A. Khan and J. Musarrat, *Int. J. Biol. Macromol.*, **33**, 49 (2003).
441. R. B. Martin, *Met. Ions Biol. Sys.*, **19**, 19 (1985).
442. C. M. Mikulski, J. Fleming and D. Fleming, *Inorg. Chim. Acta*, **144**, 9 (1988).
443. T. Ohyama and J. A. Cowan, *Inorg. Chem.*, **34**, 3083 (1995); M. Novák-Pékli, M. E.-H. Mesbah and G. Pethö, *J. Pharm. Biomed. Anal.*, **14**, 1025 (1996); L. Lambs and G. Berthon,

Inorg. Chim. Acta, **151**, 33 (1988); J. M. Wessels, W. E. Ford, W. Szymczak and S. Schneider, *J. Phys. Chem. B*, **102**, 9323 (1998).
444. F. C. S. de Paula, S. Carvalho, H. A. Duarte, E. B. Paniago, A. S. Mangrich and E. C. Pereira-Maia, *J. Inorg. Biochem.*, **76**, 221 (1999).
445. M. Jeżowska-Bojczuk, L. Lambs, H. Kozłowski and G. Berthon, *Inorg. Chem.*, **32**, 428 (1993).
446. F. C. Machado, C. Demicheli, A. Garnier-Suillerot and H. Beraldo, *J. Inorg. Biochem.*, **60**, 163 (1995); H. F. Dos Santos, E. S. Xavier, M. C. Zerner and W. B. De Almeida, *J. Mol. Struct. (Theochem)*, **527**, 193 (2000); G. Berthon, M. Brion and L. Lambs, *J. Inorg. Biochem.*, **19**, 1 (1983); M. Brion, G. Berthon and J. B. Fourtillan, *Inorg. Chim. Acta*, **55**, 47 (1981).
447. K. H. Jogun and J. J. Stezowski, *J. Am. Chem. Soc.*, **98**, 6018 (1976); M. Celotti and G. V. Fazakerley, *J. Chem. Soc. Trans. 2*, 1319 (1977); M. Schnarr, M. Matthies and W. Lohmann, *Z. Naturforsch.*, **34**, 1156 (1979).
448. Y. Jung and Y. M. Kim, *Drug Deliv.*, **15**, 31 (2008).
449. A. Yamaguchi, T. Udagawa and T. Sawai, *J. Biol. Chem.*, **265**, 4089 (1990); W. Hellen and C. Berens, *Annu. Rev. Microbiol.*, **48**, 345 (1994); J. Jin J. A. A. Guffanti, D. H. Bechhofer and T. A. Krulwich, *J. Bacteriol.*, **184**, 4722 (2002).
450. M. Takahashi, L. Altschmied and W. Hillen, *J. Mol. Biol.*, **187**, 341 (1986); P. Orth, W. Saenger and W. Hinrichs, *Biochemistry*, **38**, 191 (1999).
451. P. Orth, F. Cordes, D. Schnappinger, W. Hillen, W. Saenger and W. Hinrichs, *J. Mol. Biol.* **279**, 439 (1998).
452. W. Hinrichs, C. Kisker, M. Düvel, A. Müller, K. Tovar, W. Hillen and W. Saenger, *Science*, **264**, 418 (1994); C. Kisker, W. Hinrichs, K. Tovar, W. Hillen and W. Saenger, *J. Mol. Biol.*, **247**, 260 (1995); P. Orth, D. Schnappinger, P. E. Sum, G. A. Ellestad, W. Hillen, W. Saenger and W. Hinrichs, *J. Mol. Biol.*, **285**, 455 (1999); A. Aleksandrov, J. Proft, W. Hinrichs and T. Simonson, *Chembiochem*, **8**, 675 (2007).
453. P. Orth, D. Schnappinger, W. Hillen, W. Saenger and W. Hinrichs, *Nat. Struct. Biol.*, **7**, 215 (2000).
454. T. Lederer, G. J. Palm, P. Orth, W. Saenger, M. Takahashi, W. Hillen and W. Hinrichs, Unpublished structure submitted to the Protein Data Bank (pdb ID 2fj1).
455. (a) N. Ettner, J. W. Metzger, T. Lederer, J. D. Hulmes, C. Kisker, W. Hinrichs, G. A. Ellestad and W. Hillen, *Biochemistry*, **34**, 22 (1995).
(b) N. Ettner, W. Hillen and G. A. Ellestad, *J. Am. Chem. Soc.*, **115**, 2546 (1993).
456. J. Bergeron, M. Ammirati, D. Danley, L. James, M. Norcia, J. Retsema, C. A. Strick, W. G. Su, J. Sutcliffe and L. Wondrack, *Antimicrob. Agents Chemother.*, **40**, 2226 (1996); I. Chopra, *Curr. Opin. Pharmacol.*, **1**, 464 (2001); A. P. Johnson, *Curr. Opin. Anti-Infect. Invest. Drugs*, **2**, 164 (2000).
457. R. Kayyali, J. B. Porter, Z. D. Liu, N. A. Davies, J. H. Nugent, C. E. Cooper and R. C. Hider, *J. Biol. Chem.*, **276**, 48814 (2001); Z. D. Liu, R. Kayyali, R. C. Hider, J. B. Porter and A. E. Theobald, *J. Med. Chem.*, **45**, 631 (2002).
458. E. A. Abourashed, I. Muhammad, M. Resch, R. Bauer, F. S. el-Feraly and C. D. Hufford, *Planta Med.*, **67**, 360 (2001).
459. E. W. Oppenheim, I. M. Nasrallah, M. G. Mastri and P. J. Stover, *J. Biol. Chem.*, **275**, 19268 (2000).
460. L. Bubacco, E. Vijgenboom, C. Gobin, A. W. J. W. Tepper, J. Salgado and G. W. Canters, *J. Mol. Catal. B: Enzymatic*, **8**, 27 (2000).
461. H. Hashiguchi and H. Takahashi, *Mol. Pharmacol.*, **13**, 362 (1977).
462. M. E. Winkler, K. Lerch and E. I. Solomon, *J. Am. Chem. Soc.*, **103**, 7001 (1981).
463. R. Saruno, F. Kato and T. Ikeno, *Agric. Biol. Chem.*, **43**, 1337 (1979); G. Battaini, E. Monzani, L. Casella, L. Santagostini and R. Pagliarin, *J. Biol. Inorg. Chem.*, **5**, 262 (2000); J. S. Chen, C.-i Wei, R. S. Rolle, W. S. Otwell, M. O. Balaban and M. R. Marshall, *J. Agric. Food Chem.*, **39**, 1396 (1991).
464. S. R. Piettre, C. André, M. C. Chanal, J. B. Ducep, B. Lesur, F. Piriou, P. Raboisson, J.-M. Rondeau, C. Schelcher, P. Zimmermann and A. J. Ganzhorn, *J. Med. Chem.*, **40**, 4208 (1997).
465. A. J. Ganzhorn and J.-M. Rondeau, *Prot. Eng.*, **10**, 61 (1997).
466. S. R. Piettre, A. Ganzhorn, J. Hoflack, K. Islam and J. M. Hornsperger, *J. Am. Chem. Soc.*, **119**, 3201 (1997).

467. M. Goldstein, E. Lauber and M. R. McKereghan, *Biochem. Pharmacol.*, **13**, 1103 (1964)
468. J. C. Espin and H. J. Wichers, *J. Agric. Chem.*, **47**, 2638 (1999).
469. E. Valero, García-Moreno, R. Varón and F. García-Carmona, *J. Agric. Food Chem.*, **39**, 1043 (1991).
470. R. T. Borchard, *J. Med. Chem.*, **16**, 377 (1973).
471. S. R. Budihas, I. Gorshkova, S. Gaidamakov, A. Wamiru, M. K. Bona, M. A. Parniak, R. J. Crouch, J. B. McMahon, J. A. Beutler and S. F. J. Le Grice, *Nucl. Acids Res.*, **33**, 1249 (2005).
472. G. R. Moran, *Arch. Biochem. Biophys.*, **433**, 117 (2005).
473. G. R. Whistance and D. R. Threlfall, *Biochem. J.*, **117**, 593 (1970).
474. L. Serre, A. Sailland, D. Sy, P. Boudec, A. Rolland, E. Pebay-Peyroula and C. Cohen-Addad, *Structure*, **7**, 977 (1999).
475. I. M. Fritze, L. Linden, J. Freigang, G. Auerbach, R. Huber and S. Steinbacher, *Plant Physiol.*, **134**, 1388 (2004).
476. C. Yang, J. W. Pflugrath, D. L. Camper, M. L. Foster, D. L. Pernich and T. A. Walsh, *Biochemistry*, **43**, 10414 (2004).
477. J. Brownlee, K. Johnson-Winters, D. H. T. Harrison and G. R. Moran, *Biochemistry*, **43**, 6370 (2004).
478. D. L. Lee, C. G. Knudsen, W. J. Michaely, H.-L. Chin, N. H. Nguyen, C. G. Carter, T. H. Cromartie, B. H. Lake, J. M. Shribbs and T. Fraser, *Pestic. Sci.*, **54**, 377 (1998).
479. G. Meazza, B. E. Scheffler, M. R. Tellez, A. M. Rimando, S. O. Duke, D. Nanyarkkara, I. A. Khan, E. A. Abourashed and F. E. Dayan, *Phytochemistry*, **60**, 281 (2002).
480. F. E. Dayan, S. O. Duke, A. Sauldubois, N. Singh, C. McCurdy and C. Cantrell, *Phytochemistry*, **68**, 2004 (2007)
481. J. G. Romagni, G. Meazza, N. P. D. Nanayakkara and F. E. Dayan, *FEBS Lett.*, **480**, 301 (2000).
482. S. Lindstedt, E. Holme, E. Lock, O. Hialmarson and B. Strandvik, *Lancet*, **340**, 813 (1992); C. Phornphutkul, W. J. Introne, M. B. Perry, I. Bernardini, M. D. Murphey, D. L. Fitzpatrick, P. D Anderson, M. Huizing, Y. Anikster, L. H. Gerber and W. A. Gahl, *N. Engl. J. Med.*, **347**, 2111 (2002).
483. C. S. Wu, J. L. Huang, Y. S. Sun and D. Y. Yang, *J. Med. Chem.*, **45**, 2222 (2002).
484. M. Kavana and G. R. Moran, *Biochemistry*, **42**, 10238 (2003).
485. O. W. Choroba, D. H. Williams and J. B. Spencer, *J. Am. Chem. Soc.*, **122**, 5389 (2000); T. L. Li, O. W. Choroba, E. H. Charles, A. M. Sandercock, D. H. Williams and J. B. Spencer, *Chem. Cimmun.*, 1752 (2001).
486. B. K. Hubbard, M. G. Thomas and C. T. Walsh, *Chem Biol.*, **7**, 931 (2000).
487. J. Brownlee, P. He, G. R. Moran and D. H. T. Harrison, *Biochemistry*, **47**, 2002 (2008).
488. J. A. Conrad and G. R. Moran, *Inorg. Chim. Acta*, **361**, 1197 (2008).

CHAPTER 12

Analytical aspects of metal enolates

ELI HARLEV and SHMUEL BITTNER

Department of Chemistry, Ben-Gurion University of the Negev, P. O. Box 653, Beer-Sheva 84105, Israel
Fax: +972 77 7575886; e-mail: bittner@bgu.ac.il

and

JACOB ZABICKY

Department of Chemical Engineering, Ben-Gurion University of the Negev, P. O. Box 653, Beer-Sheva 84105, Israel
Fax: +972 8 6472969; e-mail: zabicky@bgu.ac.il

The chemistry of metal enolates
Edited by Jacob Zabicky

I. ACRONYMS

AAS	atomic absorption spectroscopy/spectrometry
acac	acetylacetonate anion
ANN	artificial neural network
bipy	2,2′-bipyridine
bzac	benzoylacetonate anion
bztfac	1-benzoyl-3,3,3-trifluoroacetonate anion
CD	circular dichroism
CE	capillary electrophoresis
CPE	carbon paste electrode
CV	cyclic voltametry
dibzac	1,3-diphenyl-1,3-propanedionate anion
dik	β-diketonate anion
dpm	dipivaloylmethanate anion
DPV	differential pulse voltametry
ECD	electron capture detection/detector
ESI-MS	electrospray ionization mass spectrum/spectrometry
FAAS	flame AAS
FID	flame ionization detection/detector
FLD	fluorescence detection/detector
fuac	2-furoylacetonate anion
futfac	1-(2-furoyl)-3,3,3-trifluoroacetonate anion
GCE	glassy carbon electrode
hfac	1,1,1,6,6,6-hexafluoro-2,4-pentanedionato anion
hfod	1,1,1,2,2,3,3-heptafluoro-7,7-dimethyl-4,6,-octanedionate anion

ICP-AES	inductively coupled plasma atomic emission spectroscopy/spectrometry
IP	ion-pair
ISE	ion-selective electrode/s
LC	liquid chromatography
LOD	limit/s of detection
LOQ	limit/s of quantitation
MALDI	matrix-assisted laser desorption/ionization
miRNA	microribonucleic acid
ODS	octadecyl-bonded silica gel
phen	1,10-phenanthroline
PLS	partial least squares
ptfa	pivaloyltrifluoroacetonate anion
pvc	poly(vinyl chloride)
RP	reversed phase
RSD	relative standard deviation
SCE	saturated calomel electrode
sds	sodium dodecylsulfate
SFC	supercritical fluid chromatography
SNR	signal-to-noise ratio
SSCE	silver–silver chloride electrode
TCD	thermal conductivity detection/detector
tfa	trifluoroacetic acid
tfac	trifluoroacetylacetonate anion
thf	tetrahydrofuran
TLC	thin layer chromatography
TOF	time of flight
tris	2-amino-2-hydroxymethyl-1,3-propanediol
ttfac	1-thenoyl-3,3,3-trifluoroacetonate anion
UPS	ultraviolet photoelectron spectroscopy
UVD	UVV detection/detector
UVV	ultraviolet-visible
XPS	X-ray photoelectron spectroscopy

II. INTRODUCTION AND SCOPE OF THE CHAPTER

Several problems have to be considered in modern practice when developing new analytical methods, as briefly discussed in other volumes of *The Chemistry of Functional Groups* series[1,2]. The classical requirements of accuracy and precision regarding performance are now part of the more inclusive concept of 'fitness for purpose'[3], which stresses the importance of validation. Consideration must also be given to occupational risks for the personnel working with the method and to the environmental risks involved in the disposal of spent samples and reagents. Optimization of operational parameters may be a complicated task when they interact in a nonlinear fashion. A chemometric approach to experimental design may be very rewarding, as in the case of optimization of the CE-UVD determination of ascorbic acid (**1**)–isoascorbic acid (**2**) mixtures[4] mentioned in Section III.C.2. When developing methods for routine application, savings in time and reagents are all-important; these may be achieved by introduction of automation in the analytical operations, reduction of the reactor volume, using sensitive instrumentation and applying computational chemometric techniques. Multiple analyte determinations can become problematic due to mutual interference, which may be avoided on applying a chromatographic separation and detection method. However, such an option is expensive in time and valuable mobile phases. Examples of a new trend are shown in Section III.C.1

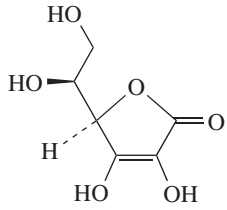

(**1**)

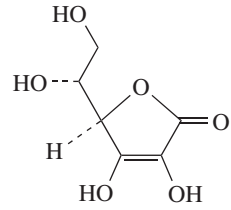

(**2**)

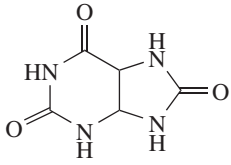

(**3**)

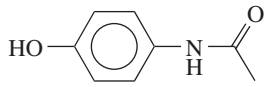

(**4**)

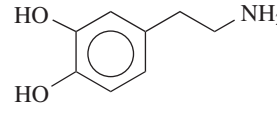

(**5**)

for the simultaneous electrochemical determination of ascorbic acid (**1**), uric acid (**3**) and paracetamol (**4**). The chosen alternative in this case was a voltametric measurement, using an 'electronic tongue' holding several small working electrodes, and applying the ANN computational technique for interpreting the results[5]; also the simultaneous electrochemical analysis of **1** and dopamine (**5**), showing strong nonlinear interference between the analytes[6] or rather close oxidation potentials[7], was solved with the aid of computational techniques.

Throughout this volume are mentioned applications of metal enolates as catalysts[8], polymer initiators[9], luminescent compounds[10] and precursors for metal or metal oxide deposition[11]. Metal enolates are also part of pharmaceuticals and other consumer products and take part in important biological processes[12]. Ascorbic acid (**1**) and derived salts such as magnesium ascorbylphosphate (**6**) have found application in modern cosmetics for their protective action against photoaging and their whitening action on the skin as synergetics of melatonin (**7**), a hormone secreted by the pineal gland[13]. Kojic acid (**8**) has found applications due to its ability of sequestering transition metal ions (e.g. the enolate complexes **9**). Thus, **8**, alone or with other antioxidants such as **1**, is used in skin bleaching formulations, as inhibitor of the Cu metalloenzyme tyrosinase participating in melanin formation[14,15]. **8** and its manganese and zinc complexes (**9**) are low-toxicity compounds with good *in vivo* radioprotective activity, similar to that of amifostine (**10**), which is administered before radiotherapy to diminish possible damage caused by γ-rays to healthy cells[16]. Besides the important role of ascorbate/ascorbic acid in biological systems, making them most studied analytes, they are also considered as the archetypal interference species when analyzing samples of biological origin[17]. Quality control and tracking the fate of these compounds in processes requires analytical methods for detection and determination of metal enolates, which are discussed in Section III.

Metal enolates found varied application in chemical analysis. An outstanding group are certain lanthanide enolates used as shift reagents in NMR spectroscopy[18]. The analytical methods discussed in Section IV are based on formation of a metal enolate for separation, detection, identification and determination of metal ions or the use of a metal enolate as ancillary reagent to improve analytical quality. Of special relevance in analytical chemistry are the metal β-diketonates, $M(dik)_n$, derivatived from deprotonated β-diketones (dikH),

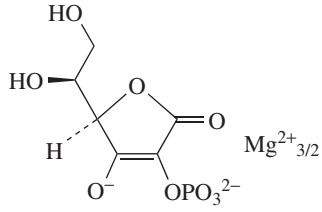

(**6**)

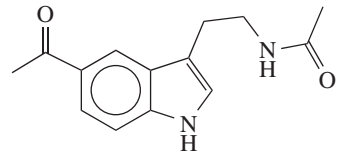

(**7**)

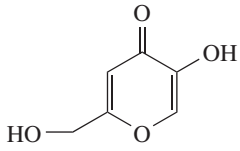

(**8**)

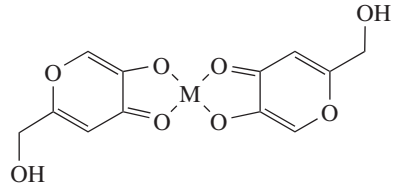

(**9**) M = Mn, Zn

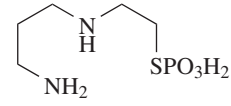

(**10**)

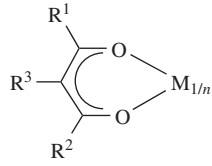

(**11**) R^3 = H unless otherwise stated

$R^1 = R^2 =$ Me (acac); $R^1 =$ Me, $R^2 =$ Ph (bzac); $R^1 =$ Mef, $R^2 =$ Ph, (bztfac);

$R^1 = R^2 =$ Ph (dibzac); $R^1 = R^2 =$ *t*-Bu (dpm); $R^1 =$ Me, $R^2 =$ 2-Fu (fuac);

$R^1 =$ Mef, $R^2 =$ 2-Fu (futfac); $R^1 = R^2 =$ Mef (hfac); $R^1 =$ *t*-Bu, $R^2 =$ *n*-Prf (hfod);

$R^1 =$ Mef, $R^2 =$ *t*-Bu (ptfa); $R^1 =$ Me, $R^2 =$ Mef (tfac); $R^1 =$ Mef, $R^2 =$ 2-Fu (ttfac)

especially when they assume a chelate configuration, as shown in the various modalities of **11**. Sometimes the metal in **11** is coordinated to additional ligands.

III. DETECTION AND DETERMINATION OF METAL ENOLATES

A. General

Enolates of many metals were synthesized in the last 50 years and were characterized and determined, applying large number of chemical, physical and spectral methods. For example, lanthnide chelate complexes of the type $Ln(dpm)_3$, $Ln(dpm)_3$py, $Ln(dpm)_3$bipy, $Ln(dpm)_3$phen as well as $Ce(dpm)_4$ have been synthesized and characterized by mp, DTA, TGA, IR, UVV, magnetic susceptibility and Weiss constants[19]. Reaction of anhydrous YCl_3, Ba metal or anhydrous $Cu(OAc)_2$ with highly pure acetylacetone (acacH), dipivaloylmethane (dpmH) and ethyl acetoacetate (etacH) in a dry atmosphere yielded the corresponding chelates of Y(III), Ba(II) and Cu(II) with acac, dpm and etac, as confirmed by IR and ^{1}H NMR spectra[20]. Various methods can be applied for analyzing enolates

and phenolic compounds (e.g. Folin–Ciocalteu, Price–Butler) in biological samples, such as fruits and cereals[1]. Other methods can assess the antioxidant capacity stemming from phenols (Trolox equivalent, diphenylpicrylhydrazyl radical, ferric reducing power). When applying such methods, it is important to consider ascorbic acid (**1**) and reducing saccharides, as their presence may significantly affect the results[21].

Lasalocid (**12**), an acyclic carboxylic ionophore produced by microorganisms, transports metal cations and biogenetic amines across natural and artificial membranes. It forms pseudocyclic complexes in which the guest cations are coordinated by donor groups of the acyclic lasalocid. This also forms outer sphere complexes with several metal amine and amine complex guests. Complexation of a metal ion with **12** is regarded as a new class of molecular recognition and has wide application in coordination chemistry and separation science. Indeed, lasalocid ionophore can extract water-soluble $Ln(acac)_3$ chelates into CCl_4 via inner sphere complexation. This offers higher extraction abilities for small Er(III) and Dy(III) complexes than for large Pr(III) and La(III) complexes[22]. Since lasalocid extracts lanthanide cations nonselectively, this 'metal complex recognition' has new and interesting possibilities in separation and sensing of valuable lanthanides.

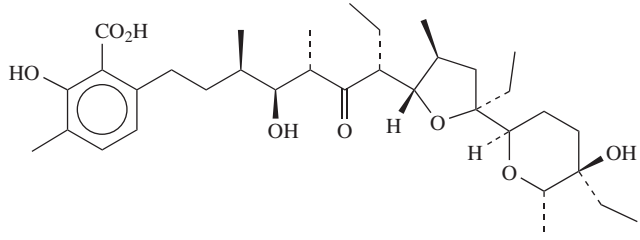

(**12**)

B. Spectral Methods

Structural analysis of metal enolates by spectral methods (IR, Raman, UVV, NMR, EPR and MS) is discussed elsewhere in this volume[23].

1. Infrared spectra

$V(acac)_3$ has several applications, including its use as a component in olefin polymerization catalysts; it is air sensitive, undergoing gradual oxidation in moist air to give $VO(acac)_2$. Commercial $V(acac)_3$ is allowed to contain not more than 2.0 wt% of $VO(acac)_2$. Several spectroscopic techniques, such as IR, ESR and NMR, have been used to study the structure and properties of $V(acac)_3$. IR and ^1H NMR spectrometries were used effectively for determination of $VO(acac)_2$ in $V(acac)_3$; however, IR showed lower LOD[24]. FT-NIR spectroscopy was used for the determination of calcium ascorbate in blister packs, tablets, plastic bottles etc.[25].

2. Ultaviolet–visible spectra

Hydroxylamine hydrochloride was used as an indicator for the determination of $Co(acac)_2$. The absorbance of the resulting colored solution was measured at 590 nm[26]. Iridium β-diketonates were fluorinated oxidatively with BrF_3 in Freon 113, followed by decomposition in 6M HCl to $IrCl_6^{2-}$ and spectrophotometric determination at 488 nm[27].

A comprehensive review of spectrophotometric methods for the determination of ascorbic acid (**1**) was presented. Most of the methods are based on the reducing action of ascorbic acid, making use of an Fe(III)–Fe(II) redox system, and to a lesser extent Cu(II)–Cu(I), V(V)–V(IV) and phosphomolybdate/phosphotungstate–molybdenum/tungsten blue redox systems[28]. A kinetic spectrophotometric method for the determination of L-ascorbic acid and thiols (RSH) was developed, whereby the absorbance of the Fe(II)–phen complex formed during the reaction of **1** or RSH with Fe(III)–phen was continuously measured at 510 nm by a double beam spectrophotometer equipped with a flow cell. The linearity range for **1** was 4–40 μM and for RSH 8–80 μM. The method was validated for pharmaceutical dosage forms[29].

A method for determination of sodium isoascorbate (see **2**) in boiler feed water, where it is used for deoxygenation, consists of following the reaction kinetics of Rhodamine B (**13**) in the presence of $KBrO_3$, measuring at 555 nm. A linear correlation exists between the catalytic effect of the analyte on the reaction rate and its concentration; Fe(III), Ca(II) and Mg(II) in the 5–200 ppm range interfere with the analysis[30]. The effects of solvents, pH, surfactants, metal ions and other food additives on the absorbance were studied for the micelle-enhanced UV spectrophotometric determination of the food preservative sodium D-isoascorbate. The optimal conditions were using water at pH 7–8 as solvent and polyvinyl alcohol as surfactant, which causes an up to 3-fold increase of the UV absorbance[31].

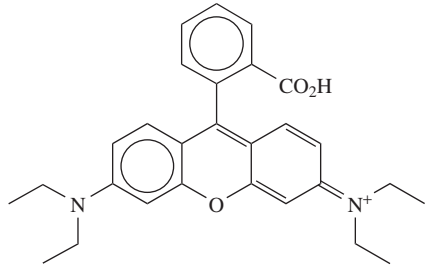

(**13**)

A multisyringe spectroscopic flow injection analysis (FIA) system was proposed for evaluating the antioxidant capacity of solutions, as a function of the solvent and the pH. The method is based on UVD at 517 nm of the scavenging capacity of the test solution in the presence of the 2,2-diphenyl-1-picrylhydrazyl free radical (**14**) during 3 min after stopping the flow. The method was validated for ascorbic acid and a series of phenolic antioxidants[32].

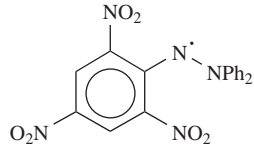

(**14**)

Ascorbic acid can be determined spectrophotometrically in colored and sugar-rich samples by a simple and highly specific method, based on the oxidation by guaiacol peroxidase, claimed to be more precise than officially adopted chemical methods[33].

Ascorbic acid concentrations can be determined fluorometrically by adding Cu(II) and treating the hydrogen peroxide formed with horseradish peroxidase in the presence of *p*-hydroxyphenylacetic acid, which forms a fluorescent dimer. The reaction is suitable for analysis of concentrations in the range from 50 μM to 4 mM ascorbic acid and can be used for pharmaceutical preparations, but is unsuitable for preparations derived from natural sources[34]. A fluorescent sensor for diols was developed, based on the temperature- and pH-sensitive copolymer of *N*-isopropylacrylamide and 4-vinylphenylboronic acid (nipaco-vpba, **15**). Certain properties of **15** have to be calibrated to determine the optimal operation conditions of concentration, pH and temperature. **15** combines with nonfluorescent Alizarin Red S (**16**) to yield a fluorescent complex **17** ($\lambda_{ex} = 460$ nm, $\lambda_{fl} = 660$ nm). This is the basis for a determination method of diols of the most varied nature, by measuring the fluorescence quenching due to competition of the analyte with **16** for boronic ester formation, as shown in equation 1. The method was applied to various diols, including ascorbic acid (**1**)[35].

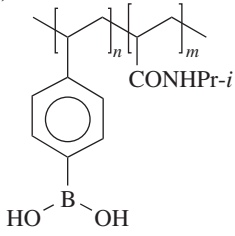

(**15**)

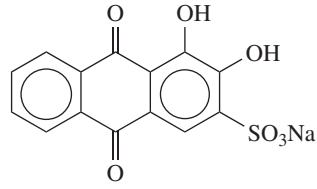

(**16**)

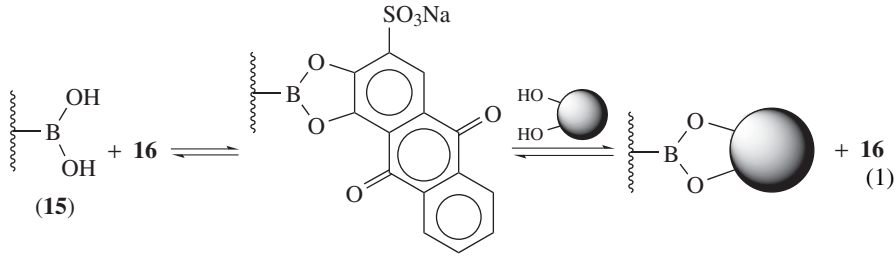

(**15**) (**17**) (1)

Many small molecules and molecular fragments exhibit relatively intense photoluminescence which may serve for identification or quantitation. Common photoluminescent fragments include HCO, OH, NH, CH, CN, SH, PO, CCl, CF, CO^+, C_2, H, C and most metal atoms. Organometallic molecules such as $Cu(tfac)_2$ undergo laser photolysis producing a pair of atomic copper emission lines with maxima at 324.8 and 327.4 nm, and a major emission at 392 nm derived from ligand fragments[36]. Soluble Mn(IV) was used as a chemiluminescence reagent for the determination of various analytes including ascorbic acid with LOD = 20 nM[37].

The volatile chelates $Ba(dpm)_2$, $Ba(ptfa)_2$ and $Ba(hfod)_2$ were studied by gas-phase UPS and characterized by thermal analysis, IR spectra and vacuum sublimation. In the UPS of these chelates obtained at >200 °C, ionization bands of π^{3-}, p^+ and p orbitals were identified at 8–10 eV. At *ca* 280 °C thermal decomposition began. The use of UPS to study Ba diketonates is complicated by the formation of oligomers in the gas phase[38].

Photoderacemizations of $Cr(acac)_3$ with circular polarized light gave very small ee values[39]. Later, photoinduced deracemization of a racemic mixture of Δ- and Λ-$Co(acac)_3$ was successfully carried out and was followed by CD measurements. With a chiral ruthenium(II) complex, Δ-$[Ru(menbpy)_3]^{2+}$ (menbpy = 4,4′-bis{(1*R*,2*S*,5*R*)-(−)-menthoxycarbonyl}-2,2′-bipyridine), in acetonitrile–H_2O (7:3 v/v), in the presence of either triethylamine or NaOH, under visible light irradiation ($420 < \lambda < 470$ nm), the Λ-isomer was obtained preferentially with 38% ee[40]. The selectivity of deracemization remarkably depends on the solvent and anion concentration. These counter anion effects were interpreted in terms that the reduction potential of $Co(acac)_3$ becomes more negative by addition of F^- or AcO^- [41].

3. Mass spectrometry

The ability to measure metal isotopic abundances rapidly and accurately using a conventional mass spectrometer provides a powerful tool for exploring trace metal metabolism. When the chelates of Cu(II) and Fe(II), which show poor sensitivity in GC, were introduced directly into the ion source of a mass spectrometer, their ionic intensity was large; however, the ratio of the molecular ion to the total ion current was smaller than that of the chelates of Rh(III) and Cr(III), showing good detection sensitivity in GC with a smaller number of fragment ions. When the sample was heated for evaporation and collection in a gas reservoir for MS, chelates of Cu(II) and Fe(II) showed great disintegration of the molecular ion and a large number of fragment ion species was produced[42].

High-precision isotope ratio measurements for a series of volatile alkaline earth and transition metal chelates was carried out using conventional GC-MS instrumentation. The chelating reagents used were tfacH and 1,1,1,2,2-pentafluoro-6,6-dimethylheptane-3,5-dione (pfdhH), and the chelated metals were Mg, Ca, Fe, Cr, Cu and Ni[43]. The ESI-MS of $Ho(acac)_3 \cdot H_2O$ showed no masses higher than those of the molecular ions, indicating a monomer structure in the gas phase. Comparison of the mass spectra of acac complexes of Ho, Nd and La showed a common mechanism of decomposition of these compounds[44]. Many other metal β-diketonates were characterized by MS or GC-MS. For example, alkaline earth complexes used as precursors for chemical vapor deposition (CVD) of thin film superconductors were characterized by MS[45]. Secondary-ion MS (SIMS) was used to sputter and determine ions from TLC or from gel electrophoresis. The key to successful SIMS analysis of these systems is use of the correct phase-transition matrix. In some cases crown ethers can be used to extract the β-diketonate complexes from the polar silica gel without excessive lateral diffusion. The ultimate spatial resolution for molecular mapping was *ca* 1 μm[46].

Six types of $Eu(dik)_3$ complexes were accurately analyzed in the absence and presence of phen, using both infusion ESI-MS and FLD. The LOD by FLD for compounds extracted with acetonitrile were 1–100 ppb[47]. Using ESI-MS, high sensitive and prompt discrimination of luminescent europium β-diketonates can be achieved. The combination of laser sampling and ion trap MS is a powerful analytical technique for the direct analysis of complex samples. Thus, the generation of both negative and positive ions by laser desorption directly within a quadrupole ion trap was applied to analyze complex samples such as $Cr(acac)_3$[48].

Resonance-enhanced multiphoton ionization (REMPI) has proved to be a versatile ionization technique for MS offering a number of advantageous features in the field of chemical analysis. Since it makes use of substance-specific excited states for the ionization process, it involves UV spectroscopy of the molecule to be ionized. Thus, it enables ionization of preselected compounds, control of the degree of fragmentation and, for a large number of substances, a high ionization efficiency. These features require that the excited molecular state(s) involved in the REMPI process not be significantly depleted

during the laser pulse. When using ultrashort laser pulses, analysis with REMPI can be achieved even with metal β-diketonates, which show extremely rapid relaxation of their excited states[49]. Ultrashort light pulses were applied for the analysis of quickly relaxing organic molecules by means of laser MS. Species undergoing fast relaxation processes cover a large part of the technically or environmentally relevant substances, including molecules containing heavy atoms, for example, the $Pt(acac)_2^+$ and $Co(acac)_3^+$ cations and others. The mass spectra of the chelates depend crucially on the duration of the applied laser pulses. Whereas under nanosecond conditions only small and unspecific fragments were detected, the picosecond REMPI-MS are dominated by the molecular ion signal accompanied by structure-specific fragments[50].

In the membrane introduction ion trap MS (MIMS) technique, a membrane composed of a microporous polypropylene hollow support fiber coated with an ultrathin (*ca* 0.5 μm) polydimethylsiloxane layer serves as the interface between the sample and the vacuum chamber of the mass spectrometer. The simultaneous diffusion of volatile and semivolatile compounds through the ultrathin polydimethylsiloxane MIMS membrane is one of the method's strengths, in that all the analytical information is obtained in a relatively short time (in the order of seconds to minutes). Lead and nickel β-diketonates could be detected by the MIMS technique[51].

4. X-ray fluorescence and absorption spectroscopies

The performance characteristics (precision, accuracy and LOD) of X-ray spectrometric procedures for the elemental analysis of organometallics were critically reviewed, paying attention to the source and elimination of random and systematic errors, as well as to sample preparation and calibration plots[52].

$Ti(acac)_2$ was rapidly and quantitatively analyzed by X-ray fluorescence (XRF) spectroscopy[53]. $Fe(acac)_2$ was similarly determined by XRF with correction for Compton scattering. An instrumental geometrical factor and an equivalent wavelength were obtained experimentally, while all the other factors were calculated with the mass absorption coefficients of Fe[54]. K_α and K_β XRF spectra of $Cr(acac)_3$ and other Cr compounds were measured with a Bragg spectrometer. The relative intensities of the $K_{\beta 1.3}$, $K_{\beta 2}$, $K_{\beta'}$ and $K_{\beta''}$ lines with respect to the K_α line confirm the chemical effect on the K_β/K_α intensity ratio obtained using a Si(Li) detector[55].

K-Edge XAS spectra of heavy atoms in solution are very sensitive to the chemical environment, including changes of the oxidation state and the coordination sphere. Thus, calculations based on the maxima and inflection points of spectra taken of a suspension of blood cells of tunicates (*Phallusia nigra* and *Ascidia ceratodes*) after exposure to $VOSO_4$ helped in the identification and quantitation of a variety of species, such as $[V(H_2O)_6]^{3+}$, $[V(SO_4)(H_2O)_5]^+$, $[V(SO_4)_2(H_2O)_4]^-$, $[V(OH)(H_2O)_5]^{2+}$, $[V(SO_4)(OH)(H_2O)_4]$, $[V(SO_4)(OH)_2(H_2O)_3]^-$, $[V_2O(H_2O)_{10}]^{4+}$, $[V(catecholate)_3]^{3-}$, $[V(acac)_3]$, $VO^{2+}{}_{aq}$, $SO_4{}^{2-}$/V(III), $K_2[VO(catecholate)_2]$ and $[VO(acac)_2]$. The latter two species are indistinguishable by XAS and the relative amounts of the complexes in solution are pH dependent[56].

C. Electrochemical Methods

1. Electroanalysis

The copper in $Cu(acac)_2$ was determined polarographically after mineralization by the closed flask combustion method[57]. Composition and stability constants were determined

for Be, Mg, Ca, Sr and Ba chelate compounds derived from acacH, bzacH, dibzacH and ttfacH by potentiometric titration in water–dioxane solutions[58]. The first stage in formation of the chelates of divalent transition metal ions was a monopositive cation with one chelate ring, followed by attachment of the second ligand and formation of a two-ring neutral complex. The highest stability was observed for Be β-diketonates. For a given element the stability increased with increasing the number of phenyl groups in the β-diketonate involved.

The ligand interchange reaction between metal β-diketonates and edta was utilized to establish the amount of metal β-diketonate by conductometry in DMF or DMSO. The β-diketonates studied were of Co(II), Cu(II), Mn(II), Fe(III) and Cr(III). The combination ratios of the metal β-diketonate with edta were 4:1, 2:1 and 1:1. Presence of less than 1% H_2O, inorganic acids or organic solvents did not affect the inflection points in the conductometric titration curves[59].

Anodic stripping voltammetry (ASV) was applied to the determination of copper traces present as $Cu(dik)_2$. The differential pulse technique was used to strip the amalgamated copper from a hanging mercury drop electrode. The experimental variables such as scan rate of electrode potential, deposition potential, deposition time and stirring speed of the solution could be optimized. The linear range of the calibration plot was 0.05–1 μM and the LOD was 0.014 μM Cu(II). A method was used for the determination of copper in breast milk and beer as typical examples of application, consisting of mineralization of the sample, extraction of Cu(II) from the aqueous solution with a 1 M solution of acacH in chloroform and ASV end analysis[60].

Ascorbic acid and Na ascorbate can be determined in an automated constant current coulometric system. Under optimal conditions, an excellent precision of $\pm$0.3% was achieved, with 95% probability[61]. Ca ascorbate can be determined by potentiometry (using Ag as indicator electrode) and constant current coulometric methods. Automatic coulometry possesses the advantage of speed and, with its satisfactory precision, is well suited to routine pharmaceutical analysis[62].

The direct redox reactions of ascorbic acid (**1**), uric acid (**3**) and dopamine (**5**) take place at bare electrodes at very similar potentials and are believed to be irreversible. Their amperometric detection usually requires high overpotentials. These and other technical problems have made the simultaneous electrochemical analysis of these important analytes a challenging goal[63]. An important factor affecting the electroanalytical quality in these cases is the buffer capacity[64]. A potentiometric sensor for L-ascorbic acid (**1**) based on the redox properties of Cu(II) ions incorporated in a poly(ethylene-co-vinyl acetate) (EVA) membrane was also developed[65]. Many modifications of the working electrode have been proposed, aiming at a variety of purposes, such as improving durability, sensitivity, specificity and ease of operation in complex matrices[66]. The more recent propositions summarized in Table 1 may serve as leading references.

A coulometric titration method was introduced for sequential determination of sulfite, thiosulfate and ascorbic acid (**1**) in solutions containing sulfite–thiosulfate or sulfite–ascorbic acid couples. Formaldehyde or acetaldehyde can be used to mask the sulfite component. Two sequential measurements of coulometric time, one for both components in the mixture and one for the sample solution in which sulfite is masked, can be used to determine the concentrations of sulfite–thiosulfate and sulfite–ascorbic acid couples. The method is linear for 0.5–60 μM **1** in the presence of 0.44–13 μM sulfite, with RSD 0.1–4% and current efficiency of *ca* 98.0%. The method can be used for determination of the presence of sulfite and **1** in real sample matrices such as mineral waters and vitamin C tablets[97].

TABLE 1. Modification of working electrodes for determination of enolates or enols[a]

Type	Modification and comments
Au	Alternating thin films of poly(allylamine hydrochloride) (pah) and poly(glutamic acid) (pga) were deposited layer by layer on the Au electrode. When pah is the capping film, ferricianide ions are incorporated onto the electrode to confer electrocatalytic properties. For example, ascorbate (**1**) in the mM concentration range is oxidized to dehydroascorbic acid (**18**, equation 2) and the catalyst is regenerated at the anode (equation 3)[68a]. A biosensor for electrochemical amplification in detection of miRNA is prepared by chemisorption of specific capture strands on the electrode surface[68b]. After tagging the miRNA with an osmium complex and hybridizing the miRNA on the electrode surface, the amperometric oxidation of ascorbate (**1**) is measured at +0.15 V vs. SSCE. The LOD is about 10 ng of specific miRNA[69].
Pt	3,4-Ethylenedioxythiophene (**19**) was deposited on the Pt electrode by potentiostatic electropolymerization. The conducting polymer (PEDOT) shows electrocatalytic activity and a sharp response in the determination of ascorbate (**1**) at pH 7, using a GCE and SSCE three-electrode setup[70]. A polyaniline film was electrodeposited on the electrode while applying a strong magnetic field. This is supposed to confer on the polymer helices a preferred chirality inducing a different voltametric behavior with the enantiomers of an analyte. The method was applied to the electroanalysis of ascorbic acid (**1**) and isoascorbic acid (**2**)[71].
$C_{graphite}$	A highly-ordered pyrolytic graphite (HOPG) electrode was polished so as to expose more edge plane than basal plane surface. Without further modification, the edge-plane pyrolytic graphite electrode was capable of carrying out an electroanalytical oxidation of ascorbic acid (**1**), dopamine (**5**) and serotonin (**20**) in phosphate buffer (pH 7) such that it has much higher electron conductivity. The oxidation potentials vs. SCE and LOD were, respectively, −0.03 V, 200 nM; 0.16 V, 90 nM and 0.28 V, 60 nM. Other carbon electrodes, such as basal-plane pyrolytic graphite electrode, unmodified GCE, boron-doped diamond electrode and carbon nanotube (CNT) electrode, could not carry out this analysis[72]. Rutin (**21**) was electropolymerized on the electrode and served as catalyst for two-electron oxidations. The electrode was tested vs. SCE for determination of epinephrine (**22**), serotonin (**20**) and ascorbic acid (**1**)[66]. The electrode was modified by adsorption of aniline and complexation with $CoCl_2$ and $K_4[Fe(CN)_6]$. The Co(II) to Co(III) oxidation served as electrocatalysis for the amperometric determination of ascorbic acid (**1**), practically unaffected by pH in the 2–10 range. The LOD was 33.3 μM **1**, with linearity from 55.2 μM to 32.3 mM. At the 0.10 mM **1** level, no interference was observed from a 10-fold concentration of uric acid (**3**), paracetamol (**4**), glucose, fructose or H_2O_2. However, dopamine (**5**) could not be resolved from **1** and the presence of a surfactant such as cetyltrimethylammonium bromide in the solution strongly abated the electrode response[73]. Some interferences and their possible correction have been reported for Prussian Blue-modified electrodes[74]. Modification with $Mn_3[Fe(CN)_6]_2$ in wax showed good electrocatalytic performance in the reduction of ascorbic acid (**1**) at pH 2–10. The LOD (SNR 3) was 22.2 μM **1**, with linearity from 55.2 μM to 14.4 mM[75]. A melanin polymeric film was developed on pyrolytic graphite working electrodes by anodization in the presence of dopamine (**5**). This was used for DPV simultaneous determination of ascorbic acid (**1**), uric acid (**3**) and dopamine (**5**), at pH 10 with excellent recoveries, no mutual interference and avoiding superficial poisoning effects. The LOD were 13 (**1**), 1.4 (**3**) and 0.11 (**5**) μM[76].
$C_{diamond}$	A boron-doped diamond electrode with Pt-foil counterelectrode vs. SCE as reference electrode was used for simultaneous PDV anodic determination of ascorbic acid (**1**) and paracetamol (**4**). The linear range for both analytes was 0.01–0.1 mM and RSD 2–3%, adequate for pharmaceutical products[77].

TABLE 1. (*continued*)

Type	Modification and comments
C_{fiber}	An electrochemically modified carbon fiber electrode was used for ascorbate determination at cellular level in the presence of catecholamines[78]. Self-referencing amperometry (SRA) methods were reviewed; they are applied for electrochemical probing at cellular levels and may extend elecroanalytical methods to the nanoscale, for analysis at subcellular and organellar levels[79].
GCE	A copper-modified GCE (glassy carbon electrode) electrode was described as sensor for the simultaneous voltametric detection of ascorbic acid (**1**), uric acid (**3**) and homovanillic acid (**23**). Other applications demonstrated for such electrode were the sensitive simultaneous detection of **3** and **23** (10 nM each) in the presence of **1** (100 nM), measurement of **1** in Vitamin C tablets and of **3** in urine and serum[80]. A GCE was modified by electrochemical deposition of a hybrid PtAu film in the presence of L-cysteine. The electrode was used for the simultaneous determination of ascorbic acid (**1**), uric acid acid (**3**) and dopamine (**5**) at pH 4.0 by CV and DPV. The linearity ranges for these analytes were 0.024–0.384, 0.021–0.336 and 0.103–1.65 mM, respectively, with RSD under 2% for all three, with good sensitivity and stability[81]. The GCE surface was covered by *o*-aminophenyl groups (**24**), as a result of electrochemical reduction of the diazonium salt derived from 4-amino-2-nitrophenol, followed by electrochemical reduction of the nitro groups. The electrocatalytic action of the modified electrode is shown in equation 4. The electrode was used for simultaneous determination of ascorbic acid (**1**) and uric acid (**3**) in urine[82]. Sequential or simultaneous electrodeposition of polyaniline and poly(3-phenylaminopropanesulfonic acid)[83] shift the anodic peak of electrooxidation of ascorbate at pH 7.2, from 0.36 V for a bare electrode to 0.00 V vs. SSCE. The electrode was used for amperometric determination of ascorbate, with a response of 1.96 nA μM^{-1}, LOD = 2.2 μM and linear range from 5 to 50 μM. Neither uric acid nor dopamine interfered with the determination. A dual carbon band electrode was modified in the same fashion[84]. An electroconducting film was developed on the electrode by electropolymerization of 4-(2-pyridylazo)resorcinol (**25**). The indistinct voltametric peaks of the bare electrode for ascorbic acid (**1**), dopamine (**5**) and uric acid (**3**) are resolved into peaks at 210, 391 and 590 mV, respectively, when working vs. SSCE in phosphate buffer at pH 4.0. The corresponding LOD are 7.5, 0.4 and 1.6 μM and the linearity ranges are 100 to 800, 5 to 50 and 20 to 100 μM[63]. A poly(4-vinylpyridine) (pvp) film was developed on the electrode. In its acidic form the pvp-H^+ film acts as weak anion exchanger, capturing $[Mo(CN)_8]^{4-}$ ions from a solution. The mechanism of redox electrocatalysis of the modified electrode in the determination of ascorbic acid (**1**) is similar to that shown in equations 2 and 3, with Mo(IV) to Mo(III) instead of Fe(III) to Fe(II) interconversion. The method was used for determination of **1** in orange juice and in commercial Vitamin C tablets[85]. A mixture for electrode preparation incorporates a cobalt complex with salophen (**26**) and tetraoctylammonium bromide. The modified electrode can be used for simultaneous determination of ascorbic acid (**1**) and dopamine (**5**)[86]. A hydrous ruthenium oxide ($RuO_x \bullet nH_2O$) film was deposited on the polished surface of the electrode by the CV technique. The modified electrode allowed simultaneous determination of ascorbic acid (**1**) and dopamine (**5**)[87]. A conducting membrane was developed over the electrode by simultaneous electropolymerization of the inclusion compound formed by 4-aminothiophenol and β-cyclodextrin (**27**) and deposition of gold nanoparticles (*ca* 10 nM). The modified electrode allowed simultaneous determination of ascorbic acid (**1**) and dopamine (**5**) at 153 and 300 mV, respectively, vs. SCE[88]. A GCE modified by L-cysteine and subsequently by self-assembled gold nanoparticles can be used for the simultaneous DPV determination of ascorbic acid (**1**) and uric acid (**3**), with linear ranges of

(*continued overleaf*)

TABLE 1. (*continued*)

Type	Modification and comments
	8.0 μM–5.5 mM and 0.60 μM–0.85 mM, respectively, with much stronger anodic currents than those with the simple GCE[89]. A GCE modified by a multilayer of alternating poly(2,5-dimethoxyaniline) and phosphotungstic acid showed enhanced electrocatalytic oxidation of ascorbic acid (**1**) by CV, attributed to the presence of tungsten particles at the interlayer surface[90]. A GCE modified by a poly(*p*-toluenesulfonic acid) (pptsa) film showed an excellent electrocatalytic effect on the oxidation of dopamine (**5**) and ascorbic acid (**1**). The favorable electrostatic interaction between the negatively charged pptsa film and the cationic species of dopamine (**5**) or the anionic species of **1** contribute to the response of **5** and **1** at this electrode. In DPV measurements, the pptsa-modified electrode can separate the **1** and **5** oxidation potentials by about 192 mV and can be used for the selective determination of **5** (LOD 0.6 μM) in the presence of up to 0.5 mM **1**[91].
CPE	A modified CPE (carbon paste electrode) was prepared from a mixture of acetylene black and cross-linked polyvinylpyrrolidone, and was used for determination of kojic acid (**8**) in foodstuffs. The LOD was 0.50 μM **8**, with linearity from 1.0 to 100 μM. No interference was observed from a 100-fold concentration of glucose, amylum and dextrin, 50-fold concentration of ascorbic acid (**1**), uric acid (**3**), dopamine (**5**), or amino acids such as glutamic acid, phenylalanine, aspartic acid, valine, cysteine and cystine. On the other hand, a 2-fold concentration of tryptophan (**28**) and a 5-fold concentration of tyrosine (**29**) affected the determination of **8** by 10%, due to the close oxidation potentials of these compounds[15]. The electrode modified by the Rupic (**30**) complex performed the electrocatalytic function by reduction of Ru(III) to Ru(II). The oxidation potentials of ascorbic acid (**1**) and dopamine (**5**) vs. SSCE were 0.30 and 0.35 V, respectively, which are too close for practical resolution of the analytes. However, by applying PLS regression calculations it was possible to estimate the concentrations of both analytes with error less than 20 and 12%, respectively, without previous separation[7]. Modified electrodes were prepared by adding to the paste either of the polyvanadate complexes **31** or **32**. The electrocatalytic action of these electrodes vs. SSCE was tested in 1 M H_2SO_4 solution, in the oxidation of ascorbic acid (**1**) and nitrite (NO_2^-) or in the reduction of bromate (BrO_3^-) and nitrite[92].
SPCE	Disposable screen-printed carbon electrodes (SPCE) have been variously modified for improved performance and selectivity. For example, after anodization (SPCE*) or oxygen plasma treatment (OPSPCE) the electrodes showed excellent sensitivity, selectivity and antifouling properties in the simultaneous determination of ascorbic acid (**1**), uric acid (**3**) and dopamine (**5**). Raman spectra and XPS analyses point to changes in surface planes and the presence of more surface bound carbon–oxygen functionalities. The low cost of SPCE* offers an easy extension to-on-the spot clinical diagnosis[93]. A disposable SPCE modified by electrografting an *o*-aminophenol film derived from the corresponding diazonium salt was used for amperometric determination of ascorbic acid (**1**), with linear response in the 2–20 μM range, LOD 0.86 μM, RSD 1.98% ($n = 8$) and good surface stability[94].
ito	A layer-by-layer coating of the indium tin oxide electrode (ito electrode) was fabricated by alternating dipping into solutions of chitosan, a poly(amino saccharide) extracted from crustacean shells, and a sulfonated metallophthalocyanine (**33**). The electrode modified by either **33a** or **33b** showed a difference of 0.51 or 0.56 V, respectively, for the oxidation potentials of ascorbic acid (**1**) and dopamine (**5**). However, neither the bare ito electrode nor the one modified with **33c** could discriminate between these analytes[95].

TABLE 1. (*continued*)

Type	Modification and comments
pvc	A permanganate ISE was prepared with a pvc membrane containing both tridodecylmethylammonium chloride and 2-nitrophenyl octyl ether or bis(2-ethylhexyl) sebacate as plasticizer and filled with a solution containing 0.02 M NaCl and 0.08 M $KMnO_4$. Continuous and reversible potentiometric determinations of the concentration of **1** can be carried out by measuring the EMF vs. SCE of the solution in the 1.0 μM–1.0 mM range, with LOD 0.22 μM[96].

[a]Guidelines for design of amperometric biosensors for clinical use are found elsewhere[67].

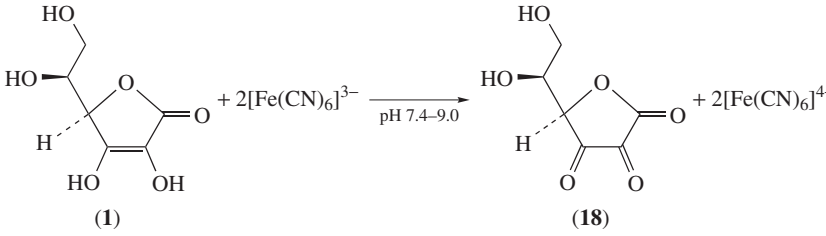

(**1**) (**18**) (2)

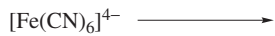

(3)

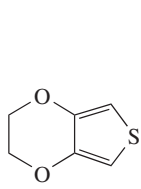

(**19**)

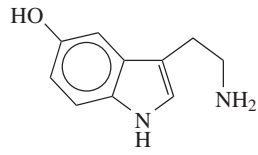

(**20**)

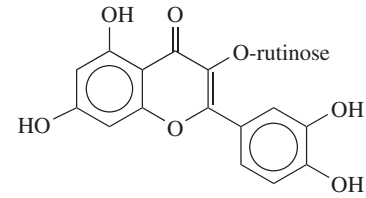

(**21**)

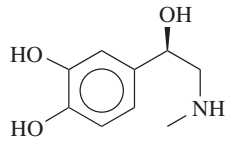

(**22**)

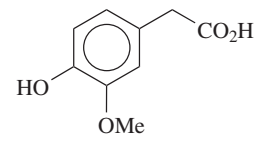

(**23**)

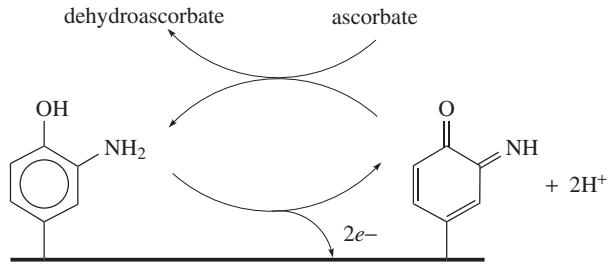

(**24**) (4)

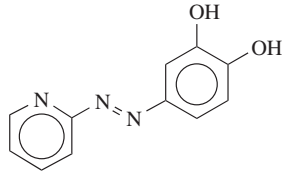

(**25**)

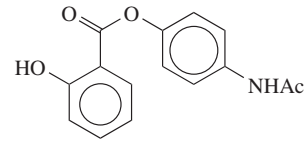

(**26**)

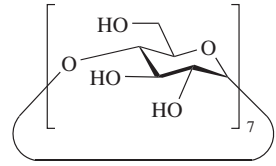

(**27**)

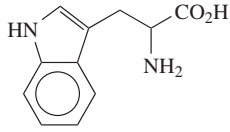

(**28**)

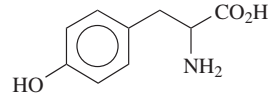

(**29**)

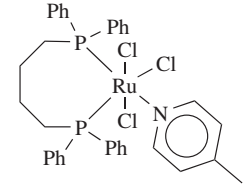

(**30**)

$H_2[Cd(phen)_3]_2\{[Cd(H_2O)(phen)_2](V_{16}O_{38}Cl)\}\bullet 2.5H_2O$

(**31**)

$H_2[Cd(bipy)_3][Cd(H_2O)_2(bipy)_2]\{[Cd(H_2O)(bipy)_2](V_{16}O_{38}Cl)\}\bullet 1.5H_2O$

(**32**)

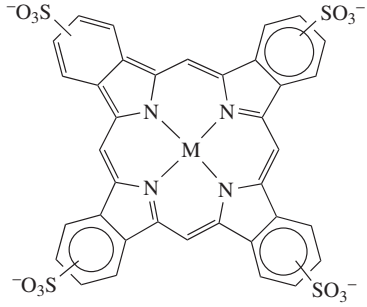

(**33**) (**a**) M = Fe
(**b**) M = Cu
(**c**) M = Ni

A cuprimetric method for the determination of ascorbic acid is based on a direct potentiometric titration with $CuSO_4$ using a copper-based mercury film electrode as the indicator electrode. The electrochemical reaction taking place is ascorbic acid reducing Cu(II) ions quantitatively to Cu(I) ions in neutral or acidic aqueous solutions. The linearity

range is 10^{-5}–10^{-1} M, with LOD = 2 μM. This method can be used whenever visual titrimetric methods are out of the question due to colored or opaque pharmaceutical solutions[98].

Methods for analysis of ascorbic acid (**1**) solutions are potentially adequate for the analysis of metal ascorbate solutions, perhaps with the proviso of acidifying the solution to achieve similar analytic conditions. A new approach towards a voltametric electronic tongue has been developed lately. Automation of the system was achieved by the use of a sequential injection analysis (SIA) system. A small detection device containing 3 working electrodes made of platinum, gold and epoxy–graphite discs was used for this purpose, and a SSCE reference electrode was integrated into the measuring cell to minimize electrical noise. Three oxidizable compounds of clinical interest, i.e. ascorbic acid (**1**), uric acid (**3**) and paracetamol (**4**), could be quantitized by the system. Employing the voltamograms as departure information, artificial neural networks (ANN) have been used as chemometric tool for modeling the system. Automation with a SIA system is presented as an advantage for easy preparation of the huge amount of standards needed by the electronic tongue systems[5]. Simultaneous analysis of dopamine (**5**) and ascorbic acid (**1**) by linear sweep voltametry (LSV) with a GCE shows a strong nonlinear interference between the analytes. Instead of applying separation methods or using modified electrodes (see Table 1), it was opted for a calibration followed by application of chemometric calculations. The statistical parameters of orthogonal signal correction (OSC) PLS were better than those of classical least squares, PLS or principal component regression (PCR), on validation of the procedure with human serum containing known amounts of the analytes[6].

The electrochemical behavior of ascorbic acid (**1**) and uric acid (**3**) in the presence of micelles and their selective determination were investigated. Aqueous cetylpyridinium bromide (cpb) and sodium dodecylbenzenesulfonate (sdbs) micellar solutions have been used. The oxidation peak potentials for **1** and **3** are separated by 270 mV in the presence of cpb in aqueous phosphate buffer solution (pH 6.8), thus allowing their selective determination, as well as the selective determination of **3** in the presence of excess of **1**. The method is simple, inexpensive and rapid with no need to modify the electrode surface by tedious procedures, and it was applied to **3** determination in samples of human urine and serum. Abnormal levels of uric acid in urine and serum are symptomatic of several diseases (gout, hyperuricaemia and Lesch-Nyhan syndrome)[99].

Ascorbic acid (**1**) is most commonly used for testing the performance of electrodes in redox systems. Thus, a Ag–Ag ascorbate selective electrode was constructed with view to use it for vitamin C determination. Its reproducibility and stability was satisfactory and ascorbate ion concentration could be determined in neutral, alkaline and alcoholic media[100]. A voltametric study was carried out for the evaluation of graphite–epoxy composite (GEC) electrodes for use in the determination of ascorbic acid and hydroquinone. They were compared with mercury and CPE in similar operating conditions of pH and supporting electrolytes. Like all redox electrodes, also GEC electrodes deteriorate on exposure to air or after repeated usage, and the surface had to be renewed for activation. GEC electrodes were found to be adequate for redox system analyses[101]. The electrocatalytic oxidation of **1** is an amplification method for determination of specific miRNA strands using the Au biosensor described in Table 1[69].

Monosegmented flow analysis (MSFA) is a flow batch system that can be used to perform true titrations without the use of standards. Each segment of sample or reagent can be accurately calibrated for volume, and on uniting two of them they can be allowed sufficient time for homogeneous mixing. The bubbles separating two segments can be of air or an inert gas. Titration of **1** with iodine is carried out as follows: A segment containing **1** is joined with one containing KI and it is recirculated in a loop until homogenization is achieved. This segment, considered as an aliquot of **1**, is introduced into a titration chamber equipped with an electrode set for electrochemical generation of I_2 (in fact I_3^-)

as titrant and an electrode set for potentiometric or biamperometric detection of the titrant. A sequence of measured pulses generates the titrant and its disappearance is followed until a slight excess remains, marking the end of titration and the beginning of the clean-up stage. This sequence can be repeated for improvement of the analytical quality. The method was validated for pharmaceutical preparations and food additives[102].

2. Electrophoresis

Chromatographic and related electrophoretic methods for the separation of transition metal complexes or their ligands were reviewed[103]. Micellar electrokinetic chromatography (MEKC) presents a new development in the field of capillary zone electrophoresis (CZE). The use of micellar solutions expands the application of CZE to electronically neutral solutes, as well as charged ones. Thus, electrically neutral β-diketonates $Cr(dik)_3$, $Co(dik)_3$, $Rd(dik)_3$, $Pt(dik)_2$ and $Pd(dik)_2$ were separated by CZE in micellar solutions of sds. A linear log–log relationship was found between the distribution coefficient and the partition coefficient of the complex between dodecane and water, which was used for prediction of both the distribution coefficients and the migration times of different metal complexes[104].

The development of methods for determination of ascorbic (**1**) and isoascorbic (**2**) acids by CE with UVD at 254 nm served to illustrate the power of chemometrics. Three operation variables were chosen for optimization: (i) The pH of the carrier solution which has a strong influence on the separation of the analytes; below pH 4.0 the electroosmotic flow (EOF) is very slow and above pH 8.5 the baseline becomes erratic. (ii) On increasing the applied voltage the time of migration is shorter and peak separation is better; however, if the voltage is excessive the Joule heating causes band broadening. Thus a compromise has to be found for which the Joule heating is acceptable. (iii) The concentration of the chosen buffer, 2-amino-2-hydroxymethyl-1,3-propanediol (tris), for which the pH is adjusted on adding HCl to the solution. This variable affects the electrical conductivity of the solution and was in the 30–50 mM range. The temperature, affecting the viscosity of the solution and thus the ion mobility, was fixed at 20 °C. The response surface methodology was applied to compare three experimental design methods of optimization, namely full factorial design (FFD), Box-Behnken design (BBD) and central composite face-centered design (CCFD). If one would like to test three values for each variable, the labor involved varies from 27 experiments for FFD, to 15 for CCFD and 13 for BBD. The optimal conditions found for the three design models were pH 7.5, 30 kV and 50 mM tris, pointing to the convenience of choosing an experimental design other than FFD for method development[4].

Clinical analysis of certain biological markers in urine, including ascorbic acid (**1**), is very important. An automatic method for solid-phase extraction coupled to CE with DA-UVD was developed and optimized, including autosampling and post-run operations to restore the instrument to readiness for the next sample. The whole cycle lasted 13.01 min, thus allowing the simultaneous determination in urine of creatine (**34**), creatinine (**35**), uric acid (**3**), *p*-aminohippuric acid (**36**) and **1**[105].

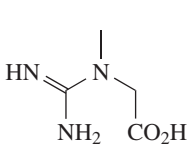

(**34**)

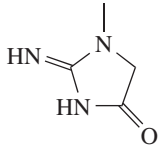

(**35**)

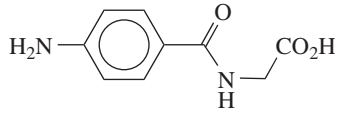

(**36**)

D. Gas Chromatography

The present section and Section IV.A.4 complement each other. The GC of metal chelates derived from monothio-β-diketones, β-diketones, β-dithioketones and β-ketoenamines was reviewed. The discussion includes column phenomena, analytical improvements and limitations and various applications[106]. A study of the GC behavior of Group 13 β-diketonates **37** shows that when the chelate contains a Mef group its volatility is enhanced, while a Ph group tends to decrease it. When R and R′ are alkyl groups the retention time of the chelates increases with the molecular weight, but it does not depend on the volatility; however, the retention time of the chelates containing a Mef group is almost inversely correlated with the volatility[107].

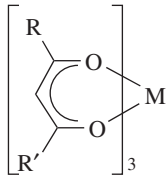

(**37**) M = Al, Ga, In

R = Me, R′ = Me (acac), Mef (tfac), Et, *i*-Pr, *t*-Bu, Ph (bzac)

R = Mef, R′ = Mef (hfac), Ph (bztfac), 2-Fu (futfac), 2-Thi (ttfac)

R = *t*-Bu, R′ = *i*-Pr, *t*-Bu (dpm); R = R′ = Ph (dibzac)

A flame spectrometric detection (FSD) system was used to study a variety of metal chelates including the $UO(tfac)_2$, $Cr(tfac)_3$, $Cr(hfac)_3$, $Al(tfac)_3$, $Cu(tfac)_2$, $Fe(hfac)_2$, $Cu(hfac)_2$, $Co(hfac)_2$ and tricarbonylchromium complexes. The GC column was connected by a heated stainless steel line to a flame spectrometer, working in a laminar flow regime with a $N_2O-C_2H_2$ premix burner that could be heated without distortion of the flame, and a monochromator provided the selective response required for the FSD. The system included a splitter to allow simultaneous FID and FSD chromatograms[108].

Sorption of $Cu(tfac)_2$ on a column depends on the amount of the compound injected, the content of the liquid phase in the bed, the nature of the support and temperature. Substantial sorption of $Cu(tfac)_2$ by glass tubing and glass-wool plugs was observed. It was also shown that sorption of the copper chelate by the bed is partialy reversible[109]. The retention data for $Cr(dik)_3$, $Co(dik)_3$ and $Al(dik)_3$ complexes were measured at various temperatures and various flow rates. The results enable one to select conditions for the GC separation of Cr, Al and Co β-diketonates. Retention of tfac and hfac of various metals on various supports were also studied[110] and were widely used for the determination of the metals. Both adsorption and partition coefficients were found to be functions of the average thickness of the film of the stationary phase[111]. Specific retention volumes, adsorption isotherms, molar heats and entropy of solution were determined from the GC data[112]. The retention of metal chelates on various stationary phases is mainly due to adsorption at the gas–liquid interface. However, the classical equation which describes the retention when mixed mechanisms occur is inappropriate to represent the behavior of such systems. This failure occurs because both adsorption and partition coefficients are functions of the average thickness of the film of the stationary phase. It was pointed out that the main problem is lack of stability under GC conditions. Dissociation of the chelates results in a smaller peak and a build-up of reactive metal ions. An improvement of the method could be achieved by addition of tfaH to the carrier gas of the GC equipped with a TCD[113] or FID[114].

GC data were reported for a series of β-diketonates bearing aryl groups. Although the chelates are thermally stable and volatile at typical column temperatures, several adverse phenomena, including peak asymmetry, baseline elevation, displacement and primary effects, were observed[115]. Column components and the extent of fluorination in the chelate were established as contributing factors to the adverse behavior. The Cr(III), Al(III), Fe(III), V(III), Cu(II) and VO_2^{2+} chelates of nonfluorinated ligands fail to elute from a wide range of liquid phases and supports, while several of the fluorinated chelates could be chromatographed successfully[116]. In contrast, Zn(II), Co(II), Co(III), Mn(II), Ni(II) and VO_2^{2+} chelates are totally retained on diverse supports, despite their adequate volatility and stability. The behavior of several β-diketonates on fused-silica wall-coated open-tubular columns is improved considerably relative to packed columns. Some elution abnormalities persist but only at the ng level. The nature of the coordinated metal ion is the dominant factor in on-column behavior and column retention, but ligand structure, injection system and stationary phase are also of importance[117].

$Cu(tfac)_2$, $Al(tfac)_3$ and $Cr(tfac)_3$ were determined by capillary GC using both FID and ECD. The limits of quantitation (LOQ) were 10^{-8}–10^{-7}% and 10^{-10}–10^{-9}% for analysis of organic and aqueous solutions, respectively[118]. The ligand in Ti β-diketonates was determined after cleaving the chelate with acetic acid and end analysis of the trimethylsilyl derivative of the liberated diketone by capillary GC[119, 120].

A GC-MS method was used in the study of the analytical characteristics of volatile $Al(dik)_3$ and $Cr(dik)_3$, dik = acac and tfac. Aluminum and chromium chelates were well separated on a fused silica capillary column of 25 m length and 0.20 mm i.d. with electron impact ionization MS detection, and yielded the unique base peak pattern corresponding to the loss of one ligand from the molecular ion. $Cr(tfac)_3$ exhibited a pair of chromatographic peaks which were found to produce nearly identical mass spectra, pointing to the existence of two geometrical isomers[121].

The alkaline-earth metal β-diketonates are less volatile than other metal β-diketonates because they exist as oligomers. For example, one Ba β-diketonate consists of a cluster of five metal ions bridged by β-diketonate carbonyl O atoms and H_2O. Several such metal β-diketonates which are used for metallorganic chemistry vapor deposition (MOCVD) of thin-film superconductors were characterized by GC-MS as well as by TGA and MS[122]. It was proved that the addition of the β-diketone to the carrier gas stream improves the GC behavior of these alkaline earth metal chelates, probably owing to adduct formation accompanying the dissociation of the oligomers[45].

Nineteen volatile dipivaloylmethanates of Th, U, Np, Pu, Zr, Hf and some rare-earth metals were prepared[123]. Their thermal stability, crystalline modifications and volatility were determined from DTA, X-ray phase analysis, tensimetric and thermal gradient sublimation data. The basic thermodynamic functions for the vapor formation were calculated. The radiolytic decomposition of several solid dipivaloylmethanates, induced by γ- or α-irradiation, was studied. Coatings obtained by the pyrolytic decomposition of volatile uranium compounds were characterized. The GC behavior of rare-earth dipivaloylmethanates and other β-diketonates on columns packed with Inerton coated with 10% Apiezon L was compared. The sorption of dpm complexes is substantially smaller than that of acac complexes. The complex is sorbed as a cationic bis(β-diketonate) accompanied by the liberation of one equivalent of dpmH[124]. The GC retention of $Ln(dpm)_3$, Ln = Ho, Yb and Lu, was examined at 200 °C on columns with 5% JXR methylsilicone elastomer on Inerton Super in the absence and presence of Pr_3PO_4 and Bu_3PO_4. The data indicate formation and decomposition of adducts between the phosphates (as medium–donor-strength ligands) and $Ln(dpm)_3$[125].

Pyrolytic sulfurization gas chromatography (PSGC) is a chemical analysis method by which several elements can be simultaneously determined in as little as 30–130 μg of

sample. It has been successfully applied to the simultaneous determination of the atomic ratio between C, H, O and N in metallorganic compounds. Good analytical results were obtained with $Fe(acac)_3$ and $Mg(acac)_2$[126–128].

E. Liquid Chromatography

The present section and Section IV.A.6 complement each other. Liquid chromatography is one of the most powerful methods for the separation of chemical compounds. The separation of the components in a mixture is based on differences in the equilibrium distribution of the components between the mobile and stationary phases. However, the differences in distribution constants of the components between the two phases are often insufficient for their complete separation. Liquid chromatography has been widely recognized as one of the methods for multielement and sensitive analysis of metal ions. Various modes of liquid chromatography have been used, including normal phase, reversed phase, ion exchange chromatography (IEC) and ion-pair reversed phase high performance liquid chromatography (IP-RP-HPLC). The success of such methods depends on a number of factors: ligand selectivity, and thermodynamic and kinetic stabilities of the complexes and components of the chromatographic system, i.e. the mobile phase and stationary phases. Supercritical fluid chromatography (SFC) is included as a LC variant, even if it operates with a gaseous carrier fluid (no liquid can exist in supercritical conditions); nevertheless, the carrier fluid acts as though it were a liquid, due to the high density attained at the high pressure of the system.

1. Column chromatography

In general, the distribution coefficient K_{av} depends on the molar volume of a metal β-diketonate. Thus, the gel chromatographic behavior was studied of the acac complexes of Co(III), Fe(III), Cr(III), Al(III), Cu(II), Ni(II) and Be(II) in the polyvinyl acetate gel (Merckogel OR-2000)–thf system[129] and of $Be(dik)_2$ and $Cr(dik)_3$, dik = acac, bzac, dibzac, tfac, futfac, ttfac and bztfac, in a column system of polystyrene gel with various organic solvents[130]. The elution characteristics K_{av}, HETP (height equivalent of a theoretical plate) and skew ratio were obtained with high precision. The behavior of metal chelates of Fe(III), Co(III) and Cr(III) with the uncomplexed β-diketones was also investigated[131]. The effects of the developing solvents (CCl_4, toluene, benzene, dichloromethane and diethyl ether) were compared in terms of solubility parameters. The adsorption behavior of $M(dik)_3$ complexes of Fe, Co, Tc, Ru and Rh as central ions in silica gel column chromatography was also examined[132]. The fundamental distribution parameters of these chelates were evaluated to find the factors affecting the separation of geometrical isomers and metal chelates possessing mixed ligands. The adsorption and distribution coefficients of $Tc(dik)_3$ complexes in a silica gel system were determined[133]. Using the relative values of the interaction energies of the substituents in a β-diketonate (G_i and G_j), the ratios of the distribution coefficients of $Cr(acac)_3$ to $Cr(dik)_3$ were evaluated. On the basis of a linear relationship between the experimental and calculated distribution cofficients, the quantitative separation of metal chelates on silica gel adsorption chromatography could be rationalized. The model for the adsorption of $Cr(dik)_3$ on silica gel was further applied to other $M(dik)_3$ complexes (e.g. M = Fe, Tc, Co, Ru and Rh) and the fundamental parameters affecting the distribution of metal chelates in silica gel column chromatography have been evaluated[134]. The acac complexes of Ru(III), Rh(III), Y(III) and La(III), and tris(1,1-diethyl-3-benzoylcarbamido)cobalt(III) (**38**) were partially resolved into enantiomers by column chromatography on a chiral stationary phase (CSP) consisting of *cis*-NO_2-*trans*-NH_2-Λ-dinitrobis(*S*-argininato)cobalt(III) nitrate monohydrate (**39**). $La(acac)_3$ is the first example of a compound that was optically resolved in this way. Enantiomers with Λ

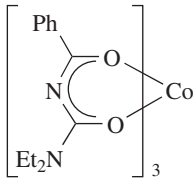

(**38**)

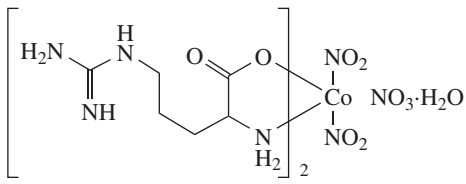

(**39**)

absolute configuration are eluted first. Y(III) and La(III) complexes undergo fast racemization. The optical inertness of the Co(III) complex is intermediate between that of Y(III) or La(III), and that of Ru(III) or Rh(III) complexes[135].

2. Zone chromatography

Zone chromatography is a variant of the zone melting method, in which the mixture being separated is introduced into a column with a solid solvent and a molten zone is passed repeatedly along the length of the column to separate mixtures into separate bands of their components. Zone chromatography has been used for the separation of mixtures of lanthanides for preparative and analytical purposes The chelates used were mixtures of hydrated β-diketonates and their adducts with 2,2′-bipyridyl (bipy) and acetylacetonimines. The distribution coefficients of different chelates and binary mixtures have been determined[136].

3. Thin layer chromatography

The dependence of the chromatographic properties of the chelates on their structure, the nature of the metals, type of donor atoms and ligand structure as a whole was studied. Also, the effect of the composition of coordinated β-diketonato ligands on R_f values of transition metals complexes[137], the effects of the geometrical configuration[138] of octahedral, square-planar[139] and *facial–meridional* isomers[140] were studied. The effects of the chelate ring size, absolute configuration[141] and the length of the coordinated ligand side chain were also considered. Separation and determination of $Co(acac)_2$ and $Co(acac)_3$ were carried out on TLC silica gel or alumina plates in the presence of poly(vinylacetate)[142, 143].

The quantitative separation and recovery of the compounds in different valences was assessed by estimating the resolved valence states spectrophotometrically. Simple and quick separation is possible with ketones, esters, alcohols and dioxane. In a study comprising twenty complexes of Cr(III), Co(III), Ru(III), Rh(III), Fe(II), Co(II), Ni(II) and Zn(II), containing such ligands as acac and bzac, the correlation between the R_f values and the radii of the metal ions did not explain the order of R_f values of complexes with central ions of similar radii. The polarization powers of the central ions proved a better parameter to explain the order of the R_f values[144]. Generally, the trend in R_f values varied considerably for the different metal ions and a parallel between the TLC and GC behavior of the chelates was apparent[145]. The R_f values of the complexes increase in the following order of ligands: acac < bzac < dibzac < ttfac < tfac < hfac. These results reflect the weakening of the strength of adsorption of the complexes to the adsorbent, caused by decreasing oxygen atom electron density[146]. Further experimentation in a single-component solvent suggests that the dominant factor is the polarization power of the central ions of the complexes assuming a separation mechanism based on adsorption[144]. However, when multicomponent solvents are used both adsorption and partition separation mechanisms are involved[147].

The TLC behavior of $Co(dik)_3$, $Cr(dik)_3$ and $Ru(dik)_3$, in which acac ligands were successively replaced with dibzac ligands, was studied. The R_f values increased with nonaqueous and decreased with aqueous solvent systems. Unmodified silica gel can be used as a sorbent for both normal phase and RP-TLC of the metal complexes. The rule of a linear dependence between the R_M values of transition metal β-diketonates and the number of substituted chelate ligands was extended[148].

The effect of the central ion of $M(dik)_3$ complexes of transition metals on their TLC R_f values on silica gel was extensively studied. Among the complexes we count M = Co, Cr and Ru chelated by dik = acac, dbzac and monothio-dibzac, either alone or in admixture, and $M(acac)_3$, M = Sc, Y, La or Nd. The dependence of retention data on the ionic radius was demonstrated. The mobility (R_f value) for dik = acac is directly proportional to the ionic radius of the central ion[149]. The effect of the electronegativity of ligator atoms on the TLC of different β-diketonato complexes was also studied. For $Co(dik)_3$, $Cr(dik)_3$ or $Ru(dik)_3$, dik = acac, dibzac and monothio-dibzac, it was found that substitution of the donor O atom by the less electronegative S atom resulted in increased mobility of the complex. In addition, a linear dependence was observed between the retardation factor R_M of the complexes and the number of acac ligands replaced by monothio-dibzac ones[150].

Separation, identification and determination of ascorbic acid, ascorbyl palmitate and sodium ascorbate were performed by TLC on layers of Kieselgel HF254. The determination was based on the UV absorption of the compounds and on the fluorescence of the layer. When the layer is excited with UV radiation of 254 μm, the fluorescence is quenched in the zones corresponding to the UV absorbing compounds. A direct measure of the concentration of the separated substances is therefore possible[151].

4. Normal phase HPLC

Separation of six β-diketonate–metal chelates by HPLC was first carried out by liquid–liquid partition chromatography involving water–ethanol–2,2,4-trimethylpentane. Of the examined acetylacetonates of Be(II), Al(III), Cr(III), Fe(III), Co(III), Ni(II), Cu(II), Zn(II), Zr(IV) and Ru(III), they separated four-component mixtures within 25 minutes. Because of dissociation of the chelates on the column, acacH had to be included in the eluent[152]. Successful separation of β-diketonate chelates by normal phase chromatography was demonstrated also by other investigators[153–155].

Electrophilic substitution reactions of metal β-diketonates led to substitution on the central carbon of the chelate ring[156]. These mixed-ligand complexes could be isolated by TLC, GC or HPLC methods[157]. Normal phase HPLC was used to monitor the electrophilic bromination and nitration of $Cr(acac)_3$, $Rh(acac)_3$ and $Co(acac)_3$, yielding mixtures of complexes $M(acac)_{3-n}L_n$ ($n = 0–3$, L = α-bromo- or α-nitroacetylacetonate) (**11**, $R^1 = R^2 = Me$, $R^3 = Br, NO_2$)[158, 159]. The Co(III) complexes were thermally unstable and hence unsuitable for GC. The Rh and Cr complexes were readily separated on an OV-101/chromosorb W column. The nitrated acetylacetonates of Co(III) could be separated using normal phase HPLC. Certain metal chelates, e.g. $Ni(dik)_2$, show anomalous elution behavior (major distortion, tailing or disappearance of peaks) in liquid–liquid partition LC. Such undesirable behavior of metal chelates has also been observed in size-exclusion chromatography (SEC). The distorted elution curves observed for $Ni(dik)_2$ and $Al(ttfac)_3$ were attributed to partial dissociation of the chelates in the SEC column. The SEC behavior of the metal chelates was investigated from the viewpoint of elution recovery. The influence of chelated metal ions, mobile phase composition, column temperature and column length was examined. The following is recommended to obtain better chromatographic behavior of metal chelates: (i) shorter columns, (ii) a fast flow rate for the mobile phase and (iii) lower column temperatures. Furthermore, adding the chelating agent to the mobile phase suppresses undesirable dissociation of the metal chelate in the column[160].

Both GC and LC behavior of metal complexes of various ligand types including salicylaldimines and Schiff bases and fluorinated β-diketones was reported. Metal ions included the lanthanides, transition metals, Pt, Pd and Zn. Dissociation and thermal instabilities were found to be the main limitations in the chromatography of such derivatives. The data indicate that pre-column derivatization and GC is unlikely to provide a viable method for the ultratrace determination of metal ions except in rare circumstances. On the other hand, LC of complexed metal ions was found as a valuable technique that combines the advantages of versatility, specificity and sensitivity with the capacity for simultaneous determination and speciation. Diastereoisomers of oxovanadium(IV) complexes of tetradentate Schiff bases could be resolved by both GC and LC[161].

5. Reverse phase HPLC

A review was published dealing with RP-HPLC separation and determination of platinum-group metals as their complexes, including chelates, and application of the method to environmental and biological analysis[162a]. RP-chromatographic separations of $Al(acac)_3$, $Cr(acac)_3$, $Cu(acac)_3$ and other compounds were studied. Resolution of *cis–trans* isomers could be also shown. Alumina and silica gel bonded phases and open-pore polyurethane columns were used with a variety of mobile phases. Microparticulate silica gel columns were suggested to be the best columns for the separation of metal complexes by LC[154]. The RP-HPLC behavior of bzac chelates of Mn(II), Be(II), Co(II), Cr(III), Rh(III), Ir(III), Pd(II) and Pt(II) was investigated using methanol–water or acetonitrile–water as mobile phases on Supelco C_{18} and Ultrasphere ODS columns. Highly symmetric peaks were obtained indicating on-column stability, in certain cases with no need to include the β-diketone in the mobile phase. However, $Cu(acac)_2$, $Ni(acac)_2$, $Fe(acac)_3$, $Co(acac)_2$, $Zn(acac)_2$ and $Pb(acac)_2$ were not resolved successfully by this technique because they decompose on column. The LOD (UVD) were in the ng levels and the linear dynamic ranges of more than two orders of magnitude[162b].

$M(acac)_3$ mixtures (M = Al, Co, Cr and Fe) were separated using RP-HPLC columns containing Lichrosorb (10 mg) with RP-2, RP-8 and RP-18 bonded phases, with MeOH–H_2O and MeCN–H_2O mobile phases. The order of elution of β-diketonates depended on the type of the column packing and on the nature and concentration of the organic modifier in the mobile phase[163]. Optimum parameters for the separation of these mixtures were established. The resolution time, depending on the column type and flow rate (1.5–2.0 $cm^3\ min^{-1}$), was 6–10 minutes. The effectiveness of the separation was independent of the column length in the 10–25 cm range; however, the column length influenced the retention time[164]. The elution behavior of platinoid metal β-diketonates was studied with the aim to elucidate their retention mechanism and optimize their RP-LC separation conditions. Four different columns were used with MeOH–H_2O and MeCN–H_2O mobile phases. The retention of uncharged platinoid metal β-diketonates is interpreted by solvophobic effect and is strongly influenced by the geometric structure of the complexes. The square-planar chelates $Pd(acac)_2$ and $Pt(acac)_2$ are retained longer than the octahedral chelates, $Rh(acac)_3$ and $Ir(acac)_3$. It is likely that square-planar chelates show greater interaction with the nonpolar stationary phase than octahedral chelates. The van't Hoff plots showed that platinoid metal β-diketonates operate on the same retention mechanism at 25–45 °C. Optimum conditions for the separation of four platinoid metal β-diketonates are: 40% MeOH, polymeric C_{18} column and 45 °C[165]. In order to clarify the mechanism of retention of several β-diketonates of chromium(III), cobalt(III) and palladium(II), their Gibbs free energies were evaluated in RP-LC on C_{18}-bonded silica gel with MeCN–H_2O mobile phase. The values obtained were compared with the liquid–liquid partition coefficients of the metal β-diketonates in the dodecane–(MeCN–H_2O) system. It enabled a

more quantitative treatment of the Gibbs free energy of the interaction of solutes with the stationary phase, which is in accordance with the additivity of Gibbs free energy[166]. Capacity factors have been measured for several β-diketonates of Cr(III) and Pd(II) on C_{18}-bonded silica stationary phases with a MeOH–H_2O mobile phase. The capacity factor of each metal complex under these conditions is related to the partition coefficient in the dodecane–(MeOH–H_2O) system[167].

IP-RP-HPLC offers multielement detection capacity, selectivity and sensitivity of analysis. Most of the reports on IP-RP-HPLC for metal analysis are based on the separation as their chelates. Precomplexation of metal ions with appropriate ligands has many advantages such as increasing selectivity between metal ions, the ability to determine speciation and increasing sensitivity for chelates with high adsorptivity. Among the many ligands successfully used for IP-RP-HPLC separation of metal ions, the azo dye 4-(2-pyridylazo)resorcinol (par) is most widely used[168]. A simple reverse flow injection set-up was used for in-line complexation of metal-par chelates prior to their separation by IP-RP-HPLC using a C_{18} Bondapak column with the mobile phase containing 37% acetonitrile, 3.0 mM acetate buffer (pH 6.0) and 6.2 mM tetrabutylammonium bromide at a flow rate of 1.0 mL min^{-1} and UVD at 440 and 530 nm. The analysis cycle including in-line complexation and separation by IP-RP-HPLC was 16 min long, which enabled to separate Cr(VI) and the par chelates of Co(II), Ni(II) and Cu(II)[169].

RP-HPLC with a C_{18} column, UVD and MeCN–H_2O (50:50) as eluent was used for determination of the solubility of noble metal β-diketonates [$Pd(acac)_2$, $Pt(acac)_2$, $Rh(acac)_3$ and $Ru(acac)_3$] in $^{SC}CO_2$. The same determination was also carried out by normal phase HPLC for $Pd(acac)_2$, $Pt(acac)_2$ and Ag(acac), using a silica column and CH_2Cl_2–MeOH–hexane (45:45:10) as eluent. The main problem is injecting the sample without evolution of bubbles that are deleterious to the system. This is achieved by injecting the sample into an eluting solvent capable of dissolving the CO_2 at the pressures of the HPLC equipment[170].

6. Supercritical fluid chromatography

Volatile fluorinated metal chelates show high solubility and good chromatographic performance in supercritical CO_2. Thus, the use of supercritical fluid chromatography (SFC) in the separation of volatile fluorinated lanthanide complexes was very appealing. The SFC performance of $La(acac)_3$, $Pr(acac)_3$ and $Eu(ttfac)_3$ was investigated using dichlorodifluoromethane as the mobile phase[171,172] and much later in more detail, with modern SFC instrumentation and supercritical CO_2 as the mobile phase. Lanthnide complexes of acac, dpm and hfod have better chromatographic performances as compared to the chelates of tfac and ttfac. The retention is a temperature-dependent function of volatility and solubility[173]. $Cu(dik)_2$ and $Mn(dik)_2$ could be separated by SFC as such or after adduct formation with tributylphosphine oxide (TBPO). Hydrated $Cu(dik)_2$ complexes exhibit strong intermolecular interactions or decomposition in SFC. Formation of the TBPO adducts can greatly improve the SFC behavior and detection sensitivity of $Cu(dik)_2$ and $Mn(dik)_2$[174].

The solubilities of β-diketonate complexes of Cu, Zn, Ni and Co in supercritical CO_2 were determined. A linear correlation was found between the stability of the metal complex and extractant dissociation. This correlation helps finding extractants optimized for both extraction of metals and the recovery of valuble chemicals. Supercritical CO_2 best extracted Cu β-diketonates and the free metal could be best recovered in nitric acid. The other metal complexes showed lower extraction levels in the decreasing order of Ni, Co and Zn. The metal removal efficiency from the stripping solution into CO_2 varied between 5 and 90% and decreased in the order Cu, Co, Ni and Zn. The overall

dissolved amount of each metal acetylacetonate complex in supercritical CO_2 decreased in the order Cu, Zn, Ni and Co[175]. The solubility of $Cr(acac)_3$ in supercritical CO_2 was much increased by the addition of alcohol modifiers, such as MeOH, EtOH and especially CF_3CH_2OH. The increased effect of the latter modifier was attributed to the formation of a specially stable hydrogen bonded complex with the chelated ion[176]. $Cr(acac)_3$ and $Cr(dpm)_3$ were separated by SFC and determined by FID (LOD = 10–250 pg) or ICP-MS (LOD = 0.9–3 pg). The reproducibility was between 1 and 4% RSD and a linear response was observed for injections in the 0.1–100 ng range with both detection methods[177].

7. Determination of ascorbates by HPLC

A HPLC method for determination of Na ascorbate and a variety of sugars (glucose, fructose, lactose, sucrose, maltose, glucono-δ-lactone) in seasonings for sausages was described using amperometric detection; glucose and lactose could not be separated[178]. Magnesium ascorbylphosphate (**6**) in cosmetic preparations was determined by RP-HPLC with UVD at 255 nm, using a Lichrosorb-NH2 column and a 1:2 MeCN/0.3 M phosphate buffer (pH 4) solution as mobile phase. The LOD was 0.4 ppm with linearity from 4 to 40 ppm[179]. A method for simultaneous determination of **6** and melatonin (**7**) is based on RP-HPLC on a C_{18} column, with UVD at 260 nm. The carrier was an aqueous solution of 0.020 M Bu_4NOH and 0.025 M KH_2PO_4 mixed with MeCN in a 77:23 volume ratio; chlorthalidone (**40**) served as internal standard. The limits of quantitation (LOQ) were 0.69 ppm **6** and 0.47 ppm **7**. The method was applied for quality control of cosmetic cream[13]. The simultaneous determination of **6**, ascorbyl glucoside (**41**), kojic acid (**8**), arbutin (**42**) and hydroquinone (**43**) was carried out by RP-HPLC with UVD at 280 nm, using a 99:1 (v/v) mixture of 0.05 M KH_2PO_4 buffer (pH 2.5) and MeOH as mobile phase and pyridoxine (**44**) as internal standard[180].

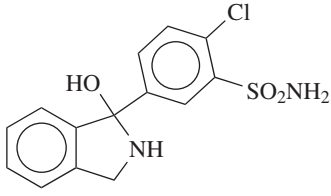

(**40**)

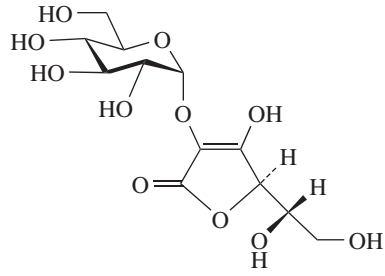

(**41**)

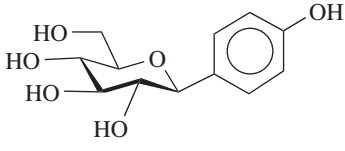

(**42**)

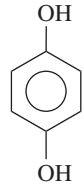

(**43**)

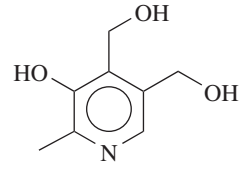

(**44**)

Ascorbic acid (**1**) has many biological functions besides its well-known antioxidant activity. It is a functional component of many pharmaceutical and cosmetic preparations. Antioxidants such as glutathione (**45**) or sodium metabisulfite ($Na_2S_2O_5$) are added

to protect the preparations activity on storage. To avoid possible interference by these additives in the determination of **1** in these preparations, it was proposed to carry out a separation by RP-HPLC with UVD at 254 nm using MeOH/MeCN containing metaphosphoric acid (pH 2.8). The method was validated for mixtures of the analyte with nicotinic acid (**46a**), **45**, oxalic acid and excipients of topical formulations such as oil in water emulsion or aqueous gel[181]. A kinetic method for determination of ascorbic acid/ascorbate (**1**) is based on measuring the initial rate of its oxidation to dehydroascorbic acid (**18**) in phosphate buffer (pH 5 to 6) catalyzed by ascorbate oxidase. The biochemical assay can be carried out in a plate reader at 265 nm, where **18** is transparent. Furthermore, the presence of **18** in a sample can also be determined after its reduction to **1** with a mercaptane such as dithiothreitol (**47**)[182].

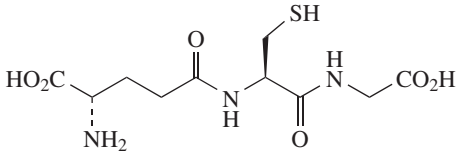

(**45**)

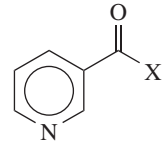

(**46**) (**a**) X = OH
(**b**) X = NH_2

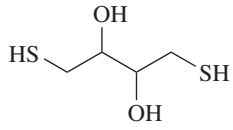

(**47**)

Ascorbyl glucoside (**48**), kojic acid (**8**) and niaciamide (**46b**) are used in commercial products as skin bleaching cosmetic formulations, where the concentration of these ingredients is regulated. A method for determination of these compounds consists of dissolving the sample in phosphate buffer solution in 40% (v/v) MeOH at pH 5.5, collecting the analytes in water after they have passed through a polycarbonate fiber microdialysis membrane, filling the sample loop of the injector with this solution and carrying out the end analysis by RP-HPLC with UVD at 254 nm, eluted by the same buffer solution. The chromatographic run was finished in about 4 min. The LOD and linearity ranges in ppm units were 0.01 and 0.068 to 304 for **48**, 0.01 and 0.071 to 284 for **8**, and 0.007 and 0.024 to 488 for **46b**, with good recovery and reproducibility[183].

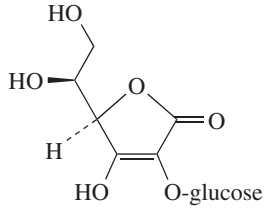

(**48**)

Evaporative light scattering detection (ELSD) can be applied in quality control for determination of analytes emerging from liquid phase separation methods, such as HPLC or ion chromatography (IC), as long as they are less volatile than the mobile phase. It has the advantage over differential refractive index detection of not being affected by gradient elution. ELSD involves three operations: (i) nebulization of the emerging stream, (ii) evaporation of the mobile phase and (iii) measurement of the intensity of the scattered light; however, the latter is not necessarily proportional to the analyte concentration[184–186]. The HPLC-ELSD method has been proposed for simultaneous determination of metallic ions

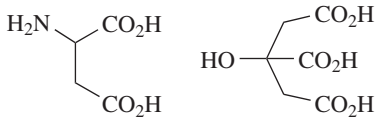

(**49**) (**50**)

and organic compounds in pharmaceutical preparations. Thus, the method was validated for determination of salts of Na(I), K(I), Ca(II), Mg(II) and Al(III) with organic acids such as ascorbic (**1**), aspartic (**49**) and citric (**50**). Each set of analytes required a special elution regime. The cations were separated on a Dionex CS-14 cation exchange resin. For example, Mg(II), Ca(II) and Al(III) were analyzed on applying a gradient elution with water containing 0.1 to 0.6% (v/v) tfa. The organic analytes and some of the cations were separated on a C_{18} RP-column. **49**, K(I) and Mg(II) were analyzed by isocratic elution with water containing 0.02% (v/v) tfa, whereas **1**, Na(I), **50** and Mg(II) required water with a gradient of tfa or nonafluoropentanoic acid. The peak areas A were calibrated for the amount m of analyte by the double logarithmic correlation ($\log A = b \log m + \log a$) where a and b are parameters of the analyte[187].

8. Separation of optical and geometrical isomers

Liquid column chromatographic methods can be used also for resolving organic and inorganic metal complex enantiomers and separating geometrical isomers. A chromatographic enantioseparation on a chiral selector consisting of a transition metal complex was first described in 1980. It was proved that neutral tris(acac) complexes of trivalent transition metals could be efficiently resolved into enantiomers on a $[(+)\text{-Co}(S\text{-Arg})_2(L)_2]^+$ ($L = NO_2^-$, Cl^-) complex acting as a chiral stationary phase[188]. The modeling of chromatographic separation of neutral $Co(acac)_3$ into enantiomers on a dinitrobis(arginine)cobalt(III) complex as a chiral selector was described. It demonstrates the predictive power of the method and its possible practical applications in designing efficient chiral stationary phases[189].

Later, a complete chromatographic resolution of $Co(acac)_3$ and $Cr(acac)_3$ on an optically active poly(triphenylmethyl methacrylate) column was accomplished. The optical data of the pure enantiomers were obtained. Extensive use was made of columns composed of clay plus metal complex adducts. Thus, optical resolution was accomplished by LC on a column packed with an ion-exchange adduct of synthetic hectorite and optically active $[Ni(II)](phen)_3$ and $[Ru(II)](phen)_3$[190]. Using these systems, $Co(acac)_3$, $Cr(acac)_3$, $Rh(acac)_3$ and $[Co(acac)_2(en)]^+$ (en = ethelenediamine) were resolved completely into enantiomers[191]. Enantiomers of these four species were separated by LC on a column packed with ion-exchange adduct of synthetic hectorite and optically active metal complexes[192]. One optically active metal complex used was tris(1,10-phenanthroline)-nickel(II), which was ion exchanged into synthetic hectorite. Racemic $Co(acac)_3$, $Cr(acac)_3$ and $Ru(acac)_3$ were also enantiomerically separated via LC using poly(*t*-butylisocyanide) as stationary phase[193].

Resolution of optically active $M(dik)_3$ and $[M(dik)_2]^+L$ complexes and their monolayer properties at an air–water interface was investigated[194]. These special complexes are chiral due to the asymmetric coordination of a central metal(III) ion. A chromatographic method to resolve $M(acac)_3$ has been developed by use of an ion-exchange adduct of a clay with optically active metal complexes. When the following eight complexes, $Cr(acacNO_2)_3$ ($acacNO_2$ = 3-nitropentane-2,4-dionato), $Co(acacNO_2)_3$, $Ru(dibzac)_3$, $Ru(hpd)_3$ (hpd = heptane-3,5-dionato), $Ru(nnd)_3$ (nnd = nonane-4,6-dionato), $Ru(dmh)_3$ (dmh = 2,6-

dimethylheptane-3,5-dionato), *fac*-Ru(tfac$_3$)$_3$ and Ru(acac)$_2$(dibzac), were eluted with a MeOH–HCCl$_3$ mixture on a column packed with the synthetic layered clay Laponite®, previously ion exchanged with [Ru(phen)$_3$]$^{2+}$, resolution was achieved for Δ,Λ-racemates of Cr(acacNO$_2$)$_3$, Co(acacNO$_2$)$_3$, Ru(hpd)$_3$, Ru(nnd)$_3$ and Ru(acac)$_2$(dibzac). The *facial* isomers of Co(bzac)$_3$ and Cr(bzac)$_3$ were retained more strongly than the *meridional* ones on a polyacrylonitrile TLC sorbent for a variety of aqueous and nonaqueous eluting solvents, pointing to stronger π-interactions of the *fac*-complexes with the sorbent[195, 196].

Certain transition metals form chiral chelates, even if the chelating ligands are achiral; e.g., in the case of M(acac)$_3$ (M = Cr, Co, Ru), two stable enantiomers, designated by prefices Δ- and Λ-, can be distinguished. Various modifications of HPLC columns capable of separating this type of racemic mixtures have been proposed based on the introduction of chiral groups or molecules that interact differently with the components of a racemic mixture. Eu(III) and Tb(III) complexes with chiral β-diketonate ligands derived from D-camphor, which can induce configurational chirality or chiroptical spectra [circularly polarized luminescence (CPL or CD)], have offered excellent opportunities for the examination of the optical activity theory as well as the chiroptical structural relation in chiral Ln(III) systems[197]. Work was done on the chiral assembly between Λ-[Cr(acac)$_2$(ox)]$^-$ and Δ-[Ln(hbpz)$_2$]$^-$ resulting in the formation of the chiral (Λ,Δ)-Cr(ox)Ln complexes, (Λ,Δ)-(acac)$_2$Cr(ox)Ln(hbpz)$_2$ (Ln = Yb and Dy, ox = oxalato, hbpz = hydrotris(pyrazol-1-yl)borato), where (Λ,Δ) is the absolute configuration around the octahedral Cr and square antiprismatic Ln moiety, respectively). The structural analysis is based on single crystal X-ray and CD spectra in comparison with those of the related mononuclear [Yb(hbpz)$_2$(*S*-pba)].

Saccharides and hydroxycarboxylic acids can substitute alkoxy groups from metal alkoxides. Thus, composites in which optically active organic compounds such as D-fructose, D-sorbitol and L-tartaric acid are highly dispersed in silica can be obtained by a sol-gel procedure using hydrolysis and condensation of tetraethoxysilane (TEOS) reacted with a saccharide[198]. During the process, ethoxy groups of the TEOS are replaced with hydroxyl groups of the saccharide. The composites obtained show higher abilities in the optical resolution of M(acac)$_3$ (e.g. Co(acac)$_3$) complexes, than those obtained by kneading and impregnation procedures, and optically active saccharides and hydroxycarboxylic acids themselves[199]. A different type of active organic–inorganic composite was also prepared by a sol-gel method. It was found that the L-tartaric acid–SiO_2 composites can resolve the racemate of M(acac)$_3$ to optically active forms[200]. The high resolution ability of the sol-gel derived composites arises from the combined effect of the silica support (adsorbing power) and the highly dispersed saccharide molecules (chiral recognition power). Cellulose tris(3,5-dichlorophenylcarbamate (CDCPC) was used as a chiral stationary phase (CSP) during HPLC. Co(acac)$_3$ and Cr(acac)$_3$ were among other chiral chemicals resolved on the CDCPC column. The applicability of CDCPC for enantioseparations in capillary liquid chromatography was also shown giving promising prospects for the screening of novel biologically active compounds for their enantiomeric composition[201]. Cyclohexylcarbamates of cellulose and amylose and their resolving abilities for enantiomers were evaluated as CPSs for HPLC. The chiral resolution capability was tested on several compounds, among them Co(acac)$_3$. The CSPs showed high resolving abilities, which are comparable to those of popular CSPs, tris(3,5-dimethylphenylcarbamate)s of cellulose and amylose[202].

HPLC enantiomeric separation of Co(acac)$_3$ was also performed with monolithic silica columns containing a covalently attached 3,5-dimethylphenylcarbamate derivative of cellulose[203]. Covalent immobilization of 3,5-dimethylphenylcarbamate derivative of cellulose was performed *in situ* onto native silica monoliths cladded in a polyether HPLC column. The covalent attachment of cellulose derivative in the range of 16–19% (w/w) was performed via an epoxide moiety. The covalent attachment of the cellulose derivative

enables this column to be used in combination with the mobile phases which are incompatible with coated-type polysaccharide columns due to solubility of chiral selector in some organic solvents. The column obtained by this technique combines the high enantiomer-resolving ability of the polysaccharide derivative with favorable dynamic properties of monolithic HPLC columns[204]. In addition, enantioseparations by HPLC were carried out using phenylcarbonate, benzoylformate, *p*-toluenesulfonylcarbamate, and benzoylcarbamates of cellulose and amylose as chiral stationary phases[205].

$Co(acac)_3$ is frequently used as a probe for enantioseparation efficiency of columns[206–208]. A monolytic capillary silica gel column was functionalized with methacrylate residues in two steps, as shown in equation 5[206], and then it was impregnated with cellulose or amylose (**51a**, **b**) which was modified so that 30% of the R groups were the methacrylate group **52** and the rest was identical to R′ (**53**). For further stability of the column, the polymeric modifier was immobilized on the silica gel by *in situ* copolymerization with an olefinic monomer such as 2,3-dimethylbutadiene. Only the column containing cellulose modified as in **51a** was able to separate the $Co(acac)_3$ racemic mixture, whereas neither cellulose nor amylose modified as in **51b** did, although they were successful in resolving other racemic mixtures[206–208].

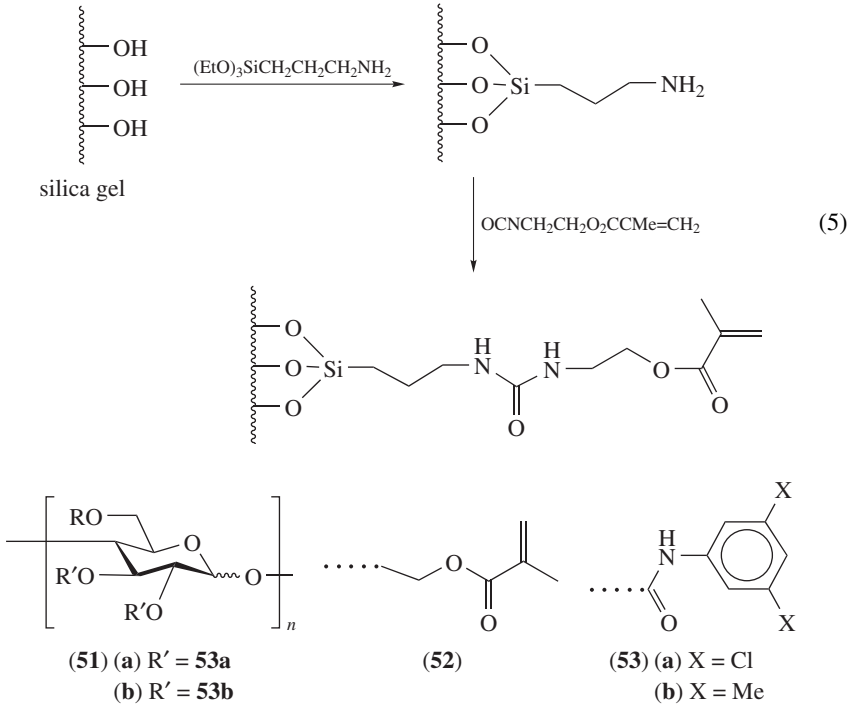

(5)

(**51**) (**a**) R′ = **53a**
(**b**) R′ = **53b**

(**52**)

(**53**) (**a**) X = Cl
(**b**) X = Me

HPLC separation of geometrical isomers of β-diketonates was also described. The retention of the *fac*- and *mer*-isomers of chromium(III) and cobalt(III) complexes with eight asymmetric β-diketonates was studied in the ODS–($MeOH–H_2O$) system. The retention order for two geometrical isomers depends on the structure of the complexing β-diketonates. Thus, the retention order *fac* < *mer* was found for complexes of the β-diketonates which possess a fluorinated functional group in each molecule. The reverse

order was found for complexes of β-diketonates without a fluorinated moiety. The retention sequence for the *fac*- and *mer*-isomers of each metal complex was the same as the increasing order of the partition coefficient values. The differences in the capacity factor between the *mer*- and *fac*-isomers is smaller than the difference in the partition coefficient value[209].

F. Miscellaneous Analytical Methods

A simple and rapid method for the iodometric determination of microgram amounts of chromium(III) in organic chelates is based on the oxidation of chromium(III) with periodate at pH 3.2, removal of the unreacted periodate by masking with molybdate and subsequent iodometric determination of the liberated iodate[210]. Iodometric titration was also used for determination of the effective isoascorbate (see **2**) concentration in fermentation processes[211]. The content of calcium ascorbate can be determined with high sensitivity by complexometric titration with edta, which is superior to iodometry[212]. The purity of β-diketonate complexes of Al, Ga, In and Ni was determined by complexometric titration with edta at pH 5.5–3, with RSD $\leqslant$ 0.01 for determining 5–30% metal ion[213]. Good analytical results were obtained by a similar procedure for the metal content of 15 lanthanide organic complexes[214].

Photoacoustic spectroscopy (PAS) is a nondestructive analytical technique in which light entering the photoacoustic cell passes through undetected if the sample is nonabsorbing, but heats up and expands the gas in the cell if the light is absorbed. This expansion makes an audible sound whenever absorption occurs and is detected by a microphone. The SNR may increase with the sample surface area. PAS determinations were carried out for hfac chelates of Sc, Y and the rare earth Ce, Pr, Nd, Eu and Er[215].

IV. METAL ENOLATES AS ANALYTICAL REAGENTS AND AIDS

A. General Methods

This part of the chapter gives an overview of different types of metal enolates, mainly β-diketonates, with emphasis on the properties that can be of interest in analytical applications. The analytical applications of rare earth β-diketonate complexes were reviewed[216].

A comparative study reviews the advantages and pitfalls of six vapor generation procedures applied when analytical methods for trace metallic elements (e.g. FAAS, ETAAS, ICP-AES and ICP-MS) involve a volatilization step: (i) Hydride generation with $NaBH_4$ is the most popular one; however, not all the transition metals form volatile hydrides, and some interferences have been observed with those that do. (ii) Generation of a metal carbonyl has been very successful in Ni ultratrace analysis. (iii) Generation of a volatile oxide is possible with certain elements and was successfully applied to Os ultratrace analysis, for which the interferences of concomitant elements and organic compounds were small, as opposed to those observed for hydride generation. (iv) Generation of volatile chelates and, in particular, β-diketonates has been extensively applied in GC; however, the method has some disadvantages, such as the necessity of sample preparation, the use of ECD that is nonspecific for the metal and is subject to contamination, and the inability to perform multielemental analysis, due to the inherent instability of the chelates of certain elements. (v) Generation of ethylated metals with $NaBEt_4$ has become a popular method for the volatilization of environmentally relevant elements (e.g. Cd, Cu, Hg, Pb, Se, Sn and Zn) prior to their quantitation or speciation; the risk of interferences with ethylated metals is lower than that with hydrides. (vi) Generation of chlorides and fluorides, especially the former, seems to be the most covenient derivatization of metals and metalloids to achieve volatility[217].

Complexation chromatography encompasses all chromatographic separations dependent on complexation, including the use of metal ions or metal complexes in the stationary phase. The versatility of complexation chromatography is due in part to its suitability in all areas of chromatography including GC, TLC, HPLC and SFC. Metal β-diketonates have been studied intensively in gas, column, liquid and thin layer chromatography, as well as in solvent extraction procedures, with the aim to find the factors that affect separation of the various metal ions. A review on chromatographic and related electrophoretic separation methods of transition metal complexes or their ligands discusses also analytical separation of metal β-diketonates by various chromatographic techniques and the incorporation of these compounds into chromatographic stationary phases to achieve a variety of effects, including chiral separations and 'synthetic antibody' action[103].

1. Optodes, photoluminescent and chemiluminescent tracers

Optode is an optical sensor device that optically measures a specific substance usually with the aid of a chemical transducer. Specific optodes consisting of glass plates coated with a permeable acrylic polymer film containing either [Cu(acac)(dmpen)]NO_3 (**54a**) or [Cu(acac)(dphpen)]NO_3 (**54b**) were prepared for the determination of H_2S in air at a level of 10 ppm. This level is considered by the National Institute for Occupational Safety and Health (NIOSH) to be about one tenth of the dangerous level for health and life. On short exposure of the optode to the contaminated atmosphere a change in color occurs, the intensity of which is proportional to the H_2S concentration and is measured with a UV spectrometer. A redox process takes place as shown in equation 6, where L represents the bidentate ligand derivatives of 1,10-phenanthroline, starting with the neutralization of the acac anion to yield acetylacetone, and followed by reduction of Cu(II) to Cu(I) and the concomitant oxidation of bisulfide anions to hydrogen disulfide[218].

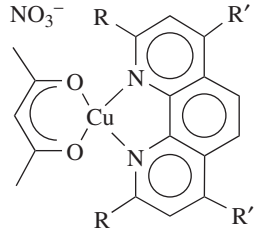

(**54**) (**a**) R = Me, R′ = H
(**b**) R = H, R′ = Ph

$$2[Cu(acac)L]NO_3 + 2H_2S \longrightarrow 2acacH + 2[LCuSH]NO_3$$
$$\longrightarrow [Cu_2L_2](NO_3)_2 + HSSH \qquad (6)$$

Some lanthanide β-diketonate complexes (**11**, M = Pr, Eu, Dy, R^1 = *n*-Pr, R^2 = *t*-Bu) have selectivity for further coordination with Cl^- ions, over F^-, Br^-, I^-, ClO_4^-, SCN^-, OH^-, AcO^-, HCO_3^-, NO_3^- and SO_4^{2-}, and are the active component of ion-selective electrodes (ISE) for Cl^-. It was proposed to take advantage of the luminescence in the visible range associated with Cl^- complexation, for the development of specific naked eye optodes (M = Eu) for this ion[219]. A sensitive fluorescence enhancement system for the determination of terbium was developed and studied. This method was applied to

the determination of trace amounts of Tb(III) in a synthetic rare earth oxide and a high purity Y_2O_3 matrix. In this system the anion derived from *N*-(2-pyridyl)-2-ketobutyramide (pykba) is a potential chelating ligand. The $Tb(pykba)_3$ complex emits intrinsic fluorescence of Tb(III) under excitation by ultraviolet light ($\lambda_{ex} = 305$ nm, $\lambda_{fl} = 496$, 549 nm). The intensity of this fluorescence is further enhanced in the presence of Et_3N and Zn(II) ions[220]. The fluorescence of $Tb(acac)_3$ nanoparticles dispersed in a polyacrylamide matrix is very strong. This is the basis of a fast and sensitive method for determination of Cr(VI) by fluorescence quenching, even in the presence of a large excess of Cr(III). The LOD is 0.8 ppb with little interference by other ions usually present in water and waste water[221].

A spectrophotometric method was developed for the quantitative evaluation of cyanide ions in the concentration range of 25 ppb by using a silica-supported $Fe(acac)_3$ column. The concentration of CN^- was calculated from the absorbance at 295 nm[222]. $VO(acac)_2$ and luminol (**55**) show a chemiluminescent reaction which served to devise a micelle-mediated method for determination of V(IV)[223,224].

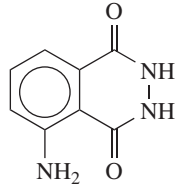

(**55**)

1,2-Enedithiolates (dithiolenes[225]) were used originally together with other ligands for production of chelates of transition metals for determination by UVD. After the discovery of photophysical properties of Pt complexes of certain 1,2-enedithiolates, they were used as phosphorescence and fluorescence dual emitters for oxygen and proton detection. The analytical applications of 1,2-enedithiolates have been reviewed[226].

Markers with red luminescence under UV light are used as tracers for shadowing pursuits in a variety of criminal cases. Luminescent markers consist of a mixture of 1% europium β-diketonates in vaseline as the carrier. The visual detection limit under UV light is 1–100 ppm. Six types of europium β-diketonates were extracted with acetonitrile and promptly identified using both fluorescence spectrophotometry and electrospray ionization mass spectrometry at the detection limits of 10–100 ppb. The markers were identified for evidence in the field of forensic science[227]. $Eu(dik)_3$ complexes emitting in red and $Tb(dik)_3$ complexes emitting in green are used as photoluminescent markers, fluoroimmonoassay labels, markers for forensic tracers and dyes of latent fingerprints. In forensic tracing analysis it is important to be able to identify the various tracers to be presented as evidence, and this is difficult with FLD because the spectra are very similar. The advantage of using a microscope laser Raman spectrometer (MLRS) over the usual microscope fluorescence spectrometer (MFS) was investigated for enolates of Eu(III) and Tb(III) without (**56a–f**) and with 1,10-phenanthroline as an additional ligand (**57a–h**). The emission spectra obtained in the MLRS were well resolved, even for the much weaker Tb(III) complexes, whereas the corresponding fluorescence spectra of the MFS appeared as a single broad peak[228].

2. Gas sensors

A capacitive-type CO_2 sensor using self-assembled organic–inorganic bilayer film operating at low temperature was described. The sensor is based on changes in capacitance

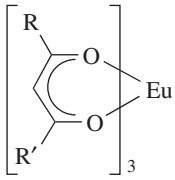

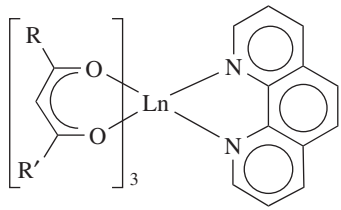

(**56**)(**a**) R = *t*-Bu, R′ = Mef
(**b**) R = *t*-Bu, R′ = *n*-Prf
(**c**) R = Ph, R′ = Mef
(**d**) R = 2-Fu, R′ = Mef
(**e**) R = 2-C_4H_3S, R′ = Mef
(**f**) R = 1-Naph, R′ = Mef

(**57**)(**a**) Ln = Eu, R = *t*-Bu, R′ = Mef
(**b**) Ln = Eu, R = *t*-Bu, R′ = *n*-Prf
(**c**) Ln = Eu, R = Ph, R′ = Mef
(**d**) Ln = Eu, R = 2-Fu, R′ = Mef
(**e**) Ln = Eu, R = 2-C_4H_3S, R′ = Mef
(**f**) Ln = Eu, R = 1-Naph, R′ = Mef
(**g**) Ln = Tb, R = *t*-Bu, R′ = Mef
(**h**) Ln = Tb, R = *t*-Bu, R′ = *n*-Prf

and resistance of a self-assembled multibilayer film containing metal acetylacetonate upon exposure to CO_2, and can be used as CO_2 sensor operable at low tempetrature[229]. A multibilayer film consisting of dimethyldidodecylammonium bromide (d.c. 1–16) and a metal acetylacetonate exhibits a large capacitance change upon exposure to CO_2 at 373 K. $Ni(acac)_2$ exhibits the largest change in capacitance, which increases linearly with increasing CO_2 concentration and hardly responds to H_2O and CH_4. Consequently, a self-assembled multibilayer film can be used as a capacitive-type CO_2 sensor at low temperatures[230]. A low-temperature gas sensor for ozone and NO_x was fabricated by laser deposition of an $In(acac)_3$ semiconducting layer, about 500 nm thick, on an alumina plate. The sensitivity of this sensor, $S = R_{sample}/R_{air}$, where R is the resistance, at the optimal measuring temperature was 470 for 100 ppb ozone at 120 °C and 50 for 130 ppm NO_x at 270 °C[231]. The gas sensors were prepared on a ceramic support by either of two techniques. By the pulsed laser deposition (PLD) technique a polymeric thin layer was deposited on alumina by 248 nm laser beam 10 Hz pulses of 0.07–0.15 J cm^{-2} energy density, on a target of $In(acac)_3$ or $Sn(acac)_2Cl_2$, at low pressure (3 Pa). In the matrix-assisted pulsed laser deposition (MAPLE) technique a 1–5 wt% solution of either chelate in acetone is frozen on the support and irradiated by the pulsed laser beam. A smoother surface is obtained by PLD than by MAPLE. The sensors have an optimal working temperature range and are operated alternatively in artificial air (20 vol% O_2 + 80 vol% N_2) and in the sample atmosphere. The signal difference between the atmospheres is calibrated for analytes such as O_2, H_2 or NO_2[232]. Deposition techniques from metal enolates were reviewed elsewhere[11].

3. Ion selective electrodes

The membrane for a Cu ISE was manufactured by adding to a solution of pvc a Cu(II) chelate (1 wt% relative to pvc of **58**, **59** or **60**), an anion excluder ($NaBPh_4$, 1%) and a plasticizer (e.g. *n*-Bu_3PO_4, 200%). After evaporation into a film, conditioning and mounting, measurements were carried out using a SCE. The linearity range was *ca* 10 μM–0.1 M Cu(II) with Nernstian response of 25–30 mV per decade and response time from 10 to 60 min, depending on the chelate and the plasticizer used[233]. A wire coated with a pvc membrane containing **58** acted as ISE for dichromate ($Cr_2O_7^{2-}$) at pH

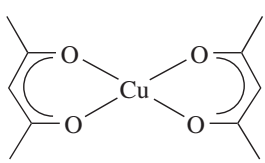

(**58**)

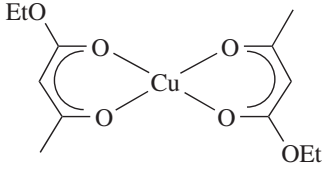

(**59**)

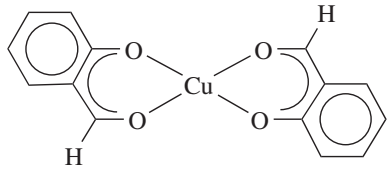

(**60**)

1.7–3.8 or chromate (CrO_4^{2-}) at pH 8.5–11.5, with Nernstian response of −29.4 and −29.2 mV per decade, respectively. The LOD was 1 μM, with good selectivity for both Cr(VI) ions and short response time. This electrode was also used for the determination of Cr in wastewater and as indicator electrode in the titration of Cr(VI) with $Pb(NO_3)_2$[234].

A Cl^- ISE was prepared with a pvc membrane containing $VO(acac)_2$. The Nernstian slope was -55.0 ± 2 mV per decade, with linear dynamic range from 25 μM to 0.10 M Cl^-. The pH 3.5–9.0 range did not affect the potentiometric measurements. The selectivity of the ISE was found to be satisfactory in the presence of 100-fold molar concentrations of AcO^-, 2-$HOC_6H_4CO_2^-$, HCO_3^-, NO_2^-, NO_3^-, ClO_4^-, F^-, CO_3^{2-} and SO_4^{2-}. However, Br^-, I^- and SCN^- interfered with the measurements[235]. Similarly, a pvc membrane containing $TiO(acac)_2$ can be used for building an iodide ISE. The Nernstian slope was 59.1 mV per decade, with LOD 3.0 μM and linear dynamic range 5 μM–0.1 M I^-. The pH 4.0–9.2 range did not affect the potentiometric measurements. The electrode could be applied for endpoint indication in the titration of I^- with $AgNO_3$[236].

Lanthanide enolates carrying lipophilic groups can be used as ionophores to fabricate Cl^- ISE membranes. Thus, electrodes with a membrane incorporating into pvc a lantanide chelate such as **61** or **62a–c**, an anion excluder such as $NaBPh_4$ and a plasticizer (dioctyl sebacate, dioctyl adipate, dibutyl phthalate, dioctyl phthalate or tributyl phosphate) have

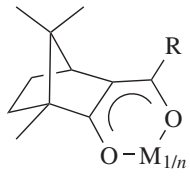

(**61**)

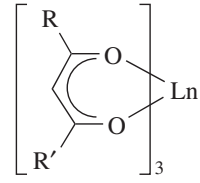

(**62**) (**a**) Ln = Pr, Eu, Yb, Dy, R = *i*-Pr, R′ = *n*-Prf
(**b**) Ln = Eu, R = R′ = *i*-Pr
(**c**) Ln = Eu, R = *i*-Pr, R′ = Mef

Nernstian response vs. SSCE of −52 to −63 mV per decade, in phosphate buffer (pH 5.8), with response time from 30 to 60 s. The LOD of these electrodes varies from 11 to 87 μM Cl^-. The selectivity for this anion was tested for N_3^-, NO_3^-, HCO_3^-, ClO_4^-, F^-, Br^-, I^-, SCN^-, AcO^-, citrate, tartarate, CO_3^{2-} and SO_4^{2-} and was found to depend on the chelate used; thus the best overall performance is obtained for **62a** (Ln = Eu); however, SCN^- interferes with Cl^- measurement. The best selectivity for Cl^- in the presence of other halides or CSN^- was shown by **61** (M = Eu, $n = 3$, R = Mef) or **62b**[219,237]. Cu(II)(acac)$_2$ (**58**) was chosen for its stability and homogeneity as reference material for the AAS determination of Cu in K_2CrO_4. The LOD (SNR 3) was 13 ppb[203].

4. Gas chromatography

The present section and Section III.D complement each other. The possibility of GC separation and determination of metal ions in the form of complexes with ligands derived from β-diketones has been the focus of extensive research. As early as 1967 it was reported about the GC of a number of volatile rare-earth β-diketonate chelates containing the ligands hfod and dpm. The volatility of these complexes increases as the ionic radii of the central metal ion decreases[238]. Later, the GC behavior of β-diketonate chelates of Cu(II), Al(III), Cr(III), Mn(II), Fe(III), Co(II), Co(III), Ni(II), Zn(II) and Ga(II) was studied. Elution and separation characteristics arise from a number of adsorptive effects. Nonpolar stationary phases give better peak characteristics than polar phases; however, the nature of the column material has little effect on the chromatography of the metal chelates. Fe(dik)$_3$ showed anomalous elution and, in general, the β-diketonates depart from ideal chromatographic behavior[239,240].

The difference in the detection sensitivities of Be(dik)$_2$, Al(dik)$_3$, Cr(dik)$_3$ and Rh(dik)$_3$, dik = acac, tfac and hfac, depends on the metal, irrespective of the ligand or detector (TCD, FID or ECD)[241]. The order of GC sensitivity is Rh(III) ⩾ Cr(III) ⩾ Be(II) > Al(III) > Cu(II) > Fe(III), is related to the ratio of molecular ions present to total ions of the chelates and is affected largely by the thermal stability rather than by the ionization efficiency in FID or ECD[42]. In a search for new chelating agents to separate metal ions by GC, some β-diketones containing the *t*-Bu group at one end and alicyclic groups, such as *c*-Pr, *c*-Bu, *c*-Pen and *c*-Hex, at the other end were synthesized. Thermogravimetric analysis of the corresponding chelates Cu(dik)$_2$, Cr(dik)$_3$ and Er(dik)$_3$ indicated that the Cu and Cr diketonates vaporized almost completely, while those of Er decomposed partially on vaporization. The thermal stability and volatility of the alicyclic β-diketonates were intermediate between those of acyclic terminal groups and aromatic ones. The *c*-Alk β-diketonates gave a clear GC peak, separated from that of the free diketone[242]. Also, the Cu and Er chelates derived from $RCOCH_2COR'$ (R = Mef, R′ = *c*-Pr, *c*-Hex) were investigated by GC and TGA. Replacement of the *t*-Bu group by a Mef increased the volatility of the chelates at a given temperature, but the Er chelates showed increased thermal decomposition, making the latter complexes unfit for Er determination by GC[243].

Dipivaloylmethanes were used to separate and determine the Ce group lanthanides by GC. Silicone XE-60 could be used as the liquid phase. Chelate mixtures of Gd–Nd, Gd–Pr, Gd–La, Eu–Pr, Eu–La and Sm–La could be separated[244]. A method was developed for the determination of Cr trace levels in serum, involving low-temperature ashing of the human serum sample, followed by treatment with tfacH to form the thermally stable and volatile Cr(tfac)$_3$ and end anlysis by GC-MED (microwave emission detector) measuring at 357.9 nm, the atomic emission line of Cr, with very good selectivity and LOD 0.9 ng L^{-1} Cr[245]. A capillary GC method was also developed for the determination of vanadium in rocks using bis(acetylpivalylmethane) ethylenediimine (**63**) as the chelating agent. The method includes complexation of the analyte, followed by solvent extraction,

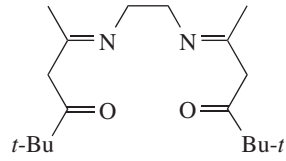

(**63**)

and then elution and separation by capillary GC. The method is effective unless high concentrations of Fe(II) exist in the mixture[246].

Metal chelate-modified polyethylene glycol (peg) liquid phase was used for GC determination of oxygen-containing compounds[247]. Mixtures of alcohols, aldehydes and ketones could be separated using this system. Thus, the chromatographic properties of stationary phases based on peg and $Ni(acac)_2$, $Al(acac)_3$ and $Cu(acac)_2$ were investigated. Separation efficiencies, sorption capacities and selectivity within a homolog series, as well as between groups for alkanes, alkenes and alkylbenzenes were reported[248]. The effect of thermal treatment of a peg stationary phase modified with $Eu(acac)_3$ on its chromatographic properties was also studied[249]. The selectivity of separation of aliphatic alcohols and α-ketones was demonstrated to increase for thermally treated phases. The separation ability of surface layers of $Ni(acac)_2$ bonded to Silochrom S-80 silica gel was also studied and the selectivity of separation was estimated for different classes of organic compounds. It was demonstrated that these sorbents are promising for the separation of complex mixtures of high-boiling aromatic compounds and oxygen-containing compounds[250].

Metal complexes such as $Ni(acac)_2$ and $Co(acac)_2$ bonded to a silica surface via β-diketonate group were used as stationary phases in chromatographic analysis of ethers and thioethers[251]. The behavior of columns with liquid phases composed of solutions of rare earth β-diketonates in squalane was studied[252]. Strong interactions were observed with the more nucleophilic organic solvents (e.g. thf), and the Er(III) fluorinated β-diketonates showed greater interaction with the nucleophiles than the nonfluorinated Er(III) chelates. Application of this method to the resolution of enantiomers was suggested here for the first time. They noted that if a chelate containing an enantiomeric ligand is part of the liquid phase, racemic analytes might be resolved. Indeed, an NMR shift reagent study showed that the chelate **61** (M = Eu, $n = 3$, R = t-Bu) preferentially coordinates the R isomer of 2-phenylethylamine of a racemic mixture. Partial resolution of neutral complexes such as $Cr(acac)_3$ and $Co(acac)_3$ was also achieved by using different optically active cobalt(III) complexes[188].

5. Complexation gas chromatography

Some statements relevant to this subject appear at the end of Section IV.A. The use of metal chelate complexes as sorbents and stationary liquid phases in GC was reviewed. Data were collected on the processes of complex formation at the phase interface and on the target production of the chelate-containing sorbents. Extensive information is given on the possibilities and advantages of using complexation at the gas–stationary phase interface in both theoretical studies and in practice. Special attention is given to the physicochemical aspect of sorption and separation with participation of the complex that forms sites of the surface. The results show that it can be effectively used in chemistry, environmental protection, medicine and in other related fields making use of chromatographic methods of analysis[253].

The application of stationary phases containing metal coordination compounds to the GC separation of organic substances has been the subject of many publications and

reviews. In one of them the 'polarity' and 'selectivity' of stationary phases containing $Pr(dik)_3$ and $Eu(dik)_3$ was qualitatively and quantitatively evaluated, employing the Rohrschnider–McReynolds classification of stationary phases, possessing the ability to form adducts with many nucleophilic compounds. Selectivity values were established for classes of solutes as follows: nitrogen bases > *n*-alcohols > ketones > *t*-alcohols > ethers[254]. The effect of surface deposition of layers of chelated Ni(II) species, such as alizarinate, dimethylglyoximate and acetylacetonate, on the retenion of various sorbates was investigated[255].

Complexation gas chromatography (CGC) is based on packings which are capable of specific π-interactions with adsorbate molecules characterized by electron-donor properties. The separation mechanism involves formation of metastable complexes, either organic or with cations of transition metals[256]. β-Diketonate complexes are interesting in CGC for at least four reasons[257]: (i) different metals can be used; (ii) different β-diketonate ligands can be employed; (iii) the metal β-diketonates can be either bonded to a silica surface via appropriate silanes or dissolved in a liquid stationary phase; (iv) a high thermal stability of the modified packings can be achieved. New packings for CGC were studied in which complexes **64** (M = Ni, Co, R = Me, Mef) are chemically bonded to silica gel. The effect of the structure and the configuration of adsorbates like olefins, cyclic and aromatic hydrocarbons on the retention of these compounds were determined. The results show good applicability of the new packings as well as high selectivity towards compounds containing π-electrons. Thus, the new packings were successfully applied for separation of mixtures of cyclic ethers and thioethers and of mixtures of furan and thiophene derivatives.

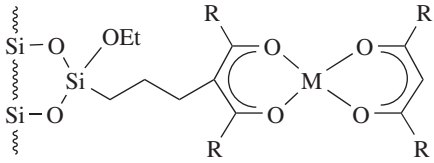

(**64**)

The practice and theory of enantioselective CGC was comprehensively reviewed. Racemic oxygen-, nitrogen- and sulfur-containing selectands can be separated without prior derivatization into enantiomers by CGC on optically active metal(II) bis[3-(perfluoroacyl)-(1*R*)-camphorate] (**61**) selectors. Peak inversion is obtained when the selectors with opposite configuration are employed. Applications pertain to chiral analysis in asymmetric synthesis, enzymatic reactions, pheromone and flavor chemistry[258].

A review appeared on the practice and theory of enantioselective CGC with optically active selectors, e.g. 3-(perfluorobutyryl)-(1*R*)-camphorate residues forming complexes on a functionalized polysiloxane stationary phase (e.g. Chirasil, **65**); SFC operates at temperatures lower than those of CGC, thus allowing better resolution, especially of thermally unstable enantiomers (e.g. those based on restricted free rotation, as is the case of dimethyl 1,1′-binaphthyl-2,2′-dicarboxylate, **66**[259]). Various analytical problems were addressed, such as determination of enantiomeric excess, assignment of absolute configuration, the elusive separation of protio- and deuterio-substituted enantiomers and the semipreparative separation of enantiomers. The following chromatographic parameters are related to the chemical and thermodynamic properties enclosed in parentheses of the enantiomeric system: (i) peak retention (chemoselectivity, $-\Delta G$), (ii) peak separation

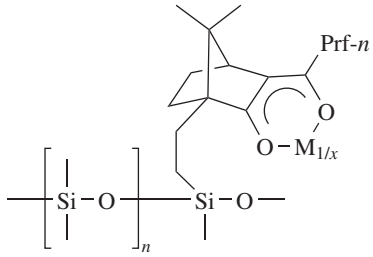

(**65**) $x = 2$, M = Ni, Mn, Zn
$x = 3$, M = Eu

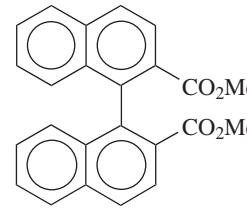

(**66**)

(enentioselectivity, $-\Delta_{D,L}G$), (iii) peak coalescence of the fourth kind (enantiomerization barrier, $\Delta G^{\neq}$), (iv) peak ratio (enantiomeric excess, ee) and (v) peak assignment (enantiomeric configuration, *R* or *S*)[258].

A review deals with the practice and theory of capillary chromatography using metal complexes or modified cyclodextrins as selectors attached to the stationary phase; it adopts a unified approach for all contemporary chromatographic methods using a single enantioselective column. Among the important findings reported are the feasibility of GC preparative enantiomeric separation and the existence of an isoenantioselective temperature, below and above of which the enantioselectivity of the column changes direction for a given racemic mixture. Several challenging problems for research were mentioned: (i) high-throughput and very fast enantiomeric analyses, (ii) trace analysis of enantiomeric impurities (e.g. at the ee = 99.998% level), (iii) search for prebiotic terrestrial and extraterrestrial homochirality, (iv) enantiomeric separations in the absence of a chiral auxiliary on planar inclined surfaces by one-directional movement, (v) determination of absolute configuration by directly visualizing small chiral molecules via Coulomb explosion, (vi) preparative GC separation of racemic five-atomic molecules (e.g. C*HClFI) as probes for measuring parity violation, (vii) chirality in environmental chemistry and (viii) unraveling mechanistic aspects of chiral recognition in enantioselective chromatography[260].

A computational procedure for the modeling of chromatographic separation of racemic $Co(acac)_3$ into enantiomers on a dinitrobis(arginine)cobalt(III) complex as a chiral selector was described. Predicted elution order calculated from the differences in total energy of interaction for Λ and Δ selectands were found to be in agreement with the experimental results. The predictive power of the method and its possible practical applications in designing efficient chiral stationary phases was demonstrated[261].

Retention of Rohrschneider–McReynolds standards of selected chiral alcohols and ketones was measured to determine the thermodynamic selectivity parameters of stationary phases containing (+)-**61** (M = Pr, Eu, Dy, Er, Yb, $n = 3$, R = Mef) dissolved in poly(dimethylsiloxane)[262, 263]. Separation of selected racemic alcohols and ketones was achieved and the determined values of thermodynamic enantioselectivity were correlated with the molecular structure of the solutes studied. The decrease of the ionic radius of lanthanides induces greater increase of complexation efficiency for the alcohols than for the ketone coordination complexes. The selectivity of the studied stationary phases follows a common trend which is rationalized in terms of opposing electronic and steric effects of the Lewis acid–base interactions between the selected alcohols, ketones and lanthanide chelates. The retention of over fifty solutes on five stationary phases containing **61** (M = Pr, Eu, Dy, Er, Yb, $n = 3$, R = Mef) dissolved in polydimethylsiloxane were later measured[264]. The initial motivation for this work was to explore the utility of a solvation parameter model proposed and developed by Abraham and coworkers[265] for complexing stationary phases containing metal coordination centers. Linear solvation

energy relationships were proposed to relate such properties as polarity, ability to form hydrogen bonds and structural arrangement of molecules to diverse processes in solution, and the behavior was correlated with changes of the Lewis acidity of the lanthanide ions.

6. Thin layer chromatography

A review on TLC of *d*-block elements and their counteranions discusses types of stationary phases, mobile phases, development modes and detection and quantitative determination techniques[266]. The colored complexes $Ni(ttfac)_2$, $Co(ttfac)_2$, $Mn(ttfac)_2$, $Cu(ttfac)_2$, $Fe(ttfac)_3$, $Ce(ttfac)_4$, $Th(ttfac)_4$ and $U(ttfac)_6$ were prepared by adding a solution of 1-thenoyl-3,3,3-trifluoroacetone (ttfacH) to a solution of the metal salts brought to pH 7.5 with sodium acetate buffer. The complexes were separated on silica gel G TLC plates. Best results were obtained with the solvent systems butanone–xylene, acetone–cyclohexane and 4-methyl-2-pentanone–xylene[267].

7. Complexation liquid chromatography

Some statements relevant to this subject appear at the end of Section IV.A. A review on chromatographic and related electrophoretic methods in the separation of transition metal complexes or their ligands discusses also analytical separation of metal β-diketonates by various chromatographic techniques and the incorporation of these compounds into chromatographic stationary phases to achieve a variety of effects, including chiral separations and 'synthetic antibody' action[103]. Studies were performed on column packings containing $Cu(acac)_2$, $Cu(hfac)_2$ and $CuCl_2$, chemically bonded via β-diketonate groups. The retention factor (k), specific retention volume (V_g) and molecular retention index (M_e) were measured and used to calculate the free energy of adsorption (ΔG_a), heat of adsorption ($-\Delta H_a$) and entropy of adsorption (ΔS_a). These parameters enable characterization of specific interactions between aromatic and cyclic hydrocarbons, ethers and thioethers, and the metal complexes chemically bonded to a silica surface[268].

Reaction of $Cu(hfac)_2$ with nitroxide 4-amido-2,2-dimethyl-5,5-dimethoxy-3-imidazoline-1-oxyl (L) in a 2:1 ratio in hexane yielded the $Cu(hfac)_2$-saturated coordination chain polymer of composition $[Cu(hfac)_2]_2L$[269]. The $M(hfac)_2$ (M = Mn, Co, Ni, Cu) complexes with nitroxide systems have been the subject of much attention for some time, since they are convenient models for the investigation of exchange interactions in heterospin systems. Thus, in $[Cu(hfac)_2]_2L$, half of the $Cu(hfac)_2$ molecules coordinate L in bidentate fashion through the amide oxygen and the imine nitrogen of the heterocycle. The other $Cu(hfac)_2$ molecules arrange the $\{Cu(hfac)_2L\}$ fragments in polymeric chains by alternate coordination of either the N or the O atom or the amide oxygens of two $\{Cu(hfac)_2L\}$ fragments to axial positions. As a result $[Cu(hfac)_2]_2L$ involves three hexacoordinated Cu ions, each with a different coordination environment. The magnetic properties of the complex are described in terms of an exchange cluster model with ferromagnetic intracluster exchange interactions.

2-Thiophenaldehyde-4-phenyl-3-thiosemicarbazone was used as a complexing reagent for liquid chromatographic determination of Co(II), Cu(II) and Fe(II) or Co(II), Ni(II), Fe(II), Cu(II) and Hg(II). The metal chelates were separated on a Microsorb C-18 RP-HPLC column, with LOD = 0.5–2.5 mg L^{-1}. The method was applied for the determination of Cu, Co and Fe in pharmaceutical preparations[270].

8. Elemental analysis involving metal enolates

Separating rare earths by converting them to volatilie chelates, usually dpm complexes, followed by fractional codistillation was described. The mixture of chelates can be fractionally distilled with a codistillant to collect enriched fractions of the chelates, from

which a rare earth salt is stripped by acidification and extraction with water[271]. The chelates of Be(II), Co(II), Ni(II), Zn(II), Al(III), Co(III), Cr(III), Fe(III), In(III), Mn(III), Sc(III), V(III), V(IV)O and Zr(IV) with tfac can be purified, without concurrent thermal decomposition, by sublimation under atmospheric pressure in a flow of He containing tfacH vapor[272]. Pivaloyltrifruoroacetone (ptfaH) was proposed as chemical modifier for the determination of trace rare earth elements in natural water by electrothermal vaporization ICP-MS, presumably to aid in the formation of volatile $Ln(ptfa)_3$ complexes[273].

Determination of the oxygen content of Al, Be, Mn and Sc β-diketonates with the Carlo Erba analyzer gave unacceptable results, caused by retention of oxygen by the oxide that is not reducible with carbon at the operating temperature of the apparatus (1100 °C)[274].

B. Specific Reagents

1. β-Diketonates

a. General considerations. The importance of metal β-diketonates in many industrial processes (e.g. the extraction and separation of metals) and as semiconductors, antioxidants, catalysts in organic reactions[8] and NMR shift reagents[18] is well established. The β-diketonates were very attractive as volatile derivatives of metals, offering possibilities for efficient separation by analytical and preparative gas chromatography. Many of them have both high volatility and thermal stability. They are formed by a wide range of metals and require no special handling techniques. In 1970, the first preparative gas chromatographic separation of metal complexes of this type was reported. Both fluorinated and nonfluorinated β-diketonates of Al, Cr and Fe have been studied and conditions were established for their complete separation. The technique was also extended to a preparative scale with up to 0.1 g chelate samples. A new way for purification of metals was established[275]. Cr has been determined in rocks, serum, plasma, urine, orchard leaves and alloys, applying GC techniques to $Cr(dik)_3$, dik = acac, hfac, hfod and tfac. A special method for the determination of Cr is based on atomizing the volatile phase generated from its β-diketonates in a silica tube. The silica tube is then heated with an air–acetylene flame. The analytical characteristics are LOD 0.15 ng, reproducibility 5.6% and linearity up to 25 ng[276].

Evaporating and cocondensing the desired metal at −196 °C, warming up and removing solvent and excess acacH in vacuum, gave the metal–acac complex in good yields, including $Ln(acac)_3$ complexes, which represent an attractive route to NMR shift reagents. The formation of β-diketonate complexes has been widely used for separating and determining metals by GC. The volatility and thermal stability of these chelates permitted the extension of a technique which initially was only applicable to organic compounds. Concurrently used with ECD, this gave rise to very sensitive methods, especially for Cr, Be and Al. However, some disadvantages were noted: (i) the necessity of using reagents free of impurities which might interfere with ECD, (ii) the elimination of excess β-diketone by back-extraction and (iii) the fact that many chelates decompose in the chromatographic column, making it impossible to elute them at trace levels. Detection systems for GC which avoid the disadvantages of ECD include MS, microwave-excited plasma, AAS and even ICP-AES, replacing the chromatographic column with a volatilization system[277]. The relative volatility and stability of various barium β-diketonates was investigated[278].

b. Acetylacetonates. Atomization of chromium β-diketonates after volatilization increases the sensitivity 54-fold as compared to the nebulization of aqueous solutions of dichromate with atomization in the flame. Cr was determined in urine samples taken from 60 diabetic patients and 21 healthy volunteers, by complexation to $Cr(acac)_3$, supercritical fluid extraction with CO_2–MeOH (200 atm, 120 °C) under static or dynamic

conditions. The GC-FID end analysis of the extract dissolved in MeOH was linear in the 0.5–43 mg L^{-1} Cr range, with LOD = 0.18 mg L^{-1} Cr. End analysis of the same MeOH solution by HPLC-UVD (350 nm) showed linearity in the 0.013–60 mg L^{-1} Cr range with LOD = 0.02 mg L^{-1} Cr[279].

The enhancement of the extraction of Ln(III) ions with ttfaH in cyclohexane or benzene by the addition of $Cr(acac)_3$ was investigated[280]. The equilibrium analysis suggested that the effect of $Cr(acac)_3$ could be ascribed to the formation of a binuclear 1:1 $La(ttfa)_3$–$Cr(acac)_3$ adduct. The formation constants of adducts along the lanthanide series decreased with the decrease of the ionic radii among the light lanthanides and were constant for their heavy counterparts. UVV, IR and ^1H NMR spectroscopic studies were also performed to explain the molecular structural differences between the light and heavy lanthanide complexes.

Al(III) solutions suitable for careful *in vivo* and *in vitro* toxicological investigation can be prepared from $AlCl_3 \cdot 6H_2O$ and other complexes, including $Al(acac)_3$, by dissolving the pure compound in tris–HCl buffer solutions. The metal concentration in the supernatant is determined spectrophotometrically under reproducible conditions[281]. $Al(acac)_3$ can be detected by ^1H NMR spectroscopy down to concentrations of 200 μM. Traces of V, Fe, Co, Mn, Cu, Ni and Cr were determined in Al, In and Zr ecetylacetonates by emission spectrography. The method involved sample decomposition in the presence of powdered graphite at 300–500 °C and excitation in a 10 A d.c. arc source in the presence of NaCl, with LOD = 0.5–1 ppm[282].

$Pd(acac)_2$ was examined as possible matrix modifier for organomercury and organoselenium in organic solvents. Indeed, the sensitivity of organomercury was found to be enhanced by applying 15 μL of an ethanol solution of $Pd(acac)_2$ to a graphite furnace, which is then heated to produce a Pd coating on the furnace. With this method, the LOD of organomercury was 0.25 ng. This method was successfully applied to the determinations of organomercury and organoselenium in an extract solution of dolphin liver[283]. Addition of $Pd(acac)_2$, among other palladium complexes, enhances the detection sensitivity of graphite furnace AAS for alkyltin compounds in organic solvents; the method was applied to determination of total tin leached from ship paints[284]. For quantitative X-ray microanalysis of metal deposits in semithin sections of biological materials, standard samples with known content of the metal element are required. The choice standards were metal acetylacetonates dissolved in epoxy resin[285].

Methods have been developed for the analysis of hydrocarbon polymers (e.g. styrene, butadiene and isoprene) by MALDI-TOF-MS, through the attachment of Ag(acac) to matrices of *trans*-3-indoleacrylic acid or 1,4-bis(2-(5-phenyloxazolyl))benzene[286]. Silver-cationized molecular ions were produced for polymers of styrene, butadiene and isoprene up to mass 125,000 Da. For lower-mass styrene polymers, the resolved oligomer molecular ions provide information concerning the end group. This technique permits the analysis of many commercially important materials such as acrylonitrile–butadiene–styrene (ABS), styrene–acrylonitrile, styrene–methyl methacrylate and styrene–isoprene copolymers. The use of the salts of transition metals other than Ag, Cu or Pd as the cationizing agents fails to cationize polystyrenes in MALDI. The ability of MALDI to reduce metals to the oxidation state +1 is critically important to polystyrene cationization, as without this reduction MALDI tends to fail to form polystyrene-metal cations. $Cu(acac)_2$ was used for the verification of the above[287].

Formation of metal–acac complexes is the basis for a method to determine the oxidation state of metal cations, by applying the MALDI-TOF-MS technique, for example, a procedure for the determination of $Co(acac)_2$ and $Co(acac)_3$[288]. Even insoluble oxides can be analyzed by sampling a fine suspension of the solid, which vaporizes in the laser plume and forms the corresponding acetyacetonate. For example, the MS of $Mn(acac)_3$ in

acetone shows strong characteristic peaks of $[Mn(acac)_3]^+$ at m/z 352 and $[Mn(acac)_5O]^+$ at m/z 566. The characteristic peak for $Mn(acac)_2 \cdot 2H_2O$ is that of $[Mn_2(acac)_3]^+$ at m/z 407, which is also the base peak, therefore the state of oxidation of Mn acetylacetonates can be distinguished[289]. Similar studies were carried out using phenolic chelating agents instead of acacH; however, the resulting spectra seem more complicated[290]. The MALDI-TOF-MS of acac and other methods were applied for the characterization of a Phillips catalyst (Cr oxide deposited on a silica matrix) used for polyethylene manufacture[291].

Thermal analysis showed that certain metal β-diketonates, such as $Al(acac)_3$, $Ga(acac)_3$ and $Cr(acac)_3$, are stable under GC conditions, up to above 170 °C. Thus, a method for GC-FID was proposed for identification and quantitation of the corresponding metal ions. This was applied for the determination of metal residues in polypropylene, by boiling a sample of the polymer in acacH, filtering the solution, evaporating to dryness, redissolving the residue and proceeding with the GC analysis. This simple procedure takes about 90 min to perform and can detect 1 to 10 ppm of metal residue in the polymer[292]. The TLC mobility on silica gel plates of complexes $M(acac)_3$, M = Sc, Y, La or Nd, as measured by the R_f values, was proportional to the ionic radius of the central ion, pointing to adsorption as the dominant mechanism for chromatographic separation[293].

Metal acetylacetonates can be used as NMR shift reagents. Thus, $Cr(acac)_3$ and $Fe(acac)_3$ can be used as paramagnetic relaxation agents to decrease the spin–lattice relaxation times of all ^{13}C signals in poly(Me methacrylate), poly(Bu methacrylate) and poly(hydroxyethyl methacrylate)[294].

When reduced glucose oxidase (GOD_{red}) is added to an aqueous mixture containing $Fe(acac)_3$, 1,10-phenanthroline (phen) and glucose the color immediately changes from pale yellow to red, due to formation of $[Fe(phen)_3]^{2+}$, that can be measured colorimetrically. DPV indicates that $[Fe(acac)_{3-n}(phen)_n]^{n+}$ cationic complexes are formed upon mixing the labile $Fe(acac)_3$ and 1,10-phenanthroline, which bind electrostatically to GOD_{red} and are easily reduced by electron transfer. This electron transfer is not affected by the presence of oxygen. The reduced complex $[Fe(acac)_{3-n}(phen)_n]^{(n-1)+}$ undergoes rapid ligand exchange to $[Fe(phen)_3]^{2+}$. Formation of this colored complex is suppressed when the salt concentration in the mixture is increased, or when anionic disodium bathophenanthrolinedisulfonate (**67**) is employed in place of 1,10-phenanthroline. *In situ* formation of mixed ligand complexes $[Fe(acac)_{3-n}(phen)_n]^{n+}$ can be used for determination of sodium D-isoascorbate by micelle-enhanced ultraviolet spectrophotometry[295].

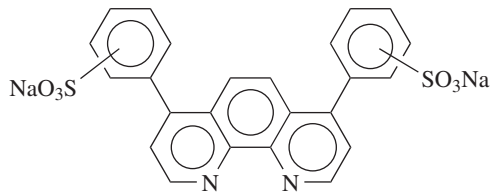

(**67**)

c. Trifluoroacetylacetonates. ICP-AES is widely used for its high sensitivity and wide dynamic range. It is applied also to determine volatile β-diketonates of Al, Be, Cr, Cu and Fe. By direct introduction of the tfac chelates into an ICP using the corresponding tfacH vapor as the carrier gas, subnanogram amounts of metal in microliter samples could be determined with RSD of a few percent[113]. Cr(III) is an essential micronutrient for humans and it is involved in important biochemical processes such as glucose tolerance metabolism and the action of insulin. Its main role is to form a glucose tolerance factor

(GTF), which acts as a cofactor of insulin in all insulin-dependent systems. Food intake is the main Cr source for humans[296–299]. 1,1,1-Trifluoro-2,4-pentadione (tfacH) is one of the most commonly used chelating agents for the GC measurement of chromium, due to its quantitative reaction with the analyte, its volatility and thermal stability and its relative inertness towards undesirable on-column reactions. Furthermore, the exceptional sensitivity of ECD to the fluorinated complex and the ease of synthesis for calibration purposes, all these have made of tfacH the most commonly used chelating agent for several decades[204].

While Cr(III) is considered to be essential in nutrition and for the maintenance of normal glucose tolerance, Cr(VI) can have acute and chronic toxic effects, including carcinogenicity. For this reason, the determination of Cr(III) and Cr(VI) in environmental samples has become very important and has led to a variety of approaches to differentiate between these species. A speciation method for Cr by electrothermal AAS (ETAAS) was developed, whereby tfacH reacts selectively with Cr(III) to form a chelate, which is volatilized at 140 °C and an aliquot of the recovered residue is placed in the graphite furnace for atomization of Cr(VI). The LOD and LOQ of the method are 0.15 and 0.52 $\mu g\,L^{-1}$ Cr(IV), respectively. The Cr(III) concentration was established by difference from total Cr[300, 301].

A procedure was developed for the determination of total and labile Cu and Fe in river surface water. It involved simultaneous solvent extraction of the metals as diethyldithiocarbamates (ddc) and tfac complexes. The complexes were extracted by isobutyl methyl ketone (ibmk) and the solution subjected to flame atomic absorption spectrometry. Variables such as pH, metal complex concentration, reaction time, ibmk volume and extraction time were optimized. Prior to the solvent extraction a microwave-assisted peroxydisulfate oxidation was used to break down the metallorganic matter complexes in the river surface waters[302]. Trifluoroacetylacetone was used as a chelation agent for the extraction and quantitative determination of total Cr in sea water. The chelation reaction was conducted in a single aqueous phase medium. Both headspace and liquid phase extractions were studied and various detection techniques, such as capillary GC-ECD, EI-MS (electron-impact MS) and ICP-MS, were tested and compared. The LOD was 11–15 $ng\,L^{-1}$ Cr for all the systems examined. The method provided accurate results with EI-MS and ICP-MS, while significant bias was experienced with ECD[303].

d. Dipivaloylmethanates. The chelates of dpmH with twenty metal ions were sublimed and the temperature condensation zones were recorded under standardized conditions. For a given metal this chelate had volatility similar to that derived from acacH, but less than those from tfacH or hfacH. The chelates derived from bzacH, bztfacH and ttfacH were less volatile than those from dpmH. For a given β-diketonate ligand, the Be chelate was the most volatile and the lanthanide and actinide chelates the least. The only volatile alkaline earth metal chelates were those of Be and Mg while the Ca, Sr and Ba chelates were not volatile. Some 64 different binary and ternary mixtures of metal dipivaloylmethanate chelates were quantitatively separated[304].

A search for new efficient techniques of rare earth element separation and purification from calcium is a current problem, as production of high-purity rare earths is of great importance in advanced technology and material science. This problem may be solved by vacuum sublimation of volatile compounds when the difference in vapor pressure of the components present is used. This technique of purification was tested for Nd and Ca separation in vacuum. The well-known volatile and thermally stable dipivaloylmethanates were taken as starting substances. It was found that the addition of pivalic acid to the $Nd(dpm)_3 + Ca(dpm)_2$ mixture caused an increase in the separation efficiency and led to pure $Nd(dpm)_3$ in the sublimate[305].

e. Miscellaneous β-diketonates. Preparation of the complex of Ln(III) with 1,1,1-trifluoro-2,4-octanedione followed by GC was proposed for detection of the rare earth elements in a sample. Thus, the chelates of Sc, Y, La, Er, Tb and Eu emerged from the column in the order of increasing cation radius[306]. 1-Thenoyl-3,3,3-trifluoroacetone (ttfaH) forms a stable red-colored complex with Fe(III). This is the basis of a method for determination of trace concentrations of ascorbic acid (**1**) in strongly acidic solution, which reduces Fe(III) to Fe(II), thus diminishing the color intensity. Measurements carried out at 405 nm ($\varepsilon = 53000\ M^{-1}\ cm^{-1}$) were linear in the 1.0–5.0 ppm **1** range. The method was validated for Vitamin C tablets, drops and multivitamin preparations[307].

The shift reagents $Eu(hfod)_3$ and $Pr(hfod)_3$ were used for the determination of aromatic carboxylic acids and of alkyl-substituted phenols by NMR. By adding $Eu(hfod)_3$ and $Pr(hfod)_3$ to the carboxylic acids in CCl_4–MeOH, a shift of each proton signal of the acid was induced, the magnitude and direction of which were affected by the configuration and chemical environment of the proton[308]. The bulk magnetic susceptibility shifts of ^1H NMR resonance signals for dpm caused by the addition of paramagnetic lanthanide(III) compounds was exploited. From that, the paramagnetic lanthanide(III) concentration in solutions could be determined[309].

Chiral $Ln(dik)_3$ complexes with ligands derived from camphor can extract zwitterionic amino acids from neutral aqueous to organic CH_2Cl_2 phases. The extraction efficiencies and enantioselectivity is largely dependent on the nature of both the coordinating ligand and the lanthanide cation[310]. The effects of axial β-diketonate ligands on chirality sensing and recognition was studied[311]. A series of Gd(III) porphyrins was prepared in which various β-diketonate ligands were introduced. The latter acted as efficient CD receptors in chirality sensing of amino acids. It was found that CD could be induced by complexation of Gd(III) porphyrinates with chiral amino acids and dipeptides. Synthetic Gd(III) porphyrins with various achiral β-diketonates as axial ligands in benzene solutions, extracted chiral α-amino acids and dipeptides from aqueous phases gave intense induced CD peaks in the Soret region, via 1:1 supercomplexation. Their CD spectral shapes were dependent on the stereochemistry at the α-positions of amino acids and of the *C*-terminal components of dipeptides. The stereochemistry of the *C*-terminal amino acid residues of the dipeptides was well sensed. Thus, when chiral 3-acetylcamphorate was introduced as an axial ligand, Gd(III) porphyrins showed CD spectral changes by supercomplexation with chiral alanylalanine. Since chiral Gd porphyrins also offered chiral differentiation of dipeptides, this type of Gd complexes has wide application in sensing of biological substrates.

Lanthanide β-diketonates containing fluorinated chiral camphor-derived ligands (**61**, M = Pr, Eu, Er, Yb, R = Mef, *n*-Prf) form highly coordinated 1:1 complexes with zwitterionic, unprotected phenylalanine, leucine, and other amino acids under neutral conditions. This allows extraction of the amino acids from their neutral aqueous solutions into dichloromethane phases[312, 313].

2. Ascorbic acid, isoascorbic acid and their salts

Magnesium ascorbyl phosphate (**6**) was used as reference compound for the RP-HPLC-UVD determination of sodium risedronate (**68**) in pharmaceutical preparations[314]. Co(II) reacts with 2,2′-bipyridylketone-2-picolylimine in the presence of Na L-ascorbate in a weakly alkaline solution to form a blue water-soluble complex with the absorption maximum at *ca* 580 nm. The absorbance at 580 nm is proportional to the concentration of Co(II) in the range 0.05–2.5 mg L^{-1}, with RSD = 0.46%. Ni(II) and Cu(II) were tolerated up to 20 and 10 mg L^{-1}, respectively, in the presence of Na citrate[315].

The method of Lindermann for phosphate determination was modified by using Na ascorbate and stannous chloride as reductants. A blue color develops within 45 min and

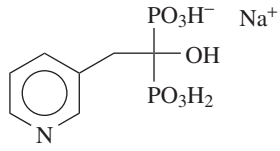

(**68**)

remained stable up to 6 h. The method is linear in the 0–1 mM orthophosphate range. The concentrations of ascorbate, buffers and ATPase affect the stability of the color[316].

Many ancillary formulations have been proposed for analytical purposes, which frequently include an ascorbate as antioxidant. Although this component has no direct function in the analytical process, it is claimed to improve the performance of the method. This is the case of sodium ascorbate added to rat bile samples while determining tetrahydrofolate[317] or while determining urinary copper ion concentration[318]. This is also the case of ascorbate added to buffers used in nucleic acid sequencing based on FLD[319].The titrimetric determination of Mn(III) or Ni(III) in presence of excess of ascorbic acid[320] and the GC-ECD determination of trihalomethane in water[321] are based on a similar approach.

A method for total extraction of RNA from leaves consists of pulverizing the leaves under liquid N_2, immediately followed by extraction with a buffer containing sodium isoascorbate (0.5 M), tris (0.1 M), ethylenediaminetetraacetic acid (10 mM), 2-mercaptoethanol (5% v/v) and sds (2% w/v). A first cleanup is carried out by liquid–liquid extraction with chloroform–isoamyl alcohol (24:1), followed by removal of DNA and proteins by a guanidinium–phenol–chloroform extraction. The method was applied to leaves of woody and herbaceous plants, such as eucalyptus (*E. camaldulensis*), Japanese apricot (*Prunua mume*), tea (*Thea sinensis*), mock orange (*Philadelphus grandiflorus*), southern magnolia (*M. grandiflora*), fragrant olive (*Osmanthus fragrans*), soybean (*Glycine max*), rice (*Oriza sativa*), buckwheat (*Fagopyrum esculentum*) and bitter melon (*Momordica charantia*). The isolated RNA was of good quality, and gel elctrophoresis showed intact rRNA bands[322].

3. Sodium croconate and rhodizonate

Disodium croconate was proposed as a reagent for determination of K. The technique is based on the formation of a pale yellow K Na croconate crystal (**69**) hydrate which changes color to bright red on dehydration. The intensity of the bright red color of the residue obtained after dehydration is proportional to the K content in the sample and can be compared with that of a standard scale. The LOD = 6 mg L^{-1} K in water, LOQ = 20 mg L^{-1} K and SRD = 0.51%, with higher sensitivity in the determination of K than with other known reagents. No interference is observed for 70-fold Mo and 80–100-fold Li, Rb, Cs and NH^+ concentrations in the determination of K[323,324]. The method was

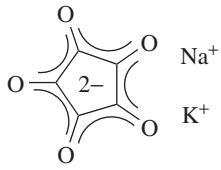

(**69**)

also applied to visual colorimetry for surface waters. The LOD = 9 mg/L with RSD = 0.29%[325]. Potassium croconate itself can be used as a reagent for the detection and determination of lithium, with LOD = 70 mg L^{-1} [326].

Sodium rhodizonate (**70**) in aqueous solution reacts with many metals and in particular with Sb, Ba and Pb, which are used in gunshot formulations, yielding red to dark brown deposits. Over sixty five years ago, Feigl and Suter introduced the use of sodium rhodizonate for detection of Pb by the pink Pb rhodizonate spot test[327]. Rhodizonate has also been used in conjunction with Ba for the determination of sulfate in soil, water and various biochemical systems. In the 1970s it was employed in histochemical procedures for Fe and Pb, and in the forensic laboratory to detect Pb residue on the hands after firing a gun. A modification of the original Pb spot test was later developed by Preer and coworkers for the detection of Pb contamination in soil at concentrations of 400–700 ppm[328]. Staining of the skin with **70** is used in forensic investigations to ascertain the shooting distance, according to the spread of the stains. However, in cadavers the skin may have undergone deterioration that makes stain recognition difficult. This can be solved without interfering with the **70** test, on application of certain triphenylmethane dyes to the surrounding tissues, such as Acid Fuchsin (**71**), Aniline Blue WS (**72**), Brilliant Green (**73**), Ethyl Green (**74**) or Light Green SF Yellowish (**75**)[329]. Forensic investigation of clothing for exposure to gunshot can be done by collecting an 'image' on a filter paper wetted with 15% aqueous acetic acid, drying and spraying with a solution of (**70**). The red spots are indicative of the presence of heavy metals and gunshot impact[330].

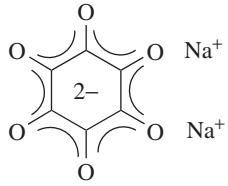

(**70**)

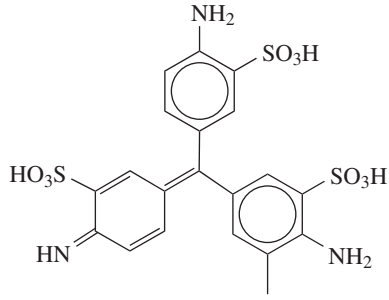

(**71**)

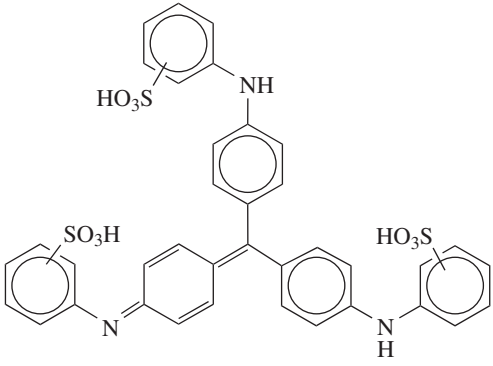

(**72**)

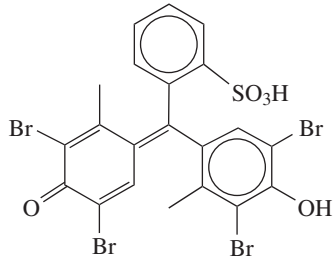

(**73**)

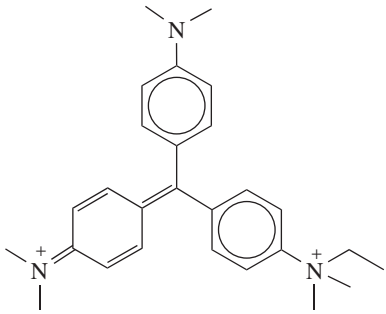

(**74**)

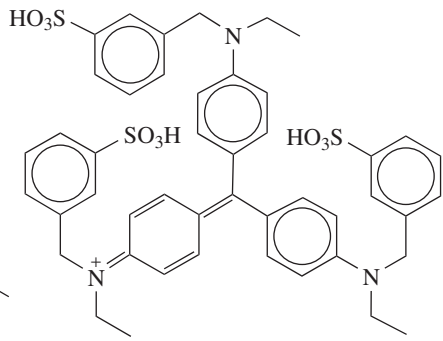

(**75**)

V. REFERENCES

1. J. Zabicky, in *The Chemistry of Phenols* (Ed. Z. Rappoport), Chap. 13, John Wiley & Sons, Ltd, Chichester, 2003, pp. 909–1014.
2. J. Zabicky, in *The Chemistry of Peroxides*, Vol. 2 (Ed. Z. Rappoport), Chap. 7, John Wiley & Sons, Ltd, Chichester, 2006, pp. 597–774.
3. Eurachem Working Group, *The fitness for purpose of analytical methods. A Laboratory Guide to Method Validation and Related Topics*, Eurachem, 1998 (http://www.eurachem.org/index.html).
4. W. J. Gong, Y. P. Zhang, S. H. Choi, Y. J. Zhang and K.-P. Lee, *Microchim. Acta*, **156**, 327 (2007).
5. A. Gutés, D. Calvo, F. Céspedes and M. del Valle, *Microchim. Acta*, **157**, 1 (2007).
6. A. Rouhollahi, R. Rajabzadeh and J. Ghasemi, *Microchim. Acta*, **157**, 139 (2007).
7. P. M. Santos, B. Sandrino, T. F. Moreira, K. Wohnrath, N. Nagata and C. A. Pessoa, *J. Braz. Chem. Soc.*, **18**, 93 (2007).
8. S. A. Westcott, in *The Chemistry of Metal Enolates* (Ed. J. Zabicky), Chap. 10, John Wiley & Sons, Ltd, Chichester, 2009, this volume.
9. P. Lecomte and R. Jérôme, in *The Chemistry of Metal Enolates* (Ed. J. Zabicky), Chap. 15, John Wiley & Sons, Ltd, Chichester, 2009, this volume.
10. H. F. Brito, O. M. L. Malta, M. C. F. C. Felinto and E. E. E. Teotonio, in *The Chemistry of Metal Enolates* (Ed. J. Zabicky), Chap. 3, John Wiley & Sons, Ltd, Chichester, 2009, this volume.
11. H. Lang and R. Buschbeck, in *The Chemistry of Metal Enolates* (Ed. J. Zabicky), Chap. 17, John Wiley & Sons, Ltd, Chichester, 2009, this volume.
12. L.-J. Ming, in *The Chemistry of Metal Enolates* (Ed. J. Zabicky), Chap. 11, John Wiley & Sons, Ltd, Chichester, 2009, this volume.
13. A. Varvaresou, E. Tsirivas, K. Iakovou, E. Gikas, Z. Papathomas, A. Vonaparti and I. Panderi, *Anal. Chim. Acta*, **573**, 284 (2006).
14. H. J. Jeon, M. Noda, M. Maruyama, Y. Matoba, T. Kumagai and M. Sugiyama, *J. Agric. Food Chem.*, **54**, 9827 (2006).
15. X. Yang and H. Zhang, *Food Chem.*, **102**, 1223 (2007).
16. S. Emami, S. J. Hosseinimehr, S. M. Taghdisi and S. Akhlaghpoor, *Bioorg. Med. Chem. Lett.*, **17**, 45 (2007).
17. S. M. Kirwan, G. Rocchitta, C. P. McMahon, J. D. Craig, S. J. Killoran, K. B. O'Brien, P. A. Serra, J. P. Lowry and R. D. O'Neill, *Sensors*, **7**, 420 (2007).
18. T. J. Wenzel and K. A. Provencher, in *The Chemistry of Metal Enolates* (Ed. J. Zabicky), Chap. 14, John Wiley & Sons, Ltd, Chichester, 2009, this volume.
19. J. Selbin, N. Hamad and N. Bhacca, *Inorg. Chem.*, **10**, 1383 (1971).
20. I. Wakeshima, K. Yamaoka, I. Kijima, K. Hirai, Y. Nagao, T. Misono and Y. Abe, *Nippon Kagaku Kaishi*, 619 (1992); *Chem. Abstr.*, **117**, 82345 (1992).
21. P. Stratil, B. Klejdus and V. Kubáň, *Talanta*, **71**, 1741 (2007).

22. H. Tsukube, H. Takeishi and Z. Yoshida, *Inorg. Chim. Acta*, **25**, 1 (1996).
23. K. Babić-Samardžija, S. P. Sovilj and V. M. Jovanović, in *The Chemistry of Metal Enolates* (Ed. J. Zabicky), Chap. 2, John Wiley & Sons, Ltd, Chichester, 2009, this volume.
24. L. A. Bruno and B.-M. Su, *Appl. Spectrosc.*, **51**, 755 (1997).
25. H. Wilson and J. Oelichmann, *Pharma Technol. J.*, **19**, 87 (1998).
26. Yu. N. Kukushkin, V. K. Krylov and V. K. Oshorova, USSR patent SU 1718063 A1 19920307 (1992); *Chem. Abstr.*, **118**, 160182 (1993).
27. V. M. Mit'kin, N. B. Morozova, V. G. Isakova and S. V. Zemskov, *Izv. Sib. Otd. Akad. Nauk SSSR, Ser. Khimi. Nauk*, 78 (1988); *Chem. Abstr.*, **109**, 221471 (1988).
28. A. P. Satya, M. Meenakshi and J. Precti, *Anal. Sci.*, **14**, 889 (1998).
29. A. Martinovic, L. Kukoc-Modun and N. Radic, *Anal. Lett.*, **40**, 805 (2007).
30. X. Guan and R. Yin, *Lihua Jianyan, Huaxue Fence*, **38**, 174 (2002); *Chem. Abstr.*, **137**, 319727 (2002).
31. Q. Ye and S. Xu, *Fenxi Huaxue*, **30**, 889 (2002); *Chem. Abstr.*, **137**, 293778 (2002).
32. L. M. Magalhães, M. A. Segundo, C. Siquet, S. Reis and J. L. F. C. Lima, *Microchim. Acta*, **157**, 113 (2007).
33. F. Tsumura, Y. Ohsako, Y. Haraguchi, H. Kumagai, H. Sakurai and K. Ishii, *J. Food Sci.*, **58**, 619 (1993).
34. W. L. Baker, J. Goode and L. Cooper, *Microchim. Acta*, **106**, 143 (1992).
35. B. Elmas, S. Senel and A. Tuncel, *React. Funct. Polym.*, **67**, 87 (2007).
36. E. L. Wehry, R. Hohmann, J. K. Gates, L. F. Gilbault, P. M. Johnson, J. S. Schendel and D. A. Radspinner, *Appl. Opt.*, **26**, 3559 (1987).
37. A. J. Brown, C. E. Lenehan, P. S. Francis, D. E. Dunstan and N. W. Barnett, *Talanta*, **71**, 1951 (2007).
38. A. I. Cherednichenko, V. I. Vovna, N. P. Kuz'mina, M. V. Chechernikova, I. G. Zaitseva, L. I. Martynenko and A. R. Kaul, *Koord. Khim.*, **18**, 566 (1992); *Chem. Abstr.*, **117**, 244544 (1992).
39. K. L. Stevenson, *J. Am. Chem. Soc.*, **94**, 6652 (1972).
40. T. Hamada, H. Ohtsuka and S. Sakaki, *Chem. Lett.*, 364 (2000).
41. T. Hamada, H. Ohtsuka and S. Sakaki, *J. Chem. Soc., Dalton Trans.*, 928 (2001).
42. K. Tanikawa, *Chem. Pharm. Bull.*, **24**, 1954 (1976).
43. D. L. Hachey, J.-C. Blais and P. D. Klein, *Anal. Chem.*, **52**, 1131 (1980).
44. N. V. Zakurin, Y. S. Nekrasov, M. D. Reshetova and A. U. Vasilkov, *Inorg. Chim. Acta*, **76**, L161 (1983).
45. S. B. Turnipseed, R. M. Barkley and R. E. Sievers, *Inorg. Chem.*, **30**, 1164 (1991).
46. M. S. Stanley, K. L. Duffin, S. J. Doherty and K. L. Busch, *Anal. Chim. Acta*, **200**, 447 (1987).
47. S. Kurata and M. Nagai, *Chem. Lett.*, 1302 (2001).
48. M. L. Alexander, P. H. Hemberger, M. E. Cisper and N. S. Nogar, *Anal. Chem.*, **65**, 1609 (1993).
49. C. Weickhardt, C. Grun, R. Heinicke, A. Meffert and J. Grotemeyer, *Rapid Commun. Mass Spectrom.*, **11**, 745 (1997).
50. C. Grun, R. Heinicke, C. Weickhardt and J. Grotemeyer, *Int. J. Mass Spectrom.*, **185/186/187**, 307 (1999).
51. M. T. Allen, M. E. Cisper, P. H. Hemberger and C. W. Wilkerson Jr., *Int. J. Mass Spectrom.*, **212**, 197 (2001).
52. A. N. Smagunova, E. N. Korzhova and T. M. Velikova, *J. Anal. Chem.*, **53**, 594 (1998).
53. K. H. Claus and C. Kruger, *Fresenius Z. Anal. Chem.*, **262**, 257 (1972).
54. T. Ui, M. Kataoka, M. Kato and E. Asada, *Bunseki Kagaku*, **37**, 538 (1988); *Chem. Abstr.*, **110**, 33064 (1988).
55. Y. Tamaki, *X-Ray Spectrom.*, **24**, 235 (1995).
56. P. Frank, R. M. K. Carlson, E. J. Carlson and K. O. Hodgson, *Coord. Chem. Rev.*, **237**, 31 (2003).
57. S. W. Bishara and F. M. El-Samman, *Microchem. J.*, **22**, 442 (1977).
58. Z. Jablonski, T. Wasag and S. Millo, *Rocz. Chem.*, **50**, 1467 (1976).
59. C. Yoshimura and T. Nishiguchi, *Nippon Kagaku Kaishi*, 716 (1984); *Chem. Abstr.*, **101**, 83139 (1984).
60. M. H. Pournaghi-Azar and M. R. Ramazani, *Electroanalysis*, **14**, 1203 (2002).

61. S. A. Moros, C. M. Hamilton, J. E. Heveran, J. J. Donahue and S. Oliveri-Vigh, *J. Pharm. Sci.*, **64**, 1229 (1975).
62. M. L. Girard, C. Dreux, J. Delattre and P. Jospin, *Ann. Pharm. Fr.*, **27**, 43 (1969).
63. J. Chen, J. Zhang, X. Lin, H. Wan and S. Zhang, *Electroanalysis*, **19**, 612 (2007).
64. J. Wang, L. Wang, Y. Wang, W. Yang, L. Jiang and E. Wang, *J. Electroanal. Chem.*, **601**, 107 (2007).
65. J. C. B. Fernandes, L. T. Kubota and G. de Oliveira, *Electroanalysis*, **11**, 475 (1999).
66. G.-P. Jin, Q.-Z. Chen, Y.-F. Ding and J.-B. He, *Electrochim. Acta*, **52**, 2535 (2007).
67. M. S. Belluzo, M. E. Ribone and C. M. Lagier, *Sensors*, **8**, 1366 (2008).
68. (a) R. Takita, K. Yoshida and J.-I. Anzai, *Sensors Actuators B*, **121**, 54 (2007).
    (b) H. Xie, C. Zhang and Z. Gao, *Anal. Chem.*, **76**, 1611 (2004).
69. Z. Gao and Y. H. Yu, *Sensors Actuators B*, **121**, 552 (2007).
70. A. Bello, M. Giannetto, G. Mori, R. Seeber, F. Terzi and C. Zanardi, *Sensors Actuators B*, **121**, 430 (2007).
71. I. Mogi and K. Watanabe, *J. Solid State Electrochem.*, **11**, 751 (2007).
72. R. T. Kachoosangi and R. G. Compton, *Anal. Bioanal. Chem.*, **387**, 2793 (2007).
73. S. Senthil Kumar and S. Sriman Narayanan, *Chem. Pharm. Bull.*, **54**, 963 (2006).
74. A. Malinauskas, G. Mickevičiūtė, R. Araminaitė and R. Garjonytė, *Chem. Anal. (Warsaw)*, **51**, 809 (2006).
75. D. Jayasri and S. S. Narayanan, *Bull. Electrochem.*, **21**, 537 (2005).
76. R. P. da Silva, A. W. O. Lima and S. H. P. Serrano, *Anal. Chim. Acta*, **612**, 89 (2008).
77. C. Radovan, C. Cofan and D. Cinghita, *Electroanalysis*, **20**, 1346 (2008).
78. F. G. Gonon, C. M. Fombarlet, M. J. Buda and J. F. Pujol, *Anal. Chem.*, **53**, 1386 (1981).
79. D. M. Porterfield, *Biosens. Bioelectron.*, **22**, 1186 (2007).
80. T. Selvaraju and R. Ramaraj, *Electrochim. Acta*, **52**, 2998 (2007).
81. S. Thiagarajan and S.-M. Chen, *Talanta*, **74**, 212 (2007).
82. H. M. Nassef, A.-E. Radi and C. O'Sullivan, *Anal. Chim. Acta*, **583**, 182 (2007).
83. D. Raffa, K. T. Leung and F. Battaglini, *Anal. Chem.*, **75**, 4983 (2003).
84. J. Yánez Heras, A. F. Forte Giacobone and F. Battaglini, *Talanta*, **71**, 1684 (2007).
85. R. Thangamuthu, S. M. Senthil Kumar and K. Chandrasekara Pillai, *Sensors Actuators B*, **120**, 745 (2007).
86. S. Shahrokhian and H. R. Zare-Mehrjardi, *Sensors Actuators B*, **121**, 530 (2007).
87. P. Shakkthivel and S.-M. Chen, *Biosens. Bioelectron.*, **22**, 1680 (2007).
88. A. I. Gopalan, K.-P. Lee, K. M. Manesh, P. Santhosh, J. H. Kim and J. S. Kanga, *Talanta*, **71**, 1774 (2007).
89. G. Hu, Y. Ma, Y. Guo and S. Shao, *Electrochim. Acta*, **53**, 6610 (2008).
90. D. Ragupathy, A. I. Gopalan, K.-P. Lee and K. M. Manesh, *Electrochem. Commun.*, **10**, 527 (2008).
91. P. F. Huang, L. Wang, J. Y. Bai, H. J. Wang, Y. Q. Zhao and S. D. Fan, *Microchim. Acta*, **157**, 41 (2007).
92. B. Dong, J. Peng, A. Tian, J. Sha, L. Li and H. Liu, *Electrochim. Acta*, **52**, 3804 (2007).
93. K. S. Prasad, G. Muthuraman and J.-M. Zen, *Electrochem. Commun.*, **10**, 559 (2008).
94. H. M. Nassef, L. Civit, A. Fragoso and C. K. O'Sullivan, *Analyst*, **133**, 1736 (2008).
95. J. R. Siqueira, Jr., L. H. S. Gasparotto, F. N. Crespilho, A. J. F. Carvalho, V. Zucolotto and O. N. Oliveira, Jr., *J. Phys. Chem. B*, **110**, 22690 (2006).
96. H. Guo, T. Yin, Q. Su and W. Qin, *Talanta*, **75**, 851 (2008).
97. H. Parham, B. Zargar and M. Alizadeh, *Asian J. Chem.*, **19**, 5123 (2007).
98. P. Riyazuddin and M. M. A. K. Nazer, *J. Pharm. Biomed. Anal.*, **16**, 545 (1997).
99. Z.-N. Gao, J. Peng and X.-X. Han, *Polish J. Chem.*, **81**, 441 (2007).
100. U. K. Pandey, B. L. Agrawal and A. K. Gurtu. *J. Electrochem. Soc. India*, **30**, 320 (1981).
101. V. N. Kiryushov, L. I. Skvortsova and T. P. Aleksandrova, *J. Anal. Chem.*, **62**, 161 (2007).
102. E. V. de Aquino and J. J. R. Rohwedder, *Anal. Bioanal. Chem.*, **386**, 1921 (2006).
103. R. E. Shepherd, *Coord. Chem. Rev.*, **247**, 159 (2003).
104. K. Saitoh, C. Kiyohara and N. Suzuki, *J. High Resol. Chromatogr.*, **14**, 245 (1991).
105. J. Ruiz-Jiménez, J. M. Mata-Granados and M. D. Luque de Castro, *Electrophoresis*, **28**, 789 (2007).
106. K. Robards, E. Patsalides and S. Dilli, *J. Chromatogr.*, **411**, 1 (1987).
107. K. Utsonumia, *Bull. Chem. Soc. Jpn.*, **44**, 2688 (1971).

108. J. D. Lodmell, *Nucl. Sci. Abstr. (report)*, **28**, 29556 (1973); *Chem. Abstr.*, **80**, 77915 (1973).
109. D. N. Sokolov, A. V. Davydov, S. Y. Prokofiev, S. S. Travnikov, E. V. Fedoseev and B. F. Myasoedov, *J. Chromatogr.*, **155**, 241 (1978).
110. S. Dilli and E. Patsalides, *J. Chromatogr.*, **176**, 305 (1979).
111. R. Fontaine, C. Pommier, C. Eon and G. Guiochon, *J. Chromatogr.*, **104**, 1 (1975).
112. J. Maslowska and S. Starzynski, *Chromatographia*, **21**, 214 (1986).
113. T. Fujinaga, T. Kuwamoto, K. Isshiki and N. Matsubara, *Spectrochim. Acta*, **38B**, 1011 (1983).
114. K. W. M. Siu, M. E. Fraser and S. S. Berman, *J. Chromatogr.*, **256**, 455 (1983).
115. S. Dilli and K. Robards, *J. Chromatogr.*, **322**, 1 (1985).
116. S. Dilli and K. Robards, *J. Chromatogr.*, **322**, 23 (1985).
117. S. Dilli, S. Miller and K. Robards, *J. Chromatogr.*, **324**, 75 (1985).
118. I. N. Glazkov, S. M. Kiseliov, Yu. S. Yashin, I. A. Revelskii, B. I. Zirko, A. F. Eleev and I. P. Efimov, *Vestn. Mosk. Univ., Ser. 2: Khim.*, **36**, 245 (1995); *Chem. Abstr.*, **123**, 245573 (1995).
119. S. Dilli and K. Robards, *J. Chromatogr.*, **312**, 109 (1984).
120. E. Kissa, *Anal. Chim. Acta*, **281**, 385 (1993).
121. W. Srichuanchuenskul, M. Rayanakorn, S. Watanesk, P. Thavornyutikarn and P. Kitsawatpaiboon, *J. Sci. Soc. Thailand*, **21**, 51 (1995); *Chem. Abstr.*, **124**, 104770 (1996).
122. S. B. Turnipseed, R. M. Barkley and R. E. Sievers, *Inorg. Chem.*, **30**, 1164 (1991).
123. V. Ya. Mishin, S. M. Solov'ev, P. P. Chinenov, A. S. Voronin, V. I. Kapitonov, E. M. Rubtsov, P. S. Soloshenkov, V. K. Isupov and Yu. Z. Prokopchuk, *Radiokhimiya*, **27**, 354 (1985); *Chem. Abstr.*, **103**, 115036 (1985).
124. N. V. Magazeeva, L. Y. Martynenko, I. A. Murav'eva, D. N. Sokolov and V. I. Spitsyn, *Izv. Akad. Nauk SSSR, Ser. Khim.*, 1813 (1986); *Chem. Abstr.*, **106**, 43028 (1987).
125. N. V. Magazeeva, L. Y. Martynenko, I. A. Murav'eva, V. I. Spitsyn and D. N. Sokolov, *Izv. Akad. Nauk SSSR, Ser. Khim.*, 1055 (1987); *Chem. Abstr.*, **108**, 15356 (1987).
126. T. Hara, K. Fujinaga and K. Tsuji, *Bull. Chem. Soc. Jpn.*, **51**, 2951 (1978).
127. T. Hara and F. Okui, *Bull. Chem. Soc. Jpn.*, **55**, 3450 (1982).
128. T. Hara and F. Okui, *Bull. Chem. Soc. Jpn.*, **56**, 1378 (1983).
129. K. Saitoh and N. Suzuki, *J. Chromatogr.*, **109**, 333 (1975).
130. H. Noda, K. Saitoh and N. Suzuki, *J. Chromatogr.*, **168**, 250 (1979).
131. K. Saitoh and N. Suzuki, *J. Chromatogr.*, **92**, 371 (1974).
132. K. Hashimoto, T. Sekine, T. Omori and K. Yoshihara, *J. Chromatogr.*, **438**, 401 (1988).
133. K. Hashimoto, T. Sekine, T. Omori and K. Yoshihara, *J. Radioanal. Nucl. Chem.*, **103**, 19 (1986).
134. T. Omori, K. Hashimoto, T. Sekine and K. Yoshihara, *J. Chromatogr.*, **438**, 401 (1988).
135. I. Hodzic, S. R. Niketic and A. Lipkovski, *Glasnik na Hemicarite i Tehnolozite na Makedonija*, **19**, 145 (2000); *Chem. Abstr.*, **135**, 380163 (2003).
136. L. M. Varlamova, O. I. Tananaeva and L. I. Martynenko, *Russ. J. Inorg. Chem.*, **27**, 364 (1982); translated from *Zh. Neorgan. Khim.*, **27**, 648 (1982).
137. Ž. Lj. Tešić, T. J. Janjić, G. N. Vučković and M. B. Ćelap, *J. Chromatogr.*, **456**, 346 (1988).
138. M. B. Ćelap, G. Vučković, M. J. Malinar, T. J. Janjić and P. N. Radivojsa, *J. Chromatogr.*, **196**, 59 (1980).
139. G. Vučković, T. J. Janjić, Ž. Lj. Tešić and M. B. Ćelap, *J. Chromatogr.*, **324**, 431 (1985).
140. T. J. Janjić, Ž. Lj. Tešić, G. Vučković and M. B. Ćelap, *J. Chromatogr.*, **404**, 307 (1987).
141. M. J. Malinar, G. Vučković, P. N. Radivojsa, T. J. Janjić and M. B. Ćelap, *J. Chromatogr.*, **249**, 65 (1982).
142. L. Schlosser and L. Levinta, *Chim. Anal. (Bucharest)*, **2**, 107 (1972).
143. K. Ravindranath and P. B Janardhan, *Curr. Sci.*, **55**, 232 (1986).
144. G. Vučković, N. Juranić, D. J. Radanović and M. B. Ćelap, *J. Chromatogr.*, **466**, 227 (1989).
145. S. Dilli and K. Robards, *J. Chromatogr.*, **270**, 313 (1983).
146. A. R. Timerbaev and O. M. Petrukin, *Anal. Chim. Acta*, **159**, 229 (1984).
147. Ž. Lj. Tešić, T. J. Janjić, G. N. Vučković and M. B. Ćelap, *J. Chromatogr.*, **456**, 346 (1988).
148. Ž. Lj. Tešić, T. J. Janjić and M. B. Ćelap, *J. Chromatogr.*, **585**, 359 (1991).
149. R. M. Baosic, D. M. Milojkovic-Opsenica and Z. Lj. Tesic, *J. Planar Chromatogr.*, **15**, 263 (2002).

150. R. M. Baosic, D. M. Milojkovic-Opsenica and Z. Lj. Tesic, *J. Planar Chromatogr.*, **17**, 250 (2004).
151. A. Martelli and G. M. Nano, *Farmaco, Ed. Prat.*, **22**, 650 (1967); *Pubmed ID* 5612786.
152. J. F. K. Huber, J. C. Kraak and H. Venning, *Anal. Chem.*, **16**, 448 (1972).
153. N. Suzuki and K. Saitoh, *Bull. Chem. Soc. Jpn.*, **50**, 2907 (1977).
154. C. A. Tollinche and T. H. Risby, *J. Chromatogr. Sci.*, **16**, 448 (1978).
155. K. Saitoh and N. Suzuki, *Anal. Chem.*, **52**, 30 (1980).
156. J. P. Collman, *Angew. Chem., Int. Ed. Engl.*, **4**, 132 (1965).
157. R. C. Mehrotra, R. Bohra and D. P. Gaur, *Metal β-Diketonates and Allied Derivatives*, Academic Press, London, 1978.
158. T. J. Cardwell and T. H. Lorman, *Inorg. Chim. Acta*, **85**, 1 (1984).
159. T. J. Cardwell, T. H. Lorman and Z. Z. Feng, *J. Chromatogr.*, **358**, 187 (1986).
160. H. Noda, K. Saitoh and N. Suzuki, *J. Chromatogr.*, **435**, 368 (1988).
161. K. Robards and E. Patsalides, *J. Chromatogr. A*, **844**, 181 (1999).
162. (a) J. Havel and A. Khramov, *Scripta Fac. Sci. Nat. Univ. Masaryk. Brun.*, **27**, 51 (1997). (b) R. C. Gurira and P. W. Carr, *J. Chromatogr. Sci.*, **20**, 461 (1982).
163. J. Maslowska and S. Starzynsky, *Chromatographia*, **28**, 519 (1989).
164. J. Maslowska and S. Starzynski, *J. Chromatogr.*, **502**, 221 (1990).
165. D. W. Lee, K. S. Kim, Y. H. Park, M. Z. Czea and K. S. Chung, *Anal. Sci. Technol.*, **6**, 107 (1993); *Chem. Abstr.*, **120**, 68099 (1994).
166. S. Tsukahara, K. Saitoh and N. Suzuki, *Chromatographia*, **51**, 553 (2000).
167. K. Saitoh, S. Tsukahara and N. Suzuki, *J. Chromatogr.*, **439**, 245 (1988).
168. S. J. Tsai and Y. Lee, *Analyst*, **116**, 615 (1991).
169. S. Srijaranai, S. Chanpaka, C. Kukusamude and K. Grudpan, *Talanta*, **68**, 1720 (2006).
170. S. Yoda, Y. Mizuno, T. Furuya, Y. Takebayashi, K. Otake, T. Tsuji and T. Hiaki, *J. Supercrit. Fluids*, **44**, 139 (2008).
171. N. M. Karayannis, A. H. Corwin, E. W. Baker, E. Klesper and J. A. Walter, *Anal. Chem.*, **40**, 1736 (1968).
172. N. M. Karayannis and A. H. Corwin, *J. Chromatogr. Sci.*, **8**, 251 (1970).
173. K. E. Laintz, S. Iso, Y. Meguro and Z. Yoshida, *J. High Resolut. Chromatogr.*, **17**, 603 (1994).
174. Y. Lin, H. Wu, C. M. Wai and N. G. Smart, *Talanta*, **52**, 695 (2000).
175. C. Kersch and G. J. Witkamp, *Solv. Extract. Ion Exch.*, **23**, 189 (2005).
176. A. Ohashi, H. Hoshino, J. Niida, H. Imura and K. Ohashi, *Bull. Chem. Soc. Jpn.*, **78**, 1804 (2005).
177. J. M. Carey, N. P. Vela and J. A. Caruso, *J. Chromatogr. A*, **622**, 329 (1994).
178. G. Hartmann, E. Juelich and G. Lind, *Fleischwirtschaft*, **74**, 637 (1994).
179. B. Hu, H. Xie and H. Hu, *Huaxue Yanjiu Yu Yingyong*, **16**, 688, 692 (2004); *Chem. Abstr.*, **144**, 266181 (2006).
180. S.-C. Huang, C.-C. Lin, M.-C. Huang and K.-C. Wen, *J. Food Drug Anal.*, **12**, 13 (2004).
181. A. M. Maia, A. R. Baby, W. J. Yasaka, E. Suenaga, T. M. Kaneko and M. V. R. Velasco, *Talanta*, **71**, 639 (2007).
182. G. Queval and G. Noctor, *Anal. Biochem.*, **363**, 58 (2007).
183. C.-H. Lin, H.-L. Wu and Y.-L. Huang, *Anal. Chim. Acta*, **581**, 102 (2007).
184. J. M. Charlesworth, *Anal. Chem.*, **50**, 1414 (1978).
185. T. H. Mourey and L. E. Oppenheimer, *Anal. Chem.*, **56**, 2427 (1984).
186. S. Cárdenas, M. Gallego and M. Valcárcel, *Anal. Chim. Acta*, **402**, 1 (1999).
187. Z. Spacil, J. Folbrova, N. Megoulas, P. Solich and M. Koupparis, *Anal. Chim. Acta*, **583**, 239 (2007).
188. M. B. Ćelap, I. M. Hodžić and T. J. Janjić, *J. Chromatogr.*, **198**, 172 (1980).
189. L. Kovi, I. M. Hod and S. R. Niketi, *J. Serb. Chem. Soc.*, **67**, 735 (2002).
190. Y. Okamoto, S. Honda, E. Yashima and H. Yuki, *Chem. Lett.*, 1221 (1983).
191. Y. Nakamura and A. Yamagishi, *J. Chromatogr.*, **482**, 165 (1989).
192. Y. Nakamura, A. Yamagishi, S. Matumoto, K. Tohkubo, Y. Ohtu and M. Yamaguchi, *J. Chromatogr.*, **482**, 165 (1989).
193. A. Yamagishi, I. Tanaka, M. Taniguchi and M. Takahashi, *J. Chem. Soc., Chem. Commun.*, 1113 (1994).
194. S. Kashiwara, M. Takahashi, M. Nakata, M. Taniguchi and A. Yamagishi, *J. Mater. Chem.*, **8**, 2253 (1998).

195. A. Yamagishi, N. Sasa and M. Taniguchi, *Langmuir*, **13**, 1689 (1997).
196. Ž. Lj. Tešić, T. J. Sabo, S. R. Trifunović and D. M. Milojković-Opsenica, *J. Chromatogr. A*, **847**, 297 (1999).
197. M. A, Subhan, T. Suzuki and S. Kaizaki, *J. Chem. Soc., Dalton Trans.*, 492 (2001).
198. F. Mizukami, H. Izutsu, T. Osaka, Y. Akiyama, N. Uiji, K. Moriya, K. Endo, K. Maeda, Y. Kiyozumi and K. Sakaguchi, *J. Chromatogr. A*, **697**, 279 (1995).
199. Y. Akiyama, F. Mitsukami, H. Izutsu, M. Sato, K. Maeda, Y. Kiyozumi and K. Sakagutchi, *J. Sol-Gel Sci. Technol.*, **13**, 421 (1998).
200. F. Mizukami, Y. Akiyama and H. Izutsu, *Supramol. Sci.*, **5**, 433 (1998).
201. B. Chankvetadze, C. Yamamoto and Y. Okamoto, *Combin. Chem. High Throughput Screen.*, **3**, 497 (2000).
202. T. Kubota, C. Yamamoto and Y. Okamoto, *J. Am. Chem. Soc.*, **122**, 4056 (2000).
203. O. I. Yurchenko, N. P. Titova and N. V. Vasil'eva, *Ukr. Khim. Zh. (Russ. Ed.)*, **70**, 119 (2004); *Chem. Abstr.*, **141**, 184180 (2004).
204. T. Ikai, R. Muraki, C. Yamamoto, M. Kamigaito and Y. Okamoto, *Chem. Lett.*, **33**, 1188 (2004).
205. T. Ikai, C. Yamamoto, M. Kamigaito and Y. Okamoto, *Chirality*, **17**, 299 (2005).
206. X.-M. Chen, C. Yamamoto and Y. Okamoto, *J. Chromatogr. A*, **1104**, 46 (2006).
207. B. Chankvetadze, T. Kubota, T. Ikai, C. Yamamoto, M. Kamigaito, N. Tanaka, K. Nakanishi and Y. Okamoto, *J. Sep. Sci.*, **29**, 1988 (2006).
208. B. Chankvetadze, C. Yamamoto, M. Kamigaito, N. Tanaka, K. Nakanishi and Y. Okamoto, *J. Chromatogr. A*, **1110**, 46 (2006).
209. S. Tsukahara, K. Saitoh and N. Suzuki, *J. Chromatogr.*, **547**, 225 (1991).
210. A. M. El-Wakil, A. B. Farag and M. S. El-Nahas, *Talanta*, **40**, 841 (1993).
211. H. Li, Y. Weng, Y. Lin, R. Guo and W. Zhang, *Niangjiu*, **31**, 59 (2004); *Chem. Abstr.*, **144**, 5574 (2006).
212. J. Liu, D. Run, H. Zhang and R. Cao, *Baiqiuen Yike Daxue Xuebao*, **26**, 467 (2000); *Chem. Abstr.*, **135**, 170842 (2001).
213. O. V. Kon'kova and N. V. Kuznetsova, *Khimicheskaya Promyshlennost, Seriya: Reaktivy i Osobo Chistye Veshchestva*, 6 (1980); *Chem. Abstr.*, **93**, 178858 (1980).
214. Y. C. Li and H. C. Lu, *Youji Huaxue*, **3**, 210 (1981); *Chem. Abstr.*, **95**, 107909 (1981).
215. Q. Su and G. Zhao, *Kidorui*, **14**, 68 (1989); *Chem. Abstr.*, **111**, 123434 (1989).
216. K. Binnenemans, in *Handbook on the Physics and Chemistry of Rare Earths*, **35** (Eds K. A. Gschneidner, Jr., J.-C. G. Bünzli and V. K. Pecharsky), Chap. 225, Elsevier B.V., Amsterdam, 2005, p. 158.
217. P. Smichowski and S. Farías, *Microchem. J.*, **67**, 147 (2000).
218. K. J. Wallace, S. R. Cordero, C. P. Tan, V. M. Lynch and E. V. Anslyn, *Sensors Actuators B*, **120**, 362 (2007).
219. R. K. Mahajan, I. Kaur, R. Kaur, S. Uchida, A. Onimaru, S. Shinodab and H. Tsukube, *Chem. Commun.*, 2238 (2003).
220. F. Dang, Y. Li and W. Liu, *Spectrochim. Acta A*, **66**, 680 (2007).
221. L. Wang, G. Bian, L. Dong, T. Xia, S. Hong and H. Chen, *Spectrochim. Acta A*, **65**, 123 (2006).
222. M. Mazhar, G. Afshan, S. Ali, S. Ikram and A. Ahmad, *J. Chem. Soc. Pakistan*, **12**, 24 (1990).
223. T. Fujiwara, T. Kyaw, Y. Okamoto and T. Kumamaru, *Anal. Sci.*, **13**, 59 (1997).
224. T. Kyaw, S. Kumooka, Y. Okamoto, T. Fujiwara and T. Kumamaru, *Anal. Sci.*, **15**, 293 (1999).
225. P. Deplano, M. L. Mercuri, A. Serpe and L. Pilia, in *The Chemistry of Metal Enolates* (Ed. J. Zabicky), Chap. 16, John Wiley & Sons, Ltd, Chichester, 2009, this volume.
226. R. S. Pilato and K. A. van Houten, in *Dithiolene Chemistry: Synthesis, Properties, and Applications* (Ed. E. I. Stiefel), in *Progress in Inorganic Chemistry* (Ed. K. D. Karlin), Vol. 52, Chap. 7, Wiley-Interscience, New York, 2004, pp. 369–397.
227. S. Kurata, H. Hirano, M. Nagai, *J. Forensic Sci.*, **47**, 797 (2002).
228. S. Kurata and M. Nagai, *Anal. Sci.*, **19**, 451 (2003).
229. T. Takagi, T. Ishihara, H. Nishiguchi and Y. Takita, *Proc. Electrochem. Soc.*, **23** (Chemical Sensors IV), 396 (1999).
230. T. Ishihara, T. Takagi, H. Mishiguchi and Y. Takita, *Chem. Sensors*, **16**, 49 (2000).

231. R. Fryček, M. Vladimír, V. Martin, V. Filip, M. Jelínek and J. Náhlík, *Sensors Actuators B*, **98**, 233 (2004).
232. R. Fryček, M. Jelínek, T. Kocourek, P. Fitl, M. Vrňata, V. Myslík and M. Vrbová, *Thin Solid Films*, **495**, 308 (2006).
233. A. K. Jain, V. K. Gupta, L. P. Singh and J. R. Raisoni, *Talanta*, **66**, 1355 (2005).
234. M. M. Ardakani, M. Salavati-Niasari and A. Dastanpour, *Bull. Electrochem.*, **20**, 193 (2004).
235. R. K. Mahajan and P. Sood, *Indian J. Chem.*, **45A**, 2446 (2006).
236. M. R. Ganjali, A. Daftari, F. Mizani and M. Salavati-Niasari, *Bull. Korean Chem. Soc.*, **24**, 23 (2003).
237. R. K. Mahajan, I. Kaur, R. Kaur, A. Onimaru, S. Shinoda and H. Tsukube, *Anal. Chem.*, **76**, 7354 (2004).
238. R. E. Sievers, K. J. Eisentraut, C. S. Springer and D. W. Meek, in *Lanthanide/Actinide Chemistry* (Ed. R. F. Gould), Advances in Chemistry Series, Vol. 71, American Chemical Society, Washington, 1967, pp. 141–154.
239. S. C. Chattoraj, C. T. Lynch and K. S. Mazdiyashi, *Inorg. Chem.*, **7**, 2501 (1968).
240. P. C. Uden and C. R. Jenkins, *Talanta*, **16**, 893 (1969).
241. K. Tanikawa, *Bunseki Kagaku*, **25**, 721 (1976); *Chem. Abstr.*, **87**, 47626 (1977).
242. A. Kito, M. Nakane and Y. Miyake, *Osaka Kogyo Gijutsu Shikensho Kiho*, **29**, 231 (1978); *Chem. Abstr.*, **90**, 161587 (1979).
243. A. Kito, M. Nakane and Y. Miyake, *Bunseki Kagaku*, **27**, 7 (1978); *Chem. Abstr.*, **89**, 52744 (1978).
244. A. Kito and Y. Miyake, *Osaka Kogyo Gijutsu Shikensho Kiho*, **25**, 93 (1974); *Chem. Abstr.*, **82**, 79965 (1975).
245. M. S. Black and R. E. Sievers, *Anal. Chem.*, **48**, 1872 (1976).
246. M. Y. Khuhawar, A. A. Memon and M. I. Bhanger, *J. Chem. Soc. Pakistan*, **22**, 267 (2000).
247. Yu. G. Slizhov, M. A. Gavrilenko, T. N. Matveeva, N. V. Pozhidaeva and N. A. Chulynina, *Zh. Prikl. Khim. (Sankt-Peterburg)*, **72**, 1648 (1999); *Chem. Abstr.*, **132**, 245601 (2000).
248. Yu. G. Slizhov, M. A. Gavrilenko, T. N. Matveeva, N. A. Chulynina and O. A. Mal'tseva, *Zh. Fiz. Khim.*, **73**, 1650 (1999); *Chem. Abstr.*, **132**, 87457 (2000).
249. Yu. G. Slizhov and M. A. Gavrilenko, *Russ. J. Phys. Chem.*, **75**, 1012 (2001).
250. Yu. G. Slizhov and M. A. Gavrilenko, *J. Anal. Chem.*, **56**, 538 (2001).
251. W. Wasiak and I. Rykowska, *Chem. Anal.*, **40**, 731 (1995).
252. B. Feibush, M. F. Richardson, R. E. Sievers and C. S. Springer, Jr, *J. Am. Chem. Soc.*, **94**, 6717 (1972).
253. Yu. G. Slizhov and M. A. Gavrilenko, *Russ. J. Coord. Chem.*, **28**, 736 (2002).
254. W. J. Kowalski, *J. Chromatogr.*, **349**, 457 (1985).
255. Yu. G. Slizhov and M. A. Gavrilenko, *Russ. J. Phys. Chem.*, **79**, 2057 (2005).
256. W. Wasiak and I. Ryokowska, *Chem. Anal. (Warsaw)*, **40**, 731 (1995).
257. W. Wasiak and I. Rykowska, *J. Chromatogr. A*, **723**, 313 (1996).
258. V. Schurig, *J. Chromatogr.*, **965**, 315 (2002).
259. V. Schurig and M. Fluck, *J. Biochem. Biophys. Meth.*, **43**, 223 (2000).
260. V. Schurig, *Chirality*, **17**, S205 (2005).
261. L. Čučković, I. M. Hodžic and S. R. Niketić, *J. Serb. Chem. Soc.*, **67**, 735 (2002).
262. M. H. Abraham, C. F. Poole and S. K. Poole, *J. Chromatogr. A*, **842**, 79 (1999).
263. W. J. Kowalski, *Chem. Anal. (Warsaw)*, **43**, 69 (1998).
264. W. J. Kowalski, *J. Chromatogr. A*, **793**, 390 (1998).
265. M. H. Abraham, *Chem. Soc. Rev.*, **22**, 73 (1993).
266. A. Mohammad, S. Tiwari, R. Yusuf and J. P. S. Chahar, *Chem. Environ. Res.*, **7**, 3 (1998).
267. K. N. Johri and K. Bakshi, *Chromatographia*, **5**, 309 (1972).
268. W. Wasiak and I. Rykowska, *Chromatographia*, **48**, 284 (1998).
269. A. B. Burdukov, V. I. Ovcharenko, R. Z. Sagdeev, A. V. Podoplelov, N. V. Pervukhina, V. N. Ikorskii, I. A. Kiriluk and I. A. Grigoriev, *Polyhedron*, **14**, 501 (1995).
270. M. Y. Khuhawar and S. N. Lanjwani, *Talanta*, **46**, 485 (1998).
271. C. W. Harris, R. E. Sievers and K. J. Eisentraut, US patent 3558440 19710126 (1971); *Chem. Abstr.*, **74**, 101249 (1971).
272. T. Fujinaga, T. Kuwamoto, Y. Nakamura and N. Matsubara, *Buneski Kagaku*, **29**, 799 (1980); *Chem. Abstr.*, **94**, 75923 (1981).
273. S. Wu, M. He, B. Hu and Z. Jiang, *Microchim. Acta*, **159**, 269 (2007).

274. G. Davies, W. J. Swindall and D. Thorburn Burns, *Anal. Proc.*, **24**, 149 (1987).
275. R. Belcher, C. R. Jenkins, W. I. Stephen and P. C. Uden, *Talanta*, **17**, 455 (1970).
276. J. R. Castillo, J. M. Mir and C. Benedicho, *Fresenius Z. Anal. Chem.*, **328**, 56 (1987).
277. R. W. Moshier and R. E. Sievers, *Gas Chromatography of Metal Chelates*, Pergamon Press, New York, 1965.
278. R. Sato, K. Takahashi, M. Yoshino, H. Kato and S. Ohshima, *Jpn. J. Appl. Phys*, **32**, 1590 (1993).
279. V. Arancibia, M. Valderrama, K. Silva and T. Tapia, *J. Chromatogr. B*, **785**, 303 (2003).
280. N. Kameta and H. Imura, *Bull. Chem. Soc. Jpn.*, **74**, 1641 (2001).
281. A. Tapparo, L. Solda, G. G. Bombi, P. Zambenedetti, P. Zatta, F. Paolo, R. Bertani and B. Corain, *Analyst*, **120**, 2425 (1995).
282. L. V. Belova, G. A. Shteinberg and V. Z. Krasil'shchik, *Reaktivy i Osobo Veshchestva*, 24 (1981); *Chem. Abstr.*, **95**, 54242 (1981).
283. H. Li, N. Hiromichi and M. Kazuko, *Anal. Sci.*, **12**, 215 (1996).
284. T. Katsura and F. Kato, *Anal. Chim. Acta*, **252**, 77 (1991).
285. T. Kurihara, T. Takehara, S. Odashima and K. I. Hirai, *J. Electron Microsc.*, **38**, 477 (1989).
286. P. O. Dank, D. E. Karr, Y. Xiong and K. G. Owens, *Rapid Commun. Mass Spectrom.*, **10**, 862 (1996).
287. H. Rashidezadeh, K. Hung and B. Guo, *Mass Spectrum.*, **4**, 429 (1998).
288. K. Matsumoto, H. Ajiro, S. Habaue and Y. Okamoto, *Rapid Commun. Mass Spectrom.*, **16**, 730 (2002).
289. K. Matsumoto, H. Ajiro, S. Habaue and Y. Okamoto, *Rapid Commun. Mass Spectrom.*, **17**, 678 (2003).
290. K. Matsumoto, A. Matsunami, H. Oyama and K. Kitagawa, *Microchem. J.*, **81**, 195 (2005).
291. P. G. Di Croce, F. Aubriet, R. Chéty-Gimondo, J.-F. Muller and P. Grange, *Rapid Commun. Mass Spectrom.*, **18**, 601 (2004).
292. Yu. G. Slizhov and M. A. Gavrilenko, *Russ. J. Appl. Chem.*, **77**, 215 (2004).
293. R. M. Baosic, D. M. Milojkovic-Opsenica and Z. Lj. Tesic, *J. Planar Chromatogr.*, **15**, 263 (2002).
294. L. G. Galya, E. F. McCord and K. Adamsons, *Int. J. Polym. Anal. Charact.*, **2**, 293 (1996).
295. M.-a. Morikawa, N. Kimizuka, M. Yoshihara and T. Endo, *Chem. Eur. J.*, **8**, 5580 (2002).
296. W. Mertz, *J. Nutr.*, **123**, 626 (1993).
297. W. Mertz, *J. Am. Coll. Nutr.*, **17**, 544 (1998).
298. R. A. Anderson, *Diabetes Metab.*, **26**, 22 (2000).
299. J. B. Vincent, *Nutr. Rev.*, **58**, 67 (2000).
300. P. Bermejo-Barrera, P. Herbello-Hermelo, M. C. Barciela-Alonso and A. Bermejo-Barrera, *At. Spectrosc.*, **24**, 22 (2003).
301. P. Bermejo-Barrera, M. C. Barciela-Alonso, B. Pérez-Fernández, A. Bermejo-Barrera, *Spectrochim. Acta, Part B*, **58**, 167 (2003).
302. P. Bermejo-Barrera, A. Moreda-Pineiro, R. González-Iglesias and A. Bermejo-Barrera, *Spectrochim. Acta, Part B*, **57B**, 1951 (2002).
303. L. Abrankó, L. Yang, R. E. Sturgeon, P. Fodor and Z. Mester, *Anal. At. Spectrom.*, **19**, 1098 (2004).
304. E. W. Berg and N. M. Herrera, *Anal. Chim. Acta*, **60**, 117 (1972).
305. I. E. Soboleva, Z. A. Tu, G. N. Kuprianova, N. P. Kuzmina and L. I. Martynenko, *J. Alloys Compd.*, **225**, 390 (1995).
306. K.-y. Pang, J. Ke, K.-j. Pang, J. Cheng and W.-Z. Bian, *Yingyong Huagong*, **32**, 51 (2003); *Chem. Abstr.*, **139**, 142886 (2003).
307. S. P. Arya and P. Jain, *Indian J. Chem.*, **42A**, 2541 (2003).
308. K. Mashimo, M. Matsukawa and T. Wainai, *Bunseki Kagaku*, **26**, 147 (1979); *Chem. Abstr.*, **90**, 214800 (1979).
309. D. M. Corsi, C. Platas-Iglesias, H. van Bekkum and J. A. Peters, *Magn. Reson. Chem.*, **39**, 723 (2001).
310. H. Tsukube, J. Uenishi, T. Kanatani, H. Itoh and O. Yonemitsu, *Kidorui*, **26**, 236 (1995); *Chem. Abstr.*, **123**, 222154 (1995).
311. H. Tamiaki, S. Unno, E. Takeuchi, N. Tameshige, S. Shinoda and H. Tsukube, *Tetrahedron*, **59**, 10477 (2003).
312. H. Tsukube, J. Uenishi, T. Kanatani, H. Itoh and O. Yonemitsu, *Chem. Commun.*, 447 (1996).

313. H. Tsukube, S. Shinoda, J. Uenishi, T. Kanatani, H. Itoh, M. Shiode, T. Iwachido and O. Yonemitsu, *Inorg. Chem.*, **37**, 1585 (1998).
314. D. Kyriakides and I. Panderi, *Anal. Chim. Acta*, **584**, 153 (2007).
315. T. Kato and K. Kano, *Bunseki Kagaku* **34**, 36 (1985); *Chem. Abstr.*, **102**, 159638 (1985).
316. K. Wignarajah, *J. Indian Chem. Soc.*, **65**, 229 (1988).
317. M. Shimoda, H-c. Shin and E-i. Kokue, *J. Vet. Med. Sci.*, **56**, 701 (1994).
318. T. Umezawa and Y. Akyoshi, *Jpn. Kokai Tokkyo Koho*, JP 05099929 A2 19930423 Heisei (1993); *Chem. Abstr.*, **119**, 90766 (1993).
319. M. Fedurco, A. Romieu and G. Turcatti, *PCT Int. Appl.*, WO 2006064199 A1 20060622 (2006); *Chem. Abstr.*, **145**, 56988 (2006).
320. M. A. Malati, *Analyst*, **112**, 511 (1987).
321. K. Takashima, N. Fujimoto, K. Tada, M. Ohgaki and T. Nakayama, *Tokushima-ken Hoken Kankyo Senta Nenpo*, **13**, 69 (1996); *Chem. Abstr.*, **124**, 269783 (1996).
322. Y. Suzuki, T. Hibino, T. Kawazu, T. Wada, T. Kihara and H. Koyama, *Biotechniques*, **34**, 988 (2003).
323. O. M. Antoshina, P. Ts. Zil'berman, L. P. Adamovich and M. S. Kravchenko, *Visn. Kharkiv Univ., Khim.*, **84**, 63 (1972); *Chem. Abstr.*, **78**, 118873, 131660 (1973).
324. M. S. Kravchenko, M. Sh. Fumarova and L. Ya. Kheifets, *Zh. Anal. Khim.*, **41**, 1371 (1986); *Chem. Abstr.*, **105**, 196866 (1986).
325. M. S. Kravchenko, M. Sh. Fumarova and E. V. Litvinenko, *Khim. Tekhnolog. Vody*, **11**, 1110 (1989); *Chem. Abstr.*, **112**, 164618 (1990).
326. M. S. Kravchenko, V. M. Ostrovskaya and M. Sh. Fumarova, *Vysokochistye Veshchestva*, 152 (1990); *Chem. Abstr.*, **114**, 239405 (1990).
327. F. Feigl and H. A. Suter, *Ind. Eng. Chem.*, **14**, 840 (1942).
328. J. R. Preer and G. B. Murchison, Jr, *Environ. Pollut.*, **12**, 1 (1986).
329. R. Zoja, A. Lazzaro, A. Battistini and G. Gentile, *Biotech. Histochem.*, **81**, 151 (2006).
330. H. Tugcu, C. Yorulmaz, Y. Karslioglu, H. B. Uner, S. Koc, C. Ozdemir, A. Ozaslan and B. Celasun, *Am. J. Forensic Med. Pathol.*, **27**, 296 (2006).

CHAPTER **13**

The chemistry of metal ynolates

MITSURU SHINDO

Institute for Materials Chemistry and Engineering, Kyushu University, Kasuga-koen, Kasuga 816-8580, Japan
Fax: +81-92-583-7875; e-mail: shindo@cm.kyushu-u.ac.jp

The chemistry of metal enolates
Edited by Jacob Zabicky

I. INTRODUCTION

Metal ynolates (**1**) have attracted much less attention than metal enolates (**2**), with only scattered reports in the literature until recently, partially due to a lack of general and convenient methods for their synthesis[1]. Metal ynolates are not only the precursors of alkynyl ethers (**3**), but also of metalated ketenes (**4**) acting as ketene (**5**) precursors, their chemistry showing interesting facets that are impossible to attain with the metal enolates. The fact that metal ynolates can act as precursors in the synthesis of other reactive species will prompt organic chemists to focus their attention on this potentially useful and exciting field. An example of the potential utility of metal ynolates is shown in equation 1, whereby a multiple step process switches twice from electrophilic to nucleophilic reagents: A metal ynolate (**1**) reacts with an electrophile to give a ketene (**5**), which reacts with a nucleophile to afford a metal enolate (**6**), which can react with an electrophile to furnish a ketone (**7**), which is attacked by a nucleophile to give an alkoxide (**8**). Thus, a smart design would enable the one-pot successive reaction sequence. If metal ynolates are synthons for complex molecules which cannot be accessed by other methods, their synthetic utility will be greatly expanded.

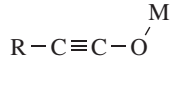

(**1**)

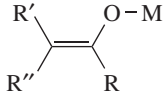

(**2**)

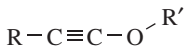

(**3**)

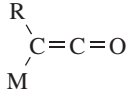

(**4**)

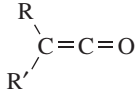

(**5**)

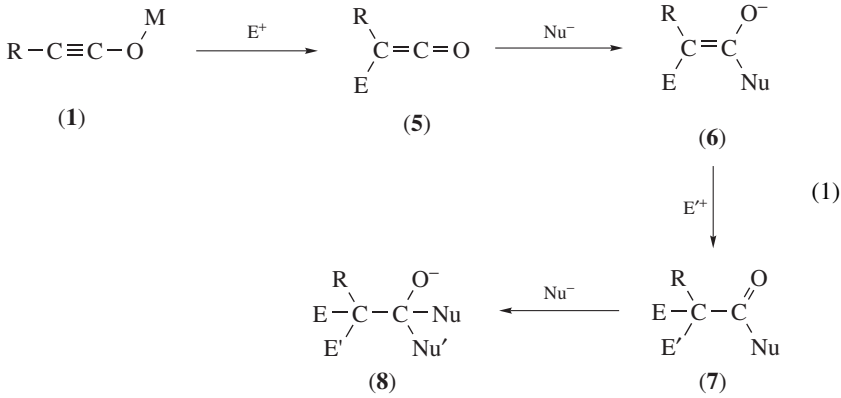

(**1**) (**5**) (**6**) (**7**) (**8**) (1)

In this chapter synthetic methods, chemical properties and synthetic applications of metal ynolates are described. In the last part, heteroatom analogues of metal ynolates are briefly discussed. The following acronyms are in use:

DMPU	*N*,*N*′-dimethyl-*N*,*N*′-propylene urea	TESCl	triethylsilyl chloride
HMPA	hexamethylphosphortriamide	Tf	triflyl (trifluoromethanesulfonyl)
LDA	lithium diisopropylamide	TIPSCl	triisopropylsilyl chloride
LHMDS	lithium hexamethyldisilazide	TIPSOTf	triisopropylsilyl trifluoromethanesulfonate
LTMP	lithium tetramethylpiperidide	TMEDA	*N*,*N*,*N*′,*N*′-tetramethylethylenediamine
NBS	*N*-bromosuccinimide	TMSCl	trimethylsilyl chloride

II. PREPARATION OF ALKALI METAL YNOLATES

Metal ynolates are not as easy to prepare in a similar fashion as metal enolates, because the intermediates may be labile monosubstituted ketenes. Several preparative methods for alkali metal ynolates have been reported, among which some have been used as intermediate steps in one-pot organic syntheses. Silyl ynolates have been prepared from lithium ynolates. There have been few reports on the other metal ynolates. Since there is no universal method to determine the yield of metal ynolates, the efficiency of preparation is estimated from the results of some of the following reactions.

A. Lithium Ynolates from Isoxazolyllithium

The first synthesis of lithium ynolates was reported by Schöllkopf in 1975. The isoxazolyllithium **10**, prepared by lithiation of 3,4-diphenylisoxazole (**9**), undergoes fragmentation to yield the lithium ynolate **11** (equation 2)[2]. The dilithium ynolate dianion **14** is also synthesized by the same protocol from 3-phenylisoxazole (**12**) via the 3-phenyl-5-isoxazolyllithium (**13**) intermediate (equation 3)[3]. The maximum yields were around 80%, judged by the yields of the β-lactones (Section IV.A).

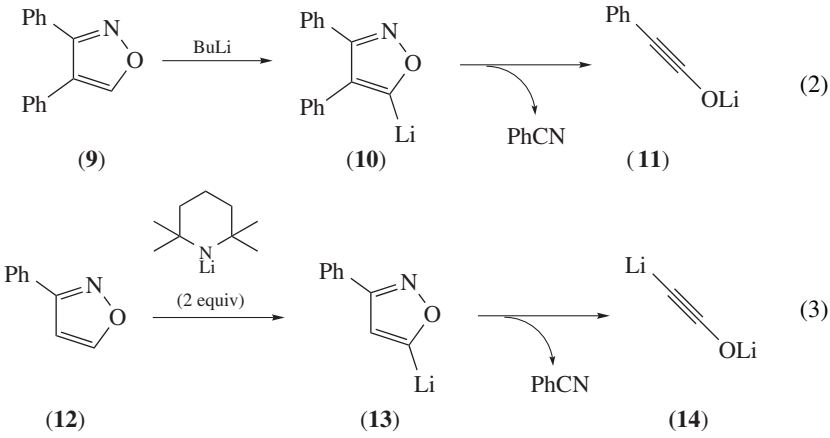

B. Rearrangement

1. Lithium ynolates from α-keto dianions derived from esters

Lithium ynolates are synthesized via the rearrangement of α-keto dianions **16**[4], which are prepared by adding dibromomethyllithium to esters **15** followed by base-induced elimination. The dianions **16** rapidly rearrange with loss of LiBr to produce the lithium ynolates **17** (equation 4). Experiments using a ^{13}C-labeled substrate suggest that the reaction is a carbon analogue of the Hofmann rearrangement. This process can be used as an alternative to the Arndt–Eistert reaction, to yield one-carbon homologated esters (**18**), after quenching with acidic alcohol[5]. γ-Lactones are homologated to give δ-hydroxy esters (equation 5)[5a]. β-Amino acids are synthesized from the corresponding α-amino esters by the homologation without loss of optical purity (equation 6)[6].

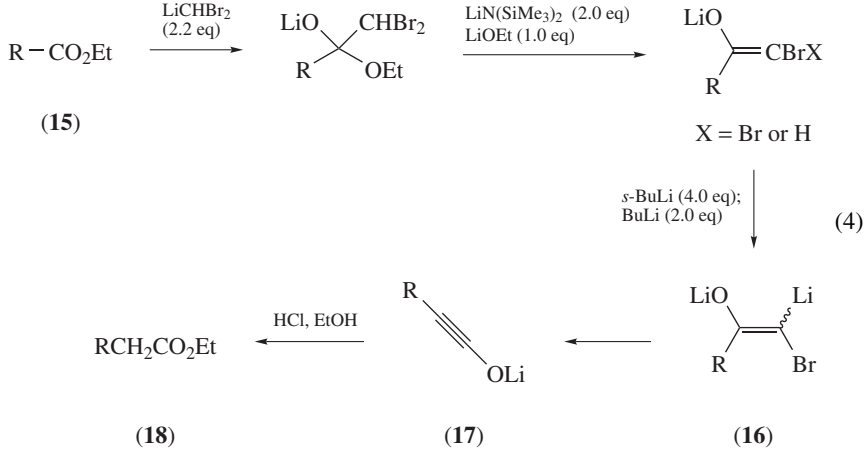

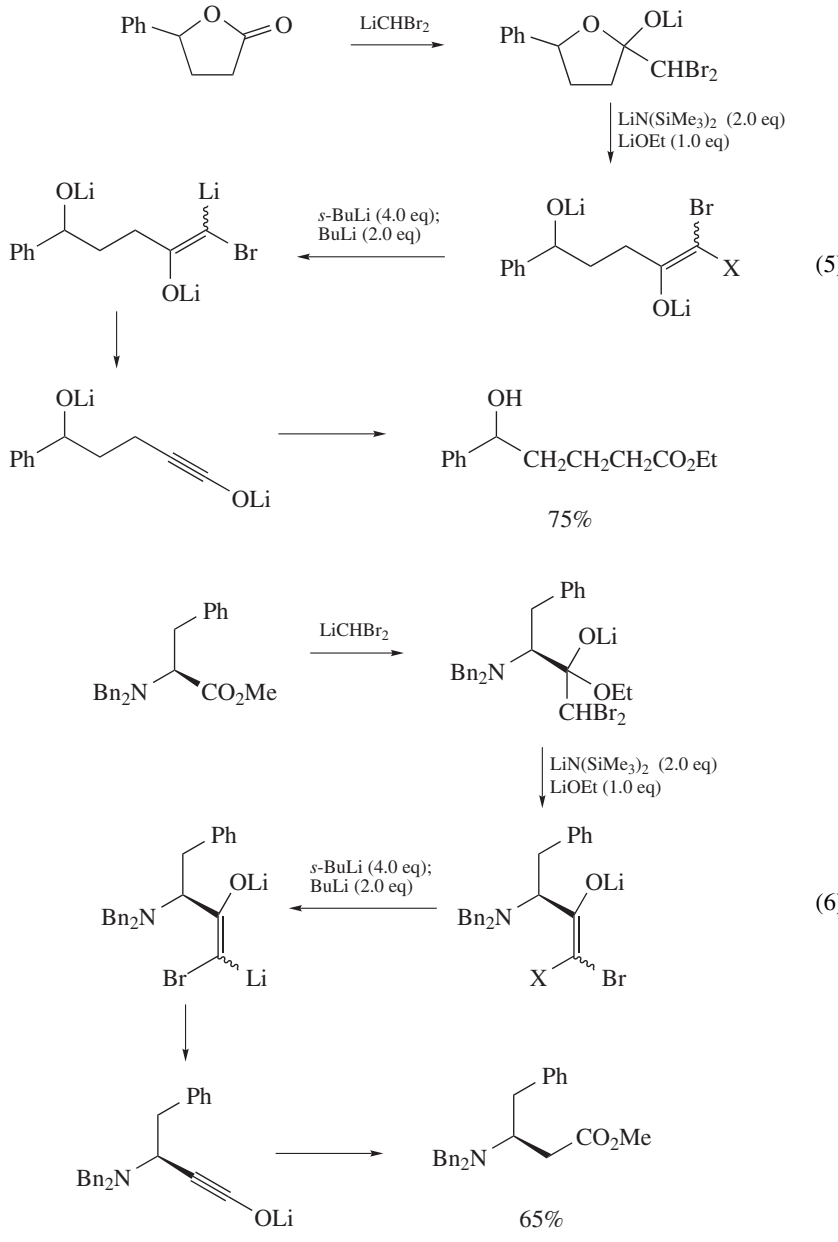
Ph
O
O
LiCHBr2
OLi
CHBr2
LiN(SiMe3)2 (2.0 eq)
LiOEt (1.0 eq)
Li
Br
s-BuLi (4.0 eq);
BuLi (2.0 eq)
X
OH
CH2CH2CH2CO2Et
75%
Bn2N
CO2Me
OEt
65%

(5)

(6)

This homologation via lithium ynolates has been used to prepare silyl ynol ethers, as described in Section V.

2. Potassium/lithium ynolates from α-chloro-α-sulfinyl ketones

The α-chloro-α-sulfinyl ketone **20** was prepared from methyl benzoate and chloromethyl phenyl sulfoxide **19** after *in situ* α-lithiation. Compound **20** is dimetallated by KH and *t*-BuLi to give the keto dianion **21**, which is converted into a potassium/lithium ynolate **22** (equation 7)[7]. The resulting metal ynolates are converted into thioesters, carboxylic acids, amides and esters (Section V).

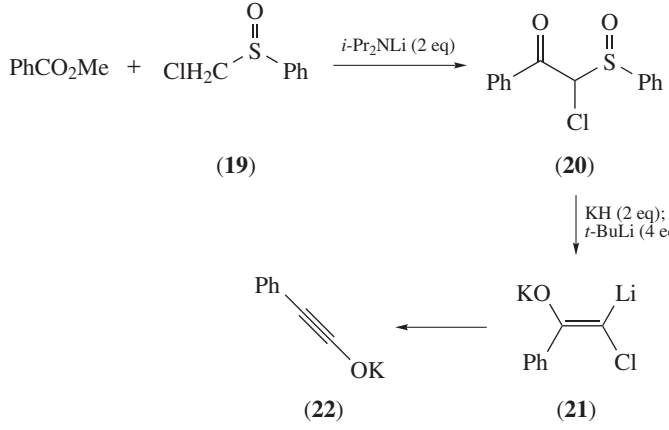

(**19**) (**20**) (**21**) (**22**) (7)

3. Lithium trimethylsilylynolate from trimethylsilyldiazomethane

The trimethylsilylynolate is prepared on treatment of trimethylsilyldiazomethane (**23**) with BuLi followed by exposure to carbon monoxide. The mechanism is explained by the fact that the lithiated silyldiazomethane (**24**) adds to carbon monoxide to give the labile α-diazoacyllithium **25**, which rearranges to the ynolate **27** via the ketene intermediate **26** (equation 8)[8].

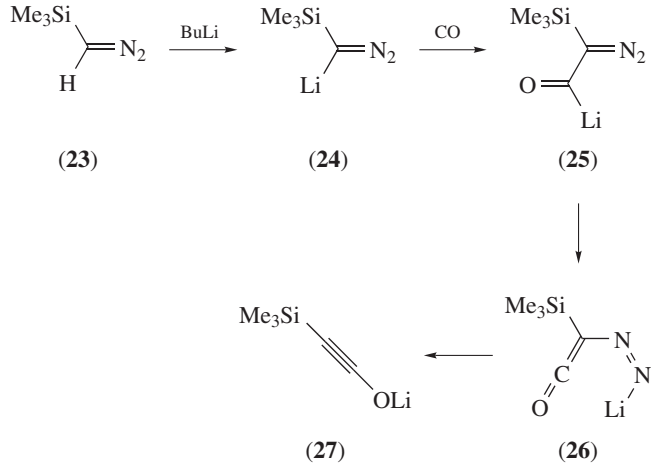

(**23**) (**24**) (**25**) (**26**) (**27**) (8)

C. Oxygenation of Terminal Alkynes

1. Oxygenation of lithium acetylides with lithium t-butylperoxide

Lithium acetylides **28** are oxygenated by lithium *t*-butylperoxide, prepared from anhydrous *t*-butylhydroperoxide[9] and LHMDS, to give lithium ynolates **29** (equation 9)[10]. This method has been used as an efficient route for the preparation of the silyl ynolates **30**[11a] (Section V). Dioxygen, *t*-butyl perborate and bis(trimethylsilyl)peroxide have been unsuccessful as oxidation reagents[11b,c].

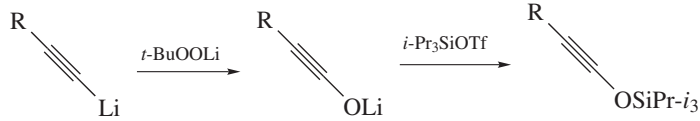

(**28**) (**29**) (**30**) (9)

2. Hypervalent organoiodine

Ynol tosylates are synthesized from terminal alkynes via a unique sequence (equation 10)[12]. The hypervalent organoiodine compound **32**, prepared by treatment of iodosobenzene diacetate with *p*-toluenesulfonic acid, reacts with the terminal alkynes **31** to give the iodonium tosylates **33**, which are then treated with 10 mol% of CuOTf or AgOTf to afford the ynol tosylates **34**. Finally, the ynol tosylates **34** are converted into lithium ynolates **35** by treatment with MeLi. The ynolates are trapped with *t*-butyldimethylsilyl chloride, triethylgermyl chloride and tributylstannyl chloride to give the silyl ynol ethers **36**, the germyl ketenes **37** and the stannyl ketene **38**[13].

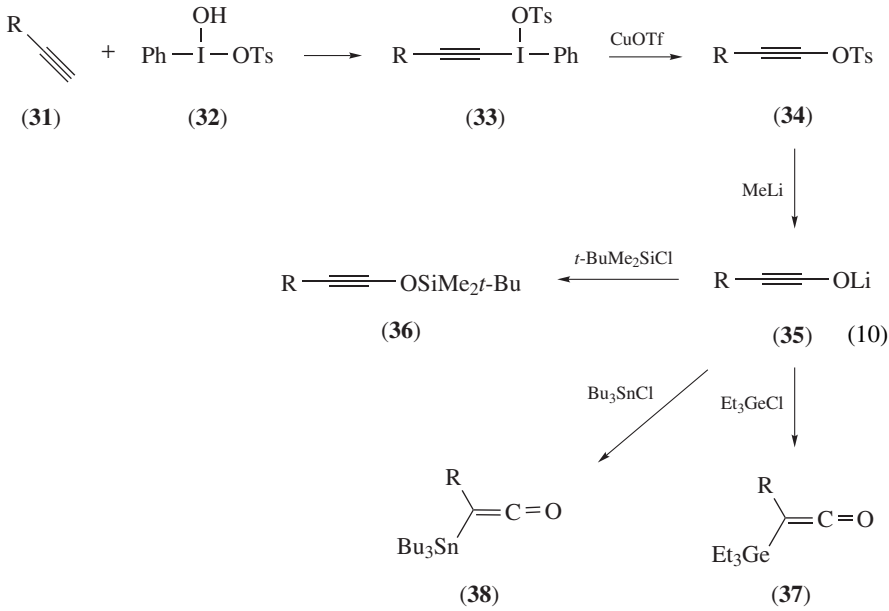

(**31**) (**32**) (**33**) (**34**) (**36**) (**35**) (10) (**38**) (**37**)

D. Metallation

1. Lithium ynolates from lithium ester enolates

Although metal ynolates are equivalents of metallated ketenes, direct metallation of ketenes is often troublesome. Metallation of the precursors of ketenes, followed by transformation into the metallated ketenes, would be a better route to metal ynolates. Based on this concept, an efficient method for the synthesis of lithium ynolates has been developed, taking advantage of the properties of ester enolates, which are easily converted into ketenes by elimination of alkoxides (equation 11)[14]. The synthetic methods for lithium ynolates via the cleavage of ester dianions are both convenient and quite general, because alkyl-, aryl- and silyl-substituted lithium ynolates can be synthesized in good yields.

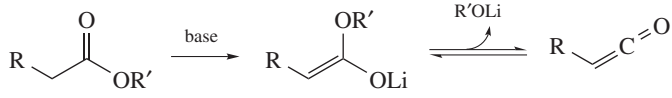

(11)

The α-bromo esters **39** are treated with LDA to form the bromo ester enolates **40**, which are subjected to lithium–halogen exchange with *t*-BuLi (3 equiv) at $-78\,^{\circ}C$. The resulting dilithium ester dianions **41** are thermally cleaved at $0\,^{\circ}C$ into the ynolates **42** in good yields (equation 12)[15]. This procedure finally regenerates LDA from diisoprpylamine and *t*-BuLi along with the lithium ynolate (equation 12′).

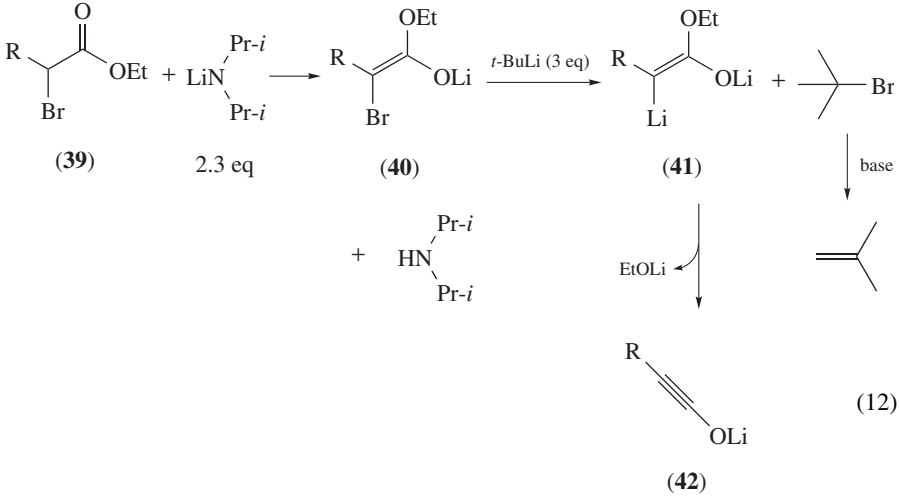

(12)

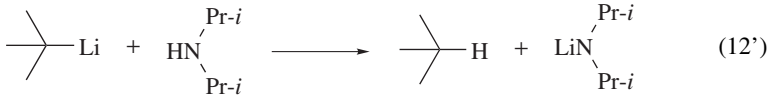

(12')

To avoid the effect of the strong base and to simplify the protocol, α,α-dibromo esters **43** are used as the starting materials, which are treated with 4 equiv of *t*-BuLi or *s*-BuLi at $-78\,^{\circ}C$. The reaction mixture is then warmed to $0\,^{\circ}C$ to produce the ynolates **44** in excellent yield (equation 13)[16]. This improved facile method can be carried out without the use of lithium amides. If compouds **43** with $R' = Ph$ are used as the starting materials,

the less basic lithium phenoxide is generated instead of lithium ethoxide. The starting dibromo esters **43** are stable compounds and are easily synthesized via bromination of the α-bromo ester enolates with 1,1,2,2-tetrafluoro- or 1,1,2,2-tetrachloro-1,2-dibromoethane (equation 14)[16b, 17] or by radical bromination (equations 15 and 16) depending on the substrates.

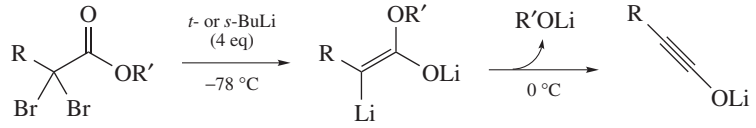

(13)

(**43**) R′ = Et, Ph (**44**)

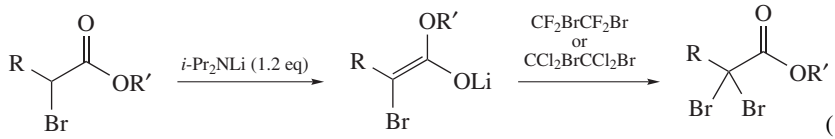

(14)

R′ = Et, Ph

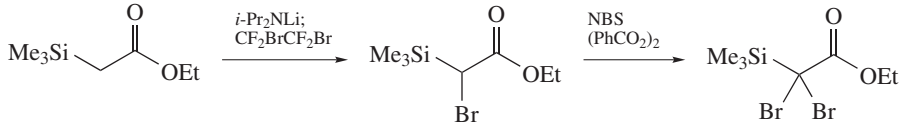

62% 75% (15)

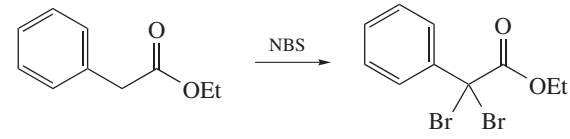

(16)

60%

Although this method is convenient in the laboratory, *t*- and *s*-BuLi are somewhat expensive and should be handled carefully, especially in a large scale. A more practical method for the synthesis of ynolates is the reductive lithiation method. The dibromo esters **43** are treated with lithium naphthalenide to give the ynolates **44** in good yield. Naphthalene-catalyzed reductive lithiation[18] of the dibromo esters can also be performed, providing the ynolates more efficiently (equation 17)[19].

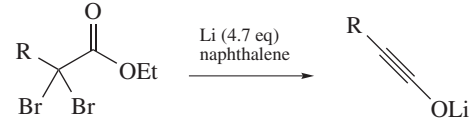

(17)

(**43**) (**44**)

2. Metallation of trialkylsilylketenes

Since metal ynolates are metallated ketene equivalents, metallation of ketenes is expected to afford metal ynolates. Direct metallation of monoalkylketenes is, however, fairly difficult due to the high lability of these ketenes (e.g. dimerization) and the strong electrophilicity of the carbonyl carbon[20]. In contrast, silylketenes are so stable that lithiation of trimethylsilylketene (**45**) with BuLi at −100 °C provides the lithium ynolate **46** in good yield (equation 18)[21]. The *t*-butyldimethylsilylketene (**47**) is also lithiated to afford the lithium ynolate **48** (equation 19)[22].

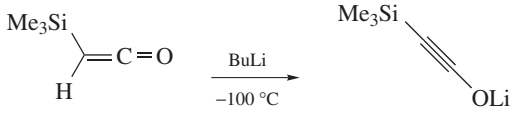

(**45**) (**46**) (18)

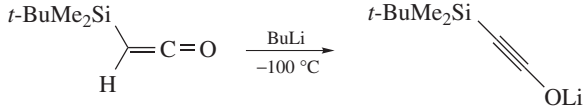

(**47**) (**48**) (19)

Transmetallation of bis(trimethylsilyl) ketene **49** by *t*-BuOK in the presence of HMPA affords the ynolate **50** (equation 20)[23]. Since it does not give the ynolate without HMPA, the trialkylsilyl group might be activated by the coordination of HMPA.

(**49**) (**50**) (20)

E. Flash Photolysis

Flash photolysis of phenylhydroxypropenone (**51**) in aqueous solution gives phenylacetic acid **53** through the ynolate **52** as a short-lived reaction intermediate (equation 21)[24]. Kinetic experiments revealed that the corresponding aryl ynols ArC≡COH are strong acids with $pK_a < 2.8$[25].

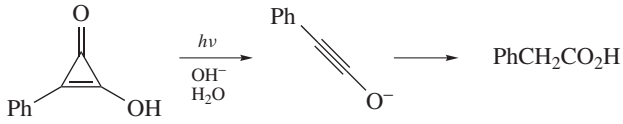

(**51**) (**52**) (**53**) (21)

F. Dilithium Ynolate

Since unsubstituted metal ynolates have a terminal alkyne, their metallation gives ynolate dianions. Schöllkopf's method affords an ynolate dianion, starting from 3-phenylisoxazole (equation 3, Section II.A)[3].

Lithiation of 2,3-dihydrofurans (**54**) followed by elimination of a 1-alkene provides dilithium ynolate (**55**) (equation 22)[26]. The properties and synthetic utility of **55** have not yet been studied.

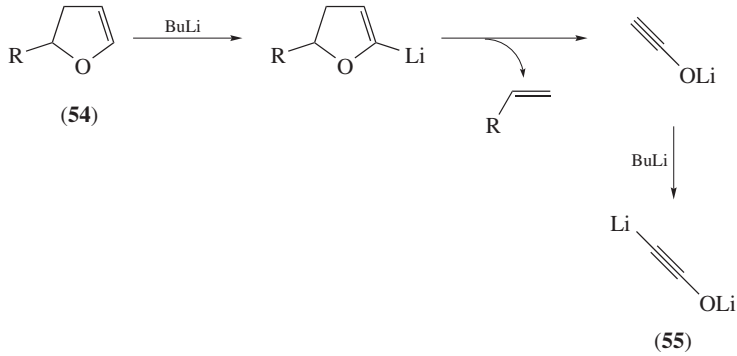

(**54**) (**55**) (22)

III. PROPERTIES OF METAL YNOLATES

Lithium ynolates are stable and keep their reactivity at 0 °C under inert gas for several days, but they decompose in 1 day at 20 °C[27]. Silyl ynolates (silyl ynol ethers) are stable for a long period and they can be purified by distillation, but they are labile to acids (Section V). The stability of ynolates of metals other than lithium is unknown.

Compared with metal enolates, there have been very few reports on the direct structural analysis and theoretical studies of ynolates. An X-ray crystal structure of a vanadium complex of lithium ynolate with a porphyrinogen ligand (**56**) is reported[28]. This metal complex was incidentally formed from $VCl_3(THF)_3$ with tetralithium salt of the octaethylporphyrinogen ligand. In this complex, the lithium cation seems to interact with the π-electrons of the ynolate. The four atoms of the ynolate group in **56** are not collinear due to a partial sp^2 character of the group in this complex.

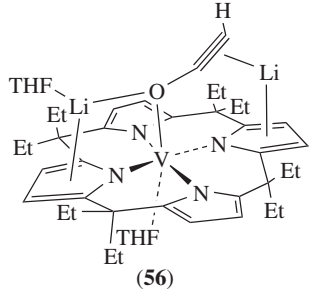

(**56**)

A calculated gas-phase structure (MP2//MP2) of an ynolate is shown in **57**, in which a C=C bond contraction, C=O bond elongation and an opening of the HCC bond angle compared with the ketene are observed. This fact suggests that the structure of the ynolate significantly contributes to the resonance hybrid of the anion structure[29].

The ^{13}C NMR spectrum of silyl-substituted potassium ynolates in THF-d_8 shows signals at 132.8 and 33.4 ppm[23], which are close to those of alkynyl ethers. The IR spectrum in THF shows a strong absorption at 2229 cm^{-1}, which is typical for alkyne[30]. These results point to a metal ynolate rather than a metallated ketene.

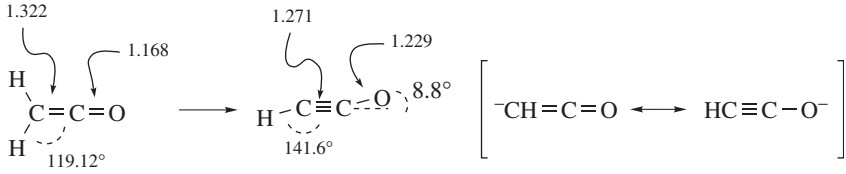

(**57**)

The ESI mass fragment ion spectra of the monomethyl glutarate anion (**58**) shows formation of ynolate anions (equation 23)[31].

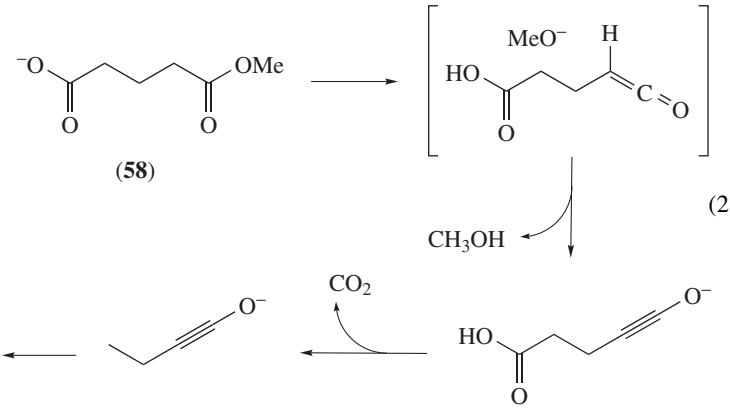

(**58**) (23)

The acidity of aryl ynols ArC≡COH is extremely strong with pK_a < 2.8, which is more acidic than unsubstituted carboxylic acid[25]. The strong acidity is also supported by theoretical calculations[24, 32].

IV. REACTIONS OF METAL YNOLATES

Since metal ynolates are ambient nucleophiles, with oxygen being a hard nucleophilic center and carbon a soft one, the position of attack at O or C would therefore depend on the hard/soft character of the electrophile (equation 24). When metal ynolates react as C-nucleophiles, they are regarded as metallated ketenes **59**. Ynolates are also considered as electron-rich alkynes. In this section, the unique reactions of metal ynolates induced by these characteristic features are summarized.

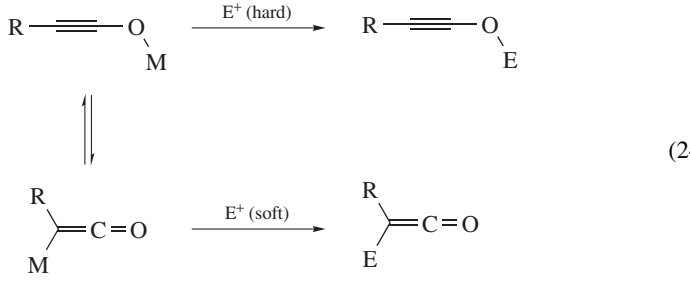

(**59**) (24)

A. Formal [2 + 2] Cycloaddition of Lithium Ynolates with Aldehydes and Ketones

Lithium ynolates easily add to aldehydes and ketones even at −78 °C to give β-lactone lithium enolates (**61**), which are stable at this temperature but undergo ring opening above −20 °C (equation 25). This reaction is a formal [2 + 2] cycloaddition, and it may occur via a stepwise mechanism through the ketene intermediate **60**. Reactions of benzaldehyde with the phenyl-substituted lithium ynolate **62** afforded the β-lactone **63** after protonation (equation 26). On the other hand, alkyl-substituted lithium ynolates (**64**) add to aldehydes to give only the 1:2 adducts **63**, even if less than 1 equivalent of aldehyde is used[16, 17], due to the higher reactivity of the β-lactone enolates (equation 27). However, ketones and sterically hindered aldehydes (e.g. pivalaldehyde) provide the 1:1 adducts (**66**, **67**) because the reactivity is lowered by steric hindrance (equations 28 and 29)[33]. The β-lactones can be decarboxylated efficiently and stereospecifically to give the olefins on heating, as shown in equation 29. The decarboxylation is accelerated by acid catalysts such as Brønstead acids, Lewis acids and silica gel[33, 34].

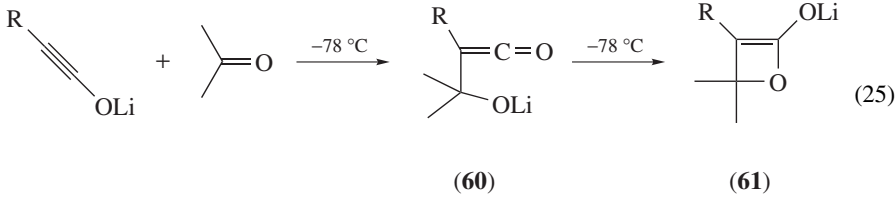

(25)

(**60**) (**61**)

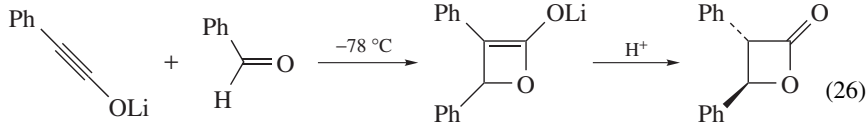

(26)

(**62**) (**63**) 60%

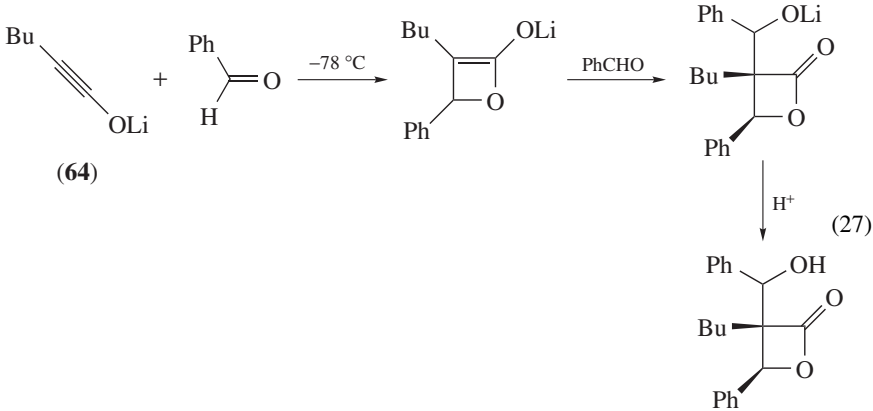

(27)

(**64**) (**65**) 85%

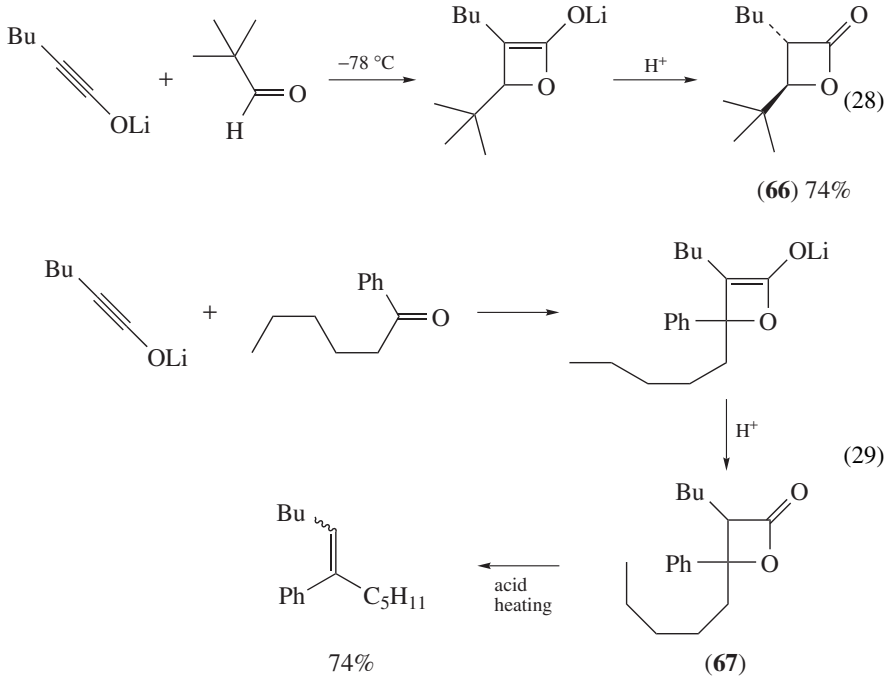

B. Lithium Ynolate-initiated Cascade Reactions Leading to Multisubstituted Carbocycles and Heterocycles

Lithium β-lactone enolates have abundant unexplored chemistry, which the ynolate chemistry could open. The β-lactone enolates prepared by cycloaddition of lithium ynolates with ketones are stable intermediates at $-78\,^{\circ}C$, but are still highly nucleophilic. Taking advantage of this reactivity, it would be possible to design a one-pot multistep synthesis (the negative–positive switching process) using lithium ynolates, as shown in equation 1. It would be even more efficient if the β-lactone enolates could be prepared by a method not involving enolization of the corresponding β-lactones. Based on this concept, novel tandem reactions involving intramolecular cyclization are developed (equation 30)[33]. The ynolate **68** adds to the γ-ketoester **69** to give the β-lactone enolate **70**, which subsequently cyclizes via the Dieckmann condensation to afford the bicyclic β-lactone **71**. This is easily decarboxylated on heating in the presence of acid to produce the 2,3-disubstituted cyclohexenones **72** in good overall yield. The direct generation of the β-lactone enolates **70** by treatment of the corresponding β-lactones **73** with LDA is unsuccessful. Therefore, ynolates allow the regioselective formation of the enolates via cycloaddition. This tandem [2 + 2] cycloaddition–Dieckmann condensation process can be applied to the syntheses of fused rings (equation 31) and naphthols (equation 32)[33b].

Several natural products, including dihydrojasmone (**74**), α-cuparenone (**75**)[33] and cucumin E (**76**)[35], were synthesized via the ynolate-initiated tandem process.

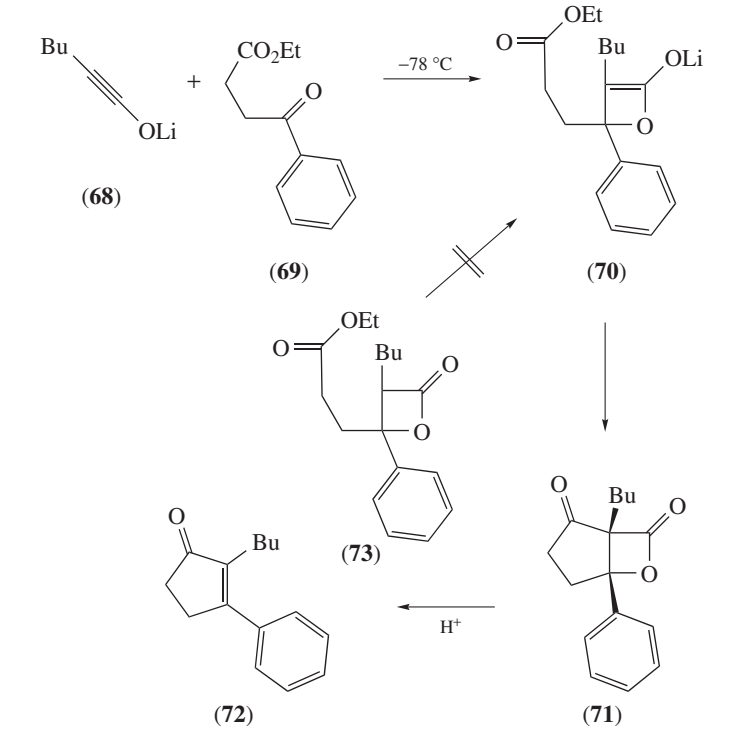
Bu
OLi
(68)
+
CO2Et
O
(69)
−78 °C
OEt
O
Bu
OLi
O
(70)
OEt
O
Bu
O
O
(73)
O
Bu
O
O
(71)
O
Bu
(72)
H+

(30)

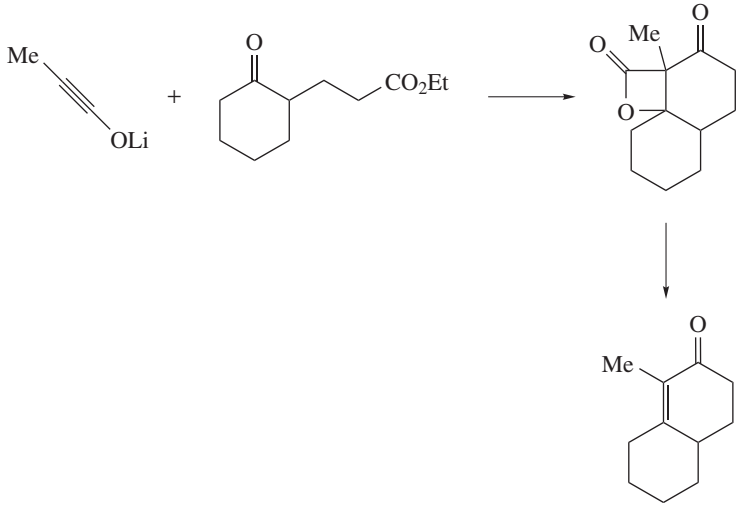
Me
OLi
+
O
CO2Et
O
Me
O
O
O
Me

(31)

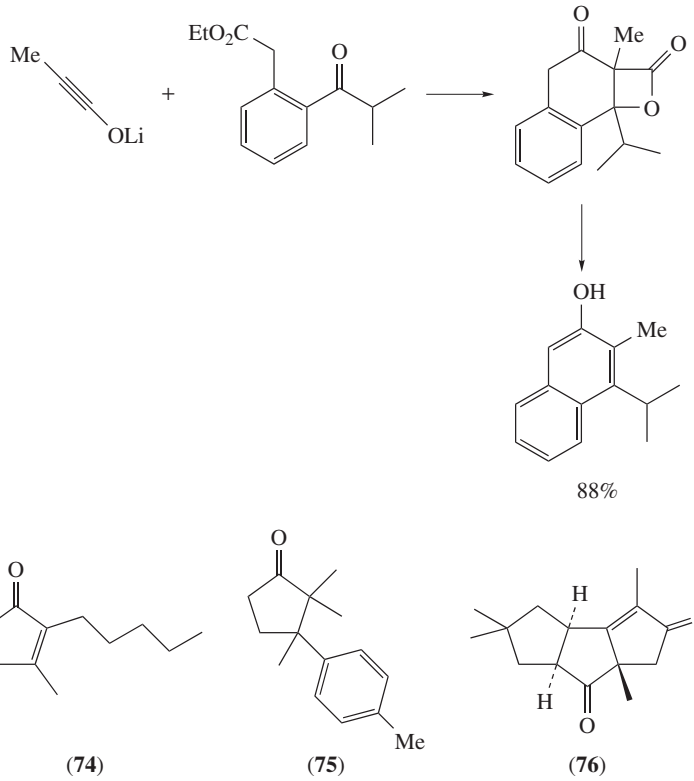

(32)

(**74**) (**75**) (**76**)

In the same way, electrophilic reactions can be applied to the tandem reaction. The ynolate-initiated tandem [2 + 2] cycloaddition–Michael reaction followed by decarboxylation furnished the polysubstituted five-, six- and seven-membered cycloalkenes in good overall yield (equation 33)[36]. The ester enolate intermediates **77** are nucleophilic, and further bond formation is possible.

Multisubstituted five-membered aromatic heterocycles are synthesized via this cascade protocol (equation 34). The cycloadditions of α-acyloxyketones **78a** with lithium ynolates afford β-lactone lithium enolates **79a**, which spontaneously cyclize to give bicyclic compounds **80a**. These intermediates, which are stable enough to be isolated, are treated with TsOH under heating to provide substituted furans **81a** via decarboxylation and dehydration. Thiophenes (e.g. **81b)** are also synthesized by the analogous scheme via intermediate **80b** using α-acylthioketones (**78b**) as a substrate. In the synthesis of pyrroles using α-acylaminoketones as a substrate, the cyclization proceeded at $-20\,^{\circ}C$, and the β-lactone was subsequently ring-opened via β-elimination to furnish pyrroles in one-pot (equation 35)[37].

C. Formal [2 + 2] Cycloaddition of Lithium Ynolates with Aldimines to Give β-Lactams

Aldimines are aza-analogues of aldehydes and are expected to react with nucleophiles in similar fashion. Since aldimines are, however, less electrophilic than the corresponding aldehydes, they often require activation and/or harsh conditions for the addition of

nucleophiles[38]. The phenyl-substituted lithium ynolate **82** reacts with aldimine **83** activated by electron-withdrawing groups (*p*-nitrophenyl etc.) to afford the 2:1 adducts **84** in good yields (equation 36)[39]. *N*-*o*-Methoxyphenylaldimine (**85**) reacts with the lithium ynolate at −78 °C to give the 2:1 adduct **86**, although the methoxy group is electron-donating (equation 37). Since *N*-*p*-methoxyphenylaldimine (**87**) is inert to the ynolate, the *N*-*o*-methoxyphenylaldimines are obviously activated by chelation with lithium[40]. The lithium ynolate **88** affords β-lactams (1:1 adduct **90**) in the reaction with aldimines activated by *N*-sulfonyl groups (**89**) at −78 °C (equation 38)[41]. Since the aldimines **83** and **85** have moderately electron-withdrawing or electron-donating groups, the β-lactam enolate intermediates would be more nucleophilic than ynolates. Therefore, the 2:1 adducts (**84** and **86**) are produced. On the other hand, in the case of equation 38, the strong electron-withdrawing group of sulfonyl stabilizes the β-lactone enolate, which is less reactive than the ynolate, and thus the 1:1 adduct is afforded.

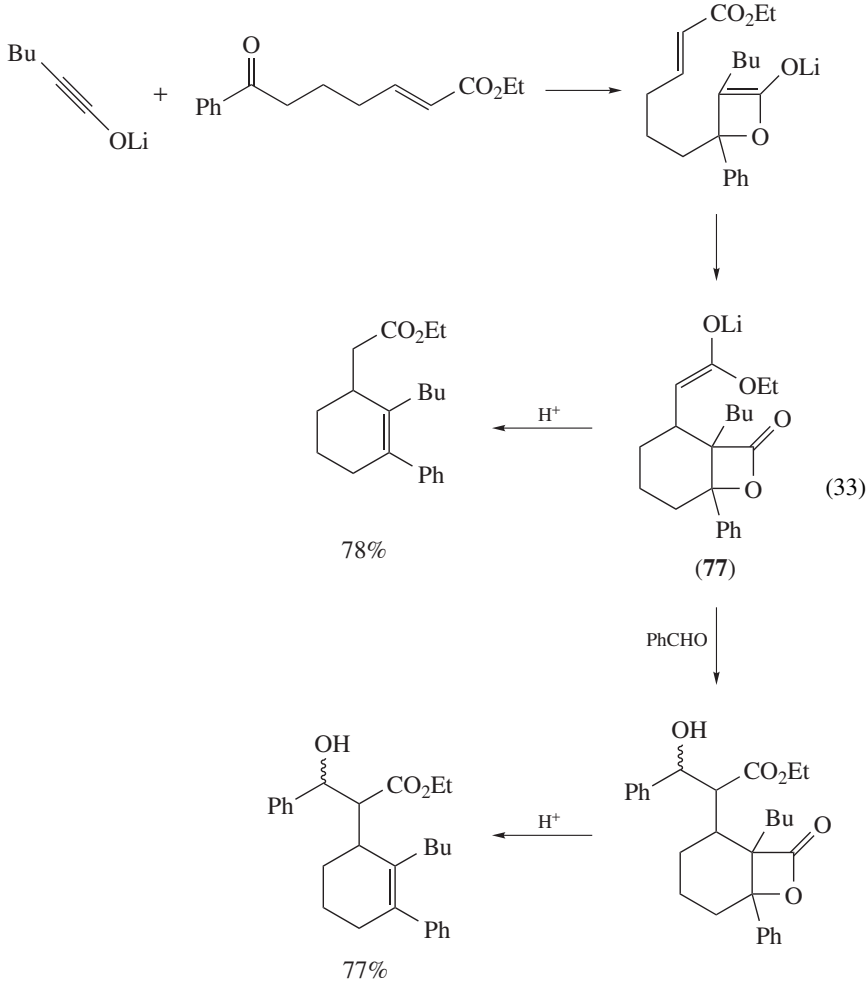

(33)

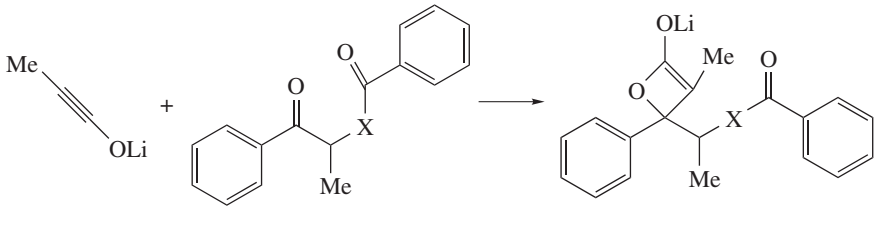

(**78**) (**a**) X = O
(**b**) X = S

(**79**) (**a**) X = O
(**b**) X = S

(34)

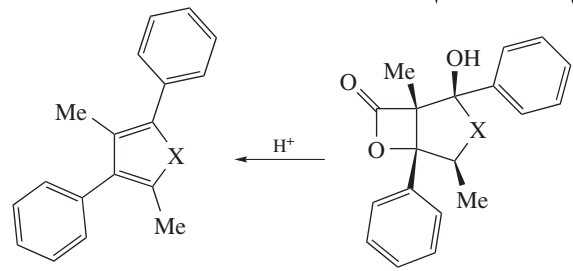

(**81**) (**a**) X = O (84%)
(**b**) X = S (85%)

(**80**) (**a**) X = O
(**b**) X = S

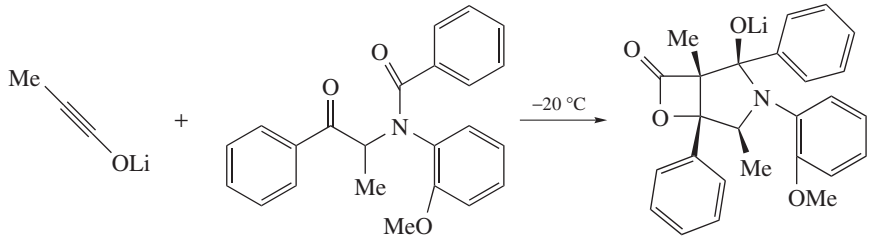

(35)

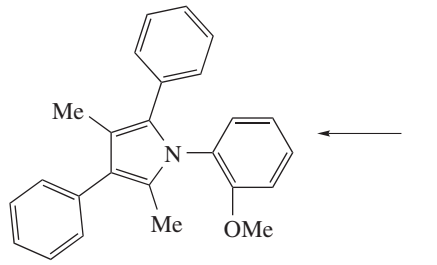

83%

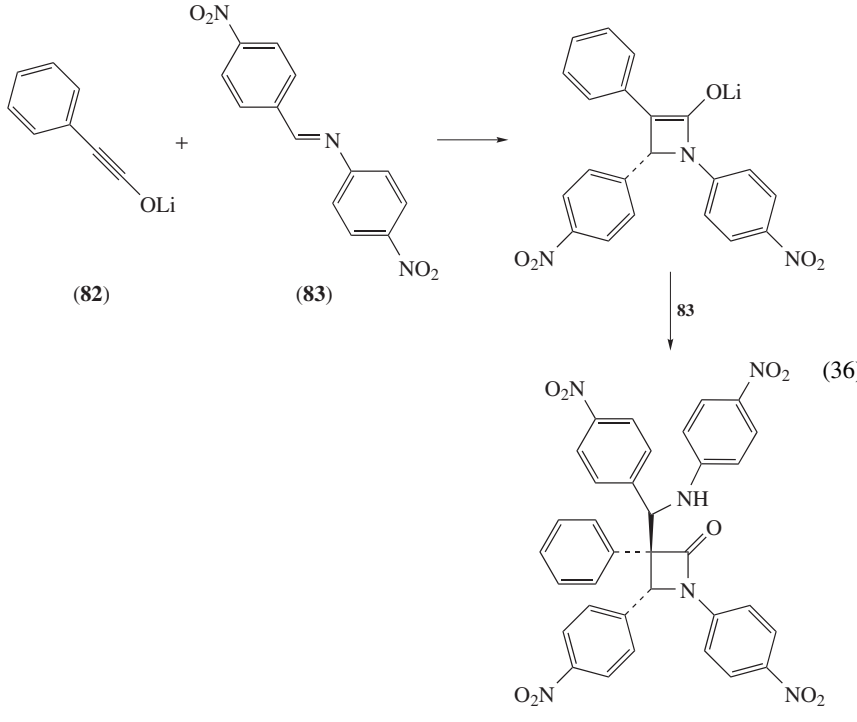
O2N
OLi
N
NO2
(82)
(83)
OLi
N
O2N
NO2
83
NO2
O2N
NH
O
N
O2N
NO2
(84) 89%

(36)

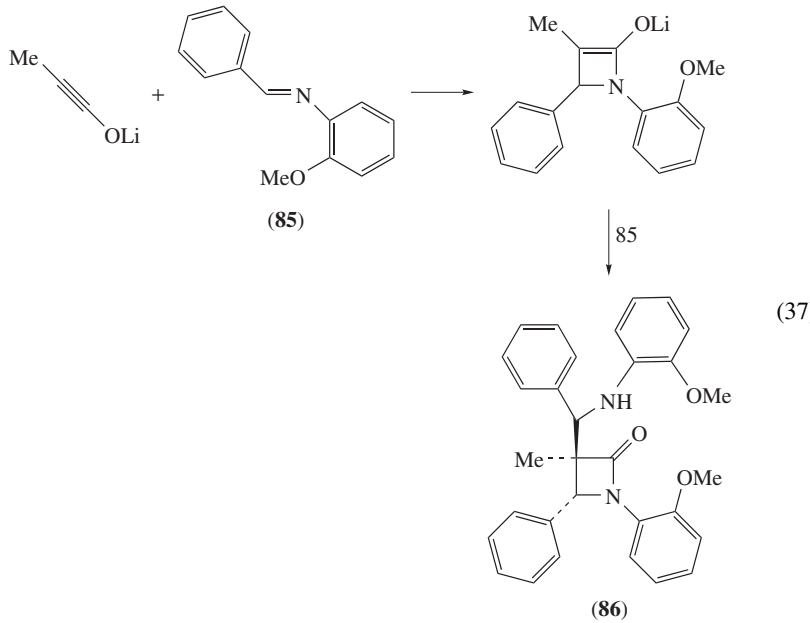
Me
OLi
N
MeO
(85)
Me
OLi
N
OMe
85
NH
OMe
O
Me
N
OMe
(86)

(37)

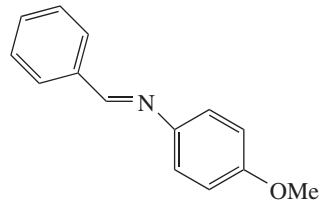

(**87**)

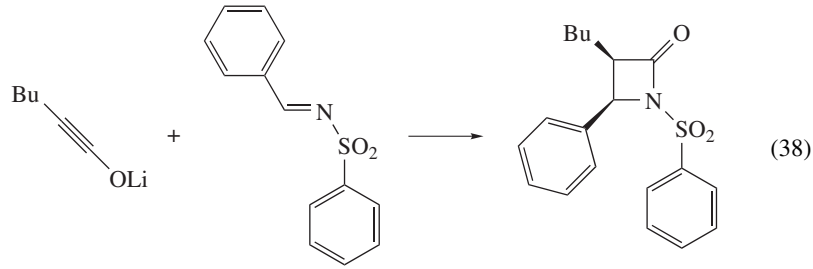

(**88**) (**89**) (**90**) (38)

D. Formal [2 + 2] Cycloaddition of Lithium Ynolates with Isocyanates to Give Azetidine-2,4-diones

Isocyanates are strong electrophiles having a C=N bond, and are used to synthesize heterocycles such as azetidine-2,4-diones[42]. Lithium ynolates add to sterically unhindered isocyanates, e.g. phenyl isocyanate (**91**) to give the azetidine-2,4-diones, such as **92** via formal [2 + 2] cycloaddition in moderate yield (equation 39)[43]. The sterically hindered 2,6-dimethylphenyl isocyanate (**93**) affords the ester **94** (equation 40). The 2,6-dimethylphenyl group would inhibit the cyclization leading to the four-membered ring, and instead lithium phenoxide, produced in the step of preparation of lithium ynolate, attacks the ketene. This result supports a stepwise mechanism of the four-membered ring formation using ynolates.

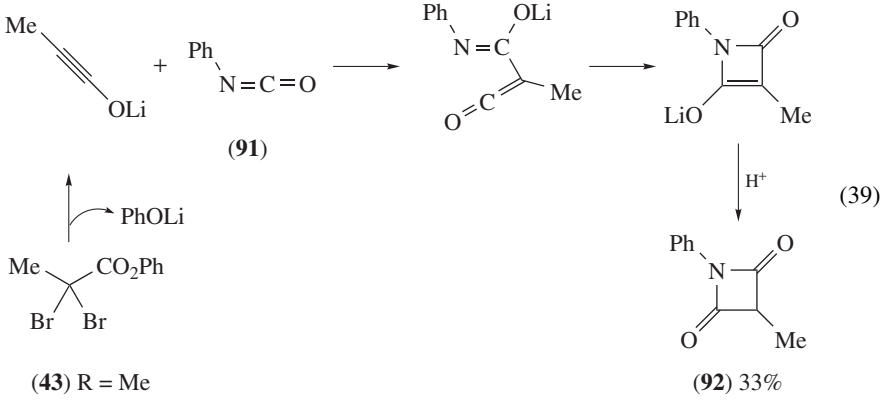

(**91**)

(**43**) R = Me

(**92**) 33% (39)

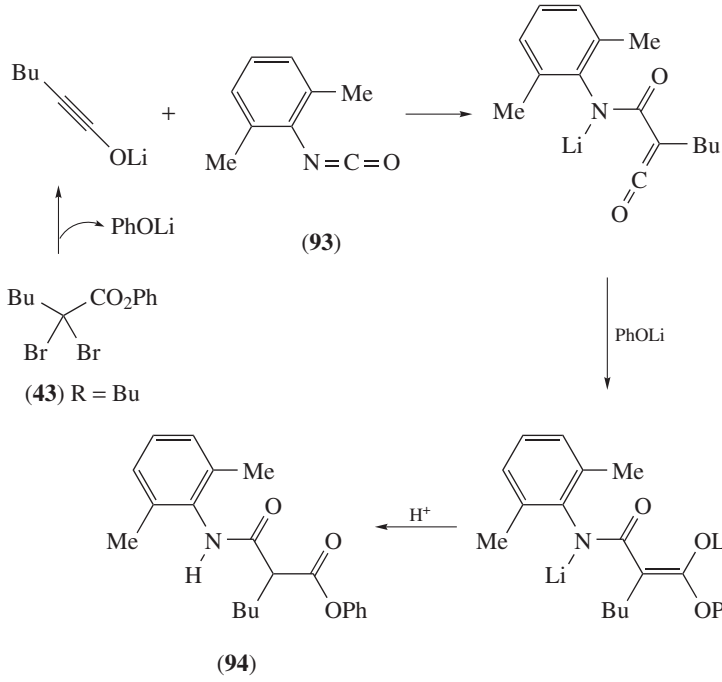

E. Formal [3 + 2] Cycloaddition of Lithium Ynolates with Nitrones to Give Isoxazolidinones

The [3 + 2] cycloaddition of 1,3-dipoles is an important method for preparing heterocyclic adducts, which may be transformed into a variety of other functionalized organic compounds. Most [3 + 2] cycloaddition of nitrones, representative 1,3-dipoles, can be classified into normal and inverse electron-demand reactions, based on the relative energies of the frontier molecular orbitals of the nitrone and the dipolarophile. The two cases are the interaction of a dipolarophile, having a low energy LUMO, with the HOMO of the nitrone, and the interaction of a dipolarophile, having a high energy HOMO, with the LUMO of a nitrone. Usually, these nitrones cycloadditions are a case of the reaction of an electron-deficient alkene (LUMO) with a 1,3-dipole (HOMO). In inverse electron-demand 1,3-dipolar cycloadditions, alkenyl ethers or ketene acetals are used as electron-rich dipolarophiles, occasionally requiring activation by Lewis acids. Lithium ynolates are expected to function as electron-rich dipolarophiles in the inverse electron-demand cycloaddition mode[44].

The anionic inverse electron-demand 1,3-dipolar cycloaddition of nitrones **95** with lithium ynolates (equation 41) proceeds at 0 °C to afford the substituted isoxazolidinones **97**. The relative configuration is determined during the protonation step of the initial isoxazolidinone enolate adduct **96**. With a thermodynamically controlled protonation, the *trans* products are mainly produced. The *in situ* alkylation of the resulting enolate adduct **96** furnishes the trisubstituted isoxazolidinone **98** with high diastereoselectivity. The isoxazolidinones are easily converted into β-amino acids (**99**, **100**) in good yield[45a].

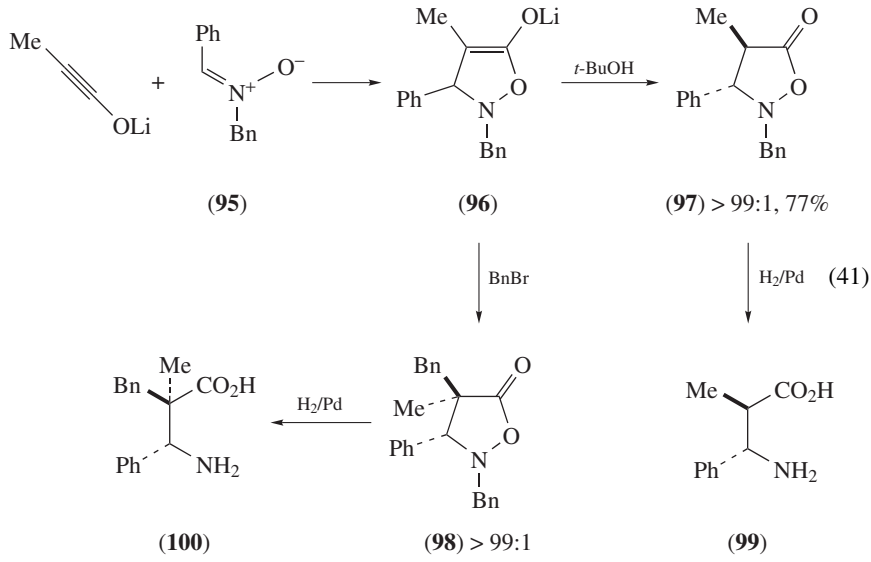

Asymmetric cycloadditions of the chiral non-racemic nitrones **101** and **103** afford the isoxazolidinones **102** and **104** respectively, with high diastereoselectivity. This process can lead to an efficient asymmetric synthesis of β-amino acids (equations 42 and 43)[45b,c]. This is the first example of asymmetric reactions with ynolates. It is noteworthy that the ynolates show higher reactivity and stereoselectivity than the corresponding lithium ester enolates and demonstrate the high potential of lithium ynolates in asymmetric reactions.

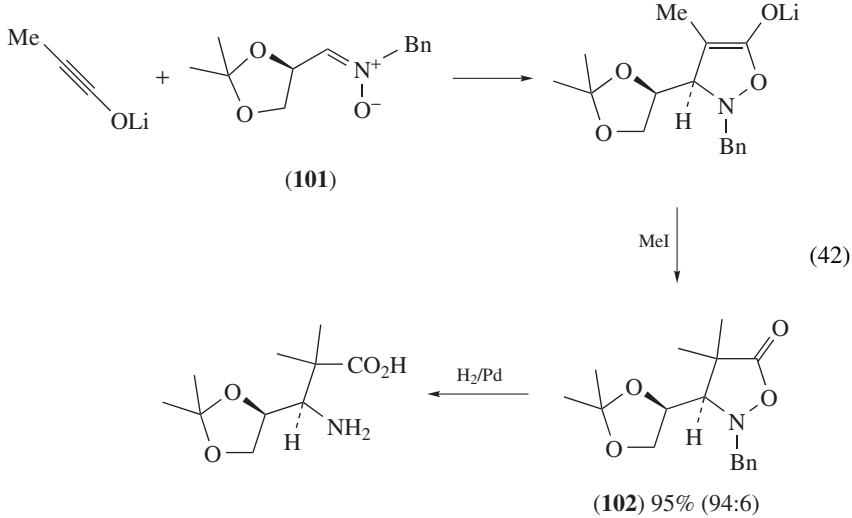

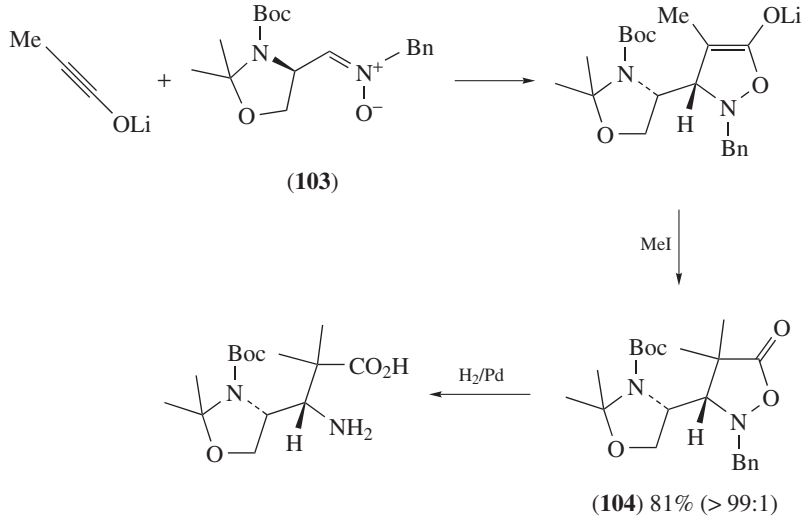

F. Formal [3 + 2] Cycloaddition of Metal Ynolates with Oxiranes and Aziridines to Give Lactones and Lactams

There has been only a few reports on reactions of small rings with metal ynolates. Oxiranes are much less electrophilic than carbonyls and sometimes need activation by Lewis acids or Lewis-acidic organometals. The lithium–trimethylaluminum ate complex of *silyl*-substituted ynolate **105** reacts with the oxirane **106** to give the γ-lactone **107** (equation 44)[8], while lithium silyl-substituted ynolates are inert to oxiranes. There have been no reports using carbon-substituted metal ynolates.

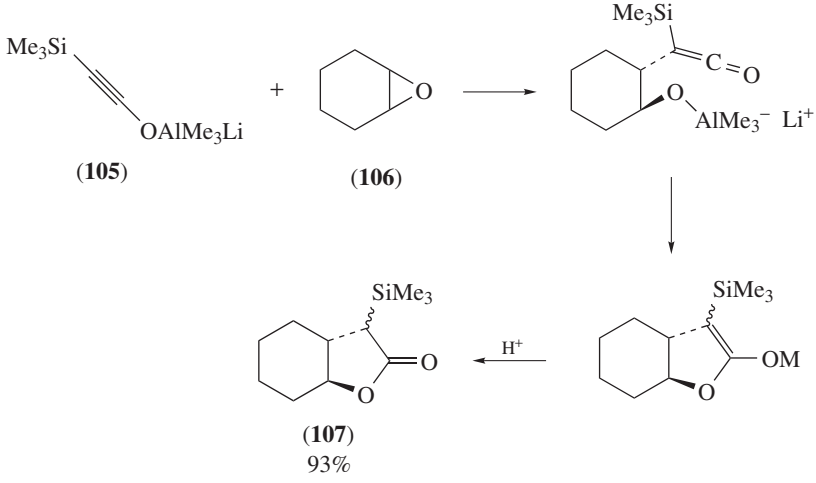

The γ-lactam **110** is prepared by the reaction of the lithium silyl-substituted ynolate **105** with the aziridine **108** activated by a *p*-toluenesulfonyl group. The initial product is the enolate **109,** which can be acidified to yield the α-silyl-γ-lactam **110**. Intermediate **109** can be trapped by aldehydes to afford the α-alkylidene-γ-lactams **111** via a Peterson reaction (equation 45)[46]. These reactions may be considered to be formal [3 + 2] cycloadditions as well as tandem reactions involving nucleophilic ring opening and cyclization.

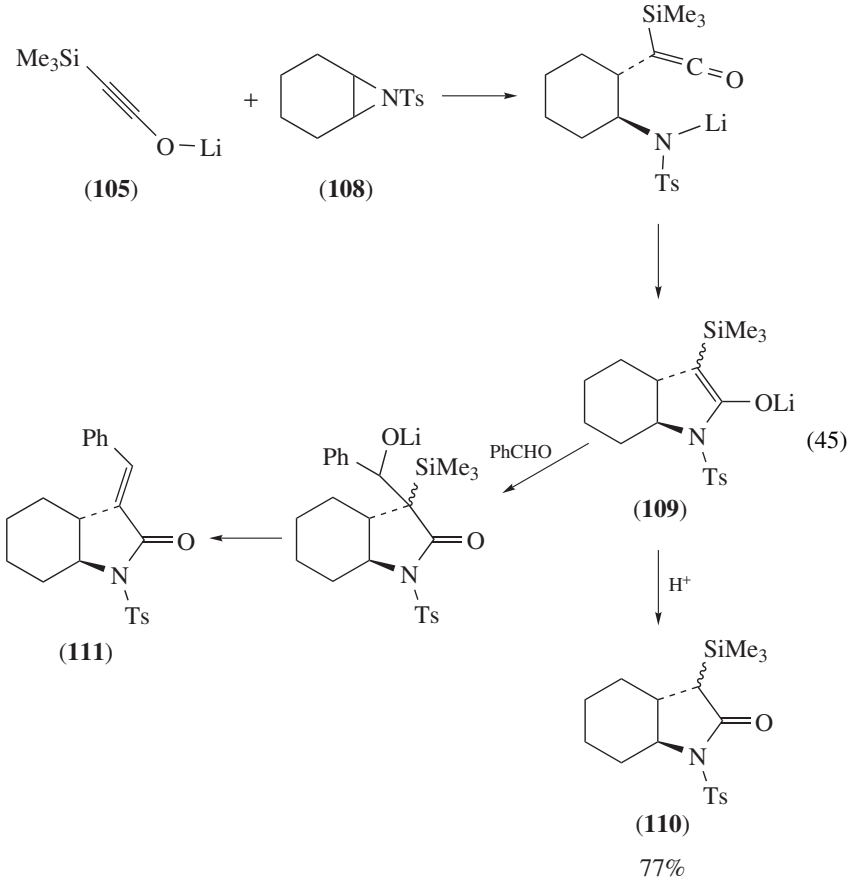

G. Formal [4 + 2] Cycloaddition of Metal Ynolates to Give Six-membered Heterocycles

Although the Michael addition of metal ynolates to α,β-unsaturated carbonyl compounds is expected to give six-membered cycloadducts, 1,2-addition to carbonyl groups usually precedes 1,4-addition. The cycloaddition of the lithium–aluminum ate complex of silyl-substituted ynolate **112** with ethyl benzylideneacetoacetate (**113**), which is doubly activated by the ester and keto functions, gives the γ-lactone **114** via a [4 + 2] type cycloaddition (equation 46). Diethyl benzylidenemalonate (**115**) affords the uncyclized ketene **116** by reaction with **112** (equation 47). This could be taken as evidence for a stepwise mechanism for equation 46[8].

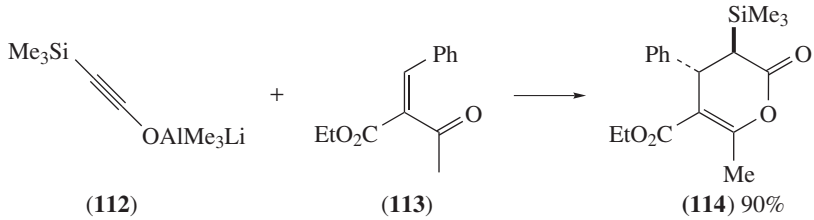

(**112**) (**113**) (**114**) 90% (46)

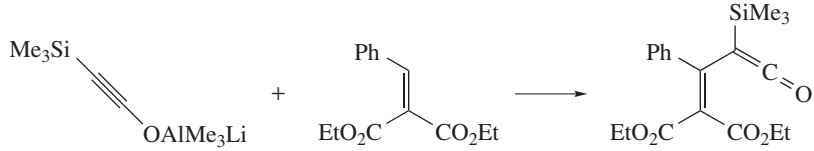

(**112**) (**115**) (**116**) 62% (47)

Styryl isocyanate (**117**) reacts with ynolates to provide the 4-hydroxypyridone **119** in moderate yield via a formal [4 + 2] cycloaddition (equation 48). This reaction also indicated the participation of the ketene intermediate **118**[43].

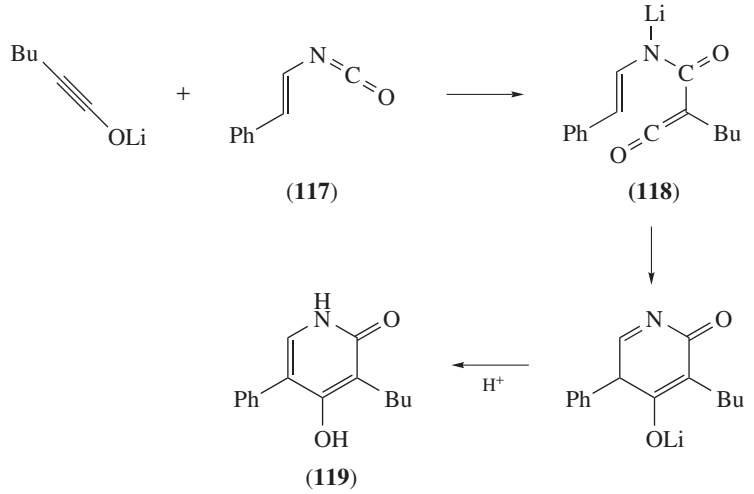

(**117**) (**118**) (48)

(**119**)

H. Formal [4 + 2] Cycloaddition of Lithium Ynolates to Vinylketenes to Give Phenols

While ketenes are too reactive to handle, silylketenes are exceptionally stable. Lithium ynolates (**120**) react with stable (trialkylsilyl)vinylketenes (**121**) to produce the highly substituted phenols **124** in a benzannulation strategy, via the ketenes **122** bearing (*Z*)-enolates. The latter undergo a 6π electrocyclic ring closure, not to β-lactone enolates but to afford the cyclohexadienones (**124**). The (*Z*)-configuration of the enolates **122** is important for the cyclization. On acidification, the cyclohexadienone intermediate **123** isomerizes to a siloxyphenol (**124**) via a 1,3-carbon–oxygen silyl shift and aromatization (equation 49)[47].

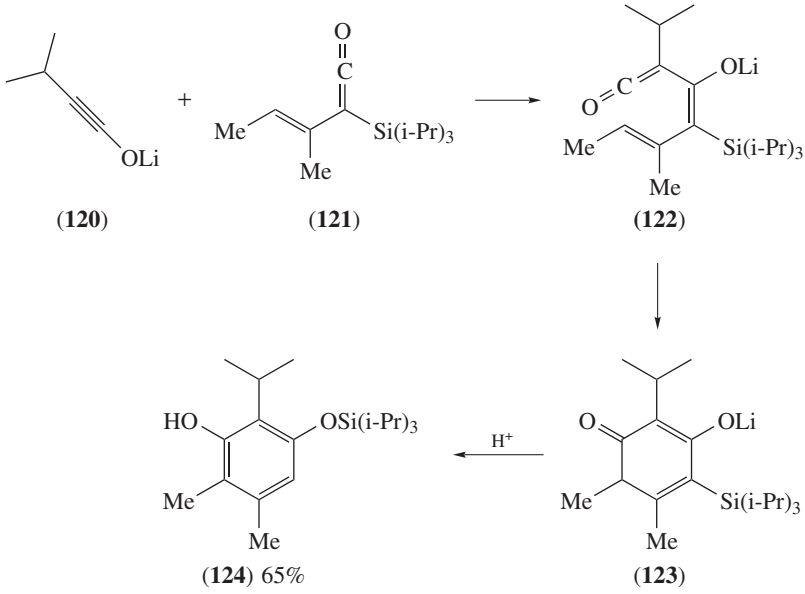

(**120**) (**121**) (**122**)

(**124**) 65% (**123**)

(49)

I. Torquoselective Olefination of Carbonyl Compounds

1. Torquoselective olefination of ketones

As described above, cycloaddition of lithium ynolates with aldehydes and ketones at −78 °C provides β-lactone lithium enolates, which are stable at −78 °C, but at higher temperatures (usually above −20 °C) the small rings are opened to give the α,β-unsaturated carboxylates[48]. Lithium ynolates add to benzaldehyde at −78 °C to give the β-lactone enolates **125**, which are ring-opened to afford the (*E*)-α,β-unsaturated carboxylic acids **126** after warming to room temperature[4]. The reaction of aldehydes with the lithium ynolate *at room temperature* affords the α,β-unsaturated carboxylic acids **126** in good yield with excellent *E*-selectivity (equation 50). This process may involve a side reaction by which intermediate **125** undergoes addition to a second benzaldehyde molecule to yield **127**, in an aldol–retroaldol equilibrium (equation 50′)[49a].

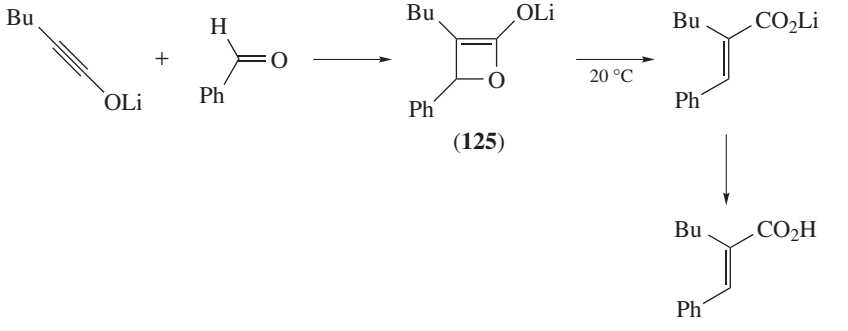

(**125**)

(**126**) 73%, *E*/*Z* > 99

(50)

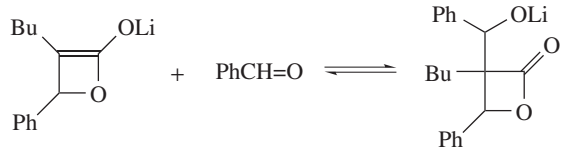

(**125**) (**127**) (50')

Stereoselective olefination of ketones giving tetrasubstituted alkenes is at present a hot topic in synthetic organic chemistry, because there have been very few reports on successful stereoselective olefination of ketones giving tetrasubstituted olefins. Olefination of unfunctionalized ketones such as acetophenone (**128**) with lithium ynolates provides tetrasubstituted olefins (**129**) in good yield (equation 51). While the Wittig and the Horner–Emmons reagents do not react with *t*-butyl phenyl ketone (**130**), the ynolate affords the corresponding olefin (**131**) in 74% yield (equation 52). These results indicate that ynolates are much better reagents for the olefination of ketones than the conventional ones. The geometrical selectivity (80:20 to 85:15) is unprecedentedly good (equation 53). In most cases, the phenyl group is preferentially *trans* to the carboxylate group, and the alkyl groups are *cis* to it. Methyl esters can be isolated by adding MeI along with HMPA or DMPU to the reaction mixture without loss of selectivity or yield[49a,b].

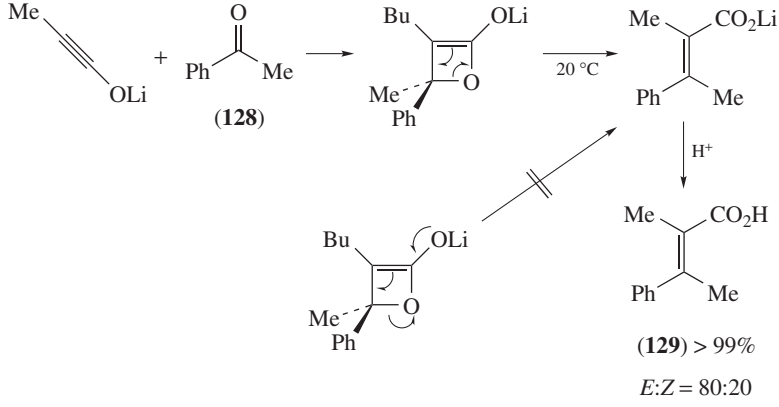

(51)

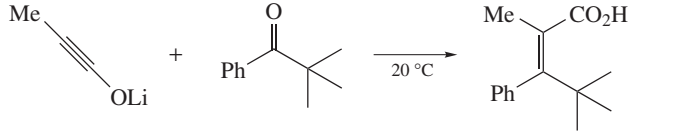

(52)

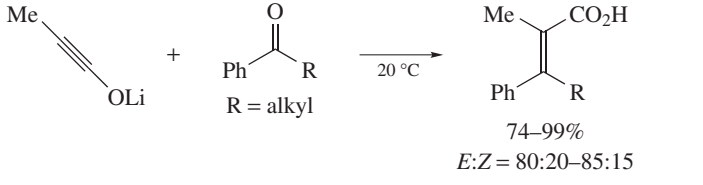

(53)

TABLE 1. Stereoelectronic effect of *para*-substituents on the olefination of acetophenones and benzophenones

	Acetophenones p-XC_6H_4COMe		Benzophenones p-XC_6H_4COPh	
X	Yield (%)	E:Z	Yield (%)	E:Z
NO_2	61	40:60	92	25:75
Cl	68	70:30	92	40:60
F	88	80:20	>99	50:50
H	82	85:15	82	—
Me	89	91:9	90	60:40
MeO	80	95:5	99	67:33
Me_2N	64	>99:1	90	83:17

The E/Z-selectivity of this olefination (equation 54) is strongly dependent on the electronic nature of the substituents (X) of the ketones (Table 1)[49c]. The acetophenones with electron-withdrawing groups at the *para*-position give lower E-selectivity, as compared to the unsubstituted compounds (X = H). On the other hand, substrates with electron-donating groups afford higher E-selectivity (up to >99:1). In the olefination of *para*-substituted benzophenones (R = Ph), in which the steric factor can be negligible, the same trend in the selectivity is observed. It is noteworthy that phenyl substituents are recognized only by remote *para*-substituents. The stereochemistry is controlled by a stereoelectronic, as well as by a steric, effect of the substituents.

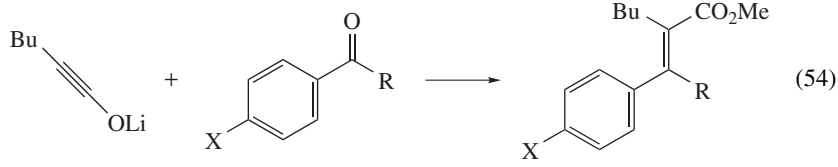

(54)

The mechanism of the ring opening of the β-lactone enolates (e.g. equation 51) is the conrotatory electrocyclic reaction of the oxetene[50], rather than the 'forbidden' β-elimination[47], and thus torquoselectivity would be operative in the selectivity[51]. Thermal ring opening of cyclobutenes (equation 55) giving butadienes has been well studied experimentally[52,53] and theoretically[54]. In this reaction, the E/Z selectivities are determined by the torquoselectivity, thus, preferentially, the electron-donating substituents (**D**) rotate outward and the electron-accepting substituents (**A**) rotate inward. The torquoselectivity is explained by the orbital interactions between the breaking C–C bond and some bond orbitals on the substituents (**132**). This concept provides a reasonable explanation for the olefination with lithium ynolates. By theoretical calculations on the transition states, the strong interactions between the disconnecting C–O σ orbital in the oxetene and the π (π^*) orbitals of the aromatic ring in the transition states are revealed[55]. Since the phenyl group has an electron-rich π-orbital, i.e. a high energy level of the occupied orbital, it is a better electron-donating group than the alkyl group. The electronic properties, however, depend on the substituents. For examples, the p-nitrophenyl substituent works as an electron acceptor in torquoselectivity. The transition state leading to the Z-olefins is stabilized by the overlap of the orbitals of the disconnecting C–O bond with the π- or π^*-orbitals, in which the energy level of the antibonding orbital is lowered by the electron-withdrawing substituents (**133**). The σ^* orbitals are also important acceptors in the torquoselectivity[56].

Since the $\sigma^*(C-CH_3)$ orbital is reported to be more electron accepting than $\sigma^*(C-H)$[57], the *t*-butyl group rotates inward preferentially (**134**)[58].

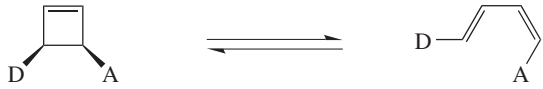

(55)

D: electron-donating group
A: electron-accepting group

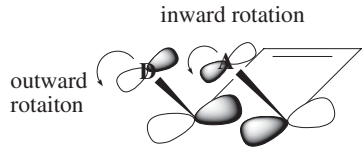

(**132**)

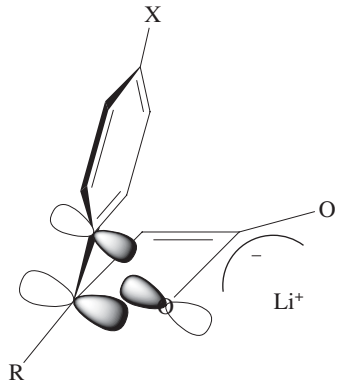

(**133**)

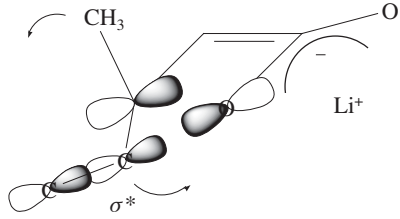

(**134**)

2. Torquoselective olefination of acylsilanes

Olefination of acylsilanes[59] is expected to become a useful method for the preparation of vinylsilanes, which are a powerful synthetic tool[60]. Olefination of the acylsilanes **135** with ynolates provides the β-silyl-α,β-unsaturated esters **136** in high yields with high *Z*-selectivity (equation 56)[61]. In most cases, the *E* isomers could not be detected by ^1H NMR and HPLC. This is the first general method for the stereoselective synthesis of tetrasubstituted olefins.

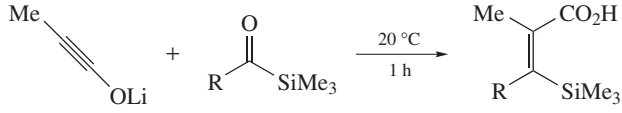

(56)

(**135**) (**136**)

R = alkyl, aryl
Z/*E* = >99

Theoretical calculations and NBO analysis suggest that this remarkable torquoselectivity is due to orbital interactions of the breaking σ(C–O)–σ*(Si–C) (**137**) in the transition state of the inward rotation during the ring opening of the β-lactone enolate. The interaction between the nonbonding orbital of oxygen and σ*(Si–C) also contributes the stabilization of that transition state (**138**)[58]. This is in good agreement with the results obtained from the ring opening of silylcyclobutenes[56].

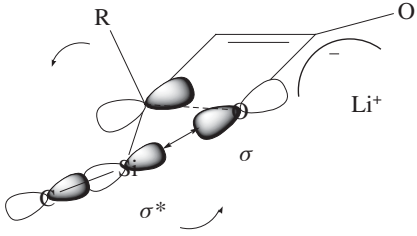

(**137**)

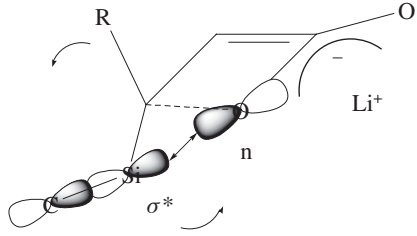

(**138**)

The importance of the torquoselective synthesis shown in equation 56 is illustrated in equations 57 to 59, for the particular case in which a multisubstituted vinylsilane (**139** = **145** = **148** = **136**, R = Bn) is converted to various kinds of multisubstituted olefins. The silyl-substituted allyl alcohol **140** is allylated to give the skipped diene **141**[62], and the iodoalkene **142**, prepared by desilyliodination of **140**[63], is subjected to metal-catalyzed cross-coupling reactions to afford the dienes **143** and **144** without *E*/*Z* isomerization (equation 57). The vinylsilane **145** thus reacts with iodine to afford the silalactone **146** with elimination of iodomethane in good yield (equation 58)[64]. Since the silicon–carbon bond is activated by the hypervalency, the C–Si bond is cleaved under mild conditions via a push–pull mechanism (**147**). The palladium-catalyzed cross coupling of the vinylsilane **148** with aryl iodides (Hiyama coupling) is also activated by hypervalency to give the coupling product **149** (equation 59) without using fluoride ion, while the inactivated vinylsilane **150** does not react[65].

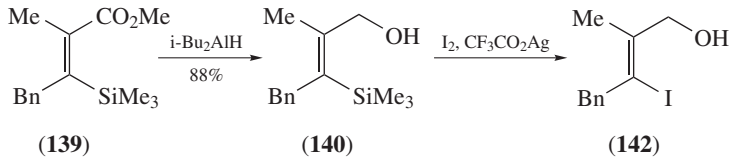

(**139**) (**140**) (**142**)

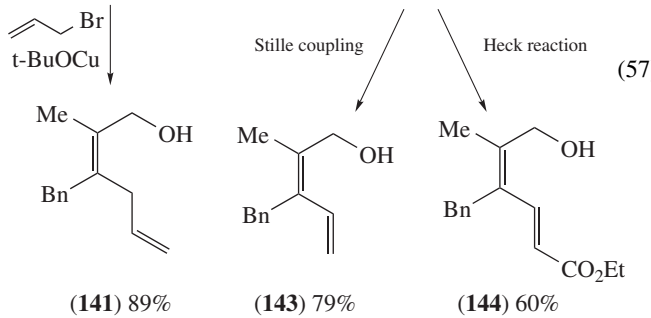

(57)

(**141**) 89% (**143**) 79% (**144**) 60%

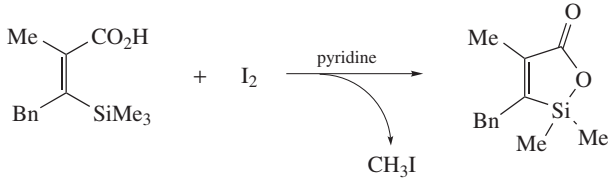

(58)

(**145**) (**146**) 90%

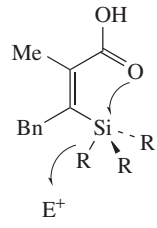

(**147**)

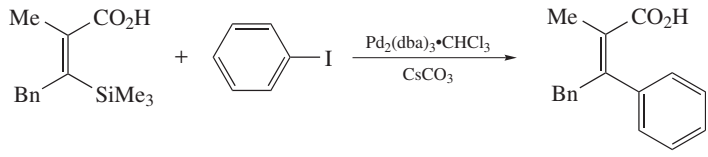

(59)

(**148**) (**149**) 72%

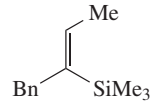

(**150**)

3. Olefination of α-oxy and α-amino ketones

Good stereocontrol in the olefination of ketones with metal ynolates requires that groups of quite different bulkiness and/or electronic properties be attached to the carbonyl group. Such is the case of the acylsilanes, whereas simpler ketones like 2-butanone are less stereospecific in this process. If both substituents on the ketones should be distinguished, strong stereocontrolling directing groups for olefination are requisite in the ketones. The α-alkoxy (**151a**) and α-trialkylsilyloxy (**151b**) acyclic ketones provide the olefins **152a** and **152b,** respectively, with high *Z*-selectivity by the torquoselective olefination with ynolates (equation 60). The α-trialkylsiloxy cyclic ketones (**153**) afford the olefins **154** with good to moderate stereoselectivity (equation 61). This selectivity depends on the conformation of the siloxy group; for example, the axially oriented siloxy group induced a high *Z*-selectivity (equation 62) but the equatorially oriented group did not (equation 63). In a similar fashion, olefination of α-amino ketones also induces good *Z*-selectivity. As shown in equation 64, the reaction of the ynolates with the α-amino ketone **155** gives the γ-amino unsaturated carboxylate, which is treated with thionyl chloride to provide the unsaturated lactam **156** in good yield, without any detection of minor isomers[66].

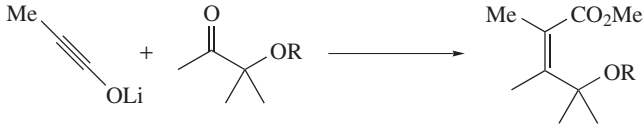

(60)

(**151**) (**a**) R = alkyl
(**b**) R = trialkylsilyl

(**152**) (**a**) R = alkyl, *Z/E* >99:1–98:2
(**b**) R = trialkylsilyl, *Z/E* >99:1–94:6

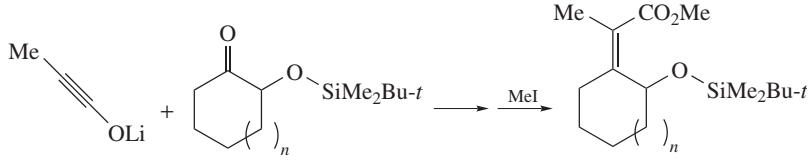

(61)

(**153**)

(**154**)

n = 1, *Z*:*E* = 83:17
n = 2, *Z*:*E* > 99:1
n = 3, *Z*:*E* = 97:3

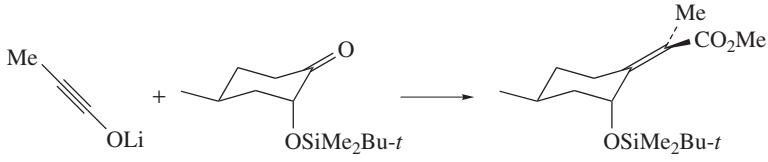

(62)

Z:*E* = 94:6

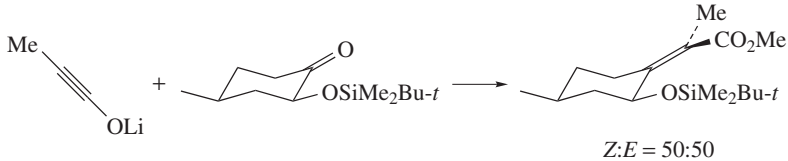

(63)

Z:*E* = 50:50

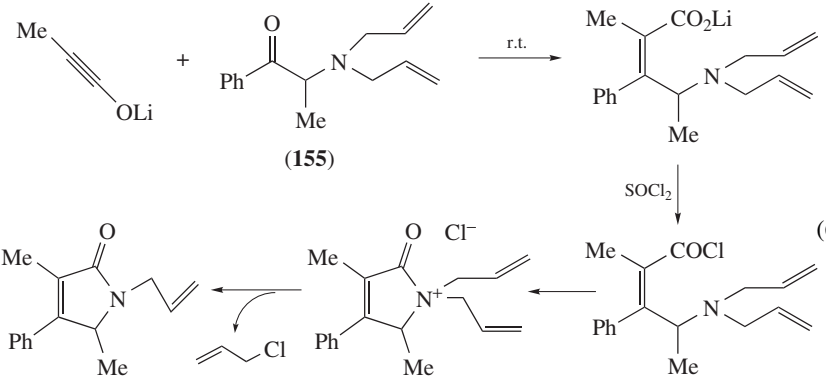

(64)

The mechanism of olefination can be deduced by consideration of orbital interactions to proceed via torquoselective olefination, rather than chelation control, for the following reasons: (1) the sterically hindered siloxy and phenoxy groups are also effective for high *E*-induction; (2) in the presence of a crown ether, the selectivity still remains high; and (3) an axially oriented siloxy group induces a high *Z*-selectivity. Theoretical calculations indicate that the transition state of inward rotation is stabilized by an orbital interaction between σ(C–O) and σ*(C–OR) (**157**)[66].

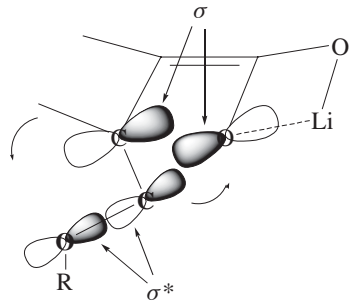

(**157**)

4. Olefination of esters

Olefination of ester carbonyl groups with metal ynolates is useful for the synthesis of enol ethers, as other methods have generally been unsuccessful in realizing olefination, due to the lower reactivity of the esters and the elimination of alkoxide. Metal carbenoids, such as Tebbe reagents, accomplish this transformation, but they are limited to the preparation of simple unfunctionalized enol ethers. The highly stereoselective synthesis of tetrasubstituted, functionalized (*E*)-enol ethers **159** via olefination of esters **158** with lithium ynolate is achieved (equation 65). Aliphatic esters afford excellent *E*-selectivities, whereas esters of aromatic carboxylic acids give good to moderate selectivity, which depends on the electronic properties of the substituents on the aromatic ring. This torquoselectivity can be elucidated from the fact that the ethoxy group preferentially rotates outwardly, because of its electron-donating property[67]. The enol ethers thus produced can be very useful in synthetic organic chemistry. For example, using β-alkoxy divinylketones **160** derived from enol ethers (**159**) in 3 steps using TBTU (**159′**) as condensing agent, a novel catalytic Nazarov reaction is reported to yield α-alkoxycyclopentenones **161** (equation 66)[68].

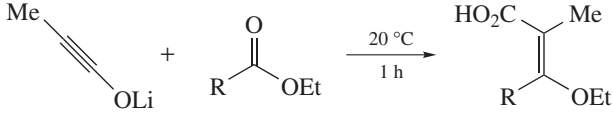

(**158**) (**159**) (65)

R = alkyl, *E*:*Z* = >99:1
R = aryl, *E*:*Z* = 77:23–99:1

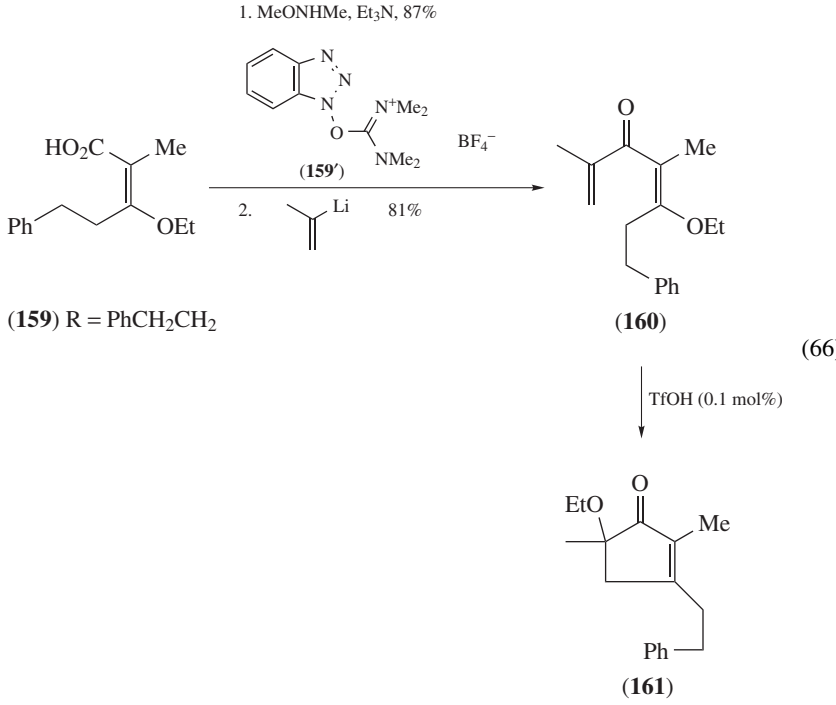

(66)

5. Homologation of thioesters

The reaction of thiol esters with lithium ynolates (equation 67) takes place by a route different than the one shown in equation 65 for alcohol esters. Thiol esters (**162**) undergo a two-carbon homologation to β-keto thiol esters **165′** in good yield. Intermediates **163** undergo a two-step rearrangement to a β-keto thiol ester enolate (**165**), via elimination of lithium thiolate to yield a ketene (**164**), followed by the nucleophilic attack of the thiolate on **164**. Finally, the homologated β-keto thioester (**165′**) is obtained on acidification of the reaction mixture[67].

6. Torquoselective olefination of aldimines

A silyl-substituted ynolate (**166**) undergoes cycloaddition to *N*-sulfonyl aldimines (**167**), followed by ring opening, to afford the α,β-unsaturated amide **168** at 20 °C (equation 68). This stereoselectivity is unusual for the torquoselective olefination. The steric interaction between bulky Me_3Si and the phenyl groups may be critical. *N*-*o*-Methoxyphenylaldimines (**170**) with ynolates (**169**) at room temperature produce α,β-unsaturated amides (**171**) in good yield with high *E*-selectivity (equation 69). Since the 2:1 adduct **172** can be detected during the reaction, the process certainly involves the retro-Mannich reaction. The processes depicted in equations 68 and 69 are torquoselective olefinations[69].

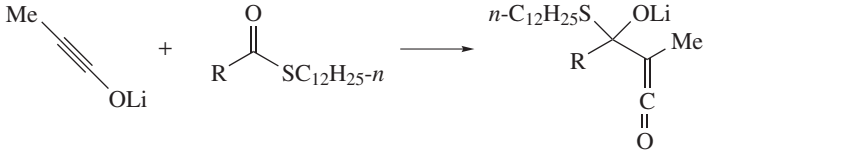

(**162**) (**163**)

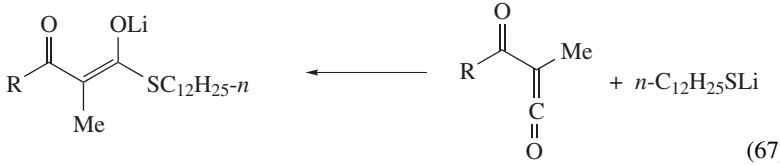

(67)

(**165**) (**164**)

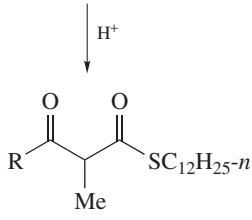

(**165′**)

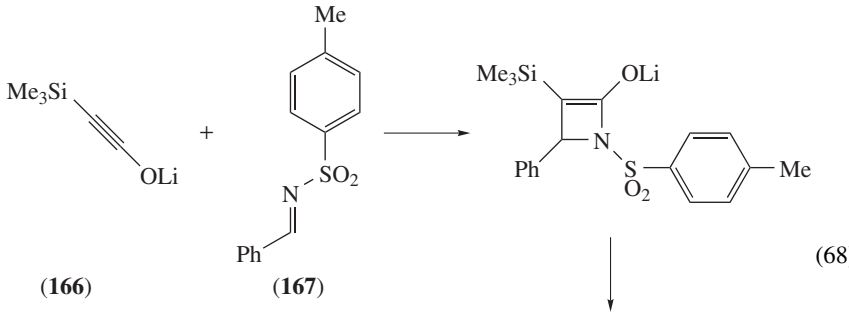

(**166**) (**167**) (**168**) 68% (*E* only)

(68)

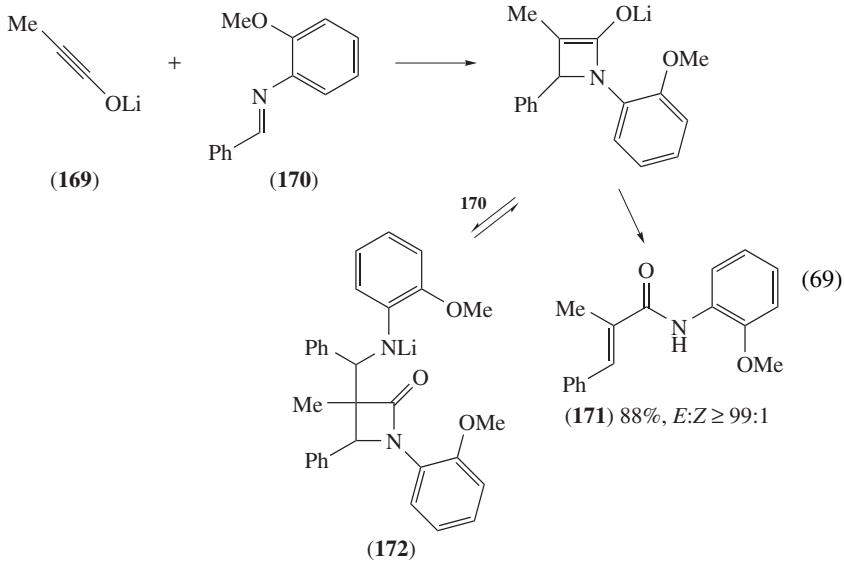

(**169**) (**170**) (**171**) 88%, $E{:}Z \geq 99{:}1$ (**172**) (69)

J. Reductive Conversion of Lithium Ynolates to Lithium Enolates

The partial reduction of the triple bond of lithium ynolates **173** by activated LiH provides the lithium *E*-enolates **174** derived from aldehydes (equation 70)[70]. This is a useful reaction, since these enolates of aldehydes are not easily prepared by the usual base treatment of aldehydes. Activated LiH is prepared *in situ* from cyclohexa-1,3-diene and lithium tetramethylpiperazide or from cyclohexa-1,3-diene and BuLi. The superactive LiH, prepared from hydrogen with BuLi-tetramethylethylenediamine, can also be used[71].

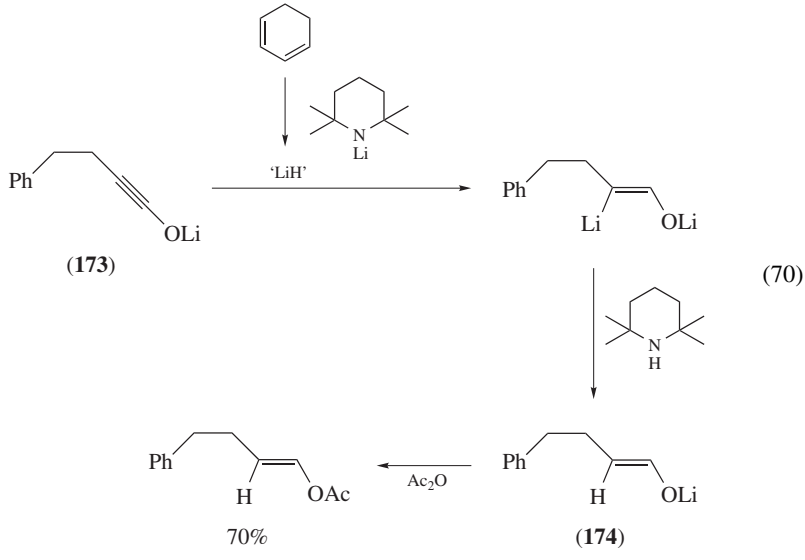

(**173**) (**174**) 70% (70)

V. PREPARATION OF SILYL YNOLATES

Since silyl ynol ethers have an electron-rich triple bond, they are useful for Lewis acid catalyzed synthetic reactions. Lithium ynolates **175** are silylated by TIPSCl or TIPSOTf and TBSCl to afford the corresponding silyl ynol ethers **176** and **177**, which are thermally stable and isolable, but sensitive toward acids (equation 71)[13, 72]. See also equations 9 and 10 in Section II.C. An experimentally improved procedure for the purification of **176** derived from Kowalski's method is described[73]. Lithium ynolate derived from Julia's method is also used for the preparation of **176**[74]. TMSCl and TESCl provide silyl ketenes **179**, however, by C-silylation. These small silyl chlorides primarily gave the silyl ynol ethers **178**, but, upon warming the reaction mixture, isomerization to the more stable silyl ketenes takes place. The soft electrophilic silyl chlorides like Ph_3SiCl afford silyl ketenes[22]. Disilyl ynol ethers, prepared from ynolate dianions, are rearranged to disilylketenes mediated by salts[26].

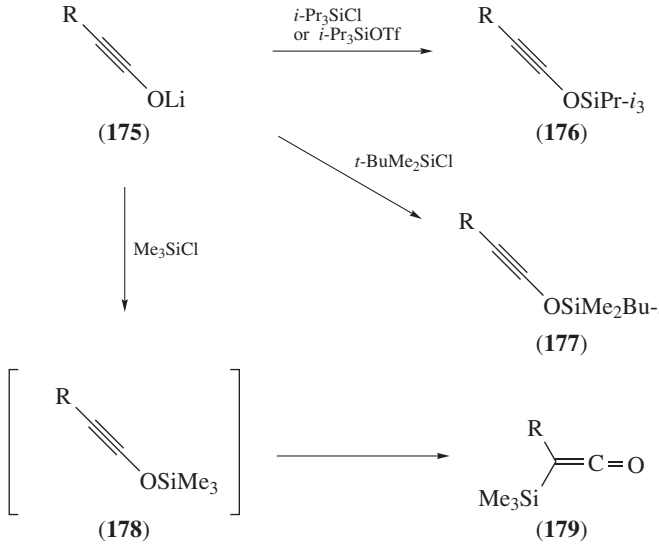

(71)

VI. REACTIVE HETEROATOM ANALOGUES OF METAL YNOLATES

Metal ynamines (metal ynamides, **180)** are aza-analogues of metal ynolates and have not been studied as well as the ynamines (**181)**[75], in spite of being much more reactive than the latter. 1,4-Diphenyl-1,2,3-triazolyllithium (**183**), prepared by lithiation of 1,4-diphenyl-1,2,3-triazole (**182**), is converted into lithium ynamine (lithium ynamide) (**184**) on thermal elimination of nitrogen (equation 72). This ynamine (**184**) is methylated in moderate yields either by methyl iodide to give a ketenimine (**185**) and a dimerization product (**186**), or

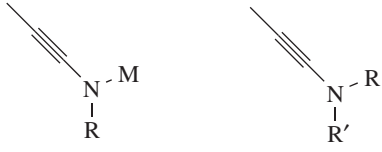

(**180**) (**181**) R, R′ = H, alkyl, aryl

by dimethyl sulfate to the *N*-methylated ynamine **187** (equation 73). Acylation of **184** can be accomplished according to equation 74 either with phenyl isocyanate to a uracil derivative (**188**), or with methyl chloroformate to an ynamide (**189**)[76].

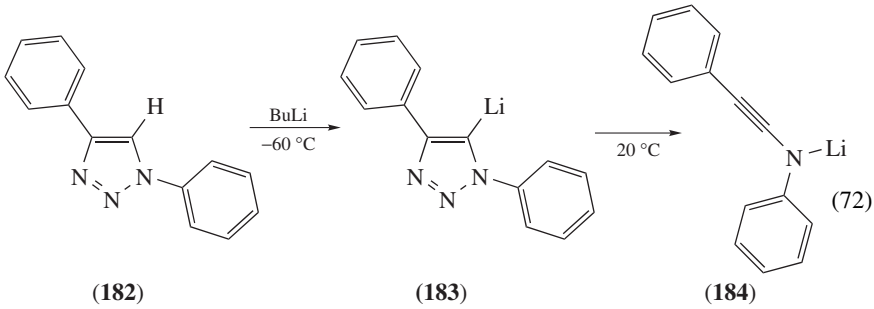

(**182**) (**183**) (**184**) (72)

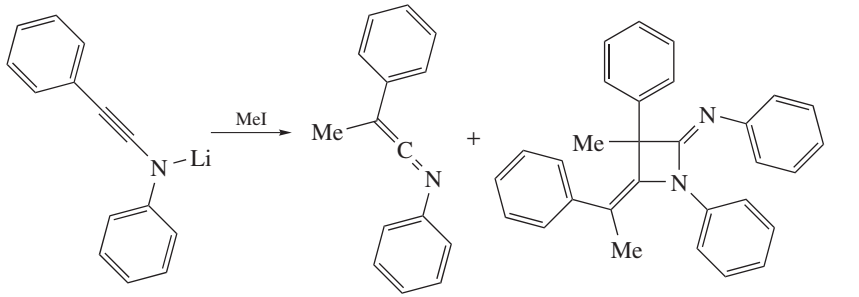

(**184**) (**185**) ~45% (**186**) (73)

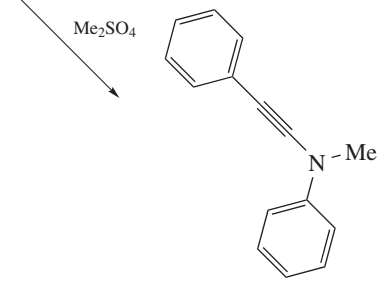

(**187**) 42%

The silylated lithium ynamine **192** is generated by metallation with BuLi of *S*-methyl *N*-phenyl-trimethylsilylethanimidothioate (**190**), via a ketenimine intermediate (**191**), as shown in equation 75. The interconversion between **191** and **192** can be discerned by silylation taking place at both the *N*- and C_β-positions to afford the *N*-silylynamide **193** and the bis(β-silyl)ketenimine **194**. In equation 76 are shown three possible synthetic

applications for **192**: with a dialkyl chlorophosphate to give the *N*-phosphorylated ynamine **195** in moderate yield; the ynamide **196** is formed with acetyl chloride in good yield; and reaction with propylene oxide affords the *N*-alkylated ynamine **197**[77].

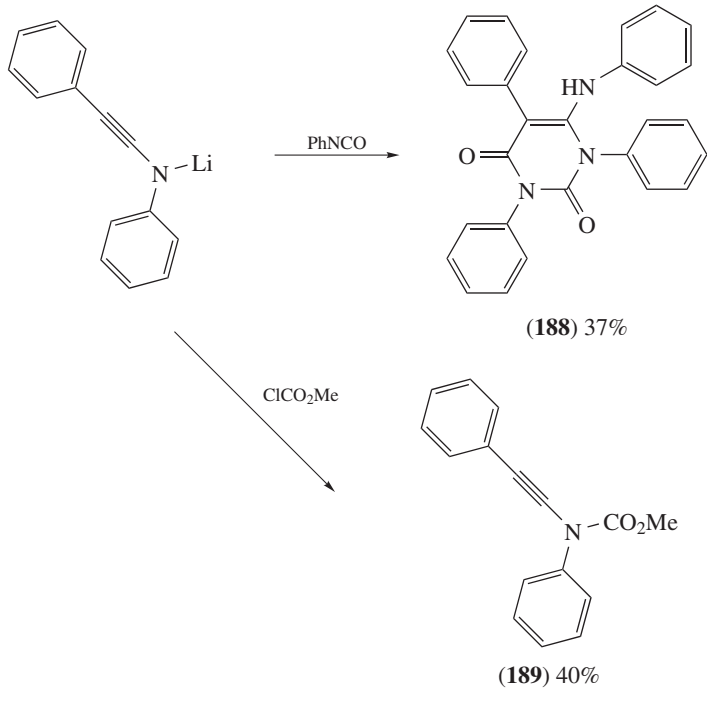

(74)

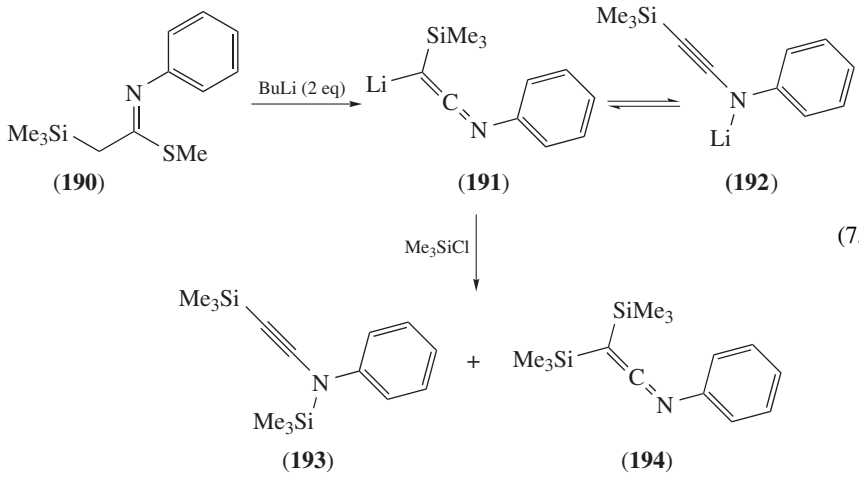

(75)

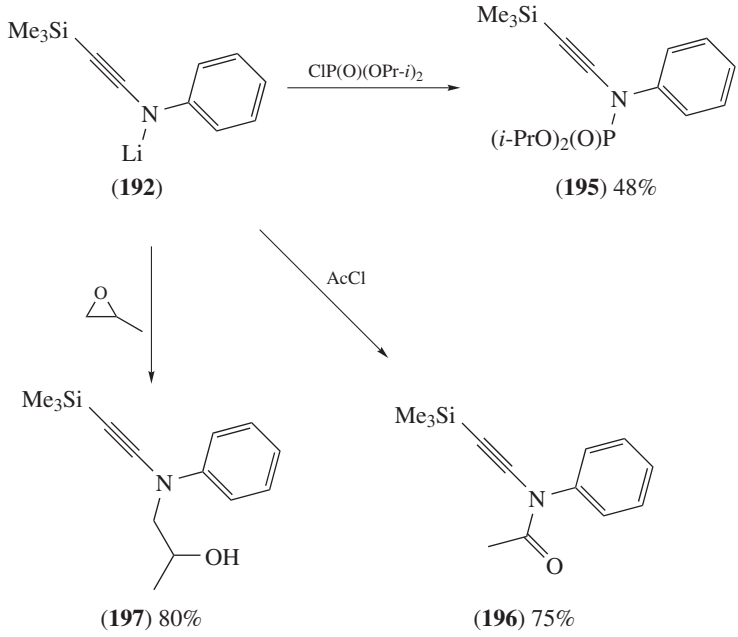

(76)

S-Analogues of lithium or sodium ynolates (thioalkynolates or alkynethiolates) are prepared from lithium or sodium acetylide and sulfur, and are trapped as alkynyl sulfides with bromoethane (equation 77)[78]. In a synthetic approach analogous to equation 72, 5-lithio-1,2,3-thiadiazoles (**198**) also afford lithium alkynethiolates (**199**) by elimination of nitrogen (equation 78)[79]. Alkynyl sulfides (**200**) are treated with lithium in ammonia to afford lithium alkynylthiolates (**199**) (equation 79)[80]. Theoretical studies on the structure of alkali metal alkynylthiolates are reported[81].

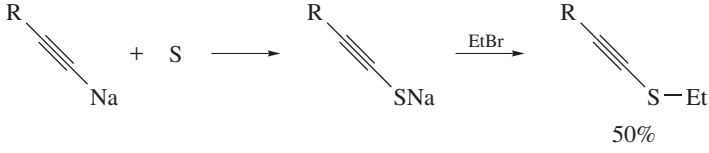

(77)

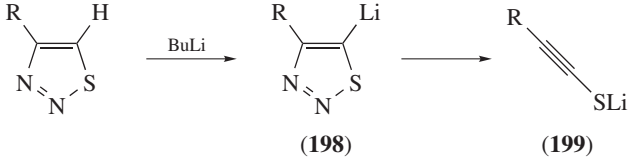

(78)

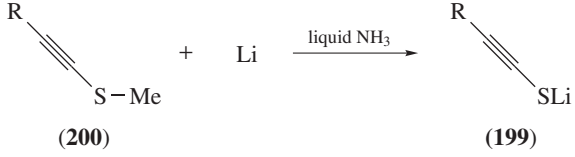

(79)

Nucleophilic reactions of lithium thioalkynolates with electrophiles mostly occur at the *S*-position to afford alkynyl sulfides. For example, *S*-silylation and *S*-stannation are shown in equation 80; the synthesis and *S*-alkylation of a quaternary ammonium thioalkynolate are shown in equation 81[82]. Exceptionally, lithium thioalkynolates add to ketones to form β-thiolactones, which are converted into alkenes on elimination of carbon oxysulfide (equation 82). Contrary to lithium ynolates, thioalkynolates do not react with aldehydes[83].

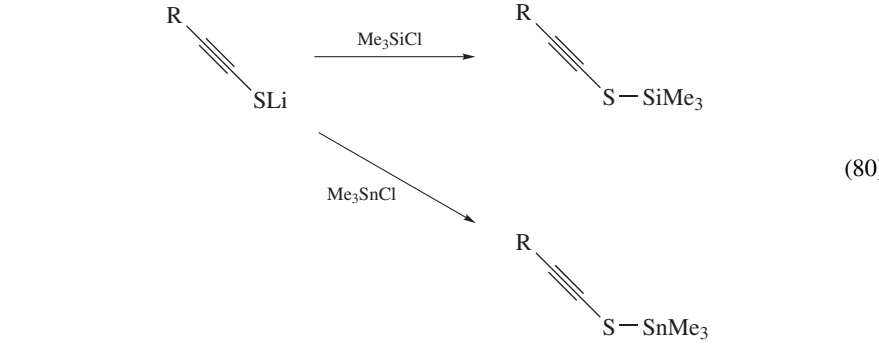

(80)

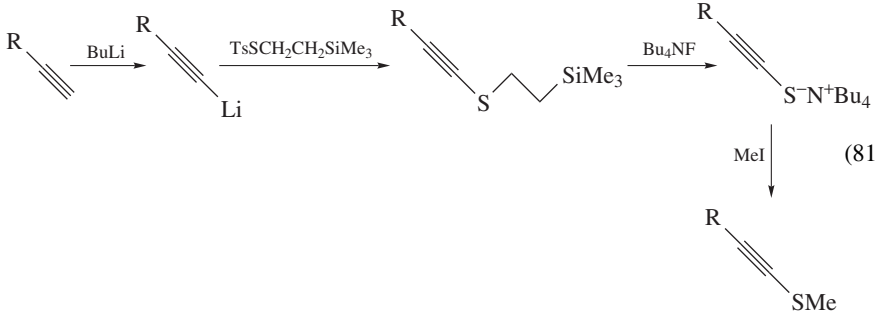

(81)

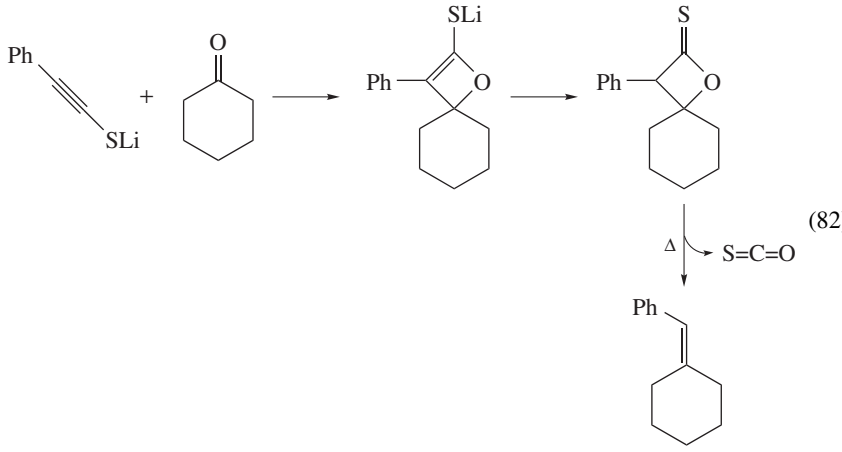

(82)

Selenium analogues of lithium ynolates are prepared by methods similar to those used to prepare sulfur analogues[78b]. Theoretical studies show that the negative charge is distributed over the whole molecule but is predominantly located on the selenium atom. The HOMO in the methyl-substituted case (**201**) has the largest coefficient on the C_β atom; the largest HOMO coefficient of the phenyl-substituted one (**202**) is on the selenium atom[84].

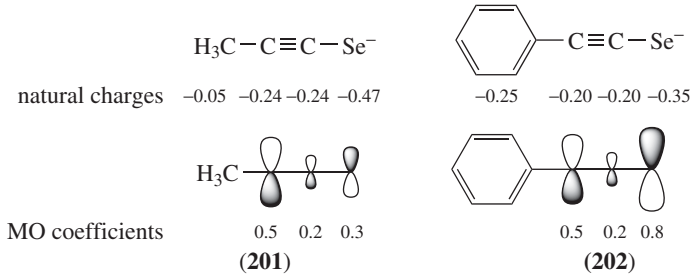

(**201**) (**202**)

Various cycloadditions and other transformations are reported using the metal selenoalkynolates carrying aromatic (**203**), aliphatic (**204**) and silyl substituents (**205**).

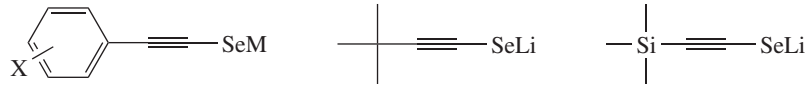

(**203**) (**a**) X = *p*-NO_2, M = K
(**b**) X = H, M = K
(**c**) X = *o*-OH, M = K
(**d**) X = H, M = Li

(**204**) (**205**)

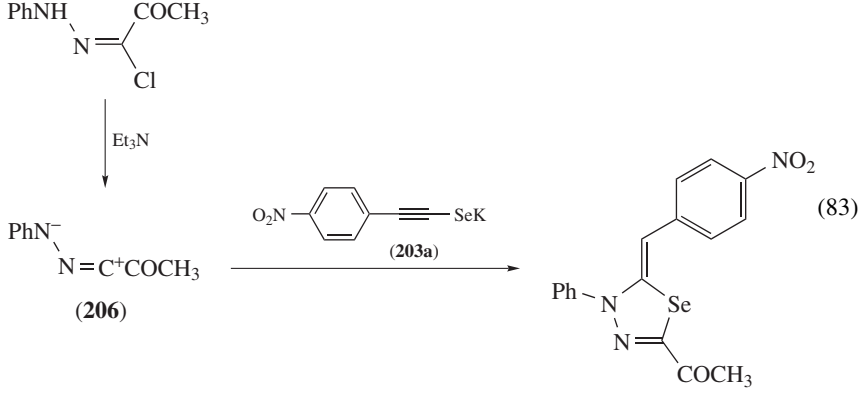

(**206**) (**203a**) (**207**) 97% (83)

The [3 + 2] cycloaddition reactions of **203a** with a nitrile imine (**206**) to give a 1,3,4-selenadiazoline (**207**) and of **203b** with phenyl isoselenocyanate (**208**) to give a 1,3-diselenole (**209**) are shown in equations 83 and 84, respectively[85,86]. An intramolecular cycloaddition takes place involving a phenolic OH group (equation 85), when **203c**,

derived from 4-(2-hydroxyphenyl)-1,2,3-selenadiazole (**210**), undergoes rearrangement to a selenoketene (**211**) and is finally converted into 2-benzylselenobenzofuran (**212**)[87,88]. Selenocyclobutenes (**214, 216**) are synthesized, respectively, by the [2 + 2] cyclaoaddition of lithium selenoalkynolate (**203d**) with diphenylketene (**213**) (equation 86)[89] or with the enone **215** (equation 87)[90]. Treatment of lithium *t*-butylselenoalkynolate (**204**) with diethylamine gives the selenoamide **217** (equation 88)[91]. Lithium selenotrimethylsilylalkynolate (**205**) undergoes allylation with allyl halides, followed by a selena–Cope rearrangement to afford an allyl(trimethylsilyl)selenoketene (**218**) (equation 89), which is stable when stored at low temperature[92].

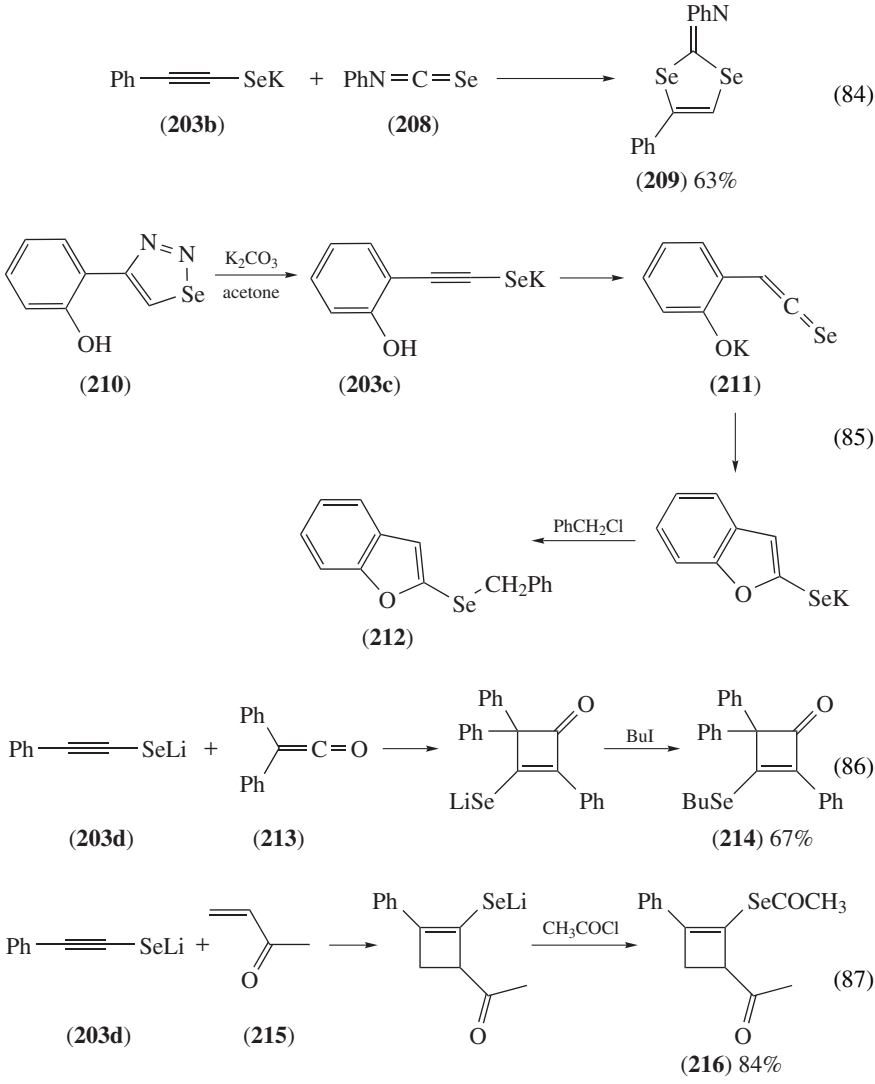

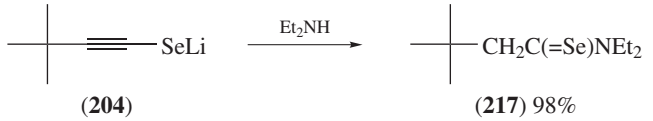

(**204**) (**217**) 98% (88)

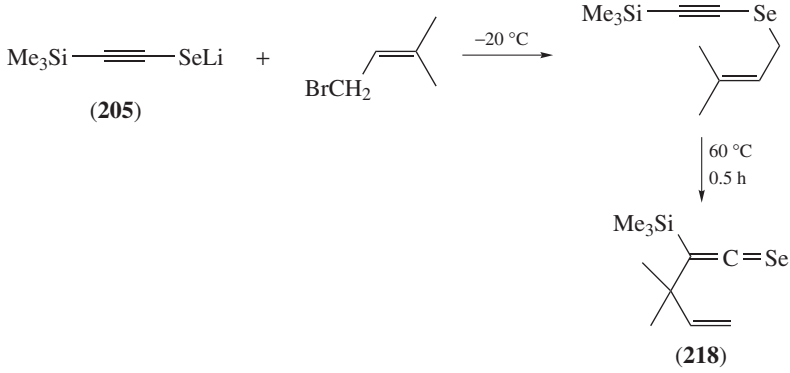

(**205**) (**218**) (89)

VII. REFERENCES

1. (a) M. Shindo, *Tetrahedron*, **63**, 10 (2007).
   (b) M. Shindo, *Synthesis*, 2275 (2003).
   (c) M. Shindo, *Yakugaku Zasshi*, **120**, 1233 (2000); *Chem. Abstr.*, **134**, 178117 (2001).
   (d) M. Shindo, *J. Synth. Org. Chem. Jpn.*, **58**, 1155 (2000).
   (e) M. Shindo, *Chem. Soc. Rev.*, **27**, 367 (1998).
2. U. Schöllkopf and I. Hoppe, *Angew. Chem., Int. Ed. Engl.*, **14**, 76 (1975).
3. I. Hoppe and U. Schöllkopf, *Justus Liebigs Ann. Chem.*, 219 (1979).
4. C. J. Kowalski and K. W. Fields, *J. Am. Chem. Soc.*, **104**, 321 (1982).
5. (a) C. J. Kowalski, M. S. Haque and K. W. Fields, *J. Am. Chem. Soc.*, **107**, 1429 (1985).
   (b) C. J. Kowalski and R. E. Reddy, *J. Org. Chem.*, **57**, 7194 (1992).
   (c) R. E. Reddy and C. J. Kowalski, *Org. Synth.*, **71**, 146 (1993).
6. D. Gray, C. Concellon and T. Gallagher, *J. Org. Chem.*, **69**, 4849 (2004).
7. (a) T. Satoh, A. Nakamura, A. Iriuchijima, Y. Hayashi and K. Kubota, *Tetrahedron*, **57**, 9689 (2001).
   (b) T. Satoh, H. Unno, Y. Mizu and Y. Hayashi, *Tetrahedron*, **53**, 7843 (1997).
   (c) T. Satoh, Y. Mizu, Y. Hayashi and K. Yamakawa, *Tetrahedron Lett.*, **35**, 133 (1994).
8. H. Kai, K. Iwamoto, N. Chatani and S. Murai, *J. Am. Chem. Soc.*, **118**, 7634 (1996).
9. J. G. Hill, B. E. Rossiter and K. B. Sharpless, *J. Org. Chem.*, **48**, 3607 (1983).
10. M. Julia, V. O. Saint-Jalmes and J. N. Verpeaux, *Synlett*, 233, (1993).
11. (a) L. Zhang and S. A. Kozmin, *J. Am. Chem. Soc.*, **126**, 10204 (2004).
    (b) L. Camici, P. Dembech, A. Ricci, G. Seconi and M. Taddei, *Tetrahedron*, **44**, 4197 (1988).
    (c) S. Florio and L. Troisi, *Tetrahedron Lett.*, **34**, 3141 (1990).
12. P. J. Stang and B. W. Surber, *J. Am. Chem. Soc.*, **107**, 1452 (1985).
13. P. J. Stang and K. Roberts, *J. Am. Chem. Soc.*, **108**, 7125 (1986).
14. (a) R. Häner, T. Laube and D. Seebach, *J. Am. Chem. Soc.*, **107**, 5396 (1985).
    (b) K. Tomioka, M. Shindo and K. Koga, *J. Org. Chem.*, **55**, 2276 (1990).
15. M. Shindo, *Tetrahedron Lett.*, **38**, 4433 (1997).
16. (a) M. Shindo, Y. Sato and K. Shishido, *Tetrahedron*, **54**, 2411 (1998).
    (b) M. Shindo, K. Matsumoto and K. Shishido, *Org. Synth.*, **84**, 11 (2007).
17. M. Shindo, Y. Sato, R. Koretsune, T. Yoshikawa, K. Matsumoto, K. Itoh and K. Shishido, *Chem. Pharm. Bull.*, **51**, 477 (2003).
18. (a) M. Yus, R. P. Herrera and A. Guijarro, A. *Chem. Eur. J.*, **8**, 2574 (2002).
    (b) M. Yus, *Synlett*, 1197 (2001).

(c) D. J. Ramon and M. Yus, *Eur. J. Org. Chem.*, 225 (2000).
(d) M. Yus, *Chem. Soc. Rev.*, 155 (1996).
19. M. Shindo, R. Koretsune, W. Yokota, K. Itoh and K. Shishido, *Tetrahedron Lett.*, **42**, 8357 (2001).
20. (a) T. T. Tidwell, *Angew. Chem., Int. Ed.*, **44**, 6812 (2005).
(b) R. K. Orr and M. A. Calter, *Tetrahedron*, **59**, 3545 (2003).
(c) A. R. Far, *Angew. Chem., Int. Ed.*, **42**, 2340 (2003).
(d) C. Palomo, J. M. Aizpurua, I. Ganboa and M. Oiarbide, *Eur. J. Org. Chem.*, 3223 (1999).
(e) M. Sato and K. Iwamoto, *J. Synth. Org. Chem. Jpn.*, **57**, 76 (1999).
(f) A. Pommier, P. Kocienski and J.-M. Pons, *J. Chem. Soc., Perkin Trans. 1*, 2105 (1998).
(g) T. T. Tidwell, *Ketenes*, John Wiley & Sons, Inc., New York, 1995.
(h) C. Wentrup, W. Heilmayer and G. Kollenz, *Synthesis*, 1219 (1994).
(i) J. A. Hyatt and P. W. Raynolds, *Org. React.*, **45**, 159 (1994).
(j) T. T. Tidwell, *Acc. Chem. Res.*, **23**, 273 (1990).
(k) B. B. Snider, *Chem. Rev.*, **88**, 793 (1988).
(l) H. R. Seikaly and T. T. Tidwell, *Tetrahedron*, **42**, 2587 (1986).
21. R. P. Woodbury, N. R. Long and M. W. Rathke, *J. Org. Chem.*, **43**, 376 (1978).
22. S. Akai, S. Kitagaki, T. Naka, K. Yamamoto, Y. Tsuzuki, K. Matsumoto and Y. Kita, *J. Chem. Soc., Perkin Trans. 1,* 1705 (1996).
23. M. Ito, E. Shirakawa and H. Takaya, *Synlett*, 1329 (2002).
24. Y. Chiang, A. J. Kresge and V. V. Popik, *J. Am. Chem. Soc.*, **117**, 9165 (1995).
25. A. J. Kresge, *Acc. Chem. Res.*, **23**, 443 (1990).
26. B. L. Groh, R. R. Magrum and T. Barton, *J. Am. Chem. Soc.*, **109**, 7568 (1987).
27. M. Shindo and T. Kumagai, unpublished results.
28. J. Jubb and S. Gambarotta, *J. Am. Chem. Soc.*, **115**, 10410 (1993).
29. C. F. Bernasconi and P. J. Wenzel, *J. Am. Chem. Soc.*, **123**, 2430 (2001).
30. M. Shindo and T. Yoshiiwa, unpublished results.
31. J. S. Grossert, P. D. Fancy and R. L. White, *Can. J. Chem.*, **83**, 1878 (2005).
32. B. J. Smith, L. Ladom and A. J. Kresge, *J. Am. Chem. Soc.*, **11**, 8297 (1989).
33. (a) M. Shindo, Y. Sato and K. Shishido, *J. Am. Chem. Soc.*, **121**, 6507 (1999).
(b) M. Shindo, Y. Sato and K. Shishido, K. *J. Org. Chem.*, **66**, 7818 (2001).
34. R. L. Danheiser and J. S. Nowick, *J. Org. Chem.*, **56**, 1176 (1991).
35. M. Shindo, Y. Sato and K. Shishido, K. *Tetrahedron Lett.*, **43**, 5039 (2002).
36. M. Shindo, K. Matsumoto, Y. Sato and K. Shishido, *Org. Lett.*, **3**, 2029 (2001).
37. M. Shindo, Y. Yoshimura, M. Hayashi, H. Soejima, T. Yoshikawa, K. Matsumoto and K. Shishido, *Org. Lett.*, **9**, 1963 (2007).
38. (a) A. E. Taggi, A. M. Hafez and T. Lectka, *Acc. Chem. Res.*, **36**, 10 (2003).
(b) G. Alvaro and D. Savoia, *Synlett*, 651 (2002).
(c) J. A. Ellman, T. D. Owens and T. P. Tang, *Acc. Chem. Res.*, **35**, 984 (2002).
39. (a) R. M. Adlington, A. G. M. Barrett, P. Quayle and A. Walker, *J. Chem. Soc., Chem. Commun.*, 404 (1981).
(b) A. G. M. Barrett and P. Quayle, *J. Chem. Soc., Perkin Trans. 1*, 2193 (1982).
40. M. Shindo, S. Oya, R. Murakami, Y. Sato and K. Shishido, *Tetrahedron Lett.*, **41**, 5943 (2000).
41. M. Shindo, S. Oya, Y. Sato and K. Shishido, *Heterocycles*, **49**, 113 (1998).
42. S. Ozaki, *Chem. Rev.*, **72**, 457 (1972).
43. M. Shindo, A. Harada, K. Matsumoto and K. Shishido, *Heterocycles*, **66**, 39 (2005).
44. (a) A. Padwa and W. H. Pearson (Eds), *Chemistry of Heterocyclic Compounds*, Vol. 58, John Wiley & Sons, Inc., New York, 2002.
(b) H. M. I. Osborn, N. Gemmell and L. M. Harwood, *J. Chem. Soc., Perkin Trans. 1*, 2419 (2002).
(c) K. V. Gothelf and K. A. Jorgensen, *Chem. Commun.*, 1449 (2000).
(d) S. Kobayashi and K. A. Jørgensen (Eds), *Cycloaddition Reactions in Organic Synthesis*, Pergamon Press, Oxford, 2002.
45. (a) M. Shindo, K. Itoh, C. Tsuchiya and K. Shishido, *Org. Lett.*, **4**, 3119 (2002).
(b) M. Shindo, K. Itoh, K. Ohtsuki, C. Tsuchiya and K. Shishido, *Synthesis*, 1441 (2003).
(c) M. Shindo, K. Ohtsuki and K. Shishido, *Tetrahedron: Asymmetry*, **16**, 2821 (2005).
46. K. Iwamoto, M. Kojima, N. Chatani and S. Murai, *J. Org. Chem.*, **66**, 169 (2001).
47. W. F. Austin, Y. Zhang and R. L. Danheiser, *Org. Lett.*, **7**, 3905 (2005).

48. J. Mulzer and T. Kerkmann, *J. Am. Chem. Soc.*, **102**, 3620 (1980).
49. (a) M. Shindo, Y. Sato and K. Shishido, *Tetrahedron Lett.*, **39**, 4857 (1998).
(b) M. Shindo, Y. Sato, T. Yoshikawa, R. Koretsune and K. Shishido, *J. Org. Chem.*, **69**, 3912 (2004).
(c) M. Shindo, Y. Sato and K. Shishido, *J. Org. Chem.*, **65**, 5443 (2000).
50. H. Yu, W. T. Chan and J. D. Goddard, *J. Am. Chem. Soc.*, **112**, 7529 (1990).
51. (a) S. Niwayama, E. A. Kallel, D. C. Spellmeyer, C. Sheu and K. N. Houk, *J. Org. Chem.*, **61**, 2813 (1996).
(b) W. R. Dolbier Jr., H. Koroniak, K. N. Houk and C. Sheu, *Acc. Chem. Res.*, **29**, 471 (1996).
52. M. J. Curry and D. R. Stevens, *J. Chem. Soc., Perkin Trans. 2*, 1391 (1980).
53. W. R. Dolbier, Jr., H. Koroniak, D. J. Burton, A. R. Bailey, G. S. Shaw and S. W. Hansen, *J. Am. Chem. Soc.*, **106**, 1871 (1984).
54. (a) W. Kirmse, N. G. Rondan and K. N. Houk, *J. Am. Chem. Soc.*, **106**, 7989 (1984).
(b) N. G. Rondan and K. N. Houk, *J. Am. Chem. Soc.*, **107**, 2099 (1985).
55. S. Mori and M. Shindo, unpublished results.
56. (a) M. Murakami, Y. Miyamoto and Y. Ito, *Angew. Chem., Int. Ed.*, **40**, 189 (2001).
(b) P. S. Lee, X. Zhang and K. N. Houk, *J. Am. Chem. Soc.*, **125**, 5072 (2003).
57. I. V. Alabugin and T. A. Zeidan, *J. Am. Chem. Soc.*, **124**, 3175 (2002).
58. S. Mori and M. Shindo, *Org. Lett.*, **6**, 3945 (2004).
59. (a) C. Najera and M. Yus, *Org. Prep. Proced. Int.*, **27**, 383 (1995).
(b) P. C. Bulman Page, S. S. Klair and S. Rosenthal, *Chem. Soc. Rev.*, **19**, 147 (1990).
(c) A. Ricci and A. Degl'Innocenti, *Synthesis*, **647** (1989).
60. I. Fleming, A. Barbero and D. Walter, *Chem. Rev.*, **97**, 2063 (1997).
61. M. Shindo, K. Matsumoto, S. Mori and K. Shishido, *J. Am. Chem. Soc.*, **124**, 6840 (2002).
62. H. Taguchi, K. Ghoroku, M. Tadaki, A. Tsubouchi and T. Takeda, *Org. Lett.*, **3**, 3811 (2001).
63. R. B. Miller and T. Reichenbach, *Tetrahedron Lett.*, 543 (1974).
64. M. Shindo, K. Matsumoto and K. Shishido, *Angew. Chem., Int. Ed.*, **43**, 104 (2004).
65. M. Shindo, K. Matsumoto and K. Shishido, *Synlett*, 176 (2005).
66. M. Shindo, T. Yoshikawa, Y. Itou, S. Mori, T. Nishii and K. Shishido, *Chem. Eur. J.*, **12**, 524 (2006).
67. M. Shindo, T. Kita, T. Kumagai, K. Matsumoto and K. Shishido, *J. Am. Chem. Soc.*, **128**, 1062 (2006).
68. M. Shindo, K. Yaji, T. Kita and K. Shishido, *Synlett*, 1096 (2007).
69. M. Shindo, S. Oya, R. Murakami, Y. Sato and K. Shishido, *Tetrahedron Lett.*, **41**, 5947 (2000).
70. (a) C. J. Kowalski and M. S. Haque, *J. Am. Chem. Soc.*, **108**, 1325 (1986).
(b) C. J. Kowalski and G. S. Lal, *J. Am. Chem. Soc.*, **108**, 5356 (1986).
(c) C. J. Kowalski and G. S. Lal, *Tetrahedron Lett.*, **28**, 2463 (1987).
71. R. Pi, T. Friedl, P. v. R. Schleyer, P. Klusener and L. Brandsma, *J. Org. Chem.*, **52**, 4299 (1987).
72. C. J. Kowalski, G. S. Lal and M. Haque, *J. Am. Chem. Soc.*, **108**, 7127 (1986).
73. R. L. Danheiser and A. L. Helgason, *J. Am. Chem. Soc.*, **116**, 9471 (1994).
74. R. F. Sweis, M. P. Schramm and S. A. Kozmin, *J. Am. Chem. Soc.*, **126**, 7442 (2004).
75. (a) J. Ficini, *Tetrahedron*, **32**, 1449 (1976).
(b) H. G. Viehe, *Angew. Chem., Int. Ed. Engl.*, **6**, 767 (1967).
76. R. Raap, *Can. J. Chem.* **49**, 1792 (1971).
77. (a) N. Lage, S. Masson and A. Thuillier, *J. Chem. Soc., Perkin Trans. 1,* 3389 (1991).
(b) C. Fromont and S. Masson, *Tetrahedron*, **55**, 5405 (1999).
78. (a) L. Brandsma, H. Wijers and J. F. Arens, *Recl. Trav. Chim. Pays-Bas*, **81**, 583 (1962).
(b) L. Brandsma, H. E. Wijers and C. Jonker, *Recl. Trav. Chim. Pays-Bas*, **83**, 208 (1964).
79. R. Raap and R. G. Micetich, *Can. J. Chem.*, **46**, 1057 (1968).
80. J. Meijer and L. Brandsma, *Recl. Trav. Chim. Pays-Bas*, **91**, 578 (1972).
81. (a) M. L. Petrov and A. V. Belyakov, *Tetrahedron Lett.*, **44**, 599 (2003).
(b) M. L. Petrov and A. V. Belyakov, *Russ. J. Gen. Chem.*, **75**, 1142 (2005).
82. (a) S. J. Harris and D. R. M. Walton, *J. Organomet. Chem.* **127**, C1 (1977).
(b) H. Takeda, S. Shimada, S. Ohnishi, F. Nakanishi and H. Matsuda, *Tetrahedron Lett.*, **39**, 3701 (1998).
(c) W.-R. Forster, R. Isecke, C. Spanka and E. Schaumann, *Synthesis*, 942 (1997).
(d) K. Takimiya, A. Moriwaki and T. Otsubo, *Synlett*, 319 (1997).

83. N. Miyaura, T. Yanagi and A. Suzuki, *Chem. Lett.*, 535 (1979).
84. R. Pietschnig, K. Merz and S. Schafer, *Heteroatom Chem.*, **16**, 169 (2005).
85. N. A. Terent'eva, M. L. Petrov, K. A. Potekhin, V. A. Galishev and Y. T. Struchkov, *Russ. J. Org. Chem.*, **30**, 1547 (1994).
86. N. I. Zmitrovich and M. L. Petrov, *Russ. J. Org. Chem.*, **32**, 1870 (1996).
87. M. L. Petrov, M. A. Abramov, W. Dehaen and S. Toppet, *Tetrahedron Lett.*, **40**, 3903 (1999).
88. M. A. Abramov, W. Dehaen, B. D'hooge, M. L. Petrov, S. Smeets, S. Toppet and M. Voets, *Tetrahedron*, **56**, 3933 (2000).
89. M. Koketsu, M. Kanoh and H. Ishihara, *Synlett*, 805 (2002).
90. M. Koketsu, K. Mizutani, T. Ogawa, A. Takahashi and H. Ishihara, *J. Org. Chem.*, **69**, 8938 (2004).
91. R. S. Sukhai, R. J. Jong and L. Brandsma, *Synthesis*, 888 (1977).
92. E. Schaumann and F.-F. Grabley, *Tetrahedron Lett.*, **21**, 4251 (1980).

CHAPTER **14**

Lanthanide enolates as nuclear magnetic resonance shift reagents

THOMAS J. WENZEL and KATELYN A. PROVENCHER

Department of Chemistry, Bates College, Lewiston, Maine 04240, USA
Fax: +1-207-786-8336; e-mail: twenzel@bates.edu

The chemistry of metal enolates
Edited by Jacob Zabicky

I. ACRONYMS

acac	2,4-pentanedionate	NOE	nuclear Overhauser effect
CSA	chiral solvating agent	phen	phenanthroline
dcm	*d*,*d*-dicampholylmethanate	PHIP	parahydrogen-induced polarization
dpm	dipivaloylmethanate	py	pyridine
fod	6,6,7,7,8,8,8-heptafluoro-2,2-dimethyl-3,5-octanedionate	tfa	1,1,1-trifluoro-2,4-pentanedionate
		tfc	3-(trifluoroacetyl)-D-camphorate
hfa	1,1,1,5,5,5-hexafluoro-2,4-pentanedionate	tpp	triphenylphosphine
hfc	3-(heptafluorobutyryl)-D-camphorate		
mtpa	α-methoxy-α-trifluoromethylphenylacetic acid		

II. INTRODUCTION

The utilization of metal β-diketonate complexes as organic-soluble NMR shift reagents was first explored in the mid-sixties with Ni(II) and Co(II) complexes of 2,4-pentanedione [$(Ni(acac)_2$ and $Co(acac)_2$][1,2]. Donor ligands such as triarylphosphines, isonitriles[1], pyridine *N*-oxides and picoline *N*-oxides[2] bind to the metal ion. Relatively small shifts were observed in the NMR spectrum of the bound donor groups. These shifts were the results of contact (through-bond) and pseudocontact (dipolar or through-space) effects.

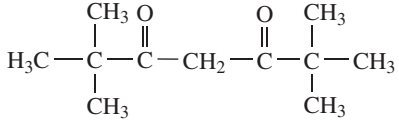

(**1**)

In 1969, Hinckley was the first one to show that a paramagnetic lanthanide tris(β-diketonate) [$Eu(dpm)_3py_2$], containing dipivaloylmethane (**1**), pyridine and Eu(III), functioned as an excellent organic-soluble NMR shift reagent[3]. Lanthanide tris(β-diketonates) cause large shifts that are mostly dipolar in origin. In Hinckley's work, suitable hard Lewis bases were able to displace the pyridine ligands and associate through a donor–acceptor interaction with the europium(III) ion. The association constants of donors with the lanthanide tris(β-diketonates) are influenced by electronic and steric effects. At the time of

Hinckley's discovery, most investigators only had access to relatively low-field NMR spectrometers and interest in lanthanide shift reagents was intense. Numerous reports expanding the understanding and applicability of lanthanide shift reagents were published. Chiral lanthanide tris(β-diketonates) were developed for the analysis of enantiomers. Binuclear lanthanide–silver reagents were developed for soft Lewis bases. Comprehensive reviews of lanthanide shift reagents have been published[4–6]. The discussion herein will provide selected examples of the utility of metal β-diketonate complexes as NMR shift reagents.

III. GENERAL CONSIDERATIONS

A. Effect of Achiral Ligands

Soon after Hinckley's discovery, it was found that $Ln(dpm)_3$ complexes were more effective NMR shift reagents than the corresponding dipyridine adducts[7]. Removing the competition of the pyridine donors enabled substrate molecules to bind more strongly to the lanthanide ion, thereby enhancing the magnitude of the shifts in the spectrum. Lanthanide complexes with many other β-diketonate ligands were evaluated for their effectiveness as NMR shift reagents[4]. Of particular note are the complexes of 6,6,7,7,8,8,8-heptafluoro-2,2-dimethyl-3,5-octanedione (**2**), [H(fod)][8].

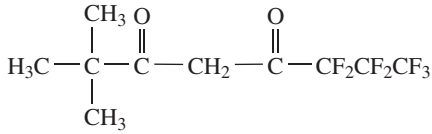

(**2**)

The $Ln(fod)_3$ chelates have three features that likely contribute to their effectiveness as NMR shift reagents. First is that the electron-withdrawing fluorine groups increase the Lewis acidity of the metal ion such that association of donors is stronger than with $Ln(dpm)_3$. Second is the remarkable solubility of the $Ln(fod)_3$ chelates in common NMR solvents. Higher solubility was especially beneficial at the time lower-field instruments were common. Third is that the fod ligand has bulky substituent groups, which seem to affect the magnitude of the shifts. Lanthanide chelates with small ligands such as acac[9,10] and 1,1,1-trifluoro-2,4-pentanedionate (tfa)[11] are rather ineffective as NMR shift reagents. Dipolar shifts are determined by the geometry of the lanthanide–substrate complex. Lanthanide tris(β-diketonate) complexes are fluxional in nature. The ligands are not locked into a set configuration and move to accommodate one or more donor molecules. The ligands also undergo exchange among different metal ions in solution[12]. Lanthanide tris(β-diketonates) with smaller ligands likely have many contributing forms, thus canceling out the dipolar shifts. Complexes with bulkier ligands likely bind donors in a more defined configuration, thus causing larger shifts than those with smaller ligands.

B. Effect of the Metal

The direction and magnitude of the shifts produced by lanthanide ions depends on their magnitude susceptibility anisotropy terms. Because the unpaired electrons of the lanthanide ions are in 4f orbitals, and these are shielded by filled 5s and 5p orbitals, the magnetic terms are essentially independent of the ion's environment, and remain constant from complex to complex. In organic solvents such as chloroform, rare earths are found

to shift resonances to higher frequency generally do so in the order Tm > Er > Yb > Eu, and to lower frequency in the order Dy > Tb > Ho > Pr > Nd > Sm[9,13]. Shifts are often too large with Tm(III) and Dy(III) such that Eu(III) is usually the ion of choice for studies in organic solvents.

C. Broadening in the NMR Spectrum

1. Uncertainty and exchange broadening

Studies with lanthanide shift reagents are subject to uncertainty and exchange broadening. Uncertainty broadening occurs because the paramagnetic lanthanide ion reduces the relaxation time of nearby nuclei. Under ideal circumstances, the substrate molecules are in fast exchange between the bound and unbound forms and the spectrum represents a time-average of both. With slow exchange, distinct peaks are observed for the bound and unbound form of the substrate. Intermediate exchange rates that are neither fast nor slow result in broadened resonances. The large size of the lanthanide–substrate complexes can slow down the exchange rate to the extent that exchange broadening is more significant at higher field strengths. Broadening with a paramagnetic lanthanide shift reagent is also proportional to the square of the shift[14]. As high field spectrometers have become more routinely available, the broadening observed in spectra with lanthanide shift reagents has limited their utility.

2. Strategies to reduce broadening

There are several strategies that can be used to reduce the broadening, especially with chiral lanthanide shift reagents, so that they can be used on high field instruments. Analysis of broadening with lanthanide shift reagents concluded that intermediate exchange rates were the more significant contribution to broadening[15]. Raising the temperature of the sample generally speeds up the exchange rate, reduces the association constant and reduces the shifts[16]. Sometimes this reduces the broadening to acceptable levels while still providing adequate shifts and chiral discrimination[17]. Sm(III) causes small shifts, and therefore less broadening. The shifts with Sm(III) chelates may be sufficient for chiral recognition studies on high field spectrometers. This was demonstrated with a series of α-amino acid methyl esters with Sm(tfc)$_3$[18]. Furthermore, the relative shifts of the enantiomers exhibited a consistent trend with absolute configuration, as discussed in Section VI.C.

Polar solvents reduce the association of substrates with the lanthanide ion by competing for binding sites and by better solvating the polar donor group. The reduced association decreases the magnitude of the shifts but also the broadening. Chiral 1,2- and 1,3-dioxygenated compounds exhibit strong chelate bonding with Eu(tfc)$_3$ and Eu(hfc)$_3$ (hfc = 3-(heptafluorobutyryl)-D-camphorate) such that the ^{1}H spectra in chloroform-*d* were broadened at 300 MHz. The broadening was reduced in acetonitrile-d_3 and acetone-d_6, and chiral recognition was observed in acetonitrile-d_3. A small amount of water in the solvent did not interfere with the chiral discrimination[19].

The *N*-methyl resonances of carnitine (**3**) were monitored in the presence of Eu(dcm)$_3$ (dcm = *d*,*d*-dicamphoylmethanate) and the Eu(III), Pr(III) and Yb(III) chelates of tfc and hfc in methanol-d_4 at 500 MHz. Eu(dcm)$_3$ was not soluble enough in methanol, but the tfc and hfc chelates achieved enantiomeric discrimination, enabling detection of 0.5% of the minor enantiomer. Signals were sharp even at high lanthanide–substrate ratios because of the fast substrate exchange in methanol[20].

For chiral recognition work, ^{13}C spectra may be better than ^{1}H spectra. Proton-decoupled ^{13}C spectra consist of only singlets, so broadening is less of a problem. Also,

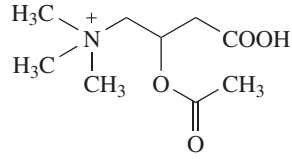

(**3**)

the larger time scale of the ^{13}C nucleus relatively to that of ^{1}H results in reduced exchange broadening. Enantiomeric discrimination was observed in the ^{13}C spectra of multistriatin (**4**)[21] and disubstituted lactams such as **4′** and **4″** [22] with $Eu(hfc)_3$ and $Eu(tfc)_3$ respectively, whereas the ^{1}H NMR spectra showed too much broadening.

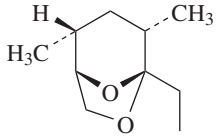

(**4**)

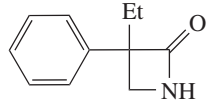

(**4′**)

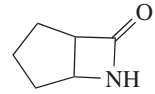

(**4″**)

Rephasing, baseline correction and Gaussian line narrowing were used as a general procedure to reduce broadening in the ^{1}H spectra (300 MHz) of a primary β-alkoxyalcohol and 1,2-cyclohexanediol with $Eu(hfc)_3$ and $Yb(hfc)_3$ at 300 MHz to acceptable levels[23].

When a spectrum has severely broadened resonances in the presence of less broadened resonances, it is possible to use a Carr–Purcell–Meiboom–Gill spin-echo sequence to remove the broadened resonances, facilitating the interpretation of the remaining signals. By setting certain parameters of the sequence, it is possible to progressively remove peaks with less and less broadening[15].

D. Shift Mechanism

Lanthanide reagents produce shifts through complexation, dipolar and contact effects. Complexation shifts are small and are measured using diamagnetic La(III) or Lu(III) chelates[24].

Dipolar shifts occur from the through-space effect of the lanthanide's magnetic field on the nucleus of interest. Dipolar shifts ($\Delta B/B$) are predictable through equations 1 and 2, initially derived by McConnell and Robertson[25]. In equation 1, r, θ and Ω are the spherical polar coordinates of the nucleus in the coordinate system of the principal magnetic axes, K and K' are constants, and the χ values are the principal molecular magnetic susceptibilities. Under conditions of axial (C_3) or higher symmetry, the magnetic terms in the second expression of equation 1 exactly cancel each other out leading to equation 2. In this simplified form of the dipolar shift equation, r is the distance between the lanthanide ion and the nucleus of interest and θ is the angle between the principal magnetic axis and the line that defines r. It is unlikely that any single lanthanide–substrate complex rigorously meets the requirement of axial symmetry, yet most fits of lanthanide shift data are done assuming there is axial symmetry, much simplifying the calculations[26,27]. The discrepancy is reconciled since the simplified equation can be used under circumstances of effective axial symmetry[26,27]. Effective axial symmetry is realized if there is a rapid interconversion among three equivalent rotamers[28]. Alternatively, effective axial symmetry is

achieved because the fluxional nature of the lanthanide complexes creates a situation in which the shifts are a time-averaged ensemble of many contributing species[26,27].

$$\frac{\Delta B}{B} = \mathrm{K}\left[\chi_{\mathrm{Z}} - \frac{1}{2}(\chi_{\mathrm{X}} + \chi_{\mathrm{Y}})\right]\frac{3\cos^2\theta - 1}{r^3} - \mathrm{K}'[\chi_{\mathrm{X}} - \chi_{\mathrm{Y}}]\frac{\sin^2\theta\cos 2\ \Omega}{\mathrm{r}^3} \quad (1)$$

$$\frac{\Delta B}{B} = K\left[\chi_{\mathrm{Z}} - \frac{1}{2}(\chi_{\mathrm{X}} + \chi_{\mathrm{Y}})\right]\frac{3\cos^2\theta - 1}{r^3} \quad (2)$$

Contact, or through-bond, shifts occur if there is a finite probability of finding the unpaired electron of the metal at the nucleus of interest. Predicting the direction and magnitude of contact shifts requires molecular orbital calculations. Contact shifts are significant in covalently bonded metal systems and are pronounced for paramagnetic transition metal complexes such as $Ni(acac)_2$ and $Co(acac)_2$[1]. Contact shifts extend over π-electron systems, and are particularly large with $Co(acac)_2$ since the Co(II) has an unpaired electron in a d-orbital that can π-bond with certain substrates[1].

The unpaired electrons of the lanthanide ions are in 4f orbitals, which are shielded by filled 5s and 5p orbitals. Electrostatic bonding dominates lanthanide ion association with ligands such that covalent bonding and contact shifts are kept to a minimum, especially with ^{1}H nuclei. Contact shifts are more common with ^{13}C nuclei. Evidence for the presence of contact shifts include 'wrong-way' shifts for certain nuclei that cannot be explained by changes in the angle term of the dipolar shift equation[29,30]. Contact shifts are especially pronounced for the ^{13}C nuclei of compounds with extended π systems such as *N*-heterocycles and anilines[31,32]. The carbon atom of carbonyl[33,34] and nitrile groups[33], as well as those directly attached to hydroxyl or amine groups, likely have contact shift contributions as well[33]. Contact shifts have also been observed for the ^{17}O signal of carbonyl oxygen atoms[34], ^{19}F signals of fluoroaromatic compounds[35] and ^{14}N atoms of *N*-heterocycles[36].

In addition to 'wrong-way' shifts, there are other methods to assess whether contact shifts occur for a nucleus. One is to compute sets of internal ratios of the shifts of protons for different metals or for directly attached ^{1}H or ^{13}C nuclei[33]. Anomalies in these ratios are indicative of a contact contribution. Chelates of gadolinium, which has an isotropic f^7 configuration, can only produce shifts by complexation or contact effects[16]. Theoretical parameters for the relative contributions of contact and dipolar shifts for different lanthanide metals can be used to construct plots that indicate whether or not the shifts of a particular nucleus are purely dipolar or have a contact contribution[5,37,38]. Theoretical parameters indicate that the proportion of contact contribution to the shifts occurs in the order Eu > Nd > Ho > Er > Tb > Dy > Tm > Yb[37,39]. Using the theoretical values of the different contact and dipolar contributions, it is possible to formulate mixed lanthanide systems of $Eu(fod)_3$ and $Pr(fod)_3$ in which the dipolar or contact contributions exactly cancel out, leading to contact- or dipolar-only shifts[40]. A thorough review[36] and evaluation[38] of different methods for accounting for contact shifts have been published.

E. Structural Fitting of Shift Data

It is possible that the measured shifts for a substrate with a lanthanide tris(β-diketonate) can be fit to a unique geometry using the simplified dipolar shift equation. While lanthanide shift data never provided a solution phase system comparable to solid-state X-ray crystallography, the utilization of dipolar shifts with lanthanide shift reagents to understand substrate geometry has been extensive.

The angle term is important when fully explaining the magnitude of the shifts in the spectra of many compounds. 'Wrong-way' shifts for one or more protons in **5**[41], *cis*-1-3-(1-naphthyl)-1,3,5,5-tetramethylcyclohexan-1-ol (**6**)[42], 3-deactylkhivorin (**7**)[43] and nitrone **8**[44] provide clear evidence for the significance of the angle term. The $3\cos^2\theta - 1$ term changes its sign at 54.736° and 125.264°. Compounds **5**–**8** have nuclei that extend out from the donor group of the substrate such that θ is larger than 54.7°.

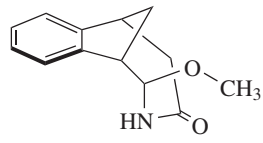

(**5**)

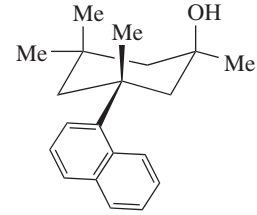

(**6**)

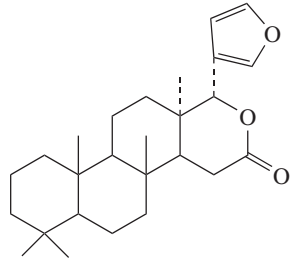

(**7**)

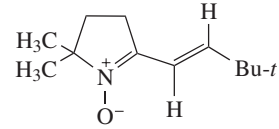

(**8**)

Fitting of shift data is typically done for 1:1 lanthanide–substrate complexes. There is ample evidence that 1:2 lanthanide–substrate complexes form in many cases, and that the proportion of the 1:1 and 1:2 species changes as a function of concentration. The stoichiometry of lanthanide–substrate complexes can be solvent dependent, with a higher likelihood of 1:2 complexes forming in a non-polar solvent such as carbon tetrachloride compared to chloroform-*d*[45].

Fitting of data requires the use of intrinsic bound shifts, which are those for the substrate in its fully complexed form, and can only involve nuclei without any contact shift contribution. Provided only a 1:1 complex forms, it is possible to use relative bound shifts, which are ratios of the shifts relative to a reference nucleus of the substrate[46]. Using both ^{1}H and ^{13}C measurements increases the size of the data set and improves the accuracy of the fit. When performing structural fitting of lanthanide shift data, it is recommended that shifts be obtained using the method of incremental dilution in which spectra for a series from high to low lanthanide–substrate ratio are recorded[47]. Methods for obtaining the association constants and bound shifts have been reviewed and evaluated[48,49]. An interesting observation is that, while substrates generally have much larger association constants with Eu(fod)$_3$ than Eu(dpm)$_3$, the intrinsic bound shifts for substrates bound to the two chelates are likely to be quite similar[50].

A potential problem when measuring lanthanide-induced shifts is the presence of scavengers such as water, and procedures to correct for the presence of scavengers have

been described[51,52]. The purity of the shift reagent is also a concern. Some batches of commercial reagents have been found to contain trace amounts of insoluble material. Also, the presence of a tetrakis chelate complex of the form $Ln(fod)_4K$ has been noted[53]. Prior to performing studies in which measured shift data will be fit to calculated values with $Ln(fod)_3$ chelates, it is advisable to purify the complex by sublimation and maintain the shift reagent in a dessiccator over P_4O_{10}.

It is essential to locate the principal magnetic axis of the lanthanide–substrate complex to determine the θ values. The principal magnetic axis is usually assumed to be collinear with the lanthanide–substrate bond, although the validity of this has been questioned in some studies[54,55].

Relaxation times measured with isotropic Gd(III) chelates can also be incorporated into the fitting process[56]. Changes in relaxation times vary only with the distance ($1/r^6$) from the gadolinium ion. Therefore, relative relaxation rates of the nuclei of the substrate provide relative distances from the gadolinium ion. Incorporation of relaxation data into the fitting process requires that the geometry of the gadolinium–substrate complex be identical to that of the other lanthanide–substrate complex used to measure shift data, which must be assumed with care[57].

Paramagnetic metal complexes with isotropic magnetic fields (Cr(III), Fe(III), Mn(II), and Gd(III)) can be used as paramagnetic relaxation reagents in ^{13}C, ^{15}N and ^{29}Si NMR spectroscopy[58,59]. These reagents cause two important effects. First, they shorten the spin–lattice relaxation time of nuclei, thereby increasing the sensitivity of ^{13}C and other nuclei with long T_1 values. The primary route of relaxation of ^{13}C nuclei involves interaction with the magnetic dipole of bonded ^1H nuclei. ^{13}C nuclei without bonded hydrogen atoms can have T_1 values as long as 100 seconds. Second, paramagnetic ions can suppress the nuclear Overhauser effect (NOE) that occurs on proton decoupling, which facilitates the integration of ^{13}C spectra. ^{15}N and ^{29}Si nuclei can have negative NOE values[58,59] which, depending on the magnitude, can cause the appearance of negative peaks or peaks of very low intensity. Suppressing the NOE makes all peaks positive and their integrated intensities correlate with chemical structure. In this application, it is preferable if the compound under study does not associate with the metal chelate. $Cr(acac)_3$ is especially noteworthy as an organic-soluble paramagnetic relaxation reagent. A more familiar present-day application of paramagnetic relaxation reagents involves the use of Gd(III) complexes as image contrast agents for magnetic resonance imaging[60–62].

The goodness of fit between observed and calculated shifts needs to be assessed, and methods of performing significance testing of lanthanide-induced shifts have been evaluated and reviewed[63]. Complexities arise when fitting lanthanide shift data for compounds with conformationally mobile groups[64]. Procedures for fitting free and hindered rotation have been described[65,66]. Reviews of the utilization of lanthanide-induced shifts for conformational analysis have been published[4,5,67], and studies to further refine the utilization of lanthanide-induced shift data for such analyses continue[38,68].

F. Integrity of Coupling Constants

The conversion of spectra from second to first order on the addition of a shift reagent in principle should allow the determination of coupling constants, although there are several processes that may influence coupling. Chemical-exchange spin-decoupling can cause collapse of the coupling[69,70]. In this situation, the extremely fast relaxation of the nucleus caused by the paramagnetic ion causes decoupling that is analogous to that of rapid chemical exchange between two environments. Electron-withdrawing effects caused by binding of the electropositive lanthanide ion to the donor atom can alter coupling constants as

well[71–73]. Finally, binding of the lanthanide can alter the conformational preference of the substrate, altering the time-averaged dihedral angles and coupling constants between nuclei.

IV. APPLICATIONS OF ACHIRAL SHIFT REAGENTS

There are many hundreds of published reports on the use of achiral lanthanide tris(β-diketonates) as NMR shift reagents. Essentially any substrate with an oxygen, nitrogen or sulfur atom is a potential candidate for analysis with lanthanide shift reagents. These include sulfur- and phosphorus-containing functional groups that have oxygen atoms. Carboxylic acids[74,75] and phenols[74] were observed to decompose lanthanide chelates of dpm, whereas solutions with chelates of fod were stable for several days and suitable for study.

Aliphatic and cyclic sulfides are weak bases but do show small shifts in the presence of $Ln(fod)_3$ chelates[76]. Alkylfluorides[77] and ethylfluorogermane[78] bind weakly to $Ln(fod)_3$ chelates through the fluorine atom and exhibit lanthanide-induced shifts. No shifts were observed in the spectra of the corresponding chloro-, bromo- and iodoalkanes[77].

A. Analysis of Metal Complexes

Metal complexes that have ligands with oxygen- and nitrogen-containing functional groups also bind to lanthanide ions. This includes some metal complexes in which oxygen atoms act as bridging units, binding simultaneously to the metal and lanthanide ion. For example, the double Schiff base obtained from an α,β-diamino compound undergoing condensation with two molecules of diacylmethane forms enolate complexes with divalent transition metal ions, e.g. Ni(II); these chelates are capable of further coordination in the presence of rare earth chelates, e.g. $Eu(fod)_3$, to yield binuclear complexes as shown in **9**[79]. $Co(acac)_3$ binds to the Eu(III) in $Eu(fod)_3$ through three bridging oxygen atoms and exhibits slow exchange at ambient probe temperatures[80].

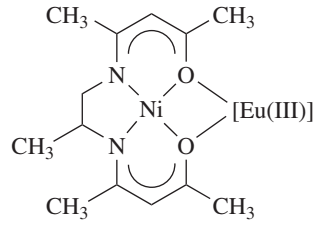

(**9**)

Certain metal complexes endowed with weak donor groups, such as $(\eta^5\text{-}C_5H_5)_2TiCl_2$ and $(C_6H_5)_3SnCl$, also show shifts in their spectra in the presence of $Ln(fod)_3$ chelates. In this case it appears likely that the halide ion associates with the lanthanide chelate to create an anionic species $Eu(fod)_3X^-$ that then forms an ion pair with the metal cation[81]. A review article on the utilization of lanthanide shift reagents for the study of metal complexes has been published[82].

B. Analysis of Organic Salts

The spectra of organic salts such as cyanine dyes, quinolinium ions and quaternary ammonium ions exhibit relatively small shifts in the presence of $Eu(fod)_3$, presumably

because of ion pairing of the organic cation with $Eu(fod)_3X^-$ [83]. Studies of ammonium[83,84], phosphonium[84] and sulfonium salts[85] noted that the larger the anion of the organic salt, the smaller the lanthanide-induced shifts.

C. Configurational Analysis of Sulfur Oxide Compounds

The utility of using lanthanide shift reagents with ^{17}O NMR spectroscopy to study the configuration of sulfones[86–89] or cyclic sulfite and sulfate diesters (**10**)[90] has been examined. Using isotopically labeled systems, it was possible to determine whether or not catalysts retained the configuration about the sulfur atom during reaction[90]. Lanthanide-induced shifts with $Eu(fod)_3$ were used to distinguish the diastereotopic oxygen atoms of 1-thiadecalin 1,1-dioxides (**11**)[86,88], six-member ring sulfones (**12**)[87,88], 3,4-epoxythiolane 1,1-dioxide (**13**)[88], the *cis*- and *trans*-epimers of 2-thiabicyclo[4.3.0]nonane 2,2-dioxide (**14**) and *trans*-8-thiabicyclo[4.3.0]nonane 8,8-dioxide (**15**)[89]. With **14**, the lanthanide ion preferentially bound at the less hindered equatorial oxygen atom[89]. A concern that arises with lanthanide shift reagent studies is what to use as a reference, especially since the paramagnetic ion changes the bulk magnetic susceptibility of the solution and may associate with and shift the resonances of the reference. The use of 1,4-dioxane as an external reference has been recommended for ^{17}O NMR studies with lanthanide shift reagents[91].

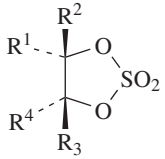

(**10**)

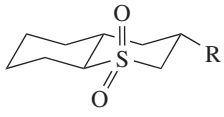

(**11**)

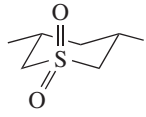

(**12**)

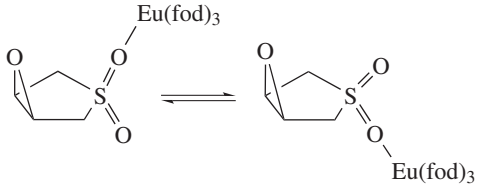

(**13**)

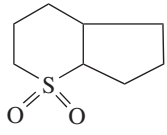

(**14**)

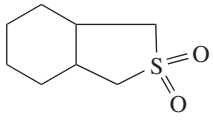

(**15**)

D. Analysis of Deuteriated Compounds

Lanthanide shift reagents have been used to determine the site of deuterium[92–95] or tritium[96] incorporation in compounds by ^1H, ^2H or ^3H NMR spectroscopy. This includes deuteriation of hexopyranosides analyzed by ^1H NMR[92], the low level incorporation of

deuterium into methyl nonanoate and other esters by ^{2}H NMR[93], 2-adamantanols by ^{1}H and ^{2}H NMR[94], and oxoporphyrins, of which **16** is one example[95]. With the oxyporphyrins, ^{1}H NMR shift data with $Eu(fod)_3$ at 300 MHz were used to confirm the assignment of the *meso* proton regions, facilitating a study of the specificity of deuterium incorporation. The product obtained after tritiation of the alkyne group of dodec-7-yn-1-ol (**17**) was analyzed using ^{1}H and ^{3}H NMR spectroscopy in the presence of $Eu(dpm)_3$. No isotope migration to the adjacent C_6 or C_9 positions was observed. The same tritiation pattern was implied when a similar functional unit was tritiated in a polymeric material that also contained phosphorylcholine groups[96].

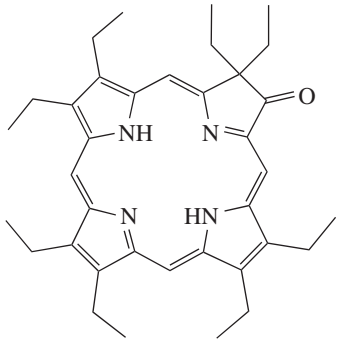

(**16**)

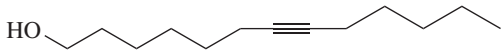

(**17**)

Another phenomenon that has been observed when studying deuteriated compounds with lanthanide shift reagents is a secondary deuterium isotope effect. In this situation, the chemical shifts of nuclei are different in a partially deuteriated versus the non-deuteriated analogue in the presence of the lanthanide chelate. This was first observed with verbanol (**18**) after deuteriation geminal to the OH group (**18′**)[97], and has since been observed for polyglycoldimethylethers with chelates of dpm[98], aliphatic alcohols deuteriated geminal to the hydroxyl group[99,100], and methyl-substituted pyridines[101], among others. In every example, the spectrum of the partially deuteriated compound exhibited the larger lanthanide shifts. The most likely explanation for this observation is that ^{2}H has a greater electropositive inductive effect than ^{1}H. This would make the donor atom more electron-rich in the deuteriated compound and increase the association constant. This explains observations with geminally substituted alcohols in which the dideuterio derivative had larger shifts than the monodeuterio derivative[99]. Also, at high lanthanide–substrate ratios, the shift differences between the deuteriated and non-deuteriated compounds diminish,

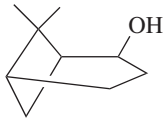

(**18**)

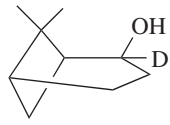

(**18′**)

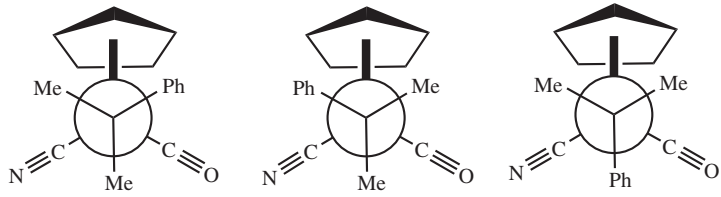

FIGURE 1. Possible orientations of phosphine derivatives of cyclopentadiene iron and nickel complexes. The Fe(II) and Ni(II) ions lie behind the circle of Newman's rendition of the complexes

presumably because both can bind to the shift reagent. With methyl-substituted pyridines, the presence of CD_3 groups at the 2- and 6-positions had a large secondary deuterium isotope effect, whereas incorporation of a CD_3 group at the 4-position had an undetectable effect[101].

E. Application to Dynamic Processes

Lanthanide shift reagents have been used to study dynamic NMR processes. One of the classic applications involves the study of rotational barriers of various amides[102, 103], thioamides[102], oximes[104] and amide oximes[105]. Lanthanide-induced shifts enabled the distinction of *cis*- and *trans*- or *syn*- and *anti*-isomers, and variable-temperature studies in the presence of the chelate were performed to determine the barrier to rotation.

A study of rotational barriers and preferred orientations (Figure 1) of phosphine derivatives of cyclopentadiene iron and nickel complexes was facilitated through an analysis of the low-temperature ^1H and ^{13}C NMR spectra in the presence of $Eu(fod)_3$[106]. Association of the europium likely occurred through binding of the nitrogen atom of the cyano group. It is important to exercise caution in such analyses since bonding of the lanthanide may perturb the dynamic process. Practical aspects of the application of lanthanide shift reagents to the study of dynamic systems such as amides have been summarized[103].

F. Analysis of Polymers

Lanthanide chelates have been used to study structural aspects of polymers. The isotactic, heterotactic and syndiotactic triads of poly(methylmethacrylate) were resolved in the presence of $Ln(dpm)_3$[107, 108] and $Ln(fod)_3$[109]. Elevated temperatures caused a sharpening of resonances and facilitated the analysis[107, 109]. Addition of $Eu(dpm)_3$ to poly(propyleneglycol) (PPG) shifted the end methyl groups away from other resonances of interior protons, such that integrated areas of the peaks could be used to determine the molecular weight of the polymer[110]. The assignment of the ^{13}C NMR spectrum of poly(2,6-dimethyl-1,4-phenylene oxide) (**19**) was revised on the basis of shift data with $Pr(fod)_3$, and integrated peak areas could then be used to determine the molecular weight[111].

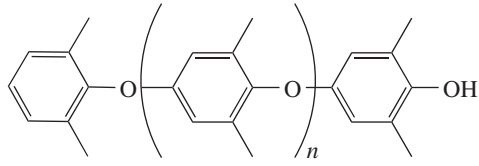

(**19**)

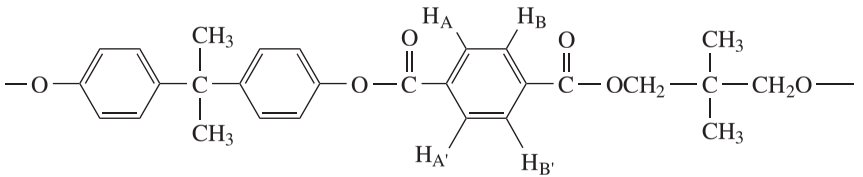

(**20**)

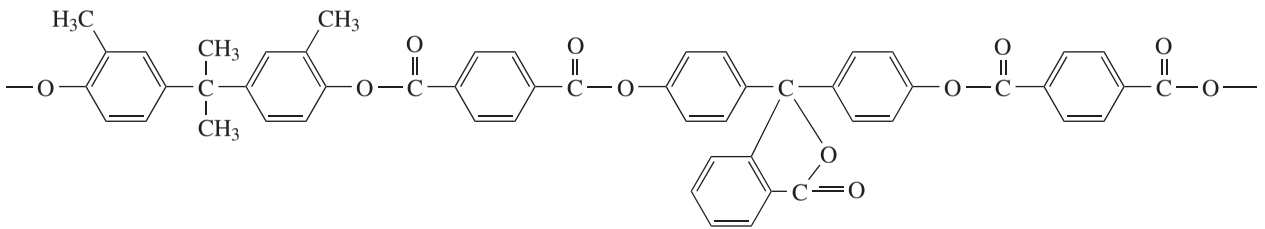

(**21**)

The coupling constant of the AA′BB′ portion of bisphenol A-neopentyl glycolterephthalate copolyesters (**20**) was determined in the presence of $Pr(fod)_3$[112]. The compositional tetrads of a 3,3′-dimethylbisphenol A-phenolphthalein copolyterephthalate (**21**) were resolved in the presence of $Eu(fod)_3$[113]. The *meso* and racemic dyads of a poly(β-substituted-β-propiolactone) were distinguishable in the ^{13}C NMR in the presence of $Eu(dpm)_3$[114]. The ^1H and ^{13}C NMR spectra of ethylene–vinyl acetate copolymers were assigned on the basis of two-dimensional NMR methods and lanthanide-induced shift data in the presence of $Eu(fod)_3$[115].

Lanthanide shift reagents have been used to analyze structural aspects of bitumen asphaltene samples[116]. Addition of $Yb(fod)_3$ shifted the resonances of hydrogen atoms α to oxygen atoms away from those α to aromatic rings, and enabled a bulk assessment of the concentrations of the two types of functionalities.

G. Analysis of Lipophillic Systems

Organic-soluble lanthanide chelates have been used to probe lipophillic systems. The compound 4-(4-dipentylamino-(*E*)-β-styryl)-1-(2,2,2-trifluoroethyl)pyridinium perchlorate (**22**) was employed as a probe in dimyristoylphosphatidylcholine vesicles. Probe molecules assembled in the inner and outer shells of the vesicle as evidenced by the presence of two signals in the ^{19}F NMR spectrum (376 MHz). Even though addition of $Eu(fod)_3$ promoted vesicle fusion, only one of the ^{19}F signals shifted. The shifted signal was likely from the probe molecule on the outer shell, as the internal ^{31}P signal of the phospholipid did not shift in the presence of $Eu(fod)_3$[117].

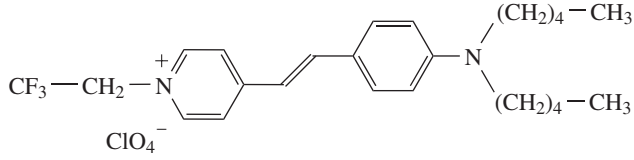

(**22**)

The self-assembly properties of amphiphillic cyclodextrins esterified at the 2- and 3-positions with lipophillic groups were examined in py-d_5 and thf-d_8 with the aid of $Eu(fod)_3$. In py-d_5 the cyclodextrin molecules dimerized as indicated in Figure 2a, and the europium ion caused shifts and broadening of the primary methylene resonances. In thf-d_8, the cyclodextrin associates had the alignment shown in Figure 2b, and the europium shifted the methyl and methylene resonances of the fatty acyl groups[118].

The permeability to ions of dioleoylphosphatidylcholine (**23**) and diphytanoyl phosphatidylcholine (**23′**) membranes was examined in the presence of $Eu(fod)_3$, $Pr(fod)_3$ and $Eu(dpm)_3$. Ion permeability of both lipid bilayers was enhanced in the presence of $Eu(fod)_3$ but not $Eu(dpm)_3$. The magnitudes of the shifts were used to gain information on the location of the $Eu(fod)_3$ in the membrane, and indicated that the europium chelate accumulated in the inner lipid layers of the two membranes and not in the central region between the two lipid layers[119].

H. Analysis of Polyfunctional Substrates

A substantial number of polyfunctional substrates have been studied with lanthanide shift reagents[4]. With two or more donor groups, there are several possible binding mechanisms for polyfunctional substrates. Binding of substrates to the lanthanide ion

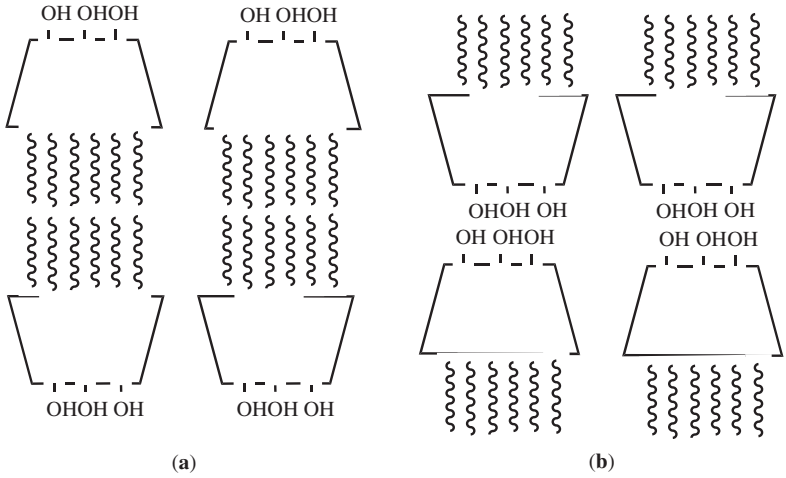

FIGURE 2. Self-assembly of amphiphillic cyclodextrin esters in (a) py-d_5 and (b) thf-d_8

is influenced by electronic and steric effects. If the donor sites of a polyfunctional substrate vary widely in either of these properties, it is possible that association occurs almost exclusively at one site. In situations when the functional groups have comparable donor properties, independent binding at each of the positions is possible and the shifts in the spectrum represent a weighted average of the two bound forms. Finally, if the donor atoms have the proper orientation, it is possible that the substrate can bond in a bidentate or even tridentate manner. Arrangement of atoms that can lead to five- or six-member rings, as in 1,2- and 1,3-dioxygenated compounds, form particularly stable chelate bonds. Examination of the binding trends of particular functional groups pointed to the order $NH_2 > OH > C{=}O > -O- > CO_2R > CN$[10] and cyclic ethers > cyclic thioethers > ketones > esters[4, 120].

In some cases it may be desirable to block a particular functional group so as to direct lanthanide association to another site. A comparison of the effect of blocking binding at hydroxyl groups by preparing trifluoroacetate, *tert*-butyldimethylsilyl ether and trimethyl silyl ether derivatives was reported[121]. The *tert*-butyldimethylsilyl ether derivative was most effective at blocking lanthanide association.

V. COUPLING OF ACHIRAL SHIFT REAGENTS TO CHIRAL DERIVATIZING AND SOLVATING AGENTS

Achiral lanthanide chelates have been used in conjunction with other chiral NMR derivatizing or solvating agents. The addition of the lanthanide enhances enantiomeric discrimination and/or causes shifts in the spectrum that show a characteristic trend with absolute configuration.

A. Chiral Derivatizing Agents

The addition of $Eu(dpm)_3$ to camphanate esters of α-deuteriated primary alcohols such as ethanol, benzyl alcohol and geraniol caused shifts in the spectrum that could be used to determine enantiomeric purity and that correlated with the absolute configuration[122].

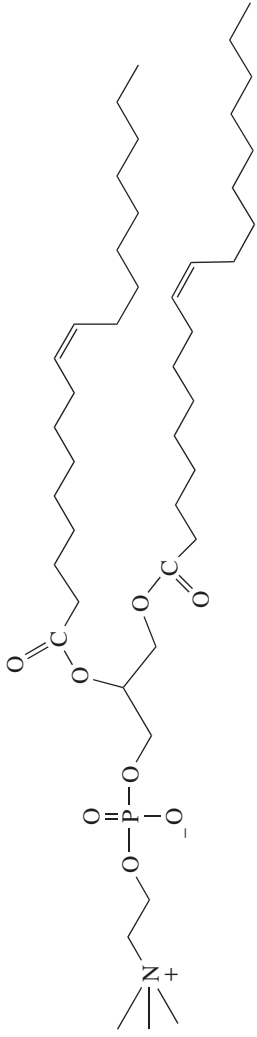

(23)

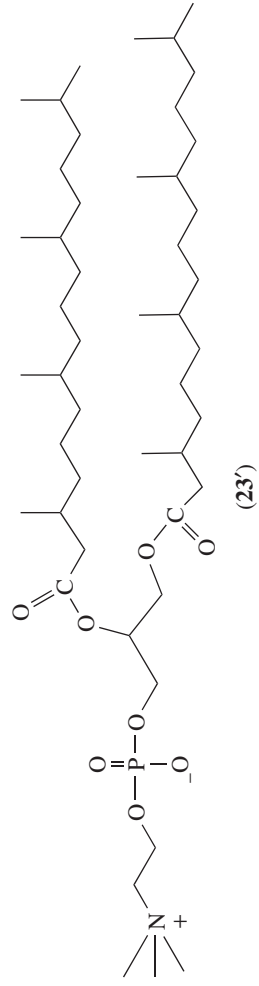

(23′)

Shifts in the spectra of camphanate esters with secondary alcohols with $Eu(fod)_3$ exhibited a consistent trend that correlated with absolute configuration[123].

The possibility of adding $Eu(fod)_3$ or $Pr(fod)_3$ to α-methoxy-α-trifluoromethylphenylacetic acid (mtpa) esters of hydroxyl- or amino-containing compounds to either assign or confirm the assignment of absolute configuration has been examined[4, 124]. Characteristic shifts of the methoxy resonance of the mtpa moiety often correlated with absolute configuration. Primary alcohols[125], secondary alcohols[126], 2- and 3-hydroxycarboxylic acid methyl esters[127], mtpa amide derivatives of amino acid esters[128], and axial chiral biaryl groups containing hydroxyl or amino groups have been studied[129].

The absolute configuration of methyl 4-methyl-6-(2-methylprop-1-enyl)cyclohexa-1,3-dienecarboxylate (**24**) was assigned on the basis of a study with $Eu(fod)_3$. **24** was first converted to its corresponding alcohol (**24′**), which was then converted to its mtpa derivative. Relative shifts of the methoxy signal of the (*S*)- and (*R*)-mtpa derivative in the presence of $Eu(fod)_3$ were used in assigning the absolute configuration. The NMR method was compared to a hydrolysis method using pancreatic lipase with the racemic ester. Porcine pancreatic lipase is known to hydrolyze the ester enantioselectively[130].

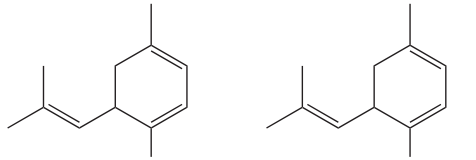

(**24**) (**24′**)

The shift of the ^{19}F resonance of the trifluoromethyl group in mtpa on adding $Eu(fod)_3$ was used to measure the enantiomeric excess of cyclopentanols, cyclohexanols and cycloheptanols[131]. However, there is ambiguity about whether the order of shifts can be used to assign the absolute stereochemistry[132]. When using mtpa-$Eu(fod)_3$ systems, a comparison to known model compounds is warranted, as assignments using only the methoxy or CF_3 resonance are based on the shifts of a single resonance.

The La(III) complex of 1,1,1,5,5,5-hexafluoro-2,4-pentanedione [$La(hfa)_3$] has been used in conjunction with mtpa derivatives of alcohols and amines to aid in the assignment of absolute configuration[133]. $La(hfa)_3$ was selected since only one signal is added to the ^1H NMR spectrum. The La(III) ion is associated in a chelate manner with the carboxyl and methoxy oxygen atoms of the mtpa derivative, as shown in Figure 3. Bonding of the La(III) causes a reversal of the relative positions of substituent groups in the mtpa derivative and the alteration in shielding by the phenyl ring can be used to verify stereochemical assignments. The validity of the method was demonstrated on several

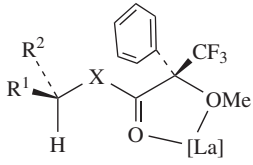

FIGURE 3. Chelate binding between the lanthanum ion in $La(hfa)_3$ and the mtpa derivatives of alcohols (X = O) and amines (X = NH, NR)

substrates, and it was especially useful for compounds with only a few ^1H resonances, for which assignments based only on the conventional means of using mtpa may be compromised[134, 135].

B. Chiral Solvating Agents (CSAs)

Achiral lanthanide chelates can also be added to CSAs such as arylperfluoroalkylcarbinols, the ethyl ester of 3,5-dinitrobenzoyl-L-leucine (**25**)[128], the 3,5-dinitrobenzoyl derivative of 1-phenylethylamine, *N*-(1-(1-naphthyl)ethyl)trifluoroacetamide (**26**)[129] and a series of 1-(1-naphthyl)ethyl urea derivatives of amino acids (**27**)[139] to enhance the enantiomeric discrimination. With sulfoxide[136] or lactone substrates[137], the europium ion preferentially associates with the substrate in the bulk solution. Provided the enantiomers have different association constants with the CSA, the isomer that shows the weaker association with the CSA shows the larger lanthanide-induced shifts. Low concentrations of lanthanide relative to the substrate and CSA lead to enhancements of enantiomeric discrimination in the NMR spectrum. If the concentration of lanthanide is too high, binding of the substrate to the lanthanide strips the substrate from the chiral solvating agent and diminishes the chiral discrimination in the NMR spectrum.

Addition of $Eu(fod)_3$ or $Pr(fod)_3$ to mixtures of enantiomeric sulfoxides and benzodiazepinones with **25** and **26** enhanced enantiomeric discrimination by an identical mechanism[138]. The method was further extended to mixtures of chiral sulfoxides, amines and alcohols with **27**. Warming the samples with lanthanide chelates to 50 °C reduced the exchange broadening to acceptable levels while retaining enantiomeric discrimination that was larger than observed with only the CSA[139].

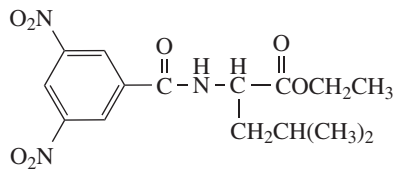

(**25**)

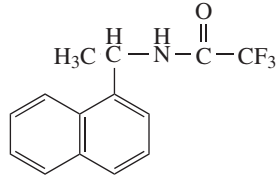

(**26**)

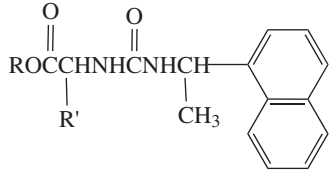

(**27**)

In subsequent work it was found that the carboxylic acid form of **25** and **27** could be solubilized in chloroform-*d* by the addition of triethylamine. Addition of $Eu(fod)_3$ caused the reverse behavior from what had been observed with the ester forms of the CSA, as the enantiomer that associated more favorably with the CSA has the larger lanthanide-induced shifts. This observation was explained by assuming that the carboxylate form of the CSA is bound to the lanthanide ion to create the species $[Ln(fod)_3CSA]^-$. The substrate then associated with the CSA in its lanthanide-bound form[140, 141].

VI. CHIRAL SHIFT REAGENTS

A. General Considerations

In 1971, Whitesides and Lewis first showed that lanthanide tris(β-diketonates) with optically pure ligands such as 3-pivaloyl-D-camphor (**28**) could be used to distinguish the spectra of enantiomers of amines, alcohols, ketones, esters and sulfoxides[142]. Many other chiral lanthanide tris(β-diketonates) were subsequently studied[4], and the complexes with 3-(trifluoroacetyl)-D-camphor (H-tfc) (**29**)[143], 3-(heptafluorobutyryl)-D-camphor (H-hfc) (**30**)[144] and D,D-dicampholylmethane (H-dcm) (**31**)[145] are noteworthy. Lanthanide complexes with these ligands are commercially available. The enhanced Lewis acidity of the metal ion caused by the electron withdrawing trifluoroacetyl and heptafluorobutyryl groups of tfc and hfc likely influence their effectiveness, although neither is consistently more effective than the other as analytical tools for chiral recognition. Chelates with dcm are remarkably effective as chiral shift reagents. For example, the enantiomeric discrimination in the methine and methyl resonances of 1-phenylethylamine, $PhCH(Me)NH_2$, in the presence of $Eu(dcm)_3$ was 4.4 and 0.7 ppm, respectively, in a 1:1 mixture[145]. Presumably, steric crowding in the $Ln(dcm)_3$ complexes creates diastereomeric lanthanide–substrate complexes with more specific geometries, which enhances the distinction of the two enantiomers.

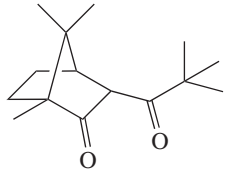

(**28**)

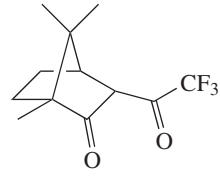

(**29**)

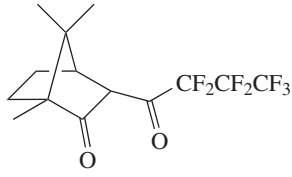

(**30**)

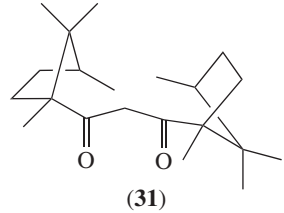

(**31**)

It is best to run a series of spectra with increasing concentrations of the chiral shift reagent, as demonstrated by the unusual behavior of the *ortho*-hydrogen resonance of 2-phenyl-2-butanol with $Eu(hfc)_3$. This resonance showed increasing enantiomeric discrimination up to a lanthanide–substrate ratio of about 0.5. At higher lanthanide–substrate ratios the nonequivalence diminished until the resonances recoalesced and then reversed their order in the spectrum. Such behavior likely reflects the dominance of a 2:1 substrate–lanthanide complex at low lanthanide concentration and a 1:1 complex at higher lanthanide concentrations. The chiral discrimination in the 2:1 and 1:1 complexes is markedly different[146]. A similar behavior was observed for 1-phenylethylamine with $Eu(dcm)_3$[145].

Chiral lanthanide tris(β-diketonates) have been used with many classes of organic compounds that have oxygen- and nitrogen-containing functional groups, as well as metal

complexes with ligands that have suitable donor groups. Review articles that provide a more extensive coverage of the range of applications of chiral lanthanide shift reagents have been published[4, 124, 147]. The rest of this section shows some of the diverse applications of chiral lanthanide tris(β-diketonates).

B. Miscellaneous Applications

Ln(tfc)$_3$ chelates were used to probe the *meso* structure of dieldrin (**32**)[148] and *meso* and chiral isomers of *cis*- (**32′**) and *trans*-4,5-dihydroxy-4,5-dihydroaldrin (**32″**)[149]. For the *meso*-compounds **32′** and **32″** in the presence of Ln(tfc)$_3$ chelates, prochiral pairs of hydrogen atoms such as H4–H5 and H3–H6 exhibit distinct resonances. The H4–H5 pair also couple to each other. For each enantiomer of the chiral compound (**32c**), the H4–H5 pair is equivalent and these appear as a singlet. In the presence of Ln(tfc)$_3$, two singlets are observed, one each for the H4–H5 pair of the (*R*)- and (*S*)-isomers. A similar analysis of the *meso* and *dl*-isomers of *cis*- and *trans*-2,3-butylene oxide was facilitated through the use of Ln(tfc)$_3$ chelates[148].

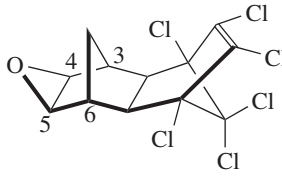

(**32**)

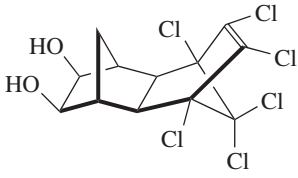

(**32′**)

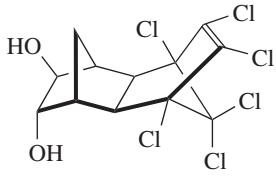

(**32″**)

The prochiral methylene hydrogen atoms α and β to the hydroxyl groups in 2-phenyl-1-ethanol (**33**) were distinguished by recording the spectrum of the *N*-(4-nitrophenylsulfonyl)-L-phenylalanyl ester in the presence of Eu(hfc)$_3$ or Yb(hfc)$_3$ at 300 MHz[150]. Being able to monitor the α and β sites would then facilitate an analysis of systems that first stereoselectively deuteriate the α-position of primary alcohols and then exhibit migration to the β-site. The utility of Ln(hfc)$_3$ at distinguishing the enantiomers of 1-deuterio alcohols has been demonstrated[151]. The relative shifts consistently correlate with the absolute configuration of the substrate.

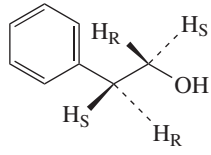

(**33**)

Compounds **34**[152] and **35**[153] are chiral by virtue of having a deuteriated substituent group. The ^{1}H and ^{2}H NMR spectra of **34** exhibited enantiomeric discrimination of the 2-methyl groups in the presence of Eu(hfc)$_3$[152]. Similarly, the *ortho*-hydrogen resonances of **35** were nonequivalent in the presence of Eu(dcm)$_3$[153].

(**34**)

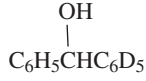

(**35**)

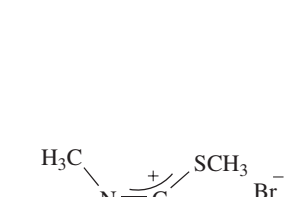

(**36**)

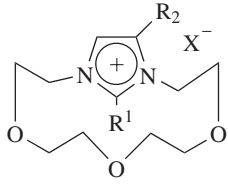

(**37**) (**a**) $R^1 = R^2 = H$
(**b**) $R^1 = Me$, $R^2 = H$
(**c**) $R^1 = R^2 = Me$

The enantiotopic protons of the prochiral methyl groups in the iminium salt **36** exhibited distinct resonances in the presence of $Eu(hfc)_3$[154]. As already discussed for achiral lanthanide β-diketonates, the system likely forms an ion pair between the organic cation and the species $[Ln(\beta\text{-dik})_3X]^-$. The spectrum of racemic **37**, which as its bromide salt has been studied as an ionic liquid, exhibits nonequivalence in the presence of $Eu(tfc)_3$ and $Eu(hfc)_3$. No splitting of the resonance occurs in the presence of $Eu(fod)_3$. In addition to the likely ion-pairing interaction of **37** with $[Ln(\beta\text{-dik})_3X]^-$, rather substantial shifts of some of the OCH_2 protons implied that the ether oxygen atoms also likely coordinated with the europium ion[155]. A similar ion-paired system explains the enantiomeric discrimination observed in the spectrum of the tris(phenanthroline) complexes of Ru(II) ($[Ru(phen)_3]Cl_2$) in the presence of $Eu(tfc)_3$[156].

Examination of the ^{13}C NMR spectrum of vinyl acetate and vinyl propionate copolymers with $Eu(hfc)_3$ or $Pr(hfc)_3$ indicated that linkages within the polymer were racemic in nature[157]. The ^1H (400 MHz) and ^{13}C (100 MHz) NMR spectra of 3-amino-1,2-dicarba-*closo*-dodecaboranes exhibited enantiomeric discrimination in the presence of $Eu(hfc)_3$[158]. The resonances broadened in the presence of the shift reagent, but it was still possible to observe signal separation for the two enantiomers.

Other nuclei besides ^1H or ^{13}C have been used to monitor enantiomeric discrimination with chiral lanthanide chelates. This includes the ^{17}O NMR spectra of chiral 2-thiabicyclo[4.3.0]nonane 2,2-dioxides (**14**) and 8,8-dioxides (**15**) with $Pr(hfc)_3$[89]. The ^{29}Si NMR spectrum of α-*C*-silylated amines and alcohols (**38**) in the presence of $Eu(tfc)_3$ was used to monitor the optical purity of these compounds[159]. A refocused-decoupled INEPT (insensitive nuclei enhanced by polarization transfer) pulse sequence was used to circumvent the long spin–lattice relaxation times of the silicon.

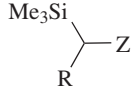

(**38**) Z = OH, NH_2

There is the potential with some substrates that the Lewis acidity of the lanthanide ion can catalyze a reaction. For example, the addition of $Eu(hfc)_3$ to a racemic mixture of dimethylpenta-2,3-dienoates (**39**) caused an enrichment of the (*S*)-isomer[160]. Over nine days the mixture converted to an 89:11 mixture. Lanthanide tris(β-diketonates) are well known catalysts for Diels–Alder reactions, and NMR spectroscopy of the reactants with $Eu(hfc)_3$ was used to understand the stereoselectivity of the europium-catalyzed cycloadditions[161].

Lanthanide chelates have been used as aids in studying the products of hydrogenation reactions monitored through parahydrogen-induced polarization (PHIP). Carrying out

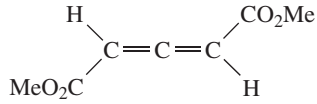

(**39**)

the hydrogenation with parahydrogen causes a significant enhancement in the hydrogen signals of the resulting products. Achiral lanthanide chelates were used to remove peak overlap in the hydrogenation of esters. Binuclear lanthanide–silver reagents were employed in the study of the hydrogenation of styrene. $Eu(tfc)_3$ was used to differentiate the chiral products of the hydrogenation of 1-phenyl-2-propen-1-ol. This procedure can be used to facilitate the study of the stereoselectivity of chiral catalysts. It was important to use low levels of lanthanide complexes, as higher concentrations quench the PHIP effect in a short period of time[162].

Chiral lanthanide chelates have been used to study compounds that are chiral but do not have an asymmetric carbon atom. 5-Oxidovinylphenanthridinium species (**40**) have two pairs of diastereomeric rotamers[163]. The number of methyl singlets of **40** doubled in the presence of $Eu(tfc)_3$, confirming the chirality under conditions of slow rotation. 1,3-Dienes such as **41** can exist in *EE, EZ* and *ZZ* forms and are chiral by virtue of slow rotation[164, 165]. The methoxy signal was conveniently monitored in the presence of $Eu(hfc)_3$ and could be used to determine the barrier to rotation. Slow rotation about the disulfide bonds of substrates of structure **42** gives rise to enantiomers, as was demonstrated by a splitting of the signals in the presence of $Eu(hfc)_3$[166].

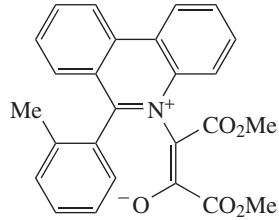

(**40**)

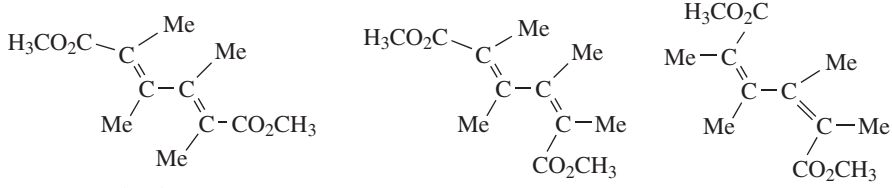

(*E,E*) (*E,Z*) (*Z,Z*)

(**41**)

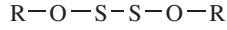

(**42**)

Methylphenylarsinous acid (**43**) is chiral under conditions of slow inversion. The resonances of the enantiomers of **43** were split in the presence of $Eu(hfc)_3$ in chloroform-*d*

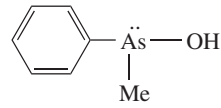

(**43**)

at 800 MHz. Shifts were very large and the *meta*- and *para*-protons of the phenyl ring were the most convenient to monitor[167].

The chirality of the (*Z*)-isomer of 2,2′-(**44a**) and 3,3′-dimethylbianthrone (**44b**) was established by observing a splitting of resonances in the presence of $Eu(hfc)_3$[168]. It was possible to distinguish the racemic pair from the *meso*-isomer as well. The methyl resonances were the most convenient to monitor. The helical chirality of annulenones, e.g. **45**, was confirmed by the doubling of certain resonances in the ^1H NMR spectrum in the presence of $Eu(dcm)_3$[169].

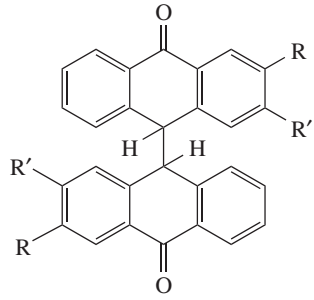

(**44**) (**a**) R = H, R′ = Me
(**b**) R = Me, R′ = H

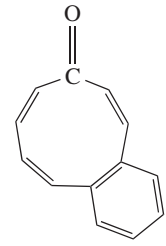

(**45**)

2,2′,6,6′-Tetrasubstituted biphenyls (**46**) exhibit axial chirality because of geometric constraints needed to reduce steric hindrance of the substituent groups. Addition of $Eu(tfc)_3$, $Pr(tfc)_3$ and $Pr(hfc)_3$ to derivatives of **46** with suitable donor groups caused enantiomeric discrimination in the ^1H NMR spectra. The (*S*)-isomer typically exhibited larger shifts in the spectrum[170].

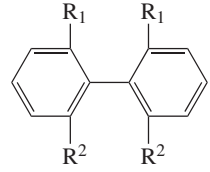

(**46**) (**a**) R^1 = OMe, R^2 = CO_2Me
(**b**) R^1 = NO_2, R^2 = CO_2Me
(**c**) R^1 = OMe, R^2 = CO_2OH

Cryptophane A (**47**) binds xenon in its cavity in $C_2D_2Cl_4$, as evidenced by the ^{129}Xe NMR spectrum of the insertion complex. In a racemic mixture of **47**, addition of $Eu(hfc)_3$ gives rise to two ^{129}Xe signals, showing an effective ‘chiralization’ of a neutral xenon atom[171].

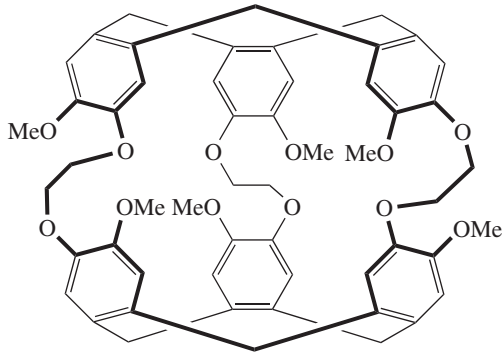

(**47**)

C. Assignment of Absolute Configuration

The geometry of chiral lanthanide tris(β-diketonates) with enantiomeric substrates is not known with enough certainty to facilitate the assignment of absolute configuration. The ligands in the complex are fluxional and alter their spatial arrangement to accommodate donor molecules. The potential of utilizing chiral lanthanide shift reagents for assigning absolute configurations is based on the observation of consistent empirical trends in relative shifts across a series of similar compounds. Caution must always be exercised when assigning absolute configurations based on empirical trends, as exceptions have been noted in many cases. It is important to compare the results to model compounds with similar structures. Such empirical trends were recently reviewed[124] and have already been noted in this chapter for the enantiomeric discrimination of α-amino acid methyl esters with $Sm(tfc)_3$[18], 1-deuterio alcohols with $Eu(hfc)_3$[151] and 2,2′,6,6′-tetrasubstituted biphenyls with tfc and hfc chelates[170].

A recent procedure for assigning the stereochemistry of secondary and tertiary alcohols using ^{13}C shifts with (*R*)- and (*S*)-$Pr(tfc)_3$ has been described[172]. ^{13}C was selected over ^{1}H because of the reduced line broadening and the presence of singlets in the spectra. Praseodymium was chosen over europium because of the reduction in contact shifts. The assignment is based on the behavior of the two carbon nuclei α to the carbon bearing the OH group, which are shown as X and Y in Figure 4. The shifts of these nuclei are measured with (*R*)- and (*S*)-$Pr(hfc)_3$ and the difference in these values determined. The

α-orientation
$\Delta\Delta\delta$ = negative

β-orientation
$\Delta\Delta\delta$ = positive

$$\Delta\Delta\delta = \Delta\delta_{(R)-Pr(tfc)_3} - \Delta\delta_{(S)-Pr(tfc)_3}$$

FIGURE 4. Correlation of $\Delta\Delta\delta$ values of ^{13}C resonances with absolute configuration of secondary and tertiary alcohols. X and Y correspond to the two carbons atoms α to the carbon with the hydroxyl group

positive or negative nature of this value consistently correlates with the configuration of the alcohol (Figure 4). The method works for α,α'-disubstituted alcohols. The hydroxyl group of diols separated by two or more carbon atoms can be treated independently and the stereostructure reliably assigned. The utility of the method was demonstrated in assigning the complete stereostructure of glisoprenin-A (**48**)[173]. The assignment was then validated by a total synthesis of the natural product[174].

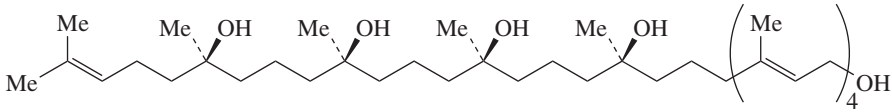

(**48**)

VII. BINUCLEAR LANTHANIDE–SILVER SHIFT REAGENTS

A. General Considerations

Lanthanide ions do not effectively associate with soft Lewis bases such as olefins, aromatics, phosphines and halogenated compounds. A strategy for generating lanthanide shift reagents for soft Lewis bases was first demonstrated by mixing silver trifluoroacetate or silver heptafluorobutyrate with $Ln(fod)_3$ to create a binuclear lanthanide–silver shift reagent[175]. The silver in the binuclear reagent associated with the soft Lewis base donor and the paramagnetic lanthanide induced shifts in the NMR spectrum. It was subsequently shown that Ag(fod) or Ag(tfa) was a far more effective silver reagent for preparing the binuclear reagent[176]. Evidence indicated that the mixture of $Ln(fod)_3$ with Ag(fod) resulted in the formation of a quadruple lanthanide chelate anion $[Ln(fod)_4]^-$ that formed an ion pair with the silver cation[177].

Lanthanide chelates of dpm were ineffective with silver β-diketonates at shifting the spectra of soft Lewis bases[178, 179]. The inability of the $Ln(dpm)_3$ chelates to form an eight-coordinate quadruple chelate anion likely explains this observation. Other silver species with β-diketone ligands containing phenyl, naphthyl and thiophene rings were evaluated for their ability to form the binuclear reagents[180, 181], and even though some pairs were more effective than Ag(fod), the commercial availability and stability of Ag(fod) relative to some of the other silver β-diketonates favor its use. The binuclear reagents have been shown to be effective for analyzing olefins, alkynes[177], aromatics, halogenated compounds and phosphines.

The shift mechanism of the binuclear reagents was examined with olefins and aromatics. Complexation shifts measured using diamagnetic $La(fod)_3$ were substantial for some resonances. Comparative internal ratios, plots obtained using theoretical dipolar and contact contributions of different lanthanides, and data with $[Gd(fod)_4]^-$ all indicated that the paramagnetic shifts of the binuclear reagents were exclusively dipolar in origin with no evidence for any contact shifts. This was not surprising given the diamagnetic silver bridge between the substrate and the lanthanide[182].

In early work with binuclear reagents at relatively low field strengths, the use of Pr(III) and Yb(III) chelates was preferable to Eu(III) as they caused larger shifts in the spectrum[176, 177]. A study aimed at determining bound shifts, association constants, and performing structural analysis located the lanthanide about 8 Å from the π bond in the binuclear–substrate complexes[183]. The larger distance between the substrate and lanthanide caused by the silver bridge, when compared to substrates that bond directly to the lanthanide, necessitated the use of larger shifting lanthanides. Pr(III) was especially effective for aromatic substrates as the upfield shifts moved the aromatic resonances into a region of the spectrum generally free of other signals[176, 179].

Association of the substrate with the silver ion of the binuclear reagent is favored in non-polar solvents. In a comparison of chloroform-*d*, cyclohexane and pentane, a shift order of pentane > cyclohexane > chloroform was observed[184].

B. Applications of Achiral Analogues

Binuclear reagents will bond to and shift the spectra of linear alkenes such as 1-hexene[177]. They can be used to distinguish (*Z*)- and (*E*)-alkenes, although the shifts show interesting behavior. The shifts in the spectrum of the (*Z*)-isomer in compounds such as 2-octene[177] and hexa-2,4-diene[185] were larger than those of the (*E*)-isomer at lanthanide–substrate ratios of less than one. The binding of silver to alkenes is sensitive to steric hindrance, such that the binding of (*Z*)-alkenes to silver is favored over (*E*)-alkenes under competitive conditions. At lanthanide–substrate ratios above one, the resonances of the (*E*)-isomer shifted further. In the absence of competitive lanthanide binding, the geometric term of the dipolar equation evidently causes larger lanthanide-induced shifts for the (*E*)-isomer. Applying these trends, $Yb(fod)_3$/Ag(fod) was used to distinguish the (*Z*)–(*Z*) and (*Z*)–(*E*) diads in polybutadienes by ^{13}C NMR spectroscopy[186].

Steric differences also explain the preferential binding of silver at the exocyclic alkene of limonene (**49**)[177, 185]. The binuclear reagents are effective at shifting the spectra of other terpenes with either an exocyclic double bond, such as β-pinene (**50**) and camphene (**51**), or an endocyclic double bond, such as α-pinene (**52**) and Δ-3-carene (**53**)[178].

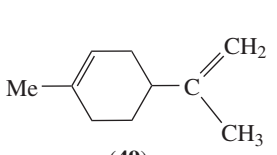

(**49**)

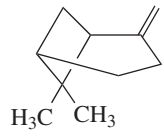

(**50**)

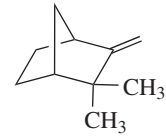

(**51**)

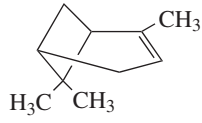

(**52**)

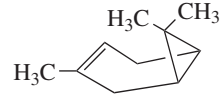

(**53**)

The binuclear reagents are effective at shifting resonances of phenyl-containing compounds such as toluene[176], *o*-, *m*- and *p*-xylene[177, 179], other methylbenzenes[179, 187] and *p*-terphenyl[176]. The shifts of the methyl resonances can be used to analyze mixtures of *o*-, *m*- and *p*-xylene and the methylbenzenes in gasoline[179]. The binuclear reagents are sensitive enough to distinguish secondary deuterium isotope effects in aromatic substrates[188]. This included differential shifts in the ^1H resonances of benzene-*d* versus benzene and *p*-xylene-d_6 (deuteriated methyl groups) versus *p*-xylene. The deuteriated compounds exhibited the largest shifts, possibly pointing to the greater inductive effect of ^2H over ^1H as the reason for the substrate to become a better donor with an enhanced association constant.

The binuclear reagents are effective at shifting the spectra of fused ring polycyclic aromatic compounds. Compounds with no substituent groups on the rings such as naphthalene, anthracene, phenanthrene and pyrene did not exhibit specific bonding to the

Ag(I) such that all resonances showed similar magnitude shifts. Incorporation of a substituent group as in 2-methylanthracene, 9-methylanthracene, 1-methylphenanthrene, 1-methylnaphthalene and acenaphthene resulted in differential shifts. The differential shifts indicated that silver bonding occurred away from the steric hindrance of the substituent group[179].

Alkyl halides such as 1-chlorocyclohexane, 1-bromopentane and 1-iodohexane associate with silver and the spectra shift in the presence of the binuclear reagents. The shifts for the organohalides were in the order I > Br > Cl, reflecting the relative softness and hence relative binding abilities of the halides to silver. Some organohalides were reactive with silver such that a silver halide precipitate formed[177].

Although only the focus of limited studies, the binuclear reagents are effective for phosphines and phosphites, as evidenced by the shifts in the spectrum of triphenylphosphine (tpp) or triphenylphosphite in the presence of $[Ln(fod)_4]Ag$. At silver–substrate ratios greater than one, the ^{31}P signal of tpp was split into two doublets. These occurred from coupling of ^{107}Ag and ^{109}Ag to the phosphorus, indicating that silver–phosphorus binding was in slow exchange. Raising the concentration of phosphine above that of the silver eventually eliminated the coupling because of fast exchange of the substrate[179].

C. Applications of Chiral Analogues

Reagents formed with chiral β-diketonate ligands such as $Ln(tfc)_3$ and $Ln(hfc)_3$ in the presence of Ag(fod) or other silver β-diketonates are effective for chiral discrimination[178, 189]. Lanthanide chelates with dcm are ineffective in the binuclear complexes, presumably because the dcm ligand is so sterically hindered that it prevents the formation of the quadruple chelate anion[181]. Silver complexes besides Ag(fod) actually form more effective chiral discriminating agents with $Pr(tfc)_3$, $Yb(tfc)_3$ and $Yb(hfc)_3$, but these complexes are not commercially available so have not been used beyond exploratory studies[178, 180, 181].

Chiral discrimination in the ^1H and/or ^{13}C NMR spectra of terpenes such as limonene (**49**), β-pinene (**50**), camphene (**51**), α-pinene (**52**), Δ-3-carene (**53**) and *epi*-β-santalene (**54**) has been observed[178, 189–191]. Other chiral olefinic substrates that show discrimination in the presence of chiral binuclear reagents include *trans*-2-menthene, 4-vinylcyclohexene, 3-methylcyclohexene, 4-*t*-butylcyclohexene, bornene[190], α-copaene (**55**)[191] and (*E*)-1-benzylidene-2,3,4(*R* or *S*)-5(*S* or *R*)-tetrabenzylcyclopenta-2-ene (**56**)[192].

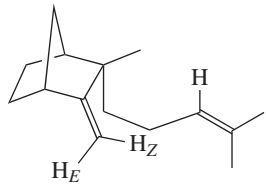

(**54**)

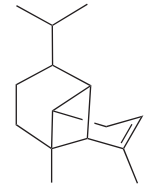

(**55**)

Chiral recognition on the order of 0.1 to 0.3 ppm was observed in the ^{13}C NMR spectrum of myrcene (**57**) and 3-methylpent-1-ene in the presence of $Pr(hfc)_3$/$Ag(fod)$[193]. The absence of any splitting of resonances in the ^{13}C spectrum of **58** was interpreted as a proof that the compound was enantiomerically pure. $Yb(hfc)_3$/Ag(fod) caused enantiomeric discrimination in the spectra of methyl[194], alkyl[195], phenyl[195] and trimethylsilyl[196]1,3-disubstituted allenes. The resonance of the methyl group at the chiral

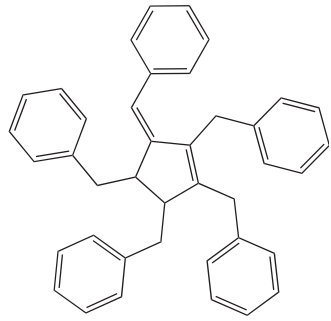

(**56**)

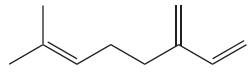

(**57**)

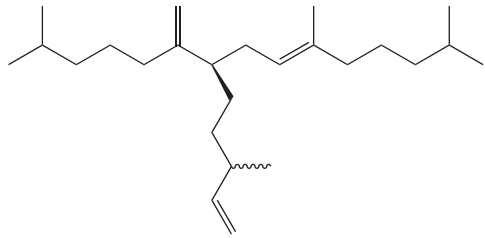

(**58**)

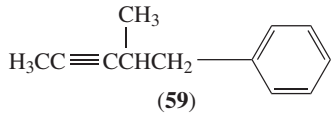

(**59**)

carbon of alkyne **59** exhibited enantiomeric discrimination in the presence of Eu(tfc)$_3$/Ag(fod)[197].

A sesquiterpene of furanodiene structure **60** is chiral because of its conformational rigidity as confirmed by a doubling of resonances in the ^{13}C NMR spectrum in the presence of Yb(hfc)$_3$/Ag(fod)[191]. The methyl groups at positions 4 and 5 in 3,4,5,6-tetramethylphenanthrene (**61**) distort out of the plane to minimize steric hindrance, causing the compound to be chiral. Enantiomeric discrimination was observed in the ^{1}H spectrum in the presence of Ln(hfc)$_3$/Ag(fod) reagents[189].

The enantiomeric purity of dibromides such as **62** was determined using Yb(hfc)$_3$/Ag(fod). Binding of the silver occurred at the bromine atoms rather than the fluorine or chlorine atoms[198].

Binuclear lanthanide–silver chelates have also been used as shift reagents for compounds with weakly basic heteroatoms that are part of π systems and do not associate strongly with lanthanide ions. With the binuclear reagents, silver association with the π electrons leads to larger shifts. Substrates of this type include compounds such as

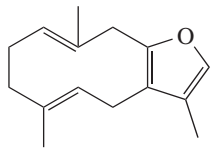

(**60**)

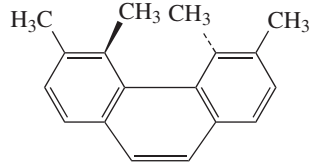

(**61**)

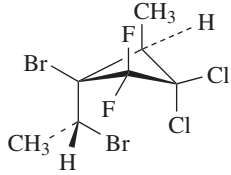

(**62**)

indole (**63**)[187, 199], pyrrole (**64**)[199], benzofuran (**65**)[185, 199], methoxybenzene[185], benzonitrile, azobenzene (**66**) and thiazole (**67**)[200]. For benzothiophene (**68**), the shifts indicated that binding of the silver likely occurred at the sulfur atom rather than with the π electrons[199].

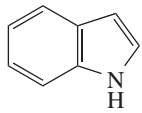

(**63**)

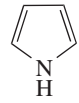

(**64**)

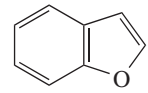

(**65**)

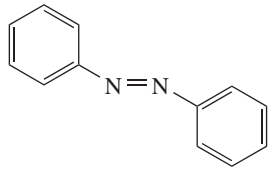

(**66**)

(**67**)

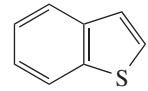

(**68**)

The spectra of **69a** and **69b** exhibited only small nonequivalence in the presence of Yb(hfc)$_3$, whereas addition of Ag(fod) caused larger nonequivalence of methyl and methoxy resonances of the R-groups at 500 MHz[201]. The binuclear dipyrromethene complex with Zn(II) (**70**) has a helical structure that renders it chiral. This was confirmed by a doubling of certain resonances in the ^{1}H NMR spectrum of the zinc complex in the presence of Eu(tfc)$_3$/Ag(fod) or Yb(tfc)$_3$/Ag(fod). Splitting of the resonances was not observed in the presence of the lanthanide chelate alone and was only observed on addition of the silver reagent[202].

D. Analysis of Organic Cations

The ion-pairing interaction of the binuclear reagents has also been exploited in the analysis of organic cations[203, 204]. Addition of the binuclear [Ln(fod)$_4$]Ag to halide salts of

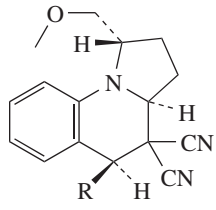

(**69**) (**a**) R = H
(**b**) R = CH_3

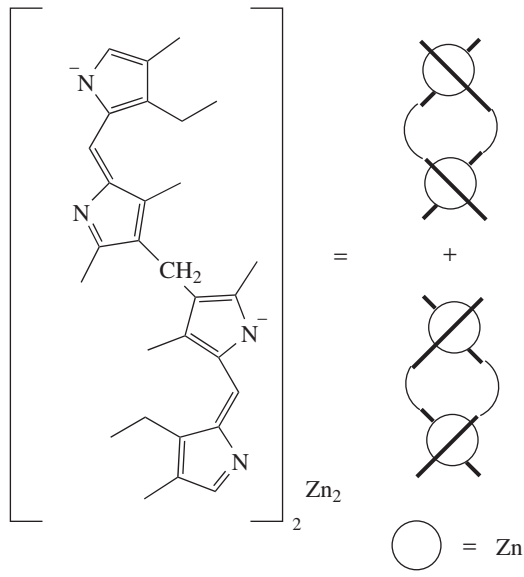

(**70**)

organic cations results in the precipitation of silver chloride. The addition of $[Ln(fod)_4]K$ caused substantially smaller shifts, indicating the need to precipitate out the silver halide to better form the ion pair[203]. For tetrafluoroborate salts, K(fod) is preferred over Ag(fod) since only KBF_4 is insoluble in chloroform-d[204]. The organic cation forms an ion pair with $[Ln(\beta\text{-diketonate})_4]^-$ and substantially larger shifts are observed in the resulting NMR spectrum than with lanthanide tris(β-diketonates) alone. The utility of $[Ln(fod)_4]^-$ as a shift reagent for sulfonium, ammonium and isothiouronium salts (**71**) has been demonstrated[203, 204].

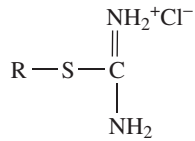

(**71**)

Substantial shifts were observed in the spectra of *N*-ethylquinolinium iodide, *N*-methylnicotinium iodide (**72**) and [3-(dimethylamino)propyl]trimethyl ammonium iodide with $[Eu(fod)_4]^-$. In the case of **72**, the relative magnitude of the shifts indicated that the cationic nitrogen was the site of association with $[Eu(fod)_4]^-$ rather than the tertiary nitrogen coordinating directly with the Eu(III)[203].

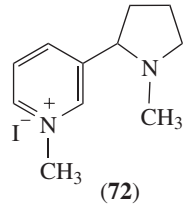

(**72**)

The ^1H NMR spectra of methyl sulfonium salts of alkyl sulfides, tetrahydrothiophene and benzothiophene (**68**) showed large shifts in the presence of $[Eu(fod)_4]^-$ [204]. A selectively deuteriated derivative of *S*-methyltetrahydrothiophenium iodide was used to confirm the assignment of the diastereotopic methylene hydrogen atoms. Studies with the *S*-methyltetrahydrothiophenium and *N*-ethylquinolinium ions indicated that 1:1 complexes formed with $[Eu(fod)_4]^-$ and that the shifts were purely dipolar in origin[205].

The analysis of isothiouronium salts, which are conveniently formed by reacting alkyl halides with thiourea, provide a way to study alkyl halides[204]. The ^1H NMR spectrum of *s*-butylisothiouronium chloride and bromide exhibited enantiomeric discrimination in the presence of $[Eu(tfc)_3(fod)]^-$ [204]. The enantiomeric purity of several alkyl methyl phenyl sulfonium ions (**73**) under conditions of slow inversion was determined using either $[Eu(tfc)_3(fod)]^-$ or $[Eu(tfc)_4]^-$ [206]. It was possible to study the inversion barrier by variable-temperature studies in the presence of the shift reagent.

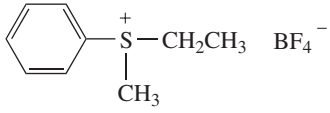

(**73**)

Achiral binuclear reagents have been added to mixtures of a chiral crown ether (**74**) and chloroform-soluble amino acid ester hydrochlorides to enhance the chiral discrimination in the NMR spectrum. The $[Ln(fod)_4]^-$ preferentially associated with the enantiomer in the bulk solution such that the enantiomer with lower association with **74** showed the larger lanthanide-induced shifts. The system also enhanced the chiral discrimination in acetonitrile-d_3, although $[Pr(fod)_4]^-$ was needed because it causes larger shifts than the

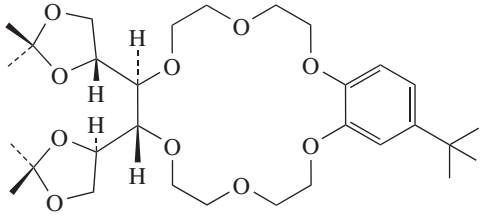

(**74**)

Eu(III) analogue. It was important to keep the concentration of lanthanide less than that of the crown ether, otherwise the lanthanide ion bound within the crown, thereby displacing the protonated amine and reducing the enantiomeric discrimination[207].

VIII. REFERENCES

1. W. D. Horrocks, Jr., R. C. Taylor and G. N. La Mar, *J. Am. Chem. Soc.*, **86**, 3031 (1964).
2. R. W. Kluiber and W. D. Horrocks, Jr., *J. Am. Chem. Soc.*, **87**, 5350 (1965).
3. C. C. Hinckley, *J. Am. Chem. Soc.*, **91**, 5160 (1969).
4. T. J. Wenzel, *NMR Shift Reagents*, CRC Press, Boca Raton, FL, 1987.
5. J. H. Forsberg, in *Handbook on the Physics and Chemistry of Rare Earths* (Eds K. A. Gschneidner and L. Eyring), Vol. **23**, Chap. 153, Elsevier, North-Holland, Amsterdam, 1996, pp. 1–68.
6. J. A. Peters, J. Huskens and D. J. Raber, *Prog. Nucl. Reson. Spectrosc.*, **28**, 283 (1996).
7. J. K. M. Sanders and D. H. Williams, *J. Chem. Soc., Chem. Commun.*, 422 (1970)
8. R. E. Rondeau and R. E. Sievers, *J. Am. Chem. Soc.*, **93**, 1522 (1971)
9. W. D. Horrocks, Jr. and J. P. Sipe, III, *J. Am. Chem. Soc.*, **93**, 6800 (1971).
10. J. K. M. Sanders and D. H. Williams, *J. Am. Chem. Soc.*, **93**, 641 (1971).
11. M. Sayeed and N. Ahmad, *J. Inorg. Nucl. Chem.*, **43**, 3197 (1981).
12. J. W. M. de Boer, P. J. D. Sakkers, C. W. Hilbers and E. de Boer, *J. Magn. Reson.*, **26**, 253 (1977).
13. R. E. Rondeau and R. E. Sievers, *Anal. Chem.*, **45**, 2145 (1973).
14. J. Reuben and J. S. Leigh, Jr., *J. Am. Chem. Soc.*, **94** 2789 (1972).
15. J. M. Bulsing, J. K. M. Sanders and L. D. Hall, *J. Chem. Soc., Chem. Commun.*, 1201 (1981).
16. K. Ajisaka and M. Kainosho, *J. Am. Chem. Soc.*, **97**, 330 (1975).
17. Z. Polívka, M. Buděšínský, J. Holubek, B. Schneider, Z. Šedivý, E. Svátek, O. Matoušová, J. Metyš, M. Valchář, R. Souček and M. Protiva, *Collect. Czech. Chem. Commun.*, **54**, 2443 (1989).
18. K. Omata, S. Aoyagi and K. Kabuto, *Tetrahedron: Asymmetry*, **15**, 2351 (2004).
19. L. M. Sweeting, D. C. Crans and G. M. Whitesides, *J. Org. Chem.*, **52**, 2273 (1987).
20. M. Kagawa, Y. Machida, H. Nishi and J. Haginaka, *J. Pharm. Biomed. Anal.*, **38**, 918 (2005).
21. G. T. Pearce, W. E. Gore and R. M. Silverstein, *J. Org. Chem.*, **41**, 2797 (1976).
22. J. Belleney, C. Bui and F. J. Carrière, *Magn. Reson. Chem.*, **28**, 606 (1990).
23. P. E. Peterson and M. Stepanian, *J. Org. Chem.*, **53**, 1907 (1988).
24. F. Sancassan, G. Petrillo and R. J. Abraham, *J. Chem. Soc., Perkin Trans. 2*, **11**, 1965 (1995).
25. H. M. McConnell and R. E. Robertson, *J. Chem. Phys.*, **29**, 1361 (1958).
26. W. D. Horrocks, Jr. and J. P. Sipe, III, *Science*, **177**, 994 (1972).
27. W. D. Horrocks, Jr., *J. Am. Chem. Soc.*, **96**, 3022 (1974).
28. J. M. Briggs, G. P. Moss, E. W. Randall and K. D. Sales, *J. Chem. Soc., Chem. Commun.*, 1180 (1972).
29. S. B. Tjan and F. R. Visser, *Tetrahedron Lett.*, **12**, 2833 (1971).
30. C. Marzin, D. Liebfritz, G. E. Hawkes and J. D. Roberts, *Proc. Natl. Acad. Sci. U.S.A.*, **70**, 562 (1973).
31. B. F. G. Johnson, J. Lewis, P. McArdle and J. R. Norton, *J. Chem. Soc., Chem. Commun.*, 535 (1972).
32. M. Hirayama, E. Edagawa and Y. Hanyu, *J. Chem. Soc., Chem. Commun.*, 1343 (1972).
33. M. Kainosho, K. Ajisaka and K. Tori, *Chem. Lett.*, 1061 (1972).
34. J. A. Peters, M. S. Nieuwenhuizen and D. J. Raber, *J. Magn. Reson.*, **65**, 417 (1985).
35. K. Ajisaka, M. Kainosho, H. Shigemoto, K. Tori, Z. W. Wolkowski and Y. Yoshimura, *Chem. Lett.*, 1205 (1973).
36. C. N. Reilley, B. W. Good and R. D. Allendoerfer, *Anal. Chem.*, **48**, 1446 (1976).
37. C. N. Reilley, B. W. Good and J. F. Desreux, *Anal. Chem.*, **47**, 2110 (1975).
38. J. H. Forsberg, R. M. Delaney, Q. Zhao, G. Harakas and R. Chandran, *Inorg. Chem.*, **34**, 3705 (1995).
39. J. Reuben, *J. Magn. Reson.*, **11**, 103 (1973)
40. M. H. Lee, *Bull. Korean Chem. Soc.*, **7**, 433 (1986).
41. P. H. Mazzocchi, H. J. Tamburin and G. R. Miller, *Tetrahedron Lett.*, **12**, 1819 (1971).

42. B. L. Shapiro, J. R. Hlubucek, G. R. Sullivan and L. F. Johnson, *J. Am. Chem. Soc.*, **93**, 3281 (1971).
43. D. E. U. Ekong, J. I. Okogun and M. Shok, *J. Chem. Soc., Perkin Trans. 1*, 653 (1972).
44. J. K. M. Sanders, S. W. Hanson and D. H. Williams, *J. Am. Chem. Soc.*, **94**, 5325 (1972).
45. V. G. Gibb, I. M. Armitage, L. D. Hall and A. G. Marshall, *J. Am. Chem. Soc.*, **94**, 8919 (1972).
46. J. W. ApSimon, H. Beierbeck and A. Fruchier, *Org. Magn. Reson.*, **8**, 483 (1976).
47. B. L. Shapiro and M. D. Johnston, Jr., *J. Am. Chem. Soc.*, **94**, 8185 (1972).
48. D. J. Raber and L. E. Hardee, *Org. Magn. Reson.*, **20**, 125 (1982).
49. D. J. Raber and J. A. Peters, *Magn. Reson. Chem.*, **23**, 621 (1985).
50. I. Armitage, G. Dunsmore, L. D. Hall and A. G. Marshall, *Can. J. Chem.*, **50**, 2119 (1972).
51. B. L. Shapiro, M. J. Shapiro, A. D. Godwin and M. D. Johnston, Jr., *J. Magn. Reson.*, **8**, 402 (1972).
52. I. Armitage and L. D. Hall, *Can. J. Chem.*, **49**, 2270 (1971).
53. J. A. Peters, P. J. Wijnand Schuyl, W. M. M. J. Bovee, J. H. Alberts and H. van Bekkum, *J. Org. Chem.*, **46**, 2784 (1981).
54. G. E. Hawkes, D. Leibfritz, D. W. Roberts and J. D. Roberts, *J. Am. Chem. Soc.*, **95**, 1659 (1973).
55. C. L. Honeybourne, *Tetrahedron Lett.*, **13**, 1095 (1972).
56. G. N. La Mar and J. W. Faller, *J. Am. Chem. Soc.*, **95**, 3817 (1973).
57. D. H. Welti, M. Linder and R. R. Ernst, *J. Am. Chem. Soc.*, **100**, 403 (1978).
58. G. C. Levy and R. A. Komoroski, *J. Am. Chem. Soc.*, **96**, 678 (1974).
59. O. A. Gansow, A. R. Burke and G. N. La Mar, *J. Chem. Soc., Chem. Commun.*, 456 (1972).
60. J. P. Basilion, S. Yeon and R. Botnar, *Curr. Top. Dev. Biol.*, **70**, 1 (2005).
61. T. Watanabe, *Nucl. Magn. Reson.*, **35**, 457 (2006).
62. P. B. Barker and D. D. M. Lin, *Prog. Nucl. Magn. Reson. Spectrosc.*, **49**, 99 (2006).
63. S. M. Rothstein, W. D. Bell and M. F. Richardson, *J. Magn. Reson.*, **41**, 310 (1980).
64. G. R. Sullivan, *J. Am. Chem. Soc.*, **98**, 7162 (1976).
65. I. M. Armitage, L. D. Hall, A. G. Marshall and L. G. Werbelow, *J. Am. Chem. Soc.*, **95**, 1437 (1973).
66. J. A. Ladd, *Magn. Reson. Chem.*, **27**, 483 (1989).
67. R. J. Abraham and F. Sancassan, in *Encyclopedia of Nuclear Magnetic Resonance*, Vol. **9**, John Wiley & Sons, Chichester, New York, 2002, pp. 578–588.
68. R. J. Abraham, M. Mobli, J. Ratti, F. Sancassan and T. A. D. Smith, *J. Phys. Org. Chem.*, **19**, 384 (2006).
69. J. Reuben and J. S. Leigh, Jr., *J. Am. Chem. Soc.*, **94**, 2789 (1972).
70. J. W. Faller and G. N. La Mar, *Tetrahedron Lett.*, **14**, 1381 (1973).
71. T. B. Patrick and P. H. Patrick, *J. Am. Chem. Soc.*, **94**, 6230 (1972).
72. B. L. Shapiro, M. D. Johnston, Jr. and R. L. R. Towns, *J. Am. Chem. Soc.*, **94**, 4381 (1972).
73. J. J. Uebel, C. Pacheco and R. M. Wing, *Tetrahedron Lett.*, **14**, 4383 (1973).
74. J. P. Shoffner, *J. Am. Chem. Soc.*, **96**, 1599 (1974).
75. M. Hajek, L. Vodicka and Z. Ksandr, *Sb. Vys. Sk. Chem.-Technol. Praze D*, **32**, 73 (1976); *Chem. Abstr.*, **86**, 15869 (1977).
76. T. C. Morrill, R. J. Opitz and R. Mozzer, *Tetrahedron Lett.*, **14**, 3715 (1973).
77. J. San Filippo, Jr, R. G. Nuzzo and L. J. Romano, *J. Am. Chem. Soc.*, **97**, 2546 (1975).
78. J. E. Bulkowski and C. H. Van Dyke, *Inorg. Nucl. Chem. Lett.*, **11**, 749 (1975).
79. L. F. Lindoy and W. E. Moody, *J. Am. Chem. Soc.*, **97**, 2275 (1975).
80. L. F. Lindoy and H. W. Louie, *J. Am. Chem. Soc.*, **101**, 841 (1979).
81. T. J. Marks, J. S. Kristoff, A. Alicii and D. F. Shriver, *J. Organomet. Chem.*, **33**, C35 (1971).
82. L. F. Lindoy, *Coord. Chem. Rev.*, **48**, 83 (1983).
83. R. E. Graves and P. I. Rose, *J. Chem. Soc., Chem. Commun.*, 630 (1973).
84. K. B. Lipkowitz, T. Chevalier, B. P. Mundy and J. J. Theodore, *Tetrahedron Lett.*, **21**, 1297 (1980).
85. R. L. Caret, A. Vennos, M. Zapf and J. J. Uebel, *Tetrahedron Lett.*, **22**, 2085 (1981).
86. T. A. Powers and S. A. Evans, Jr., *Tetrahedron Lett.*, **31**, 5835 (1990).
87. T. A. Powers, S. A. Evans, Jr., K. Pandiarajan and J. C. N. Benny, *J. Org. Chem.*, **56**, 5589 (1991).
88. T. A. Powers, L. G. Pedersen and S. A. Evans, Jr., *Phosphorus Sulfur Silicon*, **59**, 205 (1991).

89. G. Barbarella, A. Bongini, V. Cere, C. Paolucci and S. Pollicino, *J. Org. Chem.*, **58**, 6499 (1993).
90. G. Lowe and S. J. Salamone, *J. Chem. Soc., Chem. Commun.*, 1392 (1983).
91. I. P. Gerothanassis and J. Lauterwein, *Magn. Reson. Chem.*, **24**, 1034 (1986).
92. D. Horton and J. K. Thomson, *J. Chem. Soc., Chem. Commun.*, 1389 (1971).
93. P. E. Pfeffer, T. A. Foglia, P. A. Barr and R. H. Obenauf, *J. Org. Chem.*, **43**, 3429 (1978).
94. J. E. Nordlander and J. E. Haky, *J. Org. Chem.*, **45**, 4780 (1980).
95. A. M. Stolzenberg and M. A. Laliberte, *J. Org. Chem.*, **52**, 1022 (1987).
96. J. C. Russell, J. R. Jones, T. A. Vick and P. W. Stratford, *J. Labelled Compd. Radiopharm.*, **33**, 957 (1993).
97. G. V. Smith, W. A. Boyd and C. C. Hinckley, *J. Am. Chem. Soc.*, **93**, 6319 (1971).
98. A. M. Grotens, C. W. Hilbers, E. de Boer and J. Smid, *Tetrahedron Lett.*, **13**, 2067 (1972).
99. C. C. Hinckley, W. A. Boyd and G. V. Smith, *Tetrahedron Lett.*, **13**, 879 (1972).
100. J. K. M. Sanders and D. H. Williams, *J. Chem. Soc., Chem. Commun.*, 436 (1972).
101. A. T. Balaban, I. I. Stanoiu and F. Chiraleu, *J. Chem. Soc., Chem. Commun.*, 984 (1976).
102. A. H. Lewin, *Tetrahedron Lett.*, **12**, 3583 (1971).
103. H. N. Cheng and H. S. Gutowsky, *J. Phys. Chem.*, **84**, 1039 (1980).
104. A. de Savignac, A. Lattes and M. Bon, *Org. Magn. Reson.*, **6**, 528 (1974).
105. H. Gozlan, R. Michelot and R. Rips, *Tetrahedron Lett.*, **16**, 859 (1975).
106. J. W. Faller and B. V. Johnson, *J. Organomet. Chem.*, **96**, 99 (1975).
107. A. R. Katritzky and A. Smith, *Tetrahedron Lett.*, **12**, 1765 (1971).
108. Y. Inoue and T. Konno, *Makromol. Chem.*, **179**, 1311 (1978).
109. J. E. Guillet, I. R. Peat and W. F. Reynolds, *Tetrahedron Lett.*, **12**, 3493 (1971).
110. F. F. L. Ho, *Polym. Lett.*, **9**, 491 (1971).
111. J. Reuben and A. Biswas, *Macromolecules*, **24**, 648 (1991).
112. E. V. Gouinlock, R. A. Wolfe and J. C. Rosenfeld, *J. Appl. Polym. Sci.*, **20**, 949 (1976).
113. M. Matlengiewicz, *Macromolecules*, **17**, 473 (1984).
114. M. Iida, S. Hayase and T. Araki, *Macromolecules*, **11**, 490 (1978).
115. H. N. Cheng and G. H. Lee, *Polym. Bull.*, **19**, 89 (1988).
116. F. F. Shue and T. F. Yen, *Fuel*, **62**, 127 (1983).
117. B. P. Bammel, D. D. Hamilton, R. P. Haugland, H. P. Hopkins, J. Schuette, W. Szalecki and J. C. Smith, *Biochem. Biophys. Acta*, **1024**, 61 (1990).
118. P. Zhang, H. Parrot-Lopez, P. Tchoreloff, A. Baszkin, C. C. Ling, C. de Rango and A. W. Coleman, *J. Phys. Org. Chem.*, **5**, 518 (1992).
119. K. D. Schulze and H. Sprinz, *Biochim. Biophys. Acta*, **1467**, 27 (2000).
120. H. Hart and G. M. Love, *Tetrahedron Lett.*, **12**, 625 (1971).
121. D. J. Raber and G. J. Propeck, *J. Org. Chem.*, **47**, 3324 (1982).
122. H. Gerlach and B. Zagalak, *J. Chem. Soc., Chem. Commun.*, 274 (1973).
123. J. Jurczak, A. Konowal, Z. Krawczyk and A. Ejchart, *Org. Magn. Reson.*, **17**, 50 (1981).
124. T. J. Wenzel, *Discrimination of Chiral Compounds using NMR Spectroscopy*, John Wiley & Sons, Inc., New York, 2007.
125. F. Yasuhara and S. Yamaguchi, *Tetrahedron Lett.*, **18**, 4085 (1977).
126. S. Yamaguchi and F. Yasuhara, *Tetrahedron Lett.*, **18**, 89 (1977).
127. F. Yasuhara and S. Yamaguchi, *Tetrahedron Lett.*, **21**, 2827 (1980).
128. F. Yasuhara, K. Kabuto and S. Yamaguchi, *Tetrahedron Lett.*, **19**, 4289 (1978).
129. K. Kabuto, F. Yasuhara and S. Yamaguchi, *Tetrahedron Lett.*, **22**, 659 (1981).
130. E. P. Serebryakov, M. A. Shcherbakov, G. D. Gamalevich and M. I. Struchkova, *Russ. Chem. Bull., Int. Ed.*, **52**, 734 (2003).
131. E. M. Merckx, J. A. Lepoivre, G. L. Lemiere and F. C. Alderweireldt, *Org. Magn. Reson.*, **21**, 380 (1983).
132. L. Vanhoeck, J. Bossaerts, R. A. Dommisse, J. A. Lepoivre and F. C. Alderweireldt, *Org. Magn, Reson.*, **22**, 24 (1984).
133. K. Omata, T. Fujiwara and K. Kabuto, *Tetrahedron: Asymmetry*, **13**, 1655 (2002).
134. J. A. Dale and H. S. Mosher, *J. Am. Chem. Soc.*, **95**, 512 (1973).
135. T. Kusumi, Y. Fujita, I. Ohtani and H. Kakisawa, *Tetrahedron Lett.*, **32**, 2923 (1991).
136. W. H. Pirkle and D. L. Sikkenga, *J. Org. Chem.*, **40**, 3430 (1975).
137. W. H. Pirkle and D. L. Sikkenga, *J. Org. Chem.*, **42**, 1370 (1977).
138. T. J. Wenzel, C. A. Morin and A. A. Brechting, *J. Org. Chem.*, **57**, 3594 (1992).

139. T. J. Wenzel, R. D. Miles and S. E. Weinstein, *Chirality*, **9**, 1 (1997).
140. T. J. Wenzel, A. C. Bean and S. L. Dunham, *Magn. Reson. Chem.*, **35**, 392 (1997).
141. T. J. Wenzel and K. L. Brogan, *Enantiomer*, **5**, 293 (2000).
142. G. M. Whitesides and D. W. Lewis, *J. Am. Chem. Soc.*, **93**, 5914 (1971).
143. H. L. Goering, J. N. Eikenberry and G. S. Koermer, *J. Am. Chem. Soc.*, **93**, 5913 (1971).
144. R. R. Fraser, M. A. Petit and J. K. Saunders, *J. Chem. Soc., Chem. Commun.*, 1450 (1971).
145. M. D. McCreary, D. W. Lewis, D. L. Wernick and G. M. Whitesides, *J. Am. Chem. Soc.*, **96**, 1038 (1974).
146. H. L. Goering, J. N. Eikenberry, G. S. Koermer and C. J. Lattimer, *J. Am. Chem. Soc.*, **96**, 1493 (1974).
147. R. R. Fraser, *Asymmetric Synth.*, **1**, 173 (1983).
148. M. Kainosho, K. Ajisaka, W. H. Pirkle and S. D. Beare, *J. Am. Chem. Soc.*, **94**, 5924 (1972).
149. J. D. McKinney, H. B. Matthews and N. K. Wilson, *Tetrahedron Lett.*, **14**, 1895 (1973).
150. J. M. Coxon, J. R. A. Cambridge and S. G. C. Nam, *Org. Lett.*, **3**, 4225 (2001).
151. G. J. Reich, G. R. Sullivan and H. S. Mosher, *Tetrahedron Lett.*, **14**, 1505 (1973).
152. D. M. Harrison and P. Quinn, *Tetrahedron Lett.*, **24**, 831 (1983).
153. T. Makino, M. Orfanopoulos, T. You, B. Wu, C. W. Mosher and H. S. Mosher, *J. Org. Chem.*, **50**, 5357 (1985).
154. F. Lefevre, C. Rabiller, A. Mannschreck and G. J. Martin, *J. Chem. Soc., Chem. Commun.*, 942 (1979).
155. Y. Ishida, D. Sasaki, H. Miyauchi and K. Saigo, *Tetrahedron Lett.*, **45**, 9455 (2004).
156. J. K. Barton and J. S. Nowick, *J. Chem. Soc., Chem. Commun.*, 1650 (1984).
157. T. Okada, *J. Sci. Hiroshima Univ., Ser. A: Phys. and Chem.*, **45**, 215 (1981).
158. M. I. Kodess, M. A. Ezhikova, G. L. Levit, V. P. Krasnov and V. N. Charushin, *J. Organomet. Chem.*, **690**, 2766 (2005).
159. F. Fortis, B. Barbe, M. Petraud and J. P. Picard, *J. Chem. Soc., Chem. Commun.*, 527 (1999).
160. Y. Naruse, H. Watanabe, Y. Ishiyama and T. Yoshida, *J. Org. Chem.*, **62**, 3862 (1997).
161. M. M. Midland and R. W. Koops, *J. Org. Chem.*, **55**, 4647 (1990).
162. C. Ulrich and J. Bargon, *Magn. Reson. Chem.*, **38**, 33 (2000).
163. R. M. Acheson and I. S. Selby, *J. Chem. Soc., Chem. Commun.*, 537 (1973).
164. A. Mannschreck, V. Jonas, H. O. Bodecker, H. L. Elbe and G. Kobrich, *Tetrahedron Lett.*, **15**, 2153 (1974).
165. G. Becher and A. Mannschreck, *Chem. Ber.*, **116**, 264 (1983).
166. J. P. Snyder, N. Nevins, S. L. Tardif and D. N. Harpp, *J. Am. Chem. Soc.*, **119**, 12685 (1997).
167. J. S. Edmonds, T. Nakayama, T. Kondo and M. Morita, *Magn. Reson. Chem.*, **44**, 151 (2006).
168. I. Agranat, Y. Tapuhi and J. Y. Lallemand, *Nouv. J. Chem.*, **3**, 59 (1979).
169. A. G. Anastassiou and M. Hasan, *Tetrahedron Lett.*, **24**, 4279 (1983).
170. E. Diaz, E. Rojas-Davila, A. Guzman and P. Joseph-Nathan, *Org. Magn. Reson.*, **14**, 439 (1980).
171. K. Bartik, M. El Haouaj, M. Luhmer, A. Collet and J. Reisse, *ChemPhysChem*, **1**, 221 (2000).
172. I. Ghosh, H. Zeng and Y. Kishi, *Org. Lett.*, **6**, 4715 (2004).
173. I. Ghosh, Y. Kishi, H. Tomoda and S. Omura, *Org. Lett.*, **6**, 4719 (2004).
174. C. M. Adams, I. Ghosh and Y. Kishi, *Org. Lett.*, **6**, 4723 (2004).
175. D. F. Evans, J. N. Tucker and G. C. de Villardi, *J. Chem. Soc., Chem. Commun.*, 205 (1975).
176. T. J. Wenzel, T. C. Bettes, J. E. Sadlowski and R. E. Sievers, *J. Am. Chem. Soc.*, **102**, 5903 (1980).
177. T. J. Wenzel and R. E. Sievers, *Anal. Chem.*, **53**, 393 (1981).
178. T. J. Wenzel and R. E. Sievers, *J. Am. Chem. Soc.*, **104**, 382 (1982).
179. T. J. Wenzel and R. E. Sievers, *Anal. Chem.*, **54**, 1602 (1982).
180. T. J. Wenzel and D. R. Lalonde, Jr., *J. Org. Chem.*, **48**, 1951 (1983).
181. T. J. Wenzel, A. C. Ruggles and D. R. Lalonde, Jr., *Magn. Reson. Chem.*, **23**, 778 (1985).
182. T. J. Wenzel and M. D. Russett, *J. Magn. Reson.*, **75**, 493 (1987).
183. M. Hajek and D. J. Raber, *Anal. Chem.*, **58**, 1748 (1986).
184. T. J. Wenzel, *J. Org. Chem.*, **49**, 1834 (1984).
185. M. Audit, P. Demerseman, N. Goasdoue and N. Platzer, *Org. Magn. Reson.*, **21**, 698 (1983).
186. P. Dias, *Makromol. Chem., Rapid Commun.*, **11**, 299 (1990).
187. D. M. Rackham, F. M. Crutchley, D. E. Tupper and A. C. Boddy, *Spectrosc. Lett.*, **14**, 379 (1981).

188. T. J. Wenzel, *Spectrosc. Lett.*, **17**, 77 (1984).
189. W. Offermann and A. Mannschreck, *Tetrahedron Lett.*, **22**, 3227 (1981).
190. W. Offermann and A. Mannschreck, *Org. Magn, Reson.*, **22**, 355 (1984).
191. N. Baldovini, F. Tomi and J. Casanova, *Magn. Reson. Chem.*, **39**, 621 (2001).
192. A. Zschunke, P. N. Khanh and C. D. Kinh, *Adv. Nat. Sci.*, **3**, 41 (2002).
193. L. Johns, S. Belt, C. A. Lewis, S. Rowland, G. Massé, J. Robert and W. A. König, *Phytochemistry*, **53**, 607 (2000).
194. D. J. Pasto and K. D. Sugi, *J. Org. Chem.*, **56**, 4157 (1991).
195. A. Mannschreck, W. Munninger, T. Burgemeister, J. Gore and B. Cazes, *Tetrahedron*, **42**, 399 (1986).
196. P. E. Peterson and B. L. Jensen, *Tetrahedron Lett.*, **25**, 5711 (1984).
197. M. B. Wells, J. E. McConathy, P. S. White and J. L. Templeton, *Organometallics*, **21**, 5007 (2002).
198. D. J. Pasto and K. D. Sugi, *J. Org. Chem.*, **57**, 12 (1992).
199. D. M. Rackham, *Spectrosc. Lett.*, **14**, 639 (1981).
200. M. Audit, D. Davoust, N. Goasdoue and N. Platzer, *Magn. Reson. Chem.*, **23**, 33 (1985).
201. W. H. N. Nijhuis, W. Verboom, A. A. El-Fadl, G. J. van Hummel and D. N. Reinhoudt, *J. Org. Chem.*, **54**, 209 (1989).
202. A. Thompson and D. Dolphin, *Org. Lett.*, **2**, 1315 (2000).
203. T. J. Wenzel and J. Zaia, *J. Org. Chem.*, **50**, 1322 (1985).
204. T. J. Wenzel and J. Zaia, *Anal. Chem.*, **59**, 562 (1987).
205. T. J. Wenzel and K. Cameron, *Magn. Reson. Chem.*, **27**, 734 (1989).
206. T. K. Green, J. R. Whetstine and E. J. R. Son, *Tetrahedron: Asymmetry*, **8**, 3175 (1997).
207. S. E. Weinstein, M. S. Vining and T. J. Wenzel, *Magn. Reson. Chem.*, **35**, 273 (1997).

CHAPTER **15**

Metal enolates in polymer science and technology

PHILIPPE LECOMTE and ROBERT JÉRÔME

Center for Education and Research on Macromolecules (CERM), University of Liège, Sart-Tilman, B6a, 4000 Liège, Belgium
Fax: +32 4 3663497; e-mail: rjerome@ulg.ac.be

The chemistry of metal enolates
Edited by Jacob Zabicky

I. SYMBOLS AND ABBREVIATIONS

acac	acetylacetonate
12-CE-4	12-crown-4
DB-18-CE-6	6,7,9,10,17,18,20,21-octahydrodibenzo[*b*,*k*][1,4,7,10,13,16] hexaoxacyclooctadecine
DMAEMA	dimethylaminoethyl methacrylate
DP	degree of polymerization
DPE	1,1-diphenylethene
DPHLi	1,1-diphenylhexyllithium
DPMLi	diphenylmethyllithium
EiBLi	ethyl α-lithioisobutyrate
EMA	ethyl methacrylate
f	initiator efficiency
GMA	glycidyl methacrylate
GTP	group transfer polymerization
IBMA	isobornyl methacrylate
$k_{\pm}$	rate constant of contact ion pair
k_{a}	rate constant of associated species
k_{app}	apparent constant of propagation
k_{init}	constant rate of initiation
k_{prop}	constant rate of propagation
k_{term}	constant rate of termination
K_{DA}	equilibrium constant of deaggregation
K211	cryptand 211
LDA	lithium diisopropylamide
LiOEEM	lithium 2-(2-methoxyethoxy) ethoxide
MA	methyl acrylate
MiBLi	methyl 2-lithioisobutyrate
MMA	methyl methacrylate
M_{n}	number-average molecular weight
M_{w}	weight-average molecular weight
nBuA	*n*-butyl acrylate
nBuMA	*n*-butyl methacrylate
PBD	poly(butadiene)
PCL	poly(ε-caprolactone)
PEMA	poly(ethyl methacrylate)
PEO	poly(ethylene oxide)
PGMA	poly(glycidyl methacrylate)
PIBMA	poly(isobornyl methacrylate)
PLA	poly(lactide)
PMMA	poly(methyl methacrylate)
PnBuMA	polyn(*n*-butyl methacrylate)
PS	polystyrene
PtBuA	poly(*tert*-butyl acrylate)
R_{p}	rate of polymerization
TMEDA	*N*,*N*,*N*′,*N*′-tetramethyl-1,2-ethylenediamine
tBuA	*t*-butyl acrylate
tBuMA	*t*-butyl methacrylate
Vac	vinyl acetate

II. INTRODUCTION

Enolates play a key role in polymer science and technology, particularly as ligands in catalytic processes. Enolate ligated catalysts are known in organic chemistry and some of them have been extended to the chemical modification of preformed polymers with the purpose to improve their properties. These catalytic reactions will not be discussed in this review. Rather, emphasis will be placed on polymerization processes, which are initiated by organometallic compounds ligated by enolates. The major concern of the polymer chemist is indeed to design the length, the architecture and the functionality of synthetic polymers. The role of the catalyst is then crucial to control the chain growth not only in space (stereospecificity) but also in time ('livingness'). The most representative examples of control imparted to polymerization (see Sections III, IV and V) by enolate-containing cocatalysts will be the focus of attention in this review. Clearly, anionic and radical polymerizations, ring-opening polymerization of lactones and lactides and, above all, coordination polymerization of nonfunctionalized olefins, such as propene (propylene) by Ziegler–Natta-type catalysts, have gained huge benefit from the enolate chemistry.

Enolates were decisive in putting under control, for the first time, the anionic polymerization of very sensitive monomers, such as the methacrylates and acrylates (see Section VI). In this anionic polyaddition mechanism, enolates are the active species in each of the main steps, i.e. initiation (equation 1), propagation (equation 2) and termination (equation 3) where $\mathbf{I}^*$ is an active form of the initiator **I**, $\mathbf{P}^*_i$ the propagating polymer containing i monomer units **M** and **X** the terminator to yield the polymeric molecule $\mathbf{P}_i$. This is not the case, for instance, in the ring-opening polymerization of lactones and lactides, where enolates do not participate in propagation and termination although they are used as initiators[1].

$$\mathbf{I}^* + \mathbf{M} \xrightarrow{k_{\text{init}}} \mathbf{P}^*_1 \tag{1}$$

$$\mathbf{P}^*_i + \mathbf{M} \xrightarrow{k_{\text{prop}}} \mathbf{P}^*_{i+1} \tag{2}$$

$$\mathbf{P}^*_i + \mathbf{X} \xrightarrow{k_{\text{term}}} \mathbf{P}_i \tag{3}$$

The design of macromolecules, commonly called macromolecular engineering, relies on living polymerization processes. Originally, M. Szwarc said a polymerization was 'living' when it was free from termination and transfer reactions[2–5]. Therefore, initiation and propagation should be the only events in a living polymerization. Criteria for a polymerization to be considered as living are as follows: (i) Whenever the monomer conversion is complete, the chains preserve their capacity to grow further. Thus, the polymerization should be quantitatively resumed upon addition of a new monomer feed. (ii) The number-average degree of polymerization, DP, is predetermined by the initial monomer-to-initiator molar ratio at complete monomer conversion ($conv = 1$), according to equation 4, where f is the initiator efficiency. Therefore, DP must increase linearly with the monomer conversion. The slope of this linear dependence is the $[\mathbf{M}]_0/[\mathbf{I}]_0$ ratio in case of an ideal living system. Deviation from this slope indicates that either only part of the initiator has been active (higher slope) or irreversible transfer has taken place (lower slope). (iii) Whenever the initiation is fast compared to propagation ($k_{\text{init}} > k_{\text{prop}}$) and the initiation is complete, the concentration of the propagating species remains constant during polymerization (equation 5), which results in a pseudo-first order kinetics (equations 6 and 7). Thus, the linearity of the semilogarithmic plot of $[\mathbf{M}]_0/[\mathbf{M}]_t$ vs. time is commonly checked, and the apparent polymerization rate constant ($k_{\text{app}} = k_{\text{prop}}[\mathbf{P}^*]$) is directly given

by the slope of this plot. Deviation from linearity can be caused by slow initiation and irreversible terminations reactions.

$$DP = \frac{[\mathbf{M}]_0}{f \times [\mathbf{I}]_0} \times conv \tag{4}$$

$$[\mathbf{P}^*] = \text{Constant} \tag{5}$$

$$R_\text{p} = -\frac{d[\mathbf{M}]}{dt} k_\text{prop}[\mathbf{M}][\mathbf{P}^*] = k_\text{app}[\mathbf{M}] \tag{6}$$

$$\ln \frac{[\text{M}]_0}{[\text{M}]_t} = k^t_\text{app} \tag{7}$$

Living polymerization processes pave the way to the macromolecular engineering, because the reactivity that persists at the chain ends allows (i) a variety of reactive groups to be attached at that position, thus (semi-)telechelic polymers to be synthesized, (ii) the polymerization of a second type of monomer to be resumed with formation of block copolymers, (iii) star-shaped (co)polymers to be prepared by addition of the living chains onto a multifunctional compound. A combination of these strategies with the use of multifunctional initiators and/or macromonomers can increase further the range of polymer architectures and properties.

With the discovery of living polymerization by M. Szwarc in 1956[3], an unprecedented research effort was devoted to the macromolecular engineering of anionically prepared polymers such as polystyrene, polydienes and poly(ethylene oxide). For a long time, the control of the anionic polymerization of an important class of monomers, the methacrylates, could not be accomplished because of a deleterious competing nucleophilic attack of the ester carbonyl. This problem was solved in the 1980s with the invaluable assistance of metal enolates. Although controlled radical polymerization and group transfer polymerization can be valuable alternatives, the ligated anionic polymerization of methactrylates remains the major technique for tailoring of polyacrylates and polymethacrylates with a variety of well-defined architectures and functionalities.

Nevertheless, polymerizations other than the anionic ones have also been carried out using enolates as ligands of transition metal cations. Metal acetalyacetonates are indeed organometallic compounds that directly contributed to the control of radical polymerization, ring-opening polymerization and coordination polymerization of specific monomers, as discussed hereafter.

III. RADICAL POLYMERIZATION

Ethenyl acetate (vinyl acetate, Vac) is polymerizable only by radical species. Until recently, the polymerization of any monomer was out of control because of the unavoidable occurrence of irreversible termination reactions. In 1995, Matyjaszewski[6] and Sawamoto and coworkers[7] reported that the deleterious impact of these irreversible reactions could be minimized by acting on the kinetics of both the propagation and the termination reactions. Indeed, a decrease in the instantaneous concentration of radicals ($[\mathbf{M}^\bullet]$) decreases much more importantly the termination rate (proportional to $[\mathbf{M}^\bullet]^2$) than the propagation rate (proportional to $[\mathbf{M}^\bullet]$). A scheme proposed consists in converting reversibly radicals into unstable covalent species ('dormant' species). The last radically polymerizable monomer to fall under this type of kinetic control was vinyl acetate. Indeed, very recently Debuigne and coworkers proposed to polymerize Vac by 2.2′-azobis-(4-methoxy-2,4-dimethyl)valeronitrile (V-70) in the presence of cobalt(II) acetyl acetonate $[\text{Co(acac)}_2]$[8]. Under these conditions, a linear relationship is observed between

DP and the monomer conversion, and the polydispersity index is low ($M_w/M_n = 1.2$). Interestingly enough, this process is effective in bulk[8], in water suspension[9] and in aqueous miniemulsion[10]. The long-lived propagating species can be derivatized into a series of functional groups by addition of properly substituted nitroxides or nonpolymerizable olefins[11]. Moreover, PVac-*block*-PS diblock copolymers were synthesized successfully, which is an additional step in the macromolecular engineering of PVac[12].

The mechanism of $Co(acac)_2$-mediated polymerization of Vac is still an open question. On the basis of an early work by Wayland and coworkers[13a] on the controlled radical polymerization of acrylates by complexes of cobalt and porphyrins, Debuigne and coworkers proposed a mechanism based on the reversible addition of the growing radicals $\mathbf{P}^{\bullet}$ to the cobalt complex, [Co(II)], and the establishment of an equilibrium between dormant species and the free radicals (equation 8)[8]. Maria and coworkers, however, proposed that the polymerization mechanism depends on the coordination number of cobalt[13b]. Whenever the dormant species contains a six-coordinated Co in the presence of strongly binding electron donors, such as pyridine, the association process shown in equation 8 would be effective. In contrast, a degenerative transfer mechanism would be favored in case of five-coordinated Co complexes (equation 9).

$$\mathbf{P}\bullet + [\text{Co(II)}] \rightleftharpoons \mathbf{P}\text{-}[\text{Co(III)}] \tag{8}$$

$$\mathbf{P}_n\text{-}[\text{Co(III)}] + \mathbf{P}_m^{\bullet} \rightleftharpoons \mathbf{P}_n^{\bullet} + \mathbf{P}_m\text{-}[\text{Co(III)}] \tag{9}$$

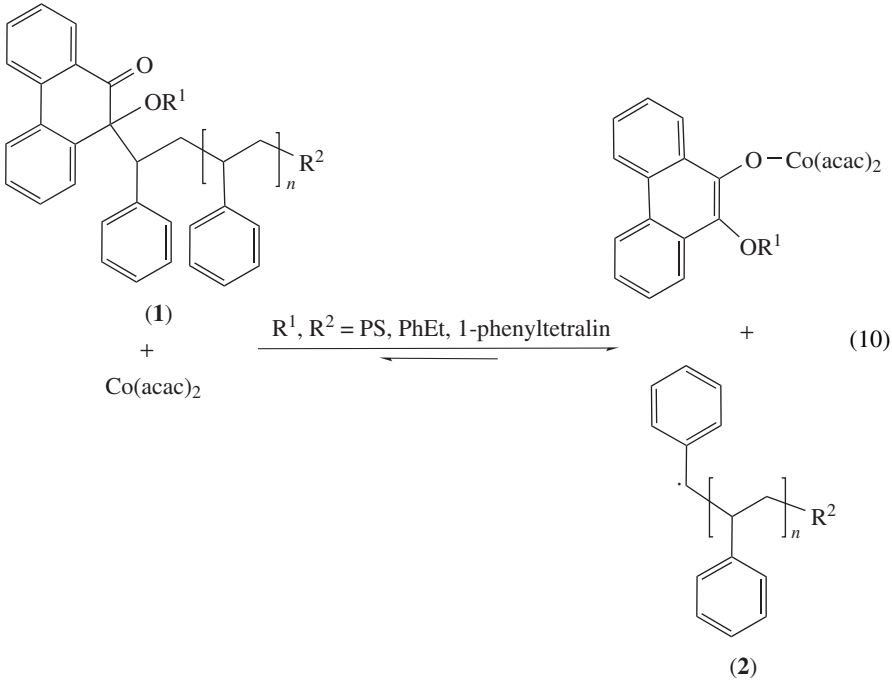

(10)

$Co(acac)_2$ proved also its efficiency in imparting control to the radical polymerization of styrene. This process, coined quinone transfer radical polymerization (QTRP), is carried out in the presence of phenanthroquinone and a catalytic amount of $Co(acac)_2$[14–16]. The origin of the control should again be found in an equilibrium between a dormant (**1**) and

an active species (**2**), as shown in equation 10. Complexes with Mn, Ni, Al cations were also tested successfully in this QTRP[17].

IV. POLYMERIZATION OF NONFUNCTIONALIZED OLEFINS

Polyolefins have a central position in the marketplace of synthetic polymers, in terms of annual production volume[18]. In the 1960s, Natta and coworkers reported that syndio-enriched polypropylene could be prepared by polymerization of propylene at $-78\,^{\circ}C$ in the presence of a mixture of vanadium tetrachloride and Et_2AlCl[19]. The molecular weight increased steadily for 25 h, and the polydispersity index ($1.4 < M_w/M_n < 1.9$) was moderately low[20]. This was the first hint of a possible control on this type of coordinative polymerization.

A truly living polymerization of propylene by a Ziegler–Natta catalyst was reported by Doi and coworkers, who substituted $V(acac)_3$ for the originally used vanadium chloride[21,22], pointing to the superiority of an enolate-type ligand. Indeed, the polymerization proceeds without detectable chain termination and transfer reactions at temperatures lower than $-65\,^{\circ}C$[21]. The molecular weight increases linearly with time and molecular weights as high as 100000 $g\,mol^{-1}$ can be obtained. The polydispersity index is unusually very low ($1.05 < M_w/M_n < 1.20$) and the syndiotacticity is very high ([r] = 0.81). The main drawback is the very low initiation efficiency (4%). Nevertheless, the structure of the enolate ligand is of prime importance, as illustrated by the quantitative initiation attained when 2-methyl-1,3-butanedionate replaces acetylacetonate[23]. Moreover, the livingness of the polymerization is maintained up to $-40\,^{\circ}C$[24].

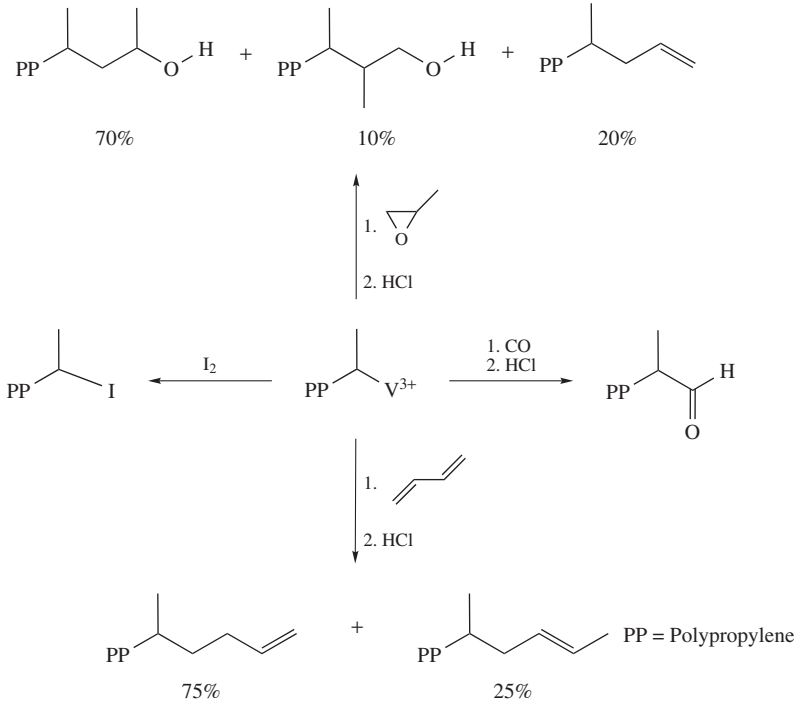

SCHEME 1. Synthesis of ω-functional syndiotactic polypropylene

The persistence of the species responsible for the chain growth made the macromolecular engineering of polypropylene a reality. Indeed, living syndiotactic polypropylene was reacted with a series of electrophiles with the purpose to prepare ω-functional chains, as illustrated in Scheme 1[25–29]. The livingness of the coordinative polymerization of propylene gave also access to copolymers. A first strategy relies on the use of ω-end capped polypropylene as a macroinitiator. For example, ω-iodo polypropylene successfully initiated the cationic polymerization of THF with formation of polypropylene-*block*-polytetrahydrofuran diblocks[25]. In another approach, Doi and coworkers added a fresh feed of methyl methacrylate (MMA) onto living polyisoprene in the presence of $V(acac)_3$/Et_2AlCl. The resumption of the polymerization resulted in a polypropylene-*block*-PMMA copolymer. A radical mechanism was proposed for the synthesis of the PMMA block[30].

The $V(acac)_3$-mediated hompolymerization of ethylene is not living and the polydispersity index is quite high (2.0)[31]. Nevertheless, ethylene can be successfully copolymerized with propylene while maintaining the livingness of the process[32]. Moreover, the enolate ligated vanadium is a catalyst for the living polymerization of 1,5-hexadiene and copolymerization with propylene[33]. It must be noted that polymerization of 1,5-hexadiene is a route to a polymer that combines constitutive 1,3-cyclopentylenemethylene units (**2′**) and vinyltetramethylene units. Therefore, pendant unsaturations are available for further functionalization.

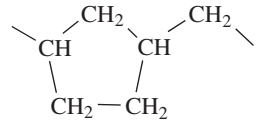

(**2′**)

V. POLYMERIZATION OF LACTONES AND LACTIDES

The ring-opening polymerizations shown in equations 11 and 12, of lactones (**3**), lactide (**5a**) and glycolide (**5b**), are a direct route to biodegradable and biocompatible aliphatic polyesters (**4,6a** and **6b**). These processes are mediated by a large number of catalysts and initiators. Among them, Al[34,35], Ca[36], Sn(II)[37], Zr[38,39] acetylacetonates were able to promote the ring-opening polymerization of ε-caprolactone (3, $n = 4$) and lactide (**5a**). The polymerization mechanism by this class of enolate mediators was disregarded for a long time. Recently, Dobrzynski[38] studied the mechanism of the ε-caprolactone (3, $n = 4$) polymerization mediated by $Zr(acac)_4$, and proposed that an *in situ* formed zirconium enolate would be the actual initiator of the the polymerization. Penczek and coworkers[34] reported that $Al(acac)_3$ is prone to mediate the polymerization of ε-caprolactone (3, $n = 4$) and lactide (**5a**), which is an extremely slow process; however, the rate is increased on addition of $Al(acac)_3$ and an alcohol. An aluminum alkoxide would be formed *in situ* as illustrated in equation 13 for *n*-butanol. Again, the actual initiator would be an alkoxide, in agreement with M_n, which is predetermined by the monomer-to-alcohol molar ratio.

(**3**) n = 1, 3, 4 (**4**) n = 1, 3, 4 (11)

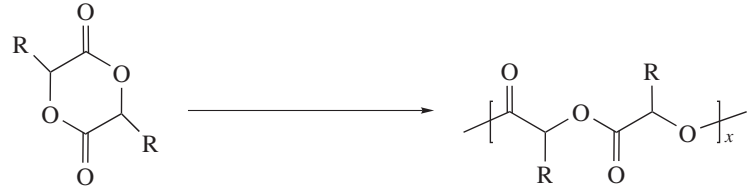

(**5**)(**a**) R = Me
(**b**) R = H

(**5**)(**a**) R = Me
(**b**) R = H

(12)

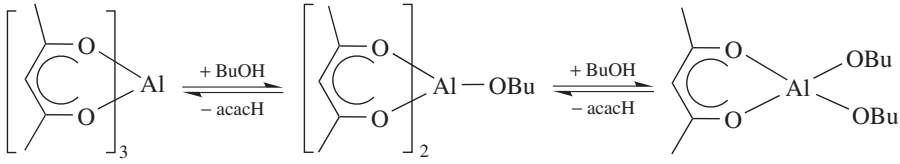

(13)

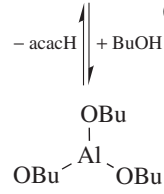

VI. ANIONIC POLYMERIZATION OF METHACRYLATES AND ACRYLATES

A. Introduction

In 1956, Szwarc and coworkers investigated the anionic polymerization of MMA initiated by sodium naphthalenide in THF at $-78\,^{\circ}C$[40]. Since then, a steadily increasing number of papers were published on this topic including a series of reviews[41–45]. The anionic polymerization of acrylates and methacrylates is a chain-growth polymerization, the propagation step of which is a Michael addition enolate to the double bond of methacrylate. As mentioned in Section II, the anionic polymerization of methacrylates is by far more complex than that of styrene. A problem arises from the propensity of enolates to form aggregates, particularly in apolar solvents. Therefore, an equilibrium is established between the aggregates and the nonassociated enolates, which are both able to propagate with different rate constants (k_a and $k_{\pm}$, respectively, equation 14). As a rule, the reactivity of the aggregated species is lower than that of the nonassociated species. The equilibrium constant K_{DA} is defined by equation 15, whereas the total concentration of the enolates is constant, as long as no irreversible termination reaction takes place (equation 16).

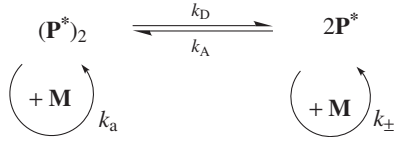

(14)

$$K_{DA} = \frac{[(\mathbf{P}^*)_2]}{[(\mathbf{P}^*]^2} = \frac{k_A}{k_D} \tag{15}$$

$$[\mathbf{P}^*] = \sum_i [\mathbf{P}_j^*] = \text{constant} \tag{16}$$

The enolate has a direct impact on the polymerization kinetics. Indeed, the kinetics order with respect to $[\mathbf{P}^*]$ is 1 when $K_{DA}[\mathbf{P}^*] \ll 1$ (equation 17) and fractional order with respect to $[\mathbf{P}^*]$ is the rule when $K_{DA}[\mathbf{P}^*] \gg 1$ (equation 18)[41]. A fractional order in initiator is thus the signature of aggregation.

$$K_{DA}[\mathbf{P}^*] \ll 1 \Rightarrow \text{polymerization rate} = k_{app}[\mathbf{P}^*] \tag{17}$$

$$K_{DA}[\mathbf{P}^*] \gg 1 \Rightarrow \text{polymerization rate} = k_{app}[(\mathbf{P}^*)_2]^{1/2} \tag{18}$$

Aggregation may also make an impact on the molecular weight distribution. Indeed, a slow equilibration between propagating species with different reactivities results in the broadening or even in the multimodality of the molecular weight distribution. The establishment of a reversible equilibrium between aggregates and nonassociated species does not fit the definition of a living system according to M. Szwarc. Nevertheless, whenever this equilibration is fast enough, polymers with a predetermined *DP* (equation 4) and possibly a low polydispersity index can be obtained. In this chapter a reversible aggregation equilibrium does not preclude livingness from a polymerization[46]. A basic problem in the anionic polymerization of acrylates and methacrylates is the occurrence of irreversible termination and transfer reactions that are hardly avoidable. Indeed, the initiator can react with the monomer not only by the Michaël addition but also by a 1,2-addition with formation of an α,β-unsaturated ketone and a new alkoxide (Scheme 2). Moreover, the initiator can react not only as a nucleophile but also as a base, as shown in Scheme 2.

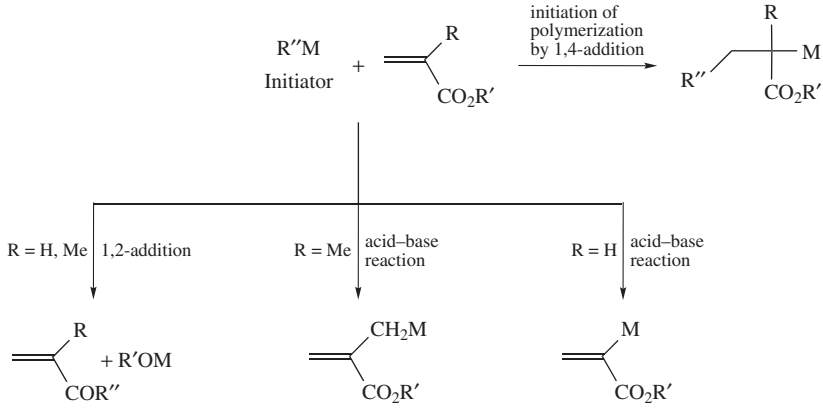

SCHEME 2. Possible reaction pathways between an organometallic initiator and acrylates or methacrylates

The situation is even more complex during polymerization, because a 1,2-addition can take place onto the ester groups of both the monomer and the monomeric units in the chains. This type of reaction can be either an intramolecular Claisen condensation, thus a backbiting reaction, with formation of cyclics (equation 19) or an intermolecular reaction

that leads to chain branching (equation 20). As a rule, the detailed mechanism of the anionic polymerization of MMA is deeply influenced by the experimental conditions as discussed hereafter.

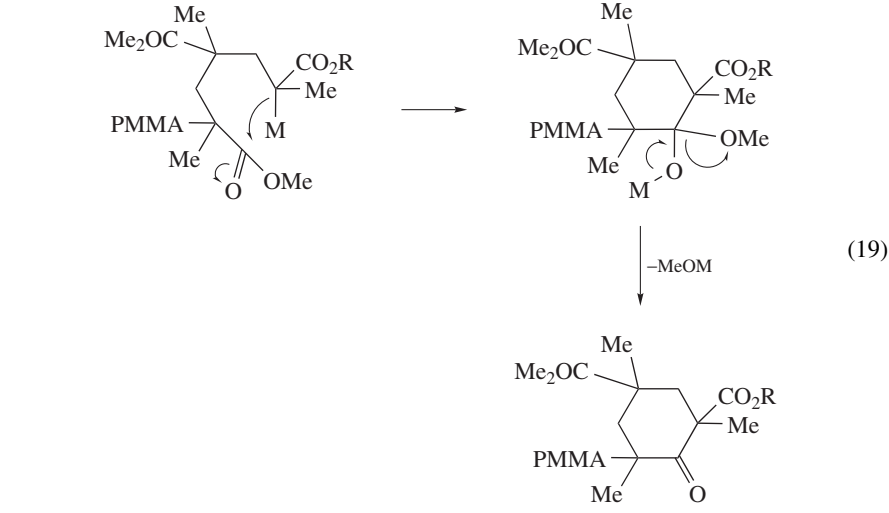

(19)

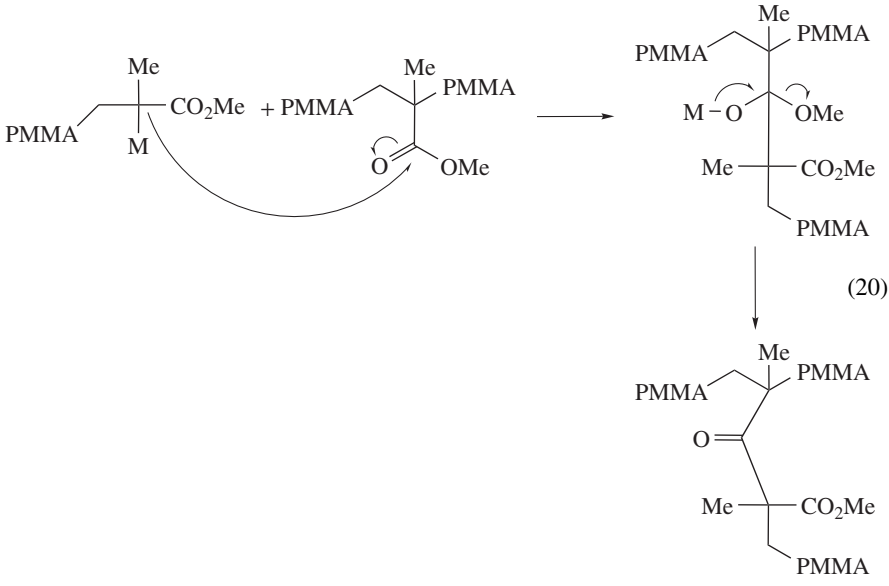

(20)

B. Anionic Polymerization in Polar Solvents

1. Influence of the initiator

The anionic polymerization of methacrylates and acrylates is poorly controlled even at low temperature, whenever initiated by alkylithium compounds, such as *n*-BuLi. In order

to restrict the undesired nucleophilic attack of the ester groups, and thus to improve the polymerization control, attention was paid to sterically hindered initiators. In their quest for PS-*block*-PMMA copolymers, Rempp and coworkers initiated the anionic polymerization of MMA by living PS chains (**7**)[47]; however, the polymerization was not under control. This problem was solved by end-capping **7** with DPE (**8**) to yield the modified macroinitiator **9**, which improved control on the MMA polymerization by a more sterically hindered diphenylalkyl anion (**9**) (equation 21). Remarkably, this premodification of the PS macroinitiator (**7**) by 1,1′-ethene-1,1-diyldibenzene (DPE **8**) was effective in improving the control on the PMMA block. It is worth mentioning that enolates are involved as propagating species only during the synthesis of the second PMMA block.

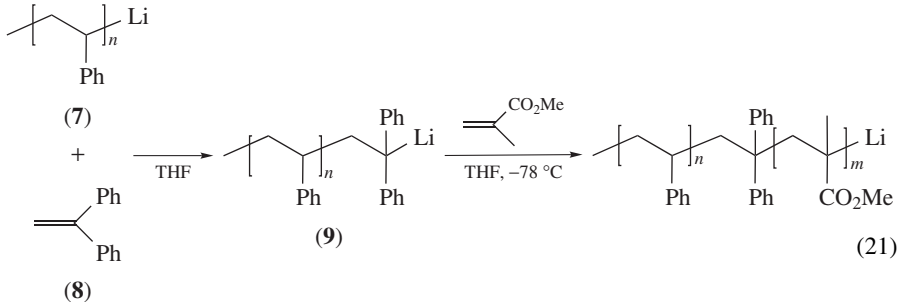

(21)

Consistently, Anderson and coworkers showed that the polymerization of MMA in THF at −78 °C is living when initiated by DPHLi (**10**), which is nothing but the model of the diphenylalkyl anion (**9**) of the PS macroinitiator used in the synthesis of PS-*block*-PMMA (equation 21). It must be noted that DPHLi (**10**) results from the direct addition of DPE (**8**) to *n*-Buli (equation 22)[48]. The molecular weight of PMMA is predetermined by the monomer-to-initiator molar ratio and the MMA conversion. The polydispersity index is low ($1.04 < M_w/M_n < 1.16$). The livingness of this polymerization was confirmed by the successful resumption of the polymerization of lauryl methacrylate (LMA), and formation of the parent PMMA-*block*-PLMA diblocks. The anionic polymerization of MMA in THF at −78 °C is thus 'living', provided that sterically hindered initiators are used.

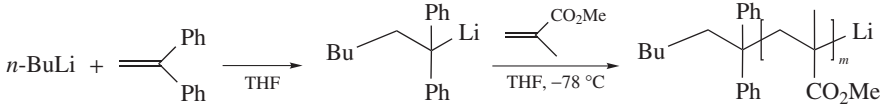

(22)

Hatada and coworkers studied the MMA polymerization initiated by benzyllithium under comparable experimental conditions. PMMA with a broad molecular distribution was obtained[49]. Baskaran and coworkers proposed that the lack of control resulted from an exceedingly high monomer concentration. Indeed, PMMA with a low polydispersity index ($M_w/M_n < 1.3$) and a predictable molecular weight was collected at lower MMA concentration[50].

Indeed, the collected PMMA was collected with a low polydispersity index ($M_w/M_n < 1.3$) and a predictable molecular weight[50].

In contrast to the polymerization of methacrylates, the anionic polymerization of acrylates is out of control in THF, at −78 °C. The steric hindrance of the monomer, e.g. tBuA, is not beneficial, as testified by a low initiation efficiency (0.56) and a high polydispersity index (2.1)[41].

Müller and coworkers studied the kinetics of the polymerization of tBuA in THF at −78 °C, which was initiated by *t*-butyl α-lithioisobutyrate[51]. The molecular weight distribution is rather broad ($M_w/M_n = 2.5$). Only after longer reaction times, side-products formed by backbiting reaction are observed.

2. Influence of the temperature

The temperature has a decisive effect on the anionic polymerization initiated by DPHLi (**10**) or benzyllithium in THF. As soon as the temperature is increased from −78 °C up to −40 °C, the livingness is lost[50]. Compared to MMA and other methacrylates, tBuMA is an exception for which the anionic polymerization remains under control at temperatures as high as 25 °C[52]. This remarkable behavior is accounted for by the steric hindrance of the ester group, which prevents side reactions from occurring at an appreciable rate.

3. Influence of the counter-ion

Müller and Jeuck considered the possible impact of the counter-ion on the polymerization kinetics of MMA in THF at −98 °C[53]. They reported a linear relationship between the interionic distance of the active species and the logarithm of k_{prop} (Figure 1). The intercept roughly corresponds to the propagation rate constant of the free anion. The deviation observed for Na^+ and K^+ was accounted for by a solvation effect, that increases the interionic distance. These results suggest that a single active species, presumably a contact ion pair, is involved in the mechanism.

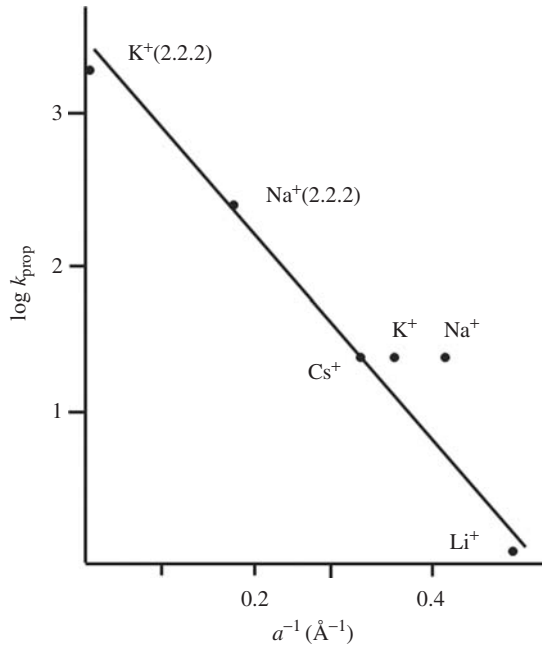

FIGURE 1. Dependence of the propagation rate (log k_{prop}) on the reciprocal interionic distance (a^{-1}). Reproduced with permission from Reference 53. Copyright Wiley-VCH Verlag GmbH & Co. KGaA

4. Stereochemical aspects

Although the anionic polymerization of MMA in THF leads to highly syndiotactic PMMA (Table 1)[54], that one of tBuMA results in an equimolar mixture of syndiotactic and heterotactic triads (Table 1). For both monomers an increase in temperature results in higher heterotacticity at the expense of the syndiotacticity[54, 55]. The chain tacticity has a direct influence on the macroscopic properties, as illustrated in Table 2 for both the glass transition (T_g) and the melting (T_m) temperatures of PMMA[56].

Enolates, which are the actual propagating species, exist in the *E* (**11**) and *Z* (**12**) configurations. The *E*/*Z* ratio of the living chain-ends can be indirectly determined by reacting the propagating enolates **11** and **12** with chlorotrimethylsilane and converting them into the corresponding ketene silylacetals **13** and **14**, which are characterized by NMR spectroscopy (equations 23 and 24)[57].

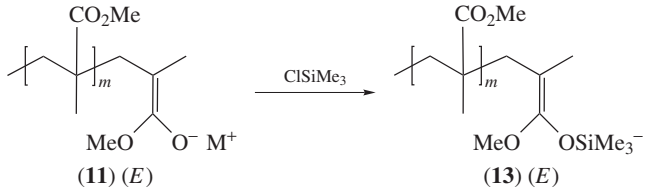

(**11**) (*E*) (**13**) (*E*) (23)

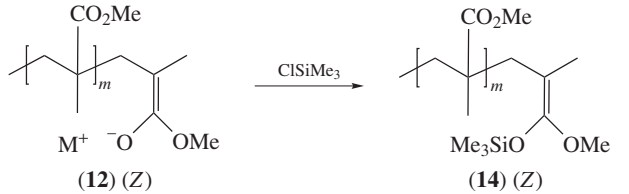

(**12**) (*Z*) (**14**) (*Z*) (24)

TABLE 1. Tacticity of PMMA and PtBMA synthesized by anionic polymerization with a Li counter-ion in THF

T (°C)	% syndiotactic triads (*rr*)[a]		% heterotactic triads (*mr*)[b]		% isotactic triads (*mm*)[c]	
	PMMA	PtBMA	PMMA	PtBMA	PMMA	PtBMA
−78	81	52	18	48	1	4
−48	72		26		2	
−20	69		28		3	
0	63	46	33	56	4	2
0		41		49		10

[a] A *rac-rac* (*rr*) triad is a chain of three consecutive monomer links of *R*,*S*,*R*- or *S*,*R*,*S*-configuration.
[b] A *meso-rac* (*mr*) triad is a chain of three consecutive monomer links of *R*,*R*,*S*- or *S*,*S*,*R*-configuration.
[c] A *meso-meso* (*mm*) triad is a chain of three consecutive monomer links of *S*,*S*,*S*- or *R*,*R*,*R* configuration.

TABLE 2. Influence of tacticity on the glass transition (T_g) and melting (T_m) temperatures of PMMA. Reproduced from Reference 56 by permission of John Wiley & Sons, Inc.

Stereoregularity[a]	M_n	T_g (°C)	T_m (°C)
Isotactic (*mm* = 100%)	7200	49	150
Syndiotactic (*rr* = 98%)	13000	108	159
Heterotactic (*mr* = 96%)	9700	91	166

[a] See footnotes to Table 1.

TABLE 3. Correlation between tacticity and Z/E isomerism for the anionic polymerization of MMA in THF at $-78\,^{\circ}C$

	Li^+	Na^+	K^+	Cs^+	$K^+(2.2.2)$
Z [a]	>99	97	60	5	10
mr [b]	18	39	56	50	31
rr [b]	81	59	28	47	67
m [c]	8	22	34	28	18
r [d]	92	78	66	72	82

[a] Configuration of the ester enolate at the living end.
[b] See footnotes to Table 1.
[c] A *meso* (m) diad consists of two consecutive links of R,R- or S,S-configuration.
[d] A *rac* (r) diad consists of two consecutive links of R,S- or S,R-configuration.

A correlation between chain tacticity and E/Z isomerism was proposed by Müller and coworkers for the polymerization of MMA in THF at $-78\,^{\circ}C$, with the major alkaline counter-ions, including crypted potassium (Table 3)[57]. Clearly, the stereochemistry of MMA polymerization is greatly influenced by the size of the cation. Indeed, the Z isomer is almost exclusively observed with the small cations Li^+ and Na^+, whereas the E isomer predominates with the large cations Cs^+ and $[K^+(2.2.2)]$[58]. Whatever the enolate involved, E or Z, formation of the *meso* diads (m) is unfavorable, more likely for thermodynamic reasons. Nevertheless, an increase in the cation radius of the Z enolate results in a higher fraction of m diads, and a higher fraction of r diads for the E enolate. The effect of the E/Z isomerism on the chain tacticity is related to the structure of the transition state of the propagation step. Although a model based on the E/Z stereoisomerism of the lithium ester enolate was proposed[57,58], further investigation is needed because the monomer coordination in the transition state is unknown and a direct proof of the E/Z isomerism of the enolate is still outstanding[43,59].

C. Anionic Polymerization in Apolar Solvents

1. Polymerization of MMA initiated by organolithium derivatives in toluene

The anionic polymerization of MMA initiated by organolithium derivatives is by far more complex in apolar solvents than in THF. Indeed, Wiles and Bywater reported that the polymerization of MMA with sterically hindered initiators in toluene is ill-controlled even when conducted at low temperature[60–62]. The strong aggregation of the active species in toluene would be responsible for the observed broad molecular weight distribution and very low initiation efficiency[63,64].

2. Polymerization of tBMA initiated by organolithium derivatives in toluene

The anionic polymerization of tBMA in toluene with a Li counter-ion is again compared to MMA and other methacrylates. Indeed, the monomer conversion is complete and the molecular weight distribution is narrow not only at $-78\,^{\circ}C$ but also at $0\,^{\circ}C$[52,65]. Nevertheless, the polymerization is not strictly living, because an important fraction of oligomers ($M_n = 650$) is collected and the initiation efficiency is low. The oligomers would be dormant chains, unable to propagate in toluene, as a result of aggregation. Nevertheless, they can be reactivated by addition of THF and resume the polymerization of freshly added monomer. The basic problem is that most of the initiator is consumed by the low molecular weight chains, which are involved in a very early pseudo-termination

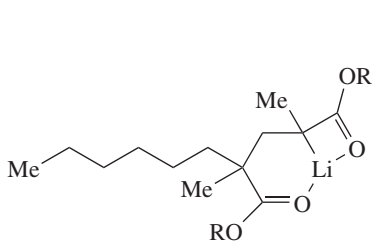

(**15**)

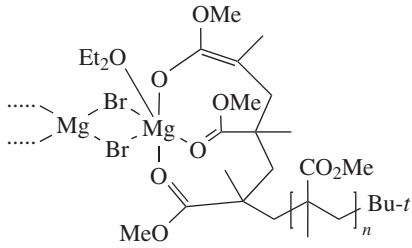

(**16**)

reaction. Consistently, when the polymerization is initiated by a macroinitiator, e.g. living anionic poly(isopropene) chains, the aggregation phenomenon is no longer effective and the initiation efficiency is close to 100%[66]. PtBMA synthesized in toluene is highly isotactic (99%)[55]. This very high stereoselectivity is usually accounted for by the intramolecular coordination of the lithium enolate (**15**)[43].

3. Polymerization of MMA in THF initiated by organomagnesium derivatives

Hatada and coworkers reported that the polymerization of MMA initiated by *t*-BuMgBr in toluene, at −78 °C, is living. The reaction is remarkably stereoselective, yielding highly isotactic PMMA ($rr > 95\%$)[56,67,68]. When less hindered organomagnesium derivatives were used as initiators (*n*-, *i*- and *s*-BuMgBr), the isotacticity decreased and the molecular weight distribution was broader[68]. Based on the NMR analysis of living oligomers, Hatada proposed an intramolecular coordination of the propagating magnesium enolate (**16**)[56]. This hexacoordination of Mg would be at the origin of the polymerization stereoselectivity.

D. Structural Investigation of Propagating Species

In order to shed light on the polymerization mechanism, the attention of several research groups was focused on the structure of the living chain-ends. A major problem is that enolates are known for condensation at a rate that depends on solvent, temperature and structure of the ester group (*t*-Bu esters being less reactive than Me esters). This undesired reaction makes the structural analysis of the chain-ends more complex[43]. In order to get rid of any contribution of the chain in the structural analysis, unimeric, dimeric and oligomeric models of the chain-ends were considered.

1. Unimeric model

α-Lithio carboxylic esters were studied by various experimental techniques, including colligative properties, NMR, IR and X-ray scattering. NMR spectroscopy confirmed that these compounds are typical ester enolates[69] (**17–19**), which can be considered as unimeric models that mimick the living chain-end of polyacrylates and polymethacrylates. Moreover, the *Z* and *E* isomers of methyl and *t*-butyl α-lithiophenylacetates, for example, could be discriminated by IR spectroscopy, with predominance of the *E* configuration in THF. *E* to *Z* isomerization was observed upon the addition of HMPA[70].

The structure of methyl 2-lithioisobutyrate (MiBLi, **18**, R = Me) was investigated by multinuclear NMR[69,71,72], confirming that MiBLi is prone to aggregation. For instance, an equilibrium between a dimer (**20**) and a tetramer (**21**) is established in THF at −78 °C ($\Delta H = -2.1$ kcal mol^{-1}, $\Delta S = -13.7$ cal mol^{-1} K^{-1}) (equation 25). At room temperature, this compound typically forms tetramers, which are however converted into dimers

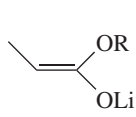

(**17**)

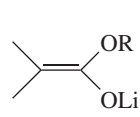

(**18**)

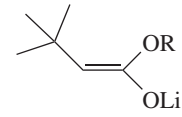

(**19**)

upon decreasing the temperature and/or the concentration. The fact that the entropy change for the dissociation is negative was accounted for in terms of steric restriction due to extra solvent molecules in the solvated dimer, relative to the tetramer[71]. The rate of exchange is slow compared to propagation[73]. The aggregation has a direct impact on the polymerization course. Indeed, semiempirical MNDO and *ab initio* calculations showed that the charge density on the α-carbon and thus the reactivity decreased with increasing the extent of the aggregation[74].

$$\underset{(\mathbf{20})}{2(\mathrm{MiBLi})_2(\mathrm{THF})_n} \rightleftharpoons \underset{(\mathbf{21})}{(\mathrm{MiBLi})_4(\mathrm{THF})_n} + n(\mathrm{THF}) \tag{25}$$

Kříž and coworkers also studied the structure of *t*-butyl 2-lithioisobutyrate (**18**, $R = t$-Bu), that mimicks the polymerization of tBuMA[75]. In THF, only one species is observed, more likely a tetramer, whatever the temperature and concentration.

As a rule, the aggregation of lithium ester enolates is mainly governed by concentration, temperature and structure of the ester group. There is thus no reason for the polymerization of methyl methacrylate and *t*-butyl methacrylate to be influenced by the same experimental parameters.

2. Dimeric model

A limitation of the unimeric model is that the possible influence of the penultimate unit is not taken into account on the reactivity of the propagating enolate. Therefore, the structure of dimeric models (**22**) was investigated[43].

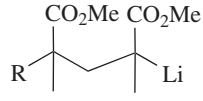

(**22**) R = Me, OMe

The intramolecular Claisen condensation of the dimeric model (**22**, R = Me) of PMMA was observed during NMR analysis, even at low temperature. This condensation results in the formation of a cyclic β-keto ester (**23**), methyl 2-lithioisobutyrate and lithium *t*-butoxide[43] (equation 26).

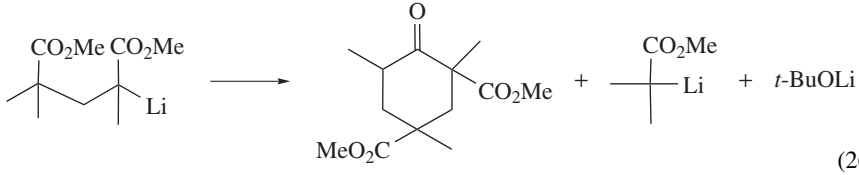

(**22**, R = Me) (**23**) (26)

A major difference between unimeric and dimeric models is the possible intramolecular interaction between the lithium enolate and the ester group of the penultimate unit. However, Bywater was unable to observe such an intramolecular complexation in case of the dimeric model of living PMMA in THF[76]. The structure of di-*t*-butyl 2-lithio-2,4,4′-trimethylglutarate (**24**), the dimeric model of living PtBuMA, was investigated. Aggregation of this ester enolate in solution was shown by measurements of apparent molecular weight[77]. IR spectroscopy suggests that the α-lithio ester and the γ-ester group are interacting[78]. By NMR spectroscopy and in agreement with *ab initio* and MNDO calculations, Kříž and coworkers found that in THF the dimeric model of PtBuMA has a strong tendency to form a complex between the Li enolate and the ester group of the penultimate unit. Actually, there would be competition between a linear complex (**24**) and a cyclic complex (**25**)[79]. The cyclic form (**25**) is monomeric in THF, in contrast to the linear complex (**24**) which is a dimer. A stabilization of *ca* 33 kJ mol^{-1} was predicted for the intramolecular coordination[79]. This situation is drastically different from that of the dimeric model of living PMMA, for which NMR analysis does not show any intramolecular complexation.

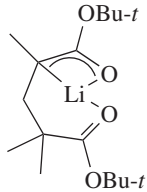

(**24**)

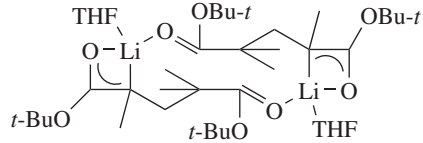

(**25**)

Zune and coworkers investigated the structure of the dimeric model of living PtBuMA in mixtures of toluene and THF[80]. Dimers were also observed as in pure THF. Moreover, partly organized pseudo-phases were detected by ^{7}Li NMR when the toluene content exceeded 50% v/v.

3. Oligomeric model

Monomeric and dimeric models do not mimic ideally living chain-ends because they ignore the influence of do β- and γ-monomeric units and the steric hindrance of the chain. It is therefore desirable to investigate the structure of propagating low molecular weight chains. However, these oligomers are more likely a mixture of living chains and dead chains as a result of unavoidable termination reactions. For instance, the occurrence of these undesired reactions made very difficult the characterization of living PMMA oligomers by multinuclear NMR spectroscopy[81]. Nevertheless, living polymerization of MMA in THF at $-78\,^{\circ}$C was studied by a series of techniques, including vibrational spectroscopy[81,82], viscometry[83], conductimetry[84,85] and kinetic measurements[86–88]. All the experimental observations were in line with the establishment of an equilibrium between nonassociated and associated dimers. In contrast to the unimeric model, formation of tetramers was unfavorable, which is expectedly an effect of the chain on the association of the propagating species.

Kinetic studies in THF at $-46\,^{\circ}$C with Li^+ and Na^+ counter-ions indicated that k_{prop} decreases with increasing [**P***], which is the signature of the coexistence of associated and nonassociated species (Scheme 3)[64,88,89]. Whenever Li^+ is the counter-ion, the reaction order is fractional and decreases from 0.75 down to 0.58, while [**P***] is increased from 10^{-4} up to 2×10^{-3} mol L^{-1}, consistent with propagating ion pairs and associated

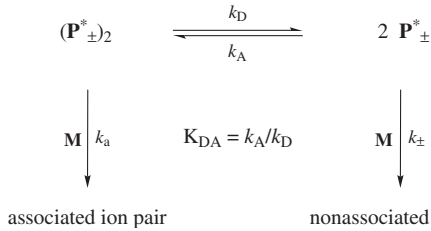

SCHEME 3. Equilibrium between associated and nonassociated ion pairs for the anionic polymerization of MMA in THF

species in comparable amount[64]. At higher temperature (−20 °C), the equilibrium between propagating ion pairs and associated species is shifted toward the less active aggregates, aggregation being thus an endothermic process[90]. It is worth noting that aggregation is an entropy-driven process, which can be accounted for by the steric restriction due to extra solvent molecules in solvated ion pairs, relative to the associated species, in line with the results on the dimer–tetramer equilibrium of MiBLi in THF[71].

The value of k_{prop} of the associated species is at least two orders of magnitude lower than k_{prop} of the nonassociated ion pairs[64]. Consistently, nonassociated ion pairs can be considered as dormant and k_a can be omitted in kinetic equations. Table 4 compares the values of various equilibrium and kinetic parameters for the polymerization of MMA, tBuMA and tBuA. Association is less important for tBMA than for MMA, more likely as a result of the bulkiness of the ester groups. In the same line, aggregation is less extensive in the polymerization of tBuMA than tBuA, because of the steric hindrance of the α-methyl subsituent[64]. Values of k_A and k_D in Table 4 were calculated according to equations 15 and 27, where a denotes the fraction of nonassociated ion pairs.

$$M_w/M_n = 1 + k_{\pm}/(ak_A) \tag{27}$$

Compared to MMA, the anionic polymerization of tBMA is living at higher temperatures due to the decreased reactivity of the enolate resulting from the higher steric hindrance[55]. Because of the rare occurrence of irreversible termination, the analysis of living oligomers was rewarding[81,91]. In contrast to the dimeric model, no intramolecular complexation of the enolate with the ester function of the penultimate unit was observed by ^{13}C NMR[91]. The equilibrium between dimeric aggregates **26** and nonaggregated species **27** (equation 28), previously reported for the dimeric model, was confirmed for the PtBMA oligomers analyzed by ^{7}Li NMR[43]. As a rule, PMMA and PtBMA chain-ends are lithium

TABLE 4. Equilibrium and kinetic parameters for the anionic polymerization of MMA, tBuMA and tBuA in THF, at −65 °C, with a Li^+ counter-ion

Parameter	MMA	tBuMA	tBuA
K_{DA} ($L\,mol^{-1}$)	0.002	0.0005	0.001
a	0.5	073	0.62
$k_{\pm}$ ($L\,mol^{-1}\,s^{-1}$)	46	8	2000
M_w/M_n	1.3	1.1	7.9
k_A ($L\,mol^{-1}\,s^{-1}$)	300	110	480
k_D (s^{-1})	0.15	0.22	0.5

enolates solvated by THF and partly aggregated.

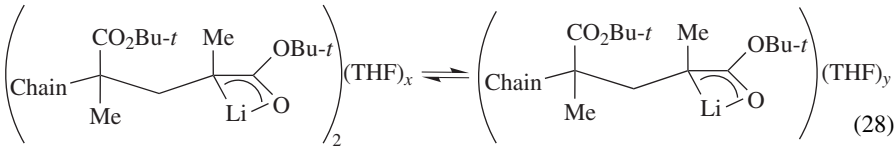

(**26**) (**27**) (28)

Whenever tBMA is polymerized in a THF/toluene mixture with an increasing toluene content, the polymerization control is less effective. According to NMR, this loss of efficiency is related to modifications in the aggregation of active species rather than to structural changes in the aggregates[80].

E. Ligated Anionic Polymerization

The first attempts, aiming at imparting control to the anionic polymerization of methacrylates initiated by organolithium derivatives, consisted of using initiators of a reactivity comparable with that of the propagating species, a highly solvating medium (e.g. THF) and a low temperature[60]. Although polymerization was controlled under these conditions, control was lost in apolar solvents[92] or at relatively high temperatures. Moreover, no control was observed for the polymerization of acrylates whatever the polarity of the solvent. As a rule, a decrease in reactivity of the propagating enolate is detrimental to the occurrence of irreversible termination. Ligation of Li enolates was proposed as a general strategy for modulating their reactivity. Indeed, the ligand may have a threefold role. First, it can change the distribution of the electron density in the metal ester enolate ion pair and, therefore, tune the reactivity. Second, the ligand can form a steric barrier, blocking access around the ion pair. Third, the ligand can modify the complexation equilibria between ion pairs and/or aggregates, the ideal situation being to end up with a unique active species. A plethora of ligands were tested, which can be classified in three main categories: μ-ligands, e.g. LiCl and *t*-BuOLi, forming polynuclear species with the metal ester enolate; σ-ligands, e.g. 12-crown-4 (**28**) and quinuclidine (**29**), forming coordinative complexes with the metal counter-ion; and $\mu-\sigma$-ligands, e.g. LiOEEM (**30**), with both possible effects.

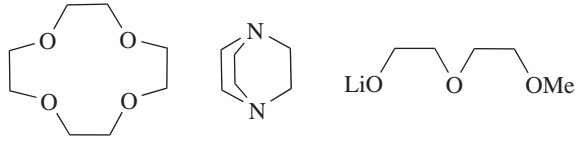

(**28**) (**29**) (**30**)

1. Inorganic salts

Ionic association equilibria can be perturbed by both organic and inorganic Li salts, depending on their Lewis acidity and steric factors.

a. Lithium chloride. The anionic polymerization of MMA and tBMA is living when carried out in THF at low temperature (−78 °C) and in the presence of lithium chloride.

The molecular weight is predetermined by the initiator-to-monomer molar ratio, and the polydispersity index is low[93]. Nevertheless, sterically hindered initiators, such as diphenylmethyllithium (DPMLi), DPHLi (10) and oligomeric α-methylstyryllithium, have to be used for good control. However, the anionic polymerization of tBMA falls under control under less demanding conditions as illustrated by the use of the less sterically hindered *s*-BuLi initiator[94]. Consistently, the control is lost when tBMA is substituted by less hindered monomers, such as MMA, GMA and DMAEMA. Interestingly enough, ligation of the adduct of *s*-BuLi and α-methylstyrene by LiCl allowed the anionic polymerization of tBuA to be controlled in THF at $-78\,^{\circ}C$ [95]. PtBuA with a narrow molecular distribution was also collected at higher temperature ($20\,^{\circ}C$)[96].

Contrary to the expected, the copolymerization of a mixture of MMA and tBuA was ill-controlled although the polymerization of each monomer is controlled under the conditions used[96, 97]. Similarly, polymerization of tBuA initiated by a living PMMA macroinitiator resulted in the expected PMMA-*block*-PtBuA diblock copolymer; however, it was contaminated by PMMA. The origin of the problems was ascribed to the detrimental backbiting reaction of the exceedingly sensitive ester function of the MMA antepenultimate unit of the moderately hindered PtBuA enolate[97]. This undesired competing reaction was no longer effective when tBuA was copolymerized with tBuMA rather than with MMA[97].

It must be noted that LiCl has no effect on the tacticity of PMMA[64]. In contrast, the isotacticity of PtBMA was increased from 9.9% to 25.5% when a threefold molar excess of LiCl was added to the initiator[98].

As shown in equation 25, MiBLi in THF is a mixture of solvated dimers **20** and tetramers **21**. Addition of LiCl results in one predominant complex of stoichiometry dependent on the relative amounts of LiCl present, as shown in equations 29 to 32[99]. A 1:1 complex, [(**24**)•(LiCl)], is formed by the dimeric model **24** with LiCl. An equilibrium is rapidly established between this complex and free LiCl. NMR relaxation times and MNDO calculations are in line with the dimeric aggregration of the 1:1 complex [(**24**)•(LiCl)][100].

$$\underset{(\mathbf{21})}{(\mathrm{MiBLi})_4} \overset{K_{eq}}{\rightleftharpoons} \underset{(\mathbf{20})}{2(\mathrm{MiBLi})_2} \xrightarrow{+\,1\mathrm{LiCl}} [(\mathrm{MiBLi})\,(\mathrm{LiCl})] \tag{29}$$

$$\underset{(\mathbf{21})}{(\mathrm{MiBLi})_4} \overset{K_{eq}}{\rightleftharpoons} \underset{(\mathbf{20})}{2(\mathrm{MiBLi})_2} \xrightarrow{+\,2\mathrm{LiCl}} [(\mathrm{MiBLi})\,(\mathrm{LiCl})_2] \tag{30}$$

$$\underset{(\mathbf{21})}{(\mathrm{MiBLi})_4} \overset{K_{eq}}{\rightleftharpoons} \underset{(\mathbf{20})}{2(\mathrm{MiBLi})_2} \xrightarrow{+\,n\mathrm{LiCl}\ (n>2)} [(\mathrm{MiBLi})\,(\mathrm{LiCl})_3] + (n-3)\mathrm{LiCl} \tag{31}$$

$$[(\mathrm{MiBLi})(\mathrm{LiCl})_3] \overset{T>55\,^{\circ}C}{\rightleftharpoons} [(\mathrm{MiBLi})(\mathrm{LiCl})_2] \tag{32}$$

Müller and coworkers studied the anionic polymerization of MMA initiated by RLi in the presence of steadily increasing amounts of LiCl[64, 96, 101]. At LiCl/RLi molar ratios lower than 1, the propagation rate increases, which was accounted for by the formation of a 1:1 complex, more reactive than the uncomplexed species. The situation changes drastically at LiCl/RLi molar ratios higher than 2. Indeed, the propagation rate then decreases with increasing content of LiCl. The same trend was observed for the polymerization of tBMA[98]. According to Müller and coworkers, formation of a less active 2:1 complex would be responsible for the detrimental kinetic effect of an excess of LiCl.

The silylation route shown in equations 23 and 24 was used to investigate the configuration of the ester enolate at the chain-end[58]. Although ligation by LiCl changed the *E*/*Z* molar ratio (11.5/88.5 instead of 0/100), no influence on the tacticity was observed[59].

Zune and coworkers studied the structure of the species propagating the anionic polymerization of tBMA by NMR spectroscopy[100]. The spectrum of the lithium ester enolate was perturbed by LiCl, as result of an equilibrium established between free lithium chloride and complexed active end-groups. The structure of the chain-end was not modified by a large excess of LiCl.

Because LiCl-mediated anionic polymerization of methacrylates is living, the addition of a second monomer to living polymethacrylate chains expectedly results in diblock copolymers, such as PtBuA-*block*-PMMA[94, 102], PtBAEMA-*block*-PMMA[103], PtBMA-*block*-PGMA[94], PtBAEMA-*block*-PtBuMA[103] and PtBMA-*block*-PDMAEMA[94].

b. Lithium perchlorate. Because of a higher Lewis acidity, $LiClO_4$ was substituted for LiCl as a ligand in the anionic polymerization of methacrylates and acrylates. Although carried out at −40 °C, the anionic polymerization of MMA initiated by DPHLi (**10**) in THF is living in the presence of $LiClO_4$[104]. The polydispersity is low ($M_w/M_n = 1.1$) and the initiation efficiency is high (>0.9). This is a substantial improvement compared to LiCl, because the livingness was then observed at −78 °C and lost at −40 °C. Moreover, the polymerization remains controlled in a mixture of toluene and THF (9/1 v/v) at −78 °C, which was not the case with LiCl as a ligand. Finally, the anionic polymerization of tBuA in THF at −78 °C is also living in the presence of 20 equivalents of $LiClO_4$ with respect to the initiator. Again, the polydispersity index is low ($M_w/M_n = 1.06$) and the initiation efficiency is high (0.96). It must be noted that a broad molecular weight distribution (2.1) and a low initiation efficiency (0.56) were observed in the absence of any ligand[104].

Baskaran and collaborators studied the kinetics of the anionic polymerization of MMA in THF at −20 °C[90]. The bilogarithmic plot of k_{app} versus [**P***] is linear with a fractional slope of 0.5, independently of the addition of a ligand. Therefore, the ligand does not prevent the propagating enolates from aggregating. Nevertheless, the apparent rate of polymerization was slower in the presence of $LiClO_4$ and decreased monotonously with increasing $LiClO_4$-to-initiator molar ratio, which was accounted for by the formation of less reactive mixed aggregates. No maximum was however observed, as was the case for the LiCl-mediated polymerization of MMA[96, 101]. The narrower molecular weight distribution of PMMA synthesized in the presence of $LiClO_4$ was explained by a faster exchange between the active species.

2. Organic salts

a. Lithium t-butoxide. *t*-BuOLi has a beneficial effect on the anionic polymerization of MMA initiated by DPHLi (**10**) in THF at −78 °C. The polydispersity index decreases from 1.35 down to 1.10 upon the addition of 10 equiv. of *t*-BuOLi. No impact on the chain tacticity was however observed[105]. At 25 °C in THF, a tenfold decrease of the rate constant of undesired cyclization compared to propagation was reported in the presence of *t*-BuOLi[106]. Moreover, the anionic polymerization of acrylates is also controlled when ligated by *t*-BuOLi, as exemplified by the polymerization of 2-ethylhexyl acrylate[107, 108] and nBuA[107, 109]. Fully acrylic block copolymers were accordingly prepared including PtBuA-*block*-PEtHA and PtBuA-*block*-PBuA copolymers[107].

The unimeric model of living PMMA ligated by *t*-BuOLi was studied by NMR. It was involved in an equilibrium between mixed tetramers[110]. The complexation rate increased with the reactivity of the complexes. For instance, the [(MiBLi)$_3$•(*t*-BuOLi)] complex was formed instantaneously, in contrast to the less reactive [(MiBLi)•(*t*-BuOLi)$_3$] complex

that took 20 h at −15 °C to be formed. The exchange between the mixed complexes (equations 33–35) is slow on the NMR time scale, although it was fast when LiCl was the ligand.

$$3\ (\text{MiBLi})_4 + (t\text{-BuOLi})_4 \rightleftharpoons 4\ (\text{MiBLi})_3.(t\text{-BuOLi}) \quad (33)$$

$$2\ (\text{MiBLi})_3{\cdot}(t\text{-BuOLi}) + (t\text{-BuOLi})_4 \rightleftharpoons 3(\text{MiBLi})_2.(t\text{-BuOLi})_2 \quad (34)$$

$$(\text{MiBLi})_2{\cdot}(t\text{-BuOLi})_2 + (t\text{-BuOLi})_4 \rightleftharpoons 2\ (\text{MiBLi}).(t\text{-BuOLi})_3 \quad (35)$$

t-BuOLi and di-*t*-butyl 2,4,4-trimethylglutarate (**24**), the dimeric model of living PtBMA, formed mixed aggregates of the A_2B_2 and AB_3 type, the molar ratio of which depends on the relative amount of *t*-BuOLi. NMR data showed the coexistence of three conformations (α, β, γ). In the γ form, the enolate is intramolecularly coordinated to the γ ester group[79]. However, the NMR analysis of living PMMA oligomers prepared by the MMA/MiBLi/*t*-BuOLi (2/1/3) system did not show signals typical of intramolecular complexation[81]. In THF at −78 °C, *t*-BuOLi has no effect on the *E*/*Z* molar ratio of the propagating enolate[59]. Consistently, no effect on the chain tacticity was observed in THF or in toluene (Table 5)[111]. However, the chain tacticity was significantly modified by *t*-BuOLi in a 9/1 toluene/THF mixture (Table 5)[111].

b. Silanolates. Zundel and coworkers reported that sBuMe$_2$SiOLi is a very efficient ligand for the living anionic polymerization of MMA initiated by *s*-BuLi in toluene at 0 °C[112]. The ligand (*s*-BuMe$_2$SiOLi) can be easily prepared *in situ* by reaction of octamethylcyclotetrasiloxane [(Me$_2$SiO)$_4$ or D$_4$] with *s*-BuLi in toluene at 20 °C (equations 36–39), thus prior to the addition of the monomer and the solvent. The livingness of the polymerization at a temperature as high as 0 °C is noteworthy. When the polymerization is carried

TABLE 5. Effect of various ligands on the stereochemistry of the MMA polymerization at −78 °C

Ligand	Initiator	Solvent	L/I[a]	*mm*[b]	*mr*[b]	*rr*[b]	*m*[c]	*r*[c]
t-BuOLi	DPMLi	THF	0	0.01	0.21	0.78	0.115	0.885
t-BuOLi	DPMLi	THF	10	0.01	0.19	0.80	0.105	0.895
t-BuOLi	DPHLi	PhMe	0	0.88	0.09	0.03	0.925	0.075
t-BuOLi	DPHLi	PhMe	10	0.87	0.09	0.04	0.915	0.085
t-BuOLi	DPMLi	PhMe/THF[d]	0	0.17	0.25	0.58	0.30	0.70
t-BuOLi	DPMLi	PhMe/THF[d]	10	0.57	0.11	0.32	0.63	0.37
12-CE-4	DPHLi	THF	0	0.01	0.21	0.78	0.11	0.89
12-CE-4	DPHLi	THF	5	0.01	0.22	0.77	0.12	0.88
12-CE-4	DPHLi	PhMe/THF[d]	0	0.17	0.25	0.59	0.30	0.70
12-CE-4	DPHLi	PhMe/THF[d]	5	0.07	0.23	0.70	0.19	0.81
12-CE-4	DPHLi	PhMe	0	0.88	0.09	0.03	0.93	0.07
12-CE-4	DPHLi	PhMe	5	0.59	0.26	0.15	0.72	0.28
K211	DPHLi	THF	2.5	0.02	0.33	0.65	0.19	0.81
K211	DPHLi	PhMe/THF[d]	2.5	0.02	0.32	0.66	0.18	0.82
K211	DPHLi	PhMe	2.5	0.02	0.32	0.66	0.18	0.82
LiOEEM	DPMLi	THF	10	0.01	0.16	0.83	0.09	0.91
LiOEEM	DPMLi	PhMe	10	0.01	0.16	0.83	0.09	0.91

[a] Ligand-to-initiator mole ratio.
[b] See footnotes to Table 1.
[c] See footnotes to Table 3.
[d] The PhMe/THF ratio is 9/1 (v/v).

out in toluene at low temperature (−78 °C), the propagating enolate remains active at least for 90 min, as shown by resumption experiments. At 20 °C, the monomer conversion is limited, the control is less efficient and the molecular weight distribution is broader. Addition of a coordinating solvent (THF, DMSO) to toluene is deleterious due to enhancement of self-termination reactions. The introduction of 2*s*-$BuMe_2SiOLi$ as a ligand paved the way to highly isotactic PMMA (85%) at a relatively high temperature (0 °C). It must be noted that initiation of the MMA polymerization by *t*-BuMgBr in toluene is an alternative route to isotactic PMMA, although a much lower temperature (−78 °C) is then required for the polymerization to be controlled[67,68].

$$s\text{-BuLi} + (Me_2SiO)_4 \longrightarrow [(s\text{-BuLi})\text{-}(Me_2SiO)_4] \quad (36)$$

$$s\text{-BuLi} + [(s\text{-BuLi})\text{-}(Me_2SiO)_4] \longrightarrow [(s\text{-BuMe})_2SiOLi + [(s\text{-BuLi})\text{-}(Me_2SiO)_3] \quad (37)$$

$$s\text{-BuLi} + [(s\text{-BuLi})\text{-}(Me_2SiO)_3] \longrightarrow [(s\text{-BuMe})_2SiOLi + [(s\text{-BuLi})\text{-}(Me_2SiO)_2] \quad (38)$$

$$s\text{-BuLi} + [(s\text{-BuLi})\text{-}(Me_2SiO)_2] \longrightarrow 2s\text{-}BuMe_2SiOLi \quad (39)$$

The ligand-to-*s*-BuLi molar ratio (R) has a key influence on the polymerization control[113]. When $R > 21$ the size exclusion chromatography fractions of PMMA are monomodal and the polydispersity index is low (<1.2). The actual concentration of the *s*-BuLi was determined by titration. At least 70% of the initiator contributed to the polymerization. One single mixed associated hexameric species, *s*-BuLi ligated to five molecules of $BuMe_2SiOLi$, was identified by ^{7}Li NMR, consistently with the large excess of ligand, which is the prerequisite for the polymerization to be controlled. When the content of ligand is not sufficiently high ($R < 21$), the control is lost, as testified by the bimodality of the molecular weight distribution of PMMA. Under these conditions, more than one mixed associated species is formed as confirmed by Li NMR[114].

Ligation by silanolates was also effective in imparting livingness to the anionic polymerization of EMA, nBuMA and isobornyl methacrylate, leading to a series of highly isotactic polymethacrylates[115]. The anionic polymerization of acrylates is also living, provided that the alkyl of the ester group is linear (e.g. nBuA)[116]. Polymerization of monomers with a bulky ester group, such as tBuMA and tBuA, is out of control[115]. Copolymerization of acrylates on the one hand or methacrylates on the other hand was successfully carried out[115]; however, the copolymerization of one methacrylate and one acrylate is out of control[115]. As a rule, the *s*-$BuMe_2SiOLi$ ligand allows a wide range of highly isotactic random and block copolymers to be prepared provided that the comonomer pair is properly selected[115].

3. Tertiary diamines

The anionic polymerization of MMA is controlled when initiated by DPHLi (**10**), in THF at −50 °C, in the presence of TMEDA. The initiation efficiency is high and the polydispersity index is low ($M_w/M_n = 1.2$)[117]. A kinetic study has showed that the slope of the bilogarithmic plot of k_{app} versus [**P***] is linear. The presence of TMEDA does not change the kinetic order (0.53) with respect to propagating enolates (THF, at −20 °C, with [TMEDA]/[initiator] >1)[118] or the polymerization rate to a significant extent. Then, TMEDA does not compete with THF for the ligation of the enolate or perturbs its state of aggregation. It must be noted that, at low ligand-to-initiator molar ratio ([TMEDA]/[initiator] <1), a small fraction of high molecular weight PMMA is formed, which suggests that a small amount of TMEDA produces highly reactive species.

Other tertiary diamines were tested as organic ligands such as TMEDA, its tetraethyl analogue, 2,2′-bipyridine, quinuclidine (**29**) and sparteine (**31**)[117]. The latter was most

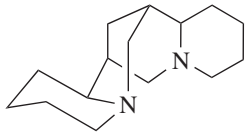

(**31**)

efficient, the anionic polymerization of MMA being kept controlled in THF at temperatures as high as 25 °C, with an initiator efficiency close to 1.

4. Crown ethers

Crown ethers such as 12-CE-4 (**28**) and DB-18-CE-6 (**32**) are well-known for their capability to chelate alkali-metal ions surrounding them with a steric barrier, which justifies that they were tested as ligands in the anionic polymerization of methacrylates and acrylates. 12-CE-4 (**28**) changes neither the molecular weight distribution of PMMA, nor the NMR spectrum of the unimeric model in THF[119, 120]. It is worth noting that the polymerization was initiated by DPHLi (**10**) in THF at −78 °C. This crown ether (**28**) is thus less complexing than THF and leaves the propagating enolate unmodified[105].

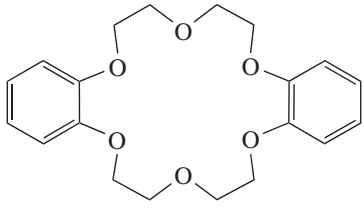

(**32**)

Consequently, the *E*/*Z* molar ratio of the propagating enolate and the chain tacticity in THF were not affected by 12-CE-4 (**28**) (Table 5)[59]. In contrast, this ligand was much less favorable to the isotactic placement in pure toluene or in a 9/1 toluene/THF mixture (Table 5)[111].

The anionic polymerization of MMA was also initiated by (diphenylmethyl)sodium ligated by several crown-ethers[121]. Substitution of the sodium counter-ion for lithium was beneficial to the livingness of the polymerization being promoted by DB-18-CE-6 (**32**); however, control was lost at 25 °C. Mainly, syndiotactic PMMA was formed at −20 °C, without significant effect of the crown-ether. At least up to −20 °C, the MMA polymerization was also living in THF, such that block copolymers were prepared by sequential polymerization of tBuA and MMA in THF at −78 °C[122]. However, when the addition order was reversed, the PtBuA-*block*-PMMA copolymer was contaminated by a small amount of homo-PMMA, as a result of backbiting of the antepenultimate ester unit of PMMA by the living PtBMA enolate.

Although these detrimental backbiting reactions were effective in the LiCl-ligated anionic copolymerization of MMA and tBuA[97], this copolymerization was living in THF at −78 °C when initiated by Ph_2CHNa ligated by DB-18-CE-6 (**32**)[122]. According to the reactivity ratios determined by the Kelen–Tüdos method ($r_{MMA} = 0.02$ and $r_{tBuA} = 8.81$), copolymers with a tapered structure were formed, as a result of the higher reactivity of tBuA.

5. Cryptands

In contrast to the crown ether **28,** the cryptand K211 (**33**) is very beneficial to the control of MMA polymerization initiated by diphenylmethyllithium in THF at −78 °C. As a result, PMMA with a very low polydispersity index (1.01) was obtained[119]. The effect of this ligand on the unimeric model, e.g. MiBLi, was studied by NMR spectroscopy. The equilibrium commonly observed in THF between tetramers and dimers is actually shifted towards a monomeric complexed species[119]. Both the *E*/*Z* molar ratio (90/10 instead of 0/100) and the chain tacticity (Table 5) are affected by the cryptand K211 (**33**) whatever the solvent used[59, 111].

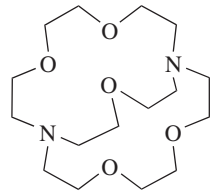

(**33**)

6. Pyridine

Anderson and coworkers showed that the polymerization of MMA initiated by *n*-BuLi is living from −78 °C up to −20 °C when carried out in a 70/30 (v/v) mixture of toluene and pyridine[48]. The beneficial effect of pyridine is maintained when THF is substituted for toluene with *s*-BuLi and *t*-BuLi as initiators. Nevertheless, the polymerization temperature must be kept below −65 °C[48]. McGrath and coworkers extended this reaction to pure pyridine at −45 °C, and they collected high molecular weight PMMA (up to 83000) with a low polydispersity index (1.1)[123].

Formation of a dihydropyridine σ-adduct at the chain-end was shown by NMR[48] and UV[123] spectral analysis. Anderson and collaborators proposed that the actual initiator would be adduct **34**, formed by reaction of *s*-BuLi with pyridine (equation 40), which implies that the α-end-group of PMMA is a dihydropyridine group[48]. This hypothesis was not experimentally confirmed. However, in the specific case of the ε-caprolactone (**3**, $n = 4$) polymerization initiated by the BuLi/pyridine adduct, no characteristic NMR signal of dihydropyridine could be detected. The polymerization mechanism was therefore revised, based on the alkyllithium as the actual initiator and the establishment of an equilibrium between an active uncomplexed enolate (**35**) and a dormant σ-complex (**36**) as the basis for polymerization control (equation 41)[123].

(**34**) (40)

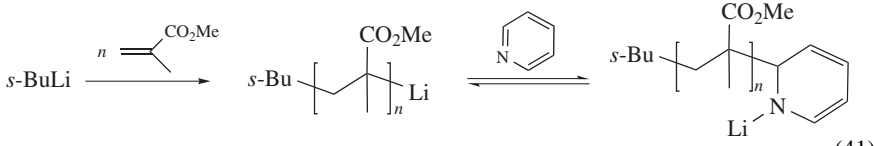

(**35**) (**36**) (41)

7. Lithium 2-(2-methoxyethoxy)ethoxide, a $\mu-\sigma$ ligand

Polyethers end-capped by a lithium alkoxide offer a unique ligation where μ complexation by the lithium alkoxide and σ complexation by the polyether can occur simultaneously[43]. The MMA polymerization in THF at $-78\,^{\circ}C$ is living in the presence of LiOEEM (**30**)[105]. In contrast to polymerization with μ-ligands, the kinetics is very fast. Indeed, only 2 minutes are necessary for the monomer conversion to be complete. Upon addition of 5 equiv. of LiOEEM (**30**), the polydispersity index is as low as 1.05. Unfortunately, the polymerization of tBMA remains uncontrolled in the presence of LiOEEM (**30**), as witnessed by a bimodal molecular weight distribution, which suggests the coexistence of at least two types of growing sites. This lack of control was accounted for by the bulkiness of the *t*-butyl group preventing effective complexation.

Complexation of the unimeric model of living PMMA by LiOEEM (**30**) was investigated by multinuclear NMR[124]. LiOEEM is actually able to deaggregate the original MiBLi aggregates with formation of a single mixed complex [(MiBLi)•$(LiOEEM)_2$], provided that more than 2 equivalents of ligand are present. Moreover, the same mixed complex is observed in a 9/1 toluene/THF mixture, which suggests that the lithium cation is strongly coordinated by LiOEEM.

The interaction of LiOEEM (**30**) with a dimeric model of living PtBMA was studied in THF at low temperature by NMR techniques. A metastable system was observed that needed several days at $-15\,^{\circ}C$ to reach equilibrium. LiOEEM is prone to self-association, which competes with formation of mixed aggregates with the dimeric model. When the LiOEEM/dimeric model molar ratio is low (up to 4), the aggregation is incomplete and several complexes coexist[125].

LiOEEM (**30**) has an effect on the E/Z molar ratio of the enolate propagating in THF ($E/Z = 11.5/88.5$ instead of 0/100) but not on the chain tacticity (Table 5)[59,111]. Nevertheless, in toluene, a substantial increase in the syndiotactic fraction is observed at the expense of the isotactic one, although the chain tacticity is the same as in THF when the ligand-to-initiator molar ratio exceeds 3 (Table 5)[111]. This stereochemical behavior is the signature of a single living species,whatever the solvent.

The LiOEEM-ligated anionic polymerization of acrylates initiated by diphenylmethyllithium is also controlled in a 90/10 toluene/THF mixture at $-78\,^{\circ}C$[105,114,126], control being as effective however as the alkyl substituent of the monomer is long, i.e. methyl < ethyl < *n*-butyl < *n*-nonyl.

The statistical anionic copolymerization of acrylates and methacrylates is also controlled in the presence of LiOEEM (**30**), as testified by the copolymerization of MMA and tBuA in THF at $-78\,^{\circ}C$[127]. Block copolymers were also prepared by the sequential polymerization of at least two methacrylates and acrylates. For instance, PMMA-*block*-PbBuA[128] and PMMA-*block*-PnNonA were synthesized[129]. The addition order of the comonomers is important. Indeed, when living PnBuA is the macroinitiator of the MMA polymerization, the expected block copolymer is contaminated by homo-PnBuA, which is not the case when the polymerization sequence is reversed. A fully acrylic-based thermoplastic elastomer, PMMA-*block*-P(2EtHA)-*block*-PMMA, was prepared by the sequential LiOEEM-ligated polymerization of MMA, 2-EtHA and MMA[130].

8. Lithium 2-(dimethylamino)ethoxide

The better σ-cation binding ability of tertiary amines compared to ethers prompted Fontanille and coworkers to investigate ligands containing lithium alkoxide and an amino group. Good control was observed for MMA polymerization initiated by DPHLi (**10**) in THF, at $0\,^{\circ}C$, in the presence of lithium 2-(dimethylamino)ethoxide[131].

F. Ate Complexes

Although the anionic polymerization of MMA initiated by alkyllithium derivatives in toluene is not living even at low temperature, Hatada and coworkers reported that a mixture of *t*-BuLi and Et_3Al led to formation of highly syndiotactic PMMA (>90%), in toluene at −78 °C, with predetermined molecular weight, high initiation efficiency and narrow molecular weight distribution, provided that the $[Al]_0/[Li]_0$ molar ratio was 3 or higher[132]. Remarkably, control is maintained when the polymerization is carried out at room temperature, provided that neither *n*-BuLi nor *s*-BuLi are used as initiators, because of detrimental reactions with the ester groups[132, 133]. This strategy was successfully extended to the anionic polymerization of other methactrylates, such as EMA, iPrMA, nBuMA, tBuMA. The polymerization livingness was confirmed by the successful synthesis of PMMA-*block*-PEMA diblock copolymer by the sequential polymerization of MMA and EMA[132].

A wide range of trialkylaluminum with different bulkiness and Lewis acidity was investigated[133–136]. They influenced differently the PMMA tacticity. Et_3Al and *i*-Bu_3Al led to syndiotactic PMMA, whereas atactic PMMA was formed in the presence of *t*-Bu_3Al. Ballard and coworkers successfully polymerized MMA in toluene at 0 °C in the presence of a mixture of *t*-BuLi and (2,6-di-*t*-butyl-4-methylphenoxy)diisobutylaluminum, that was prepared by reaction of triisobutylaluminum with 2,6-di-*t*-butyl-4-methylphenol[137]. In order to shed light on the origin of the polymerization control, a mechanistic study was undertaken by NMR techniques. In the *t*-BuLi/Et_3Al system, the actual polymerization initiator is a *t*-butyl carbanion. Actually, *t*-BuLi forms an 'ate' complex with Et_3Al[132]. Later on, Müller and coworkers analyzed the unimeric model in the presence of Et_3Al and MMA, and they confirmed the formation of a bimetallic ate complex[138, 139]. It was accordingly proposed that the propagating species is an ate complex, which exhibits a decreased nucleophilicity compared to the uncomplexed species.

The activation of the monomer by Et_3Al cannot however be disregarded. In this respect, Müller and coworkers carried out a two-step experiment. First, they polymerized MMA in toluene at −78 °C with an Al/Li molar ratio of 3.3. Finally, an excess of trialkylaluminum was added with the Al/Li molar ratio exceeding 10. This resulted in a slower propagation rate, although the concentration of the MMA•$AlEt_3$ complex was higher, in qualitative agreement with a more intense yellow color. This experiment thus suggests that the effect of Et_3Al on the MMA polymerization does not proceed through an activated monomer mechanism[138, 140].

The kinetic behavior is quite complex. The time-conversion plot shows a curvature at low conversion followed, after a kink, by a linear regime at higher conversion[138]. A first tentative explanation relied on the establishment of an intramolecular coordination of the propagating enolate by the ester group of the penultimate unit. So, the polymerization would be initiated by the ate complex, followed by the insertion of a few monomer units and the rapid conversion of the propagating ate complex into a less reactive intramolecular complex. However, a bulkier trialkylaluminum that should prevent the intramolecular complexation from occurring does not cancel the kink in the kinetic plot and does not support the proposed mechanism[141]. Another explanation involves networking of the chains as a result of the intermolecular coordination of the enolates and constitutive ester groups. Anytime they are less accessible in the gels, the enolates behave as dormant species. The actual concentration of the active enolates in the gel is thus decreased, and so is the polymerization rate. This gel effect can be suppressed by the addition of a Lewis base, such as 12-crown-4 (**28**), methyl pivalate or methyl benzoate[142], which makes the kinetics first order in monomer and the molecular weight distribution narrow.

G. Metal-free Initiators

A possible strategy to improve control of the anionic polymerization of methacrylates relies on the substitution of metal-free cations for metal cations. Ammonium and phosphonium salts were investigated as discussed hereafter.

1. Ammonium salts

Reetz studied the polymerization of nBuA initiated by tetrabutylammonium thiolates, which are easily prepared by reaction of thiols with tetrabutylammonium hydroxide[143]. Nevertheless, only polymers of molecular weight under 2000 were formed[144]. This problem was overcome by using the tetra-*n*-butylammonium salt of diethyl 2-ethylmalonate (**37**) as initiator (equation 42). PnBuA was obtained with a predictable molecular weight and a low polydispersity index ($1.1 < M_w/M_n < 1.2$).

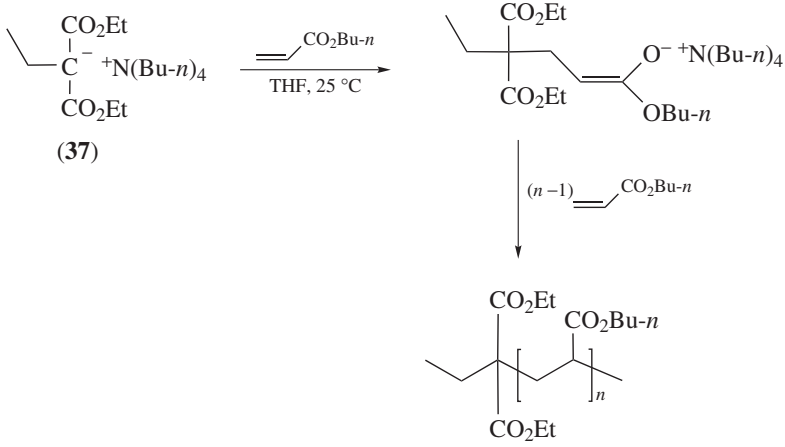

(42)

A variety of alkyl-ammonium-based initiators was tested in the polymerization of alkyl methacrylates and acrylates; however, only very limited control was observed[41]. Baskaran and coworkers initiated the polymerization of MMA by the tetrabutylammonium and the tetramethyldiethylguanidinium of the 1,1-diphenylhexyl anion, in THF at $-40\,^{\circ}C$[145]. Whereas the polymerization was very fast, the initiator efficiency was low and the molecular weight distribution was broad. The low nucleophilicity of the initiator compared to that of the propagating enolate results in a slow initiation, thus the low initiator efficiency, and a broad molecular weight distrubution. It must be noted that part of the initiator was left unreacted at the end of the polymerization. This points to initiation equilibrium and ion pairing effects being detrimental to the polymerization control[145].

Bandermann and coworkers studied the MMA polymerization initiated by **37**[146]. Whenever the initiator is contaminated by traces of diethyl 2-ethylmalonate, an inhibition period is observed, which was accounted for by a transfer reaction of the propagating enolate to diethyl 2-ethylmalonate. The polymerization cannot start until this contaminant is completely consumed. Consistently, no inhibition is observed when the initiator is highly pure. Finally, a Hoffman elimination in the propagating ammonium enolate (**38**) could occur with formation of dead chains (**39**) tri-*n*-butylamine and 1-butene (equation 43)[146].

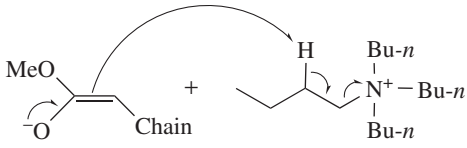

(**38**)

(43)

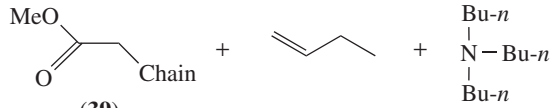

(**39**)

2. Phosphonium salts

Hogen-Esch and collaborators[147] polymerized MMA in THF at 0 °C and at 25 °C using as initiator tetraphenylphosphonium salts of various counter-ions (**40**–**45**)[147–152]. In contrast to the polymerization carried out in the presence of ammonium and guanidinium salts, the MMA polymerization initiated by tetraphenylphosphonium triphenylmethanide (Ph_3CPPh_4) is living in THF, even at room temperature, with a high initiation efficiency and a narrow molecular weight distribution ($M_w/M_n < 1.1$)[150]. The polymerization of nBuA is, however, ill-controlled under the same conditions[153].

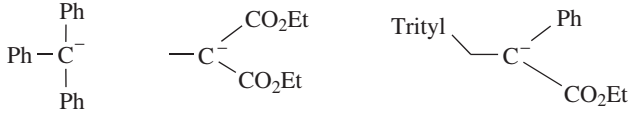

(**40**) (**41**) (**42**)

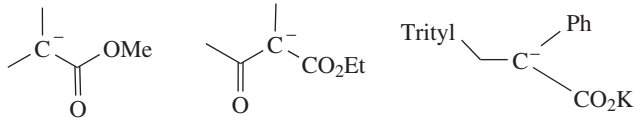

(**43**) (**44**) (**45**)

Hogen-Esch stressed that the MMA polymerization initiated by Ph_3CPPh_4 is very fast (0.3 s < half life < 1 s) with a very short induction period (0.05 to 0.2 s). Therefore, it is mandatory that the polymerization medium be very rapidly homogenized for the polymerization to be controlled. The dropwise addition of a MMA solution in THF to a solution of the phosphonium salt in the same solvent was recommended[147].

The rate of polymerization initiated by (1-naphthyl)triphenylphosphonium salts is four to five orders of magnitude slower than the one initiated by the corresponding tetraphenylphosphonium salts. Remarkably, control was maintained although no special attention was paid to the mixing of reactants[151].

Substitution of the tetraalkylphosphonium for the tetraphenylphosphonium counter-ion was detrimental to the control of the MMA polymerization. Indeed, although the molecular weight distribution was narrow, the initiator efficiency was very low (<0.18)[154]. Phosphazenes were also investigated as counter-ions, but the initiator efficiency remained quite low[155, 156]. Baskaran and Müller reported that the polymerization of MMA initiated by **45′** was very fast (0.05 s < half life < 0.15 s; $-20\,^{\circ}C < T < 20\,^{\circ}C$) and termination was negligible[157].

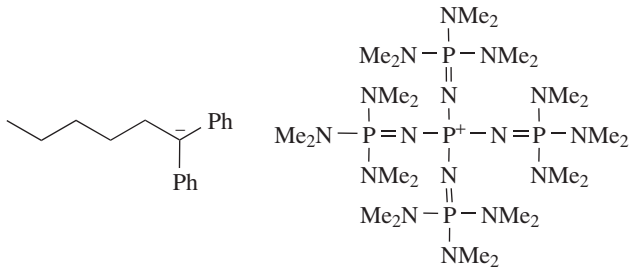

(**45′**)

A possible correlation between the structure of the phosphonium salt and polymerization control was investigated. Based on kinetic analysis[150] and NMR data[149], it was proposed that a fast equilibrium is established between the propagating enolate (**46**) and a dormant ylide (**47**) in the polymerization initiated by Ph_3CPPh_4 (equations 44 and 45).

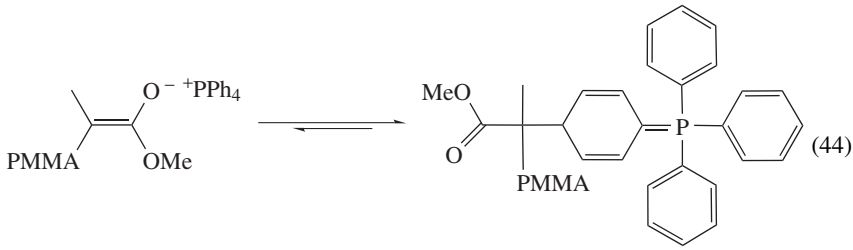

(**46**) (**47**)

$(MIB)PPh_4$, where MIB stands for the methylisobutyrate carbanion **43**, which is the unimeric model of the MMA propagating species, was synthesized and characterized by UV and NMR[149]. The aforementioned equilibrium was confirmed, in which the dormant ylide is the major species[150]. Whenever the polymerization of MMA is initiated by $(MIB)PPh_4$ in THF at 20 °C, the initiation efficiency is low (20%) and the molecular weight distribution is broad ($M_w/M_n = 2.1$). This observation was accounted for by the ylide-to-enolate isomerization, which is slower than the chain propagation[150].

In contrast to the polymerization mediated by ammonium and guanidinium salts, an equilibrium between propagating and dormant species exists and the actual concentration of the propagating species is lower, which is thought to be responsible, in part at least, for the very good polymerization control at unusually high temperatures. In agreement with this model, no ylide can be formed in case of tetraaalkylphosphonium salts and indeed the polymerization is not controlled[154]. The unique behavior of (1-naphthyl)triphenylphosphonium salts compared to tetraphenylphosphonium salts was

accounted for by the higher stability of the dormant ylide, because aromaticity is restored by the addition of the enolate to the ring.

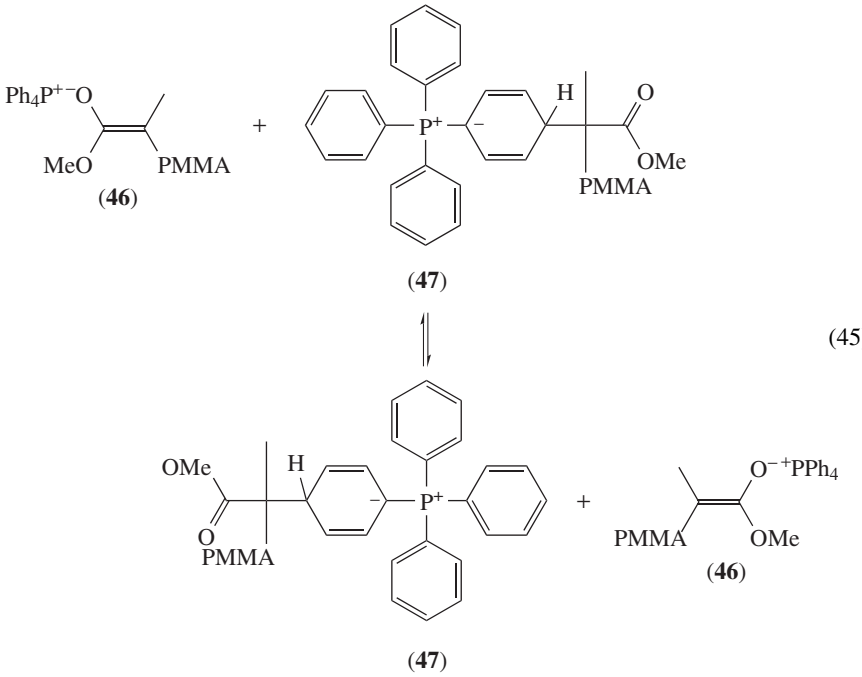

(45)

H. Group Transfer Polymerization (GTP)

Webster and coworkers discovered in the mid—1980s that the polymerization of MMA initiated by silyl ketene acetals (**48**) in the presence of $ZnBr_2$ was living (equation 46)[158–160]. Propagation proceeds through the addition of a silyl ketene acetal to an activated double bond under Lewis acid catalysis, which is nothing but the well-known Mukaiyama reaction[161]. A further breakthrough in this field was the discovery that a very small amount of bifluoride (less than 0.01% versus the initiator) is able to promote the living polymerization of methacrylates at room temperature[162]. This original process was patented by du Pont de Nemours & Company in 1983. Webster and coworkers coined the name of GTP for this polymerization as was suggested by B. M. Trost[159].

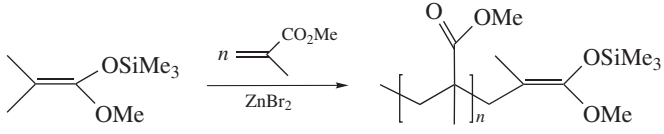

(46)

Later on, a wide range of Lewis acids and nucleophilic catalysts was shown to promote GTP. GTP mediated by Lewis acids[158] is beyond the scope of this review because no enolate is involved in the mechanism. The nucleophilic catalysts can be illustrated by bifluoride[162,163–165], fluoride[165], cyanide[163,166,167] and oxyanion salts[168], with a special

emphasis on tris(piperidino)sulfonium bifluoride that produces polymers with a narrow molecular weight distribution.

A kinetic study by Brittain and coworkers confirmed that initiation is faster than propagation, which is a prerequisite for the molecular weight distribution to be narrow[164]. Anions can be ranked in the following order of decreasing reactivity: $HF_2^- > C_6H_5CO_2^- > [PhCO_2{\cdots}H{\cdots}O_2CPh]^-$ [164].

The chain tacticity of PMMA synthesized by GTP catalyzed by nucleophiles at different temperatures was analyzed by Webster and coworkers The syndiotactic content increases from 50% at 60 °C up to 80% at −90 °C in THF, using tris(dimethylamino)sulfonium bifluoride $[(Me_2N)_3S^+\ HF_2^-]$ as catalyst[165]. In contrast to the anionic polymerization of MMA, the stereoselectivity of GTP is less sensitive to solvent. It must be noted that PMMA is less syndiotactic when the GTP is catalyzed by nucleophiles rather than by Lewis acids[165]. GTP was extended to the living polymerization of many acrylates and methacrylates, such as nBuMA, glycidyl-MA, 2-ethylhexyl-MA, $Me_3SiOCH_2CH_2$-MA, sorbyl-MA, allyl-MA, lauryl-MA), acrylates (EA, BuA), acrylonitrile, methacrylonitrile and *N*,*N*-dimethylacrylamide[165].

Several mechanisms were proposed in the scientific literature for the nuclophiles-mediated GTP. Webster and Sogah proposed a concerted associative mechanism based on the direct transfer of a pentacoordinated siliconate intermediate (**49**) from a chain to an incoming monomer (equation 47)[159, 162].

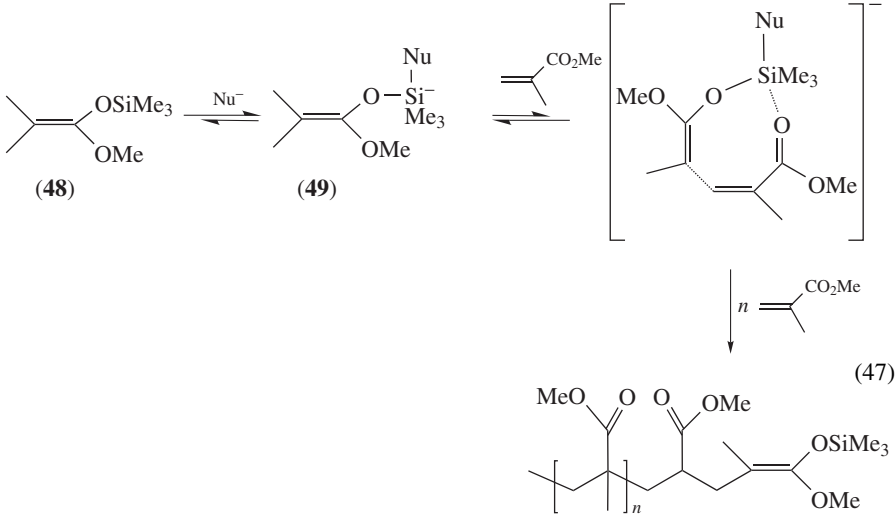

(**48**) (**49**) (47)

Based on kinetic and stereochemical considerations, Müller revised this mechanistic proposal in favor of a two-step associative mechanism[169, 170]. The monomer would be added to the α-carbon of the pentacoordinated siliconate chain (**49**) followed by migration of the silyl group to the carbonyl of the monomer (equation 48). It is then essential that the exchange of the catalyst between chain-ends is fast compared to chain propagation.

Although the silyl exchange should be typically intramolecular according to this associated mechanism, significant exchange between growing chains occurs during GTP. In order to account for this experimental observation, Quirk and coworkers proposed a dissociative mechanism, which relies on the dissociation of the pentacoordinated siliconate (**49**), followed by the Michaël addition of the released enolate (**50**) onto the monomer

and the reversible conversion of the new enolate (**51**) into a silyl ketene enolate (**52**) (equation 49)[171, 172]. This mechanism thus implies an exchange between an active species (the enolate) and a dormant species (the silyl ketene enolate). The good control imparted to GTP would then be accounted for by a decrease in the instantaneous concentration of the active species in the polymerization medium. Moreover, a fast exchange of silyl groups between chain-ends would be responsible for a narrow molecular weight distribution. Actually, GTP would take place according to different mechanisms depending on the catalysts and the experimental conditions, as shown by Müller in kinetic studies[173].

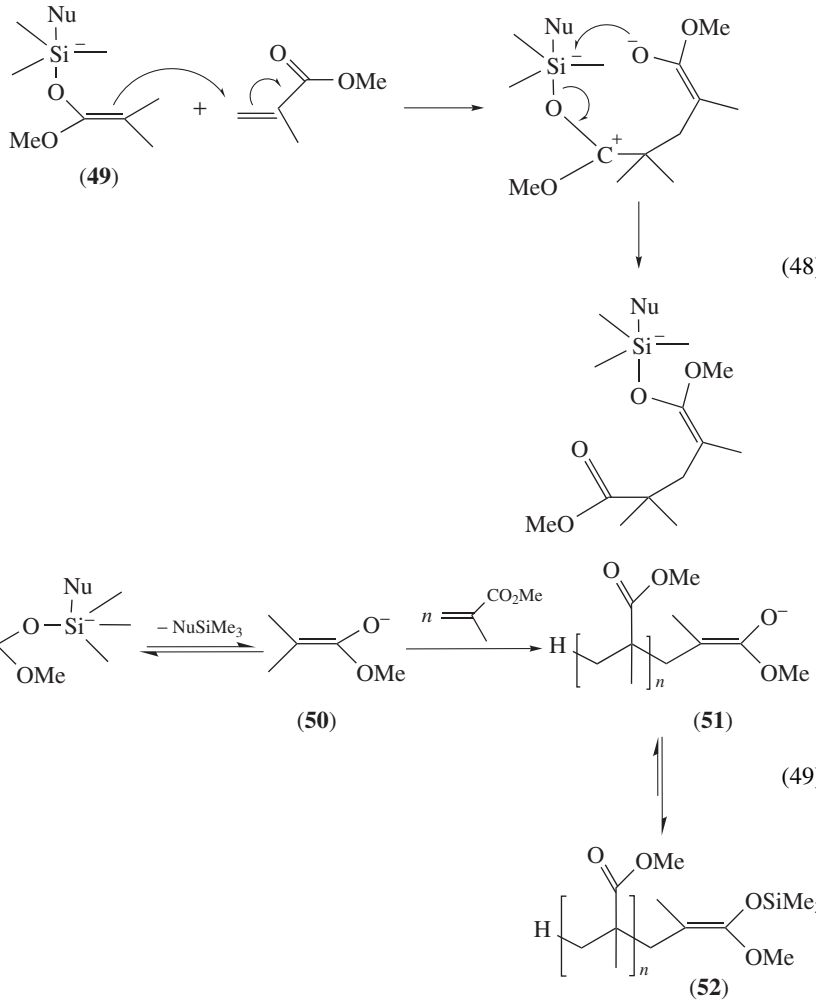

There are several similarities between classical anionic polymerization and GTP of methacylates. Indeed, side reactions observed in anionic polymerization are also observed in GTP. Brittain and Dicker showed that the intramolecular cyclization of the end-group with the ester function of the antipenultimate unit is the major termination reaction in

GTP of methacrylates[174]. Tacticity of PMMA synthesized by either anionic polymerization or mucleophile-mediated GTP is very similar[171,175]. The same conclusion holds for the reactivity ratios in random copolymerization of methacrylates and acrylates[169,176–178], for the activation energy[169,170,179a] and the frequency exponent[169,179a]. These experimental observations support that the same propagating species, i.e. enolates, are involved in both polymerization processes[41].

One main difference between anionic polymerization and GTP has to be found in the amount of enolates active in polymerization. In anionic polymerization, all the chains are end-capped by an enolate, which is the case for only a small part of the chains in GTP consistent with the very good control of GTP even at room temperature. In this respect, Brittain and Dicker showed that k_{prop}/k_{term} is by far higher in GTP (250) than in classical anionic polymerization ($k_{prop}/k_{term} = 8$)[174]. In line with slow termination compared to propagation in GTP, Bandermann and coworkers found that the amount of the nucleophilic catalyst is essential to the polymerization control. Indeed, as far as the tris(piperidino)sulfonium bifluoride-mediated GTP of MMA in THF is concerned, the polydispersity index increases with the amount of catalyst[179b].

VII. MACROMOLECULAR ENGINEERING AND ENOLATES

The advent of living anionic polymerization of acrylates and methacrylates paved the way to their macromolecular engineering. Functionalization of polyacrylates and polymethacrylates either along the chain or at the chain-end will be reviewed first. Although several examples of synthesis of fully acrylic and methacrylic diblock copolymers were already mentioned in this review, combination of the anionic polymerization of acrylates and methacrylates with the anionic polymerization of other classes of monomers is effective in extending the range of this type of polymeric materials. Moreover, the anionic polymerization can also be combined with other polymerization mechanisms, such as radical and cationic polymerization. Moreover, not only linear polymers as discussed until now can be synthesized, but also more complex architectures, such as comb- and star-shaped chains. Nevertheless, the literature dealing with the macromolecular engineering of these polymers is too extensive for a comprehensive review to be part of this chapter, and only representative examples will be mentioned. Readers interested in more detailed information are referred to specific reviews[180–183].

A. Chain End-capping by a Functional Group

Polyacrylates and polymethacrylates can be end-capped by a functional group at one chain-end according to two strategies[184], by which either the initiator bears the envisioned functional group (protected or not), or living polymer chains are reacted with a duly substituted electrophile.

1. Electrophilic activation of living polymer chains

The main limitation of this approach is that any departure from livingness because of premature termination reaction results in the partial end-functionalization of the chains. Moreover, for the derivatization reaction to be complete, conditions of ultrahigh purity are required. The chains prepared by this technique are thus ω-functional.

a. Hydroxyl end-groups. Hatada and coworkers attached ω-hydroxyl end-groups by a two-step process, based on the reaction of living PMMA chains (**53**) with allyl iodide in the presence of TMEDA, followed by the conversion of the terminal double bond

(**54**) into an alcohol (**55**) by hydroboration with 9-BBN (9-borabicyclo[3.3.3.1]nonane) followed by reaction with H_2O_2/NaOH) (equation 50)[185–188].

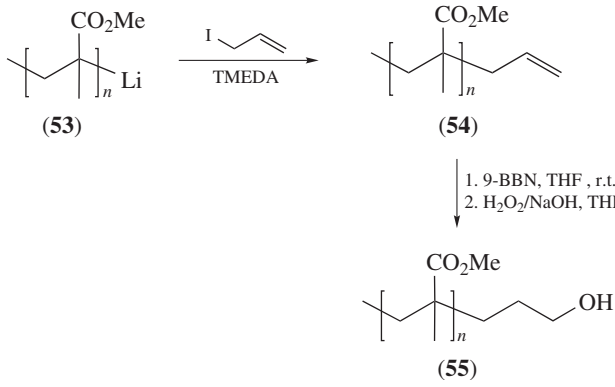

(50)

A more straightforward approach was reported by Varshney and coworkers, who reacted living anionic PtBuA with aldehydes[189]. A similar strategy was also implemented in case of polymers prepared by GTP, for the synthesis of ω-hydroxyl–PMMA. Benzaldehyde was used as the derivatizing agent[165].

b. Thiol end-groups. Varshney and coworkers derivatized living PMMA and PtBMA chains with 2-methylthiirane[190]. The actual mechanism is still unknown, although either ring-opening of thiirane (equation 51) or formation of an intermediate sulfurane (**56**) followed by elimination of propene to yield the thiol polymer **57** could occur (equation 52). Although there is a preference for this extrusion mechanism, Quirk and collaborators recently showed that polystyryl lithium reacts with 2-methylthiirane by ring-opening polymerization[191].

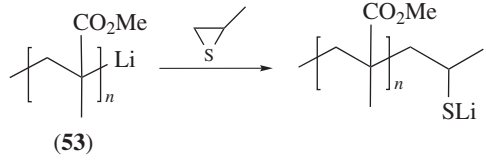

(51)

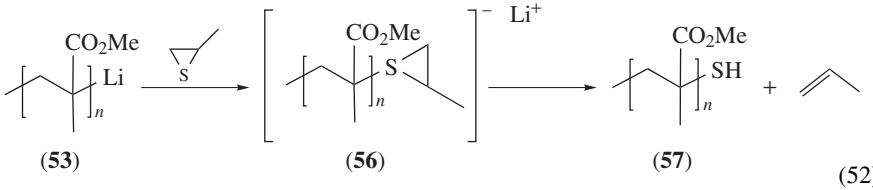

(52)

c. Carboxylic acid end-groups. For this purpose, Varshney and coworkers reacted living PtBuA with a large excess of dried carbon dioxide[189]. Whenever a difunctional initiator is used in the synthesis of PtBuA, an α,ω-dicarboxy-PtBuA is prepared, which is easily converted into a halato-telechelic polymer by neutralization of the acid end-groups with barium methoxide[89].

d. Unsaturated end-groups. Living PMMA chains were reacted with allyl bromide at −78 °C for being end-capped by an olefin[48]. The end-capping of polymethacrylates and polyacrylates by a methacrylic or an acrylic unsaturation is of great interest, because macromonomers are then available, which can be copolymerized with formation of comb-shaped polymers. However, the direct reaction of living PtBuA with methacryloyl chloride failed in forming the expected macromonomer. An alternative two-step strategy was then proposed, which relies on the reaction of living chains with an aldehyde followed by reaction of the ω-hydroxyl with methacryloyl chloride[189].

Styrene-type macromonomers were also prepared by reaction of living PtBuA and PMMA chains with *p*-vinylbenzyl chloride, iodide or bromide[48, 189], 4-(chlorodimethylsilyl)styrene[189] and 4-(chlorodimethylsilyl)-α-methylstyrene[189], respectively.

2. Initiation by a functional compound

The main advantage of this strategy is that all the chains are end-capped by the functional initiator, at least in a strictly living process. However, the functional group attached to the initiator must be protected whenever it is sensitive to nucleophilic attack. A few examples of α-functional polymethacrylates and polyacrylates are reported hereafter.

a. Amino end-group. The LiCl-ligated polymerization of MMA and tBMA was carried out by Varshney and coworkers in THF (−78 °C) or in toluene/THF (9:1 v/v, 0 °C), initiated by **59**, which is an adduct of DPE (**9**) and 2,2,5,5-tetramethyl-1-(3-lithiopropyl)-1-aza-2,5-disilacyclopentane (**58**, equation 53). The α-amino end-group was deprotected during precipitation in acidic methanol, which released polymethacrylate end-capped by a primary amino group (**60**)[190].

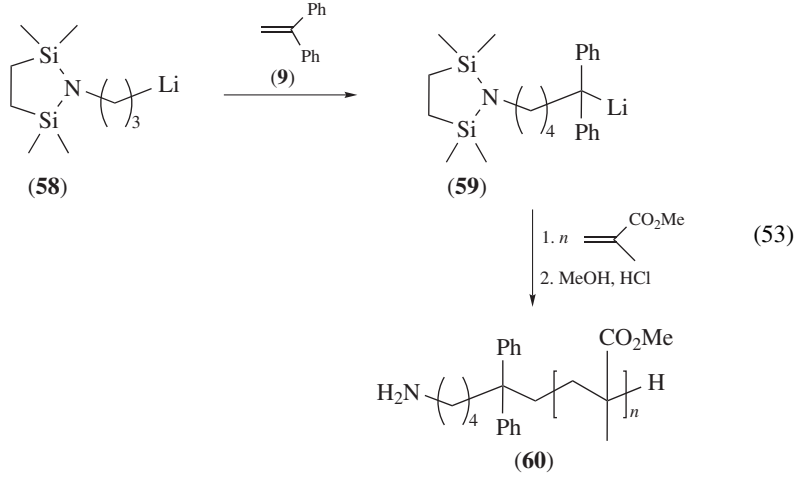

(53)

Antoun and coworkers showed that lithium diisopropylamide (LDA) is an effective initiator of the LiCl-mediated living polymerization of MMA and tBMA in THF at −78 °C[192]. Amino end-capped polymethacrylates were accordingly prepared with predetermined molecular weight and narrow molecular weight distribution[190]. Less sterically hindered lithium dialkylamides were, however, less efficient than LDA in initiating the living polymerization of methacrylates, as result of partial aggregation into 'dormant' species and parasite attack of the carbonyl groups.

b. Hydroxyl end-group. Anderson and coworkers initiated the MMA polymerization in THF at −78 °C by **62**, which is an adduct of DPE (**9**) and 3-(1-ethoxyethyloxy)propyllithium (**61**) (equation 54). Acidic deprotection of the acetal end-groups provided the targeted α-hydroxyl-PMMA (**63**) (equation 54)[48]. Coupling of living PMMA by reaction with 1,4- bis(bromomethyl)benzene followed by hydrolysis of the end-groups leads telechelic hydroxyl-PMMA, namely PMMA capped by a hydroxyl group at each chain-end[48].

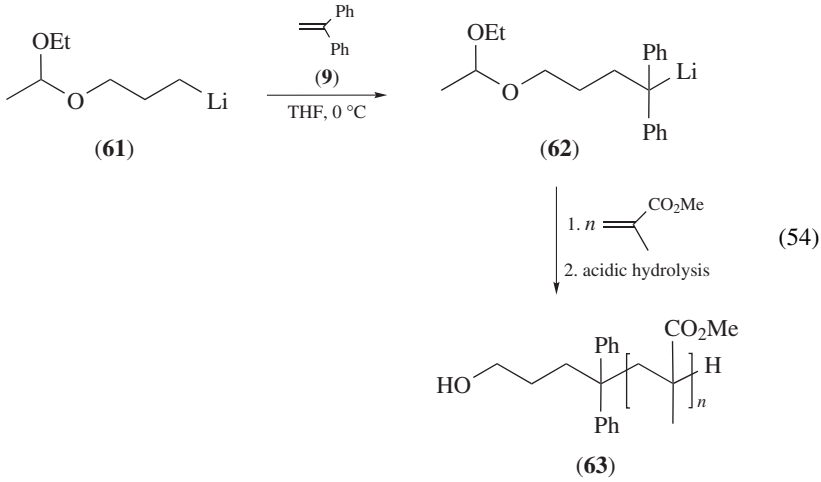

(**61**) (**62**) (**63**) (54)

Webster also prepared α-hydroxyl-PMMA by GTP initiated by $Me_2C{=}C(OSiMe_3)OCH_2CH_2OSiMe_3$[193] followed by deprotection of the α-end-group by fluoride-catalyzed methanolysis. Again, coupling of PMMA with phthaloyl fluoride prior to deprotection is a route to telechelic PMMA[193].

c. Sulfoxide end-group. Nugay and coworkers initiated the LiOEEM-ligated anionic polymerization of MMA initiated by dimsyllithium, which was generated *in situ* by reaction of *s*-BuLi and DMSO in toluene at 0 °C. PMMA end-capped by a sulfoxide was accordingly made available[194].

B. Chain Modification by Pendant Functional Groups

In order to introduce a functional group, a first route is based on the conversion of polyesters or polymers bearing pendant ester groups into the corresponding polyenolates, followed by reaction with a judiciously substituted electrophile. A second strategy is the direct polymerization of an acrylate or a methacrylate substituted by a functional group.

1. Metallation of ester-containing polymers

Poly(methyl acrylate) was reacted with LDA at −78 °C, and the corresponding polyenolate was reacted with electropiles such as benzaldehyde, benzyl chloroformate, 2-naphthoyl chloride and iodomethane (Scheme 4)[195]. The substitution yield did not, however, exceed 34%, which is much lower than the yield reported in case of low molecular weight compounds. Steric factors are a reasonable explanation for this observation.

When aliphatic polyesters are considered, lack of functional groups along the chains is a severe limitation for their application in the biomedical field or as environmentally

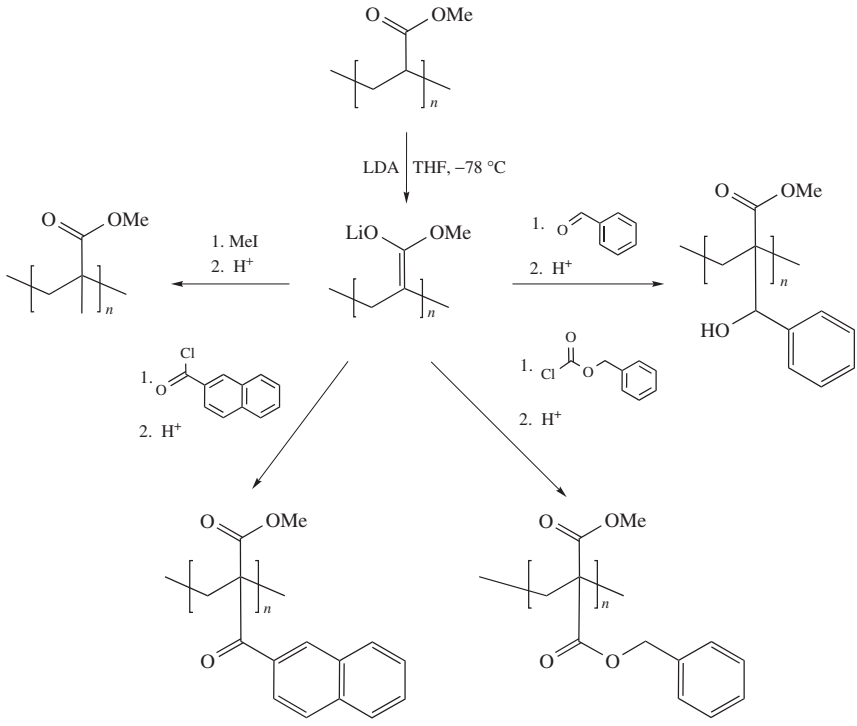

SCHEME 4. Introduction of pendant substituents in polyacrylates

friendly thermoplatics. Vert and coworkers metallated aliphatic polyesters, such as PCL (equation 55) and poly(lactic acid) (equation 56), with LDA in THF at −78 °C, followed by reaction with various electrophiles (Scheme 5)[195]. Again, the grafting yield was low, within the 10–20% range. That the ester groups are pendant or part of the backbone has no decisive effect, probably because of the unavoidable aggregation of enolates, which is unfavorable to the reaction progress. Moreover, condensation of enolates with esters can also occur and results in chain-breaking. Intermolecular condensation is thus responsible for the broadening of the molecular distribution, whereas intramolecular condensation is responsible for the formation of cyclics and a decrease in the number-average molecular weight (M_n). This chain degradation is systematically observed to an extent that depends on the experimental conditions and the structure of the polyester. As a rule, degradation is more important for copolymers of lactides (**5a**)[196] than for poly(ε-caprolactone). In spite of the limitations of this method, an advantage has to be found in the use of nontoxic organometallic compounds, which is a prerequisite for any potential biomedical applications. Vert and coworkers implemented this strategy for substituting a wide range of aliphatic polyesters by hydroxyl[195] and carboxylic acid groups[196,197], tritium[198], iodine[199] and flurorescent probes[195].

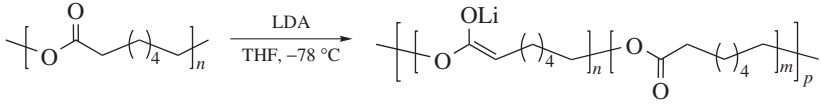

(55)

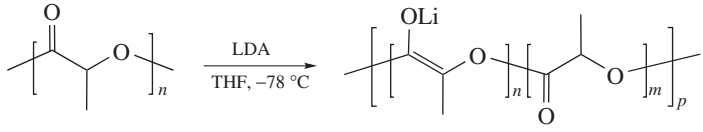

(56)

2. Polymerization of functional monomers

Polymerization or copolymerization of properly substituted methacrylates is a direct and very effective strategy for the preparation of polymers grafted by a series of substituents. For instance, polymethacrylate containing amino groups was prepared by living LiCl-mediated anionic polymerization of 2-(dimethylamino)ethyl methacrylate (DMAEMA)[200] and 2-(*t*-butylamino)ethyl methacrylate[103] in THF at −78 °C. Mixtures of DMAEMA and tBuMA were also copolymerized[200].

Methacrylates containing a functional group in the ester, such as allyl methacrylate and glycidyl methacrylate, can be directly polymerized by GTP[193], which is advantageous because no protection of the functional group is needed prior to polymerization.

In contrast to GTP, certain functional groups are not tolerant of anionic polymerization, making it necessary to protect the group prior to polymerization and to deprotect after polymerization, which makes the process more complex. For example, 2-(trimethylsilyloxy)ethyl methacrylate[165] and trimethylsilyl methacrylate[193] were anionically polymerized as precursors of poly(2-hydroxyethyl methacrylate) and poly(methacrylic acid), respectively.

C. Block Copolymers

Interest in block copolymers is based on their capacity to combine in an additive manner the properties of the constitutive blocks. They can be synthesized by coupling of the preformed blocks or by sequential polymerization of the corresponding monomers.

1. Coupling of preformed polymers

This strategy requires that the preformed polymers are end-capped by groups reactive towards a coupling agent as illustrated by Hatada and coworkers, who prepared PMMA (**67**) with a stereoblock structure. Isotactic ω-hydroxyl-PMMA (**64**) and syndiotactic ω-hydroxyl-PMMA (**66**) were coupled by reaction with sebacoyl chloride (**65**) (equation 57)[185, 186]. Nevertheless, this process is not selective because the stereodiblock was contaminated by chain-extended isotactic and syndiotactic PMMAs, respectively.

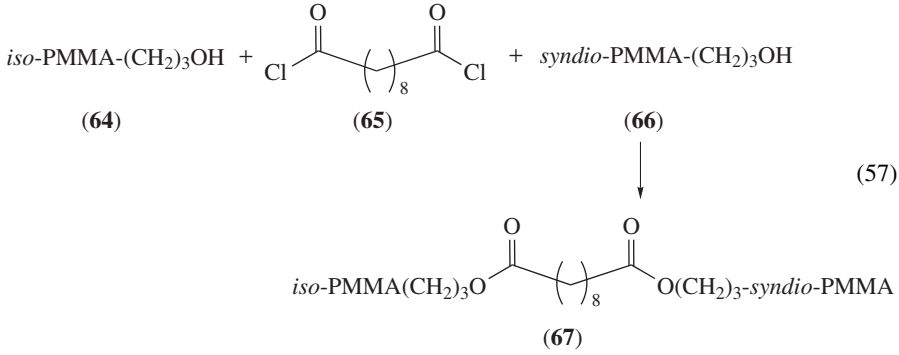

(57)

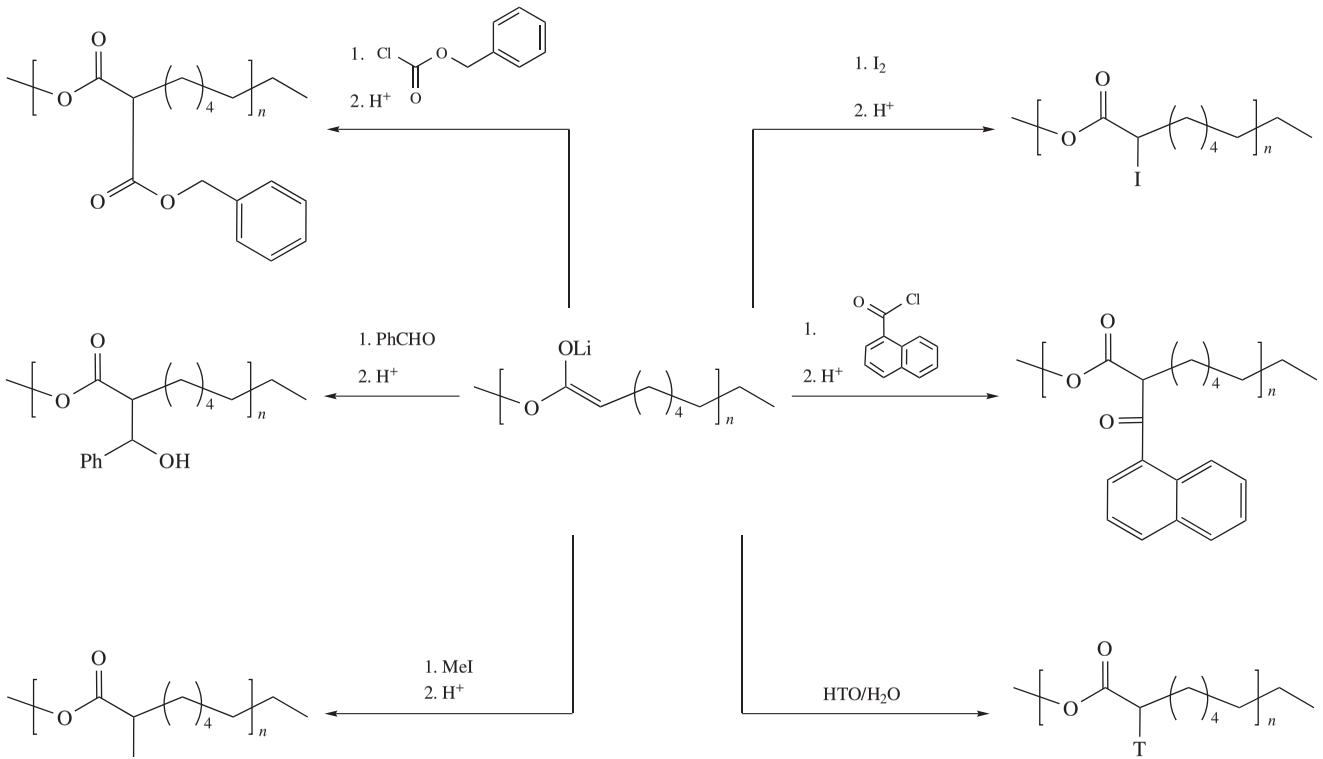

SCHEME 5. Introduction of pendant substituents in poly(ε-caprolactone) (PCL)

For coupling to be selective, the chain to be coupled must be end-capped by mutually reacting groups. For example, a living anionic polyacrylate or polymethacrylate can be directly coupled to any polymer or copolymer end-capped by a suitable electrophile. Hadjichristidis and coworkers coupled living anionic PMMA chains with the living PtBuA anion of PS-*block*-PtBuA by reaction with 1,2-bis(bromomethyl)benzene, with formation of a triblock copolymer[201].

2. Synthesis of block copolymers by sequential polymerization

Sequential polymerization of two acrylic monomers was discussed in Sections VI.E.4, VI.E.7 and VI.F. This technique was extended to three comonomers with formation of ABC-type triblock copolymers. For example, PMMA-*block*-PtBMA-*block*-PMMA triblock copolymer was synthesized by the sequential DPHLI-initiated polymerization of MMA, tBMA and MMA, respectively[202]. Symmetrical BAB-type diblock copolymers were also prepared in two steps, polymerization of the A monomer being first initiated by a difunctional compound. The B blocks formed in the second step necessarily have the same average degree of polymerization.

With the purpose of increasing the range of available block copolymers, comonomers other than methacrylates and acrylates can also be involved in sequential polymerization, provided that they are susceptible to anionic polymerization. Dienes, styrene derivatives, vinylpyridines[103,200], oxiranes and cyclosiloxanes are examples of such comonomers. The order of the sequential addition is, however, of critical importance for the synthesis to be successful. Indeed, the pK_a of the conjugated acid of the living chain-end of the first block must be at least equal to or even larger than that of the second monomer. Translated to a nucleophilicity scale, this pK_a effect results in the following order of reactivity: dienes $\geqslant$ styrenes > vinylpyridines > methacrylates and acrylates > oxiranes > siloxanes.

Zundel and coworkers proposed a very elegant strategy for circumventing the classical rule related to the order of addition of the comonomers[203–205] by boosting the reactivity of the living chain-end of the first block by converting it into a more nucleophilic species. For this purpose, they studied the polymerization of MMA initiated by Me_3SiOK as a model for the living chain-end of polysiloxane. In order to increase its reactivity, this K silanoxide end-group was converted into a silacarbanion (**69**) by reaction with 1,1,2,2-tetramethyl-1,2-disilacyclopentane (**68**) (equation 58)[204]. Silacarbanions are prone to initiate the polymerization of MMA, thus in contradiction to the classical rule. Nevertheless, the low initiation efficiency (35%) needs improvement.

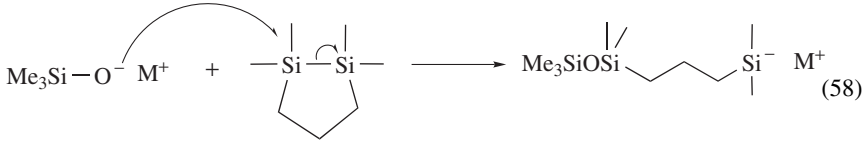

(58)

(**68**) (**69**)

a. Copolymerization of methacrylates and acrylates with styrene derivatives. Hautekeer and coworkers synthesized PS/PtBuA di- and triblock copolymers[206]. The strategy relies on the anionic polymerization of styrene initiated by mono- or difunctional initiators and resumption of polymerization with tBuA in THF at −78 °C, in the presence of LiCl.

Living PtBuMA-K enolate is not reactive enough for being an efficient macroinitiator for polymerization of the rather unreactive styrene[207]. *p*-Substitution of styrene with

an electron-withdrawing group increases the monomer reactivity and thus improves the copolymerization efficiency. Indeed, PtBuMA-K successfully initiated the polymerization of *t*-butyl 4-vinylbenzoate, of reactivity comparable to that of alkyl methacrylates[207].

b. Copolymerization of methacrylates and acrylates with dienes. Triblock copolymers of methacrylates and dienes are strong competitors of the traditional PS-*block*-PBD-*block*-PS thermoplastic elastomers, commercially available under the tradename KRATON, because they exhibit a higher service temperature. Indeed, this upper limit is dictated by the glass transition temperature (T_g) of the outer blocks, thus 70 °C for the PS blocks compared to 120 °C for syndiotactic PMMA ones. PMMA-*block*-PBD-*block*-PMMA was prepared by initiating the butadiene polymerization by either 1,3-bis(1-phenylethenyl)benzene or *m*-diisopropenylbenzene in cyclohexane at 25 °C, followed by the end-capping of the living chain-end by DPE (**9**) and finally by the MMA polymerization in THF at low temperature (−78 °C) in the presence of LiCl as ligand (Scheme 6)[208]. The strategy was extended to the polymerization of EMA[209], tBuMA[209], IBMA[209, 210] and mixtures of GMA and MMA[211], to prepare the triblock copolymers PEMA-*block*-PBD-*block*-PEMA, PtBuMA-*block*-PBD-*block*-PtBuMA, PIBMA-*block*-PBD-*block*-PIBMA and P(GMA-*co*-MMA)-*block*-PBD-*block*- P(GMA-*co*-MMA), respectively.

c. Copolymerization of methacrylates and acrylates with epoxides. Wang and coworkers showed that block copolymers of PtBuMA and PEO could be prepared by sequential anionic polymerization of tBuMA and ethylene oxide, irrespectively of the addition order. The PtBuMA block can be quantitatively hydrolyzed into poly(acrylic acid)[212a].

D. Star-shaped Copolymers

Two general strategies are possible for the synthesis of star-shaped copolymers: The arm-first method is based on the reaction of living chains with plurifunctional electrophiles carrying at least three reacting groups; alternatively, polymerization can be initiated by a multifunctional initiator according to the core-first method.

1. Synthesis of star-shaped copolymers by the arm-first method

ω-Hydroxyl-PMMA (**55**) was prepared by the hydroboration technique (equation 50) and then reacted with the trifunctional trimesoyl trichloride (**70**) with formation of a uniform three-arm star-shaped copolymer (**71**) (equation 59)[188].

Hadjichristidis and coworkers proposed a more direct approach based on grafting of living anionic PMMA onto 1,2,4,5-tetrakis(bromomethyl)benzene)[201]. A large excess of living chains was used in order to force the coupling to completion. The crude copolymerization product had to be purified by fractionation. Living polymers prepared by GTP were also coupled by polyfunctional alkylating agents and converted into star-shaped polymers[193].

Reaction of living polymer chains with a difunctional monomer is an alternative route to star-shaped polymers with a cross-linked core. The average number of arms is, however, large and ill-defined. Hadjichristidis and coworkers synthesized star-shaped PMMA by reacting living anionic PMMA with ethylene dimethacrylate[212b]. The same strategy was also implemented by Simms and Spinelli to prepare star-shaped PMMA by GTP[213]. This strategy was extended by Tsitsilianis and coworkers to the synthesis of a mikto-arm star-shaped PS/PtBuA copolymer (**73**), i.e. polymers carrying at least two different kinds of

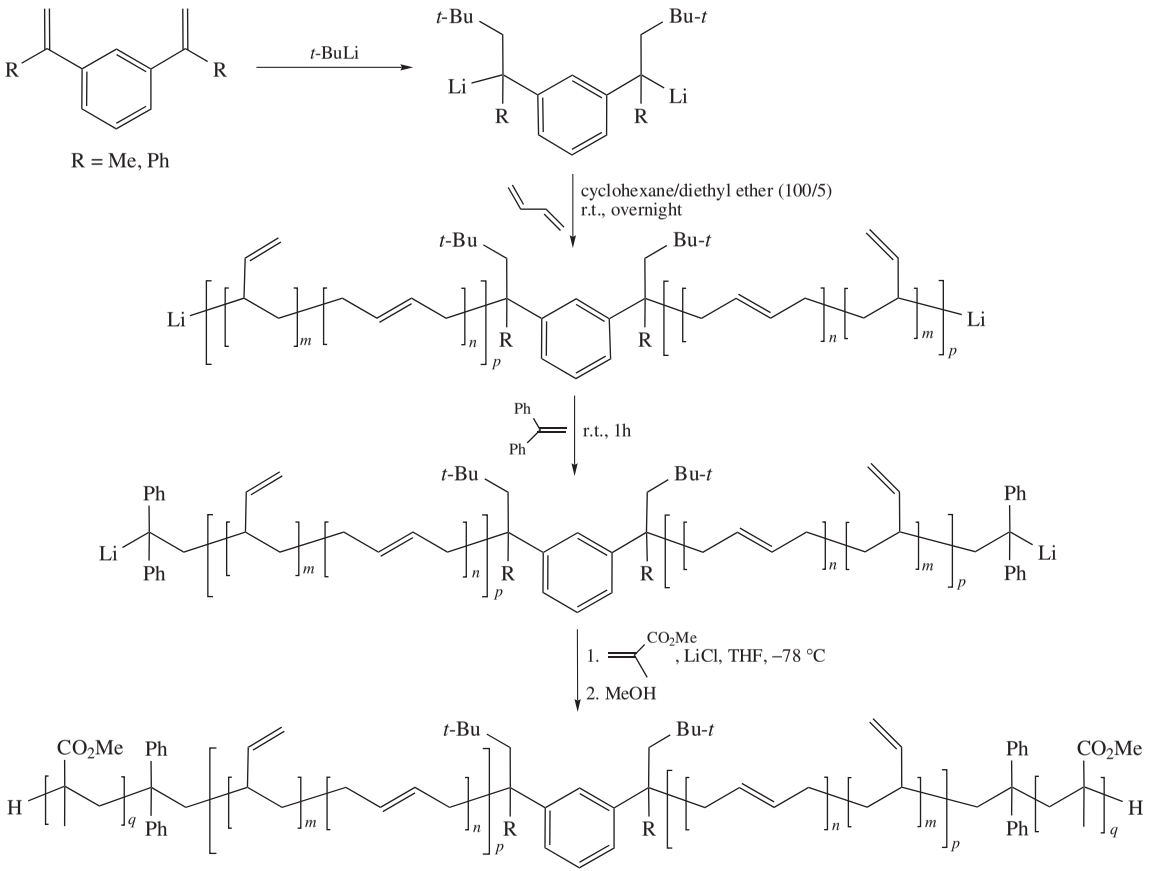

SCHEME 6. Synthesis of PMMA-*block*-PBD-*block*-PMMA triblock copolymer

arms (equation 60), by reaction of living anionic polystyrene (**72**) with divinylbenzene followed by the LiCl-mediated polymerization of tBuA[214]. It must be noted that DPE (**9**) was added before the polymerization of tBuA in order to decrease the nucleophilicity of the macroinitiator.

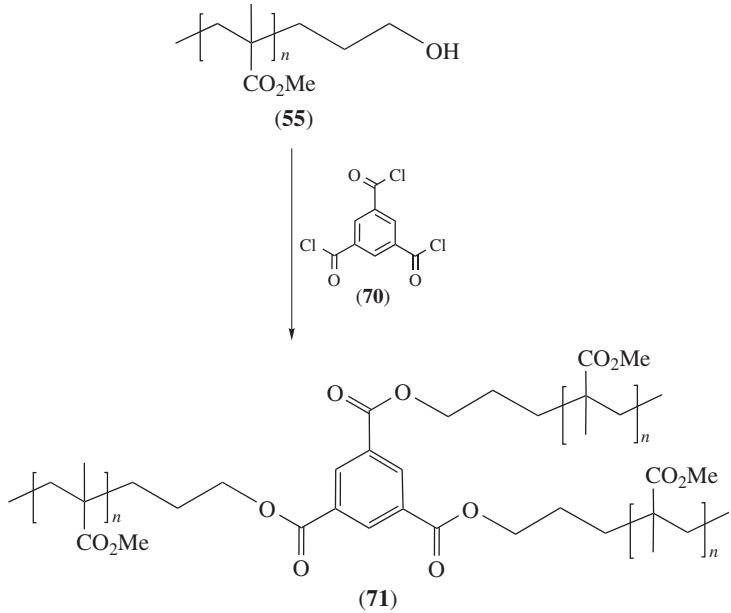

(59)

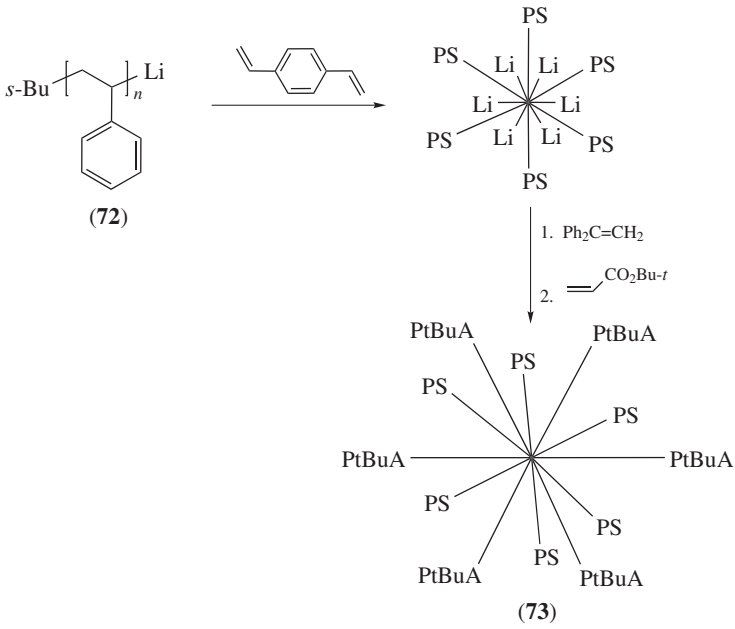

(60)

2. Synthesis of star-shaped copolymers by the core-first method

Three- and four-arm star-shaped PEA (**75** and **77**) were synthesized by GTP with tri- and tetrafunctional initiators (**74** and **76**) according to equations 61 and 62[165].

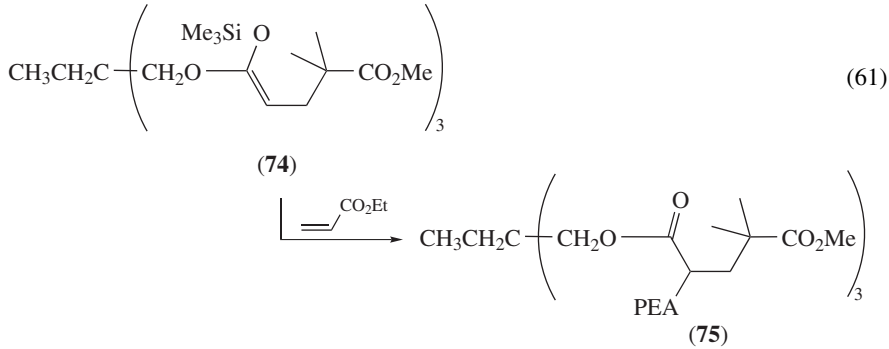

(61)

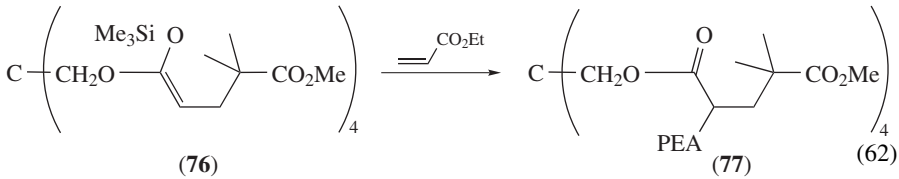

(62)

Wnek and coworkers synthesized a four-arm star-shaped PMMA with a cyclic siloxane core, as shown in equation 63[215]. Four ketene silylacetal units were first attached to 1,2,3,4-tetramethylcyclotetrasiloxane (**78**) to obtain the tetrafunctional core **79**, which was used as an initiator of the GTP of MMA with formation of the targeted four-armed star-shaped PMMA (**80**).

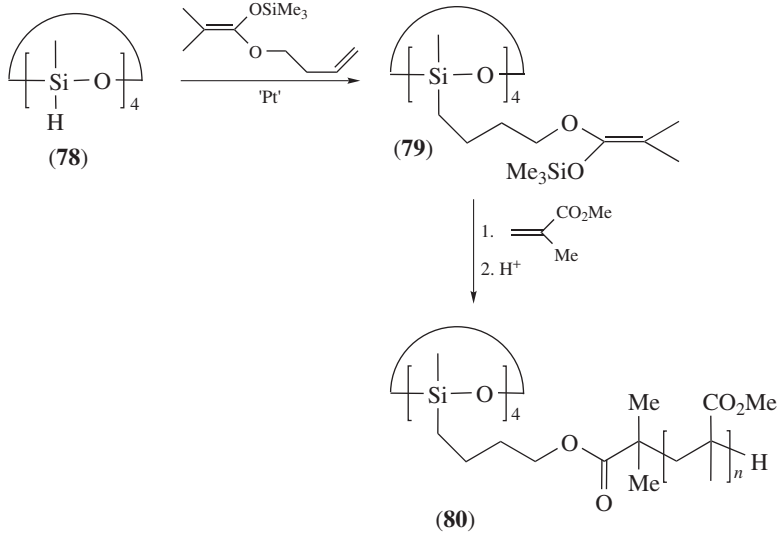

(63)

E. Comb-shaped and Graft Copolymers

Three main strategies are known for the synthesis of comb-shaped and graft polymethacrylates and polyacrylates. A first route relies on the polymerization or copolymerization of macromonomers, which are chains capped at one chain-end by a polymerizable moiety ('grafting through' process). Second, end-reactive chains can be immediately grafted onto a mutually reactive polymer backbone ('grafting onto' process). Finally, graft copolymers can be prepared by initiating the polymerization of a monomer by a macroinitiator, leading to a macromolecule that contains several pendant initiating groups along the chain ('grafting from' process).

1. The 'grafting through' process

Living anionic polymerization of methacrylates and acrylates can be used to prepare macromonomers, which can thereafter be polymerized by any technique known in the state of the art. For instance, Hatada and coworkers reacted anionic ω-hydroxyl–PMMA (**55**), which was then polymerized by radical polymerization into the corresponding comb-shaped copolymer (**81**) with 2,2′-azobis(isobutyronitrile) (AIBN) as initiator (equation 64)[187].

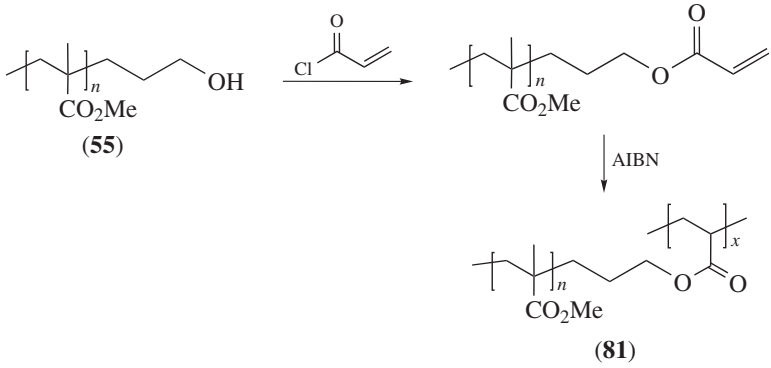

(64)

Macromonomers can be prepared by GTP, initiated by a compound containing a vinyl group inert in GTP but polymerizable by other techniques[193].

2. The 'grafting onto' process

A direct strategy relies on the grafting of any polymer duly end-capped by an electrophile onto a polyenolate. For example, Vert and collaborators prepared polyenolate **82** by reaction of PCL with LDA, that was treated with PEO end-capped by an activated bromide, to yield the grafted polymer **83** (equation 65)[216,217].

The reverse strategy consists of coupling a living polymer onto a second polymer that contains pendant electrophiles. This approach was used by Pitsikalis and coworkers, who synthesized PS-*graft*-PtBuMA (**86**) by treatment of poly(*p*-bromomethylstyrene) (**84**) with living anionic PtBuMA (**85**) (equation 66)[201]. The graft copolymer was purified by selective precipitation with hot methanol. Indeed, the graft copolymer was insoluble in this solvent, whereas the PtBuMA arms were soluble[201].

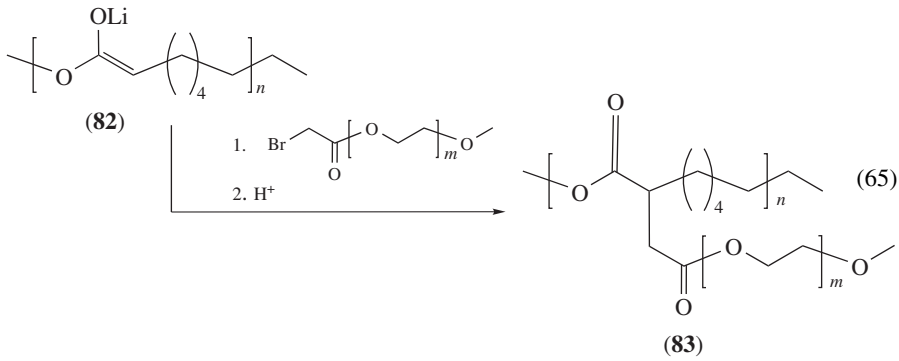

(65)

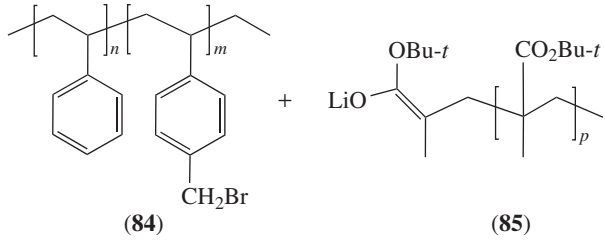

(66)

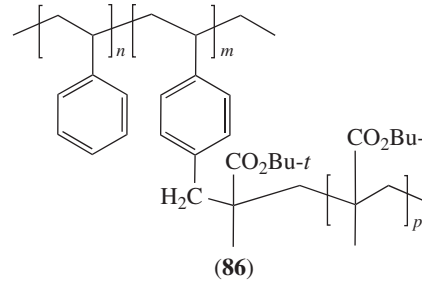

3. The 'grafting from' process

Miura and coworkers[218] and Akutsu and coworkers[219] reacted a copolymer of styrene and 2,5-bis(methoxycarbonyl-1-hexene (**87**) with LDA to yield a polyenolate (**88**), which was active in the anionic polymerization of MMA (equation 67). When less than 1 equivalent (0.75) of LDA relative to the ester groups was used, the graft copolymer **89** was formed[219]. When more than 1 equivalent of LDA was used, the molecular weight distribution was bimodal. Indeed, a mixture of homopolymer (PMMA) and graft copolymer (**89**) was formed merely because LDA is also prone to initiate the anionic polymerization of MMA[219]. It was ascertained that the styrene units of the copolymer were not involved in the grafting reaction[218].

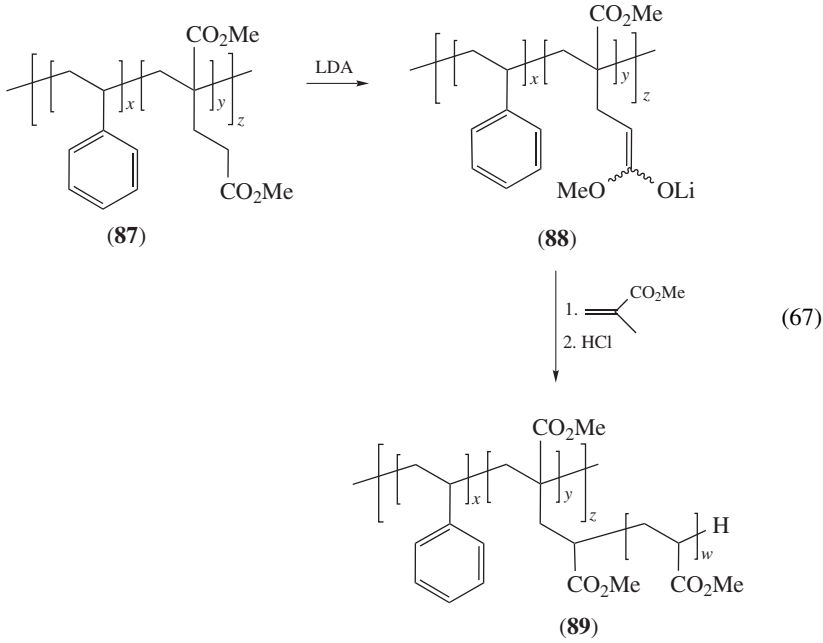

(**87**) (**88**) (**89**) (67)

Akutsu and coworkers investigated the influence of the chemical structure of the macroinitiator on the grafting efficiency of MMA. Actually, the reactivity of the copolymer depends on both steric and electronic factors. Copolymer **90** is less reactive than copolymer **91** because of the electron-donating effect of the methyl substituent. Copolymer **92** is less reactive than copolymer **91** because the acidic proton is sterically hindered by the polymer backbone. Finally, copolymer **93** is less reactive than copolymer **90** because it is more sterically crowded[219].

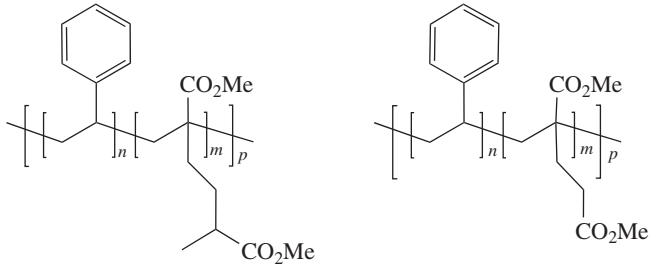

(**90**) (**91**)

When the grafting of MMA was initiated by polyenolate **94**, derived from poly(vinyl acetate) (equation 68), Inoki and coworkers applied deuterolysis to show that 26% of the acetate units were lithiated by 0.3 equivalent of LDA with respect to these units and, thus, that 87% of the original lithium was incorporated into the copolyester[220]. The average number of PMMA grafts was in the range of 1 to 7, and the average number of

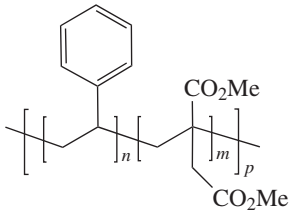

(**92**)

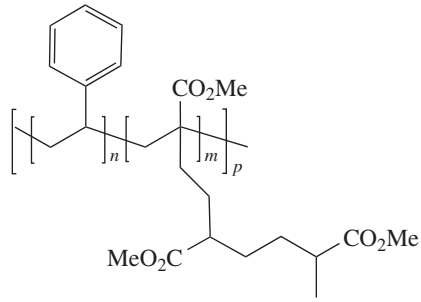

(**93**)

enolates that initiated the polymerization was very low (2.4 to 13.6%), such that only 1.9 to 11.6% of LDA actually initiated the polymerization of MMA. The low reactivity of the polyenolates was accounted for by formation of aggregates[219,220]. Moreover, condensation of a pendant enolate with unreacted ester groups leads to formation of an alcohol and a β-keto ester, as shown by IR and NMR techniques[220]. It is not clear whether this reaction is intramolecular with formation of loops or intermolecular with coupling of chains. Both reactions are likely to take place to an extent that depends on the concentration of the polymerization medium. Less than 10% of the repeating units would be involved in parasitic condensation.

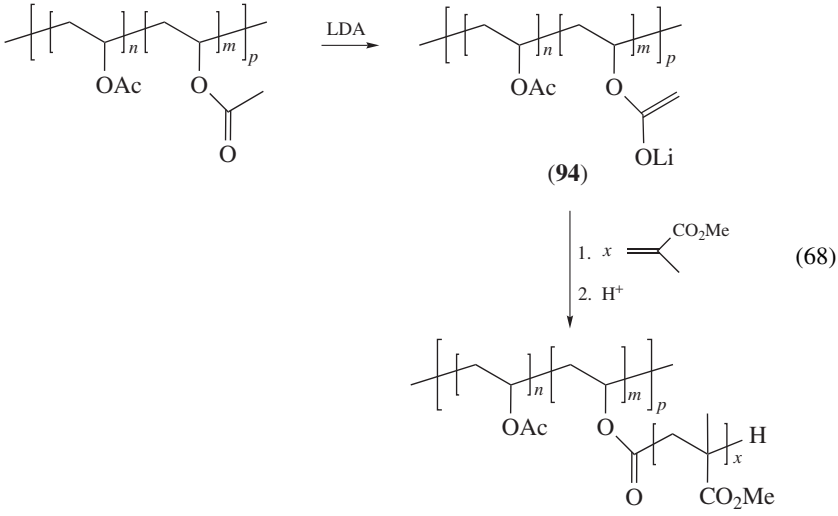

(**94**)

(68)

F. Polymer Networks

Whenever the reactive compound added to a polyenolate in the 'grafting onto' process is difunctional, a cross-linked polymer is formed. For example, amphiphilic networks (**96**) were prepared by Vert and coworkers, who reacted PCL with LDA, followed by reaction with α,ω-bis(chloroacetyl)poly(ethylene oxide) (**95**) (equation 69)[221].

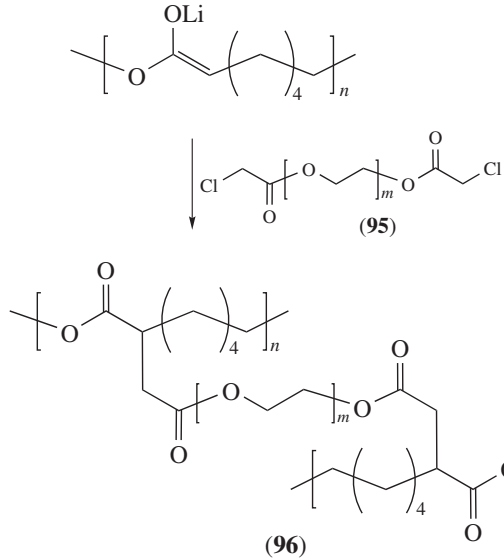

(69)

VIII. ACKNOWLEDGMENTS

The authors are grateful to the 'Politique scientifique fédérale' for financial support in the framework of the 'Pôles d'attraction interuniversitaires' (PAI VI/27). P.L. is 'Chercheur Qualifié' by the 'Fonds de la Recherche Scientifique' (FNRS). The authors thank A. Debuigne for fruitful discussions.

IX. REFERENCES

1. Ph. Lecomte and R. Jérôme, in *Encyclopedia of Polymer Science and Technology* (Ed. R. Smith), Woodhead Publishing Ltd., Abington, UK, 2005, p. 77.
2. J. Smida, M. Van Beylen and T. E. Hogen-Esch, *Prog. Polym. Sci.*, **31**, 1041 (2006).
3. M. Szwarc, *Nature*, **178**, 1168 (1956).
4. M. Szwarc, *J. Polym. Sci., Part A: Polym. Chem.*, **36**, ix (1998).
5. M. Van Beylen, S. Bywater, G. Smets, M. Szwarc and D. J. Worsfold, *Adv. Polym. Sci.*, **86**, 87 (1988).
6. J.-S. Wang and K. Matyjaszewski, *J. Am. Chem. Soc.*, **117**, 5614 (1995).
7. M. Kato, M. Kamigaito, M. Sawamoto and T. Higashimura, *Macromolecules*, **28**, 1721 (1995).
8. A. Debuigne, J.-R. Caille, C. Detrembleur and R. Jérôme, *Angew. Chem. Int. Ed.*, **44**, 1101 (2005).
9. A. Debuigne, J.-R. Caille, C. Detrembleur and R. Jérôme, *Angew. Chem. Int. Ed.*, **44**, 3439 (2005).
10. C. Detrembleur, A. Debuigne, R. Bryaskova, B. Charleux and R. Jérôme, *Macromol. Rapid Commun.*, **27**, 37 (2006).
11. A. Debuigne, J.-R. Caille and R. Jérôme, *Macromolecules*, **38**, 5452 (2005).
12. R. Bryaskova, N. Willet, A. Debuigne, R. Jérôme and C. Detrembleur, *J. Polym. Sci., Part A: Polym. Chem.*, **45**, 85 (2007).
13. (a) B. B. Wayland, G. Poszmik, S. L. Mukerjee and M. Fryd, *J. Am. Chem. Soc.* **116**, 7943 (1994).
    (b) S. Maria, H. Kanezoshi, K. Matyjaszewski and R. Poli, *Chem. Eur. J.*, **13**, 2480 (2007).

14. J.-R. Caille, A. Debuigne and R. Jérôme, *Macromolecules*, **38**, 27 (2005).
15. A. Debuigne, J.-R. Caille and R. Jérôme, *Macromolecules*, **38**, 6310 (2005).
16. A. Debuigne, J.-R. Caille and R. Jérôme, *J. Polym. Sci., Part A: Polym. Chem.*, **44**, 1233 (2006).
17. J.-R. Caille, A. Debuigne and R. Jérôme, *J. Polym. Sci., Part A: Polym. Chem.*, **43**, 2723 (2005).
18. G. J. Domski, J. M. Rose, G. W. Coates, A. D. Bolig and M. Brookhart, *Prog. Polym. Sci.*, **32**, 30 (2007).
19. A. Zambelli, G. Natta, I. Pasquon and R. Signorin, *J. Polym. Sci. C: Polym. Symp.*, 2485 (1967).
20. Y. Doi, M. Takada and T. Keii, *Bull. Soc. Chem. Jpn.*, **52**, 1802 (1979).
21. Y. Doi, S. Ueki and T. Keii, *Macromolecules*, **12**, 814 (1979).
22. Y. Doi, S. Ueki and T. Keii, *Macromol. Chem. Phys.*, **180**, 1359 (1979).
23. Y. Doi, S. Suzuki and K. Soga, *Macromol. Rapid Commun.*, **6**, 639 (1985).
24. Y. Doi, S. Suzuki and K. Soga, *Macromolecules*, **19**, 2896 (1986).
25. Y. Doi, Y. Watanabe, Y. Ueki and K. Soga, *Makromol. Chem., Rapid Commun.*, **4**, 533 (1983).
26. Y. Doi, and Keii T., *Adv. Polym. Sci.*, **73–4**, 201 (1986).
27. Y. Doi, G. Hizal and K. Soga, *Makromol. Chem., Chem. Phys.*, **188**, 1273 (1987).
28. Y. Doi, M. Murata and K. Soga, *Macromol. Rapid Commun.*, **5**, 811 (1984).
29. S. Ueki, H. Furuhashi, N. Murakami, M. Murata and Y. Doi, *Stud. Surf. Sci. Catal.*, **92**, 359 (1995).
30. Y. Doi, T. Koyama and K. Soga, *Macromol. Chem. Phys.* **186**, 11 (1985).
31. Y. Doi, S. Ueki and T. Keii, in *Coordination Polymerization* (Ed. E. J. Vandenberg), Plenum Press, New York, 1983, p. 249.
32. Y. Doi, N. Tokuhiro, S. Suzuki and K. Soga, *Makromol. Chem., Rapid Commun.*, **8**, 285 (1987).
33. Y. Doi, N. Tokuhiro and K. Soga, *Makromol. Chem., Chem. Phys.*, **190**, 643 (1989).
34. A. Kowalski, J. Libiszowski, K. Majerska, A. Duda and S. Penczek, *Polymer*, **48**, 3952 (2007).
35. J. Kasperczyk, M. Bero and G. Adamus, *Macromol. Chem. Phys.*, **194**, 907 (1993).
36. P. Dobrzynski, J. Kasperczyk, M. Bero and G. Adamus, *Macromolecules*, **32**, 4735 (1999).
37. A. J. Nijenhuis, D. W. Grijrpma and A. J. Pennings, *Macromolecules*, **25**, 6419 (1992).
38. P. Dobrzynski, *Polymer*, **48**, 2263 (2007).
39. P. Dobrzynski, *J. Polym. Sci., Part A: Polym. Chem.*, **42**, 1886 (2004).
40. M. Szwarc and A. Rembaum, *J. Polym. Sci.*, **22**, 189 (1956).
41. D. Baskaran, *Prog. Polym. Sci.*, **28**, 521 (2003).
42. R. Jérôme, P. Teyssié, B. Vuillemin, T. Zundel and C. Zune, *J. Polym. Sci., Part A: Polym. Chem.*, **37**, 1 (1999).
43. C. Zune and R. Jérôme, *Prog. Polym. Sci.*, **24**, 631 (1999).
44. P. Vlček and L. Lochmann, *Prog. Polym. Sci.*, **24**, 793 (1999).
45. D. Baskaran and A. H. E. Müller, *Prog. Polym. Sci.*, **32**, 173 (2007).
46. T. R. Darling, T. P. Davis, M. Fryd, A. A. Gridnev, D. M. Haddleton, S. D. Ittel, R. R. Matheson Jr., G. Moad and E. Rizzardo, *J. Polym. Sci., Part A: Polym. Chem.*, **38**, 1706 (2000).
47. P. Rempp, D. Freyss and M. Leng, *Bull. Soc. Chim. Fr.*, 221 (1964).
48. B. C. Anderson, G. D. Andrews, P. Arthur Jr., H. W. Jacobson, L. R. Melby, A. J. Playtis and W. H. Sharkey, *Macromolecules*, **14**, 1599 (1981).
49. K. Hatada, T. Kitayama and K. Ute, *Prog. Polym. Sci.*, **13**, 189 (1988).
50. D. Baskaran, S. Chakrapani and S. Sivaram, *Macromolecules*, **28**, 7315 (1995).
51. J. Janata, L. Lochmann and A. H. E. Müller, *Makromol. Chem., Chem. Phys.*, **191**, 2253 (1990).
52. J.-S. Wang, H. Zhang, R. Jérôme and P. Teyssié, *Macromolecules*, **28**, 1758 (1995).
53. A. H. E. Müller and H. Jeuck, *Makromol. Chem., Rapid Commun.*, **3**, 121 (1982).
54. T. E. Long, R. Subramanian, T. C. Ward and J. E. McGrath, *Polym. Prepr., Am. Chem. Soc., Div. Polym. Chem.*, **27**(2), 258 (1985).
55. T. E. Long, R. D. Allen and J. E. McGrath, *NATO Adv. Study Inst. Ser., Ser. C*, **215**, 79 (1987).

56. K. Hatada, *J. Polym. Sci., Part A: Polym. Chem.*, **37**, 245 (1999).
57. B. Baumgarten, A. H. E. Müller and T. E. Hogen-Esch, *Macromolecules*, **24**, 353 (1991).
58. T. E. Hogen-Esch, *Macromol. Symp.*, **67**, 43 (1993).
59. J.-S. Wang, R. Jérôme and P. Teyssié, *J. Phys. Org. Chem.*, **8**, 208 (1995).
60. D. M. Wiles and S. Bywater; *J. Polym. Sci., Part A: Polym. Chem.*, **2**, 1175 (1964).
61. D. M. Wiles and S. Bywater, *J. Chem. Soc., Trans. Faraday*, **61**, 150 (1965).
62. D. M. Wiles and S. Bywater, *Polymer*, **3**, 175 (1962).
63. D. M. Wiles and S. Bywater, *Chem. Ind.*, 1209 (1963).
64. D. Kunkel, A. H. E. Müller, L. Lochmann and M. Janata, *Makromol. Chem., Macromol. Symp.*, **60**, 315 (1992).
65. C. Zune, P. Dubois and R. Jérôme, *Polym. Int.*, **48**, 565 (1999).
66. P. Kilz, Ph.D. Thesis, Mainz (1990).
67. K. Hatada, K. Ute, K. Tanaka, T. Kitayama and Y. Okamoto, *Polym. J.*, **17**, 977 (1985).
68. K. Hatada, K. Ute, K. Tanaka, Y. Okamoto and T. Kitayama, *Polym. J.*, **18**, 1037 (1986).
69. L. Vancea and S. Bywater, *Macromolecules*, **14**, 1321 (1981).
70. J. Corset, F. Froment, M.-F. Lautie, N. Ratovelomanama, J. Seyden-Penne, T. Strzalko and M.-C. Roux-Schmitt, *J. Am. Chem. Soc.*, **115**, 1684 (1993).
71. J.-S. Wang, R. Jérôme, R. Warin and P. Teyssié, *Macromolecules*, **26**, 1402 (1993).
72. J. Kříž, J. Dybal, P. Vlček and M. Janata, *Macromol. Chem. Phys.*, **195**, 3039 (1994).
73. J. Dybal and J. Kříž, *Collect. Czech. Chem. Commun.*, **59**, 1699 (1994).
74. H. Weiss, A. V. Yakimansky and A. H. E. Müller, *J. Am. Chem. Soc.*, **118**, 8897 (1996).
75. J. Kříž, J. Dybal, M. Janata and P. Vlček, *Macromol. Chem. Phys.*, **196**, 3117 (1995).
76. L. Vancea and S. Bywater, *Macromolecules*, **14**, 1776 (1981).
77. V. Halaska and L. Lochmann, *Collect. Czech. Chem. Commun.*, **38**, 1780 (1973).
78. L. Lochmann and J. Trekoval, *Makromol. Chem.*, **183**, 1361 (1982).
79. J. Kříž, J. Dybal, L. Lochmann, M. Janata and P. Vlček, *Macromol. Chem. Phys.*, **197**, 1889 (1996).
80. C. Zune, P. Dubois, J. Grandjean, J. Kříž, J. Dybal, L. Lochmann, M. Janata, P. Vlček and R. Jérôme, *Macromolecules*, **32**, 5477 (1999).
81. J. Kříž, J. Dybal, M. Janata and P. Vlček, *Magn. Res. Chem.,* **32**, s8 (1994).
82. D. T. Tsvetanov, Ph. Petrova, P. H. Li and I. M. Panayotov, *Eur. Polym. J.*, **14**, 25 (1978).
83. T. Kunkel, Ph.D. Thesis, Mainz (1991).
84. J. E. Figueruelo, *Makromol. Chem.*, **131**, 63 (1970).
85. W. Fowells, C. Schuerch, F. Bovey and F. P. Hood, *J. Am. Chem. Soc.*, **89**, 1396 (1967).
86. G. Löhr and G. V. Schulz, *Makromol. Chem.*, **172**, 137 (1973).
87. G. Löhr and G. V. Schulz, *Eur. Polym. J.*, **10**, 121 (1974).
88. Ch. B. Tsvetanov, A. H. E. Müller and G. V. Schulz, *Macromolecules*, **18**, 863 (1985).
89. A. H. E. Müller, L. Lochmann and J. Trekoval, *Makromol. Chem.*, **187**, 1473 (1986).
90. D. Baskaran, A. H. E. Müller and S. Sivaram, *Macromolecules*, **32**, 1356 (1999).
91. C. Zune, P. Dubois, J. Grandjean and R. Jérôme, *Macromol. Chem. Phys.*, **200**, 562 (1999).
92. K.-E. Peikjo and H. Hocker, *Makromol. Chem., Rapid Commun.*, **3**, 243 (1982).
93. S. K. Varshney, C. Jacobs, J. P. Hautekeer, R. Fayt, R. Jérôme and P. Teyssié, *Macromolecules*, **23**, 2618 (1990).
94. S. Antoun, J. S. Wang, R. Jérôme and P. Teyssié, *Polymer*, **37**, 5755 (1996).
95. R. Fayt, R. Forte, C. Jacobs, R. Jérôme, T. Ouhadi, P. Teyssié and S. K. Varshney, *Macromolecules*, **20**, 1442 (1987).
96. D. Kunkel, A. H. E. Müller, M. Janata and L. Lochmann, *Polym. Prepr., Am. Chem. Soc.*, **32**(1), 301 (1991).
97. C. Jacobs, S. K. Varshney, J.-P. Hautekeer, R. Fayt, R. Jérôme and P. Teyssié, *Macromolecules*, **23**, 4024 (1990).
98. S. K. Varshney, Z. Gao, X. F. Zhong and A. Eisenberg, *Macromolecules*, **27**, 1076 (1994).
99. J.-S. Wang, R. Jérôme, R. Warin and P. Teyssié, *Macromolecules*, **26**, 6776 (1993).
100. C. Zune, P. Dubois, R. Jérôme, J. Kříž, J. Dybal, M. Janata, L. Lochmann and P. Vlček, *Macromolecules*, **31**, 2744 (1998).
101. D. Kunkel and A. H. E. Müller, *Polym. Prepr., Am. Chem. Soc., Div. Polym. Chem.*, **201**, 94–poly (1991).
102. S. K. Varshney, C. Jacobs, J. P. Hautekeer, Ph. Bayard, R. Jérôme, R. Fayt and P. Teyssié, *Macromolecules*, **24**, 4997 (1991).

103. S. Creutz, P. Teyssié and R. Jérôme, *J. Polym. Sci., Part A: Polym. Chem.*, **35**, 2035 (1997).
104. D. Baskaran and S. Sivaram, *Macromolecules*, **30**, 1550 (1997).
105. J.-S. Wang, R. Jérôme, R. Warin and P. Teyssié, *Macromolecules*, **26**, 5984 (1993).
106. L. Lochmann and A. H. E. Müller, *Makromol. Chem., Chem. Phys.*, **191**, 1657 (1990).
107. P. Vlček, L. Dvoranek, J. Otoupalova and M. Janata, *Macromol. Symp.*, **95**, 27 (1995).
108. P. Vlček, L. Lochmann and J. Otoupalova, *Macromol. Rapid Commun.*, **13**, 163 (1992).
109. L. Dvoranek and P. Vlček, *Polym. Bull.*, **31**, 393 (1993).
110. J.-S. Wang, R. Jérôme, R. Warin and P. Teyssié, *Macromolecules*, **27**, 1691 (1994).
111. J. S. Wang, R. Jérôme and P. Teyssié, *Macromolecules*, **27**, 4902 (1994).
112. T. Zundel, P. Teyssié and R. Jérôme, *Macromolecules*, **31**, 2344 (1998).
113. T. Zundel, C. Zune, P. Teyssié and R. Jérôme, *Macromolecules*, **31**, 4089 (1998).
114. N. Nugay, T. Nugay, R. Jérôme and P. Teyssié, *J. Polym. Sci., Part A: Polym. Chem.*, **35**, 361 (1997).
115. C. Zune, T. Zundel, P. Dubois, P. Teyssié and R. Jérôme, *J. Polym. Sci., Part A: Polym. Chem.*, **37**, 2525 (1999).
116. T. Zundel, P. Teyssié and R. Jérôme, *Macromolecules*, **31**, 5577 (1998).
117. J. Marchal, Y. Gnanou and M. Fontanille, *Macromol. Symp.*, **107**, 27 (1998).
118. D. Baskaran, A. H. E. Müller and S. Sivaram, *Macromol. Chem. Phys.*, **201**, 1901 (2000).
119. J.-S. Wang, R. Jérôme, R. Warin, H. Zhang and P. Teyssié, *Macromolecules*, **27**, 3376 (1994).
120. H. O. House, A. V. Prabbu and W. V. Phillips, *J. Org. Chem.*, **41**, 1209 (1976).
121. S. K. Varshney, R. Jérôme, Ph. Bayard, C. Jacobs, R. Fayt and P. Teyssié, *Macromolecules*, **25**, 4457 (1992).
122. J. S. Wang, R. Jérôme, Ph. Bayard, L. Baylac, M. Patin and P. Teyssié, *Macromolecules*, **27**, 4615 (1994).
123. H.-B. Gia and J. E. McGrath, in *Recent Advances in Anionic Polymers, Proceedings of an International Symposium* (Eds T. E. Hogen-Esch and J. Smid), Elsevier, New York, 1987, pp. 173–184.
124. J. S. Wang, R. Jérôme and P. Teyssié, *Macromolecules*, **27**, 4896 (1994).
125. C. Zune, P. Dubois, R. Jérôme, J. Kříž, J. Dybal, M. Janata, L. Lochmann and P. Vlček, *Macromolecules*, **31**, 2731 (1998).
126. P. Bayard, R. Jérôme, P. Teyssié, S. Varshney and J. S. Wang, *Polym. Bull.*, **32**, 381 (1994).
127. J. S. Wang, R. Jérôme, Ph. Bayard, M. Patin, P. Teyssié, B. Vuillemin and P. Heim, *Macromolecules*, **27**, 4635 (1994).
128. A. Maurer, X. Marcarian, A. H. E. Müller, C. Navarro and C. Vuillemin, *Polym. Prepr., Am. Chem. Soc.*, **38**(1), 467 (1997).
129. N. Nugay, T. Nugay, R. Jérôme and P. Teyssié, *J. Polym. Sci., Part A: Polym. Chem.*, **35**, 1543 (1997).
130. J. S. Wang, R. Jérôme, Ph. Bayard and P. Teyssié, *Macromolecules*, **27**, 4908 (1994).
131. J. Marchal, Y. Gnanou and M. Fontanille, *Polym. Prepr., Am. Chem. Soc.*, **38**(1), 473 (1997).
132. T. Kitayama, T. Shinozaki, T. Sakamoto, M. Yamamoto and K. Hatada, *Makromol. Chem., Chem. Phys.*, **Suppl 15**, 167 (1989).
133. T. Kitayama, T. Shinozaki, E. Masuda, M. Yamamoto and K. Hatada, *Polym. Bull.*, **20**, 505 (1988).
134. T. Kitayama, T. E. Masuda, M. Yamaguchi, T. Nishiura and K. Hatada, *Polym. J.*, **24**, 817 (1992).
135. M. Ikeda, T. Hirano and T. Tsuruta, *Makromol. Chem.*, **23**, 127 (1971).
136. H. Abe, K. Imai and M. Matsumoto, *J. Polym. Sci. C: Polym. Symp.*, **185**, 469 (1968).
137. D. G. H. Ballard, R. J. Bowles, D. M. Haddleton, S. N. Richards, R. Sellens and D. L. Twose, *Macromolecules*, **25**, 5907 (1992).
138. H. Schlaad and A. H. E. Müller, *Macromol. Symp.*, **95**, 13 (1995).
139. H. Schlaad, H. Kolshorn and A. H. E. Müller, *Macromol. Rapid Commun.*, **15**, 517 (1994).
140. H. Schlaad and A. H. E. Müller, *Macromol. Rapid Commun.*, **16**, 399 (1995).
141. H. Schlaad and A. H. E. Müller, *Polym. J.*, **28**, 954 (1996).
142. H. Schlaad, B. Schmitt, A. H. E. Müller, S. Jüngling and H. Weiss, *Macromolecules*, **31**, 573 (1998).
143. M. T. Reetz and R. Ostarek, *Chem. Commun.*, 213 (1988).
144. M. T. Reetz, T. Knauf, U. Minet and C. Bingel, *Angew. Chem., Int. Ed. Engl.*, **27**, 1373 (1988).

145. D. Baskaran, S. Chakrapani, S. Sivaram, T. E. Hogen-Esch and A. H. E. Müller, *Macromolecules*, **32**, 2865 (1999).
146. D. Broska, A. Fieberg, C. Heibel and F. Bandermann, *Polym. Prepr., Am. Chem. Soc.*, **38**(1), 471 (1997).
147. A. P. Zagala and T. E. Hogen-Esch, *Macromolecules*, **29**, 3038 (1996).
148. D. K. Dimov and T. E. Hogen-Esch, *Polym. Prepr., Am. Chem. Soc.*, **38**(1), 494 (1997).
149. D. Baskaran, A. H. E. Müller, H. Kolshorn, A. P. Zagala and T. E. Hogen-Esch, *Macromolecules*, **30**, 6695 (1997).
150. D. Baskaran and A. H. E. Müller, *Macromolecules*, **30**, 1869 (1997).
151. D. K. Dimov, W. N. Warner, T. E. Hogen-Esch, S. Juengling and V. Warzelhan, *Macromol. Symp.*, **157**, 171 (2000).
152. H. Konigsmann, S. Jüngling and A. H. E. Müller, *Macromol. Rapid Commun.*, **21**, 758 (2000).
153. D. K. Dimov and T. E. Hogen-Esch, *Polym. Prepr., Am. Chem. Soc.*, **38**(1), 469 (1997).
154. P. Banerjee and A. M. Mayes, *Macromolecules*, **31**, 7966 (1998).
155. T. Pietzonka and D. Seebach, *Angew. Chem., Int. Ed. Engl.*, **32**, 716 (1993).
156. H. G. Börner and W. Heitz, *Macromol. Chem. Phys.*, **199**, 1815 (1998).
157. D. Baskaran and A. H. E. Müller, *Macromol. Rapid Commun*, **21**, 390 (2000).
158. W. R. Hertler, D. Y. Sogah, O. W. Webster and B. M. Trost, *Macromolecules*, **17**, 1415 (1984).
159. O. W. Webster, *J. Polym. Sci., Part A: Polym. Chem.*, **38**, 2855 (2000).
160. O. W. Webster, *Adv. Polym. Sci.*, **167**, 1 (2004).
161. K. Narasaka, K. Saigo, Y. Aikawa and T. Mukaiyama, *Bull. Soc. Chem. Jpn.*, **49**, 779 (1976).
162. O. W. Webster, W. R. Hertler, D. Y. Sogah, W. B. Farnham and T. V. RajanBabu, *J. Am. Chem. Soc.*, **105**, 5706 (1983).
163. W. Schubert and F. Bandermann, *Makromol. Chem., Chem. Phys.,* **190**, 2721 (1989).
164. W. J. Brittain, *J. Am. Chem. Soc.*, **110**, 7440 (1988).
165. D. Y. Sogah, W. R. Hertler, O. W. Webster and G. M. Cohen, *Macromolecules*, **20**, 1473 (1987).
166. W. Schubert and F. Bandermann, *Makromol. Chem., Chem. Phys.,* **190**, 2161 (1989).
167. U. Schmalbrock, H. D. Sitz and F. Bandermann, *Makromol. Chem.*, **190**, 2713 (1989).
168. I. B. Dicker, G. M. Cohen, W. B. Farnham, W. R. Hertler, E. D. Laganis and D. Y. Sogah, *Macromolecules*, **23**, 4034 (1990).
169. A. H. E. Müller, *Makromol. Chem., Macromol. Symp.*, **32**, 87 (1990).
170. P. M. Mai and A. H. E. Müller, *Makromol. Chem., Rapid Commun.*, **8**, 247 (1987).
171. R. P. Quirk and J. S. Kim, *Makromol. Chem., Macromol. Symp.*, **67**, 351 (1993).
172. R. P. Quirk and G. P. Bidinger, *Polym. Bull.*, **22**, 63 (1989).
173. A. H. E. Müller, *Macromolecules*, **27**, 1685 (1994).
174. W. J. Brittain and I. B. Dicker, *Macromol. Symp.*, **67**, 373 (1993).
175. R. P. Quirk and J. S. Kim, *J. Phys. Org. Chem.*, **8**, 242 (1995).
176. A. D. Jenkins, E. Tsartolia, D. R. M. Walton, J. Stejskal and P. Kratochvil, *Polym. Bull.*, **20**, 97 (1988).
177. D. Haddleton, M. C. Crossman, K. H. Hunt, C. Topping, C. Waterson and K. S. Suddaby, *Macromolecules*, **30**, 3992 (1997).
178. Y. Zou, D. Lin, L. Dai, J. Zhang and R. Pan, *Polymer*, **30**, 3947 (1997).
179. (a) P. M. Mai and A. H. E. Müller, *Makromol. Chem., Rapid Commun.*, **8**, 99 (1987).
(b) W. Schubert, H.-D. Sitz and F. Brandermann, *Makromol. Chem.*, **190**, 2193 (1989).
180. N. Hadjichristidis, H. Iatrou, M. Pitsikalis and J. Mays, *Prog. Polym. Sci.*, **31**, 1068 (2006).
181. N. Hadjichristidis, M. Pitsikalis, S. Pispas and H. Iatrou, *Chem. Rev.*, **101**, 3747 (2001).
182. K. Hong, D. Uhrig and J. W. Mays, *Curr. Opin. Solid State Mater. Sci.*, **4**, 531 (1999).
183. A. Hirao and M. Hayashi, *Acta Polym.*, **50**, 219 (1999).
184. J. Jagur-Grodzinski, *React. Funct. Polym.*, **46**, 1 (2001).
185. K. Hatada, T. Nishiura, T. Kitayama, K. Ute and S. Hirotani, *Polym. J.*, **28**, 185 (1996).
186. T. Nishiura, T. Kitayama and K. Hatada, *Polym. J.*, **28**, 1021 (1996).
187. K. Hatada, T. Nishiura, T. Kitayama and S. Hirotani, *Macromol. Rapid Commun.*, **18**, 37 (1997).
188. K. Hatada, T. Nishiura, T. Kitayama and M. Tsubota, *Polym. Bull.*, **36**, 399 (1996).

189. S. K. Varshney, Ph. Bayard, C. Jacobs, R. Jérôme, R. Fayt and P. Teyssié, *Macromolecules*, **25**, 5578 (1992); 'Halato-telechelic polymer', in *IUPAC Compendium of Chemical Terminology*, **78**, 2070 (2006) (http://old.iupac.org/goldbook/HT07207.pdf).
190. S. K. Varshney, Z. Song, J. X. Zhang and R. Jérôme, *Macromol. Rapid Commun.*, **44**, 3400 (2006).
191. R. P. Quirk, M. Ocampo, M. J. Polce and C. Wesdemiotis, *Macromolecules*, **40**, 2352 (2007).
192. S. Antoun, P. Teyssié and R. Jérôme, *J. Polym. Sci., Part A: Polym. Chem.*, **35**, 3637 (1997).
193. O. W. Webster, *Makromol. Chem., Macromol. Symp.*, **33**, 133 (1990).
194. T. Nugay, N. Nugay and R. Jérôme, *Polym. Bull.*, **48**, 457 (2002).
195. S. Ponsart, J. Coudane and M. Vert, *Biomacromolecules*, **1**, 275 (2000).
196. B. Saulnier, S. Ponsart, J. Coudane, H. Garreau and M. Vert, *Macromol. Biosci.*, **4**, 232 (2004).
197. S. Gimenez, S. Ponsart, J. Coudane and M. Vert, *J. Bioactive Compatible Polym.*, **16**, 32 (2001).
198. S. Ponsart, J. Coudane, J.-L. Morgat and M. Vert, *J. Labelled Compd., Radiopharm.*, **44**, 677 (2001).
199. B. Nottelet, J. Coudane and M. Vert, *Biomaterials*, **27**, 4948 (2006).
200. S. Creutz, P. Teyssié and R. Jérôme, *Macromolecules*, **30**, 6 (1997).
201. M. Pitsikalis, S. Sioula, S. Pispas, N. Hadjichristidis, D. C. Cook, J. Li and J. W. Mays, *J. Polym. Sci., Part A: Polym. Chem.*, **37**, 4337 (1999).
202. J. D. Tong and R. Jérôme, *Polymer*, **41**, 2499 (2000).
203. R. Jérôme and J. Tong, *Curr. Opin. Solid State Mater. Sci.*, **3**, 573 (1998).
204. T. Zundel, J. Baran, M. Mazurek, J.-S. Wang, R. Jérôme and P. Teyssié, *Macromolecules*, **31**, 2724 (1998).
205. P. Teyssié, J. Baran, P. Dubois, R. Jérôme, J.-S. Wang, J. Yu and T. Zundel, *Macromol. Symp.*, **132**, 303 (1998).
206. J.-P. Hautekeer, S. K. Varshney, R. Fayt, C. Jacobs and P. Teyssié, *Macromolecules*, **23**, 3893 (1990).
207. J. Wang, Ph. Bayard, R. Jérôme, P. Teyssié and S. K. Varshney, *Macromolecules*, **26**, 2386 (1993).
208. J. M. Yu, P. Dubois, P. Teyssié and R. Jérôme, *Macromolecules*, **29**, 6090 (1996).
209. J. M. Yu, P. Dubois and R. Jérôme, *Macromolecules*, **29**, 8362 (1996).
210. J. M. Yu, P. Dubois and R. Jérôme, *Macromolecules*, **29**, 7316 (1996).
211. J. M. Yu, P. Dubois and R. Jérôme, *J. Polym. Sci., Part A: Polym. Chem.*, **35**, 3507 (1997).
212. (a) J. Wang, S. K. Varshney, R. Jérôme and P. Teyssié, *J. Polym. Sci., Part A: Polym. Chem.*, **30**, 2251 (1992).
(b) V. Efstratiadis, G. Tselikas, N. Hadjichristidis, J. Li, W. Yunan and J. W. Mays, *Polym. Int.*, **33**, 171 (1994).
213. J. A. Simms and H. J. Spinelli, *J. Coat. Technol.*, **59**, 125 (1987).
214. C. Tsitsilianis, S. Graf and P. Rempp, *Eur. Polym. J.*, **27**, 243 (1991).
215. Z. Zhu, J. Rider, Y. Yang, M. E. Gilmartin and G. E. Wnek, *Macromolecules*, **25**, 7330 (1992).
216. S. Ponsart, J. Coudane, J. McGrath and M. Vert, *J. Bioactive Compatible Polym.*, **17**, 417 (2002).
217. M.-H. Huang, J. Coudane, S. Li and M. Vert, *J. Polym. Sci., Part A: Polym. Chem.*, **43**, 4196 (2005).
218. M. Miura, F. Akutsu, M. Yamamoto, K. Naruchi and K. Nagakubo, *Macromol. Rapid Commun.*, **5**, 745 (1984).
219. F. Akutsu, M. Inoki, Y. Kasashima, Y. Shimajiri and K. Naruchi, *Macromol. Rapid Commun.*, **17**, 101 (1996).
220. M. Inoki, F. Akutsu, H. Yamaguchi, K. Naruchi and M. Miura, *Macromol. Chem. Phys.*, **195**, 2799 (1994).
221. J. Coudane, E. Laurent and M. Vert, *Macromol. Rapid Commun.*, **25**, 1865 (2004); W. Schubert, H.-D. Sitz and F. Bandermann, *Makromol. Chem., Chem. Phys.*, **190**, 2193 (1989).

CHAPTER **16**

Structure and properties of d^8 metal–dithiolene complexes

PAOLA DEPLANO, M. LAURA MERCURI, ANGELA SERPE and LUCA PILIA

Università di Cagliari, Dipartimento di Chimica Inorganica e Analitica, S.S. 554-Bivio per Sestu, I09042 Monserrato-Cagliari, Italy
Fax: +39 706754456; e-mail: deplano@unica.it

The chemistry of metal enolates
Edited by Jacob Zabicky

I. ACRONYMS

bdt	benzene-1,2-dithiolate
bdta	benzo-1,3,2-dithiazolyl
bedtttf	bis(ethylenedithio)tetrathiafulvalene
CT	charge transfer
dddt	5,6-dihydro-1,4-dithine-2,3-dithiolate
dfpdt	2,2-difluoro-1,3-propanediyldithioethylene-1,2-dithiolate
dmid	2-oxo-1,3-dithiole-4,5-dithiolate
dmit	1,3-dithiole-2-thione-4,5-dithiolate
dmstfdt	dimethyldiselenadithiafulvalenedithiolate
dsit	1,3-dithiole-2-thione-4,5-diselenolate
edt	ethylene-1,2-dithiolate
hmp	(2-pyridyl)methanolate
i.p.	in phase
mnt	maleonitriledithiolate
nlo	nonlinear optics
o.o.p.	out of phase
per	perylene
phdt	1,2-diphenylethylenedithiolate
pipdt	piperazine-2,3-dithione
SOMO	singly occupied molecular orbital
tcnq	7,7,8,8-tetracyanoquinodimethane
tdas	1,2,5-thiadiazole-3,4-dithiolate
tfadt	3-(trifluoromethyl)acrylonitrile-2,3-dithiolate
tfd	1,2-bis(trifluoromethyl)ethylenedithiolate
timdt	formally the monoanion of imidazolidine-2,4,5-trithione
tpdt	3,4-thiophenedithiolate
ttf	tetrathiafulvalene
tto	tetrathiooxalato

II. INTRODUCTION

Interest in metal–dithiolene complexes has increased since their initial synthesis to the present, because of their potential application as molecular materials with conducting[1], magnetic[2] and optical[3,4] properties and their involvement in bioinorganic processes at the active site of Mo and W metalloenzymes[5]. These applications have stimulated a multidisciplinary approach to these systems which includes theoretical studies and use of sophisticated characterization methods, furnishing a deep understanding of the structure/property relationship. This allows chemists to tailor metal–dithiolene complexes

having desired structures and functions. The tailoring is relatable to the versatility of the organic synthesis in the ligand preparation while the transition metal atom introduces further effects such as the constraints of a preferred geometry, the involvement of the metal *d* orbitals, the presence of unpaired electrons that affect the functions of the molecules.

Several reviews on these complexes are available in the literature, starting from the pioneering but still topical papers by McCleverty[6], dealing with the fundamental properties, by Mueller-Westerhoff[3], dealing mainly with their applications as near-infrared dyes, by Cassoux and Valade[7], focusing on conducting and superconducting properties of $[M(dmit)_2]^{z-}$ (M = Ni, Pd and Pt), to more recent reviews dealing with hybrid organic/inorganic CT salts with conducting/magnetic properties, such as the one by Robertson and Cronin[8], and that by Cassoux and Faulmann[1a] on the solid-state properties.

This chapter focuses on recent results concerning the class of square-planar d^8 metal–bis(dithiolene) or mixed ligand complexes, discussing their properties and applications as building blocks of molecular materials where the bulk properties are based on their component molecules interacting with each other at the supramolecular level.

III. SQUARE-PLANAR d^8 METAL DITHIOLENES

A. Background

1. Noninnocence of ligands and complexes

1,2-Enedithiolate anions are redox-active ligands (see equation 1), capable of coordinating with a variety of metals as neutral dithioketones (**1**), thioketone radical thiolate monoanions (**2**) and ene-1,2-dithiolate dianions (**3**). The complexes are named *dithiolenes* irrespective of their oxidation state to remind one that they are noninnocent ligands[9].

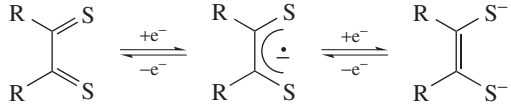

(**1**) (**2**) (**3**) (1)

In complexes of noninnocent ligands the oxidation state of the metal is not easily defined as a consequence of the uncertainty in the oxidation state of the ligand. In cases where such complexes belong to a series where the members show the same coordination geometry and are connected through reversible one-electron redox steps, additional ambiguities arise due to the difficulty in determining the spin state of the central metal. In the well known class of square-planar d^8 metal–dithiolenes of Ni(II), Pd(II) and Pt(II), the members of the series are connected through reversible one-electron redox steps which may spread from the dicationic to the dianionic form[10] as shown in equation 2.

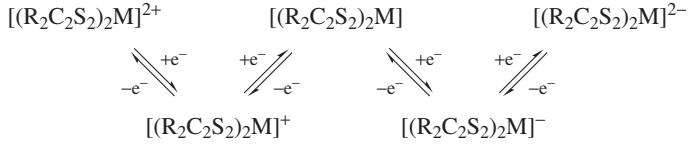

(2)

Following the Lewis formalism to summarize the bonding in these systems, classical structures involving the metal in the 2+ oxidation state and the ligands in the 1,2-dithione and 1,2-enedithiolate form, respectively, can be applied only to the diamagnetic dicationic and dianionic members of the series. For the neutral diamagnetic complex two bonding

descriptions are required: one involves a resonance hybrid (**4**) among the limiting forms where the M(II) is coordinated to one neutral dithione molecule and one dithiolate dianion, the other nonclassical Lewis description (**5**) involves the M(II) coordinated to two ligands in radical form where the spins are antiferromagnetically coupled. Similarly, nonclassical Lewis descriptions are required to describe the monocationic (**6**) and monoanionic (**7**) complexes where the M(II) is coordinated respectively to one dithione ligand and one ligand in radical form, and to one dithiolato ligand and one ligand in radical form with the spin ($S = 1/2$) highly delocalized over the molecule[11].

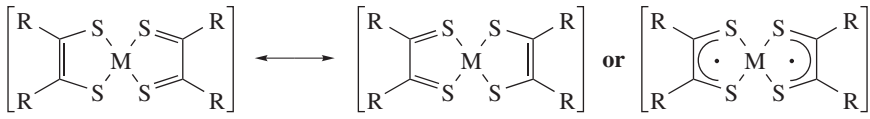

(**4**) (**5**)

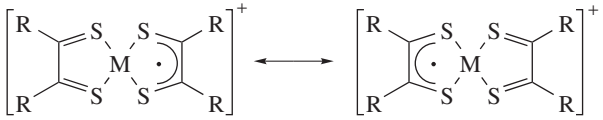

(**6**)

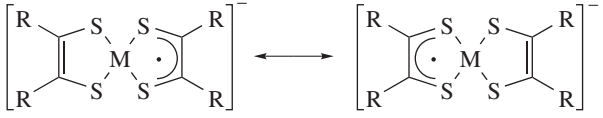

(**7**)

In the case of Au(III) (or Cu(III)) derivatives, a + charge must be added to the corresponding isoelectronic d^8 members of the series.

2. Electronic and electrochemical properties

The 2+ and 2− limits in the members of the series of the square-planar d^8 metal(II)–bis(dithiolene) complexes are due to the fairly isolated frontier π-MOs, shown in Figure 1,

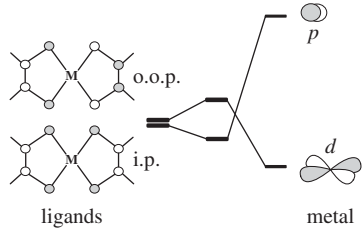

FIGURE 1. Frontier MOs in square-planar d^8 metal–dithiolene complexes formed by the in-phase (i.p.) and out-of phase (o.o.p.) combinations of C_2S_2 orbitals perturbed by the metal. The *d* metal orbitals stabilized relative to ligand orbitals lead to an 'inverted bonding scheme'. Reprinted with permission from Reference 12. Copyright 2004 American Chemical Society

which can be either empty or populated. These MOs are the in-phase (i.p.) and out-of-phase (o.o.p.) combinations of two (C_2S_2) orbitals, and are at high energy due to the C–S and S···S antibonding interactions within one ligand and between the two ligands. These orbitals are stabilized and destabilized by one high-lying p_π and a lower d_π metal orbital, respectively[12]. The d metal orbitals stabilized relative to ligand orbitals lead to an 'inverted bonding scheme', while in a 'normal bonding scheme' the d orbitals are destabilized relative to the ligand orbitals[13]. In the neutral diamagnetic term of the M(II) series only the low-lying orbital is populated and the HOMO–LUMO dipole allowed transition ($b_{1u} \rightarrow b_{2g}$ in D_{2h} symmetry) gives rise to a typical intense electronic transition which falls at low energies (NIR region). In the monoanionic paramagnetic derivative the LUMO becomes half-filled SOMO and the related HOMO–SOMO transition undergoes a bathochromic shift and a decrease in intensity, while in the dianionic derivatives a bleaching is observed because the former LUMO becomes doubly occupied. The electronic effects on the frontier orbitals of various substituents at the dithiolene core have been also quantified[3, 14]: in general, C_2S_2 π donor substituents (push) raise the energy of the HOMO and the LUMO, whose gap is lowered by a lowered interaction of the ligand orbitals with the low-lying metal orbitals, but whether or not the HOMO is pushed up at too high energy, an induced increased reactivity leading to the loss of one or two electrons can be observed, so that also this orbital is preferentially depopulated (cationic complexes). In contrast, π acceptor substituents (pull) lower the energy of both the MOs and favor the dianionic state. The electron delocalization can be further extended by selecting suitable R-substituents fixed in co-planarity with the dithiolene core, and leading to a decrease in the HOMO–LUMO gap[14]. Thus the proper choice of the R-substituents at the dithiolene moiety allows one to tune the absorption maximum of the NIR transition.

The negative or positive value of the potential $E_{1/2}{}^\circ$ for the $0 \rightarrow 1-$ reduction process can be related to the stability of the oxidized or reduced species and can be used as a marker for evaluation of the push/pull character of the substituents[12]. Complexes with increasingly stronger push substituents exhibit increasingly negative $E_{1/2}{}^\circ$, and derivatives with increasingly stronger pull substituents exhibit increasingly positive ones (Table 1). In Figure 2 the cyclic voltammograms of $[Ni(1,4\text{-}Me_2pipdt)_2]^{2+}$, $[Ni(1,3\text{-}i\text{-}Pr_2timdt)_2]$ and $[Ni(tdas)_2]^{2-}$ are reported as examples of ligands with push, nonpush/nonpull and pull character, respectively, which determines the nature of their most accessible status. The cyclic voltammogram of the dication $[Ni(1,4\text{-}Me_2pipdt)_2]^{2+}$ (Figure 2a) shows four reversible cathodic waves, ascribed to the $2+ \rightarrow 1+$, $1+ \rightarrow 0$, $0 \rightarrow 1-$ and $1- \rightarrow 2-$ processes, and represents one of the few examples of square-planar d^8 metal(II)–bis(dithiolene) complexes where four reversible redox steps are detected. The cyclic voltammogram of the neutral $[Ni(1,3\text{-}i\text{-}Pr_2timdt)_2]$ (Figure 2b) shows two reversible cathodic waves related to the $0 \rightarrow 1-$ and $1- \rightarrow 2-$ processes and a quasireversible anodic wave related to a ligand-centered oxidation process. The cyclic voltammogram of the dianion $[Ni(tdas)_2]^{2-}$ (Figure 2c) shows only one reversible anodic wave, ascribed to the $2- \rightarrow 1-$ process.

Several electrochemical data are available for the $[M(R_2C_2S_2)_2]^z$ series ($z = 2-, 1-, 0$ for M = Ni, Pd, Pt; $z = 1-, 0, 1+$ for M = Cu, Au). Unfortunately, a strict comparison of the $E_{1/2}{}^\circ$ values for the corresponding process in different systems is limited to the cases where the same solvent has been used, since the solvent may significantly affect the redox process. By using different substituents at the same ligand or different ligands at the same metal, the electronic and electrochemical properties can be further tuned. Asymmetric complexes based on two different ligands give rise to an asymmetric distribution of the charge at the $[(C_2S_2)M(C_2S_2)]$ core according to the differences in the push–pull character of the two ligands. The pull ligand (dithiolate) contributes mostly to the HOMO, the push ligand (dithione) mostly to the LUMO, and the HOMO–LUMO transition will have ligand-to-ligand charge transfer (CT) character (see Section III.C.2).

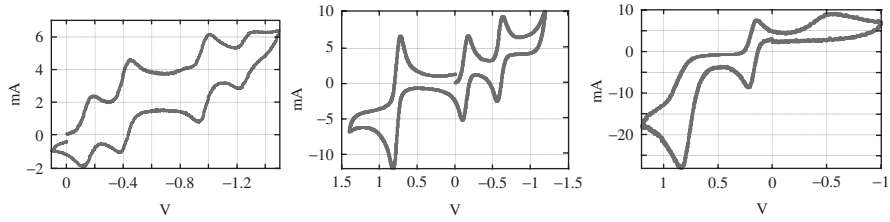

FIGURE 2. Cyclic voltammograms of $[Ni(1,4\text{-}Me_2pipdt)_2]^{2+}$ (a), $[Ni(1,3\text{-}i\text{-}Pr_2timdt)_2]$ (b) and $[Ni(tdas)_2]^{2-}$ (c) measured with a Pt *vs.* a Ag/AgCl reference electrode, in MeCN, 0.1 M Bu_4NPF_6, scan rate 100 mV s^{-1}

TABLE 1. Cyclic voltammetric data[a] of some $[Ni(L)_2]^z$ complexes

	Ligand	$E_{1/2}{}^\circ$ (V)[b] z: 0 → −	E_a (V)[c] z: − → 0	Reference
Push character	1,4-Me_2pipdt	−0.96		10
	$S_2C_2Me_2$	−0.195		11
	1,3-*i*-Pr_2timdt	−0.134[d]		15
	phdt	+0.105		16
	dddt	+0.105		16
	$S_2C_2H_2$	+0.14[e]		6
	3,5-*t*-Bu_2bdt	+0.16[f]		17
	dmit		+0.316	18
Pull character	$S_2C_2(CF_3)Ph$	+0.48		6
	$S_2C_2(CN)Ph$	+0.62		6
	tdas		+0.80	19
	$S_2C_2(CF_3)_2$	+0.97		20
	mnt		+1.11	18
	dtcr		+1.256[g]	15

[a] Measured with a Pt electrode *vs.* Ag/AgCl reference electrode, in MeCN, 0.1 M Bu_4NPF_6, scanrate 100 mV s^{-1}.

[b] For the reversible process. $[Ni(L)_2] \underset{-e^-}{\overset{+e^-}{\rightleftharpoons}} [Ni(L)_2]^-$.

[c] For the irreversible process $[Ni(L)_2]^- \xrightarrow{-e^-} [Ni(L)_2]$.

[d] Measured for this work.

[e] Estimated value.

[f] In thf solution.

[g] Quasi-reversible reduction $[Ni(L)_2]^- \underset{-e^-}{\overset{+e^-}{\rightleftharpoons}} [Ni(L)_2]^{2-}$, $E_{1/2}{}^\circ = 0.59$ V.

These introductory premises point to the relevance of the frontier π-MOs of d^8 metal–dithiolene complexes in determining their properties and related applications. The HOMO–LUMO transition at low energy turn the electrically neutral members of the series into NIR dyes, which have potential and actual applications such as converting radiation into heat, in 'smart' windows to screen the IR radiation component of daylight which causes heating, to provide protection against counterfeit in currency banknotes[4b] and in Q-switching of infrared lasers[21]. In addition, these complexes can act as polyelectrochromic

NIR dyes[22], based on the distinct NIR absorption spectra of the redox-active members of the series.

The extensive π-delocalized system of d^8 metal–dithiolene complexes is also responsible for the nonlinear optical properties (NLO) which have been recently reviewed[4b]. The interaction of radiation with the matter induces an instantaneous displacement (polarization: $P_0 = \mu = \alpha E$, where α is the linear polarizability) of the electronic density away from the nucleus at small field (linear optics). At high fields (laser light) the polarizability of the molecule can be driven beyond the linear regime and a nonlinear polarization is induced (NLO): $P_m = \alpha E + \beta E^2 + \gamma E^3 + \cdots$ and for the bulk material $P = P_0 + \chi_1 E^2 + \chi_2 E^3 + \cdots$, where β and γ are the molecular first- and second-order hyperpolarizabilities ($\alpha \gg \beta > \gamma > \cdots$) and χ_1 and χ_2 are the first- and second-order NLO susceptibilities (second- and third-order effects, respectively).

These properties are valuable for sensory devices, high-speed optical switching in telecommunication optical data processing and storage. Both symmetric and asymmetric complexes can be suitable to generate third-order NLO properties, but only asymmetric complexes at the molecular level, such as mixed-ligand complexes with push–pull ligands, and a noncentrosymmetric crystal packing for a bulk material, are required to generate second-order NLO properties. While no simple guidelines to design complexes to generate third-order NLO are available, a satisfactory structure–property relationship for second-order NLO chromophores has been furnished and will be discussed in Sections III.C.1.c and III.C.2.

Going back to the influence of the frontier orbitals on the properties of these complexes, the HOMO–LUMO gap, which decreases as the delocalization increases, has relevant consequence as to whether the single molecules arrange suitably in the solid state in such a way that the HOMO and LUMO bands can overlap each other by intermolecular interactions to produce partially filled bands. In such a way a single-component molecule system can generate a metallic or semimetallic band. Therefore, in the bulk, these building blocks can lead to electroconducting materials[1b]. Anionic complexes present as counterions of suitable radical cations, most often derived from tetrathiafulvalene (ttf) and similar molecules, can favor the formation of electroconducting materials, through intermolecular interactions which control the packing of the donor, and can be endowed with additional properties (optical, magnetic) giving rise to multifunctional hybrid organic/inorganic materials.

B. Bis(dithiolene) Complexes

1. Nonbenzenoid bis(dithiolene) complexes

So far two useful examples of three-step electron-transfer series of nickel dithiolenes: $[Ni(Me_2edt)_2]^z$ and $[Ni(3,5\text{-}(t\text{-}Bu)_2bdt)_2]^z$, $z = 2-, 1-, 0$, have been isolated and fully characterized. The ligand in the first complex belongs to the class of nonbenzenoid dithiolenes (**8**–**12**), where the π-delocalization is confined in the dithiolene core[11], and the other one to benzenoid systems[17] (**13**–**15**) (discussed in Section III.B.2). These compounds have furnished a valuable experimental tool to test the reliability of electronic structure calculations and to apply highly sophisticated techniques to the three oxidation states of the series to reach a deeper understanding of the electronic structures of these systems and to clarify points which have been the subject of debate in the past, such as oxidation number of the metals, innocent/noninnocent character of the ligand and ligand *vs.* metal oxidation[3, 6, 9, 13]. Structural data on the $[Ni(Me_2edt)_2]^z$ (**16**) series have shown that the three complexes, which are connected through reversible redox steps, have nearly planar structures with D_{2h} symmetry, and undergo a decrease of the chelate ring CC bond lengths on reduction[11]. The most significant experimental data are summarized in Table 2.

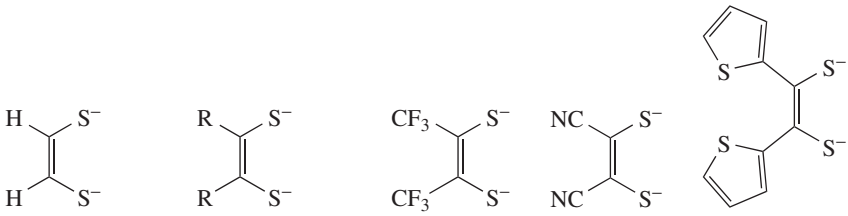

(**8**) edt (**9**) R_2edt, R = Alk, Ar (**10**) tfd (**11**) mnt (**12**) thpdt

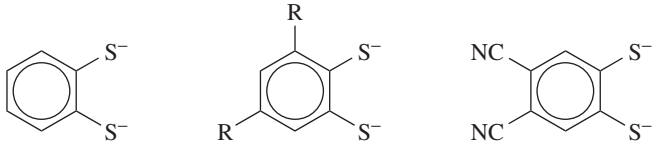

(**13**) bdt (**14**) R = Alk, Ar; 3,5-Rbdt (**15**) dcbdt

TABLE 2. Most significant experimental data for the $[Ni(S_2C_2Me_2)_2]^z$ (**16**) redox series

z [a]	$\varepsilon(\lambda_{max})$ [b]	ν(CC) (cm^{-1})	Spin	Magnetic behavior	Bond distances (see **13**, Å)
0	21500 (771)	1377, 1332	0	Diamagnetic	Bold values
1−	9700 (932)	1508	1/2	Paramagnetic	Italic values
2−	—	1595	0	Diamagnetic	Plain values

[a] $E_{1/2} = -0.15$ V for $z = 0 \rightarrow 1-$, $E_{1/2} = -1.05$ V for $z = 1- \rightarrow 2-$, in MeCN *vs.* SCE.
[b] ε in $M^{-1}\,cm^{-1}$, λ_{max} in nm.

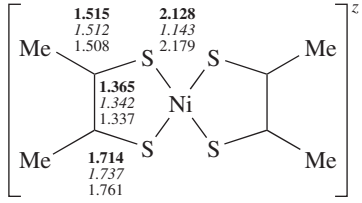

(**16**)

The geometrical parameters obtained from DFT calculations are in good agreement with structural data. In particular, the calculated distance variation d(CC) = 1.377, 1.356 and 1.347 Å for $z = 0$, 1− and 2−, respectively, is in accord with the observed shift to higher frequencies of the CC stretching vibration. This mode is easy to identify in the 1600–1300 cm^{-1} range and is not extensively mixed with other vibrational modes; therefore, it can serve as a most convenient marker for the redox state of the dithiolene ligand, as shown by spectral studies where the dependence of the ν(CC) vibration on z has been determined[23]. Very good agreement between experimental and calculated EPR parameters allow one to assign a $^2B_{2g}$ ground state of **16** for $z = 1-$, further supporting well established EPR[24] and ENDOR/ESEEM[25] studies on monoanions, which are characterized by

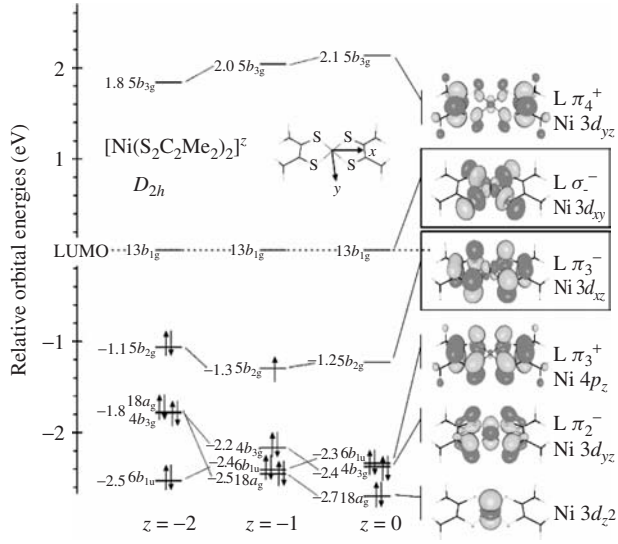

FIGURE 3. Orbital energy levels for the $[Ni(Me_2C_2S_2)_2]^z$, $z = 2-$, $1-$, 0 redox series and orbital contour plots for $z = 0$. The MO of the ligands are divided in π (out-of-plane, along the z-axis) and σ (in-plane, in the xy-plane) types. Reprinted with permission from Reference 13. Copyright 2003 American Chemical Society

covalent bonding with spin delocalized over the ligands. Holm, Solomon and coworkers[13] have further discussed the electronic structure of these complexes with the experimental support provided by the sulfur K-edge X-ray absorption spectroscopy (XAS). The orbital energy levels obtained by DFT methods are shown in Figure 3.

The orbital contour plots reported for the neutral species do not change qualitatively in the series, while the energy sequence changes. The orbitals $13b_{1g}$, $5b_{2g}$ and $6b_{1u}$ are important in describing the bonding and related properties of the series. The $13b_{1g}$ orbital (LUMO for $z = 2-$, $1-$ and LUMO $+1$ for $z = 0$) is the σ-antibonding combination of the metal and the sulfur ligand orbitals. Sulfur K-edge XAS shows that this orbital has more than 50% S character in the three oxidation states. The $5b_{2g}$ orbital (HOMO for $z = 2-$, SOMO for $z = 1-$ and LUMO for $z = 0$) is the redox active orbital composed by a π-antibonding combination of the Ni $3d_{xz}$ orbital and the S $3p_z$ ligand orbitals and this combination provides a superexchange pathway between the ligands. Also in this case theoretical and experimental sulfur K-edge XAS results converge in assigning predominant S-ligand character to this orbital for the three members of the series, and in addition are in agreement with the spin distribution obtained from EPR for the monoanion[24]. The $6b_{1u}$ (HOMO in the neutral complex, and donor orbital in the $6b_{1u} \rightarrow 5b_{2g}$ transition responsible for the NIR peak) is ligand-based, with a small contribution of the Ni $4p_z$ orbital in π-antibonding interaction with the S $3p_z$ ligand orbitals.

The overlap between the metal and ligand orbitals in the $5b_{2g}$ orbital (LUMO for $z = 0$) provides an efficient pathway for ligand-to-metal electron donation and confers electrophilic character on the ligands in neutral complexes. This finding affords a reasonable explanation for the electrophilic mechanism proposed by Wang and Steifel for the nonclassical reaction of neutral Ni–bis(dithiolene) complexes with olefins, which can be separated and purified by a novel method. The LUMO of the dithiolene complex

acceptor interacts with the HOMO of the olefin donor to give an interligand *cis*-adduct with $S_{dithiolene}C_{olefin}$ bonds[26].

The HOMO–LUMO gap in the neutral complex, which exhibits a singlet ground state, is relatively narrow (*ca* 1 eV). This gap can be related to the possibility of spin localization conferring a diradical character on the ground-state wave function. Photoelectron spectroscopy (PES) experiments from the ground state on the series $[M(mnt)_2]^z$ (M = Ni, Pd, Pt; $z = 2-, 1-, 0$) have allowed access to the lowest singlet and triplet states of the complex, yielding an experimental evaluation of the singlet–triplet splitting and providing an indication of the extent of singlet diradical character in the ground-state wave function (0.79, 0.57, 0.83 eV for M = Ni, Pd, Pt)[27]. PES data combined with DFT calculations on this series have provided further insights into molecular orbital energy levels of these systems, showing in particular that the donor orbital involved in the typical NIR transition is almost purely ligand-based (b_{1u}, with a contour plot similar to that of $6b_{1u}$ in Figure 3) since it occurs at similar energies for each species, while the acceptor orbital (b_{2g}, with a contour plot similar to that of $5b_{2g}$ in Figure 3) has metallic character and occurs at similar energies for Ni and Pt, and at lower energies for Pd, in agreement with the observed trend of the NIR peaks. Well documented examples of the dependence of this transition on the charge of the metal coordinated with a pair of identical ligand molecules have been recently reported by Wieghardt and coworkers[28]. The expected trend of the NIR transition with the charge when the metal is the same, is well illustrated in Figure 4 by the spectra of the gold(III) derivatives **17a** ($z = 1+, 0, 1-$), showing a bathochromic shift and a decrease in intensity of this peak on going from the monocation to the neutral member, and bleaching on further reduction to the monoanion. In the case of the isoelectronic but differently charged Pd(II) complexes **17b** ($z = 0, 1-, 2-$) a similar trend is observed; however, for the isoelectronic species the corresponding Pd peaks are found at shorter wavelengths. Theoretical calculations on model complexes of the gold(III) series **17c** ($z = 1+, 0, 1-, 2-$) and of palladium(II), **17d** ($z = 0$), have allowed optimizing geometrical parameters which are in good agreement with structural data when available, explaining quite satisfactorily spectroscopic and electrochemical features and pointing to the influence of the effective nuclear charge of the metal on the extent of the superexchange interaction between the ligands.

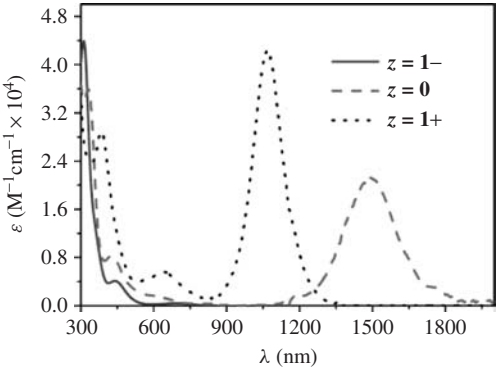

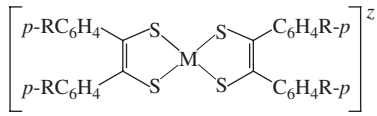

(**17**) (**a**) M = Au, R = *t*-Bu
(**b**) M = Pd, R = *t*-Bu
(**c**) M = Au, R = H
(**d**) M = Pd, R = H

FIGURE 4. Electronic spectra in CH_2Cl_2 solution of the $z = 1-, 0, 1+$ redox series of the Au(III) complexes **17a**. The peaks for the corresponding isoelectronic $z = 2-, 1-, 0$ redox series of the Pd(II) complexes **17b** are found at the following $\lambda_{max}(\varepsilon, M^{-1}\ cm^{-1})$: no NIR absorption peaks for $z = 2-$, 1250 nm (17000) for $z = 1-$ and 915 nm (3700) for $z = 0$. Reprinted with permission from Reference 28. Copyright 2007 American Chemical Society

The MOs that are important in describing the bonding in **17** are qualitatively similar to those described for **16**. However, due to the high effective nuclear charge of the metal, the Au-*d* orbitals lie very deep in energy when compared to the ligand-*p* orbitals. This strongly reduces the superexchange interaction between the ligands and the antiferromagnetic coupling between the ligand radicals. A diradical character of 88% has been calculated for $[AuL_2]^+$ from a broken symmetry DFT calculation[28]. A factor such as the presence of four doubly occupied low-lying Au-*d* orbitals and the nature of the electroactive frontier orbitals, HOMO ($2b_{2g}$ orbital, similar contour plot of $5b_{2g}$ of Figure 3) and HOMO −1 ($1b_{1u}$ orbital, similar contour plot of $6b_{1u}$ of Figure 3) for the $[AuL_2]^-$ species, which have predominant ligand character, allow the description of the $z = 1 - /0/1+$ series as Au(III) coordinated to two closed-shell dianions for $z = 1-$, radical-dianion mixed-valence delocalized ligands for $z = 0$ and singlet diradicals for $z = 1+$. The ligand character of these electroactive orbitals is in agreement with the ligand-based oxidation processes, reflected by a decrease of C–S and an increase of C–C distances when the charge changes from 1− to 1+, while the Au–S distance remains almost invariant. On the other hand, the observed increase of the Au–S distance on reduction from the monoanion to the dianion complex is in agreement with the nature of the SOMO of the dianion complex, which consists of a σ-antibonding combination of the metal and the ligand orbitals ($1b_{1g}$ orbital, similar contour plot of $13b_{1g}$ of Figure 3)[28].

2. Benzenoid bis(dithiolene) complexes

Anions **13**–**15** belong to the benzenoid class of dithiolene ligands. Most significant experimental data for complexes $[ML_2]^z$ (**18**) in various redox states (M = Ni(II), Pd(II), Pt(II), Au(III), L = 3,5-(*t*-Bu)$_2$bdt (**14**, R = *t*-Bu)) are summarized in Table 3. In the case of $[Ni(3,5\text{-}(t\text{-}Bu)_2bdt)_2]^z$ (**18**, M = Ni, $z = 2-$, 1−, 0) XRD has shown that the chelate ring C–C distance undergoes a small variation with the charge in the *o*-phenylene moiety.

TABLE 3. Most significant experimental data for the $[M(t\text{-}Bu_2bdt)_2]^z$ (**18**) redox series

M(II) ions		Au(III)		Spin	Magnetic behavior	Bond distances (see **18**, M = Ni, Å)
z	$\varepsilon(\lambda_{max})$ [a]	z	$\varepsilon(\lambda_{max})$ [a]			
0	Ni 30000 (840) Pd 50000 (850) Pt 39000 (802)	1+	unavailable	0	Diamagnetic	Bold values
1−	Ni 15000 (890) Pd 25000 (1140) Pt 19000 (900)	0	27000 (1452)	1/2	Paramagnetic	Italic values
2−	—	1−	—		Diamagnetic	Plain values

[a] ε in $M^{-1}\,cm^{-1}$, λ_{max} in nm.

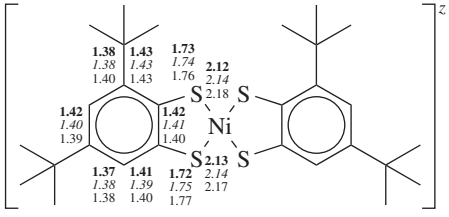

(**18**) M = Ni

It was proposed that the ligand works as an innocent dithiolate ligand[17] and consequently the formal oxidation state to the metal was assigned to be 2+, 3+ and 4+. Further experimental and theoretical studies with DFT and correlated *ab initio* methods on these systems including M = Ni(II), Pd(II), Pt(II) and the isoelectronic but differently charged Au(III) and Cu(III) complexes by Wieghardt and coworkers[29] have allowed a deeper understanding of these systems and show that also in this case the ligand is noninnocent.

In addition, the Ni, Pd, Pt triad exhibits two reversible redox waves for the $0 \rightarrow 1-$ and $1- \rightarrow 2-$ processes which fall at similar potentials. In the Au and Cu complexes the wave for the $0 \rightarrow 1-$ step falls at the same potential, while the value is more negative for the gold derivative for the $1- \rightarrow 2-$ process. The behavior of benzenoid dithiolenes is thus similar to that of nonbenzenoid systems: they belong to a series where the members are connected through reversible redox steps; the neutral terms of the Ni triad and Au monocations show strong NIR peaks, which undergo a bathochromic shift for the first reduction step and bleaching for the second reduction step. The position of the NIR peak for the isoelectronic members follows the order: λ_{max} Ni $\sim$ Pt $<$ Pd $<$ Au. The monoanions of the Ni triads and the neutral Au complexes are paramagnetic. The X-band EPR spectra of these complexes show a rhombic signal with hyperfine coupling for ^{61}Ni and for ^{195}Pt, which can be ascribed to the metal contribution to SOMO[17], while no coupling could be observed for ^{105}Pd and for ^{197}Au complexes. Theoretical calculations based on DFT explain well the experimental data. The MO and energy scheme is reported for [Au(III)(bdt)$_2$)] complexes in Figure 5. The frontier orbitals, which are important for elucidation of bonding, are similar to those of nonbenzenoid systems, except for the contribution of the C-p_z orbitals. In particular, no localized double-bond formation between C1–C6 (see Figure 5)[29a], but rather a π-interaction bonding among C2–C1–C6–C5, and C3–C4 and antibonding between C4–C5 and C2–C3, is found in the redox-active $2b_{2g}$ orbital. The lengthening of C2–C1–C6–C5, and C3–C4 and the shortening of C4–C5

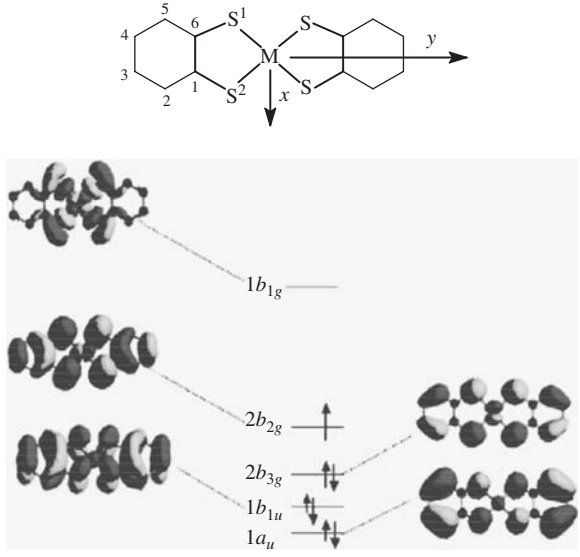

FIGURE 5. Simplified MO scheme for $[M(bdt)_2]^z$ (M = Ni(II), Pd(II), Pt(II), $z = 1-$; M = Au(III), $z = 0$). Reprinted with permission from Reference 29b. Copyright 2006 American Chemical Society

and C2–C3 observed on oxidation, is in accordance with a weak quinone-like distortion of the ligand. As the charge is delocalized over the ring, the effect on bond distances is small and is not reflected by experimental markers such as the variation of ν(CC) vibration with the charge as found for nonbenzenoid systems. This is a distinctive mark for the two classes of complexes.

In conclusion, theoretical and experimental studies for both benzenoid and nonbenzenoid metal d^8 dithiolene complexes converge in establishing the noninnocent character of the ligand and in addition show that: (i) an inverted bonding scheme with destabilized ligand orbitals relative to metal *nd* orbitals occurs, with an increasingly small contribution of the *d* metal orbital from Ni(II)–Pt(II) to Pd(II) and Au(III) to the redox-active b_{2g} orbital ($5b_{2g}$ and $2b_{2g}$ of Figures 3 and 5, respectively). This takes also in account the ligand versus metal oxidation behavior; (ii) a M(II) (Ni, Pd and Pt) or Au(III) oxidation state for the $z = 0$, 1−, 2− or 1+, 0, 1− respectively is established; (iii) that in the paramagnetic ($S = {}^1/_2$) monoanion (Ni, Pd and Pt) or neutral (Au) the spin is highly delocalized over the molecule; (iv) that in the neutral Ni triad and Au monocationic complexes limited diradical character following the order Ni ~ Pt < Pd < Au is found.

3. Complexes with ligands bearing heterocycle fused on the C_2S_2 moiety

Several d^8 metal–dithiolene complexes based on nonbenzenoid (**19**–**24**) or benzenoid (**25**, **26**) ligands, bearing heterocycle containing additional sulfur and/or nitrogen atoms fused to the C_2S_2, have been reported. The presence of these heteroatoms can promote further intermolecular interactions in the solid state. Several papers and reviews deal with the most popular complexes of this class, namely $[M(\mathbf{19})_2]^z$ ($z = 2-$, 1−, fractional charge), which can form superconducting solids[1a,7,8,30]. The family $[M(\mathbf{24})_2]^z$($z = 1-$, 0, 1+, fractional charge)[31] shows similarity to bedtttf, the organic donor that has produced so far the largest number of organic salts with superconducting properties (see Section IV). The delocalized framework, which can be further extended by proper choice of the heterocycle, narrows the HOMO–LUMO gap as the delocalization increases. When the single molecules arrange suitably in the solid state with two- or three-dimensional intermolecular interactions, a single-component molecular system with metallic or semimetallic behavior can be in hand. It has been shown that neutral Ni molecules based on extended ttf–dithiolenes are capable of forming single-component molecular metallic crystals[1b] (see Section IV). Despite the low HOMO–LUMO gap, these complexes have limited

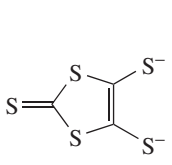
(**19**) dmit

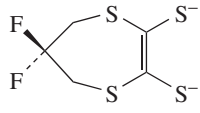
(**20**) dfpdt

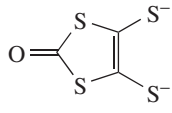
(**21**) dmid

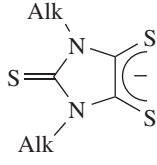
(**22**) Alk_2timdt

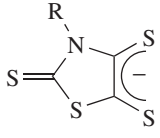
(**23**) R = Alk, Ar; Rthiazdt

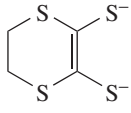
(**24**) dddt

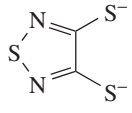
(**25**) tdas

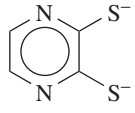
(**26**) pdt

potential as dyes for Q-switching NIR lasers, because the application requires the dye to be in solution and the complex is sparingly soluble in common solvent. Other important requirements for this application are (i) the absorption maximum as close as possible to the laser wavelength, (ii) a suitable excited-state lifetime and (iii) high thermal and photochemical stability to the laser wavelength.

Among the ligands bearing a heterocycle fused to the C_2S_2 moiety, the 1,3-Alk$_2$timdt ligand (**22**), where the electron donor N atoms of the imidazoline ring are forced into co-planarity with the dithiolene ring, proved to be valuable in shifting the low-energy transition in a region of remarkable interest for NIR dyes, while stability was maintained. Moreover, the steric hindrance of *N*-alkyl substituents prevents stacking and improves the solubility of these complexes. The symmetrical neutral complexes [M(1,3-Alk$_2$timdt)$_2$], M = Ni(II), Pd(II), Pt(II), absorb very strongly at approximately 1000 nm (ε *ca* 80000 $M^{-1}\,cm^{-1}$, so far the highest value achieved, see Figure 6), where neodymium lasers operate. These properties, coupled with their high thermal and photochemical stability at the laser wavelength, make these complexes optimal candidates for applications in Q-switching neodymium lasers[14d, 32]. The monoanion [Ni(1,3-*i*-Pr$_2$timdt)$_2$]$^{1-}$ shows the NIR peak at approximately 1400 nm (ε *ca* 40000 $M^{-1}\,cm^{-1}$)[33]. Due to their spectroelectrochemical features (see Figures 2b and 6) being the low-energy absorption tuneable with the charge on a reversible one-electron redox process, these complexes work as electrochromic switchable NIR dyes.

Interestingly, chemical oxidation of [Ni(1,3-*i*-Pr$_2$timdt)$_2$] (**27**) with a strong diiodine excess produces a ligand mixed-valence compound in which a neutral square-planar complex and an octahedral complex [Ni(I$_2$)(1,3-*i*-Pr$_2$timdt)$_2$] are bound by a sequence of diiodine molecules. In the octahedral complex the bond distances of the ligand are different from those in the monoanion and in the neutral derivatives, since the CC bond in the ring shows an increasing single-bond character [*d*(CC) 1.35(1) $z = 1-$; 1.38(1) $z = 0$; 1.49(1) z formally 2+] and the CS a larger double-bond character [*d*(CS) 1.702(10) $z = 1-$; 1.695(10) $z = 0$; 1.65(1) z formally 2+], in agreement with a ligand-centered nature of the oxidation process. It is noteworthy that the free ligand has never been isolated either as vicinal dithione or in reduced form; the sulfurization reaction of the 1,3-dialkyl-4,5-dioxoimidazolidine-2-thione works to prepare the desired ligand only in the presence of the metal, producing the neutral complexes in a one-step reaction; otherwise, the reaction products are tetrathiocino derivatives[32b].

A class of related complexes based on *N*-R-thiazdt (formally monoreduced *N*-substituted thiazolidine-2,4,5-trithione, **23**), which shows features intermediate between those of corresponding Alk$_2$timdt (**22**) and dmit (**19**) ligands, has been prepared to tune

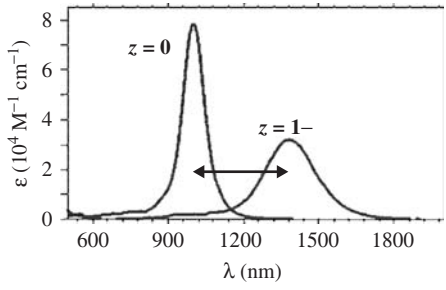

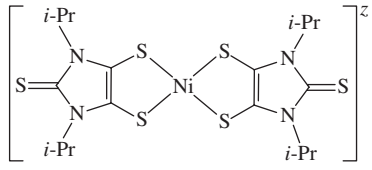

(**27**)

FIGURE 6. NIR peak of [Ni(1,3-*i*-Pr$_2$timdt)$_2$]^z (**27**) in $CHCl_3$ solutions, tuneable with the charge on reversible one-electron reduction from $z = 0$ to $z = 1-$

the spectral and electrochemical properties of these dyes for potential applications in the field of NIR lasers and photoconductors. Recently, the first structural characterization of $[M(\mathbf{23})_2]$ (M = Zn(II), Ni(II), Pd(II)) complexes has been reported[34].

The complexes in the above-described cases behave as nonbenzenoid systems and the differently charged members of the series exhibit an increase in the CC distance as z changes from a positive value to $2-$. Other complexes behave similarly to benzenoid systems in that the chelate ring CC distance of the C_2S_2 moiety is almost invariant in the variously charged species[35]. In the $[Ni(tdas)_2]^z$ complexes no significant difference in CC bond distance has been observed over the two states $z = 2-$ and $1-$ (1.435 Å in both cases), and calculated over the three states $z = 2-$, $1-$ and 0 (1.458, 1.440 and 1.443 Å, respectively). Thus, significant shift of the C=C vibration is neither expected nor observed on reduction and, consequently, this vibration cannot be used as a marker to assign the charge of the complexes, contrary to nonbenzenoid systems[36].

4. Complexes with ligands bearing additional functionality at the periphery

Suitable functionalities in the periphery of the molecule can promote interactions among molecules to favor supramolecular organization and to give ligand character to complexes, leading to bond formation with coordinatively unsaturated metal complexes. For example, Pt(II) dithioxamide (dto) complexes (**28**–**30**), which exhibit interesting properties as luminescent sensor both in solution and in the solid state activated by HCl and ammonia gases, are shown in equation 3[37]. Luminescence is ascribed to triplet Pt/S → dto CT excited states. A charge-transfer interaction between chloride and protonated dto is proposed to explain the influence of the halogen on the energy of the ligand orbitals and in promoting excited-state conversion between ligand-centered and Pt/S → dto levels. These complexes can also work as ligands toward complexes ($[M(L)_n]^+$), e.g. $[(\eta^3$-allyl)palladium$]^+$, [bis-(2-phenylpyridine)rhodium$]^+$, $[(\eta^6$-p-cymene)(chloro)ruthenium$]^+$ and similar cationic complexes, to prepare binuclear (**31**) and trinuclear (**32**) heterobimetallic complexes (equation 4)[38].

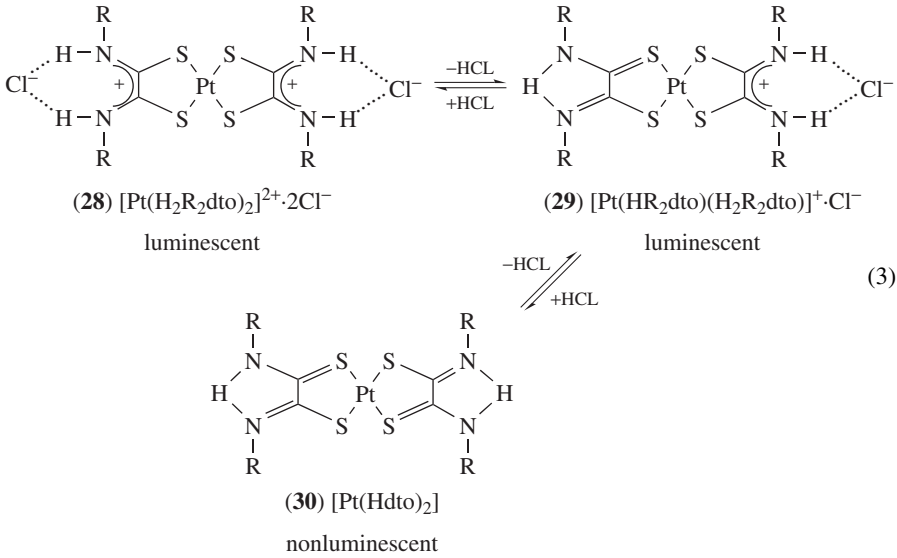

(3)

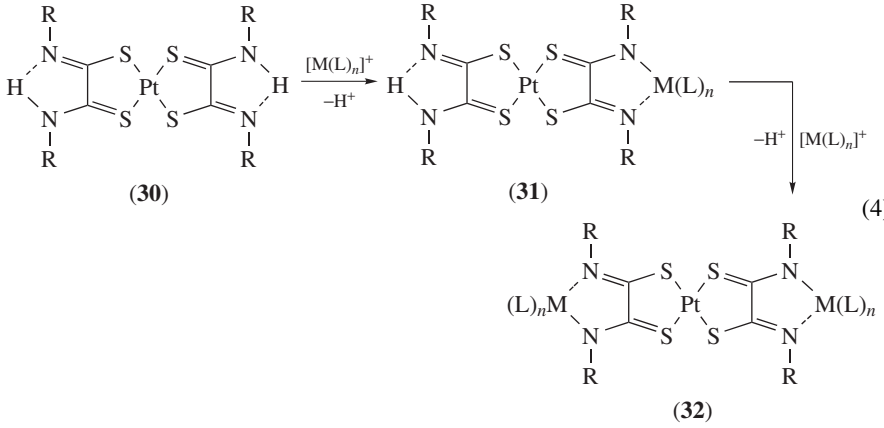

The relevance of hydrogen-bonding formation in determining the solid-state properties of nitrile-containing paramagnetic metal dithiolenes, as well as the capabilities of these complexes to work as ligands, is currently under investigation by M. Formigué's team. $[Ni(mnt)_2]^-$ has been successfully used to coordinate through the outer CN groups the metal in [Mn(III)(tpp)] (tpp = *meso*-tetraphenylporphinato) forming [Mn(III)(tpp)][Ni $(mnt)_2]_2$ unidimensional polymer chains, which exhibit antiferromagnetic interaction and order as ferrimagnets at very low temperature (2–8 K)[39]. The solid state organization of $[Ni(mnt)_2]^-$ and ammonium or pyridinium cations has been also pointed out. Bifurcated NH···NC and C4H···NC hydrogen bonds are formed favoring the dimerization of the two radical complexes (Figure 7), which show magnetic susceptibility in agreement with a singlet–triplet thermally activated behavior[40]. These studies include the use of less conventional asymmetrical ligands containing two different groups attached at the same C_2S_2 moiety.

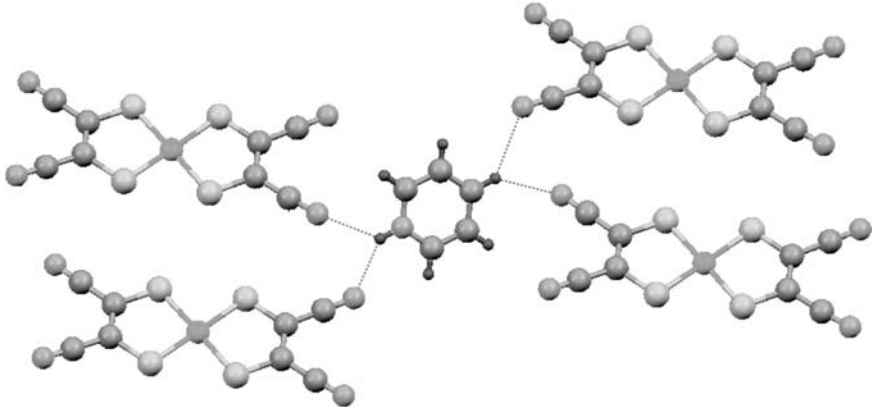

FIGURE 7. Details of hydrogen-bond network in $[pyH^+][Ni(mnt)_2]$ (pyH^+ = pyridinium). Reprinted with permission from Reference 40. Copyright 2003 American Chemical Society

With a view to preparing polymerizable complexes, thiophene-substituted nickel–dithiolene complexes [Ni(L)(L′)] have been synthesized and used to prepare films by electrochemical polymerization. The features of the complexes and of the polymers depend on the number of thiophene substituents. In particular, the complex with four thiophene substituents (L = L′ = thpdt, **12**) shows a narrower HOMO–LUMO gap as compared to complexes with two thiophene and two phenyl groups or four phenyl groups [λ_{max}, nm (ε, M^{-1} cm^{-1}) 976 (38800) L = L′ = **12**; 931 (37700) L = **12**, L′ = **9**, R = Ph; 866 (30900) L = L′ = **9**, R = Ph] and gave a polymer whose electrochemical features are similar to those of poly[1,2-di(2,5-thienylene)ethane], suggesting that similar extended chains are formed[41].

C. Mixed-ligand Complexes

1. Complexes having one dithiolene and other ligands

a. Platinum complexes having one chelating 1,1-bis(diphenyldiphosphino)ethane ligand. Platinum complexes having one heterocyclic-substituted 1,2-enedithiolato ligand and one chelating 1,1-bis(diphenyldiphosphino)ethane (dppe) or similar ligands have been reviewed recently by Pilato and Van Houten[42]. These complexes show relevant room-temperature dual-emission properties. The excited states involved in these emissions are one long-lived state one (^{3}ILCT*) with triplet character and a short-lived one with singlet character (^{1}ILCT*), producing respectively phosphorescence and fluorescence on decay. The excited states (^{3}ILCT* and ^{1}ILCT*, respectively) are achieved through an intraligand transition with charge-transfer character from the π system of 1,2-enedithiolate to the π^* system of the heterocycle. Emission occurs when the maximum positive charge is localized on the 1,2-enedithiolate sulfurs, thus coplanarity between 1,2-enedithiolate and the heterocycle is required. As shown in equations 5, this criterion is met when the heterocycle is forced into coplanarity (equation 5a) while being controlled by the steric hindrance of the R substituents in the protonated complexes (equation 5b)[43]. Given the lifetime of the triplet emission this is diffusionally quenched by agents such as dioxygen, electron donors, proton donors and hydrogen atom donors[42]. This process occurs at analyte concentrations of chemical and biological interest making these complexes suitable for use as dioxygen probes, for pH monitoring and in other applications[42]. Heteroleptic square-planar nickel and palladium complexes with dppe and unsymmetrical dithiolene ligands bearing one H-atom and one *p*-cyanophenyl or 2-thienyl or 3-thienyl group attached to the C_2S_2 moiety have been prepared and structurally characterized, but no mention is made of their luminescent properties[44].

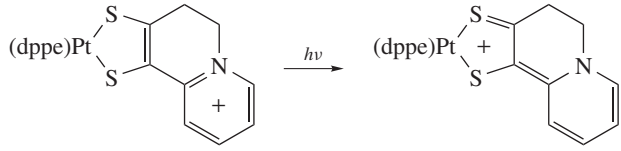

(5a)

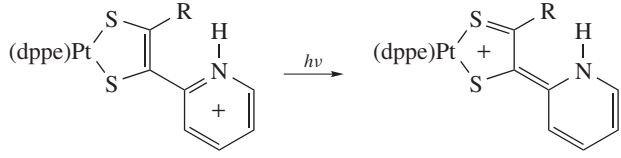

(5b)

b. Neutral radical nickel η^5-cyclopentadienidodithiolene complexes. Complexes belonging to this class, where the dithiolate ligands consist of hepta-, hexa- and penta-atomic heterocycle fused to the C_2S_2 moiety: $[S_2C_2S_2(CH_2)_2X]$ (X = CH_2, CF_2, C=CH_2, S, C=O)[45] or $[Y_2C_2X_2(CH_2)_2]$ (Y = S or Se, X = S; Y = S, X = Se)[46] or $[S_2C_2Y_2X]$ (Y = S, X = CO and CS; Y = Se; X = CS)[47], have been recently prepared and characterized. These complexes with various metals have been reviewed[48]. These complexes are redox-active and show one reversible oxidation and one reversible reduction wave: the potentials are affected by the electron-withdrawing power of the terminal group of the dithiolene ligands. The NiS_2C_2 moiety is planar and perpendicular to the Cp ring. The magnetic properties of these compounds depend on their structural features: complexes based on the seven-membered rings fused to the C_2S_2 moiety form either one-dimensional chains or a dimeric entity and those based on dmit or similar ligands present in the solid state form a set of tridimensional interactions that stabilize a 3-D antiferromagnetic ground state. DFT calculations performed on the dmit complex **33** afforded a sequence of MOs showing that the SOMO is a π orbital with a small contribution of the d_{xy} metal and Cp ring π orbitals and a predominant contribution of the dmit ligand, where the π conjugation is extended to endocyclic and exocyclic sulfur atoms of the ring (Figure 8). This explains the formation in the solid state of short intermolecular contacts through the dmit moiety and the influence of these interactions on the magnetic properties.

c. Square-planar d^8 metal diimine–dithiolene complexes. Interest in this class of complexes where the metal is coordinated with two different unsaturated chelating ligands, one more easily reduced (diimine, acceptor), the other more easily oxidized (dithiolato, donor), is far from declining. This is due to the potential applications of their peculiar properties such as solution luminescence and solvatochromism in the fields of photosentitizers or photoluminescent probes and NLO materials[4]. The Eisenberg group has performed extensive studies on the unique CT excited states of these systems[49]. This topic has been reviewed[49a]. These complexes are characterized in the visible region by a moderately strong absorption which shows negative solvatochromism. On the basis of experimental and theoretical evidence the characteristic solvatochromic absorption band, due to the $\pi \rightarrow \pi^*$ HOMO–LUMO transition, has been assigned to a mixed metal/ligand to ligand CT (MMLLCT) transition, having the HOMO mixed metal–ligand character with prevailing contribution from the dithiolene ligand, and the LUMO ligand character with prevailing diimine contribution. The composition of the frontier orbitals is in agreement with the reduction potentials which depend on the nature of the diimine whereas the oxidation potentials are mostly affected by the dithiolate ligand.

A number of platinum diimine–dithiolene complexes display long-lived solution and solid-state luminescence in ambient conditions and in frozen solvent glasses. A linear correlation has been found between emission energies and the difference in the ground-state redox potentials. These results provide the tools for tuning and systematically controlling

SOMO

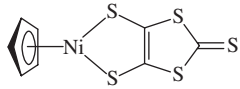

(**33**)

FIGURE 8. Singly occupied molecular orbital of [CpNi(dmit)]. Reproduced by permission of The Royal Society of Chemistry from Reference 47

the emission properties through ligand variation on changing the electron donating and accepting properties of the ligands. In addition, the influence of the metal on the excited-state properties has been investigated: the Ni(II), Pd(II) and Au(III) complexes do not show solution emission, suggesting that: (i) the third-row Pt(II) ion compared to Ni(II) and Pd(II) provides a more efficient intersystem crossing to the triplet state and lowers the nonradiative decay pathway[49a]; (ii) the increased charge on d^8 Au(III) orbitals lowers the energy of $d\sigma^*$ orbitals enough to favor a nonradiative decay involving d–d states in spite of CT–diimine states[49c].

The solvatochromism of the intense low-frequency CT absorption of the d^8 metal diimine–dithiolate complexes of Pt, Pd and Ni suggested that these complexes were second-order NLO chromophores[50]. The magnitude of the molecular first hyperpolarizability, determined from electric-field-induced second-harmonic generation experiments (EFISH) at 1.9 μm, ranges from 0 to -39×10^{-30} esu. This value depends on the CT absorption band wavelength, the oscillator strength and the variation of the dipole moment between the ground and the excited state. The resonance forms **34**–**36** are provided to depict qualitatively the HOMO, the excited state and the LUMO, respectively. In the charge-transferred state the complex has a smaller dipole moment than in the ground state, since the ligand-to-ligand axis is collinear but opposite to the ground-state dipole of the molecule. This difference, being the excited state less polar than the ground state, determines the negative solvatochromism and value of β. These properties have been interpreted following the simplification of the two-state model, which takes into account a single excited state, through the relationship: $\beta \propto \mu_{ge}^2 \times \Delta\mu / E_{ge}^2$, where β is the molecular hyperpolarizability, μ_{ge} the transition dipole moment between the first excited and the ground states, $\Delta\mu$ the difference between the dipole moment of the ground and excited states and E_{ge} the energy of the absorption band.

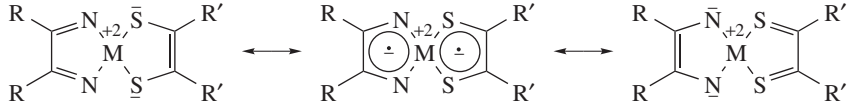

(**34**) (**35**) (**36**)

The influence of the extent of the charge-separated ground-state structure on the second-order polarizability has been investigated in platinum phenanthroline–dithiolate complexes containing sterically demanding groups (**37**, dtoc = 1,2-dithiolato-*closo*-1,2-dicarbadodecaborane) and on substituting S atoms (**38**) with O (**39**). Charge separation is in the order **37** < **38** < **39**. It was found that the chromophore bearing an O–O ligand exhibits increased charge-separated character and larger polarizability relative to the corresponding S–S one[51].

With a view to relating the second-order nonlinear properties with the charge-separated character of the complexes, an analysis of ground-state (μ_g) and excited-state (μ_e) dipole moments on a series of structurally characterized acceptor (trifluoromethyl or cyano groups) substituted nickel(diimine)(dithiolate) has been performed[52]. Most of the investigated complexes show an absorption in the visible region with medium-to-low molar absorption coefficients (in the 6000 to 13000 $M^{-1}\,cm^{-1}$ range) and a large negative solvatochromism, in accordance with the dipole moment changes between the excited and the ground state. Some of the complexes investigated exhibit absorption at longer wavelengths, with relatively large molar absorption coefficients (in the 12000 to 19000 $M^{-1}\,cm^{-1}$ range), small dipole moment change and unusually low solvatochromism. This behavior has been explained by taking into account a higher degree of π-delocalization inside the (N=C–C=N)Ni(S–C=C–S) core, influenced by the substituents and reflected

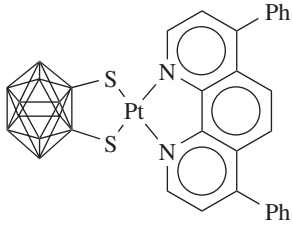

(**37**) [Pt(dpphen)(dtoc)]

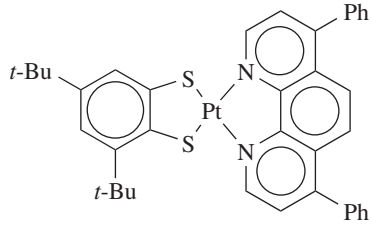

(**38**) [Pt(dpphen)(dtbdt)]

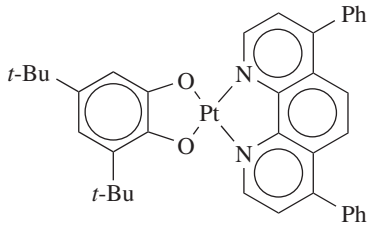

(**39**) [Pt(dpphen)(dtbc)]

by shorter NiN_2 and NiS_2 distances as compared to similar complexes exhibiting large solvatochromic shifts. This implies that the LUMO of **36** contributes to the ground-state structure, providing a cyanide-like character to these chromophores and reducing the dipole difference between the ground and the excited state (as found experimentally) $\Delta\mu$ from -4 to -6 debye.

Experimental and theoretical[53,54] investigations, based on increasingly sophisticated methods (solid-state sulfur K-edge X-ray absorption spectroscopy[53], vibrational spectra[54a], studies to relate aromaticity with CT transitions[54b] and time-dependent DFT[54c]), of the excited singlet and triplet state of [Pt(II)(diimine)(dithiolato)] systems provided additional details in the elucidation of the nature of their bonding and of the photophysical properties. The reactivity of [M(II)(diimine)(dithiolato)] (M = Ni, Pd, Pt) toward oxidation has been interpreted using the Fukui function, which provides information on the local softness and is widely used to investigate the factors that affect the reactivity of the different sites of organic molecules toward different reagents, by applying locally the hard–soft acid–base (HSAB) principle[55]. It was found that the sulfur atoms in the complexes are the preferred site for electrophilic attack, and in the M = Ni, Pd, Pt series, the sulfur atoms of nickel derivatives are less favorable to electrophilic attack. Accordingly, the photochemical oxidations of [M(bpy)(bdt)] (bpy = 2,2′-bipyridine, bdt = benzene-1,2-dithiolate), giving a monosulfinato complex when M = Pt and Pd, and a mixture of octahedral disulfonate complex and a dimetallic complex when M = Ni, have been explained. It also predicted that the nucleophilicity of the sulfur atoms would be responsible through soft–soft interactions with electrophilic centers of the crystal packing. Interestingly, the oxidation products of the neutral complexes, where diimine = 4,4′-di-*t*-butylpyridine and dithiolato was 3,6-bis(trimethylsilyl)-1,2-benzenedithiolate or 1,2-bis(4-*t*-butylphenyl)ethylene-1,2-dithiolate, have been recently obtained as monomeric monocations with a spin 1/2 ground state[53]. The monomers are in equilibrium with diamagnetic dimers, and the crystal structure of the dimer based on the ethylene-1,2-dithiolate derivative has been solved. This represents the first example of a structurally characterized diimine–dithiolene containing complex where the dithiolene ligand bears a 1− formal charge (Figure 9)[53].

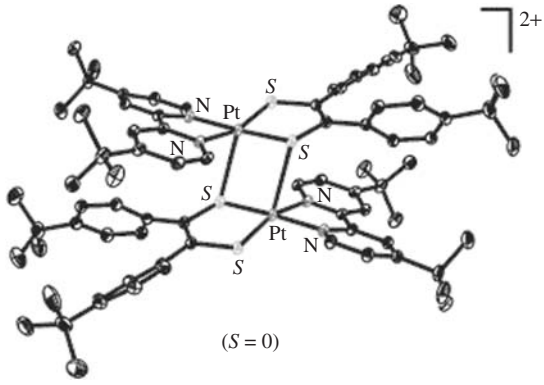

FIGURE 9. Detail of the binuclear dication in the crystal structure of $[Pt(4,4'\text{-}t\text{-}Bu_2byp)L]_2(PF_6)_2$ (L = 1,2-bis(4-*t*-butylphenyl)ethylene-1,2-dithiolate). Reprinted with permission from Reference 53. Copyright 2007 American Chemical Society

Experimental results converge in assigning the one-electron oxidation to a ligand-centered process involving the dithiolato ligand. It would be interesting to calculate the local softness parameters to verify whether the electrophilic and nucleophilic sites are in agreement with dimer formation. A partial oxidated form of dimers has been previously found as reaction product of a similar diimine–dithiolate complex [Pt(dmid)(dbbpy)] (dbbpy = 4,4′-di-*t*-butyl-2,2′-bipyridine) or similar acceptors, which undergo 2:1 donor: acceptor stacking in the solid state. X-ray data of the salt $[Pt(dmid)(dbbpy)]_2(tcnq)$ suggest partial CT from the donor $[Pt(dmid)(dbbpy)]_2$ to the acceptor tcnq[56]. Unusually for platinum diimmide–dithiolato complexes[49], [Pt(dmid)(dbbpy)] was reported as nonluminescent in the explored wavelength range.

2. Complexes with different dithiolene ligands

Relatively fewer examples of d^8 metal dithiolenes $[(R_2C_2S_2)M(S_2C_2R'_2)]$ with $R \neq R'$ than with $R = R'$ have been reported so far. Preparative methods based on symmetrical precursors as reagents are summarized for nickel in equations 6–9, where $L = R_2C_2S_2$, $L' = R'_2C_2S_2$ and $R \neq R'$; these reactions are reported to work similarly for the other d^8 divalent metals. These reactions involve ligand scrambling reactions complicated by competing redox reactions of the symmetrical precursors and/or ligand substitutions reactions. These complications were recognized since the early studies by McCleverty and coworkers[57a], who were able to isolate mixed ligand complexes by mixing the symmetrical monoanionic complexes based on the ligands L = phdt, L′ = tfd and L′ = mnt through reaction in equation 6. It has been reported[57b] that mixing symmetrical neutral precursors for L = phdt and L′ = tfd, as shown in equation 7, affords the mixed-ligand compound in shorter reaction times. Mixed-ligand complexes were also obtained through reaction in equation 8, for L = phdt and L′ = mnt, obtaining satisfactorily pure salts of the $[Ni(phdt)(mnt)]^{1-}$ and $[Ni(phdt)(tfd)]^{1-}$ anionic complexes. Fast isolation and purification of the mixed-ligand complexes was recommended to avoid formation of an equilibrium mixture of asymmetrical and symmetrical complexes[57a]. Mixed-ligand complexes show properties intermediate to those of symmetrical precursors. In Table 4 the electrochemical properties of asymmetrical $[Ni(L)(L')]^z$ complexes are compared with those of their

TABLE 4. Cyclic voltammetric data* of asymmetrical $[Ni(L)(L')]^z$ complexes and their symmetrical precursors

Compound	E_a (V) [a]	$E_{1/2}$ (V) [b]	$E_{1/2}$ (V) [c]	References
$[Ni(1,4\text{-}Me_2pipdt)_2]^{2+}$	+0.4 [d]	−0.96	−1.26	10
$[Ni(1,3\text{-}i\text{-}Pr_2timdt)_2]$	+0.78 [d]	−0.100 [e]	−0.598	15
$[Ni(tdas)_2]^{2-}$		+0.80 [a]	+0.18	19
$[Ni(dmit)_2]^{2-}$		+0.316 [a]	−0.109	18
$[Ni(mnt)_2]^{2-}$		+1.110 [a]	+0.270	18
$[Ni(dddt)_2]^{2-}$		+0.105	−0.645	58
$[Ni(1,3\text{-}i\text{-}Pr_2timdt)(dmit)]^{1-}$	+1.154	n.o. [f]	−0.402	12
$[Ni(1,3\text{-}i\text{-}Pr_2timdt)(mnt)]$	+1.160	+0.354	−0.307	12
$[Ni(1,4\text{-}Me_2pipdt)(dmit)]$	+0.590	−0.593 [e]	−1.165 [e]	12
$[Ni(1,4\text{-}Me_2pipdt)(mnt)]$	+0.900	−0.530	−0.970	59a
$[Ni(1,4\text{-}Me_2pipdt)(tdas)]$	+0.820	−0.582	−1.034	59a
$[Ni(mnt)(dmit)]^{1-}$		+0.73 [a]	+0.06	60a
$[Ni(mnt)(dddt)]^{1-}$		+0.51 [a]	−0.26	60a
$[Ni(dddt)(dmit)]^{1-}$		+0.23 [a]	−0.38	60a
$[Ni(edt)_2]^{2-}$		+0.135	−0.905	6
$[Ni(edt\text{-}CN)_2]^{2-}$		+0.695	−0.265	61
$[Ni(tfd)_2]^{2-}$		+0.53 [g]	−0.51 [g]	62
$[Ni(mnt)_2]^{2-}$		+0.63 [g]	−0.16 [g]	62
$[Ni(tfadt)_2]^{2-}$		+0.51 [g]	−0.45 [g]	62

* Measured at Pt electrode in CH_3CN, reference electrode Ag/AgCl.
[a] For the irreversible process $[ML_2]^0 \rightarrow [ML_2]^{1+} + e^-$.
[b] For the reversible process $[ML_2]^0 + e^- \rightleftharpoons [ML_2]^{1-}$.
[c] For the reversible process $[ML_2]^{1-} + e^- \rightleftharpoons [ML_2]^{2-}$.
[d] For the reversible process $[ML_2]^0 \rightleftharpoons [ML_2]^{1+} + e^-$.
[e] Quasi-reversible one-electron reduction.
[f] Not observed.
[g] Measurements performed in CH_2Cl_2 solutions; E (V) *vs.* Fc/Fc^+.

symmetrical precursors.

$$[Ni(L)_2]^{1-} + [Ni(L')_2]^{1-} \longrightarrow 2[Ni(L)(L')]^{1-} \quad (6)$$

$$[Ni(L)_2] + [Ni(L')_2] \longrightarrow 2[Ni(L)(L')] \quad (7)$$

$$[Ni(L)_2] + [Ni(L')_2]^{2-} \longrightarrow 2[Ni(L)(L')]^{1-} \quad (8)$$

$$[Ni(L)_2]^{2+} + [Ni(L')_2]^{2-} \longrightarrow 2[Ni(L)(L')] \quad (9)$$

More recently, several complexes have been obtained by equation 6 in 50–80% yields[60]: $[M(dmit)(mnt)]^{1-}$ (M = Ni, Pd and Pt); $[Ni(dddt)(mnt)]^{1-}$; $[Ni(dddse)(mnt)]^{1-}$; $[Ni(dsit)(mnt)]^{1-}$; $[Ni(dmse)(mnt)]^{1-}$; $[Ni(dddt)(dmit)]^{1-}$; $[Ni(dddse)(dmit)]^{1-}$; $[Ni(dmid)(dmit)]^{1-}$ $[Ni(tdas)(dmit)]^{1-}$; $[Ni(tdas)(dddse)]^{1-}$ (dddse = 5,6-dihydro-1,4-dithine-2,3-diselenolate, the Se analogue of dddt). The products have been purified by reversed-phase column chromatography, using aqueous acetonitrile as eluent. In this case no back reaction yielding symmetrical complexes has been observed; $[Ni(dmit)(mnt)]^{1-}$ and $[Ni(tdas)(dmit)]^{1-}$ have been used as counterions to prepare CT salts based on tetrathiafulvalene-cation derivatives. The obtained salts exhibit metallic behavior down to low temperature[60].

The method of equation 8 may work either as a two-step reaction implying a preliminary redox step with subsequent scrambling of the ligands, or simply as a metathesis. By reacting the neutral $[Ni(1,3\text{-}i\text{-}Pr_2timdt)_2]$ with the dianions $[Ni(dmit)_2]^{2-}$ and

$[Ni(mnt)_2]^{2-}$, the monoanionic asymmetrical dithiolene complexes $[Bu_4N][Ni(1,3\text{-}i\text{-}Pr_2timdt)(dmit)]$ and $[Bu_4N][Ni(1,3\text{-}i\text{-}Pr_2timdt)(mnt)]$ have been obtained in high yields[18]. In the reaction of $[Ni(1,3\text{-}i\text{-}Pr_2timdt)_2]$ and $[Ni(dmit)_2]^{2-}$, formation of symmetrical monoanionic species has been recognized spectrophotometrically (peaks at 1400 and 1130 nm for $[Ni(1,3\text{-}i\text{-}Pr_2timdt)_2]^{1-}$ and $[Ni(dmit)_2]^{1-}$, respectively). These species undergo slow ligand scrambling leading to the mixed-ligand derivative (the reaction is complete in five hours). In the corresponding reaction employing $[Ni(mnt)_2]^{2-}$, which would require a stronger oxidating species than $[Ni(1,3\text{-}i\text{-}Pr_2timdt)_2]$, no symmetrical monoanions are observed. A ligand substitution reaction may be invoked to explain the formation of the mixed-ligand derivative.

Equation 9 requires dicationic and dianionic complexes. Several stable dianionic complexes are available, while among the less common dicationic complexes, $[Ni(1,4\text{-}R_2pipdt)_2]^{2+}$ have proved to be valuable precursors in the synthesis of stable mixed-ligand complexes. This reaction is very effective, with almost quantitative yields of several mixed-ligand derivatives[59].

The alternative methods shown in equations 10[63] and 11[64] have also been used. The effectiveness of the synthetic methods in equations 6–11 depends on the availability of reagents as well as the stability of the products. The solvent may have an important role in determining the reaction products, because it affects the redox potential of the complexes and also their solubility. Formation of sparingly soluble salts may explain why, differently to the expected general trend of similar behavior in the Ni–Pd–Pt triad, the method of equation 9 does not usually lead to the mixed-ligand complexes in the Pd and Pt cases, but to salts containing a stack of alternating anion and cation complexes along one direction (see Section IV.E).

$$[Ni(mnt)(NH_3)_2] + 1,4\text{-}R_2pipdt \longrightarrow [Ni(mnt)(1,4\text{-}R_2pipdt)] + 2\ NH_3 \qquad (10)$$

$$[Pd(1,3\text{-}Et_2timdt)Br_2] + Na_2mnt \longrightarrow [Pd(1,3\text{-}Et_2timdt)(mnt)] + 2\ NaBr \qquad (11)$$

The potential of nickel mixed-ligand dithiolene complexes, containing two ligands of significantly different electron-withdrawing capability, to behave as intervalence compounds where the ligand occurs in formally different oxidation states, was recognized by Vogler and Kunkely since the early 1980s[65]. In these complexes one ligand is reducing (dithiolate, HOMO at high energy, prevailing contribution of the pull ligand), and the other is oxidizing (dithione, LUMO at low energy, prevailing contribution of the push ligand), similarly to what happens in the diimine–dithiolato case[66]. The HOMO–LUMO transition has ligand-to-ligand CT character mediated by the coordinated metal. The resonance forms **40**–**42** are shown to depict qualitatively the HOMO, the excited state and the LUMO of these complexes, similarly to the diimine–dithiolato case. Where, although asymmetric, the complexes have comparable electron-withdrawing capability of the two different ligands, they compare better with the symmetric analogues for which the overall delocalized resonance form **41** to describe the ground state is most appropriate.

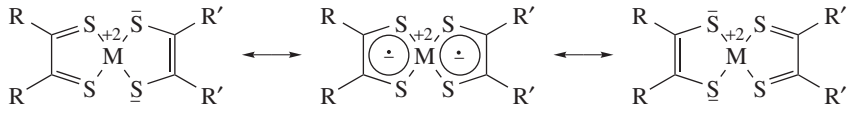

(**40**) (**41**) (**42**)

Complexes with ground state describable with the limiting form **40** show an absorption in the visible region with medium-to-low molar absorption coefficients and a large negative solvatochromism, in accordance with the dipole moment changes between the excited

TABLE 5. Optical data and dipole analysis of asymmetrical [Ni(L)(L′)] complexes

Ligands [a]	λ_{max} (nm) ε ($M^{-1}\,cm^{-1}$)	μ_{eg} (debye)	μ_g (debye)	$\mu_e - \mu_g$ (debye)	β_0 [b] (10^{-30} esu)	References
L = 1,4-(EH)$_2$pipdt [c]	829					
		3.7	16	−10	−37	63
L′ = mnt	9800					
L = 1,4-(EH)$_2$pipdt [c]	840					
		3.6	13	−8	−20	63
L′ = tdf	8700					
L = btmpedt [d]	842					
		5.9	6	1	+5	63
L′ = tfd	19000					
L = 1,3-*i*-Pr$_2$timdt	883					
		6.7	16	≈0	≈0	18
L′ = mnt	24100					
L = 1,4-*i*-Pr$_2$pipdt	965					
		5.9	13	−11	−130	59a
L′ = dmit	10900					

[a] The different nature of the two ligands in the complex allows one of them to be taken mostly as a dithione (L) and the other as a dithiolate (L′); see Section III.C.2, in particular resonance forms **40**–**42**.
[b] β_0 is the zero frequency term of β (molecular first-order hyperpolarizability).
[c] 1,4-(EH)$_2$pipdt = 1,4-bis(2-ethylhexyl)piperazine-2,3-dithione.
[d] btmpedt = 1,2-bis(3,4,5-trimethoxyphenyl)ethylene-1,2-dithiolate.

and the ground state. Complexes with ground state describable with the limiting form **41** exhibit absorption at longer wavelengths, with relatively large molar absorption coefficients (see Table 5), small dipole moment change and unusually low solvatochromism. The prevailing contribution in the ground state either of the resonance form **40** or of **41** is corroborated from the other associated spectroscopic, electrochemical properties and structural data. Electrochemical data show that in asymmetrical Ni dithiolenes with high delocalization, the reduction processes are intermediate between those of the symmetrical precursors, and in those describable as dithione–dithiolates similar values of reduction potentials for complexes bearing the same push ligand and oxidation potentials depending on the pull ligand are found, suggesting an unbalanced contribution of the two ligands to the frontier orbitals.

Also, FT-IR and Raman spectra help in evaluating the extent of electron delocalization in the two classes of complexes through the ν(C=C) marker, for which well established assignments are available, for example, 1485 cm^{-1} ($z = 2-$) and 1435 cm^{-1} ($z = 1-$)[23a, 23b] for $[Ni(mnt)_2]^z$, and 1435 cm^{-1} ($z = 2-$) and 1390 cm^{-1} ($z = 1-$)[29c] for $[Ni(dmit)_2]^z \cdot$ [Ni(1,4-Me$_2$pipdt)(mnt)] exhibits a peak at 1492 cm^{-1} and [Ni(1,4-R$_2$pipdt)(dmit)] at 1430 (R = Me) and 1440 (R = *i*-Pr) cm^{-1}, as found for the $z = 2-$ symmetrical complexes[63]. Instead, [Ni(1,3-*i*-Pr$_2$timdt)(mnt)] and [Ni(1,3-*i*-Pr$_2$timdt)(dmit)] exhibit a peak at 1425 cm^{-1} and at 1388 cm^{-1}, respectively, as found in the 1− symmetrical complexes[18]. Accordingly, dmit and mnt ligands bear more negative charge than 1,3-*i*-Pr$_2$timdt, but this asymmetrical charge distribution occurs to a lower extent than in the corresponding 1,4-R$_2$pipdt complexes. X-ray structural results provide further useful information. While there is no substantial difference between the four Ni−S coordination bond distances (2.146(2) to 2.173(2) Å), in complexes with putative ground state **40** the two vicinal C−S bonds are shorter (1.675(11) to 1.700(6) Å) and the intermediate C−C bond longer (1.433(3) to 1.50(2) Å) in the dithiolene ligands labeled L in Table 5, as compared to those labeled L′ (d(C−S) *ca* 1.734(12) Å and d(C−C) *ca* 1.34(2) Å). Structural

data available for the Ni complex with L = btmpedt and L′ = tfd with putative ground state **41** show that the C−S and C−C bonds are comparable (d(C−S) = 1.704(4) Å in L and 1.712(4) Å in L′; d(C−C) = 1.410(5) Å in L and 1.366(6) Å in L′).

A summary of optical data and of dipole analysis on representative examples appears in Table 5. Chen and coworkers explained the different behavior of unsymmetrical complexes describable mainly as dithione–dithiolato [Ni(1,4-R_2pipdt)(tdf)] (**40**) and overall delocalized [Ni(btmpedt)(tdf)] (**41**) dithiolenes[63]. Two dipoles will contribute to μ_g in these complexes: one arising from the periphery of the molecule (from the donor to the acceptor substituents), the other one originating from the metal to the dithiolato sulfurs, when the resonance form **40** is prevalent in the ground state. While the first component will remain essentially unchanged, the second dipole component will change upon excitation due to the charge-transfer transition from the dithiolate to the dithione ligand. Instead, for complexes with a nearly symmetrical charge distribution at the $(C_2S_2)Ni(S_2C_2)$ core, also the second component will remain almost unchanged. Interestingly, a different NLO response is observed for asymmetrical dithiolenes where both complexes are coordinated to one ligand bearing a potential NR donor group but inserted in a five-membered (1,3-*i*-Pr_2timdt) or six-membered ring (1,4-R_2pipdt) and to one electron-withdrawing ligand (dmit, mnt): an almost null β_0 value accompanied by a large dipole moment of the ground state, related to the presence of the dipole arising from the periphery of the molecule for the complex [Ni(1,3-*i*-Pr_2timdt)(mnt)] (**43**), and a negative β_0 with a slightly smaller dipole moment for the complex [Ni(1,4-*i*-Pr_2pipdt)(dmit)] (**44**). No experimental data for [Ni(1,3-*i*-Pr_2timdt)(dmit)] based on solvatochromic measurement are available due to the very low solubility of the species in polar solvents.

DFT calculations on model compounds **45**–**48**, where hydrogen atoms replace the alkyl groups of 1,4-R_2pipdt and 1,3-R_2timdt (Figure 10), allowed elucidation of this behavior. Moreover, analysis of the calculated first molecular hyperpolarizabilities and their components with the two-state approximation accounts for the various NLO responses in terms of the important following components: the transition dipole moment between the first excited and the ground states (μ_{ge}^2), the difference between the dipole moment of the ground and of the excited state ($\Delta\mu$) and the energy of the absorption band. The derived picture highlights the different roles of the two push and pull ligands, but also the peculiar perturbation of the π-electron density induced by the terminal CS_3 group of the dmit ligand, which induces major differences between the ground and excited states. The frontier MOs are shown in Figure 10. Similarly to symmetric complexes, the HOMOs and LUMOs of the models **45**–**48** are still i.p. and o.o.p. combinations of the critical C_2S_2 frontier π-orbital but the atomic contributions are now unbalanced, particularly when the ligand 1,4-H_2pipdt is present. In fact, the greater weight of the latter in the LUMO is evident from comparison of the HOMO and LUMO drawings of **45** and **46**. Another important aspect is the scarce contribution of the terminal CS_3 moiety of dmit to the LUMO of both complexes **45** and **47**. Thus while the p_π orbital populations change more at the core than at the peripheral atoms, the terminal S atom of the dmit ligand is significantly less populated in the excited state. Therefore, also the dipole component arising from the periphery of the molecule will change upon excitation. This explains why nonzero NLO properties are predicted for the complex **48** which exhibits the highest delocalization, thus the lower charge-separated character in the ground state, almost comparable with the symmetric analogues. The unique role of dmit ligand in perturbing the electron distribution at the dithiolene core and in inducing major differences between the ground and excited states explains the peculiarity of mixed-ligand complexes based on dmit. This shows that the simplifying assumption, that the variation of the dipolar component arising from the periphery of the molecule upon excitation is constant, is not generally applicable, and that mixed-ligand complexes based on dmit seem promising optimal candidates to induce NLO properties at the molecular level[12].

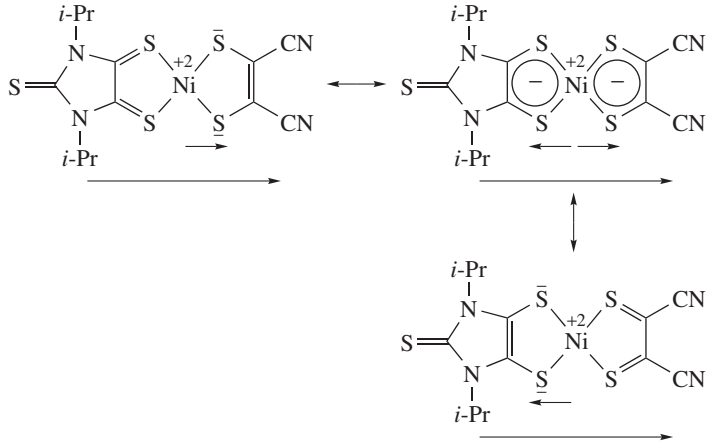

(**43**)

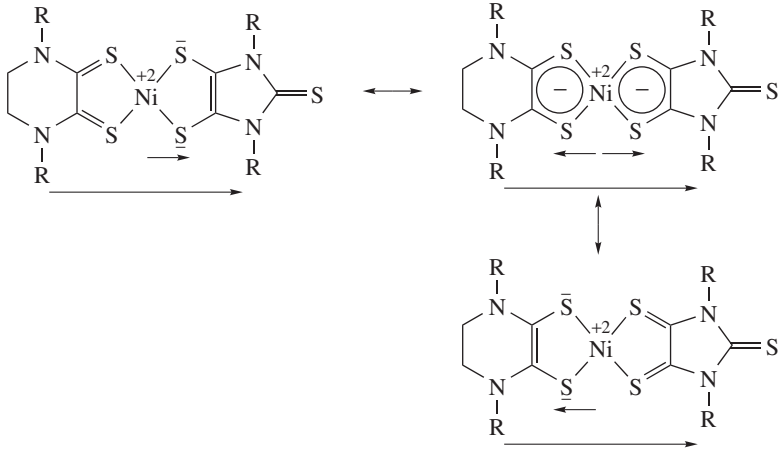

(**44**)

3. Complexes with different substituents at the same C_2S_2 moiety

Complexes based on asymmetrical dithiolenes bearing outer functional groups have been recently designed to promote formation of extended networks either through hydrogen bonds between these building blocks or through covalent bonds toward various coordinatively unsaturated metal ions with a view to building multicomponent molecular systems. For example, the nickel complex of maleamide dithiolate, containing outer CN and NH groups, forms an extended network where hydrogen bonds determine the supramolecular organization[67] (see Figure 11).

Formigué and coworkers have successfully prepared asymmetrically substituted dithiolenes such as edt-CN (edt-CN = 2-cyano-1,2-ethylenedithiolate), tfadt and their square-planar nickel (**49** and **50**) and gold complexes[61,62]. Both *cis* and *trans* isomers coexist and interconvert in solutions, while in the solid state the *trans* form is more commonly

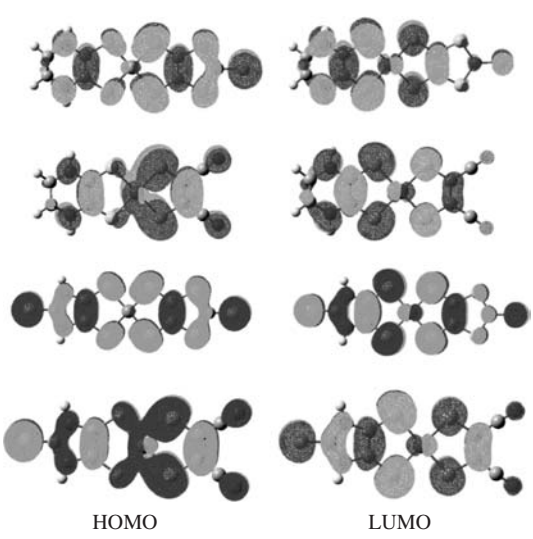

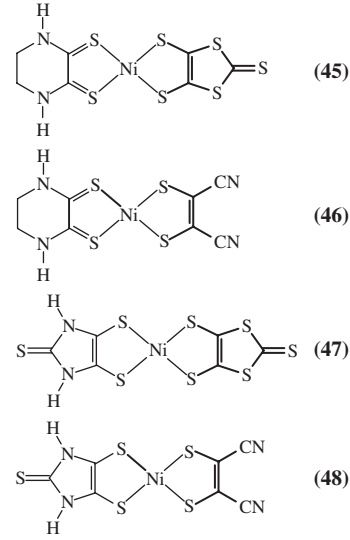

(45) **(46)** **(47)** **(48)**

FIGURE 10. Frontier orbitals of model complexes **45**–**48**, where hydrogen atoms replace the alkyl groups of ligands 1,4-R_2pipdt and 1,3-R_2timdt. Reprinted with permission from Reference 12. Copyright 2004 American Chemical Society

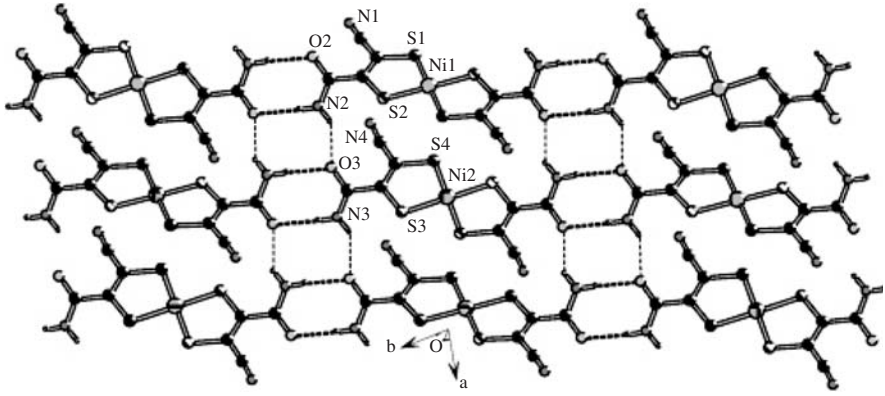

FIGURE 11. Hydrogen bonding (- - -) in $(Ph_4P)[Ni(mant)_2]$ (madt = maleamide dithiolate). Reprinted with permission from Reference 67. Copyright 2005 American Chemical Society

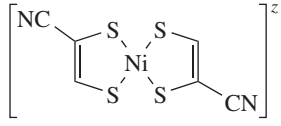

(**49**) $[Ni(edt\text{-}CN)_2]^z$, $z = 2-,1-\cdot$

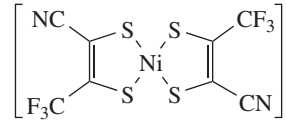

(**50**) $[Ni(tfadt)_2]^z$, $z = 2-,1-\cdot$

isolated. Both the *cis* and *trans* isomers of the square-planar Au(III) complex of tfadt have been isolated as Bu_4N^+ salts[62b].

As observed for the mixed-ligand complexes, the asymmetrically substituted dithiolenes exhibit electrochemical properties intermediate with respect to those of complexes of symmetrically substituted ligands. This provides a wider choice of paramagnetic monoanionic radical anions, while preserving coordinating properties with outer functionalities, to be used as building blocks of multifunctional materials (see Section IV). New $(Ph_4P)[Au(III)(dithiolene)_2]$ complexes with asymmetrically substituted dithiolene ligands ($RR'C_2S_2$; R = H, R′ = Ph, 2-Pyr, 3-Pyr, 4-Pyr) have been prepared and characterized. The *cis* and *trans* isomers have been isolated for the R′ = Ph and 2-Pyr; both isomers are present in solution but do not interconvert at room temperature[68]. The potential of the pyridine outer groups in promoting structural organization of these complexes has yet to be investigated.

IV. MOLECULAR CONDUCTORS, MAGNETS AND CONDUCTING/MAGNETIC HYBRID MATERIALS

A. Background

The synthesis of the first organic molecular metal (ttf)(tcnq)[69] (**51a**)(**52**) showing a metallic state down to 55 K and the subsequent discovery of superconductivity in $(tmtsf)_2PF_6$ (tmtsf = tetramethyltetraselenofulvalene, **51b**)[70], where a 2-D network was formed by short Se···Se contacts between the tmtsf stacks, focused the attention of chemists and physicists on the potential of organic molecules as building units of conducting CT salts. Since then extensive effort has been devoted to prepare new types of molecular metals or superconductors based on ttf-type π donors. A significant advance in this context appeared by using bedtttf (**53**) as organic donor, which led to many examples of 2-D organic metals and superconductors with T_c values as high as 11.5 K[71].

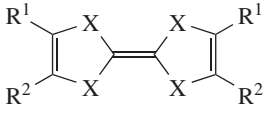

(**51**) (**a**) $R^1 = R^2$ = H, X = S; ttf
(**b**) $R^1 = R^2$ = Me, X = Se; tmtsf

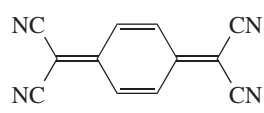

(**52**) tcnq

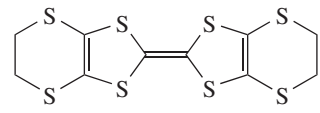

(**53**) bedtttf

The discovery in 1986 of the first molecular superconductor containing a metal–dithiolene complex $(ttf)[Ni(dmit)_2]_2$[30] (T_c = 1.6 K at P = 7 kB) and the subsequent discovery of superconductivity (T_c = 1.3 K at ambient pressure) in α-(edtttf)$[Ni(dmit)_2]$ (edtttf = ethylenedithiotetrathiafulvalene)[72] renewed interest in metal–dithiolene complexes as building blocks for new molecular conductors. These complexes can be viewed as the inorganic analogues of ttf-type donors where the transition metal replaces the central C=C bond of ttf. They are more versatile than the isosteric donors because in some cases they are directly responsible for the occurrence of the metallic or even superconducting state, while in other cases, depending on the metal, they can exhibit peculiar magnetic properties. Although in terms of molecular architecture the $[M(dmit)_2]$ molecule, where the central electron-delocalized core is extended by the sulfur-containing heterocycles, is similar to the bedtttf donor, the transverse interactions were found to be weaker than expected and unable to realize a 2-D network, and therefore the superconductivity was stablilized only at very low temperatures. The $[M(dmit)_2]$ (M = Ni, Pd) superconductors thus occupy a unique position, because almost all molecular superconductors were formed by

organic π donor molecules having ttf-like skeletons. The molecular superconductors based on $[M(dmit)_2]$ (M = Ni, Pd) complexes synthesized up to date are reported elsewhere[1a]. Other important milestones were: (i) the synthesis of two bulk ferromagnetic complexes: $(NH_4)[Ni(mnt)_2]\cdot H_2O$[73] consists of uniform stacks of planar $[Ni(mnt)_2]$ complexes separated by ammonium cations (which favor uniform stacking due to their small size) and it is an insulator showing antiferromagnetic order at $T > 100$ K, ferromagnetic coupling below this temperature and ferromagnetic ordering at $T < 5$ K; $[Cp_2^*\ Mn][Ni(mnt)_2]$[74], consisting of $\cdots C^+C^+A^-A^-C^+C^+A^-A^-\cdots$ stacks of side-by-side cations (C^+) alternating with dyads of anions (A^-), is a semiconductor with ferromagnetic ordering at $T < 2.5$ K; (ii) the synthesis of the $(per)_2[M(mnt)_2]$ (M = Fe, Co, Ni, Pd, Pt, Cu, Au; per = perylene, **54**) family[75], the first examples of paramagnetic molecular metals. In these compounds, $[M(mnt)_2]$ complexes form chains of localized spin units while the conducting properties are due to segregated perylene stacks; α-$(per)_2[M(mnt)_2]$ phases have a similar structure, with segregated stacks of perylene and $[M(mnt)_2]$ units along the stacking b-axis. They show high room-temperature conductivity along the stacking axis ranging from 700 $S\,cm^{-1}$ for M = Ni, Pt, Cu, Au to 300 $S\,cm^{-1}$ for M = Pd and 200 $S\,cm^{-1}$ for M = Fe, Co compounds. The magnetic behavior of these compounds strongly depends on the metal. These salts have been extensively investigated by Almeida and coworkers[76], in particular to study the origin of the metal-to-insulator (MI) transition and its variations, essentially depending on the nature of the metal in the dithiolene complex. A major problem associated with dithiolene complexes is their insulating instability at low temperature due to MI transition caused by Peierls-type dimerization along the chains[77] (these compounds usually crystallize forming stacks of complexes which give rise to quasi-1-D, electronic systems) preventing the occurrence of either the metallic state or superconductivity[78,79]. The Peierls distortion may be suppressed by increasing the dimensionality of the systems through lateral interactions. This can be obtained by either increasing the number of peripheral sulfur atoms in the ligand framework, or changing from sulfur to selenium ligand analogues.

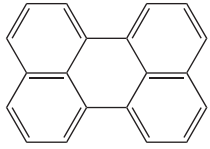

(**54**) Perylene

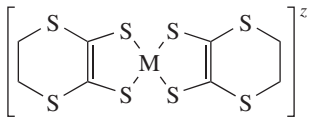

(**55**) $[M(dddt)_2]^z$, z = 2–, 1–, 0, fractional and 1+

Despite the Peierls distortion limitation, metal–dithiolene complexes can provide unique examples of novel low-dimensional materials exhibiting interesting conducting and/or magnetic properties. Some relevant examples are: (i) highly conducting and metallic single-component materials; (ii) magnetic materials such as ferromagnets, ferrimagnets, metamagnets and spin ladders (molecular systems consisting of assemblies of $S = 1/2$ chains, one next to the other) in addition to other systems suitable for the study of magnetic ordering and (iii) multifunctional hybrid materials with conducting and magnetic components. The main results achieved in these areas have been reviewed by Cassoux and Faulmann[1a] and Robertson[8] separately which focused on $[M(dmit)_2]$ and isologs, $[M(mnt)_2]$, $[M(dddt)_2]$ (**55**) systems and by Kato[80] which analyzed the electronic structure of some of these systems, especially $[M(dmit)_2]$, by discussing the two-MO picture—the interplay of the HOMO and LUMO—associated with the small HOMO–LUMO level splitting which is an essential part of the electronic structure. Geometrical aspects such as dimensionality, dimerization and frustration as well as the pressure effect on crystal and electronic structures of these systems and on their metallic and superconducting

states have been also discussed. The single-component molecular metals with extended-ttf dithiolate ligands have been recently reviewed by Kobayashi and coworkers[81].

An update of the cited reviews will be herein presented focusing on (i) the influence of intermolecular interactions, including fluorine, H-bonding and $\pi-\pi$ interactions; (ii) the role of the metal and geometrical characteristics such as size and shape of both the ligand (which can be properly tuned by chemical methods) and the counterion in determining the packing motif and thus the physical properties of the materials. Selected examples will be described of metal d^8-dithiolene-based compounds endowed with unusual structural features or physical properties when compared to analogous compounds reported in the literature. The crystal packing and physical properties of these compounds are summarized in Table 6 and clearly demonstrate why dithiolene complexes still remain the vast frontier of highly functionalized molecular systems.

B. Role of Fluorine Intermolecular Interactions

1. Fluorine segregation effects

Very weak interactions such as the fluorine van der Waals interactions are able to induce the formation of recurrent packing motifs in the solid state and also offer opportunities to isolate isostructural compounds with various electronic properties. The fluorine segregation effect has been investigated by Fourmigué and coworkers as a tool for controlling the solid-state organization of open-shell molecules, a prerequisite for controlling their electronic properties in the crystalline state. In this context, the $[Ni(dfpdt)_2]^{-\bullet}$ ($[Ni(\mathbf{20})_2]^{-\bullet}$) anionic complex was combined with the fluorinated bis(2,2-difluoropropylenedithio)-tetrathiafulvalene (bdfpdtttf) isosteric donor[97] to afford the 1:2 salt (bdfpdtttf)$[Ni(dfpdt)_2]_2$[82]. This salt shows a peculiar X-ray structure, isostructural with that of the donor, characterized by a strong segregation of the CF_2 moieties leading to the formation of a layered structure with fluorine-containing bilayers, with $F\cdots F$ distances within a layer close to twice the fluorine van der Waals radius. This compound is the first example of a salt of a ttf-type donor salt isosteric with the corresponding metal–dithiolene complex. A similar salt has been obtained through the bromine oxidation of a $[Ni(dddt)_2]^-$ complex in the presence of the isosteric bedtttf donor, but this salt is included as a very small fraction in the neutral $[Ni(dddt)_2]$ structure[98]. The structural control imposed by the fluorine segregation plays a crucial role in the formation of this salt. Single-crystal conductivity and magnetic susceptibility measurements show an insulating and diamagnetic behavior, respectively. The charge-transfer nature of this salt was inferred by Raman studies[99], which are especially sensitive to the charge state of the bedtttf molecule. In fact, an approximately linear correlation between the degree of CT and the two totally symmetric C=C stretching vibrations ν_2 and ν_3 in insulating, conducting and superconducting CT salts based on the bedtttf donor has been previously established[99].

The role of fluorine segregation control was also investigated in the preparation of the neutral $[M(dfpdt)_2]$ dithiolene complexes (M = Ni, Au)[83]. In the neutral complex $[Ni(dfpdt)_2]$ the striking segregation of the CF_2 groups forces the structure toward a 2-D layered arrangement highly unusual for neutral molecules. This 2-D layered structure is commonly observed in CT salts of the $(bedtttf)^{+\bullet}$ radical cation where it is stabilized by the overlap interactions of the open-shell species and the presence of partially filled conduction bands, but not in diamagnetic, closed-shell neutral molecules such as bedtttf[100] and $[Ni(dddt)_2]$[101]. Despite the observed 2-D layered structure, $[Ni(dfpdt)_2]$ is a closed-shell insulating compound. Similar structures could be also stabilized with open-shell molecules such as the neutral open-shell $[Au(dfpdt)_2]^{\bullet}$ complex which was obtained by electrocrystallization of the $(Bu_4N)[Au(dfpdt)_2]$ salt[83]. $[Au(dfpdt)_2]^{\bullet}$ is isostructural with the neutral bdfpdtttf donor molecule and the observed recurrent packing motif clearly

TABLE 6. Structural and physical properties of novel metal d^8 bi(1,2-dithiolene)-based compounds

Compound [a]	Packing	Electrical properties [b]	Magnetic properties [c]	References
[bdfpdtttf][Ni(**20**)$_2$]$_2$	Layered structure with fluorous bilayers	Insulator	Diamagnetic	82
[Ni(**20**)$_2$]	2-D layered structure	Insulator	—	83
[Au(**20**)$_2$]	Layered structure formed by 1-D stacks	Semiconductor ($\sigma_{rt} = 5.0 \times 10^{-2}$ S cm^{-1})	Weak Curie-type PM	83
[Au(α-tpdt)$_2$]	No structure available	Metal down to 15 K ($\sigma_{rt} = 6$ S cm^{-1})	Pauli PM (10–300 K)	84
(Bu_4N)[Ni(chdt)$_2$]	Sandwiched structure	—	AFM 1-D Heisenberg chain	85
(Bu_4N)[Ni(eodt)$_2$]	Sandwiched structure	—	Curie–Weiss PM	85
[Ni(eodt)$_2$]	No structure available	Metal down to 120 K (retained metallic state down to 6.0×10^{-1} K)	Pauli PM (120–300 K)	85
(Bu_4N)[Ni(dmstfdt)$_2$]	2-D layered structure	MI = 147 K	Curie–Weiss PM Weak F ($T_N = 20$ K)	86
(Ph_4P)$_2$[(tto)$_2$Ni$_3$(dddt)$_2$]	Layered structure	Semiconductor ($\sigma_{rt} = 1.0 \times 10^4$ S cm^{-1})	—	87
[bdta]$_2$[Cu(mnt)$_2$]	1-D ideal chain of discrete units	—	1-D Heisenberg AFM chains ($T = 2$–300 K)	88
[Pt(1,4-Me_2pipdt)$_2$] [Pt(mnt)$_2$]$_2$	Nonregular 1-D chain of anions	—	Magnetic phase transition at $T = 115$ K between an AFM alternating-exchange chain and AFM dimers	89
(Cp_2Fe)[Ni(tfadt)$_2$]	Uniform, dimerized or tetramerized chain	—	PM at $T > 250$ K; $T = 249$ K order–disorder transition (hysteresis, $\Delta T \approx 11$ K); 137 K tetramerization transition	90
[Cr(η^6-C_6H_6)$_2$] [Ni(dmox)$_2$]	3-D network formed by chains linked by H-bonds	—	Curie–Weiss PM for 1-D chains at $T > 10$ K; F transition at $T = 3.4$ K	91

(*continued overleaf*)

TABLE 6. (*continued*)

Compound [a]	Packing	Electrical properties [b]	Magnetic properties [c]	References
(*N*-(Bn)py)[Ni(α-tpdt)$_2$]	Alternated layers of anions and cations	—	Dominant F interactions Dominant AFM interactions PM down to 1.5 K	92
(*N*-(4-Br$C_6H_4CH_2$)py)[Ni(α-tpdt)$_2$]	Alternated layers of anions and cations	—	Dominant F interactions Dominant AFM interactions PM down to 1.5 K	92
(*N*-(4-F$C_6H_4CH_2$)py)[Ni(α-tpdt)$_2$]	Alternated layers of anions and cations	—	Dominant F interactions Dominant AFM interactions PM down to 1.5 K	92
[{(Mn(II)$_2$Mn(III)$_2$(hmp)$_6$(Me-CN)$_2$}{Pt(mnt)$_2$}$_4$][Pt(mnt)$_2$]$_2$	$[Mn_4]^{4-}$ units separated by 1-D double columns of $[Pt(mnt)_2]^{z-}$ units	Semiconductor ($\sigma_{rt} = 2.2 \times 10^{-1}$ S cm^{-1})	Single molecule magnet behavior	93
[Ni(dmf)$_6$][Ni(dsit)$_2$]$_2$	Chains of $[Ni(dsit)_2]_2^{2-}$ dimers surrounded by four parallel chains of $[Ni(dmf)_6]^{2+}$ cations	Semiconductor ($\sigma_{rt} = 1.0$ S cm^{-1})	Curie-type PM	94
(bedtttf)[Ni(tdas)$_2$]	Layered structure	Semiconductor ($\sigma_{rt} = 1.8 \times 10^{-2}$ S cm^{-1})	$S = 1/2$ P with weak AFM coupling	95
[Pt(1,4-Et$_2$pipdt)$_2$][Pt(mnt)$_2$]	Anion–cation 1-D stack	Photoconductor	—	96

[a] Abbreviations: bdfpdtttf = bis(2,2-difluoropropylenedithio)tetrathiafulvalene; chdt = cyclohexenotetrathiafulvalenedithiolate; dmox = 4,5-dimethoxybenzene-1,2-dithiolate; dmstfdt = dimethyldiselenadithiafulvalenedithiolate; eodt = ethylenedioxytetrathiafulvalenedithiolate.
[b] σ_{rt} is the electrical conductivity at room temperature.
[c] AFM = antiferromagnetic; F = ferromagnetic; PM = paramagnetic.

illustrates the efficiency of the CF_2 groups in promoting this kind of structure with fluorine segregation and formation of fluorine-containing bilayers. The crystal structure of $[Au(dfpdt)_2]^\bullet$ shows donor layers built from 1-D stacks along the *b* direction, very rare owing to the tendency of neutral, planar open-shell compounds to dimerize. For example, $[Au(dddt)_2]^\bullet$, of structure similar to that of bedtttf, consists of isolated diamagnetic dyads. The transport properties, measured along the stacking *b*-axis, show that $[Au(dfpdt)_2]^\bullet$ is a semiconductor with room-temperature conductivity $\sigma_{rt} = 5.0 \times 10^{-2}$ S cm^{-}1 and activation energy $E_a = 0.20$ eV and exhibits paramagnetic behavior of the Curie type. Such neutral radicals based on open-shell dithiolene complexes are thus promising candidates for the preparation of conducting single-component molecular materials.

2. Single-component molecular conductors

The realization of a molecular metal based on single-component molecules has been one of the important targets in the field of molecular conductors, since all molecular metals developed before 2000 were made of two components: the molecules forming the electronic band (designated by A) and another chemical species (designated by B); the formation of a conduction band and the generation of charge carriers by the intermolecular charge transfer between A and B seemed two essential requirements to ensure a metallic state in these systems[81].

To generate a metallic or semimetallic band in single-component molecules, the energy separation between HOMO and LUMO should be small enough to make the HOMO and LUMO bands overlap each other through 2-D or 3-D intermolecular interactions and form partially filled bands. Therefore, the molecules must have a very small HOMO–LUMO gap (ΔE) and large intermolecular interactions, especially transverse contacts. The occurrence of the metallic state in a molecular system based on a neutral species was first observed by Almeida and coworkers in $[Au(\alpha\text{-tpdt})_2]^\bullet$ (**56**, M = Au, α-tpdt = 3,4-thiophenedithiolate)[84], a member of a novel class of gold complexes with thiophenedithiolate ligands, where the peripheral thiophene sulfur atoms promote additional intermolecular S···S contacts that control the packing pattern and thus the electronic properties. Conductivity measurements performed on a polycrystalline sample show that $[Au(\alpha\text{-tpdt})_2]^\bullet$ is a metal in the 15–300 K range with high room-temperature conductivity, $\sigma_{rt} = 6$ S cm^{-1}, exceptionally large considering powder data are typically 100- to 1000-fold weaker than those observed in single crystals along their most conductive axis. This compound shows paramagnetic behavior almost independent of temperature down to 10 K, reminiscent of the Pauli paramagnetism typical of metallic systems. Unfortunately, no crystal data are available to further investigate the origin of the metallic state. Metal–dithiolenes with highly delocalized ligands such as extended-ttf donors were considered the best candidates to obtain single-component molecular conductors, since the first evidence of a very small ΔE from *ab initio* MO calculations on $[Ni(ptdt)_2]$ (**57a**, M = Ni, ptdt = bis(propylenedithio)tetrathiafulvalenedithiolate) dithiolene complex[102]. Theoretical calculations suggest that ΔE will decrease with increasing size of extended-ttf ligand system. Moreover, the ttf-like structure is crucial for obtaining large transverse intermolecular interactions because the HOMO of the ttf-like donor has the same sign on every sulfur atom and all intermolecular contacts through sulfur atoms enhance the intermolecular interaction by contributing additively[81]. Kobayashi and coworkers[1b] reported the synthesis of single-component molecular conductor $[Ni(tmdt)_2]$ (**57b,** M = Ni, tmdt = trimethylenetetrathiafulvalenedithiolate), which exhibits a stable metallic state down to very low temperature ($\sigma_{rt} = 400$ S cm^{-1}). A single-component molecular conductor incorporating magnetic moments, $[Cu(dmdt)_2]$ (**57c**, M = Cu, dmdt = dimethyltetrathiafulvalenedithiolate), has been also reported[103]. A new type of ttf ligands fused with a

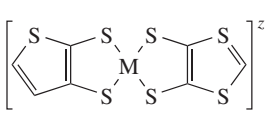

(**56**) $[M(\alpha\text{-tpdt})_2]$

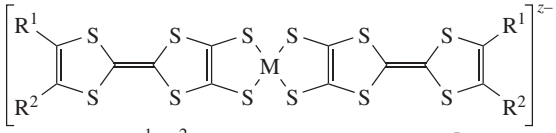

(**57**) (**a**) $R^1, R^2 = -S(CH_2)_3S-$; $[M(ptdt)_2]^{z-}$
(**b**) $R^1 \wedge R^2 = CH_2CH_2CH_2$; $[M(tmdt)_2]^{z-}$
(**c**) $R^1 = R^2 = Me$; $[M(dmdt)_2]^{z-}$

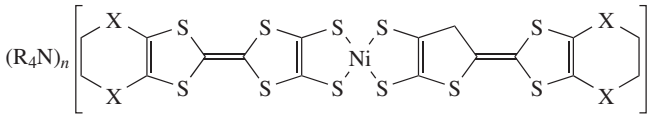

(**58**) (**a**) R = Me, X = CH_2, $n = 2$ (**d**) R = Me, X = O, $n = 2$
(**b**) R = Bu, X = CH_2, $n = 1$ (**e**) R = Bu, X = O, $n = 1$
(**c**) X = CH_2, $n = 0$ (**f**) X = O, $n = 0$

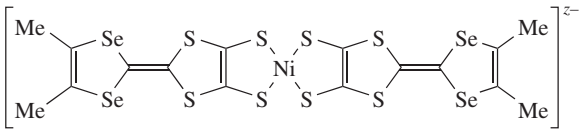

(**59**) $[Ni(dmstfdt)_2]^-$

six-membered ring such as cyclohexene and 1,4 dioxene, which possess structural flexibility similar to that of the bedtttf donor, has been used to obtain novel single-component highly conducting systems, $(R_4N)_n[Ni(chdt)_2]$ [R = Me, $n = 2$ (**58a**); R = Bu, $n = 1$ (**58b**); $n = 0$ (**58c**); chdt = cyclohexenotetrathiafulvalenedithiolate] and $(R_4N)_n[Ni(eodt)_2]$ [R = Me, $n = 2$ (**58d**); R = Bu, $n = 1$ (**58e**); $n = 0$ (**58f**); eodt = ethylenedioxytetrathiafulvalenedithiolate][85].

X-ray data were available only for **58b** and **58e**, which show sandwiched structures in which the chains or layers of the nickel complexes and cations are arranged alternately. Interchain or interlayer S $\cdots$ S contacts shorter than the van der Waals radii were observed only in the transverse direction. The magnetic behavior of **58b** is in good agreement with the Bonner–Fisher model with $J/kB = -28$ K, showing the existence of an antiferromagnetic 1-D Heisenberg chain[104] in agreement with the arrangement of anions with regular distance along the 1-D chain (*c*-axis). Complex **58e** shows Curie–Weiss paramagnetism with antiferromagnetic interactions between the $S = 1/2$ states. The neutral species **58c** and **58f** showed high room-temperature conductivity ($\sigma_{rt} = 1$ to 10 S cm^{-1}) measured on pressed pellets of samples. In this class, complex **58f** is considered to be a new single-component metal. Novel examples of highly conductive single-component molecular metals based on ttf ligands fused with tiophene moieties are reported elsewhere[105].

Recently, the new $(Bu_4N)[Ni(dmstfdt)_2]$ (**59**) (dmstfdt = dimethyldiselenadithiafulvalenedithiolate) Ni complex with stf (diselenadithiafulvalene)-type ligands has been synthesized and fully characterized[86]. This compound is a unique ambivalent molecular system exhibiting weakly metallic behavior above room temperature and weak ferromagnetism of localized spins at low temperature, despite the 1:1 stoichiometry similar to **58b** and **58e**. The crystallographically independent $[Ni(dmstfdt)_2]^-$ anions (A and B, see Figure 12) are arranged alternately along the stacking *a*-axis; the dihedral angle of 42.6°

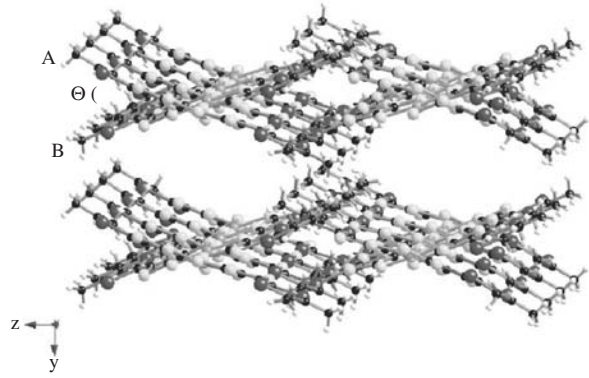

FIGURE 12. Crystal structure of $(Bu_4N)[Ni(dmstfdt)_2]$. Anion layers showing two kinds of anions A and B forming a zigzag array with a dihedral angle of 42.6(1)° between the adjacent anions along the stacking axis. Reprinted with permission from Reference 86. Copyright 2007 American Chemical Society

between the molecular planes of adjacent anions produces a weakly dimerized zigzag array which forms an anion layer parallel to the *ac*-plane. Several Se···Se contacts between the anions are present with a 2-D interaction in the anion layer.

Despite the 1:1 stoichiometry of the complex, the metallic behavior is relevant. The room-temperature conductivity is $\sigma_{rt} = 0.2\ S\,cm^{-1}$ and metallic behavior was observed down to 147 K, where transition to an insulating state occurred. The temperature dependence of the magnetic susceptibility is also very unique, and the increase in the χT product *vs.* T suggests a localization of the conduction electrons with lowering temperature at 160–280 K, where the resistivity gradually increases. The χT value was constant in the 80–150 K range and this is fitted well by the Curie–Weiss law. In conclusion, $(Bu_4N)[Ni(dmstfdt)_2]$ undergoes a transition to an insulating state as a result of localization of the conduction electrons.

Recently, Kato and coworkers[87] have prepared and fully characterized novel trinuclear Ni(II) complexes by reacting the corresponding mononuclear Ni–dithiolene complex $[Ni(S\hat{}S)_2]^z$ ($z = 0$ or $1-$, S^S = dddt, edo) (edo = 5,6-dihydro-1,4-dioxine-2,3-dithiolate) with the tetrathiooxalato (**60**, tto) ligand and a Ni(II) cation, as shown in equation 12 for the dddt ligand.

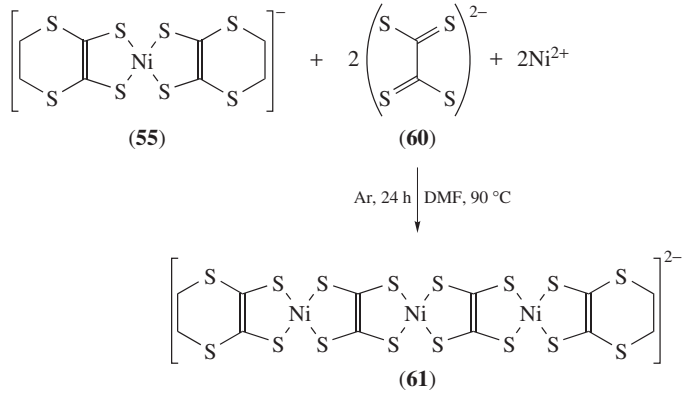

(12)

This reaction unexpectedly produced trinuclear complexes with two tto bridging ligands along with the binuclear complex. Structural results show that the anion of $(Ph_4P)_2[Ni_3(tto)_2(dddt)_2]$ (**61**) is almost planar and the coordination around Ni(1) and Ni(2) is square-planar, as expected for d^8 complexes. Theoretical calculations (*ab initio* and extended Hückel) show that this complex has a small HOMO–LUMO gap (0.15 eV) and highly symmetric HOMO and LUMO, which are similar to those of $[Ni(timdt)_2]$ (HOMO–LUMO gap = 0.10 eV), with a 3-D π band. This is reflected by the conducting properties of this salt, a semiconductor with very high room-temperature conductivity ($\sigma_{rt} = 1.0 \times 10^4$ S cm^{-1}) and very low activation energy ($E_a = 0.28$ eV). These trinuclear complexes with such an extended π-conjugated system represent a new class of highly conducting single-component molecular materials out of the mononuclear highly delocalized open-shell dithiolene complexes and metal–dithiolenes with extended-ttf donors, whose selected examples have been described at the beginning of this section.

C. Role of the Counterion

The examples of Sections IV.B.1 and IV.B.2 demonstrate the influence of the intermolecular interactions, such as fluorine and $\pi-\pi$ interactions in determining the packing motif (1-D, 2-D networks) and thus the conducting properties of dithiolene-based molecular systems. The counterion is also of key importance in controlling the packing, as it may segregate each stack to hinder further electronic communication between the complexes. Larger counterions increase the stacking distance leading to weaker intermolecular interactions, and hence decrease the conductivity, as illustrated in the $(A)_2[Cu(mnt)_2]$ series ($A^+ = Et_4N^+$, Pr_4N^+, Bu_4N^+) on variation of the size of the counterion[106], or can interrupt the regularity of the stack leading to formation of dimers and thus to a nonmagnetic ground state. Smaller counterions promote both the uniform stacking required for long-range magnetic order and strong intermolecular interaction between the dithiolene complexes. $(NH_4)[Ni(mnt)_2]\cdot H_2O$[73] is a peculiar example, which shows uniform stacking and ferromagnetic ordering at the Néel temperature $T_N = 4.5$ K. Organic counterions fully planar or containing aromatic groups have been also used to promote uniform stacking of the anions and several salts exhibiting unusual magnetic behavior have been obtained. Among them, salts based on pyridinium cations show a variety of properties such as magnetic transition from paramagnetic to diamagnetic[107], phase transitions with ferromagnetic interaction in the high-temperature phase, spin gap in the low-temperature phase and weak ferromagnetism at low-temperature[108]. Recently, unusual magnetic behavior was observed in two novel $[M(mnt)_2]$ (M = Cu, Pt) dithiolene complexes with the stable, conjugated and planar bdta (**62**) cation, which may provide S···S interactions between bdta and $Cu(mnt)_2$ through the sulfur atoms of the heterocyclic ring and $[Pt(1,4\text{-}Me_2pipdt)_2]^{2+}$ (**63**) dicationic dithiolenes discussed in Section III. These complexes, where the planarity of the central core is maintained by the Pt atom which imposes the square-planar geometry while the substituents at the peripheral N-atoms of the ligand allow for tuning the size of the cation, seem to be promising candidates to replace fully organic or fully inorganic cations in controlling the packing.

The structure of $[bdta]_2[Cu(mnt)_2]$[88] shows an alternating, diagonal stacked system in the *bc* plane, with a single $[Cu(mnt)_2]^{2-}$ anion sandwiched between two bdta cations leading to discrete units. Within each stack in the *bc* plane, these units have S···S interactions along the *a*-axis forming a 1-D chain, since no other significant S···S contacts shorter than the sum of the van der Waals radii were observed. This compound behaves as an ideal 1-D Heisenberg antiferromagnetic material in the $T = 2–300$ K range. X-ray data suggest that magnetic exchange occurred along the chain of dithiolene complexes via the nonmagnetic bdta cation; the observed strong side-by-side interaction between

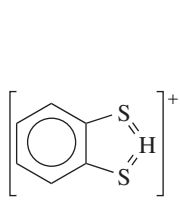

(**62**) bdta

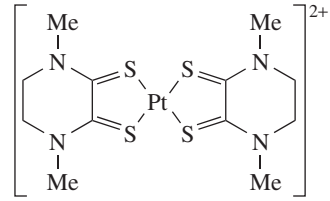

(**63**) $[Pt(1,4\text{-}Me_2pipdt)_2]^{2+}$

the sulfur atoms of the anion and cation is responsible for this unconventional pathway between magnetic centers. The novel salt $[Pt(1,4\text{-}Me_2pipdt)_2][Pt(mnt)_2]_2$[89] consists of segregated chains of anionic and dicationic $[M(1,4\text{-}R_2pipdt)_2]^{2+}$ complexes running parallel to the *c*-axis. The anionic complexes generate nonregular stacks with different distances between the planes and the cationic complexes are interposed between those stacks in a ribbon fashion; four anionic chains surround each cationic one and *vice versa* (Figure 13). Magnetic measurements show the presence of a magnetic phase transition at 115 K between the behavior of an antiferromagnetic alternating-exchange chain and the behavior of a set of antiferromagnetic dimers. The molecular structure at 103 K shows that this phase transition has only magnetic character without structural character. A magnetic phase transition between a uniform infinite chain and a dimerized chain[109] has been found in the complex [1-(4′-cyanobenzyl)pyridinium][Ni(mnt)$_2$], while several complexes based on $[M(mnt)_2]^{-\bullet}$ (M = Ni, Pt) dithiolene complexes show the magnetic behavior of an infinite chain of spins ($S = 1/2$) interacting antiferromagnetically or the behavior of antiferromagnetic dimers[110].

Magnetic phase transitions related to structural phase transitions similar to those described in neutral radical systems based on 1,3,5-trithia-2,4,6-triazapentalenyl (ttta)[111]

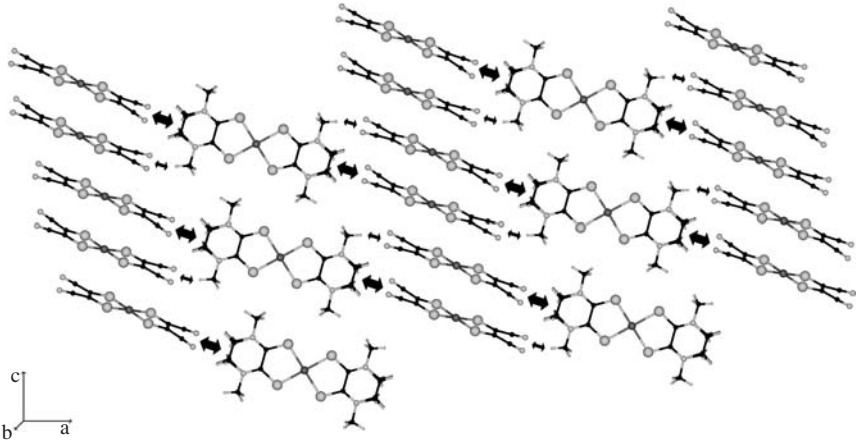

FIGURE 13. Perspective view of the crystal packing in the *ac* plane of $[Pt(Me_2pipdt)_2][Pt(mnt)_2]_2$. Interactions between the CN and the methylenic groups (⬌) and between the CN and the methyl groups (⥊) are denoted. Reprinted from *Chem. Phys. Lett.*, **421**, F. Bigoli, P. Deplano, M. L. Mercuri, L. Marchiò, L. Pilia, A. Serpe, G. Concas, F. Congiu and S. Sanna, 'Structure and Characterization of $[Pt(Me_2pipdt)_2][Pt(mnt)_2]_2$ and its Unusual Magnetic Properties Associated with a Non-Regular One-Dimensional $[Pt(mnt)_2]$ Stack', pp. 361–366. Copyright 2006, with permission from Elsevier

have been also found in $[Ni(mnt)_2]^{-\bullet}$ salts. A peculiar type of structural transition, the order–disorder transition coupled to spin transition, has recently been observed in $[Cp_2Fe][Ni(tfadt)_2]$[90], the ferricinium salt of the $[Ni(tfadt)_2]^{-\bullet}$ (**50**) dithiolene complex, containing the asymmetrically substituted tfadt ligand, incorporating the CN and the CF_3 groups characteristic of the mnt (**11**) and tfd (**10**) ligands, respectively. The CF_3 group shows conformational disorder because of the rotation around the $C-CF_3$ axis as a consequence of the segregation of the fluorinated moieties due to weak van der Waals interactions of fluorine atoms, already discussed in Section IV.B.1[112]. Such order–disorder transitions have been widely studied for their capability of affecting the conducting and magnetic properties of molecular materials based on *radical* molecules: typical examples are those related to the ordering of the ethylenic bridges of bedtttf π-donors in bedtttf salts, which have proved to control their superconducting transition[113]. The structure of $[Cp_2Fe][Ni(tfadt)_2]$ salt consists of uniform chains of dithiolene complexes stacked along the *b*-axis, separated by ferricinium dyads leading to the formation of hybrid layers parallel to the *ab* plane. The interface between these layers is formed by CF_3 and Cp moieties, pointing toward each other, which are disordered at room temperature. At $T > 250$ K this compound behaves as a Curie-type paramagnet. At lower temperatures two structural phase transitions at T *ca* 249 K, phase **A**, and T *ca* 137 K, phase **B**, affecting the magnetic susceptibility, were observed (Figure 14).

In phase **A**, uniform spin chains of $[Ni(tfadt)_2]^{-\bullet}$ anions showing weak AFM interactions and disordered CF_3 and Cp groups are present. The **A** ↔ **B** transition is associated with a dimerization of the uniform spin chains which leads to an alternate spin chain and simultaneous ordering of both the CF_3 and Cp groups that thus induces a drop of the susceptibility. The order–disorder behavior of both the CF_3 and Cp groups seems to be the driving force of the transition. The low-temperature transition leads to a third structural phase (phase **C**) consisting of antiferromagnetically coupled nickel dithiolene tetramers in a complete diamagnetic state. The occurrence of two regions of magnetic bistability in dithiolene-based systems is quite rare and has been observed only in spin-crossover systems such as dinuclear Fe(II) complexes[114], where the intermediate spin state can be stabilized while the structural sequence: uniform chain/dimerized chain/tetramerized chain, is usually observed in charge-transfer conducting salts of the $(tmttf)_2X$ type[115] but not in spin chains where full charge transfer is observed. A strong coupling between an

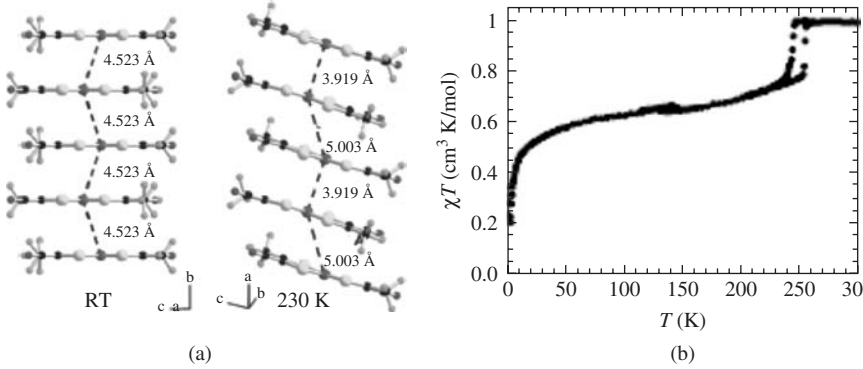

FIGURE 14. (a) A view of the dithiolene stacks in $(Cp_2Fe)[Ni(tfadt)_2]$: (Left) At 293 K, **A** phase and (right) at 230 K, **B** phase, showing the dimerization of the $[Ni(tfadt)_2]^{-\bullet}$ chain in the **B** phase. The Ni···Ni distances are marked with dashed lines. (b) Plot of χT *vs*. T in the 1.85–300 K range. Reprinted with permission from Reference 90. Copyright 2006 American Chemical Society

order–disorder transition and an electronic transition such as spin transitions, and other phenomena, has thus proved to be a useful tool for the design of molecular switches with potential applications in molecular electronics for memory or sensing applications[116].

1. Influence of H-bonding

The relevance of H-bonding in determining the solid-state properties of nitrile-containing paramagnetic metal dithiolenes has been discussed in Section III.C.3. A magnetic exchange path through hydrogen bonds which might be responsible for the occurrence of magnetic ordering has been also observed in several compounds[117–119]. Among them, the novel dithiolene complex with the organometallic bis(benzene)chromium(+) cation, bis(4,5-dimethoxybenzene-1,2-dithiolate)nickel(−), $[Cr(\eta^6\text{-}C_6H_6)_2][Ni(dmox)_2]$[91] (**64**), represents, to the best of our knowledge, the first example of a metal bis(arene) complex showing ferromagnetic ordering. It is noteworthy that magnetic ordering in organometallic compounds[120] is quite rare and studies on the corresponding $[Cr(\eta^6\text{-}C_6H_6)_2]$(tcnq) system show an ordinary paramagnetic behavior[121]. In $[Cr(\eta^6\text{-}C_6H_6)_2][Ni(dmox)_2]$, the Ni–S bond distances, which fall in the 2.13–2.16 Å range, typical for monoanionic systems[17], are in agreement with the 1–charge ascribed to the dmox complex. The Ni–S bond distance, which fall in the 2.13–2.16 Å range, typical for monoanionic systems[17], confirm the ascribed charges. The crystal structure consists of interpenetrating sublattices of anions and cations each one well separated from the other of opposite charge, where the symmetry planes defined by the cations and anions are almost perpendicular to each other. In decamethyl metallocenium/dithiolene systems these planes are almost parallel, a common structural feature of compounds showing magnetic ordering. H-bonding is crucial in determining the packing pattern. There are three shortest contacts in the structure, each one involving a hydrogen atom of one of the aromatic rings of the cations and the heteroatoms (O, S, and Ni) of the dithiolene anions, leading to chain formation and thus to a 3-D network. At $T > 10$ K, $[Cr(\eta^6\text{-}C_6H_6)_2][Ni(dmox)_2]$ (**64**) behaves as a paramagnet following the Curie–Weiss law for $S = 1/2$ on each ion ($T_{Weiss} = 8.5$ K) while magnetic susceptibility and magnetization studies show a transition to a ferromagnetically ordered phase at $T = 3.4$ K. It has been suggested that the structural motif of hydrogen bonds, especially the short contacts between anion heteroatoms (O and Ni) and cation H atoms (O–H = 2.437 Å; Ni–H = 2.908 Å) and the longer interionic S–H (3.148 and 3.260 Å) contacts, are responsible for the ferromagnetic interaction by mediating the magnetic communications between cations and anions.

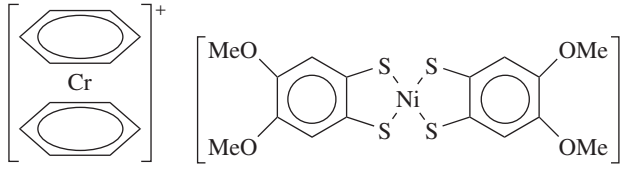

(**64**) $[Cr(\eta^6\text{-}C_6H_6)_2][Ni(dmox)_2]$

2. Influence of the substituents

A novel class of dithiolene complexes based on thiophenedithiolate ligands with interesting electrical and magnetic properties has been recently reported by Almeida and coworkers[84, 122] (Section IV.B.2). In particular, the paramagnetic $[Ni(\alpha\text{-tpdt})_2]^{-\bullet}$ (**56**, M = Ni) anionic dithiolene complex in combination with a suitable counterion has proved to be

a challenging building block for materials with unusual magnetic properties. For instance, among the several salts which have been prepared with decamethylmetallocenium cations, $[Cp^*_2Fe][Ni(\alpha\text{-tpdt})_2]$[123] shows metamagnetic behavior below 2.56 K with a critical field of 600 G, while the corresponding manganese salt, $[Cp^*_2Mn][Ni(\alpha\text{-tpdt})_2]$[123], is a frustrated magnet. When using substituted *N*-benzyl-pyridinium cations, three new salts (*N*-(4-$RC_6H_4CH_2$)py)$[Ni(\alpha\text{-tpdt})_2]$ (R = H, Br, F) have been obtained[92]. Previous studies with other dithiolene complexes[124] have shown that this type of cation favors segregated stacking of cations and anions, leading to different kinds of magnetic interactions and ordering which depend on the overlap modes of the anions in the crystal structure. The structure of all compounds consists of alternated layers of anions and cations: the anions are arranged with thiophenic sulfur atoms connected to a coordinating sulfur atom of a neighboring anion, placing the complexes almost perpendicular to their next neighbors, in zigzagging chains. The cations are positioned with the pyridine rings inserted between the thiophene rings of the anions, maximizing $\pi-\pi$ interactions but failing to promote segregated anion stacking. There are several anion–cation interactions: C···C and C···S $\pi-\pi$ interactions between the pyridine ring of the cations and the thiophene ring of the anions, S···H–C hydrogen bonds, C–Br···S short contacts through a coordinating and thiophene sulfur atom and C–F···S interactions between anions and cations which are responsible for the prevalence of the *cis* configuration, never observed so far in a $[Ni(\alpha\text{-tpdt})_2]^{-\bullet}$ dithiolene complex. The cation substitution plays a role in determining structural differences and variable amounts of *cis–trans* disorder in the anionic dithiolene complexes, related to the relative positions of the sulfur atoms of the thiophene rings. The *cis–trans* disorder affects the magnetic behavior of these compounds: (*N*-(Bn)py)$[Ni(\alpha\text{-tpdt})_2]$ shows dominant ferromagnetic interactions and, at low temperatures, typical behavior of a cluster glass as a consequence of disorder effects; (*N*-(4-$BrC_6H_4CH_2$)py)$[Ni(\alpha\text{-tpdt})_2]$ shows dominant antiferromagnetic interactions with a magnetic anomaly at *T ca* 6 K and (*N*-(4-$FC_6H_4CH_2$)py)$[Ni(\alpha\text{-tpdt})_2]$ behaves like a paramagnet down to 1.5 K. This class of compounds shows how small changes within the building blocks can significantly affect the supramolecular interactions and thus the magnetic properties.

D. Conducting/Magnetic Hybrid Materials

Bis(dithiolene)-based systems have proved to be useful components of multifunctional conducting/magnetic hybrids, a challenging class of materials which represents one of the main targets in current materials science for their potential applications in

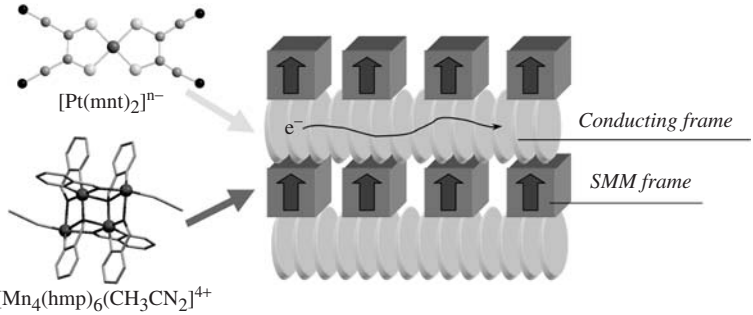

FIGURE 15. Schematic view of the $[Pt(mnt)_2]^{n-}$ conducting frame and the intercalated $[Mn_4(hmp)_6(CH_3CN)_2]^{4+}$ SMMs frame. Reprinted with permission from Reference 128. Copyright 2007 American Chemical Society

the development of molecular devices. They consist of two molecular networks, one furnishing magnetism (nonlinear optics or other properties) and the other conductivity. The combination of magnetic moments with conduction electrons in the same material may lead to a simple superposition (coexistence) of magnetic and conducting properties when the two networks are electronically independent, an essential requirement for combining properties such as ferromagnetism and conductivity which cannot coexist in naturally occurring materials, or to a mutual influence (coupling) between these properties when they interact as observed in switchable materials. Important milestones in the area of molecular magnetic conductors showing a combination of properties, apart from the first family of paramagnetic molecular metals, $(per)_2[M(mnt)_2]$ (M = Pt, Pd, Ni and Fe)[75], are based on bedtttf salts with charge-compensating anions ranging from simple mononuclear complexes $[MX_4]^{z-}$ (M = Fe(III), Cu(II); X = Cl, Br) and $[M(ox)_3]^{3-}$ (ox = oxalate) with tetrahedral and octahedral geometry, to layered structures such as the binuclear oxalate complexes $[M(II)M(III)(ox)_3]^-$ (M(II) = Mn, Co, Ni, Fe, Cu; M(III) = Fe, Cr). Three representative hybrid materials have been synthesized up to now: paramagnetic/superconductor $(bedtttf)_4[H_3OM(III)(C_2O_4)_3](PhX)$ (M(III) = Cr, Fe, Ga; X = CN, NO_2, F, Br, ...)[125], antiferromagnetic/superconductor κ-$(bets)_2[FeX_4]$ (X = Br, Cl)[126] (bets = bis(ethylenedithio)tetraselenafulvalene) and ferromagnetic/metal, the $(bedtttf)_3[MnCr(ox)_3]$[127] being the most recent and significant advance in this field. Several examples of conducting/magnetic hybrids based on bisdithiolene complexes have been reported in previously cited reviews[1a,8]. Recently, Yamashita and coworkers have reported the synthesis of a unique hybrid material based on Mn_4 single-molecule magnet (SMM) clusters in the $S_T = 9$ spin state and $[Pt(mnt)_2]^{z-}$ dithiolene complexes, $[\{(Mn(II)_2Mn(III)_2(hmp)_6(CH_3CN)_2\}\{Pt(mnt)_2\}_4][Pt(mnt)_2]_2$[128], showing SMM/semiconducting behavior (Figure 15).

Recent studies have demonstrated that the inter-SMM interaction via conducting electrons, albeit small, has a mutual influence on both SMM properties and conductivity[93].

The structure consists of $[Mn(II)_2Mn(III)_2(hmp)_6(CH_3CN)_2]^{4+}$ units (represented as a $[Mn_4]^{4+}$ cluster) separated by1-D double columns of $[Pt(mnt)_2]^{z-}$ complexes. There are two $[Pt(mnt)_2]^{z-}$ units (**A** and **B**) coordinated with the Mn(II) ion of the $[Mn_4]^{4+}$ unit forming a discrete unit, $\{[Pt(mnt)_2]_2\text{-}[Mn_4]\text{-}[Pt(mnt)_2]_2\}$. The uncoordinated $[Pt(mnt)_2]^{z-}$ (**C**) and coordinated **A** and **B** are mutually stacked along the *a*-axis (Figure 16a) to form a segregated one-dimensional double column possessing an $[\cdots \mathbf{A} \cdots \mathbf{B} \cdots \mathbf{C} \cdots]$ repeating unit (Figure 16b). Considering the charge balance and the structures of **A, B** and **C**, the $[Pt(mnt)_2]$ units show a fractional charge of −0.66. The electron transport properties of

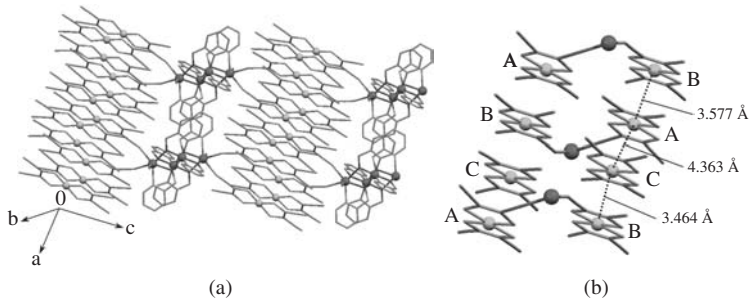

FIGURE 16. (a) Packing view of $[\{(Mn(II)_2Mn(III)_2(hmp)_6(CH_3CN)_2\}\{Pt(mnt)_2\}_4][Pt(mnt)_2]_2$, and (b) arrangement of part of $[Pt(mnt)_2]^{z-}$ moieties. Reprinted with permission from Reference 128. Copyright 2007 American Chemical Society

this salt, measured along the $[Pt(mnt)_2]^{0.66-}$ columns (stacking *a*-axis), show that it is a semiconductor down to 110 K (insulator at $T < 110$ K) with high room-temperature conductivity ($\sigma_{rt} = 0.2$ S cm^{-1}) and activation energy $E_a = 136$ meV. The temperature dependence of χT shows a typical intracluster ferromagnetic behavior, already seen in related $[Mn_4]$ clusters[129]. The magnetic behavior at low temperatures illustrates the SMM character of the $[Mn_4]^{4+}$ unit and possible interunit interactions. $[Pt(mnt)_2]^{z-}$ subunits with fractional oxidation state ($z = 0.66$ in this salt) allowing conductivity are rare and only Li salts of $[Pt(mnt)_2]^{z-}$ have been reported so far[130]. However, conductivity is present only in the temperature region where the SMM unit behaves as a general paramagnet. Moreover, both networks (SMM and conducting) act independently in the entire temperature range[131].

Among the various selenium analogs of dmit, the dsit ligand has been the most studied because the replacement of the sulfur atoms with selenium atoms in the periphery of the ligand itself or in the dithiolene core of the $[M(dmit)_2]$ complexes is expected to result in increased polarizabilities and orbital overlaps between molecules, leading to an enhancement in the dimensionality of the materials. As far as we know, few $[M(dsit)_2]$ (M = Ni, Pd) systems have been fully characterized by studies of crystallographic and electrical properties; they all consist of tightly bound dimers with closed-shell tetrahedral cations[132]. Only in the $(Me_4N)[M(dsit)_2]_2$ (M = Ni, Pd) salts, that contain the mixed-valence dimer $[M(dsit)_2]_2^{1-}$, have high room-temperature conductivities been observed (*ca* 36 and *ca* 50 S cm^{-1}, for Ni and Pd, respectively), although they behave as semiconductors. The other reported salts contain the fully charged $[Ni(dsit)_2]_2^{2-}$ anions and are insulators. Recently, a novel conducting/magnetic hybrid $[Ni(dmf)_6][Ni(dsit)_2]_2$[94] formed by the $[Ni(dsit)_2]_2^{2-}$ dianion and the $[Ni(dmf)_6]^{2+}$ cation has been reported, which combines the conducting properties (semiconductor with $\sigma_{rt} = 1.0$ S cm^{-1}) derived from the packing of the anionic $[Ni(dsit)_2]_2^{2-}$ dimers with the paramagnetic properties of octahedral $[Ni(dmf)_6]^{2+}$ cations (Curie-type behavior). This salt shows an unusual 1-D packing motif. Several short interdimer Se$\cdots$Se contacts leading to a strong 1-D character in the anionic sublattice are present. This is an unprecedented structural feature that contrasts with the lack of interdimer contacts found in the other structurally characterized $[Ni(dsit)_2]^-$ salts and affects its transport properties. The chains of $[Ni(dsit)_2]_2^{2-}$ dimers are surrounded by four parallel chains of $[Ni(dmf)_6]^{2+}$ cations and *vice versa* in such a way that this structure can be viewed as formed by chains of $[Ni(dsit)_2]_2^{2-}$ anions inserted inside the tunnels formed by four chains of $[Ni(dmf)_6]^{2+}$ cations.

Metal–dithiolene complexes of the tdas ligand have been also investigated as promising building units of conducting, magnetic and conducting/magnetic hybrids because they were proposed as potential analogs of the $[M(dmit)_2]^{z-}$ systems, but much more easily obtainable in a one-step reaction from commercial precursors. As this chapter is limited to d^8 systems, the readers are referred to elsewhere[8,133–136] for discussion on the properties of $(Bu_4N)[Fe(tdas)_2]$, $(ttf)_2[Fe(tdas)_2]$, $(bedtttf)_2[Fe(tdas)_2]$ and $(bets)_2[Fe(tdas)_2]_2$. A salt of composition $(ttf)_2[Ni(tdas)_2]$[137] has been prepared but not structurally characterized. This salt shows conducting properties unrewarding (room-temperature conductivity on a pressed pellet $\sigma_{rt} = 10^{-1}$ S cm^{-1}) when compared to $(ttf)[Ni(dmit)_2]$. Another salt, $(omttf)_2[Ni(tdas)_2]$[138] (omttf = octamethylenetetrathiafulvalene), has been obtained, and is an insulator consisting of a dimer of the omttf radical cations and the $[Ni(tdas)_2]^{2-}$ dianion. Recently, the first crystallographically and magnetically characterized salt of an open-shell cation, $(bedtttf)[Ni(tdas)_2]$, has been reported[95], with $[Ni(tdas)_2]^-$ monoanions, showing a packing pattern similar to the omttf salt in one of the layers, but totally different physical properties. This salt forms a layered structure where one layer contains dimerized bedtttf electron-donor molecules and isolated $[Ni(tdas)_2]^-$ monoanions, while the second layer contains chains of $[Ni(tdas)_2]^-$ monoanions. Conductivity measurements show that $(bedtttf)[Ni(tdas)_2]$ is a semiconductor of the Arrhenius type with

room-temperature conductivity $\sigma_{rt} = 1.8 \times 10^{-2}$ S cm^{-1} and two semiconducting regimes with activation energies of 58 and 212 meV above and below the transition temperature (*ca* 200 K), respectively. This reversible semiconducting–semiconducting transition has already been observed in other radical salts at similar temperatures and has been attributed to an ordering of the ethylene group of the bedtttf donor. Magnetic measurements show that it is a $S = 1/2$ paramagnet with weak antiferromagnetic coupling. Recently, Robertson and coworkers[139] reported on the synthesis of the new $(bdta)_2[Ni(tdas)_2]$ salt, which shows integrated anion–cation alternating stacks, the ideal motif for the formation of new functional materials. Although the magnetic properties are not remarkable, this salt shows the appropriate stacking motifs for promoting magnetic exchange and hybrid magnetic properties, and is deserving of further investigation.

E. Photoconductors

Anionic dithiolene complexes have been used to prepare IPCT (ion pair charge transfer) photoconducting salts of the type $\{(C^{2+})\ [ML_2]^{2-}\}$ (M = Ni, Pd, Pt; L^{2-} = dithiolato), where C^{2+} is a redox-active organic donor such as 4,4′- and 2,2′-bipyridinium derivatives[140]. These challenging materials have been extensively studied for their photochemical and photophysical properties, in particular the possibility to generate an electrical photocurrent which may be used in photodetector technology. An extensive investigation on these organic–inorganic CT salts by Kisch's group[140] has allowed us to understand the main factors affecting the structure/property relationship.

The supramolecular interaction between the ionic components is reflected by the presence of a strong CT band in the diffuse reflectance spectra of these salts, which exhibit electrical semiconducting behavior. When both components are planar and form a mixed donor–acceptor stack in the solid state, on applying the 'Marcus–Hush model'[141], a linear correlation between the thermal and optical electron transfer and a linear correlation between the specific electrical conductivity and the free activation enthalpy of the thermal electron transfer were found. Moreover, these CT salts showed interesting photoconducting properties. Recently, metal dithiolenes have been used as both components of IPCT salts extending the investigation from the largely studied fully organic and organic–inorganic systems to the less common fully inorganic ones[142]. The structure/property relationship of the following CT salts has been investigated[96]: $[M(1,4\text{-}R_2pipdt)_2][M(mnt)_2]$ (R = Me, M = Pd, Pt; R = Et, M = Pt)[11] and $[Pt(1,4\text{-}R_2pipdt)_2][Pt(dtcr)_2]$ (R = Me, Et; dtcr = 4,5-disulfanylcyclopent-4-ene-1,2,3-trionate, also known as dithiocroconate). These salts show strong NIR CT bands and semiconducting behavior. The structural features of both compounds are similar: approximately square-planar $[Pt(1,4\text{-}Me_2pipdt)_2]^{2+}$ dications and regular square-planar $[Pt(dtcr)_2]^{2-}$ or $[Pt(mnt)_2]^{2-}$ dianions form an infinite anion–cation 1-D stack along the *c*-axis, and a net of weak interactions between the N and O atoms of the cation and of the anion contributes to the alignment of the complexes in the stack, as shown in Figure 17; the electronic spectra of the salt and its precursors in the figure show an additional NIR peak for the salt, due to the CT transition from the dithiolate to the dithione Pt complexes[96]. The specific electrical conductivity of pressed powder pellets ranges from 10^{-11} to 10^{-5} S cm^{-1} at room temperature, follows the Arrhenius law with activation energies in the 0.2–0.6 eV range and is related to the driving force of the electron transfer process: $[C]^{2+} + [A]^{2-} \rightarrow [C]^{+} + [A]^{-}$. Preliminary photoconductivity measurements performed on the relatively more conducting samples, $([Pt(1,4\text{-}Et_2pipdt)_2][Pt(mnt)_2])$, show a gain of current during illumination, similar to what was observed in organic–inorganic $X[ML_2]$ (X^{2+} is 2,2′- or 4,4′-bipyridinium or similar derivatives, L^{2-} = dithiolato) photoconducting Kisch's salts.

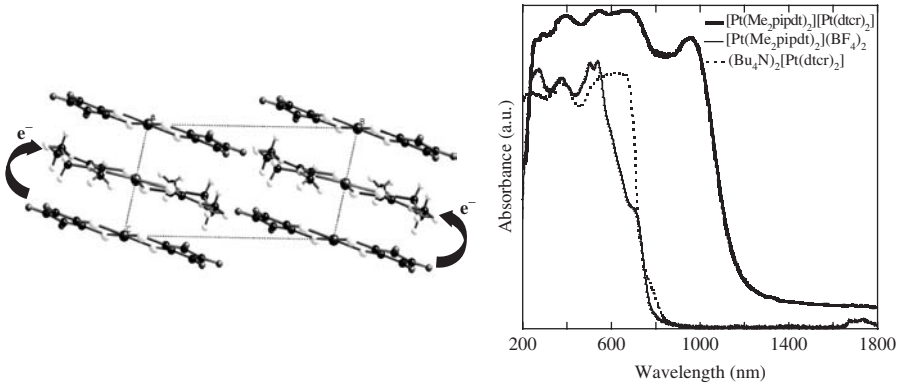

FIGURE 17. Perspective view of the crystal packing of $[Pt(Me_2pipdt)_2][Pt(dtcr)_2]$ perpendicular to the stacking axis and diffuse reflectance spectra of this salt and its precursors. Reproduced with permission of Wiley-VCH Verlag GmbH & Co. KGaA from Reference 96

V. PERSPECTIVES

Advances in the synthesis of new ligands and complexes afford novel systems with remarkable properties, such as single-component magnetic molecular conductors, which are challenging candidates for several applications in electronic, magnetic and photonic devices. Research should proceed from these results to feasability studies and development of real molecule-based devices, which often require deposition as thin films of the molecular materials, a process which represents the forefront of current science and technology[143]. Several processing techniques are available to prepare thin films: Langmuir–Blodgett (LB) films, chemical vapor deposition (CVD), physical vapor deposition (PVD), dip coating, spin coating, polymeric casting and electrodeposition. The substrates depend on the applications: (i) silicon wafers for electronics, (ii) indium tin oxide (ito) for optical devices, (iii) polymers can be suitable for several applications including magnetic devices, (iv) it has already been established that electrooptic devices can be made[144] based on chromophores incorporated into a variety of ways as LB films, self-assembled films and poled polymers[144]. Conducting LB films of $[Au(dmit)_2]$ dithiolene complex, electrical sensors such as electrodeposited films of $(Bu_4N)[Ni(dmit)_2]$ used for detecting SO_2 or NO, electrical switching and memory phenomena on devices formed by uniform thin films based on $[Ni(dmit)_2]$ and $[Ni(dmid)_2]$ dithiolene complexes have also been prepared[1a].

Significant progress has been recently achieved in film preparation of electroconducting materials, which in most cases gives rise to semiconducting behavior due to the formation of segregated domains (grains). Few examples of thin films prepared in polycrystalline form on silicon wafers by the electrocrystallization technique showing metallic behavior down to low temperatures have been reported; examples are the $(ttf)[Ni(dmit)_2]_2$ salt and the single-component neutral molecular metal $[Ni(tmdt)_2]$[145]. These films show a grain-like morphology, while films of $(per)_2[Au(mnt)_2]$, grown similarly, show a nanowire-like morphology never observed before. In all these cases lower conductivity than in single crystals was found[146]. However, recently, a superconducting transition in a fiber-like similarly prepared film of $(ttf)[Ni(dmit)_2]_2$ has been observed[147], pointing to the electrodeposition technique as a promising way to produce films on silicon wafers with the same properties as single crystals.

The advances in the processing and in the understanding of metal–dithiolene complexes are furnishing suitable tools for chemists, physicists and electronic engineers with which to convert potentially useful compounds into materials of technological relevance.

VI. ACKNOWLEDGMENTS

Fondazione Banco di Sardegna, Università di Cagliari and MIUR (PRIN–2005033820_002 'Molecular materials with magnetic, optical and electrical properties') are gratefully acknowledged for their financial support.

COST Action D35 WG D35–0011–05 'Multifunctional and Switchable Molecular Materials' has promoted collaborative links.

VII. REFERENCES

1. (a) C. Faulmann and P. Cassoux, in *Dithiolene Chemistry: Synthesis, Properties, and Applications*, *Progress in Inorganic Chemistry*, Vol. 52 (Ed. E. I. Stiefel), John Wiley & Sons, Ltd, Chichester, 2004, pp. 399–489.
   (b) H. Tanaka, Y. Okano, H. Kobayashi, W. Suzuki and A. Kobayashi, *Science*, **291**, 285 (2001).
2. A. T. Coomber, D. Beljonne, R. H. Friend, J. K. Brédas, A. Charlton, N. Robertson, A. E. Underhill, M. Kurmoo and P. Day, *Nature*, **380**, 144 (1996).
3. U. T. Mueller-Westerhoff, in *Comprehensive Coordination Chemistry* (Ed. G. Wilkinson), Pergamon, Oxford, 1987, pp. 595–631.
4. (a) W. L. Tan, W. Ji, J. L. Zuo, J. F. Bai, X. Z. You, Y. H. Lim, S. Yang, D. J. Hagan and E. W. Van Stryland, *Appl. Phys.*, **B70**, 809 (2000).
   (b) B. J. Coe, in *Comprehensive Coordination Chemistry II*, Vol. 9 (Eds J. A. McCleverty and T. J. Meyer), Elsevier-Pergamon, Oxford, 2004, pp. 621–687.
5. J. M. Tunney, J. McMaster and C. D. Garner, in *Comprehensive Coordination Chemistry II*, Vol. 8 (Eds J. A. McCleverty and T. J. Meyer), Elsevier-Pergamon, Oxford, 2004, p. 459.
6. J. A. McCleverty, *Prog. Inorg. Chem.*, **10**, 49 (1968).
7. P. Cassoux and L. Valade, in *Inorganic Materials*, 2nd edn (Eds D. W. Bruce and D. O'Hare), John Wiley & Sons, Ltd, Chichester, 1996.
8. N. Robertson and L. Cronin, *Coord. Chem. Rev.*, **227**, 93 (2002).
9. (a) G. Periyasamy, N. A. Burton, I. H. Hiller, M. A. Vincent, H. Disley, J. McMaster and C. D. Garner, *Faraday Discuss.*, **135**, 469 (2007).
   (b) M. L. Kirk, R. L. McNaughton and M. E. Helton, in *Dithiolene Chemistry: Synthesis, Properties, and Applications*, Progress in Inorganic Chemistry, Vol. 52 (Ed. E. I. Stiefel), John Wiley & Sons, Ltd, Chichester, 2004, pp. 111–212, and references therein.
10. F. Bigoli, P. Deplano, M. L. Mercuri, M. A. Pellinghelli, L. Pilia, G. Pintus, A. Serpe and E. F. Trogu, *Inorg. Chem.*, **41**, 5241 (2002).
11. B. S. Lim, D. V. Fomitchev and R. H. Holm, *Inorg. Chem.*, **40**, 4257 (2001).
12. S. Curreli, P. Deplano, C. Faulmann, A. Ienco, C. Mealli, M. L. Mercuri, L. Pilia, G. Pintus, A. Serpe and E. F. Trogu, *Inorg. Chem.*, **43**, 5069 (2004).
13. R. K. Szilagyi, B. S. Lim, T. Glaser, R. H. Holm, B. Hedman, K. O. Hodgson and E. I. Solomon, *J. Am. Chem. Soc.*, **125**, 9158 (2003).
14. (a) Z. S. Herman, R. F. Kirchner, G. H. Loew, U. T. Mueller-Westerhoff, A. Nazal and M. C. Zerner, *Inorg. Chem.*, **21**, 46 (1982).
   (b) J. Weber, C. Daul, A. Van Zelewsky, A. Goursot and E. Penigault, *Chem. Phys. Lett.*, **88**, 78 (1982).
   (c) C. Lauterbach and J. Fabian, *Eur. J. Inorg. Chem.*, 1995 (1999).
   (d) C. Aragoni, M. Arca, F. Demartin, F. A. Devillanova, A. Garau, F. Isaia, F. Lelj, V. Lippolis and G. Verani, *J. Am. Chem. Soc.*, **121**, 7098 (1999).
15. P. Deplano, M. L. Mercuri, L. Pilia and A. Serpe, unpublished results.
16. T.-M. Yao, J.-L. Zuo, F. You and X. Z. You, *Polyhedron*, **14**, 1487 (1995).
17. D. Sellmann, H. Binder, D. Häussinger, F. W. Heinemann and J. Sutter, *Inorg. Chim. Acta*, **300–302**, 829 (2000).

18. F. Bigoli, P. Cassoux, P. Deplano, M. L. Mercuri, M. A. Pellinghelli, G. Pintus, A. Serpe and E. F. Trogu, *J. Chem. Soc., Dalton Trans.*, 4639 (2000).
19. P. Deplano, L. Marchiò, M. L. Mercuri, L. Pilia, A. Serpe and E. F. Trogu, *Polyhedron*, **22**, 2175 (2003).
20. W. E. Geiger, T. E. Mines and F. C. Senftleber, *Inorg. Chem.*, **14**, 2141, (1975).
21. K. H. Drexhage and U. T. Mueller-Westerhoff, *IEEE J. Quantum Electron.*, **QR-8**, 759 (1972).
22. (a) R. J. Mortimer and N. M. Rowley, in *Comprehensive Coordination Chemistry II*, Vol. 9 (Eds J. A. McCleverty and T. J. Meyer), Elsevier-Pergamon, Oxford, 2004, pp. 581–619.
    (b) N. C. Harden, E. R. Humphrey, J. C. Jeffery, S.-M. Lee, M. Marcaccio, J. A. McCleverty, L. H. Rees and M. D. Ward, *J. Chem. Soc., Dalton. Trans.*, 2417 (1999).
    (c) M. D. Ward and J. A. McCleverty, *J. Chem. Soc., Dalton. Trans.*, 275 (2002).
23. (a) C. W. Schläpfer and K. Nakamoto, *Inorg. Chem.*, **14**, 1338 (1975).
    (b) J. L. Wootton and J. I. Zink, *J. Phys. Chem.*, **99**, 7251 (1995).
    (c) K. I. Pokhodnya, C. Faulmann, I. Malfant, R. Andreu-Solano, P. Cassoux, A. Mlayah, D. Smirnov and J. Leotin, *Synth. Met.*, **103**, 2016 (1999).
    (d) H. H. Wang, S. B. Fox, E. B. Yagubskii, L. A. Kushch, A. I. Kotov and M.-H. Whangbo, *J. Am. Chem. Soc.*, **119**, 7601 (1997).
24. R. D. Schmitt and A. H. Maki, *J. Am. Chem. Soc.*, **90**, 2288 (1968).
25. J. E. Huyett, S. B. Choudhurry, D. M. Eichborn, P. A. Bryngelson, M. J. Maronay and B. M. Hoffman, *Inorg. Chem.*, **37**, 1361 (1998).
26. K. Wang and E. I. Steifel, *Science*, **291**, 106 (2001).
27. T. Waters, H.-K. Woo, X.-B. Wang and L.-S. Wang, *J. Am. Chem. Soc.*, **128**, 4282 (2006).
28. S. Kokatam, K. Ray, J. Pap, E. Bill, W. E. Geiger, R. J. LeSuer, P. H. Rieger, T. Weyhermüller, F. Neese and K. Wieghardt, *Inorg. Chem.*, **46**, 1100 (2007).
29. (a) K. Ray, T. Weyhermüller, F. Neese and K. Wieghardt, *Inorg. Chem.*, **44**, 5345 (2005).
    (b) T. Petrenko, K. Ray, K. Wieghardt and F. Neese, *J. Am. Chem. Soc.*, **128**, 4422 (2006).
30. L. Brossard, M. Ribault, M. Bousseau, L. Valade and P. Cassoux, *C. R. Acad. Sci., Ser. II*, **302**, 205 (1986).
31. E. B. Yagubsky, A. I. Kotov, L. I. Buravov, A. G. Khomenko, V. E. Shklover, S. S. Nahapetyan, Yu. T. Struchkov, L. V. Vetoshkina and L. Yu. Ukhin, *Synth. Met.*, **35**, 271 (1990).
32. (a) F. Bigoli, P. Deplano, F. A. Devillanova, V. Lippolis, P. J. Lukes, M. L. Mercuri, M. A. Pellinghelli and E. F. Trogu, *J. Chem. Soc., Chem. Commun.*, 371 (1995).
    (b) F. Bigoli, P. Deplano, F. A. Devillanova, J. R. Ferraro, V. Lippolis, P. J. Lukes, M. L. Mercuri, M. A. Pellinghelli, E. F. Trogu and J. M. Williams, *Inorg. Chem*, **36**, 1218 (1997).
33. F. Bigoli, P. Deplano, M. L. Mercuri, M. A. Pellinghelli, G. Pintus, G. Zonnedda, E. F. Trogu, H. H. Wang and J. M. Williams, *Inorg. Chim. Acta*, **273**, 175 (1998).
34. (a) M. C. Aragoni, M. Arca, F. Demartin, F. A. Devillanova, F. Isaia, V. Lippolis, A. Mancini, L. Pala, A. M. Slawin and J. D. Woollins, *Inorg. Chem.*, **44**, 9610 (2005).
    (b) S. Eld, M. Fourmigué, T. Roisnel and D. Lorcy, *Inorg. Chem.*, **46**, 10647 (2007).
35. E. E. Edouk, M. Krawiec, Y.-S. Lee Buisson, C. J. O'Conner, D. Sun and W. H. Watson, *J. Chem. Cryst.*, **26**, 621 (1996).
36. (a) M. L. Mercuri, S. Curreli, P. Deplano, L. Pilia, A. Serpe, E. F. Trogu, J. A. Schluter, E. Coronado, C. J. Gómez-García and E. Canadell, *Journal de Physique IV*, **114**, 425 (2004).
    (b) G. Bruno, M. Almeida, D. Simão, M. L. Mercuri, L. Pilia, A. Serpe and P. Deplano, to be submitted to *Dalton Trans.* (2008).
37. (a) F. Nastasi, F. Puntoriero, N. Palmeri, S. Cavallaro, S. Campagna and S. Lanza, *Chem. Commun.*, **45**, 4740 (2007).
    (b) G. Giuffrida, M. Saitta, G. Guglielmo, S. Campagna and S. Lanza, *Inorg. Chem.*, **35**, 6816 (1996).
38. S. Lanza, G. Callipari, F. Loiseau, S. Serroni and G. Tresoldi, *Inorg. Chem.*, **44**, 6717 (2005).
39. L. Dawe, J. Miglioi, L. Turnbow, M. L. Taliaferro, W. W. Shum, J. D. Bagnato, L. N. Zakharov, A. L. Rheingold, A. M. Arif, M. Fourmigué and J. S. Miller, *Inorg. Chem.*, **44**, 7530 (2005).
40. M. Fourmigué, C. Mézière and S. Dolou, *Cryst. Growth Design*, **3**, 805 (2003).
41. C. L. Kean, D. O. Miller and P. G. Pickup, *J. Mater. Chem.*, **12**, 2949 (2002).

42. R. S. Pilato and K. A. Van Houten, in *Dithiolene Chemistry: Synthesis, Properties, and Applications*, Progress in Inorganic Chemistry, Vol. 52 (Ed. E. I. Stiefel), John Wiley & Sons, Ltd, Chichester, 2004, pp. 369–397.
43. K. A. Van Houten, D. Heath, C. Barringer, A. L. Rheingold and R. S. Pilato, *Inorg. Chem.*, **37**, 4647 (1998).
44. N. Lardiés, E. Cerrada and M. Laguna, *Polyhedron*, **25**, 2785 (2006).
45. M. Nomura, M. Geoggroy, P. Adkine and M. Fourmigué, *Eur. J. Inorg. Chem.*, 5012 (2006).
46. M. Nomura, T. Cauchy and M. Geoggroy, *Inorg. Chem.*, **20**, 8194 (2006).
47. M. Fourmigué and N. Avarvari, *Dalton Trans.*, 1365 (2005).
48. M. Fourmigué, *Coord. Chem. Rev.*, **178**, 823 (1988).
49. (a) S. D. Cummings and R. Eisenberg, in *Dithiolene Chemistry: Synthesis, Properties, and Applications*, *Progress in Inorganic Chemistry*, Vol. 52 (Ed. E. I. Stiefel), John Wiley & Sons, Ltd, Chichester, 2004, pp. 315–367.
(b) S. D. Cummings and R. Eisenberg, *J. Am. Chem. Soc.*, **118**, 1949 (1996).
(c) M. A. Mansour, R. J. Lachicotte, H. J. Gysling and R. Eisenberg, *Inorg. Chem.*, **37**, 4625 (1998).
50. S. D. Cummings, L.-T. Cheng and R. Eisenberg, *Chem. Mat.*, **9**, 440 (1997).
51. K. Base, M. T. Tierney, A. Fort, J. Muller and W. Grinstaff, *Inorg. Chem.*, **38**, 287 (1999).
52. C.-T. Chen, S.-H. Liao, K.-J. Lin, C.-H. Chen and T.-Y. J. Lin, *Inorg. Chem.*, **38**, 2734 (1999).
53. J. S. Pap, F. L. Benedito, E. Bothe, E. Bill, S. De Beer George, T. Weyhermüller and K. Wieghardt, *Inorg. Chem.*, **46**, 4187 (2007).
54. (a) C. Makedonas and C. A. Mitsopoulou, *Spectrochim. Acta, Part A*, **64**, 918 (2006).
(b) C. Makedonas and C. A. Mitsopoulou, *Eur. J. Inorg. Chem.*, 2460 (2006).
(c) C. Makedonas, C. A. Mitsopoulou, F. J. Lahoz and A. I. Balana, *Inorg. Chem.*, **42**, 8853 (2003).
55. C. Makedonas and C. A. Mitsopoulou, *Eur. J. Inorg. Chem.*, 590 (2006).
56. B. W. Smucker, J. M. Hudson, M. A. Omary and K. R. Dunbar, *Inorg. Chem.*, **42**, 4714 (2003).
57. (a) A. Davison, J. A. McCleverty, E. T. Shawl and E. J. Wharton, *J. Am. Chem. Soc.*, **89**, 830 (1967).
(b) T. R. Miller and I. G. Dance, *J. Am. Chem. Soc.*, **95**, 6970 (1973).
58. R. Kato, H. Kobayashi, A. Kobayashi and Y. Sasaki, *Bull. Chem. Soc. Jpn.*, **59**, 627 (1986).
59. (a) F. Bigoli, C.-T. Chen, W.-C. Wu, P. Deplano, M. L. Mercuri, M. A. Pellinghelli, L. Pilia, G. Pintus, A. Serpe and E. F. Trogu, *Chem. Commun.*, 2246 (2001).
(b) E. A. M. Geary, L. J. Yellowlees, S. Parsons, M. L. Mercuri, P. Deplano, S. Clark and N. Robertson, *Dalton Trans.*, 5453 (2007).
60. (a) R. Kato, Y. Kashimura, H. Sawa and Y. Okano, *Chem. Lett.*, 921 (1997).
(b) Y. Kashimura, Y. Okano, J.-I. Yamaura and R. Kato, *Synth. Met.*, **103**, 2123 (1999).
61. M. Fourmigué and J. N. Bertran, *Chem. Commun.*, 2111 (2000).
62. (a) O. Jeannin, J. Delaunay, F. Barrière and M. Fourmigué, *Inorg. Chem.*, **44**, 9763 (2005).
(b) O. Jeannin and M. Formigué, *New J. Chem.*, **30**, 1774 (2006).
63. C.-T. Chen, S.-Y Liao, K.-J. Lin and L.-L. Lai, *Adv. Mater.*, **3**, 335 (1998).
64. M. C. Aragoni, M. Arca, C. Denotti, F. A. Devillanova, E. Grigiotti, F. Isaia, F. Laschi, V. Lippolis, L. Pala, A. M. Z. Slavin, P. Zanello and J. D. Woollins, *Eur. J. Inorg. Chem.*, 1291 (2003).
65. A. Vogler and H. Kunkely, *Angew. Chem., Int. Ed. Engl.*, **21**, 77 (1982).
66. A. Vogler and H. Kunkely, *J. Am. Chem. Soc.*, **103**, 1559 (1981).
67. S. A. Baudron, N. Avarvari and P. Batail, *Inorg. Chem.*, **44**, 3380 (2005).
68. J. M. Tunney, A. J. Blake, E. S. Davis, J. McMaster, C. Wilson and C. D. Garner, *Polyhedron*, **25**, 591 (2006).
69. J. P. Ferraris, D. O. Cowan, V. Jr. Walatka and J. H. Perlstein, *J. Am. Chem. Soc.*, **95**, 948 (1973).
70. D. Jérome, M. Mazaud, M. Ribault and K. Bechgaard, *J. Phys. Lett.*, **41**, L95 (1980).
71. (a) J. M. Williams, J. R. Ferraro, R. J. Thorn, K. D. Carlson, U. Geiser, H. H. Wang, A. M. Kini and M.-H. Whangbo, in *Organic Superconductors (Including Fullerenes)* (Ed. Russell N. Grimes), Prentice-Hall, Inc., Englewood Cliffs, NJ, 1992.
(b) U. Geiser and J. A. Schlueter, *Chem. Rev.*, **104**, 5203 (2004).

72. H. Tajima, M. Inokuchi, A. Kobayashi, T. Ohta, R. Kato, H. Kobayashi and H. Kuroda, *Chem. Lett.*, 1235 (1993).
73. A. T. Coomber, D. Beljonne, R. H. Friend, J. L. Brédas, A. Charlton, N. Robertson, A. E. Underhill, M. Kurmoo and P. Day, *Nature*, **380**, 144 (1996).
74. C. Faulmann, E. Rivière, S. Dorbes, F. Senoca, E. Coronado and P. Cassoux, *Eur. J. Inorg. Chem.*, 2880 (2003).
75. (a) R. T. Henriques, L. Alcácer, in *Inorganic and Organometallic Polymers with Special Properties* (Ed. R. Laine), Kluwer Academic Publishers, Boston, 1992, pp. 163–177.
(b) V. Gama, R. T. Henriques, G. Bonfait, L. C. Pereira, J. C. Waerenborgh, I. C. Santos, M. T. Duarte, J. M. P. Cabral and M. Almeida, *Inorg. Chem.*, **31**, 2598 (1993).
(c) V. Gama, R. T. Henriques, M. Almeida and L. Alcácer, *J. Phys. Chem.*, **98**, 997 (1994).
76. (a) V. Gama, R. T. Henriques, M. Almeida and J. P. Pouget, *Synth. Met.*, **55–57**, 1677 (1993).
(b) V. Gama, R. T. Henriques, G. Bonfait, M. Almeida, S. Ravy, J. P. Pouget and L. Alcácer, *Mol. Cryst. Liq. Cryst.*, **234**, 171 (1993).
77. R. E. Peierls, *Quantum Theory of Solids*, Oxford Universiry Press, Oxford, 1955, p. 108.
78. (a) H. Kobayashi, H. Tomita, T. Naito, A. Kobayashi, F. Sakai, T. Watanabe and P. Cassoux, *J. Am. Chem. Soc.*, **118**, 368 (1996).
(b) T. Courcet, I. Malfant, K. Pokhodnia and P. Cassoux, *New J. Chem.*, 585 (1998).
(c) H. Fujiwara, E. Ojima, H. Kobayashi, T. Courcet, I. Malfant and P. Cassoux, *Eur. J. Inorg. Chem.*, 1631 (1998).
79. N. J. Harris and A. E. Underhill, *J. Chem. Soc., Dalton Trans.*, 1683 (1987).
80. R. Kato, *Chem. Rev.*, **104**, 5319 (2004).
81. A. Kobayashi, E. Fujiwara and H. Kobayashi, *Chem. Rev.*, **104**, 5243 (2004).
82. O. J. Dautel, M. Fourmigué and E. Falques, *CrystEngComm.*, **4**(45), 249 (2002).
83. O. J. Dautel, M. Fourmigué, E. Canadell and P. Auban-Senzier, *Adv. Funct. Mater.*, **12**(10), 693 (2002).
84. (a) D. Belo, H. Alves, E. B. Lopes, M. T. Duarte, V. Gama, R. T. Henriques, M. Almeida, A. Pérez-Benítez, C. Rovira and J. Veciana, *Chem. Eur. J.*, **7**, 511 (2001).
(b) D. Belo, H. Alves, E. B. Lopes, M. T. Duarte, V. Gama, R. T. Henriques, M. Almeida, A. Pérez-Benítez, C. Rovira and J. Veciana, *Synth.. Met.*, **120**, 699 (2001).
85. E. Fujiwara, A. Kobayashi, H. Fujiwara and H. Kobayashi, *Inorg. Chem.*, **43**(3), 1122 (2004).
86. E. Fujiwara, K. Yamamoto, M. Shimamura, B. Zhou, A. Kobayashi, K. Takahashi, Y. Okano, H. Cui and H. Kobayashi, *Chem. Mater.*, **19**, 553 (2007).
87. K. Kubo, A. Nakao, H. M. Yamamoto and R. Kato, *J. Am. Chem. Soc.*, **128**, 12358 (2006).
88. S. S. Staniland, W. Fujita, Y. Umezono, K. Awaga, P. J. Camp, S. J. Clark and N. Robertson, *Inorg. Chem.*, **44**(3), 546 (2005).
89. F. Bigoli, P. Deplano, M. L. Mercuri, L. Marchiò, L. Pilia, A. Serpe, G. Concas, F. Congiu and S. Sanna, *Chem. Phys. Lett.*, **421**, 361 (2006).
90. O. Jeannin, R. Clérac and M. Fourmigué, *J. Am. Chem. Soc.*, **128**, 14649 (2006).
91. N. C. Schiødt, R. Sessoli and F. C. Krebs, *Inorg. Chem.*, **43**, 1986 (2004).
92. D. Belo, M. J. Figueira, J. P. M. Nunes, I. C. Santos, L. C. Pereira, M. Almeida, V. Gama, C. Rovira and J. Veciana, *J. Mater. Chem.*, **16**, 2746 (2006).
93. (a) H. Miyasaka, K. Nakata, L. Lecren, C. Coulon, Y. Nakazawa, T. Fujisaki, K. Sugiura, M. Yamashita and R. Clérac, *J. Am. Chem. Soc.*, **128**, 3770 (2006).
(b) H. Miyasaka, K. Nakata, K. Sugiura, M. Yamashita and R. Clérac, *Angew. Chem. Int. Ed.*, **43**, 707 (2004).
94. S. Curreli, P. Deplano, M. L. Mercuri, L. Pilia, A. Serpe, F. Bigoli, M. A. Pellinghelli, E. Coronado, C. J. Gómez-García and E. Canadell, *J. Solid State Chem.*, **168**(2), 653 (2002).
95. S. Curreli, P. Deplano, M. L. Mercuri, L. Pilia, A. Serpe, J. A. Schlueter, M. A. Whited, U. Geiser, E. Coronado, C. J. Gómez-García and E. Canadell, *Inorg. Chem.*, **43**, 2049 (2004).
96. P. Deplano, M. L. Mercuri, L. Marchiò, L. Pilia, M. Salidu, A. Serpe, F. Congiu and S. Sanna, *Eur. J. Inorg. Chem.*, 1829 (2005).
97. O. J. Dautel and M. Fourmigué, *J. Org. Chem.*, **65**, 6479 (2000).
98. H. J. Keller, R. Niebl, D. Nöthe, D. Schweitzer and A. Weber, *Physica B*, **143**, 301 (1986).
99. H. H. Wang, J. R. Ferraro, J. M. Williams, U. Geiser and J. A. Schlueter, *J. Chem. Soc., Chem. Commun.*, 1893 (1994).
100. P. Guionneau, C. J. Kepert, D. Chasseau, M. R. Truter and P. Day, *Synth. Met.*, **86**, 1973 (1997).

101. H. Kim, A. Kobayashi, Y. Sasaki, R. Kato and H. Kobayashi, *Bull. Chem. Soc. Jpn.*, **61**, 579 (1988).
102. A. Kobayashi, H. Tanaka, M. Kumasaki, M. Torii, B. Narymbetov and T. Adachi, *J. Am. Chem. Soc.*, **121**, 10763 (1999).
103. H. Tanaka, A. Kobayashi and H. Kobayashi, *J. Am. Chem. Soc.*, **124**, 10002 (2002).
104. W. E. Estes, D. P. Gavel, W. E. Hatfield and D. Hodgson, *Inorg. Chem.*, **17**, 1415 (1978).
105. (a) D. Belo, M. J. Figueira, J. P. M. Nunes, I. C. Santos, M. Almeida, N. Crivillers and C. Rovira, *Inorg. Chim. Acta*, **360**, 3909 (2007).
(b) J. P. M. Nunes, M. J. Figueira, D. Belo, I. C. Santos, B. Ribeiro, E. B. Lopes, R. T. Henriques, J. Vidal-Gancedo and J. Veciana, C. Rovira and M. Almeida, *Chem. Eur. J.*, **13**, 9841 (2007).
106. K. W. Plumlee, B. M. Hoffman, J. A. Ibers and Z. G. Soos, *J. Chem. Phys.*, **63**(5), 1926 (1975).
107. J. L. Xie, X. M. Ren, Y. Song, W. W. Zhang, W. L. Liu, C. He and Q. J. Meng, *Chem. Commun.*, 2346 (2002).
108. X. M. Ren, Y. Song, W. W. Zhang, W. L. Liu, C. He and Q. J. Meng, *Chem. Commun.*, 2346 (2002).
109. J. L. Xie, X. M. Ren, C. He, Y. Song, Q. J. Meng, R. K. Kremer and Y. Yao, *Chem. Phys. Lett.*, **41**, 369 (2003).
110. X. M. Ren, H. Okudera, R. K. Kremer, C. He, Y. Song, Q. J. Meng and P. H. Wu, *Inorg. Chem.*, **43**, 2569 (2004).
111. W. Fujita, K. Awaga, R. Kondo and S. Kagoshima, *J. Am. Chem. Soc.*, **128**, 6016 (2006).
112. O. Jeannin and M. Fourmigué, *Chem. Eur. J.*, **12**, 2994 (2006).
113. M.-H. Whangbo, J. M. Williams, A. J. Schultz, T. J. Emge and M. A. Beno, *J. Am. Chem. Soc.*, **109**, 90 (1987).
114. Y. Garcia, C. M. Grunert, S. Reiman, O. van Campenhoudt and P. Gütlich, *Eur. J. Inorg. Chem.*, 3333 (2006).
115. D. Jérome, *Chem. Rev.*, **104**, 5565 (2004) and references therein.
116. (a) O. Roubeau, A. Colin, V. Schmitt and R. Clérac, *Angew. Chem. Int. Ed.*, **43**, 3283 (2004).
(b) A. Dei, D. Gatteschi, C. Sangregorio and L. Sorace, *Acc. Chem. Res.*, **37**, 827 (2004).
117. T. Okamura, Y. Takano, Y. Yoshika, N. Ueyama, A. Nakamura and K. Yamaguchi, *J. Organomet. Chem.*, **569**, 177 (1998).
118. M. Deumal, M. A. Robb and J. J. Novoa, *Poyhedron.*, **22**, 1935 (2003) and references therein.
119. J. F. Ferrer, P. M. Lahti, C. George, P. Oliete, M. Julier and F. Palacio, *Chem. Mater.*, **13**, 2447 (2001).
120. D. O'Hare and J. S. Miller, *Mol. Cryst. Liq. Cryst.*, **176**, 381 (1989).
121. A. V. Zvarykina, Yu. S. Karimov, R. B. Ljubovsky, M. K. Makova, M. L. Khidekel, I. F. Shchegolev and E. B. Yagubsky, *Mol. Cryst. Liq. Cryst.*, **11**, 217 (1970).
122. D. Belo, M. J. Figueira, J. Mendonça, I. C. Santos, M. Almeida, M. T. Duarte, R. T. Henriques, C. Rovira and J. Veciana, *Eur. J. Inorg. Chem.*, 3337 (2005).
123. D. Belo, H. Alves, S. Rabaça, L. C. Pereira, M. T. Duarte, V. Gama, R. T. Henriques, M. Almeida, E. Ribera, C. Rovira and J. Veciana, *Eur. J. Inorg. Chem.*, **9**, 3127 (2001).
124. Z. Ni, X. M. Ren, J. Ma, J. Xie, C. Ni, Z. Chen and Q. Meng, *J. Am. Chem. Soc.*, **127**, 14330 (2005).
125. (a) E. Coronado and P. Day, *Chem. Rev.*, **104**, 5419 (2004); T. Enoki and A. Miyazaki, *Chem. Rev.*, **104**, 5449 (2004).
(b) H. Kobayashi, H. B. Cui and A. Kobayashi, *Chem. Rev.*, **104**, 5265 (2004).
(c) M. Kurmoo, A. W. Graham, P. Day, S. J. Coles, M. B. Hursthouse, J. L. Caulfield, J. Singleton, F. L. Pratt, W. Hayes, L. Ducasse and P. Guionneau, *J. Am. Chem. Soc.*, **117**, 12209 (1995).
(d) L. Martin, S. S. Turner, P. Day, F. E. Mabbs and E. J. L. McInnes, *J. Chem. Soc., Chem. Commun.*, 1367 (1997).
(e) S. Rashid, S. S. Turner, P. Day, J. A. K. Howard, P. Guionneau, E. J. L. McInnes, F. E. Mabbs, R. J. H. Clark, S. Firth and T. Biggs, *J. Mater. Chem.*, **11**, 2095 (2001).
126. (a) E. Coronado, S. Curreli, C. Giménez-Saiz and C. J. Gómez-García, *J. Mater. Chem.*, **15**, 1429 (2005).
(b) S. Uji, H. Shinagawa, T. Terashima, T. Yakabe, Y. Terai, M. Tokumoto, A. Kobayashi, H. Tanaka and H. Kobayashi, *Nature*, **410**, 908 (2001).

127. E. Coronado, J. R. Galán-Mascarós, C. J. Gómez-García and V. N. Laukhin, *Nature*, **408**, 447 (2000).
128. H. Hiraga, H. Miyasaka, K. Nakata, T. Kajiwara, S. Takaishi, Y. Oshima, H. Nojiri and M. Yamashita, *Inorg. Chem.*, **46**, 9661 (2007).
129. (a) L. Lecren, W. Wernsdorfer, Y.-G. Li, O. Roubeau, H. Miyasaka and R. Clérac, *J. Am. Chem. Soc.*, **127**, 11311 (2005).
(b) L. Lecren, W. Wernsdorfer, Y.-G. Li, A. Vindigni, H. Miyasaka and R. Clérac, *J. Am. Chem. Soc.*, **129**, 5045 (2007).
130. M. M. Ahmad, D. J. Turner and A. E. Underhill, *Phys. Rev. B*, **29**, 4796 (1984).
131. H. Miyasaka and M. Yamashita, *Dalton Trans.*, 399 (2007).
132. (a) J. P. Cornelissen, J. G. Haasnoot, J. Reedijk, C. Faulmann, J.-P. Legros, P. Cassoux and P. J. Nigrey, *Inorg. Chim. Acta*, **202**, 131 (1992).
(b) A. Abramov and M. L. Petrov, *Zh. Obshch. Khim.*, **66**, 1678 (1996).
133. K. Awaga, T. Okuno, Y. Maruyama, A. Kobayashi, H. Kobayashi, S. Schenk and A. E. Underhill, *Inorg. Chem.*, **33**, 5598 (1994).
134. N. Robertson, K. Awaga, S. Parsons, A. Kobayashi and A. E. Underhill, *Adv. Mater. Opt. Electron.*, **8**, 93 (1998).
135. P. Deplano, L. Leoni, M. L. Mercuri, J. A. Schlueter, U. Geiser, H. H. Wang, A. M. Kini, J. L. Manson, C. Gómez-García, E. Coronado and M. H. Whangbo, *J. Mater. Chem.*, **12**, 3570 (2002).
136. L. Pilia, C. Faulmann, I. Malfant, V. Collière, M. L. Mercuri, P. Deplano and P. Cassoux, *Acta Crystallogr., Sect. C*, **58**, 240 (2002).
137. M. Bousseau, L. Valade, J. P. Legros, P. Cassoux, M. Garbauskas and L. V. Interrante, *J. Am. Chem. Soc.*, **108**, 1908 (1986).
138. (a) H. Yamochi, N. Sogoshi, Y. Simizu, G. Saito and K. Matsumoto, *J. Mater. Chem.*, **11**, 2216 (2001).
(b) G. Saito, H. Izukashi, M. Shibata, K. Yoshida, L. A. Kushch, T. Kondo, H. Yamochi, O. O. Drozdova, K. Matsumoto, M. Kusunoki, K.-i. Sakaguchi, N. Kojima and E. B. Yagubskii, *J. Mater. Chem.*, **10**, 893 (2000).
139. S. S. Staniland, W. Fujita, Y. Umezono, K. Awaga, S. Crawford, S. Parsons and N. Robertson, *Mol. Cryst. Liq. Cryst.* **452**, 123 (1998).
140. (a) I. Nunn, B. Eisen, R. Benedix and H. Kisch, *Inorg. Chem.*, **33**, 5079 (1994).
(b) H. Kisch, *Coord. Chem. Rev.*, **159**, 385 (1997).
(c) H. Kisch, B. Eisen, R. Dinnebier, K. Shankland, W. I. F. David and F. Knoch, *Chem. Eur. J.*, **7**, 738 (2001).
141. (a) N. S. Hush, *Prog. Inorg. Chem.*, **8**, 391 (1967).
(b) R. A. Marcus and N. Sutin, *Comments Inorg. Chem.*, **5**, 119 (1997).
142. M. Yamashita, A. Ichikawa, T. Hama, T. Ohishi, T. Manabe, H. Miyamae, D. Yoshida, S. Sugiura, H. Kitagawa, Y. Iwasa and T. Mitani, *Mol. Cryst. Liq. Cryst.*, **284**, 391 (1996).
143. J. Fraxedas, *Adv. Mater.*, **14**, 1603 (2002) and references therein.
144. R. F. Service, *Science*, **267**, 1921 (1995).
145. (a) D. de Caro, I. Malfant, J. Fraxedas, C. Faulmann, L. Valade, J. Milon, J.-F. Lamère and V. Collière, *Adv. Mater.*, **16**, 835 (2004).
(b) I. Malfant, K. Rivasseau, J. Fraxedas, C. Faulmann, D. de Caro, L. Valade, L. Kaboub, J. M. Fabre and F. Senocq, *J. Am. Chem. Soc.*, **128**, 5612 (2006).
146. J. P. Savy, D. de Caro, I. Malfant, C. Faulmann, L. Valade, M. Almeida, T. Koike, H. Fujiwara, T. Sugimoto, J. Fraxedas, T. Ondarçuhu and C. R. Pasquier, *New J. Chem.*, **31**, 519 (2007).
147. J. P. Savy, D. de Caro, L. Valade, J.-P. Legros, P. Auban-Senzier, J. Fraxedas, C. R. Pasquier and F. Senocq, *EPL*, **78**, 37005 (2007).

CHAPTER 17

Deposition of metals and metal oxides by means of metal enolates

HEINRICH LANG and ROY BUSCHBECK

Technische Universität Chemnitz, Fakultät für Naturwissenschaften, Institut für Chemie, Lehrstuhl für Anorganische Chemie, Strasse der Nationen 62, 09111 Chemnitz, Germany
Fax: +49371/531-21219; e-mails: heinrich.lang@chemie.tu-chemnitz.de; roy.buschbeck@chemie.tu-chemnitz.de

The chemistry of metal enolates
Edited by Jacob Zabicky

I. ABBREVIATIONS

AA-CVD	aerosol-assisted chemical vapor deposition
acac	2,4-pentanedionate, acetylacetonate
acen	4,4′-(1,2-ethanediyldinitrilo)bis(2-pentanoate)
acim	4-imino-2-pentanoate
AFM	atomic force microscopy
ALD	atomic layer deposition
ALE	atomic layer epitaxy
AP	atmospheric pressure
atms	allyltrimethylsilane
AVD	atomic vapor deposition
bac	1-phenyl-1,3-butanedionate
bpp	1,3-diphenyl-1,3-propanedionate
btmsa	bis(trimethylsilyl)acetylene
cod	cyclooctadiene
cot	cyclooctatetraene
CSD	chemical solution deposition
CVC	chemical vapor condensation
CVD	chemical vapor deposition
dhd	2,2-dimethyl-3,5-heptanedionate
dhfa	1,1,1,2,2,3,3,4,4,5,5,6,6,10,10,11,11,12,12,13,13,14,14,15,15,15-hexacosafluoro-7,9-pentadecanedionate
DLI	direct liquid injection
dmb	3,3-dimethyl-1-butene
dmcod	1,5-/1,6-dimethyl-1,5-cyclooctadiene
EDS	energy disperse spectroscopy
EDX	energy disperse x-ray spectroscopy
EE-CVD	electro-enhanced chemical vapor deposition
ESD	electrostatic spray deposition
fdh	6,6,6-trifluoro-2,2-dimethyl-3,5-hexanedionate
FeRAM	ferroelectric random access memory
FESEM	field emission scanning electron microscopy
FGA	forming gas annealing
fod	6,6,7,7,8,8,8-heptafluoro-2,2-dimethyl-3,5-octanedionate
glyme	ethyleneglycol dimethyl ether

hfac	1,1,1,5,5,5-hexafluoro-2,4-pentanedionate, hexafluoroacetylacetonate
hy	1-hexene-3-yne
ibpm	2,2,6-trimethyl-3,5-heptanedionate
ITO	indium-doped tin oxide
LA-CVD	laser-assisted chemical vapor deposition
LEIS	low-energy ion scattering
MBE	molecular beam epitaxy
mbo	2-methyl-3-butene-2-ol
mdop	methyl 4,4-dimethyl-3-oxopentanoate
mep	Methylethylpentaglyme
MFM	magnetic force microscopy
mhd	5-methyl-2,4-heptanedionate
mhy	2-methyl-1-hexene-3-yne
MOCVD	metal organic chemical vapor deposition
MOD	metal organic deposition
mp	4-methyl-1-pentene
mpd	2-methyl-2,4-pentanediolate
MRI	magnetic resonance imaging
nonaF	1,1,1,5,5,5-hexafluoro-4-[(2,2,2-trifluoroethyl)imino]-2-pentanoate
ofac	1,1,1,5,5,6,6,6-octafluoro-2,4-hexanedionate
OLED	organic light-emitting diode
PA-CVD	plasma-assisted chemical vapor deposition
PE-CVD	plasma-enhanced chemical vapor deposition
pentaen	Pentaethylenehexamine
phen	1,10-phenanthroline
PHTS	plugged hexagonal templated silica
PLD	pulsed laser deposition
ppm	6,6,7,7,7-pentafluoro-2,2-dimethyl-3,5-heptanedionate
pta	1,1,1-trifluoro-5,5-dimethyl-2,4-hexanedionate
PTFE	Polytetrafluoroethylene
QCM	quartz crystal microbalance
SAM	self-assembled monolayer
SCR	selective catalytic reduction
SIMS	secondary ion mass spectrometry
SMO	superconducting metal oxide
SOFC	solid oxide fuel cell
tbaoac	*t*-butyl 3-oxobutanoate
T_c	critical temperature
TCO	transparent conductive oxide
tdap	tris(2-*N*,*N*-dimethylaniline)phospine
tet	Tetraglyme
tetea	tris(2-ethoxyethyl)amine
tetraen	tetraethylenepentamine
tfac	1,1,1-trifluoro-2,4-pentanedionate
TGA	thermogravimetric analysis
thd	2,2,6,6-tetramethyl-3,5-heptanedionate
tmeda	*N*,*N*,*N*′,*N*′-tetramethylethylenediamine
tmnd	2,7,7-trimethyl-3,5-octanedionate
tmod	2,2,6,6-tetramethyl-3,5-octanedionate
tmsmb	4-trimethylsilyl-2-methyl-1-butene-3-yne

tod	2,2,8,8-tetramethyl-4,6-nonanedionate
ULSI	ultra-large-scale integration
USP	ultrasonic spray pyrolysis
VPE	vapor phase epitaxy
vtms	vinyltrimethylsilane
XPS	x-ray photoelectron spectroscopy
YSZ	yttria-stabilized zirconia

II. INTRODUCTION

This chapter is intended to cover major aspects of the deposition of metals and metal oxides and the growth of nanosized materials from metal enolate precursors. Included are most types of materials which have been deposited by gas-phase processes, such as chemical vapor deposition (CVD) and atomic layer deposition(ALD), or liquid-phase processes, such as spin-coating, electrochemical deposition and sol–gel techniques. Mononuclear main group, transition metal and rare earth metal complexes with diverse β-diketonate or β-ketoiminate ligands were used mainly as metal enolate precursors. The controlled decomposition of these compounds lead to a high variety of metal and metal oxide materials such as dense or porous thin films and nanoparticles. Based on special properties (reactivity, transparency, conductivity, magnetism etc.) a large number of applications are mentioned and discussed. Where appropriate, similarities and difference in the decomposition mechanism that are common for certain precursors will be pointed out.

This chapter is organized in three main parts. In the first one the deposition and growth techniques generally used for the preparation of metal and metal oxide films and particles will be reported. The other two parts discuss the deposition of metals and metal oxides according to their classification as main group, transition metal and rare earth metal elements.

III. DEPOSITION TECHNIQUES

Most film and particle formation techniques can be divided into gas-phase and liquid-phase deposition processes, which are briefly discussed in this section. Deposition of metal and metal oxides from metal enolate sources results from application of CVD, ALD, spin-coating, electrochemical and sol–gel methods, which are discussed in detail elsewhere[1–6].

A. Gas-phase Transfer of Precursor

1. Chemical vapor deposition

CVD is a chemical gas-phase process often used for the deposition of thin layers of various materials with thicknesses between 0.1 and 10 μm. In a typical CVD experiment the substrate (object on which the deposition is made) is exposed to volatile inorganic, organometallic or metal-organic precursors which react and/or decompose on the heated substrate surface to give the desired film on elimination of volatile byproducts formed during the decomposition process. Inert carrier gases such as argon and nitrogen are favored to enhance the rate of transport of solid and liquid compounds to the reactor chamber, and also help removing volatile decomposition products. In addition, reactive carrier gases including hydrogen, ammonia and oxygen can be used as reducing and oxidizing reagents which may participate in the decomposition process. The properties of the deposits can be controlled by factors such as pressure, gas-flow rate and decomposition temperature.

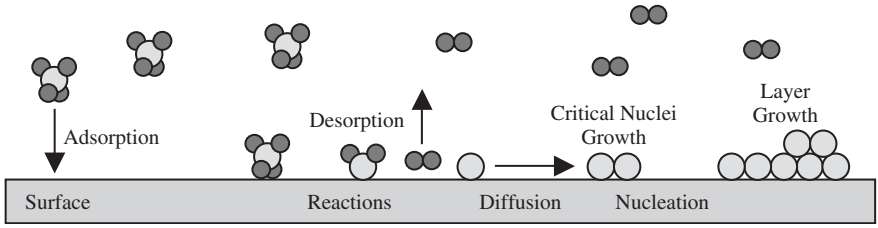

FIGURE 1. Schematic view of fundamental CVD steps

These parameters influence the mechanistic decomposition steps: adsorption–desorption, surface reactions, surface diffusion, nucleation, critical nuclei growth, layer formation and aging (Figure 1).

The reactions occurring in the gas phase or on the substrate surface responsible for the layer formation can be thermally activated by heating the CVD chamber together with the appropriate substrate (hot-wall CVD reactor), or by selective heating of the substrate (cold-wall CVD reactor). The heating and the precursor supply can be achieved by several methods. The most important ones being used for metal deposition from metal enolates are aerosol-, plasma- and laser-assisted CVD (AA-, PA- and LA-CVD, respectively). The AA-CVD technique is suitable for the use of nonvolatile or lowly volatile precursors in which the respective sources are transported to the substrate by means of an aerosol[1,7,8]. In the PE-CVD process an ionized vapor (plasma) is created to enhance the chemical reaction rates of the precursor. This is especially useful for temperature-sensitive substrates because of the lower thermal stress[1,8]. LA-CVD is a thin-film deposition process, where a focused laser beam is used to locally heat a substrate by visible or infrared light[1,8,9]. When ultraviolet light is used the metal sources undergo photolysis in the gas phase and on the substrate surface. The deposition rate of the LA-CVD process is much faster than can be achieved by conventional CVD and is a consequence of confining the reaction to a small region.

2. Atomic layer deposition

The chemistry of ALD is similar to that of CVD, except that ALD makes use of sequential precursor gas pulses to deposit a film layer-by-layer[1,4]. ALD film growth is self-limited and based on surface reactions, which makes achieving atomic-scale deposition control possible (monolayers can be obtained). In principle, the first ALD precursor is introduced into the process reactor producing only an adsorbed monolayer on the substrate surface because it cannot decompose completely without a second compound. After the second precursor is brought into the reactor chamber it reacts with the first precursor to afford the desired monolayer, as illustrated in Figure 2. Since each of such cycles produces exactly one monolayer, the thickness of the resulting film may be precisely controlled by the number of deposition cycles.

B. Spreading of Precursor Viscid Solutions

1. Spin coating

The spin-coating process allows the preparation of uniform thin films on plane substrates[10,11]. In a typical spin-coating experiment the precursor solution is placed onto the center of the substrate, which is then rotated at high speed (typically between 800

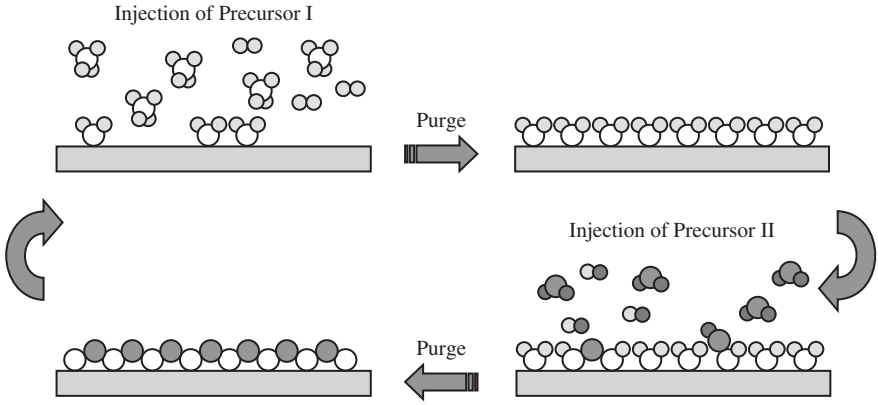

FIGURE 2. Schematic view of the ALD process

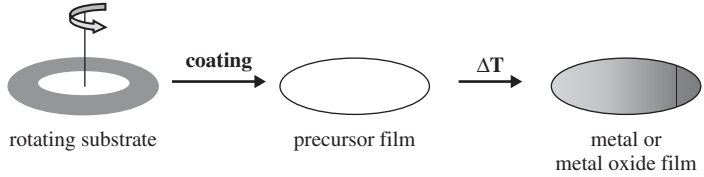

FIGURE 3. Schematic view of the spin-coating process

and 3000 rpm) spreading the solution by centrifugal force over the edge of the rotating substrate and leaving a thin film on the substrate surface (Figure 3). If the precursor is a solid or a highly viscous liquid, a solvent must be added to obtain a solution within a proper viscosity range. The final film thickness, quality, texture and other traits depend on properties of the liquid precursor, such as viscosity, drying rate and surface tension, and operational parameters chosen for the spin-coating process, such as acceleration, rotational speed and flow in the fume exhaust. The solvent is usually a volatile one and evaporates during the spinning operation. Higher spin speeds and longer spinning times lead to thinner films. Films of thickness below 10 nm can be obtained by this method.

2. Dip coating

Dip coating is a widespread procedure to create thin-film coatings of, for example, paint on a substrate piece. Therefore, the substrate is immersed into a solution of the coating material. The substrate remains there for some time to allow its complete wetting, followed by withdrawing it at constant speed. The higher the speed the thicker the film which remains on the surface. After the dip coating the coated pieces can be dried on air or baked in an oven, e.g. for the production of metal oxide films.

C. Electrochemical Deposition

Electrochemical deposition is the method of forming a thin layer on a substrate via an electrochemical reaction[12]. It can be used to obtain either cathodic films, such as

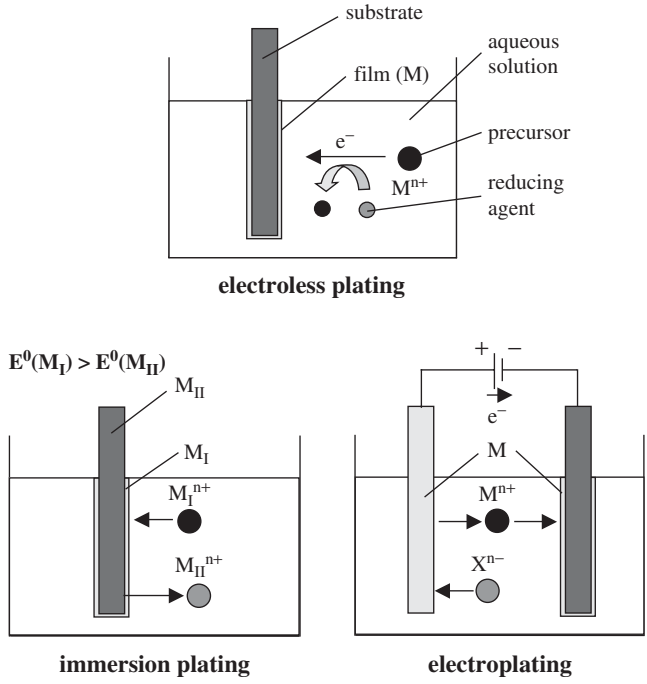

FIGURE 4. Redox methods for deposition of metal films

metals and polymers, or anodic films, such as metal oxides and polymers. In this context, electrophoresis and electropolymerization are special methods to achieve deposits with peculiar properties. These methods are used in industry for surface finishing by means of thin films (1–100 μm), endowed with attributes such as chemical or corrosion resistance and electronic conductivity. The deposit properties are influenced by different parameters such as electrolyte composition, current density and temperature.

Electroless plating, immersion plating, and electroplating are used to deposit metals onto a substrate (Figure 4)[12], wich are distinguished by the way dissolved metal ions M^{n+} become reduced and deposited as a metal M. In electroless plating the metal ions M^{n+} are reduced by chemical reagents in solution. Immersion plating involves reduction of the M^{n+} ions and deposition of M on the surface of a less noble metal substrate, which becomes oxidized and dissolved. This technique can be used to produce depositions of noble metals with a limited thickness. Electroplating requires an external current source to provide the electrons needed for the reduction process.

D. Sol–Gel Technique

The sol–gel process is a versatile solution process for making ceramic and glass materials involving the transition of a system from a colloidal suspension (sol) into a solid phase (gel)[13–15]. The resulting porous gel can be chemically purified and consolidated at high temperatures. In the classical sol–gel process, the precursor (e.g. a metal enolate or a metal alkoxide) is exposed to a series of hydrolysis and polymerization reactions to form

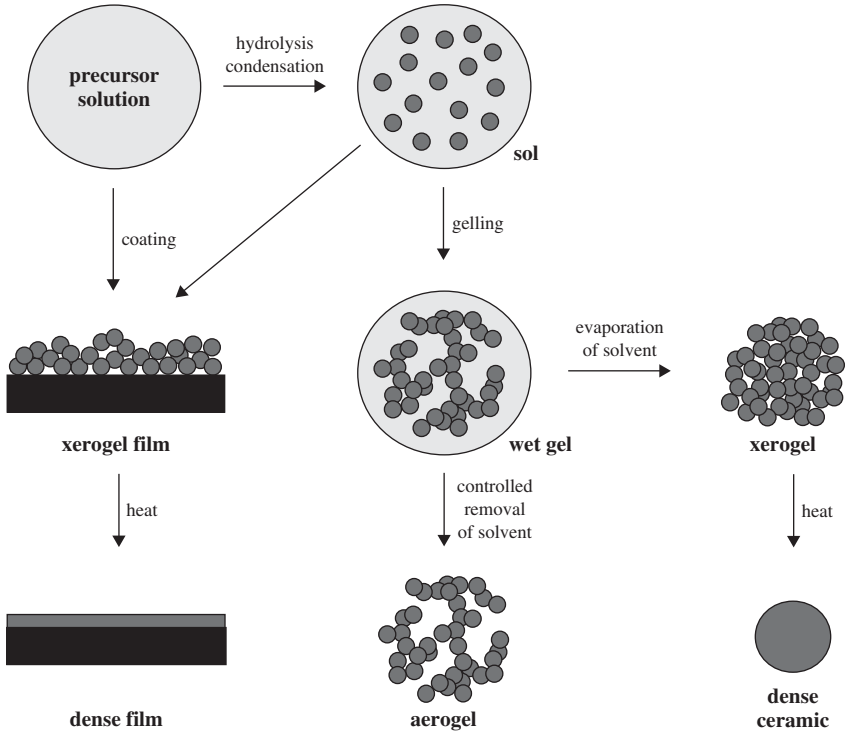

FIGURE 5. Schematic representation of the sol–gel technique

the colloidal suspension and afterwards the wet gel. Further drying converts the gel into a xerogel, which can be used to produce dense ceramic or glass materials by heat treatment (Figure 5). When the gel is dried under controlled conditions an aerogel is obtained. Thin films can be produced on a substrate by spin coating or dip coating (Section III.B).

IV. METAL DEPOSITION

Thin metallic films play an important role in diverse fields of applications, with special emphasis on micro- and nanoelectronics for which the metals Al, Cu, Ag, Au, Ti and W are essential[1,16–18]. Additional fields of commercial interests are electrodes as well as reflective, corrosion-resistant, oxidation-resistant and abrasion-resistant coatings[19]. Noble metals (periods 5 and 6 of groups 8–11 of the periodic table of the elements) are of special interest due to their manifold application in heterogeneous catalysis[20–22]. Other metals used in specialized industrial applications or as components of more complex materials such as metal alloys are Ni, Pd, Pt, Ag and Au. For example, FePt-based nanostructured materials are excellent candidates for future high-density magnetic recording media[23,24].

This section describes the formation of metals and metal alloys from metal enolate precursor sources (β-diketonates, β-ketoiminates) where chemical vapor deposition, spin coating and electrochemical deposition processes are used to generate blanket, surface selective or patterned surface structures.

A. Main Group Elements

1. Indium

In general, indium trialkyls (InR_3; R = Me, Et, ...) are used for CVD. However, these volatile compounds are very sensitive to oxygen and moisture and produce vigorous reactions when exposed to air[25]. Replacing one alkyl group in InR_3 with a β-diketonate unit gives $Me_2In(hfac)$ (**1**), a highly volatile complex, stable in air and moisture, which can be used for deposition of indium and indium-containing materials[26]. The volatility and thermal stability of this organometallic molecule was qualitatively examined by simultaneous TGA and DSC, showing that it can be handled without decomposition below 118 °C under atmospheric pressure. Indium and indium–copper alloys were deposited in a typical CVD experiment (bell jar quartz reactor, reactor pressure 0.9–2.0 Torr, bubbler temperature 60 °C, substrate temperature 300 °C, deposition time $\leqslant$10 min, no carrier gas) onto a copper substrate or platinum-coated silicon wafer[25]. The thin films were characterized by EDS and SEM. The Cu–In alloy from Cu(hfac)(mhy) and **1** showed a smooth film texture with grain sizes ranging from 0.1 to 0.2 μm and containing roughly 10% indium[25].

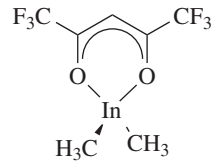

(**1**)

2. Bismuth

Formation of bismuth-containing thin films by CVD was demonstrated by Sievers and coworkers[27] using the volatile $Bi(fod)_3$ (**2**) as precursor source. In a hot-wall CVD apparatus (pyrex substrate, pressure 10^{-7}–10^{-6} Torr, precursor temperature 80–95 °C, $T_{Substrate}$ = 400–450 °C, deposition rate 10 nm min^{-1}) fluorine-free uniform layers with 73% bismuth were obtained[27]. The carbon (15%) and oxygen (12%) contaminations may be reduced or eliminated if hydrogen is used as carrier gas. No decomposition mechanism was given.

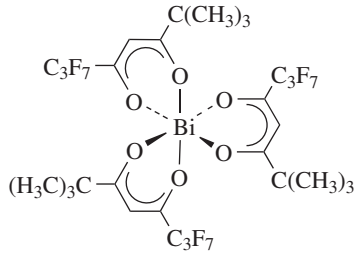

(**2**)

B. Transition Metal Elements

Many transition metal enolates are known today and most of them are applied in the deposition of metal films and in the synthesis of nanoparticles. Gas-phase deposition plays the most important role due to the enhanced volatility of the β-diketonato

complexes. Several comprehensive publications deal with this topic[1,28,29]. This section gives an overview about deposition and nanoparticle formation of metals and metal alloys from metal enolates. Pure metal films from group 3 and 4 metal enolates are not known due to their oxophilic character. They preferentially are used for the deposition of metal-oxide ceramics (Section V.B). Pure group 5 metal films and alloys are accessible from metal halides or organometallic compounds[1]; however, metal enolates from this group have not been described as CVD precursors to pure metal coatings so far.

1. Group 6 elements

As a group 6 metal enolate, $Cr(acac)_3$ has been studied by Sreedharan and coworkers[30]. Thermogravimetric and vapor pressure measurements showed that this complex can be vaporized at *ca* 230 °C without decomposition. The vapor pressure p, in Pa, can be calculated at temperature T, in K, using the equation $\log p = 14.16(\pm 0.07) - 5830(\pm 157)T^{-1}$, valid over the range 101–145 °C, from which an enthalpy of sublimation of $111.6 \pm 3.0\ \mathrm{kJ\,mol^{-1}}$ could be estimated. Based on these results $Cr(acac)_3$ was used in PA-CVD processes by the group of Dasgupta to deposit chromium onto stainless steel, silicon and quartz[31]. Thus, vapors from the precursor heated to 250 °C are carried by argon into an $Ar-H_2$ plasma (power density $70\ \mathrm{mW\,cm^{-2}}$). Decomposition takes place on a substrate heated to 550 °C, with a deposition rate of *ca* 1 μm h^{-1}. The coating films consist mostly of Cr with grain size of 10 nm and are uniform and adherent; they have a hardness of 1200 HV under loads of 100 and 200 g, which may be ascribed to the presence of strain and the nanocrystalline nature of the deposits[30].

2. Group 8 elements

a. Iron. $Fe(acac)_3$ was used as precursor for iron loading of ordered mesoporous MCM-41 by the incipient wetness impregnation procedure[32]. Thus, zeolithe MCM-41 spheres were stirred with the iron β-diketonate in toluene, followed by vacuum drying and calcination. The initial iron concentration has influence not only on the iron-loading content, but also on the mechanism of the iron-loading process (ligand exchange and hydrogen-bonding interaction mechanisms). The iron species anchored on the surface of the substrate shows a thermal decomposition behavior quite different from pure $Fe(acac)_3$. Such iron-containing mesoporous materials are of importance as catalysts for the oxidation of sulfur dioxide and hydrocarbons or the decomposition of N_2O[32].

b. Ruthenium. CVD of ruthenium using ruthenium enolate precursors has been investigated in only a few cases[33–37]. Ruthenium and RuO_2 are of particular interest for metallization in integrated circuit fabrication[33,38]. Such films can be deposited from different ruthenium precursors including coordination complex $Ru(acac)_3$ under a variety of conditions, such as deposition temperatures of 500 and 600 °C; operation under vacuum or using H_2 or O_2 as carrier gas, at pressures from 0.1 to 1.0 Torr; Si or SiO_2 served as substrate[34]. The precursor $Ru(acac)_3$, when compared to other investigated ruthenium organometallic and metalorganic compounds, provides films with high resistivities and with a carbon content reaching from 0 to 60 atom% depending on the deposition conditions. The films deposited at 500 °C showed poor adhesion, while the ones obtained at 600 °C adhered excellently on both substrates. Microstructures with grain sizes ranging from 10 to 100 nm were found[34].

In an earlier patent Crosby and coworkers described CVD processes of volatile ruthenium β-diketonates ($Ru(acac)_3$, $Ru(tfac)_3$, $Ru(hfac)_3$ etc.) on heat resistant substrates such as sintered carbides (WC/TiC/TaNbC/Co) in a low-pressure atmosphere[35].

A series of organometallic carbonyl complexes of general formula $Ru(CO)_2L_2$ (**3**), where L = acac, hfac, tfac, ofac, thd, dhd, was characterized by Liu and coworkers[36,37]. $Ru(CO)_2(hfac)_2$ (**3a**), $Ru(CO)_2(tfac)_2$ (**3b**) and $Ru(CO)_2(thd)_2$ (**3c**) were selected for CVD experiments due to their enhanced volatility. Ruthenium metal films were obtained under different deposition conditions either in the temperature range of 350–450 °C under H_2 blanketing or in the range 275–400 °C using O_2 dissolved in argon as carrier gas[37]. It must be alluded that the precise control of the oxygen partial pressure (for example, 2%) and accurate tuning of the deposition temperature are necessary for formation of pure ruthenium films. Deposition of ruthenium films was conducted using a cold-wall CVD reactor, whereby the sample reservoir was maintained at 30 °C for **3a**, 50 °C for **3b** and 70 °C for **3c** with deposition time being between 20 and 40 min. Si wafers, pyrex glass and Al_2O_3 were used as substrates. The deposited films were highly reflective, with good adhesion to the substrate. For example, complex **3a** gave films containing 95% Ru, along with 2% F and 3% O impurities, as determined by Auger and ESCA analyses (Table 1). The resistivity of these films, 48 μΩ cm, was attributed to the presence of impurities (the conductivity of bulk Ru is 7 μΩ cm). The film morphology was investigated by SEM showing smooth surfaces with neither pinholes nor cracks. The higher the deposition temperature, the rougher the surface, the larger the grain size and the thicker the film. When **3a** is used as precursor and the decomposition is carried out under pure oxygen, RuO_2 thin films are obtained (for a detailed discussion see Section V.B.6)[37].

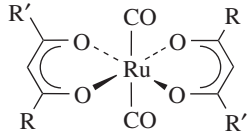

(**3**) (**a**) R = R′ = CF_3
(**b**) R = CH_3; R′ = CF_3
(**c**) R = R′ = *t*-Bu

β-Diketonate ruthenium complexes can also be used as precursors to grow Ru and RuO_2 layers by atomic vapor deposition (AVD®) on plain SiO_2/Si wafer materials and into trench structures (high *k* HfO_2/SiO_2/Si stacks, *k* = dielectric constant, Figure 6)[33]. AVD® is similar to CVD. The dissolved precursor is delivered in discrete pulses to the evaporation chamber and transported by an inert carrier gas to the showerhead, where it is mixed with a reactive gas (O_2). The deposition experiments were performed in an AIXTRON TriJet® reactor (Figure 7). The uniform ruthenium and ruthenium oxide films are strongly textured and have near bulk resistivity (Ru: 22 nm thickness, 11.5 μΩ cm;

TABLE 1. Ruthenium CVD conditions using ruthenium β-diketonates as precursors

Precursor	Evaporation temp. (°C)	Deposition temp. (°C)	Carrier gas	Reactor pressure (Torr)	Substrate	Film composition
$Ru(hfac)_2(CO)_2$ (**3a**)	30	500	—	0.5	SiO_2/Si, Al_2O_3	95% Ru, 3% O, 2% F
$Ru(tfac)_2(CO)_2$ (**3b**)	50	350	H_2	0.5	Si	94% Ru, 2% O, 4% F
$Ru(thd)_2(CO)_2$ (**3c**)	70	400	H_2	0.2	Si	97% Ru, 3% O

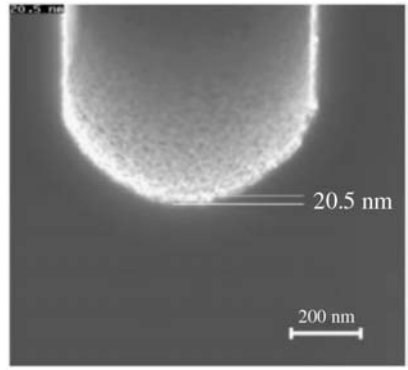

FIGURE 6. SEM micrograph of the bottom of a trench SiO_2/Si stack, coated with a 20 nm layer of Ru (coverage >90%)[33]. Reproduced from Reference 33 by permission of Elsevier

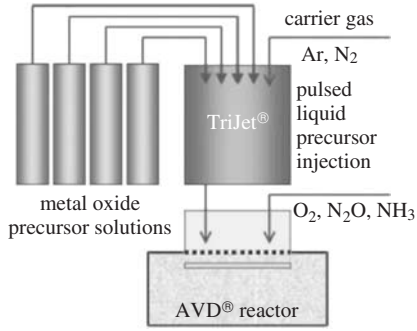

FIGURE 7. Schematic view of the TriJet AVD® reactor[33]. Reproduced from Reference 33 by permission of Elsevier

36 nm, 15.1 $\mu\Omega$ cm; RuO_2: 30 nm, 81.7 $\mu\Omega$ cm)[33]. The deviation from bulk resistivity can be explained by additional scattering of electrons at the surface and interface of these thin films. While the ruthenium grains are predominantly oriented along the (002) plane, the RuO_2 layers are nanostructured and polycrystalline. The work functions of nonannealed AVD Ru and RuO_2 films on silicon oxide are 5.06 and 5.30 eV, respectively. Treatment of the ruthenium layers by a forming gas annealing (FGA) process results in no interfacial layer growth on high-k HfO_2 gate stacks.

Lashdaf and coworkers described other ways for ruthenium deposition from $Ru(thd)_3$ on alumina and silica substrates, for example, from the gas phase by atomic layer epitaxy (ALE) and from the liquid phase by impregnation followed by reduction in a hydrogen atmosphere at temperatures as low as 140 °C[39]. Like other metal β-diketonates, $Ru(thd)_3$ is a relatively stable compound when vaporized, nonpyrophoric as well as easy to handle and to store[39]. TG measurements indicated that $Ru(thd)_3$ is more strongly bonded to alumina than to a silica surface. Mass spectrometric studies showed the formation of traces of ruthenium oxide in the impregnated samples which readily evaporate upon heating. This is a possible reason for the low ruthenium content of the ALE samples (density 0.1 Ru atom nm^{-2} on silica, 0.3 Ru atom nm^{-2} on alumina) in comparison to the impregnation

method (density 0.5–0.8 Ru atom nm^{-2} on silica, 1.9–2.8 Ru atom nm^{-2} on alumina)[39]. Reduction of the impregnated samples occurs already at 140 °C; for the ALE deposited Ru samples 300 °C is necessary to release all thd ligands. Ruthenium on alumina and silica supports are promising candidates for hydrogenation catalysis[39].

c. Osmium. Deposition of osmium metal films is mentioned only in a patent using $Os(CO)_2(acac)_2$ as precursor which decomposes at 280 °C[36], giving no additional information on the process conditions or the properties of the metal deposit.

3. Group 9 elements

a. Cobalt. High-purity thin films of cobalt can be deposited onto glass and quartz, using $Co(acac)_2$ as precursor and H_2 as carrier gas, in a hot-wall CVD reactor, at temperatures as low as 275–430 °C with a deposition rate of 100 nm min^{-1} [40]. Under the CVD conditions employed only 70% of the cobalt volatilized. Hydrogen was shown to be essential to the reduction. The films deposited had less than 0.5% C and 0.2% O. Feed-rate-limited deposition or transport-limited deposition was observed above 250 °C due to the large reaction area[40]. It was shown that the overall chemistry of the deposition process is more complicated than a direct reduction of the metal β-diketonate, because semisolid organic materials are deposited during the process, which are probably formed by catalytic reactions of the acac ligand on the cobalt surface (equation 1)[40].

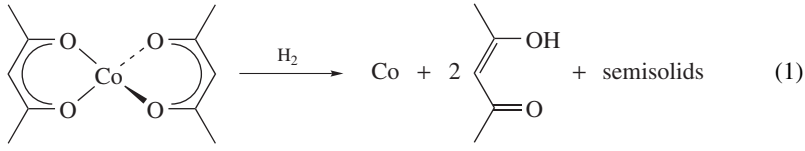

(1)

Silica-supported cobalt catalysts are accessible by ALE, after chemisorption onto silica of $Co(acac)_3$ from the gas phase with a metal loading between 5.7 and 19. 5 wt%[41]. The catalysts were tested for gas-phase toluene hydrogenation in a microreactor system.

Thin films of cobalt can be prepared by nebulized spray pyrolysis using $Co(acac)_2$ as precursor in a hydrogen atmosphere[42]. The obtained films show brilliant metallic and magnetic properties. Granular, magnetoresistant cobalt–copper alloys of composition $Co_{18}Cu_{82}$ and $Co_{50}Cu_{50}$ are accessible from $Co(acac)_2$ and $Cu(acac)_2$ mixtures under similar reaction conditions[42].

b. Rhodium. Several rhodium β-diketonates such as $Rh(acac)_3$[43], $Rh(thd)_3$[44], $Rh(CO)_2L$ (L = acac, hfac, thd)[45,46] and Rh(1,5-cod)(hfac)[47] have been used as suitable CVD precursors to deposit rhodium metal at high rates. Rhodium is favored over other noble atoms due to its lower resistivity, inertness and higher melting point for applications in electronics, for instance as diffusion barrier or seed material for copper in integrated circuits.

The group of Leskelä demonstrated the growth of metallic rhodium thin films of low resistivity (12.0 $\mu\Omega$ cm at 20 nm film thickness; bulk rhodium has 4.3 $\mu\Omega$ cm resistivity at 0 °C) and low impurity contents (0.1 atom% H, 1.6 atom% C, 2.3 atom% O) from $Rh(acac)_3$ and oxygen by ALD[43]. The film growth rate at 250 °C depends only on the $Rh(acac)_3$ pulse duration, and shows a linear dependence on the number of the deposition cycles. The films were analyzed by XRD showing a preferred (111) orientation and by SEM (Figure 8). The Rh grain size increases with increasing film thickness. The size

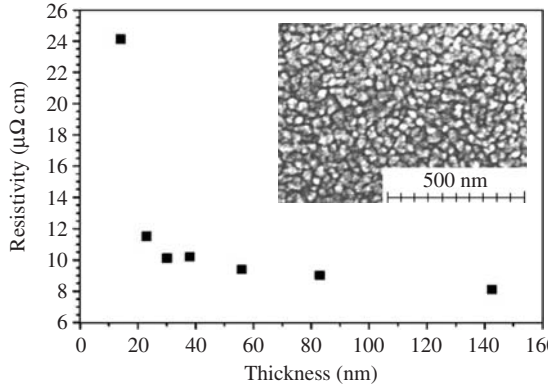

FIGURE 8. Resistivity of deposited Rh films as function of the film thickness. Inset: SEM image of a 25-nm-thick Rh film[43]. Reproduced from Reference 43 by permission of ECS—The Electrochemical Society

of the largest grains is approximately the same as the film thickness. Adhesion of the rhodium films to the Al_2O_3 substrate was acceptable. All films with thickness less than 80 nm passed the scotch tape test.

Ultrahigh vacuum CVD of rhodium films on Si and TiO_2-covered Si were carried out by Lu and coworkers using $Rh(CO)_2(acac)$ (**4a**)[45]. The metal layers obtained on Si in the temperature range of 200–500 °C contain significant amounts of carbon and oxygen contaminations which diminish during film growth. The use of TiO_2-covered silicon surfaces leads to a remarkable lowering of the initial impurities, indicating that the interaction of the precursor with the clean, reactive Si(111) surface generates the C and O found in the layers.

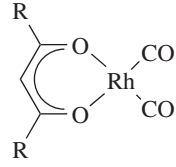

(**4**) (**a**) R = Me
(**b**) R = CF_3
(**c**) R = *t*-Bu

Direct drawing of pure rhodium lines is possible by LA-CVD, as was shown by Suhr and coworkers using $Rh(CO)_2L$ (L = acac (**4a**), hfac (**4b**), thd (**4c**)) as metal source[46]. Complex **4b** is favored over the other two species in view of the linewidth, resistivity, vapor pressure and working temperature. The decomposition pathway of the precursors includes the loss of the ligands and a successive degradation of CO and L before their total removal[46]. Deposition of a 95% purity Rh film from air stable Rh(1,5-cod)(hfac) has been reported by Baum and Larson in a patent, applying either plain CVD or LA-CVD, with substrate temperature 250–350 °C, using H_2 and He as carrier gas[47].

c. Iridium. The β-diketonate complexes $Ir(acac)_3$, $Ir(thd)_3$, $Ir(acac)_2(mhd)$ and Ir(1,5-cod)(acac) were investigated as precursors for CVD of iridium. However, little information

is available about the use of the two latter complexes for the preparation of iridium films on the surface of a carbon-containing electrode as discussed in early patents[44,47]. In contrast, Papke and Stevenson reported in 1967 that Ir(1,5-cod)(acac) is suitable for the deposition of iridium on copper substrates in high purity (85–99%) between 400 and 750 °C substrate temperature using hydrogen as carrier gas[48].

$Ir(acac)_3$ readily sublimes without decomposition at temperatures between 180 and 200 °C. White and coworkers[49] discussed low-temperature CVD of high purity, smooth, dense and homogeneous iridium films with grain sizes of 10–40 nm, on substrates such as Al_2O_3, SiO_2/Si, barium strontium titanate, TiCN and Ta_2O_5/Si. Both the substrate and oxygen play significant roles in the CVD process, for example, oxygen dissociatively adsorbs on iridium and recombinatively desorbs at 400 °C, therefore, introducing oxygen during film growth greatly suppresses carbon incorporation, increases the deposition rate and improves the film morphology, whereas the substrate has impact on the initial growth mode and the subsequent growth rate (e.g. the growth rate on TiCN is much higher than on SiO_2 surfaces). The topography of the films was compared applying AFM. It is found that on SiO_2 the roughness of the films directly depends on the initial three-dimensional growth mode on isolated islands. Iridium films were also grown on patterned wafers to examine step coverage and film morphology[49].

$Ir(acac)_3$ was also used to prepare heterogeneous catalysts by ALD of Ir on silica and alumina supports[50]. The surface-bound OH groups of the substrates were found to be responsible for the ligand exchange. The amount of the deposited iridium metal was controlled by varying different parameters, namely reaction temperature, support material and number of growing sites on the surface (by blocking with acetylacetone)[50]. $Ir(thd)_3$ can be used as precursor for CVD of iridium films on glass, using a vertical hot-wall CVD reactor (deposition temperature 350–500 °C)[51]. The profusion of CH_3 groups in the thd ligands makes this precursor more volatile than $Ir(acac)_3$, as demonstrated by TG measurements. The deposited films were found to consist of islands. The growth mechanism follows the Volmer–Weber model[51]. The crystallinity and surface morphology were determined by XRD and AFM.

4. Group 10 elements

a. Nickel. Deposition of nickel films on metallic and nonmetallic substrates is of importance for industry and advanced technology, for example, the encapsulation of graphite, metallization of ferrites, decorative and corrosion-resistant coatings, and as selective absorbers in solar thermal energy conversion[52]. Nickel is also a good material for microelectronics due to its low electrical resistivity and its high oxidation resistance.

Maruyama and Tago reported the successful deposition of highly adherent nickel thin films on borosilicate glass from $Ni(acac)_2$ by low-temperature atmospheric-pressure CVD[53]. At temperatures >250 °C, polycrystalline nickel films were obtained by hydrogen reduction. It was found that the deposition rate increases with increasing reaction temperature from 250 to 270 °C. However, at higher temperatures the precursor starts to decompose in the gas phase, leading to lower deposition rates. The resistivity (8.1–13.3 $\mu\Omega$ cm) of the films is close to that of bulk nickel (6.8–7.5 $\mu\Omega$ cm). Chelates, such as $Ni(hfac)_2$, $Ni(tfac)_2$[54], Ni acetylacetone imidate and Ni acetylacetoneethylene diimidate[55], were used for the deposition of Ni films as described in two early patents (depending on the precursor, deposition at 250 to 600 °C; hydrogen as carrier gas and reducing agent; quartz, platinum and stainless steel substrates).

A series of *N*,*N*′-bridged bis(2,4-pentanedione-iminoato) nickel(II) complexes (**5a**–**5d**) was studied by TG and DTA to determine equilibrium vapor pressures and enthalpies of sublimation and vaporization. Complexes **5a** and **5c** were found to be best suited to serve

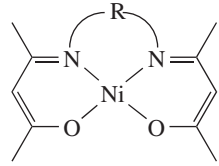

(**5**) (**a**) R = CH_2CH_2
(**b**) R = CH_2CHCH_3
(**c**) R = $CH_2CH_2CH_2$
(**d**) R = 1,2-C_6H_4

as sources for CVD of Ni in future experiments, because they can be vaporized without any significant decomposition at temperatures as low as 280 °C[56,57].

High-performance ceria-supported nickel catalysts (10 wt% Ni on CeO_2) for hydrodechlorination of chlorobenzene to benzene at 300 °C were prepared by Chary and coworkers[58], either by coprecipitation using $Ni(NO_3)_2$ or by impregnation using $Ni(NO_3)_2$ and $Ni(acac)_2$ as two alternative precursors. The dried catalysts were subjected to calcination in air at 500 °C. Catalysts prepared by coprecipitation had better catalytic performance in terms of hydrogenation activity, benzene selectivity and durability than the impregnated Ni/CeO_2 system. This is attributed to the nickel precursor used, higher dispersion of NiO crystallites having smaller particle size, and a significant interaction taking place between nickel particles and ceria during the course of reaction.

b. Palladium. Palladium is widely used in heterogeneous catalysis, for example, in hydrogenation and alkylation (Heck reaction) of olefins[59,60]. In general, Pd is deposited on a suitable support using precursors such as $Pd(thd)_2$[39], $Pd(hfac)_2$[61–63,65] and $Pd(acac)_2$[66–68], by gas-phase or liquid-phase methods, such as CVD, electroless plating and impregnation.

Girolami and Nuzzo described the surface-selective deposition of palladium from $Pd(hfac)_2$ based on a MOCVD *trans* metallation redox process (equation 2)[61–63].

$$Pd(hfac)_2 + Cu(0) \longrightarrow Pd(0) + Cu(hfac)_2 \qquad (2)$$

CVD has been conducted on diverse substrates in the range of 200–425 °C, both under vacuum (10^{-4} Torr) and hydrogen (gas flow 25 $cm^3\,min^{-1}$, pressure 10^{-2} Torr). Micron-thick films of pure palladium were only obtained when H_2 was used as carrier gas and reducing agent. The decomposition of $Pd(hfac)_2$ on copper was studied under ultrahigh vacuum conditions implying a multistep sequence (Scheme 1). The palladium precursor readily transfers its β-diketonate ligands to terrace atoms of the copper substrate whereby the Pd(II) ions are simultaneously reduced to Pd(0) yielding a palladium thin film and $Cu(hfac)_2$ (Scheme 1). The decomposition of the hfac ligands on the copper surface is self-limiting, i.e. graphitic impurities inhibit the decomposition pathway and promotes formation of $Cu(hfac)_2$. The driving force for redox *trans* metallation reaction is the favorable redox potential of the $Pd/Pd^{2+}//Cu^{2+}/Cu$ cell[62]. The activation parameters for the decomposition of the hfac chelating ligands on copper foils have been determined ($A = 1.3 \times 10^{13}\ s^{-1}$, $E_a = 36.8$ kcal mol^{-1}). The ability of surface microstructure to affect the rates of transport processes was demonstrated for this class of reaction by detailed kinetic and spectroscopic data[62,63].

The CVD decomposition behavior of binuclear $[Pd_2(PMe_3)_6](hfac)_2$ involves the disproportionation shown in equation 3[64]. Solid-state thermolysis (140 °C, vacuum) of [Pd_2

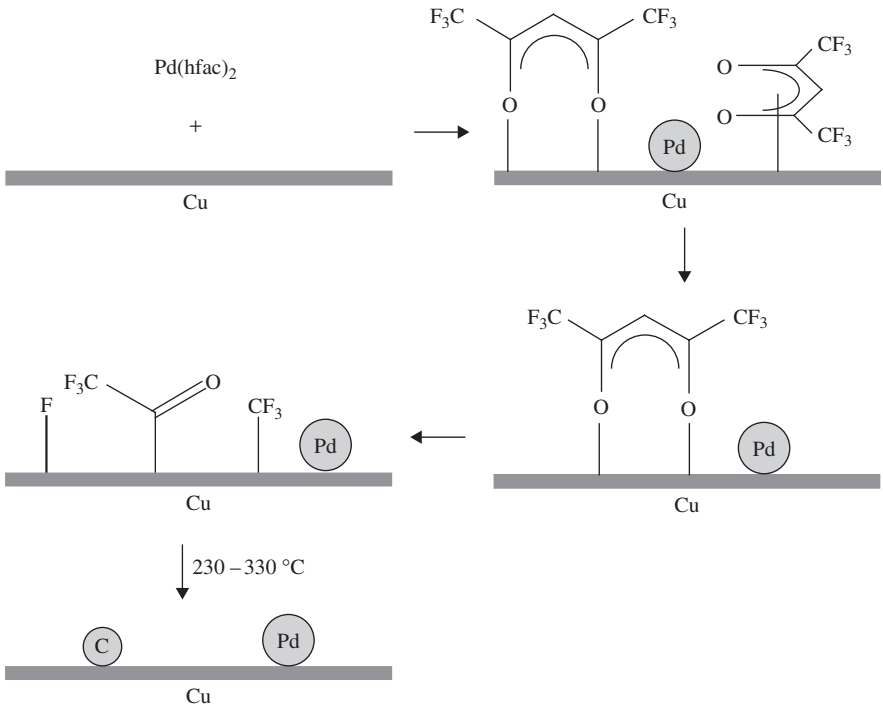

SCHEME 1. Decomposition mechanism of $Pd(hfac)_2$ on Cu under CVD conditions[62]. Reprinted with permission from Reference 62. Copyright 1996 American Chemical Society

$(PMe_3)_6](hfac)_2$ resulted in the cleavage of P−C bonds of the PMe_3 ligands to produce $[PdMe(PMe_3)_3](hfac)$, along with other palladium dimethylphosphido complexes. The P−C bond activation may generate surface-bound alkyl and dialkylphosphido intermediates, which on subsequent fragmentation may lead to the formation of C and P inclusions[64].

$$2Pd(I) \longrightarrow Pd(0) + Pd(II) \tag{3}$$

ALD of palladium films is possible by sequential exposures of the Al_2O_3 substrate to $Pd(hfac)_2$ and formalin, whereby the latter facilitates efficient nucleation of palladium[65]. Palladium film deposition proceeds via coalescence of islands with average growth rates of 0.2 Å/cycle (*ca* 0.1 Pd monolayer per cycle). The low deposition rate may result from site blocking of the surface by hfac ligands. The obtained films are cubic Pd with a roughness of 4.2 nm and resistivity of 11 $\mu\Omega$ cm at 42 nm thickness. Mesoporous anodic alumina membranes loaded with palladium (aspect ratio, *L*/*d* *ca* 1500) are promising hydrogen sensors[65].

Palladium can be deposited at low reduction temperatures on alumina or silica supports, either from the gas phase by ALE or from a solution by impregnation methods, using $Pd(thd)_2$ as precursor[39], as was described for ruthenium in Section IV.B.2.b. During ALE the precursor reacted to yield mainly metallic Pd, whereas on alumina only a small part of the impregnated metal source probably was dissociatively adsorbed yielding Pd(0). Associate adsorption describes the interaction of $Pd(thd)_2$ with the alumina and

silica supports in impregnation. Highly dispersed tunable alumina-supported palladium particles of size in the subnano range, with different physicochemical properties, were prepared by impregnation with $Pd(acac)_2$ in toluene solution as described by Thomazeau and coworkers[66].

A novel SiO_2-supported palladium metal catalyst for the ligand-free heterogeneous Heck reaction was prepared by Huang and coworkers by the reduction of $Pd(acac)_2/SiO_2$ in a hydrogen atmosphere with a 1% Pd loading[67]. It was found that the Pd/SiO_2 system is a highly active catalyst for the Heck carbon–carbon cross-coupling of bromobenzene with styrene to yield *cis*- and *trans*-stilbene. It should be noted that the activity over Pd/SiO_2 is comparable to that over a homogeneous Pd system, which can be explained by the small size of the supported palladium particles of size 12–15 nm *in-situ* generated with gentle reducing agents (CO and NMe_3 released by the decomposition of *N*,*N*-dimethylacetamide) at mild temperatures[67].

Boron nitride (130 $m^2\ g^{-1}$ surface area) was used as support for electroless plating with a low percentage (0.3–1.2 wt%) of noble metals including palladium, platinum, silver and gold[68]. In a typical experiment $Pd(acac)_2$ was reduced by hydrazine to give metal particles of *ca* 16 nm size. Preliminary catalytic tests for the total oxidation of methane in lean conditions (excess oxygen) have shown a good stability of the catalyst and a higher activity in the presence of water, but excessively high conversion temperatures (600–700 °C)[68].

c. Platinum. As nickel and palladium, also platinum has a variety of uses, for example, as heterogeneous catalyst and in alloy nanoparticles with specific magnetic properties. In this respect, only $Pt(acac)_2$ and $[Pt(acac)(Me)_3]_2$ (**6**) were used so far as precursor for deposition of platinum by CVD, vacuum pyrolysis and photolysis. Puddephatt and coworkers[69] showed that **6** can be used as volatile material for low-temperature CVD on silicon wafers in a vertical reactor at 250 °C. Films produced from this precursor showed good adherence but contained 30% C and 4% O impurities.

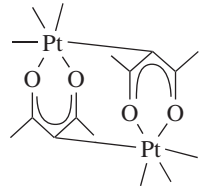

Rand[70] was the first to apply $Pt(acac)_2$ as source for platinum. The complex was vaporized at 150–200 °C in vacuum ($<2 \times 10^{-4}$ Torr) and decomposed at 500–600 °C on Si substrates, leaving films which were a 50:50 mixture of Pt and C. The high decomposition temperature makes this precursor undesirable in many applications. The high carbon content can be explained assuming comparable strengths for the Pt–O and C–C bonds, so that the β-diketonate ligands decompose simultaneously with the transition metal complex[70]. If hydrogen is present as reducing agent, $Pt(acac)_2$ will rapidly decompose to give Pt(0).

$Pt(acac)_2$ can be used as precursor for MOCVD of nanocrystalline platinum thin films on oxidized Si[71], quartz and CaF_2[72] substrates. The deposition on oxidized silicon was carried out with the substrate heated to 350 °C by oxygen-assisted pyrolysis in a low-pressure hot-wall reactor[71]. The films exhibit a preferred (111) orientation with a thickness of 12–140 nm, grain size 25 nm and a root-mean-square surface roughness of 5 nm. The growth of Pt films from $Pt(acac)_2$ occurred under a kinetically limited regime. The electrical resistivity was determined as 7.8–9 $\mu\Omega$ cm at 10 K[71]. Cross-sectional field emission scanning electron microscopy (FESEM) images showing conformal deposition

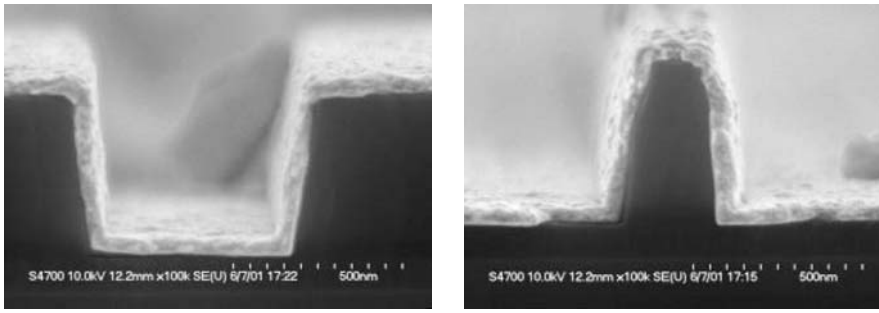

FIGURE 9. FESEM images of platinum-covered patterned SiO_2/Si substrates[71]. Reproduced from Reference 71 by permission of Wiley-VCH

of Pt onto patterned SiO_2/Si substrates are depicted in Figure 9, indicating a very dense and smooth surface morphology on the top and side-wall surfaces; the step coverage on the trench and plug varies between 85 and 95%[71]. $Pt(acac)_2$ was also used in low-pressure MOCVD of thin Pt nanostructured films on quartz and CaF_2 substrates at 420 °C[72], for possible combined electrochemical and spectroscopic applications. Independently of the reaction atmosphere (dry or wet $N_2 + O_2$, $N_2 + H_2$) the Pt films were formed as crack-free and well-adherent layers with no preferential orientation; however, they contained appreciable amounts of C and O due to incomplete β-diketonate decomposition via Pt-organic clusters[72].

Electrodes can be prepared by electrostatic spray deposition of nanocrystalline cubic Pt dense thin films on YSZ, using $Pt(acac)_2$ as precursor[73]. Investigation of the catalytic behavior of the deposited Pt as a function of the microstructural properties is currently in progress.

$Pt(acac)_2$ can be used for nanoparticle synthesis. A straightforward one-step photochemical synthesis of water-soluble Pt subnanometric particles was reported by Sortino and coworkers[74], who exposed a solution of $Pt(acac)_2$ and thioglycolic acid to visible light, where the latter reagent forms a carboxylate-terminated hydrophilic envelope to the Pt particles (equation 4). Such particles are candidates for biological applications and for 2- and 3-dimensional self-assembled nanocomposite devices[74].

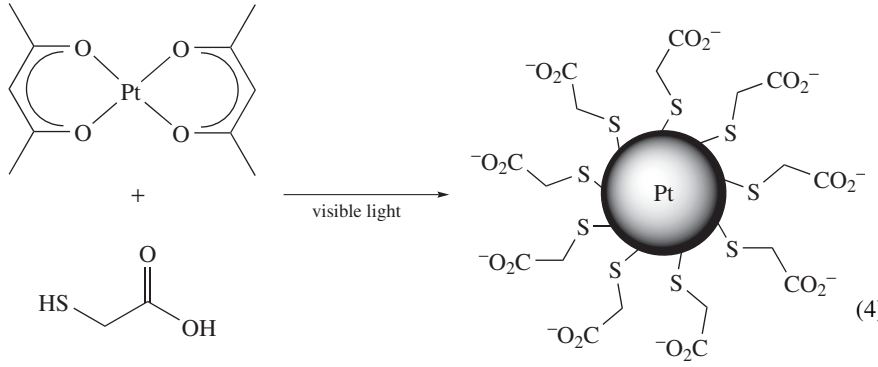

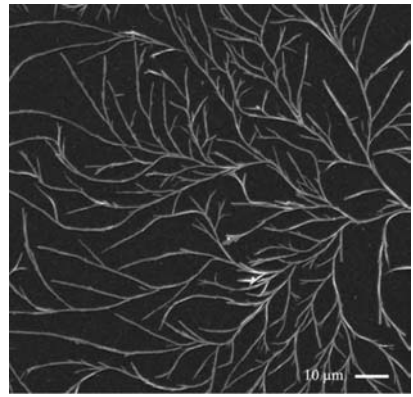

FIGURE 10. SEM of Pt fractal channels prepared by PA-CVD on SnO_2[76]. Reproduced from Reference 76 by permission of IEEE

The synthesis and activation of well-dispersed platinum nanoparticles with controlled size (3.5–11.5 nm) for fuel cell electrocatalysts was reported by Nikles and collaborators[75]. The synthesis involves the reduction of $Pt(acac)_2$ by polyalcohols using oleylamine as capping agent. The as-prepared particles were loaded on a carbon support and activated by heating in air at 185 °C. Size-dependent studies indicated that the smaller Pt particles have a significant higher intrinsic activity for methanol oxidation but a lower tolerance to CO poisoning than the larger ones.

Formation of platinum fractal-like structures is possible by PA-CVD (19% Ar, 80% O_2, 1% $SnMe_4$) on tin oxide thin films using $Pt(acac)_2$ as starting material[76]. The platinum aggregates show a dendritic structure of fractional dimension *D ca* 1.1–1.6 (Figure 10). The occurrence of such aggregates has been correlated to the concentration of the platinum precursor and to the radio-frequency power applied to the substrate electrode. Fabrication of microsensors integrated on silicon wafers with the help of photoresistors is possible[76].

Pt–SiO_2 composite films could be grown by low-temperature (300–440 °C) CVD from $Si(OEt)_4$ (teos) and $Pt(acac)_2$ in the presence of oxygen, as recently reported by DeSisto and coworkers[77]. The SiO_2 phase was amorphous and the platinum phase crystalline with average grain size of 9 nm, as determined by XRD. *In situ* FT-IR studies of the gas phase provide confirmation of the low-temperature decomposition of teos promoted by $Pt(acac)_2$. A cooperative teos-$Pt(acac)_2$ decomposition mechanism is proposed by the authors[77]. Nanostructured biphasic composite Pt–TiO_2 thin films of various Pt/Ti ratios were obtained by CVD using $Pt(acac)_2$ and $Ti(OPr\text{-}i)_4$ in an oxygen atmosphere at 400 °C[78]. The single growth process was kinetically controlled for TiO_2 and diffusion-limited for Pt. A theoretical model was developed on the basis of the two distinct types of growth that accurately predicts the composition of the mixed films[78], and was applied to prepare Pt–TiO_2-coated stainless-steel and gold electrodes[79]. The voltammetric behavior of these nanostructured electrodes has been investigated using the $[Ru(NH_3)_6]^{3+/2+}$ redox couple. These electrodes behaved as ensembles of platinum nanoelectrodes. The active sites of the composites investigated are smaller than 10 nm[79].

Three-dimensional PtRu nanostructures (i.e. $Pt_{85}Ru_{15}$, 5.9 nm particle size; $Pt_{78}Ru_{22}$, 6.7 nm) with defined shapes are available from $Pt(acac)_2$ and $Ru(acac)_3$ precursors[80]. Capping of indexed surfaces using adamantaneacetic acid and hexadecylamine led to formation

of cubic or tetrahedral nanodendrites of varied composition. These PtRu nanostructures are catalytically active in methanol oxidation.

Transition metal nanoparticles have attracted great attention due to their unique size-dependent properties and applications in diverse areas, including magnetic storage materials, catalysis, sensors and drug delivery[81–84]. Depositions of various Pt-containing alloys are summarized in Table 2. Particularly, chemically synthesized transition metal alloy

TABLE 2. Experimental conditions for synthesis and properties of platinum-containing nanoparticle alloys

Alloy	Precursors	Solvent	Stabilizer	$T_{deposition}$ (°C)	Size (nm)	References
$Pt_{47}Fe_{53}$	$Pt(acac)_2$, $Fe(CO)_5$	hexadecyl amine	1-adamantane-carboxylic acid	350–360	8	85, 86
$Pt_{51}Fe_{49}$	$Pt(acac)_2$, $Fe(CO)_5$	diphenyl ether, hexadecyl amine	1-adamantane-carboxylic acid	260	6	87
$Pt_{52}Fe_{48}$	$Pt(acac)_2$, $Fe(CO)_5$	dioctyl ether	oleic acid, oleylamine	290	3.5	88
Pt_xFe_y	$Pt(acac)_2$, $Na_2[Fe(CO)_4]$	several	oleic acid, oleylamine	297–370	1.7–7.7	89
$Pt_{75}Ru_{25}$, $Pt_{50}Ru_{50}$, $Pt_{25}Ru_{75}$	$Pt(acac)_2$, $Ru(acac)_3$	diphenyl ether	oleylamine	260	3.5–6.5	90
$Pt_{52}Co_{48}$	$Pt(acac)_2$, $[Co(CO)_3NO]$	dioctyl ether	oleic acid, oleylamine	286	7	91
$Pt_{43}Fe_{41}Cr_{16}$, $Pt_{46}Fe_{44}Cr_{10}$, $Pt_{47}Fe_{47}Cr_6$	$Pt(acac)_2$, $FeCl_2{\bullet}H_2O$, $Cr(acac)_3$	diphenyl ether	oleic acid, oleylamine	260	1.5	92
$Pt_{44}Fe_{49}Co_7$, $Pt_{43}Fe_{40}Co_{17}$, $Pt_{47}Fe_{34}Co_{19}$, $Pt_{50}Fe_{23}Co_{27}$	$Pt(acac)_2$, $Fe(CO)_5$, $Co(acac)_2$	dioctyl ether	oleic acid, oleylamine	290	3.5	88
$Pt_{42}Fe_{50}Pd_8$, $Pt_{35}Fe_{50}Pd_{15}$, $Pt_{25}Fe_{50}Pd_{25}$	$Pt(acac)_2$, $FeCl_2{\bullet}H_2O$, $Pd(acac)_2$	diphenyl ether	oleic acid, oleylamine	260	3.5	93
$[Pt_{51}Fe_{49}]_{88}Ag_{12}$	$Pt(acac)_2$, $Fe(CO)_5$, $Ag(acac)$	diphenyl ether	oleic acid, oleylamine	260	3.5	94–96
$Pt_{44}Fe_{48}Au_8$	$Pt(acac)_2$, $Fe(CO)_5$, $Au(ac)_3$	diphenyl ether, hexadecyl amine	1-adamantane-carboxylic acid	260	6	87
$Pt_{47}Fe_{48}Au_5$, $Pt_{40}Fe_{42}Au_{18}$, $Pt_{37}Fe_{38}Au_{25}$	$Pt(acac)_2$, $Fe(CO)_5$, $Au(ac)_3$	hexadecyl amine	1-adamantane-carboxylic acid	360	6	97
$[PtFe]_{100-x}Au_x$ $x = 1–24$	$Pt(acac)_2$, $Fe(CO)_5$, $Au(ac)_3$	diphenyl ether	oleic acid, oleylamine	260	3.5	98

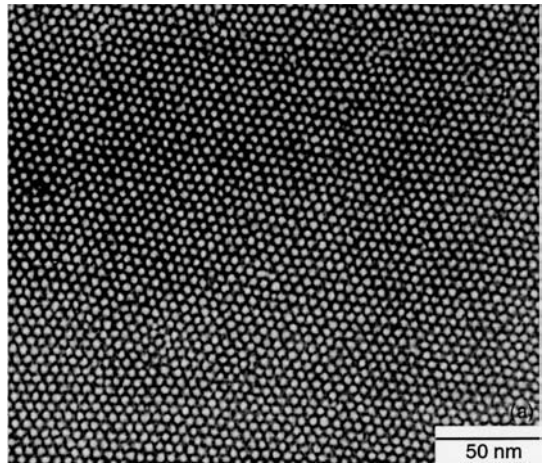

FIGURE 11. TEM image of self-assembled $[Pt_{0.47}Fe_{0.53}]_{88}Ag_{12}$ nanoparticles[96]. Reproduced from Reference 96 by permission of the American Institute of Physics

nanoparticles such as Fe_mPt_n and Co_mPt_n ($m + n = 100$) have been extensively studied by Nikles because of their chemical stability and high magnetocrystalline anisotropy[88,91]. The metal enolate precursors that have been most extensively studied for the alloys listed in Table 2 are $M(acac)_2$ (M = Pt, Co, Pd) and $M(acac)_3$ (M = Ru). The appropriate precursor components were dissolved in high-boiling organic solvents, such as dioctyl ether or diphenyl ether, were heated under continuous stirring in the presence of stabilizers including hexadecane-1,2-diol, oleic acid and oleyl amine, resulting in the formation of black suspensions containing the respective Pt_mM_n nanoparticles. By varying the surfactants, solvent and temperature the size and structural properties of the particles can be controlled[85,86,89]. A third alloy element (M′ = Cr, Co, Pd, Ag, Au) can be introduced in various proportions to incorporate within the nucleating nanoparticles of formula $Pt_mM_nM'_p$ ($m + n + p = 100$) (Table 2). These nanoparticles were characterized by elemental analysis, XRD, EDX and TEM (Figure 11). The magnetic anisotropy and switching volumes were explicitly determined from time- and temperature-dependent dynamic coercivity measurements (Figures 12 and 13)[96].

Lin and coworkers[99] systematically varied the conditions for the synthesis of Fe–Pt and Co–Pt alloy nanoparticles to gain closer insight on how the specific ligand–metal interactions affect the nucleation and growth of the nanoparticles. Thus, the concentrations of the precursors ($Pt(acac)_2$, $Fe(CO)_5$ and $Co_2(CO)_8$) and the stabilizers (oleic acid and trioctylphosphine oxide) were varied in such a way that the effect of the ligand stabilizer is amplified and becomes a dominant factor in determining the reaction pathway. As a result, the authors report that the growth of alloy nanoparticles is limited in size and constitution depending on the ligand type and the concentration.

Platinum, ruthenium and PtRu alloy nanoparticles, prepared by vacuum pyrolysis using $Pt(acac)_2$ and $Ru(acac)_3$ as precursors, were applied as anode catalysts for direct methanol oxidation[100]. The nanoparticles, uniformly dispersed on multiwalled carbon nanotubes, were all less than 3.0 nm in size and had a very narrow size distribution. The nanocomposite catalysts showed strong electrocatalytic activity for methanol oxidation, which can

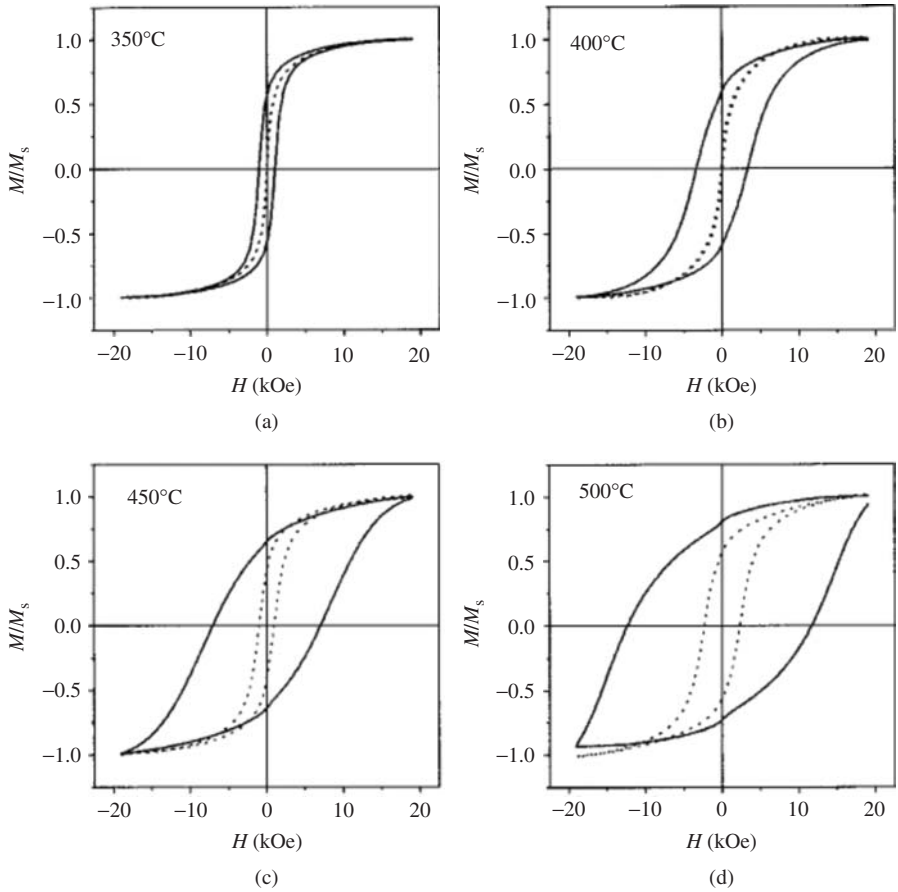

FIGURE 12. In-plane hysteresis loops of self-assembled $[Pt_{0.47}Fe_{0.53}]_{88}Ag_{12}$ (solid line) and $Fe_{53}Pt_{47}$ (dotted line) nanoparticle arrays annealed at different temperatures (H = field strength, M = magnetization, M_s = saturated magnetization)[96]. Reproduced from Reference 96 by permission of the American Institute of Physics

be explained by the formation of well-dispersed Pt–Ru alloy nanoparticles and the large surface area of the substrate[100].

5. Group 11 elements

a. Copper. Copper deposition processes play an important role in the microelectronic industry, especially for fabrication of the ULSI circuit technology[101]. Recently, copper became more valuable due to its lower resistivity (Cu 1.7 $\mu\Omega$ cm, Al 2.7 $\mu\Omega$ cm, W 5.6 $\mu\Omega$ cm), higher thermal conductivity, improved electromigration resistance (up to 4 orders of magnitude larger than aluminum) and increased resistance to stress-induced voidage, as compared to Al and W[102].

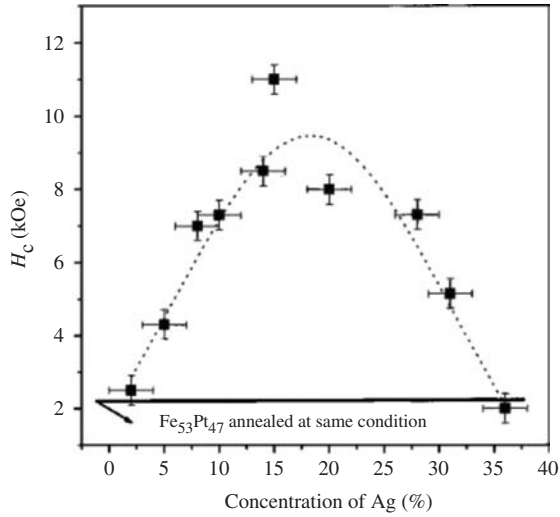

FIGURE 13. Coercitivity field strength ($\boldsymbol{H}_c$) as function of the Ag concentration for self-assembled $[Pt_{0.47}Fe_{0.53}]_{100-x}Ag_x$ nanoparticles annealed at 500 °C[96]. Reproduced from Reference 96 by permission of the American Institute of Physics

Numerous deposition methods, such as ionized metal plasma deposition, physical vapor deposition, ALD, CVD, PA-CVD, PE-CVD, electroplating and electroless plating have been used to deposit copper films on different substrates[1]. For CVD and ALD, several copper(I) and copper(II) enolates were developed which may be of interest as suitable precursors. The use of these complexes enabled the development of new technologies that are demanded to fulfill the requirements of the microelectronic industry.

i. Copper(II) precursors. In this section we discuss the current status of the deposition of copper thin films from copper(II) β-diketonates (e.g. **7a**–**7f**), and β-ketoiminates with bidentate (e.g. **8a** and **8b**) or multidentate (e.g. **9**) ligands, including adsorption studies, mechanistic considerations, growth rates, reaction conditions and film properties. Typical deposition conditions are summarized in Table 3.

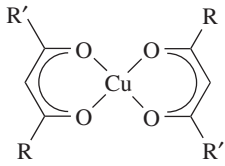

(**7**) (**a**) R = R′ = Me
(**b**) R = Me, R′ = CF_3
(**c**) R = R′ = CF_3
(**d**) R = R′ = *t*-Bu
(**e**) R = *t*-Bu, R′ = C_2F_5
(**f**) R = *t*-Bu, R′ = C_3F_7

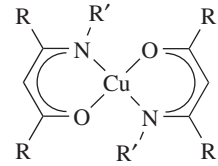

(**8**) (**a**) R = Me, R′ = H
(**b**) R = CF_3, R′ = CH_2CF_3

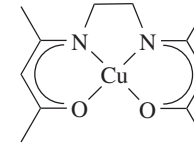

(**9**)

TABLE 3. CVD of Cu using copper(II) enolate precursors

Precursor	Evaporation temperature (°C)	Deposition temperature (°C)	Deposition rate (nm min^{-1})	Carrier gas	Reactor pressure (Torr)	Substrate	References
$Cu(acac)_2$ (**7a**)	180–200	225–250	20	H_2/Ar	760	SiO_2	103
$Cu(acac)_2$ (**7a**)	80	290–350	23	H_2	3	SAM/Si	104
$Cu(tfac)_2$ (**7b**)	135–160	250–300	—	H_2	760	glass, stainless steel	105, 106
$Cu(hfac)_2$ (**7c**)[a]	80–95	250–300	80	H_2	760	glass, stainless steel	105, 106
$Cu(hfac)_2$ (**7c**)	80–85	200	10	H_2	760	glass	107
$Cu(hfac)_2$ (**7c**)	120	340–390	4	Ar	760	SiO_2	108
$Cu(hfac)_2$ (**7c**)	30–60	250–350	120–180	H_2	10^{-3}–760	SiO_2, TiN, Al_2O_3	109
$Cu(hfac)_2$ (**7c**)	90–110	250–275	10–15	H_2	10^{-3}–760	glass	110
$Cu(hfac)_2$ (**7c**)	45–60	350	10	H_2	7–15	W, Cr, Al, Zr, $TiSi_2$	111
$Cu(hfac)_2$ (**7c**)	50–100	350–390	20–90	H_2O/H_2	15	Ta/Si	112
$Cu(hfac)_2$ (**7c**)	100	400	—	none	10	SiO_2	113
$Cu(hfac)_2$ (**7c**)	55–90	310–380	20–65	H_2	2–10	SiO_2, TiW, $TiSi_2$	114
$Cu(thd)_2$ (**7d**)	100	400	—	none	$<10^{-2}$	SiO_2	113
$Cu(ppm)_2$ (**7e**)	100	400	—	none	<0.3	SiO_2	113
$Cu(fod)_2$ (**7f**)	—	300–400	—	H_2	10^{-3}–760	SiO_2	109
$Cu(acim)_2$ (**8a**)	287	400	—	H_2	730	quartz	115
Cu(acen) (**9**)	204	450	—	H_2	730	quartz	115
$Cu(nonaF)_2$ (**8b**)	85–105	270–350	70	H_2	10–70	SiO_2, W, TiN	116

[a] This precursor is in fact a hydrate, $Cu(hfac)_2 \bullet H_2O$, containing various amounts of water.

The first reports on copper CVD came from van Hemert (1965)[105] and Moshier (1967)[106] describing the use of $Cu(tfac)_2$ (**7b**) and $Cu(hfac)_2 \bullet H_2O$ as volatile CVD precursors for deposition of copper in a hot-wall, horizontal tube reactor, under the operating conditions listed in Table 3. It should be noted that precursor **7c** requires lower temperatures for vaporization than **7b**. Various copper(II) β-diketonates listed in Table 3 became relevant for today's CVD technology. In the presence of a reducing carrier gas, such as hydrogen, the deposition process can be formulated as shown in equation 5.

$$Cu(\beta\text{-diketonate})_2 + H_2 \longrightarrow Cu(0) + 2\beta\text{-diketone} \quad (5)$$

Analogous processes can be accomplished by reducing agents other than hydrogen, such as hydrazine and carbon monoxide. Reduction with CO involves partial decomposition of the ligands giving carbon-, oxygen- and fluorine-containing organic fragments, which may be incorporated as impurities in the copper films[1]. For example, $Cu(hfac)_2$ (**7c**) produces C, O and F film contaminations on decomposition. However, higher temperatures produce more carbon film impurities due to the onset of the ligand decomposition itself[106]. It was

proposed that decomposition of the precursor proceeds by self-reduction. If the precursor is a hydrate, as in the case of $Cu(hfac)_2 \bullet H_2O$ in note[a] of Table 3, a two-step decomposition takes place, whereby ketone hfacH is eliminated affording CuO, which afterwards will be reduced by hydrogen to give metallic copper and water[105]. Summing up, the two steps can be viewed as a process in which the H_2O molecule acts essentially as a catalytic carrier for a hydrogen atom transfer.

The advantage of using hydrogen as reducing agent is that very pure copper films are formed, i.e. $Cu(hfac)_2$ (**7c**) gives copper films of purity >99%[109]. In contrast, a 10/90 mixture of H_2/Ar leads to serveral impurities including C (15%), O (10%), and F (5%)[103], while pure argon or nitrogen as carrier gases increase the oxygen content significantly (*ca* 30%); for example, **7c** decomposes in argon at 1 atm to metallic copper and Cu_2O[117]. This clearly shows that hydrogen is indispensable for protonating the enolate to desorb cleanly from the surface. In general, resistivities in the range of 1.7 to 2.4 $\mu\Omega$ cm (bulk Cu 1.67 $\mu\Omega$ cm) were found for Cu films deposited in hydrogen atmosphere from fluorinated copper(II) enolates[111, 118].

Selective depositions of copper on pre-patterned $TiSi_2$, W, Cr, Al and Zr substrate layers were also carried out successfully[111]. Adsorption studies with copper(II) β-diketonates, such as $Cu(acac)_2$ (**7a**) and $Cu(hfac)_2$ (**7c**)[119, 120], proved that the appropriate precursors adsorb dissociatively under typical CVD conditions under reducing hydrogen atmosphere, as depicted in Scheme 2.

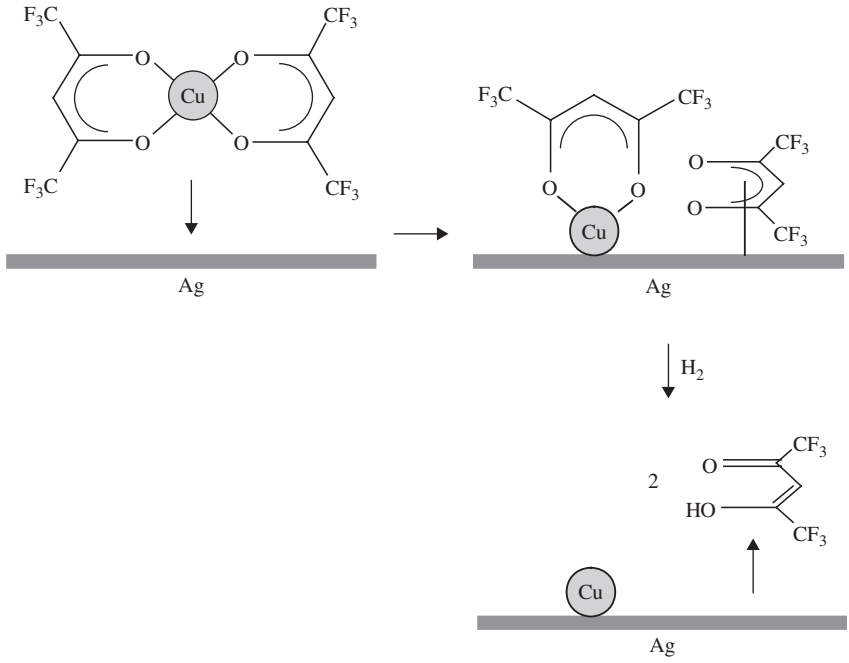

SCHEME 2. Possible mechanistic steps in the deposition of metallic copper on metallic silver substrates from copper(II) enolates[120]. Reproduced from Reference 120 by permission of Wiley-VCH

CVD of copper films was carried out on metallic substrates modified by a SAM of $HSCH_2CH_2CH_2Si(OMe)_3$ (3-mercaptopropyltrimethoxysilane) using the precursor

$Cu(hfac)_2$ (**7b**)[104]. The quality of the copper films deposited on the SAM diffusion barrier was high regarding purity and uniformity, comparable to that of films deposited on Si(100) and traditional diffusion barriers (TiN). Copper selenide binary phases can be grown from $Cu(acac)_2$ (**7a**) and trioctylphosphine selenide. Depending on the techniques applied, tetragonal Cu_2Se (aerosol-assisted CVD) or cubic $Cu_{2-x}Se$ nanoparticles capped with hexadecylamine (liquid deposition) are produced[121].

Further CVD methods to deposit metallic copper thin films are laser-assisted techniques (pyrolytic and photochemical LA-CVD) most commonly used for direct writing applications such as mask repair, circuitization and localized doping[122–124]. Diverse plasma-assisted copper CVD processes have also been reported showing the advantages of PA-CVD including higher growth rate and lower substrate temperatures which results in the possible improvement of microstructures[118, 125–127].

Besides copper(II) β-diketonates, also β-ketoiminato complexes such as $Cu(acim)_2$ (**8a**) and Cu(acen) (**9**) have been investigated as CVD precursors[115]. Hydrogen reduction is also necessary to obtain pure copper films. The disadvantage of both compounds is that they require high decomposition temperatures. Nevertheless, fluorinated $Cu(nonaF)_2$ (**8b**) needs lower temperatures for evaporation and deposition, even below those of $Cu(hfac)_2$ (Table 3)[116].

Another promising class of copper(II) β-diketonates has been synthesized by Toscano and Welch by substitution of a carbon atom by silicon[128, 129]. Copper(II) sila-β-diketonates and their fluorinated derivatives have greater volatility than the corresponding carbon–hydrogen analogues and some of them exist as liquids or low melting solids, the preferred state for industrial CVD processes. Two different deposition modes of this class of precursors are also discussed (Scheme 3)[130].

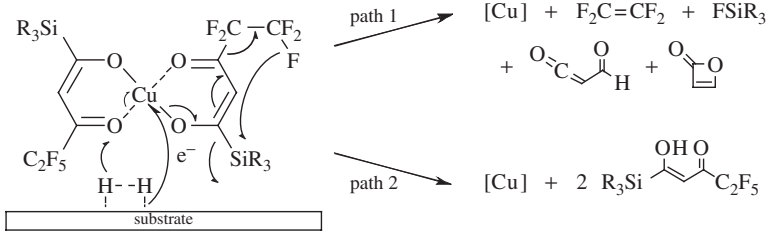

SCHEME 3. Deposition modes for Cu(II) α-fluoroalkyl-α'-trialkylsila-β-diketonates[130]. Reproduced from Reference 130 by permission of Elsevier

Laser-induced chemical liquid deposition of copper films on quartz and glass from $Cu(acac)_2$ (**7a**) as precursor was reported by Ouchi and collaborators[131]. The process is realized through the interaction of copper colloids with the appropriate surfaces. It was found that, depending on whether the laser irradiation is discontinuous (ArF laser) or continuous (KrF laser), closed copper films or nano-islands were formed. This method differs from the laser-assisted liquid-phase metallization of polymers, wherein a laser beam was used to enhance chemical reduction of copper(II) salts[131].

Sol–gel and dip-coating procedures were applied to prepare copper nanomaterials[132]. Alumina-supported copper nanoparticles from $Cu(acac)_2$ and $Al(OPr\text{-}i)_3$ were synthesized by Kantam and coworkers[132] by the aerogel procedure. The $Cu–Al_2O_3$ nanoparticles were characterized by several analytical methods and were successfully used as catalysts for the preparation of 1,2,3-triazoles by the reaction of terminal alkynes, NaN_3 and alkyl/allyl halides.

Copper-coated carbon nanotubes are accessible by decomposition of preliminary adsorbed $Cu(acac)_2$ in a hydrogen atmosphere at 1 atm and 300 °C[133]. A mechanism is proposed based on the intermediate formation of copper oxide which is reduced by hydrogen to elemental copper, whereas the acac ligand decomposes to give formaldehyde and acetone.

Metallic copper nanoparticles within covalently bonded multilayered dendritic ultrathin films made of pamam, using supercritical CO_2 as a processing medium, were described by Puniredd and Srinivasan[134]. The nanoparticles were obtained in higher yield, in a denser and more stable distribution, and showed greater stability towards polar solvent attack than the analogous products of liquid solvent processes, for example, in tetrahydrofuran, which was explained by the facile solvent separation and transport.

ii. Copper(I) precursors. Copper(I) β-diketonates of general type Cu(β-diketonate)$(L)_n$ ($n = 1, 2$), where L is a Lewis base such as phosphane, phosphite, alkene or alkyne, have been investigated extensively because such compounds can successfully be used as CVD precursors for the deposition of thin copper films. The conditions investigated for CVD using copper(I) β-diketonate precursors are summarized in Table 4.

Recently, phosphane and phosphite copper(I) carboxylates[169, 170] have become favored over copper(I) β-diketonates, since these species produce copper films of high purity with excellent electrical properties at low temperatures. However, at the time this review is being written Cu(I) β-diketonates are commercially available, e.g. Cu(hfac)(η^2-$ViSiMe_3$) (**10o**, *CupraSelect*®) and Cu(hfac)(mhy) (**10k**, *Gigacopper*®), making this class of metal enolate precursors still the most important in industrial applications.

Three- and four-coordinated Cu(I) compounds are most common; however, many one- and two-coordinated Cu(I) ones are also known[171, 172]. When less than four donor atoms are bound to the copper(I) ion the mononuclear copper(I) enolates tend to oligomerize[172]. To preserve the volatility of the precursors, the oligomerization must be prevented, for example, by using bulky and/or multidentate chelating ligands. In Table 4, Cu(I) enolate coordination compounds which can be used as precursors for CVD of copper are listed.

Copper(I) β-diketonates usually are volatile liquids in ambient conditions, decomposing at moderate temperatures between 100 and 450 °C, to leave clean copper films. Film purity strongly depends on the nature of the β-diketonate and the Lewis-base ligands. Copper deposition from these precursors takes place either by direct reduction with hydrogen present in the carrier gas, or by the disproportionation $2Cu(I) \rightarrow Cu(0) + Cu(II)$ taking place as shown in Scheme 4[1], in the wide range of conditions listed in Table 4. The high purity of the film can be explained by desorption of the neutral Lewis-base ligands L and removal of the enolate anions as Cu(β-diketonate)$_2$ in the gas phase.

DFT calculations have been performed for the L−Cu bond energies (kcal mol^{-1}) of common copper(I) β-diketonates used in CVD, such as Cu(hfac)(L) with L = PMe_3 (**10a**, 38.4), 1,5-cod (**10c**, 35.6), MeC≡CMe (**10d**, 32.1), $ViSiMe_3$ (**10o**, 33.6)[173]. It is assumed that dissociation of L is the rate-determining step for film growth due to the similarity between the bond energies and reported experimental activation energies. Good correlation with experimental observation is obtained for **10o**, with a dissociation rate constant of $1.5 \times 10^{-14} \exp(-13.5/T)$[173].

Pirolli and Teplyakov reported the deposition of copper films from the commercially available **10o** precursor (*CupraSelect*®) on a Si(100) crystal at the molecular level, combining experimental surface analytical techniques with computational analysis[174]. At −173 °C *CupraSelect*® adsorbs without noticeable decomposition. Surface annealing results in the elimination of $ViSiMe_3$ below 25 °C, while the hfac anion binds to the surface through a copper atom. Upon heating, hfac decomposes and constitutes the main source of impurities in the copper deposition process[174].

TABLE 4. Conditions for CVD of copper using copper(I) β-diketonate precursors

CVD precursor	Evaporation temp. (°C)	Deposition temp. (°C)	Deposition rate (nm min^{-1})	Carrier gas	Reactor pressure (mTorr)	Substrate	References
Cu(hfac)(PMe_3) (**10a**) Cu(hfac)(PEt_3) (**10b**) Cu(hfac)(1,5-cod) (**10c**) Cu(hfac)(2-butyne) (**10d**) Cu(hfac)(btmsa) (**10e**) Cu(hfac)(tmsmb) (**10f**)	45	100–400	20–200	none	50	Pt/SiO_2, Cu/SiO_2, W/SiO_2	135
Cu(hfac)(PMe_3) (**10a**)	45–50	150–400	10–1000	none	1	Pt/SiO_2	136
Cu(hfac)(PMe_3) (**10a**)	60	180–210	400–2000	none	50	W/SiO_2	137
Cu(hfac)(PMe_3) (**10a**)	50	200	—	none	—	PTFE	138–140
Cu(acac)[P(Bu-*n*)$_3$] (**11a**) Cu(acac)[P(Bu-*n*)$_3$]$_2$ (**12a**)	85	220	—	N_2	35×10^3	TiN/SiO_2	141
Cu(fod)(PMe_3) (**13a**) Cu(fod)(2-butyne) (**13b**) Cu(fod)(btmsa) (**13c**)	40	150–300	—	none	10	W/SiO_2	142
Cu(thd)(tdap) (**14a**) Cu(acac)(btmsa) (**11b**)	50 90	150 280	—	N_2	80×10^3	TiN/SiO_2	143
Cu(tfac)(PMe_3) (**15**)	—	100–150	200–1000	none	10	Pt/SiO_2, W/SiO_2, Cu/SiO_2	135, 144
Cu(hfac)(1,5-cod) (**10c**)	70–90	120–250	380–3750	none	10–50	W/SiO_2, Pt/SiO_2, SiO_2	145
Cu(hfac)(1,5-cod) (**10c**)	35	170–200	100	CO, H_2	—	glass	146
Cu(hfac)(1,5-cod) (**10c**) [Cu(hfac)]$_2$(cot) (**16**) Cu(hfac)(1,3-butadiene) (**10g**)	70–105	200	100	H_2	760×10^3	Si, glass	146

TABLE 4. (*continued*)

CVD precursor	Evaporation temp. (°C)	Deposition temp. (°C)	Deposition rate (nm min^{-1})	Carrier gas	Reactor pressure (mTorr)	Substrate	References
Cu(hfac)(1,5-cod) (**10c**)	62	150–250	100–500	He	70	Ta, Cu, Ag, Au, Cr, SiO_2, Si_3 W_4	147
Cu(hfac)(1,5-cod) (**10c**)	70	120	—	N_2	200	TaN/Si	148
Cu(hfac)(1,5-cod) (**10c**)	25–70	200	200	H_2	760×10^3	Si, glass	146
Cu(hfac)(CO) (**10h**)							
Cu(hfac)(dmcod) (**10i**)	50–70	180	—	H_2, He	300–700	W	149
Cu(hfac)(alkyne) (**10d**, **k**, **j**)	60	225	350–5750	He	300	Cu	150
Cu(hfac)(2-butyne) (**10d**)	65	150–210	500–9000	none	50	W/SiO_2	151
Cu(hfac)(2-butyne) (**10d**)	60	150–225	2033	He	300	Cu/Si	152
Cu(hfac)(hy) (**10j**)	70–80	140–300	200–260	He, H_2	2000	TiN/Si	153, 154
Cu(hfac)(mhy) (**10k**)							
Cu(hfac)(mhy) (**10k**)	87	100	—	He	2000	SiO_2	155, 156
Cu(hfac)(mp) (**10l**)	45	150–200	400–1500	Ar	300	TiN/Si	157
Cu(hfac)(dmb) (**10m**)	35						
Cu(hfac)(mbo) (**10n**)	—	180	—	He	1500	Ta	158
Cu(hfac)(vtms) (**10o**)	50	160	500	Ar	—	TiN, Si, Cu, SiO_2	159
Cu(hfac)(vtms) (**10o**)	40–50	120–420	1000	Ar	100	W, TiN, Ta, Al, PtSi	160
Cu(hfac)(vtms) (**10o**)	—	180–350	—	H_2/N_2	500, 800	Al/Si, Si_3N_4/Si	161
Cu(hfac)(vtms) (**10o**)	25	160–190	2000–5000	none	500	W/SiO_2	162
Cu(hfac)(atms) (**10p**)	40	60–275	—	Ar	1000–3000	TiN	163–165
Cu(hfac)(tmsmb) (**10f**)	50	145	—	N_2	35×10^3	TiN/SiO_2	166

(*continued overleaf*)

TABLE 4. (*continued*)

CVD precursor	Evaporation temp. (°C)	Deposition temp. (°C)	Deposition rate (nm min^{-1})	Carrier gas	Reactor pressure (mTorr)	Substrate	References
Cu(hfac)(1,5-cod) (**10c**) Cu(hfac)(2-butyne) (**10d**) Cu(hfac)(mhy) (**10k**) Cu(hfac)(vtms) (**10o**)	60	225	—	CO_2 [a]	13–17 × 10^7	SiO_2/Si, TiN/Si	167, 168

[a] CVD in supercritical conditions.

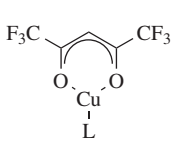

(**10a–p**)

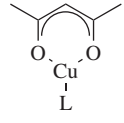

(**11a–d**)

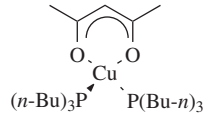

(**12**)

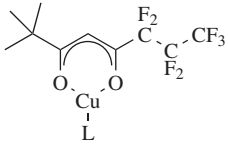

(**13a–e**)

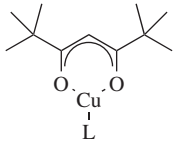

(**14a–c**)

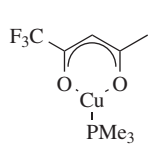

(**15**)

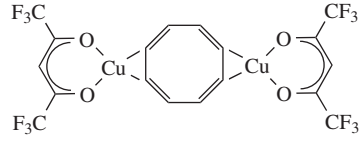

(**16**)

When CVD with copper(I) β-diketonate complexes containing a Lewis base is carried out in the presence of hydrogen[1], deposition of metallic copper occurs by direct reduction with liberation of the Lewis-base ligand and formation of the corresponding β-diketone, as was demonstrated for **10c** (equation 6)[175]. In contrast, it is found that Cu(hfac)(1,3-butadiene) (**10g**) deposits copper via disproportionation even in the presence of hydrogen[146].

$$\text{Cu(hfac)(1, 5-cod)} + {}^1/_2\text{H}_2 \longrightarrow \text{Cu(0)} + \text{hfacH} + \text{1, 5-cod} \qquad (6)$$

When CO alone is used as reducing agent, e.g. for reduction of Cu(hfac)(1,5-cod) (**10c**), the copper films are contaminated mostly with significant amounts of carbon impurities, while the use of CO/H_2 mixtures results in the formation of high-purity metallic copper films. Under the CVD conditions applied, it is proposed that the copper(I) species is transported as Cu(hfac)(CO) in the gas phase[146].

Another group of promising copper CVD precursors are β-diketonato copper(I) complexes with conjugated ene-yne donor ligands L, such as hy in **10j** and mhy in **10k**, as was shown by Doppelt and collaborators[153–156]. Complexes Cu(hfac)(L) and [Cu(hfac)]$_2$L can be prepared on mixing hy or mhy with [Cu(hfac)] in the ratios of 1:1 and 1:2, respectively. The mononuclear Cu(hfac)L (**10j** or **10k**) species possess a free olefinic unit which

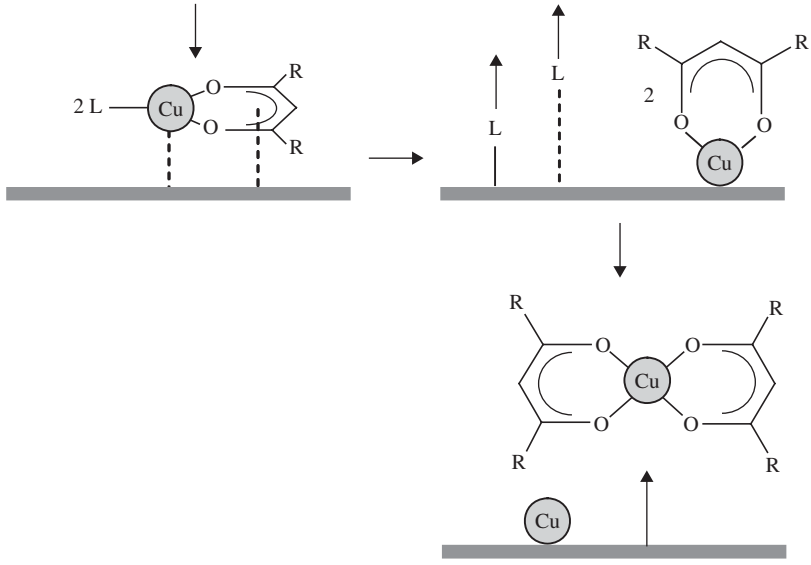

SCHEME 4. Disproportionation mechanism of $L_nCu(\beta$-diketonate) for Cu film deposition on substrates[1]. Reproduced from Reference 1 by permission of Wiley-VCH

can interact with another copper atom, for instance from the substrate surface to form the binuclear complex **10′**, which is adduced as the reason for the very low activation energy found for the surface-reaction-limited growth regime of copper films. This leads to very good filling properties that have been ascertained for **10k** as compared to other precursors[157, 158].

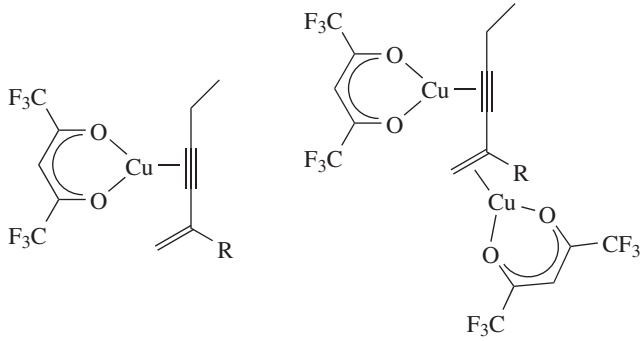

(**10**) (**j**) R = H
(**k**) R = Me

(**10′**) R = H, Me

Lang, Gessner and coworkers[166] reported improved-performance copper(I) CVD precursors containing the tmsmb ligand, as in **10f**, **11d** and **14c**. Copper films were deposited on TiN-coated oxidized silicon wafer materials from **10f** at low temperature (145 °C) and characterized by SEM and EDX. Rhee and coworkers[157] described the hfac-based copper sources Cu(hfac)(mp) (**10l**) and Cu(hfac)(dmb) (**10m**), the deposition rate of which was

about four to seven times faster than that of *CupraSelect*®. The resistivity of the thin films obtained from both precursors is 2.0 μΩ cm.

An invention dating from 2005[158] introduces β-ketoiminates (**17**, **18**) as chelating ligands which are more stable source reagents for copper deposition, resulting in enhanced adhesion properties of the obtained thin films.

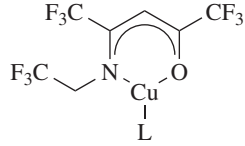

(**17**) L = PMe_3, 1,5-cod, AllOH

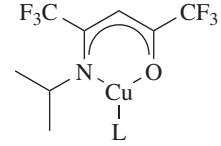

(**18**) L = PMe_3, 1,5-cod

Gessner, Lang and coworkers[141] formed thin films of copper oxide and copper from the liquid nonfluorinated copper(I) source Cu(acac)(P(*n*-Bu)$_3$)$_2$ (**12**) by low-temperature thermal ALD.

Selective deposition of copper onto patterned PTFE and similar substrates is of importance because these substrate materials have low dielectric constants[176]. The combination of PTFE with high-conductivity metals such as copper led to applications in the field of printed wiring board manufacture. A suitable precursor is Cu(hfac)(PMe_3) (**10a**)[140]. However, deposition of copper onto various patterned substrates including pyrex, SiO_2, TiN and Si_3N_4 surfaces functionalized with silanes was performed using copper(I) enolates such as Cu(hfac)(mhy) (**10 k**), whereby the films exhibit good adhesion strength and resistivities to that of elemental copper[165, 166]. After irradiation of the functionalized substrates with UV light through a mask, copper was deposited only onto the nonirradiated areas of the substrate. Ultrathin monolayers of copper prepared by this method are potentially useful for very high resolution resistors, since the lateral resolution may be of the order of molecular dimension (nanometallization).

Deposition of copper alloys such as copper/aluminum can be carried out starting from copper(I) and copper(II) enolates. Copper alloys may be of technological and scientific interest as they can help avoiding problems caused by electromigration, corrosion and poor adhesion to dielectric substrates[177].

b. Silver. Silver has the highest electrical conductivity (1.59 μΩ cm) of all metals; however, its greater cost and tarnishability has prevented it from being widely used in place of copper for electrical purposes. Besides, the fast diffusion of silver into semiconductor Si and SiO_2 device materials has limited its application for metallization. Further applications include the use of silver as a component of high-temperature superconducting ceramics[178], as silver mirrors[179] or as bactericidal coatings[180]. One of the major problems in silver CVD is the availability of suitable volatile and economical precursors, because of their sensitivity to light and low thermal stability. There have been several reports on the use of Lewis-base silver(I) β-diketonates with phosphanes, phosphites, alkenes, alkynes etc. as auxiliary ligands as suitable CVD precursors. Also, the use of silver β-diketonate salts including [Ag(tfac)] and [Ag(hfac)] as CVD metal sources is mentioned in the literature, but most of these compounds do not sublime easily and hence require unusual vaporization techniques. In contrast, the Lewis-base-stabilized silver β-diketonates listed in Table 5 are better suited as CVD precursors because of their improved stability and volatility.

As nicely shown by Puddephatt and coworkers, the complexes Ag(hfac)(PR_3) and Ag(fod)(PR_3) (R = Me, Et) are excellent CVD precursors for deposition of smooth pure silver films (grain size 0.1–0.25 μm) using moist hydrogen as carrier gas, as could be

TABLE 5. Deposition studies of silver(I) enolate CVD precursors

CVD precursor	Evaporation temp. (°C)	Deposition temp. (°C)	Deposition rate (nm min^{-1})	Carrier gas	Reactor pressure (mTorr)	Substrate	Reference
Ag(hfac)(PMe_3) Ag(hfac)(PMe_3)$_2$	20–50	250–425	—	H_2	0.1	Cu	181
Ag(hfac)(PMe_3) Ag(hfac)(PEt_3) Ag(fod)(PMe_3) Ag(fod)(PEt_3)	50–100	250–350	30	none, H_2, H_2/H_2O	50	glass, Si, Cu	182
Ag(acac)(P(Bu-*n*)$_3$)$_2$	150	200	—	N_2	$35 \bullet 10^3$	TiN/Si	183
Ag(hfac)(P(OMe)$_3$) Ag(hfac)(P(OEt)$_3$) Ag(hfac)(P(OPr-*i*)$_3$) Ag(tfac)(P(OMe)$_3$) Ag(tfac)(P(OEt)$_3$) Ag(tfac)(P(OPr-*i*)$_3$)	80	180–360	—	Ar	100–500	Si, glass	184
Ag(hfac)(C≡NMe)	80–90	250–320	—	none, H_2, H_2/H_2O	0.1–100	Si, glass	185
Ag(hfac)(SEt_2)	80	120–300	40	—	—	Cu/Si	186

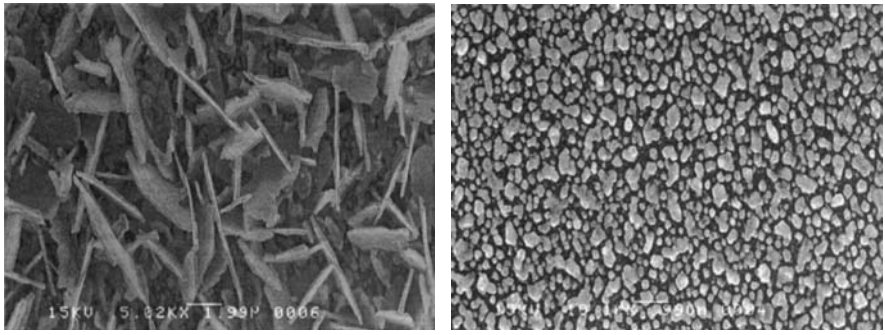

FIGURE 14. SEM images of silver films grown from Ag(fod)(PEt_3) using H_2/H_2O mixtures as carrier gas on glass applying different substrate temperatures (left: 320 °C, right: 230 °C) without annealing[182]. Reprinted with permission from Reference 182. Copyright 1995 American Chemical Society

shown by SEM (Figure 14)[182]. If no reactive carrier gas is used, the layers contain carbon impurities (5–10%) and show rough surfaces with an average grain size of 1–2 μm. The impurities were explained by the higher temperatures (370–380 °C) required for the deposition processes because the decomposition was not selective. As a consequence, in some cases fluorine, oxygen and phosphorus impurities were observed. The main products in the presence or absence of hydrogen are hfacH or fodH and PMe_3 or PEt_3. No disproportionation mechanism of the silver(I) source is observed, as it is characteristic for the analogous copper(I) species.

Next to phosphine and phosphite silver(I) enolates also methylisocyanide-stabilized species such as M(hfac)(N≡CMe) (M = Cu, Ag) can be used as suitable CVD precursors for the deposition of thin metal films on glass or silicon substrates (Table 5)[185].

A detailed mechanistic study of the decomposition process of $Ag(fod)(PEt_3)$ on a Ag(111) surface had been carried out using reflection absorption IR spectroscopy and temperature-programmed desorption techniques. From these measurements the authors conclude that the adsorbed $Ag(fod)(PEt_3)$ molecules dissociate on the surface. As byproducts, which are developed in the reaction with reducing agents like hydrogen or water, mainly the β-diketonate fodH together with HF, CO_2 and the radicals $C(CH_3)_3^{\bullet}$ and $C_3F_7^{\bullet}$ were monitored at different temperatures. Attempts to describe the reaction paths of adsorbed phases are given in equation 7[187].

$$\mathrm{Ag(fod)(PEt_3)_{(ads)}} \longrightarrow \begin{cases} \xrightarrow{T > -173\ ^\circ\mathrm{C}} \mathrm{Ag_{(ads)} + fod_{(ads)} + PEt_{3(ads)} + Ag(fod)(PEt_3)_{(ads)}} \\ \xrightarrow{-143\ ^\circ\mathrm{C\ to\ -103\ ^\circ C}} \mathrm{PEt_{3(g)} + CH_{4(g)}} \\ \xrightarrow{-73\ ^\circ\mathrm{C}} \mathrm{fodH_{(g)} + (CHO)_{\mathit{x}(ads)} + (CF)_{\mathit{y}(ads)}} \\ \xrightarrow{17\ ^\circ\mathrm{C}} \mathrm{Ag(fod)(PEt_3)_{(g)}} \\ \xrightarrow{217\ ^\circ\mathrm{C}} \mathrm{{}^{\bullet}C_3F_{7(g)} + {}^{\bullet}C(CH_3)_{3(g)} + HF_{(g)}} \\ \xrightarrow{427\ ^\circ\mathrm{C}} \mathrm{CO_{2(g)} + C_{(s)}} \end{cases} \tag{7}$$

The volatility and thermal stability in the gas phase during evaporation and transport to the substrate of selected *n*-Bu_3P silver β-diketonates has been investigated using temperature-programmed and *in-situ* mass spectrometry by Kohse-Höinghaus, Lang and coworkers[183, 188]. Examination of the fragments detected during evaporation and in a cold-wall CVD reactor allowed one to propose the gas-phase decomposition mechanisms of some silver(I) precursors. For both compounds $Ag(acac)(P(Bu\text{-}n)_3)_2$ and $Ag(hfac)(P(Bu\text{-}n)_3)_2$ the $P(Bu\text{-}n)_3$ phosphine and the respective β-diketonate fragments are detected in the temperature range of 170–330 °C, while the metal-containing fragment Bu_3PAg^+ is found at higher temperatures, 330–420 °C for $Ag(acac)(P(Bu\text{-}n)_3)_2$ and 170–290 °C for $Ag(hfac)(P(Bu\text{-}n)_3)_2$ (Figure 15)[183]. Use of a fluorinated ligand results in higher stability during evaporation but shows an uneven evaporation interval. The formation of stable evaporated adducts in the gas phase may be responsible for this behavior. Deposition experiments resulted in the formation of smooth and conductive thin silver coatings on glass substrates.

Aerosol-assisted CVD of Ag and $Ag_{1-x}Pd_x$ films, using $Ag(hfac)(SEt_2)$ and Pd(hfac-*C*)(hfac-*O*,*O*)(SEt_2) as precursors[186], and the investigation of ligand exchange reactions relevant to this[189] were performed by Hampden-Smith and Kodas. The AA-CVD experiments were carried out on Cu-coated Si wafers over a range of substrate temperatures (120–300 °C) resulting in bright, reflective, analytically pure silver films[186].

Silver and silver selenide thin films were prepared from a series of liquid silver precursors containing β-diketonates and phosphite ligands (Table 5) as demonstrated by Shim and coworkers[184]. In a typical deposition experiment, $Ag(tfac)(P(OEt)_3)$ produced very pure silver films under relatively mild conditions (170 °C) without any appreciable amount of fluorine, oxygen and phosphorus impurities. These films could easily be converted to Ag_2Se by selenium vapor deposition[184].

Highly reflective, surface-metallized, flexible polyimide films containing silver are accessible by the incorporation of [Ag(hfac)] into poly(amic acid) solutions followed by thermal curing to 300 °C[190]. The silvered films are thermally stable and maintain mechanical properties similar to those of the parent polyamide.

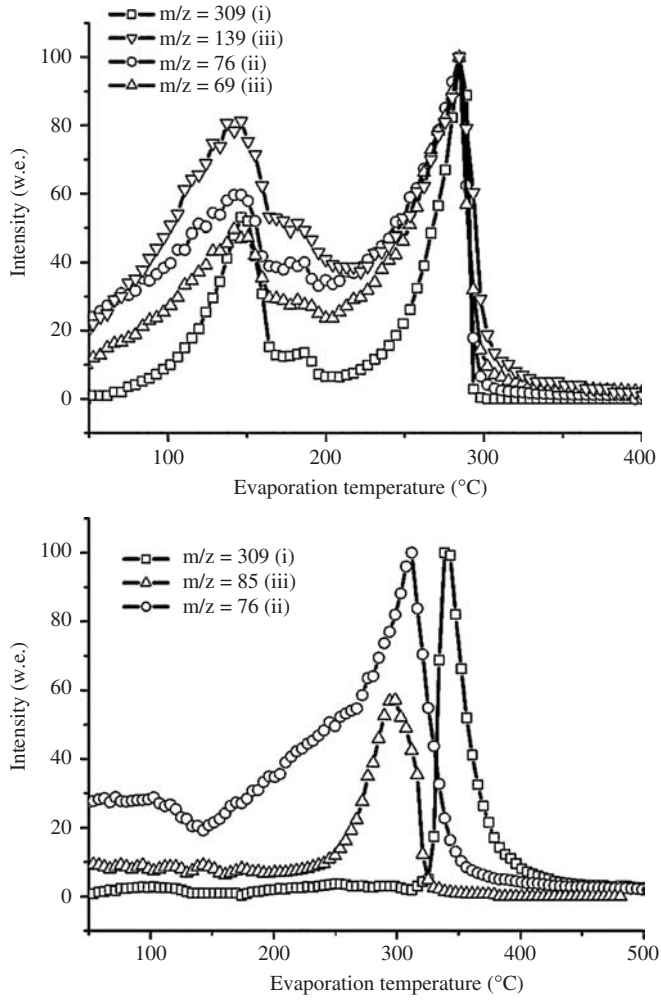

FIGURE 15. Intensity of detected fragments (MS, m/z) as a function of temperature, in the gases evolved from Ag(hfac)(P(Bu-n)$_3$)$_2$ (top): $C_{12}H_{27}AgP^+$ (309), $C_4H_2F_3O_2^+$ (139), $C_4H_9P^+$ (76), CF_3^+ (69) and Ag(acac)(P(Bu-n)$_3$)$_2$ (bottom): $C_{12}H_{27}AgP^+$ (309), $C_4H_5O_2^+$ (85), $C_4H_9P^+$ (76)[183]. Reproduced from Reference 183 by permission of Wiley-VCH

c. Gold. Gold surfaces and gold particles have recently attracted much attention due to their very promising catalytic (e.g. alcohol oxidation, epoxidation of propylene, hydrogenation), optical and electrical properties[191–193]. In the microelectronics industry gold metallization is extensively used for technological applications where absolute reliability must be maintained (e.g. electrical contacts to integrated circuits, wiring in multichip packaging modules). Compared to copper and silver, gold also possesses a low resistivity

(2.46 $\mu\Omega$ cm) but inertness to chemical corrosion. Gold is also used as an absorber in X-ray lithographic masks and for the repair of defects in thin film circuits[194]. Gold(III) β-diketonates containing two methyl groups were found to be most promising precursors for CVD of gold onto different substrate materials. Gold enolates of structural type Au(β-diketonate)$(Me)_2$ (β-diketonate = acac, hfac, tfac) are outstanding precursors because they give pure, electrically conducting gold thin films by thermal-induced decomposition, whereby the fluorinated compounds are characterized by higher vapor pressures and show faster growth rates[196]. Baum and coworkers[195–197] deposited high-quality gold films and lines by laser-induced, photothermal CVD with a focused argon ion laser, using Au(acac)$(Me)_2$, Au(hfac)$(Me)_2$ and Au(tfac)$(Me)_2$ as precursors. The deposition rates (0.1, 0.45 and 2.5 $\mu m\,s^{-1}$, respectively) are strongly dependent upon the vapor pressure. Lines deposited from these three precursors, containing 95–100% gold, have resistivities 2- to 20-fold that of bulk gold, which can be reduced to 2- to 5-fold after annealing. Plasma-enhanced CVD using Au(acac)$(Me)_2$ as metal source was applied to prepare gold alloys, such as Au/Pt, Au/Pd and Au/Pt/Pd[198]. Three different methods allow the deposition of metallic films of varying composition. They always show a metallic luster and resistivities between 100 and 200 $\mu\Omega$ cm.

Au(acac)$(Me)_2$ was used by Claus and coworkers to produce silica-supported gold nanoparticles by MOCVD[199], as a catalyst with Au content of 2.4 wt% and average Au particle size of 1.4 nm, which fits well to other supported gold catalysts prepared from alternative precursors by different routes[199]. The supported nanoparticles were applied as catalyst for low-temperature oxidation of carbon monoxide.

Grunwaldt and coworkers[200] prepared gold and gold–silver nanoparticles supported on TiO_2, Fe_2O_3/Fe_3O_4 and SiO_2 by flame spray pyrolysis from Au(acac)$(Me)_2$ and AgOBz. Depending on the support material, the size of the gold particle was in the range of 2–4 nm increasing with higher noble metal loading (0.1–1.0 wt%). Addition of silver resulted in increased particle sizes (5–10 nm). The authors mention that flame spray pyrolysis is limited when higher noble metal loadings are targeted[200]. Gold nanoparticles could also be synthesized on porous granules of γ-Al_2O_3 by chemical vapor infiltration using Au(acac)$(Me)_2$[201]. After calcination at 325 °C, small particles ($\leqslant$5 nm) of metallic gold were obtained which show a significant catalytic activity in low-temperature oxidation of CO.

V. METAL OXIDE DEPOSITION

In general, metal oxides are very common inorganic commodities, widely applied, and display an assortment of unique chemical and physical properties. They are accessible by different techniques including chemical vapor deposition and sol–gel methods. Their technological application extends from super- and semiconducting materials to electrochromic devices, optical filters, protective coatings and solar absorbers[2, 3, 202–205].

A. Main Group Elements

1. Group 2 elements

a. Magnesium. The metal oxides of alkaline earth elements have attracted much attention, i.e. MgO is thermodynamically very stable, possesses a low dielectric constant (10.0) and a low refractive index (1.74). Therefore, it is an interesting substrate material for high T_c superconducting films, perovskite-type ferroelectric coatings and protecting layers of dielectrics[206, 207]. Magnesium oxide is an inorganic insulating solid material with fcc Mg and O sublattices and low-energy neutral (100) cleavage planes. Magnesium oxide can be prepared by spray pyrolysis[208] and MOCVD techniques[209, 210]. Recently, the latter method

was applied by Boo and coworkers for the growth of crack-free and uniform MgO thin films using the simple molecular magnesium enolate precursors $Mg(acac)_2$ and $Mg(thd)_2$ and oxygen as carrier gas at 300 °C for deposition on GaAs[209] or at 500–600 °C on Si(100) and sapphire[210]. Noteworthy is that the substrate, the precursor and the substrate temperature influence the crystal growth direction and/or the crystallinity of the deposited MgO films. In addition, electrostatic spray pyrolysis (ESP) between 400–450 °C allowed the deposition of pure MgO thin films on SiO_2/Si(100) substrates with growth rates of 34 and 87 Å min^{-1} from $Mg(tmhd)_2$[208]. Only traces of carbon were found within the detection limit of XPS. The authors point out, however, that this impurity may be attributed to surface contamination and/or carbon incorporation into the MgO films.

b. Strontium. Direct liquid injection MOCVD of [$Sr(thd)_2$ x pmdeta] was used to obtain polycrystalline SrO (>9 mTorr, <350 °C) and $SrCO_3$ films (>9 mTorr, >400 °C)[211]. *In-situ* FTIR monitoring of the gas phase allowed one to propose a decomposition mechanism (Scheme 5). The ancillary ligand pmdeta is eliminated in the early stage of evaporation yielding $Sr(thd)_2$, which decomposes to produce SrO along with CO_2 and a variety of ketones above 300 °C. The CO_2 interacts with SrO to give $SrCO_3$, depending on the deposition temperature and the partial pressure of the precursor source: a higher temperature and a higher partial pressure increase the amount of $SrCO_3$. This finding can be generalized for alkaline-earth metal oxides deposited from β-diketonates[211]. These studies are mainly pertinent to MOCVD optimization and fabrication of multicomponent materials, such as $SrTiO_3$, (Ba,Sr)TiO_3 (BST), $SrBi_2Ta_2O_9$ (SBT) and $SrBaNb_2O_6$ (SBN).

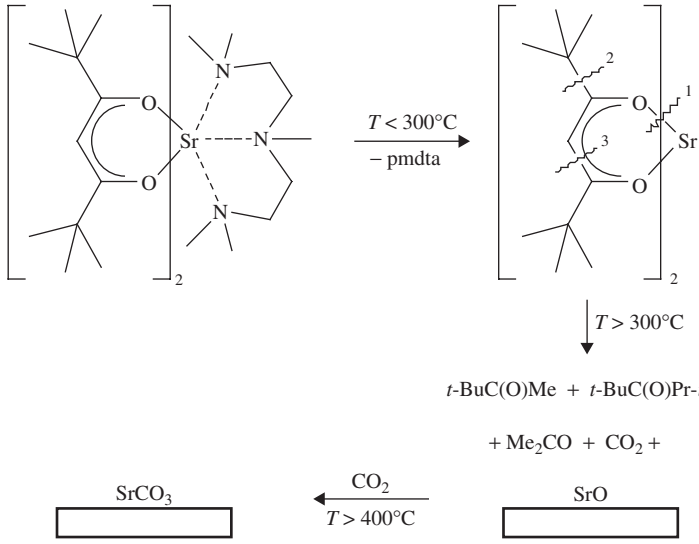

SCHEME 5. Decomposition of [$Sr(thd)_2$(pmdeta)] showing the sites (1–3) of bond cleavages[211]. Reproduced from Reference 211 by permission of Wiley-VCH

c. Barium. Alkaline-earth metal β-diketonates are less volatile than the analogous transition metal enolates, e.g. Cu(II) β-diketonates, due to their oligomeric structures[212,213] (for example, $Ba(thd)_2$ is better described by the formula [$Ba_5(thd)_9(H_2O)_3(OH)$]). On addition of an excess of free β-diketone to the carrier gas stream, these structures are

cleaved to give lower aggregation and become more volatile. Between 300–400 °C, $[Ba_5(thd)_9(H_2O)_3(OH)]$ decomposes to afford barium oxide, thd-H and other byproducts[213].

A series of volatile barium ketoiminates containing appended ether lariats (**19**, **20**; vapor pressure *ca* 1 mTorr at 150–200 °C) has been synthesized and successfully used for MOCVD by Marks and coworkers[214]. The thermolysis mechanism of these barium coordination complexes was studied applying mass spectrometry. They partially decompose during sublimation involving ligand fragmentation at the CO bond β to the ketoiminate nitrogen atom with formation of pinacolone, 2,2-dimethyl-5-imino-3-hexanone and 2-methyl-4-*t*-butylpyridine. The suitability of these complexes as MOCVD precursors of barium-oxide-containing thin films has been demonstrated through the growth of $BaPbO_3$ using $Pb(thd)_2$ as lead source[214].

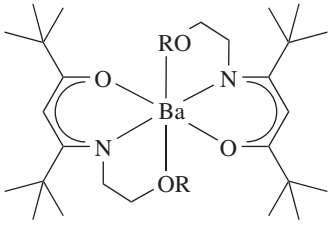

(**19**) R = Me, C_2H_4OMe, $C_2H_4OC_2H_4OMe$

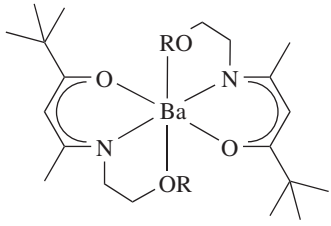

(**20**) R = Me, C_2H_4OMe, $C_2H_4OC_2H_4OMe$

2. Group 13 elements

a. Aluminum. Aluminum oxide possesses attractive chemical and physical properties. It is a relatively hard material, chemically inert, transparent in some modifications and an electrical insulator. Alumina films are therefore important as insulating layers in microelectronic devices[215], hard and antireflective coatings[216,217] and protection against oxidation. α-Alumina (corundum) is extremely hard (it is used as an abrasive), unreactive and stable at high temperature. It has a hexagonal structure consisting of a close-packed array of O^{2-} ions with Al^{3+} cations occupying octahedral interstices. γ-Alumina has a defective spinel structure, absorbs water and has amphoteric properties.

The perceived advantage of aluminum β-diketonates over other alumina precursors, such as $AlMe_3$, anhydrous $AlCl_3$ and $Al(OPr\text{-}i)_3$, includes higher stability, easier handling in the solid form and lower toxicity. Ajayi and coworkers reported about the atmospheric pressure pyrolysis of $Al(acac)_3$ under argon for deposition of amorphous Al_2O_3 films on glass and silicon[218,219]. The films were porous and highly contaminated with carbon, nevertheless, they showed good optical properties. MS evidence pointed to acetone and carbon dioxide as the major products of decomposition, the latter being responsible for the formation of the carbon impurities (for comparision see Section V.A.1.c)[220]. It was found that the higher the deposition temperature, the higher the CO_2 rate (Figure 16).

Maruyama and Arai applied low-temperature (250 °C) atmospheric pressure CVD of $Al(acac)_3$ to produce largely carbon-free aluminum oxide films on glass (borosilicate, quartz) and silicon(100) substrates in air[221]. The effect of water vapor on the growth of aluminum oxide films by low-pressure CVD from $Al(acac)_3$ have been thoroughly investigated by Kim and coworkers[222]. High water-vapor concentration improved the film purity by facilitating removal of carbon-containing ligands from the growing surface, producing pure and mirror-smooth Al_2O_3 films without affecting the film stoichiometry.

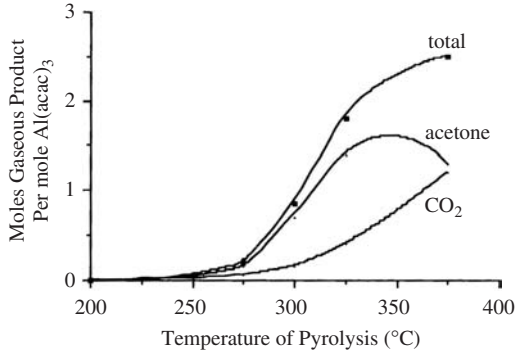

FIGURE 16. Gaseous decomposition products from aluminum acetylacetonate as a function of the temperature of pyrolysis[220]. Reprinted with permission from Reference 220. Copyright 1958 American Chemical Society

The formation of alumina from $Al(acac)_3$ during CVD processes followed two different reaction pathways, as could be shown by Rhoten and DeVore by thoroughly characterizing the evolved gases[223]. Pyrolysis of $Al(acac)_3$ in vacuum produced Al_2O_3, carbon, water vapor and diverse volatile organic molecules. The activation energy for the thermal decomposition of the aluminum precursor source is *ca* 100 kJ mol^{-1}. However, a lower-energy pathway (28 kJ mol^{-1}) involves the reaction between $Al(acac)_3$ and H_2O to produce carbon-free alumina films and acetylacetone as the main products, which is attributed to the relatively low temperatures needed for this reaction.

A study of dielectric characteristics of alumina thin films deposited on silicon substrates from $Al(acac)_3$ dissolved in dmf by spray pyrolysis between 450 and 650 °C was recently reported by Falcony and coworkers[224]. The addition of water vapor significantly improved the dielectric characteristics and smoothness of the deposits. In comparison to the CVD technique described above (see Section III.A.1) this procedure lead to considerable carbon impurities in the films. The overall resistivity of the alumina layers decreases, when both the concentration of the solution and the deposition temperature increase, which is explainable with the increase of carbon residues in the films.

Nemetz and coworkers studied the influence of the temperature difference between the precursor gas inlet and the substrate (the so-called 'gradient', ΔT) on CVD processes of $Al(acac)_3$, especially on the deposition rate and the film microstructure, at pressures between 7.5 and 30 Torr and temperatures reaching from 230 to 830 °C under oxygen[225]. It was found that at 30 Torr the alumina deposits varied from porous powders to dense films, depending on the applied temperature gradient (Figure 17). The deposition rate reaches a maximum at *ca* 600 °C and can be qualitatively described by the competition of concentration diffusion and thermophoresis of the dust particles. The powder formation on the substrate at large temperature gradients can be reduced by decreasing the total pressure.

In 2006, Carter and coworkers used combustion CVD (0.0015 M isopropanolic Al $(acac)_3$ solution, 1050–1125 °C) for the deposition of crystalline α-alumina on silica and nichrome (Ni-20Cr)[226]. The oxidation response of coated and uncoated nichrome was investigated by isothermal TGA, in air at 900–1100 °C, showing that the coated substrate has a significantly lower mass gain. Pflitsch and coworkers reported the film growth of Al_2O_3 on stainless steel by MOCVD, at atmospheric pressure and 330–500 °C, in hot-wall CVD equipment (deposition rate 0.25 μm h^{-1})[227]. Deposition at 500 °C produced

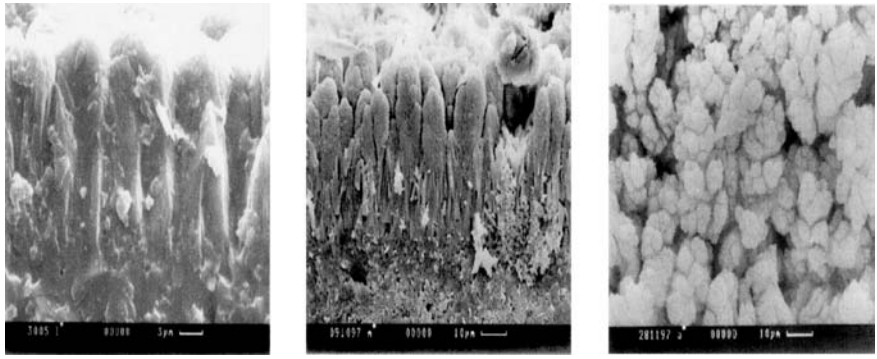

FIGURE 17. SEM cross-section of Al_2O_3 at different temperature gradients (left: $\Delta T = 0$ K, middle: $\Delta T = 30$ K, right: $\Delta T = 80$ K)[225]. Reproduced from Reference 225 by permission of Elsevier

amorphous, well adherent, completely closed and multicolored films. Annealing at 800 °C gave γ-alumina, while at 1100 °C α-alumina was formed; however, the annealed deposits were spalling[227]. In subsequent experiments alumina layers were deposited at temperatures between 500 and 1000 °C. Films produced below 800 °C were amorphous and transparent, while those grown at 1000 °C were dark and crystalline. The presence of γ-, θ- and α-alumina in the crystalline phases was demonstrated[228].

Vahlas and coworkers[229] recently tested a new delivery system based on sublimation in a fluidized bed, to improve mass and heat transport. A mixture of solid $Al(acac)_3$ (minor component) and inert alumina or silica particles was fluidized with a combination of water vapor and oxygen at 150 °C, by which amorphous Al_2O_3 films were obtained on Ti6242 alloy wafers immersed in the bed. Pauleau and Dulac compared the kinetics of vaporization of $Al(acac)_3$, $Al(tfac)_3$ and $Al(hfac)_3$ by isothermal TGA[230]. The saturation vapor pressure of $Al(hfac)_3$ is 10-fold and 100-fold higher than those of $Al(tfac)_3$ and $Al(acac)_3$, respectively.

b. Gallium. Less attention has been paid to the oxides of gallium than those of aluminum. The α- and γ-Ga_2O_3 have the same structure as their Al_2O_3 counterparts. Monoclinic β-Ga_2O_3 is the most stable crystalline modification. Nevertheless, gallium oxide has some interesting properties. It is thermally and chemically stable and possesses insulating features at 25 °C but is semiconducting at higher temperatures. Due to this and its optical properties, gallium oxide is used as insulator on GaAs and as facet coatings for GaAs-based lasers. Furthermore, Ga_2O_3 thin films find application as oxygen sensors at temperatures between 800 and 1000 °C[231].

Gallium oxide thin films can be deposited on alumina and titanium dioxide from $Ga(hfac)_3$ by MOCVD in the presence of oxygen (deposition temperature 470 °C, pressure 20 Torr, deposition rate 0.7 $\mu m\,h^{-1}$)[232]. The amorphous layers are black, smooth, well adherent to both substrates and have less than 5% C and traces of F impurities. Annealing at 700 °C led to carbon-free and transparent polycrystalline Ga_2O_3 films. SIMS investigations showed that aluminum from the alumina substrate diffuses into Ga_2O_3 at 1000 °C. However, TiO_2 buffer layers prevent this diffusion. Niinistö and coworkers applied ALE for growth of gallium oxide films using $Ga(acac)_3$ as precursor, in the presence of water or ozone[233]. The thin films were amorphous and showed only small thickness variations. The layers obtained in the presence of water contained 30 at% of carbon, whereas in the presence of ozone the Ga_2O_3 contained only 1 at% C.

Mixed γ-Ga_2O_3-Al_2O_3 oxides of different stoichiometry were prepared by the solvothermal method from $Ga(acac)_3$ and $Al(OPr\text{-}i)_3$ as starting materials and were used as catalysts for selective reduction of NO with methane[234]. The initial formation of gallium oxide nuclei controls the crystal structure of the mixed gallium–aluminum oxides. It is found that the acid density per surface area is independent of the Al:Ga feed ratio but depends on the reaction medium (diethylenetriamine, 2-methylaminoethanol, toluene, 1,5-pentanediol etc.), whereby in diethylenetriamine the catalyst had lower densities of acid sites and showed a higher methane efficiency.

c. Indium. Indium oxide is a transparent and conductive inorganic material which has a wide range of industrial and technological applications. Especially, Sn-doped In_2O_3 (ITO) is of importance for display panels and solar cell windows[235] (for further doped indium oxide materials see Section V.D).

Pyrolysis of $In(acac)_3$ in air or oxygen at 320–400 °C was carried out by Ryabova and Savitskaya as early as 1968[236], using glass, vitreous silica and mica as substrates. Amorphous In_2O_3 was formed in air at 320 °C, while at 400 °C crystalline indium oxide phases of low resistivity (10^2 Ω cm) were obtained. In pure oxygen, crystalline deposit formation occurred already at 320 °C. Reich and coworkers prepared In_2O_3 films by PE-CVD, using $In(thd)_3$ at 250–400 °C. This precursor is preferable to $InMe_3$ due to its higher stability, lower price and ability to give conducting films[237]. High-quality transparent conductive cubic-phase indium oxide thin films on quartz are accessible by a coating photolysis process using ArF excimer laser irradiation (50 mJ cm^{-2}, repetition rate 5 Hz for 5 min) employing the nontoxic $In(acac)_3$ as starting material[238]. Another single source precursor for the deposition of indium oxide thin films is dimeric $[In(acac)(Me)_2]_2$ as reported by O'Brien and coworkers[239]. Low-pressure MOCVD allowed the deposition of cubic In_2O_3 on borosilicate glass, Si(100) and GaAs(111) substrates in the temperature range from 350 to 450 °C, without introducing oxygen. For a detailed discussion of the preparation and use of mixed M–In_2O_3 (M = Sn, Zn, Cd, Mg) thin films, see Section V.D.

d. Thallium. Thallium differs from the other elements of group 13 since it has the M(I) oxide Tl_2O, besides the M(III) oxide Tl_2O_3 and a mixed oxide of composition Tl_4O_3. However, Tl_2O_3 has been deposited from thallium β-diketonate precursors[240,241]. When compared to other group 13 elements, thallium oxides possess electrical and optical properties that make them useful in transparent electrical contacts and in solar cells[242]. CVD of Tl_2O_3 thin films from Tl(acac) and $Tl(acac)(Me)_2$ single-source precursors was carried out on MgO, Al_2O_3 and Si substrates[241]. XRD analysis showed that Tl_2O, Tl_4O_3 and Tl_2CO_3 were present; in the case of the Si substrate also $Tl_8Si_5O_{14}$. Low-pressure MOCVD experiments on glass and random YSZ surfaces with the anhydrous, volatile, liquid, thermally and air-stable thallium(I) precursors Tl(hfac)(diglyme) (**21**) and Tl(hfac)(tetraglyme) (**22**) were carried out as reported by Fragalà and coworkers[240]. These 'user-friendly' thallium sources yielded thallium-containing smooth and homogeneous films of *ca* 5 μm grain size at 430 °C and 14 Torr deposition pressure without carbon and fluorine contamination.

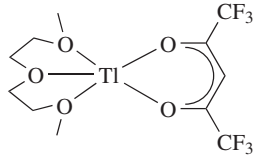

(**21**)

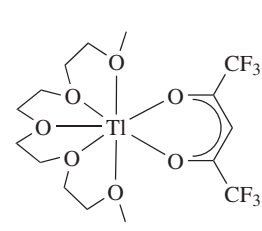

(**22**)

3. Group 14 elements

a. Tin. Tin dioxide adopts a rutile-type structure and occurs naturally as cassiterite. It is highly transparent in the visible region, highly reflective in the IR region and adheres well to diverse substrates. Beyond this, it has good chemical and mechanical stability. These properties make SnO_2 one of the most widely used inorganic basic materials for many technological applications, such as gas-sensing devices, electrodes in photovoltaic devices and conducting coatings on glass[243,244]. The number of literature sources on deposition of SnO_2 from tin halides ($SnCl_2$, SnI_4) and tetraalkyltin compounds, such as $SnMe_4$ and $Sn(Bu\text{-}n)_4$, is impressive, but less is known about the use of tin enolate precursors.

CVD of SnO_2 from tin(II) acetylacetonate studied by Maruyama and Ikuta indicated two different decomposition mechanisms, depending on the deposition temperature[245]. Below 400 °C decomposition is diffusion-controlled with a very small activation energy, while at higher temperatures the kinetic is surface-controlled with larger E_A values.

Chi and coworkers examined $Sn(acac)_2$, $Sn(tfac)_2$ and $Sn(hfac)_2$ as suitable CVD precursors of tin dioxide on substrates such as silicon, titanium nitride and glass[246]. Deposition was carried out at 300–600 °C, with oxygen as carrier gas and the rates reaching 600 Å min^{-1}. Below 400 °C all three precursors gave amorphous SnO_2 coatings, while at higher temperatures polycrystalline SnO_2 layers are observed. The deposition rates increase in the order $Sn(hfac)_2 < Sn(tfac)_2 < Sn(acac)_2$.

Feng and coworkers[247,248] prepared nanocrystalline tin oxide on monolithic mesoporous silica starting from $Sn(acac)_2Cl_2$ by simple immersing of the substrate in the precursor solution. Heat treatment (300–600 °C) leads to nanocomposites with a large specific surface area[247]. The electrical properties of these nanocomposites were also investigated. The authors found an inverse correlation between the precursor concentration and the electrical resistivities of the samples[248].

Tin dioxide thin films can be grown on silicon at room temperature by XeCl excimer laser metal-organic deposition (MOD; 100 mJ cm^2, repetition rate 10 Hz for 5 min) from a solution of $Sn(acac)_2$ in *n*-BuOH, whereby crystalline films were obtained without heat treatment[249]. Increasing the laser energy to 260 mJ cm^{-2} resulted in an improvement of the crystallinity, which is even better than that of films prepared at 900 °C without laser irradiation. Molloy and coworkers[250] used bimetallic $[Sn(dmae)_2Cd(acac)_2]_2$ (dmae = dimethylaminoethanol) as precursor for AA-CVD of amorphous SnO_2 films, containing no detectable amounts of cadmium.

b. Lead. Lead oxide, PbO, exists as the red tetragonal litharge (α-PbO, stable at room temperature) and the yellow orthorhombic massicot (β-PbO). Litharge is not only the most important oxide of lead, it is also the most widely used inorganic lead compound. Another relevant oxide is tetragonal rutile-structured PbO_2, which normally is maroon colored. Lead oxides are used in the manufacture of glass and paints; they also are an important component of many ferroelectrics, superconductors, optoelectronic devices and sensors[251,252]. Volatile lead(II) β-diketonates (**23a–g**) have been used as single-source precursors for CVD of lead oxides on different substrates[253–256].

Krisyuk and Igumenov studied the thermal properties of lead(II) β-diketonates **23a–g** by TGA and temperature-dependent vapor pressure measurements[253]. Surprisingly, only the nonfluorinated lead enolates produced films of α- and β-PbO on silicon substrates with a high refractive index using the CVD technique (2 Torr, carrier gas argon, reagent gas oxygen, source temperature 110–150 °C, substrate temperature 350–600 °C). The decomposition pathways of $Pb(thd)_2$ (**23c**) shown in equation 8 were postulated, pointing

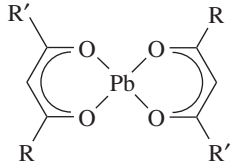

(**23**) (**a**) R = R′ = Me; $Pb(acac)_2$
(**b**) R = R′ = Mef; $Pb(hfac)_2$
(**c**) R = R′ = *t*-Bu; $Pb(thd)_2$
(**d**) R = R′ = Hexf; $Pb(dhfa)_2$
(**e**) R = Me; R′ = Mef; $Pb(tfac)_2$
(**f**) R = *t*-Bu; R′ = Mef; $Pb(pta)_2$
(**g**) R = *t*-Bu; R′ = $C(Me)_2OMe$; $Pb(mthd)_2$

out that decomposition does not occur in the gas phase. The first step in the decomposition is cleavage of one of the Pb−O bonds and further intramolecular rearrangements yielding PbO.

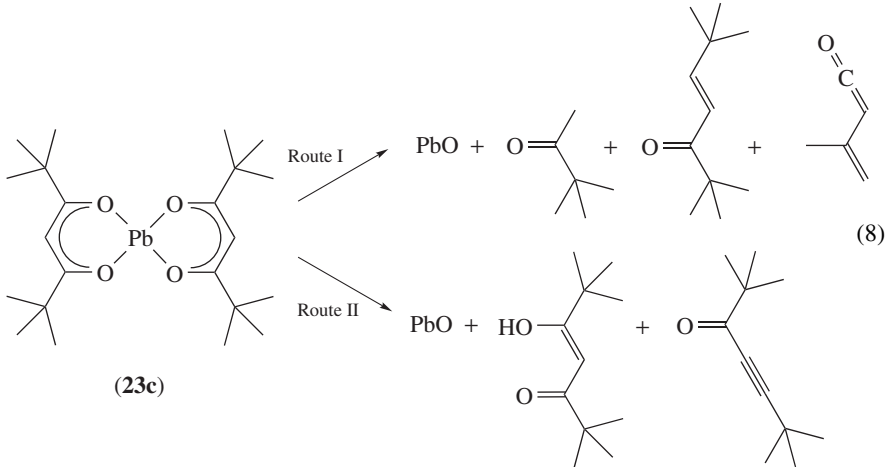

(8)

A liquid delivery CVD method was applied by Hwang and coworkers to deposit lead oxide thin films from a solution of **23c** in ethylcyclohexane[254]. Films were grown on $Pt/SiO_2/Si$ and $Ir/IrO_2/SiO_2/Si$ substrates, in the presence of oxygen, at 475–525 °C. The substrate temperature has no influence on the PbO_x layer growth on the Pt electrode substrate, while an oxidation of the iridium system along with deposition of metallic lead was observed above 500 °C. It is possible to suppress the formation of metallic lead by reducing the oxygen flow rate[254].

Samoilenkov grew carbon-free high-quality films of β-PbO on $SrTiO_3$ and α-PbO on MgO, below 400 °C substrate temperatures, using $Pb(thd)_2$ (**23c**) as precursor in the presence of water vapor and oxygen[255]. Addition of water resulted in a fivefold increase in growth rate at 300 °C, similarly to other metal enolates mentioned above

(Section V.A.2). Lee and coworkers synthesized the alkoxyalkyl-substituted β-diketonates $Pb[RC(O)CHC(O)(CH_2)_3OR']_2$ (R = *t*-Bu, Me, OMe, *i*-Pr; R′ = Me, Et), attempting to improve the volatility and stability of lead enolates[256]. However, film growth experiments showed that these compounds are not volatile enough to give satisfactory deposition rates (100–200 Å h^{-1}, as compared to 1200 Å h^{-1} for **23c**).

Lead-dioxide-coated electrodes are accessible by the sol–gel method described by Avaca, using $Pb(acac)_2$ (**23a**) and a mixture of ethanol and acetic acid as starting materials[257]. The solution was spread on a boron-doped diamond electrode body and heated at 400 °C for 1 h in argon atmosphere. PbO_2 electrodes have been widely used as anodes under extreme conditions, due to their extended anodic window in aqueous media[258].

4. Bismuth

Bismuth(III) oxide is the most important industrial compound of Bi and is found naturally as the mineral bismite. Bismuth(III) oxide has attracted interest as optical coatings, metal-insulator semiconductor capacitors, microwave integrated circuits and as material for solid oxide fuel cells[259–261]. At room temperature, monoclinic α-Bi_2O_3 is the stable form and possesses a polymeric layer structure.

Kang and Rhee[262] grew bismuth oxide films at 225–425 °C by direct liquid injection MOCVD, using $Bi(thd)_3$ dissolved in *n*-BuOAc. Temperatures above 325 °C tend to decrease the growth rate due to gas-phase dissociation processes. Annealing at temperatures up to 650 °C is necessary to obtain monoclinic α-Bi_2O_3. Temperatures above 750 °C convert α-Bi_2O_3 into cubic bismuth silicate due to the reaction with the silicon substrate.

The thermal and mass-transport properties of the MOCVD precursor $Bi(thd)_3$ were investigated by Bedoya and coworkers[263]. The authors suggested a temperature window for efficient vaporization of 190–280 °C and determined decomposition of the precursor above 350 °C.

B. Transition Metal Elements

1. Group 3 elements

a. Yttrium. Yttrium oxide is commonly used as a starting compound in both material science and inorganic chemistry. Application fields of Y_2O_3 include, for example, ceramics, optical glasses, refractory materials and protective coatings for plasma etching[264–266]. The deposition of yttrium oxide from metal–organic complexes became only lately of topical interest since it can replace SiO_2 as a dielectric material due to its high permittivity and good compatibility with silicon[267].

The deposition of Y_2O_3 on Al_2O_3 wafers is possible by CVD (230–830 °C, 7.5 Torr) from the metal–organic precursor $Y(thd)_3$ as noted by Nemetz and Wahl[225]. Worthy of mention is that at low temperatures the deposition rate follows the Arrhenius law, at mean temperatures it is almost temperature-independent (diffusion-controlled), while at high temperatures the deposition rate decreases with increasing temperature caused by homogeneous side reactions. The deposited yttrium oxide thin films have columnar structure and no powder formation was observed. The same precursor was used for high-speed laser CVD of yttria in oxygen atmosphere with deposition rates of up to 83 nm s^{-1}, which is 100- to 1000-fold those by conventional CVD[268]. The morphology of the respective films depends on the total gas pressure (0.8 to 9 Torr) and the deposition temperature (mainly determined by the laser power). Radical-enhanced ALD of smooth Y_2O_3 on Si(100) from 200–400 °C using $Y(thd)_3$ and oxygen radicals were examined by Van and Chang[269, 270]. Only submonolayer coverage of yttria was achieved per deposition cycle,

due to the bulkiness of the thd β-diketonate unit. XPS studies showed that the films were fully oxidized and that the carbon content can be decreased to 4 at% (350 °C) with increasing temperature. The surface kinetics of this deposition were studied by QCM. Arrhenius temperature-dependent plots gave the activation energies for adsorption (-0.14 ± 0.05 eV) and desorption (0.16 ± 0.03 eV).

Yttria thin films can also be deposited on Si substrates from $Y(hfac)_3$ and $Y(thd)_3$ by oxygen plasma-assisted CVD[271]. It is found that with $Y(hfac)_3$ the appropriate thin films were contaminated with fluorine, leading to unexceptional electrical properties. As discussed in Section V.A.4, next to yttrium oxide, SiO_2 and yttrium silicate are formed on the substrate surface. Pre-nitridation of the silicon surface impedes the reaction with the substrate.

b. Lanthanum. At low temperature lanthanum(III) oxide has an A-M_2O_3 hexagonal structure in which La^{3+} is 7-coordinated, while at high temperatures it possesses a C-M_2O_3 cubic crystal structure with 6-coordinated La^{3+} ions. La_2O_3 has the largest band gap of the rare earth oxides (at 4.3 eV), the lowest lattice energy and a very high dielectric constant. These properties lead to potential applications, such as dielectric layers in devices[272], gas sensors[273], and protective[274] and optical[275] coatings. CVD, ALD and spray pyrolysis are the methods of choice for the generation of lanthanum oxides from lanthanum enolates.

Polycrystalline lanthanum oxide films on Si(100) can be obtained from 0.01 M La-(acac)$_3$ solutions in 50% ethanol by pulse ultrasonic spray pyrolysis[276]. The crystalline size depends on the ratio of the spray pulse time and the time interval between pulses. Pure monoclinic films were produced with 5 s pulses followed by a 10 s interval and a substrate temperature of 550 °C, with a nozzle-to-substrate distance of 6.5 to 7.5 cm.

Growth of La_2O_3 on Si as gate dielectrics is possible using $La(thd)_3$ in an MOCVD process[277]. As pointed out in Section V.A.4, the deposited ultrathin films form an interfacial layer of lanthanum silicate with the substrate deteriorating their electrical properties; therefore, alumina was introduced as capping layer.

The groups of Rhee[278] and Jun[279] synthesized $La(thd)_3$(tetea) (**24**) and $La(thd)_3$-(tetraglyme) (**25**), which show an increased solubility compared to $La(thd)_3$, for use as precursors in direct liquid injection MOCVD. Deposition on Si(100) between 325 and 450 °C using argon as carrier gas along with oxygen as reactive gas lead to smooth dense

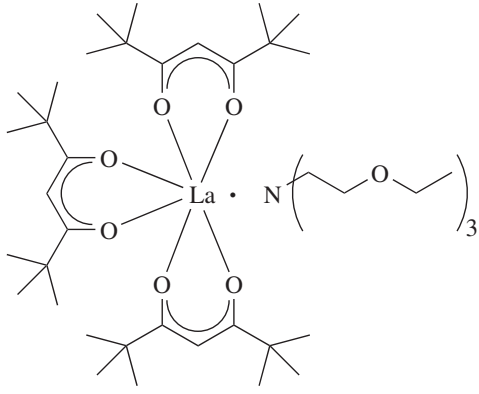

(**24**) $La(thd)_3$(tetea)

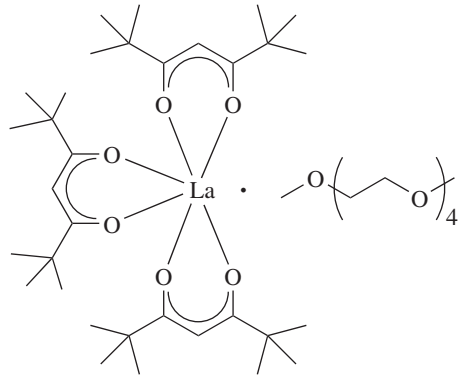

(**25**) $La(thd)_3$(tetraglyme)

films of La_2O_3. In case of complex **24** it was shown from thermal analysis that the Lewis-base ligand tetea separates at 220 °C[278]. However, a comparative study pointed to **25** as a preferable precursor owing to the better thermal stability of the obtained layers in contact with the silicon substrate, which is of importance for the annealing process[279].

ALE allowed lanthanum oxide thin film deposition from $La(thd)_3$ with ozone[280] and water[281] as oxygen sources. Films grown below 275 °C are amorphous and have the composition $La_2(O_2)CO_3$, while deposition temperatures >300 °C yielded cubic La_2O_3 with a carbon impurity of only 3 at%. All films are smooth, transparent, uniform and thin. However, the as-deposited films were found to be chemically unstable in ambient air, showing transformation to monoclinic LaO(OH) and hexagonal $La(OH)_3$. Post-annealing leads to remarkable changes in both structural and electrical properties (Figure 18). The

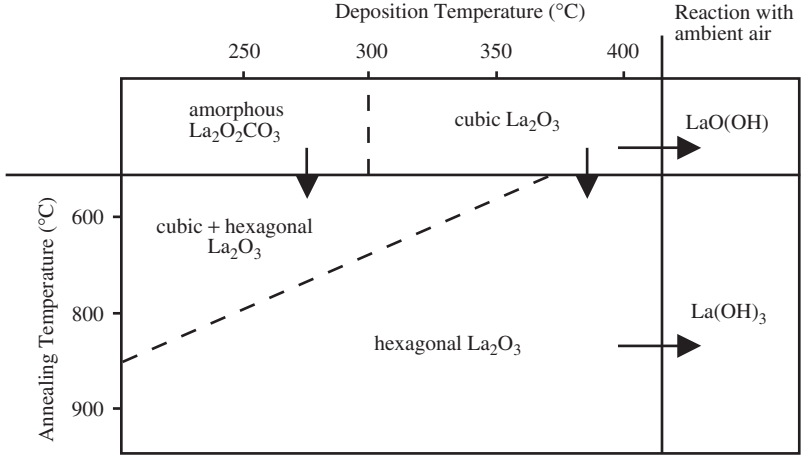

FIGURE 18. Influence of deposition and annealing temperature on lanthanum oxide film composition[280]. Reproduced from Reference 280 by permission of Elsevier

higher the annealing temperature, the more the grains of crystalline phases grow up. This results in an improved dielectric constant and leakage current density, which is attributed to the reduction of defects in the La_2O_3 film and interfaces, respectively.

2. Group 4 elements

a. Titanium. Titanium(IV) oxide exists at room temperature in the three forms anatase, brookite and rutile, all occurring in nature and containing a 6-coordinated titanium(IV) ion. Rutile is the most common form and the others transform into it on heating. Titania is the most widely used white pigment due to its brightness and excellent high refractive index, which makes it useful for anti-reflection coatings[282]. Furthermore, TiO_2 has attracted significant attention as insulator for capacitors (due to its high dielectric constant) for dynamic random access memory (DRAM) devices[282]. It shows an elevated corrosion resistance and elemental chemical stability and a very good optical transparency both in the visible and near-IR regions. As titanium oxide is exposed to UV light it becomes increasingly hydrophilic, and therefore it can be used for anti-fogging coatings and self-cleaning windows, or acquires photocatalytic properties, which can find application for the electrolysis of water[283].

Most precursors used for titanium oxide preparation, especially for film production, are based on titanium alkoxides[284]. A variety of mixed enolate–alkoxide titanium complexes exist, such as **26a**–**f**, **27**, **28** and **29a**–**e**, which are typical CVD precursors for titanium oxide.

CVD of anatase thin dielectric films on a single crystal of Si(111) was reported in the early 1970s by Patai and coworkers[285] by vaporizing **26a** at 80–100 °C in a stream of

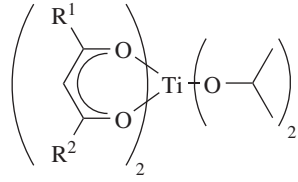

(**26a**) $R^1 = R^2 =$ Me; $Ti(acac)_2(OPr\text{-}i)_2$
(**26b**) $R^1 = R^2 = t$-Bu; $Ti(thd)_2(OPr\text{-}i)_2$
(**26c**) $R^1 = R^2 =$ Mef; $Ti(hfac)_2(OPr\text{-}i)_2$
(**26d**) $R^1 =$ Me; $R^2 =$ Ph; $Ti(bac)_2(OPr\text{-}i)_2$
(**26e**) $R^1 = R^2 =$ Ph; $Ti(bpp)_2(OPr\text{-}i)_2$
(**26f**) $R^1 =$ Me; $R^2 =$ OBu-*t*; $Ti(tbaoac)_2(OPr\text{-}i)_2$

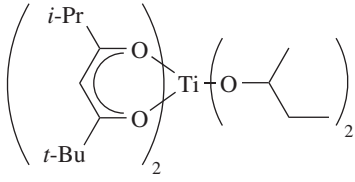

(**27**) $Ti(ibpm)_2(OPen\text{-}t)_2$

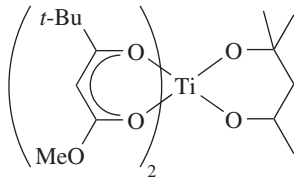

(**28**) $Ti(mdop)_2(mpd)$

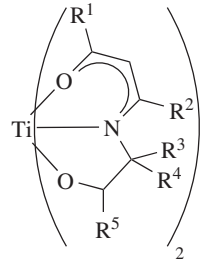

(**29a**) $R^1 = R^2 = Me$, $R^3 = R^4 = R^5 = H$
(**29b**) $R^1 = R^2 = R^5 = Me$, $R^3 = R^4 = H$
(**29c**) $R^1 = R^2 = R^3 = Me$, $R^4 = R^5 = H$
(**29d**) $R^1 = R^2 = R^3 = R^4 = Me$, $R^5 = H$
(**29e**) $R^1 = R^2 = i$-Pr, $R^3 = R^4 = H$, $R^5 = Me$

helium and oxygen with deposition at 550 °C and 650 °C. Lee and coworkers[286] examined the decomposition process of complexes **26a–e**. Initially, the OPr-*i* alkoxides dissociate followed by elimination of the substitutents of the chelating enolate ligands, and CHCO fragments of the remaining Ti-β-diketonate. β-Diketonates containing aromatic substitutents (bac, bpp) are resistant to thermal decomposition and an oxygen atmosphere must be applied to guarantee complete thermal decomposition of the precursor to TiO_2. The sublimation rates of **26b** and **26c** are faster than their decomposition rates, which makes them acceptable as precursors for CVD.

Anatase and rutile thin films can be generated from $Ti(thd)_2(OPr\text{-}i)_2$ (**26b**) by CVD and photoassisted CVD (glass, quartz and ceramic substrates; substrate temperature 360–600 °C; deposition pressure 9–76 mTorr)[287]. The photocatalytic activity of these films was studied towards the photodegradation of fenarimol. In contrast to the films obtained from $Ti(OPr\text{-}i)_4$ with **26b** as starting material, no photocatalytic effect was observed.

TiO_x films were prepared from $Ti(thd)_2(OPr\text{-}i)_2$ (**26b**) and $Ti(ibpm)_2(OPen\text{-}t)_2$ (**27**) by liquid-injection ALD using water as oxygen source at a deposition temperature of 300 °C[288]. Complex **26b** showed a lower activation energy and a higher saturated deposition rate than **27**. The deposition temperatures of both species are comparable.

A tailored precursor, $Ti(tbaoac)_2(OPr\text{-}i)_2$ (**26f**), was developed by Müller, Devi and coworkers[289]. Compared to **26b** this precursor produced anatase films with higher growth rates (10 nm min^{-1}) and lower surface roughness (<2 nm) at substrate temperatures as low as 350 °C. The fragmentation pathways shown in equations 9–11 were proposed.

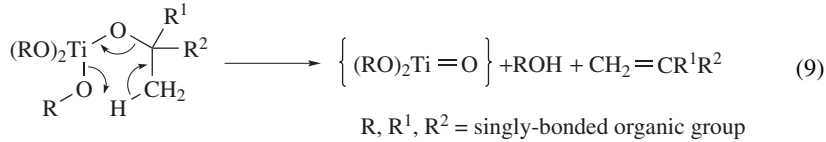

R, R^1, R^2 = singly-bonded organic group (9)

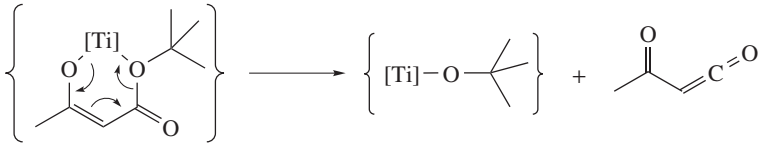

[Ti] = $Ti(tbaoac)(OPr\text{-}i)_2$ (10)

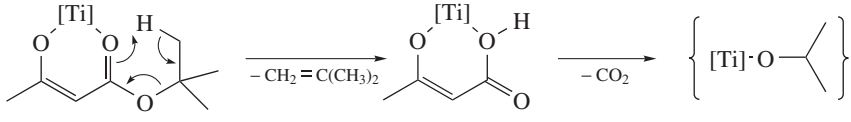

(11)

Very high deposition rates of titania were observed with the mono- or dinuclear titanium β-diketoesters Ti(mpd)(mdop)$_2$ (**28**, 17–28 nm min^{-1}) and [Ti(mpd)(mdop)(μ-OMe)]$_2$ (9–24 nm min^{-1}), 5 to 6 times higher than those of Ti(thd)$_2$(OPr-*i*)$_2$ (**26b**)[290]. The higher deposition rates can be explained by a weaker bonding of an ester moiety to titanium compared to that from a ketone. The films obtained from the dimeric species were crystalline (anatase) and showed some carbon impurity (<3%). Dimerization of complex **28** was observed when diluting with methanol, as shown in equation 12.

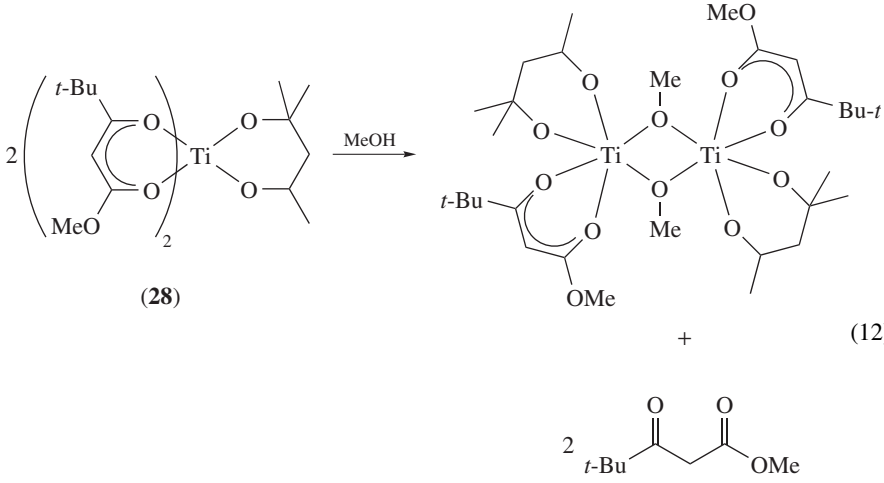

(12)

Bis(*N*-alkoxy-*p*-ketoiminate) titanium complexes (**29**) can be applied as starting materials in the deposition of TiO_2 thin films[291]. Among them, complexes **29b** and **29c** are best suited as precursors, due to their thermal stability and volatility. They provide the highest deposition rates—approximately three times higher than that with Ti(thd)$_2$(OPr-*i*)$_2$ (**26b**). Deposition of pure anatase layers was carried out at 450 °C using a liquid-injection CVD setup. The films were uniform, less crystalline and contained the usual carbon impurities (3–5%)[291].

The synthesis of TiO_2 anatase nanoparticles in supercritical CO_2 starting from Ti(acac)$_2$(OPr-*i*)$_2$ (**26a**) was recently reported by Alonso and coworkers[292]. Crystalline particles with a mean diameter of 200 nm and standard deviation of 100 nm were obtained at 150 kTorr and 300 °C using a CO_2/EtOH mixture (Figure 19). Compared to common Ti(OPr-*i*)$_4$, the β-diketonato complex was easier to handle and gave smaller particles. Increasing the reaction temperature along with decreasing the pressure also led to smaller nanoparticles.

Chemical vapor condensation (CVC) was applied by Lee[293] for the production of TiO_2 nanoparticles by decomposition of Ti(O)(acac)$_2$. In the temperature range of 800–1000 °C hollow-shell nanoparticles (10–40 nm diameter, 4–5 nm thick) of anatase–rutile mixed phases were obtained. The formation of the hollow structure is a result of the competition

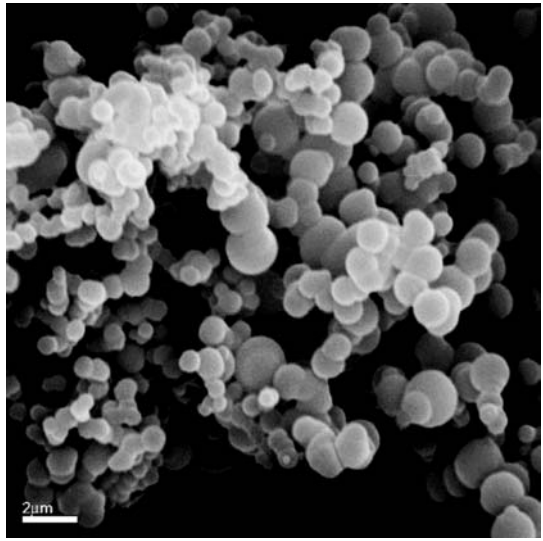

FIGURE 19. SEM image of anatase nanoparticles derived from $Ti(acac)_2(OPr\text{-}i)_2$ in CO_2/EtOH at 150 kTorr and 250 °C[292]. Reproduced from Reference 292 by permission of Elsevier

between the diffusion of TiO towards the surface and the reaction of this species with oxygen (Scheme 6). The optical transmittance of the product is 35–70% in the wavelength range of 400–800 nm, depending on the reaction temperature, which is lower than that of commercially available TiO_2 nanopowders (*ca* 80%).

b. Zirconium. Zirconium dioxide is found in nature as baddeleyite (monoclinic), which is the most stable phase at room temperature with 7-coordinated zirconium ions. Zirconium(IV) oxide is chemically stable, has a low coefficient of thermal expansion and, at 2715 °C, a high melting point. Therefore, it is a useful refractory material, being employed in the manufacture of crucibles and furnace cores. In addition, it is a most promising alternative to SiO_2 in microelectronic applications, oxygen-conductive membranes for use in fuel cells[294] and oxygen sensors[295], high-temperature thermal barriers[296] and optical coatings[297], hard protective layers[298] and ferroelectrics[299]. For high-temperature applications, the cubic phase of zirconia, which is stable at 1000 °C, must be stabilized by yttrium oxide (YSZ), resulting in superior mechanical properties.

CVD is widely used for the fabrication of zirconium oxide films starting from zirconium enolates in the presence of oxygen to avoid high carbon impurities. The organic substituents at the β-diketonate ligands have direct influence on the quality of the obtained films. While $Zr(acac)_4$ leads to high carbon impurities in the film[300] and $Zr(tfac)_4$ gives fluorine-contaminated layers[300–303], pure deposits are obtained from $Zr(thd)_4$[304,305]. The latter system requires a high deposition temperature (>600 °C), which is incompatible with the low growth temperature (<500 °C) required for deposition onto preprocessed silicon circuits in microelectronic applications. Therefore, Jones[306–308] and Baum[309] developed a new class of mixed alkoxy–enolate precursors, $Zr(thd)_2(OPr\text{-}i)_2$ and $Zr(thd)_2(OBu\text{-}t)_2$, respectively. Both metal-organic compounds deposit ZrO_2 on silicon substrates in the temperature range of 400–600 °C, whereas $Zr(thd)_2(OBu\text{-}t)_2$ produced high carbon impurities (>12 at%) in contrast to $Zr(thd)_2(OPr\text{-}i)_2$ (1.8 at%). Further physical and

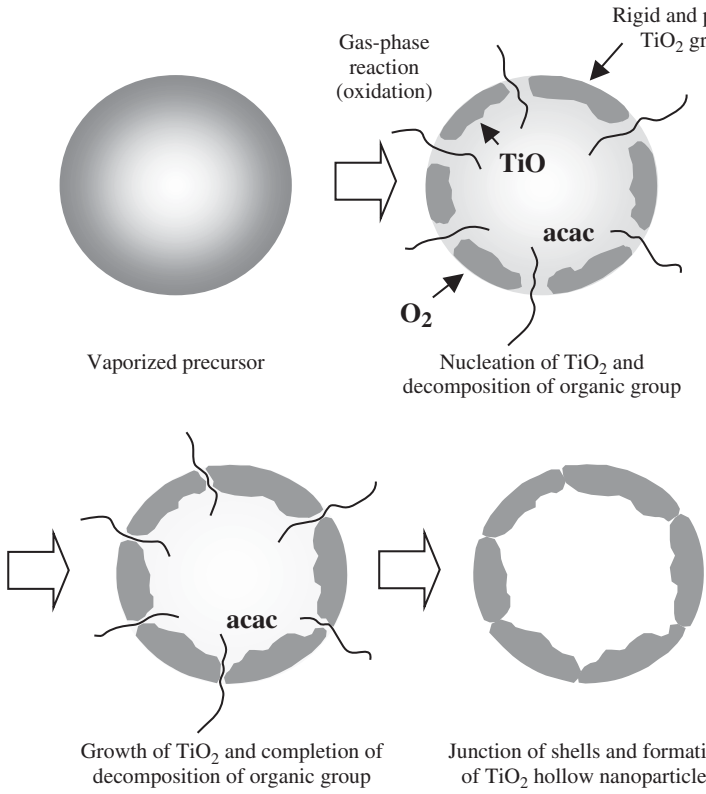

SCHEME 6. Formation of TiO_2 hollow nanoparticles from $Ti(O)(acac)_2$[293]. Reproduced from Reference 293 by permission of The Ceramic Society of Japan

electrical characterization of ZrO_2 films obtained from $Zr(thd)_2(OPr\text{-}i)_2$ were reported by Landheer and coworkers[310] Comparable layers with carbon impurities of *ca* 2 at% can be obtained using dimeric $[Zr(thd)(OPr\text{-}i)_3]_2$ as starting material, which is more volatile than $Zr(thd)_4$[307]. Especially at low temperature (350–600 °C) high growth rates (*ca* 0.2 $\mu m\,h^{-1}$) can be reached. Even higher growth rates (12 $\mu m\,h^{-1}$, 0.5 mbar) were reported by Morstein using the heteroleptic less hydrolysis sensitive zirconium complex $Zr(acac)_2(OCH(CF_3)_2)_2$[311]. Zirconia films with C and F levels between 0.25 and 0.5 at% were obtained in the temperature window from 475 to 625 °C (Figure 20). It was found that with increasing deposition temperature, the initially cubic ZrO_2 films convert progressively into the monoclinic equilibrium phase.

A volatile, and hence promising, MOCVD precursor is the comparable zirconium bis(acetylacetonato)bis(alcoholato) complex $Zr(acac)_2(OSiMe_3)_2$[312].

$Zr(tmnd)_4$ (**30**)[313] and $Zr(tod)_4$ (**31**)[314] have also been found to be suitable precursors for the deposition of monoclinic zirconia. Both species possess high deposition rates in the temperature range of 500–750 °C but, as discussed earlier for fluorine-free zirconium tetra-enolates, the disadvantage is the high carbon content of the appropriate zirconia films (i.e. **30** 7–8 at%)[314].

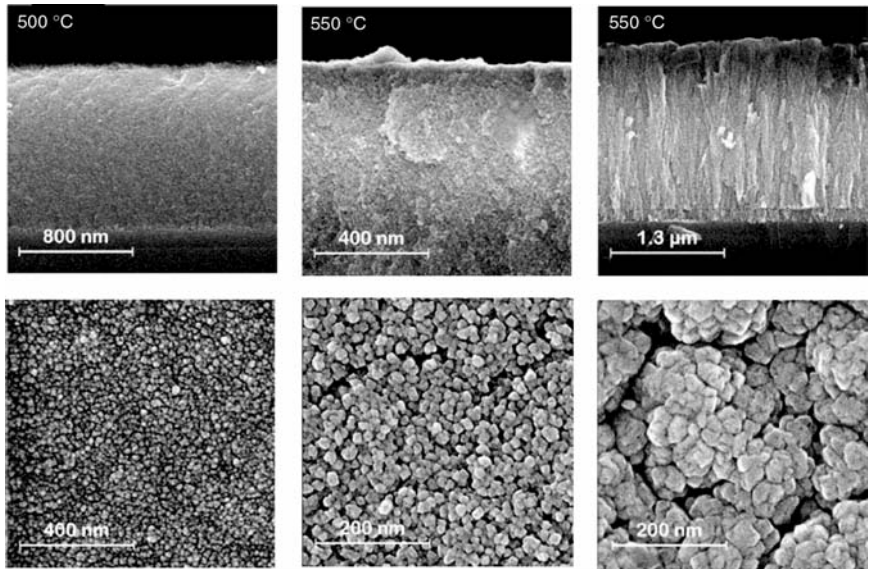

FIGURE 20. SEM images of the microstructure of zirconia films deposited from $Zr(acac)_2(OCH(CF_3)_2)_2$ at different temperatures (top cross-section of film, bottom detail of microstructure; left 500 °C, middle 550 °C, right 600 °C)[311]. Reproduced from Reference 311 by permission of Wiley-VCH

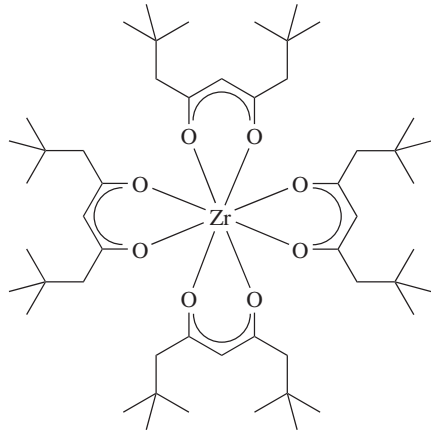

(**30**) $Zr(tmnd)_4$

Zirconia coatings can also be obtained by ESD (electrostatic spray deposition) using $Zr(acac)_4$ as metal source[315]. In a typical experiment, precursor concentrations of 0.04–0.16 mol L^{-1}, a flow rate of 0.5 mL h^{-1}, a positive high voltage from 5–10 kV, a nozzle-to-substrate distance of 27 mm and a deposition temperature range of 300–500 °C were applied. Various polymer additives were used to optimally tune the microstructure of the coating. Smooth, dense and homogeneous thin layers were deposited.

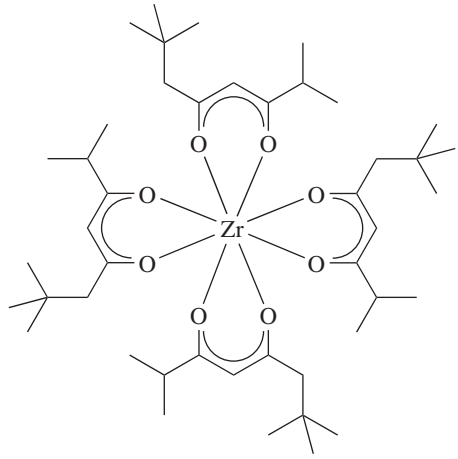

(**31**) $Zr(tod)_4$

c. Hafnium. Monoclinic hafnium oxide is isomorphic to baddeleyite and is an electrical insulator and a currently leading candidate to replace SiO_2 as a gate insulator. Zirconium and hafnium tetra-enolates show the expected similar behavior in the formation of thin metal oxide films by decomposition in the presence and absence of oxygen. For example, $Hf(acac)_4$, $Hf(tfac)_4$, $Hf(hfac)_4$[301,316], $Hf(thd)_4$[317], $Hf(tod)_4$[313] and $Hf(tmnd)_2$[314] produce (monoclinic) HfO_2 and other volatile organic compounds on heating above 300 °C. In the presence of oxygen most of the carbon is removed as CO_2 from the layers. Variations of carbon and/or fluorine film contaminations were found, depending on the nature of the substituents at the β-diketonate entities. As outlined for zirconia deposition, also the mixed alkoxy–enolate hafnium(IV) complex $Hf(thd)_2(OPr\text{-}i)_2$ is suitable as precursor for successful hafnia film production by CVD[309] and chemical solution deposition (CSD) processes (Figure 21)[318]. Hafnium oxide films produced by the latter method remain amorphous at high temperatures (600 °C).

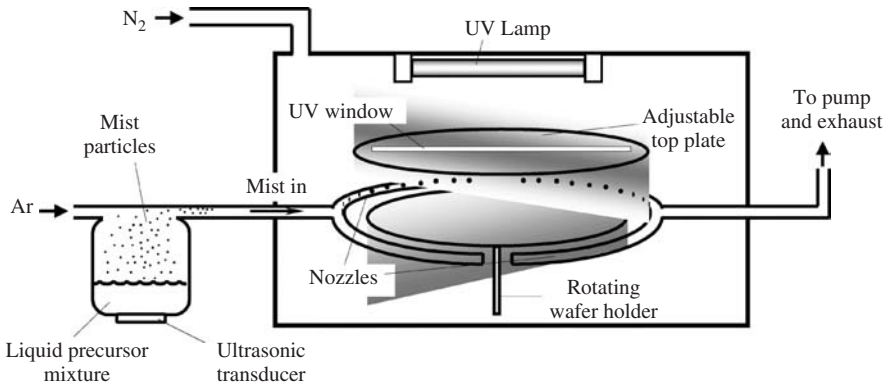

FIGURE 21. Schematic representation of a CSD system[318]. Reproduced from Reference 318 by permission of Taylor and Francis Inc. www.informaworld.com

3. Group 5 elements

a. Vanadium. Besides the four oxides of vanadium (V_2O_5, VO_2, V_2O_3 and VO) a number of other phases of intermediate composition are known. Vanadium pentoxide is both an amphoteric oxide and an oxidizing agent. The ability to reversibly lose oxygen upon heating makes it a catalyst of choice, for example, in the oxidation of SO_2 and numerous organic compounds[319, 320] in air. In addition, V_2O_5 finds use as detector material in bolometers due to its high thermal coefficient of resistance[321]. In contrast, VO_2 is a material that displays thermochromic properties and has potential application in the area of energy-efficient glazing and solar heating[322, 323].

VO_2, V_2O_5 and V_6O_{13} can be grown on glass substrates by MOCVD using stable vanadyl acetylacetonate $VO(acac)_2$ as precursor[324–326]. In the temperature window of 475–520 °C monophasic, monoclinic VO_2 films are obtained, while outside of this range other vanadium oxide phases dominate[324]. The film microstructure depends strongly on the growth temperature: a strong (200) orientation is present in films grown at 475 °C, whereas grain orientation is nearly random at 520 °C. Furthermore, the oxygen flow rate influences the stoichiometry of the films deposited, as shown in Figure 22[325]. Vanadium(IV) oxide

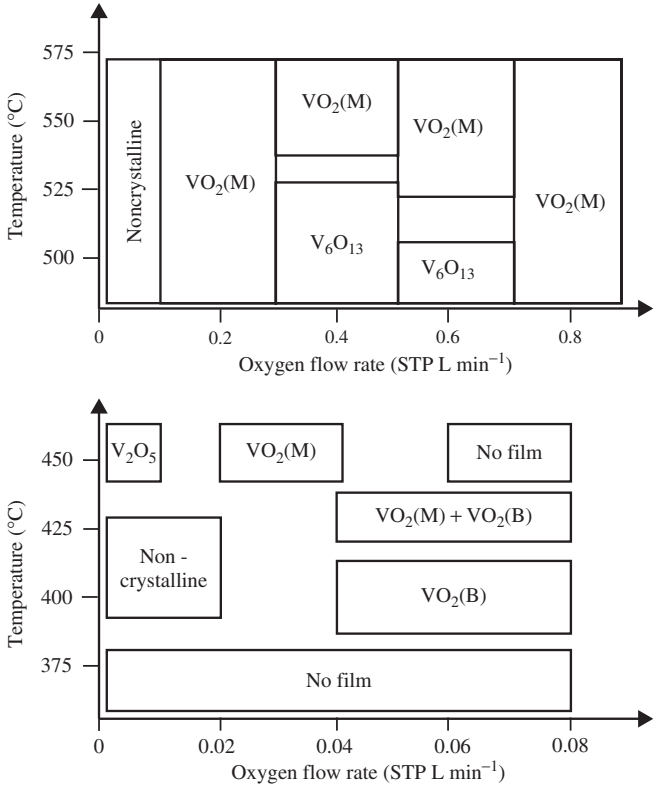

FIGURE 22. Influence of substrate temperature and oxygen flow rates on the stoichiometry of the films grown by AP-CVD (top) and DLI-CVD (bottom)[325]. M = monoclinic phase, B = metastable monoclinic phase appearing in nanocrystalline form. Reproduced from Reference 325 by permission of Wiley-VCH

films prepared in a DLI-CVD reactor exhibited considerably poorer thermochromic and morphological properties as compared to those grown by atmospheric-pressure CVD[325].

A huge number of silica- and alumina-supported vanadium oxide catalysts are obtained by the molecular designed dispersion technique as reported by Vansant and coworkers[319, 320, 327–335]. The process of this method is depicted in Scheme 7 including two different adsorption strategies (hydrogen bonding and ligand exchange). The following three processes are observed during thermolysis: (i) sublimation of the excess $VO(acac)_2$, (ii) a nonoxidative proton-assisted thermolysis of the hydrogen-bonded acac ligands and (iii) oxidative decomposition of the *non*-hydrogen-bonded ligands[330]. This procedure resulted in the high dispersion of V^{5+} species.

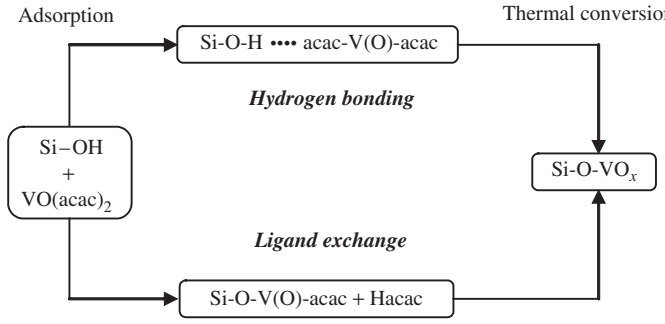

SCHEME 7. Schematic view of the molecular dispersion method for the production of vanadium oxide deposits, using $VO(acac)_2$ as metal source and silica as support[328]. Reprinted with permission from Reference 328. Copyright 1996 American Chemical Society

On silica supports all the vanadium oxide species have V in strictly tetrahedral coodination and no formation of microcrystallites was observed with a vanadium loading of 2.5 wt%, while on alumina surfaces vanadium loadings that are 5 times higher can be achieved without induced crystallinity. The use of alkylchlorosilanes as coupling agents for the preparation of hydrophobic MCM-48/VO_x catalysts was reported by van der Voort and Vansant[336, 337]. The vanadium oxide catalysts are thermally stable up to 500 °C, very resistant towards leaching in aqueous media and possess a high structural as well as hydrothermal stability. Diffusion effects in vanadium oxide catalysts on SBA-15 (an aluminosilicate molecular sieve) and its plugged analogues have been studied[332], which may be important regarding the oxidation of methanol to formaldehyde[330], the oxidative dehydrogenation of ethylbenzene to styrene in the presence of N_2O[335] and the selective catalytic reduction (SCR) of NO with ammonia to N_2[333, 334]. In general, higher vanadium oxide loadings result in higher conversions. Mixed-metal oxide catalysts of the type $VO_x–TiO_y$ on SBA-15 can also be synthesized by the molecular designed dispersion methodology[331, 334]. A higher dispersion of the metals is observed compared to the disposition of $VO(acac)_2$ on SBA-15, leading to a higher catalytic activity towards the SCR of NO with NH_3[334].

The sol–gel synthesis of a $V_2O_5–SiO_2$ catalyst and its application in the oxidative dehydrogenation of *n*-butane to give CO, CO_2 or dehydrogenated compounds was described by Sham and coworkers using $V(acac)_3$ and $Si(OEt)_4$ (teos) as precursors[338]. Calcination at 500 °C resulted in the formation of a solid with a high surface area, which allows a better dispersion of active species. Furthermore, a direct correlation between the catalytic activity and the Brönsted acidity was also observed.

b. Niobium and tantalum. Niobium and tantalum form different oxide phases but they are not so extensively characterized as those of vanadium. Their pentoxides are dense white solids and are relatively more stable and difficult to reduce. Their structures are complicated networks. In particular, Nb_2O_5 displays extensive polymorphism; however, the polymorphs of both metal oxides are by no means all analogous. Niobium and tantalum oxides each display a high dielectric constant and are employed as thin dielectric films for storage capacitors. Uses of Nb_2O_5 include catalysis, special ceramics and moisture sensors. Due to its high refractive index, Ta_2O_5 has been utilized in the fabrication of photographic lenses.

Nanocrystalline niobium(V) oxide films are accessible by an extended sol–gel method ($Nb(OEt)_5 + 2acacH + H_2O$ in ethanol solution) as reported by Brooks and coworkers[339]. Autoclaving leads to amorphous gels, from which homogeneous nanocrystalline, porous and crack-free Nb_2O_5 films can be obtained. The orthorhombic T-phase is formed on annealing at 600 °C.

Thin films of β-Ta_2O_5 with (111) orientation were prepared by Tominaga and coworkers using $Ta(thd)_4Cl$ as CVD precursor (source temperature 215 °C, reactive carrier gas 1:1 argon–oxygen, substrate quartz and Si(100) at 600–700 °C, pressure 5 Torr, deposition rate 50–150 $Å\,min^{-1}$)[340]. The films are smooth but appeared to contain a number of pits caused by columnar growth perpendicular to the substrate.

4. Group 6 elements

a. Chromium. Chromium(III) oxide, also known as chromia or chromium sesquioxide of formula Cr_2O_3, is the most stable chromium oxide. It has the corundum structure and it is semiconducting and antiferromagnetic below 35 °C. It has found wide application as a green pigment, protective coating or catalyst[341,342]. Also known are brown-black colored CrO_2 and deep-red CrO_3. Chromium(IV) oxide is metallic, conductive and ferromagnetic and found use in the manufacture of magnetic recording tapes. In contrast, chromium(VI) oxide is strongly acidic and rather covalent. Its intense oxidizing properties are widely used in organic chemistry. Cr_2O_3 coatings on steel and steel alloys were prepared by CVD of $Cr(acac)_3$ in oxygen atmosphere[343]. Variation of the deposition conditions (precursor and substrate temperature, flow rates of carrier gas argon and reactive gas oxygen) led to the formation of optimized coatings.

A series of papers was published by Vansant and coworkers dealing with the gas-phase deposition and thermal transformation of $Cr(acac)_3$ to chromia on the surface of alumina and silica supports[344–347]. $Cr(acac)_3$ binds to the hydroxyl-terminated alumina surface by hydrogen bonding and/or a donor–acceptor interaction with coordinatively unsaturated Al^{3+} ions as outlined in Figure 23[344].

On heating in nitrogen, the elimination of hydrogen-bonded enolate ligands is assisted by proton transfer below 270 °C. The residual acac ligands need higher temperatures (*ca* 400 °C) to be removed from the surface, whereby in an oxygen atmosphere the oxidation of the β-diketonate ligands occurs in a single step already at *ca* 300 °C, as could be shown by DTG measurements and diffuse reflectance FTIR spectroscopy[344]. Comparable results were observed for the deposition of $Cr(acac)_3$ on hydroxylated silica surfaces at 190 °C[345]. Mesoporous silicas, such as MCM-48, SBA-15, MCF and MSU, could be modified by the molecular designed dispersion method using $Cr(acac)_3$ in toluene solution[346]. The properly calcined materials were studied with respect to their textural properties and chemical composition. When calcination is carried out in an oxygen-containing atmosphere, oxidation of surface-bound Cr^{3+} to Cr^{6+} is observed.

b. Molybdenum. The most important oxide of molybdenum is MoO_3 (molybdena). Its structure consists of layers of linked MoO_6 units showing a complex and unique

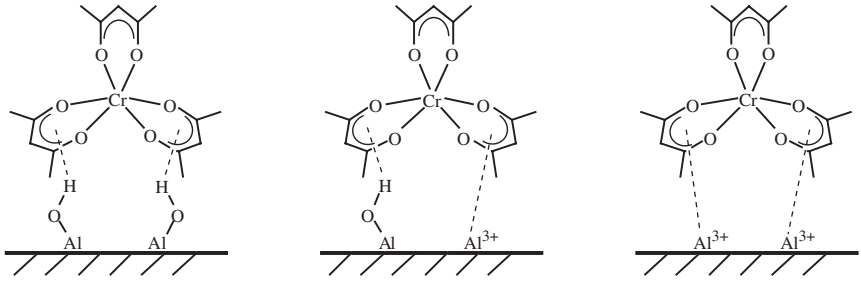

FIGURE 23. Binding of $Cr(acac)_3$ on a hydroxylated alumina surface[344]. Reproduced from Reference 344 by permission of The Royal Society of Chemistry

3-dimensional network. In contrast, less stable MoO_2 possesses a distorted rutile structure. In between these extremes lies a variety of intensely colored phases showing complex structures. Molybdenum(VI) oxide has attracted considerable attention for high-density storage devices, gas sensors, and heterogeneous and shape-selective adsorption catalysis[348, 349].

Molybdenum(VI) oxide thin films can be prepared via metal-organic CVD from volatile $MoO_2(acac)_2$ and $MoO_2(thd)_2$ single-source precursors as outlined by Fragalà[350] and Tondello[351]. $MoO_2(acac)_2$ was successfully applied as starting material for the one-step deposition of silica- and zirconia-supported MoO_3[350]. Pure MoO_3 films on silica were obtained at a high $O_2/MoO_2(acac)_2$ ratio ($P_{O_2} : P_{MoO_2(acac)_2} = 7 \times 10^{-4}$, hence, with lower deposition rates), while lower oxygen partial pressures result in the presence of some molybdenum suboxides on alumina supports. Interestingly, it is noteworthy that on zircona under identical conditions only pure MoO_3 formation is observed. $MoO_2(thd)_2$ allows the deposition of MoO_3 layers on Pt and Si(100) substrates[351]. A qualitative indication on the possible decomposition path was obtained by mass spectrometry and thermal analysis. The deposition rate was found to be feed-rate limited because of the low vapor pressure of $MoO_2(thd)_2$. At low flow rates a lower number of nucleation sites are formed, the oxidation of the Mo_xO_y species is favored and larger crystallites are obtained[351].

The properties of silica- and/or alumina-supported molybdena catalysts for propene metathesis were studied by Handzlik and coworkers[352]. These materials could be prepared by thermal spreading of $MoO_2(acac)_2$ with well-dispersed molybdenum in a wide range of its loading. The selective metathesis activity depends on the substrate and on the surface molybdenum concentration. For example, a higher activity is found for the molybdena–alumina system at high Mo loadings.

c. Tungsten. Tungsten(VI) oxide is the most stable and valuable oxide among the known tungsten oxides. As already discussed for molybdenum oxides, also a variety of tungsten oxides are known between WO_3 and WO_2. Tungsten oxide shows electrochromic properties and can be used for smart windows, optical filters and display devices[353, 354].

Volatile tungsten(IV) oxo alkoxide/β-diketonate complexes of structural type W(O)(β-diketonate)$(OR)_3$ (R = *i*-Pr, *t*-Bu; β-diketonate = acac, **32**, hfac, **33**) are excellent precursors for the low-pressure CVD of electrochromic tungsten oxide films, as shown by Chisholm and coworkers[355]. While with **32b** and **33b** the produced films were transparent and blue, **32a** and **33a** led to pale yellow layers which darkened to pale green-blue when exposed to air for several days[355]. With the exception of **33a**, all other tungsten complexes formed good-quality films with respect to adhesion and surface coverage; however, no surface selectivity for quartz, pyrex or ITO was observed.

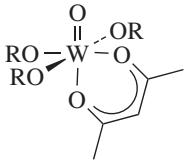

(**32a**) R = *t*-Bu
(**32b**) R = *i*-Pr

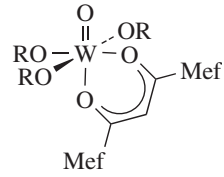

(**33a**) R = *t*-Bu
(**33b**) R = *i*-Pr

Complexing-agent-assisted sol–gel processes also allowed the preparation of tungsten(VI) oxide gels and thin films by starting from WCl_6 and ethanol followed by addition of 2,4-pentanedione, as shown by Nishide and Mizukami[356–358]. All precipitated materials (on quartz) were heated to 300–700 °C, resulting in the formation of crystalline and transparent WO_3 films (cubic, monoclinic or their mixture). The films prepared with 2,4-pentanedione as additive showed comparable refractive indices with those prepared with catechol; however, the values are lower than those of the films produced with ethylene glycol or without any additive[358]. On peeling off the films from the quartz substrate the cubic crystals of WO_3 were transformed to stable monoclinic ones.

5. Manganese

Many oxides of manganese are known, whereby the oxidation state of manganese reaches from +2 to +7. However, MnO_2 is by far the most important oxide, though it is not the most stable, decomposing to Mn_2O_3 (contains distorted MnO_6 units, antiferromagnetic < −193 °C) at *ca* 530 °C. Manganese(IV) oxide is widely used as oxidizing agent in organic and organometallic chemistry. The only stoichiometric form is β-MnO_2 (pyrolusite), which possesses the rutile-type structure. Mn_3O_4 (hausmannite, spinel structure) is obtained, when any manganese oxide is heated to 1000 °C in air. All manganese oxides are semiconductors, whereby the lowest resistivity is found for MnO_2 (0.0028 Ω cm)[359]. MnO_2 has very promising electrochromic properties, but most commonly it is applied in batteries. Furthermore, MnO_2 can be used as a heterogeneous catalyst for the oxidation of hydrocarbons[360], the oxidation and reduction of nitric oxide[361] and decomposition of ozone[362].

Liquid injection CVD (Si(100) substrate at 240–560 °C, 0.5 Torr), using a solution of $Mn(thd)_3$/thf to deposit manganese oxides with the average valence being smaller than +3, was published by Nakamura and coworkers[363]. Addition of oxygen promotes decomposition of the metal–organic precursor. Carbon-free manganese oxide films are obtained, when the substrate temperature lies between 360–480 °C. No significant influence on the atomic composition is found within this temperature range. Manganese oxide thin films also can be grown from the same precursor and using ozone as oxidizing agent by the ALD process[364]. Films were deposited on both soda-lime glass and Si(100) single crystals in the temperature window 138–210 °C, giving mainly metal oxides with manganese in the +4 oxidation state. At higher deposition temperatures the oxidation state decreases, which is consistent with the thermodynamic stability of the solid phases in the Mn–O system. The electrical resistivity of MnO_2 on soda-lime is in the 0.3–3.2 Ω cm range.

Manganese oxide–silica aerogels with a content of 7 wt% Mn were synthesized by Baiker[365]. In a typical sol–gel process $Si(OEt)_4$ and $Mn(acac)_3$ underwent a reaction to give MnO_x-SiO_2, whereby, depending on the conditions (hydrolysis, gelation conditions, calcination temperature), the structural, chemical and catalytic properties of the aerogels

changed drastically. This procedure led to formation of different manganese oxide species, ranging from crystalline Mn_3O_4 and amorphous Mn_5O_8 to highly dispersed manganese oxides. The aerogels were used for selective catalytic oxidation of NH_3. Amorphous aerogels with highly dispersed MnO_x showed high selectivity for N_2 (78%), whereas the aerogels containing crystalline Mn_3O_4 and amorphous Mn_5O_8 afforded N_2O as main product (74%). This can be correlated with the abundance of Lewis acid-bound ammonia, which was higher on the amorphous dispersed mixed oxides.

6. Group 8 elements

a. Iron. Three oxides of iron can be distinguished, but all are subject to nonstoichiometry. Fe_2O_3 exits in a number of forms, whereby the α- and γ-phases are the most important ones. The paramagnetic α-Fe_2O_3 is also known as the mineral haematite which adopts a corundum structure, while γ-Fe_2O_3 (maghemite), obtained by careful oxidation of Fe_3O_4 (magnetite), is metastable, ferromagnetic and has cubic structure. The β-Fe_2O_3 phase, which can be produced by CVD from iron(III) enolates (see below), undergoes a $\beta \rightarrow \alpha$ phase transition on annealing at 500 °C. Iron oxides are widely used, for example, as beam splitter and interference layer in optical devices (α-Fe_2O_3), as heterogeneous catalysts and, due to its high magnetic coercivity and stable ferromagnetic properties, as magnetic material in the manufacture of high-frequency transformers and high-density magnetic recording tapes[366, 367].

Iron oxide formation from iron enolates depends on the decomposition temperature and the partial oxygen pressure used in the appropriate deposition experiment. The iron β-diketonate $Fe(acac)_3$ gives Fe_2O_3 in the temperature range of 400–500 °C[368]. Replacing the chelate ligands acac by tfac significantly lowers the decomposition temperature and hence, $Fe(tfac)_3$ produces β-Fe_2O_3 (bixbyite structure) at 300 °C[369]. Fe_3O_4 has been prepared by electron cyclotron resonance PE-CVD using $Fe(acac)_3$ as the source material, hydrogen as carrier gas, an oxygen plasma and soda-lime glass as substrate at temperatures in the range of 150–350 °C[370, 371]. Magnetite growth from $Fe(thd)_3$ has been obtained via low-pressure CVD as discussed by Rastogi and Igumenov[372]. Oxidation of these thin films converts Fe_3O_4 to γ-Fe_2O_3 which shows a superior magnetic coercivity (γ-Fe_2O_3, 122 kA m^{-1}) and remanence value of 102 mT.

Lie and Kjekshus applied the ALD process with $Fe(thd)_3$ and ozone as precursors on diverse substrates in the temperature range of 160–210 °C[373]. Depending on the substrates different orientations were found: on soda-lime glass and Si(100) (001)-oriented columns of α-Fe_2O_3 with no in-plane orientation were formed, while on α-Al_2O_3(001) and MgO(100) substrates α-Fe_2O_3 and β-Fe_2O_3 structures of highly oriented columns with in-plane orientation matching that of the substrate were observed. The influence of a magnetic field on the growth of α-Fe_2O_3 on α-Al_2O_3(001) and soda-lime glass by ALD under the same conditions was studied[374]. The deposited iron oxide films are not influenced by a magnetic field on α-Al_2O_3(001), whereas the film growth on other surfaces is influenced. ALD in combination with low-energy ion scattering (LEIS) with $Fe(acac)_3$ and O_2 was performed at room temperature by Brongersma and Vansant, who studied the growth of an iron oxide overlayer on YSZ[375]. Oxidation at $T > 800$ °C causes migration of Fe_2O_3 into the bulk which limits its usefulness in surface catalytic processes. A reaction mechanism involving binding of $Fe(acac)_3$ to the YSZ surface was proposed (equation 13). The same authors also reported the use of $Fe(acac)_3$ for deposition of iron oxides on zirconia by the molecular designed dispersion method[376]. Upon reaction with ZrO_2, Zr-acac surface units are formed which are thermally unstable and transform into zirconium acetate species at 110 °C in air or above 200 °C in vacuum. During

calcination at 500 °C all organic groups are removed and zirconium/iron-hydroxyl moieties are formed.

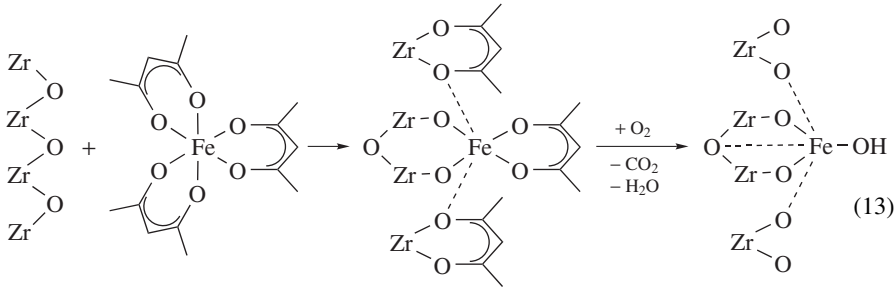

(13)

Fabrication of patterned magnetite films by soft lithography and thermal decomposition using $Fe(acac)_3$ is also possible as described by Yang and coworkers[377, 378]. The modality to obtain such structures on gold substrates is illustrated in Scheme 8. The array size could be tuned by changing the dimension of patterns on poly(dimethylsiloxane) stamps, the concentration of $Fe(acac)_3$ solution and the size of water droplets during the condensation process.

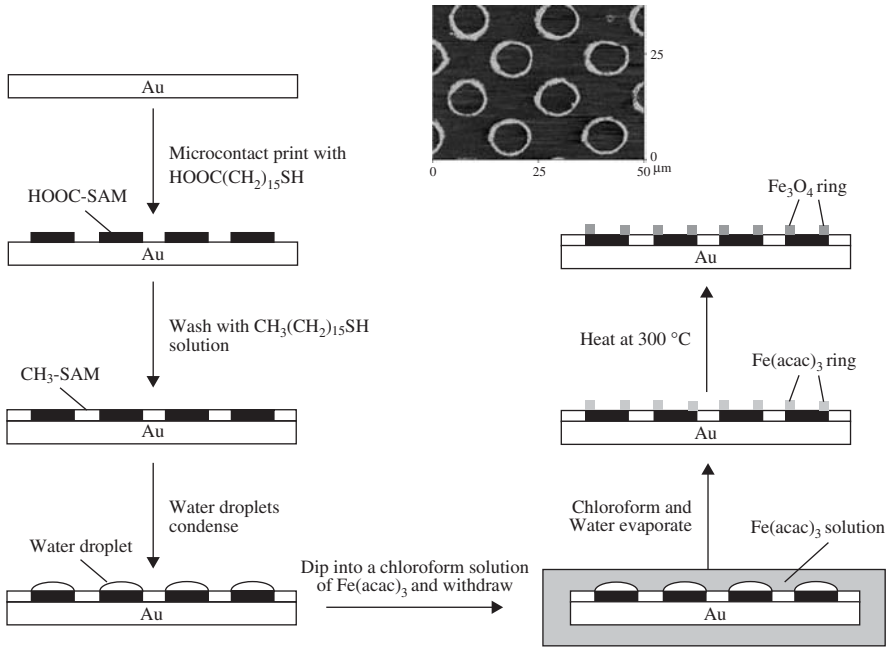

SCHEME 8. Microlithographic fabrication of magnetic rings on gold substrates, including a magnetic force microscopy (MFM) image of Fe_3O_4 rings (phase shift mode)[378]. Reproduced from Reference 378 by permission of Elsevier

The preparation, characterization and catalytic behavior of iron-oxide-modified nanosized diamonds was reported by Tsoncheva and coworkers[379, 380]. These composite

materials are accessible by using shock-wave-synthesized ultrananosized diamond blends impregnated with $Fe(acac)_3$. This operation leads to highly dispersed iron oxide particles with unique properties which can be applied as highly active and stable catalysts for the decomposition of methanol.

Various mesoporous silicas (MCM-48, SBA-15, MCF, MSU) modified with iron oxides introduced by $Fe(acac)_3$ were prepared using the molecular designed dispersion method (Section V.B.3.a)[346, 347, 381, 382]. The mechanism of interaction between the iron acetylacetonate complex and the support surface differs from that with $Cr(acac)_3$ (Section V.B.4.a) and $Cu(acac)_2$ (based on hydrogen bonding, Section V.B.8). In the case of the iron precursor a ligand exchange mechanism is operative. Catalytic activities of the iron-oxide-modified mesoporous silicas were investigated for the oxidative dehydrogenation of ethyl benzene in the presence of N_2O (nitrous oxide, laughing gas)[381], the selective reduction of NO by ammonia[382] and the reduction of N_2O with ammonia and methane[347].

A possibility to generate Fe_3O_4 nanoparticles is given by the method described by Zysler[383]. Tailoring the size of colloidal iron oxide magnetic cubic-faceted nanoparticles is possible in the range of 4–22 nm by a one-step high-temperature reaction of a $Fe(acac)_3$ solution at 250–270 °C[383]. The particle size can be easily modified by changing the surfactant/precursor ratio (Figure 24). Magnetic measurements showed the usual behavior for magnetic nanoparticle systems, i.e. super-paramagnetic and blocked regimes.

Monodisperse oleic-acid-coated magnetite nanoparticles of sizes 7 and 19 nm could be prepared by the seed-mediated high-temperature thermal decomposition of iron acetylacetonate[384]. Another group synthesized a series of highly branched and self-supporting nanostructures of magnetic nanoparticles (Figure 25)[385]. The morphology is strongly dependent on the nanoparticle concentration: at low concentrations straight rods of 80 nm average diameter and several microns length are formed, while at higher concentrations tree-like dendritic structures start appearing.

b. Ruthenium. Ruthenium has with RuO_2 and RuO_4 no oxides comparable to iron. RuO_2 is a blue-to-black solid with rutile structure, where the intense color most probably results

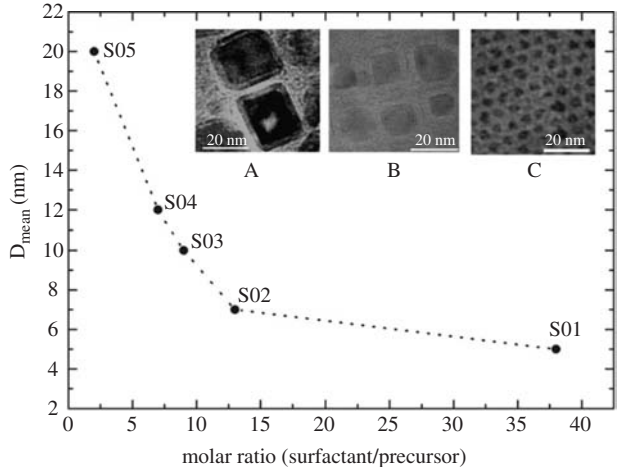

FIGURE 24. Size of iron oxide particles as a function of the surfactant/precursor molar ratio. The SEM images are of samples S05 (A), S04 (B) and S01 (C)[383]. Reproduced from Reference 383 by permission of Institute of Physics Publishing Ltd

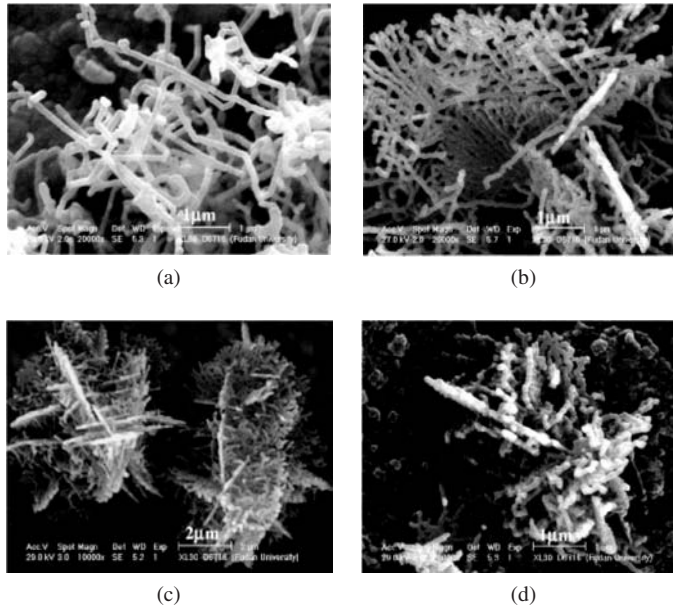

FIGURE 25. SEM images of Fe_3O_4 nanorods and nanodendrites obtained from $Fe(acac)_3$ at various concentrations: (a) 0.02 g L^{-1}, (b) 0.10 g L^{-1}, (c) 0.25 g L^{-1} and (d) 0.50 g L^{-1} [385]. Reprinted with permission from Reference 385. Copyright 2006 American Chemical Society

from small amounts of Ru^{3+} ions. Yellow RuO_4 is volatile and decomposes explosively above 100 °C to RuO_2. Ruthenium(IV) oxide displays interesting physical properties including low resistivity and thermodynamic stability. This oxide is used in integrated circuits, resistor applications and exhibits excellent diffusion barrier properties[386, 387].

The preparation of RuO_2 films on Si and SiO_2 from $Ru(acac)_3$ in the presence of oxygen is possible at 600 °C[34]. Compared to other precursors, i.e. $Ru(\eta^5\text{-}Cp)_2$, $Ru(acac)_3$ gave only inferior RuO_2 thin films (643 μΩ cm; for comparison: ruthenocene, 89.9 μΩ cm). In contrast, the deposition of dense and smooth RuO_2 films with resistivities of 45–60 μΩ cm is possible by direct liquid injection from $Ru(thd)_3$ in the presence of O_2, in *n*-butylacetate at 250 to 450 °C[388]. Higher deposition temperatures increase the resistivity of the films due to carbon incorporation. Ruthenium oxide thin films on $TiO_2(100)$ of lower resistivity (40 μΩ cm) were obtained from $Ru(thd)_3$ by CVD at 300 °C with oxygen as carrier gas[389]. The *cis*-$Ru(thd)_2(CO)_2$ precursor enables the formation of high-quality RuO_2 films (45–210 μΩ cm) with preferred (200) orientation by cold-wall MOCVD at 300 °C, as accomplished by Chi and coworkers[390, 391].

7. Cobalt

There are two stable cobalt oxides, CoO and Co_3O_4. CoO has the NaCl structure and is antiferromagnetic below 16 °C. It is used as a pigment in glasses and ceramics. When heated in air between 600 and 700 °C it converts to Co_3O_4 of spinel structure. The oxides of cobalt have a variety of applications due to excellent chemical stability and optical, electrical and magnetic properties. Especially, thin films of Co_3O_4 are very appealing as

magnetic materials, solar-selective absorbers, counterelectrodes, humidity sensors, oxygen sensors, protective coatings and buffer layers[392–394]. Also, Co_3O_4 possesses high catalytic activity, for example, in the oxidation of hydrocarbons[395].

CoO films can be prepared by PE-MOCVD using $Co(acac)_2 \cdot 2H_2O$ as source material[396]. This method is a superior technique for preparing high-quality CoO films on soda-lime, glass, Si(111), stainless steel and fused silica with good crystallinity and high orientation at low temperatures (substrate temperature 150–400 °C independently of the kind of substrate).

CVD of Co_3O_4 was carried out using different kinds of cobalt enolate precursors in the presence of oxygen or nitrous oxide. Shivashankar and coworkers applied $Co(acac)_2$ in a low-pressure MOCVD process to grow strongly oriented or epitaxial thin films of Co_3O_4 on substrates such as glass, MgO(100), Si(100), $SrTiO_3$(100) and $LaAlO_3$(100) in the temperature range of 400–550 °C[397,398]. It was observed that the activation energy for the growth of polycrystalline films on glass is significantly higher than that for epitaxial growth on $SrTiO_3$. SEM studies showed faceted grains characteristic of cubic symmetry, the faceting getting stronger at higher growth temperatures. Systematic studies were carried out with $Co(acac)_2$ using O_2 and N_2O as oxygen sources[399]. Films grown in N_2O atmosphere comprise poorly crystallized, randomly oriented grains of either Co_3O_4 or $CoO + Co_3O_4$, while in the presence of oxygen only strongly faceted, uniform-sized grains of Co_3O_4 are produced. $Co(acac)_2$ enabled deposition of 100-nm-thick smooth and polycrystalline Co_3O_4 layers onto Si(100) at 650 °C, applying pulsed-liquid injection CVD as shown by Apátiga[400]. According to the magnetic response of these films, a strong magnetic susceptibility, matching antiferromagnetic spin alignments typical of a film with low chemical inhomogeneities, was obtained (coercivity 6.61 mT, squareness ratio 0.2607, saturation magnetization 12.17 nA m^2)[400]. $Co(acac)_2$ can also be used as precursor in microwave PE-CVD for the deposition of carbon-free, nanosized CoO_x species (2–10 nm) on titania[401].

Novel self-generating liquid MOCVD precursors of type $Co(hfac)_2(MeOCH_2CH_2OMe)$[402] and $Co(hfac)_2(Me(OCH_2CH_2)_4OMe)(H_2O)_2$[403] for cobalt oxide films were reported by Gulino and Fragalá. In a typical CVD experiment using a low-pressure horizontal hot-wall reactor (substrate temperature 350 °C, 4 Torr total pressure, argon–oxygen ratio 1:1) cubic and highly oriented CoO films were deposited from $Co(hfac)_2(MeOCH_2CH_2OMe)$ on optically transparent SiO_2 substrates. In contrast, $Co(hfac)_2(Me(OCH_2CH_2)_4OMe)(H_2O)_2$ afforded Co_3O_4 thin films (deposition conditions: substrate temperature 400 °C, total pressure 2–5 Torr, argon–oxygen ratio 1:4). This cobalt oxide film shows a high absorbance in the visible range and a low emission in the IR range, making it a promising candidate for thermal solar energy conversion and for anodic electrochromic materials. Another cobalt(II) enolate adduct is formed by dissolving $Co(thd)_2$ in glyme[404]. The films deposited at 350–540 °C by pulsed liquid injection MOCVD showed a pure Co_3O_4 spinel structure; no CoO was formed as evidenced by XRD. However, XPS spectra recorded for most of the films seem to correspond to CoO. This unexpected oxidation state on the surface was ascribed to the effect of the high density of edges and corners present in the surface morphology.

A series of complexes $Co(acac)_2(L)$ and $Co(thd)_2(L)$ were synthesized by varying the bidentate ligand L from a diamino compound TMEDA (**34a**,**b**) to amino alcohols DMAE (**35a**,**b**) and DMAP (**36a**,**b**) and applied as precursors in MOCVD experiments by Abrutis and Hubert-Pfalzgraf[405,406]. Co_3O_4 films deposited on monocrystalline $LaAlO_3$, Si, MgO and sapphire from these adducts exhibited rather similar epitaxial quality and surface roughness when compared with films grown from $Co(acac)_2$, but they outperform existing cobalt CVD precursors in terms of volatility and oxidation stability. Especially, **34a** captivates because of its high deposition rate (1.6 $\mu m\,h^{-1}$ at 600 °C).

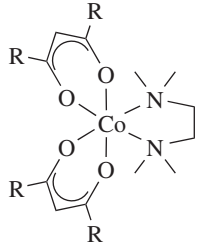

(**34**) (**a**) R = Me; $Co(acac)_2(TMEDA)$
(**b**) R = *t*-Bu; $Co(thd)_2(TMEDA)$

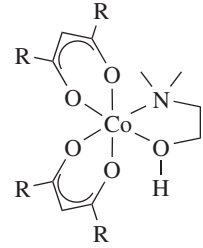

(**35**) (**a**) R = Me; $Co(acac)_2(DMAE)$
(**b**) R = *t*-Bu; $Co(thd)_2(DMAE)$

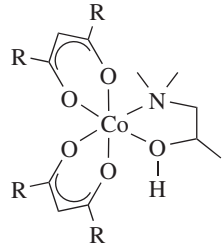

(**36**) (**a**) R = Me; $Co(acac)_2(DMAP)$
(**b**) R = *t*-Bu; $Co(thd)_2(DMAP)$

8. Nickel

Nickel(II) oxide crystallizes in the NaCl structure. Thin amorphous films of it exhibit electrochromic behavior and are antiferromagnetic at $T_N = 247\,^{\circ}C$. Nickel(II) oxide films with smooth surfaces and columnar structures of preferred (100) orientation on MgO(111), Si(111), soda lime glass, fused silica and stainless steel can be obtained by CVD[368] and PE-CVD[396] between 150 and 500 °C from $Ni(acac)_2$ in the presence of oxygen.

9. Copper

Two oxides of copper, Cu_2O (cuprous oxide, cuprite; yellow or red) and CuO (cupric oxide, black), are known of which the former is more stable at higher temperatures. The solid-state structure of copper(I) oxide is related to that of β-cristobalite with Cu(I) in linear sites and O^{2-} in tetrahedral sites. Cuprite is mainly used as red pigment in ceramics, porcelain, glazes and glasses. Additionally, it is used as antifouling agent due to its fungicidal properties. Copper(II) oxide has a monoclinic crystal structure consisting of square-planar CuO_4 units which are linked by bridging oxygen atoms into chains with cooperite structure type. It is used as a pigment in ceramics to give blue, red and green glazes. Furthermore, it has application as a *p*-type semiconductor due to its narrow band gap of 1.2 eV. Copper oxide materials find wide application in the fields of catalysis, solar cells, coatings and electronic devices[407]. In addition, copper-based mixed oxide films (for example, YBCO: Y-Ba-Cu oxides, BSCCO: Bi-Sr-Ca-Cu oxides, TBCCO: Ta-Ba-Ca-Cu oxides) have been the subject of investigations due to their applications as high-temperature superconducting materials (Section V.D.1).

While copper(I) and copper(II) enolates are mainly used for the preparation of copper thin films by CVD techniques (Section IV.B.5.a), under certain conditions (in the presence of oxygen and/or water) also copper(I) and/or copper(II) oxides can be obtained. Chisholm and Baxter proposed a mechanistic role for water and oxygen in the CVD of Cu, Cu_2O and CuO from $Cu(hfac)_2$[408]. Water is shown to provide the key step of H^+ transfer in facilitating the elimination of hfacH, while the oxygen atom of water remains in the formed copper oxide (equation 14). The *in situ* formed Cu(hfac)(OH) species can be stabilized either by coordination of another H_2O molecule (monomeric structure) or by an oligomerization giving dimers, tetramers and nonamers. The organic by-product hfacH further reacts with oxygen to yield F_3CCO_2H and $F_3CC(O)CHO$; the latter molecule gives $F_3CC(OH)_2CH(OH)_2$ in the presence of water. If hfacH is directly treated with water, $F_3CC(OH)_2CH_2C(OH)_2CF_3$ is produced.

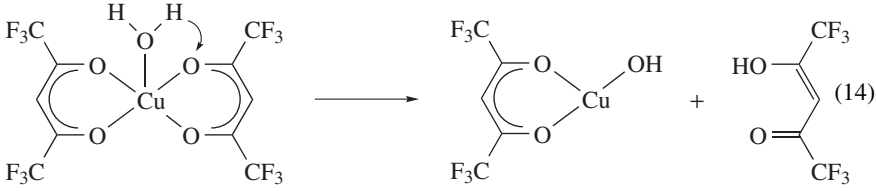

(14)

Törndahl and coworkers applied the results from these mechanistic investigations for the ALD of Cu_2O monolayers from $Cu(hfac)_2$ and water on amorphous SiO_2 and single-crystal α-Al_2O_3[409]. The introduction of the water pulse was found to be crucial for initiating the film growth on both substrates. They used the oxide monolayers for reaction with ammonia in an ALD experiment resulting in the formation of Cu_3N films.

The kinetics and reaction mechanism of the formation of copper, copper(I) oxide and copper(II) oxide films by low-pressure CVD from $Cu(acac)_2$ in the presence of oxygen was studied by the group of Fragalá[410,411]. At high P_{O_2} (2.7–6 Torr) and low $P_{Cu(acac)_2}$ (0–3 mTorr) pure Cu_2O was formed, while at low P_{O_2} and high $P_{Cu(acac)_2}$ formation of metallic copper with carbon contaminations is typical. Above 8 Torr P_{O_2}, CuO films have been grown under a reaction-rate-limited regime. A reaction mechanism based on the dissociative adsorption of $Cu(acac)_2$ on two different active sites was proposed to explain the complex kinetics of the deposition process[410]. The same group reported on the successful use of $Cu(thd)_2$ in the synthesis of free-standing, ordered homogeneous CuO nanotube arrays through a MOCVD template process at a deposition temperature of 400 °C and 1.5 Torr P_{O_2}[412]. Anodic Al_2O_3 membranes consisting of ordered hole arrangements were used as templates. The nanotubes possess an outer diameter of *ca* 250 nm, wall thickness 40 nm and a length of *ca* 1 μm (Figure 26).

Recently, a novel consecutive two-step CVD process for producing thin, smooth and conformal copper films on TaN substrates via Cu_2O deposited with $[Cu(hfac)_2 \bullet H_2O]$ was given by Lee and coworkers[413]. Ethyl alcohol was used as additive to reduce the copper oxide films. The grain size and roughness of these films range from 30–94 nm and 1.12–6.33 nm, respectively. Therefore, this technique may be of interest for the growth of high-quality seed layers for electroplating to be used in ULSI circuit fabrication. A facile mild synthesis methodology of submicron Cu_2O and CuO crystallites from metal-organic $Cu(acac)_2$ has been described by Zhang and coworkers[414]. Cubic Cu_2O crystals of size 80–260 nm were produced by hydrothermal treatment in distilled water at 180 °C. Thermolysis of $Cu(acac)_2$ in air at 300 °C gave monoclinic CuO with a grain size of 130–470 nm.

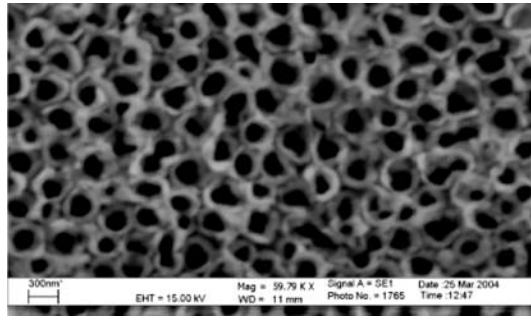

FIGURE 26. SEM image of CuO nanotubes (dark spots, seen as cross sections) grown into an electrochemically generated alumina template[412]. Reprinted with permission from Reference 412. Copyright 2004 American Chemical Society

10. Zinc

Zinc oxide (ZnO, wurtzite structure) eliminates oxygen on heating to form nonstoichiometric colored phases, $Zn_{1+x}O$ with $x \leqslant 70$ ppm. ZnO is almost transparent and is used as white pigment, polymer stabilizer, emollient in zinc ointments, creams and lotions, as well as in the production of Zn_2SiO_4 for TV screens. A major application is in the rubber industry to lower the temperatures and to raise the rate of vulcanization. Furthermore, it is an *n*-type semiconductor (band gap 3.37 eV) and shows piezoelectric properties, making zinc oxide useful for microsensor devices and micromachined actuators[415]. Other applications include gas sensors[416], solar cell windows[417] and surface acoustic devices[418]. ZnO has also been considered for spintronic application because of theoretical predictions of room-temperature ferromagnetism[419].

In general, $Zn(acac)_2$ precursors are applied for production of ZnO films and nanocrystalline particles. Low-temperature conductive ZnO films with a minimum resistivity of 2.44 Ω cm have been obtained at 550 °C by CVD in oxygen atmosphere, as reported by Natsume and coworkers[420]. Arrhenius plots of electrical conductivity exhibited linearity.

Homo- and heteroepitaxial growth of nonpolar smooth zinc oxide films on single-crystal ZnO[421] and sapphire[422] was achieved by MOCVD with $Zn(acac)_2$ at 650 °C substrate and 124 °C precursor temperature.

A method for the preparation of undoped ZnO films is by spray pyrolysis, using $Zn(acac)_2 \cdot H_2O$ between 100 and 400 °C either with a dry solvent or in the presence of excess water[423]. Above 200 °C, a change in the decomposition mechanism occurs and the films became more consolidated, transparent, have larger grains and are more conductive. Ultrafine ZnO particles of size less than 9 nm with a narrow size distribution were prepared by $Zn(acac)_2$ and NaOH in ethanolic solution[424,425]. The formation of stable ZnO nanoparticles is attributed to the stabilization of surface Zn^{2+} ions chelated by acac ligands and the presence of only a small amount of H_2O.

C. Rare Earth Metal Elements

Although Ln(III) oxides (Ln_2O_3) are preferred among the rare earth elements, Ln(II) oxides (EuO), Ln(IV) oxides (CeO_2) and oxides of mixed oxidation states Ln(II)/Ln(III) (Eu_3O_4) and Ln(III)/Ln(IV) (Pr_6O_{11}, Tb_4O_7) are also known. The lanthanide oxides adopt three structural types conventionally classified as *A*-type (favored by the lightest lanthanides), *B*-type (favored by the middle lanthanides) and *C*-type (favored by the middle

and heavy lanthanides). Lanthanide oxides Ln_2O_3 show properties similar to those of the alkaline earth oxides. Rare earth metal oxide films are an important group of materials with a high application potential in technological fields as diverse as refractory antireflection coatings, due to their high refractive indices (1.91–1.98 for the *C*-type structure)[426], protective and corrosion resistive coatings, since they are thermodynamically very stable[427], and passivation of group-III—group-V compound semiconductors[428].

Excellent overviews on the deposition methods of lanthanide and actinide oxides were published in several reviews by Niinistö[429,430], Zhang and Yan[431], Lee[432] and Yagi[433].

1. Cerium

Pale yellow cerium dioxide (ceria, ceric oxide) has the fluorite structure and is used in catalysis[434], solid oxide fuel cells (SOFC)[435], thin film optical waveguides[436], reversible oxygen storage materials for automobile catalysts[437] and for doping copper oxide superconductors[438]. The diverse cerium enolate precursors and deposition methods used in the formation of cerium oxide thin films are summarized in Table 6, whereby the most common precursor for ceria is $Ce(thd)_4$.

In 1993, Dahmen and coworkers reported about the use of $Ce(thd)_4$, $Ce(fdh)_4$, $Ce(thd)_3$(phen) and $Ce(fdh)_3$(phen) as MOCVD precursors for the preparation of CeO_2 thin films in the presence of oxygen[439]. From thermal analysis and evaporation-rate experiments the following decreasing order of volatility was established: $Ce(fdh)_4 > Ce(thd)_4 > Ce(fdh)_3(phen) \approx Ce(thd)_3(phen)$, with $Ce(thd)_4$ as the most thermally stable species. The deposited films showed high crystallinity and preferential orientation for substrate temperatures in the range of 400–500 °C[439]. No nitrogen or fluorine was incorporated in the films and only 2–4% of carbon impurities were found. Homogeneous and smooth films with columnar orientation were formed. Similar results were reported by Ami[442] and Meng[443,448], who deposited CeO_2 on Si(100), YSZ and α-Al_2O_3 substrates containing hydrogen-bonding groups on the surface. To achieve epitaxial growth of ceria a better understanding of the initial stage of film growth is necessary. A decomposition mechanism was proposed[449], where the C–Bu-*t* bond was cleaved at first, followed by cleavage of the C–H, C–O and C–C bonds.

TABLE 6. Deposition studies of cerium oxide (CeO_2) films

Precursor	Method	$T_{precursor}$ (°C)	$T_{substrate}$ (°C)	Pressure (Torr)	Atmosphere	Substrate	Reference
$Ce(thd)_4$	CVD	170–206	300–500	13–19	He/O_2	Si, SiO_2	439
	CVD	150–200	300–500	0.04–2.25	O_2	Si	440
	CVD	300	680	4	O_2	Al_2O_3	441
	CVD	170–210	500–1000	1–10	Ar/O_2	Si	442
	CVD	–	680–720	6.7–7.5	Ar/O_2	YSZ, Al_2O_3	443
	C-CVD[a]	–	1000	–	$PhMe/O_2$	Al_2O_3	444
	PE-CVD	170	150–300	1.1	Ar, Ar/O_2	Si, SiO_2	445
	ALD	140	175–375	1.5	N_2/O_3	Si, glass	446
$Ce(fdh)_4$	CVD	120–140	250–600	13–19	He/O_2	Si, SiO_2	439
$Ce(thd)_3$(phen)	CVD	180–220	400–550	13–19	He/O_2	Si, SiO_2	439
	ALD	175–180	225–350	1.5	N_2/O_3	Si, glass	446
$Ce(fdh)_3$(phen)	CVD	180–220	275–550	13–19	He/O_2	Si, SiO_2	439
$Ce(hfac)_3$(glyme)	CVD	80–140	450–600	1	O_2	TiN, Pt, Si	447

[a] Combustion CVD.

$Ce(thd)_4$ can be applied as metal source for ceria thin film formation by PE-CVD[445] and combustion–CVD (C-CVD)[444] (Table 6). Nanophase cerium oxide film deposition was carried out in a low-pressure Ar and $Ar–O_2$ plasma at low temperatures on SiO_2 and Si(100), whereby the film microstructure is influenced by the competition of the ablation and deposition processes. The CeO_{2-x} films had a Ce(IV)/Ce(III) ratio tunable as a function of the substrate temperature or the oxygen partial pressure[445]. Ceria films obtained at significantly higher temperatures by the combustion-CVD method are strongly influenced by the initial aerosol droplet size distribution[444]. Two types of film morphology were found: small aerosols and low precursor concentrations resulted in apparently dense materials, consisting of clusters nucleated in the gas phase and further grown on a substrate, while larger aerosols and/or higher precursor concentrations gave films containing polycrystalline particles with preferred (111) orientation.

The glycol ether-stabilized complexes $[Ce(hfac)_3(MeO(CH_2CH_2O)_nMe)]$ ($n = 1$, 2, 3) and $[(Ce(hfac)_3)_2(\mu\text{-}MeO(CH_2CH_2O)_4Me)]$ were used as CVD precursors for the deposition of mixed Ce(IV)/Ce(III) oxides in oxygen atmosphere[447]. The films were contaminated with fluorine; however, when either moist oxygen was used or annealing was carried out in an oxygen atmosphere at 600 °C, the films were fluorine-free. A possible mechanism for fluoride formation is shown in equation 15.

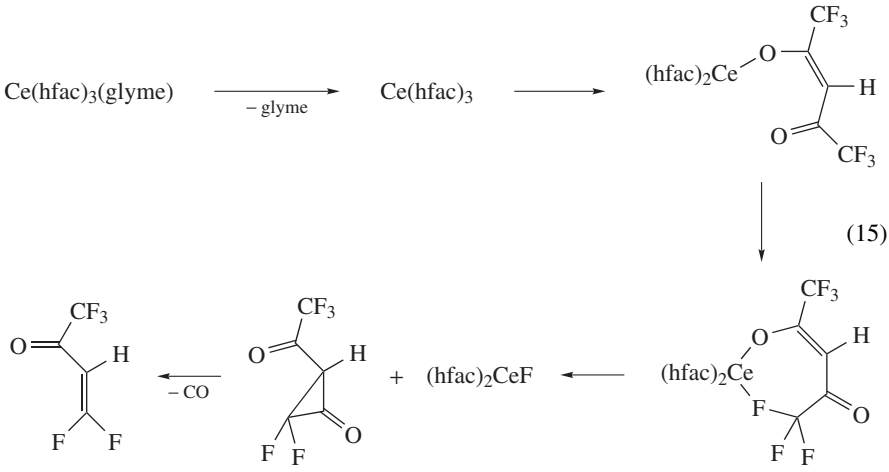

Cerium dioxide buffer layers are accessible by low-temperature ALD using $Ce(thd)_4$ and $Ce(thd)_3(phen)$ as metal sources and ozone as oxygen source, as reported by Niinistö and coworkers[446] (Table 6). The growth rates were 0.32 Å cycle^{-1} for $Ce(thd)_4$ and 0.42 Å cycle^{-1} for $Ce(thd)_3(phen)$, similar to other ALD experiments carried out at higher temperature[446]. The use of $Ce(thd)_4$ instead of $Ce(thd)_3(phen)$ is recommended because of the sensitivity of the growth rate to low reproducibility of the precursor synthesis and to the instability of $Ce(thd)_3(phen)$, as it decomposes in air within a few weeks. The films are polycrystalline with no dominating orientation, whereas for superconducting films it would be favorable to have a preferred (100) orientation.

The formation of CeO_2 and ZrO_2 nanocrystals of size 2.0–2.5 nm (CeO_2) and 2.5–3.5 nm (ZrO_2) as well as CeO_2/ZrO_2 core-shell nanocrystals (2.4 nm core, 1.2 nm shell) have been studied by Omata and coworkers applying a hot surfactant colloidal synthesis route[450], using $Ce(acac)_3$ and $Zr(OPr\text{-}i)_4$ as precursors. The core-shell nanocrystals,

which contain a high density of highly ionic conducting interfaces, may be used for the fabrication of nanostructured solid electrolytes[450].

2. Miscellaneous rare earth metals

In this section various existing lanthanide and actinide metal-organic enolate precursors for rare earth metal oxide deposition are discussed and the rationale of their selection is addressed. CVD, ALD and ultrasonic spray pyrolysis (USP) of the lanthanide or actinide enolate starting materials has been carried out under a variety of conditions as can be seen from Table 7.

A comparative study on rare earth metal oxide thin films of Nd, Sm, Eu, Gd, Dy, Ho, Er, Tm grown on Si(100) substrates by ALD was recently published by Päiväsaari, Putkonen and Niinistö (Table 7)[430], using $Ln(thd)_3$ in an ozone-containing atmosphere. From all these precursors cubic (*C*-type) and polycrystalline films were obtained except

TABLE 7. Deposition studies of lanthanide and actinide oxide films other than cerium oxide

Film	Precursor	Method	$T_{precursor}$ (°C)	$T_{substrate}$ (°C)	Pressure (Torr)	Atmosphere	Substrate	References
La_2O_3	$La(thd)_3$	CVD	170–230	570	0.75–1.5	H_2/H_2O	quartz	433
Nd_2O_3	$Nd(thd)_3$	CVD	170–230	570	0.75–1.5	H_2/H_2O	quartz	433
		ALD	161–164	200–450	1.5–2.3	N_2/O_3	Si, glass	430, 451
		CVD	130–160	800	10	Ar/O_2	MgO	452
	$Nd(tmod)_3$	CVD	130–160	800	10	Ar/O_2	MgO	452
Sm_2O_3	$Sm(thd)_3$	CVD	170–230	570	0.75–1.5	H_2/H_2O	quartz	433
		ALD	148–152	300	1.5–2.3	N_2/O_3	Si	440
	$Sm(acac)_3(phen)$	CVD	200–250	450–675	2	Ar/O_2	Si, quartz	453
Eu_2O_3	$Eu(thd)_3$	CVD	170–230	570	0.75–1.5	H_2/H_2O	quartz	433
		ALD	135	300	1.5–2.3	N_2/O_3	Si	430
	$Eu(acac)_3(phen)$	CVD	150–250	450–800	2	Ar/O_2	quartz	454
	$Eu(acac)_3$	USP	–	550	–	Air	Si	455
Gd_2O_3	$Gd(thd)_3$	CVD	170–230	570	0.75–1.5	H_2/H_2O	quartz	433
		ALD	140–160	225–400	1.5–2.3	N_2/O_3	Si	430, 456
	$Gd(acac)_3(phen)$	CVD	150–250	450–800	2	Ar/O_2	Si, quartz	454, 457
Dy_2O_3	$Dy(thd)_3$	ALD	125	300	1.5–2.3	N_2/O_3	Si	430
Ho_2O_3	$Ho(thd)_3$	CVD	170–230	570	0.75–1.5	H_2/H_2O	quartz	433
		ALD	130	300	1.5–2.3	N_2/O_3	Si	430
Er_2O_3	$Er(thd)_3$	CVD	170–230	570	0.75–1.5	H_2/H_2O	quartz	433
		ALD	130	200–450	1.5–2.3	N_2/O_3	Si, glass	430, 458
		RE-ALD	200	300	10^{-8}	O	Si	459
	$Er(acac)_3(phen)$	CVD	150–250	450–800	2	Ar/O_2	Si, quartz	454, 459
Tm_2O_3	$Tm(thd)_3$	CVD	170–230	570	0.75–1.5	H_2/H_2O	quartz	433
		ALD	125–128	300	1.5–2.3	N_2/O_3	Si	430
Yb_2O_3	$Yb(thd)_3$	CVD	170–230	570	0.75–1.5	H_2/H_2O	quartz	433
	$Yb(acac)_3(phen)$	CVD	150–250	450–800	2	Ar/O_2	quartz	454
Lu_2O_3	$Lu(thd)_3$	CVD	170–230	570	0.75–1.5	H_2/H_2O	quartz	433
ThO_2	$Th(thd)_4$	CVD	170–230	510	0.75–1.5	H_2/CCl_2F_2	quartz	433
U_3O_8	$UO_2(thd)_2$	CVD	170–230	500	0.75–1.5	Ar/O_2	quartz	433
UO_2	$UO_2(thd)_2$	CVD	170–230	500	0.75–1.5	Ar/H_2O	quartz	433
U_4O_9	$UO_2(thd)_2$	CVD	170–230	470	0.75–1.5	He/CCl_2F_2	quartz	433

for Nd_2O_3, which also contained a hexagonal phase. The films show carbon, fluorine and hydrogen contaminations of which the carbon impurity is related to the *in situ* formation of metal carbonates. In the case of Nd_2O_3 it was found that films with low carbon content were somewhat unstable and became hydrated upon storage in the ambient[451]. The electrical properties of the films were studied extensively[430]. As assumed, the ALD growth rates of the appropriate lanthanide oxides seem to follow rather linearly the ionic radii of the rare earth metal elements.

Detailed surface reaction kinetic studies in radical-enhanced ALD of Er_2O_3 from $Er(thd)_3$ and oxygen radicals were given by Van and Chang[459], applying the Langmuir–Hinshelwood model to describe the adsorption of the appropriate precursor molecule. The activation energies for adsorption and desorption were determined to be -0.24 ± 0.09 and 0.29 ± 0.03 eV, respectively. The reactions of the chemisorbed precursors with oxygen radicals were found to be saturative at 200–300 °C.

Oriented growth of lanthanide oxide thin films of Sm, Eu, Gd, Er and Yb on different substrates is possible by the low-pressure MOCVD technology from the corresponding phenanthroline adducts of rare earth metal enolates $Ln(acac)_3(phen)$ as described by Shivashankar and coworkers (Table 7)[453, 454, 457, 460]. As expected, the films grown at lower temperature (500 °C) are poorly crystalline, while those deposited above 525 °C display a significant (111) texture. Irrespective of the deposition conditions and the substrate materials, the thin films comprise cubic Ln_2O_3 phases. Optical and electrical characterizations of the films are also given. Using liquid $Nd(tmod)_3$ (melting point 134–136 °C) as CVD precursor of neodymium oxide[452] allows source temperatures below 200 °C (*ca* 80 °C lower than those of $Nd(thd)_3$). The lower melting point is attributed to the unsymmetrical ligand structure.

Nanophase europium oxide polycrystalline films can also be deposited on Si(100) by nebulization of a $Eu(acac)_3$ solution in a 50% ethanol–water mixture followed by pulse ultrasonic spray pyrolysis in flowing air[455]. The thermal decomposition was exemplarily studied using $[Sm(acac)_3(H_2O)_2]$ in the temperature range of 100–800 °C by thermogravimetry, differential thermal analysis and IR spectroscopy of the gaseous products[461]. $Sm(acac)_3$ completely decomposes to Sm_2O_3 at 750 °C via *in situ* formation of $Sm(acac)_2(OAc)$ at 150 °C, $Sm(acac)(OAc)_2$ at 235 °C, $Sm(OAc)_3$ at 270 °C, $Sm_2O(OAc)_3$ at 500 °C and $Sm_2O_2(CO_3)$ at 650 °C. As gaseous by-products propyne, acetone, carbon oxides, methane, and *iso*-butene were found. The product left after evolution of carbon oxides from $Sm_2O_2(CO_3)$ had a high surface area (47 $m^2\,g^{-1}$) and extensive porosity.

High-quality monodisperse, cubic lanthanide oxide nanocrystals (nanodiscs and nanoplates) are accessible via a nonhydrolytic approach from lanthanide acetylacetonates and benzoylacetonates[462]. The transformation from the metal-organic complexes to Ln_2O_3 was proposed to occur in two steps as depicted in Scheme 9. First a ligand exchange between the lanthanide-bonded acac ligands and the solvent oleic acid takes place, followed by the subsequent decomposition of the oleates into Ln_2O_3 catalyzed by the base oleylamine. Dynamically stable nanoplates and thermodynamically stable nanodiscs could be controllably prepared under fast/slow growth modes (Scheme 9).

Sol–gel processes are also suitable for lanthanide oxide formation, as could be shown by the use of $Tb(acac)_3$[463] and $Dy(OBu\text{-}n)_3$ in acetylacetone[464]. Tb_2O_3 crack- and pinehole-free, dense and smooth microstructured buffer layers were produced on nickel tapes by a reel-to-reel continuous sol–gel process. The authors report that the film properties can be strongly influenced by solution components, temperature, time and atmosphere. Nanocrystalline mesoporous dysprosium oxide Dy_2O_3 with narrow monomodal pore size distribution can be approached by a combined sol–gel process with a surfactant-assisted templating technique[464]. The spherical Dy_2O_3 nanoparticles were formed with aggregations.

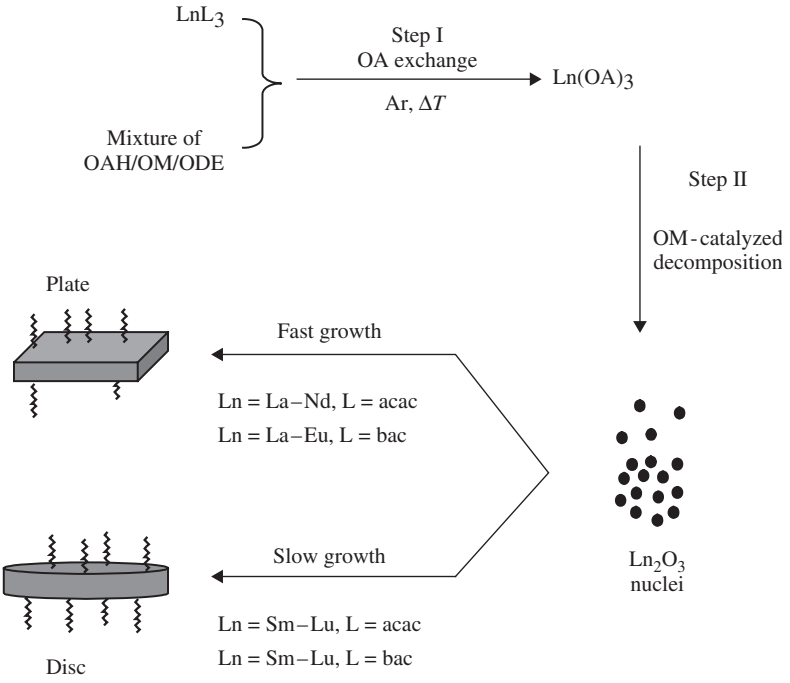

SCHEME 9. Possible mechanism for the formation of Ln_2O_3 nanoplates and nanodiscs (OAH = oleic acid, OM = oleylamine, ODE = 1-octadecene)[462]. Reprinted with permission from Reference 462. Copyright 2007 American Chemical Society

D. Mixed Metal Oxides

This section provides a comprehensive tabular summary of mixed metal oxide deposition, complementary to the books edited by Rees Jr.[2] and by Jones and O'Brien[3], focusing on the literature dealing with metal enolate precursors published after 1996.

Mixed metal oxides can be addressed as belonging to three main fields, namely superconducting metal oxides (SMOs) (Section V.D.1), transparent conductive oxides (TCOs) (Section V.D.2) and ferroelectric oxides (Section V.D.3). The synthesis procedures for mixed metal oxides include sintering, sol–gel, PLD or laser ablation, sputtering evaporation, MBE, MOVPE (metal–organic vapor-phase epitaxy), OMVPE (organometallic vapor-phase epitaxy) and CVD in particular.

1. Superconducting metal oxides (SMOs)

A superconductor is a material which conducts electricity without resistance and the exclusion of the interior magnetic field (Meissner effect) below a certain critical temperature T_C. Superconductivity occurs in a wide variety of materials, including elements, various metallic alloys and some heavily-doped semiconductors. Mixed metal oxides belong to the class of high-temperature superconductors ($T_C > 30$ K).

The discovery of high-temperature superconductivity in a lanthanum-based cuprate *perovskite* material with a transition temperature of $T_C = 35$ K by Bednorz and Müller

in 1986[465] stimulated an unprecedented enthusiasm and led to the discovery of different families of cuprates which remain superconducting at appreciably higher temperatures than those of low T_C metallic superconductors. The most important systems are Y–Ba–Cu–O (YBCO; $T_C = 93$ K)[466], Bi–Sr–Ca–Cu–O (BSCCO; $T_C = 105$ K)[467] and Tl–Ba–Ca–Cu–O (TBCCO; $T_C = 120$ K)[468]. A detailed discussion of the solid-state structure of these materials is given elsewhere[2].

Application of superconducting materials include (i) high-field superconducting magnets in various systems (NMR, MRI, particle accelerators, magnetically levitated trains, generators etc.), (ii) low-field applications (superconducting power transmission lines and superconducting resonant cavities) and (iii) electronics application (analog-to-digital converters, single-flux quantum shift registers, neural networks)[2].

The deposition of mixed metal oxides is based on the deposition techniques and precursors used for the formation of metal oxides discussed earlier in this chapter. The most important publications in the field of high-temperature superconducting materials produced from metal enolates since the date of release of Rees' book[2] in 1996 are summarized in Table 8.

2. Transparent conductive oxides (TCOs)

Indium tin oxide (ITO, In–Sn–O), the most common example of transparent conductive oxides, is a mixture of In_2O_3 and SnO_2, typically 90 wt% In_2O_3 and 10 wt% SnO_2. It is colorless and transparent in thin films and can be operated at temperatures up to 1400 °C. However, there are other metal oxides known with optical band gaps of 2.5–4.0 eV like magnesium-doped indium oxides[476] and indium or gallium doped zinc oxides[477,478]. Thin films of In and Sn oxides can be deposited on different surfaces by, for example, the CVD techniques described earlier. ITO has been the subject of intense research because of its importance in making transparent, conductive coatings for flat displays, OLEDs, solar cells etc. and is also used for various optical coatings in architectural and automotive glasses. Further applications include gas sensors, antireflection coatings and Bragg reflectors.

Since ITO is a well-investigated material, much of the research in the field of transparent conductive oxides has been directed at combining different main-group and transition metal oxides, such as MgO, ZnO and CdO, in order to improve electrical and optical properties. Recent developments made in the preparation of TCOs from metal β-diketonate precursors are given in Table 9.

3. Ferroelectric oxides

The ferroelectric effect is an electrical phenomenon. Particular materials, including the ternary oxides (Ba,Sr)TiO_3, Pb(Zr,Ti)O_3 and (Bi,La)TiO_3, exhibit a spontaneous dipole moment which can be switched between equivalent states by an external electric field. Ferroelectric thin films are of importance for the production of nonvolatile ferroelectric random access memory devices (FeRAM)[480]. Two possibilities to synthesize such mixed metal oxides are given by the CVD and ALD methods. Table 10 shows the preparation methods of such materials synthesized from metal enolates recently.

4. Miscellaneous mixed metal oxides

For the sake of completeness, a choice of further mixed metal oxides not mentioned above are summarized in Table 11.

TABLE 8. MOCVD of superconducting metal oxides (SMOs)

SMO	Precursors	References
$YBa_2Cu_3O_x$	$Y(thd)_3$, $Ba(thd)_2(pentaen)_2$, $Cu(thd)_2$	469
$YBa_2Cu_3O_x$	$Y(thd)_3$, $Ba(thd)_2(tetraen)_2$, $Cu(thd)_2$	470
$YBa_2Cu_3O_x$	$Y(thd)_3$, $Ba(thd)_2$, $Cu(thd)_2$	471
$Tl_2Ba_2Ca_{n-1}Cu_nO_x$	$Ba(hfac)_2(tet)$, $Ca(hfac)_2(tet)$, $Cu(acac)_2$; Tl_2O_3	472
$Tl_2Ba_2CaCu_2O_8$	$Ba(hfac)_2(tet)$, $Ca(hfac)_2(tet)$, $Cu(thd)_2$; Tl_2O/Tl_2O_3	473 474
$TlBa_2Ca_2Cu_3O_{9+x}$	$Ba(hfac)_2(mep)$, $Ca(hfac)_2(tet)$, $Cu(thd)_2$; TlF	475

TABLE 9. Deposition of transparent conductive oxides (TCOs)

TCO	Precursors	Deposition method	Reference
In doped SnO_2 (ITO)	$In(acac)_3$, $Sn(acac)_2Br_2$	AA-CVD	476
Mg doped In_2O_3	$In(thd)_3$, $Mg(thd)_2(tmeda)$	MOCVD	476
In doped ZnO	$Zn(thd)_2$, $In(thd)_3$	MOCVD	477
Ga doped ZnO	$Zn(acac)_2$, $Ga(acac)_3$	MOCVD	478
Sn doped In_2O_3	$In(thd)_3$, $Sn(acac)_2$	MOCVD	479

TABLE 10. Deposition of ferroelectric oxides

Ferroelectric oxide	Precursors	Deposition method	Reference
$SrTiO_3$	$TiO(thd)_2$, $Sr(thd)_2$	ALD	481
$SrTiO_3$	$TiO(thd)_2$, $Sr(thd)_2$	AA-CVD	482
$SrTiO_3$	$TiO(thd)_2$, $Sr(thd)_2$ $Ti(thd)_2(OPr\text{-}i)_2$, $Sr(thd)_2$	CVD	483
$SrTiO_3$ $BaTiO_3$	$Ti(OPr\text{-}i)_4$, $Sr(thd)_2$ $Ti(OPr\text{-}i)_4$, $Ba(thd)_2$	PE-CVD	484
$PbTiO_x$	$Ti(thd)_2(OPr\text{-}i)_2$, $Pb(tmod)_2$	ALD	485
$PbTiO_x$	$Ti(thd)_2(OPr\text{-}i)_2$, $Pb(thd)_2$	ALD	486
$Pb(Zr,Ti)O_3$	$Zr(thd)_4/Zr(dibm)_4/Zr(methd)_4$, $Ti(thd)_2(OPr\text{-}i)_2/Ti(mpd)(methd)_2$, $Pb(thd)_2/Pb(methd)_2$	LD [a]-MOCVD	487
$Bi_{4-x}Nd_xTi_3O_{12}$	$Ti(thd)_2(OPr\text{-}i)_2$, $Nd(thd)_3$, $Bi(thd)_3$	DLI-CVD	488

[a] Liquid delivery.

TABLE 11. Deposition of miscellaneous mixed metal oxides

Mixed metal oxide	Precursors	Deposition method	References
YSZ	$Zr(acac)_4$, $Y(acac)_3$	AA-CVD	489
YSZ	$Zr(acac)_4$, $Y(acac)_3$	USP	490
YSZ	$Zr(thd)_4$, $Y(thd)_3$	MOCVD	491
YSZ	$Zr(thd)_4$, $Y(thd)_3$	ALE	492
YSZ	$Zr(thd)_4$, $Y(thd)_3$	AA-CVD	493, 494
YSZ	$Zr(thd)_4$, $Y(thd)_3$	PI-MOCVD	495
YSZ	$Zr(thd)_4$, $Y(thd)_3$	MOCVD	496
Ce doped YSZ	$Zr(tfac)_4$, $Y(hfac)_3$, $Ce(thd)_4$	MOCVD	497
Ag doped YSZ	$Zr(tfac)_4$, $Y(hfac)_3$, $Ag(hfac)(C_4H_8OS)_2$	MOCVD	498
$LaAlO_3$	$Al(acac)_3$, $La(acac)_3$	MOCVD	499
$LaAlO_3$	$Al(acac)_3$, $La(thd)_3$	ALE	500
$LaAlO_3$	$Al(acac)_3$, $La(hfac)_3$(diglyme)	MOCVD	501, 502
ZrAlO	$Al(acac)_3$, $Zr(acac)_3$	pyrosol process	503
$LaGaO_3$	$La(thd)_3$, $Ga(acac)_3$	ALE	504
$Er_xGa_{2-x}O_3$	$Er(thd)_3$, $Ga(acac)_3$	ALE	505
MoO_3-Bi_2O_3	$BiPh_3$, $MoO_2(thd)_2$	MOCVD	506
$LaMnO_{3\pm x}$	$Mn(acac)_3$, $La(thd)_3$	MOCVD	507
$LaCoO_3$	$Co(thd)_2$, $La(thd)_3$	ALE	508
$LaNiO_3$	$Ni(thd)_2$, $La(thd)_3$	ALE	509
$YScO_3$	$Sc(thd)_3$, $Y(thd)_3$	ALE	510
$SrZrO_3$	$Zr(thd)_4$, $Sr(thd)_2$	MOCVD	511
$Li_xLa_yFe_zO_4$	Li(acac), $La(acac)_3$, $Fe(acac)_3$	thermal decomposition	512
$Zr_{1-x}Ce_xO_2$ NPs	$Zr(acac)_4$, $Ce(acac)_4$	thermal decomposition	513

VI. REFERENCES

1. T. Kodas and M. Hampden-Smith (Eds), *The Chemistry of Metal CVD*, VCH, Weinheim, 1994.
2. W. S. Rees (Ed.), *CVD of Nonmetals*, VCH, Weinheim, 1996.
3. A. C. Jones and P. O'Brien (Eds), *CVD of Compound Semiconductors*, VCH, Weinheim, 1996.
4. R. A. Fischer (Ed.), *Precursor Chemistry of Advanced Materials: CVD, ALD and Nanoparticles*, Springer, Berlin, 2005.
5. D. L. Smith, *Thin-Film Deposition: Principles and Practice*, McGraw-Hill, New York, 1995.
6. M. L. Hitchman and K. F. Jensen (Eds), *Chemical Vapor Deposition*, Academic Press, London, 1993.
7. K.-L. Choy (Ed.), *Aerosol-Assisted CVD*, in *Chemical Vapor Deposition*, **12**(10), 2006.
8. R. F. Bunshah (Ed.), *Handbook of Deposition Technologies for Films and Coatings*, Noyes Publications, Westwood, 1994.

9. D. B. Chrisey and G. K. Hubler (Eds), *Pulsed Laser Deposition of Thin Films*, Wiley-VCH, New York, 1994.
10. S. Middleman and A. K. Hochberg, *Process Engineering Analysis in Semiconductor Device Fabrication*, McGraw-Hill, Singapore, 1993.
11. D. W. Schubert and T. Dunkel, *Mater. Res. Innovations*, **7**, 314 (2003).
12. M. Paunovic and M. Schlesinger, *Fundamentals of Electrochemical Deposition*, Wiley-VCH, Hoboken, 2006.
13. C. J. Brinker and G. W. Scherer, *Sol–Gel Science: The Physics and Chemistry of Sol–Gel Processing*, Academic Press, San Diego, 1990.
14. J. D. Wright and N. A. J. M. Sommerdijk, *Sol–Gel Materials: Chemistry and Applications*, Taylor & Francis, London, 2001.
15. T. M. Lopez, D. Avnir and M. A. Aegerter, *Emerging Fields in Sol–Gel Science and Technology*, Kluwer Academic, Dordrecht, 2003.
16. A. Z. Rubezhov, *Platinum Met. Rev.*, **36**, 26 (1992).
17. R. Gliem and G. Schlamp, *Met. Technol.*, **41**, 34 (1987).
18. F. Malik, *Thin Solid Films*, **206**, 70 (1991).
19. W. Kern, in *Thin Film Processes* (Eds J. L. Vossen and W. Kern), Academic Press, New York, 1978.
20. J. M. Thomas and W. J. Thomas, *Principles and Practice of Heterogeneous Catalysis*, VCH, Weinheim, 1996.
21. H. U. Balser, A. Indolese, A. Schnyder, H. Steiner and M. Studer, *J. Mol. Catal. A*, **173**, 3 (2001).
22. Y. Z. Chen, C. M. Hwang and C. W. Liaw, *Appl. Catal. A*, **169**, 207 (1998).
23. S. Sun, C. B. Murray, D. Weller, L. Folks and A. Moser, *Science*, **287**, 1989 (2000).
24. S. Kang, Z. Jia, S. Shi, D. E. Nikles and J. W. Harrell, *Appl. Phys. Lett.*, **86**, 062503 (2005).
25. J. T. Leman and A. R. Barron, in *Encyclopedia of Inorganic Chemistry* (Ed. R. B. King), John Wiley & Sons, Inc., New York, 1995, pp. 1531–1542.
26. C. Xu, T. H. Baum, I. Guzei and A. L. Rheingold, *Inorg. Chem.*, **39**, 2008 (2000).
27. K. C. Brooks, S. B. Turnipseed, R. M. Barkley, R. E. Sievers, V. Tulchinsky and A. E. Kaloyeros, *Chem. Mater.*, **4**, 912 (1992).
28. R. J. Puddephatt, *Polyhedron*, **13**, 1233 (1994).
29. M. J. Hampden-Smith and T. T. Kodas, *Polyhedron*, **14**, 732 (1995).
30. R. Pankajavalli, C. Mallika, O. M. Sreedharan, V. S. Raghunathan, P. A. Premkumar and K. S. Nagaraja, *Chem. Eng. Sci.*, **57**, 3603 (2002).
31. P. A. Premkumar, P. Kuppusami, A. Dasgupta, C. Mallika, K. S. Nagaraja and V. S. Raghunathan, *Mater. Lett.*, **61**, 50 (2007).
32. S. Liu, P. Cool, L. Lu, E. Beyers, P. Van der Voort, E. F. Vansant and M. Jiang, *Micropor. Mesopor. Mater.*, **79**, 299 (2005).
33. C. Manke, O. Boissière, U. Weber, G. Barbar, P. K. Baumann, J. Lindner, M. Tapajna and K. Fröhlich, *Microelectron. Eng.*, **83**, 2277 (2006).
34. M. L. Green, M. E. Gross, L. E. Papa, K. J. Schnoes and D. Brasen, *J. Electrochem. Soc.*, **132**, 2677 (1985).
35. J. N. Crosby and R. S. Hanley, US Patent 4250210 (1981).
36. Y. Chi, F. J. Lee and C.-S. Liu, US Patent 6303809 (2001).
37. Y.-H. Lai, Y.-L. Chen, C.-S. Liu, A. J. Carty, S.-M. Peng and G.-H. Lee, *J. Mater. Chem.*, **13**, 1999 (2003).
38. J. J. Joo, J. M. Seon, Y. C. Jeon, K. Y. Oh, J. S. Roh, J. J. Kim and J. T. Choi, *J. Appl. Phys.*, **37**, 3396 (1998).
39. M. Lashdaf, T. Hatanpää, A. O. I. Krause, J. Lahtinen, M. Lindblad and M. Tiitta, *Appl. Catal. A: General*, **241**, 51 (2003).
40. R. G. Charles and P. G. Haverlack, *J. Inorg. Nucl. Chem.*, **31**, 995 (1969).
41. L. B. Backman, A. Rautiainen, M. Lindblad, O. Jylhä and A. O. I. Krause, *Appl. Catal. A: General*, **208**, 223 (2001).
42. S. Parashar, A. R. Raju and C. N. R. Rao, *Mater. Chem. Phys.*, **61**, 46 (1999).
43. T. Aaltonen, M. Ritala and M. Leskelä, *Electrochem. Solid State Lett.*, **8**, C99 (2005).
44. K. V. Kordesch, US Patent 3364074 (1968).
45. J.-P. Lu, P. W. Chu and R. Raj, *Thin Solid Films*, **208**, 172 (1992).
46. J. Messelhäuser, E. B. Flint and H. Suhr, *Adv. Mater.*, **4**, 347 (1992).

47. T. H. Baum and C. E. Larson, US Patent 5096737 (1992).
48. J. A. Papke and R. D. Stevenson, in *Proceedings of the Conference on CVD Refractory Metals* (Ed. A. C. Shaffhauser), AIME, Gatlinburg, 1967, p. 193.
49. Y.-M. Sun, J. P. Endle, K. Smith, S. Whaley, R. Mahaffy, J. G. Ekerdt, J. M. White and R. L. Hance, *Thin Solid Films*, **346**, 100 (1999).
50. R. J. Silvennoinen, O. J. T. Jylhä, M. Lindblad, J. P. Sainio, R. L. Puurunen and A. O. I. Krause, *Appl. Surf. Sci.*, **253**, 4103 (2007).
51. X. Yan, Q. Zhang and X. Fan, *Mater. Lett.*, **61**, 216 (2007).
52. F. Catlura, F. Molina, M. Sabio and F. Rodríguez, *J. Electrochem. Soc.*, **142**, 4084 (1995).
53. T. Maruyama and T. Tago, *J. Mater. Sci.*, **28**, 5345 (1993).
54. R. W. Moshier, R. E. Sievers and L. B. Spendlove, US Patent 3356527 (1967).
55. R. G. Charles and J. G. Cleary, US Patent 3594216 (1971).
56. P. A. Premkumar, R. Pankajavalli, O. M. Sreedharan, V. S. Raghunathan, K. S. Nagaraja and C. Mallika, *Mater. Lett.*, **58**, 2256 (2004).
57. S. Arockiasamy, P. A. Premkumar, O. M. Sreedharan, C. Mallika, V. S. Raghunathan and K. S. Nagaraja, *J. Mater. Sci.*, **41**, 3383 (2006).
58. K. V. R. Chary, P. V. R. Rao and V. Vishwanathan, *Catal. Commun.*, **7**, 974 (2006).
59. I. P. Beletskaya and A. V. Cheprakov, *Chem. Rev.*, **100**, 3009 (2000).
60. A. Cabot, J. Arbiol, A. Cornet, J. Morante, F. Chen and M. Liu, *Thin Solid Films*, **436**, 64 (2003).
61. W. Lin, T. H. Warren, R. G. Nuzzo and G. S. Girolami, *J. Am. Chem. Soc.*, **115**, 11644 (1993).
62. W. Lin, B. C. Wiegand, R. G. Nuzzo and G. S. Girolami, *J. Am. Chem. Soc.*, **118**, 5977 (1996).
63. W. Lin, R. G. Nuzzo and G. S. Girolami, *J. Am. Chem. Soc.*, **118**, 5988 (1996).
64. W. Lin, S. R. Wilson and G. S. Girolami, *Inorg. Chem.*, **33**, 2265 (1994).
65. J. W. Elam, A. Zinovev, C. Y. Han, H. H. Wang, U. Welp, J. N. Hryn and M. J. Pellin, *Thin Solid Films*, **515**, 1664 (2006).
66. M. Benkhaled, S. Morin, C. Pichon, C. Thomazeau, C. Verdon and D. Uzio, *Appl. Catal. A: General*, **312**, 1 (2006).
67. L. Huang, Z. Wang, T. P. Ang, J. Tan and P. K. Wong, *Catal. Lett.*, **112**, 219 (2006).
68. G. Postole, A. Gervasini, C. Guimon, A. Auroux and B. Bonnetot, *J. Phys. Chem. B*, **110**, 12572 (2006).
69. R. Kumar, S. Roy, M. Rashidi and R. J. Puddephatt, *Polyhedron*, **8**, 551 (1989).
70. M. J. Rand, *J. Electrochem. Soc.*, **120**, 686 (1973).
71. J. Goswami, C.-G. Wang, W. Cao and S. K. Dey, *Chem. Vap. Deposition*, **9**, 213 (2003).
72. S. Barison, M. Fabrizio, G. Carta, G. Rosetto, P. Zanella, D. Barreca and E. Tondello, *Thin Solid Films*, **405**, 81 (2002).
73. A. Lintanf, R. Neagu and E. Djurado, *Solid State Ionics*, **177**, 3491 (2007).
74. S. Giuffrida, G. Ventimiglia, F. L. Callari and S. Sortino, *Eur. J. Inorg. Chem.*, 4022 (2006).
75. Z. Liu, M. Shamsuzzoha, E. T. Ada, W. M. Reichert and D. E. Nikles, *J. Power Sources*, **164**, 472 (2007).
76. J. Pulpytel, C. P. Etienne and F. Arefi-Khonsari, *IEEE Trans. Plasma Sci.*, **33**, 244 (2005).
77. T. P. Martin, C. P. Tripp and J. DeSisto, *Chem. Vap. Deposition*, **11**, 170 (2005).
78. G. A. Battiston, R. Gerbasi, M. Porchia and A. Gasparotto, *Chem. Vap. Deposition*, **5**, 13 (1999).
79. S. Daniele, C. Bragato, G. A. Battiston and R. Gerbasi, *Electrochim. Acta*, **46**, 2961 (2001).
80. X. Teng, S. Maksimuk, S. Frommer and H. Yang, *Chem. Mater.*, **19**, 36 (2007).
81. D. Weller and A. Moser, *IEEE Trans. Magn.*, **35**, 4423 (1999).
82. C. B. Murray, S. Sun, H. Doyle and T. Betley, *MRS Bull.*, **26**, 985 (2001).
83. R. Narayanan and M. A. El-Sayed, *J. Phys. Chem. B*, **109**, 12663 (2005).
84. H. Gu, P. Ho, K. W. T. Tsang, L. Wang and B. Xu, *J. Am. Chem. Soc.*, **125**, 15702 (2003).
85. S. Kang, Z. Jia, S. Shi, D. E. Nikles and J. W. Harrell, *Appl. Phys. Lett.*, **86**, 062503 (2005).
86. S. Kang, Z. Jia, S. Shi, D. E. Nikles and J. W. Harrell, *J. Appl. Phys.*, **97**, 10J318 (2005).
87. Z. Jia, S. Kang, S. Shi, D. E. Nikles and J. W. Harrell, *J. Appl. Phys.*, **97**, 10J310 (2005).
88. M. Chen and D. E. Nikles, *Nano Lett.*, **2**, 211 (2002).
89. H. L. Nguyen, L. E. M. Howard, G. W. Stinton, S. R. Giblin, B. K. Tanner, I. Terry, A. K. Hughes, I. M. Ross, A. Serres and J. S. O. Evans, *Chem. Mater.*, **18**, 6414 (2006).

90. Z. Liu, E. T. Ada, M. Shamsuzzoha, G. B. Thompson and D. E. Nikles, *Chem. Mater.*, **18**, 4946 (2006).
91. M. Chen and D. E. Nikles, *J. Appl. Phys.*, **91**, 8477 (2002).
92. C. Srivastava, G. B. Tompson, J. W. Harrell and D. E. Nikles, *J. Appl. Phys.*, **99**, 054304 (2006).
93. S. Kang, Z. Jia, S. Shi, D. E. Nikles and J. W. Harrell, *J. Appl. Phys.*, **95**, 6744 (2004).
94. S. Kang, J. W. Harrell and D. E. Nikles, *Nano Lett.*, **2**, 1033 (2002).
95. S. Wang, S. S. Kang, D. E. Nikles, J. W. Harrell and X. W. Wu, *J. Magn. Magn. Mater.*, **266**, 49 (2003).
96. S. Kang, D. E. Nikles and J. W. Harrell, *J. Appl. Phys.*, **93**, 7178 (2003).
97. Z. Jia, S. Kang, D. E. Nikles and J. W. Harrell, *IEEE Trans. Magn.*, **41**, 3385 (2005).
98. S. Kang, Z. Jia, D. E. Nikles and J. W. Harrell, *IEEE Trans. Magn.*, **39**, 2753 (2003).
99. A. C. S. Samia, J. A. Schlueter, J. S. Jiang, S. D. Bader, C.-J. Qin and X.-M. Lin, *Chem. Mater.*, **18**, 5203 (2006).
100. Y.-J. Gu and W.-T. Wong, *Langmuir*, **22**, 11447 (2006).
101. P. T. Panousis, D. P. Favreau, S. M. Merchant, V. Ryan and E. A. Dein, in *Advanced Metallization for ULSI Applications* (Eds V. V. S. Rana, R. V. Joshi and I. Ohdomari), Materials Research Society, Pittsburgh, PA, 1992, pp. 3–12.
102. S. Shingubara, Y. Nakasaki and H. Kaneko, *Appl. Phys. Lett.*, **58**, 42 (1991).
103. Y. Pauleau and A. Y. Fasasi, *Chem. Mater.*, **3**, 45 (1991).
104. X. Liu, Q. Wang and S. Wu, *Chem. Vap. Deposition*, **12**, 679 (2006).
105. R. L. Van Hemert, L. B. Spendlove and R. E. Sievers, *J. Electrochem. Soc.*, **112**, 1123 (1965).
106. R. W. Moshier, R. E. Sievers and L. B. Spendlove, US Patent 3356527 (1967).
107. R. Kumar, F. R. Fronczek, A. W. Maverick, W. G. Lai and G. L. Griffin, *Chem. Mater.*, **4**, 577 (1992).
108. D. Temple and A. Reisman, *J. Electrochem. Soc.*, **136**, 3525 (1989).
109. A. E. Kaloyeros, A. Feng, J. Garhart, K. C. Brooks, S. K. Ghosh, A. N. Saxena and F. Luehers, *J. Electron. Mater.*, **19**, 271 (1990).
110. W. G. Lai, Y. Xie and G. L. Griffith, *J. Electrochem. Soc.*, **138**, 3499 (1991).
111. N. Awaya and Y. Arita, in *Digest of Technical Papers—IEEE International Solid-State Circuits Conference* (Ed. J. L. Wuorinen), IEEE, Piscataway, NY, 1989, pp. 103–104.
112. N. Awaya and Y. Arita, in *Advanced Metallization for ULSI Applications* (Eds V. V. S. Rana, R. V. Joshi and I. Ohdomari), Materials Research Society, Pittsburgh, PA, 1992, pp. 345–354.
113. Y. Hazuki, H. Yano, K. Horioka, N. Hayasaka and H. Okano, in *Tungsten and Other Advanced Metals for VLSI/ULSI Applications V* (Eds S. S. Wong and S. Furukawa), Materials Research Society, Pittsburgh, PA, 1990, pp. 351–357.
114. D.-H. Kim, R. H. Wentorf and W. N. Gill, in *Advanced Metallization and Processing for Semiconductor Devices and Circuits—II* (Eds A. Katz, S. Murarka, Y. I. Nissim and J. M. E. Harper), San Francisco Spring Meeting, Materials Research Society, Pittsburgh, PA, 1992, pp. 107–112.
115. R. G. Charles and J. G. Cleary, US Patent 3594216 (1971).
116. S. M. Fine, P. N. Dyer, J. A. T. Norman, B. A. Muratore and R. L. Iampietro, *Mater. Res. Soc. Symp. Proc.*, **204**, 415 (1990).
117. D. N. Armitage, N. I. Dunhill, R. H. West and J. O. Williams, *J. Cryst. Growth*, **108**, 683 (1991).
118. C. Oehr and H. Suhr, *Appl. Phys. A*, **45**, 151 (1988).
119. G. S. Girolami, P. M. Jeffries and L. H. Dubois, *J. Am. Chem. Soc.*, **115**, 1015 (1993).
120. S. L. Cohen, M. Liehr and S. Kasi, *Appl. Phys. Lett.*, **60**, 50 (1992).
121. Y. Hu, M. Afzaal, M. A. Malik and P. O'Brien, *J. Cryst. Growth*, **297**, 61 (2006).
122. C. R. Jones, F. A. Houle, C. A. Kovac and T. H. Baum, *Appl. Phys. Lett.*, **46**, 97 (1985).
123. F. A. Houle, C. R. Jones, T. Baum, C. Pico and C. A. Kovac, *Appl. Phys. Lett.*, **46**, 204 (1985).
124. D.-M. Mao, Z.-K. Jin and Q.-Z. Qin, *J. Appl. Phys.*, **71**, 6111 (1992).
125. N. Awaya and N. Arita, *Jpn. J. Appl. Phys.*, **30**, 1813 (1991).
126. H. Li, E. T. Eisenbraun and A. E. Kaloyeros, *J. Vac. Sci. Technol. B*, **10**, 1337 (1992).
127. J. Pelletier, R. Pantel, J. C. Oberlin and Y. Pauleau, *J. Appl. Phys.*, **70**, 3862 (1991).
128. K. K. Banger, A. Kornilov, R. U. Claessen, E. T. Eisenbraun, A. E. Kaloyeros, P. J. Toscano and J. T. Welch, *Inorg. Chem. Commun.*, **4**, 496 (2001).

129. K. K. Banger, S. C. Ngo, S. Higashiya, R. U. Claessen, K. S. Bousman, P. N. Lim, P. J. Toscano and J. T. Welch, *J. Organomet. Chem.*, **678**, 15 (2003).
130. S. Higashiya, K. K. Banger, S. C. Ngo, P. N. Lim, P. J. Toscano and J. T. Welch, *Inorg. Chim. Acta*, **351**, 291 (2003).
131. A. Ouchi, Z. Bastl, J. Bohacek, J. Subrt and J. Pola, *Surf. Coat. Technol.*, **201**, 4728 (2007).
132. M. L. Kantam, V. S. Jaya, B. Sreedhar, M. M. Rao and B. M. Choudary, *J. Mol. Catal. A: Chemical*, **256**, 273 (2006).
133. G. Wenli, Z. Yue and L. Tongxiang, *J. Mater. Sci.*, **41**, 5462 (2006).
134. S. R. Puniredd and M. P. Srinivasan, *Ind. Eng. Chem. Res.*, **46**, 464 (2007).
135. H. K. Shin, K. M. Chi, M. J. Hampden-Smith, T. T. Kodas, M. F. Paffett and J. D. Farr, *Chem. Mater.*, **4**, 788 (1992).
136. H. K. Shin, K. M. Chi, M. J. Hampden-Smith, T. T. Kodas, M. F. Paffett and J. D. Farr, *Adv. Mater.*, **3**, 246 (1991).
137. A. Jain, K. M. Chi, H. K. Shin, M. J. Hampden-Smith, T. T. Kodas, M. F. Paffett and J. D. Farr, *Metallization: Performance and Reliability Issues for VLSI and ULSI*, SPIE Conf. Proc., **23**, 1596 (1991).
138. R. R. Rye, K. M. Chi, M. J. Hampden-Smith and T. T. Kodas, *J. Electrochem. Soc.*, **139**, L60 (1992).
139. M. J. Hampden-Smith, T. T. Kodas and R. R. Rye, *Adv. Mater.*, **4**, 524 (1992).
140. R. R. Rye, J. A. Knapp, K. M. Chi, M. J. Hampden-Smith and T. T. Kodas, *J. Appl. Phys.*, **72**, 5941 (1993).
141. M. Leschke, S. E. Schulz, R. Ecke, T. Gessner and H. Lang, *Chin. J. Inorg. Chem.*, **20**, 1257 (2004).
142. K. M. Chi, T. S. Corbitt, M. J. Hampden-Smith, T. T. Kodas and E. N. Duesler, *J. Organomet. Chem.*, **449**, 181 (1993).
143. H. Lang, M. Leschke, M. Melter, B. Walfort, K. Köhler, S. E. Schulz and T. Gessner, *Z. Anorg. Allg. Chem.*, **629**, 2371 (2003).
144. K. M. Chi, A. Jain, M. J. Hampden-Smith and T. T. Kodas, *Mater. Res. Soc. Symp. Proc.*, **260**, 629 (1992).
145. A. Jain, K. M. Chi, M. J. Hampden-Smith, T. T. Kodas, M. F. Paffett and J. D. Farr, *J. Mater. Res.*, **7**, 261 (1992).
146. G. L. Griffin, W. G. Lai, A. W. Maverick, R. Kumar and P. K. Ajmera, in *Conference Proceedings ULSI—VII* (Eds V. S. Rana, R. V. Joshi and I. Ohdomari), Materials Research Society, Pittsburgh, PA, 1992, p. 367.
147. S. K. Reynolds, C. J. Smart, E. F. Baran, T. H. Baum, C. E. Larson and P. J. Brock, *Appl. Phys. Lett.*, **59**, 2332 (1991).
148. Y.-L. Kuo, C. Lee, G. Chen, K.-L. Liu and Y.-W. Yen, *Electrochem. Solid-State Lett.*, **10**, D51 (2007).
149. P. Doppelt and T. H. Baum, *MRS Bull.*, **19**, 41, (1994).
150. T. H. Baum and C. E. Larson, *J. Electrochem. Soc.*, **140**, 154 (1993).
151. A. Jain, K. M. Chi, M. J. Hampden-Smith, T. T. Kodas, M. F. Paffett and J. D. Farr, *Chem. Mater.*, **3**, 995 (1991).
152. T. H. Baum and C. E. Larson, *Chem. Mater.*, **4**, 365 (1992).
153. T.-Y. Chen, J. Vaissermann, E. Ruiz, J. P. Senateur and P. Doppelt, *Chem. Mater.*, **13**, 3993 (2001).
154. T.-Y. Chen, J. Vaissermann and P. Doppelt, *Inorg. Chem.*, **40**, 6167 (2001).
155. N. G. Semaltianos, J.-L. Pastol and P. Doppelt, *Appl. Surf. Sci.*, **222**, 102 (2004).
156. N. G. Semaltianos, J.-L. Pastol and P. Doppelt, *Surf. Sci.*, **562**, 157 (2004).
157. S.-W. Kang, S.-H. Han and S.-W. Rhee, *Thin Solid Films*, **350**, 10 (1999).
158. M. Farnia, R. S. Zorich, J. R. Thurmond and J. A. T. Norman, US Patent 6838573 (2005).
159. M. E. Gross and V. M. Donelly, in *Advanced Metallization for ULSI Applications* (Eds V. S. Rana and R. V. Joshi), Materials Research Society, Pittsburgh, PA, 1991, p. 355.
160. J. A. T. Norman, B. A. Muratore, P. N. Dyer, D. A. Roberts and A. K. Hochberg, *J. Phys. (Paris)*, **4**, C2-271 (1991).
161. G. A. Petersen, J. E. Parmeter, C. A. Apblett, M. F. Gonzales, P. M. Smith, T. R. Omstead and J. A. T. Norman, *J. Electrochem. Soc.*, **142**, 939 (1995).
162. A. Jain, K. M. Chi, M. J. Hampden-Smith, T. T. Kodas, M. F. Paffett and J. D. Farr, *J. Electrochem. Soc.*, **140**, 1434 (1993).

163. M.-Y. Park, J.-H. Son and S.-W. Rhee, *Electrochem. Solid-State Lett.*, **1**, 32 (1998).
164. J.-H. Son, M.-Y. Park and S.-W. Rhee, *Thin Solid Films*, **335**, 229 (1998).
165. M.-Y. Park, J.-H. Son, S.-W. Kang and S.-W. Rhee, *J. Mater. Res.*, **14**, 975 (1999).
166. Y. Shen, T. Rüffer, S. E. Schulz, T. Gessner, L. Wittenbecher, H.-J. Sterzel and H. Lang, *J. Organomet. Chem.*, **690**, 3878 (2005).
167. J. M. Blackburn, D. P. Long, A. Cabañas and J. J. Watkins, *Science*, **294**, 141 (2001).
168. A. Cabañas, J. M. Blackburn and J. J. Watkins, *Microelectron. Eng.*, **64**, 53 (2002).
169. L. Wittenbecher, H. Lang and Y. Shen, World Patent WO 058789A2 (2005).
170. T. Wächtler, Y. Shen, A. Jakob, R. Ecke, S. E. Schulz, L. Wittenbecher, H. J. Sterzel, K. Tiefensee, S. Oswald, S. Schulze, H. Lang, M. Hietschold and T. Gessner, 'Evaluation of Phosphite and Phosphane Stabilized Copper(I) Trifluoroacetates as Precursors for the Metal-Organic Chemical Vapor Deposition of Copper', http://archiv.tu-chemnitz.de/pub/2006/0031/data/PosterMAM2006.pdf.
171. M. J. Hampden-Smith and T. T. Kodas, *Polyhedron*, **14**, 699 (1995).
172. P. Doppelt, *Coord. Chem. Revs.*, **178–180**, 1785 (1998).
173. C. Cavallotti, V. Gupta, C. Sieber and K. F. Jensen, *Phys. Chem. Chem. Phys.*, **5**, 2818 (2003).
174. L. Pirolli and A. V. Teplyakov, *Surf. Sci.*, **600**, 3313 (2006).
175. R. Kumar, A. W. Maverick, F. R. Fronczek, G. Lai and G. L. Griffin, *Precursors for Chemical Vapor Deposition of Copper,* 201st American Chemical Society Meeting, Atlanta, April 1991, Abstract INOR256.
176. *Electronic Materials Handbook, Vol. 1, Packaging*, ASM International, Materials Park, OK, U.S.A., 1989.
177. V. H. Houlding, H. Maxwell Jr., S. M. Crochiere, D. L. Farrington, R. S. Rai and J. M. Tartaglia, *Mater. Res. Soc. Symp. Proc.*, **260**, 119 (1992).
178. D. Lee and X. Chaud, *Appl. Phys.*, **31**, 359 (1992).
179. J. Fraden, *Handbook of Modern Sensors: Physics, Design and Applications*, 2nd edn., American Institute of Physics, Woodbury, NY, 1997.
180. H. Liedberg and T. Lundeberg, *Urol. Res.*, **17**, 359 (1989).
181. W. Lin, T. H. Warren, R. G. Nuzzo and G. S. Girolami, *J. Am. Chem. Soc.*, **115**, 11644 (1993).
182. Z. Yuan, N. H. Dryden, J. J. Vittal and R. J. Puddephatt, *Chem. Mater.*, **7**, 1696 (1995).
183. H. Schmidt, A. Jakob, T. Haase, K. Kohse-Höinghaus, S. E. Schulz, T. Wächtler, T. Gessner and H. Lang, *Z. Anorg. Allg. Chem.*, **631**, 2786 (2005).
184. H.-K. Kim, H.-C. Jeong, K. S. Kim, S. H. Yoon, S. S. Lee, K. W. Seo and I.-W. Shim, *Thin Solid Films*, **478**, 72 (2005).
185. Z. Yuan, N. H. Dryden, X. Li, J. J. Vittal and R. J. Puddephatt, *J. Mater. Chem.*, **5**, 303 (1995).
186. C. Xu, M. J. Hampden-Smith and T. T. Kodas, *Adv. Mater.*, **6**, 746 (1994).
187. S. Serghini-Monim, Z. Yuan, K. Griffiths, P. R. Norton and R. J. Puddephatt, *J. Am. Chem. Soc.*, **117**, 4030 (1995).
188. T. Haase, K. Kohse-Höinghaus, N. Bahlawane, P. Djiele, A. Jakob and H. Lang, *Chem. Vap. Deposition*, **11**, 195 (2005).
189. C. Xu, M. J. Hampden-Smith, T. T. Kodas, E. N. Duesler, A. L. Rheingold and G. Yap, *Inorg. Chem.*, **34**, 4767 (1995).
190. L. M. Davis, D. S. Thompson, C. J. Dean, M. Pevzner, J. L. Scott, S. T. Broadwater, D. W. Thompson and R. E. Southward, *J. Appl. Polym. Sci.*, **103**, 2409 (2007).
191. M. Haruta, *Catal. Today*, **36**, 153 (1997).
192. M. S. Chen and D. W. Goodman, *Science*, **306**, 252 (2004).
193. D. Boyer, P. Tamarat, A. Maali, B. Lounis and M. Orrit, *Science*, **297**, 1160 (2002).
194. T. H. Baum and P. B. Comita, *Thin Solid Films*, **218**, 80 (1992).
195. T. H. Baum and C. R. Jones, *Appl. Phys. Lett.*, **47**, 538 (1985).
196. C. E. Larson, T. H. Baum and R. L. Jackson, *J. Electrochem. Soc.*, **134**, 266 (1987).
197. T. H. Baum, *J. Electrochem. Soc.*, **134**, 2616 (1987).
198. H. Suhr, A. Etspüler, E. Feurer and S. Kraus, *Plasma Chem. Plasma Process.*, **9**, 217 (1989).
199. S. Schimpf, M. Lucas, C. Mohr, U. Rodemerck, A. Brückner, J. Radnik, H. Hofmeister and P. Claus, *Catal. Today*, **72**, 63 (2002).
200. S. Hannemann, J.-D. Grunwaldt, F. Krumeich, P. Kappen and A. Baiker, *Appl. Surf. Sci.*, **252**, 7862 (2006).

201. P. P. Semyannikov, B. L. Moroz, S. V. Trubin, G. I. Zharkova, P. A. Pyryaev, M. Y. Smirnov and V. I. Bukhtiyarov, *J. Struct. Chem.*, **47**, 458 (2006).
202. Electroceramic Thin Films, Parts I and II, *MRS Bull.*, **21**, (1996).
203. A. C. Jones, *Chem. Vap. Deposition*, **4**, 169 (1998).
204. M. Niederberger, G. Garnweitner, J. Buha, J. Polleux, J. Ba and N. Pinna, *J. Sol-Gel Sci. Technol.*, **40**, 259 (2006).
205. M. Niederberger and G. Garnweitner, *Chem. Eur. J.*, **12**, 7282 (2006).
206. D. K. Fork, F. A. Ponce, J. C. Tramontana and T. H. Geballe, *Appl. Phys. Lett.*, **58**, 2994 (1991).
207. A. Masuda, Y. Yamanaka, M. Tazoe, T. Nakamura, A. Morimoto and T. Shimizu, *J. Cryst. Growth*, **158**, 84 (1996).
208. S. G. Kim, J. Y. Kim and H. J. Kim, *Thin Solid Films*, **376**, 110 (2000).
209. J.-H. Boo, K.-S. Yu, W. Koh and Y. Kim, *Mater. Lett.*, **26**, 233 (1996).
210. J.-H. Boo, S.-B. Lee, K.-S. Yu, W. Koh and Y. Kim, *Thin Solid Films*, **341**, 63 (1999).
211. C. Bedoya, G. G. Condorelli, A. Motta, A. Di Mauro, G. Anastasi, I. L. Fragala, J. G. Lisoni and D. Wouters, *Chem. Vap. Deposition*, **11**, 269 (2005).
212. G. S. Hammond, D. C. Nonhebel, C. S. Wu, *Inorg. Chem.*, **2**, 73 (1963).
213. S. B. Turnipseed, R. M. Barkley and R. E. Sievers, *Inorg. Chem.*, **30**, 1164 (1991).
214. D. L. Schulz, B. J. Hinds, D. A. Neumayer, C. L. Stern and T. J. Marks, *Chem. Mater.*, **5**, 1605 (1993).
215. J. S. Moodera and L. R. Kinder, *J. Appl. Phys.*, **79**, 4724 (1996).
216. J. E. Sundgren and H. T. G. Hentzell, *J. Vac. Sci. Technol., A, Vac. Surf. Films*, **4**, 2259 (1986).
217. B. E. Yoldas, *Appl. Opt.*, **19**, 1425 (1980).
218. O. B. Ajayi, M. S. Akanni, J. N. Lambi, H. D. Burrows, O. Osasona and B. Podor, *Thin Solid Films*, **138**, 91 (1986).
219. O. B. Ajayi, M. S. Akanni, J. N. Lambi, C. Jeynes and J. F. Watts, *Thin Solid Films*, **185**, 123 (1990).
220. J. Von Hoene, R. G. Charles and W. M. Hickam, *J. Phys. Chem.*, **62**, 1098 (1958).
221. T. Maruyama and S. Arai, *Appl. Phys. Lett.*, **60**, 322 (1992).
222. J. S. Kim, H. A. Marzouk, P. J. Reucroft, J. D. Robertson and C. E. Hamrin, Jr., *Thin Solid Films*, **230**, 156 (1993).
223. M. C. Rhoten and T. C. DeVore, *Chem. Mater.*, **9**, 1757 (1997).
224. M. Aguilar-Frutis, M. Garcia, C. Falcony, G. Plesch and S. Jimenez-Sandoval, *Thin Solid Films*, **389**, 200 (2001).
225. M. Pulver, W. Nemetz and G. Wahl, *Surf. Coat. Technol.*, **125**, 400 (2000).
226. V. S. K. G. Kelekanjeri, W. B. Carter and J. M. Hampikian, *Thin Solid Films*, **515**, 1905 (2006).
227. C. Pflitsch, A. Muhsin, U. Bergmann and B. Atakan, *Surf. Coat. Technol.*, **201**, 73 (2006).
228. C. Pflitsch, D. Viefhaus, U. Bergmann and B. Atakan, *Thin Solid Films*, **515**, 3653 (2007).
229. C. Vahlas, B. Caussat, F. Senocq, W. L. Gladfelter, L. Aloui and T. Moersch, *Chem. Vap. Deposition*, **13**, 123 (2007).
230. Y. Pauleau and O. Dulac, *Chem. Mater.*, **3**, 280 (1991).
231. M. Fleischer and H. Meixner, *Sensors Actuators B*, **6**, 257 (1992).
232. G. A. Battiston, R. Gerbasi, M. Porchia, R. Bertoncello and F. Caccavale, *Thin Solid Films*, **279**, 115 (1996).
233. M. Nieminen, L. Niinistö and E. Rauhala, *J. Mater. Sci.*, **6**, 27 (1996).
234. M. Takahashi, T. Nakatani, S. Iwamoto, T. Watanabe and M. Inoue, *Appl. Catal. B: Environmental*, **70**, 73 (2007).
235. J. N. Avaritsiotis and R. P. Howson, *Thin Solid Films*, **80**, 63 (1980).
236. L. A. Ryabova and Y. S. Savitskaya, *Thin Solid Films*, **2**, 141 (1968).
237. S. Reich, H. Suhr and B. Waimer, *Thin Solid Films*, **189**, 293 (1990).
238. T. Tsuchiya, A. Watanabe, Y. Imai, H. Niino, I. Yamaguchi, T. Manabe, T. Kumagai and S. Mizuta, *Jpn. J. Appl. Phys.*, **38**, L1112 (1999).
239. J.-H. Park, G. A. Horley, P. O'Brien, A. C. Jones and M. Motevalli, *J. Mater. Chem.*, **11**, 2346 (2001).
240. G. Malandrino, A. M. Borzi, F. Castelli, I. L. Fragalà, W. Destrù, R. Gobetto, P. Rossi and P. Dapporto, *Dalton Trans.*, 369 (2003).

241. A. D. Berry, R. T. Holm, R. L. Mowery, N. H. Turner and M. Fatemi, *Chem. Mater.*, **3**, 72 (1991).
242. R. J. Phillips, M. J. Shane and J. A. Switzer, *J. Mater. Res.*, **4**, 923 (1989).
243. W. A. Badaway, *J. Electroanal. Chem.*, **281**, 85 (1990).
244. J. P. Zheng and H. S. Kwok, *Appl. Phys. Lett.*, **63**, 1 (1993).
245. T. Maruyama and Y. Ikuta, *Solar Energy Mat. Solar Cells*, **28**, 209 (1992).
246. K.-M. Chi, C.-C. Lin, Y.-H. Lu and J.-H. Liao, *J. Chin. Chem. Soc.*, **47**, 425 (2000).
247. Y. S. Feng, S. M. Zhou, Y. Li, C. C. Li and L. D. Zhang, *Solid State Sci.*, **5**, 729 (2003).
248. Y. S. Feng, R. Yao and L. D. Zhang, *Physica B*, **350**, 348 (2004).
249. T. Tsuchiya, M. Takeda, I. Yamaguchi, T. Manabe, T. Kumagai and S. Mizuta, *Appl. Phys. A*, **79**, 1541 (2004).
250. N. Hollingsworth, G. A. Horley, M. Mazhar, M. F. Mahon, K. C. Molloy, P. W. Haycock, C. P. Myers and G. W. Critchlow, *Appl. Organomet. Chem.*, **20**, 687 (2006).
251. T. Kawahara, M. Yamamuka, T. Makita, J. Naka, A. Yuuki, N. Mikami and K. Ono, *Jpn. J. Appl. Phys.*, **33**, 5129 (1994).
252. O. Auciello and R. Ramesh, *MRS Bull.*, **21**, 21 (1996).
253. V. V. Krisyuk, A. E. Turgambaeva and I. K. Igumenov, *Chem. Vap. Deposition*, **4**, 43 (1998).
254. J. S. Zhao, J. S. Sim, H. J. Lee, D.-Y. Park and C.-S. Hwang, *J. Electrochem. Soc.*, **152**, C277 (2005).
255. S. V. Samoilenkov, *Chem. Vap. Deposition*, **12**, 206 (2006).
256. J. T. Lim, J. C. Lee, W. I. Lee and I.-M. Lee, *Bull. Korean Chem. Soc.*, **20**, 355 (1999).
257. H. B. Suffredini, G. R. Salazar-Banda, S. T. Tanimoto, M. L. Calegaro, S. A. S. Machado and L. A. Avaca, *J. Braz. Chem. Soc.*, **17**, 257 (2006).
258. M. Zhang and C. P. Wilde, *J. Electroanal. Chem.*, **390**, 59 (1995).
259. P. B. Clapham, *Br. J. Appl. Phys.*, **18**, 363 (1967).
260. E. Y. Wang and K. A. Pandelisev, *J. Appl. Phys.*, **52**, 4818 (1981).
261. A. M. Joshi, M. M. Mandhre, M. L. Jadhav, S. A. Gangal and R. N. Karekar, *Jpn. J. Appl. Phys.*, **27**, 2168 (1988).
262. S. W. Kang and S. W. Rhee, *Thin Solid Films*, **468**, 79 (2004).
263. C. Bedoya, G. G. Condorelli, S. T. Finocchiaro, A. Di Mauro, I. L. Fragalà, L. Cattaneo and S. Carella, *Chem. Vap. Deposition*, **11**, 261 (2005).
264. V. M. Koleshko and N. V. Babushkina, *Thin Solid Films*, **62**, 1 (1979).
265. A. Huignard, A. Aron, P. Aschehoug, B. Viana, J. Théry, A. Laurent and J. Perrière, *J. Mater. Chem.*, **10**, 549 (2000).
266. D. H. Riu, S. W. Lee, Y. K. Jeong and S. C. Choi, *Key Eng. Mater.*, **601**, 264 (2004).
267. M. Spankova, I. Vavra, S. Chromik, R. Luptak, J. Soltys and K. Husekova, *Mater. Sci. Eng., B, Solid State Mater. Adv.*, **116**, 30 (2005).
268. T. Goto, R. Banal and T. Kimura, *Surf. Coat. Technol.*, **201**, 5776 (2007).
269. T. T. Van and J. P. Chang, *Surf. Sci.*, **596**, 1 (2005).
270. T. T. Van and J. P. Chang, *Appl. Surf. Sci.*, **246**, 250 (2005).
271. D. Niu, R. W. Ashcraft, Z. Chen, S. Stemmer and G. N. Parsons, *J. Electrochem. Soc.*, **150**, F102 (2003).
272. T. Mahalingam, M. Radhakrishnan and C. Balasubramanian, *Thin Solid Films*, **78**, 229 (1981).
273. D. H. Kim, J. Y. Yoon, H. C. Park and K. H. Park, *Sensors Actuators B*, **62**, 61 (2000).
274. G. Bonnet, M. Lachkar, J. P. Laprin and J. C. Colson, *Solid State Ionics*, **72**, 344 (1994).
275. Y. M. Gao, P. Wu, K. Dwight and A. Wold, *J. Solid State Chem.*, **90**, 228 (1991).
276. S. Wang, W. Wang and Y. Qian, *Thin Solid Films*, **372**, 50 (2000).
277. J.-B. Cheng, A.-D. Li, Q.-Y. Shao, H.-Q. Ling, D. Wu, Y. Wang, Y.-J. Bao, M. Wang, Z.-G. Liu and N.-B. Ming, *Appl. Surf. Sci.*, **233**, 91 (2004).
278. S.-W. Kang and S.-W. Rhee, *J. Electrochem. Soc.*, **149**, C345 (2002).
279. J. Jun, J. H. Jun and D. J. Choi, *J. Mater. Sci. Lett.*, **21**, 1847 (2002).
280. M. Nieminen, M. Putkonen and L. Niinistö, *Appl. Surf. Sci.*, **174**, 155 (2001).
281. N. K. Park, D. K. Kang, B.-H. Kim, S. J. Jo and J. S. Ha, *Appl. Surf. Sci.*, **252**, 8506 (2006).
282. T. Won, S. Yoon and H. Kim, *J. Electrochem. Soc.*, **139**, 3284 (1992).
283. C. A. Grimes, O. K. Varghese and S. Ranjan, *Light, Water, Hydrogen: The Solar Generation of Hydrogen by Water Photoelectrics*, Springer, New York, 2007; K. Honda and H. Fujishima, *Nature*, **238**, 37 (1972).
284. A. C. Jones, *J. Mater. Chem.*, **12**, 2576 (2002).

285. M. Balog, M. Schieber, S. Patai and M. Michman, *J. Cryst. Growth*, **17**, 298 (1972).
286. S. T. Hong, J. T. Lim, J. C. Lee, M. Xue and I.-M. Lee, *Bull. Korean Chem. Soc.*, **17**, 637 (1996).
287. V. G. Bessergenev, R. J. F. Pereira, M. C. Mateus, I. V. Khmelinskii, D. A. Vasconcelos, R. Nicula, E. Burkel, A. M. Botelho do Rego and A. I. Saprykin, *Thin Solid Films*, **503**, 29 (2006).
288. T. Watanabe, S. Hoffmann-Eifert, C. S. Hwang and R. Waser, *J. Electrochem. Soc.*, **153**, F199 (2006).
289. R. Bhakta, R. Thomas, F. Hipler, H. F. Bettinger, J. Müller, P. Ehrhart and A. Devi, *J. Mater. Chem.*, **14**, 3231 (2004).
290. K. Woo, W. I. Lee, J. S. Lee and S. O. Kang, *Inorg. Chem.*, **42**, 2378 (2003).
291. S. H. Hong, S. K. Rim, I.-M. Lee, Y. S. Min, D. Kim and W. I. Lee, *Thin Solid Films*, **409**, 82 (2002).
292. E. Alonso, I. Montequi, S. Lucas and M. J. Cocero, *J. Supercrit. Fluids*, **39**, 453 (2007).
293. C.-W. Lee and J.-S. Lee, *J. Ceramic Soc. Jpn.*, **114**, 923 (2006).
294. K.-W. Chour, J. Chen and R. Xu, *Thin Solid Films*, **304**, 106 (1997).
295. M. H. Siadati, T. L. Ward, J. Martus, P. Atanasova, C. Xia and R. W. Schwartz, *Chem. Vap. Deposition*, **3**, 311 (1997).
296. K. S. Fancey and A. J. Matthews, *J. Vac. Sci. Technol. A*, **4**, 2656 (1986).
297. M. Ritala and M. Leskelä, *Appl. Surf. Sci.*, **75**, 333 (1994).
298. W. C. Russell and C. Strandberg, *Int. J. Refract. Met. Hard Mater.*, **14**, 51 (1996).
299. G. J. M. Dormans, M. de Keijser and P. J. van Veldhoven, *Mater. Res. Soc. Symp. Proc.*, **243**, 203 (1992).
300. S. B. Desu, T. Shi and C. K. Kwok, in *Chemical Vapor Deposition of Refractory Metals and Ceramics* (Eds T. M. Besmann and B. M. Gallois), Materials Research Society, Pittsburgh, PA, **168**, 349 (1990).
301. M. Balog, M. Schieber, M. Michman and S. Patai, *J. Electrochem. Soc.*, **126**, 1203 (1979).
302. C. S. Hwang and H. J. Kim, *J. Mat. Res.*, **8**, 1361 (1993).
303. E.-T. Kim and S.-G. Yoon, *Thin Solid Films*, **227**, 7 (1993).
304. J. Si, S. B. Desu and C.-Y. Tsai, *J. Mat. Res.*, **8**, 1721 (1993).
305. M. Pulver, G. Wahl, H. Scheytt and M. Sommer, *J. Phys. IV*, **3**, 305 (1993).
306. A. C. Jones, T. J. Leedham, P. J. Wright, M. J. Crosbie, P. A. Lane, D. J. Williams, K. A. Fleeting, D. J. Otway and P. O'Brien, *Chem. Vap. Deposition*, **4**, 46 (1998).
307. A. C. Jones, T. J. Leedham, P. J. Wright, M. J. Crosbie, D. J. Williams, K. A. Fleeting, H. O. Davies, D. J. Otway and P. O'Brien, *Chem. Vap. Deposition*, **4**, 197 (1998).
308. A. C. Jones, T. J. Leedham, P. J. Wright, D. J. Williams, M. J. Crosbie, H. O. Davies, K. A. Fleeting and P. O'Brien, *J. Eur. Ceramic Soc.*, **19**, 1431 (1999).
309. T. H. Baum, J. F. Roeder, C. Xu and B. C. Hendrix, US Patent 2002/0015790 A1 (2002).
310. H.-W. Chen, T.-Y. Huang, D. Landheer, X. Wu, S. Moisa, G. I. Sproule and T.-S. Chao, *J. Electrochem. Soc.*, **149**, F49 (2002).
311. M. Morstein, I. Pozsgai and N. D. Spencer, *Chem. Vap. Deposition*, **5**, 151 (1999).
312. M. Morstein, *Inorg. Chem.*, **38**, 125 (1999).
313. S. V. Pasko, A. Abrutis and L. G. Hubert-Pfalzgraf, *Mater. Lett.*, **59**, 261 (2005).
314. S. V. Pasko, L. G. Hubert-Pfalzgraf, A. Abrutis, P. Richard, A. Bartasyte and V. Kazlauskiene, *J. Mater. Chem.*, **14**, 1245 (2004).
315. R. Neagu, D. Perednis, A. Princivalle and E. Djurado, *Solid State Ionics*, **177**, 1451 (2006).
316. M. Balog, M. Schieber, M. Michman and S. Patai, *Thin Solid Films*, **41**, 247 (1977).
317. L. V. Yakovkina, V. N. Kichai, T. P. Smirnova, V. V. Kaichev, Y. V. Shubin, N. B. Morozova, K. V. Zherikova and I. K. Igumenov, *Inorg. Mater.*, **41**, 1300 (2005).
318. M. Miyake, X.-J. Lou, M. Zhang, F. D. Morrison, T. J. Leedham, T. Tatsuta, O. Tsuji and J. F. Scott, *Integrated Ferroelectrics*, **74**, 165 (2005).
319. Y. Segura, L. Chmielarz, P. Kustrowski, P. Cool, R. Dziembaj and E. F. Vansant, *Appl. Catal. B: Environmental*, **61**, 69 (2005).
320. P. Kustrowski, Y. Segura, L. Chmielarz, J. Surman, R. Dziembaj, P. Cool and E. F. Vansant, *Catal. Today*, **114**, 307 (2006).
321. C. Cesari, C. Leroux and G. Nihoul, *Key Eng. Mater.*, **155–156**, 227 (1998).
322. F. J. Morin, *Phys. Rev. Lett.*, **3**, 34 (1959).

323. S. M. Babulanam, T. S. Eriksson, G. A. Niklasson and C. G. Granqvist, *Sol. Energy Mater.*, **16**, 347 (1987).
324. M. B. Sahana, M. S. Dharmaprakash and S. A. Shivashankar, *J. Mater. Chem.*, **12**, 333 (2002).
325. D. Vernardou, M. E. Pemble and D. W. Sheel, *Chem. Vap. Deposition*, **12**, 263 (2006).
326. M. B. Sahana and S. A. Shivashankar, *J. Mater. Res.*, **19**, 2859 (2004).
327. P. Van Der Voort, K. Possemiers and E. F. Vansant, *J. Chem. Soc., Faraday Trans.*, **92**, 843 (1996).
328. P. Van Der Voort, I. V. Babitch, P. J. Grobet, A. A. Verberckmoes and E. F. Vansant, *J. Chem. Soc., Faraday Trans.*, **92**, 3635 (1996).
329. P. Van Der Voort, M. Morey, G. D. Stucky, M. Mathieu and E. F. Vansant, *J. Phys. Chem. B*, **102**, 585 (1998).
330. P. Van Der Voort, M. G. White and E. F. Vansant, *Langmuir*, **14**, 106 (1998).
331. M. Baltes, P. Van Der Voort, B. M. Weckhuysen, R. R. Rao, G. Catana, R. A. Schoonheydt and E. F. Vansant, *Phys. Chem. Chem. Phys.*, **2**, 2673 (2000).
332. M. Baltes, K. Cassiers, P. Van Der Voort, B. M. Weckhuysen, R. A. Schoonheydt and E. F. Vansant, *J. Catal.*, **197**, 160 (2001).
333. S. Van Doorslaer, Y. Segura and P. Cool, *J. Phys. Chem. B*, **108**, 19404 (2004).
334. V. Meynen, Y. Segura, M. Mertens, P. Cool and E. F. Vansant, *Micropor. Mesopor. Mater.*, **85**, 119 (2005).
335. Y. Segura, P. Cool, P. Kustrowski, L. Chmielarz, R. Dziembaj and E. F. Vansant, *J. Phys. Chem. B*, **109**, 12071 (2005).
336. P. Van Der Voort, M. Baltes and E. F. Vansant, *J. Phys. Chem. B*, **103**, 10102 (1999).
337. P. Van Der Voort and E. F. Vansant, *Micropor. Mesopor. Mater.,* **38**, 385 (2000).
338. V. Murgia, E. M. F. Torres, J. C. Gottifredi and E. L. Sham, *Appl. Catal. A: General*, **312**, 134 (2006).
339. F. Lenzmann, V. Shklover, K. Brooks and M. Grätzel, *J. Sol-Gel Sci. Technol.*, **19**, 175 (2000).
340. K. Tominaga, R. Muhammet, I. Kobayashi and M. Okada, *Jpn. J. Appl. Phys.*, **31**, L585 (1992).
341. M. P. McDaniel, *Adv. Catal.*, **33**, 47 (1985).
342. F. Cavani, M. Koutyrev, F. Trifirò, A. Bartolini, D. Ghisletti, R. Iezzi, A. Santucci and G. Del Piero, *J. Catal.*, **158**, 236 (1996).
343. H. I. Chbihi, S. Audisio, F. Defoort and D. Hertz, *Mat. Manuf. Process*, **6**, 469 (1991).
344. I. V. Babich, Y. V. Plyuto, P. Van Der Voort and E. F. Vansant, *J. Chem. Soc., Faraday Trans.*, **93**, 3191 (1997).
345. I. V. Babich, Y. V. Plyuto, P. Van Der Voort and E. F. Vansant, *J. Colloid Interface Sci.*, **189**, 144 (1997).
346. P. Kustrowski, L. Chmielarz, R. Dziembaj, P. Cool and E. F. Vansant, *J. Phys. Chem. B*, **109**, 11552 (2005).
347. L. Chmielarz, P. Kustrowski, M. Kruszec, R. Dziembaj, P. Cool and E. F. Vansant, *J. Porous Mat.*, **12**, 183 (2005).
348. A. M. Azad, S. G. Mhaisalkar, L. D. Birkefeld, S. A. Akbar and K. S. Goto, *J. Electrochem. Soc.*, **139**, 2913 (1992).
349. M. G. Kanatzidis and T. J. Marks, *Inorg. Chem.*, **26**, 783 (1987).
350. A. Gulino, G. G. Condorelli and I. Fragalà, *J. Mater. Chem.*, **6**, 1335 (1996).
351. B. Ballarin, E. Brescacin, G. A. Rizzi and E. Tondello, *J. Mater. Chem.*, **5**, 1147 (1995).
352. J. Handzlik, J. Ogonowski, J. Stoch, M. Mikolajczyk and P. Michorczyk, *Appl. Catal. A: General*, **312**, 213 (2006).
353. C. M. Lampert, *Sol. Energy Mater.*, **11**, 1 (1984).
354. A. Agrawal, J. P. Cronin and R. Zhung, *Sol. Energy Mater.*, **31**, 9 (1993).
355. D. V. Baxter, M. H. Chisholm, S. Doherty and N. E. Gruhn, *Chem. Commun.*, 1129 (1996).
356. T. Nishide, H. Yamaguchi and F. Mizukami, *J. Mater. Sci.*, **30**, 4946 (1995).
357. T. Nishide and F. Mizukami, *Thin Solid Films*, **259**, 212 (1995).
358. T. Nishide and F. Mizukami, *J. Sol-Gel Sci. Technol.*, **6**, 263 (1996).
359. P. H. Klose, *J. Electrochem. Soc.*, **117**, 854 (1970).
360. R. Craciun and N. Dulamita, *Catal. Lett.*, **46**, 229 (1997).
361. L. Chen, T. Horiuchi and T. Mori, *Catal. Lett.*, **60**, 237 (1999).
362. S. T. Oyama, *Catal. Rev.-Sci. Eng.*, **42**, 279 (2000).

363. T. Nakamura, R. Tai, T. Nishimura and K. Tachibana, *J. Electrochem. Soc.*, **152**, C584 (2005).
364. O. Nilsen, H. Fjellvag and Kjekshus, *Thin Solid Films*, **444**, 44 (2003).
365. P. Fabrizioli, T. Bürgi and A. Baiker, *J. Catal.*, **207**, 88 (2002).
366. M. Li, H. Schnablegger and S. Mann, *Nature*, **402**, 393 (1999).
367. Q. Guo, X. Teng, S. Rahman and H. Yang, *J. Am. Chem. Soc.*, **125**, 630 (2003).
368. L. Ben-Dor, R. Druilhe and P. Gibart, *J. Cryst. Growth*, **24/25**, 172 (1974).
369. L. Ben-Dor, E. Fischbein, I. Felner and Z. Kalman, *J. Electrochem. Soc.*, **124**, 451 (1977).
370. H. Torii, E. Fujii and M. Aoki, *J. Jpn. Soc. Powder Powder Metallurgy*, **35**, 197 (1988).
371. E. Fujii and H. Torii, *Jpn. J. Appl. Phys.*, Part 2, **32**, L1527 (1993).
372. S. Dhara, B. R. Awasthy, A. C. Rastogi, B. K. Das, N. V. Gelfond, N. E. Fedotova, A. F. Bykov and I. K. Igumenov, *J. Magn. Magn. Mater.*, **134**, 29 (1994).
373. M. Lie, H. Fjellvag and A. Kjekshus, *Thin Solid Films*, **488**, 74 (2005).
374. O. Nielsen, M. Lie, S. Foss, H. Fjellvag and A. Kjekshus, *Appl. Surf. Sci.*, **227**, 40 (2004).
375. M. De Ridder, P. C. Van De Ven, R. G. Van Welzenis, H. H. Brongersma, S. Helfensteyn, C. Creemers, P. Van Der Voort, M. Baltes, M. Mathieu and E. F. Vansant, *J. Phys. Chem. B*, **106**, 13146 (2002).
376. P. Van Der Voort, R. G. Van Welzenis, M. De Ridder, H. H. Brongersma, M. Baltes, M. Mathieu, P. C. Van De Ven, and E. F. Vansant, *Langmuir*, **18**, 4420 (2002).
377. L. An, Z. Li, W. Li, Y. Nie, Z. Chen, Y. Wang and B. Yang, *J. Magn. Magn. Mater.*, **303**, 127 (2006).
378. Y. Nie, W. Li, L. An, D. Zhu, Z. Wang and B. Yang, *Colloids Surf. A: Physicochem. Eng. Aspects*, **278**, 229 (2006).
379. T. Tsoncheva, M. Dimitrov, L. Ivanova, D. Paneva, D. Mitev, B. Tsintsarski, I. Mitov, S. Stavrev and C. Minchev, *J. Colloid Interface Sci.*, **300**, 183 (2006).
380. T. Tsoncheva, L. Ivanova, D. Paneva, M. Dimitrov, I. Mitov, S. Stavrev and C. Minchev, *J. Colloid Interface Sci.*, **302**, 492 (2006).
381. P. Kustrowski, L. Chmielarz, J. Surman, E. Bidzinska, R. Dziembaj, P. Cool and E. F. Vansant, *J. Phys. Chem. A*, **109**, 9808 (2005).
382. L. Chmielarz, P. Kustrowski, R. Dziembaj, P. Cool and E. F. Vansant, *Appl. Catal. B: Environmental*, **62**, 369 (2006).
383. J. M. Vargas and R. D. Zysler, *Nanotechnology*, **16**, 1474 (2005).
384. L. Zhang, R. He and H.-C. Gu, *Appl. Surf. Sci.*, **253**, 2611 (2006).
385. Y. Chu, J. Hu, W. Yang, C. Wang and J. Z. Zhang, *J. Phys. Chem. B*, **110**, 3135 (2006).
386. L. Krusin-Elbaum, *Thin Solid Films*, **169**, 17 (1989).
387. Q. X. Jia and W. A. Anderson, *Appl. Phys. Lett.*, **57**, 304 (1990).
388. D.-J. Lee, S.-W. Kang and S.-W. Rhee, *Thin Solid Films*, **413**, 237 (2002).
389. G. X. Miao, A. Gupta, G. Xiao and A. Anguelouch, *Thin Solid Films*, **478**, 159 (2005).
390. R.-S. Chen, Y.-S. Huang, Y.-L. Chen and Y. Chi, *Thin Solid Films*, **413**, 85 (2002).
391. Y.-H. Lai, Y.-L. Chen, Y. Chi, C.-S. Liu, A. J. Carty, S.-M. Peng and G.-H. Lee, *J. Mater. Chem.*, **13**, 1999 (2003).
392. G. E. McDonald, *Thin Solid Films*, **72**, 83 (1980).
393. P. S. Patil, L. D. Kadam and C. D. Lokhande, *Thin Solid Films*, **272**, 29 (1996).
394. E. Barrera, I. González and T. Viveros, *Solar Energy Mater. Solar Cells*, **51**, 69 (1998).
395. C. Hoffmann, A. Wolf and F. Schuth, *Angew. Chem., Int. Ed.*, **38**, 2800 (1999).
396. E. Fujii, A. Tomozawa, S. Fujii, H. Torii, M. Hattori and R. Takayama, *Jpn. J. Appl. Phys.*, Part 2, **32**, L1448 (1993).
397. K. Shalini, A. U. Mane, S. A. Shivashankar, M. Rajeswari and S. Choopun, *J. Cryst. Growth*, **231**, 242 (2001).
398. A. U. Mane, K. Shalini, A. Wohlfart, A. Devi and S. A. Shivashankar, *J. Cryst. Growth*, **240**, 157 (2002).
399. A. U. Mane and S. A. Shivashankar, *J. Cryst. Growth*, **254**, 368 (2003).
400. L. M. Apátiga and V. M. Castaño, *Thin Solid Films*, **496**, 576 (2006).
401. A. Dittmar, H. Kosslick, J.-P. Müller and M.-M. Pohl, *Surf. Coat. Technol.*, **182**, 35 (2004).
402. A. Gulino, P. Dapporto, P. Rossi, G. Anatasi and I. Fragalà, *J. Mater. Chem.*, **14**, 2549 (2004).
403. A. Gulino, P. Dapporto, P. Rossi and I. Fragalà, *Chem. Mater.*, **15**, 3748 (2003).
404. M. Burriel, G. Garcia, J. Santiso, A. Abrutis, Z. Saltyte and A. Figueras, *Chem. Vap. Deposition*, **11**, 106 (2005).

405. S. Pasko, A. Abrutis, L. G. Hubert-Pfalzgraf and V. Kubilius, *J. Cryst. Growth*, **262**, 653 (2004).
406. S. Pasko, L. G. Hubert-Pfalzgraf, A. Abrutis and J. Vaissermann, *Polyhedron*, **23**, 735 (2004).
407. J. T. Spencer, in *Progress in Inorganic Chemistry*, Vol. 41 (Ed. K. D. Karlin), John Wiley & Sons, Inc., New York, 1994, pp. 145–237.
408. J. Pinkas, J. C. Huffman, D. V. Baxter, M. H. Chisholm and K. G. Caulton, *Chem. Mater.*, **7**, 1589 (1995).
409. T. Törndahl, M. Ottosson and J.-O. Carlsson, *J. Electrochem. Soc.*, **153**, C146 (2006).
410. G. G. Condorelli, G. Malandrino and I. Fragalà, *Chem. Mater.*, **7**, 2096 (1995).
411. G. G. Condorelli, G. Malandrino and I. Fragalà, *Chem. Vap. Deposition*, **5**, 21 (1999).
412. G. Malandrino, S. T. Finocchiaro, R. Lo Nigro, C. Bongiorno, C. Spinella and I. Fragalà, *Chem. Mater.*, **16**, 5559 (2004).
413. H.-H. Lee, C. Lee, Y.-L. Kuo and Y.-W. Yen, *Thin Solid Films*, **498**, 43 (2006).
414. Y. C. Zhang, J. Y. Tang, G. L. Wang, M. Zhang and X. Y. Hu, *J. Cryst. Growth*, **294**, 278 (2006).
415. P. Waltereit, O. Brandt, A. Trampert, H. T. Grahn, J. Menninger, M. Ramsteiner, M. Reiche and K. H. Ploog, *Nature*, **406**, 2355 (2002).
416. S. Pizzini, N. Butta, D. Narducci and M. Palladino, *J. Electrochem. Soc.*, **136**, 1945 (1989).
417. J. J. Aranovich, D. Golmaya, A. L. Fahrenbruch and R. H. Bube, *J. Appl. Phys.*, **51**, 4260 (1980).
418. G. S. Kino and R. S. Wager, *J. Appl. Phys.*, **44**, 1480 (1973).
419. T. Dietl, H. Ohno, F. Matsukura, J. Cibert and D. Ferrand, *Science*, **287**, 1019 (2000).
420. Y. Natsume, H. Sakata, T. Hirayama and H. Yanagida, *J. Appl. Phys.*, **72**, 4203 (1992).
421. T. Abe, Y. Kashiwaba, S. Onodera, F. Masuoka, A. Nakagawa, H. Endo, I. Niikura and Y. Kashiwaba, *J. Cryst. Growth*, **298**, 457 (2007).
422. Y. Kashiwaba, T. Abe, S. Onodera, F. Masuoka, A. Nakagawa, H. Endo, I. Niikura and Y. Kashiwaba, *J. Cryst. Growth*, **298**, 477 (2007).
423. A. J. C. Fiddes, K. Durose, A. W. Brinkman, J. Woods, P. D. Coates and A. J. Banister, *J. Cryst. Growth*, **159**, 210 (1996).
424. M. Iwasaki, Y. Inubushi and S. Ito, *J. Mater. Sci. Lett.*, **16**, 1503 (1997).
425. Y. Inubushi, R. Takami, M. Iwasaki, H. Tada and S. Ito, *J. Colloid Interface Sci.*, **200**, 220 (1998).
426. K. J. Hubbard and D. G. Schlom, *J. Mater. Res.*, **11**, 2757 (1996).
427. G. Bonnet, M. Lachkar, J. P. Larpin and J. C. Colson, *Thin Solid Films*, **261**, 31 (1995).
428. M. Hong, J. Kwo, A. R. Kortan, J. P. Mannaerts and A. M. Sergent, *Science*, **283**, 1897 (1999).
429. M. Tiitta and L. Niinistö, *Chem. Vap. Deposition*, **3**, 167 (1997).
430. J. Päiväsaari, M. Putkonen and L. Niinistö, *Thin Solid Films*, **472**, 275 (2005).
431. R. Si, Y.-W. Zhang, H.-P. Zhou, L.-D. Sun and C.-H. Yan, *Chem. Mater.*, **19**, 18 (2007).
432. J. T. Lim, S. T. Hong, J. C. Lee and I.-M. Lee, *Bull. Korean Chem. Soc.*, **17**, 1023 (1996).
433. Y. Shiokawa, R. Amano, A. Nomura and M. Yagi, *J. Radioanal. Nucl. Chem.*, **152**, 373 (1991).
434. P. A. Weyrich, H. Trevino, W. F. Holderich and W. M. H. Sachtler, *Appl. Catal. A: General*, **163**, 31 (1997).
435. B. C. H. Steele, *Ceram. Int.*, **19**, 269 (1993).
436. P. F. Wahid, K. B. Sundaram and P. J. Sisk, *Opt. Laser Technol.*, **24**, 263 (1992).
437. N. Katuta, N. Morishima, M. Kotobuki, T. Iwase, T. Mizushima, Y. Sato and S. Matsuura, *Appl. Surf. Sci.*, **121/122**, 408 (1997).
438. J. M. Tranquada, S. M. Heald, A. R. Moodenbaugh, G. Liang and M. Croft, *Nature*, **337**, 720 (1989).
439. M. Becht, T. Gerfin and K.-H. Dahmen, *Chem. Mater.*, **5**, 137 (1993).
440. H. Mölsä and L. Niinistö, *Mater. Res. Soc. Symp. Proc.*, **335**, 341 (1994).
441. Z. Lu, R. Hiskes, S. A. DiCarolis, A. Nel, R. K. Route and R. S. Feigelson, *J. Cryst. Growth*, **156**, 227 (1995).
442. T. Ami and M. Suzuki, *Mater. Sci. Eng. B*, **54**, 84 (1998).
443. M. Pan, G. Y. Meng, H. W. Xin, C. S. Chen, D. K. Peng and Y. S. Lin, *Thin Solid Films*, **324**, 89 (1998).

444. W. B. Carter, G. W. Book, T. A. Polley, D. W. Stollberg and J. M. Hampikian, *Thin Solid Films*, **347**, 25 (1999).
445. D. Barreca, A. Gasparotto, E. Tondello, C. Sada, S. Polizzi and A. Benedetti, *Chem. Vap. Deposition*, **9**, 199 (2003).
446. J. Päiväsaari, M. Putkonen and L. Niinistö, *J. Mater. Chem.*, **12**, 1828 (2002).
447. K. D. Pollard, H. A. Jenkins and R. J. Puddephatt, *Chem. Mater.*, **12**, 701 (2000).
448. H. Z. Song, Y. Z. Jiang, C. R. Xia, G. Y. Meng and D. K. Peng, *J. Cryst. Growth*, **250**, 423 (2003).
449. H. Z. Song, H. B. Wang, J. Zhang, D. K. Peng and G. Y. Meng, *Mater. Res. Bull.*, **37**, 1487 (2002).
450. T. Omata, S. Sasai, Y. Goto, M. Ueda and S. Otsuka-Yao-Matsuo, *J. Electrochem. Soc.*, **153**, A2269 (2006).
451. A. Kosola, J. Päiväsaari, M. Putkonen and L. Niinistö, *Thin Solid Films*, **479**, 152 (2005).
452. Y. Tasaki, M. Satoh, S. Yoshizawa, H. Kataoka and H. Hidaka, *Jpn. J. Appl. Phys.*, **36**, 6871 (1997).
453. K. Shalini and S. A. Shivashankar, *Bull. Mater. Sci.*, **28**, 49 (2005).
454. M. P. Singh, S. A. Shivashankar, *J. Cryst. Growth*, **276**, 148 (2005).
455. S. Wang, W. Wang and Y. Qian, *Mater. Res. Bull.*, **35**, 2057 (2000).
456. J. Niinistö, N. Petrova, M. Putkonen, L. Niinistö, K. Arstila and T. Sajavaara, *J. Cryst. Growth*, **285**, 191 (2005).
457. M. P. Singh, C. S. Thakur, K. Shalini, S. Banerjee, N. Bhat and S. A. Shivashankar, *J. Appl. Phys.*, **96**, 5631 (2004).
458. J. Päiväsaari, M. Putkonen, T. Sajavaara and L. Niinistö, *J. Alloys Compd.*, **374**, 124 (2004).
459. T. T. Van and J. P. Chang, *Appl. Surf. Sci.*, **246**, 250 (2005).
460. M. P. Singh, C. S. Thakur, K. Shalini, N. Bhat and S. A. Shivashankar, *Appl. Phys. Lett.*, **83**, 2889 (2003).
461. H. M. Ismail, *Colloids Surf. A, Physicochem. Eng. Aspects*, **97**, 247 (1995).
462. R. Si, Y.-W. Zhang, H.-P. Zhou, L.-D. Sun and C.-H. Yan, *Chem. Mater.*, **19**, 18 (2007).
463. E. Celik and Y. S. Hascicek, *Mater. Sci. Eng. B*, **96**, 300 (2002).
464. T. Sreethawong, S. Chavadej, S. Ngamsinlapasathian and S. Yoshikawa, *J. Colloid Interface Sci.*, **300**, 219 (2006).
465. J. G. Bednorz and K. A. Müller, *Z. Phys. B*, **64**, 189 (1986).
466. M. K. Wu, F. R. Ashburn, C. J. Torng, P. H. Hor, R. L. Meng, L. Gao, Z. J. Huang, Y. Q. Wang and C. W. Chu, *Phys. Rev. Lett.*, **58**, 908 (1987).
467. H. Maeda, Y. Tanaka, M. Fukutomi and T. Asano, *Jpn. J. Appl. Phys.*, **27**, L209 (1988).
468. Z. Z. Sheng and A. M. Hermann, *Nature*, **332**, 138 (1988).
469. H. Zama, N. Tanaka and T. Morishita, *J. Cryst. Growth*, **221**, 440 (2000).
470. H. Zama, N. Tanaka and T. Morishita, *Mater. Sci. Eng.*, **B54**, 104 (1998).
471. L. Klippe and G. Wahl, *J. Alloys Compd.*, **251**, 249 (1997).
472. G. Malandrino, G. G. Condorelli, G. Lanza, I. L. Fragalà, U. Scotti di Uccio and M. Valentino, *J. Alloys Compd.*, **251**, 332 (1997).
473. G. Malandrino, L. M. S. Perdicaro, I. L. Fragalà, A. M. Testa and D. Fiorani, *Chem. Mater.*, **16**, 608 (2004).
474. G. Malandrino, A. M. Borzi, I. L. Fragalà, A. Andreone, A. Cassinese and G. Pica, *J. Mater. Chem.*, **12**, 3728 (2002).
475. R. J. McNeely, J. A. Belot, B. J. Hinds, T. J. Marks, J. L. Schindler, M. P. Chudzik, C. R. Kannewurf, X. F. Zhang and D. J. Miller, *Appl. Phys. Lett.*, **71**, 1243 (1997).
476. A. Suzuki and K. Maki, *Chem. Vap. Deposition*, **12**, 608 (2006).
477. J. Ni, L. Wang, Y. Yang, H. Yan, S. Jin, T. J. Marks, J. R. Ireland, C. R. Kannewurf, *Inorg. Chem*, **44**, 6071 (2005).
478. A. Wang, J. Dai, J. Cheng, M. P. Chudzik, T. J. Marks, R. P. H. Chang and C. R. Kannewurf, *Appl. Phys. Lett.*, **73**, 327 (1998).
479. A. R. Kaul, O. Y. Gorbenko, A. N. Botev and L. I. Burova, *Superlattices and Microstructures*, **38**, 272 (2005).
480. H. Funakubo, *Top. Appl. Phys.*, **93**, 95 (2004).
481. O. S. Kwon, S. K. Kim, M. Cho, C. S. Hwang and J. Jeong, *J. Electrochem. Soc.*, **152**, C229 (2005).

482. J. Peña, A. Martínez, F. Conde, J. M. González-Calbet and M. Vallet-Regí, *Solid State Ionics*, **101–103**, 183 (1997).
483. A. N. Golubenko, L. V. Yakovkina, T. P. Smirnova, Y. V. Shubin, N. B. Morozova and V. S. Danilovich, *Inorg. Mater.*, **40**, 516 (2004).
484. K. Itoh and O. Matsumoto, *Thin Solid Films*, **345**, 29 (1999).
485. T. Watanabe, S. Hoffmann-Eifert, C. S. Hwang and R. Waser, *J. Electrochem. Soc.*, **153**, F199 (2006).
486. T. Watanabe, S. Hoffmann-Eifert, S. Mi, C. Jia, R. Waser and C. S. Hwang, *J. Appl. Phys.*, **101**, O14114 (2007).
487. T. Shiosaki, S. Okamura, M. Miyake, Y. Otani and N. Abe, *Ferroelectrics*, **293**, 69 (2003).
488. M.-K. Song and S.-W. Rhee, *J. Electrochem. Soc.*, **153**, G992 (2006).
489. H. B. Wang, C. R. Xia, G. Y. Meng and D. K. Peng, *Mater. Lett.*, **44**, 23 (2000).
490. E. B. Ramírez, A. Huanosta, J. P. Sebastian, L. Huerta, A. Ortiz and J. C. Alonso, *J. Mater. Sci.*, **42**, 901 (2007).
491. C. Dubourdieu, S. B. Kang, Y. Q. Li, G. Kulesha and B. Gallois, *Thin Solid Films*, **339**, 165 (1999).
492. M. Putkonen, T. Sajavaara, J. Niinistö, L.-S. Johansson and L. Niinistö, *J. Mater. Chem.*, **12**, 442 (2002).
493. H. Song, C. Xia, Y. Jiang, G. Meng and D. Peng, *Mater. Lett.*, **57**, 3833 (2003).
494. Y. Jiang, J. Gao, M. Liu, Y. Wang and G. Meng, *Solid State Ionics*, **177**, 3405 (2007).
495. G. Garcia, J. Caro, J. Santiso, J. A. Pardo, A. Figueras and A. Abrutis, *Chem. Vap. Deposition*, **9**, 279 (2003).
496. R. Tu, T. Kimura and T. Goto, *Surf. Coat. Technol.*, **187**, 238 (2004).
497. M. H. Siadati, T. L. Ward, J. Martus, P. Atanasova, C. Xia and R. W. Schwartz, *Chem. Vap. Deposition*, **3**, 311 (1997).
498. C. Xia, T. L. Ward, C. Xu, P. Atanasova and R. W. Schwartz, *J. Electrochem. Soc.*, **145**, L4 (1998).
499. M. V. Cabañas, C. V. Ragel, F. Conde, J. M. González-Calbet and M. Vallet-Regí, *Solid State Ionics*, **101–103**, 191 (1997).
500. M. Nieminen, T. Sajavaara, E. Rauhala, M. Putkonen and L. Niinistö, *J. Mater. Chem.*, **11**, 2340 (2001).
501. G. Malandrino, A. Frassica and I. L. Fragalà, *Chem. Vap. Deposition*, **3**, 306 (1997).
502. G. Malandrino and I. L. Fragalà, *Chem. Mater.*, **10**, 3765 (1998).
503. M. Bizarro, J. C. Alonso and A. Ortiz, *Mater. Sci. Semicond. Proc.*, **9**, 1090 (2006).
504. M. Nieminen, S. Lehto and L. Niinistö, *J. Mater. Chem.*, **11**, 3148 (2001).
505. C. L. Dezelah IV, P. Myllymäki, J. Päiväsaari, K. Arstila, L. Niinistö and C. H. Winter, *J. Mater. Chem.*, **17**, 1308 (2007).
506. D. Barreca, G. A. Rizzi and E. Tondello, *Thin Solid Films*, **333**, 35 (1998).
507. G. L. Bertrand, G. Caboche, L.-C. Dufour, *Solid State Ionics*, **129**, 219 (2000).
508. H. Seim, M. Nieminen, L. Niinistö, H. Fjellvag and L.-S. Johansson, *Appl. Surf. Sci.*, **112**, 243 (1997).
509. H. Seim, H. Mölsä, M. Nieminen, H. Fjellvag and L. Niinistö, *J. Mater. Chem.*, **7**, 449 (1997).
510. P. Myllymäki, M. Nieminen, J. Niinistö, M. Putkonen, K. Kukli and L. Niinistö, *J. Mater. Chem.*, **16**, 563 (2006).
511. M. Andrieux, V. Viallet, M. Le Stum, L. Rapenne, M. Ghysel, C. Haut and M. Condat, *Appl. Surf. Sci.*, **222**, 351 (2004).
512. M. Vucinic-Vasic, B. Antic, A. Kremenovic, A. S. Nikolic, J. Blanusa, S. Rakic, V. Spasojevic and A. Kapor, *J. Alloys Compd.*, **428**, 322 (2007).
513. H. T. Zhang, G. Wu and X. H. Chen, *Mater. Chem. Phys.*, **101**, 415 (2007).

Author Index

This author index is designed to enable the reader to locate an author's name and work with the aid of the reference numbers appearing in the text. The page numbers are printed in normal type in ascending numerical order, followed by the reference numbers in parentheses. The numbers in *italics* refer to the pages on which the references are actually listed.

Subject Index

Entries are in letter-by-letter alphabetical order ignoring spaces and punctuation marks. Page numbers in *italic* refer to Figures and Tables not included in the relevant page ranges.

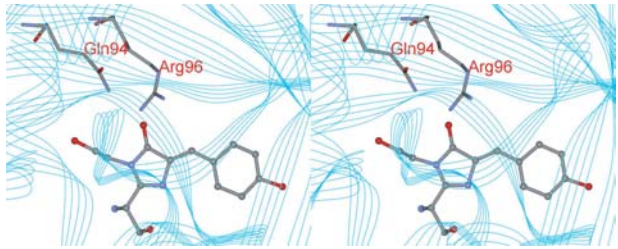

PLATE I; Section II.D, FIGURE 2

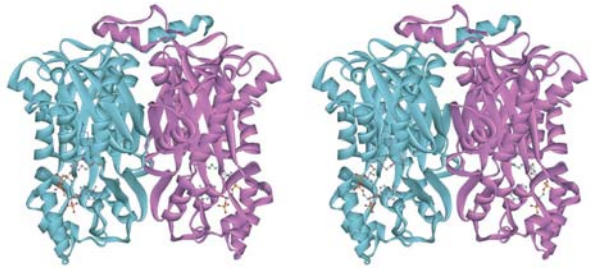

PLATE II; Section II.D, FIGURE 3A

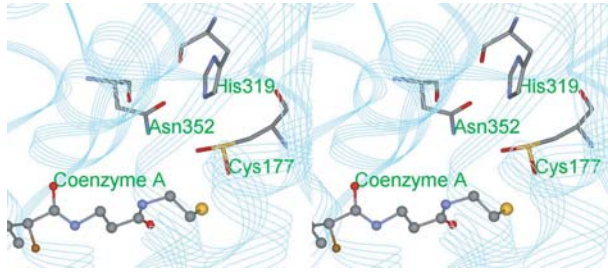

PLATE III; Section II.D, FIGURE 3B

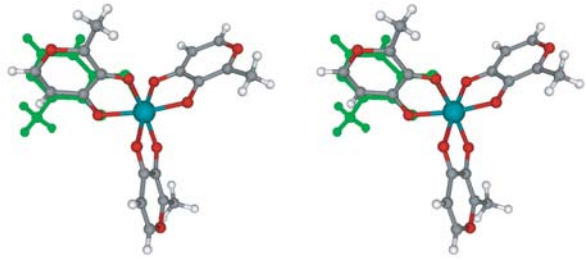

PLATE IV; Section III.B.1.d, structure **64**

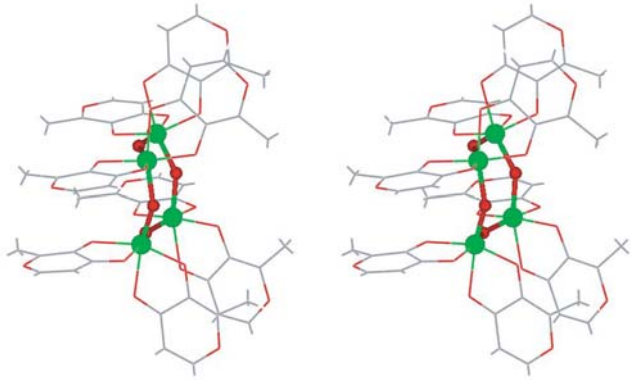

PLATE V; Section III.B.1.d, structure **66′**

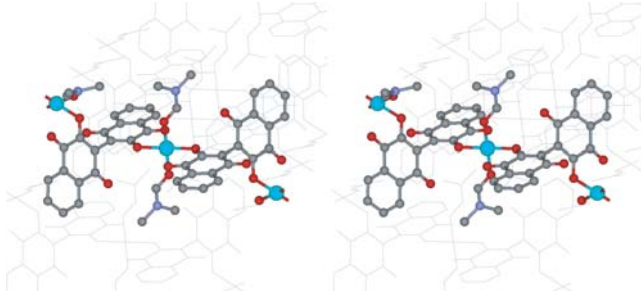

PLATE VI; Section III.B.1.f, structure **76**

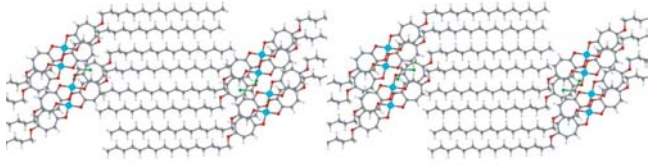

PLATE VII; Section III.B.1.g, structure **82**

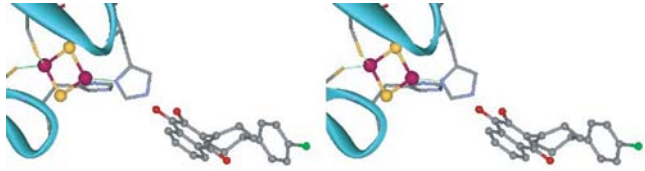

PLATE VIII; Section III.B.2.d, FIGURE 5A

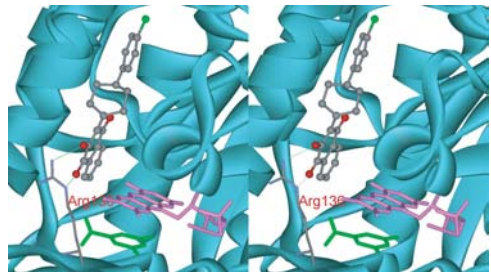

PLATE IX; Section III.B.2.d, FIGURE 5B

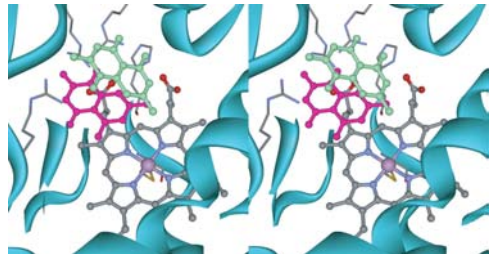

PLATE X; Section IV, FIGURE 6

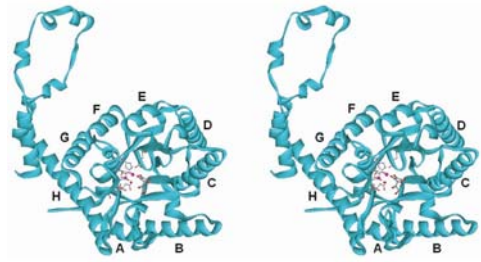

PLATE XI; Section IV.A.1, FIGURE 7A

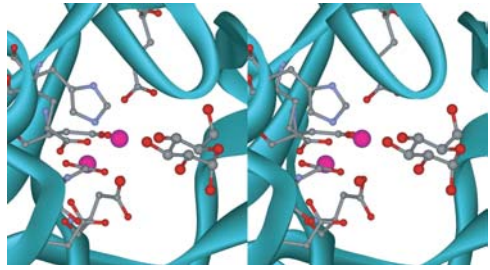

PLATE XII; Section IV.A.1, FIGURE 7B

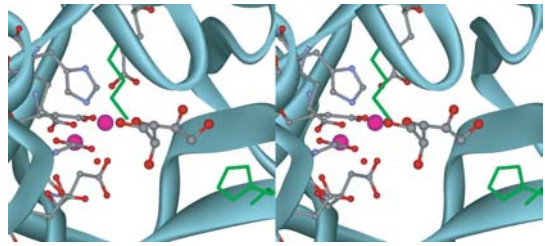

PLATE XIII; Section IV.A.1, FIGURE 7C

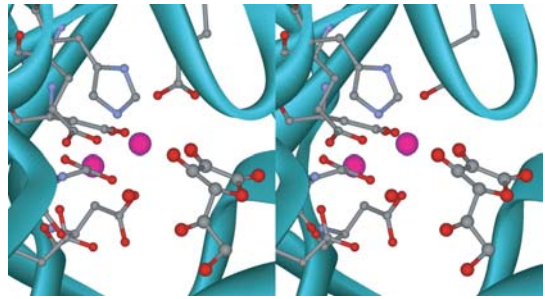

PLATE XIV; Section IV.A.1, FIGURE 7D

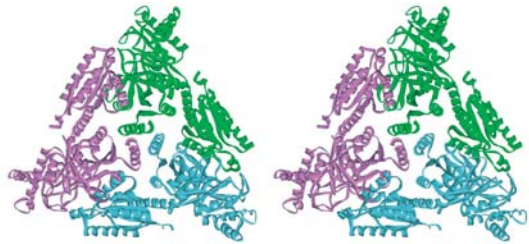

PLATE XV; Section IV.A.1, FIGURE 8A

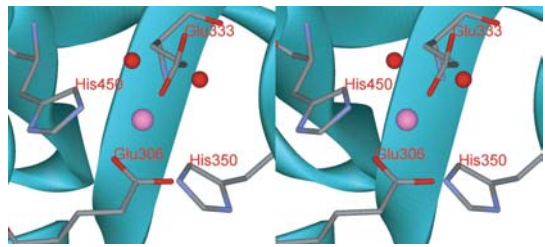

PLATE XVI; Section IV.A.1, FIGURE 8B

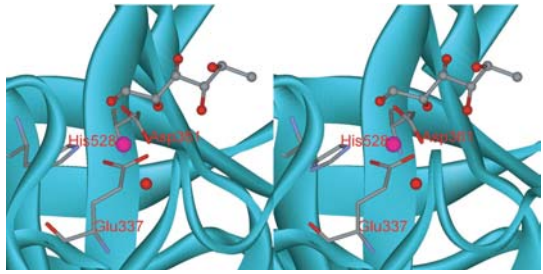

PLATE XVII; Section IV.A.1, FIGURE 8C

PLATE XVIII; Section IV.A.1, FIGURE 9A

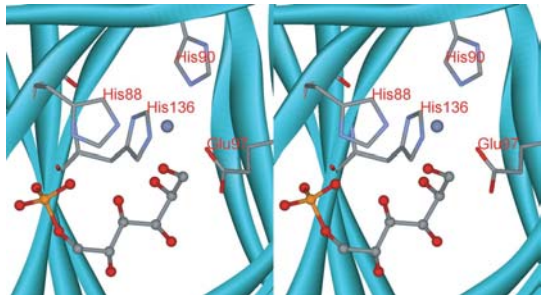

PLATE XIX; Section IV.A.1, FIGURE 9B

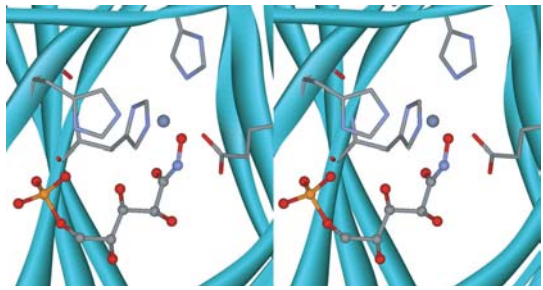

PLATE XX; Section IV.A.1, FIGURE 9C

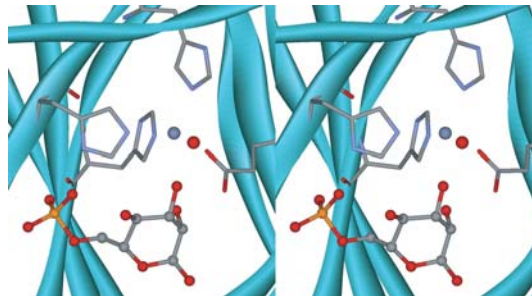

PLATE XXI; Section IV.A.1, FIGURE 9D

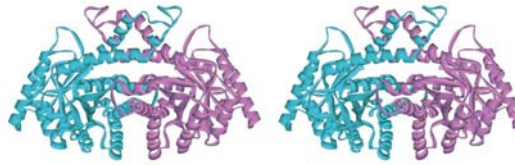

PLATE XXII; Section IV.A.2, FIGURE 10A

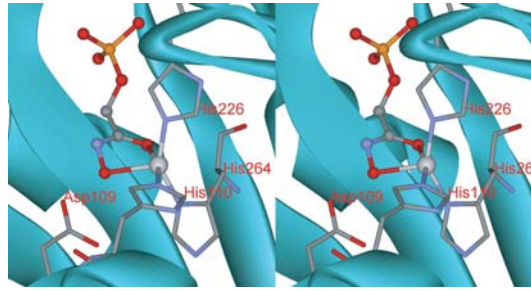

PLATE XXIII; Section IV.A.2, FIGURE 10B

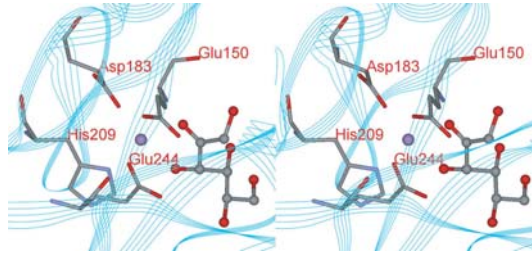

PLATE XXIV; Section IV.A.2, FIGURE 11

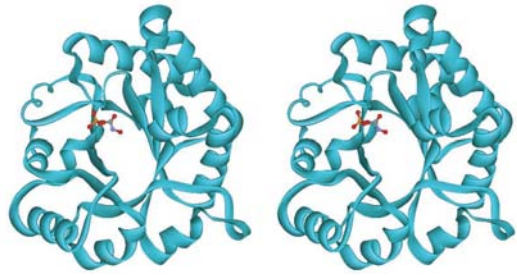

PLATE XXV; Section IV.A.3, FIGURE 12

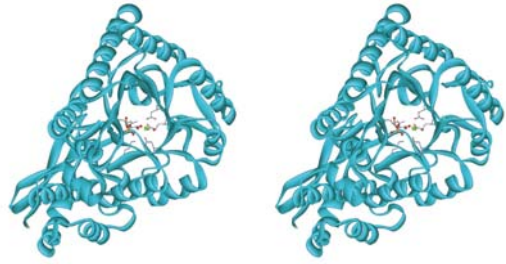

PLATE XXVI; Section IV.A.4, FIGURE 13A

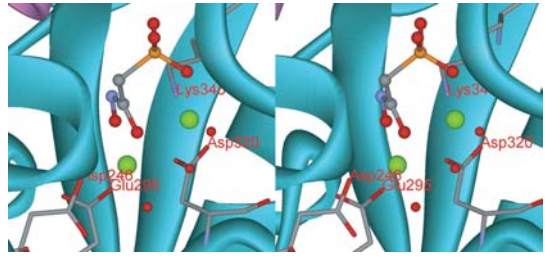

PLATE XXVII; Section IV.A.4, FIGURE 13B

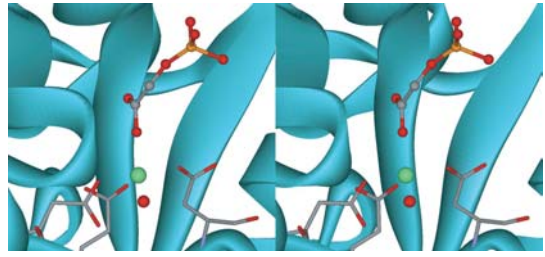

PLATE XXVIII; Section IV.A.4, FIGURE 13C

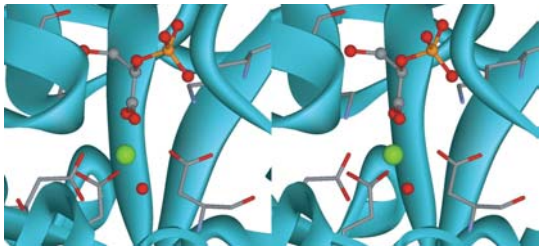

PLATE XXIX; Section IV.A.4, FIGURE 13D

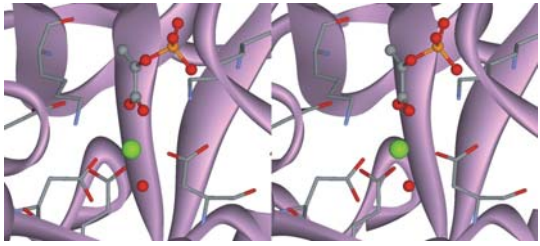

PLATE XXX; Section IV.A.4, FIGURE 13E

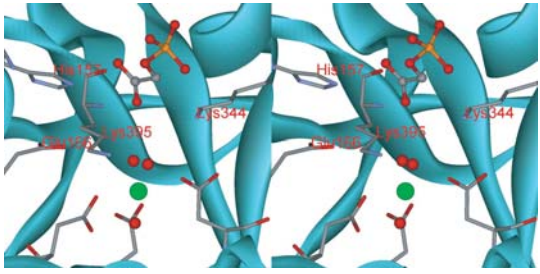

PLATE XXXI; Section IV.A.4, FIGURE 13F

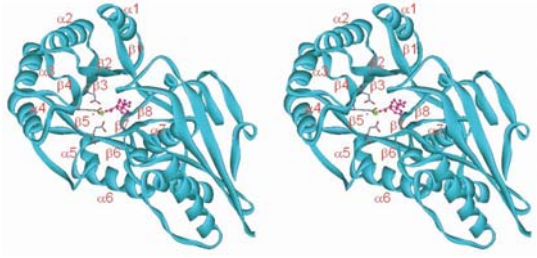

PLATE XXXII; Section IV.A.4, FIGURE 14A

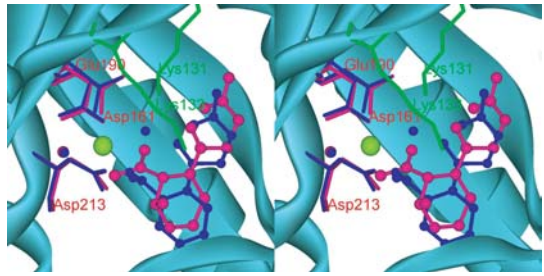

PLATE XXXIII; Section IV.A.4, FIGURE 14B

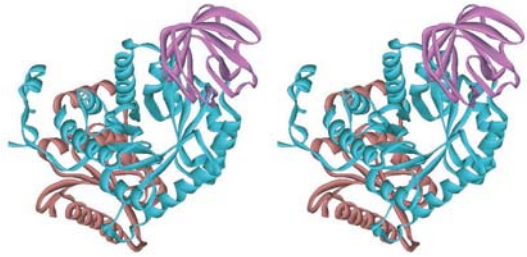

PLATE XXXIV; Section IV.A.5, FIGURE 15A

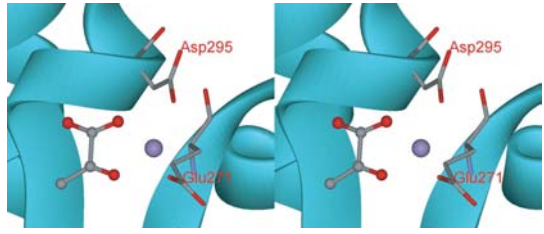

PLATE XXXV; Section IV.A.4, FIGURE 15B

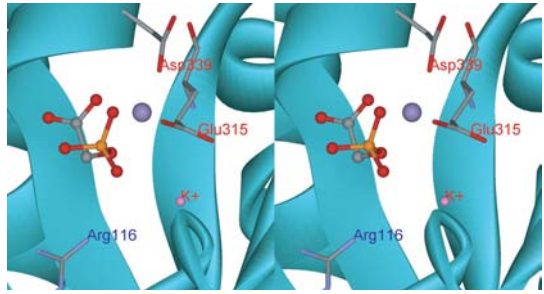

PLATE XXXVI; Section IV.A.4, FIGURE 15C

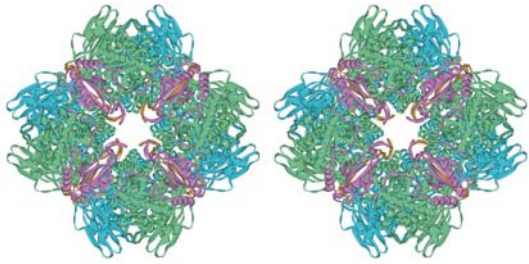

PLATE XXXVII; Section IV.B, FIGURE 16A

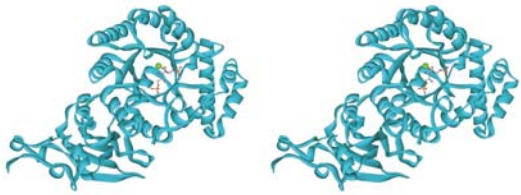

PLATE XXXVIII; Section IV.B, FIGURE 16B

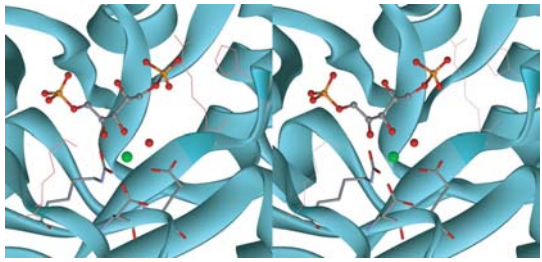

PLATE XXXIX; Section IV.B, FIGURE 16C

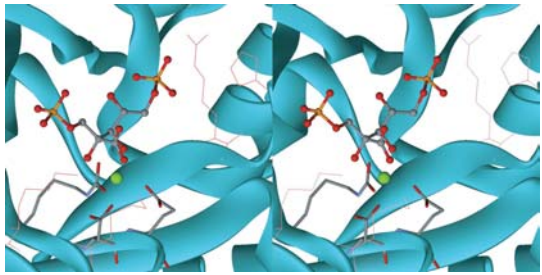

PLATE XL; Section IV.B, FIGURE 16D

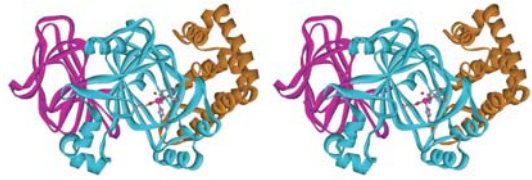

PLATE XLI; Section IV.C, FIGURE 18A

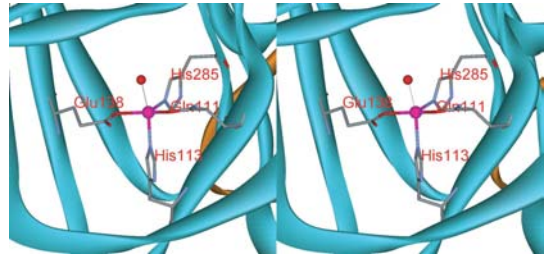

PLATE XLII; Section IV.C, FIGURE 18B

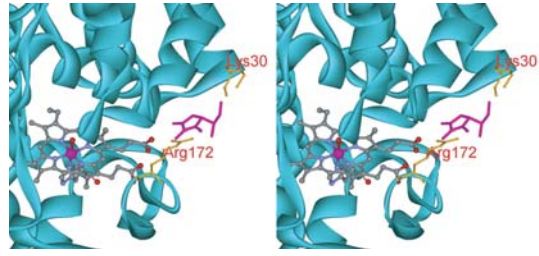

PLATE XLIII; Section IV.C, FIGURE 19

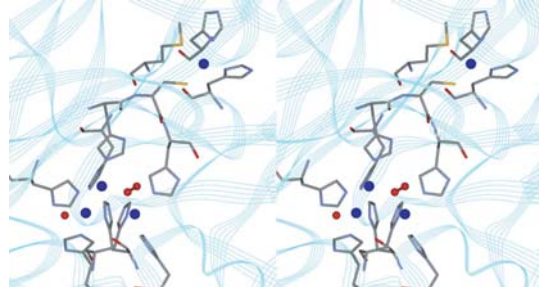

PLATE XLIV; Section IV.C, FIGURE 20

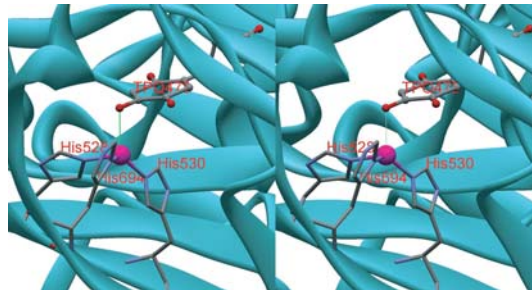

PLATE XLV; Section IV.D, FIGURE 21

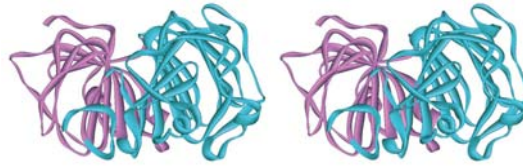

PLATE XLVI; Section IV.E, FIGURE 24A

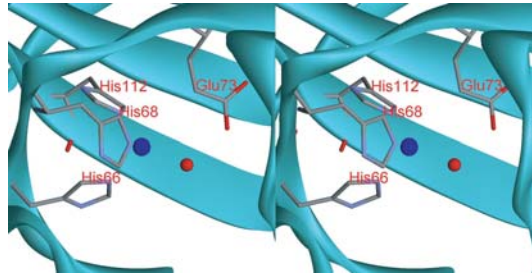

PLATE XLVII; Section IV.E, FIGURE 24B

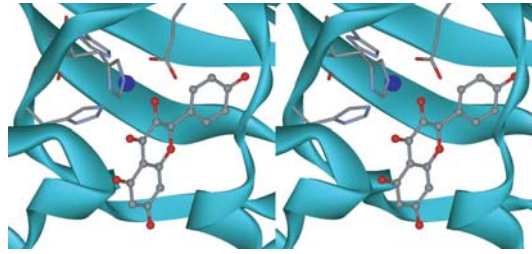

PLATE XLVIII; Section IV.E, FIGURE 24C

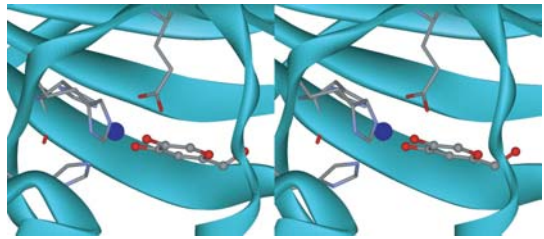

PLATE XLIX; Section IV.E, FIGURE 24D

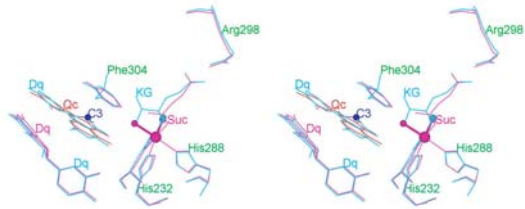

PLATE L; Section IV.E, FIGURE 24E

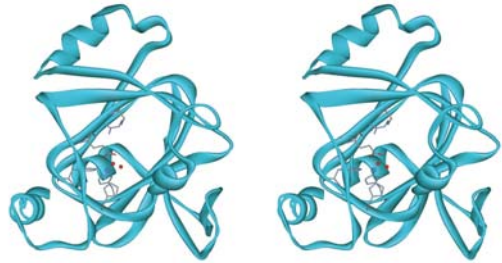

PLATE LI; Section IV.F, FIGURE 27A

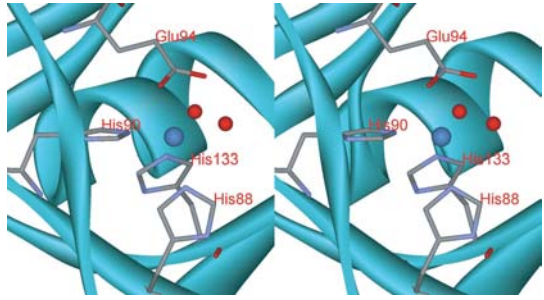

PLATE LII; Section IV.F, FIGURE 27B

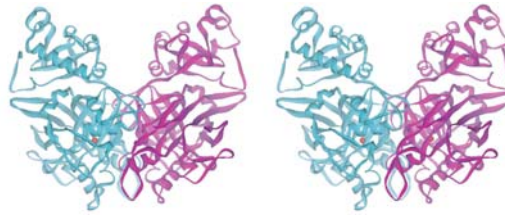

PLATE LIII; Section IV.G.1, FIGURE 29A

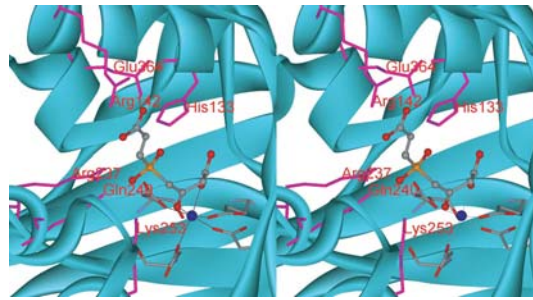

PLATE LIV; Section IV.G.1, FIGURE 29B

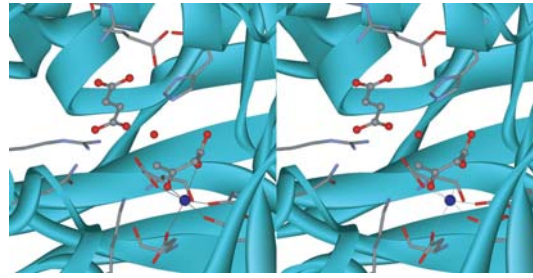

PLATE LV; Section IV.G.1, FIGURE 29C

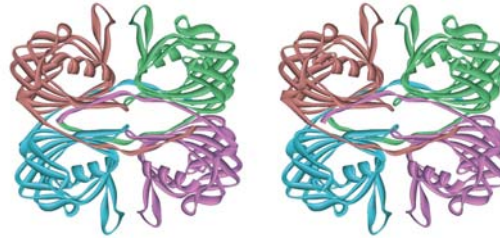

PLATE LVI; Section IV.G.2, FIGURE 30A

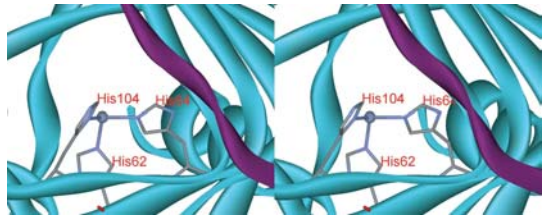

PLATE LVII; Section IV.G.2, FIGURE 30B

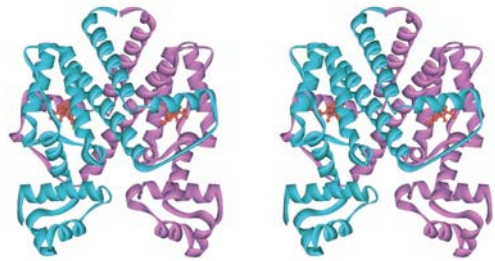

PLATE LVIII; Section IV.H, FIGURE 31A

PLATE LIX; Section IV.H, FIGURE 31B

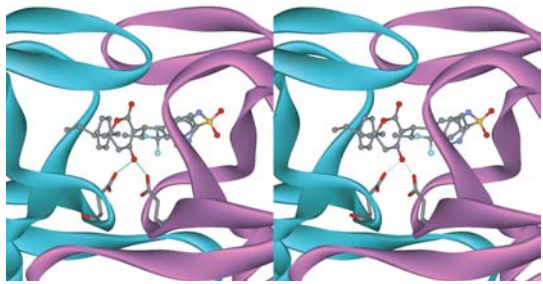

PLATE LX; Section IV.I, FIGURE 32

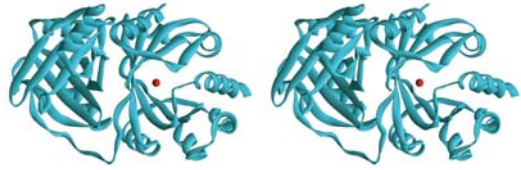

PLATE LXI; Section IV.I, FIGURE 33A

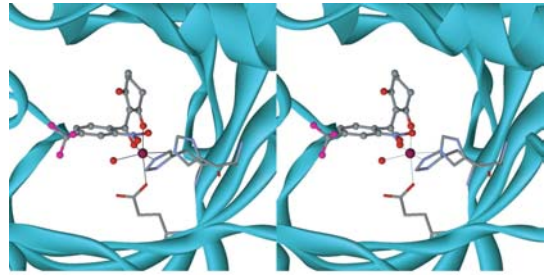

PLATE LXII; Section IV.I, FIGURE 33B

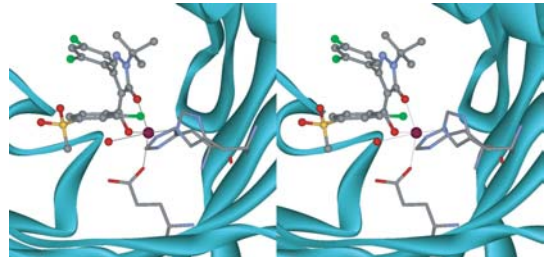

PLATE LXIII; Section IV.I, FIGURE 33C

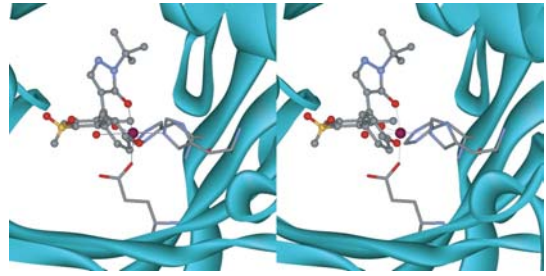

PLATE LXIV; Section IV.I, FIGURE 33D